UNIVERSITY OF CALIFORNIA
SCRIPPS INSTITUTION OF OCEANOGRAPHY

CONTRIBUTIONS

1956

APR 1958
LIBRARY
POFI
FISH & WILDLIFE
SERVICE

PERIODICAL

Calif. Univ. S.I.O.
Contributions

1956

LIBRARY
BUR. OF COMM. FISH.
HON. BIOL. LAB.

UNIVERSITY OF CALIFORNIA
SCRIPPS INSTITUTION OF OCEANOGRAPHY

CONTRIBUTIONS

1956

2090^60

This volume contains contributions from the Scripps Institution of Oceanography which appeared during 1956 in publications other than *Bulletins of the Scripps Institution of Oceanography.*

APR 1958
LIBRARY
POFI
FISH & WILDLIFE
SERVICE

THE LIBRARY
UNIVERSITY OF CALIFORNIA
SCRIPPS INSTITUTION OF OCEANOGRAPHY
LA JOLLA, CALIFORNIA

February 1958

PHOTOLITHOPRINTED BY CUSHING - MALLOY, INC.
ANN ARBOR, MICHIGAN, UNITED STATES OF AMERICA
1958

SCRIPPS INSTITUTION OF OCEANOGRAPHY
CONTRIBUTIONS, NEW SERIES
1956

Contrib. Number		Page Number
818	**STEWART, H. B., JR.** Contorted sediments in a modern coastal lagoon explained by laboratory experiments. American Association of Petroleum Geologists, Bulletin, v.40, no.1, 1956. pp.153-161.	1
819	**HUBBS, CARL L.** Scripps Institution of Oceanography, University of California. A.I.B.S. Bulletin, v.6, no.1, 1956. pp.11-13	11
820	**MAXWELL, A. E. and ROGER REVELLE.** Heat flow through the Pacific Ocean basin. Publications du Bureau Central Seismologique, Travaux Scientifiques, Series A, fascicule 19. pp.394-405	13
821	**SNODGRASS, FRANK E.** Mark IX shore wave recorder. Conference on Coastal Engineering Instruments, Proceedings. 1st, 1955. Council on Wave Research. Engineering Foundation. 1956. pp. 61-100.	25
822	**MENZIES, ROBERT J., THOMAS E. BOWMAN and FRANKLIN G. ALVERSON.** Studies of the biology of the fish parasite *Livoneca convexa* Richardson (Crustacea, Isopoda, Cymothoidae)	65
823	**ECKART, CARL and HORACE G. FERRIS.** Equations of motion of the ocean and atmosphere. Review of Modern Physics, v.28, no.1, 1956. pp.48-52	85
824	**ALEEM, ANWAR ABDEL.** Quantitative underwater study of the benthic communities inhabiting kelp beds off California. Science, v.123, no.3188, 1956. pp.183	91
825	**MENZIES, ROBERT J. and MILTON A. MILLER.** A redescription of the marine isopod crustacean "*Exosphaeroma*" *Faxoni* Richardson from Texas. Bulletin of Marine Science of the Gulf and Caribbean, v.5, no.4, 1955. pp.292-296.	93
826	**MUNK, WALTER, FRANK SNODGRASS, and GEORGE CARRIER.** Edge waves on the continental shelf. Science, v.123, no.3187, 1956. pp.127-132	99
827	**VAN DORN, WILLIAM G.** A portable tsunami recorder. American Geophysical Union, Transactions, v.37, no.1, 1956. pp.27-30.	105
828	**FERGUSON WOOD, E. J.** Diatoms in the ocean deeps. Pacific Science, v.10, no.4, 1956. pp.377-381	109
829	**JOHNSON, MARTIN W. and ROBERT J. MENZIES.** Migratory habits of the marine gribble *Limnoria tripunctata* Menzies in San Diego harbor, California. Biological Bulletin, v.110, no.1, 1956. pp.54-68.	115

Contrib. Number		Page Number
830	HAMILTON, EDWIN L. Sunken islands of the Mid-Pacific mountains. Geological Society of America, Memoir No.64. March, 1956. . .	*
831	KUNO, HISASHI, ROBERT L. FISHER and NORIYUKI NASU. Rock fragments and pebbles dredged near Jimmu seamount, northwestern Pacific. Deep-Sea Research, v.3, no.2, 1956. pp.126-133	131
832	CURRAY, JOSEPH R. The analysis of two-dimensional orientation data. Journal of Geology, v.64, no.2, 1956. pp.117-131.	141
833	CLENDENNING, K. A. and F. T. HAXO. Photosynthetic induction in marine algae. Canadian Journal of Botany, v.34, 1956. pp.214-230	157
834	BIEN, GEORGE S. and EDWARD D. GOLDBERG. The polarographic determination of ferrous and ferric iron in refractory minerals. Analytical Chemistry, v.28, no.1, 1956. pp.97-98	175
835	SHEPARD, FRANCIS P. Late Pleistocene and Recent history of the central Texas coast. Journal of Geology, v.64, no.1, 1956. pp.55-69	177
836	COX, CHARLES. Optical measurements of sea surface roughness. Conference on Engineering Instruments, Proceedings. 1st, 1955. Council on Wave Research. Engineering Foundation. 1956. pp.1-15 . .	193
837	SNODGRASS, JAMES M. and ADRIAN F. RICHARDS. Observations of underwater volcanic acoustics at Barcena volcano, San Benedicto Island, Mexico, and in Shelikof Strait, Alaska. American Geophysical Union, Transactions, v.37, no.1, 1956. pp.97-104	209
838	HUBBS, CARL L. Back from oblivion - Guadalupe fur seal: still a living species. Pacific Discovery, v.9, no.6, 1956. pp.14-21.	217
839	HUBBS, CARL L. Ways of stabilizing zoological nomenclature. International Congress of Zoology, Proceedings. XIV, Copenhagen, 1953. Copenhagen, 1956. pp.548-553.	227
839a	HEDGPETH, JOEL W. The population of hypersaline and relict lagoons. International Congress of Zoology, Proceedings. XIV, Copenhagen, 1953. Copenhagen, 1956. pp.452-453	235
839b	BUZZATI-TRAVERSO, ADRIANO A. On the growth of populations. International Congress of Zoology, Proceedings. XIV, Copenhagen, 1953. Copenhagen, 1956. pp.66-75	240
840	PARKER, ROBERT H. Macro-invertebrate assemblages as indicators of sedimentary environments in the east Mississippi delta region. American Association of Petroleum Geologists, Bulletin, v.40, no.2, 1956. pp.295-376	251
841	INMAN, D. L. and NORIYUKI NASU. Orbital velocity associated with wave action near the breaker zone. U.S. Army. Corps of Engineers. Beach Erosion Board. Technical Memorandum No.79. 1956 . .	333
842	CROMWELL, TOWNSEND and JOSEPH L. REID, JR. A study of oceanic fronts. Tellus, v.8, no.1, 1956. pp.94-101.	415

* Not available for exchange.

Contrib. Number		Page Number
843	SUESS, HANS E. Absolute chronology of the last glaciation. Science, v.123, no.3192, 1956. pp.355-357.	425
✓ 844	HORRER, PAUL L. and ROGER REVELLE. The ocean off the California coast. In "California and the Southwest", edited by Clifford Zierer. New York, Wiley and Sons, 1956	429
845	REX, ROBERT W. Microrelief produced by sea ice grounding in the Chukchi Sea near Barrow, Alaska. Arctic. (Journal of the Arctic Institute of North America), v.8, no.3, 1955. pp.177-186	447
✓ 846	KNAUSS, JOHN A. An estimate of the effect of turbulence in the ocean on the propagation of sound. Acoustical Society of America, Journal, v.28, no.3, 1956. pp.443-446.	457
847	RAKESTRAW, NORRIS W. Hermann Wattenberg: a pioneer in a new field of exploration. Journal of Chemical Education, v.33, 1956. pp.217-222	462
848	RUDNICK, PHILIP. The spectrum of the variation in latitude. American Geophysical Union, Trans., v.37, no.2, 1956. pp.137-142	469
849	BEAL, M. ALLAN and FRANCIS P. SHEPARD. A use of roundness to determine depositional environments. Journal of Sedimentary Petrology, v.26, no.1, 1956. pp.49-60	475
850	MUNK, WALTER. Polar wandering: a marathon of errors. Nature, v.177, no.4508, 1956. pp.551-554.	487
✓ 851	DUNTLEY, S. Q. and S. S. BALLARD. A program of research in the visual detectability of distant objects. In "Problems in Contemporary Optics". Florence, Italy. National Optical Institute of Italy. 1956. pp.575-584	497
852	MORITA, RICHARD Y. and CLAUDE E. ZOBELL. Effect of hydrostatic pressure on the succinic dehydrogenase system in *Escherichia coli.* Journal of Bacteriology, v.71, no.6, 1956. pp.668-672	508
853	GROVES, GORDON W. Periodic variation of sea level induced by equatorial waves in the Easterlies. Deep-Sea Research, v.3, no.4, 1956. pp.248-252	513
854	INMAN, D. L. and G. A. RUSNAK. Changes in sea level on the beach and shelf at La Jolla, California. U.S. Army. Corps of Engineers. Beach Erosion Board. Technical Memorandum no.82, 1956.	519
855	REID, JOSEPH L., JR. Observations of internal tides in October 1950. American Geophysical Union, Trans., v.37, no.3, 1956. pp.278-286	588
856	SHEPARD, F. P. and H. E. SUESS. Rate of postglacial rise of sea level. Science, v.123, no.3207, 1956. pp.1082-1083.	597
857	JOHNSON, MARTIN W. Plankton of the Beaufort and Chukchi Sea areas of the Arctic and its relation to the hydrography. Arctic Institute of North America, Technical Paper No.1, 1956.	599
858	EL WARDANI, SAYED A. Germanium in meteorites. Geochimica and Cosmochimica Acta, v.10, 1956. pp.321-322	631

Contrib. Number | Page Number

859 COX, CHARLES and WALTER MUNK. Slopes of the sea surface deduced from photographs of sun glitter. BULLETIN OF THE SCRIPPS INSTITUTION OF OCEANOGRAPHY, v.6, no.9, 1956. . . . . *

860 LEWIS, GEORGE and EDWARD D. GOLDBERG. X-ray fluorescence determination of barium, titanium, and zinc in sediments. Analytical Chemistry, v.28, no.8, 1956. pp.1282-1285. 633

861 RECHNITZER, ANDREAS B. Land birds at sea off southern California. Condor, v.58, no.5, 1956. pp.388-389 637

862 ZOBELL, CLAUDE E. and RICHARD Y. MORITA. Bacteria in the deep sea. In "Galathea Deep Sea Expedition, 1950-1952". Ed. by Brunn, Grieve, Milche, and Spärck. London, Allen and Unwin, Ltd., 1956. New York, Macmillan, 1957. pp.202-210 . . . . *

863 HUBBS, CARL and WALTER R. CROWE. Preliminary analysis of the American cyprinid fishes, seven new, referred to the genus *Hybopsis*, subgenus *Erimystax*. University of Michigan, Museum of Zoology, Occasional Papers, no.578, 1956 639

864 SILAS, E. G. The systematic position of the Indian cyprinid fish, *Cirrhinus fasciatus* Jerdon (1849), with a new name for *Barbus fasciatus* Bleeker (1853). Copeia, no.3, 1956. p.194 647

865 CRAIG, HARMON. Distribution, production rate, and possible solar origin of natural tritium. Physical Review, v.105, no.3, 1957. pp.1125-1127 649

866 RIEDEL, WILLIAM R. Sediment cores from the west Pacific. Radiolaria: a preliminary stratigraphy. Swedish Deep Sea Expedition, Reports. (Publication delayed) . . . . ---

867 MENARD, HENRY W. Archipelagic aprons. American Association of Petroleum Geologists, Bulletin, v.40, no.9, 1956. pp.2195-2210 651

868 SUESS, HANS E. Grundlagen und Ergebnisse der Radiokohlenstoff-Datierung. Angewandte Chemie, v.68, no.17-18, 1956. pp.540-546 667

869 HOLMES, ROBERT W. and THEODORE M. WIDRIG. The enumeration and collection of marine phytoplankton. Journal du Conseil, v.22, no.1, 1956. pp.21-32 675

870 LIMBAUGH, C. and W. J. NORTH. Fluorescent, benthic, Pacific coast coelenterates. Nature, v.178, 1956. pp.497-498 687

871 WOLFE, JACK B., RICHARD Y. MORITA, and HENRY I. NAKADA. Glucosamine degradation by *Escherichia coli*. I. Observations with resting cells and dry-cell preparations. Archives of Biochemistry and Biophysics, v.64, no.2, 1956. pp.480-488 689

872 NORTH, WHEELER. Scientific diving. Yale Scientific Magazine, v.31, no.3, 1956. pp.49-54 699

* Not available for exchange.

Contrib. Number — Page Number

873 BIERI, ROBERT. A method for the microscopic examination and manipulation of plankton on board ship. Journal du Conseil International pour l'Exploration de la Mer, v.22, no.1, 1956. pp.38-41. . . . 703

874 RIEDEL, WILLIAM R. and JULIUS SCHLOCKER. Radiolaria from the Franciscan group, Belmont, California. Micropaleontology, v.2, no.4, 1956. pp.357-360. 709

875 PHLEGER, FRED B Significance of living foraminiferal populations along the central Texas coast. Cushman Foundation for Foraminiferal Research, Contributions, v.7, pt.4, 1956. pp.106-151. 713

876 BULLARD, E. C., ROGER REVELLE, and A. E. MAXWELL. Heat flow through the deep-sea floor. In "Advances in Physics", v.3, 1956. pp.153-181. New York, Academic Press, 1956 . . . . *

877 PARKER, ROBERT H. and JOSEPH R. CURRAY. Fauna and bathymetry of banks on continental shelf, northwest Gulf of Mexico. American Association of Petroleum Geologists, Bulletin, v.40, no. 10, 1956. pp.2428-2439 761

878 JOHNSON, MARTIN W. The larval development of the California spiny lobster, *Panulirus interruptus* (Randall), with notes on *Panulirus gracilis* Streets. California Academy of Sciences, Proceedings, 4th Ser., v.29, no.1, 1956. pp.1-19 775

879 CURRAY, JOSEPH R. Dimensional grain orientation studies of recent coastal sands. American Association of Petroleum Geologists, Bulletin, v.40, no.10, 1956. pp.2440-2456 795

880 SNODGRASS, JAMES M. and JOHN H. CAWLEY, JR. Temperature and depth circuitry in a telerecording bathythermometer. National Electronics Conference, Proceedings, v.12, 1957. pp.74-82. 813

881 VOLKMANN, G. H., J. A. KNAUSS, and A. C. VINE. The use of parachute drogues in the measurement of subsurface ocean currents. American Geophysical Union, Transactions, v.37, no.5, 1956. pp.573-577. 823

882 FOX, DENIS L. Physical and chemical coloration in birds. Yale Scientific Magazine, v.31, no.1, 1956. pp.54, 57-58 829

883 RAITT, RUSSELL W. Seismic-refraction studies of the Pacific Ocean basin. I. Crustal thickness of the central equatorial Pacific. Geological Society of America, Bulletin, v.67, no.12, pt.1, 1956. pp.1623-1640 833

884 VAN DORN, W. G. Large-volume water samplers. American Geophysical Union, Transactions, v.37, no.6, 1956. pp.682-684 852

885 ZOBELL, CLAUDE E. Bacteria - annotated bibliography. In "Treatise on Marine Ecology and Paleoecology" v.2, Paleoecology. Geological Society of America, Memoir 67, 1957. pp.693-698 855

* Not available for exchange.

Contrib. Number		Page Number
886	LIEBERMANN, LEONARD. On the pressure dependence of sound absorption in liquids. Acoustical Society of America, Journal, v.28, no.6, 1956. pp.1253-1255.	861
887	SHEPARD, FRANCIS P. Marginal sediments of the Mississippi delta. American Association of Petroleum Geologists, Bulletin, v.40, no.11, 1956. pp.2537-2623	865
888	RECHNITZER, ANDREAS B. Foraging habits and local movements of the wood ibis in San Diego county, California. Condor, v.58, no.6, 1956. pp.427-432	957
889	LIEBERMANN, LEONARD. Extremely low-frequency electromagnetic waves. I. Reception from lightning. II. Propagation properties. Journal of Applied Physics, v.27, no.12, 1956. pp.1473-1483.	965
890	HUBBS, CARL L. Off-season, southern occurrence of the black scoter on the Pacific coast. Condor, v.58, no.6, 1956. pp.449	977
891	COCHRANE, JOHN D. The frequency distribution of surface-water characteristics in the Pacific Ocean. Deep-Sea Research, v.4, 1956. pp.45-53	979
892	SCRUTON, P. C. Oceanography of Mississippi delta sedimentary environments. American Association of Petroleum Geologists, Bulletin, v.40, no.12, 1956. pp.2864-2952	989
893	HUBBS, CARL L. The Guadalupe fur seal still lives! ZooNooz (Publication of Zoological Society of San Diego), Dec., 1956. pp.6-9	1080
894	CRAIG, HARMON, GIOVANNI BOATO, and DONALD E. WHITE. Isotopic geochemistry of thermal waters. Conference on Nuclear Processes in Geologica Settings, 2nd, Proceedings. National Academy of Sciences—National Research Council Publication #400. 1956. pp.29-38	1085
895	CRAIG, HARMON. Natural distribution of radiocarbon and the exchange time of carbon dioxide between atmosphere and sea. Tellus, v.9, no.1, 1957. pp.1-17	1097
896	KAMPA, ELIZABETH and BRIAN P. BODEN. Light generation in a sonic scattering layer. Deep-Sea Research, v.4, 1957. pp.73-92	1115
897	FAIRBRIDGE, RHODES W. The dolomite question. In "Regional Aspects of Carbonate Deposition." Journal of Sedimentary Petrology, special volume #5 (SEPM Carbonate Symposium) Tulsa, 1957. pp. 125-178	*
898	SCHAEFER, MILNER B. Tuna and tuna-bait resources in the eastern tropical Pacific Ocean. Pan American Fisherman, May, 1956. pp.10-11, 14-15, 20-21	1135
899	CROMWELL, TOWNSEND. Eastropic Expedition. Pacific Fisherman, July, 1956. pp.25-29	1143

*Not available for exchange.

UNIVERSITY OF CALIFORNIA
SCRIPPS INSTITUTION OF OCEANOGRAPHY
CONTRIBUTIONS, NEW SERIES
1956

AUTHOR INDEX

	Contrib. Number	Page Number
ALEEM, ANWAR ABDEL		
Quantitative underwater study of the benthic communities inhabiting kelp beds off California	824	91
ALVERSON, FRANKLIN G.		
(with Robert J. Menzies and Thomas E. Bowman) Studies of the biology of the fish parasite *Livoneca convexa* Richardson (Crustacean, Isopoda, Cymothoidae)	822	65
BALLARD, S. S.		
(with S. Q. Duntley) A program of research in the visual detectability of distant objects	851	497
BEAL, M. ALLAN		
(and Francis P. Shepard) A use of roundness to determine depositional environments	849	475
BIEN, GEORGE S.		
(and Edward D. Goldberg) The polarographic determination of ferrous and ferric iron in refractory minerals	834	175
BIERI, ROBERT		
A method for the microscopic examination and manipulation of plankton on board ship	873	703
BOATO, GIOVANNI		
(and Donald E. White, with Harmon Craig) Isotopic geochemistry of thermal waters	894	1085
BODEN, BRIAN P.		
(with Elizabeth Kampa) Light generation in a sonic scattering layer	896	1115
BOWMAN, THOMAS E.		
(and Franklin G. Alverson, with Robert J. Menzies) Studies of the biology of the fish parasite *Livoneca convexa* Richardson (Crustacea, Isopoda, Cymothoidae)	822	65
BULLARD, E. C.		
(and Roger Revelle and A. E. Maxwell) Heat flow through the deep-sea floor	876	*

*Not available for exchange.

	Contrib. Number	Page Number
BUZZATI-TRAVERSO, ADRIANO A.		
On the growth of populations	839b	240
CARRIER, GEORGE		
(and Frank Snodgrass, with Walter Munk) Edge waves on the continental shelf	826	99
CAWLEY, JOHN H., JR.		
(with James M. Snodgrass) Temperature and depth circuitry in a telerecording bathythermometer	880	813
CLENDENNING, K. A.		
(and F. T. Haxo) Photosynthetic induction in marine algae	833	157
COCHRANE, JOHN D.		
The frequency distribution of surface-water characteristics in the Pacific Ocean	891	979
COX, CHARLES		
Optical measurements of sea surface roughness	836	193
(and Walter Munk) Slopes of the sea surface deduced from photographs of sun glitter	859	*
CRAIG, HARMON		
Distribution, production rate, and possible solar origin of natural tritium	865	649
(and Giovanni Boato and Donald E. White) Isotopic geochemistry of thermal waters	894	1085
Natural distribution of radiocarbon and the exchange time of carbon dioxide between atmosphere and sea	895	1097
CROMWELL, TOWNSEND		
(and Joseph L. Reid, Jr.) A study of oceanic fronts	842	415
Eastropic Expedition	899	1143
CROWE, WALTER R.		
(with Carl Hubbs) Preliminary analysis of the American cyprinid fishes, seven new, referred to the genus *Hybopsis*, subgenus *Erimystax*	863	639
CURRAY, JOSEPH R.		
The analysis of two-dimensional orientation data	832	141
(with Robert H. Parker) Fauna and bathymetry of banks on continental shelf, northwest Gulf of Mexico	877	761
Dimensional grain orientation studies of Recent coastal sands	879	795
DUNTLEY, S. Q.		
(and S. S. Ballard) A program of research in the visual detectability of distant objects	851	497
ECKART, CARL		
(and Horace G. Ferris) Equations of motion of the ocean and atmosphere	823	85
EL WARDANI, SAYED A.		
Germanium in meteorites	858	631

* Not available for exchange.

	Contrib. Number	Page Number
FAIRBRIDGE, RHODES W.		
The dolomite question	897	*
FERGUSON WOOD, E. J.		
Diatoms in the ocean deeps	828	109
FERRIS, HORACE G.		
(with Carl Eckart) Equations of motion of the ocean and atmosphere	823	85
FISHER, ROBERT L.		
(and Noriyuki Nasu, with Hisashi Kuno) Rock fragments and pebbles dredged near Jimmu seamount, northwestern Pacific	831	131
FOX, DENIS L.		
Physical and chemical coloration in birds	882	829
GROVES, GORDON W.		
Periodic variation of sea level induced by equatorial waves in the Easterlies	853	513
GOLDBERG, EDWARD D.		
(with George S. Bien) The polarographic determination of ferrous and ferric iron in refractory minerals	834	175
(with George Lewis) X-ray fluorescence determination of barium, titanium, and zinc in sediments	860	633
HAMILTON, EDWIN L.		
Sunken islands of the Mid-Pacific mountains	830	*
HAXO, F. T.		
(with K. A. Clendenning) Photosynthetic induction in marine algae	833	157
HEDGPETH, JOEL W.		
The population of hypersaline and relict lagoons	839a	235
HOLMES, ROBERT W.		
(and Theodore M. Widrig) The enumeration and collection of marine phytoplankton	869	675
HORRER, PAUL L.		
(and Roger Revelle) The ocean off the California coast	844	429
HUBBS, CARL L.		
Scripps Institution of Oceanography, University of California	819	11
Back from oblivion - Guadalupe fur seal: still a living species	838	217
Ways of stabilizing zoological nomenclature	839	227
(and Walter R. Crowe) Preliminary analysis of the American cyprinid fishes, seven new, referred to the genus *Hybopsis*, subgenus *Erimystax*	863	639
Off-season, southern occurrence of the black scoter on the Pacific coast	890	977
The Guadalupe fur seal still lives!	893	1080

* Not available for exchange.

	Contrib. Number	Page Number
INMAN, DOUGLAS L.		
(and Noriyuki Nasu) Orbital velocity associated with wave action near the breaker zone	841	333
(and G. A. Rusnak) Changes in sea level on the beach and shelf at La Jolla, California	854	519
JOHNSON, MARTIN W.		
(and Robert J. Menzies) Migratory habits of the marine gribble *Limnoria tripunctata* Menzies in San Diego harbor, California	829	115
Plankton of the Beaufort and Chukchi Sea areas of the Arctic and its relation to the hydrography	857	599
The larval development of the California spiny lobster, *Panulirus interruptus* (Randall), with notes on *Panulirus gracilis* Streets	878	775
KAMPA, ELIZABETH		
(and Brian P. Boden) Light generation in a sonic scattering layer	896	1115
KNAUSS, JOHN A.		
An estimate of the effect of turbulence in the ocean on the propagation of sound	846	457
(and A. C. Vine, with G. H. Volkmann) The use of parachute drogues in the measurement of subsurface ocean currents	881	823
KUNO, HISASHI		
(and Robert L. Fisher and Noriyuki Nasu) Rock fragments and pebbles dredged near Jimmu seamount, northwestern Pacific	831	131
LEWIS, GEORGE		
(and Edward D. Goldberg) X-ray fluorescence determination of barium, titanium, and zinc in sediments	860	633
LIEBERMANN, LEONARD		
On the pressure dependence of sound absorption in liquids	886	861
Extremely low-frequency electromagnetic waves. I. Reception from lightning. II. Propagation properties	889	965
LIMBAUGH, CONRAD		
(and Wheeler J. North) Fluorescent, benthic, Pacific coast coelenterates	870	687
MAXWELL, A. E.		
(and Roger Revelle) Heat flow through the Pacific Ocean basin	820	13
(with E. C. Bullard and Roger Revelle) Heat flow through the deep-sea floor	876	*
MENARD, HENRY W.		
Archipelagic aprons	867	651
MENZIES, ROBERT J.		
(and Thomas E. Bowman and Franklin G. Alverson) Studies of the biology of the fish parasite *Livoneca convexa* Richardson (Crustacea, Isopoda, Cymothoidae)	822	65

*Not available for exchange.

	Contrib. Number	Page Number
MENZIES, ROBERT J. (Continued)		
(and Milton Miller) A redescription of the marine isopod crustacean *"Exosphaeroma" Faxoni* Richardson from Texas. . . .	825	93
(and Martin W. Johnson) Migratory habits of the marine gribble *Limnoria tripunctata* Menzies in San Diego harbor, California	829	115
MILLER, MILTON A.		
(with Robert J. Menzies) A redescription of the marine isopod crustacean *"Exosphaeroma" Faxoni* Richardson from Texas. . . .	825	93
MORITA, RICHARD Y.		
(and Claude E. ZoBell) Effect of hydrostatic pressure on the succinic dehydrogenase system in *Escherichia coli*.	852	508
(with Claude E. ZoBell) Bacteria in the deep sea.	862	*
(and Henry I. Nakada, with Jack B. Wolfe) Glucosamine degradation by *Escherichia coli*. I. Observations with resting cells and dry-cell preparations	871	689
MUNK, WALTER		
(and Frank Snodgrass and George Carrier) Edge waves on the continental shelf.	826	99
Polar wandering: a marathon of errors	850	487
(with Charles Cox) Slopes of the sea surface deduced from photographs of sun glitter	859	*
NAKADA, HENRY I.		
(with Jack B. Wolfe and Richard Y. Morita) Glucosamine degradation by *Escherichia coli*. I. Observations with resting cells and dry-cell preparations	871	689
NASU, NORIYUKI		
(with Hisashi Kuno and Robert L. Fisher) Rock fragments and pebbles dredged near Jimmu seamount, northwestern Pacific . . .	831	131
(with D. L. Inman) Orbital velocity associated with wave action near the breaker zone	841	333
NORTH, WHEELER J.		
(with Conrad Limbaugh) Fluorescent, benthic, Pacific coast coelenterates	870	687
Scientific diving	872	699
PARKER, ROBERT H.		
Macro-invertebrate assemblages as indicators of sedimentary environments in the east Mississippi delta region	840	251
(and Joseph R. Curray) Fauna and bathymetry of banks on continental shelf, northwest Gulf of Mexico	877	761
PHLEGER, FRED B		
Significance of living foraminiferal populations along the central Texas coast	875	713
RAITT, RUSSELL W.		
Seismic-refraction studies of the Pacific Ocean basin. I. Crustal thickness of the central equatorial Pacific	883	833

* Not available for exchange.

	Contrib. Number	Page Number
RAKESTRAW, NORRIS W.		
Hermann Wattenberg: a pioneer in a new field of exploration.	847	462
RECHNITZER, ANDREAS B.		
Land birds at sea off southern California	861	637
Foraging habits and local movements of the wood ibis in San Diego County, California	888	957
REID, JOSEPH L., JR.		
(with Townsend Cromwell) A study of oceanic fronts	842	415
Observations of internal tides in October 1950.	855	588
REVELLE, ROGER		
(with A. E. Maxwell) Heat flow through the Pacific Ocean basin . . .	820	13
(with Paul L. Horrer) The ocean off the California coast	844	429
(and A. E. Maxwell, with E. C. Bullard) Heat flow through the deep-sea floor	876	*
REX, ROBERT W.		
Microrelief produced by sea ice grounding in the Chukchi Sea near Barrow, Alaska	845	447
RICHARDS, ADRIAN F.		
(with James M. Snodgrass) Observations of underwater volcanic acoustics at Barcena volcano, San Benedicto Island, Mexico, and in Shelikof Strait, Alaska.	837	209
RIEDEL, WILLIAM R.		
Sediment cores from the west Pacific. Radiolaria: a preliminary stratigraphy.	866	*
(and Julius Schlocker) Radiolaria from the Franciscan group, Belmont, California	874	709
RUDNICK, PHILIP		
The spectrum of the variation in latitude	848	469
RUSNAK, G. A.		
(with D. L. Inman) Changes in sea level on the beach and shelf at La Jolla, California	854	519
SCHAEFER, MILNER B.		
Tuna and tuna-bait resources in the eastern tropical Pacific Ocean	898	1135
SCHLOCKER, JULIUS		
(with William R. Riedel) Radiolaria from the Franciscan group, Belmont, California	874	709
SCRUTON, P. C.		
Oceanography of Mississippi delta sedimentary environments	892	989
SHEPARD, FRANCIS P.		
Late Pleistocene and Recent history of the central Texas coast . . .	835	177
(with M. Allan Beal) A use of roundness to determine depositional environments.	849	475

*Not available for exchange.

	Contrib. Number	Page Number
SHEPARD, FRANCIS P. (Continued)		
(and H. E. Suess) Rate of postglacial rise of sea level.	856	597
Marginal sediments of the Mississippi delta	887	865
SILAS, E. G.		
The systematic position of the Indian cyprinid fish, *Cirrhinus fasciatus* Jerdon (1849), with a new name for *Barbus fasciatus* Bleeker (1853)	864	647
SNODGRASS, FRANK E.		
Mark IX shore wave recorder	821	25
(and George Carrier, with Walter Munk) Edge waves on the continental shelf.	826	99
SNODGRASS, JAMES M.		
(and Adrian F. Richards) Observations of underwater volcanic acoustics at Barcena volcano, San Benedicto Island, Mexico, and in Shelikof Strait, Alaska	837	209
(and John H. Cawley, Jr.) Temperature and depth circuitry in a telerecording bathythermometer.	880	813
STEWART, H. B., JR.		
Contorted sediments in a modern coastal lagoon explained by laboratory experiments	818	1
SUESS, HANS E.		
Absolute chronology of the last glaciation	843	425
(with F. P. Shepard) Rate of postglacial rise of sea level.	856	597
Grundlagen und Ergebnisse der Radiokohlenstoff-Datierung	868	667
VAN DORN, WILLIAM G.		
A portable tsunami recorder	827	105
Large-volume water samplers.	884	852
VINE, A. C.		
(with G. H. Volkmann and J. A. Knauss) The use of parachute drogues in the measurement of subsurface ocean currents.	881	823
VOLKMANN, G. H.		
(and J. A. Knauss and A. C. Vine) The use of parachute drogues in the measurement of subsurface ocean currents	881	823
WHITE, DONALD E.		
(with Harmon Craig and Giovanni Boato) Isotopic geochemistry of thermal waters	894	1085
WIDRIG, THEODORE M.		
(with Robert W. Holmes) The enumeration and collection of marine phytoplankton	869	675
WOLFE, JACK B.		
(and Richard Y. Morita and Henry I. Nakada) Glucosamine degradation by *Escherichia coli*. I. Observations with resting cells and dry-cell preparations	871	689
ZOBELL, CLAUDE E.		
(with Richard Y. Morita) Effect of hydrostatic pressure on the		

	Contrib. Number	Page Number
ZOBELL, CLAUDE E. (Continued)		
succinic dehydrogenase system in *Escherichia coli.*	852	508
(and Richard Y. Morita) Bacteria in the deep sea	862	*
Bacteria - annotated bibliography	885	855

---

* Not available for exchange.

Reproduced by Permission

Reprinted for private circulation from
THE BULLETIN OF THE AMERICAN ASSOCIATION OF PETROLEUM GEOLOGISTS
Vol. 40, No. 1, January, 1956

CONTORTED SEDIMENTS IN MODERN COASTAL LAGOON EXPLAINED BY LABORATORY EXPERIMENTS[1]

HARRIS B. STEWART, JR.[2]
La Jolla, California

INTRODUCTION

The increasing interest in the barred coastal lagoon as a favorable environment for the accumulation of potential source beds and reservoirs for petroleum led the writer to undertake an investigation of the coastal lagoon as a sedimentary environment. San Miguel Lagoon 40 miles south of the Mexican border on the Pacific coast of Baja California was chosen for the control area, and it was during the investigation of the sediments of this lagoon that the structures described in this paper were found.

San Miguel Lagoon is typical of many of the coastal lagoons on the Pacific coast of North America in that it is isolated from the ocean by a bay barrier (term proposed by Shepard, 1952) during much of the year. When the lagoon is open, a narrow channel is maintained through the barrier by tidal currents, and the lagoon water level fluctuates with the ocean tide. Tidal currents in this channel have built into the lagoon a delta 300 feet long and 100 feet wide. Comparable tidal deltas on the east coast of the United States were described by Lucke (1934). The contorted structures were observed on exposed sand flats of this tidal delta at San Miguel Lagoon.

DESCRIPTION OF DEFORMED LAYERS

Below the top 2–3 inches of flat sand laminae, the sediments are highly contorted (Figs. 1, 2, and 3). The structure is especially conspicuous because the deformation is an alternating laminae of light and dark sand. The lamination results from the sorting action of waves washing over the tidal sand flats, and the striking color alternations are due to the coincidence of color differences with differences in density. Similar laminations on California beaches were described in detail by Thompson (1937). The dark laminae are composed primarily of dark heavy minerals (magnetite and green hornblende with minor amounts of hypersthene, epidote, and garnet), whereas the lighter laminae are predominantly feldspar and quartz grains of somewhat larger size. Both light and dark sands are well sorted (Table I).

---

[1] Manuscript received, August 27, 1955. Contribution from the Scripps Institution of Oceanography, New Series No. 818.

[2] Scripps Institution of Oceanography. The writer is indebted to L.M.J.U. Van Straaten for his stimulating discussions of this phenomenon and to F. P. Shepard, M. N. Bramlette, H. W. Menard, and D. L. Inman for their critical reading of the manuscript.

Contortions are most intense in a section of laminae 8 inches thick, and individual structures average 3–5 inches across. The deformation takes various forms, but there is none of the recumbent folds typical of slump structures (Fairbridge, 1946). The most pronounced feature of these structures is that the trend of the axis of any individual fold approaches the vertical. Small angular unconformities that can not be traced horizontally for more than a few inches are common throughout the sections. Structural relationships indicate that deformation has taken place both before and after the time of these unconformities, indicating continuing or repeated application of the deforming force. Local pockets filled with non-laminated sand are found in all the sections exposed. Deformation is more intense in the upper laminae and dies out with depth. The slope of the surface of the sand flat is 1.3°.

TABLE I. COMPARISON OF SAND FROM LIGHT AND DARK LAMINAE, SAN MIGUEL LAGOON
(One sample of each)

	Light	*Dark*
Median diameter (ϕ)*	2.35	2.53
Median diameter (mm.)	0.196	0.172
Sorting ($\sigma\,\phi$)*	0.30	0.32
% Heavy minerals (S.G.>2.83)	15.3	74.0

* ϕ Measures described by Inman (1952).

The contorted sediments are restricted to the more protected parts of the tidal delta and are further limited to those areas of very loosely compacted or cavernous sands. The sediments involved contain large amounts of trapped air; and when these sediments are under water, walking across the area produces violent outbursts of air bubbles. The sand flat is subjected to regular alternating tidal cover and exposure, and the part of the delta where the structures are found is protected from the vigorous action of waves and currents.

The barrier sealed the lagoon from the ocean shortly after these observations, and rising lagoon waters inundated the area. The structures have since been covered with flat-lying sands that exhibit no deformation.

PROPOSED METHOD OF FORMATION

These highly deformed structures are believed due to the movement of pockets of trapped air that enters the sand flats during low-tide exposure. The entrapment of air in beach sands and the associated sand holes, sand domes, and cavernous sands are well known phenomena (Johnson, 1919; Palmer, 1928; Kindle, 1936; Trefethen, 1941; and Emery, 1945).

At San Miguel Lagoon, cavernous sands have been found only on the tidal delta. As the tide beings to rise, ocean water enters the channel, and the delta acts as a barrier to the direct action of waves and currents. Sedimentation takes place when the water level approaches the height of the sand flats and a wave refracted around the end of the delta spreads over these tidal flats depositing a

(2)

thin lamina of sand which is covered with more sand by the next wave and eventually inundated by the rising tide. Once the sand flat is under water, wave action in the lee of the delta is gentle, so the depth of disturbance of the sand by wave action is proportionately small (King, 1951) and the permeability is high. In this manner laminae of loosely compacted sand are built up.

As the tide recedes, water drains slowly from the gently sloping delta. More and more of the sand flat becomes exposed as the water table sinks, below the surface drawing air down into the porous sands. On other sand flats in the lagoon, the sand is more compact, even to the extent that water remains in depressions throughout low tide.

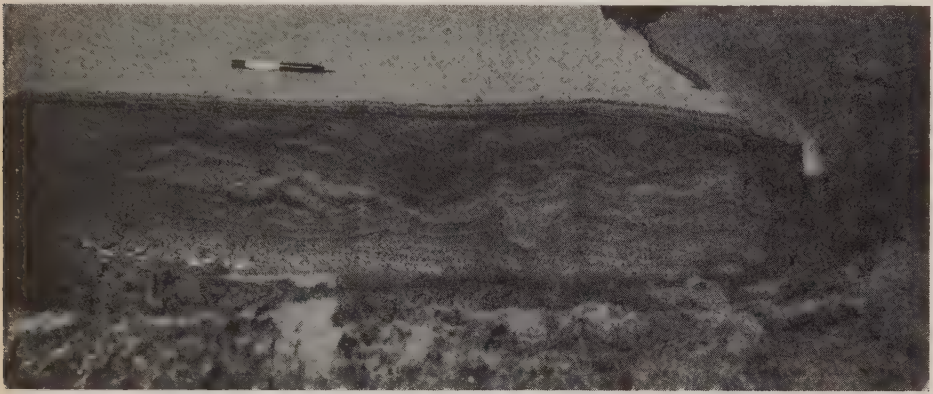

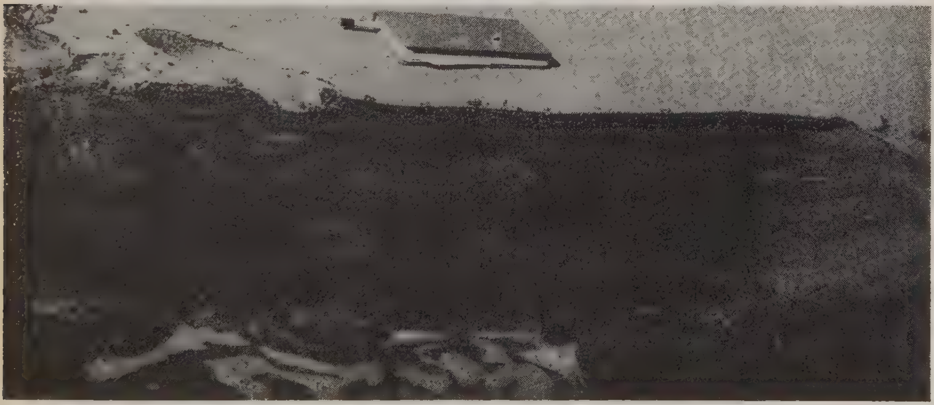

FIG. 1.—Contorted sand laminae, San Miguel Lagoon, Baja California. Section at right angles to slope of sand flat.

FIG. 2—Section parallel with slope of sand flat. Lagoon is at right. Note sand dome below notebook and water table at bottom of section.

On the incoming tide, the water table rises in the sand, tending to force the interstitial air upward. At the same time, water from the waves spreading over the tidal flats is percolating downward, filling the interstices of the upper layers

(3)

with water and making the sand less permeable to the rising air. Surging in the tidal channel causes fluctuations in the level of the water table in the adjacent porous sands, resulting in a pulsating upward motion of the pockets of trapped air. It is suggested that when a rising air pocket encounters a less permeable lamina, this is bowed upward to produce a sand dome such as that shown in Figure 2 and comparable with those described by Emery (1945). More often there would be rupture of the overlying laminae, so that sand flowed in to fill the area behind the rising air pocket. Sometimes this sand might slump as a unit, and the lamination would still be visible but distorted. At other times, turbulence behind the rising air might result in mixing that destroys the lamination and results in the observed pockets of uniform non-laminated sand. The small un-

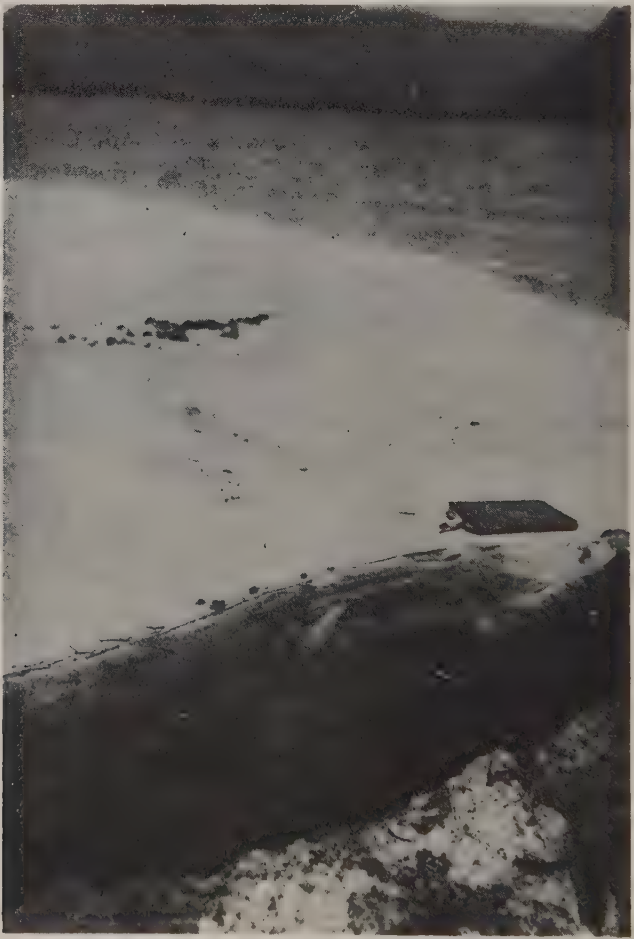

FIG. 3.—Contorted sand laminae, San Miguel Lagoon, Baja California. Lagoon in background. Tide lower than in Figure 1.

(4)

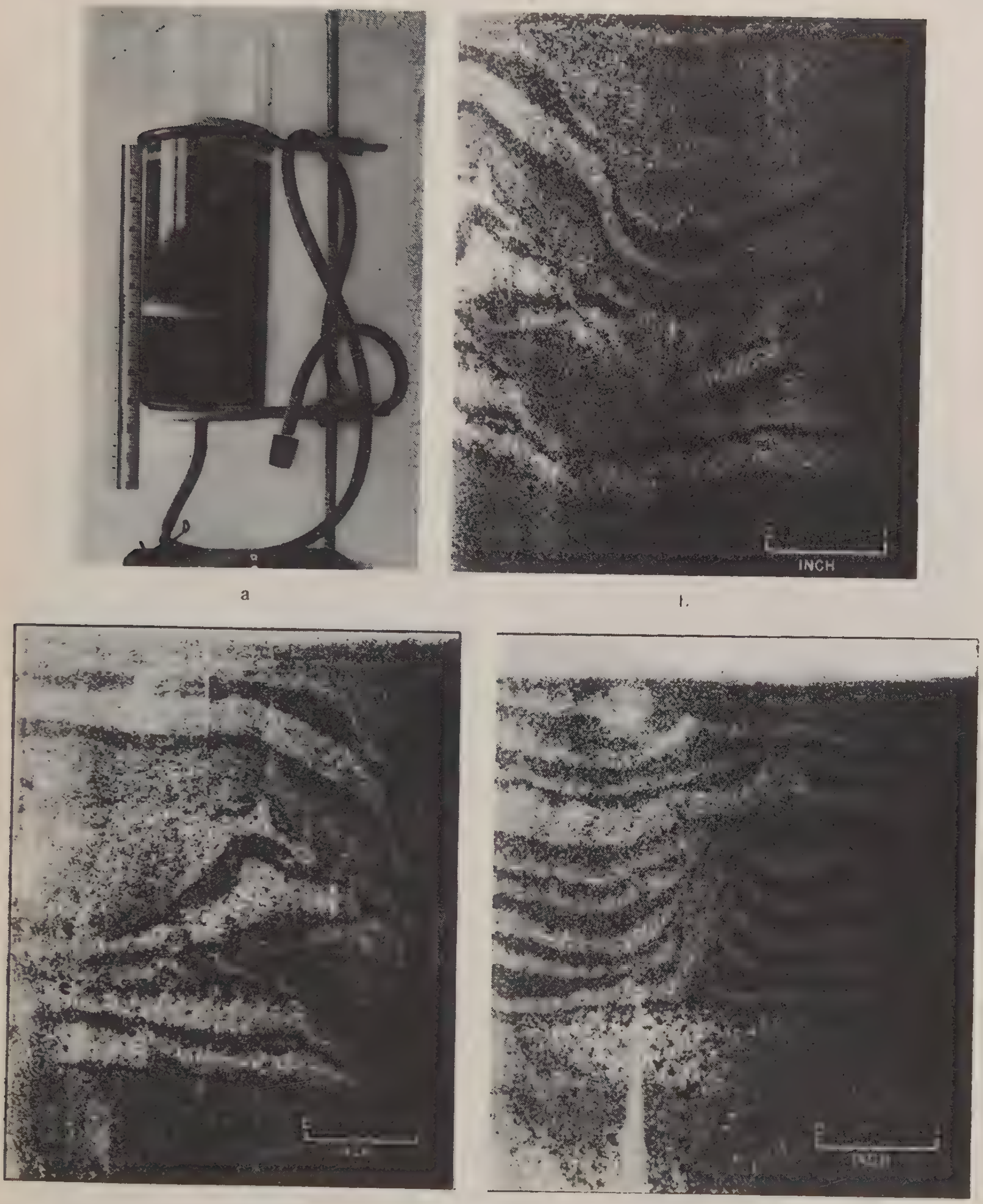

a b

c d

FIG. 4.—Contorted sediments produced in laboratory. (a) Apparatus used to make structures in b, c, and d. (b) Slump in wake of rising air pocket. Compare with Figure 3. (c) Typical contorted structures. Air bubbles in light laminae and deformation above bubble at lower right. Compare with Figure 2. (d) Rupture of laminae due to rising air pocket. Compare with structure above hammer in Figure 5b.

(5)

conformities are also believed due to this movement of sand in the wake of rising air pockets. The general direction of movement of the trapped air is vertical, accounting for the observed vertical axes of the structures, and the small scale of the features is a reflection of the size of the trapped air pockets.

During the following low tide, air is again drawn into the sand. As the water level subsequently rises, new horizontal laminae are deposited at the surface, and the churning of the sediments by trapped air continues. Vertical sections through sediments subjected to this process would expose structures such as those found at San Miguel Lagoon.

Comparable cavernous sands and alternating exposure and inundation by tides were found on tidal deltas in Sorrento Lagoon near Del Mar, California, and at Mugu Lagoon near Port Hueneme, California. Digging on these sand flats revealed that similar deformed structures were present.

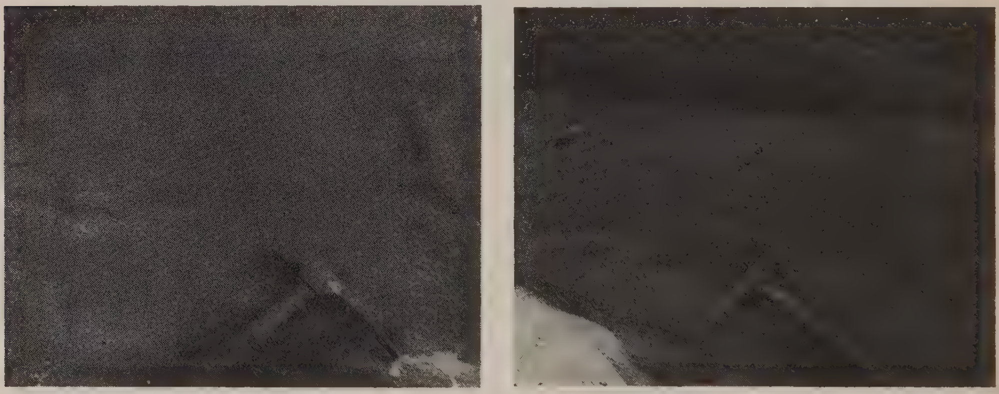
a b

Fig. 5.—Deformation in Upper Cretaceous sandstone exposed in vertical sea cliffs at La Jolla, California.

LABORATORY EXPERIMENTS

The foregoing hypothesis was developed primarily as the result of laboratory experiments with an apparatus in which laminae of alternating light and dark sand were subjected to the same processes observed in the lagoon. The apparatus (Fig. 4a) consisted of a glass cylinder 13 inches high and 4 inches in diameter into which water could be introduced both from above and below. Gravel was placed in the bottom and covered with fine wire mesh to insure even distribution of the rising water. Lamination was produced by alternately adding dark sand (median diameter 2.64ϕ or 0.160 mm.) and light sand (median diameter 2.61ϕ or 0.164 mm.) and allowing each to settle to the bottom. The cylinder was then drained of water to simulate a lowering tide, and the sand was allowed to dry. Water was then introduced at the surface to correspond with the waves washing

(6)

across the sand flats. At the same time, water was introduced from below as though from a rising tide. Bubbles began to coalesce in the coarser light-colored layers and to begin moving upward through the laminae. In order to reproduce short-period fluctuations in the height of the water table, the flow of water from below was stopped from time to time and the water partly drained from the sand. Complete tidal cover was simulated by adding more water at the surface, and new light and dark laminae were added with each "tidal cycle."

Experiments with this apparatus produced structures almost identical with those formed in the lagoons. Examples are shown in Figure 4. The origin of the non-laminated pockets and the local unconformities was not apparent in the field but was clearly revealed by these experiments. They also indicated that the more intense deformation of the upper part of the section is due to the increased plasticity of the upper sediments wet from above and to the enlarging of the air pockets by the accretion of smaller bubbles as they rise through the sediment. The term "air heave" is suggested for the process and "air-heave structures" for the resultant deformation of the sediments.

COMPARABLE STRUCTURES IN ANCIENT SEDIMENTS

On the basis of these field observations and laboratory experiments, criteria may be established for the recognition of air-heave structures preserved in the ancient sediments. These criteria include the following:

1. Small structures generally less than 8–10 inches across
2. A pronounced vertical trend to the structures
3. Unconformities only a few inches in length and pockets of non-laminated sand
4. Structures that die out with depth, and the most intense deformation is near the upper limit of the deformed section
5. Structures limited to lithotypes that are predominantly sandstone
6. Structures probably limited to a thin zone in the section because of the transient nature of the conditions necessary for their formation
7. The zone of structures generally overlain and underlain by flat-lying beds exhibiting no deformation

Vertical sea cliffs at La Jolla, California, expose Upper Cretaceous sandstones that exhibit highly contorted beds up to 2 feet thick between beds showing no deformation. Parts of these contortions show overturning more suggestive of slumping, but other sections are believed to have resulted from air heave. The latter structures (Fig. 5) fit the criteria described and occur in alternating light and dark laminae of fine-grained sandstone associated with beds containing ripple marks and filled animal burrows.

The accumulation of data on structures attributable to penecontemporaneous deformation is too large to be reviewed here, but Shrock (1948, pp. 258–80) and Beets (1946) presented excellent summaries of the literature on the subject. A study of the more recent records reveals descriptions of structures in ancient sediments that probably can be attributed to air heave.

Tanner (1953a, summarized in Tanner, 1953b) presents photographs and descriptions of contorted bedding in the Upper Pennsylvanian Virgil and Mis-

(7)

souri series in central Oklahoma that is very similar in appearance to the deformation found in San Miguel Lagoon. From Tanner's data, these are interpreted by the present writer as air-heave structures. The grain size of these Pennsylvanian sediments is in the medium-sand to silt range. The contortions have a pronounced vertical trend. Many of the deformed sandstones are basal members unconformably overlying truncated beds and therefore representing overlap—the expected relationship in a tidal delta. Cross-bedding and ripple marks are common, and the contorted sands either contain or are associated with beds containing remains of land plants. The contorted sands of the Hilltop formation grade laterally into lagoon and tidal-flat shales, further suggestive of the proper conditions for air-heave structures.

Poborski (1954) reported contorted bedding in quartz siltstone of the Triassic Virgin formation in Utah. The layers in which the deformed bedding occurs contain indeterminate tracks and numerous structures attributed to desiccation, indicating exposure above water at least for short periods. The sediments are of marine origin and are most commonly overlain by siltstones which Poborski ascribes to quiet-water deposition in a lagoon. The environment was apparently similar to that near the channel in San Miguel Lagoon, and his detailed lithologic descriptions suggest the necessary conditions for air-heave structures.

Van Straaten (1949) described deformed layers from the Archean of Finland. A photograph of contorted layers near Aitoniemi (*ibid.*, Fig. 5) shows what appear to be air-heave structures. Van Straaten states (*ibid.*, p. 15):

> It can also be seen that in the sand bed considerable internal movements have occurred, the traces of stratification being directed nearly perpendicular to the general bedding at both sides of the wedge

CONCLUSIONS

If the hypothesis proposed here is correct, the occurrence of air-heave structures in the geologic column may be interpreted as indicative of a tidal area exposed at low tide with a continuous source of sand supplied by very gentle waves. Though these conditions are found occasionally on ocean beaches, the zone of deformation in open beach deposits would be very thin, because a period of gentle waves is seldom of sufficient duration to produce any thickness of such sediments. The necessary conditions develop most commonly near the entrances to tidal estuaries and lagoons.

Though not in themselves conclusive evidence of a lagoonal environment, air-heave structures when coupled with other evidence may be of considerable use in determining the environment of deposition of ancient sediments.

BIBLIOGRAPHY

Beets, C., 1946, "Miocene Submarine Disturbances of Strata in Northern Italy," *Jour. Geol.*, Vol. 54, No. 4, pp. 229–45.

Emery, K. O., 1945, "Entrapment of Air in Beach Sand," *Jour. Sed. Petrology*, Vol. 15, No. 2, pp. 39–49.

Fairbridge, R. W., 1946, "Submarine Slumping and Location of Oil Bodies," *Bull. Amer. Assoc. Petrol. Geol.*, Vol. 30, No. 1, pp. 84–92.

(8)

INMAN, D. L., 1952, "Measures for Describing the Size Distribution of Sediments," *Jour. Sed. Petrology*, Vol. 22, No. 3, pp. 125–45.

JOHNSON, D. W., 1919, *Shore Processes and Shoreline Development.* 584 pp. Revised ed., 1938. John Wiley and Sons, New York.

KINDLE, E. M., 1936, "Dominant Factors in the Formation of Firm and Soft Beaches," *Jour. Sed. Petrology*, Vol. 6, No. 1, pp. 16–22.

KING, C. A. M., 1951, "Depth of Disturbance of Sand on Sea Beaches by Waves," *ibid.*, Vol. 21, No. 3, pp. 131–40.

LUCKE, J. B., 1934, "A Theory of Evolution of Lagoon Deposits on Shorelines of Emergence," *Jour. Geol.*, Vol. 42, No. 6, pp. 561–84.

PALMER, R. H., 1928, "Sand Holes of the Strand," *ibid.*, Vol. 36, No. 2, pp. 176–80.

POBORSKI, S. J., 1954, "Virgin Formation (Triassic) of the St. George, Utah, Area," *Bull. Geol. Soc. America*, Vol. 65, No. 10, pp. 971–1006.

SHEPARD, F. P., 1952, "Revised Nomenclature for Depositional Coastal Features," *Bull. Amer. Assoc. Petrol. Geol.*, Vol. 36, No. 10, pp. 1902–12.

SHROCK, R. R., 1948, *Sequence in Layered Rocks.* 507 pp. McGraw-Hill, New York.

TANNER, W. F., 1953a, "The Geology of Seminole County, Oklahoma," *unpublished Ph.D. Thesis*, University of Oklahoma, Norman, Oklahoma.

———, 1953b, "Facies Indicators in the Upper Pennsylvanian of Seminole County, Oklahoma," *Jour. Sed. Petrology*, Vol. 23, No. 4, pp. 220–28.

THOMPSON, W. O., 1937, "Original Structures of Beaches, Bars, and Dunes," *Bull. Geol. Soc. America*, Vol. 48, No. 6, pp. 723–51.

TREFETHEN, J. M., 1941, "Dominant Factors in the Formation of Firm and Soft Sand Beaches—a Discussion," *Jour. Sed. Petrology*, Vol. 11, No. 1, pp. 42–43.

VAN STRAATEN, L. M. J. U., 1949, "Occurrence in Finland of Structures Due to Subaqueous Sliding of Sediments," *Comptes Rendus de la Societe Geologique de Finlande*, N:o XXII, pp. 2–17.

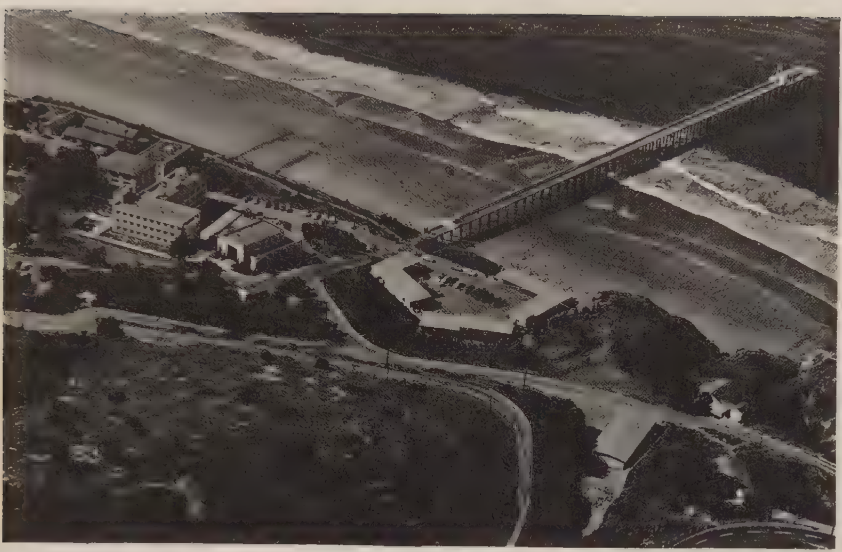

Main campus of Scripps Institution of Oceanography, University of California.

Scripps Institution of Oceanography, University of California[1]

CARL L. HUBBS, *Professor of Biology*

THE oceanographic branch of the vast University of California is at La Jolla, with an extensive annex on the grounds of the United States Navy Electronics Laboratory on Point Loma—both in the San Diego area. It is an outgrowth of the Scripps Institution for Biological Research, which was founded and so named in 1912, when the University accepted the laboratory of the Marine Biological Association of San Diego. That laboratory was the last of a series of independent marine biological stations established in Southern California by William Emerson Ritter, who continued as director of the institution until 1923. He was succeeded by Thomas Wayland Vaughan, a geologist, during whose administration (1923-1936) the institution continued to grow. In recognition of the expanded activities the name was changed in 1925 to Scripps Institution of Oceanography. Further development has been achieved under the successive directorships of Harald U. Sverdrup, world-renowned Norwegian oceanographer (1936-1948), Carl Eckart (1948-1951), and the present head, Roger Revelle.

World War II emphasized the importance of oceanography to national security and accelerated the growth of Scripps and other institutions devoted to marine sciences and to the training of marine scientists. Since the war there has grown a realization of the peacetime as well as military significance of oceanography. The value of the varied oceanic resources to the state, the nation, and the whole world has become recognized. As a result, increasing support for Scripps Institution has come from various sources: from the state that owes much to the great ocean it broadly borders; from the various military and civilian branches of the nation that depends so much on the knowledge of the sea and on the men who can develop this knowledge; and from several private agencies, such as Rockefeller Foundation and the American Petroleum Institute, that are concerned with the advancement of knowledge, either for the sake of humanity in general or for the welfare of an industry.

Over the past ten years the main parameters of the institution have increased about ten fold. The annual budget now exceeds $3,000,000; the staff approximates 500, including more than 100 scientists; the research fleet has grown from one schooner to five ocean-going ships, including two capable of transoceanic expeditions, plus various smaller craft; and shore facilities include on the 175-acre La Jolla campus five permanent buildings, one now being doubled in size, a 1,000-foot pier, and various minor and temporary structures; and at the Scripps Field Annex, thirteen buildings and adequate dock facilities. But to the staff the sea remains the Institution's main laboratory.

In many ways Scripps Institution is comparable to Woods Hole Oceanographic Institution, but differs in being an integral part of a university. For this reason the training of oceanographers has been, along with concentrated research, a main function of the California institution. Many heads and other staff members of oceanographic departments and laboratories across the nation and in several foreign nations are proudly listed among the Scripps alumni. Except for a limited number of summer apprentices, and for military personnel in short-term courses, only graduate students are enrolled. Currently few other than doctoral candidates are accommodated. Of the approximately fifty students, mostly men, who are in training, nearly all take some part in the organized research programs. The number of new students who can be accepted is limited by factors of space and time, since the institution has greatly outgrown its only moderately expanded quarters and since all members of the faculty are deep in research programs and other activities. Applications

---

[1] Contributions from the Scripps Institution of Oceanography, New Series, No. 819.

Reprinted from A.I.B.S. Bulletin, Vol. 6, No. 1, January, 1956, pp. 11-13.
Reproduced by Permission

are welcomed, however, from students with a compelling interest in some phase of oceanography and with a good foundation in basic sciences (at La Jolla the course offerings are restricted to the marine aspects of the several sciences involved in the broader interpretation of oceanography). Students are considered for acceptance at Scripps only after having been admitted by the Graduate Division of the Southern Section of the University of California (Los Angeles 24). After enrollment they may pursue an M.S. or Ph.D. degree in oceanography or an A.M. or Ph.D. degree in one of the sciences, such as zoology, botany, microbiology, or biochemistry, that are represented in the faculty on the Scripps campus.

Integrated with the Institution are the Marine Physics Laboratory and the Visibility Laboratory, which are in some respects cooperatively associated with the Navy Electronics Laboratory; the Foraminifera Laboratory, associated with the Geology Division; the Marine Life Research program, which engages in the California Cooperative Fisheries Investigation along with the state Department of Fish and Game, the Federal Fish and Wildlife Service, the California Academy of Sciences, and Stanford University; and various other standing and *ad hoc* projects. The newly organized Institute of Marine Resources, though University-wide, has its administrative and main research center at La Jolla. Its director is Charles D. Wheelock. The extensive research projects in the Gulf of Mexico undertaken under grants from the American Petroleum Institute are now administered by this Institute. Associated intimately with and housed by Scripps Institution are the South Pacific Fishery Investigations of the Fish and Wildlife Service, headed by John C. Marr, and the Inter-American Tropical Tuna Commission, of which Milner B. Schaefer is director. Close cooperation is maintained with the state Department of Fish and Game; with other branches of the University of California and with other universities, laboratories, and societies; and with various state, federal and international agencies concerned with the sea.

For the benefit of the public as well as its own staff and students, the Institution maintains the Thomas Wayland Vaughan Aquarium and Museum. In certain fields research collections are maintained. Scripps has been the authorized center for processing and storing the now voluminous bathythermograph data for the whole Pacific. A well-equipped shop has developed many oceanographic instruments and has otherwise served the instrumental needs of the staff. The Library, with more than 30,000 volumes, 60,000 reprints and pamphlets, more than 800 journals, and a large chart collection, serves the staff directly and through contact with the other libraries. The Institution compiles and distributes each year, as contributions from the Scripps Institution of Oceanography, the scientific papers published by the staff in various journals, and issues, through the University Press, the *Bulletin* of the Scripps Institution of Oceanography and Oceanic Observations of the Pacific.

In large part the strength of Scripps Institution lies in integrated attacks on the physical, chemical, geological, and biological problems of the sea. In former years the researches were largely restricted to the coastal waters of Southern California and northwestern Mexico, but more recently, especially since the war, the operations have covered much of the northern and equatorial Pacific, with extensions into the Gulf of Mexico, the Arctic Ocean, and other waters. Each year since 1950 one or more long expeditions have been undertaken by the Institution's vessels, either alone or with ships of other agencies.

Scripps is a year-round laboratory, with no special summer session and no regular summer courses. Within the limits of outgrown facilities, however, qualified investigators are welcomed and accommodated in summer as well as other seasons.

Biological activities at Scripps Institution are diverse, though all focused on marine problems. The program in biochemistry, headed by Denis L. Fox, stresses such subjects as biochromes and comparative biochemistry of marine organisms and the role of particulate organic detritus in their nutrition. Research in microbiology, under Claude E. ZoBell, has dealt with the constitution of the marine bacterial flora, with the role of bacteria as geochemical agents, and with the biochemistry of marine microorganisms. It now stresses the physiology of bacteria that live under enormous pressures at great depths of the sea. The marine botany section, led by Francis T. Haxo, emphasizes problems related to the basic productivity of the seas, but deals also with other phytoplankton problems and with the physiology and biochemistry of attached marine algae. The work in invertebrate zoology, administered by Martin W. Johnson, deals chiefly with the zooplankton, with emphasis on systematics, life histories, quantitative distribution, and relations to oceanic currents, water masses, and other ecological factors. Dr. Johnson's pioneering work on the deep scattering layer is being extended by special projects. The studies in marine vertebrates, headed by Carl L. Hubbs, deal with the systematics, ecology, and distribution, habits, and reactions of marine vertebrates, both of coastal waters and the high-seas. Included currently is a study of the ecology of man during past periods of the eruption of populations along the coast. The newest division, marine genetics, being developed by Adriano Buzzati-Traverso, deals not only with the heredity of certain marine organisms, but also with population dynamics and evolution.

The biological work is closely correlated with that of the other divisions—physicial, chemical, and geological. The chemistry division, for example, deals with nutrient cycles, with the accumulation of trace elements by organisms, and with the relations between radioactive elements and marine organisms. A new laboratory for C^{14} and O^{18} analysis will greatly benefit paleoecological researches. Biological research at Scripps is further expanded by cooperation with the associated fisheries laboratories, other state and federal fishery agencies, and such other institutions as the California Academy of Sciences and the San Diego Zoological Society.

The biological program at Scripps Institution is being rapidly accelerated by reason of a one-million dollar eight-year grant from the Rockefeller Foundation. Under this subsidy particular stress will be laid on fresh experimental attacks on marine biological problems. Several new staff members, postdoctoral fellows, predoctoral fellows, and visiting researchers will be supported. Applications are being received.

HEAT FLOW THROUGH THE PACIFIC OCEAN BASIN

by A. E. MAXWELL and Roger REVELLE,
Scripps Institution of Oceanography of the University of California.*

ABSTRACT.

Fifteen measurements of the heat flow through the Pacific Ocean floor give an average value similar to that found for the continents. Neglecting three extremely high values the average of the remaining twelve measurements is 1.25×10^{-6} cal cm^{-2} sec^{-1}. The measurements have been made in widely separated areas in the Pacific and it is thought that they are representative of true oceanic values. Considerable variations exist, suggesting that anomalies of heat flow are present under the ocean and may represent previously undetected geophysical phenomena. Heat flow values were determined by measuring separately the thermal gradient and the thermal conductivity in the bottom sediments. The sum of the errors of measurement is found from experiment and theoretical analysis to be about 10 %. Investigation of the origin of the heat indicates that past fluctuations of bottom water temperature and processes occurring in the sediments are probably negligible, and that virtually all the heat must originate beneath the Mohorovicic discontinuity. Comparison of the oceanic with the continental heat flow suggests inconsistencies in the usually assumed distribution of radioactive materials in the earth's crust and mantle if heat transfer is taking place by molecular conduction. If the earth was initially hot, the present temperature at depths of a few hundred kilometers would be markedly higher under the oceans than under the continents, and this is difficult to reconcile with other geophysical data. It is possible that convective processes of outward heat transport dominate in the oceanic area.

---

[*] Contribution from the Scripps Institution of Oceanography New Series No. 820. This work was supported by the Office of Naval Research and the Bureau of Ships of the Navy Department and by the Institute of Geophysics of the University of California.

Reproduced, by permission, from Publications du Bureau Central Seismologique International; Travaux Scientifiques, Series A. Fascicule 19.

Introduction.

The continental heat flow is usually attributed to the decay of radioactive elements in the crust. Indeed, the heat flow is thought to vary directly with the thickness of the crust and in particular with the thickness of the granitic layer, in which it is believed the radioactivity is highly concentrated. Beneath the oceans, a granitic layer is thin or absent and one might anticipate a comparatively low heat flow. The oceanic measurements do not bear out this expectation; the heat flow is found to be about the same as in the continental areas. This result is of importance in considering the earth's thermal state, because the oceanic areas cover some 70 % of the earth's surface.

Measurements.

The flux of heat through the ocean floor may be determined from measurements of the thermal gradient and conductivity within the sediments, the relation being

$$\Sigma Q = - k \frac{dt}{dx}$$

where ΣQ is the heat flux, k the thermal conductivity and $\frac{dt}{dx}$ the thermal gradient.

TABLE 1

Mid-Pacific (1950) and Capricorn (1952-53) Heat Flow Results.

Station	Water Depth (m)	Gradient ($°C m^{-1}$)	Conductivity (10^{-3} cal cm^{-1} sec^{-1} $°C^{-1}$)	Heat Flow (micro cal cm^{-2} sec^{-1})
M. P. 1	4000	.0671	1.9*	1.27
M. P. 21	4500	.0650	1.8*	1.17
M. P. 32	3900	.0350	2.1*	0.74
M. P. 35-2	4900	.0623	2.0*	1.24
M. P. 36	5040	.0661	1.8*	1.19
M. P. 38	4750	.0692	1.6*	1.11
CAP. 2-B	4310	.0760	2.48	1.88
CAP. 5-B	5000	.0723	1.87	1.35
CAP. 9-B	2700	.0630	2.40	1.51
CAP. 10-B	3900	.1250	2.07	2.58**
CAP. 31-B	4880	.0862	1.83	1.58
CAP. 33-B	4300	.0210	1.71	0.36
CAP. 40-B	3020	.2150	2.44	5.25**
CAP. 48-B	4100	.0730	2.26	1.65
CAP. 50-B	4350	.1240	1.96	2.43**
			Average	1.69
Average without values marked by**				1.25

Conductivities measured by the National Physical Laboratory, Teddington, England.

Table 1 shows the results of six measurements of heat flow made on the Scripps Institution — U. S. Navy Electronics Laboratory Mid-Pacific Expedition of 1950 (Revelle and Maxwell, 1952) and nine measurements made on the Scripps Institution's Capricorn Expedition of 1952-53. The observed thermal gradients are three or four times larger than most continental gradients and the conductivities correspondingly smaller, so that the oceanic heat flows are similar to the continental values. The average of all 15 values is 1.69 μ cal cm^{-2} sec^{-1}. Omitting three extraordinarily high values, the remaining 12 give an average of 1.25 μ cal cm^{-2} sec^{-1} with a standard deviation of 0.395 μ cal cm^{-2} sec^{-1} or 31.5 %. The individual variation is markedly higher for the Capricorn results, which represent a much larger area of investigation, than for the Mid-Pacific values. One very low value obtained on the Capricorn Expedition is retained, although some unknown large source of error may be involved.

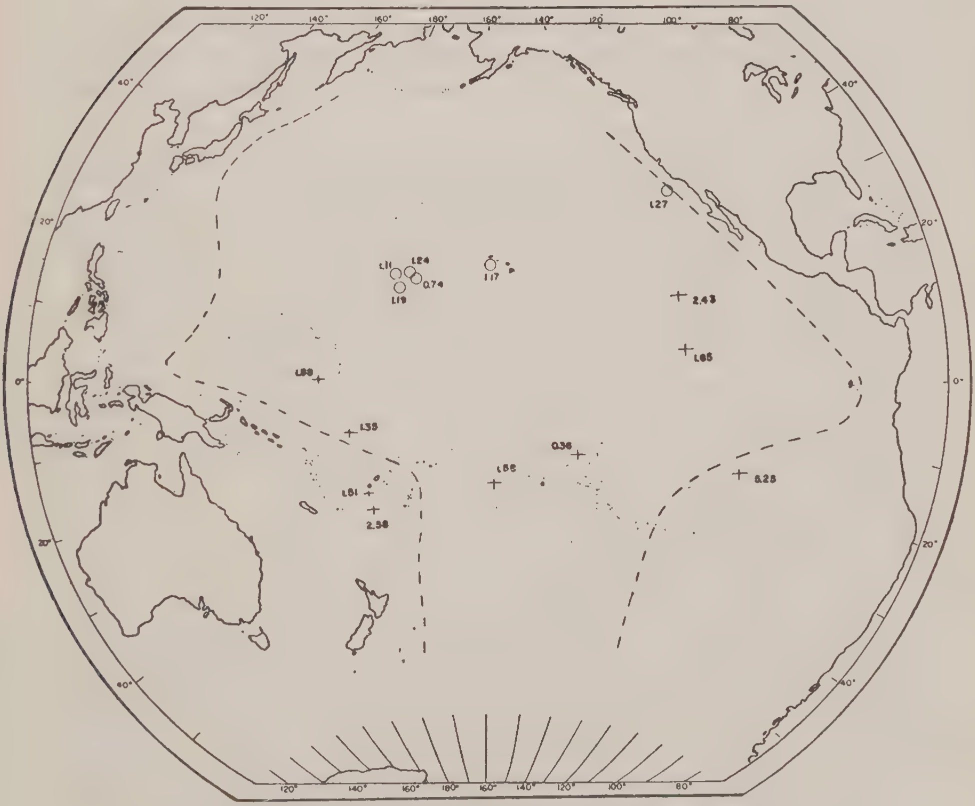
120°
140°
160°
180°
160°
140°
120
100°
80°
40°
40°
20°
20°
0°
0°
20°
20°
40°
40°
1.27
1.11
1.24
0.74
1.19
1.17
2.43
1.65
1.88
1.35
0.36
1.55
8.25
1.81
2.38
120°
140°
160°
180
160°
140°
120°
100°
80°

Fig. 1. Geographic distribution of oceanic heat flow measurements.

The geographic distribution of the results is presented in Fig. 1. Mid-Pacific values are shown as circles and the Capricorn results are represented by crosses. The heavy dashed curve gives the approximate location of the « andesite line », which at least in the South Pacific may be the boundary of the true Pacific basin. Two of the extremely high values lie on the continental side of the andesite line while the third appears to be well within the Pacific basin. For the present, we shall consider these three values as anomalous. Whether this is justified can not be determined without many more measurements. (In any case, the following interpretation will be little affected whether or not these high values are included in the average.) Obviously, the data are too meager to conclude whether a major pattern exists in the heat flow or the high values represent isolated local effects. On the other hand, the average value may be fairly representative of the entire Pacific basin.

Additional evidence on the similarity of the oceanic and continental heat flow has been obtained by Sir Edward Bullard (1954) with five measurements in the Atlantic Ocean. The Atlantic values obtained by him average somewhat less than our Pacific ones.

Sources of the heat.

All or part of the heat flow might be the result of temperature changes in the water immediately above the bottom. If the water was warmer in the past than at present a fraction of the heat introduced into the sediments would still remain and would contribute to the observed heat flow. We have satisfied ourselves that the magnitude of the temperature changes over time of one year or more necessary to account for a significant part of the heat flow would have to be much larger than available evidence permits. Consequently, the heat must originate either in the sediments or in the rocks underlying the sediments.

For convenience in discussion we may divide ΣQ, the observed heat flow, into components :

$$\Sigma Q = Q_s + Q_c + Q_m + Q_i$$

where the subscripts *s*, *c*, *m* and *i* refer to those portions of the observed heat flow arising from the heat generated in the sediments, the crust and the mantle, and from cooling of an « initially » hot earth, respectively. Computations show that various exothermal processes occurring within the sediments, including biological activity, compaction, diagenetic processes and radioactive decay, produce less than one per cent of the observed heat flow. This leaves the deeper layers of the earth as the primary source.

Raitt's (1951) seismic refraction measurements show that the Mohorovičic discontinuity lies about 7 kilometers beneath the Pacific Ocean floor. If we consider that this discontinuity marks the boundary between the earth's crust and mantle, and assume that all the material above the Mohorovicic discontinuity in the Pacific has a radioactivity similar to basalt, we find that Q_c can be only 10 % of the observed heat flow. Therefore, 90 % must have its origin in the mantle. This is in marked contrast to conditions under the continents, where it is generally believed that at least 70 % of the heat flow originates in the crust. The estimates of relatively high heat production in the continental crust are based on evidence that the Mohorovičic discontinuity is about 35 km below the surface, and that the rocks above the discontinuity are relatively high in radioactive materials. This is partly confirmed by the higher heat flows found in some mountain areas where the crust is presumably thickened (Birch 1950).

To make an estimate of the heat arising from the initial distribution of temperature, Q_i, we may assume that cooling has been taking place by conduction alone; then Q_i should be the same under both continents and oceans. In the continental case Q_c is predominant. As an upper limit for Q_c (continental), the heat generated in the continental crust might account for all the observed heat flow. As a lower limit, if the entire 35 km of the continental crust had an average radioactivity similar to basalt, Q_c (continental) would be about 0.7 μ cal cm^{-2} sec^{-1}. The heat flow resulting from radioactive decay in the mantle, Q_m (continental), must be at least 0.1 μ cal cm^{-2} sec^{-1}. Consequently Q_i must lie between 0 and 0.6 μ cal cm^{-2} sec^{-1}. The probable upper limit of Q_i, utilizing the available evidence on the distribution of radioactivity in the continental crust, is 0.3 μ cal cm^{-2} sec^{-1}. This value is represented by the dashed line in Fig. 2.

We have considered a sphere that has been cooling for 3×10^9 years with an initial temperature distribution, $a + b\,x$, and a thermal conductivity, k (constant with depth), where a is the temperature at the earth's surface and b is the increase with depth, x. As an upper limit for the initial temperature we may assume the earth to have been molten throughout, whence $a = 1300°$ C (the melting point of basalt at atmospheric pressure). Following Jeffreys (1952), we may estimate the melting point gradient from the Clausius-Clapeyron equation to be 3° C km^{-1}. This probably gives an upper limit for the change of melting point with depth. For the lower limit of the initial temperature we have assumed

$a = 650°$ and b to be the adiabatic increase in temperature with depth. Verhoogen, (1954), estimates that the adiabatic gradient is 0.5° C km^{-1}. These two cases will be referred to as the « hot » and « cool » earth.

Figure 2 shows calculated values of Q_i plotted against thermal conductivity, k. For a hot earth, the estimated upper limit of Q_i, 0.3 μ cal cm^{-2} sec^{-1}, will be obtained if the average value of k is 0.006 cal cm^{-1} sec^{-1} °C^{-1}. For a cool earth, k must be 0.035 cal cm^{-1} sec^{-1} °C^{-1}.

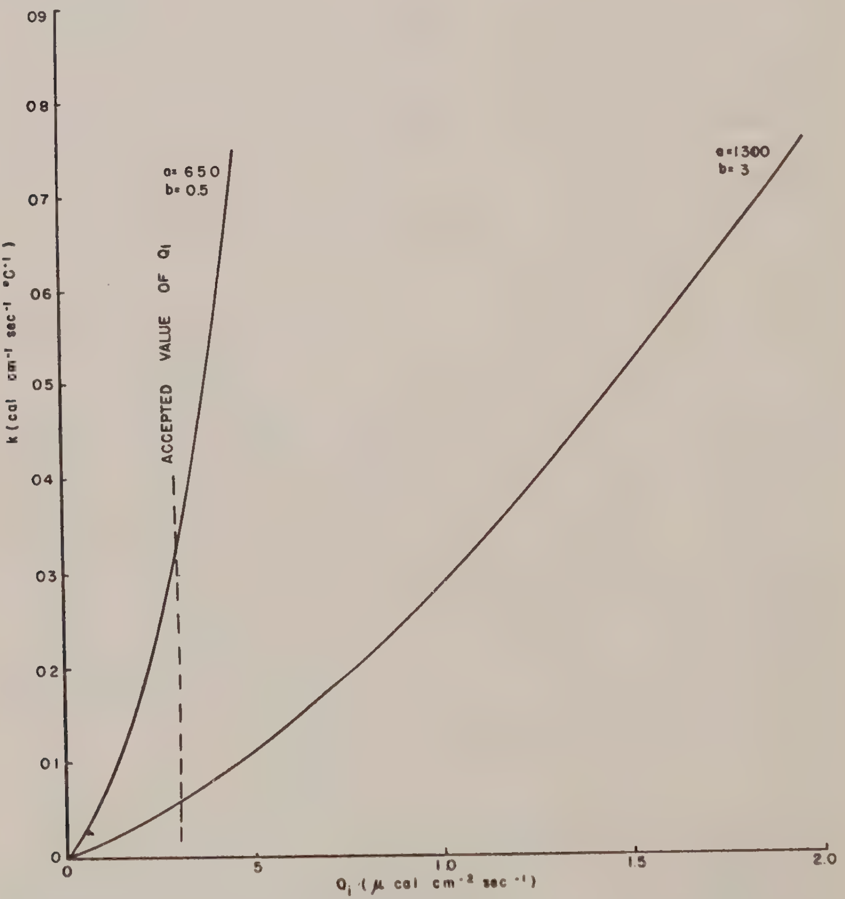

FIG. 2.
Values of Q_i as a function of the thermal conductivity for an initially « hot » and « cool » earth.

With the preceding values of Q_c and Q_i, Q_m beneath the oceans must be at least 0.8 μ cal cm^{-2} sec^{-1}. We have assumed, for simplicity, that the total radioactive heat production per unit area is just sufficient to prevent either heating or cooling of the mantle as a whole, and that this radioactivity is uniformly distributed down to a depth L, beneath which the radioactivity is negligible. The maximum depth L over which the radioactivity can be distributed to give the observed heat flow is plotted in Fig. 3 as a function of the thermal conductivity. The corresponding amounts of radioactivity per unit volume (expressed in terms of heat production H, cal cm^{-3} sec^{-1}) are also shown. If the mantle was initially at the assumed melting point at all depths, the previous considerations concerning Q_i indicate that k must approximate 0.006 cal cm^{-1}

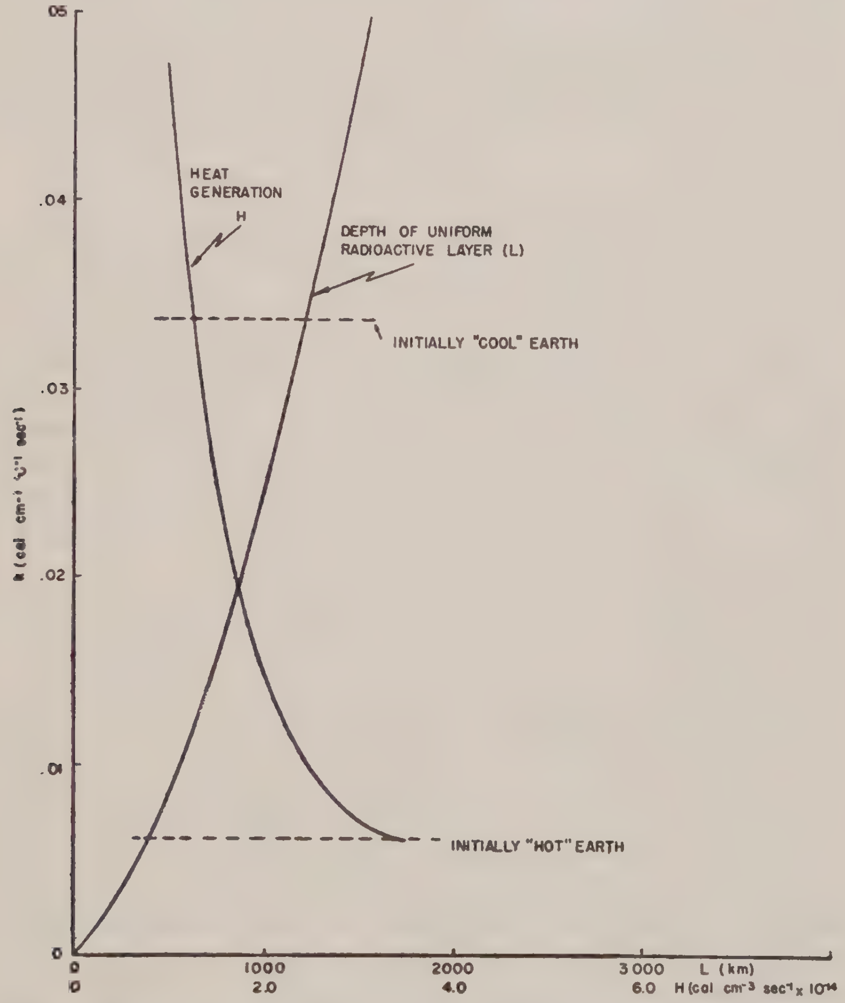

FIG. 3. Depth of uniformly distributed radioactive layer L and corresponding heat generation H as a function of the thermal conductivity.

sec^{-1} °C^{-1}. We see from Fig. 3 that L can not then be more than 400 km and H not less than 3.7×10^{-14} cal cm^{-3} sec^{-1}. This value of H appears improbably high in the light of the usual suppositions about the composition of the mantle. On the other hand, for an initially cool earth (initial surface temperature 650°, increasing adiabatically with depth $H = 1.2 \times 10^{-14}$ and $L = 1200$ km. But in this case the thermal conductivity must be quite high, although possibly not beyond the limits of Uffen's (1954) recent theoretical considerations.

It is of interest to examine the case of a hot earth in somewhat more detail. In order to prevent rapid cooling, k must be small and there must therefore be an upward concentration of the radioactivity. The limit of such an upward concentration would be a distribution of radioactivity under the oceans similar to that under the continents. This is difficult to reconcile with the depths to the Mohorovicic discontinuity, 5 to 10 km beneath the oceans and 30 to 40 km under the continents. It would appear more likely that most of the continental radioactivity is above the Mohorovicic discontinuity while the oceanic radioactivity is distributed over a greater range of depth.

Fig. 4 shows the temperature that would result from different distributions of radioactivity under the continents and oceans. For simplicity we have assumed, as before, that the radioactivity is uniformly distributed down to a given depth and zero at greater depths, and that the total radioactivity is sufficient to maintain the observed heat flow. The depths of the radioactive layers have been taken as 35, 165 and 200 km, representing a typical continental and two possible oceanic distributions, respectively. Two salient features are noted. First we see that if the radioactive layer extends to depths greater than 165 km, heating, and presumably melting, of the mantle will occur. Second, the temperatures beneath the oceans will be several hundred degrees higher than beneath the continents over a considerable range of depth. The magnitude of this difference will be somewhat smaller if exponential distributions of radioactivity are considered instead of a two-layer model. A large temperature difference in the mantle between the oceans and continents is difficult to reconcile with the data on gravity, as has been pointed out by Griggs (1954). We consider it more likely that the radioactivity is distributed over considerable depths and that high conductivities and comparatively low mantle temperatures are required.

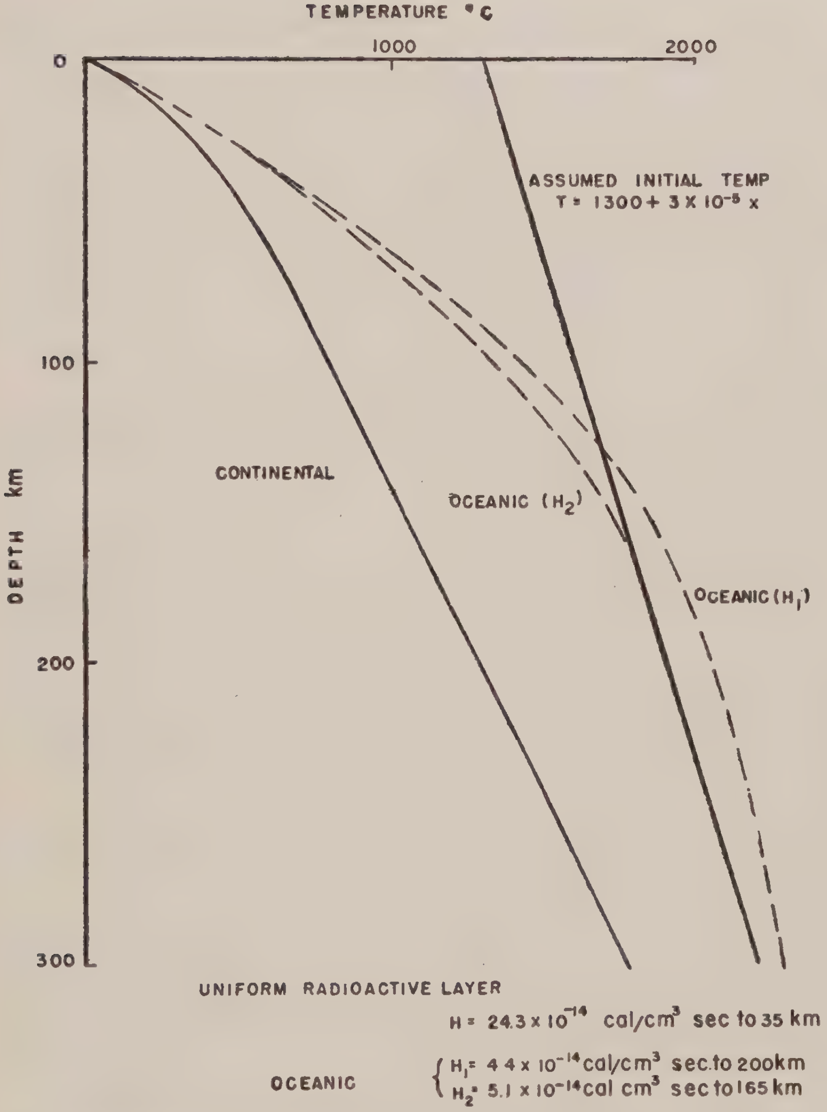

Fig. 4.
Possible temperature — depth distributions under continents and oceans.

Provided the temperature gradient within the earth is nearly adiabatic, the existence of radioactive substances at depth in the oceanic mantle might cause continuous convection there and consequently a relatively rapid upward transport of heat generated by radioactivity, while convection might be absent in a continental mantle that had been largely drained of its radioactive elements. The average heat flow originating in the continental crust and in the oceanic mantle would then be nearly the same, but if convection cells of moderate size exist under the oceans there should be a detectable pattern of variations from place to place in the heat flow through the sea floor.

If convection were not continuous but intermittent, as Griggs (1939) and others have suggested, there would be no restrictions on initial conditions and the oceanic heat flow could be a relic of a past overturn. In this case it would be coincidental that the oceanic and continental heat flows are similar.

SUMMARY.

Measurements of oceanic heat flow give an average value similar to but somewhat higher than the average for the continents. Over 90 % of the observed oceanic heat flow must come from beneath the Mohorovicic discontinuity. This is in marked contrast to the continental situation, where it is usually estimated that not more than 30 % of the heat flow originates within the continental mantle. Consequently the oceanic mantle must differ from the continental mantle either in its properties or its behavior. The oceanic heat flow and the total radioactivity per unit area under the oceans could both be the same as the continental values, provided that under the oceans one of the following three situations hold :

1. The radioactivity is concentrated near the earth's surface. Improbably high values of radioactivity are then necessary for the rocks in the outer part of the mantle.

2. The radioactivity is distributed more or less uniformly throughout a considerable thickness of the mantle. This requires a « cool » earth and relatively high thermal conductivity at all depths.

3. The heat is transported from the earth's interior by convection as well as conduction. This also requires a cool earth.

A detailed mathematical presentation of the above arguments is given by Revelle and Maxwell (1956).

REFERENCES.

1. BIRCH (F), 1950, Flow of Heat in the Front Range, Colorado, Geo. Soc. Amer. Bull., vol. 61, pp. 567-630, 16 fig.
2. BULLARD, Sir EDWARD, 1954, The Flow of Heat Through the Floor of the Atlantic Ocean, Proc. Roy, Soc. A vol. 222, pp. 408-429 17 fig.

3. Griggs (D.), 1939, Discussion on A Theory of Mountain Building, Amer. Jour. Sci., vol. 237, pp. 611-650.
4. Griggs (D.), 1954, Symposium on Earth's Mantle, Amer. Geophys. Union, Trans., vol. 35-1, pp. 93-96.
5. Jeffreys (H.), 1952, *The Earth,* 3rd edition, Cambridge Univ., 392 p.
6. Raitt (R. W.), 1951, Seismic Refraction Studies of the Pacific Ocean Basin, Paper presented at Seismol. Soc. Amer., Annual meeting March 23 and 24.
7. Revelle (R.) and Maxwell (A. E.), 1952. Heat Flow Through the Floor of the Eastern North Pacific Ocean, Nature, vol. 170, pp. 199-200.
8. Revelle (R.) and Maxwell (A. E.), 1956, Heat Flow Through the Ocean Floor IV. Bull. Geol. Soc. Amer. (in press).
9. Uffen (R. J.), 1954, A Method of Estimating the Thermal Conductivity of the Earth's Mantle (abstract), Amer. Geophys. Union, Trans., vol. 35, p. 380.
10. Verhoogen (J.), 1954, Petrological Evidence on Temperature Distribution in the Mantle of the Earth, Amer. Geophys. Union, Trans., vol. 35, p. 380.

CHAPTER 6

MARK IX SHORE WAVE RECORDER(1)

Frank E. Snodgrass

INTRODUCTION

The Mark IX shore wave recorder system is designed as a general purpose instrument for permanent installations. Its principal component is the Bourns differential pressure potentiometer, which is used as the transducer. The movement of the pressure-sensitive brass bellows is magnified by a potentiometer-contact lever which (in normal position of zero differential pressure) divides the resistance of the potentiometer windings equally. Variations of differential pressure cause the potentiometer contact arm to move across the potentiometer windings. The position variation of the potentiometer arm is converted to a proportional current by the bridge circuit and is recorded by the recording milliammeter.

The low impedance (750 ohms) and high power dissipation (1 watt) of the transducer potentiometer enables the pressure head to be used with practically any type recorder available. An Esterline-Angus recording milliammeter connected in a 24 volt Wheatstone bridge circuit, of which the pressure head forms two legs, is used by the University of California as a standard recording system.

GENERAL DESCRIPTION OF THE COMPLETE SYSTEM

A potentiometer type differential-pressure transducer was selected as the basic component around which the system was designed. This transducer is built by the Bourns Laboratories located in Riverside, California, and can be purchased complete, with calibration, ready to be installed in the pressure head. The transducer can be obtained with any sensitivity normally required in oceanographic studies (full scale deflections of 1 to 20 feet of water) with linearity and resolution of one per cent of full scale. Life tests conducted by the Bourns Laboratory indicated no fatigue or wear failure after 5 million cycles. Installations have been made in which the instrument operated satisfactorily for periods of one to two years.

The Bourns transducer, called a Model 503 Differential Pressure Gage, is 2¼ inches in diameter and 2½ inches in length with two pressure inlets at one end and three electrical terminals at the other. One pressure port connects to the inside of a bellows while the second port connects to the inside of the pressure-tight case, and therefore, to the outside of the bellows. The bellows is connected through a simple lever system to the arm of a potentiometer. As the differential pressure varies, the arm is moved along a resistance winding approximately 1/2 inch in length. One electrical terminal is connected to each end of the

---

(1) Contribution from the Scripps Institution of Oceanography, New Series No. 821.

(2)

Conference on Coastal Engineering Instruments, Proceedings, 1st, 1955. Council on Engineering Research, Engineering Foundation. Reproduced by Permission potentiometer winding and one to the potentiometer arm. The potentiometer is rated at 750 ohms with 1 watt power dissipation.

A brass casing houses the transducer (see figure 1), provides a water-tight cable connection, and by means of a slow leak and compliant chamber, provides an average or static pressure which is applied to one pressure port of the transducer. The second pressure port of the transducer is connected directly to the dynamic underwater pressure through a rubber bellows. Details of the compliant chamber, cable connection chamber and bellows chamber are discussed under "Pressure Head Design."

Armored submarine cable is used to connect the pressure head to the shore unit which consists of a power supply, a Wheatstone bridge, and a pen recorder. The power supply can be dry or wet cell batteries connected for a total output of 24 volts, or an electronic power supply operated from a standard 110 volts a-c or d-c power source. The Wheatstone bridge is mounted in the power supply unit and is a conventional circuit except for special calibration potentiometers.

BRIDGE CIRCUIT DESIGN

GENERAL CONSIDERATIONS

The problem of designing a Wheatstone bridge using a 0.5-0-0.5 milliampere recording milliammeter in the galvanometer circuit was primarily the problem of selecting circuit constants that provided a reasonable compromise between the conflicting requirements of the circuit. The requirements of the circuit were as follows: (a) the resistance of the circuit should not overdamp the recording milliammeter, (b) the ratio of bridge current to recorder current should be large to minimize recording errors, (c) a minimum of power should be supplied to the circuit in order that dry cell operation of the bridge unit is practical.

Frequency response tests indicated that a damping resistance of not less than 10,000 ohms should be connected across the Esterline-Angus recording milliammeter. Considering this resistance to be entirely contained in the meter's series resistance, g, (see figure 2) the voltage across the bridge had to be 20 volts or more in order that full scale recording could be obtained for one-half rated pressure signals. Twenty-four volts was selected for the bridge voltage so that standard batteries of 1½, 6 or 12 volts each could be used as a power source.

A value of 750 ohms was selected for the resistance of the pressure head potentiometer since the Mark III pressure head, which this unit replaces, contained a 750 ohm potentiometer. Equipment designed to operate with the Mark III pressure head therefore could be used with the improved pressure head without modification. The Bourns Laboratories designed a transducer with a special potentiometer that met these specifications (i.e., 750 ohms, 24-volt, 1-watt). Precision resistors of 500 ohms each were selected for the remaining two legs of the bridge circuit.

The equivalent damping resistance and the accuracy with which the

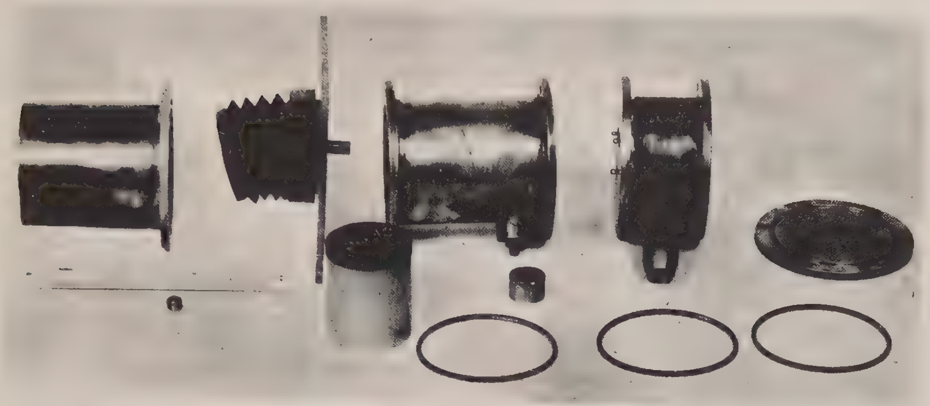

Fig. 1a. Mark IX differential pressure gage. Exploded view.

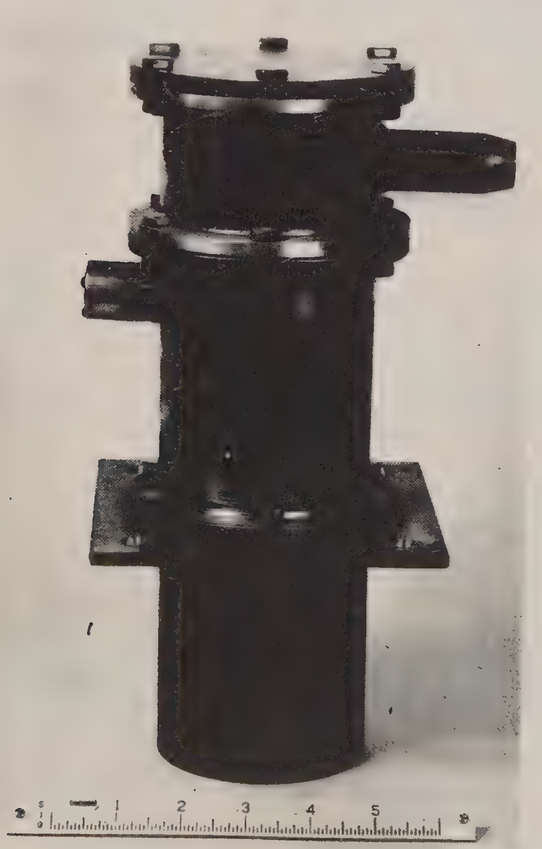

Fig. 1b. Mark IX differential pressure gage. Assembled view.

position of the potentiometer arm is recorded by the recording milliammeter are discussed in the following two sections of this report.

SENSITIVITY ADJUSTMENT

Under actual operating conditions of the circuit, the exact resistance of the pressure head potentiometer will not be 750 ohms, the calibration of the pressure head transducer (ohms per foot of sea water) will not be exactly the desired values, and the resistance of the submarine cable will vary from nearly zero to perhaps 50 ohms resistance, depending upon the length of cable required. By adjusting the current in the pressure head to a value of 32 milliamperes, the effect of the cable resistance is minimized. If a cable of high resistance is used, the voltage across the bridge is increased, maintaining the 32-milliampere current so that 24 volts always appears across the 750-ohm pressure head potentiometer. By adjusting the resistance in series with the recording milliammeter so that full scale current will flow at the desired full scale differential water pressure, the variations in potentiometer resistance and transducer calibration can be compensated. The method of making this adjustment and the error of the adjusted circuit is as follows:

The current that flows in the Esterline-Angus recorder is given by the general bridge equation

$$I_{EA} = \frac{E(bc - ad)}{ab(c + d) + bc(a + b) + g(a + b)(c + d)} \qquad (1)$$

where a, b, c, and d, g are the circuit resistance defined in the simplified diagram (see figure 2) and E is the applied voltage.

Reducing the equation to eliminate b, d, and E by substituting the conditions of the circuit (see figure 3) $a = b$, $E = I_p(c + d)$ and $d = (c + d) - c$, an equation involving the known constants of the circuit I_p, a, g, and $(c + d)$ and the independent variable, c can be formed.

$$I_{EA} = \frac{I_p \left[c - \frac{c + d}{2}\right]}{c - \frac{c^2}{c + d} + \frac{a}{2} + g} \qquad (2)$$

Since the potentiometer arm is at the mid-position of the potentiometer when zero pressure is applied to the pressure head, the independent variable is usually thought of as the displacement of the potentiometer arm from this position. Let y be the resistance between the zero pressure position of the arm and the position of the arm when a pressure, p,

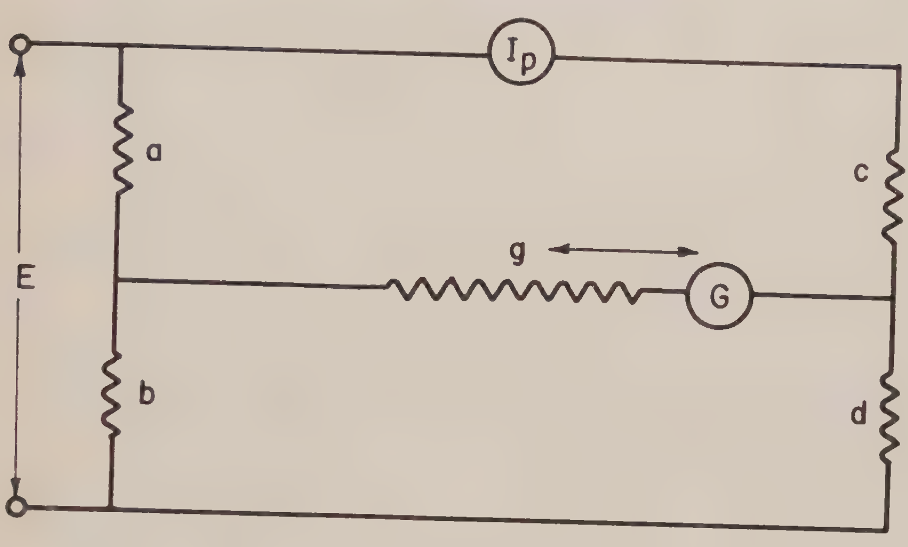

Fig. 2. Simplified bridge circuit.

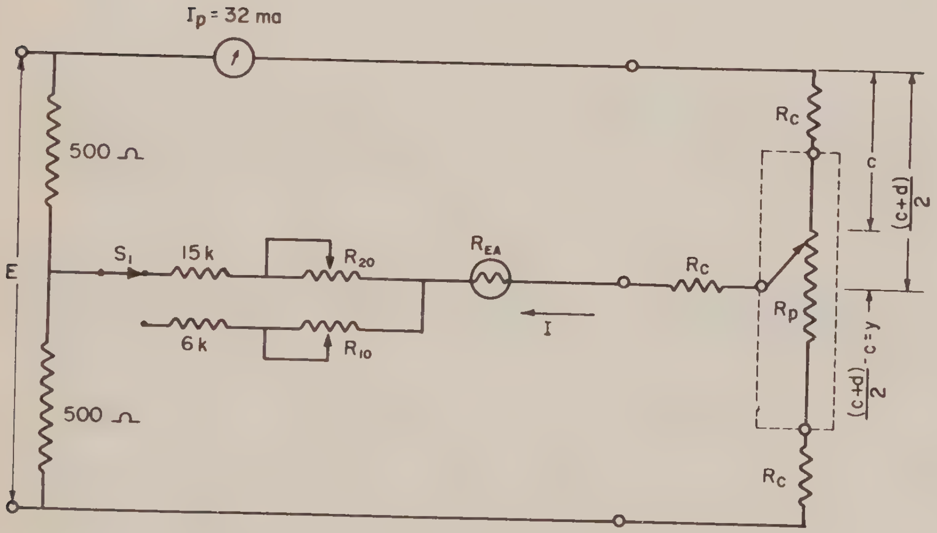
Ip = 32 ma
500 Ω
S1
15 k
R20
REA
Rc
E
6 k
R10
I
Rp
500 Ω
Rc
Rc
c
(c+d)/2
(c+d)/2 - c = y

Fig. 3. Complete bridge circuit.

is applied to the pressure head. Then

$$y = \frac{c + d}{2} - c \tag{3}$$

and

$$\alpha = \frac{y}{\frac{c + d}{2}} = 1 - \frac{c}{\frac{c + d}{2}} \tag{4}$$

where α is the fractional displacement (with respect to the circuit constant $\frac{(c + d)}{2}$) of the potentiometer arm. The independent variable, c, now can be expressed in terms of the fractional deflection of the arm and the resistance $\frac{(c + d)}{2}$.

$$c = \frac{c + d}{2} (1 - \alpha) \tag{5}$$

and

$$I_{EA} = \frac{I_p \quad \alpha \left(\frac{c+d}{2}\right)}{\frac{c+d}{4} - \alpha^2 \left(\frac{c+d}{4}\right) + \frac{a}{2} + g} \tag{6}$$

A further condition of the circuit is that full scale current will flow in the recording milliammeter when the deflection of the potentiometer arm is equal to some value, $\alpha = K$. That is, the circuit will be adjusted so that a given pressure will cause the recorder to register full scale. The system will then be calibrated and the chart width will represent a known total pressure variation.

The necessary resistance of the recording circuit, g , to satisfy the condition that full scale current, $(I_{EA})_{f.s.}$, will flow when the potentiometer arm is in the position $\alpha = K$ can be found from Equation (6):

$$(I_{EA})_{f.s.} = \frac{I_p \quad K \frac{c+d}{2}}{\frac{c+d}{4} - K^2 \left(\frac{c+d}{4}\right) + \frac{a}{2} + g} \tag{7}$$

$$g = \mu K \frac{c + d}{2} + K^2 \left(\frac{c + d}{4}\right) - \frac{c + d}{4} - \frac{a}{2} \tag{8}$$

where

$$\mu = \frac{I_p}{(I_{EA})_{f.s.}}$$

The values of the constants in Equation (8) can be defined in terms of the known circuit values as follows:

(1) $c + d = R_p + 2R_c$ (9)

R_p = resistance of the Bourns potentiometer ohms

R_c = resistance of cable between the bridge and the pressure head; ohms/conductor

(2) a = resistance of the fixed leg of the bridge - 500 ohms

(3) $$K = \frac{y_{f.s.}}{\frac{c + d}{2}} \qquad (10)$$

where $y_{f.s.}$ = resistance between the zero setting position of the potentiometer arm and the full scale position.

Also

$$y_{f.s.} = \frac{R_p}{2} \; \frac{C_d}{C_p} \qquad (11)$$

where R_p = total resistance of the Bourns potentiometer

C_p = total range of the Bourns potentiometer in feet of water

C_d = desired full scale calibration of the chart in feet of water.

K can be computed directly by substituting the formula for $y_{f.s.}$ Equation (11) in the equation for K, Equation (10).

$$K = \frac{R_p\, C_d}{(c+d)\, C_p} = \frac{R_p\, C_d}{(R_p + 2R_c)\, C_p} \qquad (12)$$

Knowing the correct resistance of the recording circuit, g, as computed by Equation 8, the resistance of the "sensitivity potentiometers" can be computed as follows:

$$R_{LOW} = g_{low} - 15{,}000 - R_c - R_{EA} \qquad (13)$$

where

R_{LOW} = resistance of the low sensitivity potentiometer in ohms

R_c = resistance of the cable between the bridge and the pressure head in ohms/conductor

R_{EA} = resistance of the Esterline Angus recorder in ohms

g = total required resistance as in Equation (8)

15000 = fixed resistance in the circuit.

Since the dial is calibrated in 100 divisions and the total resistance of the potentiometer is 10,000 ohms, the dial setting on the low sensitivity range is

$$\text{D.S. (low)} = \frac{R_{LOW}}{10{,}000}\ 100. \qquad (14)$$

The high sensitivity dial is set by computing g, Equation (8), using the correct "desired full scale calibration" C_d in Equation (12) to compute K, and using the following equations:

$$R_{HI} = g_{hi} - 6{,}000 - R_c - R_{EA} \qquad (15)$$

$$\text{D.S. (hi)} = \frac{R_{hi}}{5{,}000}\ 100.$$

SAMPLE CALCULATIONS FOR SENSITIVITY POTENTIOMETER SETTINGS

Given Values

Site: Golden Gate, San Francisco
Bourns potentiometer No. 687
C_p = 10.2 feet sea water full scale
R_p = 746 ohms
Cable resistance : R_c = 10 ohms/conductor
Esterline Angus resistance = 1325 ohms
Desired Calibration: C_d (low) = 10 ft. (± 5 ft.)
C_d (high) = 5 ft. (± 2.5 ft.)

Low Sensitivity Dial Setting

(1) $c + d = R_p - 2\ R_c = 746 + 2(10) = 766$ ohms

(2) $a = 500$ ohms

(3) $$K_{LOW} = \frac{R_p}{(c+d)}\ \frac{C_d}{C_p} = \frac{746 \times 10}{766 \times 10.2} = .955$$

(4) $$g_{low} = 64K\left(\frac{c+d}{2}\right) + K^2\left(\frac{c+d}{4}\right) - \frac{c+d}{4} - \frac{a}{2}$$

$$= 64(0.955)\left(\frac{766}{2}\right) + (0.955)^2\left(\frac{766}{4}\right) - \frac{766}{4} - \frac{500}{2} = 23{,}142$$

(5) $$R_{LOW} = g_{low} - 15{,}000 - R_c - R_{EA}$$

$$= 23{,}142 - 15{,}000 - 10 - 1{,}325 = 6{,}807 \text{ ohms}$$

(6) $$\text{D.S. (low)} = \left(\frac{R_{LOW}}{10{,}000}\right) 100 = \underline{68.0 \text{ divisions}}$$

High Sensitivity Dial Setting

(1) $c + d = R_p + 2R_c = 746 + 2(10) = 766$ ohms

(2) $a = 500$ ohms

(3) $$K_{HI} = \frac{R_p}{(c+d)} \frac{C_d}{C_p} = \frac{746 \times 5}{766 \times 10.2} = 0.478$$

(4) $$g_{hi} = 64K\left(\frac{c+d}{2}\right) + K^2\left(\frac{c+d}{4}\right) - \frac{c+d}{4} - \frac{a}{2}$$

$$= 64\,(0.478)\left(\frac{766}{2}\right) + (0.478)^2\left(\frac{766}{4}\right) - \frac{766}{4} - \frac{500}{2}$$

$$= 11{,}306 \text{ ohms}$$

(5) $$R_{HI} = g_{hi} - 6{,}000 - R_c - R_{EA}$$

$$= 11{,}306 - 6{,}000 - 10 - 1{,}325 = 3{,}971 \text{ ohms}$$

(6) $$\text{D.S. (hi)} = \frac{HI}{5{,}000} \; 100 = \frac{3{,}971}{5{,}000} 100 = \underline{79.4 \text{ divisions}}$$

Bridge Circuit Error

Substituting the value of g obtained from Equation (8) in Equation (6) the recording current for any position of the potentiometer arm can be expressed as a function of the desired full scale position of the potentiometer arm, k, and the independent variable, α , which represents the potentiometer arm position and the full scale current of the recorder, $(I_{EA})_{f.s.}$

$$I_{EA} = (I_{EA})_{f.s.} \frac{\alpha}{K} \frac{1}{1 + \frac{K}{2\mu}\left(1 - \frac{\alpha^2}{K^2}\right)} \qquad (16)$$

Assuming that the position of the potentiometer arm varies linearly with differential pressures, the recording current should vary linearly with the position of the potentiometer arm, α , being equal to $(I_{EA})_{f.s.}$ when $\alpha = K$. Letting I'_{EA} be the correct recording current, we can express the above as

$$I'_{EA} = (I_{EA})_{f.s.} \frac{\alpha}{K} \tag{17}$$

The error in the recording current, expressed as a percent of the full scale current, therefore, is

$$\frac{I'_{EA} - I_{EA}}{(I_{EA})_{f.s.}} 100 = \frac{\alpha}{K} \left[1 - \frac{1}{1 + \frac{K}{2} \quad 1 - \frac{2}{K^2}} \right] 100 \tag{18}$$

PERCENT ERROR AS A FUNCTION OF THE FULL SCALE CALIBRATION K AND THE POSITION OF THE POTENTIOMETER ARM

$\frac{\alpha}{K}$	K = 0.25	K = 0.50	K = 0.75	K = 1.00
0	0	0	0	0
0.2	0.03	0.07	0.11	0.15
0.4	0.06	0.13	0.20	0.26
0.6	0.07	0.15	0.23	0.30
0.8	0.05	0.13	0.17	0.23
1.0	0	0	0	0

POWER SUPPLY DESIGN

Regulated d-c voltage for operation of the bridge unit may be derived from 60-cycle a-c power by passing it through a full wave rectifier, a choke input filter and a voltage regulator (see Figure 4).

The voltage regulator is a series-shunt type having as reference a 22½-volt battery. A regulator circuit functions in such a way as to maintain a given ratio between the output voltage and the reference voltage.

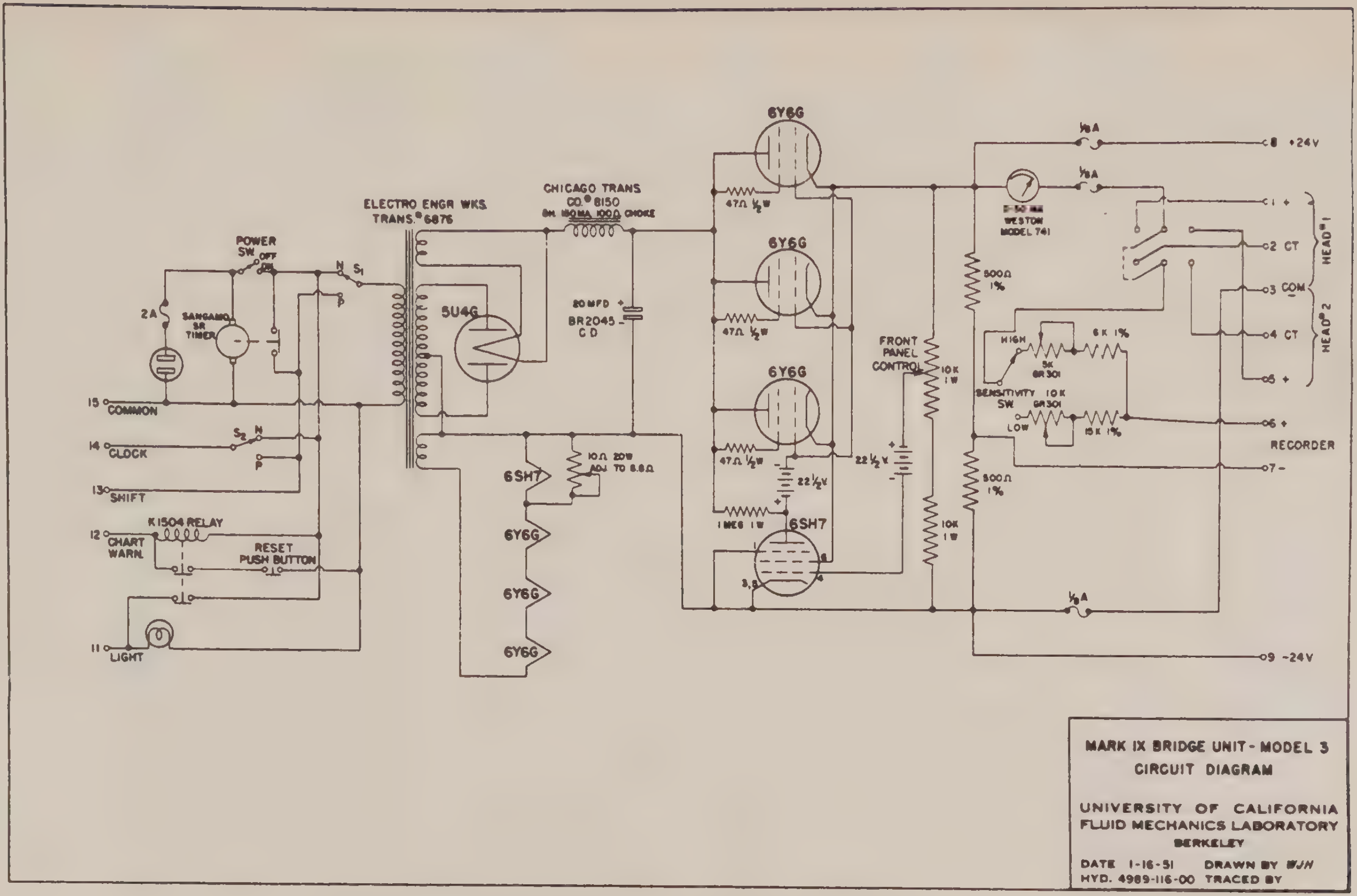
ELECTRO ENGR WKS TRANS.® 6876
CHICAGO TRANS CO.® 8150
8H. 150MA. 100Ω CHOKE
POWER SW
OFF
ON
N
S₁
P
2A
SANGAMO SR TIMER
5U4G
20 MFD
BR2045
C D
10Ω 20W ADJ. TO 8.8Ω
6SH7
6Y6G
6Y6G
6Y6G
15 COMMON
14 CLOCK
S₂
N
P
13 SHIFT
12 CHART WARN.
K1504 RELAY
RESET PUSH BUTTON
11 LIGHT
6Y6G
6Y6G
6Y6G
47Ω ½W
47Ω ½W
47Ω ½W
1 MEG 1W
6SH7
3,5
6
4
22½V
22½V
FRONT PANEL CONTROL
10K 1W
10K 1W
500Ω 1%
500Ω 1%
WESTON MODEL 741
⅛A
⅛A
⅛A
HIGH
LOW
SENSITIVITY SW.
5K GR301
10K GR301
6K 1%
15K 1%
8 +24V
1 +
2 CT
3 COM
4 CT
5 +
HEAD® 1
HEAD® 2
6 +
RECORDER
7 -
9 -24V
MARK IX BRIDGE UNIT - MODEL 3
CIRCUIT DIAGRAM
UNIVERSITY OF CALIFORNIA
FLUID MECHANICS LABORATORY
BERKELEY
DATE 1-16-51
DRAWN BY WJH
HYD. 4989-116-00
TRACED BY

Fig. 4. Mark IX power supply and bridge circuit.

The reference battery operates without load current and consequently has a life equal to the shelf life of the battery. A second battery, used as a bias in the grid circuit of the series tube, also operates at small load. These batteries should be replaced approximately once each six months or whenever the current adjustment control on the front panel can no longer be set to provide the correct bridge current.

The circuits of the power supply and regulator are of conventional design and therefore will not be discussed in regard to the theory of operation. Several special features have been included in the design, however, and these details will be discussed, as will the various controls and methods of operation.

REGULATION

Tests were conducted to determine the effectiveness of the regulator circuit. The results of these tests are shown in Figures 5 and 6. The operating range of the regulator is shown in Figure 5 and is indicated by the area below the 6Y6 G = 0 bias (90 v.a.c. input) line and the 6SH7 zero bias (130 v.a.c. input) line. Within this area the regulator is operating; with the output of the regulator adjusted to 24 v.d.c., regulation is obtained with load currents as high as 100 milliamperes. Regulation within this area was found to be of such a degree that variation in output voltage could not be detected without a differential voltmeter. As this regulation exceeded the required regulation, no attempt was made to determine the output error voltages.

Figure 6 indicates the regulation with constant current loads against power line voltage variations. The output of the regulator first was set at 38 volts (with loads of 80 to 180 ma.) and the input voltage decreased until the regulator became inoperative. As the output voltage decreased, the load was adjusted to maintain the given load current. These tests were then repeated with the regulator output adjusted to 24 v.d.c. The output voltage is shown as a straight line when the regulator is within the operating range since no differential voltmeters were used.

These tests indicate that a wide range of load currents can be supplied with large variations in input power. At the normal operating load condition of 24 v.d.c. and 56 milliamperes, an extremely wide range of power line voltage (75 v.a.c. to 130 v.a.c.) can be regulated. This is desirable since many shore sites, such as lighthouses, fishing piers, and oil piers, have very poor voltage regulation.

TRANSFORMER DESIGN

The power supply is intended to be operated from 110 volt, 60-cycle power, but also can be operated from 110 v.d.c. power. The power supply transformer has been designed so that the input voltage to the regulator

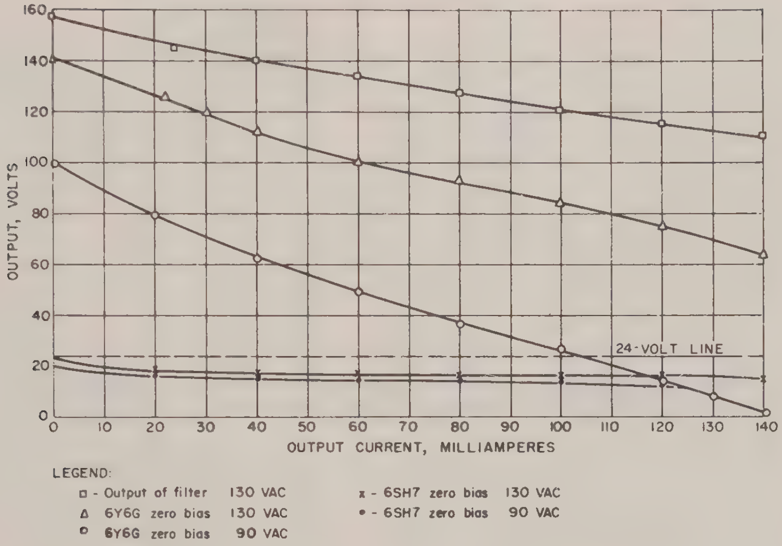

Fig. 5. Regulator characteristics.

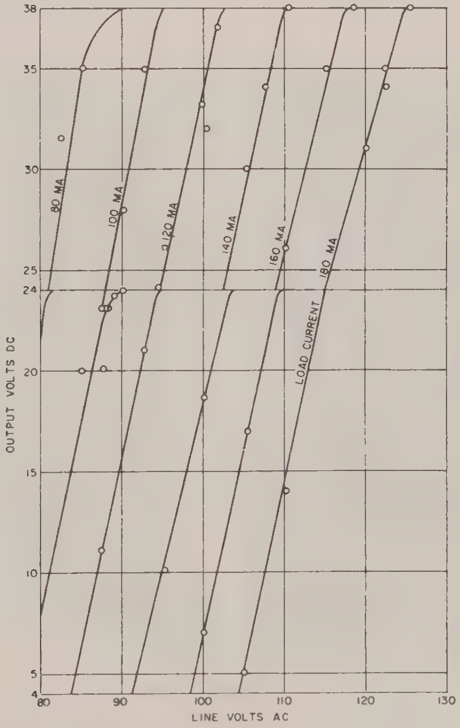

Fig. 6. Voltage regulator characteristics.

is approximately 110 v.d.c. with 110 v.a.c. applied at the power transformer primary. Thus, if only 110 v.d.c. power is available the power line can be connected to the input of the regulator with minor changes in circuit wiring, and the circuit functions normally except for the program timer.

The filaments of the regulator circuit tubes have been connected in series so that a minimum of power will be dissipated in the necessary series resistor when the circuit is operated from a 110 v.d.c. power source. A 25-volt winding is supplied on the power transformer so that the series filament connection is also used when operating the circuit from 110 v.a.c. power.

Series connection of the filament also has the advantage of protecting the pressure head in the case of tube failure. For example, if the shunt tube (6SH7) should fail, the bias on the series tubes would be lost and the output voltage would increase. With the series filament connection, the series tubes also will be made inoperative by failure of the 6SH7 filament, preventing any damage to the pressure head.

OPERATION OF THE POWER SUPPLY AND BRIDGE

FRONT PANEL CONTROLS (FIGURE 7)

Sangamo Timer

The timer, driven by a self-starting, synchronous motor, is connected directly across the a-c input line, hence it is in continuous operation regardless of the power switch position. The programming dial can be seen through the window provided in the case. The protective case cover may be removed for adjustment of the programming cams. Two cams are used to set the duration of the fast and slow speed runs. Each of these cams has four arms spaced 90° apart to provide 6-hour intervals; (other intervals may be obtained by cutting cams with more or less than the four arms; see figure 9). The duration of the fast run may be fixed to a minimum of 15 minutes by careful angular positioning of the "on" and "off" cams with respect to each other. They are securely clamped in place on the shank of the hub by a knurled nut.

In addition to automatic programming of the chart speed, a manual speed shift lever is provided which extends through a slot in the cover of the timer. This lever will shift the chart to the fast speed during any portion of the slow speed interval for additional fast sampling during storm periods. This lever should not be operated if the next fast-speed run is scheduled in less than two hours (minimum off time, 2 hours).

The dial of the timer may be set for the time of day by rotating it clockwise until the correct time is aligned with the red pointer located just below the dial.

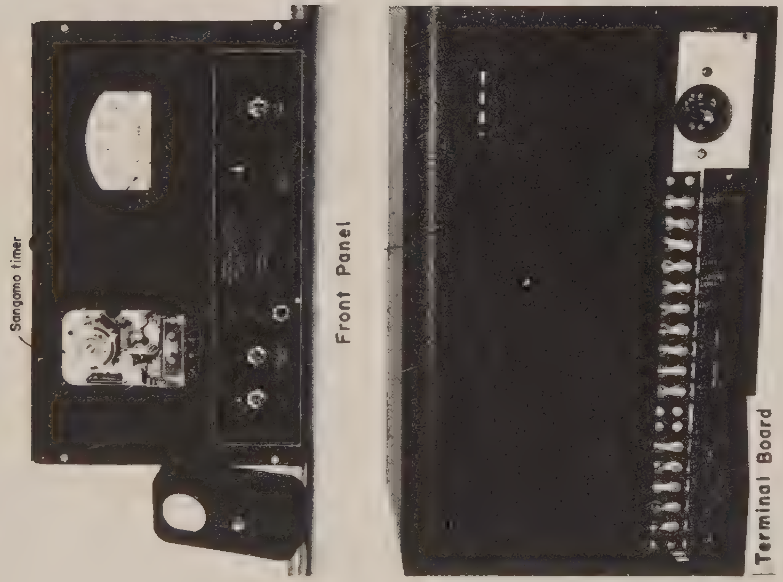
Sangamo timer
Front Panel
Terminal Board

Fig. 7. Mark IX bridge and power supply unit.

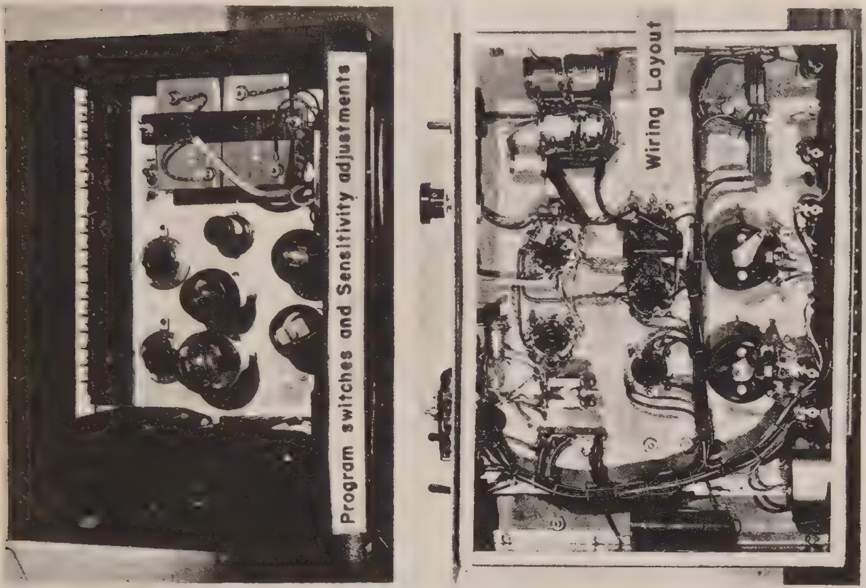
Program switches and Sensitivity adjustments
Wiring Layout

Fig. 8. Mark IX bridge and power supply unit.

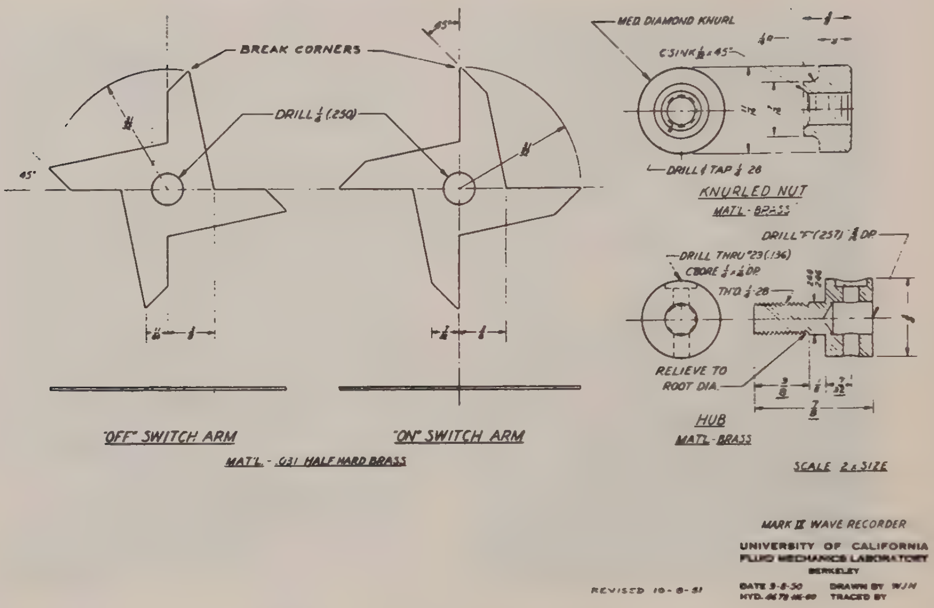
BREAK CORNERS
DRILL ¼ (.250)
45°
MED. DIAMOND KNURL
C'SINK $\frac{1}{32}$ x 45°
DRILL # TAP ¼ 28
KNURLED NUT
MAT'L - BRASS
DRILL "F" (.257) ⅛ DP.
DRILL THRU #23 (.136)
CBORE ⅛ x ⅛ DP.
THD ¼-28
RELIEVE TO ROOT DIA.
HUB
MAT'L - BRASS
"OFF" SWITCH ARM
"ON" SWITCH ARM
MAT'L - .031 HALF HARD BRASS
SCALE 2 x SIZE
MARK II WAVE RECORDER
UNIVERSITY OF CALIFORNIA
FLUID MECHANICS LABORATORY
BERKELEY
DATE 3-8-50
DRAWN BY WJH
TRACED BY
REVISED 10-8-51

Fig. 9. Timer switch details.

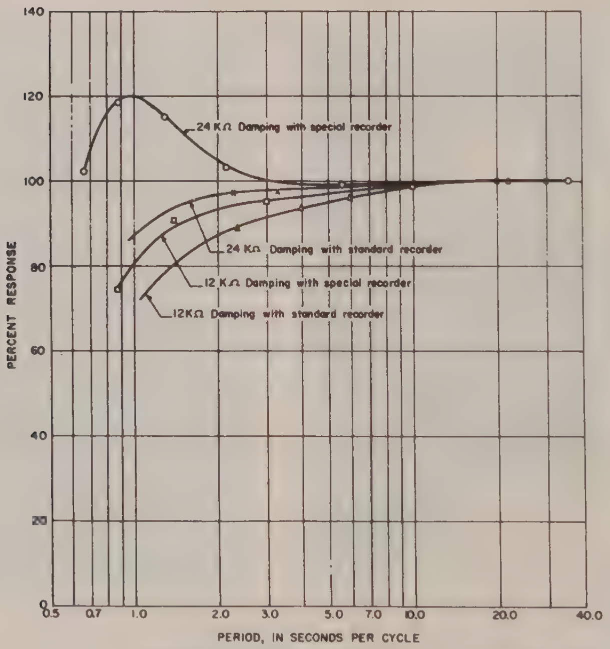

Fig. 10. Esterline-Angus Recording Milliameter frequency response.

Power Switch

With the power switch open, the only element in operation is the Sangamo timer. The rest of the circuit is inoperative including the chart movement, the power to the measuring circuit, the shift mechanism and the warning circuit. When the power switch is closed, the unit will operate according to the programming selected (see "Programming Switches").

Selector Switch

The Model III bridge and power supply unit provides for two pressure heads installed at different locations, or at the same location with one unit as a stand-by. Only one pressure head may be operated at a time. The selector switch is provided to bring one unit or the other into the bridge circuit. The two pressure heads (if two are used) are wired to the bridge circuit with a common negative lead.

Bridge Current Control

To adjust the bridge current, the potentiometer control knob is turned (clockwise for increasing, counterclockwise for decreasing) until the bridge current is 32 ma. The bridge milliammeter is located just above this potentiometer control knob on the front panel. The purpose of this adjustment is to provide the correct current in the Bourns differential pressure potentiometer. The output voltage to the bridge circuit is made sufficient by the above adjustment to compensate for the line drop in the cable from the bridge to the pressure head. The "current adjustment" is actually an adjustment of the regulated d-c output voltage of the regulator.

Sensitivity Switch

Two measuring sensitivities are built into the bridge circuit. The range switch may be placed in either of two positions corresponding to high or low sensitivity.

CHASSIS CONTROLS (FIGURE 8)

Sensitivity Adjustment

As seen in the circuit diagram, Figure 4, potentiometers are connected in series with the range switch. The purpose, location and application of these potentiometers are given below. Hereafter, their operation will be referred to as sensitivity adjustments.

The dial-skirt knobs connected to the sensitivity adjustment potentiometers are located within the Bridge and Power supply cabinet. By varying the resistance in series with the range resistors, fine adjustments are made to correct for: (a) the change in sensitivity of the bellows-potentiometer transducer due to the compliant chamber error (see compliant chamber design), and (b) variations in the manufacturer's specification of the potentiometer. The setting of the sensitivity adjustments has been discussed under that section "Bridge Circuit Design".

Programming Switches

These switches are located within the cabinet, Switch S_1 is the power programming switch, and Switch S_2 is the chart drive programming switch. In "normal" programming, the Sangamo timer actuates only series of fast speed and slow speed intervals showing the time history of the wave action during both speeds. The time durations of these fast chart speed runs and slow chart speed runs depend upon the positioning of the timer cams in the Sangamo timer. By switching both switches to the "P" position, the recording equipment will be turned off during the "off" cycle of the timer. The resulting record then will consist only of a series of fast speed runs.

Fuses

As noted in the circuit diagram, one 2-amp. and three 1/16-amp. fuses provide overload protection. The 2-amp. fuse provides protection to the input circuit, and the 1/16-amp. fuses, located in each line of the bridge circuit, provide protection to the pressure head.

TERMINAL BOARD WIRING (FIGURE 7)

All external connections to the bridge and power supply are made on the main terminal board at the back of the cabinet. Five terminals are provided for the pressure head cables with the "-" lead common. The pressure head's fusite terminals are stamped with "+" and "-" and "CT" (Center Tap) so that with color coded submarine cable there should be little confusion in making the correct connections between the pressure heads and the bridge unit.

Two other sets of terminals include the plus and minus recorder terminals connected to corresponding binding posts on the Esterline-Angus recorder, and the auxiliary 24-volt d-c terminals. The latter may be used in either of two situations:

a. In case of unavailability or failure of a-c power source, the bridge power may be supplied by dry cell batteries. The drain on the battery supply would be the total bridge current (56ma.). When batteries are used, the regulator circuit is inoperative, since the filaments of the tubes are not being supplied with power.

b. It may be desirable to use additional capacity of the power supply to operate a complementary instrument. Current may be drawn from the power supply through these connections (100 ma. maximum), in addition to that required by the pressure head.

The shift, clock and a-c common terminals are connected to corresponding terminals on the Esterline-Angus recorder with an a-c common connection to one post of each circuit.

ESTERLINE-ANGUS RECORDER

MECHANICAL FEATURES

The metering element of the Esterline-Angus recording milliammeter is a permanent magnet, moving-coil type. The instrument is housed in a portable case. The writing pen is supplied with ink fed to the point by capillary action. A center zero calibration is used and the range is plus and minus 0.5 millamperes. Chart speeds of 3/4, 1½, 3, 6 and 12 inches per hour and inches per minute are available with both 8-day spring clock and synchronous motor drives.

For use in conjunction with an automatic programming timer, an electric gear shift can be obtained to change chart speed.

FREQUENCY RESPONSE

In the standard Esterline-Angus recorder the metal bobbin on which the moving coil is wound is constructed to act as a shorted turn and cause the instrument to be critically damped. Connecting any external circuit to the recorder further increases the damping with the result that the high frequencies are attenuated. At a very nominal extra cost, Esterline-Angus recorders can be purchased with special high resistance bobbins made of nickel-silver which cause the recorders to be underdamped. These special recorders become critically damped when shunted with a resistance of 15,000 ohms.

The damping resistance of the bridge circuit is for all practical purposes the resistance of the galvanometer series resistance, g, as defined in Figure 2. Examination of the circuit diagram shown in Figure 3 indicates this resistance will vary between 12,000 ohms and 24,000 ohms for the various operating conditions of the circuit. The frequency response of both the standard and the special type recorders was measured to determine the recorder error at various frequencies. The results of these tests are shown in Figure 10.

Since the shortest period normally encountered in subsurface pressure measurements is about 5 seconds per cycle and the average period is normally between 8 and 15 seconds per cycle, the frequency response of either the special or standard recorder with damping between 12,000 ohms and 24,000 ohms is satisfactory. However, if the recorder is used to record waves of shorter period, special consideration must be given to the damping of the recorder. In this case only the special recorder can be used. If an optimum damping resistance is connected to the recorder, wave periods as short as 1.5 seconds per cycle can be recorded with little error.

PRESSURE HEAD CONSTRUCTION

MECHANICAL FEATURES

Machine shop and assembly drawings are appended. The potentiometer chamber acts as a water tight encasement surrounding the potentiometer unit. A silver soldered separation disc, provided with Fusite hermetically-sealed terminals, divides the connection chamber and the potentiometer chamber. The lower flange of the potentiometer chamber is sealed against surrounding water pressure by an O-ring gasket.

When the instrument is submerged the static pressure at this level will act on the rubber bellows clamped on the shoulder provided on the bottom of the mounting flange. The rubber bellows is filled with a silicone fluid of 500 centistoke viscosity. This fluid is forced to flow through two inlets to the potentiometer chamber.

The first of these inlets is fitted with a "slow leak" that restricts the flow of silicone fluid. Normally, the time constant of flow into the transducer is about one minute (see air dome calculations). When the unit is installed in the sea, fluid will flow between the rubber bellows and the transducer chamber until the pressure within the chamber is equal to the average pressure of the sea. The pressure of the air in the chamber acts on the outside of the bellows in the transducer.

The second inlet is connected directly to the inside of the transducer bellows with no impediment to the flow of fluid from the rubber bellows. The difference in the pressures on the two sides of the bellows (the dynamic pressure fluctuation caused by wave action) causes the bellows to be displaced.

Cable Connection

The electrical cable is connected to the instrument in a chamber located at the top of the pressure head. Since the inside of the electrical cable is at atmospheric pressure, the shore end being open to the atmosphere, the connection chamber must also be at atmospheric pressure. Standard packing glands were found to be unsatisfactory as pressure seals when an instrument was to be installed for long periods of time, due to the plastic flow of the synthetic rubbers found in most cable. A cable connection was developed which has a clamping ring inside the connection chamber for mechanical strength, and a rubber tape seal between a smooth cable nipple and the electrical cable external to the chamber. Tape seals of this type have been found to be satisfactory for periods of two years.

Rubber Bellows Chamber

An "O" ring seal has been provided in the flange of the rubber bellows chamber so that the rubber bellows chamber can be pressurized for calibration purposes. A simple plate with a gasket seal and appropriate fittings can be clamped against the bottom of the chamber by bolts through the mounting flange for this operation.

The inside of the rubber bellows chamber has been so shaped and dimensioned that the rubber bellows can be pressurized before installation.

COMPLIANT CHAMBER DESIGN

An air space is necessary in the transducer chamber to prevent hydraulic locking of the transducer bellows, and a sufficient air volume must be provided to prevent excessive pressure variation of the air volume due to variation in volume of the transducer bellows. As the bellows is deflected, its volume must necessarily vary in order that work be done on the system; this variation in bellows volume causes an equal variation in compliant air volume. The variation in air volume in turn causes a pressure variation of the air volume that opposes the initial dynamic pressure and thereby reduces the sensitivity of the instrument.

Assuming that a negligible flow of fluid through the slow leak occurs during the relatively short period of the wave generated pressure fluctuations, the differential pressure across the transducer bellows is equal to the difference between the instantaneous sea pressure and the instantaneous compliant chamber pressure.

$$(P + p_W) - (P + p_a) = p_W - p_a \qquad (19)$$

where P = average absolute water pressure at instrument

p_W = hydrodynamic pressure of waves

p_a = pressure in the compliant chamber due to the transducer bellows expanding.

The displacement of the bellows and the reading of the instrument is proportional to the differential pressure across the bellows, while the correct reading is proportional to p_W. The fractional instrument error is, therefore,

$$E = \frac{p_W - (p_W - p_a)}{p_W} = \frac{p_a}{p_W} \qquad (20)$$

(45)

The change in volume of the transducer bellows, which is equal to the volume change of the air volume, v_a, is a function of the differential pressure across the bellows and the bellows spring constant c_1

$$v_a = c_1 (p_w - p_a) = c_1 p_w (1 - E) . \qquad (21)$$

The pressure change, p_a, and the bellows volume change, v_a, are related by the gas law and can be expressed to the first approximation as

$$\frac{P}{P + p_a} = \left(\frac{V - v_a}{V}\right)^n = 1 - \frac{n\, v_a}{V} \qquad (22)$$

where n is the polytropic expansion coefficient. Now

$$v_a = \frac{V}{n} \frac{p_a}{P + p_a} \qquad (23)$$

and equating Equation (21) and Equation (23), we have

$$c_1 p_w (1 - E) = \frac{V}{n} \frac{p_a}{P + p_a} \qquad (24)$$

Equation 24 can be solved for the instrument error as a function of the bellows spring constant and the pressure and volume of the air in the compliant chamber.

$$E = \frac{1}{1 + \dfrac{V}{c_1 n P}} \qquad \text{assuming } P \cong P + p_a \qquad (25)$$

For the Mark IX pressure head the volume of the air space can not be less than 11 cubic inches nor greater than 22 cubic inches, with an optimum working volume of 17 cubic inches (see Pressurization of the Pressure Head). The ± 3.3 psi (± 7.5 feet of sea water) Bourns transducer bellows expands 0.1 cubic inches for full deflection and therefore has a spring constant of 0.1/7.5 cubic inches per foot of sea water pressure. Further, assuming n to be equal to unity for the long period pressure fluctuations of ocean waves, the instrument error can be calculated for the normal working depths.

For c = 0.1/7.5' = 0.0133 cu. in/ft of water V = 11, 17, 22 cu. in.

Depth of instrument in feet	Absolute Pressure. ft. of water	Percent decrease in sensitivity		
		E_{11}	E_{17}	E_{22}
0	33	3.8	2.5	1.9
25	58	6.5	4.4	3.4
50	88	10.6	6.4	5.1
75	108	11.6	7.8	6.1
100	133	13.8	9.4	7.5

The decrease in sensitivity of the pressure head can be compensated by adjusting the sensitivity controls (see Adjustment of Sensitivity Controls) for a correspondingly greater sensitivity. The correction can be made by assuming the Bourns pressure transducer to be correspondingly less sensitive when calculating the sensitivity control settings. Thus if a transducer with a sensitivity of 750 ohms/15 feet of water is to be installed in 50 feet of water, a sensitivity of 750 ohms/1.064 x 15 ft. would be used in the calculations.

Slow Leak Design

The purpose of the slow leak is to seal the air chamber against the pressure fluctuations generated by the waves, but at the same time to allow a sufficiently rapid flow into and out of the compliant chamber to prevent the instrument from recording tides. Considering viscous friction as the only factor restricting flow, the flow of fluid through the slow leak is proportional to the pressure across it.

$$\frac{dq}{dt} = c_2 (p_w - p_a) \tag{26}$$

where

q = quantity of fluid in the air dome (in.^3)

c_2 = slow leak constant $\left(\frac{\text{in.}^3/\text{sec}}{\text{psi}}\right)$

p_w = pressure of the water (psi)

p_a = pressure in the compliant chamber (psi)

t = time (sec.)

If the pressure head has been pressurized according to the procedure outlined in "Pressurizing the Pressure Head Unit" of this report, the air volume in the transducer chambers, V, will be 17 cubic inches with the instrument installed in the sea. The absolute pressure in the chamber, P, will be equal to the absolute pressure of the water. If an additional quantity of fluid, q, is forced into the chamber, the pressure in the chamber will be

$$p_a = \frac{P\,V}{V - q} \quad . \tag{27}$$

Therefore

$$q = V - \frac{PV}{p_a} \tag{28}$$

$$\frac{dq}{dt} = \frac{PV}{{p_a}^2}\,\frac{dp_a}{dt} \tag{29}$$

and Equation (26) can be written

$$\frac{PV}{{p_a}^2}\,\frac{dp_a}{dt} = c_2\,(p_w - p_a) \quad . \tag{30}$$

A general solution of Equation (30) can not be found easily but the special case which covers the normal operating conditions of the instrument can be solved readily. In this special case the assumption is made that the pressure fluctuation in the compliant chamber is small relative to the pressure fluctuation in the sea due to wave action, and therefore the fluctuation in the chamber is very small relative to average pressure. The pressure, p_a, then can be assumed equal to P and Equation (30) can be written

$$\frac{V}{c_2 P}\,\frac{dp_a}{dt} = p_w - p_a \quad . \tag{31}$$

If $p_w = P + p' \sin \frac{2\pi t}{T}$ where P is the average pressure and $p' \sin \frac{2\pi t}{T}$ is the pressure fluctuation due to ocean waves of period, T, Equation (31) can be solved for the response of the instrument which is equal to

$$R = \frac{\text{Pressure variation recorded by the instrument}}{\text{Actual pressure variation due to wave action}}$$

$$R = \frac{1}{\sqrt{1 + \left(\frac{T}{2\pi t_o}\right)^2}} \qquad \text{where} \quad t_o = \frac{V}{c_2 P} \qquad (32)$$

The above results can be obtained by assuming that the pressure head can be represented by an equivalent electrical circuit of a resistor (slow leak) and a condenser (of a compliant chamber) connected in series across the input signal with the output signal measured across the resistor.

The slow leak can be adjusted for a greater rate of flow than would be intuitively thought possible. The time constant of the instrument can be adjusted to be equal to the longest wave period to be recorded without loss of sensitivity. This means that normally $t_o = V/c_2P$ can be adjusted as low as 15 seconds without jeopardizing the operation of the recorder, since a wave of fifteen second period will be recorded with only a one percent loss in sensitivity. A frequency test on a Mark IX Model 2 instrument showed close agreement between Equation (32) and the operation of the recorder.

Adjusting the slow leak to as rapid a flow as possible is desirable since it will permit the pressure head to be lowered during installation at a fast rate. Also, the slow leak is less subject to plugging with the more rapid flow rates.

PRESSURIZING THE PRESSURE HEAD UNIT BEFORE INSTALLATION

GENERAL PROCEDURE

The total volume of the rubber bellows when expanded under pressure to the full extent of the lower dome has been measured and found to be equal to 24 cubic inches. If the pressure head contains 20 cubic inches of fluid, and the pressure head is pressurized, the entire volume of fluid can be forced into the expanded rubber bellows and an air pocket will exist above the fluid.

The air pocket in the pressurized rubber bellows has been provided to simplify the pressurization procedure as follows: (1) the slow leak between the air dome and the rubber bellows will not restrict appreciably the flow of air between the two chambers, and therefore will permit rapid pressurization of both chambers without damage to the Bourns transducer; (2) the fluid in the rubber bellows will be in direct contact with the air and will reach an equilibrium between the air pressure and the amount of absorbed air in the fluid in a relatively short time.

The following procedure can be used to pressurize the pressure head unit:

a. Twenty-four hours before installation, pressurize the unit to a pressure equal to the depth of the proposed installation. The fluid will then absorb air from the air-pocket above the fluid until it is saturated for the condition of the final installation. The pressure in the pressure head should be checked every few hours, and repressurized if necessary, until equilibrium is reached.

b. At the time of the installation, the actual depth of the proposed installation should be checked and the absolute pressure in the pressure head unit reduced to 0.55 of the absolute pressure of the installation depth or to the pressure as calculated in the following sections. The air in solution in the silicone fluid will not escape during this readjustment of the pressure. The readjustment of the pressure can be done any time after equilibrium, as described in part (a), has been reached.

CALCULATION OF INITIAL PRESSURE

The initial pressure must be adjusted so that the rubber bellows will collapse to the correct working volume, and the compliant chamber pressure will increase to the average pressure of the water when the pressure head unit is installed in the sea. The calculation of the initial pressure is based, therefore, on: (1) the final pressure, (2) the initial and final air volumes within the pressure head unit and (3) the initial and final temperature corresponding to the air temperature and the sea temperature. Note that the calculations do not allow for absorption of air by the fluid. It is assumed the fluid is pre-saturated as described in the previous section.

$$P_i = P_f \frac{V_f}{V_i} \frac{T_a}{T_w} \qquad (33)$$

where

P_i = absolute initial pressure

P_f = absolute final pressure

V_f = initial air volume within the pressure head unit

V_i = initial air volume within the pressure head unit

T_a = absolute temperature of the air

T_w = absolute temperature of the water.

The initial air volume within the pressure head is:

$$V_i = V_d + V_b' - V_s = 27 + 24 - 20 = 31 \text{ cu. in.}$$

where

V_d = volume of the compliant chamber = 27 cu. in.

V_b' = total volume of the pressurized rubber bellows = 24 cu. in.

V_s = total volume of silicone oil in the pressure head = 20 cu. in.

In order that the rubber bellows will not affect the instrument reading, the final air volume within the pressure head must remain within a given maximum and minimum volume. If the rubber bellows has collapsed too far, or remains pressed against the walls of the lower dome, the pressure within the bellows will not be the same as the sea pressure and an error will be introduced in the instrument reading. The maximum and minimum allowable final air volume as determined by the maximum and minimum rubber bellows volumes are as follows:

$$(V_f)_{max} = V_d + (V_b)_{max} - V_s = 27 + 15 - 20 = 22 \text{ cu. in.}$$

where

$(V_b)_{max}$ = measured maximum working volume of the rubber bellows = 15 cu. in.

$$(V_f)_{min} = V_d + (V_b)_{min} - V_s = 27 + 4 - 20 = 11 \text{ cu. in.}$$

where

$(V_b)_{min}$ = measured minimum working volume of the rubber bellows = 4 cu. in.

If the optimum working volume of the rubber bellows of 10 cubic inches is used, and the difference in absolute temperature of the air and water is small, the initial pressure can be computed as follows:

(51)

$$P_i = P_f \frac{V_d + (V_b)_{opt} - V_s}{V_d + V_b' - V_s} = P_f\left(\frac{17}{31}\right) = 0.55\ P_f \qquad (34)$$

or

$$(P_i)_{gage} = \left[0.55\ (z + 33) - 33\right]\ .44 \cong \left(\frac{z}{4} - 6.5\right)\ \text{psig} \qquad (35)$$

where

$(P_i)_{gage}$ = optimum initial gage pressure in psig

z = depth of instrument below surface of water in feet

33 = atmospheric pressure in feet of sea water

.44 = psi/foot of sea water.

After computing the optimum initial pressure, the extremes in final pressure due to tide variations, and the extremes in water temperature variations should be used to calculate the final bellows volume to be sure the volume remains within the allowable range under all conditions.

INITIAL PRESSURE FOR SHALLOW WORKING DEPTHS

Approximately 1.5 psig is needed to expand the rubber bellows to the full volume of the lower dome. With an initial pressure of 1.5 psig, the optimum working depth is about 34 feet and the minimum depth is 18 feet.

If the unit is pressurized to force all the fluid into the rubber bellows but without forcing any air into the rubber bellows, the following conditions will be found to exist:

1. Only about 17 cubic inches of fluid will be forced into the rubber bellows due to the height of the slow leak opening in the compliant chamber,
2. The pressure required to expand the rubber bellows to a volume of 17 cubic inches will be less than 0.25 psi, which can be neglected when considering the initial air pressure,
3. The initial volume of air will be $V_d - 3 = 24$ cu. in., and the initial pressure will be atmospheric; the instrument therefore will operate satisfactorily for depths between 3 and 30 feet with an optimum depth of 14 feet.

The procedure for pressurizing the head will be the same as before, except that the final pressure will be adjusted to atmospheric.

1. Twenty-four hours in advance, pressurize the unti to a pressure equal to the depth of the proposed installation.

2. At the time of installation, open the valve in the compliant chamber and allow the pressure to decrease to atmospheric.

Any air trapped in the lower bellows will escape quickly through the slow leak leaving the rubber bellows filled with silicone fluid without an air pocket. The valve should be held open approximately 10 seconds.

EQUIPMENT NECESSARY TO PRESSURIZE UNIT

By adding a pressure gage to a standard bicycle pump, and attaching an ohm-meter to the fusite terminals of the pressure head, (see Figure 11) the following procedure will prevent damage to the transducer:

1. Increase the pressure in the compliant chamber until the ohm-meter indicates zero or 750 ohms (the limit of the potentiometer) and disconnect the tire pump.

2. Allow several minutes for the pressure to equalize between the air dome and the rubber bellows as indicated by the ohm-meter reading returning to $R_p/2$ ohms (usually about 375 ohms).

3. Repeat (1) and (2) until all of the silicone fluid has been forced from the compliant chamber into the rubber bellows.

4. Pressurize the unit to the desired pressure. The ohm-meter will indicate a value near $R_p/2$ at all times during this operation, since the slow leak will be ineffective. Also the check valve in the pump will be ineffective if the pump handle is moved slowly and the pressure in head can be increased or decreased as desired.

MARKER BUOYS FOR SUBSURFACE PRESSURE HEAD

A scheme having the features of the taut-line spar-buoy type marker with long life has been developed (see Figure 12). This system utilizes: (1) a spar buoy (15 feet long, 7 inches in diameter, 149 pounds total weight); (2) a 3/8-inch chain connecting the buoy to a section of one-inch chain, which acts as a "variable anchor"; (3) a 3/8-inch lifting chain between the one-inch chain and the tripod; and (4) a 200 pound tripod. The buoy size is determined by the amount of chain to be supported, which includes a section of the large chain. The system is designed so that at a zero tide the buoy is exposed two feet; at a 6-foot tide the buoy is totally submerged. The large chain, therefore, acts as a "variable anchor" in that it reduces the motion of the spar buoy and maintains tension in the buoy chain to prevent snapping action in the chain.

By adjusting the length of the buoy chain to a length equal to the water depth (at MLLW) less 16.3 feet, the amount of one-inch anchor chain lifted off the bottom will be sufficient to submerge the buou at a 6-foot tide. This can be shown as follows (with reference to Figure 12):

Buoyant force of the spar buoy = 17.2 L_1 pounds
Weight of the anchor chain = 9.3 L_2 pounds
Weight of the buoy = 150 pounds
Weight of buoy chain (in water) = 40 pounds

Therefore

$$17.2\ L_1 = 9.3\ L_2 + 190 \tag{36}$$

and

$$L_1 + L_c + L_2 = \text{MLLW} + \text{Tide} \tag{37}$$

If the buoy submerges, L_1 will be equal to the total length of the buoy (15 feet) and the amount of anchor chain lifted off the bottom can be computed from Equation (36).

$$L = \frac{17.2(15) - 190}{9.3} = 7.3 \text{ feet} \tag{38}$$

By adjusting the length, L_c, of the buoy chain the buoy will be submerged at the desired tide stage of six feet. Equation (37) now becomes

$$L_c = \text{MLLW} + 6 - 15 - 7.3 = \text{MLLW} - 16.3 \tag{39}$$

If, for example, the buoy is to be installed in a MLLW depth of

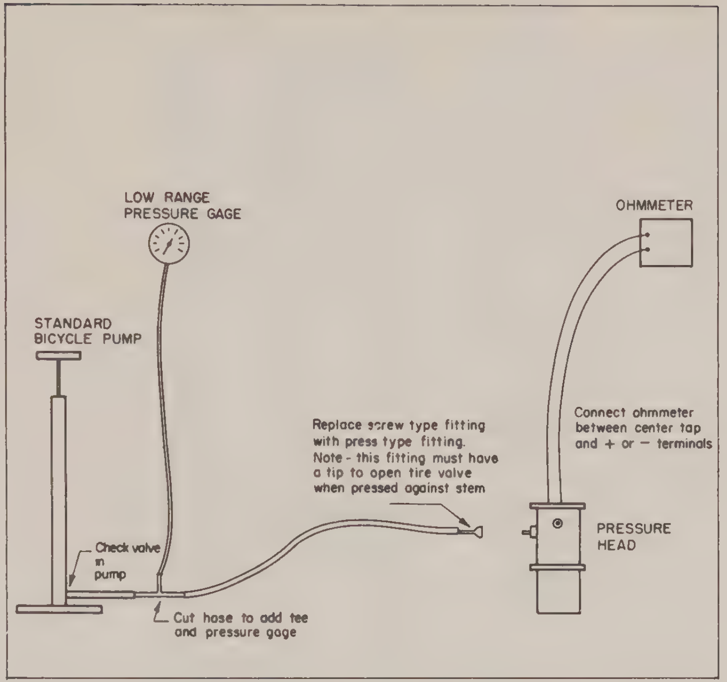
LOW RANGE PRESSURE GAGE
STANDARD BICYCLE PUMP
OHMMETER
Replace screw type fitting with press type fitting. Note - this fitting must have a tip to open tire valve when pressed against stem
Connect ohmmeter between center tap and + or − terminals
PRESSURE HEAD
Check valve in pump
Cut hose to add tee and pressure gage

Fig. 11. Equipment required to pressurize pressure head.

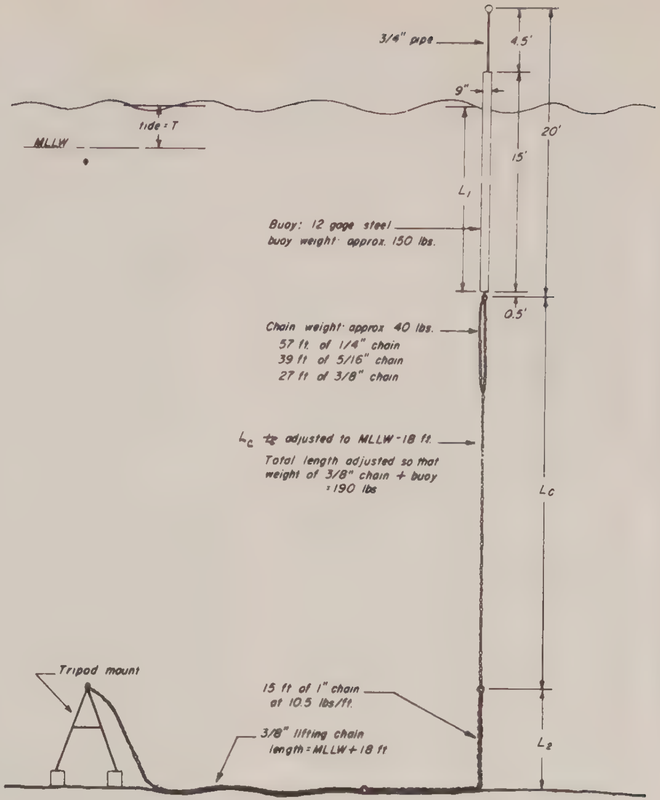
3/4" pipe
4.5'
9"
20'
15'
tide = T
MLLW
L_1
Buoy: 12 gage steel buoy weight: approx. 150 lbs.
0.5'
Chain weight: approx 40 lbs.
57 ft. of 1/4" chain
39 ft of 5/16" chain
27 ft of 3/8" chain
L_c adjusted to MLLW-18 ft.
Total length adjusted so that weight of 3/8" chain + buoy =190 lbs
L_c
Tripod mount
15 ft of 1" chain at 10.5 lbs/ft.
3/8" lifting chain length = MLLW + 18 ft
L_2

Fig. 12. Installation diagram for a spar marker with chain anchor.

40 feet, L_c would be adjusted to $40 - 16.3 = 23.7$ feet. Since 27 feet of 3/8-inch chain is required to bring the total weight of the buoy and chain to 190 lbs, 3.3 feet of chain would be doubled as shown in Figure 12. The length of buoy submerged, L_1, and the length of anchor chain lifted off the bottom, L_2, for any tide, T, can now be computed from Equations (36) and (37).

$$L_1 = 0.35\ T + 12.9 \tag{40}$$

$$L_2 = 0.65\ T + 3.4 \tag{41}$$

INSTALLATION OF SUBMARINE ELECTRICAL CABLES

The installation of the submarine electrical cable between the offshore tripod and the shore station is a relatively simple task under favorable conditions and with proper equipment. Favorable conditions include a straight beach with a sand bottom from the beach to the instrument. Under these conditions an armored cable can be laid along the bottom without anchors or additional protection and little or no cable wear will take place. The cable will quickly "sand down" so that it is not exposed to the turbulent action of the surf zone or to littoral currents that my exist at times parallel to the beach. After a few months the cables usually will be covered by sand to such depths that they cannot be recovered.

The "sanding down" takes place for two reasons; first, the fluidity of the sand (especially in the surf zone) will allow the cable to settle until it is covered to a depth of a few inches or more; and second, the movement of sand bars -- the movement of sand onshore and offshore and the movement of sand along the shore will alternately undercut and bury the cable until it may be covered to a depth of several feet.

In California during the summer when the sand moves toward the beach, the offshore cable may be very near the sand surface, or actually exposed. Directly under the summer berm on the beach the cable may be buried as much as ten feet. Conversely, during the winter the cable may be near the sand surface in the surf zone while offshore it may be buried several feet. The cable seldom, if ever, will be exposed along its entire length.

Under favorable conditions the armored cable need be used only to cross the surf zone. Unarmored cable can then be spliced to the armored cable and laid along the bottom to the instrument site. The splice normally will not have the full strength of the cable and care must be taken to prevent tension at this point. Anchoring the cable near the splice will reduce the cable tension at the splice.

When reefs exist along the beach or the bottom offshore is covered with rock and the cable cannot sand-down, special anchoring of the cable is necessary to hold the cable in place. Anchoring prevents wear of the cable on sharp edges of rocks and prevents excessive tension in the cable due to long lengths of cable being exposed to underwater currents. The problem of rocky bottoms offshore can be dealt with effectively by having divers work the cable, laying it around and between the rocks and perhaps anchoring the cable periodically with concrete blocks.

When installing cables across coral reefs the cable may be laid in the crevices, which extend across the reef face. The cable then will not be required to withstand the direct force of the breaking waves. However, they will be required to withstand large forces due to the surge currents present in the crevices, and the weight and strength of the armored electrical cable may not be sufficient. Both weight and strength can be added by lashing the electrical cable to heavy chain. The armored cable first can be attached to the chain with rings made of 3/8-inch diameter iron rod and then tightly lashed with seizing wire. The iron rings would serve as a permanent binding while the seizing wire would serve to prevent the electrical cable from being snagged on the bottom during installation.

INSTALLATION OF SUBMARINE ELECTRICAL CABLES BY SMALL CRAFT

The length of cable usually installed for a wave recorder varies between one thousand and five thousand feet depending upon how far offshore the desired depth of water can be found. Cable-laying ships cannot be used economically to install these short lengths of cable. It often is necessary to use small boats, landing craft and amphibian trucks (Navy DUKW) to perform this operation. The DUKW is more convenient than the other craft, since it can be loaded with the cable, driven to the shore site and used to lay the cable in one operation. The remarks which follow apply directly to the use of a DUKW to install the cable, but should also apply in general to the use of any small craft.

Figure 13 shows cable spool holders designed to mount 2500-foot spools of armored cable in the cargo compartment of a DUKW. The design includes a foot brake which acts on the rims of the spool to hold tension in the cable as it is being laid. Without the foot brake, the spool will spin due to the weight of the cable hanging in the water and cable may

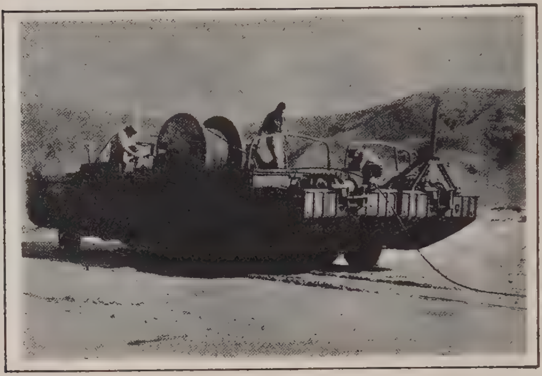

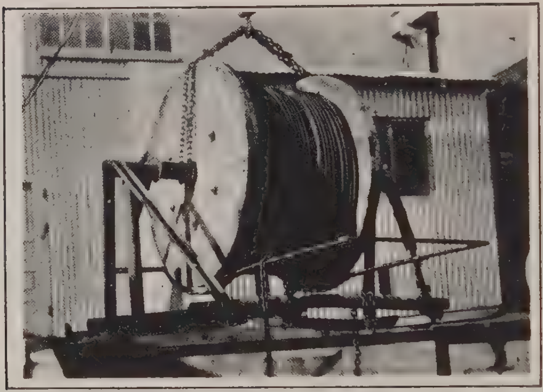

Fig. 13. Spool holder mounting 2500 feet of armored cable.

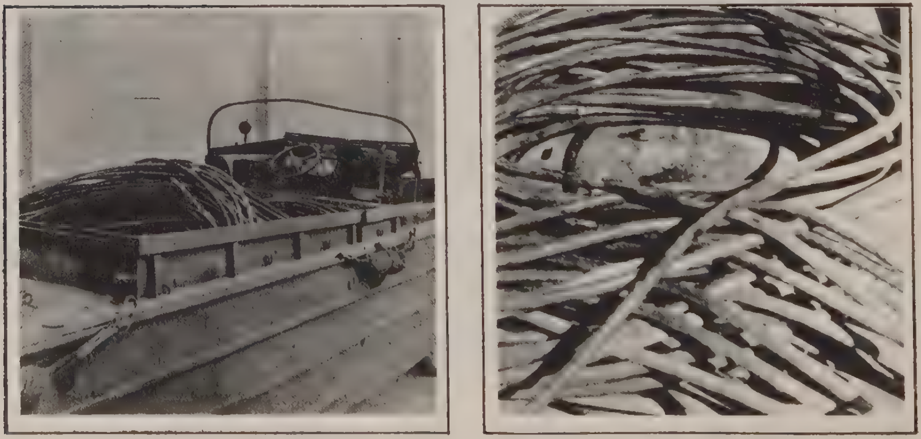

Fig. 14. 2500 feet of armored cable faked in a DUKW.

unreel faster than the craft progresses.

The cable can also be faked in the DUKW as illustrated in Figure 14. By faking the cable (coiling the cable to form a "figure 8") as shown, the cable can be payed out without twisting. A full spool of armored cable (3000 feet) can be stowed in a DUKW cargo compartment without difficulty. The disadvantages of faking cable in the cargo compartment are that: (1) there is always a possibility of the cable becoming tangled and a danger to anyone attempting to free such tangles, (2) there is no simple way to hold tension on the cable being laid, and the cable may uncoil too rapidly, (3) considerable work is involved in unspooling and recoiling the heavy armored cable.

Attempts have been made to drag a portion of the cable offshore from a spool mounted on the beach. Not more than 1000 feet of armored cable can be dragged by a floating DUKW unless floats are attached to the cable to reduce the bottom friction.

ACKNOWLEDGMENTS

This instrument was designed while the author was working for the Institute of Engineering Research, University of California, at Berkeley, California and was previously published as indicated in the reference which follows.

The author wishes to thank his colleagues, W. N. Bascom and R. L. Wiegel for their helpful suggestions. Many of the techniques used in the installation of the equipment were developed by them. The author wishes to thank M. Lincoln for preparing the illustrations.

REFERENCES

1. SNODGRASS, F. E. and STILLING, D. D., Operation manual for Mark IX shore wave recording system; Technical Report Series 3, Issue 320, IER., University of Calif., Berkeley, 16 pp, 5 plates, March 1951.

APPENDIX. MANUFACTURING DRAWINGS

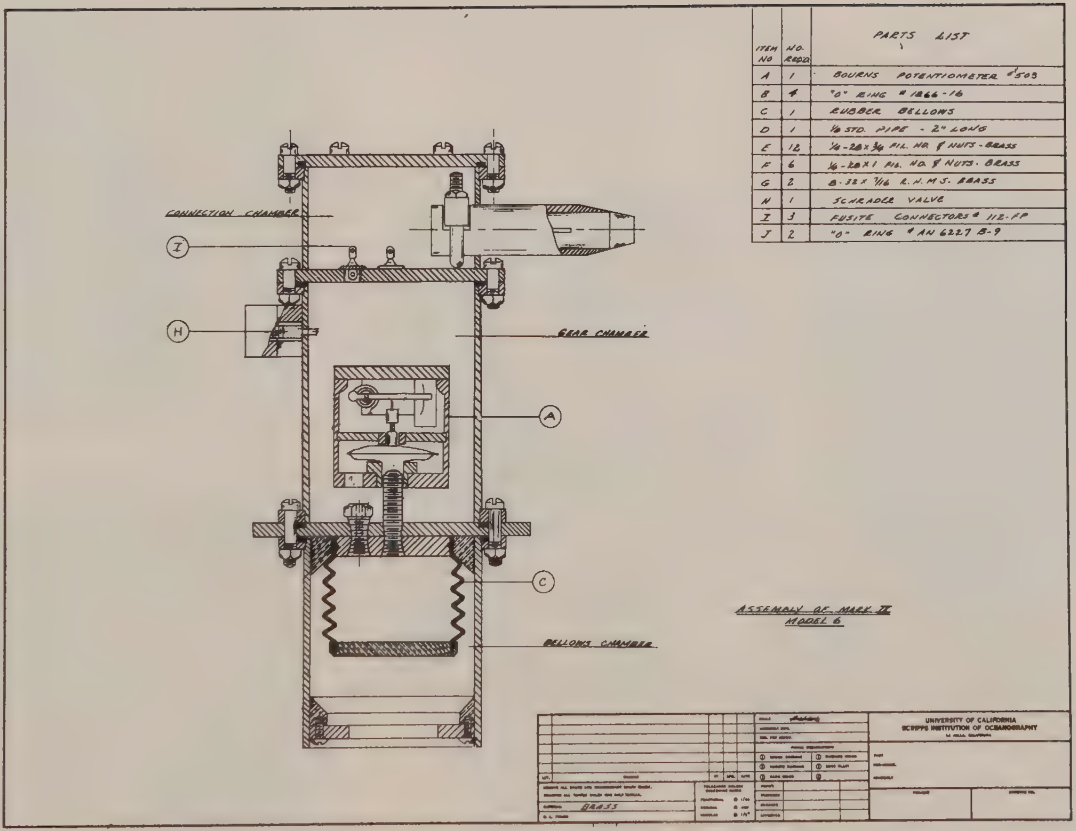

ITEM NO	NO. REQ'D	PARTS LIST
A	1	BOURNS POTENTIOMETER #503
B	4	"O" RING #1866-16
C	1	RUBBER BELLOWS
D	1	1/8 STD. PIPE - 2" LONG
E	12	1/4-28 x 3/4 FIL. HD. & NUTS - BRASS
F	6	1/4-28 x 1 FIL. HD. & NUTS. BRASS
G	2	8-32 x 7/16 R.H.M.S. BRASS
H	1	SCHRADER VALVE
I	3	FUSITE CONNECTORS # 112-FP
J	2	"O" RING # AN 6227 B-9

CONNECTION CHAMBER
I
H
GEAR CHAMBER
A
C
BELLOWS CHAMBER
ASSEMBLY OF MARK IX
MODEL 6
UNIVERSITY OF CALIFORNIA
SCRIPPS INSTITUTION OF OCEANOGRAPHY
BRASS

Fig. 15. Assembly drawing, Mark IX, Model 6.

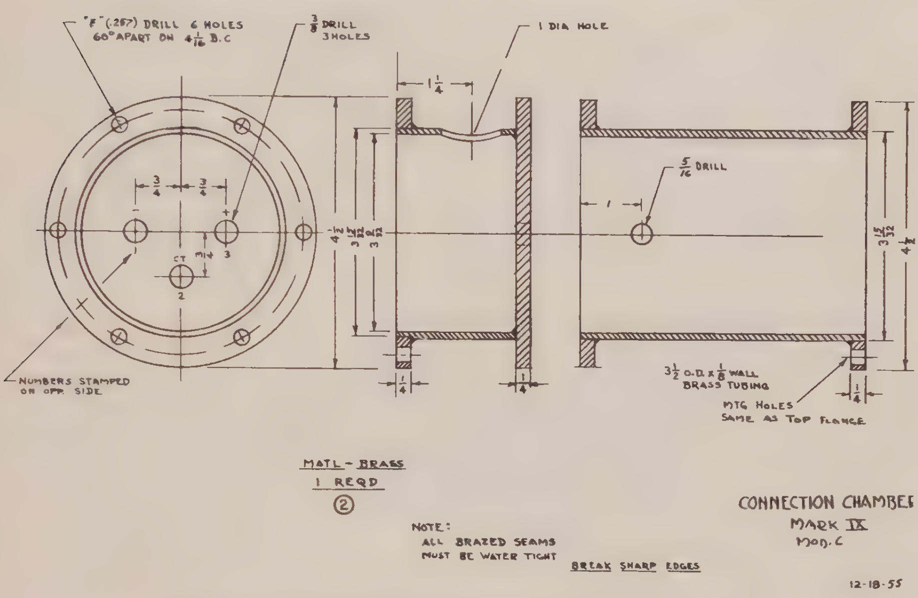
"F" (.257) DRILL 6 HOLES 60° APART ON 4 1/16 B.C
3/8 DRILL 3 HOLES
1 DIA HOLE
1 1/4
3/4
3/4
CT
1/4
3
2
4 1/2
3 15/32
3 9/32
5/16 DRILL
1
3 15/32
4 1/2
NUMBERS STAMPED ON OPP. SIDE
1/4
1/4
3 1/2 O.D. x 1/8 WALL BRASS TUBING
MTG HOLES SAME AS TOP FLANGE
1/4
MATL - BRASS
1 REQD
②
NOTE: ALL BRAZED SEAMS MUST BE WATER TIGHT
BREAK SHARP EDGES
CONNECTION CHAMBE
MARK IX
MOD. 6
12-18-55

Fig. 16. Connection chamber, Mark IX, Model 6.

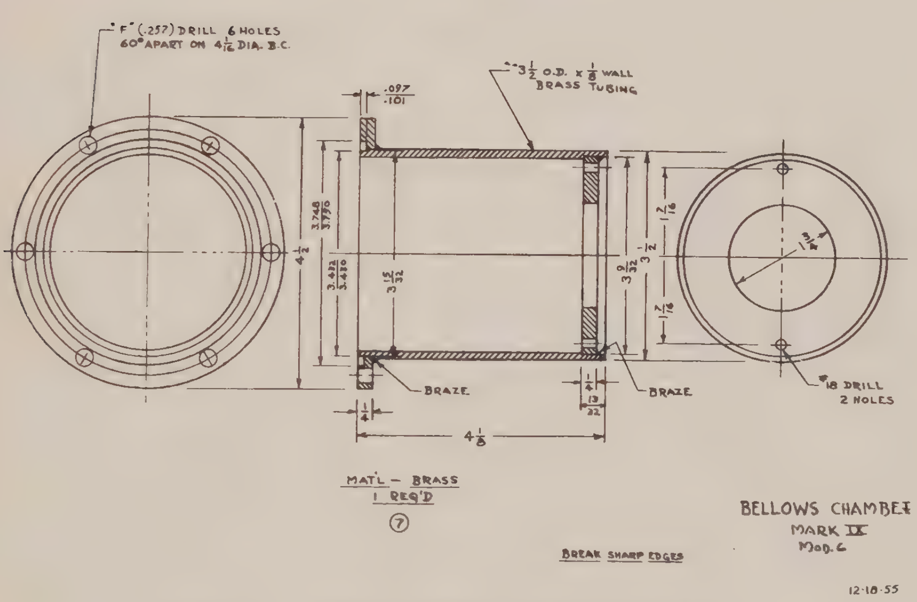
"F" (.257) DRILL 6 HOLES 60° APART ON 4 1/16 DIA. B.C.
3 1/2 O.D. x 1/8 WALL BRASS TUBING
.097 .101
4 1/2
3.748 3.750
3.422 3.430
3 15/32
3 9/32
3 1/2
1 7/16
1 7/16
1 3/4
BRAZE
BRAZE
1/4
13/32
1/4
4 1/8
#18 DRILL 2 HOLES
MAT'L - BRASS
1 REQ'D
⑦
BREAK SHARP EDGES
BELLOWS CHAMBE
MARK IX
MOD. 6
12-18-55

Fig. 17. Bellows chamber, Mark IX, Model 6.

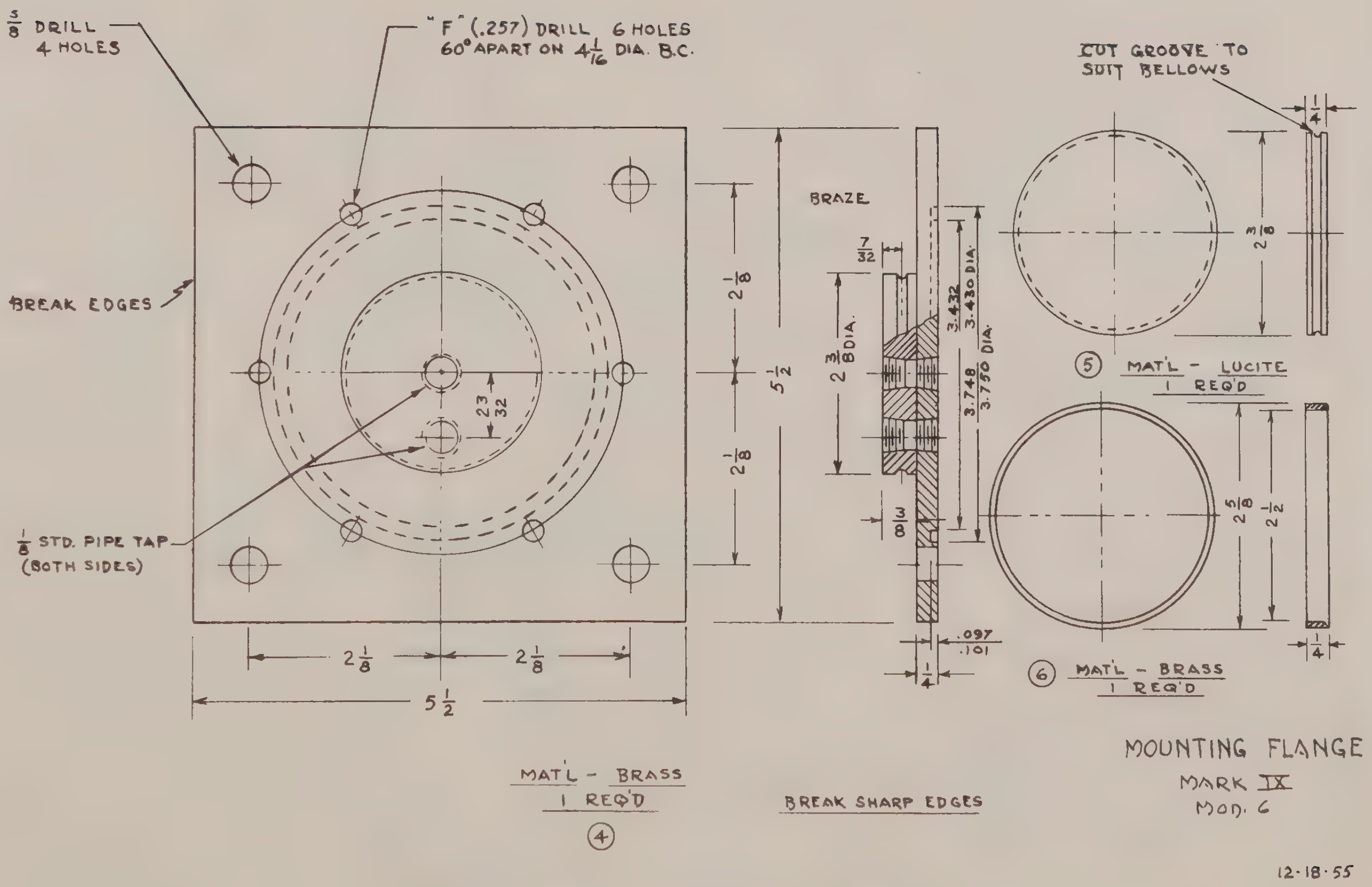
$\frac{3}{8}$ DRILL
4 HOLES
"F" (.257) DRILL 6 HOLES
60° APART ON $4\frac{1}{16}$ DIA. B.C.
BREAK EDGES
$\frac{1}{8}$ STD. PIPE TAP
(BOTH SIDES)
$\frac{23}{32}$
$2\frac{1}{8}$
$2\frac{1}{8}$
$5\frac{1}{2}$
$2\frac{1}{8}$
$2\frac{1}{8}$
$5\frac{1}{2}$
MAT'L - BRASS
1 REQ'D
④
BRAZE
$\frac{7}{32}$
$2\frac{3}{8}$ DIA.
3.432
3.430 DIA.
3.748
3.750 DIA.
$\frac{3}{8}$
.097
.101
$\frac{1}{4}$
BREAK SHARP EDGES
CUT GROOVE TO
SUIT BELLOWS
$\frac{1}{4}$
$2\frac{3}{8}$
⑤ MAT'L - LUCITE
1 REQ'D
$2\frac{5}{8}$
$2\frac{1}{2}$
$\frac{1}{4}$
⑥ MAT'L - BRASS
1 REQ'D
MOUNTING FLANGE
MARK IX
MOD. 6
12·18·55

Fig. 18. Mounting flange, Mark IX, Model 6.

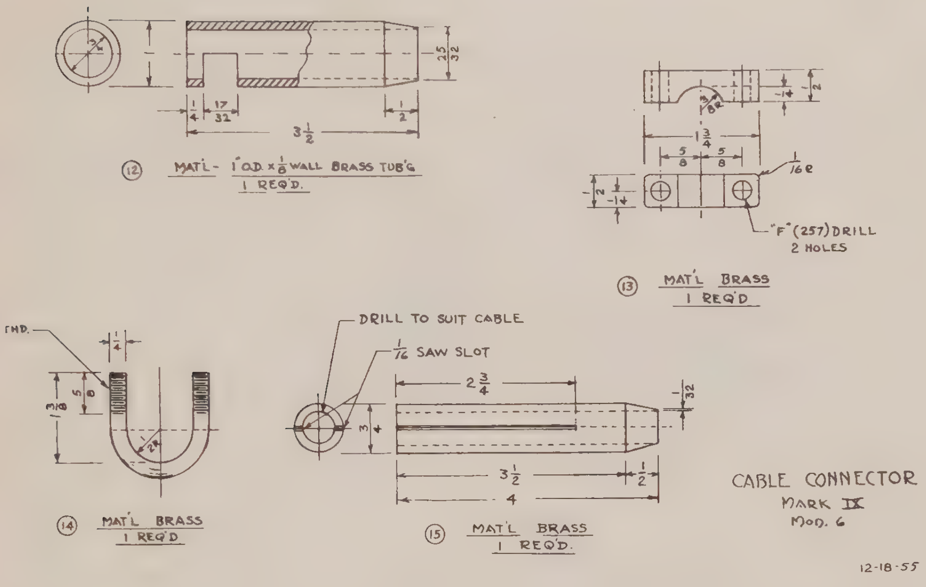
⑫ MAT'L - 1" O.D. x 1/8 WALL BRASS TUB'G
1 REQ'D.
1/4
17/32
1/2
3 1/2
25/32
⑬ MAT'L BRASS
1 REQ'D
1 3/4
5/8
5/8
1/16 R
"F" (257) DRILL
2 HOLES
THD.
1/4
5/8
1 3/8
⑭ MAT'L BRASS
1 REQ'D
DRILL TO SUIT CABLE
1/16 SAW SLOT
2 3/4
3/4
1/32
3 1/2
1/2
4
⑮ MAT'L BRASS
1 REQ'D.
CABLE CONNECTOR
MARK IX
MOD. 6
12-18-55

Fig. 19. Cable connector, Mark IX, Model 6.

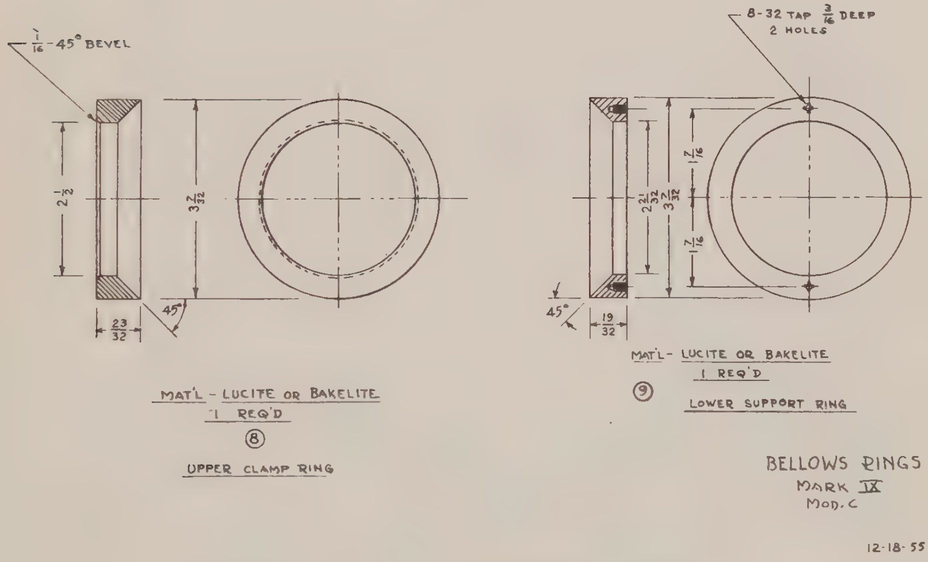
1/16 - 45° BEVEL
2 1/2
3 7/32
45°
23/32
MAT'L - LUCITE OR BAKELITE
1 REQ'D
⑧
UPPER CLAMP RING
8-32 TAP 3/16 DEEP
2 HOLES
2 21/32
3 7/32
1 7/16
1 7/16
45°
19/32
MAT'L - LUCITE OR BAKELITE
1 REQ'D
⑨
LOWER SUPPORT RING
BELLOWS RINGS
MARK IX
MOD. 6
12-18-55

Fig. 20. Bellows rings, Mark IX, Model 6.

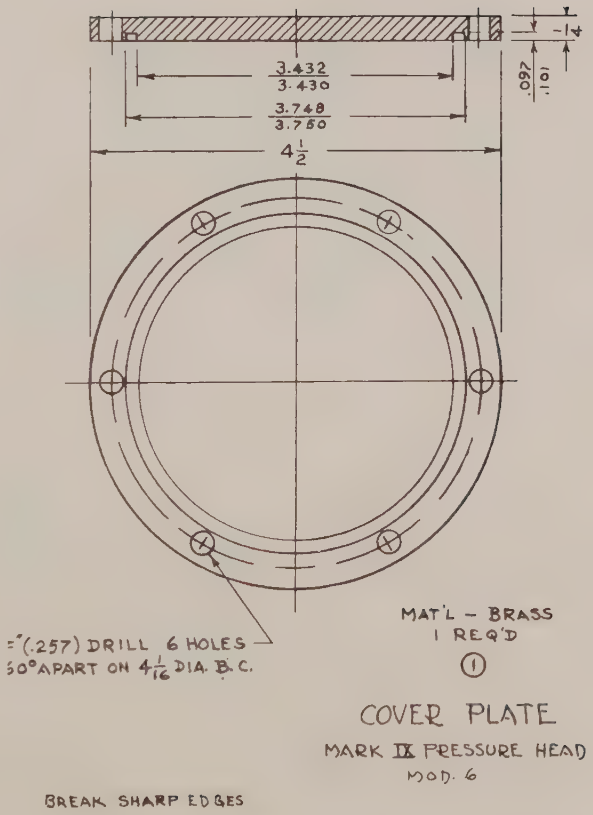
3.432
3.430
3.748
3.750
4 1/2
.097
.101
1/4
=″(.257) DRILL 6 HOLES
60° APART ON 4 1/16 DIA. B.C.
MAT'L – BRASS
1 REQ'D
①
COVER PLATE
MARK IX PRESSURE HEAD
MOD. 6
BREAK SHARP EDGES

12-18-55

Fig. 21. Cover plate, Mark IX, Model 6.

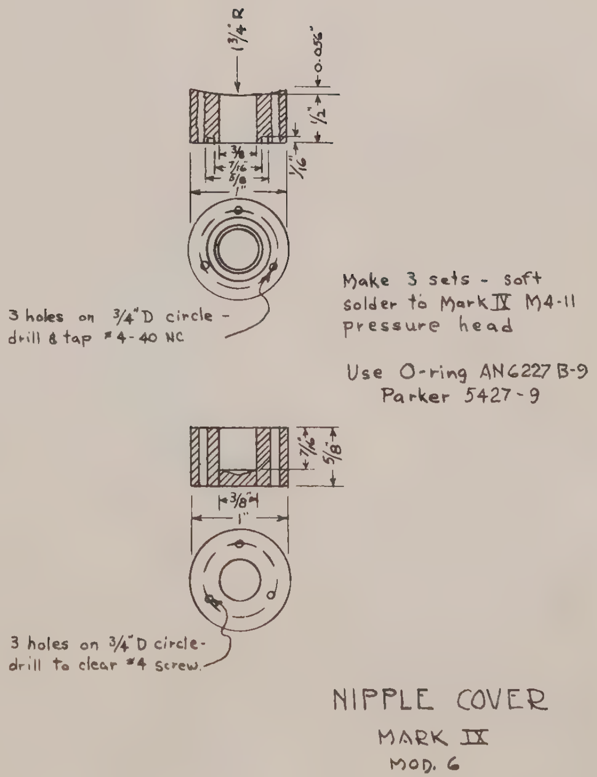
(3/4″ R
0.056″
1/2″
1/16″
3/8
7/16
5/8
1″
3 holes on 3/4″D circle -
drill & tap #4-40 NC
Make 3 sets - soft
solder to Mark IX M4-11
pressure head
Use O-ring AN6227 B-9
Parker 5427-9
7/16″
5/8″
3/8″
1″
3 holes on 3/4″D circle-
drill to clear #4 screw.
NIPPLE COVER
MARK IX
MOD. 6

12·18·55

Fig. 22. Nipple cover, Mark IX, Model 6.

THE WASMANN JOURNAL OF BIOLOGY

VOL. 13, NO. 2 FALL, 1955

Studies of the Biology of the Fish Parasite Livoneca convexa Richardson (Crustacea, Isopoda, Cymothoidae)

ROBERT J. MENZIES, *Lamont Geological Laboratory, Columbia University,*

THOMAS E. BOWMAN,[1] *University of California, Scripps Institution of Oceanography,* and

FRANKLIN G. ALVERSON, *Inter-American Tropical Tuna Commission, Scripps Institution of Oceanography.*

INTRODUCTION

The studies reported herein are based upon specimens of the marine parasitic isopod, *Livoneca convexa* Richardson, deposited in the collections of the United States National Museum. These were taken from the carangid fish, *Chloroscombrus orqueta* Jordan and Gilbert, a bait species of minor importance to the California-based tuna fleet. Members of the tuna fleet have assisted the Inter-American Tropical Tuna Commission in its bait-fish investigation by saving and delivering to the Commission samples of fish from their bait hauls. Specimens examined by us were taken from such samples.

The objectives of this investigation have been to record observations about the anatomy and life history of *Livoneca convexa* which illustrate relationships between it and its host.

The definition one selects for the term parasite of course determines whether *Livoneca* is a parasite or not. We prefer the broad definition of parasite given by Allee *et al.* (1949, p. 253) which states that the "parasite obtains noteworthy aid in the form of food, shelter, protection, or transportation. It not only does not

---

[1] Present address: Division of Marine Invertebrates, U. S. National Museum, Washington 25, D. C.

Contribution New Series No. 822, Scripps Institution of Oceanography, La Jolla, California.

Reproduced by Permission

give due return, but is more or less harmful to its host." The male stage satisfies all the requirements of a parasite given by Allee *et al. (op. cit.)*. The female stage, if not parasitic, is surely commensal for reasons we enumerate later. The young, infective stage of *Livoneca* is assumed to be free living.

In contrast, the adults of both sexes of the isopod *Olencira praegustator* (Latrobe), occupy the mouth of the menhaden and appear to cause no damage. Goode (1877, pp. 101–105) concluded that this species was a commensal and not a parasite.

SYSTEMATICS

Livoneca convexa Richardson, 1905.

Synonym: *Livoneca convexa* Richardson, 1905, pp. 445–446, figures 1–2.

Dr. W. L. Jones collected a single specimen of this species in 1885 in Panama. A host was not recorded. The type and only specimen was described by Richardson and deposited in the collection of the University of Pennsylvania. Dr. D. H. Wenrich of the Zoological Laboratory of that institution was unable to locate the specimen (*in litt.*, April, 1953). A search of the collection of the United States National Museum by Dr. Fenner A. Chace, Jr., curator of marine invertebrates, was similarly fruitless. Therefore, it seems probable that the holotype of *Livoneca convexa* has been lost. To our knowledge, the species has not been recorded since its original description. Our record of over 200 specimens, all from *Chloroscombrus orqueta,* indicates the species to be rather common and perhaps a serious fish pest.

DESCRIPTION (Figures 1–2)

Male and Ovigerous Females.

Specimens in this category range between 14 and 21 mm. in length.

Cephalon and appendages. Cephalon about 1/6 wider than long;

Figure 1. *Livoneca convexa* Richardson: A, Ovigerous female; B, Cephalon of male; C, Cephalon of virgin female; D, Cephalon of young; E, First peraeopod of young; F, Last peraeopod of young; G, Inner margin of propod and carpus of last peraeopod of young; H, Pleotelson of male; I, Pleotelson of young; J, Last peraeopod of ovigerous female; K, First peraeopod of ovigerous female. Figures with identical magnification: A; B to D, H; E, F, I; G; J, K (not known).

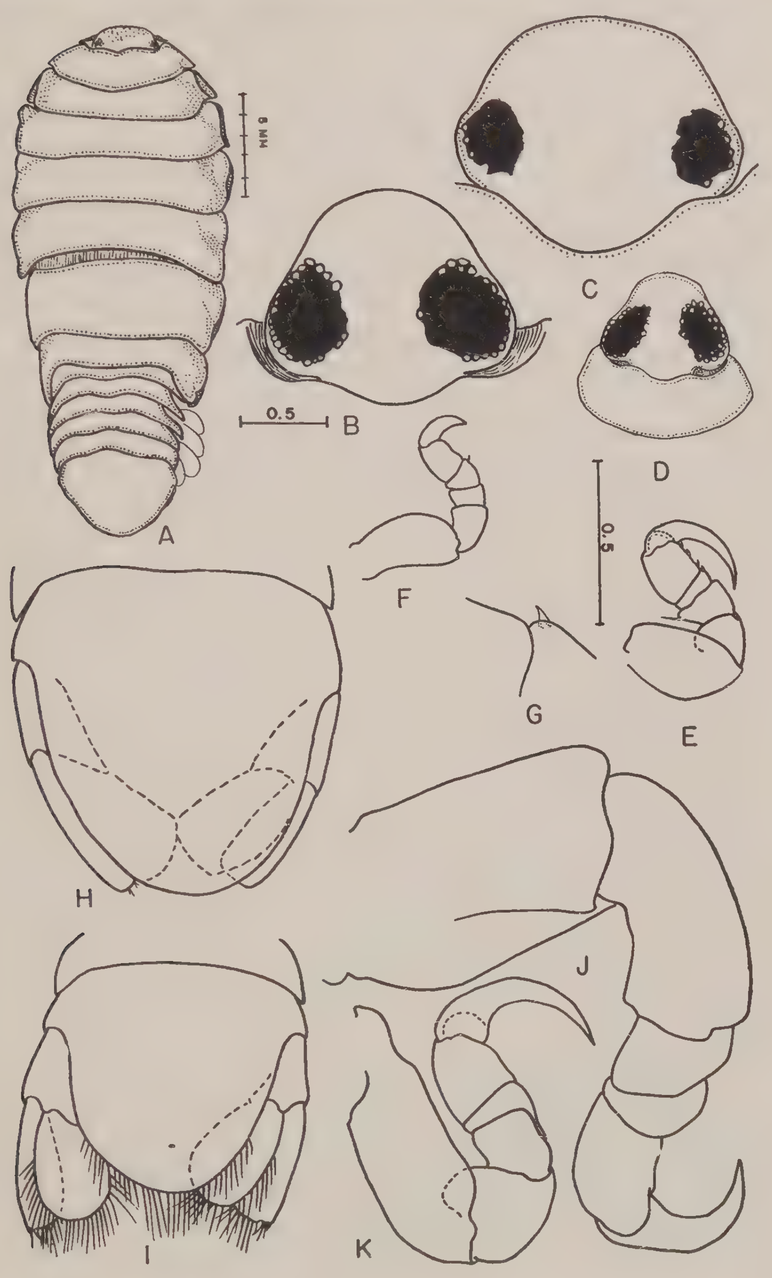
5 MM
A
0.5
B
C
D
0.5
E
F
G
H
I
J
K

frontal border evenly convex. Eyes with few evident facets and separated from each other by a distance equal to about ½ the width of the cephalon. First antenna with seven to eight articles. Second antenna with nine to ten articles. Mandibular palp with three articles, the first being the longest; apical article with three terminal setae. Mandible with darkened sclerotized incisor and a small molar process; setal row and lacinia mobilis lacking. First maxilla lacking endopod; exopod with four recurved hooks at apex. Second maxilla consisting of one article bearing a row of thirteen stout setae at apex. Maxilliped without epipod; palp with two articles; terminal article about ½ of the width of and slightly shorter than first article, bearing three stout setae at apex.

Peraeon and appendages. Peraeon about twice as long as wide. Dactyl strongly curved, longer than propod. Propod of first and seventh peraeopods without setae.

Pleon and appendages. Pleon ⅕ longer than wide. Pleotelson about ⅓ the length of pleon; distal margin smooth, lacking setae. Uropods flexed under telson so as to be scarcely discernible in dorsal view. Uropodal peduncle with a few minute setae on medial margin, distal medial angle otherwise lacking setae; exopod pointed, slightly longer and much narrower than endopod; endopod with broadly rounded apex, about twice as long as wide, both rami without setae. Pleopods all fleshy, lacking marginal setae. First pleopod with accessory lobe attached to outer margin of peduncle; endopod with accessory lobe on inner margin. Peduncle of second pleopod with two accessory lobes, the more proximal folded and incised on outer margin; endopod with an accessory lobe and an appendix masculinum. Third to fifth pleopods similar to first except that the endopods and accessory folds are progressively more fleshy and pleated.

MATURE MALES.

These specimens range between 7 and 14 mm. in length.

Cephalon and appendages. Cephalon ⅐ wider than long; frontal border more pronounced than in females. Eyes with numerous obvious facets, eyes separated from one another by a distance equal to about ⅓ the width of the cephalon. First antenna with eight articles. Second antenna with ten to eleven articles. First maxilla, maxilliped and most parts of mandible as described for female. Palp of mandible with three to four setae on apical article. Second maxilla with five to twelve setae on apical margin.

Peraeon and appendages. Peraeon about twice as long as wide. Dactyl of first peracopod similar to that of female; propod with vestiges of three stout setae on inner margin and one vestigial seta on inner margin; merus with two setae on outer distal angle. Propod, carpus, and merus of seventh peraeopod with two, three, and two stout setae respectively on inner margins. Paired penis lobes present on ventral surface of seventh somite.

Pleon and appendages. Pleon similar to female, but uropods less inflexed, hence, more visible in dorsal view. Uropodal peduncle with about ten marginal setae; exopod with about sixteen marginal setae; endopod with about twenty marginal setae. Exopod slightly larger than endopod, less pointed than that of female. Pleopods similar to those of female except that their folds and pleats are less extensive.

YOUNG SPECIMENS.

Young specimens ranged in a size between 5 and 7 mm. length.

Cephalon and appendages. Cephalon about 1/6 wider than long. Frontal border more pronounced than in male. Eyes with numerous obvious facets, eyes separated from one another by a distance equal to about 1/4 the width of cephalon. First antenna with eight articles. Second antenna with ten to eleven articles. Palp of mandible with three to five setae at apex. Other parts of mandible, first maxilla, and maxilliped similar to male. Second maxilla with a small inner lobe and a large outer lobe; lobes bear a total of four stout marginal setae.

Peraeon and appendages. Peraeon similar to male, about twice as long as wide. Dactyl of first peraeopod without dark coloring at tip; propod with three stout outward-curved setae on inner margin, carpus with one such seta on inner margin; merus with one seta on outer distal angle. Seventh peraeopod lacking or present; when present the dactyl is underdeveloped and the carpus has one stout seta on inner margin. Penis not developed.

Pleon and appendages. Pleon similar to male but uropods not inflexed; pleotelson with about thirty-six setae on distal margin. Uropodal peduncle with one marginal seta; exopod with two strong hooks at outer apical angle and about twenty plumose setae on inner margin; endopod with one stout seta at apex and about twenty-eight marginal plumose setae; exopod slightly larger than endopod, apex not pointed. Pleopods lack pleats and the appendix masculinum but bear small accessory lobes on endopods of third, fourth, and fifth pleopods as well as marginal setae on all pleopods.

REMARKS ON SYSTEMATICS.

Since Richardson had only one female specimen at her disposal, the notes on the male and young given above are additions to the description of the species. The fact, mentioned by Richardson, that the uropods of the female are inflexed below the pleotelson serves to distinguish this species from the other known species of *Livoneca*.

The descriptions of most members of the Cymothoidae are based largely on the females and accordingly it remains impossible for one to identify a species on the basis of young or male specimens alone. It would seem, however, that the microscopic details of the uropods and telson such as are here described and figured, especially of the young specimens, might offer more useful diagnostic characteristics than the often vague and subtle differences in body shape and proportions on which the diagnoses of so many of the female cymothoids depend today.

DISTRIBUTION

The type locality and apparently only prior record for *L. con-*

Figure 2. *Livoneca convexa* **Richardson: A, Maxilliped, ovigerous female; B, Apex of maxilliped, ovigerous female; C, Apex of first maxilla, young; D, Apex of first maxilla, ovigerous female; E, Uropod, ovigerous female; F, Apex of uropodal exopod, young; G, Apex of mandibular palp, male; H, Apex of maxillipedal palp, young; I, Antennae of young; J, Lateral view of mandible, male; K, Apex of second maxilla, ovigerous female; L, Second maxilla, ovigerous female; M, Mandible, inner view, with lower lip attached, ovigerous female; N, Apex of second maxilla, young; O, Apex of second antenna, ovigerous female; P, Apex of second antenna, young; Q, Lateral view of mandible, young; R, Apex of mandibular palp, young; S, Second antenna, ovigerous female; T, First antenna, ovigerous female; U, Second pleopod, young. Figures with identical magnification: A, I, L, M, T, U; B, C, D, F, H, J, K, N, S, P, O, Q, R; E.**

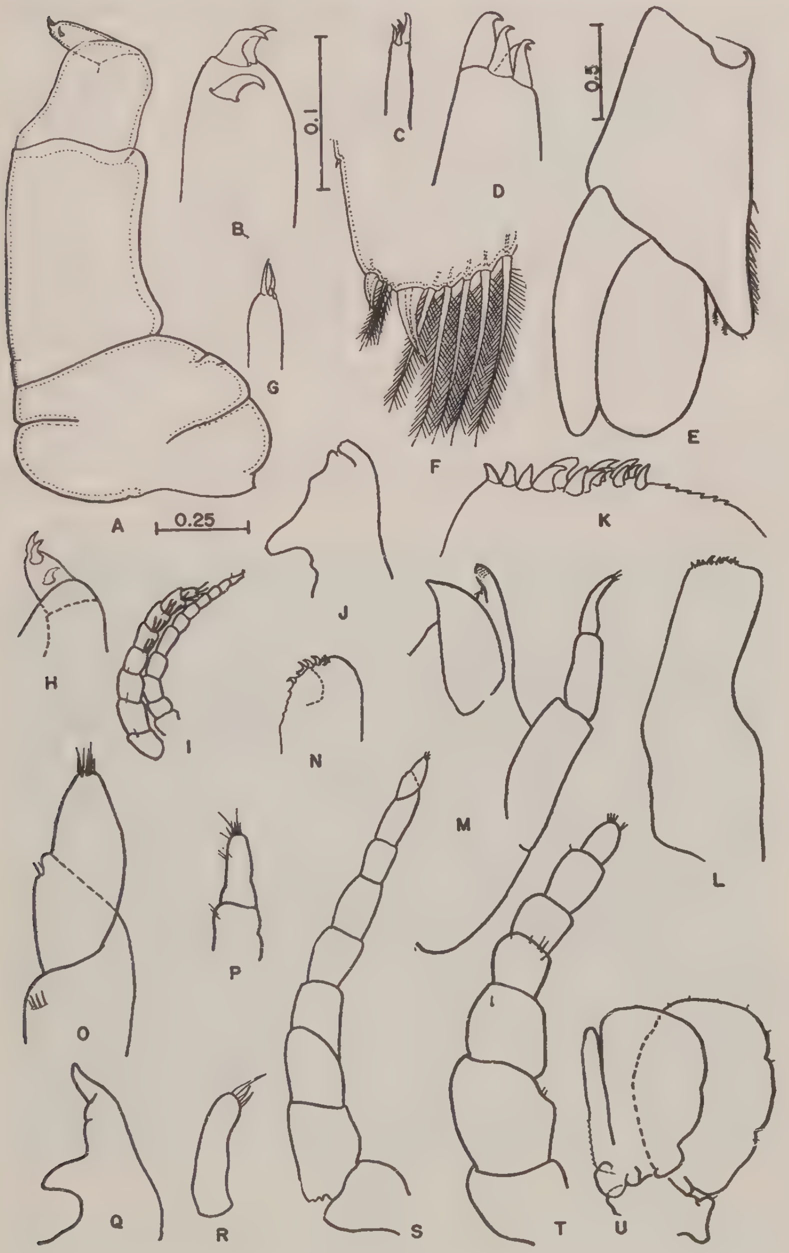
A
B
C
D
E
F
G
H
I
J
K
L
M
N
O
P
Q
R
S
T
U
0.1
0.5
0.25

vexa is Panama. Our study is based on specimens taken from three samples of *Chloroscombrus orqueta* from the following localities:

1. Jambeli Point, Gulf of Guayaquil, Ecuador, 16 November, 1951. Surface temperature 82°F. Sixty-six adults and more than 100 young.
2. Rio Anton, Gulf of Panama, 4 November, 1951. Surface temperature 81°F. One adult specimen (female).
3. Gulf of Fonseca, off entrance to San Lorenzo Bay, Honduras, 4–5 April, 1952. Surface temperature about 82°F. (mean temperature for April, 1952, in the Gulf of Fonseca, recorded by tuna clippers). About 45 specimens.

The two northernmost records for the host are near Los Angeles harbor, California (Fry, 1940) and San Quintin Bay, Baja California, Mexico (Fitch, 1949). It is thus probable that *L. convexa* occurs well to the north of the localities from which we have received specimens.

LIFE HISTORY (Figures 3–4, Table I)

Like other cymothoid isopods, *Livoneca convexa* is a protandrous hermaphrodite. While quite young, it is a male with functional testes, but also has tissue which will develop into the ovaries in the older, female stage of its life history. As the ovaries develop, the testes degenerate and some parallel changes occur in the secondary sex characters.

The protandrous nature of cymothoids was first recognized by Bullar (1876) and was confirmed by Mayer (1879). More recently this subject has been given extensive treatment by Montalenti (1941) and Legrand (1952). These investigators all worked primarily with the cymothoid, *Anilocra physodes* Linnaeus. No comparable studies have been made on American cymothoids.

The life history of *Livoneca* is summarized diagrammatically in figure 4 and is discussed below, beginning with the youngest stages.

JUVENILES (presumably free-swimming).

When the young leave the marsupium they lack the seventh peraeopods (as do the early stages of all isopods), but develop them during what is assumed to be the free-swimming period.

The pleopods, uropods, and telson are provided with numerous setae. These and the well-developed eyes are apparently adaptations for a free-swimming existence, during which the young must find a new host. It would appear that the juvenile does not feed during this period, as it still has a small supply of yolk during at least part of the free-swimming period, and its mouth parts are essentially like those of the adult.

While still a free-swimming animal, the testes begin to develop, as do the elevated paired openings or penis on the seventh peraeon somites and the appendix masculinum on the endopodite of each second pleopod.

Males.

The isopod, morphologically still a larva or perhaps a young male, settles in the gill chamber of a host. The position and orientation in the gill chamber was the same in all the specimens

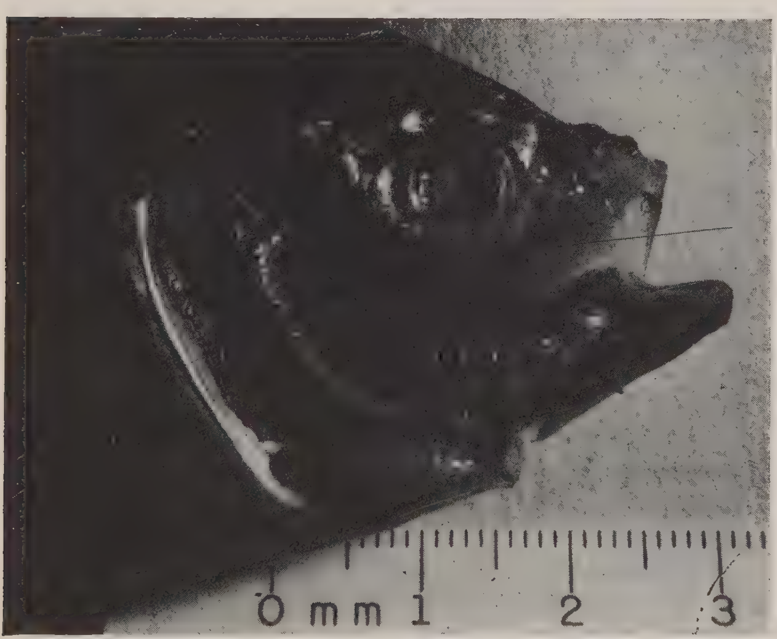

Figure 3. *Livoneca convexa* Richardson on *Chloroscombrus orqueta* (operculum removed). Male in gill chamber; female on tongue in mouth. Photograph provided through the courtesy of Mr. George Mattson, U.S. Fish and Wildlife Service.

of *Chloroscombrus* we have examined. The male was always located in the anterio-ventral part of the gill chamber, with his head directed toward the anterior end of the host fish (figure 3). At this location, the male damages the tissues of the host.

With the abandonment of the free-swimming phase, the number of eye facets becomes somewhat reduced, and many of the natatory setae present in the free-swimming juvenile are lost. The plumose setae on the telson and margins of the pleopods are lost, while those of the uropodal rami are reduced. On the other hand, the number of marginal setae on the peduncles of the uropods is increased. The pleopods show notable additions in the development of more accessory lobes and in the appearance of many pleats in the endopods, changes presumably associated with the need for a greater respiratory surface as the animal gets larger.

While still in the gill chamber, the sex characters of the mature male are fully acquired. The testes become mature, and the penis and appendix masculinum attain full development. Small ovaries are already present.

Adult Females.

The mature female is invariably found on the floor of the mouth, lying over the basibranchials and extending up onto the pharyngobranchials. When viewed laterally, the body of the female is seen to be characteristically arched. The dorsal surface is slightly concave in the region of the posterior peraeon and anterior pleon. The convexity of the ventral surface, accentuated by the swollen marsupium, fits it to the concave floor of the host's mouth. Without exception, the female *Livoneca* was oriented with her head directed toward the caudal end of the fish. This puts her in a position with her mouthparts close to the gill rakers, so that she could easily feed on the food particles strained by them.

The testes and penis are lost. The appendix masculinum of each second pleopod is reduced in size, but is retained throughout the life of the female. The ovaries, already present in the male stage, are now fully developed. In contrast to the gradual development of the ovaries, the oostegites appear to be formed during a single molt, for no specimens have been found with incompletely developed oostegites. Oostegite development is a gradual process requiring several molts in many isopods, especially the nonparasitic species.

The eye facets are further reduced in number and the eyes are smaller relative to the size of the head. The setae on the carpus and propodus of the first peraeopods are lost, as are the setae of the seventh peraeopods. The setae of the uropodal rami are further diminished in number, and the setae on the apical article of the mandibular palp are reduced from four to three. There is a marked increase in the number of setae on the second maxilla and on the uropodal peduncle. The pleopods develop many more folds and pleats than in the male and hence have a greater respiratory area per pleopod.

Discussion of Life History

Montalenti (1941) recognized eight developmental stages in *Anilocra.* Two prehatching stages (I to II) and three transitional stages (IV, VI, VII) have not been described by us but these nonetheless occur in *Livoneca* also and accordingly are located approximately in figure 4.

The fact that *Livoneca* destroys host tissue during its mascu-

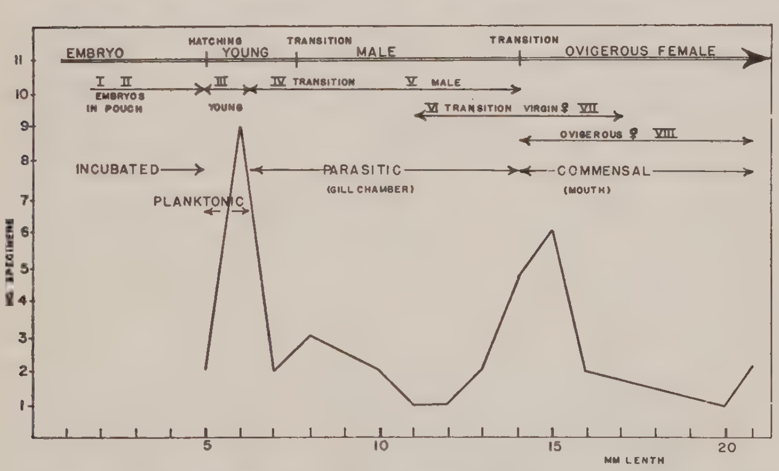

Figure 4. Size distribution of a population of 38 specimens of *Livoneca convexa* R. from Jambeli Point, Gulf of Guayaquil, Ecuador. Roman numerals indicate size groups of *Livoneca* equivalent to Montalenti's stages in the development of *Anilocra.*

line phase of development clearly indicates its parasitic nature. On the other hand, the fact that no host tissue is destroyed by the female suggests that she is at this stage only a commensal associate with her host.

Whether the male eats fish flesh is not known and the examinations made of the "stomachs" of males, and females as well, give no clues as to their food habits.

The retention of the typically masculine appendix masculinum on each second pleopod by functional females suggests that not all masculine structures behave alike with the shift in hormonal balance and indicate perhaps that more than one factor (hormone?) is involved in the loss (or development) of the male secondary sex characteristics.

HOST-PARASITE RELATIONSHIPS

Data are available on the following aspects of the relationship between the host and its parasite; the incidence of parasitism, host-parasite specificity, host-parasite size relationship, damage caused by the parasite.

Incidence of Parasitism.

Chloroscombrus orqueta is a "schooling" fish. This habit would seem to facilitate the spread of infestation by *Livoneca* due to the fact that the many young, representing the infectious stage, produced by *Livoneca* would have a greater chance of reaching a host than they would were *C. orqueta* a nonschooling species.

A population of 31 fish from the Gulf of Guayaquil showed an 80.7 per cent infection, while 100 fish from the Gulf of Fonseca showed only a 37.0 per cent infection. Parasitic isopods were not found on 97 fish from the Gulf of Panama.

Host-Parasite Specificity.

The parasite *Livoneca convexa* has been collected only from *Chloroscombrus orqueta.* The literature is of no aid in permitting a prediction that it will ultimately be found to be a highly host-specific as our data might suggest, or a non-host specific parasite. For example, *Cymothoa oestrum* (Linnaeus), *Livoneca vulgaris* Stimpson, *Livoneca ovalis* Say, and *Irona nana* Schioedte and

(76)

Meinert have been collected from two to seven different genera of fish (Richardson, 1905, pp. 254, 258, 263, 265). *Anilocra physodes* (Linnaeus) has been reported from six different genera of fish (Legrand, 1952, p. 11). Other species of cymothoids, however, having a similar life history to those mentioned have been taken from only one species of fish (*op. cit.*, pp. 214–267). Specimens of the carangid fishes *Oligoplites refulgens* Gilbert and Starks, *Selene brevoortii* (Gill), and several species of *Caranx* have been examined for parasitic isopods without our finding *Livoneca convexa* on them.

HOST-PARASITE SIZE RELATIONSHIPS.

There seems to be a definite correlation between the length of the gravid female parasite and the fork length of the host, with

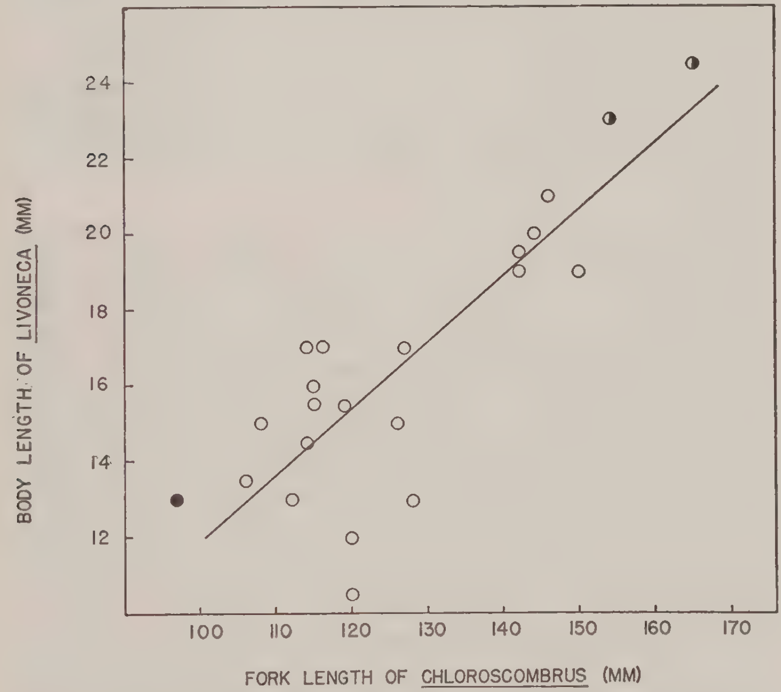

Figure 5. Regression of body length of *Livoneca* on fork length of *Chloroscombrus*. ($Y = .1747\,X - 5.556$; $r = 0.845$). Open circles, specimens from the Gulf of Guayaquil. Solid circles, Gulf of Panama. Half solid circles, Gulf of Fonseca.

large fish generally having large gravid female parasites. This relationship is shown in figure 5. It is difficult to see why this should be the case (assuming the data to be valid) but it can be suggested that the amount of space (in the mouth of the fish) available for growth determines the maximum size reached by the isopod. If this were the case, however, we should find small gravid female isopods in large as well as small fish. It is evident that more data are needed on the subject.

DAMAGE TO THE HOST.

Externally, infected fish cannot be distinguished from non-infected fish. The male, located in the gill chamber, erodes the gill filaments in a characteristic manner, destroying the distal portions of them except for the outer filaments of the first arch which are only slightly damaged. This activity leaves a cavity between the outer filaments of the first gill arch and the inner wall of the gill chamber equal to the size of the isopod.

The female, located on the tongue, appears to cause no direct injury. She might reduce the ability of the fish to feed and might compete with the fish for the food it strains from the water.

FECUNDITY OF THE PARASITE.

Specimens between 20.4 mm. and 25.5 mm. in length had between 67 and 130 eggs per pouch. Generally small specimens had fewer eggs than did the larger specimens. The frequency with which broods are produced is not known. The fecundity of many free-living isopods is often between 10 and 20 per brood or about 1/7th that of *Livoneca*. The fecundity of bopyrid parasites, which may bear several hundred eggs in one brood, is considerably higher than that of *Livoneca*. This moderate fecundity of *Livoneca* correlates with the moderate number of morphological changes undergone by *Livoneca* in its development toward a parasitic mode of life and with the fact that it is associated with a schooling species of fish.

POSSIBLE EVOLUTIONARY SIGNIFICANCE OF THE MORPHOLOGIC CHANGES IN THE DEVELOPMENT (Figures 6–7)

During ontogeny, free-living isopods tend to add structures, appendages, parts of appendages, setae, etc., until the adult stage is reached. In parasitic isopods three developmental patterns are evident:

1. Considerable reduction and loss of larval parts; e.g., dajiid and cryptoniscid isopods (ectoparasites of crustaceans).
2. Moderate reduction of larval parts accompanied by a marked increase in the complexity of the adult involving the production of structures not known in other isopods: some bopyrid isopods (parasites of crustaceans).
3. A loss of few larval parts with only a slight increase in adult complexity; e.g., most flabelliferan parasitic isopods, including *Livoneca.*

The young and male stages of *Livoneca* are rather similar in general body form to most other isopods of the suborder Flabellifera, a major group including the families Cirolanidae, Aegidae, and Cymothoidae. Of these families the Cirolanidae is generally considered to have the fullest complement of characteristics common to the entire order and accordingly is believed to be the most primitive of all isopodan families. In figure 6 are shown the characteristics used to separate the three families systematically

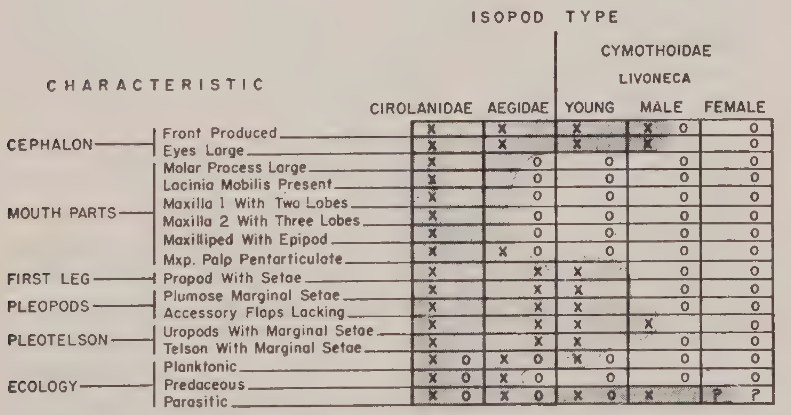

CHARACTERISTIC		ISOPOD TYPE				
				CYMOTHOIDAE		
				LIVONECA		
		CIROLANIDAE	AEGIDAE	YOUNG	MALE	FEMALE
CEPHALON	Front Produced	X	X	X	X O	O
	Eyes Large	X	X	X	X	O
MOUTH PARTS	Molar Process Large	X	O	O	O	O
	Lacinia Mobilis Present	X	O	O	O	O
	Maxilla 1 With Two Lobes	X	O	O	O	O
	Maxilla 2 With Three Lobes	X	O	O	O	O
	Maxilliped With Epipod	X	O	O	O	O
	Mxp. Palp Pentarticulate	X	X O	O	O	O
FIRST LEG	Propod With Setae	X	X	X	O	O
PLEOPODS	Plumose Marginal Setae	X	X	X	O	O
	Accessory Flaps Lacking	X	X	X	O	O
PLEOTELSON	Uropods With Marginal Setae	X	X	X	X	O
	Telson With Marginal Setae	X	X	X	O	O
ECOLOGY	Planktonic	X O	X O	X O	O	O
	Predaceous	X O	X O	O	O	O
	Parasitic	X O	X O	X O	X	? ?

Figure 6. Chart showing morphologic and ecologic relationships of the families Cirolanidae, Aegidae, and Cymothoidae (represented by three stages in the life history of *Livoneca*). + indicates character as described in column at left, O indicates a change in the structure. Stippled area links structures showing little initial change.

from one another. There the following relationships become apparent:

1. The Aegidae differ from the Cirolanidae only slightly in general body form. Differences which exist are concerned primarily with structural modifications of the mouth parts.
2. The young of *Livoneca* are so close to the aegid line that they fall within the Aegidae in key characteristics alone.
3. The male and particularly the female *Livoneca* show many characteristics separating them from either the Cirolanidae or Aegidae or their own young.

The close similarity of the young *Livoneca* with the family Aegidae suggests that *Livoneca* and the family to which it belongs, the Cymothoidae, has been derived phylogenetically from the aegid stock. These relationships are shown graphically in figure 7.

In the development of the three families there seems to have been a progressive increase in the percentage of species having a pelagic (at least in one part of the life history) and parasitic mode of life. The primitive flabelliferan is presumed to have been benthonic and free-living because the Cirolanidae (twenty species of seven genera) are largely benthonic (85 per cent) and free-living (90 per cent). The Aegidae (ten species of two genera) have only a 30 per cent benthonic and free-living representation. Finally, not one of the known American Cymothoidae (eighteen species in eleven genera) is benthonic or free-living (figure 7), all known species being both pelagic (while young) and parasitic throughout much of their life history.

The percentages on which the above generalities are based come largely from a tabulation of the data on species within the families given in Richardson (1905, pp. 81–267); however, it must be emphasized that our knowledge is yet so very incomplete that the percentages can be considered only rough approximations. We have no proof, for example, that the benthic Aegidae reported by Richardson are truly benthonic. Many might well have been jarred loose from their host or captured as the dredge was being towed to the surface. Thus we have reason to suspect that the percentage of benthonic aegids is actually too high.

(80)

SUMMARY OF OBSERVATIONS AND CONCLUSIONS

1. *Livoneca convexa* Richardson, known previously only from one adult female, is more fully described on the basis of its young, male, and female stages.
2. The isopod, like most other cymothoids, is a protandrous hermaphrodite. Its life history consists of a presumably planktonic young, a parasitic male occupying the gill chamber, and a presumably commensal female occupying the oral cavity of the fish *Chloroscombrus orqueta*.
3. In changing from an adult male to an adult female, *Livoneca* showed a loss of most but not all masculine secondary sex characteristics, suggesting perhaps that more than one sexual substance is involved in the loss (and possibly development) of the several secondary sex characteristics.
4. Incidence of parasitism varied from 0.0 to 80.7 per cent infection with the schools of fish examined.
5. *Livoneca convexa* produces 67 to 130 eggs per brood. The frequency with which broods are produced is not known.

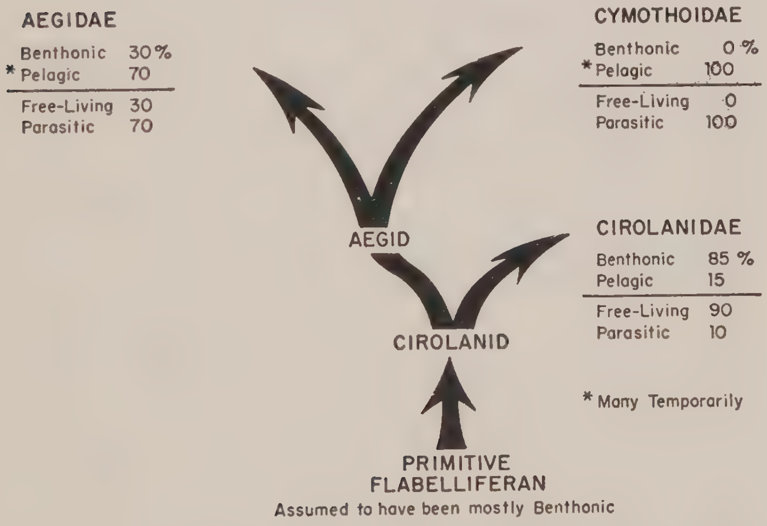
AEGIDAE
Benthonic 30%
* Pelagic 70
Free-Living 30
Parasitic 70
CYMOTHOIDAE
Benthonic 0%
* Pelagic 100
Free-Living 0
Parasitic 100
AEGID
CIROLANIDAE
Benthonic 85%
Pelagic 15
Free-Living 90
Parasitic 10
CIROLANID
* Many Temporarily
PRIMITIVE
FLABELLIFERAN
Assumed to have been mostly Benthonic

Figure 7. Schematic diagram of evolutionary and ecologic relationships between three families of flabelliferan isopods. The percentage ecologic composition of the species within the families is only a first approximation. Data were derived largely from Richardson (1905).

6. *Livoneca convexa* is possibly highly host-specific, having been found on only one species of fish.
7. The largest gravid females were found associated with the largest specimens of fish.
8. Only the masculine stage shows evidence of causing direct injury to the fish. The food of the isopod is not known. The moderate change in mouth part structure during the transition from young to male to female suggests that there is little or no change in feeding habits.
9. The observation that the young of *Livoneca* are morphologically very closely related to the family Aegidae suggest that *Livoneca* and its family Cymothoidae were derived evolutionarily from an aegid stock.
10. A benthonic habit, characteristic of the Cirolanidae today, appears to have been markely reduced in the Aegidae and lost completely in the Cymothoidae.

TABLE I. *Locus of* Livoneca convexa *R. in thirteen fish from Jambeli Point, Gulf of Guayaquil, Ecuador. Four fish with more than one isopod in gill chamber.*

Type of Development	*Location*	
	Gill Chamber	*Oral Cavity*
Young	6	0
Transitional ♂♂	4	0
Adult ♂♂	8	0
Transitional—virgin ♀♀	0	4
Ovigerous ♀♀	0	9

LITERATURE CITED

ALLEE, W. C., *et al.*

1949. Principles of animal ecology. 837 pp., W. B. Saunders Co., Philadelphia and London.

BULLAR, J. F.

1876. The generative organs of the parasitic Isopoda. Journal of Anatomy and Physiology, 11:118–128.

FITCH, JOHN E.

1949. Some unusual occurrences of fish on the Pacific Coast. California Fish and Game, 35(1):41–49; figs. 1–8.

FRY, D. H.

1940. A northern record for a Central America Pompano. California Fish and Game, 26(1):77.

GOODE, G. B.

1879. The natural and economical history of the American Menhaden. Report of the Commissioner, 1877, Part V. appendix A. The Sea Fisheries, 1–517: 31 pls.

LEGRAND, J.-J.

1952. Contribution a l'étude expérimentale et statistique de la biologie d'Anilocra physodes L. (Crustacé Isopode Cymothoïdé). Archives de Zoologie Expérimentale et Générale, 89(1):1–55.

MAYER, P.

1879. Carcinologische Mitteilungen. VI. Ueber den Hermaphroditismus bei einigen Isopoden. Mitteilungen Zoologische Station zu Neapel, I:165–179.

MONTALENTI, G.

1941. Studi Sull'ermafroditismo dei Cimotoidi. I. *Emetha Audouinii* (M. Edw.) e *Anilocra physodes* (L.). Pubblicazioni della Stazione Zoologica di Napoli, 18(3):337–94.

RICHARDSON, H. E.

1906. Description of a new species of *Livoneca* from the coast of Panama. Proceedings United States National Museum, 29 (1430):445–446, figs. 1–2.

(83)

Reprinted from Reviews of Modern Physics, Vol. 28, No. 1, 48–52, January, 1956
Printed in U. S. A.

Reproduced by Permission

Equations of Motion of the Ocean and Atmosphere[*]

Carl Eckart and Horace G. Ferris

Scripps Institution of Oceanography, University of California, La Jolla, California

The density of the air in the atmosphere, or of the water in the ocean, is a function of altitude or depth. Linear equations for the motion of such stratified fluids have been derived by many authors. Many have introduced simplifying assumptions into their derivations, with the result that it is difficult to compare one paper with another. The present review is a collection of the major systems of equations, in a uniform notation. The derivations given are those which bring out the interrelations of the various systems, and are sometimes quite different from those of the original papers. The solution of the equations is not discussed, so that the relative merits of the various systems cannot be evaluated.

INTRODUCTION

The most obvious fact about the earth's atmosphere is the variation of its density and temperature with altitude. This stratification gives it a stability that strongly influences the motion of the air. Although it is not so obvious, the earth's oceans and lakes are also stratified, and it is known that their stability (at least in the thermocline layer) is comparable to, or even greater than, that of the atmosphere.

Through the years, a very considerable but scattered literature on the motion of stratified fluids has accumulated. This includes the theory of convection as well as the theory of waves in the geophysical media. There has been little effort to systematize these theories, so that a typical paper will begin with a derivation of the equations of motion, at the same time introducing simplifying assumptions, and proceed to the discussion of special approximate solutions. The comparison of different papers is rendered difficult both by differences in the basic equations and by differences in notation.

The objective of this review is to collect the major systems of equations that have been derived, in a uniform notation, and to discuss the relations between them. It is clear that this requires the formulation of the physical assumptions from which they follow. No attempt is made to compare these assumptions in terms of validity, nor is any attempt made to preserve the arguments advanced by their original proponents. Neither is there any attempt to describe the solutions of the equations. Such attempts would have caused this review to grow beyond reasonable bounds; the interested reader must consult the original papers on these matters.

In Sec. III, the most general system of differential equations is discussed in somewhat more detail than the others. A transformation of dependent variables is found which exhibits their essential mathematical structure. This is rather simpler than has been supposed.

I. THE MOST GENERAL EQUATIONS

A. Thermodynamics

The thermodynamic properties of a pure substance are completely determined when its internal energy ϵ (erg/g) is given as a function of the specific volume v (cm^3/g) and the entropy η (erg/g deg). Then the pressure p (dyne/cm^2) and temperature θ are calculable from the equations

$$p=-\partial\epsilon/\partial v, \quad \theta=\partial\epsilon/\partial\eta. \tag{1}$$

In differential form, these are equivalent to

$$\delta p=-X\delta v+Y\delta\eta, \tag{2}$$

$$\delta\theta=-Y\delta v+Z\delta\eta, \tag{3}$$

X, Y, Z, being the second derivatives of ϵ, taken with appropriate signs.

These coefficients are also expressible in terms of the following four quantities:

c = velocity of sound,
a = coefficient of thermal expansion,
s = specific heat at constant volume,
γ = ratio of the specific heats;

with $\rho=1/v$, the expressions are

$$\begin{aligned} X&=\rho^2c^2,\\ Y&=\rho(\gamma-1)/a,\\ Z&=\theta/s. \end{aligned} \tag{4}$$

The four quantities are not independent, but are related by the equation

$$\gamma(\gamma-1)s=a^2c^2\theta, \tag{5}$$

which is equivalent to

$$XZ-Y^2=XZ/\gamma. \tag{6}$$

---

[*] Contribution from the Scripps Institution of Oceanography, New Series, No. 823. This work was partly supported by the U. S. Navy, Bureau of Ships, Contract NObsr-43356.

B. Hydrodynamics

The hydrodynamic equations are[1]

$$Du/Dt+v\nabla p+g\nabla\chi=\mathbf{f}, \quad (7)$$

$$Dv/Dt-v\nabla\cdot\mathbf{u}=0, \quad (8)$$

$$D\eta/Dt=q/\theta, \quad (9)$$

where

$\mathbf{u}$ = velocity (cm/sec),
$g\chi$ = gravitational potential (cm/sec)^2,
g = 980 cm/sec^2 (by international convention),
$\mathbf{f}$ = resultant of all nongravitational forces (dyne/g),
q = net accession of heat, (erg/g sec),
$D/Dt=\partial/\partial t+\mathbf{u}\cdot\nabla$.

In laboratory applications, the forces $\mathbf{f}$ are primarily viscous; in large scale geophysical applications, they are primarily the Coriolis force due to the earth's rotation, and the tide producing forces of the sun and moon. If the transfer of heat occurs only by conduction,

$$q=v\nabla\cdot(k\nabla\theta),$$

k being the thermal conductivity of the fluid. In meteorological applications, the transfer of heat is primarily by radiation, and the expression for q is more elaborate Many of the references discussed below either ignore $\mathbf{f}$ and q, or adopt specific forms for them. Such specializations will be mentioned only when there is a definite reason to do so.

C. The Zero-Order Solution

Following the standard scheme of perturbation theory,[2] we shall derive the linearized equations by considering the first-order perturbations of a zero-order state. This zero-order state will be one of rest in all that follows. Some of the references cited use other zero-order states[2–5] and the present discussion assumes that the equations of these references have been appropriately simplified.

The zero-order state of rest is specified when the pressure is given as a positive, monotonically decreasing function of the gravitational potential χ:

$$p=p_0(\chi). \quad (10)$$

Then the density is

$$\rho=\rho_0(\chi)=-p_0'/g, \quad (11)$$

where the accent indicates differentiation with respect to χ. Equations (1), (2), and (3) combine with these to determine θ_0 and η_0, also as functions of χ only.

It then becomes possible to express all other zero-order quantities, such as X, Y, Z, as functions of χ. Strictly, these functions should be distinguished by a subscript zero, as in the case of p_0 etc., but no confusion will result if this subscript is omitted. With this understanding, Eqs. (2) and (3) yield

$$\begin{aligned} p_0'&=-Xv_0'+Y\eta_0', \\ \theta_0'&=-Yv_0'+Z\eta_0'. \end{aligned} \quad (12)$$

D. The First-Order Equations

In the perturbed state, $v=v_0+v_1+\cdots$, $p=p_0+p_1+\cdots$, $\mathbf{u}=\mathbf{u}_1+\cdots$, and the linearized equations are to be obtained by neglecting all terms indicated by dots, as well as squares and products of quantities carrying the subscript one. Equations (1) and (2) then yield

$$\begin{aligned} p_1&=-Xv_1+Y\eta_1, \\ \theta_1&=-Yv_1+Z\eta_1. \end{aligned} \quad (13)$$

With

$$\zeta=\nabla\chi, \quad (14)$$

Eqs. (7), (8), and (9) yield

$$(\partial\mathbf{u}_1/\partial t)+p_0'v_1\zeta+v_0\nabla p_1=\mathbf{f}_1, \quad (15)$$

$$(\partial v_1/\partial t)+v_0'\mathbf{u}_1\cdot\zeta-v_0\nabla\cdot\mathbf{u}_1=0, \quad (16)$$

$$(\partial\eta_1/\partial t)+\eta_0'\mathbf{u}_1\cdot\zeta=q_1/\theta_0. \quad (17)$$

These equations suffice to determine all first-order quantities. For many applications, it is desirable to consider two other equations, obtainable from Eqs. (16) and (17) by using Eqs. (12) and (13):

$$(\partial p_1/\partial t)+p_0'u_1\cdot\zeta+Xv_0\nabla\cdot u_1=Yq_1/\theta_0, \quad (18)$$

$$(\partial\theta_1/\partial t)+\theta_0'u_1\cdot\zeta+Yv_0\nabla\cdot u_1=Zq_1/\theta_0. \quad (19)$$

Except for notation, these equations are identical with those derived by Bjerknes, Bjerknes, Solberg, and Bergeron[6] and Blokhintzev.[7] If the fluid is a perfect gas, γ is a constant and

$$\begin{aligned} c^2&=\gamma R\theta_0=\gamma p_0/\rho_0, \\ a&=1/\theta_0, \\ s&=R/(\gamma-1) \end{aligned} \quad (20)$$

Using these special values of the thermodynamic parameters, we find Eqs. (15), (16), and (17) are essentially identical with equations derived by Lamb.[8,9] They have also been used by Pekeris,[10–12] Wilkes,[13]

---

[1] C. Eckart, Phys. Rev. 58, 207 (1940).

[2] V. Bjerknes and Colaborators, *Physikalische Hydrodynamik* (Verlag Julius Springer, Berlin, 1933), Chapter VII.

[3] D. Blokhintzev, *The Acoustics of an Inhomogeneous and Moving Medium*, Translated from the Russian by R. T. Beyer and D. Mintzer, Providence, Research and Analysis Group, Physics Department, Brown University (1952).

[4] B. Haurwitz, *Perturbation Equations in Meterology* (Compendium of Meterology, American Meteorology Society, Boston, 1951), p. 401.

[5] P. Queney, *Theory of Perturbations in Stratified Currents with Applications to Air Flow Over Mountain Barriers*, University of Chicago, Department of Meteorology, Misc. Rept. No. 23, (1946).

[6] See reference 2, Sec. 84.

[7] See reference 3, p. 17.

[8] H. Lamb, *Hydrodynamics* (Cambridge University Press, New York, 1932), sixth edition, p. 547.

[9] H. Lamb, Proc. Roy. Soc. (London) A84, 551 (1890).

[10] C. L. Pekeris, Proc. Roy. Soc. (London) A158, 650 (1937).

[11] C. L. Pekeris, Proc. Roy. Soc. (London) A171, 434 (1939).

[12] C. L. Pekeris, Phys. Rev. 73, 145 (1948).

[13] M. V. Wilkes, *Oscillations of the Earth's Atmosphere* (Cambridge University Press, New York, 1949).

Haurwitz,[4] Gossard and Munk,[14] and others. Some of these writers introduce the assumption that the vertical acceleration is zero, before proceeding to the solution.

The Laplace-Rayleigh theory of sound is obtained from Eqs. (15) and (18) by neglecting p_0' and setting $\eta_1=0$ in Eq. (13).[15] Bergmann[16] and Blokhintzev[3] have considered the effect of the terms in p_0' and v_0' on the propagation of sound.

The older Newtonian theory of sound is obtained from Eqs. (15) and (18) by setting $\theta_1=0$ in Eq. (13) and eliminating η_1. This theory has been used by Laplace[17] and Rayleigh[18] for the discussion of atmospheric and oceanic tides, with the further assumption that $\theta_0'=0$. These classic researches have strongly influenced later work.[19]

Margules[20] attempted a theory of the thermal atmospheric tide, based on Eqs. (15) and (16) with $f_1=0$ and the assumption of θ_1 as a specified function of time and position. Most later work on this problem is based either on equations to be developed in Sec. II or on the unsimplified equations (15) to (19).

The simplification $v_1=0$ does not seem to have been investigated in connection with stratified fluids. It is always combined with $\rho_0'=0$, and then leads to the classical theory of the homogeneous incompressible fluid.

Neither is the simplification $p_1=0$ discussed in the literature. Instead, there is a series of papers whose apparent objective is the avoidance of this assumption while achieving some of its consequences. These will be discussed in Sec. II.

II. LOVE'S EQUATIONS AND THEIR VARIANTS

A. The Assumption of Incompressibility

Equation (2) implies

$$\begin{aligned} Y(D\eta/Dt) &= (Dp/Dt)+\rho^2c^2(Dv/Dt), \\ &= (Dp/Dt)-c^2(D\rho/Dt). \end{aligned} \tag{21}$$

Since c^2 is a large number, many writers neglect the first term on the right. With this approximation, Eqs. (4) and (5) lead to

$$\theta(D\eta/Dt) = -(\gamma s/\rho a)(D\rho/Dt). \tag{22}$$

Equation (9) then becomes

$$(D\rho/Dt) = -\rho a q/\gamma s, \tag{23}$$

and when this is combined with Eq. (8), the latter becomes

$$\nabla\cdot\mathbf{u} = aq/\gamma s. \tag{24}$$

When Eqs. (7), (24), and (23) are linearized as in Sec. I.D the result is

$$(\partial\mathbf{u}_1/\partial t)+v_0 g\rho_1\zeta+v_0\nabla p_1=\mathbf{f}, \tag{25}$$

$$\nabla\cdot\mathbf{u}_1=aq_1/\gamma s, \tag{26}$$

$$(\partial\rho_1/\partial t)+\rho_0'\mathbf{u}_1\cdot\zeta=-\rho_0 aq_1/\gamma s, \tag{27}$$

use having been made of the equations $p_0'=-\rho_0 g$, $v_1\rho_0=-\rho_1 v_0$.

These equations were derived by Love[21] and have been used by Lamb,[22] Groen,[23] Fjeldstad,[24] and others.

B. Oberbeck's Equations

Equations (2) and (3) also imply

$$-Z\delta p+Y\delta\theta=XZ\delta v/\gamma, \tag{28}$$

or

$$\rho_0 v_1=a\theta_1-\gamma p_1/\rho_0 c^2, \tag{29}$$

$$\rho_0 v_0'=a\theta_0'-\gamma p_0'/\rho_0 c^2. \tag{30}$$

Following the idea of Love's approximation, many writers neglect the second terms on the right of the last two equations, obtaining

$$\rho_0 v_1=-v_0\rho_1=a\theta_1, \tag{31}$$

$$\rho_0 v_0'=-v_0\rho_0'=a\theta_0'. \tag{32}$$

When these approximations are substituted into Eqs. (23) to (27) they become

$$(\partial\mathbf{u}_1/\partial t)-ga\theta_1\zeta+v_0\nabla p_1=\mathbf{f}_1, \tag{33}$$

$$\nabla\cdot\mathbf{u}_1=aq_1/\gamma s, \tag{34}$$

$$(\partial\theta_1/\partial t)+\theta_0'\mathbf{u}_1\cdot\zeta=q_1/\gamma s. \tag{35}$$

Overbeck[25] introduced equations similar to these into the theory of convection. However, he simplified them with two further approximations:

(1) Terms proportional to ga are to be retained, but terms proportional to a alone are to be neglected.

(2) In Eq. (35), $\theta_0'\mathbf{u}_1\cdot\zeta$ is to be neglected.

Babcock[26] and Pekeris[27] have also used these simplified equations. Rayleigh[28] has used equations that differ from Oberbeck's only in the retention of the term in θ_0', but he refers them to Boussinesque.[29] These equations are still widely quoted, e.g., by Jeffreys,[30] Pellew and Southwell,[31] and Chandrasekhar.[32]

---

[14] E. Gossard and W. Munk, J. Meteorol. 11, 259 (1954).

[15] Lord Rayleigh, *Theory of Sound* (Dover Publications, New York, 1945), Vol. II, p. 18.

[16] P. Bergmann, J. Acoust. Soc. Am. 17, 329 (1946).

[17] Laplace, *Mécanique Céleste* (English Translation by N. Bowditch, Boston, 1832), Book 4, Chapter 5.

[18] Lord Rayleigh, Phil. Mag. 29, 173 (1890).

[19] G. I. Taylor, Proc. Roy. Soc. (London) A156, 318 (1936).

[20] M. Margules, Wien. Sitzber. Ak. Wiss. 99, 204 (1890).

[21] A. E. H. Love, Proc. Math. Soc. (London) 22, 307 (1891).

[22] See reference 8, p. 378.

[23] P. Groen, *Contribution to Theory of Internal Waves* (Köninklijk Nederlands Meteorlogisch Instituut De Bild, 1948), No. 125.

[24] J. E. Fjeldstad, Geofys. Publikasjoner 10, No. 6 (1933).

[25] A. Oberbeck, Ann. Physik 7, 271 (1879).

[26] R. W. Babcock, Phys. Rev. 35, 1008 (1930).

[27] C. L. Pekeris, Monthly Notices Roy. Astron. Soc. Geophys. Supplement 3, 343 (1935).

[28] Lord Rayleigh, Phil. Mag. 32, 529 (1916).

[29] J. Boussinesque, *Théorie Analytique De La Chaleur* (Paris, 1903).

[30] H. Jeffreys, Phil. Mag. 2, 833 (1926).

[31] Anne Pellew and R. V. Southwell. Proc. Roy. Soc. (London) A176, 312 (1940).

[32] S. Chandrasekhar, Proc. Roy. Soc. (London) A217, 306 (1953).

C. Jeffreys' Equations

Jeffreys[33] has proposed a modification of Oberbeck's equations. The derivation starts from the general equations (15) to (19) rather than from Love's equations (23) to (27); moreover, Eqs. (30) and (31) are used instead of Eqs. (31) and (32). Equation (15) then reduces to

$$(\partial \mathbf{u}_1/\partial t)-ga\theta_1\zeta+v_0\nabla p_1=\mathbf{f}_1, \tag{36}$$

which is identical with Eq. (33). Equation (16) becomes

$$\nabla\cdot\mathbf{u}_1=a(\partial\theta_1/\partial t)+(a\theta_0'+\gamma g/c^2)\mathbf{u}_1\cdot\zeta.$$

Now, the adiabatic temperature gradient is defined as

$$\theta_a'=-(\gamma-1)g/ac^2, \tag{37}$$

so that this may be written

$$\nabla\cdot\mathbf{u}_1=a\{(\partial\theta_1/\partial t)+[\theta_0'-\gamma\theta_a'/(\gamma-1)]\mathbf{u}_1\cdot\zeta\}. \tag{38}$$

If this is substituted into Eq. (15), the result is

$$(\partial\theta_1/\partial t)+(\theta_0'-\theta_a')\mathbf{u}_1\cdot\zeta=q_1/\gamma s. \tag{39}$$

Jeffreys uses Oberbeck's principle (1) to simplify Eq. (38), but retains the term in $(\theta_0'-\theta_a')$. In many applications, the quantities θ_0' and θ_a' are of comparable magnitude. Other writers give Love's or Oberbeck's derivation, but substitute $\theta_0'-\theta_a'$ for θ_0' without attempting a formal justification. In meteorology, the potential temperature, θ_p, is often used. It may be defined by the equation

$$\theta_p'=\theta_0'-\theta_a',$$

and this notation is frequently employed in writing Eq. (39). The corresponding modification of the equations for oceanographic purposes is discussed by Hesselberg and Sverdrup.[34]

III. THE FIELD EQUATIONS

A. Energy and the Quadratic Integral

The energy of the fluid, in erg/g, is

$$W=\tfrac{1}{2}u^2+\epsilon+g\chi. \tag{40}$$

Equations (1), (7), (8), and (9) imply that

$$\rho(DW/Dt)+\nabla\cdot(p\mathbf{u})=\rho(\mathbf{f}\cdot\mathbf{u}+q), \tag{41}$$

which is known as the energy equation. If $\mathbf{u}=\mathbf{u}_1+\mathbf{u}_2+\cdots$, $p=p_0+p_1+p_2+\cdots$, etc., the energy $W=W_0+W_1+W_2+\cdots$, and Eq. (41) can be resolved into a set of equations, of zero, first, second . . . orders. The zero- and first-order equations, thus derived, are identically satisfied because of Eqs. (11) and (15) to (19). The expression for W_2 involves $\mathbf{u}_2$, p_2, $\cdots$ as well as squares and products of $\mathbf{u}_1$, p_1, $\cdots$. Therefore, the second-order energy equation cannot be derived from Eqs. (15) to (19), which do not involve the second-order quantities.

Equations (15), (16), and (17) do imply the equation

$$(\partial E/\partial t)+\nabla\cdot(p_1u_1)$$

$$=\rho_0\left[\mathbf{u}_1\cdot\mathbf{f}_1+p_1q_1\frac{Y}{X\theta_0}-\eta_1q_1\frac{p_0'Y}{\eta_0'X\theta_0}\right], \tag{42}$$

with

$$E=\tfrac{1}{2}\rho_0u_1^2+\frac{p_1^2}{2\rho_0c^2}-\tfrac{1}{2}\rho_0\eta_1^2\frac{p_0'Y}{\eta_0'X}. \tag{43}$$

The quantities E and ρ_0W_2 are not identical, though they have some terms (e.g., $\tfrac{1}{2}\rho_0u_1^2$) in common; neither is Eq. (42) the second-order energy equation. Nevertheless, Eq. (42) is very important in the theory of Eqs. (15) to (19) and can often be used much as an energy equation would be used.

It would be desirable to have a simple terminology that preserves this distinction; in fact, this is essential if paradoxes are to be avoided. No such terminology has been invented, and E (or some similar expression) is usually called "energy." This misnomer is convenient in many applications, and is used in acoustics without causing confusion, but only because certain fundamental problems are ignored. The expression E may be called the quadratic integral of Eqs. (15) to (19), though this is clumsy, and does not indicate the physical importance of this quantity. Some adjectival phrase, like "external energy," would be desirable.

B. The Field Equations

Equations (42), (43), and (15) to (19) are much simplified by the following transformation of variables:

$$\begin{aligned} \mathbf{U}&=\mathbf{u}_1(\rho_0c)^{\frac{1}{2}}, & \mathbf{F}&=\mathbf{f}_1(\rho_0c)^{\frac{1}{2}},\\ P&=p_1(\rho_0c)^{-\frac{1}{2}}, & G&=(q_1Y/\theta_0)(\rho_0c)^{-\frac{1}{2}},\\ Q&=(\eta_1/\eta_0')(\rho_0c)^{\frac{1}{2}}, & H&=(q_1/\eta_0'\theta_0)(\rho_0c)^{\frac{1}{2}}. \end{aligned} \tag{44}$$

Similar transformations are to be found in references 5, 14, and 16. Equations (44) are not uniquely determined, and modifications may be desirable for special purposes.

Equations (42) and (43) then become

$$(\partial E/\partial t)+\nabla\cdot(P\mathbf{U})=(\mathbf{F}\cdot\mathbf{U}+GP+N^2HQ)/c, \tag{45}$$

$$E=(U^2+P^2+N^2Q^2)/2c, \tag{46}$$

where

$$\begin{aligned} N^2&=\rho_0g\eta_0'Y/X\\ &=\eta_0'g(\gamma-1)/ac^2=-\eta_0'\theta_a'. \end{aligned} \tag{47}$$

Equations (15), (17), and (18) become

$$(\partial\mathbf{U}/\partial t)+c(\nabla+\Gamma\zeta)P-N^2Q\zeta=\mathbf{F}, \tag{48}$$

$$(\partial P/\partial t)+c(\nabla-\Gamma\zeta)\cdot\mathbf{U}=G, \tag{49}$$

$$(\partial Q/\partial t)+\mathbf{U}\cdot\zeta=H, \tag{50}$$

---

[33] H. Jeffreys, Proc. Cambridge Phil. Soc. 26, 170 (1930).

[34] Th. Hesselberg and H. U. Sverdrup, *Die Stabilitätsverhältnisse des Seewassers bei vertikalen Verchiebungen* (Bergens Museums Aarbok, 1914–1915), No. 14.

where

$$\Gamma=\tfrac{1}{2}[(\rho_0 c)'/(\rho_0 c)]+(g/c^2). \tag{51}$$

These will be called the field equations, and have a considerably simpler form than Eqs. (15) to (19), to which they are equivalent. In particular, their left sides depend only on three parameters, c, N^2, and Γ. These are generally functions only of the vertical coordinate (i.e., of χ); in the particular case of an isothermal ideal gas, all three are constants.

Equations (48), (49), and (50) are essentially self-adjoint, and if $N^2>0$, their quadratic integral is positive definite. These are important physical facts. Most of the simplifying assumptions discussed above destroy one or both of these properties of the equations. An exception is the acoustic assumption, $\eta_1=0$.

The literature does not contain a systematic account of the solutions of these equations, although special or approximate solutions are frequently implied.

C. The Parameters of the Field Equations

The parameter, c (cm/sec), is the Laplacian velocity of sound, and requires no further discussion. The parameter Γ (radians/cm) has very small values, and does not affect the qualitative character of the solutions of the equations. In the case of the oceans, $2\pi/\Gamma$ is so much greater than their depth that its quantitative influence is completely negligible. In the case of the atmosphere, the quantitative influence of Γ becomes appreciable only at altitudes greater than about 50 km; however, it does determine the behavior of the solutions at infinite altitudes, so that the approximation $\Gamma=0$ may introduce paradoxes.

The parameter N (radians/sec) is sometimes called Väisälä's frequency.[35] The sign of N^2 is that of the entropy gradient, η_0'; when this is positive, the stratification of the fluid is stable, and small disturbances have an oscillatory character. When $\eta_0'<0$, N is imaginary, and the stratification is unstable. Väisälä established these facts by simple physical considerations; they can also be derived from a study of Eqs. (48), (49), and (50). They are frequently used by meteorologists; the limiting case $N=0$ is called convective equilibrium.

Using Eq. (12), one obtains the following alternative expressions for N^2:

$$N^2=-g[(\rho_0'/\rho_0)+(g/c^2)], \tag{52}$$

$$=ga(\theta_0'-\theta_a'). \tag{53}$$

The last expression should be compared with the formulas of Sec. II.C; the appearance of the combination ga also relates it to Oberbeck's principle (1), but not in any consistent fashion.

---

[35] Vilho Väisälä, Über die Wirkung der Windschwankungen auf die Pilotbeobachtungen. Soc. Sci. Fennica, Commentationes Phys.-Math. II 19, 37 (1925).

Reprinted from SCIENCE, February 3, 1956, Vol. 123, No. 3188, page 183.

Quantitative Underwater Study of Benthic Communities Inhabiting Kelp Beds off California

By use of a Cousteau-Gagnan Aqualung and a heavy-duty diving suit, the sea bottom off La Jolla, Calif., was explored during the spring of 1955 in an attempt to assess the standing crop of the benthic animals and plants that live in association with the giant kelp, *Macrocystis pyrifera*. This method of investigation insures free movement under water and enables one to make more extensive observations of the submerged communities than one can by dredging or by diving with a helmet (*1*).

The visibility at the bottom is largely limited by the depth, the density of overlying kelp, the turbulence, and the amount of suspended matter in the water. Thus, on clear days at a depth of 20 m, the visibility ranges between 1 and 10 m.

Cross sections of the sublittoral region, which extends more than 400 m from the low-tide level to the outer edge of the kelp beds, were surveyed. The organisms dwelling on the bottom were analyzed quantitatively by the quadrant method. The quadrants used enclosed an area of ¼ m^2; for the larger kelp as well as for animals dispersed over wider areas, the number of organisms was counted along lines of 2- or 10-m length in different directions.

The results of this survey reveal a zonal distribution of the chief submerged plants and animals, which seem to be controlled chiefly by light and temperature.

Thus, on the exposed rocks below mean low-water spring tide, a community dominated by the sea grass *Phyllospadix scouleri* flourishes best under surf conditions and extends down to a depth of about 7 m, covering 80 to 100 percent of the rock surface. Epiphytes on *Phyllospadix* consist largely of *Porphyra naiadum* var. *australis*, *Melobesia mediocris*, and *Ectocarpus granulosus*; *Callithammion californicum* and *Ceramium pacificum* occur as secondary epiphytes. This community is poor in animals, and—apart from *Membranipora*, *Caprella*, hydroids, and a few small snails—the gross weight obtained in the quadrants is owing mainly to the sea grass and amounts to an average value of 3634 g/m^2.

Table 1. Standing crop (average fresh weight) of the coralline community at different depths below mean sea level.

Depth (m)	Plants (g/m^2)	Animals (g/m^2)	Total wt. (g/m^2)
1.5	4667	125	4792
7	2490	329	2819
15	1972	392	2364
22	606	377.2	983.2

A *Pterygophora-Eisenia* community flourishes where the sea grass ceases to grow, at first as widely scattered individuals intermingled with *Egregia laevigiata*, *Cystoseira osmundacea*, *Codium fragile*, *Dictyota binghami* and *Dictyopteris zonarioides*; it reaches a climax in deeper water between 10 and 20 m, where the two main Laminariales, *Pterygophora* and *Eisenia* form, together with *Laminaria farlowii*, a "forest" under the large *Macrocystis* plants.

Macrocystis pyrifera forms extensive beds ranging in width between 200 and 500 m in a depth of water from 7 to 25 m. Individuals become more crowded in the middle of the beds, with holdfasts 1 to 2 m apart. At the outer edge, *Macrocystis* becomes replaced by scattered individuals of the elk kelp, *Pelagophycus porra*, in a depth of water of 20 to 25 or 30 m.

Where *Macrocystis* grows on outcropping rocks or on boulders, it meets with competition from sea urchins, which clear whole areas of kelp; this is demonstrated by the patchy appearance of the beds at the surface. Survival of kelp plants depends largely on the enormous production of juvenils, which grow on a variety of substrata, including other algae and sea grass.

The standing crop of the *Macrocystis* plants in these beds is estimated to be between 25 and 40 tons/acre, and average annual yield is estimated to be about 4 to 6 tons/acre (fresh wt.). This was judged by observations at the bottom and on the surface, as well as by studies of aerial photographs, by weighing representative samples, and by laboratory experiments on the growth rate of kelp. Under favorable conditions, the latter ranges between 3 and 5 cm per day.

The lowermost stratum of vegetation is occupied by a coralline community that forms an extensive cover under the larger kelps. *Corallina chilensis*, *C. gracilis*, *Bossea orbigniana*, *B. gardneri*, *Lithothrix aspergillus*, and *Lithothamnion* spp. are the chief calcified algae inhabiting this substratum. The quantity and quality of organisms inhabiting this community were found to vary with depth as follows: (i) the percentage of cover by the dominant alga decreases with depth, hence the production per unit area decreases; (ii) *Bossea* preponderates over the *Corallina* beyond a depth of 15 m. These modifications are accompanied by modification in the fauna that live in association with the corallines. For example, the sea fans, red and pink abalones, the sea star *Henricia leviuscula*, together with the holothurian *Stichopus parvimensis* and the acorn barnacle *Balanus tintinnabulum*, become noticeable at 20 to 25 m; some of these appear for the first time at such depths. Table 1 gives a comparison of production of the coralline community at different depths.

It has also been found that, while the total weight of plants decreases with depth, that of the animals tends to increase. On the basis of the foregoing survey, an average figure for the standing crop of the organisms that inhabit the rocky bottom of the kelp beds, including *Macrocystis* itself, would approach 9.4 kg/m^2 of sea bottom, or approximately 38 tons/acre. These figures do not include the pelagic forms.

ANWAR ABDEL ALEEM*
Division of Marine Botany, Scripps
Institution of Oceanography and
Institute of Marine Resources,
La Jolla, California

Notes

1. Contribution from the Scripps Institution of Oceanography, new series, No. 824.

* Permanent address: Oceanography Department, Faculty of Science, Alexandria, Egypt.

28 June 1955

Reproduced by Permission

Reprinted from
BULLETIN OF MARINE SCIENCE
OF THE GULF AND CARIBBEAN
Vol. 5, No. 4, pp. 292-296
DECEMBER, 1955

A REDESCRIPTION OF THE MARINE ISOPOD CRUSTACEAN "*EXOSPHAEROMA*" *FAXONI* RICHARDSON FROM TEXAS[1]

ROBERT J. MENZIES
Lamont Geological Observatory, Columbia University
MILTON A. MILLER
Department of Zoology, University of California
Davis, California

ABSTRACT

Exosphaeroma faxoni Richardson is placed in the genus *Cymodoce* and redescribed on the basis of specimens collected at Port Isabel, Texas and the type specimen from Florida. This is the first indigenous species of *Cymodoce* reported from North America.

The species *Exosphaeroma faxoni* Richardson was described in 1905 from one male specimen taken in Florida by Professor A. S. Packard. The type is located in the Museum of Comparative Zoology at Harvard College, Cambridge, Massachusetts, Cat. No. 6732, M. C. Z.

Several specimens from Port Isabel, Texas, which suspiciously looked like the drawings of this species (Richardson, 1905, fig. 307) were sent to us for determination by their collector, Dr. Joel Hedgpeth, then with the Institute of Marine Sciences, University of Texas, Port Aransas, Texas. Several discrepancies were noted. First, the specimens from Port Isabel belonged to the genus *Cymodoce* and not to *Exosphaeroma*. This is a matter of considerable importance for its own sake since only one other species of the genus *Cymodoce* had been previously reported from North America and this species, *C. japonica* Richardson (Hatch, 1947, p. 215), is believed to have been introduced into America from Japan along with the Japanese oyster. This then constitutes the first record of an indigenous species of *Cymodoce* from North America. The second item of concern was the fact that the pleon of *E. faxoni* is figured as having four complete segments plus the lateral incisions of a partly coalesced fifth. This would be an unusual state of affairs for most sphaeromid genera and would not allow the placement of *E. faxoni* in either *Exosphaeroma* or *Cymodoce*. Richardson (op. cit., p. 292) remarked, however,

Contribution from the Department of Zoology, University of California, Davis, California and the Scripps Institution of Oceanography, New series No. 825.

"The abdomen is composed of two segments." Our specimens had a pleon (abdomen, Fig. 1E) composed of *three* segments as is usual for many sphaeromids. The first is small and concealed by the last peraeonal somites except for parts of its lateral margin. The second and third are about as Richardson describes.

Dr. Elisabeth Deichmann, Curator of Invertebrates at the Museum of Comparative Zoology at Harvard College, generously aided us in our problem by providing us with sketches of the type and by comparing the figures given here with the type. She found the type specimen to agree favorably with our figures and accordingly, we have arrived at the conclusion that Hedgpeth's Texan specimens of *Cymodoce* and Richardson's *Exosphaeroma faxoni* are probably one and the same species.

Richardson did not describe several anatomical features which are important today in isopod taxonomy and these we give in the following description.

Cymodoce faxoni (Richardson) comb. nov.

Figures 1A-J, 2A-K

Synonyms. Exosphaeroma faxoni Richardson, 1905, pp. 292-293, figs. 307-308.

Diagnosis. Pleon composed of a narrow first somite which is concealed from dorsal view except near the lateral margins by the seventh peraeonal somite, a longer second somite which is formed by the fusion at the mid-line of three pleonal somites (pleonites), and a pleotelson which is twice as long as the rest of the pleon. Last pleonite with a pair of medially located swellings at posterior margin. Pleotelson with a similar but more obvious elongated pair of swellings at central area. Posterior apical margin of pleotelson trifid. Uropodal exopod styliform, as long as endopod in female and one-third to one-half longer than endopod in male with the large males having the longest and most styliform exopods; endopod apically truncated, outer angle pointed. First antenna with first peduncular article elongate and swollen, second article as wide as long being one-third narrower and one-half as long as first; third article one-half narrower than second and four times as long as wide; fourth article small, partly concealed between third peduncular and first flagellar article; flagellum with about 10 articles. No antennular scale was found but three setae projecting between the third and fourth peduncular articles indicate where its vestige might be located. Peduncle

(94)

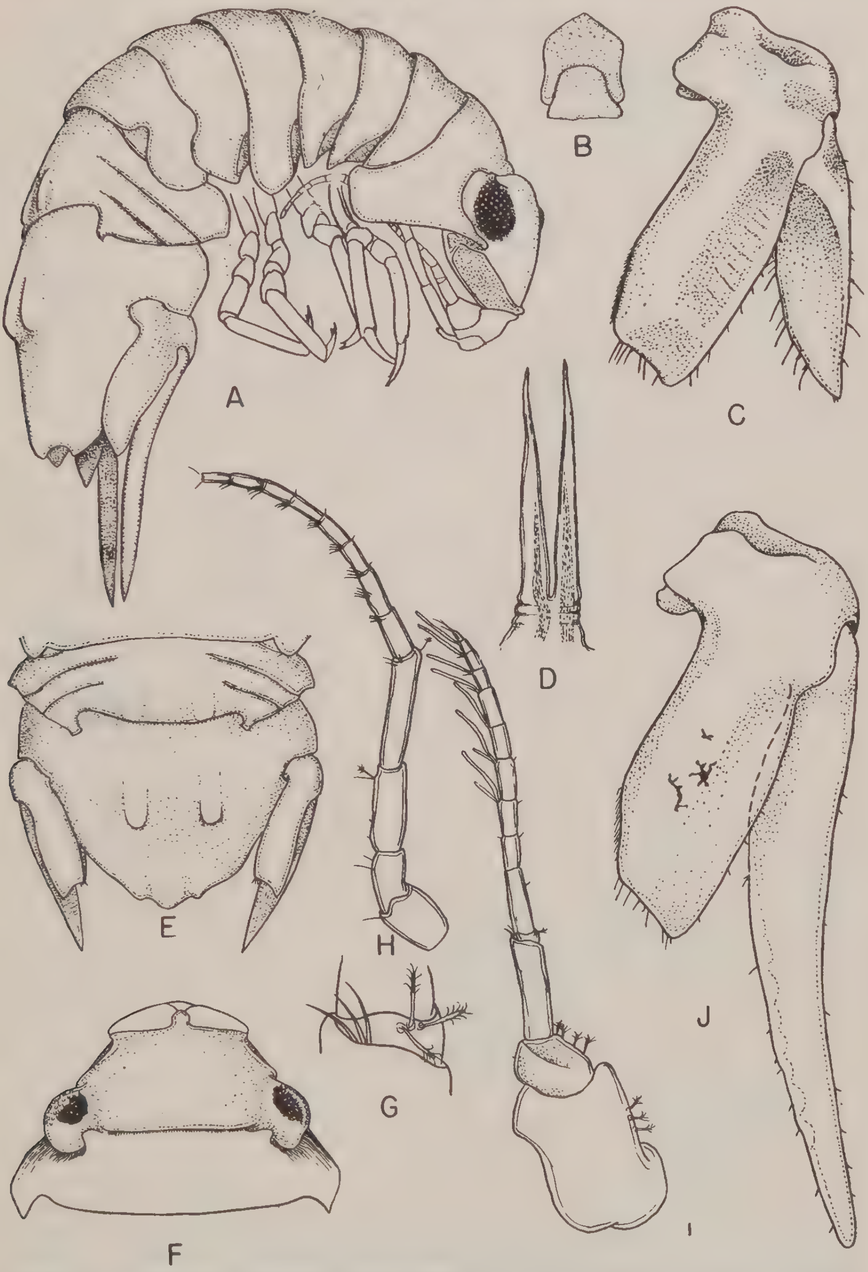

FIGURE 1. *Cymodoce faxoni* (Richardson). A. Male, lateral view, B. Clypeus and labium, C. Uropod, female, D. Genital apophyses, male, E. Pleon of young male, F. Cephalon and first peraeonal somite of female, G. Terminal peduncular article of first antenna, H. Second antenna, I. First antenna, J. Uropod of mature male.

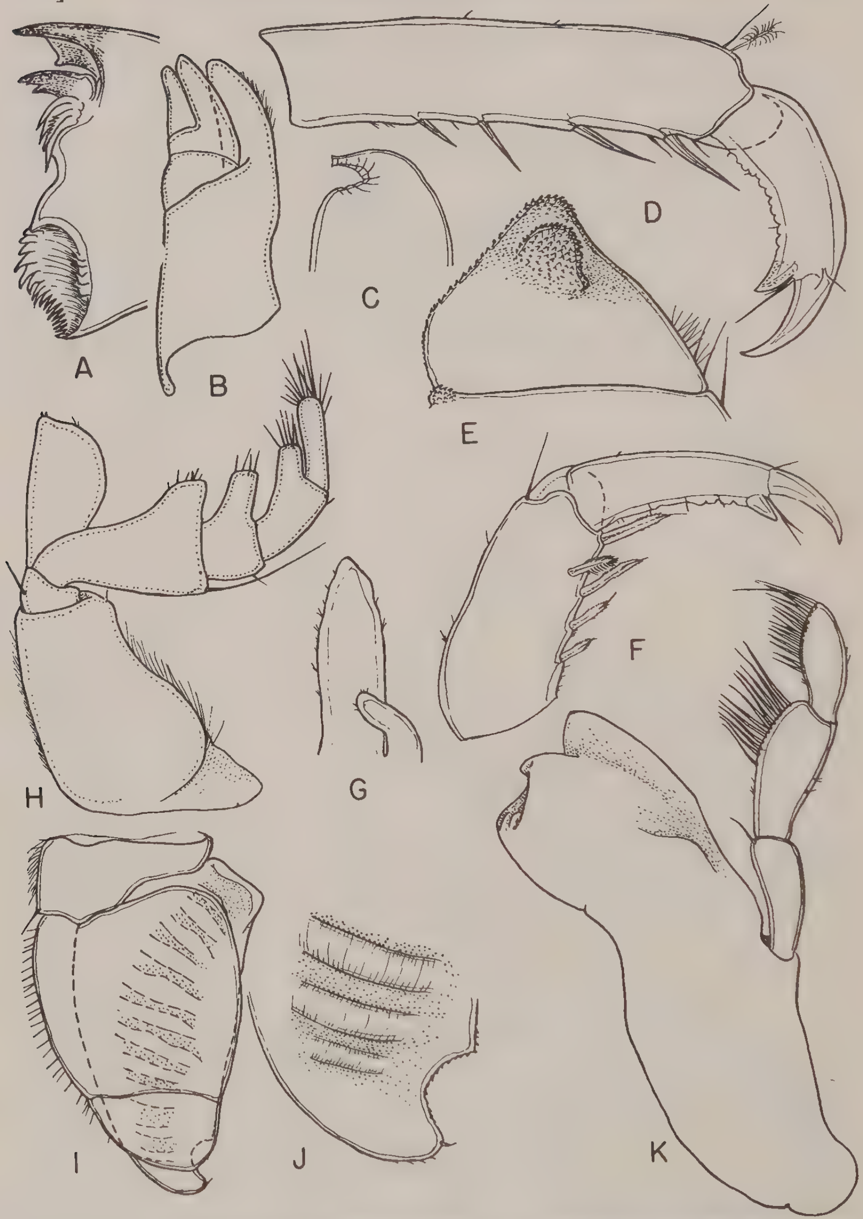

FIGURE 2. *Cymodoce faxoni* (Richardson). A. Left mandible, male, B. Second maxilla, female, C. Apex of stylus of male second pleopod, D. Seventh peraeopod, male, E. Apex of endopod of male fifth pleopod, F. Second peraeopod, male, G. First maxilla, female, H. Maxilliped of female, I. Fourth male pleopod, J. Apex of endopod of fourth male pleopod, K. right mandible of female.

of second antenna with four articles of similar width, first and second subequal in length, third one-third longer than second, fourth one-third longer than third, flagellum with 14-15 articles. In dorsal view the frontal process of the cephalon is produced and apically pointed. It projects downward medially where it meets the frontal lamina (clypeus) thus separating the first peduncular articles of the first antenna medially. Genital apophyses (penes) elongate and styliform. Appendix masculinum of second male pleopod laterally recurved at apex.

Mouth parts of female metamorphosed, showing particularly a loss of setae. Mandible of female shows a diminution of the incisive process, a loss of the lacinia mobilis and of the setae of the setal row. Male maxilliped each with one coupling hook. Endopods of fourth and fifth male pleopods fleshy, each with eleven respiratory folds. apex of fourth with a distinctive emargination medially, that of fifth with two spinulate lobes.

Measurements. Male (figured), 5.4 mm long, 2.3 mm wide at first peraeonal somite. Female (not ovigerous), 4.8 mm long, 2.0 mm wide at first peraeonal somite.

Material examined. Two males, five females, collected 11-12-47 at South Bay, Port Isabel, Texas. The specimens have been donated to the Museum of Comparative Zoology, Harvard College, Cambridge, Massachusetts.

Remarks. This species appears to be closely related to *Cymodoce acuta* Richardson (1904, pp. 38-39, figs. 8-10). It differs from it in having a less pointed pleotelson and further in having the suture of the first pleonite (the first fused somite in the coalesced "second" pleonal somite) extending farther medially than that of the second. The reverse of this is shown in Richardson's figure (op. cit.). The species also resembles *C. japonica* Richardson but it differs from that species in having one pair of elevations medially on the pleon instead of two pair.

LITERATURE CITED

HATCH, MELVILLE H.

1947. The Chelifera and Isopoda of Washington and adjacent regions. Univ. Wash. Pub. Biol. *10* (5): 155-274.

RICHARDSON, HARRIET

1904. Contributions to the natural history of the Isopoda. Proc. U. S. nat. Mus., *27* (1350): 1-89.

1905. A monograph on the isopods of North America. Bull. U. S. nat. Mus., No. 54, 727 pp.

Reprinted from SCIENCE, January 27, 1956, Vol. 123, No. 3187, pages 127–132.

Edge Waves on the Continental Shelf

Walter Munk, Frank Snodgrass, George Carrier

In 1846, Stokes derived a solution for wave motion over an inclined bank, which differs markedly from the conventional pattern of waves coming onto a sloping beach. In Stokes' solution, the crests are normal to the coast line, and they travel in a direction parallel to the coast. Amplitudes diminish rapidly from the shore seaward and are negligible at a distance of 1 wavelength. Lamb (*1*, p. 447) accordingly calls these waves "edge waves" and states that "it does not appear that the type of motion here referred to is very important." But edge waves appear to be common! Evidence comes from a variety of sources (*2*).

Gust of 6 January 1954

At 3:35 A.M. (0335) on 6 January 1954, an unusual gust was recorded at Scripps pier (Fig. 1). Pressure rose by 2 millibars, and wind speed increased abruptly from 3 to 14 miles per hour. This gust was followed by pressure and wind oscillations of 8-minute period; these have been attributed to internal waves on the atmospheric inversion layer (*3, 4*). Sea level at Scripps responded to the atmospheric pressure as an inverted barometer. This is shown by the trace of the Scripps tsunami recorder (*5*), an instrument that discriminates by means of pneumatic devices against swell and tides and that has a peak response for a period of 45 minutes. Our attention for the moment is on the simultaneously recorded (by radio link) signal from the tsunami recorder at Oceanside, 38 kilometers along the coast to the northwest. Between 3:40 A.M. (0340) and 4:50 A.M. (0450), it showed the familiar features of an impulsively generated dispersive wave train. There was no meteorologic disturbance at Oceanside that could account for the recorded wave train.

It is not difficult to compute roughly the character of edge waves that are caused by an impulsive source. Phase velocity C, wavelength L, and period T of edge waves over a beach of constant inclination β are related by the equations

$$C = (gT \sin \beta)/2\pi, \qquad L = (gT^2 \sin \beta)/2\pi \quad (1)$$

These are identical with the relationships for ordinary deepwater waves when gravity g is replaced by $g \sin \beta$. With this modification, the Cauchy-Poisson treatment of impulsively generated waves in deep water from a line source is applicable. The upper curve in Fig. 2 shows the solution copied from Lamb (*1*, p. 387). Time is in units of $(2y/g \sin \beta)^{\frac{1}{2}}$, and elevation is in units of $Q/\pi y$, where y is the distance from the disturbance and Q is the sectional area of the initially elevated fluid. The second curve is the recorded Oceanside trace corrected roughly for instrument response (on the record, the short late waves are suppressed and slightly delayed relative to the long early waves) and drawn to scale for best agreement with the theoretical curve. Zero time is taken at the first indication of the disturbance at La Jolla. On comparison, we find that

$$(2y/g \sin \beta)^{\frac{1}{2}} = 582 \text{ sec}, \quad Q/\pi y = 0.3 \text{ cm}$$

The mean slope over the continental shelf between La Jolla and Oceanside is 0.02. With this value of $\sin \beta$, we get

$$y = 33 \text{ km}, \quad Q = 3.1 \times 10^6 \text{ cm}^2$$

These values are reasonable; y is nearly the distance between Scripps and Oceanside, and Q corresponds to an initial displacement of 3 centimeters over 10 kilometers. The recorded displacement at La Jolla was about 8 centimeters.

The wave train is barely discernible on a record taken by the Mark IX wave instrument at Camp Pendleton, 3.5 kilometers northwest of Oceanside. With imagination, one can find some traces on tide records in the Los Angeles area. However, these records are hardly useful; the wave instrument is tuned to higher frequencies, and the tide gage is tuned to lower frequencies than the frequency of the disturbance under consideration.

We must point out a number of difficulties in the application of the Cauchy-Poisson theory to our problem. The continental shelf is about 5 kilometers wide, and the assumption of constant slope is tolerable only if $L/2\pi$ is less than 5 kilometers. This is true for the wave that arrived after 4 A.M. (0400), but the first arrival must have extended beyond the shelf, and the theory does not strictly apply.

It has been demonstrated by Ursell (*6*) that the Stokes solution represents only the gravest of an infinite number of possible modes of edge waves. The n'th mode has n extrema in elevation between shore and open sea, and its velocity and length are given by

$$C = [gT \sin (2n+1)\beta]/2\pi, \qquad L = [gT^2 \sin (2n+1)\beta]/2\pi \quad (2)$$

This reduces to Eq. 1 for $n = 0$. Note that the computed values of y and Q for the first harmonic are 3 times those for the zero mode and that they are inconsistent with observations. Suppose that the initial disturbance is $f(x,y)$, with x pointing seaward and y measured along the coast. If the disturbance is concentrated very near $y = 0$, then $f(x,y)$ can be written $g(x)\ \delta(y)$, where δ is the delta function. The relative amplitudes of the various modes can be found by expanding $g(x)$ in Laguerre polynomials. The predominance of the fundamental mode points to an exponential-like (at least

---

Reproduced by Permission

The authors are on the staff of the Scripps Institution of Oceanography, La Jolla, Calif. Dr. Carrier is on leave of absence from Harvard University.

monotonic) drop off with distance from shore.

The Cauchy-Poisson theory is derived for such a concentrated line source at $y = 0$, but holds reasonably well for a finite width provided that the computed wavelengths are larger than this width. The Oceanside signal ended at 4:50 A.M. (0450) with a period of 10 minutes, which corresponds to a wavelength of about 10 kilometers. This may be taken to mean that the initial disturbance was about this wide.

A search through 3 years of records did not reveal any other example of a comparable gust, nor did it reveal a similar Cauchy-Poisson type of disturbance in sea level.

Hurricanes and Squalls

On 26 August 1954, hurricane Carol formed near the Bahamas and was moving very slowly northwestward. On the morning of 30 August, the hurricane started its rapid trip up the East Coast. According to weather maps (*7*), Carol was moving at 32 knots when it passed Atlantic City 24 hours later. From the arrival times of the water-level disturbance at various tide gages (*8*), we obtain 34 knots.

Consider the characteristics of edge waves that might be generated by such a traveling disturbance. The prominent waves will have a velocity C that just equals U, the longshore component of velocity of the traveling disturbance. Precisely the same considerations determine the period and length of waves behind a vessel traveling at velocity U. Accordingly, we replace C by U in Eq. 1 and obtain

$$T = \frac{2\pi U}{g \sin \beta}, \qquad L = \frac{2\pi U^2}{g \sin \beta} \qquad (3)$$

for the period and wavelength of the fundamental edge-wave "wake." Off Atlantic City, the 30-fathom line is approximately 100 kilometers offshore, giving a slope of $\beta = 5 \times 10^{-4}$. For $U = 32$ to 34 knots, this yields $T = 5.8$ to 6.1 hr for the fundamental mode. A. C. Redfield and A. R. Miller have kindly furnished us values of observed minus predicted tide level. They indicate four waves about 2 feet high with a period of 5.5 hours (Fig. 3). Note that these waves do not show the progressive shortening in period that is so characteristic of impulsive generation (Fig. 2).

For the first harmonic ($n = 1$), the computed period is one-third of the fundamental. The records do not show any prominent oscillations of 2-hour period.

Further north, near Sandy Hook, the 30-fathom line is more nearly 120 kilometers offshore, and $\beta = 4.25 \times 10^{-4}$. The computed periods are then somewhat longer, 6.9 to 7.2 hours. The measured period at Sandy Hook was also longer, 7 hours. But it is not clear whether the change in topography actually accounts for the change in period, and we have not considered in detail what happens when slope varies gradually along the travel path.

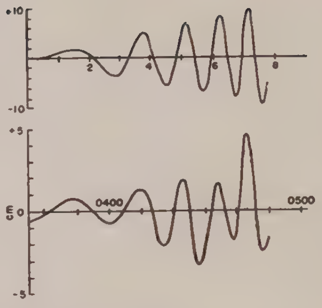

Fig. 2. The upper curve shows elevation against time at a fixed point according to the Cauchy-Poisson theory. The lower curve is the recorded water level at Oceanside corrected for instrument response.

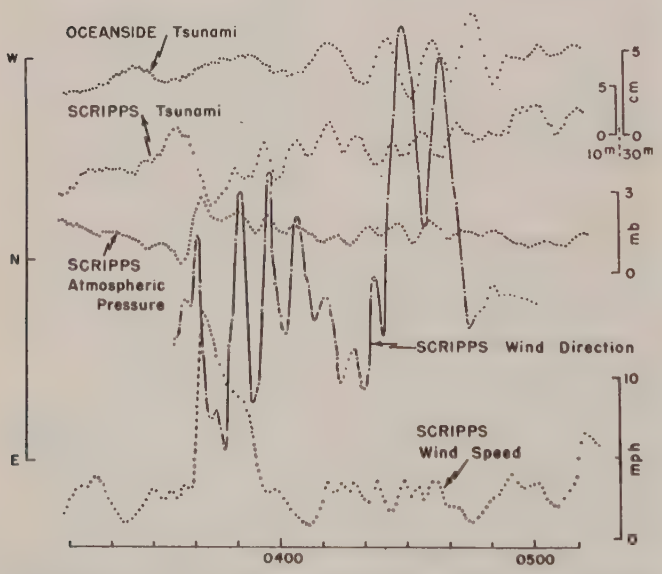

Fig. 1. Meteorologic and sea-level records of 6 January 1954. The Scripps and Oceanside tsunami recorders are peaked for sea-level oscillations of 45-minute period. The scale for oscillations of 30-minute and 10-minute periods is indicated. A gust recorded at Scripps at 3:35 A.M. (0335) is followed by a dispersive sea-level oscillation at Oceanside, 38 kilometers to the northwest.

The wavelengths are of the order of 400 kilometers. Edge waves are essentially confined to a strip within a distance $L/2\pi$ from shore; for this reason, we have based our calculations on average slopes over the first 100 kilometers. Beyond the continental shelf, the slope is far larger. To estimate the effect of this increased slope, we have worked out the theory (not given here) for an inclination β_1 to a distance x_1, followed by β_2 beyond x_1. Setting

$$x_1 = 200 \text{ km}, \ \beta_1 = 4.25 \times 10^{-4}, \ \beta_2 = 5.9 \times 10^{-4}$$

for the bottom off Sandy Hook leads to a *decrease* in computed period by roughly 2 percent. The approximation of a constant slope is adequate.

The sea-level disturbance at Atlantic City and Sandy Hook consisted of four waves and lasted until about 24 hours after the passage of the hurricane. A rough calculation of the expected duration of an edge-wave wake is as follows. Hurricane Carol started its rapid trip up the east coast on the morning of 30 August from about latitude 31°N. The hurricane arrived at Atlantic City about 24 hours later. The front of the water disturbance arrives with the hurricane; the rear travels with group velocity, which is one-half the phase velocity for edge waves. Hence the rear will take twice 24 hours, and the duration is 24 hours, as observed. For the general case, let D be travel time and Y travel distance at a velocity of U. The duration τ of the disturbance is given by

$$\tau = D \text{ or } \tau = Y/U \qquad (4)$$

These expressions are equivalent for constant U, as assumed. For Carol we set D=24 hr, Y=540 naut. mi., U=33 knots; the two expressions give $\tau = 24$ hr and $\tau = 16$ hr. The numerical values are summarized in Table 1, together with similar calculations for three other hurricanes (*9*). The values for Edna are similar to those for Carol. The hurricanes of 1938 and 1944 had similar paths and were farther out at sea than the 1954 hurricanes. We have taken their starting time when the storms' centers came over the shelf just south of Cape Hatteras. This yields durations that are considerably shorter than the observed values. To obtain agreement, one must take the starting time 12 hours earlier, when the hurricane centers were about 250 miles from shore.

It is known that the rise in water level is of the same order as that given by the inverse barometer rule: the water level rises 1 centimeter for each millibar of pressure drop. The measured rise is often larger, and the difference is attributed to winds. Here we limit ourselves to the question whether a traveling pressure spot of reasonable dimension could generate edge waves with amplitudes of the order of the inverted barometer. Consider a pressure spot

$$p = p_0 \frac{a(x+a)}{(x+a)^2 + (y-Ut)^2}$$

traveling from $y = -\infty$, $t = -\infty$ with velocity U parallel to the coast. The resemblance to actual hurricanes is poor, but the Fourier transform is simple. The isobars are nonconcentric circles. The pressure deficiency is p_0 at $x=0$, $y=Ut$, and $\frac{1}{2}p_0$ on a circle of radius a centered at $x=0$, $y=Ut$. It can be shown that the elevation of the sea surface is given to good approximation by

$$2ka(p_0/\rho g)e^{-k(x+a)} \cos k(y-Ut)$$

where $k = g \sin \beta / U^2$ is the wave number $(2\pi/L)$ of the fundamental mode of edge waves traveling with a velocity $C = U$. Only the fundamental mode is generated to the present approximation. This is, of course, a consequence of the assumed pressure pattern, but it is doubtful whether any monotone (nonwiggly) pressure pattern resembling surface isobars of hurricanes would be an effective generator of harmonics. The crest height at the coast line differs from that given by the inverted barometer rule by a factor of $2\ ka\ e^{-ka}$. This has a maximum value of $2/e$ for $ka = 1$. Thus, with wavelength having been determined by the speed of the hurricane, its effectiveness depends on the hurricane's dimension. The waves are largest when the radius of the half-pressure isobar equals

$$k^{-1} = L/2\pi = U^2/(g \sin \beta)$$

For the hurricanes under consideration here, this equals 30 to 40 miles. The observed half-pressure radius is more like 100 miles, too large for optimum generation. The afore-mentioned values give $ka = 2.5$ to 3.0, and $2\ ka\ e^{-ka} = 0.41$ to 0.30. Thus, the inverted barometer rule yields the correct order of magnitude.

The over-all agreement for the four East Coast hurricanes is good. The observed and computed periods agree, and the longest period is associated with the fastest hurricane. Duration and amplitude cause no particular difficulties. The outstanding feature is that the periods are large, and this is attributed to the very gentle bottom slope.

For contrast, we consider very briefly the disturbance caused by a traveling squall over Osaka Bay, Japan, on 29 August 1953 (*10*). Coming from the southwest at a speed of very roughly 30 knots, it gave rise to a pressure drop of 3 millibars at Wakayama. In this region, the coast tends north-south, and the longshore projection of the velocity was of the order of 40 knots. The offshore topography is irregular. We replace it by an idealized profile consisting of a constant slope to the 30-fathom line 4 miles offshore, and constant depth seaward. The theory for this geometry (not included here) gives a period of 31 minutes for a phase velocity of 40 knots. If one assumes the slope to extend indefinitely, Eq. 3 applies, and the period is 29 minutes. The observed periods along this stretch of coast line were 20 minutes at Shimatsu, 30 minutes at Kainan, and 25 minutes at Wakayama.

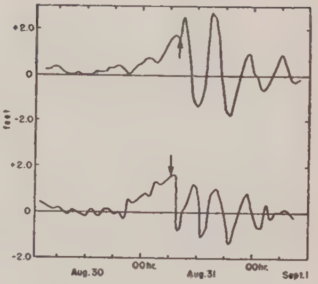

Fig. 3. Observed minus predicted tide-gage level at Atlantic City (lower curve) and Sandy Hook (upper curve) during hurricane Carol. Arrows indicate time of passage of storm center.

On comparison with Table 1, we find the velocities of the disturbance to be commensurate, but the bottom slope of Osaka Bay is 15 times larger than that off Atlantic City. In accordance with edge-wave theory, the excited periods should be one-fifteenth as large, and they are. In most regions of the world, the slope is even larger than it is off Wakayama, and the observed open-sea seiche periods are shorter. Typical values are $\beta = 0.015$ and $T = 10$ min; this requires a longshore component of velocity of 27 knots for the traveling disturbance.

Redfield and Miller (*8*) discussed the oscillatory wake under the heading "resurgences." They stated "these phenomena are of particular importance because they tend to catch one unaware, coming as they do after the storm appears to be subsiding. . . . Should a storm pass along the coast at low tide the accompanying rise in water level might be inconsequential, but the resurgence occur-

Table 1. Periods and durations of sea-level disturbances caused by four hurricanes.

Hurricane	Velocity U (knots)	Path Y (naut. mi)	Travel time D (hr)	Wave period T (hr)				Duration (hr)		
				Computed		Observed		Computed	Observed	
				$\sin\beta = 5.0 \times 10^{-4}$	$\sin\beta = 4.2 \times 10^{-4}$	Atlantic City	Sandy Hook		Atlantic City	Sandy Hook
30 Aug.–1 Sept. 1954 (Carol)	32–34	540	24	5.8–6.1	6.9–7.2	5.5	7.0	16–24	20	26
11–12 Sept. 1954 (Edna)	32	530	24	5.8	6.9	6.0	7.0	17–24	23	?
14–15 Sept. 1944	33	360	12	6.0	7.1	5.6	7.2	11–12	23	30
21–22 Sept. 1938	40	360	9	7.3	8.6		8.0	9		16

ring six hours later would arrive at high tide, and might thus prove more destructive than the original rise in water level."

The prediction of the resurgences is then a matter of practical importance, and our calculations for four hurricanes must be extended to other cases. The results shown in Table 1 give some hope that the arrival time of resurgent crests can be predicted on the basis of Eq. 3 and that the number of such crests can be estimated from Eq. 4. The amplitude will be more difficult to predict; it is of the order given by the inverted barometer rule. We expect resurgences only if the hurricane travels over the shelf for a time exceeding $T\,[= 2\pi\, U/(g \sin \beta)$, Eq. 3]. Hurricane Hazel came over the shelf at 40° incidence and quickly traveled inland. There were no resurgences.

In closing this discussion, we should point out the connection between our treatment and previous investigations. Redfield and Miller (*8*) contoured the depth h^* for which $(gh^*)^{1/2}$ equals the speed of the disturbance. They correctly emphasized that effective generation of the water-level disturbance takes place only where the shelf depth is less than h^*. Our interpretation of h^* (for constant slope) is the depth at a distance $L/2\pi$ from shore, the *mean* distance of the wave elevation. Ewing, Press, and Donn (*11*) drew similar contours to explain the disturbance caused by a squall line over Lake Michigan. They attributed the disastrous wave to the unusually high velocity of the squall. This has the effect of coupling the atmospheric disturbance to the relatively flat areas near the lake bottom rather than to the steeper edges. Edge-wave theory is not applicable to this situation, but it might be profitable to look for a normal mode solution that is.

Edge-Wave "Noise"

The causes discussed so far have dealt with clear-cut and exceptional meteorological disturbances. But the Scripps and Oceanside tsunami recorders show some activity at all times. The root-mean-square height ranges from less than 1 centimeter on quiet days to more than 5 centimeters on noisy days. There is a correlation between the general level of activity at Scripps and Oceanside, but there is no coherence between individual waves at the two stations. The records are irregular and quite similar in appearance to ordinary wave records, but the periods are about 100 times longer. M. J. Tucker of the National Institute of Oceanography, Great Britain, has kindly made a frequency analysis of some of the records. The spectra show a band of activity between periods of 10 and 30 minutes.

If this activity is the result of edge waves, then it should diminish with distance from shore in the predicted manner. To test this, we have made simultaneous recordings from a shore-based and a ship-based recorder. The portable shore unit was placed on the bottom in about 30 feet of water. The fluctuating pressure acts on a system of capillaries and air volumes that discriminate against swell and tides and give peak response for 10-minute periods. A strain-gage transducer converts the filtered pressure fluctuations into fluctuating voltages, which are transmitted by cable to a bank of shore-based resistance-capacitance filters of very long time constant. Their output is recorded in two broad frequency bands, one centered at 13-minute period, the other at 22-minute period.

This kind of instrument is not readily adapted to great depth. It is hard to provide for an adequate volume of compressed air, and even if one does, one is apt to have a thermometer on one's hand instead of a pressure recorder. We have accordingly abandoned any compliance and prefiltering at depth for the ship-based instrument. A Vibrotron transducer on the sea bottom consists essentially of a stretched wire oscillating at 15,000 to 30,000 cycles per second. The "raw" pressure fluctuations modulate this frequency, and the oscillations are counted and printed on shipboard. The instrument has been used up to depths of 2500 feet. For 1-minute counts, we can detect changes in pressure by 1 millimeter of water.

The Vibrotron output includes the effects of swell and tides as well as the effects of the intermediary frequencies that are under consideration here. For comparison of records with those of the shore-based recorder it is necessary to subject the Vibrotron output to equivalent frequency filters. This has been done numerically by forming a convolution of the record with the Fourier transform of the impedance of the shore-based recorder. Details are elaborate and will be submitted for publication elsewhere.

The observed values in Table 2 have been obtained by the crude method of selecting portions of the record for which some frequency predominates for a few cycles, and then comparing amplitudes and phases. The last columns give theoretical values. The computed ratios in the column headed "edge waves" are $\exp(-2\pi\,\Delta x/L)$, where Δx is the distance between the recorders projected along a line normal to shore and L is the wavelength of the fundamental mode, $n = 0$, for slopes of 0.02 and 0.03, respectively. The shallow-water values are computed on the assumption that wave heights are proportional to $h^{-1/4}$ and that the phase velocity equals $\sqrt{gh}$.

For nearby stations, the coherence was sufficiently good to permit positive identification of detailed features on both records, but for shorter periods at distant stations, one ought to compare spectra. The complex submarine topography off La Jolla, Calif. (Fig. 4) is as much a

Table 2. Comparison between selected portions of wave records of ship-based recorder at stated distances and depths and wave records of shore-based recorder at 1200-foot distance from the beach and 22-foot depth beneath mean lower low water; r is the ratio of offshore to near-shore amplitude, and Δt is the offshore minus near-shore arrival time of a coherent feature. For comparison, the values based on edge-wave theory and ordinary shallow-water propagation are also tabulated.

			Observed			Edge wave		Shallow water	
Station	Distance (ft)	Depth (ft)	Period (min)	r	Δt	r $\beta = 0.02$	r $\beta = 0.03$	r	Δt
A	1,450	35	2	1.0	*	0.39	0.49	0.89	8^s
			12.5	0.81	*	0.97	0.98		
B	4,700	135	2	0.65	30^s	0.00	0.00	0.64	1^m15^s
			3.5	0.65	-40^s	0.01	0.04		
			4.0	0.70	-12^s	0.02	0.08		
			16	0.85(?)	*	0.79	0.86		
C	6,500	155	3.5	0.56	2^m	0.00	0.00	0.61	1^m50^s
			4	0.62	-30^s	0.00	0.02		
			5	0.50	*	0.03	0.09		
			10.5	0.80	*	0.45	0.56		
			22.5	0.84	1^m	0.83	0.88		
D	10,200	295	2	0.37	2^m(?)	0.00	0.00	0.52	2^m15^s
			13.7	0.50	*	0.44	0.58		
E	22,900	275	2	0.40	†	0.00	0.00	0.53	3^m40^s
			12	0.18	*	0.07	0.18		
			15	0.40	*	0.19	0.33		
			22	0.43	*	0.47	0.60		
			25	0.58	*	0.55	0.67		

* The phase lag was too small to be measurable. † No coherence.

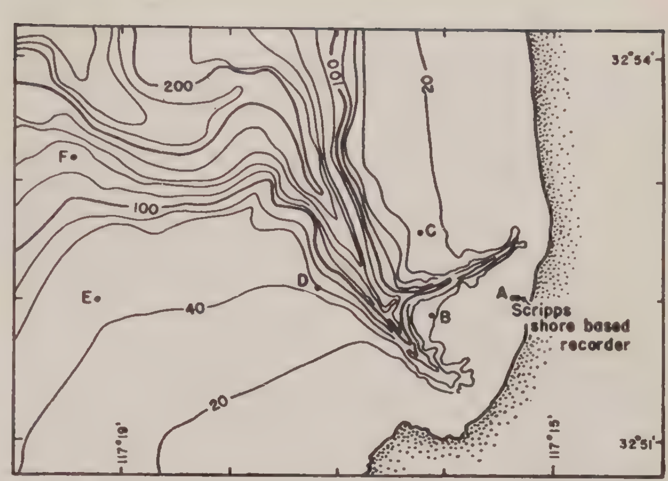

Fig. 4. Depth contours in fathoms off La Jolla, California. Positions of ship-based tsunami stations, *A* to *F*. The permanent shore-based recorder is located near station *A*, as shown.

liability to us as it is an asset to the submarine geologists. The recorded distances in Table 2 are referred to the beach at Scripps; had we measured them from the nearest land, the values would have been appreciably smaller. We are planning a series of measurements in regions with simpler topography, as well as an analysis involving co- and quadrature spectra of the two records. But even so, certain results stand out clearly from the present crude analysis.

1) There is a marked distinction between waves of period less than 5 minutes and those of period more than 10 minutes.

2) The 2- to 5-minute waves have been called surf beat (*12–14*). Their spectrum is related to the spectrum of the *envelope* of the incoming swell, and their energy just outside the surf zone is 1 percent of the wave energy. According to edge-wave theory, these waves should be all but eliminated at stations B, C, D, and E; according to the conventional shallow water theory, the amplitude should be reduced only by a factor of two at the farthest stations. The observed values are certainly not in accord with edge-wave theory. There is rough agreement with regard to amplitudes (but not with regard to phase) with shallow water theory.

3) The 10- to 30-minute waves are believed to be a quite different phenomenon. Certainly their general level of activity is found to be unrelated to that of the surf beat. Table 2 shows that the observed amplitude ratios are in general agreement with those given by edge-wave theory. Particularly at station E, a shift toward the longer periods was noticeable. The shift with distance from shore is analogous to a similar shift with *depth* in the case of ordinary surface waves.

4) Results were similar at stations B and C, which were located at opposite sides of the Scripps submarine canyon (Fig. 4).

How is the edge-wave noise generated? One is tempted to look again for some coupling between atmosphere and ocean. This time we do not look for a single impulse or a well-defined traveling disturbance, but for the random superposition of many such disturbances. A possible source is the microbarographic oscillations. The microbarograph at Scripps traces a noisy record containing frequencies of the same order as those on the sea-level record. About ten times a year, these oscillations show rather well-defined patterns with amplitudes of as much as 1 millibar. One such case is shown by the pressure and wind direction traces on Fig. 1. There is quite good evidence (*3, 4*) that these oscillations are the surface (actually bottom) manifestation of internal waves traveling on the atmospheric inversion layer with the "shallow water" velocity

$$C_a = (gh_a \Delta \ln \theta)^{1/2} \qquad (5)$$

where h_a is the height of the inversion layer, and $\Delta \ln \theta$ is the logarithmic change in potential temperature across this layer. Ultimately, these waves may be caused by a variety of meteorologic events such as cyclogeneses offshore or break-throughs of marine air (*4*).

We now suppose, without evidence, that the usual microbarographic noise in this area is also the result of internal waves on the inversion layer. Let α be their direction relative to a normal with the coast line. There is coupling with edge waves, provided that $C_a \csc \alpha = C$, or in view of Eqs. 2 and 5, if

$$T = \frac{2\pi(gh_a \Delta \ln \theta)^{1/2}}{g \sin \alpha \sin (2n+1)\beta} \qquad (6)$$

Typical values are $h_a = 400$ m, $\Delta \ln \theta = 0.075$, $\sin \beta = 0.02$. For the fundamental mode, these give $\alpha = 90°$ (glancing), $T = 8.7$ min; $\alpha = 60°$, $T = 10.0$ min; $\alpha = 30°$, $T = 17.4$ min; $\alpha = 15°$, $T = 33.5$ min.

The observed values of T are 10 to 30 minutes. The short-period limit of the spectrum is determined by the speed of the atmospheric waves. Longer periods are the results of the "scissors effect" between atmospheric wave crests and the coast line for other than glancing incidence. The computed periods can be made arbitrarily large for near-normal incidence; but for equal probability of wave direction, the spectral densities of very long periods are then very small. Without further measurements, the peculiar mechanism proposed here—that of coupling the atmospheric inversion to the continental shelf—must be regarded as speculation.

Tsunamis

So far, we have dealt with edge waves generated by atmospheric disturbances over the shelf. The reader may have wondered whether tsunamis recorded on coastal tide gages are, at least in part, edge waves excited by long waves from the open sea.

We have considered in some detail the problem of waves from the open sea (depth H_0) impinging on a coastal ledge of some specified width D and depth H_1. This geometry makes the algebra simple and the comparison with observed conditions difficult. A detailed treatment is out of place here, but we shall sketch our results. Suppose a regular wave train arrives from the open sea with a velocity $C_0 = (gH_0)^{1/2}$ from a direction α relative to the coast normal. After a time interval of several wave periods, a disturbance is built up over the shelf. The disturbance is driven along the coast line with a speed $C \csc \alpha$ that is far greater than the speed of free edge waves of comparative length.

The amplitude at the coast line depends on α and the relative dimensions of the shelf and waves. For our simple geometry, Brewster's angle

$$\arctan (C_0/C_1) = \arctan (H_0/H_1)^{1/2}$$

enters in a critical manner. For incidence more nearly glancing than Brewster's angle, the coastal amplitude is always smaller than the deep-sea amplitude. For incidence more nearly normal, it is always larger. The maximum amplification is $(H_0H_1)^{1/4}$. This occurs for normal incidence if the wavelengths are such as to give an antinode at the coast and a node at the outer edge of the shelf, in close analogy with the open organ pipe formula.

We must therefore expect that only the first few waves can give some indication of the deep-sea disturbance. Thereafter, selective amplifications of those particular frequencies that are in resonance with local topography should dominate the record. This is more or less what one observes. For example, the measured time interval between the first and second crest usually shows a systematic increase with travel time (*15*) in accordance with what is to be expected for slightly dispersive waves (*16*). But the frequencies in the interior of the record differ erratically from station to station. A spectrum analysis by M. J. Tucker of the La Jolla and Oceanside tsunami records for the Japanese tsunami of 4 March 1952 (*17*) revealed sharp peaks at periods of 30 and 21 minutes. Application of the open organ pipe formula yields resonance amplification of the continental borderland ($H_0 = 3000$ m, $H_1 = 1000$ m, $D = 260$ km) for periods of 1.2 hr, 2.5 hr, and so forth; the continental shelf ($H_0 = 1000$ m, $H_1 = 100$ m, $D = 1.5$ km) is resonant for periods of 3 minutes or less. The former periods are larger, and the latter are smaller than the periods believed to be effectively generated by tsunamis, and this may explain why the average amplitudes in the California region are only a fraction of those at Hawaii. There is no clue here for the observed spectral peaks of 30 and 21 minutes. Our interpretation is that the continental waves are due to off-resonance coupling and that the spectral peaks were already inherent in the offshore disturbance.

The important point is this: the customary procedure is to estimate deep-sea amplitudes by assuming a coastal amplification of $(H_0/H_1)^{1/4}$ according to Green's law, or some equivalent rule based on ray optics. Since we find that the amplification may be much larger or much smaller, the usual estimates of deep-sea amplitudes may be off by orders of magnitude. Useful estimates can perhaps be made from stations on isolated small islands because the wave height observed there would be nearly that of the open sea.

One more point needs to be made. Irregularities in the coast line such as bays and headlands will scatter the waves on the shelf and convert some of their energy into *free* edge waves. In this manner, the deep-sea disturbance is trapped into low-velocity propagation along the edges (*13*). A curvature in the coast line that is concave shoreward (a bay) should be effective in trapping; convex curvature would lead to a loss of trapped energy by radiation back to the open sea. Major tsunamis are followed by something like 5 days of enhanced activity, whereas the sea-level disturbance in an infinite ocean of constant depth should be a matter of hours, at most. Some of the prolongation is undoubtedly associated with reflection from continental borders, as shown by Cochrane and Arthur (*18*); some may be the result of scatter from oceanic islands and sea mounts. We suggest that some of the afterglow, at least on continental margins, results from a conversion by coastal irregularities of fast open-sea waves into slow edge waves. There is a close analogy here with the experimental demonstration by Tatel (*19*) that some of the complexity of seismic records can be traced to a conversion by surface irregularities of fast body waves into slow surface (Rayleigh) waves. But there are difficulties with this suggestion. Travel times between La Jolla and Oceanside for tsunami waves do not check out well; and how is one to account for the afterglow at Hawaii?

References and Notes

1. H. Lamb, *Hydrodynamics* (Cambridge Univ. Press, Cambridge, 1932).
2. Contribution from the Scripps Institution of Oceanography, new series No. 826. This work was supported by the Office of Naval Research and the Air Force Cambridge Research Center, contract AF (19) 604 (1163). We wish to express our appreciation to A. C. Redfield and A. R. Miller of the Woods Hole Oceanographic Institution, who furnished us with the sea-level data for the four hurricanes; to M. J. Tucker of the National Institute of Oceanography, Great Britain, who made frequency analyses of tsunami records; and to the many people who helped with the seagoing work.
3. E. Gossard and W. H. Munk, *J. Meteorol.* **11**, 259 (1954).
4. ———, *Quart. J. Roy. Meteorol. Soc.* **81**, 484 (1955).
5. W. H. Munk, H. V. Iglesias, T. R. Folsom, *Rev. Sci. Instr.* **19**, 654 (1948).
6. F. Ursell, *Proc. Roy. Soc. London* **A214**, 79 (1952).
7. J. S. Winston, *Monthly Weather Rev.* **82**, 228 and Chart X (1954).
8. A. C. Redfield and A. R. Miller, unpublished manuscript.
9. W. Malkin and G. C. Holzworth, *Monthly Weather Rev.* **82**, 267 and Chart X (1954); H. C. Sumner, *ibid.* **72**, 187 (1944).
10. T. Shimizu, *Bull. Geograph. Survey Instr.* **4**, 69 (1954).
11. M. Ewing, F. Press, W. Donn, *Science* **120**, 684 (1954).
12. M. J. Tucker, *Proc. Roy. Soc. London* **A202**, 565 (1950).
13. J. D. Isaacs, E. A. Williams, C. Eckart, *Trans. Am. Geophys. Union* **32**, 37 (1951).
14. W. H. Munk, *ibid.* **30**, 849 (1949).
15. C. K. Green, *ibid.* **27**, 490 (1946).
16. C. Eckart, *Revs. Mod. Phys.* **20**, 399 (1948).
17. W. H. Munk, *Bull. Seismol. Soc. Amer.* **43**, 219 (1953).
18. J. D. Cochrane and R. S. Arthur, *J. Marine Research Sears Foundation* **7**, 239 (1948).
19. H. E. Tatel, *J. Geophys. Research* **59**, 289 (1954).

Vol. 37, No. 1 Transactions, American Geophysical Union February 1956

A Portable Tsunami Recorder*

Wm. G. Van Dorn

Abstract—A compact self-contained long-period wave recorder has been developed for remote operation on small islands where the influence of continental land masses is minimized. The instrument can be installed in two or three days, requires no electric power, and needs only weekly attention. It can detect waves less than one cm high at its period of maximum response (1000 sec), and it attenuates both swell and tides to about three per cent of their relative amplitudes.

Introduction—From its first installation in 1948 the tsunami recorder on the Scripps Institution pier has exhibited pronounced wave activity over much of the spectrum intermediate between the swell and the tides [*Munk*, *Iglesias*, and *Folsom*, 1948]. However, only in the case of a large tsunami [*Munk*, 1953] has convincing coherence been found between the records obtained from this instrument and a similar installation at Oceanside (20 mi N of Scripps), save that both records reflect the same general signal amplitudes from day to day. That much of this activity may be locally generated has been suggested by *Munk* [1949] and *Isaacs*, *Williams*, and *Eckart* [1951], who show that once generated, it can be effectively 'trapped' as waves rebounding along the coast. Such energy as may leak off into deep water would have its already small amplitudes greatly reduced. On the other hand, according to *Cochrane* and *Arthur* [1948], most of the energy of tsunamis approaching the California coast is reflected back out to sea.

It thus appears as if the continental shelf is a poor place to study tsunamis, and that the signal-to-noise ratio might be improved by making long-period wave measurements in deep water, or on small relatively isolated islands.

While no successful deep-ocean recorder has yet been developed, this paper describes a tsunami recorder specifically designed to be transported by air to such remote islands, where it can be installed by two or three men without outside assistance and operated on a semi-permanent basis with no more attention than an ordinary tide gage. Up to the present time eight temporary installations have been operated intermittently for a total of twenty months on six Pacific islands, and it is hoped to have at least two stations operating continuously in the Pacific in the near future.

Description of the instrument—A schematic of a typical installation of the tsunami recorder is shown in Figure 1. It consists of a tripod-mounted wave filter in a protected location, connected hydraulically to the sea by a tube or pipe, and electrically to the shore recorder by a three-wire cable. No external electric power is required. The distance between the respective elements can be as great as 1000 ft, which gives considerable latitude in the choice of instrument location. While the tripod is usually constructed at the site, the remaining components are packed for shipment in a suitcase-size wooden box equipped with a plastic cover, which can serve as an all-weather shelter for the recorder.

The tube installation—The tube from the wave filter to deep water essentially places the filter in the position of being able to receive offshore signals without appreciable distortion or attenuation and still occupy a site protected from waves and surf, and available for easy maintenance.

During early experiments with these recorders no tube was used, but it was soon evident that such protected locations abound with locally generated seiches having periods within the pass band of the filter and amplitudes much larger than the signals being sought. In fact, tsunamis themselves usually excite any local resonant water masses in a way which completely masks the character of the incoming signal.

The tube used in previous installations was a half inch inside diameter, transparent, vinyl-plastic garden hose, available in continuous lengths. The depth of the free end below sea level is not critical except that air bubbles, suspended sediment, and regions where currents can produce sustained dynamic pressures should be avoided. The tube is terminated at its outer end in a screened basket to prevent ingress of organisms or material likely to obstruct the flow of water. It was found necessary to tie the hose down every three feet or so in the surf zone, which requirement somewhat taxes the ingenuity of the field

---

* Contribution from the Scripps Institution of Oceanography, New Series, No. 827.

Reproduced by Permission

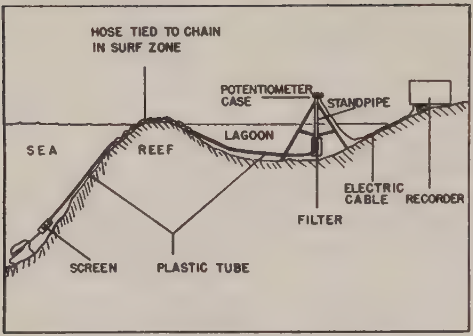
HOSE TIED TO CHAIN
IN SURF ZONE
POTENTIOMETER CASE
STANDPIPE
LAGOON
SEA
REEF
ELECTRIC CABLE
RECORDER
FILTER
SCREEN
PLASTIC TUBE

FIG. 1 – A typical tsunami recorder installation

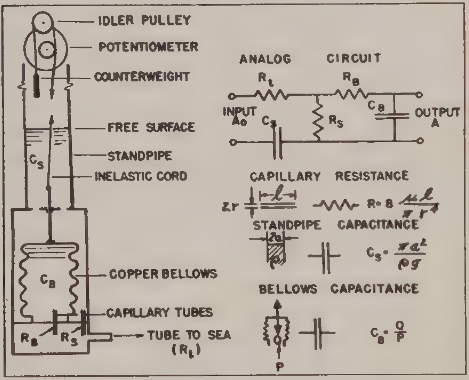
IDLER PULLEY
POTENTIOMETER
COUNTERWEIGHT
FREE SURFACE
STANDPIPE
C_S
INELASTIC CORD
C_B
COPPER BELLOWS
CAPILLARY TUBES
R_B
R_S
TUBE TO SEA
(R_t)
ANALOG CIRCUIT
R_t
R_B
INPUT
A_0
C_S
R_S
C_B
OUTPUT
A
CAPILLARY RESISTANCE
$2r$
ℓ
$R = 8\frac{\mu \ell}{\pi r^4}$
STANDPIPE CAPACITANCE
$2a$
$C_S = \frac{\pi a^2}{\rho g}$
BELLOWS CAPACITANCE
Q
P
$C_B = \frac{Q}{P}$

FIG. 2 – The wave filter and its electrical analog circuit

party. A scrap length of heavy chain makes excellent ballast, whereas coral boulders are very poor, tending to roll and pinch the tube.

The wave filter—Discrimination against unwanted signals is accomplished by the wave filter (Fig. 2). It consists of two capillaries, a copper bellows, and a standpipe arranged to form an hydraulic resistance–capacitance network as shown in the accompanying electrical analog circuit, the response characteristics of which are discussed below. Physically, the filter is a small brass canister with a removable bottom on which are mounted the copper bellows and glass capillary tubes. The canister is screwed on the lower end of a standpipe rigidly constrained to the vertical by any convenient means. The standpipe length is arbitrary save that its upper and lower ends must be respectively above and below the greatest anticipated sea level excursion. Pressure signals conducted to the filter by the hose result in vertical motions of the bellows which are converted into electrical signals by an inextensible cord passing up the standpipe around the shaft of a potentiometer, over an idler pulley, and down to a counter weight. The potentiometer is in a sealed case with a supply of desiccant to remove any slight amount of moisture coming in around the shaft seal. (One can, alternatively, where electric power is available, measure the pressure difference across the bellows with a suitable transducer, and connect its output directly to a recording potentiometer.)

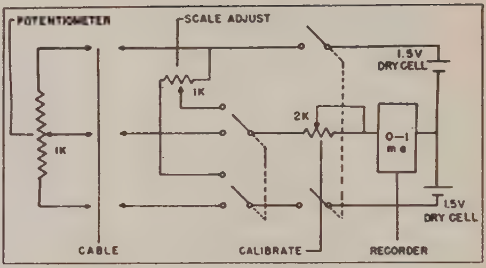
POTENTIOMETER
SCALE ADJUST
1.5V
DRY CELL
1K
2K
1K
0–1
ma
1.5V
DRY CELL
CABLE
CALIBRATE
RECORDER

FIG. 3 – The wiring diagram for the recorder

The recorder—A three-conductor cable connects the potentiometer to the control panel in the recorder case, which can be located ashore in any convenient spot. The simple bridge circuit (Fig. 3) employs four flashlight batteries in series parallel, which have a service life of about six months. Provision is made for applying a standardizing *calibrate* signal and adjusting the sensitivity to compensate for the gradual reduction in battery voltage. The Esterline Angus 0-1 ma, spring wound, strip chart recorder is manually set to center-zero. A chart speed of three inches per hour is adequate to resolve any signals that get through the filter.

Response characteristics—The amplitude response A, of the electric analog circuit (Fig. 2) to an incoming sinusoidal wave of unit amplitude A_0, as obtained by simple network theory is

$$\frac{A}{A_0} = \left[\left(1 + \frac{C_B}{C_S} + \frac{C_B}{C_S} \cdot \frac{R_B}{R_S}\right)^2 + \frac{C_B}{C_S} \cdot \frac{R_B}{R_S}\left(\frac{T'}{T} - \frac{T}{T'}\right)^2\right]^{-\frac{1}{2}} \tag{1}$$

where T is the period of the incoming wave and T' the period at maximum response, defined by

$$T' = 2\pi(R_B R_S C_B C_S)^{\frac{1}{2}} \tag{2}$$

The response function (1) is plotted in Figure 4 for the case $R_B/R_S = C_B/C_S = 1$. As with all single-stage RC filters, the amplitude response for periods long or short compared to T' falls off directly as $1/T$ or T respectively. But much can be done to control the shape of the curve (frequency cutoff) in the region $0.01 < T/T' <$

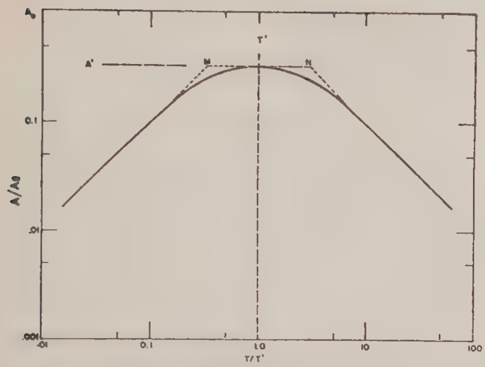

FIG. 4 – A typical amplitude response curve for the wave filter, where $R_B/R_S = C_B/C_S = 1$

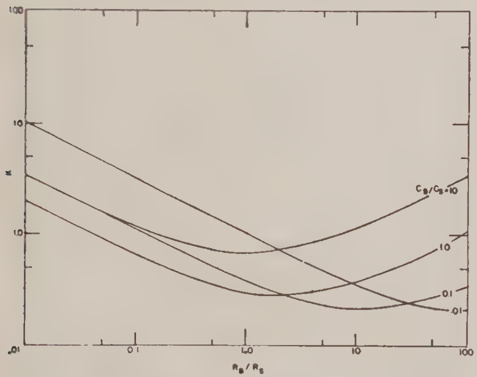

FIG. 5 – Band width K as function of the resistance ratio, for four capacitance ratios

100. If we define an *effective band width* K as that portion of the period spectrum between the intercepts at M and N (Fig. 4), K can be determined from (1) by equating the two terms on the right; namely

$$K = \frac{T'}{T} - \frac{T}{T'} = \frac{C_S}{C_B} \cdot \frac{R_S}{R_B} \cdot \left(1 + \frac{C_B}{C_S} + \frac{C_B}{C_S} \cdot \frac{R_B}{R_S}\right) \quad (3)$$

In addition the maximum amplitude A' occurs when $T = T'$

$$A' = A_0 \left(1 + \frac{C_B}{C_S} + \frac{C_B}{C_S} \cdot \frac{R_B}{R_S}\right)^{-\frac{1}{2}} \quad (4)$$

In Figures 5 and 6 K and A' are plotted against the resistance ratio R_B/R_S for various capacitance ratios C_B/C_S, and one can see by inspection how the performance of the filter varies as the circuit components are changed. It should be kept in mind that the *amplitude* discussed above refers to the pressure difference across the copper bellows. For a specific bellows the extension per unit pressure will determine the stroke available to operate a recording device.

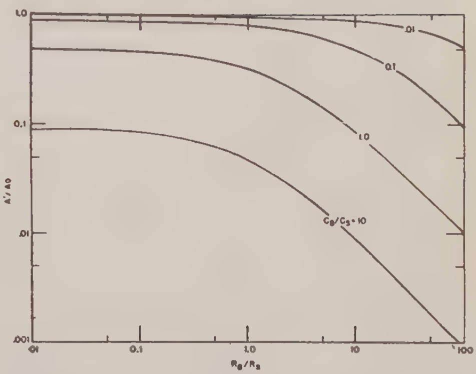

FIG. 6 – Maximum amplitude A' as a function of the resistance ratio, for four capacitance ratios

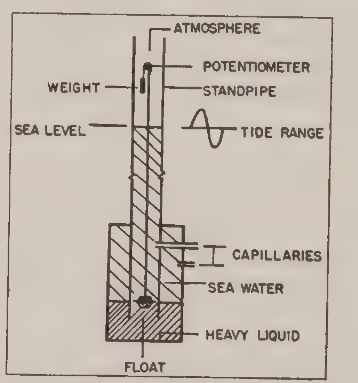

FIG. 7 – Schematic of new filter design eliminating bellows

The fluid resistance offered by the tube between the filter and the sea, shown in Figure 2 as R_t, is in series with the filter input impedance Z_f; it will reduce the amplitude response directly as the ratio R_t/Z_f. This attenuation is only important in the pass band where reactance is small, and it is sufficient to require that:

$$R_t \leq 0.1 \left[\frac{R_B \cdot R_S}{R_B + R_S}\right] \quad (5)$$

to obtain a practical compromise in component sizes without serious signal loss. Likewise, spurious signals generated along the tube by pressure changes elsewhere than at the free end are dissipated by movement of water through the seaward end of the tube before they can produce significant variations within the bellows.

Discussion—Present limited experience with island installations indicates that the long-period background noise in the open sea is very low—substantially less than one cm high. All tsunamis recorded to date have been only a few centimeters high, and they pass unnoticed on tide gages. In order to resolve such small signals present design modifications are aimed at improving the sensitivity from about 0.5 cm to about 0.5 mm wave height. Since the instrument is virtually temperature insensitive and does not respond to atmospheric pressure fluctuations, its resolution is principally governed by mechanical hysteresis in the potentiometer linkage. Moreover, the copper bellows is intrinsically a non-linear capacitance, and can itself be eliminated by substitution of a heavy liquid in the same standpipe, as shown in Figure 7. Such an improved instrument is currently undergoing tests.

Acknowledgment—This paper represents the results of research carried out by the University of California under contract with the Office of Naval Research Reproduction in whole or in part is permitted for any purpose of the United States Government.

REFERENCES

COCHRANE, J. D. AND R. S. ARTHUR, Reflection of tsunamis, *J. Mar. Res.*, **7,** 239–251, 1948.

ISAACS, J. D., E. A. WILLIAMS, AND C. ECKART, Total reflection of surface waves by deep water, *Trans. Amer. Geophys. Union*, **32,** 37–40, 1951.

MUNK, W. H., Surf beat, *Trans. Amer. Geophys.. Union*, **30,** 849–854, 1949.

MUNK, W. H., Small tsunami waves reaching California from the Japanese earthquake of March 4, 1952, *Bull. Seis. Soc. Amer.*, **43,** 219–222, 1953.

MUNK, W. H., H. V. IGLESIAS, AND T. R. FOLSOM, An instrument for recording ultra low frequency ocean waves, *Rev. Sci. Instr.*, **19,** 654–658, 1948.

Scripps Institution of Oceanography, La Jolla, California

(Communicated manuscript received October 6, 1955; open for formal discussion until July 1, 1956.)

Reprinted from PACIFIC SCIENCE, *vol. X, no. 4, October, 1956*

Diatoms in the Ocean Deeps

E. J. FERGUSON WOOD[1]

THE CONCEPTION of a rain of diatoms from the plankton to the ocean deeps is, at first thought, a reasonable one. Further thought, however, makes it appear extremely unlikely. Because diatoms occur in swarms, particularly in certain areas of the oceans, it seems to have been assumed that they descend more or less vertically to form diatomaceous ooze. In fact, in deeper waters, we could expect them to become widely dispersed, especially as their form is such as to retard vertical movement. Further, there is the question of the gradient of silica concentration with depth, and the effect of pressure thereon. Harvey (1945) states that the silica content of seawater, in general, has been found to increase with depth, and that it is probably in true rather than colloidal solution. This suggests that the diatom tests are dissolved as they fall through the water after the death of the cell.

Wiseman and Hendey (1953) found large numbers of the diatom *Ethmodiscus rex* (Rattray) Hendey in material collected from the Mariana Trench by H.M.S. "Challenger" in 1951. These authors speculate regarding the origin of the tests, pointing out that *E. rex* is rare in the plankton, and that, "there is no indication that the species is found living in the waters immediately over the deposit itself." They do not consider the possibility that the diatom is autochthonous.

During a microscopic examination of a mud sample from the Weber Deep (depth, 7,400 m.) in a search for living bacteria, I observed a number of benthic types of diatom frustules. The sample studied was collected by Claude E. ZoBell and Richard Y. Morita during the "Galathea" expedition in 1951, and has since been kept in a pressure bomb at 10,500 p.s.i. and 10°C.

MICROSCOPIC OBSERVATIONS

Some of the frustules seen appeared to contain protoplasmic material (Fig. 1), as did some *Globigerina* and *Nummulites* which were also observed. Some showed dense spherical bodies, usually four in number, which could have been microspores (Figs. 2, 3). The larger *Coscinodiscus* forms appear to have burst, as did the form shown in Figure 3, probably owing to the rapid release of pressure when the bomb was opened. The smaller *Coscinodiscus* remained intact for the most part.

The cells from some preserved material were stained with various aniline dyes and took up the stain. When stained with acridine orange and viewed under fluorescent light they fluoresced orange-red, whereas the empty frustules did not fluoresce. Hence it may be concluded that the stained cells did contain protoplasm. It is impossible that both cell and protoplasm could have been preserved intact during a slow descent of 7,400 metres from the photic zone, so the evidence that these forms are autochthonous is very strong. Further, many of the frustules of all the species

---

[1] Scripps Institution of Oceanography, La Jolla, California, U.S.A. and Marine Biological Laboratory, Cronulla, Australia. Manuscript received October 21, 1955.

Reproduced by Permission

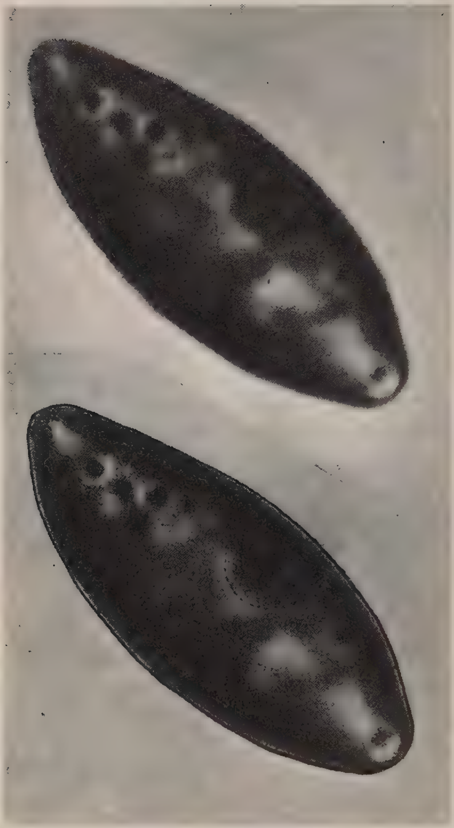

FIG. 1. A naviculoid diatom from the Weber Deep. It contained a brown pigment, vaculoes, fat(?) globules, and nucleus but no chloroplasts. Lower figure retouched. (Phase contrast.)

observed were intact, and appeared quite fresh and uneroded. No planktonic forms were observed, nor were there even fragments of such species as *Rhizosolenia*, *Chaetoceras*, etc., as one would expect from the "rain" theory.

Table 1 lists all of the "Galathea" stations from which bottom material was examined. The samples were first examined directly and again after digestion with hydrochloric acid. Cell contents were seen in material from stations 463 and 492.

In Table 2 the species of diatoms observed and the station from which they came are listed.

The samples all contained numerous sponge spicules, and the presence of these and of the sessile forms *Synedra* and *Melosira* suggest that these diatoms may be epiphytic on the sponges. It is interesting to note also that all, or nearly all, the forms mentioned in Table 2 are found as fossils, and that *Melosira granulata* and *Cocconeis pendiculus* are not recorded from seawater. Since the flora associated with the ocean deeps is unique, it would appear that we are dealing with a separate biocoenosis. Studies made by ZoBell (1952) on the bacterial flora contained in the same samples confirm this.

EXPERIMENTAL

If the diatoms are autochthonous, as I suggest, they must be living saprophytically. Recently, Lewin (1953) has described experiments in which diatoms were grown heterotrophically in the dark in a medium containing tryptone and glucose. She points out in her paper that if the diatom cultures are not pure, the bacteria outgrow the diatoms. Accordingly I obtained two cultures of her heterotrophic strains in order to test their growth under pressure, at the same time endeavouring to grow some diatoms in culture from the "Galathea" material.

All the cultures were made in the following medium—an adaptation of that suggested by Lewin:

Solution a	K_2HPO_4	0.02 g.
	$MgSO_4, 7H_2O$	0.02 g.
	$CaNO_3, 4H_2O$	0.01 g.
	Glucose	5 g.
	Tryptone	1 g.
	Distilled water	100 ml.
Solution b	Seawater	900 ml.
	Agar (if required)	15 g.

The solutions were sterilized separately and after cooling to about 50°C. were combined.

The cultures, placed in small tubes so as to leave an airspace above, were closed with neoprene stoppers, placed in pressure bombs (ZoBell and Oppenheimer, 1950) and pressurized at 1, 100, 200, and 500 atmospheres.

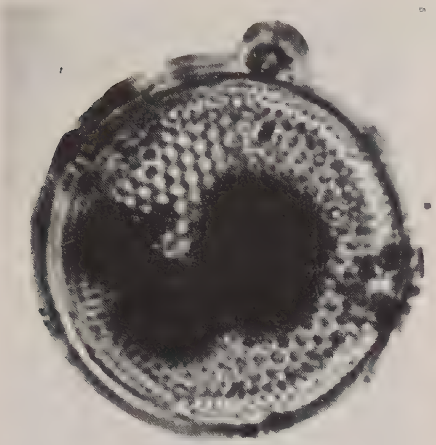

FIG. 2. *Coscinodiscus marginatus* Ehr. from Weber Deep showing dense spherical bodies (microspores?).

In addition, the "Galathea" material was pressurized at 1,000 atmospheres. In the case of the pure cultures, suspensions were made in a small amount of the medium, and 0.1 ml. was pipetted into the small tubes which were then partially filled with the medium. After 14 days, the bombs were opened, the tubes centrifuged for 15 minutes at 4,000 r.p.m., the density of the deposit estimated, and the material examined microscopically. The following observations were made.

1,000 Atmospheres Pressure

"Galathea" material only. Some *Coscinodiscus marginatus* with cell material.

500 Atmospheres Pressure

"Galathea" mud. *Coscinodiscus* containing refractile bodies and a long straight rod-like body.

Culture 6 M. Cells square with 2 to 4 green, somewhat refractile bodies, deposit density rated as 1. (Fig. 4*a*.)

Culture 13 M. Cells oval to rounded, with refractile bodies; greenish to brownish. Deposit density, 1.

200 Atmospheres Pressure

"Galathea" mud. *Coscinodiscus* with refractile bodies, and cell material between the valves.

Culture 6 M. Cells square to oblong, with greenish-brown chloroplasts. Notably heavy sediment of cells; density, 2.

Culture 13 M. Cells oval, more elongate than at 500 atmospheres. Chloroplasts brown, nucleus evident; vacuoles frequent, with particles either in Brownian movement or rotating. Cells frequently paired as though they had divided recently.

100 Atmospheres Pressure

"Galathea" mud. *Coscinodiscus* observed apparently containing cellular material; other empty tests seen.

Culture 6 M. Cells normal in appearance, i.e., like original culture. Growth heavier than at 1 atmosphere. Density, 2.

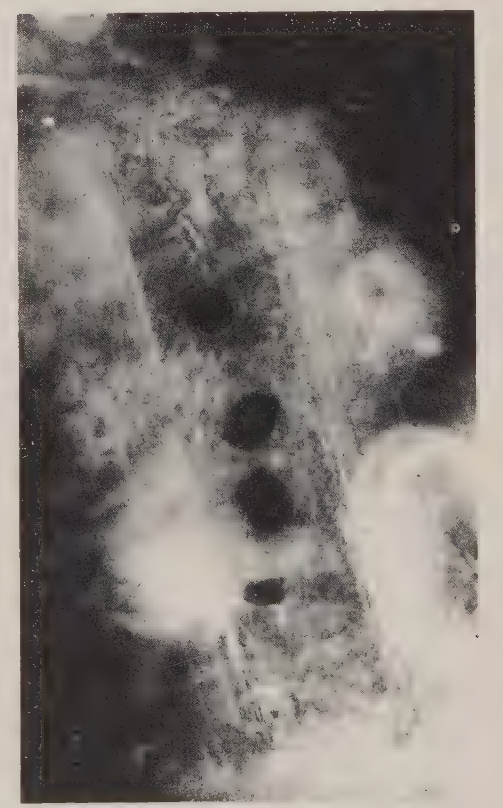

FIG. 3. Naviculoid diatom from Weber Deep which appears to have burst at side and end. (Phase contrast.)

Culture 13 M. Paired cells frequent. Cells oval, frequently with a vacuole at one end containing particles in motion. Fair growth, more than at 1 atmosphere. Density, 1–2.

1 Atmosphere Pressure

Culture 6 M. Cells similar in form to those of parent culture; poor growth. Density, 1. (Fig. 4*b*.)

Culture 13 M. Cells more oval than at high pressure. Density slightly less than at 100 atmospheres.

There appears to have been more growth at 100 and possibly at 200 atmospheres than at 1 atmosphere, but little or no growth at 500 atmospheres. Cells were more square in 6 M and circular (13 M) at high pressures.

Material from these cultures was transferred to agar slopes. Cultures 6 M grew on this medium from 1, 100, 200, and 500 atmospheres, and there was some evidence of growth of 13 M at 500 atmospheres, but the other cultures were overgrown by bacteria.

The experimental evidence suggests that diatoms taken from atmospheric pressure may grow heterotrophically or remain viable at pressures up to 500 atmospheres, and this supports the possibility of the growth of

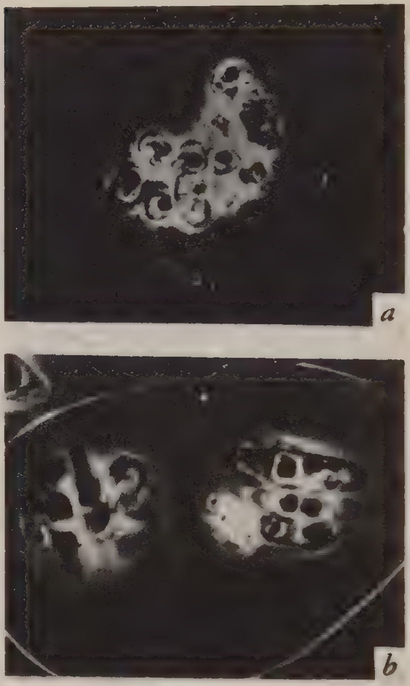

FIG. 4. Diatoms of culture 6M: *a*, Grown at 500 atmospheres pressure; *b*, grown at atmospheric pressure in bomb. (Phase contrast.)

TABLE 1

SPECIMENS OF BOTTOM MATERIAL EXAMINED COLLECTED BY THE "GALATHEA"

STATION	LOCATION		WATER DEPTH (Metres)	DATE COLLECTED	DEEP	DIATOMS PRESENT
	Lat.	Long.				
418	10°20′N	126°30′E	10,387	15/ 7/51	Mindanao	....
422	10°49′N	126°01′E	2,010	24/ 7/51	Mindanao	+
440	10°25′N	126°40′E	10,610	14/ 8/51	Mindanao	+
463	10°16′N	109°51′E	7,214	3/ 9/51	Sunda	+
492	5°31′S	131°01′E	7,445	20/ 9/51	Weber	+
496	5°36′S	131°06′E	7,465	23/ 9/51	Weber	+
497	....	....	9,000+	24/ 9/51	Weber	+
517	6°31′S	153°58′E	9,020	11/10/51	Solomons	+
517 ?	6°31′S	153°58′E	9,255	13/10/51	Solomons	....
608	44°31′S	167°50′E	390	18/ 1/52	Milford Sound	+
645	35°16′S	178°40′E	8,515–8,425	13/ 2/52	Kermadec	....
650	32°20′S	176°54′W	6,794	16/ 2/52	Kermadec	....
658	35°51′S	178°31′W	7,837–7,901	21/ 2/52	Kermadec	+
677	38°38′S	175°53′W	6,370	4/ 3/52	Kermadec–Tonga	....
678	28°30′S	175°53′W	9,437	4–5/ 3/52	Kermadec–Tonga	....
678 (water)	28°30′S	175°53′W	9,335	4–5/ 3/52	Kermadec–Tonga	....
686	20°53′S	175°31′W	10,080	11/ 3/52	Kermadec–Tonga	....

TABLE 2

Diatoms Observed in Mud Collected by the "Galathea" and Stations at Which They Were Taken

SPECIES	STATION NUMBER
Coscinodiscus marginatus Ehr.	422, 463, 492, 496, 497, 517, 517?, 608
Coscinodiscus pacificus (Grun) Rattray	440
Synedra tenera W. Sm.	463
Melosira granulata (Ehr.) Ralfs	463
M. moniliformis Mueller	497
Navicula	
Nitzschia panduriformis Greg.	463
Cocconeis pendiculus Ehr.	463
Diploneis crabro Ehr.	463
Pinnularia dactylis Ehr.	440
Ethmodiscus rex (fragts)	440
Coscinodiscus centralis Ehr.	497
Trachyneis aspera (Ehr.) Cleve	463
Pleurosigma normani Ralfs	497

abyssal diatoms at this and higher pressures.

There is a great deal to support the theory enunciated in this paper that the diatoms found in abyssal mud samples may be autochthonous, and, so far, no indication that the flora found in the ocean deeps is allochthonous. Even in shallow estuarine muds planktonic forms are rare or absent except for the heavily silicified *Coscinodiscus*, *Biddulphia*, etc.

ACKNOWLEDGMENTS

I wish to thank Dr. Claude E. ZoBell, and the Rockefeller Foundation, for providing the opportunity for me to visit the Scripps Institution of Oceanography and undertake this work, Dr. Joyce Lewin for cultures of her strains of heterotrophic diatoms, Dr. Carl H. Oppenheimer for taking the photomicrographs, and Mr. L. H. Crosby of the Marine Biological Laboratory, Cronulla, for the specific determination of the diatoms.

REFERENCES

Harvey, H. W. 1945. *Recent advances in the chemistry and biology of seawater.* vii + 164 pp. Cambridge University Press, Cambridge.

Lewin, Joyce C. 1953. Heterotrophy in diatoms. *Jour. Gen. Microbiol.* 9: 305.

Wiseman, J. D. H., and N. I. Hendey. 1953. The significance and diatom content of a deep sea floor sample from the neighbourhood of the greatest oceanic depth. *Deep-sea Res.* 1: 47.

ZoBell, C. E. 1952. Bacterial life at the bottom of the Philippine Trench. *Science* 115: 507.

ZoBell, C. E., and C. H. Oppenheimer. 1950. Some effects of hydrostatic pressure on the multiplication and morphology of marine bacteria. *Jour. Bact.* 60: 711.

Contributions from the Scripps Institution of Oceanography, New Series, No. 828

Reprinted from BIOLOGICAL BULLETIN, Vol. 110, No. 1, 54–68, February, 1956
Printed in U. S. A.
Reproduced by Permission

THE MIGRATORY HABITS OF THE MARINE GRIBBLE LIMNORIA TRIPUNCTATA MENZIES IN SAN DIEGO HARBOR, CALIFORNIA

MARTIN W. JOHNSON AND ROBERT J. MENZIES
Scripps Institution of Oceanography of the University of California, La Jolla, California

THE MIGRATORY HABITS OF THE MARINE GRIBBLE LIMNORIA TRIPUNCTATA MENZIES IN SAN DIEGO HARBOR, CALIFORNIA[1, 2]

MARTIN W. JOHNSON AND ROBERT J. MENZIES

Scripps Institution of Oceanography of the University of California, La Jolla, California

The isopod gribble *Limnoria* is a serious wood-boring pest in nearly all tropical, temperate, and boreal harbors where contamination has been established and where salinities are not markedly reduced by influx of fresh water. Typical examples of the ravishes of one or more species of this borer are offered by the findings of the San Francisco Bay Marine Piling Committee (Kofoid and Miller, 1927). During that survey only *Limnoria lignorum* (Rathke) was recognized, but Holthuis (1949) has shown that the species *L. quadripunctata* described by him as new was present in the area and had been confused with *L. lignorum.* Actually two species exist in San Francisco Bay, neither of which is *lignorum* (Menzies and Mohr, 1952).

Examination of collections from the San Diego region and elsewhere in California led Menzies (1951) to establish yet another species, *L. tripunctata* which has hitherto also been confused with *L. lignorum.*

Along the west coast of North America the geographic ranges of the three species of wood-boring *Limnoria* have been established as follows (Menzies, in manuscript): *Limnoria lignorum* (Rathke); Alaska to Point Arena, California. *Limnoria quadripunctata* Holthuis; California (41° N) to San Diego Bay. *Limnoria tripunctata* Menzies; warm parts of San Francisco Bay to Mazatlan, Mexico.

The seasonal activities of *L. lignorum* were studied at Friday Harbor, Washington, by Johnson (1935) who found that that species undergoes a pronounced seasonal swimming migration at which time new wood is attacked mainly during early spring. Sömme (1940) confirmed this type of activity for the same species in Norway and reported that a survey by Kramp in 1927 showed similar activity in Danish waters. Kramp's report, published in a Danish engineering journal, has escaped the attention of biologists in other parts of the world. He gives no figures of relative abundance or intensity of attack by *Limnoria lignorum* on new test blocks but states that at Hirtshals, Denmark, there was a pronounced maximum of attack in April. He concludes that the attacks result from periodic swarming of mainly adult individuals. Following the April swarming, the attacks occur in diminishing intensity during the summer.

It is of practical interest to know to what extent the findings relative to the northern species *L. lignorum* can be generally applied to the other species. With this in mind, the present study was designed to test *L. tripunctata,* a species of world-wide distribution in southern waters and the only one found in San Diego Bay.

---

[1] Contributions from the Scripps Institution of Oceanography, No. 829.

[2] Sponsored by the U. S. Navy Office of Naval Research, Project NR163-084, Contract Nonr-233(13).

(116)

PROCEDURE

As a means of determining the migratory habits of *Limnoria tripunctata,* wooden test blocks were suspended freely in the water in the immediate vicinity of piling known to be heavily infested with *Limnoria.*

The test blocks consisted of 5 × 8 × 1 inch Douglas fir which provided about 106 sq. in. (684 cm.^{2}) of surface that could be examined by means of a low-power binocular microscope. After having been soaked in sea water free of borers for a period of 14 days, the blocks were attached to a rope line or stainless steel wire which was suspended from the pier and held taut by a concrete weight attached to the lower end, such that the weight hung free of the bottom. Test blocks thus rigged were located about one foot from infested piling so that they could be reached only by swimming migrating animals.

Two test stations were established in San Diego Bay: Station "A" at the U. S. Naval target repair base at Point Loma and Station "B" at the Johnson and Western Pier well within the bay near the Coronado ferry landing. Owing to reconstruction and repair there was some interruption at each station. The vertical position of the blocks and approximate days of exposure for each are given in Table I.

TABLE I

Position and exposure of test blocks

Station A

Aug. 12, '52–Aug. 13, '53		Aug. 13, 53–Feb. 15, '54		Apr. 14, '54–Mar. 14, '55	
Position of blocks	Days of exposure	Position of blocks	Days of exposure	Position of blocks	Days of exposure
Floating*	60				
Floating	30	Floating	30	Floating	30
6 ft. from bottom	30	6 ft. from bottom	60	6 ft. from bottom	60
4 ft. from bottom	30	4 ft. from bottom	90	4 ft. from bottom	90

* Zero tide datum is approximately 14.6 feet above bottom. The mean tidal range was approximately 4 feet.

Station B

Aug. 15, 1952–Aug. 13, 1953		Feb. 15, 1954–Mar. 14, 1955	
Position of blocks	Days of exposure	Position of blocks	Days of exposure
Floating**	30	5 ft. from bottom	30
2 ft. from bottom	30	4 ft. from bottom	60
		3 ft. from bottom	90
		2 ft. from bottom	120

** Zero tide datum is approximately 9 feet above bottom. Tidal range same as for Station A.

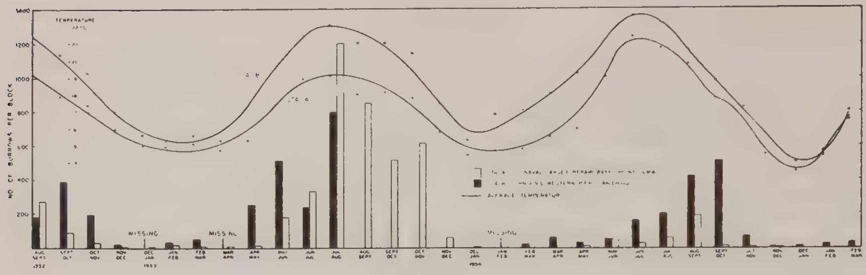

FIGURE 1. *Limnoria tripunctata.* Seasonal attack on test blocks exposed for successive 30-day intervals at Stations A and B, San Diego Bay from August, 1952 to March 14, 1955. Seasonal temperature included.

The intensity of settlement or attack on the blocks for a given period is taken to represent the intensity of migration for the period. It is determined by counting the number of burrows in the surface of the wood. Usually there are two animals, male and female, in each of the deeper burrows.

Surface temperature of the water was taken once each month at each station except for the period 15 August 1953 to 7 May 1954 when a continuous temperature recorder was in operation near Station A. Salinities in San Diego Bay fluctuate but little. The mean annual value is about 33.6‰.

Requirements for a study of this nature are: (1) nearby ample source of gribble infestation; (2) little or no interference resulting from repair or removal of piling; (3) safety from ship action, heavy seas or pilferage; (4) absence of adverse conditions due to low dissolved oxygen or low salinity.

These requirements were well met but for the already mentioned changes due to pier repair.

RESULTS

Seasonal Migrations

An examination of the severity of attack on the test blocks reveals that migration occurs to a greater or lesser degree throughout the year, but as in *L. lignorum,* there was each year a period of pronounced increase in migratory activity. In migrating the animals swim freely and a special preliminary study designed to reveal diurnal behavior in nature indicates that the greatest swimming activity takes place at night.

In Figure 1 is shown graphically the monthly seasonal fluctuations in migration between Aug. 12, 1952 and March 14, 1955 inclusive. The data used in compiling the figure were derived from the blocks submerged for successive 30-day periods with omissions as noted. Other periods of submergence, especially the 60-day periods, provided corroborative data on season of attack (Fig. 5) but the longer periods of submergence were designed mainly to provide information on rate of growth, sexual condition and reproduction.

The test blocks that were in place for 30-day periods beginning August 12, 1952, apparently caught mainly the declining portion of that year's migration.

In 1953 at Station A there was a period of active migration which extended from about the middle of May to the middle of November with a maximum during July–

August. This was also the peak 30-day period for Station B. This station was abandoned in August, 1953 when it was apparent that both stations at the various depth levels were showing a similar migratory picture; however, it was re-established when the reconstruction of piles at Station A forced a temporary abandonment of that station in January, 1954. By April, 1954 both stations were again studied until the completion of this phase of the work in March, 1955.

From the time of re-establishing of Station A in April, 1954, the attack on the blocks was relatively light but with a definite maximum occurring this time in August–September. The lighter attack may be attributed to a diminished source of infection as a result of replacement of infested piling, etc., with new pressure-treated creosoted timbers which left only a nearby infested stub and doubtless other undetected submerged wood, and some more distant infested structures. This also explains the low migratory figure shown in Figure 5 for the second year.

The main season of attack at Station B appears to be during August and September after which it diminishes rapidly to the low winter level.

The seasons of active attack on the blocks roughly coincide at the two stations, but it appears to have continued somewhat later at Station B in 1952 and began slightly earlier in 1953. The same trend is suggested in 1954. This difference may be correlated with the temperature. From Figure 1 it will be noted that a higher temperature prevailed throughout the year at Station B.

It has commonly been reported that the attack by *Limnoria lignorum* is not so great on floating or shallowly placed test blocks as it is on deeper blocks or near the bottom (Johnson and Miller, 1935; Sömme, 1940; Black and Elsey, 1948). This may be a factor of considerable importance in the relative rate of deterioration of floating or driven structures. However, our data from *Limnoria tripunctata* indicate that it shows no marked preference with respect to depth of settlement.

In order to better understand the migratory activity of *Limnoria* in light of its population biology an analysis was made of the seasonal composition of the population from the piling and from the test blocks. For this purpose the animals were studied as to size and, in the older specimens, also as to sex and reproductive condition.

Accurate measurements of the body length of *Limnoria* are usually difficult to obtain because of the natural tendency of the animals to assume a strongly bent position or for the segments to become more or less telescoped depending upon the type of preservative used or upon other factors such as ovarial development or injury. A practical substitute is therefore here made by using the pleotelson width at its widest point as an index of size. This has the advantage that we here deal with a flat rigid structure (the last segment of the body) that is not readily distorted. It has the further advantage that the size of animals in shallow burrows may often be determined without removing them from the burrow, and also the size of exuviae can be determined by this one fragment of the generally disarticulated cast.

Ten size categories can be established more or less clearly based on the width of the pleotelson.

In the literature dealing with *Limnoria*, the size index given is always in length; hence it will be useful here to provide Table II giving conversions of pleotelson widths to body lengths for the ten groups.

TABLE II

Limnoria tripunctata. Pleotelson width to body length. 180 animals measured

Size class	Mean pleotelson width, mm.	Body length, mm.		Remarks
		♂	♀	
1	0.24–0.26	0.8–1.2		Young lacking seventh pair of pereiopods
2	0.28–0.33	1.0–1.6		
3	0.35–0.40	1.1–1.6		Young with underdeveloped seventh pair of pereiopods
4	0.42–0.46	1.5–2.2	1.5–1.5	Sexual maturity reached by males
5	0.48–0.53	1.7–2.2	1.9–3.0	Females develop oostegites
6	0.55–0.60	2.1–3.0	1.8–3.0	Females become gravid
7	0.61–0.67	2.0–3.3	2.6–3.5	Includes majority of reproductive individuals, especially the females
8	0.69–0.74	2.5–3.4	3.0–3.8	
9	0.76–0.81	2.5–3.4	2.7–3.5	
10	0.82–0.86	2.5–3.2	2.5–3.8	Only few reach this size

An analysis of the population composition of a one-month test block and of old piling on the same date are given respectively in Tables III and IV. The results are quite typical, but for piling populations, there may be considerable variation in samples of one square inch in size taken adjacently in the same pile; hence, in most instances, counts were made in duplicate or triplicate.

A comparison of the percentage composition of the populations shown in Tables III and IV reveals that over 97% of the migrants are sexually mature animals of fairly large size, whereas on the piling, only about 28% are sexually mature, over 50% are newly hatched or immature animals, and 19% intermediate.

Analyses of piling samples taken monthly are given in Table V where the percentage composition of size classes are given and the mean calculated for three-month periods. Thus the variations are smoothed out to give seasonal means for

TABLE III

Limnoria tripunctata. Migrant population, Station A, Sept. 13, 1952. Numbers in size class, maturity, sex and per cent of total population (164) in test block of each month exposure

Size class	Immature	♀ (?) Young	♀ with oostegites	♀ gravid	♂
3	1				
4		2			1
5		1			16
6					12
7			21	7	25
8			12	10	11
9			18	11	10
10			2	2	2
% of Total	0.60	1.81	32.29	18.26	46.90

TABLE IV

Limnoria tripunctata. Piling population, Station A, Sept. 13, 1952. Numbers in size class, maturity, sex and per cent of total population in one square inch sample of infested wood with a total of 432 animals

Size class	7th pereiopod lacking	Immature	♀ (?) Young	♀ with oostegites	♀ gravid	♂
1	83					
2	36	39				
3		69	39			
4			39			8
5			5	4		10
6				10		7
7				7	13	23
8				8	10	7
9				4	7	4
% of Total	27.54	24.99	19.19	7.62	6.93	13.64

spring, summer, autumn, and winter. From this it appears that the piling population remains rather constant in its composition with some preponderance of the youngest class during the migratory months (June–November) and of the middle group during the winter (December–February) and relatively more adults in the spring (March–May) prior to heavy migration.

In the test block population presented in Table III, there is a slight predominance of females over males. It appears, however, from analyses of many block

TABLE V

Limnoria tripunctata. The mean percentage of size composition for monthly and seasonal periods for piling populations, 1952–1953

Size class	Spring			Seasonal mean	Summer			Seasonal mean
	March	April	May		June	July	August	
1–3	16	65.5	34	38.5	31.5	48	44	41.3
4–7	53.8	19.5	40.3	38	48	43.5	35	42.3
8–10	33.7	20	29	27.5	20.5	8.5	21	16.7
No. examined	403	783	792		545	449	300	
Size class	Autumn			Seasonal mean	Winter			Seasonal mean
	Sept.	Oct.	Nov.		Dec.	Jan.	Feb.	
1–3	69	34	47.5	50.3	17	53	33	34.3
4–7	16	51	40.3	35.8	63.5	34	54	50.7
8–10	15	15	12.3	14.1	19.6	13	13	15.2
No. examined	449	328	1282		557	153	44	

and piling samples, that the ratio of males to females on the piling is on an average about 1 to 1 for sexually mature specimens, whereas on test blocks it is often 1.3 to 1. This suggests that the males have a greater tendency to migrate than do the females, especially the younger females. Mating occurs after migration, the females becoming gravid some time after they have become established on the test block. This is evidenced by observations that (1) gravid females were found only in the longest, hence oldest burrows of the thirty-day test blocks, (2) here they occupied the blind end of the burrow while the male occupied the open end, (3) no gravid females were observed to occupy a burrow singly. This is in accord with the conclusions regarding the breeding habits of *Limnoria lignorum* (Kramp, 1927; Johnson, 1935; Sömme, 1940). Further evidence substantiating the opinion that migration precedes fertilization is found in Menzies' (1954) report which shows that females lack a sperm storage organ and the sperm produced by the male are relatively few in number and not grouped into spermatophores.

Sperm were found only in the oviduct of females which were moulting prior to deposition of eggs into the brood pouch. None were found in virgin or gravid females. Copulation probably precedes each brood production.

Factors Influencing Migration

Temperature

As shown in Figures 1 and 5 for *Limnoria tripunctata* and Figure 2 for *L. lignorum,* there is a certain correlation between the water temperature and the intensity of migration as indicated by severity of attack on the test pieces. The figures do, however, show a sharp difference in the maximum migratory period of the two species as related to the temperature curve and season of the year. *L. lignorum* reaches a peak of migratory activity on a rising temperature whereas *L. tripunctata* follows more nearly the seasonal trend of temperature with some tendency to lag behind. However, it should be pointed out that while the above appears to be typical for *L. lignorum,* at widely separated areas, data from Tromsösund, Norway, show a period of greatest migratory activity on a falling temperature. Sömme (1940) concluded that the season of migration varied with hydrographic conditions; hence each locality requires special investigation to determine the season of maximum attack on new wood. In a survey designed mainly to test the depth of attack in British Columbia waters, Black and Elsey (1948) indicate some variation in season of attack by *L. lignorum.* However, their data show that in areas such as Williams Head, Bentinick Island, and Esquimalt, which are not seriously affected by dilution, the main attack was during spring. The data used in Figure 2 A and B are derived from analysis of test blocks kindly provided us by the William F. Clapp Laboratories.

These differences in the two species may arise from specific differences in temperature requirements. Temperature *per se* may, however, not be the immediate cause of migration in either species of *Limnoria.* It is perhaps mediated through its effect on the rate of other biological activities such as growth, attainment of sexual maturity, and reproduction. Seasonal increases in these rates must lead to population pressure which is more acute at some seasons than at others.

Population pressure

In the study of *L. lignorum* at Friday Harbor (Johnson, 1935), it was hypothesized that migration results from overcrowding and approach of sexual maturity. Overcrowding is, of course, closely dependent upon the nature and availability of food supply and living space. *Limnoria,* like other wood borers, is unique in that it eats the substratum on which it lives. Limits to size and growth of the population are therefore set by the area of available wood. When conditions become intolerable due to population pressure, either a migratory movement must take place or the ratio of reproduction and growth to mortality must change. That the first takes place, we know, and there is some evidence also of the latter. The rate of growth, age of attainment of sexual maturity, and fecundity are then of prime importance in an understanding of migration.

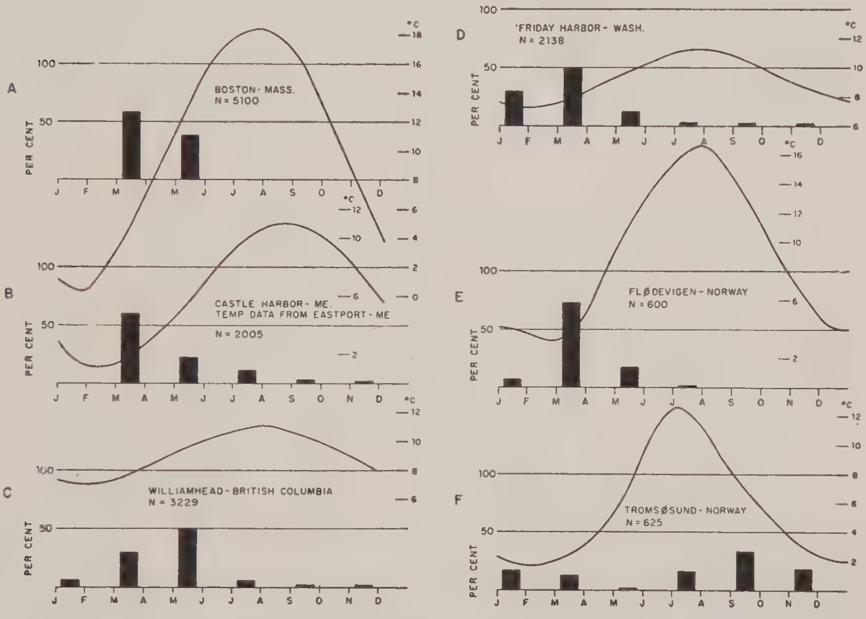

FIGURE 2. *Limnoria lignorum.* Percentage of seasonal attack in bimonthly periods in various localities. A and B data from William F. Clapp Laboratories; C from Black and Elsey, 1948; D from Johnson, 1935; E and F from Sömme, 1940. N = Yearly sum of animals on test blocks.

Fecundity Related to Overcrowding

That there is a reduction of fecundity in a crowded population is indicated in Table VI. Here it is apparent that with increased size of the female, as shown by pleotelson width, there is also an increase in the number of eggs produced. This relationship is more evident for the test-block than for the piling population. It will be noted also that the brood size of piling populations remains approximately one-half the size of that of the migrant population irrespective of size increase in the female. Thus it appears that an increased population density influences the brood size so that the rate at which young are added to a dense population may be only about one-half that at which they are added to a sparse population with plenty of wood for expansion. However, even with this adjustment, the population pressure must increase as the living space diminishes.

Fecundity Related to Temperature

The rate of development of eggs in the ovaries appears to be temperature-dependent. Brood-bearing females were found at Station A on test blocks which had been submerged for 30-day intervals all months of the year except the winter. In July and August, 1954, a brood was produced and hatched in 30 days at a temperature near 20.8° C. Test blocks submerged for 60 days showed gravid females throughout the year and hatched young most months of the year except during the spring of 1953 and in January and February, 1954. Station B yielded similar results for the 30-day exposures except that a brood was produced and hatched in less than 30 days in April and May (mean temperature 19.5° C.). The deposition of eggs and hatching of broods did not occur within 60 days at Station A during the winter or spring months of 1953–54 when temperatures ranged from 14.8 to 15.8° C. This suggests that with a temperature difference of only 5° C., it takes about twice as long to produce and incubate young during winter as it does during the summer.

TABLE VI

Limnoria tripunctata. Comparison of brood size with size in females from old wharf piles and from 30-day test blocks

Size class	Piling			Test blocks		
	No./brood Mean	No./brood Range	No. gravid ♀♀ examined	No./brood Mean	No./brood Range	No. gravid ♀♀ examined
6	4.6	1–6	11	—	—	None found
7	5.8	1–12	25	8.9	4–18	35
8	4.0	1–12	28	10.8	1–18	79
9	5.1	1–12	34	12.4	1–22	95
10	7.0	1–12	3	10.5	4–21	21

It was observed that at least during the summer months, females with hatched young also had ripe ovaries and could incubate another brood soon after the emergence of the first batch from the pouch. Frequently young and their secondary or lateral burrows were observed in a burrow of a gravid female. In the test blocks exposed for three-month periods, the following maximum numbers of broods were observed: Station A, mid-November, 1953–mid-February, 1954 (mean temperature 14.8° C.) one brood; mid-July–mid-October, 1954 (mean temperature 20.6° C.) three broods; mid-August–mid-November, 1954 (mean temperature 17.4° C.) two broods; Station B, mid-February–mid-May, 1953 (mean temperature 18.6° C.) two broods. Using size as a criterion, it appears that migrant females may have produced one or two broods prior to migration. This is indicated in Figure 3 which should be coordinated with Table II showing that females may become gravid in size class 6. Females in size class 10, the largest, were found only in migrant populations. Although migrants must frequently land on already heavily infested wood, the relative absence of the large females probably indicates that few, if any, re-establish themselves in dense populations. Thus the implication is that migration is largely an urge to seek less crowded conditions. Analysis of the population forming the basis of Figure 3 shows also that the summer and fall gravid migrants average 0.04 mm. smaller than those of other seasons and the gravid females from piling average 0.05 mm. smaller, thus indicating that sexual maturity is reached at a smaller size (hence more rapidly) during the warmer months.

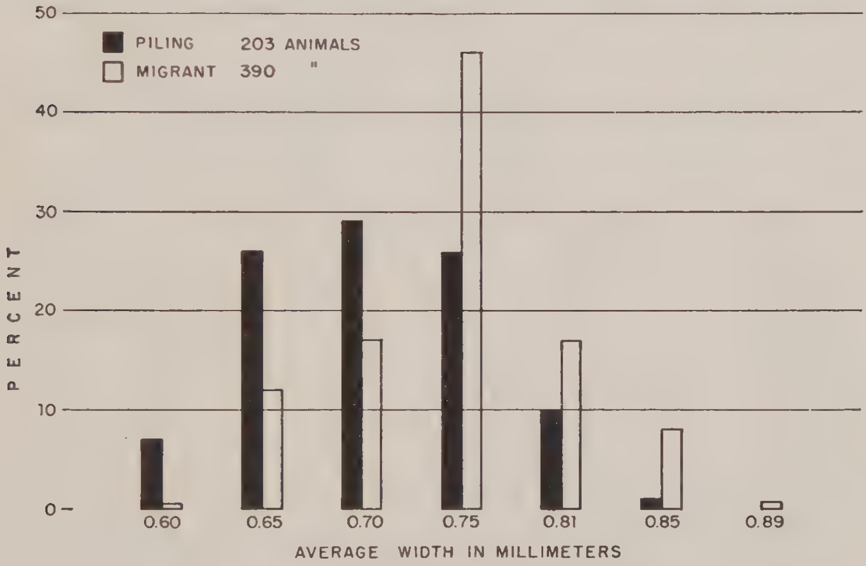

FIGURE 3. *Limnoria tripunctata*. Percentage size composition of gravid female populations.

That reproduction in *Limnoria* is influenced seasonally by temperature is further indicated by a study of the "gravidity" which may be defined as the per cent of gravid females among the adult females occurring at any time in a piling population of maximum density (Table VII).

From Table VII, it seems evident that gravidity for this species reaches its peak somewhere between 17° and 19° C., declining at temperatures above and below these values. Gravidity appears to double between 14° and 18° C. In laboratory cultures only 28% became gravid at 24° C. The broods of specimens kept at 34° C. deteriorated, suggesting that such high temperatures may unfavorably affect brood production. At Beaufort, N. C., Coker (1923) reported no gravid females at

10° C. Mawatari (1950) reports that temperatures of 2–6° C. are lethal to *Limnoria lignorum* (probably *L. tripunctata*).

In contrast the northern species *Limnoria lignorum* appears to reach its peak gravidity at about 10° C., based on data from Johnson (1935). These data (assuming a 50-50 ratio of males to females) indicate that with environmental temperatures from 7.9° to 11.1° C. the gravidity figures varied from 22% to 79%, whereas at 7.5° C., the lowest temperature encountered, it was down to 14%. Sömme (1940) reports that *Limnoria* ceases to produce eggs at temperatures of 0° C. and below. In experiments she observed that the brood of a gravid female kept at 24.7° C. failed to develop after five days; at 14.8° C. and 6.3° C. development was apparently normal but at the lower temperature about twice the time was required as at an average of 13° C.

TABLE VII

Limnoria tripunctata. Seasonal gravidity (per cent gravid females of sexually mature females, 50/50 sex ratio assumed) in piling populations, Station A, 1952–1953. Figures based on gross size-class analyses of two to three one square inch samples of wood per month

Month sample collected	Mature animals of both sexes examined	Total females	Gravid females	% Gravid	Temperature °C.	
					Range	Approx. mean
January, 1953	96	48	6	12	15.5–14.8	15
February, 1953	124	62	34	55	14.8–14.6	15
March, 1953	289	44	83	57	14.6–15.0	15
April, 1953	109	54	31	57	15.0–15.5	15
May, 1953	220	110	68	62	15.5–16.3	16
June, 1953	133	66	53	80	16.3–18.3	17
July, 1953	44	22	12	55	18.3–19.2	18
August, 1953	53	26	28	100*	19.2–19.3	19
September, 1952	121	60	42	70	18.5–17.4	18
October, 1952	57	28	17	60	17.4–16.2	16
November, 1952	154	77	55	71	16.2–15.4	16
December, 1952	104	52	2	4	15.4–14.8	15

* In this case there were obviously more females than males in the sample.

Individual and population growth

The habits and life history peculiar to *Limnoria* make it possible to determine the growth rates of individuals and to follow the development of one or more broods in nature. To accomplish this, the test block (habitat) must have remained in the water a sufficiently long time to allow the migrants to incubate their broods and for the young to grow, but not so long that young of a second generation or new migrants confuse the picture. Development is direct and when the young emerge from the brood pouch, they immediately construct their own burrows within the walls of the parent burrow. The old female followed by the male continues burrowing deeper into the wood, so that subsequent broods released are separated more or less clearly from the previously released brood.

Thus up to the time that they may desert their burrows or have burrowed too far from the parent burrow, the young produced on the block can readily be distinguished from young which might have migrated to the block. Even specimens which have become sexually mature, and no longer associated with the parent burrow can usually be distinguished from sexually mature young migrants to the blocks because they occur in significantly larger numbers than do the young (small) migrants.

Rate of Growth.

The growth rate of *Limnoria tripunctata* was determined by culturing individuals in the laboratory and from measurements of the growth of young on test blocks for two-, three-, and four-month intervals. The maximum growth rate seasonally as found in test block exposures is shown in Figure 4. An evident feature is the seasonal difference in growth rate of the young. Those emerging in winter require roughly twice as long to reach size class 5 (with 0.48–0.53 mm. pleotelson width) as do the spring young, and three times as long as the summer young. Thus increased crowding from growth of individual animals (distinguished from increased crowding resulting from addition of new individuals) would be greatest during spring and summer.

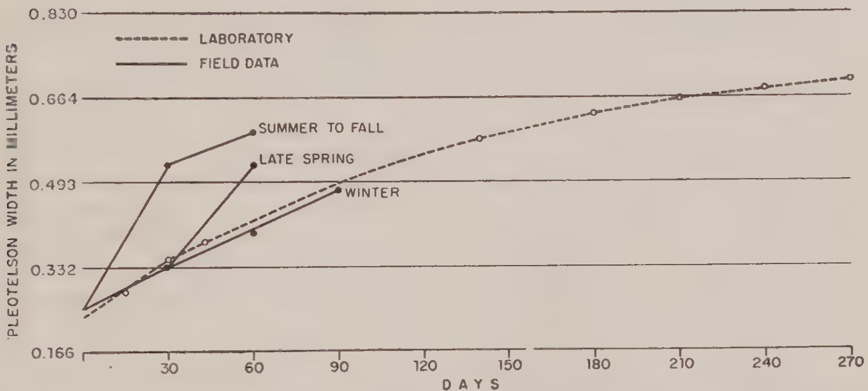

FIGURE 4. *Limnoria tripunctata.* Individual growth rate at different seasons: late spring, average temperature 19° C.; summer to fall, average temperature 22° C.; winter, average temperature 15° C.; laboratory culture average temperature 15° C. Measurements in field are from broods hatched on test blocks, those in laboratory, from individual specimens.

Population Growth.

Some idea can be had of the population growth by direct observation of the number and size of broods produced by migrant females during different portions of the year, namely on test blocks that were in place for successive 2-, 3- and 4-month periods throughout the year. In Table VIII summaries and calculations of probable annual rate of reproduction have been made, based on number of young observed in these 2- to 4-month periods.

Data from the test blocks show that a brood may be produced in a minimum of 25 days. The three- and four-month exposures indicate, however, that only one brood is produced during the winter, possibly three during the summer and at most only two during spring and fall. Thus a maximum of eight broods could conceivably result if a female can continue to produce successive broods at this rate. It has, however, been possible to follow the performance of individual females through a maximum of only three successive broods. Hence, it is not known whether or not a female that has produced three broods during the season of maximum production will continue to produce additional broods at the reduced rate at other seasons. Therefore, extrapolations must be considered with caution. Assuming an annual rate of eight broods with an average of 10 young per brood (Table VI) 100 females might produce a maximum of 8000 young. However, not all females in a population are gravid at any one time. The gravidity may be close to 100% during the mid-summer but drops as low as 4% during the winter (Table VII). An approximate mean gravidity for the year might be near 60% which would allow 100 females to produce only 4800 young per year at the rate shown for test board populations. Females in old piling populations appear to produce only about ½ this figure since their average brood size is only 5.

TABLE VIII

Limnoria tripunctata. Rate of production of young based on observed values for test block populations

Station	Duration of test block exposure	Dates of exposure	Total number of months	Number of young found per 100 mature females	Raw monthly rate	Adjusted* monthly rate	Adjusted* annual rate
A	2 months	Aug. 1952– Oct. 1953	12	380	31.6	63.2	758
A	2 months	Oct. 1953– Dec. 1954	12	717	59.7	119.4	1433
B	2 months	Feb. 1954– Feb. 1955	12	619	51.6	103.2	1238
A	3 months	April 1954– Jan. 1955	9	1009	112.1	149.1	1789
B	3 months	Feb. 1954– Jan. 1955	9	1251	139.0	185.3	2224
B	4 months	Feb. 1954– Feb. 1955	12	1585	132.0	165.0	1980
				Average annual rate			1570

* In order to approach the reproductive continuity that must occur on piling, one-month incubation time is allowed. Raw monthly rate on blocks of 2-month exposure are accordingly doubled, those of 3- and 4-month exposures are increased by ⅓ and ¼ of raw rate, respectively.

If the average annual realized reproductive performance of 100 sexually mature females is 1570 young as shown in Table VIII, the difference between this figure and the reproductive potential based on number and size of brood suggests the annual mortality on test blocks.

The reproductive rate given above may appear low compared with the potentialities suggested for *Limnoria lignorum* by Kramp (1927) who indicated four broods of 20–30 eggs per female per year. He, however, did not investigate the relative number of young resulting on the test blocks. Hence, no allowance was made for mortality. In Japan Shiino (1950) found only 1–12 eggs produced by *L. lignorum* (*tripunctata?*).

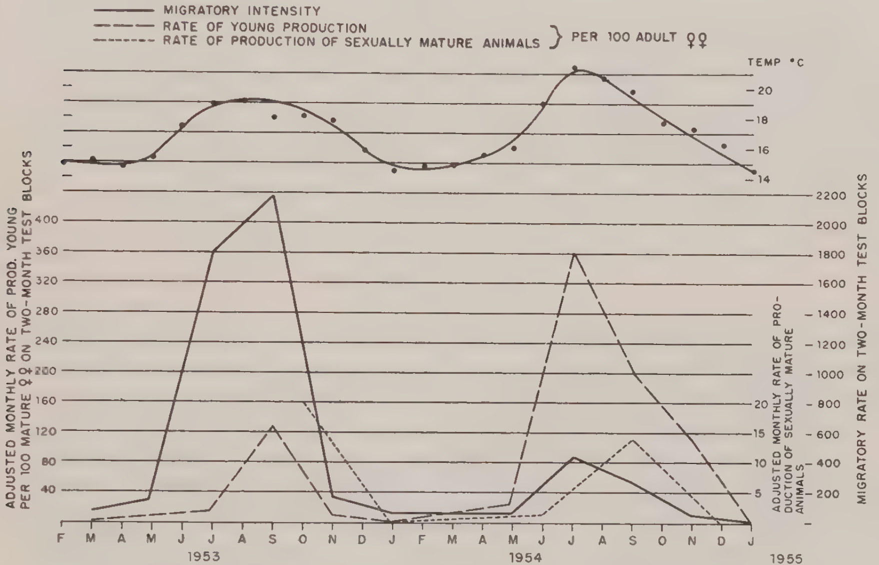

FIGURE 5. *Limnoria tripunctata.* The relationship between monthly production rates and migration in two-month periods, Station A, San Diego Bay.

The relationship between monthly production rate and migration in San Diego Bay is shown graphically in Figure 5. Interpolated to the piling, these data indicate that a marked increase would have occurred there during the months of maximal migration.

SUMMARY

1. *L. tripunctata* undergoes a definite seasonal migratory period which reaches its height approximately during the season of highest water temperatures. This differs from the earlier migratory season usually shown for *L. lignorum*.

2. The attack on new wood is about equally severe on floating and submerged blocks.

3. A comparison of the percentage composition of the 30-day test-block populations shows that about 97% of the migrants are sexually mature animals as con-

trasted with piling populations where 50% consisted of newly hatched immature animals and only about 28% sexually mature. The piling population remains fairly constant in its composition.

4. None of the females is gravid at the time of migration. Pairing takes place after establishment on the test blocks.

5. As with *L. lignorum* the factors influencing migration are probably a combination of approach to a reproductive phase and population pressure due to overcrowding in old established populations.

6. Water temperature is important in influencing migration in that the higher temperatures hasten the rate of growth and attainment of sexual maturity, production of eggs, and shorten the incubation period. Gravidity (per cent gravid females) in *L. tripunctata* evidently reaches its peak between 17° and 19° C. as contrasted with about 10° C. for *L. lignorum.*

7. The brood size of piling populations is about ½ that found in uncrowded test-block populations.

8. A single female probably produced three or more broods during the year.

9. Using size as a criterion, most migrant females appear to have produced a brood prior to migration.

10. In extrapolating the test-block data to the piling populations, there is indicated a marked population increase during the months of maximal migration.

LITERATURE CITED

Black, Edgar C., and G. R. Elsey, 1948. Incidence of wood-borers in British Columbia waters. *Bull. Fish. Res. Bd. Can.,* **80**: 1–20.

Coker, R. E., 1923. Breeding habits of *Limnoria* at Beaufort, N. C. *J. Elisha Mitchell Sci. Soc.,* **39**: 95–100.

Holthuis, L. B., 1949. The Isopoda and Tanaidacea of the Netherlands, including the description of a new species of *Limnoria. Zool. Mededelingen Reiksmuseum Van Natuurlijke Hist. te Leiden,* **30**: 163–190.

Johnson, Martin W., 1935. Seasonal migrations of the wood-borer *Limnoria lignorum* (Rathke) at Friday Harbor, Washington. *Biol. Bull.,* **69**: 427–438.

Johnson, Martin W., and Robert C. Miller, 1935. The seasonal settlement of shipworms, barnacles and other wharf-pile organisms at Friday Harbor, Washington. *Univ. of Washington Pub. in Oceanography,* **2**: 1–18.

Kofoid, C. A., and R. C. Miller, 1927. Biological Section, Final Report of the San Francisco Bay Marine Piling Committee (published by the Committee), pp. 188–343.

Kramp, P. L., 1927. Undersögelser over Paeleorm og Paelekrebs ved Hirtshals. *Ingeniören,* **36**: 329–340.

Mawatari, Shizuo, 1950. Biological and industrial study of marine borer problem in Japan. Studies on the aquatic animals of Japan (1), pp. 9–12, 45–124. In Japanese with English summary.

Menzies, Robert J., 1951. A new species of *Limnoria* (Crustacea: Isopoda) from Southern California. *Bull. So. California Acad. Sci.,* **50**: 86–88.

Menzies, Robert J., 1954. The comparative biology of reproduction in the wood-boring isopod crustacean *Limnoria. Bull. Mus. Comp. Zool.,* **112**: 364–388.

Menzies, R. J., and J. L. Mohr, 1952. The occurrence of the wood-boring crustacean *Limnoria* and of Nebaliacea in Morro Bay, California. *Wasmann J. Biol.,* **10**: 81–86.

Shiino, Sueo M., 1950. The marine wood-boring crustacea of Japan. I. Limnoriidae. *Wasmann J. Biol.,* **8**: 333–358.

Sömme, Olaug M., 1940. A study of the life history of the gribble *Limnoria lignorum* (Rathke) in Norway. *Nytt. Mag. for Naturvidenskapene,* **81**: 145–205.

Deep-Sea Research, 1956, Vol. 3, pp. 126 to 138. Pergamon Press Ltd., London.
Reproduced by Permission

Rock fragments and pebbles dredged near Jimmu Seamount, northwestern Pacific

HISASHI KUNO,* ROBERT L. FISHER† and NORIYUKI NASU*

(*Received* 24 *November* 1955)

Abstract—Fifty-five rock fragments and pebbles were dredged at 2,550-2,800 fathoms (4,650-5,100 metres) near Jimmu Seamount, 700 miles southeast of Kamchatka. Tuffaceous shale, andesitic and dacitic tuff, pyroxene-hornblende dacite-pumice, and augite-hypersthene andesite are the most abundant rock types. Minor constituents in the haul include augite-pigeonite basalt, augite-olivine basalt, olivine dolerite, quartz syenite porphyry, metabasalt, sandstone, and chert. Petrographic and chemical analyses indicate closer affinities with Kuril Islands and Kamchatka volcanic rocks than with Cenozoic Japanese or Pacific Basin types. Probably these rocks were dropped by Pleistocene icebergs carried south and east by ocean currents.

INTRODUCTION

THE University of California R/V *Spencer F. Baird* visited Jimmu Seamount in September 1953, while engaged in the Hydrographic and Biological Trans-Pacific Expedition to the Western Pacific (Fig. 1). The samples discussed below were collected by biological dredge from the northwest flank of the seamount, at a depth of 2,550-2,800 fathoms (4,650-5,100 metres). The petrographic examination of these samples was made at the Geological Institute, Tokyo University.

From the expedition fathograms, Jimmu Seamount appears to be a guyot or tablemount, with a least depth of 700 fathoms (1,280 metres) and a principal break in slope at 830 fathoms (1,520 metres). The flat top probably indicates truncation by wave action when the summit was at or very near the sea surface.

Jimmu Seamount is one peak on a north-south submarine range which DIETZ (1954, p. 1209-11) has designated the Emperor Seamounts. The south end of the range apparently joins the western end of the Hawaiian Swell. Three guyots of this range are shown on the profile in Fig. 1, from a Trans-Pacific Expedition fathogram. The summits of the three peaks are not accordant. DIETZ, among others, favours local isostatic subsidence of such peaks; according to this view the greater submergence of the southernmost guyot need not indicate greater age.

PETROGRAPHIC DESCRIPTION

Fifty-five rock fragments and pebbles were dredged from near the base of Jimmu Seamount. Nineteen are flat, angular fragments of comparatively soft rocks (Nos. 1-19, Fig. 2a), ten are well-rounded pumice (Nos. 20-29, Fig. 2b), twenty-four are well-rounded pebbles of hard rocks (Nos. 30-53, Figs. 3a and 3b), and two are ragged fragments of scoria and slag (Nos. 54 and 55, Fig. 3b). Thirty-six thin sections were cut from representative specimens of these rocks.

---

* Geological Institute, Tokyo University, Tokyo, Japan.
† Scripps Institution of Oceanography, La Jolla, California.

A. *Angular fragments* (*Fig. 2a*)

Most of the angular fragments consist of light grey or yellowish grey shale and tuff of salic andesite or dacite. Much of the shale is tuffaceous. Quartz syenite porphyry and quartz gabbro are also represented. The former consists of orthoclase-perthite, albite, quartz, and altered mafic minerals; the latter is strongly weathered.

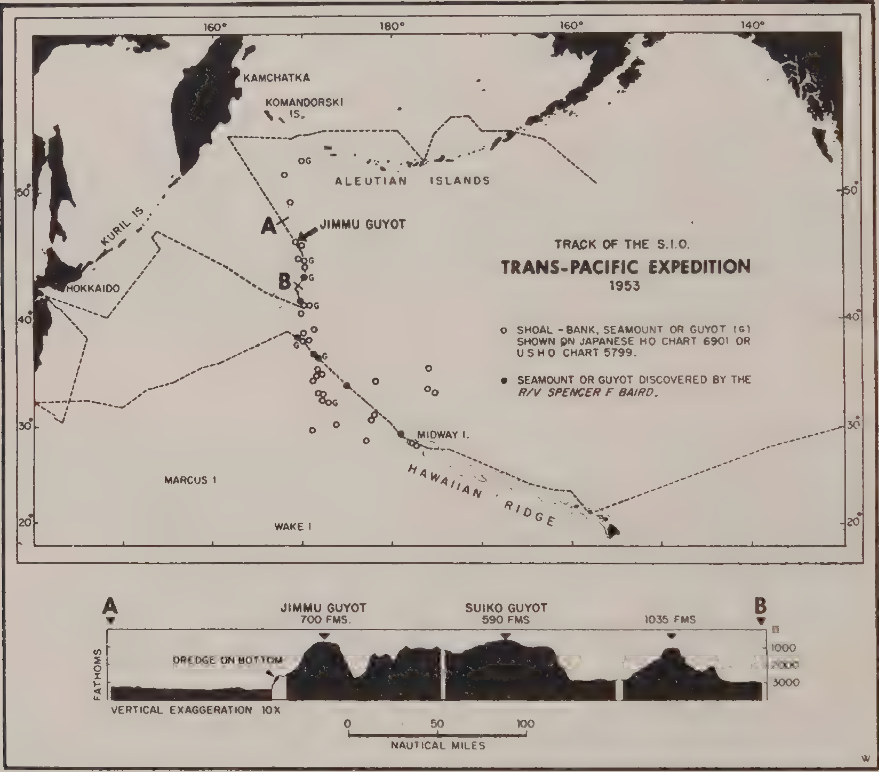
160°
180°
160°
140°
50°
40°
30°
20°
KAMCHATKA
KOMANDORSKI IS.
ALEUTIAN ISLANDS
KURIL IS
HOKKAIDO
A
B
JIMMU GUYOT
G
MIDWAY I.
MARCUS I
WAKE I
HAWAIIAN RIDGE
TRACK OF THE S.I.O.
TRANS-PACIFIC EXPEDITION
1953
○ SHOAL - BANK, SEAMOUNT OR GUYOT (G) SHOWN ON JAPANESE HO CHART 6901 OR USHO CHART 5799.
● SEAMOUNT OR GUYOT DISCOVERED BY THE R/V SPENCER F BAIRD.
A
JIMMU GUYOT 700 FMS.
SUIKO GUYOT 590 FMS
1035 FMS
B
FATHOMS
DREDGE ON BOTTOM
1000
2000
3000
VERTICAL EXAGGERATION 10X
0
50
100
NAUTICAL MILES
W

Fig. 1.

The fragments are coated with a thin black film, probably of manganese oxide. Small fragments are attached to the surface of larger pieces of the same rock. Calcareous tubes of Annelida adhere to the surfaces of some of this suite. The larger white tubes (No. 18) are those of Serpulinae, while smaller brownish ones (Nos. 12, 13, and 14) are those of *Amphicteis* sp. These tubes do not give any information as to the source of the fragments because allied species of annelida have been obtained from various parts of the Pacific Ocean, between the depths of 345 and 3,125 fathoms (oral communication by HORIKOSHI). As the tubes look very fresh and cover the surface of the black film, they were probably formed after the fragments were emplaced in their present position.

B. *Pumice* (*Fig. 2b*)

The pumice has a nearly uniform petrographic character. It is pyroxene-hornblende

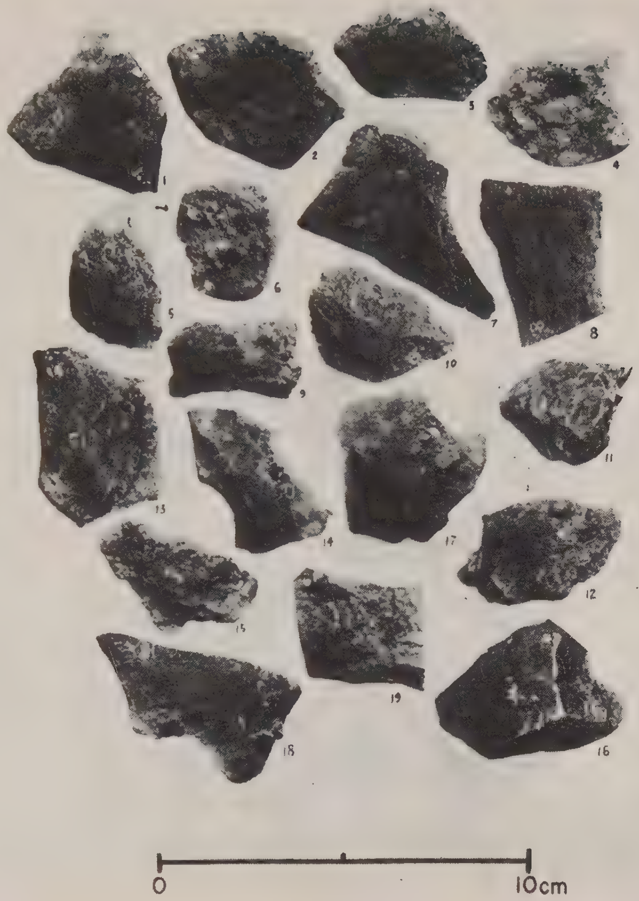
1
2
3
4
5
6
7
8
9
10
11
12
13
14
15
16
17
18
19
0
10cm

Fig. 2a.

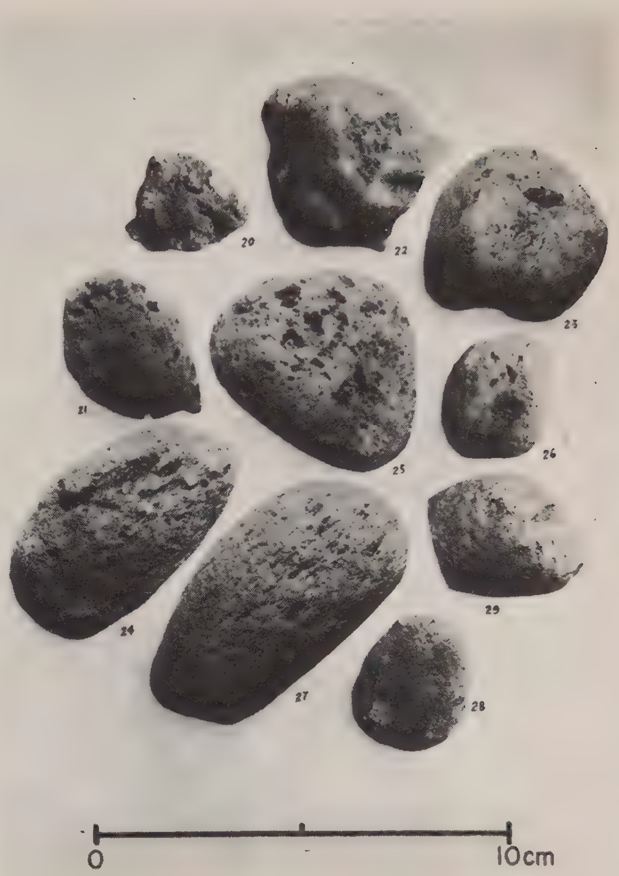
20
21
22
23
24
25
26
27
28
29
0
10cm

Fig. 2b.

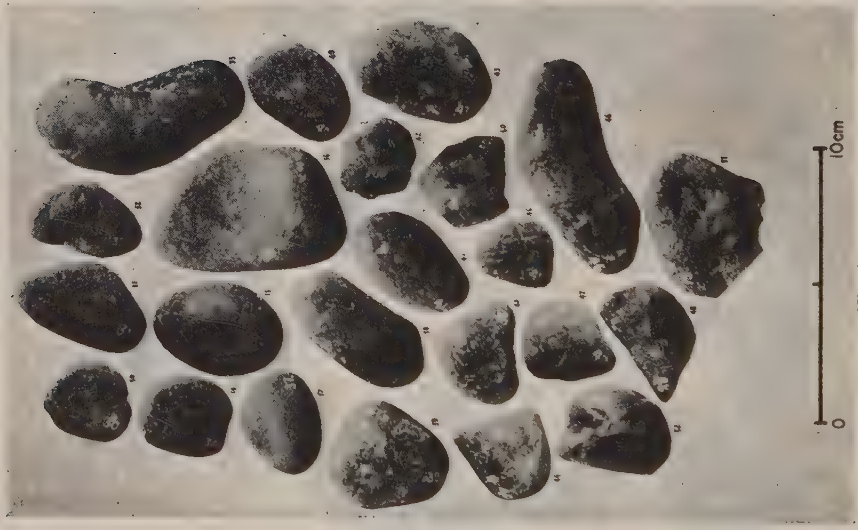

Fig. 3a.

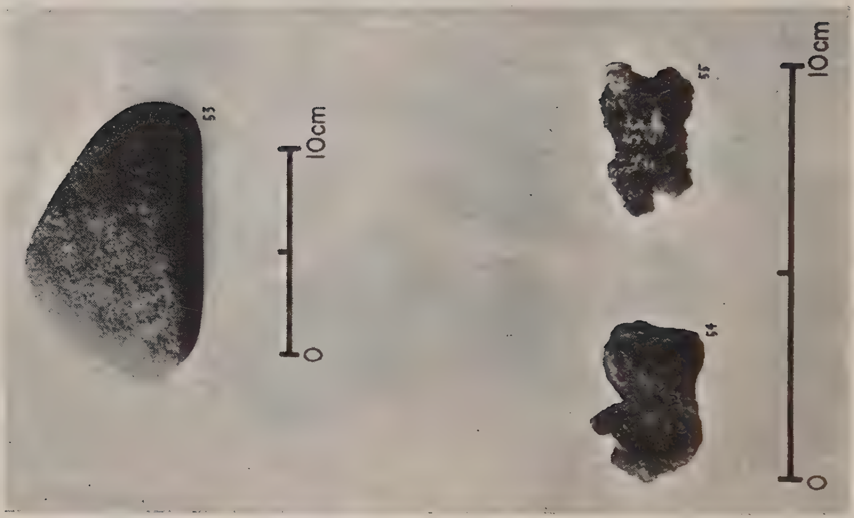
53
0
10cm
54
55
0
10cm

Fig. 3b.

dacite with phenocrysts of medium plagioclase, augite, hypersthene, green hornblende, and magnetite, although pyroxenes or hornblende are absent in some specimens. Quartz phenocrysts are only found in one of the slides. The groundmass consists of colourless glass entirely free of devitrification. A chemical analysis of one of the dacites (No. 27) is given in Table 1.

Small xenoliths of tuffaceous sandstone, biotite-hornblende gneiss, and olivine-augite-anorthite basalt are present in some specimens. Some of the cavities of the pumice are filled with radiolarian ooze which obviously was deposited after the pumice was dropped in its present position.

Table 1. *Chemical composition of the pebbles dredged from Jimmu Seamount, northwestern Pacific.*

Specimen No.	36	41	54	49	34	27
SiO_2	45·90	48·63	52·33	53·85	60·38	71·96
Al_2O_3	16·76	18·06	17·27	18·72	16·98	13·76
Fe_2O_3	5·27	4·01	4·27	3·44	2·93	0·69
FeO	5·25	7·52	4·01	4·90	3·66	1·19
MgO	7·06	5·11	5·93	4·78	3·26	0·55
CaO	10·08	11·23	10·22	8·87	6·61	2·38
Na_2O	2·98	2·15	2·80	3·24	2·93	4·38
K_2O	1·38	0·48	1·31	0·82	1·53	1·95
H_2O (+)	2·09	1·09	0·58	0·34	0·65	1·61
H_2O (−)	1·01	1·06	0·32	0·12	0·30	0·45
TiO_2	1·77	0·72	0·66	0·84	0·60	0·23
P_2O_5	0·48	0·20	0·29	0·20	0·16	0·09
MnO	0·23	0·23	0·30	0·23	0·16	0·14
Total	100·26	100·49	100·29	100·35	100·15	100·14*
			Norm			
Q	–	2·46	–	5·58	18·00	32·94
Or	8·34	2·78	7·78	5·00	8·90	11·68
Ab	23·58	17·82	23·58	27·25	24·63	36·68
An	28·36	38·36	30·86	33·92	28·91	10·84
Ne	0·85	–	–	–	–	–
C	–	–	–	–	–	0·51
Wo	7·54	6·84	7·54	3·94	1·28	–
En	5·80	12·80	14·80	12·00	8·20	1·40
Fs	0.92	9·64	3·17	5·28	3·56	1·58
Fo	8·40	–	–	–	–	–
Fa	1·43	–	–	–	–	–
Mt	7·66	5·80	6·26	4·87	4·18	0·93
Il	3·34	1·37	1·37	3·80	1·22	0·46
Ap	1·34	0·34	0·67	0·34	0·34	0·34

No. 36 Augite-olivine basalt (trachybasaltic).
No. 41 Augite-pigeonite basalt.
No. 54 Hornblende-olivine-augite andesite.
No. 49 Olivine-hypersthene-augite andesite.
No. 34 Olivine-hypersthene-augite andesite.
No. 27 Hornblende dacite-pumice.

* Including 0·76 NaCl.

Analyst : T. KATSURA.

C. *Pebbles* (*Figs.* 3*a and* 3*b*, *upper*)

The hard-rock pebbles comprise a varied suite : pyroxene andesites (8 specimens), basalts (2), altered olivine dolerite (1), metabasalt (1), tuffs (2), shales and tuffaceous shales (7), sandstone (1), and chert (2).

The andesites contain phenocrysts of labradorite, augite, hypersthene, and magnetite, occasionally with those of olivine or hornblende. Xenocrysts of quartz are found in one specimen. The groundmass constituents are plagioclase, augite, hypersthene, iron ore, and interstitial glass and quartz. In some rocks, the plagioclase is replaced by albite while the mafic minerals are changed to chlorite. Three fresh andesites (Nos. 34, 39, and 54) were selected for chemical analysis with the result given in Table 1.

One of the basalts is an augite-pigeonite basalt, containing phenocrysts of bytownite, pigeonite, augite, and a little hypersthene, in a groundmass consisting of a feathery aggregate of labradorite, augite, and iron ore, with interstitial dark brown glass. The occurrence of porphyritic pigeonite in basalt is rather unusual; in most cases porphyritic pigeonite is found in andesite and dacite representing late differentiates of tholeiitic magma (KUNO, 1950). As seen from the analysis (No. 41) given in Table 1, the rock has a high $FeO + Fe_2O_3/MgO$ ratio, low alkalies, and a little normative quartz in spite of low SiO_2. These features agree with the general characteristics of tholeiitic basalt. Basalts with similar composition but not with similar mineral assemblage are quite common in Japan.

The other basaltic specimen is an olivine- and augite-bearing type, of trachybasaltic affinity. An undersaturated, slightly alkalic rock, it contains phenocrysts of bytownite, augite, and olivine, set in a groundmass consisting of labradorite, augite, olivine, magnetite, apatite, and interstitial alkali-feldspar. The olivine is entirely replaced by chlorite or saponite. As seen from the analysis (No. 36, Table 1), the rock has low SiO_2 and relatively high alkalies, yielding a considerable amount of normative olivine and a little nepheline.

The olivine dolerite has coarse ophitic texture and consists of albitized plagioclase, titanaugite, olivine replaced by chlorite or saponite, magnetite, ilmenite, and interstitial zeolite. It has a composition probably approximate to that of the olivine-augite basalt No. 36.

All of the mafic minerals in the metabasalt have been changed to actinolite, while plagioclase is less altered. Schistosity due to parallel arrangement of the actinolite is developed along planes of shearing.

The pyrogenetic material of the tuffs (coarse tuffs) and tuffaceous shales is andesite or trachyandesite. One of the tuffs has been slightly mylonitized.

The sandstone contains angular grains of quartz, plagioclase, biotite, muscovite, and epidote, apparently derived from granitic or gneissose rocks.

The chert is a cryptocrystalline variety, consisting of extremely fine grains of quartz.

D. *Scoria and Slag* (*Fig. 3b, lower*)

The ragged fragment of scoria is glassy olivine-hornblende-augite andesite. The slag fragment probably was dropped from a steamship.

PETROGRAPHIC SIMILARITIES OF DREDGED VOLCANIC ROCKS TO INTRA-PACIFIC AND CIRCUM-PACIFIC VOLCANIC SUITES

It is evident from the above descriptions that the mineralogy and chemistry of the volcanic rocks dredged near Jimmu Seamount bear little resemblance to those of the volcanics characterizing the Intra-Pacific region, but agree almost exactly with those of the Circum-Pacific volcanic zone. Basalts similar to No. 36 in Table 1 may occur in the Intra-Pacific region, while such rocks are also found occasionally in the Circum-Pacific Zone.

To demonstrate that the chemical compositions of the rocks in question lie within the variation range of the Circum-Pacific volcanic rocks, a variation diagram for alkalies has been constructed (Fig. 4), using the compositions of the rocks of the Katmai region, Alaska (FENNER, 1926), those of Adak and Kanaga Islands, Aleutian Islands (COATS, 1952), and the average compositions of Japanese volcanic rocks (TANEDA, 1952).

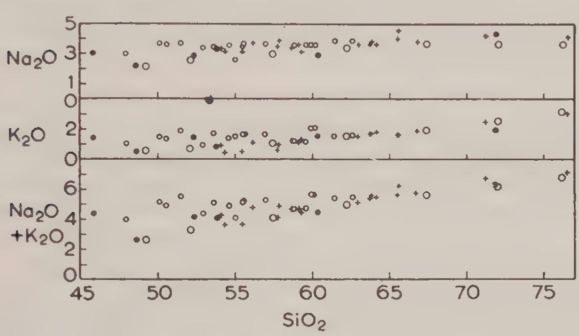

Fig. 4. Variation diagram for alkalies of the volcanic rocks dredged from Jimmu Seamount (black circles), the rocks of Katmai region (crosses), the rocks of Adak and Kanaga Islands (small open circles), and the average compositions of Japanese volcanic rocks (large open circles).

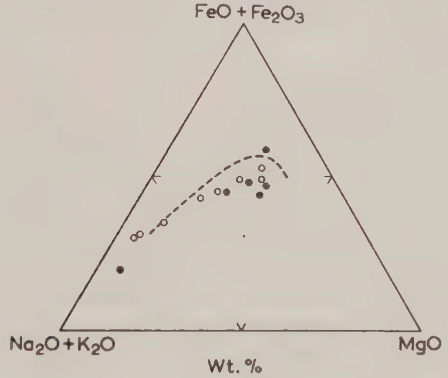

Fig. 6. Plot of the oxides ($FeO + Fe_2O_3$), MgO, and ($Na_2O + K_2O$) of the volcanic rocks dredged from Jimmu Seamount (black circles) and of Kamchatka (open circles). The broken line represents the boundary between the field of the pigeonitic rock series of Japan (above) and that of the hypersthenic rock series (below).

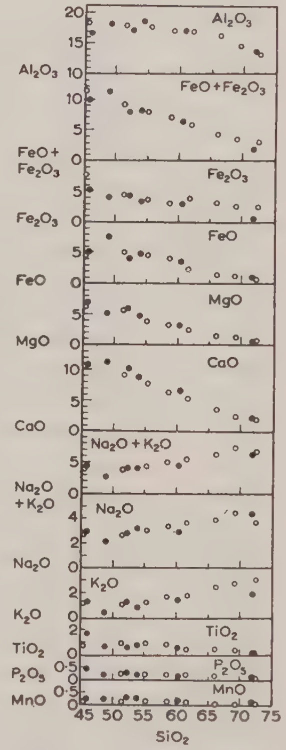

Fig. 5. Variation diagram of the volcanic rocks dredged from Jimmu Seamount (black circles) and the average volcanic rocks of Kamchatka (open circles).

In Fig. 5, the composition of the Jimmu pebbles is compared with the average compositions of volcanic rocks of Kamchatka given in Table 2. A close agreement between the compositions of the pebbles and those of the Kamchatkan rocks is evident from the figure. The augite-olivine basalt (No. 36 of Table 1) is approximate in composition to the average picrite-basalt of Kamchatka (column 1 of Table 2). The pigeonite basalt (No. 41) shows a slight departure from the trend of the Kamchatkan rocks.

The compositions of the Jimmu pebbles and the Kamchatkan rocks are plotted in the triangular diagram (Fig. 6). Except for the pigeonite basalt which lies rather close to the FeO + Fe_2O_3 corner of the triangle, the rocks of the pebbles and of Kamchatka show a trend characteristic of the calc-alkali rock series (TILLEY, 1950) or the hypersthenic rock series (KUNO, 1953). These rock series are thought to be formed through contamination of magmas by sialic materials (TILLEY, 1950; KUNO, 1950). The pigeonite basalt lies within the field of the pigeonitic rock series (KUNO, 1953) which, it is considered, is formed through fractional crystallization of tholeiitic magma (KUNO, 1950).

Table 2. *Averages of chemical analyses of volcanic rocks of Kamchatka. After* VLODAVETS (1939, 1946), *quoted in* TOMKEIEFF'S *paper* (1949).

	1	2	3	4	5	6	7	8
Number of Analyses	3	59	37	19	16	15	4	11
SiO_2	45·54	51·47	55·37	58·68	61·64	66·17	69·31	72·41
Al_2O_3	18·37	17·91	17·64	16·93	16·84	16·05	14·46	13·15
Fe_2O_3	7·69	4·44	3·77	3·03	3·93	3·09	2·47	2·54
FeO	4·46	5·01	4·57	4·15	2·31	1·34	1·31	0·78
MgO	6·27	5·74	3·96	3·20	2·32	1·33	0·71	0·56
CaO	10·61	9·12	7·72	6·30	5·23	3·62	2·45	1·98
Na_2O	2·70	2·64	3·04	3·34	3·66	3·83	4·47	3·69
K_2O	1·17	1·03	1·24	1·73	1·75	2·48	2·78	3·07
H_2O (+) H_2O (−)	2·32	1·42	1·34	1·45	1·52	1·37	1·63	1·42
TiO_2	0.75	0·87	0·96	0·83	0·48	0·47	0·38	0·28
P_2O_5	–	0·22	0·26	0·24	0·21	0·17	–	0·06
MnO	0·12	0·13	0·13	0·12	0·11	0·08	0·03	0·06
Total	100·00	100·00	100·00	100·00	100·00	100·00	100·00	100·00

1. Picrite-basalt.
2. Basalt.
3. Andesite-basalt.
4. Andesite.
5. Andesite-dacite.
6. Dacite.
7. Rhyolite-dacite.
8. Rhyolite.

The dredged volcanic rocks are also very similar in composition to those of Kuril Islands. The basalt No. 36 and the olivine-augite anorthite basalt found as xenoliths in the dacite-pumice are mineralogically very close to some lavas of Alaid Volcano, at the northern end of the island arc (KUNO, 1935).

PROBABLE SOURCE OF THE ROCK FRAGMENTS AND PEBBLES

Only two modes of origin of the rocks dredged from the flank of Jimmu Seamount need be considered. One possibility is that they are locally-derived, representing debris slumped from the top of the seamount when it was cut by wave erosion. The seamount may have been composed of a variety of rocks, volcanic, plutonic, sedimentary, and metamorphic; or it may have been a volcanic cone made up of a rather simple association of volcanic rocks, the other rock types having been torn from the basement rocks by explosive eruption and interbedded with the lavas as pyroclastic layers. On this interpretation the minerals comprising the sandstone would indicate the existence of sialic material in the source region. Likewise, as has been stated, the andesites and dacites would have been formed by incorporation of sial in the magma. However, as the existence of the sialic layer in the Jimmu region is very improbable, if not yet disproved by geophysical data, the derivation of the rock fragments and pebbles from the adjacent seamount is unlikely.

The other possibility is that these rocks were transported by Pleistocene icebergs from some region belonging to the Circum-Pacific volcanic zone and were dropped at the present location upon melting of the ice. The rounded pebbles are probably beach or river gravels which were captured by the glaciers.

In Hokkaido, at the northern end of the Japanese Islands, Pleistocene glaciers were present only on mountains higher than 1,500 metres (4,900 feet), while such glaciers appear to have existed even near sea level in the Kuril Islands (oral communication by Sasa). In Kamchatka, glaciers still exist on mountains higher than about 1,500 metres, and during Pleistocene time they extended down to the sea coast (VON REINHARD, 1915; KLEBELSBERG, 1948). It is likely therefore that icebergs derived from the Pleistocene glaciers of Kamchatka or the Kuril Islands were carried first southward by the cold ocean current and then eastward until they reached the vicinity of Jimmu Seamount. The similarity in petrographic character of the volcanic rocks found as pebbles at Jimmu to those of Kamchatka and of the Kuril Islands supports this interpretation. If oceanic circulation in the North Pacific during Pleistocene time was similar to the present pattern, possibly displaced southward slightly, icebergs originating in Alaska or the Aleutian Islands would not have reached Jimmu Seamount because of the warm current flowing eastward and southeastward.

The possibility that light pumice from volcanoes in the Japanese Islands was transported to Jimmu Seamount by the warm ocean current cannot be excluded entirely.

Acknowledgements—The writers are very much indebted to Mr. TAKASHI KATSURA of Tokyo Institute of Technology for making the chemical analyses, and to Mr. MASUOKI HORIKOSHI of Tokyo University for identification of the annelida. Their thanks are due also to Professor YASUO SASA of Hokkaido University and Dr. GAKURO IMAMURA for valuable information regarding the glaciation of Hokkaido, the Kuril Islands, and Kamchatka.

Contribution from the Scripps Institution of Oceanography, New Series No. 831. *This work represents one of the results of research carried out for the Office of Naval Research and Bureau of Ships, U.S. Navy, under contracts with the University of California.*

REFERENCES

COATS, R. R. (1952), Magmatic differentiation in Tertiary and Quarternary volcanic rocks from Adak and Kanaga Islands, Aleutian Islands, Alaska. *Bull. Geol. Soc. Amer.*, **63**, 485-514.

DIETZ, R. S. (1954), Marine geology of Northwestern Pacific: description of Japanese bathymetric chart 6901. *Bull. Geol. Soc. Amer.*, **65**, 1199-1224.

FENNER, C. N. (1926), The Katmai magmatic province. *J. Geol.*, **34**, 673-772.

KLEBELSBERG, R. (1948), *Handbuch der Gletscherkunde und Glaciologie*, 467 and 764.

KUNO, H. (1935), Petrology of Alaid Volcano, North Kurile. *Jap. J. Geol. Geogr.*, **12**, 153-162.

KUNO, H. (1950), Petrology of Hakone Volcano and the adjacent areas. *Bull. Geol. Soc. Amer.*, **61**, 957-1020.

Kuno, H. (1953), Formation of calderas and magmatic evolution. *Trans. Amer. Geophys. Union*, **34**, 267-280.
Taneda, S. (1952), New average chemical compositions of Japanese effusive rocks. *J. Geol. Soc. Japan*, **58**, 517-521.
Tilley, C. E. (1950), Some aspects of magmatic evolution. *Quart. J. Geol. Soc. London*, **106**, 37-61.
Tomkeieff, S. I. (1949), The volcanoes of Kamchatka. *Bull. Volcanologique, Ser.* 2, **8**, 87-113.
von Reinhard, A. (1915), Über die eisseitliche Vergletscherung Kamschatkas nach den Beobachtungen von W. Komarou. *Z. Ges. Erdk. Berlin*, 180-183.

Printed in Great Britain by The Salisbury Press Ltd., Publicity House, Wilton Road, Salisbury, Wilts. (95250)

Reprinted for private circulation from
THE JOURNAL OF GEOLOGY
Vol. 64, No. 2, March 1956
PRINTED IN U.S.A.
Reproduced by Permission

THE ANALYSIS OF TWO-DIMENSIONAL ORIENTATION DATA[1]

JOSEPH R. CURRAY
Scripps Institution of Oceanography, La Jolla, California

ABSTRACT

It is often useful to measure and analyze the orientations of various geological features—fabric elements, structural features, etc. Such measurements are more easily interpreted if they are summarized by statistics representing: (1) a preferred orientation direction, (2) the degree of preferred orientation, and (3) the probability that the preferred orientation is real and not merely due to chance. Application of conventional linear statistical methods, such as are used for grain-size analyses, presents some difficult problems, because orientation data are in the form of circular frequency distributions. A method of analysis which avoids these difficulties is discussed in this paper.

A logical approach to the problem is to treat the distribution directly in its circular form rather than to divide it into a linear frequency distribution. This avoids the difficulty that the mean and standard deviation of such a distribution varies with the choice of origin or dividing point. A resultant vector is obtained for the circular distribution by treating each observation as a vector and summing components. The direction of this vector is the preferred orientation direction, and the vector magnitude is a measure of the dispersion, or degree of orientation. These descriptive statistics have the advantage that they are independent of any a priori reference direction or origin. An excellent correlation exists between vector mganitude and the standard deviation calculated around the vector direction.

A test of the significance of the difference between an empirical orientation distribution and randomness is presented. Comparison shows that statistical significance is in many cases more easily attained with this test than with the chi-square and the *F* tests.

Two empirical distributions with rather low vector magnitudes (high standard deviations), taken from sand-grain orientation studies, are tested for goodness of fit against several model distributions. The best fits appear to be the circular normal distribution and a distribution obtained by wrapping an unlimited linear normal curve around the center point of a polar co-ordinate plot.

INTRODUCTION

Certain kinds of orientation data, if properly used, can be valuable in contributing to the understanding of geologic processes and past events. Studies of the orientations of fractures and fabric elements in deformed rocks have been used to interpret tectonic forces; orientations of cross-bedding and other structures, and particle long axes in undeformed sediments, have been used to interpret the directions of the depositing currents of wind or water; orientations of remnant magnetism in rocks have been used to interpret paleomagnetism and possible magnetic pole migrations during geologic time. Proper interpretation of orientation data starts with the problems of statistical analysis, because only through statistically controlled sampling, analysis, and evaluation of the results can reliable geologic inferences be drawn. An excellent review of methods of analyzing orientation data was given by Pincus (1953).

Several articles appeared in the geologic literature recently on the analysis of orientation data. Most investigators treated their data like the familiar linear normal distributions and computed mean and standard deviation or variance as descriptive statistics. Jizba (1953) and Chayes (1954) called attention to one of the difficulties which arises in such an analysis, namely, the necessity for choosing an origin in order to divide a circular distribution into a linear frequency curve. A change in the choice of origin of one class interval, or of just a few degrees, may make a considerable difference in the mean and variance calculated. In the majority of geological applications, therefore, where no base line or origin can be chosen a priori, the mean is not a good indication of preferred orientation direction, and the variance cannot be used as a reliable test of the significance of the distribution. Chayes (1954) offered a possible solution to this problem by devising a method of finding a minimum variance origin, but he also pointed out that, in the case of a good orientation, this origin could fall into a range of equally likely positions.

---

[1] Contribution from the Scripps Institution of Oceanography, New Series 832. This investigation was supported by a grant from the American Petroleum Institute, Project 51. Manuscript received March 8, 1955.

A vector method of analyzing orientation data is presented which avoids these difficulties, because the descriptive statistics used for preferred orientation direction and dispersion are independent of origin. A test of the significance of the results is also proposed which involves no additional computations but is a function only of the number of observations and the calculated dispersion.

The requirements of a method of analyzing orientation data are: (1) A measure of central tendency or preferred orientation direction which is independent of origin. (2) A measure of dispersion which is independent of origin. (3) A test of the statistical significance of the results against a model of randomness.[2] (4) A model distribution such as the circular normal or the linear normal distributions from which deviations can be tested.

Recent discussions in the literature prompted the writer to present the system outlined in the following section which has been used satisfactorily for the analysis of the preferred dimensional orientation of sand grains. Like the other methods which have been proposed it could be adapted to analysis of such orientation data as cross-bedding, fractures, fabric elements in deformed rocks, slope orientations, etc. Extension of this method to a three-dimensional study is also possible.

VECTOR METHOD

Reiche (1938) used a vector summation method of interpreting wind direction from measurements of cross-bedding in the Coconino sandstone. He computed the resultant vector direction as an indication of average wind direction and the vector magnitude, which he called "consistency ratio," as a measure of dispersion, or consistency of wind direction. This is essentially the same as the system proposed here. Krumbein (1939) applied such a vector method to orientation measurements of pebbles, but he failed to compute the magnitude of the vector as a measure of dispersion.

Each observation, be it a fracture, cross-bed, or particle long axis orientation, is considered a vector with direction and magnitude. The magnitude is generally considered unity, but it may be other than unity by weighting by cross-bed dip, by particle size or shape, etc. The north-south and east-west components of each observation vector are computed by multiplying the magnitude by the cosine and sine of the azimuth, respectively. These components are summed to give the components of the resultant vector, which again has a direction and a magnitude. The magnitude is reduced to a 0–100 per cent scale by dividing by the sum of all observation vector magnitudes (by the number of observations, if the observations are not weighted) and multiplying by 100. If, as in most practical applications, the computations are performed on the percentage of observations in each sector or group, the magnitude comes out in per cent without this last step. The calculations are outlined here:

---

[2] Pincus (1953) uses the term uniform rather than random. A uniform two-dimensional distribution is one in which each increment of angle contains the same frequency of occurrence of the angular variate. In this paper, the terms random, uniform, and rectangular distribution are used interchangeably, although G. A. Rusnak has pointed out to the writer that a random distribution is not necessarily uniform except in the case of an infinite population.

$$\text{N–S component} = \Sigma n \cos \theta \,,$$

$$\text{E–W component} = \Sigma n \sin \theta \,,$$

$$\tan \bar{\theta} = \frac{\Sigma n \sin \theta}{\Sigma n \cos \theta} \,,$$

$$r = \sqrt{(\Sigma n \sin \theta)^2 + (\Sigma n \cos \theta)^2} \,,$$

$$L = \frac{r}{\Sigma n} 100 \,,$$

where:

θ = azimuth from 0° to 360° of each observation or group of observations.

$\bar{\theta}$ = azimuth of resultant vector.

n = observation vector magnitude or, in the case of grouped data of unit vectors, it is the number of observations in each group.

r = magnitude of resultant vector.

L = magnitude of resultant vector in terms of per cent.

In the measurement of orientations of most sedimentary particles, no distinction is made of one end of the particle from the other. All measurements are, therefore, made in a range of 180°. If a 360° graph of the distribution is then desired, each grain is in effect plotted twice, once in the range measured, and again in the range 180°–360°. The resulting plot is symmetrical through the center. A resultant vector calculated on this symmetrical plot would be zero, because the diametrically opposed vectors would cancel each other. A vector calculated only on the 180° distribution would not be zero, but on the other hand, it may not reflect the true central tendency of the distribution. For example, if the 180° range lies in the eastern semicircle, the distribution has no west components at all. North components would tend to cancel south components, but no west components would be present to cancel east components; so the resultant vector would always possess a strong east component even if the true central tendency lay close to the north-south line. To remedy this (or to find the phase of the second harmonic by Fourier analysis), Krumbein (1939) doubled the angles of the observation vectors before computing the components, thus obtaining a nonsymmetric periodic distribution. This yields the vector magnitude and the tangent of twice the angle of the resultant. The calculations are:

$$\text{N–S component} = \Sigma n \cos 2\theta \,,$$

$$\text{E–W component} = \Sigma n \sin 2\theta$$

$$\tan 2\bar{\theta} = \frac{\Sigma n \sin 2\theta}{\Sigma n \cos 2\theta} \,,$$

$$r = \sqrt{(\Sigma n \sin 2\theta)^2 - (\Sigma n \cos 2\theta)^2}$$

$$L = \frac{r}{\Sigma n} 100 \,,$$

$$\bar{\theta} = \tfrac{1}{2} \arctan \frac{\Sigma n \sin 2\theta}{\Sigma n \cos 2\theta} \,.$$

These calculations can be performed on either grouped or ungrouped data. In practice, a simple and rapid scheme of working with grouped data and a desk calculator has been used with both weighted and unweighted data. Reiche (1938) used a graphical method in working with ungrouped, weighted data.

The vector direction is interpreted as a measure of the central tendency of the distribution, such as the preferred orientation direction of the long axes of sand grains. In this respect it is comparable to the mean but has the decided advantage of being independent of the reference direction or origin. The mean is very sensitive to the choice of origin, i.e., how the circular distribution is divided to make it into a linear distribution (Jizba, 1953, Chayes, 1954).

The vector magnitude varies from 0 per cent to 100 per cent. A random distribution of orientations will give a magnitude of 0 per cent, because all components cancel each other during summation. The vector direction is in this case indeterminate. A "perfect" orientation of 100 per cent means that all observation vectors have exactly the same phase, or, in the case of grouped data, they all lie within the same azimuth group. The vector magnitude is, therefore, a rather sensitive measure of dispersion and is comparable to standard deviation or variance, again with the advantage that it is independent of the choice of origin.

RELATION BETWEEN VECTOR MAGNITUDE AND STANDARD DEVIATION

If the standard deviation is computed for an orientation distribution, a tacit assumption is usually made that the distribution bears some resemblance to the gaussian linear normal, or bell-shaped curve. If we go a step further and assume, for the moment, that the distribution is exactly linear normal with a given standard deviation, and from tables find the ordinates for different parts of the distribution, we obtain figure 1, *A*. Next let us plot this as a polar co-ordinate plot by letting each ordinate in figure 1, *A* represent a radius in figure 1, *B*. The plotting was started at −360° and proceeded counterclockwise, setting the radii equal to the corresponding ordinates. From 0° to +360° the plotting is additive because the tails of the distribution overlap. The total radius for the south direction, for example, is the sum of the ordinates for plus and minus 180°.

This gives the "wrapped" normal distribution of Levy (1938) and Marcinkiewicz (1938), described by Gumbel, Greenwood, and Durand (1953).

Another way of graphically representing the distribution in figure 1, *B* is the equiareal graph of Leighly (1928), shown in figure 1, *C*. Because linear histograms and frequency curves are conventionally plotted in terms of area rather than height of ordinate, the frequency represented by any portion of the graph is proportional to the area. Hence, in order to apply an analogous significance to a polar co-ordinate type of graph, the frequencies should be represented along radii at distances from center corresponding to the square roots of the frequencies. The area of any sector or azimuth group will then represent the frequency of occurrence within that sector. A recent discussion of such graphs is given by Court (1952) and Gumbel *et al.* (1953).

The distribution in figures 1, *B* and *C* bears a qualitative resemblance to actual 0°–360° orientation distributions. The purpose of introducing this distribution is not to propose it as a model distribution at this time, but to point out some of the relationships between vector magnitude and standard deviation computed in two different ways. Model distributions are discussed in a later section.

Without a priori knowledge of the origin or mean of an orientation distribution, empirical data are obtained in a form such as 1, *B* or *C* without the inner part of the spiral. In order to analyze such data in terms of standard deviation, an origin or dividing point must be selected as 180° from the mode or vector direction, or the minimum variance origin (Chayes, 1954) must be located. After this is done, the distribution is replotted as a linear distribution. This has

(144)

been done in figure 1, *D* by plotting the radii in figure 1, *B* as the corresponding ordinates in figure 1, *D*. The inner parts of the spiral appear as disconnected tails in the linear plot, although these cannot be determined in empirical data: only the upper part of the curve from −180° to +180° can be distinguished. The distribution used in the example no longer bears much resemblance to a linear normal curve because of the vertical ends. In the example, the ordinates at plus and minus 180° are twice the height of the ordinates at these points in the original normal curve in figure 1, *A*.

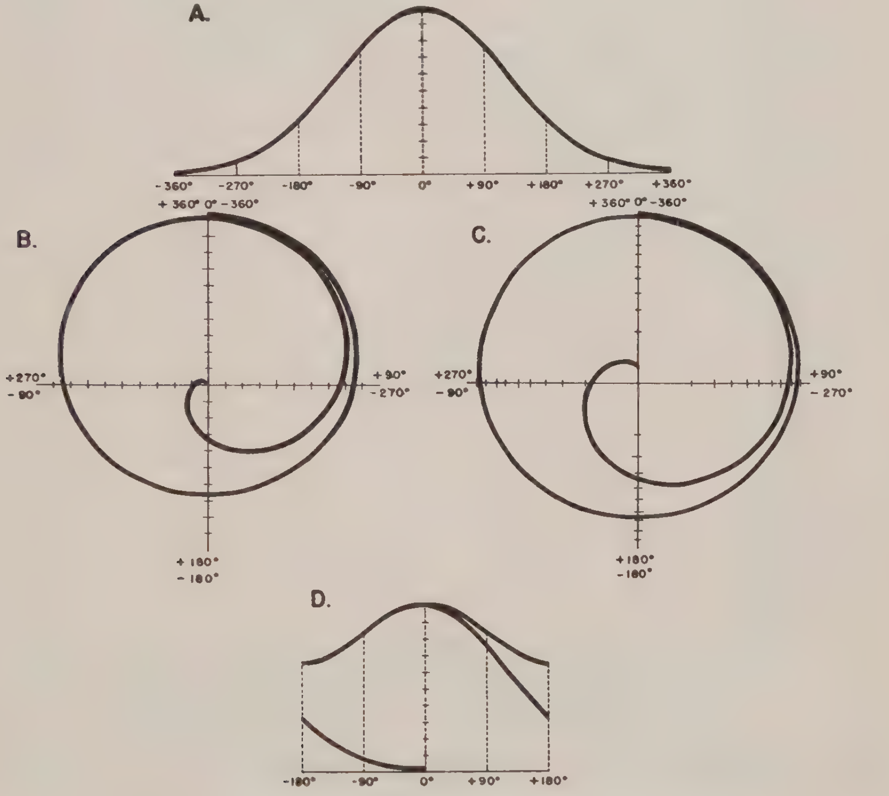

FIG. 1.—Derivation of the "wrapped" linear normal distribution

On the basis of this example, let us define some terms for use in the following sections. The standard deviation used in plotting figure 1, *A* is called the "true" standard deviation. In the example, it is: $\sigma_t = 120°$. The standard deviation calculated on the upper part of the curve in figure 1, *D* is the "calculated" standard deviation: $\sigma_c = 96.8°$. In analyzing the circular distribution in figures 1, *B* and *C*, for standard deviation, the first step is to find the vector direction (0°); set the mean equal to this; and finally compute the standard deviation around this defined mean. This, or a similar procedure, is the same as is done in analyzing an empirical distribution for standard deviation. For purposes of comparison, the vector magnitude for this distribution is: $L = 11.2$ per cent.

As a demonstration of the dangers of analyzing such distributions only by mean and standard deviation without re-sorting to a method of minimum variance (Chayes, 1954), or by positioning the mean to coincide with the vector direction, the calculations have been repeated after moving the origin or dividing point 20° to the right. The results are: $\bar{x}' =$ 15.6°, and $\sigma_c' = 97.4°$. The vector magnitude and direction are unaffected by this change in origin.

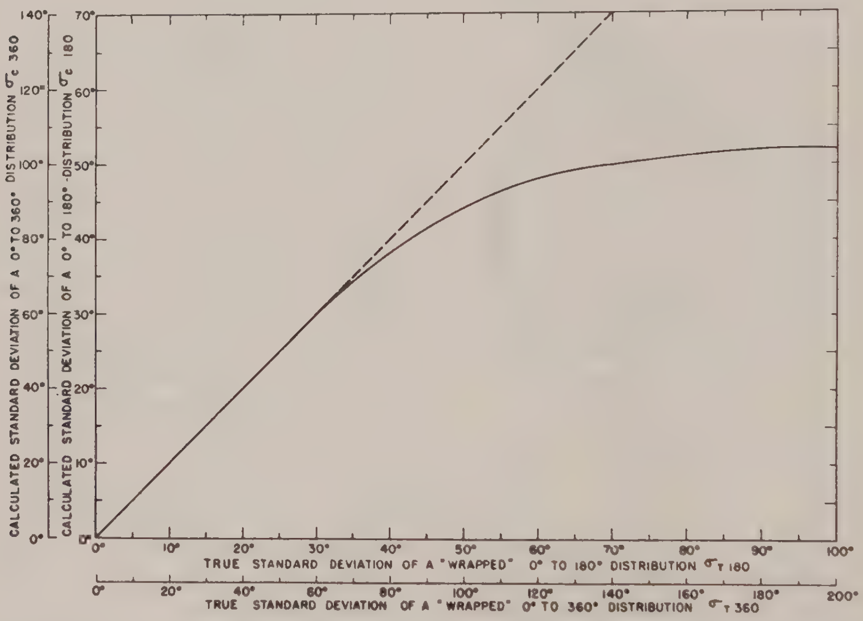

FIG. 2.—Relationship between the true standard deviation of a "wrapped" distribution and the calculated standard deviation.

In computing the standard deviation of empirical data, the result is the "calculated" standard deviation of a distribution like figure 1, *D*. If the distribution is linear normal, its actual form and standard deviation are as shown in figure 1, *A*, with the tails of the distribution extending indefinitely in both the plus and minus directions. When plotted in its circular form it is like figure 1, *B* and *C*. Therefore, the "calculated" standard deviation is only an operational substitute for the "true" standard deviation.

The differences between "true" standard deviation and "calculated" standard deviation are shown in figure 2. The diagonal straight line shows the line of perfect agreement. There is no difference below about 30° for a 180° distribution, and 60° for a 360° distribution. Below this point the tails of the distribution do not overlap, so that the plots corresponding to figures 1, *A* and *D* are identical. The calculated standard deviation approaches 52° (or 104°) as the distribution in figure 1, *D* approaches a rectangular or uniform distribution.[3]

Figure 3 shows the relationship between vector magnitude and the two standard deviations discussed previously. The curves coincide for vector magnitudes over about 60 per cent but diverge beyond that point. Also plotted are 46 points computed from two-dimensional sand-grain orientation data (measured as a 0°–180° distribution) for vector magnitude versus calculated standard deviation. In all cases the standard deviations were computed around the resultant vector. The computed trend line for the range 0–60 per cent vector magnitude is shown by means of a light solid line; one standard error on either side is shown with a light dashed line. The computed trend line, standard error of estimate, and correlation coefficient are:

---

[3] Griffiths and Rosenfeld (1953) demonstrated the derivation of the standard deviation of a rectangular distribution. This derivation need not be repeated here, but the result of the calculation is, for a distribution covering 180°, $\sigma = 51.96°$. For a distribution covering 360°, $\sigma = 103.92°$.

$$s_{c\,180} = 52.3 - 0.340\,L\,,$$

$$S_{s_c} = 0.50\,,$$

$$r = -0.994\,,$$

where:

$s_{c\,180}$ = empirical standard deviation as contrasted with theoretical standard deviation derived from an infinite population, represented by σ.

L = vector magnitude in per cent.

S_{s_c} = standard error of estimate.

r = correlation coefficient.

This computed trend line agrees very closely with the theoretical curve for calculated standard deviation and furthermore agrees closely with the theoretical maximum calculated standard deviation of 52°. This suggests that the model distribution used in the above discussion and in deriving figures 2 and 3 is suf-

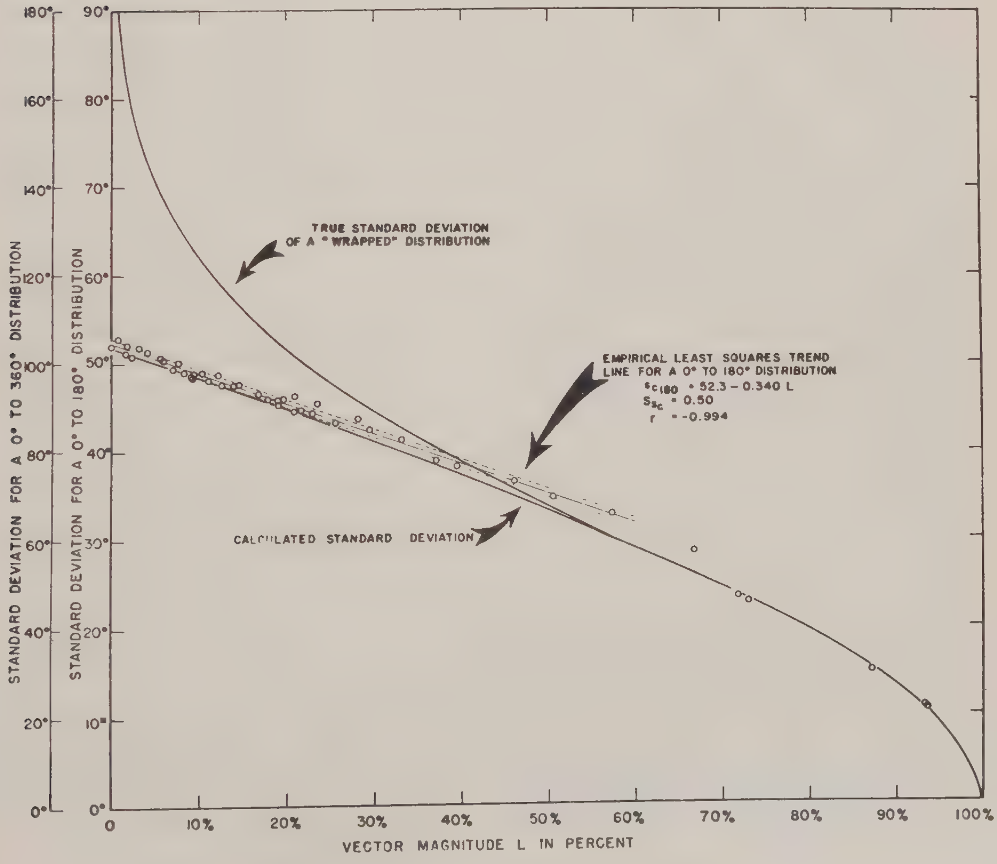

FIG. 3.—Relationship between vector magnitude and standard deviation

ficiently close to these empirical distributions to validate, in the first approximation, these theoretical aspects of the relationship between vector magnitude and standard deviation.

For purposes of analyzing dimensional orientation of the elongate sand grains in thin sections of modern sands, the writer has employed the vector direction and magnitude as routine descriptive statistics. The range of vector magnitudes for individual horizontal thin sections has been from about 1 per cent to about 30 per cent, with the great majority of magnitudes lying between 5 per cent and 20 per cent. Vector magnitudes of up to 45 per cent have been obtained for vertical thin sections.[4] Griffiths (1952) obtained a range of standard deviations of from about 51° to 35° in similar studies of vertical and horizontal thin sections, corresponding to a range of vector magnitude of 3–51 per cent. Reiche's (1938) work on cross-bed orientation yielded a range of "consistency ratio" of 0.44–0.86 for a 360° distribution (vector magnitudes of 44–86 per cent). Apparently the various geological uses of orientation data cover a wide range of azimuthal dispersion, but in any one application, the range may be more limited. The writer has been primarily interested in the lower part of the vector magnitude range. The part of the range utilized will have some bearing on the selection of a model distribution, as will be discussed in a later section.

For workers who for any reason prefer to use standard deviation rather than vector magnitude as a measure of dispersion, it is suggested that the vector direction be first computed as the mean and that the standard deviation be computed around this mean. This is somewhat comparable to Chayes' (1954) method of finding a minimum variance origin, but computationally it is perhaps easier, and it furthermore avoids the difficulty of the minimum variance origin falling into a range of possible values. Some consideration should be given to the advisability of using the "true" standard deviation if a linear normal model is to be used. One simple, although not rigorous, means of obtaining this value is to calculate the vector magnitude or the calculated standard deviation and convert to the "true" standard deviation by means of a graph such as figure 2 or figure 3. Conversion in the range of vector magnitude of 1–20 per cent can be made conveniently with a semilog graph of vector magnitude on a logarithmic scale versus "true" standard deviation on an arithmetic scale.

TEST OF SIGNIFICANCE

Several methods of testing the significance of two-dimensional orientation distributions against randomness have been proposed, but none of these published tests are felt to be entirely satisfactory.[5]

The chi-square test may be used to test the significance of the differences between a distribution and a model of randomness. The formula is:

$$\chi^2 = \Sigma\left[\frac{(f_o - f_e)^2}{f_e}\right]$$

---

[4] The calculated points in figure 3 for the range of from 30 per cent to 94 per cent were obtained from data on vertical thin sections. In a vertical plane, the elongate grains lie very nearly in the bedding or lamination planes or at an angle of imbrication. Also the more elongate grains are more perfectly aligned, so all of the very high vector magnitudes were computed for certain sphericity (in this case axial ratio) groups extracted from the total orientation distributions.

[5] Additional new tests of significance have been developed and distributed in unpublished form by J. W. Tukey and C. Eisenhart to various members of the Earth Sciences Panel of the American Statistical Association's Committee on Statistics in the Physical Sciences. These unpublished tests have not been considered here.

where: χ^2 = chi-square, f_o = the observed frequency in each group, f_e = the expected frequency in each group if the distribution is random. If the groups are of equal size, f_e is the same for all groups. The probability value is obtained from standard statistics tables knowing χ^2 and the number of degrees of freedom, usually taken to be the number of groups minus one.

The disadvantage of this test is that the deviations from randomness which produce a significant result do not necessarily represent a preferred orientation. This is true of most tests, but it appears to be more objectionable in this than in the other tests considered here because of the effect of random class to class variations.

Griffiths and Rosenfeld (1953) have proposed an *F* test as a means of evaluating the significance of orientation distributions. The *F* ratio is the ratio of the variance of a random or rectangular distribution over the variance of the observed distribution. A difficulty with this test is that, for maximum efficiency, the variance of the observed distribution should be the minimum variance, i.e., the minimum variance origin should be selected by the method of Chayes, or the mean should be taken as the summation vector direction. The test has been used successfully in many cases without this precaution, but the minimum variance is necessary when nonminimum variance fails to show significant difference from randomness.

Rayleigh (1894, p. 35–42) devised a distribution for describing random phases in sound waves. He was concerned with the resultant obtained by combining random isoperiodic vibrations of either equal amplitudes or unequal amplitudes. For either case:

$$p = e^{-r^2/n}$$

where p = probability of obtaining a greater amplitude by pure chance combination of random phases, r = resultant amplitude obtained, n = number of components or phases, e = base of natural logarithms.

The problem of combining isoperiodic vibrations and obtaining a resultant amplitude is identical to the analysis of geological orientation data, because each observation can be represented by a vector with direction and magnitude just as the vibrations are represented by a vector with phase and amplitude. The test is adapted to this application by expressing the resultant amplitude in terms of per cent as the vector magnitude:

$$L = (r/n)\,100$$

or

$$r = Ln/100\ .$$

Substituting:

$$p = e^{(-L^2 n)\,(10^{-4})}$$

where L = vector magnitude in terms of per cent, n = number of observations, p = probability of obtaining a greater amplitude by pure chance combination of random phases.

The results of the test can be expressed in a table or a graph as a function of vector magnitude and number of observations. It is most conveniently used in practice as a graph (fig. 4), because usually no standard number of observations are made per sample. As an example of the use of the graph, the probability is greater than 0.05 that a vector magnitude of 9.7 per cent or more will be obtained by pure chance in 270 observations. Any level of significance can be used, but the writer has found the 0.05 level convenient and practical for the study of sand-grain orientation. No distribution is accepted as being significantly different from randomness unless there are less than 5 chances in 100 of its being due to chance.

Sufficient data are provided in table 1 for construction of such a graph, using log-log graph paper. The vector magnitudes corresponding to the given probability levels are listed for $n = 100$, and for $n = 1{,}000$. For a given probability level, moving the decimal point two places to the right in n will move the decimal point one place to the left in L.

TABLE 1

RAYLEIGH TEST OF SIGNIFICANCE, VECTOR MAGNITUDE FOR DIFFERENT COMBINATIONS OF p AND n

p	$n=$ 100	$n=$ 1,000	p	$n=$ 100	$n=$ 1,000
10^{-20}	67.86	21.46	0.10	15.18	4.799
10^{-15}	58.77	18.58	.20	12.68	4.011
10^{-10}	47.99	15.18	.30	10.97	3.470
10^{-5}	33.93	10.73	.40	9.571	3.026
10^{-4}	30.35	9.597	.50	8.325	2.632
10^{-3}	26.28	8.311	.60	7.148	2.260
0.01	21.46	6.786	.70	5.975	1.889
.02	19.78	6.255	.80	4.722	1.493
.03	18.73	5.922	.90	3.240	1.025
.04	17.95	5.674	.95	2.258	0.7141
0.05	17.31	5.474	0.99	1.000	0.3162

For example, for $p = 0.05$, $n = 100$, $L = 17.3$ per cent; for $p = 0.05$, $n = 10{,}000$, $L = 1.73$ per cent. The values in the table were obtained by taking the natural logarithms of both sides of the equation, solving for L, and substituting the desired values of p and n.

Rayleigh (1894, p. 42) has provided the equations necessary for extending this test of significance to the analysis of three-dimensional orientation data.

Comparable results have been obtained in many cases using the chi-square and Rayleigh tests, but the F test has in all cases proved to be more sensitive. Many distributions which are indicated as being significant, or of a high order of significance, by the Rayleigh and chi-square tests are not significant or are barely significant by the F test. In no cases has the reverse been true.

The differences which have been observed between the results of the Rayleigh and chi-square tests appear to be a function of the vector magnitude and the number of observations. The Rayleigh test generally indicates a higher level of significance than chi-square for high vector magnitudes and for large numbers of observations. These differences are shown in figure 5 on a plot of number of observations versus vector magnitude. The symbol "R" represents a sample in which the Rayleigh test indicates a higher level of significance, i.e., a lower probability that the distribution could have arisen by chance sampling of a random population. The symbol "C" represents samples in which the chi-square test indicates a higher level of significance. The dots represent samples in which the tests give the same result. The data are clearly insufficient to do more than indicate general regions on the plot.

In practice the writer has found it convenient to use both chi-square and Rayleigh tests on all distributions measured. After a predetermined minimum of observations has been made, the results are checked occasionally by chi-square as the work progresses, and measurements are continued until the 0.05 level of significance is attained, or until it becomes apparent that a prohibitively large number of observations would be necessary to reach significance. The preferred orientation direction and dispersion are computed by the vector method, and the Rayleigh test is used as the final criterion of significance (except in the case of a polymodal distribution in which the vector is very weak).

Chayes (1949, p. 313) stated that disproof of a random orientation is not necessarily proof of a preferred orientation. This is true of the chi-square test, where the major contributors to the chi-square value may be random class to class variations, especially for small numbers of ob-

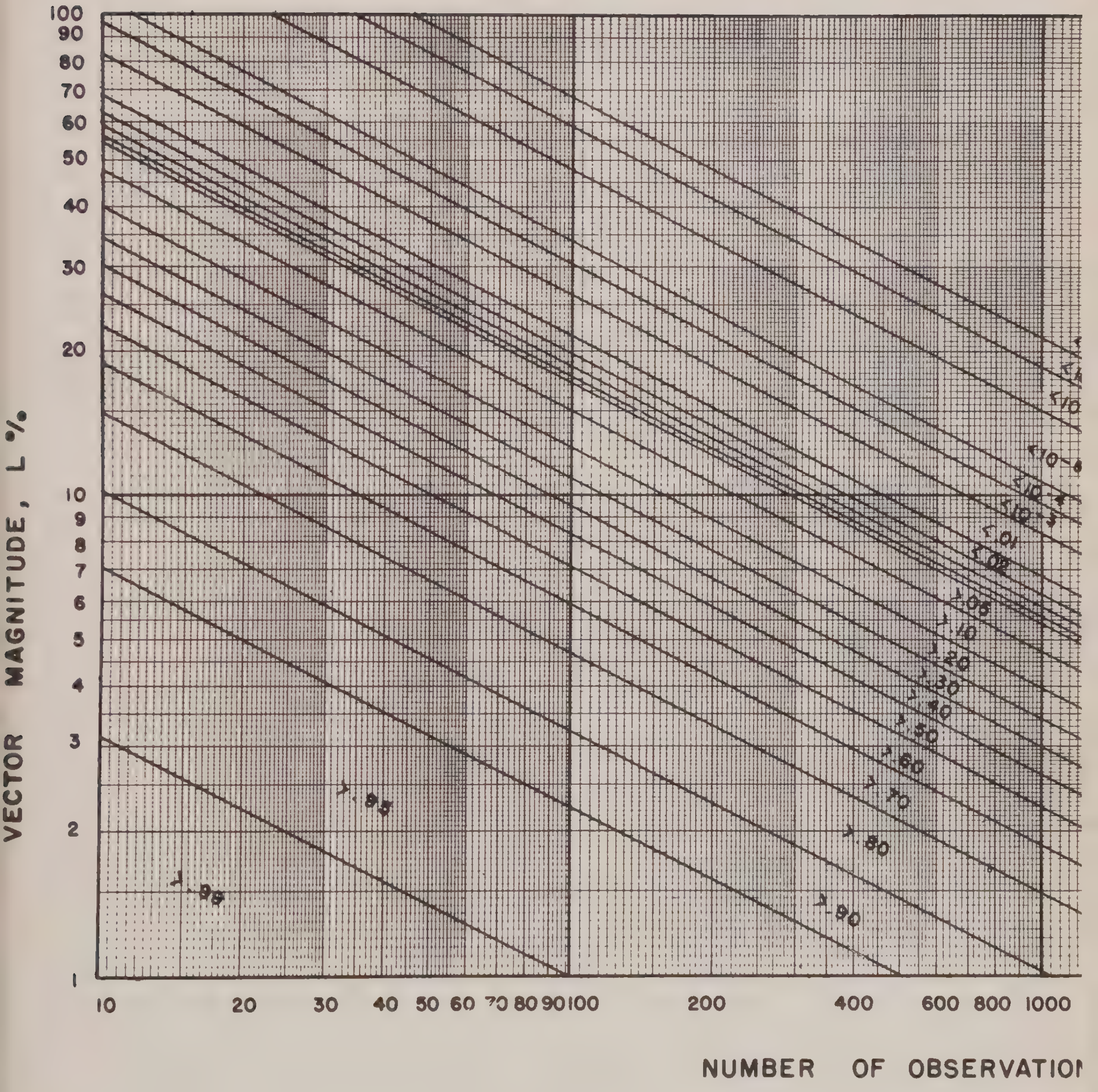

FIG. 4.—Rayleigh test of significanc

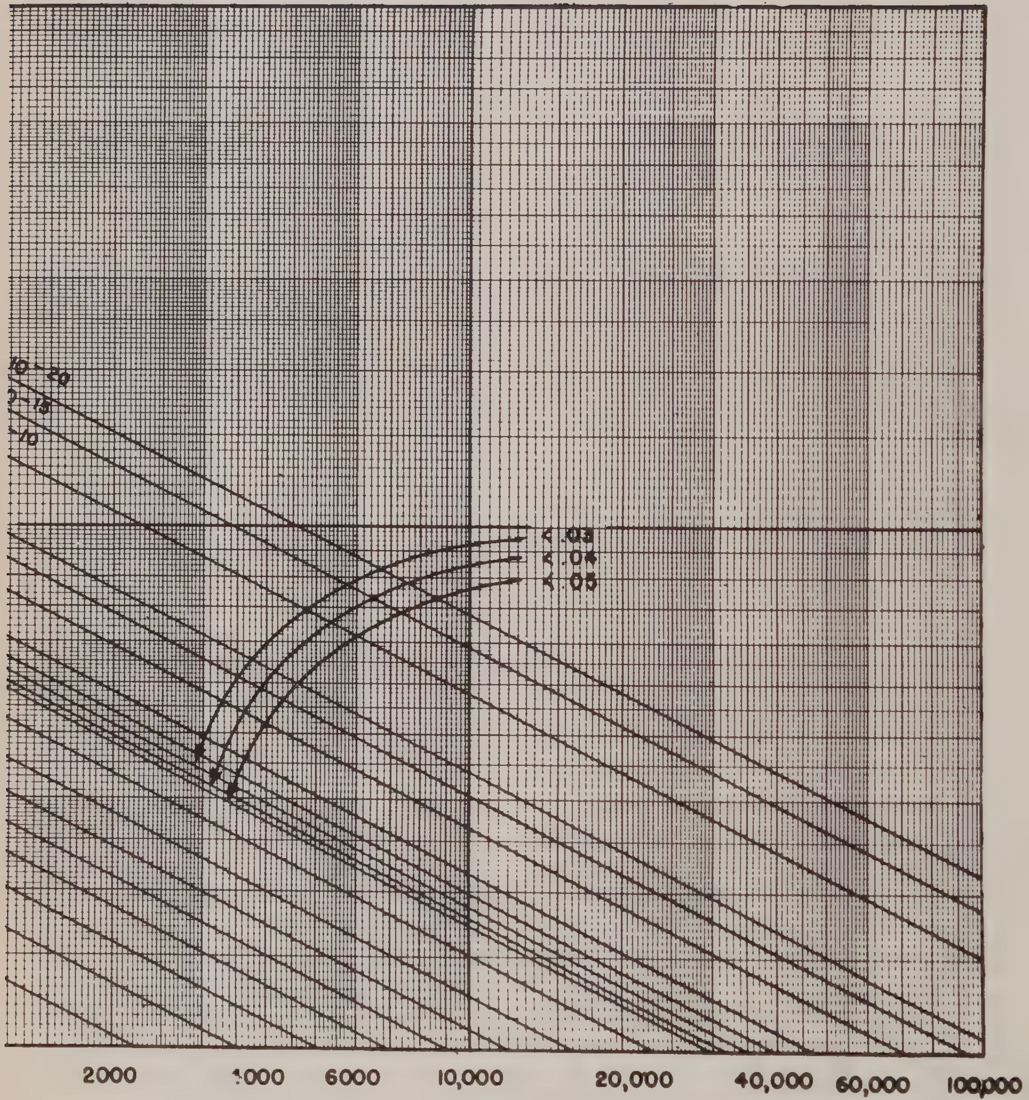
10 - 20
0 - 15
-10
A .03
A .04
A .05
2000
4000
6000
10,000
20,000
40,000
60,000
100,000

NS , n

e

servations. The statement is perhaps somewhat less true of the Rayleigh test. In this test, the individual class frequencies are not the basis for the test, but rather the cumulative effect or the vector sum. Thus a difference from randomness is indicated only for a combination of individual class frequencies which give a certain vector magnitude, or a certain preferred orientation. This is perhaps as close as we can expect to come to being able to classify a finite empirical distribution as showing preferred orientation or not showing preferred orientation.

COMPARISON WITH MODEL DISTRIBUTIONS

It is desirable to compare the measured frequency distribution with a model (Pincus, 1953) or theoretical distribution to determine whether the sample data fit the model. The goodness of fit of the data to the model can be tested with chi-square. If the empirical data can be demonstrated to fit a model, the equation of the model can then be used to describe the empirical distribution as is done with the linear normal distribution in so many applications.

The raw data and statistics for the two distributions to be tested are given in table 2. Both are composites of several samples (thin sections cut parallel to the laminations) of Recent Gulf Coast beach sand which were artificially lithified with plastic during the sampling. The orientations of the least projection elongations (Dapples and Rominger, 1945, p. 251) of a random sampling (by point counter) of the grains in the sections were measured as a 0°–180° distribution, and recorded in 10° sectors. Vector summation and tests of significance were performed on the distributions resulting from both the individual thin sections and from composites of groups of thin sections.[6]

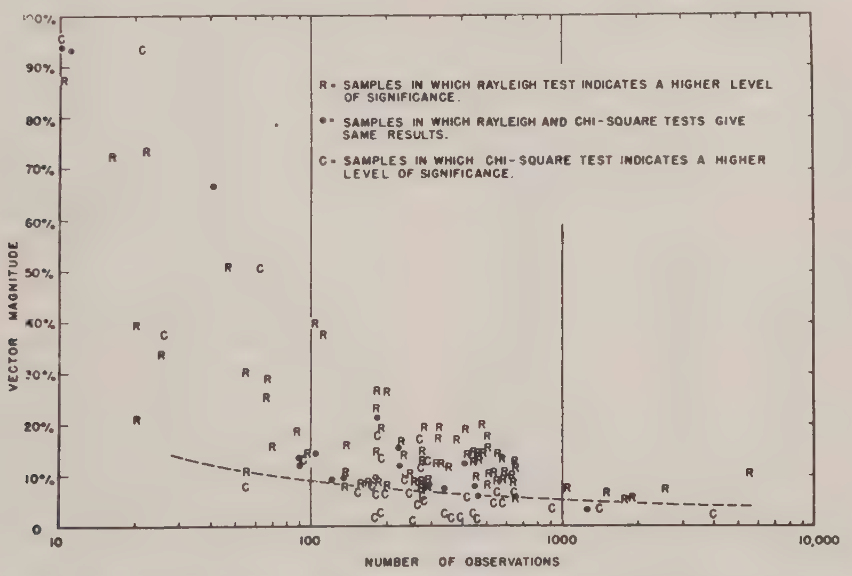

FIG. 5.—Comparison between results of Rayleigh and chi-square tests of significance

---

[6] The dimensional preferred orientation directions of sand grains tend to lie parallel to the direction of flow of the depositing medium. Thus in a sand from the wave-washed part of a beach, the preferred orientation direction is approximately

Only the composites will be considered here, as summarized in the table and illustrated in equiareal polar co-ordinate plots in figure 6, along with the models to be tested.

The results of the tests against several possible models are summarized in table 3 and are discussed more fully here:

1. Test against randomness by the Rayleigh test. Both distributions are significantly different from randomness by this test, especially the one with the higher vector magnitude and larger number of grains.

TABLE 2

SAND-GRAIN ORIENTATION RAW DATA AND STATISTICS

Sector or Statistic	Composite A	Composite B
0° Sector	59 Grains	244 Grains
10	59	262
20	48	246
30	41	290
40	40	284
50	49	314
60	58	326
70	73	340
80	50	371
90	59	401
100	74	382
110	66	332
120	69	322
130	58	295
140	68	230
150	57	256
160	58	263
170	67	281
Total	1,053 Grains	5,439 Grains
No. Samples	5	20
θ	121°	85°
L	7.78 per cent	10.21 per cent
s_t	65°	61°
s_c	49.7°	48.8°
k	0.158	0.205

2. Test against randomness by chi-square test. Both are again significantly different from randomness, but are less so than by the other test. This is the region of figure 4 in which the Rayleigh test indicates the higher order of significance.

3. Test against the circular normal distribution by chi-square. To obtain these distributions, the vector magnitude was converted to parameter *k* by reference to table 2, Gumbel *et al.* (1953). Radii for the sectors were taken from table 3 (*ibid.*) and the angles halved to obtain a 180° distribution. Testing with chi-square reveals that while neither distribution differs from the models at the 0.05 level, the fit does perhaps leave something to be desired. This failure may be due to the fact that both distributions are made up of several component distributions which should be separated and tested individually (Gumbel, 1954).

4. Test against a "wrapped" linear normal distribution by chi-square. The standard deviation ("true," s_t) of this distribution is obtained from figure 3, and ordinates for the 10° sectors are taken from standard statistical tables. Ordinates for the overlapping tails of the distributions are added as shown in figure 1. Testing with chi-square reveals that distribution B differs significantly from its model, but that distribution A does not.

5. Test against a "chopped" linear normal distribution by chi-square. The standard deviation (s_c) of this distribution was obtained from figure 3, and ordinates were taken from standard statistical tables for this standard deviation. In this distribution the tails are simply chopped off at plus and minus 90° from the vector direction. Back calculation of standard deviation from the resulting distribution will not give the same value as was utilized in setting up the model except for a standard deviation of about 30° or less. While the level of significance of the difference between the observed

---

perpendicular to the trend of the beach and hence to the long axis of the sand body. In a fluvial sand, on the other hand, the preferred orientation direction is parallel to the trend of the elongate sand body.

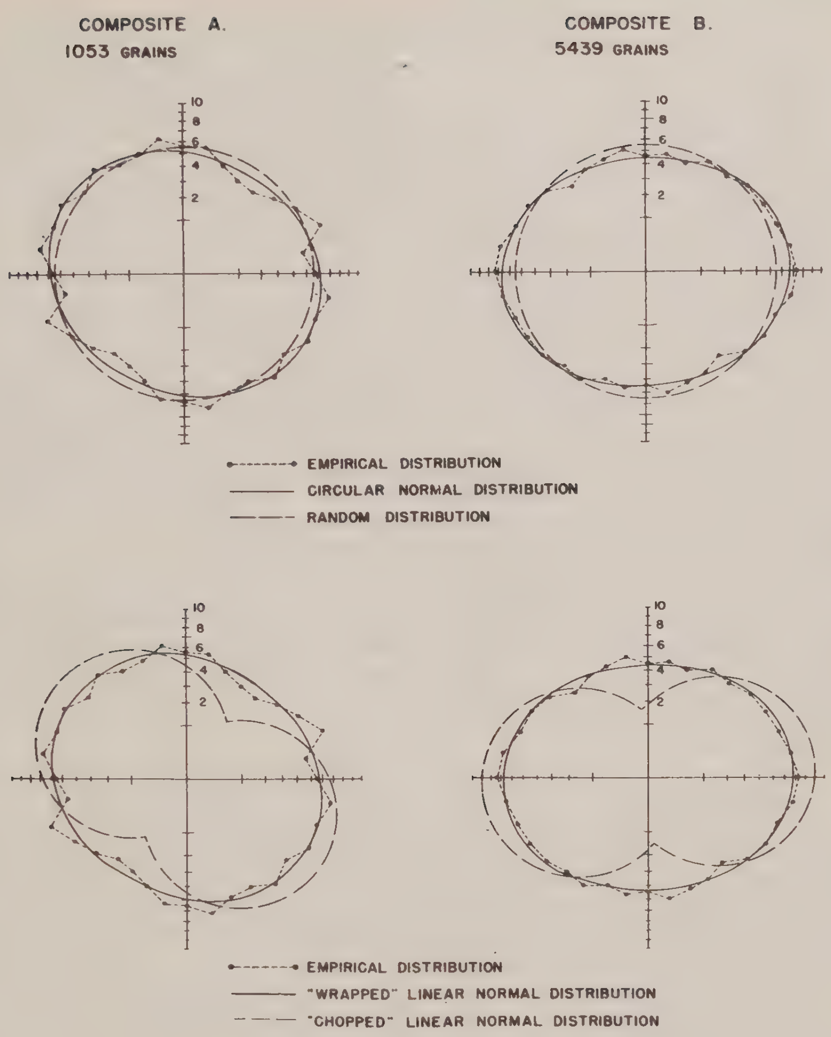

Fig. 6.—Comparison between empirical and model distributions

TABLE 3

Tests of Empirical Distributions against Model Distributions

Model and Test	Composite A χ^2	Composite A p	Composite B χ^2	Composite B p
Randomness by Rayleigh test		<0.01		$<10^{-24}$
Randomness by chi-square	29.1	$<.05$	140.1	$\ll 0.001$
Circular normal by chi-square	17.2	$<.50$	24.9	$<.10$
"Wrapped" linear normal by chi-square	17.5	$<.50$	30.1	$<.05$
"Chopped" linear normal by chi-square	137.8	$\ll 0.001$	845.8	$<<< 0.001$

distributions and the models is tremendous, it might not be too unreasonable to expect a somewhat closer agreement in the case of a very well oriented distribution (less than 30°).

It is suggested that more empirical distributions be tested against these models and others in order to determine which model distribution is most appropriate for the various kinds of orientation distributions. From the tests discussed above, it appears that the circular normal distribution and the "wrapped" linear normal distribution fit about equally well, although many more tests of goodness of fit should be tried. No tests have been made of distributions with low standard deviations but it is believed that the linear normal distributions (which coincide below about 30°) may provide satisfactory models in this range of dispersion.

CONCLUSIONS

Although there are many diverse applications of orientation studies in geology, it is believed that the same basic methods of analysis can be used for all. In the past, the tendency has been to apply the conventional methods of analyzing linear distributions to this entirely different study of circular distributions. The results of such studies are now clouded in doubt by the subsequent re-evaluation of the methods utilized. A more logical approach to the problem would be to analyze circular data directly in their circular form by a method of vector analysis. As a measure of dispersion, either the vector magnitude or the standard deviation computed around the vector direction can be used.

Use of a single test of significance and a single model distribution is not advisable until we are more familiar with the characteristics and variations possible in orientation distributions. It is hoped that other investigators will try the tests and models discussed here to help evaluate their applicability.

Extension of the vector methods and the Rayleigh test to the analysis of three-dimensional orientation studies follow as logical steps. The spherical probability distribution is a possible model.

Acknowledgments.—The writer is indebted to G. M. Webster of the Carter Oil Company for suggesting the use of the Rayleigh distribution and the circular normal distribution. The following have read the manuscript and suggested valuable changes: M. A. Rosenfeld and M. Foster of the Magnolia Petroleum Company, R. L. Miller and G. A. Rusnak of the University of Chicago, D. L. Inman and P. Rudnik of the Scripps Institution of Oceanography, and G. M. Webster of the Carter Oil Company. Other suggestions were made by F. P. Shepard, R. J. Hurley, and D. G. Moore of the Scripps Institution. All of the illustrations were prepared by J. R. Moriarty.

REFERENCES CITED

Chayes, F., 1949, Statistical analysis of two-dimensional fabric diagrams; Statistical analysis of three-dimensional fabric diagrams, p. 297–326, *in* Fairbairn, H. W., Structural petrology of deformed rocks: 344 p., Cambridge, Mass., Addison-Wesley Press.

——— 1954, Discussion: Effect of change of origin on mean and variance of two-dimensional fabrics: Am. Jour. Sci., v. 252, p. 567–570.

Court, A., 1952, Some new statistical techniques in geophysics, p. 75–85, *in* Advances in geophysics, v. 1: 362 p., New York, Academic Press, Inc.

Dapples, E. C., and Rominger, J. F., 1945, Orientation analysis of fine-grained sediments: a report of progress: Jour. Geology, v. 53, p. 246–261.

Griffiths, J. C., 1952, A review of dimensional orientation of quartz grains in sediments: Pennsylvania State College, Min. Ind. Expt. Sta. Bull. 60, p. 47–52.

——— and Rosenfeld, M. A., 1953, a further test of dimensional orientation of quartz grains in Bradford sand: Am. Jour. Sci., v. 251, p. 192–214.

Gumbel, E. J., 1954, Applications of the circular normal distribution: Jour. Am. Stat. Assoc., v. 49, p. 267–297.

——— Greenwood, J. A., and Durand, D., 1953, The circular normal distribution: Theory and tables: Jour. Am. Stat. Assoc., v. 48, p. 131–152.

Jizba, Z. V., 1953, Mean and standard deviation of certain geological data: a discussion: Am. Jour. Sci., v. 251, p. 899–906.

Krumbein, W. C., 1939, Preferred orientation of pebbles in sedimentary deposits: Jour. Geology, v. 47, p. 673–706.

Leighly, J. B., 1928, Graphic studies in climatology: The polar form of diagram in the plotting of the annual climatic cycle: Univ. Calif. Pub. in Geography (Berkeley), v. 2, p. 387–407.

Lévy, P., 1938, Sur l'arithmétique des lois de probabilités enroulées: Soc. Math. Frances, Comptes Rendus, p. 32.

Marcinkiewicz, J. M., 1938, Sur l'arithmétique des lois de probabilités enroulées: Soc. Math. Frances, Comptes Rendus, p. 34.

Pincus, H. J., 1953, The analysis of aggregates of orientation data in the earth sciences: Jour. Geology, v. 61, p. 482–509.

Rayleigh, Lord (Strutt, J. W.), 1894, The theory of sound, 2d ed., v. 1: 480 p., New York, reprinted in 1945 by Dover Publications.

Reiche, P., 1938, An analysis of cross-lamination: The Coconino sandstone: Jour. Geology, v. 46, p. 905–932.

PHOTOSYNTHETIC INDUCTION IN MARINE ALGAE

By K. A. Clendenning and F. T. Haxo

Reprinted from Canadian Journal of Botany, 34 : 214-230. 1956
Reproduced by Permission

PHOTOSYNTHETIC INDUCTION IN MARINE ALGAE[1]

BY K. A. CLENDENNING[2] AND F. T. HAXO[3]

Abstract

Effects of dark time and of oxygen supply upon photosynthetic induction in *Ulva* were investigated polarographically and manometrically. Under continuously aerobic conditions, the induction period was of about two minutes' duration following one day in darkness in flowing sea water; beyond 10 min., length of the aerobic dark period had little effect. The induction period was lengthened by dark anaerobiosis, but was not eliminated entirely by dark aeration or oxygenation treatments. Aerobic induction periods of similarly brief duration were observed in *Ulva*, *Gigartina*, and *Gelidium* fronds which corresponded with those established previously for leaves and unicellular algae. Aerobic induction is attributed to an initial lack of "CO_2-acceptor" which is regenerated photosynthetically. Interpretations are provided for the widely different induction periods and saturating carbon dioxide concentrations which had been observed in earlier studies of photosynthesis in attached marine algae.

Introduction

The apparent duration of aerobic induction periods in attached marine algae has varied greatly in studies of their photosynthesis (4, 11, 19, 23). In the earliest study of photosynthetic induction, Osterhout and Haas (19) observed that photosynthesis in *Ulva* underwent a large and progressive increase during the first hour of saturating illumination, after which it proceeded at a uniform rate. Their photosynthesis measurements were based on an indicator method for dissolved carbon dioxide, and were preceded by overnight dark treatments in flowing sea water. Equally lengthy induction periods were observed under similar conditions in *Enteromorpha*, *Hydrodictyon*, and *Spirogyra*, and in *Potamogeton* leaves (19). Blinks and Skow (4) observed induction periods of "many minutes" duration when *Ulva* was subjected to overnight anaerobic dark treatments. The induction periods otherwise were of less than two minutes' duration when samples of *Ulva* fronds and *Potamogeton* and *Ricinus* leaves were examined by the platinum electrode method for dissolved oxygen (4). Blinks and Skow concluded that photosynthetic induction is probably caused by oxygen deficiency in the preceding dark period: "An induction period is . . . . absent even after rather long dark periods, provided the plant has been kept well aerated." Tseng and Sweeney (23) observed long induction periods (20–30 min.) in the red alga *Gelidium* by the Winkler method for dissolved oxygen. The respiratory absorption of oxygen and R.Q. values which Tseng and Sweeney observed in their darkened "control" samples showed that aerobic conditions were provided during their photosynthesis measurements. Emerson and Green's manometric studies of the red alga *Gigartina* (11) were made on small samples of low respiratory activity suspended in sea water which was shaken almost continuously under air (natural sea water under air, and under 5% CO_2 in air; artificial sea water under 5% CO_2 in air, and bicarbonate-buffered artificial sea water under air). The full rate of photosynthesis was observed after from 15 to 40 min. of saturating illumination in these media.

---

[1] *Manuscript received September 28, 1955.*
Contribution from the Charles F. Kettering Foundation, Yellow Springs, Ohio; the Scripps Institution of Oceanography, University of California, La Jolla, Calif., New Series No. 833, and the Marine Biological Laboratory, Woods Hole, Mass.
[2] *Research Biochemist, Charles F. Kettering Foundation, Yellow Springs, Ohio.*
[3] *Chairman, Division of Marine Botany, Scripps Institution of Oceanography, University of California, La Jolla, Calif.*

The measurement of photosynthesis in marine algae introduces special problems. Natural sea water usually contains *ca.* 3.5% dissolved salts, 2.0×10^{-3} *M* bicarbonate, and about 1×10^{-5} *M* dissolved carbon dioxide (22). The pH varies from 7.5 to 8.4 under natural conditions (22) but is usually in the range 7.8–8.1. The magnesium and calcium carbonate contents are close to saturation (22), and carbonate precipitation is promoted by the addition of bicarbonate and by the photosynthetic removal of carbon dioxide. Photosynthesis in the ocean is not limited by the natural supply of carbon dioxide (22), but the amount of plants per unit of volume is infinitely smaller ($< 10^{-6}$) than in mass *Chlorella* cultures or in the algal suspensions ordinarily used in photosynthesis research. (Strain (21) concluded on the basis of chlorophyll analyses that there are scarcely enough algae in the oceans to form a compact surface layer one cell deep.) When the algal density is increased for laboratory studies, larger reservoirs of carbon dioxide are required. If the sea water is supplemented with minimal amounts of carbon dioxide or bicarbonate, the system is weakly buffered so that large changes in CO_2 concentration and pH occur during photosynthesis measurements. If sea water is equilibrated with 5% CO_2 in air, as in two-vessel manometry, the algae are exposed to more than 100 times greater carbon dioxide and hydrogen ion concentrations than those of the natural environment. (Photosynthesis in *Gelidium* was reduced *ca.* 30% by six hours' immersion in sea water having a pH of 6.7 (23).) If concentrated bicarbonate buffers are added, magnesium and calcium carbonates are precipitated progressively, with attending pH changes. Bicarbonate buffers cannot be used as simple aqueous solutions, as with *Chlorella*; their use in monovalent chloride solutions isotonic with sea water has been discouraged by the detrimental effects of such solutions on marine algae (3).

A suitable medium for laboratory measurements of photosynthesis in marine algae would be isotonic with natural sea water and would contain calcium and magnesium for purposes of "salt antagonism" (3), but in sufficiently reduced amounts for bicarbonate buffering at any required molarity and pH. As one part of this study, the calcium and magnesium contents of natural and artificial sea water were reduced so that bicarbonate buffers could be employed at any desired strength. The effects of substituting artificial sea water, modified in this way, for natural sea water, and the effects of bicarbonate molarity at constant pH upon steady-state photosynthesis in *Ulva* were determined. Modified polarographic and manometric methods were devised with which photosynthetic induction periods of equal duration were observed in parallel applications to samples from a single frond. The original experiments of Osterhout and Haas (19) were repeated on *Ulva* collected in the same locality, and the effects of dark treatments and of oxygen supply upon photosynthetic induction were established polarographically and manometrically. Induction in *Gelidium* (23) and *Gigartina* (11) was also re-examined.

Materials and Methods

Algae

Vegetative fronds of *Ulva lactuca* var. *rigida* (15) (or *U. rigida* (19)), collected near Woods Hole, Mass., were maintained in flowing sea water for up to two days before use in the research on methods. Disks were freshly cut from adjoining parts of the same frond in the methods' studies, and disks of unimpaired activity also were tested successively in different media. Representative samples had a fresh weight of 9.7 mgm./cm.^{2}, dry weight 2.3 mgm./cm.^{2}, and a chlorophyll content of 1.7 mgm./dm.^{2}. The fronds employed in studies of induction were selected from collections made shortly before each experiment. *Gelidium pulchrum* and *Gigartina armata* were collected near La Jolla, Calif.

Sea Water Media

Emerson and Green (11) suggested that the calcium and magnesium contents of artificial sea water might be reduced without unfavorable effects in short-term experiments, thus enabling the use of concentrated bicarbonate buffers. We have explored this possibility, using artificial sea water with the same basic formula as was employed by these workers. Upon reducing the calcium and magnesium contents to one-fourth, while maintaining the ionic strength with extra sodium or potassium chloride, carbonate precipitation did not occur in the presence of 0.025 *M* bicarbonate buffers. The concentration of dissolved carbon dioxide provided by bicarbonate buffers is increased by the sea water salts, and our studies have shown that it is seldom necessary to employ a bicarbonate concentration above 0.025 *M*. When the calcium and magnesium contents were reduced to 1/10th, 0.1 *M* bicarbonate buffers could then be employed*; the artificial sea water used in the calibration studies reported below contained only 1/10th the usual amount of calcium and magnesium.

Natural sea water was used in comparative studies of media without modification as well as after it was decarbonated by boiling with hydrochloric acid (20% vol. loss, pH 4.5): the cooled solution was adjusted to pH 7.0 with carbonate-free sodium hydroxide and diluted to original volume. Such solutions retain trace elements of natural sea water. In contrast, the artificial sea water was employed without supplementary trace elements.

---

* *Artificial sea water of reduced calcium and magnesium content has also been successfully used in photosynthesis measurements on the halophytic red alga Porphyridium cruentum, and on a wide variety of green, brown, and red marine algae (F. T. Haxo, unpublished), as well as in studies of the marine dinoflagellate Gonyaulax (16).*

(160)

Natural sea water may be used with quite concentrated bicarbonate buffers if part of the calcium and magnesium is removed beforehand with carbonate. Using sea water obtained at Woods Hole, Mass., and Miami, Fla., treatment with 0.025 *M* and 0.05 *M* Na_2CO_3 (solid) removed sufficient calcium and magnesium to allow the decarbonated filtrate to be employed with 0.015 *M* and 0.025 *M* bicarbonate buffers respectively at pH 8.5. Alternatively, residual carbonate in the clear filtrate may be used as the source of carbon dioxide by adjustment of the pH downward to 8.5 before use. These treatments involve small salinity changes which could be corrected by volume adjustment.

Carbon Dioxide Concentration

Dissolved carbon dioxide in bicarbonate-buffered artificial sea water (Table I) was calculated with Buch's dissociation constants for bicarbonate/carbonate in sea water at 25° C., chlorinity 19 : $\mathrm{p}K_{C1} = 5.939$ (9); $\mathrm{p}K'_2 = 8.95$ (8). Buch (8) has shown that the same dissociation constants may be used in estimating carbon dioxide concentrations in artificial and natural sea water of the same salinity.

The Platinum Electrode Method

In earlier applications, thallus strips were pressed against a flat platinum electrode either with a thin disk of agar (4) or with a band of cellophane which was tightened with a winding rod (14). Fruiting margins of *Ulva* thallus have a high respiration rate, and they exhibited lengthy "anaerobic-type" induction periods when examined by the platinum electrode method (15). For the present studies, this method was modified so that one side of

TABLE I

CARBON DIOXIDE CONCENTRATIONS IN BICARBONATE-BUFFERED ARTIFICIAL SEA WATER (CHLORINITY 19, 25° C., $\mathrm{p}K'_2 = 8.95$, $\mathrm{p}K_{C1} = 5.939$)

	Bicarbonate–carbonate molarity		
	0.015 *M*	0.025 *M*	0.05 *M*
pH	Dissolved CO_2, moles/liter $\times 10^{-5}$		
7.7	24.6	41.0	82.1
7.8	19.3	32.1	64.2
7.9	15.1	25.1	50.2
8.0	11.7	19.5	39.0
8.1	9.44	15.6	30.2
8.2	6.98	11.6	23.3
8.3	5.34	8.87	17.8
8.4	4.04	6.73	13.5
8.5	3.04	5.07	10.1
8.6	2.26	3.77	7.54
8.7	1.66	2.77	5.54
8.8	1.21	2.01	4.03
8.9	0.86	1.44	2.88
9.0	0.61	1.03	2.05

the thallus was in as close contact with the electrode as before, but with the other side in immediate contact with agitated sea water. The ends of thallus strips were rolled over aluminum foil and sewn to adjustable supports with which the thallus was drawn firmly against the electrode for photosynthesis measurements. During lengthy dark treatments, the thallus was released so that both its surfaces were bathed with agitated sea water. Oxygen consumption by the electrode in darkness was minimized by turning off the polarizing current except for a few minutes prior to illumination (saturating white light, *ca.* 25° C.). Galvanometer readings were made visually at minimum intervals of five seconds. The apparatus and conditions otherwise were similar to those used in earlier studies (14, 15). Our polarographic measurements differed from those of Blinks and Skow (4) in that we employed a higher (saturating) light intensity, a higher carbon dioxide concentration, and longer successive periods of illumination.

Manometric Methods

Warburg's method (27) involving intermittent illumination was modified for marine algae as follows: a small frond sample was placed in 5 ml. of artificial sea water containing at least 0.015 *M* bicarbonate/carbonate, pH 8.5–8.7. After dark equilibration (220 r.p.m., 1.6 cm. stroke), the vessels were illuminated briefly with saturating white light for different lengths of time; the illumination periods were separated by 10 min. dark intervals. After each illumination, the manometers were read successively at one minute intervals until the full yield of oxygen was observed. This method was useful in reference applications, but was unsuitable for use with lengthy dark periods.

A few measurements of photosynthesis in *Ulva* were made by the two-vessel method. Matched disks were placed in 7 ml. artificial or natural sea water contained in rectangular vessels of unequal volume. The vessels were gassed with 5% CO_2 in air, equilibrated in darkness, then illuminated with saturating light for two hours. The gas solubilities used in the two-vessel equations were $\alpha_{CO_2}^{25°} = 0.68$, $\alpha_{O_2}^{25°} = 0.022$ (22).

Direct measurements of photosynthetic capacity were made under conditions physically similar to those employed by Emerson and Green (11). A small thallus disk (1.8 cm.^{2}) was placed in a rectangular vessel with 7 ml. artificial sea water of reduced calcium and magnesium content, containing at least 0.015 *M* bicarbonate. Oxygen evolution under an atmosphere of air was determined by simple manometry at pH 8.4–8.7. For direct manometric measurements of the initial time course, the thallus area was increased, the liquid volume and vessel size was reduced, and the vessels were shaken at high speed. Narrow rings of filter paper were placed around the outer and inner edges of the main compartment of a conical vessel having a center well and venting sidearm. An annular ring of thallus, area 6 cm.^{2}, was blotted and placed on the bottom of the vessel, between the rings of filter paper. From 1 to 2 ml. of bicarbonate-buffered artificial sea water, initial pH 8.5–8.6, was placed on the thallus, and a further milliliter was placed in the sidearm. The vessel was shaken (180 2-cm. oscillations/min.) so that a ripple of sea water crossed the thallus six times each second. The liquid in contact with the thallus remained in equilibrium with that which was held loosely in the filter paper. After dark equilibration, the thallus was illuminated with saturating white light.* The time course of photosynthesis was followed at one minute intervals, and the extra milliliter of sea water was tipped in after a steady rate of photosynthesis was attained. Manometric response was very rapid and carbon dioxide exchange could be neglected under these conditions.

Results

Photosynthesis in Bicarbonate-buffered Sea Water

In selecting a medium for use in direct manometric measurements, it was necessary to determine the effect of substituting artificial for natural sea water, and to establish the bicarbonate molarity, pH, and CO_2 requirements.

When 1.8 cm.^{2} *Ulva* disks were illuminated in 7 ml. natural sea water, initial pH 7.9, the pressure increments rose during the first 20 min., after which they remained relatively constant for 40 min. The pH rose from 7.9 to 8.4–8.5 during one hour of saturating illumination, which would be associated with a decrease in the carbon dioxide concentration from *ca.* 12 to 3×10^{-6} M. The observed net rate of photosynthesis during the second and third 20 min. periods was 20–25 mm.^{3} O_2/hr./cm.^{2}, using fresh as well as recently boiled sea water. Upon incorporating 0.015 M $KHCO_3$ – 0.001 M Na_2CO_3 ("E" buffer (11)) in decarbonated sea water, the corresponding rate of photosynthesis ($H \cdot Ko_2$ for 20–60 min.) was 43–46 mm.^{3} O_2/hr./cm.^{2} in samples from the same frond. Upon incorporating "E" buffer in artificial sea water containing 1/10th calcium and magnesium, the rate of photosynthesis was again 43–46 mm.^{3} O_2/hr./cm.^{2} (duplicate measurements). Two-vessel measurements in artificial sea water under 5% CO_2 showed 39.3 mm.^{3} O_2 evolved and 39.8 mm.^{3} CO_2 absorbed per hour per cm.^{2}, again using disks from the same frond. A repetition of the above experiment on freshly harvested *Ulva* revealed approximately equal rates of photosynthesis in natural sea water under 5% CO_2, in decarbonated sea water plus "E" buffer, and in artificial sea water plus "E" buffer (55–60 mm.^{3} O_2/hr./cm.^{2}). When the initial pH of the artificial sea water was adjusted to 8.65, the rate of photosynthesis during the first hour remained the same as under 5% CO_2 in air. Artificial sea water thus could be substituted for natural sea water in experiments involving up to two hours immersion, and a saturating supply of carbon dioxide was provided by Emerson and Green's "E" buffer at an initial pH of 8.65.

---

* *Collimated light from a 1000 watt projection lamp was filtered through 3 in. of M/35 copper sulphate and through 18 in. of water before entering the vessel. No manometric response was detected upon illuminating heat-inactivated thallus under nitrogen with 5400 ft.-c. white light under these conditions. The saturating light requirement for Ulva at 25° C. was ca. 1500 ft.-c. under the manometric conditions. Reflection from the bright platinum electrode reduced the saturating light intensity to ca. 1000 ft.-c. under the conditions of the polarographic method.*

A pH of 8.5 was selected as the minimum at which gaseous CO_2 absorption could be neglected on the following basis. The apparent rates of oxygen production by *Ulva* ($H \cdot K_{O_2}$) were followed in pairs of vessels having different gas/liquid ratios and containing 0.015 *M* bicarbonate in artificial sea water, initial pH 7.9. As the medium became more alkaline, the pressure increments rose, and the apparent rates of oxygen production became the same in each vessel; at this stage, the minimum pH value was 8.3–8.4. The rate of photosynthesis remained unchanged as the pH rose to 8.7–8.8. The rate of photosynthesis observed with bicarbonate-buffered artificial sea water having an initial pH of 8.5 was as high as was observed under any other set of conditions.

Effects of bicarbonate concentration at an initial pH of 8.5 are shown in Table II. The rate of photosynthesis observed during the first hour did not differ significantly in the presence of 0.015–0.1 *M* bicarbonate. There was a small decline during the second hour at the lowest bicarbonate concentration, and a large decrease occurred during the third hour at all bicarbonate levels. The latter decrease must have been caused by the artificiality of the medium rather than by a limiting CO_2 supply. (Several hours immersion in artificial sea water has a detrimental effect on *Ulva* even in darkness.) For that reason, thallus samples were always maintained in natural sea water until shortly before the photosynthesis measurements were begun.

The Carbon Dioxide Requirement

Our studies indicate that the full rate of photosynthesis in *Ulva* (1.8 cm.^{2} in 7 ml.) is supported for one hour by 0.015 *M* bicarbonate, initial pH 8.5, and for two hours by 0.025 *M* bicarbonate. These media provide initial carbon dioxide concentrations of 3×10^{-5} *M* and 5×10^{-5} *M* respectively (Table I). A carbon dioxide concentration of 3×10^{-5} *M*, as provided by the former medium, similarly supported the full rate of photosynthesis in two red algae investigated, *Gelidium pulchrum* and *Gigartina armata*, i.e. 9 ml. and

TABLE II

PHOTOSYNTHETIC ACTIVITY OF *Ulva* FROND DISKS AT 25° C. IN ARTIFICIAL SEA WATER CONTAINING DIFFERENT AMOUNTS OF BICARBONATE, INITIAL pH 8.5 (mm.^{3} O_2/hr./cm.^{2})

Time	Bicarbonate molarity			
	0.015 *M*	0.025 *M*	0.05 *M*	0.10 *M*
1st hour	58	56	60	56
2nd hour	50	56	55	56
3rd hour	38	38	35	—
Final pH	9.0	8.9	8.8	8.6

6.9 ml. O_2/hr./gm. solids respectively. By contrast, much higher saturating carbon dioxide concentrations have been reported for related red algae as follows: for *Gelidium cartilagineum*, 10×10^{-5} *M* (Tseng and Sweeney (23)); for *Gigartina Harveyana*, 36×10^{-5} *M* (Emerson and Green (11)). The following considerations serve to reduce these discrepancies. As Emerson and Green pointed out, use of Buch's revised values for pK'_2 reduces their calculated carbon dioxide concentrations by 40%; with this revision, their saturating carbon dioxide concentration becomes $20\text{–}25 \times 10^{-5}$ *M*, which is still about ten times higher than we observed. The pH value is of critical importance in calculating the carbon dioxide concentration; Emerson and Green (11) used the initial pH values, and Tseng and Sweeney (23) used averages of the initial and final pH values. Weakly buffered sea water was used in both of these studies so that the pH rose and the carbon dioxide content fell during the photosynthesis measurements. Had the maximum pH value *during* steady-state photosynthesis been used in the calculations (11, 23), the saturating carbon dioxide concentration then would agree rather closely with our observations.

Photosynthetic Induction After Various Dark Treatments

A large *Ulva* frond was placed under 200 ft.-c. white light in flowing sea water immediately after harvest; a second frond from the same collection was halved; one half-frond was placed in flowing sea water, and the other was placed in a masked jar of natural sea water through which nitrogen was bubbled continuously after the jar was closed with a two-hole stopper; both half-fronds were maintained in total darkness at 20–25° C. Disks and strips of thallus tissue were cut and prepared for photosynthesis measurements in very dim light. Artificial sea water low in calcium and magnesium (1/10th) and containing 0.015 *M* $KHCO_3$, initial pH 8.5, was employed in the manometric and polarographic measurements (Figs. 1–4).

Manometric time courses of photosynthesis in *Ulva* that had been subjected in the Warburg vessels to one hour in darkness under air and nitrogen are shown in Fig. 1. A constant rate of photosynthesis was attained in the aerobic samples within two minutes (Fig. 1*a*). Upon illumination of the anaerobic samples, there was an initial "gush" followed by an induction period which regularly lasted for more than ten minutes. The time courses observed following one hour of dark anaerobiosis varied between the extremes shown in Fig. 1*b* and 1*c*; the full rate of photosynthesis was observed within 15 min. in some samples, others had not recovered completely after 30 min. illumination.

The initial changes in photosynthetic activity reported in Figs. 2 and 3 are of particular interest since they refer to *Ulva* that had been held in flowing sea water for a full day in darkness. The parallel manometric (Fig. 2) and polarographic (Fig. 3*a*) measurements revealed only brief induction periods of approximately two minutes' duration, after which photosynthesis proceeded steadily and quite as rapidly as in the "control" thallus that had been continuously illuminated in flowing sea water.

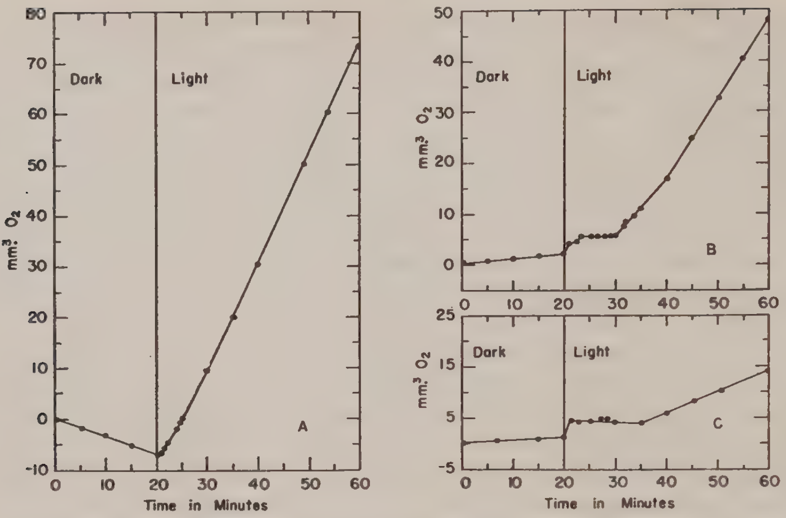

FIG. 1. Manometric time course of photosynthesis in *Ulva* after one hour in darkness (A) under an atmosphere of air, (B) and (C) under an atmosphere of nitrogen.

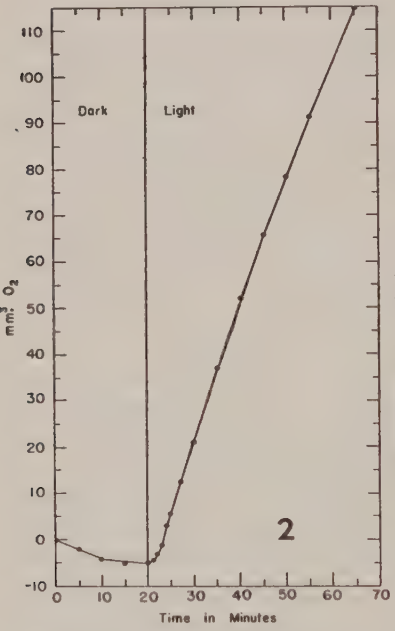

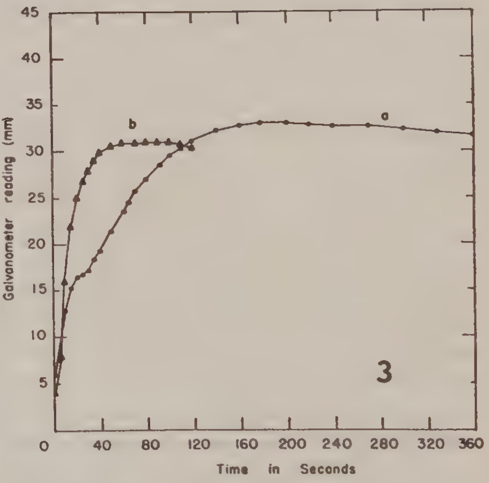

FIG. 2. Manometric time course of photosynthesis in *Ulva* after 26 hr. in darkness in flowing sea water.

FIG. 3. Initial changes in photosynthetic rate observed polarographically in *Ulva* after 26 hr. in darkness in flowing sea water (*a*) initial six-minute illumination, (*b*) second illumination following a two-minute dark interval. The time courses for subsequent illuminations (with two-minute dark intervals) closely resembled curve (*b*). The difference in time required to achieve the "steady-state" rate of oxygen production (i.e. plateau) is a measure of the induction loss after a 26 hr. vs. a two minute aerobic dark period.

Following lengthy aerobic dark pretreatments, the polarographic measurements regularly revealed a brief "oxygen gush" during the first few seconds in light (Fig. 3*a*). After the full rate of photosynthesis was attained, the thallus was subjected to a two-minute aerobic dark period, then illuminated a second time. The full rate of photosynthesis now was attained during the first minute, and the "oxygen gush" was no longer evident (Fig. 3*b*). These polarographic measurements demonstrated that lengthy aerobic dark pretreatments (up to 26 hr.) cause induction periods in *Ulva* which are not more than 90 sec. longer than following two-minute dark periods.

Manometric data for the half-frond which was held in darkness overnight under an atmosphere of nitrogen are shown in Fig. 4. One subsample was shaken for one hour in darkness under nitrogen, and a second subsample was simultaneously subjected to one hour in darkness under air. (Both were only briefly exposed to air while being transferred to the manometer vessels.) After an initial "gush", gas exchange was negligible during 40 min. illumination under nitrogen. Under an atmosphere of air, photosynthesis proceeded at a low rate after a brief initial "gush" (Fig. 4). Dark aeration of *Ulva* thallus for one hour after it had been held overnight under nitrogen thus caused a partial restoration of its capacity for photosynthesis. Hydrogen evolution apparently was responsible for the initial "gush" from anaerobic *Ulva* which was regularly observed manometrically (13).

The time courses reported in Figs. 2–4 were observed on samples from adjoining parts of a single frond in a coordinated experiment, and those reported in Fig. 1 were observed on a second frond collected at the same time. The following polarographic and manometric measurements were made independently.

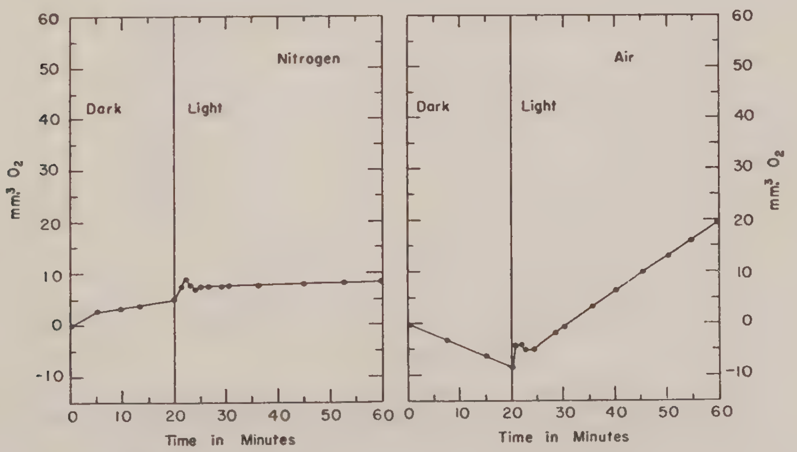

FIG. 4. Manometric time course of photosynthesis in *Ulva* after 24 hr. in darkness under an atmosphere of nitrogen; subsamples equilibrated for one hour under atmospheres of air and nitrogen.

Fig. 5 reports the initial changes in photosynthetic rate which were observed polarographically on *Ulva* that had been maintained for two hours in darkness under an atmosphere of nitrogen. (The sea water medium was gassed with nitrogen during the polarographic measurements in light and darkness.) The photosynthetic rate rose slowly during the first six minutes in light. A succession of illuminations separated by two-minute dark intervals raised the rate of oxygen production to a maximum after 15 min. illumination. Fig. 5 illustrates the marked effect of brief periods of anaerobiosis upon photosynthetic induction in *Ulva*: upon extension of the anaerobic dark interval from 2 to 10 min., the duration of the induction period was approximately doubled.

After 10 and 15 min. aerobic dark periods, the photosynthetic time courses were the same (Fig. 6) as following overnight dark treatments (Fig. 3): there was an initial oxygen "gush", a secondary peak appeared within the first minute, and the full rate of photosynthesis was attained within the second minute. After three minutes in light, the thallus was maintained in darkness for three minutes under aerobic conditions and again illuminated. The full rate of photosynthesis now was attained during the first minute. Figs. 3 and 6 demonstrate that aerobic induction in *Ulva* remains essentially the same, under the conditions of the polarographic method, upon extension of the dark treatment at room temperature from 10 min. to more than 24 hr. Fig. 7

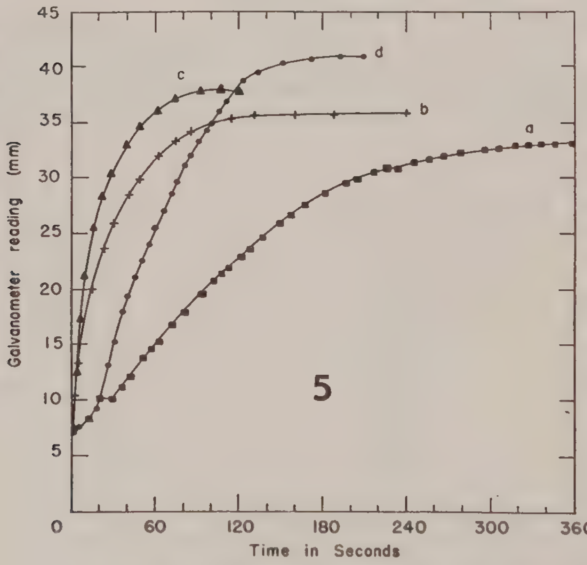

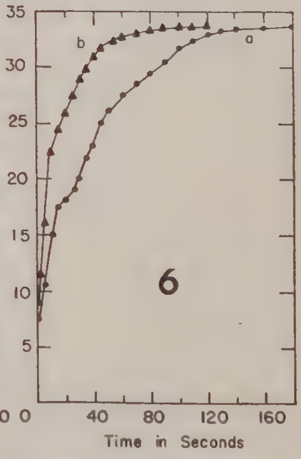

FIG. 5. Initial changes in photosynthetic rate observed polarographically in *Ulva* after two hours of dark anaerobiosis (*a*) initial six-minute illumination, (*b*) second illumination after a two-minute dark period, (*c*) third illumination after two-minute dark period, (*d*) fourth illumination after a 10-min. anaerobic dark period.

FIG. 6. Initial changes in photosynthetic rate observed polarographically in *Ulva* after 10 (or 15) min. aerobic dark periods (*a*) first illumination, (*b*) second illumination preceded by three-minute aerobic dark period.

shows that this is also true under the conditions of the manometric method: the first illumination period of Fig. 7 was preceded by a 17-hr. dark period, and the second illumination was preceded by a 20-min. dark period: the induction periods were of the same brief duration in both cases.

Photosynthetic Induction Under Pure Oxygen

Blinks and Skow (4) had indicated that photosynthetic induction in *Ulva* fronds and higher plant leaves could be entirely eliminated by thorough aeration in the preceding dark periods. Several of the accompanying figures refer to *Ulva* which was thoroughly aerated throughout the dark periods, yet brief induction periods had been observed consistently, manometrically and polarographically. Since photosynthetic induction in *Ulva* was not eliminated under our conditions by aeration, effects of pure oxygen were determined manometrically. When the thallus samples were maintained under an atmosphere of oxygen during the dark periods and during the photosynthesis measurements, the induction periods remained the same as under an atmosphere of air. This observation has been confirmed in corresponding experiments at 25° C. on two strains of *Chlorella pyrenoidosa* and on *Nostoc muscorum* (7). Experiments also were conducted in which the atmosphere of

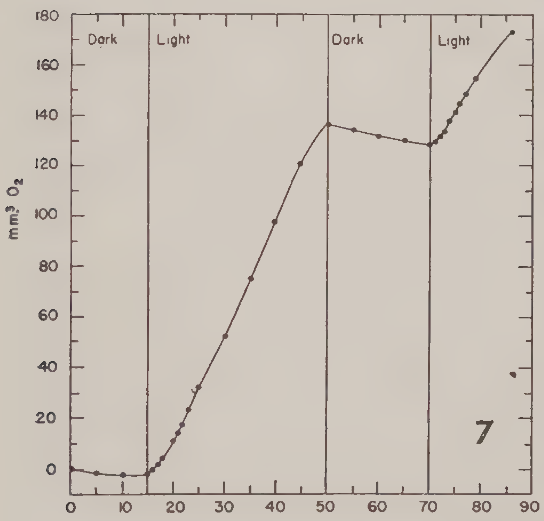

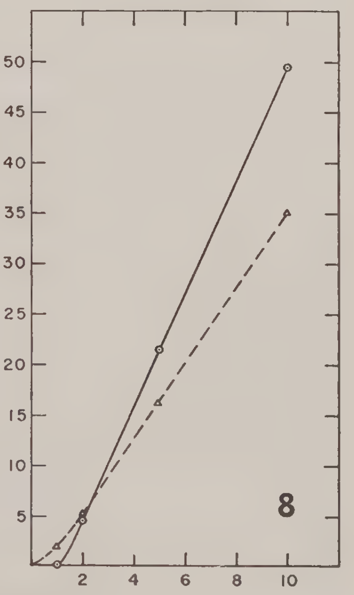

FIG. 7. Manometric time course of photosynthesis in *Ulva* after a 17 hr. aerobic dark period (first illumination) and after a 20-min. aerobic dark period (second illumination).

FIG. 8. Manometric time course of photosynthesis in *Gelidium* and *Gigartina*. Ten hour aerobic dark treatment before the first illumination (2000 ft.-c.) in artificial sea water (1/4th calcium and magnesium) 0.015 *M* $NaHCO_3$, pH 8.7, 20° C. △ - - - - - △, 270 mgm. fresh wt. of *Gigartina* (4 cm.²) ○———○, 170 mgm. fresh weight of *Gelidium*.

pure oxygen was replaced with air in darkness, 25 min. before the thallus samples were illuminated. Air was restored in these experiments to allow photosynthesis to be measured at the same oxygen tension following dark periods under air and oxygen atmospheres. In the latter experiments the induction losses ranged from 0.6–1.7 minutes of steady-state photosynthesis; those observed following dark oxygenation treatments were not significantly smaller than following 10 min. aerobic dark periods.

Photosynthetic Induction in Gelidium and Gigartina

Gelidium and *Gigartina* had exhibited lengthy induction periods in manometric (11) as well as Winkler titration measurements (23). Although satisfactory interpretations of these long induction periods were obtained in the course of our work on *Ulva*, the duration of the aerobic induction period in *Gelidium* and *Gigartina* was examined experimentally. Using our adaptation of Warburg's method, the full rate of photosynthesis was attained in both of these algae within two minutes (Fig. 8).

Discussion

The main objective of this study was to learn why such widely different induction periods had been observed in earlier studies of marine algae. For this purpose, Warburg's method involving intermittent illumination was adapted, and a direct manometric method was also devised with which induction periods of the same duration were observed as with Warburg's method and with the platinum electrode method. Our measurements of aerobic induction periods in the marine algae which were employed in earlier studies (*Ulva* (4, 19), *Gelidium* (23), *Gigartina* (11)) have shown that they do not differ appreciably from those of *Chlorella* or of higher plant leaves. In undertaking to interpret the earlier observations, it should be recalled that photosynthesis is controlled by intracellular conditions which can only be assessed indirectly.

Our studies have shown that the long induction periods observed in *Ulva* by Osterhout and Haas (19) were not caused by the overnight dark treatments in flowing sea water which preceded their photosynthesis measurements: the induction periods were found in the present study to be no longer after a full day in darkness in flowing sea water than after 10 or 20 min. aerobic dark periods; the rate of photosynthesis observed after the second minute in light also was as high as in thallus samples that had been continuously illuminated in flowing sea water. The factor or factors causing the long induction periods in the original investigations (19) must have operated after the thallus samples were transferred to the vessels used in measuring photosynthesis. Natural sea water containing alcoholic phenolphthalein was employed in the vessels (*ca.* 5×10^{-3} *M* ethanol, 3×10^{-4} *M* phenolphthalein), but Osterhout and Haas stated that photosynthesis was not affected by this internal indicator. Since the sea water was replaced periodically during the photosynthesis measurement (19) strongly limiting carbon dioxide concentrations were avoided (6). The long induction periods observed by Osterhout and Haas (19) apparently were caused by anaerobic conditions which developed within the thallus just before it was illuminated. *Ulva* samples (10–15 cm.^{2}) were coiled within small glass cylinders, capacity *ca.* 5 ml., so that the stiff thallus lined and pressed against the inner glass surface (19). The vessel was then filled with sea water, stoppered, and shaken intermittently. The cell fluid would initially be in equilibrium with aerated sea water, which contains 5 ml. dissolved oxygen/liter at 25° C. (22). The maximum amount of oxygen within the darkened thallus can be assessed from its water content, and the frequency with which it is replaced under aerobic conditions may be calculated from the respiration rate. According to our observations, the turnover time for oxygen in *Ulva* at 25° C. in darkness is from one to two minutes. Aerobic conditions could be maintained in the Osterhout-Haas experiments if the vessel contents were kept constantly in motion. With the vessels temporarily at rest, the development of an anaerobic state would become possible. Lengthy induction periods were observed regularly by the authors in *Ulva*, polarographically and manometrically, when oxygen was withheld, but not when aerobic conditions were maintained throughout the dark period.

Tseng and Sweeney (23) used large volumes of natural sea water with small *Gelidium* samples, with and without supplementary bicarbonate and carbon dioxide, at the temperature and light intensity of the natural environment. Their data show that aerobic respiration proceeded actively in their darkened control vessels, with an R.Q. value of 1.11 ± 0.28. (Respiration was about one-eighth of photosynthesis.) The corresponding vessels in which photosynthesis was measured must have been similarly supplied with oxygen. Provision was made for the continuous mixing of the vessel contents during the photosynthesis and respiration measurements, nevertheless little photosynthesis occurred during the first 15 to 20 min. of illumination (23). The completely filled vessels were apparently at rest, however, before the measurements were begun. Upon equilibration of the vessel contents, aerobic respiration would be resumed without an induction period, whereas a long photosynthetic induction period would be shown as an aftereffect of oxygen deficiency developed under static conditions. To test this interpretation, we examined *Gelidium* under continuously aerobic conditions with Warburg's method (Fig. 8). The photosynthetic induction period was of less than two minutes duration, beyond which the rate of photosynthesis was higher than was observed by Tseng and Sweeney (23).

The experiments of Emerson and Green (11) apparently were conducted under continuously aerobic conditions. *Gigartina* has a very low respiration rate, and small samples were used in 8 ml. vol. of sea water which were shaken almost continuously under air. Nevertheless, their data regularly show induction periods lasting for 15 min. upwards, as we observed on *Ulva* under Emerson and Green's conditions. These long induction periods cannot be explained either by oxygen deficiency or by "manometric lag", although the latter can be an important contributing factor. They are best understood by considering separately the conditions which are imposed in sea water equilibrated under 5% carbon dioxide, and in sea water weakly buffered with bicarbonate slightly above pH 7.5. Under 5% CO_2 in air, chemical equilibration with the natural bicarbonate (11) and physiological adaptation of the cells to unusual concentrations of carbon dioxide and hydrogen ion are probably causes of long induction periods (6). The lengthy induction periods observed in bicarbonate-buffered sea water having an initial pH of 7.5–8.0 are mainly artifacts caused by inadequate control of gaseous carbon dioxide exchange. Upon raising the initial pH to 8.5 in artificial sea water solutions containing at least 0.015 *M* bicarbonate, and introducing modifications to eliminate "manometric lag", the aerobic induction periods observed manometrically and polarographically are then of a similarly brief duration. When we examined *Gigartina* under continuously aerobic conditions (Fig. 8), the full rate of photosynthesis was attained within two minutes.

The aerobic induction periods which were observed with our modified manometric methods as well as polarographically corresponded closely with those published by Blinks and Skow (4). The principal point of difference concerns the complete elimination of photosynthetic induction by aeration (4). Assuming that aerobic induction is caused by an initial lack of "carbon dioxide acceptor" which is regenerated photosynthetically (10), absence of the brief aerobic induction period may be expected following any dark treatment in which the carbon dioxide acceptor is not depleted to a limiting concentration. Shiau and Franck (20) observed instances in which an aerobic induction period was lacking when dilute suspensions of young *Chlorella* cells were first illuminated. In the present study, brief aerobic induction periods were observed consistently in *Ulva* subjected to aerated sea water or to an atmosphere of pure oxygen during the dark period as well as when illuminated. Using Warburg's method involving intermittent illumination, photosynthetic induction was not eliminated in *Chlorella* or *Nostoc* when maintained continuously under an atmosphere of pure oxygen (7). Brief induction periods are regularly shown by continuously illuminated leaves and algae when the light intensity is suddenly increased from a limiting to a saturating level (12, 18). For these reasons, we are inclined to agree with Hill and Whittingham (17) that photosynthetic cells usually exhibit a brief aerobic induction period, no matter how thoroughly they have been aerated throughout the preceding dark period.

The following plants all have exhibited aerobic induction periods of a similarly brief duration at room temperature (20–25° C.):

Algae: *Chlorella* (5, 7, 17, 18, 26, 27), *Gelidium*, *Gigartina* (authors' observations), *Hormidium* (1), *Nostoc* (7), *Protococcus* (26), *Scenedesmus* (17), *Stichococcus* (1), *Ulothrix* (26), *Ulva* (4, author's observations).
Leaves: *Chenopodium* (17), *Holcum* (26), *Lamium* (17), *Nicotiana* (26), *Ricinus* (4), *Triticum* (18).
Needles: *Sciadopitys* (26).
Mosses: *Mnium* (17).

(172)

The existence of an aerobic induction period of brief but quite uniform duration within this wide variety of plants allows unified conclusions to be drawn concerning its cause. For reasons advanced previously (10), it is attributed to an initial lack of the CO_2-acceptor compound, now known to be ribulose diphosphate which is regenerated by photosynthesis (2). Certain differences between species are apparent with respect to transitory details, which are discussed by Van der Veen (24–26).

Photosynthetic cells differ in their ability to withstand long periods of dark anaerobiosis (28), so the anaerobic induction periods may be expected to vary widely between species. Since an induction period is lacking in the Hill reaction following anaerobic dark treatments of *Chlorella* and other algae, the site of anaerobic as well as aerobic induction phenomena must be in the process of carbon dioxide assimilation rather than of water photolysis and oxygen evolution.

References

1. Aufdemgarten, H. Zur Kenntnis der sogenannten Inductionvorgange bei der Kohlensäure assimilation. Planta, 29 : 643-678. 1939.
2. Bassham, J. A., Benson, A. A., Kay, L. D., Harris, A. Z., Wilson, A. T., and Calvin, M. The path of carbon in photosynthesis. XXI. The cyclic regeneration of carbon dioxide acceptor. J. Am. Chem. Soc. 76 : 1760-1770. 1954.
3. Blinks, L. R. Manual of phycology. *Edited by* G. M. Smith. Chronica Botanica Company, Waltham, Mass. 1951. Chap. 14. p. 270.
4. Blinks, L. R. and Skow, R. K. The time course of photosynthesis as shown by a rapid electrode method for oxygen. Proc. Natl. Acad. Sci. U.S. 24 : 420-427. 1938.
5. Brackett, R. S., Olson, R. A., and Crickard, R. G. Time course and quantum efficiency of photosynthesis in *Chlorella*. J. Gen. Physiol. 36 : 563-579. 1953.
6. Briggs, G. E. and Whittingham, C. P. Factors affecting the rate of photosynthesis of *Chlorella* at low concentrations of carbon dioxide and in high illumination. New Phytologist, 51 : 236-249. 1952.
7. Brown, T. E. Doctoral dissertation. Ohio State University, Columbus, Ohio. 1954.
8. Buch, K. On boric acid in the sea and its influence on the carbonic acid equilibrium. J. conseil intern. exploration mer, 8 : 309-325. 1933.
9. Buch, K., Harvey, H. W., Wattenberg, H., and Gripenberg, S. Über das Kohlensäuresystem im Meerwasser. Conseil permanent intern. exploration mer, Rapports et Proces-Verbaux des Réunions, 79 : 1-70. 1932.
10. Clendenning, K. A. and Ehrmantraut, H. C. Photosynthesis and Hill reactions by whole *Chlorella* cells in continuous and flashing light. Arch. Biochem. 29 : 387-403. 1950.
11. Emerson, R. and Green, L. Manometric measurements of photosynthesis in the marine alga *Gigartina*. J. Gen. Physiol. 17 : 817-843. 1934.
12. Franck, J., French, C. S., and Puck, T. T. The fluorescence of chlorophyll and photosynthesis. J. Phys. Chem. 45 : 1268-1300. 1941.
13. Frenkel, A. W. Paper read at Symposium on hydrogen transfer in Photosynthesis. Am. Chem. Soc. Meeting, Chicago. Sept., 1950.
14. Haxo, F. T. and Blinks, L. R.. Photosynthetic action spectra of marine algae. J. Gen. Physiol. 33 : 389-422. 1950.
15. Haxo, F. T. and Clendenning, K. A. Photosynthesis and phototaxis in *Ulva Lactuca* gametes. Biol. Bull. 105 : 103-114. 1953.
16. Haxo, F. T. and Sweeney, B. M. *In* Luminescence in biological systems. *Edited by* F. H. Johnson. Am. Assoc. Advance. Sci. Monograph, Washington, D.C. 1955.
17. Hill, R. and Whittingham, C. P. The induction phase of photosynthesis in *Chlorella* determined by a spectroscopic method. New Phytologist, 52 : 133-141. 1953.
18. McAlister, E. D. and Myers, J. The time course of photosynthesis and fluorescence determined simultaneously. Smithsonian Inst. Publs., Misc. Collections, 99, No. 6. 1940.

19. Osterhout, W. J. V. and Haas, A. R. C. On the dynamics of photosynthesis. J. Gen. Physiol. 1 : 1-16. 1918.

20. Shiau, Y. G. and Franck, J. Chlorophyll fluorescence and photosynthesis in algae, leaves and chloroplasts. Arch. Biochem. 14 : 253-295. 1947.

21. Strain, H. H. Manual of phycology. *Edited by* G. M. Smith. Chronica Botanica Company, Waltham, Mass. 1951. Chap. 13. p. 258.

22. Sverdup, H. V., Johnson, M. W., and Fleming, R. H. The oceans, their physics, chemistry and biology. Prentice-Hall, Inc., New York. 1946.

23. Tseng, C. K. and Sweeney, B. M. Physiological studies of *Gelidium cartilagineum*. I. Photosynthesis, with special reference to the carbon dioxide factor. Am. J. Botany, 33 : 706-715. 1946.

24. Van der Veen, R. Induction phenomena in photosynthesis. I. Physiol. Plantarum, 2 : 217-234. 1949.

25. Van der Veen, R. Induction phenomena in photosynthesis. II. Physiol. Plantarum, 2 : 287-296. 1949.

26. Van der Veen, R. Induction phenomena in photosynthesis. III. Physiol. Plantarum, 3 : 247-257. 1950.

27. Warburg, O. Über die Geschwindigkeit der photochemischen Kohlensäurezersetzung in lebenden Zellen. II. Biochem. Z. 103 : 188-217. 1920.

28. Willstatter, R. and Stoll, A. Untersuchungen über die Assimilation der Kohlensäure. Julius Springer, Berlin. 1918.

Reproduced by Permission

Reprinted from **ANALYTICAL CHEMISTRY**, Vol. 28, Page 97, January 1956
Copyright 1956 by the American Chemical Society and reprinted by permission of the copyright owner

Polarographic Determination of Ferrous and Ferric Iron in Refractory Minerals

GEORGE S. BIEN and EDWARD D. GOLDBERG

Scripps Institution of Oceanography, University of California, La Jolla, Calif.

A polarographic method for the simultaneous determination of ferrous and ferric iron in refractory minerals is described. The minerals are initially decomposed in a flux of sodium metafluoroborate. The flux is dissolved in a supporting electrolyte solution containing citrate ion, which complexes both the ferrous and ferric irons. The composite wave of oxidation and reduction of the complex ions gives an anodic current proportional to the concentration of ferrous iron and a cathodic current proportional to the concentration of ferric iron. The procedure can be applied to samples containing both organic materials and manganous compounds.

THERE are several serious limitations (*2*) in the general extensions to rock analysis of the permanganate titration of ferrous iron. First the oxidizability of manganous ion by permanganate in the presence of even limited amounts of hydrofluoric acid tends to give high results in minerals containing manganese; and second any organic matter present tends to cause high results. Further, the simultaneous determination of both ferrous and ferric iron requires a double titration with the attendant complications in the reduction of the ferric iron. A promising rapid polarographic method in which both ferrous and ferric iron are ascertained simultaneously seemed possible from the works of Stackelberg and Freyhold (*7*), Lingane (*4*, *5*), and Kolthoff and Lingane (*3*). The composite wave of oxidation and reduction of the complex ions formed between ferric and ferrous ions and oxalate ion give an anodic current proportional to the concentration of the ferrous iron and a cathodic current proportional to the concentration of the ferric iron. Lingane (*5*) indicated that citrate ion might be preferable as a complexing agent for the purpose of determining ferrous and ferric iron.

The purpose of this investigation was to develop a general polarographic method for the assay of the absolute ferric and ferrous iron contents of refractory minerals, as well as the optimal conditions for the dissolution of the mineral sample with minimal oxidation of the ferrous iron.

APPARATUS AND REAGENTS

All polarographic measurements were made on the Sargent Model XXI polarograph. Standard electrolysis cells were used with the dipping-type saturated calomel or silver-silver chloride cells as the reference anode. All measurements were made at 25° ± 0.05° C. The capillary characteristics with a mercury height of 64 cm. in the standard complexing solution on the horizontal portion of the current-voltage curve were: $m = 8.47$ mg. sec.$^{-1}$, $t = 3.5$ seconds, and $m^{2/3}t^{1/6} = 5.12$ mg.$^{2/3}$ sec.$^{-1/2}$

All reagents used were of the highest reagent grade. The distilled water was the equivalent of that produced by a triple distilling process. The supporting electrolyte solution included the complexing agent and had the following composition: sodium citrate, 0.25M; citric acid, 0.25M; and potassium nitrate, 0.50M. The pH of this solution is 4.00 and should be maintained at the same value for all solutions inasmuch as the half-wave potentials are determined by the pH (*5*). The potassium nitrate is added as the carrying electrolyte. Potassium nitrate was chosen in preference to potassium chloride, because there is a maximum in the ferric wave which was difficult to suppress when potassium chloride was used. Gelatin can be used as a maximum suppressor with potassium chloride. However, to reduce the number of reagents used in the analytical procedure, preference was given to the use of potassium nitrate. The flux used for the breakdown of the minerals was sodium metafluoroborate (*6*). This flux has advantage over sodium carbonate in that it gives no effervescence even at high temperatures in producing rapid and complete dissolution of minerals (*1*).

RECOMMENDED PROCEDURE

A weighed sample of 0.1 to 0.2 gram of powdered mineral and about six times its weight of sodium metafluoroborate are placed in a platinum crucible, the weight of which was previously ascertained. The crucible is covered with an inverted clay crucible through which nitrogen gas enters at the top. After a 5-minute nitrogen flush of the apparatus, the flux mixture is gradually brought to a fusion temperature of 1000° to 1050° C. with a Meker burner under an atmosphere of nitrogen. The fused condition is maintained for approximately 5 minutes, or until a clear homogeneous melt is obtained. The crucible is allowed to cool under a stream of nitrogen, weighed again, and the melt removed. The melt is ground under acetone and dried under a stream of nitrogen. An aliquot of 0.3 to 0.4 gram of the powder is weighed and dissolved in 50 ml. of oxygen-free complexing solution under a stream of nitrogen. An aliquot of this amount gives adequate diffusion currents for minerals containing up to 20% total iron. After the solution attains a temperature of 25.00° C., a polarogram is obtained from +0.15 to −0.35 volt (Figure 1). The zero current value is ascertained by the pen position with the dropping mercury electrode polarity switch in the "off" position.

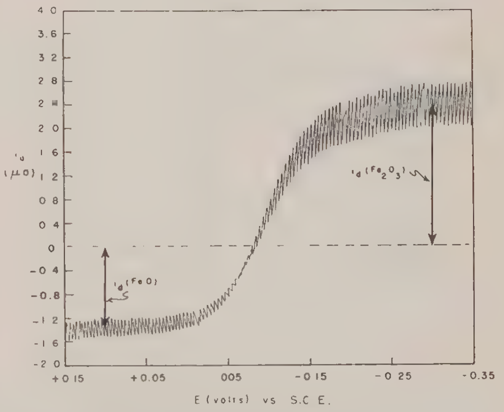

Figure 1. Typical polarogram

Solution contained both divalent and trivalent iron in the supporting electrolyte solution, which contained 0.25M citric acid, 0.25M sodium citrate, and 0.50M potassium nitrate.

To determine the respective polarographic constants, k_{FeO} and $k_{Fe_2O_3}$, for the equation of quantitative polarographic analysis, $i_d = kC$, where i_d is the diffusion current and C the concentration in question, aliquots containing the equivalent of 0 to 8.0 mg. of ferrous and ferric oxides are added to 50-ml. portions of the complexing solution. Reagent grade ferric ammonium sulfate, $Fe_2(SO_4)_3.(NH_4)_2SO_4.24H_2O$, and reagent grade ferrous ammonium sulfate, $FeSO_4.(NH_4)_2SO_4.6H_2O$, were used as standards. Weighed quantities of these salts were introduced directly into the complexing solutions.

This procedure bypasses the preparation of standard ferrous and ferric solutions; the concentration of the ferrous standard may change with time. It further eliminates the pipetting of standard solutions in which oxidation of ferrous iron may occur.

Table I. Calibration Data for Ferrous and Ferric Oxides[a]

Run	FeO Concn., Mg./ 50 Ml.	$-i_d$, µa.	$-i_d$[b], µa.	k_{FeO}	Fe_2O_3 Concn., Mg./ 50 Ml.	$+i_d$, µa.	$+i_d$[b], µa.	$k_{Fe_2O_3}$
1	0.0	0.20	0.00	...	0.0	0.06	0.00	...
2	1 25	0.96	0.76	0.610	1.13	0.64	0.58	0.515
3	1 67	1.24	1.04	0.624	1.77	0.98	0.92	0.519
4	2.05	1.53	1.33	0.648	1.97	1.06	1.00	0.507
5	2.71	1.84	1.64	0.605	3.51	1.90	1.84	0.524
6	3.54	2.46	2.26	0.639	3.71	1.93	1.87	0.520
7	3.94	2.72	2.52	0.640	3.74	2.02	1.96	0.524
8	4.82	3.26	3.06	0.635	4.21	2.30	2.24	0.533
9	6.10	3.92	3.72	0.610	6.71	3.60	3.54	0.528

[a] In 0.5*M* potassium nitrate, 0.25*M* sodium citrate, and 0.25*M* citric acid. Dropping mercury electrode *vs.* S.C.E. where $M^{2/3}t^{1/6}$ = 5.12 mg.$^{2/3}$ sec.$^{-1/2}$. Ferrous and ferric values both obtained in single runs listed above.

[b] Corrected for blank values.

The slight increase of volume due to the introduction of the solid salts into the solution is insignificant. The results of one set of these calibrations are given in Table I. The values of the *k*'s are expressed in microamperes per milligram instead of microamperes per millimole for convenience in the rapid conversion of results to the weight units used in the literature of geology. The standard deviations of k_{FeO} and $k_{Fe_2O_3}$ are 2.6 and 1.6%, respectively.

There apparently is no effect of the ferric iron produced by the oxidation of ferrous iron upon the measured ferric iron value of the sample. This is shown in Table I where each sample contained both ferrous and ferric iron. There is no trend in the values of $k_{Fe_2O_3}$ with increasing ferrous concentration.

Table II. Comparison of Polarographic and Volumetric Determinations of Ferrous Oxide Content in Weight Per Cent

Description of Sample	Polarographic, %	Volumetric, %
Glauconite	12.4	11.5
	12.5	11.1
	12.2	12.5
	11.2	11.6
	11.2	11.6
Olivine	5.01	6.29
	6.55	6.52
Saponite	4.46	4.51
Hornblende	19.88	19.89
Marcasite bearing rocks	19.15	...
	18.93	...

RESULTS

The polarographic determinations of ferrous iron were compared with the results of a permanganate titration of splits from identical samples (Table II). In the volumetric procedure the melt was dissolved in a solution containing 20 ml. of 12*N* sulfuric acid and 20 ml. of saturated boric acid solution under an atmosphere of nitrogen. The mixture was warmed slightly to effect solution. Upon cooling, 5 ml. of 86% phosphoric acid were added, and the titration was carried out. The results of these titrations are given in Table II and show reasonable agreement with the results of the polarographic method. The titration was not carried to completion for the marcasite sample inasmuch as the hydrogen sulfide formed during acidification reduced permanganate. Replicate analyses were made on the glauconite, olivine, and marcasite samples.

Table III. Determination of Ferrous and Ferric Oxides with Presence of Manganous Ion

$MnCl_2$ Added, Mg.	FeO		Fe_2O_3	
	Present, mg.	Found, mg.	Present, mg.	Found mg.
0	4.82	4.85	2.47	2.51
11.0	4.78	4.76	0.0	0.0
14.4	4.87	4.85	4.09	4.10
22.4	4.93	5.03	2.45	2.49
44.3	4.86	4.85	2.44	2.49

It was found that manganous ion does not interfere with the polarographic determination of either the ferrous or ferric iron inasmuch as the oxidation potential of the manganous ion is far removed from that of the ferrous-ferric waves. Recovery determinations of known quantities of ferrous and ferric oxides with varying quantities of manganous chloride are given in Table III.

The fusion process can be carried out with minimum oxidation of ferrous iron if done rapidly and under a nitrogen atmosphere. However, lengthy grinding periods, even under acetone, result in a reduction of the ferrous concentration (Table IV). To reduce any photochemical reduction of the citrate solutions, it is recommended to carry out the polarographic determinations in low actinic (colored) glass vessels or in the absence of strong light.

Table IV. Oxidation of Ferrous Iron During Grinding Process

Description of Sample	Per Cent	
	FeO	Fe_2O_3
Glauconite chips (directly from crucible)	12.60	6.6
Glauconite chips (broken up by light pounding in a mortar, without acetone)	12.40	7.1
Glauconite powder (ground in acetone, 20 mesh)	11.93	7.6
Glauconite powder (ground in acetone, 100 mesh)	11.22	7.7
	11.19	7.6

CONCLUSION

The use of the polarographic composite oxidation and reduction waves of ferric and ferrous ions provides a convenient method of assay in refractory materials even in the presence of manganous ion and organic matter. The use of the sodium metafluoroborate flux, with the precautions of limited light exposure, fusion time, and grinding, results in minimum oxidation of ferrous iron.

ACKNOWLEDGMENT

This investigation was supported by a grant from the American Petroleum Institute, Project 51.

LITERATURE CITED

(1) Groves, A. W., "Silicate Analysis," 2nd ed., p. 184, George Allen and Unwin, Ltd., London, 1951.
(2) Hillebrand, W. F., and Lundell, G. E. F., "Applied Inorganic Analysis," 2nd ed., p. 912, Wiley, New York, 1953.
(3) Kolthoff, I. M., and Lingane, J. J., "Polarography," 2nd ed., p. 219, Interscience, New York, 1952.
(4) Lingane, J. J., *Chem. Revs.* **29**, 17 (1941).
(5) Lingane, J. J., *J. Am. Chem. Soc.* **68**, 2448 (1946).
(6) Rowledge, H. P., *J. Roy. Soc. W. Austrália* **20**, 165 (1934).
(7) Stackelberg, M. von, and Freyhold, H. von, *Z. Elektrochem.* **46**, 120 (1940).

Received for review August 29, 1955. Accepted October 20, 1955. Contribution from Scripps Institution of Oceanography, New Series No. 834.

Printed in U. S. A.

LATE PLEISTOCENE AND RECENT HISTORY OF THE CENTRAL TEXAS COAST

FRANCIS P. SHEPARD

Reprinted for private circulation from
THE JOURNAL OF GEOLOGY
Vol. 64, No. 1, January 1956
PRINTED IN U.S.A.

Reproduced by Permission

LATE PLEISTOCENE AND RECENT HISTORY OF THE CENTRAL TEXAS COAST[1]

FRANCIS P. SHEPARD
Scripps Institution of Oceanography, La Jolla, California

ABSTRACT

As a result of the intensive study of the sediments in the bays, on the barrier islands, and on the continental shelf in an area along the central Texas coast, diagnostic characteristics of the various environments have been sufficiently determined to allow interpretations of the buried sediments of the area. The samples from a total of 27 borings extending to depths of from 15 to 85 feet have been analyzed and compared with the recent sediments. This work provides a basis for interpreting the history of the coastal area which, according to carbon 14 determinations, extends back almost 10,000 years. About 9,500 years ago the sea invaded some of the valleys cut during the lowered Pleistocene sea-levels, and sheltered bay deposits now found about 85 feet below sea-level were deposited. Barrier islands or sandy shoals grew up along the coast, keeping pace with the slow rise of sea-level, so that bays with brackish water were maintained in most of the area during the long period which followed. Evidence was found of minor shifts, only, in the position of the present barrier islands, although other post-Pleistocene barrier islands are now submerged under the inner continental shelf deposits. The sequence of formations stands in opposition to the hypothesis of a positive sea-level stand during the postglacial climatic optimum.

INTRODUCTION

As a part of the American Petroleum Institute sedimentology project, being conducted by Scripps Institution scientists with help from subcontractors in other universities, a series of borings was made in the central Texas coast area where various phases of surface sediments were being studied. These borings were made in a bay-head delta, in three bays, and on two barrier islands. The purpose of the work was to find the minor variations in sedimentation conditions since the beginning of the most recent cycle of deposition. It was anticipated that this would only involve boring to a depth of about a score of feet before encountering formations representative of Pleistocene conditions of lower sea-level, such as the gravel alluvial deposits and the leached and oxidized Beaumont clay found by Fisk (1944) and others. Contrary to predictions, however, it was necessary to continue the borings to depths of from 40 to as much as 80 feet before finding the Beaumont clay or what appeared to be a Pleistocene river deposit. No Pleistocene gravels were encountered. As a result, instead of obtaining continuous cores, as had been planned, it seemed advisable to alternate between washing and coring operations. In general we retained 2-foot cores out of every 5 feet of hole but increased the wash intervals when the operations in the bays had to be curtailed by lateness in the day, because it was considered unwise to leave the light drilling rig set up over night. In the barrier islands, where the cuttings showed there were continuous sands, relatively long wash intervals were used between cores.

Most of the drilling operations were carried on with a light rotary rig having a 3-inch diameter core barrel. These borings were supplemented by 1-inch

---

[1] Contribution from the Scripps Institution of Oceanography, New Series no. 835. This investigation was supported by a grant from the American Petroleum Institute, Project 51. Manuscript received April 11, 1955.

cores from a Porter soil sampler which we pounded manually into the delta and into portions of the islands. In three of the Porter holes, practically continuous samples were obtained from the surface down to about 30 feet, and in two of the holes made by the drilling rig, coring was continuous from 25 to 35 feet.

All cores from the drillings have been analyzed for grain size and for composition of the coarse fraction (Shepard and Moore, 1954). Very extensive studies were also made of the faunal content, the water content, the chemistry, and of the clay minerals. The details of this work can be found in another publication (Shepard and Moore, 1955).

GENERAL SETTING OF THE BORING OPERATIONS

Figure 1 shows the location of the various holes and the depth of the boring, and the depth, if attained, at which borings encountered a change indicative of the late-glacial, low sea-level stand. It will be noted that the main line of borings extends down Guadalupe Delta and along the length of San Antonio Bay and across Matagorda Island. Two lines transverse to this were developed, one of them in lower San Antonio Bay and the other along the barrier-island beaches. Various miscellaneous borings were obtained, including a scattering of holes on St. Joseph Island, three on the fringes of Aransas Bay, and one in the middle of that bay.

The main line of borings, which is related to San Antonio Bay and its delta head, crossed the present delta and extended past the low-salinity upper bay to the higher-salinity lower bay and thence across the barrier island. It is supplemented by samples furnished by Humble Oil Company from a boring made from their well platform $3\frac{1}{2}$ miles seaward of the northeast end of St. Joseph Island.

The surface sediments and the organisms related to them were examined in great detail during the work in Project 51, so that the characteristics of the depositional environments in this area are well known (see Shepard and Moore, 1955). Using these characteristics and the assemblages of organisms, it has been possible to interpret the environment in which the sediments represented by the borings were deposited.

THE GENERAL RESULTS OF THE DRILLING

The general composition of the various sediments obtained in the holes is indicated by three sections (figs. 2–4), two of them parallel to the coast and the third extending up into San Antonio Bay. Interpretations of two of these lines are given in figure 5. Examining first the section transverse to the coast (figs. 2, 5), it will be seen that the Guadalupe Delta is relatively thin and is underlain by bay deposits; the uppermost of these shows strong influence of a nearby river, whereas those underneath are suggestive of middle-bay conditions. Where the holes penetrated to the base of the bay sediments, deposits suggestive of deltaic or some type of alluvial deposition were encountered.

A detailed history of the changes which took place in the area at the lower end of the Guadalupe Delta is provided by a study of 29 samples from a 26-foot Porter hole which was cored continuously (fig. 6). The changing abundance of different constituents along with the nature of the organisms provides the sequence of events. The high wood contents and abundant Foraminifera and Ostracoda, along with a scarcity of terrigenous sands, show that the upper

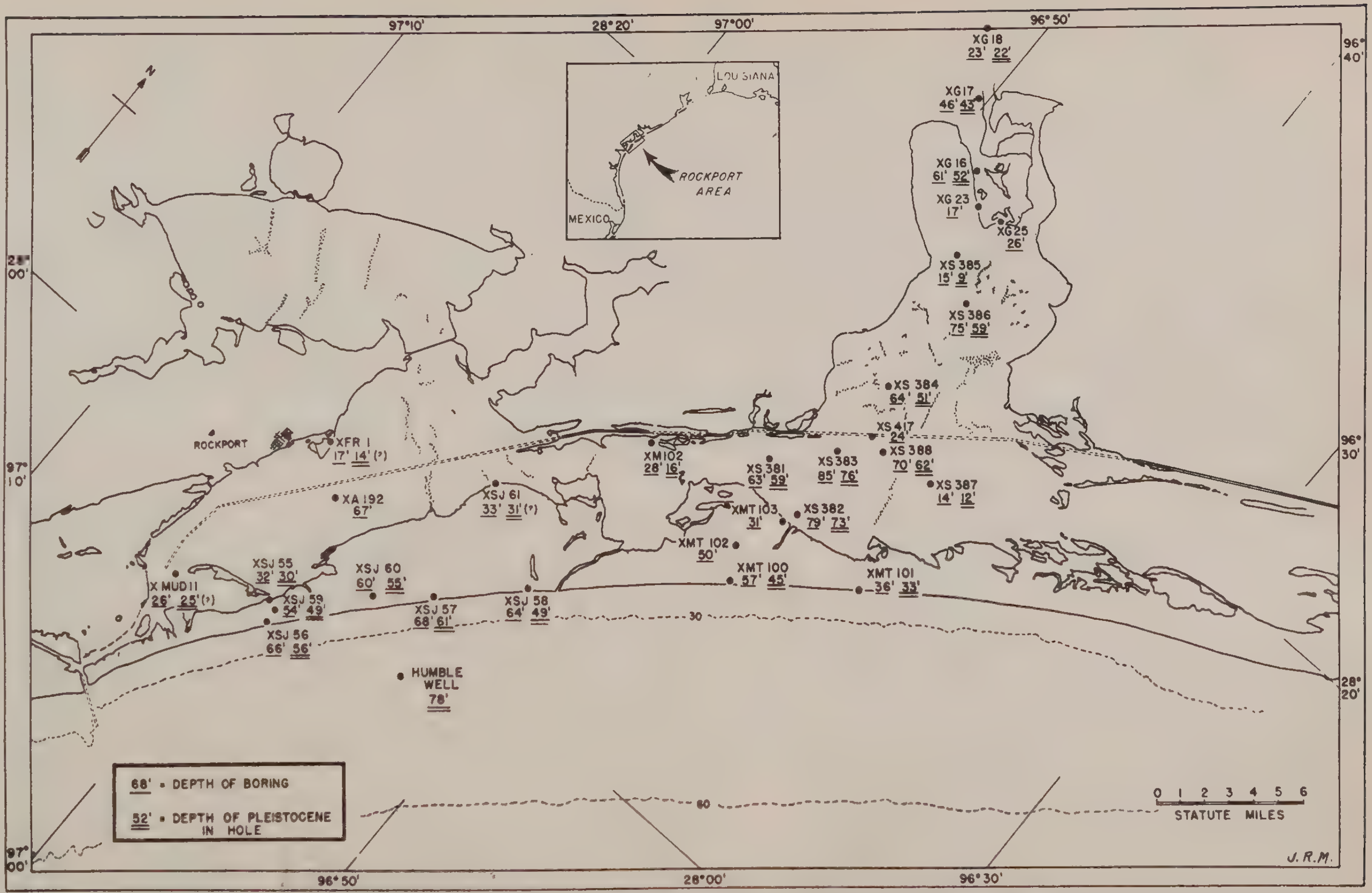
97°10'
28°20'
97°00'
96°50'
96° 40'
28° 00'
97° 10'
96° 30'
28° 20'
97° 00'
96° 50'
28°00'
96° 30'
N
LOUISIANA
MEXICO
ROCKPORT AREA
ROCKPORT
XG 18 23' 22'
XG 17 46' 43'
XG 16 61' 52'
XG 23 17'
XG 25 26'
XS 385 15' 9'
XS 386 75' 59'
XS 384 64' 51'
XS 417 24'
XS 388 70' 62'
XS 387 14' 12'
XS 383 85' 76'
XS 381 63' 59'
XS 382 79' 73'
XMT 103 31'
XMT 102 50'
XMT 100 57' 45'
XMT 101 36' 33'
XM 102 28' 16'
XFR 1 17' 14' (?)
XA 192 67'
XSJ 61 33' 31' (?)
XSJ 60 60' 55'
XSJ 55 32' 30'
XSJ 59 54' 49'
XSJ 56 66' 56'
XSJ 57 68' 61'
XSJ 58 64' 49'
X MUD 11 26' 25' (?)
HUMBLE WELL 78'
30
60
68' = DEPTH OF BORING
52' = DEPTH OF PLEISTOCENE IN HOLE
0 1 2 3 4 5 6
STATUTE MILES
J. R. M.

FIG. 1.—Locations of shallow borings in the vicinity of Rockport, Texas. Note that the depth at which the supposed Pleistocene was encountered is given for all holes except where the boring did not extend below the Recent. For general location, see inset.

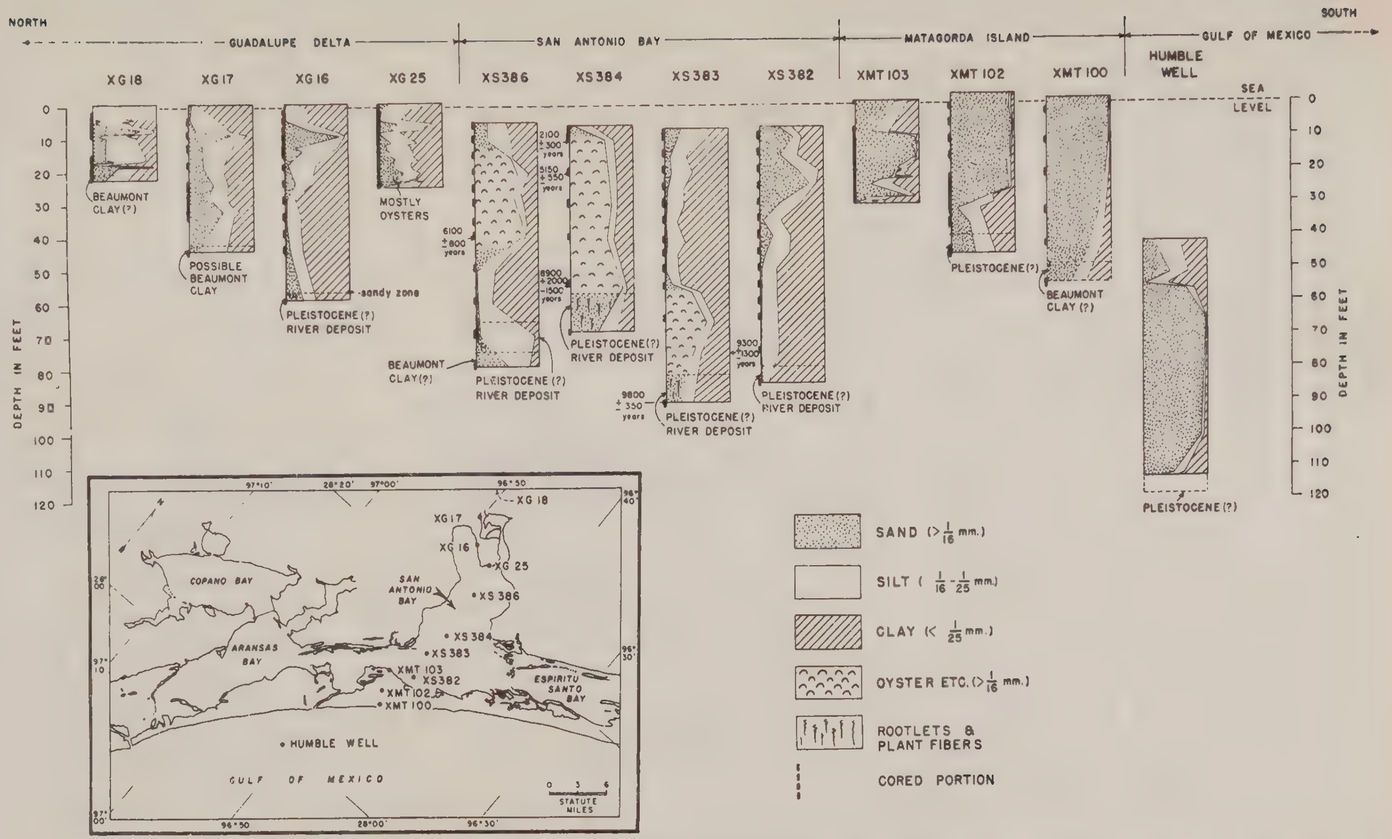
NORTH
GUADALUPE DELTA
SAN ANTONIO BAY
MATAGORDA ISLAND
GULF OF MEXICO
SOUTH
XG18
XG17
XG16
XG25
XS386
XS384
XS383
XS382
XMT103
XMT102
XMT100
HUMBLE WELL
SEA LEVEL
DEPTH IN FEET
0
10
20
30
40
50
60
70
80
90
100
110
120
BEAUMONT CLAY(?)
POSSIBLE BEAUMONT CLAY
MOSTLY OYSTERS
sandy zone
PLEISTOCENE(?) RIVER DEPOSIT
6100 ± 800 years
2100 ± 300 years
5150 ± 350 years
8900 + 2000 − 1500 years
9300 ± 1300 years
9800 ± 350 years
BEAUMONT CLAY(?)
PLEISTOCENE(?)
97°10'
28°20'
97°00'
96°50
96°40'
96°30'
28°00'
28°00
97°10
97°00'
COPANO BAY
ARANSAS BAY
SAN ANTONIO BAY
ESPIRITU SANTO BAY
HUMBLE WELL
GULF OF MEXICO
0 3 6
STATUTE MILES
SAND (> 1/16 mm.)
SILT (1/16 - 1/25 mm.)
CLAY (< 1/25 mm.)
OYSTER ETC. (> 1/16 mm.)
ROOTLETS & PLANT FIBERS
CORED PORTION

FIG. 2.—Showing the sand-silt variations in depth of hole in the borings along San Antonio Bay. Includes also the Humble boring. The dates were obtained by carbon 14, by Magnolia Field Research Laboratories.

portion represents a deposit due to waves lapping up over the end of the delta and introducing the sort of material which is in suspension at the edge of the bay. These same conditions were repeated at a depth of 8 feet, but at 7 feet the high terrigenous-sand content, found also at about the same depth in the other delta holes (fig. 2), shows that there may have been a river flood introducing more sand than usual to the area. Another possible flood may have occurred during the deposition of sediment found at a depth of 21 feet. Below 8 feet the deposits are indicative of bay deposition, although a relatively close proximity to the river is shown by the repeated finding of plant fibers. The increase of shells and an abundance of oysters at 23 feet suggest that oyster reefs indicative of the intermediate salinity of mid-bay conditions existed during the deposition of the sediment of the deeper portions of the boring.

In San Antonio Bay, holes XS 386, XS 384, and XS 383 (from north to south in figs. 2, 5) all penetrated into oyster reefs, which are also present in consider-

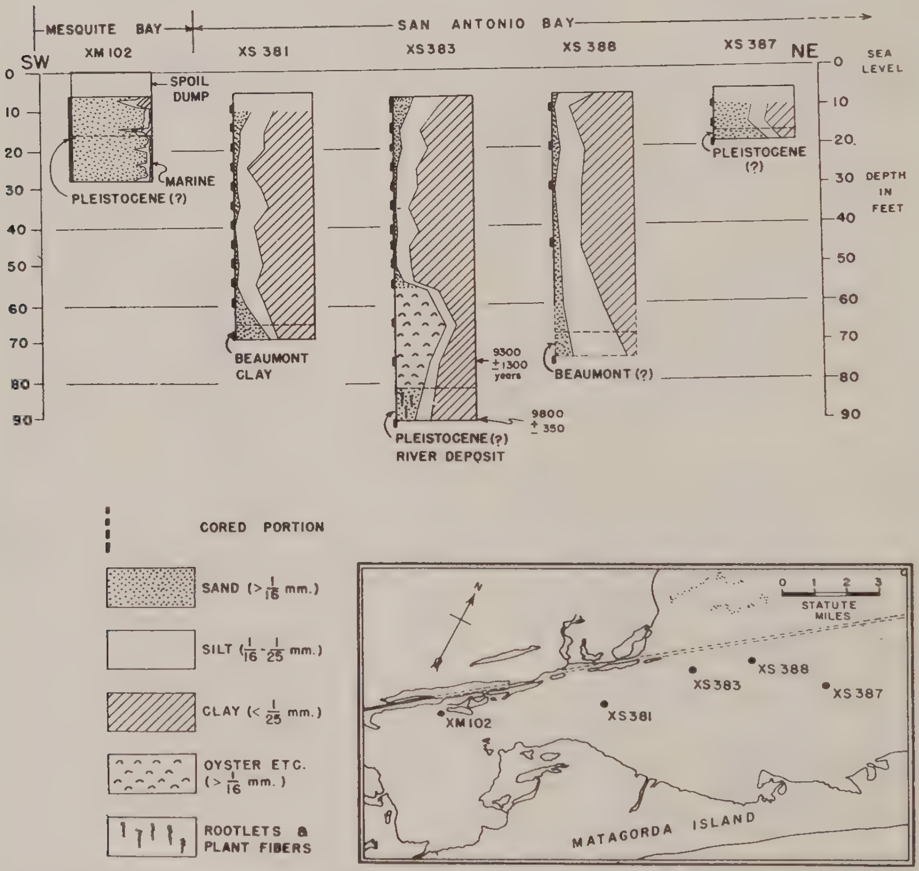
MESQUITE BAY
SAN ANTONIO BAY
XM 102
XS 381
XS383
XS 388
XS 387
SW
NE
0
10
20
30
40
50
60
70
80
90
SEA LEVEL
DEPTH IN FEET
SPOIL DUMP
MARINE
PLEISTOCENE (?)
BEAUMONT CLAY
9300 ±1300 years
9800 ± 350
PLEISTOCENE (?) RIVER DEPOSIT
BEAUMONT (?)
PLEISTOCENE (?)
CORED PORTION
SAND (>1/16 mm.)
SILT (1/16-1/25 mm.)
CLAY (<1/25 mm.)
OYSTER ETC. (>1/16 mm.)
ROOTLETS & PLANT FIBERS
N
0 1 2 3
STATUTE MILES
XS 388
XS383
XS 387
XS381
XM102
MATAGORDA ISLAND

FIG. 3.—Line of borings across lower San Antonio Bay and in upper Mesquite Bay, showing sand-silt-clay contents. Note that the deeper Pleistocene in XS 383 indicates deposition in a valley.

able abundance in the modern environments of central San Antonio Bay. These oyster-reef deposits were found near the surface in XS 386 and near the bottom of the hole in XS 383, whereas they are quite continuous in XS 384 in the middle of the bay. Since oyster reefs represent intermediate salinity, this change from north to south might suggest that the conditions creating intermediate salinity had migrated up the bay until a recent reversal took place. The abundance of oyster shells found in some of the samples from below the end of Guadalupe Delta suggests that an intermediate salinity might also have existed as far north as the delta, where low salinity now exists.[2] The holes along the central portion of San Antonio Bay, aside from their oyster-reef elements, had indications of what might be called more normal bay deposition. Similar bay deposits were found in hole XS 382, near the barrier island and at a short distance below sediments indicative of deposition near an island (see fig. 5). The bay deposits persist to a depth of 77 feet where river deposits were encountered.

Under Matagorda barrier island, the hole nearest the bay, XMT 103, pene-

---

[2] Reports, which it has not been possible to confirm, were given us that oysters had been discovered several miles farther up the delta in borings by an oil company.

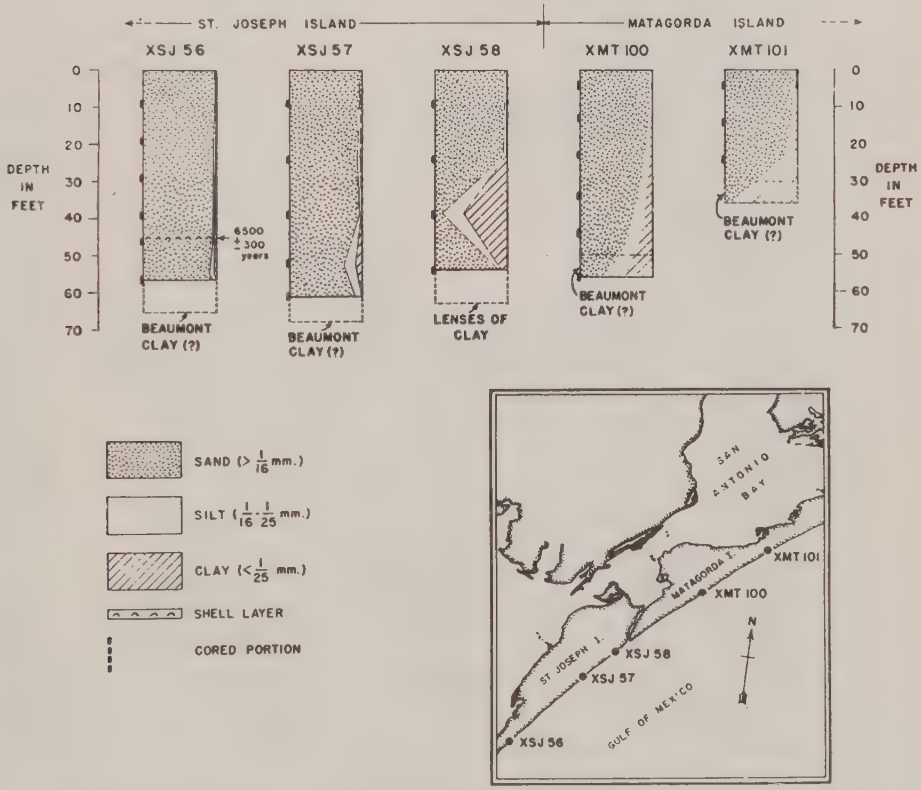
ST. JOSEPH ISLAND
MATAGORDA ISLAND
XSJ 56
XSJ 57
XSJ 58
XMT 100
XMT 101
DEPTH IN FEET
0
10
20
30
40
50
60
70
6500 ± 300 years
BEAUMONT CLAY (?)
BEAUMONT CLAY (?)
LENSES OF CLAY
BEAUMONT CLAY (?)
BEAUMONT CLAY (?)
SAND (> 1/16 mm.)
SILT (1/16 - 1/25 mm.)
CLAY (< 1/25 mm.)
SHELL LAYER
CORED PORTION
SAN ANTONIO BAY
MATAGORDA I.
ST JOSEPH I.
GULF OF MEXICO
N
XMT 101
XMT 100
XSJ 58
XSJ 57
XSJ 56

FIG. 4.—Line of borings along the beaches of St. Joseph and Matagorda islands. Note the high sand content virtually throughout the length of the holes; also, the 6,500-year age at 46 feet in XSJ 56.

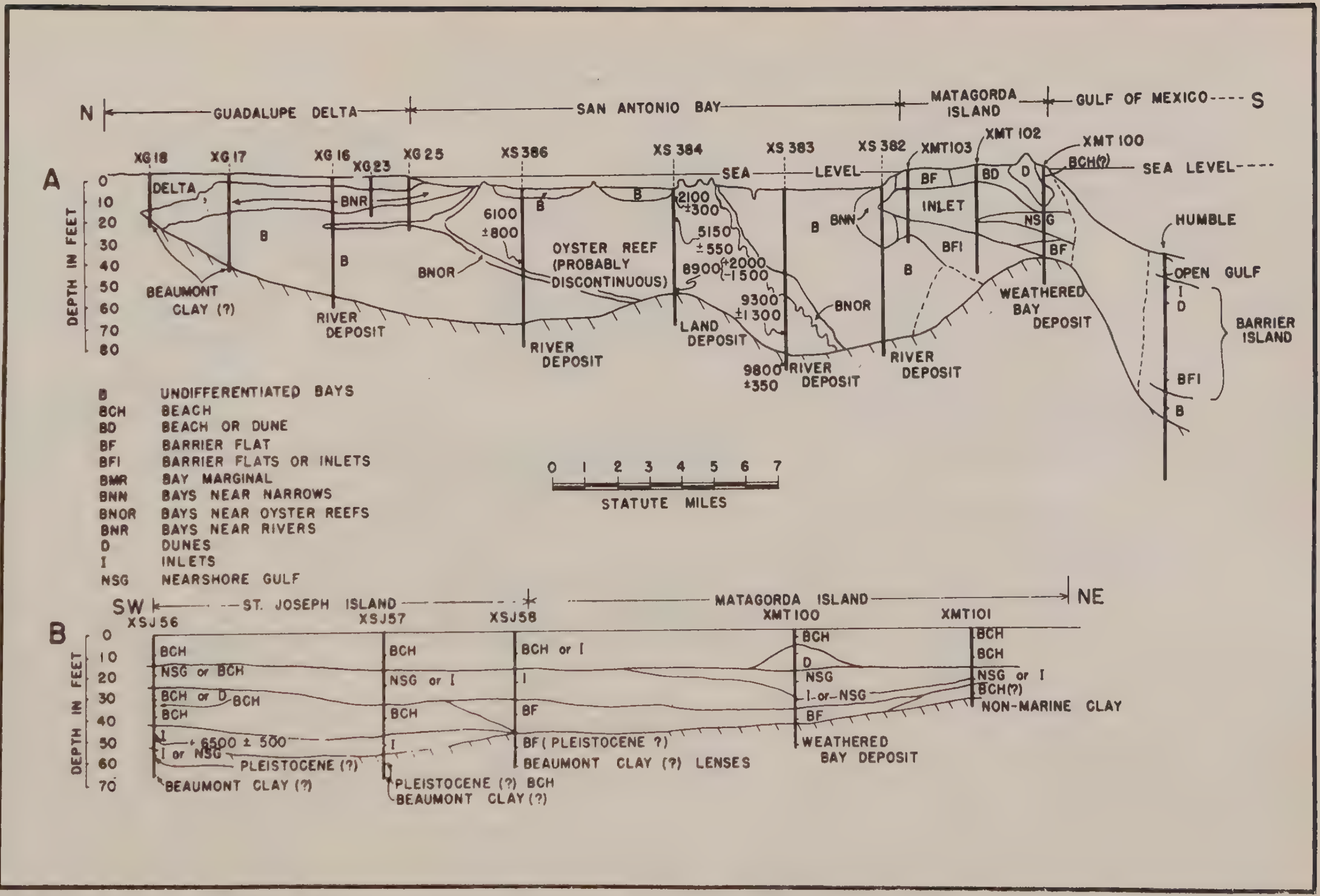
N
GUADALUPE DELTA
SAN ANTONIO BAY
MATAGORDA ISLAND
GULF OF MEXICO
S
A
DEPTH IN FEET
0
10
20
30
40
50
60
70
80
XG 18
XG 17
XG 16
XG 23
XG 25
XS 386
XS 384
XS 383
XS 382
XMT 103
XMT 102
XMT 100
SEA LEVEL
BCH(?)
DELTA
BNR
B
BEAUMONT CLAY (?)
RIVER DEPOSIT
BNOR
6100 ±800
OYSTER REEF (PROBABLY DISCONTINUOUS)
2100 ±300
5150 ±550
8900 +2000 -1500
9300 ±1300
9800 ±350
LAND DEPOSIT
BNN
BF
BD
D
INLET
NSG
BFI
WEATHERED BAY DEPOSIT
HUMBLE
OPEN GULF
I
BARRIER ISLAND
B UNDIFFERENTIATED BAYS
BCH BEACH
BD BEACH OR DUNE
BF BARRIER FLAT
BFI BARRIER FLATS OR INLETS
BMR BAY MARGINAL
BNN BAYS NEAR NARROWS
BNOR BAYS NEAR OYSTER REEFS
BNR BAYS NEAR RIVERS
D DUNES
I INLETS
NSG NEARSHORE GULF
0 1 2 3 4 5 6 7
STATUTE MILES
SW
ST. JOSEPH ISLAND
MATAGORDA ISLAND
NE
B
XSJ 56
XSJ 57
XSJ 58
XMT 100
XMT 101
BCH
NSG or BCH
BCH or D
BCH or I
NSG or I
I or NSG
I-or-NSG
6500 ± 500
PLEISTOCENE (?)
BEAUMONT CLAY (?)
PLEISTOCENE (?) BCH
BF (PLEISTOCENE ?)
BEAUMONT CLAY (?) LENSES
WEATHERED BAY DEPOSIT
BCH(?)
NON-MARINE CLAY

FIG. 5.—Interpretation of the sediments found at various depths in the holes, *A*, along San Antonio Bay, and *B*, along the beaches of St. Joseph and Matagorda islands. For locations, see figures 2 and 4. The individual samples are labeled only in section *B* because the close spacing in section *A* made this difficult, except in the case of the Humble well.

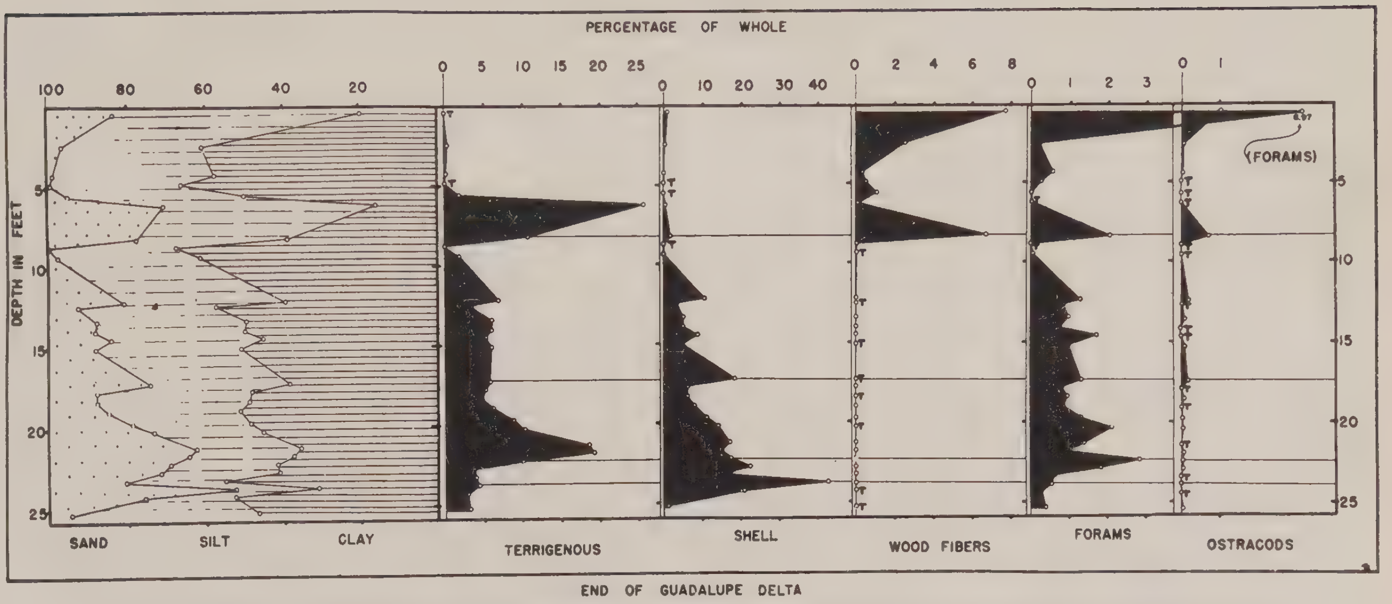

FIG. 6.—Variation of constituents and of sand-silt-clay along the length of a continuously bored hole in the end of Guadalupe Delta

trates 9 feet of muddy deposits similar to those of the inner barrier island flats and pools. This is underlain by sandy inlet deposits which extend to 17 feet, where there are muddy deposits indicative of inlets which are not connected directly to the Gulf (see Shepard and Moore, 1955). At 29 feet a bay deposit is indicated. The hole in the middle of Matagorda Island goes through barrier-island deposits, most of which seem to be characteristic of inlets, penetrating at the base into deposits that are suggestive of the present barrier flats. A hole made in the Gulf beach of Matagorda Island penetrated through thick sections of beach and dune sands into inlet deposits and, at a depth of 50 feet, reached a clay which, judging from its weathered appearance, is indicative of Pleistocene conditions. Seaward of the barrier island, the Humble Oil Company well penetrated about 12 feet only of open Gulf sediments before entering into what appears to be a barrier-island deposit. The latter, which includes some dune sand, persists to about 65 feet where bay deposits are found. At 78 feet the well penetrated what was interpreted by Humble Oil Company geologists as Pleistocene.

The transverse section of lower San Antonio and Mesquite bays (fig. 3) goes through bay sediments with thicknesses of 70–80 feet in three of the holes. Below that depth two of the holes encountered Pleistocene Beaumont clay, and the third, a river deposit with an age determined from wood fragments to be about 9,800 years. In the northeastern hole probable Pleistocene was encountered at only 12 feet. In the Mesquite Bay hole at 16 feet, deposits were found which are believed to represent the outer border of the Pleistocene barrier islands which form Live Oak and Black Jack peninsulas. The faunas and general character of the sequence indicate that this barrier island was encroaching on a marine deposit. The varying depth of the Pleistocene in this section indicates a submerged valley which became a bay when the sea came into the area. However, the nature of the deposits suggests that the bay was not directly connected with the open Gulf.

The section along the Gulf beaches of St. Joseph and Matagorda islands shows a persistence of beach, dune, or some other barrier-island environment, down to depths varying from 30 to about 60 feet, where old weathered formations high in clay were encountered—apparently representing the Beaumont stage of the late Pleistocene. The section under the beaches seems to show very clearly that deposits were formed under barrier-island conditions rather than in the open Gulf. This can be told by the general character of the faunas and by the dissimilarity of the size distribution in the sediments to that found regularly in the sandy sediments of the open Gulf near the barrier islands (see fig. 7). Also, glauconite, of which a minimum of 0.1 per cent is found in most open Gulf sediments of the vicinity, is very scarce in barrier-island sediments; a similar scarcity in the sediments of the barrier-island borings argues against an open Gulf origin. At the bottom of one hole shells were found that are characteristic of the bay beaches on the inside of the islands. A few samples, from depths up to 44 feet in the holes, had a roundness index which is found exclusively in dune sands in this area (Beal and Shepard, in press). This gives further confirmation that the islands had existed as such during the deposition of the 30–60 feet of sediment penetrated above the Pleistocene contact.

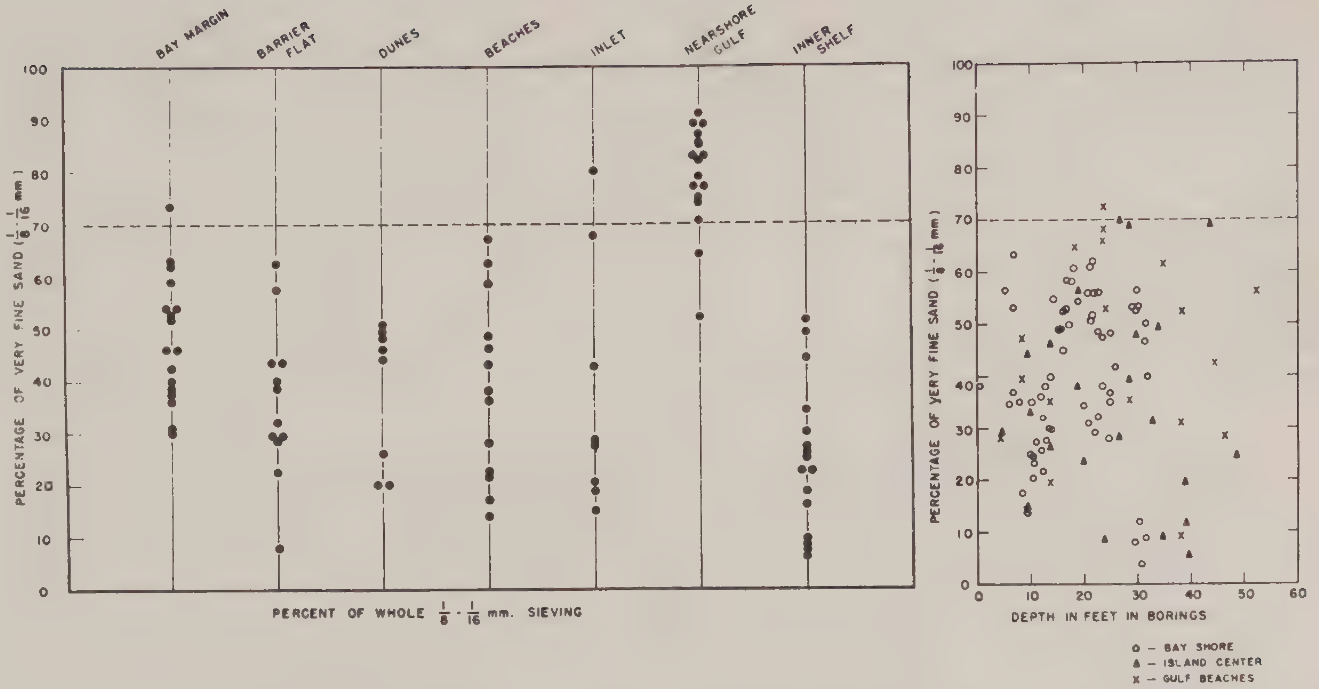

FIG. 7.—Showing the percentage of very fine sand ($\frac{1}{8}$–$\frac{1}{16}$ mm.) in (1) the sandy environments of the central Texas area, and in (2) the borings made into two barrier islands. Note that the latter have been subdivided according to the position of the boring. The general absence of percentages in the boring samples as high as those typical of the near-shore environment indicates that near-shore Gulf conditions were virtually absent during the deposition of the sediments underlying the barrier islands.

AGE DETERMINATIONS BY CARBON 14 METHOD

Through the courtesy of Magnolia Petroleum Company's Field Research Laboratory and under the direction of Dr. Nelson P. Stevens, a series of seven carbon 14 dates were determined for us from samples obtained in the borings. Four of these have been checked by a double run, and three showed consistent results with the earlier run. Six of the ages, however, are based on oyster shells which may give results a few hundred years too old, because oysters living in a carbonate-rich environment may extract some ancient carbon from solution to incorporate in their shells. Six of the determinations were made along the line of the San Antonio Bay section (figs. 2, 5). The seventh measurement came from some shells obtained at 46 feet under the thick sand section of the St. Joseph Island beach in hole XSJ 56 (figs. 4, 5). These ages show that the bay deposits date back to about 9,300 years and that barrier-island deposits go back to at least 6,500 years.[3]

At least a portion of the thick sections of recent sediments, comparable to present-day bay sediments, were deposited during the melting of the ice sheets at the end of the last glacial episode. The 9,300-year figure, deep in the oyster reef of XS 383, and the 9,800 years, based on wood fragments in the underlying river deposit, indicate that the sea came into the area around 9,500 years ago, entering the valley in San Antonio Bay about 85 feet below present sea-level.[4] The valley was presumably eroded by rivers during a still lower sea-level, like the valleys of the Louisiana area described by Fisk (1944 and 1952). Similar valleys have been found by many people along the Texas coast.

Even the very early bay deposits contain little if any evidence of access of open Gulf material. This indicates that when the sea invaded the valleys, bars were built across the mouths of the bays, producing semiclosed bays like those of the present day. The existence of oyster reefs even at the base of the bay deposits is substantial evidence that the bay was partly blocked from the open Gulf. Evidence that the barrier island was growing up during the deposition of bay material, which followed, comes from the finding of the 6,500-year age for the shells at 46 feet in the sands under St. Joseph Island. In this case also we have confirming evidence that the deposition took place at a time when the sea-level was rising.

A slow rate of deposition in the upper layers of hole XS 384 is well established by two carbon 14 dates. Actually, this may not mean that deposition in the bays as a whole was as slow as indicated by the 2,200 years for the 4½-foot sediment cover, because the date comes from oyster-reef material, and it is likely that the reefs stood then as they do now above the general level of the bay. It is probable that deposits first formed on either side, building up to the level of the oyster reef before that became covered. The study of Foraminifera abundance at the various depths in the bay borings (Moore, 1955) indicates the likelihood that deposition has gone through a series of alternations, so that it was slow prior to 7,000 years ago, rapid (as much as 2 feet per century) from 7,000 to 5,000 years ago, then slow from

---

[3] A check on this 6,500 ± 300 date was made by Dr. Hans Suess of the U.S. Geol. Survey. His analysis (W228) gives a date of 6,050 ± 300 years for the sample.

[4] There is, of course, the likelihood that the area has subsided somewhat since that time so that this does not prove that the sea stood 85 feet below the present level at that time.

5,000 to 500 years ago (as little as 0.3 foot per century) and then increasing to about 0.7 foot per century since 500 years ago.

MIGRATION OF BARRIER ISLANDS

The information from the borings provides some data concerning the direction in which the barrier islands of this area have been migrating in postglacial time. If the barriers had grown seaward over the marine deposits of the frontal slope, it seems almost certain that the characteristic near-shore Gulf sediments and faunas would have been discovered. Since only one sample of the 102 which have been investigated fits in size distribution into the near-shore Gulf environment (fig. 7), we seem to have found virtually no evidence of a seaward migration of these barrier islands. The suggestion that the seaward margins have migrated in a landward direction comes from finding that the beach material grades down into deposits more characteristic of the interior or the bay-shore of the barrier islands than of the frontal area.

The evidence from the bay-shore borings of the islands is twofold. The underlying material along the San Antonio Bay shore of Matagorda Island (XMT 103, fig. 1) is suggestive of bay deposition, indicating a migration bayward in that case. On the other hand, the borings on the north part of St. Joseph Island (XSJ 61, fig. 1), and on the tidal flat at the southeast end of Mud Island (XMud 11, fig. 1) penetrated deposits which were apparently terrestrial, because they lack the faunas found in all present-day bay or Gulf deposits.

Barrier-island material was found on top of bay deposits in the samples which were given us by Humble Oil Company from their offshore drilling. This gives further indication of a landward migration of the barrier islands, presumably during the rise in sea-level. This barrier island has been covered by the waters of the Gulf for a considerable period, as shown in the top 12 feet of marine (open Gulf) sediments.

The discovery that the barrier islands have moved more toward the land than away from it in this particular area appears to contradict the indications from a series of ridges, generally referred to as "beach ridges," which are found next to the fringing dunes on both Matagorda and St. Joseph islands. It is probable, however, that these ridges were formed as dunes, since they have the typical dune-sand roundness which is consistently higher than that of beach sand in the area. This probably indicates that the dune ridges formed inside a seaward advancing shoreline which resulted from a temporary, very slight submergence.

The findings in this central Texas area should not be used as evidence that all barrier islands necessarily migrate toward the land. In some other areas comparison of old charts and photographs with present-day conditions indicates that barrier islands have grown seaward. New islands are actually being formed along parts of the west coast of Florida and in some places have appeared subsequent to airplane photographs of 1934 and after sounding surveys of 1930 (Shepard, 1952, figs. 3, 7).

RELATION TO GLACIAL AND POST-GLACIAL SEA-LEVELS

The sequence of events indicated by the borings along the central Texas coast may provide some helpful information concerning the times and nature of the sea-level changes at the end of the Pleistocene. The Gulf Coast is probably subsiding somewhat, but it seems likely that it is more stable than the glaciated areas where large changes of level are still occurring as the result of the readjustment of the earth's crust to the loss of weight from the melted ice sheets. The carbon 14 dates, which indicate that the sea was rising and attained a level of about 80 feet below the present sea-level some 9,300 years ago, appear to correspond with the finding by Fisk (1952, p. 40) of shells dating about 9,000 years at 73 feet below sea-level in the Mississippi Delta and by Edmund Gill of a tree found at a depth of 69 feet below sea-level in a place near Melbourne, Australia, with an age of about 8,800 years.[5] Comparing the 9,500 years with glacial chronologies, the time scale provided by Flint (1953) shows the Mankato Maximum at about 10,000 years ago and Antevs (1954) gives the Valders Maximum as about 11,000 years ago. The result of the retreat of these ice masses may have brought the sea into the bays. Several Gulf Coast geologists, on the other hand, are more inclined to the idea that the ice retreated rather constantly from about 25,000 years ago (Fisk, 1952; LeBlanc and Bernard, 1954) and reached the present level about 4,000 years ago. There is no evidence from the borings which would help decide this question.

A postglacial thermal maximum (also called climatic optimum, or altithermal) is thought to have existed about 4,000–7,000 years ago (see Flint, 1953, pl. 3; Antevs, 1954, fig. 1). It is generally believed that this was a period of high sea-level as first suggested by Daly (1920). If the sea did stand 10 feet or more above its present level during this period, or during any considerable portion of the time, it would have left a record that was clearly depicted in the borings, because the bays would have been deeper and would have shoaled a few thousand years ago. Judging from the finding of abundant Foraminifera in the present-day deeper portions of Aransas Bay, it seems likely that a similar abundance of Foraminifera would have developed in the bay deposits formed during the thermal maximum if the sea-level were higher. The Foraminifera are abundant, however, during a period extending from about 500 to a maximum of 5,000 years ago. This certainly does not conform with the period considered to be the time of postglacial high sea-level. Furthermore, the rise of sea-level to a height well above the present should have extended the sea a considerable distance up the Guadalupe Valley, developing extensive bay deposits at such locations as XG 18 (fig. 2). Only a very thin post-Pleistocene bay deposit was found in that well, nor is there any indication of an unconformity. This thin bay deposit appears to have formed in very close proximity to the delta. Also, according to all indications, this very slight bay invasion was at a period much closer to the present than to the supposed postglacial thermal maximum.

The interpretations from these borings should not be given any more weight than those from any other relatively stable area from which similar information is available, but, unfortunately, most other detailed information comes from areas which have been glaciated or from the tracts marginal to glaciation. It would be very helpful to obtain more information both from the Gulf Coast and from other coastal plain areas where drilling is in progress.

---

[5] See also Swain and Prokopovich, 1954.

ACKNOWLEDGMENTS.—The writer wishes to express especial appreciation to D. G. Moore, who was in charge of much of the field work and co-operated extensively in studying the materials. In addition Frances L. Parker and Jean F. Peirson made many determinations of the environmental significance of the Foraminifera; R. H. Parker diagnosed the macro-organism environments of the samples; W. D. Johns determined the clay minerals in a number of samples, and D. M. Poole and Harry Lusk made grain-size determinations of the samples. The Magnolia Petroleum Company's Field Research Laboratory, through the courtesy of C. I. Alexander and N. P. Stevens, supplied carbon 14 age determinations, and The Humble Oil Company, through the courtesy of H. N. Fisk, supplied samples from an offshore boring. Many others have contributed directly or indirectly to the results which are summarized in this report.

REFERENCES CITED

ANTEVS, ERNST, 1954, Geochronology of the Deglacial and Neothermal ages: a reply: Jour. Geology, v. 62, p. 516–521.

BEAL, M. A., and SHEPARD, F. P., (in press), A use of roundness to determine depositional environments: Jour. Sed. Petrology.

DALY, R. A., 1920, A general sinking of sea-level in Recent time, Nat. Acad. Sci. Proc., v. 6, no. 5, p. 246–250.

FISK, H. N., 1944, Geological investigation of the alluvial valley of the lower Mississippi River, U.S. Army Corps of Engineers, 78 p.

——— 1952, Geological investigation of the Atchafalaya Basin and the problem of Mississippi River diversion, v. 1: U.S. Army Corps of Engineers, 145 p.

FLINT, R. F., 1953, Probable Wisconsin substages and late-Wisconsin events in northeastern United States and southeastern Canada: Geol. Soc. America Bull., v. 64, p. 897–920.

LEBLANC, R. J., and BERNARD, H. A., 1954, Résumé of late Recent geological history of the Gulf Coast: Geol.-mijn., nr. 6, n. s. 16e Jaarg., p. 185–194.

MOORE, D. G., 1955, Rate of deposition shown by relative abundance of Foraminifera: Am. Assoc. Petroleum Geologists Bull., v. 39, p. 1594–1600.

SHEPARD, F. P., 1952, Revised nomenclature for depositional coastal features: Am. Assoc. Petroleum Geologists Bull., v. 36, p. 1902–1912.

——— and MOORE, D. G., 1954, Sedimentary environments differentiated by coarse-fraction studies: Am. Assoc. Petroleum Geologists Bull., v. 38, p. 1792–1802.

——— — ——— 1955, Central Texas coast sedimentation: characteristics of sedimentary environment, Recent history, and diagenesis: Am. Assoc. Petroleum Geologists Bull., v. 39, p. 1463–1593.

SWAIN, F. M., and PROKOPOVICH, N., 1954, Stratigraphic distribution of lipoid substances in Cedar Creek Bog, Minnesota: Geol. Soc. America Bull., v. 65, p. 1183–1198.

CHAPTER 1

OPTICAL MEASUREMENTS OF SEA SURFACE ROUGHNESS

Charles Cox
Scripps Institution of Oceanography,*
La Jolla, California

Methods are described for interpreting, in terms of statistics of surface slopes, the distribution of brightness of glitter of the reflected sun. The methods depend on associating with every point on the sea surface that particular slope required to reflect the sun's rays toward the observer. Since the observations require no physical contact with the sea surface and the law of reflection applies even for minute ripples, the methods are particularly suited for aerial observation of low frequency waves and measurements at the high frequency and of the wave spectrum.

In the first method aerial cameras are used to find the average brightness in the vicinities of a series of points on the sea surface; from this information the probabilities of the corresponding slopes are calculated. Correction for background illumination is necessary.

In the second method a telescope and photocell combination mounted near the sea surface detects the spatial variations of brightness over a limited area of sea. The "power spectrum" of the electrical signal is shown to be closely related to the "power spectrum" (in spatial coordinates) of sea surface slopes.

In a third method photographs from high altitude are used to deduce the spectrum of long waves on the sea surface.

I. INTRODUCTION

If the sea surface were perfectly plane, the reflected image of the sun would resemble the sun itself and be fixed in position. The actual sea surface is never plane, and the sun's image is broken into myriads

---

*Contribution from the Scripps Institution of Oceanography, New Series, No. 836. This work has been sponsored by the Geophysics Research Directorate of the Air Force Cambridge Research Center, under Contract No. AF (19)604(1053).

Reproduced, by permission, from the Proceedings, 1st Conference on Engineering Instrumentation, 1955. Council on Wave Research. Engineering Foundation. 1956.

of sparkles, each a tiny distorted image of the sun (or a part of it). As the surface moves, the sparkles move and wink on and off. We shall be concerned here with relations between the spatial distribution of sparkles and the spectrum of sea surface waves which gives rise to it.

First we consider the average brightness pattern; this could be photographed, for example, by taking a long time exposure. This leads to a measure of the sea surface slope probability distribution and a technique is outlined in section II for its measurement. In section III we consider the distribution of brightness in space on a finer scale; this could be photographed by an instantaneous snapshot.

Suppose a series of snapshots is made with a camera suspended at a high altitude over the sea. At first the camera is badly out of focus, but gradually it is brought into perfect focus. Then it would be found that the first photograph yields information similar to a long time exposure while the succeeding photographs yield in addition details of sea surface waves, first low frequency ones, then those of higher and higher frequency. An ideal photograph in perfect focus would yield information on the entire spectrum of ocean waves.

Finally, in section IV we consider advantages and limitations of these optical methods of study of the sea surface.

II. TECHNIQUE OF SLOPE PROBABILITY MEASUREMENT

The method of slope probability measurement consists of two phases: (1) of identifying, from the law of reflection, with every point on the surface that particular slope required to reflect the sun's rays toward the observer; and (2) of relating the average brightness at a particular point with the probability that the corresponding slope occurs. By choosing many such points one finds the probability distribution of slopes. A full development of these phases is available (Cox and Munk, 1954a); here we shall only mention some features of a photographic technique of measuring the brightness.

Four K-17 (six-inch focal length) aerial cameras were mounted on a frame which could be lowered through the bomb bay of a B-17 airplane and leveled during flight. They were wired for synchronous exposures. Two cameras pointed vertically downward, the other two pointed to port and were inclined downward at an angle of 30° with the horizontal. With this arrangement a 25 per cent overlap exists between the vertical and tilted photographs. One of the vertical cameras and one of the tilted cameras took ordinary in-focus or image photographs (Plate I), using "variable density minus blue" filters. These photographs were used to find the attitude of the plane and to note white caps, slicks, and cloud shadows on the sea. At an altitude of 2000 feet, two points on the sea

Glitter from reflected sunlight as viewed from an aircraft flying at 2000 feet altitude. The elevation of the sun is 75°. Upper and lower left: Tilted and vertical image photographs as described in Sec. I. The superimposed grids show the angle of slope (closed curves) and the azimuth of ascent relative to the sun's azimuth (radial lines) necessary for a sea surface facet to yield a reflection. The direction of the wind is shown by arrow and a 50-foot schooner (equipped to make meteorological observations) is circled. Notice overlap between photos and shadow of plane, faintly visible within the white cross (vertical photograph). Lower right: Vertical photometric photograph taken simultaneously with image photographs. The light circle indicated by the broken arrow is the "image" of the schooner. Camera data: Six-inch focal length K-17 cameras, 9-inch x 9-inch negatives. Exposure data for Aero Super XX film: Image photographs; 1/225 sec f/22, variable density minus blue filter. Photometric photographs: 1/50 sec, 0.66 inch diameter aperture, Wratten A-25 filter.

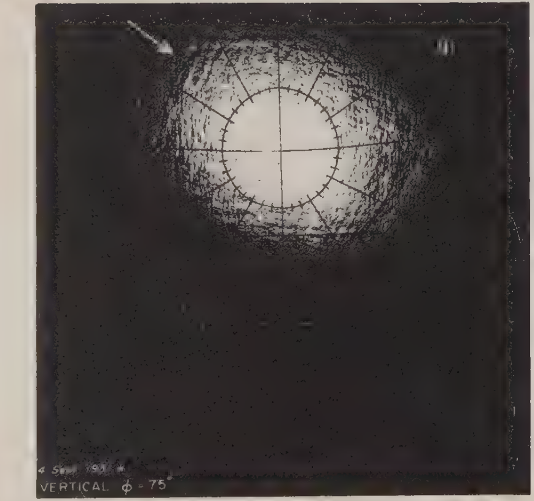

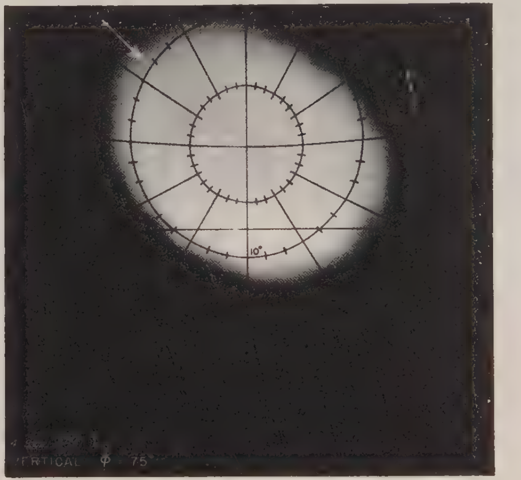

Plate I.

surface separated by more than 40 cm are resolved on the image photographs. The two remaining cameras were deliberately set out of focus by removing the lens systems. The resulting photometric photographs yield (by measurements of optical density) the average sea surface brightness and form the basis for computations of slope probabilities. In order to reduce unwanted background light, mostly blue in color, red glass filters were installed in these cameras.

During the photographic runs, the plane was steered by sun compass so that the azimuth of the tilted cameras was toward the sun. An attempt was made to avoid cloud shadows and atmospheric haze. In most cases the field of the cameras was sufficiently restricted to avoid these effects when the plane was flying at an altitude of 2000 feet.

All photographs have to be corrected for the roll, pitch and yaw of the plane. With some care in flying, these angles can all be kept to within a few degrees. They are uniquely determined from the positions on the photographs of the plane's shadow (Plate I) and of the horizon, allowance having been made for the depression of the horizon due to the earth's curvature.

The remaining problem is to relate the darkening of the photographic negative to the light incident on it. There are difficulties in using photographic techniques for measuring intensity; these result from the non-linear response of the film, the spreading of light in the film, and the failure of the reciprocity law. These difficulties are largely avoided by out-of-focus cameras: the variation of light incident over the film is so much reduced as compared to an in-focus photograph that spreading becomes negligible, and the exposure time is substantially constant all over the film. It only remains to determine the relation between density and light intensity; this can be done by comparison with calibration exposures produced by light of known intensities.

Because of the failure of the reciprocity law the calibration exposures have to be the same as the exposure on the flights. The calibration light source may consist of a concave diffusing surface (from a Federal 4"x5" cold light enlarger) illuminated by incandescent bulbs arranged in a ring within the periphery of the diffusing surface. The light is passed through a red filter in order to restrict the wave length range to that of the photometric photographs. Just before falling on the photographic film the light is intercepted by an optical wedge (a modified Eastman Kodak projection print scale) with eleven steps of differing transmission ranging from 100 to 3.7 per cent. The range of light intensities (100 to 3.7) from a single calibration can be extended by making several exposures with differing voltages on the incandescent lamps. Curves of density versus log intensity are then drawn for each exposure and fitted together by comparison of the overlapping range of densities. In this way a calibration range of light intensities of 1000 to 1 is obtained. No absolute measurement of light

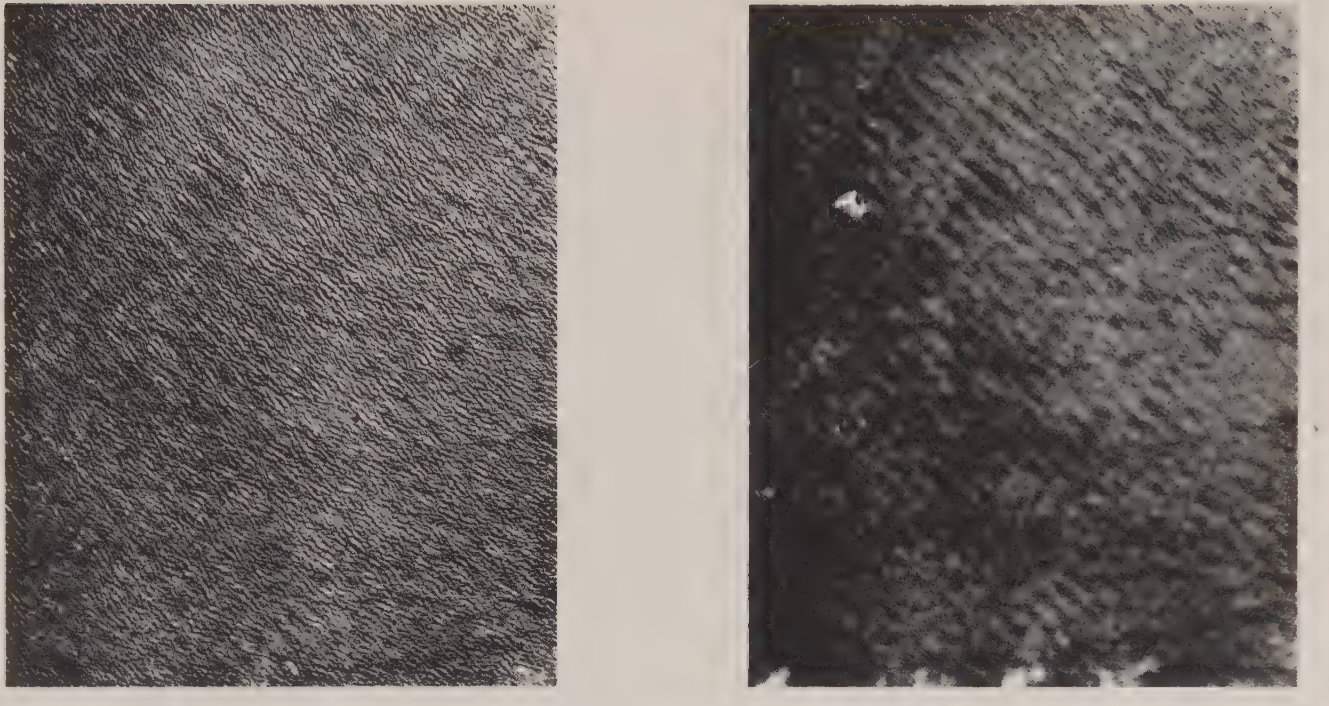

Plate II. "Edge of sun glitter pattern as viewed from 12,000 foot altitude. The tradewind swell is made visible because it alternately tilts the roughened sea surface toward and away from the camera, thus making it alternately more and less effective as a reflector. The reproduction at the right was printed out of focus from the same negative as that used in focus at left.

This "optical filtering" suppresses short wavelength variations in brightness, thus bringing out the underlying swell. For photometric work it is necessary that the original negative be exposed slightly out of focus, rather than the reproduced positive, because of certain basic faults of the photographic process. A one-inch distance on the photograph corresponds to 2000 feet on the ocean.

intensity is required to determine the probability distribution of slopes; hence the relative density-intensity scale established in this way is adequate.

Calibration exposures should be made on each roll of film just before and just after each flight. The roll film is then developed preferably in hand operated tanks using D-76 developer. On a roll containing only calibration exposures it has been found that the slopes, gamma, of the density - log intensity curves varied by less than 3 per cent except for exposures within 12 feet of the ends of the roll. Consequently, leaders of this length should be left on the ends of all photometric photograph rolls.

In addition to the reflection of the sun's rays from the sea surface, there are two other distinct sources of radiation: (1) the skylight reflected at the sea surface, and (2) the light scattered by particles beneath the sea surface. These provide the "background" against which the sun's glitter is measured.

Rough estimates can be made of the skylight. On the basis of this and a comparison with the observed background radiation on a calm day, an estimate of the scattered sunlight has been found, (Cox and Munk, 1954b). Correction for the background light is then made by subtraction, at every point of measurement on the photometric photograph, of the calculated backgrounds. Fortunately, the ratio of signal to background can be made fairly large by the use of a red filter, because sunlight is white while the skylight and scattered light is blue. Near the center of the sun glitter pattern, the ratio varies from 500:1 on a smooth sea to 15:1 on a very rough sea. But in computing the probability of the large (and infrequent) slopes, an essential limitation is imposed by the disappearance of the glitter radiation into the background of the reflected skylight and scattered sunlight.

III. SPATIAL DISTRIBUTION OF REFLECTIONS IN A RUFFLED SURFACE

In plate II, the presence of an underlying swell is apparent near the upwind edge of the glitter pattern. In the absence of the long swell the sea would be uniformly ruffled by the wind; this essentially produces the observed glitter pattern. When this ruffled surface is tilted toward and away from the observer by the swell, the resulting variations in brightness at the edges of the glitter pattern delineate the swell. And we shall find that the spatial distribution of brightness on a photograph is related not only to the low frequency part of the ocean wave spectrum, but to the high frequency part as well. The approximation of ray optics is used throughout the discussion.

The method is illustrated by a one-dimensional example.* Notation is shown in Fig. 1. The sea surface is supposed statistically uniform, hence $z(x)$ is a stationary random variable. Consider the slope of the sea surface, $s(x) = \partial z/\partial x$. According to the ray theory of optics, there will be a reflection toward the camera of rays from an element $\delta\phi$ of the source at every point on the surface where the relations

$$s_0 - \tfrac{1}{2}\delta s_0 < s \leq s_0 + \tfrac{1}{2}\delta s_0,$$

$$s_0 = \tan^{-1}[\tfrac{1}{2}(\phi - \psi)],$$

$$s_0 \pm \tfrac{1}{2}\delta s_0 = \tan^{-1}[\tfrac{1}{2}(\phi \pm \tfrac{1}{2}\delta\phi - \psi)],$$

hold, (Fig. 2), (this assumes that the aperture of the camera is vanishingly small). If the camera and light are at a great distance from the sea, $\tfrac{1}{2}(\phi - \psi)$ is a slowly varying function of x. This variation is neglected in the following treatment.

To express the brightness of the sea surface due to the element $\delta\phi$ one defines the function illustrated in Fig. 2,

$$b(s_0; x) = \begin{cases} (\delta s_0)^{-1} & \text{if } s_0 - \tfrac{1}{2}\delta s_0 < s \leq s_0 + \tfrac{1}{2}\delta s_0, \\ 0 & \text{otherwise;} \end{cases} \tag{1}$$

the intensity at position x as seen by the camera is then

$$i(s_0)\, b(s_0; x)\, \delta s_0,$$

where i is the intensity of the element of the sun after reflection in the water surface, that is, the intensity of the element $\delta\phi$ times the reflectivity of sea water. The intensity of the sun varies over its disc and the reflectivity varies with the angle of incidence; both of these variations have been included by representing i as a function of the slope of the reflecting facet, s_0.

The light intensity at the position x on the sea surface due to the entire sun is obtained by summing over all elements of the sun:

---

*I am indebted to Prof. Carl Eckart for helpful discussions of this subject. A fuller account including the generalization to two dimensions will be published elsewhere.

$$I(x) = \int_{-\infty}^{\infty} i(s_0) \; b(s_0; x) \, ds_0. \qquad (2)$$

The limits $\pm\infty$ may be used provided one sets $i(s) = 0$ for slopes such that no reflection of the sun is possible.

We may now describe the variation of intensity over the surface of the sea by its "mean displaced product" (MDP),

$$r_I(\xi) = \langle I(x) \; I(x+\xi) \rangle. \qquad (3)$$

(The symbols $\langle \, \rangle$ indicate a space or time average of the enclosed quantity. Since the sea surface is assumed statistically uniform there will be no difference in the two types of average. Another advantage of choosing conditions when the sea surface is statistically uniform is that the MDP is then a function only of the lag distance, ξ, as written.) A quantity easily calculated from the MDP is the autocorrelation of slope, $r_I(\xi) - \langle I \rangle^2$. The autocorrelation is particularly useful because it is the Fourier cosine transform of the spatial spectrum of intensity and conversely. The spectrum is readily measured by electronic methods.

Combining equations (2) and (3) one finds that

$$r_I(\xi) = \iint_{-\infty}^{\infty} i(s_1) \, i(s_2) \langle b(s_1; x) \, b(s_2; x+\xi) \rangle \, ds_1 \, ds_2. \qquad (4)$$

The dependence upon the statistics of the sea surface are evidently contained in the averaged term. It can be shown that

$$\langle b(s_1; x) \, b(s_2; x+\xi) \rangle \, ds_1 \, ds_2 = p_2(s_1, s_2; \xi) \, ds_1 \, ds_2, \qquad (5)$$

where $p_2 \, ds_1 \, ds_2$ is the joint probability that the sea have the slope s_1 within the range $\pm \frac{1}{2} ds_1$, at x and the slope s_2 within the range $\pm \frac{1}{2} ds$ at $x+\xi$.

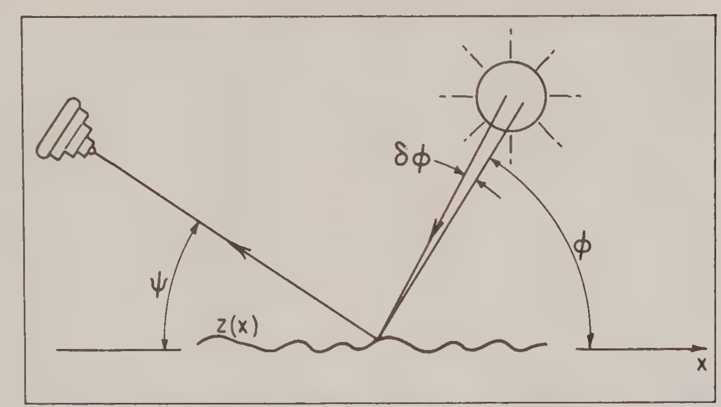

Fig. 1. Notation for one-dimensional discussion of sun glitter distribution. The elevation of the sea surface from its undisturbed level is z, a function of horizontal coordinate x. An element of a light source, the "sun", of angular size $\delta\phi$ is at an elevation ϕ. The observer's camera is at elevation ψ.

Fig. 3. The joint probability function $p_2(s_1, s_2; \xi)$. When the lag distance ξ is large so that s_1 and s_2 are scarcely correlated p_2 differs from zero largely in the region outlined by the open ellipse. For smaller lag distances the region becomes narrower as shown by the narrow ellipse. In the limit, $\xi \to 0$, p_2 develops into a "razor-back" along the diagonal line. The volume indicated by $\int_{-\infty}^{\infty} p_2 ds_1 ds_2$ remains equal to unity.

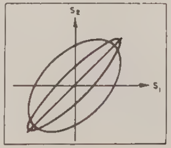

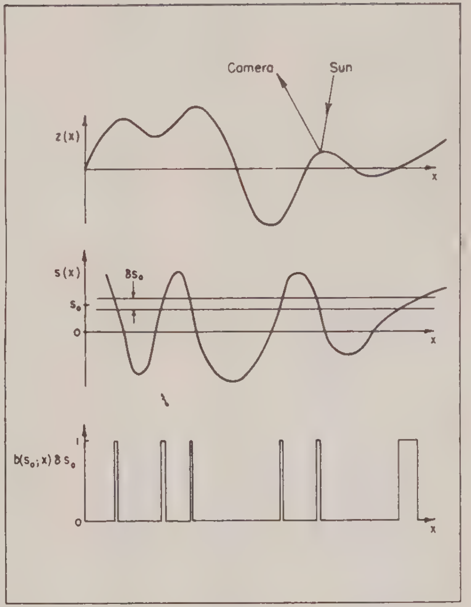

Fig. 2. The sea surface elevation, $z(x)$, is illustrated by the upper curve. The middle curve shows the corresponding sea surface slope. The two thin lines centered at slope s_0 and separated by an amount δs_0 delineate, by their intersections with the heavy line, the regions in which reflections will occur. The lower curve shows the function $b(s_0; x)$ defined by equation (1).

To proceed further one must know the form of the joint probability function. It is known that the first probability function (obtained by integrating over the entire range of one slope variable in p_2) is close to a Gaussian distribution (Cox and Munk, 1954b). This suggests that a suitable first approximation is the two-dimensional probability distribution (Rice, 1944, Sec. 2.9, 2.10)

$$p_2 = (2\pi\sigma^2)^{-1}(1-\rho^2)^{-\frac{1}{2}} \exp[-\tfrac{1}{2}(1-\rho^2)^{-1}\sigma^{-2}(s_1^2 - 2\rho s_1 s_2 + s_2^2)], \qquad (6)$$

where σ is the rms slope and $\sigma^2\rho$ is the slope autocorrelation,

$$\sigma^2 \rho(\xi) = \langle s(x)\, s(x+\xi)\rangle. \qquad (7)$$

However, it must be emphasized that a Gaussian first distribution does not require a Gaussian joint distribution. The justification can only come from experimental observations which are not yet available.

The limiting value, unity, of $\rho(\xi)$ as lag distance, ξ, tends to zero causes p_2 to develop a razor-sharp ridge along $s_1 = s_2$ as ξ tends to zero (Fig. 3). For large lag distances on the other hand p_2 is well behaved and a suitable approximation to equations (4) and (5) is

$$r_I(\xi) = \left[\int_{-\infty}^{\infty} R(t)\, dt\right]^2 p_2(s_0, s_0; \xi), \qquad (8)$$

where

$$R(t) = \int_{-\infty}^{\infty} i(s)\, i(s+t)\, ds, \qquad (9)$$

and $i(s)$ differs from zero in the neighborhood of $s = s_0$.

This result does not depend on the particular character of p_2

but only requires that $p_2(s_1,s_2)$ should not vary appreciably from $p_2(s_0,s_0)$ throughout the region in which $i(s_1)\,i(s_2)$ differs from zero. Since the angular diameter of the sun is only $\frac{1}{2}$ degree while the rms slope is of the order of ten degrees, this requirement is satisfied for ρ differing only slightly from unity.

For very large lag distances, $|\rho| << 1$, and a suitable expansion for the autocorrelation of brightness is, combining equations (6) and (8),

$$r_I(\xi) - \langle I\rangle^2 = \frac{\left[\int R(t)\,dt\right]^2}{2\pi\sigma^2} \exp\left(-\frac{s_0^2}{\sigma^2}\right)\left\{\rho\left(\frac{s_0}{\sigma}\right)^2 + \rho^2\left[\frac{1}{2}\left(\frac{s_0}{\sigma}\right)^4 - \left(\frac{s_0}{\sigma}\right)^2 + 1/2\right] + \ldots\right\}. \quad (10)$$

The first term in the curly brackets is proportional to the slope autocorrelation, the second to the square of the slope autocorrelation and so on. Hence, the autocorrelation of intensity is linearly related to the autocorrelation of slope for small enough values of the latter. The region of linearity is extended by choosing experimental conditions such that $s_0 = \pm\sigma$ for then the term within square brackets vanishes.

It is well known that the autocorrelation at long lag distances essentially determines the spectrum at low wave numbers (long wave lengths). Furthermore, the slope autocorrelation becomes small for long lag distances. Hence equation (10) demonstrates that the spatial spectrum of intensity differs from the spectrum of slopes only by a constant of proportionality for long waves.

At small lag distances the discussion has to take into account the razor-back shape of p_2. Using the Gaussian distribution, (6) it can be shown that the MDP of intensity is

$$r_I(\xi) = \frac{\sigma}{2\pi K\xi} \exp\left(-\frac{1}{2}\frac{s_0^2}{\sigma^2}\right)\int_{-\infty}^{\infty} R(t)\exp\left[-t^2/(2K^2\xi^2)\right]dt, \quad (11)$$

again provided the angular size of the light source is small compared with the rms slope, σ . Here $K^2 = \langle(\partial s/\partial x)^2\rangle$ is (approximately) the mean square curvature of the surface. The quantity $R(t)$, (equation 9), depends only on the size of the light source and distribution of intensity within it. Hence, since the spectrum at high wave numbers is largely determined by the autocorrelation at small lags, measurement of the intensity spectrum for very short wave lengths determines the rms curvature of sea surface. At intermediate wave lengths one has to use equation (9), find the autocorrelation of slopes, then take the cosine transform to find the slope spectrum.

An attempt is being made to exploit these "one-dimensional" relationships by a suitable technique. Instead of using the sun, a long horizontal tubular light source is placed close to the observer. Let the x,y plane be horizontal with the y-axis parallel to the light tube. Then a sea surface element will reflect light to the observer if the x-component of its slope, $s = \partial z/\partial x$, is appropriate regardless of the value of $\partial z/\partial y$. With this experimental arrangement the preceding analysis goes through without change except that the autocorrelations become functions of two lag components; for example,

$$r_I(\xi, \eta) = \langle I(x, y)\ I(x+\xi, y+\eta) \rangle,$$

and the term $\exp[-\frac{1}{2} t^2/(\kappa^2 \xi^2)]$ in equation (11) is replaced by

$\exp[-\frac{1}{2} t^2/(\lambda^2 \xi^2 + \mu \xi \eta + \nu^2 \eta^2)]$ where

$$\lambda^2 = \left\langle \left(\frac{\partial^2 z}{\partial x^2}\right)^2 \right\rangle, \quad \mu = \left\langle \frac{\partial^2 z}{\partial x^2} \frac{\partial^2 z}{\partial x \partial y} \right\rangle, \text{ and } \nu^2 = \left\langle \left(\frac{\partial^2 z}{\partial x \partial y}\right)^2 \right\rangle$$

are also closely related to the curvature of the sea surface. To measure the autocorrelation of intensity a photocell is mounted behind a moving curtain in the focal plane of a lens. As the curtain moves, the photocell scans the image of the sea surface through a small peep-hole in the curtain. The output of the photocell is then introduced into a spectrum analyzer. By scanning along the x direction, one finds (by taking the Fourier transform of the output) the autocorrelation with the lag component $\eta = 0$. Conversely, by scanning parallel to the y-axis, one finds the autocorrelation with $\xi = 0$.

The apparatus is conveniently mounted on a pier about 25 feet above sea level. This close approach to the sea surface is necessary to resolve the fine structure of ocean ripples, but it prevents one from studying long waves.

For the latter purpose it is necessary to have an unrestricted view over a very large uniformly illuminated area of ocean; hence, observations from a high altitude are indicated. Under the circumstances one must put up with a light source of small angular diameter such as the sun and the preceding "one-dimensional" discussion must be generalized. When this is done a joint probability distribution of the four slope components $s_{x1} = \partial z/\partial x$, $s_{y1} = \partial z/\partial y$ at the position (x_1, y_1), and of the same slope components, s_{x2} , s_{y2} at a displaced position (x_2, y_2) plays the important role corresponding to the joint distribution p_2. For a statistically uniform sea this distribution is a function of six variables:

$$p_4 = p_4(s_{x1}, s_{y1}, s_{x2}, s_{y2}; \xi, \eta),$$

where

$$\xi = x_2 - x_1 \quad \text{and} \quad \eta = y_2 - y_1 .$$

At moderate to long lag distances the MDP of intensity takes a form analogous to equation (8)

$$r_I(\xi, \eta) = \text{constant} \times p_4(s_{x0}, s_{y0}, s_{x0}, s_{y0}; \xi, \eta), \qquad (12)$$

where s_{x0} , s_{y0} are the slope components appropriate for reflection from the center of the sun. For long lag distance, where the autocorrelations of the slopes become small compared to the mean square slopes, the autocorrelation of intensity can be expanded to the first order of small quantities in the following form:

$$r_I(\xi, \eta) - \langle I \rangle^2 = \text{function of } (s_{x0}, s_{y0}) \times$$
$$\times \left(\rho_{xx} \frac{s_{x0}^2}{\sigma_x^4} + 2 \frac{\rho_{xy} s_{x0} s_{y0}}{\sigma_x^2 \sigma_y^2} + \frac{\rho_{yy} s_{y0}^2}{\sigma_y^4} \right). \qquad (13)$$

Here ρ_{xx}, ρ_{yy} are autocorrelations of s_x , s_y respectively and

ρ_{xy} is the cross correlation of s_x and s_y ; σ_x and σ_y are the rms values of s_x and s_y respectively.

Suppose one observes in a region where $|s_{xo}| \gg |s_{yo}|$. Then only the first term in parentheses contributes and one finds ρ_{xx} (or by taking the cosine transform, the spectrum of s_x). This can be summarized by the following statement: The spectrum of the two-dimensional distribution of intensity at the edges of a sun glitter pattern is proportional to the spectrum of that component of slope which increases away from the center of the glitter. This development forms a rational foundation for Barber's (1949) ingenious proposal for measuring the sea surface spectrum. Barber's technique was to use a photograph of the sea surface as a diffraction grating. The Fraunhofer diffraction pattern yields directly the spectrum of the blackening on the photographic plate. Three features of this technique are: 1) the position and shape of the light source influences the result; the most easily reproducible arrangement is to use sunlight rather than the skylight as Barber appears to have done; 2) the photographic process must be carefully controlled so that the blackening of the negative is linearly related to the light intensity. It may be desirable to set the camera slightly out of focus to reduce halation and Eberhard effects; 3) the procedure yields the spectrum of one slope component rather than of the sea surface elevation. To deduce the latter without ambiguity it is necessary to measure spectra of the two slope components, for example by photographs at two regions of a sun glitter pattern.

IV. DISCUSSION AND SUMMARY

Several techniques for optical studies of the sea surface have been outlined. They depend on the connection between the intensity of light reflected from the sea surface and the spectrum of the sea surface roughness. By measurements on a successively finer scale, the probability distribution of slopes, then the spectra of long waves, short waves, and ripples may be found.

One characteristic feature of optical techniques is that they require no contact with the sea. This is essential for the study of ripples since the slightest physical contact generates the very type of disturbance being studied. Observations of long waves are facilitated because no supporting structure on the sea bottom is necessary and measurements from aircraft over the open sea are possible.

The second feature, which may be exploited when photographs are taken, is that the two-dimensional character of ocean waves becomes measurable.

There are two approximations in the development which need further attention. The most important is the representation of probability distributions p_2 and p_4 by Gaussian forms. When the true distributions are known, the functions of slope which enter equations (10), (11), and (13) will be modified but probably not the essential content. Nevertheless, the general equations (8) and (12) indicate that the autocorrelation of intensity gives valuable information about the sea surface whatever the form of the probability.

The second approximation is that shadowing or hiding of part of the sea surface by waves, and multiple reflections, have been neglected. This effect becomes negligible when the elevation of source and observer (ϕ and ψ in Fig. 1) are both large compared to the rms slope. The condition is certainly satisfied for ϕ and ψ greater than, say, 30°.

There are also technical difficulties which should be emphasized. If photographs are used for quantitative measurement one is faced with all the difficulties of photometric photography. With any method of observation one must choose a time when the atmosphere is transparent and the sea is statistically uniform. The presence of oil slicks on the sea and variable winds may make the latter difficult. Furthermore, the methods of analysis fail at high wind speeds because an appreciable part of the sea surface is covered with foam.

In conclusion, one may state that optical studies of the sea surface offer possibilities for a two-dimensional presentation of sea surface roughness. Suitable techniques are as yet in a very early stage of development.

REFERENCES

Barber, N. F. (1949). A diffraction analysis of a photograph of the sea: Nature, vol. 164, p. 485.

Cox, C. and Munk, W. (1954a). Measurement of the roughness of the sea surface from photographs of the sun's glitter: Jour. Opt. Soc. Am., vol. 44, p. 838.

Cox, C. and Munk, W. (1954b). Statistics of the sea surface derived from sun glitter: Jour. Mar. Res., vol. 13, p. 198.

Rice, S. O. (1944). Mathematical analysis of random noise: Bell Sys. Tech. Jour., vol. 23, p. 282.

Vol. 37, No. 1 Transactions, American Geophysical Union February 1956
Reproduced by Permission

Observations of Underwater Volcanic Acoustics at Bárcena Volcano, San Benedicto Island, Mexico, and in Shelikof Strait, Alaska*

JAMES M. SNODGRASS AND ADRIAN F. RICHARDS

Abstract—Magnetic tape recorders and sonobuoy equipment have made possible a practical approach to the study of underwater volcanic acoustics. Underwater audio energy originating from Bárcena Volcano on San Benedicto Island, Mexico, was studied from plane and ship between November, 1952, and May, 1955, and tape recorded on four different occasions. The recorded sounds are of two kinds: a rumble with a pitch of approximately 125 cycles, and a higher frequency hiss. These sounds, unlike any of known biological or other origin, are discussed and a frequency analysis of the rumble is given. In order to determine the source of audio energy produced from Bárenca a triangulation method was devised by making an effectively simultaneous time and frequency analysis of selected portions of the acoustic spectrum from pairs of strategically placed sonobuoys. This technique was successfully used from shipboard in November, 1953. An unsuccessful attempt was made in August, 1953, to determine if audio energy generated from the active volcano Mt. Trident, in the Katmai National Monument, could be received in Shelikof Strait. The attempt is described to illustrate the technique used.

Introduction—The study of volcanic acoustics is in its infancy. The first recordings of volcanic sounds were made by *Perret* [1926, pp. 138–139] very early in this century who used a surface microphone, electromagnetic receiver, sapphire stylus, and a wax phonograph cylinder as his basic equipment to record underground rumblings in the Pozzuoli Solfatara near Naples.

More recently detonations of the 1950 Strombolian type of eruption of Oo-sima (O Shima), 68 miles south-southwest of Tokyo, were tape recorded by members of the NHK Broadcasting Bureau (Minakami, personal communication).

In 1952–53, *Dietz* and *Sheehy* [1954] ably demonstrated that low frequency volcanic sounds can travel great distances in the sea by correlating SOFAR records made in California with the trans-Pacific volcanic explosions of Myojin Reef located about 200 nautical miles south of Tokyo. However, these sounds, with a frequency of less than 500 cycles, were recorded as visual power levels on a drum recorder and are not audibly reproducible.

In recent years the availability of newly developed equipment has made possible a practical approach to the study of audio energy radiated from volcanoes. This paper reports on studies of underwater volcanic acoustics between November, 1952, and May, 1955, in two areas. Magnetic tape recordings were made at Bárcena Volcano on San Benedicto Island off the west coast of Mexico. A three-station listening survey across Shelikof Strait, between Kodiak Island and the Alaskan peninsula, was made in 1953 in an unsuccessful attempt to record sounds from active Mt. Trident volcano in the Valley of Ten Thousand Smokes.

Description of Bárcena Volcano—Bárcena Volcano, previously known as Boquerón or 'Big Mouth,' was born on August 1, 1952. The Volcano is situated on the southern end of three-mile-long San Benedicto Island which is located approximately 900 nautical miles south-southeast of San Diego, California, 218 miles south of the southern tip of Baja California and about 300 miles off the west coast of the Mexican mainland (Fig. 1). The birth of Bárcena and its development in 1952–53 has been summarized by *Richards* and *Dietz* [in press]. Briefly, a 1250-ft ash and cinder cone was erected within 12 days of the birth of the Volcano. Block lava half filled the crater in middle November, 1952, and in early December viscous lava pierced the eastern base of the cone and flowed out into the sea for over two months forming a delta of lava (Fig. 2 and 3). Bárcena became inactive in March, 1953. A strong emission of fumarolic steam continued to escape from the crater into 1954. Since August, 1954, only weak fumarolic activity has been observed from the crater and lava delta vent; the volcano is presumed to be dead.

Attempted SOFAR correlation—*Dietz* and *Sheehy* [1954, pp. 955–956] examined the SOFAR records at the Kaneohe, Oahu, and other stations in an attempt to correlate unknown sounds with known activity at Bárcena Volcano. They could not correlate any of the sounds received and concluded

---

* Contribution from the Scripps Institution of Oceanography, New Series, No. 837.

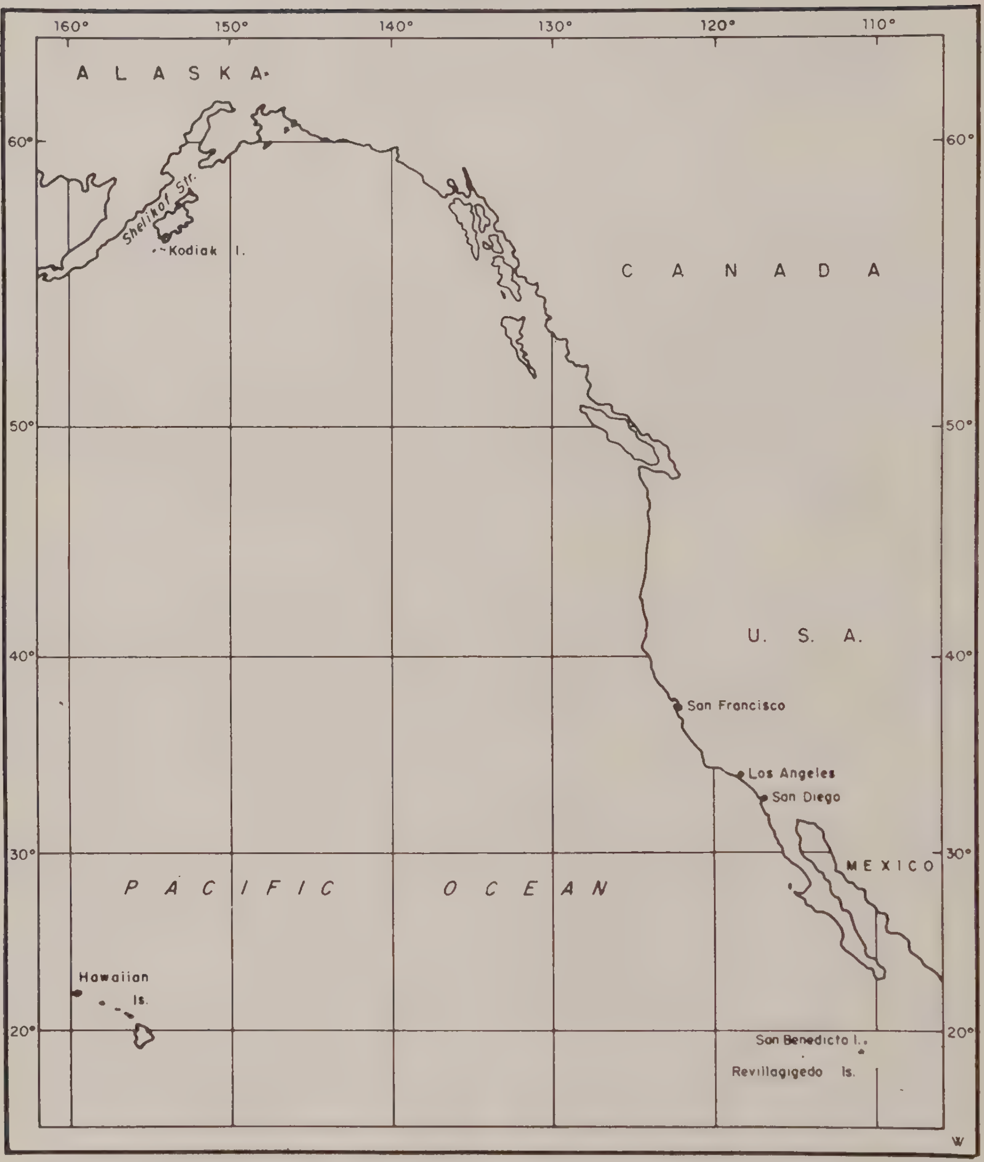
160°
150°
140°
130°
120°
110°
60°
50°
40°
30°
20°
A L A S K A
Shelikof Str.
Kodiak I.
C A N A D A
U. S. A.
San Francisco
Los Angeles
San Diego
MEXICO
P A C I F I C O C E A N
Hawaiian Is.
San Benedicto I.
Revillagigedo Is.
W

FIG. 1 – Location of San Benedicto Island, Mexico, and Shelikof Strait, Alaska

that either Bárcena was not producing sufficient energy into the water or that unknown submarine structures between the Volcano and Kaneohe prevented sound transmission.

Instrumentation—A brief summary of the instrumentation used at Bárcena Volcano is included in Table 1. The equipment used on all of the 1952–53 Navy flights consisted of Navy type AN/SSQ-2 sonobuoys, essentially small floating radio stations which contain a listening hydrophone sensitive to audio frequencies, a Navy R-316/ARR-26 sonobuoy receiver and a Magnecord model PT6-AH magnetic tape recorder and PT63-J amplifier. The tape recorder was mounted on a rubberized hair mattress to isolate it from the vibrations of the plane. Its power requirement was supplied by a 115-volt, 60-cycle dynamotor which operated from the 28-volt dc supply of the plane.

On the December, 1952, visit to Bárcena by the yacht *Observer* a stock model Zenith 75 hearing-aid

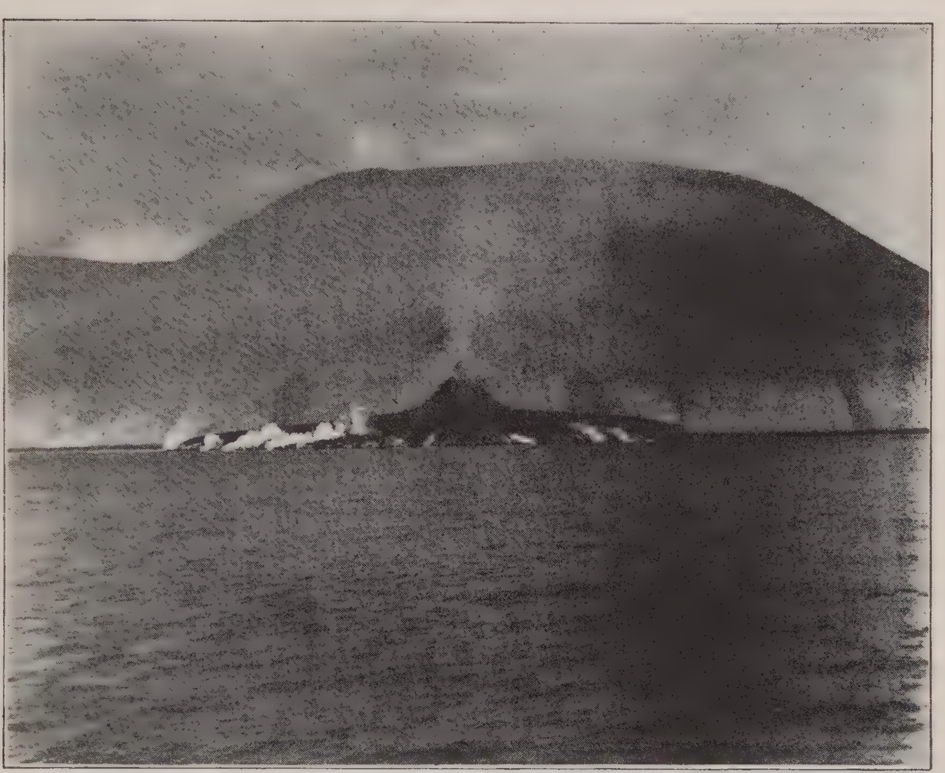

FIG. 2 – Proto-lava delta and Bárcena Volcano from the yacht *Observer*, December 10, 1952 (L. W. Walker photograph)

was slightly modified by substituting a sonobuoy hydrophone for the microphone. The hydrophone was connected to the hearing-aid through an impedance matching transformer and 100 ft of cable. This is the lightest, most portable equipment that has been used by the writers.

In March, 1953, the hydrophone-hearing-aid combination was again used at Bárcena Volcano from the Scripps Institution's research vessel *Crest*. The output from the hearing-aid at this time was fed directly into a model RP-402-A Concertone tape recorder.

Instrumentation of the triangulation technique used on the November, 1953, visit by the *R/V Crest* will be described in a separate section. A barium titanate hydrophone was also used during this visit. It was connected to a voltage amplifier and an Ampex model 403-2 tape recorder by approximately 110 ft of cable.

In May, 1955, a Navy Electronics Laboratory rochelle-salt crystal hydrophone was used with a voltage amplifier and a model RP-402-A Concertone tape recorder from on board the *R/V Crest*. The current to run the amplifier was supplied by a storage battery. The tape recorder was powered by a small gasoline generator isolated from the deck of the *Crest* by a partially inflated tire inner-tube.

The equipment used on the Shelikof Strait survey consisted of a sonobuoy hydrophone, 110 ft of cable, an impedance matching transformer, and a Stancil-Hoffman model M5A tape recorder, internally powered by batteries.

During the listening periods on the December, 1952, March, 1953, and May, 1955, expeditions to Bárcena Volcano and on the Shelikof Strait survey, all shipboard power equipment, including gyrocompass, was turned off to make the ship acoustically quiet. Experience gained on the 1953 Scripps Institution of Oceanography Trans-Pacific Expedition—when in the Bering Sea unsuccessfully listening for underwater volcanic sounds from volcanoes on the Aleutian Islands—and elsewhere has demonstrated that a ship must have all power equipment silenced for acoustic work of this type. Our studies have also demonstrated that a storage battery powered dynamotor is the most satisfactory means of supplying ac current to a high

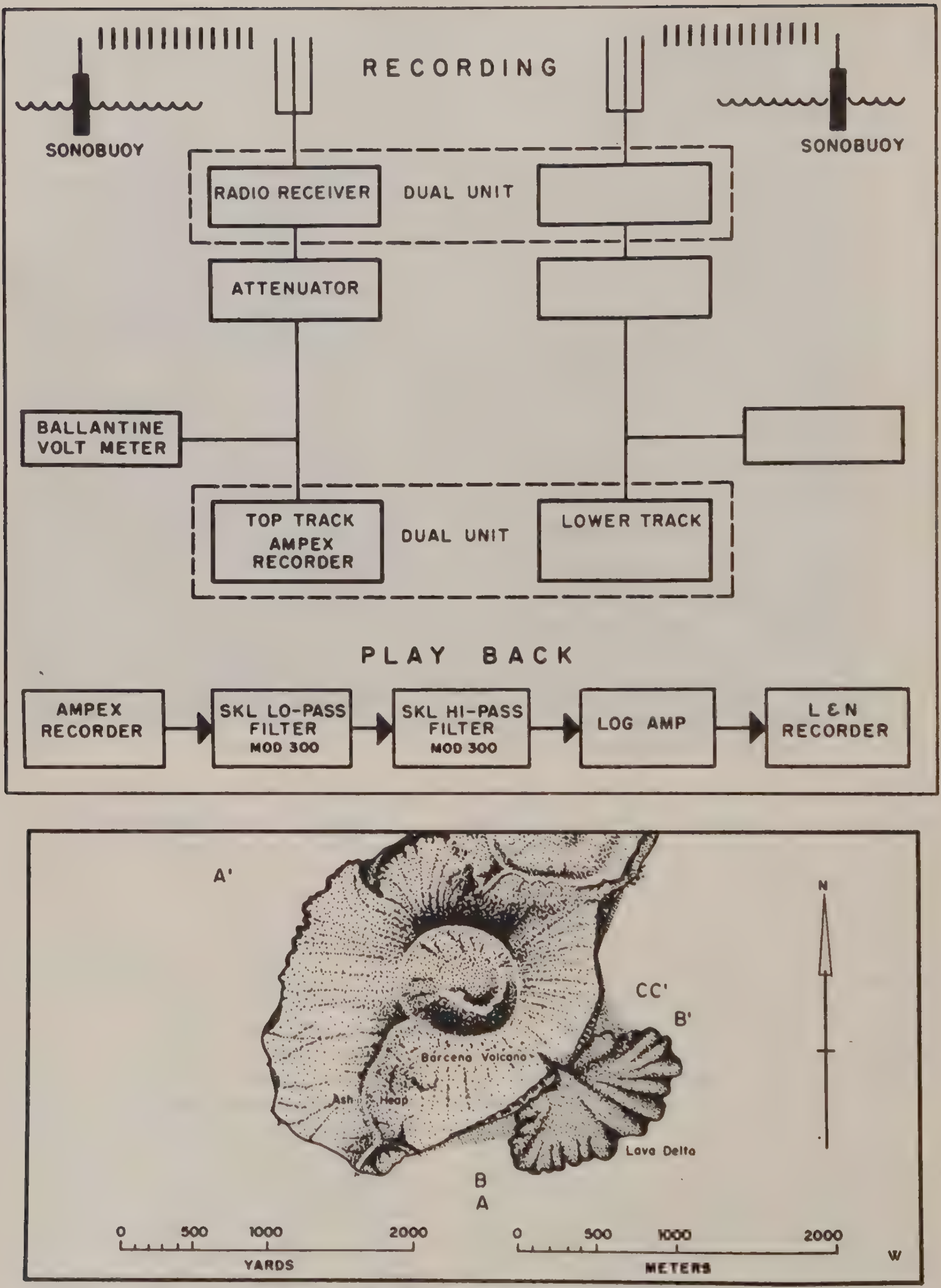
RECORDING
SONOBUOY
SONOBUOY
RADIO RECEIVER
DUAL UNIT
ATTENUATOR
BALLANTINE VOLT METER
TOP TRACK AMPEX RECORDER
DUAL UNIT
LOWER TRACK
PLAY BACK
AMPEX RECORDER
SKL LO-PASS FILTER MOD 300
SKL HI-PASS FILTER MOD 300
LOG AMP
L & N RECORDER
A'
CC'
B'
Bárcena Volcano
Ash Heap
Lava Delta
B
A
N
0
500
1000
2000
YARDS
0
500
1000
2000
METERS
W

FIG. 3 – Location of sonobuoys used in November, 1952, triangulation at Bárcena Volcano and block diagram of acoustic triangulation instrumentation

fidelity tape recorder. Special gasoline generators are often difficult to isolate acoustically from the deck of a ship, or even if isolated, may induce spurious noise into the water through the air.

Underwater acoustic observations at Bárcena Volcano—Between November, 1952, and May, 1955, observations of underwater volcanic acoustics were made at Bárcena Volcano. These obser-

TABLE 1 – *Summary of underwater acoustic observations at Bárcena Volcano*

Date	Instrumentation	Observation Craft	Tape re-corded	Sounds	Location of hydrophone or sonobuoy	Correlation and comments
Nov. 15, 1952	Sonobuoy, receiver, tape recorder	Navy PBM	Yes	Random rumble with a pitch of approx. 125 cycles	About one mile south of Bárcena volcano	No correlation with volcanic activity
Dec. 9–11, 1952	Hydrophone, modified hearing-aid	Yacht *Observer*	No	Continuous hissing	600 yd northeast of proto-lava delta	Noise of sea quenching incandescent block lava
Mar. 9–13, 1953	Hydrophone, hearing-aid, tape recorder	R/V *Paolina T*	Yes	Fish noises	500 yd southwest of lava delta	Equipment insensitive to low frequency sounds
April 16, 1953	Sonobuoy, receiver, tape recorder	Navy P4Y	No	None	About one mile south of lava delta	Power failure to tape recorder; no sounds heard when sonobuoy transmission monitored by ear
May 20, 1953	Sonobuoy, receiver, tape recorder	Navy P4Y	No	None	About one mile south of lava delta	Sonobuoys failed to work
July 13, 1953	Sonobuoy, receiver, tape recorder	Navy P4Y	Yes	Short bursts of hissing noise	About one mile south of lava delta	Sea quenching hot lava
Sep. 21, 1953	Sonobuoy, receiver, tape recorder	Navy P4Y	Yes	Rumble similar to that heard in Nov., seven-second bursts of hissing	About ½ mile south of lava delta	Rumble not correlated; hiss probably originated from sea quenching hot lava
Nov. 17–19, 1953	Sonobuoy, special recording equip., see Fig. 3	R/V *Crest*	Yes	Hissing	See Fig. 3	Triangulation for source of sounds; hiss probably due to sea quenching hot lava.
Mar. 25, 1955	Sonobuoy, special recording equip., see Fig. 3	Navy P5M	Yes	Fish noises	Same as illustrated in Fig. 3	Triangulation attempt from the air; Volcano inactive
May 1, 1955	Hydrophone, amplifier, tape recorder	R/V *Crest*	Yes	None	About ½ mile south of lava delta	Background noise produced by noisy generator too high to hear anything else; Volcano believed dead

vations are summarized in Table 1. For comparative purposes Table 2 lists the five reported observations of airborne volcanic sounds from 21 visits to the Volcano between the time of its birth on August 1, 1952, and the cessation of activity in early 1954.

The procedure on the 1952–53 flights was to drop two or three sonobuoys into the sea near the lava delta of the Volcano from altitudes of 500 to 10,000 ft. More than one sonobuoy was dropped on each flight to insure at least ten minutes of transmission time, for many of the buoys were defective, perhaps because they all had been used previously.

In December, 1952, the yacht *Observer* was anchored in 120 ft of water 600 yds from the seaward margin of the lava flow. The hydrophone was lowered to a depth of 90 ft. The only sound heard was the violent boiling noise of the sea quenching incandescent lava (Fig. 2). The level of this noise was sufficiently strong to mask completely all other underwater sounds, including normal wave and surf background noise.

In November, 1953, in conjunction with the triangulation technique a hydrophone was lowered to a depth of about 100 ft when the *R/V Crest* was near Bárcena. However, there was great difficulty in silencing the ship and essentially negative results were obtained. A similar difficulty was encountered in May, 1955.

During the time that the Volcano was visibly active, 1952–53, our equipment failed to receive volcanic sounds only twice. On the first occasion, in March, 1953, it is possible that low frequency sounds were present but below the 130 cycle lower limit of the hearing-aid. In April, 1953, no sounds attributable to volcanic activity were heard when the sonobuoy transmission was monitored by earphone. However, in November, 1952, and September, 1953, no low frequency sounds were heard when monitoring the transmission; yet these sounds were successfully tape recorded. Consequently, we feel that the absence of audible sounds, when monitoring the April transmission, does not necessarily indicate that low frequency sounds were not being generated by the Volcano.

Triangulation for source of sounds—A new triangulation technique to determine the source of

TABLE 2 – *Airborne acoustic observations at Bárcena Volcano*

Date	Sounds heard	Location of observer and comments	Activity of Bárcena at time of observation	Observer
Aug. 12, 1952	Continuous roar	Piper Cub of M/V *Intrepid* flying near Volcano	Continuous vulcanian-Peléan type eruptions	Chester Blasko
Nov. 13, 1952	Intermittent low rumble	M/V *Constitution* 8–10 miles east of volcano	Weak ash and steam eruptions, extrusion of lava into crater	Manuel Neeves, Jr.
Dec. 9, 1952	Intermittent low rumble	M/V *Star of the Sea* or *Challenger* abeam of vent of new lava breakthrough at a probable distance of 1–2 miles; observation questionable	Weak ash and steam eruption from crater, beginning of lava extrusion from basal vent	Name not known
Dec. 9–11, 1952	Loud hissing	Yacht *Observer* 600 yd off the new lava delta. Also similar hissing-grinding sounds heard from beach next to moving flow	Weak ash and steam eruption from crater, extrusion of lava into sea (see Fig. 2)	Lewis Walker and Adrian Richards
Jan. 12, 1953	Intermittent faint rumble	M/V *Cape Beverly* abeam of lava delta at a distance of ¼ mile	Very weak ash and steam eruption from crater, extrusion of lava from basal vent	Paul Lynn

the underwater volcanic sounds was devised and successfully used by the senior author from the *R/V Crest* in November, 1953. Navy AN/SSQ-2 sonobuoys were placed as shown in Figure 3. Two buoys were first placed on either side of Bárcena Volcano (A-A′), next on opposite sides of the lava delta but on the same side of the volcano (B-B′), and last off the northern end of the delta (C-C′). With this arrangement it was possible to receive both buoys simultaneously and yet remain at such distances that the miscellaneous ship noises were not picked up by the sonobuoys. Each buoy operated on different radio frequencies and the transmissions were received on a Navy R-316/ARR-26 sonobuoy receiver which served as a dual simultaneous receiving system. The receiver output was fed directly into an Ampex dual-track tape recorder, model 403-2. By this method it was possible to obtain a synchronized acoustic record from each sonobuoy with a maximum time error between the sound tracks of 50 microseconds. The block diagram of Figure 3 shows the relationship of the equipment used.

The recorded sound tracts were roughly analyzed for correlations of signals by playing them back and filtering in order to separate various portions of the acoustic spectrum. The output of the filters was fed through a logarithmic amplifier which drove a Leeds and Northrup Speedomax recorder. By replaying the tape, and recording over the same portion of the Speedomax chart, it was possible to obtain an effectively simultaneous time and frequency analysis from two buoys with respect to selected portions of the acoustic spectrum. An analysis of this type showed no correlation when the sonobuoys were placed on opposite sides of the volcano. Little correlation existed between buoys on the same side of the volcano, but on opposite sides of the lava delta. There was a high degree of correlation between buoys on the same side of the delta. At present this leads us to conclude that there was no activity within the Volcano which radiated energy within the acoustic spectrum, at least during the times when it was possible to record. Hissing sounds were heard from each buoy except the one located at A′. The localized contact of sea water with hot lava in the delta appears to be the most likely explanation of these sounds.

This same recording technique was used from the air in March, 1955. Sonobuoys, all of which worked successfully, were dropped from a low altitude at the positions of A′, B, and B′ in Figure 3. By switching receiver channels transmissions from pairs of buoys were recorded much in the same manner as previously described. No volcanic sounds were recorded; Bárcena had been dead since the previous August. However fish noises were recorded and the method was proved feasible from the air.

Underwater acoustic observations in Shelikof Strait—Mt. Trident volcano became active in

February, 1953 [*Snyder*, 1954]. From June to September the activity consisted of a quiet extrusion of lava and steady, moderately vigorous steaming [*Muller*, *Juhle*, and *Coulter*, 1954].

A very brief survey was made in Shelikof Strait (Fig. 1) on August 20, 1953, by the junior author, during a short stopover after he had left the Scripps Trans-Pacific Expedition in Adak, Alaska. An unsuccessful attempt was made to determine if audio energy produced from nearby Mt. Trident, or other volcanoes in the Valley of Ten Thousand Smokes, was present in the water of the Strait between the northwestern tip of Kodiak Island and the Katmai National Monument on the Alaskan peninsula. In order that the recordings could be correlated with the activity of Mt. Trident the late Werner Juhle and others observed the Volcano during the time of the survey.

A three station listening survey was made across Shelikof Strait on the M/V *Dennis Winn*, during the night of August 20, from Cape Raspberry on western Raspberry Island to Cape Ugyak, Kukak Bay, in eastern Katmai National Monument. The distance to Mt. Trident varied from 53 nautical miles, first station, to 34 miles, third station. All stations were made in approximately 100 fm of water at a hydrophone depth of 100 ft. The average recording time at each station was 21 minutes. While recording, the tape was only partly monitored by earphone and, since the recorder did not have a play-back mechanism, the tapes were later played back in the laboratory at Scripps.

No noises attributable to volcanic action were heard despite ideal weather conditions and a completely silent ship during the recording periods. According to a radio message received later from the party observing Mt. Trident, the Volcano emitted no noise during the recording periods and was not very active. However, seven hours after the survey was completed six loud rumbles, due to steam explosions, were produced within three hours, three of which were spaced only ten minutes apart. Unfortunately the available time and supply of tape did not permit the recording periods to be extended. In an operation of this kind it appears that recordings must definitely be made over much longer periods of time and that playback equipment should be available in the field in order to permit re-using any tape on which wanted sounds had not been recorded.

Analysis and origin of sounds recorded at Bárcena Volcano—Two kinds of volcanic sounds have been recorded at Bárcena. The first, a hissing sound heard and recorded on several occasions, we believe to have been produced when the sea came in contact with hot lava. A second, less likely, explanation is that it may have been produced by the shifting of blocks of lava as the flow settled into the unconsolidated ash beneath the delta. A similar airborne hissing-grinding sound also was heard when standing next to the moving lava flow (see Table 2).

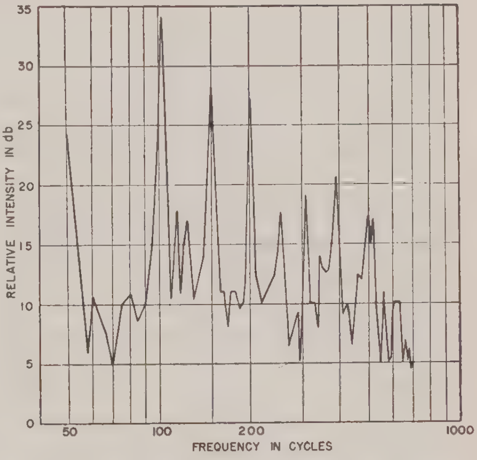

Fig. 4 – Acoustic spectrum of the rumble from Bárcena Volcano recorded November 15, 1952; arbitrary reference level of 0.015 volt to analyser is equal to 0 db

The low-frequency rumble, recorded in November, 1952, and September, 1953, has been studied by means of a detailed frequency analysis, illustrated in simplified graphic form (Fig. 4). The original frequency analysis, 49–800 cycles, was obtained from a Western Electric RA 1437 frequency spectrum analyser which is a scanning filter system of adjustable band width. The acoustic signal shows distinct energy maxima at 49, 103, 150, 203, 257, and 309 cycles. Little energy exists above 550 cycles. There is a strong harmonic progression of approximately 50 cycles. However, because of the attenuation of the sonobuoy hydrophone it is possible that 49 rather than 103 cycles represents the fundamental frequency of the rumble. The background noise level is below the arbitrary reference level (0 db) of 0.015 volts to the analyser. It is difficult to assign a special pitch to the rumble; a pitch of 125 cycles is a close approximation.

Few detailed frequency analyses have been made of biological and other sounds occurring in the ocean. Consequently we are unable at this time to make a detailed comparison with selected naturally occurring noises. For a discussion of various noises in the ocean the reader is referred to the paper by *Knudsen*, *Alford*, and *Emling* [1948].

Dobrin [1947, p. 22] graphed audio frequency against sound pressure for noises produced by six fish. His graphs show frequency maxima between approximately 200 and 500 cycles, intensity attenuation both above and below the maxima, and comparatively little energy below 100 cycles. From a U. S. Navy recording of the isolated 'boob' produced by the toadfish *Opsanus tau* a detailed frequency analysis was prepared for comparative purposes. There is little in common between the two analyses.

As far as we can tell qualitatively there does not appear to be any similarity between the volcanic sounds, sounds of known biological origin, and other sounds present in the ocean such as wave and surf noises. This is confirmed by experts in marine biology acoustics Martin W. Johnson and Marie P. Fish and by Naval personnel in the field of underwater sound all of whom report they have never heard similar sounds.

The rumble has not been correlated with visible activity. A possible explanation is that it may be related to the movement, or escape, of gas in the magma conduit or crater lava.

Summary and discussion—Sonobuoy and hydrophone investigations from ship and plane have demonstrated that audio energy generated by Bárcena Volcano could often be detected by underwater listening equipment when no sounds could be heard by observers stationed on or near the volcano at approximately the same time. This is undoubtedly because sound energy, especially in the low frequencies, is much more readily propagated in water than in air.

Although we have been concerned with underwater volcanic acoustics it should be apparent that terrestrial studies using tape recorders can be conducted by substituting sensitive contact microphones for hydrophones. Doak Cox (personal communication) has suggested that immersing a hydrophone in the water of a well near an active volcano might provide a better impedance match than direct coupling with the ground. For acoustic triangulation, using receiving equipment similar to that described in this paper, several microphones could be remotely placed in the field, connected to a central receiving station by either radio or transmission lines. Investigations of acoustic energy, especially when made for extended periods of time, may prove to be a valuable adjunct to seismic studies, the best present method of investigating the internal functions of a volcano.

We have made only qualitative measurements at Bárcena, but it should be possible to make quantitative measurements of volcanic sound energy both from land and sea.

Additional study of volcanic acoustics is highly desirable. The eminent volcanologist Frank A. Perret, the first pioneer in volcanic acoustic research, after nearly half a century of study summarized his opinion [*Perret*, 1950, p. 141] shortly before his death, by writing, "Submarine detection by microphone devices is now well known, and I consider subterranean auscultation vitally important to volcanological science."

Acknowledgments—This paper represents results of research carried out by the University of California in part under contract with the Office of Naval Research. The flights to San Benedicto Island were made for the most part with Office of Naval Research sponsorship and the assistance of Photographic Squadron 61, U. S. Navy, as part of the scientific study of Bárcena Volcano. We acknowledge with appreciation the assistance of the many people who have aided us in this study, in particular to Woodrow Krieger, for transportation on his yacht *Observer*, and Captains Zamora of the *Observer*, Perriera of the *Star of the Sea*, Valin of the *Columbia*, and Dall of the *Dennis Winn*. The Shelikof Strait survey was made possible thanks to the excellent cooperation of the 30th Engineer Base Topographic Battalion, U. S. Army, which made available their chartered U. S. Fish and Wildlife ship *Dennis Winn*. The frequency analyses were kindly made for the authors by S. H. Sessions and T. H. Wells of the U. S. Navy Electronics Laboratory. A preliminary copy of the manuscript was read by Gordon Macdonald, Howard Powers, George Snyder, Ray Wilcox, and Howel Williams, who offered helpful suggestions.

REFERENCES

DIETZ, ROBERT S. AND MILES J. SHEEHY, Transpacific detection of Myojin volcanic explosions by underwater sound, *Bul. Geol. Soc. Amer.*, **65**, 941–956, 1954.

DOBRIN, M. B., Measurements of underwater noise produced by marine life, *Science*, **105**, 19–23, 1947.

KNUDSEN, VERN O., R. S. ALFORD, AND J. W. EMLING, Underwater ambient noise, *J. Mar. Res.*, **7**, 410–429, 1948.

MULLER, ERNEST H., WERNER JUHLE, AND HENRY W. COULTER, Current activity in Katmai National Monument, *Science*, **119**, 319–321, 1954.

PERRET, FRANK A., The Vesuvius eruption of 1906; study of a volcanic cycle, Carnegie Inst. Wash., *Pub.* 339, 151, 1924.

PERRET, FRANK A., Volcanological observations, Carnegie Inst. Wash., *Pub.* 549, 162, 1950.

RICHARDS, ADRIAN F. AND ROBERT S. DIETZ, Eruption of Bárcena Volcano, San Benedicto Island, Mexico, *Proc. Eighth Pac. Sci. Congr.*, Philippines, in press.

SNYDER, GEORGE L., Eruption of Trident Volcano, Katmai National Monument, Alaska, February–June, 1953, U. S. Geol. Survey *Circ.* 318, 7 pp., 1954.

Scripps Institution of Oceanography, La Jolla, California

(Communicated manuscript received September 12, 1955; open for formal discussion until July 1, 1956.)

(216)

BACK FROM OBLIVION

GUADALUPE FUR SEAL: STILL A LIVING SPECIES

Carl L. Hubbs

Reprint from PACIFIC DISCOVERY, (Vol. IX, No. 6, November-December 1956, pp. 14–21, 11 figs.), a bimonthly publication of the California Academy of Sciences, San Francisco. Reproduced by Permission

Contributions from the Scripps Institution of Oceanography, New Series, No. 838

CARL L. HUBBS

BACK FROM OBLIVION

GUADALUPE FUR SEAL: STILL A LIVING SPECIES

THE GUADALUPE FUR SEAL — *one of the principal objects of research during several productive expeditions the California Academy of Sciences has conducted on the islands of the eastern Pacific, alone or in coöperation with other scientific organizations — has on several occasions been feared extinct, but each time a thread of continued existence has been rediscovered. The story of this species is replete with alternating fears of extermination and jubilations at rediscovery.*

The indiscriminate, unregulated, wanton destruction of this once very valuable animal has been decried by conservationists, who have realized that adequate protection would have restored the population and that a regulated harvest could then have been sustained. The saving of the species from the bitter tragedy of complete extermination may well be laid to the proclamation of Guadalupe as a wildlife sanctuary by President Obregón of Mexico in 1922, largely as the result of the evidence and pleas of conservationists under the leadership of Drs. Barton Warren Evermann and G. Dallas Hanna of the Academy staff.

Recent rediscoveries of this fur seal have again raised the hope that with thorough protection it may yet be saved. There are indications already that the tiny remnant on Guadalupe has taken the first steps on the road to recovery.

THE INITIAL DISCOVERY and the first harvesting of the Guadalupe fur seal are perhaps lost in the haze of unrecorded history, particularly obscured in this case by the rivalry of the early sealers, who, as one fur-seal herd after another was depleted, were constantly seeking new multitudes on isolated islands — and trying to keep their finds secret. As early as 1563 and 1683 either this species or its one very close relative (recent authorities differ in their conclusions on this point, though there is agreement on the general relationships) was found in almost incredible numbers

▲ Bull Guadalupe fur seal on a large lava boulder, Guadalupe Island, Baja California, June 1955. (All photographs by George E. Lindsay, San Diego Museum of Natural History)

on Más Afuera, Juan Fernández Islands, off Chile. The first recorded commercial sealing for this distinctive type of fur seal (the genus or subgenus *Arctophoca*) was in 1792, when the ship *Eliza* out of New York took 38,000 skins on Más Afuera, for sale in Canton. Six years later the *Betsey*, from the same port, took 100,000 skins, nearly all off the same island, to China.

The North American species, or population, may also have been subject to initial exploitation just before the end of the 18th century, on islands off Mexico or southern California, but no definite records quite that early seem to have been brought to light.

During 19 days in 1805 the San Benito Islands off Baja California yielded 8,338 fur seals, almost surely of this species, to the crew of the British whaler *Port au Prince*. The species seems to be extinct there, as also on the Farallons, just off San Francisco's Golden Gate, where the next known sealing was undertaken.

In 1808 Yankee sealers are recorded as having begun on the Farallons a ruthless harvest of fur seals that are now believed to have been the northern outliers of the Guadalupe species. One American vessel is reported to have here taken 130,000 in two years, beginning in 1808. Some may think that the skipper (Capt. B. Smith) was exaggerating, but such cargoes are reported elsewhere, and full credence is placed on the listed take of another party on the Farallons: 33,740 skins in 1810, 21,153 in 1811, 18,509 in 1812 (total, 73,402). Russians maintained a sealing station on these rocky islets from 1812 to 1840. At first they took 1,200 to 1,500 per year, but after 1818 the annual yield dropped to only two or three hundred.

Such was the story of the destruction of fur seals of various species on island after island, leading to complete or almost complete extirpation. The homing instinct in the fur seals is so deeply ingrained that the population on each island remained, or returned, even though facing annihilation.

It is commonly stated, but without detailed documentation, that the vast fur-seal rookeries of Guadalupe Island were slaughtered during the first two decades of the last century by Aleuts brought from Alaska by the Russians. It is not known whether Yankee or even British seafarers preceded the Russians, or to what extent they may have coöperated or competed with them in their gory game. History tells us, however, that the Russians knew Guadalupe and its fur seals, and that soon after the turn of the century they brought Alaskan natives to California for the fur harvest. And on the bleak shores of Guadalupe, which lies well off the Baja California coast about 240 miles south of San Diego, ample evidence has been found not only of the former existence of vast herds of fur seals, but also of extensive sealing operations. In many places along the rockbound coast, including two or three stretches of a half mile or more, the smooth and polished surface of the lava rock gives mute testimony to the countless generations of many thousands of fur seals that dragged their bodies and flippers over the rookeries. At four places, close to ancient rookeries thus made known, stone ruins remain of the sealing establishments. There are remains of the stone walls of

Dr. Victor B. Scheffer and Dr. Carl L. Hubbs deciphering inscriptions (like the one ABOVE) on stone house ruins near the southern end of Guadalupe Island's east shore. Mrs. Laura C. Hubbs is taking dictation from her husband. The inscription shown here, the next to the oldest one found, reads "SHIP ESSEX '35 OCT. HENRY WALDBON, BRISTOL, R. I."

living quarters and storage bins, of barricades used in driving the seals to slaughter, of cleared areas where until about a quarter century ago there still persisted wooden pegs used to stake out the hides to dry — enough, in all, to stimulate the imagination to a reconstruction of vast activity in the unrecorded past.

A thin thread of historic record was discovered on the island in June 1955. We had heard at the Mexican weather station at the south end (the only present habitation on the whole island) that there were some dated carvings on one of the ruins. These we found on the largest and best preserved of the stone-house walls of the southern sealing station on the east coast. Here, carefully engraved, are records of venturesome Yankees, who, we suspect, visited the spot and left their petroglyphic calling cards on what was probably already a deserted ruin. Among these inscriptions retaining the names of men, and of a few ships and home ports, we deciphered a number of dates, as follows: 1834, 1835, 1837, 1839, 1849, 1851, 1861?, 1869, 1873, and 1881 — and, significantly, not one during the ensuing three-quarter century. We suppose that at least some of these records are of the sealers who were taking a diminishing toll of the survivors from the early mass slaughter — a mere remnant of the vast hordes of fur seals that must have been living on the island when modern man, the world-champion predator, arrived on the scene.

Around the middle of the 19th century the resident fur seals of California and Baja California were thought to have been nearly or quite exterminated. But in 1876 the crew of a wandering schooner located fur seals on Guadalupe, the last significant stronghold of the species, in numbers rather large, but no doubt puny in comparison with the virgin abundance. Some thousands were taken by ships out of San Diego, but the kill dropped to a low ebb by 1894, the last year of a recorded commercial catch.

Again the population was feared extinct, for only a

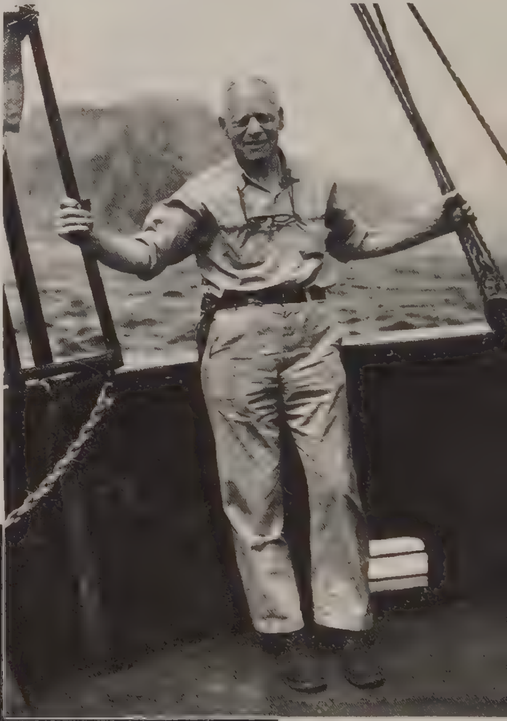

Mr. Joseph W. Sefton of San Diego aboard his research ship, the *Orca*, at Guadalupe Island, June 1955.

◄ The *Orca* off Guadalupe Island. She is now part of the research fleet of the Scripps Institution of Oceanography, Universit of California, La Jolla.

Taking off
from shore
observations,
Guadalupe,
June 1955—
llan J. Stover,
arl L. Hubbs,
Dr. Scheffer.
rs. Hubbs and
rthur Flechsig
are in the
tender.

few scattered, unverifiable, hearsay reports emanated from the islands of the two Californias in the period 1895-1926. I write "population," because until near the end of the last century it was not known that the fur seal of these islands was different from the northern fur seal, which, though greatly depleted to a low ebb about 1911, was never really near extermination. The first scientific specimens were not collected until 1892. In that year Charles Haskins Townsend, then with the U. S. Fish Commission, collected four skulls from one of the large rookery sites on Guadalupe Island. On the sole basis of these bones a famous naturalist, C. Hart Merriam, published in 1897 the description of a new species, *Arctocephalus townsendi*, which he aligned with the Southern Hemisphere fur seals and named in honor of the collector. For more than thirty years this species was known only from the skull characters. No scientist knew definitely what the beast looked like.

The definitive history of the Guadalupe fur seal was resumed in 1926 (possibly 1927). In that year two fishermen, William O. Clover and Harry Fisher, found on Guadalupe Island a small group of animals that they took to be fur seals. Clover reported his find to the president of the San Diego Zoological Society, Dr. Harry Wegeforth, who engaged the fisherman to obtain a pair of specimens. Clover succeeded in capturing two bulls, which he delivered to the San Diego Zoo on April 25, 1928. Dr. Wegeforth was overjoyed when he ventured the identification of the handsome and distinctive creatures as Guadalupe fur seals, at long last rediscovered, and now exhibited for the first (and only) time. Fortunately, the first collector of the species and a long-time student of seals, Dr. Townsend, arrived a few days later at the Zoo, with the historic collection of giant land tortoises from the Galápagos (another specialty, by the way, of the California Academy of Sciences). Dr. Townsend, the head of the New York Aquarium, verified the identification, whereupon the rediscovery was promptly announced in popular and scientific articles.

The story of the initial relocation of the fur seal on Guadalupe was verified by Mr. Joseph W. Sefton, Jr. and me on January 9, 1950, when at the Navy Hospital in San Diego we discussed the find with a sick patient, Harry Fisher, who had been Clover's companion at Guadalupe just 24 years earlier. Perhaps realizing that his days were numbered, the invalid

Bull fur seal (ABOVE) and one member of his harem (RIGHT) on Guadalupe Island, June 1955.

vividly, and we felt honestly, told us of the trip, describing in detail the spot where the fur seals had been encountered. Possibly overexcited by the tale, the poor fellow went to his fisherman's reward the very next day.

Clover, who might have been the hero of the rediscovery, turned out to be something of a villain. At first he gave for the point of capture a position where the chart shows Alijos Rocks, far south of Guadalupe. After becoming involved in a serious disagreement with Dr. Wegeforth, Clover swore that he would slaughter the whole remaining herd, which he had estimated at 60 individuals. Reportedly he killed all he could and took the hides to Panamá to sell, but was there killed in a bar-room brawl. The fate of the fur has never become known.

Somehow, either directly from Clover or indirectly, the officials of the Zoo and of the San Diego Museum of Natural History were correctly informed regarding the provenance of the two specimens (the Alijos Rocks, mere needles projecting above a shallow platform well out to sea, could not be regarded as a proper habitat for fur seals). In order to locate the reported hiding place of the seals, Mrs. Belle J. Benchley in 1930 arranged and accompanied an expedition to Guadalupe on Capt. Allan Hancock's yacht, the *Velero II*. Taking along a lady who had been Clover's companion on his 1928 trip, the party was able to identify the place where the two specimens had been collected, but neither here nor elsewhere saw any, except perhaps for one in the small sea lion rookery. But Townsend reported that some had been seen in 1929, and Lewis Wayne Walker, an accomplished if somewhat erratic naturalist, has told me that he saw a few on each of several trips to Guadalupe in the 1930's. Significantly, he gave as the location of each observation the very area where the fur seal has recently been rediscovered. I know of no subsequent observation of fur seals on Guadalupe until I first saw them there in 1954.

Following the capture of two specimens in 1928, the few sight records at Guadalupe Island and in California prior to 1949 were generally disregarded, for one reason or another, and the species once more was thought or feared to be extinct. Rediscovery came again, dramatically, in 1949. On a trip to count and

study the seals of San Nicolas Island (the most outlying of the famed Channel Islands of California), Dr. George A. Bartholomew of the University of California at Los Angeles suddenly came upon a lone bull of a strange type, somewhat segregated from the abundant sea lions. On three following trips in 1949 he saw what was probably the same animal, which he tentatively identified as the supposedly extinct Guadalupe fur seal. This field determination was confirmed by a comparison of his excellent close-up photographs with pictures of the Guadalupe fur seals in the San Diego Zoo in 1928. Somewhere, he thought, the species may well retain a small breeding population.

Dr. Bartholomew and I immediately planned to explore the shores of Guadalupe Island, the last main holdout of the species, to see if such a population might be found. For this trip, Mr. Joseph W. Sefton, Jr. graciously made available the Research Ship *Orca*, which has since joined the Scripps fleet (we did not then realize that the small ship from which Clover had collected the two Zoo specimens was also named *Orca*, though we did know that the orca or killer whale is one of the very few animals capable of catching a seal). In February of 1950 we closely examined the bold shores all around this volcanic island, but found no trace of seals that we could identify as *Arctocephalus townsendi*. We returned, much disappointed on this score, though pleased by other discoveries, including the observation of migrating northern fur seals as far south as between Guadalupe and San Benito islands. On the San Benitos not a single fur seal was detected among approximately 9,500 sea lions actually counted.

When Dr. Bartholomew, on returning to San Nicolas in 1950, could not find the one combative bull fur seal that he had seen on each of four trips in 1949, we came to fear that he might very well have seen the last living example of this once flourishing species. This feeling became more and more entrenched, during the following months and year, as during repeated trips to the islands and along isolated stretches of the mainland coast we failed to locate another specimen, despite close scrutiny of all propitious habitats encountered. Our hopes for another discovery of the species kept fading toward – but not quite to – the vanishing point.

Eventually, vigilance and hope were crowned with success. On the very last day of another expedition on the *Orca* to Guadalupe, in November, 1954, as we were preparing to leave for home, I was seized by the desire to try once again for a sight of the fur seal species that we feared to be extinct. Mr. Sefton obligingly

The bull plunged into a bath of sea foam.

Boatman Allan J. Stover has just landed Dr. Hubbs on Guadalupe to observe fur seals.

acceded to my belated request for one of the tuna tenders, in which our boatman Eddie Arebalo and I might cruise along the rocky shores closer to the rocks than the big ship would dare run. Not long before dark, after straining eyes had failed to locate any sign whatever of a fur seal, Eddie located just ahead a seal perched on a rock at the mouth of a shallow cave. This sight was at once suggestive of the fur seal, which, toward the end of the commercial harvest, reportedly was usually found in caves. We therefore turned in closer toward shore. I was soon thrilled to hear this bull seal emit a defiant roar that bore little resemblance to any of the voices I had been hearing from the sea lions or elephant seals, the only species of the tribe that were then definitely known from the island. Full of expectation we turned right into the surge, where in the early dusk I could plainly see the sharp, almost collie-like snout, coarse guard hairs overlying silky smooth fur, oversized flippers, and other characteristics of the Guadalupe fur seal. Then we heard the belligerent bleat of fur-seal cows and the plaintive whimper of their pups. In the shadows we could make out at least two cows and three pups. These voices transported me back to St. Paul Island of the Pribilof group in Bering Sea, where, during a visit in 1939, the very similar calls of the northern fur seal rang in my ears throughout day and night.

I could not restrain a shout of elation, for we had without any doubt rediscovered the Guadalupe fur seal alive — not only one individual, such as my colleague Bartholomew had seen on a California island five years before, but an active though small harem on Guadalupe, the last main habitat. The species was still alive and reproducing!

Continuing along the shore in the growing dusk we soon saw other pups on a low flat rock and several half-grown fur seals disporting in the surf, like yearlings of the fur seal in Alaska. At least 14 were counted before darkness set in. We finally reached our nocturnal rendezvous with the *Orca,* and jubilantly announced our discovery. The next morning we delayed our departure from the island to return to the cave to photograph the harem. This time none were seen on the way to the cave, but in the dark shadows of the recess we saw at least one adult fur seal and a very small pup, apparently newly born. But before we could take a photograph, our over-anxious boatman ran onto a rock in the surge, damaging the launch and forcing a return to the *Orca.*

I vowed to return for more definite observations and counts, and for a photographic record of this remnant of a once grand and flourishing population. This I did in June, 1955, accompanied by a party of scientists, including a collaborator, the famous seal specialist Dr. Victor B. Scheffer of the Fish and Wildlife Service, and an expert photographer, Dr. George E. Lindsay of Stanford University (now Executive Director of the San Diego Museum of Natural History). This time we saw more than thirty fur seals and took many still pictures, including Kodachromes, and a considerable footage of colored movies. One pair in particular patiently posed for nearly two hours, actors each worthy of an Oscar.

Four more trips have been made to study and count the fur seals on Guadalupe. In December, 1955, Dr. Raymond M. Gilmore of the U. S. Fish and Wildlife Service, with a small party on one of the Scripps vessels, visited the shoreline where we had found these animals. He estimated the number seen at 70 to 75 and John B. MacFall, Institution photographer, took motion pictures. On a return trip in June, 1956, in another Scripps vessel, Dr. Gilmore estimated the numbers seen at 92. Shortly thereafter, on an airplane flight generously provided and expertly piloted by Dr. Gifford C. Ewing, Señor Julio Berdegué of the Dirección General de Pesca e Industrias Conexas of Mexico, and I saw, again along the same five-mile stretch of coast, about 30 fur seals, of which about 20 were disporting together in the narrow band of surf. In August, with a party from Scripps Institution of Oceanography and the San Diego Museum of Natural History, I again cruised the fur-seal habitat in a small boat. We counted between 71 and 76 fur seals and got still more photographs.

Although fluctuations in the count are inevitable, because at times some animals no doubt swim out to sea, and others are concealed in caves or behind rocks, or are just overlooked because their slick blackish fur so closely resembles the black lava rock on which they rest, we do feel that the population is on the increase. I am almost certain that the animals were much fewer when I failed to see any on four trips from 1946 to 1950. It is true that we had not cruised in a small boat right off the rocks along the coast where the population has been found on each of the six trips from 1954 to 1956, but we did see some there in 1956 from the research vessels plying along shore in essentially the same track that was followed in previous years, when the shoreline was also scrutinized with binoculars.

Even allowing for wanderers at sea and for animals concealed among the rocks, we realize that the life of this species hangs on a very slender thread. Perhaps 200 to 500 individuals scattered along a small stretch of the coast of the island, survive to represent the primeval multitudes, probably a thousand-fold more numerous, that swarmed on three large rookeries and on many smaller ones. The survivors seem perilously few, but we hearten to realize the elephant seal and the gray whale have recovered marvelously from somewhat similar remnants, that the sea otters have staged a similar though less spectacular recovery from exceedingly low numbers, and that the northern fur seals of the Pribilofs under wise management have increased about 200-fold during the last half century.

Naturalists of both Mexico and the United States, backed by national and international conservation agencies, are now pleading for more secure protective measures, under which the Guadalupe fur seal may have a better chance to regain some measure of its former abundance—at least to be saved from the abysmal catastrophe of extinction.

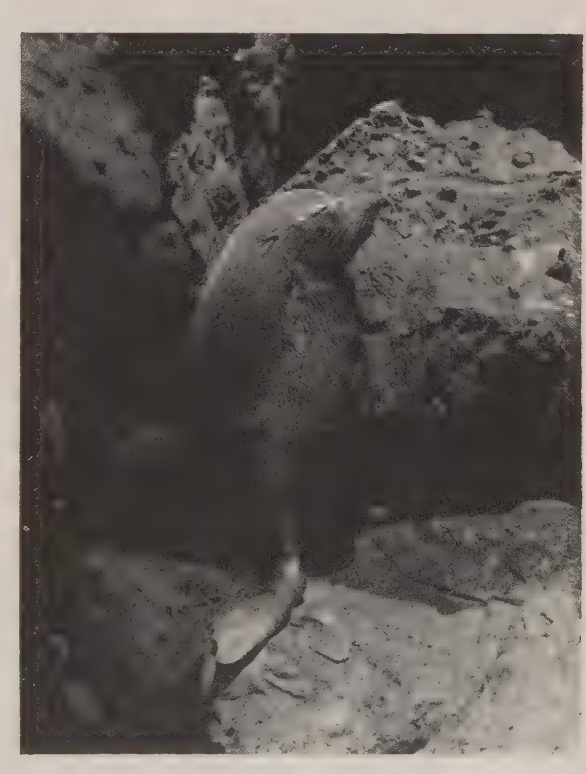

The bull Guadalupe fur seal.

Reprint from:
Proceedings XIV International Congress of Zoology, Copenhagen 1953. Copenhagen 1956.

Reproduced by Permission

WAYS OF STABILIZING ZOOLOGICAL NOMENCLATURE[1]

by Carl L. Hubbs (California)

Stability in zoological nomenclature has been accepted as an outstanding need and a prime aim, but diverse views have been held on how this need and aim may be attained. In the hope of contributing to an answer I present some ideas for consideration and discussion, and report actions that have been taken just before and during this Congress to bring about a more stable and a more universal nomenclature; that is, nomenclature more uniform in both time and space.

At the outset we should face the fact that the decisions reached five years ago at Paris have led to considerable dissention and controversy, even to suggestions that the International Rules be ignored or abandoned. At the Colloquium on Zoological Nomenclature which has preceded the present Congress a representative group of systematists from many countries has considered the pressing problems of nomenclature in fine spirit and sympathetic understanding, has retracted some of the Paris decisions that have proved most objectionable, and has reached essential agreement, preparing the way for a new grammar of systematic zoology.

Obviously, a world-wide stability in the scientific names for animals is dependent on the free interchange of the results of scientific work, through publications, societies, congresses, and individual contacts. Our nomenclature has been essentially international but will remain so only to the extent that nations retain their intellectual connections with the rest of the civilized world. Every curtain that is pulled down creates isolation, and with this, the prospect for variations in nomenclature.

A second essential for nomenclatorial uniformity is the development of systematics as a sound field of scientific work, and the recognition of the scientific nature of systematics by biologists in general. Scientific names will be appreciated and properly used to the degree that systematists and their labors warrant and receive due respect. There is need, and hope, for improvement in the field of systematics, quantitatively and qualitatively, and for a healthier attitude toward systematics by specialists in other fields —and by systematists toward those colleagues. The rapid development of systematic societies, including the Society of Systematic Zoology, with its new journal, is one demonstration of this need and hope.

---

[1] Presented at the General Meeting of the XIV International Congress of Zoology, Copenhagen, August 7, 1953. Contributions from the Scripps Institution of Oceanography, New Series, No. 839.

The attainment of mutual respect and understanding between systematists and other biologists will undoubtedly lead to a greater integration between the fields, to their mutual benefit and to the general advancement of science. Their will also ensue, to some degree, a breakdown of the barriers between the compartmentalized subsciences, and an increase in the number of workers in the promising areas between and overlapping the fields.

One main way of stabilizing names is to recognize and follow the wise principle of maintaining the *status quo* until there is good reason for effecting a change. Another way is to tolerate understandingly and to accept promptly changes that are based on sound need. We should recognize that the language of systematics, like other languages, is a living and growing entity, but we should do what we can to direct the change and growth along reasonable and orderly lines.

Though stability and universality in the names of animals is dependent in large measure on the actions and attitudes of scientists, the responsibilities and opportunities for promoting uniformity have been especially entrusted by zoologists, through their International Congresses of Zoology, in the International Commission on Zoological Nomenclature, and in the International Rules of Zoological Nomenclature that the Congresses have approved. The ways of stabilizing zoological names are therefore to a large degree the ways of the International Commission, and of the Rules that the Commission has drawn up. I shall, therefore, direct my remarks largely toward the Commission and the Rules, with particular reference to the actions taken at the present Congress.

It is obvious that the Commission can effectuate its purpose only in so far as it engenders and retains the respect and approbation of working zoologists. Such respect and favor has been and will be increasingly nurtured by common understanding of one another's points of view, by cooperation, by willingness to comprise, by mutual faith, by the more timely dispersal of new proposals, by promptness in reaching decisions and opinions, by wise and well-considered actions, by the formulation of the Rules in simple, clear, and brief terms, and by the broad and unrestricted dissemination of the Rules and other pertinent information. Along these lines much has been accomplished over the past several years, thanks largely to the energy and devotion of the present Secretary of the Commission, and much more would have been done, we may assume, had more adequate facilities and funds been available. Tasks beyond the capacity of any man to perform have doubtless prevented the Secretary from attending to multitudinous queries and requests that have been heaped upon him during the busy preparation for this meeting.

Under Mr. HEMMING's leadership the large and representative Colloquium on Zoological Nomenclature has tackled the whole problem courageously and thoughtfully, constantly keeping in mind the need for implementing the prime purpose of attaining more uniform usage. Members of the Colloquium feel deep gratitude to the Secretary for his extensive work and for his many accomplishments.

One official action that has aroused almost unanimous opposition, in America at least, has been the withholding of publication rights on the International Rules and associated material. We appreciate that the sale of the Bulletins and other official publications has been a main source of income for the Trust that has financed the work of the International Commission and that the restriction of republication may help to prevent incomplete, misleading, or erroneous statements (though such statements could largely be avoided otherwise or could be corrected). A wiser policy, many of us have thought, would be to curtail the length of the presentations and to set a price on the publications that would encourage much larger circulation, among institutions and individuals who can not afford the price that has been charged. Since the dissemination of the Rules, Opinions and discussions is a prerequisite to their understanding by zoologists in general, and is essential to compliance therewith, we hold that the unfettered republication of the Rules should be encouraged and promoted, rather than prohibited. We look on the Rules as the bible of nomenclatural procedure, and bibles should not be copyrighted. We rejoice in the announcement that Mr. Hemming proposes to issue the decisions of the Copenhagen Colloquium free to the members of this group and available to all others at a very reasonable price, and that he proposes to put this forth in brief and clear language. We rejoice even more in the indications that the recodified Rules will be prepared and issued in similar fashion.

The manner in which the nomenclatorial discussions and proposals have been presented in the Bulletin of Zoological Nomenclature has been, indeed, a widespread source of discontent. Situations that are relatively simple have been stated in lengthy semi-legal terminology that is difficult to grasp, even by English-speaking people, and is hardly conducive to wide or enthusiastic support—or at least it has seemed so to American zoologists. It would appear that, in a laudable effort to be unequivocal, the prime literary virtues of brevity, simplicity, and clarity have been forgotten. That brief, simple, and clear statements can be drawn up to express the prolonged discussions in the Bulletin has been proved in the draft of the report of the decisions of the Copenhagen Colloquium and in the resumé of the Paris Enactments (the latter prepared by Mr. W. I. FOLLETT, chairman of the nomenclature committees of the Society of Systematic Zoology and the American Society of Ichthyologists and Herpetologists). The old Rules were, it is true, too terse and in places of uncertain meaning, but were in general quite understandable, in fact a rather noble charter, capable of being augmented by precise definitions, by more complete explanations, and by statements to cover special situations. But complexities have arisen, experience has brought out many special situations not covered by the old Rules, and certain of the articles have proved bothersome and difficult.

Though designed to promote stability, several of the Paris Enactments, reported in the Bulletin, would, if confirmed, have led to endless difficulties and uncertainties. Some subjects were presented in such a way as to require a long and expanding series of exceptions. To interpret some enactments, thus complicated, would have called for the services of a new kind of lawyer. Some complications are unavoidable, in fact are required to render a rule applicable to all situations, but others are unnecessary and should by all means be avoided wherever possible. For one reason—a major reason—such complications would render the Rules unusable to the average zoologist who hasn't the time or the inclination to become a specialist in nomenclature. Thus, many general zoologists would be diverted from systematics—most unfortunately, for, as already stated, we need to encourage wide respect for and wide participation in systematics. Some of the discussions and proposals were actually so confusing as to sour some active systematic zoologists on their own field. With such feelings they would tend to abandon their systematic researches, or to ignore the Rules. Either action would be most regretable.

Compliance with the Rules—essential to stability—will be attained only to the degree that these Rules are so constructed and so worded as to command the respect and approbation of systematists around the world. The Secretary is to be warmly commended for having sought the views of committees on nomenclature and of individuals on all sides, and for having arranged the Colloquium on Zoological Nomenclature that has just preceded this Congress. He is especially to be commended for his leadership in arriving at the promising stage where we now stand.

Another way by which uniformity can be greatly advanced is through speedier action on requests for opinions. Systematists who have failed to get action on a valid request for years, or never, have not been tempted to submit another request. Those who know of such specific delays have hesitated to submit cases for opinion and have, instead, adopted on their own initiative, according to their particular point of view, either the familiar name or the unfamiliar older one. Mr. HEMMING has made the welcome announcement that speedy opinion can now be anticipated. It is to be hoped that systematists, on the basis of the new and more workable provisions, will submit for rejection long-forgotten prior names that they uncover, and take other actions conducive to uniformity. Thus one of the main occasions for instability—and for disrespect of systematists—should be avoided.

Nearly all of us will agree that absolutely strict and invariable adherence to the law of priority has been unwise and should have been avoided from the start. Had the Commission in years long past adopted a more balanced policy in this regard, and had it encouraged and passed rapidly on requests for the use of its plenary power to preserve familiar names in general usage, systematics would have maintained a more respected position and zoology would have been materially advanced. Much controversy would have been avoided and much time saved. Limitations are needed, and have been adopted. The new principle for action in preserving names and in arriving at other nomenclatorial decisions should release the load on the Commission and should advance stability. This is the principle of publishing the facts with recommendation for conservatory action, the recording of such action in the Bulletin of Zoological Nomenclature, and the approval of the recommendation if no protest is received by the Secretary of the Commission within a stated period. The initiative will be handed to zoologists, with rules to control unscrupulous systematists who would use technicalities as an excuse for proposing long unused or new names.

On the other hand, the general abandonment of the principle of priority would have led to instability as well as injustice, for workers of different regions or with different points of view would make their own selections on non-objective and ill-defined grounds. Priority should be set aside only by official action, either by Plenary Power or by the new principle just stated, only on compelling grounds, and only to avoid changes in names that are generally current among zoologists. Systematists themselves are accustomed to learning or relearning names and should not call for plenary action to retain names familiar only to them. Excessive use of the Plenary Power would lead to hasty and often unwise action, or might favor the wishes of only one group of specialists. When two or more names are commonly used for a genus or species, as in different countries, the older names should be adopted by concerted action, or, if a request for opinion has been entered, by the Commission.

Above all, let us strive to preserve the International Commission and to abide by its Rules and decisions. To do otherwise would surely lead to regional variance in nomenclature, at a time when increased stability is especially called for. One way to preserve the international scope and function of the Commission is to render it effective and wise and to insure Rules that command full adherence and universal use. The „Copenhagen Decisions“ should go far toward maintaining compliance with the Commission and its Rules.

Thus far we have considered stability from the more strictly nomenclatorial standpoint, with especial reference to priority. Such stability is particularly favored by adherence to the International Rules, and by official suspension of the Rules in special cases. Surveys of successive check-lists, as of North American fishes, however, often show that the overwhelmingly main cause for name changes lies in generic reclassification, an activity that is traditionally and we think rightly beyond the scope of the International Commission and its Rules. For many years the splitters were to blame; now, more commonly, the lumpers are to blame. Splitting and lumping create instability chiefly because of the confounding of classification with nomenclature in the Linnaean system. Every time a generic name is changed, every species in the genus must have its name altered. Every time generic limits are diminished or enlarged, one or more species must be rechristened. The more we lump, the greater the number of name changes—one argument for fine splitting. We see no way to rule against name changes due to revised classification, including revised interpretation of generic limits. Let us appeal to the good sense of systematists, urging them to be conservative in making such changes, particularly when one doubtful opinion is exchanged for another. When new and sound evidence calls for new arrangements, however, particularly in the course of thorough revisionary studies, let us stand ready to accept the necessary changes. To do otherwise would often block the orderly progress of science. Under such circumstances stability will be enhanced, if justifiable changes are generally and promptly accepted.

Discussion:

FRANCIS HEMMING: Beyond thanking Dr. HUBBS for the tribute which he had paid to the work of the International Commission on Zoological Nomenclature and acknowledging the justness of his strictures on certain shortcomings in the past, the object in addressing the present Plenary Session was to seek an expression of opinion on the merits of the suggestion which Dr. HUBBS had made for resolving the difficulty which had arisen in the preparation of the Report on the one question on which there was not substantial agreement. Dr. HUBBS' proposal was that no further attempt should be made to secure agreement on a detailed proposal and that instead there should be inserted in the Report a paragraph (1) stating that it was recommended that the *Règles* should include a provision limiting the application of the Law of Priority in such a way as to preserve any well-known name which had been in use for a considerable period from being sunk as a junior synonym of some much older name which had not been used more than a small number of times in a specified recent period of considerable length, this provision to contain also the best safeguards that could be devised to prevent the abuse of the proposed provision by unscrupulous persons, and (2) entrusting to the Commission the duty of preparing a definite provision on the foregoing lines for inclusion in the forthcoming edition of the *Règles*. It was part of Dr. HUBBS' proposal that the provision should be as brief and concise as the circumstances would permit.

BIANCO LUNO A/S KBH.

Reprint from:
Proceedings XIV International Congress of Zoology, Copenhagen 1953. Copenhagen 1956.

Reproduced by Permission

THE POPULATION OF HYPERSALINE AND RELICT LAGOONS

by Joel W. Hedgpeth (California)

Hypersaline lagoons are environments more or less directly connected with the sea, in which salinities are concentrated to values greater than $40\text{–}50\,^{0}/_{00}$ by an excess of evaporation over fresh water inflow. Such environments occur along the Gulf Coast of the United States, on the shores of the Black Sea and Sea of Azov and in subtropical areas throughout the world. The best known hypersaline lagoons are the Laguna Madre on the coast of Texas, the Sivash, on the western side of the Sea of Azov, and the Salzee near Anchialo on the Bulgarian coast. An analagous situation is found in the Bitter Lakes region of Suez Canal, where it is evident that salinities in excess of $50\,^{0}/_{00}$ do not prevent the migration of many marine organisms from the Red Sea into the Mediterranean. Some idea of the eventual end point of a hypersaline lagoon may be gained from the examples of the isolated Birket el Gessabaia in the Libyan desert, and from the Salton Sea in southern California.

The approximate upper tolerances of the various groups of marine and brackish water organisms invading hypersaline lagoons (exclusive of Insecta and Phyllopoda, which are not marine in origin), may be summarized as follows (the values are parts per thousand total salts):

Protozoa	180	Ostracoda	60–100
Hydromedusae	60	Cirripedia	60–80
Turbellaria	139	Isopoda	70
Nemertea	60	Amphipoda	90
Rotifera	60	Macrura	60
Nematoda	70	Brachyura	70
Oligochaeta	60	Pelecypoda	60–80
Polychaeta	139	Gastropoda	80
Copepoda	80	Pisces	75–85

Insofar as it can be summarized at this time, the fauna of hypersaline lagoons seems to be recruited principally from groups of organisms already well represented in the sea, and at the same time from species adapted to life in estuaries and brackish waters. Copepods, polychaetes, mollusks and fishes are particularly abundant, but several other highly succesful groups, including sponges, hydroids and echinoderms, are absent or are represented by only a few species. Thus it appears that the same faunal elements that have not been able to penetrate freshwater successfully are also limited from these hypersaline environments, although insects and phyllopods are characteristic members of the fauna of inland brines. The phyllopod Artemia seems to be limited from such marine lagoons by the predation of fishes, especially

Contributions from the Scripps Institution of Oceanography, New Series, No. 839a

cyprinodonts. The most pronounced ecological peculiarity of these hypersaline lagoons, apart from their high salinities, is the allochthonous nature of a large part of the fauna: few species reproduce successfully and the bulk of the populations, especially of the larger forms, is maintained by continuous migration, or is carried by water movements, from the neighbouring sea. The high summer temperatures of such environments, as well as the high salinities, probably inhibit the reproduction of many of the species. There also seems to be a tendency toward dwarfing of species in these environments. When the lagoons are completely cut off from the sea the difficulties of maintaining natural populations are even greater, and the fauna is reduced to a very few species, usually of entomostracans, mollusks, and cyprinodont fishes.

Discussion:

THURLOW C. NELSON: The records just shown on the slides show *Cordylophora* existing in salinity 36. In New Jersey the Delaware and Raritan Canal connecting the Atlantic Ocean with the upper Delaware River was abundant for navigation in 1933. Fifteen years later I found a submergel tree literally covered with a heavy growth of reproducing *Cordylophora* some 20 miles from the Raritan Bay and separated by three locks from tidal water. There is no possibility of ingress of tide water since this level of the canal lies more than 10 meters above mean sea level.

J. W. HEDGPETH: There are fresh water records for *Cordylophora* from the Ohio River, but it also occurs in bays on all coasts of the United States.

THURLOW C. NELSON: For over a hundred years pleasure boats many with bottoms covered by marine growths passed through and anchored in the Canal. The possibility of introduction of marine organisms was always present. The diatom *Nitschia closterium* is occasionally found now in the Canal.

T. GISLÉN: *Cordylophora* (nowadays generally called *C. caspia*) will occur in fresh water in Sweden generally near their openings in brackish water. Properly it is a brackish water animal and therefore could be expected in hypersaline water too, as also stated by Dr. HEDGPETH.

E. DAHL: Dr. HEDGPETH commented upon the fact that a few insect larvae occured in hypersaline lagoons. It was pointed out that Chironomid larvae are very common in brackish water and in the upper parts of the tidal zone. They, too, apparently occur more frequently in brackish and hypersaline media than in the sea.

M. J. DUNBAR: You mention large fish production. How large? Compared to the New Foundland banks or the North Sea? What supports the production. Can the lagoon be compared to shallow dystrophic lakes?

J. W. HEDGPETH: The production is not comparable to the great fishing banks. In the Sivash the mullet catch alone is 80–90 tons, and has been as high as 500 at least one year, while in the Laguna Madre the production of all fish has been 900 metric tons in some years. The productivity is based principally on phytoplankton and bottom invertebrates. I would say the production is roughly comparable to a dystrophic lake.

BIANCO LUNO A/S, KBH.

Reprint from:
Proceedings XIV International Congress of Zoology, Copenhagen 1953. Copenhagen 1956.

Reproduced by Permission

ON THE GROWTH OF POPULATIONS

by Adriano A. Buzzati-Traverso
(La Jolla, California, and Pavia, Italy)

Dedicated to Professor Fritz Baltzer on his seventieth birthday.

The success of living matter in colonizing the earth's surface can be described in terms of population growth. Whether we consider the primeval simple organisms or the highly complex and evolved forms which we see around us now, the appearence of a new species, its spreading over a certain area and its extinction can be represented in numerical terms. We may say that at first there were just a few individuals of a particular form, that later, finding suitable conditions over a vast territory, their number increased, that the population remained more or less of the same size over a certain period of time, and that eventually, after a decrease in number, the species disappeared completely. If we had a complete card index of all the organisms which have lived in the past with their birth and death dates, and we had a sorting machine of the right size and speed, it would be possible to give a description of the evolutionary process in terms of the numbers of individuals belonging to the various forms which were living at different times, and hence in terms of population growth and decline.

The significance of this quantitative aspect of living matter has been realized by biologists long ago. Darwin's theory of evolution by natural selection is a manner of describing the ebb and flow of the population waves in the course of time. More recently, as you well know, ecologists have been particularly aware of this phenomenon. They have succeeded in producing satisfactory analytical descriptions of population growth and have collected experimental data which seem to fit the results of mathematical calculations very well. The esthetic feelings of modern biologists are certainly satisfied by the simplicity and neatness of this mathematical approach. For once the great complexity of a biological phenomenon of this sort seems to yield to the synthetic abilities of the mathematician.

It seems to me, however, that students of population dynamics have overlooked a rather important biological factor, which certainly plays a role in such numerical equilibria, namely the genetic heterogeneity of natural popu-

Contributions from the Scripps Institution of Oceanography, New Series, No. 839b

lations. But the fault, if one can speak of faults in such matters, has not been limited to this group of biologists; a limitation of outlook has characterized also the work of geneticists interested in populations. These, in fact, while producing convincing evidence about the genetic variability of free living forms, have, in their turn, overlooked the numerical aspects of the populations they were studying. It seems worthwhile, then, to examine what conclusion can be reached if one takes both of the mentioned aspects of populations structure into account.

Let us first briefly consider the approach of students of population dynamics to the problem and their conclusions. For the sake of simplicity let us assume that the area or volume upon which the population grows is limited and that the amount and quality of available energy sources are constant. A few individuals of a certain form enter this very simplified biotope and find suitable conditions for their life and reproduction. The population, originally very small, will grow at first with no restrictions, because space and food are plentiful. The number of individuals will grow at a geometric rate of increase, the coefficient being given by the sum of factors of the species considered contributing to population growth, such as fecundity, fertility, length of life cycle, rate of development, and so on; for this complex of factors CHAPMAN has proposed the term "biotic potential", which will be used in the discussion to follow. The population, however, cannot increase indefinitely at such a rate, because sooner or later a shortage of space and food is bound to appear. To use another term of CHAPMAN, the "environmental resistance" which was nil at first becomes larger with the increase in population size, competition for food and space among the population's members takes place, the growth rate of the population diminishes and eventually a numerical equilibrium is reached. As it is well known, several mathematical descriptions of the phenomenon of population growth have been proposed by VERHULST, GOMPERTZ, PEARL and REED, and others. The growth form of the population can be slightly different under these various analytical treatments, but in every case one can find the following three basic properties of the curve: (a) the curve is characterized by an upper asymptote which approaches a finite number, which is the largest number of individuals that can be supported in the biotope; (b) the lower asymptote of the curve is zero, since one cannot imagine a negative population; (c) the rate of growth of the population is determined by the biotic potential, which is constant for the population considered.

As you know, the most extensive study of such problems has been developed by RAYMOND PEARL and his collaborators. The simple differential equation given by PEARL and REED is the following:

$$\frac{dN}{dt} = bN\frac{K-N}{N},$$

where N is the number reached by the population at any particular time, K is the maximum number of individuals which can live in the limited biotope, b is the biotic potential, and t is time. The curve includes a first part having a sigmoid shape representing the period of actual rapid increase in numbers until all the available space is occupied, and a second part where the curve is practically parallel to the abscissa, describing the period of numerical equilibrium. Actual observations carried on experimental populations of Drosophila, Paramecium, Tribolium, yeast and other forms showed good fits to curves described by this differential equation, the so-called "logistic curves". Some data taken from wild populations of a few vertebrates and invertebrates are also in fairly good agreement with such theoretical curves. Most observations deal with the sigmoid period of population growth; after the stationary number has been reached, observations in most cases have been suspended. In general it can be said that the work of students of population dynamics has been extremely useful for reaching a better insight into some ecological problems, and the logistic curve proved to be a precious tool for this type of investigation.

On the other hand, as you know, during the last 20–25 years another group of biologists became interested in the study of populations, but from a different angle. Geneticists, who for some decades had focussed their attention on the mechanisms of inheritance as studied on experimental animals in the laboratory, became curious to learn something about the genetic constitution of free living animals and plants. By simple observation of samples taken in the field, by inbreeding in the laboratory animals captured in nature, or by breeding populations under controlled conditions in an attempt to identify the factors responsible for the changes in gene or chromosome frequencies which had been observed in nature, geneticists have produced an overwhelming wealth of evidence for the presence of a great amount of genetic variability in natural populations. Even in those cases where the taxonomists had found very constant phenotypes within a species, a great reserve of hidden genetic variation turned out to be present. In every organism which has been analyzed from this angle vast arrays of visible mutations, of lethals, of chromosome mutations were discovered. Every individual living in nature, belonging to a cross breeding species, is likely to be heterozygous for many genes. The general picture which can be derived from such studies is that of a continuous dynamic flow of gene frequencies occurring in wild populations under the pressure of environmental change. The very fact that large number of genes exist in heterozygous condition seems to be useful for the organism, and therefore a great storage of genetic variability is maintained.

The observed genetic variability is not only represented by clear-cut visible mutants, which follow a simple Mendelian inheritance, like the standard laboratory mutants, but comprises as well quantitative characters of a morphological and physiological nature, which follow a multifactorial scheme of inheritance. Thus it has been found that individuals of the same species may differ in genetic traits which are directly connected with their ecological requirements; inherited differences in temperature sensitivity, in rates of growth, in resistance to drought and to diseases were demonstrated in many animals. Factors affecting survival, such as fecundity, fertility and longevity were found to fall under genetic control, and to be determined by many genes. On the whole, the picture of wild populations offered by the geneticist is one of great variability and plasticity, which enables the species or local isolate to cope with the whims of the environment.

What bearing have the results obtained by the population geneticist on the study of population growth? If we consider together the two lines of evidence presented, one conclusion seems ineluctable: the very factors which determine the shape of the curve fall under genetic control, and thereby do not have fixed values. Let us now examine, then, how this fact affects population growth.

If we consider an ideal population of an asexually reproducing organism, or of a sexually reproducing but genetically homogeneous form, with no new mutation occurring in either case, the logistic curve will hold true. Under these conditions every individual will have the same biotic potential and therefore b in the differential equation will have a constant value. As a corollary of this, the maximum number of individuals which can be supported within the biotope will have a fixed value around which the asymptote will fluctuate for an indefinite number of generations after the numerical equilibrium is reached.

But if the original population is genetically heterogeneous, that is, if its members are highly heterozygous as they certainly are under natural conditions, then the value of b, the biotic potential, and of K, the asymptote, will not be constant but will change with the increase in age of the population. Furthermore the two values will be in some way interdependent. Let us try to visualize what will happen under these circumstances. Let us imagine that we start an experimental population with a small number of individuals which are genetically different and that we follow its development for many generations. At first all the members which we have introduced in the experimental limited space will have equal chances of reproducing, and their progenies will have equal chances of surviving, for space and food are plentiful. As soon as the effects of environmental resistance become noticeable, and a struggle for a restricted and steadily decreasing number of open spaces available develops, natural selection will begin to operate. Competition for survival and reproduction will occur. Those individuals which have a genotype conferring higher viability on its carriers will have better chances of being represented by their progeny in the following generations. The ones which have, say, higher fecundity, greater fertility, a shorter developmental period, greater hardiness, will outgrow their fellows which are inferior in these various respects. Accordingly, this pressure of natural selection to produce a population having a higher fitness to the environment will determine a shift in the frequencies of those genes which partake in the determination of the various viability factors. And, as a consequence, the average biotic potential of the population will increase. Furthermore, natural selection will tend to discriminate against those individuals which, on the one hand, are poor in their ability to assimilate the available food, and, on the other hand, require much space for their activities. Hence, in spite of the fact that the available space remains limited and that the supply of food is kept constant, the total number of individuals will not remain stationary but will tend to increase as the action of natural selection becomes effective. In terms of the logistic curve, or of any other similar mathematical expression, this means that the asymptote will not be reached after the period of sigmoid growth, but rather that a continuous increase in the size of the population, even though at a rate lower than that of the first period, will occur. Since, as previously noted, free living populations are genetically heterogeneous, the process I have just described, should be the general case for population growth. The logistic curve must be considered accordingly as a limited case no longer valid when the above specified requirements of genetic homogeneity do not obtain.

It may be asked here: if this is true, why have the experimental tests of the logistic curve given satisfactory results, and what experimental evidence is available to support the presented theoretical considerations?

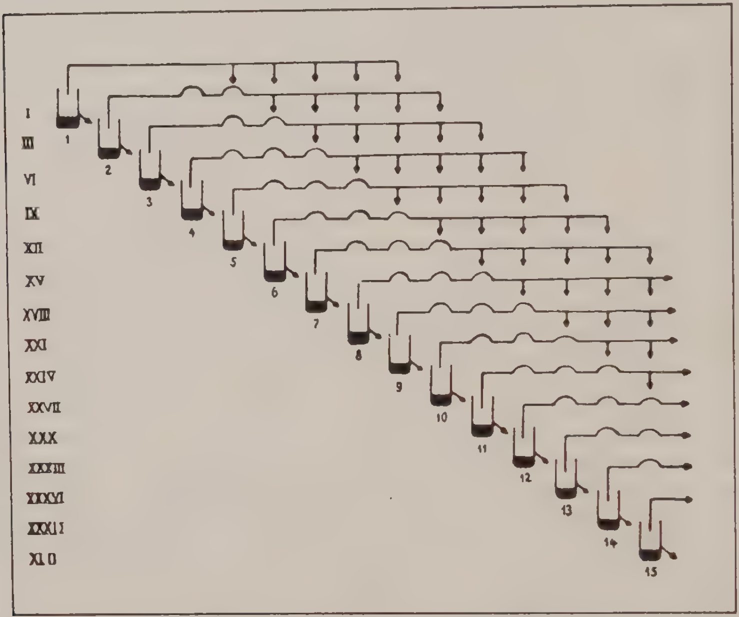

Fig. 1. Method of breeding populations of *Drosophila melanogaster*. A small number of flies is placed in the first vial (1). After three days (roman number III) the flies are removed and transferred to vial No. 2. Such transfer is repeated every three days to a new vial. As soon as the adults emerge from the first vial, these are added to the vial which contains the flies; every day the new born are added to the population, which accordingly increases in number. After 20 days, before a second generation emerges, the vials are discarded. Keeping the amount of food constant in the vials an equilibrium between the available space and food and the population's size is reached, as described in text.

As I have mentioned before, the main interest of students of population growth had been in finding out whether the actual numbers one can observe in an experimental population follow with some precision the curve which can be drawn on the basis of the differential equation of PEARL and REED. It did not seem very much worthwhile to continue the observations on the second part of the curve, when the number of individuals, after a rapid growth, tapers off, presumably reaching an approximately stationary value. Therefore very few data, if any, are available in the literature on the life of a population beyond the apparent point at which the asymptote was reached. Furthermore, most of the existing data have been derived either from unicellular, asexual organisms or from laboratory strains of insects, which were presumably highly homogeneous from the genetic viewpoint. In view of this it does not seem surprising that no discrepancy was found between the experiments and the logistic curve.

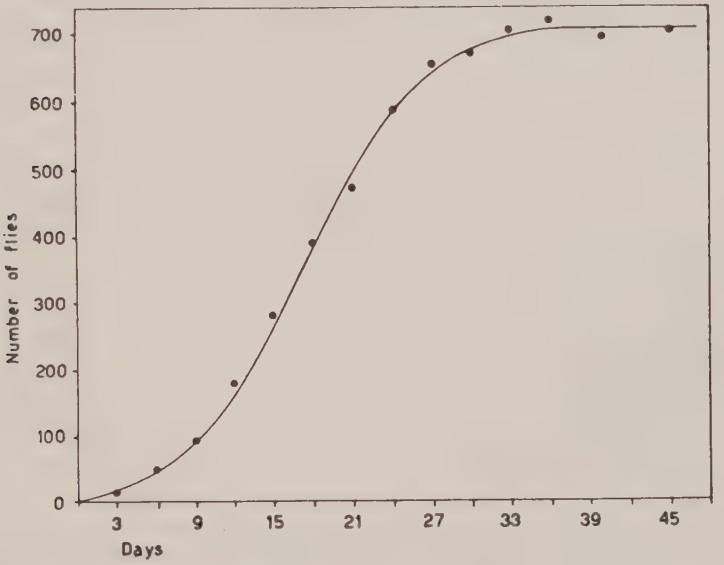

Fig. 2. The logistic curve calculated on the mean numbers of four populations of *Drosophila melanogaster*. Experimental data are represented by black dots.

As for experimental evidence supporting the previously presented considerations, I can only refer to some data derived from some populations of *Drosophila melanogaster* I have bred for other purposes. As these data I am going to discuss here are a by-product of another investigation aimed at the discovery of variations in fitness occurring in experimental populations, they are not as complete as they ought to be for a complete demonstration of my thesis. I hope, however, that they will appear convincing enough to make my thesis worthy of consideration and to stimulate other investigators to perform experiments along similar lines. Four populations of *Drosophila melanogaster* have been started by crossing two unrelated strains of this species, and have been kept under identical conditions for several generations with a constant supply of food. A method of breeding was used which was very similar to that of Pearl and which allowed the population to be maintained at a supposedly stationary number. I will not enter into a detailed description of the culturing method now, since it is irrelevant for our discussion. I will only mention that the bottles used were 12 cm. high and 3.5 cm. in diameter, and that records of the population numbers were kept at every transfer of the population from one bottle to the next, namely (see fig. 1) every three days. Two of the four populations were started about one year later than the other two. The same original strains and the same type of bottle were used in the two experimental series. The remarkable similarity of the data obtained in these two sets of parallel experiments at different times supports the conclusion that the numerical history of the populations was not fortuitous but rather determined by a mechanism of the sort described.

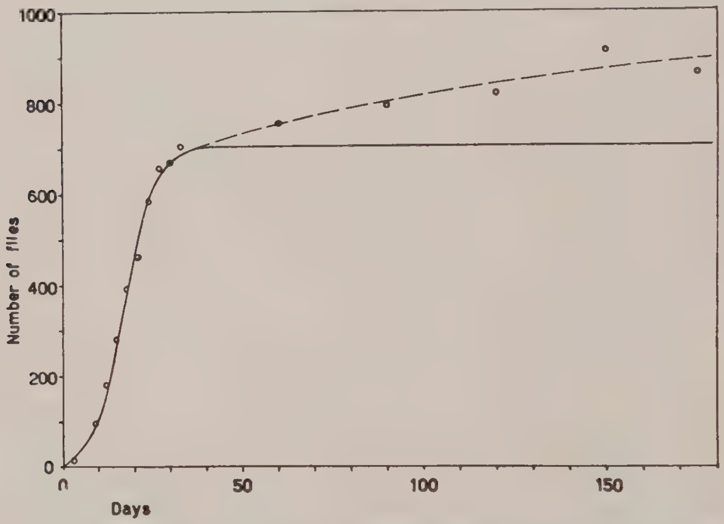

Fig. 3. Discrepancy between the calculated logistic curve (solid line) and the values observed in four populations of *Drosophila melanogaster*.

As can be seen in Figure 2, it has been possible to obtain a curve, using Pearl and Reed's logistic equation, which fits the experimental data well, that is the average numbers reached by the four populations during the first three generations. The curve has been calculated using as an asymptote the actual mean value of 704 flies reached by the populations after the first period of growth. But later a discrepancy between the calculated and the observed values became evident. In Figure 3, for the first part of the curve up to the 33rd day the same points are given which were presented in the previous figure. While these indicate the average numbers for the four populations at every counting, that is every three days, the points for the second part of the curve have been obtained averaging all the values obtained from the four populations over ten successive countings, that is over a period of thirty days. While, on the basis of the logistic curve one would expect the populations to fluctuate around the asymptotic value of 700, plus or minus, of course, minor differences due to occasional lack of constancy in culturing conditions and to sampling errors, the present data show a consistent trend toward higher values. The fact that the points shown are averages of forty observations, and that these have been obtained from two separate series of experiments run at different times makes it reasonably certain, I think, that this is not a mere coincidence between the considerations developed and the experimental data. Unfortunately no more records of this sort were kept for the four populations, for, as I said, at the time of conducting the experiment I had other problems in mind. It appears beyond doubt that after the first period of rapid growth the value of K did not remain constant. This means that the maximum number of individuals which can be supported in a limited area or volume at one time is not the same as the maximum at a later stage. Correspondingly, the value of the biotic potential of the population has been steadily increasing.

On this point I have clear-cut experimental evidence derived from observations carried on at different times on samples of flies taken from the four populations. Measurements were taken of the percentage of sterile females present in the population, of the fecundity of females, of the longevity of the adult flies, of the rate of development and of fertility, or percentage of emergence of adults from a known number of eggs. These values were compared to those of the two original strains which were crossed to start the populations. It turned out that natural selection had produced a new genotype, better adapted to the particular experimental environment, and that the improvement was manifested by a measurable increase in fitness. Detailed data about this part of this experiment will be presented elsewhere, but here I wish to stress the fact that the viability factors measured coincide with what was previously called the biotic potential. This, then, did not remain constant but increased in the course of the experiment, as one would expect considering the effect of genetic heterogeneity on population growth.

As the population increases in number and as the biotic potential becomes greater, the struggle for existence becomes more stringent. Those strong at one stage of the population development may become weak at a later stage. Such a process will necessarily eliminate the weakest genotypes at a progressive rate and thereby provoke a steady depletion of the genetic variability which was originally present. At a certain stage no more free genetic variability will be available, and then, indeed, the population number will have reached a plateau, which will not be surpassed unless new mutants appear. This, I think, ought to be checked by experiments, for, if true, it might become highly significant for ecological problems.

Let us assume that under natural conditions a similar process may occur. Over a certain area the population of a species becomes established and increases in number. After a sudden outbreak in the population's number determined by the open space, the ensuing slow increase acquires an adaptive significance in that natural selection operates to produce the most efficient genotype for that particular environment, which, for the sake of the argument, we shall assume to be constant over a long period of time. But this adaptation takes place at the expense of the genetic variability, and, after the process has gone on for some time, and the final plateau has been reached, one may assume that genetic homogeneity has been reached. If at that stage even a very minor change should take place in the environment, this may bring about the collapse of the population for it has not any longer genetic reserves which could be mobilized when the need appears. All of a sudden the population will crash and reach a very low ebb, and perhaps extinction, as a consequence of a minor environmental change, which, at a previous stage of the population's history, might have gone unnoticed. If the population disappears completely there will be an empty space which will before long be colonized again by migrants from neighbouring populations. The new immigrants will carry a new reserve of genetic variability, which will be used for a new population cycle. But even if the population does not disappear completely, if only a few individuals do survive, they will face a completely new set of environmental circumstances, for the very disappearance of a large population from its area can produce a major change in the biotope. New selective agencies will be at work then, and these may be instrumental in determining a reconstruction of the genotype. We now know in genetics that the lack of response to selection which one may observe after having achieved some progress for a desired trait can occur even when there still is some genetic variability for the selected trait present in the strain. It just happens that natural selection tries to keep a balance, a homeostatic condition in the genotype as it does at the physiological level. Once the unidirectional selective agency is removed the whole genotype may undergo a basic reconstruction which may free the genetic variability which was previously blocked and thus may allow further progress in the direction of the previous selection. Now, if a similar condition should obtain in our population, the few surviving individuals may produce progeny, which, under the new conditions, having a new set of free genetic variability present, may exploit it to start a new cycle of population growth.

I realize the highly speculative nature of the latter part of my argument, but I cannot help wondering whether a similar mechanism might not at least be in part responsible for the sudden fluctuations observed in animal populations. I know, of course, that there are many ecologic factors which could be held responsible for such variations in numbers, and that in some cases there are no doubts that the main determinant is of an environmental nature. I think, however, that even these more speculative aspects of my thesis could be checked with a proper study of experimental populations. There are many things which remain to be done, no doubt. It will be worthwhile to check on the validity of the new type of curve and on the genetic factors which may determine the slope of the second part of the curve. One could actually perform experiments starting with populations having various amounts of genetic reserves present and try to find a new type of analytical expression to fit the data. One could try to see whether there might be any way to make predictions about the time when the population will reach the final plateau, if the genetic constitution of the population is known. One could try to alter more or less drastically the environment to see whether a crash of the previously described type would occur. One could try to analyze mathematically as well as experimentally what bearing the introduction of the genetic variable may have on more complex cases of population growth, where more than one species at the same time is considered in the same milieu. In this way it will become feasible to evaluate the significance of the genetic heterogeneity for the theory of populations.

You will forgive me, I hope, if I am biased in my outlook, in that I try to emphasize such genetic mechanisms. Ecologic factors are certainly the main determinants of the growth of populations, but still I think that the genetic component should not be disregarded. It could well be that a definite interplay between environmental agencies and genetic structure would explain some of the puzzling problems of animal populations.

Contribution from the Scripps Institution of Oceanography, University of California, New Series No. 839b

Discussion:

U. D'ANCONA: I should like to point out that also VOLTERRA has analytically represented the populations' growth as a part of his mathematical theory. He has pointed out that, after reaching the asymptotic level, the populations do not maintain a constant size, but fluctuate around the asymptote.

The logistical curve, like all similar theoretical curves, presumes constant conditions and homogeneous populations. Therefore when selection is operating upon an initially heterogeneous population and does isolate a single genotype, the final condition of the population is no more the same as it was at the beginning. As a result the conditions are by far more complex and difficult to be analytically represented.

BIANCO LUNO A/S. KBH

(250)

BULLETIN OF THE AMERICAN ASSOCIATION OF PETROLEUM GEOLOGISTS
VOL. 40, NO. 2 (FEBRUARY, 1956), PP. 295-376, 32 FIGS., 8 PLS.

MACRO-INVERTEBRATE ASSEMBLAGES AS INDICATORS OF SEDIMENTARY ENVIRONMENTS IN EAST MISSISSIPPI DELTA REGION[1]

ROBERT H. PARKER[2]
La Jolla, California

ABSTRACT

As a result of a study based on three years of biological sampling in the east Mississippi Delta region, eight macro-invertebrate assemblages are recognized, each characteristic of a specific sedimentary environment ranging from the Mississippi Delta marshes to the edge of the continental shelf northeast of the Delta proper. The eight assemblages and their corresponding environments are: (I) the delta marshes, (II) delta front and lower distributaries, (III) lower Breton Sound and lower pro-delta clayey slopes, (IV) upper Breton Sound, (V) inlets, or areas of strong currents, (VI) the shallow continental shelf of the Gulf of Mexico from 0 to 12 fathoms, (VII) the deeper part of the continental shelf from approximately 13 fathoms to 60 fathoms, and (VIII) the living oyster reefs of the shallow protected bays of the Delta region. The boundaries of these environments were established by plotting the distributions of both living and dead representatives of species of invertebrates furnishing hard parts plus the distributions of living soft-bodied animals which were so abundant as to characterize regions where animals with hard parts were scarce though present.

Comparison of the distribution of the hydrographic factors with the physiography of the landmasses in this area with the macro-organism distributions made it possible to formulate criteria for the interpretation of ancient environments as far back as the Miocene on the Gulf and Atlantic coasts. Paleontologic literature shows that most of the present-day delta species have been found in the Pliocene, and most of the diagnostic forms have existed since the lower Miocene. The primary factors influencing distributions of these organisms are bottom type, salinity and temperature (especially the degree of variability), turbidity of the water, and currents. It was also found that comparative rates of deposition could be estimated by the ratio of the number of living to the number of dead, in equal-size samples. A series of marine bottom communities based on the community concept of European marine ecologists is recognized on the basis of the most abundant and widespread animals.

INTRODUCTION

This paper describes one of a series of studies of nearshore sedimentary environments in the northern Gulf of Mexico, supported by the American Petroleum Institute as Project 51, at Scripps Institution of Oceanography under the direction of Francis P. Shepard. The study was made on the east side of the Mississippi Delta in Breton Sound and beyond in the open Gulf of Mexico from the shore to approximately the 90-fathom contour (Figs. 1 and 2). The work was begun in October, 1951; biological collections and observations were made during the fall and early winter of 1951, the spring and early summer of 1952, and the last week of May and first week of June, 1953. Bottom-sediment samples for mechanical analysis yielding biological information were also obtained in the fall of 1953 and in February, 1954. Biological collections were made at more than 280 stations, and in addition 130 bottom-sediment sampling sites provided some biological data. Two maps (Figs. 3 and 4) show the locations of all stations providing biological data. Positions for most of the inshore biological stations were

---

[1] Contribution from the Scripps Institution of Oceanography, New Series No. 840. This investigation was supported by a grant from the American Petroleum Institute, Project 51. Manuscript received, August 15, 1955.

[2] Scripps Institution of Oceanography.

Reproduced by Permission

located by the use of horizontal sextant angles; the offshore stations were made by dead reckoning and are, therefore, approximate.

Acknowledgments.—For assistance in preparing the manuscript and for helpful suggestions on many aspects of this problem, the writer thanks Joel W. Hedgpeth of the Scripps Institution of Oceanography. Thanks are also due to Robert L. Miller of the University of Chicago for suggesting various methods of analyzing the field data and presenting it in statistical form. The writer is particularly grateful to Miss Joan Demond, formerly with this Project, for her assistance in identifying and establishing the synonomy of the mollusks (to be published

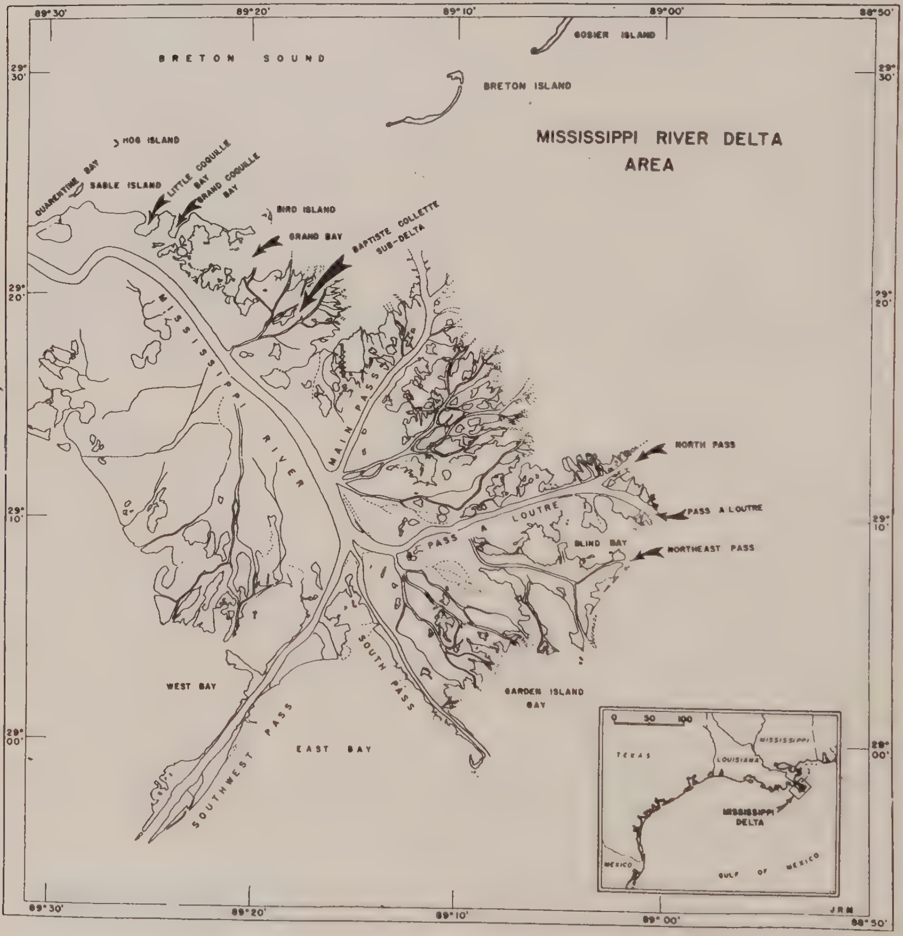
89°30'
89°20'
89°10'
89°00'
88°50'
29° 30'
29° 20'
29° 10'
29° 00'
BRETON SOUND
GOSIER ISLAND
BRETON ISLAND
MISSISSIPPI RIVER DELTA AREA
HOG ISLAND
QUARANTINE BAY
SABLE ISLAND
LITTLE COQUILLE BAY
GRAND COQUILLE BAY
BIRD ISLAND
GRAND BAY
BAPTISTE COLLETTE SUB-DELTA
MISSISSIPPI RIVER
MAIN PASS
NORTH PASS
PASS A LOUTRE
BLIND BAY
NORTHEAST PASS
SOUTH PASS
GARDEN ISLAND BAY
WEST BAY
EAST BAY
SOUTHWEST PASS
0 50 100
TEXAS
LOUISIANA
MISSISSIPPI
MISSISSIPPI DELTA
MEXICO
GULF OF MEXICO
JRM

FIG. 1.—General map and place names of east Mississippi Delta region.

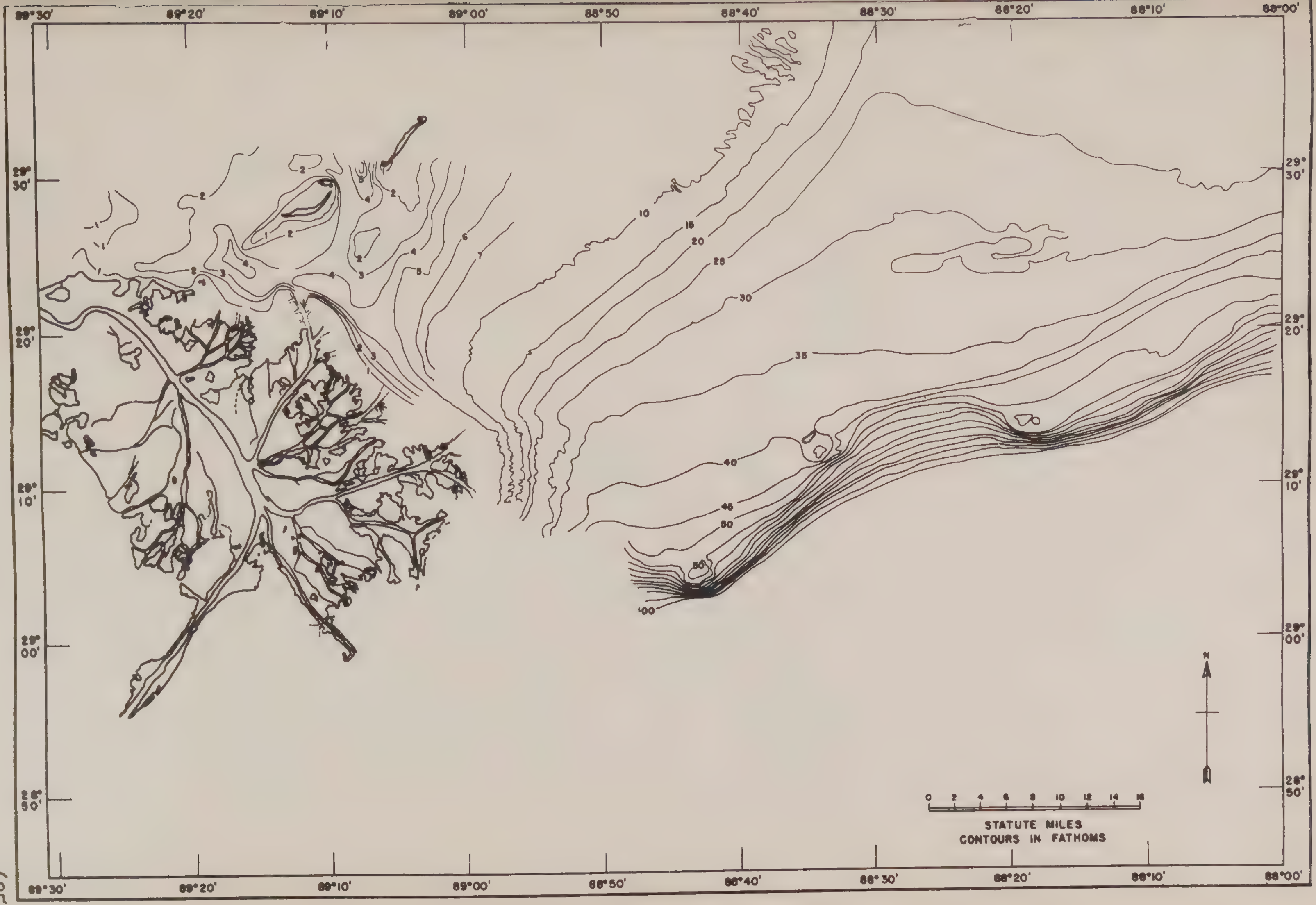
89°30'
89°20'
89°10'
89°00'
88°50'
88°40'
88°30'
88°20'
88°10'
88°00'
29° 30'
29° 20'
29° 10'
29° 00'
28° 50'
N
0 2 4 6 8 10 12 14 16
STATUTE MILES
CONTOURS IN FATHOMS
10
15
20
25
30
35
40
45
50
100

FIG. 2.—Offshore bottom contours of east Mississippi Delta area.

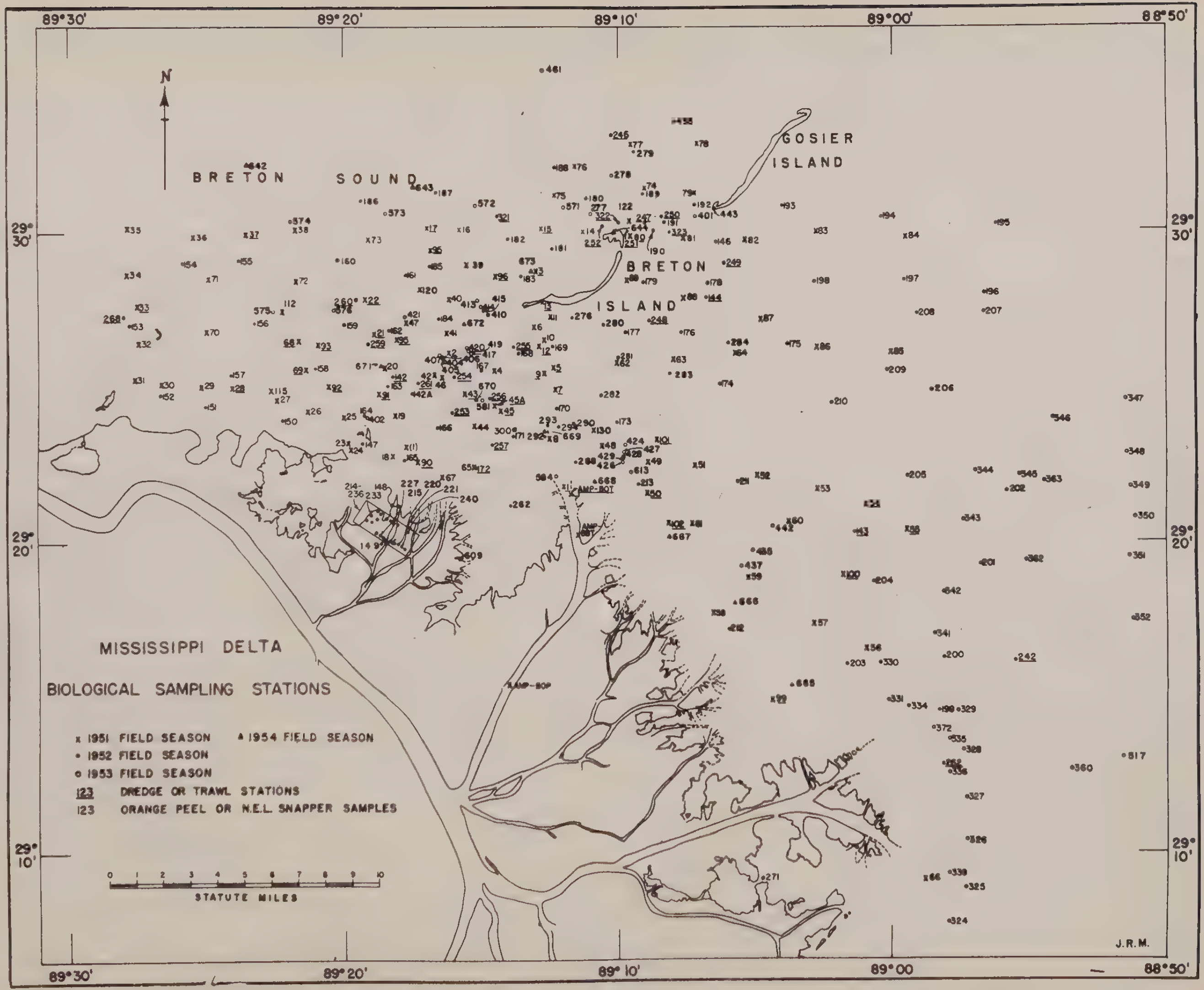
MISSISSIPPI DELTA
BIOLOGICAL SAMPLING STATIONS
x 1951 FIELD SEASON
• 1952 FIELD SEASON
○ 1953 FIELD SEASON
▲ 1954 FIELD SEASON
123 DREDGE OR TRAWL STATIONS
123 ORANGE PEEL OR N.E.L. SNAPPER SAMPLES
0 1 2 3 4 5 6 7 8 9 10
STATUTE MILES
BRETON SOUND
GOSIER ISLAND
BRETON ISLAND
N
89°30'
89°20'
89°10'
89°00'
88°50'
29° 30'
29° 20'
29° 10'
J.R.M.

FIG. 3.—Station locations of biological samples taken from 1951 to 1954 in inshore Mississippi Delta region.

separately); and also to Thomas E. Pulley of the University of Houston who identified many of the pelecypods. He also thanks Harald A. Rehder and Joseph P. E. Morrison of the Division of Mollusks, United States National Museum, and R. Tucker Abbott of the Philadelphia Academy of Natural Sciences, for help in identifying many of the mollusks, and William K. Emerson of the American Museum of Natural History for identification of the scaphopods. Appreciation is also extended to J. Wyatt Durham and Elton L. Puffer of the Museum of Paleontology at Berkeley for identification of the echinoderms and corals and for furnishing some of the photographs used in the faunal plates; and to Donald J. Reish of the Allan Hancock Foundation, University of Southern California, for identification of the polychaete worms. James R. Moriarty of the Geology Division at Scripps prepared the charts and illustrations in this paper, and Thomas E. Mahnken made most of the photographs.

Previous work.—With the exceptions of various collections of mollusks (Vanatta, 1903; Clench, 1929; Hadley, 1936; Richards, 1954), there has been little investigation of the bottom fauna of this area before or since the preliminary survey of the clam and scallop beds in the vicinity of the Chandeleur Islands and Breton Island by Spaulding (1906), and the faunistic surveys by Cary (1905) and Cary and Spaulding (1909). Many of the species of mollusks collected during the present investigation were previously recorded only in Dall's monographs (1886, 1889) on the collections near the Mississippi Delta by the *Blake* and the *Albatross*. Rehder and Abbott (1951) described several species of mollusks which were also taken near the Mississippi Delta in the same localities where project collections were made, and Richards (1954) listed many of the Delta mollusks from borings made in the region now being studied. A general history of investigations in the Gulf of Mexico may be found in Galtsoff *et al.* (1954, pp. 25–32, 203–13).

GENERAL DESCRIPTION OF AREA

The principal physiographic features of this area (Fig. 1) are the low delta plain of the Mississippi River with its active distributaries which empty into Breton Sound or directly into the Gulf of Mexico, and the small barrier islands (Breton and Gosier), which lie about 6 miles offshore. Wide inlets have formed between Breton Island and the shores of the Delta and between Breton and Gosier islands. Both of these inlets are 26–45 feet deep and are characterized by strong tidal currents. The barrier islands are narrow and of low relief, but seem to be an effective barrier to both fresh water pouring out of the Mississippi River distributaries toward the southwest and to the high-salinity waters of the open Gulf of Mexico. Breton Island has a shallow lagoon on the south side of the island with a stand of honey mangrove (*Avicennia nitida*) on the island edge of this lagoon.

Breton Sound, although it is broadly connected with the Gulf, is shallow and fairly well enclosed by land except where it joins Chandeleur Sound on the north.

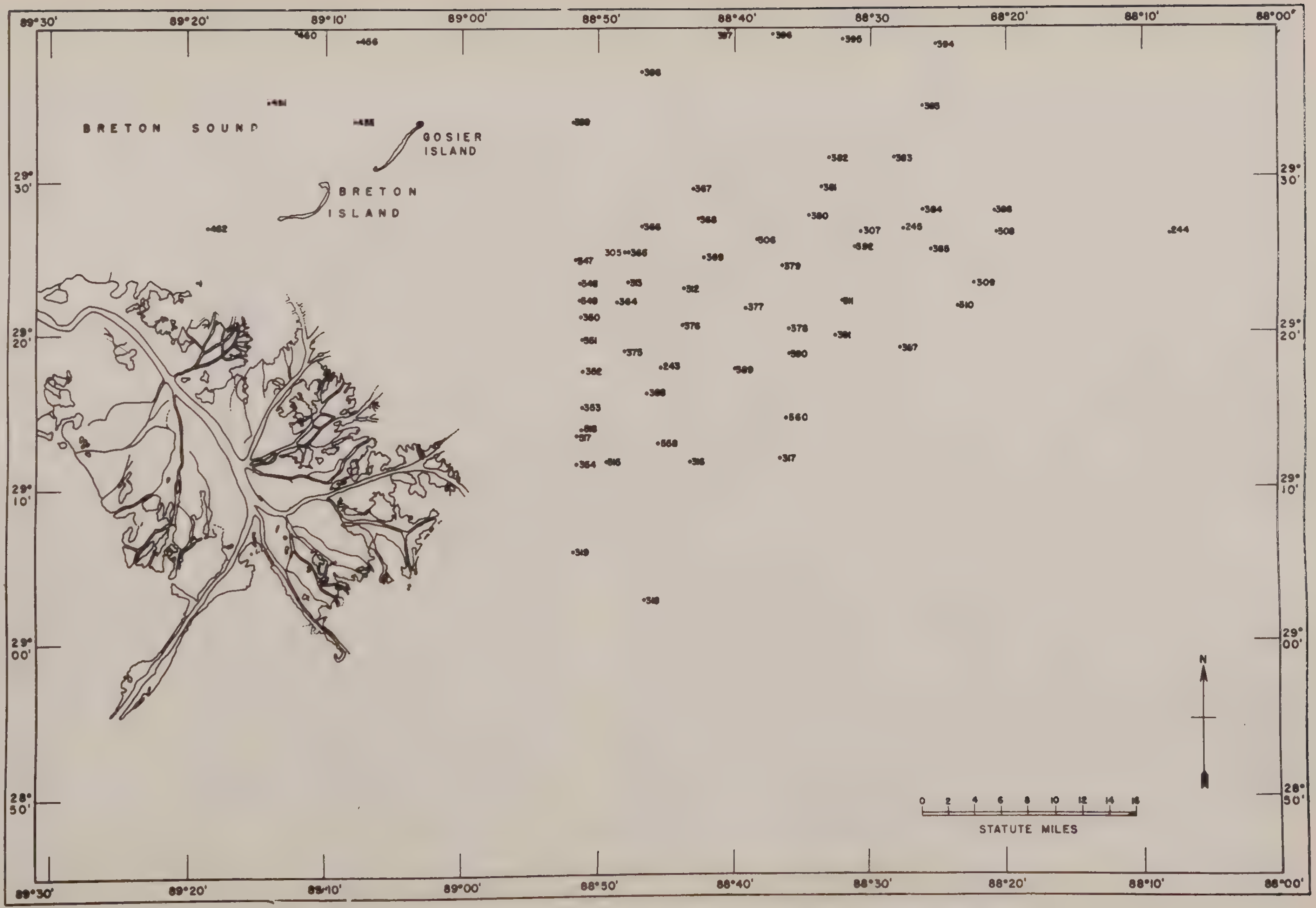
BRETON SOUND
GOSIER ISLAND
BRETON ISLAND
305
89°30'
89°20'
89°10'
89°00'
88°50'
88°40'
88°30'
88°20'
88°10'
88°00'
29° 30'
29° 20'
29° 10'
29° 00'
28° 50'
N
0 2 4 6 8 10 12 14 16
STATUTE MILES

FIG. 4.—Station locations of biological and geological sediment samples taken in offshore Delta region.

Breton Sound is 8–15 feet deep in its northwest part, increasing to 18–26 feet in the southeast part (Fig. 5). A brief physical description of the region is given in a paper by Scruton (1956).

The sediments and sedimentary processes of the area are described in detail by Scruton (1956), who proposed sediment units based on the particle size and gross appearance of the deposits. Inman (1956) has also compiled a chart of sediment types of the inshore region, based on the parameters of the size distribution of the sediments. Two maps (Figs. 6a and 6b) were also compiled for this study to show the size distribution of the sediments based on their percentages of sand, silt, and clay, by the classification described by Shepard (1954). These two maps will be shown to have close agreement with the distribution of macro-organisms.

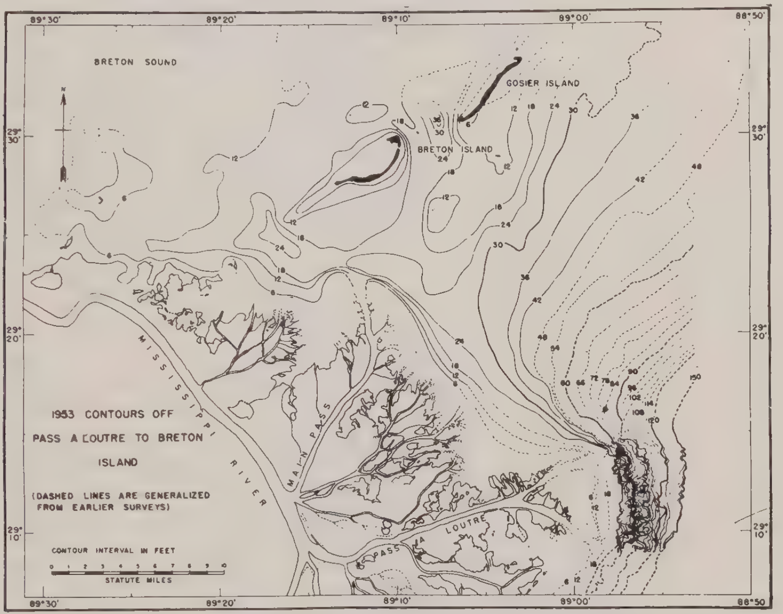

89°30'
89°20'
89°10'
89°00'
88°50'
29° 30'
29° 20'
29° 10'
BRETON SOUND
N
GOSIER ISLAND
BRETON ISLAND
MISSISSIPPI RIVER
MAIN PASS
PASS A LOUTRE
1953 CONTOURS OFF PASS A LOUTRE TO BRETON ISLAND
(DASHED LINES ARE GENERALIZED FROM EARLIER SURVEYS)
CONTOUR INTERVAL IN FEET
0 1 2 3 4 5 6 7 8 9 10
STATUTE MILES

FIG. 5.—Bottom contours of inshore Mississippi Delta region (as compiled by F. P. Shepard).

In general, both chlorinity (chlorinity rather than salinity is used here because normal ionic ratios used to calculate salinities may not hold in these areas diluted by river water) and temperature are extremely variable in this region, except in the bottom waters of the offshore parts of the Gulf of Mexico (discussed in detail by Scruton, manuscript). The northeast parts of Breton Sound are somewhat more stable and generally possess higher chlorinity and water temperature than the waters in the vicinity of the delta shores and distributaries (Figs. 7, 8, 9, and 10). According to Marcus A. Hanna of the Gulf Oil Corporation (personal

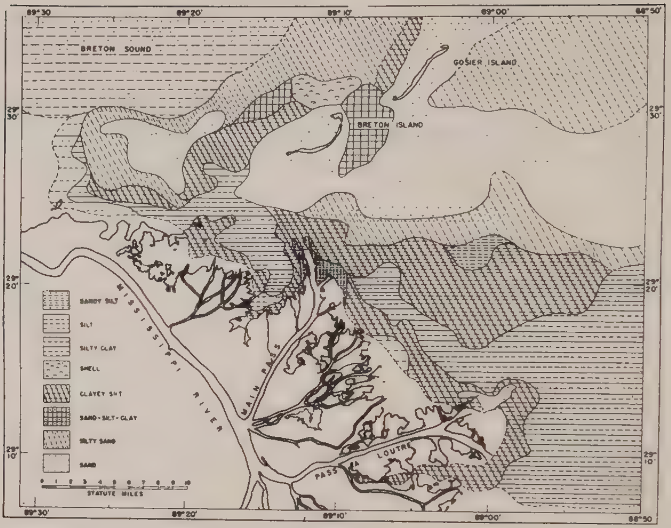
BRETON SOUND
GOSIER ISLAND
BRETON ISLAND
MISSISSIPPI RIVER
MAIN PASS
LOUTRE
PASS
SANDY SILT
SILT
SILTY CLAY
SHELL
CLAYEY SILT
SAND-SILT-CLAY
SILTY SAND
SAND
STATUTE MILES
89°30'
89°20'
89°10'
89°00'
88°50'
29° 30'
29° 20'
29° 10'

FIG. 6a.—Areal distribution of sediment types as determined by sand-silt-clay contents for inshore Delta region (compiled by Parker and D. G. Moore).

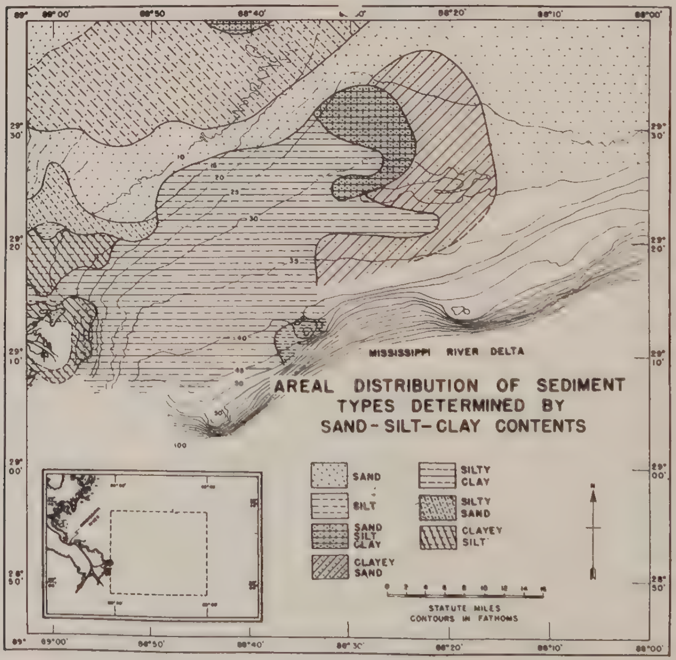
MISSISSIPPI RIVER DELTA
AREAL DISTRIBUTION OF SEDIMENT TYPES DETERMINED BY SAND-SILT-CLAY CONTENTS
SAND
SILT
SAND SILT CLAY
CLAYEY SAND
SILTY CLAY
SILTY SAND
CLAYEY SILT
STATUTE MILES
CONTOURS IN FATHOMS
89°00'
88°50'
88°40'
88°30'
88°20'
88°10'
88°00'
29° 30'
29° 20'
29° 10'
29° 00'
28° 50'
10
15
20
25
30
35
40
100

FIG. 6b.—Areal distribution of sediment types as determined by sand-silt-clay contents of offshore Delta region (compiled by Parker and D. G. Moore).

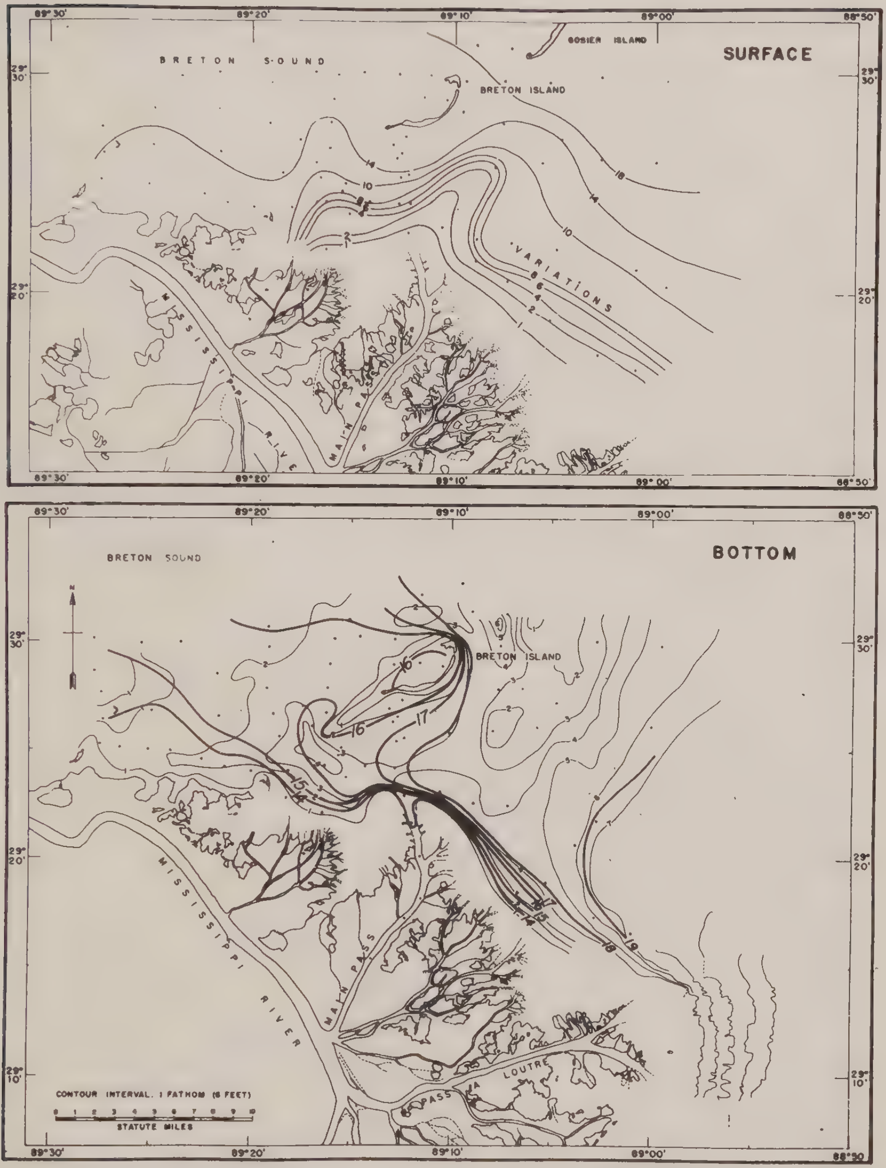
SURFACE
BRETON SOUND
GOSIER ISLAND
BRETON ISLAND
VARIATIONS
MISSISSIPPI RIVER
MAIN PASS
89°30'
89°20'
89°10'
89°00'
88°50'
29° 30'
29° 20'
29° 10'
BOTTOM
BRETON SOUND
BRETON ISLAND
MAIN PASS
MISSISSIPPI RIVER
LOUTRE
PASS
CONTOUR INTERVAL, 1 FATHOM (6 FEET)
STATUTE MILES
0
1
2
3
4
5
6
7
8
9
10

FIG. 7.—Areal distribution of chlorinities in parts per thousand as observed in fall of 1951 during time of minimum river discharge (compiled by P. C. Scruton).

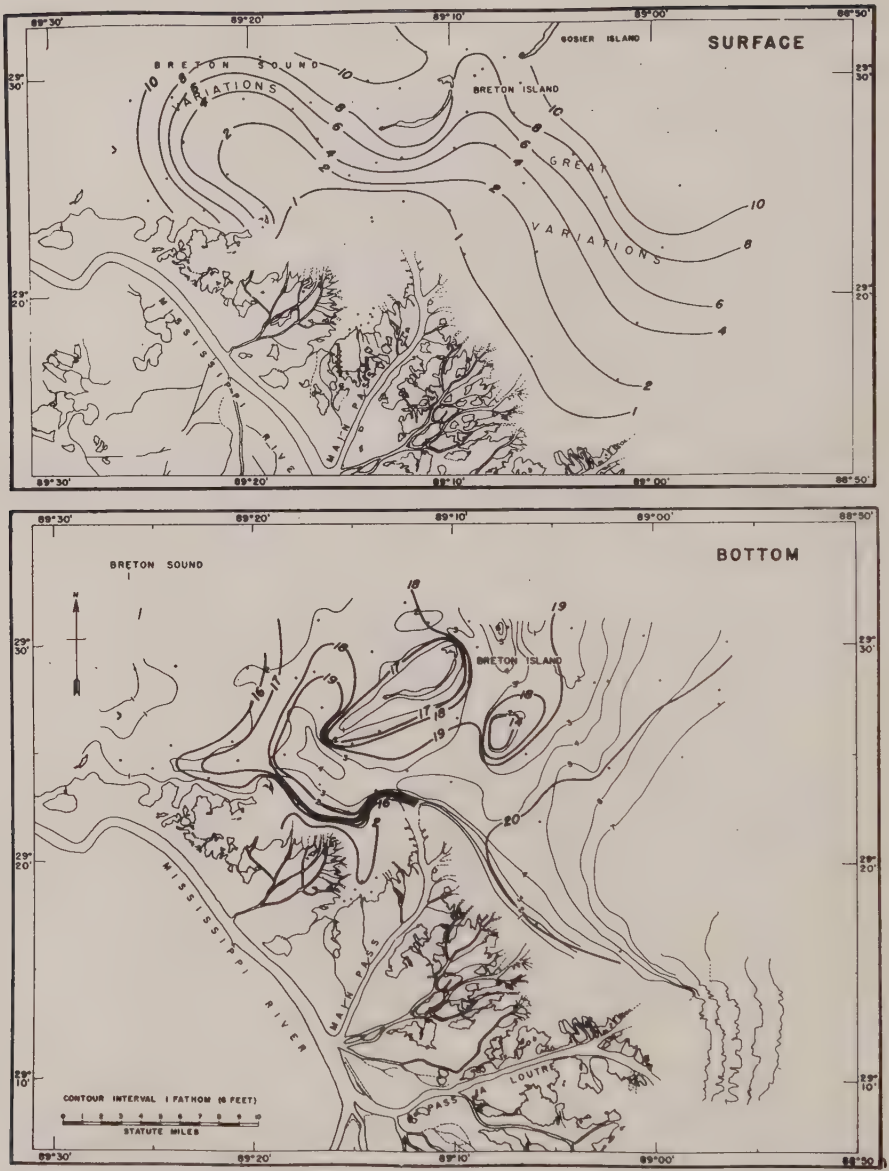
SURFACE
GOSIER ISLAND
BRETON SOUND
VARIATIONS
BRETON ISLAND
GREAT VARIATIONS
MISSISSIPPI RIVER
MAIN PASS
BOTTOM
BRETON SOUND
BRETON ISLAND
N
PASS A LOUTRE
CONTOUR INTERVAL 1 FATHOM (6 FEET)
0 1 2 3 4 5 6 7 8 9 10
STATUTE MILES
89°30'
89°20'
89°10'
89°00'
88°50'
29° 30'
29° 20'
29° 10'

FIG. 8.—Areal distribution of chlorinities in parts per thousand as observed in spring of 1952 during time of maximum river discharge (compiled by P. C. Scruton).

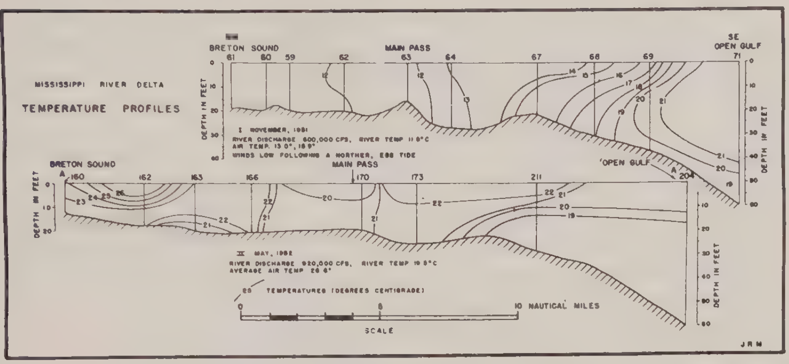

FIG. 9.—Water-temperature profiles of inshore Mississippi Delta region at times of low and high river discharge (compiled by P. C. Scruton).

communication) a semi-permanent wedge of high-salinity water impinges on the shores of the delta near Coquille and Denisse bays.

Although the chlorinities are variable in Breton Sound and in the vicinity of the delta, they are not typical of normal low-chlorinity bays, such as San An-

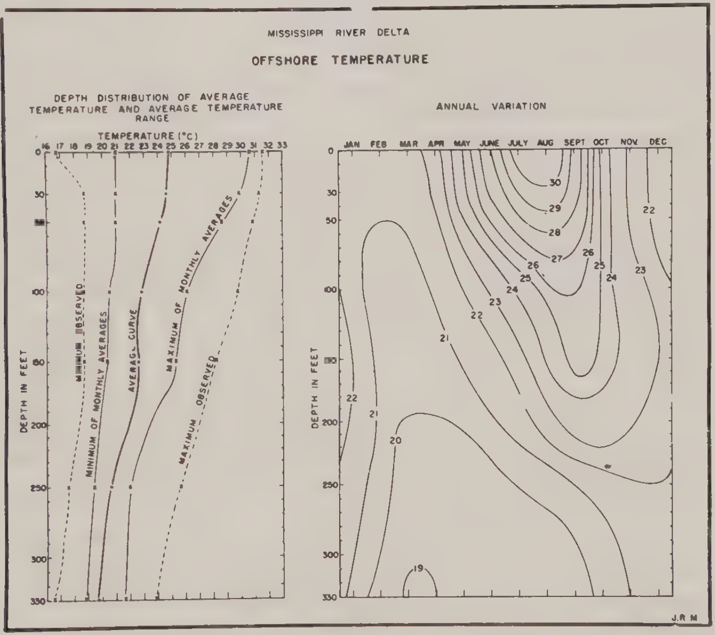

FIG. 10.—Depth distribution and annual variation of water temperatures in offshore Delta region (compiled by P. C. Scruton).

tonio and Galveston bays (Galtsoff, 1931), or Copano Bay (Collier and Hedgpeth, 1950) in Texas. The bottom chlorinities in Breton Sound seldom fall below 16 °/₀₀ (parts per thousand) even during the flood stages of the Mississippi River (Fig. 8). The only parts of the project area which have chlorinities below 5 or 6 °/₀₀ are the river distributaries less than 3–5 feet deep of the Delta front and the waters of the Delta marshes. The waters of the open Gulf of Mexico at depths greater than 12–13 fathoms (72–78 feet) seldom fall below 19 °/₀₀ chlorinity and have a very narrow range of chlorinity (19.6–20.2 °/₀₀) and temperature (20°–25°C.). Scruton (manuscript) discusses the inter-relationships of the hydrographic factors in the Delta region. Turbidity of the waters in this region may also be important in influencing the distribution of many of the invertebrates in the area. Scruton and Moore (1953) discussed turbidities in this region.

METHODS OF STUDY

Most of the biological samples were obtained with an orange-peel bucket approximately $\frac{1}{3}$ cubic foot in capacity. Because of varying hardness of the bottom sediments, samples were not of equal size; therefore, samples comparable on an unweighted basis were not obtained. On particularly hard sand bottom, a snapper grab sampler was used. Because this device took no more than a handful of sediment, several samples were taken at each station. Several dredges and trawls were used for the large animals and those organisms which were too mobile to be taken by grab samplers. Coring devices also produced valuable biological data, since comparative distribution figures could be obtained by analyzing the top 5–20 centimeters of sediments in the cores. Most of the shells from cores were collected from the sand fractions of sediment analyses from these cores.

An attempt was made to list all organisms taken at every station while in the field. Most of the material was preserved in iso-propyl alcohol for later study. From the field notes and from the condition of the preserved material it was possible to get approximate living and dead counts of all organisms at each station, although each single valve was counted as one dead individual. All major faunal groups were sorted from each sample, and all except the bryozoans, crustaceans, and fish were sent to specialists for identification. A complete list of invertebrate species and the biological station numbers at which each species was taken is listed in Table I. Most of the specimens taken in the study are at Scripps Institution of Oceanography, except the scaphopods, echinoderms, and corals, which are at the Museum of Paleontology at Berkeley. Most of the organisms used in defining the macro-organism assemblages will be illustrated in a catalogue of invertebrata of the Gulf Coast, in preparation.

From the collections in the east Mississippi Delta region the following numbers of species were found: 93 gastropods (and 7 pteropods), 116 pelecypods, 6 scaphopods, 1 chiton, 3 cephalopods, 7 anthozoa (coelenterates), 8 echinoderms, 31 polychaete worms, 8 identifiable bryozoa, and 34 crustaceans, a total of 314 species. A series of species distribution maps for the more important invertebrates

TABLE I. SPECIES AND STATION OCCURRENCES OF INVERTEBRATE ANIMALS COLLECTED IN MISSISSIPPI DELTA REGION

Species	*Biological Station Numbers at Which Species Was Collected*
MOLLUSCA	
GASTROPODA	
Diodora cayenensis	33, 62, 74, 75, 76, 246, 247, 309, 311
Fissurella barbadensis	247
Neritina reclivata	33, 35, 38, 52, 62, 74, 75, 76, 81, 122, 146a, 151, 153, 180, 188, 190, 220, 221, 227, 240, 246, 277, 278, 284, 311, 323, 398, 402, 457, 571, 642, 643, 672
Littorina irrorata	12, 13, 15, 244, 321
Littoridina sphinctostoma(?)	426, 643, 670
Modulus modulus	11
Architectonica nobilis	309
Cerithium muscarum	33
Cerithiopsis subulata	75
Bittium varium	643
Calyptraea centralis	244, 308, 309, 311, 316
Crucibulum auricula	308, 309, 311, 393
Crepidula fornicata	33, 34, 62, 68, 77, 142, 151, 244, 308, 309, 311, 321, 393
Crepidula plana	4, 13, 17, 32, 33, 34, 36, 37, 38, 62, 73, 74, 76, 80, 153, 154, 155, 157, 160, 180, 188, 251, 268, 316, 321, 322, 383, 429, 575, 642, 643
Strombus alatus	13, 244, 321, 393, 443
Polinices duplicatus	1, 2, 4, 9, 11, 12, 13, 15, 17, 20, 28, 32, 33, 35, 37, 43, 48, 52, 62, 69, 71, 77, 142, 143, 153, 154, 155, 160, 171, 181, 183, 189, 233, 246, 247, 248, 250, 251, 254, 255, 256, 257, 261, 321, 322, 323, 405, 406, 424, 642, 643, 669, 672
Polinices uberinus	244, 308, 309, 311, 316, 317, 387, 393
Natica pusilla	8, 10, 14, 43, 73, 82, 88, 171, 188, 190, 197, 248, 283, 294, 308, 309, 311, 313, 316, 321, 345, 346, 366 382, 402, 424, 584, 643, 669, 670
Natica canrena	308, 309, 311
Sinum perspectivum	189, 322, 366
Phalium granulatum	13, 244, 443
Distorsio clathrata	308, 309, 311
Sconsia striata	316, 366, 560
Tonna galea	443
Murex recurvirostrus rubidus	244, 308, 309
Murex cabritii	309
Murex florifer arenarius	309
Thais haemastoma floridana	4, 9, 12, 15, 37, 74, 189, 249, 250, 321, 323, 458
Thais haemastoma haysae	13, 143, 252, 261
Anachis (Astyris) perpicta	244, 308, 309, 311, 342, 364, 365, 367, 382, 383, 384
Anachis obesa	4, 6, 7, 8, 11, 12, 15, 17, 20, 21, 32, 33, 38, 39, 43, 48, 50, 52, 53, 55, 56, 62, 68, 69, 72, 73, 75, 76, 79, 80, 81, 82, 120, 146a, 151, 152, 153, 158, 160, 167, 168, 169, 171, 183, 188, 189, 197, 205, 206, 244, 247, 254, 257, 277, 278, 280, 288, 311, 313, 323, 345, 346, 347, 348, 350, 352, 362, 363, 366, 367, 368, 375, 382, 393, 406, 413, 415, 419, 420, 424, 428, 460, 571, 572, 573, 575, 642, 643, 669, 670, 672
Anachis iontha	244, 309, 311
Anachis avara semiplicata	7, 39, 43, 62, 70, 142, 143, 152, 154, 155, 188, 246, 247, 250, 252, 254, 321, 322, 401, 575, 581, 642, 670
Anachis avara similis	17, 76, 81, 142, 254, 257, 261, 288, 323, 393, 643, 669
Mitrella lunata	7, 142, 250, 311, 404, 642, 643, 670
Colubraria lanceolata	309
Seila adamsi	74, 76, 250, 311
Nassarius ambiguus consensus	244, 308, 309, 311, 316, 317, 366, 382, 385, 386, 387, 391, 393, 560
Nassarius acutus	2, 4, 5, 6, 7, 8, 10, 11, 12, 15, 17, 19, 20, 21, 22, 23, 25, 26, 27, 29, 30, 31, 32, 33, 35, 38, 39, 40, 41, 42, 43, 46, 49, 51, 52, 56, 61, 62, 68, 69, 70, 71, 72, 73, 76, 77, 78, 79, 82, 84, 86, 88, 142, 142a, 143, 146a, 150, 151, 152, 154, 155, 156, 157, 158, 159, 160, 161, 162, 165, 167, 168, 169, 170, 171, 172, 174, 178, 181, 182, 183, 187, 188, 190, 196, 205, 213, 246, 247, 248, 250, 254, 261, 262, 268, 276, 277, 290, 292, 293, 300, 309, 321, 322, 323, 326, 330, 331, 336, 367, 383, 384, 402, 404, 405, 406, 407, 410, 414, 417, 419, 420, 424, 426, 428, 435, 455, 459, 461, 491, 573, 581, 584, 642, 643, 666, 667, 669, 670, 671, 672, 673,
Nassarius vibex	15, 643
Cantharus cancellarius	7, 12, 15, 32, 33, 34, 35, 43, 51, 62, 73, 74, 75, 78, 80, 81, 143, 144, 146a, 155, 160, 171, 186, 188, 189, 197, 246, 247, 248, 250, 254, 277, 278, 321, 322, 323, 346, 404, 457, 571, 643
Odostomia impressa	153
Busycon contrarium	12, 13, 15, 33, 43, 62, 73, 80, 246, 247, 251, 259, 321, 443
Busycon spiratum plagosum	12, 13, 37, 45, 244, 261, 321, 443, 642
Oliva sayana	12, 33, 62, 171, 244, 308, 311, 321, 322, 346, 347, 367, 387, 399, 560
Oliva caribaeensis	311
Olivella mutica	3, 6, 10, 11, 14, 17, 22, 35, 38, 39, 40, 43, 49, 56, 62, 68, 74, 76, 87, 88, 112, 130, 167, 168, 169, 170, 171, 173, 178, 180, 181, 188, 190, 244, 276, 277, 281, 282, 283, 290, 292, 294, 308, 309, 321, 398, 410, 414, 419, 420, 424, 428, 429, 457, 571, 572, 581, 584, 642, 643, 669, 670, 672, 673
Epitonium, species	308, 643
Marginella aureocincta	308, 309, 311, 316, 391
Marginella denticulata	244, 311
Mangelia citronella	382
Mangelia serga	393
Mangelia jewetti	382
Mangelia ceroplasta	309
Melanella bilineata	316
Turbonilla hemphilli	77, 80, 154, 160, 180, 382, 642, 643
Turbonilla, species	32, 40, 53, 76, 155, 309, 311, 316, 317, 348, 349, 571, 642
Liostraca bilineata	154, 244, 311, 317
Rissoina cancellata	308
Polystira albida	393
Polystira tellea	316

TABLE I—(*continued*)

Species	*Biological Station Numbers at Which Species Was Collected*
Conus clarki	244, 308, 309, 393
Niso interrupta	183, 308, 309, 311, 316
Litiopa melanostoma	244
Liotia variabilis	316
Ancystosyrinx radiata	308, 311, 316
Janthina, species	316
Trigonostoma smithi	309
Mathilda yucatecana	244, 311, 316, 317
Aedeorbis supranitidis	316
Terebra cinerea	251, 669
Terebra dislocata	33, 75, 76, 80, 122, 180, 382, 673
Terebra protexta	10, 12, 35, 38, 62, 63, 70, 73, 76, 152, 154, 247, 398, 666, 672
Retusa canaliculata	14, 21, 27, 30, 31, 32, 40, 54, 70, 72, 73, 76, 150, 151, 154, 155, 157, 159, 160, 171, 262, 316, 428, 457, 459, 460, 571, 573, 642, 643, 672
Arene variabilis	316, 317
Acteon canadensis	309
Scaphander watsoni	309, 311, 316
Cyclichna alba	305, 316, 317, 348, 398, 643
Truncatella, species	461
Atlanta peroni	316
Pelecypoda	
Nucula proxima	244. 308, 309, 311, 316, 317, 344, 345, 348, 349, 363, 366, 367, 382, 387, 391, 393, 396, 560
Nuculana acuta (nearshore form)	15, 17, 31, 53, 54, 74, 76, 77, 82, 188, 201, 244, 257, 277, 279, 308, 309, 311, 343, 642, 643
Nuculana acuta (deep shelf form)	242, 244, 308, 309, 311, 316, 317, 319, 362, 366, 367, 382, 383, 384, 385, 387, 391, 393, 560
Nuculana eborea	5, 6, 8, 16, 17, 19, 21, 25, 27, 29, 32, 33, 34, 35, 38, 39, 40, 41, 46, 49, 57, 61, 70, 73, 74, 79, 115, 142a, 150, 151, 152, 155, 157, 159, 161, 167, 168, 170, 171, 181, 182, 205, 244, 290, 309, 311, 316, 342, 348, 349, 366, 382, 393, 419, 420, 424, 428, 429, 642, 670
Yoldia solenoides	244, 308, 309, 311, 316, 382, 384, 385, 387, 390, 391, 393, 560
Limopsis sulcata	317
Arcopsis adamsi	308
Barbatia domingensis	316
Anadara chemnitzi	13
Anadara campechiensis	4, 5, 8, 9, 10, 12, 15, 23, 27, 28, 32, 33, 37, 38, 39, 42, 49, 55, 57, 62, 68, 70, 73, 76, 80, 112, 143, 153, 154, 155, 157, 159, 160, 167, 171, 178, 180, 200, 244, 257, 268, 277, 278, 279, 293, 294, 316, 402, 419, 424, 428, 455, 642, 669, 670, 672
Anadara lienosa floridana	244, 308, 309, 311, 316, 560
Anadara transversa	3, 11, 15, 16, 28, 34, 40, 42, 43, 55, 62, 70, 74, 75, 76, 77, 80, 81, 146a, 153, 156, 159, 160, 178, 180, 188, 189, 247, 278, 290, 321, 322, 382, 402, 404, 405, 417, 424, 428, 458, 461, 642, 643
Anadara baughmani	311, 316, 366, 382, 387
Anadara brasiliana	12, 13, 16, 17, 36, 62, 64, 74, 75, 76, 155, 159, 167, 171, 178, 188, 257, 321, 322, 367, 643
Noetia ponderosa	32, 33, 45, 70, 171, 250, 443, 642
Volsella demissa granosissima	13, 251, 322, 443
Brachidontes recurvus	33, 34, 37, 74, 76, 82, 153, 180, 189, 322, 402, 642
Brachidontes exustus	246
Atrina rigida	13, 33
Atrina serrata	13, 443
Pinna carnea	348, 367
Pecten raveneli	244, 308, 309, 311, 316, 560
Pecten papyraceum	244, 309, 377
Chlamys sentis	309, 316
Chlamys benedicti	308
Aequipecten gibbus gibbus	244, 250, 308, 309, 316, 317, 382, 383, 385, 386, 387, 393, 560
Aequipecten irradians concentricus	13, 443
Aequipecten irradians amplicostatus	3, 45, 443
Cyclopecten nanus	244, 308, 309, 311, 316, 317, 382, 385, 386, 387, 393, 394, 560
Plicatula gibbosa	316, 560
Anomia simplex	12, 13, 15, 33, 62, 153, 244, 308, 309, 311, 316, 317, 363, 366, 382, 391, 393, 396, 402, 420, 455, 643
Crassostrea virginica	3, 4, 13, 15, 17, 23, 33, 34, 35, 36, 37, 43, 45, 62, 72, 74, 75, 76, 77, 82, 152, 153, 154, 155, 160, 178, 180, 188, 190, 233, 244, 247, 251, 261, 268, 277, 278, 308, 322, 323, 393, 402, 417, 419, 420, 443, 455, 461, 571, 575, 642, 672
Ostrea equestris	34, 35, 36, 38, 74, 75, 76, 151, 152, 153, 155, 160, 161, 178, 188, 190, 277, 309, 394, 398, 406, 458, 459, 642, 643
Lima pellucida	244, 311, 316, 317, 349, 393
Eucrassatella speciosa	244, 308, 309, 311
Crassinella martinicensis	33, 34, 38, 43, 74, 75, 76, 80, 82, 112, 153, 169, 180, 181, 182, 188, 190, 246, 247, 252, 277, 278, 311, 322, 386, 417, 424, 429, 458, 459, 461
Diplodonta punctata	34, 75, 180, 246, 420, 455, 458, 642
Diplodonta semiaspera	12, 14, 15, 16, 30, 32, 35, 36, 38, 62, 68, 70, 72, 74, 76, 146a, 152, 154, 155, 169, 188, 244, 316, 321, 414, 457, 642, 643
Lucina amianius	3, 10, 14, 15, 35, 41, 62, 64, 68, 74, 75, 76, 78, 80, 81, 82, 84, 85, 154, 159, 160, 169, 178, 180, 181, 183, 188, 190, 192, 246, 276, 277, 278, 281, 282, 309, 311, 316, 321, 323, 344, 345, 346, 348, 363, 366, 367, 386, 393, 398, 399, 417, 420, 457, 458, 461, 571, 575, 584, 642, 643, 672, 673
Lucina crenella	3, 10, 14, 17, 73, 74, 76, 77, 79, 82, 112, 115, 155, 159, 169, 180, 181, 183, 188, 197, 311, 316, 321, 346, 347, 402, 456, 457, 459, 571, 642, 643, 672, 673
Lucina sombrerensis	244, 308, 309, 311, 316
Lucina pennsylvanica	244
Phacoides nassula	244, 308
Divaricella quadrisulcata	244, 308, 309, 311
Echinochama cornuta	244, 308, 309, 311, 316, 386, 393

TABLE I—(*continued*)

Species	*Biological Station Numbers at Which Species Was Collected*
Chama congregata	308
Trachycardium muricatum	9, 13, 33, 34, 37, 38, 39, 62, 74, 75, 76, 80, 82, 153, 154, 155, 178, 180, 188, 189, 191, 233, 246, 247, 248, 250, 268, 278, 308, 321, 323, 406, 420, 429, 458, 642, 643, 673
Dinocardium robustum	4, 13, 15, 37, 69, 76, 181, 248, 321, 398, 443, 571
Dinocardium robustum vanhyningi	244
Laevicardium laevigatum	244, 308, 317, 367
Laevicardium fiski	244, 308, 309, 311, 316, 382, 393, 560
Laevicardium sybariticum	309
Microcardium transversum	308, 309, 316
Papyridea soleniformis	309
Gouldia cerina	244, 308, 309, 311, 316, 383, 386, 393
Pitar cordata	245, 311, 349, 382
Pitar simpsoni	244, 309
Spisula solidissima similis	62, 74, 329, 443
Mactra fragilis	250
Macrocallista maculata	244, 311, 319
Dosinia discus	3, 4, 5, 9, 10, 12, 13, 14, 15, 17, 32, 33, 35, 36, 37, 38, 42, 45, 55, 69, 70, 72, 73, 75, 76, 77, 82, 115, 152, 154, 155, 156, 157, 159, 160, 169, 173, 180, 181, 183, 188, 189, 190, 197, 244, 246, 248, 257, 268, 280, 282, 316, 321, 322, 344, 346, 347, 364, 366, 367, 383, 398, 399, 402, 410, 414, 415, 419, 420, 424, 428, 443, 455, 457, 461, 572, 574, 575, 576, 642, 643, 669, 672, 673
Cyclinella tenuis	321, 322
Antigona strigillina	244, 309, 316
Mercenaria campechiensis texana	3, 4, 11, 12, 13, 14, 15, 16, 28, 30, 32, 33, 34, 36, 37, 38, 62, 68, 70, 72, 73, 75, 76, 77, 82, 122, 152, 153, 154, 155, 159, 160, 169, 180, 182, 183, 186, 187, 188, 196, 251, 277, 278, 280, 321, 322, 420, 428, 443, 457, 458, 575, 576, 642, 643, 672, 673
Chione cancellata	12, 244
Chione intapurpurea	3, 244, 309, 346, 367, 387, 396, 398
Chione grus	244, 308, 309, 311, 386
Chione clenchi	244, 308, 309, 311, 316, 317, 319, 344, 348, 366, 367, 382, 393, 397, 560
Petricola pholadiformis	38, 70, 76, 81, 146a, 151, 323, 401
Periploma fragilis	30, 79, 161
Periploma inaequalis	38
Mulinia lateralis	3, 5, 6, 9, 10, 11, 12, 14, 15, 16, 17, 19, 21, 26, 27, 28, 29, 30, 31, 32, 33, 34, 35, 36, 37, 38, 40, 41, 42, 43, 48, 49, 50, 51, 52, 57, 58, 59, 60, 61, 62, 63, 64, 66, 68, 69, 70, 71, 72, 73, 74, 75, 76, 80, 81, 82, 87, 115, 120, 142a, 146a, 150, 151, 152, 153, 154, 155, 156, 157, 158, 159, 160, 167, 168, 169, 170, 171, 173, 174, 177, 178, 179, 180, 183, 186, 187, 188, 190, 197, 205, 213, 244, 247, 248, 276, 281, 282, 283, 284, 288, 290, 292, 293, 294, 300, 308, 309, 311, 316, 319, 321, 322, 323, 327, 331, 334, 345, 346, 382, 383, 393, 394, 402, 404, 406, 407, 410, 414, 417, 419, 420, 424, 426, 427, 428, 429, 437, 442, 455, 457, 459, 461, 642, 643, 644, 666, 669, 670, 672, 673
Rangia cuneata	13, 28, 246, 250, 268, 271, 410, 672, 673
Rangia flexuosa	15, 33, 76, 153, 246, 250, 257, 420, 443, 643, 672
Labiosa plicatella	13, 38, 252, 346, 420, 428, 443, 673
Labiosa lineata	13, 51, 443
Donax tumida	14, 16, 33, 62, 64, 82, 178, 181, 193, 244, 309, 345, 394, 402, 410, 419, 420, 672, 673
Donax denticulata(?)	72
Tagelus divisus	10, 12, 13, 15, 17, 20, 30, 32, 33, 34, 35, 36, 37, 38, 39, 62, 68, 69, 70, 72, 73, 74, 75, 76, 77, 79, 80, 82, 152, 153, 154, 155, 157, 158, 159, 160, 167, 170, 171, 178, 180, 181, 183, 186, 187, 188, 189, 246, 249, 268, 277, 279, 308, 316, 321, 322, 323, 363, 404, 407, 414, 420, 424, 429, 455, 457, 458, 461, 573, 642, 643, 670
Tagelus plebeius	37, 155, 160, 443
Semele proficua	12, 32, 33, 34, 62, 74, 75, 76, 77, 153, 154, 155, 180, 188, 246, 247, 268, 321, 322
Semele purpurescens	74, 308, 309, 321, 458
Semele bellastriata	244, 311
Abra aequalis	5, 9, 11, 12, 15, 16, 17, 20, 33, 34, 36, 37, 38, 39, 40, 41, 42, 49, 52, 53, 54, 56, 60, 62, 68, 70, 72, 74, 75, 76, 79, 80, 81, 82, 112, 146a, 151, 153, 154, 155, 157, 158, 159, 160, 161, 167, 169, 171, 173, 178, 180, 181, 186, 188, 189, 201, 244, 246, 247, 248, 252, 272, 279, 316, 321, 322, 345, 346, 348, 366, 367, 382, 404, 405, 406, 407, 414, 415, 419, 420, 424, 428, 458, 461, 642, 643, 669, 670, 672
Abra lioica	53, 61, 205, 324, 325, 326, 329, 334, 336, 341, 342, 343, 344, 345, 348, 349, 350, 362, 363, 364, 463, 642, 669, 670
Tellina alternata	1, 5, 9, 10, 12, 14, 15, 16, 32, 35, 36, 37, 40, 45, 62, 72, 73, 76, 77, 154, 155, 156, 160, 169, 171, 178, 180, 182, 183, 186, 197, 246, 247, 290, 311, 321, 322, 344, 366, 367, 398, 406, 410, 415, 420, 424, 428, 643, 669, 672
Quadrans lintea	12, 74, 197, 201, 244, 321, 367, 393, 398
Tellina versicolor	5, 6, 9, 11, 15, 16, 17, 30, 31, 35, 37, 38, 39, 40, 42, 49, 53, 54, 60, 62, 68, 70, 71, 72, 73, 74, 76, 81, 82, 84, 85, 86, 146a, 154, 157, 159, 160, 167, 169, 170, 171, 173, 177, 181, 182, 183, 186, 188, 189, 205, 206, 308, 309, 316, 321, 322, 343, 344, 345, 346, 347, 348, 349, 363, 365, 366, 367, 396, 404, 406, 413, 415, 420, 424, 428, 429, 435, 437, 457, 573, 642, 643, 669, 670, 672, 673
Tellina georgiana	244, 308, 309, 311
Tellina texana	308, 309, 316
Phylloda squamifera	244, 308, 309, 311, 316, 317, 348, 366, 386, 393
Strigilla mirabilis	62, 72, 75, 87, 88, 283, 311, 362, 382, 394, 419
Tellidora cristata	12, 15, 32, 36, 38, 76, 77, 142a, 154, 160, 187, 188, 311, 316, 321, 345, 424, 457, 643, 673
Macoma tageliformis	180, 325, 372, 674, 675
Macoma tenta	5, 12, 15, 17, 32, 38, 39, 42, 73, 79, 152, 157, 158, 160, 167, 169, 183, 188, 192, 201, 205, 244, 247, 308, 311, 316, 321, 344, 345, 348, 363, 394, 404, 407, 420, 572, 642, 643, 669, 670, 672
Macoma extenuata	244, 308, 309, 311, 317, 366, 382, 393
Macoma mitchelli	76, 149, 151, 215, 227, 609, 643, 674
Macoma constricta	37, 171
Ensis minor	6, 13, 32, 37, 42, 51, 52, 53, 73, 76, 85, 87, 154, 169, 349, 402, 417, 442, 457
Solecurtus cummingianus	308, 311

TABLE I—(*continued*)

Species	*Biological Station Numbers at Which Species Was Collected*
Panope bitruncata	443
Varicorbula operculata	244, 308, 309, 311, 316, 317, 363, 366, 367, 382, 387, 393, 560
Corbula contracta	3, 34, 73, 74, 75, 76, 80, 180, 181, 188, 277, 278, 279, 309, 642
Corbula dietziana	244, 309, 316
Corbula swiftiana	33, 38, 154, 155, 169, 188, 244, 308, 309, 311, 316, 317, 321, 322, 344, 346, 348, 363, 364, 365, 366, 367, 382, 384, 385, 386, 387, 390, 393, 396, 427, 560, 642
Cyrtopleura costata	1, 13, 14, 22, 31, 33, 37, 42, 62, 74, 76, 173, 188, 190, 244, 321, 402, 428, 443, 672
Pandora trilineata	10, 12, 14, 39, 42, 53, 62, 68, 73, 87, 154, 158, 160, 162, 169, 170, 173, 178, 183, 189, 280, 322, 402, 419, 420, 424, 642, 643, 669, 673
Pandora bushiana	308, 309, 311, 316, 366, 382, 393, 398
Cuspidaria ornatissima	244, 308, 309, 311, 316
Cuspidaria media	309, 317
Cuspidaria granulata	244, 308, 309, 311, 316
Cuspidaria jeffreysi	309
Cuspidaria costellata	244
Cuspidaria perrostrata	309
Verticordia ornata	244, 308, 309, 311, 316, 317, 345, 366, 382, 384, 386, 393, 560
SCAPHOPODA	
Dentalium laqueatum	309, 317
Dentalium texasianum	40, 76, 178, 277, 311, 316, 317, 344, 345, 347, 348, 349, 365, 366, 367, 398
Dentalium sowerbyi	244, 308, 309, 311, 316
Cadulus mayori	311, 316, 317
Cadulus carolinensis	244, 308, 309, 311, 316, 346, 347, 348, 349, 366, 367, 378, 379, 393
Cadulus arctus	244, 309, 311, 344, 382
PTEROPODA	
Cavolina uncinata	171, 201, 244, 308, 309, 311, 316, 393
Cavolina longirostris	244, 308, 309, 342, 345, 350, 362, 363, 364, 366
Euclio pyramidata	244, 309
Creseis virgula	309
Creseis acicula	309, 311, 366, 393
Diacria quadridentata	309
CHITONS	
Chaetopleura apiculata	247, 323
CEPHALOPODA	
Lolliguncula brevis	17, 20, 37, 43, 62, 69, 143, 144, 246, 249, 252, 254, 256, 257
Loligo pealei	243, 366
Argonauta argo	244
COELENTERATA	
HYDROZOA	
Hydractinia, species	321
ANTHOZOA	
ANENOMES	
Calliactis tricolor	12, 143, 244, 257, 323
HEXACORALS	
Eupsamnia floridana	308, 309, 315
Bathycyathus, species	309
Astrangia astreiformis	11, 13, 15, 16, 33, 72, 74, 75, 76, 77, 167, 188, 321, 443, 643, 672
OCTOCORALS	
Leptogorgia setacea	256
Eugorgia stheno	244, 308, 346
PENNATULIDS	
Renilla mülleri	7, 12, 43, 53, 55, 62, 89, 143, 144, 242, 248, 249, 346, 366
ECHINODERMATA	
ASTEROIDS	
Luidia clathrata	4, 12, 62, 144, 246, 247, 261, 346
Astropecten articulatus valenciennesi	243, 346, 366
OPHIUROIDS	
Hemipholis elongata	5, 12, 15, 45, 50, 188, 246, 247, 322, 323
Amphiodia limbata	9, 15, 28, 29, 33, 34, 35, 36, 38, 40, 70, 75, 76, 77, 146a, 154, 155, 168, 169, 182, 189, 211, 250, 321, 404
Ophiolepis elegans	322
Unidentified species	167, 343, 362, 364
ECHINOIDS	
Mellita quinquiesperforata	3, 4, 11, 12, 15, 43, 62, 82, 83, 246, 247, 248, 249, 250, 254, 255, 256, 278, 283, 322, 419, 420, 672, 673
Clypeaster prostratus	244, 319
Clypeaster raveneli	317

TABLE I—(*continued*)

Species	*Biological Station Numbers at Which Species Was Collected*
ANNELIDA	
POLYCHAETA	
Lepidonotus sublevis	70
Polydontis lupina	39
Sthenelais articulata	33, 81, 322, 404
Paeurythoe, species	25, 26
Aglaophamus dicirris	51, 54, 56, 57, 84, 86, 344
Glycera americana	5, 15, 33, 34, 35, 36, 39, 154, 205, 328
Marphysa sanguinea	153
Diopatra cuprea	2, 4, 5, 9, 15, 16, 21, 22, 33, 45, 50, 56, 62, 71, 77, 80, 81, 171, 174, 247, 362, 399
Lumbrineris erecta	15, 188
Lumbrineris bifilaris	26, 27, 52, 150, 200, 201
Lumbrineris, species	25, 29, 57, 322, 325, 336, 349, 366
Prionospio, species	54
Nerine agilis	150
Chaetopterus variopedatus	38, 77, 155
Spiochaetopterus oculatus	31, 70
Maldane sarsi	77
Clymenella torquata calida	154, 346, 349
Owenia fusiformis	5, 16, 321, 349
Sternapsis scutata	54
Sthenelais, species	345
Eurythoë complanata	324
Nereis, species	343, 362
Nephtys picta	404
Nephtys, species	324, 325, 336, 339, 350
Glycera dibranchiata	404
Lumbrineris? bassi	336
Ancistrosyllis bassi	324
Cossura, species	328, 335, 336, 339
Prionospio treadwelli	322, 335
Magelona (near) *cerae*	363
Branchioasychis americana	366
BRYOZOA	
Bugula neritina	2, 4, 7, 9, 12, 15, 16, 17, 20, 22, 28, 33, 37, 43, 45. 48, 51, 53, 55, 69, 70, 71, 76, 80, 81, 142, 142a, 143, 187, 188, 189, 246, 247, 248, 249, 250, 252, 254, 255, 257, 268, 321, 322, 323, 346, 428
Zoobytron, species	7, 12, 37, 43, 45, 51, 53, 55, 62, 74, 76
Schizoporella floridana	244, 308, 309, 311, 316
Schizoporella unicornis	244, 308, 309, 311, 316
Mamillopora cupula	244, 308, 309, 311, 316, 321, 346
Cupuladria canariensis	244, 308, 309, 311, 316, 321, 322, 349, 410
Smittina trispinosa	244, 308, 309, 311, 316
Membranipora, species	17, 32, 33, 74, 75, 76, 80, 81, 246, 322, 323, 424, 428, 455
ARTHROPODA	
DECAPODA	
Libinia emarginata	17, 37, 55, 246, 247, 250, 256, 321
Petrolisthes armatus	33
Heterocrypta granulata	75, 81, 246, 322, 323
Portunus spinimanus	1, 37, 247, 321, 322, 323
Portunus gibbesi	4, 7, 20, 43, 50, 69
Porcellana sayana	4, 12, 17, 323
Neopanope packardi	12, 17, 28, 33, 36, 62, 74, 171, 246, 247, 248, 250, 260, 321, 322, 323, 404
Callinectes sapidus	(1), AMP-BBT, AMP-BOT, 20, 28, 32, 53, 55, 143, 144, 242, 246, 247, 250, 252, 253, 254, 255, 256, 257, 259, 260, 261, 262, 321
Callinectes danae	(1), 37, 62, 142, 143, 242, 243, 261, 262, 268, 360
Calappa springeri	244, 365
Polyonyx macrocheles	16
Euceramus praelongus	17, 62, 322, 399
Pilumnus dasypodus	17
Persephone punctata	29
Chasmocarcinus, species	39
Ovalipes occellatus	62
Hepatus epheliticus	321
Metoporhaphis calcatus	322
Crangon heterochaelis	17, 33, 36, 74, 80, 321
Pagurus floridanus	1, 2, 12, 13, 15, 17, 33, 37, 62, 69, 71, 251, 321, 322
Pagurus longicarpus	12, 321
Clibinarius vittatus	12, 142, 321
Squilla empusa (*stomatopoda*)	1, (1), 7, 20, 53, 55, 142, 143, 242, 253, 254, 257, 259, 261, 262, 319, 360
Xiphopenaeus kroyeri	AMP-BOT, 262
Penaeus setiferus	1, (1), AMP-BOT, 12, 17, 45, 50, 55, 69, 142, 143,242, 249, 268
Penaeus duoarum	1, AMP-BOT, 7, 20, 28, 33, 37, 43, 55, 62, 142, 252
Palaemonetes, species	17
Sicyonia dorsalis	242, 319, 323
Uca mordax	214 to 239 (marsh stations)
Uca pugnax	Marsh stations
Uca pugilator	Marsh stations
Crayfish (*Cambarus*, species)	Fresh-water marsh stations
XIPHOSURA	
Limulus polyphemus	13

is included in the discussion of macro-organism assemblages. The physical and chemical data taken at each of the biological stations have been discussed in full by Scruton (*op. cit.*).

MACRO-ORGANISM ASSEMBLAGES

Seven divisions of the region were recognized on the basis of the distribution of the macro-organisms collected in this study, published distribution records of the same organisms, and consideration of the environmental factors which affect animal distribution. These seven divisions are: (I) the delta marshes; (II) delta front and lower distributaries; (III) lower Sound and pro-delta slopes; (IV) Upper Breton Sound and Chandeleur Sound; (V) inlets; (VI) shallow continental shelf of the Gulf of Mexico from the barrier islands to 12–13 fathoms; and (VII) the deep continental shelf of the Gulf of Mexico from 13 fathoms to the outer edge of the continental shelf. A possible eighth environment or assemblage is represented by the living oyster reefs, most of which are outside the project area and accordingly not discussed in any detail here. The approximate boundaries of these seven major environments and their characteristic assemblages are illustrated in Figures 11 and 12. Table I shows the station distribution of all the important faunal elements of these divisions in the east Mississippi Delta region. Table II

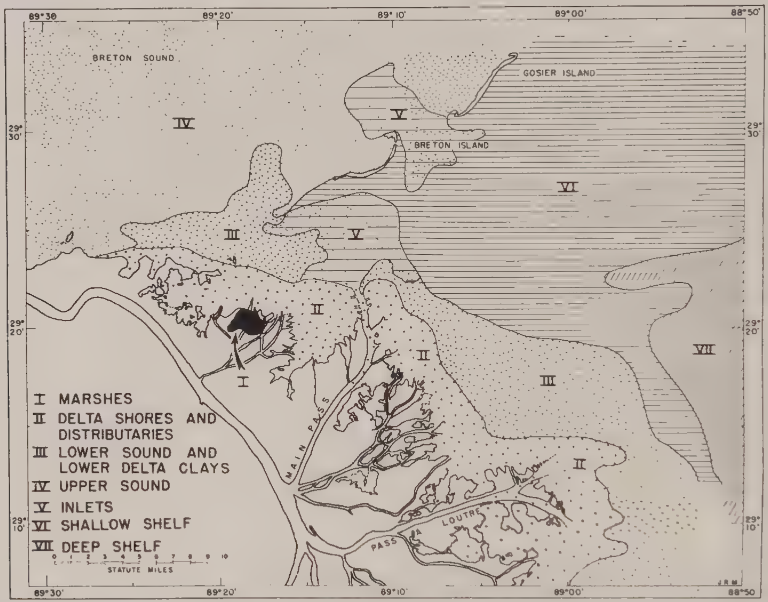
89°30
89°20'
89°10'
89°00'
88°50'
BRETON SOUND
GOSIER ISLAND
BRETON ISLAND
29° 30'
29° 20'
29° 10'
IV
V
VI
III
V
II
II
III
VII
I
II
MAIN PASS
LOUTRE
PASS
I MARSHES
II DELTA SHORES AND DISTRIBUTARIES
III LOWER SOUND AND LOWER DELTA CLAYS
IV UPPER SOUND
V INLETS
VI SHALLOW SHELF
VII DEEP SHELF
0 1 2 3 4 5 6 7 8 9 10
STATUTE MILES
J.R.M.

FIG. 11.—Areal distribution of environments as characterized by macro-invertebrate assemblages in inshore Delta region. Actually, marsh environment is of far greater extent, but area in black represents only part studied.

shows the environmental distribution of most of the common invertebrates found in these environments, with their comparative abundance living and dead, and Table III is a similar table of macro-organism distribution compiled from published data.

I. *Delta marshes.*—Although the marshes are not strictly a marine environment, they do contain macro-invertebrates which are tolerant of salt water, and which are occasionally found as remains in reworked marine deposits. The vegetation of the Mississippi Delta marshes has been discussed in detail by O'Neil (1949). The only part of the delta marsh sampled for macro-organisms was in the vicinity of Baptiste Collette Bayou. This marsh area contains both fresh- and salt-water marsh vegetation which grows in from several inches to 2 feet of water.

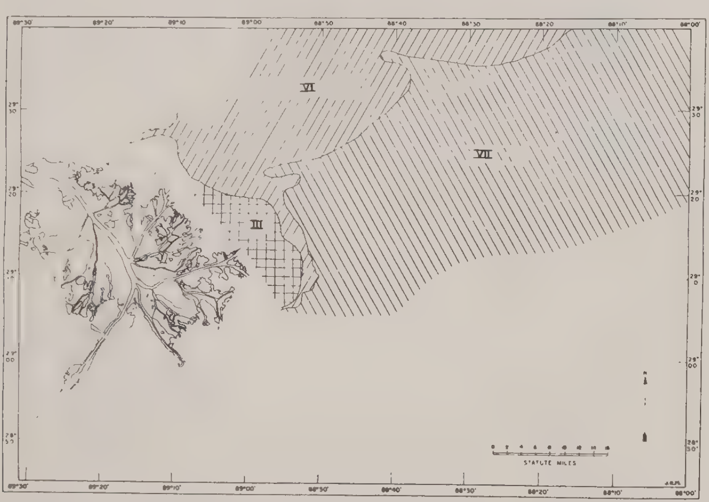

FIG. 12.—Areal distribution of environments as characterized by macro-invertebrate assemblages in offshore Delta region. (Key to Roman numerals: III, Lower sound and pro-delta slope; VI, Shallow shelf; VII, Deep shelf).

Animals which can produce fossil remains are rare in the marsh environment. The principal mollusk found in this study was *Neritina reclivata* (Say), a snail found from a few inches to a foot or so above the surface of the water on the stems of the grasses and sedges (Fig. 13a).[3] Another littoral gastropod reported from these and neighboring marshes (Hadley, 1936, p. 404; Fisk *et al.*, 1954, p. 89) is *Littorina irrorata* (Say). No living specimens of this gastropod were found, although empty shells were common in old shell deposits in Breton Sound and on the shores of the inner side of Breton Island. It has been reported to be living

---

[3] *Neritina reclivata* and *Rangia cuneata* proved to be abundant in marshes adjacent to natural levees at North Pass as determined by a reconnaissance of this area in November, 1955.

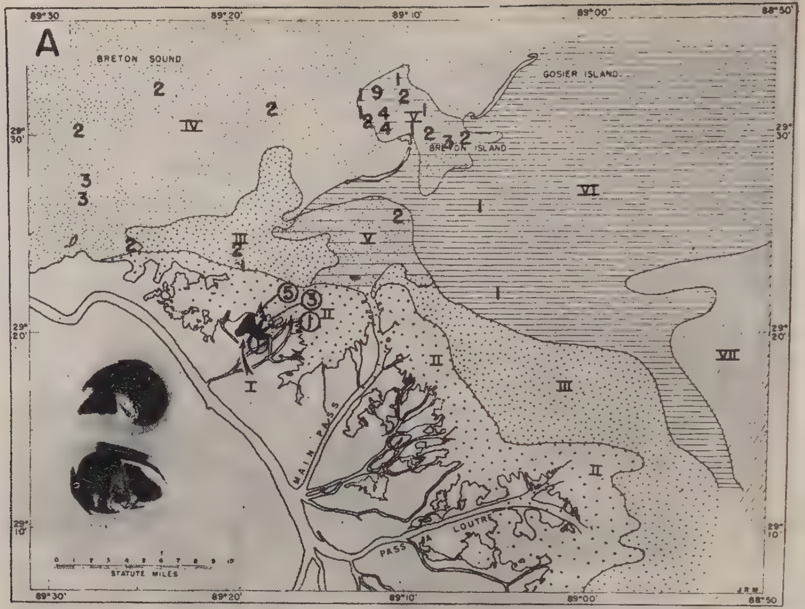
A
BRETON SOUND
GOSIER ISLAND
BRETON ISLAND
MAIN PASS
PASS A LOUTRE
I
II
III
IV
V
VI
VII
89°30'
89°20'
89°10'
89°00'
88°50'
29° 30'
29° 20'
29° 10'
STATUTE MILES
J.R.M.

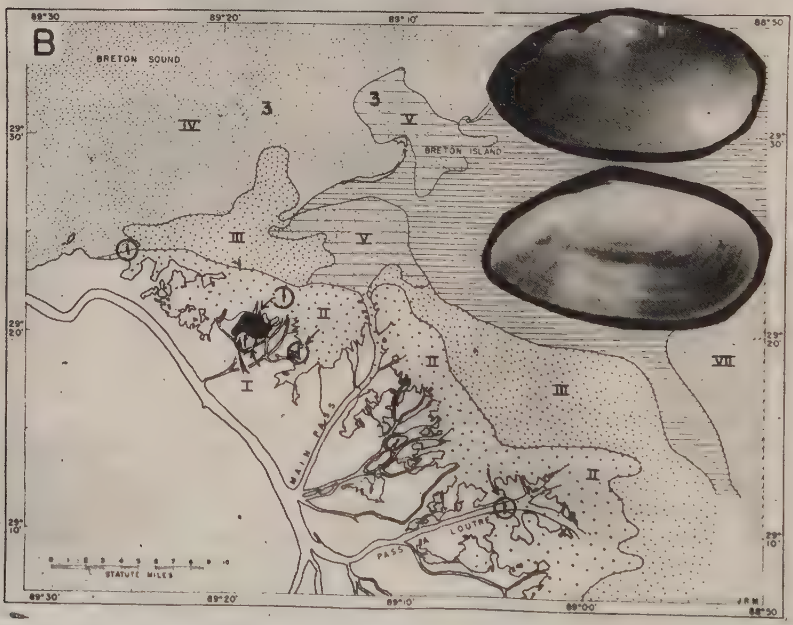
B
BRETON SOUND
BRETON ISLAND
MAIN PASS
PASS A LOUTRE
I
II
III
IV
V
VII
89°30'
89°20'
89°10'
89°00'
88°50'
29° 30'
29° 20'
29° 10'
STATUTE MILES
J.R.M.

FIG. 13a.—Distribution of marsh snail *Neritina reclivata* as related to areal distribution of environments. Circled numbers indicate living occurrences; numbers indicate number of individuals at each station.

FIG. 13b.—Distribution of pelecypod *Macoma mitchelli*, indicative of delta front and distributaries. Circled numbers indicate living occurrences.

TABLE II. DISTRIBUTION OF MARINE ORGANISMS TAKEN IN EAST MISSISSIPPI DELTA REGION

Species	*Marsh*	*Delta Front*	*Lower Sound*	*Upper Sound*	*Inlets*	*Shallow Shelf*	*Deep Shelf*
Neritina reclivata M	xxxxx		- - -	-- --	-----		
Uca, sp. C	xxxxx						
Cambarus, sp. C	xxxxx						
Littorina irrorata M	xxxxx		- - -	- - -	- - -		-
Littordina, sp. M		- -					
Macoma mitchelli M		xxxxx		- -			
Macoma tageliformis M		xxxxx				- - -	
Mulinia lateralis M		xxxxx	xxxxx	xxxxx	- - -	xxxxx	
Crassostrea virginica M		xxxxx	- x -	-----	-----	- - -	-
Rangia flexuosa M	x	-	-	-----	- - -		
Lumbrineris bifilaris P		x x x				x	
Lumbrineris erecta P		x x x				x	
Nassarius acutus M		xxxxx	xxxxx	xxxxx	xxxxx	xxxxx	
Penaeus setiferus C		xxxxx	xxxxx	xxxxx	xxxxx	xxxxx	
Portunus spinimanus C		x		x-x--			
Nuculana eborea M		-	xxxxx	x	- - -	- -	
Polinices duplicatus M		- - -	xxxxx	x-x-x	x-x-x	x-x	
Squilla empusa C			xxxxx		x x x	x x x	
Portunus gibbesi C			x x x	x	x x x		
Anachis avara similis M			xxxxx	- x -	x x		
Anachis obesa M		x-x-x	x-x-x	xxxxx	xxxxx	xxxxx	-----
Callinectes sapidus C		xxxxx	xxxxx	x x x	xxxxx	xxxxx	
Penaeus duoarum C			xxxxx	xxxxx	xxxxx	xxxxx	xxxxx
Prionospio, sp. P			xxxxx				
Diopatra cuprea P			xxxxx	x x x	xxxxx	xxxxx	
Callinectes danae C			xxxxx	x x x	xxxxx	xxxxx	
Bugula neritina B			xxxxx	xxxxx	xxxxx	xxxxx	
Thais haemastoma floridana M			x x x			xxxxx	
Abra lioica M			xxxxx	- x -		xxxxx	x-x-x
Zoobytron, sp. B			xxxxx	xxxxx	xxxxx	xxxxx	
Corbula contracta M				xxxxx			
Petrolisthes armatus C				x x x			
Crangon heterochelis C				xxxxx			
Chaetopterus variopedatus P				x x x			
Lumbrineris, sp.				x x			
Brachidontes exustus M				x			
Nassarius vibex M				x			
Diplodonta punctata M				-----			
Retusa canaliculata M			-	-----			
Periploma fragilis M				- - -			
Periploma inaequalis M				-			
Cerithium muscarum M				-			
Amphiodia limbata E			x	xxxxx	x x x	x	
Diplodonta semiaspera M				x-x-x	- - -		
Semele proficua M				--x--		-	
Sthenelais articulata P				x x	x		
Tagelus gibbus M				- x -		-	
Astrangia astreiformis CO				-----	- - -		
Donax tumida M				-----		-----	
Macoma tenta M				xxxxx	- - -	x-x-x	
Pagurus floridanus C		x		xxxxx	xxxxx		
Thais haemastoma haysae M				x-x-x	--x--	-	
Lolliguncula brevis M				xxxxx	xxxxx	xxxxx	
Libinia emarginata C				x x x	x x x	x	
Pagurus longicarpus C				x x x	x x x	x x x	
Mercenaria campechiensis texana M				x-x-x	- - -	- -	
Glycera americana P				x x x	x	x	
Tellidora cristata M			-	--x--	x -		
Brachidontes recurvus M			-	-----	-		
Ostrea equestris M				-----	- - -	- - -	
Terebra dislocata M			-	- - -	- -		
Nuculana acuta (nearshore form) M				-----	-	- - -	
Aequipecten irradians amplicostatus M				- -	-	-	
Tagelus divisus M			- -	xxxxx	x-x--	- -	
Crepidula plana M			-	xxxxx	x-x-x	-----	
Neopanope packardii C			x	xxxxx	xxxxx	x x x	
Anadara brasiliana M			-	--x--	--x--	- - -	
Ensis minor M		-		--x--	- - -	--x--	
Crassinella martinicensis M			-	--x--	- - -	-	
Lucina crenella M			-	-----	-		- - -
Moira atropos E			- - -	-----	-----	-----	
Crepidula fornicata M			-	-----		-	-----
Abra aequalis M		-	- - -	xxxxx	--x-x	-----	
Tellina alternata M		-	- -	x-x-x	--x--	--x--	
Dosinia discus M			-----	--x--	--x--	--x--	- -
Cyrtopleura costata M		- -	- - -	-----	-----	- - -	
Heterocrypta granulata C					xxxxx		
Hemipholis elongata E					xxxxx		
Mitrella lunata M					xxxxx		
Ophiolepis elegans E					xxxxx		

TABLE II—(*continued*)

Species	*Marsh*	*Delta Front*	*Lower Sound*	*Upper Sound*	*Inlets*	*Shallow Shelf*	*Deep Shelf*
Chaetopleura apiculata M					x x x		
Modulus modulus M					-		
Calliactis tricolor CO					xxxxx	x x x	
Mamillopora cupula B					x x x		-----
Cupuladria canariensis B					x x x		-- -
Diodora cayenensis M					x-x-x		
Chione cancellata M					x x-x		
Owenia fusiformis P				x	x x		
Porcellana sayana C				x x	x x x		
Turbonilla hemphilli M				-	- - -		
Rangia cuneata M		(xxxxx)		-	. -		
Sinum perspectivum M					-		
Petricola pholadiformis M				-	--x--	-	
Terebra protexta M				-	- -	-	
Olivella mutica M				-----	xxxxx	- -	
Cantharus cancellarius M				-----	xxxxx	xxxxx	
Mellita quinquiesperforata E				x -	xxxxx	xxxxx	
Anachis avara semiplicata M				-- --	xxxxx	- x -	
Busycon spiratum plagosum M				-	x x-	-	
Trachycardium muricatum M				----	x-x-x		
Anadara transversa M				x-x x	x-x-x	- x -	
Busycon contrarium M			- x	x -	x-x-x	- -	
Natica pusilla M			- -	x	x-x-x	- - -	
Lucina amiantus M			-	- x-	x-x-x	x-x x	- x -
Pandora trilineata M			- - -	- x--	xxxxx	-----	
Aglaophamus dicirrus P			x x			xxxxx	
Atrina serrata M						----	
Volsella demissa granonissima M						- -	
Aequipecten irradians concentricus M						- -	
Anadara chemnitzi M						-	
Labiosa lineata M						.	
Spisula solidissima similis M						- -	
Tonna galea M						-	
Panope bitruncata M						-	
Xiphopenaeus kroyeri C						xxxxx	xxxxx
Luidia clathrata E					x x x	xxxxx	
Renilla mülleri CO					x x x	xxxxx	
Noetia ponderosa M					- - -	--- -	
Strombus alatus M						- - -	- - -
Phalium granulatum M						- - -	- - -
Labiosa plicatella M					-	- - -	
Chione intapurpurea M				-		- - -	- -
Strigilla mirabilis M				.	-	-----	
Oliva sayana M				- - -	-	-x--	- - -
Quadrans lintea M				-	- - -	--- --	- -
Dinocardium robustum M			-	. -	-	-----	
Tellina versicolor M			- x -	--x--	--x--	xxxxx	xxxxx
Anadara campechiensis M		- - -	- - -	--x--	--x--	x-x-x	
Anomia simplex M			-	- - -	-	-----	-----
Eugorgia stheno CO							x x x
Clypeaster prostratus E							x x x
Verticordia ornata M							x-x-x
Anadara baughmani M							x -x
Eucrassatella speciosa M							-x-x-
Polystira albida M							x x
Loligo pealii M							x x
Pitar cordata M							--x--
Pecten papyraceum M							--x--
Limopsis sulcata M							- x -
Cuspidaria ornatissima M							-----
Varicorbula operculata M							-.---
Tellina texana M							-----
Macoma extenuata M							-----
Phylloda squamifera M							--x--
Laevicardium fiski M							-- -
Divaricella quadrisulcata M							-
Lucina sombrerensis M							-- -
Chlamys muscosus M							. ---
Nassarius ambiguus consensus M							--
Anadara lienosa floridana M							- ---
Yoldia solenoides M							-- -
Cyclopecten nanus M							---
Gouldia cerina M							-----
Echinochama cornuta M							-----
Marginella aureocincta M							-----
Cavolinia uncinata M							-----
Polinices uberinus M							-----
Calyptraea centralis M							-----
Dentalium sowerbyi M							-----
Chione grus M							-----

TABLE II—(*continued*)

Species	*Marsh*	*Delta Front*	*Lower Sound*	*Upper Sound*	*Inlets*	*Shallow Shelf*	*Deep Shelf*
Cuspidaria granulata M							-----
Cavolinia longirostris M							-----
Schizoporella floridana B							-----
Smittina trispinosa B							-----
Corbula swiftiana M				- - -			xxxxx
Nuculana acuta (offshore form) M						- - -	x-x-x
Chione clenchi M						-	x-x-x
Aequipecten gibbus gibbus M					-		-x-x-
Nucula proxima M						-	xxxxx
Astyris perpicta M						-	x-x -x
Dentalium texasianum M					- - -	- - -	-----
Phacoides nassula M							- - -
Cadulus carolinensis M						- - -	-----
Cadulus mayori M							- - -
Crucibulum auricula M							- - -
Corbula dietziana M							- - -
Pecten raveneli M							- - -
Macrocallista maculata M							- - -
Tellina georgiana M							- - -
Lima pellucida M							- - -
Anachis iontha M							- - -
Chlamys benedicti M							- - -
Microcardium transversum M							- - -
Cuspidaria perrostrata M							- - -
Scaphander watsoni M							- - -
Mangelia jewetti M							- - -
Melanella bilineata M							- - -
Ancystocyrinx radiata M							- - -
Pandora bushiana M							- -
Eupsamnia floridana CO							- - -
Bathycyathus, sp. CO							- -
Oliva caribaeensis M							- -
Murex recurvirostrus rubidus M							- -
Plicatula gibbosa M							x x

x = Living.	Frequency of x's and -'s indicate relative abundance.
- = Dead.	
M—Mollusks.	C—Crustacean.
E—Echinoderm.	P—Polychaete worm.
CO—Coelenterate.	B—Bryozoan.

on the vegetation on the inner side of the Chandeleur Islands by Cary and Spaulding (1909, p. 20). Cary and Spaulding found that *Rangia cuneata* Gray was common in the fresh-water marshes along the Louisiana coast, but only one living specimen of this species of pelecypod was found in the delta region during this study. Characteristic crustaceans of the marshes are two species of fiddler crab of the genus *Uca* and at least one species of crayfish (*Cambarus*) which are mentioned as preserved in marsh sediments by Fisk (1954). The fiddler crab, *Uca mordax* Smith, was also mentioned by Cary and Spaulding (p. 11) as a common inhabitant of the salt marshes of the coastal parishes. The diagnostic macroinvertebrates for the delta marshes are the following (Pl. I).

Neritina reclivata	—Common
Littorina irrorata	—Somewhat less common
Rangia cuneata	—Common in some areas
Uca pugilator	—Common in salt or brackish marshes
Uca pugnax	—Common in salt or brackish marshes
Uca mordax	—Common in salt or brackish marshes
Cambarus, sp.	—Very common in fresh-water marshes

II. *Delta front and lower distributaries.*—The delta front region with its characteristic low chlorinity (2–10 ‰), wide range of temperature (21°C.), fine, clayey silt substrate, shallow water, and proximity to the marshes is also charac-

TABLE III. DISTRIBUTION OF MARINE ORGANISMS, EAST MISSISSIPPI DELTA REGION, FROM PUBLISHED DATA

Species	*Marsh*	*Delta Front*	*Lower Sound*	*Upper Sound*	*Inlets*	*Shallow Shelf*	*Deep Shelf*
Cary and Spaulding, 1909							
GASTROPODS							
Bulla striata				x x x			
Hominoea succinea				x x x			
Melampus flavus				x x x			
Terebra cinerea				x x x			
Cancellaria reticulata						- - -	
Oliva sayana				- - -		- - -	
Fasciolaria distans						- - -	
Busycon spiratum plagosum						- - -	
Busycon contrarium						- - -	
Nassarius vibex						- - -	
Anachis avara						- - -	
Anachis obesa				xxxxx			
Mitrella lunata				x x x			
Murex fulvescens		- - -					
Murex pomum						- - -	
Thais haemastoma						xxxxx	
Epitonium sayana				x x x			
Janthina, sp.						- - -	
Distorsio clathrata						- - -	
Phalium granulatum						- - -	
Tonna galea						- - -	
Strombus alatus						- - -	
Seila terebralis						- - -	
Cerithiopsis, sp.						- - -	
Bittium nigrum				- -			
Bittium varium				- - -			
Cerithium muscarum				- - -			
Cerithidea varicosa(?)				- - -			
Modulus modulus					- - -		
Littorina irrorata	x x			x x x (on land)			
Architectonica nobilis						- - -	
Rissoina chesneli						- - -	
Crepidula fornicata						x x x	
Crepidula convexa						x x x	
Crepidula plana						x x x	
Polinices duplicatus						- - -	
Sinum perspectivum					- - -	- - -	
Neritina reclivata	x x x			x x x (on land)			
Chaetopleura apiculata				x x x			
Spirula spirula						- - -	
Lolliguncula brevis						xxxxx	
PELECYPODS							
Crassostrea virginica						- - -	
Anomia simplex				x x x			
Aequipecten irradians amplicostatus				xxxxx			
Atrina rigida				xxxxx			
Atrina serrata						x x x	
Brachidontes recurvus						- - -	
Volsella americana	x x x			x x x			
Anadara campechiensis						- - -	
Nuculana acuta (*eborea*?)			x x x				
Lucina floridana				x x x			
Dinocardium robustum						x x x	
Trachycardium muricatum					x x x	x x x	
Laevicardium laevigatum						- - -	
Callocardia texasianum						- - -	
Mercenaria campechiensis texana				xxxxx			
Macrocallista maculata						- - -	
Dosinia discus						- - -	
Petricola pholadiformis		- - -				- - -	
Donax tumida						xxxxx	
Tagelus gibbus						- - -	
Tagelus divisus				- - -		- - -	
Tellina alternata						- - -	
Rangia cuneata	xxxxx						
Spisula solidissima similis						x x x	
Mactra brasiliana		x x x				- - -	
Labiosa lineata		- - -				- - -	
Labiosa plicatella		- - -				- - -	
Ensis minor						- - -	
Pholas campechiensis						- - -	
Cyrtopleura costata						- - -	
SPONGES							
Cliona sulphurea						x x x	

TABLE III—(*continued*)

Species	*Marsh*	*Delta Front*	*Lower Sound*	*Upper Sound*	*Inlets*	*Shallow Shelf*	*Deep Shelf*
COELENTERATES							
Bougainvillea superciliaris						x x x	
Bougainvillea carolinensis						x x x	
Hydractinlia polyclina						x x x	
Porporita lineana					x x x		
Renilla mülleri						x x x	
Calliactis tricolor						x x x	
Cerianthus americanus						x x x	
ECHINODERMS							
Luidia clathrata						x x x	
Luidia alternata						x x x	
Mellita quinquiesperforata						x x x	
Moira atropos						x x x	
Ophiura brevispina				xxxxx			
POLYCHAETE WORMS							
Nereis pelagica						x x x	
Diopatra cuprea				x x x			
Chaetopterus pergamentaceous						x x x	
Arenicola, sp.						x x x	
Sabellaria vulgaris						x x x	
CRUSTACEANS							
Lepus antifera						xxxxx	x x x
Penaeus setiferus						xxxxx	xxxxx
Crangon heterochelis						x x x	x x x
Hyppolyte zostericola				x x x			
Tozeuma carolinense				x x x			
Palaemon tenuicornis			x x x				
Conchordia gibberosa				x x x			
Palaemonetes carolinensis				x x x			
Emerita talpoidea						xxxxx	
Eupogebia affinis						x x x	
Pagurus floridanus						x x x	
Clibinarius vitattus						x x x	
Uca mordax	xxxxx						
Pinnotheres maculatus				x x x			
Eupanopeus herbstii				x x x			
Eupanopeus rugosus				x x x			
Neopanope texana						x x x	
Menippe mercenaria				x x x			
Menippe nodifrons						x x x	
Callinectes sapidus			x x x	x x x	x x x	x x x	
Petrolisthes armatus			x x x	x x x	x x x	x x x	
Libinia dubia						x x x	
Hepatus ephiliticus				x x x			
Squilla empusa						x x x	
Hadley, 1936							
GASTROPODS							
Littorina irrorata	xxxxx	- - -					
Busycon contrarium		- - -					
Busycon spiratum		- - -					
Cantharus cancellarius		- - -					
Neritina reclivata		- - -					
Oliva sayana		- - -					
Polinices duplicatus		- - -					
Crepidula plana		x x x					
Thais haemastoma floridana		- - -					
PELECYPODS							
Anadara campechiensis		- - -					
Anadara brasiliana		- - -					
Cyrtopleura costata		- - -					
Dinocardium robustum		- - -					
Dosinia discus		- - -					
Ensis minor		-----					
Macoma constricta		- - -					
Mulinia lateralis		- - -					
Crassostrea virginica		-----					
Atrina, sp.		- - -					
Labiosa plicatella		- - -					
Rangia cuneata		-----					
Tagelus gibbus		- - -					
Mercenaria campechiensis texana		-----					
Periploma inaequalis		-----					

x = Living. Frequency of x's and –'s indicate relative abundance.
– = Dead.

terized by a scarcity of species and individuals of macro-organisms. Biological material from cores and the few biological stations taken in this environment indicates a distinct fauna. Living *Macoma mitchelli* Dall was collected only in this region (Fig. 13b). In Texas it has been reported to be very abundant in the waters near the Guadalupe River Delta where environmental conditions are somewhat similar (Ladd, 1951, p. 142, as *Tellina texana*; Parker, 1955). Another species, *Macoma tageliformis* Dall, was also common, living in the delta front region, especially in the vicinity of the mouth of Pass a'Loutre. At several stations during the fall of 1951 there were large numbers of very small *Mulinia lateralis* (Say) in the delta front region when the Mississippi River was at a low stage. This pelecypod can not be considered a characteristic mollusk of this area alone, since its shell was taken in varying numbers from almost every station in Breton Sound and on the shallow part of the continental shelf.[4] In certain areas near the delta shores the common commercial oyster, *Crassostrea virginica* (Gmelin) could be considered the characteristic invertebrate. Extensive reefs of living oysters were found in the large indentations or bays of the Delta, especially Quarantine, Coquille, and California bays, several miles northwest of the area studied (Fig. 1).[5] A small oyster reef was observed in Blind Bay, which lies be-

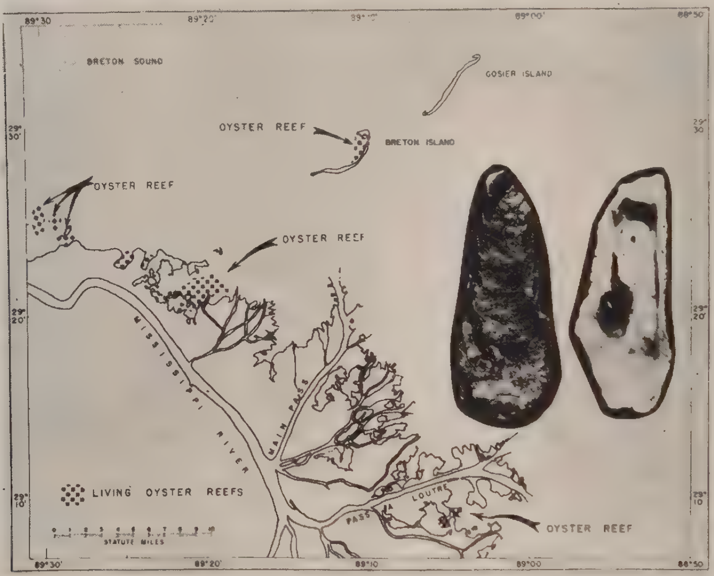
89°30'
89°20'
89°10'
89°00'
88°50'
BRETON SOUND
GOSIER ISLAND
OYSTER REEF
BRETON ISLAND
29° 30'
OYSTER REEF
OYSTER REEF
29° 20'
MISSISSIPPI RIVER
MAIN PASS
LIVING OYSTER REEFS
29° 10'
PASS A LOUTRE
OYSTER REEF
STATUTE MILES

FIG. 14.—Location of living oyster reefs (*Crassostrea virginica*) in east Mississippi Delta area.

---

[4] In November, 1955, a survey of the submarine natural levee at North Pass showed a predominance of living *Macoma mitchelli*, *Neritina reclivata*, *Rangia flexuosa*, and dead shell composed of *Mulinia lateralis*, *Petricola pholadiformis*, *Macoma constricta*, and *Rangia cuneata*.

tween Pass a'Loutre and Southeast Pass in the southern part of the Delta, and also another small reef was located behind Breton Island in the lagoon on the Sound side. Figure 14 shows the locations of living oyster reefs in the east delta region. The fauna which one might expect to be associated with oyster reefs in the delta region is similar to that described by Puffer and Emerson (1953). Although Puffer and Emerson's paper deals with the oyster-reef biota of the central Texas coast, the same species were found dead in old oyster-reef deposits in upper Breton Sound, and are illustrated in Puffer and Emerson's paper. The polychaete *Lumbrineris bifilaris* (Ehlers) was found living very close to the delta shore. Fresh shells of *Rangia cuneata* and *Rangia flexuosa* were observed in the delta front region, although no living *Rangia* was found. A similar assemblage of mollusks is discussed by Van Andel (1954, pp. 113–17) as occurring in the shallow waters surrounding the Orinoco River Delta. The characteristic macroorganism species for the delta front and lower distributaries are the following (Pl. I).

Macoma mitchelli	—Few living and dead, should be found more abundant with more intensified collecting
Macoma tageliformis	—Fairly common, living in Pass a'Loutre region
Rangia cuneata	—Probably common in certain areas
Rangia flexuosa	—Less common than *R. cuneata*
Crassostrea virginica	—Very common, forming reefs in protected areas
Lumbrineris bifilaris	—May be found abundant with better sampling
Anachis obesa	—Common, although equally as common in inlets
Littoridina sphinctostoma	—Several specimens thought to be this species were taken in delta front region, and it is one of most characteristic forms of Guadalupe River Delta region in Texas (Ladd, 1951, p. 143).

III. *Lower Breton Sound and pro-delta slopes.*—This subdivision of the Breton Sound-shallow shelf region, corresponds roughly with Scruton's "Pro-Delta silty clay" sedimentary unit (Scruton, 1956), and is based primarily on the small numbers of species and individuals which live in this fluid clayey bottom. As can be expected in a division where no topographic boundaries exist, there is no definite boundary between faunas. There is a gradation from an area where few or no animals are found to increasing populations on the north and to the rich and varied faunas of the upper sound. If a boundary exists it can be found at the farthest extent of the most turbid waters pouring out of Baptiste Collette Bayou, Main Pass, and Pass a'Loutre, producing the clayey silt and silty clay bottoms shown in the general area in Figure 11. The physical characteristics which differentiate this region from surrounding areas are: a somewhat more variable chlorinity than surrounding waters of equal depth; a very fine silty clay to clayey silt bottom; and a generally year-round occurrence of high turbidity (suspended sediments) from the river distributaries. Although little is known concerning the influence of high turbidity and fine fluid bottom upon the particular animals living in the delta region, there is some reason to believe that

---

[5] A representative sample obtained in November, 1955, from one of these reefs contained many living *Crassostrea virginica*, *Brachidontes recurvus*, *Crepidula plana*, *Martesia* sp., and barnacles.

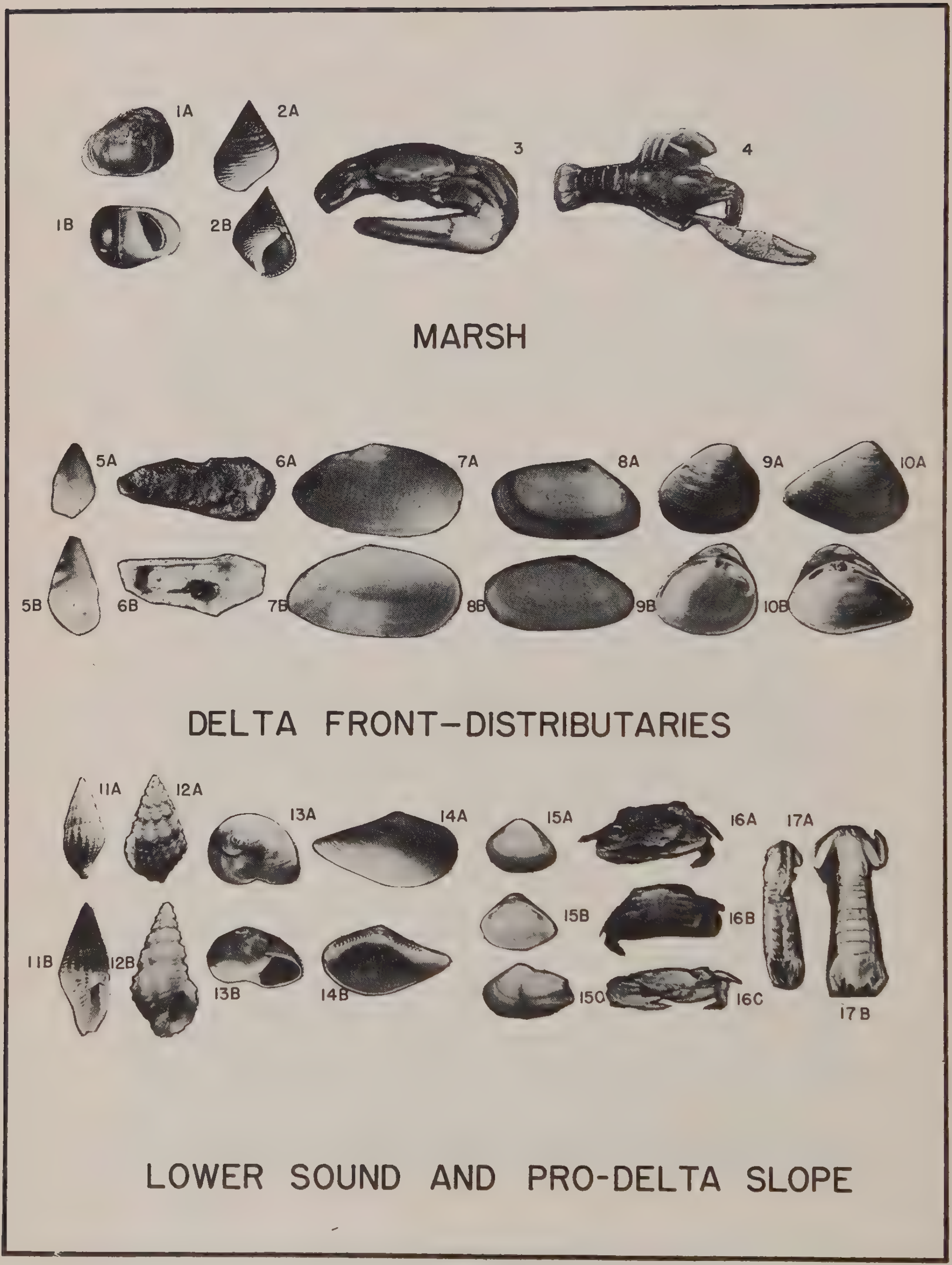
1A
2A
3
4
1B
2B
MARSH
5A
6A
7A
8A
9A
10A
5B
6B
7B
8B
9B
10B
DELTA FRONT-DISTRIBUTARIES
11A
12A
13A
14A
15A
16A
17A
15B
16B
11B
12B
13B
14B
15C
16C
17B
LOWER SOUND AND PRO-DELTA SLOPE

PLATE I

the filter-feeding of some animals and the larval settlement of many invertebrates may be inhibited by these two factors; thus only certain types of organisms may occur in the lower sound and pro-delta slope area.

Only 20 species of macro-invertebrates were found living in the lower sound and pro-delta slope area as compared with more than 50 species living in the upper sound region. A few mollusks and other invertebrates can be considered indicative for the lower sound area and are common enough to make good environmental indicators. Of these, the pelecypods, *Nuculana eborea* (Conrad) and *Mulinia lateralis*, and the two gastropods, *Polinices duplicatus* (Say) and *Anachis avara similis* (Ravenel), are the most abundant and distinctive. The distributions of *Nuculana eborea* and *Mulinia lateralis* are shown in Figure 15a and b, and those of *Polinices duplicatus* and *Squilla empusa* in Figure 16a and b. The macro-organisms which can be considered characteristic for the lower sound and pro-delta slope area are as follows (Pl. I).

Mulinia lateralis	—Extremely abundant, living on clayey slope near Main Pass. Dead throughout inshore delta region
Nuculana eborea	—Common living in northwestern part of this environment, dead throughout inshore regions of Mississippi Delta area
Polinices duplicatus	—Common living here, a few scattered in upper sound and inlet environments
Anachis a. similis	—Few living and dead, few also found in inlets
Anachis a. semiplicata	—Few, more common in near-by inlet region
Squilla empusa	—Mantis shrimp are strangely common in this region
Portunus gibbesi	—This swimming crab is also common in inlet between Breton Island and Main Pass
Nassarius acutus	—Abundant, especially where there are large populations of *Mulinia*. Not strictly characteristic of lower sound and delta, as occurs in varying numbers throughout whole delta region
Abra lioica	—Although primarily shallow-shelf species, this pelecypod is common in lower delta region in vicinity of Pass a'Loutre

---

PLATE I

I. Marsh Assemblage

Fig. 1.—*Neritina reclivata* (Say, 1822), size—11×13 mm., a. side view, b. front.
Fig. 2.—*Littorina irrorata* (Say, 1822), size—19×14 mm., a. back view, b. aperture.
Fig. 3.—*Uca*, species, size—24×17 mm., side view.
Fig. 4.—*Cambarus*, species, size—125 mm., top or dorsal.

II. Delta Front and Distributaries Assemblage

Fig. 5.—*Littoridina sphinctostoma* Abbott and Ladd, 1951, size—3×2 mm., a. back view, b. front or aperture.
Fig. 6.—*Crassostrea virginica* (Gmelin, 1790), size—170×70 mm. a. exterior, b. interior.
Fig. 7.—*Macoma mitchelli* Dall, 1895, size—21×12 mm., a. exterior, b. interior.
Fig. 8.—*Macoma tageliformis* Dall, 1900, size—44×25 mm., a. exterior, b. interior.
Fig. 9.—*Rangia cuneata* (Gray, 1831), size—42×39 mm., a. exterior, b. interior.
Fig. 10.—*Rangia flexuosa* (Conrad, 1840), size 36×30 mm., a. exterior, b. interior.

III. Lower Sound and Pro-Delta Slope Assemblage

Fig. 11.—*Anachis avara similis* (Ravenel, 1861), size—8×3 mm., a. back, b. front view.
Fig. 12.—*Nassarius acutus* (Say, 1822), size—11×4 mm., a. back, b. front view.
Fig. 13.—*Polinices duplicatus* (Say, 1822), size—39×41 mm., a. top, b. aperture.
Fig. 14.—*Nuculana eborea* (Conrad, 1846), size—11×6 mm., a. exterior, b. interior.
Fig. 15.—*Mulinia lateralis* (Say, 1822), size—10×7 mm., a. exterior, b. interior, c. typical association with barnacle, commonly occurring in the Delta Slope environment.
Fig. 16.—*Portunus gibbesi* (Stimpson, 1859), size—49×22 mm., a. dorsal, b. ventral, c. side view.
Fig. 17.—*Squilla empusa* Say, 1818, size—95 mm., a. ventral, b. dorsal side.

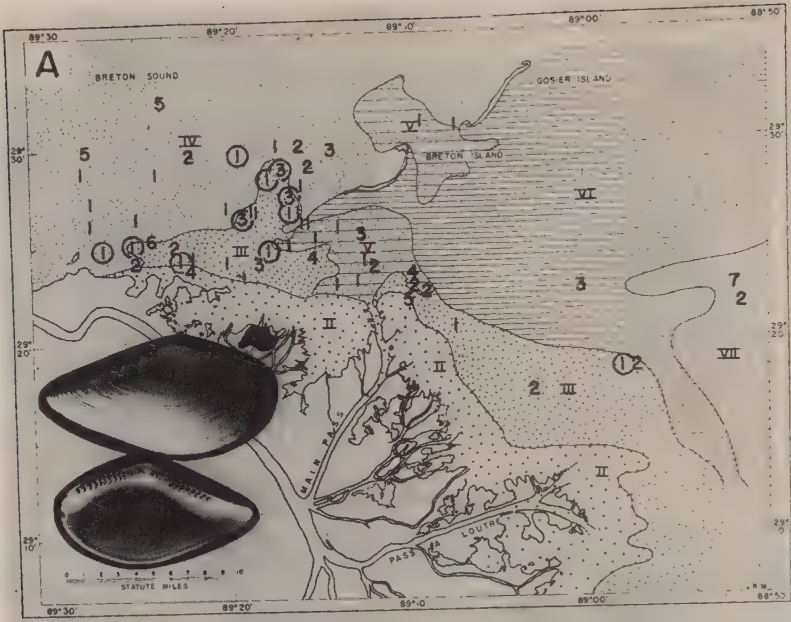
A
BRETON SOUND
GOSIER ISLAND
BRETON ISLAND
MAIN PASS
PASS A LOUTRE
I
II
III
IV
V
VI
VII
STATUTE MILES
89°30'
89°20'
89°10'
89°00'
88°50'
29° 30'
29° 20'
29° 10'

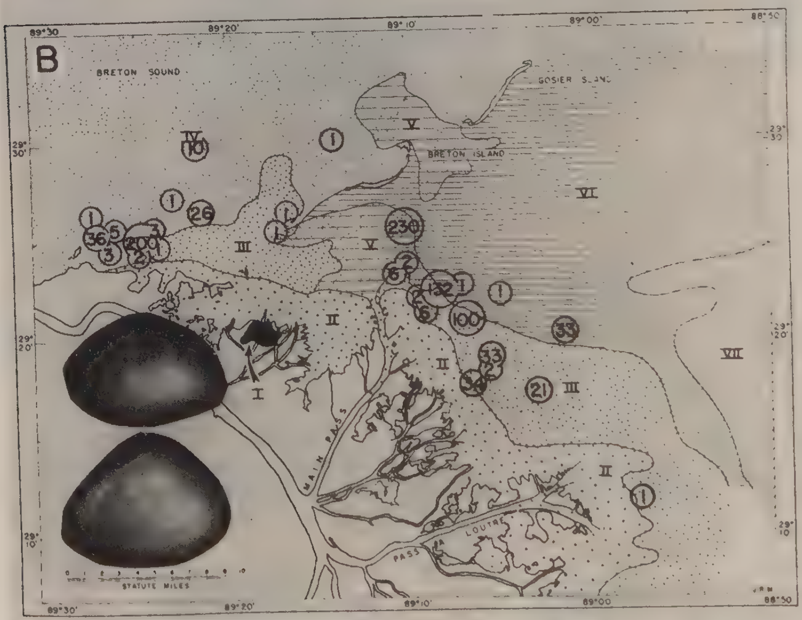
B
BRETON SOUND
GOSIER ISLAND
BRETON ISLAND
MAIN PASS
PASS A LOUTRE
I
II
III
IV
V
VI
VII
STATUTE MILES
89°30'
89°20'
89°10'
89°00'
88°50'
29° 30'
29° 20'
29° 10'

FIG. 15a.—Distribution of pelecypod, *Nuculana eborea*, indicative of lower sound and pro-delta slope. Circled numbers indicate living occurrences, uncircled numbers, dead occurrences.

FIG. 15b.—Distribution (all living) of pelecypod, *Mulinia lateralis*, indicative of lower sound and pro-delta slope environment.

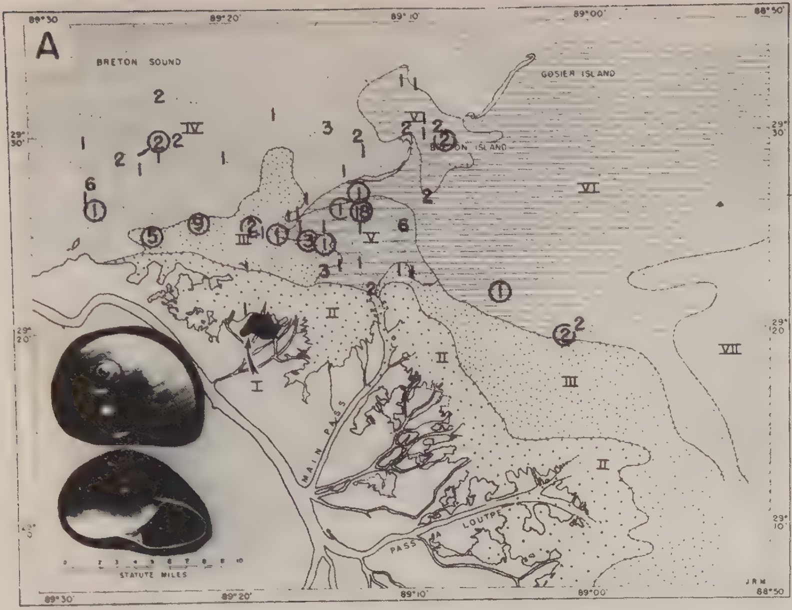
A
BRETON SOUND
GOSIER ISLAND
BRETON ISLAND
MAIN PASS
PASS A LOUTRE
I
II
III
IV
V
VI
VII
89°30'
89°20'
89°10'
89°00'
88°50'
29° 30'
29° 20'
29° 10'
STATUTE MILES

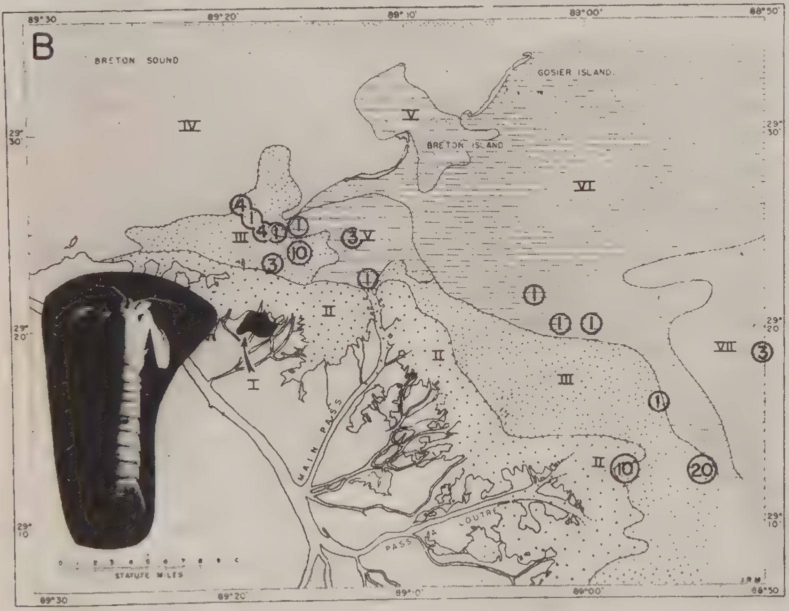
B
BRETON SOUND
GOSIER ISLAND
BRETON ISLAND
MAIN PASS
PASS A LOUTRE
I
II
III
IV
V
VI
VII
89°30'
89°20'
89°10'
89°00'
88°50'
29° 30'
29° 20'
29° 10'
STATUTE MILES

FIG. 16a.—Distribution of gastropod, *Polinices duplicatus*, indicative of lower sound and pro-delta slope environment. Circled numbers indicate living, uncircled—dead occurrences.

FIG. 16b.—Distribution of stomatopod, *Squilla empusa*, indicative of lower sound and pro-delta slope environment.

IV. *Upper Breton Sound and Chandeleur Sound.*—This part of the east Mississippi Delta area is more like the typical high-chlorinity bay environments along the Texas coast (Ladd, 1951, pp. 149, 152–54) than any other part of the Delta region. The physical characteristics of these waters resemble to some extent those of lower Aransas Bay, Matagorda, and Corpus Christi bays on the Texas coast (Galtsoff, 1931; Collier and Hedgpeth, 1950; Hedgpeth, 1953; and Parker, 1955), and many of the organisms are common to both areas. The chlorinity of the upper sound region is somewhat more constant than in the lower sound area, and normally ranges from about 10 to 19 $^{\circ}/_{00}$. These relatively unstable but rather high chlorinities apparently exclude any extensive living oyster reefs of *Crassostrea virginica* (except for a small one behind Breton Island), and also exclude many of the very low-chlorinity animals such as *Rangia* and *Macoma mitchelli*.

Many species were found only in the upper sound region, although many of these were represented by a few specimens. Of the more than 90 species of invertebrates collected in the area, 20 species were characteristic and abundant, both living and dead. Most of the species found in the upper sound environment are listed in Tables I–III. These tables also demonstrate the difference in the number and abundance of species between the two sound environments. Several distribution maps of the more characteristic upper sound animals are given: the pelecypods, *Tagelus divisus* (Spengler) (Fig. 17a) and *Abra aequalis* Say (Fig. 17b) and the gastropod, *Retusa canaliculata* (Say) (Fig. 18a), and the brittle-star, *Amphiodia limbata* (Grube) (Fig. 18b). A more complete list of the characteristic macro-invertebrates of the upper sound region follows (Pls. II–III).

MOLLUSKS
PELECYPODS

Anadara transversa	—Fairly common, few living
Noetia ponderosa	—Few, some living
Nuculana acuta	—These specimens lack characteristic ridges and shape of variety of *Nuculana acuta* consistently found offshore in 13–50 fathoms
Brachidontes recurvus	—Rather common as dead fragments
Crassostrea virginica	—Very common as dead shell reefs
Ostrea equestris	—Very common dead, mixed with dead *C. virginica*
Crassinella martinicensis	—In some localities extremely common dead, although very few found living
Diplodonta punctata	—Fairly common dead, uncommon living
Diplodonta semiaspera	—Common, both living and dead
Lucina crenella	—Common, dead
Mercenaria c. texana	—Very common dead as juveniles, few living adults, reported living in large beds back of barrier islands
Dosinia discus	—Very common dead, scarce living (juveniles), indications that living adults more common in shallow shelf region
Abra aequalis	—Common both living and dead in both upper sound and shallow shelf near barrier islands
Tagelus divisus	—Very abundant living and dead (most characteristic pelecypod)
Tagelus plebeius	—Few, one living
Semele proficua	—Common, few living
Tellina alternata	—Common, few living, probably common on shallow shelf also
Tellidora cristata	—Common, few living in both upper sound and inlets
Macoma tenta	—Abundant, living and dead, also very characteristic
Corbula contracta	—Common, few living

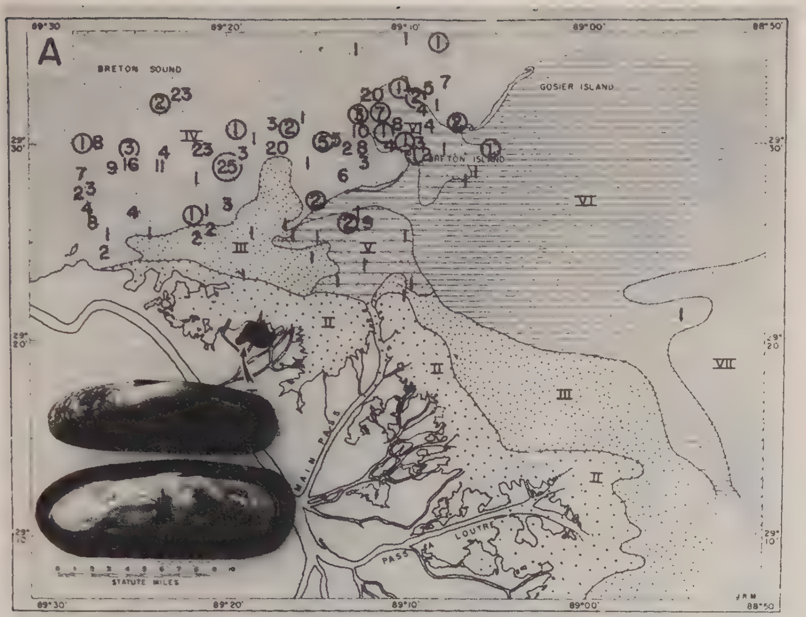
A
BRETON SOUND
GOSIER ISLAND
BRETON ISLAND
MAIN PASS
LOUTRE PASS
STATUTE MILES
I
II
III
IV
V
VI
VII
89°30'
89°20'
89°10'
89°00'
88°50'
29° 30'
29° 20'
29° 10'
J.R.M.

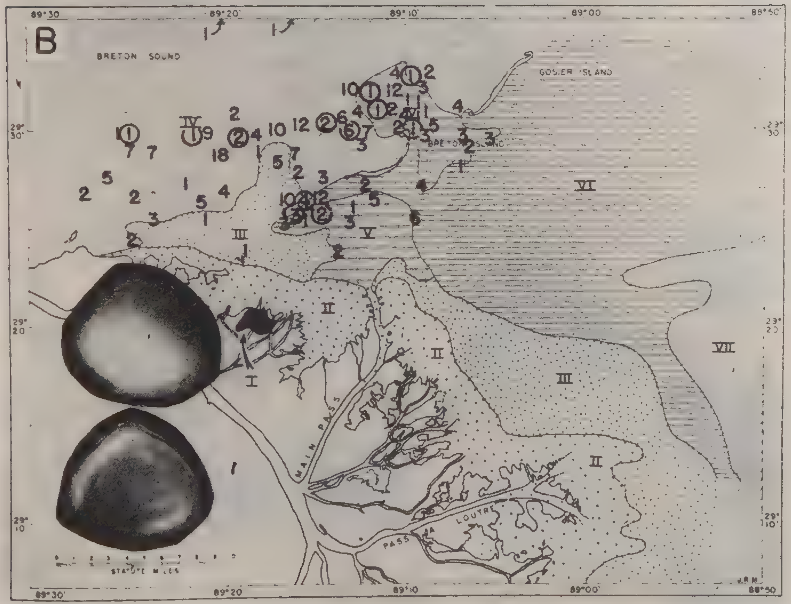
B
BRETON SOUND
GOSIER ISLAND
BRETON ISLAND
MAIN PASS
LOUTRE PASS
STATUTE MILES
I
II
III
IV
V
VI
VII
89°30'
89°20'
89°10'
89°00'
88°50'
29° 30'
29° 20'
29° 10'
J.R.M.

FIG. 17a.—Distribution of pelecypod, *Tagelus divisus*, indicative of upper sound environment.
FIG. 17b.—Distribution of pelecypod, *Abra aequalis*, indicative of upper sound environment.

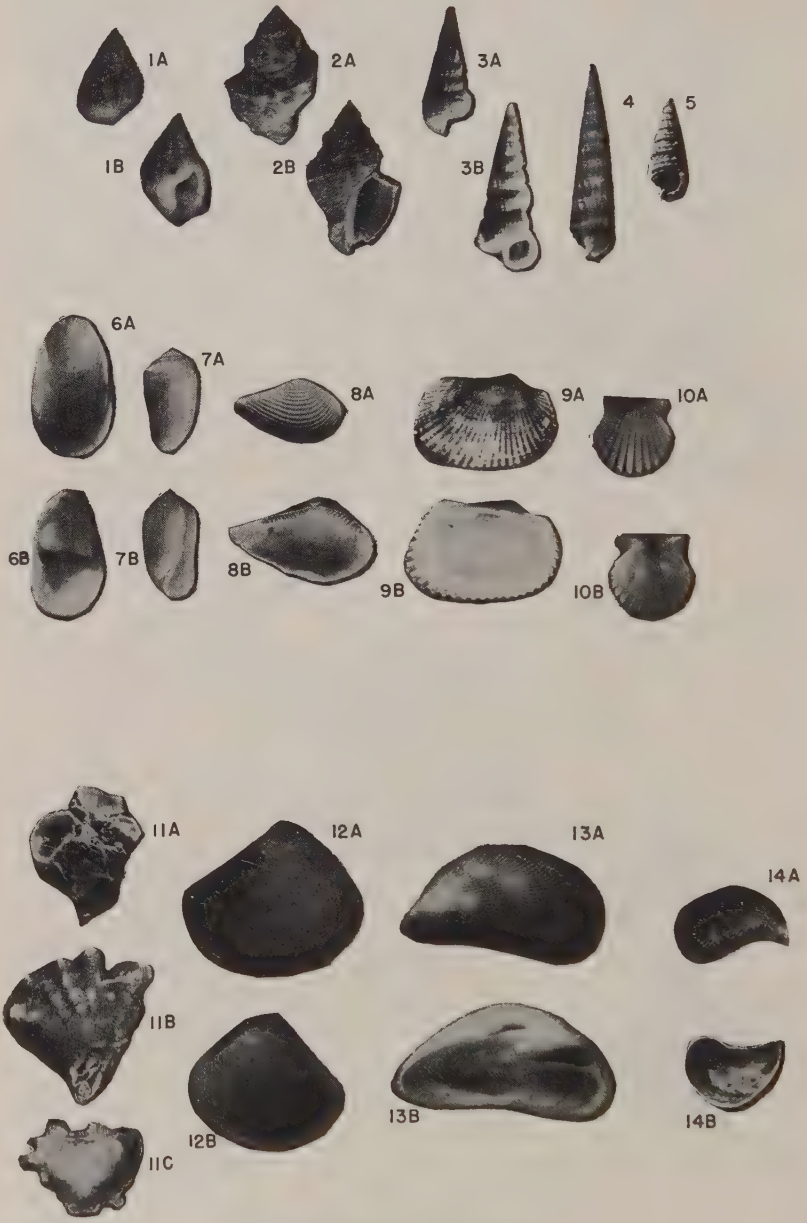
1A
2A
3A
4
5
1B
2B
3B
6A
7A
8A
9A
10A
6B
7B
8B
9B
10B
11A
12A
13A
14A
11B
13B
14B
12B
11C

UPPER SOUND

PLATE II

GASTROPODS
Crepidula plana —Abundant living and dead
Crepidula fornicata —Common dead, found also in inlets and Gulf
Nassarius vibex —Rare, living and dead in open sound, common living on inner side of Breton Island
Terebra protexta —Common dead, rare living
Turbonilla hemphilli —Common dead, also common in inlets
Retusa canaliculata —Common dead in upper sound only

POLYCHAETE WORMS
Glycera americana —Common, living
Chaetopterus variopedatus—Common, living
Sthenelais articulata —Rare, living
Lumbrineris, sp. —Rare, living

CRUSTACEANS
Petrolisthes armatus —Few, living
Crangon heterochelis —Common, living

ECHINODERMS
Amphiodia limbata —Abundant, living

COELENTERATES
Astrangia astreiformis —Common, dead

Cary and Spaulding (1909) list many organisms living in Breton and Chandeleur sounds which were not collected by the writer, but are common in the other high-salinity bays of the northern Gulf of Mexico. Those species collected as fragments by the writer and collected abundantly, living, by Cary and Spaulding are: *Epitonium sayana*, *Anomia simplex*, *Aequipecten irradians amplicostatus*, and *Atrina rigida*, the more common mollusks, and many species of crustaceans. Of particular interest is Spaulding's (1906; see Galtsoff, 1954, p. 209) report on the extensive beds of *Mercenaria campechiensis texana* and *Aequipecten irradians amplicostatus*, the commercial clam and scallop, in the lagoons behind the Chandeleur and Breton islands. No living scallops and only a few large living clams were collected on this survey, although the method of sampling may be responsible for not finding these beds.

V. *Inlets or passes.*—The inlets (Fig. 11) are distinct from the rest of the environmental regions in the delta area, both in the biological assemblage and en-

---

PLATE II

IV. UPPER SOUND ASSEMBLAGE

FIG. 1.—*Nassarius vibex* Say, 1822, size—12×8 mm., a. back, b. aperture.
FIG. 2.—*Thais haemastoma haysae* Clench, 1927, size—59×33 mm., a. back, b. front.
FIG. 3.—*Cerithidea pliculosa* (Menke, 1824), size—32×11 mm., a. back, b. front.
FIG. 4.—*Terebra dislocata* (Say, 1822), size—27×7 mm., front or aperture view.
FIG. 5.—*Cerithium muscarum* Say, 1832, size—19×7 mm., front or aperture view.
FIG. 6.—*Crepidula plana* Say, 1822, size—22×12 mm., a. exterior, b. interior.
FIG. 7.—*Retusa canaliculata* (Say, 1827), size—6×3 mm., a. back, b. aperture.
FIG. 8.—*Nuculana acuta* Conrad, 1832 (nearshore form), size—6×4 mm., a. exterior, b. interior.
FIG. 9.—*Anadara transversa* (Say, 1822), size—15×10 mm., a. exterior, b. interior.
FIG. 10.—*Aequipecten irradians amplicostatus* (Dall, 1898), size 65×63 mm., a. exterior, b. interior.
FIG. 11.—*Ostrea equestris* Say, 1834, size—a. clump—38×50 mm., b. exterior, c. interior—19×14 mm.
FIG. 12.—*Crassinella martinicensis* (d'Orbigny, 1842), size 8×7 mm., a. exterior, b. interior.
FIG. 13.—*Brachidontes exustus* (Linné, 1758), size—17×9 mm., a. exterior, b. interior.
FIG. 14.—*Brachidontes recurvus* (Rafinesque, 1820), size—16×11 mm., a. exterior, b. interior.

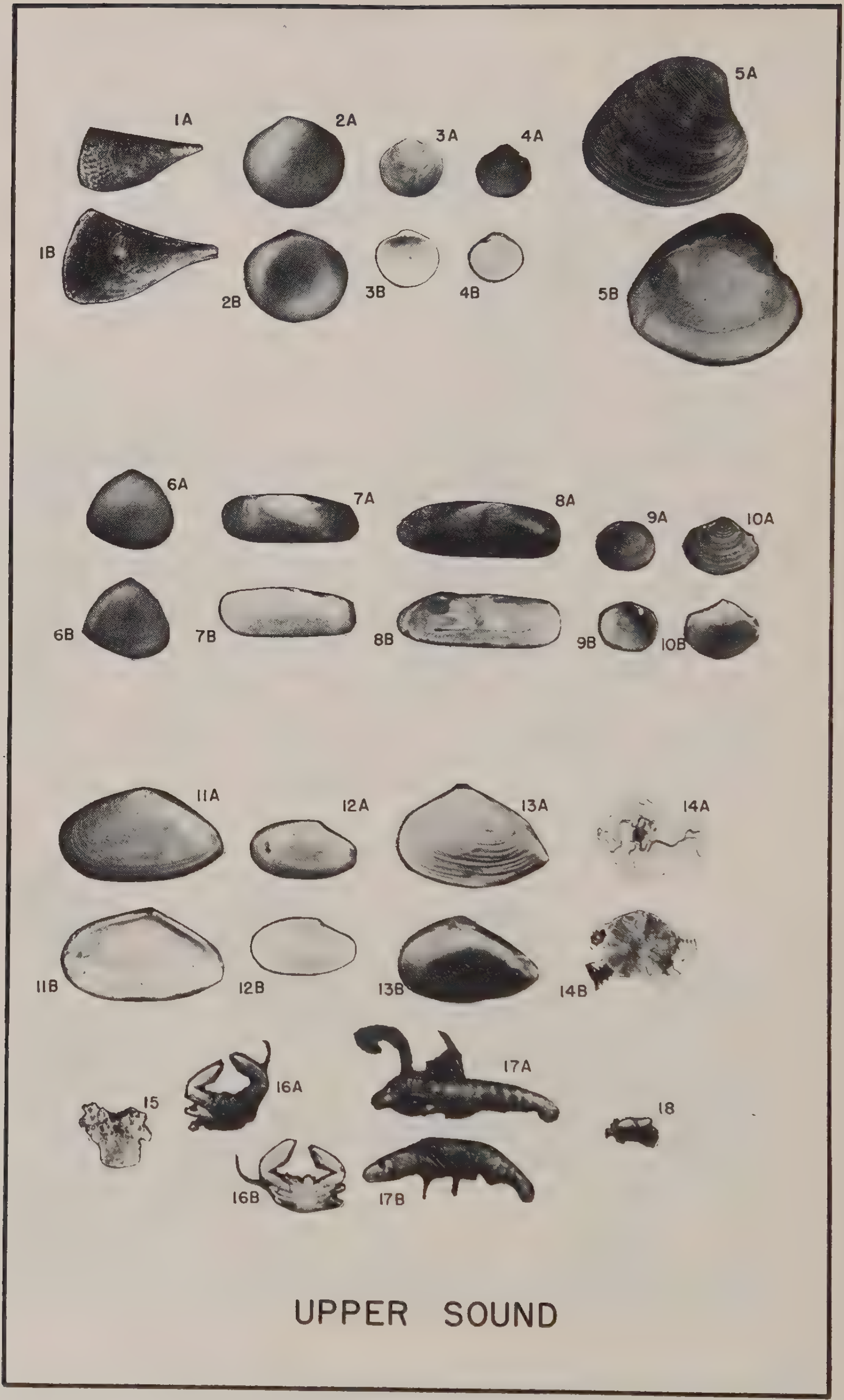
1A
2A
3A
4A
5A
1B
2B
3B
4B
5B
6A
7A
8A
9A
10A
6B
7B
8B
9B
10B
11A
12A
13A
14A
11B
12B
13B
14B
15
16A
17A
18
16B
17B
UPPER SOUND

Plate III

vironmental factors. Physically, the inlets are characterized by strong tidal currents (Scruton, manuscript), a firm bottom of sand, sandy, silty clay, and old shell material concentrated by the currents, and greater depths with narrower ranges of temperature and chlorinity than those of surrounding areas. The inlets show close faunal affinities with both the upper and lower sound environments and the shallow shelf, which is to be expected, since the currents bring water into this environment from each direction. Although faunal elements are present from environments on each side of the inlets, there are at least 12 species of macro-organisms which were found only in the inlets. Of the 100 species collected in the inlets, 56 were found alive, and 44 dead. The distribution of *Anachis avara semiplicata* (Stearns) and *Hemipholis elongata* (Say), the two species restricted mostly to inlets, is illustrated in Figure 19a and b. Two species which are not restricted entirely to the inlets and are represented by occasional individuals in other environments are the gastropod, *Olivella mutica* (Say), and the pelecypod, *Trachycardium muricatum* (Linné) (Fig. 20a and b). Those macro-invertebrates which may be considered characteristic of the inlets are the following (Pl. IV).

MOLLUSKS	
PELECYPODS	
Anadara brasiliana	—Common dead, few living
Trachycardium muricatum	—Common living and dead
Chione cancellata	—Few living
Lucina amiantus	—Abundant living and dead, but also occurs commonly in upper sound and shallow-shelf region
Petricola pholadiformis	—Few living, fairly common dead
Cyrtopleura costata	—Common dead, at times abundant as dead shell on barrier-island beaches
Pandora trilineata	—Few living, fairly common dead, but also found in upper sound near inlets
GASTROPODS	
Diodora cayenensis	—Few living, common dead
Natica pusilla	—Few living, common dead

PLATE III

IV. UPPER SOUND ASSEMBLAGE (CONTINUED)

FIG. 1.—*Atrina rigida* (Solander, 1786), size—188×108 mm., a. exterior, b. interior.
FIG. 2.—*Diplodonta punctata* (Say, 1822), size—12×11 mm., a. exterior, b. interior.
FIG. 3.—*Diplodonta semiaspera* Philippi, 1836, size—10×9 mm., a. exterior, b. interior.
FIG. 4.—*Lucina crenella* (Dall, 1901), size—5×5 mm., a. exterior, b. interior.
FIG. 5.—*Mercenaria campechiensis texana* (Dall, 1902), size—102×94 mm., a. exterior, b. interior.
FIG. 6.—*Abra aequalis* (Say, 1822), size—12×10 mm., a. exterior, b. interior.
FIG. 7.—*Tagelus plebeius* (Solander, 1786), size—42×16 mm., a. exterior, b. interior.
FIG. 8.—*Tagelus divisus* (Spengler, 1794), size—27×9 mm., a. exterior, b. interior.
FIG. 9.—*Semele proficua* (Pultney, 1799), size—13×11 mm., a. exterior, b. interior.
FIG. 10.—*Tellidora cristata* (Recluz, 1842), size—15×13 mm., a. exterior, b. interior.
FIG. 11.—*Tellina alternata* Say, 1822, size—52×29 mm., a. exterior, b. interior.
FIG. 12.—*Macoma tenta* (Say, 1834), size—10×9 mm., a. exterior, b. interior.
FIG. 13.—*Corbula contracta* Say, 1822, size—7×5 mm., a. exterior, b. interior.
FIG. 14.—*Amphiodia limbata* (Grube), size—disc diameter—6 mm., a. top, b. disc.
FIG. 15.—*Astrangia astreiformis* Milne-Edwards and Haime, size—clump or colony, 25 mm.
FIG. 16.—*Petrolisthes armatus* (Gibbes), size—10×12 carapace, a. dorsal, b. ventral.
FIG. 17.—*Crangon heterochelis* (Say), size—37 mm., a. dorsal, b. side view.
FIG. 18.—*Neopanope packardi* (Kingsley, 1789), size—8×7 (carapace), ventral view.

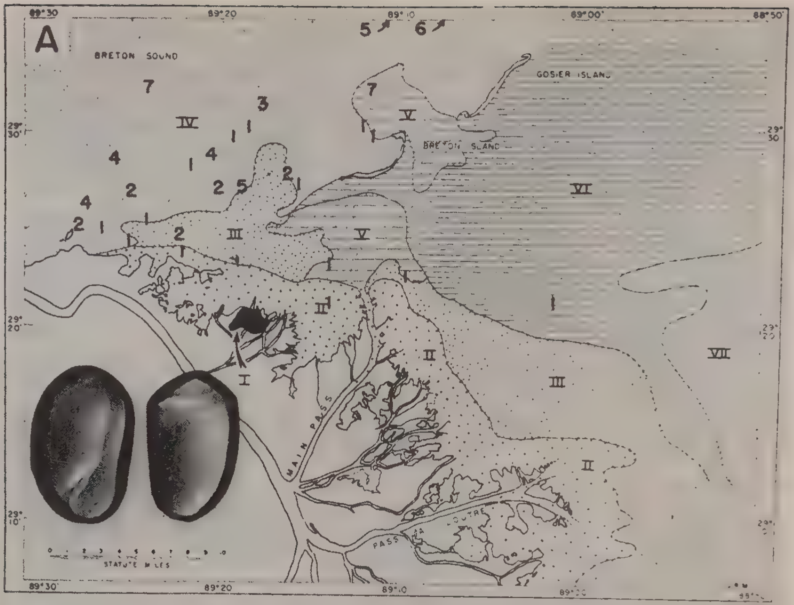
A
BRETON SOUND
GOSIER ISLAND
BRETON ISLAND
MAIN PASS
PASS A LOUTRE
I
II
III
IV
V
VI
VII
5
6
7
3
4
2
1
89°30'
89°20'
89°10'
89°00'
88°50'
29° 30'
29° 20'
29° 10'
STATUTE MILES

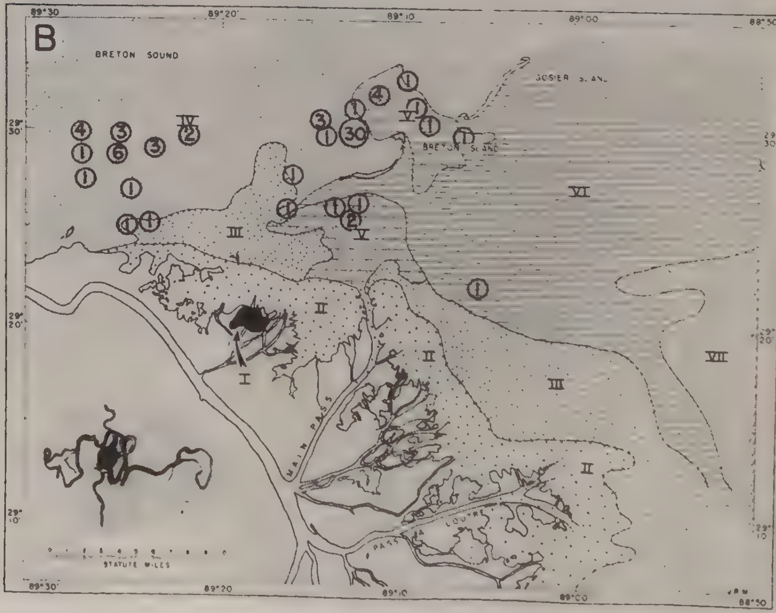
B
BRETON SOUND
GOSIER ISLAND
BRETON ISLAND
MAIN PASS
PASS A LOUTRE
I
II
III
IV
V
VI
VII
④
③
①
⑥
②
30
89°30'
89°20'
89°10'
89°00'
88°50'
29° 30'
29° 20'
29° 10'
STATUTE MILES

FIG. 18a.—Distribution of gastropod, *Retusa canaliculata* (all dead), indicative of upper sound environment.

FIG. 18b. - Distribution of brittle star, *Amphiodia limbata* (all living); indicative of upper sound environment.

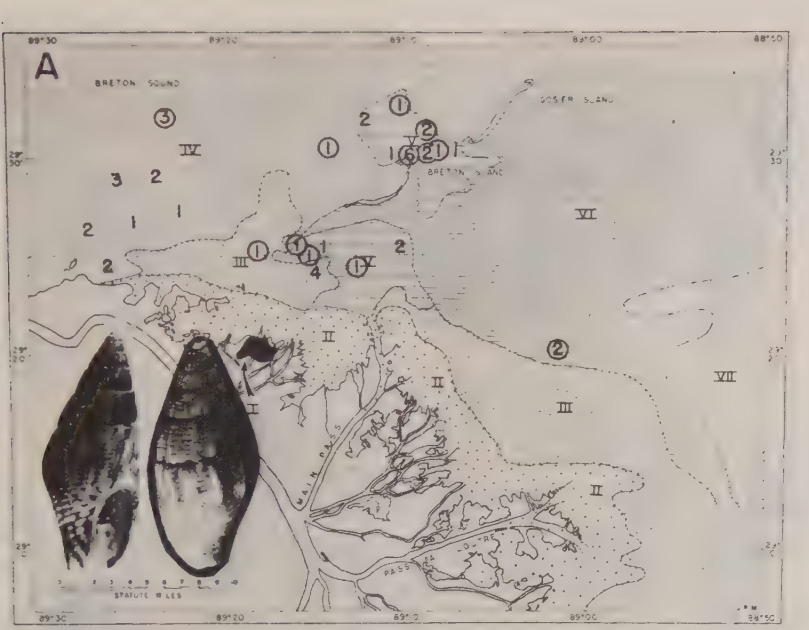
A
BRETON SOUND
GOSIER ISLAND
BRETON ISLAND
MAIN PASS
PASS A LOUTRE
STATUTE MILES
89°30
89°20
89°10
89°00
88°50
29° 30'
29° 20'
29° 10'
I
II
III
IV
V
VI
VII

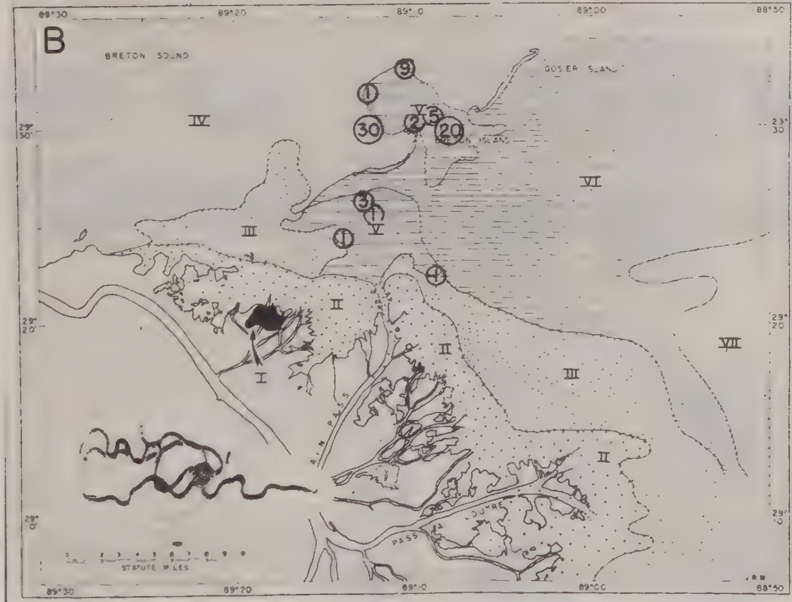
B
BRETON SOUND
GOSIER ISLAND
BRETON ISLAND
MAIN PASS
PASS A LOUTRE
STATUTE MILES
89°30
89°20
89°10
89°00
88°50
29° 30'
29° 20'
29° 10'
I
II
III
IV
V
VI
VII

Fig. 19a.—Distribution of gastropod, *Anachis avara semiplicata*, indicative of inlet environment.
Fig. 19b.—Distribution of brittle star, *Hemipholis elongata*, indicative of inlet environment (all living).

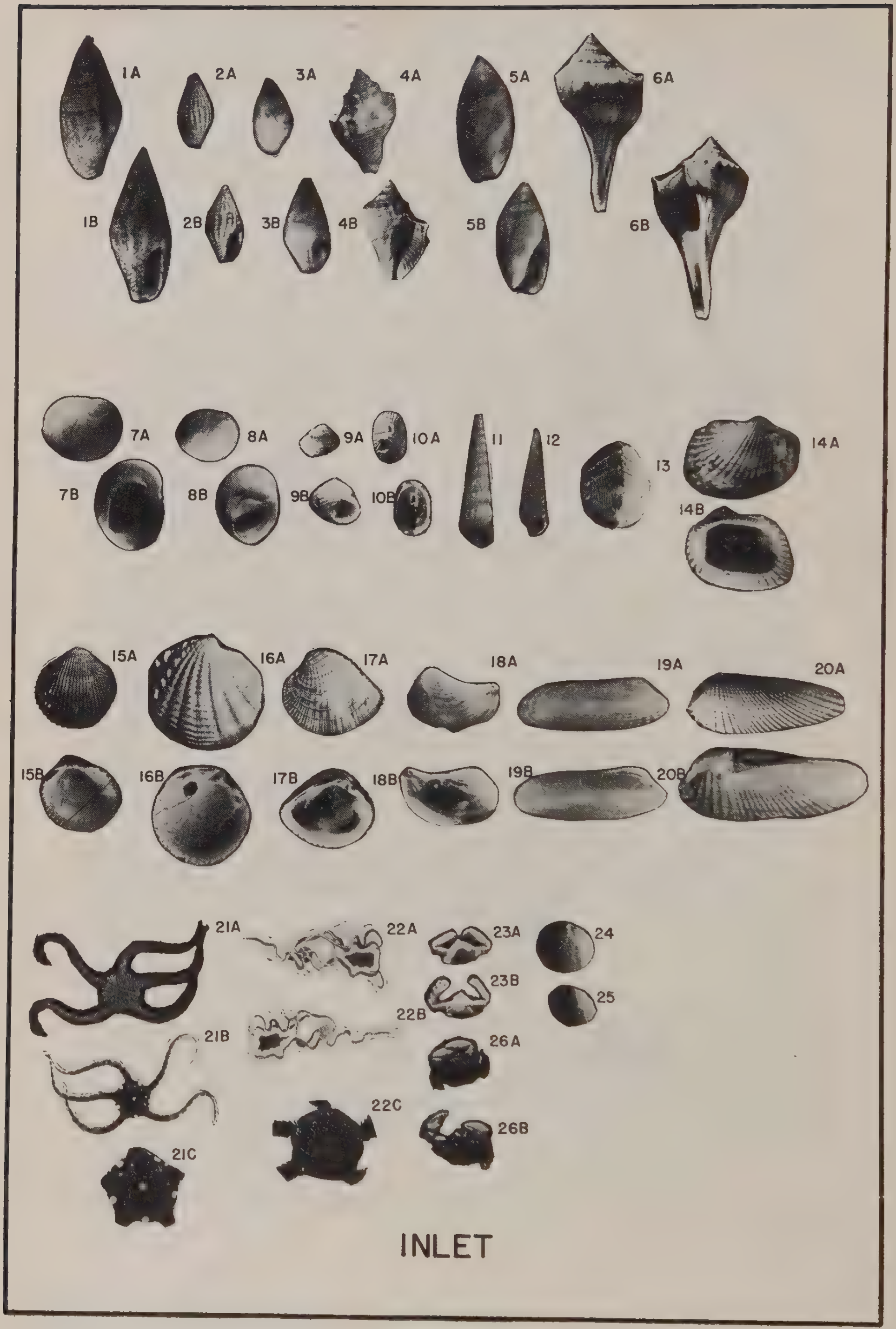
1A
2A
3A
4A
5A
6A
1B
2B
3B
4B
5B
6B
7A
8A
9A
10A
11
12
13
14A
7B
8B
9B
10B
14B
15A
16A
17A
18A
19A
20A
15B
16B
17B
18B
19B
20B
21A
22A
23A
24
23B
25
22B
21B
26A
22C
26B
21C
INLET

Plate IV

Thais haemastoma floridana—Few living, common dead, although not restricted to inlets
Anachis obesa—Common living and dead, center of population in inlets
Anachis a. semiplicata—Common living and dead
Mitrella lunata—Few living and dead
Busycon contrarium—Common living and dead, but not entirely restricted to inlet
Busycon spiratum plagosum—Less common than other species of *Busycon*, and probably is more common on shallow shelf
Sinum perspectivum—Few dead in inlets only
Olivella mutica—Abundant both living and dead with center of abundance in inlets
Turbonilla hemphilli—Common dead in inlets and upper sound

CHITONS
Chaetopleura apiculata—Few living in inlets only

ECHINODERMS
Hemipholis elongata—Abundant living
Ophiolepis elegans—Abundant living, found also in deep channels of Chandeleur Sound
Luidia clathrata, *Mellita quinquiesperforata*, and *Moira atropos* all range into inlets, although are more indicative of shallow shelf

CRUSTACEANS
Heterocrypta granulata—Common, living
Porcellana sayana—Few living

POLYCHAETE WORMS
Owenia fusiformis—Few living

COELENTERATES
Calliactis tricolor—Fairly common, attached to hermit shell

BRYOZOA
Discoporella umbellata—Few, living
Cupuladria canariensis—Few, living
Membranipora, sp.—Abundant, living

Cary and Spaulding (1909) list the following species from the inlets of the Chandeleurs: the gastropods, *Modulus modulus* and *Sinum perspectivum*; the

---

PLATE IV

V. INLET ASSEMBLAGE

FIG. 1.—*Anachis avara semiplicata* Stearns, 1873, size—11×5 mm., a. back, b. front.
FIG. 2.—*Anachis obesa* C. B. Adams, 1845, size—4×2 mm., a. back, b. aperture.
FIG. 3.—*Mitrella lunata* (Say, 1826), size—4×2 mm., a. back, b. aperture.
FIG. 4.—*Thais haemastoma floridana* (Conrad, 1837), size—47×29 mm., a. back, b. front.
FIG. 5.—*Olivella mutica* (Say, 1822), size—2×8 mm., a. back, b. aperture.
FIG. 6.—*Busycon contrarium* (Conrad, 1840), size—80×39 mm., a. back, b. aperture.
FIG. 7.—*Sinum perspectivum* (Say, 1831), size—31×31 mm., a. top, b. aperture.
FIG. 8.—*Natica pusilla* Say, 1822, size—3×4 mm., a. top view, b. aperture.
FIG. 9.—*Modulus modulus* (Linné, 1758), size—9×10 mm., a. side view, b. aperture.
FIG. 10.—*Diodora cayenensis* (Lamarck, 1822), size—12×7 mm., a. exterior, b. interior.
FIG. 11.—*Turbonilla hemphilli* (Bush, 1899), size—2×8 mm., front or aperture.
FIG. 12.—*Terebra protexta* (Conrad, 1843), size—26×6 mm., front or aperture.
FIG. 13.—*Chaetopleura apiculata* Say, 1830, size—10×7 mm., exterior or top view.
FIG. 14.—*Anadara brasiliana* (Lamarck, 1819), size—13×9 mm., a. exterior, b. interior.
FIG. 15.—*Trachycardium muricatum* (Linné, 1758), size—42×44 mm., a. exterior, b. interior.
FIG. 16.—*Lucina amiantus* (Dall, 1901), size—6×6 mm., a. exterior, b. interior.
FIG. 17.—*Chione cancellata* (Linné, 1758), size—26×22 mm., a. exterior, b. interior.
FIG. 18.—*Pandora trilineata* Say, 1822, size—20×11 mm., a. exterior, b. interior.
FIG. 19.—*Petricola pholadiformis* Lamarck, 1818, size—23×8 mm., a. exterior, b. interior.
FIG. 20.—*Cyrtopleura costata* (Linné, 1758), size—98×39 mm., a. exterior, b. interior.
FIG. 21.—*Ophiolepis elegans* (Lütken), size—disc—20 mm., arms 55 mm., a. ventral, b. dorsal, c. disc.
FIG. 22.—*Hemipholis elongata* (Say), size—disc 7 mm., a. ventral, b. dorsal, c. disc.
FIG. 23.—*Heterocrypta granulata* (Gibbes, 1849), size—15×10 (carapace), a. top, dorsal, b. ventral.
FIG. 24.—*Mamillopora cupula* Smitt, size—22 mm., colony.
FIG. 25.—*Cupuladria canariensis* Busk, size—18 mm., colony.
FIG. 26.—*Porcellana sayana* (Leach), size—12×11 mm., a dorsal, b. ventral.

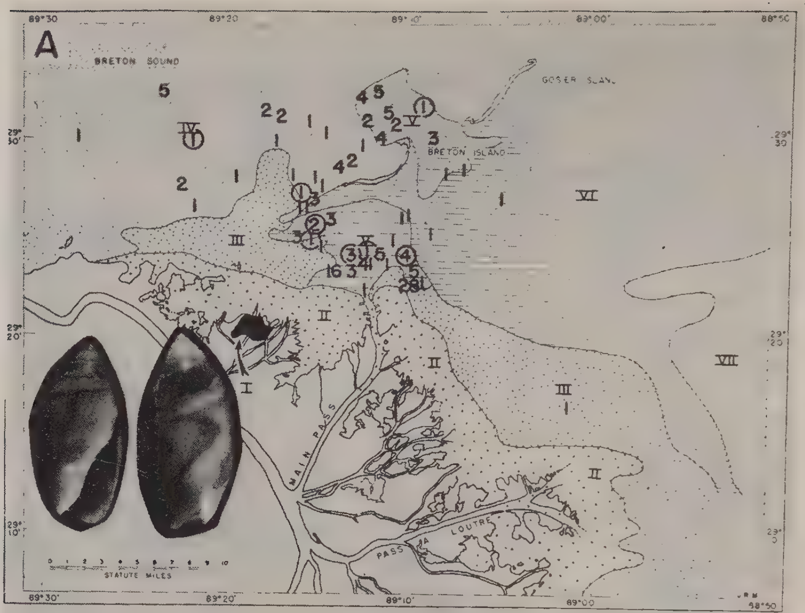
A
BRETON SOUND
GOSIER ISLAND
BRETON ISLAND
MAIN PASS
PASS A LOUTRE
STATUTE MILES
89°30'
89°20'
89°10'
89°00'
88°50'
29° 30'
29° 20'
29° 10'
I
II
III
IV
V
VI
VII

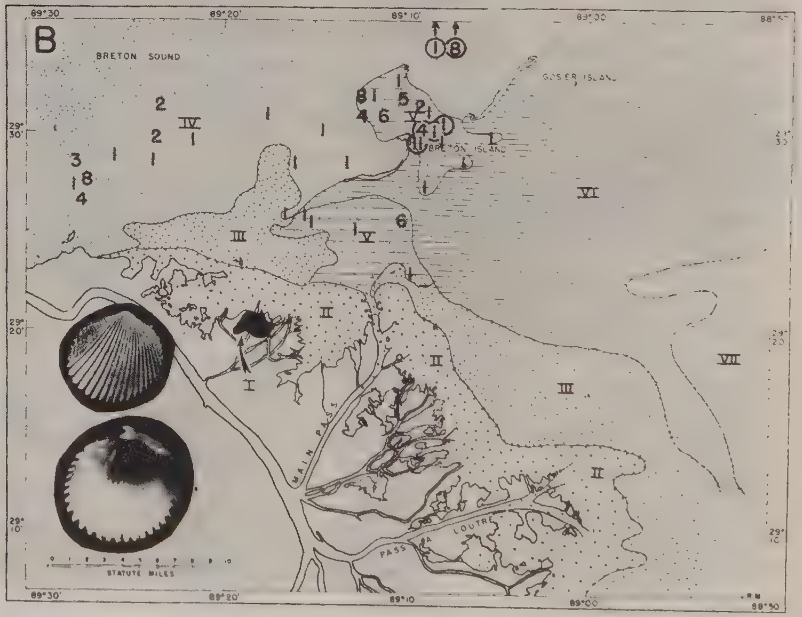
B
BRETON SOUND
GOSIER ISLAND
BRETON ISLAND
MAIN PASS
PASS A LOUTRE
STATUTE MILES
89°30'
89°20'
89°10'
89°00'
88°50'
29° 30'
29° 20'
29° 10'
I
II
III
IV
V
VI
VII

FIG. 20a.—Distribution of gastropod, *Olivella mutica*, indicative of inlet environment.

FIG. 20b.—Distribution of pelecypod, *Trachycardium muricatum*, indicative of inlet environment.

pelecypod, *Trachycardium muricatum*; and the crab, *Petrolisthes armatus* (Gibbes).

VI. *Shallow continental shelf of Gulf of Mexico from 0 to 13 fathoms, off barrier islands.*—Although no exact boundary can be drawn between the inlets and shallow continental shelf of the Gulf where the inlets are very wide, the shallow-shelf assemblage is distinct from that of the other areas. It does not extend to the vicinity of the shores of the active Mississippi Delta and other parts of the Gulf coast where rivers empty directly into the Gulf, because of the effect of the fresh water and sediments discharged directly into the open Gulf of Mexico. However, where the open Gulf meets the barrier islands and sandy peninsulas or coastline without barrier islands or large rivers, wave action forms sandy shores, and there is a typical high-salinity shallow-shelf fauna close to shore with characteristic surf-zone animals. In the typical shallow-shelf region, the chlorinities are generally above 14 °/₀₀, and usually above 17 °/₀₀, while the water temperatures are variable according to the season of the year. The fauna of this region is related to the warm-temperate waters of the Carolina coast, with occasional forms typical of the west coast of Florida (Hedgpeth, 1953; Pulley, 1953).

Although the characteristic invertebrates of the shallow-shelf region are many and varied, few were taken alive on this project because of inadequate collecting methods. The shells of many of the shallow-shelf species of mollusks often occur in large drifts on the beaches after storms, and their presence should characterize Gulf beach deposits in older formations. Eighty-one species of macro-invertebrates were collected in this area during the investigation, of which 32 species were living and 49 were dead remains. The distribution maps for some of the characteristic shallow-shelf organisms collected on this project are shown as follows: the gastropod, *Cantharus cancellarius* (Conrad) (Fig. 21a); the sea pansy, *Renilla mülleri* Kölliker (Fig. 21b); the polychaete worm, *Aglaophamus dicirris* Hartman (Fig. 22a); the starfish, *Luidia clathrata* (Say) (Fig. 22b); and the sand dollar, *Mellita quinquiesperforata* (Leske) (Fig. 23a). A pelecypod which is found in the shallow-shelf region that borders the active delta, but does not live on the sand bottoms near the barrier islands, is *Abra lioica* Dall, whose distribution is shown in Figure 23b.

The mollusks observed on the Gulf beaches in large numbers and reported living in the shallow part of the shelf by other investigators (Cary and Spaulding, 1909; Harry, 1942; Behre, 1950; Pulley, 1953; Hedgpeth, 1953; Parker, 1955) are the pelecypods, *Dinocardium robustum* (Solander), *Atrina serrata* (Sowerby), *Aequipecten irradians concentricus* (Say), *Callocardia texasiana* Dall, *Cyrtopleura costata* (Linné), *Labiosa plicatella* (Lamarck), *Labiosa lineata* Say, *Macoma constricta* Bruguière, *Spisula solidissima similis* (Say), and *Dosinia discus* (Reeve); and the gastropods, *Phalium granulatum* (Born), *Olvia sayana* Ravenel, *Tonna galea* Linné, *Murex fulvescens* Sowerby, *Murex pomum* Gmelin, and *Strombus alatus* Gmelin. Of particular interest was the presence of the valves of the giant clam, *Panope bitruncata* Conrad, a close relative of the geoduck (*P. generosa*) of the Pacific coast, on the beach of Gosier Island. According to Abbott (1954)

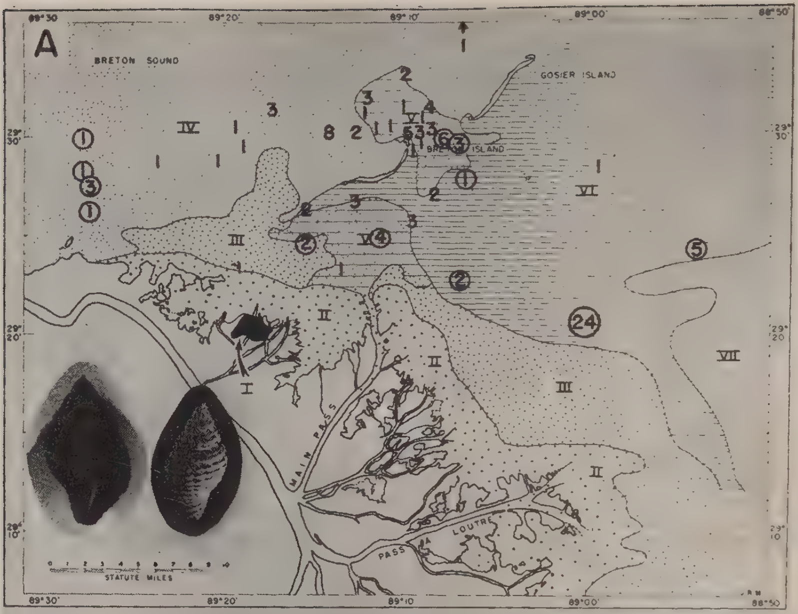
A
BRETON SOUND
GOSIER ISLAND
BRETON ISLAND
MAIN PASS
LOUTRE PASS
STATUTE MILES
I
II
III
IV
V
VI
VII
89°30'
89°20'
89°10'
89°00'
88°50'
29°30'
29°20'
29°10'

FIG. 21a.—Distribution of gastropod, *Cantharus cancellarius*, indicative of shallow-shelf and inlet environments.

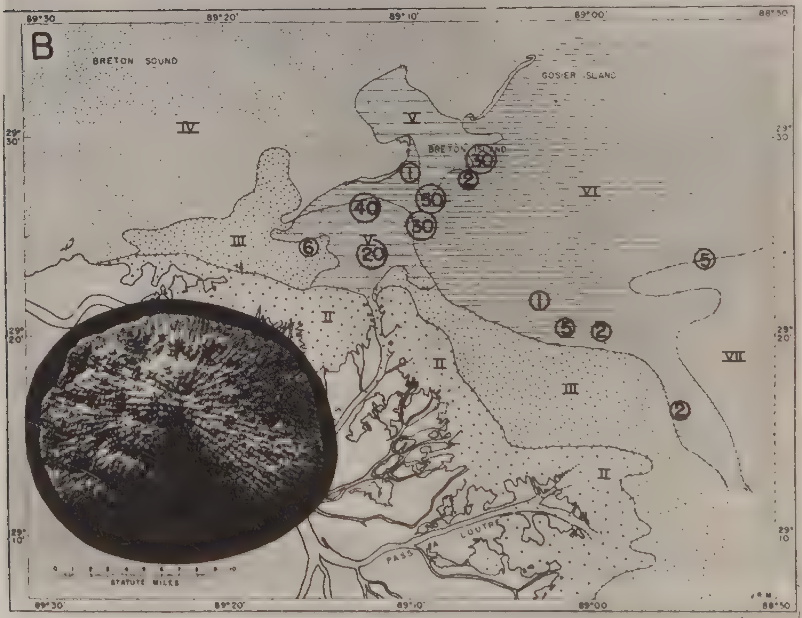
B
BRETON SOUND
GOSIER ISLAND
BRETON ISLAND
LOUTRE PASS
STATUTE MILES
I
II
III
IV
V
VI
VII
89°30'
89°20'
89°10'
89°00'
88°50'
29°30'
29°20'
29°10'

FIG. 21b.—Distribution of pennatulid, *Renilla mülleri*, indicative of shallow-shelf environment (all living).

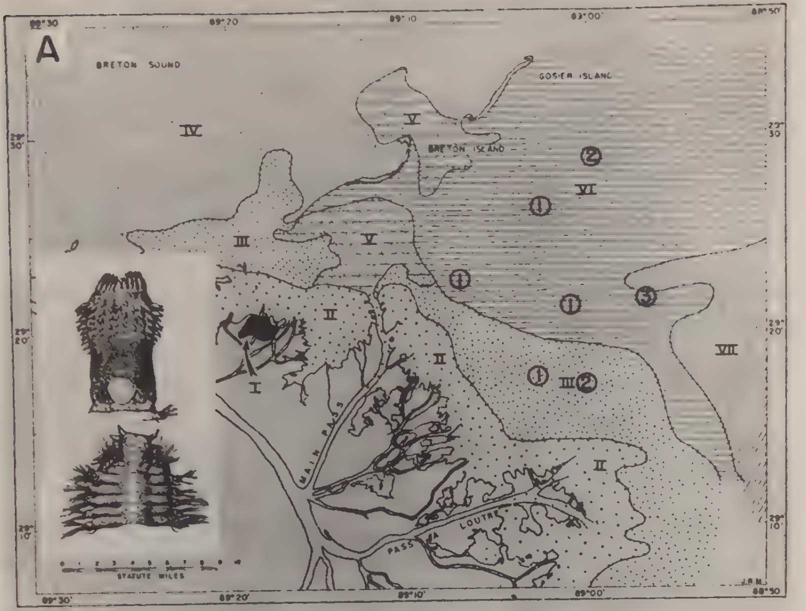
A
BRETON SOUND
GOSIER ISLAND
BRETON ISLAND
IV
V
VI
VII
III
II
I
MAIN PASS
PASS A LOUTRE
STATUTE MILES
89°30'
89°20'
89°10'
89°00'
88°50'
29°30'
29°20'
29°10'

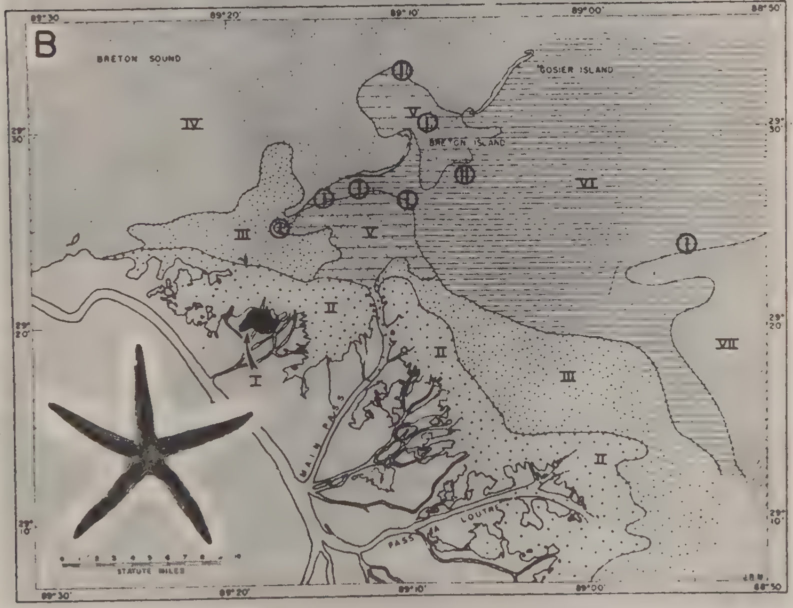
B
BRETON SOUND
GOSIER ISLAND
BRETON ISLAND
IV
V
VI
VII
III
II
I
MAIN PASS
PASS A LOUTRE
STATUTE MILES
89°30'
89°20'
89°10'
89°00'
88°50'
29°30'
29°20'
29°10'

FIG. 22a.—Distribution of polychaete worm, *Aglaophamus dicirris*, indicative of shallow-shelf environment (all living).

FIG. 22b.—Distribution of starfish, *Luidia clathrata*, indicative of shallow-shelf and inlet environments (all living).

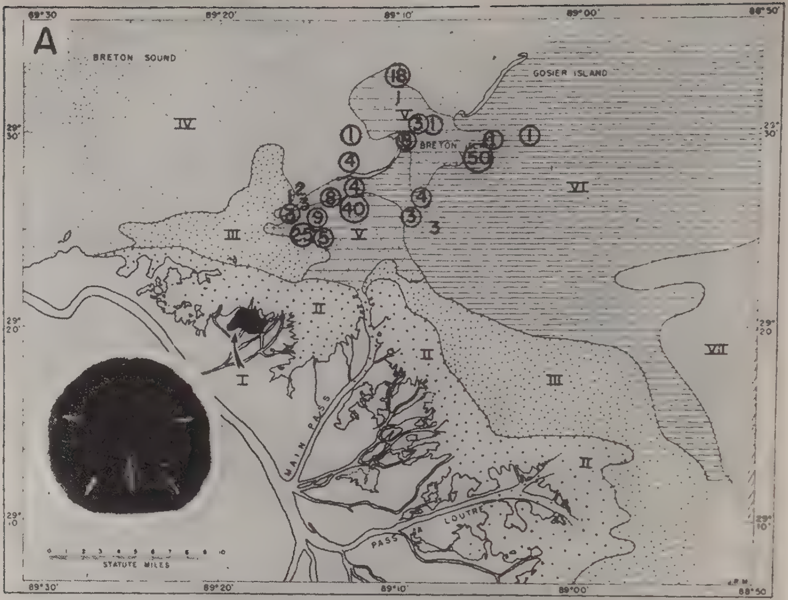
A
BRETON SOUND
GOSIER ISLAND
BRETON
IV
V
VI
VII
III
II
I
MAIN PASS
PASS A LOUTRE
STATUTE MILES
89°30'
89°20'
89°10'
89°00'
88°50'
29°30'
29°20'
29°10'

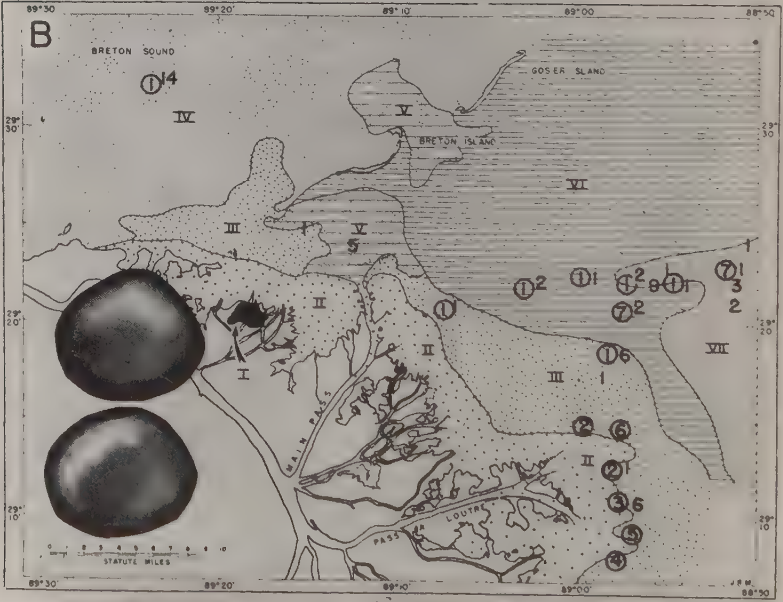
B
BRETON SOUND
GOSIER ISLAND
BRETON ISLAND
IV
V
VI
VII
III
II
I
MAIN PASS
PASS A LOUTRE
STATUTE MILES
89°30'
89°20'
89°10'
89°00'
88°50'
29°30'
29°20'
29°10'

FIG. 23a.—Distribution of sand dollar, *Mellita quinquiesperforata*, indicative of shallow-shelf and inlets.

FIG. 23b.—Distribution of pelecypod, *Abra lioica*, indicative of shallow-shelf and pro-delta slope.

this clam has never been seen alive and is thought to be extinct, but the valve from Gosier Island still had organic material in the hinge. Pulley (1953) cites an open-Gulf record of *Panope* from Port Isabel, Texas. The mollusks which are characteristic of the surf zone and sand beach are *Donax tumida* Philippi, *Terebra cinerea* (Born), and occasionally large populations of *Olivella mutica* Say. The ghost crab, *Ocypode albicans* Bosc, is also a prominent member of the sand-beach community. Its remains are common in beach drift and *Ocypode* claws are commonly preserved in old Gulf beach assemblages found deep in borings from the Texas coast. The general distribution of the other shallow-shelf invertebrates can be seen in Tables II and III. A list of the invertebrates characteristic of the nearshore Gulf follows (Pls. V–VI).

MOLLUSKS	
GASTROPODS	
Architectonica nobilis	—Uncommon in delta collections, but abundant off Rockport, Texas
Strombus alatus	—Common on Gulf beaches, common living taken by shrimp trawlers, and occasionally found in deeper parts of continental shelf
Cantharus cancellarius	—Common, living on shallow shelf, and also found on Gulf side of inlets
Busycon spiratum plagosum	—Few dead on Gulf beach, living in inlets, although farther south, this species is confined to shallow shelf and is common
Oliva sayana	—Common dead, few living
Phalium granulatum	—Common dead on Gulf beaches and living, taken by shrimp trawls in 5–15 fathoms
Tonna galea	—Rare dead on Gulf beaches, and occasionally picked up in shrimp trawls
Janthina janthina	—At times extremely abundant on Gulf beaches, is pelagic, but rafts up on beaches after storms
Murex fulvescens	—Not uncommon on Gulf beaches, rare living
Murex pomum	—Rare on Gulf beaches, seldom found living
Terebra cinerea	—Common, living in surf zone and somewhat less common out to 10 fathoms
PELECYPODS	
Nuculana acuta (nearshore)	—Common dead, although also found in upper sound and inlet
Anadara campechiensis	—Often large numbers of valves cast up on Gulf beach
Anadara chemnitzi	—Rare shells on Gulf beach
Noetia ponderosa	—Large numbers of valves on Gulf beach
Volsella demissa granosissima	—Few on Gulf beaches
Atrina serrata	—After storms, extremely abundant on Gulf beaches, seldom seen living
Aequipecten irradians concentricus	—Common scallop of Gulf beaches, but seldom taken living
Lucina amiantus	—Abundant, living but also found in inlets and upper sound
Dinocardium robostum	—Common large cockle of Gulf beach, although seldom seen living
Spisula solidissima similis	—Few found dead on Gulf beach, not seen living, except off Rockport
Callocardia texasiana	—Few, dead in dredge hauls and on Gulf beach, never taken living
Dosinia discus	—Large valves common on Gulf beach, also few large individuals taken living, very small *Dosinia* common in upper sound
Chione intapurpurea	—Few dead, also found in deep shelf region
Labiosa plicatella	—Common dead on Gulf beaches
Labiosa lineata	—Common dead on Gulf beaches, occasionally taken living on shallow shelf
Donax tumida	—Extremely abundant in surf zone of Gulf beaches, living, common dead in somewhat deeper water to 3–5 fathoms
Abra lioica	—Common living in clayey bottoms on east slope of delta and shallow shelf
Quadrans lintea	—Few dead on shallow shelf, also found in inlets

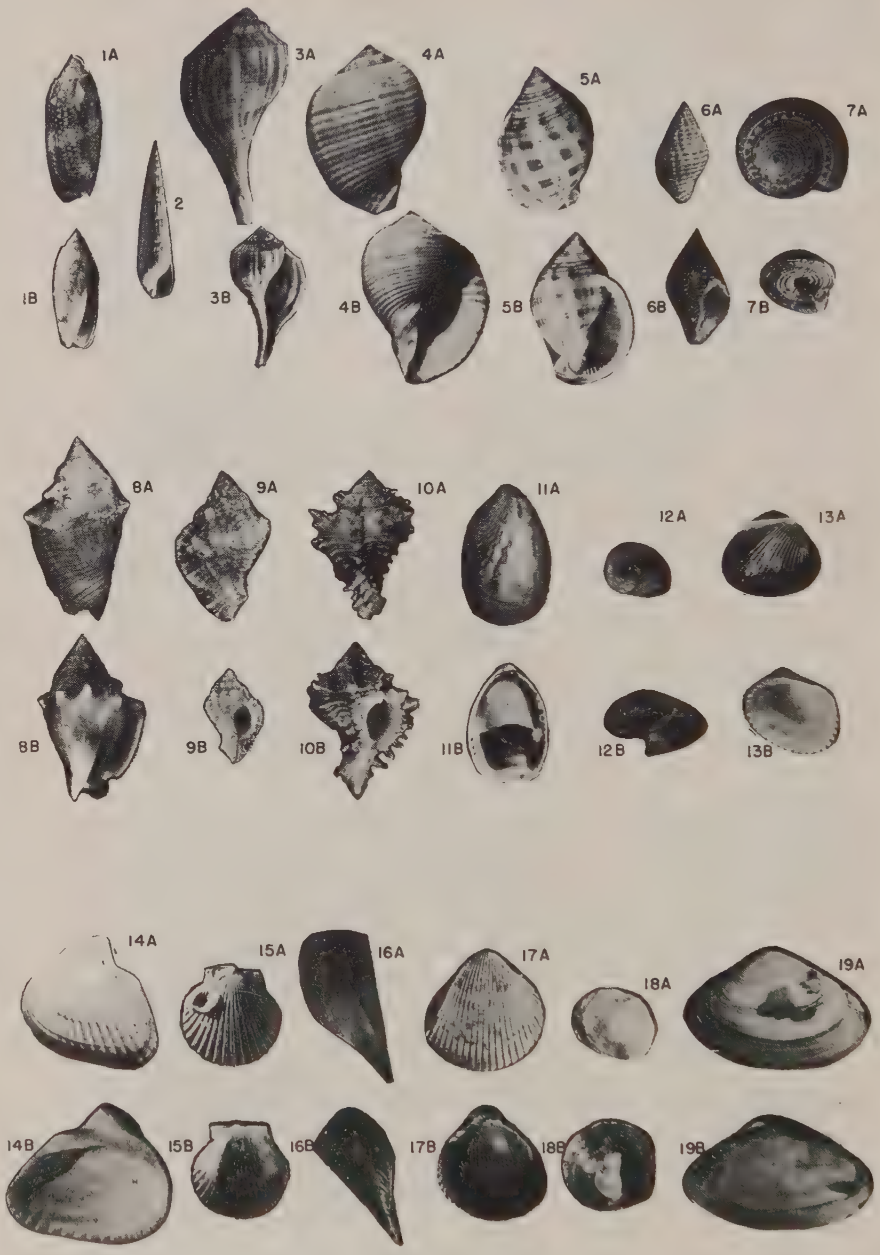
1A
3A
4A
5A
6A
7A
2
1B
3B
4B
5B
6B
7B
8A
9A
10A
11A
12A
13A
8B
9B
10B
11B
12B
13B
14A
15A
16A
17A
18A
19A
14B
15B
16B
17B
18B
19B

SHALLOW SHELF

PLATE V

Tellina versicolor	—Most abundant living on shallow shelf, although also found in upper sound and inlet
Strigilla mirabilis	—Most abundant (dead) on shallow shelf, few found in inlets and upper sound
Ensis minor	—Common living and dead on shallow shelf, although also found in inlets and upper sound to less extent
Panope bitruncata	—Found dead only on Gosier Island beach
COELENTERATES	
Renilla mülleri	—Extremely abundant on sand bottom off barrier islands to about 5 fathoms
Leptogorgia setacea	—Only dead strands found in delta, but very common on sand bottom off barrier islands on Texas coast
ECHINODERMS	
Luidia clathrata	—Common living on sand bottom near barrier islands
Luidia alternata	—Reported by Perrier (1876) as *Luidia variegata* taken alive from Gulf shores of Breton Island. Verrill (1919, p. 202) states this specimen was *L. alternata*, a species common on Texas coast
Astropecten antillensis	—Few living in outer part of shallow-shelf region, abundant, close to shore on Texas coast
Mellita quinquiesperforata	—Extremely common on sand bottom around barrier islands out to about 5 fathoms
Moira atropos	—At times, tests of this heart urchin forms large windrows on Gulf beaches, not taken living
POLYCHAETES	
Aglaophamus dicirris	—Common living on shallow shelf only
Prionospio, sp. and *Cossura*, sp.	—Extremely abundant in clayey sediments in shallow-shelf region close to delta
BRYOZOA	
Zoobytron, sp.	—At certain seasons, extremely abundant on shallow-shelf, filling shrimp trawls to exclusion of other invertebrates
CRUSTACEANS	
Ovalipes ocellatus	—Not uncommon on shallow-shelf out to at least 13 fathoms
Sicyonia dorsalis	—Abundant on shallow shelf, usually taken with other species of shrimp such as *Penaeus setiferus* and *Penaeus duorarum*, both found also in upper and lower sound. Shrimp were taken up in distributaries to head of Denise Pass in fall of 1954 according to Louisiana Department of Conservation (personal communication)

PLATE V

VI. SHALLOW SHELF ASSEMBLAGE

FIG. 1.—*Oliva sayana* Ravenel, 1834, size—43×17 mm., a. back, b. aperture.
FIG. 2.—*Terebra cinerea* (Born, 1778), size—32×7 mm., front or aperture.
FIG. 3.—*Busycon spiratum plagosum* Conrad, 1863, size—119×57 mm., a. back, b. front.
FIG. 4.—*Tonna galea* (Linné, 1758), size—51×36 mm., a. back, b. front or aperture.
FIG. 5.—*Phalium granulatum* (Born, 1778), size—59×40 mm., a. back, b. front.
FIG. 6.—*Cantharus cancellarius* (Conrad, 1846), size—30×17 mm., a. back, b. front.
FIG. 7.—*Architectonica nobilis* Röding, 1798, size—49×31 mm., a. top, b. aperture.
FIG. 8.—*Strombus alatus* Gmelin, 1790, size—85×54 mm., a. back, b. front.
FIG. 9.—*Murex pomum* (Gmelin, 1790), size—48×31 mm., a. back, b. front.
FIG. 10.—*Murex fulvescens* Sowerby, 1834, size—54×36 mm., a. back, b. front.
FIG. 11.—*Crepidula fornicata* (Linné, 1758), size—23×14 mm., a. exterior, b. interior.
FIG. 12.—*Janthina janthina* (Linné, 1758), size—16×21 mm., a. top, b. aperture.
FIG. 13.—*Anadara campechiensis* (Gmelin, 1790), size—38×30 mm., a. exterior, b. interior.
FIG. 14.—*Noetia ponderosa* (Say, 1822), size—32×28 mm., a. exterior, b. interior.
FIG. 15.—*Aequipecten irradians concentricus* (Say, 1822), size—62×44 mm., a. exterior, b. interior.
FIG. 16.—*Atrina serrata* (Sowerby, 1825), size—175×76 mm., a. exterior, b. interior.
FIG. 17.—*Dinocardium robustum* (Solander, 1786), size—96×90 mm., a. exterior, b. interior.
FIG. 18.—*Anomia simplex* d'Orbigny, 1842, size—21×20 mm., a. exterior, b. interior.
FIG. 19.—*Spisula solidissima similis* (Say, 1822), size—80×55 mm., a. exterior, b. interior.

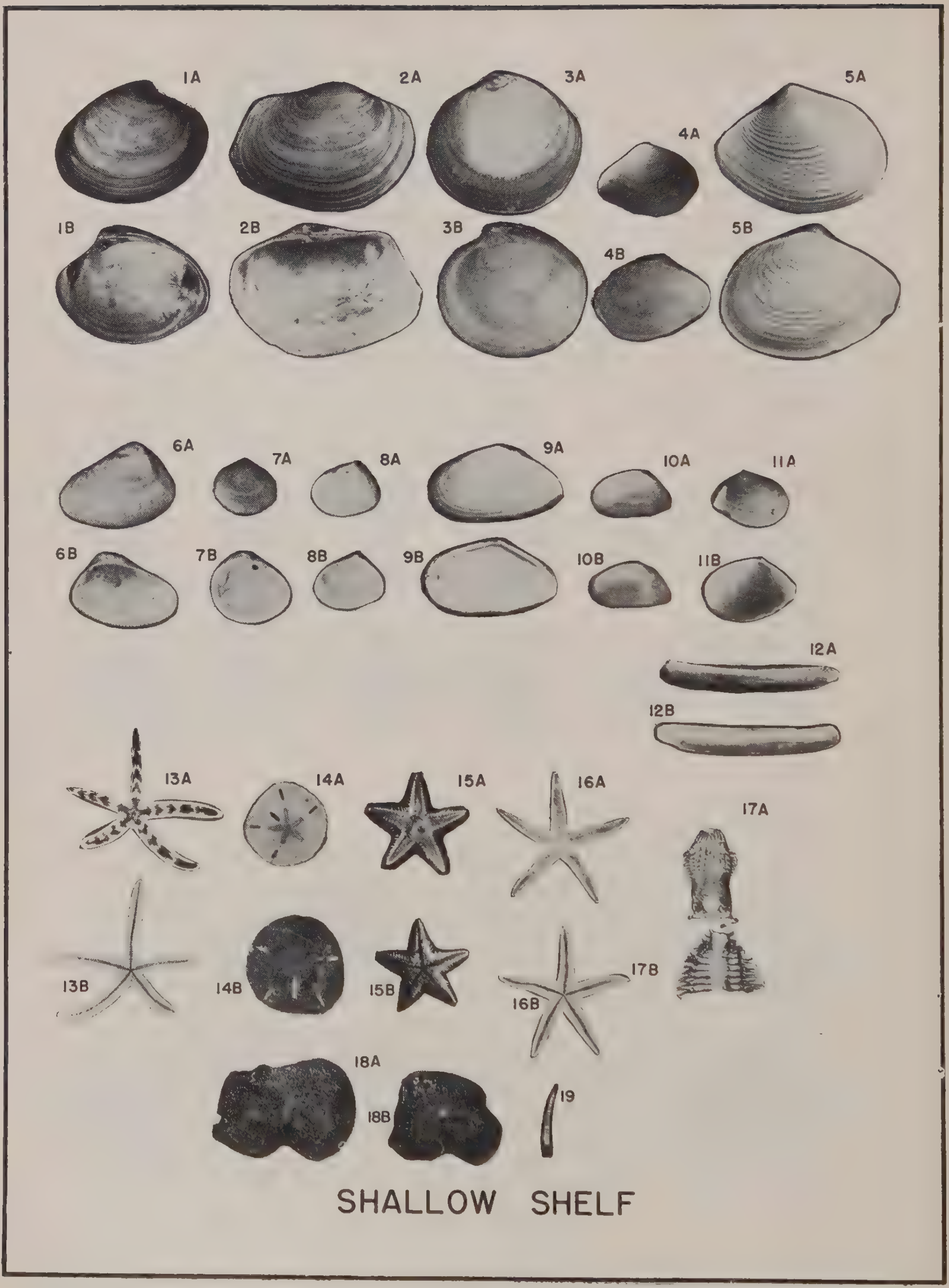
1A
2A
3A
4A
5A
1B
2B
3B
4B
5B
6A
7A
8A
9A
10A
11A
6B
7B
8B
9B
10B
11B
12A
12B
13A
14A
15A
16A
17A
13B
14B
15B
16B
17B
18A
18B
19
SHALLOW SHELF

Plate VI

XIPHOSURA	
Limulus polyphemus	—One specimen of horseshoe crab was found on Breton Island beach

VII. *Deeper continental shelf of Gulf of Mexico, from approximately 13 to 50 fathoms.*—At approximately 13 fathoms out from the barrier islands off the east Mississippi Delta, a distinct assemblage of animals is encountered. The species composing the major part of this group make an infrequent appearance at 13 fathoms, and increase in individuals per station out to at least 40 fathoms, which was the limit of biological sampling in this study (Fig. 12 shows limits of deep-shelf environment). Fresh specimens of these deep-shelf species are never found on the beaches and worn specimens are rare. A detailed description of the free-swimming epi-benthic or just-off-the-bottom assemblages of the "inshore" and "offshore" shrimp grounds off the Louisiana and Texas coasts is given by Hildebrand (1954), who characterizes the grounds inside 12–14 fathoms by the dominant organisms *Penaeus setiferus*, *Callinectes danae*, *Renilla mülleri*, and several species of fish, such as the sand sea trout, hardhead sea catfish, and croakers. The offshore grounds, extending from about 12 to 25 fathoms, were dominated by *Penaeus aztecus*, *Squilla empusa*, *Pitar cordata*, and the sea robin, *Prionotus rubio*. Hildebrand's study did not extend to the outer edge of the continental shelf, where a completely different type of fauna is found.

Since the physical-chemical conditions in the deeper Gulf of Mexico are by no means well known, the reasons for this separate assemblage beginning at 13 fathoms can only be guessed. It has been suggested by Pulley (1953), that the waters of the Gulf of Mexico at these depths seldom fall below 65°F. at any time during the year. An examination of unpublished temperature data at the United

---

PLATE VI

VI. SHALLOW SHELF ASSEMBLAGE (CONTINUED)

FIG. 1.—*Callocardia texasiana* (Dall, 1892), size—50×40 mm., a. exterior, b. interior.
FIG. 2.—*Panope bitruncata* (Conrad, 1872), size—160×106 mm., a. exterior, b. interior.
FIG. 3.—*Dosinia discus* (Reeve, 1850), size—73×71 mm., a. exterior, b. interior.
FIG. 4.—*Macoma constricta* Brugiére, 1792, size—59×41 mm., a. exterior, b. interior.
FIG. 5.—*Labiosa plicatella* (Lamarck, 1818), size—68×50 mm., a. exterior, b. interior.
FIG. 6.—*Donax tumida* Philippi, 1848, size—10×7 mm., a. exterior, b. interior.
FIG. 7.—*Strigilla mirabilis* (Philippi, 1841), size—10×9 mm., a. exterior, b. interior.
FIG. 8.—*Abra lioica* Dall, 1881, size—8×7 mm., a. exterior, b. interior.
FIG. 9.—*Tellina alternata* Say, 1822, size—52×29 mm., a. exterior, b. interior.
FIG. 10.—*Tellina versicolor* De Kay, 1843, size—12×6 mm., a. exterior, b. interior.
FIG. 11.—*Quadrans lintea* Conrad, 1837, size—16×12 mm., a. exterior, b. interior.
FIG. 12.—*Ensis minor* Dall, 1899, size—54×10 mm., a. exterior, b. interior.
FIG. 13.—*Luidia alternata* (Say, 1825), size—120×130 mm., a dorsal, b. ventral.
FIG. 14.—*Mellita quinquiesperforata* (Leske), size—53×46 mm., a. test, b. dorsal, live.
FIG. 15.—*Astropecten antillensis* Lütken, 1859, size—34 mm., a. dorsal, b. ventral.
FIG. 16.—*Luidia clathrata* (Say, 1825), size—95 mm., a. dorsal, b. ventral.
FIG. 17.—*Aglaophamus dicciris* Hartman, 1950, size—30 mm. long, a. and b. head and proboscis.*
FIG. 18.—*Renilla mülleri* Kölliker, size—75×58 mm., a. dorsal, b. ventral.
FIG. 19.—*Dentalium texasianum* Philippi, 1849, size—20 mm., side view.

* Drawing from Hartman, Olga, 1950, "Goniadidae, Glyceridae, and Nephytyidae," *Allan Hancock Expeditons*, Vol. 15, No. 1, p. 178.

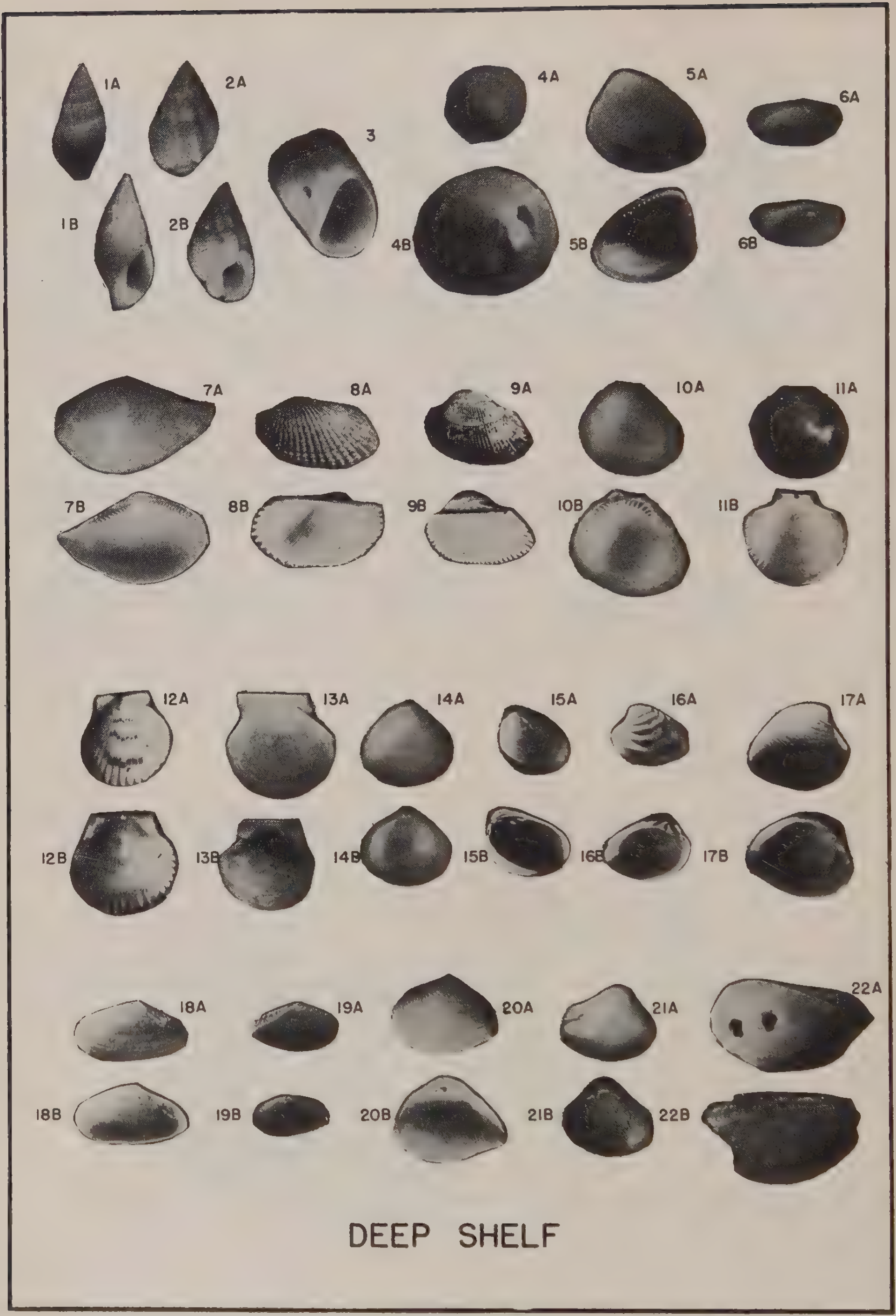
1A
2A
4A
5A
6A
3
1B
2B
4B
5B
6B
7A
8A
9A
10A
11A
7B
8B
9B
10B
11B
12A
13A
14A
15A
16A
17A
12B
13B
14B
15B
16B
17B
18A
19A
20A
21A
22A
18B
19B
20B
21B
22B
DEEP SHELF

Plate VII

States Navy Hydrographic Office substantiates this. Winter surface-water temperatures periodically fall well below 50°F. in the northern Gulf of Mexico, but it is thought that the bottom waters of the deeper shelf may be deep enough to escape the effects of intermittent seasonal cooling in the winter. The faunal affinity of this assemblage of organisms is close to West Indian or sub-tropical, since many of the species which are rare at these depths in the northern Gulf are plentiful in the shallower waters farther south.

One hundred and twenty-two species of macro-invertebrates were identified from this region, of which 21 species were found alive and 101 were found only as dead remains. Many more species of gastropods were collected, but because of the confusion existing in the systematics of certain groups, could not be identified to species. There are at least 42 good diagnostic species of macro-invertebrates from the deep-shelf region, and an equal number which appear to be good indicator species, although not as abundant as the first 42. The distributions of four mollusks repeatedly taken in offshore waters are illustrated as follows: the pelecypods *Cyclopecten nanus* Verrill and Bush (Fig. 24a), *Chione clenchi* Pulley (Fig. 24b), *Yoldia solenoides* Dall (Fig. 25a), and *Nucula proxima* Say (Fig. 25b). Two echinoderms, the cake urchin *Clypeaster prostratus* Ravenel, and the starfish *Astropecten articulatus valenciennesi* Müller and Troschel, are common living in the deeper shelf of the Gulf and fragments of another cake urchin, *Clypeaster raveneli* (A. Agassiz) were also taken offshore. Three species of corals, *Eupsammia floridana* (Pourtalès), *Eugorgia stheno* Bayer and *Bathycyathus*, sp.; one crustacean, the large boxcrab, *Calappa springeri* Rathbun; as well as many calcareous

---

PLATE VII

VII. Deep Shelf Assemblage

Fig. 1.—*Astyris perpicta* (Dall and Simpson, 1902), size—9×4 mm., a. back, b. front.
Fig. 2.—*Nassarius ambiguus consensus* Ravenel, 1861, size—8×5 mm., a. back, b. front.
Fig. 3.—*Polinices uberinus* d'Orbigny, 1842, size—6×8 mm., aperture.
Fig. 4.—*Calyptraea centralis* (Conrad, 1841), size—(large) 7×6 mm., (small) 4×3 mm. a., exterior, b. interior.
Fig. 5.—*Nucula proxima* Say, 1822, size—5×5 mm., a. exterior, b. interior.
Fig. 6.—*Yoldia solenoides* Dall, 1881, size—13×7 mm., a. exterior, b. interior.
Fig. 7.—*Nuculana acuta* Conrad, 1832 (offshore form), size—8×5 mm., a. exterior, b. interior.
Fig. 8.—*Anadara lienosa floridana* (Conrad, 1869), size—58×57 mm., a. exterior, b. interior
Fig. 9.—*Anadara baughmani* Hertlein, 1951, size—33×21 mm., a. exterior, b. interior.
Fig. 10.—*Limopsis sulcata* Verrill and Bush, 1898, size—11×10 mm., a. exterior, b. interior.
Fig. 11.—*Pecten papyraceus* (Gabb, 1873), size—58×54 mm., a. exterior, b. interior.
Fig. 12.—*Aequipecten gibbus gibbus* (Linné, 1758), size—27×26 mm., a. exterior, b. interior.
Fig. 13.—*Cyclopecten nanus* Verril and Bush, 1897, size—6×5.5 mm., a. exterior, b. interior.
Fig. 14.—*Gouldia cerina* (C. B. Adams, 1845), size—8×7 mm., a. exterior, b. interior.
Fig. 15.—*Laevicardium fiski* Richards, 1954, size—12×17 mm., a. exterior, b. interior.
Fig. 16.—*Chione clenchi* Pulley, 1952, size—18×15 mm., a. exterior, b. interior.
Fig. 17.—*Pitar cordata* Schwengel, 1951, size—43×48 mm., a. exterior, b. interior.
Fig. 18.—*Tellina georgiana* Dall, 1900, size—29×17 mm., a. exterior, b. interior.
Fig. 19.—*Phylloda squamifera* (Deshayes, 1854), size—16×10 mm., a. exterior, b. interior.
Fig. 20.—*Corbula swiftiana* C. B. Adams, 1852, size—6×4 mm., a. exterior, b. interior.
Fig. 21.—*Varicorbula operculata* (Philippi, 1848), size—9×7 mm., a. exterior, b. interior.
Fig. 22.—*Pandora bushiana* Dall, 1886, size—8×5 mm., a. exterior, b. interior.

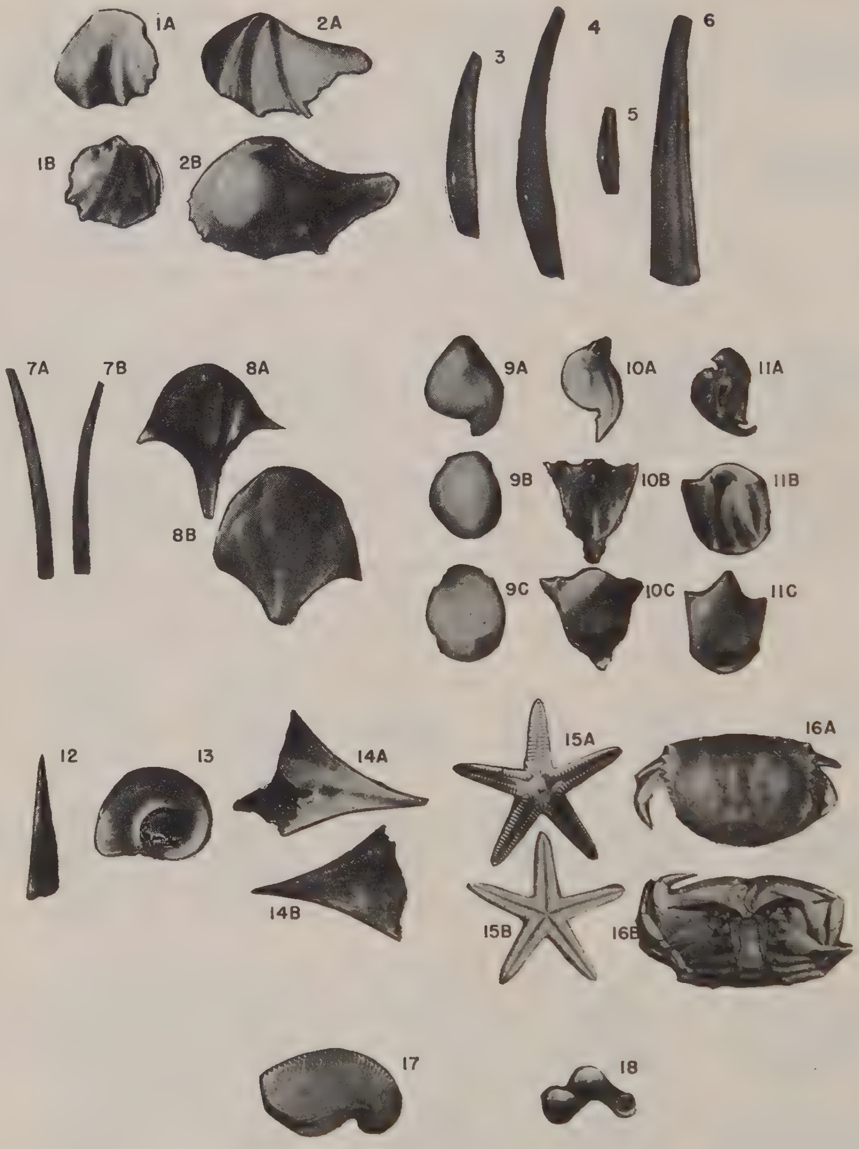
1A
2A
3
4
5
6
1B
2B
7A
7B
8A
8B
9A
10A
11A
9B
10B
11B
9C
10C
11C
12
13
14A
14B
15A
15B
16A
16B
17
18

DEEP SHELF

PLATE VIII

bryozoans, were taken in the deep-shelf region. Other mollusks which are characteristic of the deep-shelf region and frequently taken in shrimp trawls (Hildebrand, 1954) are *Anadara baughmani* Hertlein, *Anadara lienosa floridana* (Conrad), *Gouldia cerina* C. B. Adams, *Laevicardium pictum* Ravenel, *Laevicardium fiski* Richards, *Laevicardium laevigatum* Linné, *Limopsis sulcata* Verrill and Bush, *Tellina georgiana* Dall, *Nuculana acuta* (offshore variety), *Polinices uberinus* d'Orbigny, *Astyris perpicta* Dall and Stearns,[6] *Calyptraea centralis* Conrad, *Pitar cordata* Schwengel, *Pecten papyraceus* Gabb, *Corbula swiftiana* C. B. Adams, and *Cuspidaria ornatissima* (d'Orbigny). The list of all species of macro-invertebrates found in the deep-shelf environment is too long to be included separately, but most of them are indicated in Tables I and II, and representatives are illustrated in Plates VII and VIII. Several species which are common offshore near the Mississippi Delta but which were not recorded in this study are illustrated in Rehder and Abbott (1951).

ANIMAL COMMUNITY CONCEPT AS APPLIED TO MISSISSIPPI DELTA

Many European and American ecologists have attempted to define various marine environments or regions by the animal community which predominates in each particular region. Allee and Schmidt (1951), Petersen (1913), and Jones (1950) working in the more northern latitudes have introduced several classifica-

---

[6] Comparison with museum collections indicates that this is an undescribed species, and here and in text should be referred to as *Astyris*, species.

PLATE VIII

VII. Deep Shelf Assemblage (continued)

Fig. 1.—*Verticordia ornata* (d'Orbigny, 1846), size—4×4 mm., a. exterior, b. interior.
Fig. 2.—*Cuspidaria ornatissima* (d'Orbigny, 1846), size—9×6 mm., a. exterior, b. interior.
Fig. 3.—*Cadulus carolinensis* Bush, 1885, size—9×1 mm., side view.
Fig. 4.—*Cadulus arctus* Henderson, 1920, size—12×2 mm., side view.
Fig. 5.—*Cadulus mayori* Henderson, 1920, size—4×1 mm., side view.
Fig. 6.—*Dentalium laqueatum* (Verrill, 1885), size—27×5 mm., side view.
Fig. 7.—*Dentalium sowerbyi* (Guilding, 1834), size—10×.5 mm., a. and b. side views.
Fig. 8.—*Diacria trispinosa* ('Lesueur' Blainville, 1821), size—7×7 mm., a. and b. dorsal views.
Fig. 9.—*Diacria quadridentata* ('Lesueur' Blainville, 1821), size—2×1.5 mm., a. side, b. dorsal, c. ventral.
Fig. 10.—*Cavolinia ongirostris* 'Lesueur' Blainville, 1821, size—4.5×5.5 mm., a. side, b. dorsal, c. ventral.
Fig. 11.—*Cavolinia uncinata* 'Rang' d'Orbigny, 1836, size—3.5×4 mm., a. side, b. dorsal, c. ventral.
Fig. 12.—*Styliola subula* Quoy and Gaimard, 1827, size—6×1 mm., side view.
Fig. 13.—*Atlanta*, species (*A. peroni* Lesueur, 1817) ?, size—6×4 mm., dorsal view.
Fig. 14.—*Euclio pyramidata* (Linné, 1767), size—7×5 mm., a. dorsal, b. ventral.
Fig. 15.—*Astropecten articulatus valenciennesi* Müller and Troschel, size—92 mm., a. dorsal, b. ventral.
Fig. 16.—*Calappa springeri* Rathbun, 1931, size—101×67 mm. (carapace), a. dorsal, b. ventral.
Fig. 17.—*Argonauta argo* Linné, 1758, size—90×60 mm. (egg case), side view.
Fig. 18.—*Schizoporella umbellata* (Defrance), size—12 mm. diameter, 2 exterior, 1 interior colonies.

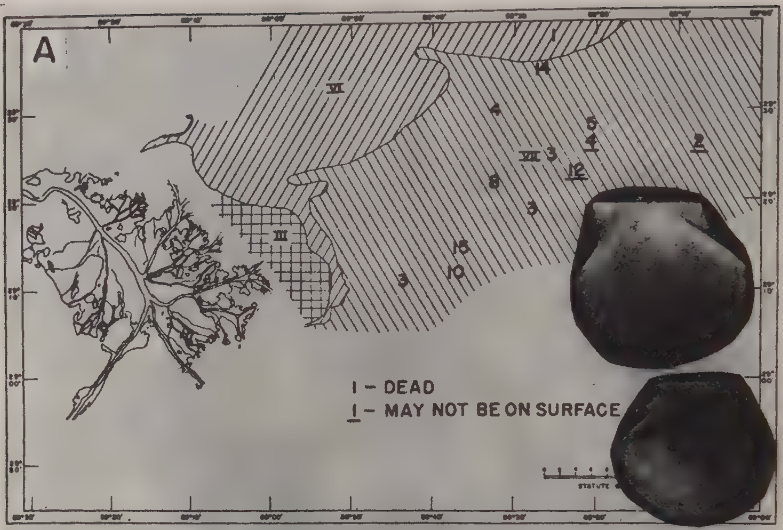
A
VI
14
4
5
4
2
VII 3
12
8
3
III
15
10
3
I - DEAD
I - MAY NOT BE ON SURFACE
STATUTE

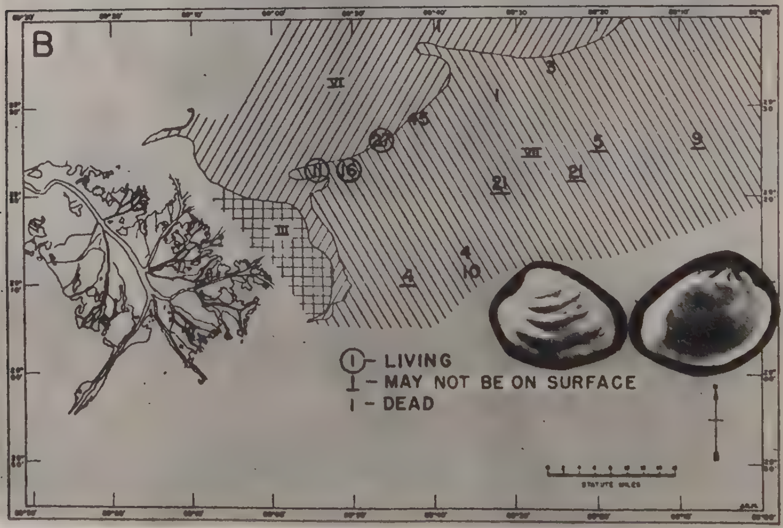
B
VI
3
1
45
27
11
16
VII
5
9
21
21
III
4
10
4
① - LIVING
I - MAY NOT BE ON SURFACE
I - DEAD
STATUTE MILES

FIG. 24a.—Distribution of pelecypod, *Cyclopecten nanus*, indicative of deep-shelf environment (all dead, underlined occurrences indicate specimens found at various depths in core samples).
FIG. 24b.—Distribution of pelecypod, *Chione clenchi*, indicative of deep-shelf environment.

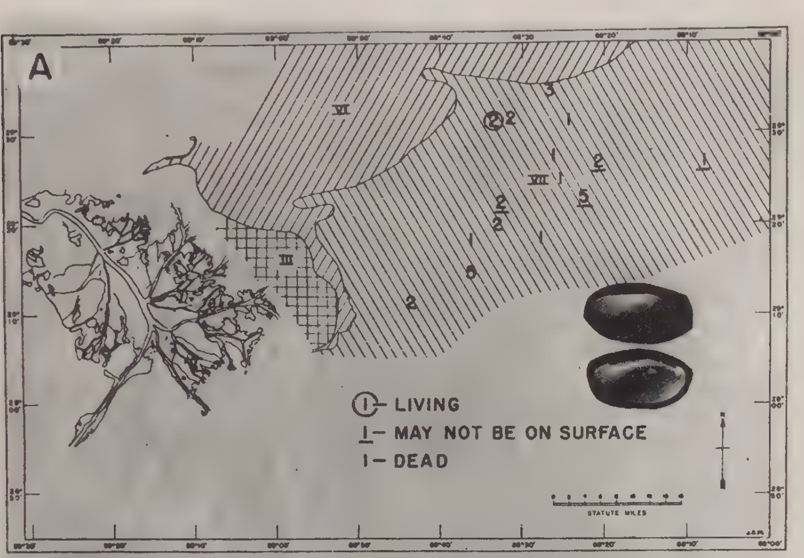
A
VI
VII
III
① – LIVING
1̲ – MAY NOT BE ON SURFACE
1 – DEAD
STATUTE MILES

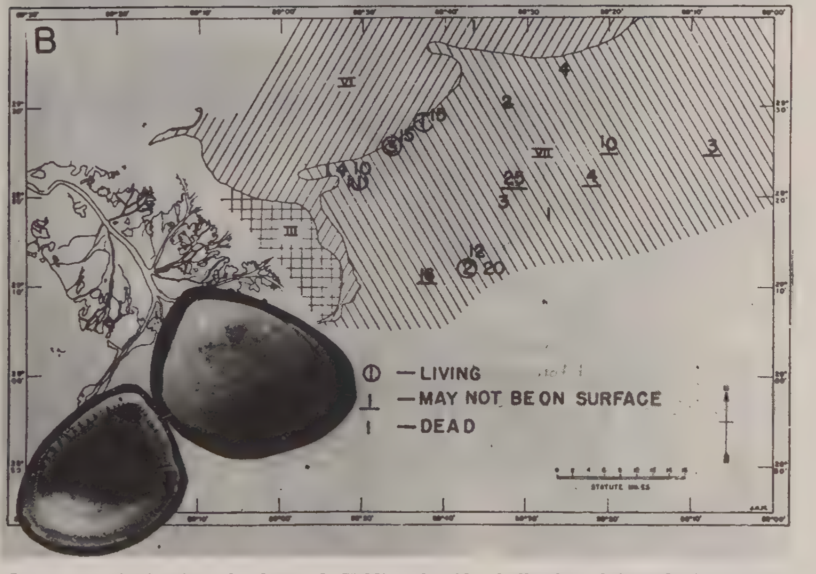
B
VI
VII
III
① – LIVING
1̲ – MAY NOT BE ON SURFACE
1 – DEAD
STATUTE MILES

FIG. 25a.—Distribution of pelecypod, *Yoldia solenoides*, indicative of deep-shelf environment.
FIG. 25b.—Distribution of pelecypod, *Nucula proxima*, indicative of deep-shelf environment.

tions of marine bottom communities based on the distribution of benthic invertebrates in relation to the character of the bottom sediments, temperature, salinity, light, and other physical and biological factors. Since more exact quantitative studies of bottom fauna than obtained by this study are needed to approximate the communities defined by Jones and Petersen, it is possible only to indicate the probable communities and dominant organisms. According to Hedgpeth in Galtsoff *et al.* (1954, pp. 207–10), the delta mud-bottom community is apparently "comparable to the *Syndosmya* (= *Abra*) community of 'shallow and protected waters of estuarine character' (Jones, 1950)." This suggestion was made before all the Delta material was analyzed, but apparently is still true, although there appears to be more than one community in this region.

Although *Mulinia lateralis* exists in large concentrations (as many as 200 per orange-peel sample) in the fine silty clay and clayey silt bottoms close to the shores of the active Delta, this species is not widespread, but localized (Fig. 15b). By referring to Table IV, which gives the number of station occurrences of the more abundant organisms in the delta region, it can also be seen that of the total 150 station occurrences of *Mulinia*, only 29 produced living specimens. However, the distribution of the dead remains of *Mulinia* (Tables I and II) shows that its shells occur at nearly every biological station in the inshore delta region. Where *Mulinia* was found living in large numbers it was present almost to the exclusion of any other invertebrates except *Nassarius acutus* and *Anachis obesa*, which are the two most abundant mollusks in station occurrences taken on this project. The other pelecypod which is rather abundant and is consistently found at every station with *Mulinia* is *Abra lioica* (Fig. 23b). If the distributions of *Mulinia*, *Abra lioica*, and *Nassarius acutus* along with those of *Polinices duplicatus* (Fig. 16a) and *Aglaophamus dicirris* (Fig. 22a) are compared, it can be seen that the probable community of the clayey bottoms near the delta is a *Mulinia-Nassarius* one in the shallow waters close to Main Pass, grading into a *Abra-Aglaophamus* one in deeper waters near Pass a'Loutre. Indications from the more detailed biological collecting in June, 1953, of the Pass a'Loutre region show that a species of *Cossura* (a polychaete) is extremely abundant in the silty clays off the mouth of Pass a'Loutre, and at some stations coated the bottom of the sifting screen to a depth of ½ inch. Individuals numbered in the thousands from one orange-peel sample. Associated with these small polychaetes in the bottom were *Abra lioica* and an occasional *Nassarius acutus*. It should be mentioned that this particular region appears to be a very productive shrimp-fishing area, since at the times of sampling concentrated trawling operations were taking place all around. It has been suggested by various workers on the Gulf of Mexico that the primary food of the commercial shrimp may be the small worms which live in the muddy or clayey bottoms where most shrimp are fished (Hedgpeth, personal communication). The observation of large numbers of polychaetes and large shrimp production from the same area supports this suggestion.

In the sand and poorly sorted sandy, silty clay bottoms in the upper sound

(3081)

Table IV. Station Occurrences of Abundant Species of Invertebrates Taken from All Stations in Mississippi Delta Region

Species	*Total Number of Station Occurrences*	*Number of Stations (Living)*	*Number of Stations (Dead)*
Gastropods			
Nassarius acutus	144	74	70
Anachis obesa	91	39	52
Olivella mutica	63	9	54
Polinices duplicatus	53	14	39
Cantharus cancellarius	41	8	33
Neritina reclivata	33	4	29
Crepidula plana	31	3	28
Retusa canaliculata	31	0	31
Natica pusilla	30	2	28
Anachis avara semiplicata	24	12	12
Oliva sayana	15	1	14
Terebra protexta	15	1	14
Busycon contrarium	14	5	9
Nassarius ambiguus consensus	14	0	14
Crepidula fornicata	13	0	13
Anachis avara similis	12	6	6
Thais haemastoma floridana	12	2	10
Astyris perpicta	11	1	10
Diodora cayenensis	9	1	8
Mitrella lunata	8	4	4
Busycon spiratum plagosum	8	1	7
Turbonilla hemphilli	8	1	7
Terebra dislocata	8	0	8
Polinices uberinus	8	0	8
Pteropods			
Cavolinia uncinata	8	0	8
Cavolinia longirostris	10	0	10
Pelecypods			
Mulinia lateralis	150	29	121
Abra aequalis	87	12	75
Tellina versicolor	86	17	69
Dosinia discus	85	4	81
Tagelus divisus	83	22	61
Lucina amiantus	63	14	49
Nuculana eborea	60	11	49
Anadara campechiensis	57	6	51
Mercenaria campechiensis texana	57	5	52
Crassostrea virginica	52	1	51
Tellina alternata	51	5	46
Anadara transversa	43	7	46
Macoma tenta	41	11	33
Trachycardium muricatum	38	5	33
Lucina crenella	34	1	33
Corbula swiftiana	33	5	28
Crassinella martinicensis	31	2	29
Pandora trilineata	30	2	28
Diplodonta semiaspera	28	4	24
Ostrea equestris	25	0	25
Anomia simplex	22	0	22
Anadara brasiliana	21	1	20
Nuculana acuta (nearshore)	21	0	21
Nuculana acuta (offshore)	20	4	16
Tellidora cristata	20	2	18
Abra lioica	24	16	8
Nucula proxima	19	4	15
Ensis minor	19	2	17
Semele proficua	19	1	18
Donax tumida	19	0	19
Cyrtopleura costata	19	0	19
Corbula contracta	16	1	15
Chione clenchi	15	3	12
Yoldia solenoides	13	1	12
Aequipecten gibbus gibbus	13	0	13
Cyclopecten nanus	13	0	13
Varicorbula operculata	13	0	13
Verticordia ornata	13	0	13
Brachidontes recurvus	12	0	12
Dinocardium robustum	12	0	12
Rangia flexuosa	11	0	11
Phylloda squamifera	10	1	9
Strigilla mirabilis	10	0	10
Rangia cuneata	9	1	8
Tellina lintea	9	0	9
Noetia ponderosa	8	1	7

Table IV—*(continued)*

Species	*Total Number of Station Occurrences*	*Number of Stations (Living)*	*Number of Stations (Dead)*
Diplodonta punctata	8	1	7
Petricola pholadiformis	8	1	7
Laevicardium fiski	8	0	8
Gouldia cerina	8	0	8
Chione intapurpurea	8	0	8
Labiosa plicatella	8	0	8
Macoma extenuata	8	0	8
Pandora bushiana	8	0	8
Macoma mitchelli	8	5	3
Scaphopods			
Dentalium texasianum	16	0	16
Cadulus carolinensis	14	0	14
Cephalopods			
Lolliguncula brevis	14	14	0
Hexacorals			
Astrangia astraeiformis	16	0	16
Pennatulids			
Renilla mülleri	13	13	0
Echinoderms (asteroids)			
Luidia clathrata	8	8	0
Ophiuroids			
Hemipholis elongata	10	10	0
Amphiodia limbata	24	24	0
Echinoids			
Mellita quinquiesperforata	24	18	6
Moira atropos	9	0	9
Polychaetes			
Diopatra cuprea	20	20	0
Glycera americana	9	9	0
Bryozoa			
Bugula neritina	46	46	0
Zoobytron, sp.	12	12	0
Membranipora, sp.	14	0	14
Cupuladria canariensis	9	3	6
Mamillipora cupula	7	2	5
Crustaceans			
Callinectes sapidus	25	23	2
Neopanope packardii	18	18	0
Squilla empusa	17	17	0
Pagurus floridanus	14	14	0
Penaeus setiferus	14	14	0
Penaeus duoarum	12	12	0
Callinectes danae	11	11	0
Libinia emarginata	8	8	0

and inlet region there are indications of a different community. Although many species of invertebrates are found in these environments, only a few are abundant enough and occur commonly enough to constitute a community. Of these, *Tagelus divisus* (Fig. 17a) is the most abundant (Table IV), occurring alive at 22 of 83 stations. Two other pelecypods which are important members of this community in numbers of individuals and station occurrences are *Tellina versicolor* and *Abra aequalis* (Table IV). Since the most common type of bottom in which this community lives is sand or a muddy sand, *Tagelus* and *Tellina* are to be expected (Allee and Schmidt, 1951, pp. 226–27). As in other communities on sand and muddy sand bottoms, there are large numbers of the brittle star, *Amphiodia* *limbata* (Fig. 18b); these occurred at 24 stations in the upper sound environment. The common polychaetes of this community are *Glycera americana* with 9 station occurrences and *Diopatra cuprea* with 20 station occurrences. This, then, is a sand or muddy sand-bottom community of shallow inshore waters and is characterized by the thin-shelled *Tellina* and *Tagelus*, a large population of brittle stars, and tube-building polychaete worms, for which the name *Tagelus-Amphiodia* community is proposed.

There is an indication that a separate community exists on the hard sand bottoms in the Gulf, adjacent to the barrier islands. The most abundant organism in this community is the sand dollar, *Mellita quinquiesperforata* (Fig. 23a), which occurred at 18 stations with as many as 50 specimens at one station. Another abundant echinoderm in this region is the asteroid *Luidia clathrata*, with 8 station occurrences and as many as 11 individuals at one station. An important member of this community is the sea pansy *Renilla mülleri* (Fig. 21b), found at 13 stations in this environment, with an average of 20–30 individuals per station. Hedgpeth in Galtsoff *et al.* (1954, p. 211) comments that *Renilla* is the most conspicuous member of the shrimp ground community and must pave the bottom in some localities. Hildebrand (1954) also mentions *Renilla* as one of the more abundant members of the "inshore" shrimp grounds. The common pelecypods of this community are *Tellina alternata*, *Macoma tenta*, *Strigilla mirabilis*, and *Ensis minor* (Table IV gives number of station occurrences), all thin-shelled members of the family Tellinidae except *Ensis*, which is closely related to the Tellinidae. This community might be designated the *Mellita-Renilla-Tellina* community of the shallow-shelf sand bottoms.

Not enough quantitative or distributional data are available to adequately describe the deep-shelf clay and sand or muddy sand-bottom community. Observations from the present study and Hildebrand's work indicate that other prominent members providing hard parts of the deep clayey bottom community are probably a starfish, *Astropecten articulatus valenciennesi*, a large crab, *Calappa springeri*, the shrimp, *Penaeus aztecus*, and two pelecypods, *Pecten papyraceus* and *Anadara baughmani*. Sand or predominantly sand bottoms are comparatively rare in the deeper waters of the northern Gulf of Mexico, and little information is available concerning the abundant invertebrates from this type of environment.

BOTTOM SEDIMENTS AS INFLUENCING DISTRIBUTION OF MACRO-ORGANISMS IN MISSISSIPPI DELTA REGION

It is generally recognized that the type of bottom sediment has a pronounced influence on the distribution of animal communities. The principal studies of relationship of organisms to bottom sediments have been made in Europe, initiated by the classic work of Petersen (1913–1915). In the United States the earliest attempt to relate marine benthic fauna distribution to substrate was by Verrill (1873), in Vineyard Sound, Massachusetts. Several papers since then have been published on distributions of invertebrates related to bottom sediments in North America, although all have been in colder waters in the Atlantic and Pacific (Sumner, Osburn, and Cole, 1911; Packard, 1918; Allee, 1923; Lee, 1944; and Pratt, 1953). Jones (1950) recently discussed the bottom communities of European waters.

In the present study, the biological station locations were first superimposed upon detailed sediment distribution charts shown in Figures 6a and 6b. It was observed that the distributions of many of the benthic macro-invertebrates agreed closely with the distribution of certain types of sediments. For example, the distribution of living *Nuculana eborea* was very closely related to the distribution of silty clays in the lower sound region (Fig. 26a), while the distributions of *Mellita quinquiesperforata* and *Renilla mülleri* were in good agreement with the distribution of hard sand bottom in the vicinity of Breton Island (Fig. 27a and b). The heavily concentrated populations of *Mulinia lateralis* (more than 30 living individuals per orange-peel grab sample) were practically all found in the clayey silt or silty clay types of sediment, and occurred primarily in the fall season (Fig. 26b). Since these heavy concentrations of *Mulinia* were found only on clayey types of bottom, and these sediments were located both in the shallow-shelf parts of the Delta shores and in the lower Sound regions (all areas of differing chlorinity and temperature), the major factor associated with the distribution of this pelecypod was apparently bottom type.

With the exception of *Mulinia* and *Nuculana eborea* at some of the stations, most of the stations occupied in silty clay areas produced few or no organisms. Typical stations with little or no biological material in them from clayey areas are: BS 22, BS 25, BS 46, BS 47, GM 54, PL 354, and PL 352 (Fig. 28a gives locations of the inshore stations with no biological material). The same is also true for the stations on the very hard sand bottom (Fig. 28a), although this may have been the function of the sampling devices which were not designed to take large biological samples in sand areas. The principal difference between the fauna on the hard sand bottoms and on the clayey bottoms was the presence of many living starfish, sand dollars, and sea pansies on the sand bottoms, although echinoid plates are common in the deep-shelf clays.

On the other hand, sampling from areas of predominantly poorly sorted sand and silty clays of varying concentrations produced a very abundant and varied invertebrate population, including many species of macro-organisms confined to this type of substrate. The distributions of two pelecypods, *Tagelus divisus* and *Macoma tenta* (Say) (Figs. 29a and b), are superimposed upon the distribution of sandy, silty clays and other poorly sorted sediments. A striking example of differences in invertebrate populations between deep-shelf clays and the deep-shelf sandy, silty clays can be observed by comparing the distribution of stations containing few or no organisms in the surface sediments, composed of silty clay, with that of similar stations located on coarser sediments (Fig. 28b). Stations from the deep-shelf silty clays produced very few or no mollusks (except pteropod and scaphopod fragments) and several echinoid spines and plates. Fisk *et al.*

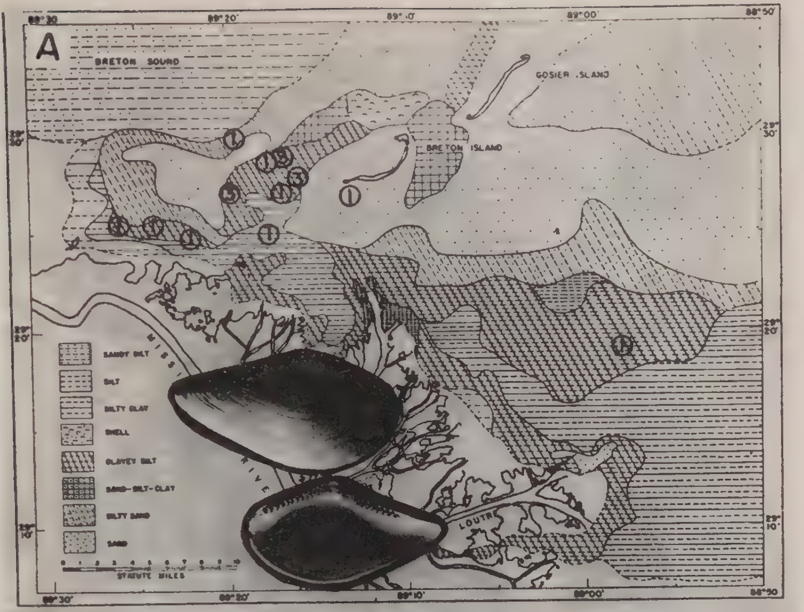
A
BRETON SOUND
GOSIER ISLAND
BRETON ISLAND
LOUTRE
SANDY SILT
SILT
SILTY CLAY
SHELL
CLAYEY SILT
SAND-SILT-CLAY
SILTY SAND
SAND
STATUTE MILES
89°30'
89°20'
89°10'
89°00'
88°50'
29°30'
29°20'
29°10'

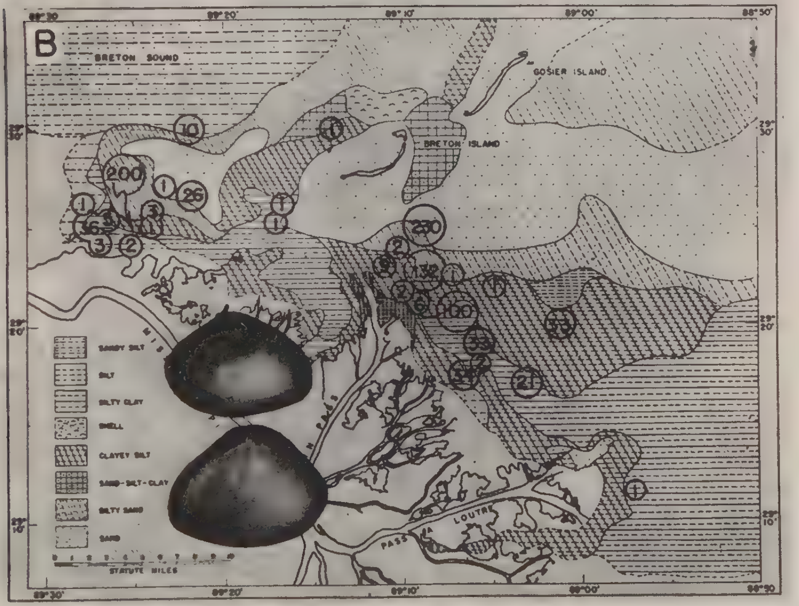
B
BRETON SOUND
GOSIER ISLAND
BRETON ISLAND
PASS A LOUTRE
SANDY SILT
SILT
SILTY CLAY
SHELL
CLAYEY SILT
SAND-SILT-CLAY
SILTY SAND
SAND
STATUTE MILES
200
230
132
100
36
33
27
26
10
89°30'
89°20'
89°10'
89°00'
88°50'
29°30'
29°20'
29°10'

FIG. 26a.—Distribution of living *Nuculana eborea* as related to distribution of sediment types in inshore Mississippi Delta region.

FIG. 26b.—Distribution of living *Mulinia lateralis* as related to distribution of sediment types in inshore Mississippi Delta region.

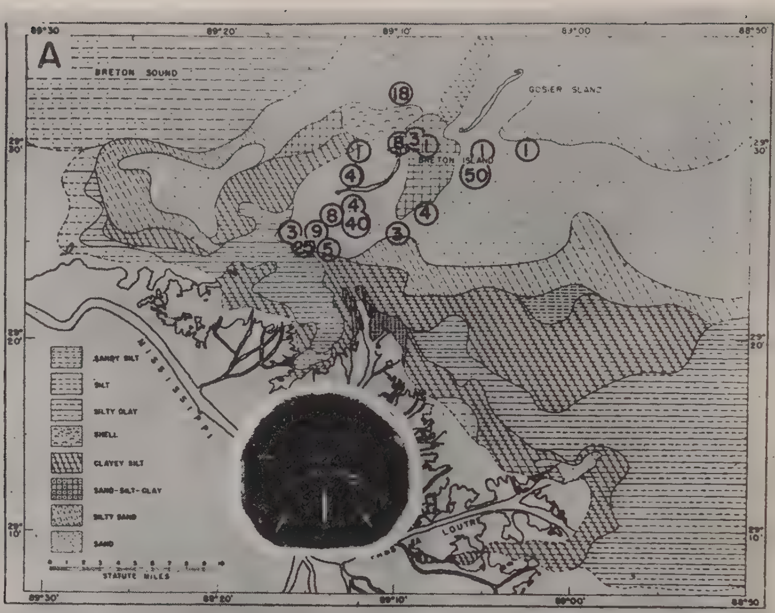
A
BRETON SOUND
GOSIER ISLAND
BRETON ISLAND
MISSISSIPPI
LOUTRE
PASS
89°30'
89°20'
89°10'
89°00'
88°50'
29°30'
29°20'
29°10'
18
1
6
3
1
1
1
50
4
4
40
8
9
3
25
5
3
4
SANDY SILT
SILT
SILTY CLAY
SHELL
CLAYEY SILT
SAND-SILT-CLAY
SILTY SAND
SAND
STATUTE MILES

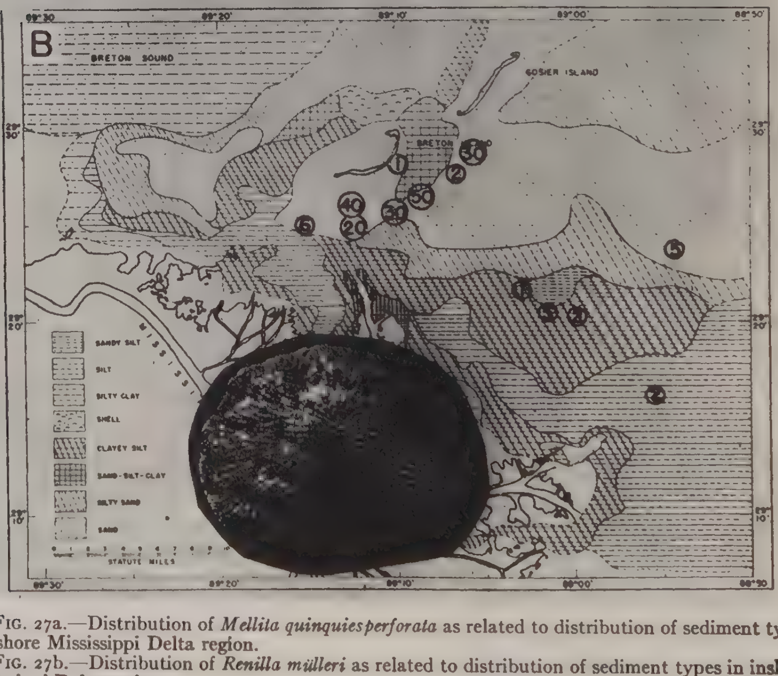
B
BRETON SOUND
GOSIER ISLAND
BRETON
MISSISSIPPI
89°30'
89°20'
89°10'
89°00'
88°50'
29°30'
29°20'
29°10'
1
50
12
50
40
20
30
5
SANDY SILT
SILT
SILTY CLAY
SHELL
CLAYEY SILT
SAND-SILT-CLAY
SILTY SAND
SAND
STATUTE MILES

FIG. 27a.—Distribution of *Mellita quinquiesperforata* as related to distribution of sediment types in inshore Mississippi Delta region.

FIG. 27b.—Distribution of *Renilla mülleri* as related to distribution of sediment types in inshore Mississippi Delta region.

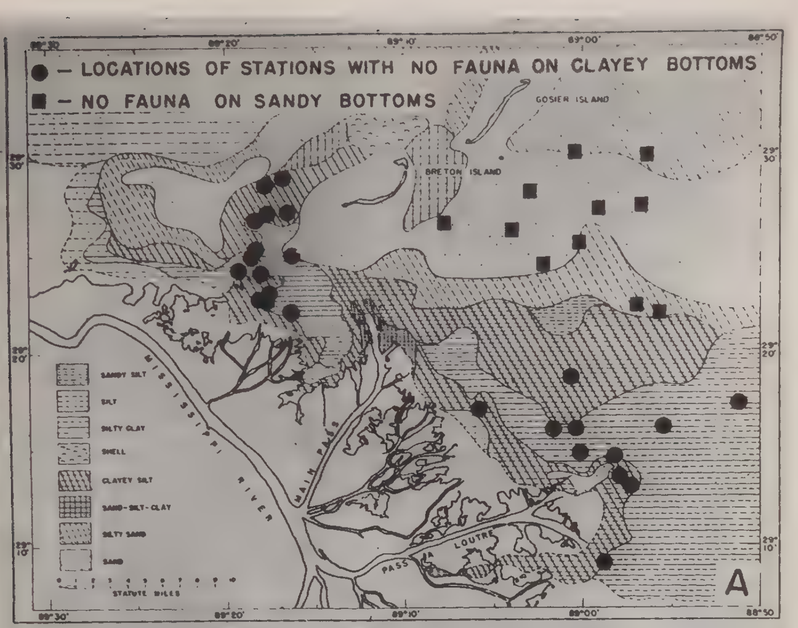
● — LOCATIONS OF STATIONS WITH NO FAUNA ON CLAYEY BOTTOMS
■ — NO FAUNA ON SANDY BOTTOMS
GOSIER ISLAND
BRETON ISLAND
MISSISSIPPI RIVER
MAIN PASS
PASS A LOUTRE
SANDY SILT
SILT
SILTY CLAY
SHELL
CLAYEY SILT
SAND-SILT-CLAY
SILTY SAND
SAND
STATUTE MILES
89°30'
89°20'
89°10'
89°00'
88°50'
29° 30'
29° 20'
29° 10'
A

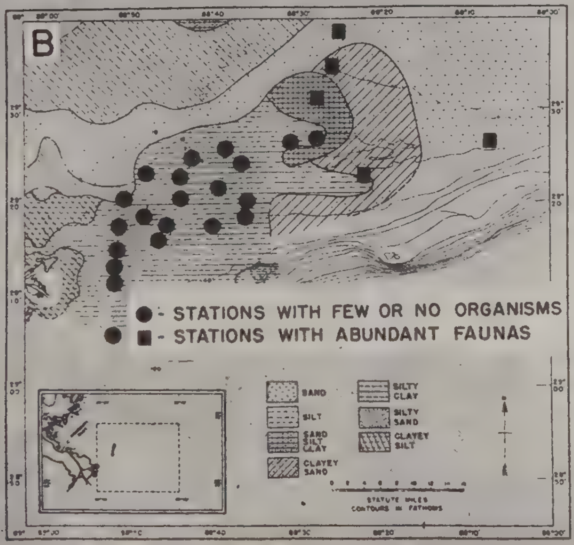
B
● - STATIONS WITH FEW OR NO ORGANISMS
■ - STATIONS WITH ABUNDANT FAUNAS
SAND
SILT
SAND SILT CLAY
CLAYEY SAND
SILTY CLAY
SILTY SAND
CLAYEY SILT
STATUTE MILES
CONTOURS IN FATHOMS
89°00'
88°50'
88°40'
88°30'
88°20'
88°10'
88°00'
29° 30'
29° 20'
29° 10'
29° 00'
28° 50'

FIG. 28a.—Relationship between sediment type and stations where no organisms were taken in inshore Delta region.

FIG. 28b.—Relationship of stations with no organisms on clayey bottoms, and stations with abundant fauna on sandy clay or sandy, silty clay bottoms.

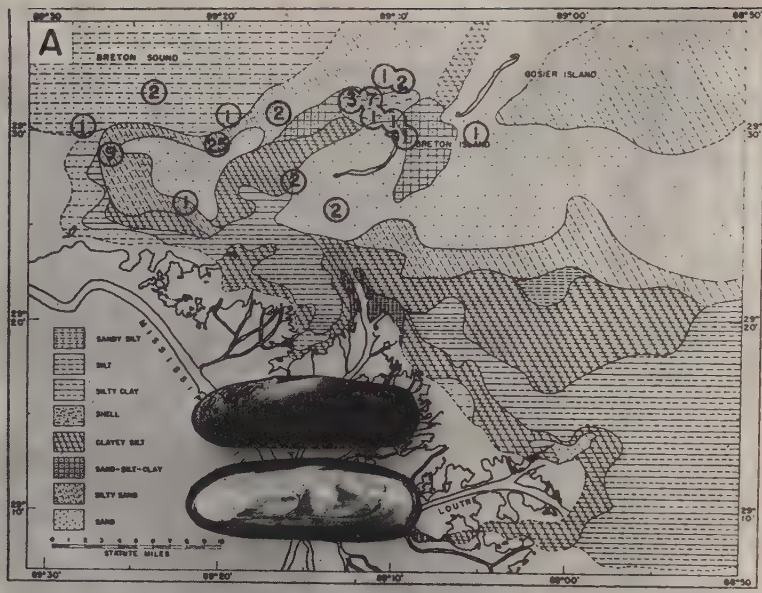
A
89°30'
89°20'
89°10'
89°00'
88°50'
29°30'
29°20'
29°10'
BRETON SOUND
GOSIER ISLAND
BRETON ISLAND
MISSISSIPPI
LOUTRE
SANDY SILT
SILT
SILTY CLAY
SHELL
CLAYEY SILT
SAND-SILT-CLAY
SILTY SAND
SAND
STATUTE MILES

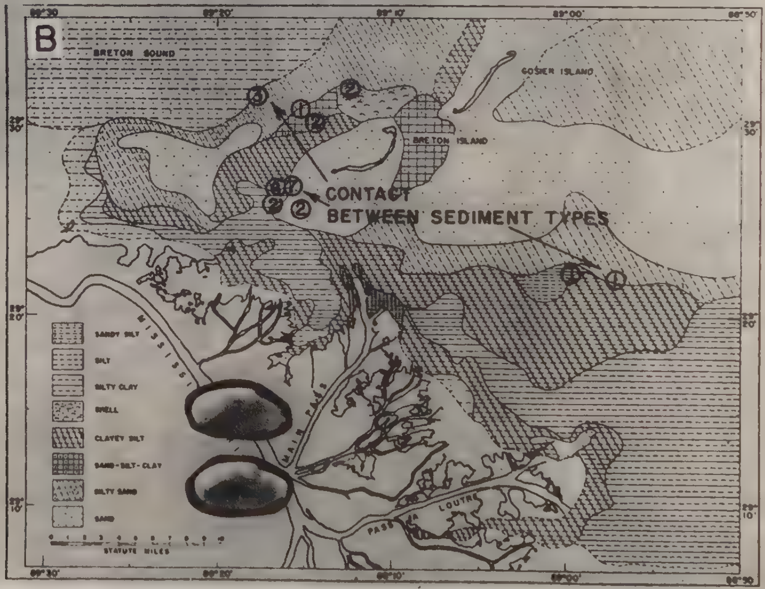
B
89°30'
89°20'
89°10'
89°00'
88°50'
29°30'
29°20'
29°10'
BRETON SOUND
GOSIER ISLAND
BRETON ISLAND
CONTACT
BETWEEN SEDIMENT TYPES
MISSISSIPPI
MAIN PASS
PASS A LOUTRE
SANDY SILT
SILT
SILTY CLAY
SHELL
CLAYEY SILT
SAND-SILT-CLAY
SILTY SAND
SAND
STATUTE MILES

FIG. 29a.—Distribution of *Tagelus divisus* as related to distribution of sediment types (poorly sorted or mixed sediments) in inshore Mississippi Delta region.

FIG. 29b.—Distribution of *Macoma tenta* as related to distribution of sediment types (particularly at contacts between sediments) in inshore Delta region.

(1954, p. 87) also mention abundant scaphopods, bryozoans, and echinoids in the clays of the outer shelf. The stations such as GM 244, GM 309, GM 383, GM 393, and GM 394 (Figs. 4 and 28b) on the coarse sediments were productive, at least in dead shell, and, where sampling techniques were successful with an orange-peel grab, an abundant living population was found.

Organisms as possible indicators of rates of deposition.—Although this study did not produce quantitative results which can be interpreted as numbers of organisms per station, comparative results were obtained with the orange-peel and biological material from the top 15 centimeters of the cores taken by the geologists. Counts of macro-organisms from orange-peel and core samples which were taken in areas of rapid deposition, such as the "pro-delta silty clay" region (Scruton, 1956), where deposition can take place at the rate of 1–2 feet per year, show either very little material living or dead, or fairly large numbers of living forms, and practically no dead material. In areas where the deposition rate is relatively slow, such as the deep-shelf coarse deposits, and the shell-sand deposits of upper Breton Sound, there were comparatively few living forms in relation to the large number of dead shells in the form of large shell deposits with very many mollusk species represented. This was especially true of the deep-shelf areas where littoral and beach deposits were exposed on the bottom at depths of 30–35 fathoms (Fig. 30). The fact that so few dead representatives of the very common living species are found on the surface in areas of rapid sedimentation can be explained by the rapid burial of those individuals as they die, while the living mollusks maintain themselves on or near the surface. Since it is not likely that the whole population dies at once, there would be a considerable layer of sediment over each individual which dies and becomes part of the sediment column. This was observed in several cores from the pro-delta slope region, where many live individuals were preserved at the top of the cores, and only a few single shells were found throughout the rest of the cores.

In areas without recent deposition, there might be the same number of living individuals in the surface sediments as in the rapid depositional area, but instead of being covered by a layer of sediment after death, those individuals would lie at the surface among the living population. Over a period of years or centuries, along with changing hydrographic conditions, there would be many generations and species representing the changing ecological conditions, making up a shell deposit. This is illustrated by some deep-shelf deposits (Fig. 30) where there were large numbers of dead specimens of species representing shallow, low-salinity environments mixed with many dead specimens and living representatives of species now living in the deep-shelf region. Table V shows the comparative numbers of living and dead macro-organisms from stations in rapid depositional and non-depositional areas.

The indication of depositional rate of sediments by the ratio of live *versus* dead organisms has been suggested by F. B Phleger, who has worked out this principle in more detailed analyses, using foraminiferal assemblages (Phleger,

TABLE V. COMPARISON OF NUMBERS OF LIVING AND DEAD MACRO-ORGANISMS FROM RAPID DEPOSITIONAL AND NON-DEPOSITIONAL AREAS, MISSISSIPPI DELTA

*Station Number**	*Number of Species*	*Number of Specimens (Living)*	*Number of Specimens (Dead)*
Stations from rapid-depositional areas: 1–2 feet depth change per year			
BS 25 BOP	4	6	1
BS 26 BOP	4	2	3
BS 27 BOP	6	9	6
BS 46 BOP	2	2	1
GM 57 BOP	5	24	3
GM 58 BOP	1	39	14
GM 61 BOP	4	106	3
BS 142a BOP	5	3	3
BS 165 BOP	1	1	0
PL 324 BOP	1	4	0
PL 325 BOP	2	6	0
PL 326 BOP	2	4	5
PL 329 BOP	2	6	1
PL 334 BOP	2	2	3
PL 342 BOP	4	2	11
MP 666 BOP	3	4	10
MP 667 BOP	1	2	0
Average, 17 stations	2.9 species	13 living specimens	3.8 dead specimens
Stations from non-depositional areas: no depth change, or scour, in 30–50 years			
BS 32 BOP	23	13	40
BS 34 BOP	19	2	60
BS 36 BOP	17	10	22
BS 38 BOP	27	25	64
BS 70 BOP	20	6	31
BS 72 BOP	15	8	38
BS 73 BOP	22	12	43
BS 74 BOP	36	19	74
BS 75 BOP	25	3	65
BS 76 BOP	47	21	151
BS 80 BOP	19	14	23
BS 81 BOP	15	10	18
BS 153 BOP	14	2	52
BS 154 BOP	28	15	128
BS 180 BOP	18	2	88
BS 171 BOP	22	10	80
BS 188 BOP	32	11	97
Average, 17 stations	23.5 species	10.8 living specimens	63.2 dead specimens

* Orange-peel grab samples.

1951, pp. 64–67, and personal communication). Phleger suggests that relative sedimentation rates can be obtained by comparing the distribution of the living benthonic Foraminifera with those of the empty tests. Moore (1955) used total numbers of Foraminifera per unit volume of sediment to determine rates of deposition, assuming a constant rate of production.

INFLUENCE OF WATER TEMPERATURE UPON DISTRIBUTION OF MACRO-INVERTEBRATES IN MISSISSIPPI DELTA REGION

Most of the biogeographic regions in the sea have been based on the distribution of animals in relation to the distribution of maximum and minimum sea temperatures (Hutchins, 1947; Allee and Schmidt, 1951, pp. 325–43; Ekman, 1953, pp. 1–308; Sverdrup, Johnson, and Fleming, 1942, pp. 799–810; and Phleger, 1951, pp. 59–63). Pulley (1953) established a series of zoögeographic provinces on the Atlantic coast and in the Gulf of Mexico based on the distribution of pelecypods in relation to mean maximum summer and mean minimum water temperatures (Fig. 31). Essentially, the criteria used in establishing Pul-

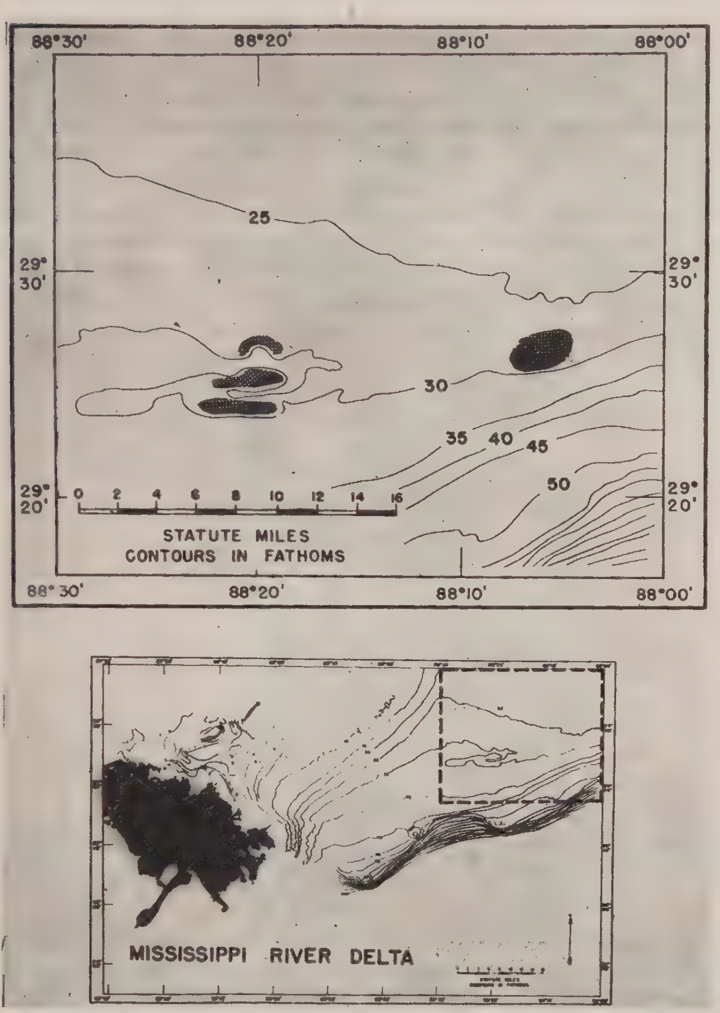
88°30'
88°20'
88°10'
88°00'
29° 30'
29° 20'
25
30
35
40
45
50
0 2 4 6 8 10 12 14 16
STATUTE MILES
CONTOURS IN FATHOMS
MISSISSIPPI RIVER DELTA

FIG. 30.—Location of deep-shelf littoral deposits containing oyster shell (*Crassostrea virginica*), marsh snails (*Littorina irrorata*), and Gulf beach clams (*Donax tumida*) from surface sediments. Note resemblance of bottom contours to barrier island or peninsula.

ley's temperature provinces are those stated in Hutchins (1947), who maintains that there are four basic types of zonation of marine animals with boundaries poleward and equatorward. These four criteria are: (1) minimum temperature for survival or winter poleward boundary, (2) minimum temperature for repopulation (reproduction) or summer poleward boundary, (3) maximum temperature for repopulation or winter equatorward boundary, and (4) maximum temperature for survival or summer equatorward boundary. Pulley found that wherever natural divisions of the coast occurred in relation to natural temperature divisions (breaks in mean minimum and mean maximum inshore temperatures, such as Cape Hatteras, Cape Canaveral, Cape Romano, Anclote Keys, the mouth of the Mississippi), he also found breaks in distribution of a large number of species of pelecypods. These breaks were usually indicated by the presence of the larval stages or juveniles in the northern part of the species range, but an absence of adults (which may not have been collected, but could have been present), indicating that the water temperatures are too cold for adult survival; and by the presence of adults alone in the southern part of these faunal breaks, indicating that the water was too warm for reproduction. According to the series of 11 faunal provinces proposed by Pulley (1953), the shallow inshore region of the east Mississippi Delta region falls into the "northeast Gulf of Mexico province," with the Anclote Keys on the west coast of Florida as its eastern boundary, and the Mississippi River Delta on the west (Fig. 31). Pulley states that the mean maximum summer water temperature for this province is between 88° and 89°F., and the range of mean winter water temperatures is approximately 57° to 60°F. On the other hand, the waters west of the Mississippi River (which contain many mol-

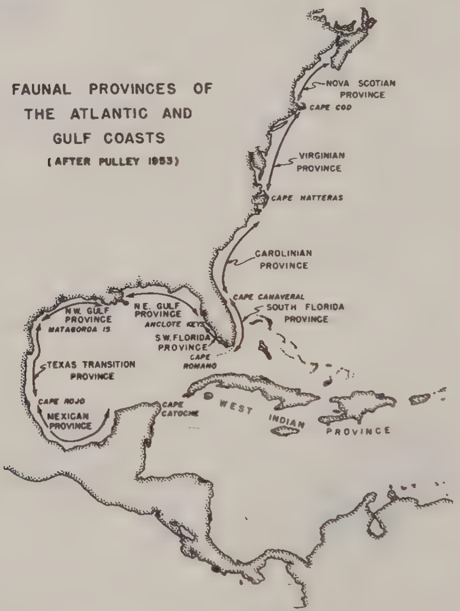
FAUNAL PROVINCES OF
THE ATLANTIC AND
GULF COASTS
(AFTER PULLEY 1953)
NOVA SCOTIAN PROVINCE
CAPE COD
VIRGINIAN PROVINCE
CAPE HATTERAS
CAROLINIAN PROVINCE
CAPE CANAVERAL
SOUTH FLORIDA PROVINCE
N.W. GULF PROVINCE
MATAGORDA IS.
N.E. GULF PROVINCE
ANCLOTE KEYS
S.W. FLORIDA PROVINCE
CAPE ROMANO
TEXAS TRANSITION PROVINCE
CAPE ROJO
MEXICAN PROVINCE
CAPE CATOCHE
WEST INDIAN PROVINCE

FIG. 31.—Location of molluscan faunal provinces on Atlantic and Gulf coasts as proposed by Pulley (1953).

lusks that were not found east of the river) were reported by Pulley to have a mean maximum water temperature of 90°F., and mean minimum winter water temperatures of between 46° and 48°F., which may account for the difference between molluscan fauna on opposite sides of the Delta. There has been some question about the application of the temperature data cited by Pulley (tide-station data from the Coast and Geodetic Survey Publication TW-1) to the distributions of animals which range out to 40–60 feet deep. Many of the tide stations are located very close to shore in sheltered localities, and water temperature data from those stations are thought to represent only very local conditions. However, Scruton (manuscript) states that the minimum observed water temperature in Breton Sound is approximately 52°F. (11°C.) and has an average maximum of 88°–89°F. (31°–32°C.), and that these extreme variations do not extend to depths greater than approximately 30–40 feet in the immediately adjacent Gulf.

There are also indications from the positions of the surface and 200-meter isotherms in the Gulf of Mexico (Fuglister, 1947 and 1954) that warm water swings closer to the shore near the delta and the northeastern Gulf than in the northwestern Gulf (Fig. 32). This hypothesis of warmer waters closer to the shore in the east Delta region is verified to some degree by the fact that many of the West Indian or subtropical mollusks are taken in 10–12 fathoms offshore of the Chandeleur Islands, while these same species are not found in less than 15–20 fathoms offshore of the Texas coast, with the exception of Sabine and Heald banks off Galveston, Texas (personal communication from Willis G. Hewatt for the Magnolia Petroleum Company, Field Research Laboratories, and Hildebrand, 1954), where warmer bottom-water isotherms are further offshore. The region just north of the Delta area also has many Florida shallow-water species, such as *Melongena corona* Gmelin and *Scaphella junonia johnstoneae* Clench,

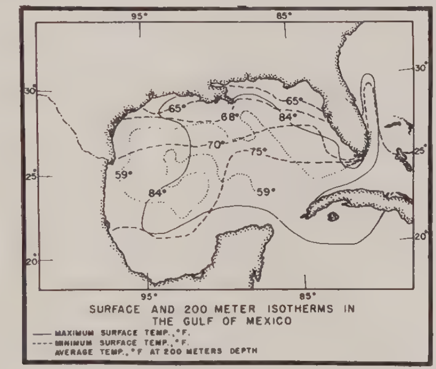
95°
85°
30°
25°
20°
65°
68°
65°
84°
70°
75°
59°
84°
59°
95°
85°
SURFACE AND 200 METER ISOTHERMS IN THE GULF OF MEXICO
—— MAXIMUM SURFACE TEMP., °F.
---- MINIMUM SURFACE TEMP., °F.
AVERAGE TEMP., °F AT 200 METERS DEPTH

FIG. 32.—Surface (maximum and minimum) and 200-meter (average) isotherms of Gulf of Mexico, showing warmer water closer to shore in east Delta region. Data taken from Fuglister (1947, 1954).

which have not been reported west of Mississippi Sound (Clench, 1953, p. 376).

If the mean minimum and mean maximum bottom-water temperatures are among the more important factors for limiting the distribution of benthic invertebrates, these factors can be used to explain in part the faunal discontinuity which appears in approximately 12–15 fathoms off the Mississippi Delta. These deep-shelf waters of the study area fall partly into Pulley's "offshore West Indian province," which consists of the outer part of the continental shelf of the northern Gulf of Mexico from 25–35 fathoms to approximately 100 fathoms. According to Pulley (1953), the temperatures at the upper level should be near 65° or 70°F. and at the lower level from 55° to 60°F. These figures were originally obtained from Phleger (1951) and have since then been verified by temperature studies of the Gulf of Mexico by Adams and Sorgnit (1951) and Scruton (manuscript). The offshore temperature data are discussed by Scruton for this project, and he indicates that the average temperature varies from approximately 78°F. at the surface to 68°F. at a depth of 330 feet (Fig. 10). The average range of temperature at the surface is 9.8°C. (49°F.) and at 330 feet about 2.5°C. (36.5°F.). The deep-shelf bottom-water extremes differ radically from those of the inshore bottom water extremes where the average bottom water can range from 52° to 89°F. (Fig. 9, and Scruton, manuscript). These temperature observations may explain the occurrence of many species of invertebrates on the outer shelf of the northern Gulf of Mexico, which occur normally in the shallow waters of southwestern Florida and the Gulf of Campeche, Mexico (Galtsoff *et al.*, 1954, pp. 472–73, and Table VI). To date, few of the species in Table VI have been found in the shallow-shelf waters of the northern Gulf of Mexico, where apparently the mean minimum winter air temperatures which are effective to at least 60 feet are too low for either survival of the adults or for reproduction.

Richards (1954) cites a number of these deep-shelf species from deep borings made in the Delta region, and explains their occurrence (as warmer-water forms) by the lack of the cooling influence of the Mississippi River waters at the time the shells were deposited, about 450 years ago. These same species are common now in water depths of from 12 to 50 fathoms along most of the northern Gulf coast; therefore, it is not necessary to attribute these species to the absence of cooler Mississippi River waters. It is probable that the thin overlying river water could not exert a cooling influence on bottom waters at these depths. Their presence may be explained on the basis of warmer deep water at the time of deposition.

DISTRIBUTION OF MARINE MACRO-INVERTEBRATES AS INFLUENCED BY SALINITY

Many workers in marine ecology have determined that certain organisms are confined to, or apparently prefer, waters of either low or high salinities. Ladd (1951), working with brackish-water and marine assemblages on the Texas coast, based his communities or facies on the distributions of marine invertebrates and Foraminifera, and found that there were relationships between the

TABLE VI. PUBLISHED* RANGE OF SOME SPECIES OF MOLLUSKS FOUND AT 15–50 FATHOMS OFF MISSISSIPPI RIVER DELTA

Species	*Depth Range off Mississippi Delta (Fathoms)*	*Published Geographic Range*
GASTROPODS		
Crucibulum auricula	25–40	Cedar Keys, Fla., to Barbados, West Indies
Polinices uberinus	20–40	N. Carolina to Caribbean (not on NW. Florida coast)
Murex recurvirostrus rubidus	25–30	South half of Florida and to Bahamas
Nassarius ambiguus consensus	15–40	N. Carolina, south Florida to Bahamas, from 0 to 100 fathoms
Oliva caribaeensis	30–40	Puerto Rico, Caribbean Sea in shallow water
Marginella aureocincta	20–40	N. Carolina to both sides of Florida and West Indies
Ancystocyrinx radiata	25–40	Cedar Keys, west Florida to West Indies
Arene variabilis	30–40	N. Carolina, east Florida and West Indies, to 20 fathoms
Acteon candens	30–60	N. Carolina, SE. Florida to Cuba in 2–6 fathoms
Scaphander watsoni	30–40	Florida Keys to Bahamas
PELECYPODS		
Pinna carnea	20–30	SE. Florida and West Indies and Mexico
Chlamys sentis	25–40	N. Carolina, SE. Florida, West Indies at low-tide mark
Aequipecten muscosus	20–40	N. Carolina, both sides of Florida to West Indies, shallow
Aequipecten gibbus gibbus	20–40	Southern Florida to West Indies and Mexico in shallow water
Cyclopecten nanus	13–40	West Indies and Mexico in shallow water
Lima pellucida	20–35	Cedar Keys, Fla., to West Indies, in shallow water
Lucina sombrerensis	20–40	Known only from Miami and Florida Keys in 20 fathoms
Phacoides nassula	30–35	South Florida, Cape San Blas to Bahamas
Divaricella quadrisulcata	30–40	East coast from Cape Cod to West Indies, in shallow water
Echinochama cornuta	13–40	Florida Keys, West Indies, and Mexico in shallow water
Laevicardium pictum	20–40	South Florida to West Indies and Mexico, 3–100 fathoms
Gouldia cerina	15–40	South Florida to West Indies and Brazil in shallow water
Pitar simpsoni	30–35	SW. Florida, Cuba, Caribbean and Veracruz, Mexico
Macrocallista maculata	30–40	Alabama to West Indies, S. Texas to Campeche banks
Chione grus	25–40	Southern Florida and Campeche banks in shallow water
Semele bellastriata	30	Florida Keys, West Indies to Brazil, in 13–16 fathoms
Phylloda squamifera	13–40	South half of Florida and Campeche banks, 1–20 fathoms
Tellina georgiana	20–40	West Indies and Florida Keys in 10 fathoms
Strigilla mirabilis	5–40	South Florida, West Indies, and Mexico
Macoma extenuata	20–40	Cape San Blas, Florida to Florida Keys
Tellina texana	20–40	S. Carolina, south Florida, Florida Keys, and West Indies
Varicorbula operculata	13–40	Florida Keys to West Indies and Port Isabel, Texas, to Campeche
Corbula dietziana	30–40	Southern Florida and Campeche banks in shallow water
Pandora bushiana	12–40	Known only from SW. Florida in 13–19 fathoms
Verticordia ornata	20–40	South half of Florida to West Indies in 2 fathoms
Cuspidaria ornatissima	25–40	Florida Keys, West Indies, and Port Isabel, Texas
Cuspidaria granulata	25–40	Known only from Miami, Fla., and West Indies

* References used:
Abbott, R. Tucker, 1954, *American Seashells.*
Dall, W. H., 1889, "A Preliminary Catalogue of Shell-Bearing Marine Mollusks," *U. S. Natl. Museum Bull. 37*
Johnson, C. W., 1934, "List of Marine Mollusca of the Atlantic Coast from Labrador to Texas," *Proc. Boston Soc. Nat. Hist.*, Vol. 40, pp. 1–204.
Pulley, Thomas E., 1953, "A Zoogeographic Study Based on the Bivalves of the Gulf of Mexico," *Ph.D. dissertation,* Harvard University.

distributions of certain species with the increasing salinity gradient from river mouth to the open Gulf of Mexico. Gunter (1950) also discussed at length the relationship between invertebrate distribution and salinity in the Texas bays. Both Ladd and Gunter arrived at the conclusion that the distribution of invertebrates in these bays was controlled primarily by salinity. Hedgpeth (1953), Puffer and Emerson (1953), and Parker (1955) also discuss the importance of salinity in influencing the distribution of Gulf coast macro-organisms.

In the Texas area, although salinity conditions are more or less stable over long periods of time, they fluctuate seasonally, and tend to fluctuate only in the upper or lower ranges over several years' duration (Parker, 1955). This is not the case in the east Mississippi Delta region, where bottom salinities in some shallow-water areas can fluctuate as much as $18\,^{\circ}/_{\circ\circ}$ in a very short time throughout the year (Geyer, 1950; Scruton, manuscript). It is also evident that no enclosed hydrographic system exists in the delta area similar to the Rockport, Texas, region, where a river empties into an enclosed bay, and communication with the Gulf waters is restricted to a few narrow, shallow inlets. The delta region is almost completely open to the discharge of the Mississippi River distributaries and to the influx of Gulf water. This results in rather broad areas of somewhat unstable salinity characteristics with no fixed boundaries. Because this region is open to the Gulf, there is only a narrow fringe of the delta shores and perhaps some of the small bays close to and between the distributaries, with conditions comparable with those of the upper bays of the Rockport area. It is only in the narrow fringe of the delta that the species which are common in the Rockport low-salinity assemblage were found, such as *Macoma mitchelli* and *Rangia cuneata*. Apparently the only areas near the delta which contain relatively stable salinity characteristics needed for the continual growth of oyster reefs such as found in the Rockport area, are the shallow protected bays such as Quarantine, Coquille, and California bays west and north of the project area (Fig. 14). The fact that small oyster reefs also exist behind Breton Island indicates that this area is also protected enough to maintain relatively stable salinities.

Salinity is also a major factor influencing the distribution of macro-invertebrates in the shallow-shelf area. The species which are confined to Gulf waters, or occasionally come into parts of the sounds near the inlets, are those which are adapted to fairly high, stable salinities. They have not been reported from the bays on other parts of the northern Gulf coast, but are common on the shallow parts of the shelf along the entire northern Gulf coast. Although Breton Sound salinities are generally high enough to permit many species of invertebrates to exist there, they are still too low and variable for those species which seem to prefer normal Gulf salinities of 32–36 °/₀₀. Harry (1942), Behre (1950), Hildebrand (1954), and Parker (1955) list many of the organisms which are found only in the higher Gulf salinities. The deep-shelf waters of typical high salinity are also characterized by pelagic open-ocean mollusks whose presence can be detected in the underlying sediments by abundant pteropod shells and an occasional egg case of *Argonauta argo* Linné, the paper nautilus, as well as a few remains of species of the gastropod genus *Janthina*.

It may be significant that there is an increasing number of species in the samples proceeding outward into the Gulf of Mexico. The marshes contained 2.1 per cent of the total number of species, or 5 species; the delta front, 9.4 per cent, or 22 species; the lower sound and pro-delta slopes, 19.7 per cent, or 46 species; the upper sound, 39.9 per cent, or 93 species; the inlets, 42.9 per cent, or 100 species; the shallow shelf, 34.8 per cent, or 81 species; and the deep shelf, 52.4 per cent, or 122 species, of all species taken. The inlet has somewhat more species than either the upper sound or shallow shelf, which is to be expected since species from both environments are found there plus endemic species. The number of index or characteristic species of invertebrates also increases from the marshes to the outer edge of the shelf, with only 2–6 species characteristic for the very nearshore areas, increasing to 30–40 index species in the stable upper sound and deep-shelf

(324)

areas. This increase in numbers of species outward into the Gulf corresponds roughly with the degree of stability of the physical factors, particularly salinity in the delta region. These factors close to the delta and its distributaries are extremely variable and tend to stabilize in narrower ranges outward from the delta, so that the deep-shelf region has the largest number of species associated with a very narrow range of salinity and temperature.

APPLICATION OF MACRO-INVERTEBRATE DISTRIBUTIONS IN MISSISSIPPI DELTA TO ANCIENT MARINE ENVIRONMENTS

It may be possible to apply several features of the distribution of macro-organisms found in the Delta area to ancient environments and fossil assemblages preserved at least to the Pleistocene and Pliocene, and probably to the Miocene of the Gulf and south Atlantic coasts. All the species considered characteristic for the Recent delta environments are known to have been present in the Pleistocene, and the majority of the species have been found in the Pliocene sediments of the Gulf coast. Maury (1920, 1922) lists 17 species of gastropods and 40 species of pelecypods found in this present study as extending to lower Miocene. Richards (1947), in a study of the deep wells on the Atlantic coast, cites 38 species of mollusks from the Pleistocene, of which 32 have been found living in the delta; 46 from the Pliocene, of which 23 were found in the delta; and 209 species from the Miocene, of which 29 were found in the delta. None of the delta species was listed from the Cretaceous, although most of the genera found in the Cretaceous have species represented in the Recent of the Delta region. Richards (1939, p. 1894), in a list of invertebrate fossils from the marine Pleistocene of Texas, indicates that more than 90 per cent of these species are living to-day along the Gulf of Mexico coast, and thus it can be seen that most of them are species which occur living in the project area. Table VII gives the published distribution in geologic time of the mollusks used here to establish the macro-organism assemblages and to define environments (the following give details on geologic ranges used in compiling this table: Gardner, 1926–1947; Dall, 1898–1903; Maury, 1920, 1922; Richards, 1939, 1947; Moore, Lalicker, and Fischer, 1952; and Shrock and Twenhofel, 1953).

Since many of the macro-invertebrates which serve to define the environments in this study have also been found as fossils as far back as the Miocene, it should be possible to reconstruct some ancient environments on the following characteristics.

1. River deltas and mainland shores with associated salt marshes could be detected in the sediments by the presence of numerous wood and plant fibers in association with the gastropods *Neritina reclivata* and *Littorina irrorata*, and possibly the claws and carapaces of various species of fiddler crabs, *Uca*, and crayfish, *Cambarus*.

2. The shorelines of deltas and river mouths or areas where chlorinity is continually reduced below 10 °/₀₀ should be characterized by the presence of the

TABLE VII. GEOLOGIC RANGE OF SPECIES AND RELATED SPECIES OF MACRO-ORGANISMS FROM EAST MISSISSIPPI DELTA REGION*

Species	*Recent*	*Pleistocene*	*Pliocene*	*Miocene*	*Range of Related Species and Genera*
Abra aequalis M	xxxxx	xxxxx	xxxxx	xxxxx	Genus to lower Oligocene
Abra lioica M	xxxxx	xxxxx			Genus to lower Oligocene
Aequipecten i. amplicostatus M	xxxxx	xxxxx	xxxxx	xxxxx	Genus to Jurassic
Aequipecten g. gibbus M	xxxxx	xxxxx	xxxxx	xxxxx	Genus to Jurassic
Aequipecten musocus M	xxxxx				Genus to Jurassic
Amphiodia limbata E	xxxxx				Related forms to Miocene
Anachis avara ssp. M	xxxxx	xxxxx			Related species and genus to Miocene
Anachis obesa M	xxxxx	xxxxx	xxxxx		Genus to Miocene
Anadara baughmani M	xxxxx				Related species to Jurassic
Anadara brasiliana M	xxxxx	xxxxx	xxxxx	xxxxx	Related species through Miocene
Anadara lienosa floridana M	xxxxx	xxxxx			Related species to Jurassic
Anadara campechiensis M	xxxxx	xxxxx	xxxxx	xxxxx	Related species through Miocene
Anadara transversa M	xxxxx	xxxxx	xxxxx	xxxxx	Genus to Jurassic
Anomia simplex M	xxxxx	xxxxx	xxxxx	xxxxx	Genus to Cretaceous
Architectonica nobilis M	xxxxx	xxxxx	xxxxx	xxxxx	Genus to Upper Cretaceous
Astrangia astraeiformis CO	xxxxx	xxxxx	xxxxx	xxxxx	Genus to Cretaceous
Astyris perpicta M	xxxxx				Genus to Miocene
Atrina rigida M	xxxxx	xxxxx			Related forms to Jurassic
Atrina serrata M	xxxxx	xxxxx	xxxxx		Related forms to Jurassic
Brachidontes exustus M	xxxxx	xxxxx	xxxxx		Genus to Triassic
Brachidontes recurvus M	xxxxx	xxxxx	xxxxx		Genus to Triassic
Bugula neritina B	xxxxx				Related forms to Cretaceous
Busycon contrarium M	xxxxx	xxxxx	xxxxx	xxxxx	Related species to Upper Cretaceous
Busycon spiratum plagosum M	xxxxx	xxxxx	xxxxx	xxxxx	Related species to Upper Cretaceous
Cadulus carolinensis	xxxxx	xxxxx			Related species to Cretaceous
Calliactis tricolor CO	xxxxx				Anemone remains(?) (*Mackenzia*) in Cambrian rocks
Callocardia texasiana M	xxxxx	xxxxx			Related genus to Paleocene
Calyptraea centralis M	xxxxx	xxxxx	xxxxx	xxxxx	Related species to Upper Cretaceous
Cantharus cancellarius M	xxxxx	xxxxx			Related forms to Eocene
Cavolinia uncinata M	xxxxx	xxxxx			Related species to Miocene
Cerithium floridanum M	xxxxx	xxxxx	xxxxx		Genus to Cretaceous
Chione cancellata M	xxxxx	xxxxx	xxxxx	xxxxx	Related forms to Jurassic
Chione clenchi M	xxxxx				Closely related species to Miocene
Chione latilirata M	xxxxx	xxxxx	xxxxx	xxxxx	Genus to Cretaceous
Clypeaster prostratus E	xxxxx				Genus to Miocene
Corbula contracta M	xxxxx	xxxxx	xxxxx		Genus to Triassic
Corbula swiftiana M	xxxxx	xxxxx	xxxxx	xxxxx	Related species to Triassic
Crassinella martinicensis M	xxxxx	xxxxx	xxxxx	xxxxx	Genus to Eocene
Crassostrea virginica M	xxxxx	xxxxx	xxxxx	xxxxx	Related forms to Triassic
Crepidula fornicata M	xxxxx	xxxxx	xxxxx	xxxxx	Genus to Upper Cretaceous
Crepidula plana M	xxxxx	xxxxx	xxxxx	xxxxx	Genus to Upper Cretaceous
Crucibulum auricula M	xxxxx	xxxxx	xxxxx	xxxxx	Genus to Miocene
Cuspidaria ornatissima M	xxxxx				Genus to Jurassic
Cyclopecten nanus M	xxxxx				Related species to Miocene
Cyrtopleura costata M	xxxxx	xxxxx	xxxxx		Genus to Jurassic
Dentalium laqueatum M	xxxxx				Related forms to Ordovician
Dentalium texasianum M	xxxxx	xxxxx			Related species to Ordovician
Dinocardium robustum M	xxxxx	xxxxx	xxxxx	xxxxx	Related forms to Upper Cretaceous
Diodora cayenensis M	xxxxx				Related species to Miocene, genus to Cretaceous
Diopatra cuprea P	xxxxx				Polychaete jaws and tubes from Cambrian
Diplodonta punctata M	xxxxx	xxxxx	xxxxx		Genus to Paleocene
Diplodonta semiaspera M	xxxxx	xxxxx	xxxxx		Genus to Paleocene
Divaricella quadrisulcata M	xxxxx	xxxxx	xxxxx	xxxxx	Genus to Upper Paleocene
Donax tumida M	xxxxx	xxxxx			Genus to Eocene
Dosinia discus M	xxxxx	xxxxx	xxxxx		Genus to Eocene
Echinochama cornuta M	xxxxx	xxxxx	xxxxx	xxxxx	Genus to Oligocene
Ensis minor M	xxxxx	xxxxx	xxxxx	xxxxx	Genus to Eocene
Glycera americana P	xxxxx				Polychaete jaws and tubes from Cambrian
Gouldia cerina M	xxxxx				Closely related species to lower Eocene
Hemipholis elongata E	xxxxx				Related forms to Miocene
Labiosa lineata M	xxxxx				Related species to Miocene
Labiosa plicatella M	xxxxx	xxxxx	xxxxx	xxxxx	Genus to Jurassic
Laevicardium laevigatum M	xxxxx	xxxxx	xxxxx	xxxxx	Genus to Triassic
Laevicardium pictum M	xxxxx				Genus to Triassic
Limopsis sulcata M	xxxxx	xxxxx	xxxxx	xxxxx	Related forms to Cretaceous
Littoridina sphinctostoma M	xxxxx	xxxxx			Related genus (*Amnicola*) to Paleocene
Littorina irrorata M	xxxxx	xxxxx			Genus to Cretaceous
Lucina amiantus M	xxxxx	xxxxx			Related species to Miocene, genus to Silurian
Lucina crenella M	xxxxx	xxxxx	xxxxx		Genus to Silurian
Lucina sombrerensis M	xxxxx	xxxxx			Genus to Silurian
Luidia clathrata E	xxxxx				Related forms to Upper Cretaceous
Lumbrineris bifilaris P	xxxxx				Polychaete jaws and tubes from Cambrian

TABLE VII—(*continued*)

Species	*Recent*	*Pleistocene*	*Pliocene*	*Miocene*	*Range of Related Species and Genera*
Macoma constricta M	xxxxx	xxxxx	xxxxx		Genus to Miocene
Macoma extenuata M	xxxxx				Related species to Miocene
Macoma mitchelli M	xxxxx	xxxxx			Genus to Miocene
Macoma tageliformis M	xxxxx	xxxxx			Genus to Miocene
Macoma tenta M	xxxxx	xxxxx	xxxxx		Related species to Miocene
Macrocallista maculata M	xxxxx	xxxxx	xxxxx	xxxxx	Related forms to Paleocene
Mangelia cerina M	xxxxx	xxxxx	xxxxx	xxxxx	Genus to Eocene
Marginella aureocincta M	xxxxx	xxxxx	xxxxx	xxxxx	Related species to Eocene
Mellita quinquiesperforata E	xxxxx	xxxxx	xxxxx	xxxxx	Genus to Miocene
Mercenaria campechiensis M	xxxxx	xxxxx	xxxxx	xxxxx	Genus to Jurassic
Mitrella lunata M	xxxxx	xxxxx	xxxxx		Related species to Eocene
Modulus modulus M	xxxxx	xxxxx			Genus to Miocene
Mulinia lateralis M	xxxxx	xxxxx	xxxxx	xxxxx	Related species to late Eocene
Nassarius acutus M	xxxxx	xxxxx	xxxxx	xxxxx	Related species to Eocene
Nassarius ambiguus consensus	xxxxx	xxxxx	xxxxx		Related species to Miocene
Nassarius vibex M	xxxxx	xxxxx	xxxxx		Related species to Miocene
Natica pusilla M	xxxxx	xxxxx	xxxxx		Genus to Triassic
Neritina reclivata M	xxxxx	xxxxx			Genus to Jurassic
Noetia ponderosa M	xxxxx	xxxxx	xxxxx	xxxxx	Related forms to Eocene
Nucula proxima M	xxxxx	xxxxx	xxxxx	xxxxx	Genus to Silurian
Nuculana acuta M	xxxxx	xxxxx	xxxxx	xxxxx	Genus to Silurian
Nuculana eborea M	xxxxx	xxxxx	xxxxx	xxxxx	Related species to Silurian
Oliva sayana M	xxxxx	xxxxx	xxxxx	xxxxx	Genus to Eocene
Olivella mutica M	xxxxx	xxxxx	xxxxx	xxxxx	Related species to Paleocene
Ostrea equestris M	xxxxx	xxxxx			Related forms to Triassic
Pandora bushiana M	xxxxx	xxxxx	xxxxx		Genus to Lower Eocene
Pandora trilineata M	xxxxx	xxxxx	xxxxx		Genus to Lower Eocene
Panope bitruncata M	xxxxx	xxxxx	xxxxx		Genus to Upper Cretaceous
Pecten papyraceous M	xxxxx	xxxxx	xxxxx	xxxxx	Related species to Cretaceous
Petricola pholadiformis M	xxxxx	xxxxx			Genus to Cretaceous
Phacoides nassula M	xxxxx	xxxxx	xxxxx	xxxxx	Genus to Silurian
Phalium granulatum M	xxxxx	xxxxx			Genus to Paleocene
Phylloda squamifera M	xxxxx				Closely related species to Miocene
Pitar cordata M	xxxxx				Related species to Paleocene
Plicatula gibbosa M	xxxxx	xxxxx			Genus to Triassic
Polinices duplicatus M	xxxxx	xxxxx	xxxxx	xxxxx	Genus to Cretaceous
Polinices uberinus M	xxxxx				Related species to Eocene
Polystira albida M	xxxxx	xxxxx	xxxxx	xxxxx	Genus to Lower Miocene
Quadrans lintea M	xxxxx	xxxxx	xxxxx	xxxxx	Related genus to Jurassic
Rangia cuneata M	xxxxx	xxxxx	xxxxx	xxxxx	Genus to Eocene(?)
Rangia flexuosa M	xxxxx	xxxxx			Genus to Eocene(?)
Renilla mülleri CO	xxxxx				Fossil Pennatulids from Triassic rocks
Retusa canaliculata M	xxxxx	xxxxx	xxxxx	xxxxx	Related species to Oligocene
Sconsia striata M	xxxxx				Related species to Eocene
Semele bellastriata M	xxxxx	xxxxx	xxxxx		Related species to Miocene
Semele proficua M	xxxxx	xxxxx	xxxxx		Related species to Eocene
Semele purpurescens M	xxxxx	xxxxx	xxxxx		Genus to Eocene
Simum perspectivum M	xxxxx	xxxxx	xxxxx	xxxxx	Genus to Upper Cretaceous
Solecurtus cummingianus M	xxxxx	xxxxx	xxxxx		Genus to Cretaceous
Spisula s. similis M	xxxxx	xxxxx	xxxxx		Genus to Upper Cretaceous
Strigilla mirabilis M	xxxxx	xxxxx	xxxxx	xxxxx	Genus to Oligocene
Strombus alatus M	xxxxx	xxxxx	xxxxx	xxxxx	Related species to Cretaceous
Tagelus divisus M	xxxxx	xxxxx	xxxxx	xxxxx	Genus to Cretaceous
Tagelus plebeius M	xxxxx	xxxxx	xxxxx	xxxxx	Genus to Cretaceous
Tellidora cristata M	xxxxx				Related genus to Miocene
Tellina alternata M	xxxxx	xxxxx	xxxxx		Genus to Jurassic
Tellina texana M	xxxxx	xxxxx			Genus to Jurassic
Tellina versicolor M	xxxxx	xxxxx			Genus to Jurassic
Terebra dislocata M	xxxxx	xxxxx	xxxxx	xxxxx	Related species to Eocene
Terebra protexta M	xxxxx	xxxxx			Related species through Tertiary
Thais haemastoma floridana M	xxxxx	xxxxx			Related genera to Eocene
Thais haemastoma haysae M	xxxxx	xxxxx			Related genera to Eocene
Tonna galea M	xxxxx				Genus to Eocene
Trachycardium muricatum M	xxxxx	xxxxx			Genus to Miocene, related genera to Cretaceous
Turbonilla hemphilli M	xxxxx				Genus to Upper Cretaceous
Varicorbula operculata M	xxxxx	xxxxx	xxxxx		Related genera to Jurassic
Verticordia ornata M	xxxxx				Genus to Paleocene
Volsella d. granossisima	xxxxx	xxxxx	xxxxx		Genus to Devonian
Yoldia solenoides M	xxxxx	xxxxx			Related species to Pennsylvanian

* References used to compile this table: Dall (1890–1903), Gardner (1926–1947), Maury (1920–1922), Richards (1939, 1947), Moore, Lalicker, and Fischer (1952), Shrock and Twenhofel (1953).

M—Mollusk.	E—Echinoderm.
C—Crustacean.	P—Polychaete worm.
B—Bryozoan.	CO—Coelenterate.

pelecypods *Rangia cuneata*, *R. flexuosa*, *Macoma mitchelli*, and *M. tageliformis*, and a small gastropod *Littoridina sphinctostoma* (mentioned by Ladd, 1951, and only tentatively identified from the Mississippi Delta by the writer).

3. Nearshore sound and gulf areas in the vicinity of large rivers where salinity is reduced and the sedimentation rate is rapid could be detected by the presence of comparatively few molluscan remains at any one level, the majority of which are *Mulinia lateralis*, *Nuculana eborea*, *Abra lioica*, and the gastropod *Nassarius acutus*.

4. Bay or sound areas with considerable gulf and river influence and widely spaced barrier islands should be characterized by the presence of many bay species such as listed in Tables I, II, and III and in the discussion of the upper sound environment, plus a considerable number of shallow shelf and inlet species, discussed under the headings of these two environments.

5. A bay or sound area which has been cut off from the Gulf by a series of uninterrupted barrier islands, should contain characteristic bay fauna (Ladd, 1951), with very little Gulf influence. If small rivers emptied into the bay or sound, causing the chlorinity to be decreased consistently below 11 °/oo, oyster reefs composed of *Crassostrea virginica* would be found. Whenever the *Crassostrea* reefs contain an abundance of *Ostrea equestris*, the gulf oyster, it can be assumed that salinities have risen either from a series of droughts or from an increase in the size of the inlets from the open Gulf (Parker, 1955).

6. Inlets between the barrier islands or areas of strong currents which bring about an interchange of high and lower salinity water should be detected by the presence of many reworked shells with such sessile or attached organisms as limpets, chitons, and calcareous bryozoans. Certain pelecypods such as *Crassinella martinicensis*, *Trachycardium muricatum*, *Chione cancellata*, *Anadara brasiliana*, *Pandora trilineata*, and *Tellidora cristata* (only in the Delta region) and gastropods such as *Natica pusilla*, *Anachis avara semiplicata*, *Olivella mutica*, *Cantharus cancellarius*, and various species of *Turbonilla*, as well as the brittle stars, *Ophiolepis elegans* and *Hemipholis elongata*, have their centers of populations in or confined to the inlets.

7. The sound or bay sides of barrier islands, close to shore are apparently characterized by beds of *Mercenaria campechiensis texana* and *Aequipecten irradians amplicostatus*, and such gastropods as *Cerithium floridanum*, *C. muscarum*, *C. variabile*, and *Cerithidea pliculosa* (Cary and Spaulding, 1909).

8. The gulf side of barrier islands which have been subjected to considerable wave or surf action creating sand beaches may be detected by shell concentrates of *Donax*, *Terebra cinerea*, *Olivella*, many valves and bits of the large shallow-shelf Gulf mollusks, plus many fragments of heart urchins and sand dollars thrown on the shores by storms.

9. The shallow continental shelf areas out to 12–13 fathoms should be characterized by a large number of mollusks and echinoderms which can withstand moderate extremes of temperature, but are seldom found in waters where the

chlorinity falls below 17 ‰ (discussions of shallow-shelf assemblage for animals characteristic of this region: Harry, 1942; Behre, 1950; Ladd, 1951; Hildebrand, 1954; and Parker, 1955).

10. Various depth contours on the continental shelf can be detected by distinct assemblages. These extend from 0 to approximately 13 fathoms, from 13 to approximately 50–60 fathoms, and from 50–100 fathoms and deeper (discussions on shelf assemblages of organisms characteristic of these depths: Rehder and Abbott, 1951; Pulley, 1953; and Dall, 1889). Since depth range appears to have a specific temperature range, these assemblages may also be used to detect possible bottom-water temperature ranges, at least in the northern Gulf of Mexico.

11. It may be possible to determine the approximate climate existing during the deposition of sediments in the ancient environments, by analyzing the species composition of the imbedded fossils, and checking these species against their present geographical distribution.

12. Reduced rates of sedimentation may be detected by shell concentrates of large numbers of valves and shell fragments, which may have died in place, representing many species and several environmental conditions. Rapid sedimentation rates should be indicated by a lack of shell material, few species, and an assemblage indicating only one set of environmental conditions at any one level in the formation.

It must be emphasized that the presence of only one or two of the organisms characteristic of a certain environment is not enough to establish the presence of this particular environment. The appearance of the entire assemblage and the comparative abundance of each species within the assemblage must be considered.

SUMMARY

1. Biological data on macro-invertebrates were obtained from 280 biological collecting stations and 130 geological (core) collecting stations. The following numbers of species of invertebrates were identified: 93 (+7 pteropods) gastropods, 116 pelecypods, 6 scaphopods, 1 chiton, 3 cephalopods, 7 anthozoans, 8 echinoderms, 31 polychaete worms, 8 bryozoans, and 34 crustaceans.

2. Seven divisions of the east Mississippi Delta region were recognized by the distribution of the macro-organisms collected in this study, from published records of invertebrates from this region, and from the distribution of the hydrographic factors in the area. The seven divisions are: (I) the delta marshes, (II) delta front and lower distributaries, (III) lower Breton Sound and pro-delta clayey slopes, (IV) upper Breton Sound, (V) inlets, or areas of strong currents, (VI) the shallow continental shelf of the Gulf of Mexico from 0 to 13 fathoms, and (VII) the deeper parts of the continental shelf from 13 fathoms to the outer edge of the shelf. A possible eighth assemblage is the living oyster reef. Tables and distribution charts are included to show the characteristic forms for each environment.

3. A series of bottom communities based upon the community concepts of Petersen, Thorson, and Jones were recognized on the basis of the most abundant and widespread animals.

4. Certain species may be used to detect the range of the environmental factors (substrate, temperature, and salinity) which are associated with the distribution of these characteristic invertebrates.

5. Most of the species with hard parts found in the Delta sediments, which have been used to characterize these environments, have existed in the past on the Gulf of Mexico coast to the Pliocene and many extend back to the lower Miocene. Since the known environmental data can be applied to the distribution of these species to-day, it should be possible to reconstruct ancient environments from fossil beds containing these species back to the Miocene.

REFERENCES

Abbott, R. Tucker, 1954, *American Seashells*. xiv, 541 pp., 40 pls. D. Van Nostrand Company, Inc. New York.

Adams, R. M., and E. F. Sorgnit, 1951, "Comparison of Summer and Winter Temperatures, Gulf of Mexico," *Dept. of Oceanogr., Texas A and M Tech. Rept. 3*, 4 pp., 3 figs.

Allee, W. C., 1923, "Studies in Marine Ecology. I. The Distribution of Common Littoral Invertebrates of the Woods Hole Region," *Biol. Bull.*, Vol. 44, pp. 167–91.

———, and Karl P. Schmidt, 1951, *Ecological Animal Geography*. xiii, 715 pp. John Wiley and Sons, Inc., New York.

Behre, Ellinor H., 1950, "Annotated List of the Fauna of the Grand Isle Region, 1928–1946," *Occas. Papers Marine Lab., Louisiana State Univ.*, No. 6. 66 pp.

Cary, L. R., 1905, "A Contribution to the Fauna of the Coast of Louisiana," *Bull. Gulf Biol. Sta.*, Vol. 6, pp. 50–59.

———, and H. Spaulding, 1909, "Further Contributions to the Marine Fauna of the Louisiana Coast," *ibid.*, No. 12. 21 pp.

Clench, W. J., 1929, "Some Land and Marine Shells from the Mississippi Delta Region," *Nautilus*, Vol. 43, pp. 34–35.

———, 1953, "The Genera *Scaphella* and *Auriniopsis* in the Western Atlantic," *Johnsonia*, Vol. 2, No. 32, pp. 376–80.

Collier, Albert, and J. W. Hedgpeth, 1950, "An Introduction to the Hydrography of the Tidal Waters of Texas," *Pub. Inst. Marine Sci.*, Vol. 1, No. 2, pp. 120–94.

Dall, W. H., 1886, "Report on the Molluska. Part I. Brachiopoda and Pelecypoda," *Bull. Comp. Zool., Harv. Coll.*, Vol. 18, pp. 171–318; 9 pls.

———, 1889a, "Report on the Molluska. Part II. Gastropoda and Scaphopoda," *ibid.*, Vol. 18, pp. 1–492; 40 pls.

———, 1889b, "A Preliminary Catalogue of Shell-Bearing Marine Mollusks and Brachiopods of the Southeastern Coast of the United States, with Illustrations of Many of the Species," *Bull. U. S. Nat. Mus.*, No. 37, pp. 1–219; 74 pls.

———, 1890–1903, "Contributions to the Tertiary Fauna of Florida," *Trans. Wagner Free Inst. Sci.*, Vol. 3 (in 6 parts). 1654 pp., 60 pls.

Ekman, Sven., 1953, *Zoogeography of the Sea*. xiv, 417 pp. Sidgwick and Jackson, Ltd., London.

Fisk, H. N., E. McFarlan, Jr., C. R. Kolb, and L. J. Wilbert, Jr., 1954, "Sedimentary Framework of the Modern Mississippi Delta," *Jour. Sed. Petrology*, Vol. 24, No. 2, pp. 76–99; 15 figs.

Fuglister, F. C., 1947, "Average Monthly Sea Surface Temperatures of the Western North Atlantic Ocean," *Pap. in Phys. Oceanog. and Meteor., Massachusetts Inst. Tech. and Woods Hole Oceanog. Inst.*, Vol. 10, No. 2, pp. 325–35.

———, 1954, "Average Temperature and Salinity at a Depth of 200 Meters in the North Atlantic," *Tellus*, Vol. 6, pp. 46–58.

Galtsoff, Paul S., 1931, "Survey of Oyster Bottoms in Texas," *U. S. Bur. Fish. Inv. Rept.*, Vol. 6, pp. 1–30; 15 figs.

——— et al., 1954, "Gulf of Mexico, Its Origin, Waters and Marine Life," *Fishery Bull., U. S. Fish and Wildlife Serv.*, Vol. 55. 89, xiv. 604 pp.

Gardner, Julia, 1926–1947, "The Molluscan Fauna of the Alum Bluff Group of Florida," *U. S. Geol. Survey Prof. Paper 142*. 656 pp., 62 pls.

GEYER, RICHARD A., 1950, "The Occurrences of Pronounced Salinity Variations in Louisiana Coastal Water," *Jour. Mar. Research*, Vol. 9, pp. 100–10.

GUNTER, GORDON, 1950, "Seasonal Population Changes and Distributions as Related to Salinity of Certain Invertebrates of the Texas Coast, Including Commercial Shrimp," *Pub. Inst. Mar. Sci.*, Vol. 1, No. 2, pp. 7–51.

HADLEY, WADE, JR., 1936, "Some Notes on the Recent Mollusca from Plaquemines and St. Bernard Parishes, Lower Mississippi River Delta," *Louisiana Dept. Conserv., Geol. Bull. 8*, pp. 403–406.

HARRY, HAROLD W., 1942, "List of Mollusca of Grand Isle, La., Recorded from the Louisiana State University Marine Laboratory, 1929–1941," *Occas. Paps. Mar. Lab., Louisiana State Univ.*, No. 1, pp. 1–13.

HEDGPETH, JOEL W., 1953, "An Introduction to the Zoogeography of the Northwestern Gulf of Mexico with Reference to the Invertebrate Fauna," *Pub. Inst. Mar. Sci.*, Vol. 3, No. 1, pp. 110–224.

HILDEBRAND, HENRY H., 1954, "A Study of the Fauna of the Brown Shrimp (*Penaeus aztecus* Ives) Grounds in the Western Gulf of Mexico," *ibid*, Vol. 3, No. 2, pp. 233–366.

HUTCHINS, LOUIS W., 1947, "The Bases for Temperature Zonation in Geographical Distribution," *Ecol. Monog.*, Vol. 17, pp. 325–35.

INMAN, DOUGLAS, 1956, "Particle Size Distribution in Nearshore Sediments," in *Finding Ancient Shorelines*, Soc. Econ. Paleon. and Miner. (in press).

JONES, N. S., 1950, "Marine Bottom Communities," *Biol. Rev.*, Vol. 25, pp. 283–313.

LADD, HARRY S., 1951, "Brackish-Water and Marine Assemblages of the Texas Coast, with Special Reference to Mollusks," *Pub. Inst. Mar. Sci.*, Vol. 2, No. 1, pp. 125–64.

LEE, RICHARD E., 1944, "A Quantitative Survey of the Invertebrate Bottom Fauna in Menemsha Bight," *Biol. Bull.*, Vol. 86, pp. 83–97.

MAURY, C. J., 1920, "Recent Mollusca of the Gulf of Mexico and Pleistocene and Pliocene Species from the Gulf States. Part I: Pelecypods," *Bulls. Amer. Paleon.*, Vol. 8, pp. 1–116; 1 pl.

———, 1922, "Recent Mollusca of the Gulf of Mexico and Pleistocene and Pliocene Species from the Gulf States. Part II: Scaphopoda, Gastropoda, Amphineura, Cephalopoda," *ibid.*, Vol. 9, pp. 32–172.

MOORE, D. G., 1955, "Rate of Deposition, Shown by Abundance of Foraminifera," *Bull. Amer. Assoc. Petrol. Geol.*, Vol. 39, No. 8 (August), pp. 1594–1600.

MOORE, RAYMOND C., C. G. LALICKER, AND A. G. FISCHER, 1952, *Invertebrate Fossils*. xiii, 766 pp. McGraw-Hill Book Company, Inc., New York.

O'NEIL, TED, 1949, *The Muskrat in the Louisiana Coastal Marshes*, Louisiana Dept. of Wild Life and Fish. xii, 152 pp.

PACKARD, E. L., 1918, "A Quantitative Analysis of the Molluscan Fauna of San Francisco Bay," *Univ. California Pub. in Zool.*, Vol. 8, No. 13, pp. 299–336.

PARKER, ROBERT H., 1955, "Changes in the Invertebrate Fauna, Apparently Attributable to Salinity Changes in the Bays of Central Texas," *Jour. Paleon.*, Vol. 29, No. 2, pp. 193–211.

PERRIER, M. EDMOND, 1876, "Revision des Stellerides du Museum: Family Asterinidae (Gray, 1840)," *Archiv. Zool. Exper. et Gener.*, Vol. 5, pp. 209–304.

PETERSEN, C. G. J., 1913, "Valuation of the Sea. II. The Animal Communities of the Sea Bottom and Their Importance for Marine Zoogeography," *Rept. Danish Biol. Sta.*, Vol. 21, pp. 3–44.

———, 1915, "On the Animal Communities of the Sea Bottom in the Skagerrak, the Christianiafjord and Danish Waters," *ibid.*, Vol. 23, pp. 3–28.

PHLEGER, FRED B, AND FRANCES L. PARKER, 1951, "Ecology of Foraminifera, Northwest Gulf of Mexico," *Geol. Soc. America Mem. 46*. ix, 64 pp.

PRATT, D. M., 1953, "Abundance and Growth of *Venus mercenaria* and *Cellocardia morrhuana* in Relation to the Character of Bottom Sediments," *Jour. Mar. Res.*, Vol. 12, pp. 60–74.

PUFFER, ELTON L., AND WILLIAM K. EMERSON, 1953, "The Molluscan Community of the Oyster Reef Biotope on the Central Texas Coast," *Jour. Paleon.*, Vol. 27, pp. 536–44; 1 pl.

PULLEY, THOMAS E., 1953, "A Zoogeographic Study Based on the Bivalves of the Gulf of Mexico," *unpub. Ph.D. dissert., Harvard Univ.* (abstract in *Ann. Rept., Amer. Malacological Union*, 1952, pp. 2–3).

REHDER, HARALD A., AND R. TUCKER ABBOTT, 1951, "Some New and Interesting Mollusks from the Deeper Waters of the Gulf of Mexico," *Rev. de la Sociedad Malacologica*, Vol. 8, pp. 53–68; 4 pls.

RICHARDS, HORACE G., 1939, "Marine Pleistocene of Texas," *Bull. Geol. Soc. America*, Vol. 50, pp. 1885–98.

———, 1947, "Invertebrate Fossils from Deep Wells along the Atlantic Coastal Plain," *Jour. Paleon.*, Vol. 21, pp. 23–37.

———, 1954, "Mollusks from the Mississippi Delta," *Notulae Naturae Acad. of Nat. Sci. Philadelphia*, No. 263. 8 pp., 1 pl.

SCRUTON, P. C., 1956, "Sediments of the Eastern Mississippi Delta," *Finding Ancient Shorelines*, Soc. Econ. Paleon. and Miner., (in press).

———, *ms.*, "Oceanography of Mississippi Delta Sedimentary Environments," (unpublished manuscript).

———, AND D. G. MOORE, 1953, "Distribution of Surface Turbidity Off Mississippi Delta," *Bull. Amer. Assoc. Petrol. Geol.*, Vol. 37, pp. 1067–74.

SHEPARD, FRANCIS P., 1954, "Nomenclature Based on Sand-Silt-Clay Ratios," *Jour. Sed. Petrology*, Vol. 24, pp. 151–58.

SHROCK, ROBERT R., AND W. H. TWENHOFEL, 1953, *Principles of Invertebrate Paleontology.* xx, 816 pp. McGraw-Hill Book Company, Inc., New York.

SPAULDING, M. H., 1906, "A Preliminary Report on the Distribution of the Scallops and Clams in the Chandeleur Islands Region, Louisiana," *Bull. Gulf Biol. Sta.*, Vol. 6, pp. 29–43.

SUMNER, FRANCIS B., RAYMOND C. OSBURN, AND LEON J. COLE, 1911, "A Biological Survey of the Waters of Woods Hole and Vicinity. Part I," *Bull. U. S. Bur. Fish.*, Vol. 31. 544 pp.

SVERDRUP, H. U., MARTIN W. JOHNSON, AND R. H. FLEMING, 1942, *The Oceans, Their Physics, Chemistry, and General Biology.* x, 1097 pp. Prentice-Hall, New York.

VAN ANDEL, T., AND H. POSTMA, 1954, "Recent Sediments of the Gulf of Paria. Rept. of Orinoco Shelf Expedition, Bol. I," *Verhandelingen der Koninklijke Nederlandse Akademie van Wetenschappen*, Afd. Natuurkunde, Eerste Reeks, Deel XX, No. 5. 245 pp. vii pls. 4 charts.

VANATTA, E. G., 1903, "A List of Shells Collected in Western Florida and Horn Island, Mississippi," *Proc. Acad. Nat. Sci., Philadelphia*, Vol. 55, pp. 756–59.

VERRILL, A. E., 1873, "Report upon the Invertebrate Animals of Vineyard Sound and the Adjacent Waters, with an Account of the Physical Character of the Region," *Rept. U. S. Comm. Fish. for 1871–1872*, Senate Miscel. Doc. No. 61, pp. 295–778; 38 pls. Supt. Documents, Govt. Printing Office, Washington, D. C.

———, 1919, "Report on the Starfishes of the West Indies, Florida, and Brazil, Including Those Obtained by the Bahama Expedition from the University of Iowa in 1893," *Bull. from Lab. Nat. Hist., Univ. Iowa*, Vol. 7, No. 1, pp. 1–232; 29 pls.

ORBITAL VELOCITY ASSOCIATED WITH WAVE ACTION NEAR THE BREAKER ZONE

TECHNICAL MEMORANDUM NO. 79
BEACH EROSION BOARD
CORPS OF ENGINEERS

MARCH 1956

FOREWORD

One of the facts of water wave mechanics about which very little is known is the water particle motion in shallow water. Yet this orbital particle motion must account to a large degree for the maintaining (if not the initiation) of material in suspension in the nearshore zone. It probably also accounts for a certain amount of the littoral movement, particularly in an onshore-offshore direction, and, by differential velocities in the two directions, the size sorting of sand in the nearshore area. This report presents the results of a field study of the maximum orbital velocities observed under wave action of varying characteristics and attempts to relate them to certain theoretical wave parameters.

This report was prepared at the Scripps Institution of Oceanography of the University of California in pursuance of contract DA-49-055-eng-3 with the Beach Erosion Board which provides, in part, for the study of wave motion in shallow water. The authors of the report, Douglas L. Inman and Noriyuki Nasu are members of the staff of that institution.

Views and conclusions stated in the report are not necessarily those of the Beach Erosion Board.

This paper represents in part
results of research carried out
by the University of California
under contract with the Office
of Naval Research.

This report is published under authority of Public Law 166, 79th Congress, approved July 31, 1945.

TABLE OF CONTENTS

Page

List of Figures & Tables ---------------------------------- b

List of Symbols --- c & d

Abstract -- 1

Introduction -- 1

Method -- 2

- Orbital Velocity Meter ---------------------------------- 6
  - Calibration --- 6
  - Errors in Measurement of Orbital Velocity ------------- 9
  - Electronics --- 10
- Wave Measurements --------------------------------------- 10
  - Wave Period --- 10
  - Wave Height --- 11
  - Depth of Water -- 11

Ideal Waves --- 13

- Airy Waves -- 15
- Stokes' Waves --- 15
- Solitary Wave Theory ------------------------------------ 16

Analysis of Data -- 18

- Wave Height and Period ---------------------------------- 27
- Orbital Velocity -- 28
  - Distribution of Maximum Onshore and Offshore Velocities -- 28
  - Comparison of Measured and Ideal Velocities ---------- 33
- Conclusions --- 41

Acknowledgments --- 41

Literature Cited -- 42

APPENDICES

Appendix IA-IF Tabulation of Wave and Orbital Velocity Measurements

Appendix II Physical Characteristics of the Orbital Velocity Meter

LIST OF FIGURES

Figure Page

1. Notation and definition of symbols ---------------- 3
2. Schematic diagram ---------------------------------- 4
3-5. Handling and operation of orbital velocity meter -- 4-5
6. Calibration curve for the orbital velocity meter -- 8
7-8. Calibration of the wave pressure record ----------- 12
9-10. Determination of still water depth ---------------- 14
11-16. Samples records of wave pressure and orbital velocity -- 19-21
17-24. Relation of wave height to wave period ------------ 22-25
25-26. Distribution of maximum orbital velocities -------- 29
27. Graph of the function $_sU = \frac{1}{2}$ NC for solitary waves- 30
28-33. Comparison of orbital velocity with solitary theory -- 34-36
34. Relation of orbital velocity to wave period ------- 37
35-40. Comparison of orbital velocity with solitary and Airy-Stokes theory ---------------------------- 38-40

LIST OF TABLES

Table

1. Summary of wave properties ------------------------ 26
2a-2b. Statistics of the distributions of horizontal orbital velocities ---------------------------- 31
3. Threshold velocity of the orbital meter system ---- 32

LIST OF SYMBOLS

In general a prefix to a symbol indicates the method used in obtaining the data; o refers to direct visual observation, a to Airy and Stokes theory, s to solitary theory, etc. Suffixes indicate the part of the wave to which the data pertains; c refers to the crest, 1 and 2 to the troughs preceding and following the crest, etc. Most symbols are defined schematically in figure 1.

a - Prefix indicating data based on equations for Airy or Stokes waves; also the coefficient of virtual mass of the orbital velocity meter (equation 1)

C - Velocity of propagation of the wave crest

d - Still water depth (equation 3, figures 9 and 10)

g - Acceleration of gravity 32.2 ft/sec^2

h_c - Depth of water under wave crest

h_1 - Depth of water under trough preceding wave crest

h_2 - Depth of water under trough following wave crest

$h = \frac{1}{2} (h_1 + h_2)$

H_1 - Wave height measured from preceding trough to crest

H_2 - Wave height measured from crest to following trough

$H = \frac{1}{2} (H_1 + H_2)$

$\bar{H}_{1/3}$ - Significant wave height; average of the highest one-third of the waves. The number of waves to be averaged was based on the average period of the ten highest waves of relatively simple profile occurring during a 20 minute interval.

$\bar{H}_{1/10}$ - Average height of the highest one-tenth of the waves

L - Wave length

m - Slope of regression line

$\left.\begin{matrix} M \\ N \end{matrix}\right\}$ - Functions in solitary wave theory defined by equations 12 and 13

o - Prefix indicating data obtained directly from visual observations of water level on staff

s^- - Prefix indicating data based on solitary wave equations

t - Time, usually measured from wave crest

T - Wave period

T_n - Neighbor period; one-half of the elapsed time between the passage of the preceding wave crest and the following wave crest

$\bar{T}_{1/3}$ - Significant wave period; average period of the highest one-third of the waves

u - Horizontal component of orbital velocity

u_c - Maximum onshore component of orbital velocity, measured near the bottom during passage of wave crest

u_1, u_2 - Maximum offshore component of orbital velocity, measured near the bottom during passage of preceding and following wave troughs respectively

$U = \left| u_c \right| + \frac{1}{2} \left| u_1 + u_2 \right|$; absolute sum of maximum crest and average trough orbital velocities

$U_1 = \left| u_c \right| + \left| u_1 \right|$; absolute sum of maximum orbital velocities under wave crest and preceding trough

$_aU = \frac{2\pi H}{T} \cdot \frac{1}{\sinh \frac{2\pi}{L} d}$; absolute sum of maximum crest and trough velocities computed at the bottom for Airy and Stokes waves

$_sU = \frac{1}{2} NC$; maximum orbital velocity computed at the bottom for a solitary wave

w_1, w_2 - Maximum up and down components of orbital velocity preceding and following passage of wave crest respectively

x - Horizontal coordinates measured from wave crest and positive in direction of propagation

z - Vertical coordinate measured positively from the bottom upwards

γ - Relative wave height, H/h

ORBITAL VELOCITY ASSOCIATED WITH WAVE ACTION NEAR THE BREAKER ZONE*

by

D. L. Inman and Noriyuki Nasu
University of California
Scripps Institution of Oceanography
La Jolla, California

ABSTRACT

The orbital velocity associated with ocean surface waves in shallow water was measured for various wave conditions at La Jolla, California, as part of a program of study of sand transport and beach erosion. The measurements were made near the bottom and just seaward of the breaker zone in water depths ranging from about five to fifteen feet and for wave heights as great as seven and one-half feet. The current measuring device consisted essentially of a cylindrical rod fixed rigidly at one end like a cantilever, and the system was so arranged that the orbital velocity could be interpreted from the bending of the rod caused by the force exerted by the moving water. Orbital velocity and wave pressure were recorded simultaneously for time intervals of about twenty minutes.

The observed maximum horizontal velocities compare favorably with velocities predicted from solitary wave theory for most waves with simple profiles when the ratio of the wave height to water depth is greater than about 0.4. The agreement with theory is somewhat better for longer period waves, and in some cases is still quite good in regions where the ratio of wave height to water depth is less than about 0.2. On the average, the onshore velocity associated with the passage of a wave crest was greater in magnitude and of shorter duration than the offshore velocity under the wave trough. The differences in crest and trough velocities varied from wave to wave, but in general correlated with the shape of the waves.

INTRODUCTION

There has been much interest recently in wave action in shallow water and in the orbital or particle motion associated with such waves. Although an understanding of the mechanics of wave motion is essential in the study of sand transportation, forces on structures and related phenomena, no adequate theory has been developed to describe the properties of waves in shallow water. Some progress, from a practical standpoint, has come from adaptation of the form and mechanics of certain ideal waves such as the solitary and Stokes' waves to limited regions nearshore. However, such application does not allow for all progressive changes as waves travel from deep to shoal water, nor for the inherent variability of wave properties in nature.

---

* Contribution from the Scripps Institution of Oceanography, New series No. 841.

Reproduced by Permission

Most experimental investigations of orbital velocity and other wave properties have been restricted to small scale model studies in wave tanks where properties such as wave period and height usually remain constant. Thus the laboratory waves are essentially ideal waves and lend themselves to comparison with theory, but like the theory lack many of the complexities of natural waves.

Recent laboratory studies of wave motion in shallow water are described by Hamada (1951), Iversen (1952), Daily and Stephan (1952), and Ippen and Kulin (1955). A brief study of the orbital velocity associated with ocean waves is given in the Interim Report of the Beach Erosion Board for 1933. This study was based on motion pictures of the exposed portion of a staff connected to a subsurface float, and its results are in good agreement with solitary wave theory as adapted to the surf zone by Munk (1949a).

An instrument was designed and built at the Scripps Institution of Oceanography to measure the orbital velocities associated with ocean surface waves nearshore. The instrument was placed near the bottom and just seaward of the breaker zone in water depths ranging from about five to fifteen feet. Fifteen series of measurements, each with a duration of approximately twenty minutes, were obtained for various wave conditions. Six of these were sufficiently complete to warrant a detailed description in this report.

METHOD

The procedure used in the measurement of the orbital velocities and related wave parameters is described in some detail here because of the many variables involved and because of the complexities of ocean waves. The notation used is defined in figure 1 and in the preceding list of symbols. The general plan of operation and the field procedures are illustrated in figures 2 through 5.

The current meter used for measuring the orbital velocities was a drag type in which the force exerted by the moving water on a rigidly mounted rod was interpreted in terms of the velocity of the water. A pressure type wave meter was used with the current meter, and the two meters mounted on a tripod designed so that the orbital current meter was relatively uninfluenced by the field of flow around the tripod (figure 4). The tripod and meters were lowered into the water from the Scripps Institution of Oceanography pier by a crane and placed a distance of 15 feet from the pier to minimize the influence of the pier pilings (figure 3). The tripod feet had weights and stabilizing rods to reduce motion of the unit while on the sand bottom. The tripod was oriented from the pier by three guy lines so that the rod element in the current meter was parallel to the crests of the waves. Since the objective of the investigation was to measure orbital currents near the bottom, the current meter was mounted 0.82 feet (25 cm.) above the bottom. This height was selected because theory indicates little change of velocity with depth in this

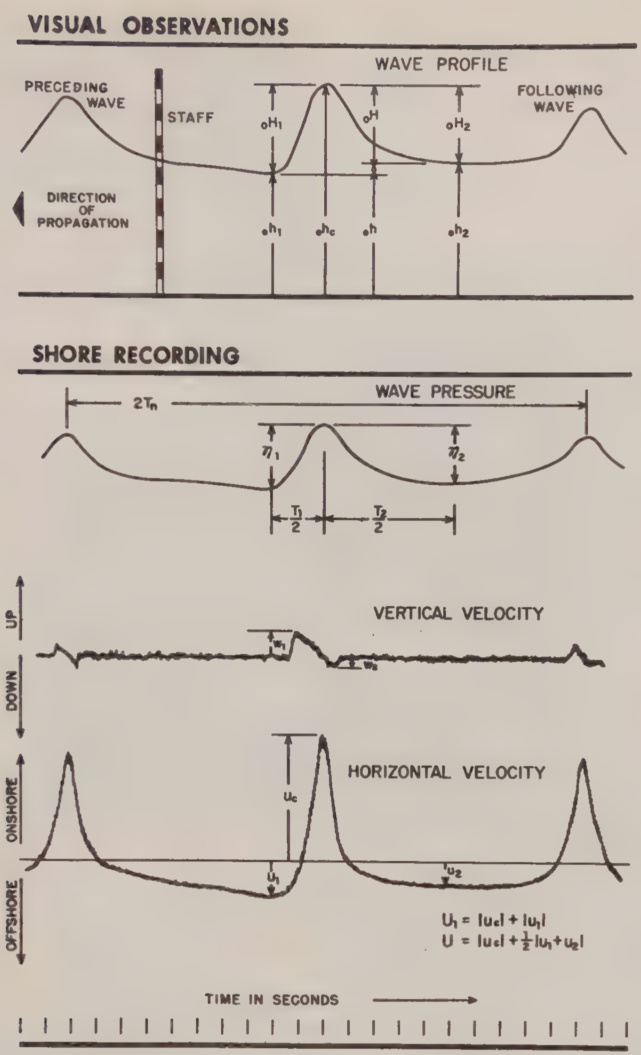
VISUAL OBSERVATIONS
WAVE PROFILE
PRECEDING WAVE
STAFF
FOLLOWING WAVE
$_oH_1$
$_oH$
$_oH_2$
DIRECTION OF PROPAGATION
$_oh_1$
$_oh_c$
$_oh$
$_oh_2$
SHORE RECORDING
WAVE PRESSURE
$2T_n$
η_1
η_2
$\frac{T_1}{2}$
$\frac{T_2}{2}$
VERTICAL VELOCITY
UP
DOWN
w_1
w_2
HORIZONTAL VELOCITY
ONSHORE
OFFSHORE
u_c
u_1
u_2
$U_1 = |u_c| + |u_1|$
$U = |u_c| + \frac{1}{2}|u_1 + u_2|$
TIME IN SECONDS

Figure 1. Notation and definition of symbols.

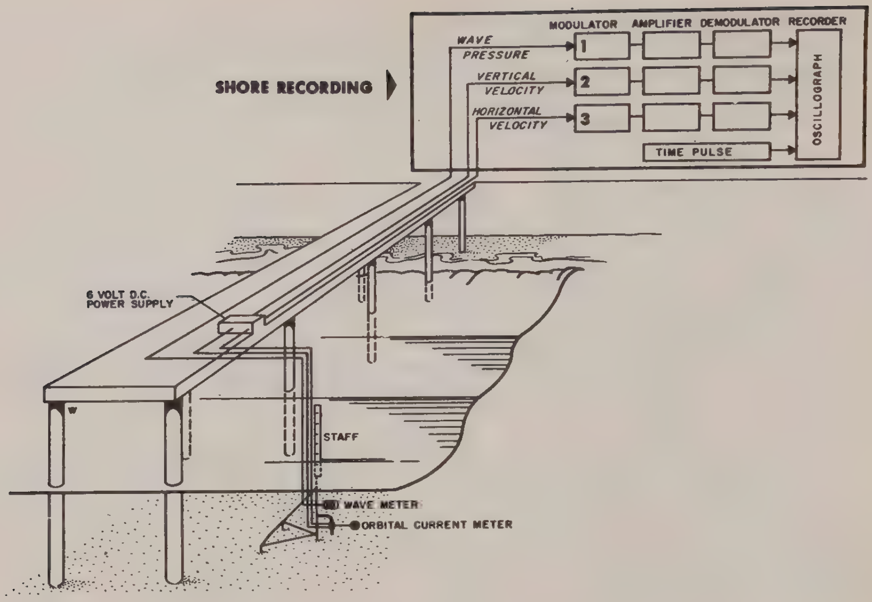
MODULATOR
AMPLIFIER
DEMODULATOR
RECORDER
WAVE PRESSURE
1
VERTICAL VELOCITY
2
HORIZONTAL VELOCITY
3
OSCILLOGRAPH
TIME PULSE
SHORE RECORDING
6 VOLT D.C. POWER SUPPLY
STAFF
WAVE METER
ORBITAL CURRENT METER

Figure 2. Schematic diagram of the system for measuring orbital velocity.

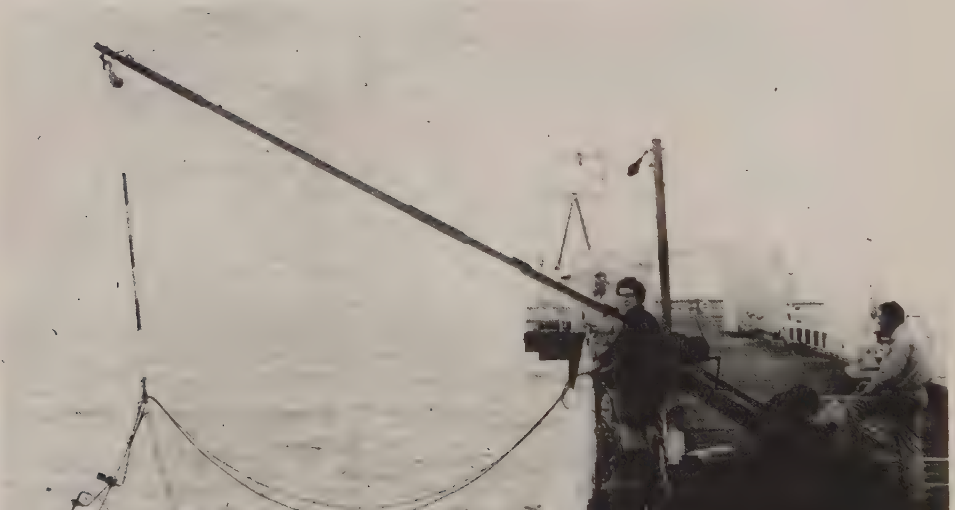

Figure 3. Lowering the orbital velocity meter from the ocean pier at the Scripps Institution of Oceanography. Note the graduated staff above the tripod and the orientation lines attached to each leg of the tripod.

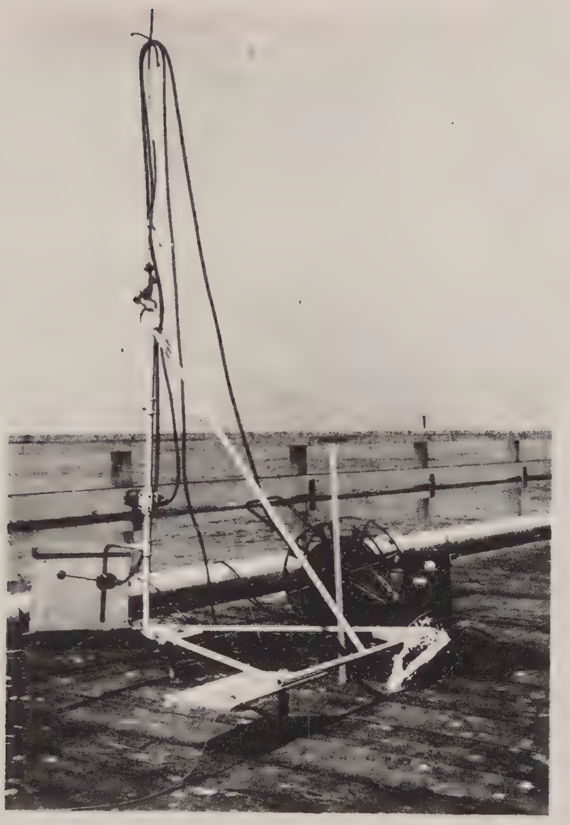

Figure 4. Details of the tripod supporting the orbital velocity meter and the wave meter. Meter box (right background) houses the voltage regulator.

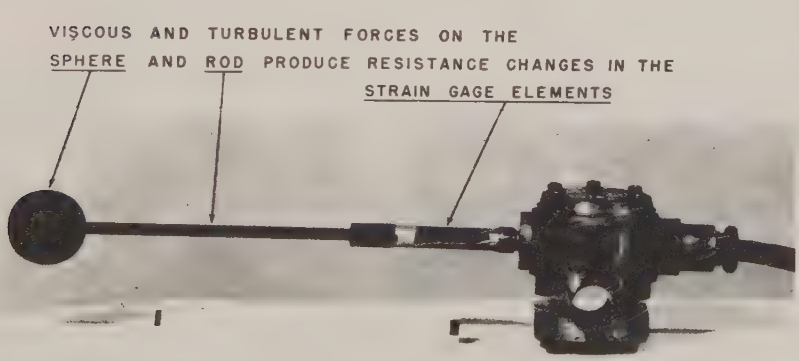
VIŞCOUS AND TURBULENT FORCES ON THE
SPHERE AND ROD PRODUCE RESISTANCE CHANGES IN THE
STRAIN GAGE ELEMENTS

Figure 5. Detail of the orbital velocity meter.

region (Munk, 1949a, plate 10), and it was thought in general to be above the zone of high concentrations of suspended sand and bottom boundary effects. The bottom sediments in this region consist of well-sorted fine sand with a median diameter of about 180 microns. In the region where the orbital velocities were measured the sand bottom had an average slope of about 1 in 35. The bottom sloped seaward from this area at the rate of 1 in 45 out to the 50-foot contour where the slope increased.

The output of the two meters, after proper modulation and amplification, was fed into a six element galvanometer type oscillograph and the horizontal and vertical components of orbital velocity, and wave pressure were recorded simultaneously as a function of time on light sensitive tape. A block diagram giving the essentials of the instrumentation procedure is shown in figure 2.

ORBITAL VELOCITY METER

Basically the instrument consisted of a small flexible beryllium-copper rod with a sphere mounted on one end and the other mounted rigidly to a support (figure 5). Four strain gauges were cemented at 90° intervals around the circumference of the supported end of the rod and connected so that the opposite pairs form two adjacent legs of a Wheatstone bridge (appendix II). Viscous and turbulent forces on the rod and sphere produce strains which change the resistance of the strain gauge elements, which in turn unbalance the bridge and produce an electrical potential which is interpreted in terms of the orbital velocity. The dimensions and physical constants of the meter and the tripod are listed in appendix II.

By using two Wheatstone bridge circuits and letting opposite pairs of strain gauges form two legs of each bridge, two components of velocity were obtained. In this study the meter was always used with the rod horizontal and parallel to the wave crests. Thus the velocities measured consisted of the vertical component and a horizontal component in the direction of wave propagation.

Calibration: When the forces acting on the orbital meter are resolved and considered to be acting on the center of the sphere, they can be expressed in the following manner:

$$f = a \frac{\partial u}{\partial t} + bu^2 \qquad (1)$$

where f is the total force considered as acting upon the center of the sphere, u is the velocity of the water relative to the meter, "a" is proportional to the virtual mass coefficient, and "b" is proportional to the drag coefficient. Within the ranges of velocity and acceleration found in the field, the values of "a" and "b" were found experimentally to be about 80 and 5.2 cgs units respectively.

Both the sphere and rod dimensions are such that their drag coefficients are nearly constant for velocities from 0.2 to over 15 ft./sec., thus making the strain proportional to the square of the velocity for steady state uniform flow within these ranges. The meter was calibrated for steady flow at the Hydro court, University of California, Berkeley, for velocities ranging from 1/3 to 3 ft./sec. The results of the laboratory calibration were in good agreement with values calculated from the physical constants and dimensions of the meter (appendix II).

Thereafter, the meter was calibrated in the field by applying forces to the end of the rod (center of the sphere) which were equivalent to the forces resulting from a given steady flow velocity around the meter. In the field the meter was placed in a large basin of still water so that the calibration would be made under buoyant forces similar to those during the measurement of orbital velocities. A typical calibration curve obtained in this manner for vertical and horizontal velocities is shown in figure 6. For this case the up and down calibrations were approximately the same, but the onshore and offshore components differed slightly. Because the meter response is proportional to the square of the velocity it is insensitive to low velocities but gives relatively good discrimination for high velocities. A measure of the lower threshold velocity is given in table 3, where the velocity required to give a 1 mm. displacement from the null positions on the orbital record is listed for each series. (See page 32 for Table 3.)

In addition to establishing the null or rest point of the meter during the field calibrations, the null point was also obtained when the instrument was in the ocean by placing a plastic sleeve over the rod and sphere. This was done to insure application of the calibration to operating conditions where the water pressure and temperature differed. Consideration was given to temperature compensation in the design of the instrument by mounting the two stationary resistance elements of the Wheatstone bridge in the waterproofed brass housing at the support end of the rod. Thus all legs of the bridge could be maintained at the same temperature.

The effects of accelerative forces on the orbital current meter were measured experimentally in the laboratory by subjecting the instrument to simple harmonic motion both in air and in water. The inertial characteristics of the moving instrument were obtained by assuming the effects of fluid drag in air to be negligible. Then since the values of f, b, u, and $\frac{\delta u}{\delta t}$ from equation (1) were known, the value of "a" was calculated from the experimental data. The value of "a" was found to vary with the period of oscillation, and to obtain an upper limiting value of about 80 gram cm. (appendix II).

As an approximation to field conditions, the experimental results of the calibrations were applied to theoretical velocity distributions. Two cases were considered, one assuming the velocity distribution to be

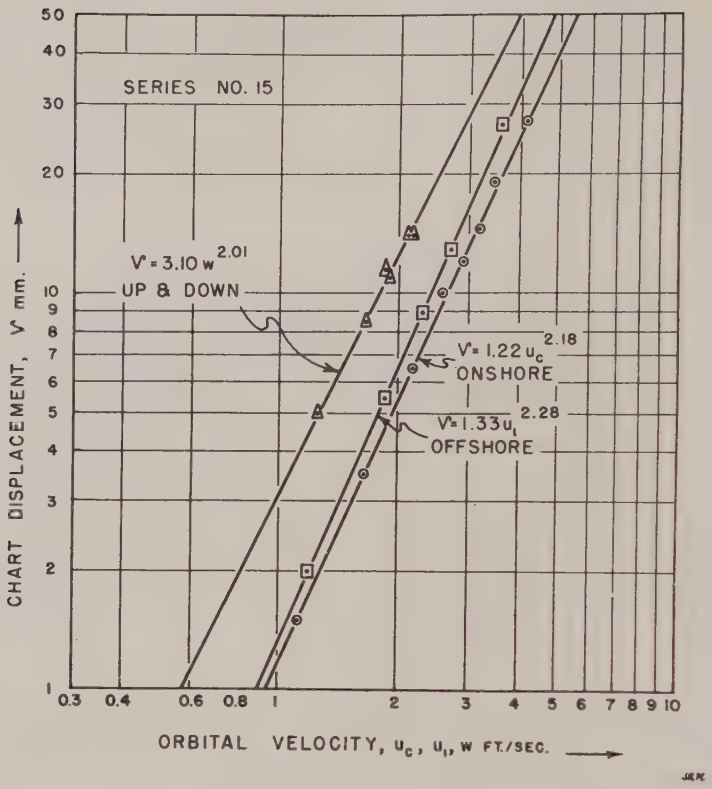

Figure 6. Typical calibration curve for the orbital velocity meter.

that for waves with sinusoidal profile as in the case of waves of small steepness, and the other that the velocity distribution was of the solitary wave type described by Munk (1949a).

In both of these theoretical cases it was found that the magnitude of the accelerative terms in the record of orbital velocity in the vicinity of the crests and troughs of the wave would be negligible compared to the magnitude of the drag or velocity effects when the wave periods are greater than five seconds. The relatively small magnitude of accelerative terms in these theoretical cases suggests that accelerative terms are also small in the case of actual waves outside of the breaker zone. However, it seems unlikely that the accelerative effects can be neglected in the region between the crest and trough of the wave where minimum velocities and maximum accelerations occur. For this reason computations involving orbital velocities, and comparisons of observed velocities with theoretical velocities were restricted to velocities measured at the crest and trough of the wave where the maximum horizontal component of force occurs. This decision to tabulate only crest and trough measurement from the records seriously restricted the scope of the study, since the continuous profile of force as a function of time could not be interpreted in terms of velocity; however, it appreciably lessened the number of assumptions which are inherent in this type of interpretation.

Thus, the record from the orbital meter is that of the forces exerted on the meter by the motion of the water, and where the record has been interpreted in terms of velocity, the assumption is made that the drag force on the meter is proportional to the square of the velocity.

Errors in Measurement of Orbital Velocity: The interpretation of maximum orbital velocity from the record of the orbital meter is predicated on the following assumptions: a) the meter response was proportional to the square of the velocity, b) the instrument was level, c) the axis of the rod in the meter was parallel to the crest of the waves, and e) the null point established during calibration is the point of zero velocity.

As discussed previously, the assumption that the meter response is proportional to the square of the velocity is probably justified for maximum velocity readings. Errors of this type are probably less than 1% and would tend to give high readings. The meter level was probably maintained within 10 degrees of horizontal at all times, so that the measured horizontal velocity would be decreased by less than 2%. However, a 10 degree tilt would result in an excess reading on the vertical velocity component equivalent to 17% of the total horizontal velocity. Since the vertical velocity components are expected to be small near the bottom, this may result in a large error in interpreting vertical velocities. Inspection of the records (figures 11-16) suggests that the meter was not always level, and for this reason detailed analysis of the vertical velocity component has not been attempted.

The error in alignment between the wave meter and the wave crest was probably no greater than 10 degrees for long crested waves and not over 15 for short crested waves. This would result in an error of 2 to 4% in orbital velocity.

Collectively these errors should result in the meter giving a lower horizontal velocity than the true one, but are probably all small compared to the general error inherent in calibrating and zeroing the meter in the field.

Electronics: A conventional carrier type amplifier, consisting of a voltage amplifier followed by a power amplifier, was used with the orbital velocity meter (figure 2). Since the electric leads were long, it was not feasible to use alternating currents to energize the strain gauge elements. Therefore, the strain gauges were powered by direct current and the direct current signal output from the Wheatstone bridge was inverted by means of a chopper or modulator so that it could be more readily amplified. For most of the work a vibrating type Stevens-Arnold #222 chopper was found to serve quite satisfactorily as a modulator. Adjustable biasing potentials were included so that the meter could be zeroed in water.

The output of the power amplifier was fed to a demodulator and filter system which furnished a direct current potential to the oscillograph recording elements. A General Electric six-element type PM-10 oscillograph was used to make a simultaneous record of the orbital meter output as well as wave pressure and a time pulse. The galvanometer elements, which record on photosensitive paper, have essentially uniform response up to 3,000 cycles per second and thus do not introduce any appreciable time errors in the measurements.

WAVE MEASUREMENTS

A continuous record of wave pressure was obtained from a thermopile wave meter mounted on the tripod with the orbital current meter. The thermopile wave meter operates on the principle of the polytropic gas law, and was used in this study because it was small, light-weight, and had simple cable requirements (Isaacs and Wiegel, 1950). The meter was calibrated during each operation by comparing the meter output with visual measurements of wave height obtained from a calibrated staff mounted directly above the instrument (figures 2 and 3).

Wave Period: The record from the wave meter was used directly as a time indicator for the passage of wave crests and for obtaining the period between crests. Because of the complexity of the waves it was necessary to define and obtain several types of wave period from the pressure record. The first period, T, was used only for evaluating wave height from the record as described in the following section. It is defined as the time interval of the rise and fall of water associated with the passage of the wave crest and was measured on the record from the minimum pressure just preceding the crest to that immediately following the crest (figure 1).

Since waves near the breaker zone are not sinusoidal and each crest tends to be somewhat independent of its neighbors, the essential time element should give the separation of each crest from preceding and following disturbances. Consequently, a "neighbor period", T_n, for a given wave crest was defined as one-half the time interval from the preceding to the following wave crests. Any disturbance less in height than one-fourth of the average of the heights of the crest under consideration and the preceding crest was omitted from consideration. The neighbor period was used in all calculations where the period of individual waves was concerned.

For general characterization of the group aspect of the waves during each observation, the significant wave period, $\bar{T}_{1/3}$, was obtained by averaging the period of the highest one-third of the waves during each series of observations. The number of waves to be averaged was based on the average period of the ten highest waves of relatively simple profile occurring during a 20-minute interval. General features of the waves during the observations are listed in table 1, and graphs of wave height versus period for each series in figures 17 through 24.

Wave Height: Although the meter operates on the principle of the polytropic gas law, the wave pressure could not be obtained directly from the record because the meter is not completely adiabatic and there is a lag in the silver-constantine thermopile. Since these discrepancies in the meter response are a function of period, the wave record was corrected and made proportional to pressure by a correction factor obtained from the calibration of the meter.

Because the interpretation of wave height from shallow water pressure records is not clear, the meter output was calibrated for wave height by obtaining the least squares best fit (regression line) of the corrected meter response as a function of the observed wave height (figures 7 and 8). In general the wave height used in this study was the average of the heights from the wave crest to the preceding and following troughs, although each was used separately in some phases of the study.

Each observational series included several hundred waves, and approximately 20% of these waves were visually measured on the graduated staff above the orbital meter tripod and used for calibrating the wave recorder. In the final analysis of most data, wave height was based on this calibration. Nomenclature and the method of computation are given in the list of symbols and figure 1.

Depth of Water: An average depth for the water during each observation was interpreted from the visual measurements of water level on the calibrated staff mounted above the orbital meter tripod. As mentioned

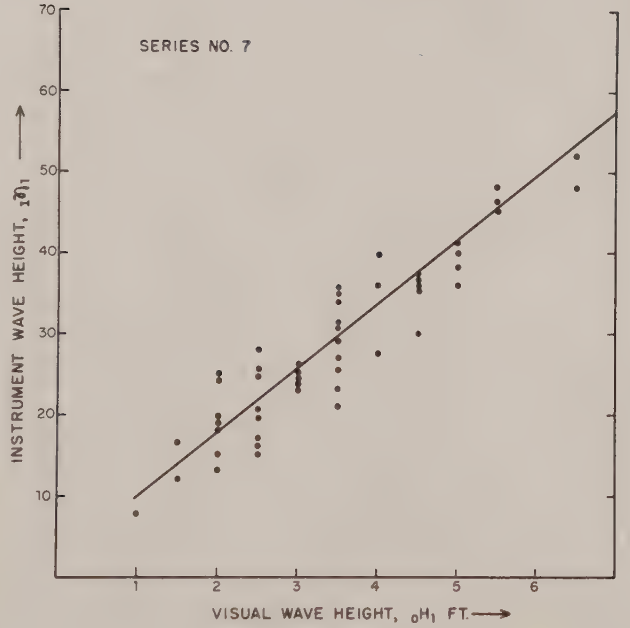

Figure 7. Calibration of the wave pressure record from the regression line of instrument wave height as a function of height from wave staff. The instrument wave height is the chart displacement of the pressure record corrected for the frequency response of the instrument.

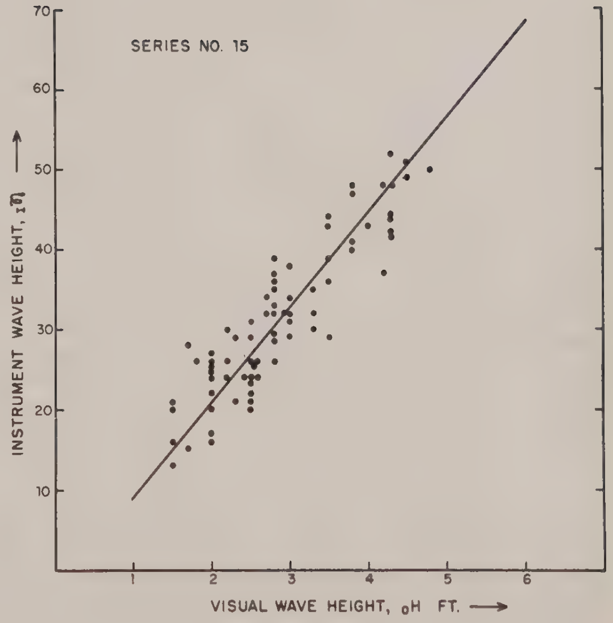

Figure 8. Calibration of the wave pressure record for series 15 (refer to figure 7).

previously, the water depth under the wave crest, ${}_oh_c$, and the preceding and following troughs, ${}_oh_1$, and ${}_oh_2$, were systematically measured for about 20% of the waves. From these measurements an average wave height, ${}_oH$, was obtained for each wave crest:

$$ {}_oH = {}_oh_c - \tfrac{1}{2}\,({}_oh_1 + {}_oh_2) \qquad (2) $$

The prefix "o" indicates that the data are obtained from visual measurements of water level on the wave staff and not from an interpretation of the wave pressure record.

The still water depth, d, was defined as the depth axis intercept of the least squares orthogonal regression line (Hald, 1952, p. 601) of ${}_oh_c$ and ${}_oH$. The equation for this line can be expressed as,

$$ {}_oh_c = m\,{}_oH + d \qquad (3) $$

where ${}_oh_c$ is the distance of the wave crest above the bottom, m is the slope of the regression line and d, is the h axis intercept. Thus d is an approximation to the average water depth as the wave height approaches zero. Graphs of ${}_oh_c$ and ${}_oH$ are shown in figures 9 and 10, and the values of d and m for each series are listed in table 1. (see page 26 for Table 1)

If equation (3) is written in the form

$$ m = \frac{{}_oh_c - d}{{}_oH} $$

it is evident that the slope of the line, m, is the ratio of that portion of the wave crest which extends above the average depth to the total wave height. The value of m was found to range from 0.76 to 0.86. This means that for a given wave height, measured from the wave trough to wave crest, approximately 76 to 86% of the height is above water level and the remaining portion, extending to the wave trough, is below.

IDEAL WAVES

In deep water, waves tend to be sinusoidal and each wave is an interdependent part of a broader pattern or group. The motion of such waves is principally dependent on their length, to a lesser extent on their height, and is independent of depth. The wave concepts of Airy and Stokes apply best to waves in deep water where wave length is the essential descriptive parameter.

In shallow water and especially near the breaker zone, the sinusoidal or continuous frequency characteristics commonly associated with waves in deep water are lost and individual waves tend to retain their identity. Here, the length of the wave is less significant, and the depth of water

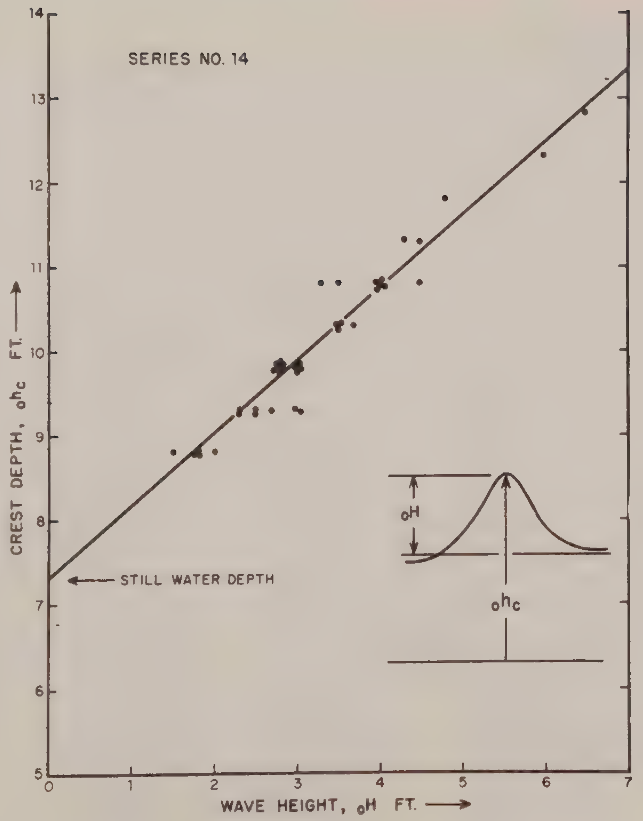

Figure 9. Determination of still water depth from the orthogonal regression line of the wave height and the depth of water under the **wave crest**. The slope of the line, m, defined by equation(3), is a measure of the proportion of the wave height which extends above still water depth. Depth, d = 7.3 ft; slope, m = 0.86.

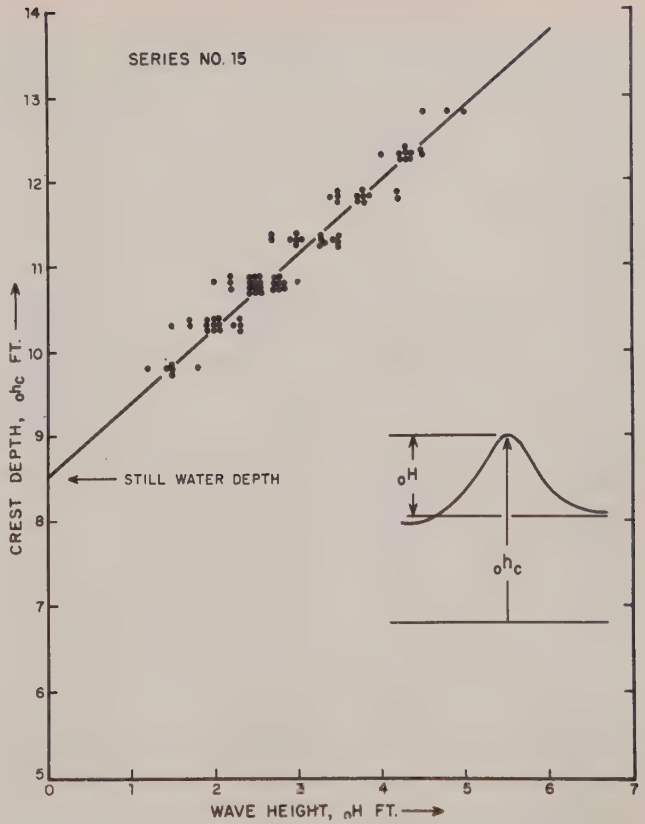

Figure 10. Determination of still water depth for series 15. Depth, d = 8.5 ft; slope of the orthogonal regression line, m = 0.85.

and height of wave become controlling factors. In profile there is a tendency for the waves to consist of isolated crests separated by relatively flat troughs. For this reason the solitary wave concept of Scott-Russell has been applied to waves near the surf zone, and has met with some degree of success. Brief summaries of the essential relations for Airy, Stokes, and solitary waves are given below.

AIRY WAVES

The equation of classical hydrodynamics gives the wave phase velocity C as a function of wave length L and depth of water d:

$$C^2 = \frac{gL}{2\pi} \tanh \frac{2\pi}{L} d \qquad (4)$$

where g is the acceleration of gravity. The instantaneous horizontal and vertical components of orbital velocity u and w are:

$$u = \frac{\pi H}{T} \frac{\cosh \frac{2\pi}{L} z}{\sinh \frac{2\pi}{L} d} \cos \frac{2\pi}{L} (x - Ct) \qquad (5)$$

$$w = \frac{\pi H}{T} \frac{\sinh \frac{2\pi}{L} z}{\sinh \frac{2\pi}{L} d} \sin \frac{2\pi}{L} (x - Ct) \qquad (6)$$

where T = L/C is the wave period, H is the wave height, z is the vertical coordinate measured from the bottom upwards, and x and t are the horizontal distance and time respectively measured from the wave crest.

The above general theory, attributed to Sir George Airy in 1845 (Lamb, 1945, p. 368), is strictly applicable to waves of infinitely small height in water of any depth. The wave profile is sinusoidal and the particle orbits are closed circles in deep water and ellipses in shallow water. Inspection of equations 5 and 6 shows that the orbital velocities vary as sine functions with time, and that the magnitudes of the maximum onshore and offshore velocities are equal. The requirement of small wave height and the resulting symmetry of orbital velocity are not in agreement with ocean surface waves near the breaker zone.

STOKES' WAVES

Of the theories for waves of finite height, that of Sir George Stokes (1847) has met with most success. The Stokes' wave has flatter troughs and steeper crests than the Airy wave. The particle orbits are not closed, but lead to a slight net transport in the direction of wave propagation.

The horizontal and vertical components of orbital velocity for Stokes' waves are, to the second approximation:*

$$u = \frac{\pi H}{T} \frac{\cosh \frac{2\pi}{L} z}{\sinh \frac{2\pi}{L} d} \cos \frac{2\pi}{L} (x-Ct) + \frac{3}{4} \frac{\pi^2 H^2}{LT} \frac{\cosh \frac{4\pi}{L} z}{(\sinh \frac{2\pi}{L} d)^4} \cos \frac{4\pi}{L} (x-Ct) \tag{7}$$

$$w = \frac{\pi H}{T} \frac{\sinh \frac{2\pi}{L} z}{\sinh \frac{2\pi}{L} d} \sin \frac{2\pi}{L} (x-Ct) + \frac{3}{4} \frac{\pi^2 H^2}{LT} \frac{\sinh \frac{4\pi}{L} z}{(\sinh \frac{2\pi}{L} d)^4} \sin \frac{4\pi}{L} (x-Ct) \tag{8}$$

Inspection of equation (7) shows that the first term, which is identical to the complete expression for the horizontal orbital velocity of the Airy wave (equation 5), is positive under the wave crest and negative under the trough, while the second term is positive under both crest and trough and negative at 1/4 and 3/4 wave lengths from the crest. The effect of this term is to increase the magnitude but shorten the duration of the orbital velocity under the crest, and decrease the magnitude but lengthen the duration of the offshore velocity under the trough. This asymmetry of the orbital velocity profile with time is more nearly like the solitary wave and is in keeping with observations of shallow water waves in nature. It should be noted, however, that the sum of the absolute values of maximum velocities under the wave crest and trough has the same magnitude for both Airy and Stokes waves. Thus along the bottom the sum of crest and trough velocities for both waves is given by:

$${}_{a}U = \left| \begin{matrix} u_{\text{crest}} \\ z = 0 \end{matrix} \right| + \left| \begin{matrix} u_{\text{trough}} \\ z = 0 \end{matrix} \right| = 2 \frac{\pi H}{T} \frac{1}{\sinh \frac{2\pi}{L} d} \tag{9}$$

This expression for the orbital velocity is in a convenient form for comparison with field observations because the effects of other velocities that may be present at the time of measurement are minimized so long as their period is long compared to that of the waves.

SOLITARY WAVE THEORY

Munk (1949a) has summarized useful relationships derived from solitary wave theory and made them accessible to numerical examples by plotting various dimensionless relationships. These relationships were used to compute theoretical velocities for comparison with those measured in the field.

Following Munk (1949a), McCowan's approximation for the horizontal orbital velocity, u, and the associated vertical velocity, w, can be expressed as:

---

*These equations result from the partial derivatives of the second order velocity potential given by Stokes (1847, eq. 18), and are identical to equations 3 and 6 of Morison and Crooke (1953). Personal communication from R. A. Fuchs, University of California, Berkeley.

$$\frac{u}{C} = N \frac{1 + \cos M \frac{z}{h} \cosh M \frac{x}{h}}{(\cos M \frac{z}{h} + \cosh M \frac{x}{h})^2} \qquad (10)$$

$$\frac{w}{C} = N \frac{\sin M \frac{z}{h} \sin M \frac{x}{h}}{(\cos M \frac{z}{h} + \cosh M \frac{x}{h})^2} \qquad (11)$$

Where $C = \sqrt{g(H + h)}$ is the velocity of propagation of the wave crest, H is the wave height, h is the depth of water under the wave trough, M and N are functions of the relative wave height, $\gamma = H/h$, and are defined by the equations

$$\gamma = \frac{N}{M} \tan \frac{1}{2} \left[M(1 + \gamma) \right] \qquad (12)$$

$$N = \frac{2}{3} \sin^2 \left[M(1 + \frac{2}{3}\gamma) \right] \qquad (13)$$

Directly beneath the wave crest both x and w are zero and equations (10) and (11) reduce to

$$(u)_{x=0} = \frac{NC}{1 + \cos M \frac{z}{h}} \qquad (14)$$

At the bottom z is zero and the velocity beneath the crest becomes

$${}_sU = (u)_{\substack{x = 0 \\ z = 0}} = \frac{1}{2} NC \qquad (15)$$

Values of ${}_sU$ for various water depths and wave heights are graphed in figure 27.

According to solitary theory, water particles are essentially at rest at distances greater than about x = 10h in front of the wave crest. As the crest approaches they move forward and upward and attain their maximum velocity at the instant the crest passes. Following the passage of the crest the velocity of the particles decreases and they move downward, eventually reaching a new rest position, a distance r in advance of their former rest position. Thus, when solitary waves travel through still water, particles undergo relatively flat trajectories with motion only in the direction of wave propagation. The velocity given by equation (15), ${}_sU$, is therefore the maximum velocity that a particle would attain at the bottom during the passage of a solitary wave in still water.

Closed or partially closed trajectories and orbital motion more nearly resembling those for shallow water waves in nature are obtained from the theory by superposing some sort of return flow on the solitary wave (Munk 1949a). If we consider a uniform velocity v opposed to the direction of propagation of a train of solitary waves, the maximum velocity at the time of crest passage will be ${}_sU$-v. If the solitary waves are far apart, the velocity under the trough will be v, and opposite in direction to that under the crest. In this case the sum of the absolute values of maximum velocities under the wave crest and trough would be ${}_sU$. Thus ${}_sU$ and ${}_aU$ are comparable in that both represent the absolute sums of crest and trough velocity for their respective types of wave motion.

ANALYSIS OF DATA

The complex character of wave motion in nature made systematic analysis of the records difficult. It was possible to obtain frequency distributions of various properties such as wave height and period and some aspects of the orbital velocity. However, in order to compare the measured values of velocities with wave theory it was necessary to neglect group characteristics and to consider each wave individually, including only those waves which had relatively simple profiles as in figure 11. The distinction between simple and complex wave profiles was necessarily arbitrary. Examples of simple waves are listed in the captions for the sample wave records. In general, compounded or double crested waves, as illustrated by the first wave in figure 16 and the last wave in figure 15, were excluded from comparison with theory, but were included in frequency distributions which were used to characterize the wave and orbital spectrum. Thus all waves were used to plot wave height-period diagrams, figures 17 through 23, and histograms showing the distributions of maximum orbital velocities, figures 25 and 26.

The simple waves were used for comparison with wave theory, figure 28 through 39, and a list of the pertinent measurements for each wave is given in appendix I.

Two techniques were used to compare the simple waves graphically with theory. The waves were compared with solitary wave theory by plotting the ratio of the observed horizontal velocity, U, to the predicted velocity ${}_sU$ (ordinate) as a function of the relative wave height H/h. The proximity of plotted points to a value of unity for the orbital velocity ratio is a measure of the agreement between measured and predicted velocities. Comparisons of this type are shown in Figures 28 through 33.

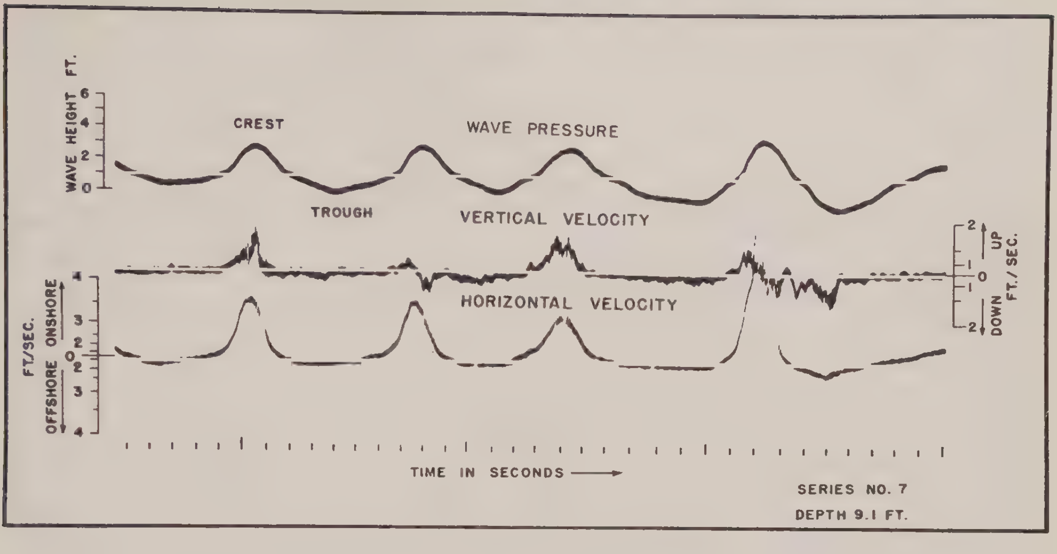

Figure 11. Sample of the record of wave pressure and orbital velocity, series No. 7. Waves number 70 through 73 are shown here. All four waves were considered to have relatively simple profiles; wave and orbital velocity values are tabulated in appendix IB.

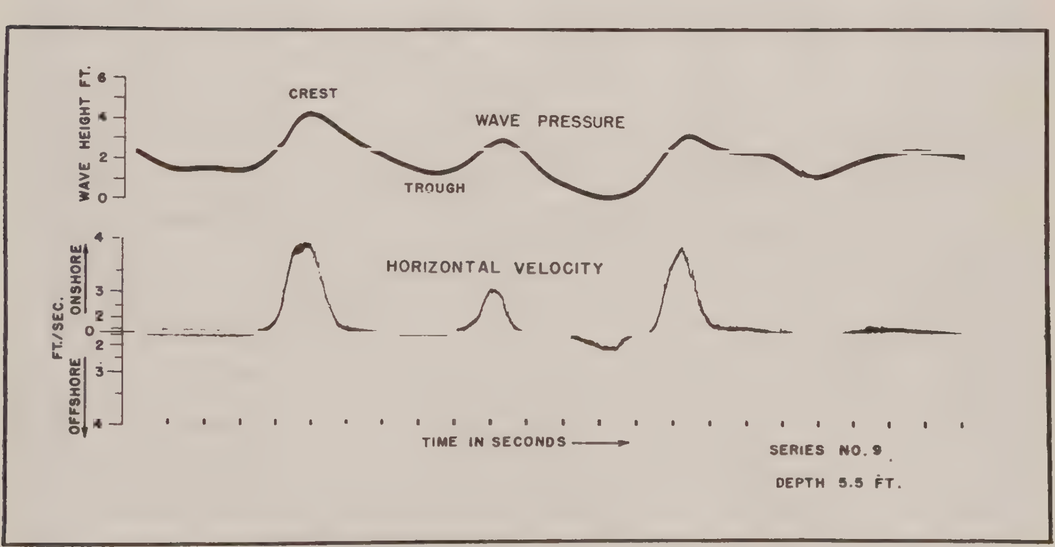

Figure 12. A portion of the record of wave pressure and horizontal component of orbital velocity, series No. 9. Waves number 243 through 246 are shown. The first two were considered to have simple profiles and their properties are listed in appendix IC.

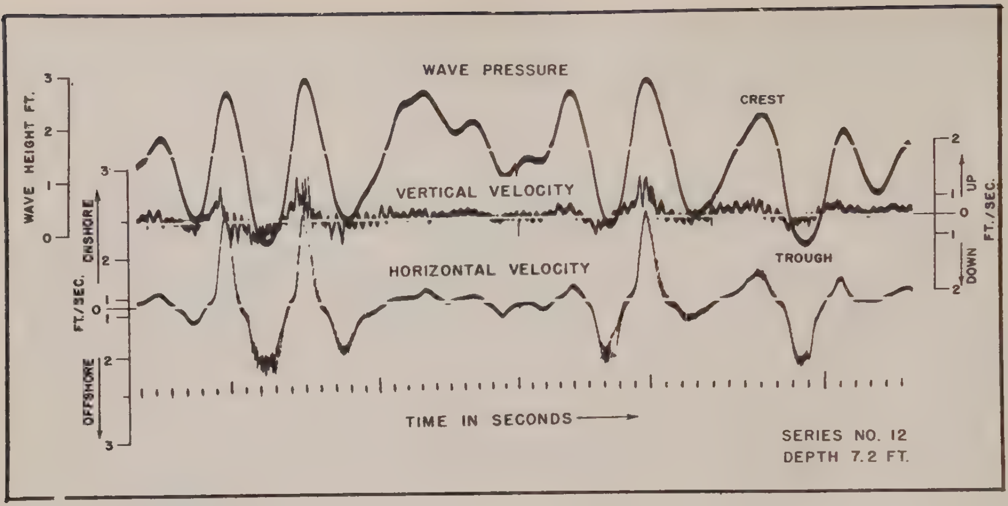

Figure 13. Sample of the record of wave pressure and orbital velocity, series No. 12, showing wave numbers 23 through 31. The first three and the last three were considered to have simple profiles and their properties are listed in appendix ID.

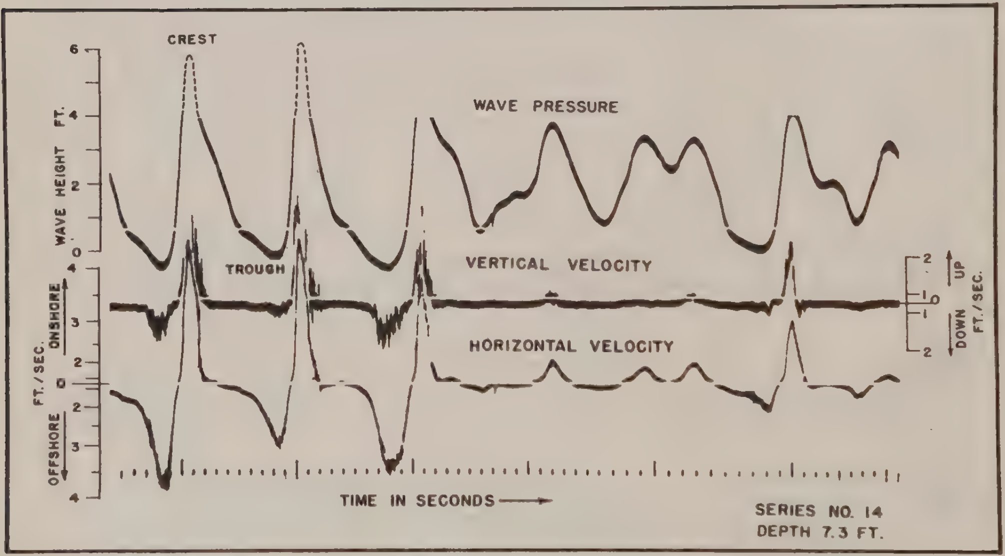

Figure 14. Sample of the record of wave pressure and orbital velocity, series No. 14, showing waves number 40 through 47. The first two, which were measured just before breaking, were considered to have relatively simple profiles and their properties are listed in appendix IE. The dashed lines indicating the crests of these two waves were based on visual measurements of wave height because the pressure record was off scale.

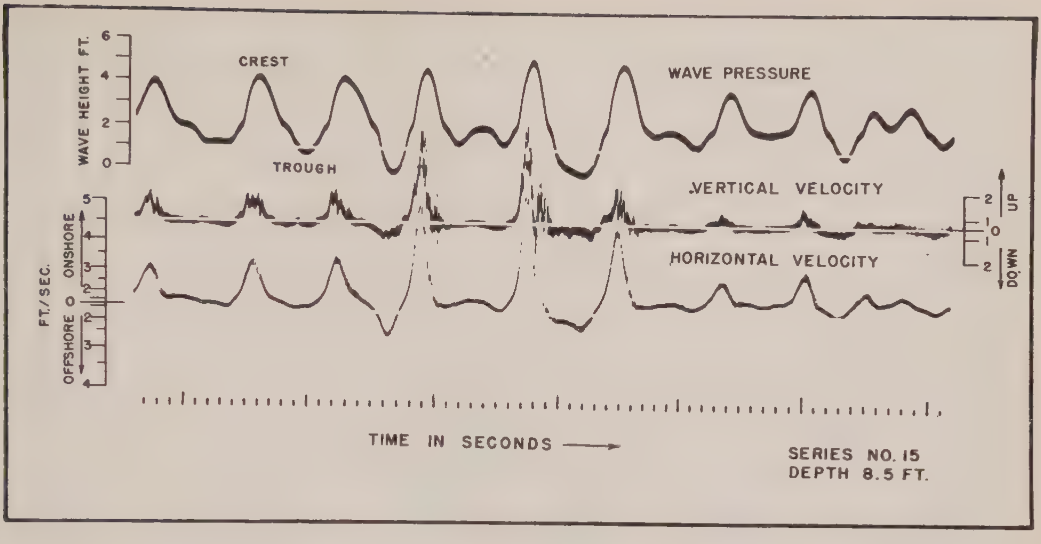

Figure 15. Sample of the record of wave pressure and orbital velocity, series No. 15, wave numbers 3 through 13. Wave numbers 4, 5, 6, 8, and 11 were considered to have simple profiles; their properties are listed in appendix IF.

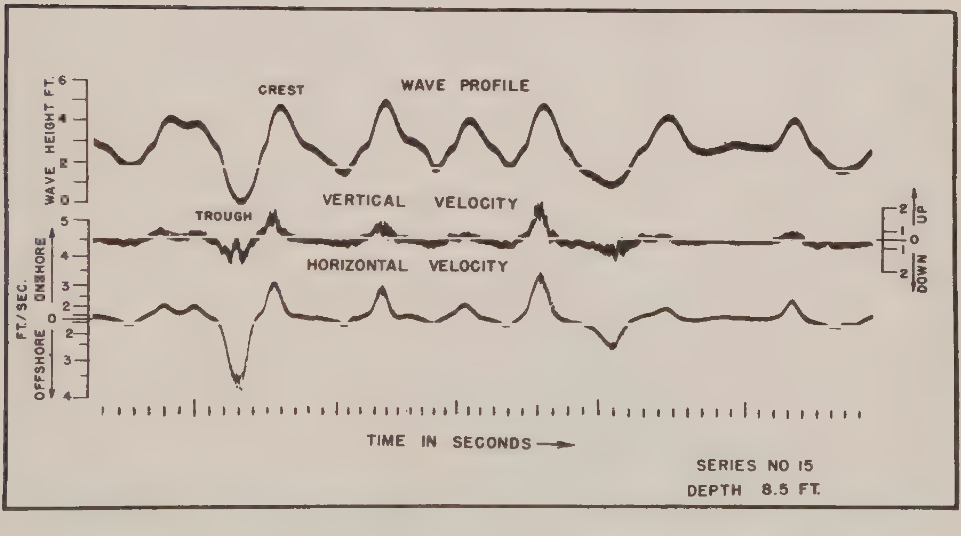

Figure 16. Sample of the record of wave pressure and orbital velocity, series No. 15, showing wave numbers 168 through 174. The second through fifth waves were considered to have simple profiles and are tabulated in appendix IF.

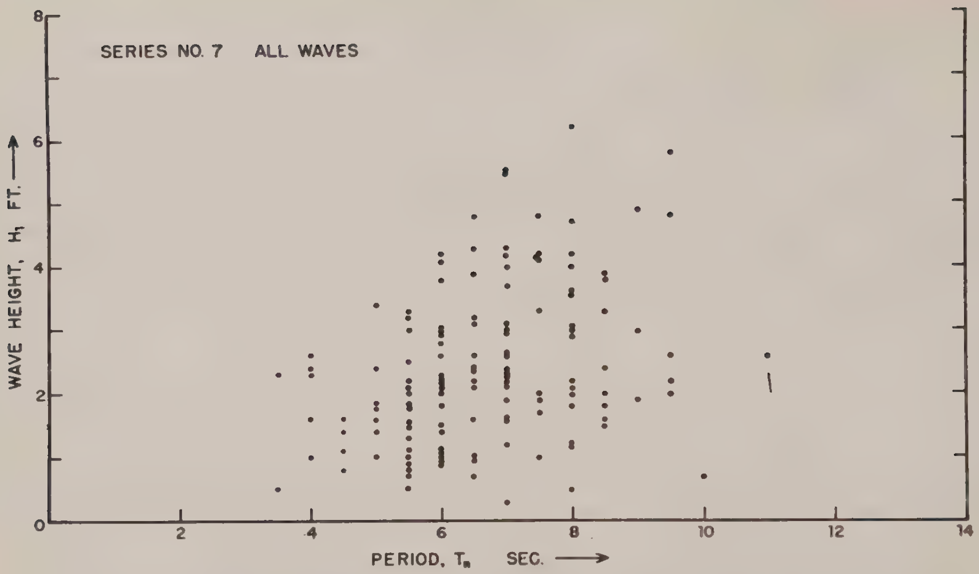

Figure 17. The relation of wave height to wave period for individual waves, series No. 7. This wave height-period diagram shows the wave height, H_1, measured from preceding trough to crest, plotted against wave period.

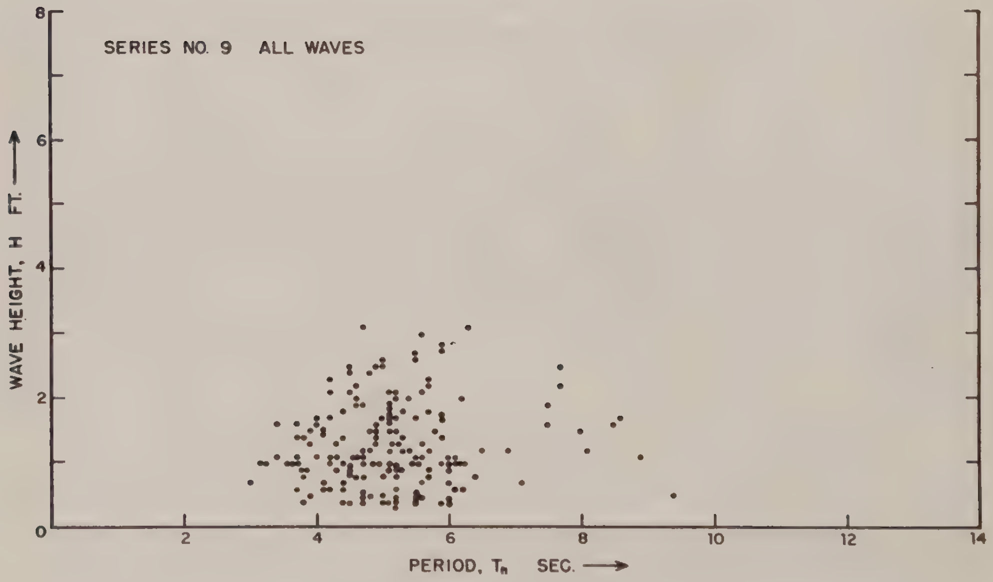

Figure 18. Wave height-period diagram for series No. 9 showing the wave height, H, averaged from crest to preceding and following trough, plotted against wave period.

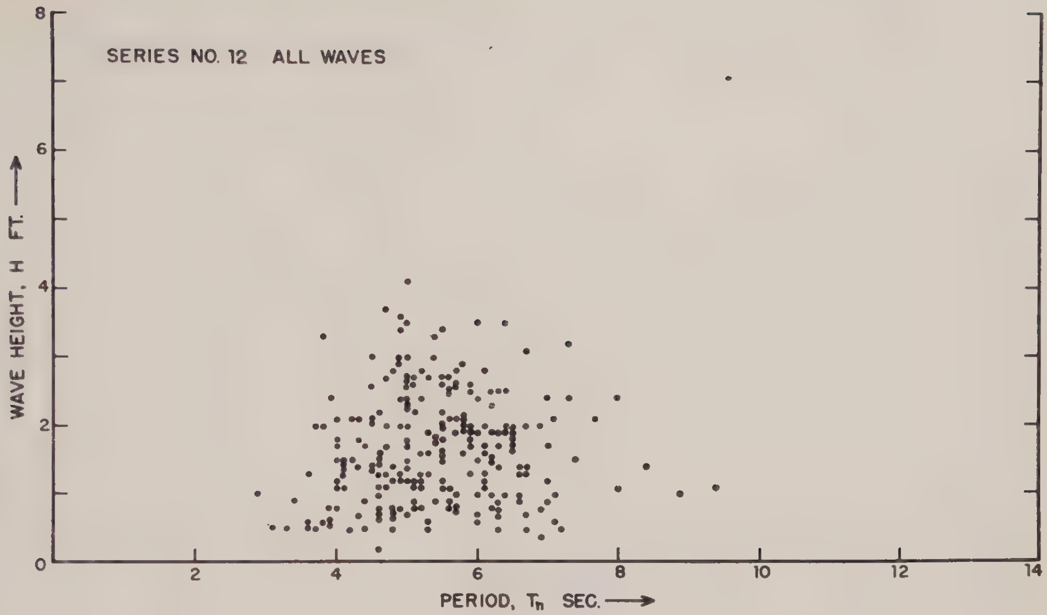

Figure 19. Wave height-period diagram for series No. 12.

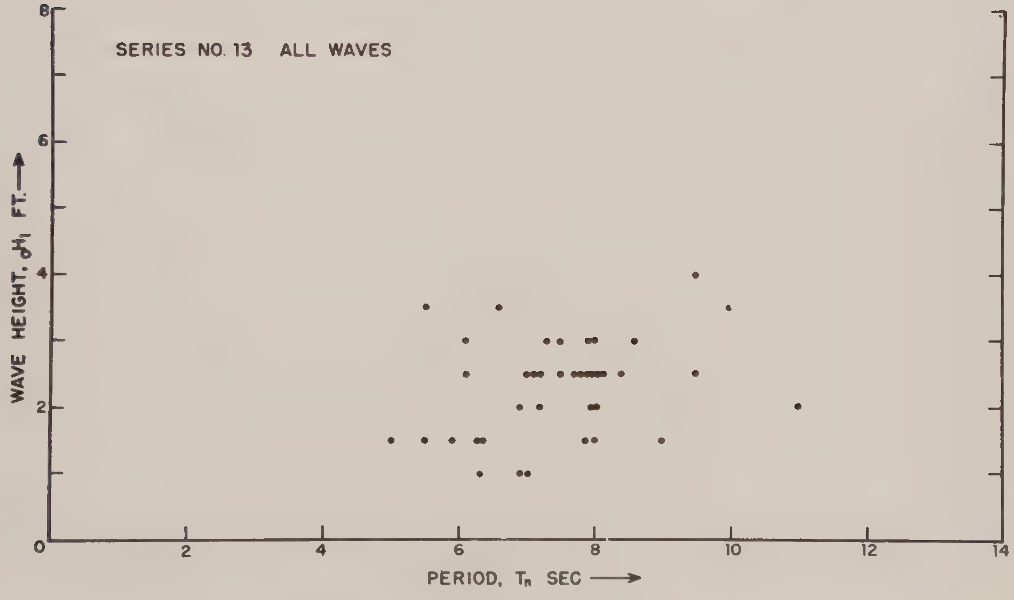

Figure 20. Wave height-period diagram for series No. 13.

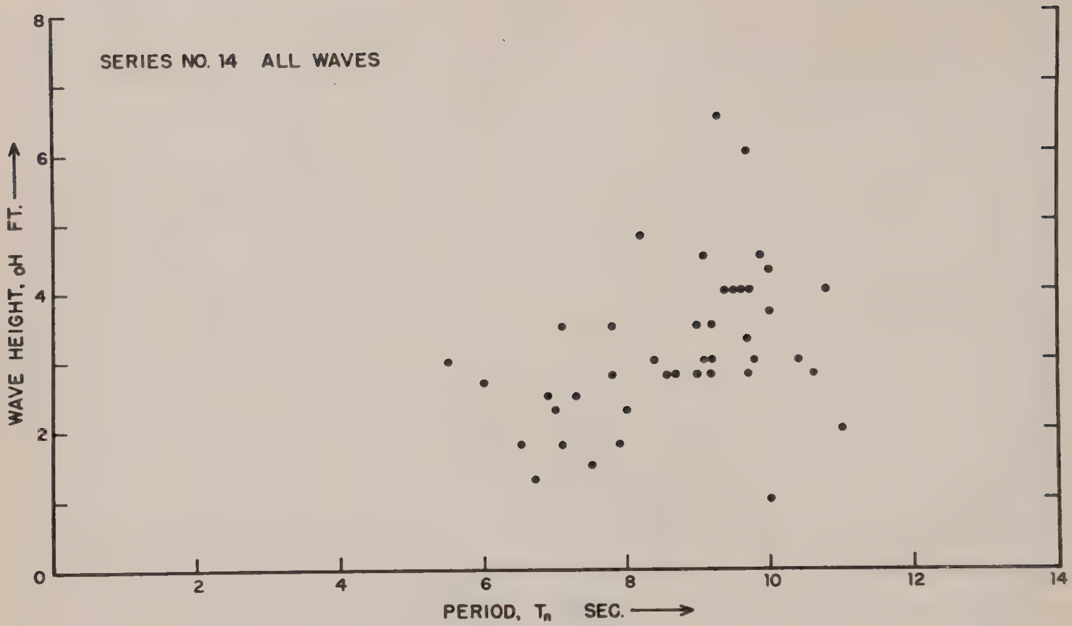

Figure 21. Wave height-period diagram for series No. 14.

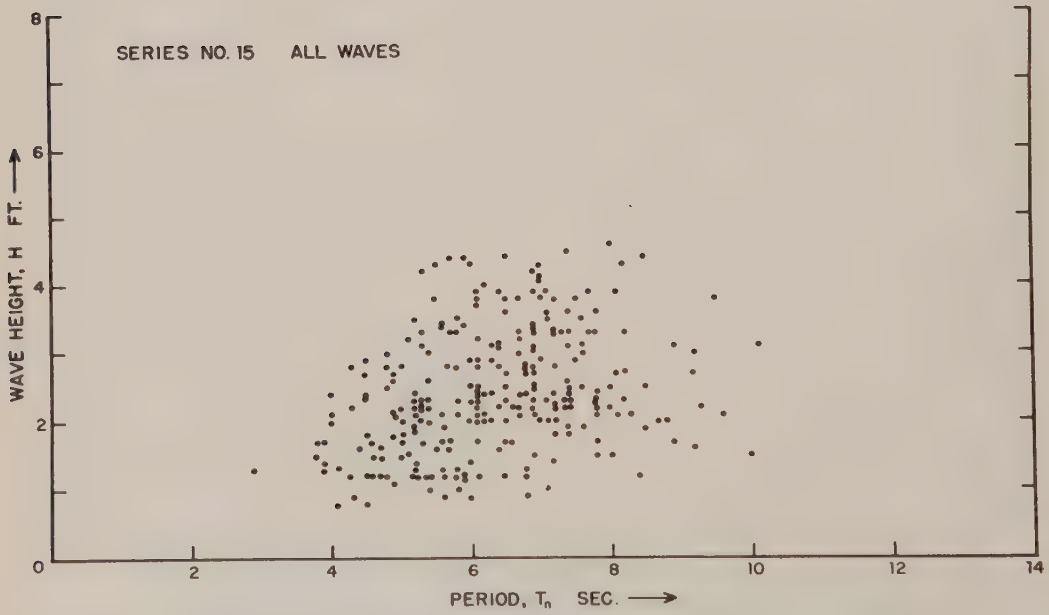

Figure 22. Wave height-period diagram for all waves in series No. 15, using the average wave height H. Compare with figures 23 and 24.

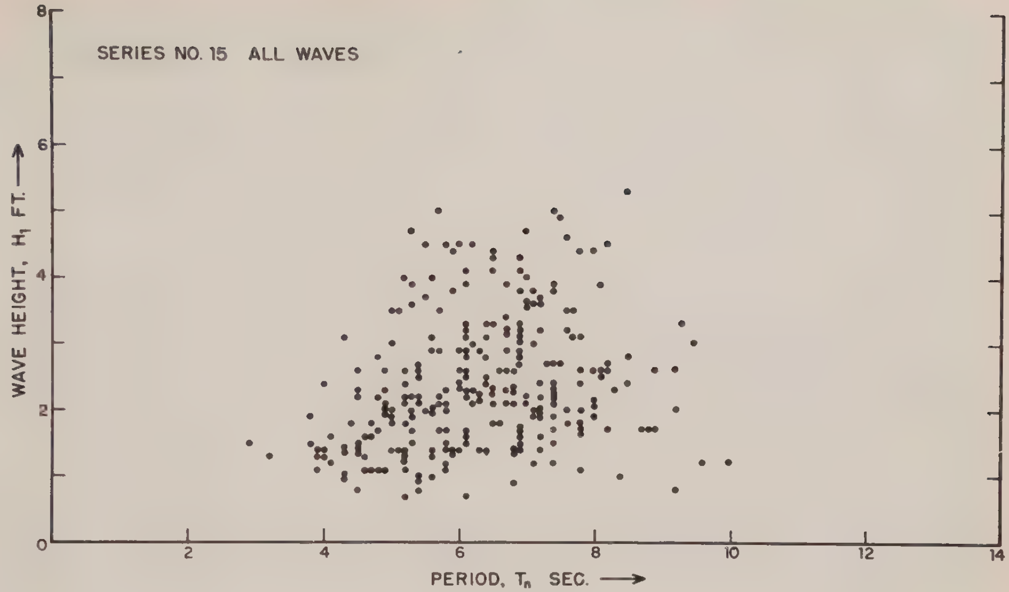

Figure 23. Wave height-period diagram for all waves in series No. 15, using the wave height H_1 measured from crest to preceding trough. Compare with figure 22.

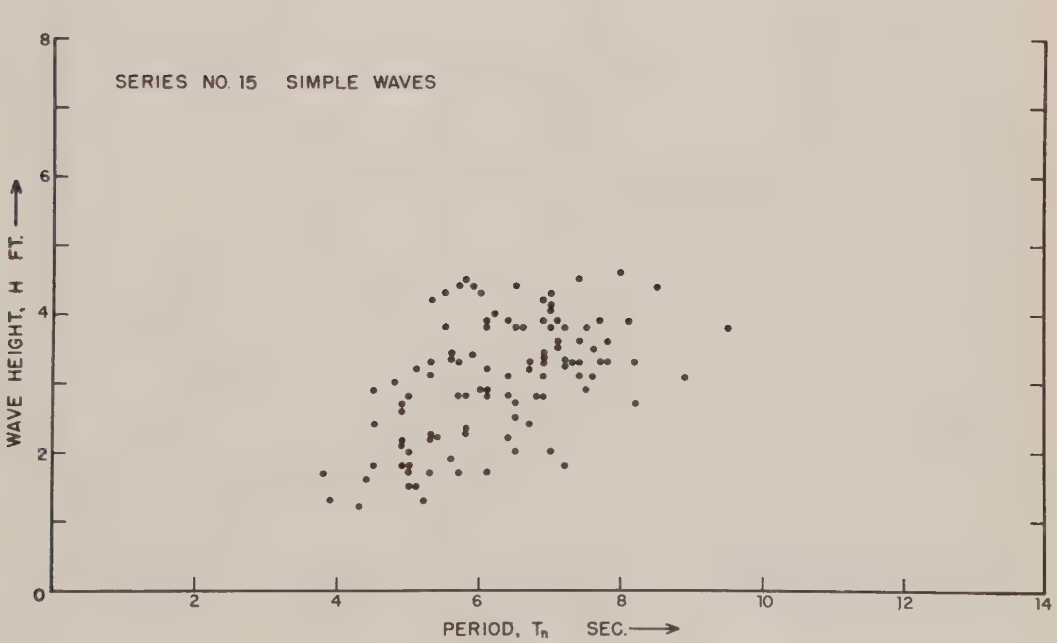

Figure 24. Wave height-period diagram for series No. 15, showing only waves with simple profiles. Data for this figure is tabulated in appendix IF.

TABLE 1. Summary of wave properties.

Series	Duration sec.	Description of Waves	Number of Waves Analyzed		Wave Period[2] $\bar{T}_{1/3}$ sec.	Wave Height[2]			Still Water Depth d ft.	Ratio[5] m	Relative Wave Height[6] $\gamma_{1/3}$
			Total	Simple		$\bar{H}_{1/3}$ ft.	$\bar{H}_{1/10}$ ft.	H_{max} ft.			
7	937	8 sec swell, shorter period superimposed	140	106	7.8	4.1	5.0	6.2	9.1	0.85	0.48
9	1083	5 sec short crested swell, 9 sec secondary	206	64	5.4	2.0	2.5	3.1	5.5	0.76	0.40
12	1358	5½ sec swell	249	185	5.5	2.7	3.2	4.1	7.2	0.79	0.41
13	1253	complex 5 and 12 sec swell	203	*[3]	~7½	~3½			7.2	0.83	0.53
14	1638	10 sec swell, shorter period secondary with tendency to ride preceding crest	213	60[4]	9.8	4.5	5.5	7.0	7.3	0.86	0.67
15	1730	7½ sec swell, tends to be short crested	280	105	6.9	3.8	4.5	5.3	8.5	0.85	0.48

[2] The number of waves to be averaged for $\bar{T}_{1/3}$, $\bar{H}_{1/3}$, and $\bar{H}_{1/10}$ was determined by averaging the periods of large well defined wave trains. The period obtained in this way approximated the value listed for the significant wave period, $\bar{T}_{1/3}$.

[3] Faulty wave pressure record. $\bar{T}_{1/3}$ and $\bar{H}_{1/3}$ estimated from visual measurements. There were few waves with simple profiles.

[4] Portions of wave pressure record off scale. Approximately 2/3 of the waves had simple profiles.

[5] Proportion of the wave crest above still water level. See equation 3.

[6] Relative wave height of the significant waves.

The absolute sum of maximum horizontal crest and trough velocities was obtained from the field data by the following relations:

$$U = u_c + \tfrac{1}{2} \left| u_1 + u_2 \right| \tag{16}$$

$$U_1 = u_c + \left| u_1 \right| \tag{17}$$

The first represents a total absolute maximum velocity from the wave crest to the average of the preceding and following troughs, and the latter from the wave crest to the preceding trough. To obtain the value of the corresponding predicted velocity $_sU$ and $_sU_1$, the wave heights were computed accordingly, and the absolute velocity obtained from the graph of equation 15 (figure 27).

A general comparison of measured velocities with ideal waves was obtained by plotting the orbital velocity as a function of wave height, and superimposing the theoretical curves for Airy-Stokes waves and solitary waves (figures 35-39). Since the solitary theory does not depend on frequency, it is represented by a single curve, while the Airy-Stokes relation requires a curve for each wave period. Curves for 3, 5, and 10-second periods were drawn for each series; the period most applicable for the various wave heights in each series can be approximated by inspection of the wave height-period diagrams.

WAVE HEIGHT AND PERIOD

The relationships between wave height and period, as shown on the height-period diagrams (figures 17-24), are similar to those obtained for ocean waves by Putz (1951, 1952), although there is a more pronounced tendency in these waves for the high waves to have longer periods. This tendency for wave height to increase with period is present in the two wave series, 7 and 14, which have the longer significant period. Those observations where the periods were shorter, such as series 9, 12, and 15, and those where complex wave trains were present, as in series 13, show no tendency for increase in period with wave height.

As mentioned in the discussion following equation (3), the slope of the line when the depth of water beneath the crest is plotted as a function of wave height is a measure of the proportion of the total wave height which occurs above still water depth. For the six series of waves analyzed the slope, m , ranged from 0.76 to 0.86 (table 1), indicating that 76% to 86% of the wave height was above still water level while 24% to 14% was below this level. These findings are in general agreement with model studies of waves near the breaker zone (Wiegel, 1950; Iversen, 1952). Comparison of the slope with the significant period, $\bar{T}_{1/3}$, (table 1) shows that greater values of m occur for series having longer periods and for those series which were measured closer to the breaker zone (high values of the relative wave height, $\gamma_{1/3}$). Thus series 14 has the longest significant period, the highest value of $\gamma_{1/3}$ and the largest value of m, whereas, series 9 has the shortest significant period, the lowest value of $\gamma_{1/3}$, and the lowest value of m. The relative influence of period and depth individually on the value of m cannot be ascertained from this data.

ORBITAL VELOCITY

In general the graph of the horizontal component of orbital velocity as a function of time resembles that of the wave pressure (figures 11-16). The data indicate that the horizontal velocity is more dependent on the rate of change in level of the water surface during the passage of a wave train than on the actual height of the wave. This is illustrated by the fourth wave crest in figure 13; the wave is almost as high as those preceding it, but shows a more gradual rise in level from the preceding trough to the crest which results in a very low crest velocity. The following wave also has a gentle slope preceding the crest and a low crest velocity, whereas the succeeding trough velocity which is associated with a rapid change in water level is exceptionally high. The asymmetry in wave profile and the associated asymmetry in the horizontal crest and trough velocity of waves very near the point of breaking is illustrated by the first two waves of figure 14 which were measured just before they broke.

Distribution of Maximum Onshore and Offshore Velocities: Histograms showing the frequency of occurrence of various values of orbital velocity under wave crest and trough are presented in figures 25 and 26, and the statistical constants such as mean, standard deviation, and root-mean-square values of the crest and trough velocities for each series are listed in tables 2a and 2b. The data are computed and presented in two ways; the first gives the distribution of the maximum orbital velocities under each wave crest and trough (figures 25, table 2a), and the second gives the distribution of maximum onshore and offshore orbital velocities between zero crossings of the horizontal velocity record (figure 26, table 2b). The first method counts as a wave crest each disturbance of the water surface which results in a maximum peak on the horizontal orbital velocity record. The second method considers only the maximum velocities which occur between changes in direction (zero crossings) of the horizontal velocity.

These two methods of presentation differ because the water in the surf zone is in a continual state of fluctuation (Munk, 1949b; Shepard and Inman, 1950, figure 11), and because there is apparently some tendency in shallow water for large waves to "trap" smaller waves, resulting in double crested waves and the accompanying double peak in onshore velocity. Double crested waves such as the fifth wave in figure 14 and the last wave in figure 15 result in trough velocities between the crests which are in an onshore direction. For these reasons

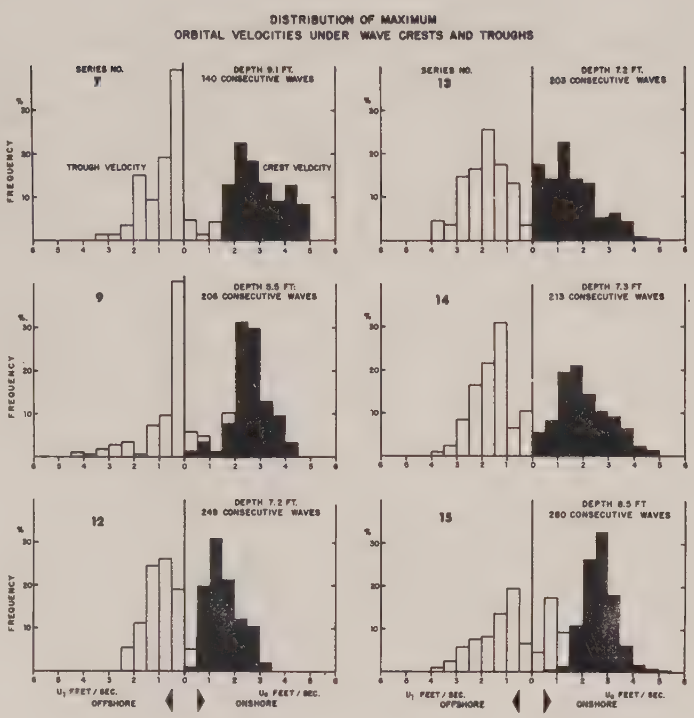

Figure 25. Histograms of the distribution of maximum horizontal orbital velocities under each wave crest (shaded) and trough (unshaded). Each disturbance of the water surface which results in a maximum peak on the horizontal velocity record is considered as a separate wave crest.

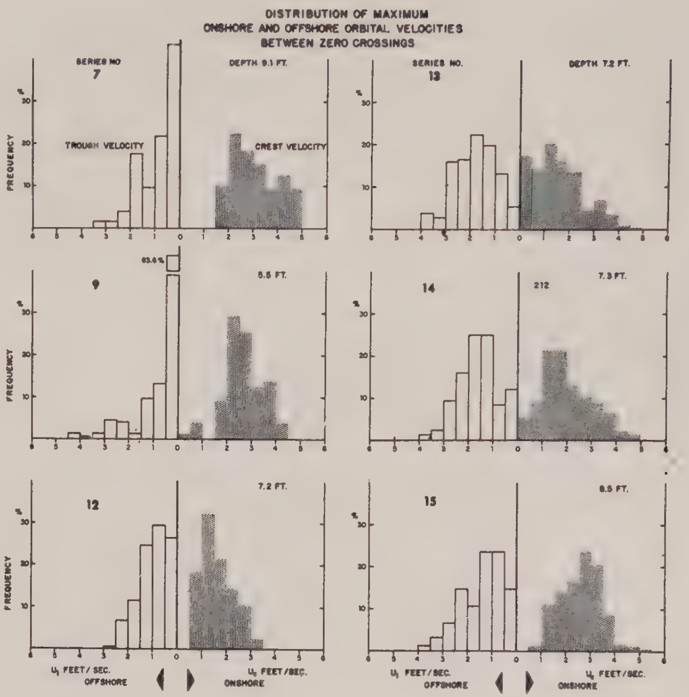

Figure 26. Histograms of the distribution of maximum horizontal orbital velocities occurring between zero crossings (changes in direction) of horizontal velocity. Onshore orbital velocities under the wave crest are shaded; offshore velocities under the wave trough are unshaded.

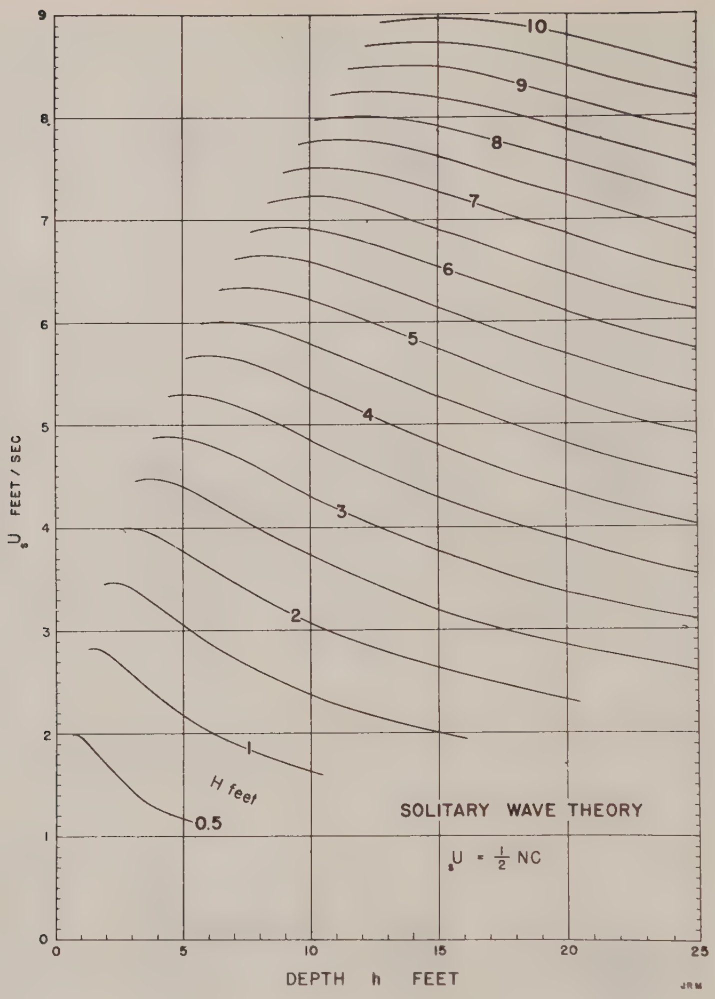

Figure 27. Isolines of wave height, H, as a function of the maximum horizontal orbital velocity at the bottom, $_sU$, and the depth of water under the wave trough, h, from equation 15. $_sU$ is the absolute sum of the maximum velocities under the wave crest and trough.

TABLE 2a. Statistics of the distribution of maximum orbital velocities under wave crests and troughs. Histograms for these velocities are plotted in figure 25.

Series	Onshore Maximum Horizontal Velocity, ft/sec				Offshore Maximum Horizontal Velocity, ft/sec			
	Mean $\bar{u}_c$	Standard* Deviation	Root-mean-square	Maximum Velocity	Mean $\bar{u}_1$	Standard Deviation	Root-mean-square	Maximum Velocity
7	3.0	0.9	3.2	4.9	0.7	0.8	1.1	3.3
9	2.6	0.8	2.7	4.2	0.1	1.4	1.4	4.3
12	1.6	0.7	1.7	3.1	0.8	0.8	1.1	2.4
13	1.6	1.0	1.9	4.6	1.8	0.8	2.0	3.9
14	2.0	1.0	2.3	4.7	1.6	0.8	1.7	3.7
15	2.7	0.6	2.8	5.1	0.6	1.4	1.5	3.8

---

* $\sqrt{\frac{1}{N}\sum(u_c - \bar{u}_c)^2}$

TABLE 2b. Statistics of the distribution of maximum horizontal onshore and offshore orbital velocities between zero crossings. Histograms of these velocities are plotted in figure 26.

Series	Onshore Maximum Horizontal Velocity, ft/sec				Offshore Maximum Horizontal Velocity, ft/sec				Ratio $\bar{u}_c/\bar{u}_1$
	Mean $\bar{u}_c$	Standard* Deviation	Root-mean-square	Maximum Velocity	Mean $\bar{u}_1$	Standard Deviation	Root-mean-square	Maximum Velocity	
7	3.1	0.7	3.2	4.9	0.9	0.7	1.2	3.3	3.4
9	2.7	0.8	2.8	4.2	0.7	0.9	1.2	4.3	3.9
12	1.6	0.7	1.7	3.1	1.0	0.6	1.1	2.4	1.6
13	1.6	1.0	1.9	4.6	1.8	0.8	2.0	3.9	0.9
14	2.0	1.0	2.3	4.7	1.6	0.8	1.8	3.7	1.3
15	2.6	0.8	2.7	5.1	1.4	0.8	1.6	3.8	1.9
								Average	2.2

---

* $\sqrt{\frac{1}{N}\sum(u_c - \bar{u}_c)^2}$

TABLE 3. Threshold velocity of the orbital velocity meter system for each series of observations. The threshold velocity is arbitrarily defined as that steady flow required to produce a 1 mm displacement from the null position on the orbital velocity record (see figure 6).

Series	Horizontal Velocity ft/sec	Vertical Velocity ft/sec
7	1.0	0.6
9	1.0	0.5
12	0.5	0.4
13	0.6	0.4
14	0.7	0.5
15	0.9	0.6

the first method of summation, which includes each velocity peak, results in the occurrence of some trough velocities on the onshore or crest side of the histogram (figure 25).

The maximum velocity under the wave crest was always onshore or in the direction of wave propagation, and for all of the wave series analyzed with the exception of series 2 and 13 the mean onshore maximum velocity exceeded the offshore velocity. The two series out of the fifteen for which the mean of the maximum trough velocities was greater than the mean of the crest velocities were both characterized by irregular and confused wave trains, in which there was a high incidence of wave crests with gentle forward slopes and steep back slopes. However, even in these cases the highest velocities measured were in an onshore direction.

Comparison of Measured and Ideal Velocities: The maximum orbital velocities of the more uniform or simple waves were compared with values computed from equations for the solitary and Airy-Stokes waves. For purposes of comparison the absolute sum of the observed maximum crest and trough velocities as defined by equation (16) and (17) were used so that longer period fluctuations in the surf zone could be neglected. Inspection of the data (figures 28-40), shows that the scatter of plotted points is fairly large for all series, and that the scatter increases with decrease in relative wave height. The increase in spread of plotted points for low waves results in part from decreased sensitivity of the orbital velocity meter at low velocities. However, it is apparent from the plotted data that the velocities measured in the field are on the average in better agreement with the solitary wave than with the Airy-Stokes relations, although portions of some series are not in good agreement with either.

Series 7 and 14, which have longer significant periods of approximately 8 and 10 seconds, are in good agreement with solitary theory (figures 28 and 31). Series 12, which consisted of a relatively uniform swell with a short significant period of 5½ seconds, had orbital velocities which averaged about 20% lower than velocities predicted from the solitary wave equations (figure 30). The observation with the shortest significant period, series 9, showed the greatest scatter in plotted points, but on the average also gave lower values than predicted (figure 29). However, this series was complex; the waves showed a tendency towards short crestedness and included wave trains with a primary period of about 5 seconds and a secondary period of 9 seconds (figure 18). The other short crested group, series 15, is in fair agreement with solitary theory for waves with relative heights greater than about 0.4, but shows a progressive departure from predicted values for lower waves (figures 32 and 33). This series also shows a tendency for the shorter period waves to be associated with lower values of orbital velocity (figure 34). All of the series of observations had significant periods longer than the minimum allowable period suggested by Munk (1949a, plate 2) for applying solitary wave theory to the surf zone.

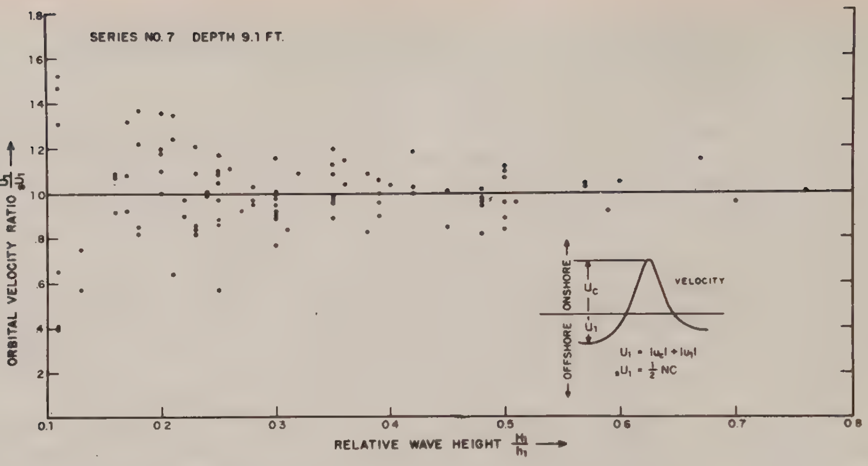

Figure 28. Comparison of the maximum horizontal orbital velocity measured near the bottom with the velocity predicted by solitary wave theory. U_1 is the absolute sum of the observed crest and preceding trough velocities as illustrated in the inset; $_sU_1$ is obtained from figure 27 by using appropriate values of H_1 and h_1. These data are for selected waves of simple profile and are tabulated in appendix IB.

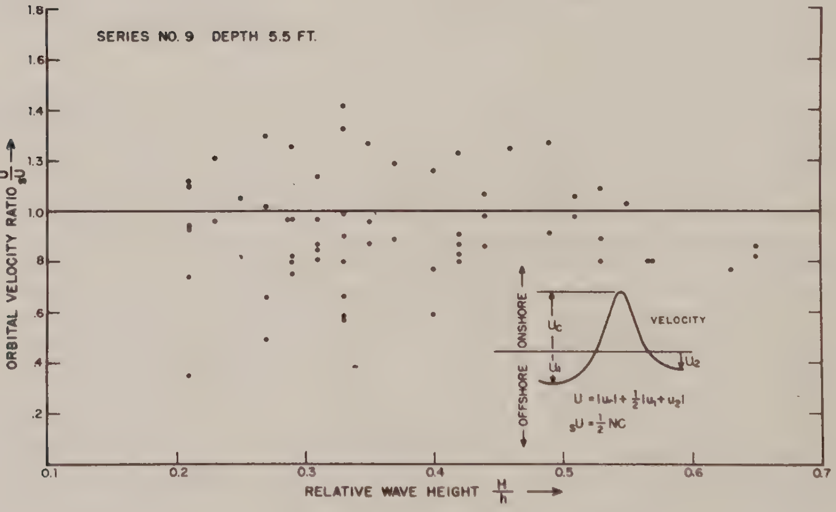

Figure 29. Comparison of the maximum horizontal orbital velocity measured near the bottom with the velocity predicted by solitary wave theory. U is the absolute sum of the observed crest and the average of the preceding and following trough velocities as illustrated in the inset; $_sU$ is obtained from figure 27 by using appropriate values of H and h. These data are for selected waves of simple profile and are tabulated in appendix IC.

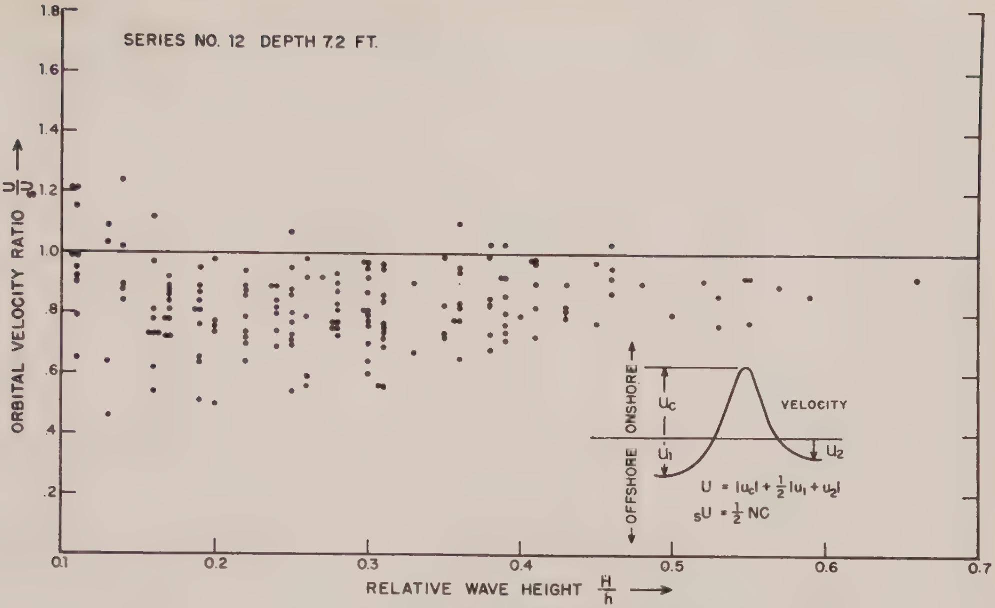

Figure 30. Comparison of the maximum horizontal orbital velocity measured near the bottom with the velocity predicted by solitary wave theory. These data are for selected waves of simple profile and are tabulated in appendix ID.

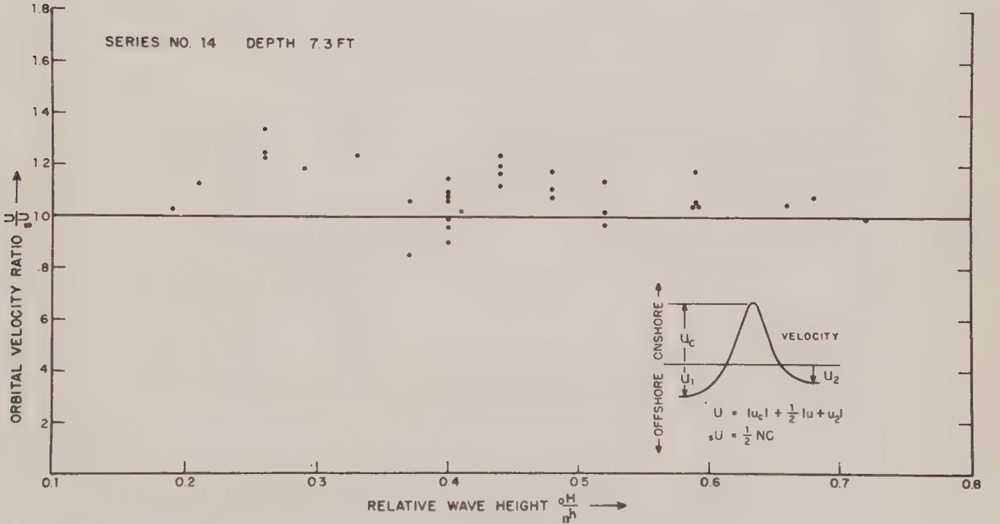

Figure 31. Comparison of the maximum horizontal orbital velocity measured near the bottom with the velocity predicted by solitary wave theory. These data are for selected waves of simple profile and are tabulated in appendix IE.

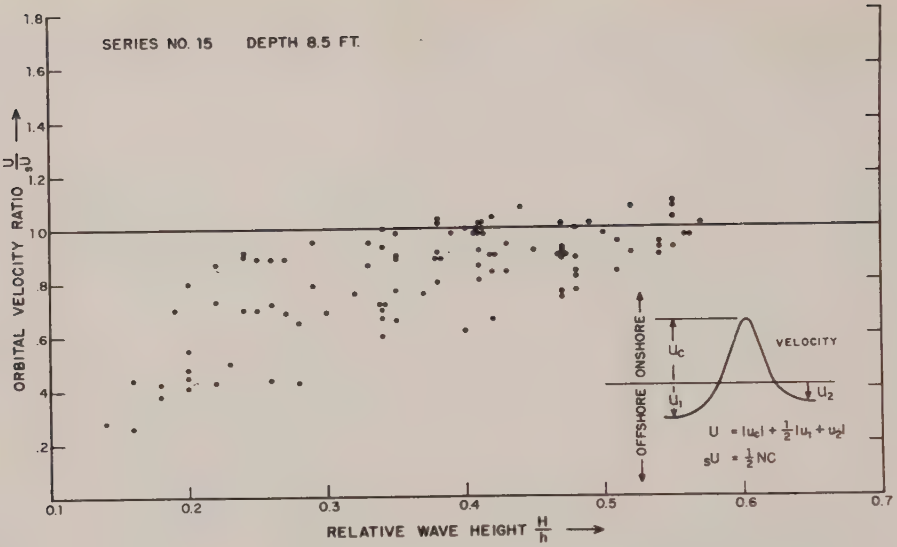

Figure 32. Comparison of the maximum horizontal orbital velocity measured near the bottom with the velocity predicted by solitary wave theory. These data are for selected waves of simple profile and are tabulated in appendix IF.

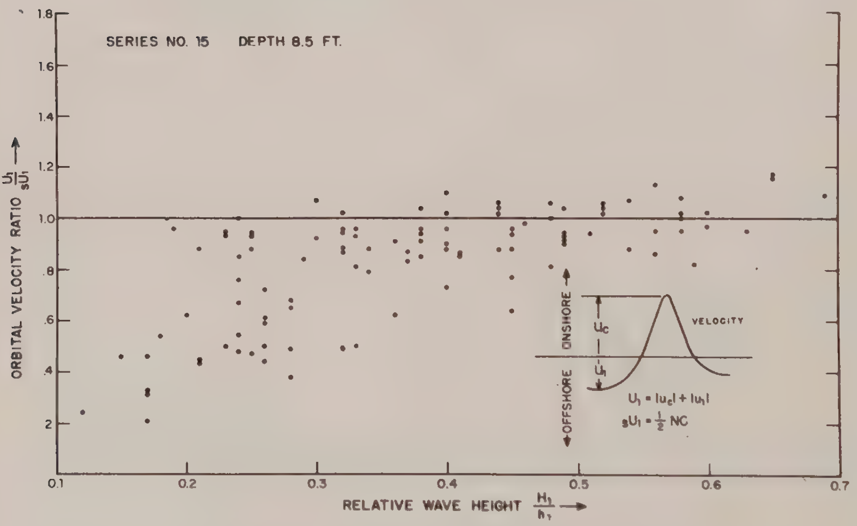

Figure 33. Comparison of the maximum horizontal orbital velocity measured near the bottom with the velocity predicted by solitary wave theory. These data are based on velocities under the wave crest and preceding trough; compare with figure 32 which is for the same wave series, but is based on the crest and the average of the preceding and following trough velocities.

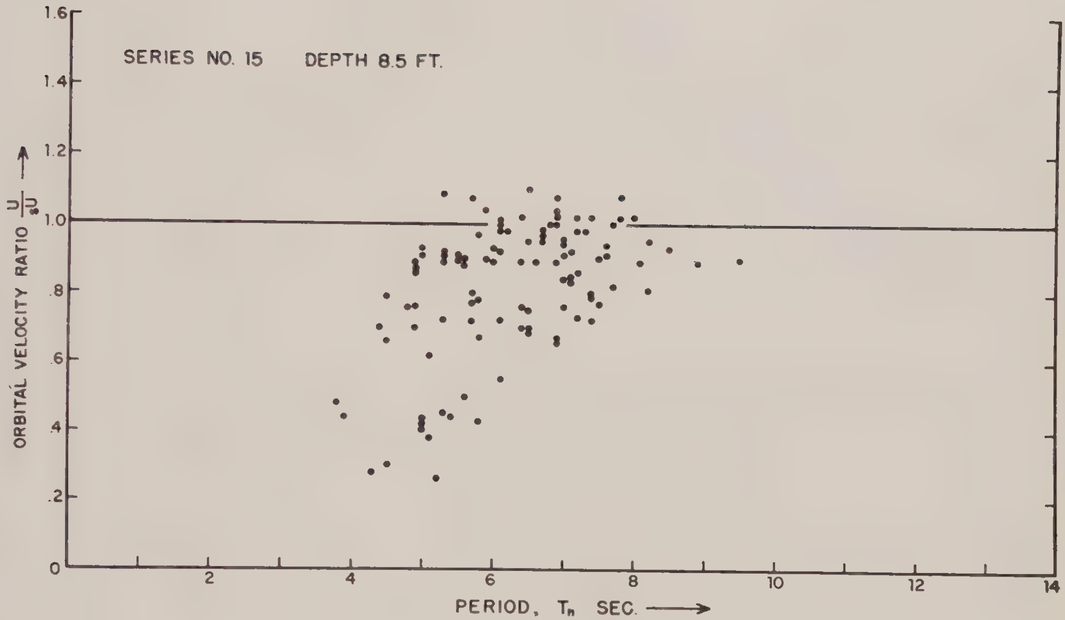

Figure 34. Relation between the ratio of observed to predicted orbital velocity and the period of individual waves, series No. 15.

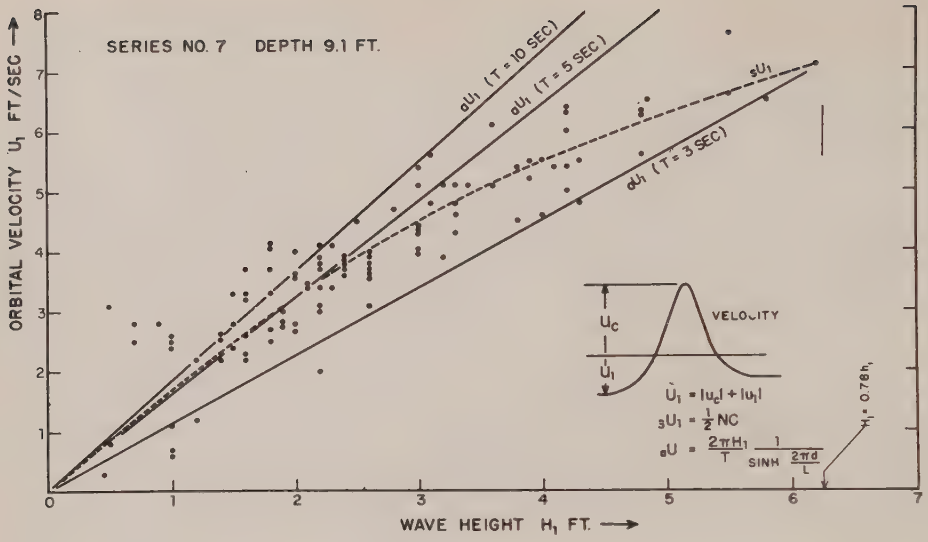

Figure 35. Relation of maximum horizontal orbital velocity to wave height, with curves based on Airy-Stokes and solitary wave theory superimposed for reference. The orbital velocity, $_aU$, from the Airy-Stokes equation, requires a separate curve for each wave period; curves for 3, 5, and 10 second periods are shown. These data are for selected waves of simple profile and are tabulated in appendix IB.

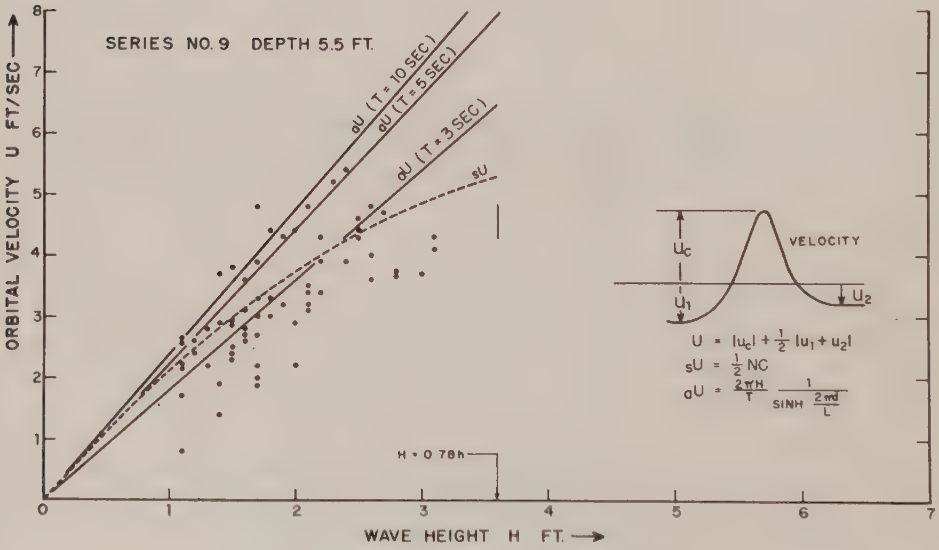

Figure 36. Relation of maximum horizontal orbital velocity to wave height, with curves based on Airy-Stokes and solitary wave theory superimposed for reference. These data are for selected waves of simple profile and are tabulated in appendix IC.

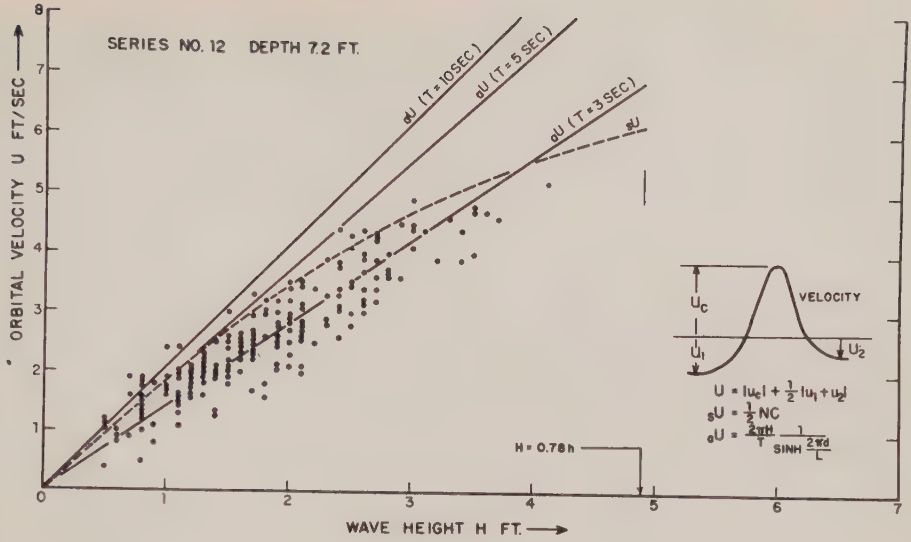

Figure 37. Relation of maximum horizontal orbital velocity to wave height, with curves based on Airy-Stokes and solitary wave theory superimposed for reference. These data are for selected waves of simple profile and are tabulated in appendix ID.

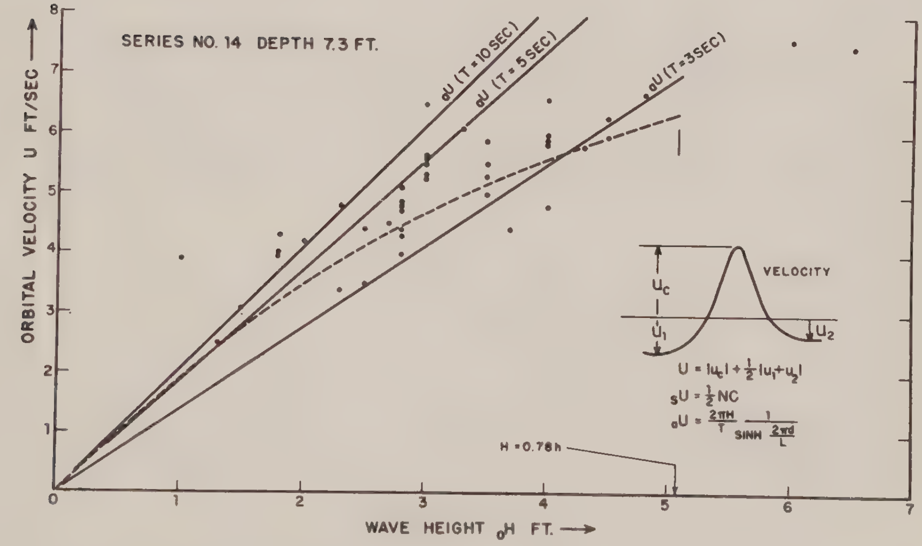

Figure 38. Relation of maximum horizontal orbital velocity to wave height, with curves based on Airy-Stokes and solitary wave theory superimposed for reference. These data are for selected waves of simple profile and are tabulated in appendix IE.

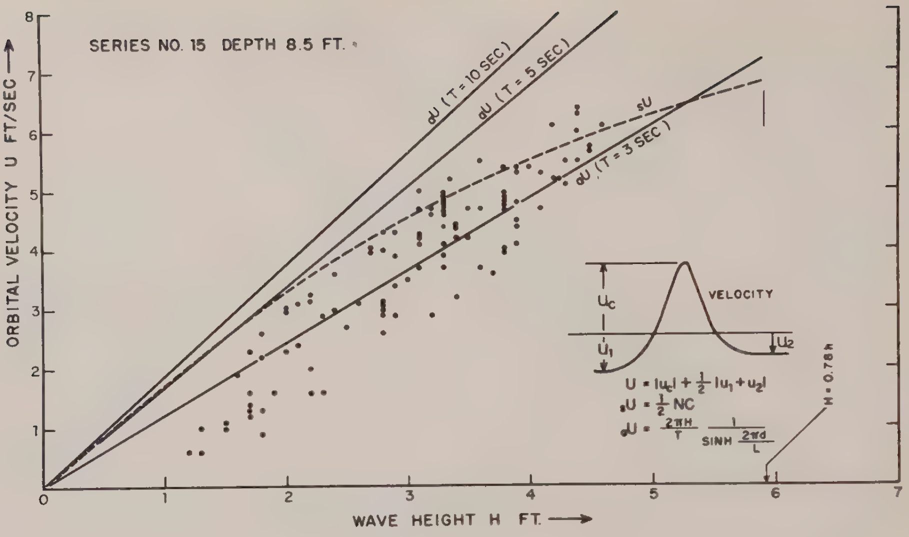

Figure 39. Relation of maximum horizontal orbital velocity to wave height, with curves based on Airy-Stokes and solitary wave theory superimposed for reference. Compare with figure 40 which is based on the absolute sum of the crest and preceding trough velocities. These data are for selected waves of simple profile and are tabulated in appendix IF.

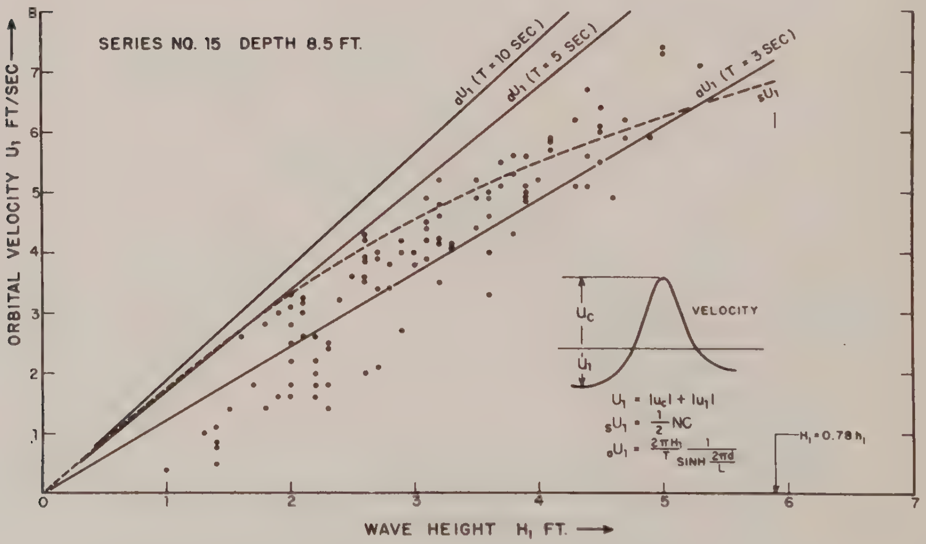

Figure 40. Relation of maximum horizontal orbital velocity to wave height, with curves based on Airy-Stokes and solitary wave theory superimposed for reference. These data are for selected waves of simple profile and are tabulated in appendix IF.

It made little difference in comparing orbital velocities with theory whether the observed velocities were measured from crest to preceding trough, crest to following trough, or crest to the average of the preceding and following trough velocities. The scatter of plotted points was less in the latter case because the averaging process is also a smoothing process. Comparison of the different methods of presentation for series 15 are shown in figures 32, 33, 39 and 40.

CONCLUSIONS

The analysis shows that the observed maximum horizontal orbital velocities in general compare more favorably with velocities predicted from solitary wave equations than from the equations of Airy and Stokes. The observed velocities were in better agreement with solitary wave theory when: 1) the wave profile was not complex, 2) the effective wave period was longer than about 6 seconds, and 3) the relative wave height was greater than about 0.2. While agreement with theory was somewhat better for the longer period waves, in general it was still quite good for most simple waves with relative wave heights greater than about 0.4.

ACKNOWLEDGMENTS

Many people on the staff of the Scripps Institution of Oceanography and elsewhere have given freely of their time and energy during the development of the orbital velocity meter and the succeeding field and laboratory investigations. The basic design of the orbital velocity meter follows the principle originally suggested by Carl Eckart. The construction of the meter and the design of the electronic components were under the supervision of James M. Snodgrass. Assistance in the field work and analysis of data was given by Jean Short, Earl Murray, and Ruth Young, and assistance with illustrations was given by Robert C. Winsett and James R. Moriarty. Valuable suggestions and guidance during the course of the study were contributed by Robert S. Arthur, Walter Munk, John Isaacs, J. D. Frautschy, and Francis X. Byrnes.

LITERATURE CITED

Airy, Sir George. 1845. "Tides and Waves". Encyclopaedia Metropolitana.

Beach Erosion Board. 1933. Interim Report, Office, Chief of Engineers, U. S. Army.

Daily, J. W., and S. C. Stephan, Jr. 1952. "The Solitary Wave". Hydrodynamics Lab., Mass. Inst. of Tech., Tech. Report No. 8.

Hald, A. 1952. Statistical Theory with Engineering Applications. John Wiley & Sons, New York

Hamada, Tokuichi. 1951. "Breakers and Beach Erosion". Transportation Technical Research Institute, Tokyo, Report No. 1

Ippen, A. T. and Gershon Kulin. 1955. "Shoaling and Breaking Characteristics of the Solitary Wave". Hydrodynamics Lab., Mass. Inst. of Tech., Tech. Report No. 15.

Isaacs, J. D., and R. L. Wiegel. 1950. "The Thermopile Wave Meter," Trans. Amer. Geoph. Union, Vol. 31, pp. 711-716

Iversen, H. W. 1952. "Laboratory Study of Breakers". Gravity Waves, National Bureau of Standards, Circular 521, pp. 9-32.

Lamb, H. 1945. Hydrodynamics 6th ed. Dover Publications, New York

Morison, J. R., and R. C. Crooke. 1953. "The Mechanics of Deep Water Shallow Water, and Breaking Waves." Beach Erosion Board, Corps of Engineers, Tech. Memo. No. 40, 14 pp.

Munk, W. H. 1949a. "The Solitary Wave Theory and its Application to Surf Problems." Ann. New York Acad. Sci., Vol. 51, Art. 3, pp. 376-424.

Munk, W. H. 1949b. "Surf Beats". Trans. Amer. Geoph. Union, Vol. 30, pp. 849-854

Putz, R. R. 1951. "Joint Variation of Wave Height and Wave Period For Ocean Swell". Univ. of California, Inst. of Engrg. Res., Tech. Rpt. HE-116-328.

Putz, R. R. 1952. "Statistical Distributions for Ocean Waves". Trans. Amer. Geoph. Union, Vol. 33, pp. 685-692

Shepard, F. P., and D. L. Inman. 1950. "Nearshore Water Circulation Related to Bottom Topography and Wave Refraction". Trans. Amer. Geoph. Union, Vol. 31, pp. 196-212.

Stokes, G. G. 1847. "On the Theory of Oscillatory Waves". Trans. Cambridge Philosophical Society, Vol. VIII, pp. 441-455.

Wiegel, R. L., and J. D. Isaacs. 1948. First Report on the Mark V (Thermopile Wave Meter), Univ. of Calif., Dept. Engrg., Tech. Rpt. HE-116-287

Wiegel, R. L. 1950. "Experimental Study of Surface Waves in Shoaling Water". Trans. Amer. Geoph. Union, Vol. 31, pp. 377-385.

APPENDIX IA - IF

Wave Properties and Horizontal Orbital Velocity Measurements
for
Selected Waves of Simple Profile

IA	Series	6
IB	Series	7
IC	Series	9
ID	Series	12
IE	Series	14
IF	Series	15

APPENDIX IA - SERIES NO. 6.

WAVE[1] NUMBER	WAVE HEIGHT		TROUGH DEPTH		PERIOD	MAXIMUM HORIZONTAL[2] ORBITAL VELOCITY		
						Crest	Trough	
	H_1 ft	H ft	h_1 ft	h ft	T_n sec	u_c ft/sec	u_1 ft/sec	u_2 ft/sec
10	6.6	7.6	10.1	9.9	10.0	4.8	2.8	4.2
11	8.6	6.9	9.8	10.0	10.0	3.7	4.2	2.9
18	5.6	6.6	10.2	10.1	9.0	4.6	2.0	3.5
19	7.7	7.1	9.9	10.0	10.0	3.7	3.5	3.4

[1] Wave number refers to the chronological sequence of wave crests within the series. Only waves with relatively simple profiles are listed.

[2] Orbital velocities under the wave crest are positive in the direction of wave propagation (onshore). Trough velocities are considered positive when the motion is in an offshore direction. Negative notation for trough velocity indicates current flowing onshore.

APPENDIX IB SERIES NO. 7

WAVE NUMBER[1]	WAVE HEIGHT		TROUGH DEPTH		PERIOD	MAXIMUM HORIZONTAL ORBITAL VELOCITY[2]		
						Crest	Trough	
	H_1 ft	H ft	h_1 ft	h ft	T_n sec	u_c ft/sec	u_1 ft/sec	u_2 ft/sec
1	4.3		8.4		6.5	4.2	1.3	1.9
2	5.5		8.2		7.0	4.7	1.9	1.8
3	2.8		8.6		6.0	2.9	1.8	0.8
4	3.0		8.6		6.0	3.6	0.8	2.3
7	2.2		8.7		8.0	2.9	0.8	0.4
8	1.8		8.7		6.0	3.3	0.4	1.5
9	3.0		8.6		7.0	3.6	1.5	1.5
10	3.0		8.6		8.0	2.8	1.5	0.4
13	1.6		8.8		7.0	3.0	-0.4	0.4
14	4.0		8.4		8.0	4.2	0.4	-1.2
16	1.8		8.7		5.0	2.9	0.4	-1.2
17	2.6		8.6		7.0	4.3	-1.2	0.4
19	6.2		8.1		8.0	4.9	2.2	1.9
22	4.0		8.4		7.0	4.7	0.8	1.8
23	4.8		8.3		6.5	4.5	1.8	2.0
24	4.2		8.4		8.0	4.4	2.0	0.4
27	3.8		8.4		6.0	4.6	0.8	1.6
28	2.4		8.6		6.5	2.3	1.6	-1.6
30	1.4		8.8		6.0	2.2	0.4	-1.6

APP. IB - 2

WAVE NUMBER	H_1	H	h_1	h	T_n	u_c	u_1	u_2
32	1.2		8.8		7.0	2.8	-1.6	1.8
33	4.8		8.3		7.5	4.5	1.8	2.9
34	3.9		8.4		6.5	2.6	2.9	0.4
35	2.1		8.7		6.5	3.0	0.4	0.8
36	3.6		8.5		8.0	4.3	0.8	0.4
40	1.6		8.8		4.0	1.8	0.4	-2.0
41	.46		8.9		3.5	2.3	-2.0	0.4
42	1.4		8.8		4.5	1.8	0.4	-1.6
43	1.0		8.8		6.0	2.7	-1.6	1.3
44	3.4		8.5		6.0	4.3	0.8	1.6
45	2.6		8.6		4.0	2.2	1.6	1.6
46	2.2		8.7		5.5	3.6	-1.6	1.8
47	5.8		8.1		9.5	4.7	1.8	1.5
50	3.0		8.6		6.0	3.3	1.1	1.5
51	3.1		8.6		6.5	3.2	1.6	1.1
52	2.6		8.6		6.5	3.2	0.4	-1.6
53	1.0		8.8		6.0	2.2	-1.6	0.4
54	1.9		8.7		7.5	2.4	0.4	0.4
55	2.0		8.7		9.5	2.3	0.4	1.8
57	3.0		8.6		5.5	3.2	2.2	0.4
58	2.2		8.7		6.0	3.7	0.4	0.4
59	1.6		8.8		6.5	2.9	0.4	0.4
60	3.3		8.5		5.5	3.9	0.4	0.8

WAVE NUMBER	H_1	H	h_1	h	T_n	u_c	u_1	u_2
61	0.9		9.0		5.5	2.0	0.8	0.4
63	1.0		8.8		---	2.2	0.4	-1.4
64	0.5		8.9		8.0	2.2	-1.4	0.8
66	1.5		8.8		5.5	2.4	0.4	-1.4
67	3.2		8.5		6.5	4.3	-0.4	0.4
68	4.8		8.2		9.5	4.8	0.8	1.8
70	2.3		8.7		7.0	3.7	0.4	0.4
71	3.0		8.6		7.0	3.6	0.4	0.4
72	2.6		8.6		7.0	3.3	0.4	0.8
73	4.1		8.4		7.5	4.6	0.8	1.8
75	2.2		8.7		6.0	3.1	0.8	0.4
76	0.7		8.9		6.5	2.1	0.4	0.4
77	1.0		8.8		6.0	2.0	0.4	0.4
78	1.0		8.8		4.0	2.1	0.4	0.4
79	2.4		8.6		4.0	3.2	0.4	0.8
80	0.5		8.9		5.5	2.3	0.8	0.8
82	2.4		8.6		6.5	3.4	0.4	0.8
83	1.8		8.7		8.5	3.3	0.8	0.8
84	3.0		8.6		9.0	4.1	0.8	1.8
85	3.2		8.5		5.5	3.3	1.8	-2.0
87	3.3		8.5		8.5	3.8	0.8	0.4
89	2.2		8.7		9.5	2.6	0.8	0.4
90	1.9		8.7		7.0	2.6	0.4	1.1

WAVE NUMBER	H_1	H	h_1	h	T_n	u_c	u_1	u_2
91	3.1		8.6		7.0	4.2	1.1	0.8
92	4.2		8.4		7.5	4.6	0.8	0.8
93	4.9		8.2		9.0	4.9	1.6	0.4
94	3.3		8.5		9.5	4.7	0.4	0.4
95	1.9		8.7		9.0	2.4	0.4	0.4
96	2.0		8.7		---	3.2	0.4	2.2
97	1.2		8.8		---	1.8	0.4	0.4
98	1.8		8.7		5.0	2.3	0.4	3.1
102	3.9		8.4		8.5	4.4	0.8	2.4
103	3.6		8.5		8.0	3.7	2.4	0.4
104	2.1		8.7		8.0	3.0	0.4	0.4
105	2.0		8.7		7.5	3.6	0.4	0.4
106	4.3		8.4		7.0	4.4	0.4	3.3
108	1.6		8.7		5.0	2.9	0.8	1.6
110	3.3		8.5		7.5	4.0	0.8	0.4
111	3.8		8.4		8.5	4.1	0.4	0.4
112	2.4		8.6		8.5	3.3	0.4	0.4
113	1.5		8.8		5.5	2.0	0.4	0.4
114	2.0		8.7		5.5	2.4	0.4	0.8
115	2.6		8.6		6.0	3.1	0.8	0.4
116	1.5		8.8		6.0	2.9	0.4	1.6
118	2.6		8.6		11.0	2.7	1.3	0.4
120	1.0		8.8		7.5	2.3	-1.6	0.8
121	2.2		8.7		6.5	3.0	0.8	0.4

WAVE NUMBER	H_1	H	h_1	h	T_n	u_c	u_i	u_2
122	1.4		8.8		5.0	2.2	0.4	0.4
123	1.6		8.8		4.5	1.9	0.4	0.8
124	2.2		8.7		6.0	2.3	0.8	1.1
125	0.7		8.9		5.5	1.7	1.1	-1.6
126	2.3		8.6		4.0	3.0	0.4	1.9
127	1.8		8.7		5.5	2.3	1.8	1.3
129	2.4		8.6		5.0	2.4	1.5	0.4
130	1.8		8.7		5.5	2.1	0.4	0.4
131	2.2		8.7		7.0	2.6	0.4	0.4
132	2.0		8.7		8.0	3.2	0.4	1.3
135	2.5		8.6		5.5	2.9	1.6	-1.6
137	2.6		8.6		9.5	2.8	0.8	0.4
143	4.2		8.4		6.0	4.5	1.8	2.7
144	5.5		8.2		7.0	4.9	2.7	1.8
145	4.2		8.4		7.5	4.2	1.8	1.3
146	4.2		8.4		7.0	3.7	1.3	0.4
147	1.6		8.7		7.0	2.8	0.4	0.8

APPENDIX IC SERIES NO. 9

WAVE 1/ NUMBER	WAVE HEIGHT		TROUGH DEPTH		PERIOD	MAXIMUM HORIZONTAL 2/ ORBITAL VELOCITY		
						Crest	Trough	
	H_1 ft	H ft	h_1 ft	h ft	T_n sec	u_c ft/sec	u_1 ft/sec	u_2 ft/sec
5	1.7	1.7	5.1	5.1	8.6	3.6	0	2.3
8	1.6	1.6	5.1	5.1	8.5	2.6	0	0
11	1.8	2.3	5.1	5.0	4.2	2.5	2.6	2.7
16	2.2	1.7	5.0	5.1	5.0	4.0	0	0
20	2.4	2.4	4.9	4.9	4.8	4.2	2.4	0
30	1.5	1.7	5.1	5.1	4.0	3.0	-2.0	0
41	1.8	2.0	5.1	5.0	5.4	3.0	0	2.9
46	1.9	1.7	5.0	5.1	5.1	2.8	2.3	-1.8
47	1.3	1.7	5.2	5.1	5.9	2.8	-1.8	0
54	1.5	2.2	5.1	5.0	7.7	4.0	-1.9	2.5
61	---	1.1	---	5.2	4.6	2.9	-2.3	0
64	1.8	1.1	5.1	5.2	3.4	3.1	0	-1.9
66	1.4	1.2	5.2	5.2	5.1	2.9	-	-0.9
79	1.9	1.9	5.0	5.1	7.5	3.8	1.0	0
86	1.7	1.6	5.1	5.1	7.5	3.6	-0.9	0
88	1.7	1.8	5.1	5.1	4.3	3.0	0	0
99	2.0	1.4	5.0	5.2	3.8	3.0	0	-2.2
102	1.8	1.5	5.1	5.2	3.9	3.8	-1.8	-0.9
104	1.3	1.1	5.2	5.2	4.2	2.8	-1.8	-2.2

WAVE NUMBER	H_1	H	h_1	h	T_n	u_c	u_1	u_2
108	2.3	1.8	4.0	5.1	5.7	3.3	3.0	-0.9
112	1.0	1.5	5.3	5.2	5.2	2.9	-2.3	4.2
118	---	2.0	---	5.0	5.2	3.4	-2.4	0
119	2.5	2.6	4.9	4.9	5.0	4.0	0	0
120	2.2	2.2	5.0	5.0	5.7	3.9	0	0
125	---	1.6	---	5.1	3.7	3.0	-2.4	1.8
129	2.1	2.1	5.0	5.0	5.1	4.1	0	-1.9
130	1.8	1.4	5.1	5.2	4.9	3.4	-1.9	-2.2
141	1.3	1.5	5.2	5.2	8.0	2.5	0	0
147	1.4	1.5	5.2	5.2	4.1	2.4	1.0	
150	3.4	3.1	4.7	4.8	6.3	4.1	0	0
152	2.3	2.1	5.0	5.0	4.2	3.2	0	0
158	2.7	2.8	4.8	4.9	5.9	3.7	0	0
159	2.3	2.0	5.0	5.0	6.2	2.9	0	0
162	2.2	2.5	5.0	4.9	4.5	3.2	0	2.2
163	2.3	2.7	5.0	4.9	5.5	3.5	0	2.4
172	---	2.6	---	4.9	4.9	3.1	1.0	0
174	1.1	1.1	5.2	5.2	4.7	2.1	1.0	0
177	1.9	1.9	5.0	5.1	4.7	3.2	0	0
183	1.6	1.5	5.1	5.2	5.8	2.4	0	1.0
184	3.1	3.0	4.8	4.8	5.6	3.7	0	0
187	2.9	2.5	4.7	4.9	7.7	3.5	2.2	0
191	2.9	2.4	4.8	4.9	4.5	3.9	0	0
192	2.1	1.1	5.0	5.2	6.0	2.6	0	0
193	1.4	1.2	5.2	5.2	4.7	2.6	0	0

APP. IC - 3

WAVE NUMBER	H_1	H	h_1	h	T_n	$u_ç$	u_1	u_2
198	1.3	1.7	5.2	5.1	5.1	2.2	1.0	0
203	---	2.2	---	5.0	4.6	3.4	0	0
204	1.5	1.5	5.1	5.2	5.1	2.3	0	0
205	2.1	1.7	5.0	5.1	4.2	2.8	0	1.0
209	1.5	1.7	5.1	5.1	5.6	2.2	0	0
212	1.5	1.4	5.1	5.2	5.3	2.9	0	0
216	1.3	1.6	5.2	5.1	4.0	2.2	1.0	0
221	3.1	3.1	4.8	4.8	5.9	3.8	0	1.0
226	2.2	2.1	5.0	5.0	5.6	2.9	0	1.0
227	2.6	2.5	4.9	4.9	4.9	3.9	1.0	0
228	2.8	2.8	4.8	4.9	5.9	3.7	0	0
229	1.6	1.3	5.1	5.2	5.2	2.2	0	0
230	1.5	1.4	5.1	5.2	4.4	3.7	0	0
232	1.0	1.1	5.3	5.2	5.5	2.2	0	0
233	2.6	2.1	4.8	5.0	4.5	3.5	0	0
236	---	1.8	---	5.1	5.3	3.3	0	0
243	2.8	2.6	4.7	4.9	5.5	3.8	1.0	1.0
244	1.7	2.1	5.1	5.0	5.2	3.0	1.0	2.6
247	1.3	1.3	5.2	5.2	4.3	2.3	0	1.0
248	1.8	1.6	5.0	5.1	3.4	3.1	1.0	0

APPENDIX ID SERIES NO. 12

WAVE NUMBER[1]	WAVE HEIGHT		TROUGH DEPTH		PERIOD	MAXIMUM HORIZONTAL ORBITAL VELOCITY[2]		
						Crest	Trough	
	H_1 ft	H ft	h_1 ft	h ft	T_n sec	u_c ft/sec	u_1 ft/sec	u_2 ft/sec
1	2.1	2.4	6.8	6.6	5.2	1.4	1.0	1.4
2	2.2	2.4	6.7	6.6	4.9	1.8	1.4	1.3
3	2.9	2.4	6.6	6.6	7.4	2.8	1.3	0.5
4	2.2	2.4	6.7	6.6	8.0	2.0	0.8	1.9
5	2.3	1.9	6.7	6.7	6.5	1.4	1.9	0.8
11	1.2	0.9	7.0	7.0	5.6	1.3	1.3	0
14	1.6	1.5	6.9	6.8	4.1	1.6	1.2	0.5
15	1.4	1.3	6.9	6.9	6.6	1.1	0.5	0.9
18	2.3	2.1	6.7	6.7	5.7	1.9	1.6	0.9
19	1.5	1.9	6.9	6.7	5.9	1.2	0.9	1.6
23	1.0	1.2	7.0	6.9	5.2	1.0	0.3	1.2
24	2.6	3.0	6.7	6.5	4.9	2.5	1.2	2.0
25	3.0	3.1	6.6	6.5	6.7	2.6	2.0	1.7
29	2.7	2.8	6.6	6.5	6.1	2.5	1.9	1.2
30	1.3	1.9	6.9	6.7	6.3	1.6	1.2	2.0
31	2.0	1.7	6.8	6.8	4.8	1.4	2.0	0.5
32	1.8	0.8	6.8	7.0	4.6	0.9	0.5	0.5
33	1.3	1.1	6.9	6.9	4.0	1.2	0.5	-0.6
35	1.5	1.3	6.9	6.9	4.7	0.9	1.7	0.8

APP. ID - 2

WAVE NUMBER	H_1	H	h_1	h	T_n	u_c	u_1	u_2
36	1.0	1.2	7.0	6.9	4.9	1.2	0.8	1.0
37	1.9	1.4	6.8	6.9	6.7	1.7	1.0	0.6
41	1.4	1.5	6.9	6.8	6.2	1.1	0.8	1.2
42	1.8	2.0	6.8	6.7	5.9	1.7	1.2	1.2
43	2.3	2.7	6.7	6.8	5.0	1.8	1.2	2.2
44	3.7	3.4	6.4	6.5	4.9	3.0	2.2	1.2
47	2.4	1.6	6.7	6.8	5.3	1.9	1.7	-0.6
48	1.8	1.0	6.8	7.0	6.2	1.3	-0.6	1.2
49	2.4	2.3	6.7	6.6	6.2	1.9	1.2	1.5
50	2.2	2.0	6.7	6.7	4.9	1.6	1.5	0.8
52	1.4	2.1	6.9	6.7	4.0	1.9	0	1.8
53	3.0	2.6	6.6	6.6	5.7	2.2	1.8	1.2
54	1.2	1.2	6.9	6.9	6.1	1.2	1.2	0.3
55	0.7	0.8	7.0	7.0	5.2	1.0	0.3	0.7
56	1.5	1.1	6.9	6.9	8.0	1.6	0.7	0.3
57	0.8	0.9	7.0	7.0	7.0	1.3	0.3	0.6
58	1.2	1.0	7.0	7.0	4.6	1.2	0.6	0.8
59	1.6	1.4	6.9	6.9	4.8	1.2	0.8	0.8
60	---	1.5	---	6.8	4.0	1.2	0.8	1.8
61	1.4	3.0	6.9	6.5	4.5	2.7	1.8	1.4
62	2.7	2.3	6.6	6.6	5.0	3.0	1.4	0.3
63	---	0.5	---	7.1	4.2	0.9	0.3	0.3
64	1.0	1.2	7.0	6.9	4.6	1.4	0.3	0.8
65	1.7	2.0	6.8	6.7	6.4	2.3	0.8	1.5

WAVE NUMBER	H_1	H	h_1	h	T_n	u_c	u_1	u_2
66	1.7	1.6	6.8	6.8	5.5	1.3	1.5	0.7
67	1.2	1.0	7.0	7.0	6.0	1.4	0.7	1.2
68	1.5	1.7	6.9	6.8	7.0	1.5	1.2	1.7
69	2.9	2.6	6.6	6.6	5.7	2.7	1.7	0.8
70	1.7	1.6	6.8	6.8	5.2	1.6	0.8	0
73	1.0	1.2	7.0	6.9	4.0	1.0	0.3	1.2
76	1.3	1.8	6.9	6.8	5.0	2.0	0	1.2
77	1.6	1.5	6.9	6.8	6.0	1.2	1.2	1.2
78	2.6	3.0	6.7	6.5	5.4	2.8	1.2	2.1
81	1.3	1.2	6.9	6.9	5.1	0.9	1.2	0.3
82	1.2	1.3	7.0	6.9	4.9	1.2	0.3	0.5
83	1.0	1.1	7.0	6.9	4.1	1.0	0.5	0.5
85	1.6	1.7	6.9	6.8	4.0	2.0	0.8	0
87	2.0	1.8	6.8	6.8	5.5	1.7	1.4	1.6
88	2.7	2.0	6.6	6.7	6.9	2.5	1.6	0.3
89	1.0	1.3	7.0	6.9	5.9	1.3	0.3	1.3
90	2.4	3.0	6.7	6.5	5.0	3.0	1.3	2.4
91	3.4	2.7	6.5	6.6	5.3	2.6	2.4	0.8
92	1.6	1.5	6.9	6.8	4.6	1.2	0.8	0.3
93	---	0.6	---	7.1	3.8	0.8	0.3	0
95	1.7	1.7	6.8	6.8	4.4	1.6	0.8	0.8
96	1.0	1.0	7.0	7.0	4.6	0.6	0.8	1.3
97	2.5	2.6	6.7	6.6	4.5	2.5	1.3	0.5
98	1.7	2.1	6.8	6.7	5.6	2.2	0.5	2.0

APP. ID - 4

WAVE NUMBER	H_1	H	h_1	h	T_n	u_c	u_1	u_2
99	2.7	2.3	6.6	6.6	6.7	1.9	2.0	0
104	1.9	2.4	6.8	6.6	5.0	2.0	0.9	1.2
105	1.5	1.2	6.9	6.9	5.0	1.2	1.2	0
106	0.9	1.2	7.0	6.9	4.8	1.5	0	1.0
107	1.4	1.1	6.9	6.9	5.6	1.1	1.0	0
108	1.4	1.4	6.9	6.9	5.0	1.0	0	0.5
109	1.6	2.0	6.9	6.7	3.7	1.5	0.5	0.7
110	2.9	2.6	6.6	6.6	5.1	2.0	0.7	1.4
111	1.5	1.6	6.9	6.8	5.8	1.2	1.4	0.5
112	2.3	2.1	6.7	6.7	5.8	2.6	0.5	1.3
113	2.3	2.0	6.7	6.7	5.5	1.6	1.3	0.5
114	0.8	0.8	7.0	7.0	6.9	1.2	0.5	0.9
117	1.5	1.8	6.9	6.8	5.4	1.5	0.7	2.3
118	2.4	2.2	6.7	6.7	5.5	2.0	2.3	0.5
119	0.4	0.5	7.1	7.1	4.8	1.0	0.5	0.8
120	2.4	2.4	6.7	6.6	6.0	3.0	0.8	2.1
121	2.4	2.4	6.7	6.6	7.0	2.1	2.1	1.4
122	1.6	1.5	6.9	6.8	6.2	1.8	1.4	0.3
123	0.8	0.6	7.0	7.1	5.3	1.0	0.3	-0.6
124	1.0	1.1	7.0	7.0	4.7	1.2	-0.6	1.4
128	2.7	2.8	6.6	6.5	5.2	2.0	1.2	2.0
129	2.8	2.9	6.6	6.5	4.9	2.1	2.0	0.9
133	2.5	2.8	6.7	6.5	5.7	2.2	1.4	1.5
134	2.1	2.1	6.8	6.7	4.2	1.5	1.5	0.7
135	1.8	2.2	6.8	6.7	4.6	1.3	0.7	1.7

WAVE NUMBER	H_1	H	h_1	h	T_n	u_c	u_1	u_2
136	2.7	2.8	6.6	6.5	4.8	2.0	1.7	1.5
139	1.5	2.0	6.9	6.7	6.1	2.0	0.7	1.2
140	2.8	2.1	6.6	6.7	4.5	2.2	1.2	0
142	2.9	3.5	6.6	6.4	6.0	2.7	2.0	2.1
143	3.6	2.5	6.4	6.6	6.3	2.4	2.1	1.4
144	3.0	3.5	6.6	6.4	6.4	3.0	1.4	2.1
145	2.8	2.9	6.6	6.5	5.8	2.6	2.1	1.8
148	1.1	1.1	7.0	6.9	5.5	1.3	0.3	0.3
150	1.0	1.4	7.0	6.9	4.1	1.6	-0.6	1.6
151	2.7	2.6	6.6	6.6	5.0	2.7	1.6	1.7
152	3.2	3.3	6.5	6.4	5.4	2.8	1.7	1.8
153	3.0	2.5	6.6	6.6	5.6	2.3	1.8	-0.7
156	1.3	1.0	6.9	7.0	6.4	1.5	0.8	-0.3
157	0.4	0.8	7.1	7.0	6.2	1.0	-0.3	1.2
158	2.3	2.5	6.7	6.6	6.2	2.5	1.2	0.9
161	1.9	1.8	6.8	6.8	4.0	1.4	1.0	-0.6
162	1.2	1.5	6.9	6.8	4.6	1.6	-0.6	1.4
163	2.2	2.3	6.7	6.6	5.0	2.0	1.4	0.3
164	1.0	0.8	7.0	7.0	3.9	0.9	0.3	0.7
165	2.6	2.7	6.6	6.6	5.6	3.0	0.7	1.9
166	1.9	2.5	6.8	6.6	6.4	1.7	1.9	0.8
167	1.3	1.7	6.9	6.8	5.9	1.8	0.8	1.1
168	1.4	1.6	6.9	6.8	6.1	1.3	1.1	1.5
169	1.3	1.3	6.9	6.9	5.3	1.2	1.5	0.9

WAVE NUMBER	H_1	H	h_1	h	T_n	u_c	u_1	u_2
170	1.3	0.8	6.9	7.0	5.6	1.3	0.8	-0.6
172	2.2	2.4	6.7	6.6	3.9	2.6	0.5	0.9
174	1.6	2.0	6.9	6.7	5.0	2.2	1.1	0
175	1.56	1.7	6.9	6.8	4.7	2.2	0	2.4
176	1.8	2.0	6.8	6.7	5.8	2.6	2.4	-0.7
179	2.0	2.1	6.8	6.7	5.8	1.8	0.3	0.3
182	1.2	1.4	6.9	6.9	6.3	1.7	0.3	0.3
187	1.8	1.7	6.8	6.8	6.5	1.6	0.3	0.9
188	2.0	2.1	6.8	6.7	5.8	1.3	0.9	0.7
191	0.7	0.7	7.0	7.0	6.3	0.9	1.3	0
196	0.9	0.7	7.0	7.0	6.0	0.9	0	0
197	1.7	1.9	6.8	6.7	5.3	1.9	0	1.2
198	2.6	2.5	6.7	6.6	5.6	2.0	1.2	1.7
199	2.5	2.7	6.7	6.6	5.5	2.3	1.7	0.9
200	1.2	1.3	6.9	6.9	5.2	1.2	0.9	0.8
201	1.8	1.4	6.8	6.9	6.6	1.6	0.8	0
204	2.1	2.0	6.8	6.7	3.8	1.6	1.6	-0.3
205	2.0	2.6	6.8	6.6	3.8	2.6	-0.3	1.3
206	2.2	2.1	6.8	6.7	4.5	1.5	1.3	1.0
207	1.6	1.4	6.9	6.9	4.5	1.2	1.0	-0.7
210	3.2	3.5	6.5	6.4	5.0	2.9	1.2	1.0
211	2.7	2.7	6.6	6.6	4.7	2.7	1.0	0
212	1.0	0.8	7.0	7.0	5.7	0.9	0	0.3
216	2.2	2.0	6.7	6.7	6.7	2.1	1.2	0.7
217	1.50	1.6	6.9	6.8	5.5	1.9	0.7	0.7

APP. ID - 7

WAVE NUMBER	H_1	H	h_1	h	T_n	u_c	u_1	u_2
218	1.4	1.3	6.9	6.9	4.6	1.0	0.7	1.5
219	2.1	1.7	6.8	6.8	6.1	1.6	1.5	0.5
221	1.2	1.9	6.9	6.7	6.2	1.2	0.5	2.2
222	3.8	3.7	6.4	6.3	4.7	3.1	2.2	0.8
223	2.3	2.6	6.7	6.6	5.9	2.3	0.8	0.9
225	1.4	1.9	6.9	6.7	6.0	1.7	0.6	1.8
226	2.0	1.6	6.8	6.8	4.6	1.8	1.8	-0.8
227	---	0.5	---	7.1	4.4	1.1	-0.8	-0.6
229	0.4	0.5	7.1	7.1	3.7	0.9	-0.7	0.9
230	1.4	0.8	6.9	7.0	5.7	1.0	0.9	-0.6
233	2.7	2.7	6.9	6.6	5.1	2.8	1.7	1.3
234	1.9	1.8	6.8	6.8	5.4	1.9	1.3	0.8
235	2.1	1.9	6.8	6.7	6.5	2.2	0.8	0
237	1.2	0.9	6.9	7.0	6.3	1.2	0	-0.7
238	1.0	0.8	7.0	7.0	4.0	1.3	-0.7	-0.9
240	---	0.9	---	7.0	4.4	1.1	-0.7	0.7
241	1.6	0.7	6.9	7.0	5.0	1.0	0.7	1.2
242	2.0	1.9	6.8	6.7	6.5	2.4	1.2	-0.3
244	2.2	2.1	6.7	6.7	7.1	2.2	1.1	0.8
245	1.2	1.3	7.0	6.9	6.1	1.2	0.8	0.7
246	1.2	0.8	7.0	7.0	6.3	1.4	0.7	0
247	1.4	1.8	6.9	6.8	5.9	1.3	0	1.1
248	1.8	1.7	6.8	6.8	6.3	1.2	1.1	1.0
249	1.8	2.0	6.8	6.7	5.5	2.3	1.0	0
251	1.0	1.1	7.0	6.9	5.2	1.2	-0.7	1.0

APP. ID - 8

WAVE NUMBER	H_1	H	h_1	h	T_n	u_c	u_1	u_2
252	1.8	1.9	6.8	6.7	6.4	2.2	1.0	0.6
253	1.5	1.5	6.9	6.8	5.5	1.6	0.6	0
254	1.0	1.1	7.0	6.9	5.1	1.1	0	0.9
257	1.5	1.7	6.9	6.8	5.0	1.4	1.4	-0.8
263	2.6	2.5	6.7	6.6	5.9	2.3	1.9	2.1
264	3.4	3.2	6.5	6.4	7.3	2.9	2.1	0
266	0.6	1.2	7.1	6.9	7.0	1.3	-0.8	2.3
267	3.6	4.1	6.4	6.2	5.0	2.9	2.3	2.4
268	3.6	3.4	6.4	6.4	5.5	2.5	2.4	0.3
269	1.0	1.5	7.0	6.8	5.0	1.6	0.3	1.0
270	2.2	2.1	6.7	6.7	4.3	1.9	1.0	0.6
271	2.9	2.6	6.6	6.6	5.5	3.0	0.6	1.3
272	1.5	1.1	6.9	6.9	6.1	1.2	1.3	0.9
273	2.7	2.7	6.6	6.6	5.9	2.6	0.9	1.8
274	1.3	1.2	6.9	6.9	5.5	1.2	1.8	-0.8
275	0.5	0.6	7.1	7.1	4.6	1.2	-0.8	0.5
276	0.7	0.8	7.0	7.0	4.8	0.9	0.5	1.3
277	2.0	2.0	6.8	6.7	4.7	1.9	1.3	1.4
278	2.9	3.4	6.6	6.4	4.9	2.9	1.4	1.6

APPENDIX IE SERIES NO. 14

WAVE[1/] NUMBER	WAVE HEIGHT		TROUGH DEPTH		PERIOD	MAXIMUM HORIZONTAL ORBITAL VELOCITY[2/]		
						Crest	Trough	
	H_1 ft	H ft	h_1 ft	h ft	T_n sec	u_c ft/sec	u_1 ft/sec	u_2 ft/sec
10	3.5	---	6.8	---	8.9	2.9	2.7	3.0
11	---	---	---	---	9.3	2.2	3.0	2.7
12	4.0	3.3	6.8	7.5	9.7	4.0	2.7	1.5
16	2.5	3.0	6.8	6.3	9.8	2.9	1.7	3.7
17	6.0	6.0	6.3	6.3	9.7	4.4	3.7	2.6
18	2.5	---	6.3	---	11.3	2.2	2.6	1.4
22	4.0	---	6.8	---	9.3	3.2	1.9	1.6
40	6.5	6.5	6.3	6.3	9.3	4.2	3.7	2.9
41	7.0	---	6.3	---	10.2	4.2	2.9	3.4
53	4.0	4.0	6.8	6.8	9.6	4.4	2.0	2.4
54	3.0	2.8	6.8	7.0	8.7	3.0	2.4	1.8
55	1.5	1.8	7.3	7.0	7.1	2.0	1.6	2.2
56	2.5	2.3	6.8	7.0	7.0	2.8	2.2	1.6
57	1.5	1.8	7.3	7.0	7.9	2.5	1.6	1.9
58	3.5	3.5	6.8	7.8	7.1	3.5	1.9	1.6
59	1.5	---	6.8	---	5.1	1.3	1.6	1.0
67	3.0	---	7.3	---	10.4	3.0	2.1	2.6
77	3.5	3.5	7.3	7.3	9.2	3.8	1.4	2.0
80	3.5	---	6.8	---	9.6	3.4	2.2	1.0
102	4.5	4.8	7.3	7.0	8.2	4.3	2.0	2.8

APP. IE - 2

WAVE NUMBER	H_1	H	h_1	h	T_n	u_c	u_1	u_2
103	4.0	4.0	6.8	6.8	9.5	3.2	2.8	2.0
105	1.5	---	6.8	---	7.7	1.2	2.0	-0.5
109	3.0	2.8	6.8	7.0	7.8	2.3	2.2	1.2
110	1.0	1.3	7.3	7.0	6.7	1.2	1.2	1.5
111	2.0	1.8	6.8	7.0	6.5	2.2	1.5	2.0
112	3.0	---	7.3	---	7.5	3.1	2.0	1.2
120	2.5	2.8	7.3	7.0	8.6	2.7	1.5	2.0
121	3.5	3.5	6.8	6.8	7.8	3.3	2.0	1.4
122	2.5	---	6.8	---	7.5	2.4	1.4	1.1
123	2.5	2.8	7.3	7.0	9.2	3.1	1.1	2.2
124	3.0	2.8	6.8	7.0	10.6	2.7	2.2	1.0
127	2.5	2.8	6.8	7.0	9.0	2.8	1.6	2.2
128	4.0	4.0	6.8	6.8	9.4	3.5	2.2	2.6
130	2.5	2.5	6.8	6.8	6.9	2.2	2.6	0.0
156	2.5	3.0	7.3	6.8	8.4	2.3	2.4	3.6
157	3.0	3.0	6.3	6.3	5.5	2.1	3.6	2.7
158	3.0	2.7	6.3	6.6	6.0	1.9	2.7	2.4
159	2.5	2.5	6.8	6.8	7.3	1.8	2.4	2.6
160	2.0	---	6.8	---	7.5	1.4	2.6	1.3
162	---	---	---	---	---	1.3	1.5	1.5
165	1.5	1.5	7.3	7.3	7.5	1.8	1.2	1.4
166	2.5	---	7.3	---	11.5	2.4	1.4	0.7
178	4.5	---	6.8	---	10.2	3.4	2.0	3.0
180	4.5	---	6.8	---	11.2	2.9	3.0	1.5
183	1.5	---	7.3	---	12.5	1.4	1.2	-0.5

APP. IE - 3

WAVE NUMBER	H_1	H	h_1	h	T_n	u_c	u_1	u_2
186	4.5	4.5	6.3	6.3	9.9	3.6	2.7	2.0
187	4.0	---	6.3	---	10.3	3.6	2.0	0.0
188	2.5	---	6.8	---	10.4	2.7	0.9	0.7
190	2.5	3.7	6.8	6.6	10.0	2.9	1.6	1.2
193	2.0	---	7.3	---	11.5	2.5	0.0	0.8
195	4.0	4.3	7.3	7.0	10.0	4.0	1.4	2.2
196	2.0	2.0	6.8	6.8	11.0	2.5	2.2	1.2
216	4.0	4.0	6.8	6.8	9.7	3.7	1.4	3.1
217	4.0	---	6.8	---	10.1	3.5	3.1	1.6
219	2.5	---	7.3	---	9.5	3.1	2.2	1.2
222	2.5	---	6.8	---	8.8	2.3	2.0	1.2
224	2.5	2.8	7.3	7.0	9.7	2.8	1.2	2.9
225	4.5	4.5	6.8	6.8	9.1	3.6	2.9	2.5
226	3.0	3.0	6.8	6.8	9.1	3.2	2.5	2.2
227	3.5	3.5	6.8	6.8	9.0	3.6	2.2	2.4
228	3.0	3.0	6.8	6.8	9.2	3.3	2.7	3.7
229	3.0	3.0	6.8	6.8	10.4	2.5	3.7	2.2

APPENDIX IF SERIES NO. 15

WAVE 1/ NUMBER	WAVE HEIGHT		TROUGH DEPTH		PERIOD	MAXIMUM HORIZONTAL 2/ ORBITAL VELOCITY		
						Crest	Trough	
	H_1 ft	H ft	h_1 ft	h ft	T_n sec	u_c ft/sec	u_1 ft/sec	u_2 ft/sec
2	2.0	1.7	8.3	8.3	5.0	2.2	-0.6	-1.4
4	2.7	2.9	8.2	8.2	7.5	3.4	0.0	0.0
5	3.2	3.8	8.1	8.1	6.6	3.5	0.0	2.5
6	5.0	4.5	7.7	8.0	7.4	4.9	2.5	-0.9
8	4.4	4.6	7.9	8.0	8.0	5.1	0.0	2.1
11	2.1	2.8	8.3	8.2	5.8	3.1	-1.5	1.2
16	3.6	3.8	8.0	8.1	7.2	4.1	0.8	1.8
19	4.7	4.1	7.8	8.0	7.0	3.9	2.3	-0.6
20	1.7	1.7	8.4	8.3	6.1	2.4	-0.6	-1.1
22	2.1	2.0	8.3	8.3	6.5	2.4	0.8	-0.6
23	2.2	3.0	8.3	8.2	4.8	2.8	-0.6	2.0
24	3.9	3.1	8.0	8.2	5.3	3.0	2.0	2.0
26	1.4	1.5	8.4	8.3	5.0	2.3	-1.5	-1.0
30	1.0	1.2	8.5	8.4	4.3	1.8	-1.4	-1.1
31	1.3	1.3	8.5	8.3	3.9	2.1	-1.1	-1.1
32	1.4	1.5	8.4	8.3	5.1	2.2	-1.1	-1.4
33	1.4	1.3	8.4	8.3	5.2	1.8	-1.0	-1.4
34	2.3	2.3	8.3	8.2	5.8	2.8	-1.4	-0.9
37	4.5	4.3	7.8	8.0	5.5	3.6	2.5	0.8
38	2.6	2.7	8.2	8.2	4.9	2.8	0.8	0.8
39	2.8	2.9	8.2	8.2	6.1	2.6	0.8	2.6

APP. IF - 2

WAVE NUMBER	H_1	H	h_1	h	T_n	u_c	u_1	u_2
40	5.3	4.4	7.7	8.0	8.5	4.5	2.6	-1.6
41	2.7	3.3	8.2	8.1	8.2	3.1	0.8	0.8
43	2.3	3.1	8.3	8.2	7.4	3.4	-1.0	1.6
45	2.9	3.4	8.1	8.1	5.6	3.3	-0.6	2.4
46	3.7	3.3	8.5	8.1	7.2	3.1	2.4	0.8
50	2.7	2.8	8.2	8.2	6.9	3.0	-0.9	0.0
51	3.6	3.8	8.0	8.1	7.0	4.0	0.0	0.0
53	1.5	1.7	8.4	8.3	5.3	2.3	-0.9	-1.0
60	2.9	2.8	8.1	8.2	5.7	2.8	1.2	-0.6
61	2.2	2.2	8.3	8.3	5.3	2.6	-0.6	-0.6
63	2.0	1.9	8.3	8.3	5.6	2.8	-1.0	-1.4
66	1.9	1.7	8.3	8.3	3.8	2.2	-0.6	-0.9
68	1.8	1.8	8.4	8.3	5.0	2.3	-0.9	-1.0
69	2.2	2.4	8.3	8.2	4.5	2.8	-1.0	1.3
70	3.8	3.4	8.0	8.1	5.9	3.0	1.3	1.4
71	4.5	4.3	7.8	8.0	6.0	3.9	1.6	0.8
78	3.5	3.3	8.0	8.1	5.7	3.1	1.8	-0.6
82	4.1	3.9	7.9	8.1	6.1	3.1	2.8	1.8
94	2.0	2.1	8.3	8.3	4.9	2.5	0.8	-0.9
97	3.1	3.3	8.1	8.1	7.7	3.0	1.4	2.3
98	4.9	3.8	7.8	8.1	7.5	3.6	2.3	0.0
99	2.2	2.8	8.3	8.2	6.1	2.6	0.0	1.0
102	4.7	4.2	7.8	8.0	5.3	3.8	2.1	0.8
107	3.5	3.2	8.0	8.1	5.1	2.8	-0.6	0.8
109	2.2	2.2	8.3	8.3	5.4	2.6	-1.0	-1.1

WAVE NUMBER	H_1	H	h_1	h	T_n	u_c	u_1	u_2
110	2.6	2.9	8.2	8.2	4.5	3.1	-1.1	0.8
111	1.8	1.6	8.4	8.3	4.4	2.0	0.8	-1.0
122	4.1	3.9	7.9	8.0	6.9	3.9	1.8	1.0
124	2.3	2.5	8.3	8.2	6.5	2.8	-1.0	0.8
133	3.5	3.9	8.0	8.1	7.7	3.6	0.8	0.8
137	3.3	3.4	8.1	8.1	6.9	3.1	1.0	-0.9
142	3.9	3.6	8.0	8.1	7.4	3.5	1.4	-0.9
144	4.3	3.8	7.9	8.1	6.5	4.1	1.0	-1.1
149	4.5	4.5	7.8	8.0	5.8	3.7	2.3	1.7
159	2.6	3.1	8.2	8.1	8.9	2.6	1.3	2.0
161	2.9	3.1	8.1	8.2	6.9	3.0	1.2	1.0
163	3.0	3.5	8.1	8.1	7.1	3.0	1.0	1.4
166	3.0	3.8	8.1	8.1	9.5	3.0	0.8	2.7
169	4.4	3.6	7.9	8.1	7.8	3.1	3.6	1.2
170	3.2	3.1	8.1	8.2	7.6	3.0	1.2	1.2
171	2.4	2.2	8.2	8.2	6.4	2.0	1.2	1.2
172	3.2	3.4	8.1	8.1	6.9	3.4	1.2	2.5
176	2.6	2.8	8.2	8.2	6.8	2.5	1.4	2.1
177	2.6	2.4	8.6	8.2	6.7	2.2	2.1	0.8
180	3.6	4.3	8.0	8.0	7.0	3.3	1.3	3.2
181	3.5	2.8	8.0	8.2	5.0	2.0	3.2	0.8
184	3.9	3.8	8.0	8.1	6.1	3.1	1.8	1.8
188	2.0	1.7	8.3	8.3	5.7	1.8	1.0	0.0
192	2.1	2.1	8.3	8.2	4.9	2.2	0.8	1.0
193	2.5	3.1	8.2	8.2	6.4	2.6	1.0	3.2

WAVE NUMBER	H_1	H	h_1	h	T_n	u_c	u_1	u_2
197	2.7	3.3	8.2	8.1	7.3	3.2	0.8	2.5
198	3.8	3.6	8.0	8.1	7.1	2.8	2.5	1.3
201	4.1	4.4	7.9	8.0	6.5	3.6	2.3	3.3
205	2.8	2.8	8.2	8.2	6.4	2.8	1.0	-0.6
208	3.6	3.9	8.0	8.1	7.1	3.3	1.7	0.8
218	2.6	2.9	8.2	8.2	6.0	2.8	0.8	1.4
219	3.1	3.4	8.1	8.1	5.6	2.8	1.4	1.7
220	4.4	4.4	7.9	8.0	5.9	3.9	1.7	2.5
223	3.7	3.8	8.0	8.1	5.5	3.0	2.1	1.7
224	3.1	3.2	8.1	8.1	6.1	2.8	1.7	2.1
225	4.0	4.1	7.9	8.0	7.0	3.1	2.1	2.4
226	3.1	3.3	8.1	8.1	7.8	2.5	2.4	2.5
227	4.3	4.2	7.9	8.0	6.9	3.7	2.5	2.3
228	3.8	3.3	8.0	8.1	7.4	3.3	2.3	1.0
236	3.9	3.9	8.0	8.1	8.1	3.1	2.0	1.4
238	3.3	2.7	8.1	8.2	6.5	2.0	2.1	2.0
239	3.2	3.2	8.1	8.1	6.7	2.8	2.0	1.6
241	1.6	1.8	8.4	8.3	7.2	1.8	0.8	0.0
243	2.0	2.2	8.6	8.2	5.3	2.3	0.8	1.0
245	4.5	4.0	7.8	8.0	6.2	3.6	2.8	0.8
248	3.2	3.3	8.1	8.1	6.9	2.2	3.0	2.1
249	4.6	3.5	7.8	8.1	7.6	2.8	2.1	1.7
254	2.0	2.3	8.3	8.2	5.8	2.5	0.0	0.8
257	3.2	3.3	8.1	8.1	7.2	3.0	1.2	1.0
262	1.9	2.0	8.3	8.3	5.0	2.0	1.0	1.0

APP. IF - 5

WAVE NUMBER	H_1	H	h_1	h	T_n	u_c	u_1	u_2
264	2.0	1.8	8.3	8.3	4.9	2.2	0.0	0.8
267	2.3	2.6	8.3	8.2	4.9	2.5	0.0	1.2
269	3.6	3.3	8.0	8.1	5.3	2.8	2.1	1.2
275	3.1	3.9	8.1	8.1	6.4	2.5	1.4	3.8
276	5.0	4.4	7.7	8.0	5.7	3.5	8.3	1.7
277	2.6	2.6	8.2	8.2	8.2	2.5	1.7	1.3
279	3.9	3.3	8.0	8.1	6.7	2.6	3.0	1.2
280	2.1	2.0	8.3	8.3	7.0	2.0	1.2	0.8

APPENDIX II

PHYSICAL CHARACTERISTICS OF THE ORBITAL VELOCITY METER

APPENDIX II

PHYSICAL CHARACTERISTICS OF THE ORBITAL VELOCITY METER

Details of the form and mounting of the orbital velocity meter and its components are shown in figures 4 and 5. A general description of its functioning is included in the text.

ROD

Composition: Beryllium-copper (98% Cu, 2% Be)

Youngs Modulus: $Y = 11 \times 10^{11}$ dynes/cm^2

Yield Strength: 6.9-10.4 dynes/cm^2

Overall length: 25 cm

Effective bending length: $L = 20$ cm

Diameter: 1/4 in. or 0.635 cm

Two pairs of parallel flats were milled on the rod surface near the supported end for mounting the strain gauge elements. The distance, r, of the extreme element of the rod from its neutral axis was 0.242 cm; the distance between flats 0.483 cm.

SPHERE

Composition: Linen bakelite

Density: Approx. 1.33 grams/cm^3.

Diameter: 4.0 cm.

STRAIN GAUGE

Type: Baldwin Locomotive Works "SR-4" bonded resistance wire strain gauge, matched, type A12-3

Resistance: 120.0 ∓ 0.2 ohms

Gauge factor: $C_f = 2.04 \mp 1\%$

Dimensions: Nominal gauge length 3/4 in.

Minimum trim width 1/8 in.

After cementing the gauges on the milled flats on the rod, a thin sleeve of "Penrose" latex drainage tubing was fitted over the assembly, and the void filled with Dow-Corning 200 series silicon oil of 100 centistokes viscosity.

INERTIAL CHARACTERISTICS OF THE ORBITAL VELOCITY METER

After the meter had been calibrated for steady flow, the effects of accelerative forces on the orbital velocity meter were measured experimentally in the laboratory by subjecting the instrument to simple harmonic motion both in air and in water. The coefficient of virtual mass, "a", as defined by equation 1 of the text, was found to be:

"a" (gram cm)	Period of Oscillation (seconds)
18	1.8
69	2.7
78	5.4

Särtryck ur Tellus nr 1, 1956
Reproduced by Permission

A Study of Oceanic Fronts[1]

By TOWNSEND CROMWELL and JOSEPH L. REID, Jr., Scripps Institution of Oceanography,
University of California

(Manuscript received 3 August 1955)

Abstract

Oceanic fronts and frontal layers are defined. Temperature data obtained at two fronts in the equatorial Pacific are presented and a particular circulation, considered basic to the existence of a front, is proposed.

Vertically isothermal warm water overlies the stable frontal layer. This suggests that vertical mixing in the isothermal water maintains the frontal layer in the same way that wind-induced vertical mixing maintains sharp thermoclines.

The data suggest that the depth of vertical mixing is different in the warm and cool water masses adjacent to one of the fronts. It is suggested that the change in vertical mixing regimes contributes to the horizontal gradients of properties across this front.

Introductory Remarks

Atmospheric "fronts" are studied daily by weather forecasters and the term is in widespread popular use. This paper is concerned with an analogous occurrence in the ocean. It is the phenomenon often called "current rip" or "tide rip" in English literature on the subject, although these terms have been applied to a number of different phenomena. Recent observations in the central tropical Pacific revealed a subsurface structure near "current rips" similar to that at atmospheric fronts and led us to adopt meteorological terminology.

The majority of investigations into the nature of oceanic fronts have been by the Japanese. Their interest centers around the fact that fish and whales are abundant along fronts (Uda, 1938, 1953, 1954). Uda (1938) has published a paper including a history of observations of fronts and many descriptions of visual manifestations of the phenomenon.

A surface front is often visible as a narrow band of agitated wavelets. This band may follow a sinuous path, and, if there is floating debris in the area, it concentrates along the front. There is frequently a sound, apparently produced by breaking wavelets, and which, on occasion, has been reported as a "roaring noise". Uda (1938) reports a front audible at a distance of three miles.

Definitions

We know of no definition of an oceanic front. It seems necessary to start with one, but it will be inadequate and will be expanded by discussion and specific examples.

A *front* will mean a band along the sea surface across which the density changes abruptly. Our measurements across fronts are of temperature by a recording thermograph. Throughout this paper, which deals with fronts in the open ocean where salinity variations are small, we will interpret abrupt temperature

---

[1] Contribution from the Scripps Institution of Oceanography, New Series No. 842.

Work initiated by the Pacific Oceanic Fishery Investigations of the U.S. Fish and Wildlife Service and completed under the auspices of the Office of Naval Research and the California Cooperative Oceanic Fisheries Investigations.

Tellus VIII (1956), 1

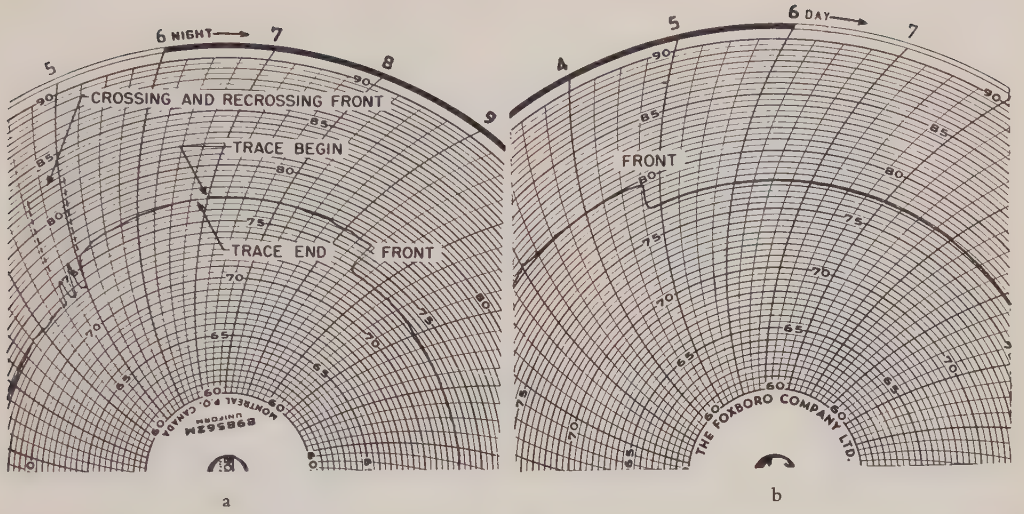

Fig. 1. Examples of surface temperature gradients in the central tropical Pacific. Ship speed during recording, about 9 knots so that each hourly interval (marked along the top) represents about 9 miles. Frontal system corresponding to trace a. appears in cross section in Fig. 3 and that corresponding to trace b., in Fig. 4.

changes as indicative of abrupt changes in density.

Perhaps the fuzziest part of the definition lies in the degree of abruptness of the density gradient required for a front to exist. Only qualitative remarks can be made about this requirement.

Fig. 1 shows thermograph records which illustrate sea surface temperature gradients encountered in the central tropical Pacific. Generally the gradient of surface temperature in this region is of the order of degrees per ten or hundred miles as can be seen in the figure. At fronts, however, the surface temperature gradient is often of the order of degrees per hundredth or tenth miles. Examples of the gradients encountered at these fronts in the central Pacific appear on the thermograph traces in the figure.

Besides density, temperature and salinity, additional properties may change abruptly across a front, including current velocity and concentrations of dissolved and suspended materials, sometimes with striking changes in water color and transparency. Only a change in density is required by the definition, however, for the existence of a front.

From the front, a stable layer inclines downward, separating a warm water mass of low density above, from a cooler one of greater density below. This transition zone will be called the *frontal layer*, a feature that is analogous to that occurring in association with atmospheric fronts. There is an upper, *warm boundary* and a lower, *cool boundary* to the frontal layer. We wish to emphasize that the frontal layer extends in three dimensions and to refer to certain characteristics of the temperature gradient across it. In particular, an important characteristic is the clarity with which the warm and cool boundaries are defined by the BT traces. For example, on bathythermograph traces 61 and 62 of Fig. 2, the warm boundary is clearly defined by a sharp curvature maximum on each trace, whereas the cool boundary is defined less clearly by minor curvature maxima. At some fronts the cool boundary is more sharply defined than it is here.

Temperature distributions near fronts

1. Bathythermograms were obtained close to a front in the equatorial Pacific on October 27, 1952, by G. I. Murphy from the Pacific Oceanic Fishery Investigations' hydrographic vessel SMITH (Fig. 2). The front was clearly visible as a band of agitated wavelets about 150 feet wide, oriented east-west. The two "cool" traces, 58 and 59, were obtained 9 miles and

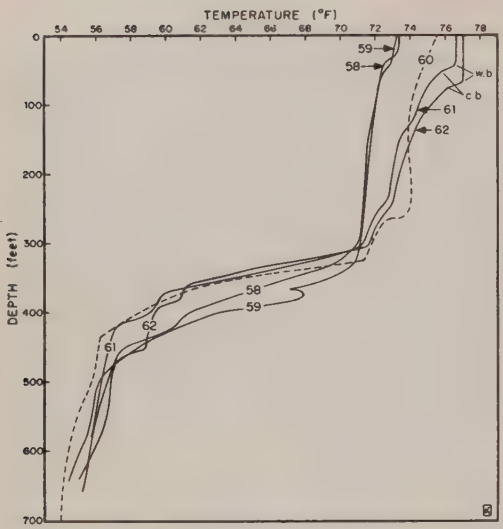

Fig. 2. BT traces on the cool side (58 and 59) and on the warm side (61 and 62) of a front. BT trace no. 60 is in the front. The warm boundary (w. b.) and cool boundary (c. b.) of the frontal layer are indicated. This frontal system appears in cross section in Fig. 3.

150 feet south of the front, respectively. Trace 60 was obtained at the northern edge of the zone of agitated wavelets. Traces 61 and 62 show the thermal structure 3 and 5 miles north of the surface front. It is apparent that the horizontal temperature change is much greater across the front than it is for many miles in either the warm or cool water masses separated by the front. There is an abrupt density change across the front.

We feel that the character of the vertical temperature gradient on the warm side of the front is significant. The warm water is vertically isothermal and the frontal layer begins abruptly at the bottom of this isothermal layer. This suggests that there is intense vertical mixing in the warm water above the frontal layer and also the further possibility that this mixing plays a part in *maintdining* the frontal layer in a manner that will be described in a later section.

Enough BTs were obtained near this front to represent the thermal distribution in cross-section (Fig. 3). The warm and cool boundaries of the frontal layer are indicated using heavy solid lines. The thin lines are isotherms. Regions where water is nearly isothermal vertically are indicated by shading. The hypothesized basic water circulation, discussed below, is indicated by arrows.

The drawing in the vicinity of the surface front may need some explanation. BT trace No. 60 (Fig. 2) shows water of 72F at 288 feet at the northern edge of the frontal zone. Water of this same temperature occurs at 98 feet on BT trace No. 59, obtained ten minutes earlier and approximately 300 feet to the south. Thus, the 72F isotherm rises 190 feet over a horizontal distance of approximately 300 feet. The actual slope of this isotherm is at least 190 ft./300 ft., or approximately 2 feet of rise per 3 feet horizontal distance.

Because of the vertical exaggeration in the section (760: 1) the 72F isotherm appears to rise vertically beneath the surface front be-

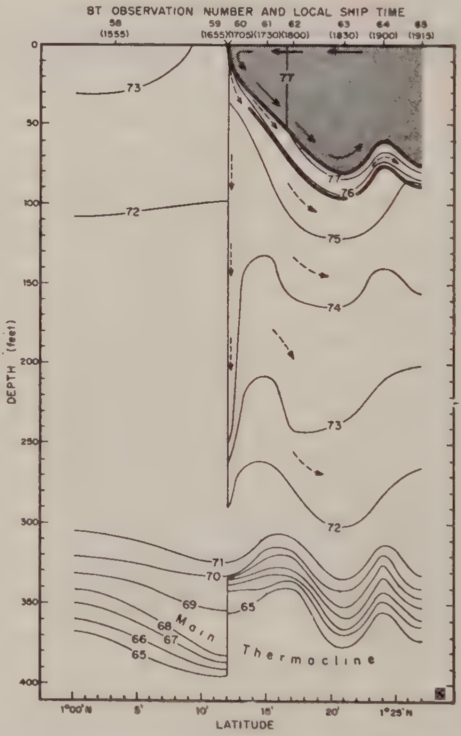

Fig. 3. Vertical temperature distribution across front at 1°12'N, 120°11'W, on October 27, 1952. Isotherms for each °F, thin lines. Frontal layer enclosed by heavy lines. Water nearly isothermal vertically, stippled. Hypothesized basic circulation indicated by arrows. The solid arrows indicate water involved in cell-like motion in this plane. Vertical exaggeration 760 : 1. Surface thermograph trace across this front appears as Fig. 1, a.

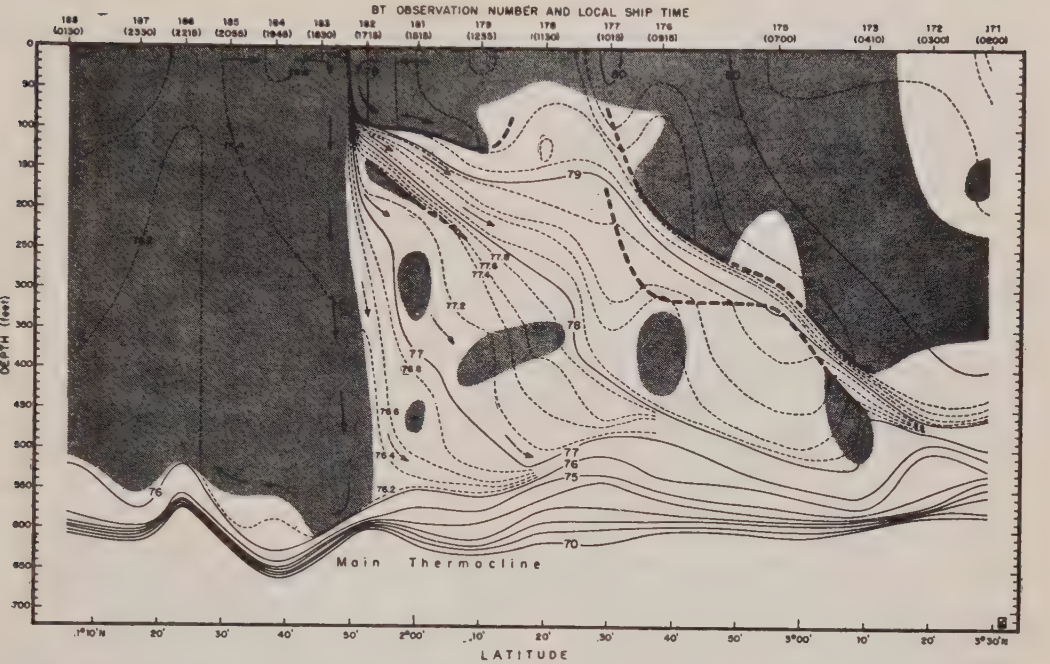

Fig. 4. Vertical temperature distribution across front at 1°50′N, 172°00′W, on February 5, 1950. Isotherms for each °F, thin lines, and for each .2F, thin dashed lines. Frontal layer enclosed by heavy lines (where clearly defined by BT observations) and heavy dashed lines (where diffusely defined). Water nearly isothermal vertically, stippled. Hypothesized basic circulation indicated by arrows. The solid arrows indicate water involved in cell-like motion in this plane. Vertical exaggeration 760:1. Surface thermograph trace across this front appears as Fig. 1, b.

tween 288 and 98 feet. Successive isotherms of higher value, found at considerable depth on BT trace No. 60 in the frontal zone, are found closer to the surface or not at all on BT trace No. 59 in the cool water. Thus, the nearly vertical line extending upward from 290 feet is made up of several isotherms, some of which intersect the sea surface at the front.

The deep penetration of warm water locally beneath the surface front is based on a single BT observation, No. 60 (compared to those nearby). It suggests the existence of a steeply inclined "frontal wall". Closely spaced BTs, obtained recently by R. A. Schwartzlose from the Scripps vessel HORIZON, at a front off Lower California, revealed no such feature. More observations are needed to determine whether or not a frontal wall is a real feature of some oceanic fronts.

2. Data were obtained near a front encountered Feb. 5, 1950. A cross section showing the thermal structure at this front was drawn by CROMWELL (1953) and has been redrawn by us in the light of additional information about fronts discussed in this paper and to show greater detail (Fig. 4). Typical BTs near this front are reproduced in Cromwell's paper. There was no observation immediately at the position of the front.

This frontal layer is more complex than the other. It appears to be "broken", 30 miles north of the surface front. In this region the frontal layer is spread upward and downward so that it occupies a large part of the surface layer. Further, the warm and cool boundaries of the frontal layer through this region are not discernible. The frontal layer is defined again, farther to the north.

As at the front in Fig. 3, the warm water adjacent to this front is nearly isothermal and the frontal layer begins abruptly at the bottom of this isothermal layer. Data obtained near two additional fronts, not presented here, revealed this same basic thermal structure.

The circulation near fronts

There are, to our knowledge, no published measurements of subsurface currents near oceanic fronts. No such measurements were made at the fronts shown in the cross sections in this paper. However, it seems to us that a reasonable speculation can be made as exhibited by arrows in the sections.

Surface convergence along fronts:

Many observers have noted that foam, kelp, and floating debris sometimes collect in conspicuous bands. It seems almost axiomatic that there is a component of surface flow directed into these zones. Feebly swimming plankton observed in fronts (Beebe, 1926; Uda, 1938) are probably concentrated there by the convergent surface flow. The physical data, in particular the abrupt temperature changes across fronts, are consistent with this idea. Surface waters of different temperatures, by virtue of their different origins, are brought into juxtaposition by the convergent flow.

Sinking at fronts:

Continuity demands that there be a flow to compensate for the horizontal convergence that occurs along fronts. This could be accomplished by sinking beneath the surface front and such flow has been observed, strong enough to sink fishing nets at fronts off Japan (Uda, 1938). Recently we observed a similar occurrence.

On November 30, 1953, the authors placed a crude drag near a front off San Diego harbor to observe its motion. The drag consisted of two mutually perpendicular 3 ft. by 3 ft. planes of 1/32 inch sheet iron, attached by 40 feet of line to a surface float (corks), pole and flag. Upon reaching the front, the pole, which previously had lain tilted, became suddenly vertical and sank slowly as though pulled from below. Although we remained in the area for an hour and watched for the flag, it was not sighted again.

Divergence at depth:

Given these two features of the flow, there must be horizontal divergence at depth. If there is a main thermocline which remains stationary, the divergence must occur somewhere in the surface layer.

These three features of flow, 1) convergence along the front, 2) sinking and 3) divergence below, are shown in the cross sections. Water which sinks in the front and which must have a temperature somewhere between that of the warm and cool water masses probably sinks to intermediate depths in and below the frontal layer as shown by the dashed arrows. In Fig. 3 a jet is indicated downward beneath the surface front, but, again, it should be mentioned that more data are needed to determine whether or not a deep penetration of warm water is a real feature beneath some oceanic fronts. In the vertically isothermal water masses, where stability would not oppose them, cell-like circulations are drawn. We have no information about where water rises to the surface to compensate for that which sinks along the front.

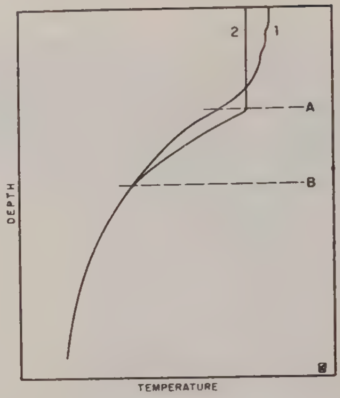

Fig. 5. Effect of wind-induced turbulence on the vertical temperature gradient in the ocean, Curve 1: Before a strong wind. Curve 2: After a strong wind has blown for some time.

An hypothesis concerning the maintenance of frontal layers

The maintenance of frontal systems involves the problem of the maintenance of the thin, stable, frontal layer in spite of diffusion across the layer which should act to destroy it. A process that may maintain the frontal layer is suggested by a different, but, presumably, related phenomenon, i.e., the maintenance of sharp thermoclines by wind-induced turbulence.

Some effects of wind-induced turbulence on the vertical temperature gradient:

Curve 1 of Fig. 5 pictures a typical vertical temperature gradient in the ocean. Curve 2

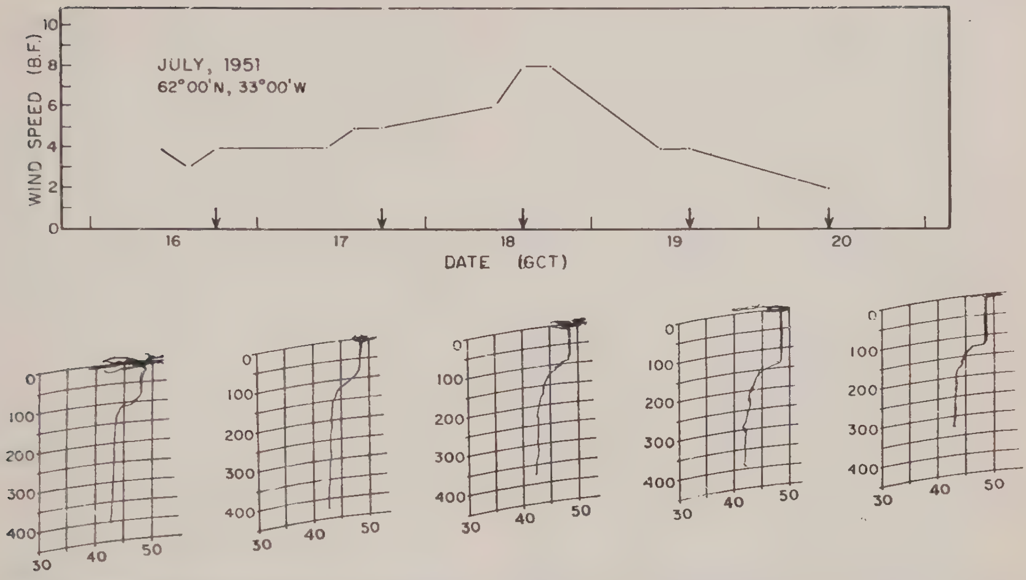

Fig. 6. Selected BTs illustrating "confined mixing" in the surface layer. Wind and BT data obtained at weather patrol station by USCGC UNIMAK. Times of BT observations indicated in wind speed diagram by arrows.

presents the gradient in the same region after a strong wind has blown for some time. This picture is virtually the same as figure 2 in H. O. Misc. 15360 prepared by Schule, *et al.* (1952).

The strong wind increases turbulence at the sea surface and, presumably, downward through the surface layer. This turbulence alters the vertical temperature gradient in three respects pertinent to the present discussion: 1. Mixing, which is made more intense by the turbulence, reduces or eliminates the gradient throughout a layer adjacent to the sea surface. This is shown schematically in the figure between the surface and depth A. 2. The gradient is *intensified* in a layer immediately subjacent to the mixed layer, as illustrated between depths A and B in the figure. 3. The transition from the surface layer to the thermocline layer becomes more abrupt, i.e., the curvature at the "knee" of the trace is increased. One or more of these events have been described by various authors (Sverdrup, *et al.*, 1942, p. 497; Anonymous, 1946; LaFond, 1954), but to our knowledge no data illustrating their occurence have been published.

Francis and Stommel (1953) used fifteen BT series obtained at weather ship stations before and after (and in some cases during) gales to show that the depth of the thermocline increases during a strong wind. These data, lent to us by the Woods Hole Oceanographic Institution, show clearly the events described in the preceding paragraph. Selected BTs from one of the series appear as Fig. 6.

What occurs, as a result of the increasing wind, might be called "confined mixing" because the turbulent mixing induced at the sea surface is bounded below by a stable layer. The stability of the confining, stable layer is increased during the process. A concise physical explanation of how or why this phenomenon occurs, has not been given.

The maintenance of frontal layers:

The correlation that appears in the cross sections among the isothermal warm water mass, the subjacent stable frontal layer and the abrupt transition between the two suggests that the frontal layers are maintained by the same process that maintains sharp thermoclines, i.e., confined mixing. The question arises as to the source of the turbulence.

The frontal layer is overlain by a mixed layer of neutral stability. Turbulence within the mixed layer is not damped by action of the Archimedean force. Turbulence created at the sea surface by the wind or by cooling and subsequent overturn can extend downward to the frontal layer. There is another source of turbulence which may be of basic importance in the maintenance of frontal layers.

Circulations like those drawn in the warm water in each section have been suggested by UDA (1938) and have been reported to occur in Lake Mead (VETTER, 1953). It is necessary, now, to postulate that the "mixed" water overlying the frontal layer is not perfectly homogeneous. One would expect heterogeneities of density to exist near the surface of this water mass by virtue of small scale variations in the factors that control the heat and water transfer processes at the boundary; for example, small scale variations in wind speed. If the warm water mass is not perfectly homogeneous, the hypothesized circulation in the warm water intermittently will bring parcels of low-density water into vertical juxtaposition beneath relatively dense water. Instability, so produced, will provide a continuing source of energy for turbulent overturn. Stommel has suggested that closed circulations, required by the presence of lateral boundaries, may be of importance in producing isothermal layers bounded by thermoclines (POLLAK, 1954). A front seems to provide a "fluid boundary" which allows this process to occur in the open ocean.

Changes in properties across fronts

Convergent flow appears to be partially responsible for the change of properties that occurs across a surface front. Surface waters, of different properties by virtue of their different origins, would be brought into juxtaposition by flows like those shown in the cross sections. Water motion hypothesized to occur near the front shown in Fig. 4 leads to an additional partial explanation for the change in properties that occurs across this front. Both the warm and cool water masses are nearly isothermal vertically. It is proposed that cell-like circulations in the warm and cool water masses lead to turbulent overturn and mixing, as already described. This overturn maintains vertically mixed layers of *differing thickness* in the warm and cool water.

Specifically, in Fig. 4, vertical mixing extends from the sea surface to a depth greater than 500 feet in the cool water south of the front and to a depth only a little greater than 100 feet in the warm water just north of the front. This vertical mixing has virtually eliminated the vertical temperature gradient. Mixing in the warm water north of the front is confined by the stable frontal layer. South of the front, vertical turbulence has extended downward to the main thermocline and it seems reasonable that the surface temperature has been lowered by mixing with this deeper water. This process may contribute to the change in temperature observed horizontally across the front.

The mixing that redistributes the temperature gradient will also redistribute gradients of other properties and will, in general, contribute to the changes in all properties horizontally across the front. For example, the resulting surface velocities in the cool and warm water masses separated by the front will, in general, be different, and thus the vertical mixing may contribute to the horizontal shear across such a front. Analogous reasoning suggests that there should be large shear across the frontal layer. Shear, then, is envisaged as possibly a *result* of the processes that maintain such a front.

Acknowledgements

We appreciate the helpful suggestions from R. B. Montgomery and F. C. Fuglister concerning some of the material and ideas in this paper. We are indebted to the Pacific Oceanic Fishery Investigations of the U. S. Fish and Wildlife Service and the Woods Hole Oceanographic Institution for lending data to us.

T. S. Austin, G. I. Murphy and W. S. Wooster read and made valuable suggestions concerning parts of the manuscript.

REFERENCES

Anonymous, 1946: The application of oceanography to subsurface warfare. *NDRC Summary Technical Reports*, Division 6, v. 6A, 106 pages.

BEEBE, WILLIAM, 1926: *The Arcturus Adventure*. New York and London. G. P. Putnam's Sons, ch. 2, pp. 41—70.

CROMWELL, TOWNSEND, 1953: Circulation in a meridional plane in the central equatorial Pacific. *Journal o Marine Research*, **12**, (2), pp. 196—213.

FRANCIS, J. D. R. and HENRY STOMMEL, 1953: How much does a gale mix the surface layers of the ocean?

Quarterly Journal of the Royal Meteorological Society, **79**, (342), pp. 534—536.

LaFond, E. C., 1954: Factors affecting Vertical Temperature Gradients in the Upper Layers of the Sea. *The Scientific Monthly*, **78**, (4), pp. 243—253.

Pollak, M. J., 1954: Notes from the conference on the thermocline of 25—27 May 1953. *The Chesapeake Bay Institute*, reference 54—2, 49 pages.

Schule, J. J., Jr., L. S. Simpson and A. Shapiro. Effects of weather upon the thermal structure of the ocean. *H. O. miscellaneous 15360*. U.S. Navy Hydrographic Office, 81 pages.

Sverdrup, H. U., M. W. Johnson and R. H. Fleming, 1942: *The Oceans*. New York. Prentice-Hall, Inc., p. 497.

Uda, Michitaka, 1938: Researches on "Siome" or Current Rip in the Seas and Oceans. *Geophysical Magazine*, **11**, (4), pp. 307—372.

— 1953: On the Convergence and Divergence in the NW Pacific in Relation to the Fishing Grounds and Productivity. *Bulletin of the Japanese Society of Scientific Fisheries*, **19**, (4), pp. 435—438.

— 1954: Studies of the Relation between the Whaling Grounds and the Hydrographical Conditions (1). *The Scientific Reports of The Whales Research Institute*, No. 9, pp. 179—187.

Vetter, C. P., 1953: Sediment problems in Lake Mead and downstream on the Colorado River. *Transactions of the American Geophysical Union*, **34**, (4), pp. 249—256.

PRINTED IN SWEDEN ESSELTE, STHLM 56

(423)

(424)

Reprinted from SCIENCE, March 2, 1956, Vol. 123, No. 3192, pages 355–357.
Reproduced by Permission

Absolute Chronology of the Last Glaciation

Hans E. Suess

Radiocarbon dating (*1*) has led to a well-established chronology of the Wisconsin stage of glaciation in North America, which was, until recently, considered to be equivalent to the Last or Würm Glaciation of Europe. The first step in this direction was the dating of wood from the Two Creeks forest bed in Wisconsin by W. F. Libby (*2*) which showed, contrary to what had been expected from other evidence such as telecorrelation of varve sequences, that the last major substage of the Wisconsin, the Mankato of North America, was equivalent to the Younger Dryas of Europe.

Since then, more than 60 individual measurements by Suess and by Rubin and Suess (*3*) at the U.S. Geological Survey in Washington, D.C., on samples from a large number of localities in North America have conclusively established the times of the next previous substages, the Cary and the Tazewell. The Tazewell substage represents, at least in the Middle West of the United States, the time of the maximum southward extent of the ice front, which was reached between 17,000 and 18,000 years ago after a more or less continuous advance over a period of more than 10,000 years (*4, 5*). The Washington radiocarbon dates are sufficiently conclusive to allow the calculation of rates of advance and retreat of the ice during that interval of time and thereafter (*6, 8*).

Continental Glacial Chronology

At least four episodes of colder climate with advancing glaciers can be assumed to have followed the Tazewell maximum with decreasing amplitude toward the present time. They are listed in Table 1 on page 356.

It appears that these oscillations have occurred at fairly regular intervals of about 3500 years. Various oscillations of still shorter periods can also be recognized. They seem to become increasingly conspicuous in postglacial time. For two pre-Tazewell substages of the Wisconsin, the Iowan and Farmdale, stratigraphic evidence and radiocarbon dates are less conclusive. Nevertheless, it seems conceivable that these episodes might represent such oscillations immediately preceding the Tazewell substage (*8*).

It can be shown, however, that the Wisconsin glacial stage of North America does not cover the whole period of the Last or Würm Glaciation as understood by European workers. Penck and Brückner (*9*) showed in 1909 that one can estimate from rates of weathering and deposition that the beginning of the Last Glaciation was about 100,000 years ago. Washington radiocarbon measurements also indicate that the last cold period must have begun much earlier than is indicated by the dates on wood from the early Wisconsin Farmdale loess deposits of Leighton (*10*) (samples W-68, W-69, W-79, W-141, and others). Interstadial forest zones in Canada and Alaska (W-100, 121, 157, 189, 76, 77, 174, and so forth) and the base of the interstadial Younger Loess II of Europe (W-173) as well as archeological remains from the Cold Mousterian were found to be older than the present range of the Washington laboratory, which is about 38,000 years.

Deep-Sea Sediments

Further evidence for a long duration of the Last Glaciation comes from the study of deep-sea sediments. The composition of these sediments, in particular their carbonate content, depends strongly on climatic conditions. A series of climatic oscillations during the Pleistocene can be recognized. The extensive work of G. Arrhenius (*11*) on the titanium content of deep-sea sediments of the Pacific Ocean gives an estimated time for the beginning of the last cold period as 100,000 years ago; this agrees with the European estimates of Penck and Brückner. The technique involved determining the titanium sedimentation rate by radiocarbon dating of codeposited carbonate sediments (*12*).

A much more quantitative and direct approach was made by C. Emiliani (*13*), who applied Urey's paleotemperature method (*14*) to a large number of samples from various Atlantic and Caribbean cores. Emiliani identified and separated pelagic Foraminifera tests, usually *Globigerinoides sacculifera* and *Globigerinoides rubra*, from samples taken in 10-centimeter intervals along the cores. The O^{18} to O^{16} ratio in the $CaCO_3$ of these tests was measured by the mass spectrometer group in Urey's laboratory (Toshiko Mayeda, Harmon Craig, and others) at the Enrico Fermi Institute for Nuclear Studies of the University of Chicago. As was shown by Urey (*14*), this ratio is essentially a function of the water temperature at the time of growth of the shells. In this way, the temperature of surface water was obtained as a function of depth below the top of each core.

The temperature records from all the cores show several regular oscillations. Emiliani finds an apparent amplitude of 7° to 8°C temperature variation. By taking into account a slight increase in the O^{18} concentration during glacial times, about 6°C actual variation of the mean temperature of the surface water is found at the locations where the cores were taken. The experiments and interpretation of the results are discussed in detail by Emiliani (*13*).

The author is a research geochemist at the Scripps Institution of Oceanography, La Jolla, California.

Table 1. Approximate time of maximum extent of glaciers in North America as determined from radiocarbon dates (*4, 5*).

Substage or advance	Time of max. extent before present (yr)	Pertinent samples
Post altithermal advance	3,000?	W-143, W-78
Cochrane	6,500 to 7,500	W-136, W-145
Mankato	10,000 to 11,000	W-42, W-83, W-49
Cary	13,500 to 14,500	W-198, W-33
Tazewell	17,000 to 18,000	W-187, W-165, W-91

Table 2. Apparent radiocarbon ages of carbonate from three deep sea cores determined at the U.S. Geological Survey (*5, 6*). The sedimentation rate for Core A 179-4 (from samples W-160 and W-159) was 2.78 cm/1000 yr or 1 cm/360 yr; the sedimentation rate for Core A 172-6 (from samples W-236 and W-247) was 3.70 cm/1000 yr or 1 cm/270 yr; the sedimentation rate for Core A 180-73 (from samples W-280 and W-278) was 2.44 cm/1000 yr or 1 cm/410 yr.

Sample No.	Depth (cm)	Material	Apparent age (yr)
Core A 179-4: lat. 16°36'N, long. 74°48'W, depth 2965 m (Caribbean Sea).			
W-160	0– 10	Total carbonate	3,950 ± 250
W-158	23– 30	Fine fraction	13,500 ± 400
W-159	23– 30	Coarse fraction	11,800 ± 300
W-134	30– 35	Total carbonate	15,700 ± 400
W-164	60– 65	Total carbonate	21,300 ± 800
W-162	70– 77	Coarse fraction	27,600 ± 1000
W-135	150–155	Total carbonate	35,000 ± 3000
W-147	260–265	Total carbonate	35,000 ± 3000
Core A 172-6: lat. 14°59'N, long. 68°51'W, depth 4160 m (Caribbean Sea)			
W-236	0– 10	Coarse fraction	3,700 ± 200
W-237	51– 61	Coarse fraction	17,500 ± 500
W-238	114–125	Coarse fraction	36,000 ± 3000
W-239	240–250	Coarse fraction	> 38,000
Core A 180-73: lat. 0°10'N, long. 23°0'W, depth 3749 m (Mid-Atlantic Ocean)			
W-280	0– 8	Coarse fraction	2,960 ± 300
W-278	30– 38	Coarse fraction	15,300 ± 300
W-276	80– 88	Coarse fraction	27,000 ± 1500

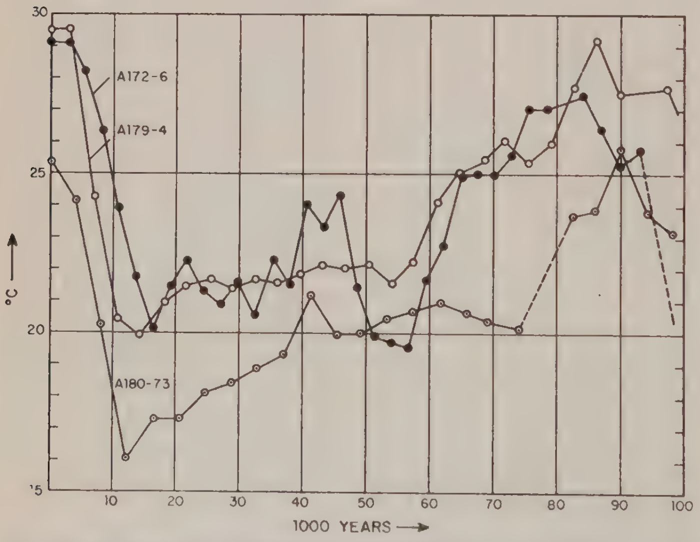

Fig. 1. Paleotemperatures of Foraminifera tests (*Globigerinoides sacculifera*) from O^{18} measurements at the University of Chicago (*13*) versus their age from C^{14} measurements at the U.S. Geological Survey (*5, 6*) for three deep-sea cores from the Lamont Geological Observatory, Palisades, New York.

Carbon-14 determinations were carried out at the U.S. Geological Survey radiocarbon laboratory on three of these cores (*5, 6*), which had been investigated for O^{18} by Emiliani, for the purpose of determining rates of deposition and, from this, the temperatures as a function of time.

The core material was supplied by D. Ericson of the Lamont Geological Observatory, who selected cores that appeared as homogeneous and as free as possible from the effects of turbidity currents, erosion, or slumping. The respective levels for C^{14} dating were selected by Emiliani on the basis of O^{18} trends.

Table 2 lists the results of these C^{14} measurements, expressed in terms of apparent ages, which were obtained by taking for present-day carbonate the C^{14} to C^{12} ratio of modern wood (*15*) and 5568 years for the C^{14} half-life (*1*). The true C^{14} to C^{12} ratios of modern sea carbonate are not accurately known, in particular with respect to possible geographic variations, but the uncertainty in the ages will, for this reason, not exceed a few hundred years. For two other reasons, the apparent ages may well deviate from the true ages to a considerably greater degree. (i) The core material may contain redeposited old carbonate incorporated in some way from stirred-up or dissolved older sediments. (ii) It may also contain some modern carbonate as a result of exchange with atmospheric CO$_2$ during the handling and drying in the laboratory.

The statistical standard error of each measurement is given in the table. It expresses the uncertainty in the C^{14} determination only, and not the uncertainty in age that results from admixture of foreign carbonate. An indication of admixture of old carbonate can be seen from the fact that the total carbonate in the fine fraction has an apparent age sometimes greater by almost 2000 years than the coarse fraction, which consists mainly of Foraminifera tests. All considerations are based on measurements from sieved fractions (greater in size than 74 microns) prepared by Ericson at the Lamont Geological Observatory. The addition of old carbonate, provided that it was constant, only affects absolute age values and not the rates of deposition that are calculated from them. Addition of young carbonate, however, affects the older dates (greater than 20,000 years) to a much greater degree than younger ones. That such an addition has, in some instances, actually taken place can be seen from the measurements for samples W-135 and W-147. The age of these layers was undoubtedly much greater than the apparent age of 35,000 years. Such an addition is insignificant for younger dates (less than 20,000 years); the younger dates were used for calculating rates of deposition.

In Fig. 1, the O^{18} temperatures (derived from *Globigerinoides sacculifera*) as determined at the University of Chicago are plotted as a function of age, which was obtained from the rate of deposition that results from C^{14} determinations at the U.S. Geological Survey. It was assumed that this rate was constant and equal to that at which the upper part of the cores was deposited. Despite the obvious uncertainties of this assumption, it can be seen that the temperature trends as a function of time in the three cores investigated so far agree surprisingly well. If the rate of deposition was different during glacial times from that during the more recent period, then this difference must have been nearly the same in the three cores.

Assuming that this difference was negligible, one finds that a period of decreasing temperatures began about 80,000 years ago. The temperature reached a minimum about 15,000 years ago; this time coincides within the accuracy of the method with the time of the maximum extent of the North American ice sheet. Thereafter, a relatively rapid temperature increase took place, leading to conditions resembling those of the present. Although no indications for fluctuations of a 3500-year period can be recognized, the record from the core material seems to parallel the continental glacial and postglacial events in a crude but unmistakable way. Extrapolating backward in time, we find that the record shows a less pronounced temperature minimum about 55,000 years ago that preceded a relatively moderate period about 45,000 years before the present. The warm period of about 90,000 years ago may be correlated with the Sangamon time of North America, and the moderate period of 45,000 years ago may be correlated with a yet unnamed oscillation that is recognized in Pleistocene stratigraphy of the northern areas of North America (*3*). With respect to European glacial chronology, the sequence resembles that proposed by Zeuner (*16*) if one correlates the temperature interstadial of 45,000 years ago with LG 2/3 and the time about 85,000 years with LG 1/2. Such correlation with the respective Würm phases may well require revision. However, a certain similarity of the temperature record in the core material with the astronomical insolation curve of Milankovitch (*17*), on which Zeuner's chronology is based, cannot be denied. This, at least, is the conclusion that Emiliani (*13*) derives from the combined temperature records of his cores, which in some instances go back to the beginning of the Pleistocene, and from sedimentation rates estimated from various methods of dating. In particular, the 40,000-year period in the obliquity of the earth's axis (*18*) seems to be reflected in these records. The minima in the obliquity, however, precede the temperature minima by nearly 10,000 years.

Summary

It appears that there is evidence for two main types of climatic fluctuations that have occurred during the Last Glaciation on two different time scales, one of the order of 40,000 years and another of the order of 3500 years. The Last Glaciation embraces at least two of the long periods (Fig. 1) upon which are superimposed oscillations of the short period (Table 1). Apparent contradictions in radiocarbon dates (*19*) are at least in part the result of miscorrelations between events on these two different time scales (*20*).

References and Notes

1. W. F. Libby, *Radiocarbon Dating* (Univ. of Chicago Press, Chicago, 1952).
2. R. F. Flint and E. S. Deevey, Jr., *Am. J. Sci.* **249**, 257 (1951).
3. R. F. Flint and M. Rubin, *Science* **121**, 649 (1955).
4. H. E. Suess, *Science* **120**, 5 (1954.)
5. M. Rubin and H. E. Suess, *Science* **121**, 481 (1955).
6. ——, *Science*, in press.
7. R. F. Flint, *Am. J. Sci.* **253**, 249 (1955).
8. L. Horberg, *J. Geol.* **63**, 278 (1955).
9. A. Penck and E. Brückner, *Die Alpen im Eiszeitalter* (Leipzig, 1909).
10. M. M. Leighton, *J. Geol.* **34**, 167 (1926).
11. G. Arrhenius, *Report of Swedish Deep-Sea Expedition 1947–48*, Vol. 5, fasc. 1, p. 198.
12. G. Arrhenius, G. Kjellberg, W. F. Libby, *Tellus* **3**, 222 (1951).
13. Cesare Emiliani, *J. Geol.* **63**, 538 (1955).
14. S. Epstein *et al.*, *Bull. Geol. Soc. Amer.* **62**, 417 (1951); **64**, 1315 (1953).
15. H. E. Suess, *Science* **122**, 415 (1955).
16. F. E. Zeuner, *Dating the Past* (Methuen, London, 1952).
17. M. Milankovitch, *Handb. Geophys.* **9**, 593 (1938).
18. A. J. J. Van Woerkom, in *Climatic Change*, H. Shapley, Ed. (Harvard Univ. Press, Cambridge, Mass., 1953).
19. E. Antevs, *J. Geol.* **63**, 495 (1955).
20. This article is a contribution from the Scripps Institution of Oceanography, new series, No. 843. Thanks are due to C. Emiliani for making his manuscript (*13*) available to me prior to its publication. The critical comments of R. Rex, M. Rubin, and C. Emiliani are appreciated.

CHAPTER

9

The Ocean off the California Coast[1]

THE COAST, ISLANDS, AND SEA FLOOR

Character of the Shoreline and Islands

Unlike the Atlantic and Gulf coasts of the United States, the shoreline of California is relatively straight and short when measured against the coastwise length of the state. This character of the shoreline has been determined by two factors: the presence of highlands and mountains near shore, and changes of sea level during the late geologic past. Along much of the coast, fossil sea shells and step-like marine terraces give evidence that the land has risen; elsewhere, partially filled estuaries reflect the rise in the sea which accompanied the end of the ice age. Rocky headlands and pocket beaches of sand or cobbles characterize the uplifted regions. Long, straight, or gently curving stretches of sandy beach extend along the shore from the mouths of many estuaries. Along some parts of the coast there are wide reaches of undulating sand dunes. In other areas low sea cliffs that cut into river alluvium form the landward margin of the beach zone. A terrace a few feet above the present mean tide line is usually present. It is probably the result of a world-wide fall of sea level during the past few thousand years.

Some of the larger estuaries form sheltered harbors. San Francisco Bay, the largest, has an area of approximately 400 square miles. Other examples of estuaries which with their barrier beaches form natural harbors are Humboldt, Morro, Newport, Mission, and San Diego bays. Los Angeles harbor is largely man-made, but in its development advantage was taken of the shelter furnished by a pre-existing estuary and barrier beach.

Islands along the California coast include the Farallons off San Francisco and the Channel Islands off southern California (Fig. 1). Together with submerged banks off central California, the Farallons lie in a northwest to southeast line parallel to the major topographic features of the coastal region. The islands off southern California are separated from the mainland by deep water (more than 700 feet); they are the summits of submerged mountain ridges. Other summits of submerged ridges have been planed off below sea level to form shallow banks, such as Tanner, Cortez, and Thirty-mile Bank (Fig. 2).

Topography of the Sea Floor

The location of the continental slope, which separates the submerged western edge of the North American continental platform from the abyssal basin of the Pacific Ocean, is roughly approximated by the 6000-foot depth contour (Fig. 1). Although the continental slope is close to shore along northern and central California, it is 160 miles from the southern California shore. Between the coast and the continental slope off southern California lie a series of submerged mountain ranges and intervening deep basins and troughs (Fig. 2). This ocean floor area has been

---

[1] Contribution from the Scripps Institution of Oceanography, New Series, No. 844.

By Paul Horrer and Roger Revelle, University of California,
Scripps Institution of Oceanography, La Jolla

Reproduced, by permission, from CALIFORNIA AND THE SOUTHWEST, ed. Clifford M. Zierer. New York, John Wiley & Sons, Inc., 1956.

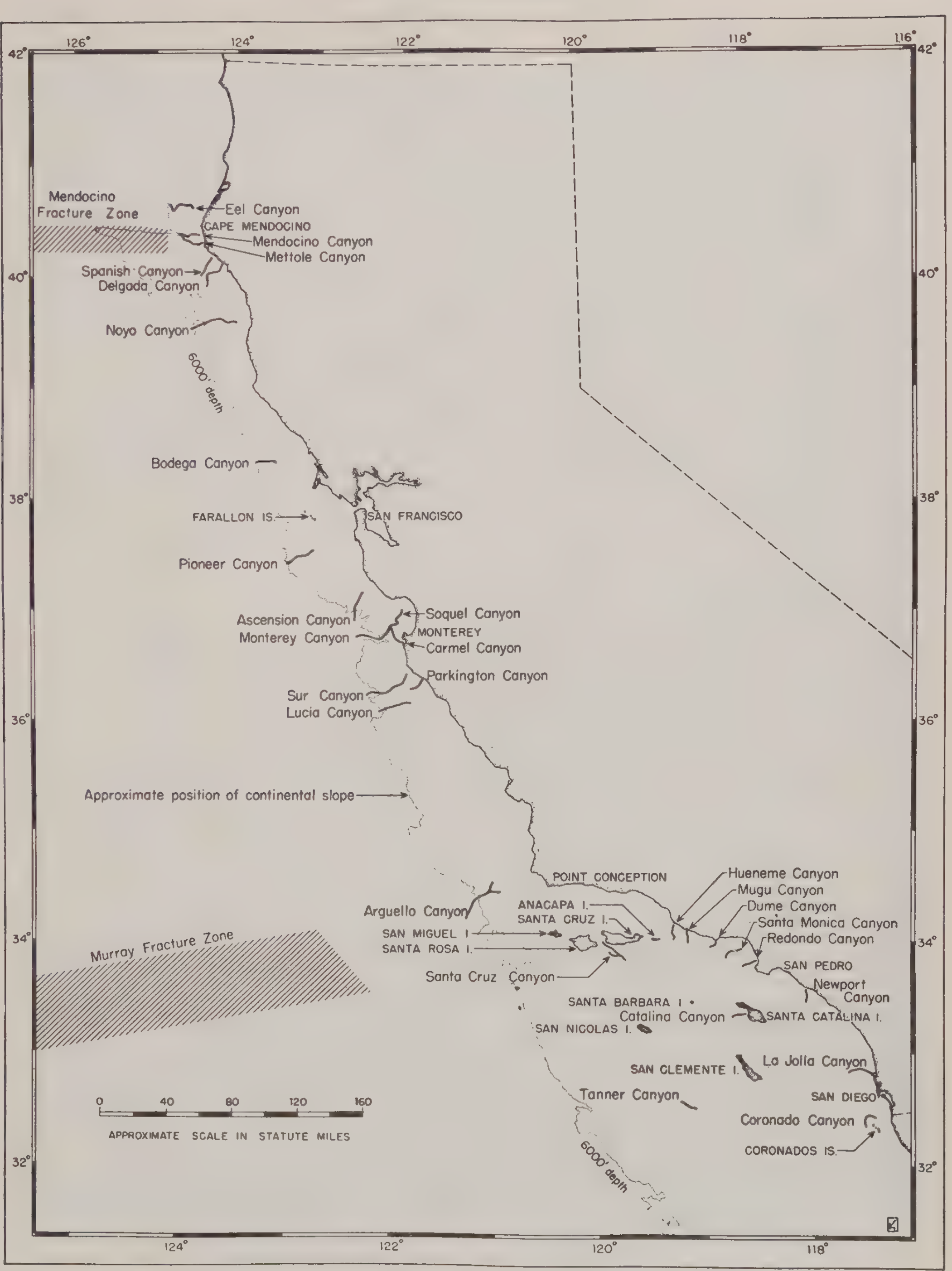
126°
124°
122°
120°
118°
116°
42°
40°
38°
36°
34°
32°
Mendocino Fracture Zone
Eel Canyon
CAPE MENDOCINO
Mendocino Canyon
Mettole Canyon
Spanish Canyon
Delgada Canyon
Noyo Canyon
6000' depth
Bodega Canyon
FARALLON IS.
SAN FRANCISCO
Pioneer Canyon
Ascension Canyon
Monterey Canyon
Soquel Canyon
MONTEREY
Carmel Canyon
Parkington Canyon
Sur Canyon
Lucia Canyon
Approximate position of continental slope
POINT CONCEPTION
Hueneme Canyon
Mugu Canyon
Dume Canyon
Santa Monica Canyon
Redondo Canyon
Arguello Canyon
ANACAPA I.
SANTA CRUZ I.
SAN MIGUEL I
SANTA ROSA I.
Murray Fracture Zone
Santa Cruz Canyon
SAN PEDRO
Newport Canyon
SANTA BARBARA I.
Catalina Canyon
SANTA CATALINA I.
SAN NICOLAS I.
SAN CLEMENTE I.
La Jolla Canyon
SAN DIEGO
Tanner Canyon
Coronado Canyon
CORONADOS IS.
6000' depth
0
40
80
120
160
APPROXIMATE SCALE IN STATUTE MILES

Figure 1. California shoreline, islands, and submerged canyons.

named "continental borderland" by Shepard and Emery.

A sudden withdrawal of the sea from the continental borderland off southern California would leave eleven or twelve sizable lakes. These would have individual surface areas up to almost 1000 square miles and depths to 2900 feet. In the United States today only the Great Lakes have larger surface areas and none is as deep. The ridges separating the lakes would be comparable in vertical and horizontal dimensions to the coastal mountain ranges of the adjacent land. But much of their summit area would be nearly flat and at about the same elevation, corresponding to the banks and flat-topped ridges, planed off by wave erosion during former lower stands of sea level.

Along the entire length of the state a gently sloping submarine terrace extends out from shore to depths of 300 to 600 feet. This is called the continental shelf. South of Point Conception the slope beyond the edge of the shelf leads to the innermost basins of the continental borderland. From San Diego to Monterey, the shelf is narrow (1 to 5 miles); north of Monterey it broadens to a maximum width of about 28 miles off San Francisco.

The continental shelf is deeply incised by a series of steep-sided submarine valleys or canyons. These are similar in many respects to river-cut canyons on land, but in general the submarine

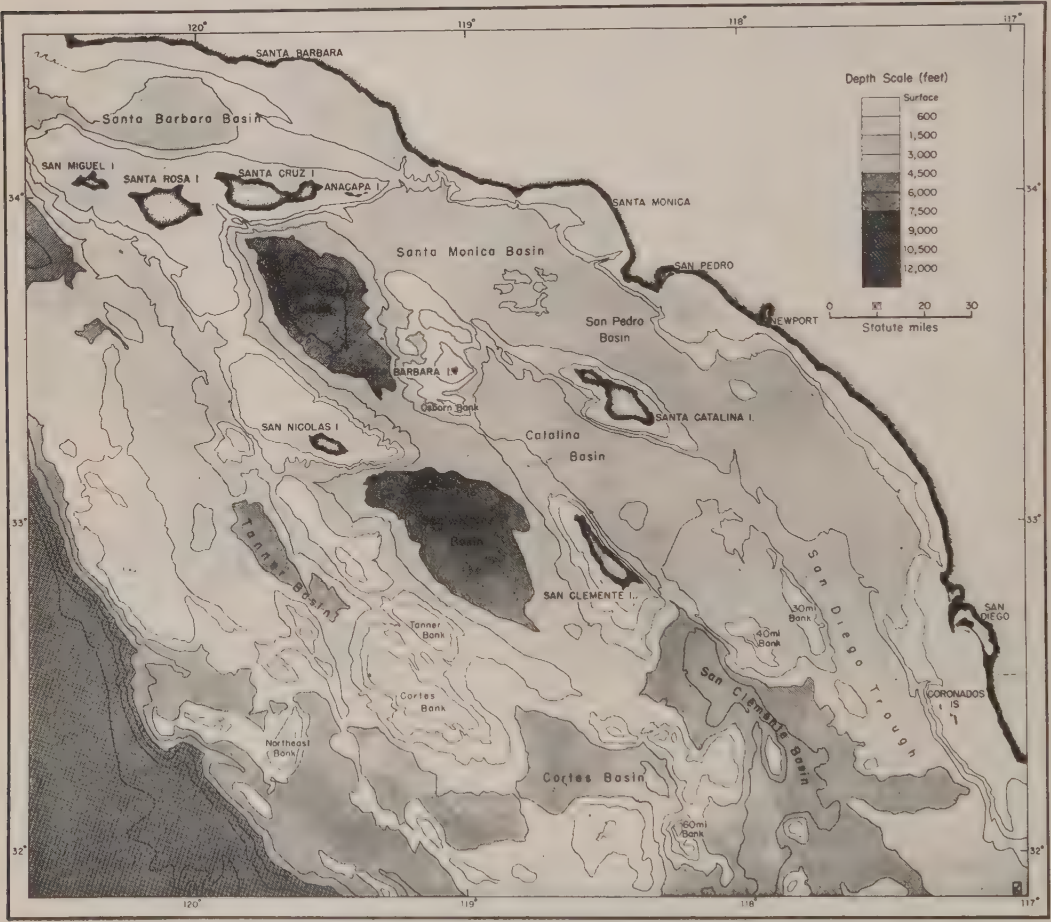
120°
119°
118°
117°
34°
33°
32°
SANTA BARBARA
Santa Barbara Basin
SAN MIGUEL I
SANTA ROSA I
SANTA CRUZ I
ANACAPA I
SANTA MONICA
Santa Monica Basin
SAN PEDRO
San Pedro Basin
NEWPORT
SANTA BARBARA I.
Osborn Bank
SANTA CATALINA I.
SAN NICOLAS I
Catalina Basin
San Nicolas Basin
Tanner Basin
SAN CLEMENTE I.
Tanner Bank
Cortes Bank
Northeast Bank
Cortes Basin
San Clemente Basin
30mi Bank
40mi Bank
60mi Bank
San Diego Trough
SAN DIEGO
CORONADOS IS
Depth Scale (feet)
Surface
600
1,500
3,000
4,500
6,000
7,500
9,000
10,500
12,000
0
20
30
Statute miles

Figure 2. Submarine topography off the coast of southern California.

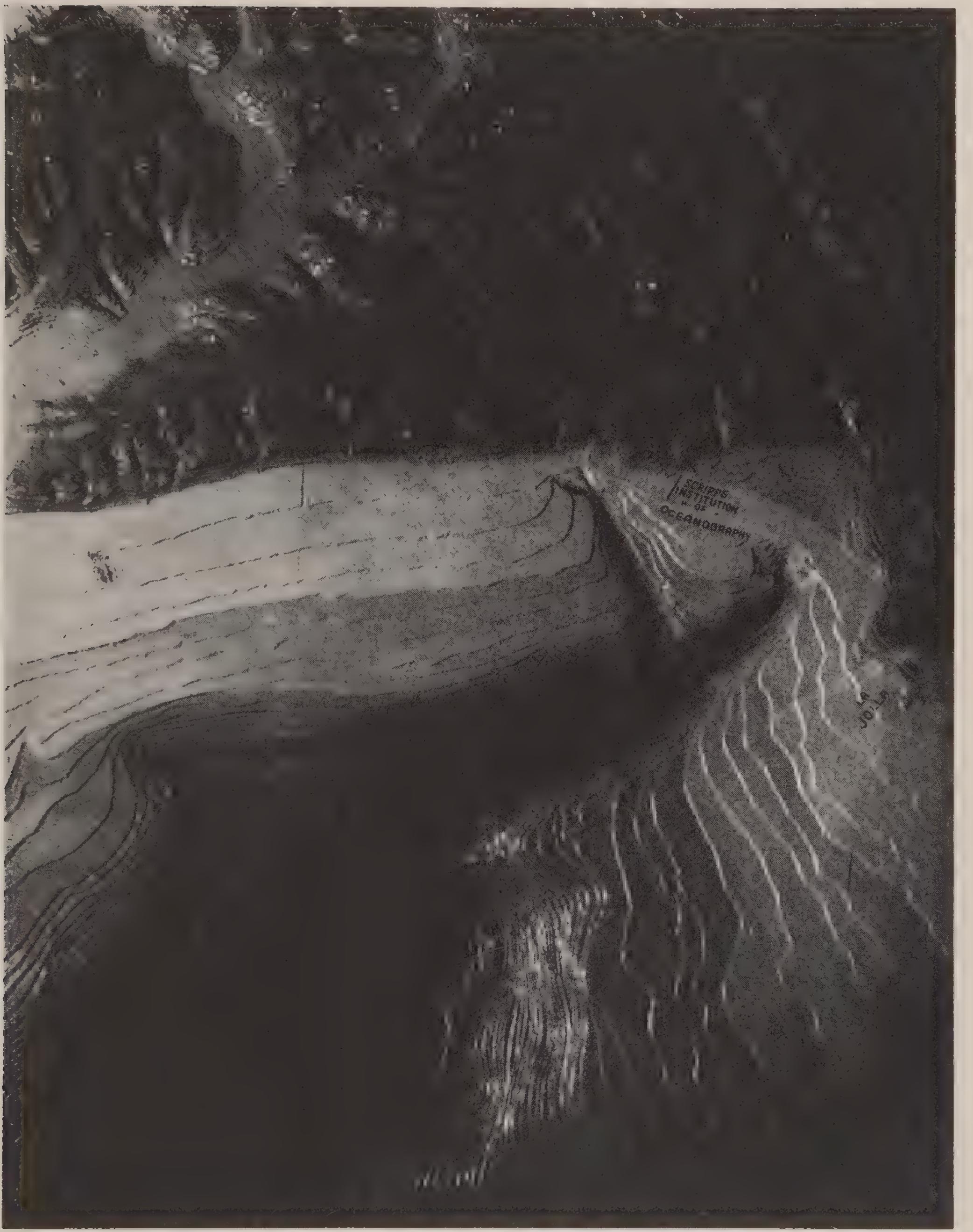
SCRIPPS INSTITUTION OF OCEANOGRAPHY
LA JOLLA

Figure 3. Model of La Jolla and Scripps submarine canyons.

canyons off California are larger and steeper than the land valleys of the adjacent coast (Fig. 3). The great submarine canyon off Monterey is as deep and its walls are as steep as the Grand Canyon of the Colorado River.

Beyond the continental slope off Cape Mendocino, a great submerged escarpment extends due west for at least 1500 miles (Fig. 1). This is called the Mendocino Fracture Zone. A similar feature, the Murray Fracture Zone, extends west by south from the base of the continental slope off Point Conception. Between these two zones of broken topography the sea floor is relatively flat and slopes gently westward from depths of about 13,000 feet at the base of the continental slope to nearly 18,000 feet east of the Hawaiian Islands. South of the Murray Fracture Zone, the deep-sea floor is pimpled with submarine volcanos, which rise as isolated peaks comparable in shape and size to Mount Shasta.

Borderland Sedimentation

Sand, silt, and clay are brought to California coastal waters by swollen streams during the winter rains. Another source of sediment is the sand and rock fragments eroded from sea cliffs by waves. Carried outward in suspension in the upper water layers, the particles of silt and clay eventually settle gently to the sea floor, where they accumulate slowly on deep slopes and in the bottoms of basins and troughs. The coarser particles (diameters greater than 0.0025 inch) are winnowed by waves and near-shore currents. Some of these particles return to land to form sand beaches and are later collected in coastal sand dunes by winds. But much of the sand moves out to the basins and troughs, traveling along the bottom at irregular intervals in deep currents or slumping under the action of gravity. Little or no sediment is accumulating at the present time on the continental and island shelves, the banks, ridges, steep submarine slopes, and submarine canyons.

Erosion and Deposition along the Shoreline

Waves and the currents they generate are the principal agencies of erosion and deposition near shore as shown by Inman. Along the California coast, the highest and steepest waves occur in winter, moving sand from the beach to deeper water and frequently denuding the rocks underlying the beach. The longer and lower waves of summer move the sand back to the foreshore, and the rocks are covered again.

When breaking waves, which carry water toward shore, approach the beach at an angle, longshore currents are generated. These currents, flowing parallel to the beach inside the breaker zone, transport sand-sized particles along the shore. The water is returned seaward, completing the circuit of water movement, by strong, narrow currents flowing out from the shore, called rip currents. Points or headlands of land and man-made obstructions influence the circulation pattern and alter the direction of the currents flowing along the shore.

The establishment and persistence of a sandy beach is the result of a delicate balance between erosion and deposition. Erosion usually predominates over deposition off headlands; deposition, both marine and terrestrial, tends to dominate along indentations between headlands.

PHYSICAL AND CHEMICAL CHARACTER OF COASTAL WATERS

Temperature and Its Variations

The near-surface waters to the west of continents are colder than those to the east of continents. The northward-flowing Kuroshio of the Western Pacific warms the coastal waters of Japan. In the Eastern Pacific the southward-flowing California current is laden with cold, subarctic water, which warms slowly as it travels down the California coast. Thus the ocean water temperatures off California are colder than those off Japan at similar latitude (Fig. 4).

The seasonal range of coastal surface water temperature is smaller than that of the overlying air temperature because of the high heat capacity of water and the ocean's sluggish circulation. In consequence, seasonal changes in air temperature tend to control the changes in ocean surface temperature. Ranges in air temperature over the ocean are greatest off east coasts where the air moves to the sea from the land.

By lowering the summer temperatures, a process called "upwelling" tends to reduce seasonal ranges in surface water temperatures to the west of continents. The wind moves the warm surface waters tens and hundreds of miles away from shore and brings colder water from depths to the surface near shore. The most pronounced effect of this phenomenon is to delay spring and early summer warming (Fig. 4).

As depth increases in the ocean the temperature becomes lower, reaching a minimum of about 35° F. below about 10,000 feet. The water temperature does not decrease uniformly with depth, however. There is almost always an upper layer of nearly uniform temperature which oceanographers call the "mixed layer." Beneath it the temperature decreases sharply for several hundred feet, and then more and more slowly to the bottom. The depth where temperature decreases most rapidly, called the "thermocline," may be only 30 or 40 feet below the surface inshore and as much as 400 feet deep several hundred miles offshore. The decrease in temperature is accompanied by a relatively rapid increase in density of the water. During World War II, when the enemy used listening devices, American submarines found the thermocline to be a tangible and highly useful structure. They were sometimes able to escape detection by the simple expedient of stopping all engines and "balancing" on the denser water beneath the thermocline.

Distribution of Density and Salinity

The density of water in the open sea is comparatively uniform, being everywhere within 2 per cent of the average value for the oceans as a whole.

Near the sea surface, the coastal waters off southern California are both more saline and warmer than off northern California. But the density in both areas is nearly the same, being

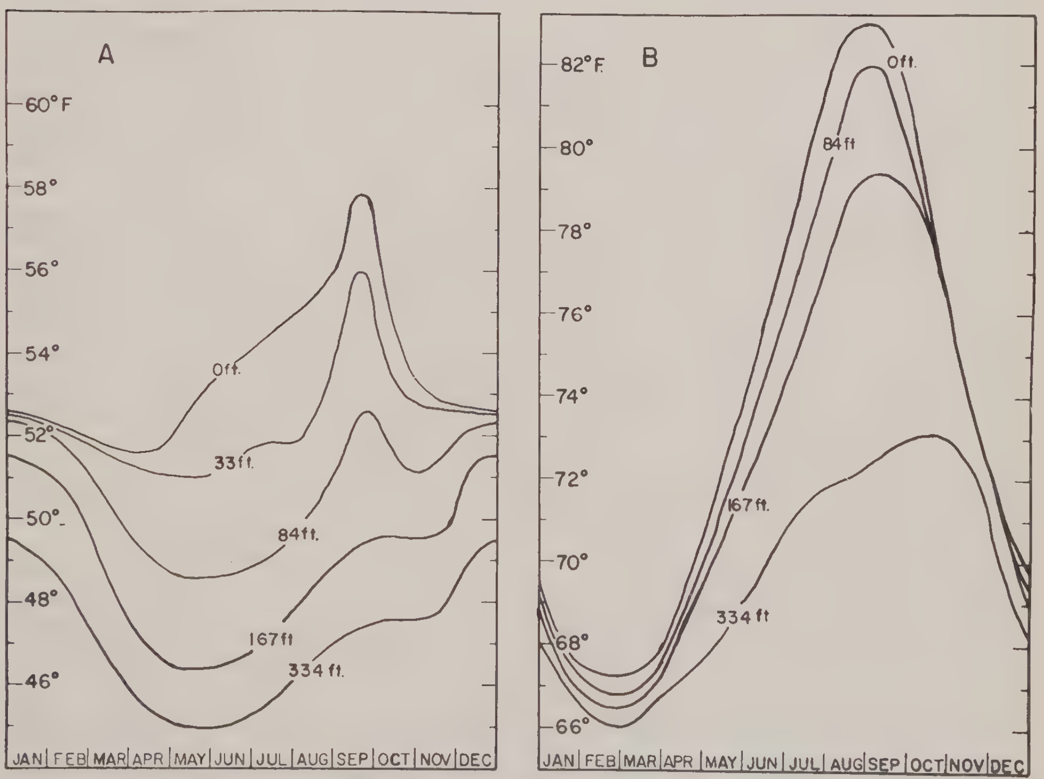

Figure 4. Annual variation in temperature at certain depths in coastal waters of California (A) and Japan (B) at about latitude 37 degrees. (Reproduced from H. U. Sverdrup, Martin W. Johnson, and Richard H. Fleming, *The Oceans: Their Physics, Chemistry, and General Biology*, Prentice-Hall, Inc., New York, 1946, with permission.)

1.024 to 1.026 times the maximum density of pure water at surface pressure. Two miles below the surface, where the waters are very cold and are more saline than the surface waters, and under a pressure of between 2 and 3 tons per square inch, the density is 1.045 times the maximum density of pure water.

There is little variation either horizontally or vertically in the amount of salt contained in the California coastal waters, except near river and stream outfalls. Surface waters average about 33.5 and deep waters about 34.7 parts per thousand. Because evaporation is greatest during summer, the highest salinity at the surface occurs in that season; rainfall and runoff produce a minimum during floods in winter. The salinity of surface waters may be lowered to 28 parts per thousand 10 miles distant from sizable rivers such as the Eel, and to nearly zero right at their mouths.

Chemical Composition

The total quantity of chemicals in sea water varies slightly from place to place, but the ratios of the most abundant elements to each other remain constant. Minor elements and compounds, such as phosphorus, nitrate, and silica, are much more variable in concentration than the major constituents of sea water. The amounts of these "trace" substances in the water layers near the surface determine whether a particular area of the sea is fertile, supporting an abundance of life, or a barren ocean desert. Some of these substances occur in such small quantities that they cannot be measured by ordinary chemical methods; their presence in sea water was first inferred from the fact that they are found in relative abundance in the tissues of certain marine plants and animals. Examples are vanadium, copper, manganese, and iodine.

Plant nutrients and growth factors are not always abundant in the upper layers of the ocean where bright sunlight penetrates and plants can grow. The average amount in subsurface sea water falls well below that in many river and lake waters. The upper water layers off California, however, are relatively high in nutrients as compared with oceanic areas far from shore. This is due to the slow surfaceward movement, or upwelling, of the deeper waters along the coast, which are rich in nutrients. Upwelling is most intense on the California coast in spring and early summer; consequently there is an intense blooming of marine plants during these seasons.

Transmission of Sound

Sound travels in water more rapidly and with much less absorption of energy than in air. (Just the opposite is true of light and other electromagnetic waves.) As a result, acoustic methods for navigation and submarine warfare have become highly developed. The speed of sound in sea water is about 4800 feet per second, compared with 1100 feet per second in air. The sound velocity is independent of wave length; it increases with increasing temperature, pressure, and salinity.

Color and Transparency

Offshore waters of relatively low plant populations are typically transparent and blue in color. In these waters a shipboard observer can see objects at depths in excess of 150 feet. Like the blue of the sky, the blue color of the offshore waters is the result of scattering of sunlight against the water molecules themselves or against suspended minute particles. In inshore areas the depth of visibility may be reduced to 6 feet along the coast and even to 3 feet or less in bays (such as the upper end of San Diego Bay) by suspended sediment as well as by plant plankton. The color of inshore waters is affected by the content of organic matter and sediments. Green water is common in coastal areas, and brown or "red" water is occasionally observed when certain microscopic plants are abundant.

CURRENTS AND TIDES OFF THE CALIFORNIA COAST

California Current

Along the West Coast of the United States flows the California current (Fig. 5), a meandering water body about 400 miles wide. It moves sluggishly (0.2 to 0.6 mile per hour) over a deep bed of almost motionless but colder and more saline water. The volume of water it carries annually to the south is 200 to 300 times that discharged each year at the mouth of the Mississippi

—one of earth's mightiest rivers. Yet the annual transport of the California current is only one-tenth that of the narrow, fast, and deep Gulf Stream in the Atlantic. It sweeps southward along the coast from the Canadian border to central and lower Baja California, where most of it turns westward to lose its identity by joining the westward-flowing North Equatorial current. The California current is the dominant feature in the ocean geography of the entire northeastern Pacific. Several lesser currents are associated with it.

California Countercurrent

Between the California current and the coast lies a complex system of countercurrents and eddies ever changing with the seasons (Fig. 6). During the winter there is often a narrow countercurrent near the coast flowing northward at 0.2 to 0.5 mile per hour. This current was responsible for numerous shipwrecks during the nineteenth century.

When the countercurrent is absent at the surface, as it often is during summer, great oceanic eddies, lazily revolving masses of water, form in the inshore regions. One such eddy is usually present off central California, but the most persistent one is located near the southern California islands according to Sverdrup and Fleming. This giant wheel of water, sometimes 100 miles or more across, rotates slowly counterclockwise. In its center, the surface waters have upwelled from intermediate depths and are enriched in the nutrient substances required for plant growth. On the southern limb of the eddy, near northern Baja California, some California current water turns toward the coast. Here the surface waters sink and their fertility is low, causing the area to be nearly a marine desert.

Wind-Induced Drift

Superimposed on the more steady currents, discussed in preceding paragraphs, are very shallow currents which change readily with the wind. In moderate to strong winds the surface waters may move at a speed of 1.5 to 2 miles per hour, generally somewhat to the right of the wind's direction. Like the prevailing winds off the California coast, these wind-driven currents are usually from the northwest. Such drift currents, often obscuring the sluggish California current and countercurrent, are of great importance in determining the set of ships.

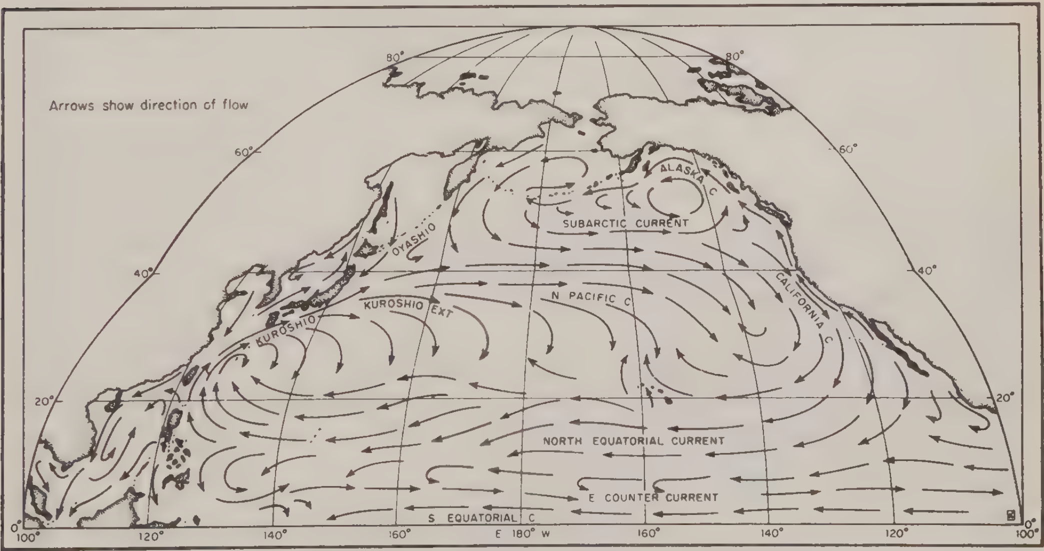

Figure 5. Surface currents of the North Pacific. (Reproduced from H. U. Sverdrup, Martin W. Johnson, and Richard H. Fleming, *The Oceans: Their Physics, Chemistry, and General Biology*, Prentice-Hall, Inc., New York, 1946, with permission.)

Mixing and Stirring Processes

When the wind blows, the sea surface is roughened and the upper layers of the sea become turbulent; that is, stirring occurs. This tends to mix and homogenize the upper water layers. Vertical mixing also results from evaporation or cooling at the surface, which causes the surface water to become denser than the underlying water. The consequent sinking of the surface water and rising of deep water to take its place are called convection.

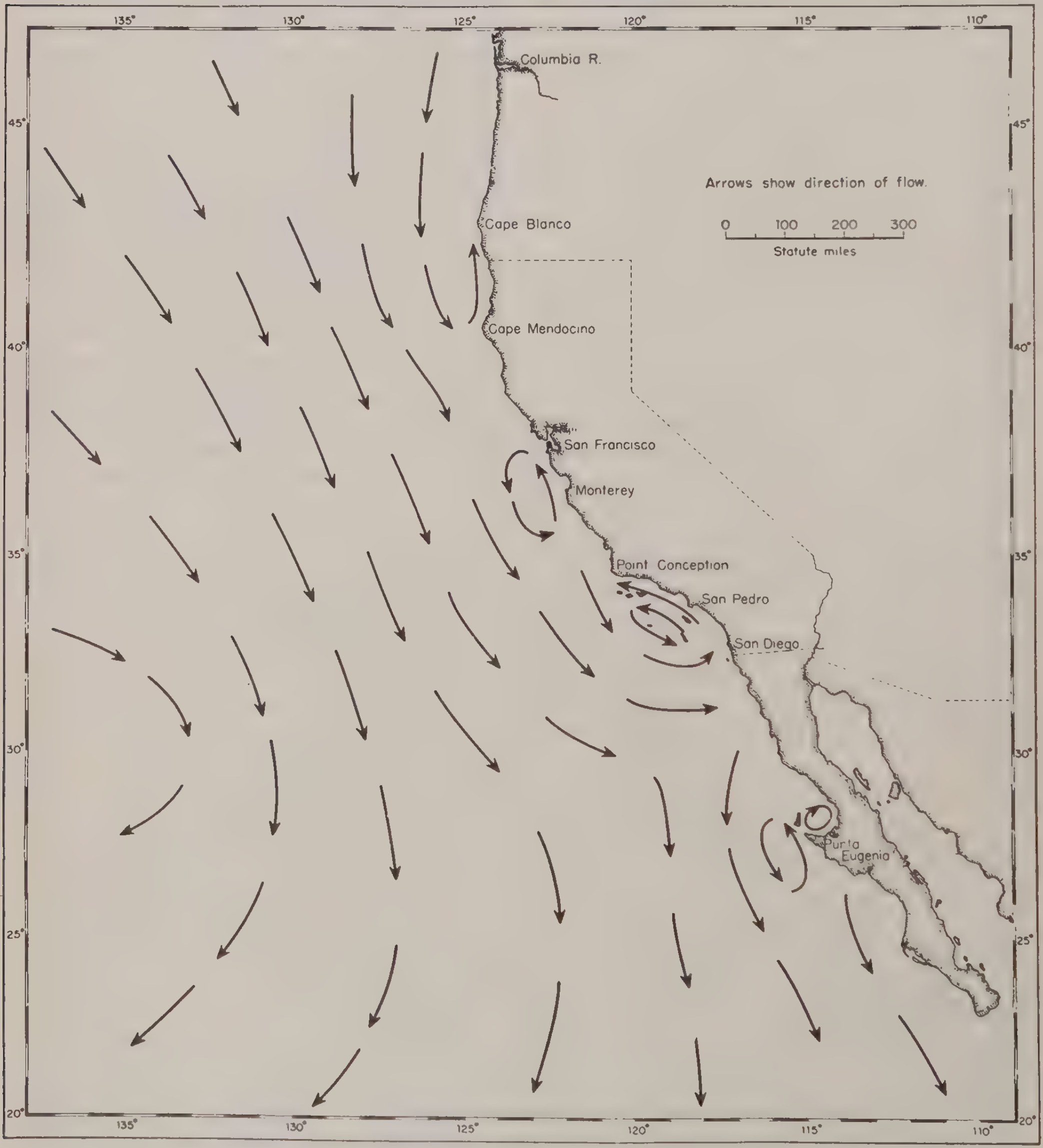
135°
130°
125°
120°
115°
110°
45°
40°
35°
30°
25°
20°
Columbia R.
Cape Blanco
Cape Mendocino
San Francisco
Monterey
Point Conception
San Pedro
San Diego
Punta Eugenia
Arrows show direction of flow.
0 100 200 300
Statute miles

Figure 6. Surface currents off the California coast.

Currents and mixing within the sea affect marine plants and animals by oxygenating subsurface water, by distributing and dispersing their supply of nutrients and food, and by dispersing wastes from their metabolic processes. Beneath the sea surface, currents determine the temperature and other characteristics of the environment. They transport spores, eggs, larvae, and adult organisms, thus setting up barriers to migration and occasionally carrying organisms to unfavorable surroundings. For example, adverse currents can carry a fish spawn into an area unsuitable to its survival.

Tides and Tidal Currents

Tides are caused by the gravitational attraction of the sun and the moon, the latter exhibiting the strongest pull upon the sea. But the character of the tides in different parts of the sea varies widely, depending on the shape of the sea basins, and large variations occur even within short geographical distances, depending on the submarine topography near shore.

All along the coast of California there are two high and two low tides each day, varying in height and relative importance at different parts of the coast. The largest tides, known as "spring" tides, occur every two weeks when the sun, moon, and earth are nearly in a straight line. The smallest occur just one week after spring tides and are known as "neap" tides. When high tides coincide with high waves, waterfront areas often become inundated and serious erosion of beaches may occur.

Tidal currents with speeds between 1 and 2 miles per hour occur in near-shore areas along the open coast, but these currents reach their greatest speed in the narrow entrances of large bays. In San Francisco Bay, for example, the tidal current races through the Golden Gate at 6 to 7 miles per hour.

WAVES OFFSHORE AND AT THE COAST

Swell and Wind Waves

Whenever wind blows over water, a complex pattern of waves is formed as shown by Russell and MacMillan. High, steep, and irregular waves

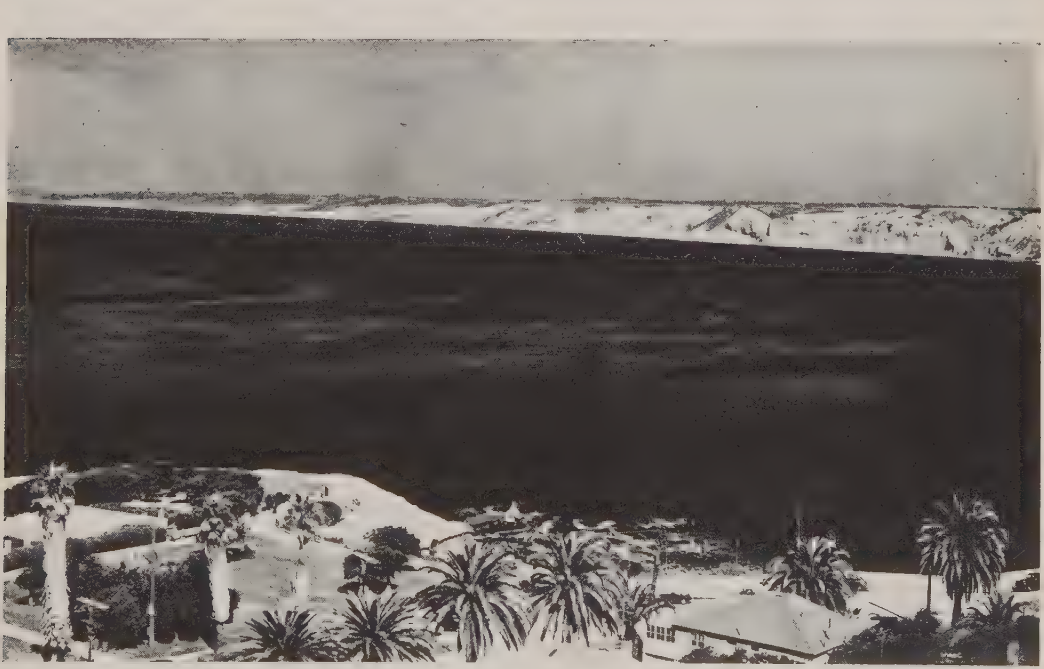

Figure 7. A series of surface slicks caused by internal waves.

(439)

are generated by stormy winds. As these waves advance out of storm areas, they are sorted into the gentler, more regular undulations known as "swell." When swell arrives in shoal water, each wave crest rises sharply from the water's surface, grows steeper and steeper until it becomes unstable and breaks, and rushes as foaming white surf up the beach.

Wave-producing winds are always present in the Pacific Ocean; consequently there is a continuous surf on the California coast. The most severe wave activity in the region usually occurs in the winter months. During summer the predominant waves reaching the coast of California travel all the way from the "roaring Forties" of the Southern Hemisphere and are called "southern swell." These have small heights in deep water and the distances between wave crests are great. They may form sizable breakers, however.

Breakers generate currents in the surf zone. These longshore currents ordinarily flow parallel to shore for several hundred yards and then turn seaward as "rip currents." The latter are dangerous to swimmers. A swimmer may escape a rip current by swimming parallel to shore. The so-called "undertow" is practically non-existent, and good swimmers need not fear entering moderate surf where no rip currents appear.

Internal Waves and Surface Slicks

Waves occur at subsurface depths in the sea along the boundaries between water layers of different density. These internal waves have low energy, fairly high amplitude, and a variety of periods ranging from seconds up to more than 24 hours. They are induced in various ways by currents, tides, winds, and earthquakes.

The convergence and divergence of the surface waters over internal waves moving toward the coast affect the surface tension and produce surface slicks arrayed in parallel lines (Fig. 7). Such slicks are visible only when the wind is very light (but not calm), so that small ripples are formed on the water surface between the slick areas.

When the wind speed increases, the large slicks are broken up into narrow bands spaced much closer together, with the long axes oriented nearly along the wind direction. These "wind cell" slicks are common in bays.

MARINE PLANTS, BACTERIA, AND ANIMALS

Mode of Marine Life

The populations of the sea contain more of the simpler forms of plants and animals than do land populations. In the simplest types the body surfaces and cavities are continually bathed in sea water; hence these creatures must respond quickly to changes in ocean conditions. But sea plants and animals are in no danger of desiccation, as plants and animals in land environments sometimes are. The sea provides easy flotation for many organisms and support to those which lack skeletal structure. Its high heat capacity prevents large changes in temperature, while its high rate of diffusion helps organisms to obtain their food and to dispose of their waste products. Sea water is a slightly alkaline buffer solution, containing abundant carbon dioxide and calcium; consequently marine plants and animals can easily construct hard parts of calcium carbonate.

Marine Plants

Marine plants are limited almost entirely to primitive species having no true root, stem, or leaf. Nevertheless, the kinds of vegetation in the sea vary in size from microscopic floating forms to the giant kelp, and include such diverse types as the sea lettuce of the mud flats and the delicately branched red seaweeds clustered on rocks and in tide pools.

Without plants as synthesizers of primary food, life in the sea would be impossible. The plants of the sea, like their terrestrial counterparts, can grow only in the presence of sunlight, carbon dioxide, water, and nutrient substances or "fertilizers." The amount of carbon dioxide per unit volume in the ocean is 300 times greater than in the air. But sufficient sunlight is present only in the brightly lighted waters near the surface; hence only a small part of the ocean can support plant life. In the surface layers the supply of nutrient substances varies widely in different areas, with the result that the production of marine plants is much higher in some ocean regions than in others. The coastal waters of California are among the more fertile regions.

Plants in the Open Sea

The plants of the open sea are planktonic (free floating), and nearly all of them are microscopic in size. Most abundant are the diatoms, which constitute 60 per cent of the total weight of all marine plants. It has been estimated that in the area from the shore out to 200 miles off the thousand-mile-long California coast, more than a billion tons of plant material are produced each year. This is nearly as much as the annual production of all the farms on earth.

In general, the waters along the northern California coast are richer in plant plankton than those to the south. But several areas off central and southern California are enriched at intervals. Close to shore, and particularly in bays, the amounts of plant plankton are high relative to those in the oceanic waters far offshore. Swarms of animal plankton graze in these fertile areas, and marine birds and fish are numerous.

The color in so-called red water, often more brown than red, is due to an abundance of dinoflagellates (microscopic plankton organisms intermediate between plants and animals). Dinoflagellates are bioluminescent, and when red water is present, the surf is seen to glow at night. At times certain poisonous dinoflagellates become so numerous that fish and invertebrates are killed. Although there have not been such spectacular "red tides" on the California coast as the recent ones in Florida, outbreaks lethal to fish have occurred from Monterey Bay to San Diego. Dinoflagellates are eaten by filter-feeding invertebrates such as mussels, and the poison may become concentrated in these animals. Some human deaths have resulted from the eating of raw mussels during summers when red water occurred; the taking of potentially poisonous shellfish is therefore prohibited by law when red water appears.

Plants in Shallow Water

Only 3 per cent of the ocean's total area is shallow enough for attached plants to obtain sufficient sunlight. In these shoal areas are found the bottom-living marine algae, varying from small unicellular plants to large red and brown forms. The kelps are a well-known example (Fig. 8). Eel grass, a seed plant related to pond weeds, also covers much of the bottom and provides a protected habitat for shore-dwelling marine animals. The large kelps grow in bands or patches outside the tidal zone, where there is active circulation of water, yet the danger of damage by breakers and sand abrasion is reduced. From just north of Point Conception to Baja California, the principal kelps are the giant *Pelagophycus* and *Macrocystis*. These "sequoias of the ocean" are among the largest of marine plants. Attached by massive holdfasts in depths of 20 to 60 feet, their stems may be as long as 100 feet; their "foliage" is as heavy as the leaves of a rubber tree. They are

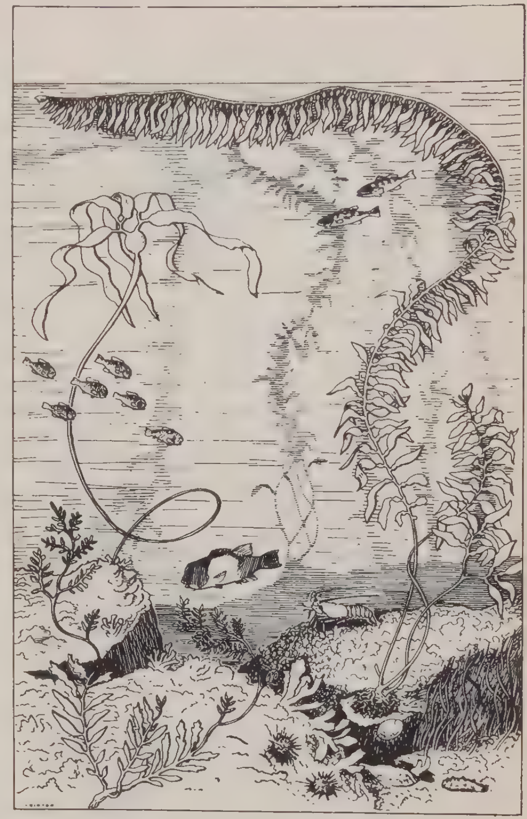

Figure 8. Plants and animals of shoal coastal waters: giant kelp, *Macrocystis;* elk kelp, *Pelagophycus;* sea fern, *Cystoseira;* bath towel alga, *Gigartina;* eelgrass, *Zostera;* kelp bass, *Paralabrax clathratus;* opaleye, *Girella nigricans;* sheepshead, *Pimelometopon pulchrum;* spiny lobster, *Panulirus interruptus;* sea urchin, *Strongylocentrotus;* abalone, *Haliotis;* sea cucumber, *Stichopus.*

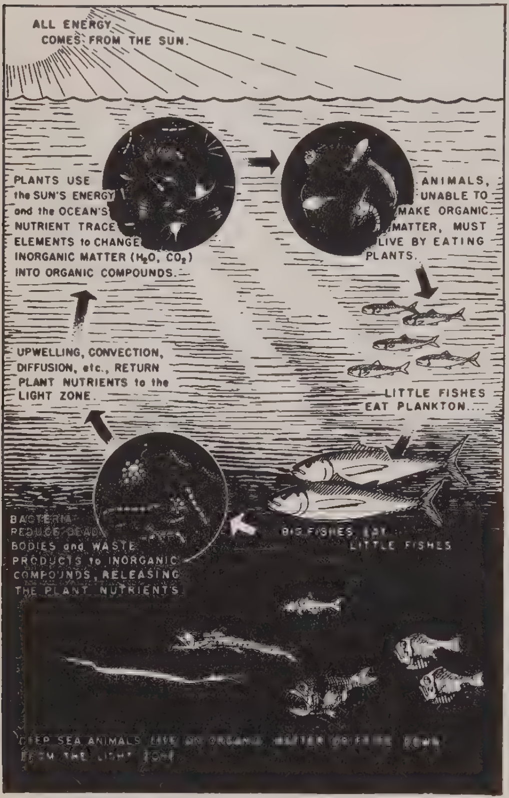
ALL ENERGY COMES FROM THE SUN.
PLANTS USE the SUN'S ENERGY and the OCEAN'S NUTRIENT TRACE ELEMENTS to CHANGE INORGANIC MATTER (H_2O, CO_2) INTO ORGANIC COMPOUNDS.
ANIMALS, UNABLE TO MAKE ORGANIC MATTER, MUST LIVE BY EATING PLANTS.
UPWELLING, CONVECTION, DIFFUSION, etc., RETURN PLANT NUTRIENTS to the LIGHT ZONE.
LITTLE FISHES EAT PLANKTON.
BACTERIA REDUCE DEAD BODIES and WASTE PRODUCTS to INORGANIC COMPOUNDS, RELEASING THE PLANT NUTRIENTS
BIG FISHES EAT LITTLE FISHES
DEEP SEA ANIMALS LIVE ON ORGANIC MATTER DRIFTING DOWN FROM THE LIGHT ZONE

Figure 9. Cycle of life in the open sea.

buoyed by rows of bladders, or by a single float the size of a grapefruit, and by the hollow stipe.

Kelp is harvested by San Diego- and San Pedro-based harvesters operating among the southern California islands and along the mainland. The growing plants are "mowed" by barges equipped with special cutting devices, and the crop is processed to obtain a variety of food and industrial products, such as algin, agar, and potash.

Marine Bacteria

Throughout the water column, bacteria are at work reducing organic matter to inorganic chemicals (Fig. 9). The latter diffuse toward the surface where they may again be used by plants, thus completing the food cycle.

The greatest concentrations of marine bacteria are found in the bottom clays and silts, but these tiny creatures are also abundant in the surface layers of high plant production as shown by ZoBell. They tend to attach themselves to any floating object, including the diatoms, dinoflagellates, and animals which constitute the plankton populations. The importance of bacteria in replenishing the nutrients utilized for plant growth cannot be overestimated. They may also serve directly as food for many marine animals.

Marine Animals in the Open Sea

In the open sea, the microscopic floating plants living in the brightly lighted subsurface waters are grazed upon by minute animals. These, in turn, are eaten by larger planktonic forms. The plankton animals are devoured by herring, mackerel, sardines, and other small fishes. The small fishes are fed upon by carnivorous fishes—salmon, tuna, shark, and many others. The excreta and dead bodies of all these creatures living in the waters near the surface settle to greater depths and there furnish food for scavengers (Fig. 9). In general, the largest numbers of animals are found in the upper layers where plants can grow and food is plentiful, or on the bottom where food particles settling from the surface are concentrated. Formerly, it was believed that life must be sparse at intermediate depths. It has recently been found, however, that animals live in considerable abundance everywhere in the ocean between depths of 1000 and 2000 feet.

At these depths the water is still dimly illuminated by sunlight filtering down from the surface, though the light intensity is too low for photosynthesis. During World War II it was discovered that populations of animals live in the daytime at these dimly lighted mid-depths in numbers sufficient to scatter and reflect the beam of sound from an echo sounder. Some of the animals in these "deep scattering layers" execute a diurnal vertical migration, rising to the surface at sunset and descending to mid-depths at sunrise. Others show no pronounced daily movement, and a few move contrary to the principal daily migration. Investigations during the last few years by various workers have shown that the deep scattering layers are a world-wide phenomenon, being present to some extent in all oceans and at all times of the year.

Large populations of commercially important pelagic (open-sea) fish are found in California coastal waters. To Californians, the most valuable fish are the tunas, but most of these are caught in Mexican, Central American, and South American waters, although landed in San Diego and San Pedro. The largest commercial catches taken off California have been of the California sardine or pilchard (*Sardinops caerulea*). In the 20 years between 1930 and 1950 the sardine catch varied from 130,000 to 700,000 tons, with population sizes estimated at 9 to 30 billion fish weighing approximately 1 to 3 million tons. In 1952–1953, the catch of this species as well as of Pacific mackerel had declined to unprecedented lows.

Animals in the Shallow Inshore Waters

Because of their great volume, the open-ocean waters contain the vast majority of marine creatures. But the shallow inshore waters are the zone of most varied life as demonstrated by Ricketts and Calvin. Here life flourishes most abundantly on the bottom. The character of the bottom, whether it be rock, sand, or mud, influences the living community, as does the degree of shelter from surf, and, in the tidal zone, the proportion of time that the animals are covered by water.

Many of the bottom dwellers are permanently attached to rocks or pilings; other animals live among the abundant bottom plants (Fig. 8); some live inside the shells and body cavities of others; many find shelter by burrowing into the sand or mud. Small crabs, shrimps, and worms live under rocks and in crevices of rocks. During their adult lives many of the invertebrate creatures of the inshore zone move slowly or not at all. Some of them, in fact, resemble plants and even have plant-like names such as sea anemone and sea cucumber. Nearly all, however, are planktonic as larvae, and the larvae can be carried by currents far from their sessile parents, thereby accomplishing widespread distribution.

For protection from surf, desiccation, and each other, most invertebrate bottom dwellers have hard external shells or skeletons. Hard parts also serve as tools for burrowing, as weapons, and as bases for muscular attachment. Some animals employ the complex organic compound, chitin, for their hard parts, but in most cases the shells or skeletons contain calcium, the element dissolved in sea water that is most easily precipitated. Calcium metabolism is influenced by the temperature of the water. Consequently the character of the bottom fauna in the relatively cold waters off California is very different from that in tropic waters. In the tropics, where calcium precipitation is easy, heavy-shelled forms and limestone reef builders predominate. Off California many animals have thin shells, and reef builders are virtually absent.

Several kinds of near-shore invertebrates are pests. Starfish and drills are rapacious predators on species of economic importance. Other forms damage wood, concrete, and even steel structures. Deterioration of wooden-hulled vessels and wooden piling results from attack by the shipworm *Teredo* and the gribble *Limnoria*. Fouling organisms, including barnacles, mussels, and tunicates, clog the intake pipes of water cooling systems and attach to steel- and wooden-hulled ships and piling.

Most of the marine invertebrates prized as food delicacies are shallow-water, bottom-living forms. These include mussels, clams, abalones, octopuses, sea urchins, shrimps, crabs, and lobsters. One invertebrate that is not a bottom dweller, the squid, is taken commercially.

Marine vertebrates, including fishes, mammals, and birds are not as abundant in shallow inshore waters, either by weight or by volume, as the invertebrates. Several of the fishes are used as food. These include such flatfish as halibut, sole, turbot, flounder, and sand dabs, and such swimming fish as sea bass, salt-water perch, barracuda, rockfish, yellowtail, California bonito, herring, sculpin, smelt, and corbina.

Marine Mammals

Many marine mammals, the big game of the sea, live in or migrate through California coastal waters. The most notable migrant is the California gray whale, which at maturity reaches lengths of 35 to 55 feet and weighs up to 30 tons. In summer it ranges northward from Kamchatka while in winter the population congregates in the lagoons of Baja California for calving and breeding. On their way southward the whales appear to navigate by landmarks on shore, and they pass within one or two miles of the headlands of southern California. Moderate numbers of humpback, finback, and sperm whales visit California waters, and some remain as summer residents. A few blue whales (the largest animals that have ever lived, attaining lengths of 80 feet and more) are occasionally observed.

Islands and rocky capes off the coasts of California and Baja California serve as rookeries and hauling grounds for large populations of sea lions. Two other species of marine mammals, the beautiful sea otter and the grotesque elephant seal, formerly inhabited the California coast but were virtually absent for many years. A surviving herd of sea otters has recently been found on the rocky coast of Monterey County and now numbers perhaps 500 individuals. One hundred sixty-eight elephant seals were recently counted on San Nicolas Island.

Marine Birds

Throughout the earth, the coastal waters are characterized by abundant bird life; in regions of high fertility, the numbers of a single species may be so great that the sky is darkened by their flight. An outstanding example is found off Peru where the Guano birds carry out one of earth's largest fisheries for their livelihood.

The birds of the California coast may be divided into different categories, depending on their way of life. Some spend most of their lives inland and occasionally visit the shore; others live in bay marshes, or on coastal cliffs, and those of a third group are pelagic, ranging far from shore and visiting land only to nest. Some are California residents, others are winter or summer migrants. The distribution of most shore species has been described by Grinnell and Miller; and Alexander has described the pelagic birds.

Notable among the pelagic species are the black-footed and the Laysan albatrosses, which nest in the Hawaiian Islands, the sooty shearwaters, which nest in islands off Cape Horn but feed in great flocks off the California coast, and several species of petrels. Western gulls, cormorants, pelicans, and murres are the most common resident birds. They are generally unable to fly long distances and rely on food sources in the near-shore waters. Sea ducks and other small shore birds are winter migrants. Summer migrants include the California and Heerman gulls and some terns. Several migrant species nest far inland around salt-water bodies such as Mono Lake, Great Salt Lake, and Salton Sea.

A boundary in the distribution of marine bird species occurs near Point Conception, coinciding with the location of greatest change in other marine animals and plants along the California coast.

DEVELOPMENT OF MARINE RESOURCES

California's long stretch of border on the Pacific is a heritage which is of increasing social and economic importance to the people of the Southwest. In addition to the aesthetic and recreational values of the seashore, the coast gives access to earth's largest underdeveloped area, covering nearly half the globe, the Pacific Ocean. The fisheries of California are one of the state's basic industries. Even at present they utilize for their raw materials fish caught many thousands of miles away from the ports of San Diego, San Pedro, Monterey, and San Francisco. But it is certain that the untapped resources of the Pacific, in food, industrial materials, power and water, and as a medium for waste disposal and transport, are far greater than those already realized.

Seaside Recreation

The beaches of California are major recreation areas, especially in the southern part of the state where water temperatures are moderate. Development of facilities and improvements to beaches and bays are being carried out by many public agencies.

The Harvest of Food from the Sea

Increasing the harvest of marine fishes and invertebrates is a complex problem, involving not only discovery of new raw materials but also development of markets and public acceptance, design of new fishing gear and vessels, and improvement in methods of processing the highly perishable food products of the sea. Several species of fish known to be abundant in California waters, such as hake and saury, are unexploited or taken only in limited numbers.

Although it may eventually be possible to use the plant plankton directly as food or raw materials, their small size and wide dispersion throughout the upper layers of the sea make this unlikely. At intermediate levels in the ocean food pyramid between the microscopic plants and the fishes are great quantities of crustacean organisms. These are larger than the plants and tend to accumulate in swarms, for example, in the deep scattering layer; consequently they offer better food prospects. Practical methods of capturing, preserving, and marketing these animals may be developed in the future. New uses may also be found for seaweeds and other attached marine plants. For example, it may be possible, through application of modern agricultural genetics, to alter the characteristics of these plants to provide better food for livestock.

Disposal of Wastes

In coastal population centers, disposal of sewage and industrial wastes in the ocean is an economical and widely used method. But it must be well planned to avoid contamination of beaches or excessive pollution of bays and to minimize damage to marine plants and animals.

One of the major problems in the development of industrial atomic power will be the disposal of radioactive wastes. It has been suggested that these be dumped in the deep waters of the ocean far from shore. Much more knowledge of the deep-water circulation and the effects of radioactivity on marine animals is needed as a guide to planning for this problem.

Petroleum and Minerals

Despite its great oil industry, California is now importing petroleum; known reserves of crude oil in the state's oil fields are being depleted faster than new ones are being discovered. This depletion and the development of methods for drilling in shallow water have given impetus to exploration for oil on the shallow continental shelf.

The area of the shelf off California above a depth of 600 feet is approximately 10,000 square statute miles. Estimates based on average yield per square mile in regions of sedimentary rock on land indicate that the sedimentary rock under the shelf contains at least 2 billion barrels of recoverable petroleum. This is about 10 per cent of the estimated ultimate production of crude oil in the state, corresponding to approximately 8 years of production at the average rate over the past 25 years from all California oil fields, or about 6 years of production at the rate attained during the last 5 years.

Table 1. Approximate Amount and Value (at Wholesale Price) of Some Chemicals in One Cubic Statute Mile of Sea Water

Magnesium	5,500,000 tons	$3,000,000,000
Calcium carbonate	4,500,000 tons	550,000,000
Bromine	260,000 tons	120,000,000
Potassium sulfate	3,500,000 tons	140,000,000
Sodium chloride	106,000,000 tons	2,300,000,000
Water	3,400,000 acre-feet	20,000,000

Low-grade deposits of cobalt, nickel, and copper lie at the bottom of the deep sea, associated with manganese and iron deposits. The problems of mining these materials, in the face of the great water pressure and depth and the roughness of the sea floor, have not been solved. Methods of mining the sodium chloride, bromine, and magnesium dissolved in the water itself, using natural evaporation and other means, have long been highly developed. The quantities and approximate values at wholesale prices of some of the more important chemicals in a cubic mile of sea water are shown in Table 1.

Valuable substances present in trace amounts in sea water may someday be reclaimed as byproducts from the mining of the ocean. For example, a cubic mile of sea water contains about 6 tons of uranium. The heat energy released by fission of this amount of uranium is equal to that produced by burning 3 billion gallons of gasoline, four months of California's oil production.

Water and Power

One of the potentially valuable constituents of sea water is the water itself (Table 1). The basic principles for the extraction of fresh water from sea water are well known. But at present it is not economically feasible to use water from the ocean for irrigation, because methods of desalting the water and pumping it to higher elevations are too expensive. Several government agencies are attempting to develop more economical methods, utilizing low-cost power. Solar distillers and low-temperature-difference distillers have proved effective in pilot plant operation, but are not yet practical on a large scale. It may eventually be possible to utilize the temperature difference between the warm surface waters and the cold deep waters of the ocean as a source of energy for desalting and pumping the water. The presence of cold water near shore in the bottoms of the submarine canyons off California makes the possibility of developing this technique promising.

The total energy of the sea's motions is only one-tenth to one-fifth that of the atmosphere, but much of the ocean's energy is concentrated near the coast and might therefore be harnessed effectively. Tides in bays and estuaries, and waves along the shore, are potential sources of power. Electric power plants utilizing tidal energy are in practical operation in Argentina and France. Having relatively small tidal ranges, California is not as well situated to utilize power from tides as some other coastal regions. Waves in the surf zone offer promise, however. The total wave energy dissipated on California shores is five to ten times as great as the electric power produced at Hoover Dam.

REFERENCES

Alexander, W. B., *Birds of the Ocean: A Handbook for Voyagers,* G. P. Putnam's Sons, New York, 1928, new and rev. ed., 1954, 306 pp., 146 illus.

California Department of Fish and Game, Marine Research Committee, California Cooperative Sardine Research Program, *Progress Report, 1 January 1951 to 30 June 1952,* 1952, 51 pp.

Grinnell, J., and A. H. Miller, "The Distribution of the Birds of California," *Pacific Coast Avifauna, 27:*1–608 (1944).

Inman, D. L., *Beach and Nearshore Processes along the Southern California Coast,* Geology of Southern California, California State Division of Mines, Bulletin 170, 1954.

Revelle, R., and F. P. Shepard, "Sediments off the California Coast," in *Recent Marine Sediments,* American Association of Petroleum Geologists, Parker D. Trask (Editor), Tulsa, 1939, pp. 245–286.

Ricketts, E. F., and J. Calvin, *Between Pacific Tides,* Stanford University Press, Stanford, 3rd. ed., 1952, 502 pp.

Russell, R. C. H., and D. H. Macmillan, *Waves and Tides,* Hutchinson's Scientific and Technical Publications, New York, 1952, 348 pp.

Shepard, F. P., *Submarine Geology,* Harper and Brothers, New York, 1948, 348 pp.

——, and K. O. Emery, *Submarine Topography off the California Coast,* Geological Society of America, Special Paper 31, 1941, 171 pp.

Sverdrup, H. U., and R. H. Fleming, "The Waters off the Coast of Southern California, March to July, 1937," Scripps Institution of Oceanography, University of California, *Bulletin 4,* University of California Press, Berkeley and Los Angeles, pp. 261–378.

——, M. W. Johnson, and R. H. Fleming, *The Oceans: their Physics, Chemistry, and General Biology,* Prentice-Hall, Inc., New York, 1946, 1087 pp.

ZoBell, C. E., *Marine Microbiology,* Chronica Botanica Co., Waltham, Mass., 1946, 240 pp.

(446)

MICROELIEF PRODUCED BY SEA ICE GROUNDING IN THE CHUKCHI SEA NEAR BARROW, ALASKA[*]

Robert W. Rex[†]

It has long been known that sea ice and glacial icebergs ground in shallow water (Transehe, 1928, p. 102) and can deform the bottom (H.O. 77, 1951, p. 31; United States Coast Pilot, 1947, p. 594). Small-scale microrelief has been noted on the inner shelf of the Beaufort Sea off the Colville River by Carsola (1952, pp. 22, 64; 1954, p. 159) who suggested that it is caused by ice grounding. Pressure ridge ice is often the last fast ice to break up and float free in the summer. Frequently the inner fast ice in water of 20 to 30 feet depth will break up while pressure ridge ice remains grounded in deeper water. Boat observations at the time of break-up are extremely hazardous and little accurate information is available as to the depths of ice groundings. In the summer of 1954 the writer studied the microrelief off Barrow, Alaska, to determine the effective range of grounding of the polar pack ice.[1] The Barrow area of the Chukchi Sea was chosen because it is the northernmost shoal area of Alaskan waters and the site of the Arctic Research Laboratory.

Method

Numerous short echo sounding traverses were carried out in a boat to establish confidence in the instruments, procedures, and the reality of the microrelief, then 6 bathymetric traverses were made, all together consisting of 14 legs. These traverses and a summary of the results obtained are shown in Fig. 1. The microrelief studied here is not the same as that described by Carsola (1954) for deeper waters of the outer continental shelf to the northwest of the Barrow area.

Depth determinations were made with a new Bludworth Model NK-6 echo sounding recorder operating at 14.25 kilocycles, for which the power supply was 12 volts from the boat's batteries. The echo sounder was the only power drain on the batteries during the period of its operation. Frequent checks from a moored boat showed that no measurable changes in depth were recorded by the instrument at any engine or generator speed encountered

---

[*] Contribution from Scripps Institution of Oceanography, New Series No. 845.

[†] Scripps Institution of Oceanography, La Jolla, California.

[1] This study was aided by a contract between the U.S. Office of Naval Research and the Arctic Institute of North America. Reproduction in whole or in part is permitted for any purpose of the United States government.

Reprinted from "ARCTIC", Journal of the Arctic Institute of North America, Volume 8, Number 3, 1955. Reproduced by Permission

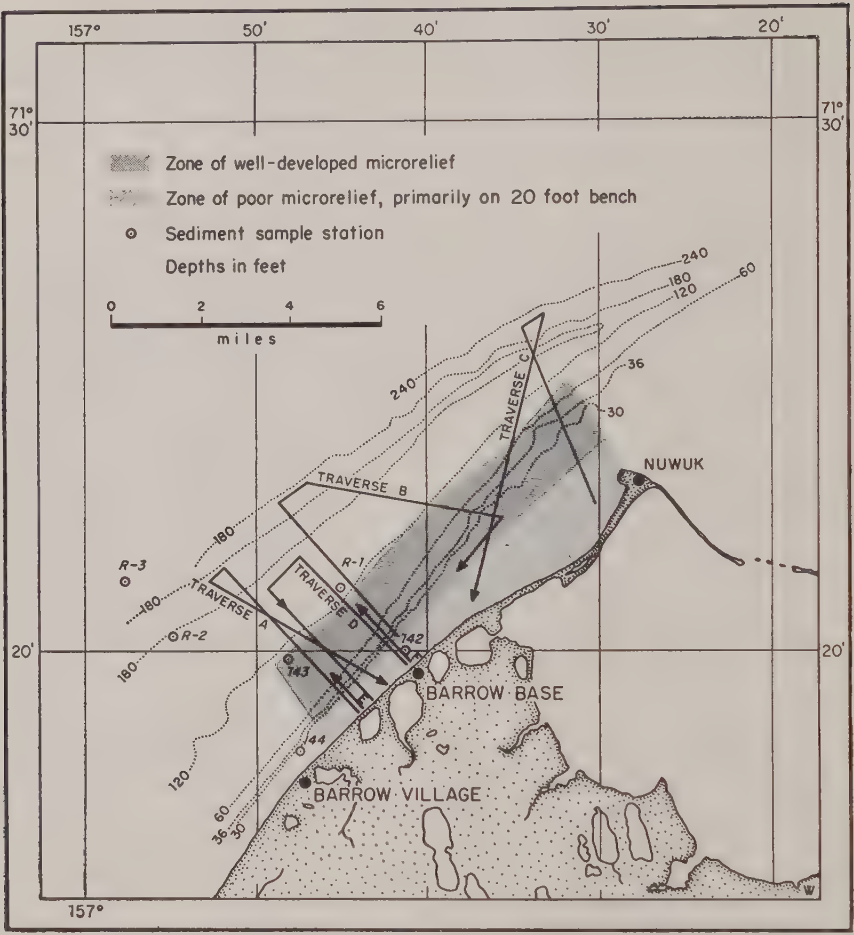
157°
50′
40′
30′
20′
71° 30′
20′
Zone of well-developed microrelief
Zone of poor microrelief, primarily on 20 foot bench
Sediment sample station
Depths in feet
0 2 4 6
miles
240
180
120
60
36
30
TRAVERSE A
TRAVERSE B
TRAVERSE C
TRAVERSE D
R-1
R-2
R-3
142
143
144
NUWUK
BARROW BASE
BARROW VILLAGE

Fig. 1. Barrow area, showing zone of sea ice grounding and location of echo sounding traverses A–F.

during the traverses. In addition, depth checks were made with a hand line. Therefore the depth fluctuations recorded are assumed real for values ± ½ foot.

Sediment samples R-1, R-2, and R-3 (Fig. 1) were obtained with a Dietz-LaFond snapper and samples 142 and 143 with a 1⅜ inch I.D. gravity corer.

Results

The traverses generally showed irregular depth fluctuations of 8 feet or less over distances of 25 to 50 feet, superimposed on a very gently sloping bottom. These depth variations occur both parallel (Fig. 2) and perpendicular (Fig. 3) to the depth contours. Figure 2 was made at a speed of ¼ knot drifting with the current parallel to the depth contours. Depth fluctuations

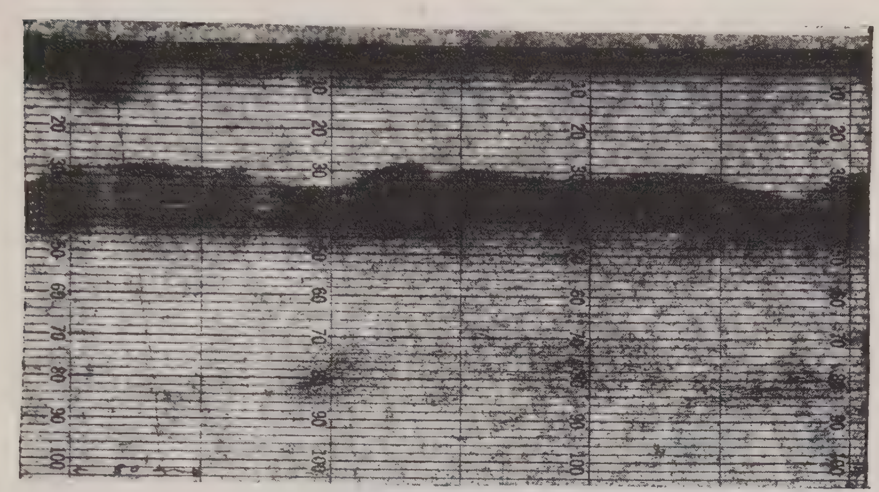

Fig. 2. Echo sounding traces, parallel to contours near Traverse F. Depth in feet. Add 2 feet to depths for transducer depth correction. Distance between vertical lines approximately 25 feet.

were determined simultaneously with the echo sounder and a hand line and agreement was ± ½ foot.

Microrelief is best developed between depths of 20 and 80 feet, where it is often 6 feet, and in one case reached 12 feet (Fig. 3). Moderate microrelief usually extends to a depth of 100 feet (Fig. 4).

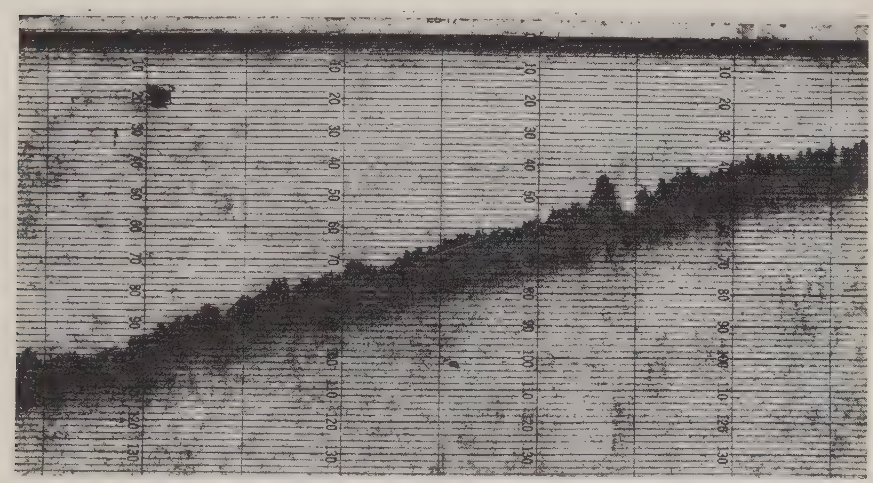

Fig. 3. Slope from 35 to 100 feet showing development of microrelief perpendicular to contours. Depth in feet. Add 2 feet to depths for transducer depth correction. Distance between vertical lines approximately 200 feet.

(449)

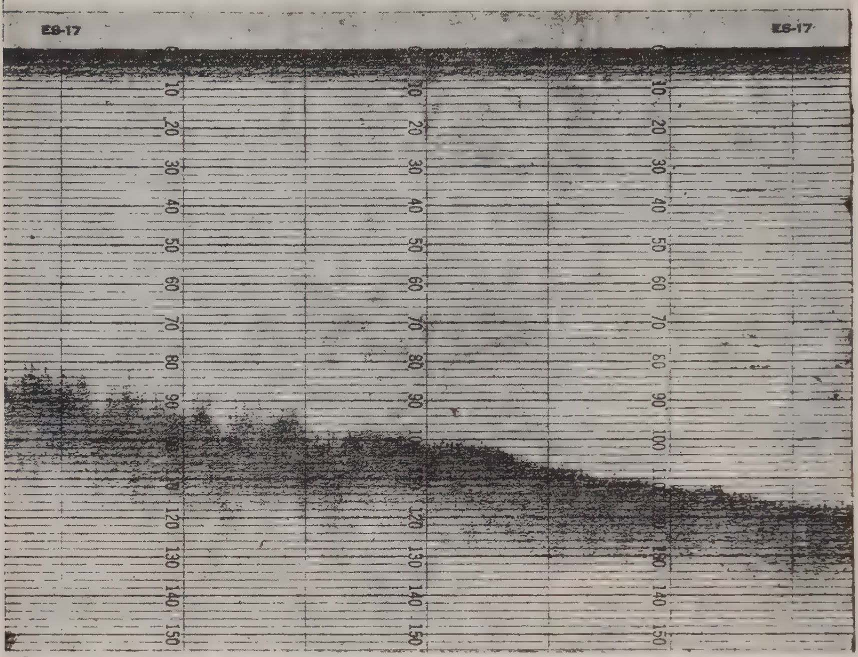

Fig. 4. Traverse D, leg 1, from 80 to 120 feet, showing the transition from microrelief above 100 feet to microrelief-free slope below. Depth in feet. Add 2 feet to depths for transducer depth correction. Distance between vertical lines approximately 80 feet.

A submerged shoreline marked by drowned river and stream valleys and a broad bench from 20 to 30 feet in depth (Fig. 5) characterizes the northern Alaska coast of the Chukchi Sea. Pack ice impinges against the outer portion of this 20-foot bench or terrace in the Barrow area and forms pressure ridges. Brash ice,[1] some pack ice, and young pancake ice fill the area above the 20-foot bench. The ice is grounded in places and remains as part of the fast ice in the spring. Moderate microrelief is developed on the 20-foot bench (Fig. 6) and pressure ridge ice extends seaward from it. Aerial photographs indicate that the main series of contiguous pressure ridges occur in water depths between 20 and 100 feet, coinciding almost exactly with the depth distribution of the microrelief. Pressure ridges also occur in various patterns in the open pack, but not as a continuous zone of crumpled ice over a mile in width and hundreds of miles in length, as is true of the fast pressure ridge ice. Fast pressure ridges have in general an arcuate pattern with overall lineation very roughly parallel to the depth contours. Pressure ridge ice forms the

---

[1] All sea ice terminology is in accord with the definitions given in the U.S. Hydrographic Office sailing directions for arctic waters, for example H.O. 77, 1951.

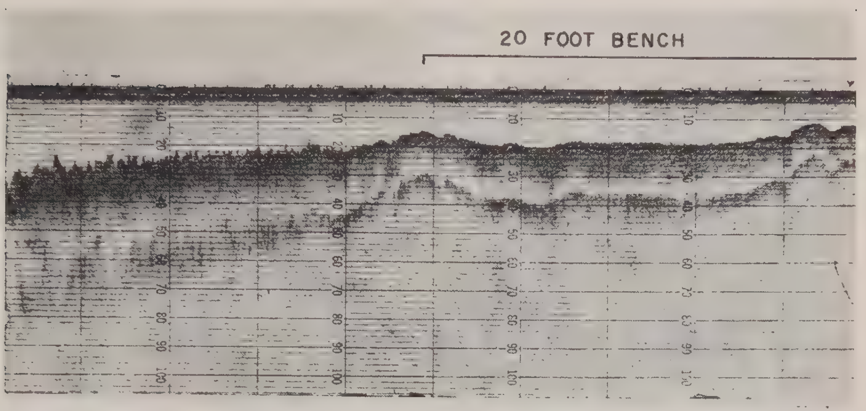

Fig. 5. Traverse from near shore bar (right), across 20-foot bench to ridge where inner pressure ridge ice grounds, downslope to 30 feet in the zone of microrelief (left), in the vicinity of Traverse F. Note relative absence of microrelief from 20-foot bench. Depth in feet. Add 2 feet to depths for transducer depth correction. Distance between the vertical lines approximately 200 feet.

principal body of fast ice in spring and early summer, sometimes containing large quantities of silt and fine sand, and occasionally it contains some mollusc shells.

Before accepting the hypothesis of pack ice grounding to explain the microrelief a number of alternate hypotheses were considered. These were: residual features of thawed permafrost, slump topography, current scouring, and sand waves.

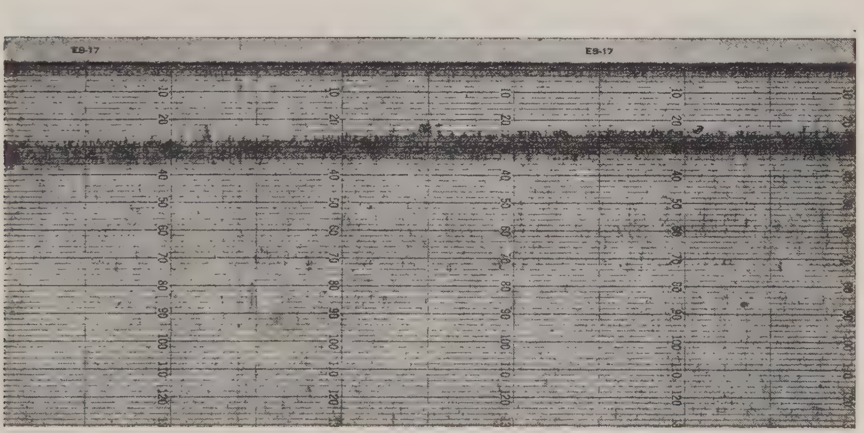

Fig. 6. Traverse C, leg 2, microrelief developed on the 20 to 30-foot bench in a level area. Depth in feet. Add 2 feet to depths for transducer depth correction. Distance between vertical lines approximately 150 feet.

Thawed permafrost as described by Hopkins in the Imuruk Lake area of the Seward Peninsula (1949) may be an explanation for some of the microrelief found in the Chukchi Sea. The thaw lakes in the Imuruk Lake area are up to several hundred feet in width and 30 feet in depth. Carsola (1954, p. 1598) suggests that possibly the microrelief observed to the northwest of the Barrow Sea Valley resulted from the thawing of Pleistocene permafrost by a rising sea. Relict thawed permafrost topography is readily buried under prograding continental shelf sediments and can be expected only in areas free of sedimentation from the time of their submergence to the present day. The East Chukchi Sea-Alaska Coastal Current carries sediments northward on and near the bottom of the shelf to the north-northeast trending Barrow Sea Valley. It therefore appears probable that Carsola's area of microrelief, to the northwest of the Barrow Sea Valley, lies in a sediment "shadow" thereby meeting the requirement of non-deposition of sediments for the present day preservation of thawed permafrost topography.

The microrelief studied in the Barrow area by the writer differs in a number of important ways from the microrelief studied by Carsola. The Barrow microrelief is of smaller dimensions; the relief is 6 feet compared to a maximum of 30 feet, and 100 feet in length compared to a maximum of 1,000 feet. It lies on the southwest side of the Barrow Sea Valley, between the valley and the present shore line, within a zone of sedimentation; and it occurs at depths between 20 feet and 100 feet, whereas Carsola's microrelief occurs at about 300 feet.

The sediments on shore consist of 150 to 200 feet of Recent and possibly Pleistocene unconsolidated silts, sands, and gravels of the Gubik formation (Payne, 1951; Gryc and others, 1951). A stratigraphic study (Rex, 1953) indicated that the upper portion of the Gubik formation in this area consists of prograding marine sands and silts overlain with littoral deposits of beach sands and gravels. A series of uplifted beach ridges (Rex, 1953) extends inland from the Barrow area. Black (1952) estimated from the growth rate of ice wedges that the age of the uplifted beach deposits near the coast is approximately 3,500 years, supporting the concept of recent sedimentation in this area at a time when sea level was within 10 to 20 feet of its present stand. Sediments forming the beach and shallow water deposits can certainly be expected to mask any residual permafrost topography in some cases less than 1,000 feet away and in water only 20 feet deep. Extensive movement of silt occurs in this area during summer storms when the water is extremely turbid. Therefore thawed permafrost is rejected as an explanation of the microrelief observed by the writer.

Slump topography described by Shepard (1948, pp. 195–8; 1955, p. 1479) is characterized by irregular undulating or hummocky relief and slump scars or valleys in the source areas. The presence of microrelief on the broad and flat 20-foot bench cannot be explained as slump topography, because slumps must have a source and slump scars are not evident in association with the microrelief on the 20-foot bench. Gravity cores, Samples 142 and 143 (Fig. 1), taken in the area of microrelief disclose a compact grey silt beneath 2 to 5 feet

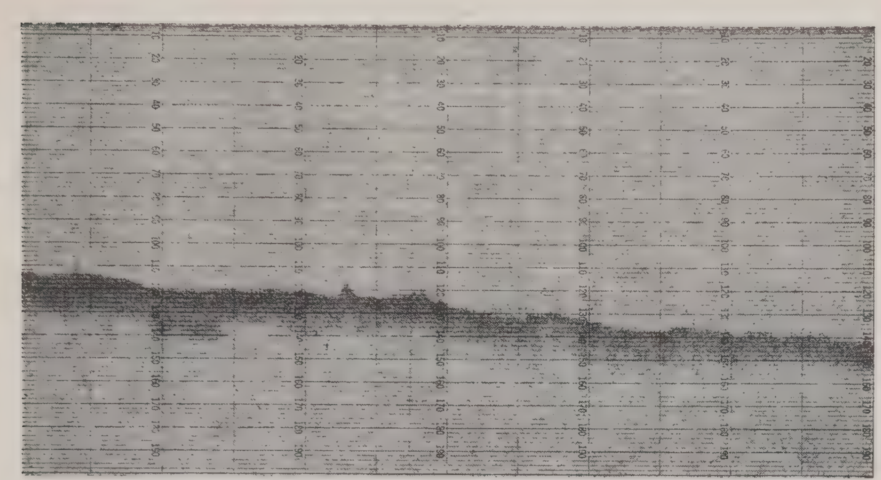

Fig. 7. Traverse B, leg 1, gently undulating relief, more like slump topography than is the shallower microrelief attributed to sea ice grounding. Depth in feet. Add 2 feet for transducer depth correction. Distance between vertical lines approximately 80 feet. Compare with Fig. 4 for scale of microrelief.

of soft grey silt. The compact sediment contains a fine structure that is usually destroyed in slump material. In addition, the extreme sharpness of the microrelief is not characteristic of slump terrain. Handline soundings show this sharpness better than do echo soundings which tend to smooth bottom irregularities. It is possible that some of the deep undulating relief below 120 feet may be slump topography (Fig. 7), but this deeper topography differs from the shallower microrelief in being of greater width and lesser relief, suggesting that a slump origin is an unsatisfactory explanation for the shallow microrelief.

Current scouring occurs in the Barrow area. Deep scour channels result where large quantities of water pass through the inlet between Elson Lagoon and the open sea at speeds sometimes exceeding four knots. The East Chukchi Sea-Alaska Coastal Current flows to the northeast over the microrelief area with an average speed of one knot and occasionally attains two to three knots with a favourable wind. This current is sometimes reversed temporarily by strong winds from the northeast and then flows to the southwest. In midsummer after ice break-up and before the first summer storm, the waters of the Chukchi Sea at Barrow are unusually clear permitting white objects on the bottom to be observed at depths of 50 feet. It was evident that no bottom veil or cloud of sediment was being moved across the 20-foot bench at times when the current flow was two knots. Microrelief disappears relatively abruptly below a depth of 100 feet. To create microrelief by current scouring a two-layer water mass is necessary, with fast moving water above 100 feet and slow moving water below. Temperature, salinity, and paravane current data do not support the presence of a two-layered system with an interface at 100 feet depth. On the contrary, the data indicate nearly isothermal water with irregularly varying salinity related to sea ice melt water and river runoff. Traverse E, made after a strong storm late in the summer, lies about 300 feet to the northeast and parallel to Traverse A (Fig. 1). The effect of the storm was very slightly noticeable in Traverse E and tended to diminish the microrelief on the 20-foot bench, not increase it. These observations effectively eliminate the possibility of current scour as a mechanism of microrelief formation.

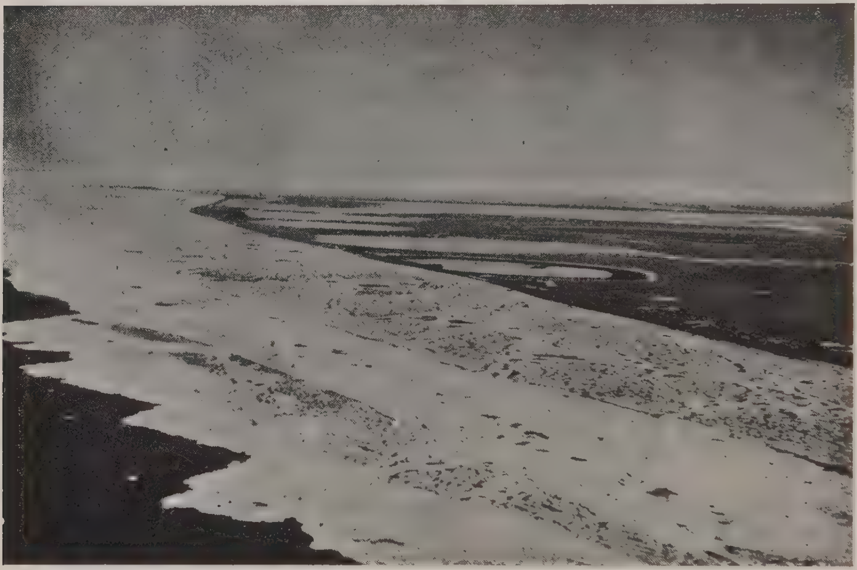

Fig. 8. Fast ice near Barrow, looking northeast from 1,500 feet, 28 June 1952. The dark puddled area near the shore (right) overlies the 20-foot bench. Two weeks later the fast ice broke up and floated free.

Sand waves cannot explain the microrelief because it is developed in an area of predominantly silt sediments and shows no symmetry, a characteristic feature of any ripple mark.

Pack ice grounding could cause the development of microrelief in a way that explains all the observed features. Fast pressure ridge ice, as indicated by aerial photographs (Fig. 8), is restricted almost completely to the zone of microrelief. The pressure ridge ice, as previously noted, sometimes contains large quantities of silt and occasionally shells. This supports the hypothesis of contact with the bottom. The sharpness of the microrelief and the scale are what one would expect if an average ice floe (4–6 feet thick and 20–100 feet in diameter) were up-ended by the pressure of other floes and driven into the bottom. The abrupt end of microrelief at 100 feet can be explained as the maximum depth at which pack ice grounds. Perhaps the relatively uniform value of this deeper limit represents a depth where a balance occurs between the buoyant force of the water on the pressure ridge ice and the load of ice floe telescoped upon ice floe by the maximum force of the polar ice pack in the Barrow area.

In 1952 the writer observed that the pressure ridge ice seaward of the 20-foot bench remained grounded for a period of more than twelve hours after the break-up of the ice over the 20-foot bench. In view of the constant coastal current in excess of one knot this observation is taken as proof that at least some pack ice grounds seaward of the 20-foot bench. The indirect and direct evidence are therefore considered to support the hypothesis of sea ice grounding to a depth of 100 feet to the exclusion of other hypotheses.

The probability of sea ice grounding as a function of time was not determined. It is suggested that, on the basis of the sharpness of the microrelief, grounding is most frequent between 20 and 80 feet. Grounding below this depth is probably less frequent and occurs with less bottom gouging than grounding within this depth range.

Ice grounding serves to mix the surface sediments, perhaps to a depth of 4 to 5 feet thereby destroying stratification, oxygenating the sediment, and considerably modifying the environment of benthonic organisms.

Aerial photographs of a coastal area taken in spring and early summer indicate the belt of pressure ridge ice and therefore the zone of ice grounding (Fig. 8). For increased accuracy photographs covering a period of several years should be used.

Subsequent to the completion of this paper MacGinitie (1955) has made a number of comments on sea ice grounding. His observations agree with those of this writer, but are of a more general nature. MacGinitie's winter observations are of special interest; he notes that the pack "ice grounds offshore where the water is 60 to more than 100 feet deep and forms what is spoken of as the 'big pressure ridge'" (p. 12). This major pressure ridge forms nine years out of ten and "from shore to a depth of over 100 feet offshore the bottom is rubbed and gouged by ice" (p. 14). Later he again mentions that "ice grounds out to a depth of 90 to 100 feet" inhibiting faunal development (p. 53) and that grounding ice may have rubbed organisms off large stones and boulders found in a rubble zone (p. 62).

The author wishes to express his appreciation for the assistance of the Director, Mr. T. Mathews, and Staff of the Arctic Research Laboratory; Dr. W. K. Lyon and Staff of the U.S. Navy Electronics Laboratory, and the considerable help both at sea and ashore of Dr. M. Schalk and Mrs. J. R. Rex. The author is indebted to H. L. Burstyn for his comments on the manuscript.

References

Black, R. F. 1952. "Growth of ice-wedge polygons in permafrost near Barrow, Alaska". (Abstract of paper presented at the November meeting of the Geological Society). *Geol. Soc. Amer. Bull.* Vol. 63, pp. 1235–6.

Carsola, A. J. 1952. 'Marine geology of the Arctic Ocean and Adjacent Seas off Alaska and Northwestern Canada'. University of California at Los Angeles, unpublished Ph.D. thesis.

——— 1954. "Microrelief on the arctic sea floor". *Amer. Assoc. Pet. Geol. Bull.* Vol. 38, No. 7, pp. 1587–1601.

Gryc, G., W. W. Patton, Jr., and T. G. Payne. 1951. "Present Cretaceous stratigraphic nomenclature of northern Alaska". *J. Wash. Acad. Sci.* Vol. 41, pp. 159–67.

Hopkins, D. M. 1949. "Thaw lakes and thaw sinks in the Imuruk Lake area, Seward Peninsula, Alaska". *J. Geol.* Vol. 57, pp. 119–31.

MacGinitie, G. E. 1955. "Distribution and ecology of the marine invertebrates of Point Barrow, Alaska". *Smithsonian Misc. Coll.* Vol. 128, No. 9, Pub. 4221, iv + 201 pp.

Payne, T. G. 1951. "Geology of the Arctic Slope of Alaska". *U.S. Geol. Surv. Oil and Gas Invest.* Map OM 126 (in 3 sheets).

Rex, R. W. 1953. 'Uplifted-beach ridges and first generation lakes in the Barrow, Alaska area'. U.S. Office of Naval Research Final Report, Section 2, Contract Nonr 225 (09), Unpublished.

Shepard, F. P. 1948. 'Submarine Geology'. New York: xvi + 338 pp.

——— 1955. "Delta-front valleys bordering Mississippi distributaries". *Geol. Soc. Amer. Bull.* Vol. 66, No. 12, Part 1, pp. 1489–1498.

Transehe, N. A. 1928. "Ice cover of the Arctic Sea, with a genetic classification of sea cover" *in* 'Problems of polar research'. *Amer. Geogr. Soc. Spec. Pub.* No. 7, pp. 91–123.

United States Coast Pilot. 1947. 'Alaska. Part 2. Yakutat Bay to Arctic Ocean'. 5th ed. Washington, D.C.: xi + 659 pp. (U.S. Coast and Geodetic Survey. Ser. No. 680).

U.S. Hydrographic Office. 1951. 'Sailing directions for northern Canada . . .'. 2nd ed. Washington, D.C.: xxvi + 582 pp. (H.O. Pub. No. 77).

(456)

Reprinted from THE JOURNAL OF THE ACOUSTICAL SOCIETY OF AMERICA, Vol. 28, No. 3, 443–446, May, 1956
Copyright, 1956 by the Acoustical Society of America.
Printed in U. S. A.

Reproduced by Permission

An Estimate of the Effect of Turbulence in the Ocean on the Propagation of Sound

JOHN A. KNAUSS
Scripps Institution of Oceanography, La Jolla, California*
(Received September 27, 1955)

A hydrophone monitoring a constant level sound source in the open ocean records a sound whose intensity fluctuates over short periods of time. Previously it has been demonstrated that much of this fluctuation can be accounted for by the temperature microstructure. It has been suggested that another cause of the observed fluctuation could be inhomogeneities in the velocity field (turbulence). This paper is an attempt to estimate the magnitude of turbulence in the ocean. The conclusion is reached that turbulence contributes very little to the fluctuation observed in the intensity of underwater sound signals.

I. INTRODUCTION

IT has been observed in the open ocean that a hydrophone monitoring a constant level sound source records a sound whose intensity fluctuates over short periods of time.[1] This is because the ocean is inhomogeneous. Liebermann[2] has observed temperature fluctuations of the order of 0.1°C from the mean within an average range of 60 cm. The intensity of this temperature microstructure appears to be independent of whether the measurements are made in "isothermal water" or in the thermocline as recorded by a bathythermograph. He has demonstrated that this observed temperature inhomogeneity is enough to account for the observed fluctuations.

There is another source of inhomogeneity in the ocean which one might guess is an important factor in causing fluctuation of sound intensity. That is the fluctuation in the velocity field—or turbulence. So far as is known no measurements of open ocean turbulence in the scale required (10 cm–10 m) have yet been made. It does appear possible, however, to make an estimate of the magnitude of the turbulent structure within this range and to satisfy oneself that the fluctuation of sound level due to turbulence is small compared to that caused by the observed temperature microstructure.

II. PREDICTIONS OF SIMILARITY THEORY

The basis for this estimate is certain predictions made from the similarity theory of turbulence. The applicability of the similarity theory to oceanic turbulence has not yet been demonstrated; however, the theory appears valid in wind tunnel experiments where satisfactory observations can be made, and it is predicted to become increasingly valid with increasing Reynolds numbers. A few observations in the atmosphere and ocean indicate that the predictions of the theory are valid for geophysical turbulence as well.[3]

The similarity theory of turbulence is predicated on certain concepts and hypotheses concerning the nature of the breakdown of turbulent eddies.

(1) The original large eddies break down into ever smaller eddies and so on until the kinetic energy is lost to heat by the viscous forces of the fluid. As the kinetic energy is passed down to ever smaller eddies the effect of viscous damping becomes increasingly important so that there is a lower limit to eddy sizes.

(2) The properties of the original large scale eddies are, in general, not isotropic. They are influenced by the characteristics of the main flow. However, it is proposed that some sort of "statistical decoupling" accompanies the transfer of energy down the eddy scale, so that the direct effect of the large scale eddies is lost as the energy is passed along, and small eddies have properties which are to some extent random. Because of the stability of the ocean, it is doubtful if small scale turbulence in the ocean is ever random except in its horizontal dimensions. It is assumed in what follows that we are only referring to horizontal turbulence. The first hypothesis of the similarity theory is that properties of this scale of turbulence (small in comparison to large scale eddies) are uniquely governed by two parameters: the viscosity of the fluid, ν, and the rate of energy dissipation per unit mass, ϵ. This latter parameter is of course a measure of the rate at which energy is passed down the turbulent scale.

For conditions where the Reynolds number is large enough, there must be a scale of turbulence in which the eddies are small compared to the original energy carrying ones but large compared to those eddies where the viscous forces play an important part. This range is called "the inertial subrange" and the second hypothesis of the similarity theory is that the properties of this scale of turbulence are governed by ϵ alone.

The scale of turbulence important in underwater sound probably falls within this inertial subrange. The characteristic length of eddies where viscosity is important is determined by $(\nu^3/\epsilon)^{\frac{1}{4}}$; ν is the kinetic viscosity (10^{-2} cm^2/sec for water). As will be demonstrated a value of $\epsilon = 10^{-3}$ ergs/g/sec appears to be reasonable for the open ocean. This value gives a length of 0.2 cm for the viscous important eddies.

The upper limit of the inertial subrange is more difficult to define. It must be small compared to the original

---

* Contribution from the Scripps Institution of Oceanography, New Series, No. 846. This paper represents the results of research carried out by the University of California under contract with the Office of Naval Research. Reproduction in whole or in part is permitted for any purpose of the United States Government.

[1] M. J. Sheehy, J. Acoust. Soc. Am. 22, 24 (1950).

[2] L. Liebermann, J. Acoust. Soc. Am. 23, 564 (1951).

[3] G. K. Batchelor, Quart. J. Roy. Meteorol. Soc. 76, 133 (1950).

(457)

large eddies. On the basis of what is known about the eddies in major currents like the Gulf Stream and the California current the scale of the large horizontal eddies is probably in excess of 10 km.

For this inertial subrange (say, 10 cm–100 m in the ocean) the theory predicts the following correlation relationship[3]

$$\langle[u(x+l)-u(x)]^2\rangle=k(\epsilon l)^{\frac{2}{3}}\left(1+\frac{1}{3}\frac{l_1^2}{l^2}\right), \qquad (1)$$

where u is the component of turbulent velocity in the x-direction, l is the absolute distance between two particles, l_1 is the component of l in the x-direction, ϵ the rate of energy dissipation, and k a dimensionless constant of order of magnitude unity. For the special case where $l_1=0$, u is then normal to a line between the two particles.

$$\langle[u(x+l)-u(x)]^2\rangle=k(\epsilon l)^{\frac{2}{3}}. \qquad (2)$$

If this line is parallel to the acoustic wave front, u can then be considered a perturbation on the velocity of sound c and can be added algebraically.

$$\langle[\Delta c(l)^2]\rangle=k(\epsilon l)^{\frac{2}{3}}. \qquad (3)$$

Another way of looking at this distribution of turbulent velocity as predicted by the similarity theory is in terms of an autocorrelation coefficient.

$$R(l)=\frac{\langle u(x)u(x+l)\rangle}{\langle u^2\rangle}. \qquad (4)$$

Equation (2) can be written in terms of $R(l)$.

$$\begin{aligned}\langle[u(x+l)-u(x)]^2\rangle &= \langle[u(x)^2-2u(x)u(x+l)+u(x+l)^2]\rangle\\ &= 2\langle[u(x)^2-u(x+l)u(x)]\rangle.\end{aligned}$$

The mean of $u(x)^2$ and $u(x+l)^2$ must be the same.

$$R(l)=1-\left[\frac{k\epsilon^{\frac{2}{3}}}{2\langle u^2\rangle}\right]l^{\frac{2}{3}}. \qquad (5)$$

The evaluation of either Eqs. (3) or (5) depends upon knowing k, $\langle u^2\rangle$, and ϵ. The constant k, is given as "order-of-magnitude" unity. The mean horizontal turbulent velocity in the open ocean may be as high as 20 cm/sec and is probably not less than 3 to 5 cm/sec. The estimate of ϵ is less certain.

III. ESTIMATE OF AVERAGE RATE OF ENERGY DISSIPATION

The average rate of energy dissipation must be equal to the average rate at which kinetic energy is added to the water. One can estimate either one or the other. There are four sources of kinetic energy in the ocean: wind driven currents, waves, tides, and convection (caused by differential heating or cooling). Each has been estimated separately.

A. Wind Driven Currents

The rate at which the kinetic energy of wind driven currents increases is

$$\frac{dE_c}{dt}=mv\frac{dv}{dt}$$

$$\tau=m\frac{dv}{dt}\bigg/A$$

$$E_c'\equiv\frac{1}{A}\frac{dE_c}{dt}=\tau v \quad \text{ergs/cm}^2\text{/sec}, \qquad (6)$$

where τ is the average wind stress per unit area A, v the velocity of the surface current, and m is the mass of the water.

From the analysis of surface currents as measured by the GEK (geomagnetic electrokinetograph) there appears to be an average background of surface currents of the order of 10 to 20 cm/sec. These are more or less at random direction to the wind at any given time, and since v in the foregoing equation is the current component in the direction of the wind the value of v should be reduced, perhaps by as much as $1/\pi$. However, since the purpose of this exercise is to show the relative unimportance of turbulence in underwater acoustics, we will assume maximum conditions. The average value of τ for the oceans is between 0.5 and 1.0 dyne/cm².[4] $E_c'=15\times1=15$ ergs/cm²/sec.

B. Waves

Perhaps as good a way as any of estimating the average rate of energy input into waves is to assume that the average height of ocean waves is 1 to 2 m and that such waves are capable of being regenerated once in 24 hr. The total energy in gravity waves per unit surface area is $E_w=\frac{1}{8}\rho gH^2$ where ρ is density, g is the acceleration of gravity, and H is the height of the waves (twice the amplitude). For the assumed values $E_w'\cong40$ ergs/cm²/sec.

Probably at least half of this energy is lost near shore when the wave is breaking.

C. Tides

The average rate of dissipation of tidal energy alone is estimated at 1.4×10^{19} ergs/sec.[5] If this were distributed equally over the surface of the oceans this figure would be, $E_T=4$ ergs/cm²/sec. However, it is believed that about 80% of this energy is dissipated in shallow seas, perhaps as much as two-thirds in the eastern Bering Sea alone. A more true representation is probably: $E_T'=1$ erg/cm²/sec open ocean, $E_T'=330$

---

[4] W. H. Munk, J. Meteorol. 7, 79 (1950).

[5] H. Jeffreys, *The Earth*, Cambridge University Press, New York, (1952).

TABLE I. Predicted rms velocity differences as a function of the difference between particles and rate of energy dissipation.

l	$\langle\Delta c^2\rangle^{\frac{1}{2}}$ $\epsilon=10^{-4}$	$\langle\Delta c^2\rangle^{\frac{1}{2}}$ $\epsilon=10^{-2}$	$\langle\Delta c^2\rangle^{\frac{1}{2}}$ $\epsilon=5\times10^{-2}$
10 cm	0.1	0.5	0.8 cm/sec
1 m	0.2	1	2 cm/sec
10 m	0.5	2	4 cm/sec
100 m	1.0	5	8 cm/sec

ergs/cm²/sec eastern Bering Sea, and $E_T'=300$ ergs/cm²/sec Irish Sea.

D. Convection

There is one other source of kinetic energy in the ocean, and that is the energy due to differential heating. There seems to be no satisfactory way of arriving at an estimate of the amount of heat energy that goes into kinetic energy, but one can perhaps infer some limits. Convective energy is found either in the large scale thermo-haline circulation or in small convective cells near the surface. The kinetic energy of the thermohaline circulation must be small compared to the kinetic energy in the tides and one would expect the rate of energy dissipation to be small also.

Convective cells near the surface should be an important factor in mixing. Although the evidence is not very good there appears to be no evidence to indicate that convective mixing is more important than wind mixing. Perhaps this is not a very satisfactory argument but it seems likely that if there were an order of magnitude more kinetic energy in convective cells than in wind driven currents this would be evident in the mixing of the surface waters.

By adding up the various sources of kinetic energy, one can make an estimate of the rate of energy dissipation: $E'=30$ to 100 ergs/cm²/sec open ocean, $E'=350$ ergs/cm²/sec eastern Bering Sea.

The rate of energy dissipation probably decreases with depth in the open ocean. Using two extremes, i.e., ϵ independent of depth and $\epsilon=0$ at all depths greater than 100 m: $\epsilon=1\text{–}3\times10^{-4}$ ergs/g/sec open ocean (ϵ independent of depth), $\epsilon=0.3\text{–}1\times10^{-2}$ ergs/g/sec open ocean ($\epsilon=0$ for $h>100$ meters), and $\epsilon=5\times10^{-2}$ ergs/g/sec eastern Bering Sea. Table I shows the predicted value of the root mean square change in sound velocity from Eq. (3) using $k=1$ and $\epsilon=10^{-4}$, 10^{-2}, and 5×10^{-2} ergs/g/sec, respectively. By way of comparison Liebermann found $\langle\Delta c^2\rangle^{\frac{1}{2}}=10$ cm/sec for $l=60$ cm.

Figure 1 shows the autocorrelation coefficient calculated from Eq. (5) for a value of $\epsilon=10^{-2}$. Liebermann's autocorrelation coefficient of temperature is plotted also.

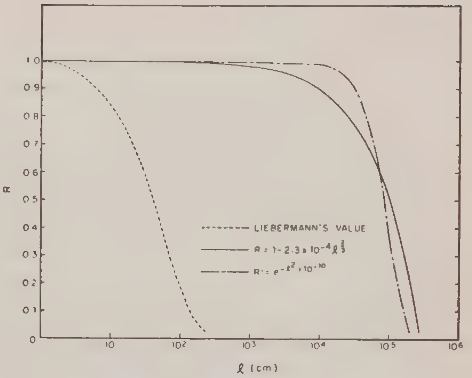

FIG. 1. Comparison of temperature inhomogeneity and turbulent velocity autocorrelation coefficients.

To the best of the author's knowledge there is but one set of published data which can be used in estimating the intensity of small scale horizontal turbulence in the ocean.[6] The relative motion of 45 pairs of small floats (slices of parsnips) was observed over a 30-sec interval from Blairmore Pier, Loch Long, Scotland. The depth of water was two meters.

The pairs were divided into wide and close pairs. The essential data are

	Close pairs	Wide pairs
$\frac{1}{2}\langle l_0+l_t\rangle$	26.7	188 cm
$\langle(l_t-l_0)^2\rangle$	384	5058 cm²

where l_0 is the initial separation along an arbitrary projection and l_t the separation along the same projection 30 seconds later.

The relationship of this experiment to the predictions of the similarity theory has been discussed by Batchelor.[3]

$$l_t=l_0+\int_0^t \delta u dt,$$

where δu is the relative motion along the projection l of the two floats. For small values of t, δu can be considered independent of time.

$$\begin{gathered} l_t=l_0+t\delta u \\ \langle(l_t-l_0)^2\rangle=t^2\langle\delta u^2\rangle. \end{gathered} \tag{7}$$

Substituting into Eq. (2)

$$\langle(l_t-l_0)^2\rangle=kt^2(\epsilon l)^{\frac{2}{3}}. \tag{8}$$

Using the observed values and a value of unity for k, $\epsilon=1\times10^{-2}$ ergs/g/sec close pairs and $\epsilon=7\times10^{-2}$ ergs/g/sec wide pairs.

The relative velocity from Eq. (7) is $\langle\delta u^2\rangle^{\frac{1}{2}}=0.6$ cm/sec close pairs and $\langle\delta u^2\rangle^{\frac{1}{2}}=2.4$ cm/sec wide pairs. The values are of the same order as that estimated by summing the various sources of kinetic energy.

The experiment has several drawbacks for estimating turbulent decay. The depth of water of two meters is quite shallow, and Blairmore Pier has piling. Both of these factors might tend to increase the rate of energy dissipation over what might be found in more truly oceanic conditions. On the other hand, a time interval of

---

[6] L. F. Richardson and H. Stommel, J. Meteorol. 5, 238 (1948).

30 sec is rather long for averaging the velocity differences.

IV. INTENSITY FLUCTUATION RESULTING FROM TURBULENCE

In his work on temperature inhomogeneities, Liebermann calculated their effect on scattering, attenuation, and refraction of sound. In all except the case of refraction he found that the calculated effect was considerably smaller than that observed and hence concluded that temperature microstructure is not important in either scattering or attenuation of sound. Since the calculated turbulent structure is of considerably less intensity than the observed temperature microstructure, there is little point in repeating here the calculations for the effect of scattering and attenuation. Furthermore, it can be readily shown that the amount of sound intensity fluctuation caused by refraction to be expected from the calculated turbulence is negligible.

Following Bergman,[7] Liebermann developed the following equation to relate variation in mean intensity I_0, to the average variation in sound velocity and the autocorrelation coefficient R.

$$\left\langle\left(\frac{\Delta I}{I_0}\right)^2\right\rangle=\frac{4r^3}{15}\left\langle\left(\frac{u}{c}\right)^2\right\rangle\int_0^\infty\frac{1}{l}\left(\frac{\partial^3 R}{\partial l^3}\right)dl, \quad (9)$$

where r is the mean distance between source and hydrophone and the other terms have their previous meanings.

In order to evaluate this integral it is necessary that the autocorrelation function be symmetrical, i.e., $\partial^3R/\partial l^3=0$ for $l=0$. This is not true of the function derived for R in Eq. (5). However, this is the same as saying that the similarity theory does not hold for very small values of l, because a nonsymmetrical function of R implies infinite shear and ignores the viscous forces. The symmetrical function $R'=\exp(-k^3\epsilon^2l^2/\langle u^2\rangle^3)$ gives a reasonable approximation of the derived function of R, Fig. 1. When Eq. (9) is evaluated with the function R', $\langle(\Delta I/I_0)^2\rangle$ is of the order of 10^{-6} for a path of 10^5 cm as compared to unity which is the value of Liebermann's.

V. CONCLUSIONS AND SUMMARY

Assuming that the similarity theory is valid for oceanic turbulence and that the scale of turbulence between 10 cm–100 m falls within the "inertial subrange" certain predictions concerning the characteristics of turbulence within this scale can be made. It is possible to predict the intensity of the turbulence knowing only the value of ϵ, the rate of energy dissipation per unit mass.

The value of ϵ is estimated from the various sources of kinetic energy: wind driven currents, waves, tides, and convection. The first three can probably be estimated to within a factor of 5. It may not be possible to estimate dissipation of kinetic energy due to convection to within an order of magnitude. The only experimental data available give a value for the rate of energy dissipation of the same order as that estimated.

Using the largest values that seem reasonable for each of these terms, it appears that turbulence is of much less importance with respect to underwater sound transmission than are the observed inhomogeneities in temperature.

VI. ACKNOWLEDGMENTS

The author is indebted to Sir Charles Wright who first posed the problem to him and to Dr. Robert Arthur and Dr. Leonard Liebermann for their encouragement and suggestions.

---

[7] P. Bergman, Phys. Rev. 70, 486 (1946).

Hermann Wattenberg

[Reprinted from Journal of Chemical Education, Vol. 33, Page 217, May, 1956.]

Copyright, 1956, by Division of Chemical Education, American Chemical Society, and reprinted by permission of the copyright owner

Reproduced by Permission

HERMANN WATTENBERG: A PIONEER IN A NEW FIELD OF EXPLORATION[1, 2]

NORRIS W. RAKESTRAW
Scripps Institution of Oceanography,
La Jolla, California

Opportunity knocks lightly, and unless one is quick to answer, she may be off and away without a backward glance. But if the door is opened with eagerness who knows what favors she may bestow?

However, opportunity, like inspiration, comes to him who is prepared. How often we hear young men complain that they never had the "breaks," whereas they simply did not have the kind of doors upon which opportunity cared to knock. It would be foolish of course, to say that virtue always has its just reward, but just as foolish to believe that brilliant careers must wait upon the lucky strokes of chance.

Nevertheless, life would be uninteresting if it were not for the unforeseen things that happen to us. The course of our lives depends upon how we react to them. Still, our preparation to react is important, for any one of these events may determine the whole subsequent course of life.

Hermann Wattenberg, a young German chemist, was thus prepared to seize his opportunity when it came, an opportunity to carve out a new kind of chemical career in a field in which there was virtually no competition. For 20 years this field expanded, but he retained a position of leadership in it, largely setting the standards of accomplishment and finally attaining the very pinnacle a few short weeks before his unfortunate death under violent circumstances. I want to tell you this story, not only because we can draw an inspiration and a moral from it but because Wattenberg's accomplishments are interesting in themselves.

EARLY LIFE

He was born in Berlin on April 16, 1901, the eldest of three brothers. The family soon moved to Essen where they lived in comfortable circumstances. The father, Ernst Wattenberg, an engineer, died in 1906, and the mother moved the family to Hannover and subsequently remarried. However, the children came to love and respect their stepfather as their own. He was an artist, and the children were raised in an atmosphere of art and music which became Hermann's avocation during his later scientific life. He had a good eye for beauty, a strong appreciation for all types of art, and a certain amount of musical talent. Nevertheless, his scientific bent appeared early, for as a boy he built himself a primitive laboratory and even made a lathe out of an old sewing machine.

In 1919 he was graduated from the Gymnasium and went to the University of Munich to study chemistry. His student years were not easy, for the family had lost all its money during the war and the subsequent inflation. Nevertheless, his persistence overcame difficulties and he obtained his Ph.D., *magna cum laude*, in 1923, having specialized in inorganic and analytical chemistry under Hönigschmid with two published papers to his credit.

He took an industrial position, with the firm of Rieder-deHaën, but quickly came to realize that this was not the life for him. Returning to the University, he obtained an appointment as assistant to Professor von Wartenberg in the Technische Hochschule in Danzig. He settled into this position happily, but not for long.

THE EXPEDITION

As early as 1919 the German Society for the Advance-

---

[1] Delivered under the title, "A career in chemistry," before the Northeastern Section of the American Chemical Society on the occasion of the James Flack Norris Award, in Boston, February 9, 1956.

[2] Contribution from the Scripps Institution of Oceanography, New Series, No. 847.

ment of Science had been planning a large-scale oceanographic expedition. It was finally decided to send it to the South Atlantic, concerning which there was already some qualitative information but where a thoroughgoing study with modern quantitative methods could yield much important knowledge about the structure and behavior of the ocean in general. The plan was to involve scientific observations of all kinds—physical, biological, geological, chemical. The last category had never received much attention on such expeditions, and the leader of the project, Dr. Alfred Merz, was insistent that for this purpose there should be chosen not an oceanographer who had learned a few chemical techniques but rather a well-trained pure chemist, adaptable enough to apply his knowledge to the problems in the entirely new field of marine chemistry or chemical oceanography. Consultation with Dr. Fritz Haber, of well known repute, confirmed this opinion and the latter undertook to find such a person. On Haber's inquiry, Professor Willstätter, head of the Chemical Institute in Munich, suggested Wattenberg who was accordingly offered the opportunity.

PREPARATION

This unexpected and flattering invitation was a complete surprise to Wattenberg and he accepted with enthusiasm. During the next few months at the Kaiser Wilhelm Institute for Physical and Electrochemistry, of which Haber was the head, he worked hard to make himself familiar with his new field of investigation. Although he had a strong feeling of responsibility for the confidence which had been placed in him, nevertheless, before the preliminary "shake-down" cruise in January, 1925, he often said that he did not know what he was going to investigate or how he was going to investigate it! He found little help in the literature. Heretofore, chemical work done at sea had been exceedingly sketchy; indeed, there was no clear conception of the nature of the chemical problems in the ocean. Analytical methods were exceedingly difficult or altogether impossible to carry out on shipboard. It was Wattenberg's task to plan a program of work and to devise the methods for carrying it out. In this, his ability to strike to the core of a problem without being diverted by inconsequentials stood him in good stead.

During the "shake-down" cruise he suffered so much from seasickness that on his return he was sorely tempted to resign from the expedition. *Mal de mer* is an occupational hazard of oceanographers, however, and its discomforts are soon forgotten. Few people are chronic sufferers; most acquire at least temporary immunity. In deciding to continue, Wattenberg could not have foreseen how this decision was the important crisis of his life.

DEPARTURE

The expedition set forth from Wilhelmshaven on Wattenberg's birthday, April 16, 1925, in the 1300-ton ship "Meteor," which for the purpose of scientific investigation had been built from the hull of a gunboat left unfinished on the ways at the end of the World War. It was more than two years before the ship returned to its home port. In the meantime, some of the most important work in the history of exploration was accomplished.

Wattenberg had of course taken part in the planning of the expedition and particularly in designing and constructing the chemical laboratory. There were no precedents to follow; indeed, no one knew how much chemical work could be done on a long expedition. Consequently, the laboratory was outfitted for many possibilities, some of which were never realized. By the time he returned, Wattenberg was the most experienced—in fact almost the *only*—chemist who practiced his profession on the rolling deck of a ship. What he had learned in the solution of practical technical difficulties as well as the natural chemical problems in the ocean set the standards for the chemists who followed in his footsteps, or, to use a better seagoing expression, in his wake.

During the course of its travels the "Meteor" visited 310 "stations" or spots located in a predetermined pattern in the South Atlantic Ocean between the latitudes of Cuba on the north and the Antarctic Continent on the south. Water was taken at these places for analysis from many depths to the bottom, as far as four and a half miles below the surface. The constituents determined, and the number of respective samples analyzed, were as follows: dissolved oxygen, 6577 determinations; pH, 6549; phosphate, 3611; CO_2-tension, 384; alkalinity, 354; iron, 17; samples taken for gold analysis, 1555. At a number of places the ship was anchored in the middle of the ocean while repeated observations were made for two or more days.

The objectives of the chemical investigation, as they eventually became definite, can be arranged as follows. The chemical analyses furnishing data involved in these objectives are given in italics.

Objectives of the Chemical Program

I. Chemistry and the Life Processes in the Sea
    A. How is the distribution of living organisms (particularly microscopic plants) related to inorganic "nutrients"? (*Determination of phosphate*)
    B. How are the processes of respiration and organic decomposition shown in the water by:
        1. Consumption of oxygen? (*Determination of dissolved oxygen*)
        2. Production of carbon dioxide? (*Determination of pH, CO_2-tension*)
II. Deposition of Calcium Carbonate
    A. Is the ocean saturated with calcium carbonate?
    B. What is the state of equilibrium between CO_2, HCO_3^-, and CO_3^{--}?
    C. Under what conditions is calcium carbonate deposited? (*Determination of pH, alkalinity, CO_2-tension*)
III. Water Movements
    A. Can the movements of water masses be followed by observing changes in the chemical composition of the water? (*Determination of dissolved oxygen*)
IV. Miscellaneous Chemical Observations
    A. (*Determination of iron*)
    B. (*Collection of samples for analysis of gold.* Carried out at the Kaiser Wilhelm Institute in Berlin)

One must remember that these analyses had to be carried out under shipboard conditions, and consequently procedures were limited to simple titrimetric and colorimetric methods. In those days colorimetry was done by visual comparison. The pH determinations, for example, were made by arranging a long series of buffer standards in tubes, adding an indicator solution, and comparing the individual working samples, similarly treated, with the standards by interpolation.

This was the first occasion upon which any large number of phosphate determinations had been made at sea. The colorimetric method used had been devised only a very few years before. This method also involved the preparation of a long set of tubes containing standard solutions, treated with molybdic acid and stannous chloride to develop color, and compared with the working samples one by one.

These colorimetric methods which now seem primitive were nevertheless developed to a high degree of precision by Wattenberg, and his results suffer little by comparison with those obtained by modern instruments, which are often difficult to maintain at sea.

PLANT NUTRIENTS

The processes by which the microscopic organisms in the sea obtain their food had long been a matter of great interest. The early conception was that the minute plants drew their nutriment and built their own structures from organic materials dissolved in the water. This idea was being seriously questioned and evidence was accumulating that inorganic compounds of nitrogen and phosphorus were the important nutrient factors, as they are in the growth of land plants. The advent of a satisfactory method for determining phosphate in the sea water made possible a large-scale investigation of this question, and one of the most important outcomes of the "Meteor" expedition was the showing that the abundance of "plankton" (the collective mass of floating microscopic living organisms) was closely related to the concentration of phosphate in the water. Surface areas often become depleted of this important nutrient, and life there becomes scarce; where the surface can be refertilized, as by the up-welling of deep water rich in phosphate, organic productivity is invariably great. We now know that the same is true of nitrate, and that "fertilizer chemistry" is the same the world over, on land and sea.

CALCIUM CARBONATE

The modifications which Wattenberg brought about in the titration method for alkalinity have made it the standard procedure, although simpler and more rapid techniques are now available since the advent of electrometric methods for determining pH. The results of this titration, along with the values for pH, make possible the calculation of the conditions of the whole carbon dioxide equilibrium once the necessary constants have been evaluated. From the carbonate concentration thus determined and a knowledge of the solubility of $CaCO_3$ in sea water, the saturation picture of this important material may be constructed. The value of this lies in the fact that about half of the sea bottom is covered with sediments made up largely of calcium carbonate, and the conditions of this sedimentation were up to that time seriously in doubt. One of Wattenberg's most notable contributions was a subsequent determination of the solubility product of $CaCO_3$, and by combining this with his analytical results he was able to show that the greater portion of the ocean, particularly its upper layers, is very highly supersaturated with calcium carbonate. He was also led to the conclusion that in the bottom of the sea in many places calcium carbonate is undergoing solution. These were new conceptions and are still the cause of much controversy.

A Chemist at Work at Sea

VENTILATION OF THE SEA

One of the most interesting features of the ocean is the distribution of dissolved oxygen in it. Not only can this be easily and accurately determined by analysis, but it participates in more different and more fundamental chemical processes than any other dissolved constituent in the water. Water at the surface is generally saturated in contact with the atmosphere, while water in the depths is deficient, as a result of oxidation processes, or sometimes contains a surplus due to photosynthesis. A peculiar phenomenon is the widespread occurrence of a depth of minimum oxygen concentration, the maintenance of which depends upon the balance between consumption and replenishment. This has been, and still is, a fruitful subject for speculation and investigation, and the 6000 or more determinations which Wattenberg made are still an important source of our knowledge about it. He was able to show a close relation between oxygen consumption and the production of carbon dioxide (from determinations of pH) and of phosphate. As a contributing influence in this process he was able to trace the movements of the principal water masses, which the oceanographers had discovered by other means in the

(465)

Atlantic basin, in currents that move at various depths from poles to equator in both directions and in both hemispheres. Transverse surface currents moving from east to west in the equatorial region were shown to produce an up-welling of deep water near the African coast, resulting in low oxygen and high phosphate concentrations near the surface with a consequent area of abundant life and high organic productivity.

LIFE AT SEA

Wattenberg was the "Benjamin" of the expedition, the youngest member of the scientific staff. Notwithstanding this, his influence was great principally because of his quiet, even temper, good practical sense, and friendly companionship—qualities which are essential for happiness on such an expedition where men are crowded together for long periods. His laboratory and quarters were popular gathering places and his counsel and advice were sought and respected even by his older comrades.

What characterized this expedition more than any previous one was the close cooperation between workers in several scientific specialties—physicists, chemists, biologists, geologists, meteorologists—all concerned with common problems.

When, after more than two years, the ship returned home the general picture of the scientific results was already apparent, for this was the first expedition of the kind during which the results of the observations were completed and worked up as it progressed. Nevertheless, the analysis of the data, the drawing of conclusions, and the writing of reports occupied the staff for the next ten years or more.

HOME AGAIN

These next years were difficult ones for Wattenberg in many ways. It was hard to settle down after such an experience as he had just had. He was given an appointment as a Fellow of the German Research Society, a position closely corresponding to our National Research Fellowships, and established himself in the Chemical Institute of the University of Munich to assemble the chemical results of the expedition. Among the other chemists in the Institute he was quite literally "a fish out of water," but the unique character of his work attracted great interest and respect and he was given the nickname "Seawater."

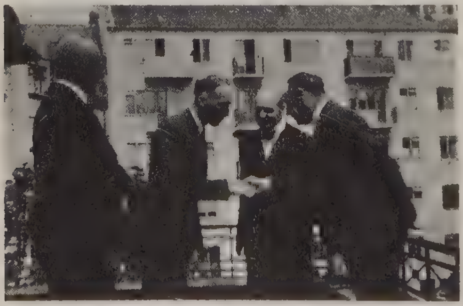

Left to Right: Hentschel, Wattenberg, Buch, Helland-Hansen. In 1934, the Year of Wattenberg's Appointment to the University of Kiel

Here he became acquainted with a young woman student whom he later married. They found mutual companionship not only in scientific interests but also in music and in their love for the outdoors. Together they tramped the mountains, in summer on foot and in winter on skis, and looked forward to the time when they could take their children on such trips. But this was to happen only once, when their eldest-born was six. Eventually their family consisted of two sons and a daughter.

Wattenberg's chemical work was finally collected in three volumes in the series of "Meteor Reports," a collection forming one of the most solid foundation walls for the oceanographic literature. The data and the conclusions have been the basis of literally hundreds of commentaries and secondary papers.

MARKING TIME

But the future for a "marine chemist" or a "chemical oceanographer" was very uncertain. There was no post for such a person at any German university. Wattenberg had never given up his hope for a teaching position in some higher academic institution, but he felt sure that he could never qualify for one on the basis of the kind of chemical research he had been doing. No appointment committee would understand or appreciate it. So he began to use his spare time for researches in pure chemistry, although he continued to dream of a laboratory or institute of some kind patterned after his experience on the "Meteor" in which scientists of many kinds could live and work together, investigating the further mysteries of the ocean. He took part in several minor expeditions, two of them into the cold waters near Iceland and Greenland, and he spent some time as a visitor in marine laboratories in England, Norway, and Finland. He was appointed to a German commission for the scientific investigation of the sea and cooperated with chemists from England and Finland in a very important study of the carbon dioxide equilibrium in the ocean. Meantime, many well-meaning friends tried to bring him back to the field of pure chemistry, offering him attractive positions at other universities. But he had been caught by the glamor of the sea and refused to leave it.

AT LAST!

Eventually the "break" came. Through Dr. Albert Defant, one of his elder colleagues on the "Meteor" and then head of the Institut für Meereskunde in Berlin, he was able to qualify for an academic appointment, first in Berlin and later at the University of Kiel. On such occasions it is required that a candidate for appointment deliver a "habilitation" lecture, intended to demonstrate his qualifications for the appointment. Wattenberg's subject for this was "The relation between the nutrient content of the sea

(466)

and plankton." I well remember Defant's pleasure in describing the skill with which Wattenberg parried the criticisms which were directed at his new but well-documented ideas.

In 1934 he was installed as head of the Laboratory of Marine Chemistry in the University of Kiel, and for the next several years his principal field of activity was in the local waters of the neighborhood. Nevertheless, in his own words, "One cannot draw boundaries in the ocean, and there is scarcely a phenomenon in it which does not exert its influence far and wide." He also carried out fundamental studies on solubilities and on trace elements in sea water. The International Council for the Exploration of the Sea charged him with the responsibility for collecting and publishing the best available methods for determining the important nutrient constituents of sea water. This work is still the only comprehensive treatise on this subject, although it failed to standardize procedures and is now rather out of date.

But these were the happiest years of his life. He was able to indulge in two of his hobbies: gardening and photography. On returning from his frequent trips to sea, he loved to spend time with his plants or long hours in his darkroom. He could concentrate on his work in the laboratory to the exclusion of everything else, with no regard for time, but when finished he could turn completely to the next thing, whether work or diversion. He was patient and considerate with students and co-workers, teaching by example rather than by word. He never gave way to anger or loud words, but was always ready to help with gentle, incidental remarks. Although his habit of life was quiet and unassuming, his decisions were clear and definite, and he was not easily influenced by others in such cases.

These many qualities, along with his scientific accomplishments, led to his promotion, first to "extraordinary" (associate) and later to "ordinary" (full) professor in the University and in its Oceanographic Institute (Institut für Meereskunde) established in 1937, of which he became head of the Hydrographic and Chemical Division. At last he saw the fulfillment of his dream of such an institute in which all the scientific disciplines cooperated in the study of the ocean.

And then came the War.

WAR!

Military mobilization must have been nearly as indiscriminate in Germany as in this country, for he was first sent with the troops as an ordinary soldier to the Polish front. But later his scientific attainments were put to the better service of his country and he became a scientific consultant to the navy, with the eventual title and rank of "Oberregierungsrat der Reich." In this capacity, between 1940 and 1944, he took part in many operations from Norway to the Mediterranean. There is no record of these.

Institut für Meereskunde, University of Kiel

The culmination of his career came in May, 1944, when he was appointed head of his Institute in Kiel. In his inaugural address he said, "Real marine science is not the incidental study of the plants, animals, and sediments in sea water, but rather the understanding of a whole organism whose parts and functions cannot be separated." This was his philosophy and his objective, and by this time he had become an oceanographer as well as a chemist.

On July 24 he and his wife were visiting friends. On their departure, he went to the laboratory to finish some work. This was the second critical decision of his life, and the last, for unfortunately he chose just the time when a bombing attack came over the city to destroy the docks and military installations. The laboratory in Kitzeberg was too close to the harbor to escape this and was totally obliterated, along with its recently appointed director. For more than a day it smoldered. At the same time the Wattenbergs lost their home and everything in it. Only she was spared, with what she carried with her.

Thus was a career in chemistry cut short, as were many careers, by the violence of war.

CONCLUSION

And what can we learn about the choice of a career from the consideration of this one? The study of the sea is not unique in its opportunity; it is but one of many fields in which the principles and practices of chemistry can be applied to the solution of natural problems. Indeed, it is not very different from the application of chemistry to industrial problems. The story does illustrate, however, how one can expand a single opportunity into a life of interesting and productive activity, provided one is prepared with the necessary technical background and personal qualities. Not every young chemist can attain the Nobel Prize, but there are other lasting rewards than the highly publicized ones. Solving problems which no one has attempted before, serving as a model for those who follow in a new sphere of activity, contributing to the advancement of a whole new branch of applied science, working at tasks of one's own choosing, inspiring

others by one's own quiet example, persisting in following a dream until it comes true, establishing a happy home with a devoted family, living a full and well-balanced life with the love and respect of those around one—these are some of the accomplishments and characteristics of the career we have just been considering. It is the kind of life to which anyone might aspire; what more can one ask? For its sudden termination at the very time when it seemed destined to be most fruitful we must blame the terrible violence of war—from which God grant we may henceforth be spared.

PUBLISHED WORKS OF HERMANN WATTENBERG

1922 "Potentiometrische Titration des Kupfers" (with E. Zintl), *Ber.*, **55**, 3366.

1923 "Potentiometrische Titration von Arsen und Antimon" (with E. Zintl), *Ber.*, **56**, 472.

1926–27 "Vier Berichte über die chemischen Arbeiten während der 'Meteor'-Fahrt," *Z. Ges. f. Erdkunde*, **1926**, 66, 264; **1927**, 137, 307.

1928 "Die chemischen Arbeiten der Deutschen Atlantischen Expedition," *Z. Ges. f. Erdk.*, Erg. Heft III, 97.

1929 "Die Phosphat- und Nitratuntersuchungen der 'Meteor'-Expedition," *Cons. Perm. Rapp. et Proc. Verb.*, **53**, 90.

"Eine einfache Methode zur direkten Bestimmung von Ammoniak in Seewasser mit Nesslers Reagenz," *Cons. Perm. Rapp. et Proc. Verb.*, **53**, 109.

"Die Durchlüftung des Atlantischen Ozeans," *J. du Cons. Perm.*, **4**, 68.

1930 "Plankton und Phosphat in der Oberflächenschicht des Südatlantischen Ozeans" (with E. Hentschel), *Ann. d. Hydrographie*, **58**, 273.

"Über die hydrographischen, chemischen und biologischen Verhältnisse an der Meeresoberfläche zwischen Island und Grönland. Ergebnisse einer Fahrt mit der Vermessungsschiff 'Meteor' im August 1929" (with G. Böhnecke and E. Hentschel), *Ann. d. Hydrog.*, **58**, 233.

"Über die Bestimmung der Alkalinität des Meerwassers. Über den Kalkgehalt des Ozeanwassers. I. Mitt.," *Ann. d. Hydrog.*, **58**, 277.

"Über zwei Bildungsweisen von Natriumnitrit und Kaliumnitrit," *Ber.*, **63**, 1667.

1931 "Über die Löslichkeit von CaCO$_3$ im Meerwasser (Vorläuf. Mitt.)," *Die Naturwissensch.*, **19**, 965.

"Die Bestimmung von Phosphat, Nitrat, Nitrit, Ammoniak und Silikat im Meerwasser," *Ann. d. Hydrog.*, **59**, 95. Correction, 428.

"Über den Kalkgehalt des Ozeanwassers. II. Mitt.: Die Verteilung im Atlantischen Ozean," *Ann. d. Hydrog.*, **59**, 273.

"Beziehungen zwischen Kalkgehalt des Meerwassers und Plankton," *Cons. Perm. Rapp. et Proc. Verb.*, **75**, 67.

"Der chemische Aufbau des Atlantischen Ozeans," *Finska Samfundets Meddelanden*, No. 2 (Helsingfors).

1932 "Liquid carbon dioxide in the depths of the ocean," *Nature*, **130**, 26.

"Beiträge zur Ozeanographie des Oberflächenwassers in der Dänemarkstrasse und Irmingersee. II. Teil" (with G. Bohnecke and B. Føyn), *Ann. d. Hydrog.*, **60**, 314.

"Die Beziehungen zwischen pH und freier Kohlensäure im Atlantischen Ozean," *Int. Rev. d. ges. Hydrobiol.*, **26**, 462.

"Über das Kohlensäuresystem im Meerwasser" (with K. Buch, H. W. Harvey, and S. Gripenberg), *Cons. Perm. Rapp. et Proc. Verb.*, **79**, 1.

1933 "Das chemische Beobachtungsmaterial und seine Gewinnung," *"Meteor"-Werk, Bd.* 8, *Tl.* 1, 1.

"Über die Titrationsalkalinität und den Kalziumkarbonatgehalt des Meerwassers," *"Meteor"-Werk, Bd.* 8, *Tl.* **2**, 122.

"Untersuchungen über den Kohlensäuredruck und die Wasserstoffionenkonzentration des Meerwassers," *"Meteor"-Werk, Bd.* 8, *Tl.* **3**, 233.

1934 "Was enthält die Tiefsee an Nährstoffen für das tierische und pflanzliche Leben?" *Tiefseebuch* (Meer in volkstüml. Darstell. 3. Bd. Berlin).

1935 "Aufgaben der chemischen Meeresforschung," *Z. f. d. ges. Naturwissensch.*, 6.

"Kalkauflösung und Wasserbewegung am Meeresboden," *Ann. d. Hydrog.*, **63**, 387.

1936 "Über die Sättigung des Seewassers an CaCO$_3$ und die anorganogene Bildung von Kalksedimenten" (with E. Timmermann), *Ann. d. Hydrog.*, **64**, 23.

"Kohlensaure und Kalziumcarbonat im Meere," *Fortforsch. d. Mineral., Kristallog. u. Petrog.*, **20**, 168.

"Der jahreszeitliche Gang des Gehaltes des Meerwassers an Planktonnährstoffen in der Kieler Bucht im Jahre 1935" (with H. Meyer), *Kieler Meeresforschungen*, **1**, 264.

1937 "Methoden zur Bestimmung von Phosphat, Silikat, Nitrit, Nitrat und Ammoniak im Seewasser," *Cons. Perm. Rapp. et Proc. Verb.*, **103**, 1.

"Die Löslichkeit von Magnesiumkarbonat und Strontiumkarbonat in Seewasser" (with E. Timmermann), *Kieler Meeresf.*, **2**, 81.

"Die chemischen Arbeiten auf der 'Meteor'-Fahrt, Febr./Mai 1937," *Ann. d. Hydrog.*, **65**, *Sept.-Beiheft*, 17.

"Die Bedeutung anorganischer Faktoren für die Ablagerung von Kalziumkarbonat im Meere," *Geol. d. Meere u. Binnengewässer*, 1.

1938 "Zur Chemie des Meerwassers: Über die in Spuren vorkommenden Elemente," *Z. f. anorg. u. allg. Chem.*, **236**, 339. (Hönigschmid-Festschrift).

"Untersuchungen über die Farbe und Durchsichtigkeit des Seewassers. I," *Kieler Meeresf.*, **2**, 293.

"Die Verteilung des Sauerstoffs im Atlantischen Ozean," *"Meteor"-Werk, Bd.*, **9**, 1. *Lief.*, 1.

"Chemie des Meeres" (Balneologe).

1939 "Das Institut für Meereskunde Kiel" (with A. Remane), *Kieler Meeresf.*, **3**, 1.

"Über den Kupfergehalt des Ozeanwassers" (with K. Kalle), *Die Naturwissensch.*, **26**, 630.

"Über die Bestimmung der Titrationsalkalinität des Seewassers," (with H. Wittig), *Kieler Meeresf.*, **3**, 258.

"Die Entstehung der sauerstoffarmen Zwischenschicht im Ozean," *Ann. d. Hydrog.*, **67**, 257.

"Einige Ergebnisse der Untersuchungsfahrten mit dem Reichsforschungsdampfer 'Poseidon' in der Westlichen Ostsee 1938," *Ber. d. Dtsch. Wiss. Komm. f. Meeresf.*, N. F., **9**, 541.

1940 "Der hydrographische Zustand der Ostsee im Sommer 1939. Ergebnisse der 'Triton'-Fahrt vom 27 Juli bis 10 August 1939," *Ann. d. Hydrog.*, **68**, 185.

1941 "Über die Grenzen zwischen Nord- und Ostseewasser," *Ann. d. Hydrog.*, **69**, 265.

"Die Verteilung des Phosphats im Atlantischen Ozean," *"Meteor"-Werk, Bd.*, **9**, 2. *Lief.*

1942 "Das Vorkommen des Eisens im Meer," *Arch. f. Lagerstättenforsch.*, **75**, 36.

1943 "Zur Chemie des Meerwassers. Neuere Untersuchungen über gelöste Gase," *Z. f. anorg. u. allg. Chem.*, **251**, 71.

"Ergänzung zu der Mitteilung: Zur Chemie des Meerwassers. Über die in Spuren vorkommenden Elemente," *Z. f. anorg. u. allg. Chem.*, **251**, 86.

"Geochemie des Weltmeeres," *Kieler Blätter*, **3**, 143.

"Neue Wege zur Messung des Salzgehaltes und der Temperatur des Meerwassers" (with J. Joseph), *Ann. d. Hydrog.*, **71**, 240.

1949 "Entwurf einer natürlichen Einteilung der Ostsee," *Kieler Meeresf.*, **6**, 10.

"Die Salzgehaltsverteilung in der Kieler Bucht und ihre Abhängigkeit von Strom- und Wetterlage," *Kieler Meeresf.*, **6**, 17.

Vol. 37, No. 2 Transactions, American Geophysical Union April 1956
Reproduced by Permission

The Spectrum of the Variation in Latitude

Philip Rudnick

(Contribution from Scripps Institution of Oceanography, University of California, New Series, No. 848)

Abstract—A Fourier series analysis of the motion of the Earth's rotation axis in the frequency range 0.74 to 1.14 cycles per year, containing 93 pct of the total power in the motion, shows: (1) an annual line without recognizable structure comprising about 22 pct of the power in the region examined; (2) the Chandler component comprising about 78 pct of the power, with band structure somewhat broader than heretofore recognized, leading to a value 9.5 yr for the amplitude decay time; (3) an annual component of excitation in agreement with previous determinations, equivalent to a root-mean-square displacement of the axis of inertial symmetry of 0.023″ of arc; (4) a continuous spectrum of excitation which is well determined in the Chandler region, at least roughly determined at other frequencies below annual, but not determined above the annual frequency. The magnitude of the continuous spectrum below annual frequency is consistent with the hypothesis that it, in association with the annual line, arises in the atmosphere, but lack of a determined spectrum at higher frequencies prevents examination of side-band symmetry.

Introduction—Variation of latitude arises from a motion of the pole of instantaneous rotation of the Earth, with respect to the Earth itself [*Jeffreys*, 1952, Chap. 7]. The motion has a west-to-east rotatory character, with a root-mean-square radius of 0.16 seconds of arc or 16 feet on the Earth's surface. Frequency analysis of the motion shows two main components, an annual term with frequency one cycle per year, and the Chandler component of lower frequency, about $\frac{5}{6}$ cycle per year. This spectrum has received considerable study, notably by *Pollak* [1927], and *Jeffreys* [1940]; an additional study, somewhat more elaborate than any preceding, is reported here.

The Chandler frequency is recognized to be that of a free motion of the rotating Earth, considered as a rather highly resonant mechanical filter whose statistically steady output is the observed motion of the pole of rotation. There must be a corresponding steady input to sustain the motion.

One mechanism of excitation is easy to visualize. The free motion of the rotation axis is a contracting spiral whose center is the inertial symmetry axis. If redistribution of mass anywhere in or on the Earth changes the position of the symmetry axis, the rotation axis will begin a new spiral motion about the new center. Thus position of the inertial axis may be considered the input to (or excitation for) the mechanical filter, and the position of the rotation axis its output. Input and output are like quantities, both being angular orientations. *Munk* and *Groves* [1952] have shown that the output may be excited by several possible mechanisms, but that the combined effect of these can be represented as an equivalent motion of the inertial axis. Such a representation will be assumed throughout this discussion.

Figure 1 shows the qualitative forms to be expected for the power spectra of input and output, and the spectral transmission of the mechanical filter. The prominence of the Chandler frequency in the output is ascribed entirely to the selective action of the filter, responding to random excitation. The input spectrum at this frequency need not, of course, be flat as shown, but no special feature is expected at the Chandler frequency. The annual term in the output, on the other hand, is ascribed entirely to a corresponding term in the input, no special behavior of the filter being expected at this frequency. Thus three successive objectives may be listed for study of the output spectrum.

(a) Near the Chandler frequency, the output spectrum gives the form of the filter resonance curve. Mechanical theory then permits extrapolation of this curve to obtain the filter response at all other frequencies. These results are used in the subsequent steps.

(b) Near the annual frequency, any structure discerned in the output spectrum also applies to the input spectrum and hence may contribute to understanding of the mechanism of excitation for the annual component.

(c) Measurement of the output spectrum at points sufficiently separated from both Chandler and annual frequencies may give information on the continuous component of excitation (part of which is responsible for the Chandler component of output) about which very little is known.

The present work was undertaken with primary

(469)

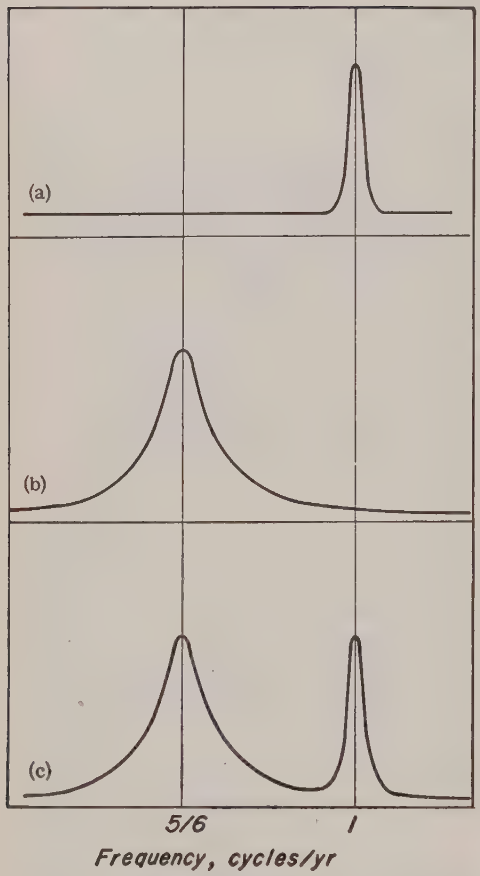

FIG. 1 – Polar motion, expected forms of spectra; (a) power spectrum of input, motion of pole of inertia; (b) spectral transmission of mechanical filter, the rotating earth; (c) power spectrum of output, motion of pole of rotation; this curve is the product of the upper two.

attention on (c), but only a little progress was found possible with presently available data. Some new information under (a) and (b) has been produced, however, and is the chief content of this report.

Notation and mathematical relations—Since the free motion of the rotation axis is a damped circular one, it is very convenient to express the spectrum analysis in terms of circular components, which in turn are conveniently described by complex exponential functions. In this system positive and negative frequencies must be distinguished, as they refer to opposite senses of rotation. This approach is embodied in the following definitions and relations.

l, m direction cosines of the Earth's rotation axis, in respective azimuths 0° and 90° E. longitude. 0.01″ of arc (or very closely one foot arc length on the Earth's surface) is the unit of measure used throughout.

$n \equiv l + im$ a single complex number giving the position of the rotation axis in two dimensions. It obeys the differential equation

$$dn/dt = i\gamma(n - n_0) \qquad (1)$$

n_0 the time-dependent complex quantity representing excitation. It may represent position of the inertial axis, or the more general quantity $[\lambda_i + \lambda_v + \lambda_a + i(\mu_i + \mu_v + \mu_a)]$ of *Munk* and *Groves* [1952]. Unit of measure is 0.01″ of arc.

t time in years.

$\gamma \equiv \omega_0 + i\alpha$ a complex constant, with ω_0 and α real and positive, such that

$$n = e^{i\gamma t} \qquad (2)$$

is a free motion of the rotation axis, possible when $n_0 \equiv 0$.

ω_0 the mid-band radian frequency, per year, of the Chandler component of motion.

$1/\alpha$ the time for e^{-1} amplitude decay of the free motion (2), in years.

ω an arbitrary radian frequency, per year, either positive or negative.

The spectral transmission of a filter described by (1) is derived by supposing steady single-frequency excitation $n_0 = e^{i\omega t}$. One then obtains $p(\omega) \equiv n/n_0 = \gamma/(\gamma - \omega)$, the complex amplitude transmission ratio, and $P(\omega) \equiv |p(\omega)|^2 = (\alpha^2 + \omega_0^2)/\{\alpha^2 + (\omega - \omega_0)^2\}$ the power transmission ratio. (A quantity having the dimensions of $|n|^2$ will be referred to throughout as a power.)

C_+, C_- real, positive amplitude constants, and

ϕ_+, ϕ_- real phase constants used in representing n as a Fourier series of circular components whose typical terms are $C_+e^{i|\omega|t+i\phi_+}$ (west-to-east) and $C_-e^{-i|\omega|t+i\phi_-}$ (east-to-west)

Y_+, Y_- similar amplitude constants, and

θ_+, θ_- similar phase constants representing specifically the annual term in n.

Y_{0+}, Y_{0-} and θ_{0+}, θ_{0-} similarly represent the annual term in n_0.

K is the harmonic number used in Fourier series.

D_+^2, D_-^2, C_{0+}^2, and ϵ defined later, in the discussion of Table 1.

The component with exact annual frequency can be written in either of two forms

$$Y_+e^{i(2\pi t+\theta_+)} + Y_-e^{-i(2\pi t-\theta_-)}$$
$$= e^{i(\theta_++\theta_-)/2}\{Y_+e^{i[2\pi t+(\theta_+-\theta_-)/2]} + Y_-e^{-i[2\pi t+(\theta_+-\theta_-)/2]}\} \quad (3)$$

The left member of (3) is a pair of circular terms. On the right their combination is shown to be an elliptical motion whose semi-major axis has the magnitude $(Y_+ + Y_-)$, lies in east longitude $(\theta_+ + \theta_-)/2$, and is occupied at time $(\theta_- - \theta_+)/4\pi$.

Fourier series analysis—The data used were 544 values of n at 0.1 year intervals covering the years 1891 through 1945. These were read from the large-scale graphs published by *Kulikov* [1950]. A partial numerical Fourier series analysis was carried through, using the method of *Danielson* and *Lanczos* [1942] with minor modification. The fundamental frequency is one cycle in 54.4 years. Because the data were smoothed most of the power was expected to be below about two cycles per year, that is, in the first 100 harmonics. In fact 93 pct of the total power was represented in the 23 harmonics actually computed, with numbers in the range $40 \leq K \leq 62$. The numerical work was carried through on l and m separately, giving cosine and sine terms for each. These were combined in a straightforward way to obtain the quantities C_+^2, C_-^2, ϕ_+, ϕ_- for circular components which are presented in Table 1, columns 2–5. The power spectrum C_+^2 is also shown by the vertical bars in Figure 2.

The annual component—If a component of exactly annual frequency is present in n, it will show itself in this analysis by substantial contributions, of like phase and known amplitude ratio, to harmonics 54 and 55, and by smaller contributions with 180° alternations of phase in neighboring harmonics both above and below. Behavior of this type is evident in ϕ_+ and less clearly in ϕ_-

TABLE 1 – *Spectrum of variation of latitude*

K 1	C_+^2 2	ϕ_+[a] 3	C_-^2 4	ϕ_-[a] 5	D_+^2 6	D_-^2 7	Av. D_-^2 8	$P_{(\lvert\omega\rvert)}$ 9	C_{o+}^2 10	Av. C_{o+}^2 11
		°		°						
40	2.39	351	0.042	35	2.39	0.042		67	0.035	
41	0.41	220	0.075	206	0.41	0.075		98	0.004	
42	7.43	35	0.177	45	7.43	0.177		159	0.046	
43	8.63	179	0.060	195	8.63	0.060	0.089	292	0.029	0.029
44	0.55	138	0.021	330	0.55	0.021		670	0.001	
45	62.23	187	0.067	114	62.23	0.067		1908	0.033	
46	47.39	265	0.006	355	47.39	0.006		1908	0.025	
47	33.72	298	0.021	213	35.37	0.014	0.027	670	0.053	0.028
48	4.61	168	0.042	125	6.32	0.052		292	0.021	
49	0.91	101	0.082	251	1.01	0.076		159	0.006	
50	1.33	123	0.380	26	2.24	0.325	0.141	98	0.022	
51	0.18	350	0.152	211	1.27	0.111	(0.081)[b]	67	0.018	0.017
52	0.37	311	0.431	50	0.65	0.359		48	0.012	
53	0.09	189	0.009	200	2.06	0.007		36	0.055	
54	26.63	6	0.168	11	0.85	0.036		28.3	0.028	
55	24.52	2	0.302	358	0.85	0.028		22.7	0.035	
56	3.53	169	0.918	139	0.33	0.729	0.203	18.6	0.014	
57	1.91	14	0.084	50	0.24	0.059	(0.032)[b]	15.5	0.012	0.026
58	0.40	165	0.125	124	0.048	0.104		13.2	. . .	
59	0.62	358	0.166	48	0.072	0.142		11.3	. . .	
60	0.25	180	0.009	155	0.006	0.004		9.8	. . .	
61	0.69	3	0.008	326	0.215	0.044		8.6	. . .	
62	0.42	192	0.056	94	0.113	0.056	0.062	7.6	. . .	0.003
Sum	229.2	. . .	3.35	. . .	180.7	2.55	. . .	. . .	. . .	. . .
Over-all averages			. . .	. . .	. . .	. . .	(0.057)[b]	. . .	. . .	0.025[c]

[a] $\phi+$ and $\phi-$ are referred to time origin at epoch 1918.7.
[b] Averages excluding K = 50, 52, 56.
[c] Average excluding K = 58 to 62.

TABLE 2 – *Supplementary spectrum values*

Source	K	D_+^2	D_-^2	$P(\lvert\omega\rvert)$	C_{0+}^2	av C_{0+}^2
Data of Table 1	68.0	0.16	0.09	4.1	0.024	
	77.7	0.05	0.02	2.0	0.000	0.012
Pollak [1927]	57.2	0.25	0.08	15.0	0.013	
	60.5	0.24	0.01	9.0	0.020	0.016
Pollak [1927]	68.0	0.44	0.10	4.1	0.092	
	77.7	0.12	0.02	2.0	0.030	0.061

for $52 \leqq K \leqq 62$. Accordingly, the circular terms for n, of exactly annual frequency, shown on the first line of Table 3 were chosen for best fit at $K = 54$ and 55. The calculated contributions of these terms to all harmonics in the range $47 \leqq K \leqq 62$ were subtracted, with consideration of phase, from the total spectrum, to give the residual power coefficients D_+^2 and D_-^2 listed in columns 6 and 7 of Table 1. The annual term is seen to account for a large part of the total power spectrum for $K \geqq 54$.

The corresponding annual term in the excitation n_0 is also given in Table 3. This has been obtained with the use of the transmission factor $P(\omega)$ whose evaluation is discussed in the next section. The elliptical character of these annual oscillations is readily derived from (3). The present formulation makes clear that while the excitation appears to contain components Y_{0+} and Y_{0-} of about the same magnitudes in the two senses, the west-to-east term Y_{0+} is derived from a much more prominent part Y_+ of the response spectrum and is therefore much more accurately established than its companion Y_{0-}. In other words, the difference in semi-axes of the annual excitation ellipse (granted $Y_{0-} > Y_{0+}$) is much better known than its orientation or eccentricity.

Independent values of the annual terms in n were also obtained by a separate calculation carried out directly on the original data, with results shown on the second line of Table 3. The agreement with the first line is not as good as was expected, but no reason for the discrepancy has been found. Results by *Jeffreys* [1940] and *Pollak* [1927] are also given for comparison.

The same calculation shows semi-annual terms with powers $C_+^2 = 0.21$ and $C_-^2 = 0.07$, together being about 0.5 pct of the annual power. These are, however, comparable with the values for a period 0.8 year, for example; the connection with the annual term is therefore doubtful.

An apparent error occurring in Jeffreys' original paper and repeated in his book [*Jeffreys*, 1952] is corrected in Table 3. In the book, one should have at the bottom of page 214, for consistency with page 210,

$$x = -0.090'' \cos\odot + 0.019'' \sin\odot$$
$$y = 0.010'' \cos\odot + 0.073'' \sin\odot$$

giving

$$\lambda = -0.002'' \cos\odot + 0.007'' \sin\odot$$
$$\mu = 0.013'' \cos\odot + 0.034'' \sin\odot$$

The annual component in n is essentially a single line and not accompanied by anything that can be recognized as associated structure.

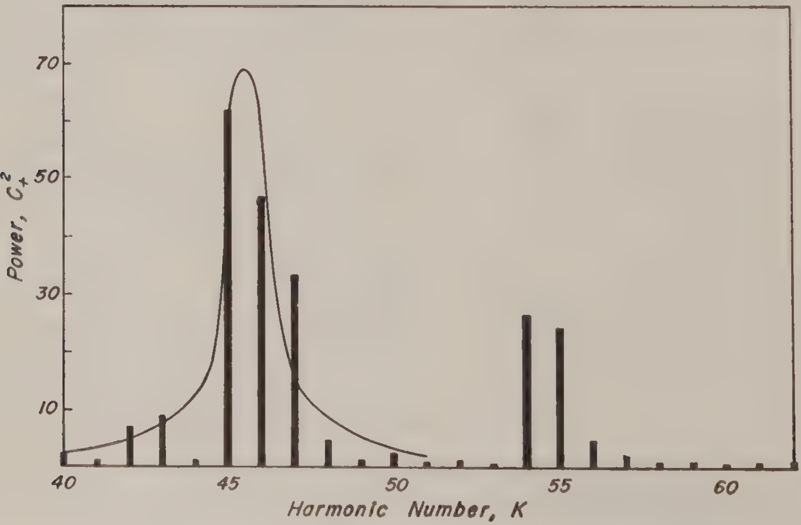

FIG. 2–Power spectrum of polar motion near Chandler and annual frequencies

TABLE 3 – *Annual components*

Source	Polar motion, n				Excitation, n_0			
	Y_+	θ_+	Y_-	θ_-	Y_{0+}	θ_{0+}	Y_{0-}	θ_{0-}
		°		°		°		°
Fourier analysis	8.0	112	0.78	−108	1.57	−75	1.7	−109
Direct calculation	7.6	112	1.00	−105	...	...	...	...
Jeffreys [1952]	8.3	111	0.96	−129	1.63	−76	2.1	−130
Pollak [1927]	8.8	116	1.00	− 84	...	...	...	...

The phase angles are referred to January 1 as time origin.

This point will be discussed further in connection with the continuous excitation spectrum.

The Chandler band—As mentioned in the introduction, the maximum in D_+^2 near $K = 45$ is attributed to a selective response of the Earth in this frequency range. Accordingly, values of center frequency and damping (ω_0 and α) were chosen to produce a power transmission ratio $P(\omega)$ as nearly as possible proportional to D_+^2 in the range $42 \leqq K \leqq 50$. The curve for $P(\omega)$ so determined is shown in Figure 2 and also in Table 1, column 9, for $\omega > 0$. The roughness of the fit seen in the figure is expected, since the power D_+^2 associated with a single harmonic should be regarded as a random variable possessing a Rayleigh distribution and consequently a standard deviation as great as its expected value. Thus even as much as 54 years of data is strikingly limited in its ability to determine the exact form of the spectrum.

The chosen parameter values are: Chandler period, $2\pi/\omega_0 = 1.196 \pm 0.007$ years $= 437 \pm 2.6$ mean solar days (corresponding to $K = 45.5 \pm 0.25$); amplitude decay time $1/\alpha = 9.5$ years $(+10\%, -20\%)$ (corresponding to half-power half-width $\Delta K = 0.9$). These values and their uncertainties were essentially determined by inspection, though an inconclusive effort at least-square fitting did furnish some guidance. The period is in agreement with previous determinations, but the decay time is materially shorter than reported by *Jeffreys* [1940], his value corresponding to $\Delta K = 0.57$. Jeffreys studied the spectrum through the autocorrelation, and while this approach has equivalent power provided the complete autocorrelation curve is examined [*Rudnick*, 1953], he used only three points therefrom. Consequently, the present result is believed superior.

Values of $P(\omega)$ for $\omega < 0$ range from 0.28 ($K = 40$) to 0.18 ($K \geqq 62$). Though they are not given explicitly in Table 1, use is made of them in the following section.

The continuous spectrum of excitation—If the three greatest values of D_-^2 (east-to-west components of n) in column 7 of Table 1 are ignored (and no interpretation is offered for them) the remainder are fairly flat with frequency, as shown in column 8. These are interpreted as observational error for two reasons. (a) Their magnitude and frequency-independence are reasonable *a priori*. (b) Assuming excitation with circular components of equal amount in the two senses, the theoretical ratio $D_-^2/D_+^2 = P(-|\omega|)/P(|\omega|)$ is far less than observed. Hence the average D_-^2 after the three exclusions, approximately 0.06, is taken as the mean power per harmonic ϵ due to observational error. In so doing we acknowledge impossibility of any direct inference of east-to-west components of excitation from the apparent response terms D_-^2.

For the west-to-east components, however, ϵ was subtracted from each D_+^2 value in column 6 and the result divided by $P(\omega)$ from column 9, giving corresponding terms C_{0+}^2 in the continuous power spectrum of the excitation, n_0, shown in columns 10 and 11. Except for the highest frequencies, $58 \leqq K \leqq 62$, this calculated excitation spectrum appears flat. In the immediate Chandler region $42 \leqq K \leqq 50$ this is only a mathematical consequence of the method by which it was obtained. At other frequencies, however, the result is considered significant.

In the region $58 \leqq K \leqq 62$, the average value of D_+^2 is little greater than ϵ and only an average value of C_{0+}^2 was computed. This is markedly below the average obtained for all lower frequencies. The difference is too marked to be a statistical accident, but is nevertheless considered wholly doubtful, in view of the supplementary values reported in Table 2. Two values of C_{0+}^2 at even higher frequencies based on the same data are possibly consistent with the $58 \leqq K \leqq 62$ range. But corresponding values from *Pollak* [1927] based on the International Latitude Service data are so markedly different as to make clear that in this sparsely occupied spectral region we are dealing with features of the data which are of doubtful significance, differing radically, as they do, between the Kulikov and the Latitude Service versions of the data. Without a critical restudy of the basic data, including reconsideration of all smoothing processes, it does not seem possible to derive significant values for the excitation spectrum above one cycle per year.

The annual component of excitation is undoubtedly traceable to mean seasonal change in the atmosphere [*Jeffreys*, 1952; *Munk* and *Groves*, 1952]. It is to be expected that the actual cycles of change in successive years will deviate from the mean, displaying amplitude and phase modulation. Consequently the spectrum line of one cycle per year frequency should be accompanied by side-band power, very probably distributed symmetrically above and below the annual line, and extending over the frequency range (1 ± 0.5) cycles per year, $27 \leqq K \leqq 82$. This appears the most plausible source, and perhaps the only plausible source, for the continuous spectrum of excitation which furnishes the energy dissipated by the Chandler component of n, the motion of the rotation axis.

Two tests may be used in considering whether the continuous excitation power below one cycle per year shown in column 11 of Table 1 is in fact a lower side-band of the annual line and consequently attributable to the atmosphere. First is its relative magnitude. This is about one pct of the annual line per harmonic or possibly 27 pct over the region of the side-band, which is reasonable. A second test is the existence of an upper side-band located symmetrically above the annual frequency. The evidence, unfortunately, is inconclusive, as pointed out in the foregoing.

Acknowledgments—The author is indebted to W. H. Munk for first calling this problem to his attention, and to Miss Gloria Slack for her efficient performance and supervision of the very extended calculations which were required. This work represents one of the results of research carried out under contract with the Bureau of Ships, Navy Department. Part of this material was presented at a Technical Conference, Institute of Geophysics, Berkeley, California, December 3, 1954.

REFERENCES

JEFFREYS, HAROLD, The variation of latitude, Mon. Not. R. Astron. Soc., **100**, 139–155, 1940.

JEFFREYS, HAROLD, *The Earth*, 3rd ed., Cambridge Univ. Press, 392 pp., 1952.

POLLAK, L. W., Das Periodogram der Polbewegung, *Gerlands Beitr. Geophys.*, **16**, 108–194, 1927.

MUNK, W., AND G. GROVES, The effect of winds and ocean currents on the annual variation in latitude, *J. Met.*, **9**, 385–396, 1952.

DANIELSON, G. C., AND C. LANCZOS, Some improvements in practical Fourier analysis and their application to x-ray scattering from liquids, *J. Franklin Inst.*, **233**, 365–380, and 435–452, 1942.

RUDNICK, P., The detection of weak signals by correlation methods, *J. Appl. Phys.*, **24**, 128–131, 1953.

KULIKOV, K. A., The motion of the poles of the Earth and the variation of latitude, *Ouspekhi Astr. Nauk*, **5**, 111, 1950. (See also OTTO STRUVE, The variation of latitude, *Sky and Telescope*, **11**, 109–111 and 142–144, 1952.)

Marine Physical Laboratory of Scripps Institution of Oceanography, University of California, La Jolla, California

(Communicated manuscript received December 20, 1955; open for formal discussion until September 1, 1956.)

JOURNAL OF SEDIMENTARY PETROLOGY, VOL. 26, NO. 1, PP. 49–60
FIGS. 1–8, MARCH, 1956

Reproduced by Permission

A USE OF ROUNDNESS TO DETERMINE DEPOSITIONAL ENVIRONMENTS[1]

M. ALLAN BEAL AND FRANCIS P. SHEPARD
Scripps Institution of Oceanography, La Jolla, California

ABSTRACT

More than 200 sand samples have been analyzed for roundness values, using roundness as curvature or roughness of surface. These have shown a consistent difference between beach and dune roundness for the same area. Because the roundness value changes at the boundary between the beach and the dunes, the difference appears to be due to selective sorting by the wind. Application of the roundness characteristic has been made to a series of borings in the barrier islands along the Texas and Louisiana coasts as an aid in determining which of the sand formations represent dunes. Dune material has been found in scattered samples from these borings down to depths of 44 feet. A series of samples taken from so-called "beach ridges" of the Texas coast have also been analyzed for roundness and have been found to represent dune sands, showing they are eolian rather than water-laid, although their linearity suggests dunes inside of a prograding shoreline.

INTRODUCTION

Roundness is a confusing term since it may refer to a surface or an outline. In relation to sand grains the curvature or roughness of the surfaces are important since they may determine the environment of deposition or the distance of transportation. Unfortunately, curvature of surfaces of small grains can not be measured conveniently although estimates can be made under the binocular microscope. Many people have recognized that roundness in the sense used here is an important characteristic of sand sediments in relation to their environments of deposition. Several articles have mentioned the greater roundness of dune than of water-laid sands[2] (see for example Russell, 1939, and Pettijohn, 1949). For the most part, this greater rounding has been ascribed to abrasion during wind transportation. For reasons presented later in this paper, the writers believe that selective sorting during transportation has caused the greater roundness of the dune sands (see Pettijohn and Lundahl, 1943). Several methods have been suggested for measuring roundness, but to date few workers have made use of roundness measurements to determine the environments in which old sediments were deposited.

In the course of extensive sampling in two Gulf Coast areas, the central Texas coast and the east Mississippi Delta, numerous sand samples have been collected. This has afforded an opportunity to determine the relationship of roundness values to environments of deposition. To check the results of the study in the Gulf Coast area, samples of beaches and adjacent dunes have been obtained from several other areas. Having found that a measurable and consistent difference exists between beach and dune roundness in all areas investigated, this information has been used as an aid in determining the depositional environments of some unknown sand deposits found in borings at various depths up to

---

[1] Contribution from the Scripps Institution of Oceanography, New Series No. 849. This investigation was supported by a grant from the American Petroleum Institute, Project 51.

[2] The contention by Mattox (1955) that wind tends to select grains of low sphericity does not necessarily disagree since his few measurements were based on a ratio of inscribed and circumscribed circles on a grain outline (Riley, 1941), and therefore gave no information on roundness in the sense of curvature of surface. For example, he would have given a high sphericity value to a six-sided flake of mica, although the true sphericity and roundness would be very low.

60 feet in the central Texas coast and from Breton Island, Louisiana. Roundness studies have also been applied to determine the origin of so-called "beach-ridges" on the barrier islands of the Texas area.

All roundness determinations in this work were made by Beal. A study of field relations was made by Shepard. Appreciation is expressed to D. G. Moore and J. R. Curray who collected many of the samples used in the study, and to J. R. Moriarty who prepared the illustrations.

METHODS OF STUDY

The $\frac{1}{8}$ to $\frac{1}{16}$ mm sieving from each of the samples was put through an Otto microsplit until only a few hundred grains remained. These were sprinkled on a black counting tray and the tray tapped lightly to orient the grains on their flattest faces. To assure randomness, traverses were made across the tray and every quartz grain entering the field of view of the microscope was classified until approximately 100 grains had been examined. Roundness values obtained for the individual grains were then averaged to obtain a value for the sample. For reasons presented below, Powers' (1953) roundness scale was used in this study.

CHOICE OF A ROUNDNESS SCALE

The work of Sorby (1880) first indicated that "shape" is a measurable parameter of sand-sized particles. In his studies he kept separate the concepts of sphericity and roundness although it remained for Wadell (1932, 1933, 1935) to define these terms in a quantitative way. Wadell's roundness formula is based on the average radius of the corners and edges of the particle compared to the radius of the maximum inscribed circle when projected to a "standard size" of 70 mm. Because of the time required to arrive at a roundness value by Wadell's method, it is not a practical method for use in any study involving large numbers of samples. His roundness formula, however, serves as a basis for the later visual comparison charts discussed below.

Krumbein (1941) published a visual comparison chart for use with pebbles. This chart is drawn from pebbles whose roundness had been determined by Wadell's method. His silhouettes are arranged arithmetically with roundness values ranging from 0.1 to 0.9. Krumbein states that the chart can be used for rapid visual estimations of sand grains under the binocular microscope if it is suitably reduced in size.

Powers (1953) published a comparison chart using photographs of clay models representing six roundness classes. Each class is represented by two models with the same roundness value; one for grains of relatively high sphericity and the other for grains of relatively low sphericity (fig. 1). He has divided his scale into class intervals arranged geometrically to

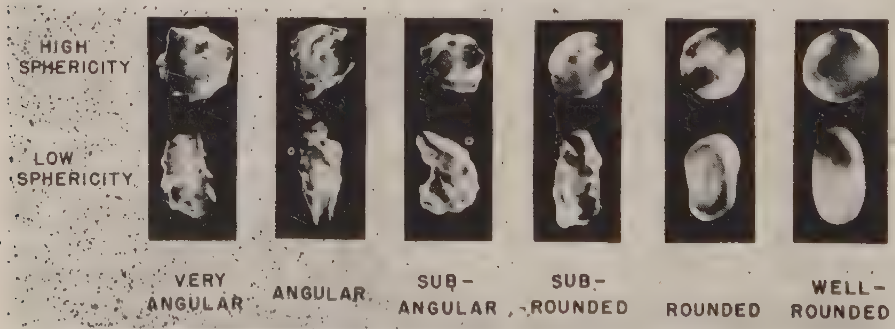

FIG. 1.—Powers' scale of roundness (1953).

provide larger divisions in the higher (more rounded) end of the scale.

Each of the two scales was considered for use in the present study. Whereas both scales are based on the Wadell method, roundness estimations made using either of the scales should give results comparable to the other. Therefore, it was felt that the selection of one of the two scales should be governed primarily by the ease with which the operator could make comparisons between the scale and the quartz particles in the field of view of the microscope. Making a selection on this basis, we felt that the Powers' roundness scale had several advantages over Krumbein's chart.

The first 16 samples of the present study were worked using Powers' method. The operator then attempted to re-work a number of the samples using the Krumbein scale. After having made estimations using the Powers' scale, which closely resembles actual quartz grains as seen under the microscope, the operator experienced difficulty in comparing the quartz particles with the silhouettes of Krumbein's scale. Possibly the difficulty was the result of using Powers' method first, thereby allowing the operator to become accustomed to the photographs used as references in that scale.

Because of the difficulty experienced in using Krumbein's scale for direct comparison of the quartz grains and silhouettes, we decided to reproduce images of the quartz grains from three of the samples as silhouettes which could then be compared with Krumbein's scale. Approximately 100 quartz grains of each sample were photographed with a Polaroid "picture in a minute" camera. The outline of each grain was then carefully traced on the photograph using a crowquill pen and India ink and the photographic image bleached away. The outlines of the grains were then filled in and the resulting silhouettes compared with a copy of Krumbein's chart which had been reduced to give image sizes as small as those obtained by the technique mentioned above.

Table I shows average roundness values for three samples from Matagorda Island in the central Texas area as determined by the Powers' method and the technique described in the preceding paragraph (Krumbein's scale).

TABLE I

	Dune	Beach Berm	Beach at Water's Edge
Powers' scale	.42	.34	.33
Krumbein's scale	.51	.37	.37

In each case the roundness value computed using Krumbein's scale was higher than the determination made with Powers' scale, and the difference between the beach and dune samples was more pronounced. As mentioned previously, both scales are based on the method of Wadell and should yield comparable results. In any study depending upon visual comparisons, the "human element" is difficult to evaluate. It is possible that the operator reacts differently to the photographs of Powers' scale than he does when using the silhouettes of Krumbein. Another possibility is that in tracing the outlines of the grains on the photographs used in the measurements by Krumbein's scale, the operator inadvertently smoothed out some of the smaller corners and raised the roundness values. In any case, the values obtained by the two methods are reasonably close and the same dune-beach roundness relationship was found.

One of our reasons for the choice of Powers' scale now appears to have been fallacious. Pettijohn (1949) pointed out that, " . . . the eye can readily distinguish slight differences in roundness when the roundness values are low, but cannot make such distinctions when the values are large." Powers accepted this as fact and arranged his geometric scale to give

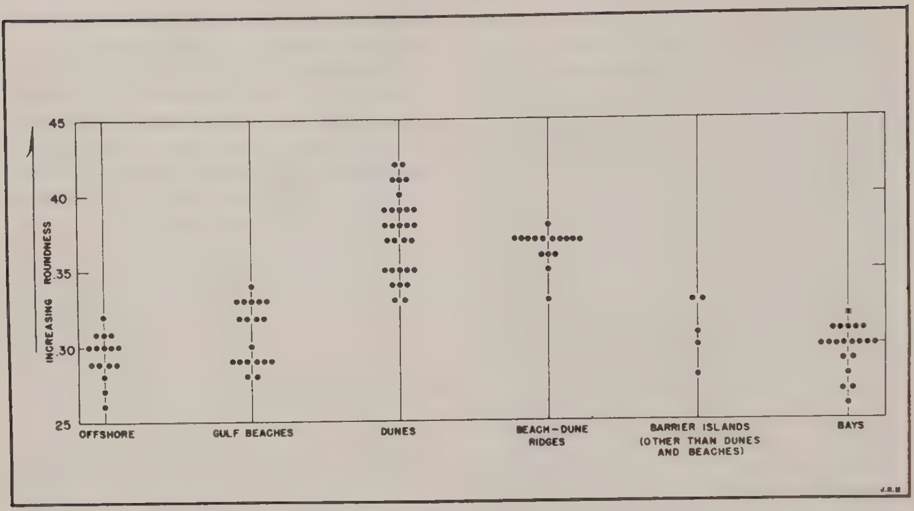

FIG. 2.—Roundness values of surface samples from sandy environments of the central Texas coastal area. For location of this area see figure 6.

larger divisions of the higher roundness values. In selecting a scale for use in the present study, the operator felt that this arrangement of the class limits offered a definite advantage over the arithmetic scale of Krumbein. However, use of Powers' scale for estimation of roundness of over 200 samples has convinced the operator that he can more easily distinguish differences in roundness when the roundness values are high. The statistical study of Rosenfeld and Griffiths (1953) published after the present study was started shows the same result; that it is easier to detect small differences in the roundness of well-rounded grains than in more angular grains. The operator now feels that in any future study, a roundness scale giving finer divisions in the higher roundness values would be desirable.

CRITICAL TESTS OF RESULTS

More than 100 samples whose origin was unknown to the operator were used for roundness measurements in this study. Nearly one-half of the roundness values shown in figure 2 and the samples from the lagoon of the Rio San Miguel, Baja California, shown in figure 3 were obtained by working with the unknown samples. This has given us confidence that the differences in roundness between dunes and adjacent beaches found in this study, though small, are real differences in the sediments and not merely a reflection of psychological "bias" on the part of the operator.

The samples were taken as they became available from the sediment laboratory after mechanical analyses had been completed, and in no case was an attempt made to work on several dune samples followed by several beach samples.

As an additional check on the validity of the roundness difference, we decided to have another operator re-work three samples to see if the dune, beach, and "beach-dune" ridge[3] roundness relationships found by Beal would be confirmed. One sample each of a dune, a beach, and a "beach-dune" ridge was micro-split, labeled with meaningless sample numbers, and given to J. R. Curray for roundness determinations by the Powers' method. Table II gives the roundness values for these three samples as determined by both operators. While the values obtained by Curray are lower in all three cases than those obtained by Beal, the relationship between the beach' dune, and "beach-dune" ridge roundness values are the same.

---

[3] So-called since origin was uncertain.

Table II

	Beal	Curray
Beach sample	0.31	0.29
Dune sample	0.36	0.33
"Beach-dune" ridge	0.37	0.35

ROUNDNESS RELATED TO GRAIN SIZE

We decided to use quartz particles in the sievings between $\frac{1}{8}$ and $\frac{1}{16}$ mm throughout our study for the following reasons:

1. Sands of this size are common in all of the samples from every environment in the central Texas coastal area.

2. By concentrating our efforts on one

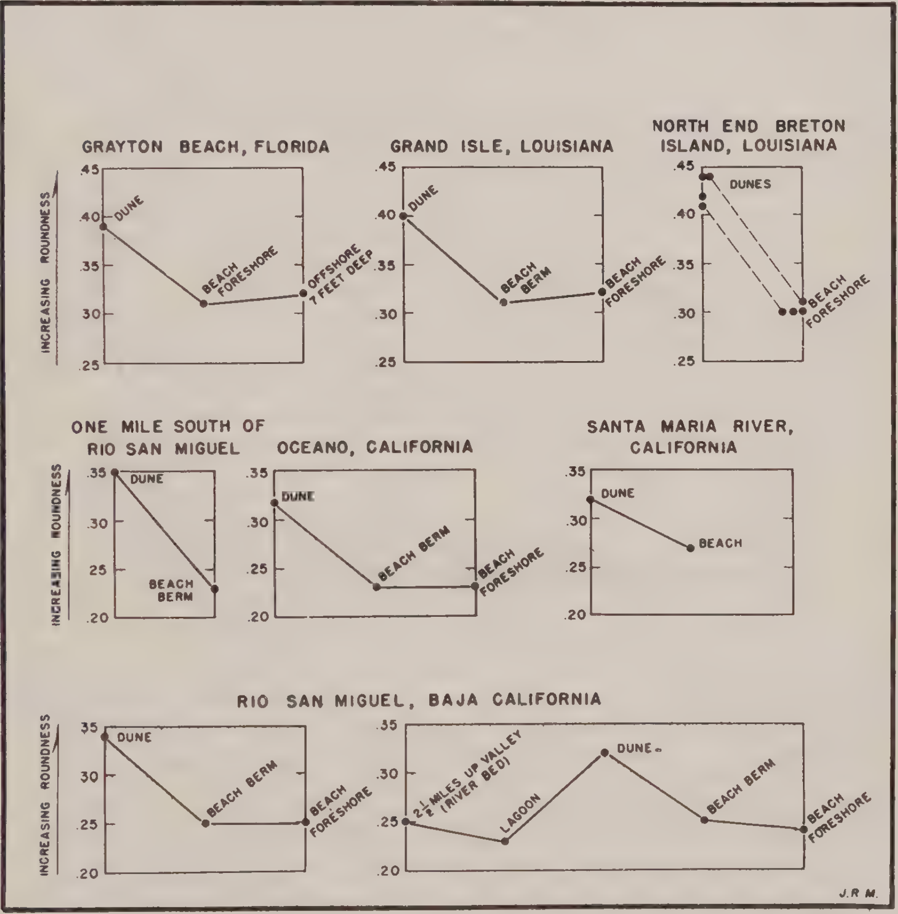

Fig. 3.—Roundness values for dune and beach surface samples from various areas other than the central Texas coast.

size fraction we were able to make roundness determinations on many more samples than would otherwise have been possible.

3. The dune and beach sands which represent most of the samples have almost identical size frequency percentages of $\frac{1}{8}$ to $\frac{1}{16}$ mm grains (Shepard and Moore, 1955, fig. 28).

Since roundness can vary with size, our choice of one sieving for study led us to investigate the size distribution of the sands within the $\frac{1}{8}$ to $\frac{1}{16}$ mm of dunes and beaches. This was accomplished by taking splits of dune and beach sands from Matagorda and St. Joseph Islands in the central Texas area and measuring diameters perpendicular to the long axis of 100 grains from each sample with a microscope equipped with a micrometer ocular. All of the techniques of eliminating "bias" used in the roundness measurements were also applied to this study. The measurements were plotted as cumulative curves of the size distribution and compared. We then looked for a difference in the size distribution that could explain the difference in roundness found in this study. Since the size distribution is the same, we feel that the difference in roundness cannot be a result of concentration in the dunes of the larger sand sizes within the $\frac{1}{8}$ to $\frac{1}{16}$ mm sievings.

COLLECTION OF FIELD SAMPLES

Although some sands for roundness measurements were obtained from the bays and the open Gulf of the areas studied, the great majority came from the barrier islands, particularly from the beaches and from the dunes. In sampling, care was taken not to collect any special concentrate represented by unusual conditions. In general the samples were taken from the top two inches of the beach or dune surface. However, in order to determine whether the tops of the dunes were different from the sand at some little distance below the surface, a series of samples was taken at a variety of depths. No consistent difference in roundness was found as a result of this check.

Because it has been commonly assumed that the sand in the dunes is rounded by abrasion, samples were collected at the outer margin of the dune directly at the contact with the beach sand. Other dune samples were taken at various distances up to three miles in from the beach source. On one occasion samples were obtained during a hurricane tide which had produced a flooding of the waters over some of the very low dunes on the upper beach, so that an opportunity was found to check the effects of a double environmental influence.

ROUNDNESS OF SURFACE SEDIMENTS

Of the 200 samples for which an average roundness value has been obtained, the majority came from beaches and dunes of St. Joseph, Matagorda, Mustang, and northern Padre islands. The roundness value of each of the samples in this central Texas area is plotted against environment in figure 2. In addition to beach and dune sands, a few sand samples were examined from the shallow open Gulf and from portions of the bays near the margins of the islands, along with a few samples from the flats on the inside of the barrier islands. It will be noted that the roundness of the dunes is quite regularly greater than in any of the other environments.

The distinction in this central Texas coastal area between the beaches and the dunes is duplicated by every other area from which we have samples (fig. 3). It will be noted, however, that the roundness on some west coast dunes is as low as in the beaches along the Gulf coast. Thus the difference is only relative rather than absolute, making it impossible to use this criterion statigraphically unless a considerable roundness study has been made of a particular sand formation.

The difference in roundness was found to occur at the immediate contact between the inner beach and the outer dune so that a distance of a few feet

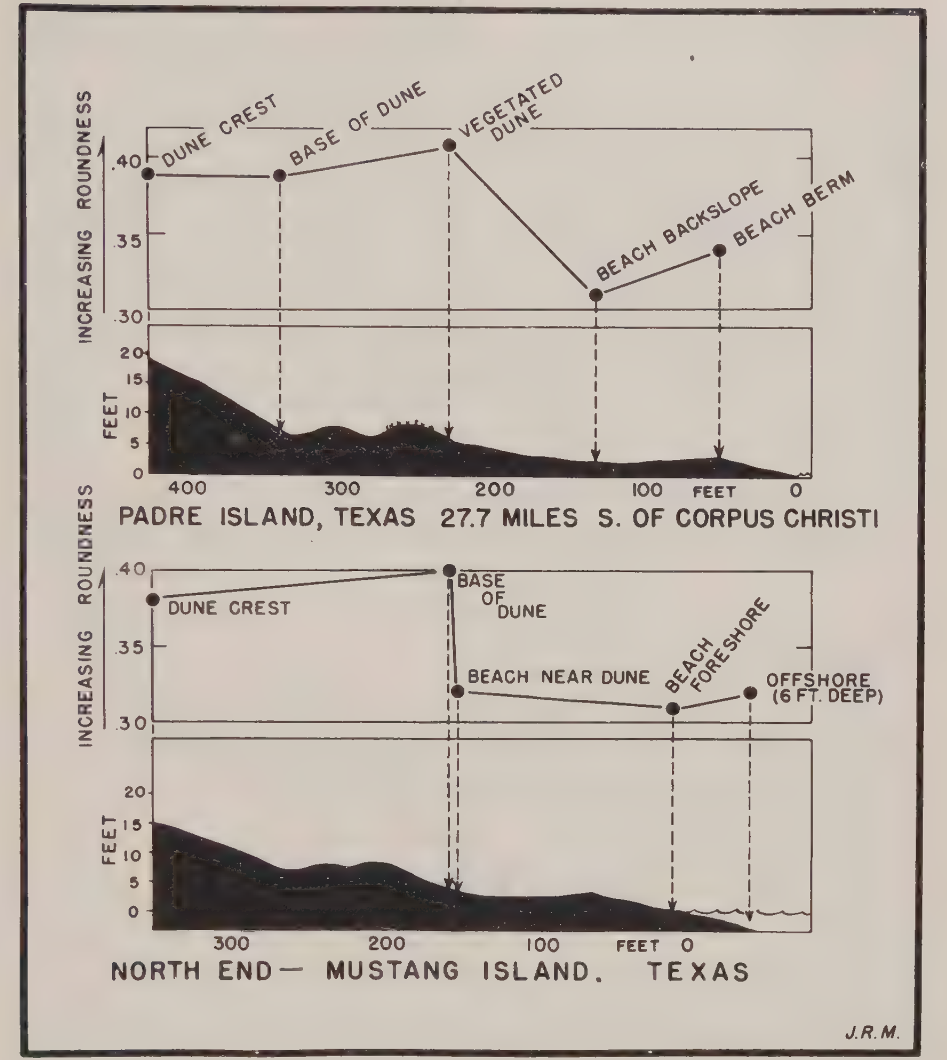

FIG. 4.—Variations of roundness along two beach-dune traverses. Note the sudden change in roundness at the beach-dune contact in the lower diagram.

makes a complete change in the roundness picture. This is shown in figure 4. In tracing the roundness away from the beach across an extensive series of dunes little change was found. Samples obtained during a hurricane tide, when the water covered a low dune on the inner beach of northern Padre Island, showed that the overrun dunes still had high roundness (fig. 5). However, the roundness here is lower than in the dune interior.

EXPLANATION OF DIFFERENCE IN ROUNDNESS

The preceding discussion shows that the roundness in the dunes is not a matter of abrasion or it would increase with distance from the beach and little or no contrast would be found at the dune beach contact. MacCarthy (1935), in working with adjacent beach and dune samples from the east coast, found that the dunes had a higher sphericity than the beaches and suggested as an explanation a selective sorting by the wind. Subsequently MacCarthy and Huddle (1938) were able to produce such a sorting in laboratory experiments. Krumbein (1942) suggests that roundness itself is not a factor in the selective sorting, but because of the correlation between sphericity and roundness a selective sorting according to sphericity results also in a roundness sorting.

Due to the rather extensive areas studied and the limited time available, sphericity determinations have not been made a part of this study. Consequently, it is not possible to draw conclusions as to whether sphericity or roundness or some combination of both is responsible for the suggested selective sorting. The results of the present study do, however, confirm the popular belief that dune sands are more rounded than the adjacent beach sands and this information could be put to use in stratigraphic studies.

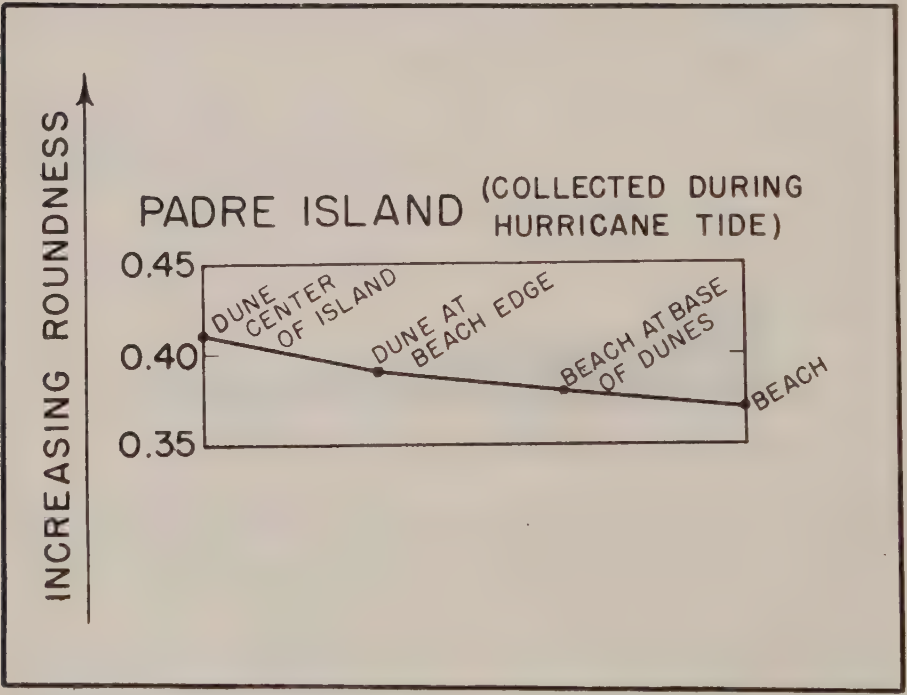

FIG. 5.—Showing a persistence of dune roundness values despite over-running of low coastal dunes by a hurricane tide. Note that the beach referred to here had been a dune prior to the hurricane.

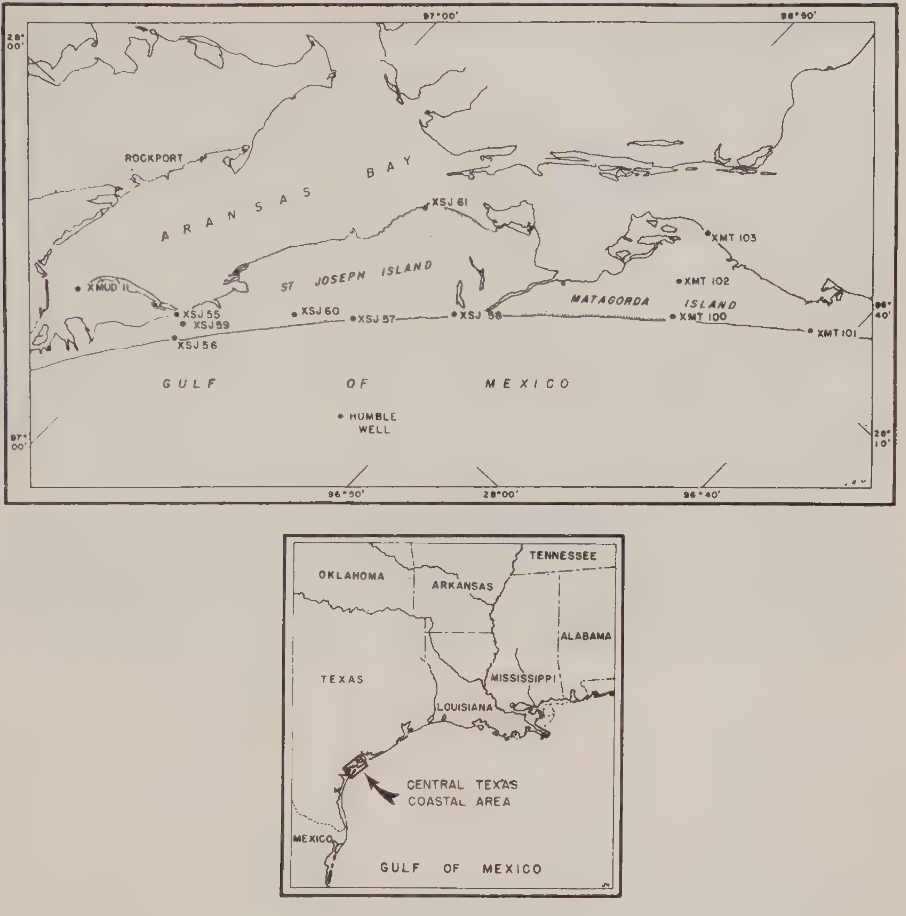
97°00'
96°50'
28° 00'
ROCKPORT
ARANSAS BAY
XSJ 61
XMT 103
ST JOSEPH ISLAND
XMUD I
XMT 102
MATAGORDA ISLAND
XSJ 55
XSJ 59
XSJ 60
XSJ 57
XSJ 58
XMT 100
XMT 101
96° 40'
XSJ 56
GULF OF MEXICO
HUMBLE WELL
97° 00'
28° 10'
96°50'
28°00'
96°40'
OKLAHOMA
TENNESSEE
ARKANSAS
ALABAMA
TEXAS
MISSISSIPPI
LOUISIANA
CENTRAL TEXAS COASTAL AREA
MEXICO
GULF OF MEXICO

FIG. 6.—Location of borings in the central Texas coastal area from which roundness values were obtained.

ROUNDNESS IN SHALLOW BORINGS

Twelve borings were made on St. Joseph and Matagorda islands (fig. 6), going to an average depth of 50 feet (Shepard and Moore, 1955). Most of the material obtained in these borings was sand. Therefore, it became important to determine roundness in many of the samples to see if they might have been deposited under dune conditions. Of 26 samples studied, five showed distinct dune roundness and two others have a roundness of 0.34 which is more likely to be in the dune category than beach. At 14 feet below the beach on Matagorda Island a distinct dune roundness was discovered at a level which is about 12 feet below present sea level. On St. Joseph Island at 29 feet below the beach a roundness of 0.34 was found in two of the holes. In a boring on the inside of the dune ridge of St. Joseph Island a sample was obtained at 44 feet which had a roundness of 0.36 and is thus quite clearly in the dune category (fig. 7a). All of these samples are of a type which could be explained as a dune deposit (Shepard and Moore, 1954).

A boring was made at Jaybird Point on the Aransas Bay side of St. Joseph Island, and one on an exposed tidal flat at the

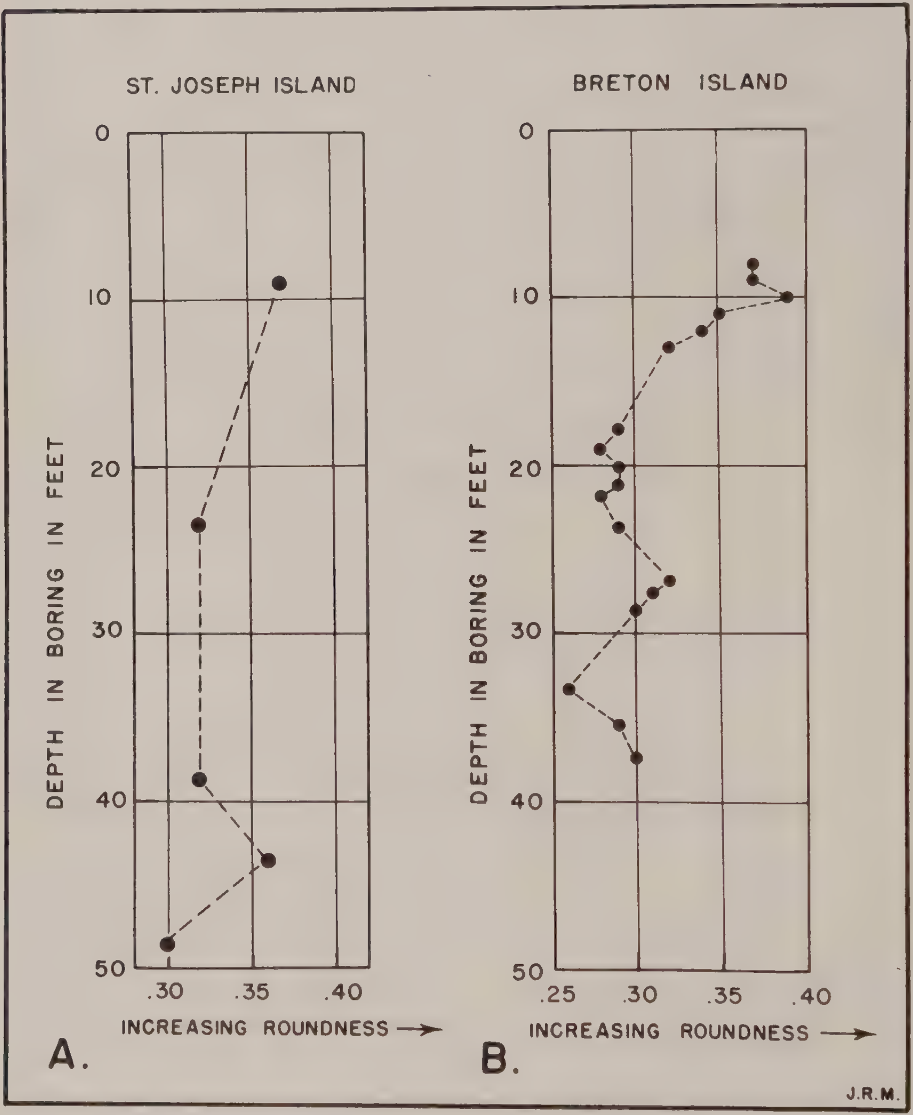

FIG. 7.—Plot of roundness values with depth in boring (A) on St. Joseph Island in the Central Texas coastal area, and (B) on Breton Island in the East Mississippi Delta area. Roundness values of surface sample greater than .33 are found to be dune sands.

(484)

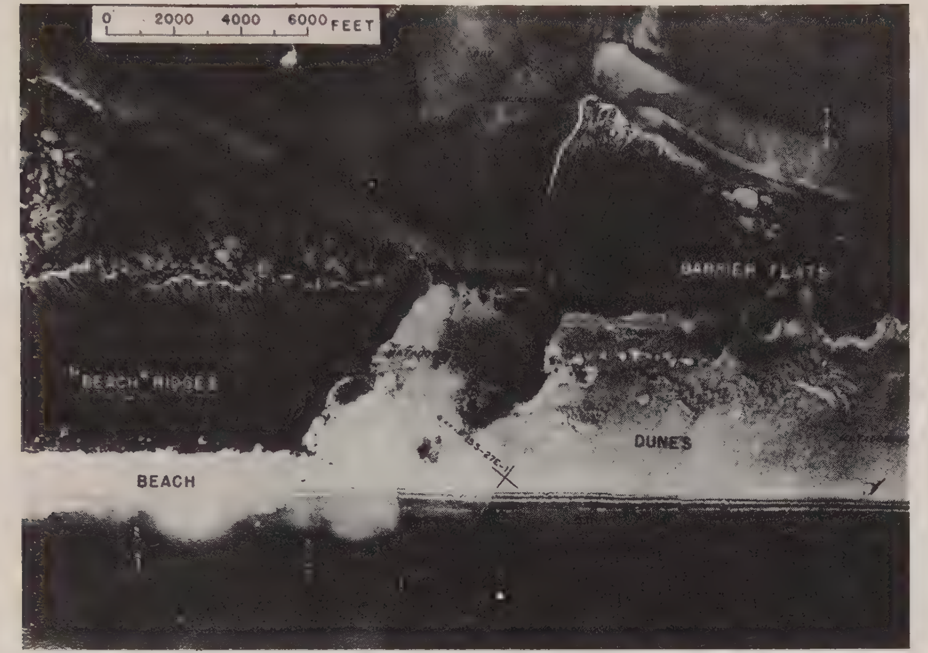

FIG. 8.—Showing the vegetated ridges on Matagorda Island which are commonly referred to as "beach" ridges, but are shown to have a dune roundness value. Note that the "beach" ridges have been overrun by dunes in some areas. (Aerial mosaic courtesy of Tobin Aerial Surveys, Inc.)

tip end of Mud Island, an extension of St. Joseph Island into Aransas Bay. Cores from both borings contained deposits which differ from typical dune sand in having about 10 percent silt and clay, but these sands showed a roundness of 0.37 at a depth of 32 feet under Jaybird Point and of 0.39 and 0.40 at depths of 16 and 17 feet respectively under Mud Island. The material lacks the faunas typical of bay deposits (figure by Parker in Shepard and Moore, 1955, fig. 38) and it would appear that either this represents a dune sand into which a certain amount of silt and clay has been blown or that dune sands have been reworked by an overwash containing some muddy sediment.

In a boring made by Humble Oil and Refining Company at a locality three and one-half miles seaward of St. Joseph Island, a sample was obtained above the Pleistocene contact at a depth of 25 feet below the ocean bottom in which a roundness of 0.42 was obtained. This sample was from a series extending through a thickness of 60 feet, all apparently formed on a barrier island or in inlets crossing such an island (Shepard and Moore, 1955, p. 1569).

Roundness studies were also made on 12 samples from two borings in the east Mississippi Delta area extending to a depth of 33 feet below the surface of Breton Island. Two samples from a depth of approximately 12 feet showed a roundness value comparable to that of the present day dune sands of Breton Island. The remainder of the sand samples from the borings yielded roundness values comparable to the present beach sands of Breton Island (fig. 7b).

BEACH RIDGES OR DUNE RIDGES

Ridges like those shown in the accompanying aerial photograph (fig. 8) are usually referred to as "beach-ridges." It is assumed by most people that they have been built on a prograding shoreline where storms have built up the sand or gravel above the general sea level. Such ridges are discussed extensively by Johnson (1919, pp. 404–453). Examination of many coastal areas has shown that storm beaches made of cobbles are quite common, but, so far as the writers know, sand is not built up into land ridges by storm waves. On the other hand, a series of submerged bars and troughs are found along many coasts and some of these may be built up at least to high tide level. Long sand ridges inside beaches are also built by the wind. Sometimes these ridges are narrow and parallel to the shore and in other places they are less ridge-like and spread over a wide area.

In order to determine whether the so-called "beach-ridges" of Matagorda and St. Joseph islands along the Texas coast were the product of piling up of sand by the waves or whether they represent dune ridges, a series of samples was obtained. These samples extended from the surface to depths of as much as seven feet in the parallel ridges and a few were obtained in the swales or valleys between ridges. An average roundness of 0.37 has been determined for these samples. The values are plotted in figure 2 and it can be seen that all but one of the samples is clearly in the dune category and the one represents a point of overlap between a dune and beach. This seems to indicate that, at least in this area, the so-called "beach-ridges" should actually be called "dune-ridges." A possible reason for there being more than one ridge could be that the beach has made a series of progradations and a dune-ridge was formed inside the beach at each stand.

REFERENCES

Johnson, D. W., 1919, Shore processes and shoreline development. John Wiley, pp. 404–453.

Krumbein, W. C., 1941, Measurement and geological significance of shape and roundness of sedimentary particles: Jour. Sedimentary Petrology, v. 11, pp. 64–72.

———, 1942, Settling-velocity and flume-behavior of nonspherical particles: Am. Geophys. Union Trans., pp. 621–633.

MacCarthy, G. R., 1935, Eolian sands: a comparison; Am. Jour. Sci., 5th ser., no. 176, v. 30, pp. 81–95.

MacCarthy, G. R., and Huddle, J. W., 1938, Shape sorting of sand grains by wind action: Am. Jour. Sci., 5th ser., no. 205, v. 35, pp. 64–73.

Mattox, R. B., 1955, Eolian shape-sorting: Jour. Sedimentary Petrology, v. 25, pp. 111–114.

Pettijohn, F. J., 1949, Sedimentary rocks. Harper, New York, pp. 422–423.

Pettijohn, F. J., and Lundahl, A. C., 1943, Shape and roundness of Lake Erie beach sands: Jour. Sedimentary Petrology, v. 13, pp. 69–78.

Powers, M. C., 1953, A new roundness scale for sedimentary particles: Jour. Sedimentary Petrology, v. 23, pp. 117–119.

Riley, N. A., 1941, Projection sphericity: Jour. Sedimentary Petrology, v. 11, pp. 94–97.

Rosenfeld, M. A., and Griffiths, J. C., 1953, An experimental test of visual comparison technique in estimating two dimensional sphericity and roundness of quartz grains: Am. Jour. Sci., v. 251, pp. 553–585.

Russell, R. D., 1939, Effects of transportation on sedimentary particles: in Recent Marine Sediments. Trask Ed., Am. Assoc. Petroleum Geologists, Tulsa, pp. 32–47.

Shepard, F. P., and Moore, D. G., 1954, Sedimentary environments differentiated by coarse-fraction studies: Am. Assoc. Petroleum Geologists Bull., v. 38, pp. 1792–1802.

———, 1955, Central Texas coast sedimentation: characteristics of sedimentary environment, recent history, and diagenesis: Am. Assoc. Petroleum Geologists Bull., v. 39, pp. 1463–1593.

Sorby, H. C., 1880, On the structure and origin of noncalcareous stratified rocks: Geol. Soc. London Quart. Jour. v. 36, pp. 46–92.

Waddell, Hakon, 1932, Volume, shape, and roundness of rock particles: Jour. Geology, v. 40, pp. 443–451.

———, 1933, Sphericity and roundness of rock particles: Jour. Geology, v. 41, pp. 310–331.

———, 1935, Volume, shape, and roundness of quartz particles: Jour. Geology, v. 43, pp. 250–280.

(*Reprinted from Nature, Vol.* 177, *pp.* 551–554, *March* 24, 1956)
Reproduced by Permission

(Scripps Institution of Oceanography, Contribution No. 850.)

POLAR WANDERING: A MARATHON OF ERRORS

By Dr. W. H. MUNK*
Department of Geodesy and Geophysics,
University of Cambridge

"THE subject of the fixity or mobility of the earth's axis of rotation in that body . . . [has] from time to time attracted the notice of mathematicians and geologists. The latter look anxiously for some grand cause capable of producing such an enormous effect as the glacial period. Impressed by the magnitude of the phenomenon, several geologists have postulated . . . a wide variability in the position of the poles on the earth; and this, again, they have sought to refer back to the upheaval and subsidence of continents." With these words George Darwin introduced his paper[1], "On the Influence of Geological Changes on the Earth's Axis of Rotation"; it occupies forty-two pages in the *Philosophical Transactions*, and its mathematical complexity is in proportion to the length. The paper was published in 1877 when Darwin was thirty-two years old; it is the first of his seventy-two papers on cosmology. Yet this was to remain the only serious study of the dynamics of polar wandering until Gold[2] reopened the problem in a succinct article in *Nature* in 1955. Gold's conclusion differs from Darwin's, but this is only the latest chapter in an extensive, and sometimes heated, controversy that has been going on for seventy years.

Darwin set himself the following problem: at time 0 some continents suddenly commence to rise, others to fall, and the movements continue at a uniform rate thereafter. What would be the position of the axis of rotation if the Earth is (*a*) a rigid solid, (*b*) a viscous fluid? We now consider that the Earth is better described as an elastic solid. Darwin did not consider this case; neither the evidence nor the elastic theory had been developed. We are here concerned only with the orientation of the axis in the body of the Earth; the orientation in space is scarcely altered. It is therefore convenient to refer to the geographical location of the poles of rotation, where the axis pierces the crust.

---

* Guggenheim Fellow on sabbatical leave from the Scripps Institution of Oceanography, University of California.

Darwin's solution (ref. 1, pp. 282–83) consists of oscillatory terms like

$$\exp(-\alpha t) \cos \omega t \qquad (1)$$

plus others that remain after the initial oscillation has become damped out. These have the components (disregarding for the moment a slight separation between axes of figure and rotation) :

$$\begin{aligned} x &= \frac{\alpha\,(\omega^2 - \alpha^2)}{\omega^2 + \alpha^2}\,u - \frac{\omega^2}{\omega^2 + \alpha^2}\,ut \\ y &= -\,\frac{2\omega\alpha^2}{\omega^2 + \alpha^2}\,u + \frac{\omega\alpha}{\omega^2 + \alpha^2}\,ut \end{aligned} \qquad (2)$$

u is a measure of the rate of upheaval, x is the polar displacement toward the centre of upheaval and y at right angles to it.

For undamped oscillations of a rigid Earth, $\alpha = 0$, and

$$x = -\,ut, \; y = 0 \qquad (3)$$

For reasonable continental upheavals, these solutions must be limited to such times that ut is of the order of a degree of latitude at most, according to Darwin ; actually one mile might be a better upper limit. In any event, there can be no appreciable polar wandering on a rigid Earth. The opposite extreme, that of great fluidity, corresponds to large α, and to

$$x = -\,\alpha u, \; y = -\,2\omega u \qquad (4)$$

so that x can be made arbitrarily large by taking α arbitrarily large.

Darwin is explicit in the interpretation of his solution : "If the earth be sensibly rigid . . . the geographical path of the axis is very nearly the same as is due merely to the geological deformations of the earth's shape ; but if the earth be more or less plastic, . . . the dynamical reactions introduced are such as more or less to modify the geographical path of the axis. In the case of great plasticity these reactions would suffice to alter entirely the character of the path". "We have therefore clearly a state of things in which the pole may wander indefinitely from its primitive position. On this hypothesis, as in successive periods the continents have risen and fallen, the pole may have worked its way, in a

(488)

devious course, some 10° or 15° away from its geographical position at consolidation, or may have made an excursion of a smaller amount and have returned to near its old position."

Whether or not there had been polar wandering was therefore not a question of dynamics, but depended on whether the Earth was taken as plastic or rigid. The decision was outside the scope of Darwin's analysis, though he favoured the latter alternative: "But Sir William Thomson has shown that the earth is sensibly rigid; and in any case the earth is not a viscous fluid, properly so-called, although it may be slightly plastic".

What was Kelvin's evidence for a rigid Earth? His original argument[3] was by way of reference to Hopkins, "who first adduced the phenomena of precession and nutation to disprove the hypothesis that the solid part of the Earth's mass is merely a thin shell". But this argument is wrong, because precession is caused by the pull of the Sun on the equatorial protuberance regardless of whether it is fluid, elastic or frozen. Kelvin was questioned on this point by Newcomb, and in a presidential address to the British Association[4] Kelvin asked his audience to cross out what he had written on this subject in "Natural Philosophy". (I found the copy in the University Library, Cambridge, to have been defaced accordingly.) Unknown to Kelvin and Newcomb, the error had already been pointed out by General Barnard[5].

Darwin[1] refers to Kelvin's retraction of precession as an argument for rigidity, but adds that Kelvin ". . . adduces, however, a number of cogent arguments on this point". Curiously enough, Kelvin refers here to a paper by George Darwin's great father[6] entitled "Observations on the Parallel Roads of Glen Roy and other parts of Lochaber in Scotland, with an attempt to prove that they are of Marine Origin", in which it is said that the Earth as a whole takes approximately the figure due to gravity and centrifugal forces, because of the fluidity of the interior and the flexibility of the crust. To this statement Kelvin raises the following two objections in his British Association presidential address[4]: (1) "But alas, for this 'attractive sensational idea' . . . that a molten interior to the globe underlies a superficial crust, its surface agitated by tidal waves, . . . the solid crust would yield so freely to the deforming influence of sun and moon that it would simply carry the waters of the ocean up and down with it, and there would be no sensible tidal rise and fall of water relatively to land . . ."; that is, unless the crust consisted of "preternaturally rigid matter", far more

(489)

rigid than steel; (2) that the "solar semiannual nutation must be largely, and the lunar fortnightly nutation enormously, affected by interior liquidity. . . . This conclusion is absolutely decisive against the geological hypothesis of a thin rigid shell full of liquid". But the argument is not decisive if we ascribe to the mantle a behaviour characteristic of many materials, whereby it responds almost as an elastic solid to disturbances of short period, but flows in response to stress of long duration. I think Darwin's suggestion was well taken[1]: "it seems quite possible that the earth may be sensibly rigid to the tidal deforming influences of the sun and moon, and yet may bring itself back from any considerable departure from a form of equilibrium to approximately that form". Kelvin's foregoing arguments may have had something to do with a letter George Darwin was to receive from his father two years later[7]: "Hurrah for the bowels of the earth and their viscosity and for the moon and for the Heavenly bodies . . . and for my son George (F.R.S very soon) . . .".

But Kelvin[4] was not yet contented with the two preceding arguments: "But now thrice to slay the slain: suppose the earth this moment to be a thin crust of rock or metal resting on liquid matter; its equilibrium would be unstable! And what of the upheavals and subsidences? They would be strikingly analogous to those of a ship which has been rammed —one portion of crust up and another down, and then all down. Now whatever may be the relative densities of rock, solid and melted, at, or about, the temperature of liquefaction, it is, I think, quite certain that cold solid rock is denser than hot melted rock; and no possible degree of rigidity in the crust could prevent it from breaking to pieces and sinking wholly below the liquid lava".

"And thrice he slew the slain"? The quotation may have been more apt than Lord Kelvin intended. For later during the feast the slain come back to plague the king, and Timotheus cries: "Those are Grecian ghosts, that in battle were slain, . . . behold how they toss their torches on high . . .".

Darwin himself seems to have been well enough convinced by Kelvin's persuasiveness[8]: "A third opinion, contended for by Sir William Thomson [Lord Kelvin], and of which I am myself an adherent, is that the earth is throughout a solid of great rigidity . . .". Thirty-one years later, when his paper was reprinted among his collected works, he wrote[9]: "The conclusions arrived at in my paper are absolutely inconsistent with the sensational speculations as to the causes and effects of the

(490)

glacial periods which some geologists have permitted themselves to make". Darwin remained on close terms with Kelvin, a friendship that had, in fact, begun with the selection of Kelvin by the Royal Society as referee for the paper here under discussion. An alternative derivation due to Kelvin is included as Appendix *C* to Darwin's paper. Kelvin, according to Darwin, "seemed to find that on these occasions the quickest way of coming to a decision was to talk over the subject with the author himself". Darwin considered that all his work on cosmogony "may be regarded as the scientific outcome of our conversations of the year 1877 ; but for me at least science in this case takes the second place".

I must refer to one more aspect of the Kelvin–Darwin discussion of polar wandering. Kelvin's arguments for a rigid Earth denied the possibility of polar wandering within the framework of Darwin's analysis. But this should not imply that Kelvin was opposed to shifting the pole over large distances. Far from it. In a passage often quoted by those who favour large polar displacements, Kelvin said[4] : "Considering, then, the great facts of the Himalayas and the Andes, and Africa and the depths of the Atlantic, and America and the depths of the Pacific, and Australia, and considering further the ellipticity of the equatorial section of the sea-level, estimated by Capt. Clarke at about 1/10 of the mean ellipticity of meridional sections of the sea level, we need no brush from the comet's tail (a wholly chimærical cause which can never have been put forward seriously except in ignorance of elementary dynamical principles) to account for a change in the earth's axis ; and we may not merely admit, but assert as highly probable, that the axis of maximum moment of inertia and the instantaneous axis of rotation, always very near one another, may have been in ancient times very far from their present geographical position, and may have gradually shifted through 10, 20, 30, 40, or more degrees without at any time any perceptible sudden disturbance of either land or water". These views were reprinted in Kelvin's "Collected Works"[10] in substantially their original form.

So far as I can see, Kelvin reasoned as follows : the surface of the Earth is divided into quadrants ; in the northern hemisphere a rise is centred at 0° longitude (say) and a fall at 180°, in the southern hemisphere a fall at 0° and a rise at 180°. For a maximum crustal displacement of 10 cm. the pole of a rigid earth is shifted by 0·1″. Then by what Kelvin calls a "simple effort of geological calculus" he finds that for a corresponding surface displacement by

10 km. the pole is moved through nearly 40° latitude. Kelvin had assumed the Earth to be sufficiently rigid to sustain a distortion commensurate with the dimensions of the equatorial bulge. Of course, this must lead to appreciable polar wandering, but it would seem to be the hard way of doing it.

We return to Darwin's solution (equation 2). It may have been noticed that the first terms in x and y have the dimensions length/(time)^2 instead of length. This is the result of a simple algebraic error made earlier in the derivation. The mistake was discovered by Lambert[11]; the corrected equations are given by Jeffreys[12]:

$$\begin{aligned} x &= \frac{\alpha\,(\omega^2 - \alpha^2)}{(\omega^2 + \alpha^2)^2}\,u - \frac{\omega^2}{\omega^2 + \alpha^2}\,ut \\ y &= -\frac{2\omega\alpha^2}{(\omega^2 + \alpha^2)^2}\,u + \frac{\omega\alpha}{\omega^2 + \alpha^2}\,ut \end{aligned} \qquad (5)$$

All terms now tend to zero as α becomes infinite. There can be no polar wandering no matter how fluid the Earth is. This conclusion contradicts the previous result (equation 4).

For simplicity we now restrict ourselves to the case $\alpha \ll \omega$. Equation (5) can then be written

$$x = (\alpha/\omega)\,(u/\omega) - ut, \qquad y = 0 \qquad (6)$$

The approximation $\alpha \ll \omega$ is amply justified by the observation that the damping of the free nutation requires many periods. Subject to the same assumptions and restrictions, I find, in an independent derivation,

$$x = (\alpha/\omega)\,(u/\omega) - ut - \tfrac{1}{2}\alpha ut^2, \qquad y = 0 \qquad (7)$$

The solutions differ by the term in t^2, and this term yields substantial polar wandering as a consequence of surprisingly small continental upheavals. Equation (7) has the pole move at a constant *acceleration* in response to a constant *velocity* of upheaval. Had Darwin chosen the simpler (and sufficient) example of a sudden vertical displacement, the result would have been a polar wandering at constant velocity. My solution agrees on all essential points with Gold's conclusions arrived at by non-analytical reasoning.

To point out the difference between Darwin's (corrected) solution, and Gold's conclusion, we must return to the basic considerations that underlie Gold's hypothesis. The pole of figure is a position where the axis of figure (about which the moment of inertia is a maximum) pierces the crust. For a rigid Earth the displacement of the pole of figure by

$x = -ut$, $y = 0$ is entirely determined by the prescribed upheaval. The pole of rotation circles the pole of figure once every ten months. In the case of a yielding Earth, there is an additional displacement of matter as the geoidal protuberance attempts to adjust to the disturbed position of the rotation axis. The total displacement of the pole of figure is then the sum of displacement of the geoidal pole and that determined by the prescribed upheaval. From dynamic considerations one finds that the velocity of the rotation pole is proportional to its separation from the pole of figure, and from elastic (or plastic) considerations that the velocity of the geoidal pole is proportional to its separation from the pole of rotation. It is, according to Gold[2], "as with the ass and the carrot hanging from a stick held by the rider". The geoidal pole pursues the rotation pole, the rotation pole pursues the pole of figure, which in turn is continuously being displaced by the geoidal pole.

Darwin's reasoning is implicit in his equations 1–4 (ref. 1, p. 282). The sum of the four equations is equivalent to the above-mentioned dynamic considerations. But equations (3) and (4) state that the geoidal pole moves at a rate proportional, not to its separation from the rotation pole, but to the separation of the rotation pole from the pole of figure. I cannot think of any reason for this type of behaviour ; it would be consistent, for example, with a stationary solution for a liquid, rotating Earth where the poles of figure and rotation are united, with the geoidal pole being elsewhere.

Darwin obtained his four equations from what he calls geometrical, rather than dynamical, considerations. The important thing is that they do not follow from a deductive argument, and he seems to have gone astray in the formulation of the last two equations. When these are modified in the above sense, then equations (7) follow once more. On the basis of the present development of the theory of elasticity, which was not available to Darwin, it is possible to proceed from fundamental principles to a solution without any break in the deductive argument, and this is, in fact, the method whereby equation (7) was derived.

We are left with three solutions : Darwin's original solution (2) made polar wandering possible ; the corrected solution (5) made it impossible ; and the modified solution (7) makes it easy. That the final outcome is not in contradiction to the original conclusion is a result of having made an even number of errors. But there is an important difference ; equation (2) requires a large value of α for polar wandering,

(493)

(7) does not, and is in fact based on the assumption that $\alpha \ll \omega$.

In the light of these developments, the many papers that have centred on Darwin's work assume grotesque proportions. Long before Darwin wrote, Comte de Buffon had founded the 'Catastrophic School' of polar wandering to account for palæoclimatic evidence. Darwin clearly hoped his paper would put certain restraints on contemporary arguments for polar wandering by Lubbock, Delabeck, Evans and others. In fact, it was followed by a renewed wave of enthusiasm for large polar displacements, which reached its peak in "Die Pendulations Theorie" of Reibisch and Simroth. Darwin's student, the astronomer Brown, countered these claims with apparent exasperation[13]: "[Darwin's] conclusion, now well known to astronomers, but frequently forgotten by geologists even at the present time is against any extensive wanderings of the pole during geological times". In 1914, Barrell[14] reviewed "The Status of Hypotheses of Polar Wanderings" as follows: "Geologists and biologists may array facts which suggest such hypotheses, but the testing of their possibility is really a problem of mathematics. . . . Notwithstanding this, a number of hypotheses concerning polar migration have been ingeniously elaborated and widely promulgated without their authors submitting them to these final tests. . . . Others, of more logical mind, recognizing the need of mathematical justification, have thought to find a qualified support in the work of Kelvin and G. H. Darwin. . . . The work of Darwin, instead of permitting hypotheses of polar wanderings, offers the most convincing proof which is available that migrations of the axis of the earth sufficiently extensive to be of geological importance have not occurred [*sic*]. . . . His [Darwin's] papers seem to have checked further speculation upon this subject in England, but, apparently unaware of its strictures, a number of continental geologists and biologists have carried forward these ideas of polar wandering to the present day. . . . Does not the history of the subject show the dangers of over-specialization within one division of science with the consequent putting forth of hypotheses regardless of the verdict of related Sciences ?"

In this controversy between physicists and geologists, the physicists, it would seem, have come out second best. They gave decisive reasons why polar wandering could not be true when it was weakly supported by palæoclimatic evidence ; and now that rather convincing palæomagnetic evidence has been discovered[15], they find equally decisive reasons why it could not be otherwise.

[1] Darwin, G. H., *Phil. Trans. Roy. Soc.*, Pt. 1. **167**, 271 (1877). Reprinted in "Scientific Papers", **3**, 1 (Cambridge, 1910).

[2] Gold, T., *Nature*, **175**, 526 (1955).

[3] Thomson. Sir W., and Tait, P. G., "Natural Philosophy", 1 (first edition), 702 (Oxford, 1867).

[4] Rep. Brit. Assoc. for the Adv. of Sci., 1–12 (1876).

[5] Barnard. J. G., *Smithsonian Contr. to Knowledge*, 240 (1871).

[6] Darwin, Charles, *Phil. Trans.*, **81** (1839).

[7] Darwin, Sir G., "Scientific Papers", **5**, xv (Cambridge, 1916).

[8] Darwin, Sir G., "Scientific Papers", **2**, 501 (Cambridge, 1908).

[9] Darwin, Sir G., "Scientific Papers", **3**, v (Cambridge, 1910).

[10] Thomson. Sir W., "Mathematical and Physical Papers", **3**, 333 (Cambridge, 1890).

[11] Lambert, W. D., *Bull. U.S. Nat. Res. Coun.*, No. 78, Chap. 16 (1931).

[12] Jeffreys, Sir H., "The Earth", 343 (Cambridge, 1952).

[13] Darwin, Sir G., "Scientific Papers", **5**, 37 (Cambridge, 1916).

[14] Barrell, J., *Science*, **40**, 333 (1914).

[15] Irving, E., thesis (Cambridge, 1954). Clegg, J. A., Almond, M., and Stubbs, P. H. S., *Phil. Mag.*, **45**, 583 (1954). Creer, K. M., thesis (Cambridge, 1955). Runcorn, S. K., "Adv. Phys.", **4**, 244 (1955).

Printed in Great Britain by Fisher, Knight & Co., Ltd., St. Albans.

Reprinted from: PROBLEMS IN CONTEMPORARY OPTICS
ISTITUTO NAZIONALE DI OTTICA, ARCETRI-FIRENZE - 1956 - Pgs. 575-584

A program of research in the visual detectability of distant objects (*)

S. Q. DUNTLEY and S. S. BALLARD
Scripps Institution of Oceanography - La Jolla, California

I. Introduction.

A new visual science has gradually evolved during the last fifteen years, and its present center of activity is located at a laboratory formed two years ago at the Scripps Institution of Oceanography of the University of California. The Visibility Laboratory, as it is known, is not really a new venture, but had its root in a succession of laboratories concerned with the same type of problems but under a variety of military and university sponsorships. During the post-war period, the work has been carried out at the Massachusetts Institute of Technology and at the University of Michigan besides the University of California. Throughout the period some of the same individuals, including the authors, have been associated with the work.

The new visual science concerns outdoor seeing, primarily from the standpoint of predicting the circumstances under which a given object can be seen at a given distance. Included are a wide variety of visual tasks: For example, the underwater breathing apparatus of Cousteau has made a new world of professional interest accessible to the staff of the Scripps Institution of Oceanography, and underwater visibility is a topic of great current interest to its fa-

---

(*) - Contribution from the Scripps Institution of Oceanography, University of California, N. 851 (New Series). This work represents results of research carried out for the Bureau of Ships, U. S. Navy, under contract with the University of California.

Reproduced by Permission

culty and students. Visibility at sea, both from the surface and from the air, plays a part in oceanography. The converse problem of the visibility of clouds, aircraft, and other objects aloft is a natural extension of Scripps interest, and all of these problems take on new and interesting aspects during twilight and at night. The visibility of lights at sea is one of the oldest practical visibility problems, and much of the pioneering work in this field was done by the various light-house services throughout the world.

II. Basic philosophy.

In order to determine how far one can follow visually a receding object it would seem a simple matter to try the experiment, and indeed this is so if the investigator has no interest beyond that particular observation. If he wishes, however, to use this test as a basis for making a general statement concerning the distances to which objects can be followed by eye, he is immediately drawn into the problem of specifying the conditions under which the observation is made, and also into the need for predicting the allowances which must be made where atmospheric and lighting conditions differ from those of the experiments. The task of documenting (a) the optical nature of the target including its lighting, (b) the atmosphere through which the image must be transmitted, and (c) the characteristics of the observer, is a formidable and intricate one. It can be accomplished only with a great deal of preparation and at considerable expense. It is more attractive, therefore, to measure representative lighting and atmospheric conditions; to measure such optical properties of the target as its reflectance, its gloss, its size, its shape; to measure the pertinent properties of the human observer; and to combine these elements by calculation.

III. Data required.

Figure 1 shows diagrammatically the essential elements involved in seeing a distant object. The object has a size, a shape, a color, a gloss, a pattern of highlights and shadows, and perhaps an inherent self-luminosity. It is illuminated by light from the sun, the moon, the stars, the sky, the ground, and other elements of its surroundings, and also, at times, by artificial sources such as searchlights. It is seen against a background which may be terrestrial or may be some aspect of the sky or of the atmosphere behind the object. Sufficient data on all of these items must be had in order that the inherent contrast of the object against its background can be calculated. The image-forming light preceding toward the observer from the object constitutes a complex optical presentation which is attenuated in its passage through the atmosphere, its information content sometimes being reduced by atmospheric inhomogeneities which give rise to effects described by the names « shimmer » or « boil ».

In traversing the atmosphere, each image-forming light beam experiences scattering, for the aerosol is composed of air molecules, water droplets, dust particles, insects, and other optical inhomogeneities. Any part of the light from the object which experiences scattering on a magnitude sufficient to direct it outside of its normal path from the object to the proper retinal element of the observer's eye is lost, in so far as the optical image is concerned. Light from the object is attenuated in every unit length of the path between the object and the observer by absorption (conversion into heat) or by the scattering processes just mentioned. Concurrently, however, each unit length of the path scatters light toward the observer, for the path is irradiated in a complex manner by the sun, the sky, and/or parts of its environment. It is axiomatic that at some level of apparent object luminance the attenuation in any given element of the path will be exactly balanced by the daylight scattered toward the observer by the path element. There is thus an *equilibrium luminance* which will be transmitted unchanged by the unit path in question. This situation is illustrated in Figure 2.

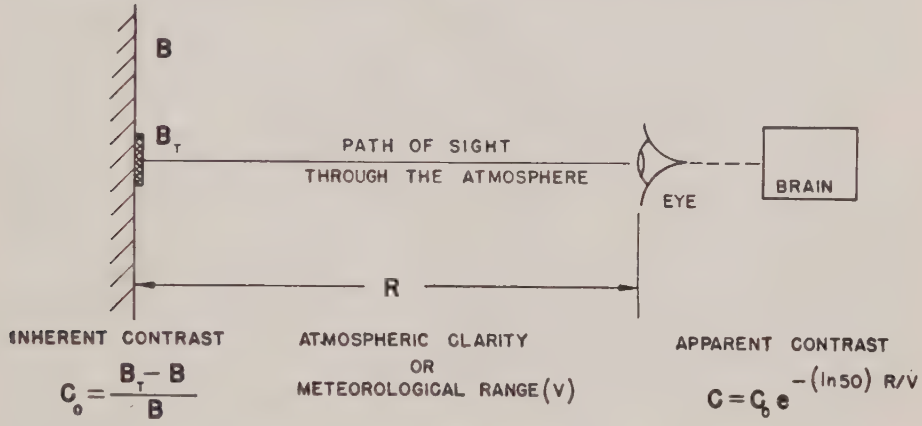

Fig. 1
Basic elements in the visibility of a distant object.

The apparent luminance of the brighter parts of the object will be reduced by the path element, whereas darker parts of the object will experience an apparent increase in luminance. Thus the apparent luminance of all parts of the object changes toward the equilibrium luminance, and the apparent contrast of the object is reduced. When the path of sight is optically homogenous, as it often is when looking out over the surface of the sea in the absence of cloud shadows, the reduction of contrast is a simple exponential and the only datum needed to specify it is a simple attenuation coefficient: this coefficient is identical with the one which would govern the attenuation of a beam of light through an otherwise unlighted atmosphere. Under more complicated circumstances, such as long inclined paths of sight through regions of cloud shadows or through haze patches, the attenuation is not such a simple function of distance, but the underlying principles are unchanged; - more data are needed but sufficient data can always be found to describe actual contrast attenuation.

The eye of the observer receives the attenuated information, and his limiting performance can be calculated only if his contrast threshold for the particular visual task at hand is known. It was discovered early in our work that the visual threshold of the eye itself is remarkably consistent from moment to moment and from day to day. This is not true of the awareness of the brain; the conscious reactions of the observer will depend upon many factors and circumstances in addition to the primary optical phenomena just discussed. Several years of study, particularly by our colleague Professor H. Richard Blackwell at the University of Michigan, have produced a background of information (¹) concerning the performance of the visual mechanism and the allowances which must be made for certain types of environmental and emotional circumstances. Contrast threshold data particularly for targets uniformly brighter or uniformly darker than their background, have been published for targets of all sizes and of many shapes, and under con-

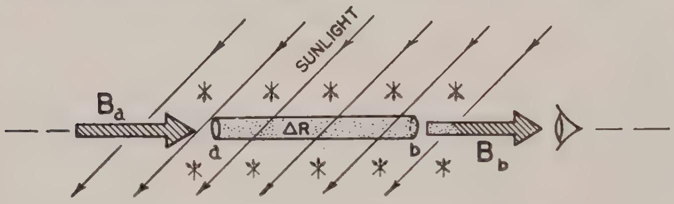

$B_b = B_a$ — LOSS DUE TO SCATTERING AND ABSORPTION

+ GAIN DUE TO SCATTERED DAYLIGHT

WHEN LOSS = GAIN, $B_b = B_a$; (EQUILIBRIUM LUMINANCE).

Fig. 2
The optical processes within the atmosphere.

(¹) - H. R. **Blackwell**, Journal of the Optical Society of America, *36*, No. 11, 624-643, November, (1946).
H. R. **Blackwell**, Illuminating Engineering, *47*, No. 11, 602-609, November (1952).

ditions ranging from brightest day to darkest night, and for observing times from several minutes down to a millisecond. Automatic laboratory equipment (²) for presenting test objects and for performing statistical analysis of observer responses has been evolved and has enabled pertinent visual data to be accumulated rapidly. This work still continues, and there are many gaps, one of the most important being the lack of information concerning targets having major portions brighter than the background and other major portions darker than the background.

IV. Practical utilization of the data.

The combination of physical data with visual data is rendered difficult because the observer's threshold of apparent contrast depends upon the angular size of the target, which in turn depends upon the distance reciprocally and linearly. The apparent contrast of the object, as we have seen, is also affected by distance, but in an exponential fashion.

The problem is best solved graphically by means of alignment diagrams or nomographs. Samples of the earliest of these, produced over a decade ago, are shown in Figures 3 and 4. Of such charts, one of the partecipating scientists, Professor Arthur C. Hardy, wrote in part: « For thousands of years, thousands of mariners have sighted thousands of ships, and have made appropriate entries in their logs. Even so, this mass of miscellaneous information is of little use in predicting the range at which a specified object will be just visible under a new set of circumstances. The .... charts .... enable the limiting range to be found under any set of prevailing conditions (³).

One interesting property of this chart is its ability to predict the performance of telescope-aided vision. In the final analysis, the function of a telescope (such as the common «binoculars») is to increase the apparent angle subtended by the object at the eye of the observer, which is equivalent to having the object physically larger. By the simple device of endowing the object with a fictitious area M^2 times as great as the area of the object itself, where M is the angular magnification of the telescope, the nomograph makes possible the prediction of the range at which the object will be seen through any perfect telescope. Actually, no telescope is perfect, for there is a loss of light and a loss of contrast due both to stray light and to aberrations. Quantitative allowances for the effect of these losses can be made by using the measured optical properties of the telescope.

(²) - H. R. Blackwell, B. S. Pritchard and J. G. Ohmart, Journal of the Optical Society of America, *44*, No. 4, 322-326, April, (1954).

(³) - S. Q. Duntley, Journal of the Optical Society of America, *38*, No. 3. 237, March, (1948).

It is interesting to compute, with the aid of the nomograph, how much magnification is required in an optical instrument to restore naked-eye capabilities, i.e., to compensate for the unavoidable amounts of stray light, luminance loss, and image quality deterioration produced by the instrument. It is found, for example, for systems like telescopes, periscopes, or rangefinders, that an angular magnification of the order of 1.3 to 1.5 is necessary to restore naked-eye seeing capabilities.

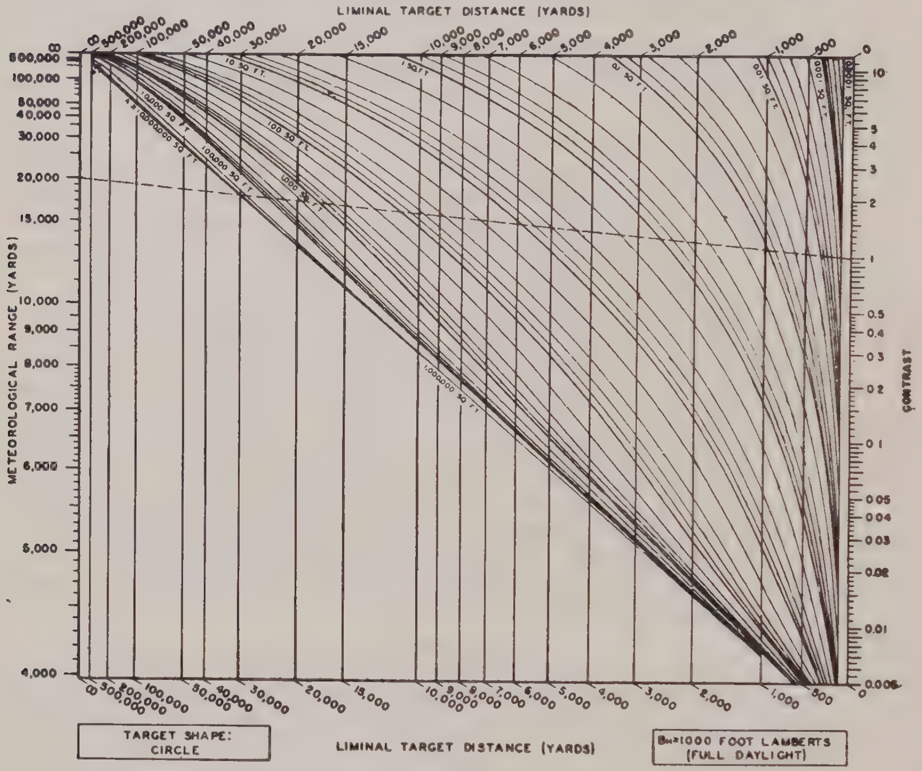

Fig. 3

A visibility nomograph for adaptation to full daylight, of luminance 1,000 foot-lamberts. The dashed line shows the set-up for determining that on a day when the meteorological range is 20,000 yards, a uniformly bright circular object of projected area 100 square feet and of inherent contrast (either positive or negative) of 0,99 can be detected at a maximum range of 11,000 yards.

V. *Field checks.*

One of the questions which is always raised by those who hear of these prediction techniques for the first time concerns the applicability of visual thresholds measured in the laboratory to outdoor seeing conditions in the real world where the scene is complex, the backgrounds are never uniform, and there are many distractions and small motions within the field of vision. In answer to this question, Professor Blackwell has conducted some very thorough experiments in which observers whose laboratory thresholds were well known performed full scale out-of-door experiments employing psychophysical techniques identical with those of the laboratory experiments but using targets that were miles distant. The results show that laboratory thresholds are indeed identical with those measured out-of-doors and represent, therefore, basic properties of the visual mechanism.

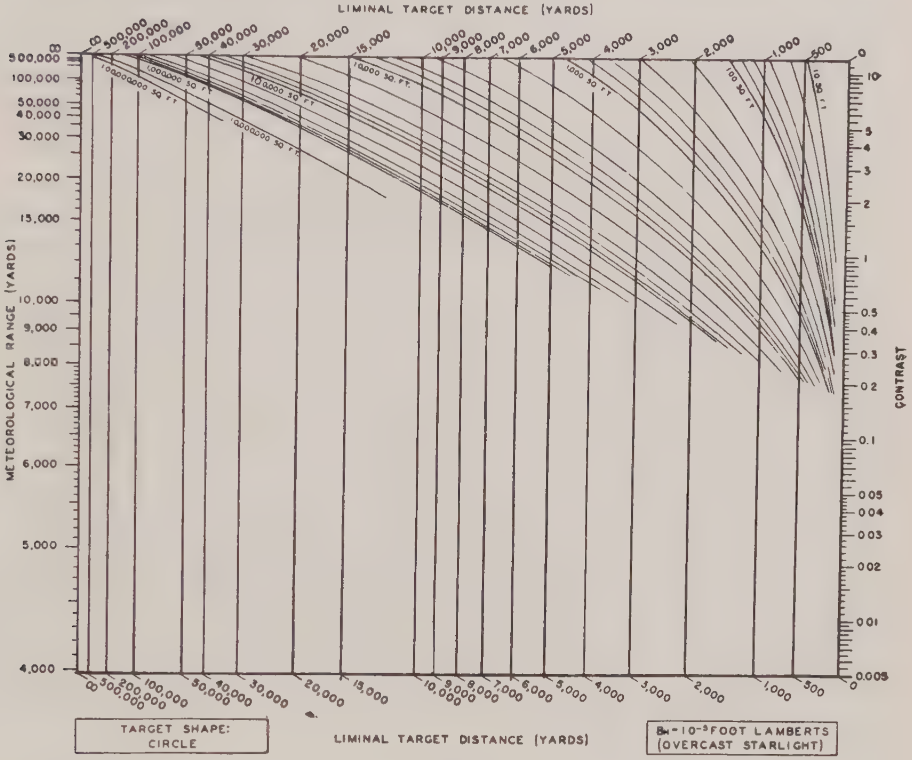

Fig. 4
A visibility nomograph for adaptation to overcast starlight (astronomical twilight), luminance 10^{-5} foot-lamberts.

Numerous field checks have been made of the ranges predicted by the nomograph charts, the most elaborate of these having been performed at sea, using both naked-eye vision and vision aided by telescopes.

VI. Current research.

The Scripps Institution of Oceanography is broadly concerned with the geophysical properties of the ocean of water and of the overlying ocean of air. The penetration of both these oceans by solar energy is a matter of basic interest, for the sun is the primary source of energy which supports life in the sea. No complete understanding of marine ecology is possible without knowledge of the permeation of the oceans by solar energy, and such knowledge is a necessary, but not sufficient, requirement for visibility calculations. The Visibility Laboratory is engaged, therefore, in a broad program of theoretical and experimental work aimed at both solar permeation and image transmission phenomena within both the ocean of air and the ocean of water.

The experimental aspects of the atmospheric program center about a large airplane which has been fitted out as flying laboratory from which the properties of the light field, the attenuation coefficient, the polar scattering diagram, and other optical and meteorological information is measured. Research in the ocean of water is made possible through the use of one or more of the five sea-going research vessels in the service of the Scripps Institution. Photoelectric underwater photometers are used for most of the work at sea, and these obtain optical data similar to those taken aloft by the airplane. It is significant that the same basic structure of differential and integral equations which describe the transmission of flux and images by the atmosphere apply also to the corresponding transmissions by the sea. This duality of media, having widely different physical properties but conforming to the same basic equations, places the experimental and theoretical program of our laboratory on an unusually favorable interlocking basis, for every optical phenomenon in the ocean has its counterpart in the atmosphere.

VII. A continuing program.

This new visual science has grown slowly over the several years, the major efforts, by far, having been devoted to creating the methods required and obtaining the data needed. By-products of several kinds have assisted in keeping the program alive and growing, and today the level of activity is higher than ever before. We expect henceforth to reap the rewards of the years of patient research and to continue the exploration of the optical phenomena of the air and water environments around us.

For example, little quantitative information is available concerning the penetration of sunlight into the sea when the sun is low in the sky and the sea is roughened by wind. This condition prevails over vast areas of the northern and southern oceans, and the budget of life-giving solar energy must drastically affect the marine productivity of these seas. Our efforts to develop a rigorous theory for this problem are based upon the result of previous researches on the statistical distribution of water wave slopes (4). It appears that we may have been successful, and a field expedition has been performing critical tests of our equations throughout the past summer.

An interesting example of a visibility range problem occurs in oceanography in connection with the widely accepted method for measuring the clarity of ocean water. This method, attributed to Secchi, consists of lowering into the sea a small white disk at the end of a line and noting the distance at which it disappears from view. Any valid calculation of the depth at which this will occur demonstrates the wide variety of intricate factors involved, and will convince even the most skeptical that the uncontrolled and casual use of the Secchi disk will produce data having little if any valid meaning. The Visibility Laboratory has, for some time, replaced the extinction type of measurement proposed by Secchi with a photometric type of device, and it is our hope that oceanographers generally will soon demand such truly valid optical techniques.

Research in the visual detectability of distant objects will not be completely solved by studies of the environment alone. Many properties of the human visual mechanism still await investigation. Outstanding among these is the very common practical problem of the visual threshold for objects of mixed contrast, i. e., objects having major portions brighter than the background and still other areas darker than the surroundings. When such an object subtends a very small visual angle only the integrated contrast matters; at very large subtense the visual detectability of pattern elements may be considered separately. At intermediate angular sizes, the eye provides a unique and reproducible detection threshold but we do not know how to predict it or how to measure it in generalizable terms. It is our firm conviction that this condition will not long prevail in the face of the research effort now being directed against it.

---

(4) - S. Q. Duntley, *Measurements of the Distribution of Water Wave Slopes.* Journal of the Optical Society of America, *44*, No. 7, 574, July, (1954).

Reproduced by Permission

Reprinted from Journal of Bacteriology
Vol. 71, No. 6, pp. 668-672, June, 1956
Printed in U.S.A.

EFFECT OF HYDROSTATIC PRESSURE ON THE SUCCINIC DEHYDROGENASE SYSTEM IN ESCHERICHIA COLI[1]

RICHARD Y. MORITA[2] AND CLAUDE E. ZOBELL

Division of Microbiology, Scripps Institution of Oceanography, University of California, La Jolla, California

Received for publication October 21, 1955

Hydrostatic pressures of the order prevailing in the deep sea (up to about 1100 atm) have been found to affect the viability, reproduction, and metabolic reaction rates of microorganisms in different ways. Certain processes are accelerated whereas others are retarded by compression. Some of these differences appear to be inherent in the protoplasm or enzymes of organisms as a function of the pressure of their habitats. Certain bacteria from the deep sea, for example (ZoBell, 1952), tolerate or actually require much higher pressures than microorganisms whose normal habitat is near 1 atm (ZoBell and Johnson, 1949).

A rational explanation of how pressure may affect biological processes is complicated by the fact that compression appears to act differently upon diverse reactions catalyzed by the same cells. For example, we find the activity of aspartase of washed cells of *Escherichia coli* to be accelerated by compression up to 680 atm, but retarded by higher pressures and stopped at 1000 atm, ostensibly owing to the inactivation of the enzyme (ZoBell and Morita, 1954). On the other hand, the activity of succinic dehydrogenase from *E. coli* appears to be retarded by a pressure of only 200 atm. Observations described in this paper indicate that the succinic dehydrogenase system in *E. coli* is inactivated by moderate pressures.

MATERIALS AND METHODS

Preparation of cells. Cells of *E. coli* were grown in a 5-gallon carboy containing 14 L of nutrient medium: glucose, 2.0 g; KH_2PO_4 2 g; K_2HPO_4, 5 g; peptone (Difco), 3 g; yeast extract (Difco), 1 g; distilled water, 1,000 ml. Following sterilization in the autoclave the pH of the medium was 7.0. It was inoculated with 1.4 L of similar medium in which *E. coli* had developed for 24 hours During the succeeding 18-hour incubation period at 22 C, the inoculated medium was agitated with filtered sterile air. Foaming was prevented by adding 0.2 g of Dow Corning AF Antifoam emulsion.

The cells were harvested in a Sharples supercentrifuge (ca 23,000 rpm), suspended in 15 L of ice cold (ca 4 C) water, and recentrifuged. The washed cells were lyophilized (−70 C at 300 μ Hg) and stored in a refrigerator over "Ascarite" *in vacuo* at 4 C.

Such lyophilized cells represent the "biological whole", a known quantity of which was used in each experiment.

Pressurization of material. Immediately prior to each series of experiments, sufficient quantities of lyophilized cells were weighed out to give 2 mg per ml in M/15 phosphate buffer (pH 7.0) solution in which they were evenly suspended. Equal aliquots of the cell suspension were pipetted into small (10 by 75 mm) test tubes. The latter were filled to capacity and closed with No. 000 neoprene stoppers, care being exercised to exclude air. The stoppered tubes were transferred at once to pressure vessels filled with hydraulic fluid equilibrated to the desired temperature in water baths. Pressure was applied for various periods of time by procedure described by ZoBell and Oppenheimer (1950).

Methylene blue reduction measurement. The Thunberg technique, described by Umbreit *et al.* (1949), was employed to measure dehydrogenase activity with methylene blue as the hydrogen acceptor. Elongated Thunberg tubes, 1.5 cm in diameter and 25 cm long, circumvented premature mixing of the bacterial suspension (in side arm) with the methylene blue succinate buffer mixture during evacuation of air, which resulted in some ebullience. In each tube was

---

[1] Contribution from the Scripps Institution of Oceanography, New Series, No. 852. This paper represents results of research carried out by the University of California under contract with the Office of Naval Research, N6onr-275(18).

[2] Present address: Department of Biology, University of Houston, Houston, Texas.

TABLE 1

Micrograms methylene blue reduced at 30 C in presence of succinate by 2 mg of lyophilized cells of E. coli stored at 5 C in vacuo

Reaction Time	7 Days' Storage	18 Days' Storage	33 Days' Storage
min	*μg*	*μg*	*μg*
0	0	0	0
3	21.2	10.3	2.9
6	34.9	16.3	6.6
9	54.3	23.2	8.6
12	76.4	32.2	8.9
15	92.9	44.6	10.3
18	108.4	52.6	12.0
21		62.9	15.2
24		74.6	17.2
27		85.2	18.0
30		99.2	19.0

placed 1 ml of 1:10,000 (0.000267 M) methylene blue, 2 ml of M/50 sodium succinate (freshly prepared for each experiment), and 2 ml of M/15 phosphate buffer (pH 7.0). In endogenous controls distilled water was substituted for the sodium succinate solution. After evacuating the air from each assembled Thunberg tube with a Cenco-Megavac pump, the tube was filled with CP nitrogen. The nitrogen was passed through a Deoxo catalytic unit to remove oxygen. Prior to adding the lyophilized cells, all solutions were boiled to exclude oxygen and cooled to 4 C. Spot tests on solutions and cell suspensions showed that in no stage of the experiments was the oxygen content as much as 0.1 ppm.

In the side arm of each tube was placed 1.0 ml of bacterial suspension (2 mg of lyophilized cells) that had been treated with different pressures at definite temperatures as indicated. The assembled Thunberg tubes were again evacuated, filled with oxygen-free nitrogen, and equilibrated in a water bath at 30 C before mixing the contents. In order to obtain comparable results in all experiments, the cells were mixed with the methylene blue-succinate buffer mixture exactly 30 minutes after they were depressurized. It would have been desirable to mix immediately after depressurization, because there may have been some regeneration or reversible recovery of dehydrogenase during this period, but it required about 30 minutes to make the necessary manipulations, including temperature-pressure equilibration of the system. As pointed out by Johnson *et al.* (1954), the effects of moderate pressures are frequently reversible, sometimes quantitatively so, as soon as pressure is released.

The amount of methylene blue reduced at intervals of 3 minutes following its mixing with the cells was determined with a Klett-Summerson photoelectric colorimeter connected to a Sola Type CVH constant voltage transformer (115 v, 1.04 amp). The zero setting was made with distilled water in a Klett tube employing a red filter (640–700 mμ). Since the Klett-Summerson potentiometer scale is logarithmic, the amount of methylene blue reduced is proportional to the Klett reading. By subtracting the Klett reading at various time intervals from the initial Klett reading, the amount of methylene blue reduced could be determined.

RESULTS

Lyophilized cells of *E. coli* undergo a gradual loss of succinic dehydrogenase activity during storage, even when refrigerated, as illustrated by the data in table 1. Consequently, it was necessary to compromise between performing all of the experiments with the same lot of lyophilized cells of increasing age and decreased activity or employing freshly prepared lots of lyophilized cells. It required about a week to prepare and standardize the cells for an experiment.

From 6 to 10 times as much methylene blue was reduced by lyophilized *E. coli* cells in the presence of succinate as by the endogenous controls without added succinate (table 2). The accelerating rate of methylene blue reduction by

TABLE 2

Micrograms methylene blue reduced by 2 mg lyophilized (9-day) cells of E. coli following 4 hours' pressurization at 30 C

Reaction Time	Treated at 1 atm		Treated at 600 atm	
	Endogenous control	With added succinate	Endogenous control	With added succinate
min	*μg*	*μg*	*μg*	*μg*
0	0	0	0	0
3	1.7	16.6	1.2	4.9
6	3.9	29.7	2.5	11.4
9	5.4	46.9	3.8	18.6
12	7.2	63.2	5.1	26.0
15	8.7	82.4	6.3	38.5
18	10.0	97.8	8.6	51.7

pressure treated cells in the presence of succinate may be due to the regeneration of succinic dehydrogenase that catalyzes the reaction:

$$\mathrm{HOOC{\cdot}CH_2{\cdot}CH_2{\cdot}COOH + MB \rightarrow HOOC{\cdot}CH{=}CH{\cdot}COOH + MB{-}H_2}$$

or the accelerating rate may be due to some other protoplasmic factor that is not understood. Since the "biological whole" was used in the experiments, the reactions were carried out anaerobically to render them independent of the action of cytochrome oxidase. The rate of acceleration with increasing reaction time was greater but the total amount of methylene blue reduced was less with lyophilized cells previously compressed at 600 atm for 4 hours.

The inactivation of succinic dehydrogenase was found to be progressively greater as the pressure was increased (figure 1). After 4 hours at 1000 atm virtually all of the succinic dehydrogenase appeared to be irreversibly inactivated. Little more methylene blue was reduced by such pressurized cells than by the endogenous controls. Pressures up to 1000 atm had little demonstrable effect on the endogenous activity at 30 C.

There is no indication that the loss of viability is responsible for the observed decreases in succinic dehydrogenase activity of cells that had been subjected to high pressure for short periods of time. The pressurized cells were found by phase microscope examination to be actively motile and morphologically normal in appearance. However, there was some diminution in the number of cells that could be demonstrated by plating procedures following compression of cell suspensions. This diminution in the number of colonies is believed to be due primarily to the clumping of cells caused by high pressure rather than due to the loss of viability. Few bacteria are killed by short exposure to moderate pressures, although a good many common forms gradually lose their viability when held for a few days at 400 to 1000 atm. ZoBell and Johnson (1949) have reported the survival of *E. coli* cultures for 2 days at 600 atm and 30 C; good growth at 600 atm and 40 C.

The effect of hydrostatic pressure on biological systems is a function of temperature. In general, the adverse effects of pressure on the viability of bacteria in nutrient media are more pronounced at low temperatures, say 0 to 20 C, than at the ordinary optimum, say 20 to 40 C, of the organisms. The optimum temperature or even the thermal death point for certain bacteria may be increased temporarily by a few

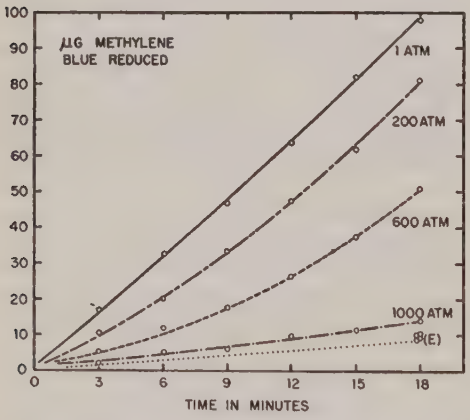

Figure 1. Micrograms of methylene blue reduced at 30 C after different periods of time by 2 mg of lyophilized (9-day) cells of *E. coli* which 30 minutes previously had been subjected to pressures of 1, 200, 600, or 1,000 atm for 4 hours at 30 C. The upper four curves represent activity with succinate as the hydrogen donor; the dotted line (*E*) at the bottom represents endogenous activity with no succinate added.

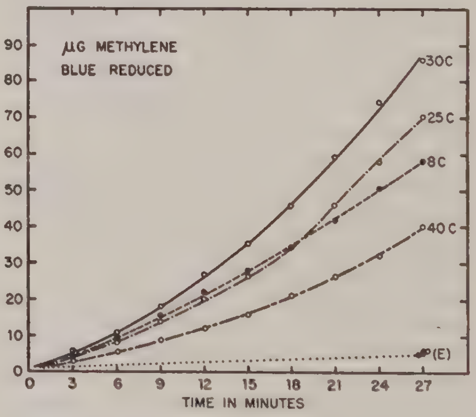

Figure 2. Micrograms of methylene blue reduced at 30 C after different periods of time by 2 mg of lyophilized (10-day) cells of *E. coli* which 30 minutes previously had been subjected to a pressure of 600 atm for 4 hours at 8, 25, 30, or 40 C. The upper four curves represent activity with succinate as the hydrogen donor; the dotted line (*E*) at the bottom represents endogenous activity with no succinate added.

TABLE 3

Micrograms methylene blue reduced at 30 C in presence of succinate by 2 mg of lyophilized (22-day) cells of E. coli previously pressurized for different periods of time at 600 atm and 30 C

Reaction Time	Period of Time Held at 600 atm		
	0 hours	1 hour	3 hours
min	*μg*	*μg*	*μg*
0	0	0	0
3	9.8	8.0	3.8
6	19.6	16.4	9.6
9	29.4	24.5	12.4
12	38.1	31.3	14.5
15	47.9	39.6	17.4

degrees during incubation at high hydrostatic pressure, but the adverse effects of pressure are aggravated by temperatures considerably in excess of the optimum of the organisms for reproduction. Similarly, the succinic dehydrogenase system of *E. coli* was found to be adversely affected by prolonged compression at temperatures that are either lower or higher than the optimum (30 C) of this strain for reproduction. During 4 hours' compression at 600 atm its succinic dehydrogenase system was inactivated more at 40 C or at 8 C than at 30 C (figure 2). Neither the rate nor the amount of endogenous activity, as indicated by methylene blue reduction in controls to which no succinate was added, was detectably affected by the temperature during 4 hours' compression at 600 atm.

The inactivation of succinic dehydrogenase increases with duration of compression. In a representative experiment (table 3) lyophilized *E. coli* cells held for 3 hours at 600 atm reduced only about half as much methylene blue as similar cells held for only 1 hour at this pressure.

DISCUSSION

Although many more observations must be made to ascertain whether the effects of hydrostatic pressure are direct or indirect, our experimental data demonstrate that moderate pressures inactivate the succinic dehydrogenase system of *E. coli*. The progressive inactivation of the succinic dehydrogenase system with time of compression makes extremely difficult any appraisal of the effects of pressure on the rate at which this enzyme system catalyzes the oxidation of succinic acid to fumaric acid in the presence of methylene blue.

According to Borrowman (1950), pressures up to 700 atm at 30 C had no effect on the rate of formic dehydrogenase activity of *E. coli* during an experimental period of 12 to 30 minutes in a pressure vessel equipped with optical windows through which methylene blue reduction could be observed. Since formic dehydrogenase, unlike succinic dehydrogenase, is a relatively stable enzyme, Borrowman heated the cells to 65 C for 5 minutes in order to denature as many interfering enzymes as possible. This is another example of different responses of enzyme systems to pressurization, perhaps attributable in part to intrinsic differences in the pressure tolerance of the enzyme system and possibly in part to differences in experimental conditions. Pressure tolerances and effects are dependent not only upon temperature and time; they are also influenced by gas tension, pH, osmotic pressure, chemical composition of the medium (Johnson *et al.*, 1954), and by other environmental factors.

Stadie and Haugaard (1945) reported the irreversible inactivation of succinic dehydrogenase system in rat tissues by 2 to 4 hours' exposure to 7 atm of oxygen. Haugaard (1946) attributed the inactivation to the oxidation of the SH group. Owing to the inactivation of succinic dehydrogenase by oxidation, particularly at high pressures, we endeavored to exclude free oxygen during the critical stages of our experiments.

SUMMARY

Employing methylene blue as the hydrogen acceptor, it has been demonstrated that the succinic dehydrogenase system associated with "biological whole" lyophilized cells of *Escherichia coli* is inactivated by moderate hydrostatic pressures.

There was some inactivation of the succinic dehydrogenase of *E. coli* at 200 atm at 30 C. The amount of inactivation increased progressively with time of compression. Approximately half of the enzyme system was inactivated after 4 hours at 600 atm and virtually all was irreversibly inactivated after 4 hours at 1000 atm.

The inactivating effects of pressure were most pronounced at temperatures either above (40 C) or below (8 C) the organism's optimum (30 C) for multiplication.

REFERENCES

BORROWMAN, S. R. 1950 Kinetics of the formic dehydrogenase system. Doctorate Dissertation, University of Utah.

HAUGAARD, N. 1946 Oxygen poisoning. XI. The relation between inactivation of enzymes by oxygen and essential sulfhydryl groups. J. Biol. Chem., **164**, 265–270.

JOHNSON, F. H., EYRING, H. AND POLISSAR, M. J. 1954 *The kinetic basis of molecular biology.* John Wiley & Sons, Inc., New York.

STADIE, W. C. AND HAUGAARD, N. 1945 Oxygen poisoning. VII. The effect of high oxygen pressure upon enzymes: succinic dehydrogenase and cytochrome oxidase. J. Biol. Chem., **161**, 153–174.

UMBREIT, W. W., BURRIS, R. H. AND STAUFFER, J. F. 1949 *Manometric techniques and tissue metabolism.* Burgess Pub. Co., Minneapolis,

ZOBELL, C. E. 1952 Bacterial life in the bottom of the Philippine Trench. Science, **115**, 507–508.

ZOBELL, C. E. AND JOHNSON, F. H. 1949 The influence of hydrostatic pressure on the growth and viability of terrestrial and marine bacteria. J. Bacteriol., **57**, 179–189.

ZOBELL, C. E. AND MORITA, R. Y. 1954 Effects of high hydrostatic pressure on physiological activities of marine microorganisms. O.N.R. Progress Report, No. 7.

ZOBELL, C. E. AND OPPENHEIMER, C. H. 1950 Some effects of hydrostatic pressure on the multiplication and morphology of marine bacteria. J. Bacteriol., **60**, 771–781.

(512)

Periodic variation of sea level induced by equatorial waves in the easterlies

GORDON W. GROVES

(*Received* 26 *March*, 1956)

Abstract—Sea-level observations at Canton Island show a regular four-day oscillation which is related to the passage of equatorial waves in the easterly winds over the island. Visual sea-level observations at Ocean Island show evidence of the same phenomenon. Records from tide gauges situated on other nearby islands show no such regular record. This gives an indication of the geographical extent of the perturbation of sea level.

INTRODUCTION

DURING a study of the day to day variation of sea level simultaneous tide records throughout a three-month interval from most of the permanent tide gauges maintained by the U.S. Coast and Geodetic Survey in the Pacific were examined (GROVES, 1956). Typical values of the root mean square deviation from the mean of these records (for spectral components having periods between two days and a week) are about 5 or 10 cm. The direct effect of the atmospheric pressure according to the " inverted barometer " law accounts for 50% to 75% of the activity in these periods.

At Canton Island, the three-month record showed a very regular oscillation which was coherent for 23 consecutive periods (Fig. 1). The amplitude (half the range) was about 3 cm on the average, and the period was 3·84 ± 0·02 days. The study was subsequently extended for 16 additional months, and during that time the oscillation was not as regular as in the original three-month record. Nevertheless, a prominent four-day oscillation was often present.

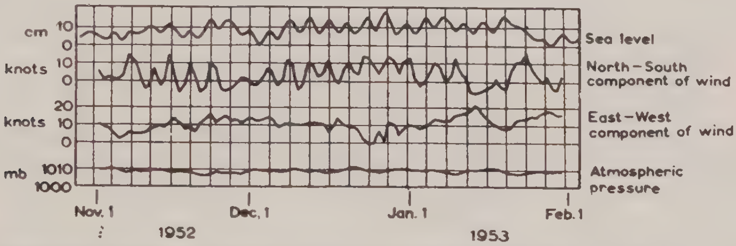

Fig. 1. Simultaneous records of sea level, surface atmospheric pressure and surface wind at Canton Island. The sea-level record is from position " *A* " (see Fig. 4). The wind and pressure records consist of (centred) averages of the eight observations made each day at three-hour intervals. The vertical lines in the figure are spaced every 3·84 days to demonstrate the remarkable coherence of phase throughout many cycles of the oscillation.

Sea-level records based on visual tide-staff observations were obtained from Ocean Island, Butaritari, and Tarawa (Fig. 2). There appears to be considerable three-to four-day activity in the Ocean Island record which may be related to the waves in the easterlies. The records from Butaritari and Tarawa appear much more irregular. At all other locations indicated by black dots in Fig. 3, there was no striking three- or four-day oscillation noted.

Contributions from the Scripps Institution of Oceanography, New Series, No. 853

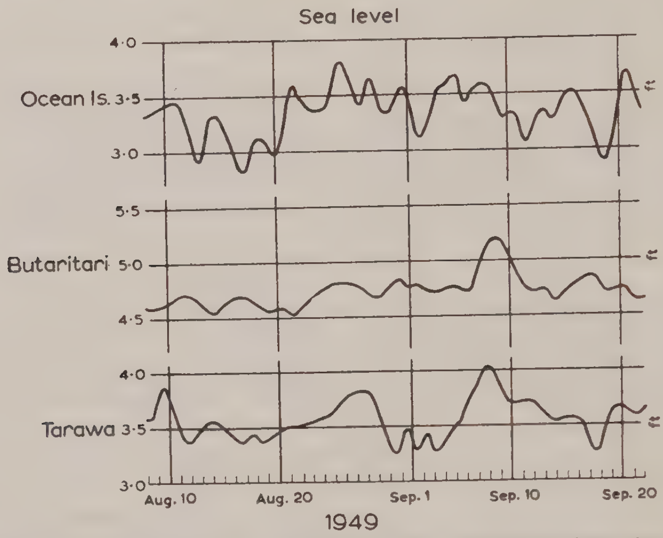

Fig. 2. Sea-level records at Ocean Island, Butaritari and Tarawa deduced from visual (tide staff observations.

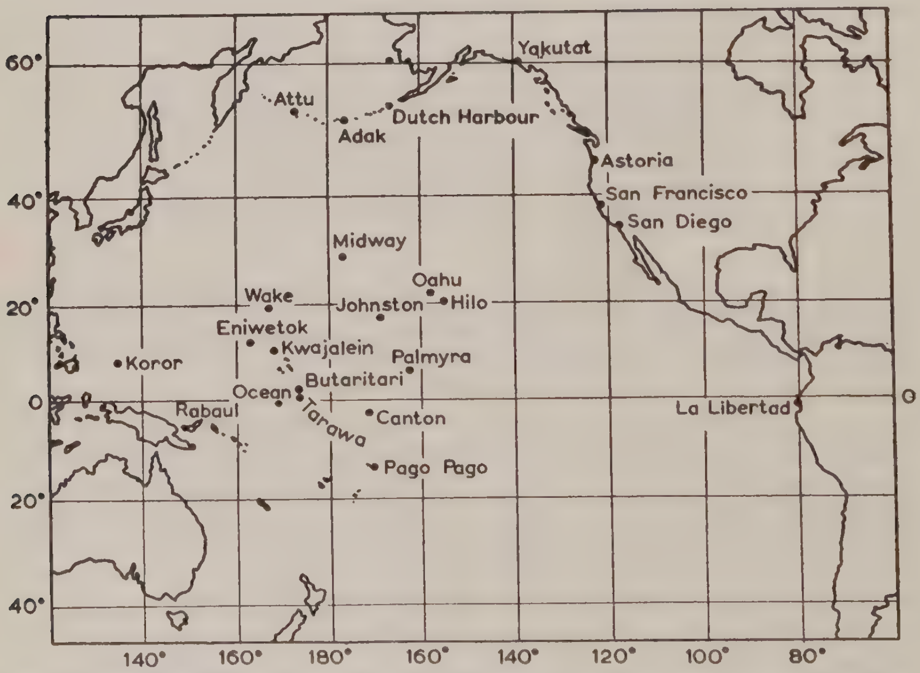
60°
40°
20°
0
20°
40°
140°
160°
180°
160°
140°
120°
100°
80°
0
Yakutat
Attu
Adak
Dutch Harbour
Astoria
San Francisco
San Diego
Midway
Oahu
Wake
Johnston
Hilo
Eniwetok
Kwajalein
Koror
Palmyra
Butaritari
Ocean
Rabaul
Tarawa
Canton
La Libertad
Pago Pago

Fig. 3. Map of Pacific Ocean area. Black dots indicate most of the places from which sea-level records in the Pacific area were studied.

THE SEA-LEVEL RECORDS

The diurnal and semidiurnal tidal constituents were eliminated from the tide-gauge data of Fig. 1 by taking appropriate weighted averages of the hourly tidal heights. The symbol C_{51} merely designates a particular weighted average used in this study, and the method has been described (GROVES, 1955). The effect has been essentially to eliminate all components whose periods are less than 24 hours while retaining those of longer periods (i.e., a low pass filter), and the result can be conveniently referred to as " sea level."

The tide gauge from which the sea-level record of Fig. 1 was obtained is located within the lagoon of Canton Island at position " *A* " (Fig. 4). This lagoon is very large and communicates with the ocean only through two very small channels. However, a tide gauge was installed outside of the reef at position " *B* " in November, 1955, and a comparison of the sea-level records in and out of the lagoon was made. The records appeared identical with respect to the four-day oscillation of sea level, even though the diurnal and semidiurnal tides were markedly different. Tide measurements made by the U.S. Navy outside the reef at position " *C* " in 1944 before any gauge was placed in the lagoon also show evidence of the four-day oscillation.

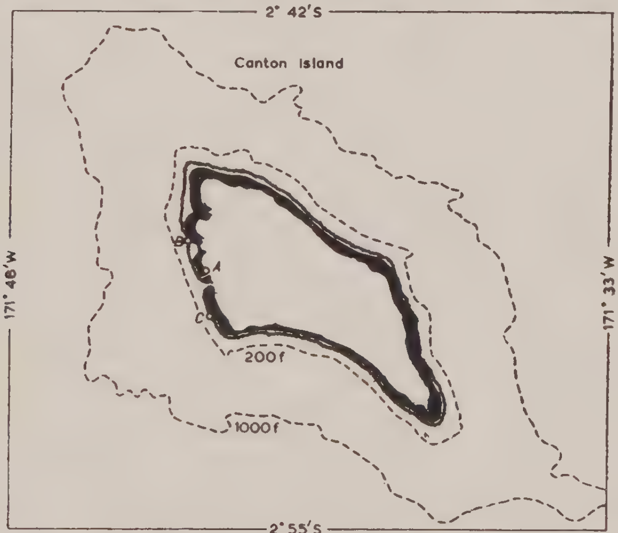

Fig. 4. Map of Canton Island showing : *A*, the location of the U.S. Coast and Geodetic Survey's tide gauge ; *B*, the location of a water-level recorder installed November 1955 ; and *C* the location of a tide gauge temporarily installed by the U.S. Navy in 1944.

The sea-level records of Fig. 2 were obtained from the Hydrographic Office of the British Admiralty and consist of the means of the four tidal extrema (from visual observation) of each lunar day.

RELATION OF SEA LEVEL TO WIND

A detailed discussion of the equatorial waves is given by PALMER (1952). According to PALMER, these waves develop somewhere in the great void between the Line Islands and the Galapagos and progress westward at about 11 knots, becoming unstable and shedding vortices (which sometimes attain hurricane intensity) after they pass the Gilbert Islands. Their wavelength is approximately 15° longtitude. At any fixed (geographical) position in their path, then, a wind oscillation whose period is approximately four days will be observed.

Comparison of surface wind and pressure data with the sea-level record at Canton Island for November, 1952 to January, 1953 reveals a convincing correspondence between oscillations of sea level and of wind (Fig. 1). The pressure fluctuations are too small to have an important direct effect on the ocean. The large oscillation of the north component of the surface wind is approximately in phase with sea level. Periodogram analysis (Fig. 5) for a 3·84 day period shows that the sea-level oscillation leads the oscillation of the north component of the surface wind by about 7 hours, on the average. In Fig. 1, the sea-level oscillation appears more regular than the wind oscillation. This effect is not entirely the result of the difference of methods in treating the sea-level and wind data.

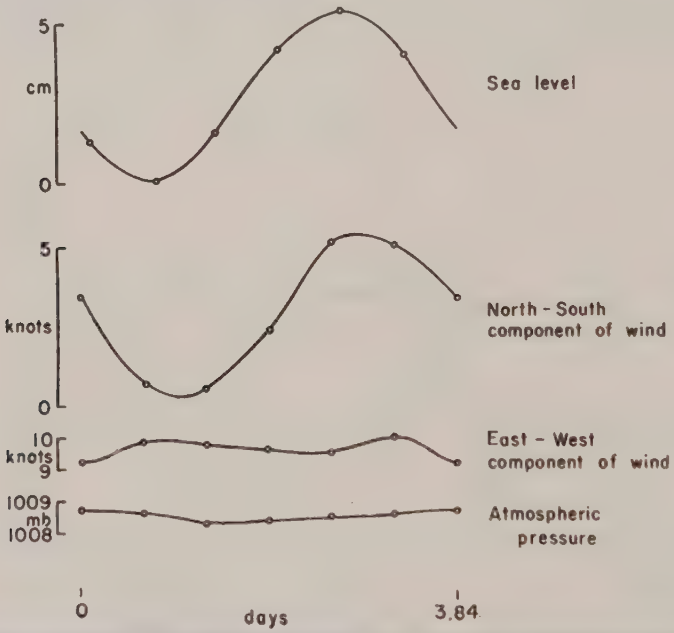

Fig. 5. Periodogram analysis of the variables shown in Fig. 1 carried out over 23 consecutive periods of 3·84 days, showing the average relative phase during this time.

CONCLUSIONS

The foregoing evidence indicates that the observed sea-level fluctuations at Canton Island are coupled to progressive waves in the easterly winds. The greater regularity of the sea-level oscillation may be the result of a free period (as yet undiscovered) in this region of the ocean very near four days, which is in forced resonance with the wind wave. Alternatively, the integrated wind stress over a large area of the ocean may oscillate in a regular fashion and be responsible for the sea-level oscillation.

One might expect that there would exist an oceanic wave of similar general character and geographic extent to the wave in the easterlies. If this were the case, the oceanic wave would extend from about 140°W to about 160°E and have a fairly restricted north-south extent. The only available data that may be contradiction to this hypothesis are the sea-level records from Butaritari and Tarawa in the Gilbert Islands, which do not show strong evidence of a four-day wave.

It is curious that the four-day waves seemingly skip the Gilbert Islands and reappear at Ocean Island. This may be the result of the following factors :

a. The Gilbert Island chain may present an obstacle to the four-day ocean wave, which must reform west of the Gilberts to appear at Ocean Island.

b. Both Butaritari and Tarawa may be too far north to be in the path of the ocean wave. Of course, the ocean currents of the equatorial system and the position of their boundaries must play a very important role in the dynamics of these ocean waves.

The recently-installed tide gauge at Christmas Island should give interesting information concerning this four-day oscillation.

Acknowledgements—The author would like to express this thanks to Prof. WALTER MUNK for his advice and encouragement of this study, to Dr. WILLIAM G. VAN DORN for his valuable help in installing the water-level recorder at Canton Island in November, 1955 and to Mr. EARL RHOADS for his help in maintaining this recorder, to the Civil Aeronautics Administration for their support of the installation project at Canton Island, to the Hydrographic Office of the British Admiralty and to the U.S. Coast and Geodetic Survey for making available the tidal data, to Mr. LESLIE SMITH and his group at the National Weather Records Center at Asheville, North Carolina, for making available the weather data, to Mrs. DOROTHY SHUMWAY and her group at the U.S. Navy Electronics Laboratory for carrying out the sea-level computations, and to Dr. CLARENCE PALMER of the Oahu Research Centre for his helpful advice.

Contribution from the Scripps Institution of Oceanography, New Series. This paper represents results of research carried out by the University of California under contract with the Office of Naval Research.

REFERENCES

GROVES, G. W. (1955), Numerical filters for discrimination against tidal periodicities, *Trans. Amer. Geophys.* Union **36** (6), 1073-1084.
GROVES, G. W. (In press), Day to day variation of sea level, *Meterorol. Monogr.*
PALMER, CLARENCE E. (1952), Tropical meteorology, *Q.J.R. Meteorol. Soc.*, **78** (336), 126-164.

Printed in Great Britain by The Salisbury Press Ltd., Publicity House, Wilton Road, Salisbury, Wilts. (99077)

CHANGES IN SAND LEVEL ON THE BEACH AND SHELF AT LA JOLLA, CALIFORNIA

TECHNICAL MEMORANDUM NO. 82
BEACH EROSION BOARD
CORPS OF ENGINEERS

JULY 1956

FOREWORD

Accurate determination of sand level changes over the nearshore area is important in making engineering analysis of littoral movement -- for both civil and military purposes. Derivation of the relation between these changes and the causative wave, water level, and tide forces would permit prediction of future change. Extremely accurate measurement of this change has been made for a three-year period by periodic diver observation of the sand level against a series of stationary reference rods driven into the sand bottom. This report presents the results of these observations. The report also shows comparison with results obtained by electronic sounding methods, demonstrating that unless great care is taken, large daily differences may be erroneously observed in acoustic measurements.

This report was prepared at the Scripps Institution of Oceanography of the University of California in pursuance of contracts with the Beach Erosion Board and the Office of Naval Research. The authors of the report, D. L. Inman, and G. A. Rusnak, are members of the staff of that institution.

Views and conclusions stated in this report are not necessarily those of the Beach Erosion Board.

This report is published under authority of Public Law 166, 79th Congress, approved July 31, 1945.

TABLE OF CONTENTS

Page No.

Abstract -- 1

Introduction -- 1

Acknowledgements -------------------------------------- 30

Method -- 2

    Positioning --------------------------------------- 4
    Reference Rods ------------------------------------ 4
    Acoustic Sounding --------------------------------- 10

Statistical Treatment of Data ------------------------- 10

    Analysis of Variance ------------------------------ 12
    Sign Test for Runs -------------------------------- 17
    Estimates of Correlation -------------------------- 18

Intrepretation -- 19

    Sand Level Changes on D Range --------------------- 21

        Reliability of measurements ------------------- 21
        Magnitude of sand level changes --------------- 23
        Correlation between stations ------------------ 24
        Sand size ------------------------------------- 24

    Sand Level Changes on B Range --------------------- 26
    Acoustic Sounding --------------------------------- 26

Summary and Conclusions ------------------------------- 29

Literature Cited -------------------------------------- 30

Appendix IA-ID Individual Rod Measurements, D Range --- I-1

Appendix IIA-IID Analysis of Variance Summary, D Range- II-1

Appendix IIIA-IIIB Sediment Size, D Range ------------- III-1

Appendix IV Wave and Tide Data ------------------------ IV-1

LIST OF FIGURES

Figure — Page No.

1. Index chart -- 3
2. Method of positioning ---------------------------- 3
3. Technique used in measuring reference rods ------ 5
4. Accuracy of positioning ------------------------- 6
5. Underwater photograph of reference rod ---------- 6
6. Swimmer equipped with SCUBA and measuring device- 8
7. Changes in sand level with time ----------------- 9
8. Changes in beach profile during tidal cycles ---- 9
9. Comparison of acoustic sounding and reference rods -- 11
10. Correlation between sand level changes at the 30 and 70-foot depths -------------------------- 20

LIST OF TABLES

Table — Page No.

1. Analysis of variance; station at 70-foot depth --
   Part A. Data and computations ----------------- 14
   Part B. Summary of analysis of variance -------- 15
2. Summary of statistical results, D range --------- 22
3. Seasonal average of sand level, D range --------- 25
4. Outline of acoustic sounding errors ------------- 28

CHANGES IN SAND LEVEL ON THE BEACH AND SHELF AT LA JOLLA, CALIFORNIA*

by
D. L. INMAN and G. A. RUSNAK
University of California
Scripps Institution of Oceanography
La Jolla, California

ABSTRACT

Changes in the level of the sandy bottom were measured periodically over an interval of almost three years at stations extending from near the surf zone to a depth of 70 feet. A reference level was established at each station by forcing six rods, spaced at intervals of 10 feet, into the bottom and changes in sand level were based on the average of the differences in length of rod exposed from survey to survey. Measurements, which were performed by swimmers equipped with self-contained underwater breathing apparatus, resulted in a standard error of about ±0.05 foot per survey in the determination of net sand level.

The total range in sand level probably exceeds 2 feet at the 18-foot deep station, where changes in excess of 0.6 foot were measured before the reference rods were lost. The magnitude of change decreases with increasing depth; changes of 0.29, 0.16, and 0.15 foot were measured at stations where the depth of water was 30, 52, and 70 feet respectively. Estimates of sand level variation, made for monthly and seasonal periods, indicate that significant changes occur between monthly periods at the 30 and 70-foot depths, and that significant seasonal changes occur at the 30 and 52-foot depths. At the deepest station overall seasonal variations are relatively small in comparison with changes of shorter period.

Comparison of acoustic soundings with reference rod measurements indicated that the accuracy of the acoustic sounding method was of the order of ± ½ foot for these operating conditions.

INTRODUCTION

The qualitative evaluation of the deposition and erosion of sediments near shore is usually based on differences obtained by comparing successive topographic surveys. In general the surveys are quite accurate for those portions of beach which are above water level, where standard leveling and positioning techniques can be employed.

---

*Contribution from the Scripps Institution of Oceanography, New Series No. 854.

Reproduced by Permission

Below water level the depth to the bottom is usually measured acoustically or with sounding lead and the bottom elevation estimated by correcting that depth for tides, waves, and various other effects. This method of hydrographic survey is relatively inaccurate as compared to the precise leveling techniques which are carried out above water.

Seasonal and long term changes in the level of nearshore sediments commonly are greatest along the narrow section of beach foreshore which falls within the intertidal zone. The magnitude of change in level decreases seaward, probably reaching a minimum on the broad flat shelves extending away from the beaches. Since the shelf areas are large in comparison with the narrow strip of beach bordering them, relatively small errors in determining sand level on the shelf may result in very large errors in estimating the total sand budget.

Attempts to evaluate the accuracy of hydrographic surveys have been made on several occasions, but the reliability of such investigations has been subject to uncertainty because of the lack of an accurate level upon which to base the surveys. The advent of self-contained breathing apparatus (SCUBA), which allows swimmers to move about freely and to make measurements and observations underwater, has provided a means of establishing underwater levels and accurately measuring changes from this level. A level is established by forcing a long rod a sufficient distance into the sandy bottom and in such a manner as to assure its remaining in a stationary position so that it does not move when material is deposited or eroded from the area. Thus, ideally, a direct comparison of the level of the exposed portion of the reference rod on two successive surveys will give the net value of erosion or deposition between surveys. A series of four stations using reference rods of this type was established on the sandy shelf off La Jolla in order to determine accurately the magnitude of erosion and deposition and to evaluate the accuracy of hydrographic surveys which use acoustical methods. Three of these stations were sampled periodically during an interval of almost three years. In addition to these stations, a series of reference rods was placed along a beach profile extending through the surf zone in order to measure small changes in sand level which occur during short intervals of time such as half-tidal cycles.

METHOD

A series of four stations were established on a range running normal to the coast line and extending from near the breaker zone out to the level portions of the sandy shelf (figure 1). Locations were selected where the depth of water was approximately 20, 30, 50, and 70 feet to allow a progressive comparison in changes of sand level from the surf zone, where fluctuations in level were known to be large, out to greater depths on the shelf. In the final analysis the exact location of the stations was determined by the proximity of good visual ranges and cross-ranges, since ease of positioning is an important factor in the economy of field operations.

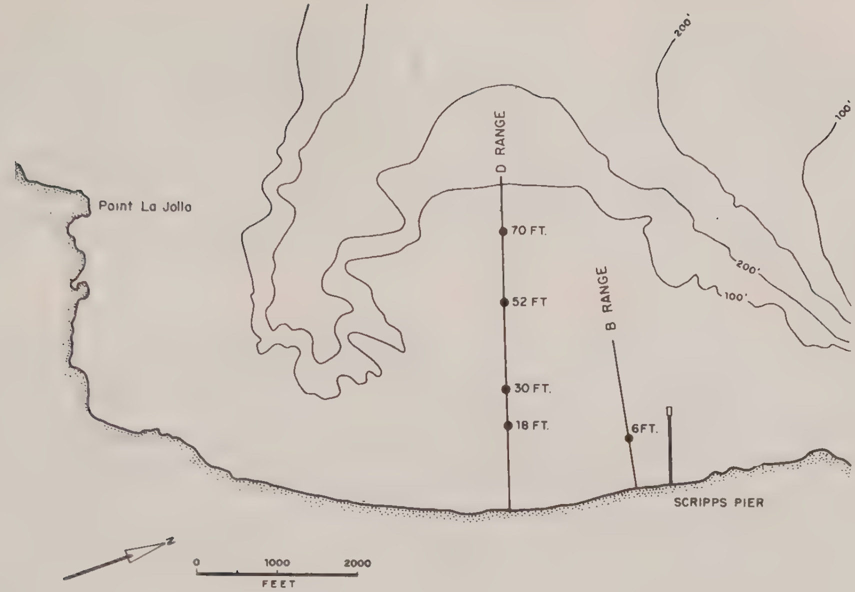
Point La Jolla
D RANGE
70 FT.
52 FT
30 FT.
18 FT.
B RANGE
6FT.
SCRIPPS PIER
200'
100'
200'
100'
N
0
1000
2000
FEET

Index chart showing the location of ranges and stations. Six reference rods were placed at each station on D range. Single rods were placed at 20-ft. intervals along a profile through the surf zone on B range. Depths are in feet below mean lower low water.

FIGURE I · INDEX CHART

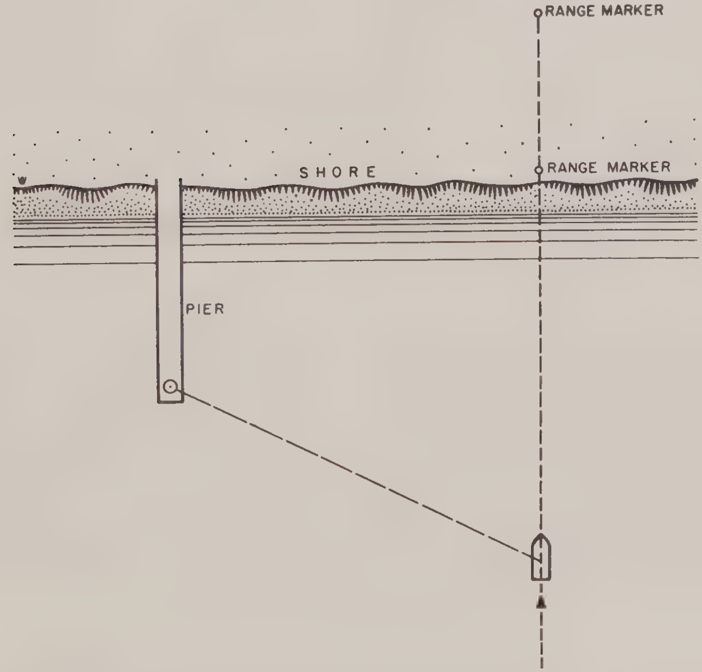
RANGE MARKER
SHORE
RANGE MARKER
PIER

The four stations on D range were located by running shoreward along a visual range to positions determined by the angle between the range and the pier. The angle was measured by sextant from the boat.

FIGURE 2 · METHOD OF POSITIONING

(525)

It was the intention in the experimental design of the field work to increase reliability of observation by making the number of independent measurements at any one station and time as large as practical, and by sampling each station frequently. Initially six reference rods were placed at each station, and on the average they were measured from one to two times per month. Because the changes in sand level, especially in deeper water, were small, the data were subjected to various statistical analyses in order to evaluate the contributing factors. The procedures used in processing the data are described in a separate section.

POSITIONING

During surveys the station locations were determined by range and horizontal sextant angle. A range was obtained by aligning visually two range markers on shore and the small craft proceeded shoreward along this range until the appropriate angle was obtained between the range and the end of the Scripps pier, at which point a marker was dropped in the water (figure 2). The marker consisted of a small cylindrical float with line wrapped around it and a ten-pound lead attached to the free end of the line. The lead sounded rapidly, causing the cylinder to spin in the water as the line unwound. Swimmers equipped with SCUBA were then guided to the location of the station by following the line to the bottom (figure 3).

This method of positioning proved to be accurate and quick and provided the swimmers with a visual reference upon which to orientate themselves. As a measure of accuracy, the rest position of the sounding lead relative to the six reference rods is shown for the 45 observations made at the 30-foot deep station (figure 4). The position of the sounding lead reflects the effects of waves and currents as well as the error in positioning at the time the marker float was placed in the water. Even so, the sounding lead landed within a radius of 5 feet of the target (reference rod number 1) about 50% of the time and within a radius of 10 feet about 80% of the time. The radius of error was slightly greater at 52-foot and 70-foot depths.

REFERENCE RODS

The basic problem was to find a means of establishing a stationary reference level near the bottom from which fluctuations of the sandy bottom could be measured. The solution used here was to force rods into the bottom in such a manner as to assure their remaining stationary when material is eroded or deposited in the area. For this purpose, brass rods 3/8 inch in diameter and 4 feet long were pounded approximately 3 feet into the bottom with a light sledge hammer. Circular brass rings were silver-soldered around the lower portion of the rods so that once emplaced in the sand they could not easily be raised or lowered. Deformed steel reinforcing rods were also tested, but their

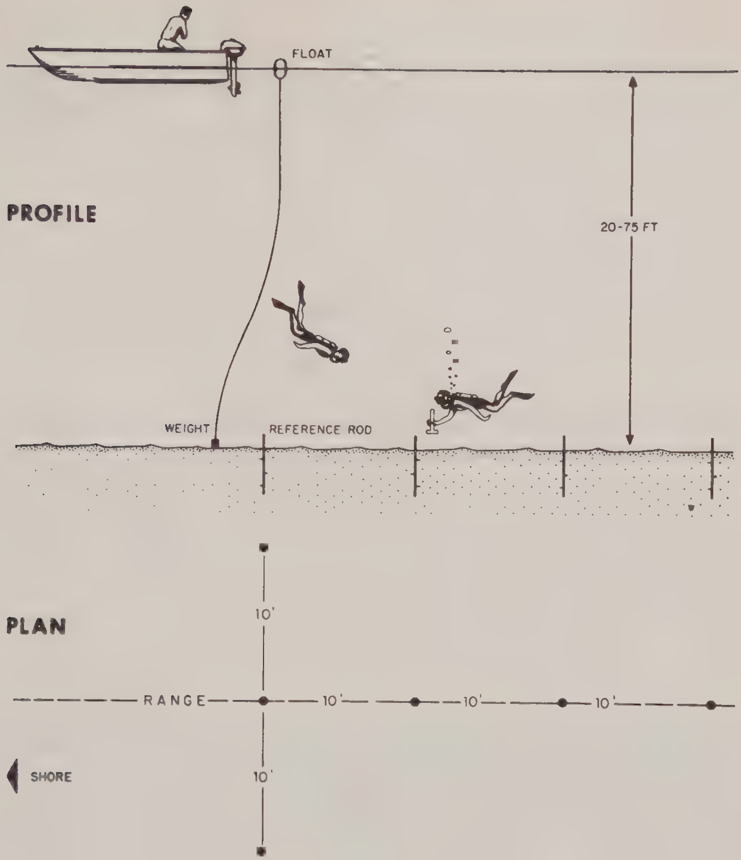
FLOAT
PROFILE
20-75 FT
WEIGHT
REFERENCE ROD
10'
PLAN
RANGE
10'
10'
10'
SHORE
10'

Schematic diagram illustrating the technique used in locating the station and measuring the reference rods. Six rods were placed in the sandy bottom at each of the four stations on D range; three across the range and four along the range. The station locations are shown in figure I.

FIGURE 3 · TECHNIQUE USED IN MEASURING REFERENCE RODS

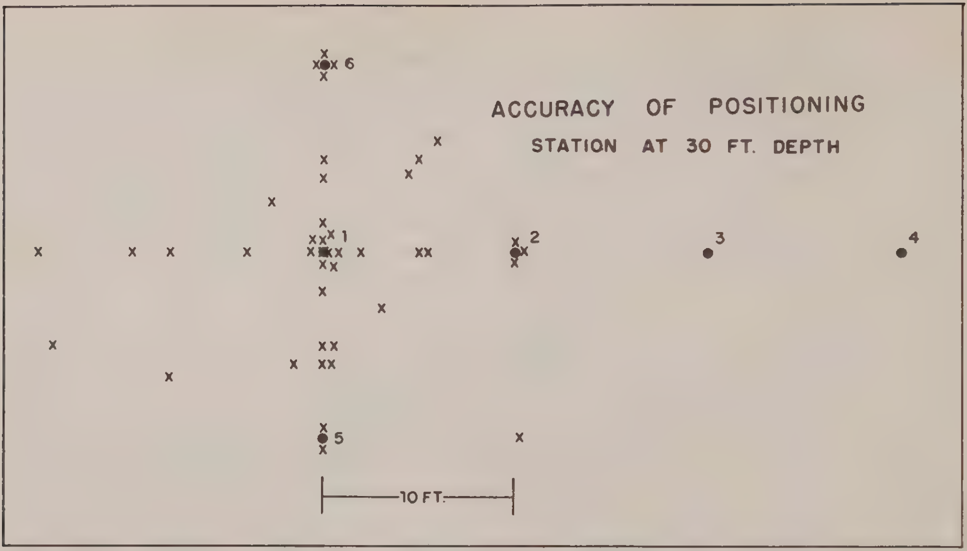

Accuracy of positioning indicated by the rest position of the sounding lead for each of the 45 observations at the 30-foot depth. The position of the sounding lead, shown by X, reflects the effect of waves and currents as well as the error in positioning the boat.

FIGURE 4 · ACCURACY OF POSITIONING

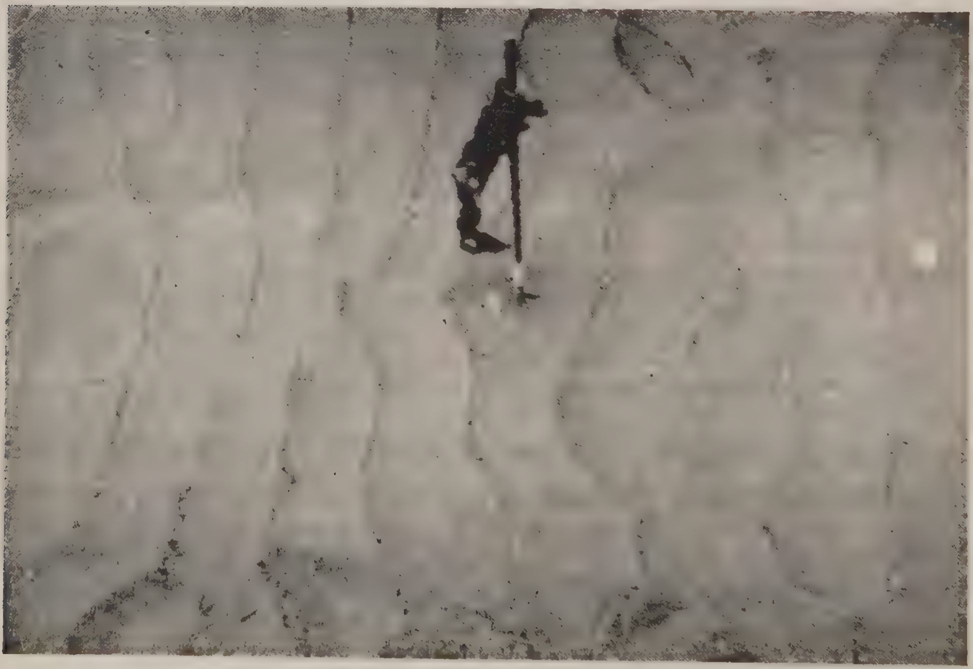

Underwater photograph of one of six reference rods at the station in 30 feet of water. The rod is 3/8-inch diameter brass; approximately 1 foot is exposed, and 3 feet are buried in the sand. The dark object is a plastic tag with growing hydroid. Note the slight scour depression at the base of the rod.

FIGURE 5 · UNDERWATER PHOTOGRAPH OF REFERENCE ROD use was discontinued because it was found that hydroids and other organisms grew profusely on the steel, whereas the brass was found to be relatively free from fouling organisms. Fouling on the steel rods made measurement more difficult and increased the stress exerted on the rod by the moving water and the degree of scour at the base of the rod. In general, only a very slight scour depression formed in the sand at the base of the brass rods, as shown in figure 5.

Six rods were forced into the bottom at each of the four stations on D range. They were placed 10 feet apart in a "T" formation, with four rods along the range and three across (figure 3). The distance between rods was sufficient to eliminate the possibility of significant hydraulic interference or influence between rods.

After the rods had been in place several days and were in equilibrium with their environment, the station was again visited and the length of each rod carefully measured. This length was recorded as the reference length for that rod and is the length upon which future changes in sand level were based. For each successive survey the new length of rod was subtracted from the reference length, and the mean value of the differences for the six rods used as a measure of the new sand level. The differences from reference length for each rod during each survey, together with the mean difference and standard deviation, are listed in Appendix IA-ID. The mean difference is graphed as a function of time in figure 7. The particle size distribution analyses of the sand samples collected by the swimmers at each station are listed in Appendix IIIA-IIID.

The length of rod was measured by placing a plexiglas device upright on the sand alongside the rod and marking the device with a grease pencil. The measuring device, which consisted of a 2-foot long strip of plexiglas with an 8-inch wide by 1-inch thick strip of wood at its base, resembled a draftsman's "T" square (figure 6). The base was wide and thick so as to bridge or cover holes that might be present at the base of the rod and to avoid settling into the sand when placed beside the rod.

The lengths of each of the six rods at each station were marked on the device. When the swimmer returned to the surface, these lengths were measured to the nearest hundredth of a foot and recorded for processing as described above.

During the summer of 1953 a series of reference rods were placed at 20-foot intervals along a profile through the surf zone on B range (figure 1). The line extended from the upper portion of the beach foreshore out to a depth of approximately 6 feet below MLLW (figure 8). The section of beach above water level was surveyed by transit, and the portion under water by swimmers and reference rods in the manner outlined for the stations on D range, excepting that only one

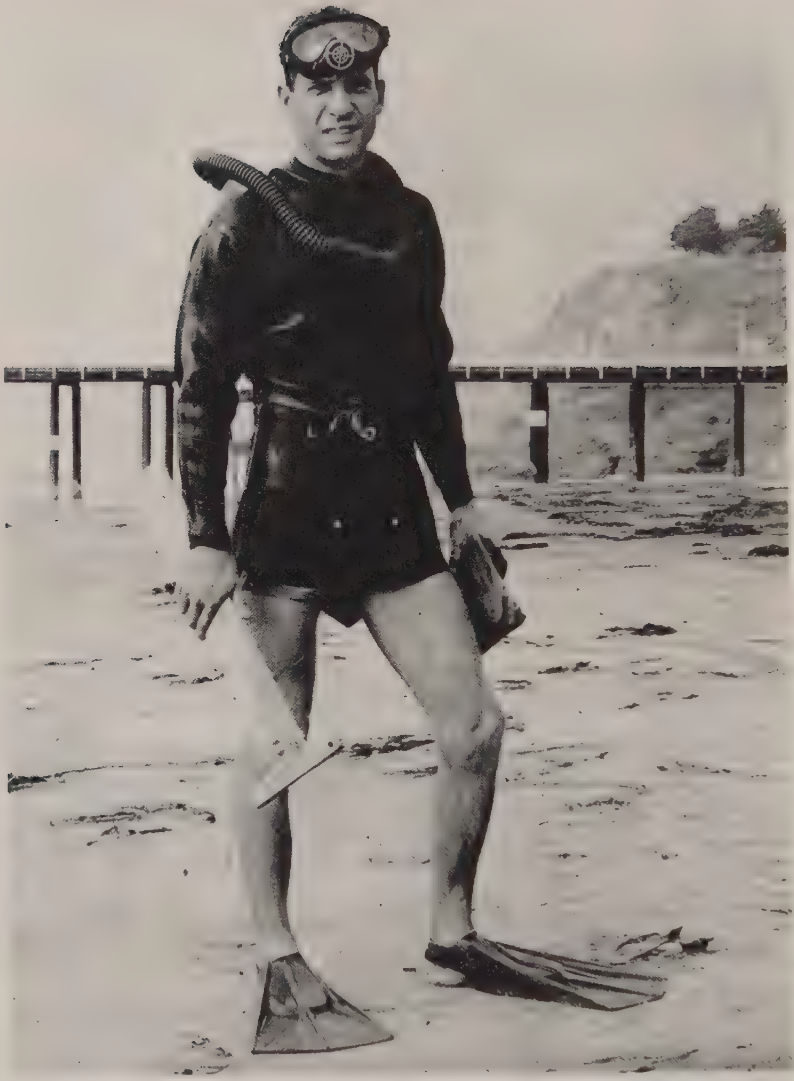

Swimmer equipped with self-contained breathing apparatus (SCUBA), exposure suit, and plexiglas device used in obtaining the length of reference rods. The length is marked on the plexiglas with grease pencil (attached to device by clip) and measured after returning to the surface.

FIGURE 6 · SWIMMER EQUIPPED WITH SCUBA AND MEASURING DEVICE

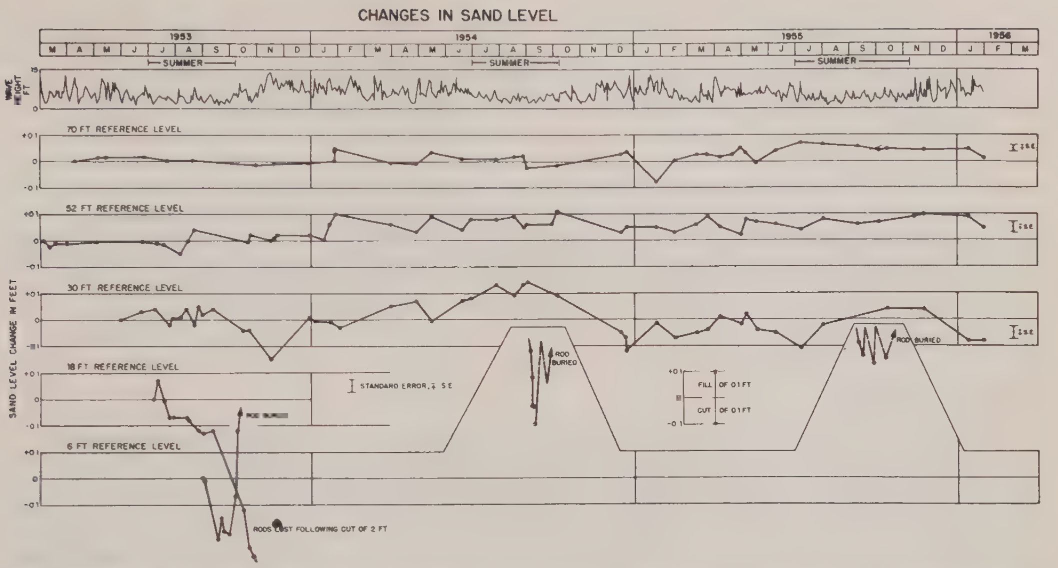

Changes in sand level with time. The stations at depths of 18, 30, 52, and 70 feet are on D range and the fluctuations in sand level are based on the mean of six reference rods at each station. The magnitude of two values of the standard error, ± S.E., is shown as a measure of reliability of the observations. The station at a depth of 6 feet was on B range and consisted of a single reference rod which was completely covered with sand during the winter. The wave heights are for significant breakers at the point of wave convergence near D range.

FIGURE 7 · CHANGES IN SAND LEVEL WITH TIME

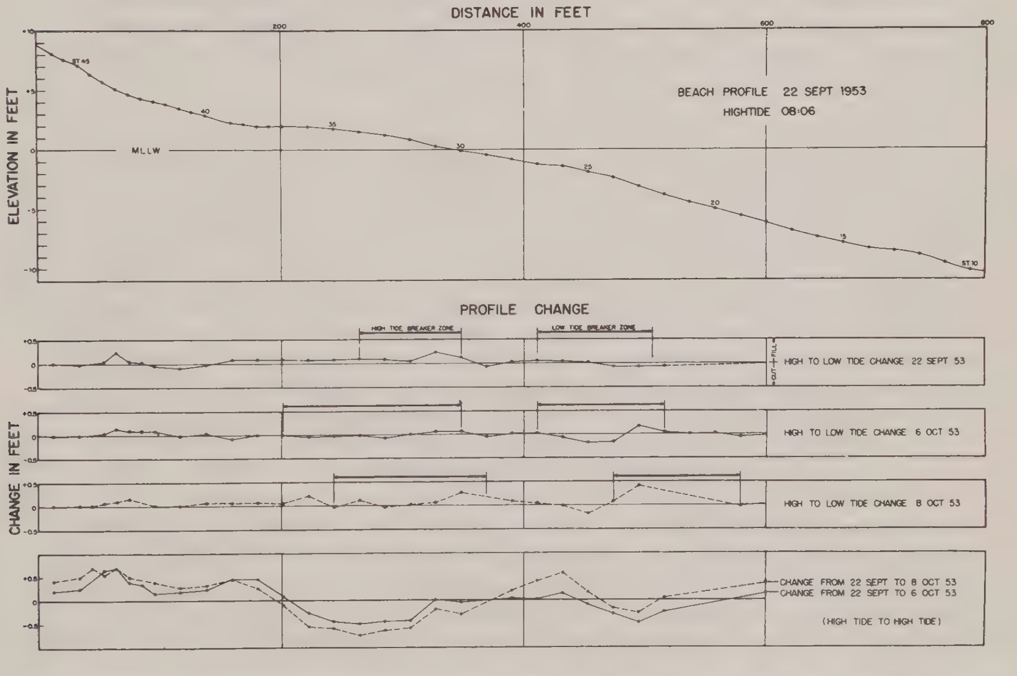

Changes in sand level on B range between time of high and low tide on three separate days. Lower graph shows the change in profile between the first day's survey and those of the succeeding days. Wave and tide conditions are listed in Appendix IV.

FIGURE 8 · CHANGES IN BEACH PROFILES DURING TIDAL CYCLES reference rod was used per station. Positioning was performed by the swimmer in the water using a visual range and a series of cross ranges. The pilings of the Scripps pier provided convenient, evenly spaced markers, which when aligned with a distant marker, made accurate visual cross ranges.

The profile of closely spaced rods through the surf zone was established in order to measure small changes in sand level which occur during half-tidal cycles. Complete surveys were made at the time of high tide and at the following low tide on three days. The changes in sand level are graphed in figure 8, and the tide and wave conditions are listed in Appendix IV.

ACOUSTIC SOUNDING

During the summer and fall of 1953 hydrographic surveys were made along D range concurrently with the reference rod measurements in order to evaluate the accuracy of the acoustic sounding method. The hydrographic surveys were made from an amphibious vehicle (DUKW) equipped with a Bludworth NK - 2 fathometer and a sounding element rigidly mounted to the side of the DUKW approximately a foot and a half below water level. This fathometer is equipped with gain, frequency, and power controls, marker bar, and has a record scale of 6½ inches equal to 60 feet in depth. The fathometer was calibrated with a lead line which was graduated in tenths of a foot and held vertically in the water beside the sounding element. Approximately six checks were made at each of two depths while the DUKW was in still water. Calibrations were made in water depths of approximately 15 and 30 feet in areas where the bottom was flat and sandy (Shepard and Inman, 1951).

Positioning was performed by visual range and horizontal sextant angles as described previously, and the fathogram was marked at the time of passage over each station. Approximately five sounding runs were made along the range just prior to measuring the reference rods at each station.

The data from the fathogram were corrected for depth and reduced to the datum of MLLW by reference to a tide record from the U. S. Coast and Geodetic Survey tide gauge on the end of Scripps pier (figure 1). A comparison between the acoustic survey and the reference rod measurements for the station at the 30-foot depth is shown in figure 9.

STATISTICAL TREATMENT OF DATA

The primary consideration of any experimental study is generally that of separating the several factors involved in the experiment. In the present study it was important to separate the variability of sand level changes into the several contributing groups of factors under study. To do this, a large group of measures of sand level were collected

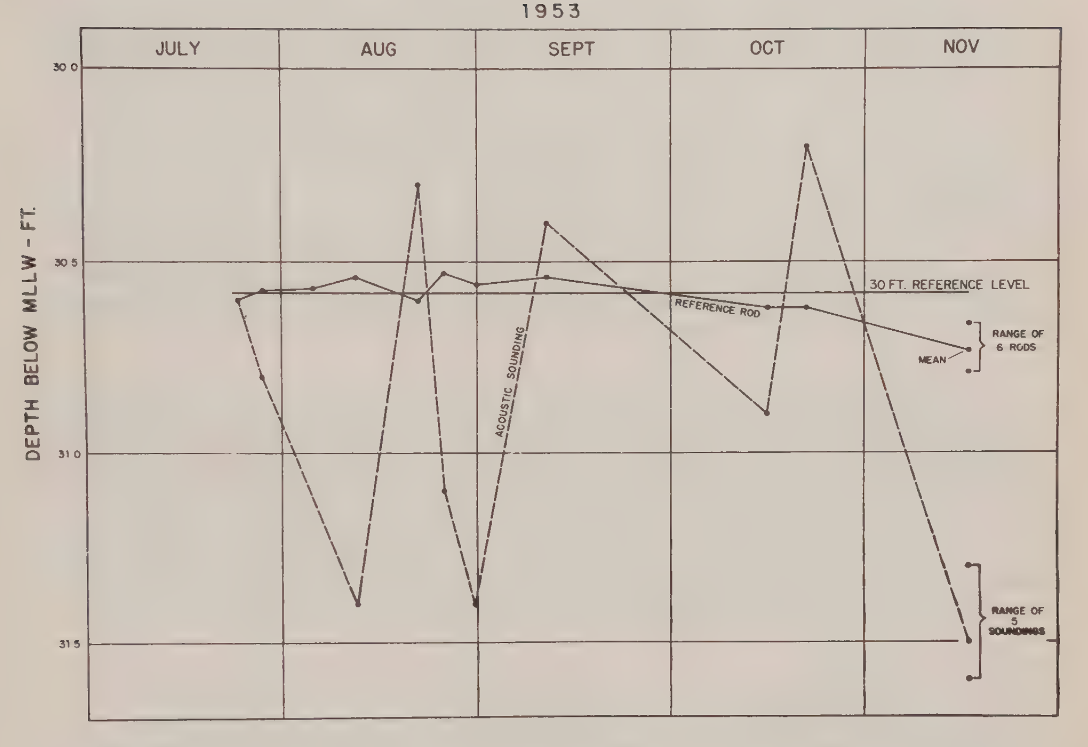

Comparison between sand levels obtained by acoustic sounding and reference rods at the 30-foot deep station on D range. Each point represents the mean of approximately 5 acoustic sounding runs or 6 reference rod measurements. Within a single day the range of acoustic soundings is only 3 to 5 times greater than the range in rod measurements. However, between days the acoustic soundings give fluctuations which would result in large errors.

FIGURE 9 · COMPARISON OF ACOUSTIC SOUNDING AND REFERENCE RODS at specific points in space and time. Then a choice of statistical procedures was made such that the information obtained could be utilized in the most efficient manner.

The natural limitations in this study, such as adverse weather conditions, did not permit the experimental design to be carried out to its best advantage. It is known, for example, that the data are somewhat biased because the measures could not be collected in a completely random manner. Nonetheless, although errors may result because the assumptions underlying the statistical theory have not been completely fulfilled, the statistical theory will not be rejected but will be applied with the condition that caution be used in its interpretation (Fisher, 1949, p. 16). If these limitations are kept in mind, the statistical applications are somewhat justified in that they may lead to the recognition of the causes of departures. As has been pointed out by Olson and Potter (1954), one must use judgment in passing over preliminary stages of analysis more rapidly than statistical rigor would permit in order to focus attention on later critical problems requiring statistical analysis.

With this point of view, several questions were asked in the study of sand level changes. These were: (1) what is the accuracy with which the sand level, at a given depth and at a given time, could be measured; (2) what are the monthly and seasonal variations of sand level; (3) is there a trend in the changes of sand level with time; and, finally; (4) is there a relation between the sand level changes at various depths? The choice of statistical tests used for obtaining estimated answers to these questions was the analysis of variance, the sign test of trend, and the estimate of correlation.

ANALYSIS OF VARIANCE

In a normally distributed population the form of the distribution is completely described by the mean μ and the variance σ^2. A random sample of n items from this population gives an estimate of these parameters in the form of the sample mean $\bar{x}$ and the sample variance s^2 (Dixon and Massey, 1951, pp. 32-35).

$$(1) \qquad \bar{x} = \frac{\Sigma x}{n}$$

$$(2) \qquad s^2 = \frac{\Sigma x^2 - (\Sigma x)^2/n}{n-1}$$

The fundamental principle upon which the analysis of variance is based is that the variance of the independent factors contributing to the population variance are additive. Therefore, the total population variance is the sum of the independent factors contributing to this variance. In the present study it was desired to separate the independent factors of sand level variability due to local irregularities

(534)

in sand level (plus measurement error) from those due to variations with time. By grouping the data in a hierarchical scheme, it was possible to separate and evaluate the magnitude of these variations.[1]

The assumptions underlying the analysis of variance are that the observations are from a normally distributed population and that the variance of each group is the same. Dixon and Massey (1951, p. 126) point out, however, that the results of the analysis are changed very little by moderate violations of the assumptions of normal distribution and equal variance.

Example of Analysis of Variance for the Station at 70-Foot Depth. For cases in which the random deviations are normally distributed, the computation of variance is conveniently made by utilizing the conventional form of the analysis of variance table (Eisenhart, et al., 1947, p. 311). The sources of variation are broken down into those (1) between k rods, (2) within j months, (3) between i months, and (4) between h seasons. Arranging the data so that these sources of variation could be separated results in the hierarchical order presented in table 1.

Computational procedure for the first step in the analysis of variance is indicated by the column headings and the summations following table I, part A. The summations are made with a calculating machine and entered directly in this part of the table. The sum totals of these columns are then entered in the analysis of variance table, part B, as lower level sum and higher level sum from the respective columns. The difference of these sums for each source is the sum of the squared deviations and corresponds to the numerator of equation (2). The sum of these squared deviations is then divided by the degrees of freedom to obtain the mean square or variance.

The number of degrees of freedom between rods is the number of rods per observation minus one (k-1), summed over all observations, and is equal to 199 for this station. Within months the number of degrees of freedom is the number of observations per month minus one (j-1), summed over all months and is equal to 11. This same procedure is followed for each successively higher level of sampling (Snedecor, 1946, p. 233).

The mean square between rods is assumed to be due to random sampling fluctuations around the true mean of the group with a true variance σ_k^2. The mean square within months, however, is dependent both upon the between rods variance, σ_k^2, affecting the individual measurements involved in the mean, and on the additional variance component, σ_j^2, due to the fluctuation of sample means around the group mean X_j. The long-run expected value of the mean square within months is equal to

---

[1] The reader is referred to standard statistical texts such as Dixon and Massey (1951, Chaps. 8 and 10), Snedecor (1946, Chaps. 10 and 11) or the lucid digest of Olson and Potter (1954) for the complete details of this method of analysis.

Table 1. Analysis of variance for unequal samples of sand level change; station at 70 ft depth.

Part A. Data and computations.

Between Seasons (h)	Between Months (i)	Within Months (j)	Between Rods (k)						$\sum_k x$	$\sum_k x^2$	$\sum_j\left[\frac{(\sum_k x)^2}{N_k}\right]$	$\sum_i\left[\frac{(\sum_{jk} x)^2}{N_j}\right]$
			1	2	3	4	5	6				
1	1	4 May '53	+.01	-.02	+.01	+.04	+.01	+.04	+.09	.0039	.00270	.00432
		13 May '53	+.05	-.02	0	+.03	+.03	0	+.09	.0047		
	2	26 June '53	+.02	--	0	+.03	+.04	0	+.09	.0029	.00162	
2	3	22 July '53	+.03	+.01	0	-.04	+.03	-.01	+.02	.0036	.00006	.00008
	4	19 Aug. '53	+.04	0	+.03	-.06	0	0	+.01	.0061	.00001	
3	5	30 Oct. '53	-.02	-.03	+.03	-.01	-.02	-.04	-.09	.0043	.00135	.02575
	6	19 Nov. '53	-.02	-.06	+.04	-.01	0	-.02	-.07	.0061	.00081	
	7	28 Dec. '53	-.02	-.02	+.03	-.02	-.04	+.02	-.05	.0041	.00041	
	8	26 Jan. '54	+.02	-.03	+.04	+.01	-.02	-.01	+.01	.0035	.02175	
		27 Jan. '54	+.01	+.04	+.05	+.06	+.07	+.01	+.24	.0128		
		28 Jan. '54	+.04	+.02	+.06	+.06	+.05	+.04	+.27	.0133		
	9	29 Mar. '54	-.01	-.02	+.03	-.01	-.03	+.02	-.02	.0028	.00006	
	10	27 Apr. '54	-.03	-.04	+.03	+.02	-.05	+.01	-.06	.0064	.00060	
	11	14 May '54	+.04	+.03	+.02	+.07	+.02	+.02	+.20	.0086	.00666	
	12	18 June '54	0	-.03	+.03	+.03	+.02	+.02	+.07	.0035	.00081	
4	13	26 July '54	0	-.02	+.03	-.02	+.06	0	+.05	.0053	.00041	.00907
	14	16 Aug. '54	-.03	-.03	+.05	+.01	+.08	+.03	+.11	.0117	.00440	
		26 Aug. '54	+.03	-.04	+.01	0	+.07	+.05	+.12	.0100		
	15	1 Sep. '54	+.02	-.20	0	-.07	+.06	+.03	+.16	.0498	.00426	
5	16	4 Oct. '54	-.07	-.06	+.01	0	+.02	0	-.10	.0090	.00166	.09686
	17	15 Dec. '54	-.02	+.04	+.07	+.05	-.01	+.03	+.16	.0104	.01308	
		21 Dec. '54	+.03	+.05	+.06	+.02	+.05	+.02	+.23	.0103		
	18	25 Jan. '55	-.15	-.01	-.10	-.20	-.03	+.01	+.48	.0736	.03840	
	19	15 Feb. '55	+.06	0	+.07	-.20	+.02	+.07	+.02	.0538	.00006	
	20	10 Mar. '55	+.06	-.01	+.03	0	+.02	+.07	+.17	.0099	.00962	
		22 Mar. '55	+.03	0	+.06	-.01	+.02	+.07	+.17	.0099		
	21	6 Apr. '55	0	+.01	+.06	+.02	-.05	+.07	+.11	.0135	.02388	
		20 Apr. '55	+.04	+.02	+.07	+.08	-.05	+.01	+.17	.0159		
		29 Apr. '55	+.02	+.09	+.05	+.06	+.07	+.03	+.32	.0195		
	22	5 May '55	+.02	-.04	+.04	+.06	+.05	+.07	+.20	.0146	.00672	
		16 May '55	+.02	-.01	+.02	-.05	-.05	+.05	-.02	.0084		
	23	8 June '55	+.09	-.03	+.05	+.03	+.07	+.04	+.25	.0189	.01041	
6	24	6 July '55	+.14	+.01	+.03	+.10	+.08	+.07	+.43	.0419	.03081	.10087
	25	1 Aug. '55	+.11	+.01	+.04	+.05	+.06	+.12	+.39	.0343	.02535	
	26	10 Sep. '55	+.11	0	+.08	+.03	+.01	+.12	+.35	.0339	.02041	
	27	3 Oct. '55	+.06	0	+.09	+.02	+.05	+.03	+.25	.0155	.02442	
		12 Oct. '55	+.06	+.02	+.09	+.06	+.06	-.03	+.29	.0202		
	28	23 Nov. '55	+.05	-.02	+.06	+.07	+.05	+.05	+.26	.0164	.01126	
7	29	13 Jan. '56	+.06	+.01	+.03	+.04	+.06	+.09	+.29	.0179	.01508	.02266
		30 Jan. '56	+.03	-.01	+.02	+.04	+.01	-.01	+.08	.0032		
								Total	+4.43	.6144	.27707	.25961

$$\sum_h\left[\frac{(\Sigma_{ijk}x)^2}{N_i}\right] = \frac{(.27)^2}{17} + \frac{(.03)^2}{12} + \ldots \frac{(\Sigma_{ijk}x)^2}{N_i} = .14709$$

$$\frac{(\Sigma_{hijk}x)^2}{N_h} = \frac{(4.43)^2}{239} = .08211$$

Table 1. Analysis of variance for unequal samples of sand level change. Station at 70 ft depth.

Part B. Analysis of variance

	Between Rods	Within Months	Between Months	Between Seasons
Lower Level Sum	0.6144	0.27707	0.25961	0.14709
Higher Level Sum	0.27707	0.25961	0.14709	0.08211
Sum Squared Deviations	0.33733	0.01746	0.11252	0.06488
Degrees of Freedom	199	11	22	6
Mean Square	0.00169	0.00158	0.00511	0.01081
Lower Component		0.00169	0.00158	0.00511
Difference		-0.00011	0.00353	0.00570
Effective Subsample		5.97489	8.55393	31.52301
Component Estimate, s^2	0.00169	0	0.00041	0.00018
F		0.93491*	3.23417**	2.11545*

* Not significantly different from variations of shorter period.

** Significant at the 0.01 level; therefore highly significant.

($\sigma_k^2 + k\,\sigma_j^2$), where k is the known number of individuals which share in the particular sample value of this distribution (Olson and Potter, 1954, pp. 37-38).

The test of significance associated with the analysis of variance in this form is considered as the test of the hypothesis that the two mean squares σ_k^2 and $\sigma_k^2 + k\,\sigma_j^2$ are equal. This is equivalent to asking whether the contribution of σ_j^2 is equal to zero or whether there is a significant contribution to the mean square due to this factor σ_j^2. The F-test is used to test this hypothesis. The value of F is the ratio of the within months mean square to the between rods mean square; and, if this ratio exceeds the tabled values of F at a specified level of significance, then the hypothesis of equality of mean squares is rejected (Olson,and Potter, 1954, p. 38; Dixon and Massey, 1951, chap. 10; Snedecor, 1946, p. 231).

From the values in part B of table 1, the computed value of F is equal to 0.93491 and is less than 1. It is concluded therefore that the mean squares are approximately equal and that there is no significant contribution due to σ_j^2. If the F value exceeded the tabulated values (Dixon and Massey, 1951, pp. 310-313), the component estimate of σ_j^2

could have been computed from $\dfrac{(\sigma_k^2 + k\,\sigma_j^2) - \sigma_k^2}{k}$, as was the case for the other stations. In the present example, k is the effective subsample size. The reason for this is that the samples contributing to this mean square were not equal in size and k had to be computed as an effective subsample size. The effective subsample size is equal to 5.97489 and is computed from the following relation (Snedecor, 1946, pp. 234, 241):

$$k = \frac{\sum_j k - \dfrac{\sum_j (k)^2}{\sum_j k}}{(j-1)} \qquad (3)$$

This same procedure is followed for the next succeeding higher level of sampling to obtain the contribution in that group. In the present example, the difference happened to result in a minus value and it is concluded that the variance at this level, σ_j^2, is equal to zero. Since σ_j^2 should not be less than zero, this discrepancy may represent a sampling variation due to some unusually divergent measures in the rods (Olson and Potter, 1954, p. 40). The practical significance of this result is that the variability within months is negligible compared to the variability between rods.

Another way of estimating the variance among individual rod measures in an observation is to compute the pooled estimate or average variance.

The formula for this estimate is given by Dixon and Massey (1951, pp. 91-92) as

$$(4) \qquad s_p^2 = \frac{(n_1-1)s_1^2 + (n_2-1)s_2^2 + \ldots + (n_k-1)s_k^2}{n_1 + n_2 + \ldots + n_k - k}$$

for k samples of variance. For the 70-foot station the pooled estimate of variance between rods is equal to 0.00169. The pooled estimate may be lower than that obtained in the analysis preceding because it is the average variance computed around each sample mean rather than around the mean of the group of all observations. It is felt that use of the pooled estimate is a better estimate for between rod variability. It is this value which has been used in obtaining the standard error discussed in the interpretation.

THE SIGN TEST FOR RUNS

The nonparametric sign test was used for determining the existence of a trend to the changes in sand level with time. This test does not involve the statistical parameters of the population distributions; it simply compares the distribution of values without specifying the form of the distributions (Dixon and Massey, 1951, p. 247). Furthermore, it is only necessary to assume that the observations represent a random sample.

For present purposes it was desired to know whether the changes in sand level with time had any cyclic trend or whether these changes were random. To test this, the procedure is to determine the median value of the ordered sequence of given mean values of sand level with time. All values above the median are then designated by a plus sign and all values below the median by a minus sign. The question is whether or not the positive values are distributed in a random manner among the negative values. The one or more adjacent similar signs are denoted as runs with the result that a run is started as soon as the sign changes (from plus to minus or from minus to plus). If the number of runs is very high, it would indicate a rapid periodic or cyclic trend. On the other hand, if the number of runs is very low, the sequence would be nearly monotonic (hence of slow period).

The test is based on the criterion for making one of three decisions for each group of observations (Hald, 1952, p. 749; Eisenhart, _et_ _al_., 1947, p. 419).

(1) Accept the hypothesis that there is a trend.
(2) Reject the hypothesis of trend.
(3) Continue sampling. There may be a trend but the observations are not sufficiently refined to bring this trend out in the analysis.

Example of Sign Test from Station at 70-Foot Depth. The median is determined by taking the mean values of the raw data from Appendix ID and arranging these in order of increasing values. This median value is +.02. Now taking the original serial sequence and designating the values above the median as plus and the values below as minus, the following is obtained:

Sign		Sign	
-	1	+	6
-		+	
-		-	7
-		-	
-		+	8
-		+	
-		-	9
-		+	10
-		+	
+	2	+	
+		-	11
-	3	+	12
-		+	
+	4	+	
-	5	+	
-		+	
-		+	
md.		+	
-		+	
-		-	13
		13	

Number of items = 40
Total number of runs = 13

Table 11 in Dixon and Massey (1951, p. 325) shows that the upper limit of runs to be expected from a pure random arrangement is 27, while the lower limit to be expected is 14. Values either above or below these tabled values would not be expected to occur more than 2.5 per cent of the time; i.e., there is a risk of being wrong in the decision 2.5 per cent of the time. Since the number of observed runs lies below the lower limit, it is concluded that there is a trend and the number of runs is abnormally smaller than would be expected from a simple random variation of data.

ESTIMATES OF CORRELATION

In order to determine the relationship between changes in sand level from one station to another, estimates of the correlation between stations were made. The test used is designed to determine whether or not the changes between stations are independent of each other. If these changes are not independent, it is desirable to know whether the correlation between them is positive or negative; i.e., either there is simultaneous deposition of sand at the two stations in question, or there is deposition of sand at one station and erosion of sand at the other.

The relatively simple statistic used here to estimate the correlation is the tetrachoric r, described in Dixon and Massey (1951, pp. 233-235). The procedure is to make a graphic plot of one mean value of sand level against the other, for all mean values observed between the two stations on a simultaneous date. After all the values are plotted in this manner, the plotted points are divided equally by a horizontal line and a vertical line. If, then, the number of points in the upper right and lower left quadrants is greater than in the other two quadrants, the correlation is positive. If the opposite is true, the correlation is negative. This procedure is very useful in the exploratory stages of a study, such as the present one, to determine whether the factors are associated.

Example of Correlation between Stations at 70 and 30-Foot Depths. By taking the data from the table in Appendix IB and ID, and collecting all mean sand level changes observed on simultaneous dates for the 70 and 30-foot depth stations, the graphic plot of figure 10 is obtained. The total number of points in the plot is 26. Dividing these points by a horizontal and a vertical line so that an equal number of points lie above and below the horizontal line and an equal number of points lie on either side of the vertical line, the graphic plot is divided into four quadrants. The number of points in each of these quadrants is then designated by n_1, n_2, n_3, and n_4. The value of

$$\frac{n_1 + n_3}{n_1 + n_2 + n_3 + n_4} \quad \text{or} \quad \frac{n_2 + n_4}{n_1 + n_2 + n_3 + n_4}$$

is then computed, whichever is larger. In this case the second relation is the larger and results in a value of 0.769. This value is then entered in figure 2 of Dixon and Massey (1951, p. 234) to obtain the estimate of correlation. The estimate arrived at from this procedure is -0.75 for the correlation coefficient. It is concluded that these stations are not independent of each other. The correlation is negative; i.e., when the sand is built up at one station, there is a loss at the other.

INTERPRETATION

Of the several distinct factors involved in a study of this kind, it is difficult to isolate the local irregularities of the bottom from those changes which are significant. That is, the local irregularities of the bottom may be as large as the net changes in sand level one is trying to measure. Consequently such irregularities may completely mask the minor changes in sand level. The primary purpose of the present study was an attempt to evaluate the magnitude of the separate factors of variability involved in sand level changes.

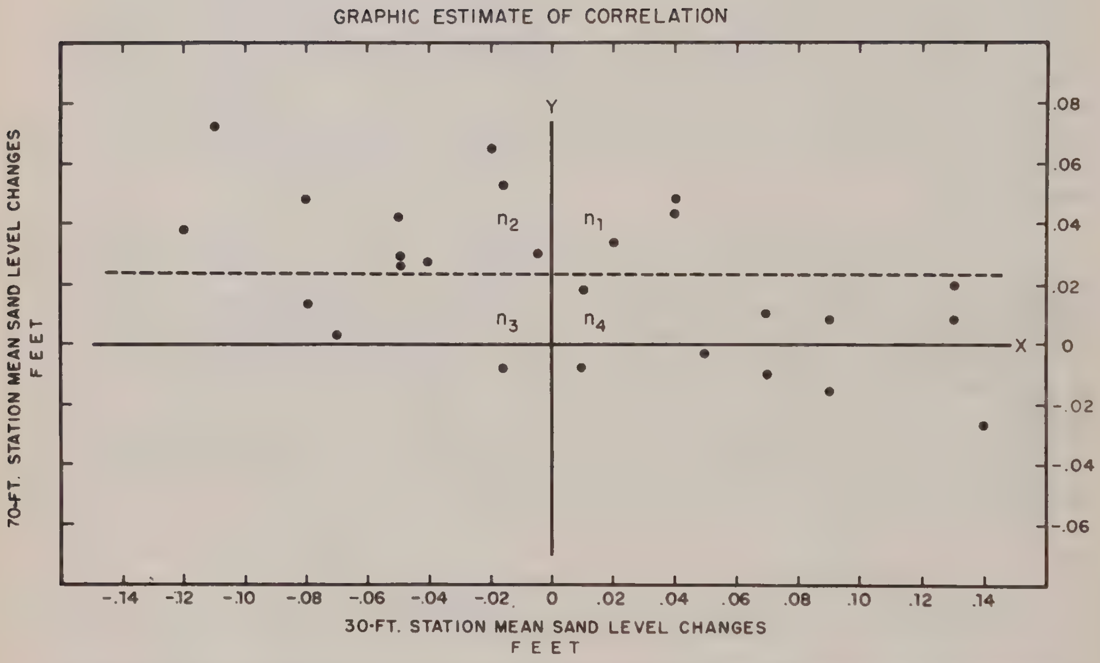

Graphic method of estimating the correlation between sand levels at the 30 and 70-foot depth stations on D range.

FIGURE 10 · CORRELATION BETWEEN SAND LEVEL CHANGES AT THE 30 AND 70-FOOT DEPTHS

Another serious consideration which could be made is the factor of costs. One might spend the entire time in a survey by making a large number of very precise measures from day to day. If, however, the changes of major importance are not day to day occurrences, but monthly or yearly occurrences, it would be less costly to take fewer day to day measures and still get the desired information. Before making such decisions, it is necessary that the sources of variation and their magnitudes be evaluated. In studies where this is done, it is possible to better allocate or budget sampling time so that in the future more information can be arrived at with a smaller cost in time and effort (Eisenhart, et al., 1947, p. 269). Suggestions are made for better budgeting of sampling in the discussion to follow and in the conclusions.

Earlier studies have indicated that the major changes in sand level on the beaches and in adjacent shallow waters tend to be systematic and can be related to the character of wave motion, tidal cycles, and to seasonal variations representing the combined effects of tides and waves. Initially it was intended that an attempt be made to correlate the sand level changes at the four stations on D range directly with local wave and tide characteristics. However, the changes were smaller than anticipated and it early became apparent that one must look to more recondite parameters than can be extrapolated from simple wave parameters. Therefore no attempt was made to correlate day to day wave action with sand level changes, but rather a gross seasonal distinction based on wave height was made. Summer was arbitrarily defined as those months or portions of months during which significant breaker height exceeded 5 feet less than one-third of the time, and winter was defined as the intervening period during which the breaker height exceeded 5 feet more than one-third of the time. For this purpose the breaker height at the wave convergence zone near D range was selected. The envelope of the significant breaker heights is plotted as a function of time in figure 7 and the summer seasons are indicated.

SAND LEVEL CHANGES ON D RANGE

The major part of this study was devoted to a study of sand level changes on D range. The large number of measurements and the control afforded by this area allowed for a relatively rigorous statistical evaluation of sand level changes. The statistical methods used have already been outlined in the previous section. The results of these analyses are presented in Appendix I and II and are summarized in table 2.

Reliability of Reference Rod Measurements. An estimate of sand level at a given depth is the mean value of a group of measures and this mean value is dependent upon the local irregularities at that station. The precision with which the mean value estimates the sand level is dependent upon the magnitude of these local irregularities. The standard error is a measure of this precision and can be computed for one observation. However, a better estimate is to compute an average standard

Table 2. Summary of statistical results, D range.

Station Depth (ft)	Total Number of Surveys	Duration of Survey in Months	Standard Error of Measurement $SE = \frac{S}{\sqrt{n}}$ (ft)	Range in Mean Sand Level (ft)	Standard Deviation of Sand Level Changes (ft)			Cyclic Trend
					Within Months	Between Months	Between Seasons	
18	11	4	.061	.62	0.055	0.040*	--	--
30	45	32	.067	.29	0*	0.048	0.042	Seasonal
52	49	35	.050	.16	0.015*	0.003*	0.033	Yes**
70	40	33	.033	.15	0*	0.020	0.013*	Yes**

* Not significantly different from variations of shorter period.
** Cycles more frequent than seasonal, but less frequent than monthly.

Correlation Between Stations		
Between Stations	Estimated Correlation Coefficient	Statistically Significant
30 52	+0.36	Weak
30 70	-0.75	Yes
52 70	+0.60	Yes

error pooled from all observations. The standard errors computed for each station in this manner, from 18 feet to 70 feet, decrease progressively away from shore (table 2). This indicates that either the local bottom irregularities or the error in measuring, or both, decrease away from shore. It is believed that while conditions nearer shore made measurements somewhat more difficult, these influences are minor compared to the actual bottom irregularities. The average standard error of observation for the four stations is approximately 0.05 foot and is a confidence limit within which the mean sand level falls. This means that if the changes in sand level which one is trying to measure are of this order of magnitude, they will be masked by this error.

Magnitude of Sand Level Changes. The magnitude of the significant changes in sand level decreases with increasing depth and is found to be very small in depths of 30 feet and greater. The changes in sand level range from 0.15 foot at depths of 70 feet to values in excess of 0.6 foot in water depths of 18 feet (table 2). The results of the analysis of variance for the station at the depth of 18 feet are not valid for statistical inference between seasons because of the limited data[2]. However, these results give an order of magnitude of the variability within and between months.

For the other three stations on D range, there is a general decrease in the magnitude of the between season variability from station to station seaward. The component estimate of the between months variability at the 30-foot depth shows that there is a fluctuation of approximately 0.05 foot around the average level of sand, and indicates a range of about 0.10 foot for the changes. This range is equivalent to twice the standard deviation (table 2), where the standard deviation is the square root of the variance component. The estimate of the between months variation at the 70-foot depth is about half that at the 30-foot depth and the variation at the 52-foot depth is negligible.

The practical significance of the zero within months variation at the 30 and 70-foot depths and the negligible variation at the 52-foot depth is that the within months variations here are very small relative to the between rods variation (table 2). Therefore these variations are masked by the variation which takes place between rods. Consequently, it is apparent that more frequent measures in time would have to be made before these within month effects could be isolated and evaluated.

The results in the analysis of trend indicate that the changes in sand level are not random but cyclic in nature (table 2). The test used, however, is by nature not efficient for indicating seasonal trends in the presence of pronounced variations of shorter period. Thus, for example, at the 30-foot station, there is a trend in sand level with season which could be observed on the graph (figure 1), and which is further indicated by the average sand level height for each season (table 3), but which did not show up in the trend test. For this station the sand level tends to be high (deposition) during the summer and low (erosion) during the winter. The deeper stations did not show measurable seasonal trends, of cyclic nature but they did show shorter period cycles.

---

[2] The reference rods at this station were lost following a series of high waves in November, 1953. Acoustic soundings at this station indicated an erosion of sand of 2 feet.

Correlation of Sand Level Changes between Stations. It was desirable to know whether or not the changes in sand level between the various stations were related. The estimates of correlation previously described indicated (as in the example shown) that the correlation between the 70-foot station and the 30-foot station was inverse (or negative). That is, when sand was eroded at the 70-foot station, there was deposition at the 30-foot station; and, conversely, when there was deposition at the 70-foot station, there was erosion of sand at the 30-foot station. Between the 70-foot and the 52-foot depths there was a positive correlation; when sand was deposited at the 70-foot station, it was also built up at the 52-foot station. Between the 30-foot station and the 52-foot station, however, there was no strong correlation.

The fairly strong negative correlation between changes in sand level at the 30 and 70-foot depths, the somewhat weaker positive correlation between the 52 and 70-foot depths, and the very weak correlation between the 30 and 52-foot depths suggests that changes at the 52-foot station are transitional or borderline. That is to say, erosion at the 30-foot level is frequently accompanied by deposition at the 70-foot level and may or may not be accompanied by deposition at the 52-foot level.

No attempt was made to correlate the changes at the 18-foot depth with the other stations. The reason for this was that the number of observations from the 18-foot station was very limited in extent and did not allow for estimates of correlation.

Sand Size. A sample of the bottom sediment was obtained by the swimmers during each of the surveys on D range. The size distribution characteristics of the samples are listed in Appendix IIIA-B. The method of analysis and a detailed description of the character and composition of sediments obtained in this area during 1949 and 1950 are given in Inman, 1953.

The median diameter of the sediments averaged about 150 microns at the 18-foot depth, 120 microns at the 30-foot depth and 110 microns at the 52 and 70-foot depths. The size of the sand remained relatively constant at the three deeper stations during the first 18 months of the study, but fluctuated erratically during several periods beginning in

Table 3. Seasonal average of sand levels, D range.

Season	Station at 30-ft. depth		Station at 52-ft. depth		Station at 70-ft. depth	
	Number of Surveys	Average Sand Level (ft)	Number of Surveys	Average Sand Level (ft)	Number of Surveys	Average Sand Level (ft)
Winter 1952-1953	1	+.03	5	-.01	3	+.02
Summer 1953	9	+.02	5	-.01	2	0
Winter 1953-1954	12	0	14	+.04	10	+.01
Summer 1954	5	+.12	6	+.08	5	0
Winter 1954-1955	13	-.05	11	+.05	12	+.02
Summer 1955	2	+.01	5	+.07	5	+.06
Winter 1955-1956	3	-.04	3	+.08	3	+.03
Average Summer	16	+.05	16	+.05	12	+.02
Average Winter	29	-.02	33	+.04	28	+.02
Mean Sand Level	45	0	49	+.04	40	+.02

December, 1954. No simple correlation between sand size and sand level change was observed, although the large changes in sand size were commonly associated with greater than usual changes in sand level.

SAND LEVEL CHANGES ON B RANGE

The sand level changes associated with the tidal cycle were measured by placing a series of reference rods at intervals of 20 feet along a profile extending through the surf zone and onto the beach foreshore on B range. Three series of surveys, each consisting of a high-tide profile followed by a profile during the succeeding low tide, were made. The differences in sand level between tidal cycles within a day and the differences in level between days are shown in figure 8. The surveys were made during spring tides with ranges from high to low water level of about 6 feet. The significant breaker heights ranged from about 2 to 4 feet (Appendix IV).

Although these surveys represent a very small sample, there is some indication of systematic changes in profile related to the position of high and low tide breaker zones. All three survey series show deposition on the upper portions of the beach foreshore between the high and the following low tide, and the two October surveys show a tendency for a bar and trough to form in the zone of low tide breakers. It is interesting to note that for these surveys the magnitude of sand level change between high and low tide was one-half as great as the magnitude of the total change for the two-week period between the first and second surveys.

Several of the seaward reference rods have remained in position for over two years. They are completely covered with sand each winter and bared again for short periods during summer when the sand migrates landward and is deposited on the beach foreshore. The summer fluctuations in sand level at the deepest station on B range, approximately 6 feet below MLLW, are graphed together with the changes on D range in figure 7.

Experience indicated that accurate measurement of reference rods was limited to surf conditions where the breaking waves did not exceed 5 feet in height. For such conditions it is estimated that the accuracy of measurement is of the order of ±0.05 foot. This is the same order of magnitude as the standard error in level obtained for the deeper water stations on D range, which was based on the measurement of six rods. The similarity in the magnitude of error results from differences in the nature of the problem on the two ranges. The problem on D range was to determine the mean level for an area from six measurements of an irregular bottom, while on B range the interest was on the sand level at the position of a single reference rod.

ACOUSTIC SOUNDING

The evaluation of the accuracy of the acoustic method of hydrographic survey was one of the objectives of the investigation. It has been demonstrated that depths obtained by echo sounding are reproducible when repeated soundings are made during the same day (Shepard and Inman, 1951; Saville and Caldwell, 1953). This finding resulted in optimism in the estimation of the reliability of hydrographic surveys. In the previous studies comparison of sounding data over periods longer than a day could not be used to evaluate the reliability of the method because of the uncertainty in the amount of true change in sand level.

The total or compounded errors involved in reducing an uncorrected sounding to some absolute datum can be roughly divided into errors incurred in (1) measuring the instantaneous depth of water, (2) positioning, and (3) resolving the corrected depth to datum. For convenience these errors are listed in outline form in table 4. Inspection of this table shows that many of the factors leading to error tend to remain constant during the course of a single survey; wave and tide conditions are similar, the same operator bias is in effect, etc. On the other hand, day to day observations may involve differences in personnel, state of the sea, and instrument characteristics. Near the surf zone, surf beat (Munk, 1949) may produce fluctuations of sea level, of the order of one-tenth of the wave height, which are not coherent over the area of the survey. Also, so subtle a factor as moisture of the fathogram paper can change the degree of halation and clarity of the trace and hence the accuracy of the fathogram.

A series of echo sounding surveys were conducted concurrent with the reference rod measurements on station D. In general, five echo sounding runs were made on each station and the data from these reduced in the manner described previously. The mean values of each day's observations from the station at the 30-foot depth are shown together with the results from the reference rod measurements in figure 9. For purposes of illustration, a value of the reference level was assumed such that the depths from the acoustic sounding and from the reference rod measurements coincided on the first day of the comparison, 23 July 1953.

It is apparent from figure 9 that the daily ranges in acoustic soundings and reference rods were relatively small, the scatter of acoustic sounding being in general three to four times greater than that of the reference rods. However, the day to day or the survey to survey variation in acoustic soundings is much greater than that for the reference rods. If it is assumed that the reference rods give a reliable measure of the real changes in sand level, then it can be concluded that the accuracy of the acoustic method of survey under these experimental conditions is of the order of ± ½ foot. Similar accuracy was obtained for the stations of 52 and 70-foot depths.

Table 4. Outline of factors leading to error in the reduction of acoustic sounding data to basic datum.

1. Errors in measuring depth.
    a. Calibration of instrument
    b. Stability of instrument
    c. Background noise: wave conditions, clarity of record
    d. Operator variables: control of gain, frequency and power of sounder, systematic errors in reading record.
2. Errors in positioning.
    a. Operator errors
    b. State of sea; pitch and roll of vessel
    c. Slope of bottom
3. Errors in correcting measured depth to absolute datum (from tide gage).
    a. Background noise of tide record: waves, clarity of record
    b. Anomalies in recorded level: water level change in tide well caused by water velocity against orifice, etc.
    c. Incoherent changes in sea level: surf beat, surges, etc.

SUMMARY AND CONCLUSIONS

1. A technique was developed for establishing a reference level on the bottom from which small net changes in sand level of the sand could be measured. The reference level was established by forcing six rods into the sandy bottom and then the changes in sand level were based upon the differences in lengths of rod exposed from survey to survey. Measurements, which were made by swimmers equipped with self-contained underwater breathing apparatus, resulted in a standard error of about ±0.05 foot per survey.

2. The total range in sand level probably exceeds 2 feet at the 18-foot deep station and changes in excess of 0.6 foot were measured before the reference rods were lost. The range decreases with increasing depth; ranges in net sand level of 0.29, 0.16, and 0.15 foot were measured at stations where the depth of water was 30, 52, and 70 feet respectively.

3. Statistical evaluation of sand level changes demonstrates that there is a general decrease in the magnitude of the variability in sand level from station to station seaward. This implies that the local bottom irregularities at each station (as measured by the variability between the six reference rods), as well as the frequency and magnitude of net change in sand level at the station, decrease with increasing depth.

4. A seasonal trend in sand level change was observed at the station at 30-foot depth where the sand level was high in the summer and low in the winter. At the deeper stations, 52 and 70 feet, seasonal trends were masked by fluctuations of shorter period.

5. There is a significant correlation between changes in sand level from stations at various depths. Changes at one depth are accompanied by changes at another; and, their relation may be direct or inverse, depending upon the stations involved.

6. A comparison of sand level changes between tidal cycles, obtained from reference rods placed along a traverse through the surf zone, showed systematic changes to occur in the beach profile near the position of high and low tide breaker zones. For the six surveys, the magnitude of sand level change between high and low tide was approximately one-half as great as the total change during the two week period.

7. Comparison of acoustic soundings with reference rod measurements indicated that the day to day accuracy of the acoustic sounding method was of the order of ± $\frac{1}{2}$ foot, although soundings during one day of survey operation may be relatively precise in terms of reproducibility.

ACKNOWLEDGEMENTS

The field phase of the investigation was largely the work of Earl Murray, who was in charge of the boat and made all of the reference rod measurements. Assistance in the field work and analysis of data was given by Jean Short, and assistance with illustrations was given by Robert C. Winsett. Valuable suggestions and guidance during the course of the study were contributed by Robert S. Arthur, Jeffrey D. Frautschy, George F. McEwen, **Robert L. Miller and J. S. Kahn.**

LITERATURE CITED

1. Dixon, W. J. and F. J. Massey. 1951. Introduction to statistical analysis. McGraw-Hill, New York, 370 pp.

2. Eisenhart, C., M. W. Hastay, and W. A. Wallis. 1947. Techniques of statistical analysis. McGraw-Hill, New York, 473 pp.

3. Fisher, R. A. 1949. Statistical methods for research workers. Oliver and Boyd, London.

4. Hald, A. 1952. Statistical theory with engineering applications. John Wiley and Sons, Inc., New York, p. 749.

5. Inman, D. L. 1952. "Measures for describing the size distribution of sediments". Jour. Sed. Petrol., Vol. 22, pp. 125-145.

6. Inman, D. L. 1953. "Areal and seasonal variations in beach and nearshore sediments at La Jolla, California." Beach Erosion Board, Corps of Engineers, Tech. Memo. No. 39, 134 pp.

7. Munk, W. H. 1949. "Surf beats." Trans. Amer. Geoph. Union, Vol. 30, pp. 849-854.

8. Olson, J. S. and P. E. Potter. 1954. "Variance components of cross-bedding in some basal Pennsylvanian sandstone of the eastern interior basin; statistical applications." Jour. Geology, Vol. 62, pp. 26-48.

9. Saville, Thorndike, Jr. and J. M. Caldwell. 1953. "Accuracy of hydrographic surveying in and near the surf zone." Beach Erosion Board, Corps of Engineers, Tech. Memo. No. 32, 28 pp.

10. Shepard, F. P. and D. L. Inman. 1951. "Sand movement on the shallow inter-canyon shelf at La Jolla, California." Beach Erosion Board, Corps of Engineers, Tech. Memo. No. 26, 29 pp.

11. Snedecor, G. W. 1946. Statistical methods. The Iowa State College Press, Ames, Iowa, 485 pp.

APPENDIX IA-ID

Deviations of Individual Rod Measurements from Their Reference Level, D Range

IA Station at 18-ft. depth
IB Station at 30-ft. depth
IC Station at 52-ft. depth
ID Station at 70-ft. depth

APPENDIX IA - STATION AT 18-FT. DEPTH

DATE	DIFFERENCE FROM REFERENCE LEVEL IN FT.						MEAN	STANDARD DEVIATION
	Rod 1	Rod 2	Rod 3	Rod 4	Rod 5	Rod 6	$\bar{x}$	s
10 July '53	+.04	+.13	+.08	+.06	+.04	+.04	+.06	.036
17 July '53	-.04	-.01	+.02	-.03	+.01	-.03	-.01	.088
23 July '53	-.08	-.01	-.09	-.05	-.07	-.12	-.07	.037
27 July '53	-.07	-.06	-.09	-.08	-.04	-.11	-.08	.024
12 Aug. '53	-.09	-.07	-.07	-.05	-.07	--	-.07	.014
14 Aug. '53	-.11	-.06	-.06	-.12	-.06	--	-.08	.030
25 Aug. '53	-.13	-.09	-.08	-.16	-.18	--	-.13	.043
31 Aug. '53	-.10	-.12	-.12	-.12	-.22	--	-.14	.048
11 Sep. '53	-.18	-.13	-.08	-.08	-.12	--	-.12	.041
15 Oct. '53	-.48	-.38	-.39	-.37	-.48	--	-.42	.055
21 Oct. '53	-.56	-.44	-.52	-.47	-.80	--	-.56	.143

APPENDIX IB - STATION AT 30-FT. DEPTH

DATE	DIFFERENCE FROM REFERENCE LEVEL IN FT.						MEAN	STANDARD DEVIATION
	Rod 1	Rod 2	Rod 3	Rod 4	Rod 5	Rod 6	$\bar{x}$	s
22 June '53	+.02	+.05	+.03	+.05	+.01	0	+.03	.020
7 July '53	0	--	+.04	+.10	+.05	+.03	+.04	.037
23 July '53	-.08	-.02	+.01	-.03	+.02	-.04	-.02	.037
27 July '53	0	+.03	-.01	+.02	-.02	-.02	0	.021
5 Aug. '53	-.06	+.02	0	+.03	+.01	+.04	+.01	.036
12 Aug. '53	+.01	+.05	+.03	+.08	+.01	+.02	+.04	.027
21 Aug. '53	-.02	-.01	-.04	+.01	-.08	-.03	-.02	.030
25 Aug. '53	+.06	+.05	+.08	+.08	+.03	0	+.05	.031
31 Aug. '53	-.01	+.06	-.05	+.07	-.01	+.04	+.02	.047
11 Sep. '53	+.02	+.07	+.07	+.04	+.03	+.01	+.04	.025
15 Oct. '53	-.06	-.03	-.04	0	-.09	-.03	-.04	.030
21 Oct. '53	-.08	-.03	-.08	+.03	-.06	-.02	-.04	.042
16 Nov. '53	-.21	-.12	-.15	-.11	-.21	-.08	-.15	.054
28 Dec. '53	+.01	+.02	+.02	+.09	-.07	-.03	+.01	.054
5 Jan. '54	-.02	+.01	0	+.04	-.04	-.04	-.01	.031

APPENDIX IB - 2

DATE	DIFFERENCE FROM REFERENCE LEVEL IN FT.						MEAN	STANDARD DEVIATION
	Rod 1	Rod 2	Rod 3	Rod 4	Rod 5	Rod 6	$\bar{x}$	s
22 Jan. '54	-.01	+.04	-.02	+.03	-.05	-.07	-.01	.043
2 Feb. '54	-.03	-.02	-.02	-.02	-.07	-.02	-.03	.020
29 Mar. '54	+.02	0	+.20	+.04	+.01	0	+.05	.077
27 Apr. '54	+.11	+.08	+.20	+.09	+.04	-.08	+.07	.092
14 May '54	-.17	+.08	-.05	+.16	-.06	+.02	0	.116
18 June '54	+.08	+.19	+.01	+.16	+.03	-.06	+.07	.095
28 June '54	+.09	-.08	+.22	+.13	+.06	+.04	+.08	.099
26 July '54	+.11	+.10	+.28	+.13	+.08	+.07	+.13	.077
16 Aug. '54	+.02	+.10	+.22	+.11	+.06	0	+.09	.079
26 Aug. '54	+.06	+.15	+.25	+.14	+.07	+.07	+.13	.073
1 Sep. '54	+.12	+.16	+.24	+.16	+.08	+.06	+.14	.065
4 Oct. '54	+.11	+.10	+.24	-.04	+.03	+.05	+.09	.094
15 Dec. '54	-.05	-.03	+.11	-.09	-.07	-.16	-.05	.089
20 Dec. '54	-.10	-.05	+.04	--	-.09	-.17	-.07	.077
21 Dec. '54	-.08	--	--	--	-.19	-.09	-.12	.060

APPENDIX IB - 3

DATE	DIFFERENCE FROM REFERENCE LEVEL IN FT.						MEAN	STANDARD DEVIATION
	Rod 1	Rod 2	Rod 3	Rod 4	Rod 5	Rod 6	$\bar{x}$	S
25 Jan. '55	-.05	0	+.10	-.04	-.02	-.09	-.02	.065
15 Feb. '55	-.05	-.07	+.05	-.06	-.17	-.12	-.07	.074
10 Mar. '55	-.07	-.05	+.08	-.07	-.07	-.10	-.05	.064
22 Mar. '55	-.05	-.04	+.10	-.07	-.06	-.13	-.04	.077
6 Apr. '55	-.03	-.01	+.12	+.01	0	-.03	+.01	.056
29 Apr. '55	-.02	-.03	+.10	-.05	-.01	-.09	-.02	.064
5 May '55	-.01	+.02	+.15	+.09	-.07	-.05	+.02	.084
17 May '55	-.07	-.03	0	-.03	-.06	-.09	-.04	.033
8 June '55	-.07	-.15	+.12	0	--	-.15	-.05	.118
6 July '55	-.10	-.07	+.01	-.05	-.15	-.31	-.11	.110
1 Aug. '55	-.05	+.03	+.03	-.04	-.04	-.04	-.02	.038
12 Oct. '55	-.10	-.01	+.23	+.07	+.09	-.07	+.04	.121
23 Nov. '55	-.03	+.05	+.20	0	-.01	+.05	+.04	.083
13 Jan. '56	-.14	-.11	-.03	-.09	-.02	-.12	-.08	.048
30 Jan. '56	-.12	-.12	+.05	-.13	-.09	-.10	-.08	.068

APPENDIX IC - STATION AT 52-FT. DEPTH

DATE	DIFFERENCE FROM REFERENCE LEVEL IN FT.						MEAN	STANDARD DEVIATION
	Rod 1	Rod 2	Rod 3	Rod 4	Rod 5	Rod 6	$\bar{x}$	s
11 Mar. '53	-.01	-.01	-.01	-.01	-.07	-.02	-.02	.024
18 Mar. '53	-.01	-.01	-.02	+.01	+.01	-.05	-.01	.022
31 Mar. '53	0	0	-.02	0	0	-.05	-.01	.020
4 May '53	+.04	-.01	-.02	+.01	-.01	-.04	-.01	.027
24 June '53	+.04	-.03	-.03	+.04	-.03	--	0	.038
10 July '53	+.04	-.03	0	+.02	-.01	-.08	-.01	.042
17 July '53	+.04	-.01	0	+.02	-.06	-.09	-.02	.049
5 Aug. '53	-.03	-.04	0	0	-.08	-.14	-.05	.054
14 Aug. '53	+.05	-.02	+.03	+.02	-.02	-.08	0	.047
21 Aug. '53	+.10	+.03	+.09	+.05	0	-.04	+.04	.053
20 Oct. '53	+.05	0	-.03	+.08	-.05	-.08	-.01	.061
23 Oct. '53	+.06	0	0	+.15	-.03	-.05	+.02	.073
16 Nov. '53	+.03	-.01	+.02	+.09	-.01	-.12	0	.069
19 Nov. '53	-.01	-.01	+.05	+.05	+.04	-.07	+.01	.047
23 Nov. '53	0	-.01	+.04	+.09	+.04	-.07	+.02	.055
28 Dec. '53	0	0	+.01	+.08	+.05	-.04	+.02	.042

APPENDIX IC - 2

DATE	DIFFERENCE FROM REFERENCE LEVEL IN FT.						MEAN	STANDARD DEVIATION
	Rod 1	Rod 2	Rod 3	Rod 4	Rod 5	Rod 6	$\bar{x}$	s
14 Jan. '54	+.01	+.01	+.03	+.02	-.03	-.03	0	.018
21 Jan. '54	+.09	+.04	+.04	+.13	+.05	+.02	+.06	.040
28 Jan. '54	+.17	+.07	+.10	+.15	+.04	+.05	+.10	.053
29 Mar. '54	--	+.03	-.01	+.12	+.05	+.09	+.06	.051
27 Apr. '54	--	-.01	-.01	+.11	+.09	-.01	+.03	.060
14 May '54	--	+.03	+.07	+.15	+.12	+.07	+.09	.047
18 June '54	--	+.13	-.01	+.02	+.07	-.02	+.04	.062
28 June '54	--	+.05	+.09	+.13	+.13	+.02	+.08	.049
26 July '54	--	+.07	+.09	+.13	+.09	+.03	+.08	.036
16 Aug. '54	--	+.06	+.08	+.17	+.11	+.01	+.09	.059
26 Aug. '54	--	+.03	+.07	+.15	+.09	+.02	+.05	.052
1 Sep. '54	--	+.03	+.06	+.15	+.09	+.07	+.06	.045
28 Sep. '54	--	+.09	+.07	+.11	+.05	0	+.06	.042
4 Oct. '54	--	+.05	+.09	+.13	+.06	+.22	+.11	.069
15 Dec. '54	--	-.02	+.04	+.12	+.04	-.05	+.03	.065

APPENDIX IC - 3

DATE	DIFFERENCE FROM REFERENCE LEVEL IN FT.						MEAN	STANDARD DEVIATION
	Rod 1	Rod 2	Rod 3	Rod 4	Rod 5	Rod 6	$\bar{x}$	s
21 Dec. '54	--	+.04	+.07	+.08	+.08	-.01	+.05	.038
25 Jan. '55	--	0	+.09	+.11	-.01	+.05	+.05	.053
15 Feb. '55	--	+.02	+.07	+.07	-.01	+.01	+.03	.036
10 Mar. '55	--	+.05	+.05	+.11	+.06	+.01	+.06	.036
22 Mar. '55	--	+.04	+.09	+.21	+.10	+.02	+.09	.074
6 Apr. '55	--	-.01	+.07	+.17	+.05	-.04	+.05	.081
29 Apr. '55	--	+.04	-.03	+.07	+.08	-.05	+.02	.059
5 May '55	--	+.09	+.02	+.12	+.12	+.05	+.08	.044
17 May '55	--	0	+.04	+.12	+.09	+.08	+.07	.047
8 June '55	--	0	+.05	+.10	+.07	+.09	+.06	.040
6 July '55	--	-.01	+.12	+.12	+.07	+.02	+.04	.059
1 Aug. '55	--	+.03	+.12	+.16	+.06	+.04	+.08	.056
10 Sep. '55	--	+.07	+.02	+.06	+.10	+.06	+.06	.029

APPENDIX IC - 4

DATE	DIFFERENCE FROM REFERENCE LEVEL IN FT.						MEAN	STANDARD DEVIATION
	Rod 1	Rod 2	Rod 3	Rod 4	Rod 5	Rod 6	$\bar{x}$	s
3 Oct. '55	--	+.10	+.02	+.14	+.12	-.03	+.07	.072
12 Oct. '55	--	+.09	+.13	+.07	+.05	+.11	+.09	.032
23 Nov. '55	--	+.04	+.09	+.18	+.13	+.06	+.10	.056
13 Jan. '56	--	+.07	+.05	+.17	+.09	+.05	+.09	.050
30 Jan. '56	--	+.04	+.01	+.07	+.01	+.13	+.05	.050

APPENDIX ID - STATION AT 70-FT. DEPTH

DATE	DIFFERENCE FROM REFERENCE LEVEL IN FT.						MEAN	STANDARD DEVIATION
	Rod 1	Rod 2	Rod 3	Rod 4	Rod 5	Rod 6	$\bar{x}$	s
4 May '53	+.01	-.02	+.01	+.04	+.01	+.04	+.02	.022
13 May '53	+.05	-.02	0	+.03	+.03	0	+.02	.026
26 June '53	+.02	--	0	+.03	+.04	0	+.02	.018
22 July '53	+.03	+.01	0	-.04	+.03	-.01	0	.026
19 Aug. '53	+.04	0	+.03	-.06	0	0	0	.034
30 Oct. '53	-.02	-.03	+.03	-.01	-.02	-.04	-.02	.024
19 Nov. '53	-.02	-.06	+.04	-.01	0	-.02	-.01	.032
28 Dec. '53	-.02	-.02	+.03	-.02	-.04	+.02	-.01	.027
26 Jan. '54	+.02	-.03	+.04	+.01	-.02	-.01	0	.026
27 Jan. '54	+.01	+.04	+.05	+.06	+.07	+.01	+.04	.025
28 Jan. '54	+.04	+.02	+.06	+.06	+.05	+.04	+.04	.015
29 Mar. '54	-.01	-.02	+.03	-.01	-.03	+.02	0	.023
27 Apr. '54	-.03	-.04	+.03	+.02	-.05	+.01	-.01	.034
14 May '54	+.04	+.03	+.02	+.07	+.02	+.02	+.03	.020

APPENDIX ID - 2

DATE	DIFFERENCE FROM REFERENCE LEVEL IN FT.						MEAN	STANDARD DEVIATION
	Rod 1	Rod 2	Rod 3	Rod 4	Rod 5	Rod 6	$\bar{x}$	s
18 June '54	0	-.03	+.03	+.03	+.02	+.02	+.01	.023
26 July '54	0	-.02	+.03	-.02	+.06	0	+.01	.031
16 Aug. '54	-.03	-.03	+.05	+.01	+.08	+.03	+.02	.044
26 Aug. '54	+.03	-.04	+.01	0	+.07	+.05	+.02	.039
1 Sep. '54	+.02	-.20	0	-.07	+.06	+.03	-.03	.095
4 Oct. '54	-.07	-.06	+.01	0	+.02	0	-.02	.038
15 Dec. '54	-.02	+.04	+.07	+.05	-.01	+.03	+.03	.035
21 Dec. '54	+.03	+.05	+.06	+.02	+.05	+.02	+.04	.017
25 Jan. '55	-.15	-.01	-.10	-.20	-.03	+.01	-.08	.084
15 Feb. '55	+.06	0	+.07	-.20	+.02	+.07	0	.103
10 Mar. '55	+.06	-.01	+.03	0	+.02	+.07	+.03	.032
22 Mar. '55	+.03	0	+.06	-.01	+.02	+.07	+.03	.032
6 Apr. '55	0	+.01	+.06	+.02	-.05	+.07	+.02	.048
20 Apr. '55	+.04	+.02	+.07	+.08	-.05	+.01	+.03	.047
29 Apr. '55	+.02	+.09	+.05	+.06	+.07	+.03	+.05	.022
5 May '55	+.02	-.04	+.04	+.06	+.05	+.07	+.03	.040

APPENDIX ID - 3

DATE	DIFFERENCE FROM REFERENCE LEVEL IN FT.						MEAN	STANDARD DEVIATION
	Rod 1	Rod 2	Rod 3	Rod 4	Rod 5	Rod 6	$\bar{x}$	s
16 May '55	+.02	-.01	+.02	-.05	-.05	+.05	0	.041
8 June '55	+.09	-.03	+.05	+.03	+.07	+.04	+.04	.041
6 July '55	+.14	+.01	+.03	+.10	+.08	+.07	+.07	.047
1 Aug. '55	+.11	+.01	+.04	+.05	+.06	+.12	+.06	.042
10 Sep. '55	+.11	0	+.08	+.03	+.01	+.12	+.06	.052
3 Oct. '55	+.06	0	+.09	+.02	+.05	+.03	+.04	.032
12 Oct. '55	+.06	+.02	+.09	+.06	+.06	-.03	+.05	.035
23 Nov. '55	+.05	-.02	+.06	+.07	+.05	+.05	+.04	.032
13 Jan. '56	+.06	+.01	+.03	+.04	+.06	+.09	+.05	.028
30 Jan. '56	+.03	-.01	+.02	+.04	+.01	-.01	+.01	.020

APPENDIX IIA - IID

Summary

Analysis of Variance, D Range

IIA Station at 18-ft. depth

IIB Station at 30-ft. depth

IIC Station at 52-ft. depth

IID Station at 70-ft. depth
(see table 1, part B)

APPENDIX IIA - STATION AT 18-FT DEPTH

SUMMARY

ANALYSIS OF VARIANCE

	Between Rods	Within Months	Between Months
Lower Level Sum	3.00760	2.83052	2.69021
Higher Level Sum	2.83052	2.69021	2.60412
Sum Squared Deviations	0.17708	0.14031	0.08609
Degrees of Freedom	48	7	2
Mean Square	0.00368	0.02004	0.04305
Lower Component		0.00368	0.02004
Difference		0.01636	0.02301
Effective Subsample		5.42857	14.28571
Component Estimate, s^2	0.00368	0.00301	0.00161
F		5.44565**	2.15019*

* Not significantly different from variations of shorter period.

** Significant at the 0.01 level; therefore highly significant.

APPENDIX IIB - STATION AT 30-FT DEPTH

SUMMARY

ANALYSIS OF VARIANCE

	Between Rods	Within Months	Between Months	Between Seasons
Lower Level Sum	2.06310	1.04648	0.99129	0.52808
Higher Level Sum	1.04648	0.99129	0.52808	0.00057
Sum Squared Deviations	1.01662	0.05519	0.46321	0.52751
Degrees of Freedom	219	16	22	6
Mean Square	0.00464	0.00344	0.02105	0.08791
Lower Component		0.00464	0.00344	0.02105
Difference		-0.00120	0.01761	0.06686
Effective Subsample		5.86570	7.52719	37.39962
Component Estimate, S^2	0.00464	0	0.00233	0.00178
F		0.74137*	6.11918**	4.17624**

* Not significantly different from variations of shorter period.

** Significant at the 0.01 level; therefore highly significant.

APPENDIX IIC - STATION AT 52-FT DEPTH

SUMMARY

ANALYSIS OF VARIANCE

	Between Rods	Within Months	Between Months	Between Seasons
Lower Level Sum	1.39220	0.84612	0.77338	0.68151
Higher Level Sum	0.84612	0.77338	0.68151	0.43288
Sum Squared Deviations	0.54608	0.07274	0.09187	0.24863
Degrees of Freedom	214	19	23	6
Mean Square	0.00255	0.00382	0.00399	0.04143
Lower Component		0.00255	0.00382	0.00399
Difference		0.00127	0.00017	0.03744
Effective Subsample		5.25692	8.69122	34.68441
Component Estimate, S^2	0.00255	0.00024	0.00001	0.00107
F		1.49803*	1.04450*	10.38345**

* Not significantly different from variations of shorter period.

** SIgnificant at the 0.01 level; therefore highly significant.

APPENDIX IID - Station at 70-ft. depth

See table 1, part B (page 15)

APPENDIX IIIA - IIID

Sediment Size, D Range

IIIA	Station at 18-ft. depth
IIIB	Station at 30-ft. depth
IIIC	Station at 52-ft. depth
IIID	Station at 70-ft. depth

APPENDIX IIIA. STATION AT 18-FT. DEPTH

Date	Median Diameter in Microns	Phi Size Distribution Measures*		
		Median Diameter Md_ϕ	Deviation Measure σ_o	Skewness Measure α_o
17 July '53	153	2.71	.38	-.03
23 July '53T	146	2.78	.38	-.05
23 July '53C	154	2.70	.38	-.05
12 Aug. '53	146	2.78	.42	-.05
14 Aug. '53	145	2.79	.40	-.05
25 Aug. '53	152	2.72	.45	0
31 Aug. '53	151	2.73	.42	-.07
11 Sep. '53	147	2.77	.42	-.07
15 Oct. '53	157	2.67	.38	-.03
21 Oct. '53	137	2.87	.45	-.09

---

* The phi size-distribution measures (Inman, 1952) are defined as:

$$Md_\phi = \phi_{50}$$

$$\sigma_o = \tfrac{1}{2}(\phi_{84} - \phi_{16})$$

$$\alpha_o = \frac{M_\phi - Md_\phi}{\sigma_o}$$

where $M_\phi = \frac{1}{2}(\phi_{16} + \phi_{84})$ is the phi mean diameter and ϕ_{16}, ϕ_{50}, and ϕ_{84} are diameters in phi units corresponding to the 16th, 50th, and 84th percentiles of the cumulative weight - percent (coarser) curve. $\phi = -\log_2$ (diameter in millimeters).

APPENDIX IIIB- STATION AT 30-FT. DEPTH

Date	Median Diameter in Microns	Phi Size Distribution Measures*		
		Median Diameter Md_ϕ	Deviation Measure σ_ϕ	Skewness Measure α_ϕ
23 July '53	124	3.01	.46	-.06
27 July '53	117	3.09	.46	-.07
5 Aug. '53	120	3.06	.47	-.11
12 Aug. '53	117	3.10	.46	-.04
21 Aug. '53	118	3.08	.48	-.04
25 Aug. '53	124	3.01	.48	-.02
31 Aug. '53	128	2.96	.47	-.04
15 Oct. '53	126	2.99	.50	-.02
16 Nov. '53	114	3.13	.47	-.17
28 Dec. '53	117	3.10	.50	-.12
5 Jan. '54	122	3.04	.55	-.13
22 Jan. '54	136	2.88	.47	-.02
2 Feb. '54	124	3.01	.47	-.02
27 Apr. '54	127	2.98	.51	-.06
14 May '54	122	3.03	.45	-.07
18 June '54	121	3.05	.45	-.07
28 June '54	117	3.10	.51	0
26 July '54	117	3.10	.46	0
16 Aug. '54	121	3.05	.46	-.07
26 Aug. '54	115	3.12	.44	-.02
1 Sep. '54	118	3.08	.45	-.06
28 Sep. '54	120	3.06	.45	0
4 Oct. '54	122	3.04	.47	-.10

APPENDIX IIIB- 2

Date	Microns	Md_ϕ	σ_ϕ	α_ϕ
15 Dec. '54	118	3.08	.48	-.02
20 Dec. '54	138	2.86	.47	+.04
21 Dec. '54	125	3.00	.47	+.04
25 Jan. '55	103	3.28	.40	-.10
15 Feb. '55	115	3.12	.48	-.12
10 Mar. '55	128	2.96	.42	-.11
22 Mar. '55	115	3.12	.50	-.04
6 Apr. '55	113	3.14	.45	-.30
29 Apr. '55	125	3.00	.45	-.04
5 May '55	129	2.95	.44	-.02
17 May '55	122	3.03	.45	-.07
8 June '55	115	3.12	.40	-.05
6 July '55	122	3.03	.41	-.10
1 Aug. '55	144	2.80	.45	0
12 Oct. '55	125	3.00	.42	+.05
23 Nov. '55	113	3.14	.45	-.22
13 Jan. '56	127	2.98	.50	-.04
30 Jan. '56	109	3.20	.48	-.30

APPENDIX IIIC- STATION AT 52-FT. DEPTH

Date	Median Diameter in Microns	Phi Size Distribution Measures*		
		Median Diameter Md_ϕ	Deviation Measure σ_ϕ	Skewness Measure α_ϕ
10 July '53	106	3.24	.39	-.15
5 Aug. '53	107	3.23	.42	-.12
20 Oct. '53	102	3.29	.38	-.13
16 Nov. '53	102	3.29	.38	-.08
19 Nov. '53	106	3.24	.38	-.05
28 Dec. '53	102	3.30	.36	-.17
14 Jan. '54	105	3.25	.42	-.14
28 Jan. '54	106	3.24	.38	-.10
29 Mar. '54	107	3.23	.41	-.10
27 Apr. '54	107	3.22	.40	-.05
14 May '54	109	3.20	.40	-.05
18 June '54	104	3.26	.38	-.10
28 June '54	107	3.23	.44	-.20
26 July '54	103	3.28	.42	-.14
16 Aug. '54	107	3.23	.41	-.14
26 Aug. '54	107	3.22	.42	-.10
1 Sep. '54	102	3.30	.40	-.20
28 Sep. '54	108	3.21	.44	0
4 Oct. '54	99	3.33	.37	-.16
15 Dec. '54	109	3.20	.38	-.13
21 Dec. '54	102	3.30	.35	-.08
25 Jan. '55	120	3.06	.46	-.04

APPENDIX IIIC- 2

Date	Microns	Md_ϕ	σ_ϕ	α_ϕ
15 Feb. '55	113	3.14	.48	-.04
10 Mar. '55	107	3.22	.43	-.11
22 Mar. '55	112	3.16	.42	-.09
6 Apr. '55	106	3.24	.36	-.36
29 Apr. '55	109	3.20	.40	-.10
5 May '55	130	2.94	.54	0
17 May '55	117	3.09	.45	-.07
8 June '55	113	3.15	.38	-.03
6 July '55	117	3.10	.39	-.30
1 Aug. '55	110	3.19	.34	0
10 Sep. '55	109	3.20	.34	-.12
3 Oct. '55	113	3.15	.36	-.08
12 Oct. '55	102	3.29	.37	-.16
13 Jan. '56	118	3.08	.42	-.10
30 Jan. '56	117	3.10	.36	-.08

APPENDIX IIDD- STATION AT 70-FT. DEPTH

Date	Median Diameter in Microns	Phi Size Distribution Measures*		
		Median Diameter Md_ϕ	Deviation Measure σ_ϕ	Skewness Measure α_ϕ
22 July '53	109	3.20	.38	-.10
19 Nov. '53	109	3.20	.37	-.13
28 Dec. '53	106	3.24	.39	-.08
26 Jan. '54	106	3.24	.38	-.13
27 Jan. '54	109	3.20	.44	-.05
28 Jan. '54	107	3.23	.38	-.08
29 Mar. '54	111	3.17	.42	-.17
27 Apr. '54	117	3.10	.42	-.10
14 May '54	113	3.15	.41	-.02
18 June '54	114	3.13	.38	-.03
26 July '54	109	3.20	.40	-.12
16 Aug. '54	111	3.17	.38	+.03
26 Aug. '54	112	3.16	.42	-.09
1 Sep. '54	110	3.18	.41	-.05
28 Sep. '54	108	3.21	.41	0
4 Oct. '54	111	3.17	.42	-.17
15 Dec. '54	105	3.25	.42	-.07
21 Dec. '54	118	3.08	.40	-.10
25 Jan. '55	121	3.05	.44	-.11
15 Feb. '55	103	3.28	.39	-.13
10 Mar. '55	113	3.15	.42	-.12

APPENDIX IIID- 2

Date	Microns	Md_ϕ	σ_ϕ	α_ϕ
22 Mar. '55	110	3.18	.37	-.10
23 Mar. '55	112	3.16	.40	-.02
6 Apr. '55	109	3.20	.36	-.16
20 Apr. '55	110	3.18	.38	-.05
29 Apr. '55	134	2.90	.25	-.20
5 May '55	124	3.01	.42	-.07
16 May '55	117	3.10	.40	-.05
8 June '55	112	3.16	.36	-.06
6 July '55	134	2.90	.32	-.06
1 Aug. '55	129	2.95	.42	-.02
10 Sep. '55	113	3.15	.37	+.03
3 Oct. '55	122	3.03	.42	-.07
12 Oct. '55	119	3.07	.39	-.10
23 Nov. '55	125	3.00	.40	-.05
13 Jan. '56	125	3.00	.45	-.04
30 Jan. '56	122	3.03	.38	-.18

APPENDIX IV
WAVE AND TIDE DATA

APPENDIX IV

Wave and tide data for the beach profile measurements on B range, shown in figure 8.

Date	Survey	Tide*			Significant Waves**	
		Time	High (ft)	Low (ft)	Breaker Height (ft)	Period (sec)
22 Sep. '53		0212		-0.4		
	High →	0806	5.6		2.5	7
	Low →	1430		0.1		
		2024	6.1			
6 Oct. '53		0206		1.0		
	High →	0754	5.3		1.9	10
	Low →	1424		0.9	3.0	12
		2012	4.8			
8 Oct. '53		0242		1.4		
	High →	0836	5.5		3.1	10
	Low →	1530		0.4	4.1	
		2124	4.2			

* Time and height of tide from the U. S. Coast and Geodetic Survey gage on the ocean pier at the Scripps Institution of Oceanography. Datum is MLLW.

** The significant breaker height is the average of the highest one-third of the waves. The number of waves averaged was based on the average period of the groups of highest waves.

Observations of Internal Tides in October 1950*

Joseph L. Reid, Jr.

Abstract—Over six days of anchor station hydrographic data from each of three vessels on a line 280 mi long were analyzed for internal waves of tidal (and other) periods. Waves of semidiurnal period with amplitudes greater than 30 ft were found at the nearshore station (40 mi offshore in 1080 fm), but little evidence of these waves or any other periodic phenomena was found at the stations farther offshore though there was considerable vertical fluctuation of isotherms. It is suggested that the waves found originate near the coast in the action of the surface tides and that, since the length of such waves, if free, is short, they either dissipate before proceeding far offshore or, more likely, are so distorted by the varying density structure and water velocity that they are no longer recognized.

Introduction—The effect of internal waves of tidal period upon the interpretation of dynamic topography has concerned various authors, among them *Seiwell* [1939] and *Defant* [1950ab]. *Rudnick* and *Cochrane* [1951] have examined three long series of data from points far from shore and found but little evidence of tidal periods. *Haurwitz* [1954] has demonstrated that short series (24 to 72 hr) can hardly yield conclusive results since the amplitudes may be the result of random fluctuations. *Rudnick* and *Cochrane* [1951] suggest that some limitation exists as to place and manner of occurrence of internal tidal waves, and that they may be generated at ocean boundaries. *Arthur* [1954] has examined temperature data from two piers and from an area within four kilometers of one of them, and found oscillations which suggest the possibility of tidal periodicities, though not as regular as the surface tides, and which would be consistent with an internal wave mechanism. *Haurwitz* [1950] has shown that internal tidal waves may have lengths of the order of 20 to 40 mi. *Rattray* [1954] has considered the effect of eddy viscosity upon such waves and concluded that their amplitude would be reduced by one-half at distances of from 120 to 15,000 km, depending mostly upon eddy viscosity, depth of the shallower layer (in a two-layer system), and the density difference.

Observations discussed in this paper bear upon the place of origin and subsequent behavior of certain internal tidal waves.

Observations of internal tides in October 1950—Beginning October 11, 1950, three vessels occupied positions at distances of 40, 160, and 320 nautical mi offshore on a line running 240° true from Point Sur, California, at depths of 1080, 2350, and 2415 fm respectively (Fig. 1). The nearshore vessel was anchored for seven days. The others were kept on station for eight days by celestial navigation. Hourly bathythermograph (BT) lowerings were made and hydrographic casts at intervals of three hours were taken for temperature, salinity, and oxygen determinations. Casts at Greenwich noon and midnight were made to 1000 m, others to 300 m. Wind varied over the area and period from calm to Beaufort force 6, but was mostly less than force 4.

The purpose of the cruise was to observe the internal waves, particularly those of tidal character, and to provide information for the interpretation of dynamic topography over the area.

Figures 2 and 3 show representative data from the three stations and the semidiurnal part of the predicted tide at the nearest part of the coast (with no phase adjustment but an arbitrary amplitude-scale ratio of 20/1). At the nearshore station the rise and fall of the thermocline immediately suggests semidiurnal tidal behavior. No such behavior is apparent to the eye at the outer stations. A harmonic analysis has been performed and a reality test employed for periods of 12.4206 (M_2), 12 (S_2), and 24 hr (K_1). Data used were depths of thermocline and isotherms from the

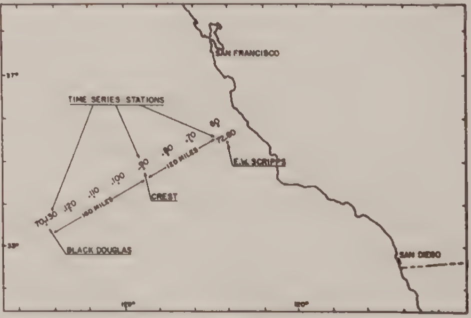

Fig. 1 – CCOFI Cruise 5011 (MLR 19), November, 1950

---

* Contribution from the Scripps Institution of Oceanography, New Series, No. 855.

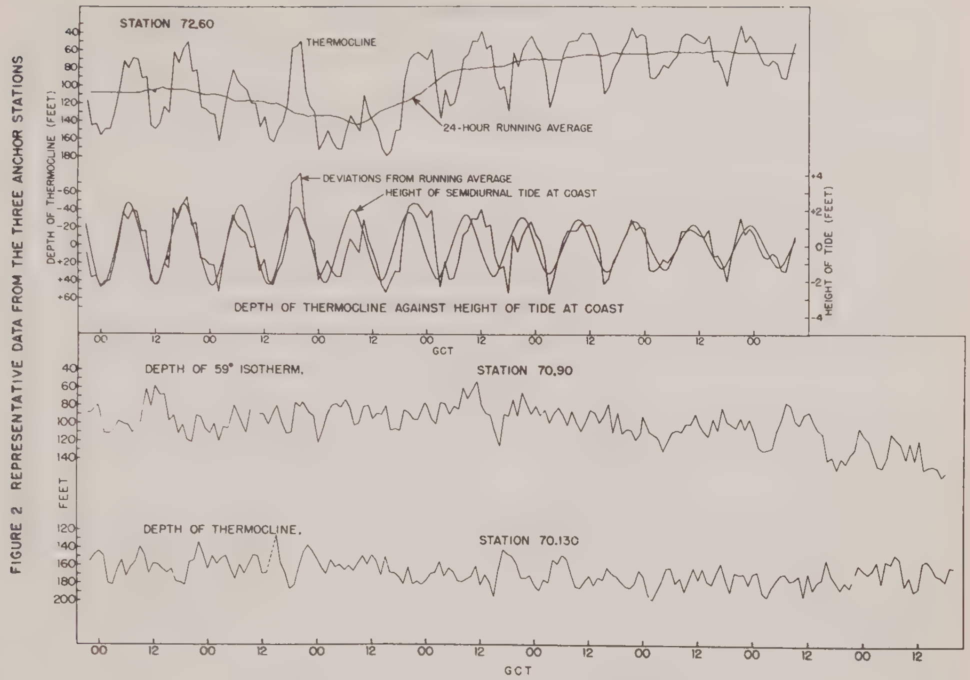

FIG. 2 – Representative data from the three anchor stations

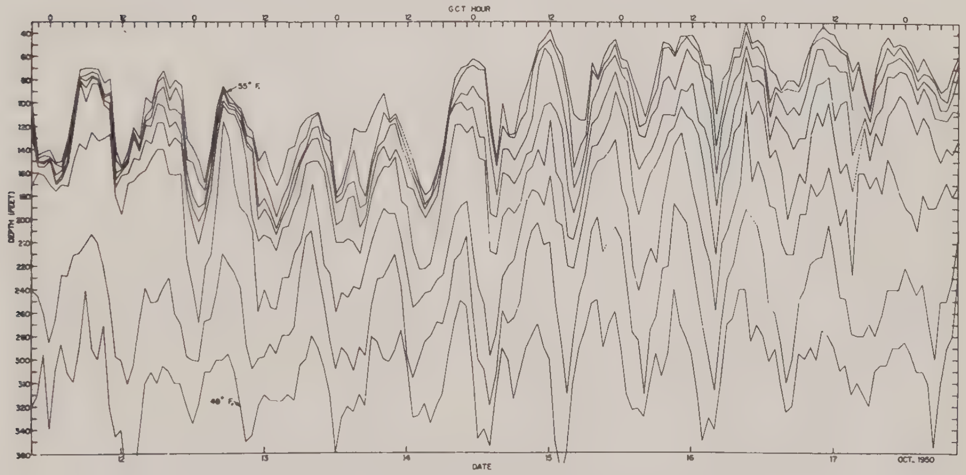

FIG. 3 – Oscillation of isotherms (from bathythermograph), station 72.60

BT depths of isotherms of the interpolated data of the reversing thermometers, and the dynamic height anomaly 0/300 db.

Method of analysis and reality test—Tables 1 to 6 give the amplitude A and also the quantities E, k^2, and p as used by *Haurwitz* [1954] in the expectancy method described by *Stumpff* [1940] and *Chapman* and *Bartels* [1940]. For derivations see the last two, and for a brief discussion of the applicability of the method to this sort of data see *Haurwitz* [1954]. Roughly, the method shows the probability that the amplitude A might have been obtained from random rather than periodic fluctuations in the data. If the data are divided

TABLE 1 – *Analysis for 12.4206-hr period (M_2), Station 72.60 (inshore), lat. 35°35.5′N, long. 122°07.5′W*

Datum	Average depth	A	E	RMS	k^2	p	Phase at 21h00m GCT Oct. 11, 1950
From BT							
	ft	ft	ft	ft			
Thermocline	101	29.4	9.1	39.2	9.54	0.000071	−10°
TCdev	0	31.8	10.1	27.7	9.86	0.000053	−11°
55°F	94	29.8	9.3	37.8	9.56	0.000068	−16°
52°F	134	33.6	9.8	37.0	9.76	0.000058	−16°
49°F	270	48.2	14.5	41.0	10.90	0.000018	3°
From reversing thermometers							
13°C	88	23.2	8.8	43.0	6.72	0.0012	−11°
12°C	104	34.8	10.4	41.6	9.03	0.00011	−14°
11°C	135	32.8	10.2	38.7	9.81	0.000055	−13°
10°C	217	40.0	12.5	44.3	9.92	0.000050	3°
9°C	332	24.0	9.2	31.1	8.68	0.000018	29°
8°C	590	22.0	10.2	30.4	4.44	0.012	118°
7°C	895	9.5	11.2	55.1	0.74	0.48	188°
From reversing thermometers and Nansen bottles							
	dyn m	dyn m	dyn m	dyn m			
ΔD 0/300	0.581	0.0070[a]	0.0029	0.010	5.89	0.0028	12°

[a] Separating M_2 and S_2 by the method of least squares described in the text this value becomes 0.0111 dynamic meters.

into n intervals of the period examined and each of the n intervals analyzed for the coefficients in

$$y = a_i \cos mt + b_i \sin mt$$

where $m = 2\pi/\text{period}$, the expectancy E is defined as $1/n\sqrt{\Sigma a_i^2 + \Sigma b_i^2}$. Then k is the ratio of A to E, and $p = e^{-k^2}$ is the probability that the amplitude A obtained in the analysis might have been obtained from random data having the expectancy E.

In the method of stepwise analysis described in the appendix the a_i and b_i are at once available for both the lunar and solar semidiurnal evaluations.

Results at the nearshore station and separation of M_2 and S_2—For the nearshore station the probability test indicates a real M_2 wave in the thermocline and at all depths down to at least 332 ft. Six and one-half days of data are not enough to separate clearly the constituents M_2 and S_2, but the amplitude from the M_2 analysis was the greater. Figure 2 shows the daily amplitude of the thermocline (TC dev, the deviation from the 24-hr running mean) to be waning with the predicted tide, with a high value somewhere near the time of new moon (13h33m GCT October 11) when M_2 and S_2 should be in phase, declining toward the first quarter (04h18m GCT October 18). The amplitude and phase for S_2 in Table 2 (19.1 ft and 276°) cannot be accepted as different from the values (19.3 ft and 258°) which one would get by analyzing 156 hr of the M_2 wave values (31.8 ft and 349°) for a 12-hr period. However, by neglecting all other constituents the amplitudes of each separate 12 hr can be fitted to the beat cycle of M_2 and S_2 waves in phase at the beginning of the series. Using the method of least squares one obtains amplitudes of 28.0 ft for M_2 and 12.3 ft for S_2. The ratio is 2.3 as compared with 2.2 for the equilibrium tide, 2.4 for the Los Angeles tide, and 3.8 for Morro, Morro Bay, the station plotted. (The expectancy method cannot be applied for S_2 because the E values will be dominated by the large M_2 in the data.)

However, the values obtained by separating M_2 and S_2 as above are a satisfactory fit to the data. Figure 4 indicates that a better fit might have been obtained by averaging amplitudes over two lengths instead of one, but the demonstration seemed adequate without this. The three worst points on the curve seemed to be real. The data were re-examined but there was no reason to doubt them.

Figure 5 shows a similar treatment of the amplitude of the dynamic height ΔD 0/300 db. There is more scatter in the points but the trend is in good agreement. It must be remembered that the accuracy of computation of dynamic height is limited by such errors as depth-determination of bottles, number of bottles available on the cast, how well the bottles were spaced to measure the critical parts of the curve, the accuracy of determination of salinity, and the final trapezoidal integration of the values of specific volume anomaly at each standard depth. For these reasons the scatter of dynamic height amplitudes should be expected to exceed those of the depth of thermocline, whose errors, if there is a good thermocline, can stem only from the depth-sensing element of the instrument.

By the same reasoning, the depths of those isotherms below the range of the bathythermograph are subject to greater error, and since these isotherms are in the region where the vertical gradients are much smaller, the values of amplitude and probability of the 9°C isotherm and below are probably less accurate than those above.

We may conclude, then, that there were present both an M_2 and an S_2 component in the thermocline and at all depths down to 332 ft and possibly deeper.

Results at the two outer stations—The outer

TABLE 2 – *Analysis for 12- and 24-hr periods, Station 72.60*

Datum	12-hr period (S_2)					24-hr period				
	A	E	k^2	p	Phase at 21h00m GCT Oct. 11, 1950	A	E	k^2	p	Phase at 21h00m GCT Oct. 11, 1950
From BT										
	ft	ft				ft	ft			
Thermocline.....	20.6	9.1	4.99	0.0068	−80°	4.7	3.9	1.44	0.23	15°
TCdev..........	19.1	10.1	4.29	0.014	−84°	...	...	...	...	...
55°F............	19.1	9.3	4.67	0.0094	−84°	...	...	...	...	...
52°F............	22.2	9.8	5.13	0.0059	−85°	...	...	...	...	...
49°F............	32.6	14.5	6.03	0.0024	−84°	...	...	...	...	...
From reversing thermometers										
13°C............	13.5	8.8	2.26	0.10	−76°	5.0	10.7	0.31	0.73	−4°
12°C............	21.2	10.4	4.30	0.014	−88°	...	...	...	...	...
11°C............	21.2	10.2	4.43	0.12	−85°	2.0	3.9	0.26	0.77	92°
10°C............	34.3	12.5	7.77	0.00043	−69°	...	...	...	...	...
9°C............	22.8	9.2	6.64	0.0013	−61°	...	...	...	...	...
8°C............	13.9	10.2	1.92	0.15	27°	2.8	3.9	0.54	0.58	−40°
7°C............	6.1	11.2	.32	0.73	−22°	...	...	...	...	...
From reversing thermometers and Nansen bottles										
	dyn m	dyn m				dyn m	dyn m			
ΔD 0/300.......	0.0058[a]	0.0029	3.98	0.019	−39°	0.0045	0.0036	1.56	0.21	−4°

[a] Separating M_2 and S_2 by the method of least squares, this value becomes 0.0065 dynamic meters.

TABLE 3 – *Analysis for 12.4206-hr period (M_2), Station 70.90 (center), lat. 34°51′N, long. 124°33′W*

Datum	Average depth	A	E	RMS	k^2	p	Phase at 21h00m GCT Oct. 11, 1950
From BT							
	ft	ft	ft	ft			
Thermocline..	67	1.2	3.4	18.2	0.13	0.88	166°
59°F..........	101	4.2	3.8	21.5	1.22	0.30	6°
From reversing thermometers							
16°C..........	85	3.3	2.6	19.6	0.69	0.50	48°
12°C..........	117	6.0	4.5	26.1	1.77	0.16	4°
10°C..........	229	3.2	5.3	32.0	0.35	0.70	316°
9°C..........	420	4.3	7.2	29.5	0.36	0.70	226°
8.5°C..........	658	8.1	9.0	31.6	0.81	0.44	194°
8°C..........	952	1.1	7.8	35.5	1.82	0.16	250°
From reversing thermometers and Nansen bottles							
	dyn m	dyn m	dyn m	dyn m			
ΔD 0/300......	0.604	0.00055	0.0025	0.009	0.04	0.96	200°

stations (Tables 3 to 6) show very little evidence of periodic behavior in any of the three tidal periods tested. A periodogram analysis was run upon the thermoclines for periods from six to 27 hr (including the period of inertial rotation) with no significant amplitudes being indicated. The root mean squares of the variation of the depth of the thermoclines at the two outer stations were somewhat less than at Station 72.60, but at lower depths they were more nearly equal, and the RMS of the variation of dynamic height above 300 db were nearly equal at all three positions. Thus the energy of fluctuation does not seem to be very much less at the outer stations, but the clearly defined waves of the inner station are not found offshore in any recognizable form.

Wave length and speed—Haurwitz [1950] has derived a theoretical expression (in which he considers the rotation of the Earth) for the relationship between the period, wave length, density structure, and depth in a two-layer system. Writing it to express L as a function of the other quantities

$$\frac{2\pi}{L} = \sqrt{\frac{(\sigma^2 - \lambda^2)\,(h' + h'')}{gh'h''\,(1 - \rho'/\rho'')}}$$

where

L = wave length
$\sigma = 2\pi/T$, T = period
$\lambda = 2\omega \sin \phi$, the Coriolis parameter
ω = Earth's rotation
ϕ = latitude

h', ρ' = the depth and density of the upper layer
h'', ρ'' = the depth and density of the lower layer

TABLE 4 – *Analysis for 12- and 24-hr periods, Station 70.90*

	12-hr period (S_2)				24-hr period				
Datum	A	k^2	p	Phase at 21h00m GCT Oct. 11, 1950	A	E	k^2	p	Phase at 21h00m GCT Oct. 11, 1950
From BT									
	ft				ft	ft			
Thermocline	4.6	0.84	0.43	−43°	7.0	3.8	3.41	0.022	46°
59°F	7.8	4.27	0.014	241°	4.6	3.5	1.64	0.19	83°
From reversing thermometers									
16°C	5.6	1.80	0.50	237°	3.5	4.2	0.69	0.50	65°
12°C	4.2	0.88	0.41	227°	6.4	5.1	1.62	0.20	90°
10°C	9.5	3.25	0.04	203°	11.3	9.6	1.44	0.25	136°
9°C	7.2	0.98	0.38	225°	8.5	7.8	1.25	0.30	227°
8.5°C	4.9	0.35	0.70	78°	5.9	9.3	0.41	0.67	299°
8°C	2.2	0.08	0.92	13°	5.4	9.9	0.34	0.74	59°
From reversing thermometers and Nansen bottles									
	dyn m				dyn m	dyn m			
ΔD 0/300	0.0042	2.45	0.09	239°	0.0021	0.0035	0.38	0.70	208°

Using values from the nearshore station (and estimating $1 - \rho'/\rho''$ at from 0.001 to 0.003 since we do not have a two-layer system) L is from 17.3 to 42.5 mi and the velocity from 1.40 to 2.36 knots.

Rattray [1954] has considered the effect of eddy viscosity upon such waves, and has found that the length is slightly decreased. A damping coefficient is derived. Entering the data at the inner station in his expression, the amplitude is found to be reduced by one-half at a distance of from 136 to 1360 mi (taking eddy viscosity at from 1 to 100 cm²/sec). This alone would not account for the lack of coherence of the data at the first two stations, as can be seen from the amplitudes of the dynamic height variations listed in Tables 1 to 4. (When the vertical density gradients vary horizontally, as in these data, the amplitudes in feet of the depths of isotherms at two stations may not be comparable measures of wave height, and it is thought best to compare amplitudes of dynamic height.)

In any case the waves are not indicated clearly enough at the two outer stations for the velocity to be computed from phase differences. No coherence is found between stations. This is not inconsistent with the theoretical wave lengths of 20 to 40 mi. If there are several wave crests between stations (as in this case) traveling through areas of different and changing density structure and layer depth and across a moving stream, then they may be distorted and attenuated [*Rattray*, 1954] to the extent of not being recognizable.

TABLE 5 – *Analysis for 12.4206-hr period (M_2), Station 70.130 (offshore), lat. 33°33′N, long. 127°16.5′W*

Datum	Average depth	A	E	RMS	k^2	p	Phase at 21h00m GCT Oct. 11, 1950
From BT							
	ft	ft	ft	ft			
Thermocline	167	3.2	2.3	13.4	1.96	0.14	196°
60°F	180	2.1	3.6	20.9	0.31	0.74	211°
From reversing thermometers							
17°C	175	2.7	4.3	17.1	0.43	0.64	78°
15°C	224	5.9	5.4	25.5	1.16	0.31	16°
13°C	310	2.8	6.6	29.8	0.20	0.82	296°
11°C	404	14.7	8.0	35.7	3.40	0.033	316°
10°C	470	13.4	7.9	31.0	2.82	0.060	291°
9°C	617	15.8	8.0	29.5	3.69	0.025	293°
8°C	855	6.6	7.4	37.0	0.70	0.50	−19°
From reversing thermometers and Nansen bottles							
	dyn m	dyn m	dyn m	dyn m			
ΔD 0/300	0.813	0.0032	0.0033	0.011	0.95	0.41	278°

Tidal effects in the dynamic height—Of the three stations, at only the nearshore one were internal waves of tidal period observed. Here the semidiurnal tidal amplitudes describe the larger part of the fluctuation. The author knows of no other data in the literature which yield such striking evidence of the existence of tidal internal waves.

TABLE 6 – *Analysis for 12- and 24-hr periods, Station 70.130*

Datum	12-hr period (S_2)				24-hr period				
	A	k^2	p	Phase at 21h00m GCT Oct. 11, 1950	A	E	k^2	p	Phase at 21h00m GCT Oct. 11, 1950
From BT									
	ft				ft	ft			
Thermocline	0.7	0.09	0.91	124°	2.9	2.2	1.81	0.16	−48
60°F	2.2	0.36	0.70	44°	4.7	4.3	1.17	0.31	−79°
From reversing thermometers									
17°C	4.2	0.93	0.39	129°	5.3	3.7	2.10	0.12	72°
15°C	0.7	0.018	0.98	−8°	3.5	7.2	0.25	0.78	148°
13°C	5.1	0.62	0.54	97°	2.8	4.9	0.30	0.74	148°
11°C	7.4	0.87	0.42	277°	1.3	9.2	0.021	0.98	268°
10°C	11.2	1.97	0.14	229°	1.3	10.0	0.020	0.98	120°
9°C	13.3	2.14	0.12	240°	5.8	7.9	0.53	0.59	148°
8°C	4.8	0.42	0.66	192°	7.8	12.6	0.90	0.41	54°
From reversing thermometers and Nansen bottles									
	dyn m				dyn m	dyn m			
ΔD 0/300	0.0059	2.84	0.059	202°	0.0034	0.003	1.22	0.30	124°

The measured waves are smooth enough to suggest that they might be recognized in non-serial data, such as BT's taken hourly from vessels underway near and parallel to the coast. Such data might show whether the waves measured here are transient or permanent phenomena, and whether they are found all along the coastline.

Space variations of dynamic height—Table 7 shows dynamic heights at nine stations along the line of the anchor stations, taken at the end of the time series. It is the sort of time-space series of data which *Defant* [1950b] had suggested was seriously roughened by short-period time variations. The observed differences from station to station, 40 mi and about five hours apart, range from 1.7 to 18.2 dynamic cm. At three points along the line we know something about the time variation, from the analysis of the anchor stations.

The largest values in the table are the 18.2 and 13.6 cm by which the value at Station 70.80 exceeds the values at 70.70 and 70.90. Examination of the data shows a different water mass at 70.80, with warmer, less saline water in the upper 250 m than at either of the adjacent stations. The density in the upper layers is far too different from that of the adjacent stations for this dynamic height difference to be the result of a short-period vertical fluctuation of the order of any of those observed at the serial stations. A gradient of 18 cm in 40 mi would be equivalent to a geostrophic surface current of about 0.8 knots, an unusually high value in this region.

That this is space- rather than time-variation is suggested by the dynamic topography of other cruises in this area, where the dynamics are occasionally complex, and somewhat different water masses may be found close together. In these cases usually one of the types will contour as a 'cloud' or closed circle surrounded by a relatively sharp gradient of temperature and salinity.

If these clouds are in geostrophic equilibrium they are eddies, rotating rapidly in the center of a broad, slowly moving current. Such an eddy has been observed [*Fuglister* and *Worthington*, 1951] on the edge of the Gulf Stream, where the momentum is much higher. But if they are not in geostrophic balance they may be non-rotating and moving with the same slow velocity as the rest of the current. In any case, the value of dynamic height at Station 70.80 exceeds the adjacent values by much more than could be explained by any of the time changes on the table, periodic or random.

Time-space variation of dynamic height—The other increments are much more nearly equal. The total change in dynamic height from 72.60 to 70.130 is 23.2 cm. The average change is 3.3 cm. per 40-mi station interval. This is a little more than the root mean square of the greatest changes during 12 hr (column 8), and a little less than the greatest change during any 12 hr (column 7).

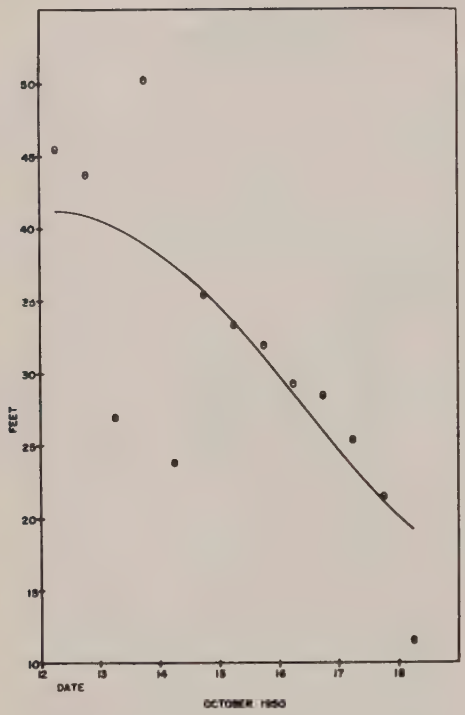

FIG. 4 – Amplitude of M_2 at thermocline

Column 9 shows the root mean square of deviations from the 12-hr means, and column 10 the part of the variations which might have been periodic and hence accounted for in interpretation.

The greatest differences at the time series stations occurred from three to seven days apart. It was not expected that such changes could be eliminated, nor was it desired, since they represent real phenomena and the stations are usually taken not more than six hours apart. At the ends of lines, of course, these intervals may be exceeded by another six hours since the distance between station lines is greater than that between stations on a line, and where the cruise patterns of two ships adjoin the interval may be several days. On occasion two weeks have passed between covering adjacent lines 40 to 120 mi apart. Since these results have become available more serious attempts have been made to work adjacent vessels either away from each other, letting them start together on adjacent lines, or toward each other working until they meet.

Time variations in dynamic height at a station are important if they are of the order of magnitude of the 'average' dynamic height increment to the adjacent stations. Therefore stations should be spaced with a knowledge of the gradient and time variation of dynamic height in each locality as well as according to other considerations. These other considerations may well require a closer spacing of stations than would seem justified for valid interpretation of dynamic height. An example is found in programs where biological sampling may be needed sometimes at ten-mile intervals, and certain hydrographic data desired for each sample.

Suggestions for further work—The results show that at the time of this cruise, at least, corrections to dynamic height could not be made at the outer stations on the basis of known phase and period, as *Defant* [1950ab] had hoped.

To find the distance at which internal tidal waves might keep coherence and to measure the speed it is suggested that two vessels begin quite close together, and only after coherence is established increase the distance.

Conclusions—Clearly defined tidal internal waves were found 40 mi offshore in deep water (1000 fm). They did not appear 120 mi farther out in a recognizable shape, although the non-periodic fluctuations in dynamic height were as great even at 280 mi offshore.

The phase of the measured tidal internal wave was the same as that of the surface tidal wave at the coast 40 mi away, and the amplitude varied with that of the surface tidal wave.

It may therefore be supposed that these tidal

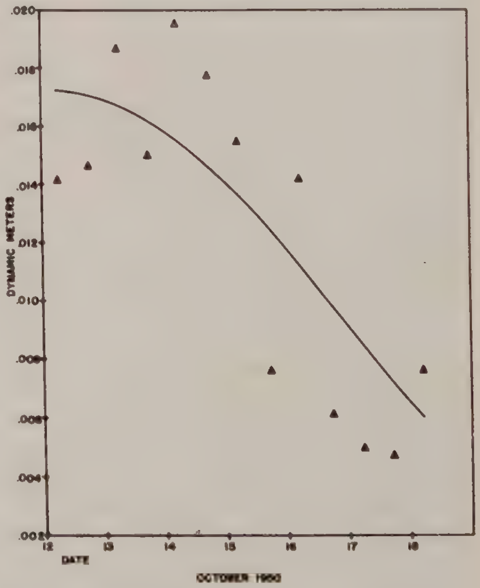

FIG. 5 – Amplitude of dynamic height 0/300 decibars

TABLE 7 – *Dynamic heights, 0/300 db, for the nine stations of Figure 1*

Station	Distance	Time of cast or series	ΔD 0/300	Difference	Greatest range during time series	Greatest range during any 12 hrs.	RMS of 12-hr ranges	RMS of deviations from 12-hr mean	Amplitude of M_2
1	2	3	4	5	6	7	8	9	10
	mi	Oct h m	dyn m	dyn m	dyn m	dyn m	dyn m	dyn m	dyn m
72.60		12 00 00							
		to	0.581[a]		0.074	0.034	0.026	0.010	0.0111[b]
		18 09 00			(Oct 13–16)	(Oct 12)			
72.60		18 09 00	0.545						
	30			0.003					
70.60		20 07 49	0.548						
	40			0.056					
70.70		20 03 25	0.604						
	40			0.182					
70.80		19 22 57	0.786						
	40			−0.136					
70.90		19 18 00	0.650						
70.90		11 21 00							
		to	0.604[a]		0.085	0.050	0.029	0.009	0.0005
		19 18 00			(Oct 12–19)	(Oct 12)			
70.90		19 18 00	0.650						
	40			0.001					
70.100		20 09 28	0.651						
	40			0.098					
70.110		20 04 29	0.749						
	40			0.047					
70.120		19 23 18	0.796						
	40			0.036					
70.130		19 18 00	0.832						
70.130		11 21 00							
		to	0.813[a]		0.057	0.051	0.024	0.011	0.0032
		19 18 00			(Oct 14–17)	(Oct 12)			

[a] Average value for the time series.

[b] Separating M_2 and S_2 by the method described in the text.

internal waves originate near the shore in the surface tides. That they were not found farther out may be the result of attenuation over so many wave lengths due to frictional loss. More likely, since the speed of advance is so low and is dependent upon a complex and constantly varying density structure, and the waves must cross an irregular current, they may be so severely distorted after two or three lengths that they are no longer recognizable as periodic phenomena, even though their energy has not yet been spent.

If these waves are really formed near the coast by the action of the surface tide and have the simple phase relationship shown in this case, then it may be possible to examine long distances of the coast for this phenomenon from data already available.

Other measurements of internal waves in the deep ocean at great distances offshore have shown considerable vertical fluctuations but only in rare cases (and then usually only over short series of measurements) has it been possible to ascribe a periodicity to them. It may be possible that some part of these vertical fluctuations could originate near the coasts, near islands and seamounts or banks, through the action of the surface tides in shallow water.

Acknowledgment—I wish to express my appreciation to Robert S. Arthur for many stimulating discussions and suggestions.

This paper represents one of the results of research conducted in the California Cooperative Oceanic Fisheries Investigations, a program sponsored by the Marine Research Committee and carried out cooperatively by the Scripps Institution of Oceanography of the University of California, the Bureau of Marine Fisheries of the California Department of Fish and Game, the South Pacific Fishery Investigations of the United States Fish and Wildlife Service, the Hopkins Marine Station

of Stanford University, and the California Academy of Sciences.

APPENDIX

Analyzing data tabulated at solar hour intervals for the lunar semi-diurnal period of 12.4206 hours—Certain criteria [*Haurwitz*, 1954] for the reality of the amplitudes associated with a certain period involve determining the amplitude of each cycle separately so that a stepwise analysis is necessary. The extra labor can be reduced if the stepwise analysis can be made to serve for two slightly different periods such as the M_2 and S_2 constituents. This can be done because if one cycle of a 12.4206-hr curve is analyzed for a 12-hr curve the 12.4206-hr amplitude is closely approximated and the differences may be accounted for. Then each 12 hr of the data can be analyzed separately and the resultant set of curves may be then referred to a common time origin and averaged for the final evaluation of the lunar semidiurnal.

In the rare cases where the data justify it, variation of daily amplitudes may be used to separate two constituents.

Numerical evaluation of the coefficients—Any 12 hr of a curve of 12.4206-hr period may be fairly well represented by a 12-hr curve. That is, if

$$y = f(t) = a \cos mt + b \sin mt \qquad (1)$$

where $m = 2\pi/12.4206$, t in hours, we can approximate it by

$$y' = a' \cos nt + b' \sin nt,$$

where $n = 2\pi/12$, by defining

$$\left.\begin{aligned} 6a' &= \int_{-6}^{6} f(t) \cos nt \, dt \\ 6b' &= \int_{-6}^{6} f(t) \sin nt \, dt \end{aligned}\right\} \qquad (2)$$

We see that $a' = 0.9801\, a$, $b' = 1.0141\, b$. If (1) be rewritten to refer to a time L rather than to $t = 0$, it will be, if $t_L = t - L$

$$\begin{aligned} y &= a \cos m(t_L + L) + b \sin m(t_L + L) \\ &= (a \cos mL + b \sin mL) \cos mt_L \\ &\quad + (b \cos mL - a \sin mL) \sin mt_L \qquad (3) \end{aligned}$$

we may determine the approximate curve y_L' for the interval $-6 \leq t_L \leq 6$ by substituting (3) into (2). The resulting coefficients, which depend upon L, are related to a and b by

$$\left.\begin{aligned} a_L' &= 0.9801\,(a \cos mL + b \sin mL) \\ b_L' &= 1.0141\,(b \cos mL - a \sin mL) \end{aligned}\right\} \qquad (4)$$

These can be solved for a and b, designated a_L and b_L since in the data they will vary with L, and

$$a_L = 1.0203\, a_L' \cos mL - 0.9861\, b_L' \sin mL \qquad (5a)$$

$$b_L = 0.9861\, b_L' \cos mL + 1.0203\, a_L' \sin mL. \qquad (5b)$$

In practice a_L' and b_L' are determined from the data by direct harmonic analyses as in (2) and then a_L and b_L determined from (5a) and (5b).

REFERENCES

ARTHUR, ROBERT S., Oscillations in sea temperature at Scripps and Oceanside Piers, *Deep-Sea Res.*, **2,** 107–121, 1954.

CHAPMAN, SYDNEY AND J. BARTELS, *Geomagnetism*, **2,** 545–605, Oxford, 1940.

DEFANT, A., On the origin of internal tide waves in the open sea, *J. Mar. Res.*, **9,** 111–119, 1950a.

DEFANT, A., Reality and illusion in oceanographic surveys, *J. Mar. Res.*, **9,** 120–138, 1950b.

FUGLISTER, F. C., AND L. V. WORTHINGTON, Some results of a multiple ship survey of the Gulf Stream, *Tellus*, **3,** 1–14, 1951.

HAURWITZ, BERNARD, Internal tidal waves of tidal character, *Trans. Amer. Geophys. Union*, **31,** 47–52, 1950.

HAURWITZ, BERNARD, The occurrence of internal tides in the ocean, *Arch. Met.*, Vienna, **A7,** 406–424, 1954.

RATTRAY, MAURICE J., Propagation and dissipation of long internal waves, *Dept. Oceanography, Univ. Wash. Tech. Rep. 27*, Ref. 54-11, March 1954 (unpublished).

RUDNICK, PHILIP AND J. D. COCHRANE, Diurnal fluctuations in bathythermograms, *J. Mar. Res.*, **10,** 257–262, 1951.

SEIWELL, H. R., The effect of short period variations of temperature and salinity on calculations in dynamic topography, *Pap. Phys. Oceanogr.*, **7**(3), 32 pp., 1939.

STUMPFF, K., Ermittlung und Realität von Periodizitäten, Korrelations-Rechnung, *Handbuch der Geophysik*, **10**(1), Berlin, 1940.

Scripps Institution of Oceanography, La Jolla, California.

(Communicated manuscript received February 13, 1956; open for formal discussion until November 1, 1956.)

(596)

Reprinted from Science, June 15, 1956, Vol. 123, No. 3207, pages 1082–1083.

Rate of Postglacial Rise of Sea Level

The results of careful studies of peat and shell material from Velsen in North Holland reported by van Straaten (*1*), and radiocarbon measurements on this material by deVries and Barendsen (*2*) have led to a fairly adequate knowledge of the approximate sea stand as a function of time for the Dutch coast over the past 8000 years. These authors represent their results by a figure showing radiocarbon age of shell and peat versus depth of the sample horizon relative to the present strand line. The same is shown in this report (*3*) in Fig. 1; we have added measurements from other localities for comparison. Most of the added measurements were made by the Magnolia Petroleum Laboratory, Houston, Tex., on material that was obtained from bays, barrier islands, and the continental shelf of the Texas and Louisiana coasts (*4*). The sources of other dates are indicated in the figure caption.

With the exception of several dates that were determined by the Lamont Geological Observatory, the measurements appear to show approximately equal rates in the rise of the sea level at the various localities. This may indicate that the observations reflect the actual eustatic change that accompanied the melting of the last ice sheets rather than the effects of local tectonic movements or compaction. It is obvious, however, that many more measurements from a variety of locations must be made before it will be possible to distinguish conclusively between eustatism, tectonic movements, and compaction.

A possible temporary halt in the rise of the sea level some 7000 or 8000 years ago seems to be indicated by samples from both North Holland and the Gulf Coast. Such a halt may conceivably correspond to the Cochrane halt in the retreat of the ice (*5*).

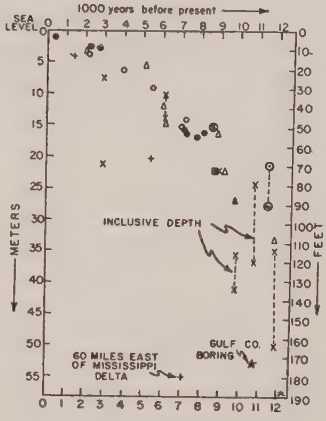

Fig. 1. Radiocarbon ages relative to depths below present sea level. Samples of wood and shells are believed to have been deposited essentially at sea level. No correction has been made for compaction or subsidence from other causes. ■, wood (Suess, U.S. Geological Survey, Australia, *9*); ○, shells, and ●, peat (deVries and Barendsen, Holland); △, shells, and ▲, wood (Magnolia Petroleum Laboratory, Texas Gulf); +, shells, and ×, wood (Kulp, Lamont Geological Observatory, Mississippi Delta); ⊙, wood (Kulp, Bermuda); ★, shells (Humble Oil Company, Texas Shelf).

The picture becomes confused prior to the last 10,000 years, which may be due to imperfection of the data, or, possibly, to an oscillation of the sea stand connected with the Mankato readvance of the ice sheets around the Great Lakes (*6*). Evidence for or against changes in the rate of eustatic rise in correlation with oscillations of the ice sheets might prove helpful in determining whether or not glacial readvances were synchronous on different continents and in the two hemispheres.

Perhaps the most interesting question connected with these observations is that of the supposed postglacial higher sea stand during the "climatic optimum" (*7*). Neither the samples from the Gulf Coast nor those from North Holland give any indication of a postglacial sea level higher than that of the present. As yet no evidence from carbon-14 measurements has been produced that would prove such a high sea level, and a sample (W-185) of shells from one of the low terraces from Western Australia (+10 to 12 ft), which was expected to date this sea stand, gave an age of more than 30,000 years.

Any assistance in securing samples for radiocarbon determinations that would date a sea level as accurately and as conclusively as possible and hence give a bearing on the afore-mentioned problems would be greatly appreciated.

F. P. Shepard
H. E. Suess
*Scripps Institution of Oceanography,
La Jolla, California*

References

1. L. M. J. U. van Straaten, *Geol. en Mijnbouw* 16, 247 (1954).
2. H. L. deVries and G. W. Barendsen, *Nature* 174, 1138 (1954).
3. Contribution from the Scripps Institution of Oceanography, new series, No. 856. This investigation was supported in part by a grant from the American Petroleum Institute, project 51, and by a contract between the Office of Naval Research and the University of California.
4. F. P. Shepard and D. G. Moore, *Bull. Am. Assoc. Petroleum Geol.* 39, 1463 (1955).
5. H. E. Suess, *Science* 123, 355 (1956).
6. L. Horberg, *J. Geol.* 63, 278 (1955); R. F. Flint and M. Rubin, *Science* 121, 649 (1955).
7. Plant fossils indicate that during a short period about 5000 years ago the climate may have been warmer than it is now. See R. F. Flint, *Glacial Geology and the Pleistocene Epoch* (Wiley, New York, 1947), pp. 187–191.
8. H. N. Fisk and E. McFarlan, Jr., *Geol. Soc. Amer. Spec. Paper* No. 62 (1955), pp. 279–302; J. L. Kulp, *Sci. Monthly* 75, 5 (1952).
9. H. E. Suess, *Science* 120, 467 (1954).

21 December 1955

Reproduced by Permission

ARCTIC INSTITUTE OF NORTH AMERICA

TECHNICAL PAPER NO. 1

THE PLANKTON OF THE BEAUFORT AND CHUKCHI SEA AREAS OF THE ARCTIC AND ITS RELATION TO THE HYDROGRAPHY

By

MARTIN W. JOHNSON

PUBLISHED JULY 1956
Reproduced by Permission

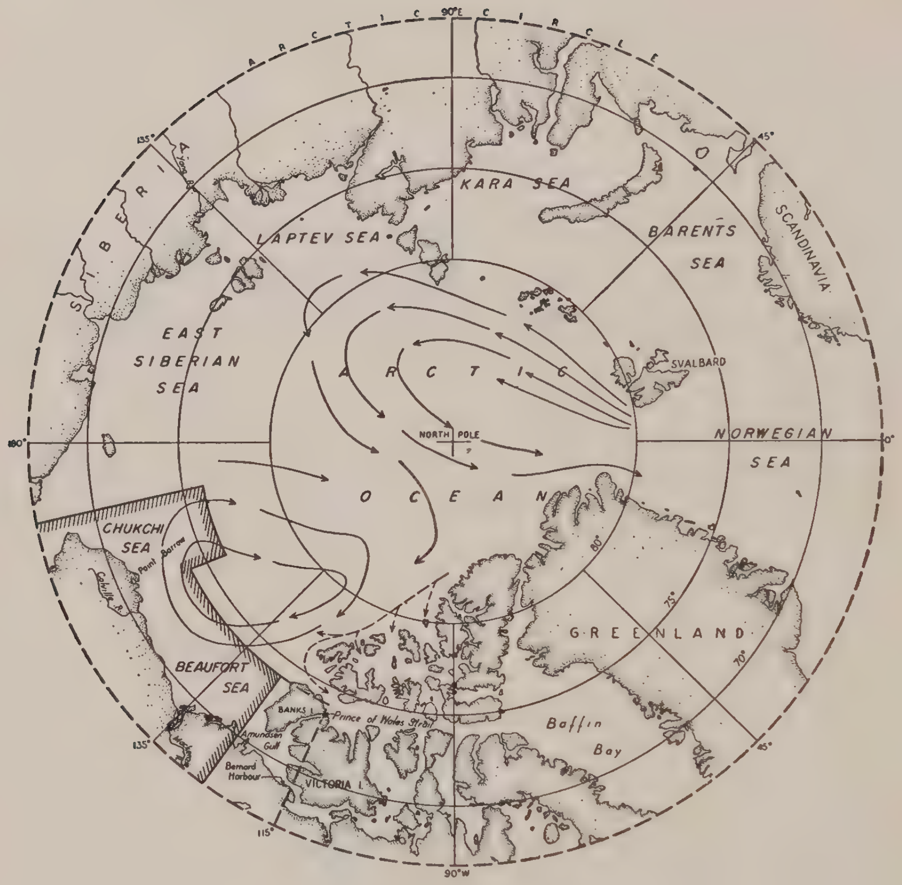
ARCTIC CIRCLE
90°E
135°
45°
SIBERIA
KARA SEA
LAPTEV SEA
BARENTS SEA
SCANDINAVIA
SVALBARD
EAST SIBERIAN SEA
ARCTIC OCEAN
NORTH POLE
180°
0°
NORWEGIAN SEA
CHUKCHI SEA
Point Barrow
Colville R.
80°
75°
70°
GREENLAND
BEAUFORT SEA
BANKS I.
Prince of Wales Strait
Amundsen Gulf
Bernard Harbour
VICTORIA I.
Baffin Bay
135°
45°
115°
90°W

Fig. 1. Arctic regions showing area considered in this study. The water circulation in the Polar Basin is based on Worthington's (1953) modification of Nansen's picture to include the cyclonic eddy. The dashed arrows are from Dunbar (1951).

THE PLANKTON OF THE CHUKCHI AND BEAUFORT SEA AREAS OF THE ARCTIC AND ITS RELATION TO THE HYDROGRAPHY*

Martin W. Johnson†

Within the last decade there has been a great surge of interest in arctic research which has been prompted in part by a hope for greater use of the resources of the Arctic, including those associated with the sea. Even if the expectations prove greater than warranted in some instances, much research is needed to evaluate the potentialities and variabilities in the arctic marine fauna. The urgent problems and implications involved have been well discussed by Dunbar (1953) who stresses particularly the need for research in the Beaufort Sea. Marine biological research important to our knowledge of both the Chukchi and Beaufort seas has been carried out from the Arctic Research Laboratory at Point Barrow, but this has not been concerned directly with the marine plankton. Some pioneering investigations have been made of the ecology of the marine zooplankton of the Bering and Chukchi seas (Johnson, 1934, 1938, 1953). These investigations have provided information on the composition and reproduction of endemic forms and have also indicated a northward drift of characteristically Bering Sea and north Pacific copepods through the Bering Strait into the Chukchi Sea. A Russian plankton survey carried out in this area and reported upon by Stepanova (1937) has also indicated a northward drift of plankton through Bering Strait.

The present paper extends our information on the plankton much farther into the Arctic Ocean than did the earlier accounts and penetrates into hitherto unexplored waters of the Arctic (Fig. 1). It is based mainly on two extensive oceanographic surveys made by the U.S.S. *Burton Island*, a naval icebreaker, in the Chukchi and Beaufort seas during August 1950 and August and September 1951. In 1950, 73 oceanographic stations were occupied for the study of physical, chemical, and biological conditions. Plankton hauls were made at 50 widely distributed stations covering the area between 125°W. and 164°W., and from 70°N. and northward into the pack ice to nearly 74°N. These hauls consisted of vertical tows made from various depths (usually 100 to 0 metres) with a one-half-metre Nansen-type plankton net, the upper and lower parts being constructed respectively of No. 2 and No. 10 bolting silk. In 1951 a total of 56 stations were occupied for plankton samples with the one-half-metre net drawn vertically from 100 to 0 metres. The area covered was roughly the same as that for 1950 but extended into higher latitudes and

---

*Contributions from Scripps Institution of Oceanography New Series, No. 857.

†Professor of Marine Biology, Scripps Institution of Oceanography, University of California, La Jolla, California.

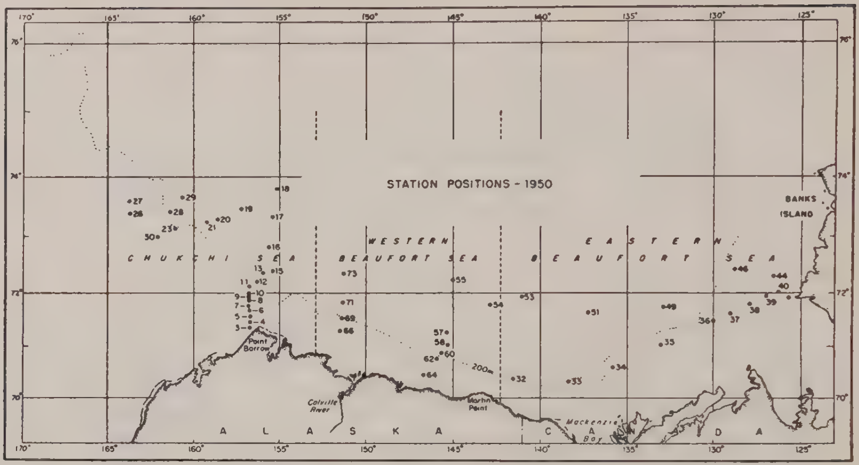
STATION POSITIONS - 1950
CHUKCHI SEA
WESTERN BEAUFORT SEA
EASTERN BEAUFORT SEA
BANKS ISLAND
Point Barrow
Colville River
Barter Point
Mackenzie Bay
ALASKA
CANADA
200m
170°
165°
160°
155°
150°
145°
140°
135°
130°
125°
76°
74°
72°
70°

Fig. 2. U.S.S. *Burton Island* 1950 plankton station positions and approximate location of 200-metre contour (after Carsola, 1954).

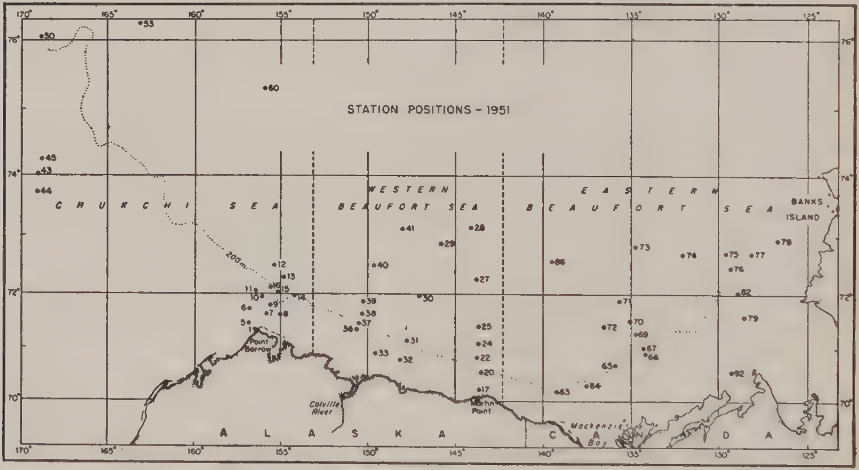
STATION POSITIONS - 1951
CHUKCHI SEA
WESTERN BEAUFORT SEA
EASTERN BEAUFORT SEA
BANKS ISLAND
Point Barrow
Colville River
Barter Point
Mackenzie Bay
ALASKA
CANADA
200m
170°
165°
160°
155°
150°
145°
140°
135°
130°
125°
76°
74°
72°
70°

Fig. 3. U.S.S. *Burton Island* 1951 plankton station positions and approximate location of 200-metre contour (after Carsola, 1954).

5° farther to the west. The station positions are shown in Figs. 2 and 3. The depth intervals sampled are given in Tables 1 to 14. In 1953 samples were obtained at 30 stations in Amundsen Gulf and Prince of Wales Strait.

The analyses of the plankton samples given in Tables 1 to 14 are based on a complete enumeration of the less abundant organisms, and for the abundant forms on counts of an aliquot part of the sample multiplied by the appropriate factor and, when needed, standardized to 0–100-metre vertical hauls (excepting hauls in Tables 4 and 11) which is the most frequent depth interval sampled, especially in 1951. Some of the organisms not included in the tables are discussed in the text. The distribution of selected forms that show restriction in geographical range is given in Figs. 4 to 10.

From a study of the range of certain species and the relative abundance of certain pelagic species and larvae, it will be seen that during the period of the survey the area falls rather sharply into a western and an eastern section. These sections correspond to the northern Chukchi Sea and the Beaufort Sea. Biologically, the boundary between these areas appears to lie in the region off Point Barrow with a transition zone, which in 1950 extended eastward into the Beaufort Sea to the next line of stations (numbers 66 to 73), especially to stations 71 and 73. In 1951 the areas were also clearly distinct but with somewhat greater penetration of the Chukchi Sea elements obliquely into the western Beaufort Sea, including stations just to the east and southeast of Point Barrow as far as Martin Point. On this basis the whole area covered can be divided more or less clearly into three parts: Chukchi Sea, western Beaufort Sea, and eastern Beaufort Sea as indicated in Figs. 2 and 3.

In presenting the results it will be convenient to consider the fauna in two parts: 1) The copepods which constituted by far the greater bulk of the plankton and 2) The miscellaneous plankton.

This exceptional survey was made possible through the cooperation of the U.S. Navy during the exploratory cruises of the icebreaker U.S.S. *Burton Island*. I am greatly indebted to the officers and men and to the scientists aboard who, under the leadership of Dr. Clifford A. Barnes of the University of Washington and Dr. Waldo K. Lyon of the Navy Electronics Laboratory, made the net collections. Among those contributing specifically to the collecting should be mentioned especially Mr. Eugene LaFond in 1950 and Mr. Alfred A. Carsola in 1951, both of the Navy Electronics Laboratory, and Dr. Warren Wooster in 1950 and Mr. Robert Bieri in 1953, both of the Scripps Institution of Oceanography. Miss Linda Haithcock assisted in the calculations and in preparing the tables and figures.

Copepods

No attempt will be made to give in detail the known geographic range of all of the different species found during this survey. There are a number of systematic and biological reports that include this information for certain of the species dealt with. Some of these sources are mentioned elsewhere in the text, especially useful are: G. O. Sars (1900, 1903, 1918), van Breeman (1908), With (1915), Farran (1926), Rose (1933), Jespersen (1934), Wilson (1950), and Vervoort (1951). These reports, covering different parts of the world, show how very extensive is the range of several of the species that flourish best in arctic waters. In the lower latitudes these arctic species are either migrants, transported by currents from the north, or inhabitants of the deeper, colder waters, where they may live and reproduce.

Species characteristic of the Bering Sea found in the area

Several of the stations occupied in the northern Chukchi Sea and western Beaufort Sea yielded a few copepod species that thrive normally in the Bering Sea and to the south. Among those that occurred in small numbers in the more offshore waters within the Arctic Circle are especially *Eucalanus bungii* Giesbrecht (northern variety *bungii*), and *Metridia lucens* Boeck (Figs. 4–6).

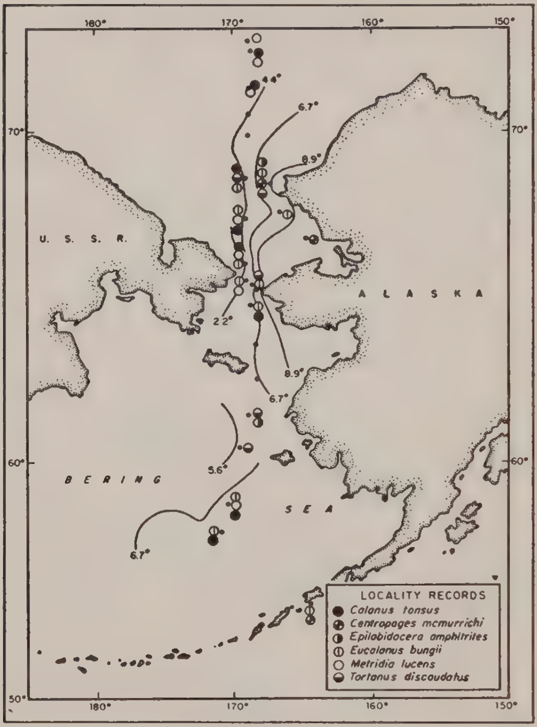
180°
170°
160°
150°
70°
60°
50°
U. S. S. R.
A L A S K A
B E R I N G
S E A
6.7°
8.9°
2.2°
8.9°
6.7°
5.6°
6.7°
LOCALITY RECORDS
● Calanus tonsus
Centropages mcmurrichi
◑ Epilabidocera amphitrites
Eucalanus bungii
○ Metridia lucens
Tortanus discaudatus

Fig. 4. Copepod distribution. Locality records U.S.S. *Nereus* 1947; surface isotherms °C from Johnson (1953).

Eucalanus bungii is a large, numerically important Pacific species that extends well down the west coast of North America as sub-species *californica*, and is also present on the Asiatic coast. *Metridia lucens* is usually less abundant along the west coast but is well represented there and elsewhere in the Pacific and in the Atlantic but is not considered arctic in its northern range. Only adult or sub-mature specimens of these two species were found as expatriate stragglers in the northern range whereas previous surveys (Johnson, 1934) have shown them, particularly *Eucalanus*, to be actively reproducing in the Bering Sea and Bering Strait. In 1951 one adult male of *Eucalanus bungii* was found at Station 20 off Martin Point far beyond its expected range.

Calanus tonsus Brady was not found as far north as were the previous two species, but it is clearly a northern extension of the more southern fauna. Each year it occurred near Point Barrow only. In 1950 a single specimen was taken at Station 5, whereas in 1951 it occurred at six stations grouped just north of Point Barrow (Figs. 5 and 6). Elsewhere the species is reported from both the Atlantic and Pacific. It is often very abundant in the Bering Sea and in the inshore and offshore waters on the west coast of Canada and the United States and is also reported from the northwest Pacific by Brodskiy (1952).

Calanus cristatus Krøyer likewise appears to be a visitor from the southern fauna. It occurred in our samples only twice. In 1950 a single Stage V

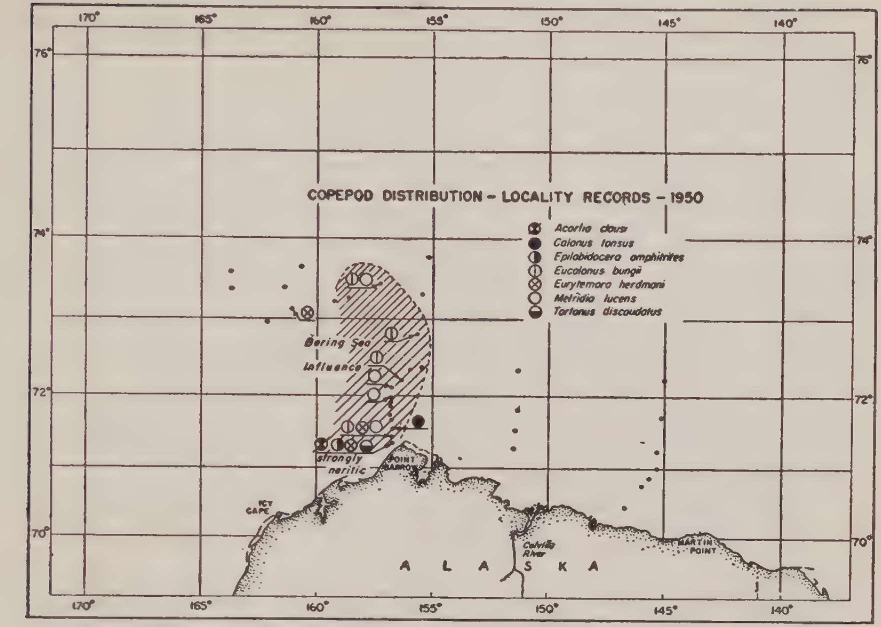
COPEPOD DISTRIBUTION – LOCALITY RECORDS – 1950
Acartia clausi
Calanus tonsus
Epilabidocera amphitrites
Eucalanus bungii
Eurytemora herdmani
Metridia lucens
Tortanus discaudatus
Bering Sea influence
strongly neritic
POINT BARROW
ICY CAPE
Colville River
MARTIN POINT
A L A S K A
170°
165°
160°
155°
150°
145°
140°
76°
74°
72°
70°

Fig. 5. Copepod distribution 1950. Locality records for seven species.

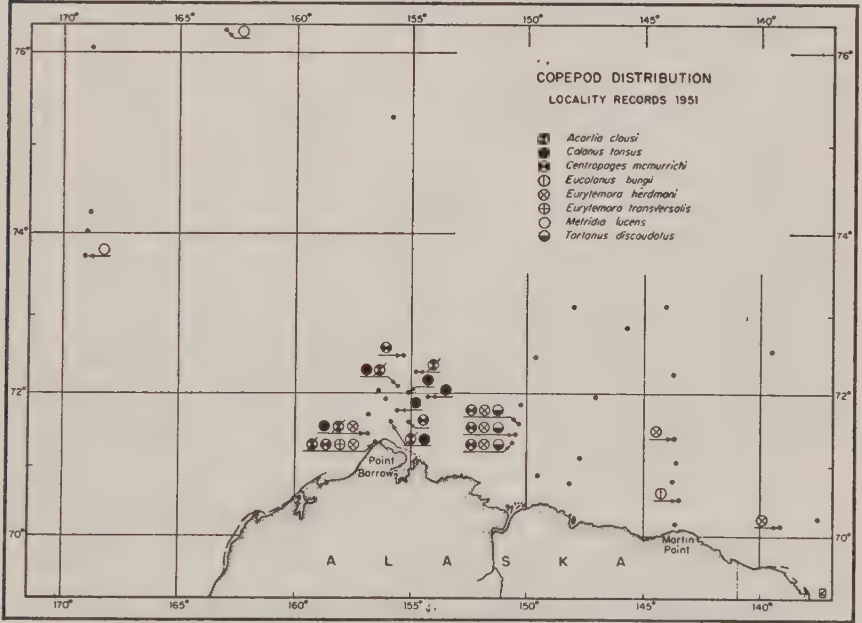
COPEPOD DISTRIBUTION
LOCALITY RECORDS 1951
Acartia clausi
Calanus tonsus
Centropages mcmurrichi
Eucalanus bungii
Eurytemora herdmani
Eurytemora transversalis
Metridia lucens
Tortanus discaudatus
Point Barrow
Martin Point
A L A S K A
170°
165°
160°
155°
150°
145°
140°
76°
74°
72°
70°

Fig. 6. Copepod distribution 1951. Locality records for eight species.

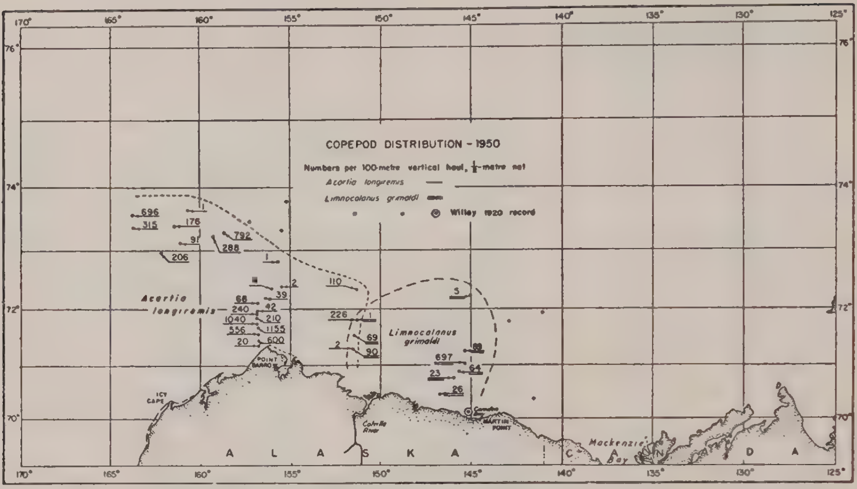
COPEPOD DISTRIBUTION - 1950
Numbers per 100-metre vertical haul, ½-metre net
Acartia longiremis
Limnocalanus grimaldi
Willey 1920 record
Acartia longiremis
Limnocalanus grimaldi
696
315
176
91
206
792
288
1
110
2
39
68
42
240
210
1040
1155
556
600
20
226
1
69
2
90
3
697
64
23
26
POINT BARROW
ICY CAPE
Colville River
MARTIN POINT
Mackenzie Bay
A L A S K A
170°
165°
160°
155°
150°
145°
140°
135°
130°
125°
76°
74°
72°
70°

Fig. 7. Copepod distribution 1950. Locality records for *Acartia longiremis* and *Limnocalanus grimaldi.*

female was surprisingly taken at Station 53 at 71°57N., 140°59W. This specimen measured 10 millimetres in length which is nearly 1.5 millimetres longer than usually reported for this stage of the species. The second specimen was found in 1951 at Station 7, off Point Barrow. The species is abundant in the Bering Sea and southward in offshore waters to Point Conception, California. It is also present off Japan (Mori, 1937) and in the North Atlantic.

Acartia longiremis (Lilljeborg), although often found in coastal areas, may also be included with the characteristically offshore species but, unlike the other species mentioned, it occurred at virtually all of the stations in the Chukchi Sea south of 75°N. In the earlier surveys in the Bering Sea and Bering Strait it occurred at 55 per cent and 85 per cent of the *Chelan* and *Nereus* stations respectively. From this we can conclude that it is quite at home in both the Bering Sea and well up into the Chukchi Sea. From the latter it appears to be swept for some distance into the western Beaufort Sea where it was present in diminishing numbers and reached as far east as Mackenzie Bay (Figs. 7 and 8). The Canadian Arctic expedition (Willey, 1920) found it at Bernard Harbour in Dolphin and Union Strait where it appears to have been reproducing. It was present also in very small numbers in collections made by Mr. Robert Bieri aboard the U.S.S. *Burton Island* in Amundsen Gulf and Prince of Wales Strait in 1953 where four out of thirty stations were positive, with a total of 8 specimens ranging in copepodid stages from III to adult. *Acartia longiremis* is considered an arctic circumpolar species and its tolerance of offshore waters should enable it to live in most of the Beaufort Sea. The probable reason for its absence in a large part of the eastern section will be discussed later.

The more strongly neritic character of the nearshore stations just to the west and north of Point Barrow is shown by the presence of *Acartia clausi*

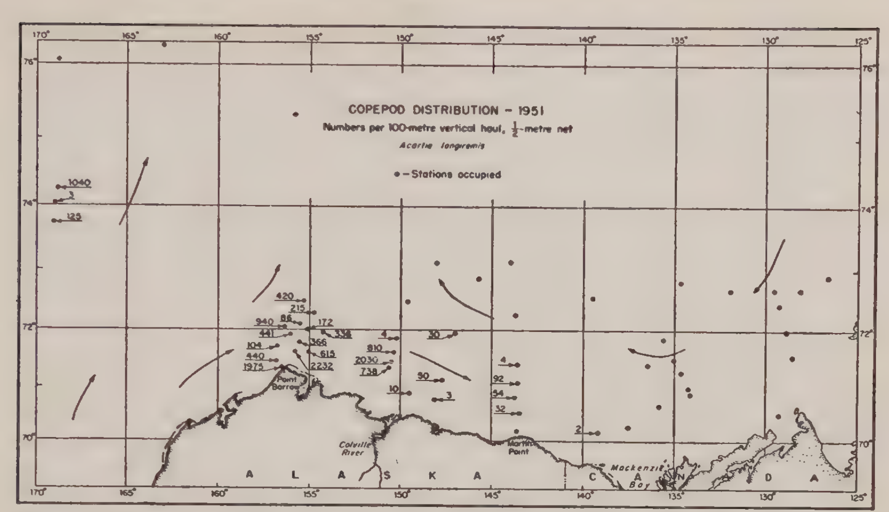
COPEPOD DISTRIBUTION - 1951
Numbers per 100-metre vertical haul, ½-metre net
Acartia longiremis
• - Stations occupied
170°
165°
160°
155°
150°
145°
140°
135°
130°
125°
76°
74°
72°
70°
1040
3
125
420
215
940
86
172
441
338
104
366
440
615
1975
2232
4
30
810
2030
738
10
30
3
4
92
54
32
2
Point Barrow
Colville River
Martin Point
Mackenzie Bay
A L A S K A
C A N A D A

Fig. 8. Copepod distribution 1951. Locality records for *Acartia longiremis*. The long arrows indicate general circulation as suggested by copepod distribution.

Giesbrecht, *Centropages mcmurrichi* Willey, *Epilabidocera amphitrites* (McMurrich), *Eurytemora herdmani* Thompson and Scott, *Eurytemora transversalis* Campbell, and *Tortanus discaudatus* (Thompson and Scott). Most of these species are at times abundant in the coastal waters of western Canada and the United States and also in the shallower eastern part of the Bering Sea and well north of Bering Strait on the Alaskan side (Esterly, 1924; Willey, 1920; Campbell, 1929; Johnson, 1953). These species strongly suggest a Bering Sea influence though *Eurytemora herdmani* is known to inhabit nearshore water east of Point Barrow as far as Dolphin and Union Strait (Willey, 1920). (Cf. Figs. 4–6).

Gurney (1933) considers that *Eurytemora transversalis* and several other species are synonymous with *Eurytemora americana* Williams. The female fifth feet are quite indistinguishable except for some differences in the length and shape of the spine on the penultimate segment. The species are no doubt closely akin but Campbell's (1930) species is retained here since further study is desirable especially on the males from the type areas. *Eurytemora kieferi* Smirnov (1931) which occurs off Kamchatka and in the Sea of Okhotsk is, however, probably the same as Campbell's species since the fifth feet of the males appear to be identical, whereas the original description of *Eurytemora americana* Williams (1906) and that given by Wilson (1932) indicate differences that may be specific.

Species characteristic of both Chukchi and Beaufort seas

There are a number of copepod species that are common to most of the Chukchi and Beaufort sea areas. Reference to the tables will show that some of these are the dominant species numerically and therefore the most important in the biological economy of the area of this survey. A number are widespread elsewhere in the Arctic while others, for example *Calanus finmarchicus*

(Gunnerus), also extend well into lower latitudes, especially in the deeper waters.

Calanus finmarchicus occurred at nearly 100 per cent of the stations. Only three stations off Point Barrow failed to yield the species. This and the two following species are by far the most abundant of the large copepods encountered.

Calanus hyperboreus Krøyer is a characteristic arctic species which occurred at 92 per cent of stations in 1950 and 73 per cent of stations in 1951. It may have been present at additional stations since the juvenile copepodid stages I and II were not closely examined and may therefore have been lumped with "*Calanus* spp. juveniles" in the tables. In the early stages they are separated only with difficulty from *Calanus finmarchicus* as pointed out by With (1915) and Jespersen (1939).

Metridia longa (Lubbock) proved to be a very important copepod in the region of the survey. It was present at most stations except those near Point Barrow. Though definitely an arctic species, it has been reported from Japanese waters (Marukawa, 1928), from the Vancouver Island region (Campbell, 1929), and off the Washington coast (Davis, 1949). Brodskiy (1952) does not report it from the northwest Pacific nor have I seen the species in many collections from the north Pacific.

Pseudocalanus minutus (Krøyer) was found at all but six stations in 1950 and four stations in 1951, and was certainly the most generally abundant of the microcalanids. Sars (1900) established a second species *Pseudocalanus major* to receive a form larger than *Pseudocalanus minutus.* In the present survey some large forms were also present but no attempt was made to distinguish the two in the analysis of the catches. With (1915) made a careful analysis of the two species and *Pseudocalanus gracilis* G. O. Sars but was unable to find valid distinctions. In the tables it is lumped together with *Microcalanus pygmaeus* as "microcalanids".

Microcalanus pygmaeus (G. O. Sars) was the second most abundant microcalanid, except at stations in the ice pack where it was often the most abundant. It was widely distributed in the Beaufort Sea where it occurred at all but two of the stations in 1950. In the Chukchi Sea it was absent mainly from the coastal stations off Point Barrow. It is a widespread species in the Arctic (Sars, 1900) but was not taken at any of the stations occupied by the Canadian Arctic expedition (Willey, 1920); the probable reason is that the stations were all situated too near shore. In the present survey the offshore stations were the most productive, however, it was commonly present in samples taken by the U.S.S. *Burton Island* in Amundsen Gulf and Prince of Wales Strait in 1953.

Oithona spp. and *Oncaea* spp. are among the numerically important tiny copepods. The species involved appear to be mainly *Oithona similis* Claus and *Oncaea borealis* G. O. Sars, both of which are widespread in the Arctic (Sars, 1900, 1903, 1918; Linko, 1913; Willey, 1920).

Pareuchaeta norvegica (Boeck) occurred at many stations throughout the area but at fewer stations and in diminished numbers in the Chukchi Sea, especially near Point Barrow. It was nowhere abundant but its large size and persistent presence could make it of some significance in the marine economy.

Rarer species

A number of copepod species were caught in small numbers more or less sporadically in the regular hauls. Among the species not discussed above are the following: *Chiridius obtusifrons* (G. O. Sars), *Cyclopina schneideri* T. Scott, *Gaidius brevispinus* (G. O. Sars), *Gaidius tenuispinus* (G. O. Sars), *Heterorhabdus norvegicus* (Boeck), *Limnocalanus grimaldi* (de Guerne), *Scaphocalanus magnus* (T. Scott), *Scolecithricella minor* (Brady), and *Scolecithrix brevicornis* G. O. Sars. Except for *Limnocalanus* there is little need at this time for discussion of the individual species (*see* below) the occurrence of which is shown in Tables 1 to 7.

Several of the regular hauls taken during 1950 ranged in depth up to 230 metres. During that year, however, two stations, No. 18 and No. 71, were occupied for especially deep hauls (up to 700 metres) with closing nets to sample different depth intervals as given in Table 4. The following copepods were caught only in the deepest interval of these hauls and presumably represent a part of the deepwater fauna to be expected in many places within the Polar Basin: *Haloptilus acutifrons* (Giesbrecht), *Mormonilla minor* Giesbrecht, *Spinocalanus abyssalis* Giesbrecht, *Spinocalanus magnus* Wolfenden, and *Xanthocalanus propinquus* G. O. Sars.

Nauplii

The nauplius larvae of copepods occurred throughout the area and while quite patchy, they were often present in considerable numbers giving evidence of active copepod reproduction during the period of sampling. The average number adjusted to 0–100-metre hauls per station (including Stations 18 and 71 for 1950) for areas by years was: Chukchi Sea–2,225 (1950), 2,510 (1951); western Beaufort Sea–1,863 (1950), 1,486 (1951); eastern Beaufort Sea–849 (1950), 842 (1951). The copepod larvae occur mainly in the surface waters (Table 4).

Miscellaneous Plankton

Holoplankton

The amphipods (which will form part of a separate report) and the ostracods were scattered irregularly over most of the area. From Table 11, it appears that the ostracods prefer the deep water and, like certain copepods, may not have been adequately sampled by the shallower, regular hauls. *Conchoecia maxima* Brady and Norman was the dominant ostracod.

In 1951 *Podon* and *Evadne* (not in tables) were abundant at Station 1 and common at Station 8. A few were observed at Station 64 and at Stations 36, 37, and 38. None were counted in 1950.

The Euphausiacea were poorly represented in the catches, especially in the adult stage. The collections do, however, greatly extend the range of the species found. *Thysanoëssa inermis* (Krøyer) was found at three stations in the Chukchi Sea but not elsewhere. *Thysanoëssa raschii* (M. Sars) appears to be the main euphausiid of the area, occurring at seven stations in the Chukchi Sea and three stations in the western Beaufort Sea. *Thysanoëssa longipes* Brandt occurred but once in the Chukchi Sea. No adult euphausiids were caught in the eastern Beaufort Sea and only two furcilia stages were found at Station 63 (1951). The larval stages of euphausiids were best repre-

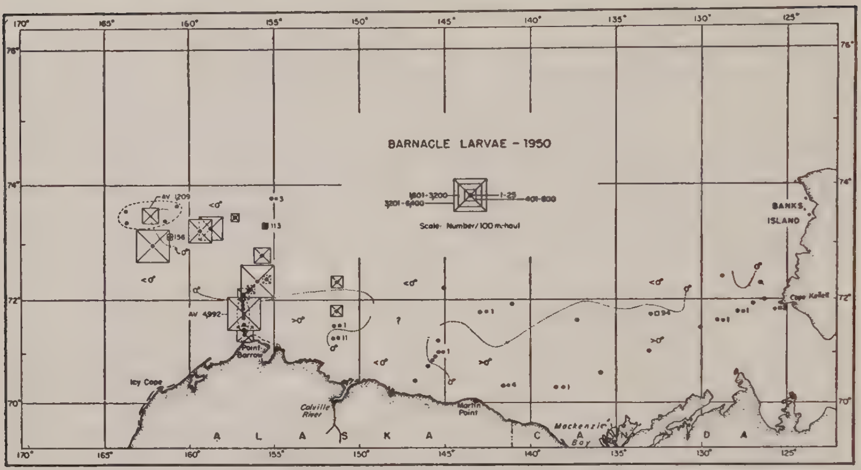
BARNACLE LARVAE – 1950
1801-3200
3201-6400
1-25
401-800
Scale: Number/100 m-haul
AV 1209
AV 4992
156
113
Point Barrow
Icy Cape
Colville River
Martin Point
Mackenzie Bay
BANKS ISLAND
Cape Kellett
A L A S K A
C A N A D A
170°
165°
160°
155°
150°
145°
140°
135°
130°
125°
76°
74°
72°
70°

Fig. 9. Barnacle larvae 1950, total nauplii and cyprids combined. Where several station points are encircled by a dashed line, the square that has its centre nearest the centre of the station points is the average value for those stations. The dotted line shows approximate position of 0°C surface isotherm.

sented in 1951 when most stations in the Chukchi Sea and western Beaufort Sea yielded a few larvae.

The euphausiid species mentioned above are the only ones recorded by Schmitt (1919), from the Canadian Arctic expedition collections. It is of interest to note that none of these euphausiid species were reported from the collections made by the *Fram* (Sars, 1900), but *Thysanoëssa raschii* has been reported from various localities in the eastern Arctic as far north as Svalbard and *Thysanoëssa inermis* to 69°44N. (Stephensen, 1933). The *Sedov* apparently took no euphausiids whatever (Bogorov, 1946).

Chaetognaths were well represented at many of the stations in both the Chukchi and Beaufort seas. Their occurrence will be covered in a separate report.

Medusae, especially *Aglantha* were common in most of the area.

Meroplankton

The temporary planktonic stages of bottom-living animals were best represented by barnacle larvae. Both naupliar and cyprid stages were abundant in the Chukchi Sea in 1950 and in 1951, especially the latter year when they extended also in considerable numbers into the western Beaufort Sea at the more coastal stations (Figs. 9 and 10). Only scattered specimens, mostly cyprid stages, were present in the eastern Beaufort Sea, with the exception of Station 49 (1950) which appeared anomalous in yielding 94 larvae.

The summary of cyprid and naupliar stages of barnacles given in Table 15, provides some information on the biology of the area under survey. It appears that:—

1. In 1951 there seems to have been a far greater production of barnacle larvae than in 1950. The period of collecting was almost identical for both

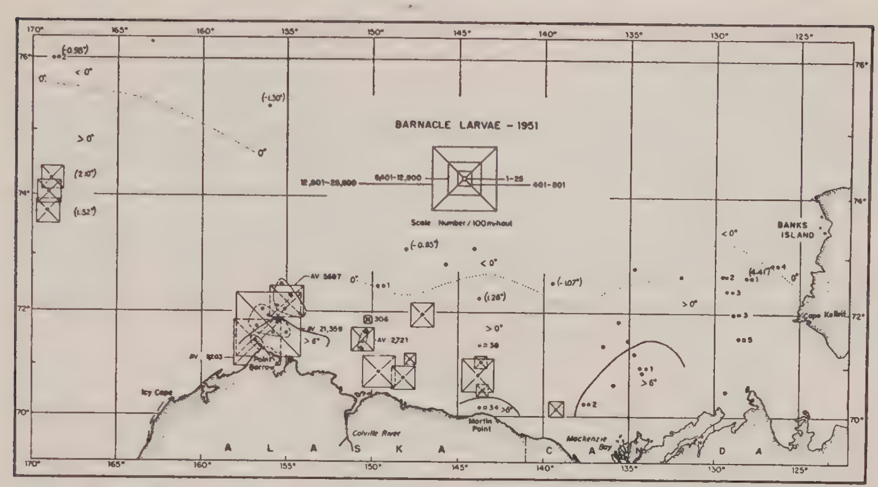
BARNACLE LARVAE - 1951
12,801-25,600
6401-12,800
1-25
401-801
Scale Number/100m-haul
BANKS ISLAND
Cape Kellett
Point Barrow
Icy Cape
Colville River
Martin Point
Mackenzie Bay
A L A S K A
C A N A D A
AV 5687
AV 21,359
AV 2721
AV 8203
304
< 0°
> 0°
> 6°
(-0.98°)
(-1.30°)
(2.10°)
(1.52°)
(-0.83°)
(1.26°)
(-1.07°)
(4.41°)
170°
165°
160°
155°
150°
145°
140°
135°
130°
125°
76°
74°
72°
70°

Fig. 10. Barnacle larvae 1951, total nauplii and cyprids combined. Where several station points are encircled by a dashed line, the square that has its centre nearest the centre of the station points is the average value for those stations. The dotted line shows approximate position of 0°C surface isotherm.

years for the western Beaufort Sea area and for the Chukchi Sea area, except for the six far offshore stations, 43, 44, 45, 50, 53, and 60 which were taken from 3–7 September 1951. In the eastern Beaufort Sea there is a discrepancy of nearly a month in collecting time, but in any event, the number of larvae taken in each year was very small, except for Station 63 (1951) near Mackenzie Bay.

2. It would appear that the reproductive season was somewhat more advanced when the 1951 samples were collected since the cyprid stage follows the naupliar stage in the development of barnacles. However, there may have been an early release of larvae in the far eastern Beaufort Sea in 1950 which gave rise to the significant number of cyprids found at Station 49.

Lamellibranch larvae were most abundant during the 1951 cruise. The following summary shows the average number netted per station by areas. When the number of larvae at a station was so small that it was indicated in the tables by only a plus sign (+), this is considered as one specimen in calculating the averages. This will doubtless usually err in minimizing the numbers actually present but the error cannot be very significant. In arriving at the average for the western Beaufort Sea in 1950, the larvae taken at Station 71 are included, but since only two stations in that section yielded larvae, the figure merely emphasizes their relative scarcity.

Average Number of Lamellibranch Larvae per Station

1950			*1951*		
Chukchi Sea	Western Beaufort Sea	Eastern Beaufort Sea	Chukchi Sea	Western Beaufort Sea	Eastern Beaufort Sea
160	10.4	6	3192	492	15

Only an occasional lamellibranch larva was observed in the collections made by the *Burton Island* at thirty stations in Amundsen Gulf and Prince of Wales Strait in 1953.

Reference to Tables 8 to 13 will show clearly that not only barnacle and lamellibranch larvae but also crab zoaeae, macruran larvae, annelid larvae, and echinoderm larvae (mainly ophioplutii) were most abundant in the Chukchi Sea area. The eastern Beaufort Sea yielded relatively few of these larvae.

The larvae and eggs of fish were strangely absent from the hauls. Only one fish larva was found at Station 3 (1950) and one young *Liparis koefoedi* Parr at Station 71 (1950). The latter was identified by Dr. Norman Wilimovsky with a statement that it is the first record of the species from arctic Alaska.

Discussion

In addition to what has been said in brief regarding the individual species, a number of interpretations and generalizations can be made.

Hydrographic implications

The geographic distribution of the holoplankton taken gives evidence of a northward flow of water from the Bering Sea into the Chukchi Sea. This flow appears to be detectable biologically northward to at least latitude 76°N.

Figure 4 shows the locality records for the collections taken during the U.S.S. *Nereus* 1947 cruise in the Bering and Chukchi seas. This figure, together with Figs. 5 and 6 for the 1950–1 surveys, shows the continuity of the following species with the Bering Sea fauna: *Calanus cristatus*, *Calanus tonsus*, *Eucalanus bungii*, and *Metridia lucens*. All of these probably drift into the Chukchi Sea area with little or no local reproduction to replenish the stock in the more northern reaches. The numbers occurring at the U.S.S. *Nereus* stations in 1947 and also the locality records and numbers for the 1934 U.S. Coast Guard cutter *Chelan*, are given by Johnson (1953). There are also a number of characteristically neritic copepod species that are pressed northward near the coast and to the east around Point Barrow, as indicated in the discussion under the species (*see* Figs. 5 and 6). These biological observations corroborate the hydrographic reports which also indicate a northward flow through Bering Strait during the summer (Barnes and Thompson, 1938; LaFond and Pritchard, 1952).

LaFond and Pritchard reporting on the U.S.S. *Nereus* 1947 data, state that the Bering Sea water flowing northward tends to follow the Alaskan coast but that at the northernmost stations near 72°N., 170°W. "the more saline and relatively warm water found at mid-depths seems to have originated in the Bering Sea . . ." (1952, p. 82). That this is probably the case is borne out by finding *Calanus tonsus* and *Metridia lucens* at these stations in 1947 (Fig. 4). The present report on the 1950–1 cruise gives biological evidence of Bering Sea water considerably farther to the north.

It should be pointed out also that for the summer of 1949, Saur, Tully, and LaFond (1954) obtained evidence indicating a flow of water from the northeastern Siberian coast to a point directly north of Bering Strait at the latitude of Kotzebue Sound. This flow would be expected to transport certain plankters from the Siberian coast but the contribution to the area covered by the present study is probably relatively small since the major current through Bering Strait is in the eastern half of the strait and according to the above investigations the Siberian coastal water appears to be deflected to the northwest towards Herald Shoal.

Sverdrup's (1950) summary of the circulation in the Polar Basin indicates a westward surface flow north of Alaska and eastern Siberia. Presumably subarctic organisms surviving long enough to drift far into the northern part of the Chukchi Sea would eventually be caught within this flow and either succumb or be carried out of the region to the west.

Evidently, a considerable amount of the northward-flowing water swings eastward in the region of Point Barrow, carrying elements of the plankton for some distance into western Beaufort Sea, especially near the shore. The distribution of species shown in Figs. 5 to 10 strongly suggests that the eastward flow was more pronounced in 1951 than in 1950 when its most obvious extension was only to the series of stations off the Colville River.

During 1950 the distribution of *Limnocalanus grimaldi* proved very interesting. This is a remarkable species closely akin to certain other species of the genus living in freshwater bodies that in the past may have been connected with the sea. It was encountered only in 1950 when it occurred in appreciable numbers at nine adjacent stations sampled in a restricted area of the western Beaufort Sea, between Point Barrow and Martin Point. This area lies off the mouth of the Colville River extending far off shore, as shown in Fig. 7. In 1913 the species was taken at one station by the Canadian Arctic expedition (Willey, 1920), near shore at Collinson Point in Camden Bay to the east of the Colville River. Since the species has estuarine affinities in some other parts of the world, it is not surprising to find it off the river mouth where its presence might indicate a spread of river water outward towards the north and east. But the salinity distribution does not readily support this view. The surface salinities at the stations where *Limnocalanus* occurred ranged from 28.04‰ to 31.65‰, and excepting the innermost station at each line, there is a general decrease in salinity with distance from shore. The picture may, however, be confused by offshore water formed from melting ice, as indicated by lower temperatures.

The absence of *Limnocalanus* from Stations 32, 33, 34, and 35, off the mouth of the Mackenzie River and Mackenzie Bay, is somewhat puzzling in view of the extensive distribution off the Colville River. This may suggest a westward flow of water (not sampled) from the Mackenzie along the shore to the area where the species was actually found. In support of this, at Station 32 the salinity was only 16.19‰. However, a better explanation may be that the Mackenzie discharge flowed to the east so near the shore that it was not sampled even at the innermost stations in that section.

Elsewhere in the world *Limnocalanus grimaldi* occurs in the Gulf of Bothnia, the Baltic and Kara seas, off Svalbard, in the estuary of the Yana River in Siberia, and strangely, also in the Caspian Sea where Sars (1897) considered it a relic of a glacial fauna in that area.

A freshwater species, *Limnocalanus johanseni*, was described by Marsh (1920) from freshwater collections near Collinson Point, and Comita and Edmondson (1953) found it to be the dominant copepod in a lake near Point Barrow.

During the summer months, some of the more neritic copepod species do find conditions favourable for limited reproduction. For instance, the disc-like egg cases and at least one nauplius larva of *Tortanus discaudatus* were found east of Point Barrow. This species and several others which are common to abundant along the east coast of Canada and northeastern United States may have a more or less continuous though probably intermittent distribution near shore in the arctic region, depending upon variations in climatic conditions and strength of arctic currents at the coast.

Coastal collections made by the Canadian Arctic expedition working from the west bears this out, at least eastward to Bernard Harbour, where Willey (1920) reported the following species with which we are concerned: *Acartia longiremis* and *Eurytemora herdmani.* A similar eastern extension of the range is shown for *Acartia* by the *Burton Island* collections for 1953, as mentioned above.

As a part of the biological picture, it was pointed out earlier that certain more or less neritic copepod species and the larvae of barnacles occur as an oblique extension southeastward into the Beaufort Sea. *Acartia* is similarly distributed in the regular hauls to about Mackenzie Bay, and, similarly, the extension was greater in 1951 than in the previous year. The surface temperatures as plotted by Carsola (unpublished MS.) from the 1950 and 1951 cruise data also show a more pronounced extension of warm water into western Beaufort Sea in the latter year (Fig. 11).

The distribution of *Acartia longiremis* (Figs. 7 and 8) presents an interesting problem and appears to throw some light on the general prevailing circulation of the water from the north or northeast, from the Arctic Ocean into the offshore eastern Beaufort Sea. In considering its transport and survival in the far north it is significant that the species lives in the surface layers (*see* Table 4) where it is subject to surface currents and to the variations in salinity and temperature found in the vicinity of melting ice. The species is considered arctic with a wide southern extension, and from its distribution elsewhere during this survey, one might assume, *a priori*, that as far as temperature or salinity conditions are concerned during the summer, it should thrive in the eastern Beaufort Sea as well as it does in the Chukchi Sea. In 1950 the surface temperatures at the eight most northwesterly stations in the Chukchi Sea where *Acartia longiremis* occurred ranged from 0.79°C at Station 28 to -1.35°C at Station 27 where nearly 700 specimens were taken. No *Acartia* were taken at Stations 17, 18, and 19 where temperatures were -1.46 to -1.54°C (*see* Figs. 9 and 10 for general surface temperature conditions). Salinities in the Chukchi Sea ranged from 24.35‰ to 28.77‰. In the eastern Beaufort Sea for the same year most of the area surveyed was characterized by surface temperatures above 0°C, with ranges from 0.80 to 2.38°C (temperatures to 5.31°C were noted at stations off Mackenzie Bay); surface salinities ranged from 23.24‰ to 30.80‰.

Despite these similarities in temperatures and salinities, *Acartia longiremis* was absent from both the 1950 and 1951 collections taken in the eastern Beaufort Sea. It was also absent from the most northerly stations in the Chukchi Sea and western Beaufort Sea. This pattern of distribution with its diminution in numbers to the east and disappearance in the northern Chukchi Sea suggests that the conditions in the Arctic Ocean are sufficiently inimical to *Acartia longiremis* to eliminate it from the plankton north of latitude 75°N. during the years sampled. Similarly, Sars (1900) found *Acartia longiremis* only in the

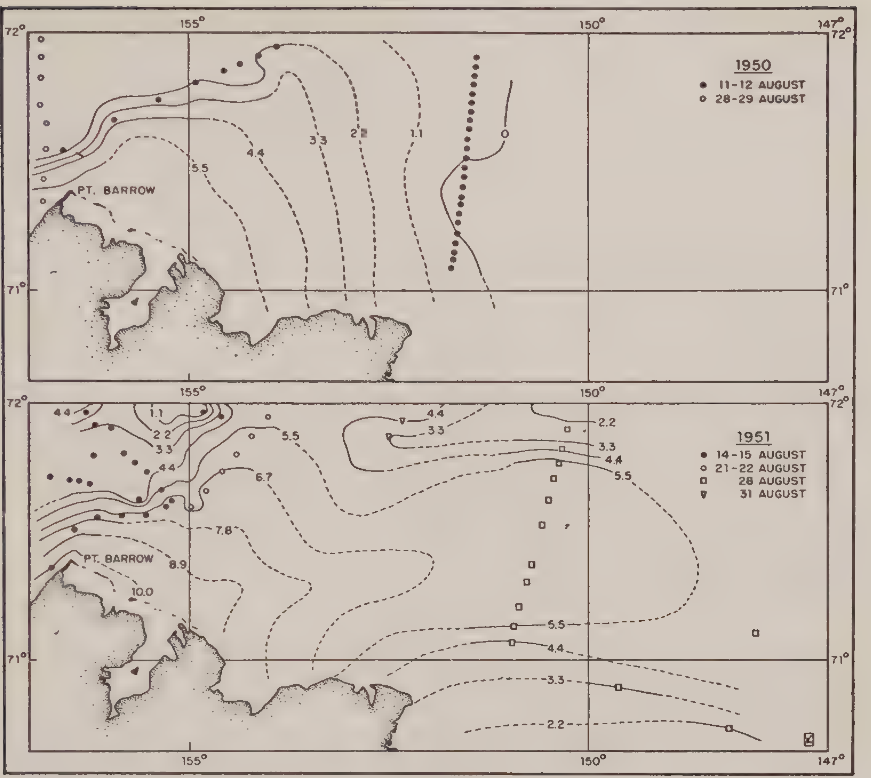

Fig. 11. Surface temperatures (°C) in the region of Point Barrow, 1950 and 1951.

first of Nansen's collections when the *Fram* was still near the Novosibirskiye Ostrova. No further specimens were found once the *Fram* had penetrated well into the Arctic Ocean. Likewise, Bogorov (1946) reports no *Acartia* from the *Sedov* drift across the Polar Basin.

Since the species apparently cannot survive in the Arctic Ocean, it is clear that a flow of water from that ocean must be barren of the species as it enters the Beaufort Sea in a great clockwise movement, swinging into the eastern portion and turning again northwestward east of Point Barrow as pictured by Dunbar (1953) and Worthington (1953). Whether or not there is a distinct eastern eddy as indicated by Worthington or a single large cyclonic flow around the perimeter of the basin as postulated by Nansen (1902) is perhaps not significant in this instance as long as the surface flow entering the Beaufort Sea is from the far north.

Thus *Acartia longiremis* is a subarctic species rather than a true arctic species if we use Dunbar's (1951) distinction between arctic and subarctic areas. According to his definition, the marine arctic is formed of those areas in which unmixed water of polar origin is found in the surface layers (200–300 metres). This water is characterized by low salinity and low temperatures, as compared with the marine subarctic in which the surface layers consist of a mixture of arctic and Atlantic or Pacific waters, and therefore have higher salinities and temperatures.

It should not be inferred that the Arctic Ocean is barren though evidently it is relatively unproductive as observed by Nansen and others. In so far as this may be reflected by the present collections, the area of smallest standing crop of zooplankton was generally in the eastern Beaufort Sea, but such copepods as *Calanus finmarchicus*, *Calanus hyperboreus*, *Metridia longa*, and *Microcalanus pygmaeus* were everywhere common as shown in Tables 1 to 7, and sometimes were abundant.

In the Beaufort Sea the holoplankton was the most important part of the zooplankton. This contrasts with the Chukchi Sea where the meroplankton is also important, showing the more neritic character of the water. However, in 1953, even in the nearshore waters of Amundsen Gulf and Prince of Wales Strait there were only a few barnacle larvae (mostly cyprids) and annelid larvae. Only two or three lamellibranch larvae were observed in the total collection from that area. This dearth of larvae could, of course, indicate that the height of spawning was passed and not that the benthic population is sparse in the area, or in some instances it may indicate that there are present fewer benthic species producing pelagic larvae than to the west, for it is well known as discussed by Thorson (1950) that most arctic invertebrates do not produce pelagic larvae. In this event, the environment in the eastern part of this survey is more typically arctic than is the western.

In evaluating the factors that bring about a richer plankton in the Chukchi Sea and part of the western Beaufort Sea than in the eastern Beaufort Sea, the relative areas of shallow water must be remembered. From Fig. 2 it will be seen that the 200-metre contour lies much farther offshore in the Chukchi Sea than in the eastern Beaufort Sea. This greater area of shallow to moderate depths doubtless accounts largely for the greater abundance of meroplankton to the west, where bottom conditions would favour production of benthic adults with planktonic larvae. The flow of water from a more favourable area must also be a significant factor. Outflow from the Mackenzie River may also suppress production of the more stenohaline species in parts of the Beaufort Sea area.

The net employed on these surveys was too coarse to sample the phytoplankton adequately but despite this, the relative amounts caught indicated that in 1950 there was obviously a burst of blooming of diatoms (mostly *Coscinodiscus* but also *Thalassiosira* and *Chaetoceros*) extending from Point Barrow to Station 30. Elsewhere that year phytoplankton was moderately sparse. In 1951 the waters just off Point Barrow were not richly populated, but there was a burst of filamentous diatoms at Stations 44 and 45 and considerable concentrations at Stations 50, 53, and 60, the farthest north sampled. In the Beaufort Sea in 1951 there was in progress a moderate burst of filamentous diatoms (and *Coscinodiscus*) from Station 17 to Station 28, and from Stations 75 to 79 there was an abundance of filamentous forms, mostly *Chaetoceros*. Among the dinoflagellates, *Ceratium* sp. was widespread, especially in the Beaufort Sea where at some stations it was abundant.

Just what these biological differences in plankton between the Chukchi and Beaufort seas mean to the production of higher marine life of direct economic importance needs further study. It may be significant that the walrus, for example, favours the western area. This may well be associated with a greater production of benthic life for food as strongly indicated by the preponderance of lamellibranch larvae. Baleen whales on the other hand may find adequate forage on the larger holoplankton in the Beaufort Sea.

Summary

This report is based on zooplankton collections made by the U.S.S. *Burton Island* during the summers of 1950 and 1951. It covers a section of the Arctic Ocean bordering Alaska and a part of Canada and extends to 76°22N. in the Chukchi Sea. Fifty widely dispersed stations were occupied in 1950 and 56 in 1951. Partial analysis was also made of plankton from 30 stations occupied in Amundsen Gulf and Prince of Wales Strait in 1953.

Thirty-three species of copepods are listed in tables and figures giving their numerical abundance and distribution. The distribution of several of these species indicates a flow of water from the Bering Sea and Strait to a latitude of about 76°N. and around Point Barrow into western Beaufort Sea. This flow was apparently more pronounced in 1951 than in 1950.

One Arctic copepod, *Acartia longiremis*, occurred at virtually all of the stations in the Chukchi Sea but, except for a coastal strip just east of Point Barrow, it is absent from the Beaufort Sea. This absence from the Beaufort Sea is accounted for by a flow of surface water from the Polar Basin where *Acartia longiremis* is apparently unable to survive.

The following copepods are common to both the Chukchi and Beaufort seas and are numerically the most important copepods of the whole area: *Calanus finmarchicus*, *Calanus hyperboreus*, *Metridia longa*, *Microcalanus pygmaeus*, *Oithona* spp., *Oncaea* spp., and *Pseudocalanus minutus*.

A study of the miscellaneous plankton was of interest in revealing a preponderance of larvae of benthic organisms especially barnacle nauplii and cyprids in the Chukchi Sea area. This is probably correlated with the greater extent there of relatively shallow water and with the direction of prevailing water currents.

Table 1. Copepods: Chukchi Sea area — 1950. Number per haul adjusted to 0–100-metre vertical tow. (+ = present).

Station Depth sampled in metres	3 0–5	4 0–58	5 0–100	6 0–100	7 0–61	8 0–72	9 0–90	10 0–109	11 0–150	12 0–230	13 0–46	15 0–122	16 0–91	17 0–107	19 0–100	20 0–100	21 0–100	23 0–145	26 0–69	27 0–137	28 0–100	29 0–91	30 0–90
Acartia clausi	78																						
Acartia longiremis	20	600	556	1155	1040	210	240	42	68	39	4	2	1			792	288	91	315	696	176	1	206
Calanus finmarchicus		840	+	110	624	630	180	375	136	39	818	228	1053	377	370	132	45	234	48	7	18	528	103
Calanus hyperboreus				112	20	200	150	175	102	43	18	48	381	75	278	2	3	52	1	12	5	6	309
Calanus tonsus			1																				
Calanus spp. juveniles			202	715	30	80	150	75	103	158	500	50	45	25	648	616	144	182	236	371	220	1232	464
Chiridius obtusifrons									1	1													
Epilabidocera amphitrites	+																						
Eucalanus bungii		1								1			1		1								
Eurytemora herdmani	100	1																2					
Gaidius tenuispinus										1													
Heterorhabdus norvegicus										59													
Metridia longa					1		2	3	305	276	273		8	75	370	20	48	26		1	2	12	4
Metridia lucens		1						2	1						1								
Oithona spp.	951	2460	1162	1485	2010	1050	360	667	271	276	1637	715	254	754	2778	1804	624	247	158	1624	1760	1496	1030
Oncaea spp.	+	300	202	385	139	420	+	489	136	315	273	1	363	75	648	352		39		186	220	264	464
Pareuchaeta norvegica								2	1	5		1		5	3		3	1		2	2	1	
Scaphocalanus magnus									1	2					2								
Tortanus discaudatus	1																						
Microcalanids*	178	7320	5657	9625	7207	9730	4260	4587	5729	1319	7911	10107	3267	4549	5834	4488	1920	1261	709	5197	2200	3080	7056
Copepod nauplii	50	360	3434	5060	2356	1470	840	959	2441	1084	10776	3770	980	415	2408	5016	576	637	867	1902	1012	2200	4686

*Includes *Microcalanus pygmaeus* and *Pseudocalanus minutus*.

Table 2. Copepods: western Beaufort Sea — 1950.
Number per haul adjusted to 0–100-metre vertical tow. (= + present).

Station Depth sampled in metres	54 0–100	55 0–100	57 0–100	58 0–100	60 0–91	62 0–61	64 0–27	66 0–46	69 0–100	73 0–100
Acartia longiremis								2		110
Calanus finmarchicus	198	78	8	82	21	30	229	51	72	183
Calanus hyperboreus	30	16	13	59	24	59	38	62	93	90
Calanus spp. juveniles		117	31		+	+	229	29	52	548
Chiridius obtusifrons							7			
Cyclopina schneideri		11								
Gaidius tenuispinus	2					2				
Heterorhabdus norvegicus	3	6			1					
Limnocalanus grimaldi		5	89	697	64	23	26	90	69	
Metridia longa	119	26	57	246	36	46	59	191	50	53
Oithona spp.	4859	2808	744	1681	3574	1650	803	2031	3090	913
Oncaea spp.	514	663	217	656	1400	512	2753	1562	1803	803
Pareuchaeta norvegica	8	10	4	8	21	10	1	11	17	8
Scolecithricella minor	4									1
Microcalanids*	1896	5811	31	492	1216	796	7800	3592	1597	3030
Copepod nauplii	672	741	496	205	2063	170	2065	547	2987	1752

*Includes *Microcalanus pygmaeus* and *Pseudocalanus minutus*.

Table 3. Copepods: eastern Beaufort Sea — 1950. Number per haul adjusted to 0–100-metre vertical tow.
(+ = present).

Station Depth sampled in metres	32 0–46	33 0–91	34 0–46	35 0–91	36 0–91	37 0–100	38 0–100	39 0–100	40 0–15	41 0–67	44 0–30	46 0–100	49 0–100	51 0–86	53 0–100
Calanus cristatus															1
Calanus finmarchicus	445	81	42	10	195	101	29	172	53	648	135	75	658	63	94
Calanus hyperboreus	295	31	205	101	221	108	15	6		15	12	52	288	51	79
Calanus spp. juveniles	267	+	441	155	390	100	161	129	13	360	13	+	+		94
Metridia longa		106	22	1	1		589	344	46	17		75	3	18	2
Oithona spp.	4722	502	8427	3698	5889	3232	3585	4601	845	2232	3986	1200	10528	3772	3055
Oncaea spp.	1693	+	824	478	819	657	749	516		648	867	638	1034	349	893
Pareuchaeta norvegica	11	5		1	3		8	4		2		3	1	10	8
Microcalanids*	1782	167	6229	1523	625	506	+	86		144	+	188	1034	443	799
Copepod nauplii	1604		733	914	1443	1263	535	387	1056	828	693	488	1833	634	329

*Includes *Microcalanus pygmaeus* and *Pseudocalanus minutus*.

Table 4. Copepods in deep tows — 1950. Not adjusted to standard tow.

Station Depth sampled in metres	18 1–110	18 190–597	71 0–50	71 145–250	71 430–700
Acartia longiremis			225	1	
Calanus finmarchicus			1062	52	10
Calanus hyperboreus	20	10	680	19	59
Chiridius obtusifrons					3
Gaidius tenuispinus				17	3
Haloptilus acutifrons		1			
Heterorhabdus compactus (?)		1			
Heterorhabdus norvegicus		1			1
Limnocalanus grimaldi					1
Metridia longa	4	162		155	223
Mormonilla minor		122			
Oithona spp.	533		5076	206	59
Oncaea spp.		243	301	155	1362
Pareuchaeta norvegica	3	1			5
Scaphocalanus magnus		2			1
Spinocalanus abyssalis		1		26	
Spinocalanus magnus		1			
Xanthocalanus propinquus		1			
Microcalanids	249	41	4286	688	459
Copepod nauplii	107	+	4399	146	118

Table 5. Copepods: Chukchi Sea area — 1951. Number per haul adjusted to 0–100-metre vertical tow. (+ = present).

Station Depth sampled in metres	1 0–36	5 0–100	6 0–63	7 0–100	8 0–50	9 0–100	10 0–60	11 0–100	12 0–100	13 0–100	14 0–100	15 0–100	16 0–100	43 0–100	44 0–100	45 0–100	50 0–100	53 0–100	60 0–100
Acartia clausi	7511	110		2						+			+						
Acartia longiremis	1975	440	104	2232	615	366	441	940	420	215	336	172	86	3	125	1040			
Calanus cristatus				1															
Calanus finmarchicus		770	413	5	82	549	840	940	1050	559	966	1505	215	1960	1000	1560	104	15	28
Calanus hyperboreus			2	4		1					2	9		784	15	1	120	35	55
Calanus tonsus		330		800		549					+	1	+						
Calanus spp. juveniles		1100	1156	2604	164	2196	525	987	1400	215	420	1505	172	315	200	+	208	31	60
Centropages mcmurrichi	977				82				1										
Chiridius sp. juveniles															1				
Eurytemora herdmani	1	+																	
Eurytemora transversalis	1																		
Metridia longa						+	105	141	210	258	126	43	+	71	1	390	156	11	
Metridia lucens															1			1	
Oithona spp.	9044	770	2311	2232	12054	1098	3790	2303	1750	731	2814	1849	430	6272	2375	4680	3588	1260	3286
Oncaea spp.			1073	248	82	366	11	376	70	86	168	215	215	2058	625	1300	1508	630	1060
Pareuchaeta norvegica			1					1		3					1	1	7	1	5
Scolecithricella minor																		5	
Microcalanids*	6255	12980	7470	12980	1968	12078	2835	6721	7000	3698	7182	6278	2795	4802	4000	6760	936	1530	2332
Copepod nauplii	10511	6380	2064	4092	1804	2196	1995	2867	1890	688	2520	903	344	1078	2125	2990	1560	630	1060

*Includes *Microcalanus pygmaeus* and *Pseudocalanus minutus*.

Table 6. Copepods: western Beaufort Sea — 1951. Number per haul adjusted to 0–100-metre vertical tow. (+ = present).

Station Depth sampled in metres	17 0–16	20 0–50	22 0–100	24 0–100	25 0–100	27 0–100	28 0–100	29 0–100	30 0–100	31 0–100	32 0–100	33 0–100	36 0–100	37 0–100	38 0–100	39 0–100	40 0–100	41 0–100
Acartia longiremis		32	54	92	4				30	50	3	10	738	2030	810	4		
Calanus finmarchicus	25	320	1512	552	114	56	104	21	270	110	779	9348	328	1566	270	188	36	31
Calanus hyperboreus	200	300	168	12	25	24	64	13	11	1							108	20
Calanus spp. juveniles		384	540	184	76	84	52	8	30	15	10	+	14	27	10	3	6	220
Centropages mcmurrichi													2	3	5			
Chiridius obtusifrons	20	2													1			
Eucalanus bungii		1																
Eurytemora herdmani					1								1	3	4			
Gaidius tenuispinus																	1	
Heterorhabdus norvegicus				1	1		1											
Metridia longa	144	8	216	92	38	84	9	4	90	1			1	4	15	12	288	22
Oithona spp.	2200	832	3240	2576	3800	3780	5044	336	5715	825	410	738	656	3422	2970	235	2196	968
Oncaea spp.	2200	256	378	782	608	1232	1924	84	1170	220	123	+	+	58	+	24	1476	660
Pareuchaeta norvegica		2	4		9	5	10	3	9					1		3	27	11
Scaphocalanus magnus																	3	
Scolecithricella minor						1	10	2										
Scolecithrix brevicornis																		1
Tortanus discaudatus													1	1	1			
Microcalanids*	12925	2012	4644	828	418	392	4734	210	2160	2750	1025	246	2419	11484	9100	659	2700	1582
Copepod nauplii	9075	1152	1620	1334	1216	392	1092	42	990	165	82	308	902	4524	2610	118	684	440

*Includes *Microcalanus pygmaeus* and *Pseudocalanus minutus.*

Table 7. Copepods: eastern Beaufort Sea — 1951. Number per haul adjusted to 0–100-metre vertical tow. (+ = present).

Station Depth sampled in metres	63 0–100	64 0–100	65 0–100	66 0–100	67 0–100	69 0–100	70 0–100	71 0–100	72 0–100	73 0–100	74 0–100	75 0–100	76 0–100	77 0–100	78 0–100	79 0–100	82 0–100	86 0–100	92 0–100
Acartia longiremis	2																		
Calanus finmarchicus	280	296	36	14	231	30	31	112	35	28	70	50	210	340	488	32	95	27	23
Calanus hyperboreus		2	1	17	+	14	14	168	50	84	136	324	+	85	+	23	50	28	3
Calanus spp. juveniles	280	222	36	65	77	24	184	112	244	51	369	1080	840	680	1220	504	193	10	83
Chiridius obtusifrons								3	2		1	1							
Eurytemora herdmani	2																		
Gaidius brevispinus									1										
Gaidius tenuispinus		1	2						6		1	2					5		
Heterorhabdus norvegicus									3			2							
Metridia longa	315	21	252		1			224	244		98	756	17	85	244		483	9	3
Oithona spp.	6370	3478	1404	715	2156	1800	4224	13944	4514	3315	2522	9072	3465	3485	1403	6328	2512	2548	6308
Oncaea spp.	1470	666	72	293	655	975	1024	2576	1708	765	984	2376	840	595	549	1400	773	672	1204
Pareuchaeta norvegica	9	1		2	4	19	14	14	10	6	11	5				2	2	10	8
Scaphocalanus magnus									3		1	1							
Scolecithricella minor		3	2		1			12	8	2	4	6					24		
Microcalanids*	3220	5180	216	427	732	900	768	5376	3782	1785	3752	4536	945	765	915	1176	435	840	748
Copepod nauplii	1960	888	252	195	154	600	576	728	1708	1326	1230	1512	1260	1020	793	560	145	420	664

*Includes *Microcalanus pygmaeus* and *Pseudocalanus minutus*.

Table 8. Miscellaneous plankton: Chukchi Sea area — 1950. Number per haul adjusted to 0–100-metre vertical tow. (+ = present).

Station Depth sampled in metres	3 0–5	4 0–58	5 0–100	6 0–100	7 0–61	8 0–72	9 0–90	10 0–109	11 0–150	12 0–230	13 0–46	15 0–122	16 0–91	17 0–107	19 0–100	20 0–100	21 0–100	23 0–145	26 0–69	27 0–137	28 0–100	29 0–91	30 0–90
Amphipods		1				76	3	5	1	6	9	2	13	6	15	6	6			3	7	1	1
Barnacle nauplii	333	420	3080	770	1663	1820	300	1126	305	217	2319	98	653	+	278	1760	1248	104	552	1485	836	968	3966
Barnacle cyprids	804	3300	2474	7810	2079	4900	3120	2085	237	118	2182	162	544	113	1	1188	1056	52	236	278	308	176	721
Crab zoeae	16	+	18	11			2		4	1								1	4		1	2	1
Thysanoëssa inermis				1					1														
Thysanoëssa longipes														1									
Thysanoëssa raschii				2		1		1	1					1									
Euphausiid nauplii			+			70																	
Euphausiid furcilia		8		1				1										1					
Macruran larvae	6	+	8	57	43	575	14	5	6		2	4	3			4		3	5	2	1	1	8
Ostracods								1	+	8					3			1					1
Annelid larvae		120	51	165	901	1050	360	542	68	39	+	65	182				96	91	+	232	+	264	875
Larvaceans		840	101	825	693	210	240	250		118	6002	780	400	151	648	396	144	65	158	557	264	88	1494
Echinoplutii					+																		
Ophioplutii				715	208	280	120	83			+	65	1				+	26	+	46		176	
Lamellibranch larvae	59	+		55	485	1050	420	417		+	+	65			556	220	+	65	+	186	88		+
Limacina helicina	+						+	125		39	273		182		463	88				93	264	176	

Table 9. Miscellaneous plankton: western Beaufort Sea — 1950. Number per haul adjusted to 0–100-metre vertical tow. (+ = present).

Station Depth sampled in metres	54 0–100	55 0–100	57 0–100	58 0–100	60 0–91	62 0–61	64 0–27	66 0–46	69 0–100	73 0–100
Amphipods	7			5	7	3	3	22	23	6
Barnacle nauplii										37
Barnacle cyprids	+			+				11	1	402
Crab zoeae										1
Thysanoëssa raschii				2			1			
Euphausiid furcilia										2
Macruran larvae								+		
Ostracods	8	10	13	19		13	2			2
Annelid larvae							+	+		+
Larvaceans	158	78	+	31	147	+	+		155	110
Lamellibranch larvae	+									
Limacina helicina	237	195	93	246	221	114		156	103	183

Table 10. Miscellaneous plankton: eastern Beaufort Sea — 1950. Number per haul adjusted to 0–100-metre vertical tow. (+ = present).

Station Depth sampled in metres	32 0–46	33 0–91	34 0–46	35 0–91	36 0–91	37 0–100	38 0–100	39 0–100	40 0–15	41 0–67	44 0–30	46 0–100	49 0–100	51 0–86	53 0–100
Amphipods	4	1	7	2	3	1						6		10	2
Barnacle nauplii	2	1				1				2					
Barnacle cyprids	2						1						94		
Ostracods		13	2				2							2	4
Annelid larvae		+	275		+				+						
Larvaceans	+	+	733	+	273			258			+	150	+	+	282
Ophioplutii			+	+		+									
Lamellibranch larvae		+		87	+					+	+		+		
Limacina helicina	+	+	550	87	897	303	161	301	+	468	+	38	1269	159	94

Table 11. Miscellaneous plankton in deep tows — 1950. Not adjusted to standard tow.

Station Depth sampled in metres	18 0–110	18 190–597	71 0–50	71 145–250	71 430–700
Amphipods		1			3
Barnacle nauplii	1		1		
Barnacle cyprids		2	226	26	1
Crab zoeae			4		
Euphausiid furcilia			2		
Macruran larvae			10		
Ostracods		12		60	104
Annelid larvae			150	17	+
Larvaceans			1391	10	44
Ophioplutii			1		
Lamellibranch larvae			113		
Limacina helicina		+	338		

Table 12. Miscellaneous plankton: Chukchi Sea area — 1951. Number per haul adjusted to 0–100-metre vertical tow. (+ = present).

Station Depth sampled in metres	1 0–36	5 0–100	6 0–63	7 0–100	8 0–50	9 0–100	10 0–60	11 0–100	12 0–100	13 0–100	14 0–100	15 0–100	16 0–100	43 0–100	44 0–100	45 0–100	50 0–100	53 0–100	60 0–100
Amphipods	3	2				2		1			4	10			2	3	11	4	2
Barnacle nauplii	7822	3960	1321	13888	3772	4392	1575	846	1960	344	462	129	774	2	1				
Barnacle cyprids	244	6380	11060	39432	1476	6954	19845	23594	7630	7095	6258	2021	1763	2450	1625	2860	2		
Crab zoeae		21	10	2	4	117	32	5	3	2			2	2	2	5			
Thysanoëssa inermis		1																	
Thysanoëssa raschii				1										1					
Euphausiid nauplii				7															
Euphausiid furcilia		4	11		2	35	12	12	8		6	1	5	2	9	3			
Macruran larvae		20	3	22	8	35	5	5	12	10	3	1	3	1	1	2			
Ostracods			3							2							4	2	
Annelid larvae	5133	770	660	1736	574	1098	420	376	560	860	210	172	43		375				
Larvaceans		1760	+	2108	1230	1464	630	470	1050		420	215		196		520	+		+
Echinoplutii	7089				820				+	43									
Ophioplutii		220			1640				+	43					375				
Lamellibranch larvae	24689	1760	4622	6448	5904	2562	4095	4136	2310	1376	840	129	430	98	1125	130			
Limacina helicina						+								392	125	390	4	+	477

Table 13. Miscellaneous plankton: western Beaufort Sea — 1951. Number per haul adjusted to 0–100-metre vertical tow. (+ = present).

Station Depth sampled in metres	17 0–16	20 0–50	22 0–100	24 0–100	25 0–100	27 0–100	28 0–100	29 0–100	30 0–100	31 0–100	32 0–100	33 0–100	36 0–100	37 0–100	38 0–100	39 0–100	40 0–100	41 0–100
Amphipods		2	7	6	5	2			5				1		1	1		
Barnacle nauplii	34		1							55	3		123	290	180			
Barnacle cyprids		512	6264	644	38				2475	440	2870	4797	1517	2900	3150	306	+	
Crab zoeae					2							6	3					
Thysanoëssa raschii			1															
Euphausiid furcilia		2	4	2					7	1	16	23	3	13	2	1		
Macruran larvae			4							2	4	2	7	12	4	1		
Ostracods			13	31	10	1			6								28	5
Annelid larvae	+	128	54							+	+		+	174	180	24		
Larvaceans	+	128	+			56	208	21	45	110	82	+	451	638	540	141		12
Echinoplutii										1			82	174				
Ophioplutii	38	+	54											58				
Lamellibranch larvae		64	756	46					1080	220	82	246	902	3654	1800	+		
Limacina helicina							156	168	225	110		13				24	648	176

Table 14. Miscellaneous plankton: eastern Beaufort Sea — 1951. Number per haul adjusted to 0–100-metre vertical tow. (+ = present).

Station Depth sampled in metres	63 0–100	64 0–100	65 0–100	66 0–100	67 0–100	69 0–100	70 0–100	71 0–100	72 0–100	73 0–100	74 0–100	75 0–100	76 0–100	77 0–100	78 0–100	79 0–100	82 0–100	86 0–100	92 0–100
Amphipods								15	21	1	8	10			1	2	6		
Barnacle cyprids	980	2			1							2	3	1	4	5	3		
Euphausiid furcilia	2																		
Ostracods			6		+			22	19		18	10					3	2	
Annelid larvae		+												+					
Larvaceans	105	148		163	270	825	384	448	610	306	2275		630	765	976	1064	435	112	208
Echinoplutii												+							
Ophioplutii		1		+								+	+	+					
Lamellibranch larvae	280	+	+	+	+	+					+		+	+		+	+		
Limacina helicina	315	222	360	423	308	975	960	224	854	153	+	864	840	1360	488	392	725	224	125

Table 15. Barnacles: summary of naupliar and cyprid stages.

	1950			1951		
Area	Chukchi Sea	Western Beaufort Sea	Eastern Beaufort Sea	Chukchi Sea	Western Beaufort Sea	Eastern Beaufort Sea
Period	Aug. 11–16	Aug. 25–30	Aug. 18–23	Aug. 12–15 Sept. 3–7	Aug. 23–29	Sept. 14–21
Nauplii	24301	37	6	41248	683	0
Cyprids	33944	414	97	140689	25913	1001
Ratio nauplii/cyprids	0.72:1.00	0.09:1.00	0.06:1.00	0.29:1.00	0.03:1.00	0.00:1.00
Av. no. per station	2532	45.1	6.86	9576	1478	52.68

References

Barnes, C. A. and T. G. Thompson. 1938. 'Physical and chemical investigations in Bering Sea and portions of the North Pacific Ocean'. *Univ. Wash. Publ. Oceanog.* Vol. 3, No. 2, pp. 35–79.

Bogorov, V. 1946. "Zooplankton collected by the *Sedov* Expedition 1937–1939". *Trudy,* Vol. 3, pp. 356–70.

Brodskiy, K. A. 1952. "Deepwater copepods (Calanoidea) of the northwest part of the Pacific Ocean" *in* 'Deepwater fauna of the northwest part of the Pacific Ocean'. *Akad. nauk S.S.S.R. Issledovaniya Dal'nevostochnykh Morey S.S.S.R.* No. 3, pp. 37–87.

Campbell, Mildred H. 1929. "Some free-swimming copepods of the Vancouver Island region". *Trans. Roy. Soc. Can.* Vol. 23, Ser. III, Sect. V, pp. 303–32.

1930. "Some free-swimming copepods of the Vancouver Island region. II". *Trans. Roy. Soc. Can.* Vol. 24, Ser. III, Sect. V, pp. 177–82.

Carsola, Alfred J. 1954. "Recent marine sediments from Alaskan and northwest Canadian Arctic". *Bull. Amer. Ass. Pet. Geol.* Vol. 38, No. 7, pp. 1,552–86.

Comita, G. W. and W. T. Edmondson. 1953. "Some aspects of the limnology of an arctic lake". *Stanford Univ. Publ., Univ. Ser., Biol. Sci.* Vol. 11, pp. 7–13.

Davis, C. C. 1949. 'The pelagic Copepoda of the northeastern Pacific Ocean'. *Univ. Wash. Publ. Biol.* Vol. 14, 117 pp.

Dunbar, M. J. 1951. 'Eastern Arctic waters'. *Fish. Res. Bd. Can. Bull.* No. 88, 131 pp.

1953. "Arctic and subarctic marine ecology: immediate problems". *Arctic,* Vol. 6, No. 2, pp. 75–90.

Esterly, C. O. 1924. "The free-swimming Copepoda of San Francisco Bay". *Univ. Calif. Publ. Zool.* Vol. 26, No. 5, pp. 81–129.

Farran, G. P. 1926. "Biscayan plankton collected during a cruise of H.M.S. 'Research,' 1900.–Part XIV. The Copepoda". *J. Linn. Soc.* Vol. 36, No. 243, pp. 219–310.

Gurney, Robert. 1933. 'British fresh-water Copepoda'. London: Ray Society, Vol. 3, xxix + 384 pp.

Jespersen, P. 1934. 'The Godthaab Expedition 1928. Copepoda'. *Medd. om Grønl.* Vol. 79, No. 10, 166 pp.

1939. 'Investigations on the copepod fauna in east Greenland waters'. *Medd. om Grønl.* Vol. 119, No. 9, 106 pp.

Johnson, Martin W. 1934. "The production and distribution of zooplankton in the surface waters of Bering Sea and Bering Strait, Part II" *in* 'Report of oceanographic cruise U.S. Coast Guard Cutter *Chelan*–1934'. *Mimeographed Rept.* pp. 45–82.

1938. "Concerning the copepod *Eucalanus elongatus* Dana and its varieties in the northeast Pacific". *Bull. Scripps Inst. Oceanog., Univ. Calif. Tech. Ser.* Vol. 4, No. 6, pp. 165–80.

1953. "Studies on plankton of the Bering and Chukchi seas and adjacent areas". *Proc. 7th Pacific Sci. Congr.* (1949), Vol. 4, 'Zoology', pp. 480–500.

Lafond, E. C. and D. W. Pritchard. 1952. "Physical oceanographic investigations in the eastern Bering and Chukchi seas during the summer of 1947". *J. Marine Res.* Vol. 11, No. 1, pp. 69–86.

Linko, A. K. 1913. 'Zooplankton de la mer glacile de Siberie, etc.' *Mém. Acad. Sci. St. Petersburg,* Sér. 8, Vol. 29, No. 4, 54 pp.

Marsh, C. D. 1920. "The fresh water Copepoda of the Canadian Arctic Expedition 1913–18". *Rept. Can. Arctic Exped. 1913–18,* Vol. 7, 'Crustacea', Part J, "Freshwater Copepoda", 25 pp.

Marukawa, H. 1928. "On the plankton of the Japan Sea". *Annot. Oceanogr. Res.* Vol. 2, No. 1, pp. 9–13.

Mori, Takamochi. 1937. 'The pelagic Copepoda from the neighboring waters of Japan'. Tokyo: Yôkendô Company, 150 pp.

Nansen, Fridtjof. 1902. 'The oceanography of the North Polar Basin'. *Norw. North Polar Exped. 1893–1896. Sci. Res.* Vol. 3, No. 9, 427 pp.

Rose, M. 1933. 'Copépodes Pélagiques'. *Faune de France,* Vol. 26, 374 pp.

Sars, G. O. 1897. "Pelagic Entomostraca of the Caspian Sea". *Ann. du Musée Zool. de l'Acad. Imp. des Sci. de St. Petersburg,* pp. 38–73.

1900. 'Crustacea'. *Norw. North Polar Exped. 1893–1896. Sci. Res.* Vol. 1, No. 5, 137 pp.

1903. 'An account of the crustacea of Norway, Vol. 4: Copepoda Calanoida'. Bergen Museum, 171 pp.

1918. 'An account of the crustacea of Norway, Vol. 4: Copepoda Cyclopoida'. Bergen Museum, 225 pp.

Saur, J. F. T., J. P. Tully, and E. C. Lafond. 1954. 'Oceanographic cruise to the Bering and Chukchi seas summer 1949. Part IV. Physical oceanographic studies: Vol. I. Descriptive report'. *U.S. Navy Electronics Lab. Rept.* 416, 31 pp.

Schmitt, W. L. 1919. "The Schizopod Crustaceans of the Canadian Arctic Expedition, 1913–18". *Rept. Can. Arctic Exped. 1913–18,* Vol. 7, 'Crustacea', Part B, "Schizopod Crustaceans", 8 pp.

Smirnov, Sergius. 1931. "Zur Kenntnis der Copepodengattung *Eurytemora* Giesbr." *Zool. Anzeiger,* Vol. 98, Nos. 5/8, pp. 194–201.

Stepanova, V. 1937. 'Biologische Zeichnungen der Stromungen im Norlichen Teil des Bering und im Sudlichen Teil des Tschuktschen Meeres'. *Publ. Hydrological Inst. of Leningrad,* Vol./No. 5, pp. 175–216.

Stephensen, K. 1933. 'The Godthaab Expedition. 1928. Schizopoda'. *Medd. om Grønl.* Vol. 79, No. 9, 20 pp.

Sverdrup, H. U. 1950. "Physical oceanography of the North Polar Sea". *Arctic,* Vol. 3, No. 3, pp. 178–86.

Thorson, Gunnar. 1950. "Reproductive and larval ecology of marine bottom invertebrates". *Biological Reviews,* Vol. 25, No. 1, pp. 1–45.

van Breeman, P. J. 1908. 'Copepoden. Nordisches Plankton'. Vol. 4, No. 8, 263 pp.

Vervoort, W. 1951. 'Plankton Copepods from the Atlantic sector of the Antarctic'. *Verh. der Koninklijke Nederlandse Akad. van Wetens. A.F.D. Natur.* Tweede Sectie, Vol. 47, No. 4, 156 pp.

Willey, Arthur. 1920. "Report on the marine Copepoda collected during the Canadian Arctic Expedition". *Rept. Can. Arctic Exped. 1913–18,* Vol. 7, 'Crustacea', Part K, "Marine Copepoda", 46 pp.

Williams, L. W. 1906. "Notes on marine Copepoda of Rhode Island". *Amer. Nat.* Vol. 40, No. 477, pp. 639–60.

Wilson, C. B. 1932. 'The copepods of the Woods Hole region Massachusetts'. *U.S. Nat. Mus. Bull.* 158, 635 pp.

1950. 'Copepods gathered by the United States Fisheries Steamer "Albatross" from 1887 to 1909, chiefly in the Pacific Ocean'. *U.S. Nat. Mus. Bull.* 100, Vol. 14, Part 4, pp. 141–441.

With, Carl. 1915. 'Copepoda I. Calanoida Amphascandria'. *Danish Ingolf-Expedition,* Vol. 3, No. 4, 260 pp.

Worthington, L. V. 1953. "Oceanographic results of Project Skijump I and Skijump II in the Polar Sea, 1951–1952". *Trans. Amer. Geophys. Union,* Vol. 34, No. 4, pp. 543–51.

Reprinted from Geochimica et Cosmochimica Acta, 1956, Volume 10, pp. 321–322.
Pergamon Press, London.
Reproduced by Permission

Germanium in meteorites

(*Received* 19 *April* 1956)

Eight chondrites (including two composites) and seven meteorites were analysed for germanium. The meteorites analysed and their germanium content are recorded in the following table.

Meteorite	Ge (p.p.m.)		Meteorite	Ge (p.p.m.)
Chondrites			Irons‡	
Composite I (7 chondrites)*	10·3	10·9	Tlacotepec	<1·0
Composite II (7 chondrites)†	9·4	9·6	Duchesne	<1·0
Cope, Colo.	9·2	9·0	Toluca	271
Melrose, N. Mex.	9·3	9·6	Henbury	273
Arriba, Colo.	9·2	9·0	Edmonton	38
Ladder Creek, Kan.	6·6		Magura	519
Plainview, Texas	12·0		Cañon Diablo	352
Roy, N. Mex.	8·8			

Meteoritic material was put into complete solution by treatment with hydrofluoric acid followed by fusion of the residue with potassium pyrosulphate. Germanium is first separated by distilling the $GeCl_4$ from constant boiling HCl and then determined by measuring the absorbance of its phenylfluorone complex.

If, following Urey (*The Planets*, 1952, Yale University Press), we take chondrites to represent average cosmic matter (excluding the volatile elements) the present analyses give 9 p.p.m. for the cosmic abundance of germanium. Previous data on the meteoritic abundance of germanium (V. M. Goldschmidt, *Geochemistry*, 1954, p. 380) are probably too high.

Chondrites appear to be uniform in their germanium content and it seems probable that the average value of 9 p.p.m. for the cosmic abundance of Ge is not far from the truth. Present data (see table) for Ge in chondrites and in iron meteorites indicate that the distribution of Ge in meteorites is determined by conditions under which meteorites were formed. The difference in the range of Ge in iron meteorites and in the iron phase of chondrites may have an important bearing on the origin of meteorites.§ This work is part of a study of the geochemistry of Ge which the author hopes to publish in the future.

I am indebted to Dr. E. B. Sandell, who provided the chondritic material, and Mr. W. Nichiporuk for placing the irons at my disposal.

Scripps Institution of Oceanography
La Jolla, California

Sayed A. Wardani

---

[*] Arriba, Colo.; Beenham, N. Mex.; Cope, Colo.; Coterfield, Neb.; Morland, N. Mex.; Plainview, Texas; Roy, N. Mex.

[†] Alamogordo, N. Mex.; Estacado, Texas; Gladstone, N. Mex.; Kingfisher, Okla.; Gruver, Texas; Ladder Creek, Kan.; Melrose, N. Mex.

[‡] Because of very limited samples, error may be ±10%.

[§] Preliminary fractionation of chondrites into the silicate and metal phases indicates that Ge is concentrated in the latter phase.

Contributions from the Scripps Institution of Oceanography, New Series, No. 858

(632)

Reprinted from **ANALYTICAL CHEMISTRY**, Vol. 28, Page 1282, August 1956
Copyright 1956 by the American Chemical Society and reprinted by permission of the copyright owner
Reproduced by Permission

X-Ray Fluorescence Determination of Barium, Titanium, and Zinc in Sediments

GEORGE J. LEWIS, Jr., and EDWARD D. GOLDBERG
Scripps Institution of Oceanography, La Jolla, Calif.

X-ray fluorescence analysis has been applied to the rapid and quantitative assay of barium, titanium, and zinc in marine sediments. Internal standards were used to minimize matrix effects in the samples, which ranged in composition from nearly pure calcium carbonate to glauconite and deep-sea clays, which have compositions similar to materials encountered in ordinary silicate analysis. Arsenic was employed as the internal standard for zinc, and lanthanum served for both barium and titanium. The barium $L\alpha_1$ and titanium $K\alpha$ peaks, which had the highest usable sensitivities, overlapped and empirical corrections to compensate for this effect were ascertained. The lower limits of detectability were 0.01% for titanium and barium and 0.004% for zinc.

STUDIES on the geochemistry of marine sediments have necessitated the determination of such minor elements as barium, titanium, and zinc in clay and calcareous materials. X-ray fluorescent techniques appeared advantageous for a number of reasons. With the selection of proper internal standards (*1*), the methods can be applied to a large variety of mineral types. The nondestructive nature of the technique does not demand the sacrificing of the small amounts of sample available for analysis. Finally, the method is rapid and reasonably simple. This paper considers some of the problems encountered in the quantitative x-ray spectrographic assay of titanium, barium, and zinc in marine sediments of widely varying composition.

Table I. Composition of Typical Marine Clay and Mock Clay Used in Preparation of Standards

	Weight % of Constituents	
	Marine clay	Synthetic clay
SiO_2	60	59
Al_2O_3	15	17
Fe_2O_3	7	8
Na_2O	5	3
K_2O	4	5
MgO	4	2
CaO	4	5
MnO	1	1

INSTRUMENTATION

A Norelco x-ray spectrograph with a 50-kv. tungsten tube (Machlett OEG-50), an argon-filled Geiger tube detector, and a lithium fluoride analyzing crystal were used. For the barium and titanium determinations a helium path was constructed from a polyethylene bag and attached to the apparatus in essentially the manner described by Davis and Van Nordstrand (*2*). Helium flow rates of at least 700 ml. per minute were used to obtain maximum reproducibility of results. A tenfold increase in sensitivity for the barium $L\alpha_1$ and the titanium $K\alpha$ radiation resulted from the substitution of a helium path for an air path. An aluminum planchet designed to hold about 1 gram of sample was machined to fit the sample holder provided with the instrument. The x-ray tube was operated at 45 kv. and 35 ma.

EXPERIMENTAL

Standards. Reagent grade chemicals were used throughout the investigation. Standard zinc samples were prepared by the addition of zinc acetate dihydrate to portions of a mock marine clay of the composition given in Table I, on a water-free basis. Barium and titanium primary standards were made by the addition of barium carbonate and titanium dioxide to calcium carbonate.

Internal Standards. The choice of an internal standard for a given element depends not only upon the desirable characteristic of having an x-ray fluorescence peak adjacent to the peak of the element in question but also upon the following criteria: (1) ready availability in an inexpensive and stable form; (2) sufficient peak separation from the element in question to make background measurements possible; (3) absence from the matrix

Table II. X-Ray Fluorescence Peak and Background Wave Lengths of Elements and Internal Standards

(Lithium fluoride used as analyzing crystal)

Element	Emission	Wave Length, A.	Degrees 2θ Peak	Degrees 2θ Background
Zinc	$K\alpha$	1.437	41.81	40.96 46.00
Arsenic	$K\alpha$	1.177	33.98	33.00 35.00
Barium	$L\alpha_1$	2.776	87.16	85.00 89.00
Titanium	$K\alpha$	2.750	86.08	85.00 89.00
Lanthanum	$L\alpha_1$	2.665	82.86	81.50 85.00

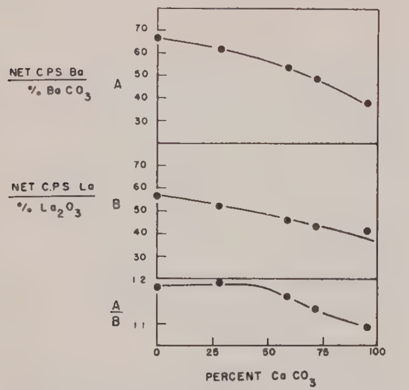

Figure 1. Effect of carbonate concentration upon fluorescent intensities of barium and lanthanum

Carbonate diluted with mock clay

under investigation as well as from the x-ray target; and (4) no absorption or enhancement effects with the element under consideration (see below). Lanthanum, the periodic table neighbor of barium, fulfilled the above requirements most completely for both barium and titanium. Arsenic was chosen as the internal standard for zinc, inasmuch as neither gallium nor germanium was available and copper was a contaminant in the target of the x-ray tube.

Preparation of Samples and Standards. The standards and sediment samples were initially ground to 300 mesh. After the addition of the internal standard to a given sample, the mixture was ground for at least 20 minutes in a machine-operated mullite mortar. Homogeneity was tested by intensity measurements of the element in question in different portions of the sample. In no case was there any indication of insufficient mixing.

The internal standard was added to the sediment or standard samples in amounts such that its peak had an intensity near that of the element in the upper concentration ranges. Arsenic trioxide addition amounted to about 0.6% of the sample weight for zinc concentrations of 0.004 to 0.6%. For titanium and barium concentration ranges of 0.01 to 2.0%, the amount of lanthanum trioxide standard amounted to approximately 2.5% of the sample weight.

Lines. The lines used in the analytical work are given in Table II. The *Kα* line of barium could not be adequately excited at the 50-kv. x-ray tube operating potential and hence recourse was made to an *L* line of this element. Times for fixed counts of 25,600 at the fluorescence peaks and 6400 at the background positions were taken. The background was determined on both sides of the peaks and from these measurements the background at the peak was calculated by interpolation. Background measurements made on mock clays free of the element to be analyzed indicated that such interpolations were valid.

Calculations. The net counting rates per unit weight per cent of the element and of the corresponding internal standard were obtained. Linear calibration curves on log-log paper resulted from plotting the weight per cent of the element against net counts per second of element/net counts per second of internal standard per weight per cent of internal standard.

RESULTS AND DISCUSSION

Barium and Titanium Determination. Although the use of internal standards in x-ray fluorescence spectroscopy largely reduces matrix effects upon the peak intensity of an element of given concentration, enhancement or absorption of one or both of the members of a line pair must be considered. This problem has been discussed recently by Adler and Axelrod (*1*), who have divided these effects into two categories: absorption effects and excitation effects.

Preferential absorption may occur if a matrix element has an absorption edge between the internal standard line and the line of the element being determined or on the long wave-length side of these two lines. Even with the proper choice of an internal standard, the intensity ratio may show a significant difference.

Preferential excitation may be caused by a matrix element which has a fluorescence line falling between the absorption edges of the internal standard and element being measured or on the short wave-length side of both. Excitation effects are usually smaller than those due to preferential absorption but may affect the results appreciably.

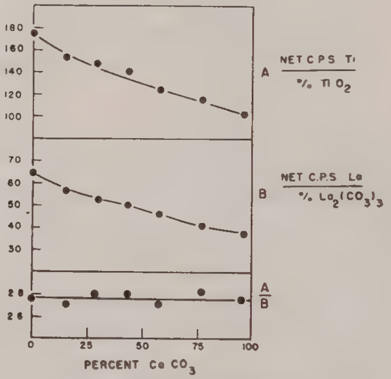

Figure 2. Effect of carbonate concentration upon fluorescent intensities of titanium and lanthanum

Carbonate diluted with mock clay

In marine sediments the calcium concentration, expressed as calcium carbonate, varies from a few to nearly 100%. As the *K* absorption edge of calcium is 3.070 A. and the measured peaks of barium, titanium, and lanthanum are less than this value, it was necessary to investigate the absorption effect of calcium upon the emission of the studied elements and their internal standard. The two upper curves in Figure 1 show the intensity of the barium and lanthanum lines as a function of calcium carbonate content in the mock clay. In the presence of 95% calcium carbonate, the barium intensity is only about 55% of the value in the carbonate-free clay mixture. The lanthanum intensity is diminished to a slightly lesser degree with increasing calcium content. This result is not unexpected, inasmuch as absorption by the matrix element decreases with decreasing wave length of the exciting peak. There is approximately a 10% variation in the barium-lanthanum ratio between 0 and 100% calcium carbonate. From this curve corrections are applied in analysis to the values of the barium concentration taken from the calibration curve, which was prepared in a pure calcium carbonate matrix, to correspond to the actual calcium carbonate content of the samples.

The curves in Figure 1 may reflect two effects. First, the major constituents of the clay (silicon, aluminum, potassium, sodium, and magnesium) have *K* absorption edges at higher wave-length values and hence absorb barium and lanthanum radiation to a smaller extent than calcium. Secondly, iron in the clay mixture has a *Kα* line at 1.937 A., which may preferentially enhance the intensity of lanthanum (L_{III} absorption edge is 2.259 A.) over barium (L_{III} absorption edge is 2.363 A.) Thus, the greater the clay content the lower the barium-lanthanum intensity ratio due to iron excitation.

Figure 2 shows the intensity of titanium and lanthanum as a function of the calcium carbonate concentration. The titanium-lanthanum ratio shown in the bottom curve is constant throughout the range of calcium carbonate concentrations in the clay. This may result from the compensation of two effects: (1) the preferential absorption of titanium over lanthanum radiation by calcium resulting in a decreasing titanium-lanthanum ratio with increasing calcium carbonate, and (2) the preferential enhancement of lanthanum $L\alpha_1$ emission over titanium $K\alpha$ emission by iron, which results in a decreasing titanium-lanthanum ratio with decreasing calcium carbonate. Hence, within experimental error the titanium-lanthanum intensity ratio is independent of calcium carbonate content.

The barium and titanium peaks used in the analysis were not completely resolved. A mutual intensity enhancement results which requires an empirical correction when both elements are present in a given sample. Titanium increases the barium intensity to a greater extent than barium affects the titanium values, but for most of the sediments encountered corrections for both elements were significant. Figure 3 shows barium standard curves in the presence of varying quantities of titanium. It emphasizes the large relative error which would occur in low barium samples if the presence of moderate amounts of titanium were neglected. The correction is linear and amounts to an absolute value of −0.045% barium oxide per 1.0% titanium oxide in the range of 0.01 to 2.0% barium oxide and titanium oxide. The barium $L\gamma_1$ line, although it is in a clear part of the spectrum, was not used, as its intensity was too low for many of the samples analyzed.

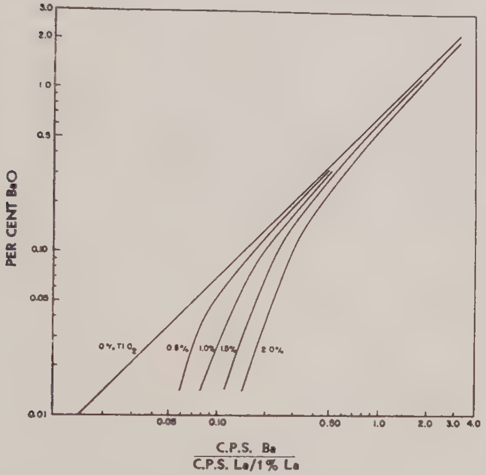

Figure 3. Barium calibration curves in presence of varying amounts of titanium

Matrix, calcium carbonate

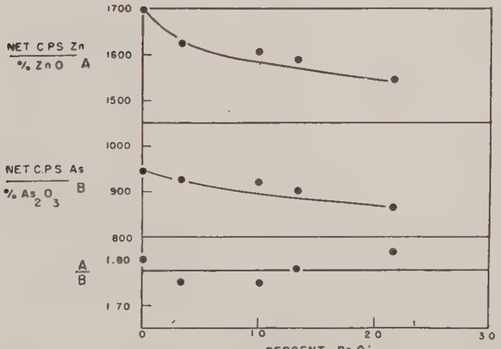

Figure 4. Fluorescent intensities of zinc and arsenic as a function of barium content

Matrix, mock clay

Corrections for barium interference upon titanium are smaller, amounting to −0.01% titanium oxide per 1.0% barium oxide within the same ranges noted above.

Titanium was determined in five calcareous sediment samples of varying calcium carbonate content by spectrophotometry (*3*) and x-ray fluorescent techniques. A comparison of the results is given in Table III.

Zinc Determination. Zinc was determined only in the clay sediments, inasmuch as these samples always contained more than 0.004% zinc, the lower limit of assay. Davis and Van Nordstrand (*2*) had shown that the presence of 0.6% barium oxide decreases the intensity of the zinc $K\alpha$ radiation by about 30% in lubricating oils. Barium is present in marine clays in amounts up to 2.0%. Figure 4 shows the absorption effect to be slightly greater than 10% for zinc as well as arsenic. The zinc-arsenic intensity ratio is independent of the barium content. It is not surprising that barium absorbs strongly in lubricating oils but not in the sediments under consideration. The oil matrix contains low atomic number elements, which are weak absorbers, and barium becomes a major contributor to the absorption effect. In sediments, where more highly absorbing elements are present, the absorption by barium is somewhat overshadowed.

Iron with a K absorption edge of 1.744 A. should readily absorb zinc $K\alpha$ radiation (1.437 A.). The data in Table IV confirm this. However, arsenic is also absorbed to the same degree, so that the intensity ratio is not altered appreciably by wide variations in iron content.

As previously noted, arsenic was used as an internal standard in preference to the periodic table neighbors of zinc because of considerations of availability and x-ray target impurities. Arsenic $K\alpha$ radiation (1.177 A.) can be absorbed by zinc. However, by the use of a near constant weight per cent addition of the internal standard to the calibration standards, as well as the sediments, this small effect is eliminated (Figure 5).

Table III. Determination of Titanium in Sediments

Sediment Type	Number	TiO_2, % X-ray	TiO_2, % Spectrophotometry	$CaCO_3$, %
Calcareous sediments	58-5	0.09	0.08	78
	58-70	0.30	0.33	30
	58-130	0.33	0.33	25
	58-149	0.13	0.14	72
	58-471	0.33	0.30	20
Glauconite	15006B	0.18	0.19	0
	15019	0.27	0.29	0
	15030B	0.10	0.09	0

Table IV. Absorption of Zinc $K\alpha$ Radiation by Iron in Mock Clays

ZnO, %	As_2O_3, %	Zn/% ZnO, C.P.S. *A*	As/% As_2O_3, C.P.S. *B*	*A/B*	Fe_2O_3, %
0.0425	0.518	2380	1092	2.18	6.9
0.0410	0.500	2195	986	2.22	10.3
0.0396	0.483	2045	942	2.17	13.0
0.0381	0 464	1942	880	2.21	16.4
0.0368	0.449	1810	806	2.25	19.5

Table V. X-Ray and Emission Spectrographic Determination of Zinc in Pacific Ocean Pelagic Clays

Sample	Zinc Oxide, %	
	X-ray	Emission
30 BG 24	0.014	0.011
31 BG 32	0.017	0.013
49 BP 52	0.018	0.022
49 BP 140	0.027	0.024
50 BP 16	0.018	0.017
50 BP 760	0.036	0.031

Results of zinc determinations on six red clays were assayed both by x-ray fluorescence and by the emission spectrographic method of Wedepohl (*4, 5*) in Göttingen. The results are given in Table V.

The reproducibility of an analysis on a given sample was governed by the random errors resulting from the counting techniques. For the lanthanum and barium determination, the absolute counting error varied from 10 to 4%, where the elements varied in concentration from 0.1 to 2.0%. In the case of zinc, the counting error varied from 15 to 4%, where the zinc concentration ranged from 0.004 to 0.6%.

ACKNOWLEDGMENT

This work was sponsored by the Office of Naval Research and the American Petroleum Institute, Project 51, under contracts with the University of California.

LITERATURE CITED

(1) Adler, I., Axelrod, J. M., *Spectrochim. Acta* 7, 91–9 (1955).
(2) Davis, E. N., Van Nordstrand, R. A., ANAL. CHEM. 26, 973–7 (1954).
(3) Sandell, E. B., "Colorimetric Determination of Traces of Metals," p. 575, Interscience, New York, 1950.
(4) Wedepohl, K. H., *Geochim. et Cosmochim. Acta* 3, 93–142 (1953).
(5) Wedepohl, K. H., personal communication.

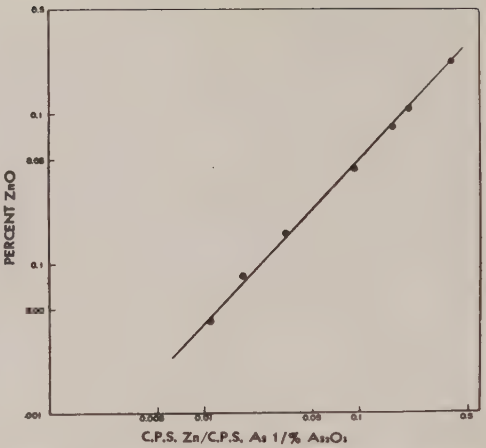

Figure 5. Calibration curve for zinc in clay sediments

RECEIVED for review December 5, 1955. Accepted May 9, 1956. Contribution from Scripps Institution of Oceanography, No. 860.

PRINTED IN U. S. A.

636)

Reprinted from The Condor, Volume 58, September-October, 1956, Number 5, pp. 388–389
Reproduced by Permission

Land Birds at Sea Off Southern California.—A number of occurrences of land birds at sea off southern California were recorded in May of 1951 (Wisner, Condor, 54, 1952:62–63). On September 25, 1953, an entirely different group of land birds was observed on board the research vessel E. W. Scripps at latitude 32° 34.6′N., longitude 117° 21.5′W. The nearest points of land were Point Loma, 8 miles northeast and the Coronados Islands, 8.5 miles to the south. The ship was surrounded by a heavy fog, and visibility aboard was reduced to about one-half mile. The foggy condition had prevailed for several days prior to these observations. The sea was calm and the air temperature about 72°F. The ship was at anchor during the night at this location prior to the following recordings.

The observations were made between 7:30 a.m. and 9:30 a.m. The first bird, a Long-billed Marsh Wren (*Telmatodytes palustris*, probably *plesius*; specimen damaged in capture) was found feeding on a moth that had become lodged in some electrical cable on deck. The wren's actions indicated that it had already become adapted to shipboard life, as it flitted about with complete composure. At the same time a Brewer Sparrow (*Spizella breweri*) and a Western Tanager (*Piranga ludoviciana*) were observed to be aboard. The sparrow seemed to be shy and retired to a secluded spot when disturbed. The tanager flitted into the air from time to time to capture insects. Its condition, however, was apparently weakened by the sojourn at sea, since it was easily captured by hand. The wren and the sparrow were less easily taken. While the writer was in pursuit of them, a Warbling Vireo (*Vireo gilvus swainsonii*) and a Ruby-crowned Kinglet (*Regulus calendula cineraceus*) appeared. Fortunately, the vireo soon flew by at close range and was captured by hand while in flight. The kinglet was taken in a similar manner.

On top of the deck house, a Mourning Dove (*Zenaidura macroura*) had alighted. When frightened, it circled the ship repeatedly but returned unnoticed. The dove lacked its upper tail coverts and was easily recognized as the same bird when rediscovered. It did not return from a second flight.

The specimens of the tanager, vireo, kinglet, and wren are deposited at the San Diego Natural History Museum, where the identifications were verified by Mr. Laurence M. Huey.—Andreas B. Rechnitzer, *Scripps Institution of Oceanography, La Jolla, California, April 10, 1956.*

Contributions from the Scripps Institution of Oceanography, New Series, No. 861

Number 578 August 24, 1956

OCCASIONAL PAPERS OF THE MUSEUM OF
ZOOLOGY
UNIVERSITY OF MICHIGAN
Ann Arbor, Michigan

PRELIMINARY ANALYSIS OF THE AMERICAN CYPRINID FISHES, SEVEN NEW, REFERRED TO THE GENUS *HYBOPSIS*, SUBGENUS *ERIMYSTAX*[*]

By Carl L. Hubbs and Walter R. Crowe

For many years we have studied the eastern North American cyprinid fishes that were recently referred to the genus *Erimystax* Jordan. Earlier, this assortment of species had been included in the genus *Hybopsis*. In the present swing of the pendulum these species are again placed in *Hybopsis*, though they may be retained in *Erimystax* as a subgenus. For several reasons the re-expanded genus *Hybopsis* rests on an unsteady basis, but it is not our purpose to attempt a generic evaluation.

The differential diagnoses to follow are presented in analytical form. The rubrics in the key that pertain to each form may be visualized in the outline of classification that heads the analysis. Thus, for *Hybopsis insignis eristigma* it will be at once apparent that the diagnosis comprises items 1b, 3b, 4b, 5b, 7b, and 9b. In addition, the diagnosis of each form may be taken to include the following features of *Erimystax*, common to all: A single small barbel is developed in the terminal or nearly terminal position (over or behind the end of the gape). The scales lack basal radii. The hooked pharyngeal teeth are uniserial, and number four on each side. The nuptial tubercles are minute or even obsolete on the top of the head (never enlarged as in *Nocomis*). The species are all small (none longer than 100 mm. to caudal) and delicate. Except in *H. harperi*, the barbel is large and consistently developed, sensory papillae are conspicuous about the mouth and on the lower surface of the head, the mouth is nearly horizontal, descending at an angle of less than 20°, the upper lip is included, and the lower lip is much included. The rather large eye is definitely wider than the suborbital. The color is dark (least so in *H. monacha*) and, typically, is more or less banded, speckled, or blotched.

We reserve for our proposed general revision a more extended

---

[*] Contributions from the Scripps Institution of Oceanography, New Series, No. 863, and the Michigan Institute for Fisheries Research. Reproduced by Permission

description of each form, figures, distributional maps showing all known record-stations as well as the range in detail, full synonymies, and other pertinent material.

ANALYSIS OF THE SPECIES AND SUBSPECIES OF HYBOPSIS REFERRED TO THE SUBGENUS ERIMYSTAX

(Constituting differential diagnoses)

Outline of Classification

- 1a.—*Hybopsis harperi*
  - 2a.—*H. h. harperi*
  - 2b.—*H. h. subterranea*
- 1b
  - 3a.—*H. monacha*
  - 3b
    - 4a.—*H. cahni*
    - 4b
      - 5a.—*H. dissimilis*
        - 6a.—*H. d. harryi*
        - 6b.—*H. d. dissimilis*
      - 5b
        - 7a.—*H. x-punctata*
          - 8a.—*H. x. x-punctata*
          - 8b.—*H. x. trautmani*
        - 7b.—*H. insignis*
          - 9a.—*H. i. insignis*
          - 9b.—*H. i. eristigma*

1.

a. *Scales* large, 32 to 38 in lateral line (very rarely 38). *Mouth* more or less oblique (gape 20° to 44° from horizontal). *Sensory papillae* very small and inconspicuous on mouth and lower part of head. *Barbel* generally minute, occasionally lacking on one or both sides. *Mandibular rami* broad, very narrowly separated medially. Dark *lateral band* conspicuous on body and head, bounded above by a *light streak* that passes through the nostrils to form an arc around the muzzle; a lengthwise *light streak* along mid-line of frontal region. *Size* smaller (maximum known standard length 55 mm.). *Additional characters, contrasting with items 3a and 3b.—Anal rays* almost always 8 (rarely 7 or 9). *Basicaudal spot* small and inconspicuous. *Dorsal fin* without pigment on interradial membranes. *Gill membranes* very narrowly conjoined (width of isthmus, between lower ends of gill openings, 9.6 to 23.0 in head). *(H. harperi.)* 2

b. *Scales* of moderate to small size, 38 to 62 in lateral line (very rarely 38). *Mouth* nearly horizontal (angle of gape with horizontal less than 20°). *Sensory papillae* prominent on mouth and lower surface of head. *Barbel* almost always well developed. *Mandibular rami* narrower, separated medially by a space nearly as wide as, to much wider than, either ramus. No conspicuous dark *lateral band* and no definite *light streaks* on body or head. *Size* larger (maximum known standard length 67 to 97 mm. in different forms; adults typically longer than 55 mm.). 3

2.(1a)

a. *Mouth* less oblique (gape 20° to 38° from horizontal, usually less than 35°). *Snout* longer (3.1 to 3.8 in head, usually 3.2 to 3.4). *Eye* averaging larger (usually 3.2 to 3.6 in head). *Springs and spring-fed creeks in northern Florida and adjacent parts of Georgia and Alabama.* .... *H. h. harperi*

b. *Mouth* more oblique (gape 33° to 44° from horizontal, usually more than 36°). *Snout* shorter (3.5 to 4.1, usually 3.6 to 3.9). *Eye* averaging smaller (usually 3.5 to 4.1). *Sinks and caves in the Ocala Limestone of Payne Prairie, Florida.* .... *H. h. subterranea*

3.(1b)

a. *Anal rays* almost always 8 (rarely 7). *Scales* 52 to 62. *Basicaudal spot* large and conspicuous. *Dorsal fin* in adult with dark pigment between last 2 or 3 rays (as in *Notropis whipplei* and relatives). *Gill membranes* narrowly conjoined (width of isthmus, between lower ends of gill openings, 6.5 to 16.0 in head). *Eye* usually 3.9 to 4.7 in head. *Additional characters, contrasting with items 4a and 4b.—Coloration* without dark blotches or specklings; sides with a tendency toward a silvery band. *Caudal-peduncle depth* 0.8 to 1.2 in snout. *Tennessee River system, in Tennessee, Virginia, North Carolina, Georgia, and Alabama.* .... *H. monacha*

b. *Anal rays* typically 7 (rarely 6). *Scales* 38 to 51. *Basicaudal spot* small and inconspicuous. *Dorsal fin* free of pigment on interradial membranes. *Gill membranes* more or less widely conjoined (width of isthmus, 2.6 to 5.5 in head). *Eye* usually 3.3 to 4.0. 4

4.(3b)

a. *Coloration* plain, without dark blotches or specklings; posterior part of body with a median shading produced by a series of dark V's, one on each myomere. *Caudal peduncle* slenderer (its depth 1.4 to 1.7 in snout). *Additional characters, contrasting with items 5a and 5b.—Scales* 40 to 46. *Body* slender and not notably terete; caudal-peduncle depth 3.3 to 4.0 in head. *Head length* 3.7 to 3.9. *Snout* long (2.3 to 2.6). *Isthmus width* usually 3.3 to 3.9 (range, 3.3 to 4.3). *Lips* moderate. Maximum known *standard length* 69 mm. *Clinch and Powell rivers, upper Tennessee system, in Tennessee.* .. *H. cahni*

b. *Coloration* variegated with conspicuous dark blotches or specklings; median dark shading usually lacking or weak in adults. *Caudal peduncle* less attenuate (its length 1.0 to 1.4 in snout). 5

5.(4b)

a. *Scales* in lateral line usually 46 to 49 (range, 43 to 51). *Body* typically slenderer and definitely more terete; caudal-peduncle depth usually 3.1 to 3.6 (range, 2.3 to 3.9). *Head* averaging shorter (3.7 to 4.6, usually 3.9 to 4.3). *Snout* averaging shorter (2.5 to 3.2 in head, usually 2.7 to 2.9). *Isthmus width*, between lower ends of gill openings, usually 3.6 to 4.6 in head (range, 3.2 to 5.5). *Lips* rather thin. Maximum known *standard length* 97 mm.; adults usually longer than 70 mm. *Additional characters, contrasting with items 7a and 7b.—Dark color pattern:* mid-side with a row of oval blotches, generally smaller than the pupil; middorsal line with a row of spots. *Eye* usually 3.5 to 4.0 (range, 3.1 to 4.2). *(H. dissimilis.)* 6

b. *Scales* usually 40 to 43 (range, 38 to 46). *Body* typically deeper and less terete; caudal-peduncle depth usually 2.7 to 3.3 (range, 2.4 to 3.6). *Head* averaging longer (3.4 to 4.3, usually 3.7 to 4.1). *Snout* averaging longer (2.2 to 3.1, usually 2.4 to 2.8). *Isthmus width* usually 2.7 to 3.6 (range, 2.6 to 4.1). *Lips* rather thick. Maximum known *standard length* 73 to 76 mm. (in different species); adults seldom longer than 70 mm. 7

6.(5a)

a. *Upper lip* rather shield-shaped; narrow on anterolateral edge, but expanded near mid-line. Lateral *dark blotches* usually smaller, more intense, and more numerous (usually more than 10). *Stepped proportions* usually: head length 4.0 to 4.5; caudal-peduncle depth 2.7 to 3.2; snout 2.5 to 2.7. *Ozark Upland, in southern Missouri and east-central Oklahoma.* ...... *H. dissimilis harryi*

b. *Upper lip* narrow throughout, horseshoe-shaped. Lateral *dark blotches* usually larger, less intense, and less numerous (usually fewer than 10). *Stepped proportions* usually: head length 3.8 to 4.2; caudal-peduncle depth 3.0 to 3.6; snout 2.8 to 3.0. *Ohio and Tennessee river systems, in Indiana, Ohio, New York, Pennsylvania, West Virginia, Virginia, Kentucky, Tennessee, and North Carolina.* .... *H. d. dissimilis*

7.(5b)

a. *Dark color pattern:* mid-side without a row of definite blotches, but with numerous scattered irregular X-shaped specklings; middorsal line without a row of definite spots. *Eye* typically smaller, usually 3.3 to 3.8 in head (range, 2.9 to 4.1). *Additional characters, contrasting with items 9a and 9b.—Upper lip* moderately expanded at mid-line (the width there 3.5 to 5.0 into upper-jaw length). *Mouth* of moderate size (upper jaw 3.0 to 4.0 in head, usually 3.3 to 3.7). *(H. x-punctata.)* 8

b. *Dark color pattern:* sides with a median row of large, rather intense, more or less rectangular blotches, mostly larger than the pupil, and with scattered, rounded specks; middorsal line with a more or less evident row of spots. *Eye* typically larger, usually 2.9 to 3.5 (range, 2.9 to 3.8). *(H. insignis.)* 9

8.(7a)

a. *Muzzle* relatively blunt, straight, and short. *Snout* in adult approximately as long as postorbital; in half-grown, definitely shorter than postorbital. *Caudal peduncle* usually deeper (least depth averaging about 0.1 less than snout length). *Ozark Upland, in the northwestern half of Arkansas, northeastern Oklahoma, southeastern Kansas, and the southern half of Missouri; with scattered populations in the Mississippi drainages of Illinois, Wisconsin, Iowa, and southeastern Minnesota.* .... *H. x. x-punctata*

b. *Muzzle* relatively pointed, down-curved, and long. *Snout* in adult typically longer than postorbital; in half-grown, about as long as postorbital. *Caudal peduncle* usually slender (least depth averaging about 0.3 less than snout length). *Ohio River basin, in Illinois, Indiana, Ohio, New York, Pennsylvania, and Kentucky (avoiding the Cumberland and Tennessee systems); isolated populations, perhaps now extinct, in Thames River, Ontario, and questionably in the Lake Erie drainage of northern Ohio.* .... *H. x. trautmani*

9.(7b)

a. *Upper lip* scarcely expanded on the mid-line (the width there 3.7 to 6.5, usually more than 4.0, in upper-jaw length). *Mouth* relatively small (upper-jaw length 3.5 to 4.3 in head, usually 3.7 to 4.0). *Cumberland River system in Kentucky and Tennessee and lower parts of Tennessee River system from Kentucky through the middle third of Tennessee to northern Alabama.* .... *H. insignis insignis*

b. *Upper lip* notably expanded on the mid-line (the width there 2.6 to 4.4, usually less than 4.0, in upper jaw). *Mouth* usually larger (upper-jaw length 2.9 to 3.6 in head, usually 3.2 to 3.4). *Upper parts of Tennessee River system, in the Appalachian Mountains of Tennessee, Georgia, North Carolina, and Virginia; in the Hiwassee, Little Tennessee, French Broad, and Holston drainages.* .... *H. i. eristigma*

1. *Hybopsis harperi* (Fowler)

Redeye Chub

This very distinct species was described as *Notropis harperi* by Fowler (1941: 231–33, Figs. 6–7). It is divisible into two subspecies.

1a. *Hybopsis harperi harperi* (Fowler)

1b. ***Hybopsis harperi subterranea,*** new subspecies

The name *Erimystax harperi subterraneus* was published by Bangham (1941: 294, 305) as a *nomen nudum.*

The holotype, UMMZ 133551, 33.8 mm. in standard length, was collected in Jerome Sink, Alachua County, Florida, by Miller, Walker, Marshall, and party from the University of Florida, on April 4, 1941, with 111 other specimens 15 to 41 mm. long. Other collections are from several sinks and caves, which, like the type locality, are in the Ocala Limestone of Payne Prairie, Florida.

2. *Hybopsis monacha* (Cope)

Spotfin Chub

This very distinct species, described as *Ceratichthys monachus* by Cope (1869: 226–27, 240, Pl. 23, Fig. 2), was made the type of a distinct genus, *Erimonax,* by Jordan (1924: 52). Since *Hybopsis* is of feminine gender and since Cope definitely indicated the adjectival form, the specific name is spelled *monacha.* Cope spelled the name *monachus* correctly in the key, in the faunal list, and on the plate, but gave it as *monacus* in the text.

3. ***Hybopsis cahni,*** new species
Slender Chub

The holotype, UMMZ 157708, an adult 62.3 mm. in standard length, was collected with 4 specimens 49 to 51 mm. long, by Reeve M. and Marion K. Bailey on September 8, 1939, in Powell River, 3 miles southeast of Harrogate at U. S. Highway 25E, Claiborne County, Tennessee. Four other examples, UMMZ 103462–63, 57 to 69 mm. long, were collected by A. R. Cahn, for whom the species is named, on March 10, 1936, in Clinch River below Norris Dam, Anderson County, Tennessee. Five other specimens, USNM 70580, 56 to 60 mm. long, were collected in 1893 at Walkers Ford, 12 miles southwest of Tazewell, Tennessee, by Barton Warren Evermann; these were reported as *Hybopsis monaca* by Evermann and Hildebrand (1916: 445). These are apparently the only known specimens of the species.

4. *Hybopsis dissimilis* (Kirtland)
Streamline Chub

This is obviously the species that Kirtland (1841: 341–42, Pl. 4, Fig. 2) described as *Luxilus dissimilis,* though this name has usually been misapplied to the gravel chub, herein named *H. x-punctata.* The streamline chub has usually been called *Hybopsis watauga* Jordan and Evermann. This species, like *x-punctata,* has become differentiated into a western and an eastern subspecies.

4a. ***Hybopsis dissimilis harryi,*** new subspecies

The holotype, UMMZ 167083, an adult 81.5 mm. in standard length, was collected on August 7, 1940, by G. V. Harry and Mitro Pellock in White River, 3 miles southeast of Mano, Barry County, Missouri, with a 73-mm. specimen (No. 151368). The other examples examined include one probably wrongly listed as from Sallisaw, Oklahoma, collected by S. E. Meek (USNM 73591), and numerous specimens from northern Arkansas and southern Missouri.

This subspecies is named for George V. Harry, in recognition of his extensive survey of the fishes of Missouri.

4b. *Hybopsis dissimilis dissimilis* (Kirtland)

5. ***Hybopsis x-punctata,*** new species
Gravel Chub

Two subspecies, with ranges indicated in the key, are distinguishable.

5a. ***Hybopsis x-punctata x-punctata,*** new subspecies

Holotype (of species and subspecies), UMMZ 152359, an adult 67.7 mm. in standard length, was collected on August 28, 1940, by Harry and Pellock in Starks Fork of Gasconade River, 8 miles south of Richland, Pulaski County, Missouri. We have studied numerous other specimens from Missouri, Arkansas, Oklahoma, Kansas, Iowa, and Minnesota, in which states the characters of the subspecies are essentially constant and distinctive. Referred material from Illinois and southern Wisconsin should be subjected to study of possible intergradation with the following subspecies.

5b. ***Hybopsis x-punctata trautmani,*** new subspecies

Holotype, UMMZ 177278, an adult 70 mm. long, was collected by Milton B. Trautman and Edward L. Wickliff on October 20, 1939, in Waldoning River, Newcastle Township, Coshocton County, Ohio, with 6 other specimens (UMMZ 177279). Many other examples, also in the Museum of Zoology of the University of Michigan, are from the Big Wabash River at St. Francisville, Lawrence County, Illinois (UMMZ 167084) and from numerous other localities in the Ohio River drainage, in Indiana and Ohio. Additional material is from Thames River, Ontario, and from the Ohio River drainage in Pennsylvania and Kentucky. Dr. E. C. Raney informs us that it also occurs in New York.

This subspecies is named in honor of Milton B. Trautman of Ohio State University, in recognition of his life-long thorough investigation of the fishes of Ohio.

6. ***Hybopsis insignis,*** new species
Blotched Chub

In this species also two subspecies are distinguishable.

6a. ***Hybopsis insignis insignis,*** new subspecies

Holotype (of species and subspecies), UMMZ 157702, an adult 59 mm. long, from Tennessee River at head of Blood River Island, Calloway County, Kentucky, was collected by Tarzwell and Howell on

October 22, 1942, on a survey by the Tennessee Valley Authority. Other specimens in the Museum of Zoology of the University of Michigan and in the United States National Museum are from various localities in the Cumberland and Duck river drainages and in the Tennessee River system as far upstream as northern Alabama and the Sequatchie River in Tennessee.

Specimens from the Powell and Clinch rivers in Tennessee and Virginia are nicely intermediate between the two subspecies and are, therefore, identified as intergrades.

6b. ***Hybopsis insignis eristigma,*** new subspecies

Holotype, UMMZ 129320, an adult specimen 62 mm. in standard length, was collected with 2 other specimens 41 and 62 mm. long (UMMZ 177282), on August 31, 1937, by Carl L. Hubbs and party, in West Prong of Little Pigeon River, about halfway between Gatlinburg and Sevierville, Sevier County, Tennessee, at Highway 71, crossing 2 miles below Pigeon Forge, at an elevation of 1,000 feet. Other specimens are from various localities in the Appalachian Mountains on the east side of the Tennessee River drainage basin, in Tennessee, Georgia, North Carolina, and Virginia.

The subspecific name is proposed as a substantive.

LITERATURE CITED

BANGHAM, RALPH V.
1941 Parasites of Fresh-water Fish of Southern Florida. Proc. Fla. Acad. Sci., 5 (1940): 289–307.

COPE, EDWARD D.
1869 On the Distribution of Fresh-water Fishes in the Alleghany Region of Southwestern Virginia. Journ. Acad. Nat. Sci. Phila., (2) 6: 207–47, Pls. 22–25.

EVERMANN, BARTON WARREN, and SAMUEL F. HILDEBRAND
1916 Notes on the Fishes of East Tennessee. Bull. U. S. Bur. Fish., 34 (1914): 431–51, Figs. 1–13.

FOWLER, HENRY W.
1941 A Collection of Fresh-water Fishes Obtained in Florida, 1939–1940, by Francis Harper. Proc. Acad. Nat. Sci. Phila., 92 (1940): 227–44, Figs. 1–13.

JORDAN, DAVID STARR
1924 Concerning the Genus Hybopsis of Agassiz. Copeia, No. 130: 51–52.

KIRTLAND, JARED P.
1841 Descriptions of the Fishes of the Ohio River and Its Tributaries. Boston Journ. Nat. Hist., 3 (1840): 338–52, Pls. 4–6.

Received for publication June 19, 1956

(646)

Reprinted from COPEIA, 1956, No. 3, p. 194, August 29
Printed in U.S.A.

Reproduced by Permission

THE SYSTEMATIC POSITION OF THE INDIAN CYPRINID FISH, *CIRRHINUS FASCIATUS* JERDON (1849), WITH A NEW NAME FOR *BARBUS FASCIATUS* BLEEKER (1853).—Jerdon (1948, Madras Jour. Litt. and Sci., 15: 305) placed a heterogeneous assemblage of eleven species under the genus *Cirrhinus* Oken. One of these, *Cirrhinus fasciatus,* he described from the headwaters of the Cauvery River and from Malabar. Günther (1868) listed *C. fasciatus* Jerdon as one of the insufficiently characterized species of *Tylognathus* Heckel. Although brief, the description of *C. fasciatus* is sufficiently clear to help in assigning the species to its proper systematic position. The writer's extensive collections from Jerdon's type localities have facilitated this task. Undoubtedly, *C. fasciatus* and two other nominal species, namely *Labeo melanampyx* Day (1865) from the Travancore Hills and *Barbus grayi* Day (1867) from the Bowany and Kallar rivers (tributaries of the Cauvery River) at the base of the Neilgherries, represent one and the same species. Day (1876) seems to have been aware of this, for he recognized *Barbus melanampyx,* with *C. fasciatus* and *B. grayi* as its synonyms. Evidently the earlier-proposed name *fasciatus* was not used to designate the species, as he considered it preoccupied by *Barbus fasciatus* Bleeker (1853, Nat. Tijdschr. Ned. Indies, 5: 190) from the East Indies.

C. fasciatus Jerdon and *B. fasciatus* Bleeker are at present both referable to the genus *Puntius* Hamilton, but are specifically distinct. It is highly doubtful whether any eventual splitting of the genus *Puntius* on characters like the barbels would separate these species. Hence, under the International Rules of Zoological Nomenclature, *fasciatus* Jerdon, which has priority over *fasciatus* Bleeker, will have to be considered as valid. This leaves Bleeker's species without a name, for which the specific name *Puntius eugrammus* sp. nov., is proposed here. For a detailed description of *Puntius eugrammus* sp. nov., reference may be made to the description of *Puntius fasciatus* (Bleeker) as given by Weber and de Beaufort (1916, Fish. Indo-Austral. Archipel., 3: 184–185).

Puntius fasciatus (Jerdon)

Cirrhinus fasciatus Jerdon 1849, Madras Jour. Litt. and Sci., 15: 305 (type locality, Malabar).

Labeo melanampyx Day 1865, Proc. Zool. Soc. London: 298 (type locality, Mundakayam, Travancore).

Puntius melanampyx Day 1865, Fish. Malabar: 210, pl. 16, fig. 1.

Barbus grayi Day 1867, Proc. Zool. Soc. London: 293 (type locality, Bowany and Kallar rivers at the base of the Neilgherries).

Barbus arulius (*nec* Jerdon) Günther 1868, Cat. Fish. Brit. Mus., 7: 133.

Barbus melanampyx Day 1876, Fish. India: 570, pl. 139, fig. 1. Beaven, 1877, Handbook Freshwater Fish. India: 49. Day, 1889, Fauna Brit. India, Fish, 1: 316. Jenkins, 1909, Rec. Ind. Mus., 3: 298. Pillay, 1929, Jour. Bombay Nat. Hist. Soc., 33: 357. John, 1936, ibid, 38: 711. Misra, 1938, Rec. Ind. Mus., 40: 258.

Barbus (*Puntius*) *melanampyx* Hora and Law 1941, Rec. Ind. Mus., 43: 793. Silas, 1949, Jour. Bombay Nat. Hist. Soc., 48: 793; 1951, ibid, 49: 673; 50: 326.

The natural distribution of *Puntius fasciatus* (Jerdon) in Peninsular India is the upper reaches of the Cauvery drainage and further southward to the Cape; also the western watersheds draining South Kanara, Malabar, and Travancore-Cochin.—E. G. SILAS, *Scripps Institution of Oceanography, University of California, La Jolla, California.*

Contributions from the Scripps Institution of Oceanography, New Series, No. 864

Reprinted from THE PHYSICAL REVIEW, Vol. 105, No. 3, 1125–1127, February 1, 1957
Printed in U. S. A.
Reproduced by Permission

Distribution, Production Rate, and Possible Solar Origin of Natural Tritium*

HARMON CRAIG
Scripps Institution of Oceanography,
University of California, La Jolla, California

(Received November 19, 1956)

LIBBY and co-workers have estimated the production rate of natural tritium as $\bar{Q}=0.14$ T atom/cm^2 of earth surface (cm$_e^2$)-sec, based on their measurements of the tritium content of natural waters.[1,2] $\bar{Q}$ was calculated separately from material balance considerations over (1) the oceans, and (2) the continents, equating the cosmic-ray production rate with the net loss from the oceanic and continental atmospheres by precipitation; the values obtained were, respectively, 0.12 and 0.16, in good agreement.[2] A $\bar{Q}$ value of 0.14, coupled with an average surface ocean concentration (pre-thermonuclear tests) of 0.24 atom T per 10^{18} atoms H (0.24 tritium unit or T.U.), was calculated as indicating uniform mixing of the sea to a depth of about 100 meters, assuming no T to be stored below this depth.[2]

Tritium production by high-energy protons on nitrogen and oxygen has been measured; the cross sections are about 30 mb with excellent agreement between two sets of data.[3,4] From these measurements and considerations of the cosmic-ray primary flux and neutron contribution, $\bar{Q}$ is calculated, independently of observed concentrations, to be approximately[3] 0.2 T atom/cm$_e^2$ sec, and, more precisely,[4] $0.14_{-0.03}^{+0.10}$, in agreement with the rate indicated by the natural concentrations.

However, the tritium production rate must be a good deal higher than the figures quoted above. The average residence time of water below the oceanic thermocline is very probably less than 500 years, and certainly less than 1000 years, as determined by oceanographic measurements,[5,6] data on the heat flux through the ocean floor,[7] and measurements of, and calculations based on, the distribution of radiocarbon in the atmosphere and sea.[8–10] These times correspond to residence times in the mixed layer of the sea of 10–20 years, comparable to the 18-year mean life of tritium. Equations relating the atmospheric production rate of a radioactive isotope to its concentration in the atmosphere, in the sea above and below the thermocline, and to the various mixing rates involved, were derived and applied to the distribution of radiocarbon,[9] and of tritium.[10] The tritium calculations show that for reasonable limits on the average deep-sea residence time of water of 100–500 years, the tritium flux into the sea ($\bar{Q}$ units) must be from 5.4 to 1.7 times the tritium concentration in surface sea water (T units). Taking the surface concentration as 0.24 T units,[2] the tritium flux into the sea should be between 1.3 and 0.4 T atom/cm$_e^2$ sec.

Accordingly, the T production rate over the North American continent was recalculated, using Libby's data[2] but taking into account removal of T from the continent by the outgoing water vapor flux,[11] as well as by runoff. The average net T production in the North American atmosphere is found to be about 1.2±0.5 atom/cm$_e^2$ sec, the main uncertainty being the storage time of continental water.

To calculate $\bar{Q}$, the effects of geomagnetic latitude, and of holdup in the stratosphere consistent with the 10-year stratospheric residence time of Sr^{90} from weapons tests, reported by Libby,[12] must be considered. About half of the cosmic-ray production probably takes place above the tropopause, and horizontal mixing in the stratosphere appears to be rapid enough to overcome geomagnetic effects in that region.[12] $\bar{Q}$ was calculated by two different assumptions:

(1) All T is made by cosmic rays (assuming an undetected mechanism), half above, and half below, the tropopause, with a 10-year holding time in the stratosphere and geomagnetic correction to be applied only to the tropospheric production. Then $\bar{Q}$ (total world average) is 1.0, and the net flux of T into the sea is 0.8, both in atoms/cm$_e^2$ sec.

(2) Only 0.2 T atom/cm$_e^2$ sec are produced by cosmic rays, as indicated by experimental data, the remainder being accreted from an extraterrestrial source into the stratosphere. With correction factors similar to those used in (1), then $\bar{Q}$ (from accretion plus cosmic rays) is 1.7, with a net flux into the sea of about 1.0 atom/cm$_e^2$ sec.

From these figures the average residence time of water below the oceanic mixed layer is calculated to be about 150–200 years, in good agreement with the few reliable C^{14} data,[8,9] measurements of the secular decrease of dissolved oxygen in deep Atlantic water,[6] and the oceanographic estimates.[5] Moreover, a direct calculation of the T/H ratio in tropospheric molecular hydrogen, based on the mixing rate through the tropopause and the water vapor content of the stratosphere, predicts a T concentration of the order of 10^5 T units, in excellent agreement with recent extensive measurements by Begemann and Libby (personal communication). The low production rate calculated from the measured transfer of T into the sea by oceanic precipitation,[2] indicates that most of the tritium enters the sea by direct molecular exchange across the sea surface. The world inventory of natural tritium is found to be about 20 kg, or 200 megacuries, most of which is in the deep sea with a predicted concentration of about 0.015 T units.

Details of the present study will be published elsewhere. The purpose of this note is to point out that approximately 1 ± 0.5 T atom/cm$_e^2$ sec, i.e., the bulk of the world production, cannot be accounted for by present estimates of the contribution from cosmic rays; the discrepancy is about one order of magnitude. The cross section for production by protons on N_2 and O_2 has been found to be the same, within experimental error, at 450 Mev and 2.2 Bev[4]; thus it appears unlikely that cosmic-ray production can account for the tritium flux into the atmosphere. Tritium production in rocks by neutrons on lithium has been shown to be negligible.[13] Moreover, a lower limit for the production rate of He^3, computed from an estimated terrestrial production and escape rate of He^4, may be as much as 10 atoms/cm$_e^2$ sec,[14] an order of magnitude higher yet than the presently computed tritium production rate.

If these elements are being accreted by solar emission, it may well be that the production of light elements on the surfaces of stars is a more widespread and common occurrence than has been estimated as possible by the proponents of the idea,[15] and serious attention should be given to experimental attempts to detect accretion of these and other light elements. Solar contribution of heavy nuclei ($Z \gtrsim 10$) has recently been suggested[16] as an explanation of an observed daily variation in intensity without an associated neutron intensity variation.

A discussion of possible explanations of the high T flux will be communicated by the writer and B. Feld, who suggested the possible solar origin on the basis of his preliminary confidence in the present evaluation of cosmic-ray contributions.[17] I wish to thank Bruno Rossi for discussions on the primary cosmic-ray flux, and F. Begemann and M. Rubin for unpublished data on tritium and carbon 14.

* Contribution from the Scripps Institution of Oceanography, New Series, No. 865. This paper represents in part the results of a general study carried out while the writer was a member of a National Academy of Sciences Study Group on oceanographic effects of nuclear phenomena. Part of this research was supported by the Office of Naval Research.

[1] S. Kaufman and W. F. Libby, Phys. Rev. **93**, 1337 (1954).

[2] H. von Buttlar and W. F. Libby, J. Inorg. Nuclear Chem. **1**, 75 (1955).

[3] E. L. Fireman and F. S. Rowland, Phys. Rev. **97**, 780 (1955).

[4] Currie, Libby, and Wolfgang, Phys. Rev. **101**, 1557 (1956).

[5] W. Wooster and B. Ketchum, Final Report, National Academy of Sciences Committee on Effects of Atomic Radiation on Oceanography and Fisheries (to be published).

[6] L. V. Worthington, Deep-Sea Research **1**, 244 (1954).

[7] R. Revelle and A. E. Maxwell, Nature **170**, 199 (1952).

[8] Unpublished C^{14} measurements on deep sea water by M. Rubin, U. S. Geological Survey Radiocarbon Laboratory, kindly communicated to the writer. (See references 9 and 10.)

[9] H. Craig, Tellus (to be published).

[10] H. Craig, reference 5.

[11] Benton, Estoque, and Dominitz, Science Report No. 1, Civil Engineering Department, Johns Hopkins University, 1953 (unpublished).

[12] W. F. Libby, Science **123**, 656 (1956); Proc. Nat. Acad. Sci. **42**, 365 (1956).

[13] P. Morrison and J. Pine, Ann. N. Y. Acad. Sci. **62**, 69 (1955).

[14] K. Mayne, Geochim. et Cosmochim. Acta **9**, 174 (1956).

[15] Fowler, Burbidge, and Burbidge, Astrophys. J. Suppl. **2**, 167 (1955).

[16] M. Koshiba and M. Schein, Phys. Rev. **103**, 1820 (1956).

[17] *Note added in proof.*—The results of these calculations were discussed with F. Begemann and W. F. Libby during the summer of 1956; they now find that their recent data on the tritium balance in the Mississippi Valley, taking into account outward vapor transport of tritium as discussed above, indicate a production rate over that area equal to the value calculated above for North America. Recently J. Arnold has also concluded from consideration of the present calculations that tritium is probably being accreted from the sun.

Reproduced by Permission

BULLETIN OF THE AMERICAN ASSOCIATION OF PETROLEUM GEOLOGISTS
VOL. 40, NO. 9 (SEPTEMBER, 1956), PP. 2195-2210, 8 FIGS.

ARCHIPELAGIC APRONS[1]

HENRY W. MENARD[2]
La Jolla, California

ABSTRACT

Most of the floor of the Pacific basin is hilly with an average relief of roughly 1,000 feet, but about 10 per cent is smooth. About $\frac{4}{5}$ of the smooth area (4×10^6 square miles) is distributed around groups of existing or drowned ancient islands and has the form of aprons which are here called "archipelagic aprons." In the central and western Pacific, aprons encircle the Caroline, Cook, Ellis, Gilbert, Line, Marquesas, and Marshall islands and the guyots of the Mid-Pacific Mountains, Emperor Seamounts, and the Magellan Seamounts. The apron around the southern part of the Hawaiian Islands is exceptionally thin and has been deformed. In the eastern Pacific the Revillagigedo Islands and isolated Clipperton Island lack extensive aprons, and the Galapagos apron is thin.

Seismic refraction measurements show that volcanic rocks are kilometers thick in the vicinity of all islands where studies have been made. This material forms the bulk of the archipelagic aprons and buries the pre-existing hilly terrane of the sea floor so as to form a relatively smooth plain. The perfection of leveling and smoothness of the aprons indicates deposition of sediment by turbidity currents.

INTRODUCTION

About 90 per cent of the sea floor of the Pacific basin is a hilly terrane with a relief measured in hundreds of feet—a seemingly endless succession of hills, valleys, ridges, and troughs. The remaining 10 per cent of the sea floor is smooth, of which 2 per cent is distributed near the margins of continents, and 8 per cent is distributed around island groups. The smooth sea floor around each island group has the form of an apron.

Abyssal smooth areas other than aprons have been recognized in many places in the oceans of the world. Wherever pertinent evidence is available it indicates that the smooth areas are produced by the burial of a pre-existing hilly terrane (Heezen, Ewing, and Ericson, 1954, p. 131; Browne, 1954, p. 399; Menard, 1955, p. 236). Aprons exhibit the features used elsewhere as criteria for partial burial of a hilly terrane, namely, steep-sided hills rising abruptly from smooth plains, apparent ponding of sediment behind ridges acting as dams, and the absence of deeps below the level of the smooth surface. Consequently, it appears probable that aprons have buried an older terrane of hills.

Deposition of denudation products from the islands is an obvious means of constructing an apron, and such deposits have already been recognized on the sea floor. Some such products contribute to the volcanic muds surrounding the Galapagos, Hawaiian, and Marquesas islands (Murray and Lee, 1909, Map 2), and are found near the drowned ancient islands of the Mid-Pacific Mountains (Hamilton, 1953, pp. 216–17). Likewise, abyssal "alluvial aprons" have been identified as topographic forms on echograms of the Hawaiian Islands (Dietz and Menard, 1953, p. 111) and the Mid-Pacific Mountains (Dietz, Menard, and Hamilton, 1954, p. 271). However, denudation products are not the only ma-

---

[1] Navy Electronic Laboratory Professional Contribution No. 39. Scripps Institution of Oceanography Contribution No. 867. Manuscript received, December 21, 1955.

[2] Scripps Institution of Oceanography. This work was done while the writer was with the U. S. Navy Electronics Laboratory. M. N. Bramlette, R. L. Fisher, E. L. Hamilton, H. H. Hess, and C. B. Officer have been kind enough to read and comment on the manuscript.

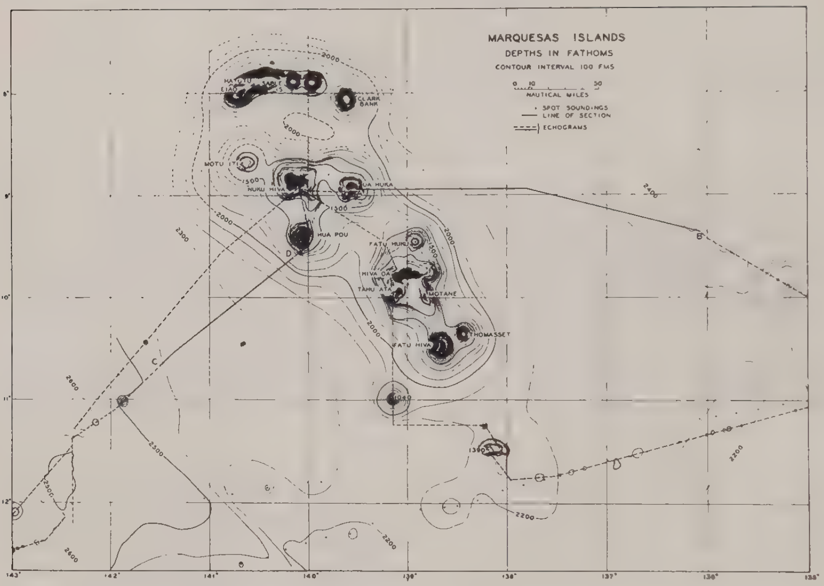
MARQUESAS ISLANDS
DEPTHS IN FATHOMS
CONTOUR INTERVAL 100 FMS
0 10 50
NAUTICAL MILES
SPOT SOUNDINGS
LINE OF SECTION
ECHOGRAMS
HATUTU
EIAO
SABLE
CLARK BANK
MOTU ITI
NUKU HIVA
UA HUKA
HUA POU
FATU HUKU
HIVA OA
TAHU ATA
MOTANE
THOMASSET
FATU HIVA
2000
1500
2300
2400
2600
2500
2200
1040
1390
B
C
D
143°
142°
141°
140°
139°
138°
137°
136°
135°
8°
9°
10°
11°
12°

FIG. 1.—Bathymetry of Marquesas Islands and apron. Lettered sections shown in Figure 3.

terials particularly associated with volcanic islands and capable of burying an irregular sea floor. The existence of a vast lens of volcanic rocks in the vicinity of the Hawaiian Islands was deduced by Betz and Hess (1942, pp. 108–11). Exceptional thicknesses of volcanics have since been found near several island groups by seismic observations. Gaskell (1954, pp. 358–59) recognized a "type B" crustal structure around islands including Hawaii chiefly on the presence of several thousand feet of volcanics; volcanic rocks were not found at "type A" seismic stations which are in the oceanic basins but distant from islands. The seismic stations made on the Mid-Pacific and Capricorn expeditions show that rocks with a velocity of 5 km./sec. (correlative with known volcanics in some places) do exist away from islands, but in general and in the northeastern Pacific in particular the material is thinner than it is near islands (Raitt, personal communication, 1955).

The aprons around islands are large, widespread, and distinctive features deserving a name. The writer here proposes "archipelagic apron" for the material distributed around island groups on the deep sea floor, and also as a topographic term for its smooth surface. A layer of material need not have a smooth surface, but one is rarely found without the other.

DESCRIPTION

TOPOGRAPHY

Profiles of most archipelagic aprons are distinctive long smooth curves in contrast to the steep sides of volcanic islands and the characteristic hilly terrane of the Pacific basin (Figs. 2, 3) which surrounds the aprons in most places. The upper parts of most aprons have slopes of 1°–2° and some are indented by deep-sea channels. At distances of 40–50 nautical miles from the shelf break, the slope of a typical apron is about 0.002.[3] The part of the apron 100–110 miles east of the Marquesas Islands has a slope of less than 0.0005 and for the next 10 miles east it is level. The outer parts of some aprons would qualify as abyssal plains according to the definition of Heezen, Ewing, and Ericson (1954, p. 123).

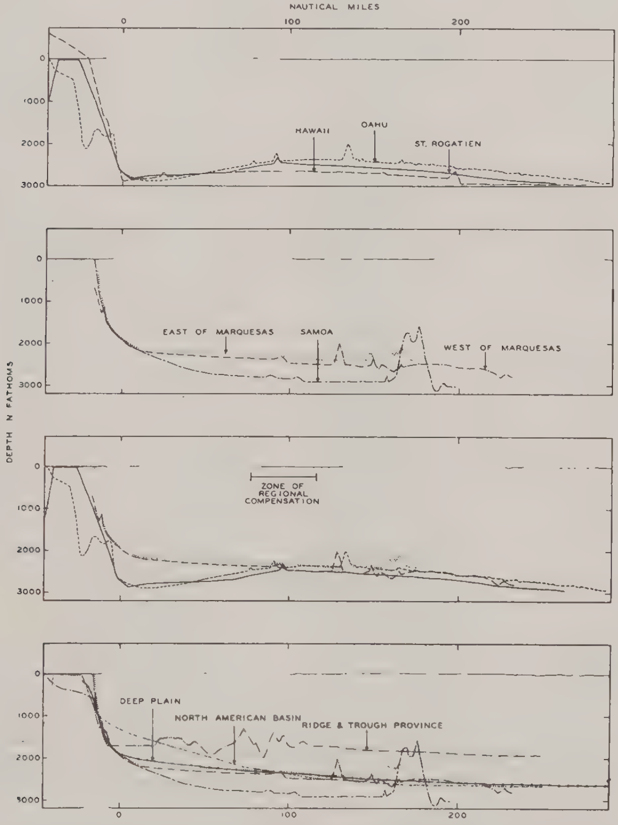

Fig. 2.—Top. Comparison of sea-floor profiles of Hawaiian Deep and Arch and some archipelagic aprons. Crest of arch is same distance from islands as seamounts which rise abruptly from, and stand high above, edge of archipelagic aprons. Bottom. Archipelagic aprons compared with continental slope and rise off North America. Most slopes show similarity and smoothness.

---

[3] Very gentle slopes are conveniently written as decimal fractions in the style of hydraulic engineers. The number is the tangent of the slope, and for slopes of a few minutes, it is also the sine of the slope, and the slope expressed in radians.

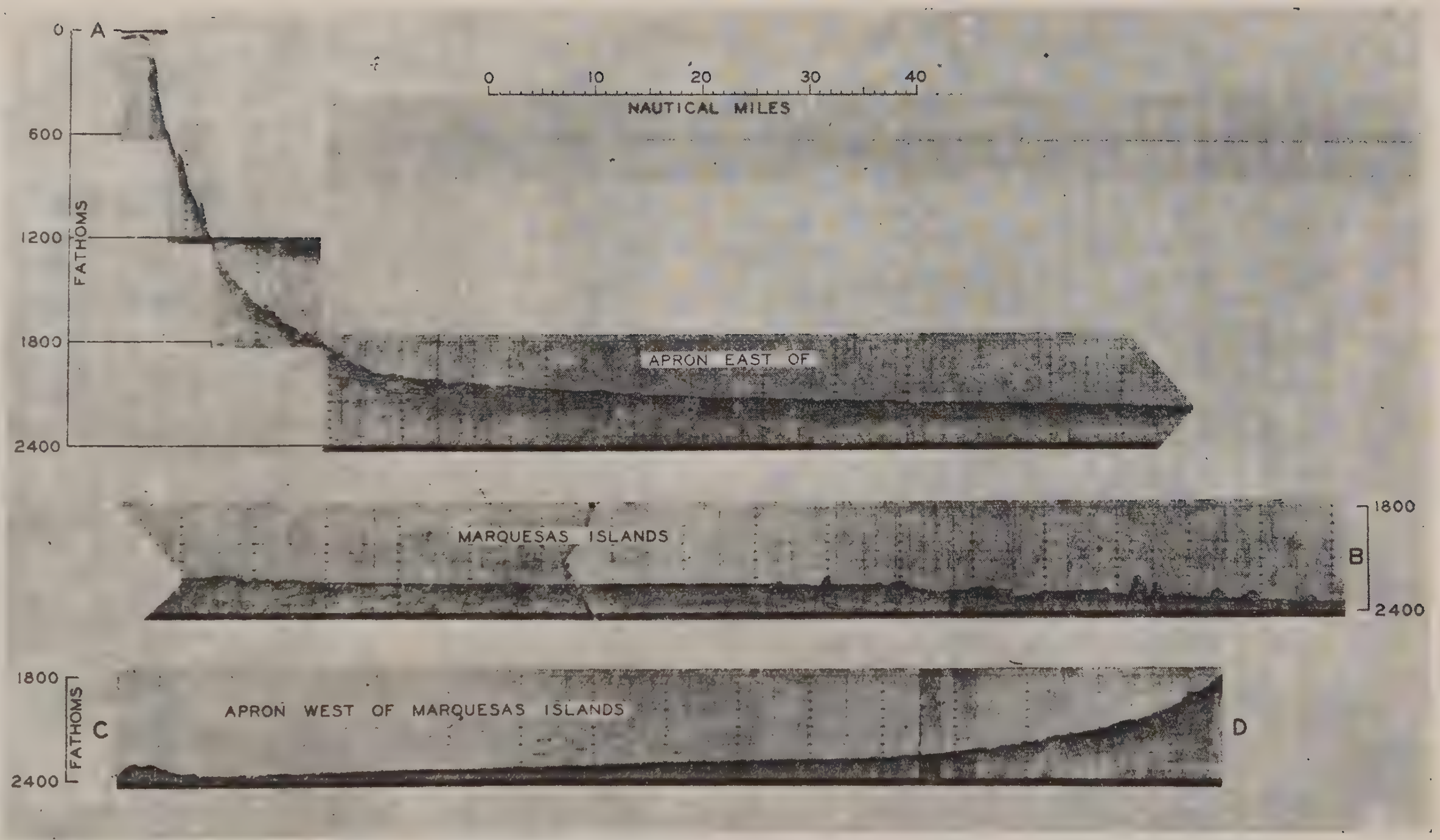

FIG. 3.- Echograms of aprons. (Figure 6C shows very irregular low relief.) Hills near B stand well above perfectly level outer edge of apron. Apron appears to be ponded

Echograms of the moat and arch southeast of the islands of Oahu and Hawaii (Dietz and Menard, 1953, Pl. 1) (Fig. 2) indicate that an apron has been deformed. In this area the sea floor is typically smooth from the base of the islands to the crest of the arch and typically rough beyond the crest of the arch. An unusual number of hills rising from the smooth sea floor indicates that the apron is not as thick as it is around most other archipelagoes. The most noteworthy characteristic of the area is that the smooth sea floor slopes downward toward the islands rather than away from them. Material spreading out from the island along the sea floor would be unable to move up the slope which may be taken as evidence that aprons are not necessarily formed in this manner. However, it is more probable that the smooth sea floor once sloped downward from the island and has since subsided. Well developed terraces at depths of a few hundred fathoms around the southern Hawaiian Islands (Dietz and Menard, 1953, pp. 106–07) show that subsidence has occurred since the islands first become islands. If the deep terraces were restored to their former position near sea-level, the smooth apron would slope downward from the islands. A small apron has begun to spread out from Oahu since subsidence distorted the equilibrium slope of the first; presumably, in time, an equilibrium slope will be restored from the islands to the crest of the arch.

In plan view (Figs. 1, 4) the aprons encircle whole archipelagoes and may also separate individual islands. The smooth slope is rarely interrupted by sea-

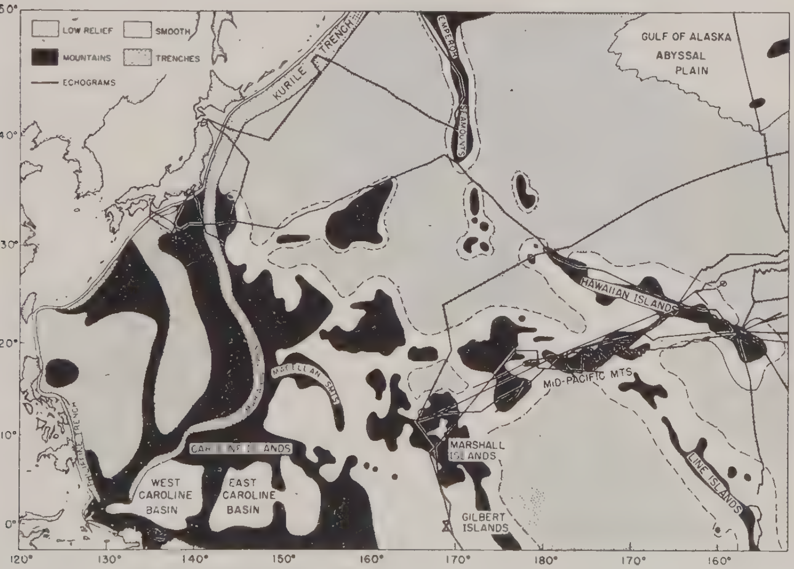
LOW RELIEF
SMOOTH
MOUNTAINS
TRENCHES
ECHOGRAMS
KURILE TRENCH
EMPEROR SEAMOUNTS
GULF OF ALASKA ABYSSAL PLAIN
HAWAIIAN ISLANDS
MID-PACIFIC MTS
MAGELLAN SMTS
CAROLINE ISLANDS
MARSHALL ISLANDS
GILBERT ISLANDS
LINE ISLANDS
WEST CAROLINE BASIN
EAST CAROLINE BASIN
PHILIPPINE TRENCH
50°
40°
30°
20°
10°
0°
120°
130°
140°
150°
160°
170°
180°
170°
160°

FIG. 4.—Distribution of archipelagic aprons in North Pacific basin.

mounts or hills. In contrast, large seamounts are unusually common at the outer edge of the aprons.

DISTRIBUTION

Echograms from Scripps Institution of Oceanography and Navy Electronics Laboratory expeditions (Figs. 4, 5) show aprons around all the sounded archipelagoes of the western Pacific, namely: the Cook, Ellis, Gilbert, Hawaiian, Line, Marquesas, Marshall, Samoan, Society, and Tuamotu islands, and also around the drowned ancient islands (guyots) of the Mid-Pacific Mountains and the Emperor Seamounts. Typical isolated aprons are about 150 miles wide, but much broader smooth areas are formed where archipelagoes of islands or seamounts intersect or otherwise bound a limited area. Aprons grade into extensive plains in the vicinity of the Caroline Islands (Hess, 1948, p. 424), between the Caroline and Marshall islands, and around the guyots of the Magellan Seamounts (Dietz, 1954, p. 1212).

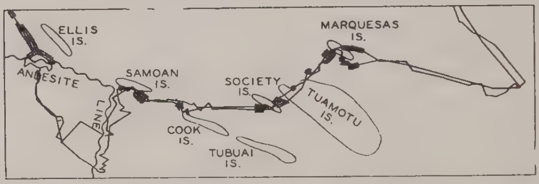

FIG. 5.—Distribution of archipelagic aprons (heavy lines) along track of Capricorn Expedition in the southwestern Pacific basin.

The sounded islands and archipelagoes in the eastern Pacific are not surrounded by well developed aprons (Fig. 4). If any aprons exist around the Revillagigedo Islands or isolated Clipperton Island, they are too thin to mask the normal hilly relief of the deep sea floor. The Galapagos Islands appear most exceptional in that an apron is indicated by smoothing and rounding of the hilly terrane in the vicinity of the islands but it is not thick enough to bury the hills and form a typical long smooth curve. The Galapagos may represent an intermediate stage in the development of an apron, or possibly the two available sounding lines crossed exceptional parts of an otherwise smooth apron. A very prominent apron surrounds the Hawaiian Islands in most places, for example, but east of Oahu on the main shipping lanes the apron is interrupted by a group of seamounts.

Smooth sea floor surrounds the seamounts, including many guyots, in the Gulf of Alaska Seamount province but apparently in large part because sediment derived from the continent has been spread out by turbidity currents to form a vast plain (Menard, 1955, pp. 239–45). The plain slopes past many seamounts rather than away from them like an apron. Other seamounts rise from ill-defined low swells that may be aprons. No morphologically identifiable aprons have been

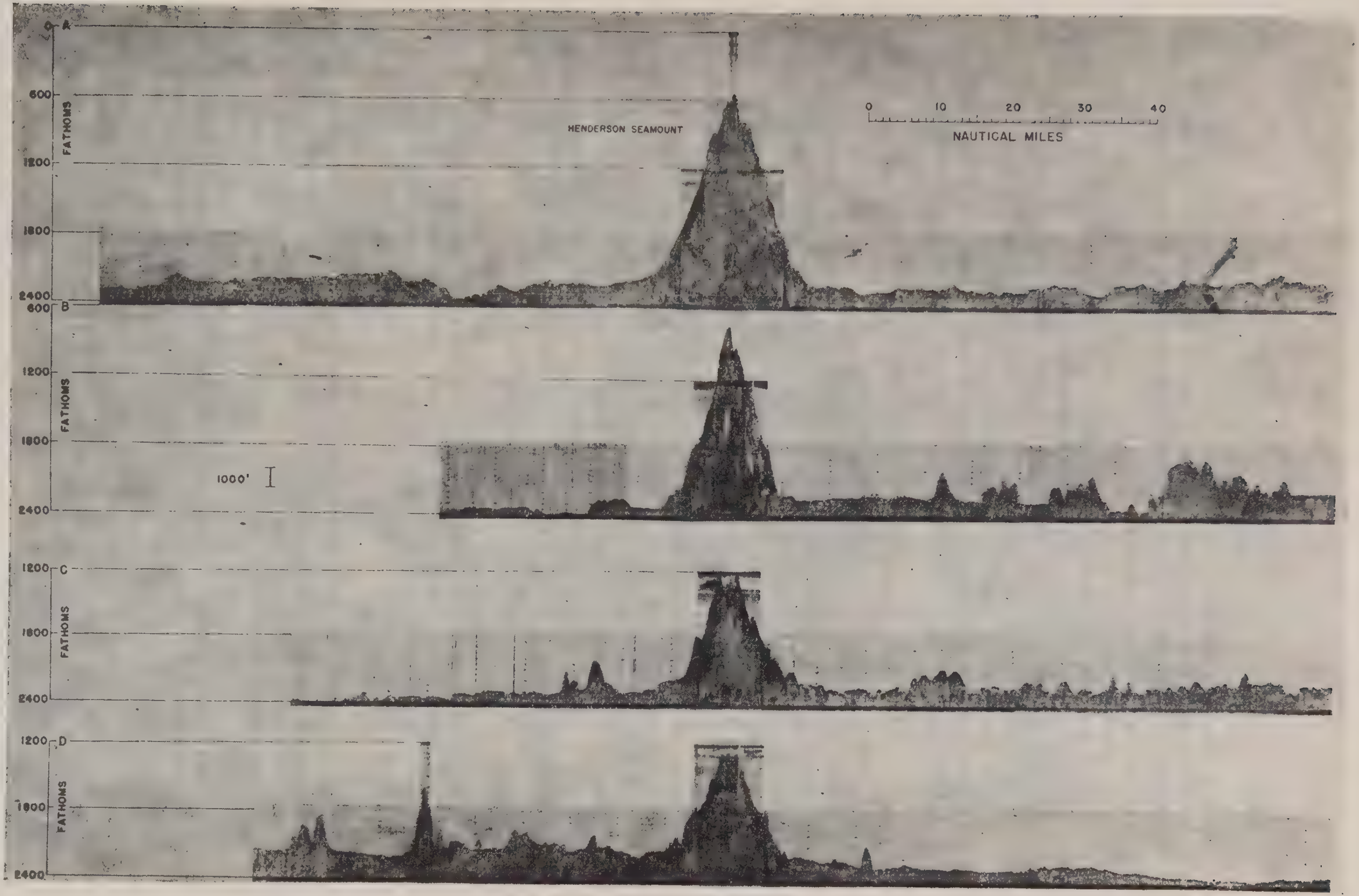

Fig. 6.—Echograms showing irregular low relief adjacent to seamounts in Baja California Seamount province.

found around the many seamounts in the Baja California Seamount province (Menard, 1955, Fig. 2, p. 239), although a slight smoothing of the low relief around Henderson Seamount suggests some localized deposition (Fig. 6).

AREA

The aggregate area of archipelagic aprons in the Pacific basin is roughly 4×10^6 square nautical miles. Figure 4 summarizes most of the positive information on which this estimate is based (areas where soundings show no aprons are not shown); the other important positive source is the echograms of the Capricorn Expedition in the southern hemisphere. Accurate estimates can not be derived from the amount of information available, and an error of $\pm 10^6$ square miles is not improbable. The greatest source of error is the almost unknown extent of archipelagic aprons in the South Pacific. The Capricorn Expedition is the sole source of useful information in most of this area, and echograms show aprons around the Cook, Marquesas, Samoan, Society, and Tuamotu islands (Fig. 5). Only the relatively small group of the Marquesas Islands was explored along enough widely spaced lines to give a reasonably accurate picture of the apron. Most of the other identified archipelagic aprons in the South Pacific are known only from a pair of profiles spaced perhaps a score of miles apart. The low relief of the sea floor around the Gambier, Phoenix, Tubuai, and Union archipelagoes and around Easter and Pitcairn islands has not been explored at all with recording echo sounders. Considering the well developed and extensive aprons discovered by the Capricorn Expedition, the estimate of 0.5×10^6 square miles for all undiscovered or unexplored archipelagic aprons in the South Pacific probably is a minimum.

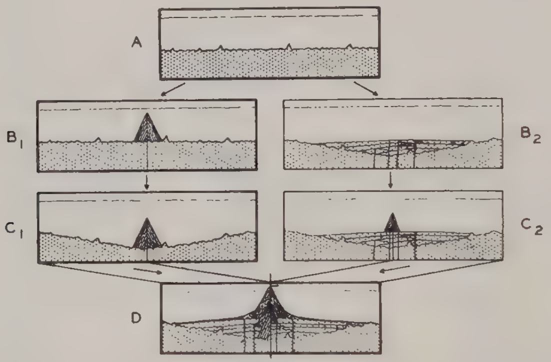

FIG. 7.—Possible sequences of development of archipelagic aprons. In A, B_1, C_1, D sequence, a line of submarine volcanoes (seen in cross section) develops on a rough sea floor, the load depresses the crust, and lava and sediment fill in the depression. All stages in this sequence have been found on sea floor. In other sequence, a lava plain covers irregular sea floor, a line of volcanoes grows on plain, and apron develops. Stages B_2 and C_2 have not been observed.

In the North Pacific, low relief in the area south of the Mid-Pacific Mountains and bounded by the Line and Marshall islands is unsounded. It is considered to be hilly (Fig. 4) in estimating the total smooth area, but, considering its position, much of it may be smooth which would increase the total smooth area by 0.2–0.5×10^6 square miles. On the other hand, many of the archipelagic aprons known from only a few profiles may be interrupted by hilly areas like the one east of Oahu in the Hawaiian Islands. Likewise some of the supposed smooth plains at the junctions of aprons may not exist. At the junction of the Marshall Islands and the Mid-Pacific Mountains, for example, the aprons are relatively narrow in some places and are separated by hilly areas. Unknown hilly areas would decrease the estimated total smooth area but, judged by existing echograms, the effect would not be large.

ESTIMATES OF MINIMUM THICKNESS AND VOLUME

RELIEF OF BURIED SURFACE

Echograms of the Swedish *Albatross* and the Mid-Pacific expeditions show that for any given 100 miles of track the relief of the hilly terrane clusters around a value of 1,000 feet (Koczy, 1954, p. 181; Dietz, Menard, and Hamilton, 1954, p. 270), and the much more extensive network of large-scale echograms now available confirms it for the whole Pacific at least as far south as the Tropic of Capricorn. The figure is correct within a few hundred feet, and pending a detailed statistical study it may be used as the average relief of exposed hilly areas in the Pacific. Some regional variations in relief appear to exist but they remain to be defined. Nevertheless, it is probable that a profile along a distance as great as the width of an archipelagic apron would show a relief of 1,000 feet if it were taken in a hilly area of the sea floor. This relief indicates the minimum thickness of aprons.

DEFORMATION OF SEA FLOOR AROUND ISLANDS

The minimum thickness and volume of an archipelagic apron may be a function not only of the relief of a pre-existing hilly terrane but also the pre-existing average slope of the sea floor and its subsequent deformation. An upward slope toward an island would require a cover only as thick as the pre-existing relief to produce the graded slope of an apron. A moat would require much more fill to form a graded slope.

That some gentle elevation of the sea floor may be associated with an archipelago is indicated by the existence of the Hawaiian Swell (Betz and Hess, 1942, p. 106; Dietz and Menard, 1953, pp. 104–06) but the swell is about 600 miles wide and all or almost all of the elevation occurs at the outer edges so that the central area is level on the average. Even on the crest of the Hawaiian Swell, the sea floor is depressed rather than elevated in the areas directly surrounding seamounts where aprons would be located if they existed (Dietz and Menard, 1953, Fig. 5). Elsewhere, the sea floor has been found to slope downward toward the base of seamounts in areas like the Baja California Seamount province where aprons are lacking and the hilly terrane is exposed (Figs. 6, 8). Inasmuch as the hilly sea floor does not slope upward in the vicinity of any of the seamounts where it can be seen, it is improbable that it slopes upward under archipelagic aprons where it can not be seen because of burial.

Both level and downward sloping hilly areas have been found around seamounts and might presumably exist under archipelagic aprons. If level, however, profiles of aprons would be expected to show smaller and smaller peaks (on the average) nearer the archipelago because of increasing depth of burial. The actual profiles show no such topography, and hills of any size rising from the apron are rare. Echograms thus suggest that the sea floor is bowed downward so that the almost perfectly level distal part of the apron covers any hills completely despite the fact that beyond the apron the hills stand distinctly above the level of the apron (Figs. 1–3).

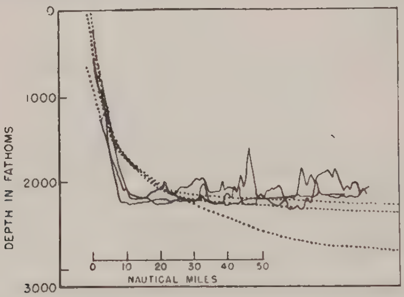

FIG. 8.—Three profiles of archipelagic aprons (dotted) compared with three profiles of irregular sea floor in vicinity of seamounts in Baja California Seamount province.

Profiles of archipelagic aprons thus give indirect indications in support of more positive evidence that the sea floor is bowed downward in the vicinity of many islands and seamounts. Some seamounts are ringed by moats in the Gulf of Alaska (Menard and Dietz, 1951, pp. 1267–68), central Pacific (Dietz, Menard, and Hamilton, 1954, p. 269), and in the Baja California Seamount province. The existence of the Hawaiian moat was cited by Vening Meinesz (1948, p. 99) as a confirmation of his interpretation of his gravity observations wherein the load of the Hawaiian Islands is compensated regionally by a downbowing of the crust. This moat is clearly visible on echograms. Gravity observations in other areas indicate a similar regional compensation and imply a downbowing. Local crustal depressions, which may be part of a discontinuous moat, have been found bordering Bermuda by seismic-refraction studies (Officer, Ewing, and Wuenschel, 1952, pp. 800–04), and similar studies suggest that the crust has been depressed around Bikini (Raitt, 1952, p. 22, Fig. 18). In brief, every type of observation available indicates that the crust is depressed in the vicinity of a large oceanic volcano.

DEPTH OF BURIAL OF HILLY SEA FLOOR

Consideration of the average relief of sea-floor hills indicates a thickness of burying material of at least 1,000 feet in order to produce a smooth apron. The much greater thickness required to fill in any depression which might exist at the base of an archipelago is more difficult to evaluate but two lines of evidence suggest that it is at least several thousand feet.

The fill in one place off Bermuda amounts to 15,000 feet of consolidated sediments and volcanics plus 2,500 feet of "unconsolidated sediment" (Officer, Ewing, and Wuenschel, 1952, Fig. 19, p. 803) although average depths are less than half as much. Near the Hawaiian Islands consolidated sediment or volcanic material is 5,000–10,000 feet thick (Gaskell, 1954, pp. 358–59), and volcanics are about 5,000–7,000 feet thick around Bikini Atoll (Raitt, 1952, Fig. 18).

Another indication of the thickness of fill can be obtained by comparing profiles of archipelagic aprons and profiles of the moat around the Hawaiian Islands (Fig. 2). The smooth sea floor around Hawaii is a partly developed apron which apparently covered most hills and was then depressed. About 4,000 feet of additional fill would be required to produce the normal profile of an archipelagic apron. If, as evidence indicates, the load of a group of volcanic islands depresses the crust, it may be tentatively assumed that the amount of depression is roughly uniform for all linear groups in the Pacific basin. This follows because the thickness and composition of the crust are remarkably constant (Raitt, in Shipboard Report, Capricorn Expedition, 1953, p. 23; Gaskell, 1954, p. 358), and the nature of the load and, prior to yielding, even the amount of load is relatively constant. It may be more than coincidence, therefore, that the Marquesan and Samoan aprons appear to be ponded and that the dam that would produce the ponding is at the same distance from the islands as the crest of the Hawaiian Arch is from the Hawaiian Islands. Both distances agree with the width of regional compensation of the Hawaiian Islands (Vening Meinesz, 1948, p. 99). A thickness of at least 4,000 feet for the Marquesan and Samoan aprons is suggested by this comparison.

Repeated or continued subsidence of archipelagoes and their aprons such as may have occurred at the Hawaiian Islands would produce a composite apron of indefinite thickness but certainly greater than the thickness of a single apron deduced by reasoning from topography. This may explain why the depth of sediment and volcanics measured seismically is so great.

MINIMUM VOLUME

An order of magnitude estimate of the minimum volume of material in the archipelagic aprons of the Pacific is about 10^6 cubic nautical miles (4×10^6 cubic kilometers). If the thickness is not the minimum 1,000 feet suggested by consideration of the burial of low relief but the 4,000 feet indicated by surface wave dispersion in some places (Oliver, Ewing, and Press, 1955, p. 933), or the 5,000–

15,000 feet indicated by seismic measurement, the volume would be correspondingly greater.

The approximate minimum volume of material in the apron around the Marquesas Islands lies between 3×10^3 and 2×10^4 cubic miles depending on the assumed configuration of the buried initial sea floor and the extent of the apron in sectors where it has not been explored. The volume is 1.1×10^4 cubic miles according to the most plausible assumptions of an apron of uniform width around the entire archipelago, a crustal downbowing corresponding to that found off Hawaii, and a saw-toothed pattern of buried relief in which the hills and valleys have similar cross sections. With the same assumptions, except that the buried relief is considered to consist of a single 1,000-foot hill rising from an irregular plain (Fig. 6 shows an example), the volume is 2.1×10^4 cubic miles.

It is interesting to compare the volume of the material in the Marquesas archipelagic apron with the volume of the Marquesas volcanoes, because the topography and surficial material show that the surface of the apron has been shaped, in large part, by turbidity-current deposition, and it seems plausible that most of the material below the surface had the same origin. The present islands are deeply dissected, but an estimate of the maximum possible volume before dissection can be obtained by extrapolating the submarine slopes upward to a point (Fig. 1). This approach includes any material eroded away during lowered stands of the sea because all banks and shelf areas are restored. The maximum possible former volume of the subaerial part of the Marquesas volcanoes according to this method is 350 cubic miles. The volume of the submarine part of the volcanoes is 8,400 cubic miles if the base is taken as 2,500 fathoms below sea-level (Fig. 1). The computations indicate that the most plausible minimum volume of the apron is 30–60 times the maximum volume of the subaerial part of the Marquesas volcanoes, and 1–3 times larger than the total volume of the submarine part of the volcanoes. It appears that most of the material in the apron has not been derived from erosion of the islands.

COMPOSITION

If the whole of the apron is not turbidity-current deposits derived from the erosion of islands, other possible components may be considered to see if their aggregate volume is adequate to bury the pre-existing terrane. The variety of materials available on and around Pacific basin volcanoes is limited compared to continents or continental islands. Possible sedimentary materials are pelagic organic remains, products of submarine erosion, subaerial volcanic ash and dust, and submarine volcanic ash. Submarine lava flows may also add large amounts of material to an apron.

Globigerina ooze is widely distributed on the surfaces of aprons, and undoubtedly pelagic organisms rain down continually while the aprons are built. However, they also rain down in many other large areas that are hilly rather than smooth; the East Pacific Rise and the area east of the Marquesas archipelagic apron, for example, are covered with calcareous ooze. The hills there are smoothed and rounded compared with other parts of the Pacific but are highly irregular compared with an apron. If an important fraction of the aprons is pelagic organic detritus, the production of the detritus must have been accelerated in the vicinity of the apron. Subaerial and littoral processes introduce nutrients into the sea, and the waters near islands and shoals are notable for the concentration of pelagic organisms, but there is no reason to believe that the rate of pelagic sedimentation is several times more rapid than away from islands. Moreover, the width, smoothness, and sharp boundaries of the apron would pose the improbable requirement that pelagic sedimentation be relatively rapid for 100–150 miles from an archipelago and slow down within a very short distance. In addition, aprons appear to be symmetrically disposed around archipelagoes instead of conforming with the strong and steady current patterns of the tropical Pacific, and the apron around the Emperor Seamounts is in water too deep for calcareous ooze to form. It is unlikely that more than a small fraction of the volume of an archipelagic apron is of pelagic origin.

Coral fragments have been found on the upper slopes of aprons (Murray and Lee, 1909, p. 156), but coral and other reef material is not required to construct an apron. The Marquesas apron is fully developed despite the virtual absence of living or fossil reefs on the Marquesas Islands. Likewise the guyots of the Mid-Pacific Mountains have only small patches of coral (Hamilton, 1953, p. 206) but the mountains are surrounded by an extensive apron. The volume of reef capping is much larger in an archipelago of coral atolls such as the Marshall Islands but even there rough estimates based on borings and seismic measurements indicate that the volume of the capping is at least an order of magnitude smaller than the apron. Coral reefs are not a necessary source of material in an apron and it is unlikely they contribute any large fraction to the volume.

Wind-borne volcanic ash and dust are very widely distributed on the sea floor and undoubtedly are deposited in archipelagic aprons. However, most of the arguments opposed to a dominant composition of pelagic organisms apply as well to ash and dust. In addition, quantitative considerations show that the vast lava volcanoes forming the islands and seamounts would be little more than conduits for a much larger volume of ash which would be required. The observably small volume of ash in a normal Pacific basin volcanic island indicates ash falls are comparatively rare.

No single source of the sediment discussed appears competent to supply more than a small fraction of the volume of an archipelagic apron. The aggregate volume from all the sources does not bear analysis but it does not appear to amount to as much as half. Most of the material in an apron apparently is not sediment —by elimination it must be submarine lava flows and ash.

This conclusion may be questioned on the grounds that seismic-refraction and -reflection measurements around Bermuda indicate a volume of "unconsolidated sediment" that is much larger than the maximum volume of the restored island.

If the subaerial part of Bermuda volcano is restored by extrapolating the submarine slopes upward to a point, the maximum volume eroded away is roughly 260 cubic miles. The volume of "unconsolidated sediment" in a 60° sector southeast of Bermuda may be computed from an isopach map of the area (Officer, Ewing, and Wuenschel, 1952, Fig. 19, p. 803). It is at least 7–8 times as great as the volume of the former subaerial volcano. However, this sediment grades westward into the much thicker deposits under the abyssal plain and continental rise off North America (Officer, 1955, Figs. 3, 4, p. 259). The continent rather than the island may be the dominant source.

Volcanic ash and lava from the central vents that formed the volcanic islands or seamounts can immediately be eliminated as an important source of unusually large quantities of volcanics. The lavas that flowed out of the vent and built up the steep sides of the volcano can hardly have spread out for an additional 120–150 miles beyond the base of the volcano and over slopes of 0.002. Stearns (1946, p. 17) has suggested that submarine volcanoes as they build upward may produce sizeable volumes of ash because of the chilling effect of the sea water. If so, the volume is not ordinarily enough to bury the surrounding hilly topography and form aprons because none is found around seamounts (Fig. 6) other than guyots.

Submarine fissure flows are the most plausible source of the volcanics. They have been proposed to explain the vast amount of volcanic material found on the Bermuda Rise by seismic methods (Gaskell, 1954, p. 360; Officer, 1955, p. 255). Fissure flows might reasonably be expected around a line of volcanoes and the volume of material produced by fissures on land would be adequate to bury the hilly terrane which disappears under archipelagic aprons. The Columbia basalts for example welled out of fissures and covered 100,000 square miles of hilly topography with 35,000 cubic miles of lava. Individual flows were as large as 360–480 feet thick and with areas of several thousand square miles (Waters, 1955, pp. 707–08).

SEQUENCE OF DEVELOPMENT

The volume of material required for burial indicates that the normal hilly terrane of the sea floor is covered by lava flows originating from fissures in the vicinity of archipelagoes. Core samples show that the lava flows are covered, at least in many places, by pelagic sediments and turbidity current deposits. The extremely gentle slopes of the apron and the presence of deep-sea channels suggest that turbidity-current deposits dominate.

The principle undiscussed questions about archipelagic aprons concern the sequence of development, particularly whether the fissure flows or the volcanoes are formed first. Presumably the sea floor is hilly before the deformation which results in the archipelago begins (Fig. 7A). The initial change is either the construction of a line of large submarine volcanoes at central vents or of a lava plain from fissure flows—or penecontemporaneous development of the two. Scores of large seamounts and also Clipperton Island and the Revillagigedo Islands rise from an irregular sea floor, so that this stage of development is observable. In contrast no single example of a large smooth plain has been found in the Pacific which is not either an abyssal plain connected by a smooth slope to a continent or an archipelagic apron fringing a group of volcanoes. In the next stage the volcanoes grow larger and older and the surrounding crust is bent downward by the load. This stage is commonly observed on fathograms and the requirement of a load great enough to bend the crust may explain why aprons are found only around islands or former islands despite the fact that erosion of the island is not adequate to produce the apron. Subsequently fissures form in the depression at the base of the line of volcanoes and lava flows fill in the depressed area of the crust. The same topography and structure could also develop starting with a lava plain and with subsequent development of a line of volcanoes but, if so, it would be difficult to explain why the lines of volcanoes are centered in the plains and why the plains ordinarily have about the same width. Both follow directly if the lava collects in a depression formed by relatively uniform loads distributed in various places on a relatively uniform crust which probably has a relatively uniform strength. In the final stage subaerial and littoral erosion of the volcanoes yields a sizeable amount of terrigenous débris, turbidity currents transport and deposit this material on the lava plains, and the apron assumes the form which is normally observed. Volcanoes may still be active during this stage.

This sequence is, of course, simplified in that pelagic sediment would rain onto the sea floor between lava flows, and turbidity currents and slumps would deposit material in the apron at any time after the volcanoes first began to grow. Moreover a sizeable amount of ash might be expected as a result of chilling of submarine lava flows. The sequence of development may also be interrupted by faulting as may have occurred at Hawaii.

BIBLIOGRAPHY

BETZ, FREDERICK, AND HESS, H. H., 1942, "The Floor of the North Pacific Ocean," *Geogr. Rev.*, Vol. 32, pp. 99–116.
BROWNE, B. C., 1954, "Gravity Measurements and Oceanic Structure," *Proc. Royal Soc.*, Ser. A, pp. 398–400.
CAPRICORN EXPEDITION, SHIPBOARD REPORT, 1953, Univ. California, Scripps Inst. Oceanography, Ref. 53–15.
DIETZ, R. S., 1954, "Marine Geology of Northwestern Pacific: Description of Japanese Bathymetric Chart 6901," *Bull. Geol. Soc. America*, Vol. 65, pp. 1199–1224.
———, AND MENARD, H. W., 1953, "Hawaiian Swell, Deep, and Arch, and Subsidence of the Hawaiian Islands," *Jour. Geology*, Vol. 61, pp. 99–113.
———, ———, AND HAMILTON, E. L., 1954, "Echograms of the Mid-Pacific Expedition," *Deep-Sea Research*, Vol. 1, pp. 258–72.
GASKELL, T. F., 1954, "Seismic Refraction Work by H.M.S. *Challenger* in the Deep Oceans," *Proc. Royal Soc.*, Ser. A, Vol. 222, pp. 356–61.
HAMILTON, E. L., 1953, "Upper Cretaceous, Tertiary, and Recent Planktonic Foraminifera from Mid-Pacific Flat-Topped Seamounts," *Jour. Paleon.*, Vol. 27, pp. 204–37.,
HEEZEN, B. C., EWING, MAURICE, AND ERICSON, D. B., 1954, "Reconnaissance Survey of the Abyssal Plain South of Newfoundland," *Deep-Sea Research*, Vol. 2, pp. 122–33.
HESS, H. H., 1948, "Major Structural Features of the Western North Pacific, "*Bull. Geol. Soc. America*, Vol. 59, pp. 417–46.
KOCZY, F. F., 1954, "A Survey on Deep-Sea Features Taken during the Swedish Deep-Sea Expedition," *Deep-Sea Research*, Vol. 1, pp. 176–84.

MENARD, H. W., 1955, "Deep-Sea Channels, Topography, and Sedimentation," *Bull. Amer. Assoc. Petrol. Geol.*, Vol. 39, pp. 236–55.

———, AND DIETZ, R. S., 1951, "Submarine Geology of the Gulf of Alaska," *Bull. Geol. Soc. America*, Vol. 62, pp. 1263–85.

MURRAY, JOHN, AND LEE, G. V., 1909, "The Depth and Marine Deposits of the Pacific," *Mem. Mus. Comp. Zoology*, Vol. 38, 169 pp.

OFFICER, C. B., 1955, "Geologic Interpretation of a Series of Seismic Reflection Profiles from Bermuda to the Continental Margins," *Deep-Sea Research*, Vol. 2, pp. 253–60.

———, EWING, MAURICE, AND WUENSCHEL, P. C., 1952, "Seismic Refraction Measurements in the Atlantic Ocean. Pt. IV: Bermuda, Bermuda Rise, and Nares Basin," *Bull. Geol. Soc. America*, Vol. 63, pp. 777–808.

PETTERSSON, HANS, 1954, *The Ocean Floor*. Yale Univ. Press, New Haven.

RAITT, R. W., 1952, "The 1950 Seismic Refraction Studies of Bikini and Kwajalein Atolls and Sylvania Guyot," Univ. California, Marine Physical Lab., Scripps Inst. Oceanography, Ref. 52-38.

STEARNS, H. T., 1946, "Geology of the Hawaiian Islands," *Terr. Hawaii Div. Hydrography Bull. 8.*

VENING MEINESZ, F. A., 1948, *Gravity Expeditions at Sea*, Vol. IV. Netherlands Geod. Comm., Delft.

WATERS, A. C., 1955, "Volcanic Rocks and the Tectonic Cycle," in "Crust of the Earth," *Geol. Soc. America Spec. Paper 62*, pp. 703–22.

ANGEWANDTE CHEMIE
HERAUSGEGEBEN VON DER GESELLSCHAFT DEUTSCHER CHEMIKER
68. Jahrgang / Nr. 17/18, 1956 / Seite 540–546
Fortsetzung der Zeitschrift „Die Chemie“ · Verlag Chemie, GmbH., Weinheim/Bergstraße

SONDERDRUCK

(667)

Grundlagen und Ergebnisse der Radiokohlenstoff-Datierung

Von Prof. Dr. H. E. SUESS

*Scripps Institution of Oceanography, University of California, La Jolla, Californien**)

^{14}C-Bestimmungen haben nicht nur kulturhistorisch wichtige Datierungen Kohlenstoff-haltiger Funde aus den vergangenen 35000 Jahren ermöglicht, sondern u. a. auch zu neuen Erkenntnissen über die geochemische Verteilung des Kohlenstoffes, Klimaänderungen der Erde und insbesondere den Ablauf der Eiszeiten geführt. Die Grundlagen der Methodik, Ausführungsweisen entsprechender ^{14}C-Analysen, Fehlermöglichkeiten und Ergebnisse werden dargestellt.

Einleitung

Die Existenz eines in der Natur vorkommenden radioaktiven Kohlenstoff-Isotops von relativ langer Lebensdauer ist für den Forscher ein außerordentlicher Glücksfall. Sie gibt ihm gleichsam einen Zauberstab in die Hand, der es ihm ermöglicht, die Geheimnisse der jüngsten geologischen Geschichte und der mit ihr verknüpften gewaltigen Klimaänderungen am Ausklang der Eiszeit und den damit einhergehenden Aufstieg der menschlichen Kulturen zu enträtseln.

Daß das radioaktive Kohlenstoff-Isotop besser zu Altersbestimmungen geeignet ist, als ein Isotop irgend eines anderen Elements, ist dem besonderen Umstand zu verdanken, daß der Kohlenstoff in zwei Bindungsformen in der Natur weit verbreitet auftritt: in reduzierter organischer Form und als Kohlensäure bzw. als Carbonat. Der sich durch Höhenstrahlungsprozesse über freie Neutronen und atmosphärischem Stickstoff bildende Radiokohlenstoff findet sich auf der Erdoberfläche vor allem im CO_2 der Atmosphäre und in den Bicarbonaten der Ozeane. Durch Photosynthese der Pflanzen wird er in organische Stoffe übergeführt. Isotopenaustausch organisch gebundenen Kohlenstoffs mit Kohlendioxyd und Carbonat ist im allgemeinen nur durch biochemische Prozesse möglich.

Während bei radioaktiven Altersbestimmungen mit Hilfe von Isotopen anderer Elemente die Frage einer präzisen Definition des Begriffes des „Alters" oft ein verwickeltes Problem darstellt, ist das Alter von Holz und anderen Pflanzenresten stets wohl definiert als die Zeitspanne, die seit der Bildung der betreffenden Substanz durch Photosynthese bis zum Zeitpunkt der Radiokohlenstoff-Bestimmung verflossen ist. Über diese Zeitspanne hin nimmt die spezifische Kohlenstoff-Aktivität in einer der Halbwertszeit des Radiokohlenstoffes entsprechenden Weise ab, so daß aus der spezifischen Aktivität des Pflanzenmaterials der Gegenwart (I_o) und der einer gegebenen Probe (I_x) das Alter der Probe (A_x) ohne weiteres berechnet werden kann:

$$A_x = \frac{T_{1/2}}{0{,}693} \ln \frac{I_o}{I_x}$$

wenn die Halbwertszeit $T_{1/2}$ bekannt ist.

In gleicher Weise können tierische Produkte, wie Knochen und Geweihe, zur Datierung verwendet werden, da ihre organischen Aufbaustoffe stets letzten Endes auf pflanzliche Nahrungsstoffe zurückgeführt werden können. Die Datierung von Carbonaten, wie Muscheln ist unter Umständen gleichfalls möglich, jedoch ist hier bei der Auswertung der Meßergebnisse Vorsicht geboten, da die Möglichkeit eines Austausches von Carbonat-Ionen mit jüngerem oder älterem Material nicht immer ausgeschlossen werden kann. Unter Umständen gibt eine Isotopenanalyse des Sauerstoffs im Carbonat die Möglichkeit, die Frage nach einem solchen Austausch nachzuprüfen.

Die Entdeckung des radioaktiven Kohlenstoff-Isotopes ^{14}C in der Natur und die Entwicklung der Methode der Kohlenstoff-Datierung verdanken wir *W. F. Libby*, der bereits 1946 darauf hinwies1)), daß die durch die Höhenstrahlung gebildeten Neutronen in der Atmosphäre wegen des relativ hohen Wirkungsquerschnitts2)) der Reaktion ^{14}N (n,p), ^{14}C von $1{,}7 \cdot 10^{-24}$ cm^2 praktisch quantitativ zur Bildung von Radiokohlenstoff der Masse 14 führen müssen. Die Anwendung eines experimentellen Kunstgriffes, der Ausschaltung des größten Teils des Höhenstrahlungsuntergrundes im Zählrohr durch Antikoinzidenzmessungen, ermöglichte 1947 *Libby* und seinen Mitarbeitern3)) den experimentellen Nachweis von natürlichem Radiokohlenstoff. In den darauffolgenden Jahren entwickelten sie die Datierungsmethode und bestimmten das Alter von Hunderten von Proben4)).

Die Halbwertszeit von ^{14}C ist von *Libby* und Mitarbeitern sowie zahlreichen anderen Forschern sorgfältig gemessen worden. Als gewogenes Mittel gab *Libby* 1952 ihren Wert zu 5568 ± 45 Jahren an. Sämtliche gegenwärtig in der Literatur angegebenen Datierungsergebnisse sind auf Grund dieser Halbwertszeit ermittelt.

Bestimmungsmethoden von ^{14}C

Die erste, in Chicago entwickelte experimentelle Methode zur Bestimmung von natürlichem Radiokohlenstoff ist von *Libby* ausführlich beschrieben worden. Man reduzierte das CO_2 aus dem Probenmaterial mit Magnesium zu elementarem Kohlenstoff, der als feuchte Paste an der gesamten Innenwand eines Geiger-Zählrohres aufgetragen wurde. Ein Schirmgitter im Zählrohr verhinderte Schwankungen in den Meßergebnissen, die sonst durch ungleichmäßiges Auftragen hervorgerufen werden können. Die Nachahmung dieser Methode in anderen Laboratorien ergab jedoch erhebliche Schwierigkeiten, besonders wegen der Gefahr einer Verunreinigung des Probenkohlenstoffes mit radioaktiven Teilchen aus der Luft, die in den letzten Jahren besonders kritisch geworden ist.

Gegenwärtig wird das natürliche ^{14}C fast ausschließlich durch Messung der Aktivität einer gasförmigen Kohlenstoff-Verbindung im Proportionalzählrohr bestimmt. Es

---

*) Veröffentlichung der „Scripps Institution of Oceanography", neue Serie Nr. 868.

1)) *W. F. Libby*, Physic. Rev. *69*, 671 [1946].
2)) *J. H. Coon* u. *R. A. Nobles*, ebenda *75*, 1358 [1949].
3)) *E. C. Anderson, W. F. Libby, S. Weinhouse, A. F. Reid, A. D. Kirshenbaum* u. *A. V. Grosse*, Science [Washington] *105*, 576 [1947]; Physic. Rev. *72*, 93 [1947].
4)) *W. F. Libby:* Radiocarbon Dating, zweite Aufl., University of Chicago Press, Chicago 1955.

Reproduced by Permission

war seit langem bekannt, daß Kohlenwasserstoffe sich als Füllgase von Zählrohren vorzüglich eignen, wenn man mit — gegenüber dem Geiger-Zählrohr — relativ geringer Zähldrahtspannung und entsprechend höherer Verstärkung der wesentlich kleineren und in ihrer Größe der Gasionisation proportionalen Stromstößen arbeitet. Auch ist es, wie die holländischen Forscher *de Vries* und *Barensen*[5]) zeigen konnten, möglich, Kohlendioxyd als Füllgas zu verwenden, wenn man es durch sorgfältige Reinigung von den letzten Spuren von Beimengungen befreit, die Elektronenaffinität zeigen, wie Sauerstoff und Wasserdampf. Ein anderer Weg zur Verwendung von CO_2 ist von *Craine* eingeschlagen worden[6]). Die *Libby*sche Methode, den Zählrohruntergrund bis auf einen geringen Bruchteil dadurch auszuschalten, daß man das Meßrohr mit einem Kranz von Höhenstrahlzählern umgibt, ist in allen Fällen beibehalten worden. Die durch Höhenstrahlungsmesonen ausgelösten Stöße treten im Meßrohr und in den umgebenden Zählern gleichzeitig auf und werden durch eine geeignete Verstärkerschaltung eliminiert. Ein Eisenpanzer von etwa 20 cm Dicke verhindert das Eindringen von γ-Quanten.

Ein im Laboratorium aus einer Probe verhältnismäßig rasch und bequem herstellbarer Kohlenwasserstoff ist Acetylen. Dieses Gas wird seit 1953 an der U. S. Geological Survey in Washington, D. C., zur ^{14}C-Bestimmung verwendet[7]). Man erhält das Acetylen durch Reduktion von Strontiumcarbonat mit Magnesium zum Carbid und nachfolgender Hydrolyse. Das Verfahren ist etwa ein Jahr später vom ^{14}C-Laboratorium (Geochronometric Laboratory) der Yale University, New Haven, Conn., übernommen worden[8]). An jeder dieser Stationen wird gegenwärtig etwa eine Datierung pro Arbeitstag ausgeführt. Wenn man von den älteren Bestimmungen *Libby*s absieht, dann beträgt die Anzahl der von diesen beiden Laboratorien zur Zeit veröffentlichten Bestimmungen ein mehrfaches derer, die von allen anderen Stationen der Welt zusammengenommen seit ihrem Bestehen publiziert wurden.

Methan wird als Zählgas im Laboratorium der Magnolia Oil Company, Houston, Texas, verwendet. Dieses Gas dürfte im Zählrohr dem Acetylen gegenüber keinerlei Vor- oder Nachteile besitzen und seine Herstellung aus dem Probenmaterial dürfte mit etwas geringerem Arbeitsaufwand möglich sein. Die Kosten der Anlage und die Betriebskosten müssen jedoch wegen des Arbeitens bei höheren Drucken, wegen der bei der Reduktion von CO_2 durch H_2 zu CH_4 nötigen Umlaufpumpen, und wegen der Unmöglichkeit einer vollständigen Kondensation des Methans mit flüssigem Stickstoff, höher geschätzt werden als die bei Anwendung von Acetylen.

Mit Kohlendioxyd als Zählgas sind außer von *de Vries* und *Barendsen*[5, 9]) in Holland auch von *Rafter* und *Fergusson*[10]) in Neuseeland und im Laboratorium der Universität Heidelberg vorzügliche Ergebnisse erhalten worden. Weitere Laboratorien, an denen die Verwendung von CO_2 als Zählgas geplant ist oder bereits angewandt wird, befinden sich u. a. an den Hochschulen in Kopenhagen, Stockholm, Pittsburg (Penn.), Lamont (N. Y.) und an dem Forschungsinstitut der Humbel Oil Co. in Houston (Texas)[11]). Dem Vorteil einer gewissen Zeitersparnis bei der chemischen Reinigung des Kohlendioxydes im Vergleich zu der Umwandlung zu Acetylen steht der Nachteil gegenüber, daß wegen der außerordentlichen Empfindlichkeit des CO_2 gegen Verunreinigungen eine sorgfältige laufende Kontrolle der Arbeitsweise notwendig ist, die die Mitarbeit eines erstrangigen Physikers erfordert.

Eine weitere Möglichkeit zur ^{14}C-Bestimmung bietet das Verfahren der Szintillationszählung an geeigneten Flüssigkeiten. Da dieses Verfahren Messungen an wesentlich größeren Probemengen gestattet, und überdies der Untergrund, auf gleiche Probenmenge bezogen, kleiner ist als der der besten Gaszählrohre, ist es im Prinzip möglich, größere Meßgenauigkeiten zu erreichen[12]). Die chemische Überführung des Probekohlenstoffes in eine bei Zimmertemperatur flüssige, sich für Szintillationszählungen eignende Verbindung, wie z. B. in einen höheren Kohlenwasserstoff, ist jedoch mühevoll und zeitraubend.

Genauigkeit

Die Genauigkeit einer ^{14}C-Bestimmung und der sich daraus ergebenden Datierung wird durch mehrere Fehlerquellen bestimmt:

1.) der statistische Fehler
2.) der Meßfehler
3.) der sich durch Verunreinigung der Probe mit älterem oder jüngerem Material ergebende Fehler
4.) der durch Isotopentrenneffekte bedingte Fehler.

Der statistische Fehler ergibt sich aus der Tatsache, daß der Elementarakt des radioaktiven Zerfalls ein akausaler Prozeß und jedes Meßergebnis statistischen Schwankungen unterworfen ist. Die Theorie dieser Schwankungen zeigt, daß bei einer gegebenen Einzelmessung bei der N Elementarakte als Zählrohrstöße beobachtet wurden, das Ergebnis mit einer Wahrscheinlichkeit von 68% um nicht mehr als $\sqrt{N}$ vom wahren Wert, d. h. vom Mittelwert einer unendlichen Anzahl von Messungen abweicht. Zu Messungen, deren Fehler in rund $^2/_3$ der Fälle 1% nicht übersteigt, müssen daher jeweils 10000 Elementarakte beobachtet werden. Die Wahrscheinlichkeit, daß in einem solchen Falle der statistische Fehler 2% nicht übersteigt, beträgt 95,4%, daß er kleiner als 3% ist 99,7% usw.

In Datierungslisten ist es üblich, als Fehlergrenzen stets den sich aus dem statistischen Fehler unter Berücksichtigung des Zählrohruntergrundes ergebenden Standardfehler anzugeben. Diese Fehlergrenzen müssen im Mittel in einem Drittel der Fälle überschritten werden, und zwar für 4,6% der Messungen um mehr als ihren doppelten Betrag. Sie enthalten keine Fehler anderen Ursprungs. Um die durch den statistischen Fehler bedingte Genauigkeit zu verdoppeln, muß viermal so lange beobachtet werden.

Fehler in der eigentlichen physikalischen Messung können von Schwankungen in der Empfindlichkeit der Zählrohre und der Verstärker, von Schwankungen in der natürlichen Höhenstrahlintensität und von radioaktiven Verunreinigungen herrühren. Im allgemeinen ist es leicht, mit dem Gaszähler an jüngerem Kohlenstoff in Probenmengen von über 1 g mit einer Genauigkeit von 1% zu messen. Werden größere Genauigkeiten gefordert, dann steigen die Schwierigkeiten rasch an und es ist selbst bei größtem Arbeitsaufwand nur selten möglich, Ergebnisse zu erhalten, deren Werte innerhalb eines Fehlers von weniger als 0,5% verläßlich erscheinen. Da der Radiokohlenstoff in etwas über sechs Halbwertszeiten auf 1% seiner ursprünglichen Konzentration abklingt, liegt die bequem erreichbare Grenze der Altersbestimmungen bei etwa 35000 Jahren.

---

[5]) *H. de Vries* u. *G. W. Barendsen*, Physica *18*, 652 [1952]; *19*, 987 [1953].

[6]) *H. R. Crane*, Science [Washington] *122*, 689 [1955].

[7]) *H. E. Suess*, Science [Washington] *120*, 5 [1954].

[8]) *R. S. Preston*, *E. Person* u. *E. S. Deevey*, ebenda *122*, 954 [1955].

[9]) *H. L. de Vries* u. *G. W. Barendsen*, Nature [London] *174*, 1138 [1954].

[10]) *G. J. Fergusson*, New Zealand J. Sci. Techn. *B 35*, 90 [1953]; Nucleonics *13*, 18 [1955]; *T. A. Rafter* u. *G. J. Fergusson*, New Zealand J. Sci. Techn. *B 35*, 127 [1953]; *B 36*, 371 [1955].

[11]) *Hilde Levi*, Nature [London] *176*, 727 [1955].

[12]) *J. R. Arnold*, Science [Washington] *113*, 155 [1954].

Als radioaktive Verunreinigung des Zählgases kommen vor allem Radium-Emanation, Krypton 81 sowie bei Verwendung eines Kohlenwasserstoffes, auch Tritium in Frage. Radium-Emanation, deren Halbwertszeit 3,5 Tage beträgt, kann am sichersten dadurch entfernt werden, indem man sie im gereinigten Probengas für zwei bis drei Wochen abklingen läßt, ehe man die Messung vornimmt. ^{81}Kr mit 8 Jahren Halbwertszeit ist als Produkt künstlicher Uran-Spaltung im atmosphärischen Krypton enthalten[13], jedoch gegenwärtig in noch zu geringer Konzentration, um merklich zu stören. Ernstere Schwierigkeiten haben sich im Laboratorium der U.S. Geological Survey im Frühjahr 1954 dadurch ergeben, daß, was damals nicht bekannt war, die Tritium-Konzentration im Leitungswasser auf zeitweilig rund das 1000fache ihres natürlichen Wertes angestiegen war. Bei der Herstellung des Acetylens wird dort jetzt Brunnenwasser aus geologisch älteren Schichten verwendet, dem kaum Regenwasser der letzten Jahre beigemengt ist.

Geochemie des Radiokohlenstoffes

Beim Auftreffen der Höhenstrahlteilchen, hauptsächlich Protonen von einer Energie von mehr als 10^9 eV, auf die Erdatmosphäre, werden Kernbruchstücke gebildet, die Mesonen, Protonen, α-Teilchen, schwerere Kerne und auch Neutronen enthalten. Das Maximum der Neutronen-Produktion liegt bei etwa 30 km Höhe. Die Menge hängt stark von der geomagnetischen Breite ab und ist an den Polen größer als am Äquator. Die mittlere Neutronen-Produktion für alle Breitegrade, integriert über die Gesamthöhe der Atmosphäre, beträgt nach *Ladenburg*[14] etwa 2,4 Neutronen pro cm² und Sekunde.

Wegen des hohen Wirkungsquerschnittes der Reaktion ^{14}N (n,p) ^{14}C von etwa $1{,}7 \cdot 10^{-24}$ cm² führen praktisch alle so gebildeten Neutronen zur Bildung von ^{14}C. Im stationären Zustand ist die Anzahl der pro Zeiteinheit sich bildenden ^{14}C-Kerne gleich der der zerfallenden, so daß der auf einem cm² der Erdoberfläche vorhandene Kohlenstoff eine durchschnittliche Radioaktivität von 2,4 Zerfällen pro Sekunde (144 pro Minute) zeigen sollte.

Geochemische ^{14}C-Verteilung

Die geochemische Verteilung des Radiokohlenstoffes umfaßt jedoch nicht den gesamten auf der Erde vorhandenen Kohlenstoff, sondern beschränkt sich auf ein gewisses „Austauschreservoir". In erster Näherung kann angenommen werden, daß sich die Vermischung innerhalb dieser Reservoire beliebig rasch vollzieht, so daß eine gleichförmige Verteilung des ^{14}C auf die verschiedenen Komponenten des Reservoires vorliegt.

Tabelle 1 gibt die einzelnen Komponenten dieses Austauschreservoires für Kohlenstoff und die in ihnen enthaltenen Kohlenstoff-Mengen berechnet als CO_2 an[15, 16].

Eine gleichmäßige Verteilung der ^{14}C-Aktivität von 144 dpm (Zerfällen pro Minute) auf die 7,8 g Kohlenstoff des Reservoirs pro cm² Erdoberfläche läßt eine spezifische ^{14}C-Aktivität von $144/7{,}8 = 18{,}5$ dpm erwarten. Experimentell werden Werte von 12 bis 15 dpm gefunden. Der Unterschied ist etwas größer als die Unsicherheit in der Abschätzung der Höhenstrahlenproduktion erwarten läßt und wohl auch zum Teil darauf zurückzuführen, daß das betrachtete Austauschreservoir nicht ein streng abgeschlossenes System darstellt, weil ein Bruchteil des ^{14}C durch Grundwässer in Kalke und andere fossile Carbonate übergeführt wird.

	Menge CO_2 in g	
	10^{18} g gesamte Erde	pro cm² Oberfl.
CO_2 der Atmosphäre	2,35	0,46
am Lande:		
lebende org. Substanzen	0,1	0,02
tote org. Substanzen	2,6	0,5
im Meer:		
Organischer Kohlenstoff	10	0.2
anorg. Kohlenstoff	130	25
Gesamtmenge im Reservoir ...	145	28

Tabelle 1

Mit dem von uns experimentell gefundenen Wert für die spezifische Aktivität des Reservoir-Kohlenstoffes von 14,7 dpm und der von *Libby* angegebenen Halbwertszeit von 5580 Jahren erhält man für das atomare ^{14}C/^{12}C-Verhältnis $1{,}23 \cdot 10^{-13}$. Die insgesamt auf der Erde vorhandene Radiokohlenstoff-Menge beträgt daher etwa 80 Tonnen.

Verschiebungen der ^{14}C-Verteilung

Aus einer Reihe von Gründen muß jedoch mit merklichen Abweichungen von dem idealisierten Zustande einer völlig gleichförmigen Verteilung des Radiokohlenstoffes innerhalb des Austauschreservoires gerechnet werden. Drei Gründe sind von allgemeiner Bedeutung und experimentell untersucht worden:

1.) Unterschiede im chemischen Verhalten von ^{12}C und ^{14}C (Isotopentrenneffekte).

2.) Merkliche Verzögerungen in der Verteilung des in der Atmosphäre entstehenden Radiokohlenstoffes auf die Komponenten des Reservoires.

3.) Künstliche Zufuhr von ^{14}C-freiem CO_2 durch die Verbrennung von Kohle und Erdöl.

Der geringe Massenunterschied der Kohlenstoff-Isotope ^{12}C und ^{14}C verursacht einen geringfügigen Unterschied in den chemischen Eigenschaften dieser beiden Isotope. Dies zeigt sich in Unterschieden in der thermodynamischen Gleichgewichtsverteilung dieser Isotope auf verschiedene Stoffe und in Unterschieden von Reaktionsgeschwindigkeitskonstanten, wie z. B. in denen, die bei der pflanzlichen Photosynthese eine Rolle spielen. Während die Isotopenverteilungskonstanten für Gasgleichgewichte leicht aus den betreffenden Molekeldaten berechnet werden können, ist man bei den Daten für Lösungen und Festkörper sowie bei kinetischen Effekten auf experimentelle Bestimmungen angewiesen. Am einfachsten und genauesten erhält man über diese Daten durch massenspektroskopische Bestimmung des Isotopes ^{13}C, bzw. des ^{13}C/^{12}C-Verhältnisses Auskunft. Die Schwankungen dieses Verhältnisses sind recht genau halb so groß wie die Isotopentrenneffekte, die für das ^{14}C zu erwarten sind[17].

Durch massenspektroskopische Messung des ^{13}C/^{12}C-Verhältnisses ist es daher möglich, allen Isotopentrenneffekten in der Natur oder im Laboratorium Rechnung zu tragen. Die erreichbare Genauigkeit dieser Messungen ist viel größer, als die der radiometrischen ^{14}C-Bestimmungen. Im Laboratorium der University of Chicago werden Messungen mit einer Genauigkeit von 0,02% ausgeführt.

---

[13] *H. De Vries* u. *G. W. Barendsen*, Appl. scl. Res. *B 5*, 387 [1956].

[14] *R. Ladenburg*, Physic. Rev. *86*, 128 [1952]; s. a. *R. K. Sobermann*, Physic. Rev. *102*, 1399 [1956].

[15] *W. W. Rubey*, Bull. Geol. Soc. Amer. *62*, 1111 [1951]. *H. W. Sverdrup*, *M. W. Johnson* u. *R. H. Fleming*: The Oceans, New York Prentice-Hall Inc. 1942.

[16] *G. E. Hutchinson*: The Earth as a Planet; Herausgeber *G. Kuiper*, Chicago, Univers. Press, Kapitel 8, 1954.

[17] *H. Craig*, J. Geology *62*, 115 [1954].

Die experimentell festgestellten Schwankungen im ^{13}C/^{12}C-Verhältnis der in der Natur vorkommenden Kohlenstoff-Verbindungen erreichen mitunter bis zu 4%. Besonders auffallend ist ein systematischer Unterschied dieses Verhältnisses in pflanzlichen organischen Verbindungen und in Carbonaten. Die Carbonate sind im Mittel um 2,5% reicher an ^{13}C als Holz und andere Pflanzenprodukte. Der ^{14}C-Gehalt von Muschelschalen sollte daher bei gleichem Alter um etwa 5% höher sein als der von Holz.

Dieser Unterschied schien anfangs eine experimentelle Bestätigung zu finden[18]), jedoch zeigte eine genaue Nachprüfung[7,8]), daß dies zumindest bei einem Vergleich von Meeresmuscheln mit Holz nicht zutrifft. Der experimentell gefundene ^{14}C-Gehalt von Muscheln ist innerhalb von Grenzen von etwa 1% der gleiche wie der von Holz, d. h. um etwa 5% niedriger als die Normierung auf gleichem ^{13}C-Gehalt erfordert[19]). Der Befund läßt keine andere Deutung zu als die, daß man dem Carbonat an den Küsten der Meere in der Tat ein „Alter" von etwa 400 Jahren zuzuschreiben hat. Über die Geschwindigkeit des Austausches zwischen der Kohlensäure der Atmosphäre und den in den Meeren gelösten Carbonaten war bis vor kurzem so gut wie nichts bekannt. *E. G. Hutchinson*[16]) stellte fest, daß ein Vergleich mit Meßergebnissen von Modellversuchen ihren Wert bis auf einen Faktor 1000 unbestimmt läßt.

Die Frage ist von besonderem Interesse wegen der Möglichkeit der Beeinflussung des Gesamtklimas der Erde durch Schwankungen des Kohlensäure-Gehaltes der Atmosphäre.

Die erwähnten Radiokohlenstoff-Bestimmungen zeigen nun unmittelbar, daß der Kohlensäure-Austausch zwischen Ozean und Atmosphäre verglichen mit der Zerfallsgeschwindigkeit des ^{14}C verhältnismäßig rasch verlaufen muß. Genauere Aussagen lassen sich auf zwei Wegen herleiten[20, 21]): 1.) Durch die Bestimmung des scheinbaren Alters des Carbonates im Meerwasser und 2.) durch Messung der durch Zufuhr von ^{14}C-freiem CO_2 durch künstliche Verbrennung fossiler Brennstoffe bedingten Abnahme der ^{14}C-Aktivität während der letzten 60 Jahre.

Bezeichnet man mit $\tau_{(\mathrm{Atm})}$ die Zeit in Jahren, die eine CO_2-Molekel im Mittel in der Atmosphäre verbringt, ehe sie im Ozean gelöst wird, und mit $\tau_{(\mathrm{See})}$ die Zeit, die ein Kohlenstoff-Atom als Bestandteil des marinen Reservoirs im Mittel benötigt, bis es als CO_2 an die Luft abgegeben wird, dann ist $\tau_{(\mathrm{Atm})}/\tau_{(\mathrm{See})}$ gleich dem Mengenverhältnis des in der Atmosphäre und im Meere befindlichen Kohlenstoffes. Die in Tabelle 1 angegebenen Daten geben für dieses Verhältnis den Wert von rund $^1/_{60}$. Das Vorhandensein organischer Materie zu Lande und im Meere ändert diese Überlegung nicht wesentlich.

Die für Muschelschalen und Meerestiere und Pflanzen von uns[19]) an drei Proben aus dem Atlantik und von *Rafter*[22]) durch sechs Messungen an marinem Material aus der Umgegend von Neuseeland gefundenen Werte für das scheinbare Alter liegen zwischen 250 und 550 Jahren. Hierbei wurde Isotopentrenneffekten durch massenspektroskopische ^{13}C-Bestimmungen Rechnung getragen. Im Mittel liegt das Alter dieses marinen Materials bei etwa 400 Jahren. Nimmt man an, daß dieser Wert dem durchschnittlichen scheinbaren Alter des Kohlenstoffes des Meeres entspricht, dann ergibt sich eine mittlere Aufenthaltsdauer einer CO_2-Molekel in der Atmosphäre $\tau_{(\mathrm{Atm})} = 7$ Jahre: Dieser Wert stellt eine untere Grenze dar, denn das mittlere Alter marinen Kohlenstoffes dürfte wegen der erforderlichen Durchmischung der Ozeane größer sein als 400 Jahre.

Über die Durchmischungszeiten der Ozeane war bis vor kurzem so gut wie nichts bekannt. Radiokohlenstoff-Bestimmungen von in Tiefseewasser gelöstem Carbonat-Kohlenstoff schienen erst auf das Vorkommen von über 1000 Jahre alten Wassermassen schließen zu lassen. Neuere Bestimmungen machen es wahrscheinlich, daß diese ersten Messungen fehlerhaft waren, und der wahre Unterschied zwischen dem ^{14}C-Alter der Meeresoberfläche und den Tiefen nur wenige hundert Jahre beträgt[23]). Dieser kleinere Wert erscheint auch auf Grund ozeanographischer Überlegungen plausibler[4]).

Die zweite Methode, über diese Fragen Aufschluß zu bekommen, ist gegeben durch die Verfolgung des Einflusses der künstlichen Zufuhr von ^{14}C-freiem CO_2 in die Atmosphäre auf die spezifische ^{14}C-Aktivität atmosphärischen Kohlendioxyds. Von den Anfängen einer mit der zunehmenden Industrialisierung einhergehenden ausgedehnten Kohlenförderung gegen Ende des 19. Jahrhunderts bis zum heutigen Tage sind insgesamt etwa 12% des in der Atmosphäre vorhandenen Kohlendioxyds an die Luft abgegeben worden.

Der britische Meteorologe *Callendar*[24]) glaubte aus einem Vergleich älterer experimenteller Daten mit jüngeren CO_2-Bestimmungen in Luft entnehmen zu können, daß im wesentlichen all dieses CO_2 in der Atmosphäre verblieben ist und diskutiert die Möglichkeit, daß eine solche Zunahme von atmosphärischem CO_2 den beobachteten leichten Anstieg der Temperatur in höheren Breitegraden verursacht haben könnte. Eine neue, statistische Auswertung des gesamten experimentellen Materials durch *Slocum*[25]) führte jedoch zu dem Ergebnis, daß durch direkten Vergleich von CO_2-Analysen aus der Zeit um die Jahrhundertwende mit solchen jüngeren Datums keine Anzeichen für oder gegen eine Zunahme des Kohlendioxydes in der Atmosphäre gewonnen werden können.

Nimmt man an, daß der Austausch von CO_2 zwischen der Atmosphäre und den Ozeanen langsam verläuft, verglichen mit der Zeitspanne von rund 60 Jahren seit dem Beginn der künstlichen CO_2-Zufuhr, dann sollte die spezifische ^{14}C-Aktivität der Atmosphäre seit Ende des 19. Jahrhunderts um etwa 12% abgenommen haben. Verläuft hingegen dieser Austausch rasch, dann sollte praktisch keine Abnahme der ^{14}C-Aktivität stattgefunden haben. Als Material zur Messung der atmosphärischen ^{14}C-Aktivität kann sehr bequem Holz verwendet werden, dessen Jahresringe unmittelbar den Zeitpunkt der organischen Fixierung des Kohlenstoffes während der Lebensdauer eines Baumes ergeben. Mögliche Isotopentrenneffekte im Verlaufe der Photosynthese müssen natürlich durch ^{13}C-Bestimmungen erfaßt und korrigiert werden.

Die wenigen bisher untersuchten Proben von Holz aus dem 19. Jahrhundert und deren Vergleich mit Holzproben der letzten Jahre zeigen nun in der Tat, daß über diesen Zeitraum hin die ^{14}C-Aktivität abgenommen hat, jedoch bedeutend geringer, als der Menge des an die Atmosphäre abgegebenen CO_2 entsprechen würde. An der Ostküste der Vereinigten Staaten wurden für drei Probenpaare Aktivitätsabnahmen von 3 bis 4% gefunden. Für je einen Baum aus Kalifornien, Alaska und Peru war der Effekt jedoch bedeutend geringer und betrug im Mittel etwa 1,5%. Die höheren Werte sind vermutlich auf lokale Erhöhungen des CO_2-Gehaltes der Luft durch die naheliegenden Industrie-Gebiete zurückzuführen.

---

[18]) *J. L. Kulp*, Atomics *4*, 96 [1953].
[19]) *H. E. Suess*, Science [Washington] *122*, 415 [1955].
[20]) *R. Revelle* u. *H. E. Suess*, Tellus, im Druck.
[21]) *J. R. Anderson* u. *E. C. Arnold*, Tellus, im Druck.
[22]) *T. A. Rafter*, New Zealand J. Sci., Techn. *B 37*, 20 [1955].
[23]) *M. Rubin*, priv. Mitteilg.
[24]) *E. S. Callendar*, Quart. J. Royal Meteorol. Soc. *64*, 223 [1938]; Weather *4*, 310 [1949].
[25]) *G. Slocum*, Monthly Weather Rev. Oct. *1955*, S. 225.

Aus diesen Befunden kann nun abermals die Austauschzeit von CO_2 zwischen der Atmosphäre und den Ozeanen berechnet werden, nur ergibt sich in diesem Falle, wenn man wie oben die Biosphäre sowie Mischungszeiten im Ozean vernachlässigt, ein oberer Grenzwert für $\tau_{(Atm)}$ von etwa 7 Jahren.

Eine genauere Rechnung mit Berücksichtigung aller geochemischen Faktoren, soweit sie bekannt sind, zeigt, daß auf Grund der bisher vorliegenden ^{14}C-Bestimmungen an Holz und marinem Material die mittlere Zeit $\tau_{(Atm)}$, die eine CO_2-Molekel in der Atmosphäre verbringt, bevor sie im Meere gelöst wird von der Größenordnung von 10 Jahren ist. Weitere Überlegungen, bei denen auch die Änderung des CO_2-Partialdruckes von Meerwasser mit zunehmender Carbonat-Konzentration zu berücksichtigen sind, zeigen, daß gegenwärtig die Zunahme des CO_2-Gehaltes der Atmosphäre als Folge künstlicher Kohle- und Erdölverbrennung nur wenige Prozente betragen kann. Die Möglichkeit einer größeren Zunahme als eine Folge anderer Ursachen ist jedoch hiermit nicht ausgeschlossen. Für kommende Jahrzehnte muß mit einem beträchtlichen, vielleicht exponentiellen Anstieg des Verbrauches fossiler Brennstoffe gerechnet werden, der dann zu einem bedeutsameren Anstieg des CO_2-Gehaltes der Luft führen könnte[20]).

Einige Ergebnisse der Radiokohlenstoff-Datierungen

Bei der Berechnung des Alters einer Probe aus dem gemessenen ^{14}C-Gehalt können die erwähnten geochemischen Faktoren ohne weiteres berücksichtigt werden. Für Isotopentrenneffekte kann auf Grund von ^{13}C-Bestimmungen korrigiert werden. Zur Vermeidung von Einflüssen der künstlichen Kohleverbrennung verwendet man zur Standardisierung Holz aus dem 19. Jahrhundert. Die so vermiedenen Fehler übersteigen jedoch kaum 200 Jahre. Sie sind für ältere Proben nicht wesentlich.

Der Berechnung liegen jedoch zwei Annahmen zugrunde, die sicherlich nur eine brauchbare Näherung darstellen. Erstens wird angenommen, daß die Höhenstrahlungsintensität über die letzten 50000 Jahre hin konstant geblieben ist. Zweitens wird das Austauschreservoir des Radiokohlenstoffs — im wesentlichen der Carbonat-Gehalt der Meere — als über diesen Zeitraum hin konstant betrachtet.

Die Höhenstrahlintensität wird in hohem Maße durch das Magnetfeld der Erde beeinflußt. In der Tat liegen Anzeichen dafür vor, daß dieses Magnetfeld selbst während der letzten Jahrtausende beträchtlichen Schwankungen unterworfen war. Das ^{14}C-Inventar der Erde stellt jedoch wegen der mittleren Lebensdauer des Radiokohlenstoffes von 8000 Jahren über Zeiträume dieser Größenordnung hin einen Mittelwert dar, der nur durch Schwankungen in der Höhenstrahlung mit vergleichbar großer Zeitkonstante systematischen Änderungen unterworfen ist.

In Bezug auf die Frage der Konstanz des Austauschreservoires des Radiokohlenstoffes mag von Interesse sein, daß das Volumen der Ozeane durch Bildung der Eiskappen an den Polen in Zeiten starker Vereisung um etwa 5% vermindert war[26]). Andererseits ist die Löslichkeit von Calciumcarbonat in Meerwasser bei niedrigeren Temperaturen etwas erhöht. Immerhin muß mit geringen Änderungen des Kohlenstoff-Austauschreservoires von der Größenordnung einiger Prozente während des von der Datierungsmethode umfaßten Zeitraumes gerechnet werden.

Wenn auch die Ergebnisse der Datierungen von Proben bekannten Alters bisher keinerlei systematische Abweichungen erkennen ließen, so besteht doch die Möglichkeit, daß wegen der oben erwähnten Unsicherheiten die durch Radiokohlenstoff-Datierungen gegebene Zeitskala eine gewisse Verzerrung aufweist. Es ist jedoch unwahrscheinlich, daß diese Verzerrung Abweichungen vom wahren Alter von mehr als einigen Prozenten entspricht.

Eiszeit und menschliche Besiedelung

Vielleicht die interessanteste Frage, die durch Radiokohlenstoff-Datierungen weitgehend gelöst worden ist, ist die der absoluten Chronologie der letzten Eiszeit. In Europa haben in den letzten 50 Jahren die Arbeiten zahlreicher Forscher[27]) hierfür das folgende Bild ergeben: Aus Abschätzungen von Erosions- und Sedimentationsgeschwindigkeiten schließt man, daß die letzte Eiszeit, in Europa „Würm“ oder „Warte“ genannt, vor rund 100000 Jahren begonnen habe. Diese Zeit war von mindestens einer milderen Epoche unterbrochen. Man spricht daher von Würm I und Würm II mit einem dazwischen liegenden wärmeren Zeitabschnitt. Der allgemeine Rückzug des Eises begann vor etwa 20000 Jahren. Der Rückzug war mehrmals durch Wiedervorrücken oder Stillstände der Eisfront unterbrochen, deren zeitlicher Ablauf durch die Arbeiten *De Geers*[27]) bekannt ist, die sich auf das Abzählen der Bänderablagerungen (Warven) in den glazialen Binnenseen Skandinaviens stützen. Besonders sind die Klimaschwankungen der Zeit seit dem letzten größeren Kälterückschlag, der jüngeren Dryas, durch diese Arbeiten zeitlich genau festgelegt worden.

In Nordamerika kannte man im wesentlichen vier Moränenzüge, die die letzte Vereisung, dort „Wisconsin“ genannt, zurückgelassen hatte. In Analogie zu den europäischen Verhältnissen war man geneigt, den ältesten dieser Moränenzüge an den Beginn der letzten Eiszeit zu legen, den jüngsten Moränen, den Valders Moränen (Mankato), schrieb man ein Alter von etwa 25000 Jahren zu, das der Zeit knapp vor dem Beginne des allgemeinen Rückzuges des Eises entspricht. Ein Studium der Bänderablagerungen amerikanischer Seen schien eine solche Zuordnung zu rechtfertigen[28]). In Europa ist es schwierig geeignete Proben der dort vorherrschenden Tundra-Vegetation zu finden, die den Stand der Eisfront unmittelbar datieren. In Nordamerika hingegen, wo das Eis viel weiter südlich bis in bewaldete Gegenden vorgerückt war, findet man nicht selten Holzreste von Bäumen die unmittelbar durch das vorrückende Eis zerstört worden waren. Es scheint, daß im Moränenschutt begrabenes Holz in der Regel aus der Zeit unmittelbar vor der Ankunft der Eisfront stammt, weil das Eis und seine Ablagerungen konservierend wirken und Holzreste sonst in wenigen hundert Jahren verschwinden.

Während die wenigen bisher gemessenen Proben aus Europa das vorher gewonnene Bild der späteren Phasen der letzten Eiszeit im Großen und Ganzen in glänzender Weise bestätigen, führten die Radiokohlenstoff-Bestimmungen amerikanischen Materials zu einem äußerst überraschenden Ergebnis. Es zeigte sich, daß der älteste der vier Moränenzüge (Iowa) ein Alter von kaum mehr als 20000 Jahren besitzt. Der folgende, zweite Eisvorstoß der Wisconsin-Periode (Tazewell), führte am weitesten nach Süden und erreichte seine bedeutendste Ausdehnung vor etwa 17500 Jahren. Das Maximum des dritten Vorstoßes (Cary) erfolgte vor rund 14000 Jahren. Der vierte, jüngste Moränenzug entspricht seinem Alter nach ungefähr der jüngeren Dryaszeit Europas, deren Höhepunkt vor etwa 10500 Jahren erreicht war. Ein weiterer Kälterückschlag, der einen Stillstand im Rückzug des Eises in der Gegend von Cochrane (Kanada) zur Folge hatte, scheint vor etwa 7000 Jahren stattgefunden zu haben.

---

[26]) *P. Woldstedt*: Das Eiszeitalter; 1. Bd., Enke Verlag, Stuttgart 1954; *R. F. Flint:* Glacial Geologie, 2. Aufl. New York u. London 1948.

[27]) Lit. bei *F. Zeuner*: Dating the Past, 3. Aufl., London 1952.

[28]) *E. Antevs*, J. Geology *63*, 495 [1955].

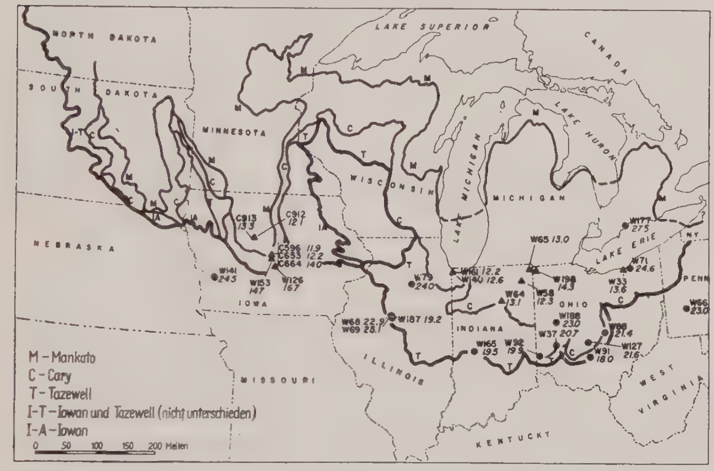
NORTH DAKOTA
SOUTH DAKOTA
MINNESOTA
NEBRASKA
IOWA
WISCONSIN
MICHIGAN
LAKE SUPERIOR
CANADA
LAKE HURON
LAKE MICHIGAN
LAKE ERIE
N.Y.
PENN
OHIO
INDIANA
ILLINOIS
MISSOURI
KENTUCKY
WEST VIRGINIA
M
C
T
I-T
I-A
C913 13.3
C912 12.1
C596 11.9
C653 12.2
C664 14.0
W141 24.5
W153 14.7
W126 16.7
W79 24.0
W161 12.2
W140 12.6
W65 13.0
W177 27.5
W71 24.6
W198 14.3
W33 13.6
W64 13.1
W58 12.3
W188 23.0
W66 23.0
W68 22.9
W69 25.1
W187 19.2
W165 19.5
W92 19.5
W37 20.7
W99 21.4
W127 21.6
W91 18.0
M – Mankato
C – Cary
T – Tazewell
I-T – Iowan und Tazewell (nicht unterschieden)
I-A – Iowan
0 50 100 150 200 Meilen

A745.1

Bild 1
Moränenzüge im mittleren Westen der Vereinigten Staaten. Es sind die Fundorte der Proben (Holz) eingezeichnet (gefüllte Kreise für Proben, die die Ankunft des Eises, Dreiecke für solche, die den Rückzug des Eises datieren), ferner Probenummer (W für Bestimmungen in Washington, C für Bestimmungen in Chicago) und gefundenes Alter in Jahrtausenden (schräge Ziffern). (Nach *R. F. Flint* und *Meyer Rubin*, Science [Washington] *121*, 649 [1955])

Diese Klimaschwankungen scheinen somit mit einer Periode von etwa 3500 Jahren stattgefunden zu haben. Möglicherweise waren die Zeitabschnitte wärmeren Klimas durch je einen weiteren Kälterückschlag unterteilt, so daß man von Klimawechsel mit einer Periode von etwa 1700 Jahren sprechen könnte. Über den Zeitpunkt des Rückzuges des Eises unterrichten Proben aus Ablagerungen in Tümpeln, die durch Toteisblöcke gebildet wurden. In Bild 1 sind derartige Proben als Dreiecke eingezeichnet. Diese kurzperiodischen Schwankungen erscheinen am Ausklang der letzten Eiszeit dem Klimawechsel mit wesentlich größerer Zeitkonstante überlagert. Auch über derartige langsamere Schwankungen sind wir in groben Zügen unterrichtet. Aus dem nördlichen Kanada und Alaska stammende Proben haben entweder ein jüngeres Alter als 7000 Jahre, oder ein Alter von mehr als 35000 Jahren jenseits der Grenzen der Methode ergeben. Unter den Proben hohen Alters fanden sich jedoch auch solche, die zweifellos Ablagerungen der letzten Eiszeit entstammten. Dies deutet darauf hin, daß der Zeitraum, der von amerikanischen Forschern als „Wisconsin" bezeichnet wird, nicht die ganze letzte Eiszeit umfaßt. Es ist naheliegend, den Ursprung dieser Proben in die Zeit eines milderen Klimas zu verlegen, das nach europäischen Beobachtungen den Ablauf der letzten Eiszeit unterbrochen hat.

Ein weiterer Befund, der für eine Unterbrechung der letzten Eiszeit durch eine mildere Periode spricht, ergibt sich aus dem Studium von Tiefseesedimenten. Diese Sedimente ergeben auch die Möglichkeit einer über die Grenzen der ^{14}C-Datierungen hinausreichenden Extrapolation der Zeitskala, wenn man annimmt, daß größere Schwankungen der Sedimentationsgeschwindigkeit nicht stattgefunden haben. Die Methode der Bestimmung von Wassertemperaturen aus dem ^{18}O-Gehalt von Calciumcarbonat nach *Urey*[29]) kann angewendet werden, um Änderungen in der Oberflächentemperatur des Meeres über den Zeitraum der Ablagerung einer Sedimentschicht zu verfolgen. Dies ist von *Emiliani*[30]) für drei Bohrkerne durchgeführt worden. Hierzu wurde der ^{18}O-Gehalt der Schalen von nahe der Meeresoberfläche lebenden Foraminiferen massenspektroskopisch gemessen und daraus die Wassertemperatur als Funktion des Abstandes von der Sedimentoberfläche bestimmt. Durch ^{14}C-Bestimmungen am Carbonat der Schalen wurde sodann die Sedimentationsgeschwindigkeit für die drei Bohrungen bestimmt und so die Temperatur als Funktion der Zeit erhalten. Die Ergebnisse sind in Bild 2 wiedergegeben. Mit der Annahme

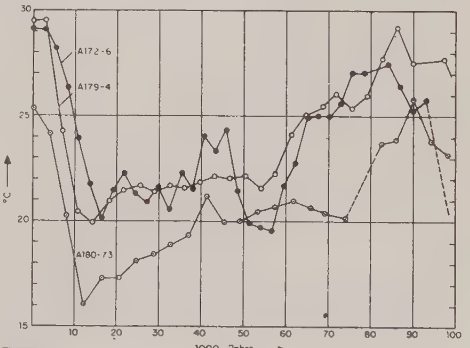

A745.3

Bild 2
Paläo-Temperaturen aus ^{18}O-Messungen der Universität von Chicago an Faraminiferen-Proben (Tiefsee-Bohrkerne) entsprechend dem Alter aus ^{14}C-Messungen an der U. S. Geological Suroey. Nach *H. Suess*, Science [Washington] *123*, 355 [1956], (vgl. Text).

---

29) *S. Epstein* u. Mitarb., Bull. Geol. Soc. Amer. *62*, 417 [1951]; *64*, 1315 [1953].
30) *C. Emiliani*, J. Geology *63*, 538 [1955].

konstanter Sedimentationsgeschwindigkeit findet man, daß die letzte kalte Periode vor rund 70000 Jahren begonnen hat. Vor etwa 40000 bis 50000 Jahren war das Klima etwas wärmer, jedoch kälter als heute. Die drei Meßreihen zeigen deutlich die rasche Erwärmung, die vor rund 15000 Jahren begann und zu dem Klima der Gegenwart führte. Hiernach ist anzunehmen, daß die Unterbrechung der letzten Eiszeit durch milderes Klima etwa vor 40000 bis 50000 Jahren stattfand.

Eine weitere Gruppe von Radiokohlenstoff-Datierungen bezieht sich auf den durch das Abschmelzen des Polareises seit dem Ausklang der letzten Eiszeit hervorgerufenen Anstieg des Meeresspiegels. Die diesbezüglichen, gegenwärtig vorliegenden Ergebnisse sind in Bild 3 dargestellt. Obwohl die Ergebnisse für Proben aus Holland und aus dem Gebiet des Golfs von Mexico auffallend gut übereinstimmen, ist es schwierig, eindeutig zwischen lokalen tektonischen Küstenbewegungen und dem weltweiten Anstieg des Meeres zu unterscheiden. Eine viel größere Zahl von Messungen aus den verschiedensten Teilen der Welt wird nötig sein, ehe der zeitliche Ablauf der postglazialen Hebung des Meeresspiegels in allen Einzelheiten festliegen wird.

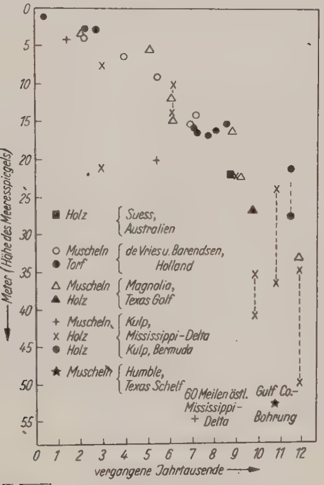

Bild 3

Durch das Schmelzen von Polareis hervorgerufener Anstieg des Meeresspiegels in den letzten 10000 Jahren (nach *Shepart* u. *Suess*, Science [Washington] *123*, 1082 [1956]). Im wesentlichen nach Datierungen von *De Vries* u. *Barendsen* für Proben aus Holland sowie des Magnolia Laboratoriums, Houston, Texas für die Küste des Golfs von Mexiko

Mit dem Ablauf glazialer Klimaperioden eng verknüpft ist die Vorgeschichte des Menschen. Europa war bis in die Würm I folgende gemäßigte Interstadialzeit vom Homo Neandertalensis bewohnt, während der dieser vom Homo Sapiens verdrängt wurde. Nach der durch Radiokohlenstoff-Datierungen gewonnenen Zeitskala geschah dies vor etwa 40000 bis 50000 Jahren. Ein Anzeichen für das Überleben neandertaloider Menschen in Nordafrika bis vor etwa 34000 Jahren bietet die Datierung eines Höhlenwohnplatzes aus der Cyrenaika[31]) (W-85). Dieser Zeit schließt sich in Europa die Periode des Aurignac-Menschen an. Für das Perigordien IV, eine Kulturstufe die dem jüngeren Aurignac zugerechnet wird, ergab eine Datierung rund 24000 Jahre (W-151). Für Holzkohle-Material aus der berühmten Lascaux-Grotte erhielt *Libby* ein Alter von 15500 ± 900 Jahren (C-406). Leider sind die Deutungen dieser wichtigen Messung und wohl auch ihre Genauigkeit unbestimmt. Für das Magdalenien, eine Kulturstufe, die aus dem Aurignacien hervorgegangen sein soll sowie für die Hamburger Stufe, der ein gleiches Alter zugeschrieben wurde, sind etwas jüngere Alterswerte erhalten worden, als erwartet worden war. So haben z. B. Proben von Geweihen aus den von *A. Rust* entdeckten Weiheteichen der Ahrensburger Gegend in Holstein für das Alter der Hamburger Kulturstufe sowohl im Laboratorium der Universität Heidelberg[32]) als auch an der U. S. Geological Survey in Washington[33]) Alter von recht genau 12000 Jahren ergeben. Der Übergang zu mesolitischen Kulturen scheint in Europa während oder bald nach dem Kälterückschlag der jüngeren Dryaszeit, also vor etwa 9000 bis 10000 Jahren vor sich gegangen zu sein. Die Zeitgeschichte der weiteren Entwicklung war seit längerem in groben Zügen bekannt. Zu ihrer Verfeinerung haben Radiokohlenstoff-Datierungen bisher nur in seltenen Fällen beitragen können, teils wegen der verhältnismäßig geringen Zahl gut belegter Proben, teils weil bei jüngeren Daten Fehler von etwa 200 Jahren viel stärker ins Gewicht fallen als bei älteren.

Für Nordamerika ist die Frage, ob es während der letzten Eiszeit dort überhaupt Menschen gegeben hat, noch immer nicht mit Sicherheit beantwortet worden. Zwar gibt es einige Anzeichen dafür, wie z. B. die Datierung von Holzkohle aus einer Feuerstelle bei La Jolla, Californien, die 21500 ± 700 Jahre ergab (W-142), jedoch enthält diese Feuerstelle sonst keinerlei Spuren einer menschlichen Besiedelung. Die ältesten Datierungen, die zweifellos frühen Indianersiedlungen entstammen, ergeben Alterswerte von etwa 11000 Jahren, also etwa der Zeit des der jüngeren Dryaszeit entsprechendem Mankato. Die Besiedelung geschah wohl von Asien her über die Beringstraße. Für die Verfolgung der weiteren Geschichte der Indianerstämme haben bereits heute Radiokohlenstoff-Datierungen wertvolle Dienste geleistet[4]).

Zusammenfassung

Gegenwärtig sind von allen Laboratorien der Welt insgesamt etwa 1000 Bestimmungen natürlichen Radiokohlenstoffs ausgeführt worden, die in einem ungewöhnlich breiten Bereich der Forschung zur Klärung offener Fragen beigetragen haben. Beispiele hierfür wurden besprochen. Der Bereich umfaßt Gebiete der Astronomie, der Physik der Höhenstrahlen, der Geochemie, Metereologie, Geologie, Paleontologie und der Vor- und Frühgeschichte des Menschen. Für diese Gebiete der Naturwissenschaften ist die Entdeckung des natürlichen Radiokohlenstoffs durch *W. F. Libby* wohl eine der bedeutsamsten unseres Atomzeitalters. Die vielen offenen Fragen, die in dem vorstehenden Bericht berührt wurden, zeigen jedoch, daß die Anwendung der Methode heute erst in ihren Anfängen steht. Die weitere Entwicklung wird eine ungewöhnlich enge Zusammenarbeit von Fachleuten der verschiedenen Forschungsgebiete notwendig machen.

Eingegangen am 9. Juli 1956 [A 745]

---

[31]) *C. B. M. McBurney*, *J. C. Trevor* u. *L. H. Wells*, Nature [London] *172*, 889 [1953].

[32]) *O. Münnich*, priv. Mitteilg.

[33]) *M. Rubin* u. *H. E. Suess*, Science [Washington] *123*, 442 [1956].

The Enumeration and Collection of Marine Phytoplankton[1]

By

Robert W. Holmes and **Theodore M. Widrig**[2])

Introduction

Ecologically speaking, we recognize two general types of descriptive phytoplankton investigations—the general survey and the time-area study. Perhaps the more common is the former, usually considered to be essentially synoptic, in which the areal distributions of species and populations, or plant pigments, are described and frequently related to physical, chemical, and biological parameters (see, for instance, BRAARUD, GAARDER, and GRØNTVED, 1953; GRAN, 1929a; or STEEMANN NIELSEN, 1934). Time-area studies concern fluctuations in abundance of species, populations, or pigments, at one or more locations with respect to time. Such fluctuations are frequently correlated with variations in conservative and non-conservative properties of the environment (see, for instance, GAARDER, 1938; GRAN, 1929b; HALLDAL, 1953; HOLMES, 1956; RILEY, 1946; or STEEMANN NIELSEN, 1951). The correlations and conclusions in many such studies have been made by the inspection of numerical data and graphs. To employ such techniques is to assume that the probability of the observed correlation being due to chance is insignificantly small. In many instances this has apparently been true, but uncertainty as to the validity of conclusions will always remain until some objective, quantitative estimate of error can be determined. If the probable-error concept, in one form or another, had been employed, considèrable strength would have been added to the conclusions.

Since comparisons and correlations in such ecological studies frequently involve the abundance of phytoplankton as one parameter, it was decided

---

[1]) Contribution from the Scripps Institution of Oceanography, N.S., No. 869. The paper is published by permission of the Director, U.S. Fish and Wildlife Service.

[2]) Of the Scripps Institution of Oceanography, La Jolla, and the U.S. Fish and Wildlife Service, La Jolla, respectively.

Reproduced, by permission, from the Journal du Conseil, v.XXII, no.1, 1956. pp.21-32.

to employ statistical methods to study the precision of a phytonplankton enumeration technique and to evaluate the adequacy of sampling as it is normally carried out. Certain concepts emerge from these studies which will be of aid in deciding how best to sample marine phytoplankton.

Enumeration

It is not our purpose to discuss the relative merits of various counting techniques; instead, we propose to investigate the precision of one of the most commonly employed techniques—the sedimentation method of Utermöhl (1936). This technique involves the estimation of phytoplankton abundance in an unconcentrated water sample by the enumeration of organisms contained in one or more aliquots of that sample. This is accomplished by pouring aliquots from a well agitated sample into volumetric cylinders, allowing the organisms to settle, and counting them with the aid of the inverted microscope.

The essential problem in evaluating such a method is to determine whether the organisms in the aliquot have been selected at random and are counted without bias (in the statistical section that follows these two sources of error are undifferentiated). Once the degree of contagion ("clumping") is known for a species, it is possible to assign limits to the probable number of that species contained in the original sample. The inquiry was made in

Table 1

	Volume of aliquot (ml.)	Number of aliquots counted	Total number of organisms counted	Average number in each aliquot	Variance s^2	$\left(\frac{s^2}{x}\right)$	Estimated λ^2
Ceratium furca	2	20	226	11·30	6·54	0·58	Negative
– –	10	–	989	49·45	27·00	0·55	–
Ceratium fusus	2	–	106	5·30	3·91	0·74	–
– –	10	–	501	25·05	42·36	1·69	0·028
Ceratium tripos	2	–	1435	71·75	57·78	0·81	Negative
– –	10	–	6501	325·05	243·94	0·75	–
Dinophysis caudata	2	–	280	14·00	23·58	1·68	0·049
– –	10	–	1288	64·40	181·62	2·80	0·028
Peridinium Stenii	2	–	164	8·20	5·75	0·70	Negative
– –	10	–	669	33·45	72·05	2·15	0.035
Prorocentrum micans ..	2	–	2	0·10	0·09	0·95	0·001
– – ..	10	–	13	0·65	0·66	1·01	0·001
Radiolarian sp.	2	–	17	0·85	0·55	0·65	0·001
– –	10	–	75	3·75	3·25	0·87	0·001
Chaetoceros borealis f. *concavicornis*	2	–	10	0·50	0·90	1·79	0.001
– – –	10	–	16	0·80	0·38	0·47	0.001
Nitzschia seriata	2	–	182	9·10	43·57	4·79	0·62–0·72
– –	10	–	591	29·55	194·94	5·07	0·19
Thalassiosira gravida ..	2	–	22	1·10	4·73	4·30	6·7–8·9
– – ..	10	–	27	1·35	6·87	5·09	10–11

the following manner. A phytoplankton sample was collected with a No. 20-mesh silk net, preserved, diluted to 1500 ml., and placed in a 2-litre boiling flask. After thorough agitation of the flask, samples were poured into a 2 ml. and a 10 ml. volumetric counting cylinder, allowed to settle, and counted¹). This was repeated until a total of twenty 2 ml. and 10 ml. aliquots had been counted (see Table 4). Of the species present in the aliquots only ten were chosen for enumeration—six dinoflagellates (*Ceratium furca*, *C. fusus*, *C. tripos*, *Dinophysis caudata*, *Peridinium Stenii*, and *Prorocentrum micans*), a radiolarian (which could not be identified by species but which belongs to the sub-order Acantharia), and three diatoms (*Chaetoceros borealis* f. *concavicornis*, *Nitzschia seriata*, and *Thalassiosira gravida*).

The hypothesis that the individual organisms were selected at random (and counted without bias) was considered not false, with a probability of 0·95 that the decisions were correct, if the value of the quantity $\frac{s^2}{\bar{x}}$ fell at or below 1·6 for the 20 samples²). An examination of the value of this quantity (Table 1) reveals that the organisms differed from one another in their degree of contagion in the cylinders; *D. caudata*, *N. seriata*, and *T. gravida* required the rejection of our hypothesis in both the 2 and 10 ml. aliquots; *C. fusus*, *P. Stenii*, and *Ch. borealis* f. *concavicornis* required that our hypothesis be rejected in either the 2 ml. or 10 ml. aliquots; and finally *C. furca*, *C. tripos*, *P. micans*, and the radiolarian did not require the rejection of the hypothesis.

In those instances in which our hypothesis is not in doubt, it becomes a simple matter to assign upper and lower limits to the probable number contained in the original sample from the number counted in the aliquot. We presume that the organisms in the aliquots are distributed in the Binomial frequency function. To facilitate such determinations, two graphs have been prepared (Figs. 1 and 2) from data based on the work of W. L. Stevens and presented by Fisher and Yates (1949)³). Upper and lower expectation levels can also be determined for organisms that required the rejection of our hypothesis in both aliquots. These species occurred both as single cells

---

¹) After counting, the material contained in the cylinders was discarded, in as much as it could not be returned quantitatively to the boiling flask.

²) In this paper the following symbols are defined as follows:—

s^2 is the estimated variance,
σ_x^2, the limit of s_x^2 as N goes to the population size,
x, the sample count,
$\bar{x}$, the arithmetic mean,
N, the number of samples.

The expected value of s^2, if the hypothesis were true, was taken as $\bar{x}$. The ratio s^2/x should then be distributed as $\frac{\varkappa^2}{N-1}$, with N-1 degrees of freedom; $\varkappa^2/19$ for 19 degrees of freedom is approximately 1·6.

³) The curves in these graphs give the upper and lower numbers that would be contained in the sample for a given aliquot count for 95 % confidence. These limits are appropriate when the volume of the organisms contained in the aliquot is very small in proportion to the total volume of the sample—which is the case when unconcentrated water samples of moderate size (greater than about 100 ml.) are used. The limits are conservative if this proportion is not small.

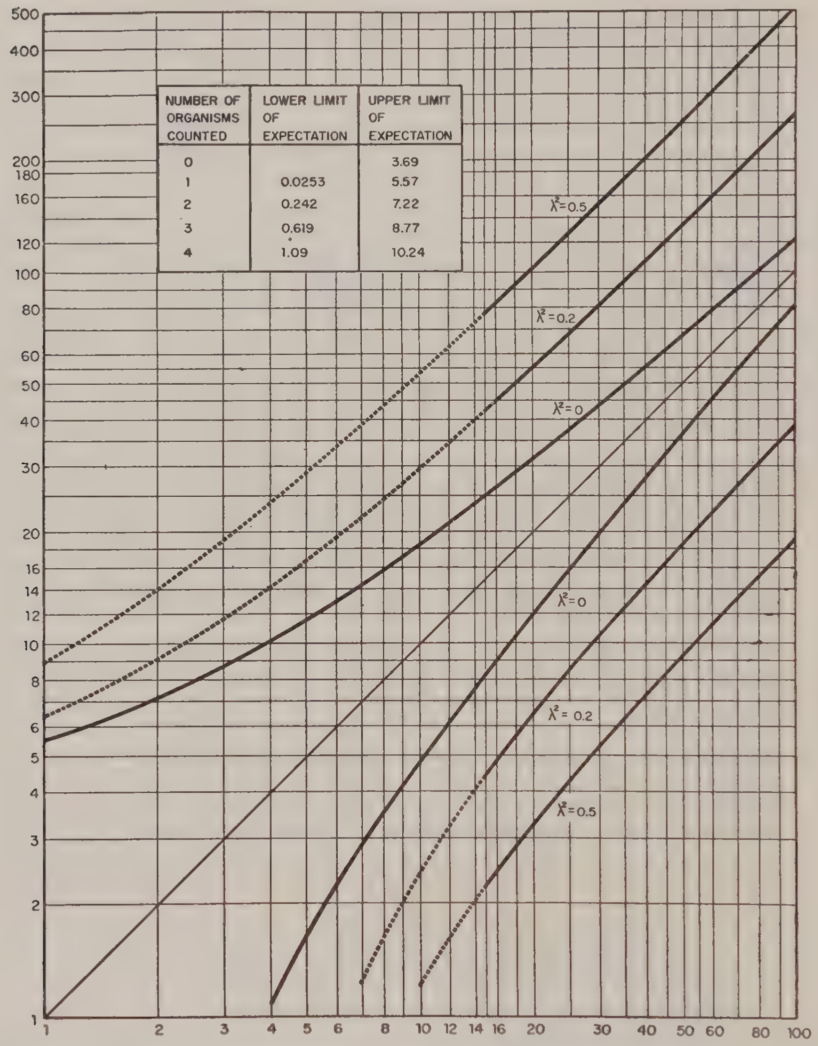

NUMBER OF ORGANISMS COUNTED	LOWER LIMIT OF EXPECTATION	UPPER LIMIT OF EXPECTATION
0		3.69
1	0.0253	5.57
2	0.242	7.22
3	0.619	8.77
4	1.09	10.24

Figure 1. The limits of expectation for Binomial and Poisson distributions at a 95% level of confidence for 3 degrees of contagion ($\lambda^2 = 0$, $\lambda^2 = 0{\cdot}2$, $\lambda^2 = 0{\cdot}5$). N from 0 to 100.

Figure 2. The limits of expectation for Binomial and Poisson distributions at a 95% level of confidence for 3 degrees of contagion ($\lambda^2 = 0$, $\lambda^2 = 0{\cdot}2$, $\lambda^2 = 0{\cdot}5$). N from 100 to 10,000.

→

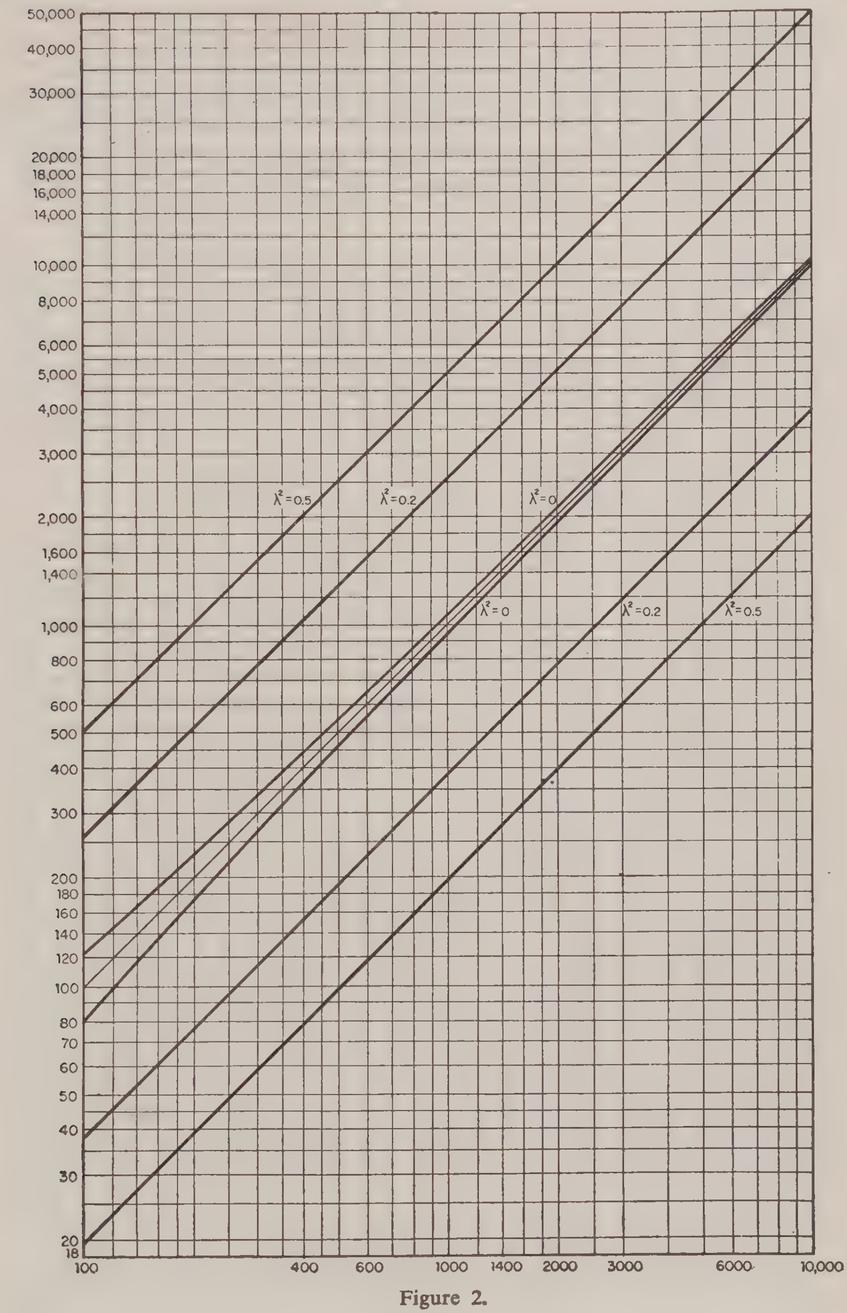
50,000
40,000
30,000
20,000
18,000
16,000
14,000
10,000
8,000
6,000
5,000
4,000
3,000
2,000
1,600
1,400
1,000
800
600
500
400
300
200
180
160
140
120
100
80
70
60
50
40
30
20
18
100
400
600
1000
1400
2000
3000
6000
10,000
λ^2=0.5
λ^2=0.2
λ^2=0
λ^2=0
λ^2=0.2
λ^2=0.5

Figure 2.

3

and in groups of two or more cells singly and in pairs in the case of *D. caudata*, and singly, and in chains of two or more individuals in *N. seriata* and *T. gravida*. This means that our hypothesis needs to be rejected because of their high degree of contagion in the original sample, even though the sample was thoroughly shaken before aliquots were taken. Such clumped organisms, under some general assumptions, can be expected to follow the Negative Binomial frequency function. The degree of contagion will be described by the coefficient

λ^2, in $\sigma_x^2 = x + \lambda^2 \bar{x}^2$, or by k, in $\sigma_{\bar{x}}^2 = x + \frac{\bar{x}^2}{k}$: the greater the degree of contagion the higher the value of λ^2. Methods for the calculation of k are given by Anscombe (1949), and Bliss and Fisher (1953). The approximate value of λ^2 is given in Table 1 for each species in each of the two aliquot volumes. Unfortunately the efficiency of the estimation of λ^2 varied, because three methods of calculation were employed, the choice depending upon the number of organisms counted and the value of λ^2; the tendency toward contagion in one aliquot but not in the other must be ascribed to chance. In actual practice it is probably reasonable to assume the Binomial distribution when $\frac{s^2}{\bar{x}}$ somewhat exceeds 1·6, providing λ^2 remains low—the estimated precision will be only slightly too great. In this paper a value of λ^2 equal to or less than 0·05 is considered the critical point of departure from the Binomial frequency function. However, when the degree of contagion is marked (greater than 0·05, by definition), it should not be ignored. In Figures 1 and 2 limits of the expectation for values of λ^2 of 0·2 and 0·5 are given[1]). Regardless of the number counted in the aliquots, these curves reveal the difficulty of obtaining accurate estimates of sample abundance with these clumping species, even with λ^2 as low as 0·05. A truly precise estimate of such clumping species can be obtained only by counting all such organisms in the entire sample. With different species of the chain-forming type, the degree of contagion can be expected to vary. This variation reflects the constancy of the number of cells within each chain. Thus, if the numbers vary only slightly from chain to chain, as was the case with *D. caudata*, then the degree of contagion is less than if the numbers per chain vary considerably, as was the case with *T. gravida*. *N. seriata* in this instance fell in between these two extremes. This reasoning implies that we believe the chains themselves to be sub-sampled randomly. We believe this to be the case even though the evidence is indirect. Prof. J. Neyman has pointed out (personal communication) that there is a very good possibility that this is indeed the case. It should be pointed out that a summation of the number of occurrences of a few or of many species in one or more aliquots of a sample does not yield a very precise estimate of

---

[1]) The limits were calculated with the following expression (after Anscombe, 1949):—

$$\left[\text{antilog}_{10}\left[\log_{10}\left(\text{count} + \frac{1}{2\lambda^2}\right) \pm 2\sqrt{0{\cdot}1886 \text{ trigamma}\left(\frac{1}{\lambda^2}\right)}\right]\right] - \frac{1}{2\lambda^2}$$

the total abundance of such species in the sample if the proportion and/or abundance of clumping species is large.

Most marine phytoplankton species are not chain-forming, but unfortunately many important genera and species do exhibit the chain-forming habit (for instance, *Chaetoceros*, *Rhizosolenia*, *Thalassiosira*, *Nitzschia*, etc.). Thus the estimation of sample abundance may or may not be difficult with the UTERMÖHL technique, the degree of difficulty depending upon the composition of the sample.

In this study all but two of the species investigated were considered to be randomly sampled, even though two of these showed slight contagion[1]). In addition to providing useful information about limits of expectation for aliquot counts, Figures 1 and 2 also show that it is advisable to count, if possible, at least between 15 and 30 representatives of any of the non-clumping species, as the percentage error of the estimate increases rapidly as the count falls below this region. This is not necessarily the case with clumping species (see Figs. 1 and 2).

The Comparison of Samples from Different Areas

Once we are able to determine upper and lower limits of expectation of a count, we can decide objectively when differences exist between samples. *Such differences are appropriate only to the sample, however, and if we wish to consider our sample as representative of an area of the sea or any volume larger than the sample volume, the situation is quite different.* In considering sample attributes to be areal attributes, we must consider additionally how well one or more samples characterizes the larger region.

This problem was approached in a manner similar to that employed in the enumeration section. It was deemed necessary to determine, first, whether or not the phytoplankton are generally distributed according to the Binomial frequency function or are contagious. Once this is known, it is possible to estimate the degree of contagion, if any, and under some general assumptions determine how great the differences between samples need be before they can be considered significant.

Data from two different sources have been employed in this particular study. In the first example the phytoplankton samples were collected in the Channel Island area off southern California by vessels and personnel of the California Co-operative Oceanic Fisheries Investigations during the first five months of 1953. The samples were collected at approximately bi-monthly intervals in Nansen bottles at 10 m. depth at four stations roughly 20 miles apart lying along a N.E.–S.W. line approximately midway between Santa Cruz and San Nicolas Islands. Of the species present in this material, several were arbitrarily selected for study (see Table 2); of these, *Pontosphaera Huxleyi* and *Nitzschia seriata* and the composite group Gymnodiniaceae were thought to be ubiquitous. The value of λ^2 is given for all the species,

---

[1]) In the material employed in this study it so happened that *Ch. borealis* f. *concavicornis* occurred only as individuals and in pairs. This is surprising and is not generally the case with this chain-forming species.

Table 2

	Σx	Zeros	$\bar{x}$	s^2	$\frac{s^2}{\bar{x}}$	Estimated λ^2
Exuviaella baltica	55	9	2·037	10·96	5·380	1·0–1·1
Gymnodiaceae	335	0	12·407	86·37	6·961	·357–·435
Pontosphaera Huxleyi	1433	0	53·074	2221·14	41·850	·625–·715
Nitzschia seriata	893	2	33·07	2171·92	65·68	1·67–2·5
Pennate diatom	66	10	2·444	16·41	6·71	1·6

N = 27

but for only two (*Pontosphaera Huxleyi* and the composite group, Gymnodiniaceae) were the limits of expectation calculated, since these alone satisfied ANSCOMBE's (1949) conditions (a mean greater than 15 and λ^2 between 0·2 and 0·5). It should be remembered that the value of λ^2 is an estimate of the total degree of contagion—both that in the aliquot and that within the sea. We believe that in the case of *Exuviaella baltica*, the Gymnodiniaceae *Pontosphaera Huxleyi*, and the pennate diatom the aliquots were randomly chosen, since they are not chain-forming organisms (see p. 27), and therefore that the value for these is truly an estimate of the degree of contagion that they manifest in the sea. *Nitzschia seriata*, on the other hand, is not randomly sub-sampled in the procedure for taking aliquots (see p. 23) and the value for λ^2 is difficult to interpret. As expected, the degree of contagion is higher when the effects of taking aliquots and the distribution in the sea are combined than when only the contagion exhibited in taking aliquots is considered. However, the actual amount of contagion due to distribution in the sea was not evaluated; it is certainly lower than 1·67–2·5.

An inspection of the values of λ^2 (Table 2) for the different groups leaves little doubt that under the conditions of the test, the organisms were not distributed at random. If they followed the Negative Binomial frequency function, the difference in precision of sample counts, which depends on the degree of contagion, can be seen from a glance at Figures 1 and 2. While we cannot at present give the limits of expectation for a value of λ^2 greater than 0·5 there is no doubt that they are much more extreme than those given for $\lambda^2 = 0·5$ (Figures 1 and 2). Under the conditions of this test, even with cosmopolitan species, the differences in abundance that are required for significance, when a single sample from each area serves as the basis for comparison, are so great that only the crudest comparisons are possible.

In the second example we have employed some of the results of a study made by HASLE (1954) in Oslo Fjord. In this instance the methods of enumeration were identical with ours; only the area and sampling plan were different. HASLE collected four surface water samples at each of six stations during the same day in the middle of that portion of the fjord lying westward of and between Moss and Fredrikstad. Two samples were taken 25 m. apart 100 m. to the west of the fjord centre and 25 m. apart 100 m. to the east of the centre of the fjord. This sampling plan was repeated six times at 5 Km. intervals along the major axis of the fjord. Thus, in all, 30 samples were collected. The results of analysis of these data are presented in Table 3.

Table 3

	Σx	$\bar{x}$	s^2	Estimated λ^2
Ceratium furca	1828	76·17	1156·6	0·19
Ceratium fusus	516	21·50	209·6	0·41
Dinophysis acuta	1406	58·58	955·4	0·26
Dinophysis borealis	787	32·79	446·8	0·38
Goniaulax polyedra	1574	65·58	1543·2	0·34
Prorocentrum micans	15596	649·83	151157·8	0·32

When compared with the previous example (see Table 2), the results of this analysis reveal a lower and generally more consistent degree of contagion. None the less, contagion still exists. Unfortunately the comparison between these two sets of data cannot be rigorous. However, these data do illustrate the fact that contagion exists in two differing sets of circumstances. The Oslo Fjord data also show that the clumps are small and probably closely spaced.

These data pose many problems, some of which are under study. For the present we merely wish to indicate that contagious distributions are probably quite common in the sea, and to examine the consequences of such distributions with respect to the comparison of samples and the design of sampling programmes.

These data reveal that tests of comparisons between phytoplankton and environmental attributes, or between populations, should be made with the transformed plankton abundance measure, i. e., $\log_{10} (n + \frac{1}{2}k)$. This transformation changes the sampling distributions of organisms in the Negative Binomial into nearly normal distributions. While the tests must be made with reference to the transformed data, conclusions are more intuitively meaningful if the raw data equivalents of the transformed means, variances, and confidence limits are also stated. For purely descriptive purposes, only the re-transformed statistics are necessary. Even though the re-transformed means, for example, are different from the raw data means, the former have properties that make them more representative of the populations than the latter. Again, the confidence limits in terms of the re-transformed data are not equidistant from the means; none the less they accurately describe a region within which the true mean should be expected to fall.

The recognition of contagion along with some idea of its degree has an obvious implication; with only a single sample in an area one cannot describe a population very accurately, either with respect to composition or abundance. Similarly, for a difference between two areas to be significant it often needs to be based upon the examination of more than just two samples. Thus, if we wish to characterize an area, we must take more than one sample at random from within that area. In general, the precision of a population estimate increases in proportion to the square root of the number of samples; an estimate in an area would be 4 times better if we used 16 randomly spaced samples. The limits of expectation decrease for a given degree of contagion when more than one sample is counted; in the above example, the limits of expectation are decreased by $\frac{1}{4}$ of that given for a single estimate for the same value of λ^2. Fortunately for the investigator,

Table 4

Number of individuals counted in the 2 ml. aliquots

Aliquot No.	1	2	3	4	5	6	7	8	9	10	11	12	13	14	15	16	17	18	19	20
Genus and species																				
Ceratium furca	16	13	9	8	9	10	8	10	11	10	8	14	12	10	10	14	16	13	11	14
Ceratium fusus	7	6	8	1	6	7	7	4	3	6	3	6	2	6	8	7	6	4	5	4
Ceratium tripos	72	72	75	66	55	74	66	74	70	70	82	77	63	62	64	75	77	74	88	79
Dinophysis caudata	10	12	19	15	8	16	12	22	14	12	19	11	12	3	9	14	18	14	23	17
Peridinium Stenii	15	7	10	9	9	6	8	8	6	13	6	7	10	7	7	6	7	8	6	9
Prorocentrum micans	1	0	0	0	0	0	0	0	0	0	1	0	0	0	0	0	0	0	0	0
Radiolarian	1	1	1	2	1	3	0	0	0	0	1	1	0	1	1	0	1	1	1	1
Chaetoceros borealis f. *concavicornis*	0	0	4	0	0	0	0	1	0	0	0	0	1	1	0	1	1	1	0	0
Nitzschia seriata	12	12	15	9	6	5	10	12	26	13	14	0	0	18	1	3	11	2	7	6
Thalassiosira gravida	0	3	0	0	2	0	4	0	0	0	0	0	0	7	0	0	0	0	6	0

Number of individuals counted in the 10 ml. aliquots

Aliquot No.	1	2	3	4	5	6	7	8	9	10	11	12	13	14	15	16	17	18	19	20
Genus and species																				
Ceratium furca	52	57	48	49	52	45	53	49	45	45	41	52	48	58	51	40	40	42	56	53
Ceratium fusus	35	26	19	20	37	21	30	22	27	15	32	27	29	28	23	15	28	13	28	26
Ceratium tripos	300	333	312	345	343	339	336	332	336	337	329	330	326	305	347	326	301	304	313	307
Dinophysis caudata	53	61	54	73	72	69	57	64	66	62	69	54	99	48	63	54	78	91	50	51
Peridinium Stenii	33	37	39	34	35	29	30	27	34	43	41	59	31	19	27	36	37	28	25	25
Prorocentrum micans	0	0	1	0	0	1	0	1	2	1	2	1	0	0	0	0	1	0	1	1
Radiolarian	5	2	4	0	3	3	6	4	3	4	5	4	4	3	7	2	3	1	5	7
Chaetoceros borealis f. *concavicornis*	0	0	2	1	1	1	1	1	2	1	0	1	0	1	0	0	1	1	1	1
Nitzschia seriata	9	30	21	33	32	37	37	25	48	47	36	37	55	21	27	18	8	21	27	22
Thalassiosira gravida	0	0	0	0	5	0	0	0	5	0	0	0	0	0	8	0	7	0	0	2

the enumeration of additional samples need not take more time; the samples can be combined and counted as one, and the precision of the estimate still increases with the number of samples. More of the ship's time would be required of course for the additional collections. An integrating sampler¹) designed to be towed behind a vessel would resolve, to a great extent, the demand for extra time. The depth sampled by such a sampler need not be restricted to the surface; by the use of the cable depressor (U.S. Pat. No. 168999) depths down to about 50 m. can be conveniently sampled with the vessel travelling at a speed of about 8 knots.

Summary and Conclusions

1. The precision with which marine phytoplankton abundance can be estimated in a sample by the UTERMÖHL sedimentation method was investigated. In general, aliquot parts of non-chain-forming species and species which occur as individuals, or together as pairs of individuals, are selected at random from the sample by the procedure described and are counted without bias. The degree of precision of the estimate of sample abundance is a function of the number of organisms counted in the aliquot. It is suggested that a minimum of 15–30 specimens of any one organism be counted if possible. The individuals in the chains of chain-forming species, on the other hand, are not selected at random when aliquots are taken, and while the accuracy of the estimate also increases with the number of organisms counted, it does so at a much slower rate. The best estimate of the abundance of such species can only be obtained by counting all the individuals in the entire sample.
2. A method is used which permits the calculation of the limits of expectation for an aliquot count with varying degrees of contagion. A graph is also presented which facilitates such determinations, once the degree of contagion is known.
3. The distribution in nature of a few species of phytoplankton was investigated. These species were found not to be distributed at random. Such inhomogeneity makes it unrealistic to consider sample attributes as precise estimates of areal attributes. If we desire to characterize an area accurately with respect to phytoplankton content and abundance, and then to compare this area with another, more than a single sample

---

¹) An integrating sampler, designed to work under these conditions, has been designed and built at the Scripps Institution of Oceanography with financial aid from the Bureau of Ships (Contract NObsr-43356, NE-120221-6). (See Progress Report on Oceanographic Instrumentation, April-June 1953, University of California, Scripps Institution of Oceanography, August 15, 1953.) Several field trials have been made and the instrument has apparently operated satisfactorily, although statistical studies designed to test its efficiency have not been completed.

As the device moves through the water a propeller-driven pump removes a charge of distilled water from behind the free-moving piston and sea water enters through a narrow orifice in the instrument's head. The piston's rate of travel is determined by the sampler's rate of travel through the water. Since an infinite number of samples are collected, the sample is fully representative, and yields a good estimate of the average condition along the line traversed.

from each area must be employed. Fortunately for the investigator, the enumeration of additional samples need not occupy additional time, since the samples may be quantitatively combined with one another before enumeration, or, alternatively, some type of integrated sample might be collected while the vessel is under way.

Bibliography

ANSCOMBE, F. J., 1949. "The Statistical Analysis of Insect Counts Based on the Negative Binomial Distribution". Biometrics, **5**, pp. 165–173.

BLISS, C. I., and FISHER, R. A., 1953. "Fitting the Negative Binomial Distribution to Biological Data." Biometrics, **9**, 2, pp. 176–200.

BRAARUD, T., GAARDER, K. R., and GRØNTVED, Jul., 1953. "The phytoplankton of the North Sea and adjacent waters in May 1948." Cons. Perm. Internat. Explor. Mer, Rapp. et Proc.-Verb., **133**, pp. 1–87.

FISHER, R. A., and YATES, F., 1949. "Statistical Tables for Biological, Agricultural, and Medical Research." Hafner Publ. Co., New York. 112 pp.

GAARDER, K. R., 1938. "Phytoplankton studies from Tromsø district 1930–31." Tromsø Mus. Årshft., Naturhist. Avd. 11, **55**, 1, pp. 1–159.

GRAN, H. H., 1929a. "Quantitative plankton investigations carried out during the expedition with the 'Michael Sars', July–September 1924". Cons. Internat. Explor. Mer, Rapp. et Proc.-Verb., **56**, 5, pp. 1–49.

GRAN, H. H., 1929b. "Investigation of the production of plankton outside the Romsdalsfjord 1926–1927". Cons. Internat. Explor. Mer, Rapp. et Proc.-Verb , **56**, 6, pp. 5–110.

HALLDAL, Per, 1953. "Phytoplankton investigations from weather ship M in the Norwegian Sea, 1948–49." Norske Vidensk. Akad., Hvalråd. Skr., 38, pp. 1–91.

HASLE, Grethe R., 1954. "The reliability of single observations in phytoplankton surveys". Nytt Mag. Bot., 2, pp. 121 [illegible] 6.

HOLMES, R. W., 1956. "The annual cycle of phytoplankton in the Labrador Sea, 1950–51." Bull. Bingham Oceanogr. Coll., **16**, Art. 1, pp. 1–74.

RILEY, G. A., 1946. "Factors controlling phytoplankton populations on Georges Bank". J. Mar. Res., **6**, 1, pp. 54–73.

STEEMANN NIELSEN, E., 1934. "Untersuchungen über die Verbreitung, Biologie und Variation der Ceratien im südlichen Stillen Ozean". Dana-Rep., **4**, pp. 1–67.

STEEMANN NIELSEN, E., 1951. "The marine vegetation of the Isefjord. A study on ecology and production". Medd. Komm. Danmarks Fisk.- og Havunders,, Ser. Plankton, **5**, **4**, pp. 1–114.

UTERMÖHL, H. "Quantitative Methoden zur Untersuchung des Nannoplanktons". Abderheldens Handbuch der Arbeitsmethoden, Abt. IX, Tl. 2/11, pp. 1879–1937.

(*Reprinted from Nature, Vol.* 178, *pp.* 497–498, *Sept.* 1, 1956)
Reproduced by Permission

Fluorescent, Benthic, Pacific Coast Coelenterates*

ORANGE fluorescing pigments have been studied extensively in red algae[1,2], where the fluorescence becomes apparent in the moribund plant ; but such pigments would appear to be rare in the animal kingdom (see Klüver[3] for evidence of a red-fluorescing pigment in mammals). At depths greater than 10 m. where sunlight becomes deficient in the longer orange and red wave-lengths, divers have sometimes observed brilliantly luminous orange and red animals. Marden[4] noted the phenomenon while photographing a large unidentified anemone in the Red Sea at 20 m., and suggested the animal might have a fluorescent pigment. Our investigations show that certain animals do indeed possess the ability to fluoresce.

During many hours of diving in Californian and Mexican waters, we have found three fluorescent forms, all coelenterates belonging to the sub-class Zoantharia : *Corynactis californicus*, order Actinaria ; *Balanophyllia elegans*, order Madreporaria ; *Cerianthus* sp., order Ceriantharia. The anemone observed by Marden in the Red Sea was an actinarian. *Corynactis* is an aggregating form, while the others are solitary. Only occasional specimens of *Cerianthus* and *Balanophyllia* fluoresce ; but entire small colonies of *Corynactis* (presumably derived asexually from the same individual) may possess the ability, although nearby colonies may fail in this respect. The situation seems reminiscent of pigmentation in the anemone *Metridium*, studied by Fox and Pantin[5], where colour can vary widely from specimen to specimen, yet exhibit constancy in a given individual and is presumably under genetic control. Environment might influence fluorescence, however, if a dietary pigment precursor is needed. It is not known if the intensity of fluorescence under natural conditions changes during the life of an individual ; but the amount of fluorescent coloration in specimens of *Balanophyllia* and *Corynactis* kept for two months in our aquarium has not changed appreciably.

Whole specimens of *Balanophyllia* and *Corynactis*, as well as comminuted tissues, were subjected to various physical and chemical tests. Most of the specimens used exhibited a striking orange or red coloration at the time of collection from depths of 20 m. or more. Fresh tissues examined microscopically (× 500) gave no sign of symbiotic algae. Animals exhibited no luminescence when observed in a darkroom. When exposed, however, to well-filtered ultra-violet, violet, blue or green light, the luminous colour observed at the time of collection reappeared. Orange and red light did not excite the fluorescence. The two species, as well as individuals of the same species, differed somewhat in the colours of emitted light ; but this could perhaps be caused by variations in concentration of other non-fluorescent body pigments, as well as by differences in the fluorescent pigments themselves. The intensity of emitted light varied directly with the intensity of the exciting light. Specimens that did not exhibit colour on the ocean floor did not fluoresce in the laboratory.

---

* Contribution from the University of California, Scripps Institution of Oceanography, New Series, No. 870.

Whole or comminuted animals did not yield any orange fluorescent pigment to either acetone or ethanol. Intact specimens of *Corynactis* kept under acetone for two months have retained their fluorescence apparently undiminished, although they yielded considerable amounts of an orange-coloured pigment, probably carotenoid in nature. Boiling water irreversibly quenches the fluorescence in whole animals after one or two minutes, leaving a dull orangish specimen in the test tubes. The pigment, therefore, is apparently heat-labile, but is distinguished from the algal fluorescent pigment, phycoerythrin, by the stability of the fluorescence to acetone.

Further work is in progress in an attempt to isolate and characterize the fluorescent pigments, to determine their emission spectra, and to study their distribution in the animal kingdom.

This work was carried out during the tenure by one of us (W. J. N.) of a post-doctoral fellowship in marine biology. Grateful acknowledgment is made to Prof. Denis L. Fox, Prof. Carl L. Hubbs, Dr. Francis T. Haxo, and to Messrs. J. Stewart, H. Scotten and R. Ghelardi for advice and assistance. We are indebted to the Division of Marine Botany for the loan of equipment to produce monochromatic light.

C. LIMBAUGH
W. J. NORTH

Scripps Institution of Oceanography,
University of California,
La Jolla, California.

---

[1] Lemburg, R., and Legge, J. W., "Hematin Compounds and Bile Pigments" (Interscience, 1949).

[2] O'hEocha, C., Ph.D. thesis, University of California, 1955.

[3] Klüver, H., *Science*, **99**, 482 (1944).

[4] Marden, L., *Nat. Geog. Mag.*, **109**, 162 (1956).

[5] Fox, D. L., and Pantin, C. F. A., *Phil. Trans. Roy. Soc.*, B, **230**, 415 (1941).

Printed in Great Britain by Fisher, Knight & Co., Ltd., St. Albans.

Reprinted from Archives of Biochemistry and Biophysics, Volume 64, No. 2, October, 1956
Academic Press Inc. Reproduced by Permission *Printed in U.S.A.*

Glucosamine Degradation by *Escherichia coli*. I. Observations with Resting Cells and Dry-Cell Preparations

Jack B. Wolfe, Richard Y. Morita and Henry I. Nakada

ARCHIVES OF BIOCHEMISTRY AND BIOPHYSICS **64**, 480–488 (1956)

Glucosamine Degradation by *Escherichia coli*. I. Observations with Resting Cells and Dry-Cell Preparations

Jack B. Wolfe,[2] Richard Y. Morita[3] and Henry I. Nakada

From the Scripps Clinic and Research Foundation, La Jolla; and the Scripps Institution of Oceanography (Contribution New Series No. 871), University of California, La Jolla, California

Received March 19, 1956

Introduction

The metabolism of glucosamine and its acetyl derivative by microorganisms has been observed by many investigators. However, little is known about the pathway of degradation of this amino sugar. Lutwak-Mann (1) reported that washed suspensions of *Escherichia coli*, *Streptococcus faecalis*, and *Proteus vulgaris* decomposed glucosamine with the formation of ammonia and other products. During this decomposition of glucosamine it was noted that oxygen consumption occurred prior to the detection of ammonia and that the quantity of ammonia produced was less than the amount of glucosamine disappearing. These results indicated to Lutwak-Mann that amino sugars are first converted by oxidation into an unknown product which then undergoes deamination. Rosenberg (2) investigating the effects of imidazole buffer and sodium azide on glucosamine degradation considered his results to indicate two possible aerobic pathways for glucosamine oxidation. This author proposed that a phosphorylated compound common to the normal carbohydrate metabolic pathway was involved in one of the two pathways. Oka and Murachi (3), using washed suspensions of *E. coli*, found that inhibitors of terminal respiration such as cyanide and arsenate strongly

---

[1] This investigation was supported in part by research grant #291 (C2) from the Division of Research Grants and Fellowships of the National Institutes of Health, U. S. Public Health Service.

[2] Charles Willard Stimson Postdoctoral Fellow in Biochemistry.

[3] Present address: Department of Bacteriology, University of Houston, Houston, Texas.

(690)

depressed glucosamine oxidation but not ammonia formation from this amino sugar. Rogers (4), studying the breakdown of *N*-acetylglucosamine by various strains of streptococci, found that metabolic inhibitors that inhibit the formation of lactate also inhibited the deamination and the disappearance of *N*-acetylglucosamine.

The involvement of phosphorylated intermediates in the degradation of glucosamine was first suggested by the experiments of Harpur and Quastel (5). These workers found that brain extracts phosphorylated glucosamine in the presence of adenosine triphosphate. The participation of phosphorylated hexoses in the biosynthesis of glucosamine has also been reported by Leloir and Cardini (6). Recently Soodak (7) reported that *N*-acetylglucosamine degradation by purified enzyme preparations from *E. coli* resulted in the formation of fructose 6-PO_4, glucose 6-PO_4, and glucosamine 6-PO_4. This author suggests that fructose 6-PO_4 is the immediate product of glucosamine 6-PO_4 deamination since fructose 6-PO_4 formation which accounted for 50% of the *N*-acetylglucosamine disappearing was accompanied by a corresponding amount of ammonia.

In the present investigation an attempt was made to confirm and extend some of the earlier work. This study was concerned with the degradation of radioactive glucosamine and normal glucosamine 6-PO_4 by resting cells and dry cell preparations.

METHODS

A strain of *E. coli* obtained from the stock culture collection of the Scripps Institution of Oceanography, University of California, La Jolla, California, was the experimental organism. All cultures were grown in a liquid medium of the following composition: 0.2% glucose, 0.5% K_2HPO_4, 0.2% KH_2PO_4, 0.1% NH_4Cl, and 0.005% yeast extract in tap water, pH 7.0. Fourteen liters of culture medium in a 5-gal. carboy was routinely employed. The contents of the flask were constantly aerated and agitated by passage of sterile air through the flasks. Five per cent by volume of a 24-hr. culture served as the inoculum. Incubation was at room temperature for 16 hr. Cells were harvested with a Sharples centrifuge, washed with distilled water, and either lyophilized for immediate use in resting cell experiments or slowly dried *in vacuo* over anhydrous calcium sulfate when dried cell preparations were desired.

Substrate oxidation was followed by conventional manometric techniques. In the experiments where radioactive glucosamine was used, sufficient trichloroacetic acid to give a final concentration of 5% was added to stop the reaction and to release carbon dioxide from the reaction mixture. The respiratory carbon dioxide was collected in alkali and then precipitated as $BaCO_3$ after addition of sufficient carrier bicarbonate so that radioactive assays could be carried out at infinite thickness. Ammonia determinations were in accordance with the procedures of Braganca, Quastel, and Schucher (8).

For the isolation of glucosamine and glucosamine 6-PO_4, the deproteinized solution was extracted with sufficient ethyl ether to remove the trichloroâcetic acid. The solution was then passed through a Dow 50- × 12 column (50–100 mesh) in the acid form and washed with 100 ml. of water. The effluent of the solution and the washings were collected in 10-ml. fractions for glucosamine 6-PO_4 analysis. Under these conditions, glucosamine remained on the column and glucosamine 6-PO_4 appeared in the third and fourth fraction as detected by nesslerization and total phosphate determinations. Elution of the glucosamine was carried out using 1 *N* HCl. The fractions containing glucosamine 6-PO_4 were adjusted to approximately pH 8 with ammonium hydroxide and incubated at 35° with intestinal phosphatase for 3 hr. The reaction mixture was then heated and neutralized, and the glucosamine was isolated as previously described.

Radioactive uniformly labeled glucosamine (glucosamine-U-C^{14}) was synthesized essentially according to the procedure of Heyns and Meinecke (9). Approximately 100 ml. of dry ammonia was condensed into a 150-ml. round-bottom flask containing 2 g. of fructose-U-C^{14} and 1 g. of NH_4Cl. The excess ammonia was driven off by a slow stream of dry N_2 over a period of 3 hr.; then the remaining ammonia was removed *in vacuo* overnight. The dry residue was dissolved in 25 ml. water, and the ammonia and glucosamine were absorbed on an acid form Duolite-C-3 ion-exchange column. The column was washed thoroughly with water to remove unreacted fructose. The glucosamine was eluted with 300 ml. of 1 *N* HCl, and the eluate was condensed to about 10 ml. by vacuum distillation. The crystals were filtered and washed with 6 *N* HCl. These crystals were not radioactive and were discarded. Five volumes of absolute alcohol were added, and after several hours the glucosamine and NH_4Cl were filtered. The salicylaldehyde derivative of glucosamine was made by the method of Irvine and Earl (10). The salicylidene derivative melted at 186° (corrected m.p. of known, 186°; and m.p. reported by Irvine and Earl, 183.5°).

The salicylidene derivative was hydrolyzed by refluxing for ½ hr. with 1.5 *N* HCl in 80% aqueous alcohol. On cooling, glucosamine.HCl crystals formed (95.5% purity). Recrystallization gave crystals that assayed 99% pure by the Miller and Van Slyke (11) reducing-sugar method and by a modification of the Elson and Morgan colorimetric method for the determination of glucosamine (12). The optical rotation of the synthetic glucosamine gave values of $[\alpha]_D^{24} = +79.1$ (conc. = 4.89, time = 15 min.), whereas twice-crystallized glucosamine.HCl (Eastman) gave values of $[\alpha]_D^{24} = +79.5$ (conc. = 4.91, time = 15 min.). Final yield of glucosamine-U-C^{14} was 159.7 mg. which assayed at 1.9×10^4 counts/min. when counted as $BaCO_3$ at infinite thickness.

Glucosamine 6-PO_4 was enzymatically prepared by the method of Brown (13) and by an adaptation of the chemical procedure described by Seegmiller and Horecker (14) for the preparation of glucose 6-PO_4 from glucose.

All radioactive determinations were carried out at infinite thickness with $BaCO_3$ obtained directly or by wet oxidation. The values are expressed in terms of the per cent of the total added activity recovered.

Results and Discussion

The ability of a lyophilized cell suspension of glucose-grown *E. coli* to produce ammonia from glucosamine is shown by the data in Fig. 1. The results indicate that glucose-grown lyophilized cells of *E. coli* produce ammonia from glucosamine without a lag period. This must mean that the enzyme system(s) responsible for the production of ammonia from glucosamine is constitutive rather than adaptive. This constitutive ability of *E. coli* to metabolize glucosamine has been observed by other workers (3).

Table I gives a comparison of the ammonia formed, oxygen consumed, and isotopic respiratory carbon dioxide obtained when glucosamine-U-C^{14} was incompletely oxidized by lyophilized cell suspensions of *E. coli.* From the data it can be observed that on a per cent theoretical basis the formation of ammonia exceeds the total oxygen uptake and that the respiratory carbon dioxide is approximately equivalent to the ammonia formed. These results indicate that a fermentative type of reaction is partly contributing to the respiratory carbon dioxide and that the production of ammonia from glucosamine may not be dependent on molecular oxygen.

Further evidence for an anaerobic pathway for the degradation of glucosamine was obtained when oxygen consumption and ammonia

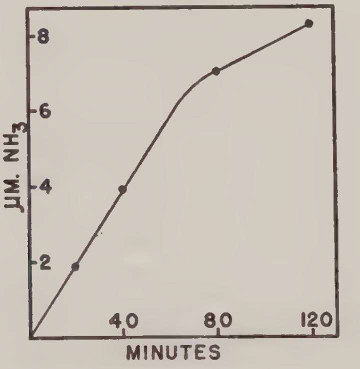

Fig. 1. The ability of *E. coli* lyophilized cells to produce ammonia from glucosamine. The reaction mixture contained 10 mg. of *E. coli* lyophilized cells, 20 µmoles glucosamine.HCl, and 0.01 *M* phosphate buffer pH 7.5 to a total volume of 2.5 ml. Incubation was for 120 min. at 37° in an air atmosphere. Ammonia values are corrected for endogenous ammonia formation.

TABLE I

The Ability of E. coli *Lyophilized Cells to Oxidize Glucosamine-U-C^{14}*

The reaction mixture contained 10 mg. *E. coli* lyophilized cells, 20 μmoles glucosamine.HCl, and 0.01 *M* phosphate buffer pH 7.5 to a total volume of 2.5 ml. Incubation was for 200 min. at 37° in an air atmosphere.

Expt.	Oxygen consumed[a]		$C^{14}O_2$ recovered		NH_4 produced[b]	
	μmoles	*% theory*	*μmoles*	*% of theory*	*μmoles*	*% of theory*
1	14.6	12.2	21.3	35.5	7.7	38.5
2	11.2	9.4	18.1	30.2	7.3	36.5

[a] Not corrected for endogenous oxygen consumption.

[b] Corrected for endogenous ammonia formation.

formation were compared during the oxidation of glucosamine by dried cell preparations in the presence of various concentrations of fluoride. The results given in Fig. 2 clearly indicate that ammonia production from glucosamine can proceed at concentrations of fluoride that completely suppress oxidation.

Previous workers have reported that small amounts of glucose inhibited the formation of ammonia from glucosamine (1, 3). The results given in Table II confirm the inhibitory nature of glucose on glucosamine utilization. It can be seen that both ammonia production and

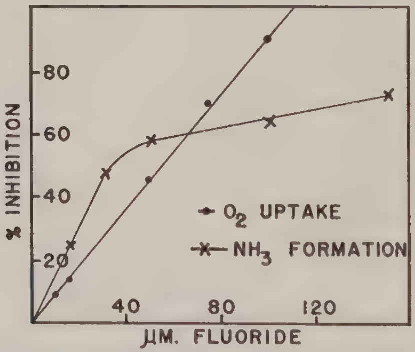

FIG. 2. The effect of fluoride on the metabolism of glucosamine by dried cell preparations of *E. coli*. The reaction mixture contained 10 mg. of *E. coli* dried cells, 20 μmoles glucosamine.HCl, and concentrations of fluoride as indicated with 0.01 *M* phosphate buffer to a total volume of 2.5 ml. Incubation was at 37° for 120 min. in an air atmosphere. Both ammonia and oxidation values given are corrected for endogenous.

TABLE II

The Effect of Glucose on Glucosamine-U-C^{14} Oxidation

Reaction mixture contained 10 mg. of dried cells, 10 μmoles glucosamine.HCl, and 0.01 *M* phosphate buffer pH 7.5 to a total volume of 2.5 ml. Incubation 37° for 180 min. in an air atmosphere.

	Per cent conversion to NH_4[a]	Per cent conversion to $C^{14}O_2$
Glucosamine	46.7	14.2
Glucosamine + 5 μmoles glucose	8.0	1.4
Glucosamine + 10 μmoles glucose	2.0	0.5
Glucosamine + 15 μmoles glucose	0	0

[a] Corrected for endogenous ammonia formation.

isotopic carbon dioxide formation are greatly decreased in the presence of small amounts of glucose. This must mean that glucose is inhibiting glucosamine utilization at a substrate level where the amine group is intact and prior to carbon dioxide production.

It is known that both yeast and brain hexokinase will phosphorylate glucosamine in the presence of ATP to form glucosamine 6-PO_4 (13, 15). This compound was, therefore, tested as a possible intermediate in glucosamine degradation. The ability of *E. coli* dried cells to metabolize glucosamine 6-PO_4 in the presence and absence of fluoride is shown by the data in Table III. The results indicate that ammonia production readily proceeds with glucosamine 6-PO_4 as a substrate. In addition, it is quite apparent that the enzyme system(s) responsible for the production of ammonia from glucosamine 6-PO_4 is not detectably sensitive to fluoride.

In order to investigate further the inhibitory effect of glucose on glucosamine utilization, the dried cell preparation was incubated with

TABLE III

The Effect of Fluoride on Ammonia Formation from Glucosamine 6-PO_4

Reaction mixture contained 10 mg. dried cells, 10 μmoles glucosamine 6-PO_4, 100 μmoles sodium fluoride, and 0.01 *M* phosphate buffer pH 7.5 to a total volume of 2.5 ml. Incubation 37°, air atmosphere for indicated times (Expt. 1 = 120 min.; Expt. 2 = 180 min.).

	Per cent conversion to ammonia[a]	
	Control	Control + fluoride
Expt. 1	29.0	31.0
Expt. 2	30.0	28.0

[a] Corrected for endogenous ammonia formation.

TABLE IV

The Effect of Glucose and Fluoride on the Metabolism of Glucosamine-U-C^{14}

The reaction mixture contained 10 mg. dried cells, 20 μmoles glucosamine-U-C^{14}, and, where indicated, 100 μmoles fluoride, 20 μmoles glucose, and 0.01 *M* phosphate buffer pH 7.5 to a total volume of 2.5 ml. Incubations were at 37° for 120 min. in an air atmosphere.

Additions	Per cent of total added counts		
	Glucosamine recovered	Glucosamine 6-PO_4 found	Respired $C^{14}O_2$
Glucosamine	39.2	0.87	7.8
Glucosamine + glucose	80.6	0.29	0.3
Glucosamine + fluoride	48.7	2.35	1.56
Glucosamine + fluoride + glucose	90.3	0.1	0.1

glucosamine-U-C^{14} alone and in the presence of glucose and fluoride together or singly. At the completion of the incubation period, 20 mg. of normal glucosamine and 20 mg. of glucosamine 6-PO_4 carrier were added to the reaction mixture, and the total radioactivity was determined in the recovered glucosamine, glucosamine 6-PO_4, and the respiratory carbon dioxide. The results of this determination (Table IV) indicate that in the presence of fluoride, glucosamine utilization and carbon dioxide production decreased, whereas glucosamine 6-PO_4 formation increased. These results would be expected if glucosamine degradation proceeded through the Embden-Meyerhof glycolytic pathways which fluoride is known to inhibit (16). The presence of glucose resulted in a decrease of glucosamine utilization, glucosamine 6-PO_4 formation,

TABLE V

The Effect of Glucose on Ammonia Formation from Glucosamine 6-PO_4

Reaction mixture contained 10 mg. dried cells, 10 μmoles glucosamine 6-PO_4 and concentrations of glucose, as indicated, in 0.01 *M* phosphate buffer pH 7.5 to a total volume of 2.5 ml. Incubation was for 2 hr. at 37° in an air atmosphere.

Additions	Per cent conversion to NH_3[a]	
Glucosamine 6-PO_4	31.2	30.6
Glucosamine 6-PO_4 + 5 μmoles glucose	30.0	22.6
Glucosamine 6-PO_4 + 15 μmoles glucose	30.0	30.6
Glucosamine 6-PO_4 + 30 μmoles glucose	32.7	
Glucosamine 6-PO_4 + 60 μmoles glucose	29.0	

[a] Corrected for endogenous ammonia formation.

and radioactive respiratory carbon dioxide production (Table IV). This effect of glucose was enhanced under conditions where glucosamine 6-PO_4 removal through oxidation is suppressed by the presence of fluoride. These results strongly suggest that glucose inhibits glucosamine utilization prior to the formation of glucosamine 6-PO_4, presumably at the kinase reaction. This would indicate that the phosphorylation of glucosamine does not require a special kinase and that the phosphorylation of glucosamine is carried out by the same kinase responsible for the phosphorylation of glucose. This conclusion is further supported by the results given in Table V, where the ability of dried cell preparations to produce ammonia from glucosamine 6-PO_4 in the presence of glucose and fluoride is presented. It can be seen that ammonia production from glucosamine 6-PO_4 proceeds uninhibited under high concentration of glucose.

The data presented suggest that an anaerobic degradation pathway exists for glucosamine which is dependent upon an initial phosphorylation to give glucosamine 6-PO_4. This latter compound then is metabolized to ammonia and carbon dioxide. Evidence for the participation of glucosamine 6-PO_4 as an intermediate has also been recently obtained with cell-free extracts of *E. coli* by Asahina and Yamaha (17). The ability of fluoride to cause an increase of glucosamine 6-PO_4 under conditions where ammonia production from this compound is not detectably inhibited would be expected if the intermediate formed after ammonia removal is a phosphorylated compound common to the Embden-Meyerhof glycolytic pathway. Evidence for the nature of this compound, however, is lacking.

ACKNOWLEDGMENT

The authors are grateful for the advice and encouragement of Dr. Arne N. Wick.

SUMMARY

The metabolism of normal glucosamine and glucosamine-U-C^{14} by resting cell suspensions and dried cell preparations of *Escherichia coli* was investigated. The results indicate that an anaerobic degradation pathway for glucosamine exists which is dependent upon an initial phosphorylation of glucosamine to give glucosamine 6-PO_4. Glucosamine 6-PO_4 then serves as a substrate for further degradation to ammonia and a product presumably common to the Embden-Meyerhof glycolytic pathway.

The inhibitory effect of glucose on glucosamine utilization was also studied. It was found that the presence of glucose decreased glucosamine utilization and glucosamine 6-PO_4 formation. The presence of glucose, however, had no effect on ammonia production from a glucosamine 6-PO_4 substrate. These results were interpreted to mean that a competition exists between glucose and glucosamine for the same hexokinase.

REFERENCES

1. LUTWAK-MANN, C., *Biochem. J.* **35**, 610 (1941).
2. ROSENBERG, A. J., *Compt. rend.* **226**, 1751 (1948).
3. OKA, Y., AND MURACHI, T., *J. Biochem.* (Japan) **41**, 107 (1954).
4. ROGERS, H. J., *Biochem. J.* **45**, 87 (1949).
5. HARPUR, R. P., AND QUASTEL, J. H., *Nature* **164**, 693 (1949).
6. LELOIR, L. F., AND CARDINI, C. E., *Biochim. et Biophys. Acta* **12**, 15 (1953).
7. SOODAK, M., *Bacteriol. Proc.* **1955**, 131.
8. BRAGANCA, B. M., QUASTEL, J. H., AND SCHUCHER, R., *Arch. Biochem. and Biophys.* **52**, 18 (1954).
9. HEYNS, K., AND MEINECKE, K. H., *Chem. Ber.* **86**, 1453 (1953).
10. IRVINE, J. C., AND EARL, J. C., *J. Chem. Soc.* **131**, 2376 (1922).
11. MILLER, B. F., AND VAN SLYKE, D. D., *J. Biol. Chem.* **114**, 583 (1936).
12. WICK, A. N., DRURY, D. R., NAKADA, H. I., BARNET, H. N., AND MORITA, T. N., *J. Biol. Chem.* **213**, 907 (1955).
13. BROWN, D. H., *Biochim. et Biophys. Acta* **7**, 487 (1951).
14. SEEGMILLER, J. E., AND HORECKER, B. L., *J. Biol. Chem.* **192**, 175 (1952).
15. SOLS, A., AND CRANE, R. K., *J. Biol. Chem.* **210**, 581 (1954).
16. WARBURG, O., AND CHRISTIAN, W., *Biochem. Z.* **310**, 384 (1941).
17. ASAHINA, M., AND YAMAHA, T., *J. Jap. Biochem. Soc.* **26**, 671 (1955).

Reprinted from the Yale Scientific Magazine
Vol. XXXI, No. 3, December, 1956
Reproduced by Permission

Scientific Diving

by **WHEELER J. NORTH**
Scripps Institution of Oceanography

The author reviews the recently developed training program of this novel facet of marine biological investigation. He stresses the importance of the safety factors involved, and also demonstrates the contribution of diving to scientific inquiry.

Man has used diving techniques since ancient times for exploring the submarine world, but only recently have refinements in equipment permitted extensive underwater investigations to be conducted. The invention of the Aqua-lung by the Frenchmen Gagnan and Cousteau has made available a relatively safe, inexpensive, and readily manageable underwater apparatus resulting in a tremendous increase in diving activities of all kinds. Equipment of this kind, where the supply of air or other breathing gas is compressed in tanks strapped to the back of the diver, has been designated as SCUBA (Self-Contained Underwater Breathing Apparatus) to distinguish it from apparatus requiring a hose extending to the surface where a pump supplies the breathing gas. SCUBA permits the diver to swim freely in any direction he may choose, unencumbered by attachments to surface tenders.

Local Advantages

The Southern California region is especially favorable for diving; the local waters are always of moderate temperature and are rich in biological material; the sea floor is highly varied, providing a multitude of different environments, often of great beauty and general interest. Perhaps of even greater importance, however, is the location in the San Diego area of two large organizations devoted to the study of the sea, The University of California's Scripps Institution of Oceanography, and the U. S. Navy Electronics Laboratory. Both of these organizations encourage diving for scientific purposes and close collaboration is maintained between the two.

From 50 to 100 scientists in many disciplines dive throughout the year, usually logging over 2500 dives annually, which involves around 10,000 man hours of diving time plus associated labor. The safety record is very impressive, since to date there have been no major accidents to personnel trained at Scripps, although diving is ordinarily viewed as a hazardous occupation. Credit for the record can be given to strict supervision of diving activities by committees of experienced divers. Diving studies and activities are aided by facilities made available by the sponsoring organizations. Such facilities may include the diving apparatus itself, as well as nets, corers, bottles, underwater cameras, or other required equipment; necessary transportation may range from a small skiff to a large ocean-going vessel. At frequent intervals, cruises are dispatched to remote regions of the Pacific—from the Alaskan Gulf to Antarctica, from the Sea of Cortez to Japan or the South Sea Islands—and they may be accompanied by a complement of diver-scientists, included to record and observe at first hand some of the mysteries of the little-known oceanic environments.

The Scripps Institution of Oceanography is the southernmost campus of the University of California, and is the largest station in the world engaged in studies of the sea. It is located almost within a stone's throw from the rim of a spectacular submarine canyon that cuts a deep gash across our western continental shelf. Scientific diving at the Institution began about ten years ago when a "hard hat" (non-SCUBA) diver was employed to study geological aspects of the above-mentioned canyon. In 1950 the Division of Marine Vertebrates acquired the Institution's first Aqua-lung, which proved so successful that virtually every division now boasts of at least one diver-scientist.

Administration of the Diving Program has now been allocated to the Institute of Marine Resources, a sister organization to Scripps, whose purpose is to develop the practical and economic aspects of the discoveries of marine scientists. Regulation of diving activities is done by the Divers' Certifying Board, composed of five experienced divers appointed from the various Divisions of the Institution.

Training Program

Training courses lasting about two weeks are held three or four times annually. The prospective student must pass a thorough physical examination and fulfill certain preliminary requirements designed to eliminate poor swimmers or persons whose physiological and psychological limitations may render them unfit for deep diving. For example, the prospective student must be able to swim 1000 feet on the ocean surface in 18 minutes; he must breathe pure oxygen in a decompression chamber at 3 atmospheres pressure for 30 minutes without ill effects.

The course consists of lectures on a wide variety of pertinent subjects as well as training in actual practice with SCUBA in a swimming pool. The student is instructed in the physics and physiology of diving; he is taught how to recognize and cope with varying conditions of waves, currents, and bottom topography; he learns useful first-aid practices and is required to know the signs, symptoms, causes and cure of the common divers' disorders; he must understand the function, maintenance, and repair of his diving apparatus and other frequently used equipment; he is lectured on the harmful and useful biological organisms which he is apt to encounter in the Pacific Ocean; and finally he is given a thorough written examination on the above material. In the pool the student learns to feel completely at home underwater. He becomes accustomed to solving problems while submerged; he is taught how to clear completely flooded apparatus without surfacing; he learns how to share his air supply with a partner who has exhausted his supply (tandem breathing); the instructors plague him with sudden "emergency" situations to check any tendencies he may have to panic and to test his ability to think quickly and clearly; he is required to ditch and recover his equipment and he learns the value of the "buddy system."

After completing the formal course, the student makes several monitored ocean dives at the end of the Scripps Pier in 20 feet of water, demonstrating his ability to perform all of the techniques mastered in the swimming pool under the vastly more difficult conditions imposed by the ocean.

Further Certification

When the diver's instructors are satisfied with his competence, he is then permitted to dive with designated divers to depths not exceeding 25 feet. When he has completed 12 ocean dives and logged a total of at least 4 hours' underwater time, he is eligible to receive his first certification card, allowing him to dive to 25 feet, always accompanied by a diver who is similarly qualified. He may dive to 60 feet if accompanied by a diver who is certified to 60 feet or deeper. When the trainee has completed 12 dives between 25 and 60 feet, logging 4 further hours of time underwater, he becomes eligible for certification to 60 feet. Similar certification is required for depths of 100 and 130 feet. To achieve certification for the 150 and 200 foot levels, only 4 dives in each range are necessary and no time requirement exists. In the latter ranges the trainee learns to guard against nitrogen narcosis and decompression sickness ("bends").

Certification is awarded by the Diver's Certifying Board, mentioned above, and during the course of his training the apprentice is expected to dive with various members of the Board in order that his capabilities and limitations may be assessed. The close personal contact thus maintained between members of the Board and the diving personnel is felt to be of great importance in minimizing hazards.

A number of general safety rules exist. The most noteworthy are: a diver must always be accompanied by a partner or buddy; the dive must be terminated at once if visual or audible contact with the buddy is lost; to retain certification, a diver must log 12 dives annually.

In addition to local scientists, men and women from all other campuses of the University of California, as well as personnel from the Navy Electronics Laboratory may receive diving instruction at Scripps.

When the student finishes his formal training and commences diving on one or another of the University research projects he becomes acquainted with strange and fascinating environments involving a wealth of new physical and psychological experiences. As he gains knowledge and becomes certified to deeper and deeper levels, he finds that at each lower depth range he enters a new, unfamiliar region, different in many respects from the higher levels he previously has encountered.

UNDERWATER CHARACTERISTICS

In the 0-25 foot range the neophyte finds himself in a world wherein the influence of gravity is much reduced. He is changed from a creature formerly restricted to movements over a surface, to a being capable of moving readily in three dimensions. He is, however, exposed to other forces such as currents and wave surge, and he must learn to anticipate and to compensate for them. He becomes accustomed to motion in a medium many times denser than air. He swims over rocky or sandy bottoms, and perhaps in shallow inlet and bay environments, and he becomes familiar with life in the subtidal zones.

In the 25-60 foot range, the diver in the La Jolla area encounters some of the long stretches of sand "desert"; he enters the kelp forests, and he can explore the rim of the submarine canyon. Wave and current motion is much reduced at this level, and the red component of daylight is almost entirely absorbed by the overlying water, hence the eye perceives only a blue world.

At depths of 60 to 100 feet the diver enters a realm of stillness. No water motion is ordinarily perceived unless there should be a strong current close to the bottom. Daylight is much reduced, and the diver becomes acclimated to swimming in quite cold water. The lower edges of the kelp beds lie in this range and the sea floor in these areas is scalloped into fantastic shapes by the activities of mollusks and echinoderms. The diver can now get well down into the upper reaches of the canyons and perhaps experiences a unique kind of claustrophobia or feeling of great isolation for the first time in his life. He explores steep gorges, hundred-foot cliffs, caves, pinnacles, and the like, and he may feast his aesthetic senses upon gardens of fluorescent anemones or canyon walls covered with lace-like Gorgonian coral.

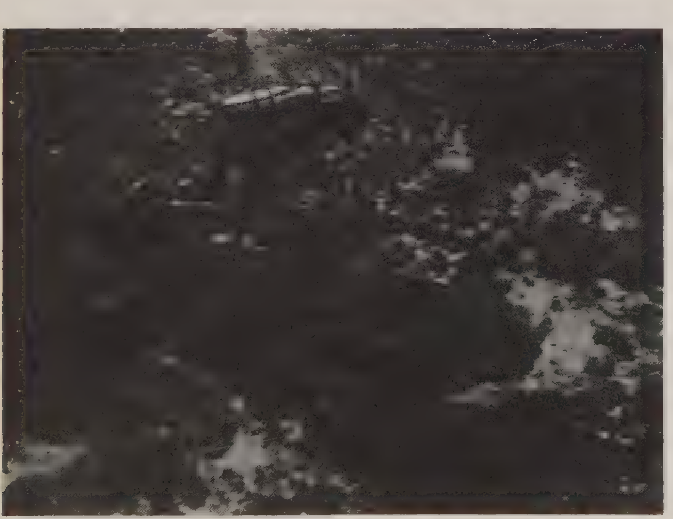

Dr. Walter H. Munk examines coral growth on Alexa Bank at a depth of 100 feet in the South Pacific during the University's "Capricorn" expedition. Munk is Professor of Geophysics at the Scripps Institution of Oceanography.

It requires considerable fortitude as well as a thick, foam rubber suit to do productive scientific work in the chilling depths below 100 feet. Illumination is reduced to twilight levels, hazards arising from decompression sickness must be avoided, and mental activities may be retarded by the effects of nitrogen narcosis. Such dives must be carefully planned to avoid accidents and to assure that the required work be accomplished. The adventurous few who become certified to descend to these depths are rewarded by glimpses of the edge of a bizarre environment that extends over nearly ¾ of the surface of our planet.

ACCOMPLISHMENTS

What are some of the results in the new field of scientific diving? Not the least of the accomplishments is the general diving program itself with its low incidence of accidents. It has evolved over a period of six years and represents the thought and work of many persons. It is still in the process of development.

An intangible product of the program is the novel outlook it has given to the many marine scientists who have received diving training at Scripps. By way of illustration, imagine the type of physician that would be produced if medical education were limited to observations on dead tissues and organs, pickled in bottles of formalin. How hopeless it would be for such a doctor to understand and deal successfully with an illness in a whole, live human being. Yet until recently a comparable situation existed in the marine sciences. Much of our knowledge depended upon "dead" observations, observations that portray a given situation at only one point in space and often at only one instant of time. The ocean, however, is almost as variable, dynamic, and unpredictable a medium as protoplasm and the advent of SCUBA provided a method whereby the research worker could make a beginning towards a first-hand appreciation of the object of his study. The education of oceanographic students can now be accomplished with much more vividness and a fuller meaning given to the volumes of statistical data and the complex charts. Subtle relationships that are laboriously or perhaps never detected by the fathometer or the sampling device, or which do not necessarily accompany the specimen into the storage bottle, may be obvious to the scientific diver at a mere glance. The diver does not, however, replace conventional instrumentation and techniques, rather he refines and adds to existing knowledge, or facilitates measurements previously impossible.

Much of the work that is done underneath the ocean's surface is merely a collection of material or information for subsequent analysis in the laboratory. The collecting process is almost always, however, more efficiently, intelligently, and, if necessary, more selectively done by a diver than by an instrument alone.

An ecological study of the kelp beds near La Jolla has been conducted by divers for several years, funds for the research being supplied by the Kelco Company of San Diego, a firm that harvests the kelp for commercially extractable products. Divers install and check various oceanographic instruments along the coast locally.

A controversy arose recently over the use of underwater explosives for commercial seismic offshore studies, since it was believed by some that this program might involve extensive damage to fish populations. Research conducted at Scripps, using SCUBA, indicated negligible damage provided only certain types of explosive were employed.

Often diving members of the staff of both Scripps and the Navy Electronics Laboratory are consulted by industrial groups or civic organizations. The effect of sewer outfalls on local marine conditions has been investigated at several locations along the coast. A group of our geological specialists has formed an organization known as Geological Diving Consultants and are available for special studies requiring SCUBA.

The above has dealt only with the work being done in the San Diego region and no mention has been made of the many other scientific and engineering diving activities that exist on a worldwide basis, extending even into freshwater environments. From the little that has been said, however, it can be seen that SCUBA is contributing greatly to the increase of man's knowledge; nevertheless the potentialities of existing equipment have probably not been fully realized or exploited. Divers are continually developing new techniques and discoveries are constantly being made of phenomena previously overlooked. But in terms of what remains to be learned in the marine sciences, the surface has just barely been scratched. It is necessary not only to extend the type of investigations described above to other shallow areas of the seas, but in order to comprehend the entire ocean, it will probably also be necessary to swim and explore at depths far greater than present facilities allow. The equipment to do this is as yet only in the dream stage; our current knowledge of physics and physiology is wholly inadequate to cope with inventions of this sort, but surely this should not be allowed to restrict our imagination. A century ago only Jules Verne dared dream of a time in the future when I might go home after a routine day's work and say to my wife, "I found a magnificent Brachiopod at 185 feet today."

---

* Contribution from the University of California, Scripps Institution of Oceanography, New Series No. 872.

Wheeler J. North was born in California in 1922. He received a B.S. degree in Electrical Engineering from the California Institute of Technology in 1944. After spending two years in the service and two years as an electronics engineer with the U. S. Navy Electronics Laboratory, he returned to his alma mater to earn a B.S. degree in Biology in 1950. Dr. North did his graduate studies at the University of California's Scripps Institution of Oceanography and received M.S. and Ph.D. degrees in Biological Oceanography in 1953. He spent a postdoctoral year at Cambridge, England, and is currently a member of the staff at the Scripps Institution of Oceanography as a Rockefeller Postdoctoral Research Fellow.

He is an alternate member of the University of California Divers' Certifying Board, and an active diver and diving instructor. His chief underwater researches are concerned with ecological studies at the 100 to 200 foot levels in the La Jolla submarine canyon. In conjunction with this, Dr. North is also pursuing a research interest in the photosensory physiology of eyeless animals.

Reprinted, by permission, from
Journal du Conseil International
pour l'Exploration de la Mer.
Vol.XXII, No.1, 1956.

A Method for the Microscopic Examination and Manipulation of Plankton on Board Ship

By

Robert Bieri,
Lamont Geological Observatory, Palisades, New York[1] [2]

Introduction

In certain regions of the Pacific there are sharp boundaries to the plankton faunas. The causes of these boundaries, indicated by the abrupt disappearance of certain species and the equally abrupt appearance of other species, are still not known. In order to study these boundary regions and the environmental factors associated with them in more detail, it is desirable to have some way of examining the zooplankton while at sea. RUSSELL (1935: 517), who apparently was the first to have attempted synoptic plankton studies at sea, did not use a microscope as the changes he was studying could be seen with the unaided eye. In the inshore region this is frequently the case, but in the oceanic realm faunal boundaries, although quite sharp, are not readily distinguished without the use of a microscope. Although some microscopic examination of plankton has been done at sea, there appear to be few published descriptions of the methods used.

The following paragraphs describe a device, the under-way plankton tray, made for the examination of plankton on board ship. With this apparatus it has been possible while at sea to examine and manipulate with probes and pipettes, at magnifications up to 100 ×, not only living and preserved zooplankton, but also the larger phytoplankton. Besides being useful for determining the kind and number of organisms present in the water, the tray should prove useful in other types of studies. Objects such

---

[1] Contrib. Scripps Inst. Oceanogr., N.S., 873.
[2] Contrib. Lamont Geol. Observ., 185, Biol. Progr., 9.

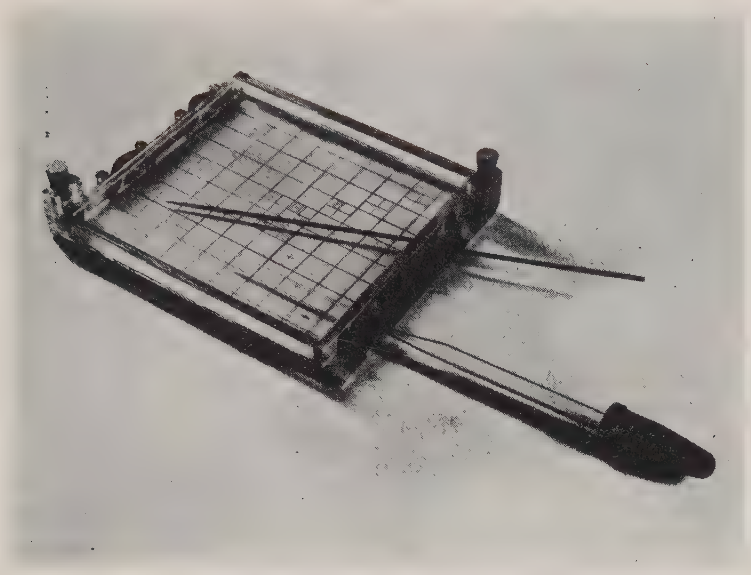

Figure 1. Under-way plankton tray with lid in place and a probe and pipette inserted through two of the entrance ports.

as large diatoms, small copepods, and fish eggs can be removed from plankton samples while alive and isolated for further study. Dissections of living organisms could probably be performed for physiological, embryological, or anatomical studies.

Description and Methods

The device is essentially an acrylic plastic tray and lid. At two opposite corners are air vents, and along two sides are entrance ports. A tray that has been in use for several months is shown in Figure 1. The dimensions are given in Figure 2. The lid, not shown in Figure 2, is a piece of $\frac{1}{8}$-inch plastic $4\frac{3}{16}$-inches (10·7 cm.) square with a $\frac{1}{8}$ by $\frac{1}{16}$-inch groove cut around its edges.

In operation the entrance ports on each side are covered by a taut rubber band. After the edges of the cover have been coated with stopcock grease, the tray is set on a table hung on shockmounted gimbals. Sixty millilitres of the sample to be examined are poured into the tray and the cover is put firmly in place. The table is then balanced so that the air bubble under the cover moves to one of the air vents. The other air vent is stoppered and the tray completely filled by means of a pipette. When the remaining air vent is stoppered, the tray can be lifted from the table to the stage of a microscope which has been firmly clamped to a suitable bench. The microscope and tray then roll and pitch with the ship.

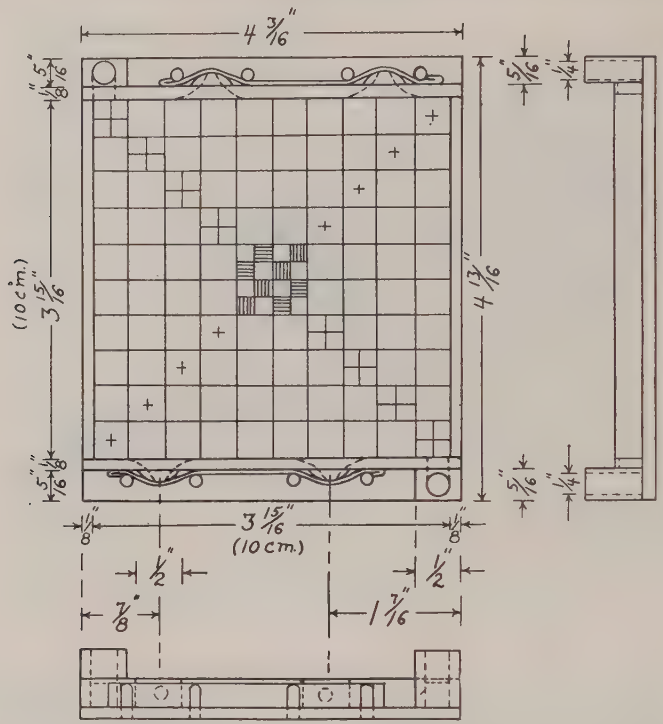

Figure 2. Dimensions of the under-way plankton tray. Lid not shown.

Probes about 6 inches long, made of $\frac{1}{16}$-inch diameter stainless-steel welding rod can be easily inserted through the side ports if they are lightly coated with stopcock grease. Glass pipettes (about 2 millimetres outside diameter) can also be readily inserted through the ports and used to remove small organisms. In Figure 3 the tray, microscope, and table set on gimbals are shown as used on board the research vessel "Vema". The device has been used successfully on the R/V "Baird" in moderate seas (28° maximum roll) and on board the R/V "Vema" in light seas (15° maximum roll). Although one can feel considerable vibration on both these ships, vibration of the microscope was not objectionable except occasionally at 100 × magnification.

Acknowledgements

The prototype of the under-way plankton tray described here was made and tested while the author was at the Scripps Institution of Oceanography. The instrument was improved and brought to its present stage of development at the Lamont Geological Observatory with the aid of funds from a grant of the Rockefeller Foundation for research in deep-sea biology (RF54087).

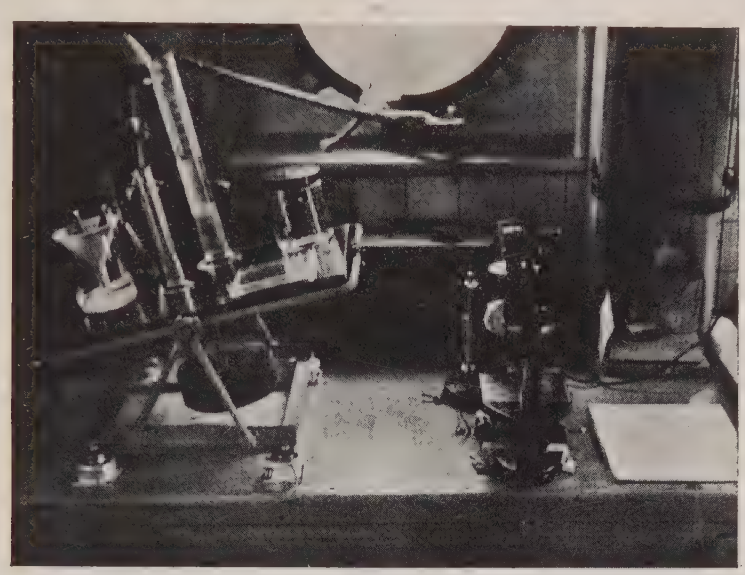

Figure 3. Under-way plankton tray on gimbal table filled and ready to be transferred to the microscope stage.

Reference

Russell, F. S. "Observations on the distribution of plankton animal indicators made on Col. E. T. Peel's yacht 'St. George' in the mouth of the English Channel, July 1935." Journ. Mar. Biol. Assoc. U. K., **20**, 3, pp. 507–522. 1936.

ABSTRACT: *Radiolaria recently found in shale of the Franciscan group (Jurassic and Cretaceous) in California are somewhat better preserved than those previously found in cherts of this group. Seven forms are described, figured, and identified generically.*

Radiolaria from the Franciscan group, Belmont, California

WILLIAM R. RIEDEL AND JULIUS SCHLOCKER
Scripps Institution of Oceanography, La Jolla, California, and
U. S. Geological Survey, Menlo Park, California

INTRODUCTION

Radiolaria were found in shale of the Franciscan group exposed in 1951 during excavation for industrial construction east of Belmont, California. Before excavation started, the site was a low hill of bedrock about 60 acres in area, that rose about 100 feet above the alluvium and tidal marsh deposits on the west shore of San Francisco Bay approximately 15 miles southeast of San Francisco, in the N½ NE¼ sec. 11, T. 5 S., R. 4 W. Lawson (1914) indicated on the geologic map of the San Mateo quadrangle (15-minute series) that the bedrock of which the radiolarian shale is a part is the Sausalito chert of the Franciscan group.

The Radiolaria were found in the shale 1150 feet southeast of Belmont Creek and about 1000 feet southwest of Bayshore freeway. The shale is in beds 4 inches to 2 feet thick and is interbedded with greywacke, radiolarian chert, and highly altered greenstone, all dipping northeast between 15° and 20°. The shale is moderate red to dark yellowish brown; some of it is laminated, consisting of alternating thin laminae of dark yellowish-brown and grayish-orange color. The Radiolaria are easily seen with the hand lens as rounded pellets. A prominent fault located 100 feet southwest of the radiolarian shale cuts northwesterly across the area and dips 40° to 50° northeast. Bedrock southwest of the fault is exposed over about 30 acres and is an olive gray, well-cemented conglomerate of well-rounded pebbles 1½ inches in average size, with a maximum size of 13 inches, in a matrix of coarse-grained sandstone. The dip of the conglomerate is northeast. Lawson (1914) designated this conglomerate "probably Knoxville formation" on the geologic map of the San Mateo quadrangle.

The Radiolaria of this shale of the Franciscan group can be isolated from the matrix by soaking the rock first in gasoline and then in water, and subsequently sieving. Their identification is hindered by their relatively poor state of preservation. No delicate tests, nor even the spines of the more robust forms, have been preserved, and those that are present are filled with iron-stained silica, which obscures internal details. Further difficulties have been introduced by lateral compression of the tests, which occurred during the compaction of the shale. Conical forms lying flat on a microscope slide therefore appear flared at a wider angle than they must originally have had, and it is difficult to distinguish between originally spherical, ellipsoidal, and discoidal skeletons. More of their structure can be determined, however, than in those few forms figured and generically determined by Hinde (1894) from chert of the Franciscan group.

Apart from Hinde's record, the only description of Radiolaria of Mesozoic age from California is that of Campbell and Clark (1944), who described a well-preserved assemblage from a small limestone sample which is probably of the same age as the Moreno shale. There is little similarity between the assemblage from the shale of the Franciscan group and that described by Campbell and Clark.

Accurate dating of the assemblage in the shale of the Franciscan group is impossible at present because of the relatively poor state of preservation and the small number of descriptions of faunas of Mesozoic age with which it might be compared. In the following discussion of forms present in the shale, it will be observed that there are similarities with some species recorded

Reproduced by Permission

from the Jurassic, and with others from the Cretaceous, of other parts of the world. The Radiolaria therefore at present throw no light on the question of whether this shale is Jurassic or Cretaceous in age.

Figured specimens will be deposited in the collections of the United States National Museum, Washington, D. C.

SYSTEMATIC DESCRIPTIONS

Class RADIOLARIA

Order SPUMELLARIA

Suborder **Sphaerellaria**

Tests belonging to this group are abundant in the assemblage, but the impossibility of determining details, such as the number of concentric shells and the nature of the spines, prevents identification of most of them. None with spongy skeletons was found, probably because of their having been dissolved or otherwise obliterated. One form can be tentatively identified generically.

Genus **Conosphaera** Haeckel, 1862
Text-figure 1

Tests belonging to this genus are rather common in the assemblage. They are spherical, thick-walled, bearing low conical to hemispherical elevations, and the entire surface has small subcircular pores. Diameter 140-210μ.

Tan Sin Hok (1927, p. 36, pl. 6, fig. 10) has described a similar large species, *Conosphaera tuberosa,* from sedimentary rocks of Mesozoic age on Rotti Island, near Timor. Parona (1890, pp. 148-149, pl. 1, figs. 9-10) described two rather similar species, *Conosphaera fossilis* and *Conosphaera antiqua,* from the Jurassic near Laveno in northern Italy. *Conosphaera mammillata* Hinde (1908, pp. 718-719, pl. 5, fig. 10), described from Triassic(?) rocks of Rotti Island and East Ceram, East Indies, and *Conosphaera sphaeroconus* Rüst (1898, pp. 13-14, pl. 4, fig. 8), from the Jurassic near Laveno and the Neocomian near St. Cassian, northern Italy, appear to differ from the form from the Franciscan group in their more regular arrangement of protuberances and pores. *Conosphaera sphaeroconus* has also been recorded, though somewhat doubtfully, by Heitzer (1930, p. 386, pl. 27, fig. 4) from the middle Jurassic of the Sonnwend Mountains, in the Austrian Tyrol.

Order NASSELLARIA

Suborder **Cyrtellaria**

Members of this group, and particularly forms belonging to the genus *Dictyomitra,* are common in the assemblage, but the difficulty of distinguishing segmental divisions and the probable loss of spines hinders even generic identifications. Only those forms that are most common, or of which the characters can be determined with some certainty, are discussed below.

Genus **Cryptocephalus** Haeckel, 1882(?)
Text-figure 2

A few specimens of distinctive form are assigned doubtfully to this genus (in the emended sense of Campbell, 1954), although the apical portion is indistinct or broken off in every specimen found. The cephalis appears to be small, spherical; there is no collar stricture. The thorax is narrow apically, rapidly broadening to become campanulate. Approximately sixteen to twenty longitudinal ribs extend along the thoracic wall, separating small circular pores in longitudinal rows. The mouth is somewhat constricted by a peristomial ring. Total length 160-190μ, breadth 125-145μ.

This form seems to resemble closely *Sethamphora pulchra* Squinabol (1904, pp. 213-214, pl. 5, fig. 8) from the Cretaceous of Euganei, in northern Italy. *S. squinaboli* Hinde (1908, p. 723, pl. 6, fig. 6), described from Triassic(?) rocks on Rotti Island, near Timor, differs from the form from the Franciscan group in its smaller size and fewer longitudinal ribs.

Genus **Dicolocapsa** Haeckel, 1882
Text-figure 3

Common tests apparently belonging to this genus possess a large subspherical thorax (breadth 175-235μ) surmounted by a small hemispherical cephalis, which projects only 10-15μ. Thoracic pores are subcircular, usually rather regularly hexagonally arranged; there are thirteen to seventeen on a half circumference. No mouth was found on examples that could be examined from the base. This is probably the form that Hinde placed in the genus *Sethocapsa,* although neither his description nor his figure indicates the presence of an apical horn.

This form is very similar to *Dicolocapsa microcephala* Heitzer (1930, pp. 394-395, pl. 28, figs. 43a-b), described from the middle Jurassic of the Sonnwend Mountains, in the Austrian Tyrol. *Dicolocapsa kalilimnii* Vinassa (1901, p. 506, pl. 1, fig. 36), described from the Cretaceous of Karpathos Island, near Crete, somewhat resembles the form from the Franciscan group, but appears to have fewer thoracic pores. *Dicolocapsa cephalocrypta* Tan Sin Hok (1927, p. 44, pl. 8, fig. 42), from rocks of Mesozoic age on Rotti Island, near Timor, is similar, but apparently the cephalis is enclosed to a greater extent by the thorax.

Genus **Tricolocampe** Haeckel, 1882
Text-figure 4

Individuals belonging to this genus are not common in the assemblage, but six specimens examined showed the following characters: Entire test thick-walled and generally

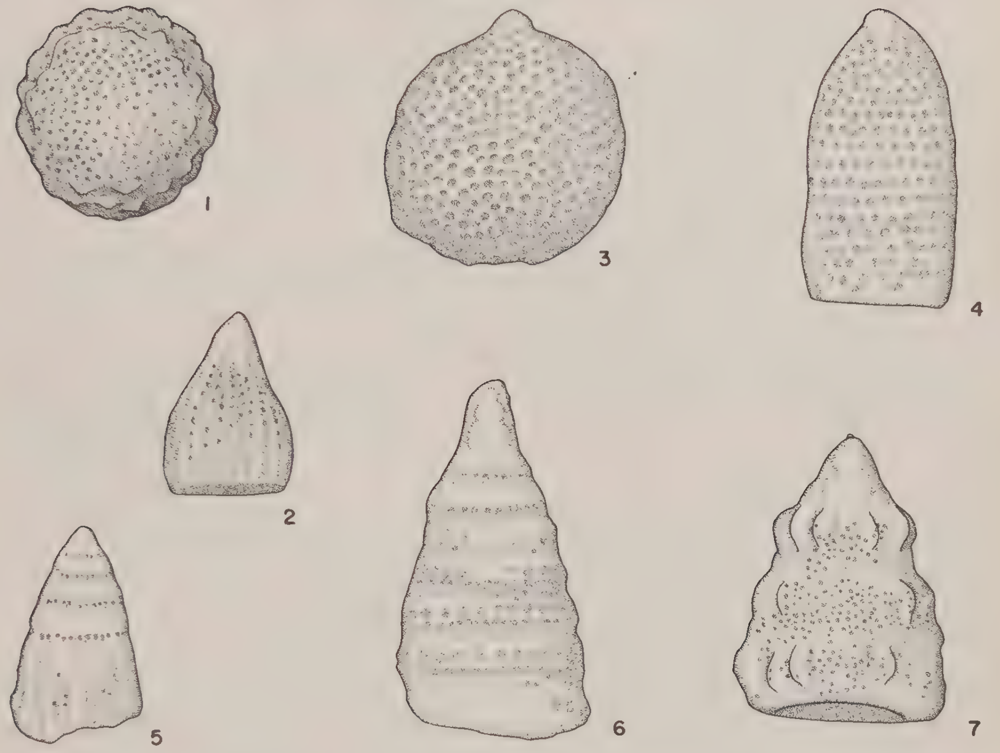

TEXT-FIGURES 1-7

1, *Conosphaera* sp.; 2, *Cryptocephalus?* sp.; 3, *Dicolocapsa* sp.; 4, *Tricolocampa* sp.; 5, *Dictyomitra* sp. *a;* 6, *Dictyomitra* sp. *b;* 7, *Dictyomitra* sp. *c.* All from shale of the Franciscan group; Belmont, California. All × 200.

cylindro-conical. Cephalis small, spherical, almost completely enclosed in the long cylindro-conical thorax. Abdomen short; no lumbar stricture. Thoracic and abdominal pores similar, subcircular, arranged hexagonally with usually pronounced transverse alignment. The thorax has eleven to seventeen transverse rows of pores; at the base of the segment there are approximately twelve to fourteen pores on a half circumference. Total length 170-300μ, breadth 105-185μ. There are no described species closely resembling this form.

Genus **Dictyomitra** Zittel, 1876

Specimens belonging to this genus are common in the assemblage, and sufficient structural details are preserved to make possible the tentative separation of three species.

Dictyomitra sp. **a**

Text-figure 5

Test rather narrowly conical, with smooth outline only occasionally modified by slight segmental bulges. Cephalis spherical; no collar stricture. The next four or five segments successively increasing somewhat in length, marked off by transverse rows of small subcircular pores; there are ten to fifteen pores on a half circumference. Longitudinal ribs usually present between pores of the transverse rows, but these are not continuous across the proximal segments. Beyond these four or five transverse rows of pores, no further segmental divisions can be distinguished. The longitudinal ribs become continuous and more pronounced, and in a few individuals the ribs separate pores that are approximately rectangularly arranged. Total length 145-285μ, breadth 75-140μ. There are no described species closely resembling this form.

Dictyomitra sp. b

Text-figure 6

Test conical, with all segments except the first two or three marked by annular swellings. Cephalis subspherical, with no stricture between it and the small poreless thorax. Third segment also usually poreless. The following two to four segments usually have a single row of small subcircular pores near their bases. Then follow three to five narrow segments, each with a row of large subcircular pores medially and a row of small pores distally. In a few specimens, small pores can be distinguished in the constrictions between the segments. Total length 255-330μ, breadth 155-185μ.

Dictyomitra hornatissima Squinabol (1904, pp. 230-231, pl. 9, fig. 12), described from the Cretaceous of Euganei, in northern Italy, appears to be very similar to this form from the Franciscan group, although some details cannot be compared because of the poor preservation of the latter.

Dictyomitra sp. c

Text-figure 7

Test conical, with outline modified by three or four annular series of rounded protuberances that probably correspond to individual distal segments. Small subspherical cephalis and ovate thorax enclosed in the thick-walled, conical shell apex. The first row of protuberances, immediately following the thorax, is very pronounced, and the subsequent, almost equidistant series are usually less prominent. Pores small, subcircular, in some individuals restricted to the zones between rows of protuberances, in others visible also on the protuberances themselves. Total length 250-300μ, breadth 180-190μ.

No described species closely resembles this form. *Dictyomitra elegans* Squinabol (1904, pp. 232-233, pl. 10, fig. 5), described from the Cretaceous of Euganei, northern Italy, shows some similarities with the form from the Franciscan group, but segments subsequent to the third lack protuberances, and pores are present on the cephalis and thorax.

Contribution from the Scripps Institution of Oceanography, new series, no. 874. Publication authorized by the Director, U. S. Geological Survey.

BIBLIOGRAPHY

CAMPBELL, A. S.
1954 – *Radiolaria.* In: MOORE, R. C., AND CAMPBELL, A. S., *Treatise on invertebrate paleontology.* Lawrence: University of Kansas Press, part D, Protista 3, pp. 11-163.

CAMPBELL, A. S., AND CLARK, B. L.
1944 – *Radiolaria from Upper Cretaceous of middle California.* Geol. Soc. Amer., Spec. Paper no. 57, 61 pp., 8 pls.

HEITZER, I.
1930 – *Die Radiolarienfauna der mitteljurassischen Kieselmergel im Sonnwendgebirge.* Austria, Geol. Bundesanst., Jahrb., vol. 80, pp. 381-406, pls. 27-29.

HINDE, G. J.
1894 – *Note on the radiolarian chert from Angel Island, and from Buri-Buri Ridge, San Mateo County, California.* California, Univ., Dept. Geol. Sci., Bull., vol. 1, pp. 235-240, pl. 14.
1908 – *Radiolaria from Triassic and other rocks of the Dutch East Indian Archipelago.* Jaarb. Mijnw. Ned. Oost-Indië, vol. 37 (ed. franç.), pp. 709-751, pls. 5-10.

LAWSON, A. C.
1914 – *San Francisco, California.* U. S. Geol. Survey, Geol. Atlas, Folio 193, 24 pp. (library edition).

PARONA, C. F.
1890 – *Radiolarie nei noduli selciosi del calcare giurese di Cittiglio presso Laveno.* Soc. Geol. Ital., Boll., vol. 9, pp. 132-175, pls. 1-6.

RÜST, D.
1898 – *Neue Beiträge zur Kenntniss der fossilen Radiolarien aus Gesteinen des Jura und der Kreide.* Palaeontographica, vol. 45, pp. 1-67, pls. 1-19.

SQUINABOL, S.
1904 – *Radiolarie cretacee degli Euganei.* R. Accad. Sci. Lett. Arti Padova, Atti Mem., new ser., vol. 18, pp. 171-244, 10 pls.

TAN SIN HOK
1927 – *Over de samenstelling en het ontstaan van krijt- en mergel-gesteenten van de Molukken.* Jaarb. Mijnw. Ned. Oost-Indië, Verh., 1926, 165 pp., 16 pls.

VINASSA DE REGNY, P.
1901 – *Radiolari cretacei dell'Isola di Karpathos.* R. Accad. Sci. Ist. Bologna, Mem., ser. 5, vol. 9, pp. 497-512, 1 pl.

158. SIGNIFICANCE OF LIVING FORAMINIFERAL POPULATIONS ALONG THE CENTRAL TEXAS COAST

FRED B. PHLEGER
Scripps Institution of Oceanography,
La Jolla, California

Reprinted from CONTRIBUTIONS FROM THE CUSHMAN FOUNDATION FOR FORAMINIFERAL RESEARCH
VOLUME VII, PART 4, OCTOBER, 1956
NORTON PRINTING CO., Ithaca, N.Y., U.S.A.

Reproduced by Permission

CONTRIBUTIONS FROM THE CUSHMAN FOUNDATION
FOR FORAMINIFERAL RESEARCH

VOLUME VII, PART 4, OCTOBER, 1956

158. SIGNIFICANCE OF LIVING FORAMINIFERAL POPULATIONS ALONG THE CENTRAL TEXAS COAST

FRED B PHLEGER

Scripps Institution of Oceanography,

La Jolla, California

ABSTRACT

1. Living and total populations from 34 stations in San Antonio, Mesquite, and Aransas bays, and from 176 stations on the adjacent continental shelf have been studied. The faunal patterns in the bays are similar in both the live and total populations.

2. Living populations average 50-200/10 ml. wet sediment. The largest bay populations are near the mouth of the Guadalupe River, and size of the open-ocean populations increases in the direction of the Colorado and Brazos rivers; this is comparable to the high living populations off the mouth of the Mississippi River. These data suggest that high living populations may be characteristic off river mouths.

3. Live-total ratios suggest fast deposition in upper San Antonio Bay, little or no sedimentation in the lower bays, and faster sedimentation in the nearshore open ocean than offshore.

4. Open-ocean biofacies boundaries are recognized at 20-30 m., 50-70 m., and 100 m. It is suggested that these facies are related to the nearshore turbulent zone and to the boundary between nearshore and offshore water masses.

5. Dead populations in the open ocean generally extend deeper than live ones, suggesting either down-slope distribution by gravity or emplacement during a previous environment.

INTRODUCTION

Several papers have been published discussing various phases of the oceanography and sedimentology along the central Texas coast in connection with research supported by American Petroleum Institute, Project 51. The present study reports the distributions of living populations of Foraminifera from San Antonio Bay, Mesquite Bay, Aransas Bay, and the adjacent continental shelf to 110 m., and interprets these distributions in terms of faunal and sedimentary facies, sediment transport, and relative rates of deposition.

Parker, Phleger, and Peirson(1953) and Post (1951) described the Foraminifera from numerous sediment samples in this area and have established the basic patterns of faunal distribution; the living population was not included in these reports. The present study includes living bay populations and numerous additional samples collected from the continental shelf offshore from the barrier island in environments only partly covered in the previous studies.

ACKNOWLEDGMENTS

This investigation was supported by a grant from the American Petroleum Institute, Project 51. The samples were collected by E. Dean Milow, Robert R. Lankford, and David G. Moore. Identifications of the Foraminifera were by Jean P. Hosmer, E. Dean Milow and Takayasu Uchio. Robert R. Lankford and Jean P. Hosmer assisted in preparation of the illustrations.

DESCRIPTION OF THE AREA

The area sampled is on the central coast of Texas in the northwest Gulf of Mexico, from approximately 26°00′-28°20′ N. Lat., and 96°00′-97°20′ W. Long. Locations of the stations and geography of the area are shown in Figures 1 and 2.

The bays are separated from the open ocean by a continuous, sandy barrier island which is breached by a small inlet at the position of Mesquite Bay. Other inlets are Aransas Pass in the southwest and Pass Cavallo in the northeast; these two inlets are the only continuous avenues of communication for water between the bays and the open ocean. The only fresh water stream of any conse-

---

Contribution from the Scripps Institution of Oceanography, New Series, No. 875; Contribution from the Marine Foraminifera Laboratory, No. 24.

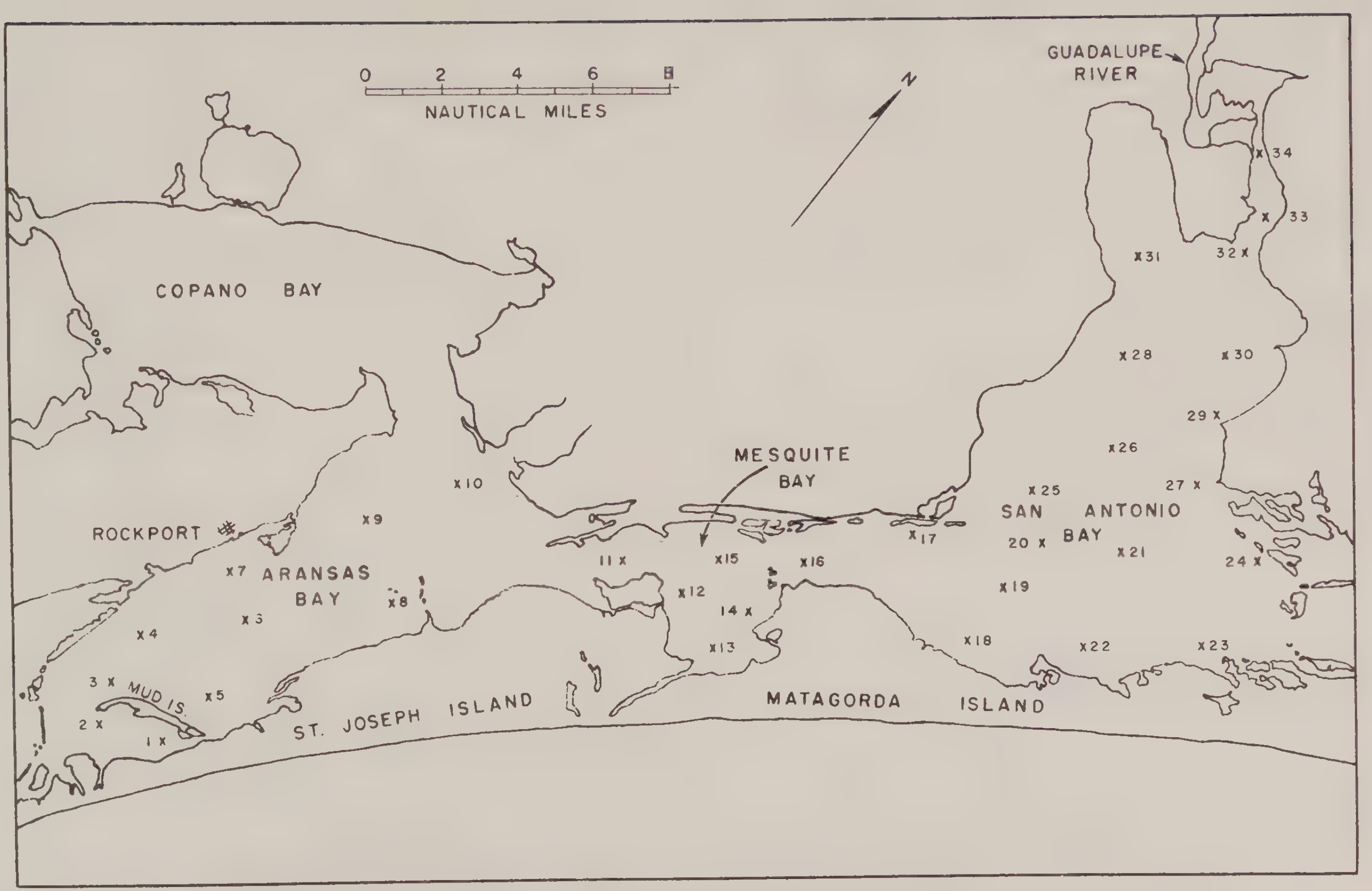
0 2 4 6 8
NAUTICAL MILES
N
GUADALUPE RIVER
COPANO BAY
ROCKPORT
ARANSAS BAY
MESQUITE BAY
SAN ANTONIO BAY
ST. JOSEPH ISLAND
MATAGORDA ISLAND
MUD IS.
1 x
2 x
3 x
x 3
x 4
x 5
x 7
x 8
x 9
x 10
11 x
x 12
x 13
14 x
x 15
x 16
x 17
x 18
x 19
20 x
x 21
x 22
x 23
24 x
x 25
x 26
27 x
x 28
29 x
x 30
x 31
32 x
x 33
x 34

Figure 1. Locations of stations in the bays.

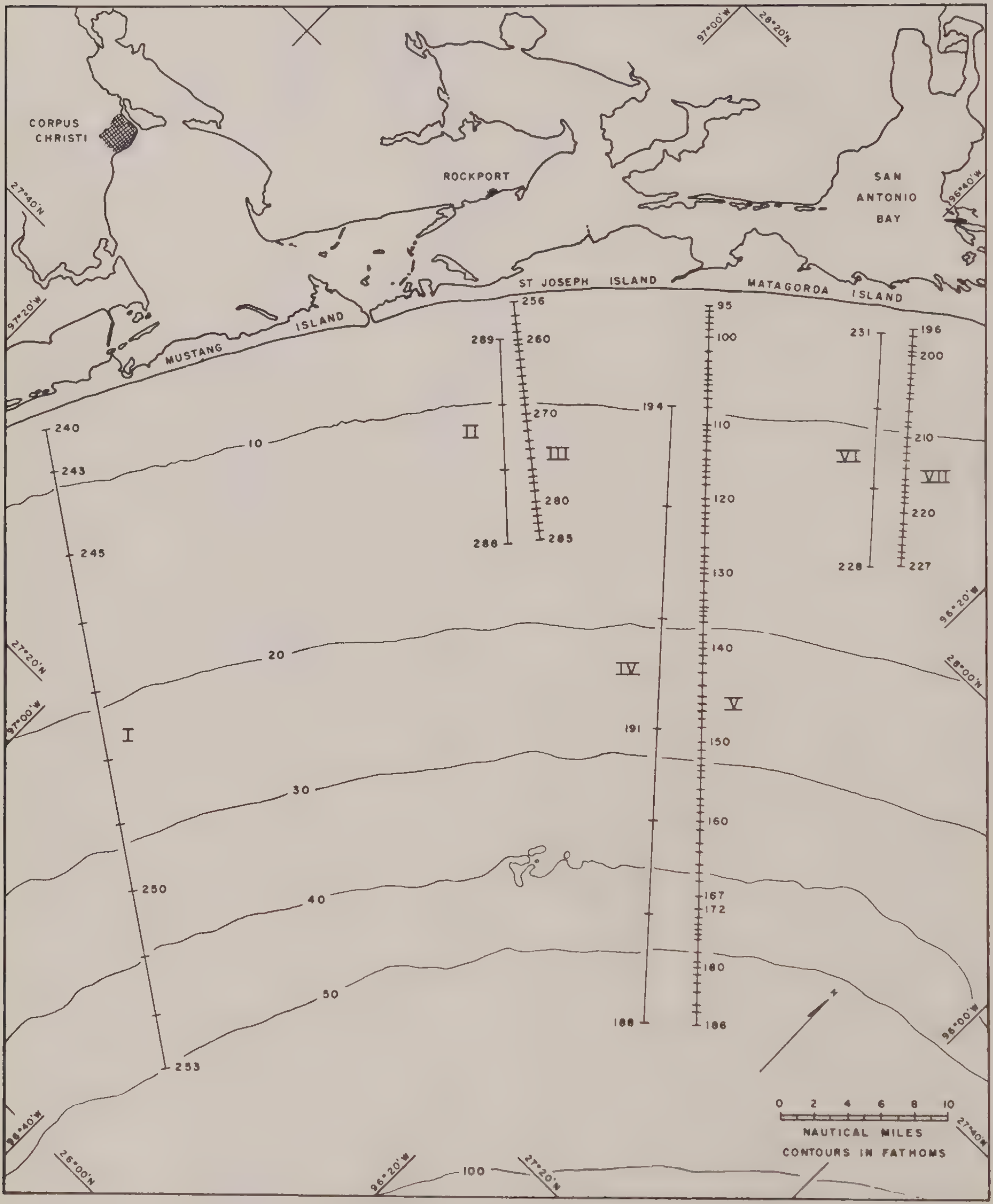
CORPUS CHRISTI
ROCKPORT
SAN ANTONIO BAY
ST JOSEPH ISLAND
MATAGORDA ISLAND
MUSTANG ISLAND
97°00'W
28°20'N
27°40'N
97°20'W
96°40'W
27°20'N
97°00'W
96°20'W
28°00'N
96°00'W
96°40'W
28°00'N
96°20'W
27°20'N
27°40'N
I
II
III
IV
V
VI
VII
240
243
245
250
253
289
288
256
260
270
280
285
194
191
188
95
100
110
120
130
140
150
160
167
172
180
186
231
228
196
200
210
220
227
10
20
30
40
50
100
0 2 4 6 8 10
NAUTICAL MILES
CONTOURS IN FATHOMS

Figure 2. Locations of stations in offshore traverses.

quence is the Guadalupe River which flows into the northeast corner of San Antonio Bay. This has formed a small delta in upper San Antonio Bay. The bays are shallow; San Antonio Bay averages five to six feet in depth, with large areas much shoaler, Mesquite Bay is less than approximately four feet deep, and in Aransas Bay the greatest depth is 11 feet. The continental shelf is about 40-45 miles wide in this area and is gently sloping seaward with occasional irregular, mound-like forms on the outer shelf apparently composed of shell and algal material (Parker and Curray, in press).

Inman and Chamberlain (1955) and Shepard and Moore (1955) have described the sediments from this area. In general there are silty clays in the center of most of the bays and these grade laterally into a narrow zone of sand at the margins. In addition, there are several small areas of oyster reef and reef debris, especially in San Antonio Bay. Sands extend out to approximately 30 foot depths in the open ocean. Most of the rest of the continental shelf is composed of sand-silt-clay or silty clay, except for local patches of shell material on the outer shelf.

Temperatures and chlorinities of the bays are summarized briefly by Parker, *et al.* (1953, p. 3). This is an area of great variation in weather and land runoff and these are reflected in water temperatures and chlorinities. Hedgpeth (1951) found that the temperatures in Aransas Bay ranged from approximately 13°C to 31°C; the actual extremes are probably 5-10°C greater than these values, possibly with actual minima of 5-8°C and a maximum of approximately 35°C. Galtsoff (1931) reports lower chlorinities in the bays during January-February, 1926, than have been recorded during the course of the present project. The lowest chlorinity, 2.2 o/oo, occurs in upper San Antonio Bay; there is a progressive increase to the southeastern part of San Antonio Bay, where 8.3 o/oo occurs. Chlorinities increase from 5.5 o/oo in southwest San Antonio Bay to a high of 14.9 o/oo at the entrance to Aransas Pass in the extreme southwest. Galtsoff's chlorinity pattern is reproduced in Figure 3.

Entirely different chlorinity values were obtained during July-August, 1951, at the time of the first survey by members of American Petroleum Institute, Project 51. A low of 8 o/oo was found at the northeast corner of San Antonio Bay at the mouth of the Guadalupe River. There was a rapid increase to a high value of 23 o/oo in southwest San Antonio Bay and even the very shallow northwest part of the bay had chlorinities of 14 o/oo to 18 o/oo. All of Aransas and Mesquite bays had chlorinities of 22 o/oo or higher. The open-ocean chlorinities during the summer of 1951 were slightly higher than 20 o/oo. These distributions are plotted on Figure 4.

It is believed that the chlorinity distributions shown in Figures 3 and 4 represent the approximate extremes to be expected in the bays of this area. The low values in 1926 reflect heavy runoff. The 1951 data were collected during a dry period when runoff was at a minimum and the principal source of water into the bays was from the open ocean. The high chlorinities reflect evaporation of the open-ocean water. The nearshore open-ocean values obtained at that time were the same as offshore oceanic chlorinity values reported by Phleger (1951) and Parr (1935), showing that there was no dilution of the nearshore water.

Chlorinities were taken during June, 1954, at the time of sampling of the sediment (Fig. 5). These values are intermediate between the extremes noted for 1926 and 1951. The lowest chlorinity is in northeastern San Antonio Bay where 3.9 o/oo was measured, and this grades to high values of approximately 20 o/oo in southeast San Antonio Bay, Mesquite Bay, and lower Aransas Bay. One interesting feature is that the chlorinities in the eastern third of San Antonio Bay were much higher than those in the middle and western parts in 1954. This suggests that the outflow diluted by runoff from the Guadalupe River affected only the middle and western parts of the bay. The eastern part of the bay appears to be isolated from the main bay circulation by an oyster reef which occurs in this area; on the basis of chlorinity distribution the water in the eastern area seems to come from the western entrances to Espiritu Santo Bay in the southeast.

Parr (1935) reports nearshore open-ocean chlorinites in 1932 of approximately 17 o/oo—18.5 o/oo in the same general area, and this may be considered a low value for the nearshore area. This is the expected condition during a time of high run-off. Under such conditions it seems likely that the low chlorinity upper water might extend for a considerable distance offshore. Water of reduced chlorinity may extend to the bottom on the inner half of the continental shelf.

METHOD OF STUDY

Sediment samples were collected during late June, 1954, with a short coring tube described by Phleger (1951). This sampler obtains sediment approximately 10 sq. cm. in area, and having a wet volume of approximately 10 ml. The upper centimeter of undisturbed sediment was placed in a jar with neutralized formalin for study of the living foraminiferal population. In the laboratory the sample was washed free of sediment finer than 0.074 mm. and the residue stained with rose Bengal for identification of living specimens (Walton, 1952). All living specimens were identified while the sample was wet. After drying, the total population (living and dead specimens) was identified and counted; in most samples only a fraction of the total population was counted, 300 specimens or more, and totals were calculated from the known fraction.

Sediment samples were collected from 34 stations in San Antonio, Mesquite and Aransas bays. These stations were so spaced that there is a reasonable coverage of the principal biofacies. One hundred and seventy-six samples have been studied from the continental shelf in this area. Most of these were collected from two traverses extending to approximately 27 m., and a third traverse out to 110 m.; samples were collected at approximately one-half mile intervals along these three traverses. A few samples were taken along four additional traverses. The locations of stations in the bays and on the continental shelf are shown in Figures 1 and 2.

BAY POPULATIONS OF FORAMINIFERA

Total Populations

Total populations (living and dead) at most stations in lower San Antonio, Mesquite, and Aransas bays are more than 10,000/sample (per 10ml.) and frequently much more than that number, *i.e.*, 34,700 specimens at station 20 in lower San Antonio Bay (see Fig. 6). Populations at eight of these 26 stations, however, are considerably lower than the average. Stations 3 and 23 (Fig. 1) are in clean sand suggesting vigorous currents or turbulence which may not be conducive to growth and deposition of large populations. Stations 2, 11, 16, and 24 are in locations where currents may be effective in preventing deposition. Deposition may be more rapid at station 6 than at other Aransas Bay stations. There is no apparent explanation for the low total population at station 14 on the east side of Mesquite Bay, unless it is the low production rate as indicated by the small living population at that station.

Total populations are significantly lower in upper San Antonio Bay, with the low populations extending as far south as station 26. It is believed that these low populations can be explained by the relatively rapid sedimentation in this part of the area, as discussed more fully below. Station 34, nearest to the mouth of the Guadalupe River, has a very high population (22,800) and this is directly correlated with the extremely high living population at that place (Fig. 6).

Living Population

The size of the living population varies from approximately 50-200/10ml. wet sediment at most stations. Extremely low populations occur at three stations in lowermost Aransas Bay and at one station in upper Aransas Bay. A very large living population is recorded from station 5, inside Mud Island. The largest living population of Foraminifera (2579) is recorded from station 34 nearest the effluent of the Guadalupe River, and a very high population was found at nearby station 33.

The previous study of total populations (Parker, *et al.*, 1953) from numerous stations within the bays showed that the most abundant forms were *Ammobaculites salsus* vars. and *A. dilatatus*, species of *Elphidium*, especially *E. gunteri*, and *"Rotalia" beccarii* vars. The bay facies was distinguished from the open-ocean "facies" ("open gulf") and an upper bay "subfacies" was differentiated in upper San Antonio Bay. In addition, fringing, island, and delta marshes contained characteristic faunas. In the present study the same basic faunal pattern is recognized in the living population, but some differences in range are observed in the living and total populations.

Living-Total Population Ratios

The importance of the ratio of living and total populations of Foraminifera as a tool for estimating relative rates of deposition has been discussed by Phleger (1951, p. 65; 1955, p. 733) and Walton (1955). The standing crop of living specimens is related at any given time to the rate of production of Foraminifera but the total number of tests (living and dead) in the sediment has accumulated over a period of time. It may be assumed that the rate of accumulation of empty tests is independent of the rate of deposition of inorganically derived sediment since each has a different source. When there is very slow deposition of inorganic sediment there will be a greater abundance of dead tests included with the sediment than if the inorganic sedimentation were rapid. In the latter case the inorganic sediment will dilute the accumulation of dead tests and the ratio of living to living-plus-dead tests will be relatively higher. The assumption must be made, of course, that the rate of accumulation of inorganic sediment does not affect the number of forms living at the sediment surface although it is possible that a very rapid rate of sedimentation might have an effect. The ratios of living to total (living and dead) populations are expressed here in percent.

The living-total population ratios in the bays fall into two geographic groups (Fig. 7). In lower San Antonio Bay, Mesquite Bay and Aransas Bay these ratios are low, generally one percent or less, with two percent at three stations and three percent at one station. In upper San Antonio Bay the ratios are higher, ranging from two to fifteen percent. The highest ratios are at the stations just off the Guadalupe Delta, 15 percent at station 32, 11 percent at station 33, and 11 percent at station 34. These ratios suggest that deposition of sediment is very slow in the lower bays and much faster in upper San Antonio Bay with the highest rate of deposition nearest the Guadalupe River.

SHELF FAUNAS

Total and Living Populations

The total populations at the continental shelf stations (see Tables 5, 8, 9, 11) generally are smaller than those in the bays, ranging from a few hundred to a few thousand per sample. Higher populations, up to 10,000 or more per sample, occur at numerous stations on the outer half of the long traverse. There appears to be a general increase in population size at several stations farther offshore. On the other hand, at many of the stations farthest offshore there are relatively small populations but these may not represent a trend and may show only local variation. There is considerable variation in population size from sample to sample and this probably is to be expected. The population sizes in both the bays and nearshore compare favorably with those reported by Parker, *et al.* (1953).

The range in size of the living population (Tables 3, 4, 6, 7, 10) is similar to the range observed in the bay samples, being approximately 50-150/sample. A few samples contained relatively large living populations: 938 at station 198, 340 at station 217, 492 at station 218, and 325 at station 157. The samples on the northeasternmost traverse have a higher average living population (average 103/station) than those in the other traverses. The samples in the southwesternmost traverse of widely spaced stations have the lowest living population with an average of 21/station. The next adjacent traverse has an average of 44/station, and the longest traverse averages 61 living specimens/station. There are very small living populations at the stations on the outer end of the long traverse, deeper than approximately 50 fathoms (91 m.).

The living-total population ratios are quite variable, ranging from less than one percent to 25 percent, but two observations may be made. There are higher ratios nearshore than offshore; this is most striking at the outermost end of the long traverse where beyond a depth of approximately 45 fathoms the ratios are very low. The average is generally higher shoreward of about 15 fathoms than deeper. The ratios are higher in the northeast than in the southwest part of the area; this is especially apparent in comparison of the values of the southwestern traverse, which are very small, with those of the northeastern traverse, which average considerably larger.

Depth Ranges

Generalized depth ranges of most of the species in the offshore traverses are shown in Figures 17-20. These data on which these figures are based are listed in Tables 3-11. Depth ranges of both the living and total populations are shown for each species. These figures are arranged according to increasing depth of the shallow limit of each species. Approximate relative abundance is indicated by the heaviness of the range lines; the shallow limit of sampling was approximately 4 m. These ranges are based on consideration of the percent of total population within a sample, frequency trends between samples, consistency of occurrence in depth, and relative number of samples in which each species was present.

A few generalizations may be made from examination of the depth distributions shown on Figures 17-20. It appears that each species has its own characteristic depth distribution which differs from the ranges of most or all other species. The following general facies boundaries are apparent: 20-30 m., 50-70 m., and 100 m. ±. It appears possible to further subdivide the depth ranges on the basis of single species or small groups of species. In most forms the total (including dead) populations have a greater deep range than the living population; the shallow limits in the more abundant species are essentially similar. None of the boundaries is sharp but there are gradations between ranges.

Forms which seem to be most indicative of the inner turbulent zone, down to 20-30 m. ±, are: *Ammobaculites dilatatus, Buliminella elegantissima,* probably certain species of *Elphidium, Gaudryina exilis, Quinqueloculina compta, Q. lamarckiana, Q. seminulum, "Rotalia" beccarii* vars. in abundance, and *"R." rolshauseni.* Other forms also occur but their ranges are more widespread.

Forms apparently characteristic of the inner shelf, shoaler than 50-70 m., are: *Bolivina lowmani, B. striatula, Eggerella* sp., *Elphidium advena, E. incertum mexicanum, E. matagordanum, E. poeyanum, Nonionella atlantica, N. opima, Nouria polymorphinoides,* and *N.* sp.

Forms restricted to the outer shelf deeper than approximately 50-70 m., or more abundant there and which may also occur beyond the shelf are: *Bigenerina* sp., *Bolivina fragilis, Cibicides* aff. *C. floridanus, C. mollis, Eponides regularis, Gaudryina* cf. *G. aequa, Lenticulina peregrina, Nonion formosum, Uvigerina parvula,* and *Valvulineria minuta.*

Species restricted to depths greater than approximately 90-100 m. are: *Bulimina spicata, Cassidulina curvata, C. norcrossi australis, Pullenia quinqueloba, Sphaeroidina bulloides,* and *Uvigerina laevis.*

DISTRIBUTION OF SPECIES

Illustrations of species are not given, but these are adequately illustrated in recent and readily available papers of Parker, *et al.* (1953), Phleger and Parker (1951), and Phleger (1954). References to illustrations for each species are given in the following section. The species are listed in alphabetical order.

Ammobaculites dilatatus Cushman and Bronnimann

Ammobaculites dilatatus Cushman and Bronnimann, 1948, Contr. Cushman Lab. Foram. Res., vol. 24, pt. 2, p. 39, pl. 7, figs. 10, 11; Parker, *et al.,* 1953, Cushman Found. Foram. Res., Spec. Publ. 2, p. 5, pl. 1, figs. 13, 15.

At less than 1% in majority of samples 17-28 m., and one specimen at 31 m.; a few living forms at same depth.

Ammobaculites dilatatus (Fig. 8) occurs in low frequencies at a few bay stations principally in the lower bays. A few living specimens were found at seven stations and empty tests occurred at a few additional stations.

Ammobaculites exiguus Cushman and Bronnimann

Ammobaculites exiguus Cushman and Bronnimann, 1948, Contr. Cushman Lab. Foram. Res., vol. 24, pt. 2, p. 38, pl. 7, figs. 7, 8; Parker, *et al,* 1953, Cushman Found. Foram. Res., Spec. Publ. 2, p. 5, pl. 1, fig. 16.

Four single living specimens 11-15 m. Dead population at majority of stations 9-33 m.; at less than 1% at occasional stations down to 62 m.

Ammobaculites salsus Cushman and Bronnimann and variants

Ammobaculites salsus Cushman and Bronnimann, 1948, Contr. Cushman Lab. Foram. Res., vol. 24, pt. 1, p. 16, pl. 3, figs. 7-9; Parker, *et al.,* 1953, Cushman Found. Foram. Res., Spec. Publ. 2, p. 5, pl. 1, figs. 17-25.

Living *Ammobaculites salsus* and variants. (Fig. 9) are present in significant frequencies at all but six bay stations. The largest populations and frequencies of living specimens are at the two stations nearest the Guadalupe River, and the extremely high living population at station 34 is composed mostly of this species. Frequencies of the living populations are comparable to frequencies of the total populations at most places indicating that the latter are good representatives of the present distributions. The lowest frequencies of both living and dead specimens are near inlets, in lower Aransas Bay and at the entrance to Espiritu Santo Bay, and the highest frequencies are throughout upper San Antonio Bay. This suggests that *A. salsus* is primarily adapted to the bay water mass and does not flourish under conditions obtaining in the open-ocean water mass.

Ammoscalaria pseudospiralis (Williamson)

Proteonina pseudospirale Williamson, 1858, Rec. Foram. Great Britain, p. 2, pl. 1, figs. 2, 3.

Ammoscalaria pseudospiralis (Williamson). Parker, *et al.,* 1953, Cushman Found. Foram. Res., Spec. Publ. 2, p. 6, pl. 1, figs. 29, 35.

Most stations at 4-108 m., with frequencies mostly less than 1% but some up to 4% on inner shelf. Living specimens occur at most stations in this depth range.

Living *Ammoscalaria pseudospiralis* is largely confined to the lower bays although it is present at three stations in the southeastern part of upper San Antonio Bay. Chlorinity distributions (Fig. 5) suggest that the water at these stations may be of lower bay type.

Angulogerina bella Phleger and Parker

Angulogerina bella Phleger and Parker, 1951, Mem. 46, Geol. Soc. Amer., pt. 2, p. 12, pl. 6, figs. 7, 8.

At most stations deeper than 40 or 45 m. in frequencies of less than 1-5%. A few records up to 24 m. Living specimens at most stations 24-105 m.

Bigenerina irregularis Phleger and Parker

Bigenerina irregularis Phleger and Parker, 1951, Mem. 46, Geol. Soc. Amer., pt. 2, p. 4, pl. 1, figs. 16-21.

Occurs at 4-110 m. Frequencies average 1-6% of total population and less at shallow and deep limits. Living specimens in abundance at most stations 7-101 m.

Bolivina fragilis Phleger and Parker

Bolivina fragilis Phleger and Parker, 1951, Mem. 46, Geol. Soc. Amer., pt. 2, p. 13, pl. 6, figs. 14, 23, 24a, b.

Living forms abundant from 53-99 m. Total population less than 1%, 48-79 m. and more than 1% deeper than 80 m. Four questionable records 12-22 m.

Bolivina lowmani Phleger and Parker

Bolivina lowmani Phleger and Parker, 1951, Mem. 46, Geol. Soc. Amer., pt. 2, p. 13, pl. 6, figs. 20a, b, 21.

Occurs rarely, less than 1%, at most stations 9-90 m. Living specimens are relatively common at 9-28 m. and occasional specimens occur as deep as 110 m.

Bolivina pulchella primitiva Cushman

Bolivina pulchella (d'Orbigny) var. *primitiva* Cushman, 1930, Fla. State Geol. Surv., Bull. 4, p. 47, pl. 8, figs. 12a, b.

Bolivina pulchella primitiva Cushman. Parker, *et al.*, 1953, Cushman Found. Foram. Res., Spec. Publ. 2, p. 6, pl. 4, figs. 2, 3.

Generally 1% or less from 11-35 m.; 1% or more 35-75 m.

Bolivina striatula Cushman

Bolivina striatula Cushman, 1922 Carnegie Inst. Washington, Publ. 311, p. 27, pl. 3, fig. 10; Parker, *et al.*, 1953, Cushman Found. Foram. Res., Spec. Publ. 2, p. 6, pl. 4, figs. 4, 5.

Less than 1% at numerous stations 7-71 m. Living specimens are at several stations 7-27 m., in abundance at two stations.

Living *Bolivina striatula* (Fig. 10) occur in low frequencies at several lower bay stations. The dead populations appear to reflect the living distributions in a general way.

Bolivina striatula spinata Cushman

Bolivina striatula Cushman var. *spinata* Cushman, 1936, Cushman Lab. Foram. Res., Spec. Publ. 6, p. 59, pl. 8, figs. 9a, b.

Bolivina striatula spinata Cushman. Parker, 1954, Bull. Mus. Comp. Zool., vol. 111, no. 10, p. 516, pl. 7, fig. 29.

Much more abundant on the outer than on the inner shelf; it occurs at all stations deeper than about 48 m. up to 4% frequency and is only at scattered stations on the inner shelf up to 15 m. The living population is very abundant at 56-75 m. and sparser elsewhere.

Bolivina subspinescens Cushman

Bolivina subspinescens Cushman, 1922, Bull. U.S. Nat. Hist. Mus., vol. 104, pt. 3, p. 48, pl. 7, fig. 5; Parker, 1954, Bull. Mus. Comp. Zool., vol. 111, no. 10, p. 517, pl. 7, figs. 30, 35.

At 1-2% in most samples deeper than 61 m., but is rare at a few stations as shallow as 20 m. Occasional living specimens 61-110 m.

Buccella hannai (Phleger and Parker)

Eponides hannai Phleger and Parker, 1951, Mem. 46, Geol. Soc. Amer., pt. 2, p. 21, pl. 10, figs. 11a. b, 12a, b, 13a, b, 14a, b.

All frequencies 1% or less between 7 m. and 101 m. but present at majority of stations. Occasional living specimens 10-59 m.

Bulimina marginata d'Orbigny

Bulimina marginata d'Orbigny, 1826, Ann. Sci. Nat., vol. 7, no. 4, p. 269, pl. 12, figs. 10-12; Parker, 1954, Bull. Mus. Comp. Zool., vol. 111, no. 10, p. 510, pl. 6, fig. 20.

At several stations 15-110 m. at less than 1%. A few living specimens 18-42 m.

Bulimina spicata Phleger and Parker

Bulimina spicata Phleger and Parker, 1951, Mem. 46, Geol. Soc. Amer., pt. 2, p. 16, pl. 7, figs. 25a-c, 30, 31.

Occurs at 1-2% at 99 m. and deeper.

Bulimina tenuis Phleger and Parker

Bulimina tenuis Phleger and Parker, 1951, Mem. 46, Geol. Soc. Amer., pt. 2, p. 16, pl. 7, figs. 32a, b, 34a, b.

Occurs at a few stations at less than 1%, at occasional stations from 13-45 m., and at most stations from 46-102 m.

Buliminella cf. B. bassendorfensis Cushman and Parker

Buliminella bassendorfensis Cushman and Parker, 1937, Contr. Cushman Lab. Foram. Res., vol. 13, pt. 1, p. 40, pl. 4, figs. 13a, b.

Buliminella sp. cf. *B. bassendorfensis* Cushman and Parker. Parker, *et al.*, 1953, Cushman Found. Foram. Res., Spec. Publ. 2, p. 6, pl. 4, figs. 6, 7.

At most stations 15-90 m., 1% or less, with a few specimens 8-105 m. Living specimens common at most stations 16-33 m. and occur 9-48 m.

Buliminella elegantissima (d'Orbigny)

Bulimina elegantissima d'Orbigny, 1839, Voy. Amér. Mérid., vol. 5, pt. 5, "Foraminifères," p. 51, pl. 7, figs. 13, 14.

Buliminella elegantissima (d'Orbigny). Parker, *et al.*, 1953, Cushman Found. Foram. Res., Spec. Publ. 2, p. 6, pl. 4, figs. 8. 9.

Rare at a few stations 7-36 m., 1% or less. A few living specimens 7-23 m.

Cancris oblonga (Williamson)

Rotalina oblonga Williamson, 1858, Rec. Foram. Great Britain, p. 51, pl. 4, figs. 98-100.

Cancris oblonga (Williamson). Parker, 1954, Bull. Mus. Comp. Zool., vol. 111, no. 10, p. 532, pl. 10, figs. 13, 14.

Occurs 10-110 m., but dead population most common 35-110 m. where it is up to 2% of the population. Living specimens found 10-108 m., but very abundant between 48 and 73 m.

Cassidulina curvata Phleger and Parker

Cassidulina curvata Phleger and Parker, 1951, Mem. 46, Geol. Soc. Amer., pt. 2, p. 26, pl. 14, figs. 5a, b.

Less than 1% at four stations deeper than 99 m.

Cassidulina neocarinata Thalmann

Cassidulina laevigata d'Orbigny var. *carinata* Cushman, 1922 (not Silvestri, 1896), Bull. U.S. Nat. Mus., vol. 104, pt. 3, p. 124, pl. 25, figs. 6, 7.

Cassidulina neocarinata Thalmann, 1950, Contr. Cushman Found. Foram. Res., vol. 1, pts. 3, 4, p. 44; Parker, 1954, Bull. Mus. Comp. Zool., vol. 111, no. 10, p. 536, pl. 11, fig. 3.

1% or less at three stations from 101-108 m.

Cassidulina subglobosa H. B. Brady

Cassidulina subglobosa H. B. Brady, 1881, Quart. Journ. Micr. Sci., n. s., vol. 21, p. 60; H. B. Brady, 1884, Rept. Voy. CHALLENGER, Zool., vol. 9, p. 430, pl. 54, figs. 17a-c; Parker, 1954, Bull. Mus. Comp. Zool., vol. 111, no. 10, p. 536, pl. 11, figs. 4-9.

More abundant deeper than about 50 m. where it is up to 6% of the population. The few records as shallow as 15 m. may be incorrectly identified. Living specimens deeper than about 50 m., with one exception.

Cibicides aff. C. floridanus (Cushman)

Truncatulina floridana Cushman, 1918, Bull. 676, U.S. Geol. Surv., p. 62, pl. 19, fig. 2.

Cibicides aff. *floridanus* (Cushman). Parker, 1954, Bull. Mus. Comp. Zool., vol. 111, no. 10, p. 541, pl. 12, figs. 5, 9.

All records deeper than 64 m. with populations up to 15% deeper than about 85 m. Living specimens common at most stations within the entire depth range.

Cibicides mollis Phleger and Parker

Cibicides mollis Phleger and Parker, 1951, Mem. 46, Geol. Soc. Amer., pt. 2, p. 30, pl. 16, figs. 7a, b, 8a, b, 9a, b.

1% or less of the fauna at numerous stations deeper than 59 m.

"Discorbis" bulbosa Parker

"Discorbis" bulbosa Parker, 1954, Bull. Mus. Comp. Zool., vol. 111, no. 10, p. 523, pl. 8, figs. 10-12.

All occurrences are deeper than about 20 m., with occasional frequencies up to 2%. A few living specimens 22-49 m.

Eggerella sp.

Restricted to 15-36 m. at 1% or less, but at numerous stations. Living populations are similar.

Elphidium advena (Cushman)

Polystomella advena Cushman, 1922, Carnegie Inst. Washington, Publ. 311, p. 56, pl. 9, figs. 11, 12.

Elphidium advenum (Cushman). Parker, *et al.*, 1953, Cushman Found. Foram. Res., Spec. Publ. 2, p. 7, pl. 3, fig. 11.

Recorded at less than 1% at several stations from 11-54 m.; a few living specimens are found at 11-27 m.

Elphidium discoidale (d'Orbigny)

Polystomella discoidale d'Orbigny, 1839, in de la Sagra, Hist. Phys. Pol. Nat. Cuba, "Foraminifères," p. 56, pl. 6, figs. 23, 24.

Elphidium discoidale (Orbigny). Parker, *et al.*, 1953, Cushman Found. Foram. Res., Spec. Publ. 2, p. 7, pl. 3, figs. 13, 14.

Occurs at most stations with total populations 5-20% down to 64 m. and less than 6% from 65-105 m. Living specimens occur at several, but not all, stations 4-64 m., and they are not so relatively abundant as total population.

Elphidium gunteri Cole

Elphidium gunteri Cole, 1931, Fla. State Geol. Surv., Bull. 6, p. 34, pl. 4, figs. 9, 10; Parker, *et al.*, 1953, Cushman Found. Foram. Res., Spec. Publ. 2, p. 8, pl. 3, figs. 18, 19.

Constitutes 5-20% of the total population at all stations down to 48 m., and 5% or less 49-102 m. Living specimens are confined to the upper 48 m. and occur at about half the stations.

Living specimens of *Elphidium gunteri* (Fig. 11) are present at most bay stations except those on the northeast side of San Antonio Bay (stations 29, 30, 32, 33, 34). This species is a much larger fraction of the total than of the living population at most stations. Such contrast in population frequencies suggests either that the June, 1954, sampling does not represent average conditions or that conditions may have recently changed in the area to modify the distribution of living *E. gunteri*. It does not seem likely that there was concentration of specimens by physical processes because of widespread high frequencies of empty tests.

Elphidium incertum mexicanum Kornfeld

Elphidium incertum Williamson var. *mexicana* Kornfeld, 1931, Contr. Geol. Dept. Stanford Univ., vol. 1, no. 3, p. 89, pl. 16, figs. 1a, b, 2a, b.

Elphidium incertum mexicanum Kornfeld. Parker, *et al.*, 1953, Cushman Found. Foram. Res., Spec. Publ. 2, p. 8, pl. 3, figs. 20, 21.

1% or less at a few stations between 4 and 41 m. One living specimen was found at 24 m.

Elphidium matagordanum (Kornfeld)

Nonion depressula (Walker and Jacob) var. *matagordana* Kornfeld, 1931, Contr. Dept. Geol., Stanford Univ., vol. 1, no. 3, p. 87, pl. 13, figs. 2a, b.

Elphidium matagordanum (Kornfeld). Parker, *et al.*, 1953, Cushman Found. Foram. Res., Spec. Publ. 2, p. 8, pl. 3, figs. 24, 25.

At 1% or less at occasional stations 4-40 m.; three living specimens 15-35 m. Living specimens of *Elphidium matagordanum* were recorded from only seven bay stations, but it occurs as 1-3% of the dead populations at all stations (Fig. 12).

Elphidium poeyanum (d'Orbigny)

Polystomella poeyana d'Orbigny, 1839, in de la Sagra, Hist. Phys. Pol. Nat. Cuba, "Foraminifères," p. 55, pl. 6, figs. 25, 26.

Elphidium poeyanum (d'Orbigny). Parker, *et al.*, 1953, Cushman Found. Foram. Res., Spec. Publ. 2, p. 9, pl. 3, fig. 26.

At the majority of stations 4-54 m. at 1% or less of the total population. Occasional living specimens at 10 stations 7-44 m.

Elphidium poeyanum (Fig. 13) has a distribution in the bays similar to that of *E. gunteri* but the frequencies are much lower. Small living populations are at the majority of stations throughout the area except on the east side of San Antonio Bay. It is 1-6% of the dead population and is present at all stations.

Epistominella vitrea Parker

Epistominella vitrea Parker, in Parker, *et al.*, 1953, Cushman Found. Foram. Res., Spec. Publ. 2, p. 9, pl. 4, figs. 34-36, 40, 41.

This species is essentially restricted to deeper than 15 m. where it occurs at most stations at 2-8%. Living population well-represented 15-69 m., with one specimen at 102 m.

Eponides antillarum (d'Orbigny)

Rotalina antillarum d'Orbigny, 1839, in de la Sagra, Hist. Phys. Pol. Nat. Cuba, "Foraminifères," p. 75, pl. 5, figs. 4-6.

Eponides antillarum (d'Orbigny). Parker, 1954, Bull. Mus. Comp. Zool., vol. 111, no. 10, p. 528, pl. 9, figs. 14, 15.

Very rare at a few stations 4-99 m., with most at about 50-80 m. Living and total distribution similar.

Eponides regularis Phleger and Parker

Eponides regularis Phleger and Parker, 1951, Mem. 46, Geol. Soc. Amer., pt. 2, p. 21, pl. 11, figs. 3a, b, 4a-c.

There are 10 living specimens of this species at 70-101 m.

Eponides turgidus Phleger and Parker

Eponides turgidus Phleger and Parker, 1951, Mem. 46, Geol. Soc. Amer., pt. 2, p. 22, pl. 11, figs. 9a, b.

Occurs as single specimens at most stations from 77-99 m. No living specimens seen.

Eponides umbonatus (Reuss)

Rotalina umbonata Reuss, 1851, Zeitschr. Deutsch. Geol. Ges., vol. 3, p. 75, pl. 5, figs. 35a-c.

Pseudoeponides umbonatus (Reuss). Parker, 1954, Bull. Mus. Comp. Zool., vol. 111, no. 10, p. 530, pl. 9, figs. 20, 21.

Present at about half the stations in the long traverse from 66-110 m. Two living specimens at 75 and 84 m.

Gaudryina cf. **G. aequa** Cushman

Gaudryina aequa Cushman, 1947, Contr. Cushman Lab. Foram. Res., vol. 23, pt. 4, p. 87, pl. 18, figs. 18-21.

Gaudryina cf. *aequa* Cushman. Phleger and Parker, 1951, Mem. 46, Geol. Soc. Amer., pt. 2, p. 6, pl. 2, figs. 11, 12.

Found at 62-90 m., mostly living specimens, and a very small fraction of the population.

Gaudryina exilis Cushman and Bronnimann

Gaudryina exilis Cushman and Bronnimann, 1948, Contr. Cushman Lab. Foram. Res., vol. 24, pt. 2, p. 40, pl. 7, figs. 15, 16; Parker, *et al.*, 1953, Cushman Found. Foram. Res., Spec. Publ. 2, p. 9, pl. 1, figs. 37, 38.

Essentially restricted to a few stations at 9-28 m. in frequencies less than 1%. Two occurrences down to 41 m.

Hanzawaia strattoni (Applin)

Truncatulina americana Cushman var. *strattoni* Applin, 1925, in Applin, Ellisor, and Kniker, Bull. Amer. Assoc. Petr. Geol., vol. 9, p. 99, pl. 3, fig. 3.

Cibicidina strattoni (Applin). Parker, *et al.*, 1953, Cushman Found. Foram. Res., Spec. Publ. 2, p. 7, pl. 4, figs. 38, 39.

One of the abundant forms on the continental shelf, averaging 5-10% of the total population from 10-110 m. The living population is abundant from about 25 m. to 77 m., and occurs to 90 m.

Lagena and related species

Species of this group occur at several stations from 16-108 m., and are most abundant from about 65-99 m.

Lenticulina peregrina (Schwager)

Cristellaria peregrina Schwager, 1866, Novara Exped., Geol. Theil., vol. 2, p. 245, pl. 7, fig. 89.

Lenticulina peregrina (Schwager). Parker, 1954, Bull. Mus. Comp. Zool., vol. 111, no. 10, p. 504, pl. 5, fig. 18.

Very rare at a few stations 61-105 m.

Family MILIOLIDAE

Both living and dead Miliolidae (Fig. 16) are confined to the lower bays where they occur in low and moderate frequencies. The highest frequencies are in lower Aransas Bay seaward from Mud Island.

Nonion formosus (Seguenza)

Nonionina formosa Seguenza, 1880, Atti R. Acad. Lincei, ser. 3, vol. 6, p. 73, pl. 7, figs. 6, 6a.

Nonion formosum (Seguenza). Parker, 1954, Bull. Mus. Comp. Zool., vol. 111, no. 10, p. 506, pl. 6, fig. 3.

Less than 1% of the population deeper than 73 m. Living specimens reflect the distribution of dead specimens.

Nonionella atlantica Cushman

Nonionella atlantica Cushman, 1947, Contr. Cushman Lab. Foram. Res., vol. 23, pt. 4, p. 90, pl. 20, figs. 4, 5; Parker, *et al.*, 1953, Cushman Found. Foram. Res., Spec. Publ. 2, p. 11, pl. 3, figs. 30, 31.

Total population averages 1-6% from 10-75 m., and is less frequent to 110 m. Living population relatively abundant 10-73 m.

Nonionella opima Cushman

Nonionella opima Cushman, 1947, Contr. Cushman Lab. Foram. Res., vol. 23, pt. 4, p. 90, pl. 20, figs. 1-3; Parker, *et al.*, 1953, Cushman Found. Foram. Res., Spec. Publ. 2, p. 11, pl. 3, figs. 32, 33.

Common at most stations 1-5%, 7-80 m. and less frequent to 110 m. Living specimens abundant and at most stations 7-79 m.

Nouria polymorphinoides Heron-Allen and Earland

Nouria polymorphinoides Heron-Allen and Earland, 1914, Trans. Zool. Soc. London, vol. 20, pt. 12, p. 376, pl. 37, figs. 1-15; Parker, *et al.*, 1953, Cushman Found. Foram. Res., Spec. Publ. 2, p. 11, pl. 3, figs. 1, 2.

This species is mostly represented by living specimens with only occasional empty tests. Most of the fragile arenaceous tests appear to be destroyed when the animal dies. This species is most frequent at 15-40 m. but is present to 66 m.

Palmerinella palmerae Bermudez

Palmerinella palmerae Bermudez, 1934, Mem. Soc. Cubana Hist. Nat., vol. 8, no. 2, p. 84, text figs. 1-3; Parker, *et al.*, 1953, Contr. Cushman Found. Foram. Res., Spec. Publ. 2, p. 11, pl. 4, figs. 42-44.

Empty tests of *Palmerinella palmerae* (Fig. 14) are widely distributed throughout the bays in low frequencies except in southeastern San Antonio Bay. The living population was found in some abundance at Stations 32-34 off the Guadalupe Delta, at three other stations in upper San Antonio Bay, and at two stations in Aransas Bay.

Planulina exorna Phleger and Parker

Planulina exorna Phleger and Parker, 1951, Mem. 46, Geol. Soc. Amer., pt. 2, p. 32, pl. 18, figs. 5a, b, 6a, b, 7a, b, 8a, b.

In most samples at 38-108 m., deeper at 1% or less, and in a few samples as shallow as 22 m. Four living specimens 42-68 m.

Proteonina atlantica Cushman

Proteonina atlantica Cushman, 1944, Cushman Lab. Foram. Res., Spec. Publ. 12, p. 5, pl. 1, fig. 4; Parker. *et al.*, 1953, Cushman Found. Foram. Res., Spec. Publ. 2, p. 11, pl. 1, fig. 4.

Occurs in most samples at 20-80 m. at 1-5% average frequencies, and present at 12-110 m. Living specimens occur through entire range.

Pullenia quinqueloba (Reuss)

Nonionina quinqueloba Reuss, 1851, Zeitschr. Deutsch. Geol. Ges., vol. 3, p. 71, pl. 5, fig. 31.

Pullenia quinqueloba (Reuss). Parker, 1954, Bull. Mus. Comp. Zool., vol. 111, no. 10, p. 538, pl. 11, fig. 16.

A few living and dead specimens present in samples 99 m. and deeper.

Pyrgo nasutus Cushman

Pyrgo nasutus Cushman, 1935, Smithsonian Misc. Coll., vol. 91, no. 21, p. 7, pl. 3, figs. 1-4.

Pyrgo cf. *nasutus* Cushman. Parker, 1954, Bull. Mus. Comp. Zool., vol. 111, no. 10, p. 501, pl. 5, fig. 4.

Occurs mostly as single specimens in most stations from 73-108 m. with three occurrences at 38-48 m. Seven living specimens at 38-73 m.

Quinqueloculina compta Cushman

Quinqueloculina compta Cushman, 1947, Contr. Cushman Lab. Foram. Res., vol. 23, pt. 4, p. 87, pl. 19, fig. 2.

Quinqueloculina sp. cf. *Q. compta* Cushman. Parker, *et al.*, 1953, Cushman Found. Foram. Res., Spec., Publ. 2, p. 12, pl. 2, figs. 5, 6.

Low frequencies at 10 stations from 11-30 m. Eleven living specimens.

Quinqueloculina lamarckiana d'Orbigny

Quinqueloculina lamarckiana d'Orbigny, 1839, in de la Sagra, Hist. Phys. Pol. Nat. Cuba, "Foraminifères," p. 189, pl. 11, figs. 14; 15; Parker, *et al.*, 1953, Cushman Found. Foram. Res., Spec. Publ. 2, p. 12, pl. 2, figs. 11, 12.

Single specimens in samples at 11-30 m. Four living specimens.

Quinqueloculina seminulum (Linne)

Serpula seminulum Linne, 1767, Syst. Nat., ed. 12, p. 1264.

Quinqueloculina seminulum (Linné). Parker, *et al.*, 1953, Cushman Found. Foram. Res., Spec. Publ. 2, p. 12, pl. 2, figs. 18, 19.

Occurs in very low frequencies at 4-20 m. One living specimen.

Rectobolivina advena (Cushman)

Siphogenerina advena Cushman, 1922, Carnegie Inst. Washington, Publ. 311, p. 35, pl. 5, fig. 2.

Rectobolivina advena (Cushman). Parker, *et al.*, 1953, Cushman Found. Foram. Res., Spec. Publ. 2, p. 13, pl. 4, figs. 10, 11.

Total population 2-4% and at most stations 30-110 m., with frequencies less than 1% 8-30. Occasional living specimens 33-62 m.

Reophax gracilis (Kiaer)

Nodulina gracilis Kiaer, 1900, Rept. Norwegian Fish. Mar. Invest., vol. 1, no. 7, p. 24, text fig. 2.

Reophax gracilis (Kiaer). Parker, 1952, Bull. Mus. Comp. Zool., vol. 106, no. 9, p. 397, pl. 2, fig. 1.

A few living specimens recorded 20-84 m. No empty tests seen, probably because of their fragile construction.

Reussella atlantica Cushman

Reussella spinulosa (Reuss) var. *atlantica* Cushman, 1947, Contr. Cushman Lab. Foram. Res., vol. 23, pt. 4, p. 91, pl. 20, figs. 6, 7.

Reussella atlantica Cushman. Parker, *et al.*, 1953, Cushman Found. Foram. Res., Spec. Publ. 2, p. 13, pl. 4, figs. 12, 13.

Present in most samples at 9-110 m., but most common at 30-110 m. where it averages 2-5% of the total population. Shallow occurrences are 2% or less.

Robulus spp.

At most stations deeper than 71 m. at less than 1% of total population. Occurs at 10 stations 22-69 m.

Rosalina floridana (Cushman)

Discorbis floridanus Cushman, 1922, Carnegie Inst. Washington, Publ. 311, p. 39, pl. 5, figs. 11, 12.

Rosalina floridana (Cushman). Parker, 1954, Bull. Mus. Comp. Zool., vol. 111, no. 10, p. 524, pl. 8, figs. 19, 20.

Generally 1% or less at most stations 10-80 m. Living specimens at only 10 stations 10-24 m.

Rosalina suezensis (Said)

Discorbis suezensis Said, 1949, Cushman Lab. Foram. Res., Spec. Publ. 26, p. 36, pl. 3, fig. 34.

Rosalina suezensis (Said). Parker, 1954, Bull. Mus. Comp. Zool., vol. 111, no. 10, p. 525, pl. 8, figs. 21, 26, 27.

Dead population 2-4% at all stations in long traverse deeper than 78 m. with scattered single specimens as shallow as 23 m. Living specimens at 38 m. and 42 m.

"Rotalia" beccarii (Linné) variants

"Rotalia" beccarii (Linné) var. A. Parker, *et al.*, 1953, Cushman Found. Foram. Res., Spec. Publ. 2, p. 13, pl. 4, figs. 20-22.

"Rotalia" beccarii (Linné) var. B. Parker, *et al.*, 1953, Cushman Found. Foram. Res., Spec. Publ. 2, p. 13, pl. 4, figs. 25-28.

"Rotalia" beccarii var. A. is abundant at all stations 4-37 m. with average frequency of 10-25%. Living specimens also abundant in this depth range. Common 38-75 m., and recorded at 1% or less to 110 m. Living specimens as deep as 77 m.

Range and frequencies of *"R." beccarii* var. B.

essentially similar to *"R" beccarii* var. A. except recorded to only 99 m. It is believed that these two variants constitute the same population.

The variants of this species are the dominant living forms at 25 of the 34 bay stations and at most stations both the living and the total populations constitute more than 50% of the fauna. They are present in abundance at all stations but one; at station 3 this species group was not recorded living, but is a large fraction of the dead population.

"Rotalia" pauciloculata Phleger and Parker

Rotalia pauciloculata Phleger and Parker, 1951, Mem. 46, Geol. Soc. Amer., pt. 2, p. 23, pl. 12, figs. 8a, b, 9a, b.

In most samples 10-75 m., frequencies generally 1% or less but up to 4%. Specimens present to 110 m. Living specimens in several samples 15-42 m. and at five stations 44-75 m.

"Rotalia" rolshauseni Cushman and Bermudez

Rotalia rolshauseni Cushman and Bermudez, 1946, Contr. Cushman Lab. Foram. Res., vol. 22, pt. 4, p. 119, pl. 19, figs. 11-13.

"Rotalia" rolshauseni Cushman and Bermudez. Parker, *et al.*, 1953, Cushman Found. Foram. Res., Spec. Publ. 2, p. 14, pl. 4, figs. 32, 33.

This species has the most restricted range of any species of the genus in this area, 7-37 m., with one specimen at 44 m. Average frequencies 1% or less. Living specimens 14-27 m.

Seabrookia earlandi Wright

Seabrookia earlandi Wright, 1891, Proc. Roy. Irish Acad., ser. 3, vol. 1 (1889-91), no. 4, p. 477, pl. 20, figs. 6, 7; Parker, 1954, Bull. Mus. Comp. Zool., vol. 111, no. 10, p. 538, pl. 11, fig. 13.

1% or less at most stations 52-90 m. Two specimens at 27-30 m. Eight living specimens 63-81 m.

Sigmoilina distorta Phleger and Parker

Sigmoilina distorta Phleger and Parker, 1951, Mem. 46, Geol. Soc. Amer., pt. 2, p. 8, pl. 4, figs. 3-5.

Generally confined to 85 m. or deeper. One living specimen at 66 m.

Siphonina pulchra Cushman

Siphonina pulchra Cushman, 1919, Carnegie Inst. Washington, Publ. 291, p. 24, pl. 14, figs. 7a-c; Phleger and Parker, 1951, Mem. 46, Geol. Soc. Amer., pt. 2, p. 24, pl. 12, figs. 15a, b.

Occurrences are 42 m. and deeper, more constant 68 m. and deeper. Frequencies are 1% or less.

Sphaeroidina bulloides d'Orbigny

Sphaeroidina bulloides d'Orbigny, 1826, Ann. Sci. Nat., vol. 7, p. 267, no. 1; Parker, 1954, Bull. Mus. Comp. Zool., vol. 111, no. 10, p. 539, pl. 11, fig. 18.

Six occurrences at 99 m. and deeper; four living specimens.

Stetsonia minuta Parker

Stetsonia minuta Parker, 1954, Bull. Mus. Comp. Zool., vol. 111, no. 10, p. 534, pl. 10, figs. 27-29.

1% or less at most stations from 45-84 m., six occurrences at 16-33 m., and one specimen at 101 m. Living specimens at 16 m., 23 m., and 66 m.

Textularia mayori Cushman

Textularia mayori Cushman, 1922, Carnegie Inst. Washington, Publ. 311, p. 23, pl. 2, fig. 3.

Textularia sp. cf. *T. mayori* Cushman. Parker, *et al.*, 1953, Cushman Found. Foram. Res., Spec. Publ. 2, p. 14, pl. 1, fig. 36.

Occurs at most stations in frequencies of 1% or less from 12-102 m. Living population confined to 23-85 m. depth.

Uvigerina auberiana d'Orbigny

Uvigerina auberiana d'Orbigny, 1839, in de la Sagra, Hist. Phys. Pol. Nat. Cuba, "Foraminifères," p. 106, pl. 2, figs. 23, 24; Parker, 1954, Bull. Mus. Comp. Zool., vol. 111, no. 10, p. 519, pl. 7, fig. 38; pl. 8, fig. 1

Seven specimens occur in the long traverse from 66-96 m.

Uvigerina laevis Goës

Uvigerina auberiana d'Orbigny. Goës, 1883 (not d'Orbigny, 1839), Kongl. Svensk. Vet. Akad. Handl., vol. 19, no. 4, p. 60, pl. 4, figs. 71-74.

Uvigerina auberiana d'Orbigny var. *laevis* Goës, 1896, Bull. Mus. Comp. Zool., vol. 29, p. 51.

Uvigerina laevis Goës. Parker, 1954, Bull. Mus. Comp. Zool., vol. 111, no. 10, p. 520, pl. 8, fig. 4.

Live and dead specimens occur at 85 m. or deeper. Occurrences at 108 m. and 110 m. are 12 and 15% of total population.

Uvigerina parvula Cushman

Uvigerina peregrina Cushman var. *parvula* Cushman, 1923, Bull. U.S. Nat. Mus., vol. 104, pt. 4, p. 168, pl. 42, fig. 11.

Uvigerina parvula Cushman. Parker, 1954, Bull. Mus. Comp. Zool., vol. 111, no. 10, p. 521, pl. 8, fig. 6.

At all stations deeper than about 50 m., and at 77 m. and deeper constitutes 10-25% of the total population. Living specimens have a similar range, 58-110 m. It is reported at occasional stations as shallow as 12 m.

Valvulineria minuta Parker

Valvulineria minuta Parker, 1954, Bull. Mus. Comp. Zool., vol. 111, no. 10, p. 527, pl. 9, figs. 4-6.

No living specimens found. Single specimens at 68 m. and deeper at the majority of stations.

Virgulina pontoni Cushman

Virgulina pontoni Cushman, 1932, Contr. Cushman Lab. Foram. Res., vol. 8, pt. 1, p. 17, pl. 3, fig. 7; Parker, *et al.*, 1953, Cushman Found. Foram. Res., Spec. Publ. 2, p. 15, pl. 4, figs. 14, 15.

Present at almost all stations, at less than 1% shoaler than 15 m., 1-5% at 16-22 m., 5-15% at 23-75 m., and 1-5% at 75-110 m. Living specimens abundant and have similar relative frequencies.

Virgulina spinicostata Phleger and Parker

Virgulina spinicostata Phleger and Parker, 1951, Mem. 46, Geol. Soc. Amer., pt. 2, p. 19, pl. 9, figs. 11a, b, 12a, b, 13a, b, 14.

Most common at about 40-80 m. with average frequencies 2-4% and present at most stations. Occurs in all samples at 85-99 m. at 1% or less. Generally 1% or less at 11-40 m. Ten living specimens at 23-39 m.

DISCUSSION

Relative Rates of Sedimentation

The live-total ratios of the benthonic Foraminifera in this area suggest high rates of sedimentation in upper San Antonio Bay and very low sedimentation in the lower bays. The apparent rates increase toward the mouth of the Guadalupe River. The low presumed rates in the lower bays suggest that either all the sediment being brought in by the river is being deposited in the upper bay or that sediment is by-passing the lower bays and being deposited on the shelf.

Live-total population ratios on most of the inner shelf indicate a rate of deposition faster than in the lower bays and slower than in upper San Antonio Bay. The ratios increase toward the northeast, with very low ones in the southwest traverse (stations 240-251) and the highest ones in the northeast traverse (stations 196-227). The presumed higher rates of sedimentation in the northeast suggest a source of supply in that direction. This source may be from the Brazos and Colorado rivers which are approximately 90 and 40 miles to the northeast. Bullard (1942) has demonstrated a southeast movement of beach sands in this area, based on heavy mineral suites, indicating a southwest set to the water near the coast.

The sediment at present being deposited in upper San Antonio Bay in association with the delta of the Guadalupe River may be confined to that brought in during normal low-water river flow. One of the characteristics of the area is intensive floods which occur at irregular intervals, and these must introduce a large amount of sediment. Much or most of this sediment may by-pass the bays and be carried through the passes and over the barrier island during an extremely high runoff.

Shepard (1953) has compared the U. S. Coast and Geodetic Survey soundings made during the last century with those made in the 1930's, and has indicated shoaling at the rate of approximately one foot per century. The slow rate of sedimentation in the lower bays based on the living-total foraminiferal faunas applies only to the upper 1 cm. of sediment sampled. This suggests a recent decrease in rate of deposition in the lower bays, if both of these methods are valid.

The live-total ratios are very low at all stations on the outer edge of traverse III, from approximately stations 175-186 at the outer edge of the continental self. This suggests that most or all of the sediment is being trapped inside this zone, but more data are needed from other traverses to verify this.

Production of Benthonic Foraminifera

There is no reliable information on how fast these forms are produced. Preliminary analyses of seasonal surveys of the standing crop in the bays of this area, however, seem to indicate that the more common forms are reproducing at all seasons. Preliminary experiments by John S. Bradshaw of the Marine Foraminifera Laboratory show that one common bay species will go through a reproductive cycle in about five weeks under laboratory conditions. Continental shelf forms may reproduce and be supplied to the sediment at a slower rate than those in the bays. The large total bay populations thus may be partly a result of high production rates in this environment.

There is considerable variation in the amount of standing crop between some closely spaced samples, as in offshore traverses III, V, and VII. This may be partly a result of the method of sampling, in which only 10 sq. cm. of sediment 1 cm. in thickness is used. Collecting a larger sample makes laboratory study of the live fauna unduly time-consuming and laborious and it has been considered desirable to study a large number of samples instead of a few large ones. Preliminary study has shown that several suites of samples collected from the same stations at different times have populations which are similar in size. Variation in population size over short distances, as in the offshore traverses, may be a normal pattern.

Certain general features of the size of the living population are of considerable interest as reflecting relative production rates. Much the largest living population is in San Antonio Bay at station 34 near the effluent of the Guadalupe River where 2579 live specimens were found. Station 33, near station 34, also contained a large population with 302 specimens. These stations are three to four miles away from the present river mouth. Very large living populations are reported four to eight miles off the distributary mouths in the southeast Mississippi Delta area (Phleger, 1955, p. 730, fig. 8). These data suggest that the large populations reflect the presence of river mouths and that there is a high organic production near rivers, in contrast to a generally accepted belief among some geologists that production is low off river mouths. Such a high production rate may be reflected in the size of the total population if sedimentation is not too rapid. The high population at station 34 in San Antonio Bay reflects the high production there and not a slow rate of deposition. The stations with high production off the Mississippi Delta do not contain unusually large total populations; this is due to the very rapid sedimentation occurring at that place (*op. cit.*, p. 733, fig. 11).

The offshore living populations show a general trend in size if numerical averages are made of the populations in each traverse. The average population increases toward the northeast, as follows:

Traverse I	21/sample
Traverse III	44/sample
Traverse V	61/sample
Traverse VII	103/sample

It is possible that the larger production in the northeast is due to the influence of the water from the Brazos and Colorado rivers, since there is evidence of a southwestward movement of water. This may be similar, therefore, to the situation off the Mississippi and Guadalupe rivers.

Post-Depositional Transport of Faunas

The distributions of living and dead populations in the bays are quite similar and it is concluded that the dead population of each species reflects its living distribution. Differences are noted mainly where frequencies are low.

In the open-ocean traverses, on the other hand, the dead populations of most species have a much wider depth distribution than living forms of the same species. Where a species is rare the probability of obtaining a living specimen is less than where a species is abundant. Dead forms are more widespread through depth than living forms, however, in both rare and abundant species. This marked wider distribution is generally restricted to the deeper ends of their ranges.

The following examples illustrate these differences in range: living "*Rotalia*" *beccarii* is abundant from the inner ends of the traverses to approximately 40 m. and is rare to approximately 80 m.; dead forms are abundant to approximately 45 m., and are common to rare to the end of traverse V at 110 m. Living *Elphidium discoidale* is rare from the inner ends of the traverses to approximately 65 m. but dead forms occur commonly to a depth of about 107 m. Living *Hanzawaia strattoni* is abundant from about 22 m. to 77 m. and rare to 90 m.; the dead population is abundant to the end of traverse V at 110 m.

Two possible explanations are suggested for these differences in depth distribution. It is possible that these faunas have moved downslope by the force of gravity, in the form of turbidity or other currents. There is also the possibility that these faunas are residual from a former environment, when sea-level was lower or when other ecological factors were similar to those at present on the inner shelf.

Causes of Shelf Zonation

It does not seem profitable to speculate on the individual environmental factors which may cause shelf depth zonation. It appears, however, that these different assemblages do reflect different characteristics of the water in a general way. The nearshore benthonic fauna, down to 20-30 m., is adapted to an environment whose distinguishing feature appears to be wave turbulence. At La Jolla, California, diving observations have shown that severe turbulence is always observed to a depth of about 10 m. and is frequently present to a depth of about 30 m. (Inman, personal communication). The depth 50-70 m. which divides the "inner" shelf benthonic assemblage from the "outer" shelf one is probably the boundary between the effect of offshore water masses and nearshore water masses affecting the bottom. The offshore, oceanic water probably is rather consistently present beyond this position. Presence of abundant planktonic Foraminifera in the outer shelf sediments is evidence in this connection since these forms are adapted to offshore water.

REFERENCES

Bullard, F. M., 1942, Source of beach and river sands on Gulf Coast of Texas, Bull. Geol. Soc. Amer., vol. 53, no. 7, pp. 1021-1043.

Galtsoff, P. S., 1931, Survey of oyster bottoms in Texas, U. S. Bur. Fish. Invest. Rept., no. 6, pp. 1-30.

Hedgpeth, J. W., 1951, in Report of the committee on a treatise on marine ecology and paleoecology, no. 11, pp. 49-56.

Inman, D. L., and Chamberlain, T. K., 1955, Particle-size distribution in nearshore sediments, Soc. Econ. Pal. and Min., Spec. Publ. 3, pp. 106-126.

Parker, F. L., Phleger, F. B, and Peirson, J. F., 1953, Ecology of Foraminifera from San Antonio Bay and environs, southwest Texas, Cushman Found. Foram. Res., Spec. Publ. no. 2, pp. 1-75.

Parr, A. E., 1935, Report on hydrographic observations in the Gulf of Mexico and adjacent straits made during the Yale Oceanographic Expedition on the MABEL TAYLOR in 1932, Bull. Bingham Oceanog. Coll., vol. V, pp. 1-93.

Phleger, F. B, 1951, Ecology of Foraminifera, northwest Gulf of Mexico, Pt. 1. Foraminifera distribution, Mem. 46, Geol. Soc. Amer., pp. 1-88.

————, 1954, Ecology of Foraminifera and associated micro-organisms from Mississippi Sound and environs, Bull. Amer. Assoc. Petr. Geol., vol. 38, no. 4, pp. 584-647.

————, 1955, Ecology of Foraminifera in southeast Mississippi Delta area, Bull. Amer. Assoc. Petr. Geol., vol. 39, pp. 712-752.

————, and Parker, F. L., 1951, Ecology of Foraminifera, northwest Gulf of Mexico, Pt. II, Foraminifera species, Mem. 46, Geol. Soc. Amer., pp. 1-64.

Post, R. J., 1951, Foraminifera of the south Texas coast, Publ. Inst. Marine Sci., vol. 2, no. 1, pp. 165-176.

Shepard, F. P., 1953, Sedimentation rates in Texas estuaries and lagoons, Bull. Amer. Assoc. Petr. Geol., vol. 37, no. 8, pp. 1919-1934.

———— and Moore, D. G., 1955, Central Texas coast sedimentation: characteristics of sedimentary environment, recent history, and diagenesis, Bull. Amer. Assoc. Petr. Geol., vol. 39, pp. 1463-1593.

Walton, W. R., 1952, Techniques for recognition of living Foraminifera, Cushman Found. Foram. Res., vol. III, pt. 2, pp. 56-60.

————, 1955, Ecology of living benthonic Foraminifera, Todos Santos Bay, Baja California, Jour. Pal., vol. 29, pp. 952-1018.

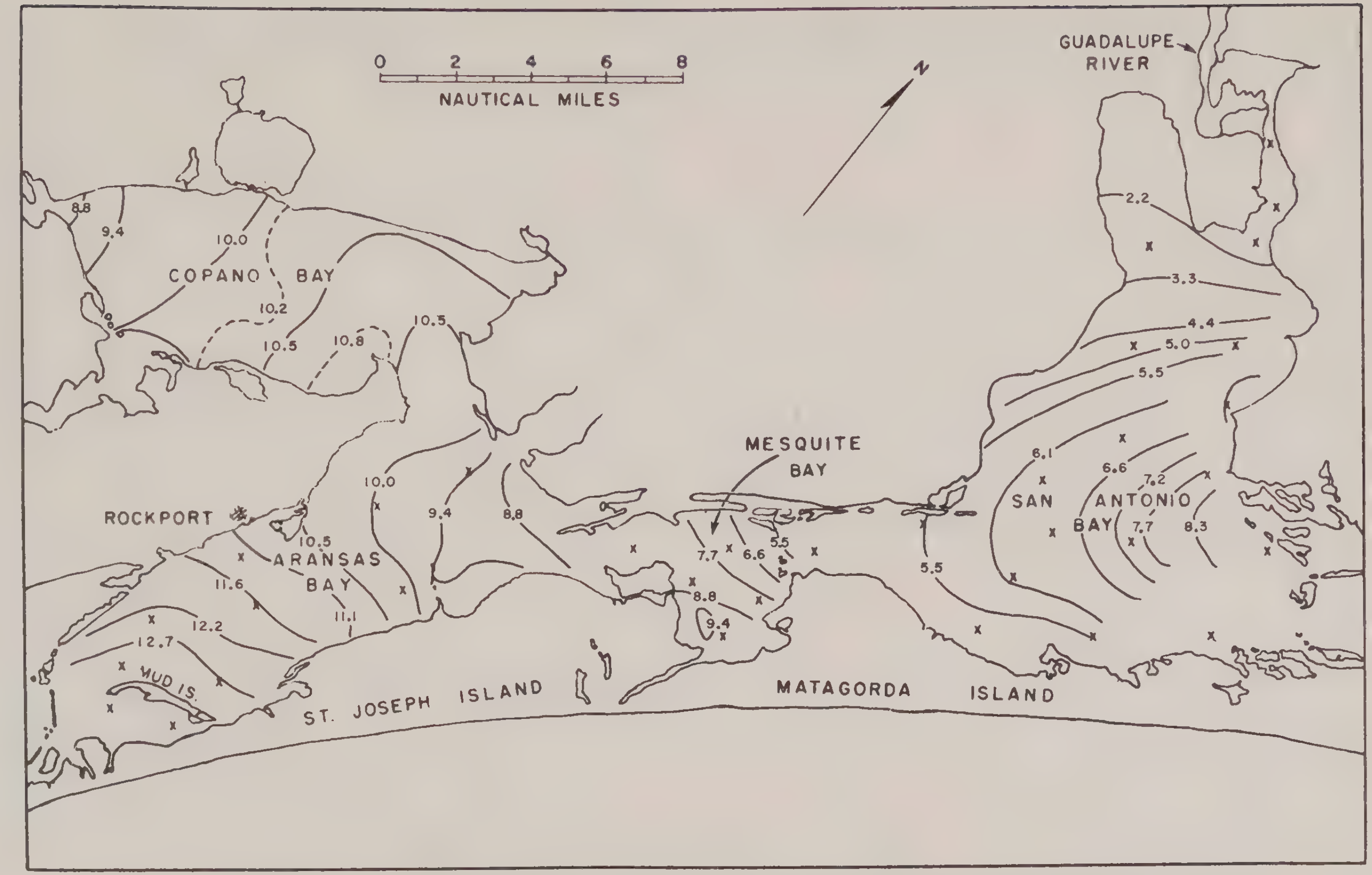
0 2 4 6 8
NAUTICAL MILES
N
GUADALUPE RIVER
COPANO BAY
ROCKPORT
ARANSAS BAY
MESQUITE BAY
SAN ANTONIO BAY
MUD IS.
ST. JOSEPH ISLAND
MATAGORDA ISLAND
8.8
9.4
10.0
10.2
10.5
10.8
10.5
10.0
9.4
8.8
10.5
11.6
11.1
12.2
12.7
7.7
6.6
5.5
8.8
9.4
5.5
2.2
3.3
4.4
5.0
5.5
6.1
6.6
7.2
7.7
8.3

Figure 3. Chlorinities in parts per thousand of water in the bays during January and February, 1926. After Galtsoff (1931).

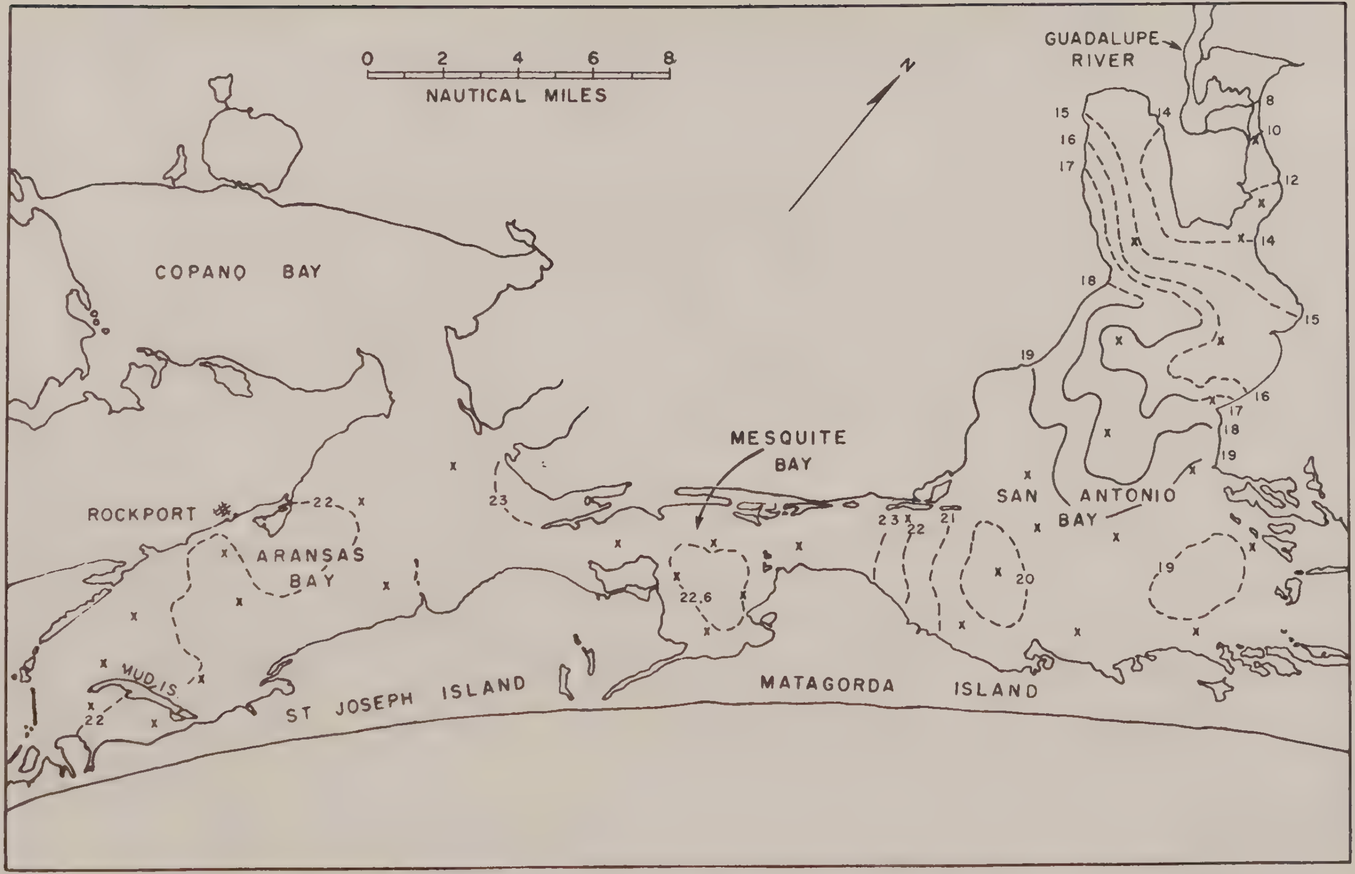
0 2 4 6 8
NAUTICAL MILES
N
GUADALUPE RIVER
COPANO BAY
ROCKPORT
ARANSAS BAY
MUD IS.
ST JOSEPH ISLAND
MESQUITE BAY
MATAGORDA ISLAND
SAN ANTONIO BAY
8
10
12
14
15
16
17
18
19
20
21
22
22.6
23

Figure 4. Chlorinities in parts per thousand of water in the bays during July and August, 1951.

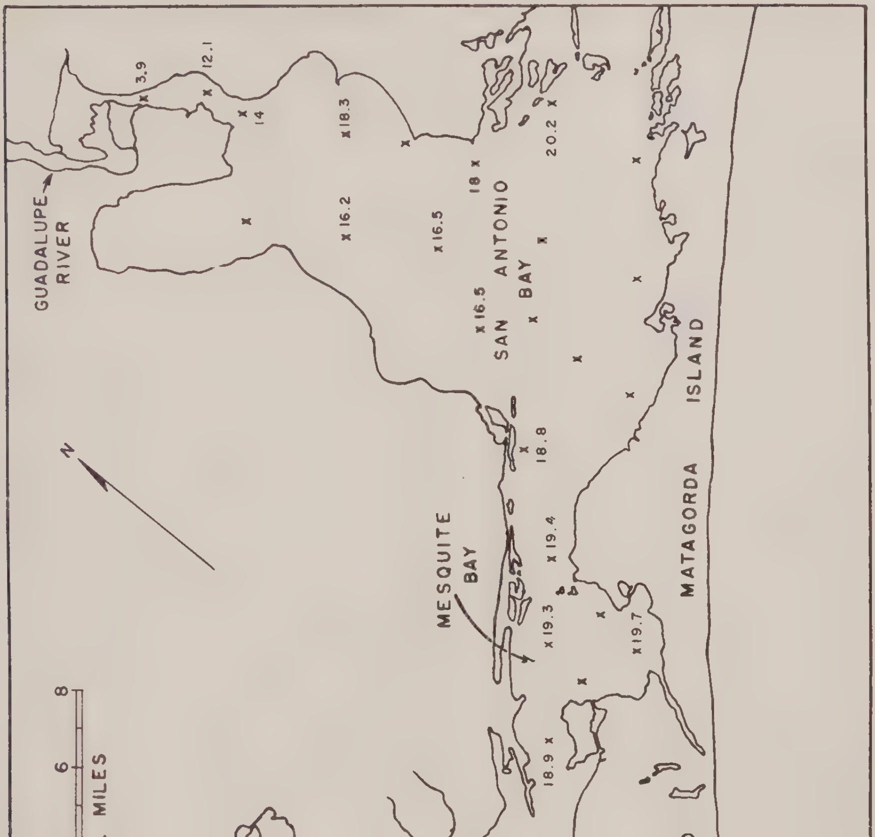
GUADALUPE RIVER
3.9
12.1
14
18.3
16.2
16.5
18
20.2
SAN ANTONIO BAY
16.5
18.8
MESQUITE BAY
19.4
19.3
19.7
MATAGORDA ISLAND
18.9
17.3
17.3
ARANSAS BAY
19
20.4
ROCKPORT
MUD IS.
19.7
ST JOSEPH ISLAND
COPANO BAY
N
0
2
4
6
8
NAUTICAL MILES

Figure 5. Chlorinities in parts per thousand of water in the bays during June, 1954.

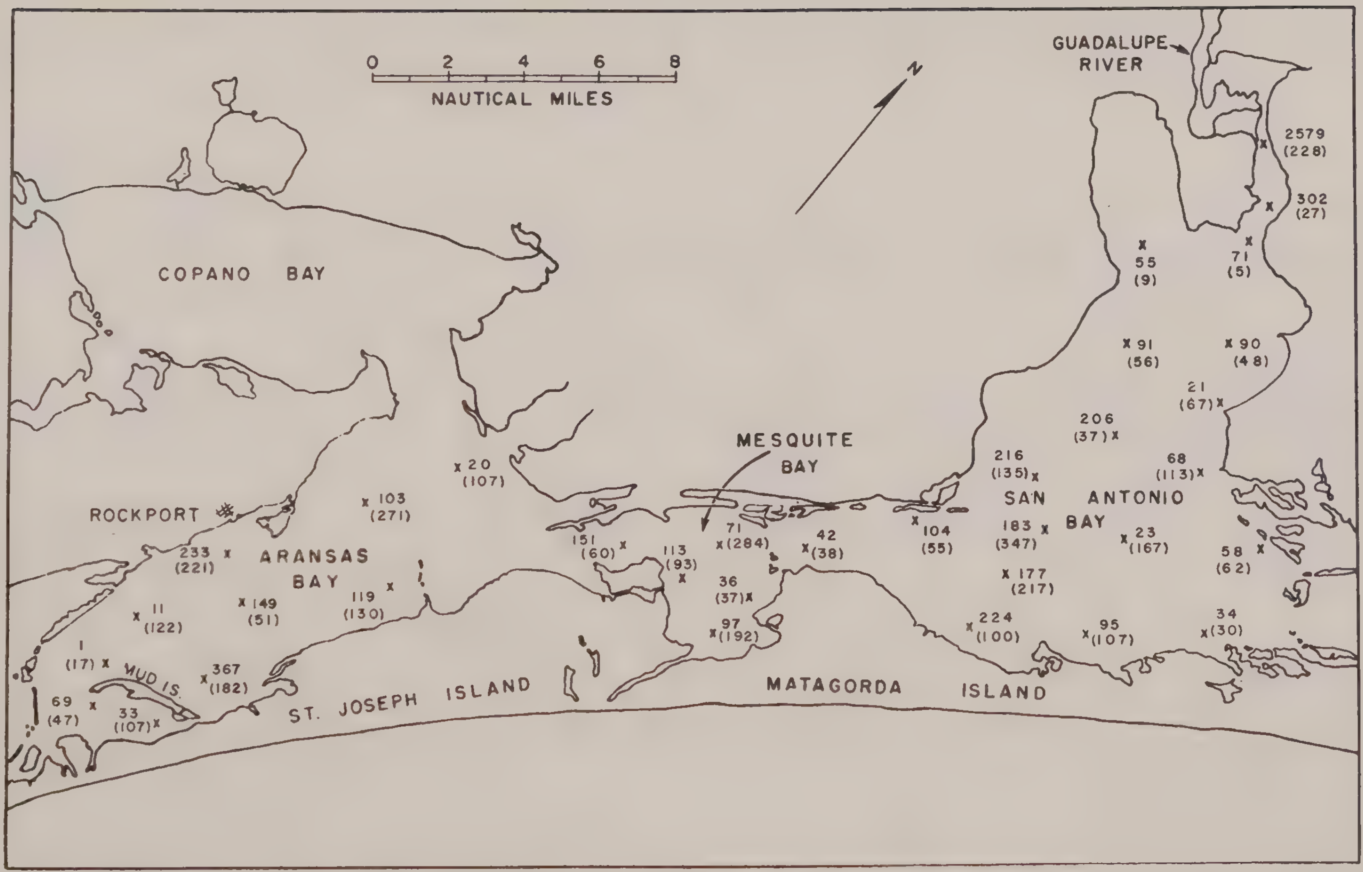
0 2 4 6 8
NAUTICAL MILES
N
GUADALUPE RIVER
COPANO BAY
ROCKPORT
ARANSAS BAY
MESQUITE BAY
SAN ANTONIO BAY
MUD IS.
ST. JOSEPH ISLAND
MATAGORDA ISLAND
2579 (228)
302 (27)
55 (9)
71 (5)
91 (56)
90 (48)
21 (67)
206 (37)
216 (135)
68 (113)
183 (347)
23 (167)
58 (62)
177 (217)
104 (55)
224 (100)
95 (107)
34 (30)
71 (284)
42 (38)
36 (37)
97 (192)
113 (93)
151 (60)
20 (107)
103 (271)
233 (221)
119 (130)
149 (51)
11 (122)
1 (17)
367 (182)
69 (47)
33 (107)

Figure 6. Actual number of living specimens of Foraminifera per uniform-size sample (outside of parentheses). Total population per uniform sample (in parentheses) in hundreds of specimens.

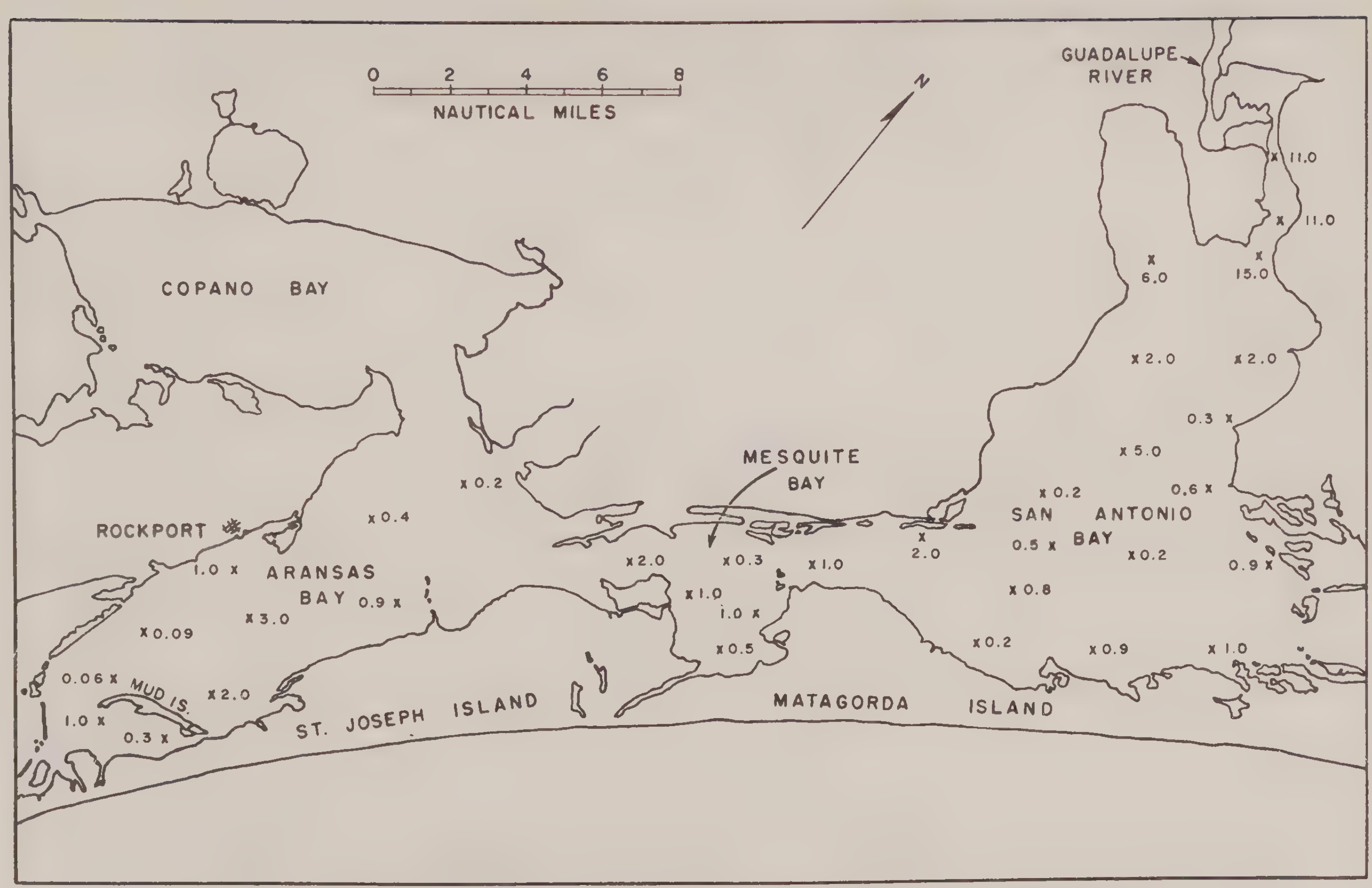
0 2 4 6 8
NAUTICAL MILES
N
GUADALUPE RIVER
COPANO BAY
ROCKPORT
ARANSAS BAY
MESQUITE BAY
SAN ANTONIO BAY
ST. JOSEPH ISLAND
MATAGORDA ISLAND
MUD IS.
11.0
11.0
6.0
15.0
2.0
2.0
0.3
5.0
0.2
0.6
0.5
0.2
0.9
0.8
2.0
0.2
0.9
1.0
0.2
0.4
2.0
0.3
1.0
1.0
1.0
0.5
1.0
0.9
3.0
0.09
0.06
2.0
1.0
0.3

Figure 7. Ratio of the living to total population in percent.

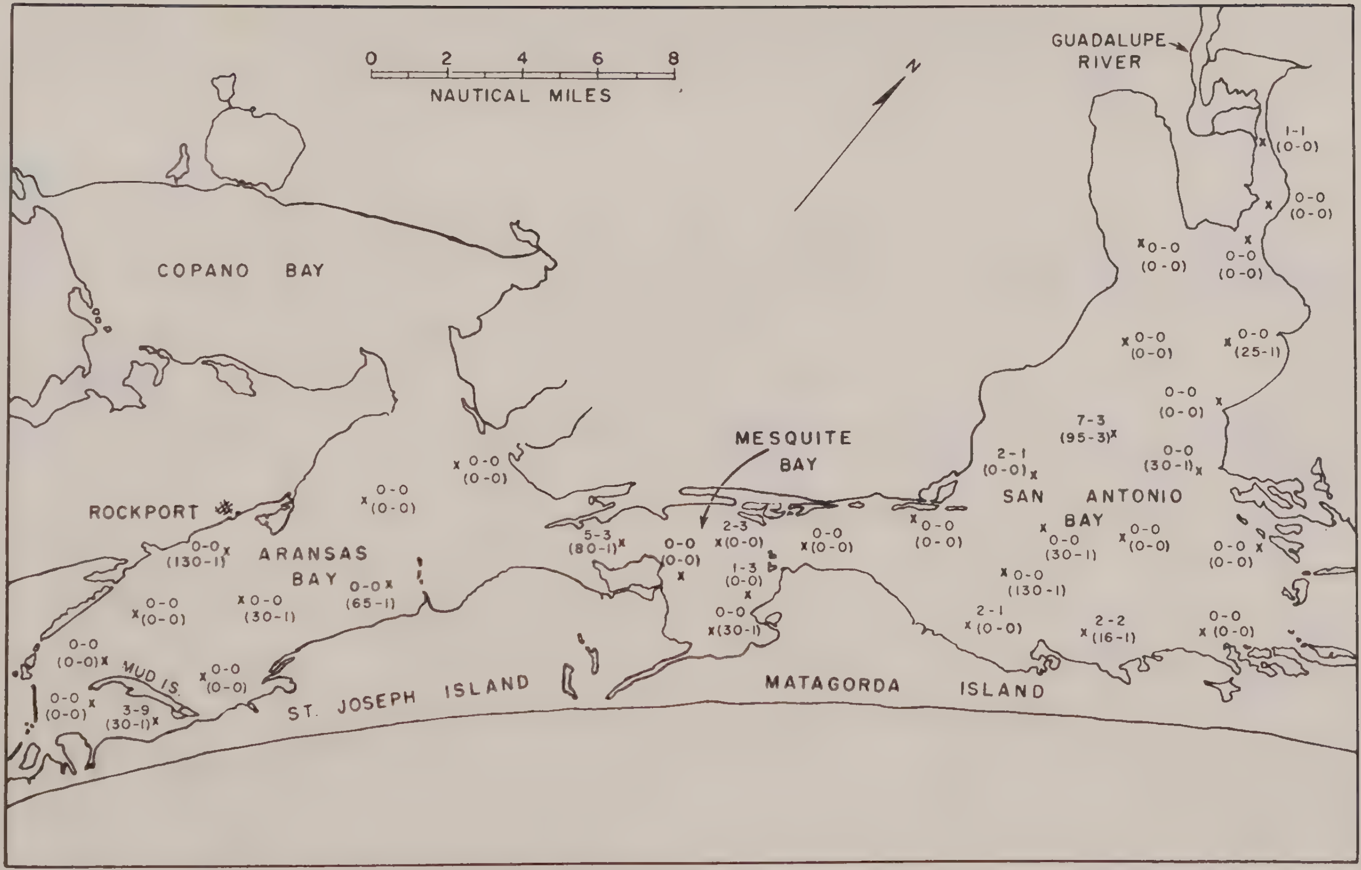
0 2 4 6 8
NAUTICAL MILES
N
GUADALUPE RIVER
COPANO BAY
ROCKPORT
ARANSAS BAY
MESQUITE BAY
SAN ANTONIO BAY
ST. JOSEPH ISLAND
MATAGORDA ISLAND
MUD IS.
1-1 (0-0)
0-0 (0-0)
0-0 (25-1)
7-3 (95-3)
2-1 (0-0)
0-0 (30-1)
0-0 (130-1)
2-2 (16-1)
2-1 (0-0)
5-3 (80-1)
2-3 (0-0)
1-3 (0-0)
0-0 (30-1)
0-0 (130-1)
0-0 (65-1)
0-0 (30-1)
3-9 (30-1)

Figure 8. Distribution of *Ammobaculites dilatatus* Cushman and Bronnimann. Living populations not in parentheses: first number, number of specimens; second number, percent of total living population. Total populations in parentheses; first number, number of specimens; second number, percent of total population.

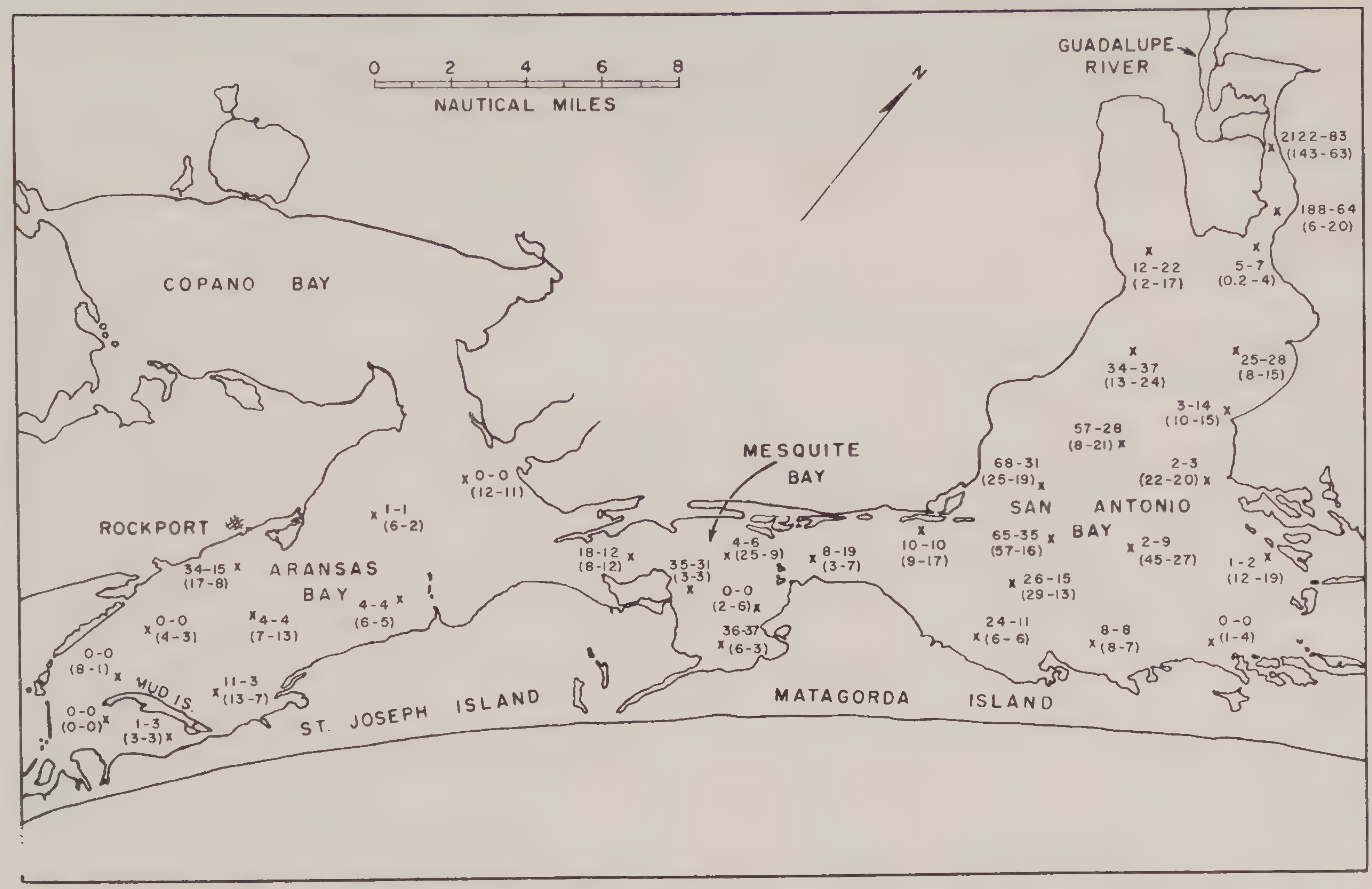
0 2 4 6 8
NAUTICAL MILES
N
GUADALUPE RIVER
COPANO BAY
ROCKPORT
ARANSAS BAY
MESQUITE BAY
SAN ANTONIO BAY
MUD IS.
ST. JOSEPH ISLAND
MATAGORDA ISLAND
2122-83 (143-63)
188-64 (6-20)
12-22 (2-17)
5-7 (0.2-4)
34-37 (13-24)
25-28 (8-15)
3-14 (10-15)
57-28 (8-21)
68-31 (25-19)
2-3 (22-20)
65-35 (57-16)
2-9 (45-27)
1-2 (12-19)
26-15 (29-13)
24-11 (6-6)
8-8 (8-7)
0-0 (1-4)
10-10 (9-17)
8-19 (3-7)
4-6 (25-9)
35-31 (3-3)
0-0 (2-6)
36-37 (6-3)
18-12 (8-12)
0-0 (12-11)
1-1 (6-2)
34-15 (17-8)
4-4 (6-5)
4-4 (7-13)
0-0 (4-3)
0-0 (8-1)
11-3 (13-7)
0-0 (0-0)
1-3 (3-3)

Figure 9. Distribution of *Ammobaculites salsus* Cushman and Bronnimann and variants. Living populations not in parentheses: first number, number of specimens; second number, percent of total living population. Total populations in parentheses: first number, number of specimens in hundreds; second number, percent of total population.

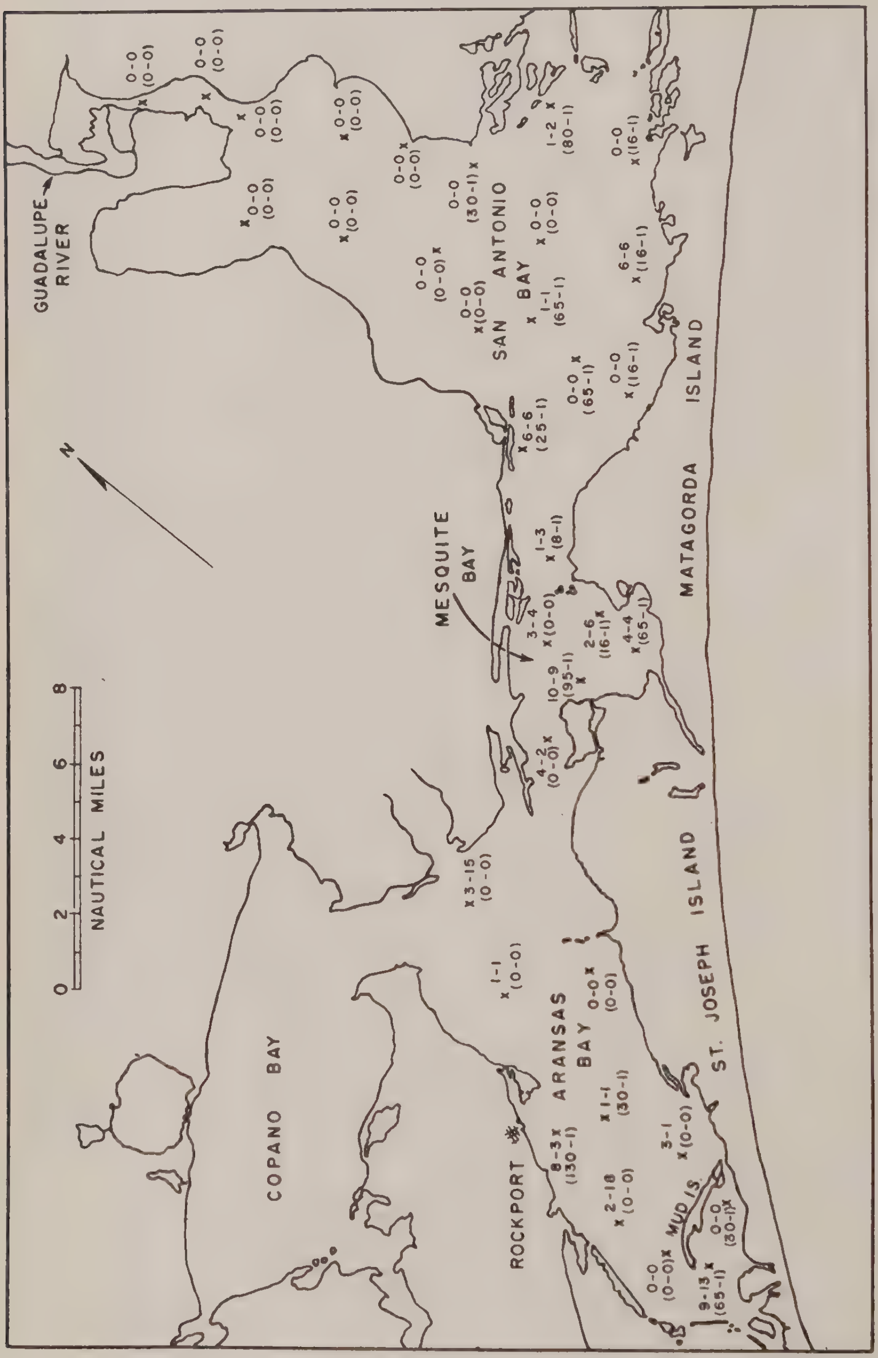
GUADALUPE RIVER
0 2 4 6 8
NAUTICAL MILES
N
COPANO BAY
ROCKPORT
ARANSAS BAY
MESQUITE BAY
SAN ANTONIO BAY
MATAGORDA ISLAND
ST. JOSEPH ISLAND
MUD IS.
0-0 (0-0)
0-0 (0-0)
0-0 (0-0)
0-0 (0-0)
0-0 (0-0)
0-0 (0-0)
0-0 (0-0)
0-0 (30-1)
1-2 (80-1)
0-0 (0-0)
0-0 (0-0)
0-0 (0-0)
0-0 (16-1)
1-1 (65-1)
6-6 (16-1)
0-0 (65-1)
0-0 (16-1)
6-6 (25-1)
1-3 (8-1)
3-4 (0-0)
2-6 (16-1)
4-4 (65-1)
10-9 (95-1)
4-2 (0-0)
3-15 (0-0)
1-1 (0-0)
0-0 (0-0)
1-1 (30-1)
8-3 (130-1)
3-1 (0-0)
2-18 (0-0)
0-0 (30-1)
0-0 (0-0)
9-13 (65-1)

Figure 10. Distribution of *Bolivina striatula* Cushman. Living populations not in parentheses: first number, number of specimens; second number, percent of total living population. Total populations in parentheses: first number, number of specimens; second number, percent of total population.

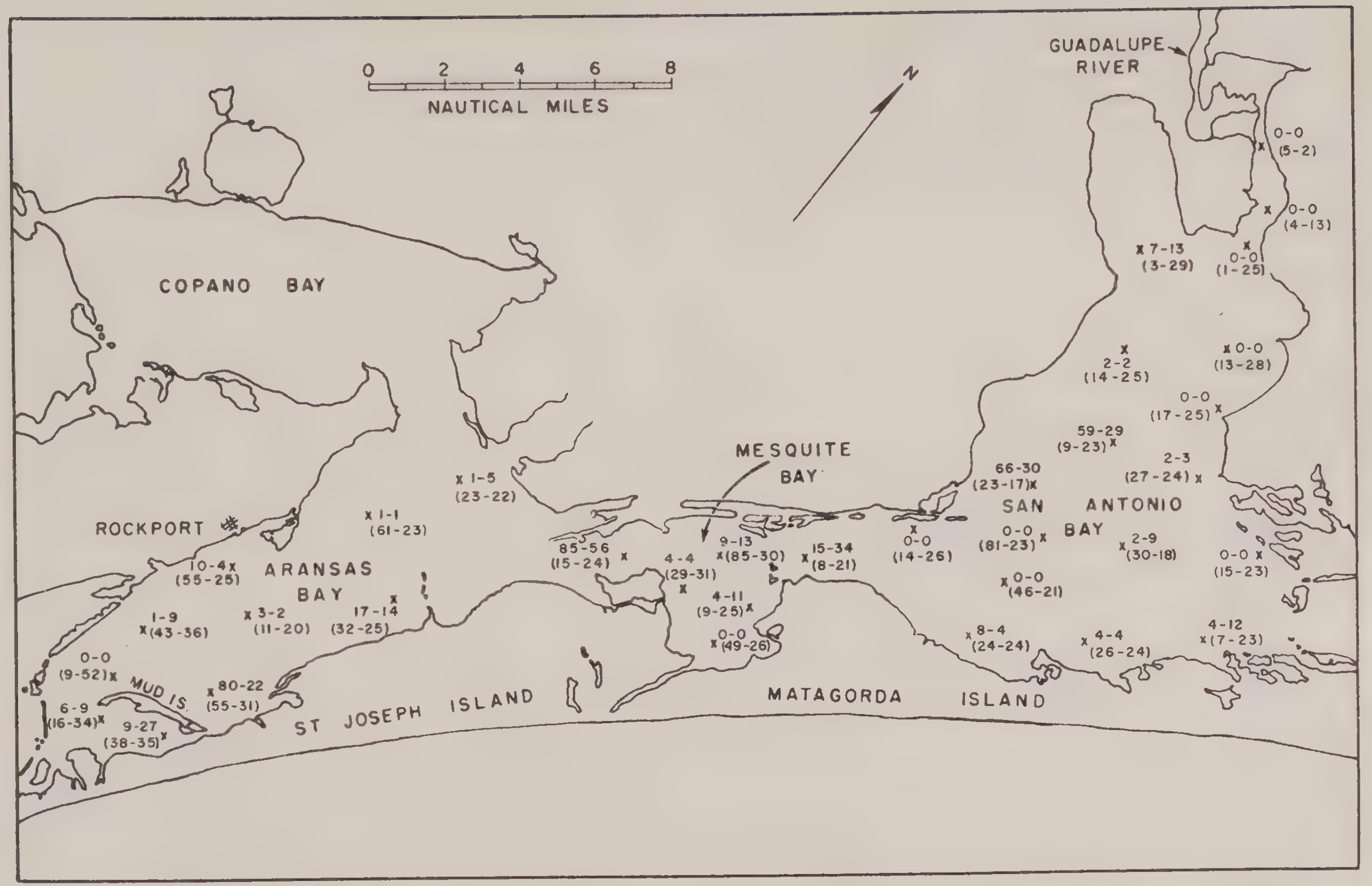
0 2 4 6 8
NAUTICAL MILES
N
GUADALUPE RIVER
COPANO BAY
ROCKPORT
ARANSAS BAY
MESQUITE BAY
SAN ANTONIO BAY
MUD IS.
ST JOSEPH ISLAND
MATAGORDA ISLAND
0-0 (5-2)
0-0 (4-13)
7-13 (3-29)
0-0 (1-25)
2-2 (14-25)
0-0 (13-28)
0-0 (17-25)
59-29 (9-23)
2-3 (27-24)
66-30 (23-17)
0-0 (81-23)
2-9 (30-18)
0-0 (15-23)
0-0 (46-21)
0-0 (14-26)
15-34 (8-21)
9-13 (85-30)
4-4 (29-31)
4-11 (9-25)
0-0 (49-26)
8-4 (24-24)
4-4 (26-24)
4-12 (7-23)
85-56 (15-24)
1-5 (23-22)
1-1 (61-23)
10-4 (55-25)
17-14 (32-25)
3-2 (11-20)
1-9 (43-36)
0-0 (9-52)
80-22 (55-31)
6-9 (16-34)
9-27 (38-35)

Figure 11. Distribution of *Elphidium gunteri* Cole. Living populations not in parentheses: first number, number of specimens; second number, percent of total living population. Total populations in parentheses: first number, number of specimens in hundreds; second number, percent of total population.

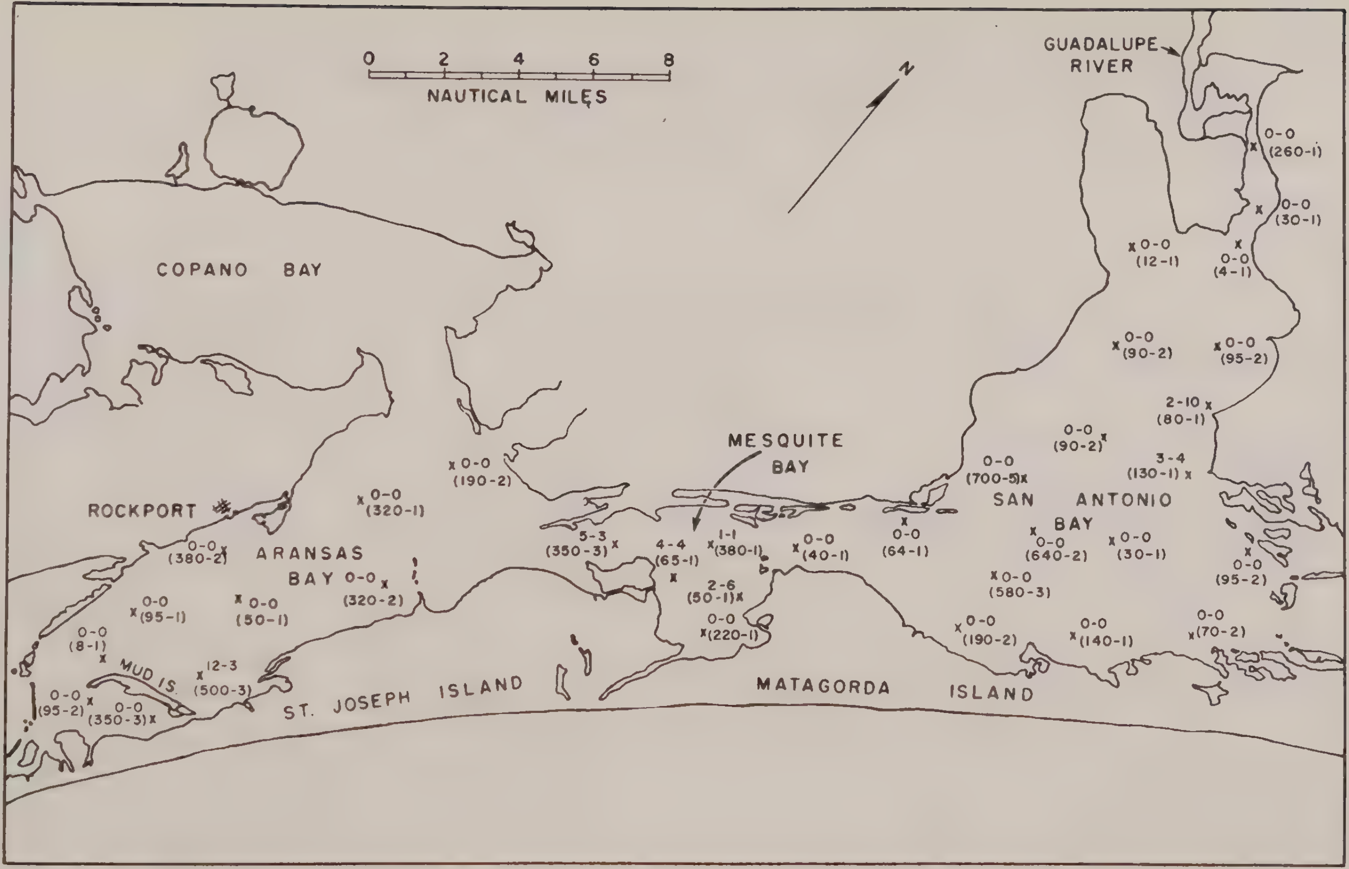
0 2 4 6 8
NAUTICAL MILES
N
GUADALUPE RIVER
COPANO BAY
ROCKPORT
ARANSAS BAY
MESQUITE BAY
SAN ANTONIO BAY
ST. JOSEPH ISLAND
MATAGORDA ISLAND
MUD IS.
0-0 (260-1)
0-0 (30-1)
0-0 (12-1)
0-0 (4-1)
0-0 (90-2)
0-0 (95-2)
2-10 (80-1)
0-0 (90-2)
3-4 (130-1)
0-0 (700-5)
0-0 (640-2)
0-0 (30-1)
0-0 (580-3)
0-0 (95-2)
0-0 (190-2)
0-0 (140-1)
0-0 (70-2)
0-0 (64-1)
0-0 (40-1)
1-1 (380-1)
4-4 (65-1)
2-6 (50-1)
0-0 (220-1)
5-3 (350-3)
0-0 (190-2)
0-0 (320-1)
0-0 (380-2)
0-0 (320-2)
0-0 (50-1)
0-0 (95-1)
0-0 (8-1)
12-3 (500-3)
0-0 (95-2)
0-0 (350-3)

Figure 12. Distribution of *Elphidium matagordanum* (Kornfeld). Living populations not in parentheses: first number, number of specimens; second number, percent of total living population. Total populations in parentheses: first number, number of specimens; second number, percent of total population.

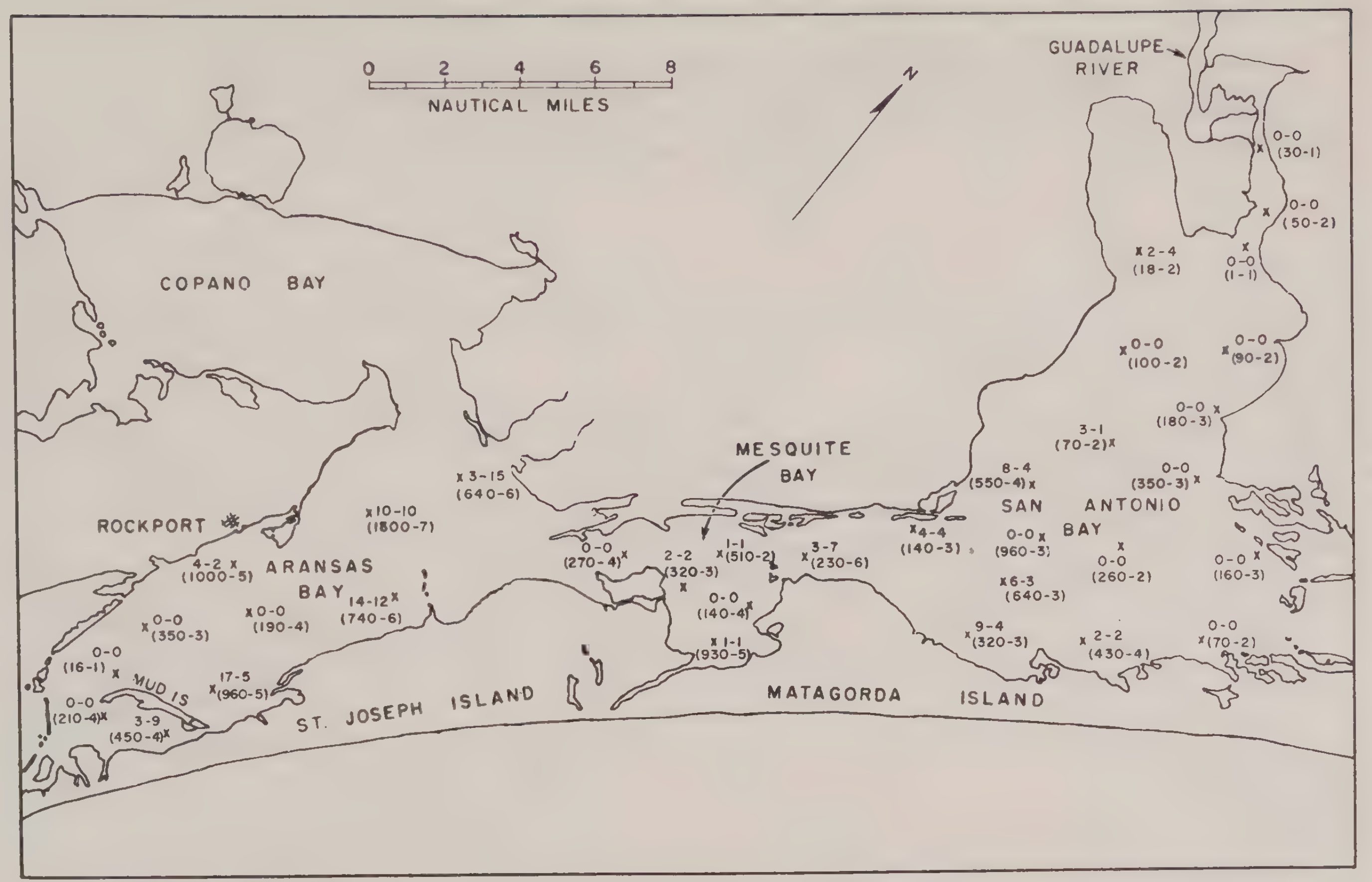
0 2 4 6 8
NAUTICAL MILES
N
GUADALUPE RIVER
COPANO BAY
ROCKPORT
ARANSAS BAY
MESQUITE BAY
SAN ANTONIO BAY
ST. JOSEPH ISLAND
MATAGORDA ISLAND
MUD IS
0-0 (30-1)
0-0 (50-2)
2-4 (18-2)
0-0 (1-1)
0-0 (100-2)
0-0 (90-2)
0-0 (180-3)
3-1 (70-2)
8-4 (550-4)
0-0 (350-3)
4-4 (140-3)
0-0 (960-3)
6-3 (640-3)
0-0 (260-2)
0-0 (160-3)
9-4 (320-3)
2-2 (430-4)
0-0 (70-2)
3-15 (640-6)
10-10 (1800-7)
0-0 (270-4)
2-2 (320-3)
1-1 (510-2)
3-7 (230-6)
0-0 (140-4)
1-1 (930-5)
4-2 (1000-5)
0-0 (190-4)
14-12 (740-6)
0-0 (350-3)
0-0 (16-1)
17-5 (960-5)
0-0 (210-4)
3-9 (450-4)

Figure 13. Distribution of *Elphidium poeyanum* (d'Orbigny). Living populations not in parentheses: first number, number of specimens; second number, percent of total living population. Total populations in parentheses: first number, number of specimens; second number, percent of total population.

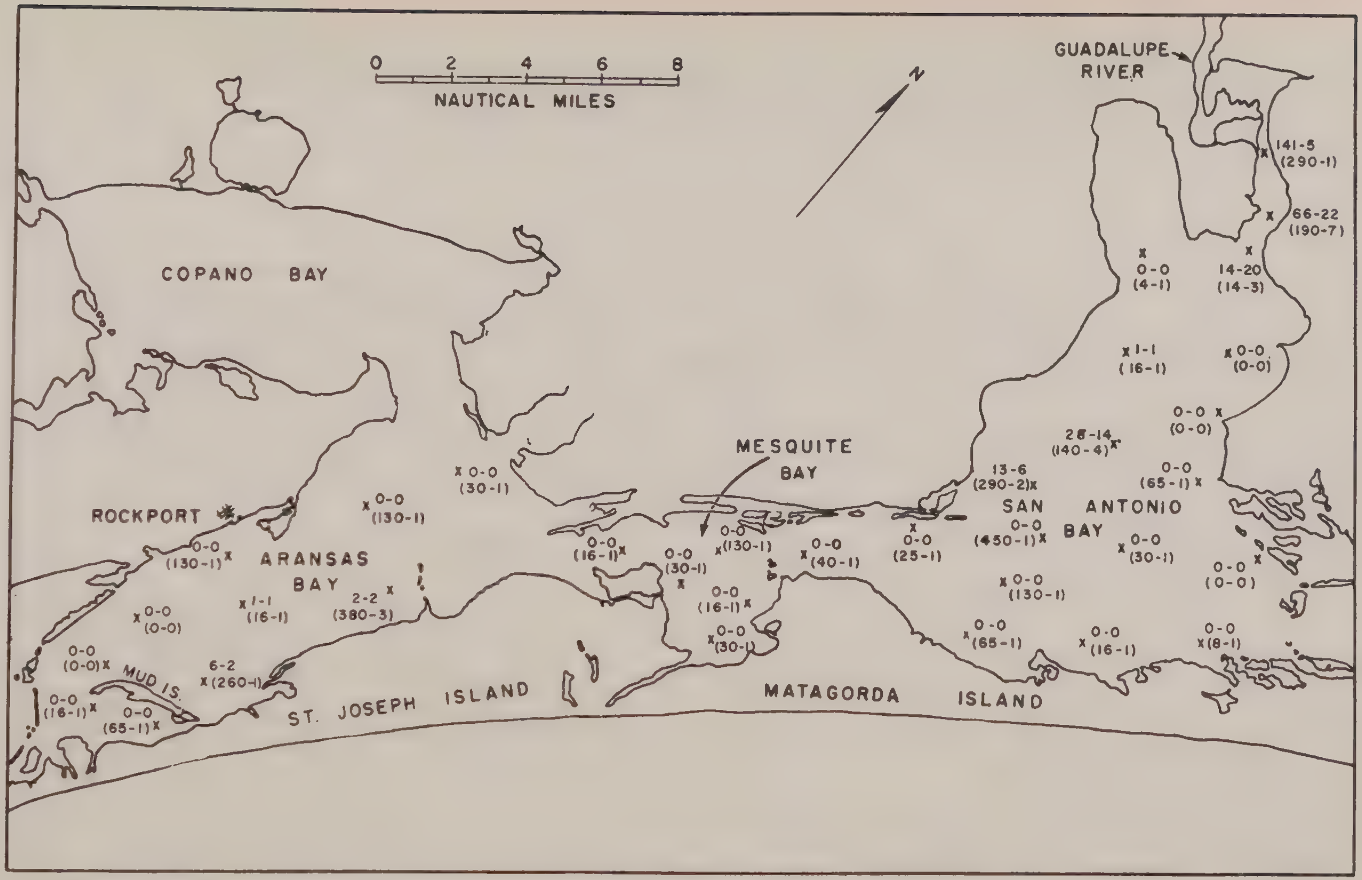
0 2 4 6 8
NAUTICAL MILES
N
GUADALUPE RIVER
141-5 (290-1)
66-22 (190-7)
0-0 (4-1)
14-20 (14-3)
1-1 (16-1)
0-0 (0-0)
0-0 (0-0)
28-14 (140-4)
0-0 (65-1)
13-6 (290-2)
SAN ANTONIO BAY
0-0 (450-1)
0-0 (30-1)
0-0 (0-0)
0-0 (130-1)
0-0 (65-1)
0-0 (16-1)
0-0 (8-1)
0-0 (25-1)
MESQUITE BAY
0-0 (130-1)
0-0 (40-1)
0-0 (30-1)
0-0 (16-1)
0-0 (30-1)
0-0 (16-1)
COPANO BAY
0-0 (30-1)
0-0 (130-1)
ROCKPORT
0-0 (130-1)
ARANSAS BAY
1-1 (16-1)
2-2 (380-3)
0-0 (0-0)
0-0 (0-0)
MUD IS.
6-2 (260-1)
0-0 (16-1)
0-0 (65-1)
ST. JOSEPH ISLAND
MATAGORDA ISLAND

Figure 14. Distribution of *Palmerinella palmerae* Bermudez. Living populations not in parentheses: first number, number of specimens; second number, percent of total living population. Total populations in parentheses: first number, number of specimens; second number, percent of total population.

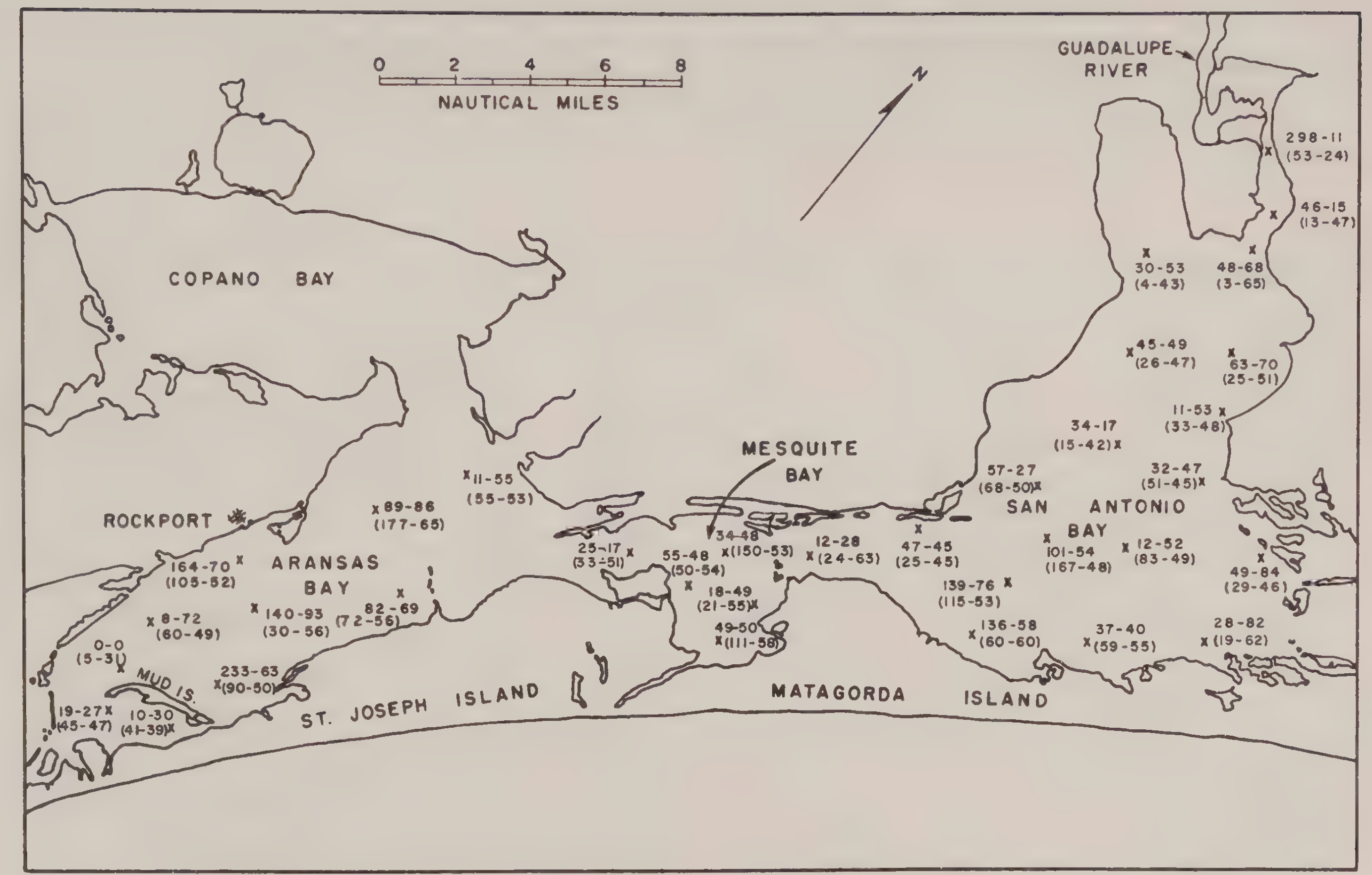
0 2 4 6 8
NAUTICAL MILES
N
GUADALUPE RIVER
COPANO BAY
ROCKPORT
ARANSAS BAY
MESQUITE BAY
SAN ANTONIO BAY
ST. JOSEPH ISLAND
MATAGORDA ISLAND
MUD IS.
298-11 (53-24)
46-15 (13-47)
30-53 (4-43)
48-68 (3-65)
45-49 (26-47)
63-70 (25-51)
11-53 (33-48)
34-17 (15-42)
57-27 (68-50)
32-47 (51-45)
101-54 (167-48)
12-52 (83-49)
49-84 (29-46)
139-76 (115-53)
136-58 (60-60)
37-40 (59-55)
28-82 (19-62)
47-45 (25-45)
12-28 (24-63)
34-48
(150-53)
55-48 (50-54)
18-49 (21-55)
49-50 (111-58)
25-17 (33-51)
11-55 (55-53)
89-86 (177-65)
164-70 (105-52)
140-93 (30-56)
82-69 (72-56)
8-72 (60-49)
0-0 (5-31)
233-63 (90-50)
19-27 (45-47)
10-30 (41-39)

Figure 15. Distribution of *"Rotalia" beccarii* (Linné) variants. Living populations not in parentheses: first number, number of specimens; second number, percent of total living population. Total populations in parentheses: first number, number of specimens in hundreds; second number, percent of total population.

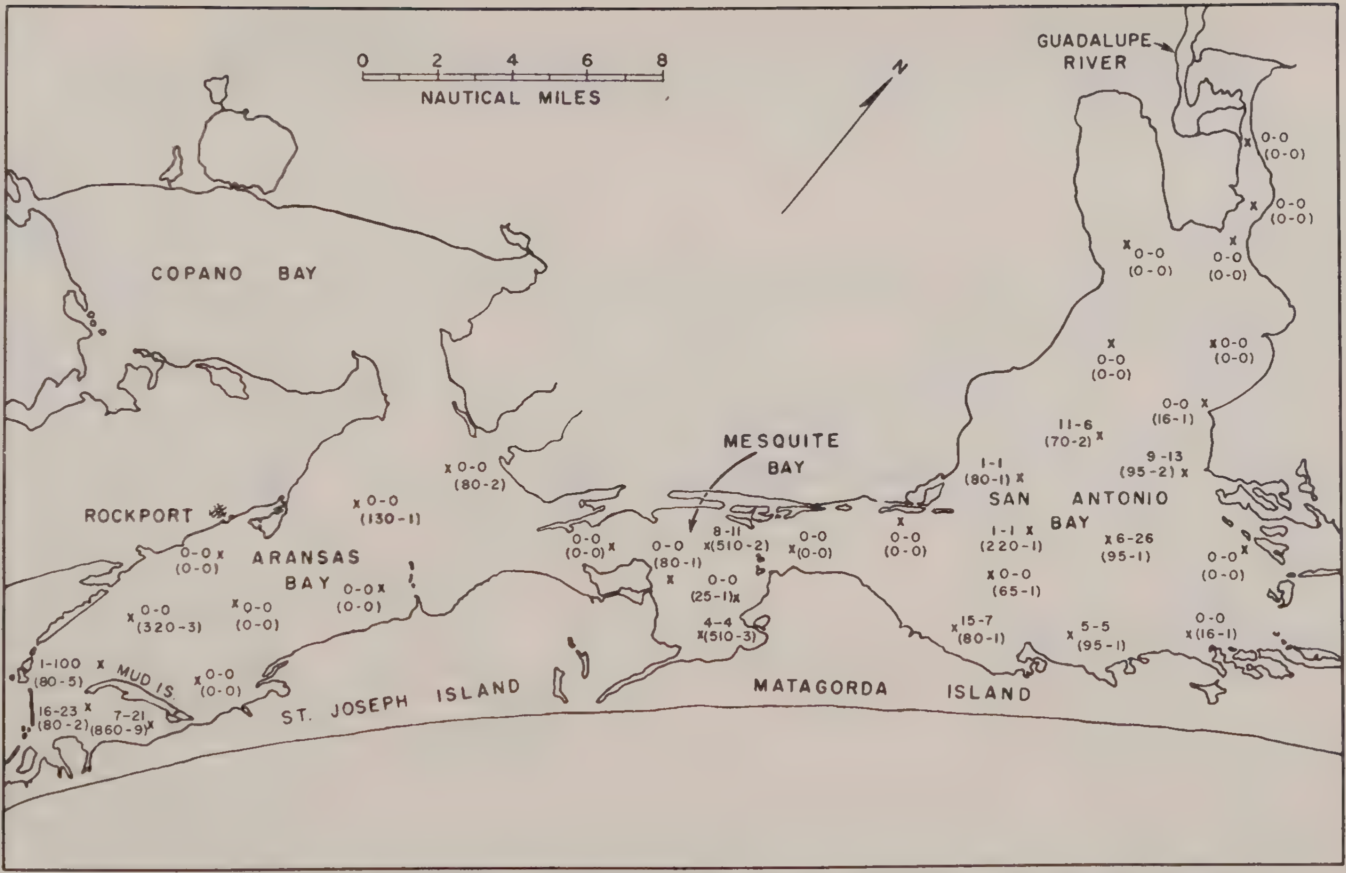
GUADALUPE RIVER
0 2 4 6 8
NAUTICAL MILES
N
COPANO BAY
ROCKPORT
ARANSAS BAY
MESQUITE BAY
SAN ANTONIO BAY
MUD IS.
ST. JOSEPH ISLAND
MATAGORDA ISLAND
0-0 (0-0)
0-0 (0-0)
0-0 (0-0)
0-0 (0-0)
0-0 (0-0)
0-0 (0-0)
0-0 (16-1)
11-6 (70-2)
9-13 (95-2)
1-1 (80-1)
1-1 (220-1)
6-26 (95-1)
0-0 (0-0)
0-0 (65-1)
15-7 (80-1)
5-5 (95-1)
0-0 (16-1)
0-0 (0-0)
0-0 (0-0)
8-11 (510-2)
0-0 (80-1)
0-0 (25-1)
4-4 (510-3)
0-0 (0-0)
0-0 (80-2)
0-0 (130-1)
0-0 (0-0)
0-0 (0-0)
0-0 (0-0)
0-0 (320-3)
0-0 (0-0)
0-0 (0-0)
1-100 (80-5)
16-23 (80-2)
7-21 (860-9)

Figure 16. Distribution of Miliolidae. Living populations not in parentheses: first number, number of specimens; second number, percent of total living population. Total populations in parentheses: first number, number of specimens; second number, percent of total population.

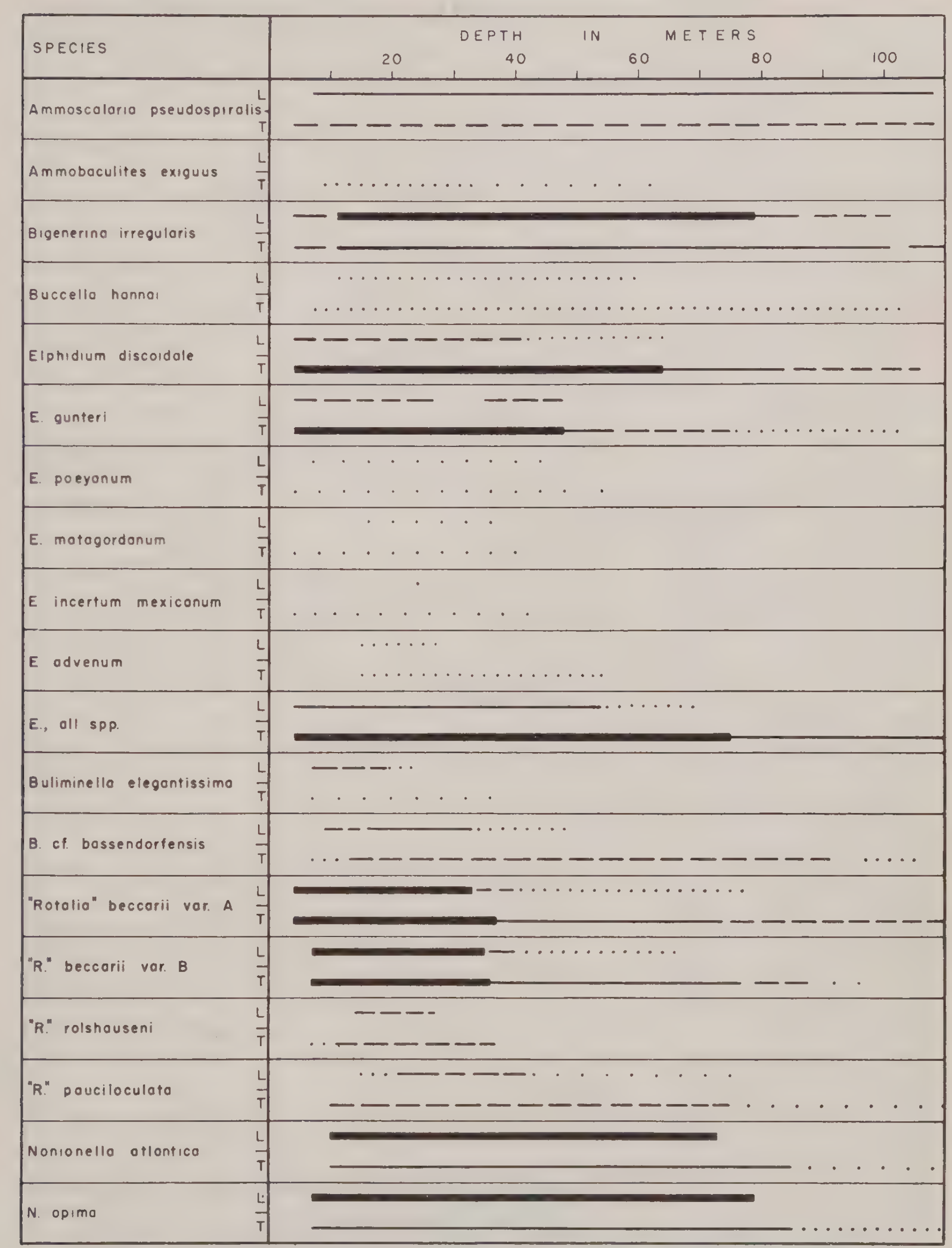

Figure 17. Generalized depth ranges of benthonic Foraminifera in offshore traverses. L = living population, T = total population. Heaviness of line indicates relative abundance.

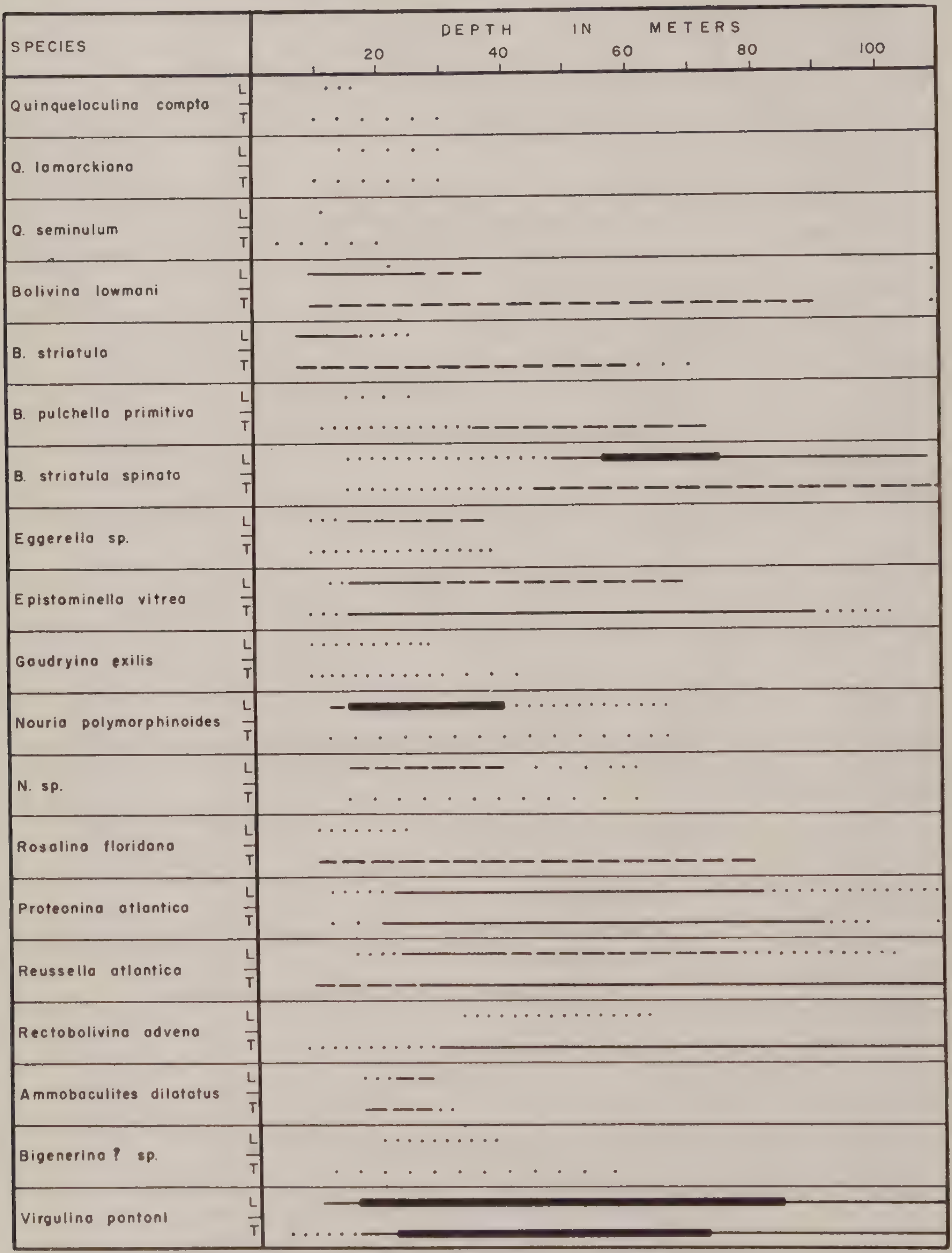

Figure 18. Generalized depth ranges of benthonic Foraminifera in offshore traverses. L = living population, T = total population. Heaviness of line indicates relative abundance.

(746)

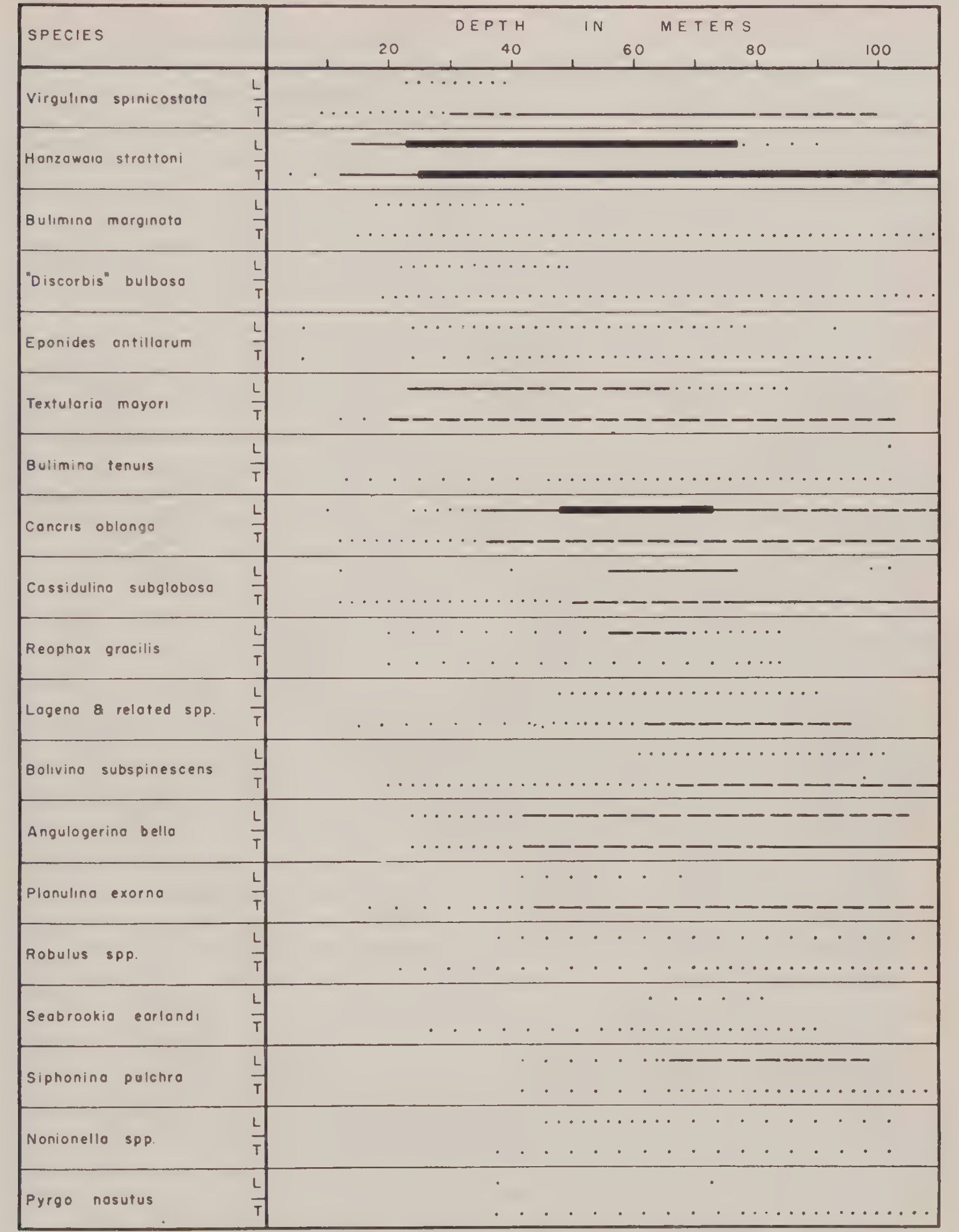

Figure 19. Generalized depth ranges of benthonic Foraminifera in offshore traverses. L = living population, T = total population. Heaviness of line indicates relative abundance.

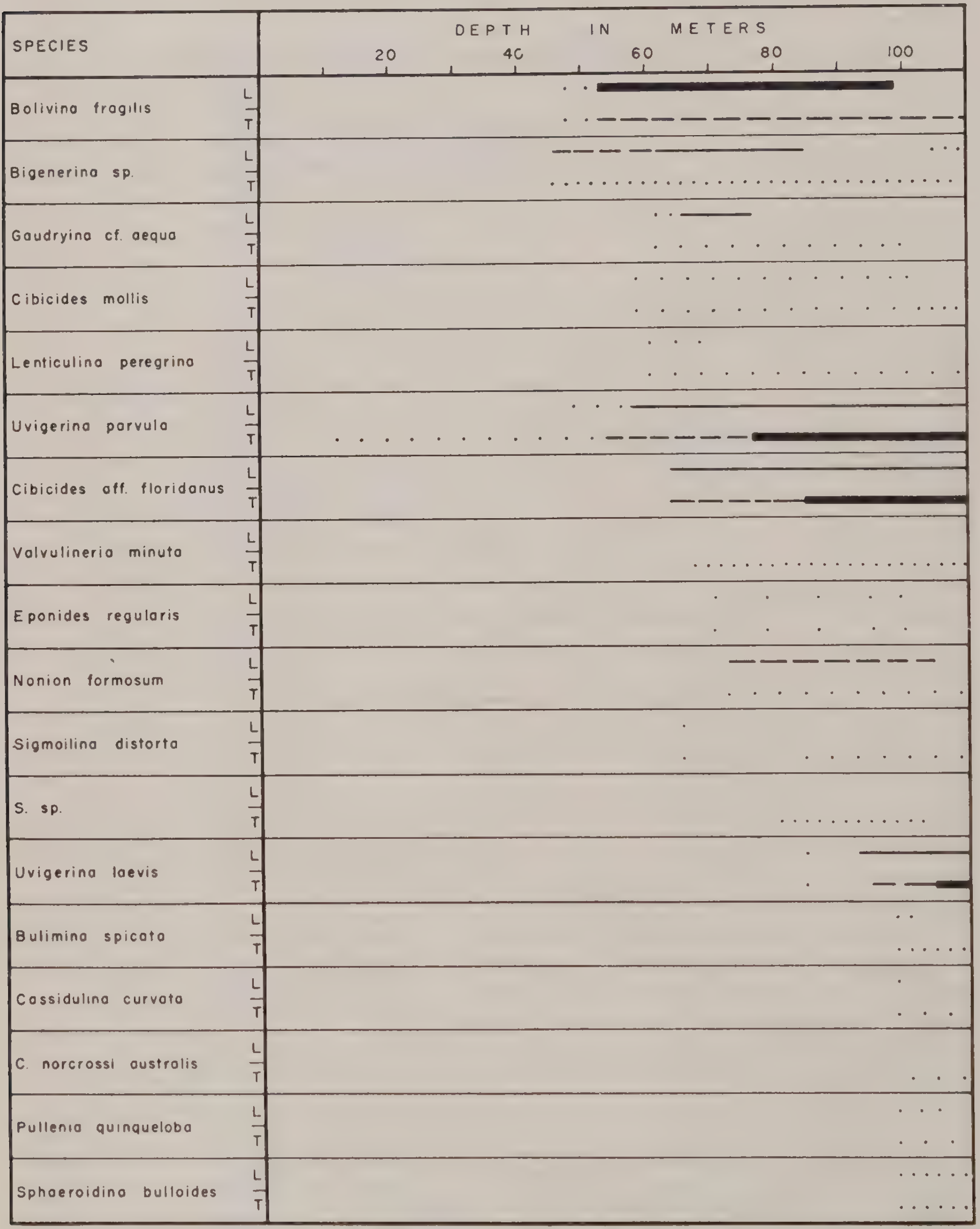

Figure 20. Generalized depth ranges of benthonic Foraminifera in offshore traverses. L = living population, T = total population. Heaviness of line indicates relative abundance.

STATION	1	2	3	4	5	6	7	8	9	10	11	12	13	14	15	16	17	18	19	20	21	22	23	24	25	26	27	28	29	30	31	32	33	34
LIVING POPULATION	33	69	1	1	367	149	233	119	103	20	151	113	97	36	71	42	104	224	187	183	23	94	34	58	216	206	68	91	21	90	55	71	302	2579
Ammobaculites dilatatus	3										5			1	2			2				2			2	7								1
A. exiguus																				2														
A. salsus & vars	1				11	4	34	4	1		18	35	36		4	8	10	24	26	65	2	8		1	68	57	2	34	3	25	12	5	188	2122
Ammoscalaria pseudospiralis		3									5			9	6	2	32	27	8	12		23	1	6	1		9		4	1	1			
Bolivina lowmani							3											1	5								2							
B. striatula		9		2	3	1	8		1	3	4	10	4	2	3	1	6			1		6		1										
Buliminella elegantissima		14					5					2	1																					
Elphidium discoidale		2													2						1													
E. galvestonense																										5		3			3			
E. gunteri	9	6		1	80	3	10	17	1	1	85	4		4	9	15		8			2	4	4		66	59	2	2			7			
E. matagordanum					12						5	4		2	1												3		2					
E. poeyanum	3				17		4	14	10	3		2	1		1	3	4	9	6			2			8	3		6			2			
E. translucens											3				1		1	1	1	1		3					4							
E. cf. tumidum																																2	2	
E. spp																1	3		1					1		2	5							
Gaudryina exilis																	1					1												
Lagena & related spp.					5							1	2																					
Miliammina fusca											1											3							1			2		9
Miliolidae	4		1																			2												
Palmerinella palmerae					6	1		2																	13	28		1				14	66	141
Pseudoclavulina gracilis									1																									
Quinqueloculina compta													4																					
Q. cultrata		2																1		1						2								
Q. lamarckiana															5			2			5													
Q. poeyana	3																	2				3												
Q. seminulum.		14													3			10			1				1	9								
Reophax gracilis							1																											
R. nana																		1	1															
"Rotalia" beccarii var. A	9	12		6	107	69	97	67	49		16	48	42	13	24	3	28	48	120	84	7	25	15	28	37	25	14	34	1	49	6	31	17	8
"R." beccarii var. B	1	7		2	126	71	67	15	40	11	9	7	7	5	10	9	19	88	19	17	5	12	13	21	20	9	18	11	10	14	22	7	3	19
"R." beccarii var. C																														1	2	10	26	271
Triloculinella obliquinoda																											9							
Trochammina inflata																							1											
Miscellaneous spp.							4			2																								8

Table 1. Living populations of Foraminifera in samples from the bays, in numbers of specimens.

STATION	1	2	3	4	5	6	7	8	9	10	11	12	13	14	15	16	17	18	19	20	21	22	23	24	25	26	27	28	29	30	31	32	33	34
TOTAL POPULATION	11000	4700	1700	12000	18000	5100	22000	13000	27000	11000	6000	9300	19000	3700	28000	3800	6500	10000	22000	35000	17000	11000	3000	6200	13000	3700	11000	5600	6700	4800	930	470	27000	23000
Ammobaculites dilatatus	.3					.6	.6	.5			1		.2						.6	.2		.2				3	.3							
A. exiguus														.2																				
A. salsus & vars.	3		.5	3	7	13	8	5	2	11	12	3	3	6	9	7	17	6	13	17	27	7	4	19	19	21	20	23	15	15	17	4	20	63
A. sp. A											.2									.1		.3				.2		.3	1		.2	.4	1	
A. sp. B																				.1	.4						.3	.7		.3	.4			1
Ammoscalaria pseudospiralis	3			.5				.2		.3	1	.3	.7	1	.9		2	.8	.9	1	.8	2	.5	1			.3		.7					
Bolivina lowmani							.3																											
B. striatula	.3	1				.6	.6					1	.3	.4		.2	.4	.2	.3	.1		.2	.5	1			.3							
Buliminella cf. bassendorfensis				.3																.1														
B. elegantissima													.2																					
Elphidium advenum	.3																					.2												
E. delicatulum	.3						.9			.3	.5		.3	.6		.2		1		.1		.3	2	2			.3		1	.5	5		8	7
E. discoidale	.9	7	1	3			.6		.2	.9	.7	.3	.7	.6					.6			.4							.2					
E. galvestonense			7	.5				.2		.3	.2		.3	.4	.7			.5	.3	.1	1	.3	.5	.3			.6	.1	.2		.4			
E. gunteri	35	34	52	35	31	21	25	25	23	22	24	31	26	25	30	21	26	24	21	24	18	24	23	23	17	23	24	25	26	28	30	25	13	2
E incertum mexicanum	1	2		.3			.6			.3	.2	1		.2						.1														
E cf koeboeense	.3			.5			.9	.7		1	.7	2	2	2	1	1	3	.6	1	.1	.4	2	1	1	.9	.2	1	.1	1	.8		.8	1	
E. matagordanum	3	2	.5	.8	3	1	2	2	1	2	3	.7	1	1	1	1	1	2	3	2	.2	1	2	2	5	2	1	2	1	2	1	.8	1	1
E. poeyanum	4	4	1	3	5	4	5	6	7	6	4	3	5	4	2	6	3	3	3	3	2	4	2	3	4	2	3	2	3	2	2	.2	2	.1
E. translucens														.2																				
E. cf tumidum	.6		1	1	2	.3	.6	2	.7	.9	.7	1	.2	.4	.2		.7		1	.1	.4	.6			.2									
E spp.				.3		.3	.9			1							.9		.3	.1	.2	.7		.8			.9		2		.2			
Gaudryina exilis						.3													.3					.5										
Hanzawaia strattoni		.3											.2	.2				.2										.1						
Lagena & related spp.					1	.3	.6			.3						.2							.3				.3			.2				
Massilina peruviana			.5							.6			.5																					
Miliammina fusca											.2			.2							.2											.2		.4
Miliolidae	.3	.7	2	.5									.3		.7														.2					
Nonionella atlantica																						.2												
N. opima							.3																											
Palmerinella palmerae	.6	.3			1	.3	.6	3	.5	.3	.2	.3	.2	.4	.4	1	.4	.6	.6	1	.2	.2	.3		2	4	.6	.3			.4	3	7	1
Quinqueloculina compta													.3		.2																			
Q. cultrata	.3																	.2																
Q. funafutiensis	1											1			.7			.2			.4													
Q. poeyana	3		2										.5					.3			.2	.2												
Q. rhodiensis	.6													.2													.3							
Q. seminulum	.3	1	.5	2						.3		.3	.8					.2				.3	.3				.3							
Reussella atlantica													.2																					
Rosalina floridana	.3																					.2												
"Rotalia" beccarii var. A	32	43	30	35	39	39	34	45	46	37	42	45	44	41	41	39	32	45	35	33	43	43	50	30	15	26	33	25	36	40	22	54	25	5
"R." beccarii var. B	7	4	1	14	11	19	18	10	19	15	9	10	13	15	12	23	13	15	18	17	6	12	12	16	36	16	12	20	12	10	19	9	19	17
"R." beccarii var. C																						.6	1	.3		.4		1	.7	.8	2	2	3	2
Triloculina sidebottomi	3								.5	.6			.2	.4	.2				.3	.1		.4	.3				1							
Triloculinella obliquinoda																									.1	2								
Trochammina comprimata																	.1																	
Miscellaneous spp.							.3							.2		.2	.1		.3															

Table 2. Benthonic Foraminifera in samples from the bays, in percent of total population.

STATION	240	243	245	246	247	248	249	250	251	252	253	289	288	287	286	194	193	192	191	190	189	188	231	230	229	228
DEPTH IN METERS	10	16	23	27	33	39	48	57	67	77	90	13	18	23	27	18	25	35	49	64	84	110	11	17	23	27
LIVING POPULATION	12	47	2	3	2	49	39	36	2	28	20	46	15	164	20	18	31	62	52	47	12	16	34	33	14	176
Ammobaculites dilatatus																	1									3
A. exiguus																							1			
Ammoscalaria pseudospiralis			1									4	4	1		2	1	2	1	1	1		7	4		14
Angulogerina bella								5											2	1						
Bigenerina irregularis												3	3	4	1	2	4	3	4	1			2	1	1	18
B. sp.										6																
B.? sp.																										2
Bolivina fragilis										1										1	2					
B. lowmani	1	3										5		10	2	1	1					1	1	5	2	25
B. striatula																							2	1		1
B. striatula spinata								1		9	1								5	20	2					
B. subspinescens																						1				
Buccella hannai							2																			
Bulimina marginata																	1									
Buliminella cf. bassendorfensis		5				1								10				1								2
B. elegantissima														1										1		
Cancris oblonga						2	3	6		2								2	3	3	1					2
Cassidulina subglobosa										1																
Cibicides aff. floridanus											6									1	1	6				
"Discorbis" bulbosa																		1	1							
Eggerella sp.			1											2	1		2									1
Elphidium advenum																										1
E discoidale		3		2									2			5	1			1				1	1	1
E. gunteri												2	1	6	1	2							1			1
E. poeyanum														1				1								
E. spp.	2											2						1					1			1
Epistominella vitrea														23	1		4									6
Eponides antillarum																			2							1
Hanzawaia strattoni		1			2		1	5			1			2	5	3	3	10	5	2				1	3	23
Lagena & related spp.						2															1					
Nonion formosum											4															
Nonionella atlantica		3												2			1	1	4							8
N. opima		3								2		6		37						1				9		
Nouria polymorphinoides						3		1						26				6								6
N. sp.						2								6			1	3								2
Proteonina atlantica						3	30	7	1		4						1	9	11	3		1		1	2	9
Pullenia quinqueloba																					1					
Rectobolivina advena						1	1												1							
Reophax gracilis																				2						
Reussella atlantica						6	1	2			2				1		1	3								6
Rosalina floridana								1																		
"Rotalia" beccarii var. A	3	7		1								2		2	1	3	4	2					3	3	3	4
"R." beccarii var B	6	18				2						22	1	14	3		1	2					16	5	2	
"R" pauciloculata															3		3									8
"R." rolshauseni													2	1												
Seabrookia earlandi										1										1						
Sphaeroidina bulloides																						1				
Textularia mayori															1					1						6
Uvigerina parvula																			1	1	2	1				
Virgulina pontoni		3				27		3		6			2	16			1	14	11	4		2		1		21
V. spinicostata											1															
Miscellaneous spp.		1					1	5	1		1							1	1	3	1	3				4

Table 3. Living benthonic Foraminifera, in numbers of specimens, from offshore traverses I, II, IV, and VI.

STATION	256	257	258	259	260	261	262	263	264	265	266	267	268	269	270	271	272	273	274	275	276	277	278	279	280	281	282	283	284	285
DEPTH IN METERS	4	7	9	10	11	12	13	13	14	15	16	16	17	18	18	19	20	20	21	21	22	22	24	24	24	25	26	26	27	28
LIVING POPULATION	9	39	13	14	11	64	83	15	76	166	139	25	77	8	73	11	13	40	16	97	16	29	19	44	24	25	36	12	17	150
Ammobaculites dilatatus																							2			1				
A. exiguus							1		1																					
Ammoscalaria pseudospiralis			1		1	2	6	4	7	32	8	1			1			1	2	2									1	1
Bigenerina irregularis					2	14	9	6	13	43	17	2	1	3	26	2	3	4		4	1	2	3	1	5	3	4		2	24
B.? sp.																				1										
Bolivina lowmani						3	5			6	5	3						2		1	1			1					1	2
B. pulchella primitiva										1																				
B. striatula					2	2	3		3	2	3																			
Buccella hannai						4			5	1																				
Bulimina marginata															1			1												
Buliminella cf. bassendorfensis							1			1		1	2	2	2	1	3	3	3	17	4	9	2	3	2	3	7		1	4
B. elegantissima		3	1		3																									
Cancris oblonga				1																				1						
Eggerella sp.																		2		2										
Elphidium advenum										1																				
E. discoidale	1	1					2		3		2		2															1		1
E. gunteri	2					2			2	6	3	3	6		4	1	1	1		1		2				1				3
E. matagordanum																								1						
E. poeyanum		1																												
E. spp.		3		1																			1							
Epistominella vitrea											1		3		2				2	11	1		2	8	1	8	5	4	1	13
Eponides antillarum	1																													
Gaudryina exilis			1																					1			1		1	2
Hanzawaia strattoni									7	4	3	6	1		1					1			1		1		2	5	1	
Miliolidae									4		5																			1
Nonionella atlantica									1	1	2	1	7								2	1			2		1			3
N. opima		2		2						1	13		3							6		1	1	5	3	1			1	14
Nouria polymorphinoides											1		13		2	1		9	2	8	2	5	1	3					2	10
N. sp.										1			6				2	5		12				5	1					5
Proteonina atlantica																		1		1					1	1	1		2	2
"P." sp.			1			2																		1			2		1	9
Quinqueloculina compta						1			5		4																			
Q. lamarckiana									2		1																			
Reussella atlantica											1	1			1									2					1	2
Rosalina floridana						1																								
"Rotalia" beccarii var. A	5	4		2	2	1	8	1	10	25	12	4	2		7	4	1	7	2	8	1	4	3	3	3	3	3		1	5
"R." beccarii var. B		25	9	8	1	32	45	4	9	38	47	1	23	3	24	1	2	2	4	8	1	3	2	2	3	2	1	1	1	19
"R." pauciloculata										1		1								1										4
"R." rolshauseni											7						1									1	2			
Textularia cf. mayori																														2
Virgulina pontoni							1		2	1	4	1	7		2	1		2	1	12	3	2	1	6	2	1	6	1		24
Miscellaneous spp.							2		2	1			1							1				1			1			

Table 4. Living benthonic Foraminifera, in numbers of specimens, from offshore traverse III.

STATION	256	257	258	259	260	261	262	263	264	265	266	267	268	269	270	271	272	273	274	275	276	277	278	279	280	281	282	284	285
DEPTH IN METERS	4	7	9	10	11	12	13	13	14	15	16	16	17	18	18	19	20	20	21	21	22	22	24	24	24	25	26	27	28
TOTAL POPULATION	1800	4000	140	1000	340	3700	3200	2100	23000	5000	5200	6300	870	1600	1800	1100	870	920	3100	750	1500	620	1800	1000	2400	1600	2700	2600	1700
Ammobaculites dilatatus																				.3			.5	1	.3	1	.3	.6	.7
A. exiguus			12	.8	2				.3		.3				.9	.4	.9				.5	.6	.7	.2	.3			.3	
Ammoscalaria pseudospiralis	.5	.4	6	.8		.2	4	2	.8	2	2	.8	.5	6	1	2	3	2	.8	1	1	2	2	.2	.7	.7	3	1	1
Bigenerina irregularis	.5	.4		.8		3	2	1	5	4	6	4	5	3	5	3	1	.9	4	2	3	1	5	3	4	2	2	3	4
B.? sp.																		.4				.3							
Bolivina fragilis																			.3										
B. lowmani						.9				.3	.3	.3									.3		.2			.2		.3	
B. pulchella primitiva						.4			.6	.6	.3	.5	.5	.5	.9	1	.9	.4	.5	2	1	.3	.5	1	2	.5	.9	.9	1
B. striatula						.4			1	.6	.6								.3				.7			.5			
B. striatula spinata											.6											.3		.2					
Buccella hannai		.4				.9			.3		.6	.3		.5	.4	.4		.4	.3		1			.2			.3	.3	
Bulimina marginata																	.5									.2	.3		.2
Buliminella cf. bassendorfensis						.2		1		.3				1	.9	.4	1	3	.5	3	2	2	2	.8	1	2	.6	2	3
B. elegantissima		.4		.8		.2																			.3				
Cassidulina subglobosa										.3															.3				
"Discorbis" bulbosa																									.7			.3	
Eggerella sp.																			.3	.5	.3	.3	.5	1		.5	.3	2	1
Elphidium advenum						.4						.3			.9				.3		.3			.4	.3	.2		.3	
E. discoidale	16	13		27		13	17	16	7	14	12	20	14	18	17	16	16	22	17	11	16	14	13	14	18	12	18	16	16
E. gunteri	21	26		21	2	15	7	12	17	15	12	12	15	8	12	12	11	4	5	5	7	6	9	12	9	9	7	3	5
E. matagordanum	.5	.4			2																								
E. poeyanum		.4					1		.6		.9	.5	.5		.9		.9		1	.3	.5				.3	1	.3	.6	
E. spp.	7	9		5		4	1	3	3	.6	2	1	.5	.5	2	.7	.5	.4	.5	1	2	1	.7	.2			.3	2	1
Epistominella vitrea											.9	.5	.9		.4				2	2	2	.6	3	2	2	7	2	3	5
Gaudryina exilis			6			.2						.3								.5	.3	.3		.4		.2		.9	
Hanzawaia strattoni	1	2				2		2	1	3	3	5	1	3	3	2	2	4	12	3	3	2	5	4	8	5	5	4	5
Lagena & related spp.												.3					.5			.3				.2					
Miliolidae				1		.7			.8		1	.3	.9																
Nonionella atlantica				.8			1	.4	2	2	3	2	3	.5	2	2	.5	3	3	2	3	1	1	4	4	4	4	2	5
N. opima		.4							3	.6	2	.8	1	.5	.4	2	.5		2	.8	2		2	1	4	1	1	2	1
Nouria polymorphinoides													2		.9		.5	1	.3	1	.5		.2	.8		.2	.3	.6	.7
N. sp.															.4					1				.4	.3		.3		.2
Planulina exorna													.5																
Proteonina atlantica											.3	.5		2	.4	.7	2	3		2	3	4	7	1	2	1	3	.6	1
"P." sp.						.2																				.2	.3		1
Quinqueloculina compta									.6		.3																		
Q. lamarkiana									.3		.6																		
Q. seminulum		.4				.7			.3																				
Rectobolivina advena								.4	.6						.4	.7	.5	.9	.8	.5	.8	.6	.2	1	1	.7	.6	.9	1
Reussella atlantica						.2	.5	.8	.6	.6	1	2	.5	.5	1	1	2	.9	2	2	.5	1		2	2	1	1		3
Robulus spp.																					.3								
Rosalina concinna											.3																	.3	
R. floridana	.5					.2		.4	.8		.9	.3	.5		.4	1	.9	.4	1	1	.3	.3	.2	.4	1	.2	.6		
"Rotalia" beccarii var. A	45	34	70	29	94	30	43	48	25	26	17	22	16	32	21	27	32	36	18	24	25	41	22	20	14	18	24	27	17
"R." beccarii var. B	8	13	6	11		25	23	11	27	27	28	24	30	22	21	22	19	15	20	26	18	18	16	18	15	20	17	15	13
"R." pauciloculata				.8		.2		.4			1	.5	.9		.4	.4	.9		2	.5	.5	.6	2	2	2	4	3	4	4
"R." rolshauseni						.4	.5	.8	1	1	2	.5	.5		.4	.4			1	.3		.3		1					.2
Stetsonia minuta																.7													
Textularia mayori											.3									.3			.2	.2	.3	.5		.3	
Uvigerina parvula											.3	.3						.4											
Virgulina complanata																							.2						
V. pontoni				1		.9		.4	.8	1	.6	1	5	2	5	4	2	2	5	6	5	3	6	6	5	6	4	6	9
V. spinicostata						.2				.3		.5	.9		.4						.3			1	2	.7	.3	1	1
Miscellaneous spp.									.3	.3				.5			.5		.5		.8								

Table 5. Benthonic Foraminifera, in percent of total population, from offshore traverse III.

STATION	95	96	97	98	99	100	101	102	103	104	105	106	107	108	109	110	111	112	113	114	115	116	117	118	119	120	121	122	123	124	125	126	127	128	129	130	131	132	133	134	135	136	137	138
DEPTH IN METERS	4	8	10	11	11	12	14	14	15	16	16	17	17	18	18	19	20	20	20	21	21	22	22	23	24	24	25	26	26	26	27	28	28	29	30	31	31	33	33	33	35	36	37	37
LIVING POPULATION	4	15	10	120	14	42	54	35	53	37	37	133	44	37	68	9	6	11	31	64	0	2	11	3	68	16	13	36	25	22	29	84	63	18	16	42	48	4	71	56	51	69	38	71
Ammobaculites dilatatus																																2												
A. exiguus			1																																									
Ammoscalaria pseudospiralis			1	3		7	6	11	5	6		1	7		2	1	4	2	2						1	1	1	2	1		2				1		1		1		1	1		1
Angulogerina bella																																									1		1	
Bigenerina irregularis				1	1	2	5	7	9	5	2	4	16	2	1			4	6	4			1		4	1	2	11	1	3	3	10	12	1	3	3	2	1	7	7	4	11	3	8
B.? sp.																																				1			2					
Bolivina lowmani				6		3	7		1	2		1							2	2													4	1		1			1					1
B. striatula			1	1	1	1	6		1		1	11	2					1							1																			
B. striatula spinata																																					1							
Buccella hannai												4													1								2										1	
Bulimina marginata																				1					1															1		1		
Buliminella cf bossendorfensis							1	1	1	1		4	1		1					3					1			2	2	1	2			1		2			2	1				
B elegantissima		1	4		1	1	1					2																																
Cancris oblonga																																	1								1		1	1
"Discorbis" bulbosa																										1									1									
Eggerella sp											2								1														1	1		1	5		4			2		
Elphidium discoidale		2		2	3	2						1			1	1									1	3		3						1						1		2	1	2
E gunteri	1			2		2				3	2	3			7	1				1					1		1	2			1										1	1	1	1
E matagordanum									1																																			
E. poeyanum		2				1		1																																				
E spp			1		1																				5	2						3									1			
Epistominella vitrea											1	10	1	4	7				2	12			5	1	11		1	3				16	6	3					4	4	1	3		4
Goudryina exilis					1											1																												
Hanzawaia strattoni								2			1								1						2	1	2	3	4	6		2	2	1	2	11	5	3	6	2	4	13	2	6
Miliolidae					1	1	1		1			1	1		12																				1									
Nonionella atlantica					1	5	1			2	4	11	3	3	4				2	3					2	2			1		1	5	3		4	1	3		2	3	3	2	3	5
N opima		1		4	2	1		3	7	4	5	24	3	7	11	2			7	15			1		3				2		5	3			1		2		3	5	5	1	5	4
Nouria polymorphinoides									1		1	13	2	12	8				2	12			1		7	1		1	3	3	2	11	7	1			7		3	1	1	4	2	
N. sp																												1					1			1	2		2	5		4		
Proteonina atlantica						1																		1	1	1		1	1	1		2	1			1	1		1	1	4	5	1	3
"P" sp		2		1																					1					1	2	1		1			1		1	1			1	
Quinqueloculina compta							1																																					
Q. lamarckiana																																		1	1									
Rectobolivina advena																																							1	1				1
Reophax gracilis																																							1					
Reussella atlantica																													1			2				3	2			4		1	4	1
Rosalina floridana							2																																					
"Rotalia" beccarii var. A	3	1		7			1	3	5	1	7	7		1	1	1	1		1	1					2			2	4	3			1	1	2	3	2		2	3	1			2
"R" beccarii var B		6	2	92	2	15	21	6	17	7	8	28	3	6	11	1	1	4	2	3		1	3		6	2	5		1	1	1	1	9	2		4			7		4	1		
"R." pauciloculata																			1	1		1			7	1		2	3			3				3	1		1	1	2	1		
"R" rolshauseni							1	1	4	1	1	1			1																													
Textularia mayori																									2			2	1		2	1	3			2	1		2		2	6		7
Virgulina pontoni										5	2	7	5	2	1	1			2	6				1	8		1	1		3	8	21	8	2		5	12		18	14	14	9	12	23
V spinicostata																																1	2	1						1	1			
Miscellaneous spp				1																																						1		1

Table 6. Living benthonic Foraminifera, in numbers of specimens, from the inner end of offshore traverse V.

STATION	139	140	141	142	143	144	145	146	147	148	149	150	151	152	153	154	155	156	157	158	159	160	161	162	163	164	165	166	167	172	173	174	175	176	177	178	179	180	181	182	183	184	185	186
DEPTH IN METERS	38	39	40	41	42	44	45	46	48	49	50	52	53	54	56	57	58	59	61	62	63	65	66	68	69	71	73	75	77	79	81	84	85	88	90	91	93	96	99	101	102	105	108	110
LIVING POPULATION	171	121	216	74	26	31	8	11	198	12	55	51	38	32	112	80	75	234	325	126	64	57	463	149	155	134	157	126	91	39	14	61	37	13	9	6	19	16	47	30	12	24	12	2
Ammoscalaria pseudospiralis	1	1		1		2	1	1	1	2			1			1	1	2	2		3		4	2	6	9	5	9	3	1	1	5						1			1	1	1	
Angulogerina bella	3				1	3	1	1	1		1			1	2	4	1	3	1	2	1	1	4	5	2	2	2	2				1	1	1					2	1		1		
Bigenerina irregularis	8	8	8	1			2		3	1	1	3		1	17	8	3	15	3	2	2	3	13	6	13	22	4	10	22	5	1	1		1			1		3	3				
B. sp.								1	1				1			1				2	1	3	1	2	1	2	1	1		1	2	5										1		1
B.? sp.	2																																											
Bolivina fragilis									1				3	2	7	3	7	36	58	15	4	4	66	9	13		19	1		4	1	4	16		3	1	1	2	8					
B. lowmani																1		1																										
B pulchella primitiva																											4																	
B striatula spinata	1		3	2					3	1	7		3	1	12	4	12	37	63	41	13	14	87	46	31	39	25	35	2	5	2	9		3			2	1	2				1	
B subspinescens																			1	2			1	1	2	1							1											
Buccella hannai	1	1		2													1	1																										
Bulimina marginata					1																																							
B tenuis																																									1			
Buliminella cf. bossendorfensis			2						1																																			
Cancris oblonga	6	1	16			1		1	25		8	2	6	5	9	11	13	34	49	19	12	8	113	22	14	9	31	5	6	2	1	4	1					3	3		1	1	1	
Cassidulina subglobosa			1												1			2	10			1	4	1	1	2	2	1	2										1		1			
Cibicides aff. floridanus																							7	3	5	7	13	11	7	2	2	14	1	5			3		2	6			3	
C mollis																		2				2	1				1													2				
"Discorbis" bulbosa	1	1							2																																			
Elphidium discoidale	2	3	2	1					1			1							1																									
E gunteri	2	2				1			2																																			
E poeyanum	1		1			2																																						
E spp									1					2									1		1																			
Epistominella vitrea	4	1	4			2			1					1		1		1	1	3		1	2		2															1				
Eponides antillarum				3								1			2			1					1	3		3	3	2	2	1							1							
E regularis																										1		1		2		1							4	1				
E umbonatus																												1				1												
Gaudryina cf. aequa																				1			3	2		2		7	12															
Hanzawaia strattoni	14	8	6	5	3		2		4	2	3	7		2	8	3		5	2	1		1	11	3	15	9	5	13	22			5		1		2	1	1		1				
Lagenidae									1	2								1	2	1			2		1		3			3		1	1		1									
Miliolidae	4					1			3													1	2	2			2			3		1												
Nonion formosum																											3				1		1	1	1	1	1	2		1	1	2		
Nonionella atlantica	14	6	11	3	1	1		1	32		2	8	4	2	19	4	4	25	27	8	2	3	24	6	9	1	3																	
N. opima	14	14	20	12	3	2			12		2		3		3		7	21	9	5	1	1	4	6	3	2	10	1		1														
N. spp									1				1	3	2	2			1	1			1					1												1				
Nouria polymorphinoides	5	2	9	1		1					1	1	1				1		4	1			1																					
N sp	3	1	2													2	1		1																									
Planulina exorna					1								1		1									1																				
Proteonina atlantica	6	5	2		1	4	2	4	10	2	8	2	3	7	4	6	2	1	5	2	2	2	3	2	2	1		2		1	1				1							1		
"P" sp			1																																									
Pullenia quinqueloba																																							2			2		
Pyrgo nasutus	4	2																									1																	
Rectobolivina advena	1		3	1	1				2		2		2	1						1																								
Reophax gracilis									1			1			4		4	1		1	1		2	4	1						1	1												
R scorpiurus															3	1			2	2		1		1																				
Reussella atlantica	2	3	3	1				1					1	1	1	3		2	2	1			2	1		2			1											2	1			
Robulus spp.	1	1							1									1	1				1				1									1						3		
Rosalina suezensis	2				1																																							
"Rotalia" beccarii var A	1	1	1						3			1											4			4			2															
"R" beccarii var. B		2	1						2		1		1			1			1				4																					
"R." pauciloculata	5	4	1	2	2							1	1					1									1	1																
Seabrookia earlandi																					2		2				1				1													
Siphonina bradyana																			1	1	2																			2				
S. pulchra					1								1					2					4	4	4	2	2	4	4	3		1	1			1			3					1
Stetsonia minuta																							2																					
Textularia mayori	10	7	8	3	4				2		1					8	1		3	3	1		1						1				1											
Uvigerina laevis	1																																1				3	3	1	2	2	2	3	
U. parvula																	1	4	1		4		20		1	4	3	2	3	4		1	4	1			3	2	6	5	1	1	3	
Virgulina pontoni	51	45	111	35	6	11			80	2	18	19	5	2	17	16	11	35	72	10	7	9	55	15	25	7	3	7				3	7		2		2	1	1		1	2		
V. spinicostata		2																				1																						
Miscellaneous spp	1			1					2			4		1			5		2	1	6	1	10	2	3	3	10	9	2	1		3	1				1		9	2	2	7		

Table 7. Living benthonic Foraminifera, in numbers of specimens, from the outer end of offshore traverse V.

STATION	95	96	97	98	99	100	101	102	103	104	105	106	107	108	109	110	111	112	113	114	115	116
DEPTH IN METERS	4	8	10	11	11	12	14	14	15	16	16	17	17	18	18	19	20	20	20	21	21	22
TOTAL POPULATION	410	230	280	940	2500	810	2600	3400	1700	2000	670	1700	2600	1300	880	1600	4000	1300	1600	3300	330	1300
Ammobaculites dilatatus														.3		.2			.5	.5		.2
A. exiguus			1		.6								.6			.7	.2	.6	2	.7	.6	.2
Ammoscalaria pseudospiralis	.5	.9	1	2	.6	2	.8	2	1	3	1	.2	4	3	4	1	4	2	1	1	.6	.3
Angulogerina bella																						
Bigenerina irregularis	.5	.9	.7	3	3	5	4	6	9	4	6	4	6	4	7	6	5	7	4	5	.6	2
B. sp.																						
B.? sp.																						
Bolivina lowmani			.7			.5	.3			.4	.6			.3			.6			.2		
B. pulchella primitiva							.3				.3	.7		.3	.5	.5	.6	2	2	1	.6	.6
B. striatula				.4		1	.6	1	.2	.2	1	.9	.3	.3		.4	.4			.7	.6	.6
B. striatula spinata									.2			.2		.6	.5						.6	
B. subspinescens																			.3			
Buccella hannai				.4	.3	.5		.2	.5		.3	.2								.2		
Bulimina marginata										.2		.2						.3	.3			.2
B. tenuis							.2									.2						
Buliminella cf. bassendorfensis		2	.7				.2			.4	.9	2	.6			.7	.4	.6	1	.2	.6	.9
B. elegantissima			1			.5	.3	.5														
Cancris oblonga									.2			.2										
Cassidulina subglobosa										.2												
"Discorbis" bulbosa																				.2		2
Eggerella sp.																				.2		
Elphidium advenum				.4			.2							.9					.3	5		.8
E. discoidale	48	14	22	9	14	13	17	24	24	14	11	7	17	12	19	13	25	17	14	11	19	13
E. gunteri	7	43	24	25	21	22	16	11	18	13	17	15	12	16	10	15	9	8	8	9	8	7
E. incertum mexicanum	4	3			1		.2	1														
E. matagordanum	.5		1		.6	.5	.3			.2												
E. poeyanum	1	.9	1	.4	1	.5	.5	1	.9	2	1	2	.9	.6	.9	.7	.6	.9	1	.5	3	2
E. spp.	.5		3		1	1	.5	.2	1	.8	.9	.2						.6		.7	.6	.6
Epistominella vitrea										.2	.3		.9	.6	1	1	.8	3	2	4	2	3
Eponides antillarum																						
Gaudryina exilis					1			.2						.9		.2	.2					
Hanzawaia strattoni	1	.9	2	3	2	3	4	2	5	5	3	2	4	5	2	4	5	6	5	5	7	6
Lagena & related spp.										.2								.3				.2
Miliolidae		2		1	4	1	3	2	2	.4				.6	.9	.2	.2				3	
Nonionella atlantica				.4	.3	1	3	.5		2	3	3	2	4	3	3	3	4	3	5	3	6
N. opima				.4	.4		1	.7	.2	3	5	2	1	5	5	1	1	1	.8	1	3	2
Nouria polymorphinoides												.5		.6						.5		
N. sp.																						
Planulina exorna																						
Proteonina atlantica													.6	.3	.5		4	1	3	1	2	.6
"P" sp.																						
Quinqueloculina compta					1	2	1	2														
Q. lamarckiana					.3		1	1	.2								.2					
Q. seminulum	2				5	.5	2	1	2	.2							.4					
Rectobolivina advena		.9					.2		.2	.2			.3		.5	.7		.9	.3	.7		1
Reussella atlantica						.5	.5	.5	.5	.4	.9	.9	.6	.9	2	.2	1	.9	.5	2		2
Robulus spp.																						.2
Rosalina concinna																						
R. floridana				.4		.5	.3	.2	.5		.6	1	.9	9		1		.3	.8	2		.8
R. suezensis																						
"Rotalia" beccarii var. A	25	25	31	22	21	33	13	17	12	16	10	11	11	12	13	13	20	7	17	10	12	11
"R." beccarii var. B	8	7	11	30	20	10	26	24	16	28	35	45	33	27	25	30	14	29	24	27	20	27
"R." pauciloculata	1					.5	.3		.2	.2			.6	1		1		3	2	1	2	1
"R" rolshauseni				.4	.6	.5	3	2	3	3	1		2	.9	.9	.2	2	.3		.5	.6	1
Seabrookia earlandi																						
Stetsonia minuta																						
Textularia mayori									.2							.2	.4		1	.5	1	.5
Trifarina bradyi																						
Uvigerina parvula						.5								.6								
Virgulina complanata																						
V. pontoni	.5				.3		.3	.2	2	2	.9	2	1	.9	4	5	2	4	4	6	7	7
V. spinicostata																			.5	.2	.6	.5
Miscellaneous spp.				1	.6					.6			.3	.3				.3	2	2	2	1

STATION	117	118	119	120	121	122	123	124	125	126	127	128	129	130	131	132	133	134	135	136	137	138
DEPTH IN METERS	22	23	24	24	25	26	26	26	27	28	28	29	30	31	31	33	33	33	34	36	37	37
TOTAL POPULATION	1100	1700	2400	4600	6700	3800	1700	1300	2500	3500	2500	5100	4500	2500	2200	4900	5300	2300	5300	5800	2700	7100
Ammobaculites dilatatus	.2	.7	.7	.3	.2	.4		.3						.3								
A. exiguus	.5	.5	.3	.3	.5		.9	1	.3		.6	.3	.2	.3	.7	.3		.3				
Ammoscalaria pseudospiralis	1		.7	1	.5	.9	.9	2	2		2	1	.5	.6	1	1	1	.7	2	.6	1	
Angulogerina bella																			.3			
Bigenerina irregularis	4	3	3	2	4	2	3	2	1	3	4	3	2	2	4	3	2	5	2	1	3	3
B. sp.					.2																	
B.? sp.												.3						.2	.3			.9
Bolivina lowmani	.2				.5					.2		.3					.6		.3	.8		
B. pulchella primitiva	.7	.7	.7	.7	.2	.4	.9		1	.7	1	.6	2	1	.7	1	.6	2	1	3	1	1
B. striatula	.7	1	.3	.2	.5			.3		.2			.2			.3	.3	.3	.3			
B. striatula spinata											.6						.3	.7				
B. subspinescens		.2		.2						.2												
Buccella hannai	.4	.2		.3						.9	.3	.3					.3	3	.3	.3		
Bulimina marginata	.7	.2		.3	.7			.3			.6			.3	.4		1	.2			.3	
B. tenuis		.2														.3						
Buliminella cf. bassendorfensis	2	.7	.7	.3	.2	.4	2	3	2	1	1	.3	1	2	1	2	1	2	.9	.8	.9	.4
B. elegantissima				.2			.5											.2		.3		
Cancris oblonga		.2		.2				.3	.3			.3	.4		.4			.4	.6	.6	1	
Cassidulina subglobosa										.2			.2						3			.4
"Discorbis" bulbosa		.5			.5		.5					.3	.7	.3	.4	.3		.5	.6	6		.4
Eggerella sp.		.2		.5				.3		.2	.6	.3		.6	.7	.7	1			.6		.4
Elphidium advenum	.4								.6	.7	.6	.3	.5		.7	.3		.2	.3	.8		
E. discoidale	11	6	20	16	10	18	13	16	6	9	9	14	6	11	15	15	10	8	10	10	14	9
E. gunteri	8	5	7	8	8	9	7	2	11	7	4	8	4	11	7	9	5	3	9	8	10	9
E. incertum mexicanum																						
E. matagordanum																						
E. poeyanum	.9	2	1	1	.2		.9	.6	.6	.7	1	1	.4	.3	.4	.3		.2	.6			
E. spp.	.7	2	3	2	.5	.4	.9		3	3	3	3	.7		1	.7	2	8	1	1	.3	1
Epistominella vitrea	4	4	5	5	3	4	3	2	8	9	6	8	9	2	4	4	8	3	3	5	2	3
Eponides antillarum																			.3			
Gaudryina exilis														1								
Hanzawaia strattoni	4	5	3	6	10	12	6	4	6	6	6	9	6	3	6	5	5	8	10	10	10	10
Lagena & related spp.	.2	1								.2	.3	.6	.7	.3			.6	.7				
Miliolidae		.2									.3		.2									
Nonionella atlantica	4	4	3	3	4	4	6	4	3	3	5	4	4	5	3	7	6	6	6	6	6	5
N. opima	4	11	1	3	2	1		1	2	2	.6	4	3	2	.7	1	3	2	.9	.8	1	.9
Nouria polymorphinoides	.2							.3									.3					
N. sp.																		.2				
Planulina exorna	.2								.3	.2			.2		.7	.7	.3					
Proteonina atlantica	.5	.2	.7	3	2	2	.9	5	1	2	1	1	.9	5	3	3	2	2	4	4	1	2
"P" sp.	.2							.3		.2		.3					.3				.3	
Quinqueloculina compta	.2												.2									
Q. lamarckiana																						
Q. seminulum																						
Rectobolivina advena			2	.7	.2		.5	.6	2	1	1	.3	3	2	2	3	2	3	3	3	2	6
Reussella atlantica	2	1	2	.9	1	2	.9		2	3	2	3	3	4	2	4	4	4	6	4	5	5
Robulus spp.											.3						.3					
Rosalina concinna				.2	.5							.3						.2				
R. floridana	.7	1	.3	.7	.7	.9		1	.3	.5	1	.6	1	.3	.4	.7	7	.3				1
R. suezensis		.2											.2									
"Rotalia" beccarii var. A	10	7	13	12	9	15	22	21	17	20	16	13	6	21	17	15	9	8	10	12	15	9
"R." beccarii var. B	30	31	22	20	31	20	22	23	15	12	18	8	18	10	14	9	14	9	8	12	10	13
"R." pauciloculata	1	.2	2	2	.5	.9	3	1	3	2	4	3	3	3	3	1	3	4	6	3	1	3
"R" rolshauseni	.2	.2	.3	.7	.5	.4				.2	.3	.3	.2		.4		.3	.2	.6	.6		.4
Seabrookia earlandi													.2									
Stetsonia minuta													.2				.6					
Textularia mayori	4	.2	3	.5	2	2		1		.9	2	2	2	.3	1	1	2	1	.6	.3	.6	2
Trifarina bradyi																				.3		.4
Uvigerina parvula																		.2				.4
Virgulina complanata				.2									.4									
V. pontoni	5	8	6	8	5	3	5	7	11	8	7	7	10	9	7	8	8	10	11	9	13	11
V. spinicostata	.9	1	1	1	1	.9		.6	.6	2	.6	2	3	.3	2	2	3	3	.9	1	1	2
Miscellaneous spp.	1	1	1		.4		.5		.3				.2	.6	.7	1	.9	.4	.3	.6		

Table 8. Benthonic Foraminifera, in percent of total population, from the inner end of offshore traverse V.

STATION	139	140	141	142	143	144	145	146	147	148	149	150	151	152	153	154	155	156	157	158	159	160	161	162	163	164	165	166	167	172	173	174	175	176	177	178	179	180	181	182	183	184	185	186
DEPTH IN METERS	38	39	40	41	42	44	45	46	48	49	50	52	53	54	56	57	58	59	61	62	63	65	66	68	69	71	73	75	77	79	81	84	85	88	90	91	93	96	99	101	102	105	108	110
TOTAL POPULATION	6700	6500	4500	4500	8300	4000	3700	4700	4500	9200	13000	12000	7000	6800	8300	20000	8300	3700	1300	4900	3300	13000	4600	5800	2500	3800	11000	4700	2600	1200	5600	2000	10000	9800	9200	4700	5300	2700	13000	2200	2900	5600	1700	2000
Ammobaculites exiguus	.2						.4							.2						.3																								
Ammoscalaria pseudospiralis		.5	.3	.4	1	2	.4	.3		.7	.2	1	.5		.2	.2	.6	.7	.3	.7			.3			.4	1	2	.6	.3	.3											.3	1	
Angulogerina bella	.5	.2	.3	.5	1	.8	.2	.3		.3	.5	1	.9	.5	.8	.3	1	1		.7	.7	.2	.7	1	1	1	1	1	2	1	3	2	7	4	5	3	4	4	4	7	8	4	4	4
Bigenerina irregularis	2	3	3	3	4	2	1	2	1	3	2	2	4	4	3	3	2	2	3	1	3	1	3	2	4	3	4	5	3	3	5	3	4	1	5	4	2	5	6	2	.5	.6	1	2
B. sp																																				.3								
B? sp							.2									.2																												
Bolivina fragilis										.7			.2	.2	.8			1	2	.3	.2	.2	.7	.5	.3		.3	.3	.6	.7		3	1	2	2	3	5	4	4	4	4	1	3	2
B. lowmani		.5					.2				.5				.6	.6	.6	.2			.5	.5	.7				.3	.7	.3		.3	.8		.7	.3									
B. pulchella primitiva	2	1	2	3	2	3	3	3	2	3	2	1	2	4	2	4	3	4	2	3	2	5	4	2	3	3	2	1	1	2	.3	.8	.6		1								.5	
B. striatula	.2	.2		.2								.5		.2	.8	.3	.2	.2				1	.7			.4																		
B. striatula spinata		.2	.5	.4					.4	.3		.3	.2		.4	.5	.8	.7	4	2	.7	.2	2	2	5	5	2	3	3	4	4	2	4	.7	2	1	2	4	2	1	2	1	2	1
B. subspinescens								.3					.5					.7	.9	1			1	1	1	.8	.9	1	2	.7	.6	2	3	2	2	1	1	2	1	1	2	1	1	2
Buccella hannai	.5	.2	.3	.7	.4	8	.7	2	1	.7	1	1	.2	.2	1	.5	.2	.2	.9		.2			.3		.3	.3					.8	1	.3	.7	.3		1		.4	.5			
Bulimina marginata			.2	.4		.8	4		.4		.2			.7	1		.2	.2	.3	.7	.7	.5		.5	.6			.3		.7	.3		.3	.3	.7		.6	.6	.5	.4		2		.4
B. spicata																																								2	.5		.5	1
B. tenuis				.2				.3	.4	.3		.5		.5	.4	.6	.6	.7	.3	.3	.2			.3		.2	.3	.7		.3			1	.7	.3	.7	1	.6	.5					
Buliminella cf. bassendorfensis	1	.5	2	.5	1	.4	.7		.4	1	.5	.5	1		1	2	.6	1	2	1	1	.5	1	2	.3	.4	.6	.3	.6	1	.9	.8	.6	.7	.3	.3				.4		.6		
Cancris oblonga	.2		1	.5	.8	.4	1	1	1	.7	.7	4	.5	1	1	2	1	2	3	2	.2	2	2	1	2	3	1	2	.9	2	1	2	2	2	2	2	2	2	2	1	2	2		4
Cassidulina curvata																																									.5	.3	.5	
C. subglobosa			.2	.2	.4	.4			.4			1	.2	.7	.8	.8	1	.4	1	.7	2	2	2	3	2	3	2	3	6	6	5	3	4	6	3	3	2	4	3	6	5	5	6	10
Cibicides deprimus																																1	.6	.7	1	1				.7				
C. aff. floridanus																							.3	.3		.8		2	.3	.3	3	4	2	6	7	9	5	8	15	6	5	14	4	5
C. mollis																							.7			.2		2	.3	.7	1				.7	.7	.6	.9	1	.7		.6	.5	
"Discorbis" bulbosa	.5	.5	.2	.2	1	.8	.2	.3	.7	1	1	.3	.9	.5	1		.6	.2	1	.3	2	1	3	1	.6	2		2	1	2	.6		.6	1		1	.6	.3	1	.7		.9		.8
Eggerella sp																.2	.2																											
Elphidium advenum		.5	.2		.4		.4	.3			.2			.5																						.3								
E. discoidale	7	11	7	9	8	11	12	13	4	9	9	9	10	6	8	6	7	5	7	4	5	5	1	4	4	6	3	2	3	2	2	3	1	.7	.3	1	.6			1	2	4		
E. gunteri	3	8	2	3	5	9	8	3	6	4	5	5	4	2	3	1	2	.7	3	2	2	2	2	.8	2	1	3	2	.6		1	.4		.3						4	.5			
E. incertum mexicanum			.2		.2																																							
E. matagordanum		.2	.2																																									
E. poeyanum	.5	.5	.9	.2	.4		.2			.3	.7			.2																														
E. spp	10	4	9	6	5	3	3	2	4	3	4	4	4	5	5	7	7	8	5	8	8	11	8	10	7	5	6	8	5	4	6	8	4	8	7	9	5	4	6	.7	2	.9	4	4
Epistominella vitrea	3	5	4	3	4	5	3	2	5	2	3	4	2	2	4	3	5	6	3	7	3	7	3	4	4	5	3	3	5	5	5	2	3	2	2		1	.3			1			
Eponides antillarum				.4								.3									.2			.3				.3	.3		.3			.3		.3			.5					
E. turgidus																													.9	1	.3	.4	.3	.6	.3	.3			.5					
E. umbonatus																							.3		.3			2	.3	1	.9	1	.6			.3	.6					.3	.5	.4
Gaudryina cf. aequa																										.2	.3	.7	.3				.3		.3									
G. exilis				.2																																								
Hanzawaia strattoni	8	5	10	10	9	6	6	9	14	8	10	11	12	13	8	6	10	5	6	9	6	2	5	4	3	4	6	5	4	3	4	4	9	10	6	9	10	8	8	2	4	5	4	5
Lagena & related spp.	.7	1					.7	.7	1	.7	.5	1	.5	.7	.4	1	1	2	.9	1	3	2	3	3	3	5	4	5	4	7	2	6	1	2	2	1	2		2				1	
Lagenidae			.3	.2	.6											.2					1							.3	.6		.6	.8		1	.7	1	3	.6	1		2	1	4	.8
Lenticulina peregrina																									.3	.2	.3			.3	.6			.3	.7				1	.4		.3		
Miliolidae	.2												.2				.8						1	1		.6	2	.7	2	3	2	2	1	2	2	3	4	2	1	.4	2		.5	.4
Nonion formosum																													.3	.3	.3			.3	.7	.7		.3	1		1	.6		.4
Nonionella atlantica	7	7	8	8	7	8	6	7	8	11	6	9	12	9	6	10	5	8	7	7	8	6	5	4	6	6	6	8	4	3	3	2	3	1	1	2	.6	3	1	2	1	1		.8
N. opima	2	2	4	4	2		.4	1	.4	.7	2	2	3	3	2	3	4	6	.9	6	7	3	4	7	8	5	2	3	4	5	3	2	3	1	1	1	.6	1	.5	.7	1	.9		.2
N. spp.	.4		.5		.4				.4		1	.5			.8	.6	.4		1	1	.5	1	3	1	1	.8	.9	2	4	3	1	3	2	1	1			.6	1					
Nouria polymorphinoides			.5	.4							.2						.2																											
N. sp.	.2																																											
Planulina exorna	.4	.5	.3	1	1	.4	.2	1	2	1	1	.5	2	2	1	.6	2	1	2	1	1	.5	1	.8	.6	.2	3	1		1	1	.4	2	3	2	2	2	1	1	1	1	.3	2	
Proteonina atlantica	3	2	2	2	1	1	4	3	3	3	5	2	2	2	2	2	3	2	3	3	.7		1		2	2	2	.7	.3	2	1	1	.6	1									.5	.4
Pullenia quinqueloba																																							.5	.7	.5	.6	3	
Pyrgo nasutus									.7													.2					.3			.7	.3		.6		1	1	1	1	1	3			.5	
Rectobolivina advena	2	4	2	3	4	2	5	4	4	4	4	5	3	6	4	3	3	1	3	.7	3	1	3	4	.6	1	3	.3	.6	1	3	2	2	3	2	.3	1	2	1	1	4	1	.5	
Reophax scorpiurus													.2	.2				.2	.6	.3	.2					.4																		
Reussella atlantica	5	5	2	3	4	7	9	7	5	6	8	7	5	5	4	3	3	2	6	4	3	1	3	5	2	3	3	3	2	.3	4	2	3	5	5	5	5	5	1	4	4	3	1	1
Robulus spp		.2							.4						.2		.2		.3							.2	.3	.3	.9	1	.9		.3	.7	.3	.7	.6	.6	.5	.4	.5	3	2	2
Rosalina concinna												.3									.2	2	.3	1		.2			.3		1													
R. floridana	1	2	1	2	2	1	1	1	1	.3	2	1	1	3	2	1	.2	1	2	.7			.3	.5		.4	.9		.3		.3													
R. suezensis															.2								.3			.2	1			3	2	4	3	3	2	2	4	4	3	1	4	2	.5	2
"Rotalia" beccarii var. A	4	6	4	6	6	5	6	7	4	7	6	3	5	4	6	6	3	2	2	5	2	4	4	3	2	2	2	1	2	.7	2	.8	1	.7	1	.3	1		1		1	1	1	.8
"R." beccarii var. B	8	10	7	6	8	11	9	7	5	7	4	5	5	5	4	7	8	8	5	5	6	9	5	4	8	3	3	3	3	1	1	2	.3	.3				.3						
"R" pauciloculata	4	4	3	5	1	3	3	1	2	.7	.2		.7	1	.6	.2	1	1	.3	.3	.5	.7	.3		.3	.2	.3	.3					.3					.3						.8
"R." rolshauseni						.4																																						
Seabrookia earlandi												.3			.6		.4	1	.3	.3	.5	2	1	.8	1	3		3	.6	1	.3	2	.3		.3									
Sigmoilina distorta																																	.3		.3	.3			1	2		.9		4
S. sp																															.6		.3		.7	.3	.6	1	.5		2			
Siphonina bradyana																																								.7				.8
S. pulchra																	.4			1	.5			.3	.3	.4	.3		.3	.7	.9	.4	1	.7	1	1	.6	.3	1	.4		2	.5	
Sphaeroidina bulloides																																									.5	1		1
Stetsonia minuta							.2		1		.2	1	.5	.5	.6		1	.2	.6	.3	.2	.7	.7		.6	.8	1	.7	.3	1		.4								.4				
Textularia mayori	2	1	.9	.4	.8	2	.2	.7	2	2	1	1	2	1	.6	.2	1	.4	.9	.7	.7	.5	.7	.5	.6		2	1			1	.4	1	1	1	.7		.3	2	.4	2			
Uvigerina laevis									.4														.3										.6	1	1	1	.6	1	1	2	4	4	12	15
U. parvula				.2	.2									.2	.2	.5	.4	1	.9	2	2	.2	3	1	1	4	3	3	18	12	10	17	13	17	19	16	23	20	17	23	18	19	31	21
Valvulineria minuta																								.5	.3					2	.3	.4	.3			.3		.3		.4	.5		.5	1
Virgulina complanata															.2	.5	.4			.3	.2		.7													.3								
V. pontoni	17	10	18	16	10	11	14	16	13	15	13	10	11	12	16	18	12	20	13	14	16	18	13	17	15	10	12	7	5	6	6	3	7	4	3	4	5	4	3	5	2	5	1	2
V. spinicostata	3	3	3	2	8	2	.6	4	4	2	2	4	2	3	4	3	3	3	2	2	4	5	2	4	5	3	6	4	2	1	2	2	1	.7	.3	2	.6	.3	.5					
Miscellaneous spp.	1	1	.2						1	1	3	1	1	.9	2	1	3		3	.6	2	2	3	.8	1	4	4	3	4	4	5	2	2	.3	1	3	2	1	1	9	9	10	6	2

Table 9. Benthonic Foraminifera, in percent of total population, from the outer end of offshore traverse V.

STATION	196	197	198	199	200	201	202	203	204	205	206	207	208	209	210	211	212	213	214	215	216	217	218	219	220	221	222	223	224	225	226	227
DEPTH IN METERS	7	9	10	10	11	12	12	14	15	15	16	16	17	18	19	20	20	20	21	22	22	23	23	24	24	25	25	26	26	26	27	27
LIVING POPULATION	29	142	938	91	77	112	35	47	132	67	36	47	67	92	38	185	58	58	162	190	125	340	492	75	85	28	62	44	77	79	60	70
Ammobaculites dilatatus													1								1	2			1	1	2					
A. exiguus										1																						
Ammoscalaria pseudospiralis	1	2	1	7	11	11	1	3		2	2	5			1		3	1		2		7	9	1	3		2	6	6	8	3	1
Angulogerina bella																								1					2		1	
Bigenerina irregularis	1	5	1	9	2	7	1	4	5	2		8	4	1	14	2	15	1	30	16	27	22	38	15	10	3	6		12	7	10	8
B.? sp.																	1					2	1		1	1		1	1			
Bolivina fragilis																						1										
B. lowmani		10	24	10	7	19	4	4	4	15	5	4	2			5	1	1	1	11	10	21	55		3		2		4	4	6	1
B. pulchella primitiva																				1			3	1			1					
B. striatula	1	6	16	2	1	3										1							1								1	1
B. striatula spinata										1										1			1							1		
Buccella hannai													8	1		3	1	2	1	2	5	4	5									
Bulimina marginata																															1	1
Buliminella cf. bassendorfensis		1	1		2			1	5		5	1	6	29	3	29		13	10	14	5	15	16	2	1	1					1	
B elegantissima		7	1	4	1			1						1		3																
Cancris oblonga																															1	
Cassidulina subglobosa						1																										
"Discorbis" bulbosa																					3			3	1			1		3	1	2
Eggerella sp.									2	1		1			1	2	1		3	3	1	4	6			1		3		1		2
Elphidium advenum																						1	3		1		1					
E. discoidale		1		2	2	2			2	1								2		2	10	3	6	3	4	2	1		2	3	1	
E. gunteri		3	5						5	2		1	3	1		2	1			1		12	14		2	1	2			1		3
E. poeyanum			1	1																												
E. spp.				1																	2				1	1	1		1	1		
Epistominella vitrea							1		9	1	4	1	7	2		14	4	8		9	4	30	51	2	7	4	6		5	1	2	3
Eponides antillarum																									1				2			
Gaudryina exilis																									1			1				
Hanzawaia strattoni										3	1	5	2	2	2	2	6		3	1	9	16	41	4	7	4	15		12	14	13	18
Miliolidae		2			1	2																										
Nonionella atlantica				6	4		2	1	8	3						5		1	1	6		8	21	1	1							1
N. opima	5	5		9	2	4	8	2	28	8	3	2	10	38	12	68	2	16	50	41	1	63	29	9	1	1	3		3	4		2
Nouria polymorphinoides						1	1		1			2	6	9		13	7	2	11	9	4	14	18	4				2		4		
N. sp.														1							1				1							
Proteonina atlantica										1										4	9	12	4	6	17	1	3	26	4	3		1
"P." sp.	1																			1		1	3	1			1		2			
Quinqueloculina seminulum					1																											
Reophax gracilis																1				1		1	2									
Reussella atlantica																					1	1	2	1	3	1			2	4	6	7
Rosalina floridana			1	1	4	2		2														1	2		3							
"Rotalia" beccarii var. A	1	16	98	4	2	5	1	2	24	13	2	7	4	1	1	4	4		8	1	12	3	17	3	1	1	11	4	2	4	3	6
"R." beccarii var. B	19	84	786	35	36	54	15	26	36	13	13	10	11	6	3	15	6	4	6	12		12	39	4		1	2		8	3	4	7
"R." pauciloculata																	1		1	3	9	17	15	1	9	1				3	3	
"R." rolshauseni							1		2				1			1			1				1				2		2			1
Stetsonia minuta											1											1	7									
Textularia mayori																						2	7	1	2	1					2	
Virgulina complanata																							1									
V. pontoni			2			1		1							1	13	4	7	36	49	11	60	72	12	3	2	1		6	9		4
V. spinicostata																						1									1	
Miscellaneous spp.			1		1				1				2			2	1					3	2						1	1		1

Table 10. Living benthonic Foraminifera, in numbers of specimens, from offshore traverse VII.

STATION	196	197	198	199	200	201	202	204	205	206	207	208	209	210	211	212	213	214	215	216	217	218	219	220	221	222	223	224	225	226	227
DEPTH IN METERS	7	9	10	10	11	12	12	15	15	16	16	17	18	19	20	20	20	21	22	22	23	23	24	24	25	25	26	26	26	27	27
TOTAL POPULATION	2400	1000	38000	4000	2600	4500	3100	870	3700	1800	1300	1300	250	3000	300	5200	440	3400	4900	5000	4400	4500	2600	5400	6700	5000	880	1500	2500	6600	4400
Ammobaculites dilatatus											.3	.3		.5		.3	.5	2	.7	2	1	.7	1	1	.2	.3	3	.3	.3		.2
A. exiguus		.4	.3						.2	.2		.9					.2		.3	1		.4	.3	.6		.3	3	1	1		.5
Ammoscalaria pseudospiralis		2		2	3	4	2	.2	4	2	.9	2	2	1	.7	2	2	5	3	2	2	2	3	2	1	1	14	4	3	1	1
Bigenerina irregularis	1	2	i	6	6	3	5	4	5	6	5	4	4	8	4	8	9	7	3	4	5	5	8	6	5	5		8	4	5	4
B. sp.						.4																.2					.5	.3			
Bolivina fragilis							.5		.4																						
B. lowmani		1	.3	.8	.3		.3	.5	1	.2		.3			.7	.3					.7	1		.3					.3	.5	.7
B. pulchella primitiva					.3		.3		.4	.2	.3	.3	.4	.5	.3	.6	.5		.7	.3	2	2	.9	.3	2	2				2	1
B. striatula	.7	2	.7	.4		1	.8		.2	.2		.3		.3			.2	.5				.5	.3	.3	.2	.9		.5	1	.2	.4
B. striatula spinata																	.2		.3				.3							.2	
Buccella hannai						.4	.8	.2	.2	.2		2		.3	.3	.3		.5		.3	.4	.5			1					.2	.4
Bulimina marginata								.2				.3	.8							.3										.2	
Buliminella cf. bassendorfensis				.4				2	.2	.9	.9	.6	10		8	.6	2	2	.3	1	.7	1	.6	.6	.5	.3		2	.3	.2	1
B elegantissima		.8								.2			.4													.3					
Cancris oblonga														.3	.3		.2		.7				.3	.3						.5	
Cassidulina subglobosa																									.2						
"Discorbis" bulbosa														.3												.6				.2	.2
Eggerella sp.																		.5		.9	.7	.4	2								.4
Elphidium advenum			.3							.2		.6		.3	.7		.2		.3	.3	.7	.4		.3	.5	.3			.3	.2	
E. discoidale	14	10	3	15	17	20	9	9	16	16	19	13	11	19	8	10	16	24	18	12	9	9	12	14	12	13		5	11	11	8
E. gunteri	21	19	11	23	21	22	15	16	17	19	12	14	12	11	7	12	13	4	10	13	13	8	6	5	8	6	.5	7	10	7	7
E. incertum mexicanum				.8	.3	.4																									
E. matagordanum	1	.8	.3						.4																						
E. poeyanum	.3	.8	.7	.8	.6	.7	.8		.4		.3				.3	.3	.2	.5				.4		.3	.2	.6			.3	.7	
E. spp.	4	1	2	3	2	.4	2	2	1	1	.6	1	.4	.8	.7	2	.7	.5		1	.7	.5	.9	1	2	.9			.3	.2	.4
Epistominella vitrea		.4						2	1	.7		2	2	1	8	2	2	1	3	.6	4	5	2	3	5	3		3	3	3	5
Eponides antillarum																															.4
Gaudryina exilis							.5			.7				.3			.2			.3							2	.3			.4
Hanzawaia strattoni				.4	2	1	.5	1	3	4	7	4	6	9	3	6	7	4	6	8	4	8	6	7	6	7		7	7	12	6
Lagena & related spp.											.3															.3				.2	
Miliolidae	.7		.7		.6	.7		.5	.2	.2	.3	.3		.3		.3															
Nonionella atlantica			.3		.6	.4	.8	2	1	1	.6	2	2	3	4	.9	2	1	2	3	3	4	.9	2	2	.9	.5	3	3	4	3
N. opima	.7	2	.3			.4	1	6	.9	2	2	2	15	3	8	.3	3	2	3	.3	1	1	.3	.6	3	2		1	.6	.2	1
Nouria polymorphinoides												1	.8		3		.5	.5	.3		.4	.2	.3				1				
N. sp.																				.3											
Planulina exorna													.4										.3		.2	.6					.5
Proteonina atlantica									.4	.7	.6			.8		.3	.7	3	3	2	2	3	7	16	2	8	71	15	9		11
"P." sp.									.2																		.9	.3			
Quinqueloculina compta			.3																												
Q. lamarckiana			.7																												
Q. seminulum			2		.3		.3																								
Rectobolivina advena					.3				.2	.7							.2	.5	.3	.3	1	1	1	.6	.5	2		.3	3	3	.9
Reussella atlantica		.4		.4			.5	.2	.4	.9	.3	.6	.8	.5		2	2	.9	2	.6	1	1	.3	.3	3	3		.8	.6	3	2
Rosalina concinna									.2								.2														.2
R. floridana		.4	.7	.4	.3		.5			.2	.3		.8	.8	.3	.3	.2	.5	.3	1	3	2	.3	1	.7	1			.3	.2	.4
R. suezensis																															.2
"Rotalia" beccarii var. A	33	33	24	30	18	20	19	17	15	12	17	16	10	16	8	18	14	10	14	20	21	15	18	14	13	15	2	20	17	15	18
"R." beccarii var. B	22	23	50	17	27	23	39	35	30	27	30	28	17	17	25	27	17	22	20	19	17	18	18	14	18	14	.9	9	14	16	13
"R." pauciloculata								.2		.7		.3	.4	.5	1	3	.9	3	2	1	1	3	2	3	5	1		2	2	2	2
"R." rolshauseni	.7	.4			.6	1	.5	.7	.4	1	.9	2	2	1	.3	.6	1		1		.7	.4	.3		.2	2		.8		.2	
Stetsonia minuta																						.2		.3							
Textularia mayori	.3					.4			.2	.2	.6	.6		1		2	1	1	.7	.3	.4	.9	.6	.9	.5			.8		2	2
Virgulina complanata																		.5												.2	
V. pontoni		.4				.4		.5	.4	1	.6	.6	1	2	5	1	3	4	5	4	4	4	7	4	8	6		8	8	8	8
V. spinicostata		.4								.7				.3	.3		.2				.4	.4		.6		2			.6	1	.4
Miscellaneous spp.	.3		.6			.7		.7		.2		.3	.4	1	2					.3							.5		.3		

Table 11. Benthonic Foraminifera, in percent of total population, from offshore traverse VII.

FAUNA AND BATHYMETRY OF BANKS ON CONTINENTAL SHELF, NORTHWEST GULF OF MEXICO

BY

ROBERT H. PARKER AND JOSEPH R. CURRAY

Reprinted for private circulation from
THE BULLETIN OF THE AMERICAN ASSOCIATION OF PETROLEUM GEOLOGISTS
Vol. 40, No. 10, October, 1956
Reproduced by permission.

BULLETIN OF THE AMERICAN ASSOCIATION OF PETROLEUM GEOLOGISTS
VOL. 40, NO. 10 (OCTOBER, 1956), PP. 2428-2439, 6 FIGS., 1 PLATE

FAUNA AND BATHYMETRY OF BANKS ON CONTINENTAL SHELF, NORTHWEST GULF OF MEXICO[1]

ROBERT H. PARKER AND JOSEPH R. CURRAY[2]
La Jolla, California

ABSTRACT

Considerable new information has been obtained on the bathymetry and fauna of several calcareous banks on the continental shelf of the northwest Gulf of Mexico. A compilation of depths to tops and bases of 130 banks on the shelf revealed primary modes of depth occurrences at 9, 31, and 45 fathoms. These modes correspond with well developed terraces at the same depths on the banks studied in detail. Several of the banks were characterized by semi-ring depressions, steep central pinnacles, and flat terraces at several depths.

The fauna collected on these banks at depths of between 24 and 31 fathoms are characteristic of intertidal depths in the West Indies and Caribbean. Many of the mollusks from these banks exhibited sub-specific differences from the species which have been collected from their normal range in the West Indies. Despite the existence of dead reef coral, no living forms were collected. Living lithothamnioids were common on all banks. Evidence suggests that the tops of these banks were in shallow intertidal waters at a time when over-all water temperatures were warmer than at present, and when populations of these faunas were continuous to the West Indies. As sea-level and hydrographic conditions changed, the original fauna became isolated and the corals which appear to form the primary organic capping ceased their growth, leaving horizontal surfaces. The presence of large crystals of gypsum and inclusions of anhydrite from the flanks of one bank may have a bearing on the original topographic high at this place.

INTRODUCTION

A feature peculiar to the outer continental shelf of the northwest Gulf of Mexico is the series of pinnacle-like banks or topographic highs rising abruptly from the generally smooth, sediment-covered bottom. These banks, sometimes called coral heads, have been discussed by Shepard (1937), Mattison (1948), Carsey (1950), Williams (1951), Stetson (1953), Goedicke (1955), and others, but except for a short discussion of the corals and algae and a profile and description of Flower Garden Banks by Stetson (1953, pp. 20–21), no lists of fauna or detailed bathymetry have been published. The data presented in this paper represent recently obtained information on the bathymetry and fauna of these features which may be related to their origin.

BATHYMETRY

Contours of two banks (Fig. 1), known locally as Flower Garden Banks, were published by Carsey (1950, p. 377) and have been reproduced in subsequent

---

[1] Manuscript received, May 2, 1956. Contribution from the Scripps Institution of Oceanography, New Series No. 877. This investigation was supported by a grant from the American Petroleum Institute, Project 51.

[2] Scripps Institution of Oceanography, University of California.

Valuable assistance in the identification of biological material was given by William J. Clench, Ruth D. Turner, Henry C. Stetson, and Elisabeth Deichman of the Museum of Comparative Zoology, Harvard University; Harald A. Rehder and William P. Morrison of the Division of Mollusks of the U. S. National Museum; and R. Tucker Abbott of the Academy of Natural Sciences of Philadelphia. Assistance and advice during the work and preparation of the manuscript were given by Francis P. Shepard of the Scripps Institution. Assistance in the field work was given by William A. Jones, Master of the Trawler *Neva J.*, David G. Moore of the U. S. Naval Electronics Laboratory, San Diego, California, and David M. Poole of Scripps Institution. David B. Ericson of Lamont Geological Observatory, Columbia University, generously furnished core material and information relating to their own recent studies of some banks off Galveston, Texas. James R. Moriarty and Thomas E. Mahnken prepared the illustrations and plates.

(762)

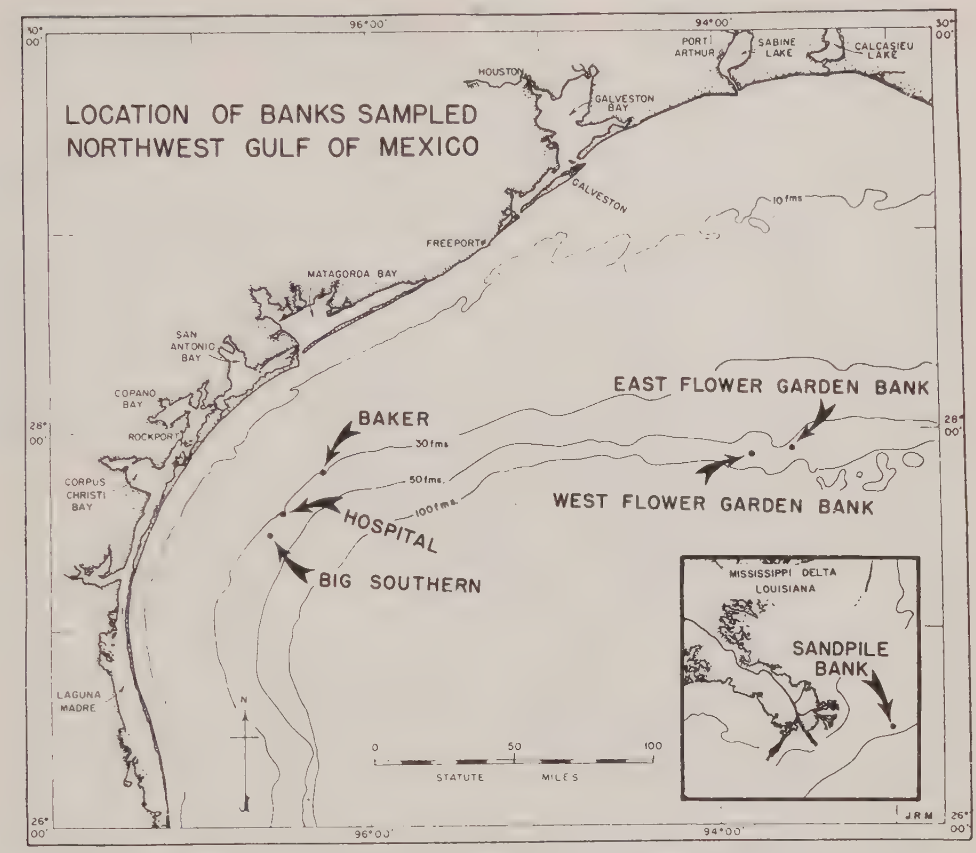
LOCATION OF BANKS SAMPLED
NORTHWEST GULF OF MEXICO
30° 00'
96°00'
94°00'
PORT ARTHUR
SABINE LAKE
CALCASIEU LAKE
HOUSTON
GALVESTON BAY
GALVESTON
10 fms
FREEPORT
MATAGORDA BAY
SAN ANTONIO BAY
COPANO BAY
ROCKPORT
28° 00'
CORPUS CHRISTI BAY
BAKER
30 fms
50 fms
100 fms
HOSPITAL
BIG SOUTHERN
EAST FLOWER GARDEN BANK
WEST FLOWER GARDEN BANK
MISSISSIPPI DELTA
LOUISIANA
SANDPILE BANK
LAGUNA MADRE
N
0
50
100
STATUTE MILES
JRM
26° 00'

FIG. 1.—Locations of banks sampled, northwest Gulf of Mexico.

papers. In May, 1955, a bathymetric survey was made on the trawler *Neva J.*, and the sounding lines were combined with soundings from the U. S. Coast and Geodetic Survey unpublished *Chart 6291*. The topography of these two banks which lie on the break in slope between the continental shelf and the continental slope is shown in Figures 2 and 3. Features of West Flower Garden Bank (Fig. 2) include: major tops at about 11, 30, and 40 fathoms; a steep central pinnacle (greater than 20° slope) on the highest peak with a relatively flat top at 11 fathoms; well developed terraces at about 45 fathoms; a poorly developed terrace at about 25 fathoms; and a depression at the foot of the slope on the north and west sides. Features of East Flower Garden Bank (Fig. 3) include: a steep central pinnacle (greater than 20° slope) at the top with a relatively flat top at about 10 fathoms; a well developed terrace at about 30 fathoms; and a depression at the base of the slope on the east side.

In June, 1954, northeast-southwest echo-sounding profiles were run on some of the smaller banks located off Aransas Pass, Texas, along the 40-fathom con-

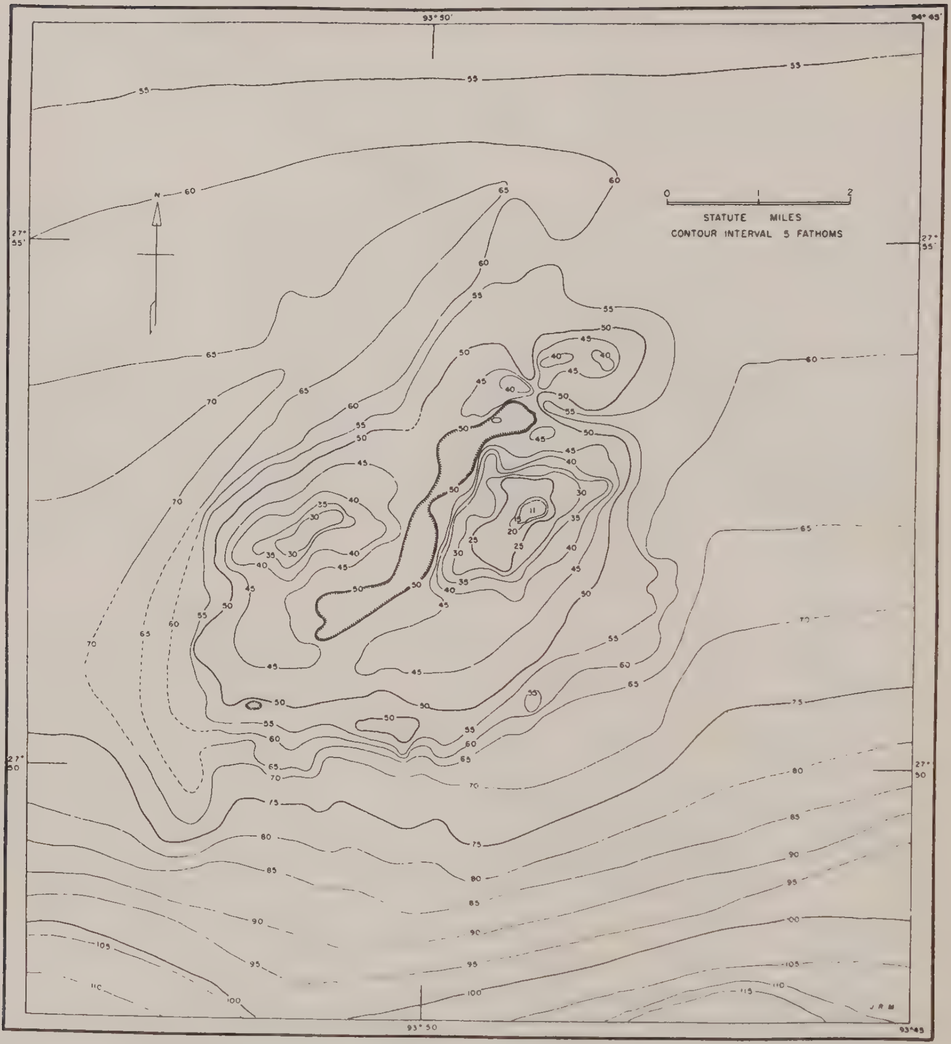
93° 50'
93° 45'
27° 55'
27° 50'
N
0
1
2
STATUTE MILES
CONTOUR INTERVAL 5 FATHOMS
J R M

FIG. 2.—Bathymetry of West Flower Garden Bank, off Galveston, Texas.

tour (Fig. 1). Profiles of three of these banks, locally named Baker, Big Southern' and Hospital Banks (Fig. 4), show marginal depressions on both sides. There is also a suggestion of terraces on the flanks, although the existence of such features can not be established from single profiles.

A compilation of depths to the tops and bases of 130 banks was made from U. S. Coast and Geodetic Survey unpublished sounding charts between the Mississippi Delta and the Mexican border. Only banks with more than 2 fathoms

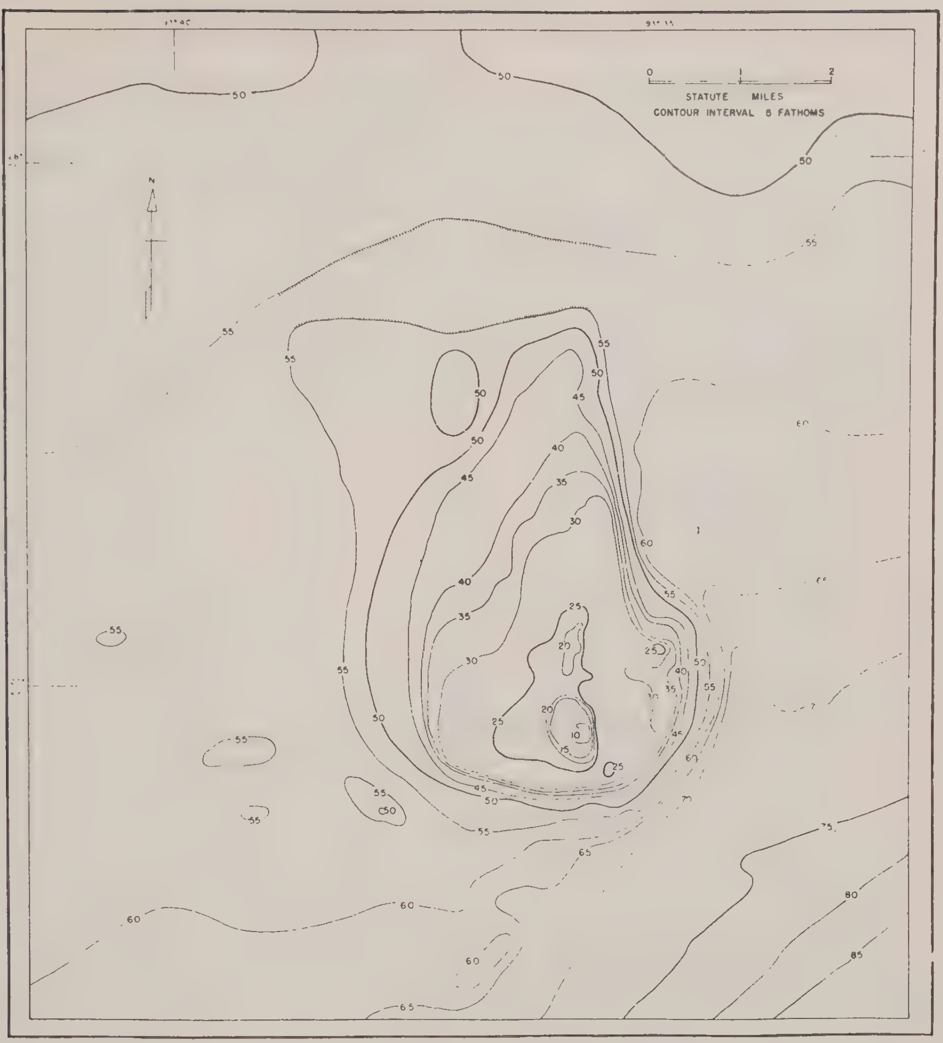
0
1
2
STATUTE MILES
CONTOUR INTERVAL 5 FATHOMS
N
50
55
60
65
70
75
80
85
45
40
35
30
25
20
15
10

FIG. 3.—Bathymetry of East Flower Garden Bank, off Galveston, Texas.

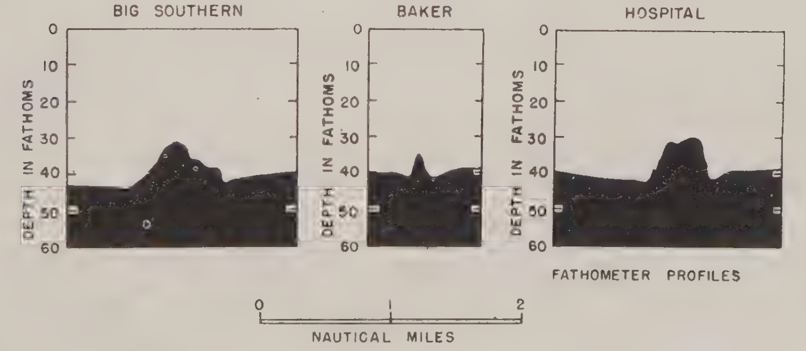

FIG. 4.—Profiles of banks off Aransas Pass, Texas. Locations on Figure 1.

relief which rise above 100 fathoms and have bases in more than 10 fathoms were considered. This tabulation, therefore, includes some low sediment- and shell-covered mounds on the continental shelf as well as the so-called coral heads which are concentrated on the outer shelf. A histogram (Fig. 5) showing the distribution of depths to the tops of these banks has three principal modes of the most commonly occurring depths. These modes are nine fathoms, about 31 to 34 fathoms, and about 45 to 48 fathoms. It is significant that the modes on this histogram very closely approximate the depths of the best developed terraces on the banks studied in detail (Flower Garden Banks), namely, about 30 and 45 fathoms; and the tops of these banks are in the nine-fathom mode.

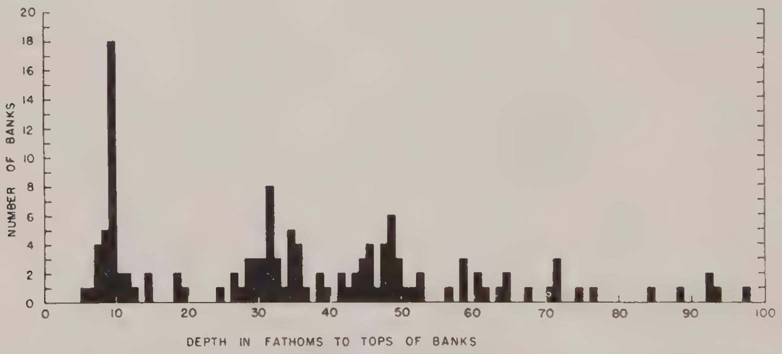

Fig. 5.—Histogram showing depth in fathoms to tops of 130 banks on continental shelf, northwest Gulf of Mexico.

FAUNA

Biological dredge samples were taken from Baker, Big Southern, West and East Flower Garden banks, and from one bank off the Mississippi Delta in 48 fathoms, Sandpile Bank, shown in the inset on Figure 1. A total of 137 species of mollusks was obtained from all of the banks in the northwestern Gulf, and one species of living coral was taken from East Flower Garden Bank. There were fragments and small colonies of dead corals obtained from the other banks which have not yet been identified. Stetson obtained five species of reef corals from the Flower Garden Banks as cited in Table I. Several species of pelecypods were contained in the material taken by Stetson from these banks, which were checked by the senior writer at the Department of Mollusks, Museum of Comparative Zoology, Harvard University, and included in Table I. One large ophiuroid (brittle star), tentatively identified as *Ophioderma rubicundum* Lütken, 1856, was taken on West Flower Garden Bank. A tabulation of all fauna from four of the banks in the northwestern Gulf of Mexico, with notes on other localities where these species have been taken, appears in Table I. A large number of the same mollusk species was also taken on Sandpile Bank, which is outside of the area under discussion. The surface of this bank, unlike the others, is composed

Fauna from Calcareous Banks off Texas and Louisiana

Species	*Baker Bank* (*31 fms.*)	*Big Southern* (*30 fms.*)	*West Flower Garden* (*24 fms.*)	*East Flower Garden* (*30 fms.*)	*Other Occurrences* (*Depth*)
MOLLUSKS					
Abra lioica Dall 1881		D			North Carolina to West Indies—3–6 fms.
Acmaea pustulata Heilbling 1779			D		Florida Keys to W. I.—Shallow water.
Acteon, new species		D			
Aequipecten muscosus Wood 1828	D				North Carolina to W.I.—Shallow water.
Anachis translirata Ravenel 1861	D	D			Mass. to N.E. Florida—Shallow water.
Anachis, new species	D				
Anomia simplex Orbigny 1842	D				New York to West Indies—Shallow water.
Antigona strigillina Dall 1902	D	D	D		SE. Florida to W. I.—20 to 70 fms.
Arca umbonata Lamarck 1819	D				North Carolina to W. I.—Shallow water.
Arca zebra Swainson 1833	A	D			North Carolina to W. I.—Shallow water.
Arcopsis adamsi E. A. Smith 1888	A	D	A		North Carolina to Brazil—Shallow water.
Arcopsis a. conradiana Dall 1886	D	D			North Carolina to Florida—25 fms.
Arene gemma Toumey and Holmes 1856	D		D		North Carolina to Brazil—12–22 fms.
Astraea caelata Gmelin 1789			A		SE. Florida to W. I.—Shallow water.
Barbatia cancellaria Lamarck 1819	D		A	A*	S. Florida to W. I.—Shallow water.
Barbatia candida Gmelin 1790	D	D			North Carolina to Brazil—Shallow water.
Barbatia domingensis Lamarck 1819	D	D	A*	A*	N. C. to West Indies—Rocks at low tide.
Barbatia tenera C. B. Adams 1845	D		D		Florida to West Indies—Shallow water.
Botula fusca Gmelin 1792			A*	A*	S. C. to West Indies—Shallow on rocks.
Bulla eburnea Dall 1881?	D				N. Carolina to W. I.—103–337 fms.
Calliostoma jujubinum rawsoni Dall 1889	D		D		Lower Keys to W. I.—1 to 10 fms.
Calyptraea centralis Conrad 1841		D			North Carolina to W. I.—Shallow water.
Cerithiopsis exile C. B. Adams 1850		D			Jamaica—Littoral Zone (1–5 fms.).
Cerithiopsis flavum C. B. Adams 1850			A		Jamaica—Littoral Zone (1–5 fms.).
Cerithiopsis greeni C. B. Adams 1839		D			Mass. to West Indies—3 to 10 fms.
Cerithiopsis latum C. B. Adams 1850			A		Jamaica—Shallow water.
Cerithiopsis subulatum Montagu 1808	A	A	A		West Indies—2 to 15 fms.
Cerithium literatum Born 1780			A	A	S. Florida to W. I.—Shallow water.
Cerodrillia thea Dall 1883		D			S. Florida—Sand bars in inside waters.
Chama congregata Conrad 1833	A	D	A		North Carolina to W.I.—1 to 7 fms.
Chama macerophylla Gmelin 1792	D	D	D		Florida to W. I.—Shallow, protected.
Chione grus Holmes 1858	D				North Carolina to Yucatan—12 to 63 fms.
Chlamys benedicti Verrill and Bush 1897	D	D			West Indies—25 to 72 fms.
Conus stearnsi Conrad 1869	D		D		Florida to Yucatan—4 to 6 fms.
Corbula aequivalvis Philippi 1836		D			Porto Rico—Shallow water.
Corbula cymella Dall 1881	D	A			Florida Keys—Shallow water.
Corbula dietziana C. B. Adams 1852			D		North Carolina to W. I.—2 to 18 fms.
Corbula swiftiana C. B. Adams 1852	D				North Carolina to W. I.—6 to 100 fms.
Crassinella martinicensis Orbigny 1842	D	D			Mass. to West Indies—Shallow water.
Crenella divaricata Orbigny 1842				A	North Carolina to W. I.—20 to 50 fms.
Crepidula plana Say 1822			D		Canada to Texas—1 to 3 fms.
Cuspidaria ornatissima Orbigny 1842	D				North Carolina to W. I.—2 to 100 fms.
Cuspidaria perrostrata Dall 1881		D			Mass. to West Indies—58 to 500 fms.
Cyclocardia armilla Dall 1903		D			NW. Florida to Texas—24 to 169 fms.
Cyclostrema amabilis Dall 1889			A		Cuba, West Indies—Shore to 150 fms.
Cythara bartletti Dall 1889	D				Key West to W. I.—16 to 450 fms.
Dentalium laqueatum Verrill 1885		D			North Carolina to W. I.—10 to 193 fms.
Dentalium, species		D			
Diodora cayenensis Lamarck 1822	D	D			Maryland to Brazil—½ to 3 fms.
Distorsio clathrata Lamarch 1816	D	D			N. C. to Colombia, S. A.—22 to 124 fms.
Drillia acestra Dall 1889?	D				Florida Straits, W. I.—Over 400 fms.
Drillia detecta Dall 1881?	D	D			Gulf of Mexico—339 fms.
Drupa didyma Schwengel 1943	D		A		SE. Florida—5 to 35 fms.
Emarginula phrixodes Dall, 1927	D		D		North Carolina to W. I.—20 to 129 fms.
Emarginula sicula Gray 1825	D				Mediterranean, West Indies—8 to 250 fms.
Erato maugeriae Gray 1832	D				Florida to West Indies—2 fms.
Glyphostoma gratula Dall 1881		D			Florida to W. I.—227 to 247 fms.
Gouldia cerina C. B. Adams 1845	A	A			Florida to W. I.—Shallow water.
Haminoea succinea Conrad 1846?		D			Florida—Shores to 2 fms.
Hiatella arctica Linné 1767	D	D			Greenland to W. I.—1 to 100 fms.
Lemintina decussata Gmelin 1791	D	D			S. Florida to W. I.—Low tide to 3 fms.
Lima pellucida C. B. Adams 1846	A	A			N. C. to West Indies—Shallow water.
Lima tenera Sowerby 1846	D	D	D		S. Florida to W. I.—Shallow at low tide.
Liotia bairdi Dall 1889	D	A			N. C., Fla. Keys, Yucatan—15 to 127 fms.
Liotia, new species			A		Taken only off Texas
Lithophaga aristata Dillwyn 1817			A*		S. Florida to West Indies, La Jolla to Peru in coral in shallow water.
Lithophaga bisulcata Orbigny 1842				A*	N. C. to West Indies—Shallow water.
Litiopa melanostoma Rang 1829		D			Pelagic in warm seas.
Lucapina sowerbii Sowerby 1835			A		Florida Keys to Brazil—Under rocks at low tide.
Macoma extenuata Dall 1900	D	D			Gulf of Mexico in 32 fms.
Mangelia psila Bush 1885?	D	D			North Carolina to W. I.—16 fms.
Mangelia, species	D				Taken only off Texas
Mathilda scitula Dall 1889	D	D			North Carolina to W. I.—49 to 294 fms.
Melanella arcuata C. B. Adams 1850	D				North Carolina to W. I.—Shallow water.
Melanella bilineata Alder 1848			D		North Carolina to W. I.—No depth given.
Melanella patula Dall & Simpson 1900		D			Georgia to Porto Rico—Shallow water.

Species	*Baker Bank (31 fms.)*	*Big Southern (30 fms.)*	*West Flower Garden (24 fms.)*	*East Flower Garden (30 fms.)*	*Other Occurrences (Depth)*
Microcardium transversum Rehder & Abbott 1951	D	D	A		Gulf of Mexico—20 to 60 fms.
Mitra nodulosa Gmelin 1790	D	D	A		N. C. to West Indies—Low tide, under rocks.
Mitrella lunata, new subspecies	D	D			*M. lunata* is a bay form.
Murex, juvenile	D		D		Taken only off Texas.
Musculus coralliophagus Gmelin 1790			A*		Florida to W. I.—2 to 7 fms.
Musculus opifex Say 1822	A	D			North Carolina to Brazil—Shallow water.
Nassarina glypta Bush 1885	D	D			N.C. to Florida Keys—14 to 63 fms.
Nassarius ambiguus Pultney 1794	D	D			N.C. to West Indies—Low tide line to 6 fms.
Natica canrena Linné 1758	D	D			N.C. to West Indies—Low tide line.
Nucula crenulata A. Adams 1856	D				N.C. to West Indies—30 to 250 fms.
Nuculana jamaicensis Orbigny 1842	D				N.C. to West Indies—54 to 640 fms.
Odostomia seminuda C. B. Adams 1839	D				Nova Scotia to Fla.—Shore to 12 fms.
Papyridea soleniformis Bruguiere 1784		D			S. Florida to Brazil—Low tide to 4 fms.
Pecten papyraceus Gabb 1873	D	D			Gulf of Mexico to W. I.—30 to 60 fms.
Peristichia toreta Dall 1889	D	D			N. C. to Florida—2 to 22 fms.
Peristichia, species		D			Taken only off Texas.
Pitar fulminata Menke 1830	D	D			N. C. to Brazil—1 to 6 fms.
Plicatula gibbosa Lamarck 1801	D	D		A*	N. C. to West Indies—Intertidal—20 fms.
Pododesmus rudis Broderip 1834	D				Florida to W.I.—Intertidal to 3 fms.
Polinices, species	D				Taken only off Texas.
Prunum, species			D		Taken only off Texas.
Pteria colymbus Röding 1798	D				N. C. to W. I.—Intertidal to 4 fms.
Pycnodonta hyotis Linné 1758		D			Florida to W. I.—20 to 50 fms.
Pyramidella crenulata Holmes 1859			D		S. Carolina to W. I.—1 to 6 fms.
Pyramidella, species	D				Taken only off Texas.
Pyrunculus caelatus Bush 1885	D	D			North Carolina to Florida—15 to 43 fms.
Rhizorus acutus Orbigny 1841	D	D			North Carolina to W. I.—15 to 124 fms.
Rimula aequisculpta Dall 1927		D			S. Florida to W. I.—1 to 25 fms.
Ringicula semistriata Orbigny 1842	D				North Carolina to W. I.—34 to 107 fms.
Rissoina browniana Orbigny 1842			D		North Carolina to W. I.—Grassy bottom in littoral zone.
Rissoina cancellata Philippi 1847	D	D	D		Florida to W. I.—Eel grass, 1–2 fms.
Rissoina chesneli Michaud 1832	D	D			North Carolina to W. I.—Shallow intertidal.
Rissoina elegantissima Orbigny 1842			D		Cuba to West Indies—Shallow water.
Rissoina multicostata C. B. Adams 1850		D			Florida to West Indies—Intertidal.
Rocellaria hians Gmelin 1790	D	D			N. C. to W. I.—Coral in shallow water.
Scaphander watsoni Dall 1881	D				N. C. to Cuba—63 to 324 fms.
Seila adamsi H. C. Lea 1845	D	D			Mass. to West Indies—1 to 6 fms.
Spondylus americanus Herman 1781				A*	Florida to W. I.—5 to 24 fms.
Teinostoma, new species		D			Taken only off Texas
Teinostoma, new species			A		Genus found S. Fla. to W. I.—Shallow water under rocks.
Trinostoma, new species			D		
Tellina promera Dall 1900	D				Fla. to Trinidad—Shallow, intertidal.
Tellina radiata Linné 1758		D			S. Carolina to W. I.—Shallow sandy.
Tellina versicolor Dekay 1843	D				Rhode Island to W. I.—1 to 10 fms.
Tenagodus squamatus Blainville 1827		D			Florida to W. I.—20 to 160 fms.
Thyasira trisinuata Orbigny 1842	D				Nova Scotia to W. I.—15 to 90 fms.
Trachycardium magnum Linné 1758		D		A*	Lower Keys to W. I.—Shallow water.
Triphora intermedia C. B. Adams 1850	D	D	A		Jamaica—Shallow water.
Triphora melanura C. B. Adams 1850	D		A		N. C. to West Indies—Shallow water.
Triphora pulchella C. B. Adams 1850	D		D		Florida to W. I.—1 to 40 fms.
Triphora turristhomae Orbigny 1842			A		N. C. to West Indies—Shallow water.
Triphora, species	D		A		Taken only off Texas.
Trivia suffusa Gray 1832	D				S. Florida to W. I.—1 to 14 fms.
Turbonilla incisa Bush 1849		D			SW. Florida—No depth given.
Turritella exoleta Linné 1758	D	A			S. Florida to W. I.—5 to 7 fms.
Varicorbula operculata Philippi 1848	D	A			N. C. to West Indies—5 to 250 fms.
Vermicularia spirata Philippi 1836	D	D	A		S. Florida to W. I.—1 to 14 fms.
Vitrinella multistriata Verrill 1884	D				N. C. to West Indies—3 to 142 fms.
Williamia krebsi Mörch 1877	D		A		Fla. Keys to W. I.—10 to 30 fms.
Yoldia solenoides Dall 1881	D	D			Gulf of Mexico—20 to 118 fms.
Zeidora biglowei Farfante 1947			D		S. Cuba—175 to 225 fms. (dead) only taken once.
ECHINODERM					
Ophioderma rubicundum Lütken 1856			A		Cape Florida, Bahamas and W. I.—9–12 fms.
CORALS					
Madracis mirabilis Duchassaing and Michelotti, 1861			D*	A*	Florida Keys to West Indies—0–400 fms.
Porites astroeoides Lamarck 1816			D*		Bermuda, S. Florida, W. I. to Brazil—0–20 fms.
Montastrea annularis Ellis and Solander, 1786			D*		Florida to West Indies, C. America—Outer edges of reefs.
Manicina gyrosa Ellis and Solander 1786			D*		Florida and Caribbean—0–10 fms.
Diploria strigosa Dana 1846			D*		Bermuda, Florida, West Indies—Massive reef builder.

D—Indicates dead occurrences.
A—Indicates taken alive.
* —Taken by Stetson, Feb. to March, 1947.

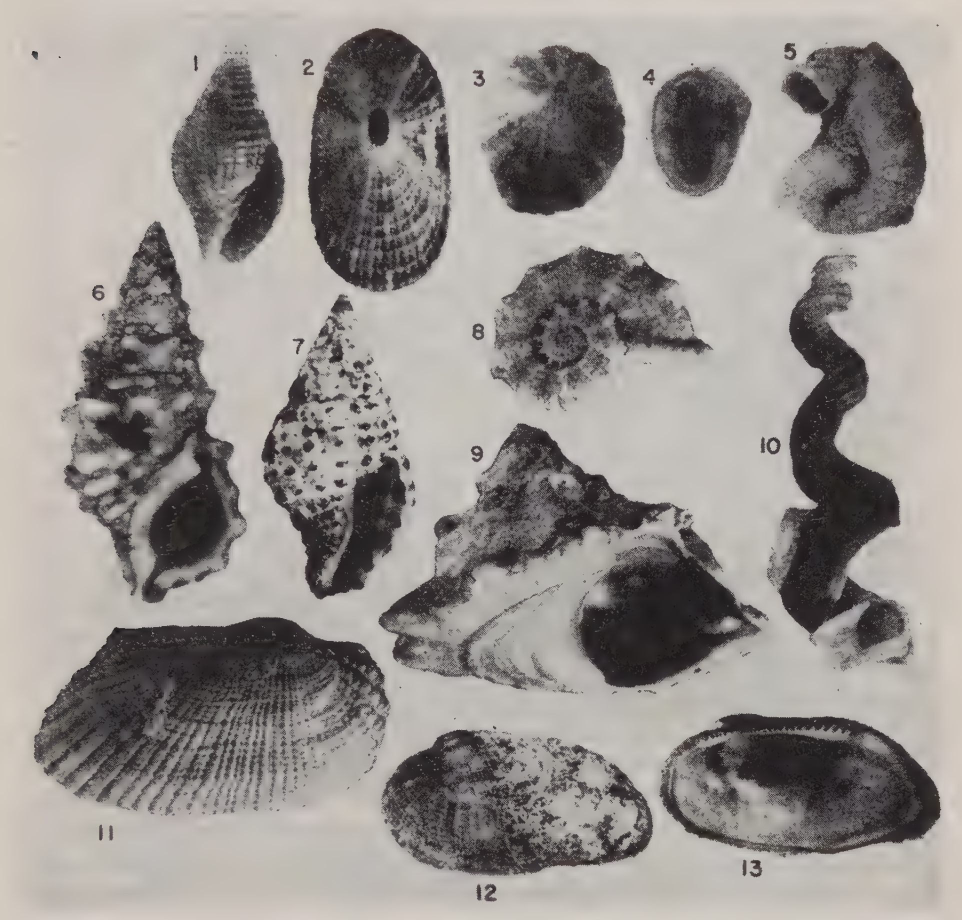

PL. I.—Typical mollusk fauna from calcareous banks, continental shelf off Texas.

FIG. 1.—*Mitra nodulosa* Gmelin, 1790, aperture view. Size —7 mm.×3.5 mm., Station J-325.

FIG. 2.—*Lucapina sowerbii* Sowerby, 1835, dorsal or exterior view. Size—13 mm.×7 mm., Station J-325.

FIGS. 3 and 4.—*Williamia krebsi* Morch, 1877, Fig. 3 exterior or dorsal view, Fig. 4 interior view. Size—2 mm.×5 mm., Station J-325.

FIG. 5.—*Lemintina decussata* Gmelin, 1791, side view (fragment). Size—15 mm.×12 mm., Station J-169.

FIG. 6.—*Cerithium literatum* Born, 1780, aperture view. Size—32 mm.×16 mm., Station J-325.

FIG. 7.—*Drupa didyma* Schwengel, 1943, aperture view. Size—9 mm. ×4.5 mm., Station J-325.

FIG. 8.—*Cyclostrema amabilis* Dall, 1889, top, or dorsal view. Size—3 mm. ×7 mm., Station J-325.

FIG. 9.—*Astraea caelata* Gmelin, 1789, aperture view. Size—5 mm.×10 mm., Station J-325.

FIG. 10.—*Vermicularia spirata* Philippi, 1836, side view. Size—30 mm.×10 mm. Station GM-/28.

FIG. 11—*Barbatia candida* Gmelin, 1790, exterior view. Size—17 mm.×9 mm., Station J-169.

FIGS. 12 and 13—*Barbatia cancellaria* Lamarck, 1819, Fig. 12 exterior view, Fig. 13 interior view. Size—18 mm.×9 mm., Station, J-325.

primarily of silty sand rather than calcareous débris. Plate I shows some of the more common mollusks found on the banks, and most of the living mollusks. All specimens illustrated are in the collection at Scripps Institution.

Interpretation of fauna.—It is significant that practically all the living and dead species of animals are either restricted to or have their centers of population in the West Indies or the Bahamas and many have not been previously collected in the Gulf of Mexico. Of the 137 species of mollusks taken, 52 have bever neen reported north of the central part of the Florida coast, and most of these range only along the east coast rather than along the west coast of Florida. Another striking observation is that 71 of the species normally live in less than 12 fathoms, with a large proportion usually living in intertidal or bay waters. All samples from the banks were taken in depths between 24 and 31 fathoms, or considerably deeper than their normal depth range. It was also observed that the bank representatives of the forms which are generally found in shallow water (0–5 fathoms) in the West Indies were almost all sub-specifically different, at least in their morphology. For example, most of these bank forms were considerably smaller, although they appeared to be mature specimens. Many of the bank specimens are more spinose and have somewhat different ornamentation than the "normal" populations in the West Indies. These comparisons were made by checking the bank specimens with all available representatives in the U. S. National Museum, Academy of Natural Sciences of Philadelphia, and the Museum of Comparative Zoology at Harvard. From these observations it might be inferred that the banks and their fauna were at some time in the past connected ecologically with the warm, shallow-water populations on the south.

Besides the mollusks, the other prominent inhabitants of the banks are the abundant living lithothamnioids and bryozoans. Practically all the débris in the samples was composed of small fragments of lithothamnioids and many colonies of calcareous bryozoans such as *Smittina*, *Schizoporella*, and *Mamillopora*. On Flower Garden Banks, the calcareous algae was in the form of large balls, composed of many concentric layers as shown in Figure 6. These lithothamnioid balls are identical with those taken by Stetson (1953, pp. 21–22) on the same banks and Challenger Bank off Bermuda. They are also very similar to the algal mats observed on Alexa Bank in the South Pacific, north of the Fiji Islands, which was explored by Scripps Institution vessels on the "Capricorn" expedition in 1952–53 (Roger R. Revelle, personal communication, and Capricorn Shipboard Report, pp. 42–43). These three widely separated banks (Flower Garden, Challenger, and Alexa) have several features in common. There are no large masses of living reef-forming corals; the platforms of these banks are below the depths where corals usually form the largest reef masses; and each is characterized by the presence of rounded lithothamnioid balls or mats.

The only living corals taken from any of the Gulf of Mexico banks by the Scripps Institution field parties were large numbers of small colonies of *Madracis mirabilis* (Dushassaing and Michelotti, 1861) (Fig. 6). This coral is considered

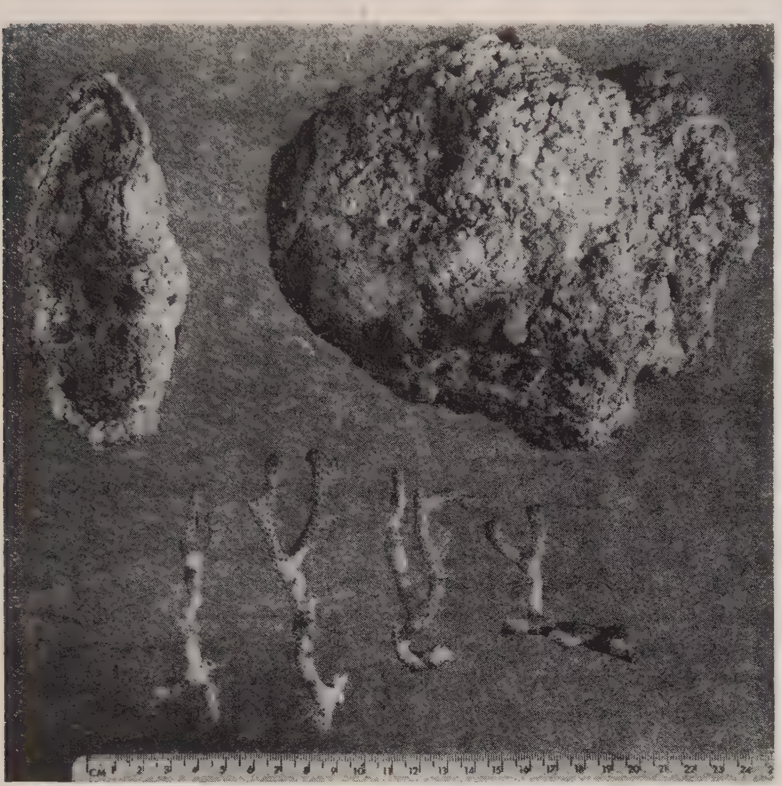

FIG. 6.—Lithothamnion balls from 24 fathoms, West Flower Garden Bank, and coral, *Madracis mirabilis*, from 30 fathoms, East Flower Garden Bank.

an encrusting species and apparently does not grow rapidly enough or abundantly enough to form large reef complexes. Smith (in Galtsoff, 1954, p. 294) gives the depth range of the genus *Madracis* as 0 to 800 meters and temperature range from 10° to 27°C. *Madracis mirabilis* occurs most abundantly in the West Indies and in sparse numbers in the Florida Keys, and has been found in the Pleistocene of Florida and lower Miocene of Cuba (Vaughan, 1919, p. 345). Although Stetson (1953, p. 21) reported several reef-forming corals such as *Montastrea*, *Manicina*, and *Porites* from the Flower Garden Banks, examination of these specimens now in the Museum of Comparative Zoology indicated that they had been collected dead. Neither from the literature nor from personal communication with workers in the northwestern Gulf have the writers been able to substantiate reports of living reef corals on these banks.

DISCUSSION

Several investigators have offered explanations for the origin of these banks, dating from Shepard (1937) who suggested that these banks may be related to salt-dome structures. Others have explained them on the basis of biohermal structures which have kept pace with changing sea-levels (Stetson, 1953), while recently Goedicke (1955, p. 152) came to the conclusion "that the pinnacles are mainly due to tectonic activity [controlling the location of salt domes] and partially due to differential erosion." Although direct evidence of the origin of the banks (emplacement of the rocks) awaits seismic studies and additional geological studies, there are clues in the data presented here as to shaping of the banks subsequent to their formation. The fact that the tops of the banks fall into distinct modes, and that the tops of deeper banks correlate well with terraces on those banks with more relief and shoaler tops, suggests erosion at various stands of sea-level, although it can not be stated when these stands might have occurred.

The faunal evidence on the banks studied intensively suggests that at one time the tops of the banks were in very shallow, almost intertidal water, at a time when the over all average water temperature was considerably warmer than at the present. This fauna certainly represents a population now isolated from the main centers of abundance in southeast Florida to the West Indies. It is also distinctly different from the fauna of the surrounding level-bottom communities. Both the assemblage of mollusks found on the banks and the presence of dead reef-forming corals suggest that the growth of the organic capping of the banks started during a much lower stage of sea-level when the water was considerably warmer. The populations of bank mollusks were then continuous around the Gulf edge to the West Indies. As the sea-level and hydrographic conditions changed, the corals were not able to maintain their colonies close to sea-level, and in some cases died off completely. Many of the mollusks which were originally living in very shallow water became isolated from the parent stock, and, in adapting to the changing conditions, exhibited morphological changes. The lithothamnioids, on the other hand, are far more resistant to temperature and depth changes, and became the primary surviving contributors to the organic capping.

REFERENCES

Carsey, J. Ben, 1950, "Geology of Gulf Coastal Area and Continental Shelf," *Bull. Amer. Assoc. Petrol. Geol.*, Vol. 34, No. 3, pp. 361–85.

Clark, H. L., 1933, "A Handbook of Littoral Echinoderms of Porto Rico and Other West Indian Islands," *Sci. Survey of Porto Rico and the Virgin Isl., New York Acad. Sci.*, Vol. 16, Pt. 1. 147 pp., 7 pls.

Galtsoff, Paul S., et al., 1954, "Gulf of Mexico Its Origin, Waters and Marine Life," *Fishery Bull., U.S. Fish and Wildlife Serv.*, Vol. 55, No. 89. xiv, 604 pp.

Goedicke, T. R., 1955, "Origin of the Pinnacles on the Continental Shelf and Slope of the Gulf of Mexico," *Texas Jour. Sci.*, Vol. 7, No. 2, pp. 149–59.

Mattison, George C., 1948, "Bottom Configuration in the Gulf of Mexico," *Jour. Coast and Geod. Survey*, No. 1, pp. 76–81.

Shepard, F. P., 1937, "Salt Domes Related to Mississippi Submarine Trough," *Bull. Geol. Soc. America*, Vol. 48, pp. 1349–62.

Shipboard Report, Capricorn Expedition, 1953, *Scripps Institution of Oceanography Reference 53-15*. 60 pp. (mimeo. report).

SMITH, PAUL A., 1948, "Comment" (on "Bottom Configuration in the Gulf of Mexico"), *Jour. Coast and Geod. Survey*, No. 1, pp. 81–82.

STETSON, HENRY C., 1953, "The Sediments of the Western Gulf of Mexico. Part I—The Continental Terrace of the Western Gulf of Mexico: Its Surface Sediments, Origin and Development," *Papers in Physical Oceanography and Meteorology of Massachusetts Inst. Tech. and Woods Hole Oceanog. Inst.*, Vol. 12, No. 4. 45 pp.

VAUGHAN, T. WAYLAND, 1919, "Fossil Corals from Central America, Cuba, and Porto Rico, with an Account of the American Tertiary, Pleistocene and Recent Coral Reefs," *Bull. U. S. Nat. Mus.*, No. 103, pp. 189–524, Pls. 69–152.

WEAVER, PAUL, 1950, "Variations in History of Continental Shelves," *Bull. Amer. Assoc. Petrol. Geol.*, Vol. 34, No. 3, pp. 351–60.

WILLIAMS, HARRY F., 1951, "The Gulf of Mexico Adjacent to Texas," *Texas Jour. Sci.*, Vol. 3, No. 2, pp. 237–50.

PROCEEDINGS
OF THE
CALIFORNIA ACADEMY OF SCIENCES
Fourth Series
Vol. XXIX, No. 1, pp. 1–19, 22 figs. November 26, 1956
Reproduced by Permission

THE LARVAL DEVELOPMENT OF THE CALIFORNIA SPINY LOBSTER, *PANULIRUS INTERRUPTUS* (RANDALL), WITH NOTES ON *PANULIRUS GRACILIS* STREETS[1]

BY

MARTIN W. JOHNSON

Scripps Institution of Oceanography
University of California, La Jolla, California

INTRODUCTION

The California spiny lobster, *Panulirus interruptus* (Randall), is the only lobster occurring on the coast of California. Its main distributional range is usually considered to be from slightly north of Point Conception, California, to the Gulf of Tehuantepec, Mexico.

For many years it has been a highly prized item in the fisheries of California and is considered eleventh in importance by value among the fisheries of the state (Wilson, 1948). The amount of research accorded the lobster has, however, not been commensurate with this economic importance or with its biological interest.

During its life history, the spiny lobster passes through a series of eleven floating larval "phyllosoma" stages in which the body is highly transparent and exceedingly compressed dorsoventrally. The last phyllosoma stage metamorphoses to a "puerulus" stage in which the animal is still transparent but structurally similar to the adult. The puerulus of some species may be found in plankton, but evidently it soon deposits calcium in the carapace and seeks the bottom to live in concealment.

---

[1] Contribution from Scripps Institution of Oceanography, New Series, No. 878.

Allen (1916) carried out certain fundamental observations on the adult animals particularly in the vicinity of Santa Barbara, the Channel Islands, and La Jolla. His findings are especially pertinent to the present study in showing that the berried females may carry 5,000 to 500,000 eggs each, depending upon size, and that the spawning season extends from March to August with its maximum activity in May, June, and July. He concluded that a period of from nine to ten weeks is probably required for hatching. The young hatched readily in aquaria, but attempts at rearing

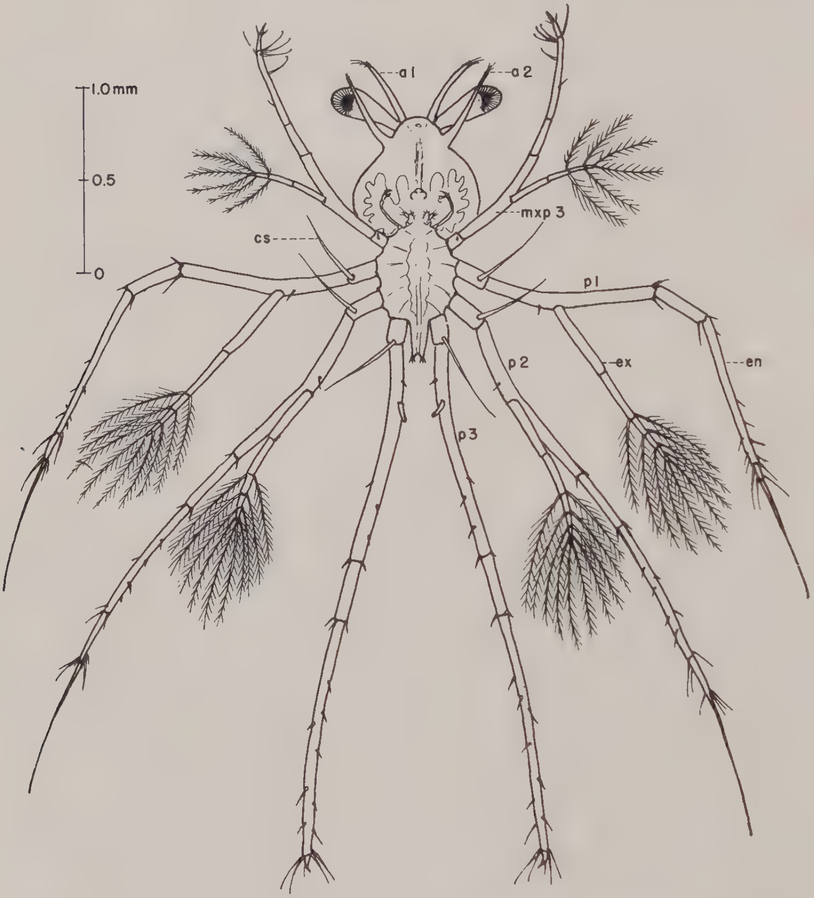

1

Figure 1. Stage I of *Panulirus interruptus* phyllosoma hatched in aquarium. Labels: *a 1*, first antenna; *a 2*, second antenna; *cs*, coxal spine; *en*, endopod; *ex*, exopod; *mxp 3*, third maxilliped; *p 1*, *p 2*, *p 3*, first, second, and third legs.

the larvae were futile. Other investigators have had similar experiences in attempts at rearing the phyllosoma larvae of other species. In a recent study, Lindberg (1955) found a maximum of 800,000 eggs produced by large females. The spawning season was essentially the same as indicated by Allen (1916).

With regard to our knowledge of the biology of phyllosoma larvae in nature, rather little is known because of their scarcity, coupled with the lack of complete and identified developmental series. Their offshore or oceanic distribution also adds to the difficulty.

In 1919 Schmitt published a brief note on phyllosoma larvae caught off the coast of southern California. Larvae of several sizes were observed. The details of structure and stages of development were, however, not worked out in any case, but a photograph was included showing a large specimen which appears to represent either the tenth or the eleventh phyllosoma stage.

A practical understanding of the biology of the California spiny lobster will require information regarding the abundance and extent of dispersal of its planktonic larvae from various areas within the geographical range of the species. It is probable that many of the larvae produced in the northern range of adult distribution are lost by drifting away from the area with the California Current. Unless many of the northern larvae are returned by some circuitous route in large local eddies, the maintenance of the local stock would depend in considerable measure upon recruitment of larvae from more southern waters, probably with the Davidson Current. A knowledge of the duration of the planktonic larval stages and the rate and direction of ocean currents is highly important in this connection, but we have no direct information on how long the larvae live in the plankton, though studies now in progress of the seasonal distribution of the stages point to a planktonic period of several months.

The series of phyllosomas examined from plankton collections along the California coast to south of Cedros Island have not revealed any significant irregularity in structure, shape, or size, of the various developmental stages, indicating that only one species is involved in the northern range. However, *Panulirus gracilis* (until recently known as *Panulirus inflatus* (Bouvier)) does overlap the southern range of *Panulirus interruptus* at least in small numbers and enters into the commercial catch of Mexico (Chase and Dumont, 1949). In a review of the conflicting synonymy of *P. inflatus*, Holthuis (1954) has concluded that the species is a synonym of *P. gracilis* Streets. The latter, being the older name, must be used.

The larvae of *P. gracilis* may be expected to drift northward should they be caught in the Davidson Current, especially during its maximum development along the coast. For this reason, among others, it is essential that the larval structure be known in detail in order to facilitate definite identification of the planktonic stages of the two species. This identification can now be made as a result of a study of larvae caught within the range of *P. gracilis* south of Point Eugenia and within the Gulf of California. The larvae of the two species are distinguishable on small but definite structural characteristics, which will be briefly mentioned here and reported upon in detail later.

A survey of the seasonal and spatial distribution of the larvae is in progress.

THE PHYLLOSOMA STAGES OF P. INTERRUPTUS

Large numbers of the first phyllosoma stage were obtained in 1940 by hatching of eggs from a berried female kept in an aquarium (figure 1). Subsequent stages (figures 2 to 18) were all obtained from plankton hauls, especially from collections made along the coasts of southern and Baja California in connection with the Marine Life Research Program of the California Cooperative Oceanic Fisheries Investigations.

Careful anatomical analysis of large numbers of larvae reveals eleven rather poorly defined developmental stages as summarized in table I. There is a considerable range in size within each "stage," especially in the later stages, and specimens are often observed in which structures such as newly added legs, exopods, gills, second maxillae, and first maxillipeds show noticeable range in size or shape or even degree of segmentation. Whether or not this signifies a molt within the stage is not known, but it may be significant that the more advanced occur in the upper-size range for the stage represented.

The fore-body (cephalic shield) of *Panulirus interruptus* is pear-shaped in outline in the early stages, and is much wider than the hind-body (thorax) during the first and second stages. But in the third stage, the hind-body has attained the width of the fore-body and remains thus during the subsequent stages. The pear-shaped fore-body of the earlier stages later becomes more uniformly oval as shown in figure 18. In no stage is the posterior margin of the hind-body deeply indented.

In stage I, the eyes are not stalked, but in stages II to XI, they are on definite slender stalks which increase steadily in length with each molt. In all stages there is present a median eye spot.

The *first antennae* (antennules) exceed in length the *second antennae* (antennae) during the first four stages, after which the second antennae

---

Figures 2–5. Stages of *Panulirus interruptus* phyllosoma (continued). Labels: *p 3*, *p 4*, third and fourth legs. The distal ends of lengthy appendages showing no significant changes from stage to stage have been omitted in these and subsequent figures.

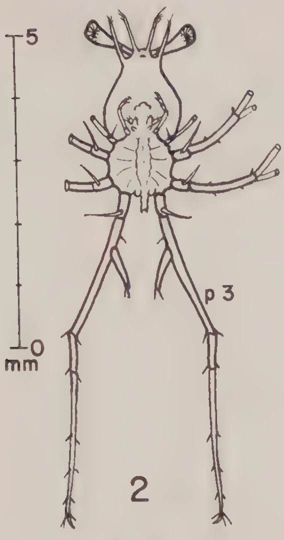

2

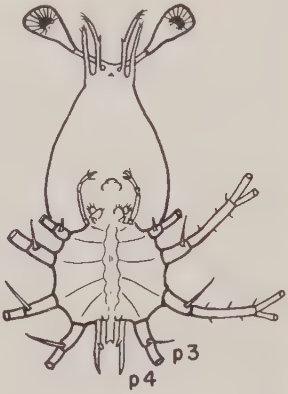

4

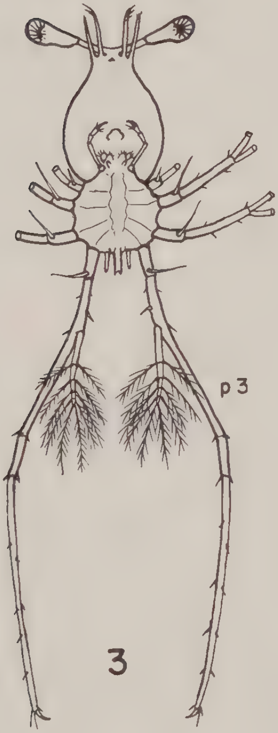

3

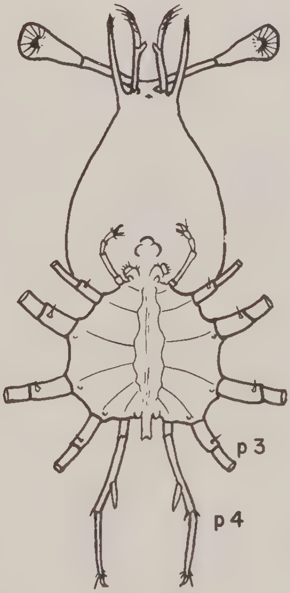

5

Figure 2. Stage II.
Figure 3. Stage III.

Figure 4. Stage IV.
Figure 5. Stage V.

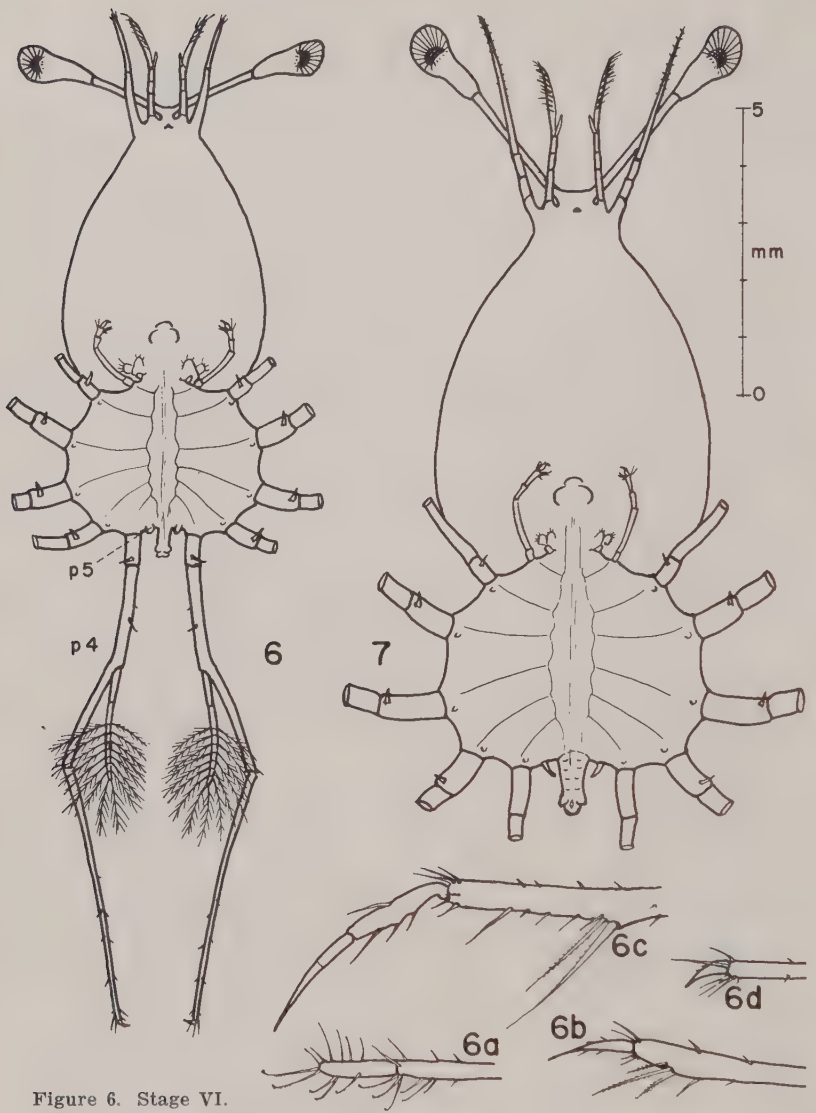

Figure 6. Stage VI.
Figure 6a. Stage VI, Tip of third maxilliped.
Figure 6b. Stage VI, Tip of first leg.
Figure 6c. Stage VI, Tip of third leg.

Figure 7. Stage VII.

Figures 6–7. Stages of *Panulirus interruptus* phyllosoma (continued). Labels: *p 4*, *p 5*, fourth and fifth legs.

progress rapidly with each successive stage until in stage XI they exceed in length the fore- and hind-body combined.

In stage I, the distal end of the first antenna bears a tuft of 4 setae and in each subsequent stage additional tufts are added proximally as transverse rows of setae. The endopod is first evident as a low bud in stage IV. In following stages it elongates, becoming a true branch, but remains small throughout the development and is not a free segment until stage VIII. Beginning in stage VI (sometimes stage VII), there are three segments in the peduncle, the first segment being equal to the combined lengths of segments two and three which are subequal. These proportions remain about the same in the next two stages, but in stages VIII–XI the third segment is somewhat longer than the second though both combined still equal the length of the first segment.

The second antennal peduncle becomes three segmented in the seventh or eighth stage. These segments remain about equal, the third being slightly the longest.

The structure of the *mandibles* and the first *maxillae* in stage XI is shown in figure 16. These appendages are very short and strong. The mandibular blade, when viewed from the ventral side of the larva, is seen from the edge. In figure 16, it is tilted slightly and the labrum lifted to show the broad scoop-shaped blade with the stronger teeth at the outer and inner angles. The two branches of the first maxillae are armed respectively with three strong hooks and three flexible setae, but prior to stages VII and VIII there are only two hooks and setae. There is present a small vestigial palp bearing two setae. In stage I the palp is prominent but diminishes in intermediate stages and later again enlarges.

Thus these mouthparts, together with the second maxillipeds which are armed at the tips with small claws and heavy setae (figure 15) indicate that the larva must feed upon particulate material gathered without the aid of a real filtering device.

The *second maxillae* in the first stage are composed of two segments, the distal one being much narrower. Each segment bears four long setae which in intermediate, and later stages are lost or shortened. There is but little change in this size relationship (figure 11) until about the sixth stage and in ensuing stages when the segments become noticeably flattened and the distal segment increases greatly in breadth especially posteriorly (figures 12–15). Similarly the first maxillipeds are at first simple buds which in the later stages gradually increase to three-lobed appendages (figure 15).

The *second maxillipeds* are functional feeding appendages in all stages. There is no change from the first until the eighth stage when an exopod bud appears. In stage IX, this bud becomes separated as a short segment which in the next stage elongates and bears 2 to 4 setae at the tip and a gill bud appears on the distal portion of the coxa. In stage IX, the exopod has become setose with five or six pairs of setae, the gill has become leaf-like, and a second gill bud has appeared on the proximal portion of the coxa.

The *third maxillipeds* are very long and the exopod is already present and setose in the first stage. With each successive stage there is, however, an increase in the number of segments in the exopods. The number of segments as shown by the number of pairs of setae appears to be regular for each of the earlier stages, but become irregular in the later. The range in numbers of exopod segments for the third maxillipeds and the first and second legs for stages I to XI is respectively: 4 to 25; 6 to 32; and 6 to 33.

The principal features of the development of the legs, especially the third, fourth, and fifth pairs, are adequately covered in table I which, together with the figures, will show the changes taking place with each stage. In contrast to the rapid development of the fourth legs, the fifth pair remain as very small buds through stages III to VII, and never exceed the abdomen in length. In no stage of the development of the legs is there present a strong spine at the distal end of the second basipods as shown for *Panulirus gracilis* (figure 22).

The inner branches of the legs are readily lost so that a complete attached set of legs has not been found beyond the sixth stage, but judging from loose appendages found in the jar with the later stages the end segments do not change after stage VI (figures 6a–6d).

Coxal spines are present in the first to ninth stages, but are usually all lost in the tenth, and are never present in the eleventh.

In stage X *gills* are present on the dorsal distal end of the coxal segment of the maxillipeds and legs and in stage XI they occur also on the proximal portion of the coxa at the juncture of the carapace and on the dorsal margin of the thorax at the base of these thoracic appendages.

In stages V to XI, there are present spines on the ventral surface of the thorax at the bases of the third maxillipeds and each of the legs.

The *abdomen,* in stages I to V, remains about the same with two small points at the tip. Complete segmentation occurs in the ninth stage though earlier indications of segments may be seen as blocks of tissue under the skin.

The *uropods* become evident as buds in the sixth stage. They increase in size and definition with each successive stage and in stage IX are well-formed biramous appendages, but the rami are not separated from the basipods and their outer edges are entire. Upon reaching the tenth stage, the uropods are completely segmented and a small notch with a marginal

---

Figures 8–17. Stages of *Panulirus interruptus* phyllosoma (continued). Labels: *ex,* exopod; *g,* gill; *mx 2,* second maxilla; *mxp 1, mxp 2,* first and second maxillipeds; *p 4, p 5,* fourth and fifth legs.

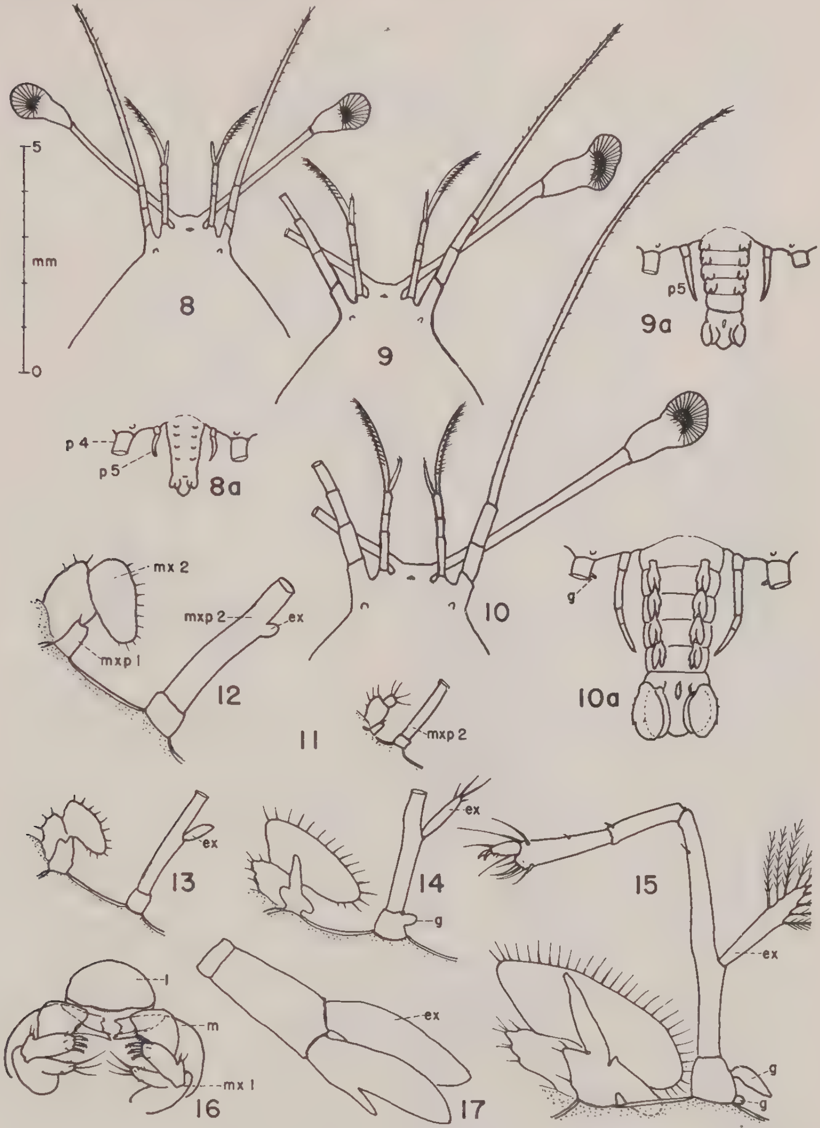
5
mm
0
8
9
p5
9a
p 4
p 5
8a
mx 2
mxp 2
ex
mxp 1
12
10
g
10a
11
mxp 2
ex
13
ex
14
g
15
ex
l
m
ex
mx 1
16
17
g
g

Figure 8. Stage VIII, anterior end.
Figure 8a. Stage VIII, posterior end.
Figure 9. Stage IX, anterior end.
Figure 9a. Stage IX, posterior end.
Figure 10. Stage X, anterior end.
Figure 10a. Stage X, posterior end.
(Figures 8–10a drawn to same scale.)

Figures 11–12. Stages IV and VIII, second maxilla with first and second maxillipeds.
Figure 13. Stage IX, same, reduced scale.
Figure 14. Stage X, same.
Figure 15. Stage XI, same.
Figure 16. Stage XI, mouth parts: labrum *(l)*; mandible *(m)*; first maxilla *(mx 1)*.

Figure 17. Stage XI, pleopod.

TABLE I

Panulirus interruptus—Phyllosoma stages

SUMMARY OF USEFUL DISTINGUISHING CHARACTERISTICS

Stage	*length mm.*	*a 1*	*a 2*	*mxp 2*	*mxp 3*	*leg 1, 2*	*leg 3*	*leg 4*	*leg 5*	*pleopods*	*uropods*
I	1.2– 1.5	1 seg.	1 seg.		ex. seto. cs. (small)	ex. seto. cs.	cs.	0	0	0	0
II	2.4– 2.8	1 seg.	1 seg.		same	same	cs. ex. 1 seg.	bud	0	0	0
III	3.3– 3.8	1 seg.	1 seg.		same	same	cs. ex. seto.	1 seg.	bud	0	0
IV	4.6– 5.2	1 seg. en. bud	1 seg.		same	same	same	1 (2) seg. ex. bud	bud	0	0
V	6.0– 6.8	2 seg. en. bud	1 seg.		same	same	same	3 seg. ex. 1 seg.	bud.	0	0
VI	7.9– 8.5	basis 2–3 seg. en. 1 seg.	2 seg. +		same	same	same	4 seg. ex. seto.	bud	0	low buds
VII	9.4–11.0	basis 3 seg. en. 1 seg.	4 seg. +		same	same	same	same	1 seg.	buds	buds (sometimes cleft)
VIII	12.9–16.0	same	same	ex. bud	same	same	same but no cs.	same	2 (1) seg.	buds cleft	buds cleft
IX	16.0–19.5	same	same	ex. bud or 1 seg.	same	same	same	same	2 seg.	long buds cleft	biramous complete
X	19.0–24.3	same	same	ex. 1 seg. 1 g. bud	same 1 g. bud	same but no cs. 1 g. bud	same 1 g. bud	same 1 g. bud	4 seg.	unseg. biramous	same
XI	26 –31.2	same	same	ex. seto. 2 g.	same but no cs. 2 g.	same but 2 g.	same 2 g.	same 2 g.	4 seg. and claw	segmented biramous	same

a 1 = first antennae
a 2 = second antennae
cs = coxal spine present
en = endopod
ex = exopod

g = gill (s) on coxa
0 = wanting
s = segment (excluding claw)
seto. = setose
+ = longer than a 1

See text and figures for further details.

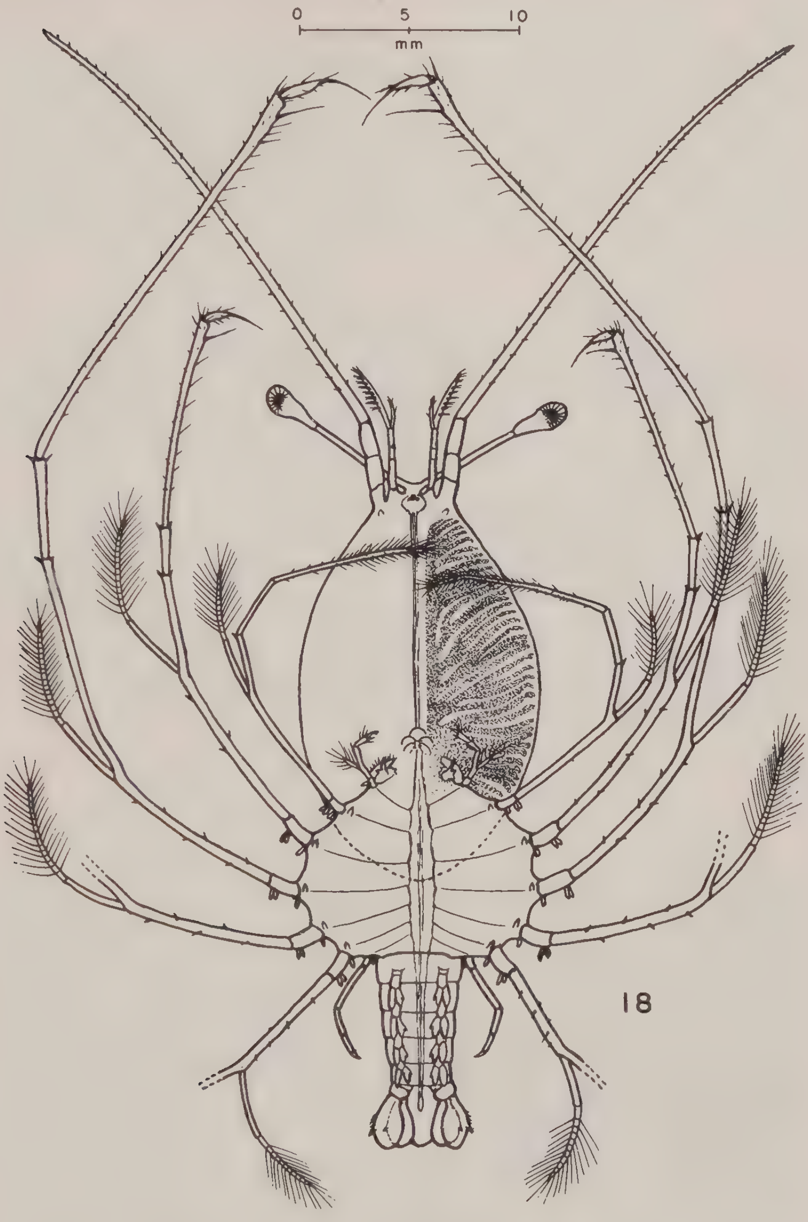

Figure 18. Stage XI of *Panulirus interruptus* phyllosoma.

spine occurs on the outer margin of each branch (figure 10a). In the last stage, this notch and spine are more pronounced.

The *pleopods* appear first in the eighth stage, but they may be indicated earlier under the skin. In stage IX, they may appear either as blunt notched projections or somewhat more advanced, more elongated and flattened structures. In the next stage, they are more leaf-like and a notch appears on the inner margin of the endopod. Complete segmentation occurs in the last stage and the notch on the inner border now sets off a well-defined blunt spine-like process (figure 17).

The Phyllosoma of Panulirus gracilis

Phyllosoma larvae of another species of *Panulirus* have been collected on 10 separate cruises at a total of 19 stations lying off Baja California, and on two cruises at eight stations in the Gulf of California. These larvae are being referred to *Panulirus gracilis,* the only other species known from the West Coast.

From figure 22, it will be seen that this larva resembles that of *Panulirus interruptus* but in distinction from that species, possesses a strong spine at the distal end of the basipod on the posterior dorsal side of the segment closely adjacent to the exopod of each of the first three pairs of legs (figure 22 sp.). The complete series of larvae have not yet been found, but the spine persists as a distinguishing characteristic up through at least the eighth stage. Other differences have also been observed, but more material is needed for further study.

The Puerulus Stage of Panulirus interruptus

(Figures 19–21)

During the metamorphosis from the last phyllosoma stage to the puerulus, the cephalic shield of the phyllosoma is greatly reduced in length and width. The thoracic region is also narrowed and fuses with the cephalic shield to form the cephalothorax. Thus the two erstwhile leaf-like distinct anterior regions of the larvae now appear as one region (figure 19). This, however, remains to some degree dorsoventrally compressed and adult spination is beginning to appear on the dorsal surface. The abdomen has become slightly broader and noticeably longer. Other conspicuous changes include loss of the exopods of the thoracic appendages, reduction in the

---

Figure 19. Puerulus stage of *Panulirus interruptus*, dorsal view.
Figure 20. Puerulus of *P. interruptus*, diagrammatic habit sketch.
Figure 21. Puerulus of *P. interruptus*, first pleopods.

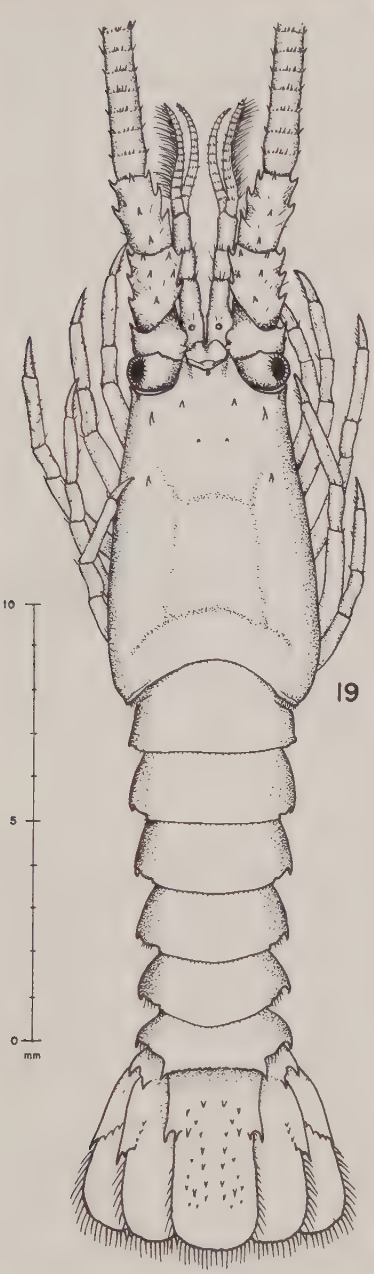

19

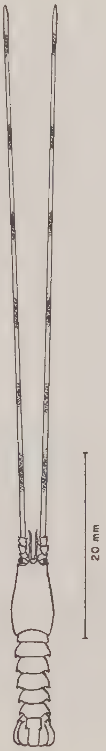

20

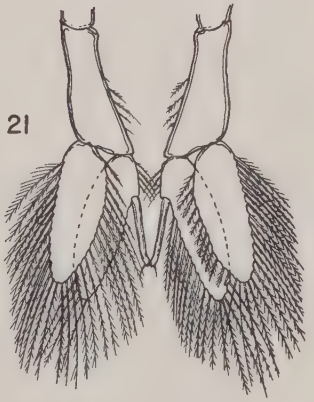

21

length of the eye stalks, and a greatly increased length of the second antennae to three times the body length.

The puerulus, while similar in appearance to the adult, is wholly transparent except for the eyes and pigment bands at intervals along the second antennae, and the walking legs are carried more laterally (figures 19 and 20). The larval median eye is still present and statocysts occur in the first segment of the first antennae.

The larval peripodal exopods which served as swimming organs in the phyllosoma stage are wanting and the animal is now apparently in the process of deserting the planktonic habit, but before deserting this pelagic existence the pleopods have developed into efficient swimming appendages. They have become heavily setose and each endopod bears a strong coupling process provided with hooks to interlock with a similar process of the opposite endopod (figure 21). Thus, in swimming, the appendages lend support to each other for more efficient propulsion.

Only a few specimens of the puerulus stage have been caught and these only from near-shore sampling at La Jolla, April, 1947; in Baja California at Bahia San Roque, September, 1949; and at Cedros Island, August, 1952, where John McGowan of Scripps Institution dip-netted four specimens. The animals are attracted to a light at night and most specimens have been caught in this way. The transverse dorsal grooves characteristic of the abdominal segments of *Panulirus interruptus* in older stages were not yet formed in the specimens. The size ranged from 20 to 21 mm. This agrees with the size reported by Gilchrist (1916) for *Jasus lalandii* in which phyllosoma of 33 to 35 mm. produced puerulus stages ranging from 22 to 26 mm. in length.

DISCUSSION

It has generally been assumed that the phyllosoma larvae are planktonic up to the puerulus stage. However, in experimental cultures Gilchrist (1916) found that after about six days the first phyllosoma larvae of *Jasus lalandii* avoid light and return to the bottom. But the evidence is not clear on this point for he mentions the possibility of larvae seeking the bottom following each molt. Von Bonde and Marchand (1935) make a similar statement regarding the first phyllosoma of that species, and Kinoshita (1934) indicates the same for *Panulirus japonicus*. In no case was the duration of the whole series of phyllosoma stages known.

Studies made on *Panulirus longipes* in Australian waters led Sheard (1949) to conclude that early phyllosomas are found in surface waters; the mid and late stages in mid to surface waters (migrating diurnally); and the late phyllosoma and puerulus stages in surface water. The duration of larval life was estimated to be about five months.

The phyllosoma larvae of the California spiny lobster have not been taken in large numbers per haul in the plankton off the southern California coast. Usually they are widely dispersed and when present occur as one or a few individuals at a station. Stage I may, however, be quite abundant during August and September at coastal stations, especially off Baja California. The maximum concentration observed (cruise 28 station 105.32) was 488 per 1000 cubic meters of water strained by a 1-meter net. Data from analysis of plankton collected monthly over a period of several years from north of Point Conception to the tip of Baja California, and compris-

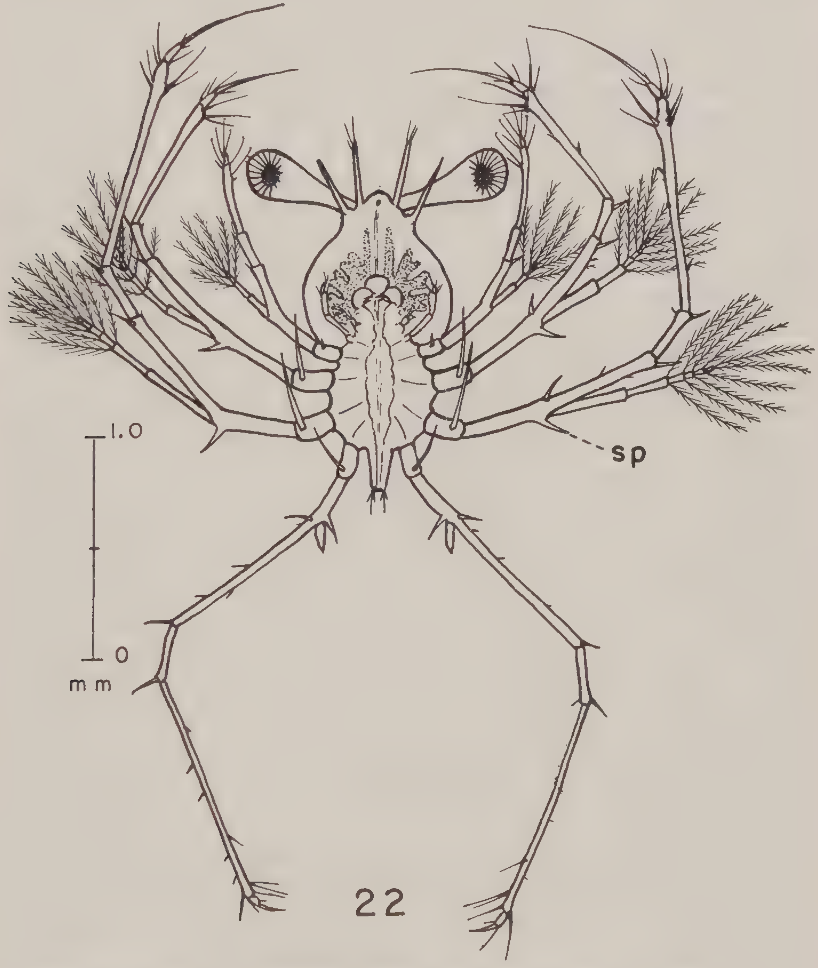

Figure 22. Stage I of *Panulirus gracilis* phyllosoma. Label: *sp*, spine.

ing hundreds of stations with routine sampling from 140–0 meters with a 1-meter net, show that complete cruises over the whole area sometimes yield no larvae whatever or only one to five late-stage individuals during January through May. More complete analysis of these data is needed and will be given in a later report. The finding of later stages floating above the 140-meter level in waters of depth ranging to several hundred meters and over 300 miles from shallow water shows that at least many of the larvae of our species do not seek the bottom regularly in the phyllosoma stages.

The scarcity of the larvae in general may, however, indicate in part a tendency of the larvae to seek levels so near the bottom that they are not adequately sampled by most of our plankton towing. That this may be so, at least in shallow water, is suggested by the finding of twenty specimens in a dredge haul made by Robert Bieri and John Bradshaw of Scripps Institution with a small specially constructed net dragged along the bottom for a distance of 17 meters at a depth of 13 meters. These larvae were, however, all in stage I and may have been just recently released in the area and not yet undergone dispersal by swimming or water currents. Midwater-trawl hauls of long duration taken at depths ranging to 1500 meters or more over very deep water have yielded later stage larvae. The depth of actual catch, however, is not known and the amount of water screened in these hauls is relatively enormous when compared with that screened during the 1-meter net hauls. In view of the many deep hauls that have not yielded larvae, no conclusions can be made from these instances relative to the depth of concentration or habit of seeking the bottom.

Nakamura (1940) working with the Japanese species, *Panulirus japonicus,* states that the embryonic period is passed through in about one month and he deduced from related data that the phyllosoma stages require about the same length of time to reach the puerulus stage. This seems much too short a period.

The status of the systematics of phyllosoma larvae was reviewed by Gurney (1936) in his analysis of the *Discovery* collection which in some 400 specimens contained about a dozen different generic or specific forms. Owing to lack of complete series, however, characters used for recognition of several genera, including *Panulirus,* were given with considerable reservation. The present complete series of larvae of *Panulirus interruptus* is therefore of special use toward establishing the characters which delineate that genus.

The larval structure of *Panulirus interruptus* agrees in general with that of larvae known or believed to belong to other species of the genus. There is, however, a notable difference, no doubt specific, in the relative widths of the main divisions of the body of the older larvae.

On the basis of material available to him, Gurney (1936) concluded provisionally that in the genus *Panulirus* the hind-body is wider, sometimes much wider, than the fore-body. This diagnostic characteristic was established for later stages on Gurney's *Panulirus* larvae A, B *(P. argus),* and D. Later Lebour (1950) and Lewis (1951), dealing with *Panulirus argus,* verify that the hind-body of that species becomes noticeably broader in the later stages. In *Panulirus interruptus,* however, the character does not hold, for in this species the hind-body has attained the width of the fore-body in stage III and remains equal in width throughout the ensuing stages. Thus the diagnostic description must be amended to accommodate not only the young stages of *Panulirus argus* as pointed out by Lebour (1950) but also the later stages of the present species. This makes it a rather unreliable generic characteristic, but useful specifically.

Just what larval details must be stressed in the diagnosis of the species of *Panulirus* are, of course, not fully established as yet and it is likely that useful characters have been overlooked or omitted in the descriptions of series or isolated stages of larvae. Among the characters that may have some specific use are the spines observed in *Panulirus interruptus* on the ventral side of the thorax at the base of each leg. Such spines are not shown or mentioned for other species, but Lewis (1951) in figure 4 B. and C. does show a series of structures suggesting low knobs on the ventral mid-line of the thorax in later stages of *Panulirus argus.* The presence and degree of persistence of coxal spines on the legs and third maxilliped appear also to vary with species within the same genus. In *Panulirus argus* no coxal spine develops on the third maxilliped and those on the legs persist only through the fifth stage, whereas in *Panulirus interruptus* the third maxilliped and all but the fourth and fifth pairs of legs bear these spines up through the ninth stage. There may be some variability in the later stages. The presence of a spine at the distal end of the basipod adjacent to the exopod of the first three pairs of legs as mentioned in the text for *P. gracilis* serves to separate that species from *P. interruptus,* but other characters such as relatively wider fore-body may be needed to separate it from Gurney's phyllosoma *Panulirus* A.

An obvious difficulty in establishing certainty in the systematics of phyllosoma larvae arises either from a considerable variability in the larval structures of some species or from erroneous descriptions as shown by the following unexplained discrepancies. Kinoshita (1934) states that in stage I *Panulirus japonicus* has no exopod on the third maxilliped and yet Nakazawa (1917) in figure I shows the exopod to be present in this stage. Crawford and De Smidt (1922) in figure 273 show no exopod on this appendage in stage I of *Panulirus argus* yet subsequent workers agree that the exopod is present.

SUMMARY

The spiny lobster, *Panuliris interruptus* (Randall), passes through eleven rather poorly defined phyllosoma larval stages. The larvae are planktonic during these stages which require several months for completion.

Through metamorphosis, the last phyllosoma stage becomes the puerulus stage which resembles the adult and becomes benthonic.

All of the phyllosoma stages and the puerulus stage are described and figured.

A second species of phyllosoma referred to *Panulirus gracilis* Streets was found overlapping the range of *P. interruptus* off Baja California, and in the Gulf of California. A description is given of this larva enabling its separation from *P. interruptus.*

LITERATURE CITED

ALLEN, B. M.
1916. Notes on the spiny lobster *(Panulirus interruptus)* of the California Coast. *University of California Publications in Zoology*, vol. 16, no. 12, pp. 139–152.

CHASE JR., F. A., and W. H. DUMONT
1949. Spiny lobsters — identification, world distribution, and U. S. trade, *Commercial Fisheries Review*, vol. 11, no. 5, pp. 1–12.

CRAWFORD, D. R., and W. J. J. DE SMIDT
1922. The spiny lobster, *Panulirus argus*, of Southern Florida: Its natural history and utilization. *Bulletin of the U. S. Bureau of Fisheries*, vol. 38, pp. 282–309.

GILCHRIST, J. D. F.
1916. Larval and post larval stages of *Jasus lalandii* (Milne Edw.) Ortman. *Journal of the Linnean Society of Zoology*, vol. 33, no. 223, pp. 101–125.

GURNEY, ROBERT
1936. Larvae of decapod crustacea Part III. Phyllosoma. *Discovery Reports*, vol. 12, pp. 400–440.

HOLTHUIS, L. B.
1954. On a collection of decapod crustacea from the republic of El Salvador (Central America). *Zoologische Verhandlingen, Rijksmuseum van Natuurlijke Historie*, No. 23, pp. 2–43.

KINOSHITA, TORAICHIRO
1934. On the artificial propagation of *Panulirus japonicus* (De Haan) and some account of its larvae. *Proceedings of the Fifth Pacific Science Congress*, 1933, vol. 5, pp. 4191–3.

LEBOUR, MARIE V.
1950. Notes on some larval decapods (Crustacea) from Bermuda. *Proceedings of the Zoological Society of London*, vol. 120, Part II, pp. 369–379.

LEWIS, JOHN B.
1951. The Phyllosoma larvae of the spiny lobster *Panulirus argus*. *Bulletin of Marine Sciences of the Gulf and Caribbean*, vol. 1, no. 2, pp. 89–103.

LINDBERG, ROBERT G.
1955. Growth, population dynamics and field behavior in the spiny lobster, *Panulirus interruptus* (Randall). *University of California Publications in Zoology*, vol. 59, no. 6, pp. 157–248.

NAKAMURA, SYUYA
1940. Ecological studies of the spiny lobster, *Panulirus japonicus* (v. Siebold), with special reference to its conservation. *Journal of the Imperial Fisheries Institute* (Tokyo), vol. 34, no. 1, pp. 101–113.

NAKAZAWA, K.
1917. On the metamorphosis of *Panulirus japonicus* (in Japanese). *Dobutsugaku Zasshi Tokyo*, vol. 29, pp. 259–267.

SCHMITT, WALDO L.
1919. Early stages of the spiny lobster taken by the boat "Albacore," *California Fish and Game*, vol. 5, no. 1, pp. 24–25.

SHEARD, KEITH
1949. The marine crayfishes (spiny lobsters), family Palinuridae, of western Australia, with particular reference to the fisheries on the western Australian crayfish (*Panulirus longipes*). *Commonwealth Scientific and Industrial Research Organization, Australia, Bulletin* No. 247, pp. 5–45.

VON BONDE, CECIL, and J. M. MARCHAND
1935. The natural history and utilization of the Cape Crawfish, kreef or spiny lobster, *Jasus (Palinurus) lalandii* (Milne Edwards) Ortman. *Department of Commerce and Industry, Fisheries and Marine Biological Survey, Fishery Bulletin* No. 1, pp. 5–54.

WILSON, ROBERT C.
1948. A review of the southern California spiny lobster fishery. *California Fish and Game*, vol. 34, no. 2, pp. 71–80.

DIMENSIONAL GRAIN ORIENTATION STUDIES OF RECENT COASTAL SANDS

BY

JOSEPH-R. CURRAY

Reprinted for private circulation from
THE BULLETIN OF THE AMERICAN ASSOCIATION OF PETROLEUM GEOLOGISTS
Vol. 40, No. 10, October, 1956

BULLETIN OF THE AMERICAN ASSOCIATION OF PETROLEUM GEOLOGISTS
VOL. 40, NO. 10 (OCTOBER, 1956), PP. 2440-2456, 8 FIGS.

DIMENSIONAL GRAIN ORIENTATION STUDIES OF RECENT COASTAL SANDS[1]

JOSEPH R. CURRAY[2]
La Jolla, California

ABSTRACT

Sand-grain-orientation measurements have been made on 110 undisturbed samples of artificially lithified Recent coastal sands to demonstrate the preferred orientation direction of elongate grains. The data presented show that there is a strong tendency for elongate grains to align themselves with their long dimensions parallel with the direction of the depositing current of air or water. This direction is parallel with the backwash direction of waves on a beach and, therefore, averages approximately perpendicular to the beach trend, although some deviation may be caused by a longshore current. Characteristic patterns showing the local fluctuations in current direction are found in hooked spits and washover deltas. The preferred orientation direction of wind-deposited sands is approximately parallel with the wind direction, and for a composite of a large number of samples appears to approach the prevailing wind direction. The perferred orientation of randomly selected wind- and wave-deposited samples from Recent elongate coastal sand bodies isolated from the ocean by progradation averages approximately perpendicular to the trend of the sand bodies.

Possible applications of grain orientation studies are to determine the direction of current of air or water which deposited an ancient sand, to predict trends of subsurface shoestring sands of known coastal origin by study of oriented cores, and to aid in the evaluation of other directional mass properties in sediments.

INTRODUCTION

Sand grains are generally not perfect spheres, but are instead irregularly shaped, slightly elongate particles. When these elongate particles are deposited, they tend to come to rest in a position of maximum stability relative to the forces acting upon them by currents of air or water: i.e., under most conditions, they tend to come to rest with their long dimensions parallel with the direction of flow. In this position they offer less resistance to the flow of the depositing medium around them than they do with their long axes aligned normal to the current direction. When a grain rests on the bottom in an unstable position, there is a great probability that it will be moved again by the current before it is buried. This movement, in the case of well sorted sands, is a pivoting movement against other grains. A hydrodynamic treatment is beyond the scope of the present paper and has been given by Rusnak (1955).

Most elongate sand bodies are formed and shaped by the same currents that produce a preferred orientation of the grains composing the sand body. A relationship may then be expected between the alignment of the long dimension of the sand body and the preferred orientation direction of the component grains. A river sand bar or channel fill is usually elongate parallel with the current direc-

---

[1] Manuscript received, April 9, 1956. This investigation was initiated at the Research Laboratory of the Carter Oil Company, Tulsa, Oklahoma, and completed under a grant from the American Petroleum Institute, Project 51, at the Scripps Institution of Oceanography. Contribution from the Scripps Institution of Oceanography, New Series 879.

[2] Scripps Institution of Oceanography, University of California.

The writer is grateful to the following, who have assisted in collection of the samples, helped to guide the laboratory work, and offered constructive suggestions during preparation of the manuscript: P. A. Dickey, A. L. Kidwell, M. W. Leighton, and R. E. Rohn of the Carter Research Laboratory, and G. A. Rusnak, F. P. Shepard, D. L. Inman, and M. A. Beal of the Scripps Institution of Oceanography. J. R. Moriarty prepared most of the illustrations.

Reproduced by permission

tion, with the preferred grain orientation direction approximately parallel with the long axis of the sand body (Rusnak, 1955, and unpublished data by the writer). A beach deposit or a longshore sand bar, on the other hand, is aligned with its long dimension perpendicular to the direction of the depositing current, that is, the uprush and backwash of the waves. In this case, then, we would expect the preferred sand-grain-orientation direction to be approximately perpendicular to the trend of the sand body. Application can thus be made of this relationship in predicting the trend of subsurface shoestring sands of known origin by a study of the grain orientation of samples from an oriented core (Nanz, 1955).

The present study deals with the preferred grain orientation obtained in undisturbed samples of artificially lithified sands collected from a variety of modern beaches and Recent abandoned beaches.

METHODS OF ANALYSIS

SAMPLE PREPARATION

To obtain undisturbed samples of loose sand, an artificial lithifying agent must be used to bond the grains during the sampling procedure. The collection technique used in this study was to take short oriented cores in thin-wall core tubes, such as tin cans or short sections of 3-inch-diameter stovepipe. These cores were carefully removed from the site of sampling and allowed partly to dry. A catalyzed thermosetting plastic, Selectron (Brown and Patnode, 1953), was used for impregnation (this resin can be thinned to almost any desired viscosity with styrene). The impregnation can be accomplished by gravity flow in a highly permeable sand, but the application of pressure or evacuation of the sample may be necessary for a dirty sand. Upon completion of the lithification procedure, thin sections were cut parallel with, or perpendicular to, the laminations in the sand. The present study has been primarily of "horizontal" thin sections cut parallel with the laminations or bedding planes in the sand.

MEASUREMENT OF GRAINS

Measurement of grain orientation in thin sections can be accomplished either directly through the petrographic microscope or by projection of the grain images. The latter technique has been used for most of the samples in this study by utilizing a microscope light table in which the image of the field of the thin section is projected up onto the underside of the glass top of the table. Remote control cables, attached to the fine focus, the mechanical stage, and to the analyzer prism of the microscope, aid the operational handling. A magnification of about 300 diameters was used for the fine and very fine grain sands studied, and only grains larger than $\frac{1}{16}$ mm. and smaller than 1 mm. were considered.

Selection of grains for measurement has been made in this study with a point counter built into the mechanical stage of the microscope (Chayes, 1949). An alternate method of selecting grains is to measure all grains in a number of randomly selected fields in the thin section. The former method of sampling gives an area (approximating a volume or weight) distribution of grains, whereas the latter gives a number distribution, a distinction which has recently been discussed by Roethlisberger (1955). The advantage of the volume distribution is that it effectively gives more weight to the larger grains in the sample rather than the more numerous small grains. Regardless of which technique is used, however, it can not be overemphasized that operator bias must be held to an absolute minimum by use of an objective, random technique of selecting grains.

Some difficulty may be encountered by selection of all grains along a linear traverse as was done by Schwarzacher (1951). This sampling pattern should be avoided because of the greater chance of encountering grains oriented normal to the traverse direction than parallel with it.

The orientation of each grain is measured as the direction in which the two most closely spaced parallel lines can be drawn tangent to the outline of the grain, the least projection orientation of Dapples and Rominger (1945). These observations are grouped into 10° or 20° sectors. On most of the recently measured samples the size and the shape of the grain outlines have been measured in addition to orientation. The size is expressed either as the long intercept measured parallel with the orientation direction or as the width measured as the spacing between the parallel tangents; and the two-dimensional "sphericity" is expressed as the ratio of the width intercept over the long intercept. No orientation has been considered in this study unless the intercept ratio is less than 0.95. The relationships between orientation, size, and shape are currently being investigated.

COMPUTATION OF DIRECTION AND DEGREE OF PREFERRED ORIENTATION

As a means of statistical expression of the direction and degree of preferred orientation of the sand grains measured, a simple two-dimensional scheme of vector analysis has been employed. This technique, modified from Reiche (1938) and Krumbein (1939), has recently been described in more detail than can be given here (Curray, 1956). The system is briefly to consider an individual grain-orientation observation as a vector with direction and with unit magnitude. Because no distinction is made of one end of the grain from the other, the range of observations is from 0° to 180°. In order to express this as a periodic distribution, the angles are doubled and the vectors are summed by components. The resultant vector direction (*half* the angle obtained in the summation) is interpreted as the preferred orientation direction. The resultant vector magnitude, expressed in per cent by dividing by the total number of observations and multiplying by 100, is interpreted as the degree of preferred orientation. The higher the vector magnitude, the better the preferred orientation of elongate grains. A high vector magnitude of preferred orientation corresponds with a low standard deviation (Curray, 1956).

When several samples are measured from one locality, a composite is formed by vector summation of the individual sample resultant vectors. This is, in effect, an enlargement of the sample size giving equal weight to each subsample.

TEST OF STATISTICAL SIGNIFICANCE OF RESULTS

In any group of samples analyzed for preferred orientation, a wide range of vector magnitudes (or degrees of orientation) may occur. A question then arises as to which of these sample distributions show a real preferred orientation present in the sample and which are due to chance sampling of grains from a sand with no preferred orientation. In some distributions, subjective examination of the data may suffice to estimate the validity of the result, but many borderline cases may be encountered, and without a quantitative test it is impossible to give proper consideration to both the number of observations and to the degree of orientation. A weak preferred orientation, for example, may be established as significant by a large number of observations, while fewer observations may leave the validity of the preferred orientation in doubt.

The Rayleigh test of significance (Curray, 1956) has been used as the final criterion for the significance of preferred orientations. This test, a function of vector magnitude and number of observations, indicates the probability of a greater vector magnitude being obtained by pure chance combination of random angles. No distribution has been accepted as being significantly different from uniformity unless the probability is less than 0.05; that is, there are less than five chances in one hundred that it could have arisen due to pure chance.

DISCUSSION OF RESULTS

SOUTHWESTERN LOUISIANA

The coastal region of the southwestern corner of Louisiana consists of marsh and mud-flat deposits slightly above sea-level. Lying in these deposits is a partly interconnected system of active beaches and abandoned beaches, locally called cheniers. The crests of the chenier ridges reach a maximum of 5–10 feet above sea-level, offering the only habitable parts of the area. The name chenier is applied from the French word for "oak" because of the luxuriant growth of live oaks found on some of the ridges. The alternating deposition of sand beaches and mud flat has been explained by Howe *et al.* (1935), and Fisk (1955), by variation in the rate of deposition in the area. During periods of rapid deposition, for example, at times of closer proximity of the Mississippi Delta, deposition predominated over wave action and mud flats were built forward into the Gulf. During periods of decreased deposition, on the other hand, as to-day when the Mississippi Delta is contributing less sediment to this part of the coast, wave action winnows the sediment and piles up beach ridges of the available coarse material. Wind reworks some of this sand into low dunes along the present shoreline, although examination of the cheniers suggests that wave action was the principal agent of deposition. It is interesting to note that during deposition of some of the older cheniers farthest from the present shoreline, not much sand was available in the area, and reworked shells are the principal constituent of the ridges.

Grain-orientation measurements were made on sands from the beaches and cheniers to determine the relationship between the preferred grain-orientation

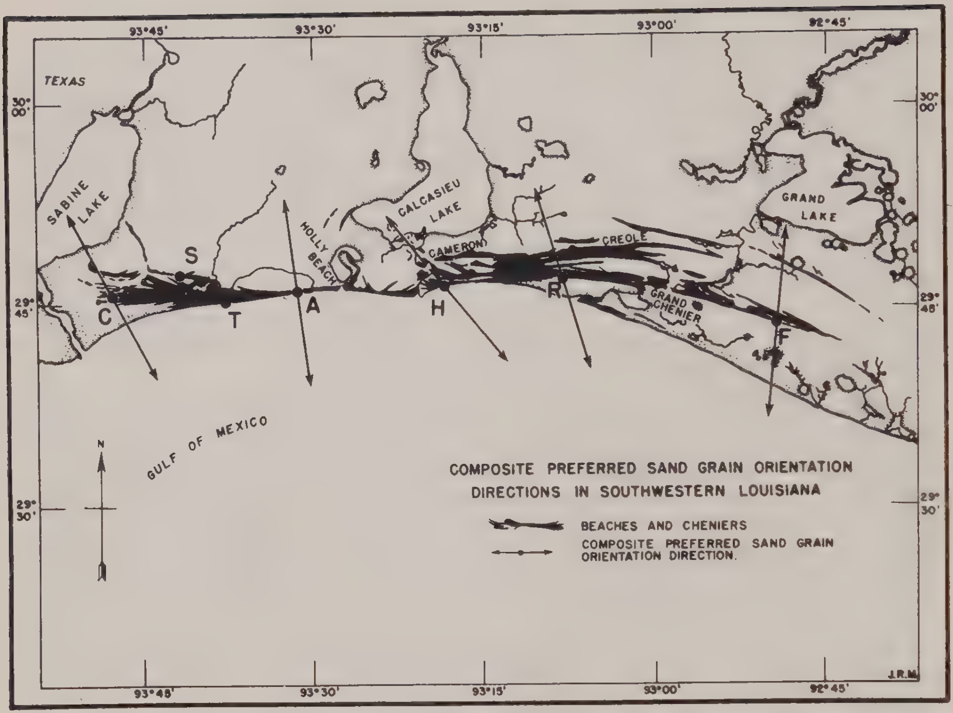
93°45'
93°30'
93°15'
93°00'
92°45'
30° 00'
29° 45'
29° 30'
TEXAS
SABINE LAKE
HOLLY BEACH
CALCASIEU LAKE
CAMERON
CREOLE
GRAND LAKE
GRAND CHENIER
GULF OF MEXICO
N
S
C
T
A
H
R
F
COMPOSITE PREFERRED SAND GRAIN ORIENTATION DIRECTIONS IN SOUTHWESTERN LOUISIANA
BEACHES AND CHENIERS
COMPOSITE PREFERRED SAND GRAIN ORIENTATION DIRECTION.
J.R.M.

FIG. 1.—Composite preferred sand-grain-orientation directions in southwestern Louisiana.

directions and the trends of the elongate sand bodies, and to test the uniformity of this relationship on samples from various parts of the sand body. Analyses, made on a total of 33 thin sections from this area, are shown graphically in Figure 1 and are summarized in Table I. The results are shown in the figure as

TABLE I. SUMMARY OF GRAIN-ORIENTATION DATA FOR LOUISIANA SAMPLES

Locality	*No. Thin Sections*	*Number Grains Measured*	*Vector Azimuth*	*Angle from Trend*[1]	*Vector Magnitude*	*Probability*[2]	*Significant*[3]
			(*Degrees*)	(*Degrees*)	(*Per Cent*)		
A	12	6,020	173	88	7.94	$<10^{-15}$	Yes
C	5	2,384	152	67	6.79	$<10^{-4}$	Yes
F	5	2,628	5	80	8.45	$<10^{-6}$	Yes
H	7	3,789	141	61	5.61	$<10^{-5}$	Yes
R	2	900	164	74	12.37	$<10^{-6}$	Yes
S	1	549	165	70	3.96	$>.40$	No
T	1	630	149	64	5.03	$>.10$	No
Composite relative to trends	33	16,900	—	77	6.89	$<10^{-20}$	Yes

[1] Angle measured clockwise from trend of shoreline to preferred orientation vector.

[2] Probability that this vector or a larger one could have arisen by chance sampling of grains without true preferred orientation.

[3] Vector is accepted as significant if probability is <0.05.

composite vector directions for the five localities in the area for which the preferred orientation is statistically significant. Reference to this figure and to the fifth column in the table shows the relationship between the preferred orientation direction of the sand grains and the trend of the sand bodies. The apparent tendency is, as expected, for the elongate sand grains to align themselves perpendicular to the trends of the beaches.

The composite preferred grain orientation for the entire area was computed by vector summation by using the trends of the individual sand bodies as reference directions. The relationship to be determined is the angle between the grain orientation direction and the sand-body trend, not compass north. For this reason the angles to be used as vector directions in forming the composite are the angles between the preferred grain-orientation directions and the individual sand body trend (the angle listed in column 5 of Table I). The composite vector deviates only 13° from the expected perpendicularity.

To determine the consistency of preferred orientation direction both laterally across the beach and in a vertical sequence below the surface of the beach, a special suite of samples was analyzed from the present beach at locality A (Fig. 2). The azimuths listed for the preferred orientations of individual samples are

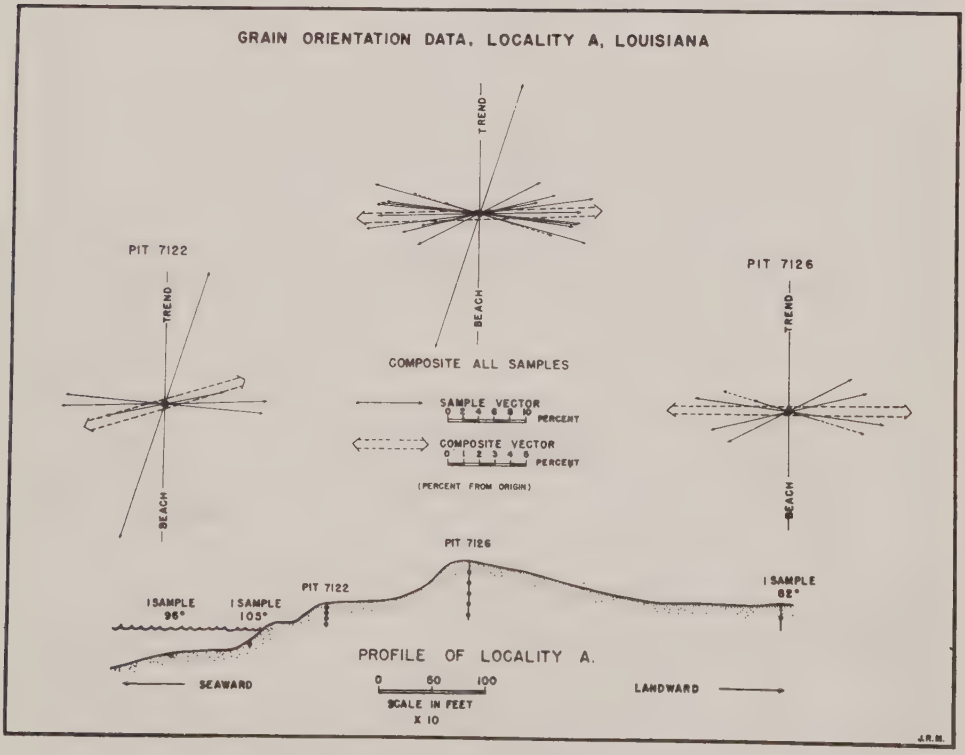
GRAIN ORIENTATION DATA, LOCALITY A, LOUISIANA
TREND
BEACH
PIT 7122
TREND
BEACH
PIT 7126
TREND
BEACH
COMPOSITE ALL SAMPLES
SAMPLE VECTOR
0 2 4 6 8 10 PERCENT
COMPOSITE VECTOR
0 1 2 3 4 5 PERCENT
(PERCENT FROM ORIGIN)
PIT 7126
PIT 7122
1 SAMPLE 96°
1 SAMPLE 105°
1 SAMPLE 82°
PROFILE OF LOCALITY A.
SEAWARD
0 50 100
SCALE IN FEET X 10
LANDWARD
J.R.M.

FIG. 2.—Grain-orientation data, Locality A, Louisiana.

measured clockwise from the trend of the beach. The composite distributions are shown for sample pits 7122, 7126, and for a composite of all twelve samples from the locality. These composites show vectors for the individual thin sections as light arrows and vectors for the composites as double-dashed arrows. The variation in preferred orientation direction between samples can be seen, but there is an apparent consistency in composite preferred orientation direction in different parts of the sand body.

During the collection of the samples from southwestern Louisiana, no distinction was made between sands deposited by waves and those deposited by wind. Some of the sands from the modern beach were clearly laid down by the action of wind, but most of the samples from the cheniers appeared from examination of the bedding and shell content to have been deposited by wave action. In many cases it was not possible at the time to identify the agent of deposition, although a possible technique for making this distinction has since been developed by Beal and Shepard (1956). The composites, therefore, represent the type of random sampling to be expected in encountering such sand bodies in a well core, that is, as mixtures of wind- and wave-deposited sands. It is notable, then, that the composite preferred orientation direction averages approximately perpendicular to the trends of the sand bodies.

TEXAS SAMPLES

A suite of samples was collected from the beaches and barrier islands of the Texas coast to attempt to answer some of the questions which had arisen during the study of the Louisiana samples. These questions were: what is the effect of a strong longshore current on the preferred orientation of sand grains on various parts of the beach, and what orientation characteristics are to be expected in sands known to have been deposited by wind? Hence, all samples were identified by direct observation at the time of collection as to the agent of deposition, and observations of the wind direction and wave uprush and backwash directions were made.

TABLE II. SUMMARY OF GRAIN-ORIENTATION DATA FOR TEXAS SAMPLES

Wave-Deposited Sands

Locality	*No. Thin Sections*	*Number Grains Measured*	*Vector Azimuth*	*Angle from Trend*	*Vector Magnitude*	*Probability*	*Significant*
			(*Degrees*)	(*Degrees*)	(*Per Cent*)		
Boca Chica	5	2,138	103	103	8.26	$<10^{-6}$	Yes
Padre Island	12	4,554	122	110	4.89	$<10^{-4}$	Yes
Mustang Island	10	2,092	116	81	8.29	$<10^{-5}$	Yes
Matagorda	2	908	135	80	3.74	$>.20$	No
Galveston	4	1,723	124	89	5.51	$<.01$	Yes
Sabine	1	450	8	113	12.27	$<.01$	Yes
Composite relative to trends	34	11,865	—	95	5.93	$<10^{-15}$	Yes

The results of the measurements on the wave-deposited sands collected from the foreshore and berm of the beaches are listed in Table II and shown graphically in Figure 3 as composite vector directions. These results seem to indicate that regardless of deviations present in any samples in these composites due to longshore currents, the "average" preferred orientation is still approximately perpendicular to the beach trend.

In studying the effects of longshore currents on a suite of samples, each sample must be considered individually because the backwash direction (the last current to act upon the sand) is different for each sample after each wave. At this stage of the investigation only a qualitative correlation can be made. This comparison strongly suggests that the backwash of the wave, at least on the foreshore of these fine-sand beaches, is the current which orients the sand grains and that the preferred orientation direction is roughly parallel with the backwash direction. The same conclusion is also suggested by an incomplete study of "imbrication" or preferred orientation in vertical thin sections of sands from

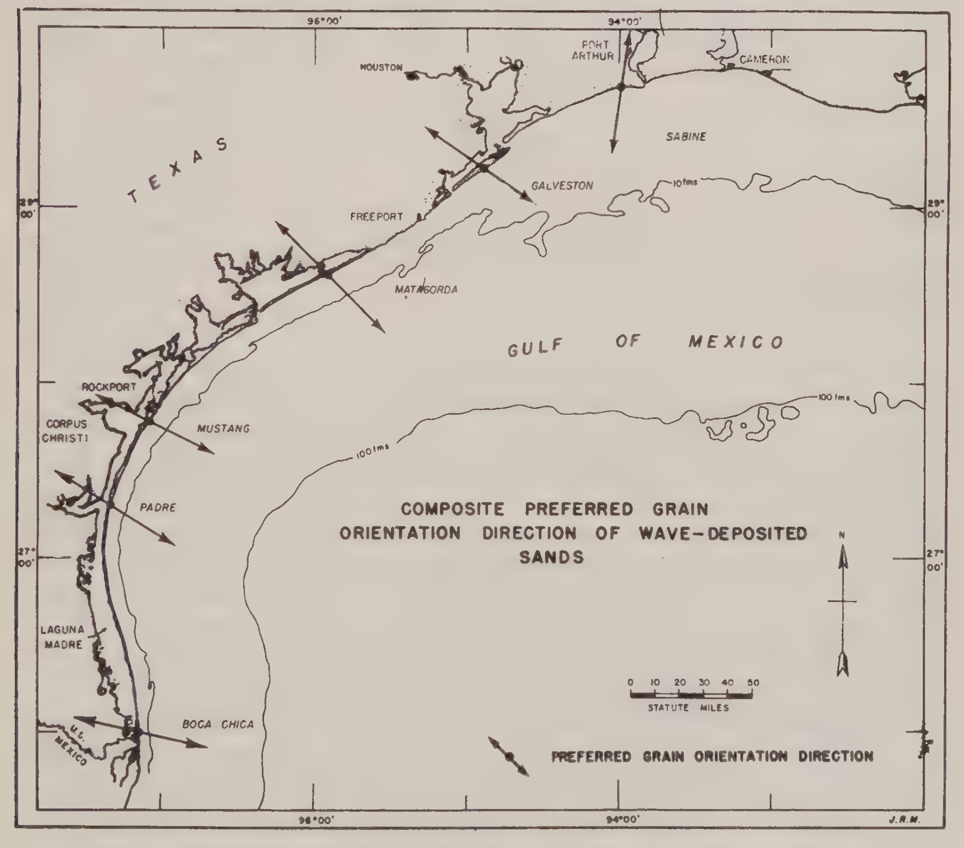
96°00'
94°00'
FORT ARTHUR
HOUSTON
CAMERON
TEXAS
SABINE
GALVESTON
10 fms
29° 00'
29° 00'
FREEPORT
MATAGORDA
GULF OF MEXICO
ROCKPORT
100 fms
CORPUS CHRISTI
MUSTANG
100 fms
PADRE
COMPOSITE PREFERRED GRAIN ORIENTATION DIRECTION OF WAVE-DEPOSITED SANDS
N
27° 00'
27° 00'
LAGUNA MADRE
0 10 20 30 40 50
STATUTE MILES
BOCA CHICA
U.S.
MEXICO
PREFERRED GRAIN ORIENTATION DIRECTION
96°00'
94°00'
J.R.M.

FIG. 3.—Composite preferred grain-orientation directions of wave-deposited sands.

the foreshore of the beach, in which the preferred orientation direction dips landward relative to the laminations in the sand. The opposite result might reasonably be expected in a highly permeable beach, such as a coarse sand or a pebble beach, because the surface backwash may be very weak or non-existent. Imbrication dipping seaward relative to the surface of cobble beaches can be observed qualitatively.

Effects of longshore current (preferred orientation parallel with the oblique backwash direction) have been noticed most strongly in samples from the foreshore of the beach, but these effects have also been noticed in some samples from the crest and surface of a seaward-sloping berm.

The results of measurements on the wind-blown sands from the Texas coast are summarized in Table III and are shown graphically in Figure 4 relative to the prevailing wind directions in the area. These samples were collected from the dry, back parts of the beaches and from the dunes behind the beaches. The prevailing winds shown were calculated from the percentage of time during which the wind blew from each point of the compass during a 2-year period from 1950 to 1952. Because no distinction was made of north from south or east from west in the grain-orientation work, and because no imbrication studies were made of these samples, the wind averages were similarly computed. North and south winds were combined in the calculations, north-northeast and south-southwest winds were combined, *et cetera*, because in terms of sand-grain orientation these diametrically opposite winds produce the same effect.

TABLE III. SUMMARY OF GRAIN-ORIENTATION DATA FOR TEXAS SAMPLES

Wind-Deposited Sands

Locality	*No. Thin Sections*	*Number Grains Measured*	*Vector Azimuth*	*Angle from Prevailing Wind*	*Vector Magnitude*	*Probability*	*Significant*
			(*Degrees*)	(*Degrees*)	(*Per Cent*)		
Boca Chica	3	1,409	178	37	3.57	$>.10$	No
Padre Island	6	1,883	144	7	8.58	$< 10^{-6}$	Yes
Mustang Island	3	594	122	29	9.21	$<.01$	Yes
Matagorda	1	502	113	42	7.68	$<.05$	Yes
Galveston	2	828	60	80	6.06	$<.05$	Yes
Sabine	1	450	91	83	8.38	$<.05$	Yes
Compositive relative to prevailing wind	16	5,666	—	16	3.62	$< 10^{-3}$	Yes

From inspection of the results, it can be seen that there is more variability in preferred orientation direction in wind-blown than in water-deposited sands. Any individual thin section of wind-blown sand may possess a strong preferred orientation direction which may be quite different in direction from the adjacent sample. This high sample-to-sample variation can be expected because of fluctuations in wind direction. The composite vector direction, on the other hand, appears to approach parallelism with the direction of the prevailing wind if a large number of samples are analyzed. The composite of all 16 samples (Table III, Fig. 4) on the Texas coast has a statistically significant preferred orientation which deviates only 16° from the "average" prevailing wind direction. This composite was prepared relative to prevailing wind direction by using the angle between the preferred grain orientation and the local prevailing wind direction as the component vector azimuth, thus giving an average deviation from local wind direction. Further verification of these conclusions was obtained by the qualitative correlation between wind direction at the time of sampling and the preferred grain orientation of samples taken from the surface sands. Such a comparison was not possible in many samples because the thin sections were taken from several millimeters below the surface of the sand.

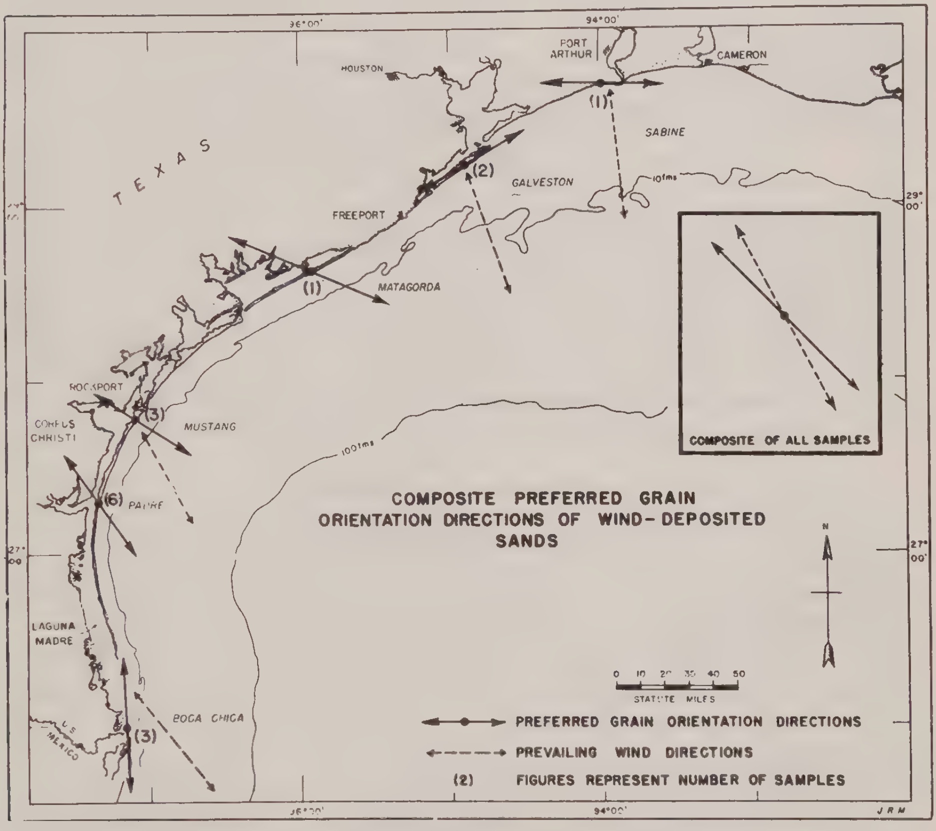
96°00'
94°00'
PORT ARTHUR
CAMERON
HOUSTON
(1)
SABINE
(2)
GALVESTON
10fms
29° 00'
TEXAS
FREEPORT
(1)
MATAGORDA
ROCKPORT
CORPUS CHRISTI
(3)
MUSTANG
100fms
(6)
PADRE
27° 00'
LAGUNA MADRE
BOCA CHICA
U.S.
MEXICO
(3)
COMPOSITE OF ALL SAMPLES
COMPOSITE PREFERRED GRAIN ORIENTATION DIRECTIONS OF WIND-DEPOSITED SANDS
N
0 10 20 30 40 50
STATUTE MILES
PREFERRED GRAIN ORIENTATION DIRECTIONS
PREVAILING WIND DIRECTIONS
(2) FIGURES REPRESENT NUMBER OF SAMPLES
94°00'
J.R.M.

FIG. 4.—Composite preferred grain-orientation directions of wind-deposited sands.

TABLE IV. SUMMARY OF GRAIN-ORIENTATION DATA IN OTHER AREAS

Locality	*No. Thin Sections*	*Number Grains Measured*	*Vector Azimuth*	*Angle from Trend*	*Vector Magnitude*	*Probability*	*Significant*
			(*Degrees*)	(*Degrees*)	(*Per Cent*)		
North Carolina							
Waves	2	900	135	90	10.06	$<10^{-3}$	Yes
Wind	2	1,260	136	91	3.08	$>.30$	No
All	5	2,404	129	84	6.20	$<10^{-3}$	Yes
Scripps beach	8	2,072	90	75	8.55	$<10^{-5}$	Yes
Washover delta	5	1,856		See Figure 6 for results.			
Galveston hook	4	1,359		See Figure 7 for results.			
Hooked chenier	6	2,378		See Figure 8 for results.			

NORTH CAROLINA SAMPLES

Sand-grain orientation was measured on five samples from Topsail Beach, a barrier island about 700 feet wide at the point of sampling, located north of Wilmington, North Carolina. The results of these measurements are listed in Table IV and shown in Figure 5, along with a diagrammatic profile of the barrier

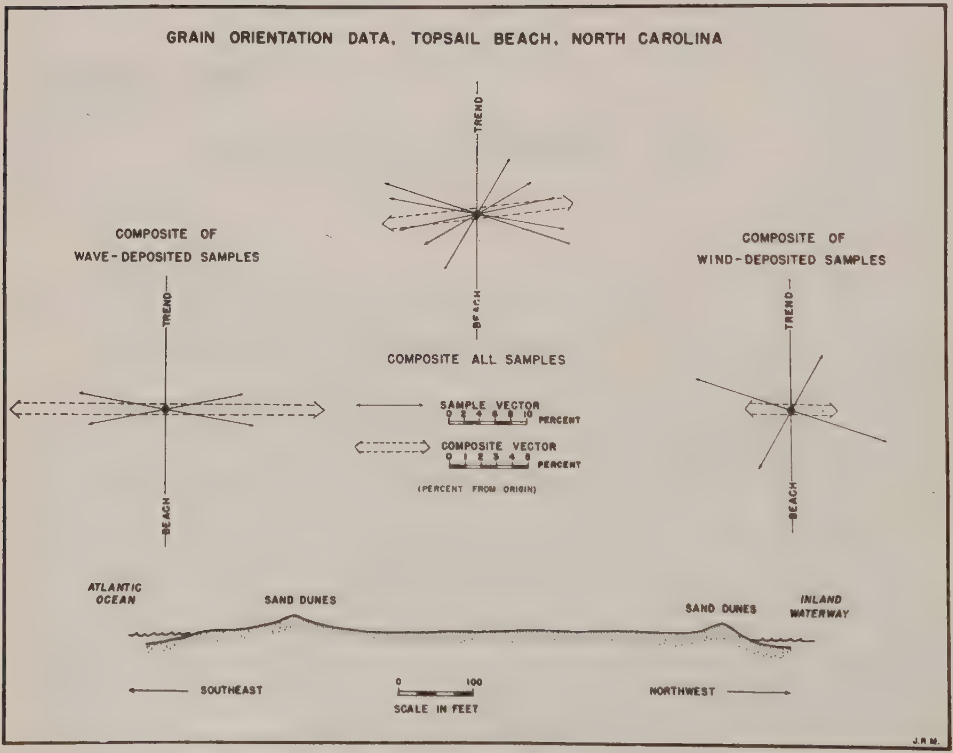
GRAIN ORIENTATION DATA, TOPSAIL BEACH, NORTH CAROLINA
TREND
BEACH
COMPOSITE ALL SAMPLES
COMPOSITE OF WAVE-DEPOSITED SAMPLES
TREND
BEACH
COMPOSITE OF WIND-DEPOSITED SAMPLES
TREND
BEACH
SAMPLE VECTOR
0 2 4 6 8 10 PERCENT
COMPOSITE VECTOR
0 1 2 3 4 5 PERCENT
(PERCENT FROM ORIGIN)
ATLANTIC OCEAN
SAND DUNES
SAND DUNES
INLAND WATERWAY
SOUTHEAST
0 100
SCALE IN FEET
NORTHWEST
J.R.M.

FIG. 5.—Grain-orientation data, Topsail Beach, North Carolina.

island. Two of the samples were collected from the foreshore of the beach and are shown as a composite on the left side of the figure. This composite has a vector angle of 90° from the trend of the beach. The two samples collected from the dunes are shown in a composite on the right side of the figure. While this dune composite also lies very nearly perpendicular to the beach trend, the vector magnitude is so low that the vector is not statistically significant. The fifth sample, collected from the sand flat on the landward side of the barrier, did not show a significant preferred orientation.

The composite for all five samples is shown in the top center of the diagram. Most of the deviation from 90° is caused by the addition of the sand-flat sample to the other samples already discussed. It is important, however, that this heterogeneous group of samples gives a fairly good estimate of the perpendicular to the trend of the sand body.

CALIFORNIA SAMPLES

Measurements were made on a suite of eight samples from the beach at the Scripps Institution of Oceanography, La Jolla, California. The samples were collected at a time when no berm existed on the beach and the entire beach was awash during the highest tides. All samples are, therefore, wave-deposited sands. The results are listed in Table IV, and show that the composite preferred orientation direction deviates from perpendicular to the beach trend by 15°.

SPECIAL BEACH SUB-ENVIRONMENTS

Three suites of samples were collected to determine the characteristic orientation patterns in some minor beach sub-environments on the Texas and Louisiana coasts. The areas from which these samples were collected are a washover delta behind the beach south of Grand Chenier, Louisiana (Fig. 1), the hooked southwest end of Galveston Island at San Luis Pass (Fig. 2), and the hooked end of a chenier south of Cameron, Louisiana (Fig. 1). The results of these analyses are shown in Figures 6, 7, and 8.

The washover delta, shown in a sketch map in Figure 6, is a thin petal-shaped deposit of sand behind a channel cut through the beach ridge and sloping landward over the surface of the marsh. As the name implies, it was formed by storm waves washing over and cutting through the crest of the beach ridge and carrying sand back into the marsh. On the basis of the results of the sand-grain orientations shown in the figure, it can be suggested that the preferred grain orientation is parallel with the channels in the sand and is radial out from the main channel supplying the sand.

The sketch map in Figure 7 shows the shape of the hooked end of Galveston Island at the time of collection of the samples and the preferred orientations obtained in the samples analyzed. Sample 10,080 shows a preferred orientation normal to the beach trend. Sample 10,075 apparently shows the effect of the offshore bar in protecting the foreshore from direct wave attack. At the time of

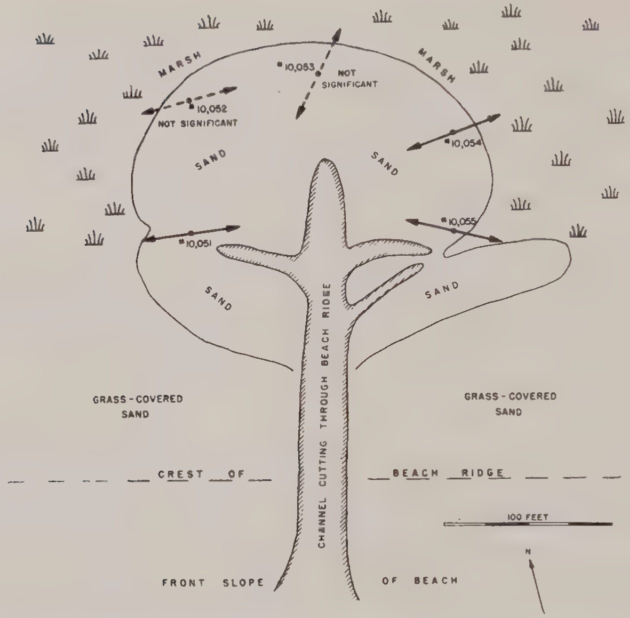
MARSH
10,053
NOT SIGNIFICANT
MARSH
10,052
NOT SIGNIFICANT
SAND
SAND
10,054
10,055
10,051
SAND
SAND
CHANNEL CUTTING THROUGH BEACH RIDGE
GRASS-COVERED SAND
GRASS-COVERED SAND
CREST OF BEACH RIDGE
100 FEET
N
FRONT SLOPE OF BEACH

FIG. 6.—Grain-orientation data, Washover Delta, south of Grand Chenier, Louisiana.

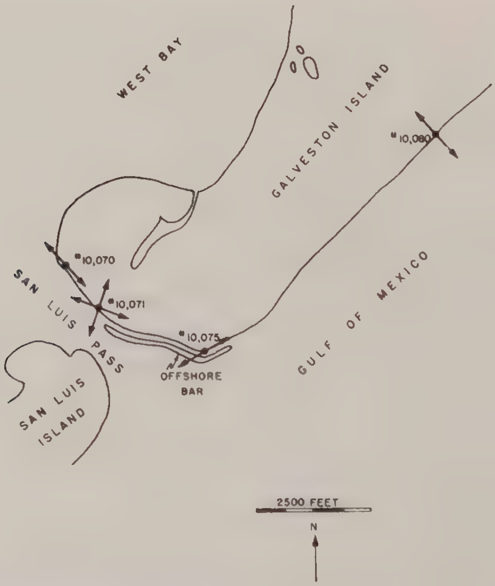
WEST BAY
GALVESTON ISLAND
10,080
10,070
SAN LUIS PASS
10,071
10,075
OFFSHORE BAR
GULF OF MEXICO
SAN LUIS ISLAND
2500 FEET
N

FIG. 7.—Grain-orientation data, southwest end of Galveston Island, Texas.

sampling, a current was running westward between the beach and the bar because of wave action. At the end of the bar, sample 10,071 shows a well developed bimodal distribution, perhaps caused by the joint effects of the current behind the bar and the refracted waves coming around the end of the bar. Sample 10,070 shows an orientation apparently caused by tidal currents sweeping through the pass.

The hooked end of the chenier south of Cameron is outlined in Figure 8. This hook, one of a series of parallel hooks in the area, is believed to have been formed by the action of the east to west longshore currents on the east bank of a former mouth of the Calcasieu River. Here, again, the sample located on the straight part of the beach is oriented normal to the beach trend. Samples 10,006 and 10,005 may have been oriented in a manner similar to the corresponding sample (10,075) on Galveston Island. Samples 10,004 and 10,003 are aligned normal to the trend of the hook, suggesting the effect of small wind waves in the channel of the river.

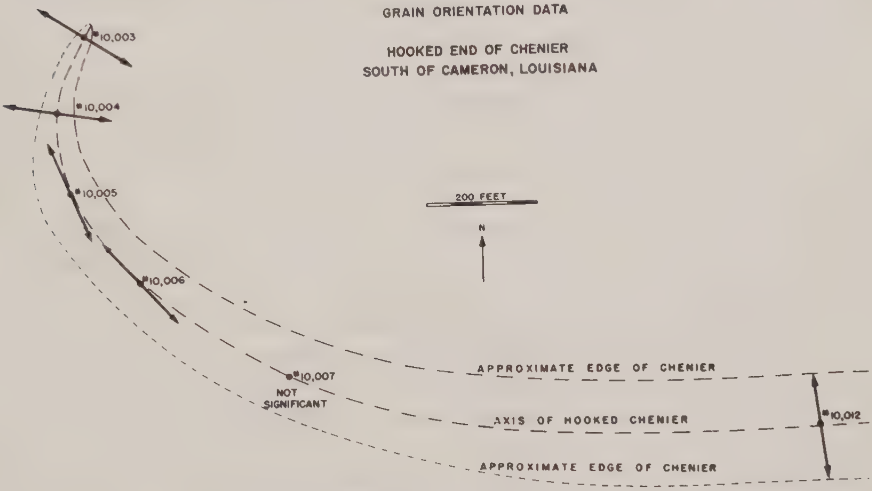
GRAIN ORIENTATION DATA
HOOKED END OF CHENIER
SOUTH OF CAMERON, LOUISIANA
10,003
10,004
10,005
10,006
10,007
NOT SIGNIFICANT
10,012
200 FEET
N
APPROXIMATE EDGE OF CHENIER
AXIS OF HOOKED CHENIER
APPROXIMATE EDGE OF CHENIER

FIG. 8.—Grain-orientation data, hooked end of chenier, south of Cameron, Louisiana.

From consideration of these two hooked spits, it is suggested that similar patterns may form in other hooked spits and barrier island inlets, but that the patterns may differ (as these have) according to the relative influences of tidal currents, wave action refracted from the sea, and wind waves commonly present in coastal lagoons, inlets, and rivers. It is clear that more work remains to be done before the grain-orientation patterns of such sub-environments can be considered established.

APPLICATIONS

The results of the study have demonstrated characteristics of preferred sand-grain-orientation patterns found in various environments of deposition on some Recent and modern shoestring sands. This is, of course, an incomplete survey of sand-grain orientation in Recent sands because so few of the present environments of deposition of sand have been considered here. Nevertheless, possible applications of sand-grain orientation may be anticipated from the results of this and other studies of sand-grain orientation.

1. The transport direction may be determined in a sand deposit, and hence the source area may be predicted. This may be applied to the study of fluvial or eolian deposits or deposits that have been interpreted as deeper-water, turbidity-current sands (Kopstein, 1954).

2. If the origin or environment of deposition of a shoestring sand is known, the trend of the long axis of the sand body may be predicted from a study of sand-grain orientation. If the sand is a fluvial sand, the trend will be parallel with the preferred grain-orientation direction; if it is a wave-deposited sand it will be approximately perpendicular.

3. Conversely, if the relationship between preferred sand-grain-orientation direction and sand-body long axis is known, the origin of the sand body may be indicated as either of the fluvial or littoral types.

4. The direction of prevailing wind during deposition of an eolion sand may be estimated as an aid in paleometeorological and paleogeographical studies.

5. Preferred sand-grain orientation may be correlated with other directional mass properties of sediments such as directional permeability (Griffiths, 1950), electrical, magnetic, and sound velocity anisotropies. Deformational fabrics, cementation, and structure may also affect these mass properties. Evaluation of depositional fabric in undeformed rocks, however, may lead to better understanding of other directional properties and to better means of evaluating and applying them on a field scale. Conversely, the correlation may lead to a simpler, indirect, laboratory technique of determining preferred sand-grain orientation.

For purposes of interpreting sand-grain orientation in the second application listed in the preceding paragraphs, the sands must be evaluated as to their absolute environments of deposition, or else the results must be interpreted in terms of heterogeneous composites of mixed wind- and wave-deposited sands. Table V lists such heterogeneous composites prepared by vector summation of all of the samples analyzed at the localities representing both wind- and wave-deposited sands. Some of the composites, from Louisiana and North Carolina, are repeated from previous tables. Examination of the results shows that most of the vectors are significant and give a fairly good estimate of the perpendicular to the trends of the sand bodies from which they were collected. As might be expected, the vectors are not as strong and not as close to perpendicularity as vectors for wave-deposited sands alone, but it is important to the applicability of the technique that the addition of a limited number of wind-deposited samples did not seriously affect the reliability of the estimates. These heterogeneous com-

TABLE V. HETEROGENOUS COMPOSITES OF GRAIN ORIENTATION

Location	*No. Thin Sections*	*Number Grains Measured*	*Vector Azimuth*	*Angle from Trend*	*Vector Magnitude*	*Probability*	*Significant*
			(*Degrees*)	(*Degrees*)	(*Per Cent*)		
Louisiana—all	33	16,900	—	77	6.89	$<10^{-20}$	Yes
A	12	6,020	173	88	7.94	$<10^{-15}$	Yes
C	5	2,384	151	67	6.79	$<10^{-4}$	Yes
F	5	2,628	5	80	8.45	$<10^{-6}$	Yes
H	7	3,789	141	61	5.61	$<10^{-5}$	Yes
Texas—all	50	17,531	—	100	4.75	$<10^{-15}$	Yes
Boca Chica	8	3,547	108	108	4.06	$<.01$	Yes
Padre Island	18	6,437	132	120	5.68	$<10^{-6}$	Yes
Mustang Island	13	2,686	117	82	8.47	$<10^{-5}$	Yes
Matagorda	3	1,410	124	69	4.69	$<.05$	Yes
Galveston	6	2,551	133	98	5.17	$<.01$	Yes
Sabine	2	900	32	137	2.30	$>.60$	No
North Carolina	5	2,404	129	84	6.20	$<10^{-3}$	Yes

posites resemble the composites to be expected in well-core samples from coastal shoestring sands.

In general, the stronger vectors show less deviation from perpendicularity than do the weaker ones. The reliability of the estimate is then apparently related qualitatively to the vector magnitude and will be determined by several factors (in order of increasing importance): (1) the variability in local wind direction and velocity; (2) the deviation from perpendicular of the wave-deposited preferred orientation direction caused by such effects as longshore currents, beach cusps, proximity of inlets, *et cetera;* (3) the angle between the prevailing wind direction and the perpendicular to the sand body; and (4) the width of the sand body and the volumetric importance of the wave-deposited *versus* all other sands in the sand body. The reliability of the estimate will be greater in the case of a narrow shoestring sand body consisting principally of wave-deposited sands. Each of these factors must be taken into consideration in evaluating the results of sand-grain-orientation measurements in a coastal sand body.

Although it may be possible to obtain a fairly good estimate of the trend of a coastal sand body from a heterogeneous composite, a better estimate can be expected by considering only wave-deposited sands. For this, the environments of deposition in ancient sands must be identified by other geological or biological criteria. A means of differentiating coastal sands from fluvial sands must also be employed when the origin of the shoestring in question is not already known from other geological considerations.

REFERENCES

BEAL, M. A., AND SHEPARD, F. P., 1956, "A Use of Roundness to Determine Depositional Environments," *Jour. Sed. Petrology*, Vol. 26, pp. 49–60.

BROWN, W. E., AND PATNODE, H. W., 1953, "Plastic Lithification of Sands in Situ," *Bull. Amer. Assoc. Petrol. Geol.*, Vol. 37, pp. 152–62.

Chayes, F., 1949, "A Simple Point Counter for Thin-Section Analysis," *Amer. Mineralogist*, Vol. 34, pp. 1–12.

Curray, J. R., 1956, "The Analysis of Two-Dimensional Orientation Data," *Jour. Geol.*, Vol. 64, pp. 117–31.

Dapples, E. C., and Rominger, J. F., 1945, "Orientation Analysis of Fine-Grained Clastic Sediments: a Report of Progress," *ibid.*, Vol. 53, pp. 246–61.

Fisk, H. N., 1955, "Sand Facies of Recent Mississippi Delta Deposits," *Proc. Fourth World Petrol. Congr.*, Sec. 1/C.

Griffiths, J. C., "Directional Permeability and Dimensional Orientation in Bradford Sand," *Producers Monthly*, Vol. 14, pp. 26–32.

Howe, H. V., Russell, R. J., McGuirt, J. H., and Craft, B. C., 1935, "Reports on the Geology of Cameron and Vermillion Parishes," *Louisiana Dept. Conserv., Geol. Bull. 6.* 242 pp.

Kopstein, F. P. H. W., 1954, "Graded Bedding of the Harlech Dome," *Ph.D. Thesis, Univ. Groningen, Pub. 81.* 97 pp.

Krumbein, W. C., 1939, "Preferred Orientation of Pebbles in Sedimentary Deposits," *Jour. Geol.*, Vol. 47, pp. 673–706.

Nanz, R. H., 1955, "Grain Orientation in Beach Sands: a Possible Means for Predicting Reservoir Trend" (abst.), *Program Soc. Econ. Paleon. and Mineralogists 29th Ann. Meeting*, New York.

Reiche, P., 1938, "An Analysis of Cross-Lamination: the Coconino Sandstone," *Jour. Geol.*, Vol. 46, pp. 905–32.

Roethlisberger, H., 1955, "An Adequate Method of Grain-Size Determination in Sections," *ibid.*, Vol. 63, pp. 579–84.

Rusnak, G. A., 1955, "The Orientation of Sand Grains under Conditions of Unidirectional Fluid Flow," unpubl. *Ph.D. Thesis, Univ. Chicago.* 55 pp.

Schwarzacher, W., 1951, "Grain Orientation in Sands and Sandstones," *Jour. Sed. Petrology*, Vol. 21, pp. 162–72.

TEMPERATURE AND DEPTH CIRCUITRY IN A TELERECORDING BATHYTHERMOMETER[a]

JAMES M. SNODGRASS and JOHN H. CAWLEY, JR.

Special Developments Division, Scripps Institution of Oceanography, University of California,
La Jolla, California

Abstract.—A mechanical Bathythermograph (BT) was developed prior to World War II for plotting ocean temperature as a function of pressure (depth). A recent device for obtaining much finer detail for use in oceanographic research has been developed. It consists of a Vibroton pressure-sensitive element and a transistorized amplifier to obtain frequency as a function of pressure, and a miniaturized temperature sensitive Wein Bridge Oscillator with a temperature sensitivity of 40 cycles per degree centigrade. This combined frequency information is telemetered to the surface via a single conductor cable.

Surface instrumentation including frequency separation, demodulation, and recording of this data on an X-Y data plotter and on magnetic tape is covered. A brief discussion of results is made.

I. INTRODUCTION

It has long been felt that an instrument to measure ocean temperature as a function of depth, and to record the result continuously, would be extremely useful in some oceanographic studies. Spilhaus (1938, 1940) developed a mechanical instrument called a Bathythermograph (BT). In its present form it is useful to a depth of about 900 feet. It consists of a smoked glass slide with a temperature-responsive bourdon activated stylus resting on its surface. The slide itself is moved by a pressure-sensitive element, the deflection being a function of pressure. The instrument, which is housed in a streamlined brass tube, is lowered from the ship while underway, thus giving a profile recording of water temperature versus pressure. Accuracy of better than ±0.5 degrees centigrade and ± five feet depth in 450 feet is generally realized in the average service instrument.

Much present day oceanographic work requires much higher resolution and continuous profile recording. Resolution of the order of one foot in 1000 in depth and temperature resolution of 0.1 degree centigrade or better are necessary. The block diagram of Fig. 1 illustrates one approach to this overall problem.

II. PRESSURE-SENSITIVE CIRCUITRY

A type 101 Vibrotron, manufactured by the Byron Jackson Company, in conjunction with a transistorized feedback amplifier, comprises the pressure-sensitive channel. The frequency range of the particular unit selected for this work is approximately 9600 cps to 11,240 cps.

---

[a] Contributions from the Scripps Institution of Oceanography, New Series, No. 880. This work was supported in part by funds from the Office of Naval Research and from the Bureau of Ships, U.S. Navy. Reproduction in part or entirety is permitted for any purposes of the United States Government.

Reproduced, by permission, from Proc., Nat'l.
Electronics Conference, 1956. Vol.12.
Chicago, Nat'l. Electronics Conference, Inc., 1957.

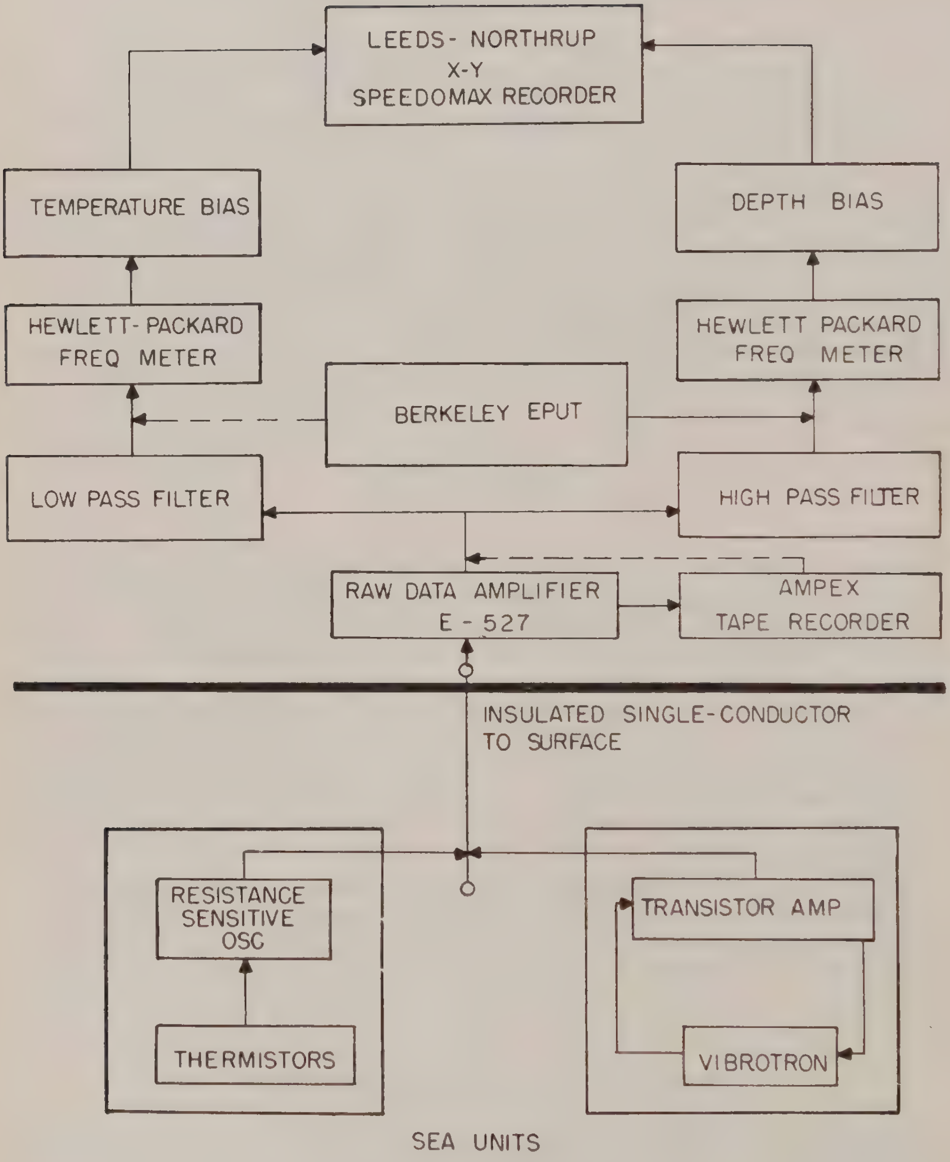
LEEDS- NORTHRUP
X-Y
SPEEDOMAX RECORDER
TEMPERATURE BIAS
DEPTH BIAS
HEWLETT- PACKARD
FREQ METER
HEWLETT PACKARD
FREQ METER
BERKELEY EPUT
LOW PASS FILTER
HIGH PASS FILTER
RAW DATA AMPLIFIER
E - 527
AMPEX
TAPE RECORDER
INSULATED SINGLE-CONDUCTOR
TO SURFACE
RESISTANCE
SENSITIVE
OSC
THERMISTORS
TRANSISTOR AMP
VIBROTRON
SEA UNITS

Fig. 1—Block diagram.

Figure 2 illustrates the circuitry for the three-stage transistor amplifier. Because the vibrating-wire and static-wire impedances are relatively low, a step-up transformer is utilized. The grounded-emitter first stage is resistance-capacitance, coupled to the grounded-emitter second stage, which is in turn, directly coupled to the grounded-collector output stage. A properly phased positive-feedback loop is fed from the low-impedance emitter of Tr_3 to the center-

(814)

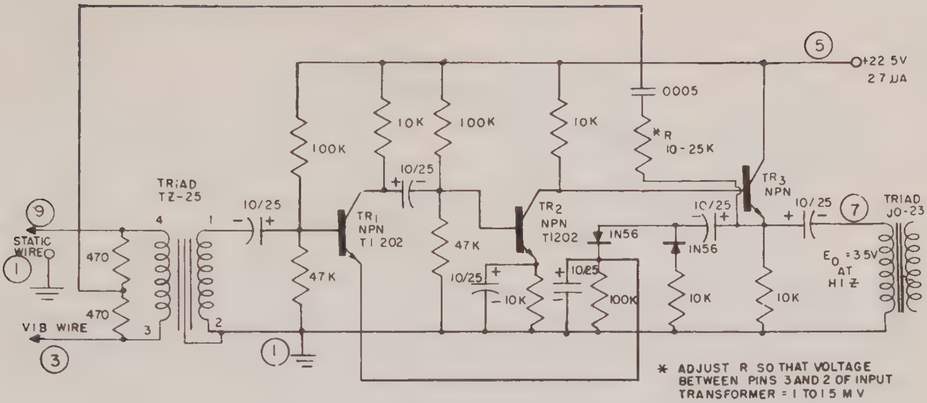
⑤
+22.5V
27 μA
.0005
10K
100K
100K
10K
*R
10-25K
10/25
TRIAD
TZ-25
10/25
TR1
NPN
TI 202
TR2
NPN
TI202
TR3
NPN
10/25
10/25
TRIAD
JO-23
⑨
⑦
4
1
STATIC
WIRE
①
470
47K
47K
IN56
IN56
E0 = 3.5V
AT
HI Z
470
10/25
10K
10/25
100K
10K
10K
VIB WIRE
3
2
③
①

∗ ADJUST R SO THAT VOLTAGE BETWEEN PINS 3 AND 2 OF INPUT TRANSFORMER = 1 TO 1.5 MV

Fig. 2—Pressure-sensitive transistor amplifier.

tap of two resistances bridged across the primary of the input transformer. As Vibrotrons of different frequency ranges and efficiencies are selected, the values of the two components in the resistance-capacitance network may have to be varied for proper phase.

An automatic gain-control network is necessary in order to drive the Vibrotron at constant amplitude. Because the relationship between amplitude and frequency of vibration is exponential, it is necessary to maintain the amplitude constant for a given stability. A voltage of between one and two millivolts measured across the vibrating wire is considered satisfactory.

It has been shown by W. Shockley, et.al., that the emitter resistance of a grounded-emitter type amplifier will vary according to the following expressions:

$$r_e = \frac{KT}{qI_e}$$

where K = Boltzman's constant
T = °K
q = Electron charge
r_e = Emitter resistance
I_e = Emitter current

therefore $r_e \cong \frac{.025}{I_e}$ at 24 degrees centigrade

R. F. Shea, et. al., have shown this equation to be more nearly equal to:

$$r_e = \frac{r_{e1}}{I_e}$$

where r_{e1} = Emitter resistance at
I_e = 1 milliamp

If one carries this one step further and assumes:

$$r_e\, r_b + << r_L << r_c(1-a)$$

then it can be shown:

$$A_v = \frac{-ar_L}{r_e + r_b(1-a)}$$

if $a \cong 1$ and is constant

$I_e < 1$ milliamp

then $r_b(1-a) << r_e$

and $$A_v \cong \frac{-r_L}{\frac{r_{e1}}{I_e}} \cong \frac{-I_e r_L}{r_{e1}} \cong \frac{r_L}{r_e}$$

It may be seen that under the conditions chosen, the gain of the first grounded emitter stage is essentially dependent upon the value of r_e. If I_e is varied over a range of 75 to 20 microamps, the graph of Fig. 3 shows the variation in voltage gain of the first stage versus input voltage. The solid line is the measured value and the dotted line is the computed value of A_v. The measured value of r_e at one milliampere for the T. I. 202 used was 33 ohms. The variation in the measured and computed values of A_v is due in part to the assumptions made in deriving the equation for voltage gain.

The graph of Fig. 4 plots output voltage as a function of input voltage for the three-stage amplifier. Also plotted is emitter current of the first stage as a function of input voltage. The overall result of the automatic gain control action is less than 1/2 db change in output voltage for a three db change in the input voltage at values over one millivolt input.

The temperature stability of the amplifier is considered adequate for this application. Sea water temperature generally is found in the range of zero to 28 degrees centigrade. Bias stabilization is generally established by the large emitter resistors and the voltage dividers in the base circuits of the first two stages. The degree of temperature stability was measured in actual tests from five degrees centigrade to 55 degrees centigrade. Figure 5 shows the results of output voltage versus temperature. Only very minor distortion was noticed over this range.

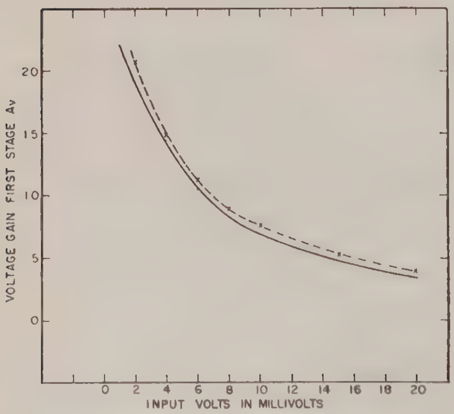

Fig. 3—Graph: A_v first stage—input voltage solid—measured value broken—computed.

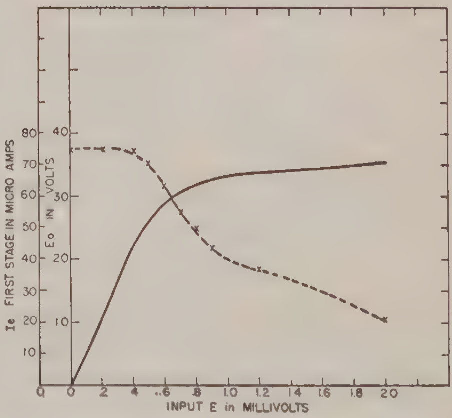

Fig. 4—Graph: E_o versus E_n of three stage amplifier I_e versus E_n of first stage.

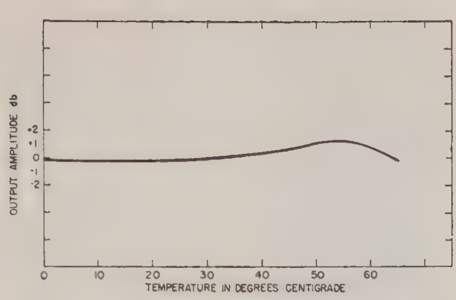

Fig. 5—Graph: E_0 versus temperature.

The output voltage is approximately 0.5 volt when working into a loaded 500 ohm line.

III. TEMPERATURE-SENSITIVE CIRCUITRY

The temperature-sensitive oscillator is of the Wein Bridge type, in which Western Electric 6014A thermistors are substituted for the resistive elements in the reactive arms of the bridge. This type oscillator was chosen because of its simplicity and dependable performance. Its one disadvantage is that separate filament batteries are necessary when using filament-type tubes. The circuit is shown in Fig. 6.

The bridge balance and oscillator frequency is set by the following equations:

$$R_1 = 2r$$

$$f_o = \frac{1.59 \times 10^{-1}}{\sqrt{C^2R^2}}$$

where f_o = Frequency of oscillation
R_1 = Negative feedback resistor
r = Lamp resistance
R = Thermistor resistance
C = Capacity in each half of positive feedback arm

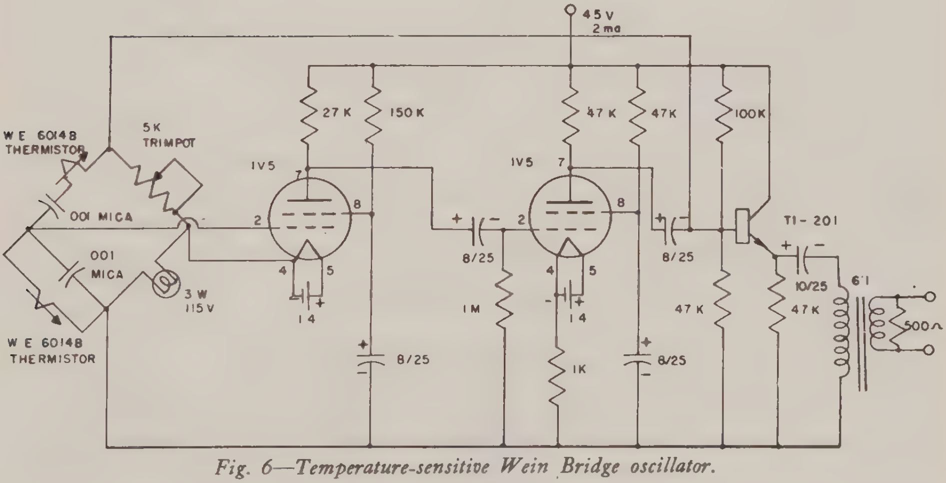
45 V
2 ma
W E 6014B
THERMISTOR
5 K
TRIMPOT
.001 MICA
.001
MICA
3 W
115 V
W E 6014B
THERMISTOR
1V5
27 K
150 K
7
8
2
4
5
1.4
8/25
1V5
47 K
47K
100K
+
−
8/25
1M
7
8
2
4
5
1.4
1K
8/25
8/25
TI- 201
10/25
47 K
47K
6:1
500Ω

Fig. 6—Temperature-sensitive Wein Bridge oscillator.

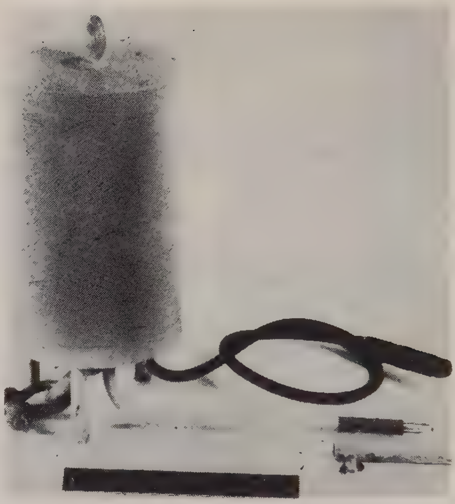

Fig. 8—Temperature unit in pressurized case showing temperature probe and 6014-A thermistors.

The temperature coefficient of resistance for the thermistor chosen is −3.9 percent per degree centigrade. Unfortunately, the resistance versus temperature characteristic is nonlinear as shown by the following equation:

$$R = R_o \epsilon^{B(1/T-1/T_0)}$$

where R_o = Resistance at reference temperature °K

B = Dependent on thermistor material

When the resistance of the reactive arms is allowed to vary according to this relationship, the frequency versus temperature graph of Fig. 7 is formed. An average sensitivity of about 40 cycles per degree centigrade is established.

The circuitry is quite standard in most respects. The tubes chosen use 40 milliamp filaments, making economic battery operation feasible. The grounded-collector transistor output stage serves to isolate the output circuitry from the oscillator section. An output voltage of 0.5 volt is available when loaded by a 500-ohm line.

The temperature stability of this oscillator is satisfactory for this application. When properly adjusted, a frequency variation of one to two cps over an eight-hour period at constant temperature is normal.

Over a temperature range of five to 50 degrees centigrade, a frequency change due to temperature of four to five cps was observed in laboratory tests.

The speed of response is important. The instrument itself was lowered and raised through the water at a rate of 2.5 feet per second. A thermal time constant of one second or less is necessary in order to resolve all the detail present. A step-function change in temperature will result in a frequency equilibrium within two seconds in sea water. This time has been cut to the order of one second on occasion by grinding down the glass surface of the thermistor beads.

IV. INSTRUMENT HOUSINGS

Both the pressure-sensitive transistor amplifier and the temperature-sensitive oscillator are encapsulated in a silica-filled epoxy resin. Plug-in construction is used to simplify maintenance and construction.

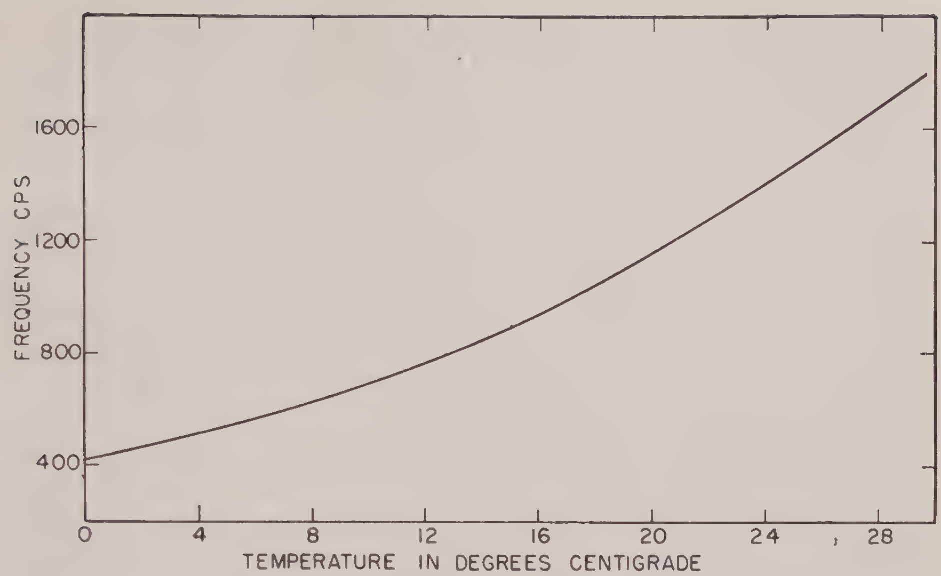

Fig. 7—Frequency versus temperature of Wein Bridge oscillator.

The two instrument housings are pressure tight and designed for a maximum pressure of 5000 pounds per square inch with an adequate safety factor. The instrument was divided into pressure and temperature units and individually housed so that they might be used separately if desired. The cases are of five-inch inside diameter, 0.312 inch wall stainless-steel tube. The end plates are of one inch brass with "O" ring pressure seals. Packing glands are used to bring out Joy Manufacturing Company long skirt push-pull plugs with four-foot leads.

The outputs of the pressure and temperature units are coupled one side to the instrument case and the other to a single-wire polyethylene-insulated cable. The cable is a 19-strand steel wire with a tensile strength of about 2800 pounds. The polyethylene jacket brings the overall diameter of the cable to approximately 0.32 inch. The polyethylene jacket also performs the extremely important job of giving the cable buoyancy. This allows the cable to support much greater instrument loads at greater depths, since the cable itself is almost weightless in sea water.

At the surface the signal is taken off the research vessel's winch via slip-rings. A sea return to the instrument is used with a zinc plate serving as the ground return connection.

V. SURFACE INSTRUMENTATION

The surface instrumentation, as shown by the block diagram, consists of a broad-band amplifier capable of handling frequencies up to 15 kilocycles. The frequencies are then separated by a high-pass and a low-pass filter and passed to a Hewlett Packard Model 500B demodulator. The resulting d-c outputs are now functions of pressure and temperature.

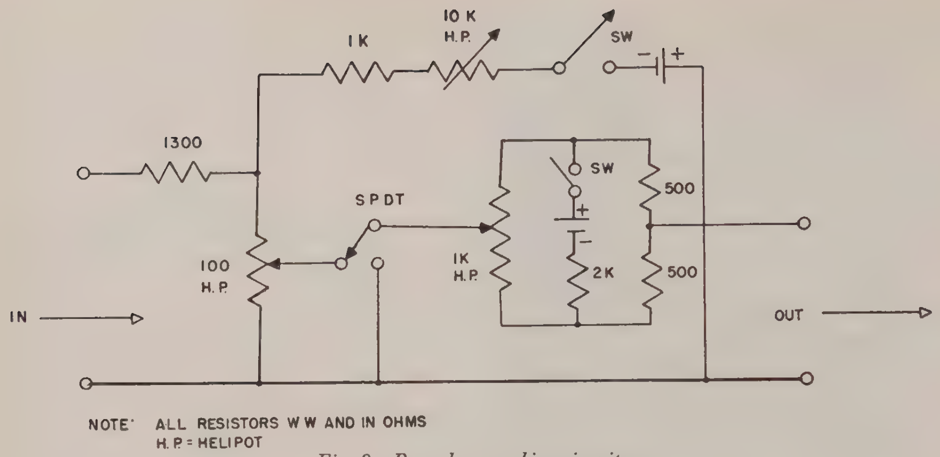

Fig. 9—Recorder zero-bias circuit.

To make these parameters suitable for recording on a Leeds and Northrup X-Y function plotter, a circuit to set the zero bias and the scale factor is a necessity. It is shown in Fig. 9. This zero-offset method is used to set at center scale on the recorder the mid-range of both the temperature and pressure functions. This eases the tedious work of laboriously setting the ranges so that the entire recorder chart width may be covered.

Pressure signal is applied to the X-axis and temperature signal to the Y-axis. This makes it possible to roll the chart manually after each successive run, thus completing a family of Bathythermometer curves.

The two channels were also recorded on a magnetic tape recorder. The combined frequency information was taken off at the output of the isolation amplifier in the deck unit. A dual-channel recorder was used with the combined temperature and pressure information recorded on one channel and a constant 5000 cps signal on the other. The advantages of this type data storage and play-back are self-evident and work is being continued to perfect this phase of the instrumentation problem.

VI. RESULTS OF TESTS

This instrument has been used at sea with good results. Figure 10 is a continuous Bathythermometer plot taken at sea off San Diego, California. The research vessel was drifting very slowly. Over the narrow range covered, the temperature scale is very nearly linear. The detail of the plot is self-evident. Small positive and negative temperature gradients are readily apparent and possible sound channels are indicated.

VII. OVERALL ACCURACY OF SYSTEM

The Vibrotron has an absolute resolution of approximately 0.003 inch at the 2.5 foot lowering rate generally used. The overall system is limited by the time constant of the Hewlett Packard 500B frequency meter. The resulting resolution of the overall pressure (depth) system is therefore of the order of 0.3 inch.

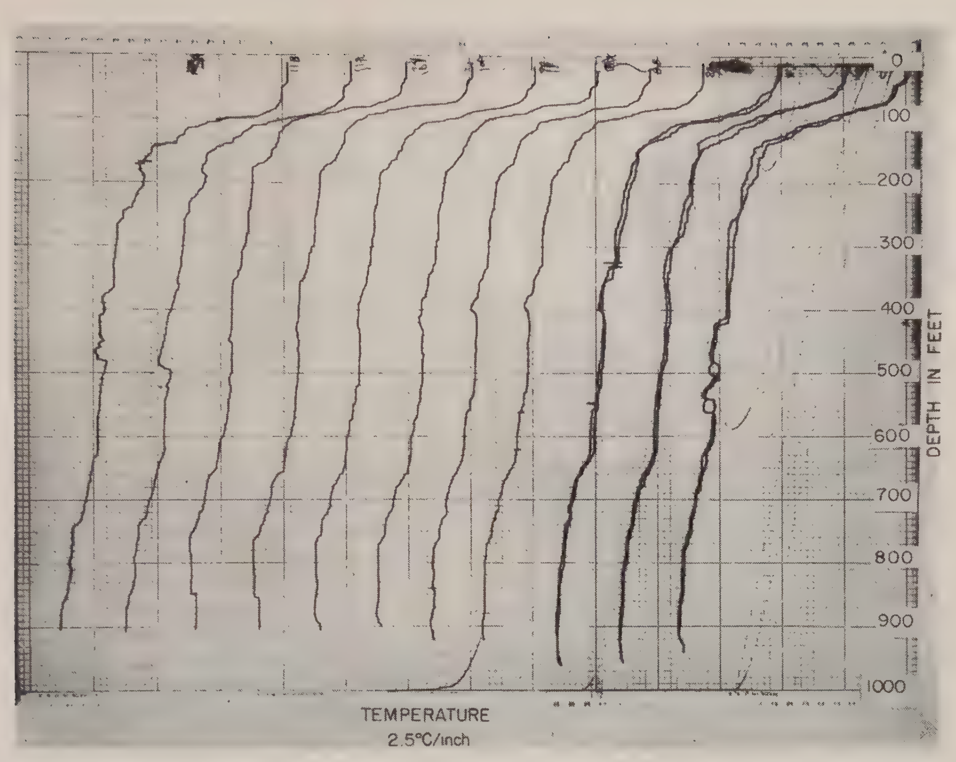

Fig. 10—X-Y plot of Bathythermometer (BT) curves.

Absolute accuracy in depth is better than ± 0.25 percent or ± 2.5 feet in 1000. The temperature sensitivity is approximately 40 cycles per degree centigrade. When these parameters are converted to direct current and applied to the function plotter with a ten inch chart width, a depth variation of ± 2.5 feet per 1000 can easily be read. If ten degrees of temperature are applied to ten inches of chart, a temperature variation of .050 degrees centigrade can be accurately plotted. Reproduction of pressure and temperature takes place without significant hysteresis effects. This was checked while at sea, where surface temperature and pressure can be accurately measured.

ACKNOWLEDGMENTS

This work was carried out at the Special Developments Division of the Scripps Institution of Oceanography of the University of California, La Jolla, California, and was supported by funds from the Office of Naval Research and the Bureau of Ships, United States Navy. The authors wish to extend their gratitude to all those who took part in this problem, and in particular to G. T. Barlow and R. M. Blei for their generous help and assistance in the construction of the equipment.

Reprinted from Volume XII
PROCEEDINGS OF THE NATIONAL ELECTRONICS CONFERENCE
Hotel Sherman, Chicago, Illinois, October 1, 2, 3, 1956.

(822)

Reproduced by Permission
Vol. 37, No. 5 Transactions, American Geophysical Union October 1956

The Use of Parachute Drogues in the Measurement of Subsurface Ocean Currents*

Gordon Volkmann, John Knauss, and Allyn Vine

Abstract—A technique for the measurement of subsurface currents is described in which a standard parachute is used at depth as a sea anchor for a small surface float. By tracing a series of drogues set at various depths, a current profile may be obtained. Hydrodynamic corrections (amounting to about ten per cent of the shear) have been computed and other refinements incorporated which make this a feasible method for measuring the main structure of the major ocean currents down to depths where the current is five to ten per cent that of the surface current.

Introduction—There have been few measurements of subsurface currents in the open ocean, as indicated by *Bowden* [1954] in his survey of the literature. On the other hand there is no shortage of papers describing current-measuring devices. *Böhnecke* [1954] listed some half a hundred different instruments and ended by quoting *Fleming* [1952] who suggested that what was needed were fewer new instruments and more measurements. The present technique has been developed over a period of three cruises in three years, and has been used for a relatively large number of subsurface current observations by ourselves and others, the results of which will be published in the future. Like other methods it has certain limitations, but it is a cheap and easy technique which has been successfully used.

The method is that of the free-floating drogue which is one of the oldest, having been used by the *Challenger* Expedition, 1873–1876 [*Thomson* and *Murray*, 1885, p. 79]. It also appears to be one of the least used, since in Bowden's summary of subsurface-current observations in deep water, all measurements were made with propeller-type instruments. However, the drogue technique has been used in recent years by *Stommel* [1954] and by *Cromwell* and others [1954].

In brief the drogue system consists of a standard aviator's parachute suspended by a weighted wire from a surface float (Fig. 1). The ideal subsurface drogue is one in which the ratio of drogue surface area to float and wire surface area is infinitely large since, as described below, a correction must be applied to the trajectory of the drogue system based on the drag of these appendages. In this respect the recent work of *Swallow* [1955], who has devised a neutrally buoyant drogue with no surface float, is the ideal. Our drogue system was designed with three points in mind. (1) The drag of the wire and surface floats should be small compared to the drag of the sea anchor. (2) The parachute must be given every chance to open and to remain open under water, and the other components and the techniques should be reliable enough so that they could be used with a high percentage of successes. When possible, positive identification of a proper or malfunctioning drogue should be provided. (3) The drogue system should be cheap enough to be considered expendable.

The work reported on was started by Vine, in March and April 1951, on R/V *Atlantis* in the Cayman Sea and continued in April 1953 on R/V *Spencer F. Baird* off Southern California and on EASTROPIC in October to December 1955 on R/V *Horizon* and *Spencer F. Baird*.

Parachute—The standard flat circular aviators' parachutes used as drogues were obtained from the armed forces over-age supply. They are also available on the civilian surplus market, although care should be taken with the latter source because parachutes are sometimes sold without shrouds to prevent re-use. The parachutes used have an effective cross section of 200 sq ft when completely open, and they are almost weightless in water, making it possible to use a relatively small surface float. Furthermore they can be launched unopened (our technique was to stuff them into large mailing tubes and 'pour' them over the side). The problem of launching an already opened or rigid frame-work type of drogue of similar cross section is formidable.

Very few pounds of force are required to open a parachute in the air, and once open it stays open. The same appears to be true when parachutes are used as deep-sea drogues. To check this, parachutes were observed underwater by SCUBA-equipped divers. The only difficulty was the tendency for the

---

* Contribution from the Scripps Institution of Oceanography, New Series No. 881. Contribution Number 856 of the Woods Hole Oceanographic Institution.

(823)

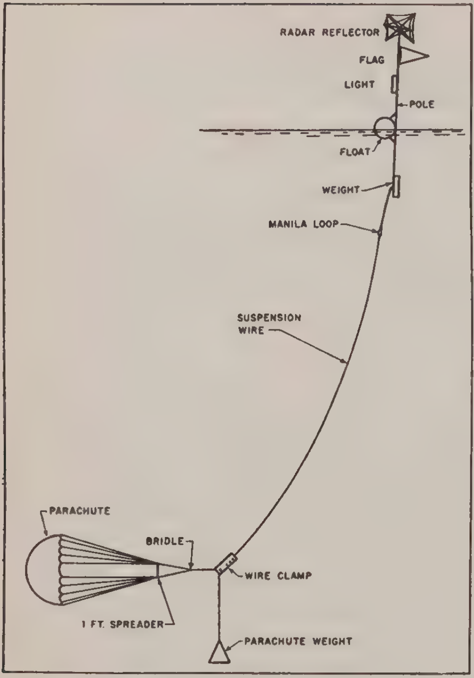

Fig. 1 – The parachute drogue system

shrouds to twist before the parachute opened as it fell through the water. In the tests conducted the parachute never failed to open, but the opening time was delayed by twisting, and a greater initial force was required. This difficulty was alleviated by inserting a spreader bar between the two groups of shrouds. Any twisting was taken up by the line which ran from the spreader bar to the wire (Fig. 1).

Wire and rigging—The suspension wire used was 0.030- or 0.040-in music wire, and while it has definite disadvantages, it was satisfactory for these purposes. The disadvantages are that it kinks easily, and, when it does, it only has about 20 pct of its original strength. It also corrodes quickly, as may be seen from the fact that 0.030-in wire generally parted after 24 hr with about a 30-lb pull on it. The advantages are that it is cheap, light, non-twisting under tension, and available in long lengths. If a laid wire is used, a good ball bearing swivel at the parachute end is recommended. The wire was in our instance the limiting factor in the length of life of the drogue, which was 24 to 36 hr. The use of either heavier wire or galvanized wire would lengthen this life considerably.

Since there is no need to reel in on this type of rig, a simple spindle and brake suffice as a winch. On two of the three cruises the front axle of an automobile complete with brake was used with great success. On the last cruise the music wire was supplied on wheel rims purchased to fit the automobile axle. The addition of small plywood flanges to prevent the wire from slipping off this drum makes a cheap and effective rig. The purchase of wire on drums rather than coils is strongly recommended because rewinding from coils requires special equipment and is lengthy and tedious.

A few of the many methods of holding music wire are shown in Figure 2. The cheek clamp is the strongest and most convenient, since it can be applied while the wire is under tension. It can also be clamped quickly, an asset when wire tension is high and mounting rapidly.

To ease the strain on the wire during drogue launching, the surface buoy with wire attached was put over first. The ship then steamed away until the proper amount of wire was out and then stopped while the parachute was 'poured.' This eliminated any tendency to sea-anchor the ship on 0.040-in music wire to an open parachute. Since music wire has a tendency to fatigue when bent on a short radius, manila leaders were used whenever practicable. Manila, marline, and friction tape were used copiously to prevent chafing and to lash the components together.

Floats—A different type of float was used on each of the three cruises: extra strong meteorological balloons in gunny sacks, canvas-covered balsa wood floats (Navy dan-buoys), and 14-inch Japanese glass fishing floats. The balloons are the cheapest and easiest to stow but are the least durable. The

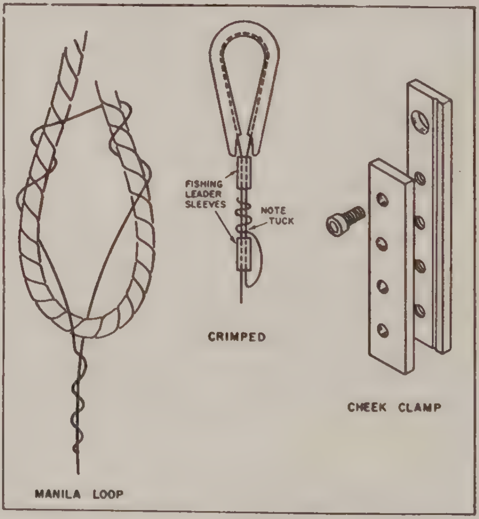

Fig. 2 – Various techniques for securing music wire

fishing floats proved the most satisfactory, but the storage of a hundred or more glass floats on a small ship can be a problem. Usually a single glass float provided enough buoyancy. The float was lashed to a bamboo pole, to the top of which were attached flags, a light, and a radar reflector. The suspension wire was attached to the bottom of the pole, and it was necessary for the parachute with its attached 20-lb weight to sink to its full depth before the pole would stand completely upright. The pole was so weighted that before the addition of the 20-lb load, it would lie at an angle of about 30° with the surface. Thus one could tell when the drogue system was properly set by watching the pole swing to an upright position, and one could also tell when something was amiss (usually a parted wire) when the pole flopped down. This type of positive identification of the fact that the drogue was properly set or that it had broken loose saved considerable time on the most recent cruise.

It can take as long as an hour for a parachute drogue and 20-lb attached weight to sink to 200 m. To eliminate the long time required for an open parachute to sink to the greater depths, additional weights were secured by means of a simple time release to the apex of the chute, which then descended closed. Here as a signalling device an additional float was attached between the upper end of the wire and the surface buoy. When the parachute was at depth, this float would be submerged under the additional weight of the release weights, but it would reappear when these weights were released. Also, when something parted, this second float would pop high out of the water and thus give a positive signal that something was amiss.

Measurement techniques—Currents at various depths were measured by tracing the movements of the various floats. Of the two general ways in which this can be done, neither is completely satisfactory: one is to measure the movement of the drogue over the surface by standard navigational techniques, that is, celestial fixes or Loran; the second is to measure the movement relative to some reference point, that is, an anchored ship, buoy, or some other easily observable reference.

The conditions were different on each of the three cruises and different techniques were used to solve this problem. Loran coverage was inadequate in each area as it is over most of the oceans of the world, and celestial navigation has certain obvious limitations with respect to accuracy, time between fixes, and the uncertainties of cloud formation. In the Cayman Sea, where we were often within sight of land, piloting techniques were used. When land fixes were not available the same surface-float, piano-wire rig was attached to an anchor and used as a reference buoy. The circular area of possible positions created by the necessary scope (we used a wire-length to water-depth ratio of 1.1 to 1) is reduced to a segment of a circle by a steady current, and this uncertainty can be considerably reduced by time averaging.

During the 1953 cruise of the *Spencer F. Baird* off Lower California where the currents were weak a slightly heavier version of the anchored buoy was used, and celestial navigation was employed to check possible lifting or dragging of the anchor.

On the EASTROPIC Expedition into the eastern part of the Equatorial Current and Countercurrent system a parachute drogue at 2000 m was used as the reference buoy. In this area of strong currents, it was felt that any slight drift of the water at 2000 m could be tolerated. An upper limit of this drift was established by celestial fixes but was never found to be more than predicted (see next section) and may have been less.

The range and bearing from the reference point to the other drogues was measured by one of three methods: (1) By timing the vessel up and down current along an average fixed course, taking bow and beam bearings or angles of depression from the horizon to establish the distance of the buoys from this course. (2) By timing the vessel from the reference buoy to each buoy and return, along a course parallel to the visual bearing between the two. (3) By standing by the reference-buoy and measuring range and bearing by radar.

The last method is, of course, the most efficient and the most accurate. Unfortunately the radar was not working properly on any of the three ships used by the authors. (EASTROPIC was a two-ship cruise and radar was used by Townsend Cromwell on the other vessel to great advantage.)

Corrections to observations—Since the velocity of the surface water is in general different from that of the water at the depth of the parachute, there is a flow of water past the surface buoy. This implies a slower flow of water by the parachute, since there must be a balance of the horizontal forces on the drogue system. These horizontal forces are given by

$$F = \tfrac{1}{2}\rho C_D A V^2 \qquad (1)$$

where F is the force, C_D a non-dimensional drag coefficient, ρ the density of the fluid, A the cross sectional area, and V the relative velocity of the fluid.

(The equation for the horizontal force created by a sinusoidal motion, for example, surface waves, of

(825)

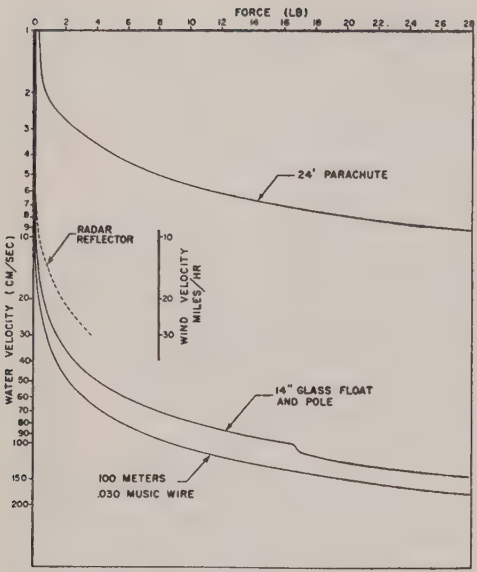

Fig. 3 – Drag forces on various components of the drogue system (note different scale for radar reflector in air)

orbital velocity U superimposed on a steady current V and integrated over one cycle is $F = (\frac{1}{2})\ \rho\ C_D A\ (V^2 + U^2/2)$. For the shallower depths the parachute may be within the region of wave motion and complicate the picture phase-wise. For the greater depths it is not clear how much of the oscillatory force is transmitted down the wire to the parachute.)

Figure 3 has a plot of force as a function of speed through the water for a 24-ft circular flat parachute computed from (1). The area of such a parachute is 200 sq ft. (The diameter must be reduced by a third in calculating the area of the parachute, according to the USAF *Parachute Handbook*, 1951.) The drag coefficient was assumed to be 1.5, although this may be subject to some error. The coefficient is a function of the porosity of the material as well as the geometry. For a completely imporous chute, it is 1.7; for a standard chute in air it is 1.3 [*Heinrich*, 1954]. The porosity of the parachute material is less for sea water than for air, but no measurements have been made of its effect on the drag coefficient.

Also plotted in Figure 3 are the forces at different speeds computed for a surface float consisting of a 14-in float and 8 ft of bamboo pole, both submerged, 100 m of 0.030-in music wire, and a two-ft Navy lifeboat radar reflector in air. The curves for the float and wire were calculated using the appropriate drag coefficients in *Rouse* [1946]; the curve for the radar reflector (type MX-138/A) is based upon measured values of drag.

To calculate completely the forces on the parachute and hence the speed at which it moves through the water, it is necessary to know exactly the forces on the float and wire. This is in general not possible, nor in many cases is it necessary if the ratio of drogue to float area is large enough. From Figure 3 one can see that a current which flows at 50 cm/sec to a depth of 100 m will drag a parachute at 200 m through the water at about 4.5 cm/sec, assuming no current at 200 m. It has been our experience that a first-order correction such as this will correct the measurements to a couple of centimeters per second and that both the uncertanties in observation as well as short-period changes in the current make it impracticable to try to reduce the error any more.

The standard flat parachute is unstable. As it falls through the air it falls at an angle of about 22° with the vertical. This angle of stability is again a function of the porosity of the chute and is 45° for a completely imporous parachute [*Heinrich*, 1954]. Hence the direction of the 4.5 cm/sec correction of the previous example could be as much as 22° to 45° in error. It is believed, however, that this directional correction is negligible. In the first place an uncertainty of even 45° on a 5 cm/sec correction to a 50 cm/sec current does not change the resultant by more than ±4°. Secondly, underwater observations of parachutes used as drogues indicate that if there is a directional preference for the towed parachute it is in the downward direction.

The actual depth of the parachute drogue can be estimated by assuming the wire to be a rigid member and the forces in equilibrium (hence the depth of the 200-m drogue with a 20-lb weight and pulled by a 6-lb force would be $d = 200 \cos \phi$ where $\phi = \tan^{-1} 6/20$ so that $d = 191$ m), or by the more rigorous method of *Pode* [1951], where the forces on the flexible wire are also considered. In this example, assuming 0.030-in wire, the calculated depth is 189 m. As long as ϕ is a relatively small angle the two methods give about the same results.

Discussions and conclusions—The techniques and equipment described have been used successfully in the measurement of surface and subsurface ocean currents in both the Atlantic and the Pacific. On Eastropic, continual tracking of as many as five drogues at various depths with reference to the 2000-m drogue was done by radar, and up to four drogues were tracked at once by continuously running between them and the reference drogue. It was nearly always possible to get a satisfactory picture of the vertical current structure down to several hundred m during the daylight hours.

The shear measured in these cruises was nearly always between 10 and 100 cm/sec. The little experience we had in three-knot (150 cm/sec) shear indicated that perhaps the drogue system would have to be sturdier to be used in the Kuroshio or the Gulf Stream.

It seems clear from the force computations in Figure 3 that in areas of even modest surface currents the correction which must be applied due to shear may easily exceed the velocities which other workers have shown to exist at greater depths. This suggests that the usefulness of this technique may be limited to depths where the current is more than 5 to 10 pct that of the surface current.

However, for the task of measuring the structure of the major ocean currents where an error of a few centimeters per second can be accepted, it is believed that the technique as described is a useful one.

Acknowledgment—This paper represents results of work carried out by the University of California and the Woods Hole Oceanographic Institution under contract with the Office of Naval Research.

REFERENCES

BÖHNECKE, G., Principles of measuring currents, International Association of Physical Oceanography, IUGG, General Assembly at Rome. *Procès-Verbaux* **6**, Sep., 1954.

BOWDEN, K. F., The direct measurement of subsurface currents in the oceans, *Deep Sea Research*, **2**, 33–47, 1954.

CROMWELL, T., R. B. MONTGOMERY, AND E. D. STROUP, Equatorial undercurrent in the Pacific Ocean revealed by new methods, *Science*, **119**, 648–649, 1954.

FLEMING, R. H., Discussion in *Symposium on Oceanographic Instrumentation*, Nat. Res. Counc. Pub. 309, 231 pp., 1952.

HEINRICH, H. G., *The effects of porosity of design and performance characteristics of parachutes*, USAF Equipment Lab., Wright Air Dev. Center, 11 pp., 1954.

PODE, L., *Tables for computing the equilibrium configuration of a flexible cable in a uniform stream*, USN David Taylor Model Basin Rep. 687, 33 pp., 1951.

ROUSE, H., *Elementary mechanics of fluids*, John Wiley and Sons, 376 pp., 1946.

STOMMEL, H., Serial observations of drift currents in the central North Atlantic Ocean, *Tellus*, **6**, 203–214, 1954.

SWALLOW, J. C., A neutral-buoyant float for measuring deep currents, *Deep-Sea Research*, **3**, 74–81, 1955.

THOMSON, C. WYVILLE, AND JOHN MURRAY, *Report on the Scientific Results of the Voyage of HMS Challenger*, Narrative, 1110 pp., 1885.

USAF Parachute Handbook, ATI 35 532, 78 pp., 1951.

Scripps Institution of Oceanography (G. V. and J. K.), *La Jolla, California, and Woods Hole Oceanographic Institution* (A. V.), *Woods Hole, Massachusetts.*

(Manuscript received April 18, 1956; presented at the Thirty-Seventh Annual Meeting, April 30, 1956; open for formal discussion until March 1, 1957.)

Physical and Chemical Coloration In Birds

by DENIS L. FOX

Professor of Marine Biochemistry, Scripps Institution of Oceanography

Reprinted from

YALE SCIENTIFIC MAGAZINE

Vol. XXXI, No. 1

October, 1956

Reproduced by Permission

Physical and Chemical Coloration In Birds

by DENIS L. FOX

Professor of Marine Biochemistry, Scripps Institution of Oceanography

Coloration in birds may be the result of either optical effects or chemical compounds in the birds' diets. The author here discusses both types, and explains some of the experiments which have been undertaken to verify them.

COLOR in the living world has excited man's wonder and active curiosity since his earliest days. In no other living things are the assorted colors, shades and contrasts more beautiful and striking than among the birds, notably in their feathers.

However, notwithstanding the vast assortments of colors exhibited by birds, these many different manifestations have their origins in but three or four basic physical or chemical attributes, or in combinations of these.

Briefly, the foundations of integumentary and feather coloration may be listed thus:

1. Schemochromes: physical (optical, or structural) colors
2. Biochromes: true pigmentary (chemical) colors
3. Combinations of schemochromic and biochromic coloration.

In group 1 there are three principle subclasses: white, blue, and iridescent colors.

Whiteness, e.g. in the feathers of white domestic fowl, gulls, some peafowl, the snow egret, snowy owl and in countless other examples including the white downy plumage of newly hatched young, results from the scattered reflection of total incident sunlight or other source of white illumination. This light-scattering arises from the presence of innumerable extremely minute air spaces (solid froth) within the alveolar cells of the feather barbules, or smallest structural elements. No colored molecules are present. The whiteness of light-scattering is exhibited by many other air-containing structures, such as plant aerenchyma cells, white blossoms and dry stem pith, snow, flour and the like. White human or other mammalian hair is another outstanding example. Some species of Arctic birds (e.g. willow grouse and ptarmigans) and northern mammals such as certain foxes, weasels and stoats assume their white air-filled livery during the winter, thus rendering themselves less visible to predators or prey.

Blue colors are displayed by feathers of jays, psitticines, kingfishers, and many other birds, through a mechanism similar to that in white feathers but differing therefrom only (1) in the degree of fine subdivision of the enclosed air vessels within the barbules, and (2) in the fact that a dark pigment (melanin) underlies the light-scattering units. Blue feathers involve no blue chemical compounds at all, but the air saces within the solid keratinaceous protein of the barbules are of extremely minute dimensions, approximating those of light waves in the visible spectrum (less than 0.7 μ) and not resolvable even with the use of a high-power microscope.

When white light impinges on such a feather, the longer rays (red, orange, yellow and much of the green) are not reflected as in total scattering by a white feather; instead, these light components penetrate the material entering the underlying screen of dark pigment, where they are absorbed and thus transformed into heat energy, while the short blue rays are reflected by the very minute intervening air bubbles, back into the view of the observer. Inspection of a blue feather by transmitted, rather than by reflected light, i.e. by looking *through* its under surface toward the light, gives the viewer no blue rays but only a shade of gray or brownish gray. The blue rays have failed to penetrate the feather, but have instead been reflected back toward the light source, and are still readily appreciated by an observer standing opposite, viewing its upper illuminated surface. The blueness of feathers is confined to their outer, exposed surfaces; the inner surface next to the bird's body, shows dark, or sometimes reddish or yellow colors.

To demonstrate the foamy or spongy structure of the blue-scattering medium within feather barbules by a simple experiment, a whole plume may be struck on an anvil with a hammer, whereupon the struck portions turn black. Or it may be immersed, usually for some hours or days, in a fluid having a refractive index very close to that of the solid feather-keratin (ca. 1.54). As the fluid (e.g. cresol or phenol in alcohol) penetrates, gradually replacing the air within the submicroscopic intrabarbular foam work, the whole feather assumes a jet black appearance, since the melanin pigment in the basal layers is now being viewed through a liquid-filled, colorless, transparent "sponge." Such a "blackened" feather, when now leached free of the foreign fluid with fresh alcohol, and then dried, exhibits the original blue color, since air has now re-entered the minute spaces within the barbules.

Iridescence, commonly called changeable, "metallic," or sometimes (erroneously) "rainbow" coloration, is encountered in the plumes of many species, notably in hummingbirds, peafowl, doves and pigeons. These brilliant, changeable chromatic aspects are assignable to interference of light waves being reflected from laminated structures within the feather barbs. Incident light enters and is reflected through longitudinal stacks of extremely thin, very tightly appressed, flat films of keratin comprising the barb of the feather. These proteinaceous laminae are themselves unpigmented, just as are the alveolar structures in white or in blue feathers, and, like the colorless water-soap-air constituents of a bubble, or the oil-and-water layers of a film on black pavement, they disintegrate white light into its several spectral components in the same way as does pearl or nacre, by the alternating reinforcement and extinction of light beams, reflected from very thin layers, separated each from the next by fractional multiples of the wavelength of visible light.

Like blue feathers, iridescent ones exhibit their characteristic chromatic effects only when viewed by light reflected from their upper (or outer) surfaces; when light is viewed through the under side, which bears a layer of dark pigment, the whole feather merely appears a dark shade.

The manifestation of blue colors, by Tyndall-scattering, and of iridescent aspects, by interference, has in each case a basic dependency upon structural units so exceedingly small in size (i.e. whether in the form of minute, separated airspaces, or in deposits of extremely thin, flat films) as to lie within the range of visible light-wave dimensions, i.e. less than about 0.6 μ or about 1/42,500 inch. In iridescent feathers, the separate reflection of each light fraction produces the characteristic color changes seen on altering the angle of vision.

Adult South American Macaw, Ara ararauna. *From a painting by Dr. Henry Kritzler, from living specimens at the San Diego Zoo.*

The true biochromes, or natural pigments, involve colored molecules, as contrasted with the relatively colorless materials discussed above, whose submicroscopic architecture is responsible for the schemochromic or optical color manifestations. Unlike schemochromic colors, true pigmentary colors are not subject to change by mechanical means, such as pressure, torsion, grinding or hammering.

Red, orange or yellow feathers display chemical compounds originally acquired in the bird's diet. The commonest members of this color class are in the carotenoid group of fat-soluble, nitrogen-free pigments occurring nearly universally in plants and animals. Carotenoids are synthesized by all green plants, and by many fungi and bacteria. Animals, being incapable of the manufacture of these pigments *de novo,* must obtain them directly or indirectly from plant sources. Carotenoid colors typify the appearance of carrot roots, citrus fruits, certain squashes, melons, and many other fruits, innumerable petals such as those of the dandelion, sunflower or marigold, as well as butter fat, adipose tissue, eggs and other materials of herbivorous animals, living on plants rich in the pigments.

All are familiar with the yellow pigmentation of legs, ears, iris and egg-yolk of the domestic fowl, which consumes grass, fruits and other plant materials. The red and yellow feathers of flickers, cardinals, orioles, bishop birds and finches, such as canaries, are additional examples. It is well known by bird fanciers that canaries will develop rich colors in their newly growing feathers if their diet be supplemented by the red carotenoids of paprika.

Water birds such as spoonbills *(Ajaia ajaja)* and flamingos *(Phoenicopterus ruber)* acquire their beautiful pigmentation from natural diets rich in small shrimp-like crustaceans and other arthropods which, like their larger relatives, such as crabs, crayfish and lobsters, store a unique red carotenoid, astaxanthin. Captive flamingos, if fed a diet deficient in their natural sources of pigmentation, gradually lose their rich colors, their plumes and exposed skin becoming successively paler. A flock of flamingos in the San Diego Zoo have accordingly received in their finely comminuted, assorted menu, a supplement of finely ground crustacean shells and red salmon flesh, both rich in astaxanthin. This has resulted in a striking return of the pink and vermilion coloration of their newly grown feathers and of the exposed skin of legs, feet and lower bill mandible. The principle carotenoid present in the crustacean material administered in the food has been recovered and chemically identified in the skin and plumes of flamingoes which had become casualties in our Zoo.

The red carotenoid coloration of facial or other skin in these and in other birds (e.g. in the facial integument of the pheasant, *Phasianus colchicus)* should not be confused with the blood-red skin of combs, naked faces or necks of many birds such as vultures, buzzards and the male turkey. This latter aspect arises from the presence of the common blood pigment, hemoglobin, viewed through the thin transparent skin, but not encountered in plumage, save in the quills of pin feathers. The blue skin of the turkeycock, guinea-fowl, cassowary and other birds is a manifestation of Tyndall-scattering by finely dispersed, submicroscopic tissue components within the fluid medium. Purple intermediary areas are the result of blue Tyndall-scattering superimposed on the hemoglobin red.

The red feathers of the African fruit-eating turaco yield a unique biochrome, turacin, wherein copper is chemically conjugated with urochrome, a heme porphyrin compound. Mildly alkaline water, brought into contact with the red feathers of this bird, whether in nature or by human design, leaches the turacin free, leaving the feather pale and rendering the water blood-red in color. Neutralization immediately precipitates the copper uroporphyrin in bright red flocks. Green feathers of the same bird carry turacoverdin, an oxidized derivative of turacin. The turaco appears to use its growing feathers as a channel for excreting excess dietary copper.

Some birds of the parrot family develop feathers bearing green or yellow-green fluorescent porphyrins derived presumably from the degradation of heme (blood) pigments within the body.

Black feathers (e.g. of ravens, blackbirds, etc.) contain relatively large quantities of the dark, endogenous, universally occurring compound melanin, elaborated in the skins and hair of many animals, including humans. Melanins are generated from the chemical oxidation of the important amino acid tyrosine and other phenolic compounds, followed by increasing polymerization. Brown, reddish or tawny feathers also contain deposits of melanin in various degrees of oxidation. The commoner birds of prey, such as hawks, owls and eagles, exhibit melanistic feather colors and patterns, but rarely if ever carotenoid pigmentation.

Many bird species commonly display combinations of both structural and pigmentary colors. A few illustrative examples may suffice.

Gray feathers exhibit intimately mixed whites and blacks, each originating independently as previously described. "Powdery" blue aspects are the result of integrated white-scattering and finer blue-scattering elements within the barbules.

Bars, spots, streaks or otherwise mottled patterns display delimited areas of black or brown, alternating with white or blue structural colors, or with yellow, orange or other pigmentary deposits.

Green feathers, save for the instances cited above, commonly arise from the combined features of blue scattering through a thin overlying yellow pigmented cuticular layer, typified in some macaws such as *Ara ararauna.* Through chemical leaching of the cuticular yellow pigment, such a green feather is rendered blue in color. Purple colors are similarly brought about by blue scattering through a thin red pigmentary covering.

Sexual dichromatism is readily recognizable in many bird species. The male in many cases displays far richer and more conspicuous coloration than does the female. This is true whether the plumage be iridescent as in peafowl, bird-of-paradise, turkey, etc., blue as in jays or pigmentary (cardinal, pheasant). This is often, but not always, accompanied by sexual dimorphism, wherein the male is larger or adorned with larger combs or wattles, or with longer, heavier feathers.

It is perhaps logical to anticipate some usefulness in sexual dichromatism in the perpetuation of the species, if one contemplates the potential advantages of brilliant colors for both advertisement and threatening of rivals in the male, and the relatively drab, obscuring coloration of female feathers which should contribute toward concealment while brooding her eggs or young.

References

1. H. B. Cott, *Adaptive Coloration in Animals,* Oxford University Press, New York (1940).
2. D. L. Fox, *Animal Biochromes,* Cambridge University Press, London and New York (1953).
3. D. L. Fox, *Nature,* 175, 942. (1955)

Contribution from the Scripps Institution of Oceanography, University of California. New Series No. 882.

Denis L. Fox is Professor of Marine Biochemistry in the University of California's Scripps Institution of Oceanography, at La Jolla, California. He serves on the Research Council of the San Diego Zoo. Born in England, he came to this country at an early age, receiving his education in California. After receiving his Bachelor's degree in chemistry at the University of California in 1925, he spent four years as a chemist with the Research and Development Department of the Standard Oil Company of California before taking up graduate work at Stanford where he received his Ph.D. in biological sciences (biochemistry) in 1931. He has just completed his 25th year on the faculty of the University of California. He spent the year 1938-39 at the Cambridge University in England as a Rockefeller Foundation Research Fellow, and held a Guggenheim Foundation Fellowship in 1945-46. Among a total of some 90 publications, about half deal with naturally occurring pigments. Among the latter are several reviews, two articles for encyclopediae and a book "Animal Biochromes and Structural Colours," published in 1953 by the Cambridge University Press.

Reproduced by Permission

BULLETIN OF THE GEOLOGICAL SOCIETY OF AMERICA
VOL. 67, PP. 1623-1640, 13 FIGS. DECEMBER 1956

SEISMIC-REFRACTION STUDIES OF THE PACIFIC OCEAN BASIN

PART I: CRUSTAL THICKNESS OF THE CENTRAL EQUATORIAL PACIFIC

BY RUSSELL W. RAITT

ABSTRACT

On the MID-PACIFIC and CAPRICORN expeditions seismic-refraction observations were made at 42 stations scattered widely within an area of the Central Equatorial Pacific Ocean extending from latitudes 22° S. to 28° N. and longitudes 162° E. to 112° W. At 29 of these stations velocities of about 8 km/sec. or more were reached at the depth of greatest penetration of the refracted waves. The mean of these velocities was 8.24 km/sec.

The crustal thickness, defined as the depth below the sea floor at which the 8 km/sec. velocity is reached, ranges from 4.8 km to 13.0 km. The distribution of thicknesses is bimodal with seven anomalous stations giving values between 10 and 13 km. The group of 22 stations believed to be typical of the deep Pacific Basin has an average thickness of 6.31 km with a standard deviation of 1.01 km.

CONTENTS

Page
Introduction 1623
Acknowledgments 1624
Station locations 1625
Operations 1628
Travel-time data 1629
Velocities 1630
Layer thicknesses 1635
Nature of the layers 1636
Crustal thickness 1637
References cited 1638

ILLUSTRATIONS

Figure Page
1. Location of seismic-refraction stations of the MID-PACIFIC and CAPRICORN expeditions 1624
2. Plan of operations of the reversed seismic profile at Station M1 1626
3. Plan of operations of split profile at Station M7 1626
4. Sample of a complete oscillogram of seismic waves recorded at short range on the MID-PACIFIC expedition 1627
5. Sample oscillograms of the low-frequency seismic-refracted waves recorded at long range 1628
6. Travel-time plots of station M1 1629
7. Travel-time plots of station M7 1630
8. Travel-time plots of station M10 1631
9. Travel-time plots of station C2 1632
10. Travel-time plots of station C8 1632
11. Travel-time plots of station C12 1633
12. Travel-time plots of station C13 1633
13. Crustal thickness of the central equatorial Pacific as a function of sea-floor elevation 1638

TABLES

Table Page
1. Location and sea depth of MID-PACIFIC stations 1625
2. Location and sea depth of CAPRICORN stations 1625
3. Layer velocities of MID-PACIFIC stations 1634
4. Layer velocities of CAPRICORN stations 1634
5. Layer thicknesses of MID-PACIFIC stations 1635
6. Layer thicknesses of CAPRICORN stations 1636

INTRODUCTION

Since the fall of 1948, seismic-refraction studies of the Pacific Ocean bottom have been made in a region extending from San Diego to the Marshall Islands and south almost to the Tropic of Capricorn. The work includes several types of problems and is separated roughly into three geographic regions: (1) the deep Pacific Basin proper; (2) atolls and islands; (3) the continental margin of North America and Central America. The present paper contains some results in category (1) obtained on two expeditions into the Central Equatorial Pacific: the MID-PACIFIC expedition of 1950 and the CAPRICORN expedition of 1952–1953 (Revelle, 1954).

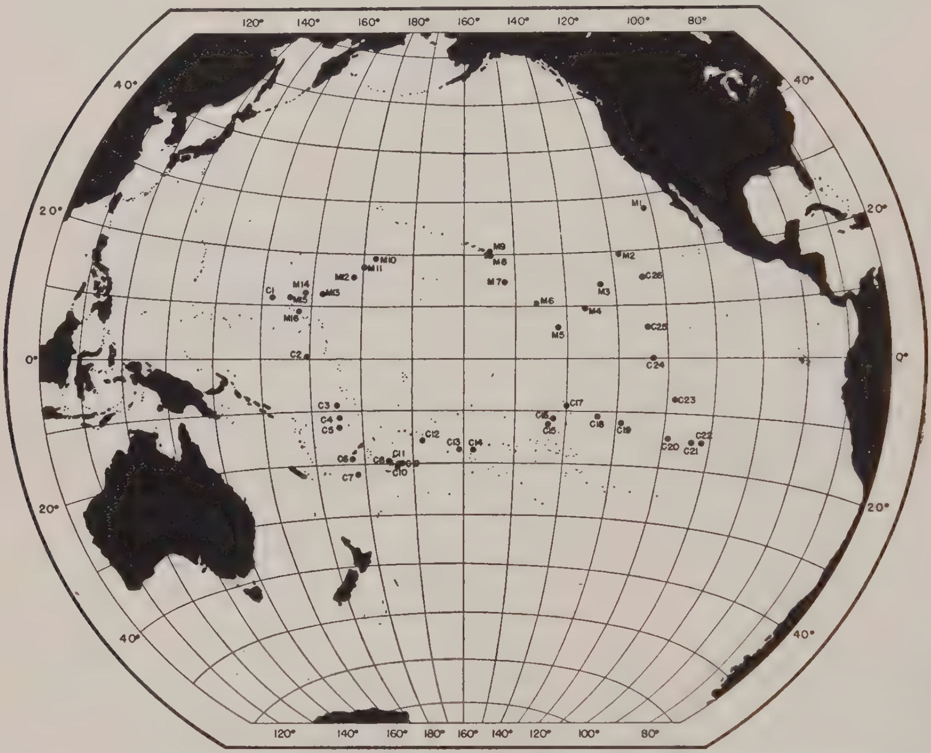

FIGURE 1.—SEISMIC-REFRACTION STATIONS OF THE MID-PACIFIC AND CAPRICORN EXPEDITIONS

ACKNOWLEDGMENTS

A seismic-refraction program of the magnitude of that conducted on the MID-PACIFIC and CAPRICORN expeditions requires the help of many people.

The leader of both expeditions was Roger Revelle, Director of Scripps Institution of Oceanography. His interest and help throughout the work at sea, as well as in the analysis of the data, were major factors in its success.

The officers and crew of the USS EPCE(R) 857, R/V HORIZON and R/V SPENCER F. BAIRD were of great help in all phases of the sea operations. The commanding officers of 857 and HORIZON on the MID-PACIFIC expedition were Lt. Comdr. D. J. McMillan (USN) and James L. Faughn, respectively. The commanding officers of HORIZON and BAIRD on the CAPRICORN expedition were Noel L. Ferris and Laurence E. Davis.

On the MID-PACIFIC expedition, Daniel K. Gibson supervised the firing operations, assisted by Chief Gunner's Mate Albert Obregon. On the CAPRICORN expedition, Willard C. North supervised the firing operations, and Maxwell Silverman of U. S. Navy Electronics Laboratory was in charge of the firing of explosives, assisted by Edward J. Taylor.

Members of the recording and firing groups were Jeffery D. Frautschy, Edwin M. Hamilton, Richard P. von Herzen, Winter D. Horton, Jr., Alan C. Jones, A. D. Raff, T. Wayne Runyan, Richard J. Smith.

The travel-time data were read, plotted, and analyzed by Gloria J. Slack, Gwendolyn A.

Roy, Clara B. Crane, Shirley R. Shivers, and Frieda K. James.

TABLE 1.—MID-PACIFIC STATIONS

Station	Date, 1950	Latitude, N.	Longtitude	Sea depth in m
M1	29 July	27° 24′	121° 35′ W.	4176
M2	2 Aug.	19° 22′	128° 30′ W.	4829
M3	6 Aug.	13° 46′	133° 41′ W.	4908
M4	9 Aug.	9° 38′	136° 19′ W.	4804
M5	13 Aug.	5° 51′	141° 51′ W.	4811
M6	16 Aug.	10° 43′	145° 53′ W.	5249
M7	19 Aug.	14° 41′	151° 54′ W.	5797
M8	21 Aug.	20° 02′	155° 11′ W.	338
M9	22 Aug.	20° 26′	154° 54′ W.	5199
M10	16 Sept.	19° 02′	177° 19′ W.	4833
M11	17 Sept.	17° 20′	179° 58′ W.	4929
M12	19 Sept.	15° 34′	177° 40′ E.	4200
M13	21 Sept.	12° 39′	172° 10′ E.	5547
M14	22 Sept.	12° 27′	168° 22′ E.	4927
M15	8 Oct.	11° 12′	165° 10′ E.	4458
M16	1 Oct.	8° 55′	167° 41′ E.	42

Valuable suggestions for improvements of the manuscript were received from M. N. Bramlette and George G. Shor, Jr. of Scripps Institution of Oceanography, and from M. N. Hill of Cambridge University.

STATION LOCATIONS

The locations of all the areas where seismic-refraction work was done on MID-PACIFIC and CAPRICORN expeditions are shown in Figure 1. Latitudes and longitudes of the approximate centers of the working areas are tabulated in Tables 1 and 2. MID-PACIFIC stations are prefixed with the letter M, and CAPRICORN stations with the letter C. Four areas, M8, M16, C4, and C17 represent shallow-water studies in the vicinities of the Island of Hawaii, Kwajalein Atoll, Alexa Bank, and Nukuhiva Island, respectively. They are not included in the present study. Two areas, M15 and C1, were the sites of extensive refraction observations in both shallow and deep water at Bikini and Eniwetok

TABLE 2.—CAPRICORN STATIONS

Station	Date	Latitude	Longitude	Sea depth in m
C1	20 Nov. 1952	11° 20′ N.	161° 35′ E.	3862
C2	2 Dec.	00° 47′ N.	169° 11′ E.	4414
C3	6 "	9° 01′ S.	174° 56′ E.	5171
C4	9 "	11° 34′ S.	175° 24′ E.	31
C5	10 "	13° 36′ S.	174° 56′ E.	2463
C6	18 "	18° 59′ S.	177° 34′ E.	2617
C7	20 "	21° 55′ S.	178° 33′ E.	4134
C8	28 "	19° 37′ S.	174° 54′ W.	1740
C9	30 "	19° 57′ S.	172° 33′ W.	6099
C10	1 Jan. 1953	20° 30′ S.	173° 20′ W.	9176
C11	2 "	20° 02′ S.	173° 07′ W.	8860
C12	10 "	16° 16′ S.	168° 31′ W.	5137
C13	13 "	17° 28′ S.	160° 59′ W.	4850
C14	14 "	17° 32′ S.	158° 40′ W.	5212
C15	22 "	12° 47′ S.	143° 33′ W.	4624
C16	23 "	11° 20′ S.	142° 25′ W.	4590
C17	25 "	8° 57′ S.	140° 01′ W.	77
C18	28 "	10° 45′ S.	133° 35′ W.	4188
C19	30 "	11° 46′ S.	128° 57′ W.	4073
C20	2 Feb.	14° 16′ S.	119° 10′ W.	3575
C21	4 "	14° 59′ S.	113° 46′ W.	2915
C22	5 "	14° 47′ S.	112° 12′ W.	3155
C23	8 "	7° 20′ S.	118° 40′ W.	4330
C24	11 "	00° 11′ N.	123° 26′ W.	4463
C25	13 "	5° 47′ N.	123° 59′ W.	4264
C26	16 "	14° 58′ N.	124° 12′ W.	4393

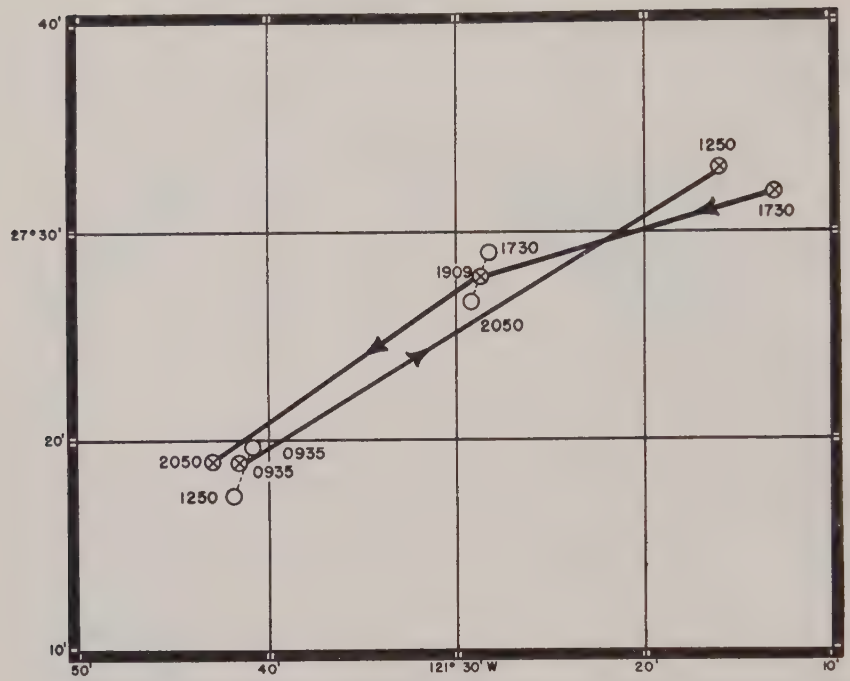
40'
27° 30'
20'
10'
50'
40'
121° 30' W
20'
10'
1250
1730
1730
1909
2050
0935
2050
0935
1250

FIGURE 2.—PLAN OF OPERATIONS OF THE REVERSED SEISMIC PROFILE AT STATION M1, JULY 29, 1950

○- - - -○ Drift track of receiving ship
⊗——⊗ Track of firing ship

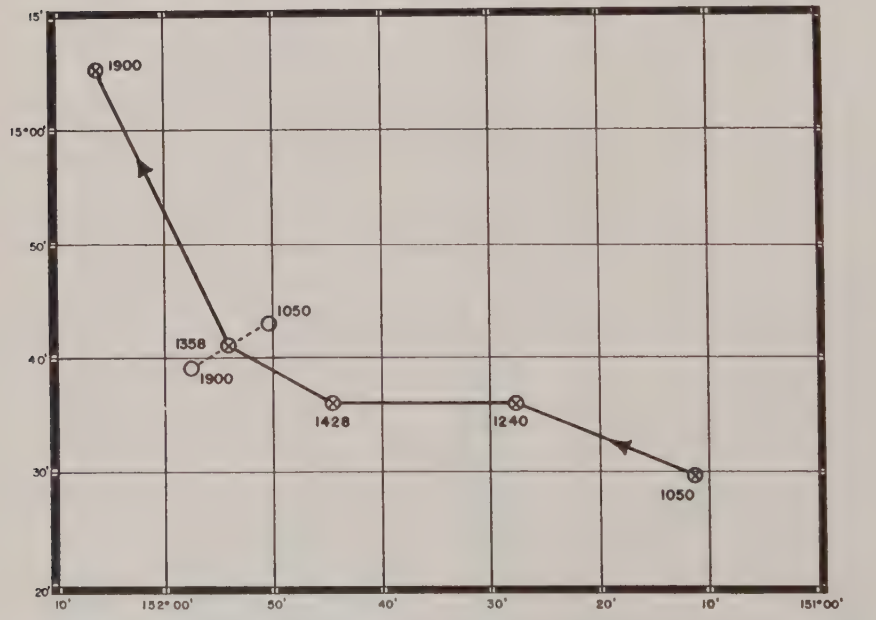
15'
15°00'
50'
40'
30'
20'
10'
152° 00'
50'
40'
30'
20'
10'
151°00'
1900
1050
1358
1900
1428
1240
1050

L-43

FIGURE 3.—PLAN OF OPERATIONS OF SPLIT PROFILE AT STATION M7, AUGUST 19, 1950

○- - - -○ Drift track of receiving ship
⊗——⊗ Track of firing ship

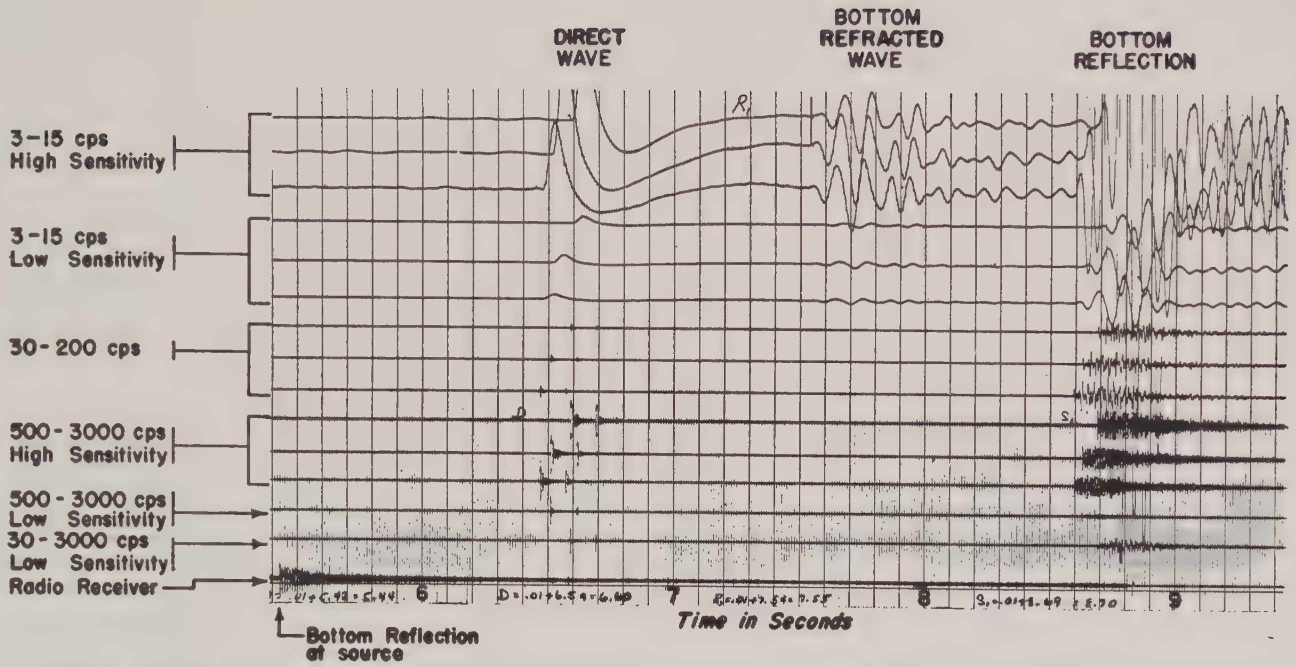

FIGURE 4.—SAMPLE OF A COMPLETE OSCILLOGRAM OF SEISMIC WAVES RECORDED AT SHORT RANGE ON THE MID-PACIFIC EXPEDITION
Length of three-hydrophone spread—600 feet
Charge—3½ pounds TNT
Shot distance—5.5 nautical miles
Ocean depth—2255 fathoms

atolls. The complete results from these two areas are reported elsewhere (Raitt, 1954; in press). In the present study, only the deep-water data observed near Bikini and Eniwetok are included. Stations C8, C9, C10, and C11 are in the Tonga area and are included in a separate study of the Tonga Trench (Raitt, Fisher, and Mason, 1955). Two other stations were near islands: M9, near the Island of Hawaii, and C6 near Viti Levu in the Fiji Islands.

The remaining 30 of the 42 stations were distributed along the course of the expeditions in positions away from islands or island groups. Efforts were made to locate these positions in flat areas in order to free the measurements from the perturbations of rough topography. These efforts, however, were rarely successful, owing to the rough bottom generally found in the Pacific and to the paucity of prior soundings in the regions explored.

OPERATIONS

At all stations two ships were used. On the MID-PACIFIC expedition, USS EPCE(R) 857 served as firing ship throughout the operation, and R/V HORIZON was the receiving ship. On the CAPRICORN expedition, R/V HORIZON was the firing ship, and R/V SPENCER F. BAIRD was the receiving ship.

Two types of seismic runs were recorded, reversed profiles (Fig. 2) and split profiles (Fig. 3). Open circles and dashed lines indicate the line of drift of the receiving ship R/V HORIZON; the crossed circles and solid lines show the lines run by the shooting ship, USS EPCE(R) 857, at a speed of 9 knots. The operation represents an attempt to record a true reversed profile in which charges are fired along a single line through two receiving positions. Failure to achieve true reversal is caused partly by wind- and current-induced drift of the receiving and sending ships and partly by poor navigational control which depends primarily on star fixes made several hours before or several hours after the operation.

Where receiving ships can be anchored and good position control can be achieved, reversed profiles are used to good advantage (Raitt, 1954). In the deep sea, however, the firing lines rarely coincide and much of the value of the reversal is lost. It is nearly as accurate and gives greater coverage to record a split profile. Many more split profiles than reversed profiles were recorded in the study here presented.

The sources of the seismic waves were TNT bombs made up from demolition charges, in sizes commonly between half a pound and 80 pounds. A few larger charges up to 450 pounds were fired. The charges were dropped while the firing ship was under way and were fired at a predetermined depth between 100 and 200 feet with slow-burning fuse cut to appropriate length.

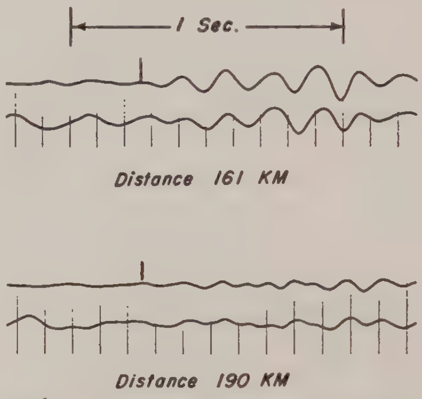

FIGURE 5.—SAMPLE OSCILLOGRAMS OF THE LOW-FREQUENCY SEISMIC-REFRACTED WAVES RECORDED AT LONG RANGE

The waves from the shots were received on pressure-sensitive hydrophones suspended from surface buoys at a depth of about 200 feet. They were recorded photographically on a multichannel oscillograph with several bands of frequencies for each hydrophone. The filters were chosen not only to enhance the refracted-wave record but also to aid in identifying the water-borne sound used to determine shot-hydrophone distances. Velocities for the latter purpose were read from Kuwahara's (1939) tables, using temperatures and salinities measured in the locality of the observations. Timing accuracy of the oscillograph was checked frequently by comparison with WWV time signals.

An example of the kind of record obtained at short range is shown in Figure 4. It was recorded during the MID-PACIFIC expedition, on which three hydrophones were used for most shots. On the CAPRICORN expedition, four hydrophones were used, but the filtering arrangements were similar.

As the range is increased, the bottom-re-

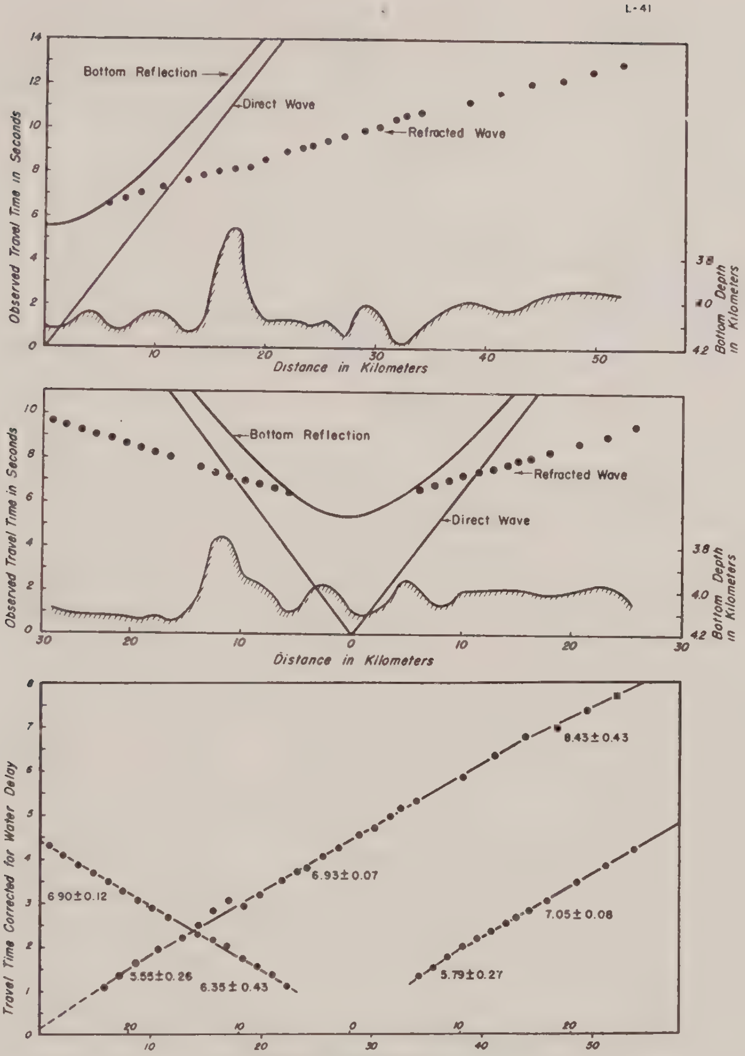

FIGURE 6.—TRAVEL-TIME PLOTS OF STATION M1

fracted sound waves become weak, and even if the shots are increased to the largest that can be conveniently thrown overside, the beginnings of many are hard to identify. Figure 5 illustrates the low-frequency traces of oscillograms of two shots of 80 pounds each at CAPRICORN station C12, recorded near the limit of detection of first arrivals.

TRAVEL-TIME DATA

In general, the records show an almost continuous succession of waves for many seconds after the first arrival. Some later arrivals can be traced from shot to shot. Those most consistently observed are multiply refracted waves arriving at intervals roughly equal to the intercept time. These waves have also been observed in the Atlantic Ocean (Ewing *et al.*, 1954). At some stations, at long range, refracted crustal waves are observed as strong second arrivals after a weak mantle wave. Less frequently, a mantle wave is observed following closely after the crust wave at ranges shorter than the crossover. At a few stations, waves appear to travel as shear waves in the crust beneath the sediments (Ewing *et al.*, 1954).

In the present study, only first arrivals have been utilized. Examples of the observed travel-time data are shown in Figures 6 to 12. M1 and M7 are the stations for which the plans of operation are shown in Figures 2 and 3. The remainder are split profiles roughly similar to Figure 3. These examples illustrate the distances of the runs, the number of shots fired, and the variety of forms of the travel-time plots. They also show the roughness of bottom in many places and the variety of topographic forms, as well as the range of bottom depths.

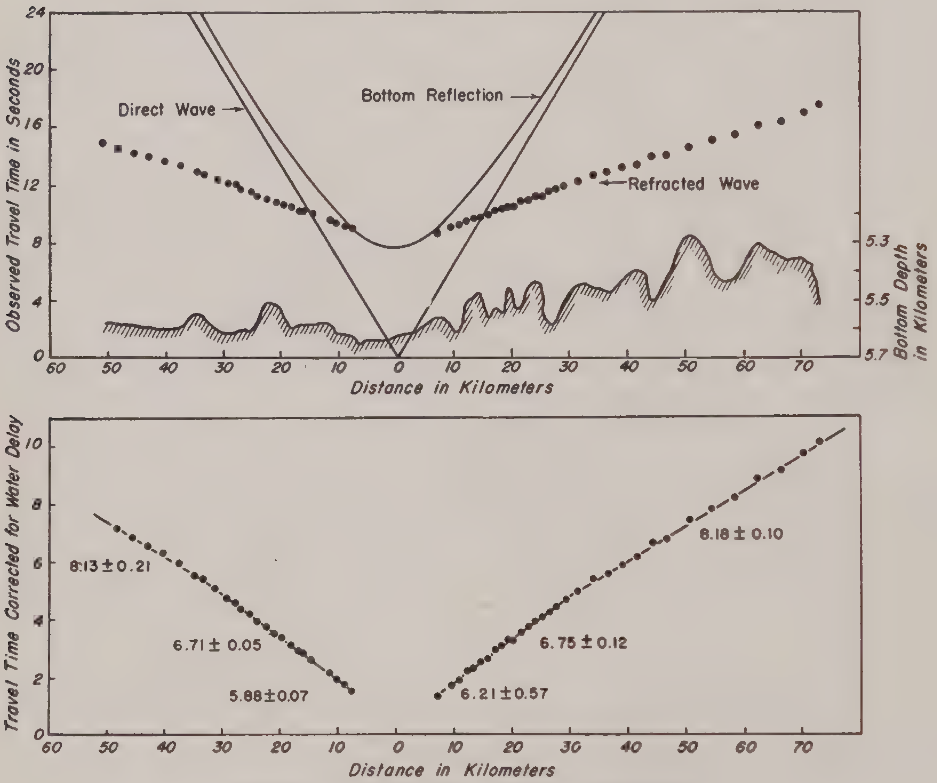

FIGURE 7.—TRAVEL-TIME PLOTS OF STATION M7

Because the bottom depths vary from station to station as well as along the lines of the profiles, differences between travel-time plots in different areas are usually caused more by differences in sea depth and topography than by differences in crustal structure.

To facilitate the comparison of profiles taken in different areas, the first step in the data analysis is to correct each refracted-wave travel time for water delay at source and receiver. In the Figures, the travel times corrected for water delay are shown in the lower graphs. These corrected points give approximately the travel times that would have been observed if the shots and receivers had been placed on the bottom directly under their positions. Velocities are determined from the corrected plots.

VELOCITIES

In the examples in Figures 6 to 12, most of the travel time data can be represented by three linear segments with velocities (in km/sec.) determined by least squares. The standard errors of the least-square determination are indicated.

Except in Figure 10, the maximum apparent velocities of all examples are more than 8 km/sec.; the examples in these Figures are representative of nearly all the deep-water stations. In some, the segment indicating 8 km/sec. velocity was not observed, because the profile was short, the noise level was high, or the waves were too weak. In others, the short segment of lower velocity at the shortest shot distances was not observed.

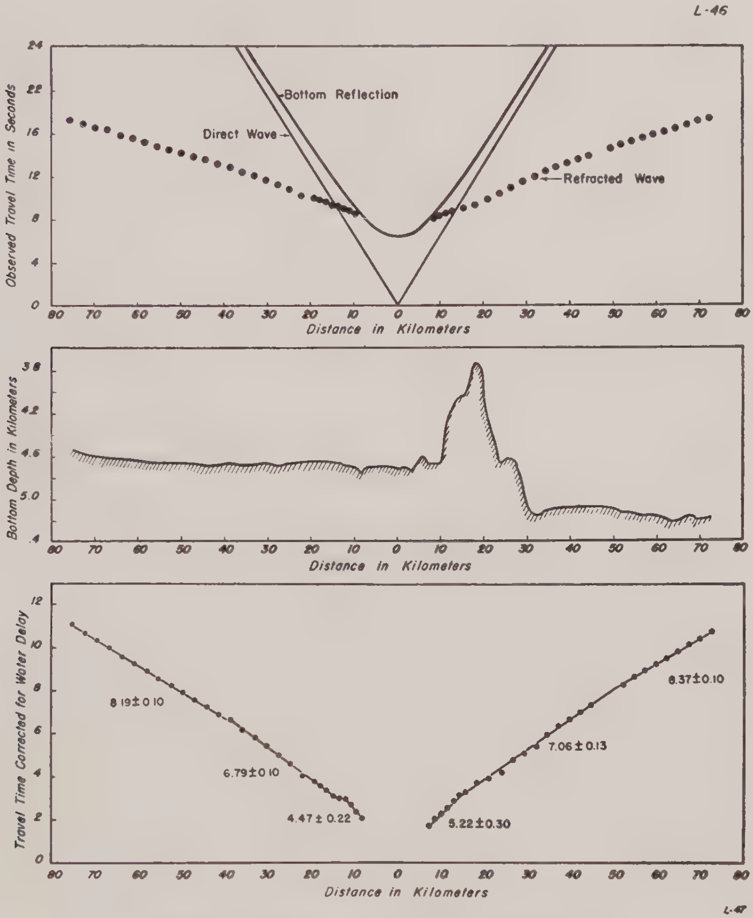

Figure 8.—Travel-Time Plots of Station M10

At each station, the velocities were determined from the average of the slopes of corresponding segments of the travel-time distance plots. The result is the harmonic mean of the apparent velocities. At the stations where split profiles were recorded the average was taken of the two halves of the profile. At others, such as the reversed profile of Figure 2, three or four segments were included in some of the averages.

At nearly all stations, the short-range segment had a finite intercept at zero range, indicating that this segment, whose velocity is about 5 km/sec., represents a layer beneath the ocean floor covered with a layer of sediment. The velocity of the sediment was not determined from the refraction studies, because waves propagated through the sediment in deep water were not observed as first arrivals. Some unpublished estimates of velocities determined from reflection profiles give values of

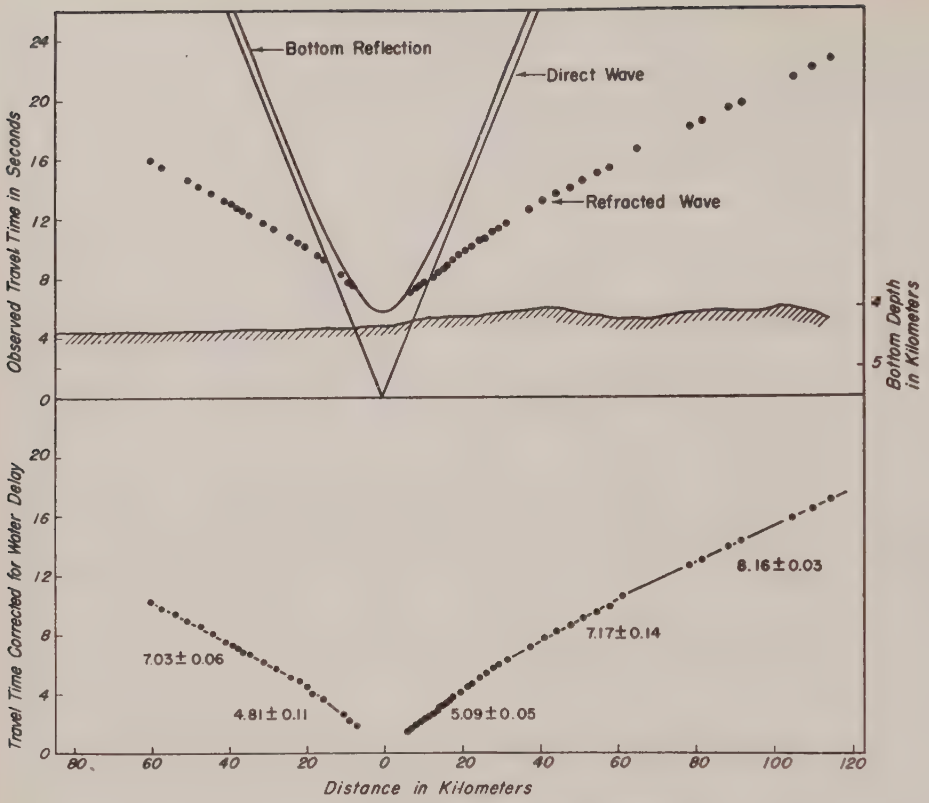

Figure 9.—Travel-Time Plots of Station C2

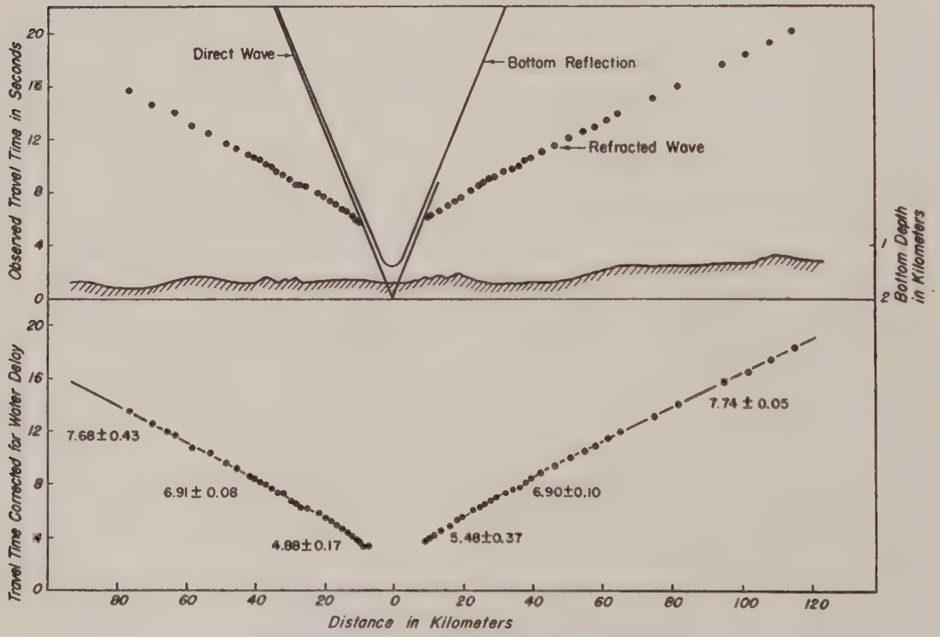

Figure 10.—Travel-Time Plots of Station C8

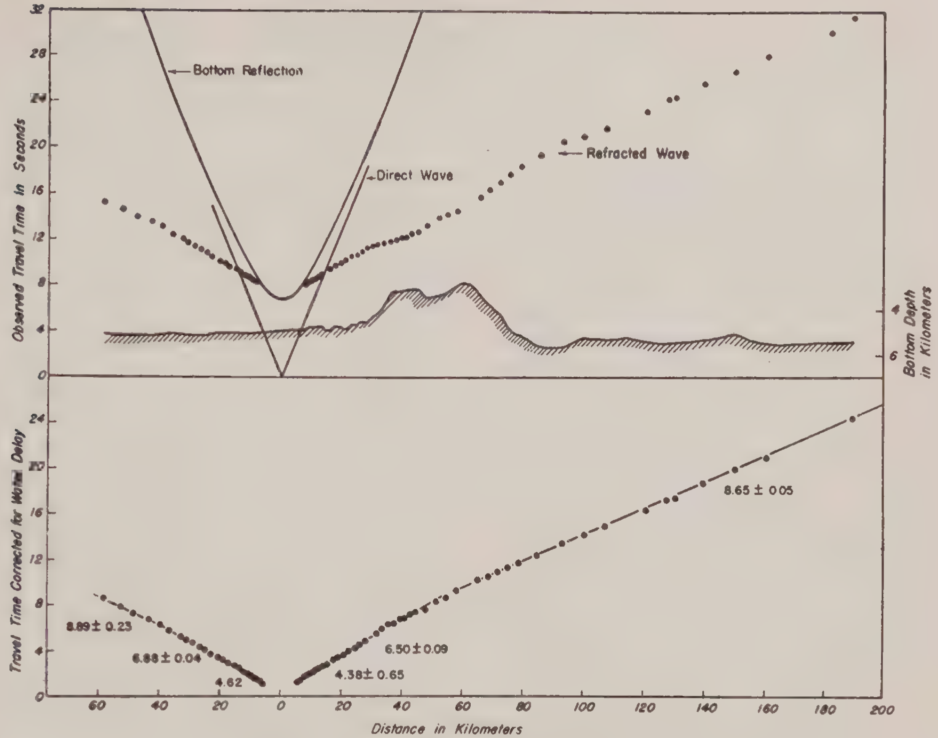

FIGURE 11.—TRAVEL-TIME PLOTS OF STATION C12

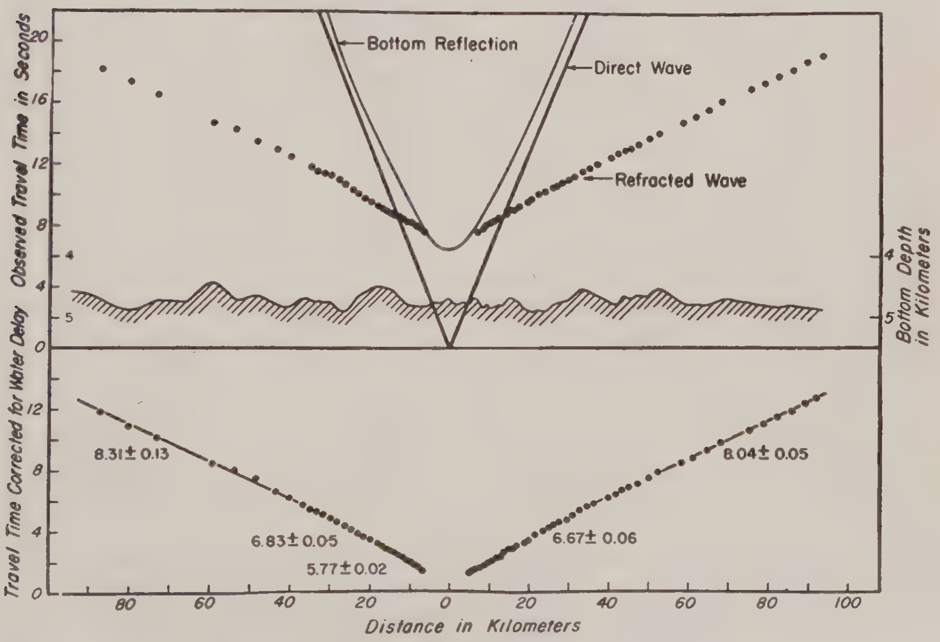

FIGURE 12.—TRAVEL-TIME PLOTS OF STATION C13

Table 3.—Mid-Pacific Velocities

Station	Second layer km/sec.	Third layer km/sec.	Fourth layer km/sec.
M1	5.88 ± 0.23	6.96 ± 0.08	8.41 ± 0.43
M2	5.97 ± 0.25	6.88 ± 0.09	8.05 ± 0.12
M3	....	6.70 ± 0.10	....
M4	5.76 ± 0.37	6.74 ± 0.10	....
M5	6.32 ± 0.20	6.79 ± 0.05	....
M6	....	6.58 ± 0.15	8.24 ± 0.12
M7	6.04 ± 0.29	6.73 ± 0.07	8.15 ± 0.12
M9	4.26 ± 0.44	6.57 ± 0.20	7.92 ± 0.12
M10	4.81 ± 0.37	6.92 ± 0.13	8.28 ± 0.09
M11	4.86 ± 0.27	7.02 ± 0.15	....
M12	4.92 ± 0.22	6.63 ± 0.06	....
M13	6.24 ± 0.10	6.83 ± 0.06	....
M14	4.39 ± 0.23	6.92 ± 0.10	8.42 ± 0.12
M15	5.16 ± 0.16	6.56 ± 0.15	8.28 ± 0.21
Mean	5.38	6.77	8.22
Standard deviation	0.73	0.15	0.17

Table 4.—Capricorn Velocities

Station	Second layer km/sec.	Third layer km/sec.	Fourth layer km/sec.
C1	4.15 ± 0.06 5.59 ± 0.08†	6.90 ± 0.10	8.09 ± 0.23
C2	4.98 ± 0.11	7.10 ± 0.08	8.16 ± 0.03
C3	5.73 ± 0.09	6.72 ± 0.40	8.14 ± 0.12
C5	4.55 ± 0.76*	6.43 ± 0.30	8.14 ± 0.06
C6	5.37 ± 0.33	6.55 ± 0.32	8.51 ± 0.43*
C7	5.00 ± 0.57	7.04 ± 0.04	8.42 ± 0.29
C8	5.17 ± 0.29	6.92 ± 0.08	7.71 ± 0.21*
C9	3.93*	6.42 ± 0.06	8.25 ± 0.12
C10, 11	5.31 ± 0.35	6.69 ± 0.33	8.29 ± 0.10
C12	4.49 ± 0.65*	6.68 ± 0.19	8.77 ± 0.12
C13	5.77	6.75 ± 0.08	8.17 ± 0.13
C14	4.64 ± 0.28*	6.45 ± 0.13	8.21 ± 0.11
C15	4.48 ± 0.10	6.81 ± 0.26	8.43 ± 0.28
C16	5.51 ± 0.36	6.69 ± 0.20	8.34 ± 0.09
C18	5.04 ± 0.24	6.91 ± 0.06	8.14 ± 0.20
C19	5.22 ± 0.26	6.69 ± 0.10	8.00 ± 0.05
C20	4.35 ± 0.12*	6.48 ± 0.17	8.12 ± 0.07
C21	4.82 ± 0.27	6.88 ± 0.07	7.66 ± 0.04*
C22	5.11 ± 0.54	7.03 ± 0.09	7.36 ± 0.22*
C23	6.02 ± 0.15	6.90 ± 0.14	8.30 ± 0.28
C24	4.92 ± 0.86	6.84 ± 0.16	8.21 ± 0.10
C25	5.78 ± 0.25	6.90 ± 0.03	8.16 ± 0.06
C26	4.52 ± 0.21	6.78 ± 0.08	8.46 ± 0.20
Mean	5.09	6.76	8.25
Standard deviation	0.52	0.20	0.18

* Omitted from averages and standard deviations.

† At Eniwetok two layers were observed whose velocities were comparable to the second layer.

about 2 to 2½ km/sec. for the average velocity to the base of the sediment. The present average of these determinations is 2.15 km/sec., a value assumed for all the stations in this paper. This value will be compared with the values of 1.5 to 2.3 km/sec. observed in the western Atlantic Ocean (Ewing, Sutton, and Officer, 1954; Katz and Ewing, 1956), and the value of 2.1 km/sec. obtained in the eastern Atlantic (Hill and Laughton, 1954) and in the Pacific (J. C. Swallow, 1954, Cambridge Univ., Ph.D. Thesis). It is unlikely that the assumed value of 2.15 km/sec. will differ from the average vertical velocity of the unconsolidated sediment by more than 20 per cent. The resultant error of sediment thickness is less than 100 m in most cases.

The mean velocities and estimated standard errors for each station are tabulated in Tables 3 and 4. The standard errors were estimated from the differences of the slopes entering into the mean-velocity determination and are generally larger than the standard errors calculated from the residuals of the least-square determinations of slope. In estimating the standard errors of the velocities, it was assumed that the individual determinations making up the station average were statistically independent. A systematic trend of structure, such as a linear thickening or constant slope of interfaces extending over the area, would cause the estimated error to be too large.

For all layers, the range of variation of velocities is greater than the estimated standard errors of measurement. In the third and fourth layers, this effect is large enough to be statistically significant but not large enough to prove that the effect is real and not due to random errors of measurement of velocity. In the second layer, however, the variation is so large that there is little doubt that it is real, in spite of the large error in velocity measurement.

The variation in the second layer is particularly evident in the MID-PACIFIC data where there are systematic regional effects. Stations M1 to M7 east of Hawaii have a higher velocity of the second layer than those in the region of the Hawaiian Islands, the Mid-Pacific Mountains (Dietz *et al.*, 1954), and the Marshall Islands to the west. The single exception to this separation is station M13, which lies between the Mid-Pacific Mountains and the Marshall Islands and appears to resemble the eastern Pacific in velocity structure.

There is no simple geographical division of the CAPRICORN velocities for the second layer. However, the two highest values of second-layer velocity obtained on the CAPRICORN expedition are at stations C23 and C25, which are not far from the region of high velocity of the MID-PACIFIC expedition.

TABLE 5.—MID-PACIFIC LAYER THICKESSES

Station	First layer km	Second layer km	Third layer km	Total thickness km
M1	0.26	0.93	6.24	7.43
M2	0.17	1.42	4.31	5.90
M3*	0.31	0.70	....	....
M4	0.45	0.35	....	....
M5	0.57	1.16	....	....
M6*	0.20	0.72	4.42	5.35
M7	0.32	0.81	4.14	5.27
M9	0.24	2.27	4.70	7.22
M10	0.34	2.21	5.66	8.22
M11	0.42	2.18	....	....
M12	0.40	2.59	....	....
M13	0.62	1.57	....	....
M14	0.57	2.60	3.14	6.31
M15	1.07	1.90	5.69	8.66

* Velocity of 5.99 km/sec. assumed for second layer

LAYER THICKNESSES

Calculation of the velocity-depth structure from the observed travel times was based on a simplified model of layers of constant velocity as determined from the travel-time plots. Methods have been summarized in several geophysical textbooks (Nettleton, 1940; Dix, 1952; Dobrin, 1952). This model represents a simplification of the actual situation, where velocities probably vary continuously with depth and possibly with horizontal distance, but it is a rough approximation and provides a basis for comparison of results.

No attempt was made to work out horizontal changes in structure within the areas of observation at each station. The purpose of the present study is to describe the Pacific Basin as an entity, and only average layer thicknesses were determined.

The results of the layer-thickness calculations are presented in Tables 5 and 6. All thicknesses of the first layer, the unconsolidated sediment, were calculated with an assumed velocity of 2.15 km/sec. In the following cases where the velocity data were poor or missing, or for special reasons, such as rough topography, records were probably unreliable, average velocities from other stations were used to calculate layer thicknesses. In the MID-PACIFIC results, a velocity of 5.99 km/sec. was assumed for the second layer at stations M3 and M6. This velocity is the average for this layer for the other stations in the eastern portion of this cruise, stations M1, M2, M4, M5, and M7. At stations C5, C9, C12, C14, and C20, a velocity of 5.09 km/sec. was assumed for the second layer. This velocity is the average for this layer at the other CAPRICORN stations. Otherwise, the velocities used in the layer calculations are those tabulated in Tables 3 and 4.

TABLE 6.—CAPRICORN LAYER THICKNESSES

Station	First layer km	Second layer km	Third layer km	Total thickness km
C1*	0.95	2.41 3.43	5.76	12.55
C2	0.20	5.40	7.41	13.01
C3	0.31	2.10	4.23	6.64
C5†	0.42	0.95	4.28	5.64
C6	0.90	2.47	9.16	12.53
C7	1.14	2.02	7.41	10.57
C8	2.12	2.80	....	.....
C9†	0.41	0.45	5.27	6.14
C10, 11†	NIL	2.90	8.26	11.16
C12	0.16	1.51	9.58	11.25
C13	0.35	0.86	4.90	6.11
C14†	0.07	1.16	4.62	5.86
C15	0.24	1.54	5.37	7.15
C16	0.24	1.31	5.90	7.46
C18	0.20	1.59	4.57	6.35
C19	0.22	0.81	4.60	5.64
C20†	0.27	0.73	4.24	5.24
C21	0.28	1.06	....	.....
C22	0.22	1.16	....	.....
C23	0.34	1.20	3.31	4.85
C24	0.38	1.18	4.03	5.59
C25	0.53	0.66	4.19	5.38
C26	0.03	1.26	5.12	6.41

* At Eniwetok the two layers were included in the velocity range of the second layer.

† Velocity of 5.09 km/sec. assumed for second layer

At stations C8, C21, and C22 the maximum velocities of 7.71, 7.66, and 7.36 km/sec. were not considered large enough to prove that penetration to the base of the crust had been achieved. Consequently, estimates of third-layer thickness are not given for these stations.

At the two stations, M3 and M6, where the short-range refraction data were too poor to establish the existence of the second layer, intercepts were calculated by assuming that the first arrivals at the shortest range had travelled through the second layer at the assumed velocity of 5.99 km/sec. In view of the position of M3 and M6 within the relatively homogeneous group M1 to M7, this procedure is more realistic than assuming that the second layer does not exist.

NATURE OF THE LAYERS

FIRST LAYER: The only layer which can be positively identified everywhere by sampling and observation is the upper layer, the blanket of unconsolidated sediment which covers most of the sea floor. The value of 2.15 km/sec. estimated for its average velocity indicates a substantial increase with depth in the sediment, as samples from the sea floor have shown values differing little from that of water, 1.5 km/sec. (Shumway, 1956; Laughton, 1954; Officer, 1955).

SECOND LAYER: The large range of velocities of the second layer indicates that it may consist of a variety of materials. At Eniwetok (station C1) samples of volcanic rock were taken on the atoll with a core drill at a depth of about 1300 m (Ladd *et al.*, 1953). Its velocity as measured by refraction (Raitt, in press) was near the lower end of the range of the second-layer values, about 4 km/sec.

The higher values of the second-layer velocities, most consistently observed at the MID-PACIFIC stations east of Hawaii, are in the 6 km/sec. range, comparable to sialic or granitic velocities characteristic of continental areas.

From these observations it could be concluded that certain areas, such as the region between Hawaii and the North American continent to the east, have a thin layer of sial about 1 km thick lying between the unconsolidated sediment and the principal crustal layer (the third layer). In other regions, such as the Mid-Pacific Mountains and the Marshall Islands, the layer between the sediments and the main crust could be largely volcanic and about 2 km thick.

These deductions are speculative. Many other types of rocks, such as limestones, schists, chert, and other forms of consolidated sediment could have the velocities observed in the second layer.

THIRD LAYER: The third layer is the principal one of the Pacific oceanic crust. It forms the most conspicuous segment within the inner 60 km of the travel-time plots and it is observed at all the Pacific stations west of the continental slope. If a similar layer has widespread occurrence beneath the continents, it is buried under a thick layer of material of lower velocity and could be concealed by earlier arrivals through the upper layers or through the mantle.

The layer is not known to outcrop anywhere in the Pacific and it has not been directly identified. Its velocity is intermediate between that of granite and that of dunite, and it is probably an intermediate type, more basic than granite, less basic than dunite. It is often called the simatic or "basaltic" layer. In crystalline structure, it would probably be similar to gabbro, as it would be unlikely to have the fine-grained structure of basalts.

The variation of its velocity, if real, indicates that it is not everywhere uniform. However, there is no systematic difference between the average values obtained on the MID-PACIFIC and CAPRICORN expeditions. Hence, the variations are localized, and over large areas the velocity seems to be uniform.

FOURTH LAYER: At most stations, the velocity of the outermost segments of the travel-time plots reached a value of about 8 km/sec. or more, believed to be characteristic of the upper mantle immediately below the Mohorovičić discontinuity. At stations C8, C21, and C22, fourth-layer velocities were 7.71, 7.66, and 7.36 km/sec. respectively. These were believed to be too low to be characteristic of the base of the crust and were not used in determining the fourth-layer average velocities or the thicknesses of the third layer. Of the velocities considered indicative of paths in the mantle, the lowest was 7.92 km/sec. at M9.

Excluding the three anomalous values, the averages of the fourth-layer velocities were 8.22 km/sec. for the MID-PACIFIC stations and 8.25 km/sec. for the CAPRICORN stations. These values are close to the upper-mantle velocities observed in continental areas from blasts and rock bursts (Gutenberg, 1955). It is therefore reasonable to assume by analogy with continental results that the fourth layer, except for the anomalous stations C8, C21, and C22, underlies the oceanic crust. The variability of its velocity, if real, indicates that it is not homogeneous. However, as in the third layer, there is no significant difference in the averages of the MID-PACIFIC and CAPRICORN velocities, showing that over large areas the mantle is uniform.

CRUSTAL THICKNESS

The crust consists of the material above the mantle. Its thickness is obtained by adding the thicknesses of the first three layers. These thicknesses are tabulated in the last columns of Tables 5 and 6.

Only stations at which a velocity of at least 7.9 km/sec. was reached were used in this crustal-thickness determination. The three anomalous stations, C8, C21, and C22 were not used for this determination because they are probably too low to represent the base of the crust, and the crustal thickness was not estimated for these stations. All three are in anomalous positions with respect to the true Pacific Basin. C8 is in the Tonga Islands, and C21 and C22 are on the Albatross Plateau. These elevated regions show an abnormally low velocity beneath the third layer rather than an increase in depth of the fourth layer. This indicates that isostatic compensation is not accomplished in these areas by a simple increase in the thickness of the first three layers. The lower velocity at stations C21 and C22 may be associated with an effect observed by Oliver, Ewing, and Press (1955) who found that surface waves crossing this region had lower velocities than generally observed in the Pacific Basin.

In Figure 13, all the crustal thicknesses are plotted as a function of the elevation of the sea floor with respect to sea level. A few representative values of continental crustal thicknesses

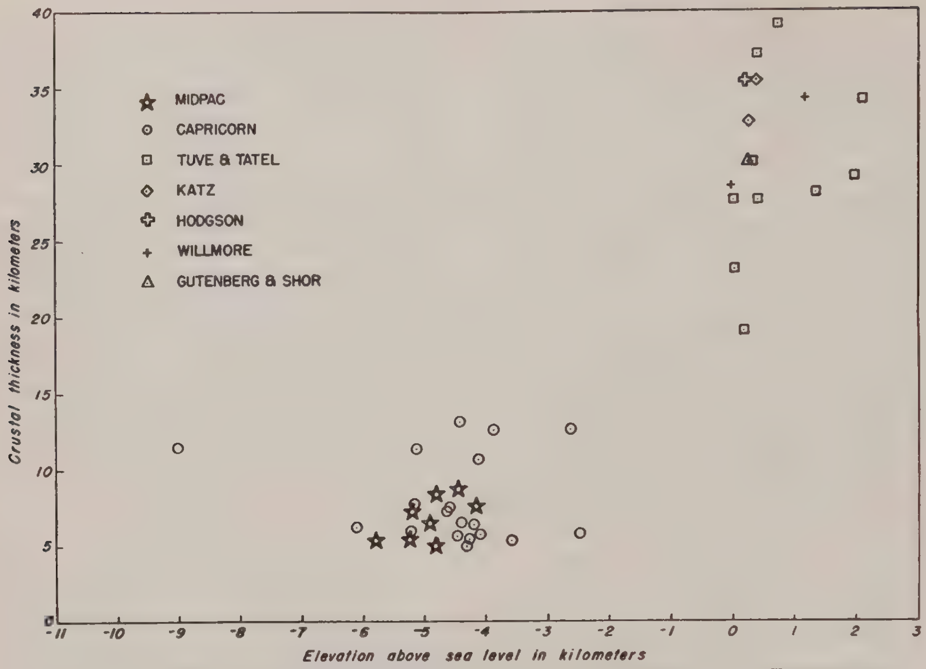

FIGURE 13.—CRUSTAL THICKNESS OF THE CENTRAL EQUATORIAL PACIFIC AS A FUNCTION OF SEA-FLOOR ELEVATION

Some continental determinations are shown for comparison.

determined by blast and rock-burst observations (Tatel and Tuve, 1955; Katz, 1953; Hodgson, 1953; Willmore, 1949; Willmore *et al* 1952; Gutenberg, 1952; Shor, 1955) are also plotted.

Although there is a systematic difference between oceanic and continental crust, there is no systematic dependence on elevation within the continental region or within the Pacific oceanic region, an observation which has been noted for the continental areas by Tatel and Tuve (1955).

The oceanic measurements cluster into two groups, with thicknesses greater or less than 10 km. The first group consists of stations C1, C2, C6, C7, C10, C11, and C12. All these stations are near the western border of the region studied and are probably anomalous with respect to the Pacific Basin proper. The remaining 22 stations are closely grouped, and their mean thickness is 6.31 km, with a standard deviation of 1.01 km.

REFERENCES CITED

Dietz, R. S., Menard, H. W., and Hamilton, E. L., 1954, Echograms of the Mid-Pacific expedition: Deep-Sea Research, v. 1, p. 258–272

Dix, C. H., 1952, Seismic prospecting for oil: N. Y., Harper Brothers, 414 p.

Dobrin, Milton B., 1952, Introduction to geophysical prospecting: N. Y., McGraw-Hill Book Co., 435 p.

Ewing, M., Sutton, G. H., and Officer, C. B., Jr., 1954, Seismic refraction measurements in the Atlantic Ocean, Part VI: Typical deep stations, North America Basin: Seismol. Soc. America Bull., v. 42, p. 21–38

Gutenberg, B., 1952, Waves from blasts recorded in southern California: Am. Geophys. Union Trans., v. 33, p. 427–431

Hill, M. N., and Laughton, A. S., 1954, Seismic observations in the eastern Atlantic, 1952: Royal Soc. London Proc., ser. A, v. 222, p. 348–356

Hodgson, J. H., 1953, A seismic survey in the Canadian Shield, I, II: Ottawa, Dominion Observatory Pubs., v. 16, p. 113–163, 169–181

Katz, S., 1953, Seismic study of crustal structure in Pennsylvania and New York: Lamont Geol. Observatory Tech. Rept. 32, 23 p.

Katz, S., and Ewing, M., 1956, Seismic-refraction measurements in the Atlantic Ocean. Part VII: Geol. Soc. America Bull., v. 67, p. 475–510

Kuwahara, S., 1939, Velocity of sound in sea water and calculation of the velocity for use in sonic sounding: Hydrog. Rev., v. 16, p. 127–140

Ladd, H. S., Ingerson, E., Townsend, R. C., Russell, M., and Stephenson, H. K., 1953, Drilling on Eniwetok Atoll, Marshall Islands: Am. Assoc. Petroleum Geologists Bull., v. 37, p. 2257–2280

Laughton, A. S., 1954, Laboratory measurements of

seismic velocities in ocean sediments: Royal Soc. London Proc., ser. A., v. 222, p. 336–341
Nettleton, L. L., 1940, Geophysical prospecting for oil: N. Y., McGraw-Hill Book Co., 444 p.
Officer, C. B., Jr., 1955, A deep-sea reflection profile: Geophysics, v. 20, p. 270–282
Oliver, J., Ewing, M., and Press, F., 1955, Crustal structure and surface-wave dispersion: Geol. Soc. America Bull., v. 66, p. 913–946
Raitt, R. W., 1954, Seismic refraction studies of Bikini and Kwajalein atolls and Sylvania guyot: U. S. Geol. Survey Prof. Paper 260-K, 21 p.
—— In press, Subsurface structure of Eniwetok Atoll from seismic refraction observations: U. S. Geol. Survey Prof. Paper 260-S
Raitt, R. W., Fisher, R. L., and Mason, R. G., 1955, Tonga Trench, p. 237–254 *in* Poldervaart, A. (Editor), Crust of the earth: Geol. Soc. America Special Paper 62, 762 p.
Revelle, R. R., 1954, The earth beneath the sea, p. 306–329 *in* Modern physics for engineers: N. Y., McGraw-Hill Book Co., 499 p.
Shor, G. G., Jr., 1955, Deep reflections from southern California blasts: Am. Geophys. Union Trans., v. 36, p. 133–138
Shumway, G. A., Jr., 1956, Resonance chamber sound velocity measurements: Geophysics, v. 21, p. 305–319
Tatel, H. E., and Tuve, M. A., 1955, Seismic exploration of a continental crust, p. 35–50 *in* Poldervaart, A. (Editor), Crust of the earth: Geol. Soc. America Special Paper 62, 762 p.
Willmore, P. L., 1949, Seismic experiments on the north German explosions, 1946 to 1947: Philos. Soc. London Trans., ser. A., v. 242, p. 123–151
Willmore, P. L., Hales, A. L., and Gane, P. G., 1952, A seismic investigation of crustal structure in the western Transvaal: Seismol. Soc. America Bull., v. 42, p. 53–80

Scripps Institution of Oceanography, University of California, La Jolla, California

Manuscript Received by the Secretary of the Society, October 31, 1955

Scripps Institution of Oceanography Contribution, New Series, No. 883

Contract NONR 23305, Office of Naval Research

Contract NObsr-43356, NE 120221-5, Bureau of Ships

(849)

Vol. 37, No. 6 Transactions, American Geophysical Union December 1956

Reproduced by Permission

Large-Volume Water Samplers*

W. G. Van Dorn

Abstract—Two new sea-water samplers have been developed to collect water in larger volumes (one and 12 gal) than the conventional Nansen bottle. Both are constructed of plastic which is relatively inert chemically, are free-flushing, and can be either messenger- or bottom-actuated.

The one-gallon sampler—The one-gallon (four-liter) sampler is simply a clear 4.5-inch diameter plastic (Plexiglas) tube, 15 inches long, clamped to the hydrographic wire by a wing nut (Fig. 1). The tube is sealed at both ends by 'plumber's friends,' known to the trade as 'force cups,' held in place by an appropriate length of heavy elastic surgical tubing. The rubber tubing is secured to the force cup by a $\frac{1}{4}$-28 NF brass machine screw, whose head is inserted about $\frac{1}{2}$ inch into the tubing and held by a ligature of nylon thread. An 11/16-inch diameter brass washer is slipped over the bolt, which then passes through a hole made in the rubber diaphragm of the force cup and is held on the other side by a nut over a $1\frac{1}{4}$-inch diameter micarta washer. Tightening the nut upsets the rubber tubing to form a tight, non-metallic seal.

In the cocked (pre-tripped) position (Fig. 2), the cups are drawn around to the sides of the tube by stretching the elastic, and they are held there by short loops of stainless steel wire cable slipped over a trigger pin. During descent the open-ended tube offers virtually no restriction to the flow of water through it. When tripped by a messenger, the cups (and auxiliary messenger, as desired) are released and snap snugly into the ends of the tube to make a tight seal. After removal from the wire, the sampler can be hung from a rack and left as long as desired without fear of leakage, even with vigorous shaking.

Draining and venting are effected through short latex hoses equipped with pinchcocks, although plastic plugs or petcocks could as easily be installed. The transparent plastic body permits visual inspection of the contents and the liquid level remaining after partial emptying.

Since Plexiglas is a fairly poor conductor of heat, a thermometer within the tube will read within a degree or two of the *in situ* temperature of the sample if it reaches the surface without unusual delay. The capacity of this sampler can be increased simply by increasing the length of the tube, but at lengths of more than three feet (about three gallons) the internal hydrostatic pressure after venting is sufficient to break the lower seal and cause leakage when the sampler is out of water.

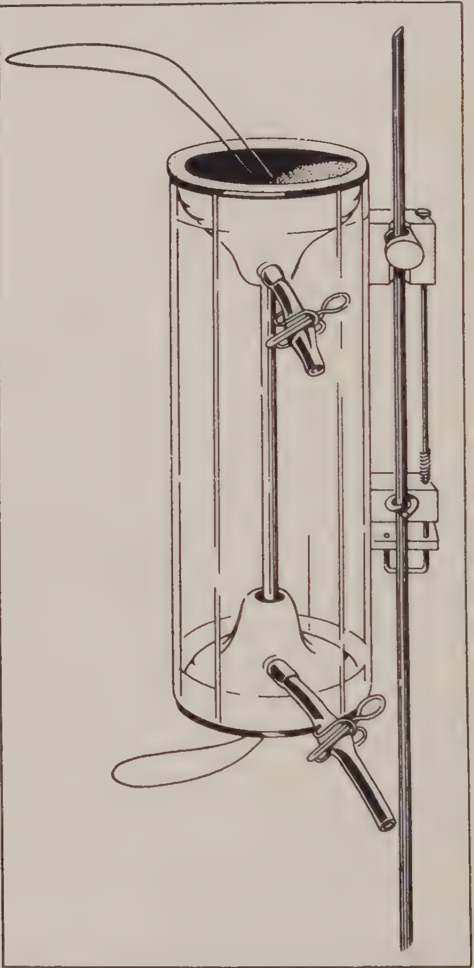

Fig. 1 – One-gallon water sampler, closed; the hydrographic wire first passes through the split ring on the lower support and then lies in a groove in the upper support and in a matching groove in the head of a bolt passing through this support; it is clamped firmly by tightening a wing-nut on the other end of the bolt

---

* Contribution from the Scripps Institution of Oceanography, New Series, No. 884

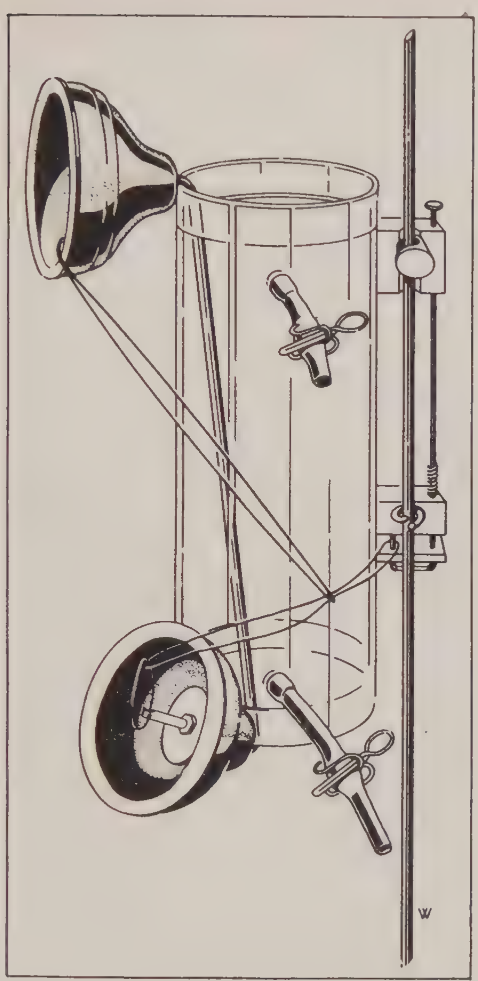

FIG. 2. – One-gallon water sampler in pre-tripped position; impact of the messenger on the upper end of the spring-loaded J-shaped trigger rod releases the stainless steel wire loops held by the short arm of the trigger rod in a V-shaped groove in the lower support

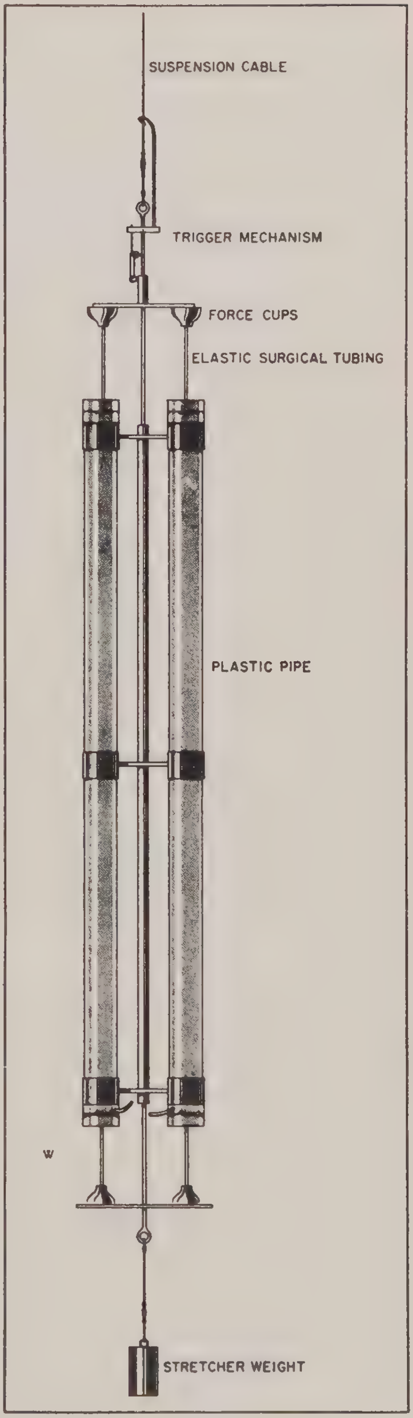
SUSPENSION CABLE
TRIGGER MECHANISM
FORCE CUPS
ELASTIC SURGICAL TUBING
PLASTIC PIPE
W
STRETCHER WEIGHT

FIG. 3

FIG. 3 – Twelve-gallon water sampler in cocked position; a link joined by an eye to the crosspiece holding the upper force cups passes over a pelican hook on the $\frac{3}{4}$-inch bar; the end of the pelican hook in turn is restrained by the left arm of the horizontal link of the trigger mechanism; when the messenger strikes the push rod looped around the suspension cable above the swivel, the right arm of the link is pushed downward, freeing the pelican hook, which in turn frees the link; the rod supporting the tube frame is not shown

Although designed for water sampling, these samplers have proved useful also as biological and sediment collecting devices. They can be lowered by hand or with light fishing tackle, since they weigh very little submerged.

The 12-gallon sampler—In order to provide large volume deep-water samples for carbon-14 analysis, a 12-gal (50-l) sampler was designed for, and used successfully on, the Scripps Institution's recent Eastropic Expedition. Eight samples were taken from depths as great as 3000 m and transferred anaerobically by nitrogen displacement on deck into suitable storage containers.

The deep sampler (Fig. 3) is hung on the end of the winch cable on which it is to be lowered, and a 100-lb stretcher weight is added below it. Swivels above and below the sampler permit rotation of the cable or weight independently. The sampler consists of two ten-foot lengths of five-inch Uscolite plastic pipe terminated in cemented couplings machined to receive the same plumber's force cups used on the one-gallon sampler. The twin pipes are clamped to a brass frame, which is free to slide on a $\frac{3}{4}$-inch diameter stainless steel bar. The bar has eyes at its ends so that it can be shackled to the cable and stretcher weight. Figure 3 shows the sampler in the open position. The lower pair of force cups is mounted on a crosspiece bolted to the center bar; the upper pair is similarly mounted but on a crosspiece which slides on the bar so that it can be drawn upward and latched to the trigger mechanism. As the crosspiece is drawn upward, a short rod picks up the tube frame about midway in its travel and lifts the tubes free of the lower cups so that they hang halfway between the upper and lower cups. In addition to gravity, closing tension is again provided by pre-stressed surgical rubber tubing between the respective pairs of cups. The trigger consists of a pelican hook that engages a link in the upper cup crosspiece and is retained by a latch. The hook is opened when a messenger strikes the push rod that bypasses the upper swivel and loops around the suspension wire. Upon release, tubes drop onto the lower cups, and the upper cups drop into the upper ends of the tubes. Alignment of the respective elements is insured by a guide slot in the tube frame and by adequate looseness or play in the cup mountings.

Experience with the 12-gal sampler indicates that an assembly of several short tubes would offer several advantages over the present design. A six-tube unit of the same capacity would reduce the over-all length from 15 to 9 ft, thus improving shipboard handling and stowage, as well as reducing the out-of-water hydrostatic pressure at the lower end by 70 pct. Pressure-actuated tripping devices might be used on the several tubes to permit sampling at a series of selected depths.

Acknowledgment—The author wishes especially to acknowledge the many helpful suggestions and technical assistance of C. S. Fleming, who constructed the prototype models of both samplers. This paper represents results of research carried out by the University of California under contract with the Office of Naval Research and the Bureau of Ships of the Navy Department.

Scripps Institution of Oceanography, La Jolla, California

(Communicated manuscript received April 4, 1956; open for formal discussion until May 1, 1957.)

(854)

Geol. Soc. America
p. 693–698

Memoir 67, 1957
Made in U. S. A.

Bacteria

CLAUDE E. ZOBELL

Microbiologist, University of California, Scripps Institution of Oceanography, La Jolla, California

Obtaining unequivocal evidence for the presence of bacteria or their remains in geological formations is attended by almost insurmountable difficulties. Many bacteria are so small they are barely within range of the resolving power of the best compound microscope, and, even when observed by the skilled microscopist, most bacteria appear as amorphous specks. The second big difficulty is preventing the bacterial contamination of the geological formations to be examined for the presence of fossil bacteria, because bacteria or their spores are almost ubiquitous. These difficulties have been overcome, however, by a few persevering people whose observations collectively, if not individually, have produced conclusive proof of the antiquity of bacteria and allied microorganisms.

Since most bacterial species are distinguished primarily by their physiological activities, fossil forms generally can be characterized only by their shape, size, and arrangement. This restricts the number of fossil forms that can be recognized as bacteria to those species with a distinctive shape or arrangement, such as streptococci or streptobacilli, for example, which appear as strings of spherical or rod-shaped cells of uniform size. In some instances the presence of fossil bacteria has been substantiated by pathological lesions persisting in the fossilized remains of plants or animals with which the bacteria were associated.

Besides the fragmentary reports on the occurrence of fossil bacteria in limestones, cherts, iron ores, oil shales, coal, bones, coprolites, and other materials dating back to the Cambrian period or earlier, there are a good many reports on the presence of living bacteria in peat deposits, petroliferous sediments, sulfur deposits, marine muds, and other sedimentary materials thousands of years old. The extent to which these bacteria have been physiologically active or buried in a state of suspended animation is problematical, but they do represent interesting forms of life of considerable antiquity. A few key references to such observations are included in this bibliography.

Also included are a few of the principal papers reviewing the literature on fossil fungi. While technically bacteria are classified as fission fungi, most of the papers dealing with fossil fungi are concerned almost exclusively with the higher fungi. Representatives of 39 families of higher fungi have been detected in various fossil rocks.

Whether the minute objects described as fossil bacteria by various investigators who have made meticulous microscopic examinations of ancient rocks are real or imaginary may be open to question in some cases, but the reports and illustrations of such workers as Moodie (1923), Renault (1895–1901), and Walcott (1915) should convince even the most skeptical student of the antiquity of bacteria. The electron microfossils delineated by the electron micrographs of Barton and Jones (1948) are also undoubtedly the remains of bacteria. The electron microscope and phase-contrast microscopes perfected in recent years offer new tools for the investigation of microfossils.

BARTON, H. M. (AND JONES, D. J.). Electron microfossils: Science, vol. 108, pp. 745–746, 1948.

Electron microscope revealed the presence of many rod-shaped and spherical objects believed by authors to be fossilized bacteria or spores of bacteria, fungi, and algae in samples of Oligocene formation from oil-well drillings 8,000 to 11,000 feet deep. Similar objects were also observed in samples from Cenozoic, Mesozoic, and Paleozoic formations.

BASTIN, E. S. 1. The problem of the natural reduction of sulphates: Bull. Amer. Assoc. Petrol. Geol., vol. 10, pp. 1270–1299, 1926.

Sulfate reducers recovered from 28 Illinois oil wells ranging in depth from 400 to 1,860 feet and in 15 California oil wells ranging in depth from 760 to 2,500 feet. 20 references.

2. (AND GREER, F. E.). Additional data on sulphate-reducing bacteria in soils and waters of Illinois oil fields: Bull. Amer. Assoc. Petrol. Geol., vol. 14, pp. 153–159, 1930.

Sulfate-reducing bacteria found in samples from six producing oil wells, five of the samples being from Bridgeport sand 900 to 1,000 feet deep and one being from McClosky sand at a depth of 1,850 feet.

BEGAK, D. A. Qualitative determination of bacteria in a highmoor peat: Pedology, vol. 21, pp. 64–75, 1926.

Bacteria present throughout peat profiles, direct microscopic procedures showing the presence of up to 715,000,000 per gram of moist peat.

BERGH, S. V. (Fossilized sulphur bacteria in aluminum schists at Kinnekulle, Sweden): Geol. Fören. Forh., vol. 50, pp. 413–418, 1928.

Fossil sulfur bacteria demonstrated in aluminum schists by photomicrographs giving magnifications ranging from 250 to 2,000 diameters. The schists consisted of claylike, sedimentary, bituminous rock composed of mica, quartz, feldspars, calcite, and pyrite.

BERRY, E. W. 1. Remarkable fossil fungi: Mycologia, vol. 8, pp. 73–79, 1916.

Fossil fungi found in virtually all geological

Reproduced, by permission, from Treatise on Marine Ecology and Paleoecology, vol.2, Geol.Soc.America, Memoir 67, 1957. pp.693-698.

horizons, the Carboniferous flora being best known. Three new species in Tertiary petrified wood described.

2. Pathological conditions among fossil plants: Chapter III in Paleopathology by R. L. Moodie, Univ. Ill. Press, Urbana, Ill., pp. 99–114, 1923.

Despite the difficulties of detecting fossil microbes, histological examination of fossil plants has produced evidence that parasitic and saprophytic fungi occurred as far back as terrestrial floras have been found, certainly as early as Carboniferous times. Spot fungi have been observed on fossil foliage from the Devonian to the present. 46 references.

Björling, P. R. (and Gissing, F. T.). Peat: Its use and manufacture: Charles Griffin & Co., London, pp. 173, 1907.

Anaerobic bacteria, molds, yeasts, and higher fungi are the chief agents of decomposition of organic matter in peat deposits. They may be preserved by acids formed by bacteria. Distribution and origin of peat.

Cayeaux, L. Existence de bactéries dans les roches sédimentaires anciennes, sutures que les phosphates: Soc. Géol. France, C. R. Somm. des Séances, Fasc., vol. 10, pp. 115–116, 1937.

Infrared photographs reveal presence of fossil bacteria in Lower Cretaceous, Jurassic, Devonian, and Silurian oölitic iron ores from France. Iron ore from the Huronian of Minnesota also showed bacteria. Fossil bacteria demonstrated in chalk, marl, and sandstone from the Paris Basin, in Cambrian shale from the Ardennes, and in Precambrian schists from Normandy and British Columbia.

Dorff, P. Die Eisenorganismen. II. Biologie des Eisen- und Mangankreislaufs: Verlagsgesellschaft für Ackerbau, pp. 106, 1935.

Part played by bacteria in the cycles of iron and manganese in nature and review of evidence for the occurrence of fossil forms in sedimentary deposits. 305 references.

Ellis, D. Fossil micro-organisms from the Jurassic and Cretaceous rocks of Great Britain: Proc. Roy. Soc. Edinburgh, vol. 35, pp. 110–133, 1915.

Many fossil fungi but no iron bacteria found in thin sections of ferruginous rocks. Fossil bacteria observed in rocks from Gault, Folkestone. Fossil actinomycetes found in ferruginous limestone. Described *Phycomycetes frodinghamii* as a new species of fossil fungi believed to have played a part in formation of iron.

Farrell, M. A. (and Turner, H. G.). Bacteria in anthracite coal: Jour. Bact., vol. 23, pp. 155–162, 1932.

Staphylococcus and a sporulating rod found in coal like that examined by Lipman (1932), but authors attributed presence of bacteria to fractures and fissures that permitted recent contamination by surface waters.

Fuchs, Frieda. (and Fuchs, W. and Reid, J. J.). Microbiology of coal. Biological decomposition of hydroxycarboxylic acids obtained from bituminous coal: Fuel, vol. 21, pp. 96–102, 1942.

From review of earlier literature the authors conclude that bacteria are indigenous to certain uncontaminated coal formations. They show that aqueous extracts from bituminous coal provide a good medium for bacterial growth. 36 references.

Fuchs, W. Thermodynamics and coal formation: Mineral Industries Expt. Station, Tech. Paper 67, Penn. State College, pp. 1–13, 1941.

Importance of bacteria in the early stages of coal formation stressed. 32 references.

Gahl, R. (and Anderson, Belle). Sulphate-reducing bacteria in California oil waters: Centralbl. f. Bakt., II Abt., vol. 73, pp. 331–338, 1928.

Sulfate-reducing bacteria found in 17 out of 40 oil wells, some from depths as great as 3,090 feet. The bacteria appeared to be indigenous to the oil-bearing formation.

Ginsburg-Karagitscheva, T. L. Microflora of oil waters and oil-bearing formations and biochemical processes caused by it: Bull. Amer. Assoc. Petrol. Geol., vol. 17, pp. 52–65, 1933.

Sulfate-reducing bacteria found in 14 out of 15 samples of oil sands from the Grozny oil-field formation, believed to be indigenous species. 18 references.

Glaessner, M. F. Principles of micropalaeontology: John Wiley & Sons, N. Y., pp. 296, 1947.

Microfossils, including microscopic animals, algae, fungi, etc., with a paragraph stating that fossil bacteria have been found in oil shales, iron ores, limestones, cherts, plant remains, bones, and coprolites. Emphasis is on fossil foraminifera. 821 references.

Gruner, J. W. The origin of sedimentary iron formations: The Biwabik formation of the Mesabi Range: Econ. Geol., vol. 17, pp. 407–460, 1922.

Some evidence for the occurrence of fossil iron bacteria in chert. Bacteria believed by author to have contributed to formation of sedimentary iron formations.

Hunt, W. F. The origin of the sulphur deposits of Sicily: Econ. Geol. vol. 10, pp. 543–579, 1915.

Sulfur formation attributed partly to reduction of hydrogen sulfide produced by sulfate-reducing bacteria.

Kaunhowen, F. Über einige Mikroorganismen der fossilen Brennstoffe: Zeitschr. prakt. Geol., vol. 9, pp. 97–110, 1901.

Description of fossilized bacteria found in coal.

Lemiere, L. Transformation des végétaux en combustibles fossiles. Essai sur le rôle des ferments: Internatl. Congress Geol., 1900, Paris, vol. 8, pp. 502–520, 1901.

Bogheads and cannels rich in remains of microbes. Bacteria and their enzymes believed to be the principal factors in carbonization of vegetable matter to give peat and lignite.

Lieske, R. (and Hofmann, E.). Untersuchungen über die Mikrobiologie der Kohlen und ihrer natürlichen Lagerstätten. 2. Mitteilung: Die Mikroflora der Steinkohlengruben: Brennstoffchemie, vol. 9, pp. 282–285, 1928.

Spore-forming, iron, and sulfur bacteria as well as cocci commonly occur in bituminous coal mines of the Ruhr district, some at depths of 400 to 750 meters, believed to be indigenous species.

Lipman, C. B. 1. Living microörganisms in ancient rocks: Jour. Bact. vol. 22, pp. 183–198, 1931.

Bacterial spores, believed to be relics of ancient bacteria originally in peat, demonstrated in Pennsylvania coal deposits from a depth of 1800 feet. The author claimed that there was no evidence of percolating water, (a claim which was refuted by Farrell and Turner in 1932).

2. Further evidence on the amazing longevity of bacteria: Science, vol. 79, pp. 230–231, 1934.

Living bacteria and endospores found in protected adobes, some of which were nearly a thousand years old.

3. Longevity in organisms: Science in the University, Univ. Calif. Press, Berkeley, Calif., pp. 211–230, 1944.

Viable bacteria, mostly spore formers, reported to be present in soil samples 65 years old, in mud bricks 1,000 to 1,400 years old, and in pre-Cambrian limestone. Author concludes that life is not a state but rather a pattern which, in some instances, can exist indefinitely.

Meschinelli, A. Fungorum Fossilium omnium hucusque cognitorum Iconographia: A. Fabris, Vicenza, Italy, pp. 144, 1902.

A fairly complete illustrated list of real and imaginary fossil fungus forms described prior to 1900, including a comprehensive review of the literature.

Molisch, H. Die Eisenbakterien: G. Fischer, Jena, pp. 83, 1910.

The remains of the iron bacteria, *Gallionella* and *Leptothrix*, were found in only four out of 61 samples of iron ore examined microscopically.

Moodie, R. L. 1. Thread moulds and bacteria in the Devonian: Science, vol. 51, pp. 14–15, 1920.

Micrococcus- and diplococcus-like fossils found in osseous lacunae of Permian animal spine. Bacterial and fungus fossils found associated with remains of ancient vertebrates.

2. Paleopathology. An introduction to the study of ancient evidences of disease: University of Illinois Press, Urbana, Ill., pp. 567, 1923.

A comprehensive review of the literature on fossil bacteria, with particular reference to microbes associated with infected animals of great antiquity.

Moore, E. S. Coal: Its properties, analysis, classification, geology, extraction, uses and distribution: John Wiley & Sons, New York, pp. 473, 1940.

Reference is made to presence of bacteria in peat deposits and the part played by bacteria in the early stages of coal formation. Fossil flora of coal include representatives of Thallophytes, Bryophytes, and Pteriodophytes. Calcareous concentrations surrounding coal balls may have been precipitated by bacteria.

Mott, R. A. The origin and composition of coals: Fuel, vol. 21, pp. 129–135, 1942; vol. 22, pp. 20–26, 1943.

Activities of anaerobic bacteria believed to play an important part in coal formation. 26 references.

Osborn, H. F. The origin and evolution of life: Charles Scribner's Sons, New York, pp. 322, 1917.

Bacteria are admirably adapted to be the most primitive inhabitants of the primordial earth. Beds of iron ore in certain pre-Cambrian stratified rocks believed to be of bacterial origin.

Pia, J. Die vorzeitlichen Spaltpilze und ihre Lebensspuren: Palaeobiologica, vol. 1, pp. 457–474, 1928.

Evidence of bacterial activity in sediments of various ages.

Polynov, B. B. (and Muir, A.). The cycle of weathering: Thomas Murby & Co., London, pp. 1–220, 1937.

Review of evidence that bacteria have contributed to the modification of the earth's crust throughout the geological ages. Microbiological weathering of rocks occurs in biosphere where there is a co-mingling of lithosphere, hydrosphere, and atmosphere.

Renualt, B. 1. Sur quelques Micrococcus du Stéphanien, Terrain Houiller Supérieur: Compt. rend. Acad. Sci., vol. 120, pp. 217–220, 1895.

Descriptions of fossilized *Micrococcus guignardi*, *M. hymenophagus*, and *Bacillus vorax* which occur abundantly in anthracite coal. The fossil forms appeared to be associated with the cellulose structure of plant remains in coal.

2. Sur quelques bactéries Dévoniennes: Compt. rend. Acad. Sci., vol. 122, pp. 1226–1227, 1896.

Fossil bacteria in remains of wood in Devonian coal distinguished from pyrites and other microscopic particles by morphology, arrangement, and structure. Two varieties of *Micrococcus devonicus* described.

3. Les Bactériacées de la houille: Compt. rend. Acad. Sci., vol. 123, pp. 953–955, 1896.

Diplococci, micrococci, streptobacilli, and other forms of fossil bacteria observed in silicified remains of wood in coal from St. Etienne, d'Autun, and elsewhere. *Micrococcus hymenophagus*, *M. carbo*, and *Bacillus carbo* described. The bacteria were believed by the author to be specific forms indigenous to coal, which contributed to coal formation by their biochemical activities.

4. Les Bactériacées des bogheads: Compt. rend. Acad. Sci., vol. 124, pp. 1315–1318, 1897.

Fossilized remains of several varieties of *Micrococcus petrolei* observed in samples of bogheads from France, Australia, England, and Russia. Fossil bacteria observed in interior of algal remains magnified 450 to 1,200.

5. Les microorganisms des lignites: Compt. rend. Acad. Sci., vol. 126, pp. 1828–1831, 1898.

Micrococci and other fossil bacteria found to be widely distributed in lignites. Fragments of fungus mycelia and spores also noted in lignites.

6. Sur quelques microorganisms des combustible fossiles: Bull. Soc. de l'Industrie Minerale, vol. 13, pp. 865–1169, 1899.

Summary of 20 years' work on bacterial fossils found in peats, lignites, bituminous schists, bogheads, cannels, and anthracite coals. Names, descriptions, and illustrations of many fossil bacteria and fungi given. Micrococci and spore-forming rods were most abundant.

7. Sur quelques microorganisms des combustibles fossiles: Bull. Soc. de l'Industrie Minerale, vol. 14, pp. 6–159, 1900.
Fossil fungi and bacteria in ancient bituminous schists preserved by silicification. Several species of fossil bacteria found in fragments of bones and scales in coproliths characterized by size, shape, arrangement, structure, and color. Bogheads and cannels believed to consist largely of spore remains and microscopic algae.

8. Du rôle de quelques bactériacées fossiles au point de vue géologique: Congrès Geol. Internat., VIII Paris 1900, vol. 1, pp. 646–663, 1901.
Reports occurrence of several new species of fossilized bacteria in coal. Fossil fungi and bacteria also observed in bone fragments, carapaces, fish scales, and plant remains in ancient sediments. Fossil forms petrified as calcium carbonate, calcium phosphate, or silica.

Tausson, W. O. On the evolution of microorganisms during the geological periods: Arkh. Biol. nauk, vol. 43 (ser. 2–3), pp. 267–286, 1936.
Summary of evidence, recorded in 187 references, for the occurrence of fossil bacteria, actinomycetes, and fungi in ferrous ore, limestones, coals, and other geological formations dating from the Algonkian Period. (In Russian with English summary.)

Thiessen, R. 1. Microscopic study of coal: U. S. Dept. Interior, Bur. Mines, Bull. 38, pp. 187–380, 1913.
Though devoted primarily to a discussion of the microscopic structure and chemical composition of peat, lignite, and higher coals, this article alludes to the presence in peat deposits of anaerobic bacteria which are believed to contribute to the coalification process.

2. (and Johnson, R. C.). An analysis of a peat profile: Jour. Indus. & Eng. Chem., Anal. Ed., vol. 1, pp. 216–220, 1929.
Evidence for the existence and activity of bacteria in peat at all depths. Bacteria believed by the author to play an important part in peat and coal formation.

3. (and Strickler, H. S.). Distribution of microorganisms in four peat deposits: U. S. Dept. Int., Bur. Mines Coop. Bull. 61, 1934.
Living bacteria demonstrated in peat deposits at all depths examined. Fungi and actinomycetes were present only in the upper strata.

Van Tieghem, P. Sur le ferment butyrique (*Bacillus amylobacter*) à l'époque de la houille: Compt. rend Acad. Sci., vol. 89, pp. 1102–1104, 1879.
Fossil bacteria found in silicified vegetable remains in coal from St. Etienne, France. The cellulose membranes showed traces of decomposition resembling effects produced by *Bacillus amylobacter*.

Waksman, S. A. 1. (and Stevens, K. R.). Contribution to the chemical composition of peat: V. The role of microorganisms in peat formation and decomposition: Soil Sci., vol. 28, pp. 315–340, 1929.
Appreciable numbers of bacteria present throughout the entire peat profile to greatest depths examined, 570 cm. Direct microscopic examination detected presence of dead as well as living cells. Investigation included peats from Florida, New Jersey, and Maine. 47 references.

2. (and Purvis, E. R.). The microbiological population of peat: Soil Sci., vol. 34, pp. 95–114, 1932.
Numerous autochthonous bacteria in peats deposited many centuries ago. Observations indicate that microbes, primarily bacteria, are chiefly responsible for peat formation and transformation. 12 references.

3. The peats of New Jersey and their utilization. Part A. Nature and origin of peat. Composition and utilization: N. J. Agric. Exper. Sta., Bull. 55, pp. 1–155, 1942.
Bacteria occur in peat deposits at all depths sampled. Actinomycetes are most abundant near surface and disappear at a depth of 120 to 150 cm. Abundance of fungi decreases with depth until none occur at a depth of 75 to 90 cm. Transformations taking place in peat bogs are primarily microbiological in nature. 339 references complete with titles.

Walcott, C. D. 1. Discovery of Algonkian bacteria: Proc. Nat. Acad. Sci., vol. 1, pp. 256–257, 1915.
Fossil micrococci reported to be present in thin sections cut from algal remains of Newland limestone in Beltian series of Algonkian (pre-Paleozoic) rocks from Montana. Bacteria occurred as single cells and in short chains.

2. Evidence of primitive life: Annual Report Smithsonian Inst. 1915, pp. 235–255, 1916.
Outline of evidence for the presence of bacteria and disease in primitive organisms found in pre-Cambrian formations.

White, D. (and Thiessen, R.). The origin of coal: U. S. Dept. Interior, Bur. Mines, Bull. 38, pp. 1–390, 1913.
Bacteria shown to occur in peat bogs to depth of at least 9 meters and they may persist at much greater depths. Bacteria believed to contribute to the early stages of coal formation.

Wilson, L. R. Spores and pollen as microfossils: Bot. Rev., vol. 10, pp. 499–523, 1944.
Spores of various microorganisms and pollens abundantly preserved as microfossils in sedimentary rocks dating from Paleozoic time to the present. 102 references complete with titles.

Wolf, F. A. (and Wolf, F. T.). Fossil fungi: Chapter 22 in The Fungi, John Wiley & Sons, N. Y., vol. II, pp. 474–489, 1947.
Summary of 39 families of fossil fungi which

have been reported to be present in material from various geological formations. 21 references.

ZoBell, C. E. 1. Changes produced by microorganisms in sediments after deposition: Jour. Sed. Petrology, vol. 12, pp. 127–136, 1942.

Recent marine sediments rich in bacteria at all depths sampled. Evidence suggests that such bacteria may be important geochemical agents. 50 references.

2. Action of microorganisms on hydrocarbons: Bact. Rev., vol. 10, pp. 1–49, 1946.

Samples of "paraffin dirt" of appreciable antiquity found to contain large number of bacteria or their remains. Review of literature on petroleum microbiology. 182 references.

3. Marine bacteriology: Ann. Rev. Biochem., vol. 16, pp. 565–586, 1947.

Bacteria present in marine mud at core deptns exceeding 350 cm. The characteristics of marine bacteria are reviewed. 198 references.

4. To what depths are bacteria alive in marine bottom deposits: Proc. 4th Internat. Congr. Microbiol., Copenhagen, vol. 4, pp. 174–175, 1947.

Viable bacteria demonstrated throughout the profile of long cores of marine mud collected from the deep sea, including material that had been buried for more than 100,000 years.

5. Bacteriological and sedimentation phases of the transformation of organic material into petroleum: API Research on Occurrence & Recovery of Petroleum, vol. 3, pp. 100–106, 1949.

Bacteria found in recent marine sediment samples at depths as great as 177 feet. Autochthonous forms found in samples of limestone-anhydrite-sulfur formation from depth of 1,560 feet.

Contribution from the Scripps Institution of Oceanography, New Series No. 885.

Manuscript Received by the Editor April 2, 1951.

Reprinted from THE JOURNAL OF THE ACOUSTICAL SOCIETY OF AMERICA, Vol. 28, No. 6, 1253–1255, November, 1956
Copyright, 1956 by the Acoustical Society of America.
Printed in U. S. A.
Reproduced by Permission

On the Pressure Dependence of Sound Absorption in Liquids*

LEONARD LIEBERMANN
University of California, Marine Physical Laboratory of the Scripps Institution of Oceanography, La Jolla, California
(Received April 21, 1956)

The theory of the dependence of sound absorption on pressure is given for liquids in which absorption significantly depends on the two coefficients of viscosity: bulk viscosity and shear viscosity. The bulk viscosity, and therefore sound absorption, is shown to be related to the equation of state. The equation of state is derived for a liquid model in which the volume is determined by molecular distribution within two states. This equation of state possesses two characteristic constants; these can be numerically evaluated for an actual liquid by comparing the theoretical equation of state with pressure-volume relations available in tables. As an example, the characteristic constants of water are evaluated and used to compute the effect of pressure on sound absorption. The theoretical prediction is in agreement with published observations. As a further example, ethyl alcohol is also treated.

INTRODUCTION

THE viscous properties of liquids are characterized by two coefficients of viscosity: shear and bulk viscosity. The absorption of sound depends on both. Shear viscosity is familiar; bulk viscosity refers to the viscous property manifested in purely dilatational (or compressional) motion. It is likely that the coefficients of bulk and shear viscosity are of the same order of magnitude in nearly all liquids; in water, the bulk viscosity is known to be three times greater than shear viscosity. It is also known that in associated liquids such as water, and the alcohols, viscous absorption accounts entirely for the observed acoustic absorption.

Litovitz and Carnevale[1] have observed the variation of sound absorption in water with increasing pressure. By subtracting the known effect of pressure on the shear viscosity they were able to deduce the effect of pressure on the bulk viscosity coefficient. The variation of acoustic absorption with pressure is not inconsiderable: a diminution of nearly one-half is exhibited at 2000 kg/cm² pressure.

The discussion below gives the theory of the effect of pressure on the bulk viscosity of an idealized liquid. As a practical application the theoretical behavior is compared with acoustical observations in water.

THE TWO STATE LIQUID MODEL

Suppose an ideal liquid exists whose volume depends solely on the distribution of molecules between two states; e.g., two internal molecular configurations representing loose and close packing. Individual molecules are incompressible; volume changes occur solely because of transitions between the two packing states. Let V_0 be the molar volume (the volume of one mole of molecules) in the loosely packed state; ΔV is the change in molar volume in transition to the other state. In general, the molecular population will be distributed between the two states; N is the fraction in the close packed state. Hence the molar volume of the liquid is specified by

$$V=V_0-N\Delta V, \tag{1}$$

with V_0 and ΔV always positive; thus as N increases the volume V diminishes.

It is useful to define a parameter which is more familiar when applied to chemical reactions: the equilibrium constant, K. In chemical terminology, the two state reaction just described is a unimolecular reaction with the equilibrium constant given by

$$K=N/(1-N)$$

or

$$K=(1-N)/N.$$

The choice of these two expressions is conventionally determined by selecting that whose numerator represents the higher energy state population. Here the energy of these two states is unspecified but as is shown below, K is unambiguously determined by other considerations.

Elastic and viscous properties of the liquid follow from K by thermodynamic considerations. The reaction isochore is

$$(\partial \ln K/\partial P)_T=(-\Delta V/RT), \tag{2}$$

where P is the pressure; R is the gas constant and T the absolute temperature. The compressibility, β, of the fluid is defined by $-dV/VdP$. Equation (2) leads to

$$\beta=(\partial V/\partial \ln K)(\Delta V/VRT). \tag{3}$$

Integration of the reaction isochore gives

$$K_0/K=\exp(P\Delta V/RT) \tag{4}$$

with K_0 the constant of integration. Hence from Eq. (4), $dP/dK<0$. But it is true for all liquids that, $dP/dV<0$; thus from Eq. (1), $dP/dN>0$. Therefore, $dK/dN<0$. In this manner the choice of K is unambiguously determined to be

$$K=(1-N)/N$$

---

* This research received support from the Bureau of Ships, U. S. Navy. Contribution from the Scripps Institution of Oceanography, New Series No. 886.

[1] T. A. Litovitz and E. H. Carnevale, J. Appl. Phys. 26, 816 (1955).

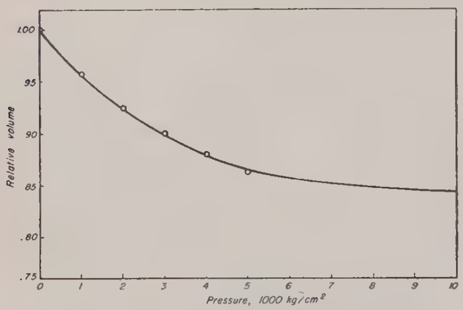

FIG. 1. Comparison of the equation of state (solid line) with compressibility data (circles) for water at 0°C. The two characteristic constants of the equation of state $V_0=1.38V_A$ and $\Delta V=0.54V_A$, were chosen by fitting the data.

or utilizing Eq. (1),

$$K=(\Delta V-V_0+V)/(V_0-V).$$

Thus the equation of state of the two state liquid is from Eq. (4),

$$[(V_0-V)/(\Delta V-V_0+V)] \times[(\Delta V-V_0+V_A)/(V_0-V_A)] =\exp(P\Delta V/RT), \quad (5)$$

where V_A is the molar volume at 0 pressure (for practical purposes, atmospheric pressure). A method for numerically evaluating the characteristic constants, V_0 and ΔV, for real liquids, is discussed in a later section. Examples are given which illustrate that Eq. (5) is a surprisingly good representation for the equation of state of real liquids at elevated pressures.

BULK VISCOSITY

The time dependent properties of the two state liquid are readily elucidated using the familiar terminology of chemical reactions. If k is the reaction rate from the state N to the state $1-N$, then at equilibrium, according to the law of mass action

$$dN/dt=0=kN-k(1-N)/K.$$

The application of pressure will shift the equilibrium an amount δN_0. The rate of redistribution to the new equilibrium is given by

$$d(\delta N)/dt=[k(1+K)/K](\delta N-\delta N_0).$$

Changing the variable to V by means of Eq. (1), the rate becomes

$$d(\delta V)/dt=[k(1+K)/K](\delta V-\delta V_0).$$

The equilibrium shift in volume is $\delta V_0=-\beta V\delta P$ where δP is the applied pressure; it will be recalled that β was defined as the isothermal *static* compressibility. Hence the foregoing equation may be written in the form

$$\delta P=[K/k(1+K)\beta V]d(\delta V)/dt-\delta V/V\beta. \quad (6)$$

This represents the viscoelastic equation of the two state liquid. By comparison the general theory of elasticity of fluids gives for uniform dilatation,[2]

$$\delta P=\phi d(\delta V)/Vdt-\delta V/V\beta \quad (7)$$

where ϕ is the bulk viscosity.

Comparison of Eq. (6) and Eq. (7) gives the condition of identity as

$$\phi=K/\beta k(1+K). \quad (8)$$

Thus in the case of the two state liquid the bulk viscosity is identified with the finite transition probability, or relaxation time between the two states.

THE PRESSURE EFFECT OF BULK VISCOSITY

According to Eq. (8) bulk viscosity depends on three parameters, K, β, and k. The effect of pressure on β and K is obvious from the previous discussion. The effect of pressure on the reaction rate, k, remains unknown. Following van't Hoff, the effect of pressure on k is given by

$$k_p=k\exp(-P\Delta V_c/RT), \quad (9)$$

where k_p is the reaction rate at elevated pressure. In the van't Hoff theory ΔV_c is a constant; ΔV_c may be interpreted as the molar change in volume in the activated state. In general the sign of ΔV_c can be either negative or positive; most reactions are increased in velocity by the application of pressure. Just as the free energy of activation is measured by examining the variation of reaction rate with temperature, the activation volume change, ΔV_c, can be found by studying the variation of k_p with pressure.

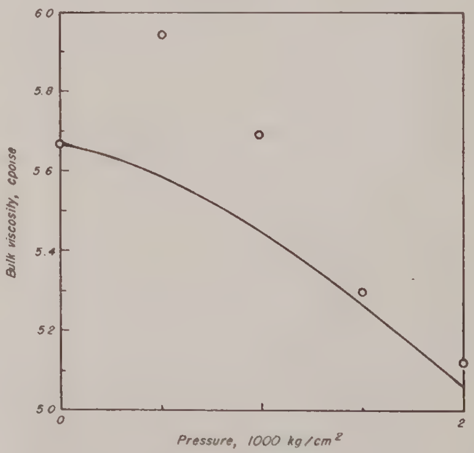

FIG. 2. The theoretical variation with pressure of the bulk viscosity of water compared with the experimental evaluation (circles) of Litovitz and Carnevale. The apparent maximum in viscosity suggested by the data may be experimental error.

---

[2] For example see, H. Lamb, *Hydrodynamics* (Dover Publications, New York, 1945), pp. 571, 645.

Hence the variation of bulk viscosity with pressure can be represented by

$$\phi_p = \frac{(\Delta V - V_0 + V)}{\beta k \exp - \Delta V_c P/RT}. \qquad (10)$$

Three constants are required to predict the effect. In the following section evaluation of these constants is discussed.

APPLICATION

The equation of state of a liquid, given in Eq. (5), can be compared with the observations of Bridgman.[3] Figure 1 gives the comparison for water at 0°C. The characteristic parameters V_0 and ΔV were chosen by arbitrarily fitting the curve at pressures of 1000 and 4000 kg/cm^2. This agreement is certainly adequate in view of the idealization on which the theory is based. In this manner V_0 and ΔV can be obtained for a wide variety of liquids. It is to be noted that both parameters are temperature dependent and must be evaluated at the desired temperature.

In the absence of prior knowledge of ΔV_c for water, the assumption is made that ΔV_c is negligible; thus k_p is assumed to be independent of pressure.† The justification for this assumption is given in Fig. 2, which gives the theoretical change in bulk viscosity with pressure together with the data of Litovitz and Carnevale. The theoretical bulk viscosity was calculated by means of Eq. (10) with β taken from published tables. The agreement is reasonable inasmuch as the bulk viscosity is evaluated as a ratio of two numbers whose magnitudes vary widely with pressure.

All measurements of bulk viscosity are fundamentally acoustic absorption experiments. Viscous absorption is given by

$$\alpha/\omega^2 = (\phi + 4\eta/3)/2\rho c^3.$$

Substituting the above expression for ϕ, viscous absorption becomes

$$\alpha \sim (\beta/V)^{\frac{1}{2}}[(\Delta V - V_0 + V) - 4\eta\beta/3]. \qquad (11)$$

The ratio of the specific heats is neglected as being sufficiently close to unity. Figure 3 gives the calculated pressure dependence of sound absorption using Eq. (11) together with observations. Pressure variations of the compressibility, β, and shear viscosity, η, are taken from published tables. The agreement of the theory with experiment is certainly within experimental error. That this agreement is significant can be seen from inspection of Eq. (11): The first term in the brackets involving the constants V_0 and ΔV is a factor 3 greater than the term involving the shear viscosity. Hence the variation of absorption with pressure is sensitive to the values of these constants.

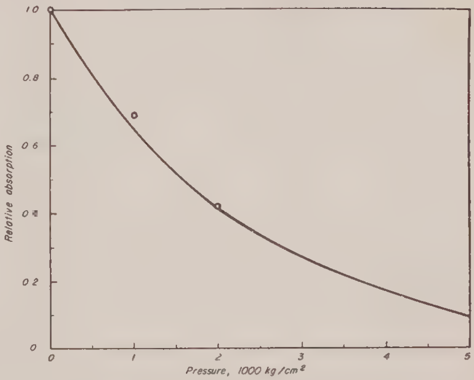

FIG. 3. Predicted change in sound absorption with pressure (solid line) compared with the observations (circles) of Litovitz and Carnevale for water at 0°C. The constants used for prediction are those deduced from Fig. 1.

Viscosity is also the important acoustic absorption mechanism in the alcohols; the effect of pressure on sound absorption has been observed in these liquids by Carnevale and Litovitz.[4] Application of this theory to ethyl alcohol results in the following: The two constants V_0 and ΔV evaluated from Bridgman's data are $1.15V_A$ and $0.32V_A$, respectively. When these values are used in Eq. (10) to compare the predicted bulk viscosity variation with the data it is found that, unlike water, ΔV_c cannot be negligible; there is a considerable diminution of the reaction rate, k_p (and increase in bulk viscosity) with increasing pressure. A good fit with acoustic data is obtained with $\Delta V_c = 10$ cc.

---

[3] P. W. Bridgman, *Physics of High Pressures* (G. Bell and Sons, London, 1949).

† This assumption does not imply that the familiar relaxation time, τ, is independent of pressure: $\tau = K/(1+K)k$.

[4] E. H. Carnevale and T. A. Litovitz, J. Acoust. Soc. Am. 27, 547 (1955).

MARGINAL SEDIMENTS OF MISSISSIPPI DELTA

BY

FRANCIS P. SHEPARD

Reprinted for private circulation from
The Bulletin of the American Association of Petroleum Geologists
Vol. 40, No. 11, November, 1956

(865)

CONTENTS

ABSTRACT 2537

INTRODUCTION 2538

ACKNOWLEDGMENTS 2538

SUBMARINE TOPOGRAPHY 2539

- General Description and Forward Growth 2539
- Delta-Front Gullies 2543

WAVES, CURRENTS, AND SALINITY 2547

EARLIER STUDIES OF THE DELTA MARGIN SEDIMENTS 2548

SEDIMENT ENVIRONMENTS 2549

SURFACE SEDIMENT DISTRIBUTION 2552

- Particle Size Relations 2552
- Sand-Silt-Clay Distributions 2556
- Relative Abundance of Fine and Very Fine Sand 2562
- Coarse-Fraction Studies 2562
    - Wood (fibers, seeds, etc.) 2564
    - Aggregates 2567
    - Mica 2569
    - Foraminifera (largely calcareous) 2570
    - Shells (largely mollusks) 2572
    - Echinoids 2578
    - Ostracods 2578
    - Glauconite 2581
- Sediment Variation Along Profiles 2582
- Seasonal Changes at North Pass 2592
- Possible Seasonal Changes at Main Pass 2595
- Heavy Mineral Content 2595
- Clay Minerals 2598
- Volcanic Shards 2598
- Calcium Carbonate Content 2600

MINOR STRUCTURES 2601

SUMMARY OF SEDIMENT CHARACTERISTICS OF DEPOSITIONAL ENVIRONMENTS 2605

- Topset Bed Deposits 2605
- Foreset Slope Deposits 2610
- Bottomset Beds 2611
- Old Shelf Deposits 2612
- Reworked Mississippi Delta Deposits 2612
- Island Deposits 2612
- Open-Inlet Deposits 2613
- Open-Lagoon Deposits 2613

RATES OF DEPOSITION 2613

COMPARISON WITH OTHER DELTAS 2615

- Atchafalaya Submarine Delta 2615
- Orinoco Delta 2616
- Fraser Delta 2617
- Yukon Delta 2617
- Asiatic Deltas 2618
- Rhone Delta 2619
- Rhine Delta 2620

CONCLUSIONS 2620

BIBLIOGRAPHY 2622

Volume 40 Number 11

BULLETIN
of the
AMERICAN ASSOCIATION OF
PETROLEUM GEOLOGISTS

NOVEMBER, 1956

MARGINAL SEDIMENTS OF MISSISSIPPI DELTA[1]

FRANCIS P. SHEPARD[2]
La Jolla, California

ABSTRACT

To obtain a better grasp of the litho-facies and bio-facies of the delta-to-marine transition, a study has been made of the sedimentary environments bordering the eastern, actively growing distributaries of the Mississippi birdfoot delta. Approximately 1,000 samples, mostly cores, were obtained from the distributary mouths, the continental shelf to the east of the delta, the continental slope to depths of 550 feet, and Breton Sound with its bordering Breton and Gosier islands. For comparative purposes samples have also been obtained in the vicinity of South and Southwest passes. The present paper discusses primarily the characteristics of the surface sediment, leaving for a future report a discussion of a relatively shallow third-dimensional phase of the study which is not yet complete.

It has been found that the sedimentary environments follow several natural subdivisions. Thus, the subaërial delta and the surrounding shallow-water platform, both of which represent the topset beds of the classic type of delta, have distinctive sediment characteristics such as a dominance of silt over clay. Sand is moderately abundant in samples taken along most of the river channels and across the adjoining platforms, although silt is usually more common. Sand percentages on the platform apparently vary according to river stages, the finer sediments increasing during low water. The sediments of the marsh areas of at least the outer delta are easily differentiated from all other environments by the abundance of roots and the absence of the lamination which characterize the submerged bordering platforms. Laminations are also found to some extent in the levee and channel deposits. A general low content of Foraminifera and mollusks in the coarse fraction (sand) and an almost complete absence of echinoids and ostracods characterize all of these topset facies of the delta. An abundance of woody materials, aggregates (largely ferruginous), and mica is found as on the bordering slope.

The deposits formed on the slopes beyond the platform margins are representative of the foreset bed type of environment in classical deltas, except that these slopes have very low angles of inclination, rarely exceeding one per cent. The slope deposits differ from platform deposits in their high clay content and in the marked decrease in lamination. Wood fibers, aggregates, and mica are even more abundant in the coarse fractions of the typical slope deposits than on the platforms. Faunally, the slopes represent a transitional zone between the comparatively sterile topset beds and the abundant organisms of the bottomset beds. Foraminifera become abundant near the base of the slope east of the delta and various types of mollusks appear in appreciable quantities.

The shelf deposits beyond the slope, constituting the bottomset beds, are very largely a product of the present Mississippi Delta out to a distance of about 30 miles east-northeast of Pass a Loutre. These sediments are poorly stratified and consist predominantly of clay, but have an abundance of silt, and show a gradual increase in the sand content toward their eastern margin. The coarse-fraction

---

[1] Contribution from the Scripps Institution of Oceanography, New Series No. 887. This investigation was supported by a grant from the American Petroleum Institute, Project 51. Manuscript received, July 30, 1956.

[2] Scripps Institution of Oceanography, University of California.

Reproduced by Permission

constituents of the bottomset beds show a surprisingly large quantity of Foraminifera, echinoids, and macroorganisms. Glauconite becomes relatively common in contrast to the zones nearer the delta.

Bordering these bottomset beds there are old sediments, probably related to the sea-level lowering during Pleistocene glacial stages. These deposits, which are found both on the south and on the east, contain the eastern Gulf mineral assemblages derived from the southern Appalachians. Their faunas are a mixture of the present-day planktonic Foraminifera and macroorganisms, mostly worn, which are clearly related to the former lowered sea-levels. The percentages of silt and clay are far lower than in the deposits that are influenced by the present delta. Also the wood fibers, aggregates, and mica have virtually disappeared.

North of the tongue of bottomset beds the relatively shallow platform, mostly under 10 fathoms, is covered by sandy sediments which represent the reworked deposits of recent Mississippi Delta lobes known as the Plaquemines and St. Bernard deltas. This is faunally a very barren area. The sediments consist almost entirely of terrigenous minerals of which mica, common directly off the delta, is very scarce. The present island sediments are virutally identical with those of the submerged part of the reworked Mississippi Delta. Inlet types of deposits are found in the tideways between Breton Island and the delta and between Breton and Gosier islands. These represent a combination of the sediments derived from the active passes of the delta with those carried down from Breton Sound, or introduced from the island platforms. Breton Sound deposits are variable in character, but have many of the characteristics of bay sediments along the Texas coast. These Sound deposits differ from most of the deposits that are marginal to the delta by an absence of the ferruginous aggregates that are common in the latter. Faunally the Sound province is quite distinct from the areas in the open Gulf and most resembles those of the Texas bays on the west. The artificially controlled South and Southwest passes are ringed by sediment zones very much like those off the eastern passes. These delta-front slope sediments of the south delta are closely related to the slope deposits of the eastern delta, although at comparable depths the sand content is somewhat higher, particularly off Southwest Pass.

INTRODUCTION

The margins of the Mississippi Delta were chosen as an area of intensive sediment study by the sedimentology project of the American Petroleum Institute because earlier studies, mostly by scientists from the Louisiana State University, had indicated that this was an area where sedimentation was proceeding at an amazingly fast rate and because the geosynclinal nature of the sedimentation accompanied by continuing subsidence gives every indication that the sediments of to-day will become the sedimentary rocks of to-morrow. Much has been learned and is still being learned about the delta itself by other groups, but the area bordering the delta has been given only a reconnaissance study. The purpose of the present investigation has been to gather sufficient information on the sediments and general ecological conditions in this border area to make it possible for stratigraphers to recognize litho-facies in ancient sediments which were deposited under similar conditions. Five years of field studies involving eleven field seasons and the intensive analysis of the sediment samples and their organisms by various new methods developed by the group associated with the project have provided the means of characterizing the various sedimentary environments.

ACKNOWLEDGMENTS

The work reported here represents the concerted effort of a considerable staff at Scripps Institution of Oceanography. Most of the field work was conducted under the direction of P. C. Scruton. A reconnaissance study of the sediments was made earlier by Scruton (1955), but a complete analysis of the sediments was prevented by his leaving to accept a position with the Stanolind Oil and Gas Company. Since Scruton left the project, the staff have made three short field studies for the purpose of filling in gaps in the information particularly at the mouth of North Pass, a major distributary. These trips have been led respectively by D. G. Moore, J. R. Curray, and the present writer. Some of the samples from Southwest and South passes were provided for us by the Humble Oil and Refining Company and the United States Engineers, New Orleans District. The cooperation of departments of the Louisiana Wildlife and Fisheries Commission in providing boats and crews for many of these trips is gratefully acknowledged.

The gathering of data for the present paper has been greatly assisted by J. R. Curray, G. A. Rusnak, and R. H. Parker. Many helpful suggestions have come from M. A. Hanna, Tj. Van Andel, and D. L. Inman. Data regarding Ostracoda were kindly supplied by Mrs. Doris Malkin Curtis, and regarding clay minerals by R. E. Grim. The size analyses of the sediments have been made by D. M. Poole and H. W. Lusk. Poole has also made some heavy-mineral determinations and Lusk has studied the ratios of quartz and feldspar in some of the sediments. Special studies of the particle-size distributions were made by Inman and Chamberlain (1955). Maps showing the sand-silt-clay relations were originally constructed by R. H. Parker and D. G. Moore, but have since been modified by the present writer. R. R. Lankford has been helpful in gathering data for the Foraminifera discussion. The descriptions of the cores were made primarily by P. C. Scruton assisted by D. M. Poole. Poole and Lusk also obtained numerous photographs of cores which have been used in various aspects of the present study. Chemical analyses have been made by George Bien. Appreciation is also expressed for the able drafting of J. R. Moriarty and T. H. Mahnken and for the careful plotting of data curves and computations of analysis data by Ruth Young and Elizabeth Sanborn.

SUBMARINE TOPOGRAPHY

GENERAL DESCRIPTION AND FORWARD GROWTH

The topography of the sea floor around the Mississippi Delta has been described by many writers, notably Russell (1936) and Fisk and others (1954). The sea floor differs somewhat in character from that found off most other large rivers which enter directly into the sea because, unlike all other rivers, the Mississippi has built a delta across the entire continental shelf (Fig. 1). As a result, much of the sediment being carried out of three main distributaries (Southwest Pass, South Pass, and Pass a Loutre) is being deposited on a forward-building continental slope (Shepard, 1955, Fig. 5). On the other hand, sediment is also being deposited on a relatively flat continental shelf east of Main Pass, where a large delta has been built into the Gulf in recent years (Fig. 2). Similar shelf deposition is occurring off Grand Pass on the west side of the delta. In addition a large part of the sediment from Pass a Loutre and Southwest Pass is contributed to the shelves on either side of the delta. As a result there are two types of prograding sea-floor topography associated with the Mississippi Delta. The difference between the two types is very striking as can be seen in Figures 1 and 3.

The series of distributaries which have built forward during the last century on the east flank of the Mississippi birdfoot delta have encroached across a platform onto a gently sloping trough which was bounded by Breton Island and adjacent shoals on the northeast and by the delta on the southwest. In 1860 the slope on the side toward the delta was 4–5 feet per mile so that the series of distributaries, of which Main Pass is the most prominent, were built out onto a

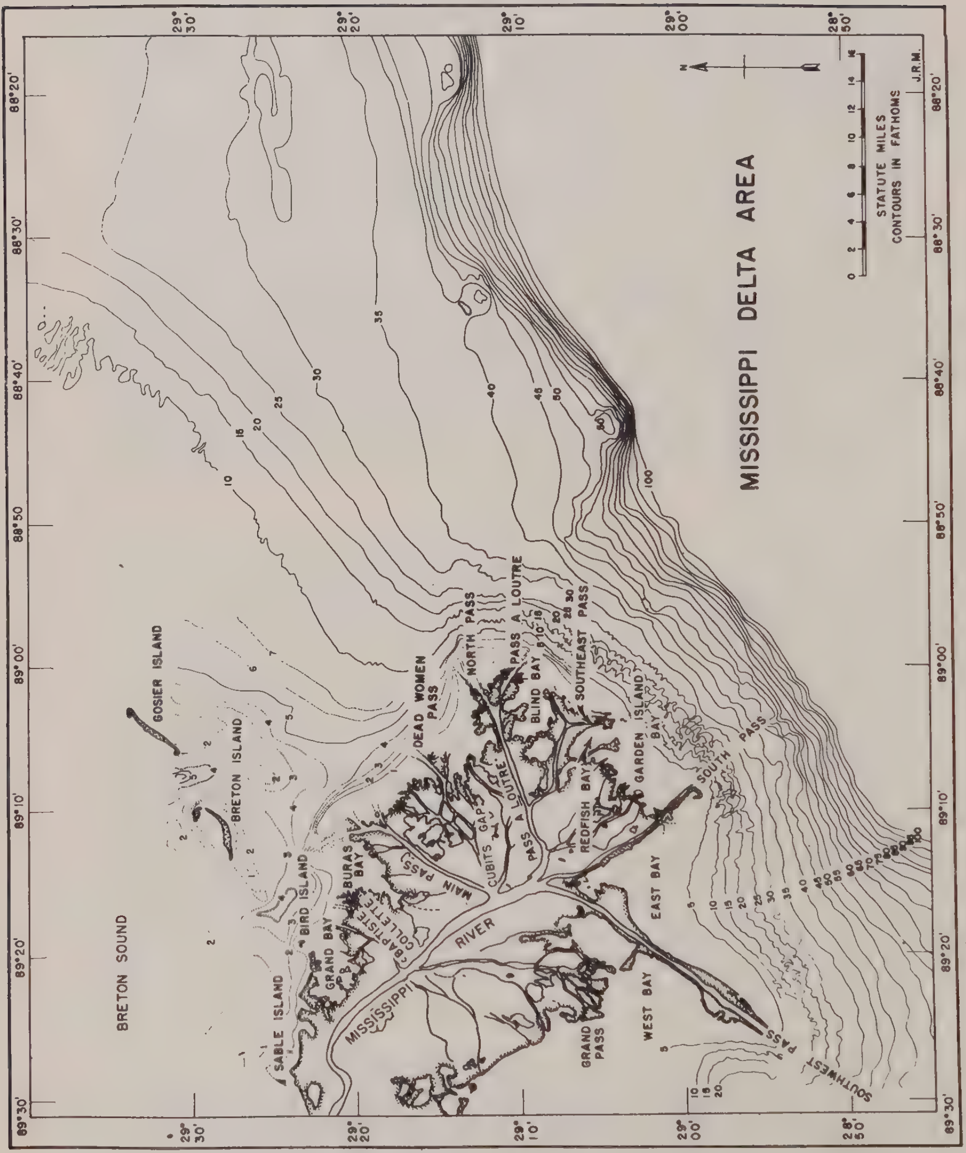
MISSISSIPPI DELTA AREA
STATUTE MILES
CONTOURS IN FATHOMS
J.R.M.
N
BRETON SOUND
GOSIER ISLAND
BRETON ISLAND
SABLE ISLAND
BIRD ISLAND
GRAND BAY
BURAS BAY
BAPTISTE COLLETTE
MAIN PASS
MISSISSIPPI RIVER
CUBITS GAP
DEAD WOMEN PASS
NORTH PASS
PASS A LOUTRE
BLIND BAY
SOUTHEAST PASS
GARDEN ISLAND BAY
REDFISH BAY
SOUTH PASS
EAST BAY
WEST BAY
GRAND PASS
SOUTHWEST PASS
29° 30'
29° 20'
29° 10'
29° 00'
28° 50'
88°20'
88°30'
88°40'
88°50'
89°00'
89°10'
89°20'
89°30'

FIG. 1.—Topography of sea floor marginal to Mississippi Delta. One-fathom contour intervals in part of area, and 5 fathoms elsewhere. All place names are included.

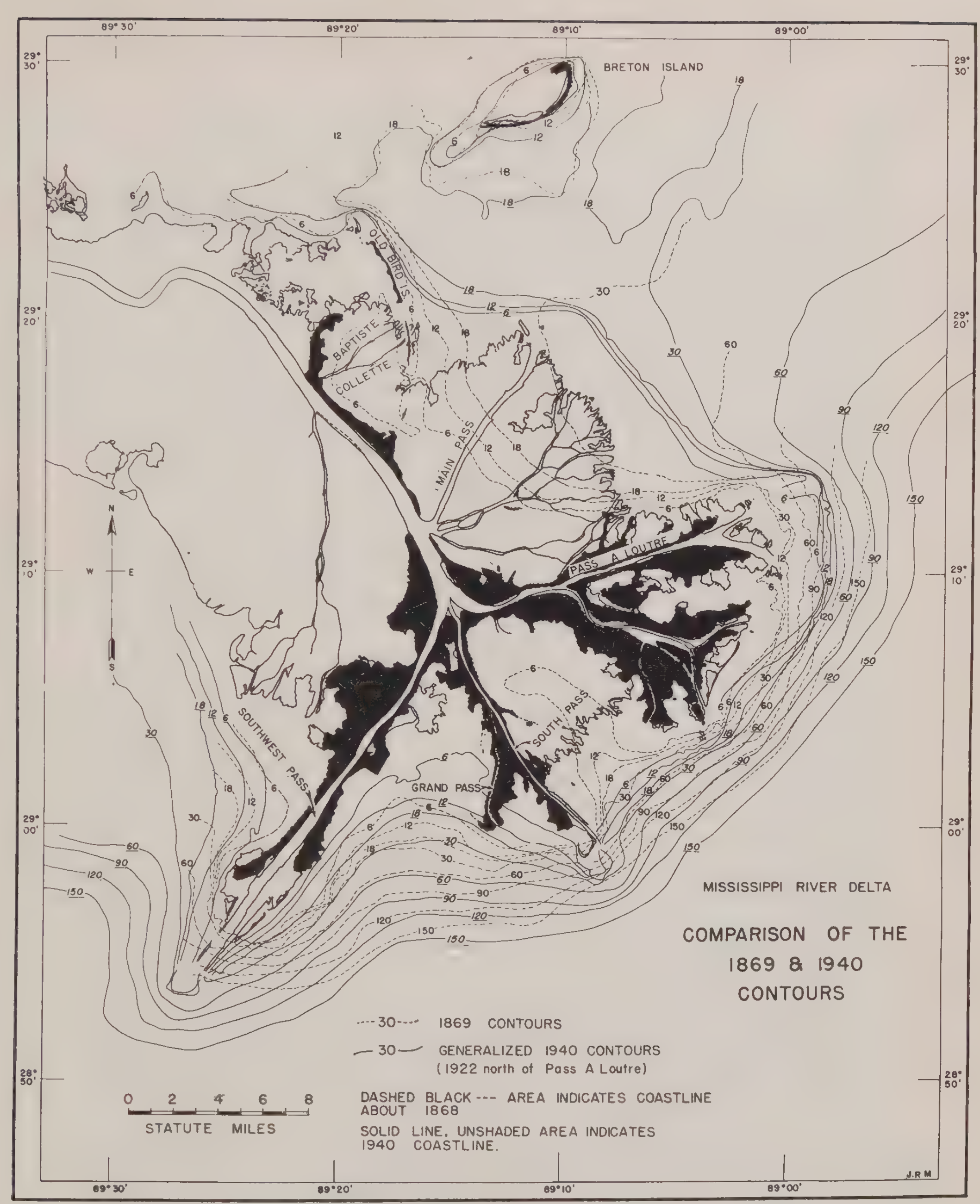
89° 30'
89°20'
89°10'
89°00'
29° 30'
29° 20'
29° 10'
29° 00'
28° 50'
BRETON ISLAND
OLD BIRD IS.
BAPTISTE
COLLETTE
MAIN PASS
PASS A LOUTRE
SOUTH PASS
SOUTHWEST PASS
GRAND PASS
N
S
E
W
MISSISSIPPI RIVER DELTA
COMPARISON OF THE 1869 & 1940 CONTOURS
---30--- 1869 CONTOURS
—30— GENERALIZED 1940 CONTOURS (1922 north of Pass A Loutre)
DASHED BLACK --- AREA INDICATES COASTLINE ABOUT 1868
SOLID LINE, UNSHADED AREA INDICATES 1940 COASTLINE.
0 2 4 6 8
STATUTE MILES
J.R.M.

FIG. 2.—Showing growth of Mississippi Delta since 1869 and depth changes. Because the 1869 soundings are not sufficiently detailed to show gullies, the 1940 contours were generalized on slope whereas true contours are indicated in Fig. 1 and Fig. 3.

very gentle slope in contrast to the principal distributaries which have been building onto a much steeper slope. As Main Pass and associated deltas have built forward they have increased the seaward slope to about 20 feet to the mile. Despite this forward building, however, the center of the trough has not decreased in depth despite this great growth of the distributaries on one side; in fact, comparison of the old and new soundings indicates that the trough may actually be a little deeper at the present time. The maximum fill is at the outer end of Main Pass and along the front of a series of distributaries toward the southeast. At Main Pass the fill from 1860 to 1952 amounted to almost 40 feet, an amount which increases southward where it reaches more than 100 feet in the area where the large distributaries are building out onto the continental slope (Fig. 2, and Shepard and Moody, 1953, Fig. 6).

Off Main Pass the forward growth of the deltas caused a blanketing by muddy sediments of the sand bodies which formerly supplied the chain of barrier islands known as Bird Islands. These islands, which formerly extended to the north side of Main Pass (Fig. 2) have gradually disappeared, leaving only a small part of Bird Island on the north.

Accompanying the forward building of the distributaries, a shallow submerged terrace is formed which may be referred to as a "delta-front platform." In most areas this platform does not exceed about 12 feet in depth below sea-level. Off the Mississippi distributaries this platform has a width of 2–3 miles in most places. If one includes as a part of the platform the interdistributary bay-like indentations between passes such as Blind Bay and Buras Bay,[3] a much greater width exists. However, these indentations seem to be physiographically somewhat separate from the platform.

The platforms are variable in character. Directly off the channels, such as North Pass (Fig. 35), they are creased by the river currents so that channels extend well beyond the margin of the land. In most places these channels are flanked by submerged natural levees. In addition, numerous mud lumps rise as small islands or shoals. These are found off the main passes, being especially well developed off Pass a Loutre. On the other hand, none of these mud lumps has been found off the northern distributaries which are building out onto shallower parts of the shelf. The mud lumps, first referred to by Hilgard (1871), have been well described recently by Morgan (1951, 1952) who attributes them to upthrust due to static pressure of the growing bar.

At the outer edge of the delta-front platform there is a rather sharp break in slope. The change of slope is particularly impressive off the main passes which are being built out into deep water. The upper part of this platform margin has inclinations of about 5 per cent, but beyond this narrow lip the slope decreases to only 1 per cent adjacent to the three largest passes. Outside the passes that are building out onto the shallow shelf such as Main Pass, Baptiste Collette, and Grand Pass the slope is considerably less, averaging about 0.3 per cent.

---

[3] These form a part of the "interdistributary" troughs referred to by Fisk and others (1954).

A strait now about 5 miles across separates the delta from Breton Island. The deepest part of this strait, which lies relatively near the remnant Bird Island, has a depth of somewhat more than 30 feet. Toward the northeast, shoals extend into Breton Island and are very changeable in position. However, the oldest U. S. Coast and Geodetic Survey charts of the area made in 1838 indicate a Breton Island which is not very different in size and location from its present counterpart.

East of Breton Island there is a channel reaching depths of 30 feet. Farther east a shallow bank borders this channel and this is surmounted by Gosier Island, the southwesternmost outpost of the Chandeleur Island arc. Unlike Breton Island, Gosier Island has changed enormously in recent years, so that it is now almost as large as Breton Island, whereas at the time of the 1922 survey (shown until recently on the published charts) it was only 2,000 feet in extent. Farther east the shelf deepens gradually to 60 feet with an average slope of about 3 feet to the mile. A series of small ridges and troughs is found about 10 miles east of Gosier Island. Farther east the slope increases to 15 feet per mile down to depths of about 130 feet and then flattens. The outer or southern part of the shelf in this area is mostly flat but there are a few submerged hills at the shelf margin which are similar to those found west of the delta (Shepard, 1937; Parker and Curray, 1956).

Northwest of Breton Island and Bird Island lies Breton Sound which extends north into Chandeleur Sound, the two sounds constituting a shallow body of water protected by the Chandeleur and Breton island arcs. In this area the bottom is relatively flat. The average depth is about 11 feet and except at the north and south entrances the water does not exceed 17 feet.

The most irregular topography on the periphery of the delta is found extending almost continuously from Pass a Loutre to Southwest Pass (Fig. 3). Here the Mississippi has built a series of distributaries across the continental shelf so that, except in the embayments, the sea floor is a part of the continental slope. The average inclination, however, is lower than that of most continental slopes and averages close to 1 per cent. In the vicinity of South Pass this slope extends apparently without interruption down to the deep floor of the Gulf of Mexico. Off Southwest Pass, the topography out to 50 fathoms is comparable with that off South Pass, but beyond that depth there is a relatively gentle slope out to about 80 fathoms, forming a broad nose with one pronounced hill. Beyond this nose the slope is continuous to the Sigsbee Deep (Ewing *et al.*, 1955).

DELTA-FRONT GULLIES

The slope near shore in this general area is cut transversely by innumerable "gullies" with widths of about ½ mile and depths up to about 50 feet below their surroundings (Shepard, 1955). These "gullies" are most pronounced off the actively building distributaries, being especially well developed off South Pass, although one of the largest is several miles west of this distributary where the slopes are somewhat more gentle. The "gullies" are not as well developed off

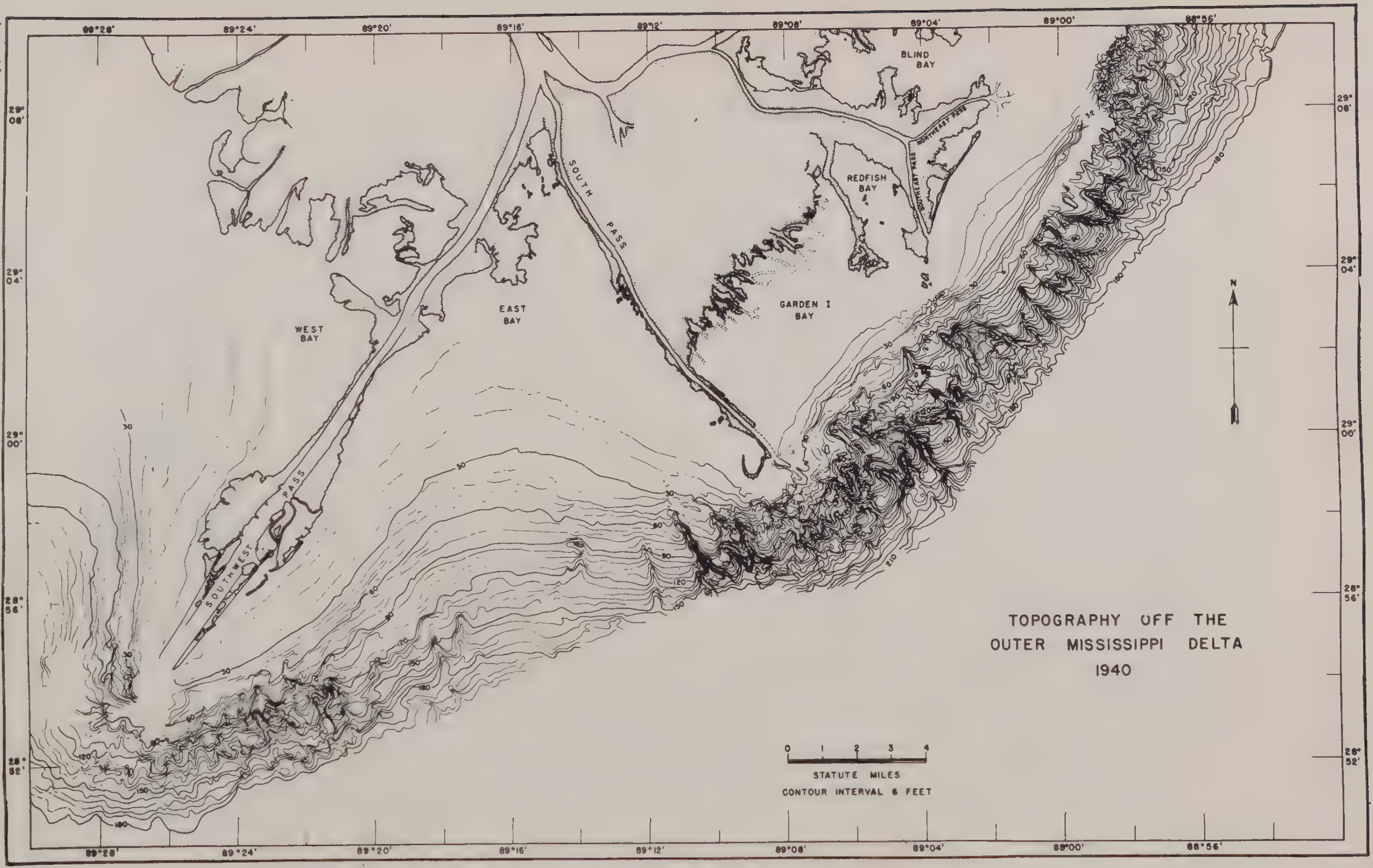
TOPOGRAPHY OFF THE
OUTER MISSISSIPPI DELTA
1940
BLIND BAY
REDFISH BAY
GARDEN I BAY
EAST BAY
WEST BAY
SOUTH PASS
SOUTHWEST PASS
NORTHEAST PASS
SOUTHEAST PASS
N
0 1 2 3 4
STATUTE MILES
CONTOUR INTERVAL 6 FEET
89°28'
89°24'
89°20'
89°16'
89°12'
89°08'
89°04'
89°00'
88°56'
29° 08'
29° 04'
29° 00'
28° 56'
28° 52'
30
60
90
120
150
180
210

Fig. 3.—Submarine gullies along foreset slope of advancing Mississippi Delta. Relation of gullies to distributaries is indicated.

Southwest Pass, despite its great forward growth, as off the entire area from South Pass to Pass a Loutre. They are virtually missing on the slope on the west side of Southwest Pass and are definitely absent north of North Pass and off the western side of the delta.

The gullies head at a variety of depths, although the majority start close to the 30-foot contour. Off East Bay (between South and Southwest passes), on the other hand, two of them do not extend inside depths of 120 feet. Most of the valleys terminate seaward at depths of 150–220 feet and there is little sign of them along the outer slope. However, the sounding lines are more widely spaced beyond about 200-foot depths so that some gullies may have been missed.

Some details of the gullies are indicated in Figure 4. It may be seen from this figure that the slopes, both of the sides and of the floor, are rather discontinuous and that in some places ridges or fan-like features occur as a seaward prolongation of the valleys. Numerous basin depressions and a few small hills were found along the length of the valleys. It is difficult to compute side slopes from U. S. Coast and Geodetic Survey records, but our fathograms indicate that the valley sides have slopes up to about 15°. The 1 per cent gradients of the valley floors are similar to those of the regional slope, except locally where there is a steepening up to 3 or 4 per cent.

An origin for the submarine gullies has been suggested (Shepard, 1955) which consists principally of an earthflow type of mass movement. Turbidity currents, which were at first considered as a possible origin, seem to be less probable because of the absence of any indication of a concentration of coarse material on the floor of the gullies such as is found in submarine canyons. The slope sediments contain ample sand and silt so that this concentration should certainly have developed if currents of any appreciable velocity had existed. Furthermore, a turbidity-current explanation is difficult to reconcile with the dying-out of the gullies at about 200 feet on the slope. This is in contrast to the continuation of deep-ocean shallow valleys, presumably related to turbidity currents, beyond numerous submarine canyons. Turdibity currents apparently move along the deep-ocean valleys which have much more gentle gradients than those of the Mississippi gullies, but it is possible that the gradients are too gentle to develop the type of submarine slide necessary to produce turbidity currents. According to Emery and Terry (1956) the slides in the steeper gullies off Palos Verdes Hills in southern California produced turbidity currents.

Relative to sedimentation, the gullies are of significance because they develop where the slope is locally steepened by the advance of the bars at the mouths of the distributaries. As the slopes build forward, old gullies are filled and new ones form elsewhere (Shepard, 1955, Fig. 6). Alternation of slump and fill should produce unconformities in the stratigraphy. Beds with an inclination greater than that of the foreset slope must develop where deposition has occurred on the relatively steep gully walls. The gullies also indicate a mode by which material is being transferred downslope. This type of mass movement apparently

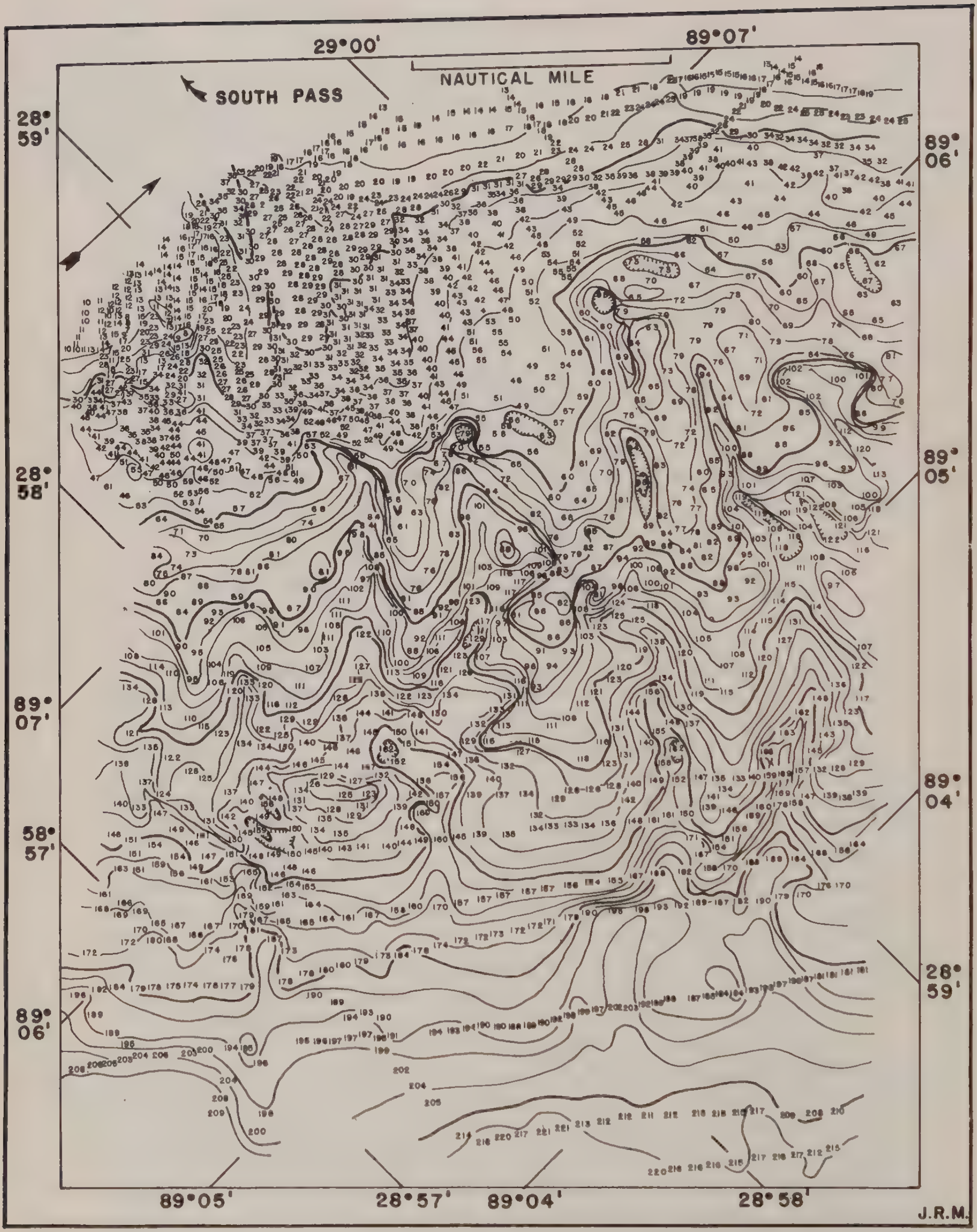
29°00'
89°07'
NAUTICAL MILE
SOUTH PASS
28° 59'
89° 06'
28° 58'
89° 05'
89° 07'
89° 04'
58° 57'
28° 59'
89° 06'
89°05'
28°57'
89°04'
28°58'
J.R.M.

FIG. 4.—Detail of gully near mouth of South Pass showing soundings. Hills and depressions in gullies are shown and dying-out of gullies at moderate depths.

prevents the slope material from becoming stable at inclinations of much greater than 1 per cent.

WAVES, CURRENTS, AND SALINITY

Because Scruton (in press) has assembled a large amount of material concerning the general physical oceanography of the Mississippi Delta sedimentary environments, only a very brief résumé is given here. Scruton has discussed the current patterns as they are related to the flow out of the distributaries of the Mississippi Delta. Scruton's data come from U. S. Hydrographic Office compilations of ship records, from the U. S. Weather Bureau, and from his own measurements and observations of the currents both in the Gulf and in the distributary mouths. Scruton found that the effluent from the river spreads widely as a "plume" over the Gulf (also Scruton and Moore, 1953). The present writer, in flying from Tampa to the delta during a flood stage and at the end of a northwest blow, observed a muddy plume as far as 200 miles east of the delta. These plumes represent a thin film of turbid water with an outer edge so thin that the wake of a vessel will stir up the relatively clean Gulf water from underneath.

During low-river stages the relatively heavy saline water of the open Gulf actually flows up the channels of the distributaries, coming particularly up the deep dredged South and Southwest passes (Holle, 1952). This salt wedge was also observed by Scruton to move rather rapidly up into Pass a Loutre during one low-water stage. The salt wedge has considerable effect on the sedimentation since it decreases velocity, as well as having an electrolytic effect favoring the deposition of the clay particles where the higher salinity is encountered. As a result the mouths of the river during low water become areas of considerable deposition despite the surface outflow.

Beyond the river mouths jet streams from the distributaries, discussed recently by Bates (1953), carry material seaward but soon lose most of their velocity so that most of the sand-size sediment is deposited as bars at the stream mouths. Beyond the bars residual velocity from the jet may be a moderately important factor in the migration of the plume, but according to Scruton the effect of any strong wind on the surface currents becomes the dominant influence a few miles beyond the passes. Along this coast the regional drift (semi-permanent current) south of the delta has a northerly component which divides at the delta so that tongues go east and west. These tongues also influence the general currents and hence the transportation of sediment. Furthermore, tidal currents, as Scruton has found, transport large volumes of water through the inlet between the delta and Breton Island and hence up into Breton Sound. The tide, which only rises about 6 inches in the area, produces rather small currents. The tidal-current velocity is considerably influenced by the wind. Despite these conflicting influences, Scruton has come to the conclusion that during times of high river discharge a current component from the river mouths has some residual momentum at a distance up to about 25 miles seaward of the largest distributaries.

The waves around the delta are low, commonly not more than 2 or 3 feet in height, and of short period. The only large waves are those associated with hurricanes which occur so rarely as to have little effect on sedimentation in this area. The more usual storm waves exercise a control on the depths of the shallow platforms especially in the area surrounding the exposed parts of the delta. In protected areas such as Breton Sound waves have even less effect on the bottom although they concentrate some of the sand into bars at the margins of the delta.

EARLIER STUDIES OF DELTA MARGIN SEDIMENTS

Several investigations have been made of sedimentary material found in the vicinity of the Mississippi Delta. Trowbridge (1930) was the first to analyze and interpret the sediments in this area. R. J. Russell (1936) collected many samples from the delta area and has made the most complete study of the delta geomorphology. Analysis of Russell's samples was made by Dohm (1936, pp. 339–96). A good summary of this earlier work was compiled by R. J. Russell and R. D. Russell (1939). Cores from the area collected by R. D. Russell and grab samples from the U. S. Fish and Wildlife and the U. S. Coast and Geodetic Survey were investigated for mineral composition by Goldstein (1942). The latter found that the heavy minerals show a distinct difference in regime along a general north-south line skirting the east delta and the Chandeleurs at an average distance of about 15 miles. This line represents the border between Mississippi River heavy-mineral suites and those of the eastern Gulf and suggests an eastern limit of sediments from Pass a Loutre and Main Pass. Goldstein found that the Mississippi River suite extends several times farther west of the delta than it does east. The investigations of Barataria Bay (Krumbein and Aberdeen, 1937) provided valuable information concerning an enclosed bay within the older part of the Mississippi Delta.

The extensive work by Fisk (1944 and 1952) and by Fisk and others (1954, 1955) has added much valuable information to all phases of delta development particularly to the subsurface or delta framework. In these works the recent sediments were discussed only briefly, but many of the important facies referred to in the present paper have been outlined. Thus Fisk emphasized the importance of the sandy "bar fingers" which are built forward by the distributaries leaving "interdistributary troughs" to be filled with clayey sediments. Fisk and his collaborators have also called attention to the silty clays of the delta-front slope and referred to Gulf bottom clayey deposits as existing at greater depths.

Further studies of the Missisippi Delta were included in a recent symposium, "Finding Ancient Shorelines" (1955). In this, Thompson (1955) has presented interesting information from the area on the western side of the delta where conditions are quite distinct from the birdfoot delta. The article by Scruton (1955) in the same symposium was based largely on a reconnaissance study of the same samples considered in the present report and before the complete analyses of this and much additional material had been made. The Scruton paper also provided ideas about the progressive advance of the delta-front environments with overlap as the delta is built forward into the Gulf, and Scruton presented useful data on rates of deposition. These aspects are not considered to any extent in the present paper because plans are being made to obtain a series of short borings which should provide the project with a much better source of information in the near future. Scruton (1955) presented a series of core photographs which show the minor structures, such as laminations, which are characteristic of various environments of deposition in the delta area. Parker (1956, pp. 355–362) discussed the sediments of the same area in relation to the distribution of the macro-organisms.

SEDIMENT ENVIRONMENTS

Several attempts have been made to classify the sediment environments and units related to the Mississippi Delta. Fisk and others (1954) refer to onshore environments which include distributary channels, natural levees, marshes, and interdistributary troughs; and offshore environments which include distributary mouth bars and pro-delta zones. Their sedimentary units include bar fingers, clay wedges, and pro-delta marine wedges. Their diagrams showing the results of their interesting three-dimensional studies present a convincing demonstration of the concept of leaf-like patterns of advancing bar fingers of sand interspersed with clay wedges.

Scruton (1955) proposed a classification of sediment units based on his field studies and a megascopic examination of cores. He did not differentiate between the types of deposits on the subaerial delta, referring to them only as "marsh deposits," and he grouped together the sediments formed in front of the pass mouths with those in the "interdistributary bays" as "delta-front silts and sands." On the slopes beyond he referred to the sedimentary units as "pro-delta silty clays" and to the deposits on the shelf beyond the slope as "offshore clays." The latter are rimmed on the north by his "marginal deposits," a mixture of sand and clay, which in turn are bordered on the north and east by his "sands." For two localities Scruton has introduced the term "older deposits" for sediments which he considered as having been formed under conditions no longer existing. The offshore clays, marginal deposits, and sands are differentiated into "Mississippi River suite" and "Eastern Gulf suite," following the determinations on mineral composition made by Goldstein (1942).

Neither of these classifications appears to be entirely satisfactory for the purpose of the present study although each contains features which are incorporated into the proposed classification which follows. Fisk and his collaborators made no attempt to extend their studies as far east as the present investigations. Furthermore their terms "sand-bar finger" and "clay wedges" imply two radically opposed types of deposits which may well apply to earlier stages of the delta but are not well confirmed by our extensive analyses of the sediments in the advancing distributaries and interdistributary bays. Scruton's classification suffers to some degree from size terminology, as can be seen from his own triangle diagram of sand-silt-clay for his units (Scruton, 1955, Fig. 6). Furthermore, his classification would be applicable only to this particular area whereas a classification such as that by Fisk and McFarlan, though perhaps not sufficiently inclusive, refers to delta features which may be found elsewhere. In constructing the present classification, a possible application to other deltas is kept very much in mind. The sediment environments of the delta area have been developed with special attention to the topography. Within the margins of the delta only about 70 samples have been obtained, all near the coast, so that the divisions here are based on much less information than are those from the sea floor. Natural provinces of the delta, however, appear to include the river channels, the natural levees, and the extensive marshes which lie beyond these low ridges, divisions which are entirely in accord with those of various earlier workers.

The submerged areas bordering the deltas have a large group of subdivisions. The outline of these environments is indicated in Figure 5 as far as was possible. First is the platform which lies directly adjacent to the forward-building passes. In general, the platforms have outer margins varying from 6 to 12 feet in depth. On the inner platforms the river channels show a submarine continuation with depths up to 25 feet (in undredged areas), but shoaling seaward. These channels are bordered by submerged continuations of the natural levees, although the latter are somewhat different in sediment character from the levee sediments on the landward part of the delta. At the outer end of the channels the submerged natural levees connect with an arc-like shoal or lunate bar (especially Bates, 1953). The platforms are complicated in their topography by the presence of mud lumps which rise as small islands or shoals above the general platform level.

Where the delta lobes have built forward in such a way as to enclose bays, such as Blind Bay (south of Pass a Loutre), Buras Bay (west of Main Pass), and Redfish Bay (south of Southeast Pass), a special environment is found which is somewhat related to the platforms. Although these have been included as a part of the "interdistributary troughs" by other investigators, the word trough does not appear to be justified here because of the very shallow water and the irregular outline of these bays so that they are here referred to as "interdistributary bays." The bays, being virtually free from river and tidal currents and largely protected from the waves of the open Gulf, represent natural settling basins for the sediments washed over the levees during the floods or introduced through small distributary channels branching from the main passes.

Beyond the platform is a slope which is designated here as the "pro-delta slope." Off the northern Baptiste Collette and Main Pass deltas these slopes are very narrow and somewhat indefinite, but they become more and more conspicuous toward the south and west. They are about 5 miles in width off Pass a Loutre but toward the south extend down to the base of the continental slope. At the base of the slopes off the zone from Pass a Loutre to Dead Women Pass, there is a relatively flat stretch of continental shelf. Where this shelf has been in-

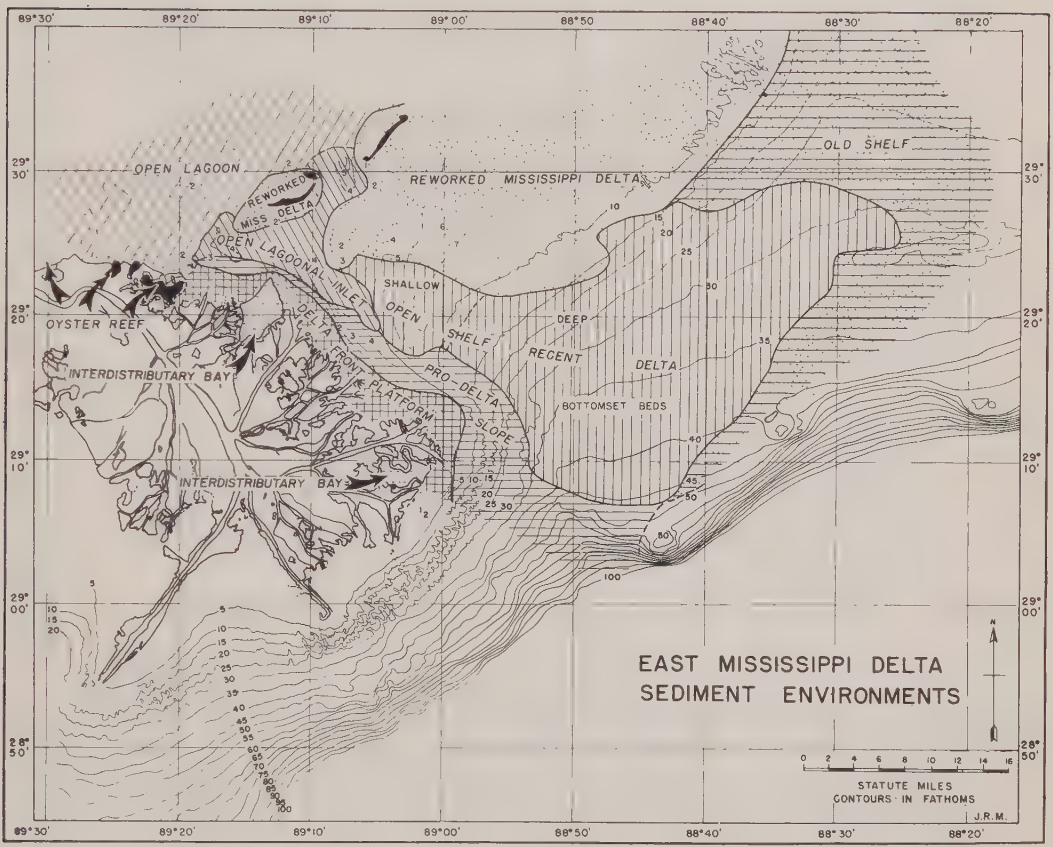
89°30'
89°20'
89°10'
89°00'
88°50
88°40'
88°30'
88°20'
29° 30'
29° 20'
29° 10'
29° 00'
28° 50'
OPEN LAGOON
REWORKED MISS DELTA
OPEN LAGOONAL-INLET
REWORKED MISSISSIPPI DELTA
OLD SHELF
SHALLOW OPEN SHELF
DEEP RECENT DELTA
BOTTOMSET BEDS
OYSTER REEF
INTERDISTRIBUTARY BAY
DELTA FRONT PLATFORM
PRO-DELTA SLOPE
INTERDISTRIBUTARY BAY
EAST MISSISSIPPI DELTA SEDIMENT ENVIRONMENTS
N
0 2 4 6 8 10 12 14 16
STATUTE MILES
CONTOURS IN FATHOMS
J.R.M.

FIG. 5.—Sediment environments proposed for area east and north of birdfoot delta.

fluenced by the recent sediment transport from the passes of the Mississippi Delta, it is referred to as "open shelf with recent delta influence" although the term "bottomset beds" seems to apply equally well. Because of faunal and lithological differences related to currents and water temperature, it seems advisable to subdivide this "open shelf" classification further according to depth. The small pocket at the northwest, where depths are less than about 11 fathoms, is considered as the shallow part of this shelf and the rest as the deep part.

On the east and southeast the "open shelf with recent delta influence" is bordered by a zone which is referred to as "old shelf deposits" which have little in common with Mississippi Delta sediments. The boundary between the two environments is very gradational and has for the most part no topographic relationship. On the shallow shelf north of the area with "bottomset beds" there is a broad reworked zone bordered on the south approximately by the 10-fathom contour and including some hilly areas on the east. Partly on the basis of heavy-mineral studies, this is classed as the "Reworked Mississippi Delta area." Breton and Gosier islands represent a rise above the surface of the platforms of this reworked and now submerged delta area. The channels between the islands and between Breton Island and the delta constitute another environment which is affected by the currents which move through them. By analogy with the environments for the central Texas coast (Shepard and Moore, 1955a, Fig. 25), the term "open inlet" seemed applicable.

Breton Sound is a lagoon connected to the open Gulf by large inlets, so that this is referred to as the "open lagoonal area." A small subdivision within Breton Sound is constituted by the oyster reefs which could be considered as a sub-environment, whereas the protected area inside the curve of Breton Island constitutes another minor subdivision, both of them having distinctive faunas.

It should be realized that the boundaries between these various environments are somewhat indefinite and difficult to locate in many places. It seems necessary, however, to use somewhat imperfect subdivisions of this sort partly because they permit the comparison of the Mississippi Delta deposits with those which exist off many other deltas.

SURFACE SEDIMENT DISTRIBUTION

A series of maps have been constructed from the results of 900 sediment particle-size analyses and 270 "coarse-fraction" analyses of constituents from the surface sediments of the various samples obtained in the delta area. The stations from which samples have been analyzed are shown in Figure 6. In discussing the distribution of sediment characteristics, special consideration is given both to the proposed sediment environments and to the distance from the distributary mouths.

PARTICLE-SIZE RELATIONS

The analysis of the sediments for particle size by Poole and Lusk was made according to the settling-velocity type of analysis described for the central Texas area (Shepard and Moore, 1955a, p. 1479). The median diameters of 860 samples (mostly at depths within the cores of 0–5 cms.) were obtained in the course of this work. These have been plotted on a map and contours (isopleths) have been drawn at 2ϕ intervals with the addition of the 3ϕ contour which appears to have special significance (Fig. 7). In referring to this map it should be remembered that 4ϕ (.062 mm.) is the standard dividing line used by most geologists between very fine sand and silt, and 8ϕ (4 microns) is the dividing line between silt and clay.

The isopleth map shows interesting relationships to the sediment environment of the delta. Considering first the area off North Pass, we find an extremely variable zone at the mouth of the pass, varying between median values of less

(884)

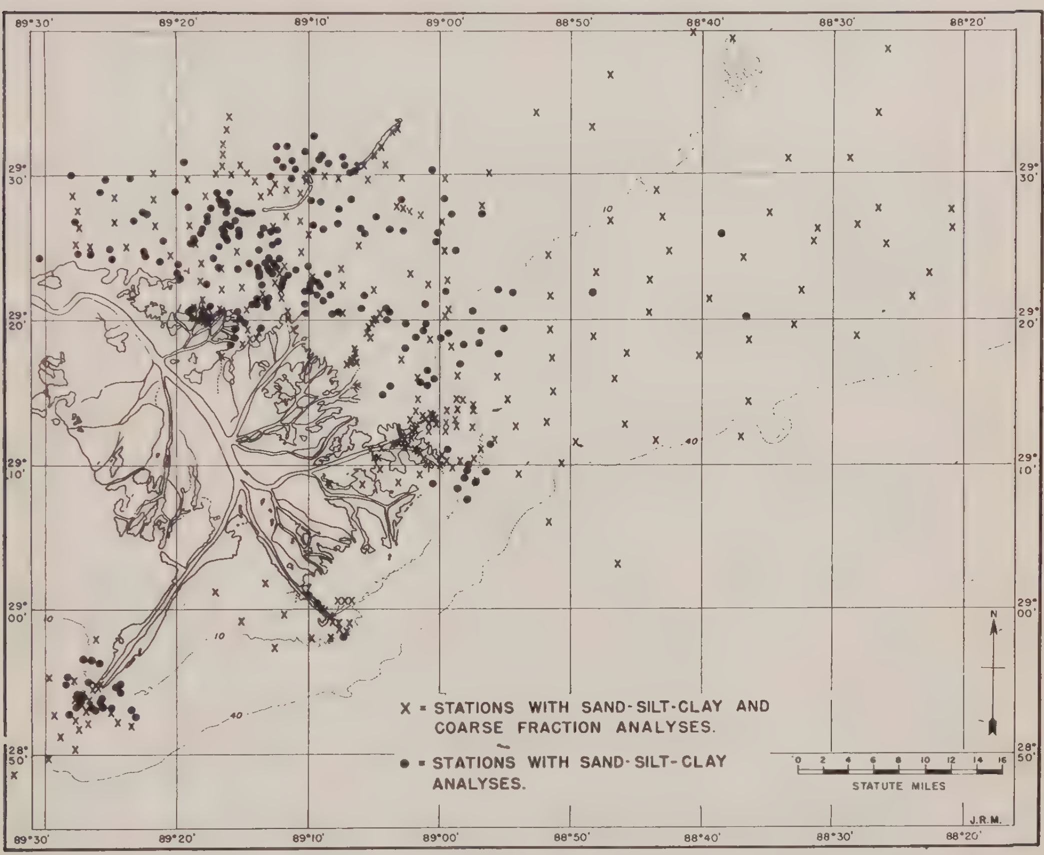
89°30'
89°20'
89°10'
89°00'
88°50'
88°40'
88°30'
88°20'
29° 30'
29° 20'
29° 10'
29° 00'
28° 50'
10
40
N
X = STATIONS WITH SAND-SILT-CLAY AND COARSE FRACTION ANALYSES.
● = STATIONS WITH SAND-SILT-CLAY ANALYSES.
0 2 4 6 8 10 12 14 16
STATUTE MILES
J.R.M.

FIG. 6.—Locations of stations from which sediments have been analyzed. In vicinity of Pass a Loutre and Main Pass it was impossible to show all points.

than 4ϕ (sand) and values greater than 8ϕ (clay). Beyond this platform the isopleths are much more regular and they show first a decrease in median grain size from about 6ϕ to approximately 11ϕ, and then a gradual increase so that a tongue of fine sediment with increasing median diameter sizes extends for 30 miles or more east-northeast of North Pass. In this large tract more than half of the samples have a median diameter in the clay size. Off Pass a Loutre the zone of high but variable median diameters has less extent, but the 8ϕ dividing line between clay and silt median diameters lies a short distance beyond the outer bar and the sediments have a median diameter in the clay size in all of the outer part. Off North Pass, on the other hand, a silt zone extends directly out beyond

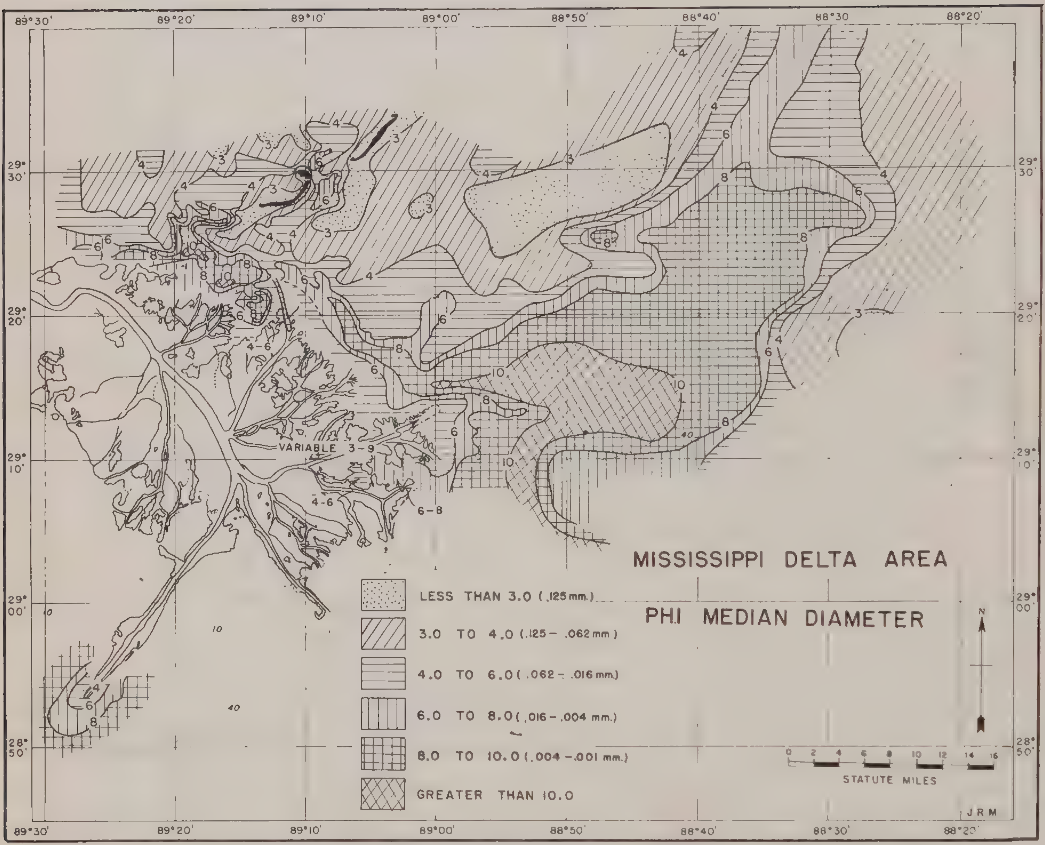
89°30'
89°20'
89°10'
89°00'
88°50'
88°40'
88°30'
88°20'
29° 30'
29° 20'
29° 10'
29° 00'
28° 50'
VARIABLE 3-9
4-6
6-8
MISSISSIPPI DELTA AREA
PHI MEDIAN DIAMETER
LESS THAN 3.0 (.125 mm.)
3.0 TO 4.0 (.125 - .062 mm)
4.0 TO 6.0 (.062 - .016 mm.)
6.0 TO 8.0 (.016 - .004 mm.)
8.0 TO 10.0 (.004 - .001 mm.)
GREATER THAN 10.0
N
0 2 4 6 8 10 12 14 16
STATUTE MILES
JRM

FIG. 7.—Variation in median diameter of sediments shown by isopleths. Relation of isopleths to distributary mouths is clearly indicated.

the pass for almost 10 miles. Farther north the situation is much more complex. A series of samples in Main Pass have median diameters in the coarse silt range, but medians in the finer silt range are found in the center of the interdistributary bay west of the pass. Finer silt is also found east of the pass. Off Baptiste Collette there are some areas where the median diameters lie in the clay range, but in Breton Sound the medians are almost exclusively in the fine sand and coarse silt range. Zones of coarser sand with less than 3ϕ median diameter surround the islands and are found in fairly extensive areas on the platform of reworked Mississippi Delta sediments on the east. Elsewhere in this reworked sediment, the medians lie in the very fine sand classification, that is, between 3ϕ and 4ϕ.

Another approach to the problem, based on the size-distribution characteristics of the sediments was devised by Inman and Chamberlain (1955). Here the sediments were classified according to their median diameter, sorting (deviation), and skewness. As part of a more general study, Inman and Chamberlain prepared a map of the Mississippi Delta area, using 239 samples to show the sediment types based on this system (Fig. 8). This type of map represents an improvement over the map consisting only of median diameters and for some conditions is far more significant. In this special map "Type I" sediments are the best sorted and the coarsest. These sands are found on Breton and Gosier islands. "Type II" sediments are finer and more poorly sorted than beach sands, having median diameters of silt to fine-sand size. This type of sediment extends over the reworked Mississippi Delta sediments on the east. "Type II B" samples coming from the perimeter of an interdistributary bay, west of Main Pass, are

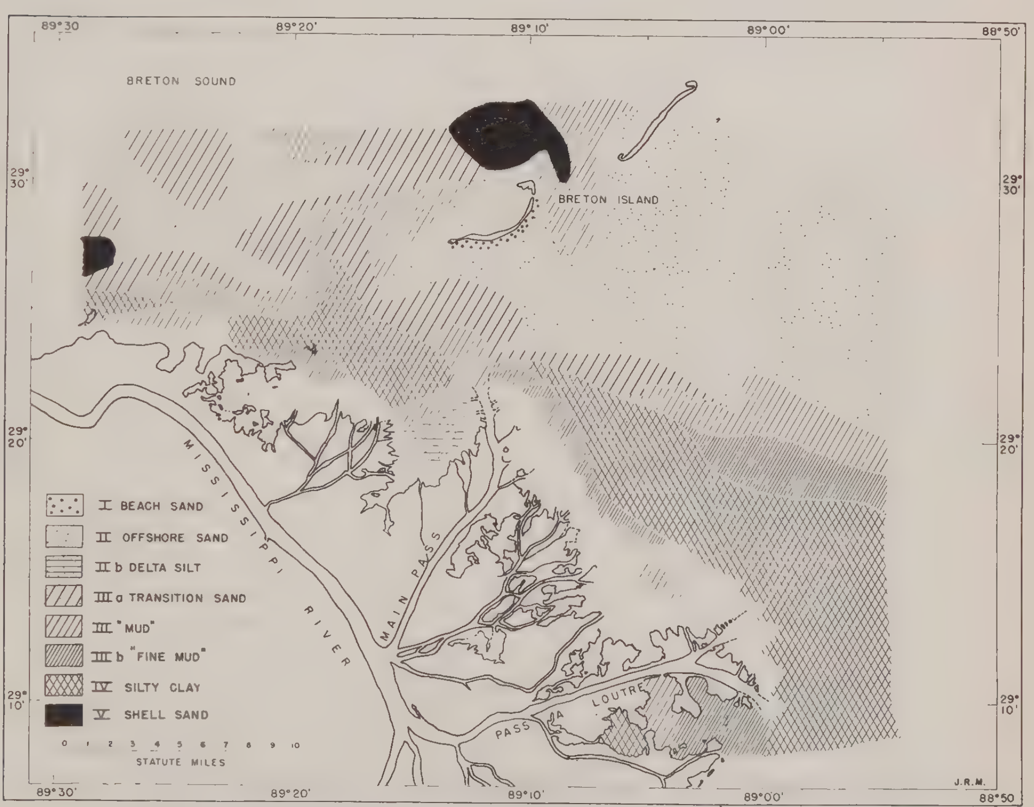
89°30
89°20'
89°10'
89°00'
88°50'
BRETON SOUND
BRETON ISLAND
29° 30'
29° 20'
29° 10'
MISSISSIPPI RIVER
MAIN PASS
PASS A LOUTRE
I BEACH SAND
II OFFSHORE SAND
II b DELTA SILT
III a TRANSITION SAND
III "MUD"
III b "FINE MUD"
IV SILTY CLAY
V SHELL SAND
0 1 2 3 4 5 6 7 8 9 10
STATUTE MILES
J.R.M.

FIG. 8a.—Area distribution of sediment types based on median diameter, phi deviation, and phi skewness. From Inman and Chamberlain (1955, Fig. 12).

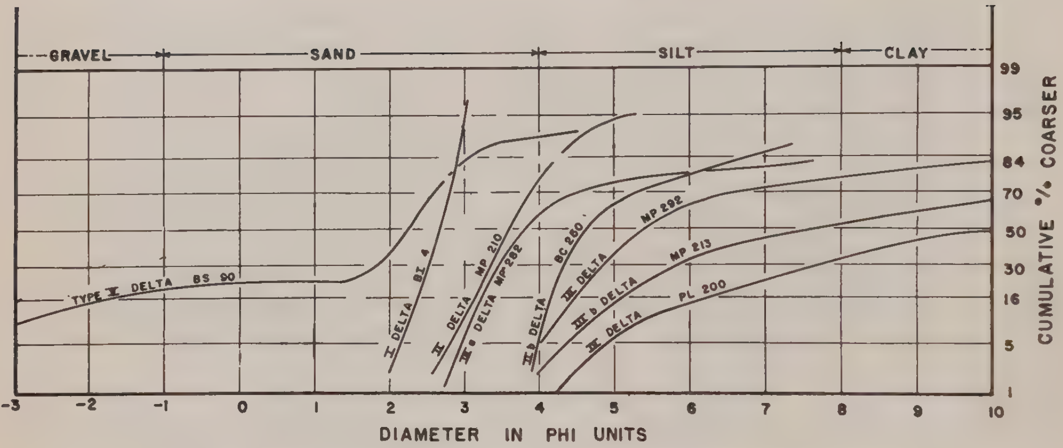

FIG. 8b.—Typical cumulative curves of delta sediments of types shown in Fig. 8A. From Inman and Chamberlain (1955, Fig. 3).

unique in being extremely well sorted for a silt-size sediment. "Type III" sediments (referred to as "mud" by Inman and Chamberlain, but according to our classification (Shepard, 1954) mostly a clayey silt) are characterized by a median diameter averaging around 5ϕ, very poor sorting, and positive skewness. They referred also to a transitional "Type III A" which lies between sand and silt. Inman and Chamberlain considered this type of sediment the result of mixing of river-borne "muds" with offshore sand. Their "Type IV," which is a silty clay, represents the fine sediments deposited in the deep quiet water off Pass a Loutre. This last type has a large phi deviation (poorly sorted), and the phi skewness is rather close to zero. This is in contrast to the "Type III" sediments with their relatively high positive skewness. The sorting in this fourth group is similar to "Type III," and poorer than "Types I and II." "Type V" represents a special category for shell sands which are related partly to the oyster reefs in Breton Sound northwest of Baptiste Collette subdelta and also to the shelly sands north of Breton Island where shells are concentrated by strong tidal currents re-working Gulf and Sound shells.

SAND-SILT-CLAY DISTRIBUTIONS

Size relationships are also indicated on three maps constructed to show respectively the percentage variations of sand, silt, and clay. The sand abundance map (Fig. 9) indicates a consistent zonation around the main passes.[4] Sand percentages are high but variable in the river channels.[5] Sand is somewhat less abundant on the levees except on parts of their submarine continuation, and it is

---

[4] This is shown to good advantage in a series of profiles made out from the main passes (Figs. 24 to 33).

[5] See also Figure 41 for variation of sand, silt, and clay by environment.

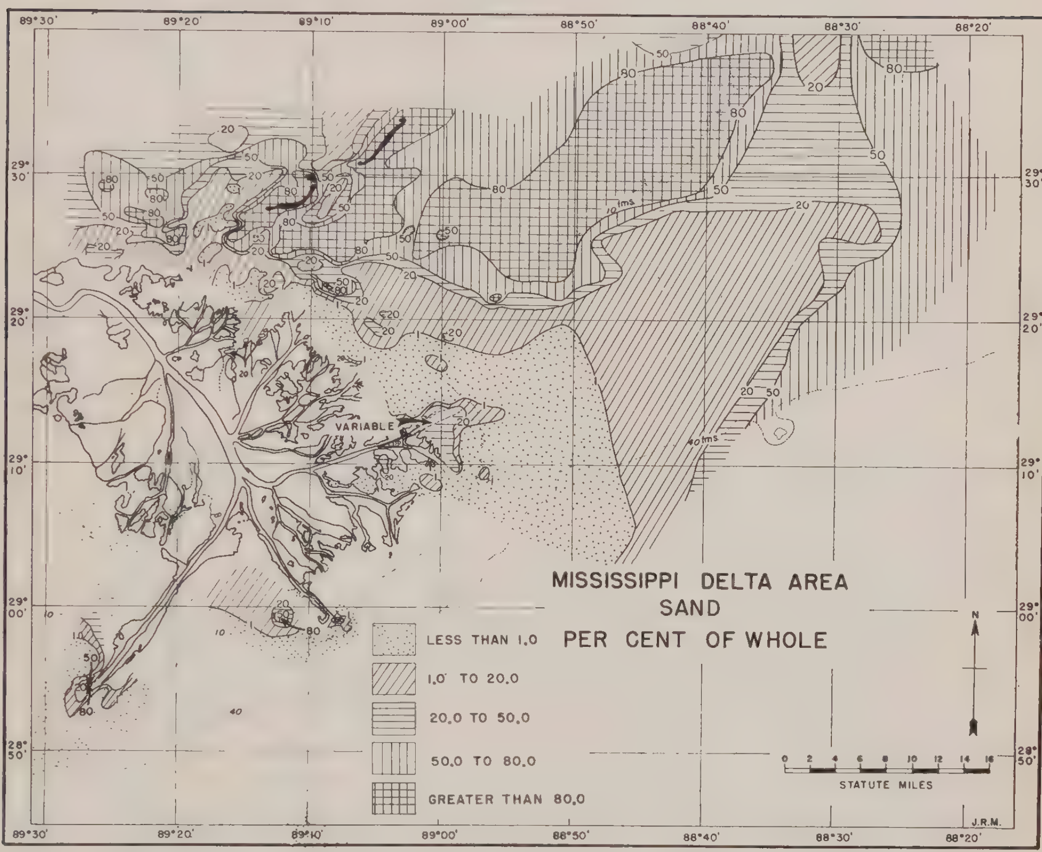
MISSISSIPPI DELTA AREA
SAND
PER CENT OF WHOLE
LESS THAN 1.0
1.0 TO 20.0
20.0 TO 50.0
50.0 TO 80.0
GREATER THAN 80.0
VARIABLE
10 fms
40 fms
N
0 2 4 6 8 10 12 14 16
STATUTE MILES
J.R.M.
89°30'
89°20'
89°10'
89°00'
88°50'
88°40'
88°30'
88°20'
29° 30'
29° 20'
29° 10'
29° 00'
28° 50'

FIG. 9.—Variation in sand content shown by contours based on percentage of sand. Decrease of sand followed by increase away from eastern passes is indicated. Fig. 10 provides depth relationship and Figures 35 and 37 show percentages off North and Main Pass including month of sampling.

only moderately abundant on the marshes. On the platforms out beyond the delta margin the sand is as abundant and variable as in the river channels. It is particularly common on the bars off the rivers where it may be more than 90 per cent, but is relatively scarce in the interdistributary bays. Delta-front slopes are low in sand content, very commonly less than 1 per cent, although tongues of higher sand content extend out onto the slopes off each of the main passes and the sand extends to a somewhat greater depth directly off the artificially deepened Southwest Pass, where as much as 60 per cent sand is found at a depth of about 26 feet, and 33 per cent at 52 feet. These relations are shown to best advantage in Figure 10 where sand content is plotted against depth.

The sand content on the slopes reaches a minimum for the entire area. Out

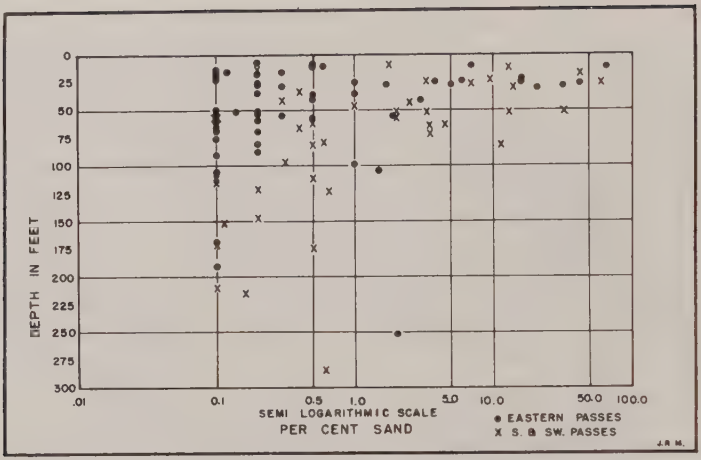

FIG. 10.—Variation of sand content plotted against depth for slopes off eastern passes and off South and Southwest passes. Very low percentages of sand are found even in shallow water.

in the bottomset-bed area of the shelf beyond the slope off North Pass and Dead Women Pass area, the sand increases away from the delta rather than decreasing, because of the tidal currents. The boundary between the bottomset beds of the recent delta and "old shelf deposits" is marked by a large increase in the sand content even where the water has a greater depth. The sand content in the shallow "reworked Mississippi Delta" area is even higher especially on the platforms near Gosier and Breton islands, where waves and currents have worn and cut the fine material.

Sand is relatively scarce in the inlet between the island platforms and is variable in the inlet between the delta and Breton Island. A tongue with low sand extends north from Baptiste Collette and northwest from Main Pass into Breton Sound, but elsewhere in Breton Sound relatively high sand contents have been found.

The average silt content in the sediments (Fig. 11) is far higher than sand in all of the environments dominated by sediment derived from the present rivers. In the delta and on the adjacent platforms silt exceeds both clay and sand. Like sand, the silt abundance is closely related to distributary mouths. In the delta-front platform there are layers of coarse silt, as well as sand, interbedded with silty clays. The silty layers are so abundant as to increase greatly the silt content of the top 5 centimeters used in the analyses. The high silt content in the shallow shelf area, centering 10 miles north of North Pass, represents mottled silty masses found consistently in the cores of this area. The same is true of the zones of abundant silt in Breton Sound. The silt content is in general higher around the Mississippi Delta than along other parts of the Gulf Coast (Shepard and Moore, 1955a, Fig. 26). Near the delta there are extensive areas with more than 40 per

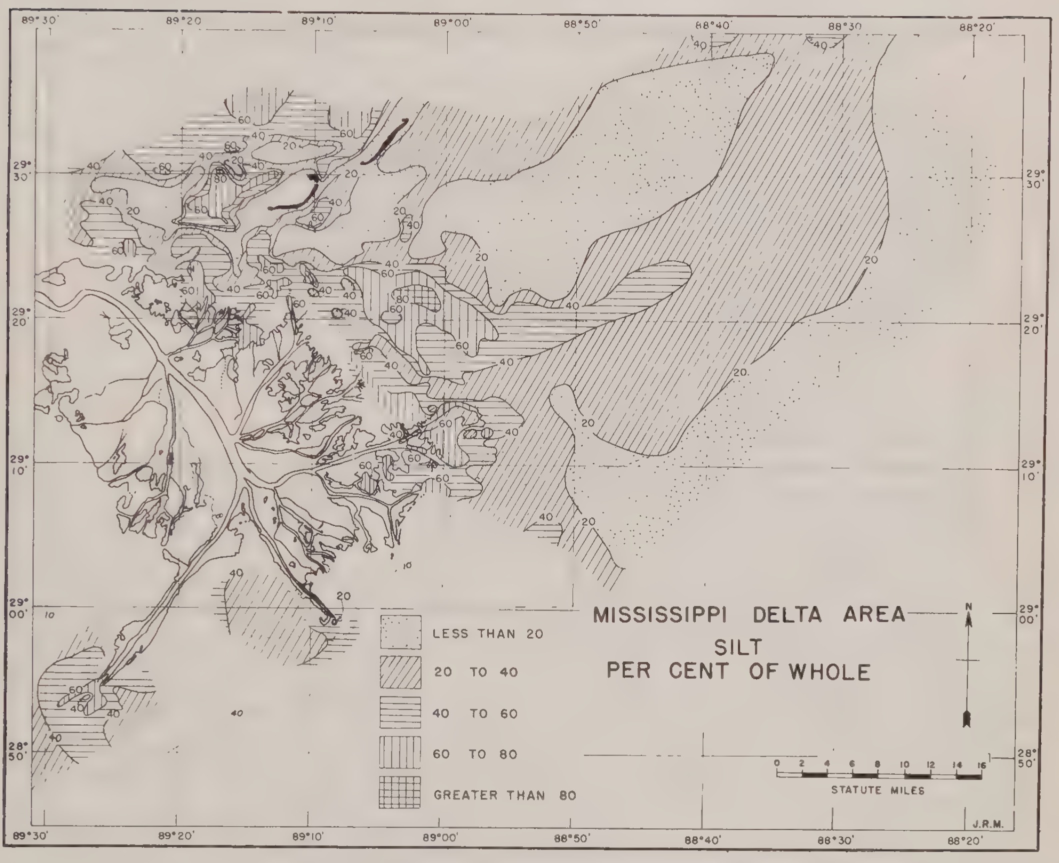
MISSISSIPPI DELTA AREA
SILT
PER CENT OF WHOLE
LESS THAN 20
20 TO 40
40 TO 60
60 TO 80
GREATER THAN 80
N
0 2 4 6 8 10 12 14 16
STATUTE MILES
J.R.M.
89°30'
89°20'
89°10'
89°00'
88°50'
88°40'
88°30'
88°20'
29° 30'
29° 20'
29° 10'
29° 00'
28° 50'

FIG. 11.—Variation in silt content of sediments marginal to Delta, varying from high concentration near distributaries to low values off shore.

cent silt, whereas along the rest of the Gulf Coast such percentages are very rare on the shelf and even rarer in the bays.

The map showing abundance of clay (Fig. 12) contains values that are to some extent inverse to that of the sand map. In a portion of the east part of the clay map, however, sand and clay are both relatively high, and the silt content low. The zone of highest clay is found near the base of the slope off the Pass a Loutre mouths and on the shelf directly beyond. A rapid increase in clay takes place just beyond the platform and the increase continues down the slope outside each of the principal distributaries, but is more gradual on the slope between river mouths, as, for example, in the zone between North Pass and Pass a Loutre. Off all of the passes there appears to be a consistent 50–70 per cent clay

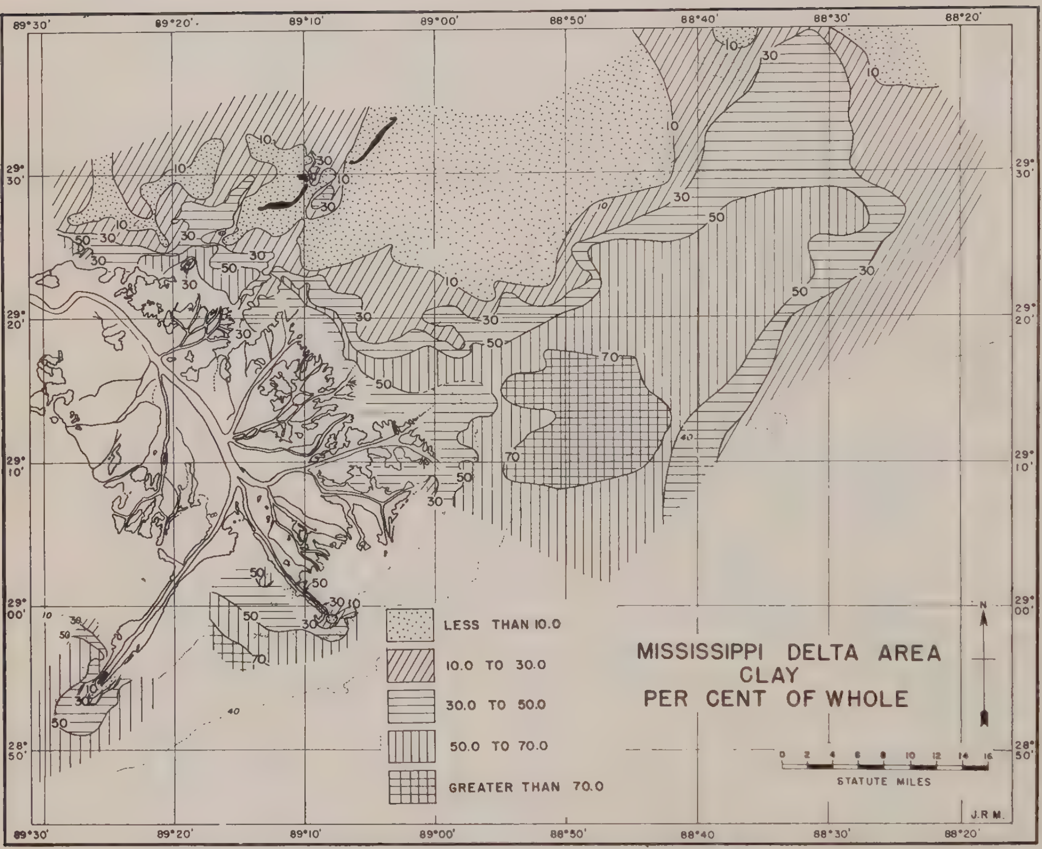
89°30'
89°20'
89°10'
89°00'
88°50'
88°40'
88°30'
88°20'
29° 30'
29° 20'
29° 10'
29° 00'
28° 50'
LESS THAN 10.0
10.0 TO 30.0
30.0 TO 50.0
50.0 TO 70.0
GREATER THAN 70.0
MISSISSIPPI DELTA AREA
CLAY
PER CENT OF WHOLE
N
0 2 4 6 8 10 12 14 16
STATUTE MILES
J.R.M.

Fig. 12.—Variation in clay content of sediments marginal to delta.

zone found within a few miles of the river mouths and forming a band around the distributaries. This "band" of high clay is much narrower off Main Pass where the currents coming up into the strait between the delta and Breton Island have had a winnowing effect. On the flanks of each of the prominences of low clay off the passes there are zones of very high clay and in some places these come very close to the outer levees. Thus there are percentages as high as 60 about a mile off both Southwest and South passes and more than 70 within 2 miles of the north levee of North Pass. Off the east levee of Main Pass the clay attains 70 per cent within 1½ miles of the mouth. These marginal high percentages of clay, however, are not maintained in the inner ends of the interdistributary bays. Actually the heads of both Blind Bay and Buras Bay have percentages of clay around 10, so that it is not advisable to refer to these bays as "clay wedges" (Fisk *et al.*, 1954, p. 92).

The samples taken in the river channels, on the levees, and in the marshes are fairly consistent in clay content. In all but one location, clay is less than 60 per cent and the median content is 26 per cent.

A map which represents an integration of the sand, silt, and clay maps (Fig. 13) is based on the nomenclature favored by the majority of a group of well known sedimentationists who were polled on the subject (Shepard, 1954). In this map also a banded structure is found around the advancing distributaries, with sandy silt bordered by clayey silt and in turn by silty clay. East of Pass a Loutre the silty clay area has an extent of almost 30 miles but it is in turn bordered by coarser sediment which (following the outer boundary in a counterclockwise direction) ranges from a sandy clay through sand-silt-clay to sandy silt. The sediment of the "reworked Mississippi Delta" area east of the islands is

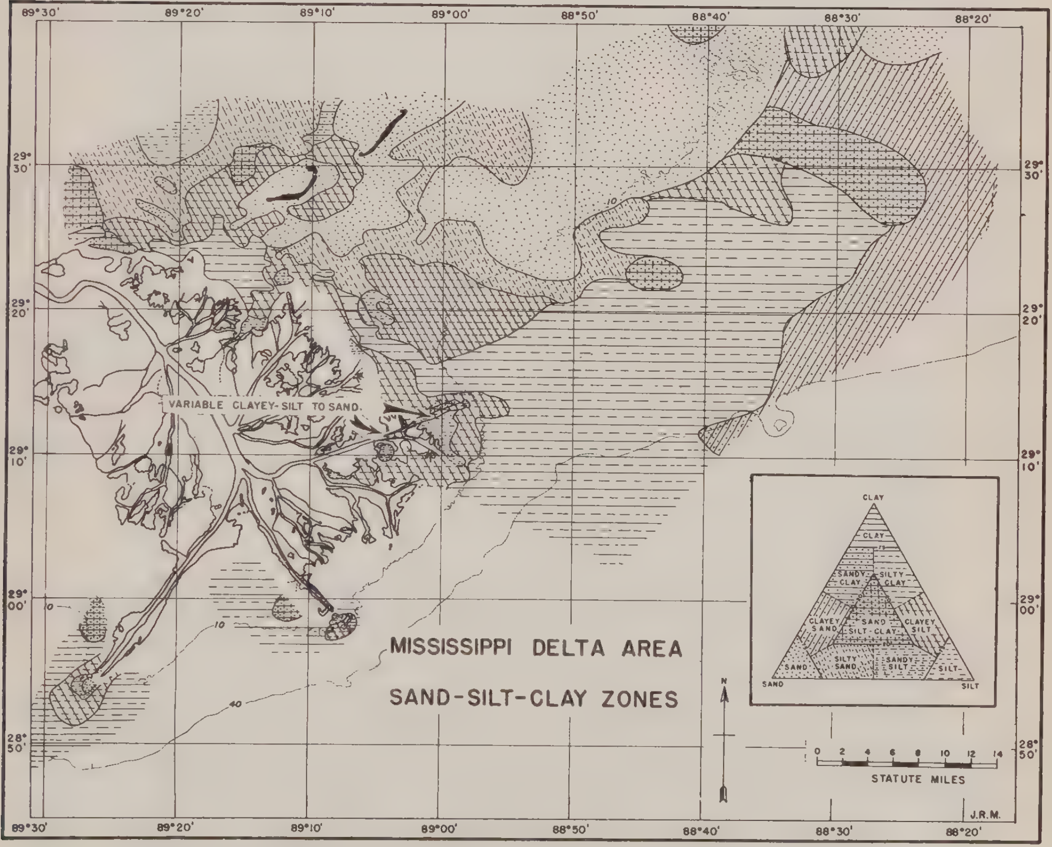
89°30'
89°20'
89°10'
89°00'
88°50'
88°40'
88°30'
88°20'
29° 30'
29° 20'
29° 10'
29° 00'
28° 50'
10
40
VARIABLE CLAYEY-SILT TO SAND.
MISSISSIPPI DELTA AREA
SAND-SILT-CLAY ZONES
N
CLAY
CLAY
75
SANDY CLAY
SILTY CLAY
20
SAND SILT-CLAY
CLAYEY SAND
CLAYEY SILT
SAND
SILTY SAND
SANDY SILT
SILT
SAND
SILT
0 2 4 6 8 10 12 14
STATUTE MILES
J.R.M.

FIG. 13.—Sediment distribution based on sand-silt-clay content in area marginal to delta. For interpretation of symbols, see triangle diagram.

mostly sand, containing less than 20 per cent silt and clay in most places. At the east, Breton Sound sediments consist mostly of silt and sand. The inlet areas are even more variable, with much of the zone between Breton Island and Gosier Island consisting of clayey silt, whereas between Breton Island and the delta there is a mixture of almost all of the types of sediments of the entire area.

RELATIVE ABUNDANCE OF FINE AND VERY FINE SAND

In studying the deposits off the central Texas coast the principal difference found between barrier island beach sands and the sands in the open Gulf directly outside the islands was that the former have almost equal amounts of fine and very fine sand, whereas the latter have a great excess of very fine sand (Shepard and Moore, 1955a, Fig. 51). For further checks on this criterion for distinguishing environments, the ratios of fine sand to very fine sand ($2-3\phi/3-4\phi$) fractions were checked in about 300 samples from the delta area. These were plotted, and contours have been drawn from these ratios (Fig. 14). Surprisingly consistent relations were found. Almost all of the samples from the islands and from the "reworked Mississippi Delta" area at the east have higher percentages of fine sand than of very fine sand. A similar greater abundance of the fine sand is found in the "old shelf deposits" east and southeast of the great arc of clayey sediments that spreads easterly from the Pass a Loutre distributaries. Other small areas where fine sand is in excess occur in Breton Sound, in Main Pass, in North Pass, and at the mouth of South Pass[6] on the spit and on the submerged levee. Otherwise the entire apron of deposits around the delta has a considerable excess of very fine sand.

The interpretation which is suggested by the distribution of the areas with more fine than very fine sand is that the river is introducing an ample supply of fine sand. Then, that the waves along the delta front are producing beaches which concentrate this fine sand on the shore but carrying out much of the very fine sand beyond the confines of the land where it is deposited outside of the influence of strong wave or current action. If this interpretation is correct, the relatively deep water zones where fine sand still predominates consist of old beach deposits not yet adjusted to their new environments. Such an interpretation is in line with most of the faunal evidence.

Another area with sand coarser than typical shelf sand is found near the outer shelf edge off the Galveston area. This sediment also is distinctive in character from the bordering shelf deposits and is presumably an old beach.

COARSE-FRACTION STUDIES

"Coarse-fraction" analyses as developed at Scripps Institution (Shepard and Moore, 1954) consist of classification and quantitative evaluation of types of constituents in sieved sizes of the coarse fraction. These sievings follow the

---

[6] Trowbridge (1930, Figs. 9 and 10) showed two bar-mouth samples off South and Southwest passes, respectively, with more fine than very fine sand.

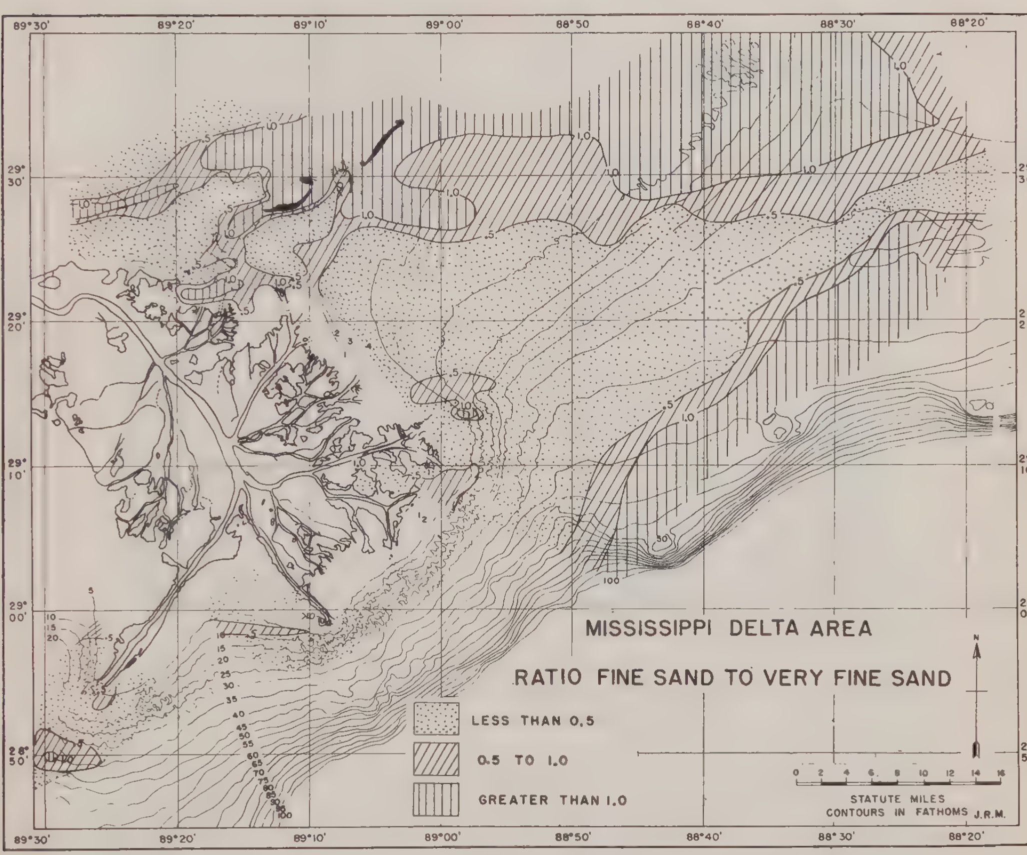
MISSISSIPPI DELTA AREA
RATIO FINE SAND TO VERY FINE SAND
LESS THAN 0.5
0.5 TO 1.0
GREATER THAN 1.0
STATUTE MILES
CONTOURS IN FATHOMS
J.R.M.
N
89°30'
89°20'
89°10'
89°00'
88°50'
88°40'
88°30'
88°20'
29° 30'
29° 20'
29° 10'
29° 00'
28° 50'

FIG. 14.—Relative abundance of fine sand compared with very fine sand. Relationh of zones with excess of fine sand to reworked Mississippi Delta and old shelf areas is clearly indicated.

standard Wentworth divisions of $\frac{1}{8}$–$\frac{1}{16}$ mm. (4–3ϕ), $\frac{1}{4}$–$\frac{1}{8}$ mm. (3–2ϕ), $\frac{1}{2}$–$\frac{1}{4}$ mm. (2–1ϕ), 1–$\frac{1}{2}$ mm. (1–0ϕ), and larger than 1 mm. If sievings are too large for a microscope tray, they are split by several sample-splitting techniques into amounts just large enough to cover the surface of a gridded tray without having any buried grains. A "Denominator Counter" is then used with a keyboard which is easy to operate by the touch system while looking through the binocular microscope. This procedure develops a statistical method which seems sufficiently reproducible to separate sediments from the various environments.' Ordinarily 100 grains are believed to be sufficient for the purpose but when the constituents are variable, the counting is carried on to 200 or more. After each sieve size has been counted, the total percentages for the entire sample are computed by using the weight percentage of each sieving. The maps included in this report are based on the results of these total percentages, the entire weight of the sand fraction of each sample considered as 100 per cent.

In the present study the following constituents were selected as most significant: terrigenous (land-derived minerals such as quartz, feldspar, and ferromagnesians); mica (which is counted separately from other terrigenous minerals because it has special hydraulic significance due to its platy character); wood (including fibers, seeds, and other land-plant materials); aggregates; glauconite; and four types of organic remains including mollusk shells (called shells), echinoids, Foraminifera, and ostracods. In addition, relatively rare constituents such as pyrite, gypsum, diatoms, and bryozoans are counted where present. On the other hand, volcanic shards, which are fairly common in most of the sediments, are included with the terrigenous because they are rather difficult to separate from terrigenous in making the coarse-fraction analyses. They were studied separately and are discussed elsewhere in the paper.

Because the contacts between environments are somewhat gradational in most parts of the area, it seemed advisable to develop a series of maps with contours showing percentage of the coarse fraction for the main constituents (Figs. 15–22). The distribution of analyzed samples used for this purpose is shown in Figure 6. All of these analyses were from near-surface sediments. Although there are some irregular zones where contouring was difficult, notably at the mouths of the rivers, most of the values fit into a simple pattern so that the contours appear meaningful, and only rarely is there a sample which falls completely out of character with its surroundings. In choosing the contours for each principal constituent, values were picked which showed the variation for each constituent. Therefore the contour intervals vary.[7]

Wood (fibers, seeds, et cetera).—Next in abundance to the terrigenous materials in the coarse fractions of the area are plant fibers, seeds, and other woody materials (Pl. I, Fig. 1) transported into the area by the rivers. The general abundance of wood around the delta stands in contrast to most of the environments in the central Texas area where no wood was found in the great majority of the coarse fractions although wood materials appear in the sediments which are marginal to the bay deltas (Shepard and Moore, 1955a, p. 1531). A trip down any of the Mississippi passes will serve to demonstrate the abundance of wood along the distributaries of the birdfoot delta, so it is not at all surprising to find high percentages in the coarse fraction in the belts around the river mouths. In the map showing abundance of wood (Fig. 15) there is a clear relation between the contours and the river distributaries, particularly for the two branches of Pass a Loutre. The tongue of woody material which can be traced for more than 30 miles east-northeast of the Pass a Loutre mouths is particularly striking. The 1 per cent contour falls fairly close to the boundary between the slope and the

---

[7] For those wishing to know more about the values in any particular area, the information may be obtained by communicating with the writer.

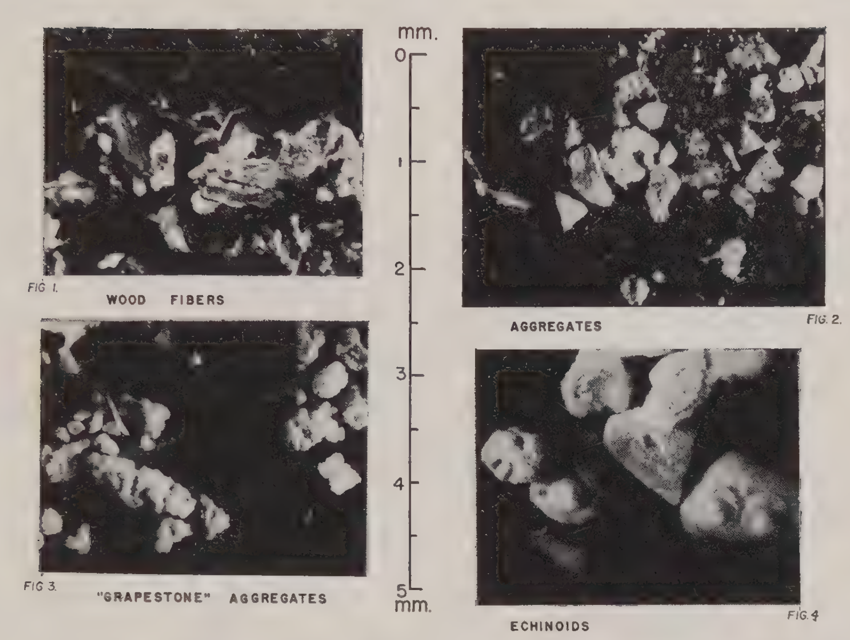

PL. I.—Photomicrographs of sieved samples from Mississippi Delta area.

FIG. 1. Wood fibers in ¼–½-mm. sieving in sample from Southwest Pass.

FIG. 2. Aggregate and wood fibers in ¼–½-mm. sieving from Blind Bay. Aggregates have orange color.

FIG. 3. Peculiar type of aggregate having quartz grains and calcareous cement, from ¼–½-mm. sieving of sample from Buras Bay near Main Pass.

FIG. 4. Typical echinoid plates showing base of spine and sugary texture from ½–1-mm. sieving of open-shelf sample.

bottomset shelf beds. Tongues of high wood content also extend north from Main Pass up through the inlet between Breton and Gosier islands and north from Baptiste Collette into Breton Sound. Another tongue extends out to the limit of sampling off Southwest Pass and off South Pass. An appreciable wood content on the shelf was found about 70 miles west of Southwest Pass.[8] Three samples 40–50 miles west of the pass have wood percentages of 2.2, 5.2, and 37.3 in the coarse fraction.

One of the striking features about the abundance of wood east of the delta is the increased percentages found on the slopes a few miles beyond several of the mouths. Wood reaches its highest percentages about 4 miles outside Pass a Loutre and Dead Women Pass and about a mile off Baptiste Collette. Similarly, highest wood content is found about 2 miles from the mouth of South Pass, and

---

[8] These samples were obtained during a cruise made by A.P.I. Project 51 in an investigation of the continental shelf west of the delta to be reported later.

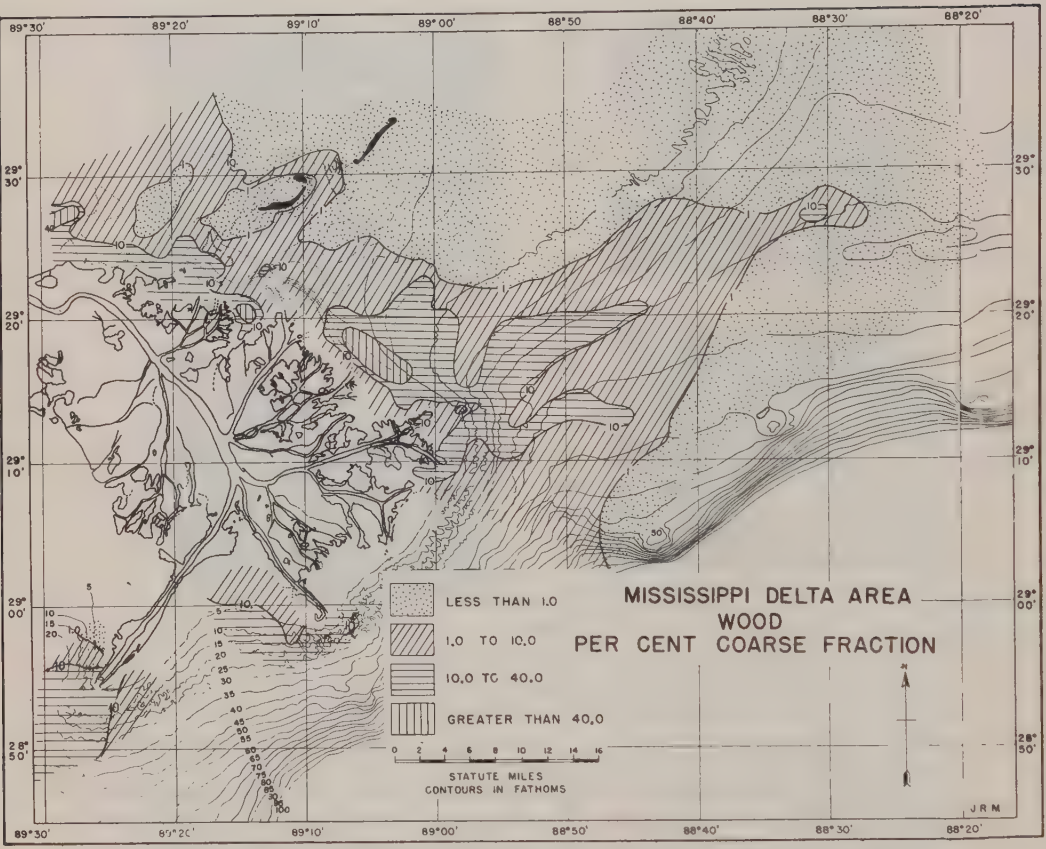
MISSISSIPPI DELTA AREA
WOOD
PER CENT COARSE FRACTION
LESS THAN 1.0
1.0 TO 10.0
10.0 TO 40.0
GREATER THAN 40.0
0 2 4 6 8 10 12 14 16
STATUTE MILES
CONTOURS IN FATHOMS
89°30'
89°20'
89°10'
89°00'
88°50'
88°40'
88°30'
88°20'
29° 30'
29° 20'
29° 10'
29° 00'
28° 50'
N
J R M

Fig. 15.—Abundance of land plant constituents (wood) in coarse fraction. Indicates large tongue of woody materials extending well east of Pass a Loutre.

off Southwest Pass it increases a short distance beyond the river-mouth bar. Evidently the waterlogged wood which is being carried down the channels does not lodge in as large quantities on the platform and bars as on the slopes beyond where the waves and currents are less vigorous. The deposition of wood on these slopes must be enormous in order to have wood constitute such a large percentage of the coarse fraction in an area where there is an extremely rapid deposition rate such as 100 feet in 70 years (Shepard, 1955).

The river channels are variable in wood content but for the most part the wood content is not as high in the channels as on the slopes beyond the platforms. Exceptions are found in parts of Pass a Loutre and North Pass where in one sample the wood content attains the record value of 80 per cent of the coarse fraction (Fig. 36). In general, where the river bottom has a high sand content the wood is scarce. The levees and the marshes have somewhat higher wood content than the channels.

Wood is very scarce in the old shelf deposits and in the reworked Mississippi Delta deposits, but it is found in the majority of the samples at least in small quantities.

Aggregates.—Examination of numerous sediments deposited near river mouths along the Gulf Coast shows that many grains are cemented together as aggregates (Pl. I, Fig. 2). After treatment of the sediments with sodium hexametaphosphate (the standard system for preparing the coarse fractions for microscopic examination), the looser assemblages are disaggregated but many rather firmly knit aggregates are left in the various sievings. These consist of clayey masses, more or less firmly knit together, and include numerous sand grains as well as silt-size particles, and commonly include masses of wood material. Some of the aggregates consist of "grapestone" groups (Pl. I, Fig. 3). It seems likely that in sedimentary rocks formed from these deposits, the aggregates could still be detected as rock fragments. Those that had been cemented together with iron oxide would be most easily recognized because of their color in contrast to the surrounding sediments.

In many respects the aggregates (Fig. 16) have a distribution similar to that found for the woody materials, suggesting a possible causal relation. Thus they increase in abundance in many places a short distance out from the mouths of the passes and in general they reach their greatest abundance on the delta-front platforms and on the pro-delta slopes, both off the eastern passes and off the artificial South and Southwest passes. Several of these samples have more than 50 per cent of their coarse fraction as aggregates, and one sample in Blind Bay has a total of 72 per cent aggregate.

Long tongues where the samples have relatively high aggregate content extend about 30 miles east of the Pass a Loutre mouths, but the aggregate percentages are less consistent than those of wood in this same area. Aggregates occur in most stream-channel deposits but are more abundant in the natural levees and most abundant in the marsh deposits.

The principal colors of aggregates are orange, yellow, and white (colorless). The white aggregates tested have calcium carbonate cement, and the others presumably are due to ferruginous cements with varying degrees of oxidation. The color distribution has a very distinct relation to the environments. Thus the typical aggregate found in the river channels is colorless with only an occasional yellow or orange aggregate. On the natural levees some orange-colored aggregates appear but the colorless aggregates are somewhat more abundant. In the marsh samples of Baptiste Collette, on the other hand, the aggregates are predominantly ferruginous with an orange color. On the bars and platforms most of the aggregates are ferruginous and a particular abundance of the orange colors is found in the interdistributary bay deposits. Off Southwest Pass, where vir-

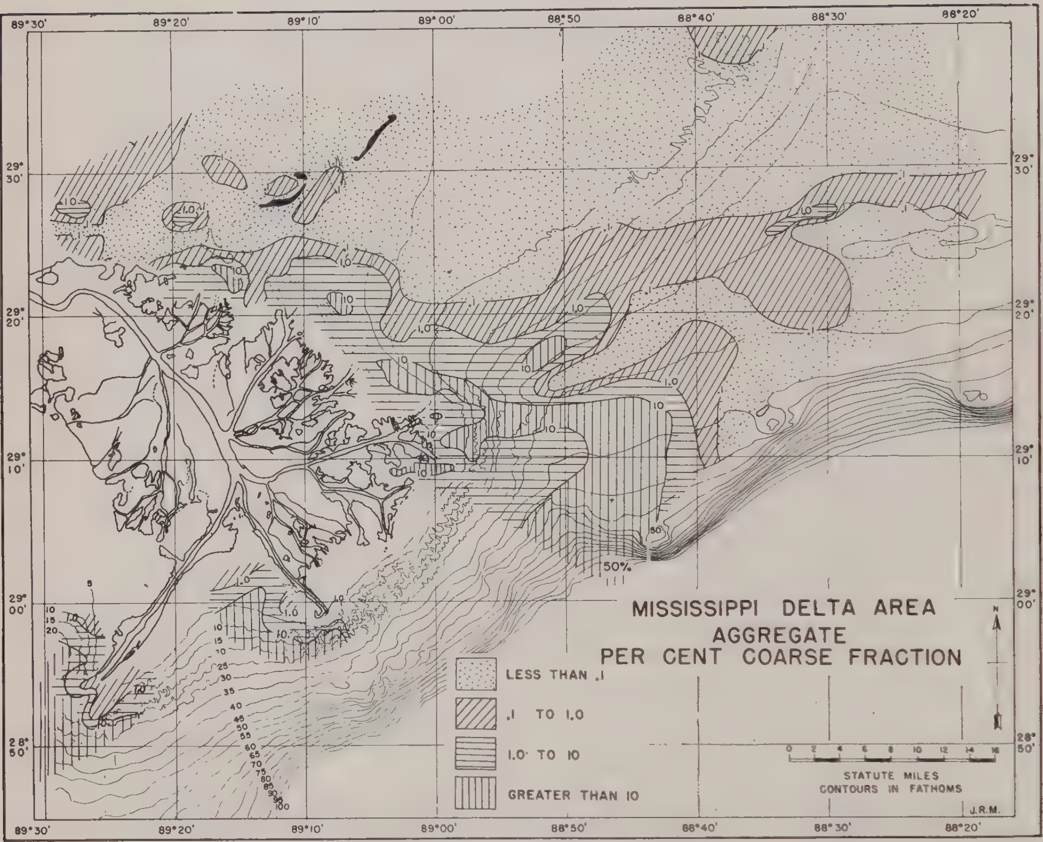
MISSISSIPPI DELTA AREA
AGGREGATE
PER CENT COARSE FRACTION
LESS THAN .1
.1 TO 1.0
1.0 TO 10
GREATER THAN 10
STATUTE MILES
CONTOURS IN FATHOMS
J.R.M.
50%
89°30'
89°20'
89°10'
89°00'
88°50'
88°40'
88°30'
88°20'
29° 30'
29° 20'
29° 10'
29° 00'
28° 50'
N

FIG. 16.—Abundance of aggregates in coarse fraction. General resemblance to wood distribution and relation to distributaries are indicated.

tually all of the samples were obtained from the slope surrounding the bar at the mouth of the river, all of the samples contain orange aggregates although a few yellow and white aggregates are included also in some of the samples. East of the Pass a Loutre mouths the orange aggregates predominate on the platform. Orange aggregates are dominant along the delta margin at Baptiste Collette, but except near the delta the rather rare aggregates found in Breton Sound are almost all white or colorless. Southeast of Pass a Loutre the orange-colored aggregates were found in a sample obtained at a depth of 550 feet on the slope. On the shelf 50 miles west of the birdfoot delta a sample contained orange to reddish aggregates in a depth of 120 feet. Thus, these ferruginous aggregates may be either transported to very considerable distances from their delta source, or may be formed in the wood-bearing deltaic sediments after deposition. In any case the orange ferruginous colors generally develop after the material has been transported out of the river channel either into the marshes or onto the platform, slope, or shelf beyond.

Mica.—The only other abundant constituent which shows a close relation to the delta deposits is mica (Fig. 17). This consists predominantly of muscovite. In many respects the distribution of mica abundance is similar to that of wood and aggregates. The tongue where mica exceeds 1 per cent extends 30 miles east of Pass a Loutre with approximately the same outline as the tongue with more than 1 per cent wood. Other tongues extend up into Breton Sound where mica is relatively more abundant than wood or aggregates. Unlike the latter, mica

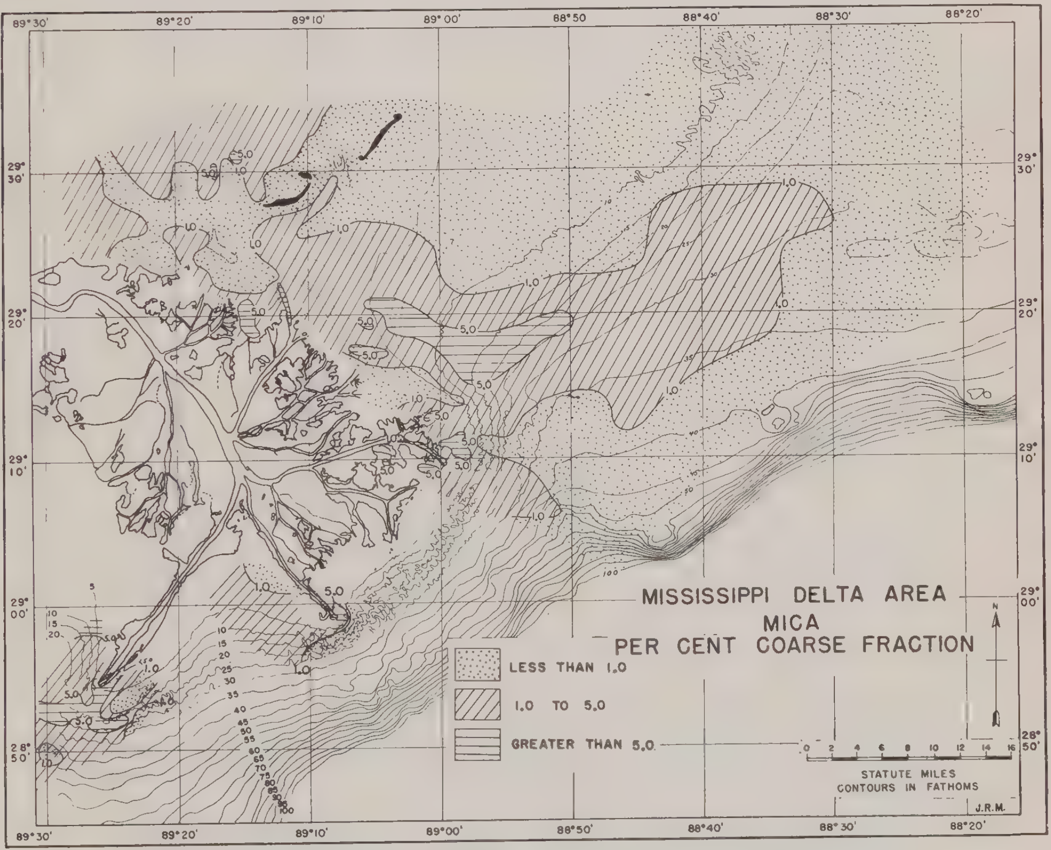
89°30'
89°20'
89°10'
89°00'
88°50'
88°40'
88°30'
88°20'
29° 30'
29° 20'
29° 10'
29° 00'
28° 50'
MISSISSIPPI DELTA AREA
MICA
PER CENT COARSE FRACTION
LESS THAN 1.0
1.0 TO 5.0
GREATER THAN 5.0
N
0 2 4 6 8 10 12 14 16
STATUTE MILES
CONTOURS IN FATHOMS
J.R.M.

FIG. 17.—Abundance of mica in coarse fraction. Similarity of distribution to that of wood and aggregates may be observed.

does not increase consistently in abundance on the slopes outside the platform edge. Areas high in mica, however, do occur in a zone about 8 miles off the sector of the delta from Dead Women Pass to North Pass. Mica is also abundant in most of the distributary channels and on the natural levees but less abundant in the marshes. It is particularly scarce in the "old shelf deposits." This scarcity may be a result of the derivation of the sediment from southern Appalachian rivers which do not contain nearly as many mica flakes of sand size as the Mississippi. The mica is also scarce in the reworked Mississippi Delta deposits, although here presumably the sediment was derived from the St. Bernard Delta (Russell, 1936, p. 71, and Scruton, 1955, Pl. I). The mica could have been removed from these old delta deposits by attrition of the currents and vigorous wave action in the shallow water. In view of the general abundance of mica around the passes it is somewhat surprising to find an area within 3 miles of Pass a Loutre in which the mica is extremely scarce. The explanation of this anomaly is not evident.

Foraminifera (largely calcareous).—In considering the Foraminifera in the coarse fraction it is important to remember that the use of sodium hexametaphosphate may cause the disaggregation of many of the arenaceous Foraminifera, although many of the arenaceous types on the outer shelf, which are better cemented than those near shore or in bays, survive the treatment. The map of Foraminifera abundance in the coarse fraction (Fig. 18) should be considered essentially as a map of the abundance of calcareous types of Foraminifera. For a more complete picture of the Foraminifera, including the arenaceous varieties, the reader is referred to Phleger (1955). Unlike the wood, aggregate, and mica constituents, the calcareous Foraminifera are virtually missing in and around the distributary mouths. The Foraminifera are also relatively scarce on the slopes where the previously discussed constituents are abundant. Near the base of the slope, however, the Foraminifera increase in a remarkably short distance so that the most abundant Foraminifera are found on the inner part of the shelf beyond the slope. Here the Foraminifera reach a maximum, consisting of 42 per cent of the coarse fraction. The Foraminifera on the deeper shelf have a large percentage of planktonics, and the ratio of planktonics to benthonics increases roughly with the distance from the delta. The relation of Foraminifera abundance to the various passes, though largely inverse to those of wood, aggregate, and mica constituents, nevertheless conforms in outline to the passes. Thus, east of the Pass a Loutre mouths, a concentric band very low in Foraminifera is bordered by a great tongue with abundant Foraminifera. This in turn is partly ringed by belts with progressively decreasing Foraminifera. Similar concentric bands occur off Southwest and South passes and off both Main Pass and Baptiste Collette.

Very low foraminiferal content is the rule in the "old shelf deposit" area and they are equally scarce or entirely missing in the "reworked Mississippi Delta deposits." The relative scarcity of Foraminifera in Breton Sound, however, is

(902)

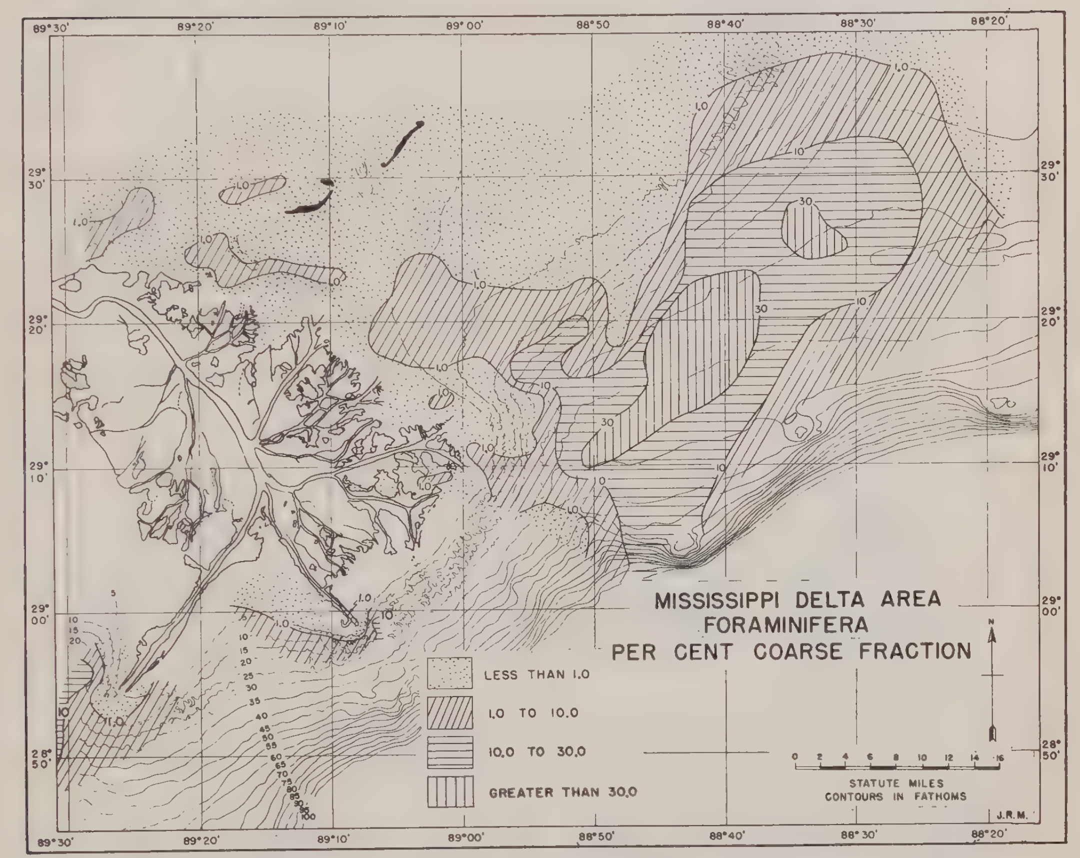
MISSISSIPPI DELTA AREA
FORAMINIFERA
PER CENT COARSE FRACTION
LESS THAN 1.0
1.0 TO 10.0
10.0 TO 30.0
GREATER THAN 30.0
STATUTE MILES
CONTOURS IN FATHOMS
0 2 4 6 8 10 12 14 16
N
J.R.M.
89°30'
89°20'
89°10'
89°00'
88°50'
88°40'
88°30'
88°20'
29° 30'
29° 20'
29° 10'
29° 00'
28° 50'
1.0
10
30

FIG. 18.—Abundance of Foraminifera in coarse fraction. Elimination of many arenaceous Foraminifera in preparing samples makes this map essentially an abundance of calcareous Foraminifera. Foraminifera, unlike wood, aggregate, and mica fractions, are very scarce near delta, and increase tremendously at base of slope east of Pass a Loutre.

somewhat illusory because rather numerous arenaceous Foraminifera occur in this area (Phleger, 1955, Figs. 14–16).

The finding of Foraminifera in some river samples, especially near the mouths, was at first believed to mean that these were of fossil origin, but examination of the live Foraminifera in North Pass and Pass a Loutre by R. R. Lankford shows clearly that living Foraminifera penetrate these distributaries, possibly coming up with the salt wedge into the river mouths. Two of the levee samples also showed a fair number of Foraminifera. The majority of the channels, however, did not have any Foraminifera in the coarse-fraction counts. Furthermore, no

Foraminifera were observed in the marsh deposits, but this again is illusory because arenaceous Foraminifera predominate in these areas.

The general scarcity of Foraminifera over a moderately wide belt off the pass mouths is in line with the scarcity of Foraminifera on the shelf 50 miles west of Southwest Pass. Still farther west an abundance of Foraminifera, particularly planktonic, is found in the outer shelf sediments.

The typical species of Foraminifera related to certain of the sedimentary environments are indicated in Plate II prepared by R. R. Lankford. As Phleger (1955) has demonstrated, the Foraminifera are clearly related to the salinity patterns around the delta, and a distinct difference exists between the open-shelf and the Breton Sound Foraminifera, with a transitional zone occurring in the inlet environment between these two areas.

Shells (*largely mollusks*).—Macroorganisms of the east delta area have been discussed by Parker (1956), who found assemblages that fitted into environmental patterns which are not too different from those suggested for the sediments in the present paper. This is not surprising since Parker found a close correlation of organism distribution with sediment type. Thus he found marsh, sound, and inlet environments, and a contrast in fauna between shallow and deep shelf at approximately 11 fathoms. His "Delta shores and distributary" environment corresponds in some degree with the delta-front platform and river channels, and the "lower sound" and "lower delta clays" correspond with the prodelta slope. These zones of faunal assemblages, like the contours in the sand-silt-clay maps, form concentric bands around the distributaries, notably Pass a Loutre and North Pass.

The coarse-fraction studies throw further light on this faunal pattern by supplying percentages of shells (predominantly mollusks) found in the various coarse fractions (Fig. 19). This map may be compared with a diagram which Parker has prepared showing the number of living organisms in his various samples (Fig. 20). These centers of abundance correspond roughly with the centers of large population of Foraminifera (Phleger, 1955, p. 733). The map (Fig. 19) based on the coarse-fraction studies shows that shells are rare around all of the passes. The same is true of the river channel stations and of most of those in the marshes. Levees on the other hand, as far as examined, appear to have a fair abundance of shells which may be concentrated by currents in this zone.

Farther seaward the shells increase toward the base of the slope and are moderately abundant (5–20 per cent of the coarse fraction) in much of the shelf area 20 miles or more east of the delta. The areas of highest shell content are found in the southern tip of the inlet environment east of Main Pass and in the tongue extending northwest of the inlet environment between Gosier and Breton islands. In the latter, a true shell-sand is found locally, and can be attributed to the relatively strong currents which sweep back and forth between the islands. A high shell content is also indicated on the west side of Breton Sound, as would be expected from the reworking of old oyster reefs.

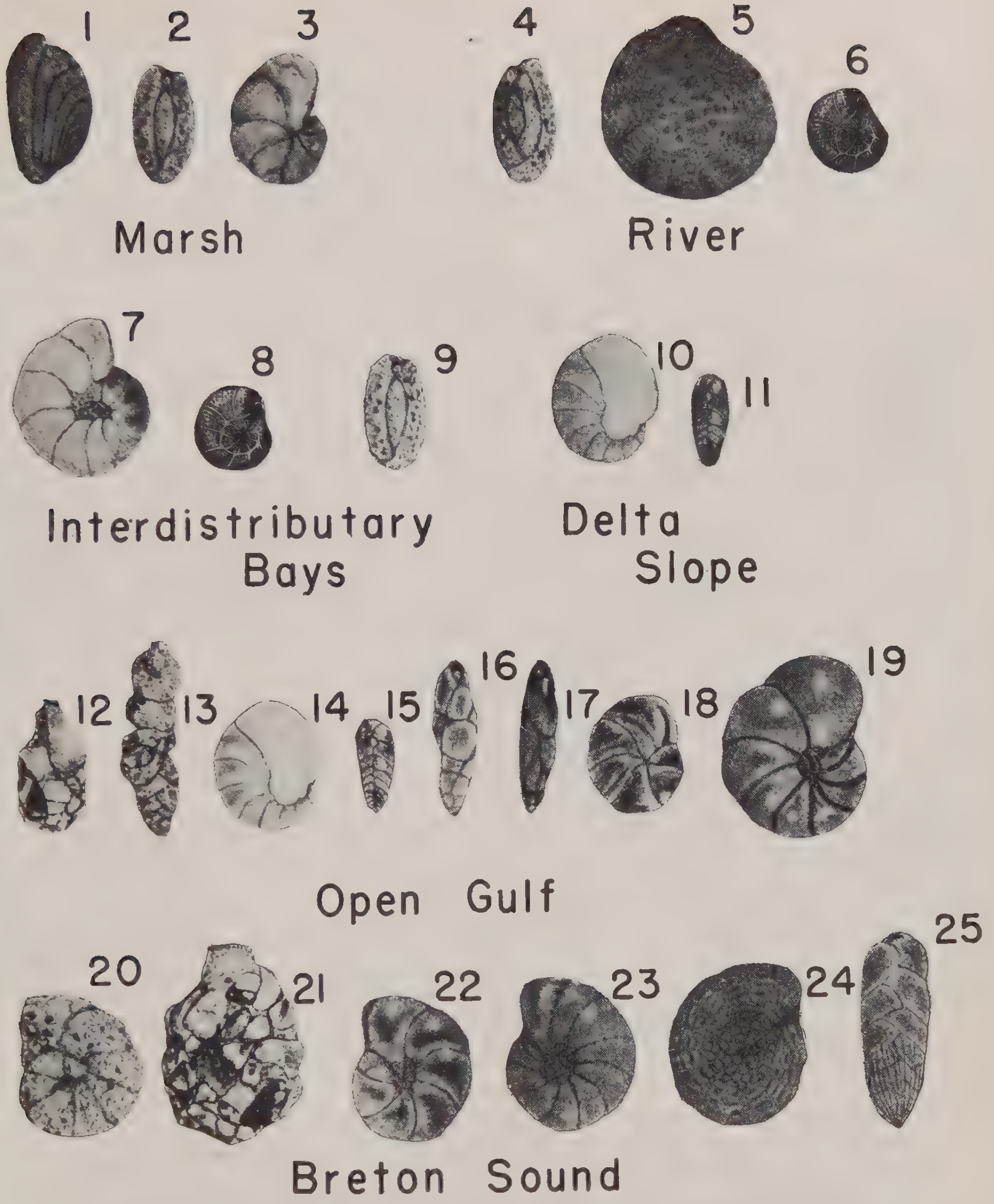
1
2
3
4
5
6
Marsh
River
7
8
9
10
11
Interdistributary Bays
Delta Slope
12
13
14
15
16
17
18
19
Open Gulf
20
21
22
23
24
25
Breton Sound

Pl. II.—Foraminifera particularly characteristic of sedimentary environments in vicinity of Mississippi Delta. Open Gulf assemblage is found mostly in bottomset beds.
Prepared by R. R. Lankford.

Fig.	*Name*
1	*Ammoastuta inepta*
2	*Miliammina fusca*
3	*Trochammina macrescens*
4	*Miliammina fusca*
5	*Elphidium gunteri*
6	*Eponidella gardenislandensis*
7	*Elphidium delicatulum*
8	*Eponidella gardenislandensis*
9	*Miliammina fusca*
10	*Nonionella opima*
11	*Bolivina lowmani*
12	*Proteonina atlantica*
13	*Bigenerina irregularis*
14	*Nonionella opima*
15	*Bolivina lowmani*
16	*Buliminella* sp. cf. *B. bassendorfensis*
17	*Virgulina pontoni*
18	*Epistominella vitrea*
19	*Hanzawaia strattoni*
20	*Ammobaculites dilatatus*
21	*Ammoscalaria pseudospiralis*
22	*Elphidium matagordanum*
23	*Elphidium incertum mexicanum*
24	*Elphidium gunteri*
25	*Bolivina striatula*

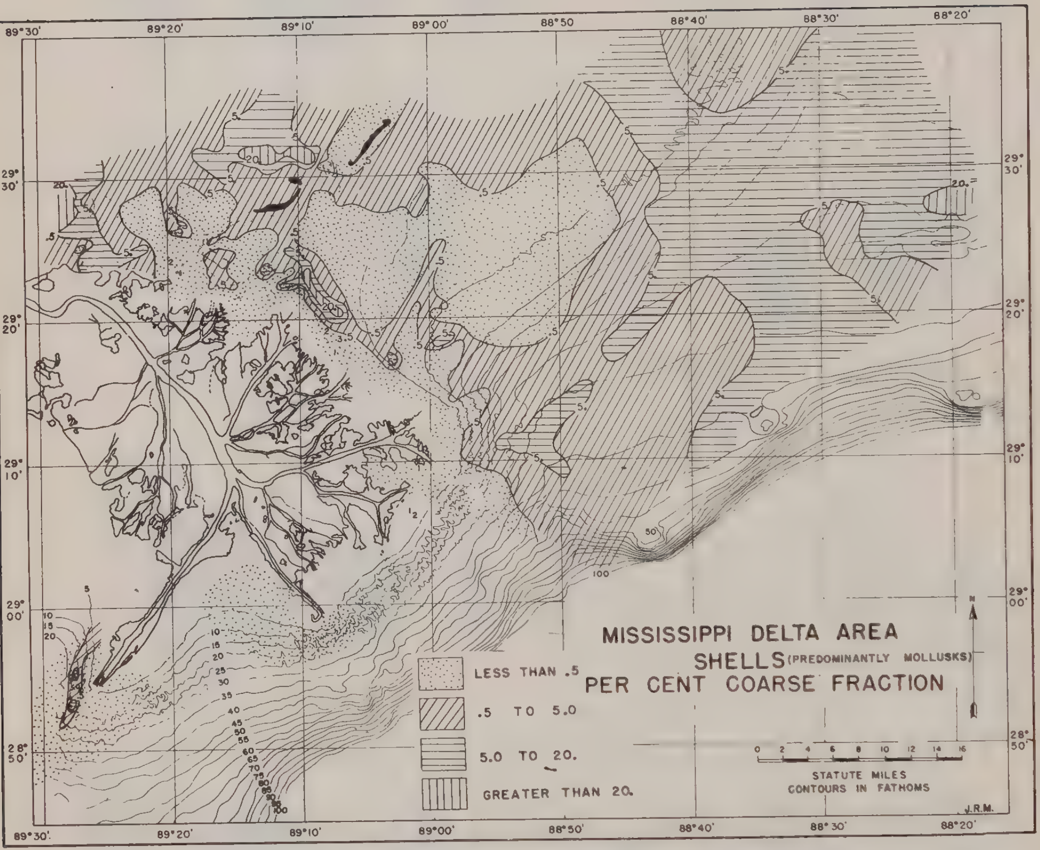
MISSISSIPPI DELTA AREA
SHELLS (PREDOMINANTLY MOLLUSKS)
PER CENT COARSE FRACTION
LESS THAN .5
.5 TO 5.0
5.0 TO 20.
GREATER THAN 20.
0 2 4 6 8 10 12 14 16
STATUTE MILES
CONTOURS IN FATHOMS
J.R.M.
N
89°30'
89°20'
89°10'
89°00'
88°50'
88°40'
88°30'
88°20'
29° 30'
29° 20'
29° 10'
29° 00'
28° 50'
100
50

FIG. 19.—Abundance of shells (predominantly mollusks) in coarse fraction. Like Foraminifera, low percentages are found around distributaries and highest percentages at some distance from delta (compare Fig. 20).

Another zone of abundant shells is found at the eastern margin of the area studied, where an old formation (probably Pleistocene), consisting of a mixture of shells and sand with a moderate abundance of silt and clay, is exposed locally at the shelf surface and is found below the surface in the long cores beneath the covering of delta-derived sediments in areas farther west. The macroorganisms in this shelly sand on the outer shelf are believed by Parker to represent an older environment, characteristic of relatively shallow, warmer water, or even of estuarine conditions because of the presence of such shells as *Crassostrea virginica*, the bay oyster, marsh snails, *Neritina reclivata*, and the little surf clam, *Donax tumida*. A C^{14} determination on some of these shells by J. L. Kulp (arranged

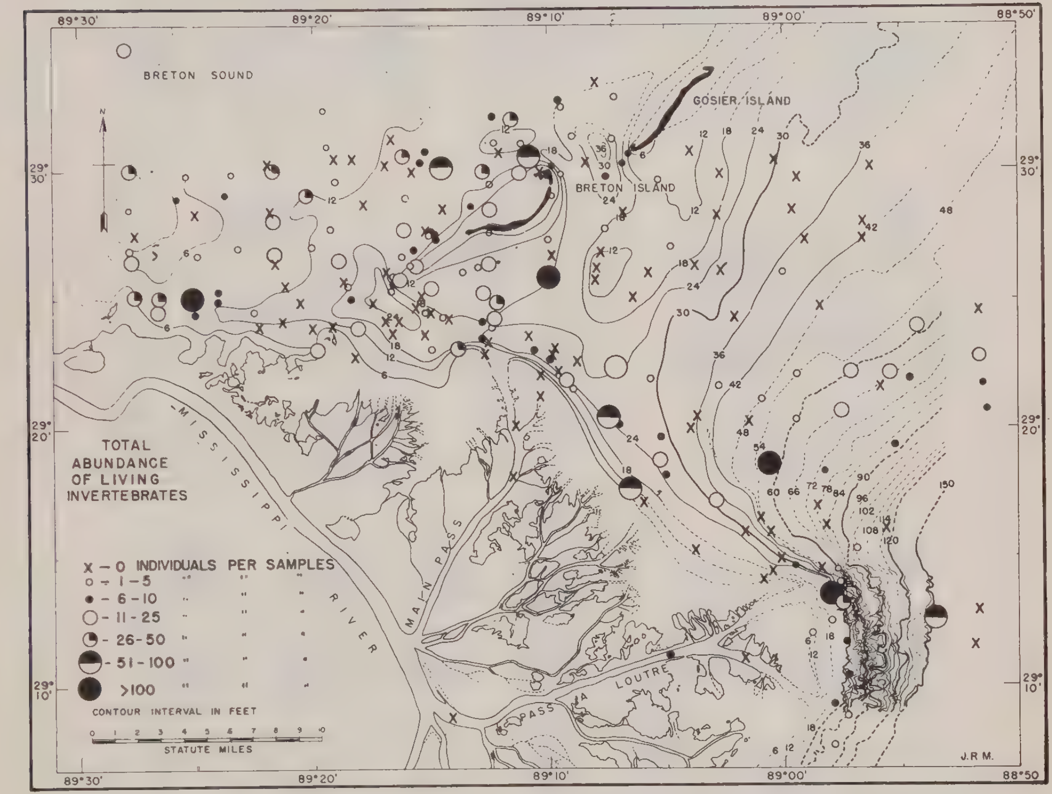
89°30'
89°20'
89°10'
89°00'
88°50'
29° 30'
29° 20'
29° 10'
N
BRETON SOUND
GOSIER ISLAND
BRETON ISLAND
MISSISSIPPI RIVER
MAIN PASS
PASS A LOUTRE
TOTAL ABUNDANCE OF LIVING INVERTEBRATES
X – 0 INDIVIDUALS PER SAMPLES
○ – 1-5 " " "
● – 6-10 " " "
○ – 11-25 " " "
◔ – 26-50 " " "
◒ – 51-100 " " "
● >100 " " "
CONTOUR INTERVAL IN FEET
0 1 2 3 4 5 6 7 8 9 10
STATUTE MILES
J.R.M.

FIG. 20.—Counts of number of living invertebrates in individual samples made by R. H. Parker. Some differences may be noted from Fig. 19, partly in relation to high abundance of living individuals in areas relatively near distributaries where productivity appears to be high.

through the courtesy of the Humble Oil and Refining Company) showed an age of about 7,000 years.

Some significant invertebrate representatives of the sediment environment are given in Plates III and IV, prepared by Parker. Although the boundaries of Parker's environments do not match exactly those boundaries of the sediment environments proposed here, certain organisms can be considered as more or less indicative of, but not restricted to, these environments. For instance, although the interdistributary bays are part of Parker's "delta shores" environment, there is a significant difference in the numbers of organisms in the delta-front platform and interdistributary bay deposits. The latter are characterized by larger numbers of the pelecypods, *Rangia* and *Macoma mitchelli*, and the delta-front platform is characterized in general by very large populations of

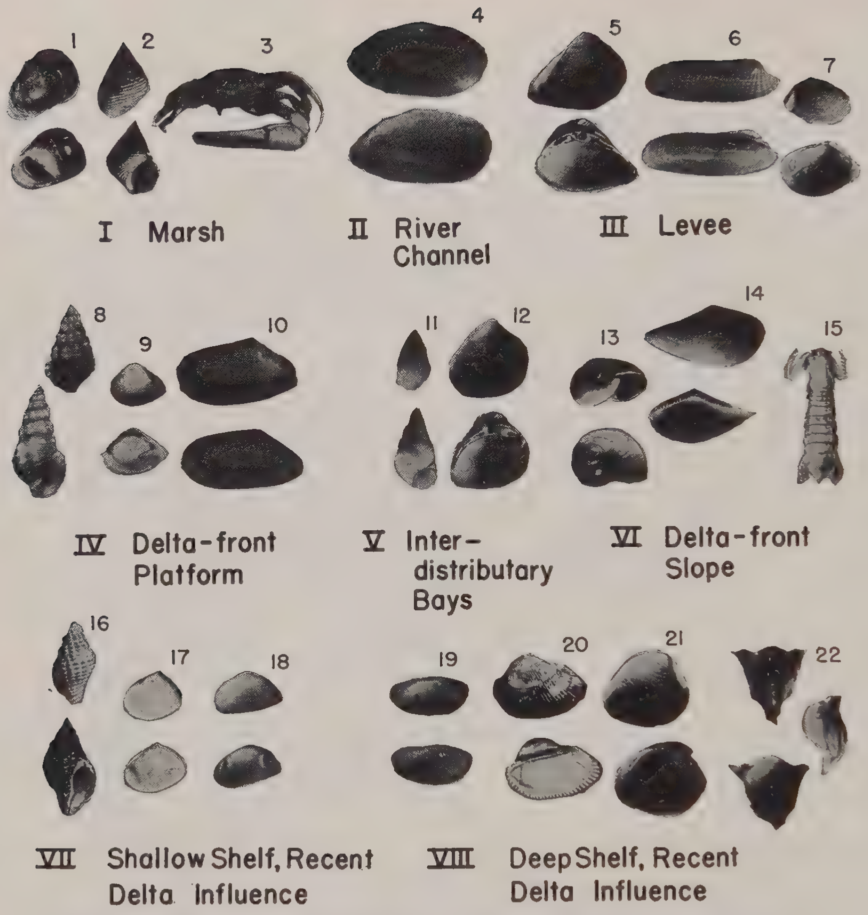
1
2
3
4
5
6
7
I Marsh
II River Channel
III Levee
8
9
10
11
12
13
14
15
IV Delta-front Platform
V Inter-distributary Bays
VI Delta-front Slope
16
17
18
19
20
21
22
VII Shallow Shelf, Recent Delta Influence
VIII Deep Shelf, Recent Delta Influence

Pl. III.—Assemblages of macroorganisms characteristic of sedimentary environments of Mississippi Delta area. Prepared by R. H. Parker.

I. Marsh
Fig. 1.—*Neritina reclivata* (Say, 1822), size—11×13 mm., side, aperture.
Fig. 2.—*Littorina irrorata* (Say, 1822), size—19×14 mm., side, aperture.
Fig. 3.—*Uca*, species, size—24×17 mm., front view.
II. River Channel
Fig. 4.—*Macoma mitchelli* Dall, 1895, size—21×12 mm., exterior, interior.
III. Levee
Fig. 5.—*Rangia flexuosa* (Conrad, 1840), size—36×30 mm., exterior, interior.
Fig. 6.—*Petricola pholadiformis* Lamarck, 1818, size—23×8 mm., exterior, interior.
Fig. 7.—*Quadrans lintea* Conrad, 1837, size—16×12 mm., exterior, interior.
IV. Delta-Front Platform
Fig. 8.—*Nassarius acutus* (Say, 1822), size—11×4 mm., side aperture.
Fig. 9.—*Mulinia lateralis* (Say, 1822), size—10×7 mm., exterior, interior.
Fig. 10.—*Macoma tageliformis* Dall, 1900, size—44×25 mm., exterior, interior.
V. Interdistributary Bays
Fig. 11.—*Littoridina sphinctostoma* Abbott and Ladd, 1951, size—3×2 mm., side, aperture.
Fig. 12.—*Rangia cuneata* (Gray, 1831), size—42×39 mm., exterior, interior.
VI. Delta-Front Slope
Fig. 13.—*Polinices duplicatus* (Say, 1822), size—39×41 mm., aperture, top.
Fig. 14.—*Nuculana concentrica* Say, 1832, size—11×6 mm., exterior, interior.
Fig. 15.—*Squilla empusa* Say, 1818, size—95 mm.. dorsal.
VII. Shallow Shelf, Recent Delta Influence
Fig. 16.—*Cantharus cancellarius* (Conrad, 1846), size—30×17 mm., side, aperture.
Fig. 17.—*Abra lioica* Dall, 1881, size—8×7 mm., exterior, interior.
Fig. 18.—*Tellina versicolor* De Kay, 1843, size—12×6 mm., exterior, interior.
VIII. Deep Shelf, Recent Delta Influence
Fig. 19.—*Yoldia solenoides* Dall, 1881, size—13×7 mm., exterior, interior.
Fig. 20.—*Anadara baughmani* Hertlein, 1951, size—33×21 mm., exterior, interior.
Fig. 21.—*Pitar cordata* Schwengel, 1951, size—43×48 mm., exterior, interior.
Fig. 22.—*Cavolinia longirostris* "Lesueur" Blainville, 1821, size—4.5×.55 mm., dorsal, side, ventral.

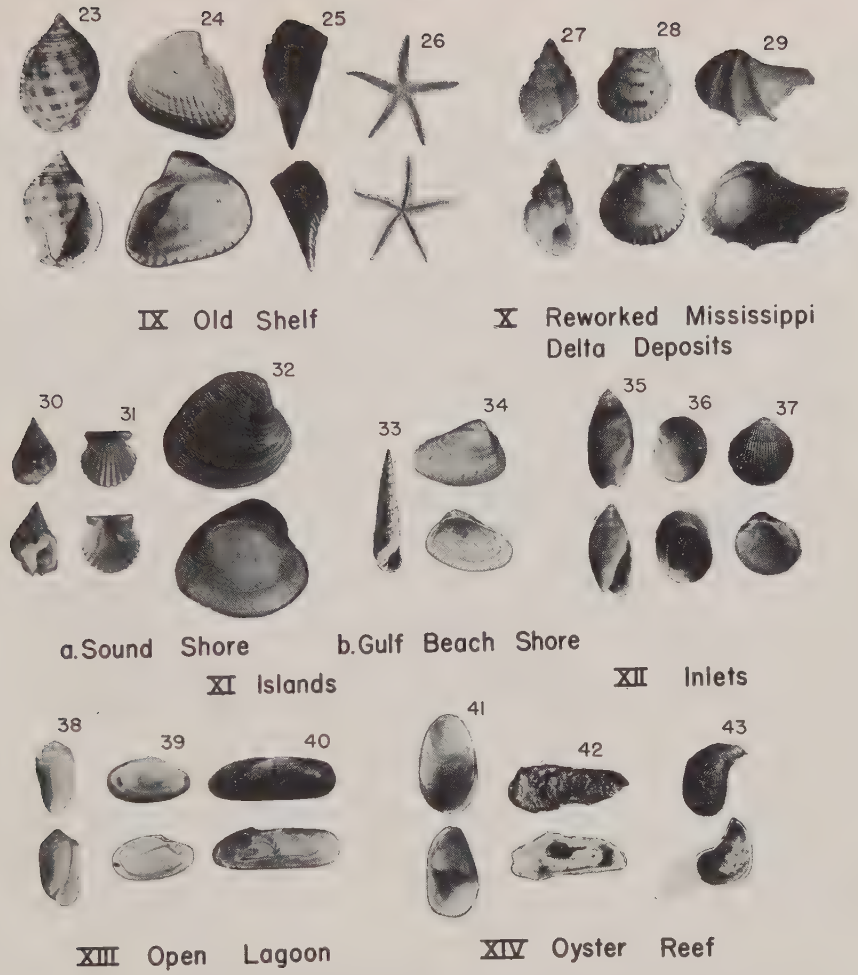
23
24
25
26
27
28
29
IX Old Shelf
X Reworked Mississippi Delta Deposits
30
31
32
33
34
35
36
37
a. Sound Shore
b. Gulf Beach Shore
XI Islands
XII Inlets
38
39
40
41
42
43
XIII Open Lagoon
XIV Oyster Reef

PL. IV.—Assemblages of macroorganisms characteristic of sedimentary environments of Mississippi Delta area. Prepared by R. H. Parker.

IX. OLD SHELF
FIG. 23.—*Phalium granulatum* (Born, 1778), size—59×40 mm., side, aperture.
FIG. 24.—*Noetia ponderosa* (Say, 1822), size—32×28 mm., exterior, interior.
FIG. 25.—*Atrina serrata* (Sowerby, 1825), size—175×76 mm., exterior, interior.
FIG. 26.—*Luidia clathrata* (Say, 1825), size—95 mm., dorsal, ventral.

X. REWORKED MISSISSIPPI DELTA DEPOSITS
FIG. 27.—*Nassarius ambiguus consensus* Ravenel, 1861, size—8×5 mm., side, aperture.
FIG. 28.—*Aequipecten gibbus gibbus* (Linné, 1758), size—27×26 mm., exterior, interior.
FIG. 29.—*Cuspidaria ornatissima* (d'Orbigny, 1846), size—9×6 mm., exterior, interior.

XI. ISLANDS
a. Sound Shore
FIG. 30.—*Nassarius vibex* Say, 1822, size—12×8 mm., side, aperture.
FIG. 31.—*Aequipecten irradians amplicostatus* (Dall, 1898), size—65×63 mm., exterior, interior.
FIG. 32.—*Mercenaria campechiensis texana* (Dall, 1902), size—102×94 mm., exterior, interior.
b. Gulf Beach Shore
FIG. 33.—*Terebra cinerea* (Born, 1778), size—32×7 mm., aperture.
FIG. 34.—*Donax tumida* Philippi, 1848, size—10×7 mm., exterior, interior.

XII. INLETS
FIG. 35.—*Olivella mutica* (Say, 1822), size—2×8 mm., side, aperture.
FIG. 36.—*Sinum perspectivum* (Say, 1831), size—31×31 mm., top, aperture.
FIG. 37.—*Trachycardium muricatum* (Linné. 1758), size—42×44 mm., exterior, interior.

XIII. OPEN LAGOON
FIG. 38.—*Retusa canaliculata* (Say, 1827), size—6×3 mm., side, aperture.
FIG. 39.—*Macoma tenta* (Say, 1834), size—10×9 mm., exterior, interior.
FIG. 40.—*Tagelus divisus* (Spengler, 1794), size—27×9 mm., exterior, interior.

XIV. OYSTER REEF
FIG. 41.—*Crepidula plana* Say, 1822, size—22×12 mm., exterior, interior.
FIG. 42.—*Crassostrea virginica* (Gmelin, 1790), size—170×70 mm., exterior, interior.
FIG. 43.—*Brachidontes recurvus* (Rafinesque, 1820), size—16×11 mm., exterior, interior.

small *Mulinia lateralis* and the gastropod, *Nassarius acutus*. In respect to fauna, the islands can be differentiated from the open lagoonal and old shelf deposits by the presence of beds of clams and scallops on the bay sides of the islands and by populations of *Donax* and *Terebra cinerea* on the Gulf or surf sides of the islands.

Echinoids.—In the central Texas area the presence or absence of Echinodermata, mostly echinoid spines and plates (Pl. I. Fig. 4),[9] was found to be a very good criterion for differentiating bay sediments and those of open Gulf (Shepard and Moore, 1955a, Fig. 28). Echinoid remains were found with varying abundance in the open-shelf sediments and proved to be extremely rare in the Texas bays. The inlets constituted a gradational zone between the two. In the delta area also echinoid remains have proved to be diagnostic, although the boundary line between scarce and relatively abundant echinoids, instead of occurring at the shoreline, curves seaward off each of the passes (Fig. 21).[10] Thus a zone with virtually no echinoids in the coarse fraction is found to extend as much as 14 miles east of North Pass and, with one exception, to the limits of sampling off both South Pass and Southwest Pass. Similarly, within the subaerial delta no echinoid remains were found in the sediments. East of the Pass a Loutre distributaries, beyond the zone of very scare echinoids, there is a rather sudden increase to a zone with the highest echinoids of the entire area. The latter is in essentially the same area, beyond the base of the slope, where the Foraminifera are also very abundant.

In the inlets, intermediate amounts of echinoids are found where the tidal currents are favorable for their existence. Breton Sound, like the bays of the central Texas coast, is low in echinoids although more of them are found in this open sound than might be anticipated from the relatively low salinity. Actually large populations of living sand dollars are found on the sand flats on the Sound side of Breton Island which may account for the presence of echinoid remains in that area.

Ostracods.—Because of the relatively abundant ostracods found near some of the deltas of the central Texas coast (Shepard and Moore, 1955a, p. 1502) it was a surprise to find so few ostracods in the coarse fractions of the Mississippi Delta area (Fig. 44). The only environments where the ostracods are represented in appreciable numbers are in the deeper portions of the bottomset beds and in the "old shelf" deposits. A few also occur in the inlets and open lagoons. Elsewhere the numbers are so small that they were not encountered in the coarse-fraction studies.

The Ostracoda have been studied by Doris Malkin Curtis who is preparing a report of this work. She has found that several very distinct environments can be recognized from the species (Pl. V). These environments include a marsh

---

[9] Distinguished in small fragments by their resemblance to sintered glass.

[10] For distribution of living echinoderms, see Parker (1956, pp. 315–317).

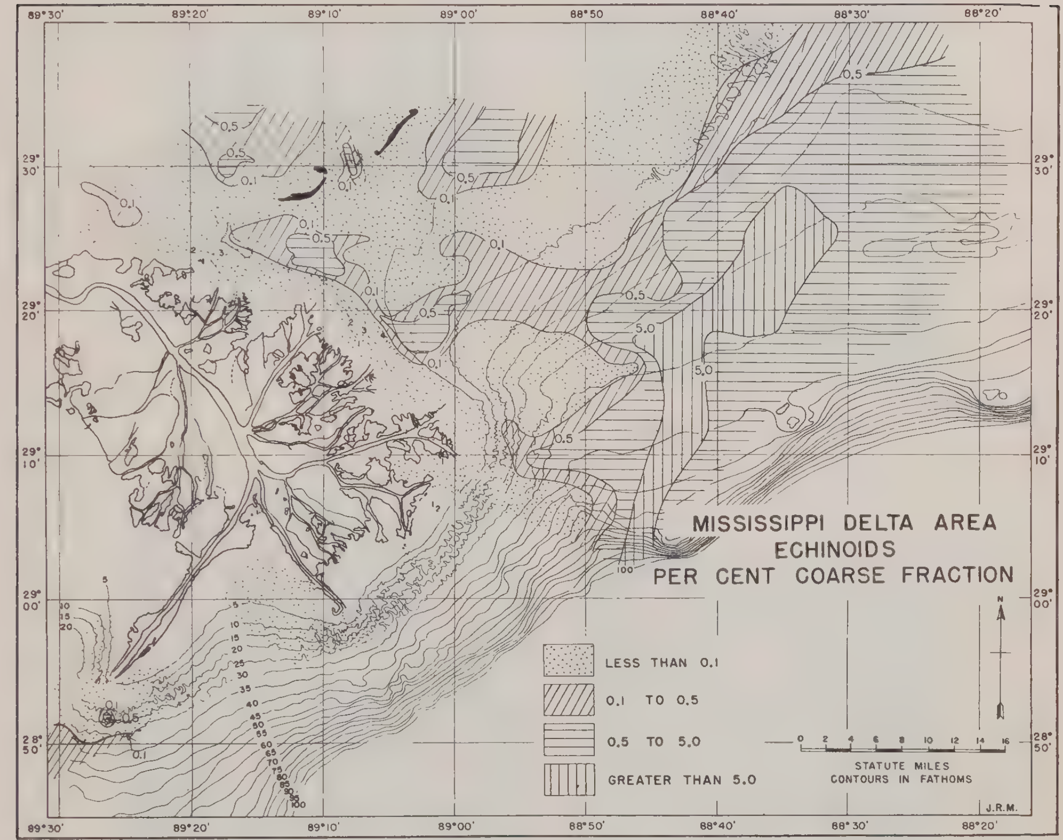
MISSISSIPPI DELTA AREA
ECHINOIDS
PER CENT COARSE FRACTION
LESS THAN 0.1
0.1 TO 0.5
0.5 TO 5.0
GREATER THAN 5.0
0 2 4 6 8 10 12 14 16
STATUTE MILES
CONTOURS IN FATHOMS
N
J.R.M.
89°30'
89°20'
89°10'
89°00'
88°50'
88°40'
88°30'
88°20'
29° 30'
29° 20'
29° 10'
29° 00'
28° 50'
0.1
0.5
5.0
100

FIG. 21.—Abundance of echinoids in coarse fraction. Distribution has close similarity to Foraminifera in relation to distributaries.

facies, one from Breton Sound, a nearshore facies of the open Gulf, and two offshore facies, one from about 10 to 50 fathoms and the other between 50 and 100 fathoms. One of the striking differences in these facies is the distribution and relative abundance of immature carapaces with a range of 50–93 per cent in the sound and nearshore samples and generally less than 50 per cent in the offshore samples. Mrs. Curtis also found that the living populations were extremely low at the times of collections, although live ostracods are found in all environments and are relatively more common in the marsh environment where the total population is very low.

A study of three samples from the same location showed Mrs. Curtis that there were considerable differences in the fauna and led her to conclude that as-

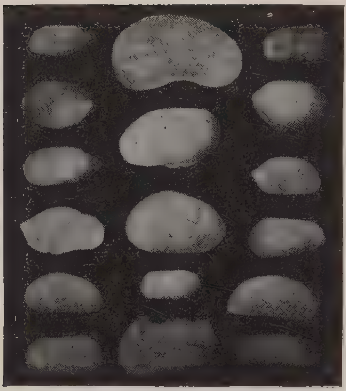

BRETON SOUND

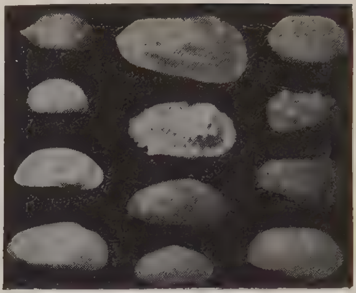

NEARSHORE OPEN GULF

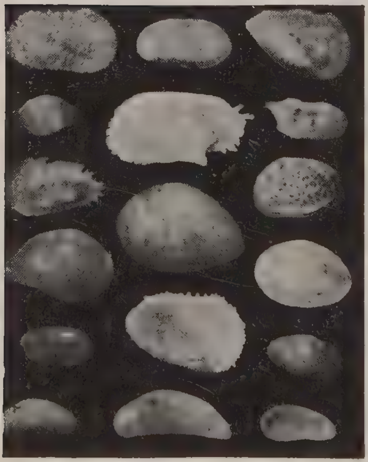

OFFSHORE OPEN GULF (10-50 fms.)

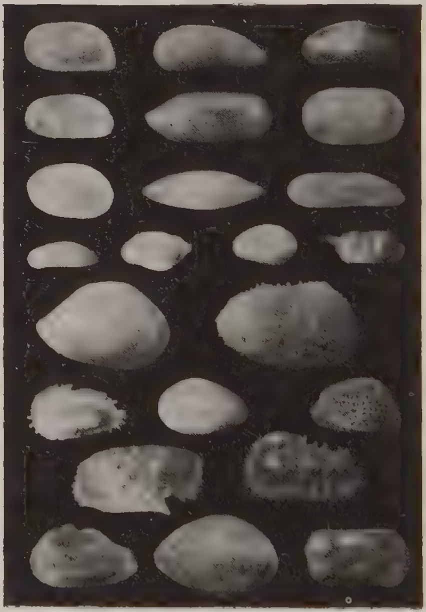

OFFSHORE OPEN GULF (50-100 fms.)

Pl. V.—Ostracod assemblages from Mississippi Delta area. Prepared by Doris Malkin Curtis.

semblages rather than individual species and groups of samples rather than individual samples should be used where possible to diagnose environments.

Glauconite.—Like echinoids, glauconite in the sediments of the central Texas area was found to constitute a criterion for open Gulf. In the delta area, however, glauconite shows relationships which are in many ways similar to those of the echinoids (Fig. 22). Glauconite is virtually missing in very extensive bands around the periphery of the various passes. It increases to a maximum very near the base of the slope east of the Pass a Loutre distributaries and becomes less abundant at greater distances east of the delta. Glauconite is found in a part of the inlet environment between Main Pass and Breton Sound but does not occur in the rest of this environment. Glauconite is scarce in Breton Sound but, like echinoids, it is not as scarce in the sound as in the Texas bays. Also, glauconite is

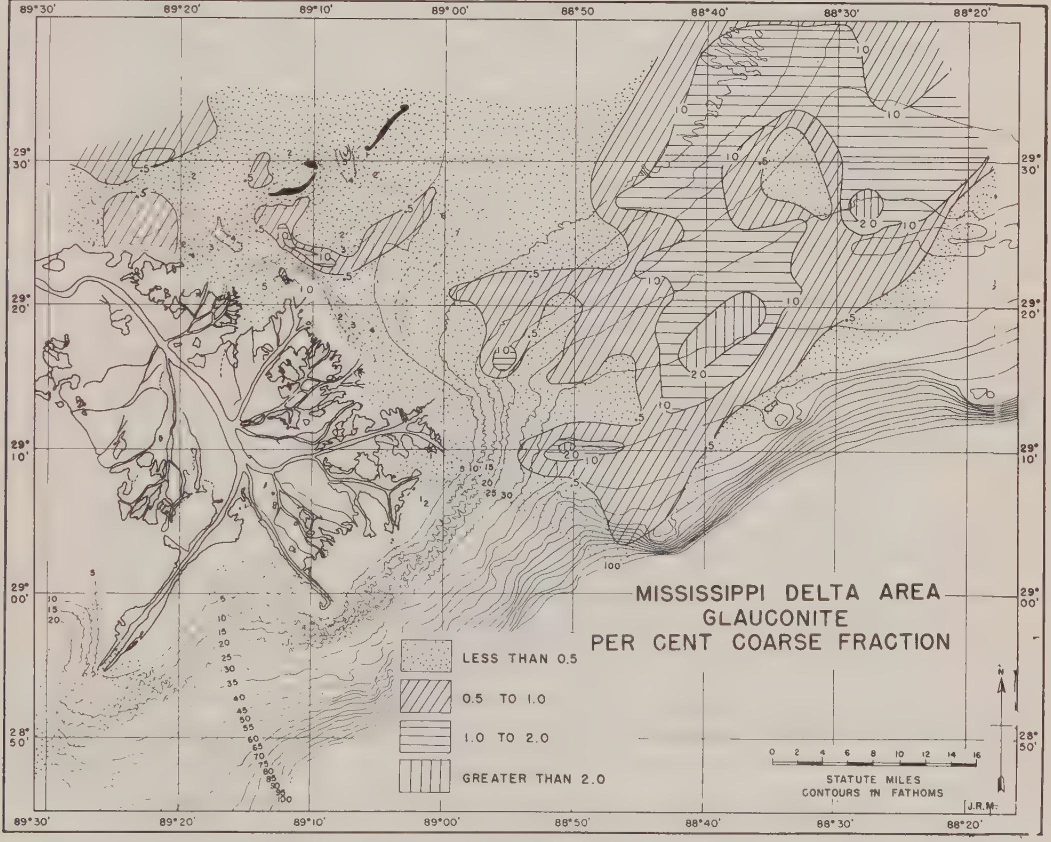
89°30'
89°20'
89°10'
89°00'
88°50
88°40'
88°30'
88°20'
29° 30'
29° 20'
29° 10'
29° 00'
28° 50'
MISSISSIPPI DELTA AREA
GLAUCONITE
PER CENT COARSE FRACTION
LESS THAN 0.5
0.5 TO 1.0
1.0 TO 2.0
GREATER THAN 2.0
0 2 4 6 8 10 12 14 16
STATUTE MILES
CONTOURS IN FATHOMS
N
J.R.M.

FIG. 22.—Abundance of glauconite in coarse fraction. Low contents are seen near all distributaries and in general in areas of rapid deposition.

found in small percentages in channel samples from the mouths of South Pass and Main Pass. This river-floor glauconite is lighter green in color than that found typically on the open shelf. Because of the scarcity of this "river" glauconite, it has not yet been possible to perform spectroscopic analyses to determine whether it is different from the glauconite of the open shelf.[11] West of the delta, outer-shelf samples show that the scarcity of glauconite extends as far as 70 miles before a somewhat normal outer-shelf abundance is found. This provides further evidence of a greater extent of the river influence in the westerly direction than toward the east.

SEDIMENT VARIATION ALONG PROFILES

A series of profiles have been made in order to indicate the variation of sand-silt-clay ratios in the sediments and of the coarse-fraction constituents with distance from the delta and depth. These profiles were located off the principal passes (Fig. 23) and additional profiles were made off Breton Island into Breton Sound, and in the offshore area (east of the delta) from east to west and from north to south. Each profile (Figs. 24–34) shows the variation in sand-silt-clay content of the samples (top bracket), the depth variation along the profile (second bracket), the percentage of the major constituents in the coarse fraction (third bracket), and the variation in most of the minor constituents at a scale enlarged to ten times that of the major constituents (bottom bracket).

The profile off Baptiste Collette (Fig. 24) includes samples within the delta and extends north to Breton Sound passing close to Bird Island. There is not very much difference in the sand-silt-clay ratios or in the terrigenous and wood contents between the two samples from the delta marsh and that of the platform and slope sample beyond. The sand is consistently small in percentage, the wood consistently large, and the terrigenous relatively small. However, the minor constituents show an increase in mica directly outside the delta part of the profile, and at the same station Foraminifera first come into the picture, whereas aggregates fall off sharply. Northward into Breton Sound, the sand content increases, the clay and silt decrease, the wood content decreases, and the shells, after an increase, fall off again. The northernmost sample is almost entirely terrigenous. The Foraminifera reach a peak in the middle of the profile but are not represented in the two northern samples, perhaps because of the destruction of the arenaceous forms in preparing the samples.

The Main Pass profile (Fig. 25) extends from the lower river channel across the bar and thence across the inlet and up onto the Breton Island platform. The channel of this moderately large distributary yielded samples high in silt but with a low sand content. The coarse fraction has an unusually large quantity of wood and mica; hence, it is relatively low in other terrigenous minerals. The

---

[11] Glauconite from various areas is being given wet chemical and spectroscopic analyses at Scripps Institution by E. D. Goldberg as a part of A.P.I. Project 51.

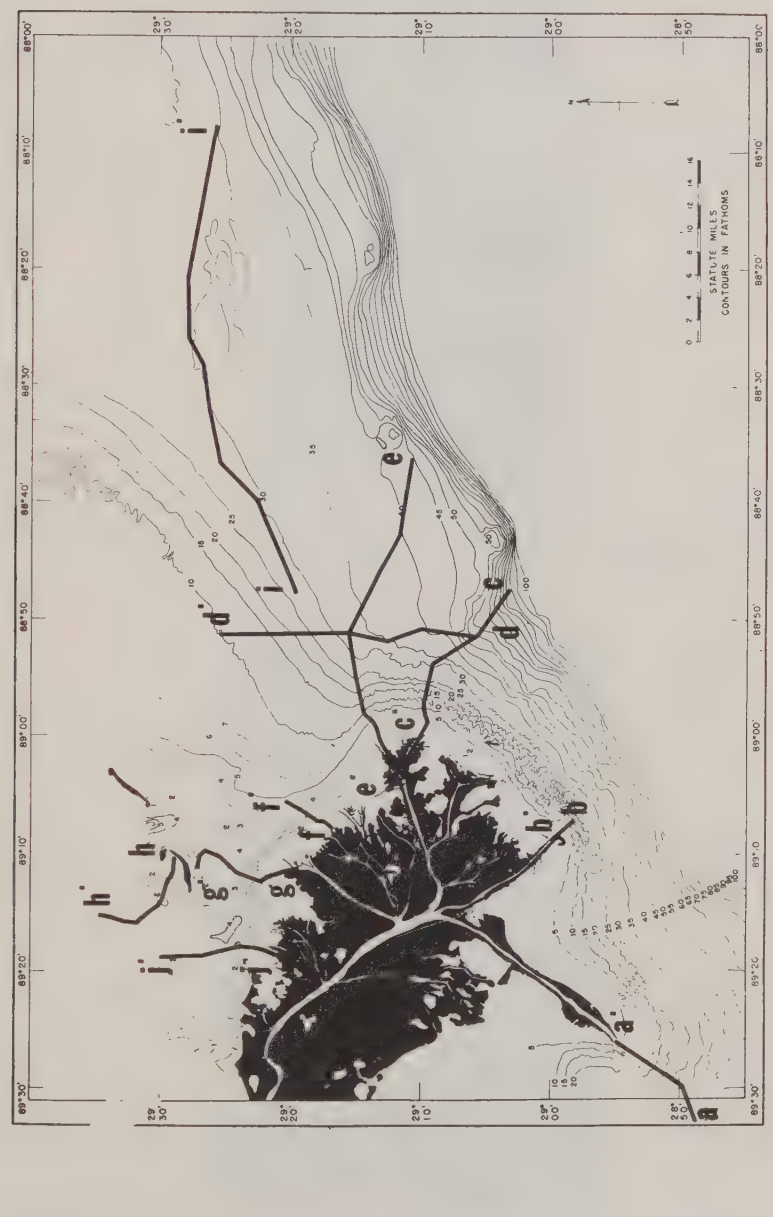
a
a'
b
b'
c
c'
d
d'
e
e'
f
f'
g
g'
h
h'
i
i'
j
j'
STATUTE MILES
CONTOURS IN FATHOMS
0 2 4 6 8 10 12 14 16
N
88°00'
88°10'
88°20'
88°30'
88°40'
88°50'
89°00'
89°10'
89°20'
89°30'
29° 30'
29° 20'
29° 10'
29° 00'
28° 50'

FIG. 23.—Location of profiles shown in Figs. 24–33.

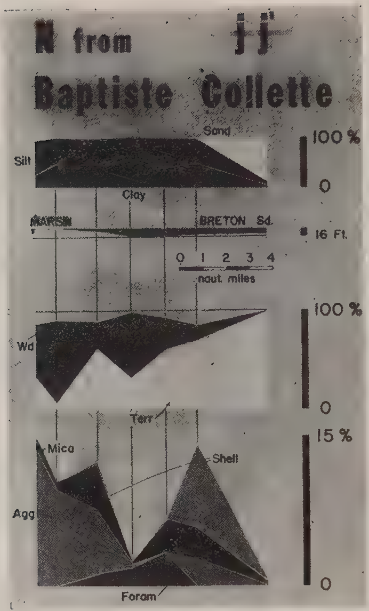

FIG. 24.—Profile north from Baptiste Collette subdelta into Breton Sound. Percentage of sand silt, and clay shown in upper bracket; depth profile in second bracket; major constituents of coarse fraction in third bracket; and minor constituents (scale times 10) in lower bracket. For locations, see Fig. 23.

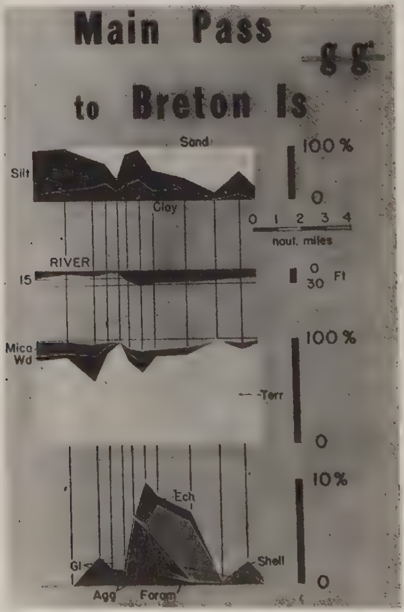

FIG. 25.—Profile north from Main Pass (including river bed samples) across bar and inlet and up onto platform adjacent to Breton Island. For explanation, see Fig. 24.

abundant aggregates of Baptiste Collette subdelta are not duplicated here. The sediment changes radically on the bar (at the mouth of the river), showing a great increase in sand which consists largely of terrigenous minerals. Glauconite is present both in the river and well out in the sound between the islands. In the deeper water of the inlet beyond the bar, Foraminifera become a moderately aboundant constituent and echinoids appear in small quantities. Approaching the Breton Island platform, the sand content becomes large and terrigenous minerals make up almost the entire coarse fraction.

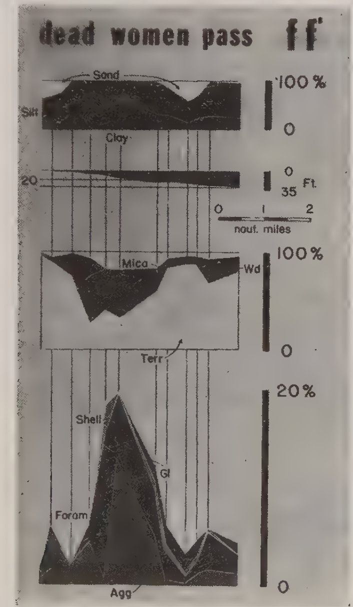

FIG. 26.—Profile northeast of Dead Women Pass. Profile starts on platform and extends down slope, crossing zone with some tidal influence in relation to currents moving into Breton Sound. For explanation, see Fig. 24.

The next profile is off a small pass, between Main Pass and North Pass (Fig. 26). The profile begins a short distance outside Dead Women Pass and extends across a very shallow platform (including the three inner samples) and then down a gentle slope into the southern extremity of the inlet area where tidal currents coming in and out of Breton Sound become significant. There is a double-phase change along this profile. The sand, which is abundant on the platform, becomes very scarce on the slope but increases again at the terrace, apparently in relation to the tidal currents related to the inlet to the north. The terrigenous minerals are dominant on the platform, whereas wood becomes the major constituent on the upper slope. Lower on the slope both aggregates and Foraminifera become significant among the minor constituents. Mica is relatively abundant along most of the profile; hence it is included among the major constituents. Glauconite becomes important on the terrace where the tidal currents are significant, and decrease the deposition rate.

North Pass, one of two major distributaries of Pass a Loutre, is represented in the next profile (Fig. 27). Here the river profile and the profile across the bar have been subdivided in a special diagram to indicate the variation of sand-silt-clay between low- and high-water stages (Fig. 34). It may be seen that the sediments in this deep and more powerful distributary (shown on the left-hand side of the profile) have more sand than those of Main Pass, but the constituents of the coarse fraction are somewhat comparable in having a high terrigenous content and relatively abundant wood, although the mica is less abundant (shown here as a minor constituent). Foraminifera are found in most of the river samples. Aggregates are somewhat less abundant than in Main Pass. The most striking feature of the profile is the major change which takes place after coming to the edge of the bar and proceeding down the slope. Here, the percentages of wood,

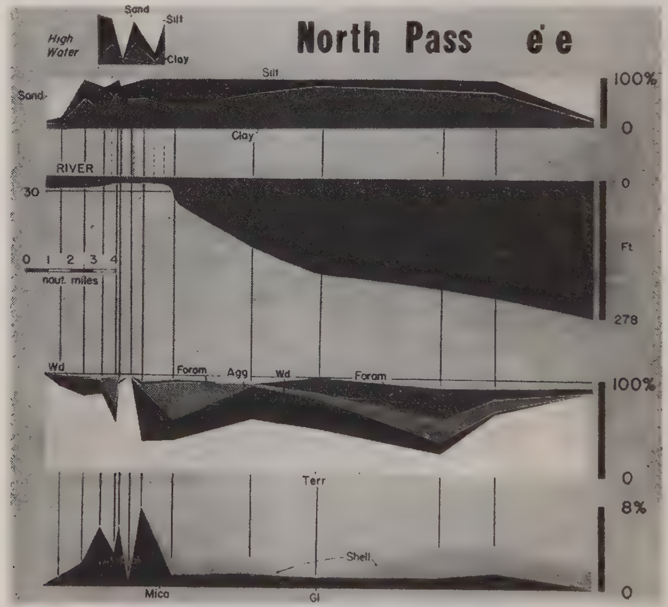

FIG. 27.—Profile extending east and then southeast from North Pass. In part showing river channel and bar, comparative sand-silt-clay percentages of high-water river stage (above) and low water (main profile) are indicated. See also Figure 34. Outer profile crosses slope, bottomset beds, and old shelf deposits, respectively. For explanation, see Fig. 24.

aggregates, and mica greatly increase. Near the base of the slope[12] where the open-shelf bottomset beds are encountered, the Foraminifera show a tremendous increase, reaching the largest percentage of the entire area. The last sample of the profile has crossed into the "old shelf deposits," accounting for the large increase in the sand content and for the decrease of many of the constituents.

The next profile (Fig. 28) is essentially an eastward continuation of the inner part of the North Pass profile, but is offset slightly to the north and extends east along the contour of the shelf beyond the foreset slope. It may be seen that the sand content along this line is very small on the west, but increases eastward rather gradually and then rather abruptly where the profile passes into the "old shelf deposits." The major constituents, starting at the west with very high Foraminifera, show a gradual increase of the terrigenous minerals and a decrease of the Foraminifera. The shells are relatively abundant along the profile particularly in the "old shelf deposits." Among the minor constituents, the echinoids replace wood as the most abundant except in the two western samples where

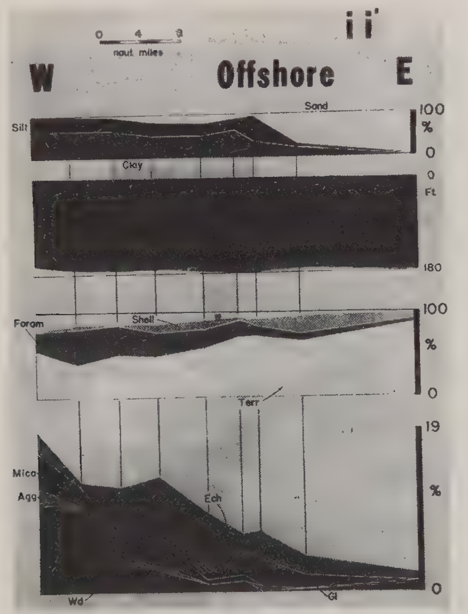

FIG. 28.—Offshore profile along shelf north-northeast of North Pass. Profile is mostly in bottomset beds, but toward right, passes into old shelf deposits. For explanation, see Fig. 24.

---

[12] Somewhat of a slope appears to continue beyond the slope deposits in this profile because of the change in direction (also Fig. 28).

wood dominates. Both wood and echinoids decrease distinctly in the eastern samples. The glauconite, which was negligible on the slope (Fig. 27), becomes of some importance in the bottomset beds beyond, but decreases again at the eastern extremity. The aggregates and mica, which were important on the slope, become negligible on the shelf especially toward the east.

The next profile starts in Pass a Loutre in the river channel (Fig. 29) where there is a high sand content, largely terrigenous. The third sample, which is on a shoal downstream from a sand bar, is low in sand, and has a coarse fraction with a large wood content and considerable mica. The next two samples are from the shallow platform, a little north of the outer channel. These show decreasing sand seaward and the coarse-fraction constituents show increasing wood and decreasing mica. Down the slope, the sand diminishes to a negligible quantity and clay becomes the major-size fraction. In the coarse fraction, wood increases tremendously as do aggregates, and both continue to be major constituents along the rest of the profile which extends down the slope to 550 feet in depth (the deepest sample in the delta area). Foraminifera are abundant on this slope, showing a general increase outward. A negligible amount of glauconite is found on the deeper

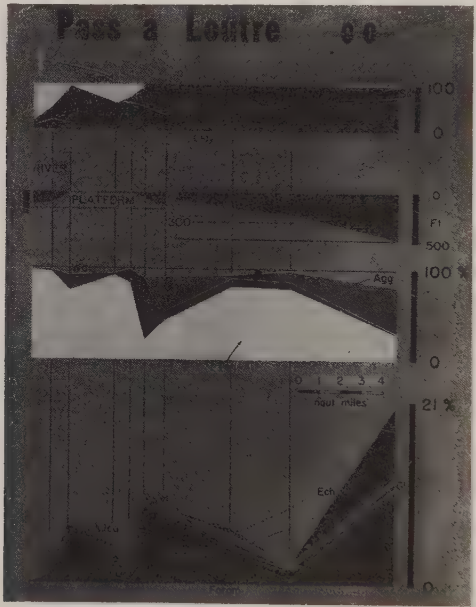

FIG. 29.—Profile extending out of Pass a Loutre and crossing platform slightly north of channel and then down slope. (Note change in scale of depth profile.) For explanation, see Fig. 24.

slope. Shells are also relatively scarce. Echinoids on the other hand become important in the deep outer station.

The South Pass profile (Fig. 30) was made along a jettied pass where there has been extensive dredging. Here the river samples have in most respects the same characteristics as in both Main Pass and North Pass. Sand content is relatively low, although the silt is abundant. Terrigenous minerals are the main constituent of the coarse fraction, with wood and mica also important. Foraminifera are found in all three of the river stations here, and one of the stations has an appreciable content of glauconite. On a relatively deep part of the river bar shown here, the sand increases and becomes dominant,[13] as does also the terrigenous part of the sand. The wood and most of the minor constituents are missing in this bar sample. On the slope beyond the bar, the wood and mica become abundant again and the aggregates are common in the samples of the outer stations.

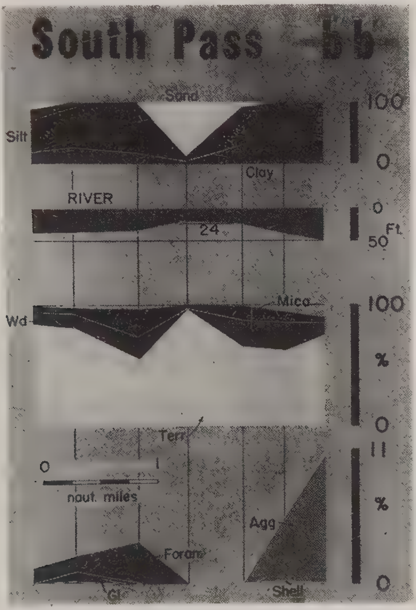

FIG. 30.—Profile extending out of South Pass and across relatively deep bar. High sand content and high percentage of terrigenous on bar are indicated. For explanation, see Fig. 24.

The profile along the artificially controlled Southwest Pass (Fig. 31) starts in the river near the outer limit of the jetties, crosses the bar, and proceeds down

[13] Trowbridge (1930, Fig. 9) shows an even higher content of sand on the bar at a shoaler depth, 11 feet.

the slope. At the pass mouth, silt predominates, the sand content is low, and the constituents include considerable wood, aggregates, and mica. In both bar samples, sand is dominant and consists almost entirely of terrigenous minerals. On the upper slope these sediments are largely silt but this gives way to clay at greater depth. Similarly the large content of terrigenous on the upper slope decreases at depths where wood, aggregates, mica, Foraminifera, and shells become abundant but variable.

Another profile, not related to any distributary, extends in a general northwesterly direction from Breton Island into Breton Sound (Fig. 32). In many respects this line resembles the northern part of the profile off Baptiste Collette (Fig. 24). The sand content is high near the island and low but variable out in the Sound where it is replaced by a high silt content. The most conspicuous features of the coarse fraction are the predominance of terrigenous minerals and the relatively high wood content found in most of the samples despite their distance from the principal Mississippi distributaries. Mollusk shells (shown in the finer constituents) are not much less abundant than wood. Mica is also a relatively abundant constituent of the Sound deposits. Foraminifera are scarce, but no

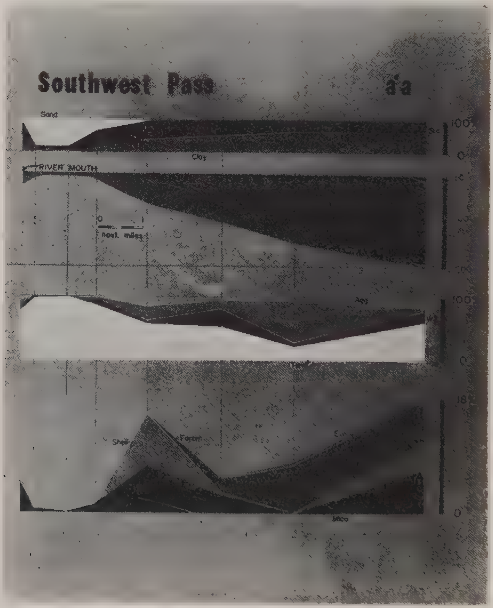

FIG. 31.—Profile starting at mouth of Southwest Pass, crossing bar, and extending down slope beyond. Bar sediment resembles that in South Pass. Explanation, in Figure 24. Samples provided by Humble Oil and Refining Company, courtesy of H. N. Fisk and U. S. Engineers.

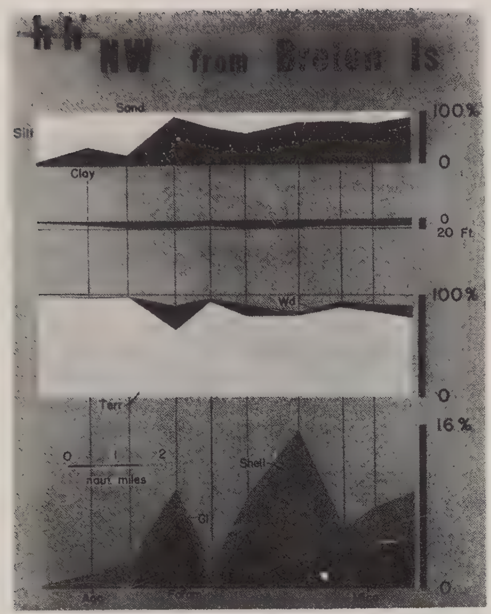

FIG. 32.—Profile in Breton Sound, northwest from Breton Island. For explanation, see Fig. 24.

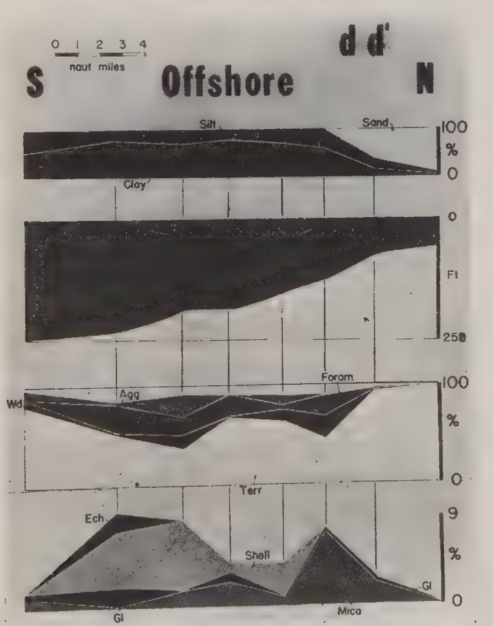

FIG. 33.—Offshore profile east of delta, extending across bottomset beds and into reworked Mississippi Delta area (two northern samples). For explanation, see Fig. 24.

doubt would be better represented if the common arenaceous forms of the sound were preserved.

A profile extending in a general north-south direction shows the variation in the shelf sediments at a distance of 10–15 miles east from the delta (Fig. 33). In this shelf profile, which shoals toward the north, the clay content remains high until a fairly shallow platform is reached at the north end where sand becomes the predominant size. Foraminifera, which are important constituents of the coarse fraction on the south, show a large decrease in the sandy sediments toward the north. Echinoids are found only at the southern end and both shells and glauconite show a general decrease in a northerly direction. Mica, on the other hand, reaches a maximum in the intermediate depths but is very scarce in the sandy area.

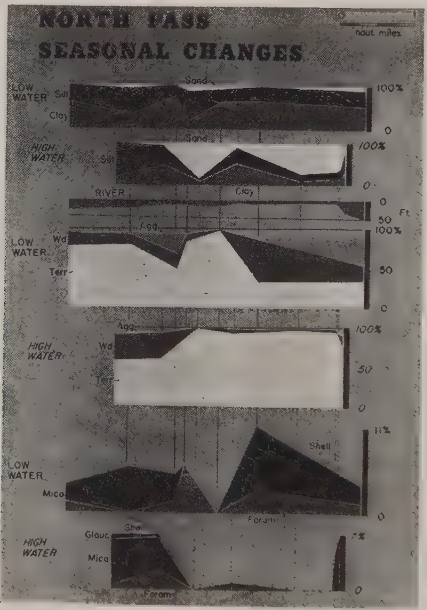

FIG. 34.—Seasonal changes along profiles extending out of North Pass across bar. Higher sand content is indicated during high water, and loss of wood, aggregate, and mica constituents (see also Figs. 35 and 36). For explanation, see Fig. 24.

SEASONAL CHANGES AT NORTH PASS

The only area where sufficient samples were obtained to determine the high-water and low-water stage variations in the bottom-sediment characteristics at a river mouth was at North Pass (Fig. 34). In the river samples, the sand-silt-clay content does not appear to have been greatly altered by the stage changes, but on the bar crest the sand seems to have become more abundant during the high-water stage, although it is not consistently high. Furthermore, during low water a few samples with high sand content were found out of the line of the profile (Figs. 35 and 36). The coarse fraction also changes seasonally along the profile. The terrigenous minerals are much more abundant on the bar during high water with a loss of wood, aggregates, and mica from low-water conditions. This probably indicates that the wood, aggregate, and mica constituents are winnowed out of the sediments during the high water. On the other hand, some of the low-water samples not along the line of profile also have a concentration of terrigenous minerals (Fig. 36).

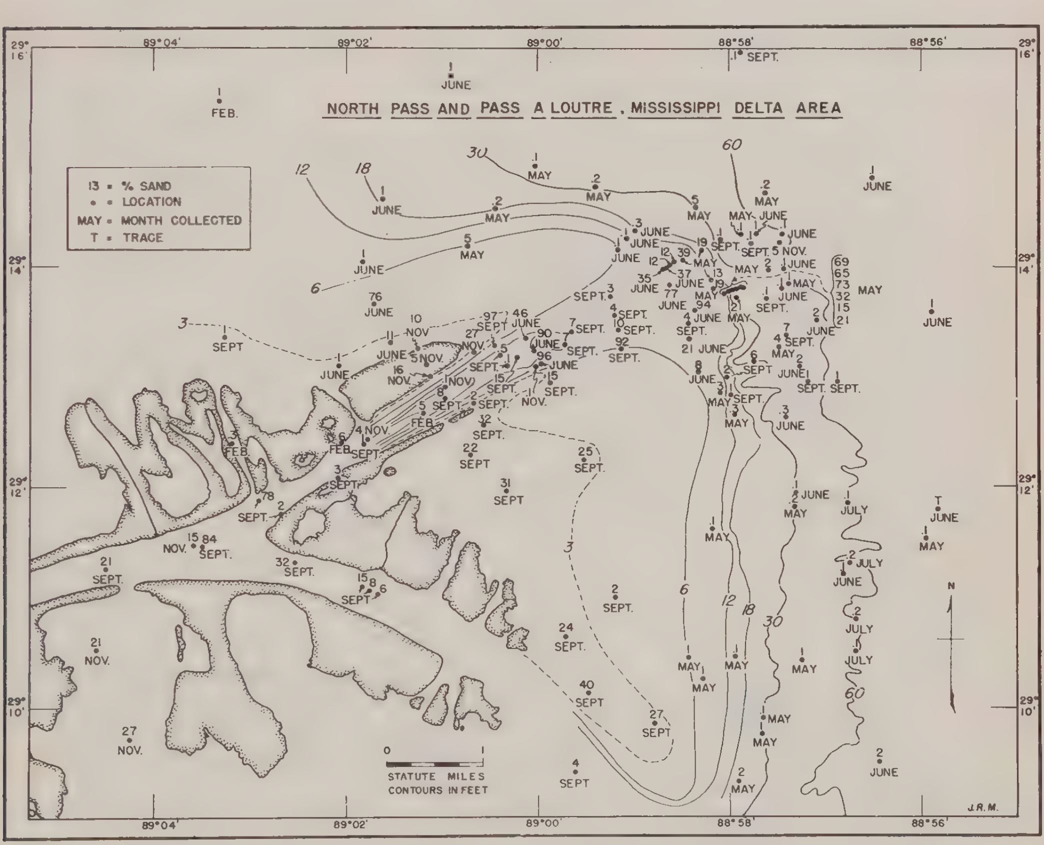
NORTH PASS AND PASS A LOUTRE, MISSISSIPPI DELTA AREA
13 = % SAND
• = LOCATION
MAY = MONTH COLLECTED
T = TRACE
89°04'
89°02'
89°00'
88°58'
88°56'
29° 16'
29° 14'
29° 12'
29° 10'
0
1
STATUTE MILES
CONTOURS IN FEET
N
J.R.M.

FIG. 35.—Detail of sand percentages around mouths of North Pass and Pass a Loutre showing relation of sand content to month of year in which sample was collected. High stage of river water comes between December and June, low water from July through November. Topography based on recent surveys, mostly by P. C. Scruton.

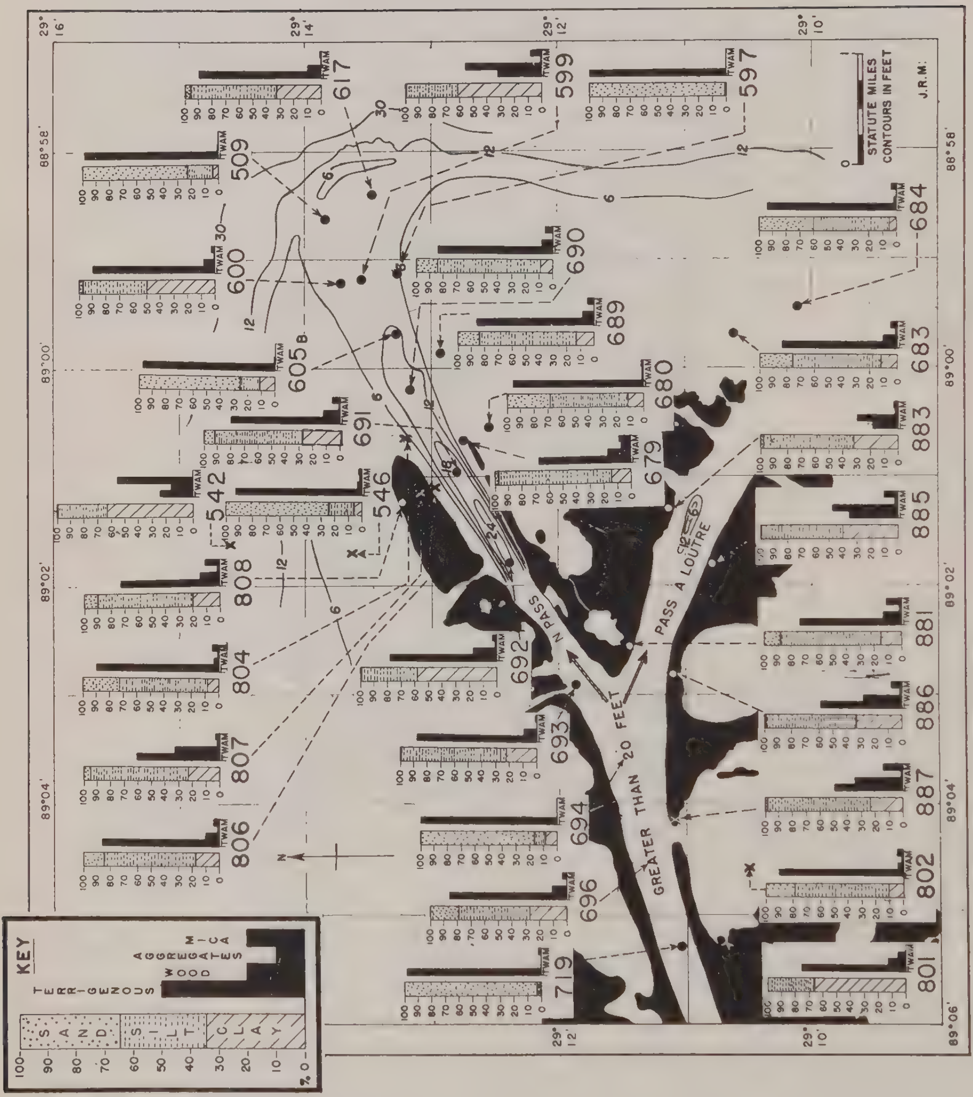
KEY
SAND
SILT
CLAY
TERRIGENOUS
WOOD
AGGREGATES
MICA
TWAM
N PASS
PASS A LOUTRE
GREATER THAN 20 FEET
STATUTE MILES
CONTOURS IN FEET
J.R.M.
617
599
597
509
600
690
684
605B
689
683
691
680
542
546
679
883
885
808
692
881
804
886
693
807
694
887
806
696
802
719
801
29° 16'
29° 14'
29° 12'
29° 10'
88°58'
89°00'
89°02'
89°04'
89°06'

Fig. 36.—Enlargement of North Pass and Pass a Loutre showing variation in sand-silt-clay content and histograms of terrigenous, wood, aggregate, and mica percentages of coarse fraction. All samples, except those on levees, taken during low water.

Perhaps most surprising about the samples collected during the high-water stage are the size variability and the relatively large amounts of both silt and clay. This spotty character of the sediment during high water was attested by R. R. Lankford, who was looking for soft bottom in the entrance to North Pass to obtain samples for live Foraminifera counts. He noticed that the bottom changed repeatedly from hard to soft as he moved over the outer channel and inner part of the bar. He found the same wide variation of bottom character in the river channel up to the juncture of Pass a Loutre.

POSSIBLE SEASONAL CHANGES AT MAIN PASS

The vicinity of Main Pass represents another area where samples representative of the high-water and low-water stages are sufficiently abundant so that they may show the seasonal variation (Fig. 37). Here, however, locations are less certain so that the data should be used with reservations. Comparisons should be made only where samples of two different seasons lie along the same contour and at about the same distance from the mouth of the pass. Furthermore the rather large variations in near-by samples of the same season show that only a group tendency can be considered as significant.

The indications are that directly off Main Pass there is no consistent seasonal difference, but at distances of 2–4 miles from the pass the sand content appears to be higher during the flood season (mostly obtained in May). At greater distances the variations seemed to be random. Taking all cases for the whole map represented by Figure 37, it is found that 20 samples have more sand in the flood season, 9 samples have a higher sand content than their neighbors in the low-water stage, and 11 are approximately the same. This appears to be in agreement with the findings at North Pass, but it is opposed to what was discovered by R. D. Russell (personal communication) in earlier studies of the delta. He found that the sediments were coarser during low water, suggesting that winnowing takes place at this stage. It is possible, however, the winnowing takes place during low water in some areas where the principal currents are tidal, whereas winnowing during high water may occur near the river mouths where the jet current is the controlling influence.

HEAVY-MINERAL CONTENT

Goldstein (1942), after a study of the heavy minerals of the continental shelf in the northern Gulf of Mexico, drew a line about 17 miles east of Pass a Loutre between the eastern Gulf heavy-mineral suites and the Mississippi heavy-mineral suites. These two provinces, according to Goldstein, are chiefly differentiated by the change in the content of staurolite and kyanite. Because of the 20 years or more since Goldstein's samples were collected, it seemed advisable to run a series of the new samples to check the situation. Twenty-two analyses were made by D. M. Poole to show the variation in the combined percentage of staurolite and kyanite in the total of the heavy minerals (Fig. 38). He used the $\frac{1}{8}$–$\frac{1}{16}$-mm. frac-

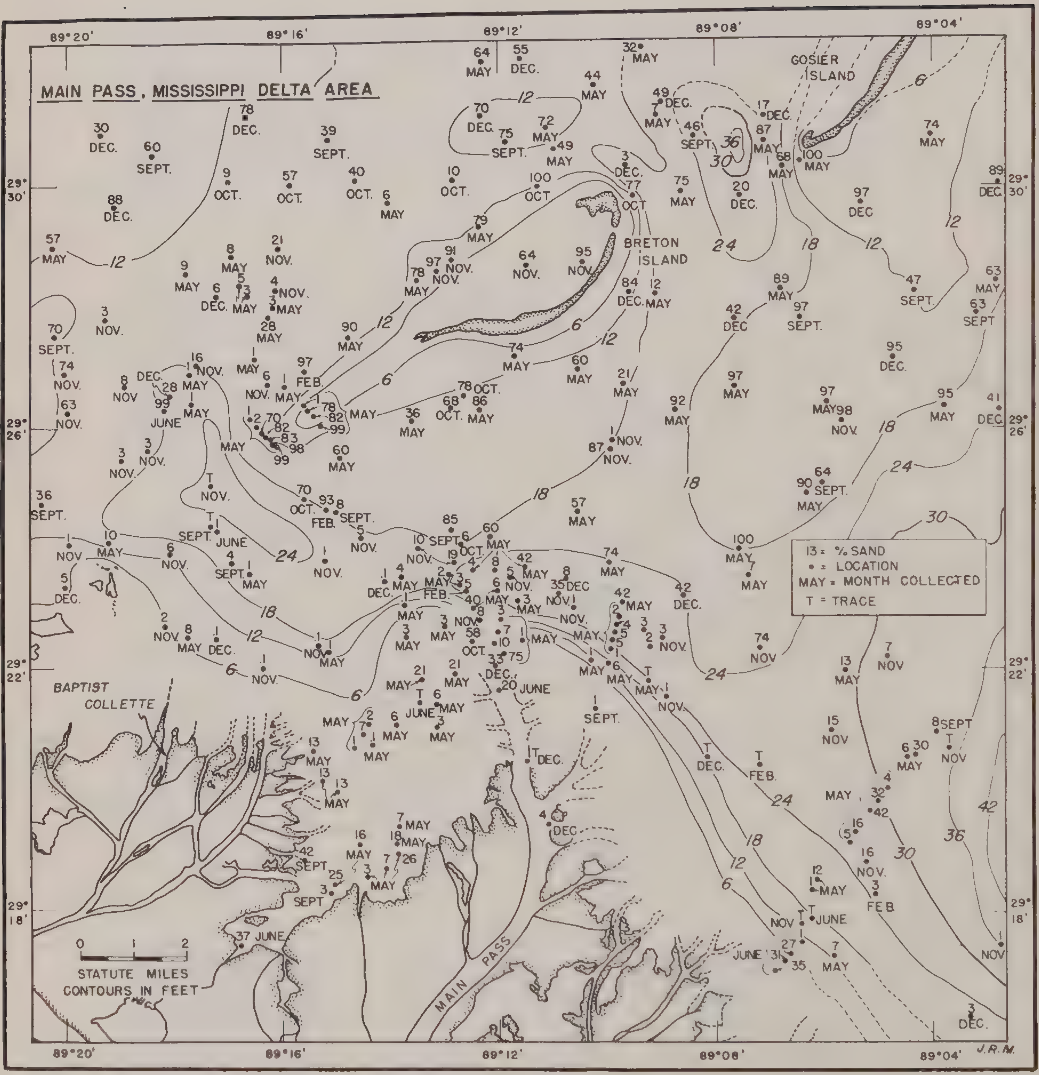
MAIN PASS, MISSISSIPPI DELTA AREA
89°20'
89°16'
89°12'
89°08'
89°04'
29° 30'
29° 26'
29° 22'
29° 18'
GOSIER ISLAND
BRETON ISLAND
BAPTISTE COLLETTE
MAIN PASS
13 = % SAND
• = LOCATION
MAY = MONTH COLLECTED
T = TRACE
0 1 2
STATUTE MILES
CONTOURS IN FEET
J.R.M.

FIG. 37.—Detail of sand percentages in vicinity of Main Pass, Baptiste Collette, and Breton Island. Month of year included for each sample makes possible some comparisons between sand contents of high- and low-river water stages, as in Fig. 35.

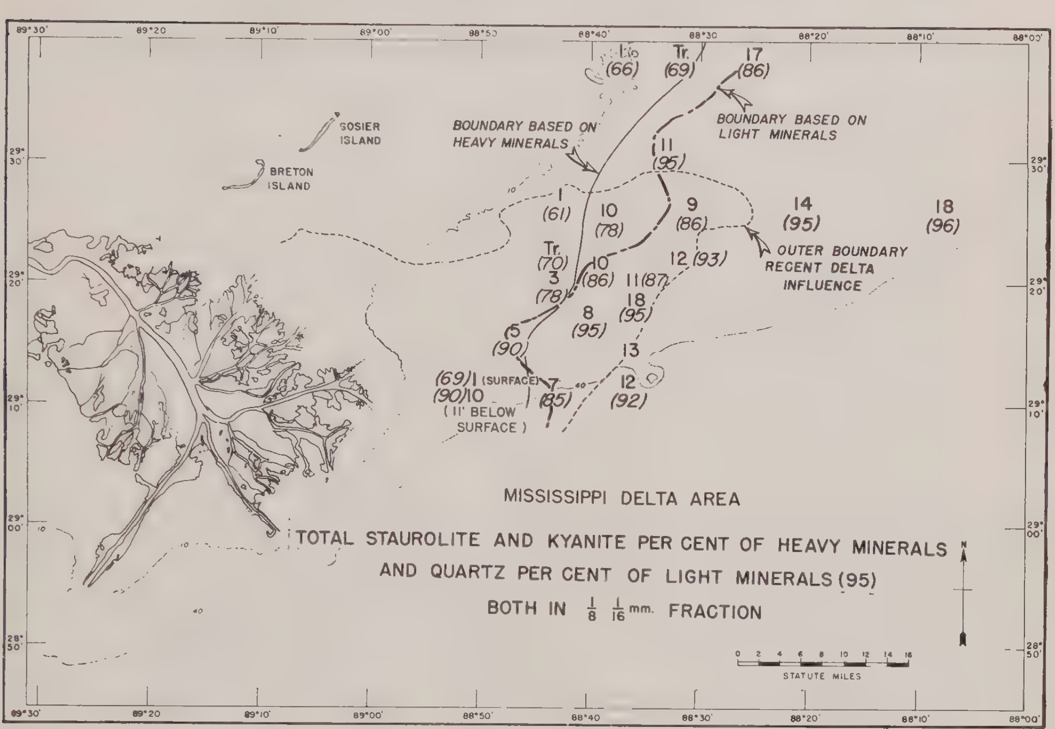
89°30'
89°20
89°10'
89°00'
88°50
88°40'
88°30
88°20'
88°10'
88°00'
29° 30'
29° 20'
29° 10'
29° 00'
28° 50'
GOSIER ISLAND
BRETON ISLAND
BOUNDARY BASED ON HEAVY MINERALS
BOUNDARY BASED ON LIGHT MINERALS
OUTER BOUNDARY RECENT DELTA INFLUENCE
16 (66)
Tr. (69)
17 (86)
11 (95)
1 (61)
10 (78)
9 (86)
14 (95)
18 (96)
Tr. (70)
10 (86)
12 (93)
3 (78)
11 (87)
18 (95)
8 (95)
5 (90)
13
(69) 1 (SURFACE)
(90) 10 (11' BELOW SURFACE)
7 (85)
12 (92)
10
40
MISSISSIPPI DELTA AREA
TOTAL STAUROLITE AND KYANITE PER CENT OF HEAVY MINERALS AND QUARTZ PER CENT OF LIGHT MINERALS (95)
BOTH IN $\frac{1}{8}$ $\frac{1}{16}$ mm. FRACTION
N
0 2 4 6 8 10 12 14 16
STATUTE MILES

Fig. 38.—Changes between the east Gulf mineral suites and Mississippi River mineral suites. Boundary for staurolite and kyanite lies somewhat east of that for light minerals in northern area. Two samples were studied from core near Pass a Loutre. One from core depth of 11 feet shows relatively abundant staurolite and high percentage of quartz characteristic of east Gulf suite, whereas surface sample represents delta suite.

tion because this provided the largest source of these minerals. The data show a remarkably good agreement with Goldstein's map and suggest that in the 20 years since the earlier samples were taken the situation has changed very little. For comparison with the typical eastern Gulf suite we obtained an analysis of sand from Ship Island. This showed a combined percentage of staurolite and kyanite of 22 per cent, which is comparable with the higher percentages on the shelf area 25 miles east of the birdfoot delta.

A study of the light minerals in the same samples by Harry Lusk, using the stain technique (Russell, 1935), has shown that the ratio between quartz and feldspar is equally useful in differentiating the east Gulf and Mississippi River suites. This is indicated by plotting the percentage of quartz (Fig. 38) since quartz and feldspar make up nearly 100 per cent of the light minerals. The samples high in staurolite and kyanite are also high in quartz. Drawing a boundary at the 85 per cent contour, we have a line that lies close to the boundary drawn for the heavy minerals. In one place the high quartz area has a salient extending into what would represent the Mississippi River suite on the basis of staurolite and kyanite. Otherwise the two indicators show close agreement.

The dividing line between the east Gulf and the Mississippi River suites crosses well over the boundary at the outer edge of the tongue of sediment having an abundance of wood fibers, aggregates, and mica which must be derived from the Mississippi River. This tongue of deltaic sediment has a thickness of at least 2 meters at some of the stations with high surface values of staurolite and kyanite, and the heavy minerals were taken only from the top 5 centimeters. Apparently the only interpretation of this anomaly is that from time to time these minerals, despite their densities (around 3.6), are carried west along the shelf so as to mingle with the eastward-moving bottomset beds of the present delta. This transportation takes place out to depths of at least 200 feet.

CLAY MINERALS

Clay minerals from the Mississippi Delta area were studied by R. E. Grim and W. D. Johns. These investigations are being reported separately. Figure 39 shows the variation in montmorillonite found by Grim and Johns in this area. Montmorillonite is moderately high (5 to 5.5 parts in 10) in and near the various distributaries. A short distance outside the distributaries the montmorillonite percentages decrease with some corresponding increase in illite and chlorite-kaolinite. The montmorillonite is variable in the area east and northeast of the delta where some values are found averaging even higher than those in and near the delta whereas others are distinctly lower.

At depth in the cores the clay minerals vary only slightly and with no consistency. These results indicate to the present writer that the analysis of the clay minerals of ancient delta sediments may not be very helpful in diagnosing environments. Such a conclusion appears to reenforce the findings from the Gulf of Paria reported by van Andel and Postma (1954, p. 79).

VOLCANIC SHARDS

One of the interesting constituents of the terrigenous part of the coarse fractions is vitric volcanic ash in the form of curved angular shards formed from bursting bubbles of volcanic glass. These were studied by J. R. Curray. He found the index of refraction of this glass to be between 1.49 and 1.50, indicating derivation from an acidic or intermediate composition magma. The index of refraction and morphology of all shards examined to date from surface or near-surface sediments from the delta area appear to be similar. The abundance of shards in the coarse fractions of samples from all parts of the delta has shown no systematic variation with environment, but a random variation in amount from a small fraction of 1 per cent to about 2 per cent of the coarse fraction.

If the ash content of the sediments was derived from relatively recent ash

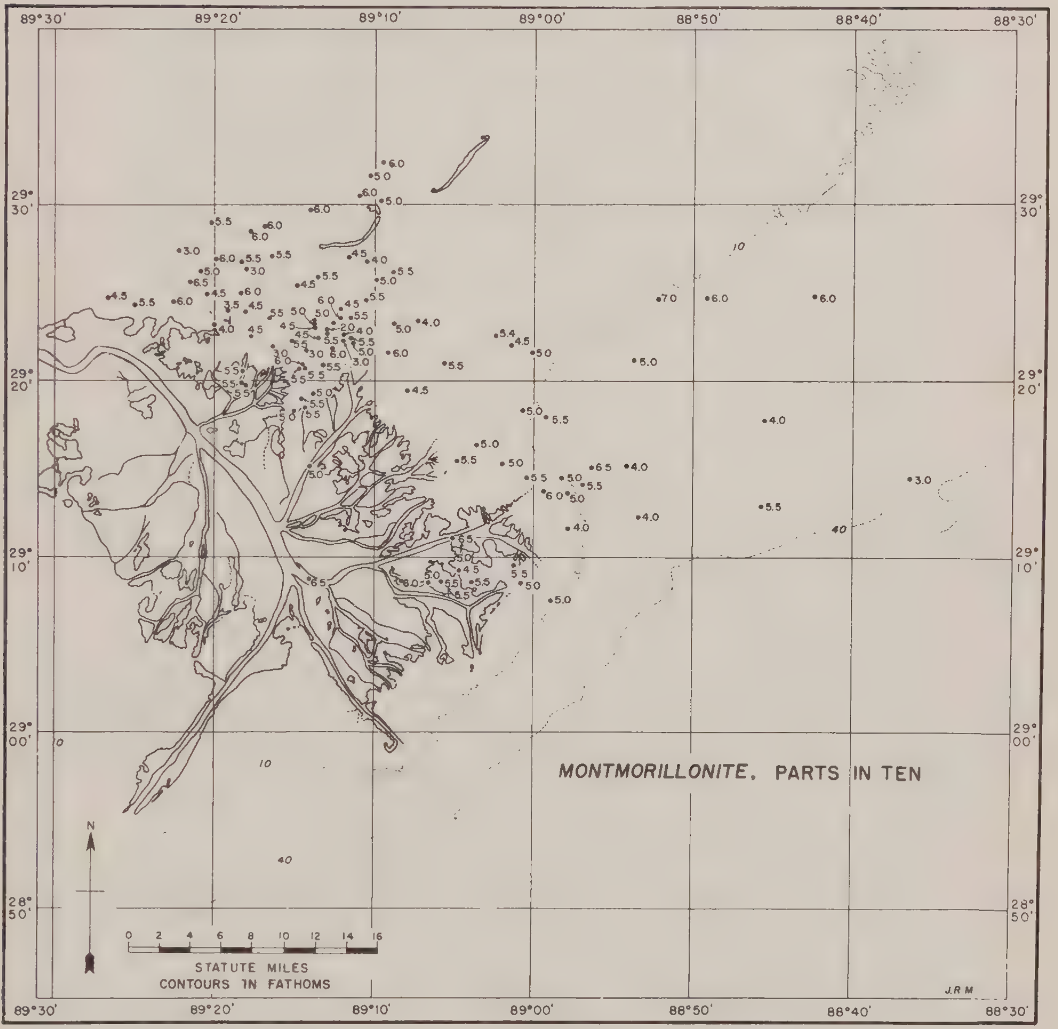
89°30'
89°20'
89°10'
89°00'
88°50'
88°40'
88°30'
29° 30'
29° 20'
29° 10'
29° 00'
28° 50'
MONTMORILLONITE, PARTS IN TEN
N
0 2 4 6 8 10 12 14 16
STATUTE MILES
CONTOURS IN FATHOMS
10
40
J.R.M.

FIG. 39.—Variation of montmorillonite among clay minerals (expressed in parts of 10) from work for A.P.I. Project 51 by R. E. Grim and W. D. Johns.

falls of volcanism in Mexico or Central America, the shards should be far more abundant in the areas of slow deposition. Since this is not the case, it is believed that these shards represent a part of the terrigenous load of the river eroded from volcanic ash deposits in the drainage area.

CALCIUM CARBONATE CONTENT

The calcium carbonate content of a selected group of sediments was determined by George Bien, using the manometrical measurements of the carbon dioxide evolved as a gas when the sample was digested in normal sulphuric acid. This is corrected to standard temperature and pressure and converted to carbonate as calcium carbonate, by the formula $0.1605\ VP/TW = \%CaCO_3$, where V is observed volume, P is pressure corrected for water-vapor pressure at room temperature, T is the room temperature in degrees Kelvin, and W is the weight of the sample used. Prior to analysis the conspicuous shell fragments were removed so that the shells from shell sands and oyster-reef debris are largely eliminated.

The results of the calcium carbonate analyses are shown in Figure 40. Certain

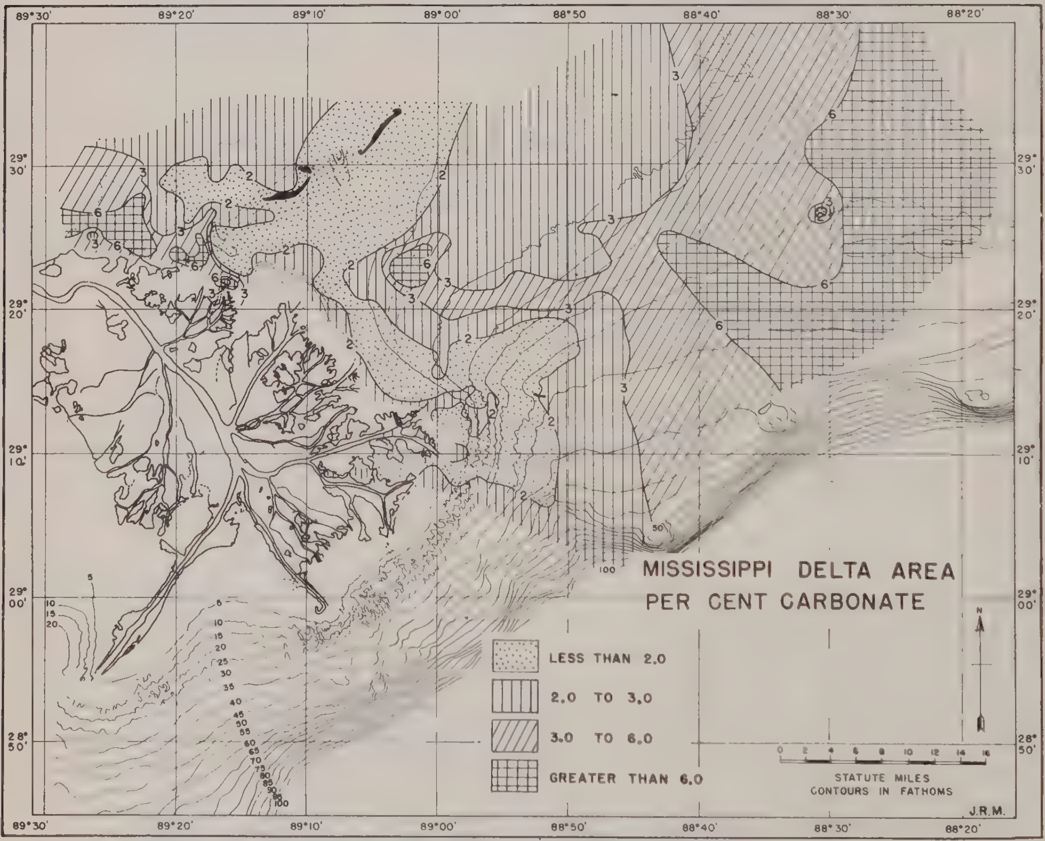
89°30'
89°20'
89°10'
89°00'
88°50'
88°40'
88°30'
88°20'
29° 30'
29° 20'
29° 10'
29° 00'
28° 50'
MISSISSIPPI DELTA AREA
PER CENT CARBONATE
LESS THAN 2.0
2.0 TO 3.0
3.0 TO 6.0
GREATER THAN 6.0
N
0 2 4 6 8 10 12 14 16
STATUTE MILES
CONTOURS IN FATHOMS
J.R.M.
2
3
6
100
50

Fig. 40.—Percentages of calcium carbonate in area east and north of Mississippi Delta. These percentages are comparable with those for Foraminifera and echinoids (Figs. 18 and 21).

definite trends are indicated. Thus, there appear to be $CaCO_3$ values slightly in excess of 2 per cent directly seaward of the eastern passes, but the values drop below 2 per cent in the indentations between the passes. The low values are particularly well illustrated for North Pass, where Blind Bay to the south of the levees has values of less than 2 per cent, where a tongue of equally low carbonate is found between Pass a Loutre and North Pass, and where the values are also below 2 per cent north of the submerged part of the North Pass levee. Outside of the area where there are appreciable river currents derived from the distributaries there is a zone of variable width, but in places more than 5 miles wide, where the values are somewhat less than 2 per cent. At greater distances seaward the values increase. Off Pass a Loutre high values are found in the bottomset beds on the shelf beyond the slope and equally high values are found in parts of Breton Sound. The values on the platforms around Breton and Goisier islands are low but somewhat higher values are found in the easterly continuation of reworked Mississippi Delta sediment. Virtually no information is available from the strait between Breton and Gosier islands so that the influence of this inlet can not be evaluated. In the inlet between Breton Island and the Mississippi Delta, however, the values are slightly higher than are those of the surrounding area.

Very few samples were examined within the delta. The river samples vary between 2 and 12 per cent $CaCO_3$. Baptiste Collette marsh samples have lower values ranging from 1 to 2½ per cent.

The significance of the calcium carbonate values is not entirely clear. As might be expected, the values are considerably higher in most areas where deposition of clastic material is slow, whereas they are low in the slope areas beyond the passes where deposition is proceeding rapidly. A slight increase in the values at the upper ends of the interdistributary bays may also be related to slower deposition at these positions than in the lower bays. The areas of high foraminiferal content are high in calcium carbonate, and other high carbonate areas are located in the vicinity of the shell reefs of Breton Sound. The low values of calcium carbonate are not necessarily related to the sediment particle sizes since they are found both in the clayey areas off the Pass a Loutre distributaries and in the sandy island platform areas.

MINOR STRUCTURES

From photographs of approximately 200 of the cores it has been possible to obtain some idea of the nature of stratification or of other minor structural characteristics of the sediments in the delta area. In the description which follows, the same classification is used as for the central Texas coast (Shepard and Moore, 1955a, Fig. 29). In the delta the minor structures vary according to the environment of deposition. Only a few cores were obtained in the river channels, but these are fairly consistent in showing relatively thin layers of coarse silt or fine sand interbedded with smooth clayey sediments. Two cores appear to be dominantly sand but with some clayey lumps, and another core shows lumps of sand in a clayey matrix. The marsh cores are distinctive in having a rather structureless mass traversed by numerous roots (Pl. VI, Fig. 1). In the middle of the North Pass levee a similar marshy structure was found and the same is true of a broad levee on the side of Baptiste Collette. Actually marshy conditions prevail at these points. Most of the other levee cores show either lamination or lenses of silt and clayey material (Pl. VI, Fig. 2), but it should be recalled that these levee cores were obtained entirely in the outer perimeter of the delta.

On the platforms outside the distributaries almost all of the cores are laminated, although a few have merely sand with clayey mottling or clay with sandy mottling. Two of them contain sand stringers. A typical laminated type is illustrated in Pl. VI, Fig. 3, where an 8-barrel coring device, which we have called an "octadent," was used to give lateral continuity. The interdistributary bays have almost the same pattern as the platforms with lamination in most of the cores. Several, however, have no laminae and instead have lenses or lumps of sand or silt in the otherwise clayey sediments. Laminations very much like those of the platforms and interdistributary bays are found beneath the marsh deposits of Baptiste Collette subdelta (Pl. VII, Fig. 1) at a depth of a few feet. These also include cross-bedding in some cores. Since it is known that Baptiste Collette has recently built over what was, according to old charts, essentially a pro-delta platform, the finding of laminations in these cores is as expected.

A decided change in the stratification was found beyond the edge of the platform. Of nine core photographs taken on the slope beyond North Pass and Pass a Loutre, the entire core length shows structureless clayey material. Apparently the laminated sediments do not extend much, if any, beyond the edge of the platform in this area. Somewhat farther north two cores on the slope show a few widely spaced silt or sand layers in a clayey matrix. Cores on the slope off South Pass, on the other hand, show thin silty or sandy partings between the clayey sediments. This same pattern is found both in the slope gullies and on the intervening ridges (Shepard, 1955).

Out beyond the slope, in the bottomset beds of the deep shelf, most of the cores are also structureless with a smooth clayey appearance (Pl. VII, Fig. 2). In some of the outer areas, however, silty lenses or lumps are found in the cores and one core showed a dark band with some silty mottling in the clayey material. Beyond the slope the shallow parts of the shelf (less than 11 fathoms) have predominantly mottled cores with silt or sand masses in a clayey matrix. One sandy core had clay mottling, another had a sand lump in clayey sediments, and still another a silt or sand lense. Thus the appearance of the shallow cores in this bottomset shelf area is quite different from that of the deep part.

Numerous photographs were made of cores from the inlet between Main Pass and Breton Island. These show mostly clayey material with lenses or layers of silt. Mottling is found in some of the cores and silt or sand lumps in clayey material in others.

Numerous cores from Breton Sound were photographed. Almost all of these

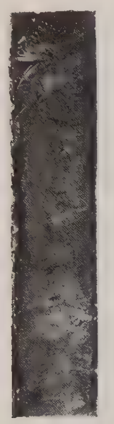

Fig. 1

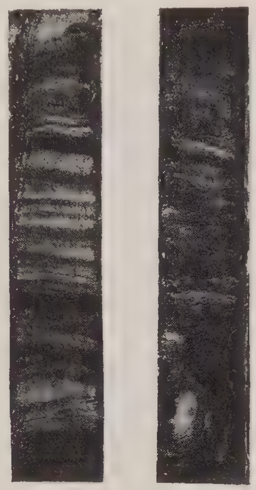

Fig. 2

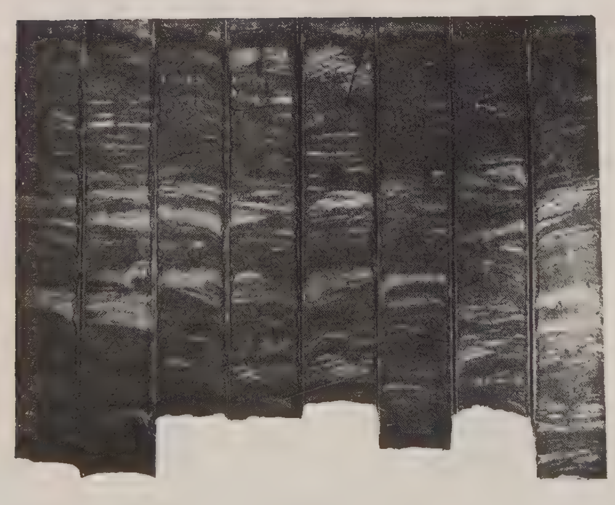

Fig. 3

Pl. VI.—Minor structures characteristic of delta area.

Fig. 1.—Structureless core from marsh environment of Baptiste Collette subdelta with abundance of plant remains.

Fig. 2.—Two cores from levee of North Pass showing typical laminations.

Fig. 3.—Eight aligned cores taken by "octadent" showing continuity of laminations from platform area between North Pass and Pass a Loutre. Each core shows slight bending on sides due to coring operation.

Fig. 1

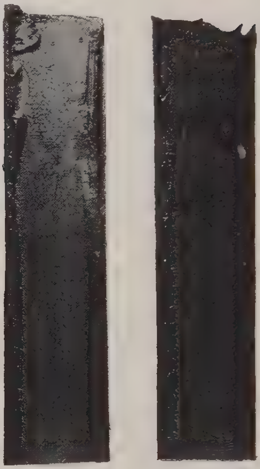

Fig. 2

Fig. 3

Fig. 4

Pl. VII.—Minor structures characteristic of delta area.

Fig. 1.—Laminations and cross-bedding shown in deposits of platform environment beneath marsh deposits of Baptiste Collette subdelta.
Fig. 2.—Typical structureless clayey core from bottomset beds.
Fig. 3.—Core showing clayey sediments "mottled" with sand from Breton Sound.
Fig. 4.—Clayey core with thin stringers of sand from Breton Sound.

show a sand mass with mottling of clay or clayey sediments mottled with sand, (Pl. VII, Fig. 3). This is somewhat like the cores found in Mesquite Bay along the central Texas coast.[14] In Breton Sound several of the cores have thin stringers of sand in clayey material (Pl. VII, Fig. 4).

The other zones do not have any core photographs available and their structure is known only from Scruton's field and laboratory notes.

SUMMARY OF SEDIMENT CHARACTERISTICS OF DEPOSITIONAL ENVIRONMENTS

The series of maps and sections (Figs. 7–34) have indicated the changing characteristics of the sediments as related to distances from the delta, depths, of water, and other influences. A summary of the characteristics of the sediments in each of the sedimentary environments (Fig. 5) is shown in plottings of the range of various parameters in the samples of each environment (Figs. 41–44). In these diagrams, lines connecting the quartiles indicate changes of the parameters in going from one environment to another. In order to show these changes to best advantage, it was found advisable to use semi-logarithmic graphs for those parameters which showed wide divergence in the smaller percentages and to use equi-dimensional graphs for the parameters which have a wide range in percentage.

TOPSET BED DEPOSITS

In the topset bed environments, sand percentages (Fig. 41) show that the river channels have only slightly higher values than those of the levees and marshes, whereas most of the sediments from the platforms directly outside the distributaries have more sand than is found in any of the subaerial delta environments, and numerous platform samples are largely sand. The interdistributary bays, on the other hand, are comparable with the river environment in their sand content. The silt (Fig. 41) of the topset beds is rather consistently more abundant than sand in all topset bed environments, rarely less than 50 per cent. The average clay (Fig. 41) is also somewhat more abundant than sand in the topset beds, but the clay usually has much smaller percentages than silt.

In the coarse fraction the subaerial delta environments show more wood (Fig. 43) than either platform or interdistributary bays. The levee and the marsh aggregates (Fig. 43) which are largely ferruginous, are comparable in abundance and character with those of the platform and the interdistributary bays, but in the river channels, aggregates (largely calcareous) have distinctly smaller percentages than those found in any of the other topset bed environments. Mica (Fig. 42) is more common in the bays than on the platforms, and is least common on the marshes of the five topset bed environments. Glauconite (Fig. 42) is extremely scarce in all of these environments, but, perhaps by coincidence,[15] is found more commonly along the river channels than in the other delta environments.

---

[14] Mesquite Bay is similar to Breton Sound in being near an inlet (Shepard and Moore, 1955b, Fig. 5C).

[15] Since our number of samples on the subaerial delta is rather small.

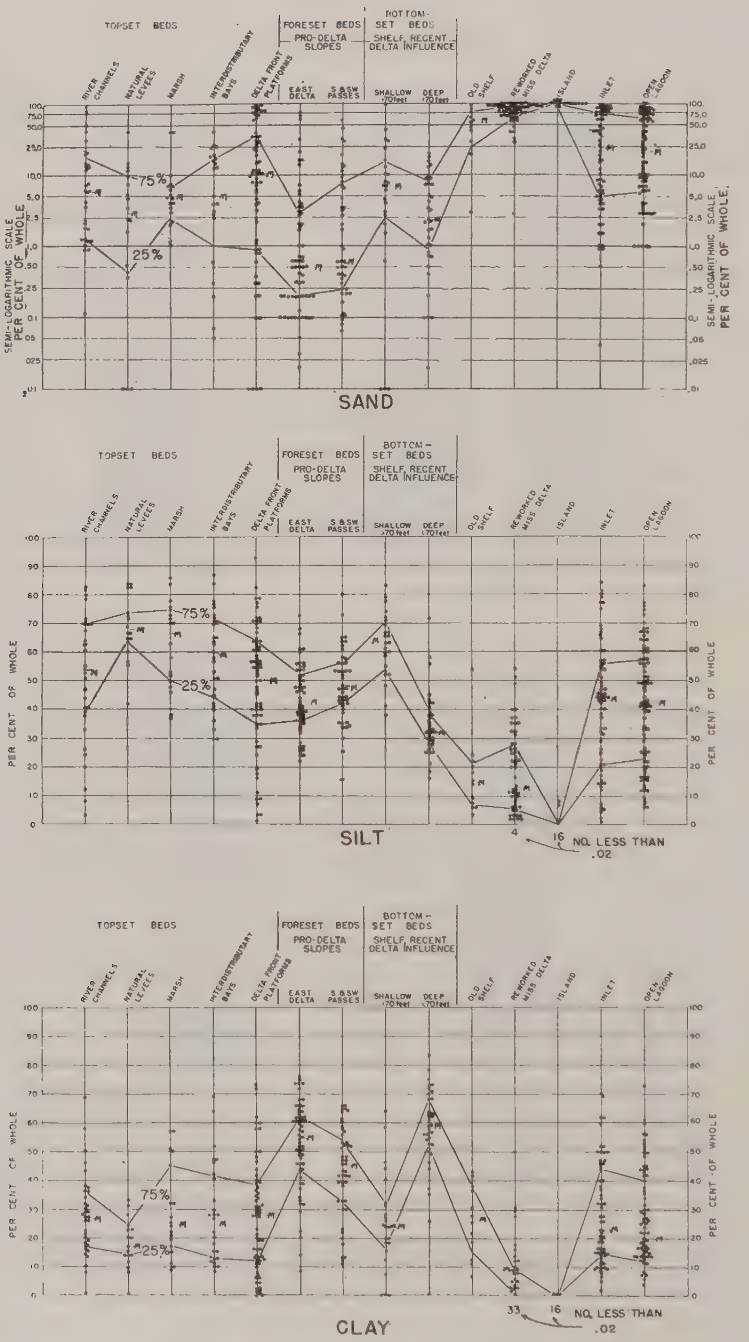

FIG. 41.—Abundance of sand, silt, and clay related to environments. All samples are included. Lines show quartiles and median point indicated by M. Numbers with less than 0.02 per cent silt and clay are shown at base of diagrams. Sand percentages shown on semi-logarithmic scale because of abundance of samples with low percentages.

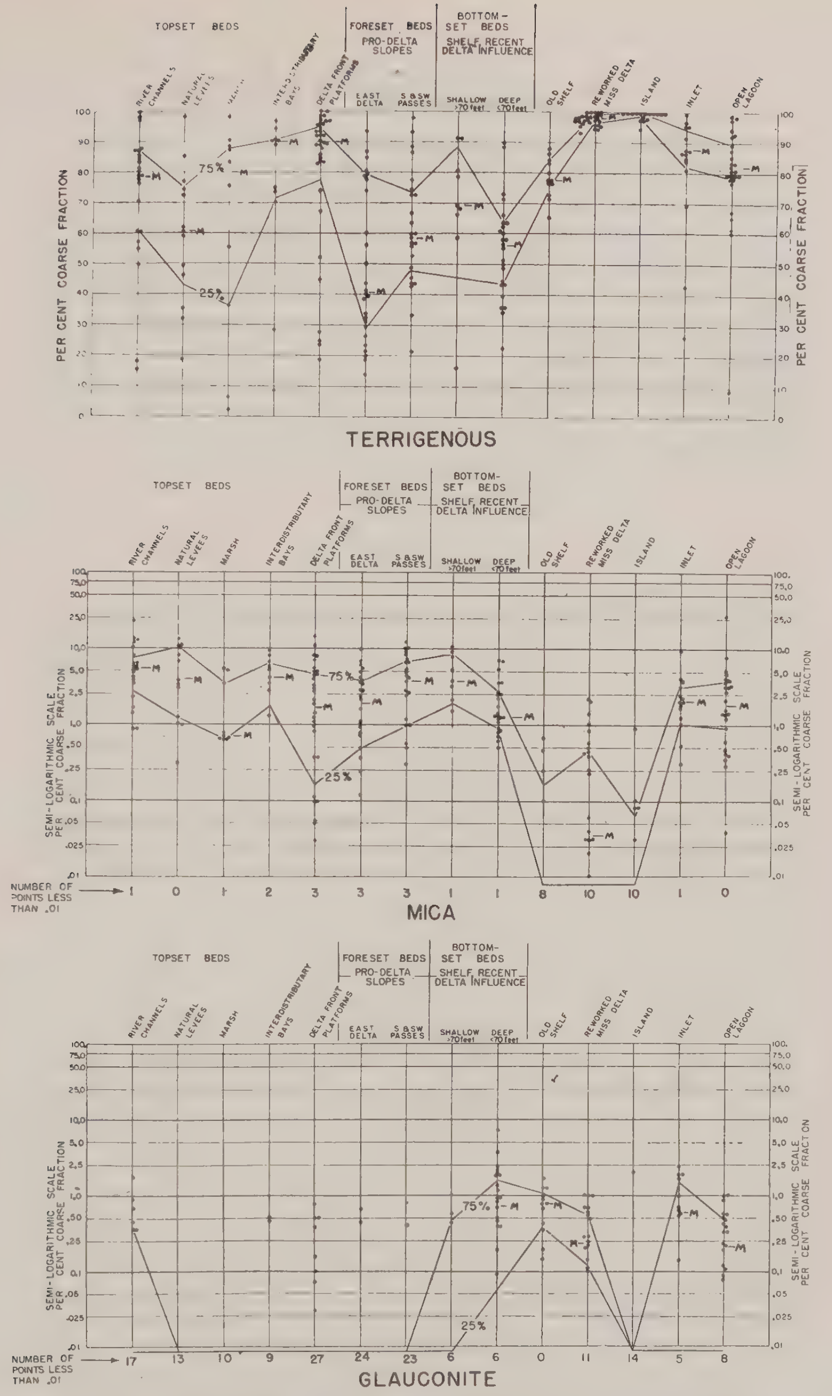

Fig. 42.—Abundance of terrigenous minerals, mica, and glauconite related to environments. Symbols same as in Fig. 40. Percentages refer to coarse fraction, and semi-logarithmic scales are used for mica and glauconite. Where lower quartile passes below the line, it indicates that it lies within points less than 0.01. Mica and glauconite plotted on semi-logarithmic scales.

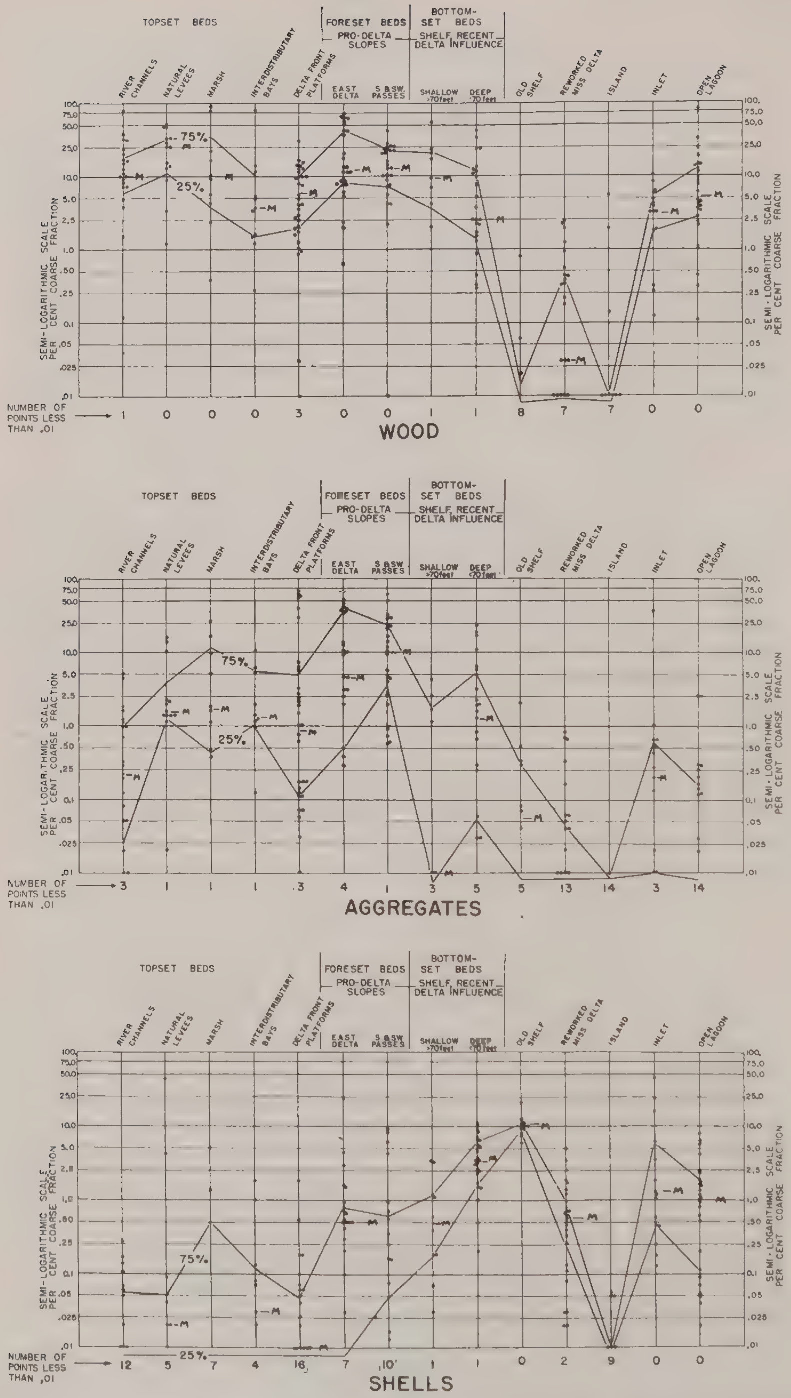

FIG. 43.—Abundance of wood, aggregates, and shells related to environments. Symbols same as in preceding diagrams. Percentages refer to coarse fraction, and all graphs are on semi-logarithmic scale.

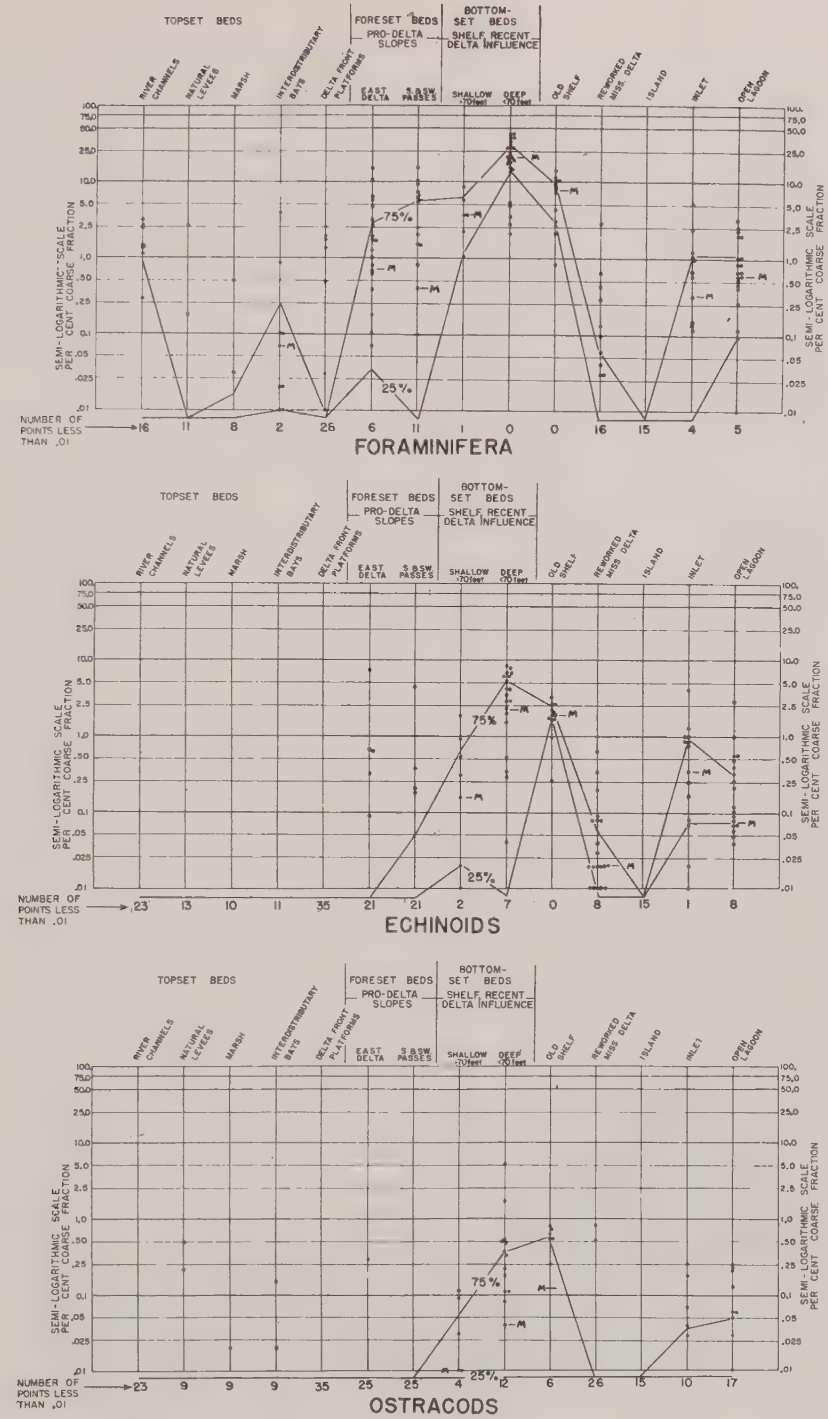

FIG. 44.—Abundance of Foraminifera, echinoids, and ostracods related to environments. Symbols same as in preceding diagrams. All scales semi-logarithmic.

Only traces of glauconite were found in the levee, marsh, and interdistributary bay samples. Foraminifera (Fig. 44) are rare in all of the topset environments, but like glauconite are found more commonly in the river channels than in the other delta environments, and in somewhat smaller quantities in the interdistributary bays. They are surprisingly rare on the platforms. The mollusk shells (Fig. 43) are also rare in all of these environments, but are slightly more common in the interdistributary bays and in the levees. In the latter they are probably concentrated by winnowing during flood stages. Echinoids and ostracods (Fig. 44), are almost entirely lacking in all five of these environments, although one sample with ostracods was found in an interdistributary bay and one in a marsh, each with approximately 0.02 per cent of ostracods.

The stratification affords a means of differentiating the marsh deposits from the other topset beds since the marsh samples show a consistent absence of stratification and an abundance of rootlets. The well developed lamination of the platforms and interdistributary bay deposits can be differentiated at least from the river channel cores, although not necessarily from the natural levee cores where some of the samples have lamination. The finding of cross-bedding among these laminations may also be expected.

FORESET SLOPE DEPOSITS

The platform sediments are distinctly different from the slope sediments which lie contiguous to them, and the difference occurs generally within a short distance. This contrast shows in the percentages of sand, silt, and clay. The sand decreases strikingly from a median of 11 per cent to about 0.5 per cent off both the eastern and southern passes (Fig. 41). The silt percentages decrease from about 55 per cent on the platform to 45 per cent in the slope sediments. The clays have median percentages which increase from 28 for the platforms to 55 for the eastern slopes and to 45 for the southern slopes.

The slope deposits have coarse fractions that are also in great contrast to those of the platform and subaerial delta sediments. The striking feature of the slope deposits is the surprisingly low median percentage for terrigenous materials, which is 41 per cent for the eastern delta slope and 61 per cent for South Pass and Southwest Pass, making a mean point in the low fifties. This is in contrast to medians around 89 per cent in the bays and on the platforms. Wood shows a distinct increase in percentage on the slopes, about 15 per cent for the slopes and only 4 per cent for the platform. Aggregates also increase on the slope and are significantly higher than in any of the five topset bed environments so that the 25 percentile is close to the median for the topset environments. Mica, on the other hand, being only slightly more abundant on the slopes than on the platforms, does not constitute a good means of differentiating these two environments. Foraminifera are more abundant, particularly on the slopes off the eastern passes, increasing from a median that is less than 0.01 per cent on the platforms to 0.4 per cent on the slopes. The speciation of the slope Foraminifera is also quite different from that found in river samples (Pl. II). The shells have increased very considerably on the slope in contrast to the topset bed environments. A few echinoids appear in the slope samples, although they are still very scarce.

The structural differences between the platform and slope are impressive in most of the cores. The laminations characteristic of the platform have virtually disappeared on the slopes. Most cores show several feet with no stratification, and only in a few are there partings of silty layers. These thin silt partings are found particularly off South Pass where they occur both in the gullies and on the ridges so that they are not due to turbidity currents which would follow the gullies. Unconformable relations of beds filling the gullies could be expected in many slope deposits although they have not been discovered in our cores.

BOTTOMSET BEDS

Beyond the slope the bottomset deposits on the shelf east of the delta display some contrast to those of the adjacent slopes, although in many samples it might be difficult to differentiate the two. The average sand content is definitely higher in these shelf deposits, so that the 25 percentile lies above the median for the slope. Sand is particularly abundant in the shallow part of this shelf, with a median of 9 per cent, in contrast to 2 per cent for the part at depths greater than 11 fathoms. The clay percentage is higher on the deep shelf area but on the shallow shelf it is distinctly lower. Compared with the slope the silt content increases in the shallow shelf and decreases for the deep shelf.

In the coarse fraction wood content and aggregates decrease in the bottomset shelf deposits, whereas the mica per cents are about the same. Beyond the slope glauconite has a median on the deeper shelf of 0.7 per cent, whereas it is less than 0.01 per cent on the slopes. On the shallow shelf, however, the glauconite is still as scarce as on the slopes. The Foraminifera have increased enormously on the shelf compared with the slope, especially in the deeper areas, where 26 per cent is the median value. Foraminifera are more abundant here than in any of the other environments, which may be helpful in recognizing bottomset beds in ancient sediments. Ostracods have appeared to some extent in these bottomset deposits but they are still somewhat scarce. Pteropods and scaphopods, which are absent in the slope deposits, were found in most of the bottomset deposits. Echinoids which were still scarce on the slope show a decided increase, having more than 2 per cent in the deeper shelf but only 0.2 per cent on the shallow shelf. The deep shelf is also the environment where the echinoids are the most abundant in the area. Shells have increased considerably compared with the slope, although again the increase is much less pronounced on the shallow shelf.

The scarcity of stratification and the general homogeneity, found in many slope cores, characterize bottomset beds of the deep shelf. The shallow shelf, however, has a mottling in the cores rarely found on the slope. It is not unlikely that consolidation would develop a parting or other indication of bedding within the deposits of the apparently unstratified bottomset and foreset beds.

OLD SHELF DEPOSITS

A very striking contrast exists between the "old shelf deposits" and the bottomset shelf deposits. Sand increases enormously in the former so that it constitutes almost 60 per cent on the average compared with only about 2 per cent in the latter. The silt shows a sharp decrease beyond the bottomset beds and the clay decreases to an even greater degree.

The coarse fraction of the "old shelf deposits" is radically different from that of any of the recent delta-derived sediments. Terrigenous material is by far the most abundant constituent, whereas wood, aggregates, and mica are found very sparingly if at all. Glauconite, on the other hand, has almost the same percentages in the old shelf deposits as in the bottomset beds of the deep shelf. Foraminifera are still present but are much less abundant than in the deep-shelf bottomset beds. Echinoids have decreased only slightly and they are still fairly common. Shells show a decided increase, with a mean slightly in excess of 10 per cent in contrast to 3.5 per cent for the deep-shelf bottomset deposits. This increase does not imply more living shells but rather that the old shelf deposits contain numerous fossil shells mixed with the sandy materials. The ostracods, presumably of recent generation, have increased slightly over those of the bottomset beds.

REWORKED MISSISSIPPI DELTA DEPOSITS

The "reworked Mississippi Delta deposits," which are found on the platforms around Gosier and Breton islands and extend as much as 20 miles east of the island, are strikingly different from all of the other environments, principally in having very high percentages of sand, mostly greater than 80 per cent, whereas the silt is correspondingly scarce, especially in the island platform area, and the clay is even scarcer, not being found in most of the samples. Coarse fractions of this environment consist almost entirely of terrigenous minerals, although in most samples wood is present in small percentages, averaging around 0.3. Aggregates and mica are scarcer even than in the "old shelf deposits." Glauconite is found in the majority of samples, especially in the eastern part of the environment, well away from the islands and their surrounding platforms. Foraminifera are extremely scarce, being largely absent near the islands. Echinoids of recent origin are found in most of the samples but with median values of only 0.02 per cent. Shells also of recent origin are more common, averaging about 1 per cent. Ostracods were found only in two of the samples. Thus these reworked early Mississippi Delta samples are most striking in having a general scarcity of most of the constituents that are common in the environments related to the present delta.

ISLAND DEPOSITS

The island samples, consisting largely of beach and dune sands, are similar to those of the island platforms except that they contain even less of the organisms and consist almost 100 per cent of terrigenous minerals. They are predominantly sand with almost no silt or clay except for small percentages in the flats and marshes inside the beaches and dunes. The beach and dune sands can be recognized by the relatively greater roundness of the latter (Beal and Shepard, 1956).

OPEN-INLET DEPOSITS

The inlet samples are somewhat intermediate in character between the sandy reworked Mississippi Delta deposits, on the one hand, and the sediments of the slope around the Mississippi Delta, on the other. They resemble in some respects the sediments of the delta-front platforms. In sand content the inlet deposits have a median that is close to that of the delta-front platforms, whereas the silt content is comparable with the slope deposits, with a median of 43 per cent. The clay of the inlets, however, is very much scarcer than the clay in the slope deposits.

In the coarse fraction of the inlet samples, terrigenous minerals, wood, and mica are all abundant with percentages comparable with those in the delta-front platform sediments. Aggregates, on the other hand, are distinctly scarcer in the inlet sediments than on the delta-front platforms, and glauconite is much more common in the inlet samples. Glauconite percentages of inlet samples are comparable with those of the deep bottomset beds, but Foraminifera, echinoids, and ostracods are definitely scarcer in the inlets than in the bottomset deposits. Shells vary widely in abundance in the inlets. The shells include numerous oysters, possibly reworked from older formations. Structurally, many of the cores have layers, lenses, and lumps of sand or coarse silt in a clayey matrix. One orange-peel sample contained clay balls probably slightly covered, and another had gypsum crystals clearly reworked.

OPEN-LAGOON DEPOSITS

The open-lagoon environment off Breton Sound differs very little from the inlet environment in particle size. The coarse-fraction is also similar in most respects. Aggregates, however, are decidedly scarcer in the lagoonal environment and consist of rather firmly cemented materials lacking the ferruginous colors so common in the loosely consolidated aggregates of most of the other environments. The echinoids are distinctly scarcer than in the inlets, as is also the glauconite which shows a median of 0.2 compared with 0.6 for the inlets. The core photographs show a great preponderance of sandy or coarse silt sediments with clay mottling or of clayey sediments with sand mottling.

The separation of inlet and open-lagoon deposits can be made best by faunas (Phleger, 1955, and Parker, 1956). Coarse-fraction and particle-size characteristics alone may not be sufficiently distinctive to separate the two. These two environments, however, may be more easily differentiated by coarse-fraction characteristics in other deltas where the inlets have much stronger currents and hence more sorting and coarser sediments than in the adjacent lagoons.

RATES OF DEPOSITION

Not very much is added here to the discussion of rates of deposition by Scruton (1955, pp. 44–48). He has shown that these rates change rapidly going outward from the perimeter of the delta, being highest near or at the front of the platforms and decreasing down the slopes out onto the shelf or toward the island platforms and Breton Sound. He has shown also that the rates change inversely to the clay content for the first 4 or 5 miles out from the delta. Scruton's description and diagrams, however, refer to his sediment units so that it seems advisable in the present paper to refer to the rates in relation to the sedimentary environments included here.

Figure 2 contains the most significant information on depositional rates, with a comparison of the contours from soundings made in about 1868 with contours from recent surveys. These contours indicate that very large deposition has taken place on the delta front platform adjacent to the growing Main Pass and Baptiste Collette, but that the largest depth changes are on the delta-front slopes beyond Pass a Loutre, South Pass, and Southwest Pass. In Main Pass and the other Cubits Gap distributaries the delta has built forward somewhat beyond the delta-front platform, encroaching slightly onto the slope and into the inlet. At the edge of the present delta there has been a fill of about 30 feet in 70 years[16] (Fig. 2).

In the advancing slope off Pass a Loutre, South Pass, and Southwest Pass, the maximum shoaling has amounted to slightly more than 100 feet in 70–80 years (Fig. 2; Shepard, 1955, Fig. 5; and Shepard and Moody, 1953, Fig. 6). There is some indication that approximately this rate of shoaling has been occurring out to depths of as much as 750 feet.

After the platform is built almost to sea-level as a result of the forward-building of the slope, most of the new sediment is by-passed by the waves and currents. Active deposition continues, however, on the sides of the platform channels adjacent to active distributaries so that natural levees are built up to the surface. Flood waters spilling over the levees may also deposit enough sediment in the interdistributary bays to fill them and develop a marsh environment. The growth in this stage is counteracted to a very considerable extent by settling of the surface due to the compaction of the sediments and presumably also because of a general sinking of the lower Mississippi Delta.

The bottomset beds found out beyond the slope east of the delta are too distant from the flatland to give accuracy to old soundings and hence allow any estimation of growth during the interval since earlier surveys. Several of our cores, however, have penetrated through the bottomset beds into formations clearly related to the "old shelf deposits." Thus at the base of the slope 10 miles east of Pass a Loutre a thickness of 11 feet of bottomset beds with a Mississippi River mineral suite overlies "old shelf deposits" with an eastern Gulf mineral suite (Fig. 38). Farther east, at a distance of 30 miles from the passes, a thickness of 7 feet of bottomset beds covers the old sandy formation. About 10 miles farther east the bottomset beds are only 4 feet thick, and a near-by core contained the sandy formation just below the surface. Accordingly, since the rise in sea-level (7,000–10,000 years ago) which left the old shelf deposits at the surface, there has been an appreciable development of bottomset beds. It is probable that this rate has become much faster as the distributaries have grown forward. In any case, the rate of deposition of bottomset beds must have been far slower than the growth of the foreset beds beyond the distributaries.

---

[16] The actual rate of deposition in all cases is somewhat larger than indicated by depth changes because the outer delta is subsiding (Russell, 1936, pp. 47–63; Fisk and McFarlan, 1955).

It is almost impossible to know what rates of deposition have taken place in the open-lagoon environment of Breton Sound and in the inlet environments. Comparison with old soundings in parts of the inlets seems to indicate that the bottom may be actually deeper than it was about 1868, perhaps due to subsidence but in view of the great difficulty which the earlier surveyors must have encountered in obtaining good positions in this area of low relief and shifting currents, the reliability of this possible deepening is open to question. Most of the cores seem to indicate that deposition has been going on in recent times both in the inlets and in Breton Sound, although a few of the cores penetrate what appear to be subaerial delta formations formed prior to the disappearance of much of the St. Bernard Delta, of which Breton Island and Gosier Island represent remnants (Russell, 1936, p. 71). Two of our borings in Breton Island indicated the delta formations with marsh characteristics at a depth of about 30 feet. It is difficult to say how much time was occupied by this amount of deposition on top of this supposedly post-glacial delta, but the delta beds have marsh characteristics, so that they apparently were formed subaerially and now have a covering of about 30 feet, partly shallow marine and partly dune sands, although below present sea-level (Beal and Shepard, 1956, Fig. 7).

COMPARISON WITH OTHER DELTAS

Because very little study has been made of the sediments bordering the major deltas of the world, it is not easy to compare the sediment types bordering other deltas with those around the Mississippi Delta. There are a few reports, however, which have been helpful, and rather detailed soundings are available from the vicinity of many deltas, so that it is possible to make some comparisons between the Mississippi Delta and those existing elsewhere.

ATCHAFALAYA SUBMARINE DELTA

With reference to the part of the Mississippi Delta west of the birdfoot delta, an interesting discussion of the situation off the Atchafalaya River, which now transports about 30 per cent of Mississippi River water (Fisk, 1952 p. 2), has appeared recently (Thompson, 1955). Here, as a result of the flow of the large Atchafalaya River into Grand Lake and the rapid building of the delta into that lake, almost all of the sand-size sediments being transported to the Gulf along this major distributary are deposited in the lake, so that for the most part only silt and clay are carried through the lake and out onto the sea floor. According to Thompson, however, there is an enormous quantity of this fine material being introduced to the Gulf through Atchafalaya Bay and this is forming a delta on the sea floor with a platform comparable at least in depth with those off the main branches of the birdfoot delta. This Atchafalaya submarine delta has a slope of 0.7 foot per mile, and is bordered by a delta-front slope of 3 feet per mile, a low inclination but nevertheless a foreset slope. This delta, according to the comparisons made by Thompson, has been growing forward actively so that it has advanced its foreset slope about 5 miles since 1889, but without any evident shoaling on the platform surface during the forward building. The strong currents flowing along the base of this slope prevent deposition beyond this submarine delta. Accordingly, because of the intervention of Grand Lake at the river mouth, there is a very special type of delta deposition in this area which consists entirely of foreset deposits with very gentle inclination.

ORINOCO DELTA

The huge delta forming at the mouth of the Orinoco River appears to have some points in common with the Mississippi, although the actual outline of the delta is quite different from the large passes, and more comparable with the smaller such as Main Pass, Baptiste Collette, and Grand Pass. The situation is illustrated in Figure 45, where with the help of Tj. H. van Andel (personal communication), attempts have been made to superimpose some Mississippi Delta environmental terms on the Orinoco area. Thus off the southern delta there is a shallow delta-front platform about 20 miles wide with an outer limit at about 25 feet. This platform has submerged channels terminating in bars slightly deeper

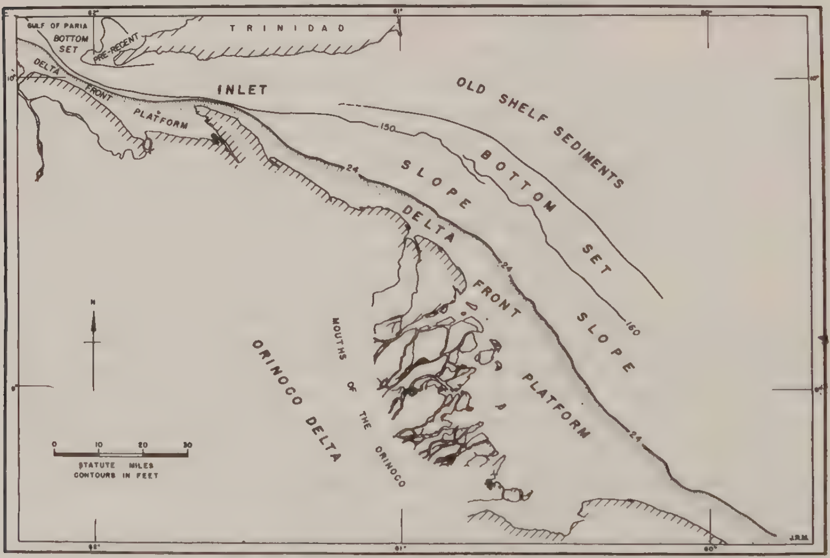
62°
61°
60°
10°
GULF OF PARIA
BOTTOM SET
PRE-RECENT
TRINIDAD
DELTA FRONT PLATFORM
INLET
OLD SHELF SEDIMENTS
150
24
SLOPE
BOTTOM SET
DELTA FRONT PLATFORM
160
SLOPE
ORINOCO DELTA
MOUTHS OF THE ORINOCO
N
0 10 20 30
STATUTE MILES
CONTOURS IN FEET
J.R.M.

FIG. 45.—Comparison of environments of Orinoco Delta area with those of the Mississippi. Data from Tj. H. van Andel (personal communication) and from U. S. Hydrographic Office charts.

than those of the Mississippi Delta. A delta-front slope extends down to approximately 180 feet. A shelf of gentle inclination is found beyond the slope, but the currents are so strong here that the fine clays from the Orinoco are largely bypassed so that there is only a narrow zone of bottomset deposits, and "old shelf deposits" partly belonging to the Pleistocene glacial stages are found beyond. Much of the sediment is swept northwest through the Serpents Mouth, the strait between the delta and Trinidad Island. Beyond in the Gulf of Paria some of these sediments are deposited as bottomset beds. The Gulf of Paria includes also a well developed delta-front platform, especially off the Boca Vagre where a stream of considerable flow enters (van Andel and Postma, 1954, p. 18).

FRASER DELTA

The Fraser is one of the largest rivers of Canada and drains an extensive area of the western Cordillera. This river enters the Strait of Georgia just south of Vancouver (Fig. 46). Sedimentation of the Fraser Delta has been described by Johnston (1921, 1922). Physiographically the margin of this delta can be compared in many respects with the Mississippi Delta sedimentary environments. Thus the channel-traversed shallow banks which have formed on either side of the rapidly advancing Fraser Delta are clear-cut examples of delta-front platforms. The general trend of the foreset slope is comparatively straight, but like the slope southeast from Pass a Loutre, the Fraser slope is found to contain numerous valleys comparable with those off the Mississippi (Fig. 46, inset). The inclination of the Fraser slope, however, is much greater than that off the Mississippi, averaging about 10 per cent to the floor of the Strait of Georgia. Beyond the slope the deep floor can be classified in part as an area of bottomset deposits. Photographs of a series of cores taken from the platform down to the deep floor (Johnson, 1922, Fig. 1) show laminations similar to those in the platform cores found in the Mississippi Delta area. A decided decrease of the laminations is found in the slope cores, and no stratification is found near the bottom of the slope and on the deep floor of the strait where sediments are found which are comparable with those shown in the cores of the Mississippi Delta bottomset beds.

YUKON DELTA

The Yukon Delta, which has been built out for many miles into the Bering Sea appears to have a number of points in common with the Mississippi. A broad delta-front platform extends almost continuously along the front of the distributaries and has a width of about 12 miles. Judged from available soundings, this platform terminates at a depth of about 12 feet. Channels, comparable with those in the Mississippi Delta, cross the platform off the distributaries. Typical bars occur at the outside of these Yukon channels. In the channels the chart symbols indicate sand, whereas on the outer parts of the delta-front platform silt is given as the bottom character. The foreset slope has an inclination of somewhat less than 1 per cent, and extends down to a depth of approximately 50

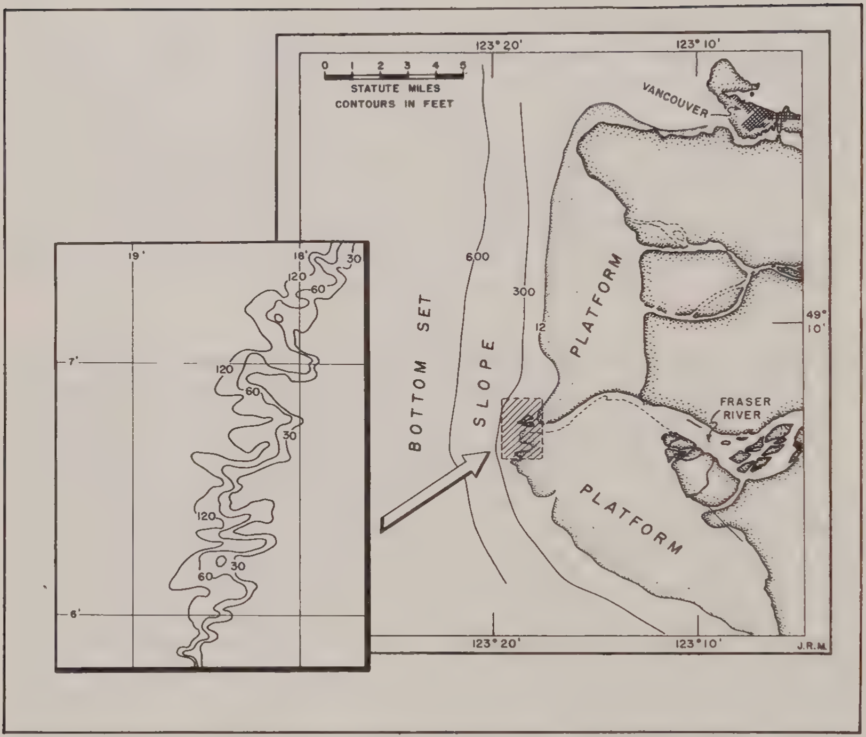
0 1 2 3 4 5
STATUTE MILES
CONTOURS IN FEET
123° 20'
123° 10'
VANCOUVER
PLATFORM
600
300
12
BOTTOM SET
SLOPE
49° 10'
FRASER RIVER
PLATFORM
123° 20'
123° 10'
J.R.M.
19'
18'
30
120
60
7'
120
60
30
120
30
60
6'

FIG. 46.—Comparison of environments of Fraser Delta with those of Mississippi. Inset shows details of slope gullies which are similar to those off Mississippi Delta (Fig. 3). Data from Canadian Hydrographic Office charts.

feet. The bottom character on the slope is labelled "mud" although some "hard bottom" is also indicated. Out beyond the foreset slope, the shelf has a very gentle slope and over a rather extensive area the chart shows sand or hard bottom, suggesting the absence of any bottomset beds from the delta, possibly due to currents like those off the Atchafalaya.

ASIATIC DELTAS

During the war, requirements of the U. S. Navy led to the compilation of bottom-character symbols on all available charts from the vicinity of the large rivers of Asia (Shepard *et al.*, 1949). Several of these rivers have built great deltas into the ocean, notably the Ganges, the Irrawaddy, and the Yangtze Kiang. Around each of these deltas certain features are indicated which suggest a parallel with the Mississippi Delta environments. Most notable are the sandy shoals around the mouths of these great muddy rivers. These are comparable with the

the Mississippi delta-front platform, and extend to approximately the same depths, terminating at 10–30 feet.

Off the huge Ganges Delta, the delta-front platform extends out about 20 miles and has a sandy bottom. On the east, off a typical delta-flank depression (Russell, 1936, Fig. 3) is a series of elongate banks forming a special type of platform. The platform off the Ganges is bordered by a gentle slope extending to about 250 feet. According to the charts, the upper part of the slope is covered with sand but becomes muddy at greater depths. There are some indications that this slope off the Ganges is bordered by a shelf with fine-grained bottomset beds like those east of the Mississippi. Along a part of the outer shelf margin there are places where "sand" bottom suggests that "old shelf deposits" are present.

Off the Irrawaddy Delta of Burma, the sandy delta-front platform is narrower, not exceeding about 10 miles in width. Here, also, a marginal depression to the east is bordered by elongate banks. Outside of the platform of the Irrawaddy the slope has a 1 per cent inclination like that off the major Mississippi passes. The bottom on the slope is indicated as "soft mud." The relatively flat floor of the Gulf of Martaban to the east appears to represent bottomset-bed deposition, but at the outer shelf margin another broad sand belt is found which is probably comparable with the "old shelf deposits" east of the Mississippi Delta. Similarly, southwest of the Irrawaddy, sandy areas on the outer shelf are interspersed with patches of coral bottom; hence, they could be interpreted as "old shelf deposits," remnants of the Pleistocene low stands of sea-level. The relatively strong currents in this area apparently keep these "old deposits" from being covered.

The chart information at the mouth of the Yangtze Kiang River which flows out of central China is not very abundant, but there appear to be wide shoals north of the river mouth, probably about 40 miles across in some places. So far as information is available, these shoals appear to be sandy, and the sand extends somewhat east of the shoals down the slope to the gently inclined outer shelf. Just south of the river and outside of a delta-flank depression, muddy bottom extends out about 100 miles from shore where it is bordered by an outer shelf covered with sand. The same mud and sand belts skirt most of the east coast of Asia (Shepard *et al.*, 1949, Figs. 15 and 18). This outer sand shelf appears to be comparable with the "old shelf deposits" east of the Mississippi Delta, whereas the muddy area presumably constitutes the bottomset beds.

RHONE DELTA

The sediments of the Rhone Delta, which have been described recently by Kruit (1955), have a few points of comparison with those of the Mississippi Delta. The Rhone, like the Mississippi, is a rapidly advancing delta (Kruit, 1955, Fig. 36). In discussing the submarine delta slope, Kruit (1955, p. 44) referred to the shoal-water sediments as having a fluvial marine environment which is characterized by the distinctive grain-size distribution. This is shown by a sample with fine sand at a depth of 3 meters, which represents the outer part of the delta-front platform. The sediments on the delta-front slope have changed radically so that they are clayey silts or silty clays like those off the Mississippi. On the continental shelf at some distance from the delta-front slope, the sediments are clearly not related to the Rhone Delta and may be comparable with the "old shelf deposits" of the Mississippi Delta area.

RHINE DELTA

The delta of the Rhine is actually a product of several rivers. This delta differs from those discussed previously because all of the distributary mouths are deeply indented, as discussed by Barrell (1912, p. 389). The indentation is apparently due to drowning. Despite this subsidence, there are platforms which terminate at a distance of 5 or 6 miles outside of the various delta islands where the depths are about 12 feet.[17] These "delta-front platforms" are, as elsewhere, cut by channels with bars at the channel mouths. Beyond the delta-front platform the slope descends to about 60 feet in 2 miles, with 0.5 per cent slope.

CONCLUSIONS

The bands of sediment which surround the actively growing distributaries of the Mississippi birdfoot delta are developing sedimentary formations with many characteristics which should leave their imprint after they become buried. Many of the criteria used for recognizing these environments in the recent sediments can probably be used in interpreting sedimentary rocks formed under similar conditions. Deposition along the margins of the Mississsippi Delta is occurring at a rate far greater than in most other recent sediment environments. Many other large rivers are building somewhat comparable deltas also at very fast rates. Accordingly it is probable that a large per cent of recent sediments are deltaic. Possibly the reason that so few large deltas have been recognized among the clastic sediments of ancient formations is because of a lack of familiarity with the sediment characteristics in the present-day deltaic encroachments. Furthermore, the failure to recognize deltas may have been in part because the steep foreset beds of textbook diagrams were anticipated, whereas in most of the large deltas of the world, including the Mississippi, the foreset slopes are very gentle, few more than 1 per cent, so that the angle of discordance between foreset beds and both bottomset and topset beds may be very slight. Finally, the massive poorly stratified character of the muddy deposits forming the bottomset beds, and perhaps also the foreset beds may have added to the difficulty.

By evidence now available from large deltas, it is suggested that topset beds formed in the vicinity of marine shorelines might be recognized by their content of an abundance of land plants and aggregates with only a scattering of marine fossils; by the presence of laminated zones with alternating fine and coarse sediments associated with the structureless root-filled marsh deposits; and by large changes in grain size within short distances laterally and vertically. In outline the topset beds should tend to be lobate and should possess elongate sandy lenses both transverse to the lobe margin (channel beds) and tangent to the lobe margin (spits due to reworking of abandoned levees). Foreset beds might be recognized partly by their high content of the land plants and aggregates, suggesting nearness to a river, but can be separated from the topset beds by having a much greater homogeneity of predominantly fine clastic sediments interrupted by rather rare partings of coarser material. The marine fossils would continue to be scarce because of rapidity of deposition which would offset a rather high productivity to be expected in this environment (judged from studies in progress at Scripps Institution). In outline these foreset beds should form a roughly concentric apron around the topset beds. Bottomset beds might be recognized again by having land plants and aggregates like the topset and foreset beds and by having predominantly fine massive sediments like the foreset beds, but unlike the others they should have a high content of marine fossils due to relatively slow deposition and perhaps also to high productivity. They should also contain an appreciable quantity of glauconite, unlike the topset and foreset beds. Also, mottling could be expected because of the slow deposition which would allow bottom-dwelling organisms to work over the sediments and distort any stratification.

---

[17] The sediments here are poorly known because of excessive danger of work in the area due to the remnants of large mine fields left from both World Wars I and II.

Most of the mass of sediment surrounding the growing Mississippi Delta consists of silt and clay. The only clean sands are those that have been reworked from the levees and the bars of the delta front by the waves into spits and shoals along parts of the delta. The only major sand bodies have formed where delta-building is not now active. This origin applies to the great masses of sand northeast of the birdfoot delta, which rise to the surface as Breton and the Chandeleur islands. These clean sand masses are known to have thicknesses of at least 30 feet and may be one of the major sites of oil concentration in ancient deposits. Sand is also quite abundant locally in the topset beds of the growing Mississippi delta, especially where those beds are being deposited in river channels of the distributaries and in the bars forming at the mouths of these distributaries. However, almost all of these sandy formations of the present day contain a considerable percentage of both silt and clay. The sandy zones of the river mouth bars and channels are very spotty in character and become more extensive in high-water than in low-water stages of the river.

Since the Mississippi Delta deposits can be differentiated readily from the older shelf deposits, it is possible to ascertain the extent of the bottomset beds. East of Pass a Loutre, formations clearly derived from the present delta are recognized at a distance of more than 30 miles where they overlap onto older shelf deposits. By means of long cores the presence of the old shelf deposits has been traced to within 12 miles of the subaerial delta where the thickness of the bottomset beds amounts to 11 feet. Although the bulk of these encroaching bottomset beds is derived from the delta, both heavy-mineral and light-mineral studies show that there is some migration of very fine sand in a westerly direction even at shelf depths as great as 200 feet. This adds to the growing evidence that sand can be transported on the outer shelf below the depths of effective wave influence.[18]

The elongate tongue of deltaic sediments east of Pass a Loutre is roughly parallel with the flow direction in this major distributary. Although this suggests an important influence by the jet flow coming from the river orifice, it may represent merely the predominant current set up by various influences during high river stages. The failure of the outer end of the sediment tongue to swing to the right appears to indicate that Coriolis force is not an important factor in this sediment distribution.

BIBLIOGRAPHY

Barrell, Joseph, 1912, "Criteria for the Recognition of Ancient Delta Deposits," *Bull. Geol. Soc. America*, Vol. 23, No. 3, pp. 377–446.

Bates, C. C., 1953, "Rational Theory of Delta Formation," *Bull. Amer. Assoc. Petrol. Geol.*, Vol. 37, No. 9, pp. 2119–62.

Beal, M. A., and Shepard, F. P., 1956, "A Use of Roundness to Determine Depositional Environments," *Jour. Sed. Petrology*, Vol. 26, No. 1, pp. 49–60.

Dohm, C. F., 1936, "Petrography of Two Mississippi River Subdeltas," *Louisiana Geol. Survey Bull. 8* (Lower Mississippi River Delta), pp. 339–96.

Drew, G. H., 1914, "On the Precipitation of Calcium Carbonate in the Sea by Marine Bacteria, and on the Action of Denitrifying Bacteria in Tropical and Temperate Seas," *Pap. Tortugas Lab.*, Vol. V, Pub. 182, pp. 7–45.

Eardley, A. J., 1938, "Sediments of Great Salt Lake Utah," *Bull. Amer. Assoc. Petrol. Geol.*, Vol. 22, pp. 1305–1411.

Emery, K. O., and Terry, R. D., 1956, "A Submarine Slope of Southern California," *Jour. Geol.*, Vol. 64, No. 3, pp. 271–80.

Ewing, Maurice, Worzel, J. L., Ericson, D. B., and Heezen, B. C., 1955, "Geophysical and Geological Investigations in the Gulf of Mexico, Part I," *Geophysics*, Vol. 20, No. 1, pp. 1–18.

"Finding Ancient Shorelines, A Symposium," 1955, *Soc. Econ. Paleon. and Mineral. Spec. Pub. 3.* 129 pp.

Fisk, H. N., 1944, "Geological Investigation of the Alluvial Valley of the Lower Mississippi River," *Mississippi River Commission.* 78 pp.

———, 1952, "Geological Investigation of the Atchafalaya Basin and the Problem of Mississippi River Diversion," *ibid.*

———, McFarlan, E., Jr., Kolb, C. R., and Wilbert, L. J., Jr., 1954, "Sedimentary Framework of the Modern Mississippi Delta," *Jour. Sed. Petrology*, Vol. 24, No. 2, pp. 76–99.

Fisk, H. N., and McFarlan, E., Jr., 1955, "Late Quaternary Deltaic Deposits of the Mississippi River," from "The Crust of the Earth," *Geol. Soc. America Spec. Paper 62*, pp. 279–302.

Goldstein, August, Jr., 1942, "Sedimentary Petrologic Provinces of the Northern Gulf of Mexico," *Jour. Sed. Petrology*, Vol. 12, No. 2, pp. 77–84.

Hilgard, E. W., 1871, "On the Geology of the Delta, and the Mudlumps of the Passes of the Mississippi," *Amer. Jour. Sci.*, 3d Ser., Vol. 1, pp. 238–46, 356–68, 425–34.

Holle, C. G., 1952, "Sedimentation at the Mouth of the Mississippi River," *Proc. 2d Conf. Coastal Engineering* (Houston, Texas, Nov., 1951), Chap. 10, pp. 111–29. Published by the Engineering Foundation, University of California.

Illing, L. V., 1954, "Bahaman Calcareous Sands," *Bull. Amer. Assoc. Petrol. Geol.*, Vol. 38, No. 1, pp. 1–95.

Inman, D. L., and Chamberlain, T. K., 1955, "Particle-Size Distribution in Nearshore Sediments," *Soc. Econ. Paleon. and Mineral. Spec. Pub. 3*, pp. 106–27.

Johnston, W. A., 1921, "Sedimentation of the Fraser River Delta," *Canada Geol. Survey Mem. 125.* 46 pp.

———, 1922, "The Character of the Stratification of the Sediments in the Recent Delta of Fraser River, British Columbia, Canada," *Jour. Geol.*, Vol 30, No. 2, pp. 115–29.

Kruit, Cornelis, 1955, "Sediments of the Rhone Delta: Grain Size and Microfauna," *Rijksuniversiteit te Groningen.* 141 pp. Published by Mouton and Company. 'S-Gravenhage.

---

[18] In this area occasional hurricanes will probably cause active stirring of the bottom at 200 feet.

Krumbein, W. C., and Aberdeen, Esther, 1937, "The Sediments of Barataria Bay," *Jour. Sed. Petrology*, Vol. 7, pp. 3–17.

Ludwick, J. C., and Walton, W. R., 1956, "Shelf-Edge Calcareous Prominences in the Northeastern Gulf of Mexico" (abst.), *A.A.P.G.-S.E.P.M. Ann. Meeting Program*, p. 68.

Morgan, J. P., 1951, "Report on the Mudlumps at the Mouths of the Mississippi River; Part I, The Occurrence and Origin of the Mudlumps at the Mouths of the Mississippi River" (unpublished report), *New Orleans District Corps of Engineers*. 127 pp.

———, 1952, "Mudlumps at the Mouths of the Mississippi River," *Proc. 2d Conf. Coastal Engineering* (Houston, Texas, Nov., 1951), Chap. 11, pp. 130–44. Published by the Engineering Foundation, University of California.

Murray, J. W., 1954, "The Deposition of Calcite and Aragonite in Caves," *Jour. Geol.*, Vol. 62, No 5, pp. 481–92.

Parker, R. H., 1956, "Macro-Invertebrate Assemblages as Indicators of Sedimentary Environments in East Mississippi Delta Region," *Bull. Amer. Assoc. Petrol. Geol.*, Vol. 40, No. 2, pp. 295–376.

———, and Curray, J. R., 1956, "Fauna and Bathymetry of Banks on Continental Shelf, Northwest Gulf of Mexico," *ibid.*, Vol. 40, No. 10, pp. 2428–39.

Phleger, F. B, 1955, "Ecology of Foraminifera in Southeastern Mississippi Delta Area," *ibid.*, Vol. 39, No. 5, pp. 712–52.

Russell, R. D., 1935, "Frequency Percentage Determinations of Detrital Quartz and Feldspar," *Jour. Sed. Petrology*, Vol. 5, No. 3, pp. 109–14.

Russell, R. J., 1936, "Physiography of Lower Mississippi River Delta," *Louisiana Geol. Survey Bull. 8* (Lower Mississippi River Delta), pp. 3–199.

———, and Russell, R. D., 1939, "Mississippi River Delta Sedimentation," *Recent Marine Sediments*, Amer. Assoc. Petrol. Geol., pp. 153–77.

Scruton, P. C., 1955, "Sediments of the Eastern Mississippi Delta," *Soc. Econ. Paleon. and Mineral. Spec. Pub. 3*, pp. 21–50.

———, 1956, "Oceanography of Mississippi Delta Sedimentary Environments," *Bull. Amer. Assoc. Petrol. Geol.*, Vol. 40, No. 12.

———, and Moore, D. G., 1953, "Distribution of Surface Turbidity off Mississippi Delta," *ibid.*, Vol. 37, No. 5, pp. 1067–74.

Shepard, F. P., 1937, "Salt Domes Related to Mississippi Submarine Trough," *Bull. Geol. Soc. America*, Vol. 48, pp. 1349–62.

———, 1954, "Nomenclature Based on Sand-Silt-Clay Ratios," *Jour. Sed. Petrology*, Vol. 24, No. 3, pp. 151–58.

———, 1955, "Delta-Front Valleys Bordering the Mississippi Distributaries," *Bull. Geol. Soc. America*, Vol. 66, No. 12, pp. 1489–98.

———, Emery, K. O., and Gould, H. R., 1949, "Distribution of Sediments on East Asiatic Continental Shelf," *Allan Hancock Foundation Publications, Univ. Southern California, Occas. Paper 9*. 64 pp.

Shepard, F. P., and Moody, C. L., 1953, "Study of Near-Shore Recent Sediments and Their Environments in the Northern Gulf of Mexico. The First Two Years," *A.P.I. Research Project 51*. Paper for Presentation to a Group Session on Fundamental Research on Occurrence and Recovery of Petroleum, during the 33rd Annual Meeting of the A.P.I., Conrad Hilton Hotel, Chicago, Illinois, November 9, 1953.

Shepard, F. P., and Moore, D. G., 1954, "Sedimentary Environments Differentiated by Coarse-Fraction Studies," *Bull. Amer. Assoc. Petrol. Geol.*, Vol. 38, No. 8, pp. 1792–1802.

———, and ———, 1955a, "Central Texas Coast Sedimentation: Characteristics of Sedimentary Environment, Recent History, and Diagenesis," *ibid.*, Vol. 39, No. 8, pp. 1463–1593.

———, and ———, 1955b, "Sediment Zones Bordering the Barrier Islands of Central Texas Coast," *Soc. Econ. Paleon. and Mineral. Spec. Pub. 3*, pp. 78–96.

Thompson, W. C., 1955, "Sandless Coastal Terrain of the Atchafalaya Bay Area, Louisiana," *ibid.*, pp. 52–76.

Treadwell, R. C., 1955, "Trafficability and Navigability of Delta-Type Coasts, Trafficability and Navigability of Louisiana Coastal Marshes: Sedimentology and Ecology of Southeast Coastal Louisiana," *Louisiana State Univ. Tech. Rept. 6*. 78 pp.

Trowbridge, A. C., 1930, "Building of Mississippi Delta," *Bull. Amer. Assoc. Petrol. Geol.*, Vol. 14, pp. 867–901.

Van Andel, Tj., and Postma, H., 1954, "Recent Sediments of the Gulf of Paria," *Reports of Orinoco Shelf Expedition*, Vol. I. 245 pp. North-Holland Publishing Company, Amsterdam.

FORAGING HABITS AND LOCAL MOVEMENTS OF THE WOOD IBIS IN SAN DIEGO COUNTY, CALIFORNIA

By ANDREAS B. RECHNITZER

Reprinted from THE CONDOR, Volume 58, November-December, 1956, Number 6, pp. 427–432
Contributions from the Scripps Institution of Oceanography, New Series, No. 888
Reproduced by Permission

(958)

FORAGING HABITS AND LOCAL MOVEMENTS OF THE WOOD IBIS IN SAN DIEGO COUNTY, CALIFORNIA

By ANDREAS B. RECHNITZER

Published records and personal observations indicate that each summer a few Wood Ibises (*Mycteria americana*) visit southern California, particularly the Imperial Valley marshes, Imperial County, and the coastal lagoons of San Diego County. Occasional stragglers have been recorded farther north: Long Beach (Law, 1912); Bixby, Los Angeles County (Daggett, 1903); San Bernardino Valley (Feudge, 1903); Daggett, San Bernardino County (Lamb, 1912); Santa Barbara (Rett, 1954); San Francisco Bay (Cooper, 1887). These annual migrants which are thought to come from the coast of western Mexico, where the species is common, appear in late June or early July and depart by mid-October. The numbers recorded vary considerably from year to year as shown in table 1. Except for the years from 1953 to 1955, when a definite effort was made to locate all individuals within the limits of San Diego County, it is suspected that the recorded numbers are underestimates of the numbers present in the county. Surveys made weekly or biweekly in the summers from 1953 to 1955 showed that the Lt. Maxton Brown Sanctuary (Buena Vista Lagoon), between Oceanside and Carlsbad, is the major foraging area for the Wood Ibis. The Santa Marguerita River mouth, north of Oceanside, and the San Elijo Lagoon at Cardiff are used as foraging areas to a lesser extent. The other lagoons and bays shown in figure 1 are now used only very infrequently. All of these areas have been occupied in the past (Lawrence Huey, personal communication), but probably they have been rendered unsuitable by dredging, filling, and sewage disposal. No Wood Ibises have been recorded recently for lakes Sutherland, Henshaw, Sweetwater, El Capitan, Lower Otay, Hodges, Wohlford, and San Vicente, and none had been observed at these lakes by representatives of the Department of Fish and Game whom I questioned. This is of interest because these lakes would seem to be logical "stop-over" areas if the birds observed in the coastal lagoons come from the Imperial Valley marshes.

Audubon (1835:129) described the rather spectacular feeding and flight habits which are characteristic of the species:

"To procure its food, the Wood Ibis walks through shallow muddy lakes or bayous in numbers. As soon as they have discovered a place abounding in fish, they dance as it were all through it, until the water becomes thick with the mud stirred from the bottom by their feet. The fishes, on rising to the surface, are instantly struck by the beaks of the Ibises, . . . [and], on being deprived of life, they turn over and so remain. In the course of ten or fifteen minutes, hundreds of fishes, frogs, young alligators, and water-snakes cover the surface, and the birds greedily swallow them until they are completely gorged, after which they walk to the nearest margins, place themselves in long rows, with their breasts all turned toward the sun, in the manner of Pelicans and Vultures, and thus remain for an hour or so. When digestion is partially accomplished, they all take to wing, rise in special circlings to an immense height and sail about for an hour or more, performing the most beautiful evolutions that can well be conceived."

Daggett (1903) examined the full crop contents of one bird taken at Bixby, California and found only aquatic insects. Grinnell, Bryant, and Storer (1918) listed the stomach contents of three Wood Ibises taken in Imperial County, California. One contained 3 tadpoles, 4 water beetles, 2 paddle bugs, and some moss [algae?] and slime; another, 9 tadpoles, a water beetle, 9 dragon fly larvae, and a carp; the third held 10 carp, a catfish, 2 bony tails [*Gila robusta*], and a water cricket. Bryant (1919) reported on another bird with 10 seeds of the screw bean, 2 seeds of mesquite, parts of 4 water beetles and some finely comminuted vegetable material. Holt and Sutton (1926) recorded the stomach contents of some adult birds collected at Alligator Lake, Florida. They found small fishes, reported as *Mollienisia latipinna, Cyprinodon variegatus, Gambusia affinis, Lepomis holbrooki,* and *Adinia multifasciata,* to be present.

Because conditions for observation in the San Diego lagoons are particularly favorable, it has been possible in the present study to identify larger items of food without sacrificing birds. In the limited and confined marsh channels of San Elijo Lagoon the major constituent of the diet is a fish, the topsmelt *Atherinops affinis littoralis*. As the Wood Ibis is a rather indiscriminant fish-eater, it is possible that it takes other fish inhabitants of these channels, namely the California killifish, *Fundulus p. parvipinnis*; tidewater goby, *Eucyclogobius newberryi*; arrow goby, *Clevelandia ios*; longjaw mudsucker, *Gillichthys mirabilis*; and probably the shadow goby, *Quietula y-cauda*. Carcasses of all those fishes, except the shadow goby, were found along the banks of the watercourses following a feeding foray by the ibis. In the freshwater San Dieguito Reservoir near Rancho Santa Fe, Wood Ibises were observed eating young black bass, *Micropterus salmoides,* and catfish, *Ictalurus* sp.

Table 1

Maximum Number of Wood Ibises Observed in San Diego County

Year	Number of ibises	Reference[1]
1946	150+	Audubon Field Notes, 1947, 1:20.
1947	22	Audubon Field Notes, 1948, 1:23.
1948	8	Personal observations.
1949	2	Audubon Field Notes, 1950, 1:34.
1950	2	Audubon Field Notes, 1951, 1:38.
1951	70	Personal observations.
1952	57	Audubon Field Notes, 1953, 1:36.
1953	300+	Personal observations.
1954	36	Personal observations.
1955	71	Personal observations.

---

[1] Published sight records and my personal observations agree closely for all years concerned. Personal observations are entered for those years wherein my cumulative total for a single day's survey indicated more birds or represented a more synoptic observation.

Ordinarily the birds were observed to eat their catch immediately after capture, but toward the end of a feeding period they began to appear satiated and would, at times, release their victims although continuing to hunt in the company of the flock with seemingly the same diligence and enthusiasm. On one occasion several thousand decaying carcasses of the topsmelt, killifish, and gobies were found in a single winddrift in the San Elijo Lagoon. Scarred and mutilated bodies suggested that they were victims of ibises, which were observed feeding in the immediate area on the previous day. Live schools of fish still remained in the area at the time of this observation, indicating that the mass mortality was probably not due to other adverse causes.

In feeding, the ibises cooperate by walking in groups, often abreast, or nearly so, through the narrow meandering drainage channels of the marshes. This method effectively extends the ranks of a flock across the entire channel width, which seldom exceeds 30 feet. At times the "marching" group is two or more birds deep. They usually start their feeding forays near the mouth of a channel or at the junction of two channels. From this point the ibises walk slowly and deliberately toward the shallow and nar-

(960)

rowing origin. The casual, non-stalking gait of the ibises effectively muddies the water, but it is doubtful that this is a necessary preliminary to catching prey in water that is already roiled or continually turbid. This foot and leg movement disturbs the water enough to herd the schooling-type fishes into shallow and more restricted areas where they are then killed and taken in large numbers. The use of foot activity for feeding may also serve to direct swimming prey animals to the beak (Rand, 1956).

Foraging in the more open waters of the San Dieguito Reservoir or the Lt. Maxton Brown Sanctuary is performed in a comparable manner, the birds working the shallows of these areas in groups of 20 or more.

When feeding in groups, the Wood Ibises do not dart the head at their prey but instead employ a groping method. With the head turned to the side, the partly open beak is immersed in water to a depth of several inches and is then passed through the water sideways like a pair of tongs. Movement of the beak through the water is accomplished either by swinging the head in a semicircular arc or by walking forward with the head turned to the right or left. When contact with a fish is made, the beak is snapped shut and invariably the bird is successful in securing a squirming morsel. It appears that the tactile sensitivity of either the tongue or the tissue lining the inner surface of the bill is remarkably developed to permit such effective feeding under relatively adverse conditions. When birds feed singly, they resort to a visual technique and take their prey by stalking and darting with the bill.

The feeding periods are usually from pre-dawn to about three hours after sunrise and for a comparable period prior to and following sunset. After feeding, the birds usually retire to dry ground near the last feeding site, where they remain during the daylight hours. Birds separated from the flock sometimes continue to feed for longer periods. After feeding, short sortie flights are made to re-establish the flock. In the early summer, shortly after their arrival, they are very gregarious and all post-feeding resting is done as a unit. Dispersal, however, becomes more common later in the season, particularly during the month of September.

Although the feeding activities of the Wood Ibises produced a surplus of fish, no other birds were noted associating with them at this time. It was particularly noticeable that the gulls (*Larus heermanni* and *L. californicus*) which were fishing at other points in the lagoon stayed away from the Wood Ibis and did not serve as a "clean-up" detail for the fish left to spoil. The Great Blue Herons (*Ardea herodias*), American Egrets (*Casmerodius albus*), Snowy Egrets (*Egretta thula*), Black-necked Stilts (*Himantopus mexicanus*) and terns (*Sterna antillarum* and *Thalasseus maximus*) which were present in the lagoons also seemed to avoid the immediate vicinity of the ibis.

Following the partial digestion of a meal the ibis reportedly takes to the air to soar (Audubon, 1835). Here again the behavior of the Wood Ibises as observed in southern California does not follow the described pattern. The short flights made by the summer visitors have been mentioned above, but the more spectacular soaring flights have been restricted almost entirely to the end of the summer. Soaring in gyres the ibises rise to heights that require binoculars to keep them in sight. On overcast days, they often disappear into the cloud cover. I have observed the spectacular plummeting dive from these high altitude flights only once (Rechnitzer, 1954). Following these flights the birds were not observed to return to the lagoon, indicating that they probably continued over the coastal range, either into the Imperial Valley or to the Gulf of California.

Dawn and dusk flights were a conspicuous part of the daily activities prior to the 1955 visit. Throughout previous summers the ibises regularly vacated San Elijo Lagoon at dusk and flew to the drainage area of the San Dieguito River (air distance about two miles). The flock usually rose into the air in tandem, and staggered their numbers so

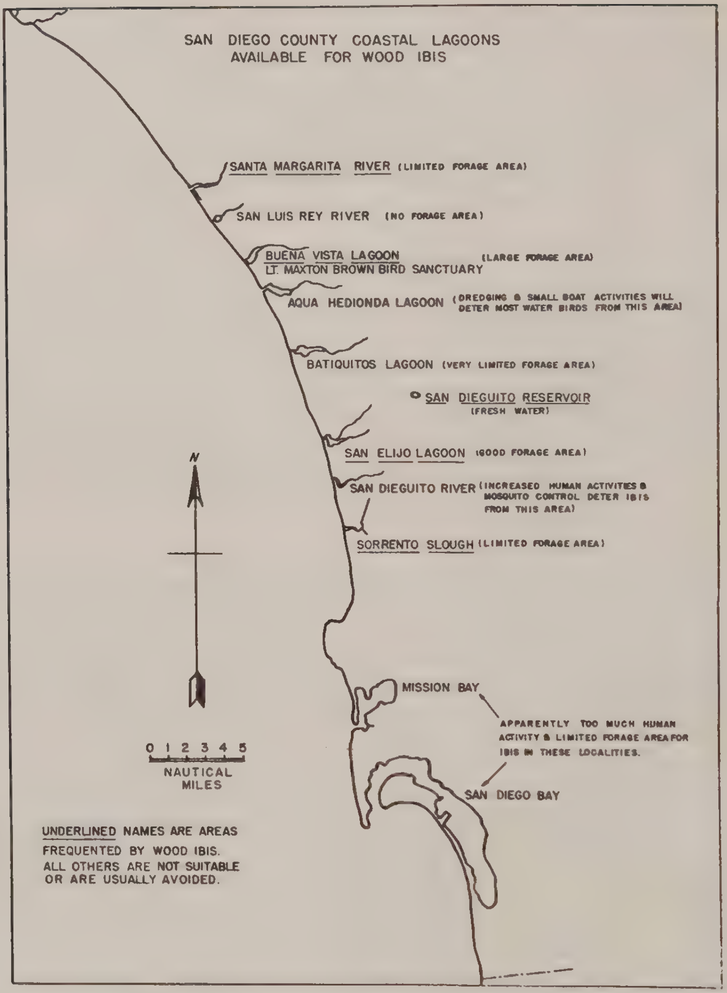
SAN DIEGO COUNTY COASTAL LAGOONS
AVAILABLE FOR WOOD IBIS
SANTA MARGARITA RIVER (LIMITED FORAGE AREA)
SAN LUIS REY RIVER (NO FORAGE AREA)
BUENA VISTA LAGOON
LT. MAXTON BROWN BIRD SANCTUARY
(LARGE FORAGE AREA)
AQUA HEDIONDA LAGOON (DREDGING & SMALL BOAT ACTIVITIES WILL DETER MOST WATER BIRDS FROM THIS AREA)
BATIQUITOS LAGOON (VERY LIMITED FORAGE AREA)
SAN DIEGUITO RESERVOIR (FRESH WATER)
SAN ELIJO LAGOON (GOOD FORAGE AREA)
SAN DIEGUITO RIVER (INCREASED HUMAN ACTIVITIES & MOSQUITO CONTROL DETER IBIS FROM THIS AREA)
SORRENTO SLOUGH (LIMITED FORAGE AREA)
N
MISSION BAY
APPARENTLY TOO MUCH HUMAN ACTIVITY & LIMITED FORAGE AREA FOR IBIS IN THESE LOCALITIES.
SAN DIEGO BAY
0 1 2 3 4 5
NAUTICAL MILES
UNDERLINED NAMES ARE AREAS FREQUENTED BY WOOD IBIS.
ALL OTHERS ARE NOT SUITABLE OR ARE USUALLY AVOIDED.

Fig. 1. Principal marsh and lagoon areas of San Diego County, California. Only San Elijo and Buena Vista lagoons, and the mouth of the Santa Marguerita River continue to attract Wood Ibises.

that the procession was intermittent but confined to a relatively short period of each day, once near sunset and again on the following morning for the return flight. The birds gained only enough altitude to permit short glides and to pass over the low ridge of hills adjacent to the lagoon. No flights other than these intra- and inter-lagoon flights were noted. In 1955 the inter-lagoon flights were completely interrupted. An increase in aircraft activities, coupled with a heavy application of a strong insecticide to the impounded waters of the lower San Dieguito drainage area probably discouraged the birds from this former summer habitat. All of the Wood Ibises remained within the San Elijo Lagoon until July 28, 1955. At this time they were frightened out of the marsh area by a "controlled brush fire," which engulfed all of the watercourse with dense smoke and destroyed the lush stand of the marsh weed *Salicornia* that blanketed the exposed areas of the lagoon. Subsequent visits to the lagoon revealed a complete exodus of Wood Ibises until early October, when the southward migration began. At this later time the birds stayed in the lagoon for only a single day or less.

After the abandonment of San Elijo Lagoon on July 28, 1955, a group of 48 birds temporarily relocated in the San Dieguito Reservoir, which is situated inland about five miles from the lagoon and relatively close to the main drainage channel that feeds the lagoon during the winter run-off (if any). After three weeks the reservoir was devoid of ibises. The number of birds in the Lt. Maxton Brown Sanctuary and the Santa Marguerita River mouth had, at this time, attained a cumulative total comparable to that observed earlier in the season at the more southerly San Elijo Lagoon.

Photographs of Wood Ibis in Florida (Bent, 1926) indicate their preference for tall trees as roosting sites. Although all the areas visited in San Diego County have trees nearby, I have yet to see a Wood Ibis occupy the apparently suitable trees, while the Great Blue Heron, American Egret, and Snowy Egret often rest in tall eucalyptus trees.

Each fall the ibises begin to move south gradually when there is a drop in the night temperatures. The daytime temperatures remain fairly high, and that there is an apparent reluctance in this movement southward, is evidenced by the occupation of the marsh or lagoon next to the south for a day or two before the ibises move on. Most of the birds leave the coastal lagoons of San Diego County after reaching San Elijo Lagoon, but a few stop four miles to the south, temporarily, at Sorrento Slough.

SUMMARY

Wood Ibises continue to visit southern California coastal lagoons as summer migrants, probably from the west coast of Mexico. They are conspicuous among the aquatic birds because of their size and their white plumage, and because of the general paucity of vegetation and obstructions in the marsh areas visited. The Wood Ibis, despite the awkward appearance of its large bill, is a very efficient feeder, particularly on small fishes and aquatic insects. The beak is immersed several inches into the turbid water and held agape while being passed to and fro like a large pair of forceps. Upon contact with a fish the bill is snapped shut. The ibises feed in flocks of 20 or more, which permits them to span the narrow drainage channels of the lagoons and thereby effectively to herd the fish into shallow water. Flight activities are not a conspicuous part of their behavior while in southern California, but soaring to great heights has been observed toward the end of summer. The amount of available forage space is being reduced by urban development along the coast, and only one sanctuary area remains as the principal area visited by Wood Ibises.

LITERATURE CITED

Audubon, J. J.
1835. Ornithological biography, or an account of the habits of the birds of the United States of America. Vol. 3.
Bent, A. C.
1926. Life histories of North American marsh birds. U. S. Nat. Mus. Bull. 135.
Bryant, H. C.
1919. Evidence as to the food of the wood ibis. Condor, 21:236–237.
Cooper, J. G.
1887. Additions to the birds of Ventura County, California. Auk, 4:85–94.
Daggett, F. S.
1903. Wood ibis in southern California. Condor, 5:18–19.

(963)

Feudge, J. B.
1903. The wood ibis near San Bernardino. Condor, 5:79.
Grinnell, J., Bryant, H. C., and Storer, T. I.
1918. The game birds of California (University of California Press, Berkeley).
Holt, E. G., and Sutton, G. M.
1926. Notes on birds observed in southern Florida. Ann. Carnegie Mus., 16:409–439.
Lamb, C.
1912. Birds of a Mohave Desert oasis. Condor, 14:32–40.
Law, J. E.
1912. Wood ibis near Long Beach. Condor, 14:41.
Rand, A. L.
1956. Foot-stirring as a feeding habit of wood ibis and other birds. Amer. Midl. Nat., 55:96–100.
Rechnitzer, A. B.
1954. Status of the wood ibis in San Diego County, California. Condor, 56:309–310.
Rett, E. Z.
1954. Audubon Field Notes, 8:41.

Scripps Institution of Oceanography, University of California, La Jolla, California, April 15, 1956.

Reprinted from JOURNAL OF APPLIED PHYSICS, Vol. 27, No. 12, 1473–1483, December, 1956
Copyright 1956 by the American Institute of Physics
Printed in U. S. A.
Reproduced by Permission

Extremely Low-Frequency Electromagnetic Waves.[*] I. Reception from Lightning

LEONARD LIEBERMANN
University of California, Marine Physical Laboratory of the Scripps Institution of Oceanography, La Jolla, California
(Received June 23, 1956)

Extremely low-frequency (ELF) radio waves (10–500 cycles) originating in lightning were received over distances in excess of 15 000 km. Transmission conditions were equally good, day or night. Propagation distances were ascertained by analysis of higher frequency components (>1700 cycles) according to known methods. The receiving antenna employed an arrangement of grounded electrodes which uniquely determined the azimuthal direction of the source. Two distinct classes of ELF pulses are described which are attributed to different conditions of propagation.

INTRODUCTION

IT is well known that lightning generates radio static, or atmospherics. The detectable upper frequency limit in a pulse generated by lightning extends well into the 100-mc band. The low-frequency end of the pulse spectrum is less familiar. The present work is concerned with reception below 10 kc with particular emphasis on frequencies below 500 cycles.

Under typical night conditions a received pulse has a distinct tonal quality, or whistle. The pulse is usually received as a long train of oscillations with gradually increasing period; the longest period of oscillation is always in the neighborhood of 1700 cycles. The duration of the received pulse may be as long as 100 msec although the originating pulse was less than 0.1 msec.[†] During the day the received pulse is typically of much shorter duration, of the order of 5 msec and hence exhibits no tonal quality.

The cut-off frequency of 1700 cycles is by no means the lower limit of the spectrum. The atmospheric pulse also exhibits considerable amplitude in the frequency range below a few hundred cycles. Figure 1 shows a pulse typical of those received at night; the initial portion is in the vicinity of 5 kc with quasi-periodic components diminishing to the cut-off frequency of 1700 cycles; superimposed on the quasi-periodic components are seen considerably lower frequency components in the vicinity of 10 to 600 cycles.

The transmission conditions responsible for frequency cutoff at 1700 cycles and for the tonal phenomena have already been adequately studied and except for details are well understood.[1,2] The transmission properties at extremely low frequencies, below 500 cycles (ELF band) remain unknown, although observations of ELF propagation are not new; the presence of the "slow tail" in atmospherics reception has long been recognized.[3] It is true however that past observations of ELF components were largely incidental to reception of the higher frequencies; neither the antennas nor the receivers were adequate for reception in the ELF band.

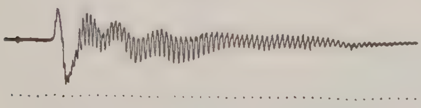

FIG. 1. Pulse received at night from a single lightning stroke 3000 km distant (time marks: 1 msec).

The present study has as its objective the detailed observations of individual pulse wave forms in the ELF band. Significant pulse characteristics are observed with new reception techniques. A detailed knowledge of pulse wave forms is extremely important for the analytical treatment of ELF propagation to be given in a later work.

RECEPTION TECHNIQUE FOR EXTREMELY LOW FREQUENCIES

Nearly all high-current lightning strokes are essentially vertical, between cloud and ground. Consequently, the radiated electric field will propagate with vertical polarization. Reception of this field is readily achieved with several possible antenna types of which the following are three examples: (a) conventional

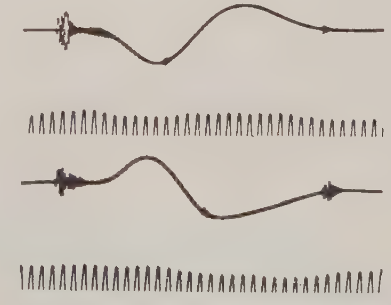

FIG. 2. Two daytime pulses possessing opposite polarity. Both were received within a short interval on the same antenna dipole, signifying opposite travel direction (time marks: 0.5 msec).

---

[*] This work received support from the Bureau of Ships, Navy Department. Contribution from the Scripps Institution of Oceanography, New Series, No. 889.

[†] Occasionally in certain localities, extremely long whistlers 50 times the above duration are observed, L. R. O. Storey, Trans. Roy. Soc. (London) A908, 246 (1953). The origin of these very long whistlers is not definitely understood.

[1] E. V. Appleton and F. W. Chapman, Proc. Roy. Soc. (London) A158, 1 (1937).

[2] Laby, Nicholls, Nickson, and Webster, Nature 139, 837 (1937).

[3] Watson-Watt, Heard, and Lutkin, Proc. Roy. Soc. (London) A162, 267 (1937).

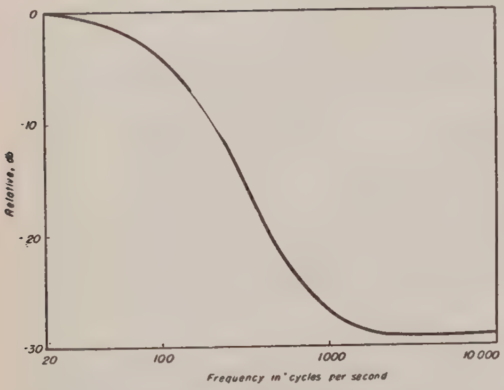

FIG. 3. Frequency response of receiving amplifiers. The low-frequency response is deliberately enhanced.

vertically polarized antenna, consisting of a horizontal wire elevated above the ground; (b) a loop antenna in a vertical plane; and (c) an unconventional dipole, termed a ground dipole.

Of these three, the ground dipole was employed for the majority of the observations. In practice, it consists of two grounded electrodes separated by a distance of 15 to 150 m. Contact potentials and polarization effects were found to be negligible with most metals; 3 cm diam vertical brass rods buried to a depth of 50 to 100 cm were most commonly employed as electrodes.

The principle of the ground dipole antenna is as follows: A propagating vertical electric field possesses a slight forward tilt in the vicinity of the earth's surface because of the partial conductivity of the earth at these frequencies. The horizontal field component although small, is nonvanishing in the earth. Measured by the ground dipole under average soil conditions this field is approximately 1% of the vertical electric field in the frequency region, 100 cycles. Although the received signal voltage is small, of the order of 10 μv, the impedance is also low (of the order of 100 ohms) so that amplifier design presents no difficulties.

The ground dipole antenna is directional. As far as can be determined it exhibits the cosine pattern to be expected from a dipole antenna. Reception from a combination of two fixed dipoles at right angles was used to determine the direction of the lightning source. Ordinarily, a loop or dipole combination used for direction finding introduces a 180° directional ambiguity. This ambiguity is removed by the transient nature of the source; normal lightning flashes occur with the cloud negative with respect to ground. This polarity is rarely, if ever, known to reverse. Hence the polarity of the received transient possesses directional information which removes the antenna ambiguity. Figure 2 illustrates two daytime pulses received on the same antenna having opposite polarity in the initial low-frequency component; these are interpreted as arriving from opposite directions.

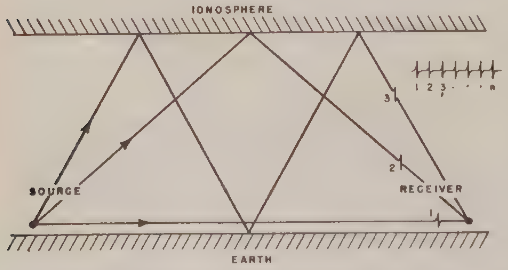

FIG. 4. Geometrical explanation of the generation of a nearly periodic signal (tonal pulse), from a single lightning pulse.

Receivers utilized for all operations were conventional wide-band amplifiers of 119 db maximum gain having a frequency band from 10 to 8000 cycles. The frequency response was deliberately enhanced in the low-frequency region as shown in Fig. 3.

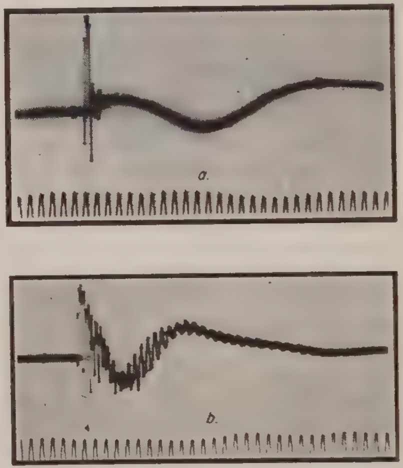

FIG. 5. Comparison of transmission at day and night; (a) day (b) night (time marks: 0.5 msec).

LIGHTNING LOCATION

The analytical interpretation of propagation phenomena is dependent on a knowledge of source distance. An estimate of the distance traveled is obtained utilizing the analysis originally suggested by Laby.[2] According to this purely geometrical approach, a single pulse may travel by many different reflection paths to the receiver. Each additional reflection introduces further delay; the last arrival suffers the largest number of reflections. The summation of all of the individual pulse arrivals from a single lightning flash resembles a nearly periodic signal of diminishing frequency as shown in Fig. 4.

It can be readily shown from geometrical considerations that if τ_n is the time delay of the nth pulse with respect to the first arrival, then the distance s is to a

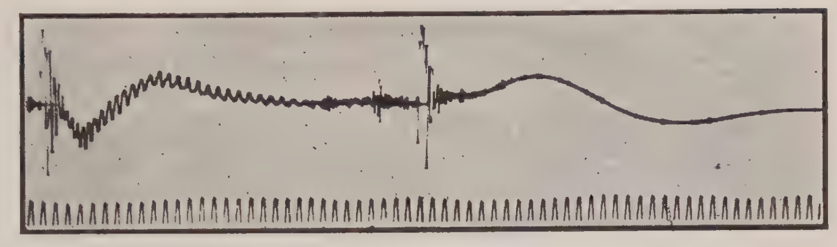

FIG. 6. Nearly simultaneous reception of day and night pulses at sundown. The night pulse (left) originated in the east; the day pulse in the west (time marks: 0.5 msec).

good approximation

$$s=c\tau_n/\{[1-c^2(\tau_n-\tau_{n-1})^2/4h^2]^{-\frac{1}{2}}-1\}, \qquad (1)$$

where c is the velocity of light and h the height of the reflecting layer.

Provided the height is known, the distance can be determined from a measurement of delay time of two successive pulses with respect to the first arrival.

Close to the tail of the pulse, where τ_n is relatively large, dispersion becomes negligible and the distance determination inaccurate. However in this case $c^2(\tau_n-\tau_{n-1})^2/4h^2$ approaches unity and

$$h \doteq c(\tau_n-\tau_{n-1})/2(\tau_n, \text{ large}) \qquad (2)$$

which conveniently gives the height of the reflection layer.‡

Near the front of the pulse the quantity $c^2(\tau_n-\tau_{n-1})^2/4h^2$ is small compared to unity and the distance formula reduces to

$$s \doteq 8h^2\tau/c(\tau_n-\tau_{n-1})^2. \qquad (3)$$

It is noted that the distance determination depends on the square of the height. A night pulse is reflected from an average layer height of 90 km according to present observations utilizing Eq. (2).§ The daytime pulse reflector is found to be located at approximately 60 km height (D layer). These two height figures were used throughout for distance determination.

OBSERVATIONS

Pulse reception exhibits several types of systematic variation summarized as follows.

Diurnal Spectrum Variations

Transmission of the tonal frequencies is greatly enhanced during night compared to day as shown by Fig. 5. During daylight hours frequently only the relatively high-frequency beginning of the pulse is evident, the tail being completely absent. The transition between day and night effect is fairly abrupt, the onset of the tonal quality coinciding with local sundown. At sundown (or sunrise) both day and night types may be received almost simultaneously; the day type originates in the west (or east) and the night type in the east (or west). An example of this occurrence at sundown is given in Fig. 6.

In a later paper it will be shown that this diurnal variation of transmission conditions is a result of reflection from the higher conductivity layer (E layer) at night and the lower conductivity (D layer) during the day. Because of the high rate of ionic recombination within the D layer its boundaries coincide closely with the lines of sunrise and sunset.

On the other hand, it is noted that *the extremely low frequency (ELF) band is subject to little, if any, diurnal variation.* This lack of sensitivity of ELF frequencies to the conductivity of the reflecting layers is also discussed in the later paper.

Diurnal Variation in Reception

On the average, approximately 20 pps are received above the noise level; the number of pulses received

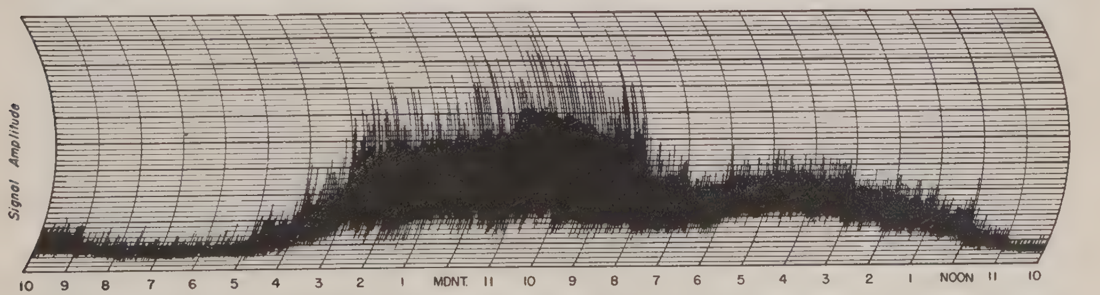

FIG. 7. A typical 24-hour recording of lightning reception in which individual pulses are unresolved. The level increases markedly at sundown and remains high until sunrise. The antenna was nondirectional.

---

‡ Owing to increased attenuation during daylight hours the region of small dispersion is observed only at night.

§ This height coincides with the E layer which has been explored with high-frequency radio sounding as well as by rockets.

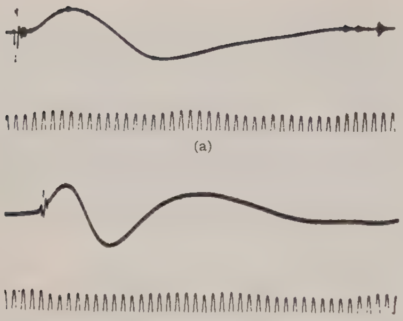
(a)

(b)

FIG. 8. Illustrates the two classifications of ELF pulses; (a) Type I, typified by a single cycle oscillation in which the first half-cycle is fairly abrupt followed by a considerably larger half-period, (b) Type II, exhibits 3 or more half-cycles. Although these are day examples, the distinction also holds for night pulses (time marks: 0.5 msec).

exhibits no *obvious* diurnal variation.‖ However, a marked variation in the average radio energy received exists as is shown in Fig. 7. Typically, at 10:00 A.M., local time, the level begins to increase, reaching a daylight maximum at mid-afternoon, the time of continental thunderstorm activity; thereafter the level diminishes somewhat. At sundown, 8:00 P.M., there is a marked increase as the tonal frequency transmission is improved; during the night the level remains high, gradually diminishing toward early morning; at sunrise, 5:00 A.M., the level falls abruptly.

Type I and II Pulses

Pulse reception in the ELF band can be divided into two classifications as illustrated in Fig. 8. Type I pulses are characterized by a relatively abrupt half-cycle onset terminated by a considerably lengthened half-cycle; the two half-cycles represent the complete pulse. Type II pulses exhibit more than two half-cycles; typically these possess three half-cycles, but occasionally more. It has not been possible to correlate the occurrence of these two types with temporal or spatial factors. Both types commonly occur. Both may be observed within the same hour although not from the same locality simultaneously. Inasmuch as these two types can hardly represent different initial lightning pulses, they must represent different propagation conditions within this frequency band.

A number of significant properties of these two types of propagation can be deduced by a Fourier analysis of the pulse shapes. This analysis is the subject of another paper.

Pulse Observations

Table I is a sample analysis of a brief reception period during a typical observation night. Fortuitously, all of these pulses are of type II; either type is ordinarily received.

TABLE I. Brief sample of atmospheric reception (June, 1954). Observations were made in the Anza Desert, California. Although this sample contains only type II pulses, type I pulses are also commonly observed.

Time (P.S.T.)	Pulse classification	Range (km)	General direction
12:01	II	3700	South
12:03	II	12000	South
12:04	II	12000	Northeast
12:06	II	4200	South
12:06	II	15000	North
12:08	II	3700	South
12:08	II	5100	South
12:09	II	5000	South

All observations were made in a remote area in the Anza Desert, California. Reception near to populated areas was hampered by interference from power lines.

ACKNOWLEDGMENTS

The author was assisted in all field observations by Mr. Stanley Lai, who also was responsible for the design and construction of the receiving equipment.

‖ Careful statistical analysis of thirty day samples by Holzer and Deal, Institute of Geophysics, University of California, (private communication) has recently demonstrated that a diurnal variation exists which can be correlated with world-wide thunderstorm activity.

Extremely Low-Frequency Electromagnetic Waves.* II. Propagation Properties

LEONARD LIEBERMANN
University of California, Marine Physical Laboratory of the Scripps Institution of Oceanography, La Jolla, California

(Received June 23, 1956)

Properties of electromagnetic propagation at extremely low frequencies (below 500 cycles) are deduced from analysis of pulse distortion. The source of the transmitted pulse is lightning. Two distinct transmission types are analyzed. Normal, or type I, propagation is shown to behave as if the earth's surface and ionosphere constitute a wave guide composed of two plane parallel surfaces, with one surface partially conducting. This wave guide has no low-frequency limit on progagation; attenuation formulas are given. The transmission properties of type II, or anomalous propagation, are derived and seen to be inexplicable by means of this wave-guide model. The analysis leads to a determination of the effective conductivity of the ionospheric reflector at these frequencies: the daytime reflecting layer (D layer) conductivity is 10^4 esu; the nighttime conductivity (E layer) is 5×10^4 esu; both results are far lower than deduced by other means.

INTRODUCTION

THE pulse of current in a lightning discharge results in the generation of an electromagnetic pulse. Distant reception of this pulse yields a wave form surprisingly different from a lightning pulse. Whereas the immense current in the stroke lasts only a few tens of microseconds, the pulse length on reception from a few thousand kilometers distance is a hundred times longer. The various frequencies present in the original pulse are dispersed, with lower frequencies traveling with slower velocities. Two well-defined frequency bands are apparent from inspection of a received pulse, as illustrated in a previous paper[1]: a band having a low-frequency cutoff at 1700 cycles and an extremely low-frequency region (ELF band) beginning at 500 cycles and extending as low as can be observed.

The previous paper reviewed the initial success of the elementary theory of multiple reflection[2] in explaining the frequency cut-off phenomenon. An alternative explanation, giving identical results, assumed that the earth's surface and the ionosphere constitute a wave guide with both surfaces considered perfect conductors. Neither explanation was able to account for low-frequency propagation below the cut-off frequency.

A decade later, Hales,[3] and later Budden,[4] proposed as an explanation of propagation below cutoff, a modified wave-guide model in which one surface was partially conducting. Both authors gave solutions to this wave guide, apparently unaware that similar solutions had appeared years earlier in text books on wave guides.[5] The published solutions to this wave guide are given in the form of the dependence of velocity (or attenuation) on frequency. Although it is qualitatively apparent from these solutions that frequencies below cutoff can be propagated, these formulas do not permit comparison with observation. It has not been demonstrated that observed ELF transmission bears more than a qualitative resemblance to propagation in a modified wave guide.

In order to be able to compare the solutions found in texts with observations, it is necessary to evaluate either of two Fourier integrals: an integral leading to the predicted wave form of a pulse in the modified wave guide; or an integral leading to the spectrum of an actual received pulse. Actually, both procedures are used here, but for different purposes. The theoretical wave form in a modified wave quide is utilized in comparing pulse reception classed as normal, or type I reception; the spectrum is evaluated for the anomalous, or type II pulses.

The discussion begins with a test of the modified wave guide model: the predicted wave form of a pulse. However, the Fourier integral leading to the pulse can only be evaluated by approximate methods. In order to establish these approximations a portion of the published theory of the modified wave guide is repeated. The evaluation of the wave form of a pulse has been attempted by Budden using numerical means, but unfortunately his calculations are erroneous.

MODIFIED WAVE-GUIDE MODEL

The transmission model for the propagation of extremely low-frequency radio waves consists of two parallel plane surfaces of infinite extent. One surface is perfectly conducting, the other a partial conductor. Thus, it is assumed that the earth is a perfect conductor with ionosphere consisting of a single partially conducting surface at a fixed height; the radius of curvature of the earth is neglected.† This wave guide is characterized by two parameters: the height h of the ionosphere and its conductivity σ. The electric field excitation is assumed to be always vertical; in wave-guide terminology the solutions are confined to the TM modes. The above boundary conditions can be shown to lead

---

* This work received support from the Bureau of Ships, Navy Department. Contribution from the Scripps Institution of Oceanography, New Series, No. 889.

[1] L. Liebermann, J. Appl. Phys. **27**, 1473 (1956).

[2] Laby, Nicholls, Nickson, and Webster, Nature **139**, 837 (1937).

[3] A. L. Hales, Proc. Roy. Soc. (London) **A193**, 60 (1948).

[4] K. G. Budden, Phil. Mag. **42**, 1 (1951).

[5] See, for example, J. C. Slater, *Microwave Transmission* (McGraw-Hill Book Company, Inc., New York, 1942), p. 142.

† In a later paper Budden [Phil. Mag. 43, 1179 (1952)] has shown that neglect of the earth's curvature and earth's magnetic field does not significantly alter the wave-guide properties at extremely low frequencies.

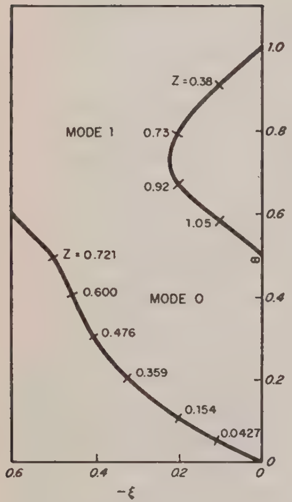

FIG. 1. Numerical values of g for the first two propagation modes; $g=\xi+\mu i$. The parameter Z is related to the impedance of the ionospheric wave guide.

to a single equation of consistency‡:

$$g \tanh(\pi g)=iZ \exp(5\pi i/4), \tag{1}$$

where

$$g\equiv (h/\pi)(k^2-\omega^2/c^2)^{\frac{1}{2}}$$

and

$$Z\equiv\omega^{\frac{3}{2}}h/2\pi^{\frac{3}{2}}c\sigma^{\frac{1}{2}},$$

where σ is in esu; the velocity in free space is c; k is the angular wave number, $2\pi/\lambda$. In general, g and therefore k is complex; thus $k=k_r+ik_i$. The real quantity, k_r, is related to the phase velocity, $k_r=\omega/v$; the magnitude of the imaginary part, k_i, is equal to the absorption coefficient defined by the familiar expression:

$$E=E_0 \exp(-as),\ a=-k_i, \tag{2}$$

where s is the travel distance.

For each value of the parameter Z, there exists an infinity of characteristic values for g. Each of these solutions corresponds to a normal mode of propagation. Except for special cases, it has not been possible to find these solutions analytically. Numerical evaluation of the two lowest (of primary interest here) is given in Fig. 1; the imaginary part of g is denoted μ, the real part ξ. The lowest solution is termed mode 0, the second is termed mode 1. Reasons for this designation are obvious from the discussion below.

The phase velocity for mode 1 is given in Fig. 2, evaluated for $Z=1.35\times10^{-7}\omega^{\frac{3}{2}}$; this value utilizes the conductivity of the E layer given later. Attenuation is plotted on the same curve above. It is noted that mode 1 exhibits a frequency cutoff at the velocity minimum. As was discussed in the previous section, a prominent characteristic of observed pulses is a cutoff at 1700 cycles. Further identification is given in the discussion below.

Mode 1 Propagation with a Highly Conducting Ionosphere

A high conducting ionosphere is one in which, $Z\ll1$.§ In this case analytic solutions for g are readily obtained: from Eq. (1),

$$\tanh(\pi g)=(iZ/g) \exp(5\pi i/4)\doteq n\pi i+\pi g, \tag{3}$$

where n is an integer. When $n=1$, the solution

$$g=i[1-(Zi/\pi) \exp(5\pi i/4)] \tag{4}$$

obtains. For a perfectly conducting ionosphere, $Z=0$, the solution is $g=i$. Referring to the numerical evaluation given in Fig. 1 this identifies the solution with that termed mode 1, explaining the mode designation. The phase velocity, v, above the cut-off frequency is

$$c^2/v^2=1-\pi^2c^2/\omega^2h^2. \tag{5}$$

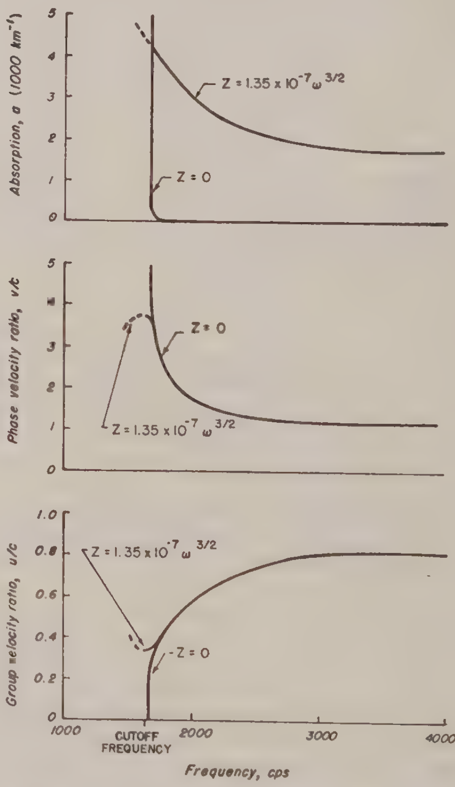

FIG. 2. Transmission properties of mode 1, primarily responsible for propagation of the tonal pulse with cutoff at 1700 cycles. The group velocity ratio is derived from, $u=d\omega/dk$; $Z=0$, signifies a perfectly conducting ionosphere.

---

‡ This expression is valid when the frequency is sufficiently small that Maxwell's polarization term is negligible (curl $H=4\pi\sigma E$).

§ The true ionosphere, with conductivity values given later, is actually highly conducting by this criterion, for frequencies less than twice cutoff.

The group velocity is obtained from the relation, $u=d\omega/dk$. Thus

$$c/u=(1-\pi^2c^2/\omega^2h^2)^{-\frac{1}{2}}. \tag{6}$$

Equations (5) and (6) are compared with numerical evaluation of the partially conducting ionosphere in Fig. 2. It is seen that except for the region near cutoff, the perfectly conducting wave guide is indistinguishable from the modified wave guide for mode 1 transmission.

The above equation can be utilized to obtain the travel distance by means of the stationary phase relation, $s/u-s/c=\tau$; τ is the delay measured from the front of the pulse of the component, ω. The resulting relationship is essentially identical with that derived solely from geometrical considerations. In this explanation (ray picture) the tonal properties of pulses result from multiple arrivals; each arrival originates in a different number of reflections. Analogously, mode 1 can be interpreted as one in which wave fronts rebound alternately between earth and ionosphere. The multiple reflection interference results in an antinode of vertical electric field at the earth's surface and another at the ionospheric boundary as shown in Fig. 3.

Mode 1 propagation is also closely related to that described by Pekeris[6] for the transmission of low-frequency acoustic waves in shallow water. In that case the sea surface and bottom serve as the two reflecting boundaries of the wave guides. However, Pekeris assumes that the sea bottom possesses no dissipation in his solution. This lack of dissipation permits propagation at frequencies below the group velocity minimum, impossible in the present case. Waves belonging to this low-frequency branch apparently have been observed in undersea sound propagation.

Mode 0 Propagation

The phase velocity for mode 0, given in Fig. 4, is evaluated numerically for $Z=1.8\times10^{-7}\omega^{\frac{1}{2}}$, corresponding to the conductivity of the D layer given later; attenuation is plotted immediately above. Contrary to mode 1, mode 0 has no velocity minimum nor frequency cutoff; transmission actually improves as the frequency diminishes. A schematic diagram of the electric field of mode 0 given in Fig. 5 may clarify its physical nature. Although sometimes referred to as the "principal wave," this mode is usually ignored in wave-guide discussions; probably because mode 0 does not exist in a wave guide with a single closed boundary surface (e.g., rectangular or circular cross section.)

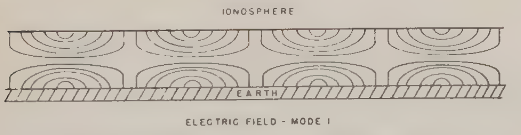

FIG. 3. Electric field distribution in mode 1.

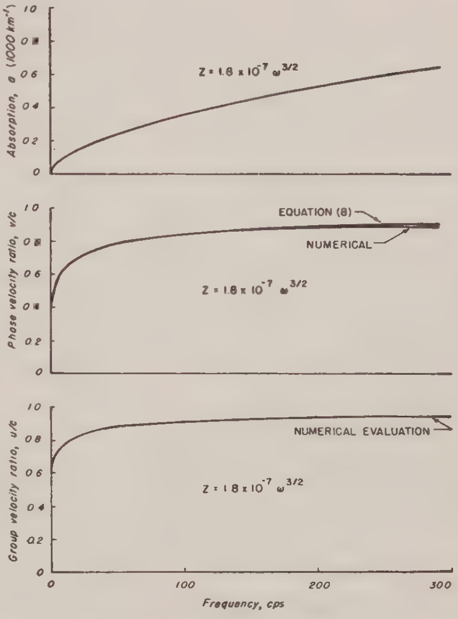

FIG. 4. Mode 0, responsible for propagation at extremely low frequencies below the mode 1 cutoff.

Mode 0 may also be treated analytically for the case of the highly conducting ionosphere, $Z\ll1$. When $n=0$, Eq. (3) becomes

$$g=(Z/\pi)^{\frac{1}{2}}\exp(7\pi i/8), \tag{7}$$

hence the wave number

$$k=(\omega/c)[1+c(1+i)/2h(2\pi\omega\sigma)^{\frac{1}{2}}]^{\frac{1}{2}}. \tag{8}$$

This expression is compared with numerical evaluation for the same value of Z in Fig. 4. When $Z=0$, (perfectly conducting ionosphere) then according to Eq. (8), $k=\omega/c$ and no dispersion exists. Stated in another way, without dissipation in one of the boundaries there is no dispersion and the wave travels in the medium as if it were unbounded. In the next section it is shown that mode 0 is responsible for reception of ELF components (<500 cycles) from lightning.

PULSE TRANSMISSION VIA MODE 0 PROPAGATION

The passage of huge current in the main stroke (return stroke) of a lightning flash is essentially complete in less than 100 μsec.[7] Consequently the current pulse can be considered a δ function having essentially a constant frequency spectrum in the region of interest, below 500 cycles. The antenna length, from cloud to ground is small compared to these wavelengths and can be considered a vertical dipole. Although the current spectrum of the dipole is independent of frequency, the

---

[6] C. L. Pekeris, Geol. Soc. Am., Memoir 27, New York (1948).

[7] H. R. Byers, *Thunderstorm Electricity* (University of Chicago Press, Chicago, 1953).

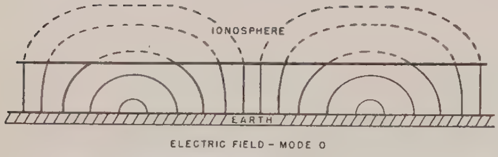

FIG. 5. Electric field distribution in mode 0. Contrary to mode 1 the field need not be vertical at the ionospheric boundary.

radiated spectrum is not, the frequency dependence being determined by boundary conditions. For example, in empty space the radiated spectrum would be of the form, $R(\omega)=R_0\omega$; with the dipole located between plane conductors as in this wave guide, the spectrum is to good approximation, $R(\omega)=R_0\omega^{\frac{1}{2}}$ for all modes, as can be shown from Watson's work.[8]

The radiated spectrum, $R(\omega)$ determines the received spectrum, $E(\omega)$ through the admittance, or transfer function, H: $R(\omega)H=E(\omega)$. The admittance function is well known in electric circuit theory; its use is less familiar in wave propagation.[9] For plane waves

$$H=\exp(-iks). \tag{9}$$

A relationship between the received spectrum and the shape of the received pulse is given by the Fourier integral,

$$G(t)=\int_{-\infty}^{\infty} E(\omega)\exp(i\omega t)d\omega$$
$$=\int_{-\infty}^{\infty} R_0\omega^{\frac{1}{2}}\exp[i(-ks+\omega t)]d\omega.$$

The quantity t in the above expression is measured from the time of origin of the pulse. For observational comparison it is useful to introduce a new time variable, τ, measured from the front of the pulse which travels at velocity c. Thus

$$G(\tau)=\int_{-\infty}^{\infty} R_0\omega^{\frac{1}{2}}\exp i[s(\omega/c-k)+\omega\tau]d\omega. \tag{10}$$

For small values of Z (high conductivity) the wave number k, Eq. (8), is approximated by

$$k=(\omega/c)[1+c(1-i)/4h(2\pi\omega\sigma)^{\frac{1}{2}}] \tag{11}$$

which leads to

$$G(\tau)=\int_{-\infty}^{\infty} R_0\omega^{\frac{1}{2}}\exp(i\omega s/c)$$
$$\times[c(i-1)/4h(2\pi\omega\sigma)^{\frac{1}{2}}+\omega\tau]d\omega. \tag{12}$$

This Fourier integral may be found in tables in different form.[10] Its solution is

$$G(\tau)=[(s^2/32\pi\sigma h^2\tau)-1](s/8\pi\tau^{\frac{3}{2}}h\sigma^{\frac{1}{2}})$$
$$\times\exp(s^2/64\pi\sigma h^2\tau). \tag{13}$$

A similar expression has been obtained by Schumann[11] by another approach not based on wave-guide solutions.

A test of the modified wave-guide theory is the comparison of Eq. (13) with the wave form of observed pulses. However, all recorded pulses were deliberately made with a receiver having a nonlinear frequency response[1] (in order to emphasize low frequencies). To facilitate comparison, Eq. (13) is plotted in modified form in Fig. 6, with the frequency response of the receiver incorporated. A photograph of a typical received pulse is adjacent for comparison. The agreement is clear. Nearly all pulses in the type I classification, regardless of propagation distance, exhibit this wave form.

Another form of Eq. (13) is more suitable for quantitative testing. If the measured parameter τ_0 is defined as the time of axis crossing of the received pulse, (see Fig. 6) then,

$$s=4h(2\pi\sigma\tau_0)^{\frac{1}{2}}. \tag{14}$$

If the source distance s and the height of the ionosphere h are known, Eq. (14) leads directly to the conductivity σ of the ionosphere. If the theory is correct σ computed in this manner should be reasonably independent of the propagation distance. This is found to be true in general, (exceptions are occasionally noted) provided propagation distances are in excess of a few thousand kilometers. The ionospheric conductivity derived in this manner is discussed in detail in a later section.

ANOMALOUS PULSE TRANSMISSION IN MODE 0

The preceding illustrates that the simple earth-ionosphere modified wave guide represents a good model of the transmission of type I pulses. However, this elementary model does not explain reception of the anomalous type II pulses, nor has any modification of the model been found which possesses these properties.

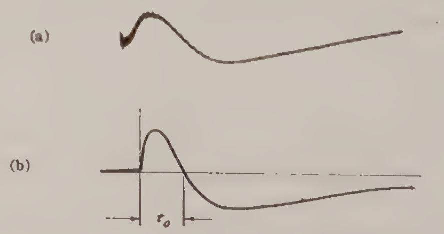

FIG. 6. Comparison of a typical observed type I pulse with that given by Eq. (13). The axis crossing time, τ_0, according to theory, is proportional to the square root of the travel distance.

---

[8] G. N. Watson, Proc. Roy. Soc. (London) A95, 546 (1919).

[9] C. Eckart, Revs. Modern Phys. 20, 399 (1948).

[10] G. A. Campbell and R. M. Foster, *Fourier Integrals for Practical Applications* (D. Van Nostrand Company, Inc., New York, 1948).

[11] W. O. Schumann, Z. angew. Phys. 4, 474 (1952).

In spite of the lack of models, some propagation properties can be deduced. In the preceding section, the initial spectrum and the phase velocity were given; the shape of the received pulse $G(\tau)$, was obtained from these two parameters by means of the Fourier integral. Here, the initial spectrum is given as before; the shape of the received pulse is also given from observation. Hence the mate to the above Fourier integral,

$$E(\omega)=\int^{\infty} G(\tau)\exp(i\omega\tau)d\tau,$$

can be used to obtain k and the phase velocity from Eq. (10),

$$E(\omega)=R_0\omega^{\frac{1}{2}}H=R_0\omega^{\frac{1}{2}}\exp[i(s\omega/c-ks)]. \qquad (15)$$

ANALYTICAL REPRESENTATION OF TYPE II PULSES

In order to evaluate the above Fourier integral, $G(\tau)$, must be expressed analytically. It has been found, purely empirically, that except for the amplitude factor, type II pulses are represented by the expression.

$$G(\tau)=\sin\Phi=\sin[\gamma\ln(\tau/\tau_0)]. \qquad (16)$$

As an example, the analysis of a typical observed pulse is shown in Fig. 7. The ordinate is $\log\tau$ and the abscissa is Φ. Values of the time τ are read at phase intervals of $\pi/2$, i.e., a maximum, minimum, and zero. The fit with Eq. (16) is evident; nearly all pulses of this type show a similar fit.

Thus each type II pulse is characterized by two empirical parameters; the slope, γ, of the analysis plot; and, τ_0, analogous to the first axis crossing parameter given above for type I pulses. Obviously the above analytical expression becomes inappropriate as τ approaches zero, but no difficulty is introduced inasmuch as only the inconsequential higher frequencies are affected in the spectrum.

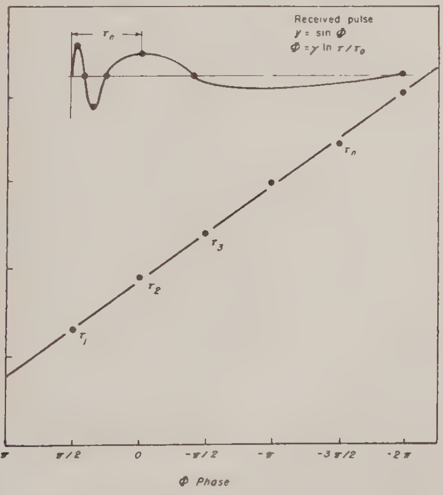

FIG. 7. Analysis of a typical type II pulse. Nearly all type II pulses can be represented by the function $y=\sin\Phi$, where $\Phi=\gamma\ln\tau/\tau_0$. The arrival time τ_n, measured from the front of the pulse represents maximum, 0, minimum, etc., in successive order. The parameter γ is the reciprocal slope of the line.

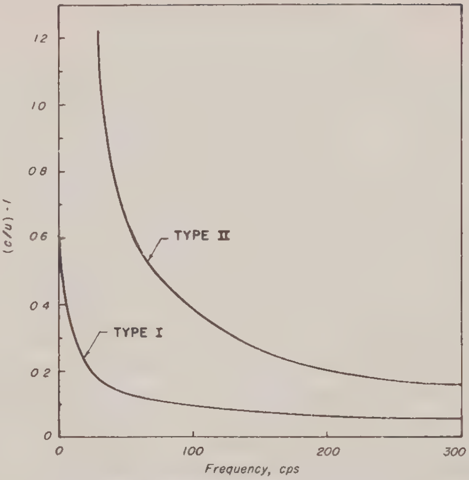

FIG. 8. Comparison of dispersion in type I and type II propagation. Type II is represented simply, by an hyperbola. Physical differences in the ionosphere responsible for these different transmission properties are unknown.

PHASE AND GROUP VELOCITY OF TYPE II PULSES

The Fourier integral determining E is now

$$E(\omega)=\int_0^{\infty}\sin[\gamma\ln(\tau/\tau_0)]\exp(i\omega\tau)d\tau. \qquad (17)$$

A solution is found in the form $E(\omega)=A(\omega)\exp(i\theta)$ where $A(\omega)$ is the familiar amplitude spectrum; θ is a real quantity, termed the phase spectrum. Comparing θ with Eq. (15) it is seen that

$$\theta=s(\omega/c-k).$$

Hence integration of Eq. (17) gives

$$1-c/v=(c/\omega s)(\gamma\ln(\omega\tau_0)+3\pi/4-\gamma\ln\gamma+\gamma). \qquad (18)$$

The details of the integration are given in the appendix. The group velocity ratio derived from Eq. (18) is then

$$c/u-1=c\gamma/\omega s. \qquad (19)$$

This simple hyperbolic relationship of group velocity with frequency is compared with the group velocity for type I transmission in Fig. 8. Type II dispersion is everywhere greater, and the group velocity ratio, c/u, larger at lower frequencies.

In Eq. (19) the group velocity depends solely on the frequency. Consequently, the ratio γ/s must be a constant. Thus the parameter γ, which is obtained from a received pulse by simple analysis, can be used for range determination.

APPLICATIONS

Conductivity of the Ionosphere

The mode 0 relationship between the observed parameter τ_0 and the travel distance given by Eq. (14) has been used to obtain the conductivity of the ionosphere. The travel distance was obtained independently from mode 1 pulses inasmuch as their group velocities do not depend significantly on conductivity (see Fig. 2). The procedure for calculating the distance has already been given.[1]

The average conductivity value of the E layer (night reflector) is calculated to be 5.0×10^4 esu. The conductivity of the D layer (daytime reflector) is 10^4 esu. The E layer conductivity is nearly two orders of magnitude less than that given by Bremmer.[12] However previous estimates are based on considerably higher frequencies (>10 kc) which exhibit greater penetration than the lower frequencies used here; the layer conductivity is known to increase with increasing height. Probably each frequency measures the conductivity of its effective layer boundary. The night estimate is based on the analysis of pulses whose paths are known to have been entirely in darkness; daytime pulses were similarly selected. In all cases day and night reflector heights were taken to be 60 km and 90 km, respectively. Inasmuch as the present theory is based on plane-wave propagation the evaluation data were limited to night pulses having ranges in excess of 8000 km. Daytime pulses were of necessity limited to a range of 3000 km, this being the maximum at which the mode 1 distance analysis could be made.

Type II Pulses

It is of interest to check the result of Eq. (19) implying a linear relationship between $1/\gamma$ and the travel distance for type II pulses. The travel distance was determined from mode 1 as above. The pulse parameter γ is determined from measurement of pulses according to the procedure outlined in an earlier section. Figure 9 gives $1/\gamma$ *versus* distance for a group of pulses of different ranges observed during the same evening. Although there is fair proportionality some wide deviations exist which may imply local variations in the ionosphere.

Diurnal Variations in Absorption

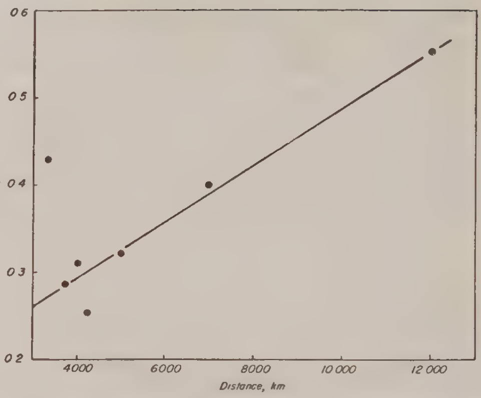

FIG. 9. A group of randomly selected type II pulses whose travel distances are supposedly known (from mode 1 analysis). Type II analysis predicts proportionality of travel distance, and $1/\gamma$. The lack of proportionality exhibited by some of the pulses above could result from spatial or temporal variations of ionospheric properties.

Observation indicates that the tonal pulses (mode 1 propagation) are received almost exclusively during the night whereas the ELF band (mode 0 propagation) is relatively unaffected by diurnal changes.[1] This difference in propagation is explained by the magnitude of the absorption in the two modes. An approximate absorption coefficient for mode 0 can be derived from Eq. (11)[‖]:

$$a=-k_i\doteq\omega^{\frac{1}{2}}/2^{5/2}\pi^{\frac{1}{2}}h\sigma^{\frac{1}{2}}. \tag{20}$$

Hence the increase at night of ionospheric height h and conductivity σ decreases the absorption coefficient by one-third. However the magnitude of the absorption, both day and night, is sufficiently low that propagation is relatively unaffected, in spite of the diurnal change. For example, the transmission loss for daytime transmission at 50 cycles according to either Fig. 4 or Eq. (20) is 2 db per thousand kilometers, a relatively small loss.

The absorption coefficient of mode 1 propagation exhibits a similar diurnal variation.[¶] However, the magnitude of mode 1 absorption is an order of magnitude higher than mode 0 as can be seen by comparing Fig. 2 and Fig. 4. For this reason the effect of the diurnal absorption variation is more apparent, particularly in the frequency range near cutoff.

It is to be noted that the absorption given in Fig. 2 appears somewhat large (e.g., 15 db/1000 km at twice cut-off frequency) in view of occasional reception of these frequencies as far as 10 000 km. It may not be true as was assumed in this calculation, that the conductivity obtained from ELF observations is effective at mode 1 frequencies. As was discussed earlier, the effective conductivity at higher frequencies may be greater, resulting in lower absorption.

It can be shown that Eq. (17) leads to a type II

---

[12] H. Bremmer, *Terrestial Radio Waves* (Elsevier Publishing Company, New York, 1949).

[‖] This approximation is based on the conditions: $c/2h(2\pi\omega\sigma)^{\frac{1}{2}}\ll1$ and $Z\ll1$. With the above D-layer conductivity it is applicable in the frequency band 40 to 600 cycles.

[¶] An approximate absorption formula for mode 1 may be derived from Eq. (4):

$$a=-k_i\doteq(\omega^{\frac{1}{2}}/hc)[8\pi\sigma(\omega^2/c^2-\pi^2/h^2)]^{-\frac{1}{2}}$$

applicable in the frequency band 1.2 to 2 times the cut-off frequency.

absorption similar to that in type I propagation. In this case the first half-cycle of the pulse, of higher frequency than succeeding cycles, may be greatly reduced, or eliminated in long distance transmission. Hence type II pulses exhibiting a gap or missing half-cycle at the start of the pulse might be expected. Some of the pulses shown in earlier work[1] appear to exhibit a missing half-cycle.

APPENDIX

The simple analytical formula for type II pulses, $\sin\gamma \ln\tau/\tau_0$, although convenient for data comparison is an awkward form for analytical treatment. It can be reformulated as

$$\sin\gamma \ln\tau/\tau_0 \equiv (1/2i)[(\tau/\tau_0)^{i\gamma} - (\tau/\tau_0)^{-i\gamma}].$$

Thus Eq. (17) becomes

$$E(\omega) = \int_0^\infty (1/2i)[(\tau/\tau_0)^{i\gamma} - (\tau/\tau_0)^{-i\gamma}] \exp i\omega\tau d\tau,$$

a form found in tables.[10] The phase and group velocities are derived from this integral as described previously.

Surprisingly, the method of stationary phase can also be utilized to obtain the group velocity although the usual criterion for application would ordinarily discourage its use. The stationary phase condition applied to $G(\tau) = \sin\gamma \ln\tau/\tau_0 = \sin\Phi$ is

$$d\Phi/dt = \omega = \gamma/\tau, \quad \text{or} \quad \Phi = \gamma \ln\gamma/\omega\tau_0.$$

The quantity θ utilized in the text is related to Φ as

$$\theta = \Phi - \omega\tau = \gamma \ln\gamma/\omega\tau_0 - \gamma$$

which is identical with that given in Eq. (18) except for a constant factor; both lead to the same group velocities.

CONCLUSIONS

Extremely low frequency propagation has in common with higher transmission frequencies, a familiar characteristic: variability. At times, extremely low frequencies propagate as if in a "modified" wave guide; at other times the propagation mechanism is altered, resulting in the "anomalous" propagation described above. These variations in propagation undoubtedly can be ascribed to variations in the electrical properties of the ionosphere. Necessarily, the electrical properties must vary over wide areas, for the data represent long distance propagation. In addition, it is only the lower boundary and not the body of the ionosphere which is significant, for these low frequencies exhibit little penetration.

Although the effect of ionospheric variability on propagation has been emphasized, it will be recalled that the phenomenon is rather subtle. Variability is not evidenced by large amplitude fluctuation or "fading" as encountered at high frequencies. By comparison with high frequencies, ELF propagation is unusually reliable, both day and night. Low attenuation permits long distance propagation. Unfortunately for communication applications, the problem of a transmission antenna appears insurmountable.

Reprinted from The Condor, Volume 58, November-December, 1956, Number 6, pp. 448–449

Off-season, Southern Occurrence of the Black Scoter on the Pacific Coast.—In a recent number of the Condor (57, 1955:121–122) I reported two observations of the Black or American Scoter (*Oidemia nigra*) from the northern coast of Baja California—the first records for México. The one seen in August was thought to be a non-migrating individual. These observations and this inference have now been confirmed.

On May 27, 1956, I clearly identified a lone drake of this species that was diving in the surf just north of Punta San Jacinto, Baja California, at approximately latitude 30° 50′ N. This record extends the range of the species about 24 miles and provides a date intermediate between those of the previous observations in México (April 10 and August 8).

On July 4, 1956, between Cardiff and Solano Beach, San Diego County, California, I saw another lone drake of this species. Like the May bird, it appeared to be in good condition. One peculiarity was that the conspicuous protuberance on the basal half of its bill above was unusually light (whitish-yellow, instead of orange-yellow). It was first seen on the wet beach in company with one Hudsonian Curlew and one Marbled Godwit. Presently it flapped into what may be called the marginal flat-water, just within the surf, where it seemed to feed, presumably on sandcrabs (*Emerita*). Later it flew into the surf and then swam outside.

This July bird was almost surely a non-migrant. The records for May, July, and August tend to bridge over the interval between the known overwintering records (November to April) for California summarized by Grinnell and Miller (Pac. Coast Avif. No. 27, 1944:90–91). It now seems almost certain that on the Pacific Coast, as on the Atlantic, individual Black Scoters occasionally remain south through the summer.

It may well be that the Black Scoter is more prone to this over-summering than the other scoters, for I have not recognized this species during the winter about San Diego and in Baja California, when Surf Scoters swarm and when White-winged Scoters are fairly common. And these last two species are very scarce in summer. Perhaps the summering Black Scoters wander about and thus reach points south of their normal wintering range.—Carl L. Hubbs, *Scripps Institution of Oceanography, La Jolla, California, July 5, 1956.*

Contributions from the Scripps Institution of Oceanography, New Series, No. 890
Reproduced by Permission

Reproduced by Permission
Deep-Sea Research, 1956, Vol. , pp. 45 to 53. Pergamon Press Ltd., London.

The frequency distribution of surface-water characteristics in the Pacific Ocean

JOHN D. COCHRANE

Abstract—The frequency distributions of surface-water characteristics in the Pacific Ocean are presented in a series of temperature-salinity diagrams. The frequencies are estimated from maps of mean surface temperature and salinity in February and August. Six twodimensional distributions are obtained, one each for February, August, and the year in the North Pacific, and one for each of these periods in the South Pacific. Prominent features of the distributions are discussed.

ALTHOUGH many maps and tabulations have been prepared to show the geographical distribution of average sea-surface temperature and salinity, few attempts have been made to describe the prevalence of different temperatures and salinities at the sea surface. The aim of the present study is to determine the prevalence of these properties at the surface of the Pacific Ocean. Six frequency distributions are derived, one each for February, August, and the year in the North Pacific, and one for each of the same periods in the South Pacific.

Nearly all previous studies of prevalence have been confined to temperature. Sir JOHN MURRAY (1898) obtained for each ocean the area of sea surface having maximum and minimum temperature within 10°F intervals. SPILHAUS (1942) computed the percentage of ocean surface having annual mean temperatures within various 5°C temperature intervals. A very complete series of sea-surface temperature distributions based on modern charts is given in a manuscript prepared by W. H. LITTLEWOOD of the US Navy Hydrographic Office*. Distributions of area among 5°F temperature intervals are presented for February and August in the world ocean and in each ocean separately.

Prevalence of both temperatures and salinities over large areas of the ocean surface does not appear to have been considered previously. The method, used by HELLAND-HANSEN (1926) and others, of plotting large numbers of serial observations of temperature and salinity from a given area as a scatter diagram (in temperature-salinity co-ordinates) gives some suggestion of the twodimensional frequency distribution. But, of course, the observations are almost never uniformly spaced horizontally or vertically. While not directly concerned with prevalence, WÜST, BROGMUS and NOODT (1954) presented related information. They showed, in a series of temperature-salinity diagrams, the average annual temperatures and salinities for each 5° zone of the world ocean and of each ocean separately. MONTGOMERY (1955) dealt quantitatively with the twodimensional frequency distribution of surface temperature and salinity at Weather Ship J.

In discussing the present study, it is convenient to introduce a few definitions. As in MONTGOMERY'S paper, the term characterstic denotes a point on the temperature-salinity diagram. Characteristic class refers to the area on the diagram included in a specified temperature and specified salinity interval. The frequency of a characteristic class means its prevalence in extent and duration within the region and period considered.

---

*This manuscript, entitled " Surface Water Temperature Distribution of the World", and dated April 1955, was brought to the writer's attention by Mr. JOHN LYMAN, Chief, Division of Oceanography, US Navy Hydrographic Office.

The boundaries of the North and South Pacific Oceans follow those given in *Die Grenzen der Ozeane und ihre Nebenmeere* (Anon., 1939). Adjacent seas are included. Sea-surface water in both ice-free and ice-covered areas is considered. In the latter areas, the term " sea surface " becomes ambiguous. Here it is used to denote the under-surface of the ice.

Ideally, an estimate of the frequency distribution of characteristics for a selected period and region would be based on a long, uniform series of observations from many fixed points spaced in relation to average gradients. Such ideal data do not exist, and even approaching them with existing observations involves considerable difficulty. Consequently, as a quick method of obtaining a first approximation, the distributions of the present study are based on information available in published form, maps of average conditions. While this procedure has obvious limitations, it seems unlikely that the salient features of the distributions so derived are untrue.

SCHOTT's (1935) maps of temperature and salinity are used as basic information except for the Antarctic region. There the more recent information in DEACON's (1937) maps of salinity and MACKINTOSH's (1946) maps of temperature seem preferable. Because of the scantiness of data from the Antarctic, especially in ice-covered areas, contributions of this region seem least reliably evaluated.

The temperature range was divided into a series of 2°C intervals beginning with $-2°$ to 0°C, and the salinity range into intervals of 0·4‰ beginning with 29·2 to 29·6‰. This resulted in 16 intervals to cover the temperature range and 19 intervals to cover most of the salinity range encountered in both oceans. Areas having salinities below 29·2 and above 37·0‰ are negligibly small.

Between 20° and 50° latitude, both north and south, regions of large horizontal gradient, the ocean surface was divided into areas 2½° latitude by 5° longitude ; in other latitudes, into areas 5° latitude by 5° longitude. Near coast lines and in a few regions of large horizontal gradient, the above areas were subdivided into as many as four equal sections. Both for the North and for the South Pacific, the total of all these small areas agrees to 3 figures with the values given by WÜST, BROGMUS, and NOODT (1954, page 139).

For February and for August, the area mean characteristics of each small area were estimated visually in terms of the centre values of the characteristic classes. The area distributions were obtained by summing the small areas within each characteristic class. These area distributions are used as approximations to the frequency distributions, although frequency as defined above includes duration as well as extent. While somewhat too concentrated, the approximations seem reasonably good, since the local range of characteristics during a month is generally not nearly so large as the total range for an ocean, but is comparable in size with the class intervals used (2°C and 0·4‰).

For the year, however, duration must be taken into account in the frequency distributions. Unfortunately, local distributions are very inadequately known. MONTGOMERY (1955) obtained the distribution at Weather Ship J in the North Atlantic. But this does not seem to be typical of large areas of the Pacific Ocean. As a first approximation, it was assumed in the present study that the characteristics at a fixed location all lie between the February and August mean values and occur with equal frequency. This gives distributions which are flatter than the actual distributions and cover a smaller range, since characteristics outside of the extreme monthly means actually occur.

The frequency distributions for the winter month, the summer month, and the year are presented in the temperature-salinity diagrams of Figs. 1, 2, and 3, respectively. Smooth isopleths were entered in each diagram to suggest the shape of the continuous frequency surface $z = f(S, T)$. They also serve to emphasize the differences between the North and South Pacific, and between winter and summer. While the isopleths were drawn so as to be smooth, they fulfill roughly the requirement that for each characteristic class the average ordinate of the frequency function $f(S, T)$ be equal to the discrete frequency for the class. Expressed symbolically, the requirement is that

$$N_{ij} = \frac{1}{\Delta S \cdot \Delta T} \int_{S_i}^{S_i+\Delta S} \int_{T_j}^{T_j+\Delta T} f(S, T)\, dT dS,$$

where N_{ij} is the frequency of the characteristic class defined by the salinity interval extending from S_i to $S_i + \Delta S$ and the temperature interval extending from T_j to $T_j + \Delta T$. The isopleths thus appear as contours based on the discrete frequency values.

All of the frequency distributions have one general form, a ridge of higher frequencies running from low temperature and low salinity to high temperature and high salinity, and then to lower salinity at about the same temperature. The ridge might be described as having the shape of a " seven " lying on its right side. (The means for 5° zones of the North and South Pacific given by WÜST, BROGMUS, and NOODT (1954) fall nearly along the ridge lines of the annual distributions.) Along the ridge, there are two or three appreciable peaks. The strongest of these occurs in all cases at the angle of the " seven," that is, at rather high temperature and salinity. (Although the South Pacific distribution for August has its highest value at low temperature, the bulk of high frequencies are at high temperature). The range of frequency values between peaks and low points along the ridge is quite large. A striking feature common to all the distributions is the fact that temperatures and salinities between the two branches of the ridge have nearly zero frequencies.

There are, of course, many marked differences between the distributions for the North and South Pacific, in addition to the well known difference in salinity range. (1) The maximum at high temperature is much stronger in the North Pacific distribution than is the one for the South Pacific. For the former, both August and February have single characteristic classes with frequencies higher than 14 per cent! This clearly results from the fact that the North Pacific is wide at low latitudes, where temperatures are generally high, and narrow at high latitudes. (2) The South Pacific distributions have marked maxima at low temperature because of the inclusion of the Antarctic area. (3) The North Pacific distributions, on the other hand, have distinct secondary frequency maxima at high temperature and low salinity because of the extensive areas of low salinity near the coasts at low latitudes in the Northern Hemisphere and near the intertropical convergence zone which usually lies in the Northern Hemisphere.

An interesting quantitative comparison between the distributions can be made by computing for each distribution the proportion of the total frequency enclosed

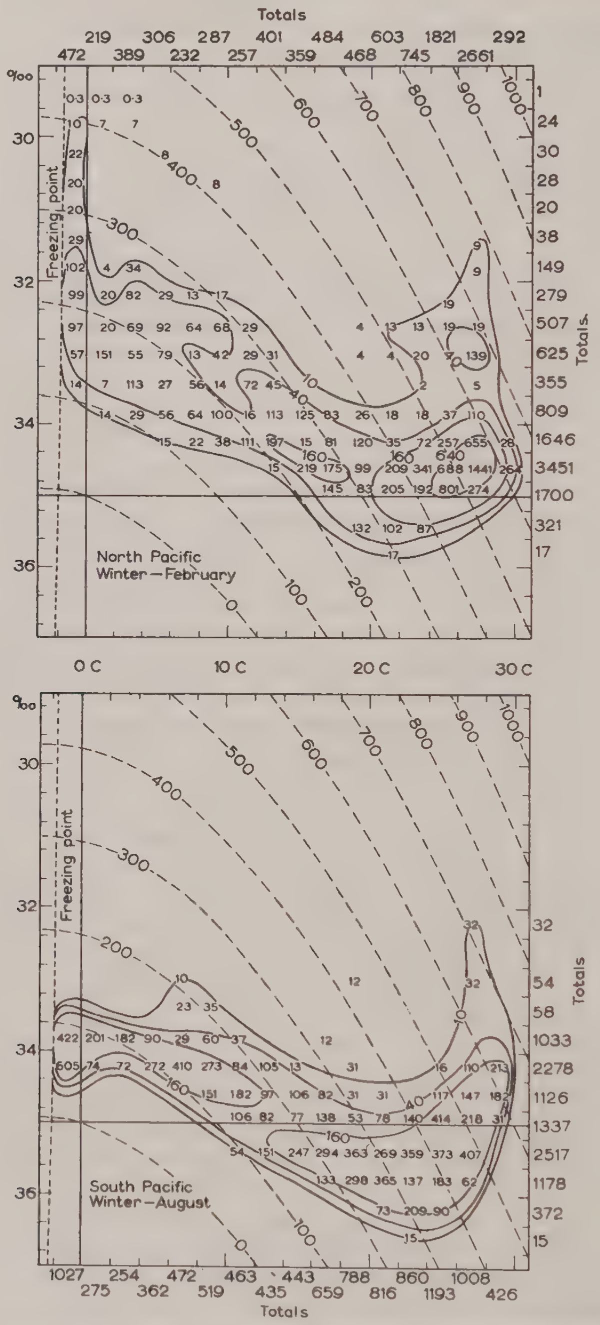

Fig. 1. Temperature-salinity diagrams showing the frequencies of surface-water characteristics for winter, February in the North Pacific, and August in the South Pacific Ocean. In each diagram, the sum of the frequencies is 10,000. Smooth isopleths of frequency are entered as full drawn curves. The frequency values may be converted to area by multiplying by 816 km2 for the North Pacific or by 981 km2 for the South Pacific. Isopleths of anomaly of specific volume are shown as dashed curves. Their values are given in centiliters per ton (metric).

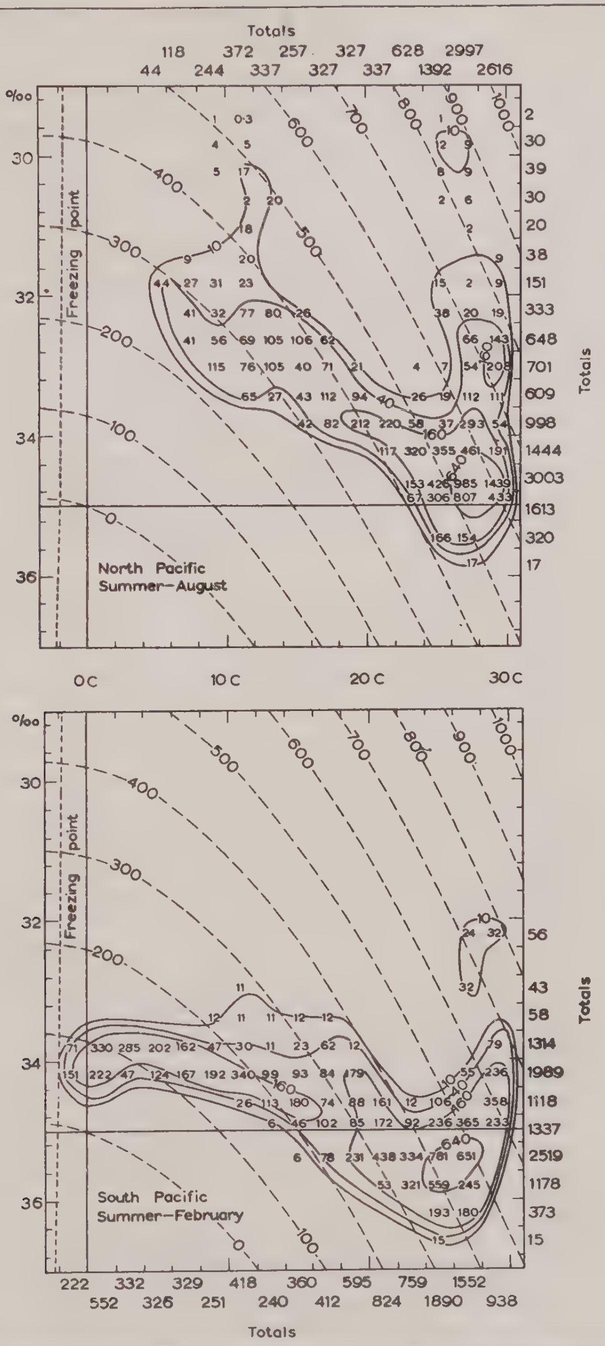

Fig. 2. Temperature-salinity diagrams showing the frequencies of surface-water characteristics for summer, August in the North Pacific, and February in the South Pacific Ocean. In each diagram, the sum of the frequencies is 10,000. Smooth isopleths of frequency are entered as full drawn curves. The frequency values may be converted to area by multiplying by 816 km² for the North Pacific or by 981 km² for the South Pacific. Isopleths of anomaly of specific volume are shown as dashed curves. Their values are given in centiliters per ton (metric).

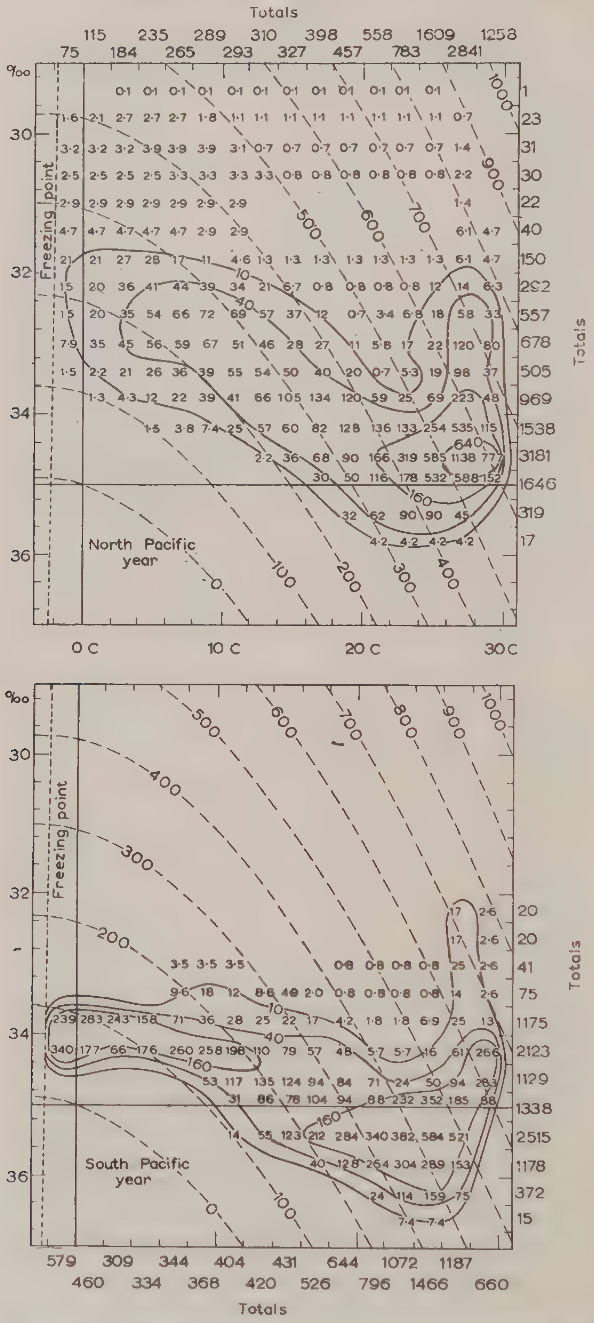

Fig. 3. Temperature-salinity diagrams showing the frequencies of surface-water characteristics for the year in the North and South Pacific Oceans. In each diagram, the sum of the frequencies is 10,000. Smooth isopleths of frequency are entered as full drawn curves. Isopleths of the anomaly of specific volume are shown as dashed curves. Their values are given in centiliters per ton (metric).

within given frequency isopleths. For want of a name, this quantity was called "beta" by MONTGOMERY (1955), who obtained isopleths enclosing stated proportions of the total. The approximate proportions for the isopleths entered in Figs. 1, 2, and 3 are given in Table 1. In both oceans, the distributions are most concentrated in the summer month, less concentrated in the winter, and, of course, least concentrated for the year. However, the oceans differ markedly in peakedness. Much of the North Pacific distribution is concentrated very near the modes, 19% of the total lying within the 640 isopleth even in the annual distribution. The concentration very near the modes of the South Pacific distributions is much less. In summer, 20% lies within the 640 isopleth compared with 34% for the North Pacific. And in the winter and annual distributions for the South Pacific, there is no 640 isopleth. On the other hand, the South Pacific shows consistently higher proportions within the 160 isopleth.

Table 1. *Proportion of the total frequency enclosed within selected frequency isopleths in per cent.*

Frequency Isopleth	*North Pacific*			*South Pacific*		
	August	*February*	*Year*	*February*	*August*	*Year*
640	34	25	19	20	0	0
160	64	55	46	80	74	72
40	90	85	80	92	88	88
10	95	92	90	93	92	91

Many smaller features of the frequency distributions might be sorted out and related to features of the geographical distributions. Some caution, however, must be exercised in interpreting the very small features because of limitations in the source information and the methods used. The actual distributions are undoubtedly smoother than those presented here. It is partly for this reason that smooth isopleths of frequency were entered in the diagrams. Some bumpiness, however, is to be expected in the actual distributions, since water with a narrow and unusual range of characteristics may occur in relatively isolated portions of the ocean.

The onedimensional frequency distributions of temperature and salinity obtained by summing columns and rows, respectively, in each of the temperature-salinity diagrams of Figs. 1, 2, and 3 are entered along the outer edges of the diagrams. The distributions of anomaly of specific volume are given in table 2. They were derived by adding the frequencies lying between the isosteres shown in Figs. 1, 2, and 3. Because of this indirect method of derivation, the accuracy of these distributions is less than that of the temperature and salinity distributions.

All of the distributions of temperature have a strong mode at high temperature. All but the North Pacific annual distribution have a second, smaller mode at low temperature. This mode is marked in the South Pacific distributions because of the inclusion of the Pacific Antarctic region. It is distinct, though small, even in the North Pacific, where its temperature undergoes considerable seasonal variation. A third, very weak mode occurs between 8° and 12°C in the South Pacific distributions. A faint suggestion of this mode occurs in the North Pacific distribution for February.

The distributions given by LITTLEWOOD are similar to those presented here. Even the third mode appears in the South Pacific distribution.

All of the salinity distributions are bimodal. The North Pacific has a strong mode at rather high salinity and a weak one at relatively low salinity. In the South Pacific distributions, the range of salinity is much smaller, the modes are closer together, and the mode at higher salinity is only slightly more intense than the one at lower salinity. For the South Pacific, the modes correspond to the two principal modes of the twodimensional distribution. But for the North Pacific, only the strong salinity mode corresponds to the principal twodimensional mode. The weaker mode at lower salinity results from both the high and low temperature branches of the twodimensional distribution.

Table 2. Frequency distribution of specific volume anomaly, in per cent.

	Anomaly of Specific Volume, in cl/ton								
	0 to 100	100 to 200	200 to 300	300 to 400	400 to 500	500 to 600	600 to 700	700 to 800	800 to 900
North Pacific									
February	0·1	10·0	21·2	13·3	21·3	28·7	5·2	0·2	0·0
August	0·0	0·0	4·9	11·2	20·4	32·7	25·0	5·1	0·7
Year	0·0	3·7	13·6	16·2	21·2	32·3	11·3	1·5	0·2
South Pacific									
February	6·5	17·6	11·1	28·1	22·5	8·3	5·3	0·6	0·0
August	15·0	24·4	21·4	14·1	15·4	6·1	3·3	0·3	0·0
Year	10·0	20·4	17·3	19·9	20·6	6·1	5·4	0·3	0·0

The distribution of specific volume anomaly is bimodal except for August and the year in the North Pacific. The modes correspond to modes in the two-dimensional distributions except that the high-temperature, low-salinity mode of the North Pacific distribution does not result in a mode in the specific volume anomaly distribution, but only in a tailing off toward high values.

Perhaps the principal value of this inventory of temperature and salinity conditions at the surface of the Pacific Ocean is that it puts into perspective some of the many details encountered in working with sea-water characteristics. A systematic classification of Pacific Ocean waters can hardly be made without this and a similar inventory of subsurface temperatures and salinities. Such information is essential to a quantitative study of the evolution and maintenance of water characteristics.

Acknowledgement—The writer wishes to record his gratitude to Dr. R. B. MONTGOMERY who suggested the subject of this study.

Scripps Institution of Oceanography, University of California.
La Jolla, California.

Present affiliation: Department of Oceanography and Meteorology, Agricultural and Mechanical College of Texas.

Contribution No. 28 *from the Chesapeake Bay Institute, The Johns Hopkins University, Baltimore* 18, *Maryland, where this study was supported by a research grant from the National Science Foundation. Contribution of the Scripps Institution of Oceanography, New Series, No.* 891. *The work reported on herein also represents results of research sponsored in part by the Office of Naval Research under contract with the University of California.*

REFERENCES

ANON (1939), Die Grenzen der Ozeane und ihrer Nebenmeere. *Ann. d. Hydrogr. u. Mar. Meteorol.* Beiheft zum Maiheft, 11 pp., 2 encl.

DEACON G. E. R. (1937), The hydrology of the Southern Ocean. *Discovery Repts.* **15**, 1-24, pls. I-XLIV.

HELLAND-HANSEN B. and NANSEN F. (1926), The eastern North Atlantic. *Geofys. Publ.* **4** (2), 76 pp., 71 pls.

MACKINTOSH N. A. (1946), The Antarctic convergence and the distribution of surface temperatures in Antarctic waters. *Discovery Repts.* **23**, 177-212.

MONTGOMERY R. B. (1955), Characteristics of surface water at Weather Ship *J. Pap. Mar. Biol. and Oceanogr., Deep-Sea Res.* Suppl. to Vol. 3, 331-334.

MURRAY JOHN (1899), The temperature of the floor of the ocean and of the surface waters of the ocean. *Geograph. J.* **14**, 34-51, 3 maps.

SCHOTT G. (1935), *Geographie des Indischen und Stillen Ozeans.* C. Boysen, Hamburg, 413 pp.

SPILHAUS A. F. (1942), Maps of the whole world ocean. *Geogr. Rev.* **32** (3), 431-435.

WÜST G., BROGMUS W. and NOODT E. (1954), Die zonale Verteilung von Salzgehalt, Niederschlag, Verdunstung, Temperatur und Dichte an der Oberfläche der Ozeane. *Kieler Meeresforsch.* **10** (2), 137-161.

Printed in Great Britain by The Salisbury Press Ltd., Publicity House, Wilton Road Salisbury, Wilts. (1112)

OCEANOGRAPHY OF MISSISSIPPI DELTA SEDIMENTARY ENVIRONMENTS

BY

P. C. SCRUTON

Reprinted for private circulation from
THE BULLETIN OF THE AMERICAN ASSOCIATION OF PETROLEUM GEOLOGISTS
Vol. 40, No. 12, December, 1956
Reproduced by Permission

BULLETIN OF THE AMERICAN ASSOCIATION OF PETROLEUM GEOLOGISTS
VOL. 40, NO. 12 (DECEMBER, 1956), PP. 2864-2952, 44 FIGS.

OCEANOGRAPHY OF MISSISSIPPI DELTA SEDIMENTARY ENVIRONMENTS[1]

P. C. SCRUTON[2]
Tulsa, Oklahoma

ABSTRACT

The Mississippi, one of the world's great rivers, has transported a vast quantity of sediment to the Gulf of Mexico during its history. Understanding the oceanography around the Mississippi's mouth increases our understanding of the sediments which have formed there and also the oceanography of other similar areas where fresh water meets and flows into the sea.

Despite the size of the Mississippi, it is small relative to the entire Gulf of Mexico, and ocean currents off its mouth can be compared with currents in a large tank off a very small rubber hose. The large body of water flows first one way and then another and carries with it the minor volume of hose discharge. Currents due to hose discharge are relatively small swirls localized about the orifice.

The regional gulf current pattern provides the background on which are superimposed local conditions off the delta. Regional or semi-permanent currents are produced both by winds blowing over the entire gulf and by regional density differences acted upon by gravity. Density differences are due to fresh water input at many places and to gulf-wide evaporation, heating, and cooling. The semi-permanent current flows northward in the central gulf, and on approaching land south of the delta, apparently divides into two tongues. These tongues diverge and flow eastward and westward away from the delta.

In addition to the regional currents, there are local currents produced by: (1) tides, (2) winds, and (3) river discharge. Any single current measurement is a vector containing components produced by all these causes. Tidal currents affect the entire water column; in inshore waters they alternate in direction and speed with changes in normal tide-producing forces, but in the open gulf they probably are rotary. Wind-driven currents are caused directly by stress on the sea surface and also by piling of water against a boundary such as the shore. Locally they change direction with the winds and are of about the speed usually attributed to wind currents.

Currents in the gulf produced by river discharge are the swirls off the small hose. They are the result of residual momentum of issuing river water, hydraulic head, and density differences between river and sea water. The direction in which these currents flow usually is determined by the direction

---

[1] Contribution from the Scripps Institution of Oceanography, New Series, No. 892. This investigation was supported by a grant from the American Petroleum Institute, Project 51. Manuscript received, August 21, 1956.

[2] Stanolind Oil and Gas Company.

Many people shared in the planning and contributed to the work for this report. Acknowledgment and appreciation are extended to each for his part. F. P. Shepard, director of Project 51, A. R. Denison and C. L. Moody, Project 51 Advisory and Steering Committee chairmen, R. R. Revelle and C. D. Wheelock, Scripps Scientific Committee chairmen, the members of each of these committees and especially R. S. Arthur, C. S. Cox, G. C. Ewing, D. G. Moore, W. H. Munk, and F. B Phleger, all took part in many discussions and made important suggestions. Arthur, Moore, Phleger, Revelle, and Shepard, all at Scripps, read and commented on the manuscript. The manuscript also was read by P. A. Dickey of the Carter Oil Company, N. L. Thomas of the Pure Oil Company, and N. A. Riley of California Research Corporation. These men performed their official, critical function as members of the Scripps scientific staff and Project 51's Publications Review Committee and a closer one as friendly advisors.

Moore, R. H. Parker, S. A. Andrews, J. R. Curray, and J. W. Pitre, captain of M/V *Deanna L.*, and D. Green, captain of M/V *Rosemary*, helped with field work. These men made vital contributions, often under trying circumstances. The Louisiana Department of Fish and Game made available one of its fully equipped vessels, field help, and other facilities for a series of observations. U. G. Whitehouse of Texas A. and M. College supervised analysis of early material. Under his direction Lela M. Jeffreys made many chemical determinations, and A. N. Brown and W. T. Williams prepared a preliminary study of the inshore area. A. E. Maxwell of the Scripps Institution also studied early results. G. S. Bien supervised the many laboratory analyses made at the Scripps Institution by Mary Barstow. J. R. Moriarity, Marjorie Brown, Bernadine Joyce, Elizabeth Sanborn, and Ruth Young helped with drafting and in numerous other ways.

Finally, special thanks are due to the Stanolind Oil and Gas Company and to H. T. Morley, F. C. Osment, and G. L. Taylor for cheerfully making time, help, and facilities available to complete the report.

of tidal, wind, or semi-permanent currents; their speed is related first to the volume of river discharge. Residual momentum currents persist seaward from the largest distributaries to a maximum distance of about 25 miles. Hydraulic head and density differences produce the usual two-layer estuarine circulation found in other areas where fresh water flows into the sea, but there are important differences from other areas because of the relatively large volume of discharge and the geography of the system.

In general, repetition of local circulation features is brought about by repetition of similar conditions of tide, wind, and river discharge. However, in the area south of the delta between the two diverging current tongues, the east- or west-directed component of the current is related mainly to local winds. Because of this, data on average monthly winds and river discharges can be used to estimate river water and sediment distribution seaward in the gulf. About 55–65 per cent of the river water is distributed westward, about 25–35 per cent goes east, and the remainder (about 10 per cent) goes south. The river delivers a huge but still unknown amount of sediment to the gulf each year. Most of this load is carried during the high discharge months of late winter and spring when the winds are persistent easterlies, and because of this as much as 70–75 per cent of the Mississippi's suspended load may start westward in the gulf. A large part of the total clastic load is deposited on the sea floor immediately around the delta, and it is only partly fractionated by size.

Interesting hydraulic processes also occur within the distributaries. Channels of the lower distributaries are defined seaward to the bars at all times. The bar crests and seaward ends of the natural levees constitute the discharge orifices of the distributaries. During low river stages of late summer and fall there is intrusion of salt water into the bottoms of the channels under the river water. This bottom water is called the "salt wedge," and it oscillates with the tide but apparently has a small upstream current on the average. When the salt wedge is present, bed load can not be transported downstream and the amount of suspended load diminishes. Only during high river is the full channel volume required to transport fresh water; only then can bed load be moved out to the sea. Principal topographic features of the lower distributaries are: (1) the channel-mouth bars, (2) the channel-bottom ramps sloping upward toward the sea, and (3) the typical bell-shaped mouths formed by outward flaring of the natural levees. These features are all related in origin, and they are shaped by both deposition and erosion during, and in response to, seasonal high river stages where light river water flows over dense salt water.

Waves in the gulf usually are small, and the largest occur seasonally. Frequency of wave-stirring of the sea floor decreases with increasing water depth and occurs at greater depths mostly during fall and winter or during the rare hurricanes. Greatest turbidity in the shallow water around the delta occurs during fall and winter storms when some of the earlier deposited load is resuspended. Salt content and temperature of the inshore water are highly variable and are related to characteristics of both river and gulf waters. Temperature in the protected sounds also is related closely to local air temperature and insolation.

Turbidity currents on the delta's face apparently take place, but probably only under the special hydrographic conditions of fall and winter. During these seasons temperature and chlorinity are uniform vertically below a thin surface layer, there is little or no density stratification in the water column and the concentration of suspended matter frequently is high.

The delta's oceanography is the sum of effects of the gulf, the river, and the atmosphere. These elements combine to create a complex natural sedimentation system which at present is not amenable to theoretical analysis.

INTRODUCTION

This is one of a series of papers on shallow-water sediments and their environments of deposition in the northern Gulf of Mexico. Investigation for these reports is being carried out at the Scripps Institution of Oceanography of the University of California under sponsorship of the American Petroleum Institute. The purpose of this work is to further understanding of older sedimentary rocks through study of their now-forming modern counterparts.

Two areas in the Gulf of Mexico are receiving special study. One is an area of open sea, barrier islands, and bays and lagoons on the central Texas coast near the town of Rockport. F. P. Shepard and D. G. Moore (1955) recently described many results of the work to date in this area. The other area is the eastern side of the Mississippi River Delta.

A generalized description of the delta's sediments and environments of deposition was given by Scruton (1955). The present paper is a more detailed description of a phase of the earlier report. This paper treats parts of the oceanography of the Mississippi Delta's sedimentary environments in such detail as the data now permit. In a continuing project, such a report at this time serves a triple purpose. First, it provides background and new data for interested workers in related fields; second, it summarizes existing information and makes it more useable to other workers in the same field; and third, it is a progress report and points out aspects that need additional study.

Particular phases of the delta's oceanography that are considered here are: the currents, waves, and salt content, temperature, and suspended sediment. Studies of each of these contribute to understanding the others, so that their order of presentation is not of great importance. Because currents are the unifying theme, they are considered first, and are followed by the other topics in the indicated order. These topics are not considered in equal detail because of different amounts of data.

There are no short cuts to a full understanding of the delta's oceanography and sedimentation. The field observations were all quantitative, insofar as possible. Treatment of the data is empirical, and because of the many variables that affect each quantity, none of the subjects is simple. Theory must advance far to explain field conditions.

CURRENTS

Currents around the Mississippi Delta are of interest because they distribute clastic sediments of all kinds, and because they influence both salt content and temperature of the water. Therefore, they are important to organic as well as inorganic sedimentation.

In addition, the currents of this area are of interest for themselves. Around the Mississippi Delta a large river meets the sea and flows into it; it is one example of other similar areas scattered over the world. When viewed in detail, current patterns of these regions are extremely complex and are highly variable, both from place to place at any one time and from time to time at any one place. Knowledge about one such area helps understand the others.

The Mississippi Delta region has been subdivided into two areas for discussion: an inshore area and an offshore area. The reasons for this subdivision are two-fold: causes of currents are partly different between the areas, and the data are different, so that it is inconvenient to discuss them together. The inshore area includes Breton Sound, the more or less restricted waters surrounding Breton Island seaward to depths of 6–8 fathoms (36–48 feet), and the shallower waters in, and seaward of, distributary mouths north and east of the delta (Fig. 1). The offshore area includes the open Gulf of Mexico seaward of these depths. Such a subdivision is arbitrary and can not be adhered to rigidly around that part of the delta facing directly on the open gulf where the inshore area grades into the offshore with no boundaries.

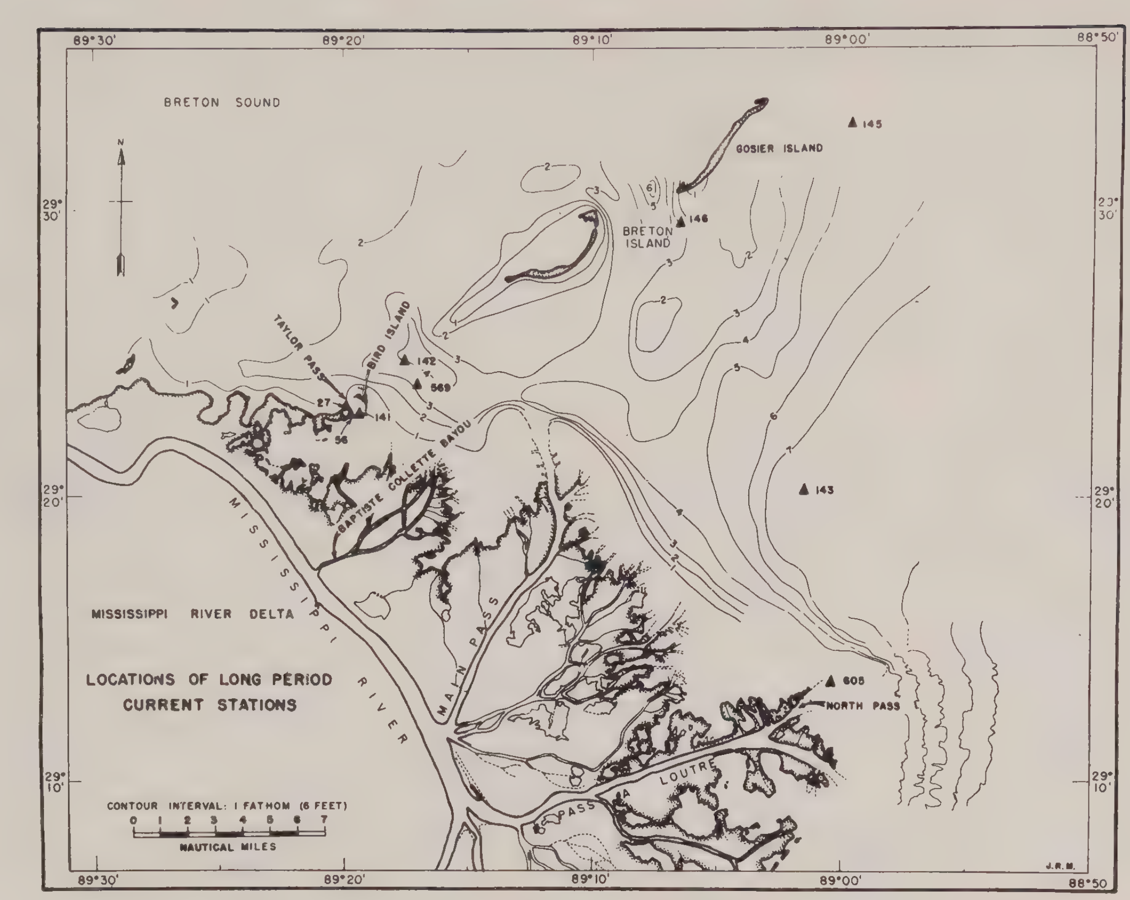
89°30'
89°20'
89°10'
89°00'
88°50'
29° 30'
29° 20'
29° 10'
N
BRETON SOUND
GOSIER ISLAND
145
146
BRETON ISLAND
TAYLOR PASS
BIRD ISLAND
142
569
27
141
56
COLLETTE BAYOU
BAPTISTE COLLETTE
143
MISSISSIPPI RIVER
MAIN PASS
608
NORTH PASS
PASS A LOUTRE
MISSISSIPPI RIVER DELTA
LOCATIONS OF LONG PERIOD
CURRENT STATIONS
CONTOUR INTERVAL: 1 FATHOM (6 FEET)
0 1 2 3 4 5 6 7
NAUTICAL MILES
J.R.M.

FIG. 1.—Place names, principal topographic features of inshore area, and locations of long-period observation stations.

The same basic approach to studying currents has been used for both subareas. The prevailing pattern of currents is described. Then, within limits of the data, the principal components of the currents are isolated, identified, discussed, and evaluated to estimate the roles played by each in the prevailing pattern.

Recently Bates (1953) published a lengthy article on currents off the Mississippi Delta. His approach to the problem and most of his conclusions are different from those described here. The interested reader is invited to compare the discussions.

CURRENTS, INSHORE AREA

SOURCES OF DATA

There are no published data on currents in the inshore area north and east of the delta. In order to study the currents of this area; a large number of measurements were made. At each point of measurement, observations of current speed and direction were obtained, both at the surface and at several subsurface depths. Measurements were made from an anchored vessel using a compass and the current cross developed by Prichard and Burt (1951). Sea dye, drift bottles, and chlorinity and suspended sediment distributions also provided data on currents.

Current stations distributed throughout the inshore area were occupied to determine the areal current pattern, and long-period anchor stations were occupied at selected localities to determine variations in the areal current pattern with time. Over 100 current stations, distributed over the area, were occupied in October and November, 1951, and about 75 stations, similarly distributed, were occupied in April and May, 1952. In addition, 28 current stations were located in and directly seaward of the mouth of North Pass during June and September, 1953. Two long-period current stations were occupied in 1951, five in 1952, and two in 1953. The periods of consecutive observations at these anchor stations ranged from 22 to 40 hours. A total of approximately 1,250 separate current measurements was made.

Other supplementary observations also were made at each of these stations. Among these were: (1) wind speed and direction (measured with hand anemometer held approximately 8 feet above sea surface unless noted otherwise), (2) water and air temperature, (3) chlorinity (salinity), and (4) turbidity (a measure of suspended matter).

GENERAL DESCRIPTION

Current stations distributed to determine the areal pattern were not made synoptically and currents were measured under a variety of tide, wind, and river discharge conditions. Results for 1951 and 1952 are shown in Figures 2 and 3; arrows indicate direction and speed. Upper diagrams show the surface currents, and lower diagrams show bottom currents; currents at intermediate depths were not included.

Measurements of bottom currents (lower diagrams, Figs. 2, 3) show that there

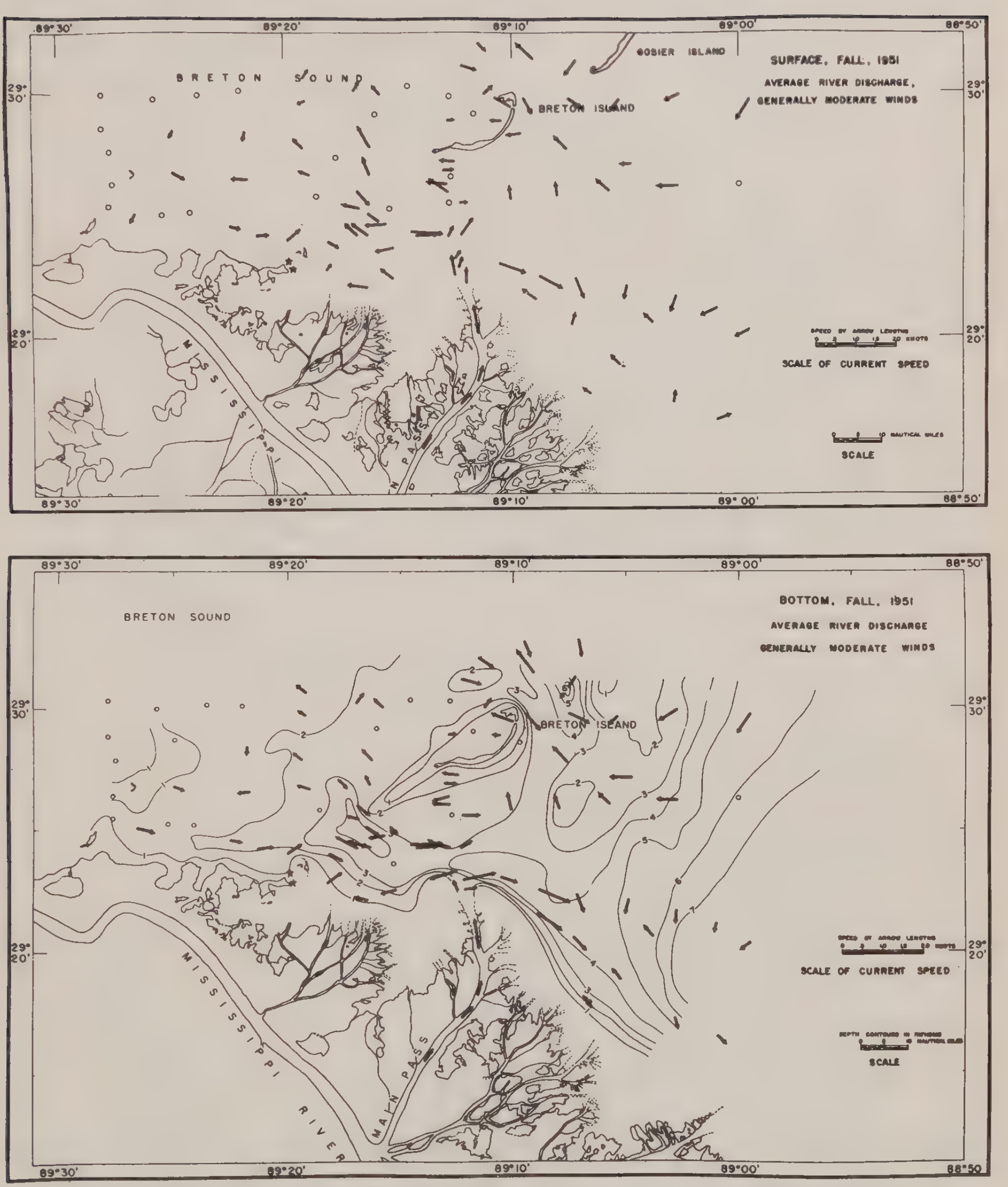
SURFACE, FALL, 1951
AVERAGE RIVER DISCHARGE,
GENERALLY MODERATE WINDS
BRETON SOUND
GOSIER ISLAND
BRETON ISLAND
MISSISSIPPI
MAIN PASS
SPEED BY ARROW LENGTHS
0 5 10 15 20 KNOTS
SCALE OF CURRENT SPEED
0 5 10 NAUTICAL MILES
SCALE
BOTTOM, FALL, 1951
AVERAGE RIVER DISCHARGE
GENERALLY MODERATE WINDS
MISSISSIPPI RIVER
DEPTH CONTOURS IN FATHOMS
89°30'
89°20'
89°10'
89°00'
88°50'
29° 30'
29° 20'

FIG. 2.—Measured currents at surface and bottom, fall, 1951. Length and direction of arrows indicate speed and direction of currents. Zero indicates no measurable currents when station occupied.

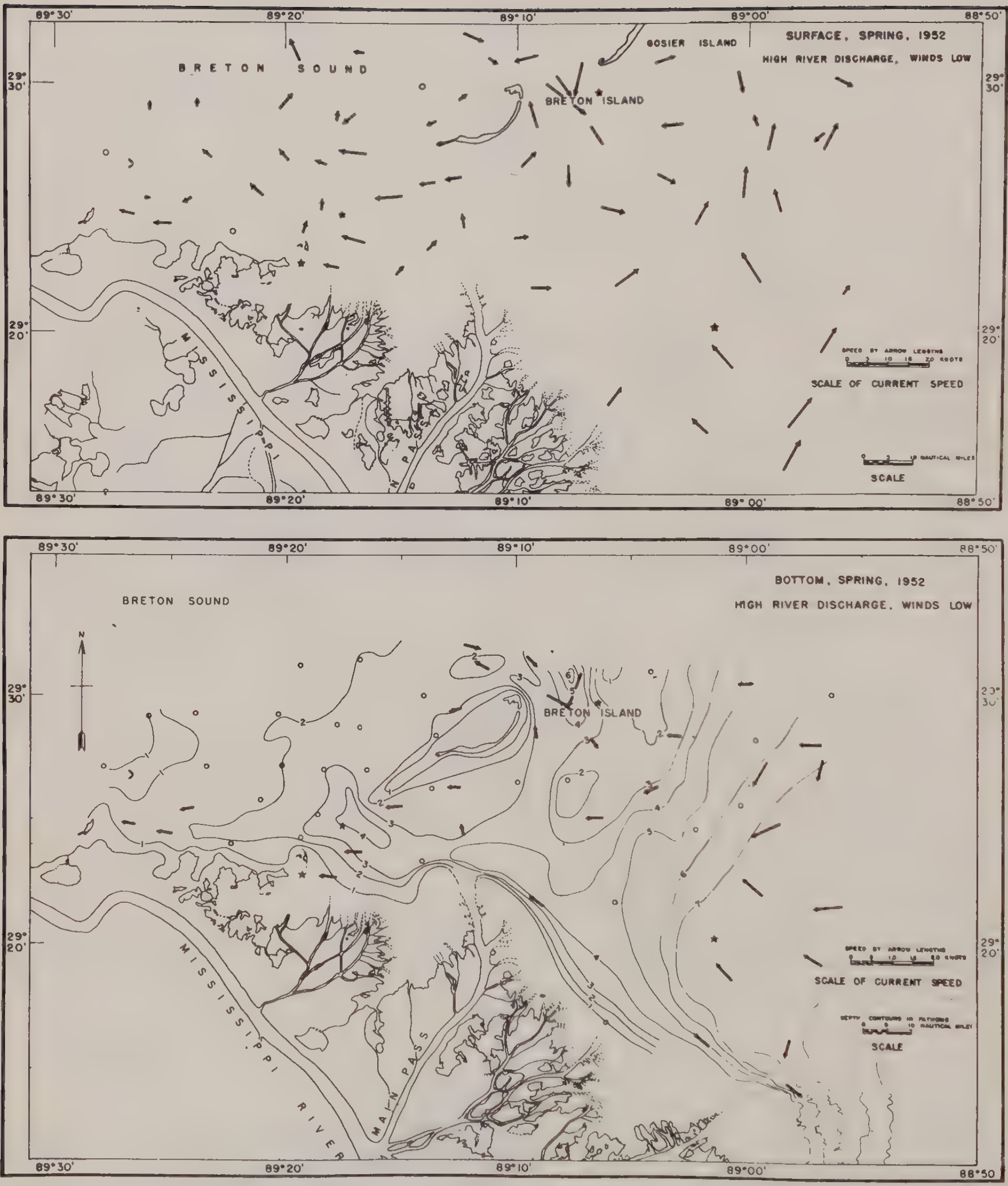

89°30'
89°20'
89°10'
89°00'
88°50'
29° 30'
29° 20'
SURFACE, SPRING, 1952
HIGH RIVER DISCHARGE, WINDS LOW
BRETON SOUND
GOSIER ISLAND
BRETON ISLAND
MISSISSIPPI
MAIN PASS
SPEED BY ARROW LENGTHS
SCALE OF CURRENT SPEED
NAUTICAL MILES
SCALE
BOTTOM, SPRING, 1952
HIGH RIVER DISCHARGE, WINDS LOW
BRETON SOUND
BRETON ISLAND
N
MISSISSIPPI RIVER
MAIN PASS
DEPTH CONTOURS IN FATHOMS
1
2
3
4
5
6
7

FIG. 3.—Measured currents at surface and bottom, spring, 1952. Length and direction of arrows indicate speed and direction of currents. Zero indicates no measurable currents when station occupied.

are preferred current directions in different parts of the area. In Breton Sound current set tends to be either toward or away from the inlets (Fig. 1 gives place names). In the inlets between Breton and Gosier islands and Breton Island, Main Pass, and Bird Island, flow is pronounced either toward the open sea or toward the sound. East of Main Pass the flow usually is either in a southeasterly or northwesterly direction, and in the shallow channel east of Breton Island currents tend to be approximately north or south. Currents over the submarine ridge south of Gosier Island usually are toward land or away from it, and farther east in deeper water, the currents are directed nearly parallel with bottom contours.

Speeds of bottom currents usually are low in areas of flat, uniform, bottom topography such as Breton Sound. However, current speeds tend to be high in more constricted areas such as the inlets northeast and southwest of Breton Island and between Main Pass and Breton Island.

Surface currents have preferred flow directions very much like those of the bottom currents (Figs. 2, 3). This is best shown by the 1951 results (Fig. 2).

Normally directions of flow of surface and subsurface currents are subparallel or parallel, and they differ mainly in speed, the surface water usually moving faster. However, under some conditions near the river mouths and in the inlets, directions of flow of surface and subsurface layers may be at high angles to each other, or even directly opposite. This is best shown by 1952 observations near Main Pass mouth (Fig. 3), at stations 143 and 146 (Figs. 1, 4), and in North Pass mouth (Figs. 12, 13, 14).

Surface currents outside distributary mouths differ most from underlying currents in both speed and direction when either river discharge or winds are high. Under either of these conditions the surface currents usually are restricted to a thin layer, about 1–6 feet thick, which moves at speeds appreciably higher than those in the underlying layer. Inside distributary mouths, on the other hand, significant differences in speed and any differences in direction between surface and bottom layers occur only under moderate to low river discharges. These differences become extreme and persistent only at low river stages (Figs. 12, 14). These differences in behavior are discussed more fully.

Long-period current stations provide data that help interpret the areal observations (Fig. 4). Station 142 was made in the inlet between Breton and Bird islands (Fig. 1), station 143 was made east of Main Pass mouth, and station 146 was made in the inlet between Breton and Gosier islands. Plots of current against time (Fig. 4) show how speeds varied and directions shifted and the compass roses show the actual current directions. Ebb and flood refer to the times predicted by the Coast Survey Tide Table for the change of tide at Pass a Loutre. Actual times of beginning of ebb or beginning of flood occurred when the current passed zero speed and changed direction.

Station 142 (inlet between Breton and Bird islands) shows that the current flows approximately northwest into Breton Sound on the flood and in an op-

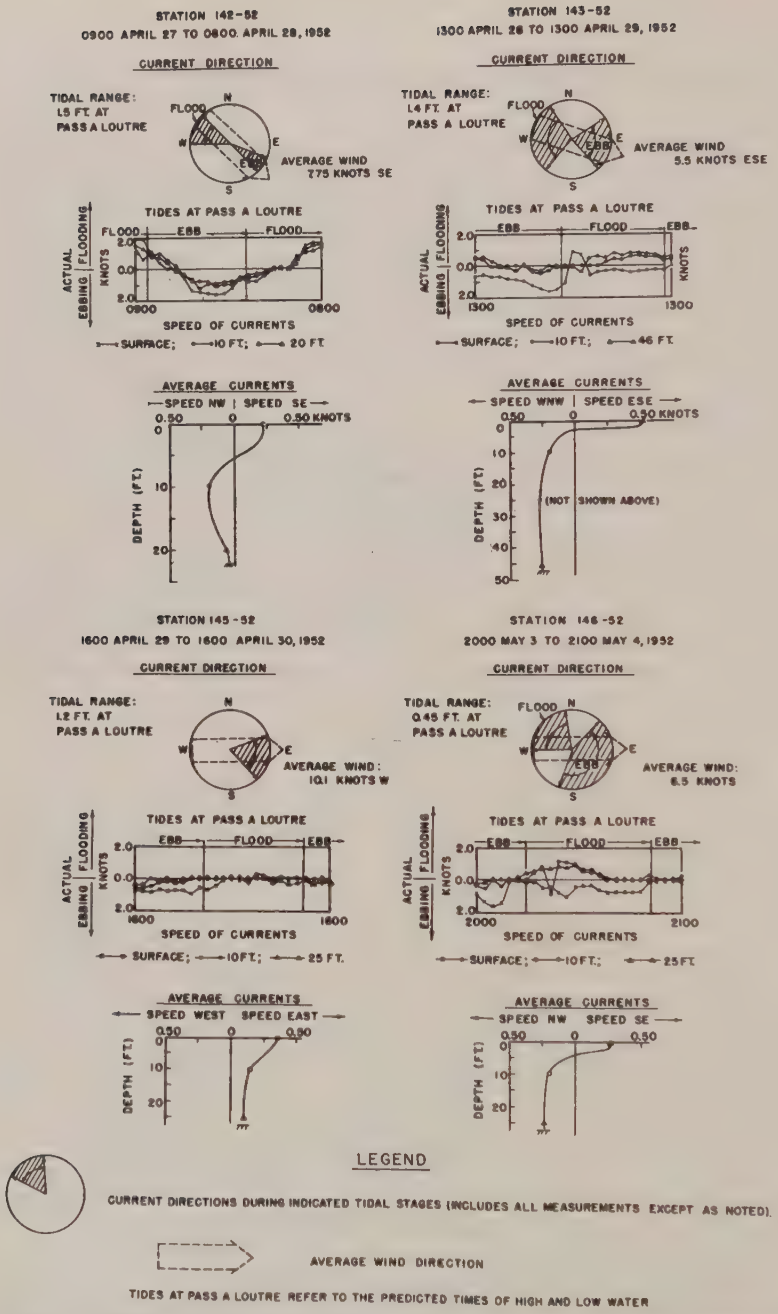

FIG. 4.—Current and wind results from long-period observation stations (Fig. 1). Average wind speed and direction shown by dashed arrows in compass roses. Hourly current speeds at different levels shown on current vs. time plots, range of current directions during flood and ebb tide shown by cross-hatching on compass roses, and profiles of average current on speed vs. depth plots. Tides at Pass a Loutre refer to times predicted by Tide Tables; actual flooding and ebbing begin when speed curve crosses zero base line.

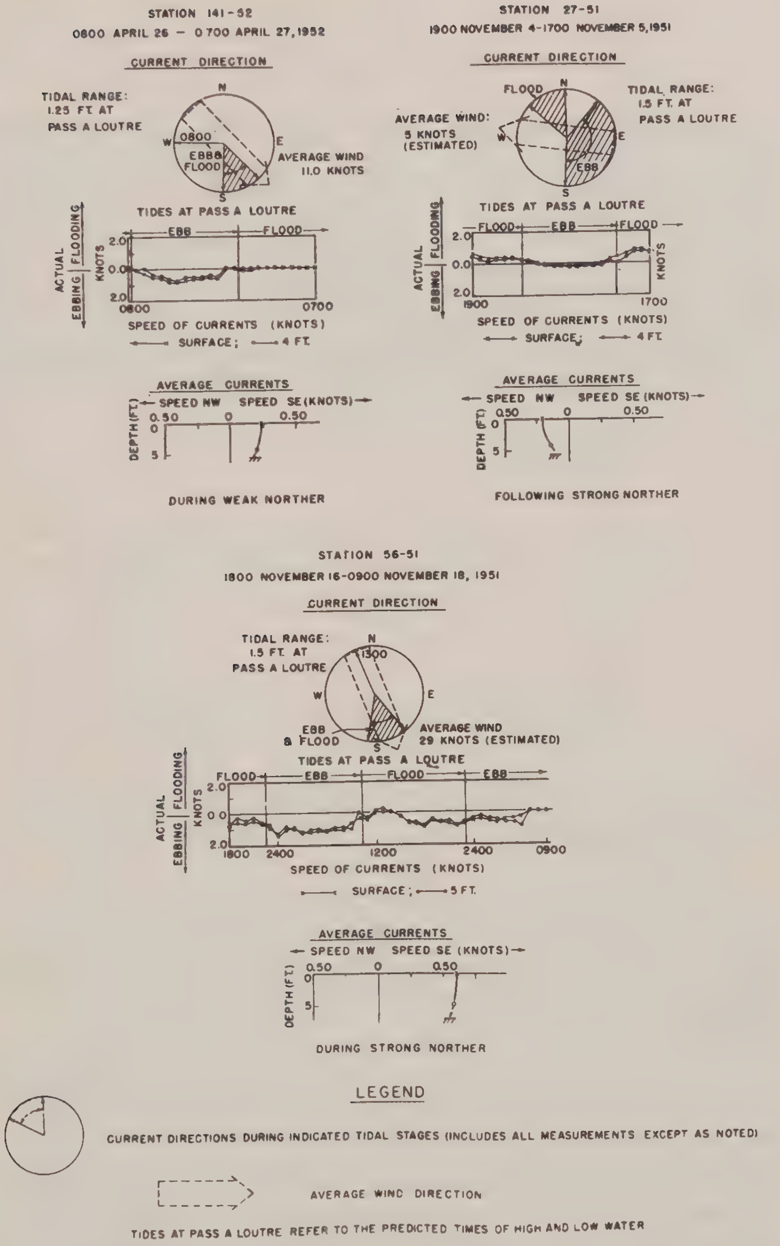

FIG. 5.—Effects of storms on currents. Current and wind results from long-period observation stations (Fig. 1). Average wind speed and direction shown by dashed arrows in compass roses. Hourly current speeds at different levels shown on current vs. time plots, range of current directions during flood and ebb tide by cross-hatching on compass roses, and profiles of average current on speed vs. depth plots. Tides at Pass a Loutre refer to times predicted by Tide Tables; actual flooding and ebbing begin when speed curve crosses zero base line.

posite direction, approximately southeast toward the open sea, on the ebb. At station 143, in deeper, more open water east of Main Pass mouth, the current during flood tide flows westward and during the ebb eastward, but there is considerable variation in both flood and ebb directions. At station 146, just out of the Breton-Gosier inlet, flood-tide current flows northwest into Breton Sound and ebb-tide current flows northeast, east, or south toward open water. There is considerable variation in ebb-tide flow direction because the station was located near the open sea in unrestricted waters.

These long-period stations show that the preferred current directions observed during areal surveys are due in large measure to tidal currents flowing between the open sea and the sounds and other inshore water bodies. Any apparent lack of pattern or system to the currents in Figures 2 and 3 is created by the random nature of the sampling program. Ebb currents may have been measured on one day while at an adjacent station, made the next day, the flood currents were measured.

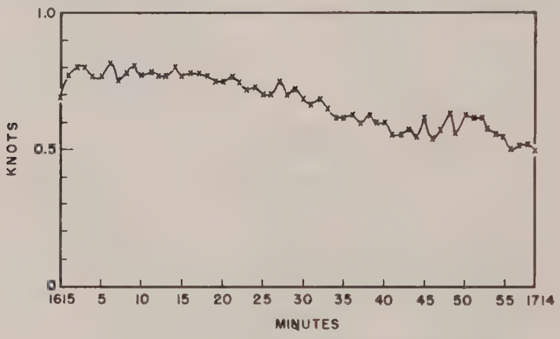

STATION 27–51, 11–5–51; CURRENT DIRECTION: NORTHWEST

FIG. 6.—Surface current measurements every minute. Hourly observations record the trend of current speed changes, and short-period fluctuations are relatively minor.

Figures 31 and 32 in a later section show charts of surface chlorinity distribution, as observed in 1951 and 1952. Low chlorinity values are the result of dilution of sea water by river discharge. These charts were prepared to show maximum seaward extent of fresh-water distribution during the periods of observation. Thus, the tongues of fresh water extending into Breton Sound were produced when fresh water flowed northwest and north on the flood tide and the broad bands of fresh water east of Main Pass were accentuated by larger volumes of river water flowing in that direction on the ebb tide. (See also section on Salt Content.)

Similarly the lobes of high turbidity extending into Breton Sound shown in Figures 41 and 42 (reproduced from Scruton and Moore, 1953) are produced partly by tidal currents.

These data have been used to draw Figure 7, a generalization of the circulation pattern of the bottom and surface waters in the inshore area. It shows the most probable current directions on both the flood and ebb tides as well as relative speeds of the currents. Where the currents reciprocate with changes of tide, as between Breton and Bird islands, current arrows are double-headed. In the surface layer directly off Main Pass mouth, a northwesterly current direction prevails on the flood tide and an easterly direction prevails on the ebb. Under these conditions the arrows are single-headed and show direction of flow on both flood and ebb. Length of the arrows indicates approximately relative current speeds between different parts of the area. Inshore the tidal currents oscillate back and forth and determine direction of river-water distribution, as modified by other factors.

CURRENT-PRODUCING AGENTS

It is impossible to learn the cause of a current from a single measurement at one place, because any current contains components related to all the different forces that affect the water mass. Causes of currents can be partly isolated and evaluated by making a number of serial observations at a single station over a period of time, and a more complete understanding can be obtained by several observations at several stations.

Hourly current measurements at long-period stations (Figs. 4, 5) and those distributed over the area (Figs. 2, 3) show the typical tidal-current alternation of flow direction in both surface and bottom waters. This alternation is diurnal in accordance with the diurnal character of tides in this part of the Gulf of Mexico, and flow normally is toward the sounds on the flood and toward the sea on the ebb. There can be no question that the principal components of the observed currents are due to tides.

If the current measurements for each long-period station are averaged to remove the tidal components insofar as possible, there still is a residual current at each station (Figs. 4, 5). In all instances, residual current in the surface layer was in the direction of the wind, and in most instances it was toward the open sea as well. At depths below the surface layer there also was a residual current, but it normally was of lower speed, was opposite in direction to the surface current, and usually was directed away from the sea.

If tidal currents were the only currents, there would be no net transfer of water over a tidal cycle. As long as the Mississippi continues to flow, there obviously also must be components of the currents that produce the net seaward transfer of river water.

When the wind blows, it transmits some of its energy to the water. In this way the wind causes the water to move and produces currents. A surface current in open water of 2–3 per cent of the average wind speed usually is predicted. This

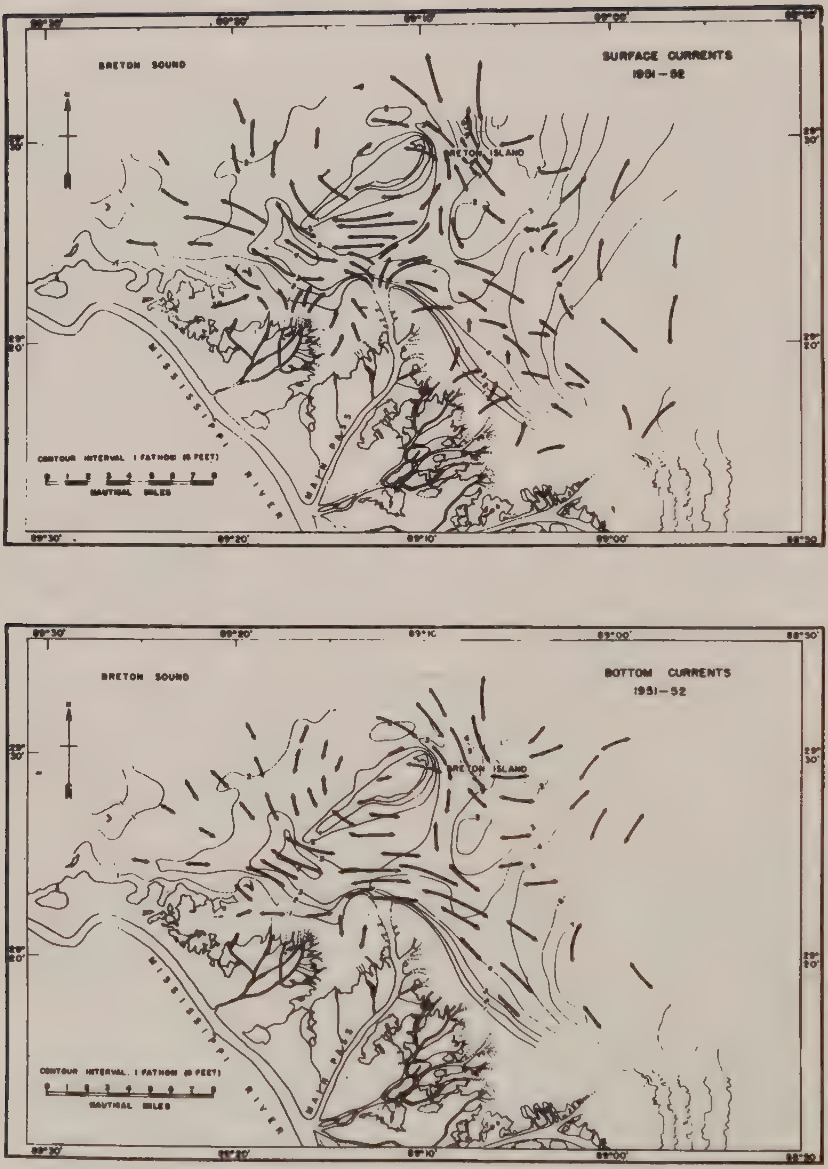
BRETON SOUND
SURFACE CURRENTS
1951–52
BRETON ISLAND
MISSISSIPPI RIVER
MAIN PASS
CONTOUR INTERVAL 1 FATHOM (6 FEET)
0 1 2 3 4 5 6 7 8
NAUTICAL MILES
89°30'
89°20'
89°10'
89°00'
88°50'
29°30'
29°20'
BRETON SOUND
BOTTOM CURRENTS
1951–52
BRETON ISLAND
MISSISSIPPI RIVER
MAIN PASS
CONTOUR INTERVAL 1 FATHOM (6 FEET)
0 1 2 3 4 5 6 7 8
NAUTICAL MILES
89°30'
89°20'
89°10'
89°00'
88°50'
29°30'
29°20'

FIG. 7.—Generalized pattern of inshore currents. Currents usually flow seaward on ebb tide, landward and toward Breton Sound on the flood. Where this occurs, arrows (indicating most likely current direction and relative strength), are double-headed. Surface currents near distributary mouths may differ in direction between flood and ebb. Where this occurs, arrows are single-headed.

is based on empirical relations developed through many observations (Sverdrup *et al.*, 1946, p. 494; U. S. Coast and Geodetic Survey Current Tables, 1951, p. 164).

Figure 8 shows the average residual surface currents from each of the long-period stations plotted against average wind speeds measured during the same periods of observation. The empirical predictions of current speeds produced by winds (2–3%) also are shown. All of the residual current components from several of the long-period stations are contained by the empirical predictions of current speed from wind. Three stations, however, had an additional component which, at station 143, was approximately twice as great as the predicted wind component. The excess of residual current in the brackish surface layer at these stations seems to be directly related to river discharge and a seaward transfer of fresh water, although at station 146 some of the apparent excess residual current may be due to secondary effects of wind.

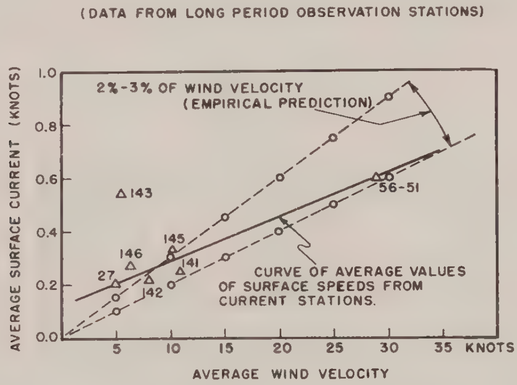

FIG. 8.—Average surface currents plotted against average wind speeds from long-period stations. Dashed lines enclose 2%–3% of wind speed. Wind speeds at stations 27 and 56 estimated.

These data show that currents generated by three agents dominate the inshore area. These current-producing agents are: (1) tides, (2) winds, and (3) river discharge. Other causes of currents seem to have relatively negligible effect.

Both wind currents and currents due to fresh-water discharge result in net transport of both fresh water and sediment and therefore are important factors in producing sediment distributions. Tidal currents also are an important agent for primary distribution of sediment, even though in restricted waters they are oscillatory and may not produce a net transport of water. Unlike solutions, suspensions tend to separate into their different components because of gravity. Thus, tidal currents that are transporting suspended sediment lose some of their load during the tidal oscillation. The net effect on sediment distribution is not the vector sum of two opposite actions; independent of other agents, tidal currents produce a primary, lateral, sediment distribution around the source that depends largely on the length and directions of the tidal excursion.

TIDAL CURRENTS

Tidal currents affect the lateral transport of water required to produce the rise and fall of the tide, and they flow in response to attractions of the moon and sun. In restricted areas they alternate in direction with changes in tide, but in the open sea they usually are rotary. The currents are associated with waves of long period and usually are uniform in speed throughout the water column.

Tides near the Mississippi Delta are diurnal, similar to those at Pensacola, Florida, that is, there usually is only one high and one low water in a day. A typical tidal curve at Pass a Loutre is shown in Figure 9. The tidal range at Pass a Loutre varies from about 2.5 feet to 0.2 foot and averages about 1.3 feet. The principal cause of variation in the tidal range of diurnal tides in the Gulf of Mexico is the changing declination of the moon (Marmer, 1954).

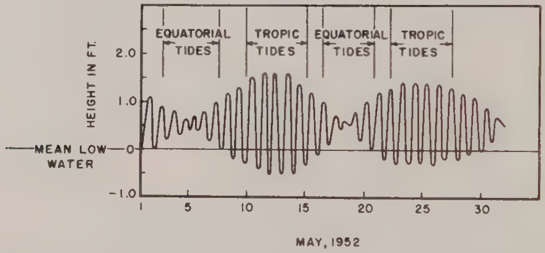

FIG. 9.—Typical curve of predicted tides at Pass a Loutre, showing variations in tidal range from day to day and fortnight to fortnight. Tide predictions are altered mainly by unpredictable variations in wind and river discharge.

At any one point the speed of tidal currents varies from hour to hour and from day to day. Tidal current speed through the cross section of a channel entrance to a more or less restricted body of water is related to the volume of water that must pass through the section to raise or lower the sea surface inside the channel by the required amount; it also is related to the time available for this transfer. The volume of water is determined by (1) the drainage area behind the section, which remains constant for practical purposes, and by (2) the tidal range, which varies widely. Figure 9, a typical tidal curve for one month at Pass a Loutre, shows the daily variations in tidal range which culminate in maxima (tropic tides) and minima (equatorial tides) at fortnightly intervals. The range also varies between successive tropic and successive equatorial tides (Fig. 9).

The time available for transfer of this varying volume of water also is a variable. In the diurnal, or daily, type of tide the average retardation in time between successive high waters or successive low waters is 50 minutes, as with the more familiar semi-daily type of tide. However, from one day to the next the retardation may vary from this average by several hours either way. This apparent irregularity is not a matter of chance but is due to the interaction of the different tidal components (Marmer, 1954).

These are factors that complicate the tidal current regimen. In general, the range of tidal current speeds is related to the total range of tides. Thus during periods of large tidal range (tropic tides) currents usually are large, while during periods of low tidal range (equatorial tides) currents are correspondingly smaller. These differences were observed at long-period current stations. Station 143 (Figs. 1, 4) was made during tropic tides (tidal range at Pass a Loutre: 1.5 feet) and currents at all depths, both ebbing and flooding, exceeded 1 knot (1 knot = 51.5 cm./sec.) and in some instances were almost 2 knots. In contrast, at nearby station 569 (Fig. 1), made during equatorial tides (tidal range at Pass a Loutre: 0.2 foot), currents did not exceed 0.6 knot and mostly were very low-speed drifts.

Hour-to-hour differences in tidal current speeds are due to the ever-changing stand of the tide. Speeds are minimum at maximum high and low water and are maximum midway between the extremes of tidal range. Station 142 (Fig. 4) best shows a typical time curve of tidal current speed. Maximum high water occurred at about 1230 when speeds at all levels were zero and the current direction changed. Ebb tide began, current speeds increased to maxima at about the midpoint of the ebb period, and then decreased to zero again at maximum low water, when current direction changed again. Figure 6 was drawn from current measurements made every minute and shows in detail how hourly measurements reflect the current.

Speeds of tidal currents at similar heights of the tide also vary areally. Especially high current speeds, due mostly to channel restriction, occur in the inlet between Breton and Gosier islands and in the inlets between Main Pass and Breton and Bird islands (Fig. 1). Current speeds are lower in the open water of Breton Sound (Figs. 2, 3).

The times at which high or low water actually occur depart widely from the predicted times at Pass a Loutre (Figs. 4, 5). This is mostly because of changing and unpredictable winds and river discharge.

WIND CURRENTS

The primary cause of wind currents is the stress exerted on the sea surface by air in motion, but an associated cause is the mass transport of waves. Freeman (1953, 1954) recently suggested that winds also can create current in a two-layer ocean by changing lateral density distribution through differential mixing of the surface and deeper layers. He computed the transport of such currents (in the surface layer only) may amount to 10–20 per cent of transport due to wind stress. In addition, currents that may extend down to considerable depths are produced and maintained by the wind when it piles up water against a coast or against an internal boundary in the ocean.

Figure 10 gives monthly average wind speeds, regardless of wind direction, at Burrwood, Louisiana, near the southern end of Southwest Pass (Fig. 17) for the period 1942–1945. These averages are based on almost 17,000 hourly observations. The average annual wind speed is 9.1 knots, and monthly averages range from a maximum of 11.4 knots in March to a minimum of 6.6 knots in June. Figure 8, the plot of residual current speed against average wind speed at long-period stations, shows that the wind currents of the inshore delta area are no less than the empirical prediction of 2–3 per cent of the wind speed. Thus, it appears that on the average there is a component of current in the surface waters that is due to winds, that ranges in speed from about 0.2–0.35 knot, and is variable in direction. This average wind current is additive to any other currents, and is positive when in the same direction and negative when in the opposite direction. It is at maximum during March and at minimum during June.

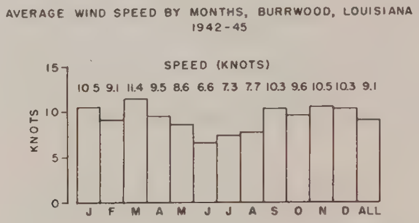

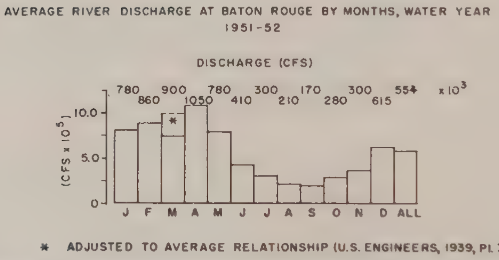

FIG. 10.—Average wind speeds and river discharge. Wind speeds obtained from U. S. Weather Bureau. Averages at Burrwood based on 16,787 observations. River discharges are monthly averages for water year 1951–52 (October to October) from New Orleans office, U. S. Engineers.

Figure 20 gives monthly resultant winds at Burrwood based on the same 1942–1945 data. The monthly resultant winds range in speed from about 5.5 knots in November to 1.6 knots in August and in direction from ENE[3] in December and January to SSW in July. The resultant of all winds for 1942–1945 was 2.3 knots from ENE toward WSW. The resultants show that the winds off

---

[3] It is customary to give wind direction as the direction *from which* the wind blows. Currents customarily are indicated by the direction *toward which* they flow.

Burrwood blow surface water mostly toward the west during all months except July.

Effects of storms.—Averages and resultants do not necessarily convey an accurate picture of instantaneous conditions, as many important details may be concealed. For example, at Burrwood the resultant wind for November is one of the largest (Fig. 20) and is made up generally of easterly winds with less frequent but much stronger northwesterlies and northerlies. The resultant for March, the month of highest average wind speeds, is appreciably less. However, the principal difference between these months is in the greater strength of the March easterlies (Fig. 18).

The period of strong northerlies and northwesterlies usually commences in late September and continues until April or early May. These winds are strongest and most frequent from November into March, and their effects on water movement are great.

Figure 5 shows the current results from three long-period stations made near Bird Island during and following "northers." During the observation period at station 56 wind speeds ranged from about 20 to 35 knots, and direction was almost constant. Tides at this time were tropic. Despite the large tidal range, the water flowed seaward before the wind during the entire 40-hour period of observation. The average current speed was greater than 0.5 knot. Because of the accompanying high waves, the seaward flowing water was heavily charged with suspended sediment stirred from the bottom of Breton Sound. At station 141 (Fig. 5), made in April during a weak norther (average wind speed 11 knots), the current flowed seaward during the period of ebbing tide, but the flood current that normally would follow was canceled by the northwest wind. Average surface current was about 0.25 knot, SSE (seaward).

Removal of surface water from partly enclosed areas by strong winds lowers their water levels. This can be observed all along the Gulf Coast during northers. This tendency apparently is offset partly during the storm by a compensating current in deeper water that flows into the affected area. Station 142 (Figs. 1, 4) was made in 22 feet of water in Breton Island-Bird Island inlet during the final stages of the weak April norther, and it shows an average current directed into Breton Sound below a depth of about 6 feet. Station 27 (Fig. 5), made immediately following a strong norther, also shows an average current into the sound. This current is somewhat stronger than would be expected from the existing winds and may have resulted partly from the hydraulic head produced by partial emptying of Breton Sound during the storm.

Effects of wind on current direction.—Hourly measurements of current velocity show that they fluctuate in direction as well as in speed (Figs. 4, 5). The amount of fluctuation from the average current direction also apparently is related to wind. Apart from alternation of current direction with alternation of tides, deviations of current directions from the direction of average wind are much less when the winds are strong than when they are weak, and usually are much less

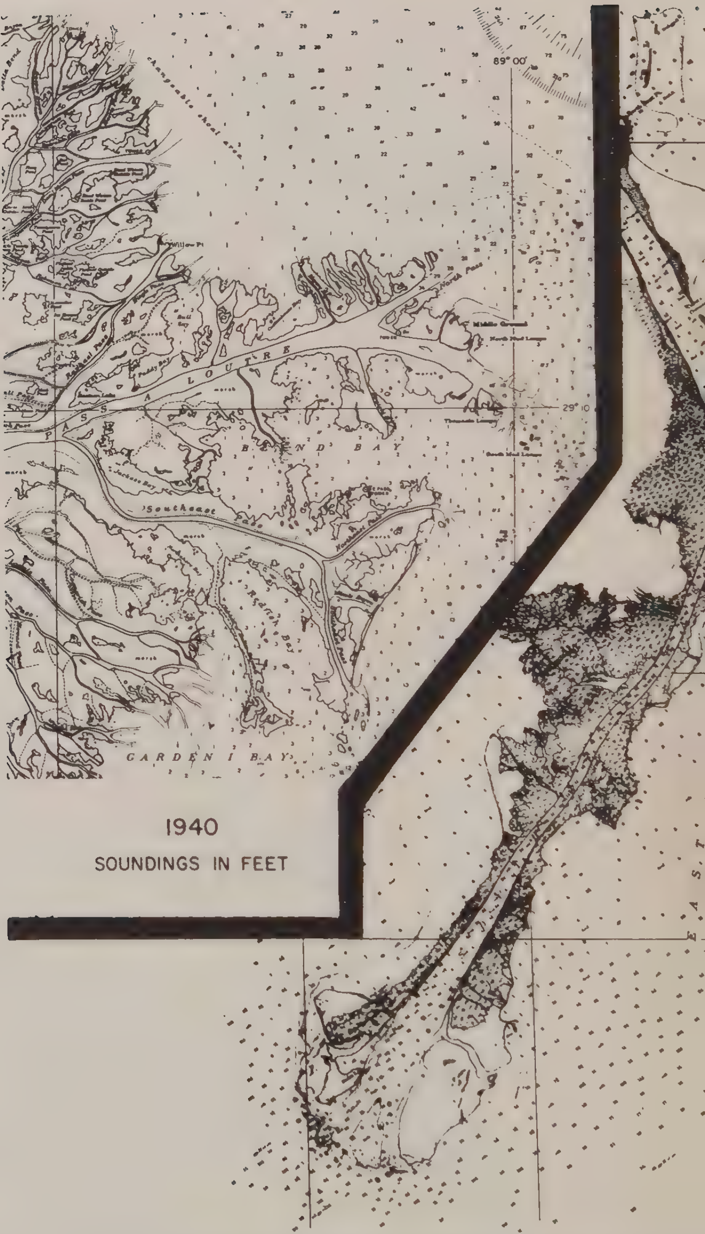
1940
SOUNDINGS IN FEET
89° 00'
29° 10'
PASS A LOUTRE
BLIND BAY
Southeast Pass
Redfish Bay
GARDEN I BAY
Willow Pt
Middle Ground
North Pass

FIG. 11.—Form of undredged distributary mouths. Note position of channel-mouth bars, te
seaward direction. These f

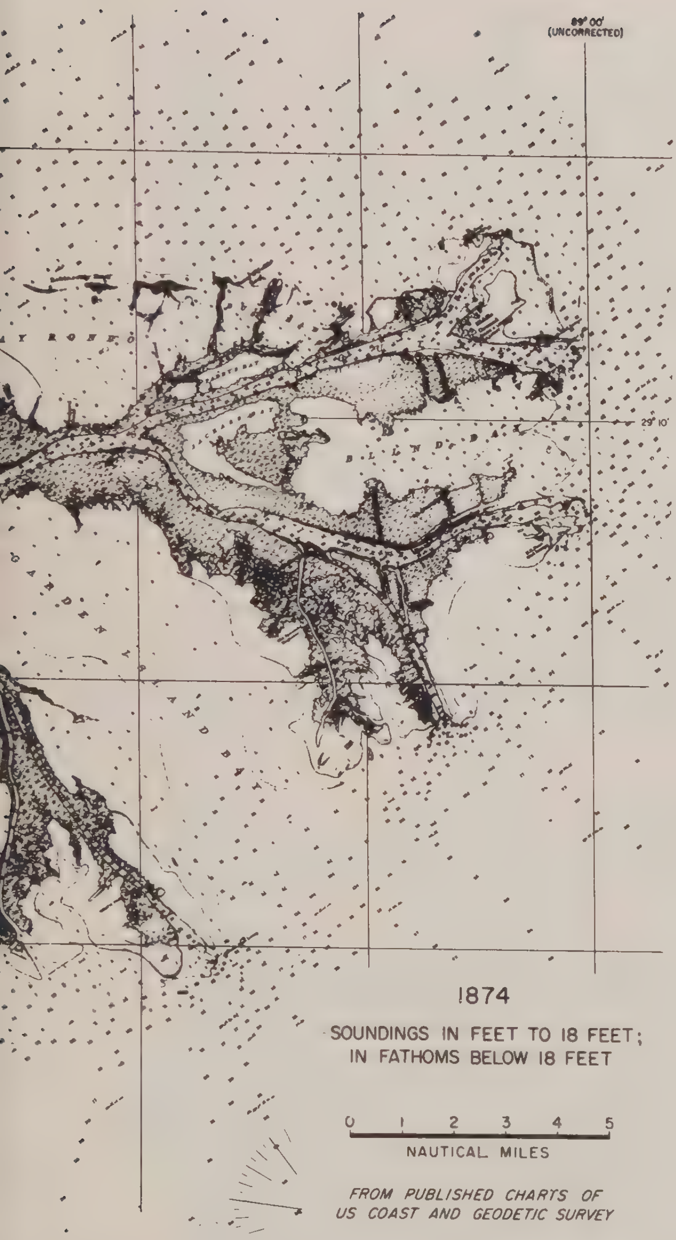
89° 00'
(UNCORRECTED)
29° 10'
BAY RONDO
BLIND BAY
GARDEN ISLAND BAY
1874
SOUNDINGS IN FEET TO 18 FEET;
IN FATHOMS BELOW 18 FEET
0 1 2 3 4 5
NAUTICAL MILES
FROM PUBLISHED CHARTS OF
US COAST AND GEODETIC SURVEY

natural levees producing a belled shape, and channel-bottom ramps sloping upward in
at Southwest Pass.

when the current and wind are in the same direction than when they are opposed. This is illustrated by a comparison of stations 56, 27 (Fig. 5), and 143 (Fig. 4). Current directions at 56 fluctuated through only 40°, and wind speed averaged almost 30 knots. At station 27 winds were light toward the west. The ebb tide flowed opposite to the wind and fluctuated through 140°, while the flood tide, flowing with the wind, had a range of only 45°. At station 143 (Fig. 4) flood tide opposed the light winds and fluctuated through 105°, while the ebb tide, flowing with the wind, fluctuated through 80°.

Station 146 (Fig. 4), made in open water south of Gosier Island (Fig. 1), shows that other factors must be considered, however, since the greatest angular fluctuation here occurred when ebb tide and winds generally were in the same direction.

In the shallow water of the inshore area none of the measurements shows any persistent tendency for the water to flow to the right of wind direction. Tidal currents, wind directions, land boundaries, and channel configurations apparently control current directions.

Changes in wind direction and speed produce corresponding changes in currents. As with tidal currents, changes of wind current result in a primary distribution of suspended sediment about the sediment source. This net distribution is not the long-time vector sum of wind currents. Rather it is the net result of day-to-day conditions whose effects only partly are understood through long-term averages and vectors. The results of winds blowing in one direction on a sedimenting system are irreversible; they are not offset by following actions, even though the following actions are equal or greater in magnitude and opposite in direction.

CURRENTS DUE TO FRESH-WATER DISCHARGE

The problem is to determine the nature of currents related to river discharge: what causes them and what limits or controls them. The currents behave differently in distributary channels than they do after river water discharges into the gulf.

In distributary channels and near the mouths.—Under moderately high discharge conditions (Fig. 12, left-hand profiles) the entire volume of the distributary channel upstream from the bar was filled with seaward-flowing water. Current speeds at all levels increased downstream toward the bar, were highest just seaward of the bar crest, and decreased rapidly with increasing distance seaward (Fig. 12). Highest speeds at the surface occurred just seaward of the bar crest where the vertical chlorinity gradient was the sharpest. This increase in current speed over the bar demonstrates that the distributary channel exerts control on flow throughout the channel length. It also shows that the wide, shallow channel over the bar is a relatively inefficient conduit (see caption, Fig. 12).

Downstream in the gulf there was a decrease in sharpness of the vertical chlorinity gradient corresponding with the decrease in surface current speed. Going seaward, thickness of the surface layer of fresh and brackish water thinned

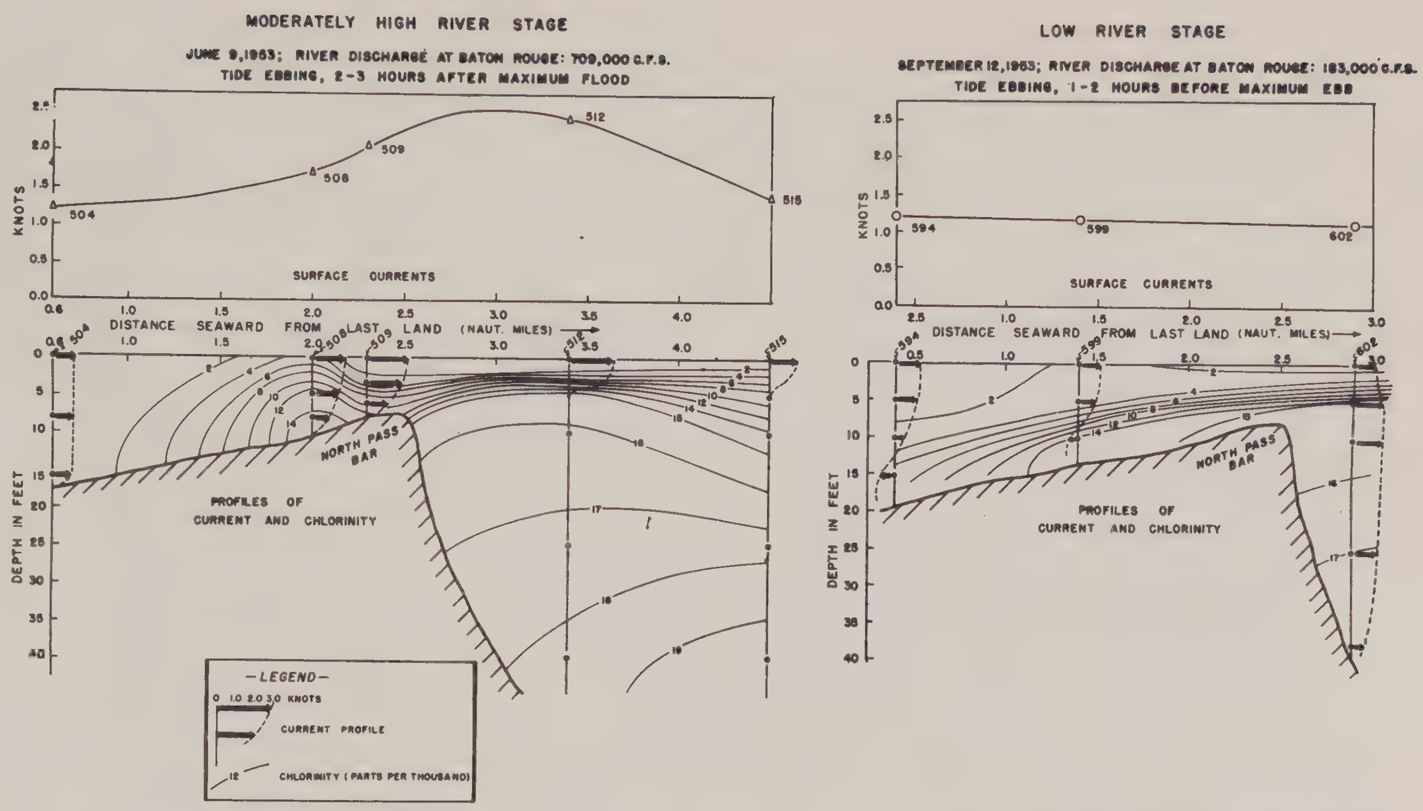

Fig. 12.—Profiles of current speed and chlorinity in North Pass and seaward of bar. Upper diagrams are plots of surface speeds along channel axis. Left-hand diagrams (moderately high river) show river flow "feeling" the bar. Flow is accelerated over bar. Since mass remains constant, force must be increased. This can only result from increase of pressure due to partial ponding upstream from bar. Maximum current speed occurs slightly downstream from bar crest, normal for continuous flow over sharp edge and surface of discontinuity. Tremendous eddies form immediately downstream from bar crest, the sharp edge. Salt water intruded during previous high tide but was rapidly flushed on ebb. Right-hand profiles show current is not affected by bar at low river. River water rides out over salt wedge, and speeds decrease smoothly in channel and over bar. Deep gulf water, flowing faster than issuing river water, carried river water south and west. Compare with suspended matter profiles, Fig. 43.

from a maximum of about 8 feet, its chlorinity increased, and chlorinity of the underlying water decreased. At most stations seaward of the bar there was no measurable current at depths of 5 feet and below.

Figure 13 shows the areal distribution of currents measured at the same times the profiles were made. Under moderately high discharge conditions (spring, 1953), current velocities seaward of the bar were variable, but there was a general lateral spreading of surface water. Turbid fresh water was widely distributed on either side of the distributary mouth. The course in the gulf followed by the thread of maximum current speed was sinuous, and there was a general set toward the east and south.

No channel axis current and chlorinity profiles were made when river discharge was very high; nevertheless, numerous single observations in several distributary mouths demonstrated conclusively that under very high discharge conditions no sea water enters undredged channels, and fresh water flows seaward at all depths, regardless of tide.

At low river stage on the channel axis the surface fresh water flowed seaward over a layer of denser, upstream-moving salt water (Fig. 12). There was a smooth continuous decrease of current speed in the surface water in the channel and over the bar. Seaward of the bar the surface layer of fresh water became thinner (Fig. 12) and spread laterally (Fig. 13, late summer, 1953). At the time

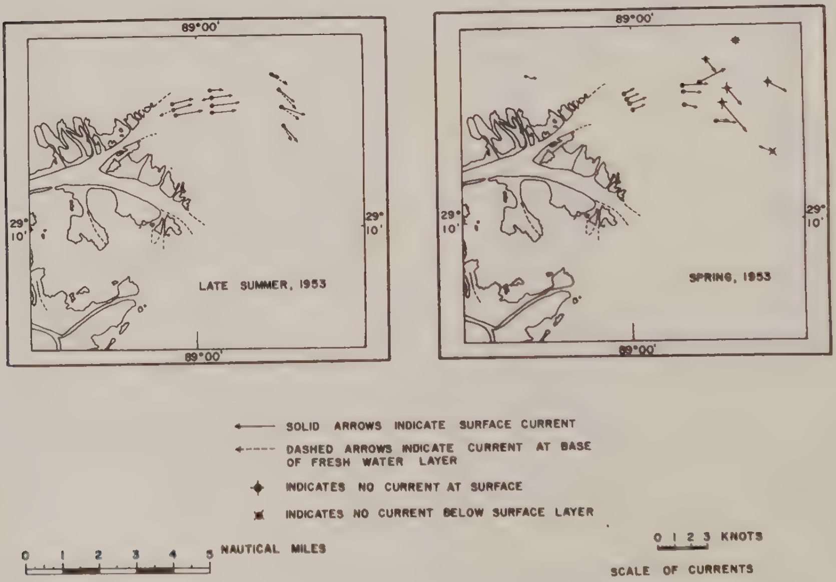
89°00'
29° 10'
29° 10'
LATE SUMMER, 1953
89°00'
89°00'
29° 10'
29° 10'
SPRING, 1953
89°00'
SOLID ARROWS INDICATE SURFACE CURRENT
DASHED ARROWS INDICATE CURRENT AT BASE OF FRESH WATER LAYER
INDICATES NO CURRENT AT SURFACE
INDICATES NO CURRENT BELOW SURFACE LAYER
0 1 2 3 4 5 NAUTICAL MILES
0 1 2 3 KNOTS
SCALE OF CURRENTS

FIG. 13.—Distribution of currents in North Pass and seaward of bar during low river (late summer, 1953) and moderately high river (spring, 1953).

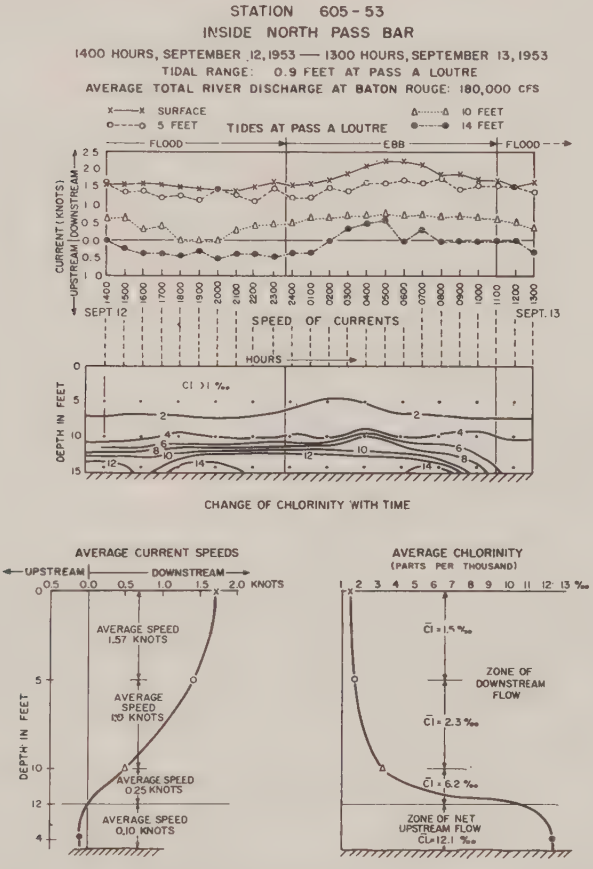

FIG. 14.—Salt-wedge observations. Hourly changes and averages of current speed and chlorinity at different depths inside North Pass bar during low river. Tides at Pass a Loutre refer to times predicted by Tide Tables.

these measurements were made there was a pronounced deep current in the gulf flowing southward (maximum of 1.3 knots near the surface, decreasing with depth to 0.7 knot near the bottom). This current was part of the large-scale circulation in the northeastern gulf and existed at all depths. Direction of the effluent river current merged close to the distributary mouth with the direction of the underlying open gulf current (Fig. 13).

The salt wedge.—At high river discharges the distributary channels are completely filled at all times with fresh water flowing seaward out to and over the crests of the bars. However, when river discharges are low, only a small fraction of the volume of the channels is required to transmit the fresh water sea ward. Heavy salt water buoys up the river water and flows into the river channel, where it may extend upstream for many miles. This layer of salt water underlying fresh river water is called the salt wedge.

When the salt wedge is present the surface water flows seaward, but currents in the underlying salt water ebb and flood with changes in the tide and normally are gentle.

The low-river profile of Figure 12 shows that the salt wedge was present at the time the measurements were made. Currents in the bottom water were upstream, and those in the surface layer were downstream. The measurements for Figure 14 were obtained at a North Pass long period observation station under similar low river stages. This figure shows hourly currents at 0, 5, 10, and 14 feet, average currents, changes of chlorinity with time, and average chlorinity.[4] Wind speed averaged about 2 knots during the station.

Current speeds were highest in the surface water and were downstream at all

---

[4] These measurements make it possible to calculate approximately the discharge of North Pass and the proportion of total river discharge carried by it.

(1) Effective width of channel at station 605 = 90,000 cm.
(2) Average effective depth of channel = 300 cm.
(3) Average downstream speed = 55 cm./sec.

$$55 \times 300 = 16.5 \text{ L/sec./cm. downstream}$$

$$(16.5) \times (9 \times 10^4) = 1.485 \times 10^6 \text{ L/sec.}$$

$$= 53{,}000 \text{ CFS, total discharge at North Pass.}$$

At the time of this station, Mississippi discharge past Baton Rouge was about 183,000 CFS (cubic feet per second), the salt wedge extended upstream at least as far as Buras, Louisiana, and the outflowing river water contained an average of 2.6 g./L of chloride. Therefore total discharge in the surface layer includes river water and intruded seawater. If we assume there was a steady state, and that the chlorinity was due entirely to intruded water (of $12\,^{\circ}/_{00}$ on the average, Fig. 14), then,

$$16.5 \text{ L/sec./cm.} \times 2.6 \text{ g./L} = 43 \text{ g./sec. discharged,}$$

or

$$\frac{43 \text{ g./sec.}}{12\,^{\circ}/_{00}} = 3.6 \text{ L/sec. sea water discharged}$$

therefore,

$$\frac{3.6}{16.5}, \text{ or } 22\% \text{ of discharge is sea water,}$$

and there is

$$53{,}000 - (.22 \times 53{,}000) = 41{,}000 \text{ CFS of river water discharged}$$

$$\frac{41{,}000}{183{,}000} \cong 20\% \textit{ of total river discharge.}$$

The U. S. Engineers variously estimate the discharge of Pass a Loutre at Head of Passes to be 35–40% of total river flow (U. S. Engineers, 1939, p. 6; Holle, 1952, p. 119). Pass a Loutre Crevasse and Southeast Pass are relatively small, and the mouth of Pass a Loutre is obstructed by mud lumps. Therefore, the figure of about 20% seems to be reasonable and is more likely to be too great than too small.

These data also show that about 10 liters of sea water are discharged through North Pass for each liter that enters. The excess must enter through the deeper distributaries, probably mainly through South and Southwest Passes which are dredged for navigation. Mixing probably occurred mostly in the river above Head of Passes.

times. They were at maximum during the period of ebb tide, and averaged about 1.75 knots downstream. In the bottom water, current was directed upstream during the flood period and during part of the ebb period. It reversed and flowed downstream for 4 hours when the downstream current above was highest, but averaged about 0.20 knot upstream at the bottom (14 feet). Currents were intermediate at intermediate depths.

Chlorinity changes at each level were small from hour to hour. Surface chlorinity was uniform, about one to two parts per thousand; chlorinity in the bottom water was greatest near the middle of the flood period and least at the end of the ebb, just prior to beginning of flood tide.

These observations show the salt wedge to be a layer of salt water that oscillated up and down stream with tidal changes. In addition to the tidal oscillation, it had an average current directed upstream for one day. If the wedge was in a steady state at this time, the net upstream movement probably was caused by salt water flowing into the distributary to replace losses at its top through mixing with the outflowing surface layer of river water.

The phenomenon of salt-water intrusion also has been found in Main Pass, Pass a Loutre, and Baptiste Collette Bayou (Fisherman's Pass). It occurs regularly in undredged distributaries and is not restricted to dredged passes.

Although no long-term serial observations on the salt wedge in the Mississippi have been reported on before, intrusion of salt water into undredged distributary mouths and far up-river was described by all early workers in the delta since the original surveys (Humphreys and Abbot, 1876, pp. 476–78, and App. A, Repts. to Capt. Talcott by Sidell and Meade, 1838, and App. G, Repts. of Forshey in 1851 and Fuller in 1859–60; Ellet, 1850; Hilgard, 1871; Forshey, 1877). More recently Dent (1928) described some features of the salt intrusion, and Russell (1936) pointed out its effect on river chlorinities as far upstream as Baton Rouge. Rhodes (1950) and Simmons (1952) described the behavior of the salt water from experiments on models of Southwest Pass. Stommel and Farmer (1952) and Farmer and Morgan (1953) undertook theoretical studies of salt-water intrusion into Southwest Pass. Holle (1952) described other observational data, and Bates (1953) discussed the phenomenon.

There is a range of river discharges between high stages (when the wedge is never present) and low stages (when it is always present) where the salt wedge is alternately intruded and extruded by variations of tide and wind. This range was called "Transitional" by Humphreys and Abbot (1876, p. 477). Data for Figure 12, Moderately High Discharge, were collected under transitional conditions. The profile shows the salt wedge actually being extruded from North Pass by fresh-water discharge and ebbing tide. Samples collected 2 hours later just inside the bar contained no salt water.

The river discharge volumes that determine which condition shall exist differ between distributaries and for differing tide and wind conditions. High tides promote salt-wedge intrusion. Small distributaries such as Baptiste Collette

Bayou tend to admit salt water at higher total river discharges than do larger distributaries. Greater maximum depths over the bar also permit salt intrusion at higher river stages. Thus, at Pass a Loutre salt water enters through the deep scour channels flanking mud lumps at river discharges high enough to prevent its entrance over shoaler North Pass bar. Favorable winds also cause intrusion of salt water, and under some conditions, may cause an upstream current at the river surface (Humphreys and Abbot, 1876, App. G, p. 617).

From study of undredged distributaries, it seems that salt-water intrusion is prevented by river discharges above about 750,000 to 800,000 CFS[5] (cubic feet per second), and that the salt wedge is present continuously in the distributaries when river discharge is below about 300,000–250,000 CFS. The transitional condition exists when river discharges are intermediate. Variations in size of distributary, in maximum depth over the bar, in wind, and in tide affect these values. The inefficient channel over the bar is the critical point; it is the "valve" through which any salt water must enter.

By comparison, Blackman and Lindner (1952) found that Mobile River discharges greater than 50,000 CFS excluded the salt wedge from this river. There does not seem to be a transitional stage in the Mobile River.

Hydraulics of distributary mouths.—Figure 11 was made from the U. S. Coast and Geodetic Survey charts of the Mississippi Delta issued in 1874 and 1940. These charts were made prior to any large-scale improvements for navigation and show undisturbed natural levees and bars at all the major Mississippi distributaries. Natural levees (the channel sides) decrease in height toward the sea and eventually slope below sea-level. They continue to slope seaward but define channels seaward as far as the bars. At the seaward ends of the channels, the levees flare widely outward from the channel axes, and the distributary mouths have a belled shape. This is best seen at Southwest Pass on the 1874 chart, but is clearly apparent at the others (as, North Pass, 1940). At Southwest Pass the outward flarings of natural levees began well upstream from the point where the levees pass below gulf level.

Although our detailed observations were made at North Pass, they undoubtedly represent conditions at all the simple distributary mouths, since the forms of undredged distributary mouths are the same. Upstream from the bars, flow is in confining channels; in the gulf downstream from them, river water spreads laterally and thins. Flow in the distributaries is confined by the sides of the channels and may also be confined by the bottoms. Under high-discharge conditions the bottom and sides of the channel constitute the boundaries. Under low-discharge conditions the boundaries are the sides of the channel and the underlying layer of salt water. Although the bars have the form of sills in longitudinal profile, nevertheless at the outer ends of the distributaries they are the deepest parts of the channels, are on the current axes, and are the loci of maximum fresh-water discharge.

---

[5] Holle states (1952) that approximately this same volume of flow completely fills Southwest Pass.

It has been shown that the channel over the bar is a relatively inefficient one, however, causing the discharge during high river to be accelerated over the bar. Since the mass of issuing river water remains relatively constant over short periods of time, this local acceleration must be due to a local concentration of force. Local concentration of force can only come from partial ponding behind the bar. Partial ponding alters the field of pressure in the river, flattening the pressure gradient upstream and steepening it directly over the bar.

These considerations also show that the bar crest and seaward limits of the submarine natural levees constitute the discharge orifices for the distributaries. The orifices are best defined in flood stage, and the areas immediately seaward of the bar crests are the sites of wild turbulence, great eddies, and awesome whirls, produced when the full force of a mighty river first meets the sea.

Topographic features at distributary mouths.—The topographic features of distributary mouths are produced by existing hydraulic conditions. Bed load of the river can only be transported when the salt wedge is absent or when it is being expelled, because there is little or no seaward bottom current in distributary channels when it is present. Times of high river and no salt wedge are the only times of extensive dredging by the U. S. Engineers at the mouths of South and Southwest passes. At times of low discharges, suspended sediment settles from overlying river water into the sluggish salt wedge throughout the entire length of the wedge. Below the upstream end of the wedge this is fine-grained sediment, and it forms a soft watery deposit, both on the channel bottom and where it collects in the gulf seaward of the bar. Upstream from the bar most of this sediment is a temporary deposit that is swept into the gulf by the strong seaward bottom currents of the next high river stages.

Distributary mouth bars are similar to wind-blown sand dunes in origin and behavior. The only sediment permanently added to the bar is carried out of the channel and deposited on the bar's seaward-sloping face. At high river very near the top of this face some deposition is from traction, but farther seaward and at low river, deposition is all from suspension. Thus there is great seasonal fluctuation in the particle size of sediment added to the bar. Coarser material is added during high river stages, and fine material is added during low water. This kind of deposition builds the bar seaward, and the seaward face corresponds with the downwind depositional face of a wind-blown dune. Inside the channel, the bottom slopes smoothly upward in the downstream direction and crests at the bar. This downstream slope is the plane upon which river water ascends to meet dense gulf water. The smooth upward slope to the sea is like the upwind side of a dune —during high river it is an erosion surface and a ramp up which bed load moves, and during low river it is a temporary deposition surface for fine sediment. The ramp continually advances downstream as the bar advances seaward and the channel elongates, and the rate of downstream advance of the ramp is the same as seaward bar advance and channel elongation (Humphreys and Abbot, 1876; Forshey, 1877).

The bell-shaped outward flarings of natural levees at their seaward ends are depositional features. They form along the margins of maximum current in response to two situations. First, at similar current speeds, the channel must progressively widen downstream as it shoals toward the bar crest in order to accommodate the same volume of discharge. Second, in the gulf, dense sea water below buoys up the entering lighter river water and causes the surface layer to spread laterally. This spreads out still farther the margins of maximum current.

The flaring natural levees advance downstream just as do the bar and ramp, and the channels narrow upstream (Fig. 11). Erosional deepening of the channel with seaward advance of the bar and ramp improves its transporting efficiency by decreasing boundary friction. The thread of maximum current gradually narrows and moves in toward the channel axis. Deposition of sediment occurs on the margins of the channel. In this way the distributary channel adjusts itself from a wide, shallow, inefficient conduit at the mouth to a relatively deep and narrow efficient conduit upstream (Fig. 11). Narrowing of channels upstream from the bars because of deposition probably occurs mainly during lower river stages.

The current data and related occurrences discussed show that the shapes and sizes of distributary mouths develop during and in response to high river discharge. Only during high river discharge is full channel volume needed to carry river flow. Only then is the entire channel perimeter in contact with river water swiftly flowing downstream. Bar depth is determined by the amount and character of river load and by density differences between river and gulf water, both of which tend to close the channel, and by the force (volume and speed) of emerging river water which tends to keep it open. It is an equilibrium depth produced by a balance between forces tending to choke the channel and those tending to maintain it. Because it represents an equilibrium, bar depth is sensitive to any differences or changes in controlling factors. The most pronounced variable between distributaries is volume of discharge; bar depth bears a direct relation to distributary discharge, varying from a few inches for small distributaries to approximately 10 feet for Southwest Pass (Fig. 11, 1874). Discharge of any particular distributary also may change with time. Recognition of this equilibrium shows why older distributaries such as Balize Bayou and Southeast Pass choked up when part of their flow was diverted. The bar width also is related to the same factors. These related topographic features—distributary mouth bars and flaring natural levees—are equilibrium land forms produced by deposition and erosion to meet hydraulic conditions where light sediment-laden water flows into and over dense water.

At the mouth of Pass a Loutre and some other distributaries, mud lumps complicate the conditions (Fig. 11). Where mud lumps occur on the submarine natural levees, they help to define the channel. Where they occur on or near the bars, they impede discharge, but usually are flanked by deep, narrow, scour channels. These conditions at the mouth of Pass a Loutre cause more complex discharge relationships than at North Pass mouth.

Large simple distributaries apparently tend to elongate seaward in a more or less straight line as a simple, unbifurcated channel. Both Southwest and South passes have followed this tendency for several hundred years (Fisk, 1952). Apparently simple bifurcation occurs occasionally, however, as where Pass a Loutre divided into North Pass and Pass a Loutre (Fig. 11). Simple distributary bifurcation seems to be something of an accident. It may be caused by mud lumps at the mouth splitting the channel (as at Pass a Loutre now), or perhaps by a large log jam collecting on the bar and disrupting flow (Trowbridge, 1930).

Many of the bifurcations of major distributaries have had a much more complicated history than this, as pointed out by Russell (1936, pp. 27–40). They apparently have been produced over some period of time by several events. For example, study of very old charts shows that Balize Bayou (now choked up) was once a major distributary of the Pass a Loutre system. Southeast Pass, below the head of Balize Bayou, also carried much of the water. During this time Pass a Loutre, below the head of Southeast Pass, was an unimportant crevasse similar to Cubitts Gap (Fig. 11). The crevasse, which is now lower Pass a Loutre, increased its discharge and was extended seaward rapidly, and Southeast Pass (including Balize Bayou) then began to diminish in importance. This history of bifurcation and the development of lower Pass a Loutre is not apparent from inspection of a modern chart; it may be representative of a common mode of origin of large bifurcations.

SEAWARD OF DISTRIBUTARY MOUTHS, RESIDUAL MOMENTUM CURRENTS

Fresh water emerges over the distributary mouth bar into the gulf with an initial speed that normally is between 0.5 and 3.0 knots, depending on river discharge and state of tide. Off some distributaries, this range of speeds often occurs in one tidal day.

The momentum associated with its issuing speed is a property of the river water. Therefore, downstream continuation of speed due to conserved momentum depends on preserving the fresh surface layer. The distance downstream in the gulf to which the issuing speed (or some part of it) due to momentum is maintained depends on the effectiveness of factors that mix fresh and sea water and interchange their properties. For example, a sample of mixed water containing 6 parts per thousand of chlorinity is composed of about two parts of river water and one part of sea water. Since change in salt content is an index to change in momentum, the initial momentum of the river water has altered by at least one-third to conform with the sea, and to this extent its behavior has changed, independent of other factors.

Vertical stability in the water column reduces vertical mixing, and is produced by large density differences. There is little stability in a water column with low density differences, and vertical mixing occurs easily. Figure 15 consists of temperature-chlorinity diagrams from data collected near Main Pass mouth. It shows the differences of density structure, and therefore vertical stability, that occur in this area under different conditions of wind and river discharge. (σ_t is related to the water density since $\sigma_t = (\rho_{Cl,T,O} - 1)1000$, where $\rho_{Cl,T,O}$ is the water density at chlorinity Cl, temperature T, and atmospheric pressure; see Fig. 26).

At high river discharge and low wind (station 143, Fig. 15) vertical stability was pronounced. Surface chlorinities ranged from about $3^{\circ}/_{oo}$ to $9^{\circ}/_{oo}$ (about $\frac{1}{7}$ to $\frac{1}{2}$ sea water), and surface flow, confined to a layer $1\frac{1}{2}$ to 3 feet thick, was directed seaward most of the time (Fig. 4). There was a net landward drift in the bottom water. Under the same high river conditions but with moderate

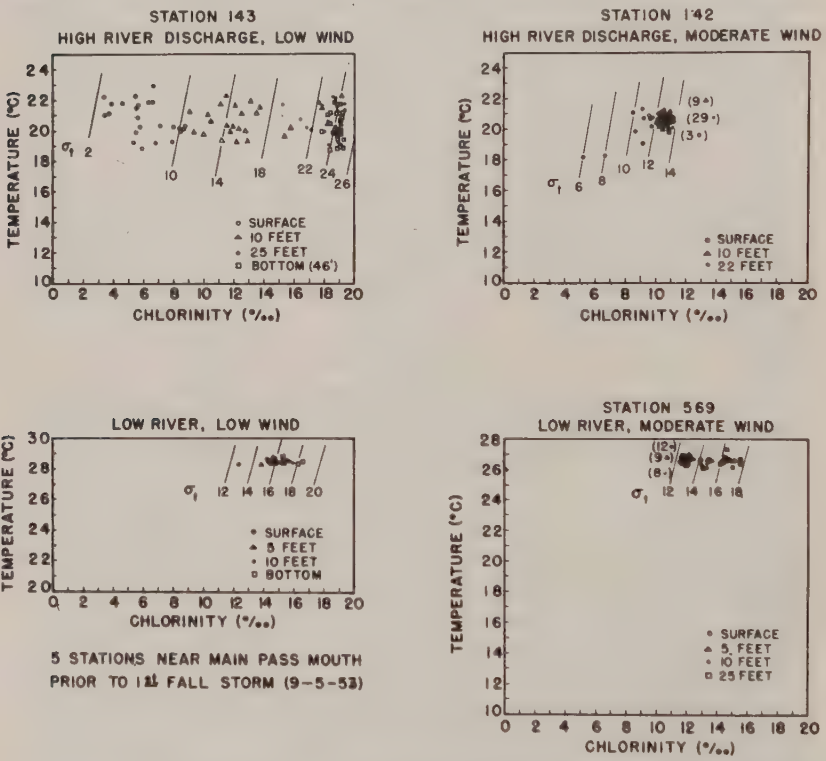

FIG. 15.—Variations of density structure near Main Pass mouth. Large differences of σ_t between depths indicate stable vertical density structure; small σ_t differences between depths indicate unstable structure.

winds (station 142), the water column was well mixed and had little vertical stability. The net seaward drift in the surface water at station 142 apparently was due to wind and was compensated by soundward drift at depth. When the river was low, the water column had little vertical stability with either low or moderate winds (station 569 and 5 stations near Main Pass mouth).

Figure 28 in a later section shows changes of chlorinity with time at stations 142 and 143. The wind had been strong, but lessened to moderate during the first part of the time when station 142 was occupied, continued to lessen toward the end of station 142, and was low during station 143, which immediately followed. A rapid redevelopment of vertical stability accompanied the lessening of wind; this is shown in Figure 28 as a progressive redevelopment of a strong chlorinity gradient. By the end of station 143, the chlorinity gradient was very strong, about 1.3°/oo per foot.

Vertical wind mixing is accomplished by waves, wind stress, and the turbulence of wind currents. These data demonstrate that when the wind is stronger than moderate, the fresh surface layer is destroyed near Main Pass mouth regardless of the volume of river water being discharged. However, it is soon recreated after cessation of the wind when discharge is high. When river discharge is low, the surface layer is mixed with sea water and destroyed very near Main Pass mouth regardless of wind strength.

The profiles of Figure 12 show downstream differences in speed of the surface effluents when the river was high and when it was low. These differences apparently depend on relative speeds of the surface and deeper waters. At moderately high river stage there was no current in the gulf, and the speed of fresh water issuing from the distributary was high relative to the underlying water (Fig. 12, left-hand diagrams). High relative speed between the two layers causes friction, great vertical turbulence, and promotes rapid vertical mixing of fresh and salt water.[6] Current speeds in the surface layers decrease rapidly seaward under these conditions, and the surface layer of fresh water quickly loses its identity.

At low river, there was a pronounced south-directed current in the gulf (Figs. 12, 13). When the speed of tidal or other ocean currents is high, they control the direction of flow of the surface layer (see also Figs. 2, 3 near Main Pass). Because there is correspondence of flow directions of surface and deeper layers, relative speed of the two layers is reduced greatly. This reduces friction between the layers, reduces the vertical turbulence and the rate of vertical mixing, and therefore reduces the rate of destruction of the surface layer. When there is a current in the gulf, the thin surface layer may persist downstream for a considerable distance, floating on moving gulf water. Depending on speed of the gulf current, speed of the surface layer may be similar to, or *even greater than*, issuing speed for many miles downstream..

Data for the chlorinity profiles (Figs. 29 and 30) were collected when temperatures were uniform. Therefore, these chlorinity profiles also are approximate density profiles. They show changes that occur from place to place and time to time near Main Pass mouth. During the May, 1952, traverse (Fig. 29), winds were low, river discharge was high, and currents were flowing northwest and north through the inlets into Breton Sound. The density gradient was strong directly off Main Pass mouth where most of the fresh water flowed in, but decreased progressively in the directions of flow. The chlorinity profile in Figure 30 was made parallel with, and in the same area as, profile *AA′* of Figure 29, but river discharge was about average (600,000 CFS) and the tide was ebbing toward the open gulf. This profile also shows that the density structure was most pronounced directly off Main Pass and progressively decreased downstream.

---

[6] The absolute values of the chlorinity (density) gradient are high at these staions, but, more important, the downstream rate of gradient decrease is high.

Such decrease in vertical stability downstream from the distributary mouth is caused by mixing that is partly due to friction between layers of different velocity and partly due to vertical turbulence of the tidal current. The surface layer ultimately is destroyed by mixing induced by any motion, but it is destroyed most quickly when the motion is large relative to that of the underlying salt water.

Therefore, the principal agents or happenings that destroy the low-density surface layer and/or dissipate its momentum are: (1) lateral spreading and thinning of fresh water seaward of the distributary mouth bar, (2) vertical and lateral mixing due to winds, and (3) mixing through turbulence caused by water motion, particularly when there is a gradient of velocity between the surface layer and the underlying sea water. The reverse conditions, namely, no wind and no velocity gradient, tend to preserve the surface layer established by river discharge. Scruton and Moore (1953) showed that the discharge from each major distributary tends to persist as a discrete plume downstream in the gulf when the plumes go east. From these conclusions, it can be seen that the distance seaward each plume persists is related to the volume discharge of its particular distributary.

Destruction of the surface layer dissipates its initial momentum, and residual momentum currents become insignificant. When conditions are unfavorable for its preservation, the surface layer is destroyed completely within less than one mile downstream from Main Pass mouth. Momentum currents become undetectable within a few feet of the mouths of the very small distributaries.

When the left-hand profile at North Pass for Figure 12 was made, river discharge was moderately high and winds were light, but there was no deep current in the gulf. Therefore, conditions were not ideal for preservation of the surface layer. Current speed was due mainly to momentum where the measurements were made, and if the curve of surface speed against distance (Fig. 12, upper left diagram) is extrapolated, it intersects the line of zero speed about 5–10 miles seaward of the distributary mouth. This suggests that residual momentum currents persisted seaward about 5–10 miles under these conditions, although this estimate may be subject to considerable error.

When conditions off large distributaries are favorable for surface-layer preservation, a current due to the residual momentum of fresh water persists farther than this downstream. The Pass a Loutre system (North Pass and Pass a Loutre) is the largest of the Mississippi's distributaries (35–40% of total river discharge versus 30% for Southwest Pass, U. S. Engineers, 1939; Holle, 1952), and the Pass a Loutre system acts as a unit in developing a plume (Scruton and Moore, 1953, Fig. 1; this report, Fig. 42). Relative motion between the surface layer of fresher water and the adjacent and underlying sea water produces features termed convergence or foam lines (*op. cit.*, p. 1070). They usually are caused by a higher speed in the fresher-water surface layer relative to the adjacent sea water, due partly to residual momentum. Convergence lines were observed from an aircraft seaward to a distance of about 20 miles in the turbid plume off the Pass a Loutre system. They were not seen farther downstream than this.

These observations are interpreted to mean that adjustments of speed between the surface layer and deeper water were completed within about 20 miles downstream from the largest distributary. Farther downstream than this, relative speed between water layers was small. The observations were made when conditions generally were favorable for preservation of the surface layer. River discharge was high (880,000 CFS), winds were moderate from the southwest, and both ocean current and river discharge were directed toward the northeast.

These data together suggest that about 20–25 miles downstream in the gulf is the maximum distance to which residual momentum currents persist. This is a very great distance for such effects to extend, even off the Mississippi, and they extend this far only because of favorable conditions. On the average, the distance undoubtedly is much less than this.

SEAWARD OF DISTRIBUTARY MOUTHS, CURRENTS FROM DENSITY DIFFERENCES AND HYDRAULIC HEAD

It has been shown that there is a component of surface currents that is the result of residual fresh-water momentum. This component persists in the gulf to a maximum of about 20–25 miles downstream from mouths of the largest distributaries, but the distance probably is much less than this on the average. There is a continuous supply of fresh water, however, and therefore there must be a continuous seaward distribution.

In recent years, a literature has developed from detailed study of inshore and estuarine areas off smaller rivers than the Mississippi where fresh water flows into and mixes with the sea. Among many notable works are the descriptions by Tully (1937, 1949) and Fjarlie (1950, 1953) of various mixing areas in western Canada such as off the Fraser River, by Ketchum and his co-workers (Ketchum, 1951a, 1951b; Ketchum *et al.*, 1951), by Prichard (1952), and by Roelofs and Bumpus (1953) of areas on the East Coast of the United States, and by the U. S. Engineers (Rhodes, 1950) of a number of regions on both the East and Gulf coasts of the United States. Stommel and Farmer compiled descriptions and analyses of similar areas from all over the world from published and unpublished sources for their general synthesis and interpretation (Stommel and Farmer, 1952a, Pts. I, III). General syntheses have been prepared also by Tully (1952), Ketchum (1953), and Stommel (1953). A brief description was given by Scruton (1953) in discussing evaporite deposition.

These studies all have shown that areas where mixing of fresh and salt water occurs have a similar current pattern. There is two-layer circulation that is produced by hydraulic head and density differences. This circulation is superimposed on other water movements such as tidal or wind currents. Net transport in the less dense surface layer is directed away from the fresh-water source, and net transport in the more dense bottom layer is directed toward the fresh-water source. Salt exchange occurs from the bottom to the surface layer by random mixing without net transfer of water; salt also is removed from the lower layer to the upper by vertical flow of salt water. Because of this, both salt content and volume of the surface layer increase seaward while salt content and volume of the bottom layer decrease landward. The net seaward transport of water and salt by the surface current is balanced over a period of time by the transport due to river discharge, landward directed bottom current, and diffusion of salt (ignoring other effects such as precipitation and evaporation).

In estuaries enclosed by land on three sides, a seaward increase occurs in either speed of the surface current or in thickness of the surface layer to transport the greater volume of surface water resulting from mixing. This maintains system continuity. Longitudinal and vertical fluctuations of the salt gradient occur in the estuaries with variations of tide, fresh-water input, and wind. Differences in circulation characteristics between estuaries depend chiefly on differences of local boundary conditions, fresh-water discharge, tides, and winds. These differences are not fundamental, but are only differences of rates and range of variation.

This two-layer type of circulation is called estuarine because it was described first in estuaries. The term refers to a pattern of circulation, however, and not to geography of the system. Stommel and Farmer (1952, Pt. III) classified estuarine circulation on the basis of vertical stratification of the salinity profile. They recognize four simple types and give examples: (1) the vertically mixed estuary (salinity homogeneous vertically, increases seaward, *e.g.*, Severn, Raritan, Sacramento, and San Joaquin rivers); (2) the slightly stratified estuary (slight vertical stratification, salinity increases seaward, *e.g.*, River Tees, James Estuary, Moros Estuary, Charleston and Savannah harbors, and the Connecticut River); (3) the highly stratified estuary (well developed salinity stratification, salinity increases seaward, *e.g.*, Alberni Inlet, Muchalot Inlet, and Osterfjord); and (4) the salt wedge estuary (with the most pronounced vertical salinity structure, *e.g.*, Southwest Pass, Mississippi River).

In the inshore area northeast of the Mississippi Delta, the following characteristics of the circulation pattern have been demonstrated.

1. A two-layer circulation system superimposed upon tidal oscillations and wind currents. The average surface current flows seaward and the average deep current is directed landward.

2. A seaward increase of surface chlorinity and a landward decrease of bottom-water chlorinity (Figs. 29, 30).

3. A net transport of fresh water seaward at the surface and a transport of salt water landward at the bottom.[7]

4. Variation of bottom chlorinity with changing tide, increasing on flood tide, decreasing on ebb tide (Figs. 28, 29, 30).

5. Variation in the degree of vertical salinity stratification, depending on the volume of river discharge and wind speed (Figs. 15, 28, 29, 30).

On the basis of these findings, it is concluded that the water circulation in the inshore area northeast of the Mississippi Delta is of the estuarine type and is similar to circulation systems in the estuaries of smaller rivers. Figure 16 shows the principal features of the circulation system as indicated from study of the current, chlorinity, and turbidity observations, the bottom topography, and other field observations.

Differences from previously described estuaries exist, however, because of the large size of some of the distributaries, the multiple sources of fresh water, and the several connections with the open sea.

The bottom current flows toward the source of fresh water because of a horizontal pressure gradient produced and maintained by mixing of salt. Bottom water also is lifted and removed at the surface with more sea water flowing in to replace this removed volume. This vertical exchange between fluids of different densities requires energy, which off smaller rivers is supplied mainly by tides and winds. Off the large Mississippi distributaries, tides and winds are active mixers also, but in addition, much of the energy required to elevate the heavy bottom water comes from the energy of discharged fresh water. It is transmitted by interlayer friction and vertical turbulence. Thus, the pattern of isochlors off North Pass in Figure 12 (lower left diagram) shows two-layer circulation. At this time, dense saline water was flowing slowly in at the bottom, being mixed, elevated, and discharged at the surface largely from energy of issuing North Pass water.

In estuaries of smaller rivers, fresh water normally is discharged from a single source at the upper end of the estuary. The salinity gradient in the surface waters that occurs under these conditions is approximately parallel with the circulation axis and the geographic axis of the estuary. Lines of equal salinity are oriented approximately perpendicular to the circulation axis. However, northeast of the Mississippi Delta this is not so. The fresh water is supplied from many sources along a more or less continuous front that is located along one side of and approximately parallel with the primary circulation axis (Fig. 16). Figures 31 and 32 are maps of chlorinity distribution in this area, and they show that under these conditions lines of equal chlorinity at the surface are oriented at a very low angle, almost parallel, with the circulation axis. The chlorinity (salinity) gradient is at a high angle to the circulation axis. This distribution apparently is similar to that found by van Andel and Postma (1954, Figs. 12, 14, 72) off the Orinoco River. The bottom water salt gradient in the primary circulation axis is typical of those in other areas and is parallel with the circulation (Figs. 31, 32).

---

[7] Because of the geography of this area, it is impossible to obtain reliable data on the budgets of water and salt with only a single vessel from which to measure. However, the observed surface transport must be a net transport. We can not prove a net bottom transport.

In many areas of estuarine circulation, there is only one connection with the open sea. However, northeast of the Mississippi Delta, there is a primary connection and several secondary connections (Fig. 16). The secondary connections are

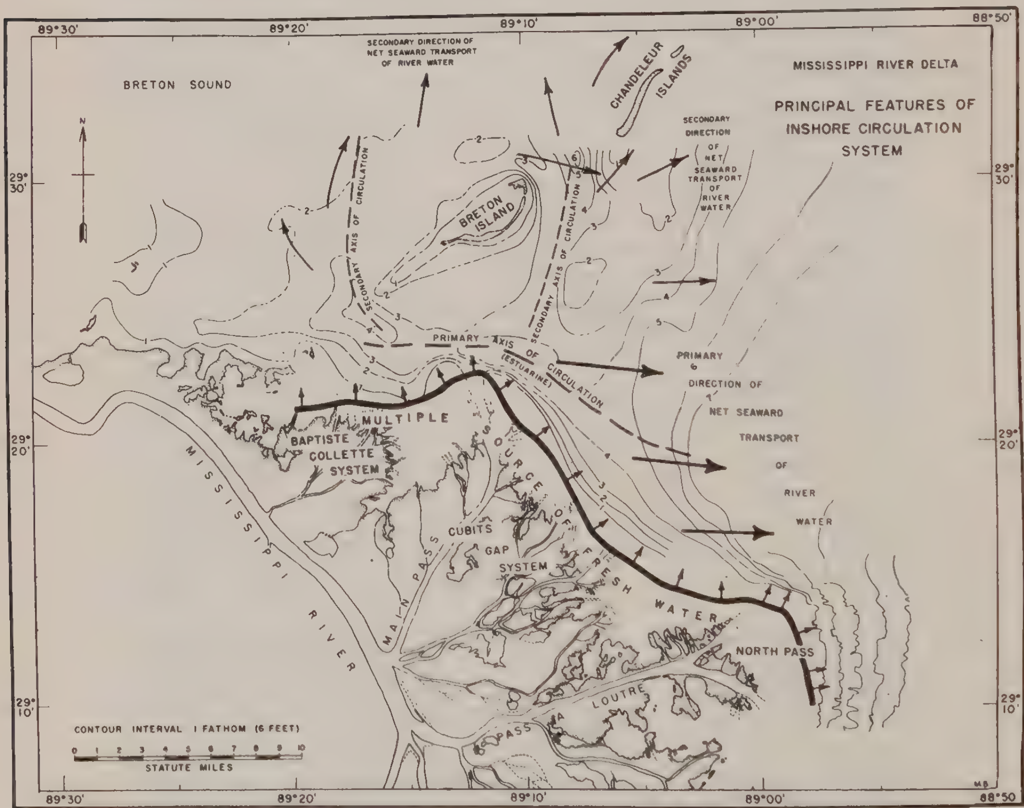
89°30'
89°20'
89°10'
89°00'
88°50'
29° 30'
29° 20'
29° 10'
BRETON SOUND
N
SECONDARY DIRECTION OF NET SEAWARD TRANSPORT OF RIVER WATER
CHANDELEUR ISLANDS
MISSISSIPPI RIVER DELTA
PRINCIPAL FEATURES OF INSHORE CIRCULATION SYSTEM
SECONDARY DIRECTION OF NET SEAWARD TRANSPORT OF RIVER WATER
BRETON ISLAND
SECONDARY AXIS OF CIRCULATION
SECONDARY AXIS OF CIRCULATION
PRIMARY AXIS OF (ESTUARINE) CIRCULATION
PRIMARY DIRECTION OF NET SEAWARD TRANSPORT OF RIVER WATER
MULTIPLE SOURCE OF FRESH WATER
BAPTISTE COLLETTE SYSTEM
CUBITS GAP SYSTEM
MAIN PASS
MISSISSIPPI RIVER
NORTH PASS
PASS A LOUTRE
CONTOUR INTERVAL 1 FATHOM (6 FEET)
0 1 2 3 4 5 6 7 8 9 10
STATUTE MILES

FIG. 16.—Principal elements of inshore circulation system. Many sources of fresh water merge to a line source parallel with primary axis of circulation, the deep channel. Circulation in primary axis is estuarine. Secondary axes of circulation distribute less river water; circulation in them may also be estuarine, but this has not been proved.

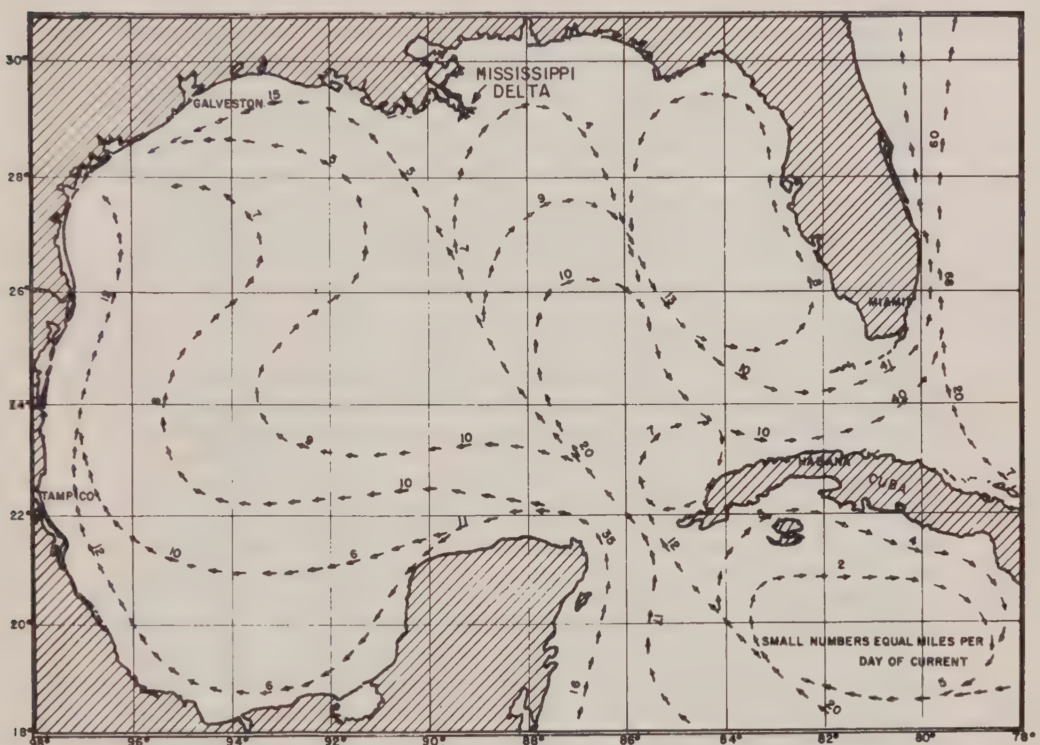
MISSISSIPPI DELTA
GALVESTON
TAMPICO
MIAMI
HABANA
CUBA
SMALL NUMBERS EQUAL MILES PER DAY OF CURRENT
30°
28°
26°
24°
22°
20°
18°
98°
96°
94°
92°
90°
88°
86°
84°
82°
80°
78°

FIG. 16a.—General circulation in the Gulf of Mexico during June. Note diverging current tongues south of Mississippi Delta. (From Leipper, 1954)

northward through Breton and Chandeleur sounds and just south of Gosier Island, and they are relatively indirect. Circulation probably is estuarine in the secondary connections also, but the data are insufficient to determine this with certainty.

Classification of two-layer circulation in the primary circulation axis depends on existing conditions of wind, river discharge, and tides. When river discharge is high and winds are low, a highly stratified estuarine pattern exists. Under other conditions, chlorinity stratification ranges from slight to vertically mixed within the depth range encountered. Circulation in distributary mouths is of the salt-wedge type when fresh water does not occupy the entire channel volume. Stratification of the circulation changes rapidly because of the dependence on wind and discharge and because these factors change over short periods of time.

Tidal currents and wind largely are responsible for current direction, although hydraulic head from water piled up inshore may offset their effects. Therefore, the axes of circulation change from time to time. The primary axis of circulation probably transports some fresh water seaward all of the time, because it is the shortest and most direct route to the open gulf, is the locus of principal tidal currents, and is wide and relatively deep. The secondary circulation axes never transport the volume of fresh water carried by the primary axis because of their shallow depth and indirect connection with the sea. Their use is favored by easterly and southerly winds, and they normally are abandoned entirely during northerlies. Large tidal range favors the secondary axis west of Breton Island by more effectively orienting river discharge in that direction on the flood tide. The axis between Breton and Gosier islands is favored by low tidal range.

OFFSHORE CURRENTS IN OPEN GULF

Offshore currents in the Gulf of Mexico seaward of the Mississippi Delta are important because they distribute river water and suspended fine-grain sediments over a large area. The direction taken by river outfall seaward of the river mouths rarely, if ever, opposes the direction of the existing general current set in the gulf. However, the distance seaward that is required to establish parallelism of flow direction between issuing river water and the underlying gulf current varies. Oceanic currents also influence heavily the physical properties of sea water around the delta.

The main problem is to estimate the seaward distribution of river water and fine-grained sediments. Currents in the open gulf, like those of the inshore region, contain several components. The principal ones are: (1) tidal, (2) semi-permanent, (3) wind, and (4) river discharge currents; the direction and speed of any observed current are the resultant of these components. Because the currents of this area are known only in a general way, estimates of river water and sediment distribution must be based on better known quantities such as average wind or average river discharge. In order to make these estimates, we must evaluate the relative part each of the principal current components plays in determining direction and speed of gulf currents.

SOURCES OF DATA

No complete oceanographic studies of the currents have been made in the northern Gulf of Mexico, although several hydrographic traverses were made by Parr (1935). For this reason it is necessary to rely on current observations of ships at sea. The observations are not entirely adequate, but they have been compiled onto charts by the U. S. Hydrographic Office (1952). They are the only source of extensive quantitative data on currents in the Gulf of Mexico seaward of the Mississippi Delta. These charts show resultant currents for each 1° square in the northern gulf and were made from all available observations prior to 1935. Data used for the Hydrographic Office current charts were obtained from observations of the amount and direction of drift experienced by vessels between successive position fixes. The resultants on the Hydrographic Office charts are a combination principally of: (1) semi-permanent current, (2) wind current, and (3) current due to river discharge. They also include some effect of ships' leeway. Tidal components are not contained in these resultants.[8]

Other earlier and less detailed charts have been prepared from similar types of data by the Hydrographic Office and the British (Soley, 1914; British Meteorological Office, 1939).

Current observations also have been made by different groups studying parts of the area. Most of these observations were made over short periods of time relatively near shore for the U. S. Engineers to help plan maintenance of navigation channels. Such observations commenced with the initial Talcott Survey of the Mississippi Delta in 1838 and have been made periodically to the present. Work of the Scripps group is of this type. The main value of these observations is in interpreting instantaneous conditions from long-term resultant data of the current charts. The U. S. Weather Bureau and the New Orleans Office of the U. S. Engineers provided wind and river discharge data, respectively.

GENERAL DESCRIPTION

Sverdrup, Johnson, and Fleming described the current pattern in the Gulf of Mexico largely from the drift of vessels and some oceanographic observations (Sverdrup *et al.*, 1946, pp.637–42, Chart VII). They showed that there is a northward drift into the gulf from Yucatan Strait and that this drift divides south of the Mississippi Delta. Tongues of the drift go both east and west and contribute to the large semi-permanent eddies of the northeastern and northwestern gulf. The positions of these eddies are determined partly by coastal and bottom contours.

More recent and extensive information confirms these interpretations. The northward drift and its division into two parts is clearly shown by dividing tongues of both salinity and temperature in Fuglister's charts of the 200-meter level in the gulf (Fuglister, 1953). The current charts of the Hydrographic Office (H. O. Misc. Pub. 10–690, 1–12, 1952) show the same features. These charts were most recently discussed by Leipper (1954) in a summary of knowledge on gulf currents. Figure 16a was taken directly from Leipper (1954) and shows the general gulf circulation in surface waters during the month of June. All available data suggest that the northward drift divides about 100–150 miles south of the Mississippi Delta and that flow goes north and east and north and west (Fig. 16a). Resultants on the Hydrographic Office charts also show that the north-south axis of drift shifts from time to time. The axis is farther east on the average during the months of May, June, July, and August than during the remainder of the year. These charts also show that during March, September, November, and December there is a countercurrent on the northern flank of the eastward directed drift. This countercurrent flows toward the west immediately south of the Mississippi Delta.

---

[8] Tidal currents are excluded from these resultants by: (1) the rotary nature of open-ocean tidal currents, (2) the number of random observations from which the results are computed, (3) the length of time over which ships' drifts were measured (between astronomical fixes, usually obtained at sunrise, noon, and sunset), and (4) data selection exercised by the Hydrographic Office (they state (H. O. Misc. Pub. 10–690, 1–12): "Observations were not considered reliable where tidal currents prevailed, where wind, sea, or swell of force 6 or above were recorded; where vessel's draft or trim would cause excessive leeway; or where doubt existed as to meaning of the word 'nil' in the report.").

AVERAGE CONDITIONS

In order to evaluate the parts played by the different components in distributing river water and sediment, the monthly resultant currents were compiled from off Grand Isle and Burrwood, Louisiana, and Pensacola, Florida. Wind measurements by months for a number of years at each of these points and monthly Mississippi River discharges were collected to compare with the current data. Figure 17 shows the locations of areas of current and wind measurements. Figures 18 and 19 show monthly resultant currents at Burrwood and Grand Isle, Louisiana, and also wind speeds and directions. Figure 20 shows resultant winds at Grand Isle, Burrwood, and Pensacola by months. The patterns of monthly wind resultants at Grand Isle and Pensacola differ very little from the pattern at Burrwood. Figures 18, 19, and 20 also give annual current and wind resultants. A glance at these figures shows that the annual resultants conceal significant monthly variations. Monthly averages of river discharge shown in Figure 10 are from water year 1951–1952 (October, 1951–October, 1952), and are approximately average values (U. S. Engineers, 1939), with the exception of February. February discharge was adjusted to conform to the average relationship between months.

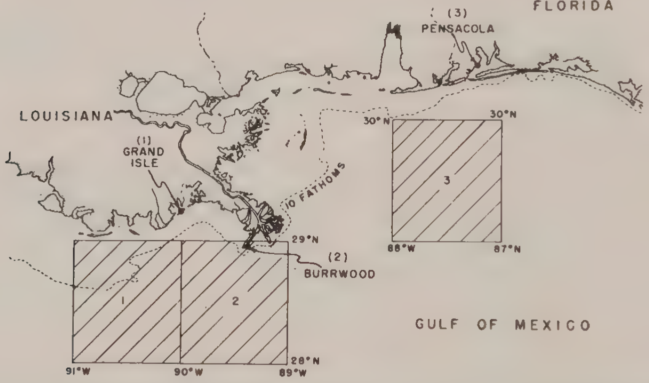

FIG. 17.—Areas in gulf (cross hatched) where current observations were compiled; points on land where wind observations were made.

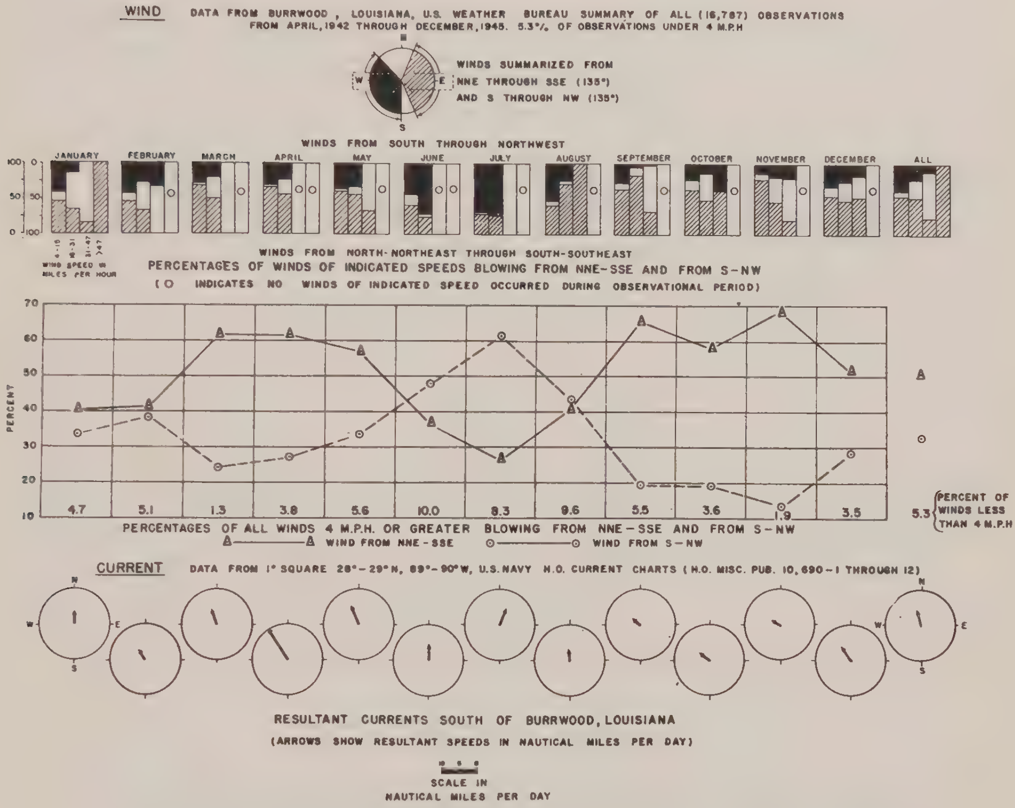

FIG. 18.—Annual variations of wind and current. Summary of wind observations from Burrwood, Louisiana, and resultant currents from Area 2 (Fig. 17). Wind summaries compiled from north-northeast through south-southeast (cross-hatched on compass rose and histograms) and south through northwest (solid on compass rose and histograms). Current arrows show direction and speed of monthly resultants.

South of the delta resultant currents are directed mainly toward the north; they contain both east- and west-directed components, but these are relatively small (Fig. 18). To the west, south of Grand Isle, the north- and west-directed components of current resultant are about equal except during summer months when resultants are mostly north (Fig. 19). South of Grand Isle there are no months with an east-directed component of resultant current.

The persistent northward drift south of the delta is opposed to the wind for about half of the year and favored by it during the remainder (Fig. 20). Since this northward drift is a direct continuation or extension of current coming from the south, there is every reason to believe it is part of the large-scale semi-

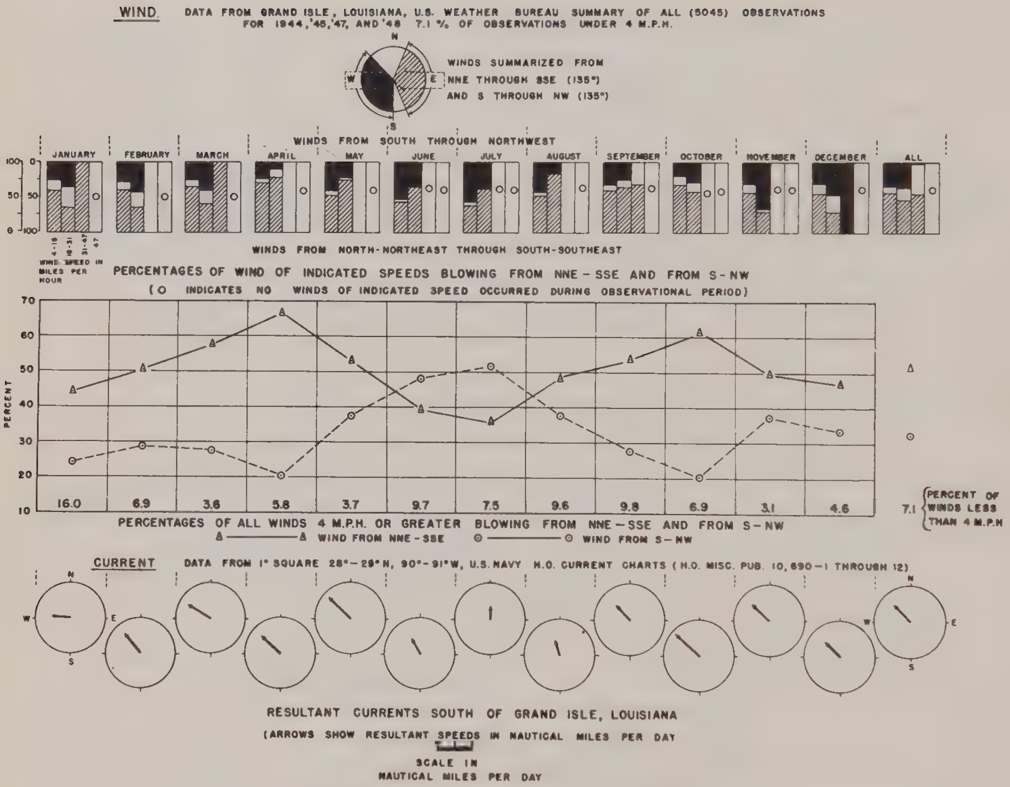

FIG. 19.—Annual variations of wind and current. Summary of wind observations from Grand Isle, Louisiana, and resultant currents from Area 1 (Fig. 17). Wind summaries compiled from north-northeast through south-southeast (cross-hatched on compass rose and histograms) and south through northwest (solid on compass rose and histograms). Current arrows show direction and speed of montly resultants.

permanent feature originally described by Sverdrup *et al.* (1946). This current owes its velocity mainly to regional winds and to the density distribution in the Gulf of Mexico brought about by regional heating, cooling, evaporation, and precipitation. This semi-permanent current is only modified by local conditions.

The effect of the persistent north-directed component of current is to prevent or limit southward movement of turbid Mississippi River water. The persistent north-directed current therefore requires that river water move either to the eastward or to the westward in the gulf (Fig. 16a). Because of this, east-directed and west-directed components of resultant current are the components that largely distribute the turbid river water. East and west components of the resultant current at Grand Isle, Burrwood, and Pensacola vary from month to month in both direction and speed. This makes it possible to estimate relative influences of wind, river discharge, and semi-permanent current on them and on disposal of river water and fine sediment.

Effects of wind.—Figure 21 is a plot of current speed and direction against wind speed and direction at Grand Isle, Burrwood, and Pensacola. Current resultants are expressed in nautical miles per day; wind resultants are expressed in knots (nautical miles per hour). Curves are best fit by eye, but agree closely with least squares curves.

In all cases there is the scatter of points to be expected from the nature of the data. There appears, however, to be a persistent relationship between resultant wind speed and resultant current speed. The greatest dependence on wind occurs at Burrwood ($r = .675$), the least scatter of data occurs at Grand Isle ($r = .681$), and the least dependence and greatest scatter occur at Pensacola ($r = .611$). These correlation coefficients are all fairly high, and the statistical probability is over 98 per cent that the indicated correlations at Burrwood and Grand Isle are significant. At Pensacola the probability is over 95 per cent. There also is good agreement between the direction of wind and current, especially in the Burrwood and Grand Isle areas, where current and wind components are all in the same direction and changes of current direction occur only during months when wind direction changes.

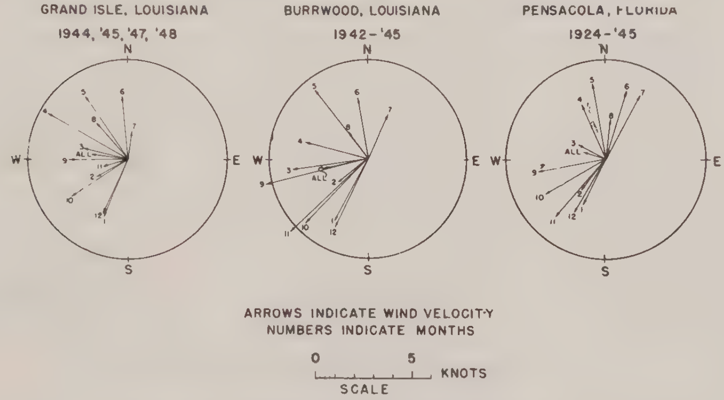

FIG. 20.—Direction and speed of monthly wind resultants at Grand Isle and Burrwood, Louisiana, and Pensacola, Florida.

The Burrwood plot also shows the normally expected relationship between current and wind speeds; the current speed is about 2–3 per cent of wind speed. Excellent agreement with this expected relation occurs at Burrwood during March, September, and November, when the westward-flowing countercurrent exists and winds blow most persistently from the east (Figs. 18, 20). Good agreement also occurs during May, June, and August. The current reverses its prevailing direction and flows toward the east on the average only during July. July is the only month at Burrwood when the resultant wind is toward the east (Fig. 20).

The intercept of the Burrwood best-fit curve suggests that the resultant current contains an east-directed semi-permanent component. This east component is weak, only about 1 nautical mile per day, and generally is offset by other factors.

The relationship between wind and current is present off Grand Isle, but it does not follow the expected relationship of current to wind as closely as at Burrwood. During July there is neither a west nor an east component of resultant current. At Grand Isle, like Burrwood, July is the only month when there is an east-directed wind component (Fig. 20). The best-fit curve is offset from the origin, and the intercept suggests a semi-permanent westward current component of 1–2 nautical miles per day.

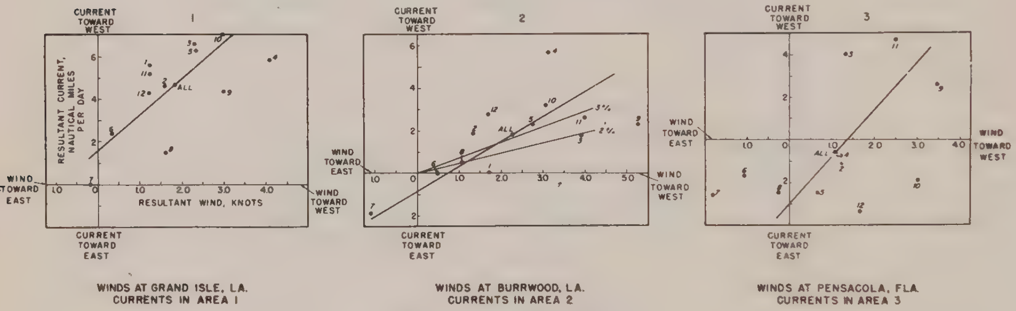

WINDS AT GRAND ISLE, LA. CURRENTS IN AREA 1

WINDS AT BURRWOOD, LA. CURRENTS IN AREA 2

WINDS AT PENSACOLA, FLA. CURRENTS IN AREA 3

WINDS FROM U.S WEATHER BUREAU
GRAND ISLE: 1944, '45, '47, '48
BURRWOOD : 1942-'45
PENSACOLA : 1924-'45

RESULTANT CURRENTS FROM U.S.N. H.O. MISC. PUB. 10-690, 1-12

FIG. 21.—Plots of east or west component of monthly resultant current against east or west components of monthly resultant wind for Grand Isle and Area 1, Burrwood and Area 2, and Pensacola and Area 3. Correlation coefficients are: Plot 1, $r=.681$; Plot 2, $r=.675$; Plot 3, $r=.611$. Thin lines on Plot 2 enclose 2% to 3% of wind speed.

In the area off Pensacola, Florida, there is an east-directed component of the resultant current during all months except March, September, and November, months of persistent easterlies and the west-flowing countercurrent. Points are scattered, but the best-fit curve intercept suggests an average easterly component of drift of about 2–3 nautical miles per day.

In evaluating these correlations between wind and current, it must be remembered that they are improved to some unknown extent by ships' leeway produced directly by the wind. This effect undoubtedly is present despite Hydrographic Office data selection (see footnote No. 8).

Effects of river discharge.—River discharge can be expected to affect the gulf currents by creating sloping pressure surfaces because of both altered density distribution and hydraulic head. The speed of any current thus established should vary directly with the volume of river discharge. The direction of such currents theoretically should be toward the west (right) under steady-state conditions because of earth's rotation. Momentum of river water is dissipated by mixing with sea water near the distributary mouths and makes no significant contribution to current speed at any distance from the river.

Figure 22 is a plot of east-west components of monthly resultant current as a function of monthly average river discharge. Again current components are expressed in nautical miles per day; river discharge is cubic feet per second $\times 10^5$, measured at Baton Rouge, Louisiana.

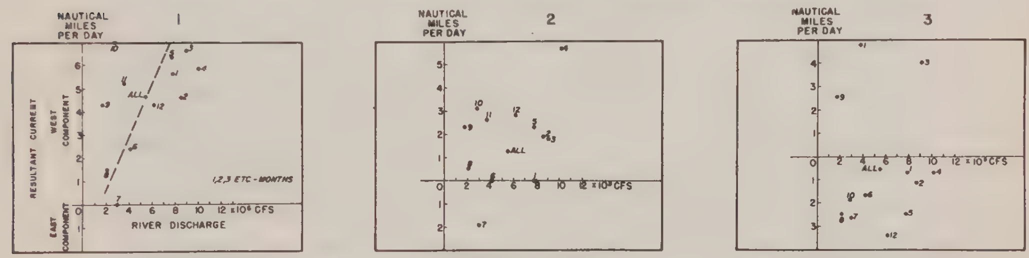

GRAND ISLE, LA.
AREA 1 (28°-29°N; 90°-91°W)

BURRWOOD, LA.
AREA 2 (28°-29°N; 89°-90°W)

PENSACOLA, FLA.
AREA 3 (29°-30°N; 87°-88°W)

RIVER DISCHARGE AT BATON ROUGE, LOUISIANA, AVERAGED BY MONTHS FOR WATER YEAR 1951-'52 (OCTOBER TO OCTOBER)

FROM U.S. ENGINEERS-N.O. OFFICE

RESULTANT CURRENTS FROM U.S.N. H.O. MISC. PUB. 10-690, 1-12

FIG. 22.—Plots of east or west component of monthly resultant current against river discharge for Areas 1, 2, and 3. Correlation coefficients are: Plot 1, $r=.522$; Plot 2, $r=.407$ (due largely to April and July); Plot 3, $r=.019$.

There is no relationship south of Pensacola between the resultant currents and the volume of river discharge ($r=.019$). Both magnitude and direction of the east-west current component seem to be independent of river discharge in this area.

South of Burrwood there is a wide scattering of points, but the data suggest some relationship between current speed and river discharge ($r=.407$ and is due largely to points for April and July). River discharge, however, can not account for the alteration of current direction (flowing toward the east) that occurs in July.

The area south of Grand Isle is in the direct path of distribution of a large part of the Mississippi's water and is where effects of river water on the currents should be most pronounced. A relationship between current speed and river discharge appears to exist in this area ($r=.522$, 90%–95% probability of significance) and is indicated by the dashed curve in Figure 22. However, river discharge can not be called on to explain the absence of west-directed current during the month of July.

These data suggest: (1) that current speed is increased by river discharge in areas that are favorably located, but (2) that river discharge exerts little influence on primary determination of current direction.

Semi-permanent currents.—The plots of current resultant against wind resultant (Fig. 21) give some indication of the speed and direction of the average east and west component of semi-permanent current. Although this method of evaluation is not an ordinary one, the results suggested by the plots are consistent with what is known of gulf conditions and considerations of system continuity. The semi-permanent component is known to be small compared with some other oceanic areas, it is known to be mainly north-directed, and it is known to divide south of the coast. The plot off Pensacola (east of the divergence area) shows an east-directed current, east-west semi-permanent current is very small in the divergence area off Burrwood, and off Grand Isle west of the divergence area, the average current is shown west-directed.

The west-directed current probably strengthens toward the west. Parr made oceanographic sections perpendicular to the coast as far west as Galveston, Texas, in March and April, 1932 (Parr, 1935). His data show fresh-water dilution as far west as Galveston and suggest a west-flowing current near the coast. If currents were westerly, dilution off Galveston is due, of course, to the combined effects of all large rivers east of Galveston. These include the Atchafalaya, Calcasieu, Sabine, Neches, and Trinity, as well as the Mississippi. The Mississippi River is only one of the many elements in the Gulf of Mexico that produce the current pattern.

INSTANTANEOUS CONDITIONS

The relationships off the Mississippi Delta described in the preceding paragraphs are derived from the results of long-term averages; therefore, they do not necessarily reflect instantaneous conditions. Fluctuations in speed and direction of semi-permanent currents and winds, variations of river discharge, and tides produce currents in the gulf which frequently are entirely opposite to the currents described by the long-term average.

This is true particularly when long-term vector magnitudes are small, as in the east-west component of resultant current south of Burrwood during most months (Fig. 18). These small vectors represent the summation of a large number of individual observations, many of which are of large magnitude. In such an instance, a small vector indicates a near-balance between opposing tendencies.

However, the direction of gulf currents determines the direction in which river water is distributed. As demonstrated in connection with oscillating inshore tidal currents, the lateral distribution of sediments settling from suspension is related to fluctuations about the mean condition as well as to the mean, since suspended matter settles during such fluctuations and the reaction is irreversible.

It has been shown that direction and most of the speed of east or west components of resultant currents south of Burrwood are functions of the resultant winds. This is because of the split or divergence south of the delta which occurs in the north-directed semi-permanent drift. Unfortunately, the relationships for instantaneous conditions are not as clear-cut because of local variations and lack of sufficient offshore data.

The U. S. Engineers investigate currents to many miles seaward of the principal distributaries in connection with development of plans for improving navigation facilities. Their early studies are reported on by Humphreys and Abbot (1876, p. 483, and App. A., Repts. of Sidell and Meade, pp. 495–508). These and other reports, based on careful analyses of the available data, later were examined and summarized by Forshey (1877, pp. 146–47) who also did much work in the area. He found the reports to be unanimous in their opinion. As his conclusion with respect to the persistent rumor of a westward littoral current in the gulf, Forshey quoted J. E. Hilgard, long an assistant in the Coast Survey on the Gulf of Mexico (op. cit. p. 147): "No currents, other than the transitory mutable wind and tidal currents, were known to the Coast Survey."

Data obtained by the U. S. Engineers at Southwest Pass from wind and current studies during 1943–1945 and field observations by Scripps personnel during 1951, 1952, and 1953 (Scruton and Moore, 1953) bear out Forshey's conclusions with some modifications. First, the winds which establish strong local currents are not necessarily local winds. Strong west-flowing currents off the delta are set in motion by high easterly winds occurring as far away as the west coast of Florida. As might be expected under these conditions, periods as long as 2 or 3 days may elapse before the currents are felt off the delta. Second, strong currents, once established in the gulf, may persist before an opposing wind. The period of opposition apparently depends on the relative velocities of wind and current and the persistence of the opposing wind. For example, if the wind speed is low and blows for only a short time, the current may not alter direction. Similarly, strong currents, once established, may flow with gradually lessening speed for some time if winds cease. Third, aerial observations show that frequently in the bight directly west of the delta (Fig. 17, between Burrwood and Grand Isle) there is an east-directed countercurrent along the coast when gulf currents to seaward are west-directed. A similar, but west-directed, eddy may be set up east of the delta when currents seaward are strong toward the east.

Currents at all levels above the bottom in the open gulf seaward of the delta have been observed to range in speed from zero to approximately 2 knots. The maximum speed of open-gulf currents is not known, but their range of speeds is similar to the speed range of currents issuing from the river mouths, which is about 0.5–3 knots.

FINDINGS OF OTHERS IN SIMILAR AREAS

Within the past few years a number of other oceanic areas similar to that off the Mississippi River have been studied and observed. Results on the currents in these areas now are available and provide additional background information. These studies include the work of Ketchum *et al.* (1951) off the Hudson River, and Hachey and Fothergill (1953) off Halifax, Nova Scotia. Jerlov (1951) gives some data on the relationship between oceanic currents and distribution of turbidity off the Amazon River. Van-Andel and Postma (1954) described distribution of Orinoco River water, and Cameron (1953) described distribution of McKenzie River water.

Ketchum, Redfield, and Ayers studied circulation in the New York Bight off the Hudson River. They state (1951, p. 43): "The volume of the oceanic counter drift entering the outer boundary of the surveyed area ranged from 47 to 224 times as great as the volume of river flow. The rapid flushing of (New York Bight) may be directly ascribed to the large volume of the oceanic circulation."

Hachey and Fothergill (1953) studied in detail 1,500 simultaneous current and wind measurements made at Sambro Lightship off Halifax, Nova Scotia. They state (1953, p. 14): "A given surface current at Sambro Lightship is a complex mixture of wind current, tidal current, and semi-permanent current. The surface current, both in direction and magnitude, is strongly influenced by the wind force and direction when the wind is greater than 8.7 knots. When the wind is less than 8.7 knots, the surface current is either from the northeast, east, or west-southwest" (the semi-permanent current directions). No large rivers discharge in this region. The average relationships found between wind and current are reproduced in Figure 23. They found that the surface current was 1.7 per cent of the wind speed, averaged by drift pole through the upper 15 feet of water.

Jerlov (1951, pp. 22, 29) pointed out the correspondence between the northwest direction of the Amazon River discharge seaward of that river and direction of the Equatorial Current. Orinoco River water also is distributed toward the north and west by the Equatorial Current (van Andel and Postma, 1954). Cameron (1953) also found some relation between the current and winds and river discharge off the McKenzie River in northern Canada, although his studies have not been completed. Recently F. P. Shepard reported (personal communication) a close relationship exists between wind direction and direction of Rhone River discharge.

DISCUSSION OF FINDINGS AND CONCLUSIONS

These data, though far from adequate, are the best evidence available on conditions in the Gulf of Mexico near the Mississippi Delta. They show that currents and distribution of river water in the gulf (and therefore river-derived suspended sediment) are related primarily to wind and semi-permanent currents. A current due to sloping pressure surfaces produced by land drainage apparently may augment the two primary factors if direction of current initially produced by the primary factors is favorable.

In general these data are interpreted to mean that water from the Mississippi River is distributed according to the gulf circulation; that this circulation is gulf-wide in origin; and that gulf circulation is mainly the product of winds and density changes from regional heating, cooling, evaporation, precipitation, and runoff. Although the Mississippi is a large river, it is not large relative to the entire Gulf of Mexico. Only to the extent that the Mississippi River constitutes a part of the gulf circulation system does it exert control over seaward distribution of its own discharge.

An analogy may help to visualize the relationships. The Gulf of Mexico can be compared with a tank about 32 feet long, 24 feet wide, and 10 feet deep. On this scale the Mississippi is like a small rubber hose only $\frac{1}{4}$ inch wide and $\frac{3}{16}$ inch deep. Water issues from the small rubber hose at about the same speed as the tank currents and is carried first one way and then another by the larger body of moving water.

When viewed in detail, hydrographic conditions in the shallow water and in the open gulf surrounding the Mississippi Delta are extremely complex and highly variable. Repetition of circulation features is brought about by repetition of similar conditions of wind, tide, semi-permanent current, and river discharge. Much more work is required to place on an adequate quantitative basis the different relations that have been discussed between these variables.

DISTRIBUTION OF RIVER WATER AND SEDIMENT IN GULF

The correspondence between wind and current directions furnishes the basis for estimating proportions of river water distributed eastward and westward in the gulf. The monthly wind summary at Burrwood, knowledge of the local wind behavior, and the monthly distribution of river discharge provide the data.

Figure 23 shows average relations between wind direction and resulting current direction at Sambro Lightship (Hachey and Fothergill, 1953). They found (1953, p. 4) when the winds were from the open sea the average current direction was approximately 21° to the right of the wind. This average value was used to compile the data in Figures 18 and 19. These figures summarize the winds that can be expected to produce an eastward or westward component of the current near the Mississippi Delta. According to the findings of Hachey and Fothergill, the arc of winds causing westward drifts is indicated in the compass rose by cross-hatching; the arc causing eastward drifts is in black. The frequencies of winds of various speeds above 4 mph. by arcs and the frequencies of all winds greater than 4 mph. are shown. Winds from north-northwest through north are not included directly and constitute the remainder of the winds.

The wind summary at Burrwood, Louisiana (Fig. 18), gives the indication

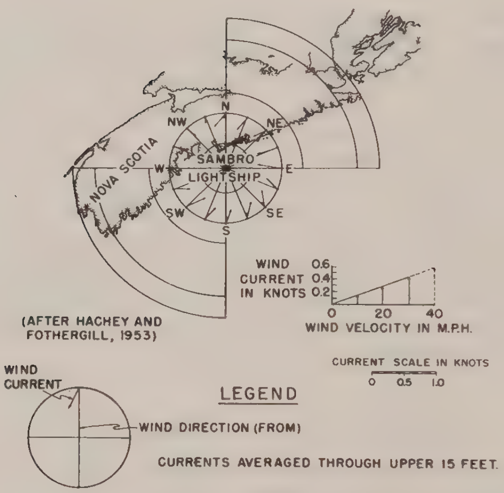
N
NW
NE
W
E
SW
SE
S
NOVA SCOTIA
SAMBRO
LIGHTSHIP
WIND
CURRENT
IN KNOTS
0.6
0.4
0.2
0
20
40
WIND VELOCITY IN M.P.H.
(AFTER HACHEY AND FOTHERGILL, 1953)
CURRENT SCALE IN KNOTS
0 0.5 1.0
WIND
CURRENT
LEGEND
WIND DIRECTION (FROM)
CURRENTS AVERAGED THROUGH UPPER 15 FEET.

FIG. 23.—Relations between wind and surface current found by Hachey and Fothergill at Sambro Lightship, Halifax, Nova Scotia. Compass rose shows direction relationships for 16 compass points. Rays indicate average wind direction (from); short arrows indicate corresponding average current direction. Wind versus current plot gives speed relationships. When wind was from open sea, current direction averaged about 21° to right of wind; current speed (upper 15 feet) averaged about 1.7% of wind speed.

of frequency of west- or east-flowing currents directly south of the Mississippi Delta. This must be modified by the usual nature of shifts in wind direction. The strong northerlies of fall and winter tend periodically to offset the persistent northerly semi-permanent current and to cause south-flowing surface currents in the open gulf which distribute river water in this direction. Also, as was pointed out in connection with the inshore circulation, on the northeast flank of the delta northerlies produce a current flowing parallel with shore toward the southeast and the open gulf. Following northerlies, the wind generally shifts toward the east and may blow from this direction for some time, causing some of this surface water then to move westward.

Table I is a summary of river discharge and winds by months to help estimate the proportions of annual river discharge that go eastward and westward. It was prepared from data in Figure 10 and Figure 18. On the basis of values in Table I and a consideration of the general behavior of the winds and currents, it seems likely that about 55–65 per cent of the river water is distributed westward, 35–25 per cent is distributed eastward, and about 10 per cent initially goes south, blown by strong northers. Later distribution of this 10 per cent can not be accounted for, but probably much of it also goes west before the east wind that usually follows northers.

These estimates, based on annual wind and river discharge variations, closely agree with Dent's field observations (Dent, 1921; also cited by Russell, 1936, p. 144). Dent collected 187 observations on current direction south of the delta, made between September, 1915, and December, 1919. Sixty-three per cent (117) of the observations showed a west-flowing current, and 37 per cent (70) of the observations showed the current flowing toward the east. No field observations could be made on south-flowing currents.

TABLE I. DISTRIBUTION OF RIVER WATER

Month	*A*[1] *River Discharge (% of Annual)*	*B*[2] *% Winds >4 MPH Toward West*	*C*[2] *% Winds >4 MPH Toward East*	*AxB*	*AxC*
J	11.6	40	34	4.6	3.9
F	12.8	41	39	5.3	5.0
M	13.4	62	25	8.3	3.3
A	15.6	62	28	9.7	4.4
M	11.6	57	34	6.6	3.9
J	6.1	36	48	2.2	2.9
J	4.5	26	62	1.2	2.8
A	3.1	41	44	1.3	1.4
S	2.5	65	20	1.6	0.5
O	4.2	58	19	2.5	0.8
N	5.4	69	14	3.7	0.8
D	9.2	52	29	4.8	2.7
Totals	100.0	50.6 (Average)	33.0 (Average)	51.8	32.4

5.3% of Winds <4 MPH; 11.1% of Winds from NW-NNE (mostly strong).

[1] Taken from River Discharge Summary, Figure 10.

[2] Taken from Burrwood Wind Summary, Figure 18.

Inequality of river-water distribution, largely caused by the winds, probably produces an even greater inequality of sediment distribution. During flood times, the Mississippi carries a greater than average concentration of sediments in its load. About 53 per cent of the annual river discharge occurs during February, March, April, and May, four months of west-directed average current. It is possible, therefore, that as much as 70–75 per cent of the annual sediment load of the Mississippi initially moves westward after it is delivered to the Gulf of Mexico.

Inequality of sediment distribution has effects on the configuration of the coast line. Humphreys and Abbot (1876, p. 483) first made reference to this, and it is well known to present-day Army Engineers who design the navigation channels at the distributary mouths with this in mind.

Perhaps the effects are best shown by seaward over-extension of one bank at the distributary mouth, a phenomenon that occurs around the entire Mississippi Delta. Along the southern and southeastern sectors of the delta the *right-hand* banks of the distributaries are over-extended seaward, whereas on the north and northeast, most of the *left-hand* banks are over-extended. Figure 11 shows the configurations of the active major distributaries in the delta prior to any extensive channel construction. Southwest Pass, Grand Pass, South Pass, Southeast Pass, Pass a Loutre, and North Pass follow this relation and have their southern or western (*right-hand*) banks over-extended; Northeast Pass does not. Along the northeastern side of the delta between 1951 and 1953 the same uniformity held, and all of the major distributaries had the northern or western (*left-hand*) banks over-extended. This was observed by Scripps personnel and confirmed by aerial mosaics furnished by Tobin Aerial Surveys, Inc., made from photographs taken in 1951. Major distributaries on the northeastern side where land on the western (*left-hand*) banks was over-extended seaward were (Fig. 11): (1) in the Baptiste Collette system: Fisherman's Pass (the main distributary), Kimbel Pass, and Emeline Pass; (2) in the Cubitts Gap system: Main Pass, Dead Women Pass, and Raphael Pass; (3) in the Pass a Loutre system: North Pass (changed since 1874) and Northeast Pass. The present relationship at Pass a Loutre is not clear because of mud lumps.

Along the northeastern flank of the delta, seaward over-extension of one bank is less marked and more changeable than on the southern flank, probably because distributaries are smaller and alternating tidal currents make discharge directions more variable. Thus, in October, 1955, the eastern bank of Main Pass had become slightly over-extended. In the areas of numerous small distributaries around the delta, no clear consistent relation exists because of anastomosing channels.

Inequality of sediment distribution also may have an effect on larger land surfaces. Some of the large volume of fine-grained sediment that is carried westward eventually is driven into the Louisiana marshes (Humphreys and Abbot, 1876; O'Neil, 1949; Morgan *et al.*, 1953). This continuing supply of detritus may partly explain why old delta surfaces at the west are emergent, while much of the St. Bernard Delta on the north has sunk below sea-level.

COMMENTS ON THEORETICAL DELTA FORMATION

The foregoing observations on hydraulics of distributary mouths, on currents over the bar and their variability, and on the seaward persistence of fresh water and its direction of distribution permit comment on some aspects of the theoretical delta formation advanced by Bates (1953) and discussed by Crickmay and Bates (1955). The curve of current speed over North Pass Bar (Fig. 12, high discharge) is typical for fluid discharged as a jet or over a weir (Rouse, 1950; Prandtl, 1952). These data support Bates' contention that there is some form of jet flow from the mouths of the distributaries.

Bates (*op. cit.*) further suggested that the orifice for this flow was "last land," and that jet flow was responsible for forming the distributary-mouth bar approximately four channel widths seaward of last land. According to this hypothesis, the bar is built by deposition at a point where the current speed falls below a critical speed. In the upper left diagram of Figure 12 the curve of surface current speed (which varies from hour to hour and day to day, Fig. 14) reaches a maximum seaward of the bar. The position of this speed maximum seaward of the bar and the absence of pronounced speed changes at low river show that the bar is responsible for the acceleration. Thus, field data demonstrate that the channel-mouth bar is part of the orifice and is the primary cause of jet characteristics at the distributary mouth. Therefore it can not be the result of jet characteristics as was suggested by Bates.

Bedload transportation furnishes another line of field evidence which shows that the bar is part of the orifice. Bates (*op. cit.*) assumes that the transported sediment is in suspension and is carried in this way so long as the current speed is above a critical speed. However, the data presented in subsequent paragraphs on distribution of suspended matter (Fig. 43) show there is a pronounced vertical gradient of suspended sediment over the bar with most of the sediment near the bottom. Probably this gradient is a manifestation of the usual river transportation regimen in which much material is carried by suspension, but much also is transported by saltation and rolling. This bedload material tends to be the coarsest that is moving, and it is frequently in contact with the solid bottom. In this kind of transportation there tends to be equilibrium between particles moving and those at rest; that is, some particles constantly are dropped while the same amount of others are picked up and moved. Transportation or deposition of the saltating and rolling (bed) load is dependent on the presence or absence of a current-affected bottom—not on a critical current speed in the surface layer. In the distributaries bedload moves up the channel-bottom ramp and is deposited on the seaward slope of the bar where the river current departs from the bottom. The point of departure of the river current from its confining channel is the distributary orifice. This point is the bar crest.

Bates (*op. cit.*) also suggested on theoretical grounds that some fraction of the issuing speed of Mississippi River water persists to a very great distance seaward (200–2000 channel widths) because of jet characteristics at the channel mouths and that the direction of river-water distribution is determined by earth's rotation. These suggestions were made after the following simplifying assumptions were introduced: that the Gulf of Mexico is a (1) currentless, (2) tideless, (3) wave-free (*i.e.*, windless) basin which is in a steady state (equilibrium). In view of the magnitude of these various factors described from field observations, Bates' assumptions do not appear to be warranted. Neither of the suggestions based on them can have practical significance in this area, because of the controlling effects of the constantly changing tides, winds, and gulf currents.

WAVES

Wave action has an important effect on sediments largely because it causes secondary movement and sorting of previously deposited particles. Such results may be due entirely to wave action or to the combined action of waves and other currents. Waves also mix the water column and therefore also influence primary deposition of sediment being transported in suspension.

Wave effects on the bottom are due largely to the horizontal component of motion of water particles associated with passage of the wave. In moderately shallow water the amplitude of the horizontal component is dependent on both length (period) and height of the wave, and amplitude at the bottom decreases exponentially with increasing depth of water. For this reason, only the largest (both long period and high) waves stir the bottom at any considerable depth.

No detailed long-term wave studies are available in the north-central Gulf of Mexico. However, the Humble Oil and Refining Company and the Beach Erosion Board of the U. S. Engineers conducted a joint study in 1948–1949 from a drilling platform off Grand Isle, Louisiana, and Mason (1952, Fig. 3) gives some of the results. Our wave observations off the delta are not statistically significant.

Results of the study reported by Mason were recomputed to show cumulative frequencies of wave sizes by period and height and monthly distribution of the larger waves. Figures 24 and 25 are the curves for the Grand Isle area. Wave periods normally ranged from 2 to 6 seconds with a median of approximately 4.4 seconds (Fig. 24). Waves with periods longer than 6 seconds occurred during most months (no data were available for January and February), but none longer than 10 seconds were reported. Waves of periods longer than 6 seconds occurred most frequently during March through May and after October (Fig. 25).

Wave heights normally ranged from 0 to 3 feet, median wave height was 0.9 foot (Fig. 24), and no waves higher than 8 feet were reported. The time of most frequent high waves began in October (Fig. 25), no waves higher than 5 feet occurred in the period of March through August, and most waves during this time were less than 3 feet in height. Frequencies of calms by months ranged from 1 to 8 per cent, averaged 3.3 per cent, and were distributed randomly by months.

At Burrwood, average winds are somewhat stronger than at Grand Isle, and the eastern side of the delta is more exposed to prevailing winds (Figs. 17, 20). Therefore, Mason's results from Grand Isle probably are minimal for those parts of the delta exposed to the open gulf, although the relative distribution of wave heights and periods probably is similar. In the shallow protected sounds north of the delta, wave periods are much shorter than those in Figure 24 with a maximum of approximately 2.5–3.5 seconds. Wave heights in these waters seldom exceed 4–5 feet, even during strong northerly winds. This is probably a result of shallow depths and short fetch of the sounds, since both of these factors restrict the size of waves (Bigelow and Edmondson, 1947, pp. 58–60).

Directions of wave-approach north and east of the delta are related to directions of generating winds, but approach directions are modified by refraction over the sloping bottom. Prevailing wave-approach directions are easterly, with either north or south components depending on the winds. The strong northeasterly winds of fall produce large waves in the open gulf which sweep toward the southwest. These waves frequently break along the submarine ridge which is a southward extension of Gosier Island (minimum depth 7–7.5 feet, Fig. 1) and are dissipated against the delta and in the area between the submarine ridge and the mouth of Main Pass. Smaller waves from the east break on Breton Island, on the bar extending southwest from Breton Island, or are dissipated against the deltaic embankment. Fall and winter northers produce the largest south-or-southeast-moving waves that occur in Breton and Chandeleur sounds, but these break or are dissipated in the sounds behind the barrier islands and do not develop any real size until some distance downwind (seaward) of these islands.

Waves of greater dimensions than those observed in the Humble-Beach Erosion Board study are associated with gulf hurricanes. Maximum size of these waves is problematical, but they undoubtedly disturb the bottom over most of the continental shelf. Their frequency of occurrence is low, however. The paths of only 27 hurricanes since 1900 (including the 1953 Pensacola hurricane) were such as probably to affect the eastern side of the Mississippi Delta (Tannehill, 1950). Of these, only about 17 passed close enough to cause really large waves in the area (Mason, 1952, Fig. 5; Escoffier, 1952, Fig. 2). Directions of approach of these large waves are southeasterly to northeasterly, and they undoubtedly break and are dissipated in a manner similar to that described for waves during fall northeasters. Long period swells developed by storms in the open Atlantic are excluded from the landlocked Gulf of Mexico.

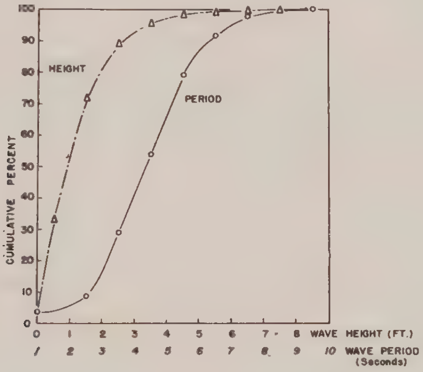

FIG. 24.—Ten-month cumulative frequency of wave heights and periods off Grand Isle, Louisiana. Data from drilling platform 8 miles off Grand Isle, recomputed from Mason (1952).

These wave data and other factors such as hurricane frequency show that waves of a size which could be expected to stir the bottom appreciably at the prevailing depth of the continental shelf in this area occur here on the average only about every 3–4 years. However, small waves occur about 95 per cent of the time, and they are capable of stirring the very shallowest bottoms around the delta (Fig. 24). Between these two extremes are waves of all intermediate sizes and bottoms at all intermediate depths. Figure 24 shows that the frequency of occurrence of waves that can affect the bottom progressively increases as water depth decreases.

Furthermore, the largest waves have a seasonal distribution. Figure 25 shows that almost all waves that are both high and have long period occur from September through at least December and probably into March (there are no data for the critical months January and February). The largest waves, associated with hurricanes, are most likely in September, but may occur from June through October. The seasonal distribution is lost when waves of smaller size are considered, and the smallest waves occur almost all the time.

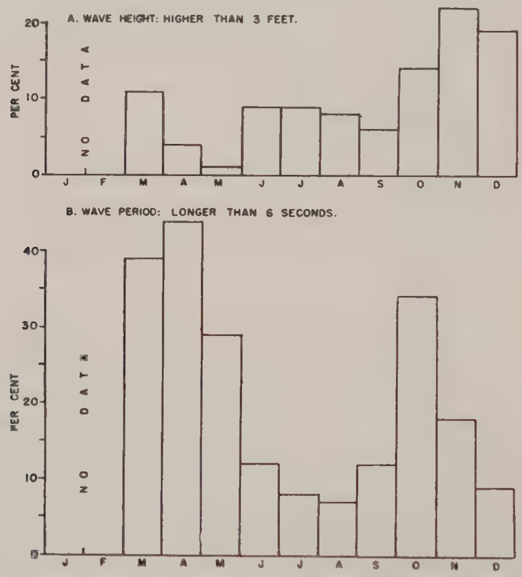

FIG. 25.—Shows seasonal distribution of larger waves off Grand Isle, Louisiana. Most waves are small, but higher waves with long period occur most frequently, beginning in late September, extending probably through January and February into March. Data from drilling platform 8 miles off Grand Isle, recomputed from Mason (1952).

SALT CONTENT

Salt content of the water surrounding the Mississippi Delta was studied because it is a tracer of river water and because of its effects on organisms. Differences of salt content are both a result and a cause of circulation in this area. Salt content changes as the result of flow and mixing of river and gulf water by breaking waves and all types of currents. In the upper layers differing water densities are largely due to variations of salt content and cause pressure surfaces to slope. The sloping pressure surfaces combine with the action of gravity to produce currents.

A high content of dissolved salts is one of the characteristics of the oceans that differentiates them from most bodies of water on land. Marine organisms are adjusted physiologically to high salt content, so that variations from normal marine concentration, either periodic or permanent, may alter faunas and floras.

Salt content usually is expressed as salinity, representing the total amount of solid material in grams dissolved in one kilogram of sea water. Because of the difficulty in analyzing for total dissolved salts, salinity is determined by analysis for chloride ion (and chloride equivalents, chiefly bromide and iodide). Chloride is titrated against silver nitrate with potassium chromate as indicator, and the results are termed chlorinity but expressed as salinity. This usage is based on the empirical relation: salinity $= 0.030 + 1.8050 \times$ chlorinity (Sverdrup *et al.*, 1946, pp. 50–51). The equation holds because of the constancy of ionic ratios in sea water and is good within narrow limits for a wide range of concentrations. Departures from the relationship occur at low concentrations, however, and they may be substantial when ionic ratios of diluting water differ materially from those of sea water. The proportions of dissolved substances in the Mississippi River are considerably different from the proportions in sea water (Clarke, 1920, p. 76), and many water samples obtained around the delta were of low concentration.

Therefore, because of errors that might be introduced were the customary relation used, and to avoid use of a double scale, all salt-content data are reported here as chlorinity (including chloride equivalents). Chlorinity is expressed as grams per kilogram (parts per thousand) for which the symbol $^{\circ}/_{\circ\circ}$ is used. Figure 26 shows the normal relationship between chlorinity and salinity, and the approximate range of uncertainty (Woods Hole Ocean. Inst., 1946).

At atmospheric pressure sea water density is a function of salinity and temperature. It is expressed here as σ_t, where $\sigma_t = (\rho_{(\mathrm{Cl},\mathrm{T},0)} - 1)1000$ and $\rho_{(\mathrm{Cl},\mathrm{T},0)}$ = water density of the indicated chlorinity, temperature, and atmospheric pressure. Figure 26 contains a diagram, also prepared from data published by Woods Hole Oceanographic Institute (1946), to show the relationships. For purposes of illustrating density differences (Fig. 15), the normal relationship of density to temperature and salinity (rather than chlorinity) was assumed to hold. Errors introduced by this assumption are small compared with density differences and do not exist in the open gulf where salt content is high.[9]

Data for study of chlorinity in the inshore region are entirely from our col-

---

[9] Suspended matter also affects bulk water density. Observations of suspended matter ranged from a maximum of 0.84 gram per liter to nil in inshore and open gulf waters, and the amount is not necessarily inversely related to chlorinity. The average suspended matter concentration probably is less than 0.1 gram per liter and therefore its effect on density is small relative to dissolved substances. Under special conditions, however, weight of suspended matter may become a significant factor (see subsequent paragraphs on Suspended Matter).

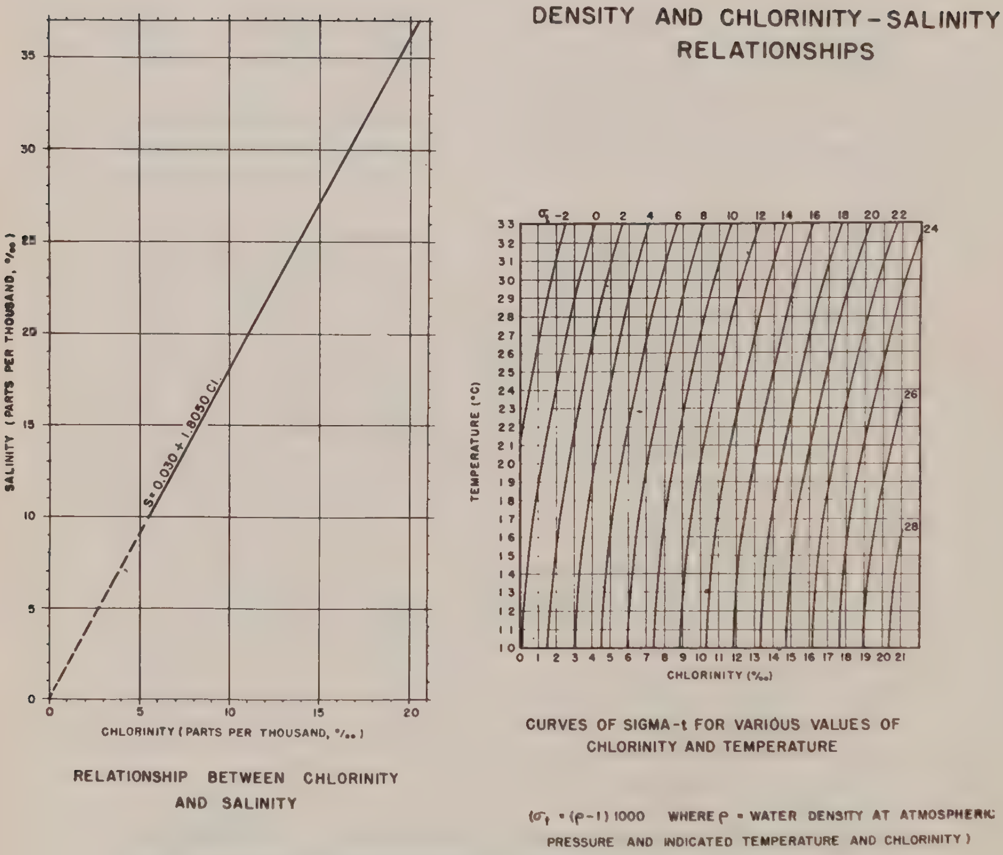

RELATIONSHIP BETWEEN CHLORINITY AND SALINITY

CURVES OF SIGMA-t FOR VARIOUS VALUES OF CHLORINITY AND TEMPERATURE

($\sigma_t = (\rho - 1)\,1000$ WHERE ρ = WATER DENSITY AT ATMOSPHERIC PRESSURE AND INDICATED TEMPERATURE AND CHLORINITY)

FIG. 26.—Conversion between chlorinity and salinity and chlorinity-temperature to σ_t.

lections. Approximately 1,500 observations were made, mostly in the inshore area, but also offshore on the continental shelf. Observations were obtained at all seasons of the year in conjunction with current and temperature measurements. Geyer (1955) recently published valuable data on the hydrography of near-by Redfish and Blind bays. In the area offshore from the delta, charts of surface salinity are included by Riley (1937); Geyer (1950) studied salinity variations with time at seven offshore drilling platforms several miles west of the delta. Parr (1935) included profiles of salinity in the Gulf of Mexico, Shaw (1913) recorded scattered observations, and Hedgpeth (1953) discussed salinities in gulf coastal waters as they affect the faunas.

DISTRIBUTION OF CHLORINITY

Changes of chlorinity may be large both at the surface and below, particularly in the inshore region, and they occur frequently and rapidly. Figure 27 shows the depth distribution of all available chlorinity observations around the delta. About 99 per cent of the observations fall between the solid and the dotted curves; the remainder fall between the dotted and dashed curves. Figure 27 shows that the amount of chlorinity variation decreases rapidly with depth to about 50 feet. Below 50 feet chlorinity usually is almost constant; values range from 19.6 to 20.2°/$_{00}$ and usually are between 20.0 and 20.2°/$_{00}$. High chlorinity is found almost to the surface where no dilution of sea water has occurred and indicates the chlorinity of undiluted gulf water.

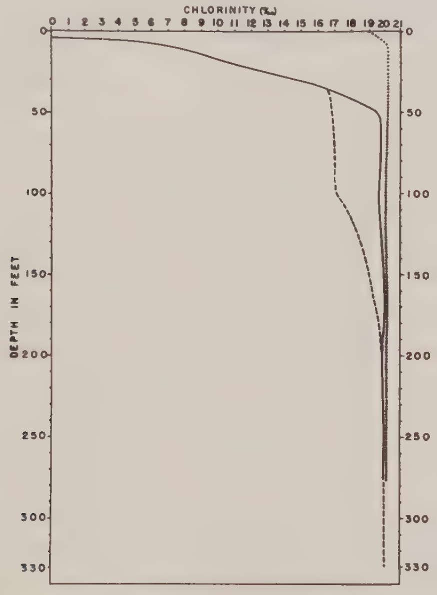

FIG. 27.—Depth distribution of available chlorinity observations. 99% of observations fall between solid and dotted curves. Remaining 1% fall between dashed and solid curves.

Fresh water is mixed to greater depths than 50 feet, however. A few deep observations were made during a September storm, and they showed reduced chlorinities to almost 200 feet (Fig. 27).

Inshore.—In the surface waters northwest of Main Pass chlorinities usually decrease on the flood tide and increase on the ebb, while to the east, surface chlorinity decreases on the ebb tide and increases on the flood. The largest changes of chlorinity that it is possible to have in the upper 50 feet (Fig. 27) do not occur at any one place, even over a period of time. Chlorinity of any particular area is related to its position with respect to sources of fresh water, to the current system, and to the winds. These factors were discussed under currents. It remains therefore, mainly to describe the chlorinity regimens of various areas, as this may affect their faunas. These areas are: (1) near Main Pass mouth, (2) in Breton Sound, and (3) east of Main Pass in deeper water.

Figure 28 is hourly variations of chlorinity at long-period observation stations in the area near Main Pass made during ebb and flood tide under different winds and river discharges (for locations, see Fig. 1). Figures 29 and 30 are profiles of chlorinity in the same areas at both flood and ebb tide, also under differing winds and discharges.

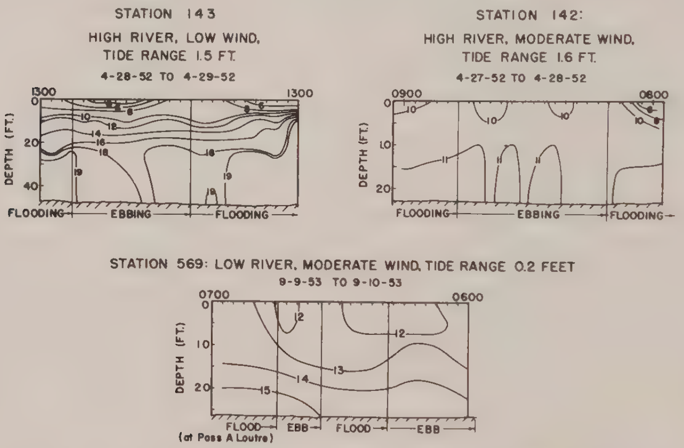

FIG. 28.—Changes of chlorinity profile with time at long-period stations. Flooding and ebbing refer to observed tidal changes except for station 569 where tidal changes could not be detected due to small range. Notice development of pronounced vertical chlorinity profile beginning near end of station 142 and continuing through station 143.

In the bottom water near Main Pass chlorinity usually increases at a particular point with the flood tide and decreases with the ebb (stations 142 and 569, Fig. 28). The hourly or short-term change in chlorinity on the bottom at any depth is not large and appears to be related first to length of tidal excursion and the chlorinity at comparable depths upstream from the point (Figs. 29, 30). This is because mixing by wind and waves is effective to the bottom inshore, and chlorinities may be relatively uniform at any particular depth over a period of one to several days.

When winds are low, bottom chlorinities are high, and when the wind is moderate or stronger, chlorinities are depressed. Under similar wind speeds, bottom chlorinity was 10°/₀₀ at high river discharge (station 142), while bottom chlorinity was 13–14°/₀₀ in the same area when the river was low (station 569). This shows that the extent of chlorinity depression under similar wind conditions is related to river discharge.

Although short-period bottom chlorinity fluctuations in stations 142 and 569 near Main Pass were relatively small, longer-period fluctuations of wind and discharge produce larger changes, more or less random in time (for example,

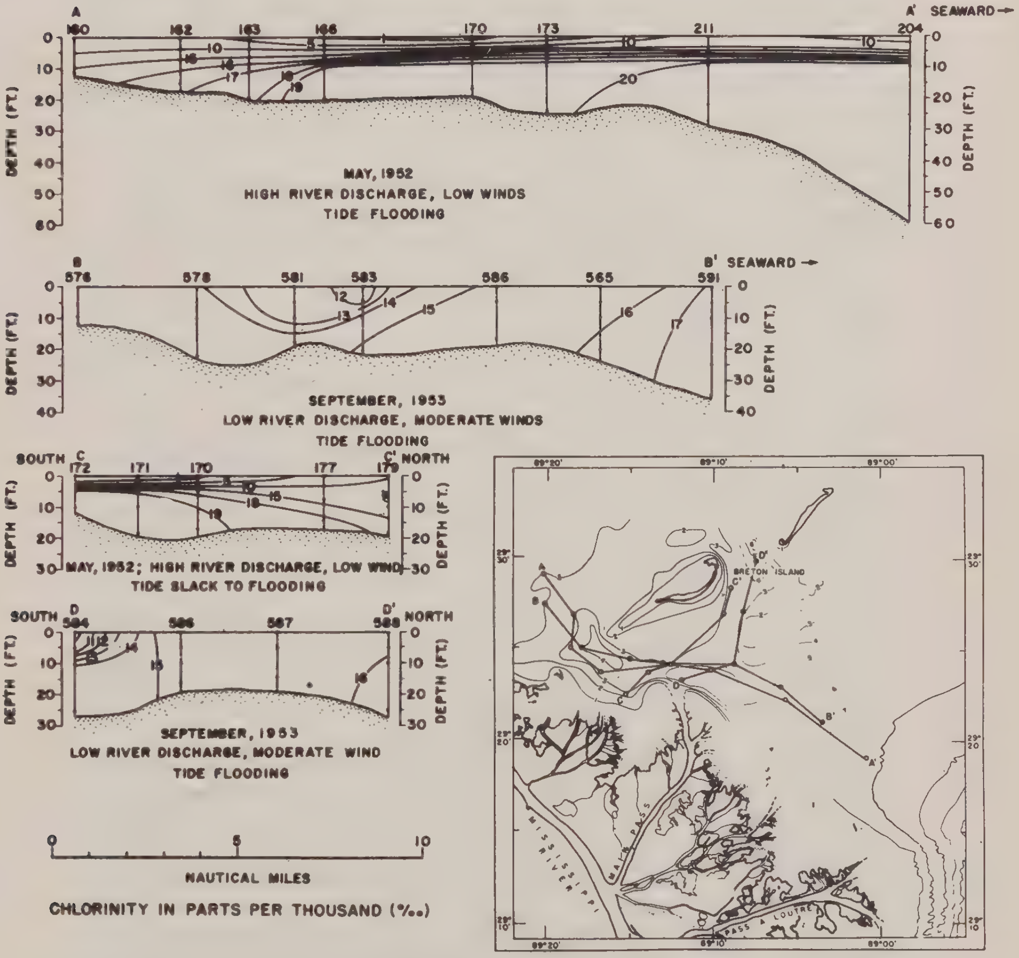

Fig. 29.—Variations in vertical chlorinity distribution caused by differences in wind and river discharge.

compare stations 142, 569, and the profiles of Figs. 29 and 30). Since their magnitude depends on both river discharge and wind, bottom chlorinity changes are greatest in the high discharge windy months of winter and early spring and are about 10°/₀₀.

The profiles of Figures 29 and 30 show the differences in bottom chlorinity between the area off Main Pass, Breton Sound, and the area east of Main Pass. In Breton Sound variations of bottom chlorinity are smaller than near the mouth of Main Pass because of distance from the fresh-water sources and the current pattern. Bottom chlorinities in the sound are depressed below normal gulf concentrations at all times, however, because of the shallow water and mixing induced by wind and tidal currents. The extreme range of bottom chlorinities in Breton Sound as a whole is large, but at any one location the range is probably only about 5°/₀₀. Thus, any local region in Breton Sound differs from the area off Main Pass by having smaller bottom-chlorinity changes and chlorinities depressed below open gulf levels. The change of regimens is gradational into and and within Breton Sound.

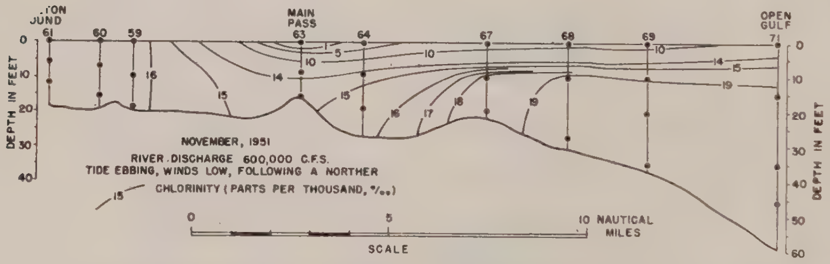

FIG. 30.—Chlorinity profile. Compare with chlorinity profiles *AA′* and *BB′* of Fig. 29.

Directly south of Breton Island tidal and other currents prevent great dilution of sea water (see Figs. 7, 31, 32, esp. surface charts). For this reason chlorinity changes here are less than those off Main Pass directly along the primary axis of circulation, and the chlorinity regimen is similar to that of Breton Sound proper.

Eastward from Main Pass mouth toward the open gulf, downward mixing of fresh water occurs similar to Breton Sound, but because of increasing depth toward the east, bottom-water chlorinity is less affected. Bottom chlorinities increase within a short distance seaward to normal open-gulf concentrations and are subject to only minor changes. Figures 29 and 30 show that the depth to which chlorinity fluctuations in the bottom water persist is about 40–50 feet along the primary axis of circulation. Bottom-water chlorinity changes usually are between 2 and 5 parts per thousand and decrease with depth. This regimen extends seaward from about Longitude 89° W. to 89° 05′ W., from about the same area as the limit of rapid winter temperature changes. The gulf east of Main Pass differs from the area directly off Main Pass in having a much smaller range of chlorinities, in having less frequent and shorter-period variations, and in having the usual bottom chlorinity of normal gulf concentration or approaching it. These two areas also grade into each other.

In the bays and shallow water around the shores of the delta, fluctuations of bottom chlorinity are produced by varying river discharge and wind, as in other parts of the area. The range of chlorinities is about 5–10°/₀₀. Because of the shallow water, these areas are particularly sensitive to changes of wind, and because of nearness to fresh-water sources, chlorinities are always depressed far below normal gulf concentrations (see also Geyer, 1955).

Figure 31 shows surface and bottom chlorinity at approximately average river discharge and during variable winds (Fall, 1951), and Figure 32 shows chlorinities during low wind and high river discharge (spring, 1952). Surface contours were drawn to illustrate maximum seaward and soundward spread of low chlorinity water. Therefore this picture is a composite of flood tide in Breton Sound and ebb tide east of Main Pass. Areas where the largest variations occur with tidal fluctuations are indicated; contours migrate seaward and landward with tide changes; because the surface contours show maximum spread of fresh water, changes cause chlorinities to increase in these areas.

On the bottom-water charts, maximum observed landward intrusion of high-chlorinity water is shown. Maximum intrusion occurs on flood tide, and change in the bottom water with the ebb tide produces lower chlorinities. Maximum observed differences are shown between surface and bottom chlorinities. The patterns of chlorinity distribution on these charts at different seasons are the same, although the absolute concentrations are widely different in some areas.

From these observations and charts it is possible to estimate the maximum chlorinities that occur in various parts of the inshore area. For the deeper water, bottom chlorinities found in the spring of 1952 (Fig. 32) are representative. For shallow water in Breton Sound and along the delta shore, however, the concentrations in spring are too low because of high river. In the shallow water of inner Breton Sound and in the bays near the small distributary mouths, the 1951 bottom contours (Fig. 31) probably more nearly represent maximum chlorinity.

Minimum bottom chlorinities occur during periods of high winds at high river stages, and observations under these conditions are not abundant. Bottom chlorinity at station 142 (Fig. 28) of about 10°/₀₀ probably is near the minimum for the channel bottom between Main Pass and Breton Island, and bottom chlorinities in inner Breton Sound (Fig, 32, spring, 1952) probably are near the normal minimum for this area, although under flood conditions, near-by Bohemia Spillway is opened and this probably reduces concentrations even farther. The ranges of chlorinity discussed for the three different areas can be applied to maximum concentrations to interpret absolute ranges. There are no sharp lines of division separating areas of different chlorinity regimen.

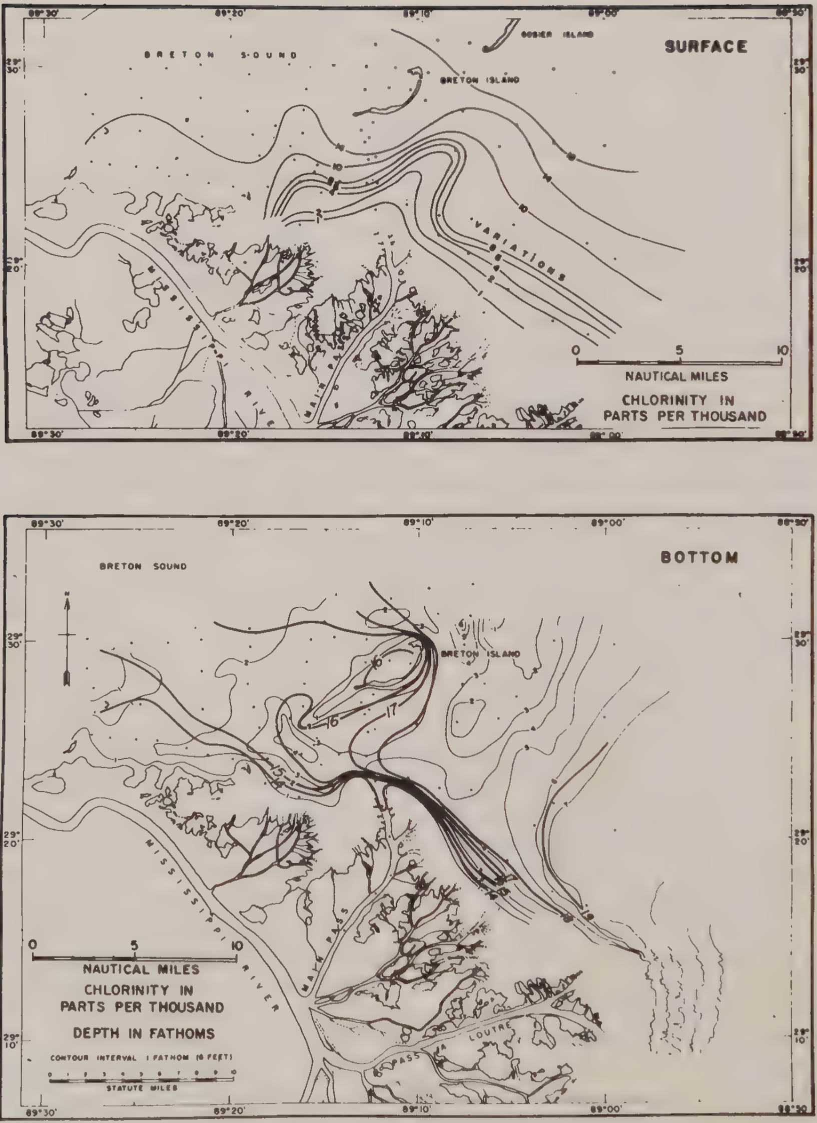
SURFACE
BRETON SOUND
GOSIER ISLAND
BRETON ISLAND
VARIATIONS
MISSISSIPPI RIVER
MAIN PASS
0 5 10
NAUTICAL MILES
CHLORINITY IN PARTS PER THOUSAND
89°30'
89°20'
89°10'
89°00'
88°50'
29° 30'
29° 20'
BOTTOM
BRETON SOUND
BRETON ISLAND
N
MISSISSIPPI RIVER
MAIN PASS
PASS A LOUTRE
0 5 10
NAUTICAL MILES
CHLORINITY IN PARTS PER THOUSAND
DEPTH IN FATHOMS
CONTOUR INTERVAL 1 FATHOM (6 FEET)
STATUTE MILES
29° 10'

FIG. 31.—Inshore chlorinity distribution, fall, 1951, average river discharge, variable winds. Bottom chart is maximum observed chlorinities, usually occurring on flood tide in this area. Surface chart is composite of minimum observed chlorinities. These usually occur on flood tide in Breton Sound and on ebb tide east of Main Pass. Chlorinity changes are most pronounced in area of "variations." Low chlorinity lobe extending into Breton Sound also is subject to considerable variation. Changes in these areas were toward higher chlorinities. Compare with Fig. 32.

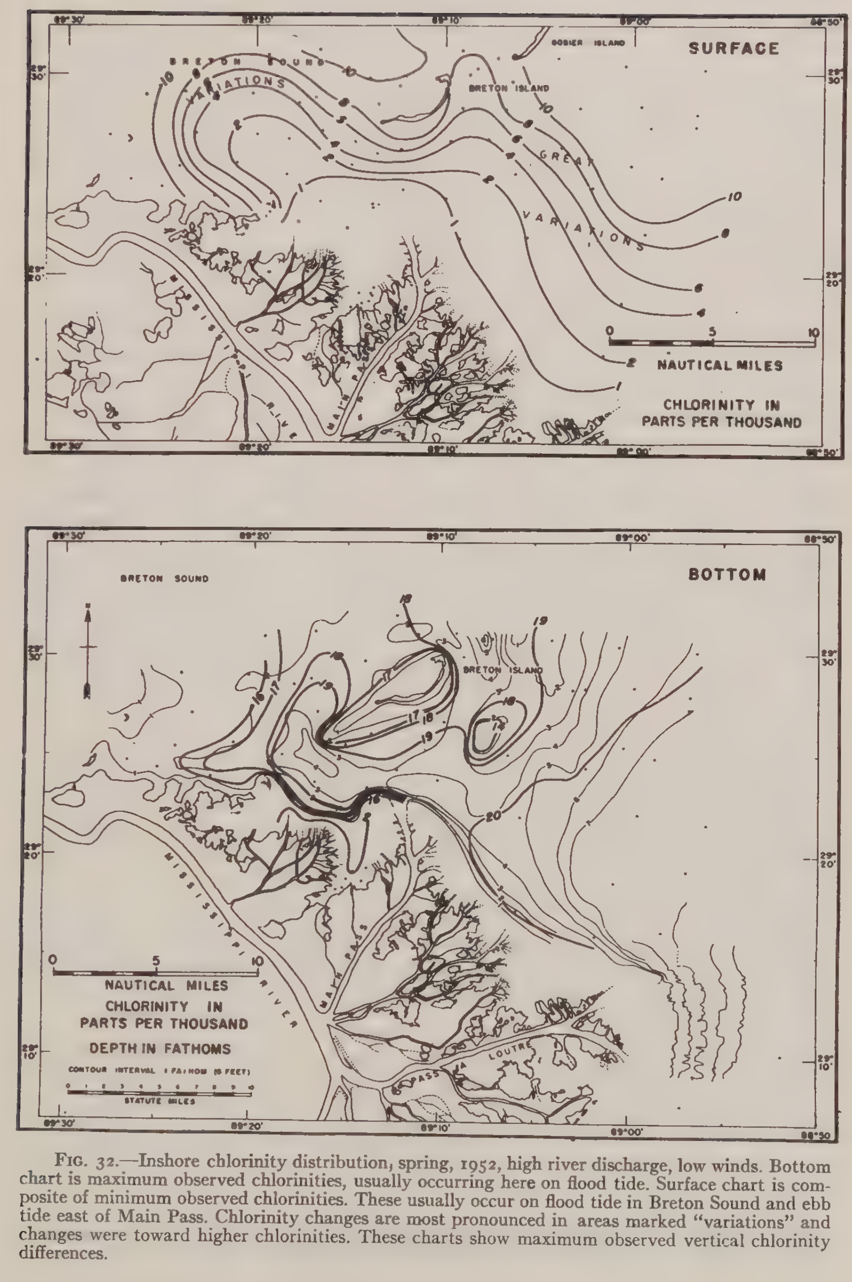
SURFACE
BRETON SOUND
VARIATIONS
BRETON ISLAND
GOSIER ISLAND
GREAT VARIATIONS
MISSISSIPPI RIVER
MAIN PASS
NAUTICAL MILES
CHLORINITY IN PARTS PER THOUSAND
89°30'
89°20'
89°10'
89°00'
88°50'
29°30'
29°20'
BOTTOM
BRETON SOUND
BRETON ISLAND
MISSISSIPPI RIVER
MAIN PASS
LOUTRE
A PASS
NAUTICAL MILES
CHLORINITY IN PARTS PER THOUSAND
DEPTH IN FATHOMS
CONTOUR INTERVAL 1 FATHOM (6 FEET)
STATUTE MILES
29°10'

FIG. 32.—Inshore chlorinity distribution, spring, 1952, high river discharge, low winds. Bottom chart is maximum observed chlorinities, usually occurring here on flood tide. Surface chart is composite of minimum observed chlorinities. These usually occur on flood tide in Breton Sound and ebb tide east of Main Pass. Chlorinity changes are most pronounced in areas marked "variations" and changes were toward higher chlorinities. These charts show maximum observed vertical chlorinity differences.

Offshore.—Chlorinity seaward of the delta on the continental shelf is the normal open-gulf chlorinity as modified by river discharge. The normal undiluted chlorinity of gulf water on the shelf is 19.6–20.2°/₀₀ and is constant with depth (Fig. 27). Dilution by fresh water lowers these values, and lowered chlorinities may extend over a large area to considerable depths.

Seaward distribution of the fresh water is produced by the areal current system previously discussed. Surface salinity charts in March and April (Parr, 1935; Riley, 1937) show major tongues of reduced salinity extending westward from the delta; Riley also found reduced salinities toward the east and north. No systematic large-scale surveys have been conducted off the delta at other seasons of the year, but differences from these observations would be encountered, depending on existing current conditions. Undoubtedly, the long tongues of turbid water extending to the east in May, 1952 (Scruton and Moore, 1953), were also tongues of lowered surface chlorinity.

Geyer (1950) investigated short-term fluctuations of salinity in surface waters (mean depth of 10 feet) on the shelf over a period of 14 months. Observations were made from 7 drilling platforms, a maximum of 60 miles west of the delta, and measurements were made by titration. He found the changes to be large and frequent. The maximum range of salinity (expressed here as chlorinity) was 13°/₀₀ (from 8°/₀₀ to 21°/₀₀) and occurred during the spring; during June and July the range was about 9°/₀₀ (from 11.5 °/₀₀ to 20.5 °/₀₀). He points out that reduced surface salinities are caused in part by more local runoff, but was able to correlate average monthly values with discharge from the near-by Mississippi River (*op. cit.*, Fig. 4). As Geyer points out, variations in depth of measurement and in the vertical chlorinity profile complicate this relationship, however, so that other factors also must be considered in more detailed analysis.

Changes of chlorinity occur at greater depths on the shelf also. The dashed line of Figure 27 encloses the reduced chlorinities encountered east of the delta in September after a period of strong northeasterly winds. Chlorinities of 17.2°/₀₀ were encountered at a depth of 100 feet, and some dilution was found to almost 200 feet. Parr (1935) found that some dilution persisted to 220 feet on a traverse made 24 miles west of the delta. Observations recorded by Shaw (1913) also show dilution of gulf water to depths of 75–100 feet. There is no doubt, therefore, that chlorinity variations occur in the deeper water of the shelf, but their extent and frequency are unknown.

HYDROGEN ION CONCENTRATION

A large number of measurements of hydrogen ion concentration in the water were made during the fall of 1951 and the spring of 1952, by use of a Beckman pH meter. Samples were mostly from water depths of less than 35 feet. The results were plotted against chlorinity, and those for the spring of 1952 are shown in Figure 33. pH measurements are uncorrected for temperature, but this correction is of the magnitude of the error of measurement. There seems to be little

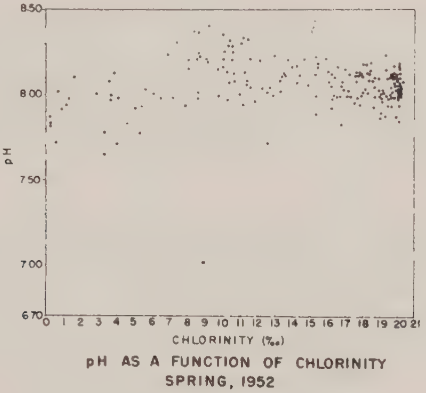

pH AS A FUNCTION OF CHLORINITY
SPRING, 1952

FIG. 33.—Hydrogen ion concentration plotted as function of chlorinity.

change of pH with change in chlorinity; differences produced by other factors such as biological activity apparently exceed differences related to chlorinity. Relationships in the fall of 1951 were similar to those in Figure 33, but the spread of pH measurements was greater in 1951 and a few low (6.7–7.0) values were observed in low-chlorinity water near the delta.

TEMPERATURE

Temperature in the shallow inshore waters is subject to great changes in a short time. This is also true of the offshore water at comparable depths, but to a much less extent. For this reason temperature is of little value in tracing water movement, and the chief purpose of this discussion is to supply background for ecological studies of the larger and smaller invertebrate faunas. Main interest is in the temperature regimen, the average annual cycles, and the extremes, both areally and at different depths.

Again it is necessary to subdivide the delta region into inshore and offshore areas. The offshore area is much simpler and more uniform.

Most of the temperature data were collected with the bathythermograph, a device for making a continuous record of temperature against depth. Approximately 470 bathythermograms were taken during the eight months of February, April, May, June, September, October, November, and December. Most of them were in the inshore area. Additional observations in the offshore area were secured from U. S. Navy Hydrographic Office records.

Temperature-depth studies of the few other data in the northeastern Gulf of Mexico were made by Adams and Sorgnit (1951) who considered differences between summer and winter temperature and thermal structure and by Fuglister (1947, 1953) who treated the monthly average surface temperatures and average temperatures at 200 meters. Slocum (1935) gives average monthly surface temperatures approximately 100 miles south of the delta, and the Current Charts of Central American Waters (U.S.N. Hydrographic Office) give monthly average surface isotherms in the Gulf of Mexico at 5°F. intervals. Hedgpeth (1953) discussed temperatures along the entire Gulf Coast, and Leipper (1954) also recently summarized most of the available offshore information.

OFFSHORE TEMPERATURE

Study of temperature of the shelf waters east of the delta is based on records of the Hydrographic Office supplemented by other information. An average of approximately 20 observations per month was used to prepare the curves of temperature distribution; averages at each depth of record (depths indicated in Fig. 34) were corrected by smoothing the annual curve at that depth (Fuglister, 1947). Surface averages obtained in this way agree within an average of 0.7°C.

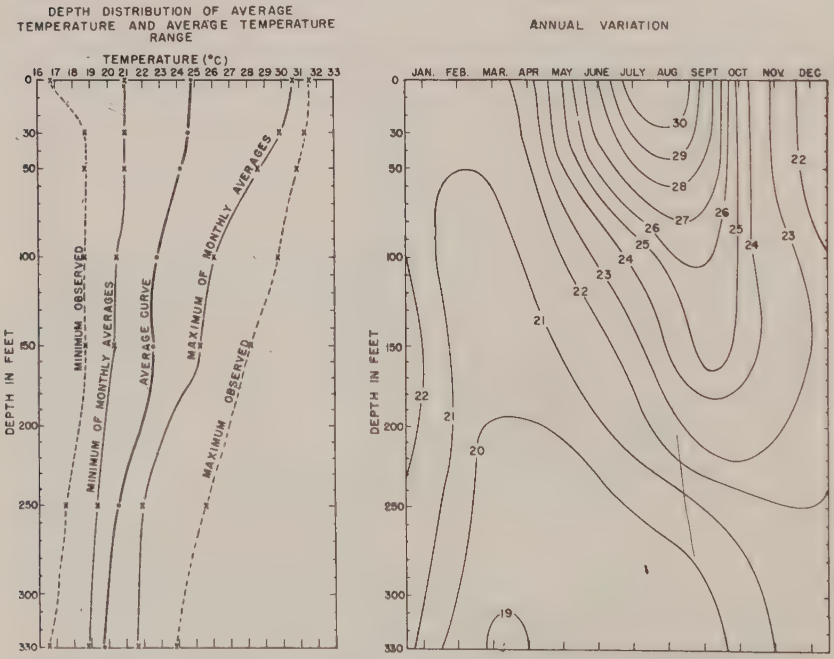
DEPTH DISTRIBUTION OF AVERAGE TEMPERATURE AND AVERAGE TEMPERATURE RANGE

ANNUAL VARIATION

FIG. 34.—Offshore temperature. Depth distribution of average temperatures in Gulf of Mexico east of Mississippi Delta. Left diagram is average depth-temperature curve, average maximum and minimum depth-temperature curves, and observed extremes. Right diagram is annual cycle of average temperature to 330 feet. Average vertical temperature structure at any time can be obtained from this diagram.

with Fuglister's monthly surface temperatures in the area. Slocum's (1935) surface averages were taken near Latitude 26° North, and show a smaller annual range.

Figure 34 consists of temperatures to a depth of 330 feet on the shelf east of the delta, and shows curves of average temperature, maximum and minimum monthly averages, and the maximum and minimum observed extremes at depths of record. This figure does not show thermal structure at a given time. It also contains the annual cycle of monthly average temperature to 330 feet. Average temperature ranges from about 25°C. at the surface to 20°C. at 330 feet. The average range of temperature at the surface is 9.8°, and the extreme observed range is about 14.8°. At 330 feet the average range is 2.5° and the extreme observed range is 7.3°. Temperature extremes are buffered by stored heat and heat capacity of the water. January, February, and March are the coldest months, with temperatures averaging about 21°. July, August, and September are the warmest months on the average.

The annual cycle of temperature is partly the result of currents bringing into the area water of certain temperature characteristics (advection), and partly the result of local changes produced by surface heating and cooling, and mixing. The cycle off the delta is similar to that of many other regions. Heating of the water commences in March and continues through the summer months with progressive deepening and warming of the surface layer. In September the change is reversed, and vertical mixing is induced by strong winds, waves, and cooling. The surface layer thickens rapidly and decreases in temperature. Continued intermittent strong winds and cooling during the fall produce a surface layer that is almost isothermal to 330 feet by December. Temperature in this layer continues to decrease until about February.

The lowering of temperature in deeper water during spring probably is due to currents. However, the temperature increase in the deeper water from October through December when the water column is essentially isothermal is caused, at least partly, by downward mixing of warm surface water and is part of the seasonal variation.

INSHORE TEMPERATURE

Temperature changes in the shallow, restricted, inshore area are relatively large, and may be rapid and frequent. Because of these changes, the relative scarcity of observations, and the several controls of temperature in the area, it is necessary to relate the data to better known cycles to get reliable annual temperature regimens in the inshore area. To do this, the factors controlling temperature here must be examined.

Temperature and temperature changes in the inshore area are related to: (1) offshore water temperature, (2) air temperature and surface effects such as solar radiation, and (3) Mississippi River temperature. Geyer (1955) discussed the effects of some of these factors on Redfish and Blind bays. At any given depth, the temperature varies over the area according to which of these factors predominates, so that no single curve can represent adequately the entire inshore area.

Figure 35 gives the annual cycle of air temperature at New Orleans based on monthly averages from 1900 to 1952 (U. S. Weather Bureau) and the annual cycle of Mississippi River water based on monthly averages from 1915 to 1938 (Hirsch, 1939). The annual air and river temperature cycles are similar, but the river extremes are greater and the curves are offset slightly, with average river temperature lagging behind average air temperature at the minima. This is chiefly because of climate in the Mississippi drainage basin and conservative nature of river temperature. As a result of the spreading of cold river water in the gulf in spring, leafing of vegetation in the lower delta is behind other parts of southern Louisiana by about a month (P. Viosca, personal communication). Extremely dense ground fogs occur regularly during periods of warm onshore winds in the late fall and winter, also because of the cold river water.

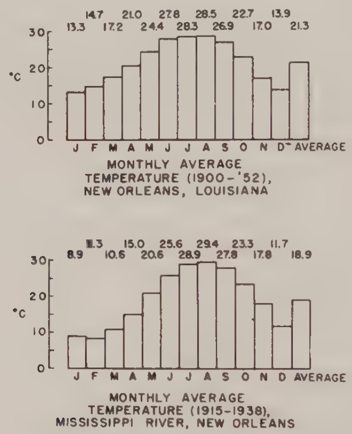

MONTHLY AVERAGE TEMPERATURE (1900-'52), NEW ORLEANS, LOUISIANA

MONTHLY AVERAGE TEMPERATURE (1915-1938), MISSISSIPPI RIVER, NEW ORLEANS

FIG. 35.—Annual cycles of monthly average air temperature at New Orleans (top diagram) and monthly average river temperature (bottom diagram).

River temperature does not change greatly until the water is spread out over the gulf and exposed to surface and mixing effects. Therefore close around the shores of the delta the annual curve of river temperature describes the average temperature range. The depth to which this curve can be used is small, however, probably a maximum of 2–3 feet except off the larger distributaries. Below this depth, dilution with salt water of different temperature alters the temperature accordingly, generally increasing the minimum temperature.

In Breton Sound water temperature seems to be influenced most by surface effects (air temperature and solar radiation) and by interchange with the open

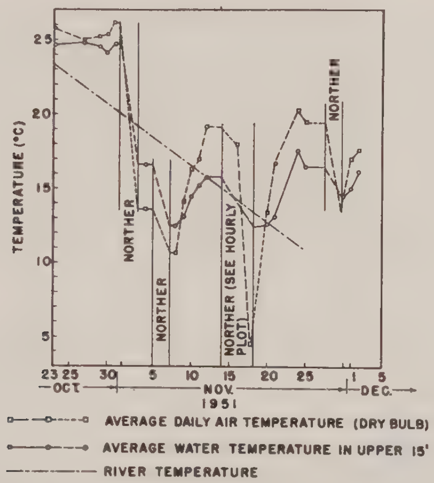

FIG. 36.—Variations of daily average temperature. Changes in inshore surface water temperatures associated with autumn storms. Air temperature falls rapidly during storms and is followed by surface temperature. Air and surface temperature increase slowly after storms. (Surface temperature curve broken when direct observations not available). Hourly temperature plots (Fig. 37) show changes in detail. River temperature curve is approximate but gives observed temperature change.

sea. Surface effects are shown on Figures 36 and 37. Figure 36 gives the periods of storms, changes of daily average air and surface temperature of the inshore waters, and the approximate river temperature during November and parts of October and December, 1951. Air temperature during "northers" dropped rapidly, remained low during the periods of northerly wind, and increased as the

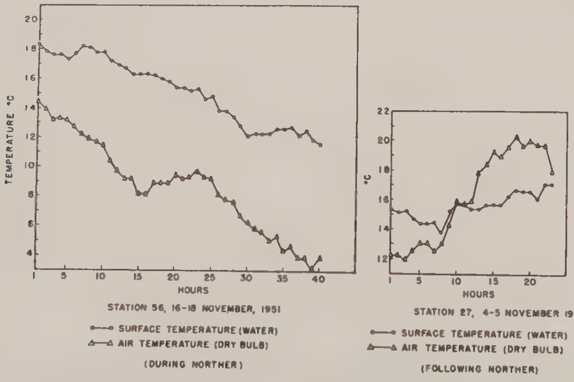

FIG. 37.—Hour-to-hour changes of air and surface water temperature during and following autumn storms, Breton Sound. See also Fig. 36.

wind shifted toward the east and south. The drop in air temperatures produced a correspondingly rapid, though retarded, drop in water temperature. Stirring by wind and waves extended the temperature change downward through the entire water column. Figure 37 shows by hourly readings the lowering of surface temperature during a single period of cooling. Water temperature reached a minimum value, however, and was always greater than the air temperature by several degrees. Figure 37 also shows air and surface temperature increasing after a northerly storm. Increase in water temperature may precede and equal or even exceed changes in air temperature.

Figure 38 shows effects of interchange with the open sea. The profiles are cross sections of temperature from Breton Sound (on the left) to the open gulf. Both profiles are in about the same position and are located in Figure 29. In the upper profile water temperature in Breton Sound east to the longitude of Main Pass averaged only 12.5°C., but in the open-gulf water temperature in the upper 40 feet averaged 21.5°C. Between these extremes there was a relatively uniform temperature gradient, temperature increasing seaward. The lower profile, A–A′, was made in early May and shows the opposite condition. Temperature in the surface water of the open gulf averaged about 20.5°C., but in Breton Sound the surface temperature ranged to over 26.0°; temperatures increased toward the sound, although the gradient was not uniform because of discharge of cool river water.

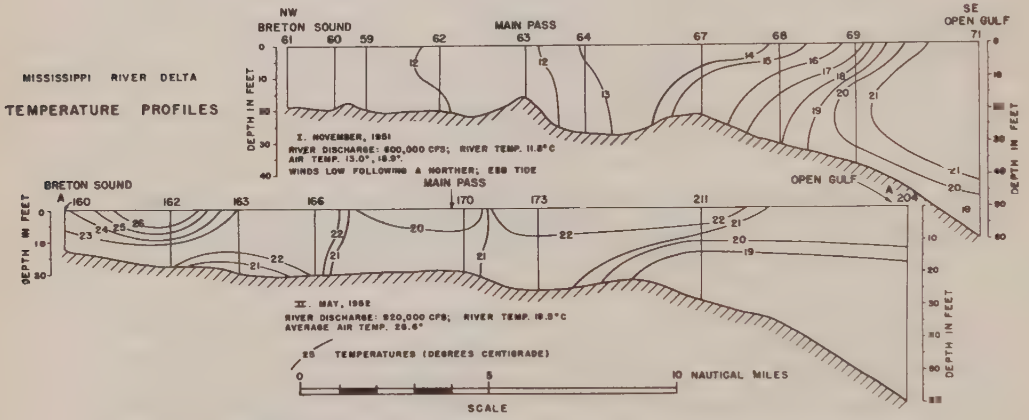

FIG. 38.—Temperature profiles from Breton Sound eastward to open gulf under different conditions (for position of profiles, see profiles *AA′* and *BB′*, Fig. 29).

These data show how surface effects and prevailing gulf temperatures determine temperatures in the shallow sound. Water temperature tends to follow air temperature cycles, but is buffered at all times through exchange with the open gulf. During winter storms the buffering effect of stored heat in the gulf water establishes a minimum temperature which depends on the rate of cooling and the rate of warm bottom-water intrusion through the deeper inlets to replace surface water removed by wind currents. Over most of Breton Sound this minimum seems to be about 11°C., although in innermost shallow bays a thin skim of ice may rarely develop (Hedgpeth, 1953). The effects of rapid temperature changes in the sound do not seem to extend to a depth greater than approximately 30–40 feet in the adjacent gulf, and even here the change is much reduced (Fig. 38, Sec. 1). The longitude of this point is about 89° 05′ W.

Following the storms, temperature in the sound rises, due mainly to exchange of chilled sound water for warmer gulf water, although insolation and warm gulf winds exert some influence. The rate at which the rise in temperature occurs suggests that the flushing period of Breton Sound on the average is about 2–4 days.

During the summer, heat capacity of gulf water exerts a buffering effect of opposite type. Sound water is heated mainly by solar radiation, but also by contact with the air. An average maximum of about 31°–32° in the surface water is imposed, however, because of exchange with the gulf. Vertical stratification usually is stronger in the summer than at other times, so that bottom temperatures in Breton Sound proper probably seldom reach 32°.

Because of the importance of surface heating and cooling and exchange with the sea, the river seems to have relatively little influence on Breton Sound tem-

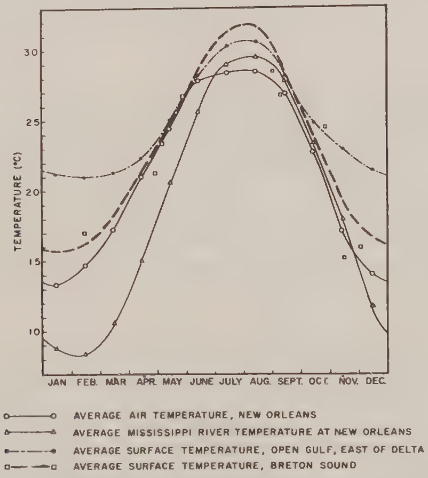

FIG. 39.—Comparison of annual cycles of average air, river, and surface-water temperatures in Breton Sound and Gulf of Mexico east of délta. Breton Sound average temperature cycle lies between air and gulf temperatures except during summer months when it exceeds them.

peratures. The effects of river temperature are present to the bottom near Main Pass mouth when the water column is vertically unstable, however.

Figure 39 shows curves of average river and air temperatures at New Orleans and average surface temperature in the open gulf east of the delta. Also shown are monthly averages of all the available surface temperatures in Breton Sound. A curve of average annual sound temperature is fitted to these monthly averages of Breton Sound temperature in accordance with considerations just described. The curve of average sound surface temperature falls between the air and gulf curves except during the hottest months.

Figure 40 gives depth distribution of measured and estimated temperature averages and extremes for near the delta shore, Breton Sound, and the open gulf. These distributions apply only to the designated areas; between these areas intermediate temperatures prevail that depend largely on position of the locality relative to these areas.

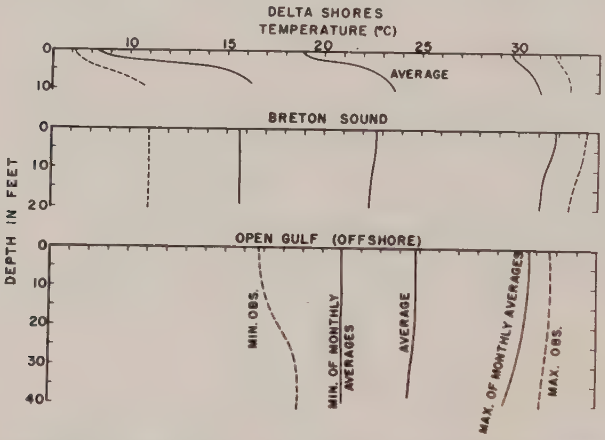

FIG. 40.—Showing depth distribution of estimated average shallow-water temperatures, estimated average monthly extremes, and estimated extremes for main subdivisions of inshore area. Compare with observed values in open gulf in lower diagram (from Fig. 34).

SUSPENDED MATTER

Sediment transported to the Gulf of Mexico by the Mississippi River makes up by far the largest proportion of the delta's bulk. The amounts and kinds of solid and dissolved sediments carried by the river and their proportions still are not accurately known (U. S. Engineers, letter of 1952; Russell, 1936, p. 137). Table II and the following discussion give the most recent information available on amounts of sediments and size proportions in the Mississippi load. They were prepared from data supplied by the New Orleans office of the Corps of Engineers,

U. S. Army, in a letter of March 31, 1952. These results are based largely on a 1938 study of suspended materials transported through the passes (U. S. Engineers, 1939) and on studies of suspended sediment samples from the Mississippi River at Baton Rouge currently being conducted by the U. S. Engineers.

In the 1938 study no samples of suspended sediment in transport contained material coarser than the very fine sand particle size. Moreover, only a small percentage of the material fell within the very fine sand range. A typical suspended sediment sample from the 1938 study would consist of 2 per cent very fine sand (0.125 mm.–0.0625 mm.), 48 per cent silt (0.0625 mm.–0.0039 mm.), and 50 per cent clay (finer than 0.0039 mm.). Size analyses of sediments from the river bed and the passes showed that the largest particles were retained on a 3.327-mm. sieve and that all particles were finer than 4.669 mm. The largest size particle contained in most of the samples was between 1.168 mm. and 1.651 mm. All samples of the river bed contained sediment down to clay size. There were no observations on the composition of the larger particles, but they may have been woody material.

TABLE II. MISSISSIPPI RIVER SEDIMENT TRANSPORTED

Flow	*Concentration of Suspended Material*		*Discharge of Bed and Suspended Material*		
	Parts Sed. Per Million Parts of Water	*Lbs. Per Cubic Foot of Water*	*Lbs. Per Sec.*	*Tons Per Day*	*Cu. Yds. Per Day*
Maximum	1,600	.100	156,000	6,800,000	42,000,000
Flood			125,000	5,400,000	33,000,000
Mean	850	.053	33,000	1,400,000	870,000
Low			2,000	100,000	60,000
Min. observed	200	.012	800	30,000	19,000

Total annual sediment discharge—500,000,000 tons or 310,000,000 cubic yards which would be equivalent to a cube 2,000 feet on a side, or 20,000 acres 10 feet deep, or 1 mile square and 300 feet high.

Based on observations, the bed load is estimated at 25% of the measured suspended material.

From data supplied by the district engineer, New Orleans Office, Corps of Engineers, U. S. Army, in a letter of March 31, 1952.

Uncertainty as to amount of sediment transported by the river is due largely to the difficulty of estimating bed load,[10] to constantly changing suspended load, and to varying relationship between discharge volume and suspended load (Elliott, 1932, p. 117). The figure of 1,400,000 tons of sediment per day (approximately 500,000,000 tons per year)[10] given by the engineers in 1952 is smaller than the estimate of 2,000,000 tons per day given by Russell and Russell (1939).

[10] For example, the U. S. Engineers at New Orleans currently estimate bed load at 25 per cent of the measured suspended load. However, E. W. Lane of the University of Iowa Hydraulic Laboratory and E. W. Eden of the U. S. Engineers in Rock Island, Illinois, computed from measurements on sand waves that the bed load of the Mississippi during high water ranged from only 0.2 to 1.5 per cent of the suspended load, and was usually less than 1 per cent (Lane and Eden, 1940, Table VI, p. 288). They considered these values higher than average annual values, because they believe there is little or no bed load movement during a large part of the time. Lane and Eden computed the average annual sediment load of the river to be about 350,000,000 tons (1940, p. 282), or approximately 70 per cent of the U. S. Engineers' estimate.

This figure may decrease still further as precision of measurements and knowledge of the relationships involved increase.

There is a tremendous volume of terrigenous sediment transported,[11] however, which is discharged through the various distributaries into the Gulf of Mexico. The distributaries carry sediment load about in proportion to their water discharge. Thus, in the present delta, Southwest Pass discharges approximately 30 per cent of the sediment, South Pass about 17 per cent, the Pass a Loutre system about 35 per cent, and Cubitts Gap, the Jump, Baptiste Collette Bayou, and other distributaries about 18 per cent (U. S. Engineers, 1939). In the gulf the load is distributed, fractionated, and deposited.

Data bearing on the seaward distribution of suspended load and the process of fractionation in the gulf are based on secchi-disc observations and sample collections in 1951, 1952, and 1953, and various observations during airplane flights. The secchi disc is a white disc 30 cm. in diameter which is lowered into the water until it can no longer be seen (Sverdrup *et al.*, 1946, p. 82). The depth of extinction is the reading; low readings indicate a large amount of suspended material. Readings from this device are crude for a number of reasons. They have proved to be quantitatively unreliable but do indicate relative amounts of suspended material in a general way. Samples collected for measuring amounts of suspended material were of gallon size, were filtered in the laboratory, dried, and weighed. Amounts are expressed as grams of dry sediment per liter of water. Results of aerial observations were summarized by Scruton and Moore (1953). Studies of particle size distribution of suspended sediment have not been made.

DISTRIBUTION

Areal.—Results of secchi-disc observations are shown in Figure 41. Values represent the depths below sea surface to which the secchi disc was visible. The patterns of high turbidity (mainly due to suspended sediment) are similar to patterns of surface chlorinity shown in Figures 31 and 32, with high turbidity in areas of low chlorinity. These maps show the highest turbidity occurs around the delta shores at both seasons of the year and decreases with increasing distance from the distributaries. High turbidity extended farther offshore at high river in the spring than at lower river in the fall. Lobes of high turbidity extended northward into Breton Sound approximately along the axes of the lobes of lowered chlorinity. Areas of great variation of turbidity coincide with areas of great chlorinity changes (Figs. 31, 32).

Figure 42, reproduced from Scruton and Moore (1953), shows the synoptic pattern of surface turbidity both inshore and in the open gulf to the east. Highest turbidity surrounded the shore, but was prolonged into great plumes extending seaward a maximum of about 65 miles off the largest distributaries. Concen-

---

[11] The great total of transported sediment is due to the large discharge of water, since the concentration of sediment is surprisingly low, even at flood stages (see Table II). Professor Forshey found from measurements carried on for a year that only about one inch of dried sediment separated from a column of river water 186 feet high (Humphreys and Abbot, 1876, pp. 139–40; Forshey, 1877).

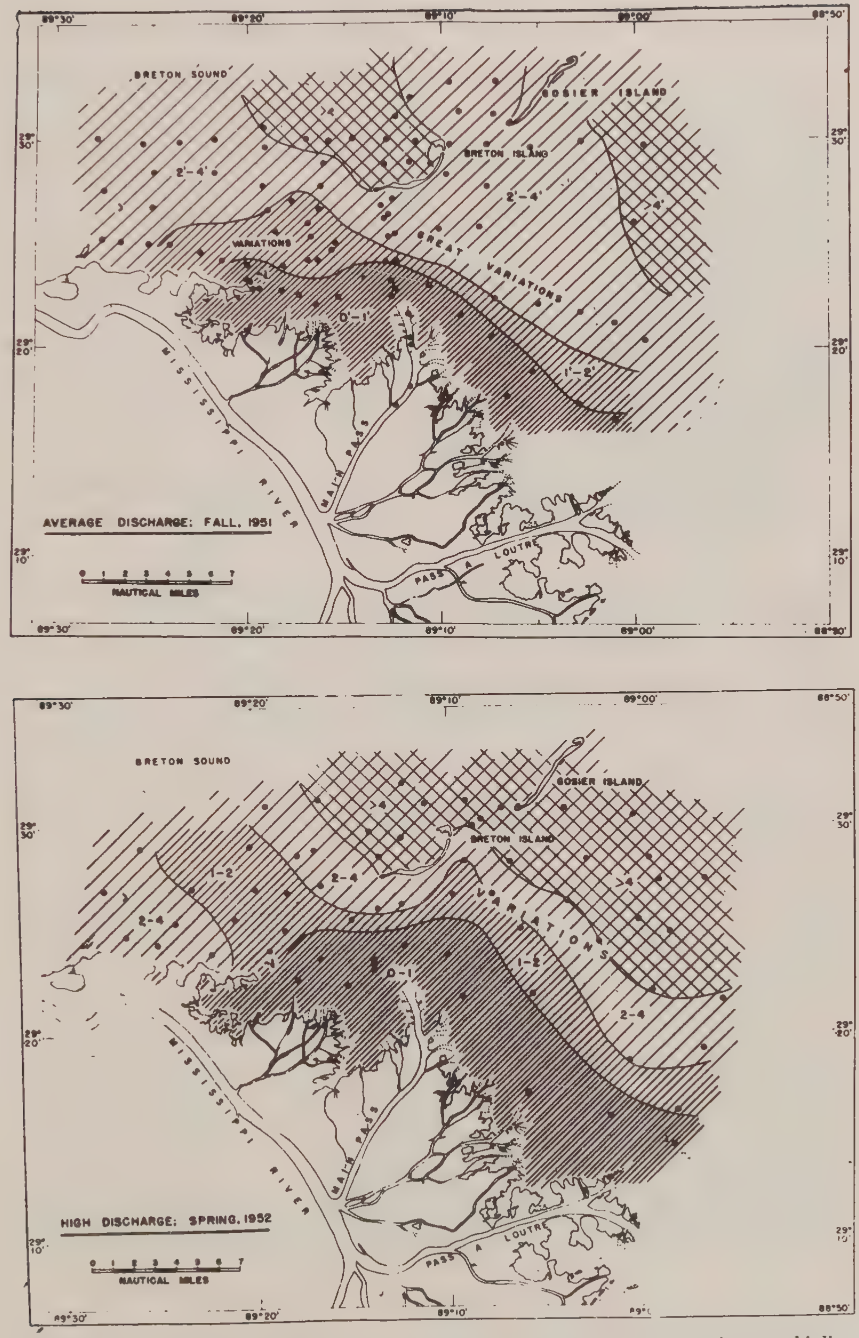
89°30'
89°20'
89°10'
89°00'
88°50'
29° 30'
29° 20'
29° 10'
BRETON SOUND
GOSIER ISLAND
BRETON ISLAND
>4'
2'-4'
2'-4'
>4'
VARIATIONS
GREAT VARIATIONS
0'-1'
1'-2'
MISSISSIPPI RIVER
MAIN PASS
PASS A LOUTRE
AVERAGE DISCHARGE: FALL, 1951
0 1 2 3 4 5 6 7
NAUTICAL MILES
BRETON SOUND
GOSIER ISLAND
BRETON ISLAND
>4
1-2
2-4
2-4
VARIATIONS
>4
0-1
1-2
2-4
MISSISSIPPI RIVER
MAIN PASS
PASS A LOUTRE
HIGH DISCHARGE; SPRING, 1952
0 1 2 3 4 5 6 7
NAUTICAL MILES

FIG. 41.—Distribution of suspended matter in surface waters of inshore area, from secchi disc observations. Compare with distribution of surface chlorinity (Figs. 31, 32). Legend: dots = observation stations. Diagonal patterns indicate visibility: close spacing, 0–1 ft.; wider, 1–2 ft,; widest, 2–4 ft.; crossed lines 4+ ft.

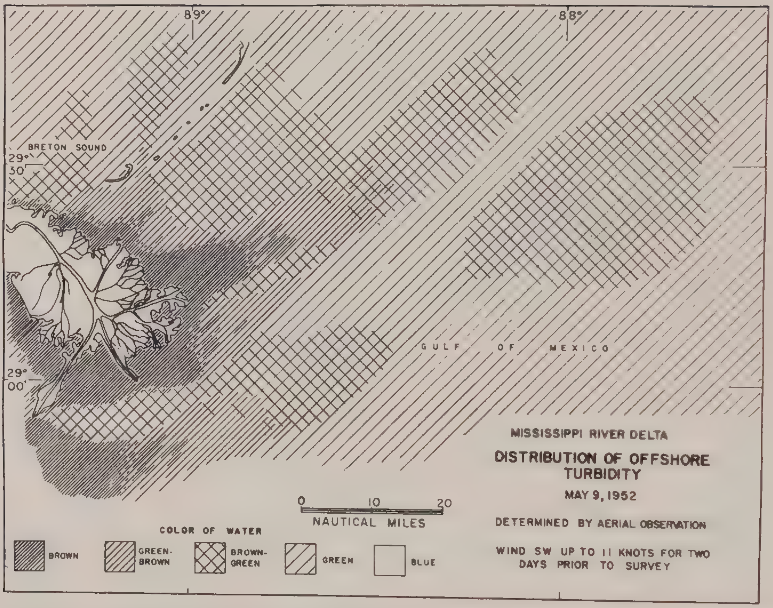
89°
88°
BRETON SOUND
29° 30'
29° 00'
GULF OF MEXICO
MISSISSIPPI RIVER DELTA
DISTRIBUTION OF OFFSHORE TURBIDITY
MAY 9, 1952
0 10 20
NAUTICAL MILES
DETERMINED BY AERIAL OBSERVATION
WIND SW UP TO 11 KNOTS FOR TWO DAYS PRIOR TO SURVEY
COLOR OF WATER
BROWN
GREEN-BROWN
BROWN-GREEN
GREEN
BLUE

FIG. 42.—Distribution of suspended matter in surface water around and seaward of Mississippi Delta. Plume seaward of Pass a Loutre distributary system was approximately 65 miles long. Note turbidity extending into Breton Sound. (After Scruton and Moore, 1953)

tration of suspended matter in these plumes decreased with increasing distance from the distributaries as shown by the change of color along their axes. A decrease in the size composition of suspended matter also can be indicated by these changes in color.

The relationship between chlorinity distribution and the current pattern has been shown and described (Figs. 7, 31, 32). A similar close relation exists between distribution of suspended matter being initially derived from the river and the currents, and the primary distribution of suspended matter is downstream from the river mouths in accordance with the existing currents.

The areal pattern of turbidity in the fall of 1951 is less well defined than in the spring of 1952 (Fig. 41). This is partly due to lower concentrations in the river, but also reflects the effects of wave action on shallow bottoms resuspending previously deposited sediments. Although concentrations of suspended sediment in the river are highest during the flood seasons, concentrations in the shallow gulf are highest intermittently during the storms of fall and winter and may exceed by many times the flood-season concentrations at the same location. For example, 0.6–0.7 gram per liter of suspended sediment was measured at station 56 (Fig. 1) during a norther where normally, even at flood stage, the concentration was very much less than this. During a period of small waves, 0.04 gram per liter of sediments was being carried by Main Pass, while the shallow water adjacent to Main Pass was highly roiled by these waves and suspended concentration was 0.12 gram per liter, or three times as great. This resuspended sediment is carried away and deposited elsewhere. Under conditions of moderate to high wind from the northerly semi-circle the pattern of turbidity on the northeastern flank of the delta tends to represent the topography, with greatest turbidity in shallowest water, but this of course is blurred by currents sweeping resuspended sediment downstream.

Vertical.—Figure 43 shows profiles of suspended matter at North Pass mouth at different river stages. Current and chlorinity distributions along these same profiles are shown in Figure 12. Contours in Figure 43 are discontinuous because of the erratic nature of the distributions.

At the moderately high discharge in June, suspended sediment upstream in the river averaged about 0.4 gram per liter and was distributed uniformly at the depths sampled. Downstream at the bar crest there was a pronounced vertical concentration gradient; the bottom concentration was 0.84 gram per liter,

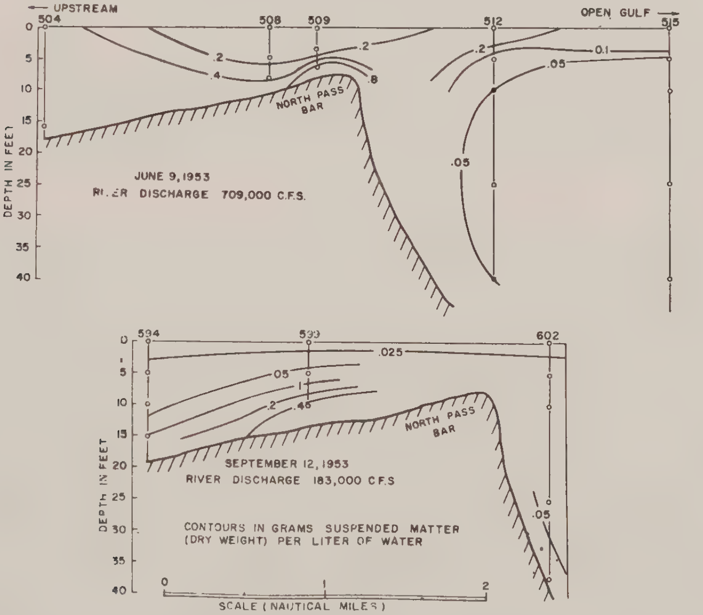

FIG. 43.—Vertical distribution of suspended matter in and near North Pass mouth at different river discharges. Note highest observed concentration is on bar crest during moderately high river. Compare with current speed and chlorinity profiles (Fig. 12).

and at the surface it was only 0.11 gram per liter. Still farther downstream (in the gulf, seaward of the bar, station 512), the surface concentration was 0.21 gram per liter, decreasing to 0.04 gram per liter at 25 feet, and 0.05 gram per liter at 40 feet. Currents in the channel were downstream at all depths, and greatest variations of concentration occurred in the bottom waters.

During low discharge in September (Fig. 43) surface concentrations were uniform and slightly greater than 0.02 gram per liter. Concentration increased rapidly with depth, however, and was a maximum of about 0.7 gram per liter in the upstream-moving bottom water. Seaward of the bar there also was an increase of suspended matter with increasing depth.

Figure 44 shows suspended matter concentrations along a traverse normal to shore between Main Pass and North Pass mouths. Waves were low at the time of sampling, and suspended sediment was being supplied from the Cubitts Gap distributary system. The tide was flooding, so that some material from North Pass probably was present also. Concentration of material was highest nearest shore and at the surface and bottom. The concentration decreased offshore, but pronounced maxima were maintained at the surface and in the saline deep waters.

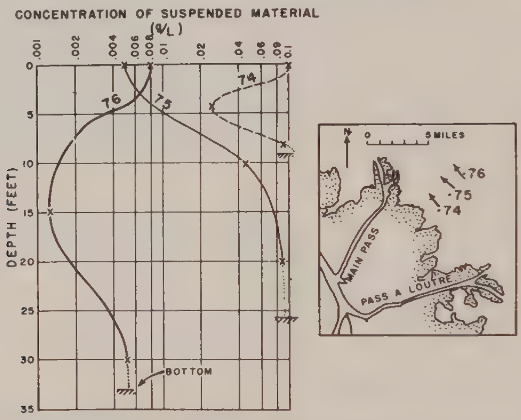

FIG. 44.—Vertical distribution of suspended matter northeast of delta. Concentration in grams per liter, dry weight. Note surface and bottom maxima persist away from shore. Arrows on index map show current directions at time of sampling.

These profiles, the secchi-disc observations, and the map of offshore turbidity show that a turbidity maximum is maintained in the surface layers and that it may persist to considerable distances downstream from the distributary mouths. Settling of sediment in the gulf therefore is initiated from this layer over wide areas. Although vertical turbulence and mixing must affect the relationships, sediment from this surface layer is fractionated in general according to particle-settling velocities, with larger particles settling closer to shore than finer particles.

This fractionation does not effect a clean separation of particle sizes, however. Because of the great amount of suspended sediment throughout the water column near shore at all times, some material of all sizes is reaching the bottom simultaneously.

The water near the delta shores is continuously turbid; at greater distances seaward, amount of suspended matter changes with changes of the currents, but it is always less abundant than near shore because of previous upstream settling. For these reasons, the seaward-sloping bottom relatively near the shores of the delta is the locus of the greatest amount of deposition.

The profiles of suspended sediment (Figs. 43, 44) suggest the manner in which still another process may be activated to distribute and fractionate the sediment. In all these profiles there was a relatively large amount of suspended sediment in the bottom saline water. Salt content of surface water near the delta is so low that none of the observed concentrations of suspended matter could change density distribution enough to produce vertical instability in the water column. However, below the surface layer, chlorinity is much higher and may be uniform or nearly so with depth. Since temperatures normally also are vertically uniform on the shelf from September to April, stability of the water column can be very low (Figs. 15, 26, 27, 34). Under these special conditions, an increase of suspended matter by a small amount, either from wave stirring or from bottom transport over the distributary bars, could cause a density increase sufficient to start a turbidity current flowing down the front of the deltaic embankment. Such currents have not been observed in the field, but the numerous small valleys and depressions on the face of the delta off the larger distributaries (Shepard, 1955) also suggest this process or a similar one is active.

SUMMARY AND CONCLUSIONS

Currents.—In general, currents off the Mississippi Delta in the Gulf of Mexico are like those off a small hose discharging onto the surface water of a large tank. The tank currents oscillate back and forth and carry with them the relatively small effluent from the hose.

When viewed in detail, measured currents are extremely complex resultants of components due mostly to tides, winds, semi-permanent currents, and river discharge. The components of these resultants vary in their relative importance in accordance with variations of these causal agents over daily and longer periods. They also vary due to position with respect to major and minor topographic features, sources of fresh water, and exposure on the open gulf.

In the partially restricted inshore waters north and east of the delta, the oscillating tidal current component usually is largest. The tidal currents vary in speed because of changes of tide range and because of differing channel cross sections. Superimposed on tidal currents are currents due to both wind and river discharge. Semi-permanent currents probably have only indirect effects inshore.

Wind currents flow in the general direction of the wind as modified by topography, and when they are isolated, they are about of the speed normally expected of currents due to wind. During fall, winter, and early spring intermittent strong northerly winds produce strong currents flowing southeast toward the gulf, but during the remainder of the time, winds develop currents generally toward the west. The component of current in the surface waters due to wind averages approximately 0.2–0.35 knot.

In the distributaries of the river upstream from the channel bars, the downstream-flowing currents may entirely fill the channel or only a part of it. River discharges greater than 750,000–800,000 CFS are required to fill completely the channels. When the entire channel volume is not required to carry the discharge, a gentle current of saline water called the salt wedge exists. This current oscillates with the tide, but has net upstream flow. Entrance of the salt wedge into the distributaries is through a "valve," the channel mouth bar, and is favored by low river discharge, deep bar, high tide, and onshore winds. Salt water enters most freely through the deep-dredged distributaries, but also enters all others that have been investigated under approximately the same conditions. Salt intruded through the deeper distributaries is mixed with river water above Head of Passes and discharged through all distributaries.

The distributary channel is defined at all times seaward to the distributary mouth bar. Channel definition is produced laterally by the submarine natural levees, and on the bottom by the solid channel floor or a floor of intruded salt water. The discharge orifices of distributaries are defined by their bars and the seaward ends of their natural levees to the bar depth. Topographic features at the channel mouths, the bars, the flared natural levees, and the channel-bottom ramps, are related to each other and are formed during and in response to high river stages.

Seaward of the bars speeds of currents due to river discharge are the result of (1) residual momentum and (2) hydraulic head and density differences. River discharge issues from the distributary mouths at speeds ranging usually from about 0.5 to 3.0 knots, depending on the height of sea-level and the volume of discharge. Speed of the discharged water may increase or decrease seaward of the bar, depending on the relationship with existing gulf currents.

The component of issuing speed due to residual momentum persists seaward in proportion to the amount of mixing with underlying sea water. Destruction of the surface layer and loss of its momentum are promoted by (1) thinning of the surface layer which commences when lateral restraint of channel walls is relaxed, (2) mixing due to any motion and particularly shearing motion between the surface layer and underlying water, and (3) by winds producing both wave and current mixing. Conversely, preservation of the surface layer is promoted by (1) high river discharge, (2) low winds, and (3) absence of motion. Because river discharge is continuous, absence of motion is impossible, but usually when gulf currents exist, relative motion is reduced. Under favorable conditions of high discharge and strong gulf currents, a current component probably due to residual momentum persists to a maximum of about 25 miles seaward of the largest distributaries. Under unfavorable conditions of no gulf current, low discharge, or high winds, mixing occurs rapidly and the residual momentum current is dissipated close to the mouths, the distance depending on the size of the distributary.

Currents seaward of the distributary mouths due to hydraulic head and density differences are similar to those which are found off similar areas that have been studied in detail. There is a two-layer estuarine type current system in the inshore area, with river water transported seaward in the mixed surface layer and salt water transported landward in the underlying layer. The vertical salinity structure ranges from the highly stratified type to the vertically mixed type, depending on river discharge, winds, and. tides, and may change from one to the other very rapidly. Ignoring wind currents, current speed in the surface layer is highest when the highly stratified salinity structure exists and may temporarily offset the normal tidal currents. Usually estuarine type circulation is slow and can be recognized only by averaging a number of measurements at one location.

The inshore area north and east of the delta differs from many other estuarine areas in three respects. First, it has a principal axis of estuarine type circulation and two, or possibly more, secondary axes in which circulation also may be estuarine. The principal axis transports fresh water seaward all or most of the time because of geography and channel characteristics; the secondary axes are periodically abandoned for these same reasons and because of their orientation. Second, outflowing river water contributes appreciable energy to drive the system, and third, the salinity gradient in surface waters is nearly parallel with the primary circulation axis.

In the region exposed to the open gulf and seaward of the delta, currents are a combination of semi-permanent currents, wind currents, currents due to river discharge, and tidal currents. Tidal currents in open water generally are rotary and of small net effect, but they could not be considered due to the nature of the data. In the bays around the delta, tidal currents are oscillatory similar to those in the inshore region on the north and east.

South of the delta the semi-permanent current has a north component of the resultant drift during all months. Because of land this current (a relatively slow drift) divides, and tongues go both west and east along the coast. The persistent (though not permanent) northerly set has the effect of preventing or restricting southward distribution of river water and requires that this distribution be principally along the coast toward the east or west.

In the open gulf south of the delta the magnitude and direction of west- or east-flowing component of resultant drift is controlled principally by the wind. Farther east or west, the effects of wind are additive to the semi-permanent drift. A counter drift which flows westward around the coast just north of the east-flowing branch is developed during months of strong and persistent easterly winds. During the time of strong northerlies the northward semi-permanent drift is overcome periodically and some river water is distributed toward the south.

The direction taken by river discharge is controlled by the direction of existing current in the gulf. Because of the control exerted by the wind on current direction south of the delta, distribution toward the east or west is related fundamentally to the wind. The distance seaward of the distributary mouths required to establish correspondence of flow direction between river effluent and gulf current is dependent on the relative speeds of the two currents. In the restricted inshore area, this relationship is modified by the necessity of delivering the fresh water to the open gulf, and indirectly by the existing currents in the open gulf. During the rare periods when there is no current in the gulf for some time, fresh water spreads over a large area seaward of the distributaries; there may be a slow drift westward under these conditions, although this has not been demonstrated.

The fractions of river water that are distributed eastward or westward are related to frequency of winds from the various directions, changes of winds, and variation of river discharge. Consideration of these factors suggests approximately 55–65 per cent of the river discharge is directed westward, 25–35 per cent is directed eastward, and 10 per cent initially goes south. This inequality of water distribution produces an inequality of sediment distribution that is even greater, and as much as 70–75 per cent of the sediment may initially go west. This has caused the western banks of the distributaries to be extended farthest seaward all around the delta.

Some effect of discharged river water in increasing resultant current speed can be detected west and south of the delta, but not east. The increase of resultant speed probably is due to sloping pressure surfaces, with a component of the resulting current directed westward.

The Mississippi River contributes only a small part to the gulf circulation system which is determined by the net gulf-wide effects of winds, heating, cooling, evaporation, precipitation, and runoff. Only to the extent that the Mississippi River is a part of this system does it control the distribution of its own water.

Waves.—Waves around the delta usually are less than 2–3 feet in height and are of short period. Large waves longer than 6 seconds and higher than 3 feet occur relatively infrequently, mostly during fall and winter; the largest waves are associated with hurricanes, and occur in this area on the average every 3–4 years. Thus the frequency with which the bottom is agitated by waves decreases with increasing water depth. Furthermore, the frequency of appreciable bottom agitation by waves varies seasonally at depths greater than the shallowest.

The largest waves approach the coast from the eastern semi-circle, and are refracted and dissipated before entering the inshore area. During northerly storms, waves in Breton Sound get to be relatively large, but are restricted in height by fetch and water depth, and are dissipated against the inner flanks of the barrier islands.

Salt content.—Undiluted gulf water east of the delta has a chlorinity of 19.6–22.2‰, and exhibits little change with depth on the continental shelf when river effects are not present. Where dilution of sea water by river water occurs, large differences from normal gulf concentrations are produced. These differences are most pronounced and frequent in the water above 40–50 feet, but persist to greater depths.

Areal and vertical distributions of chlorinity are the result of the current pattern and mixing. Density differences due to chlorinity also result in currents.

Areas of somewhat differing chlorinity regimen exist. In the inshore region all such areas are characterized by large-scale chlorinity variations and are gradational into each other. On the open continental shelf below a depth of 40–50 feet chlorinity normally is high and uniform, but some dilution may occur to at least 220 feet. The extent and frequency of the changes are unknown.

Hydrogen ion concentration in the water at two seasons was uniformly high and showed little dependence on chlorinity. A greater range of pH values and the lowest values occurred in the fall.

Water temperature.—Water temperature in the open gulf on the shelf east of the delta has a normal annual cycle which is the product of both local seasonal climatic changes and gulf currents. The annual range of monthly average temperatures at the surface is about 10°C. and decreases to about 2.5°C. at 330 feet. Seasonal effects predominate in the surface layer, are pronounced to a depth of about 160 feet, but can be recognized to 330 feet. Below the level of pronounced seasonal effects, temperature changes associated with gulf currents are more apparent.

The annual cycle of Mississippi River water temperature is due to climatic characteristics of the drainage basin and the conservative nature of river temperature. The average annual temperature range is about 21°C., but the river cycle represents conditions in the gulf only in the shallowest water closely surrounding the delta.

Temperature in Breton Sound is highly variable, is related mainly to surface effects and the cycle of gulf temperatures, and is represented by a curve that is intermediate between average air temperature and average surface temperature in the gulf. However, the extreme high is probably 1°–3° higher than the other two. The annual average range is about 16°C.

In bottom water of areas between Breton Sound, the open gulf, and the delta shore, the cycle of average temperature lies between the cycles of these three primary areas and depends largely on locality relative to each of them. There are no sharp changes between adjacent areas.

The effects of rapid fall and winter cooling in Breton Sound apparently do not chill the water to a depth of more than 30–40 feet in the open gulf, even immediately adjacent to the sound.

Suspended matter.—A huge amount of sediment is brought to the gulf by the Mississippi River, where it is widely distributed according to the existing currents, fractionated in general according to settling velocities, and deposited.

This fractionation is incomplete, however, because the water column is charged with particles of all different sizes, some of each size reaching the bottom simultaneously.

The sea floor adjacent to the delta shore is the locus of the greatest deposition because particles are continuously settling from the highly turbid water. At greater distances from shore, turbidity changes with the currents and is never as great as near shore because of upstream settling.

Highest turbidity occurs in the shallow water of the gulf during fall and winter storms because of the waves and may greatly exceed concentrations at the same location during flood stages. This is resuspended sediment which in part is removed and deposited elsewhere.

The data suggest turbidity currents may develop under the special hydrographic conditions of fall and winter in shallow water of uniform density below the surface layer. The density increase is due to suspended matter. Fall and winter wave action or river bed load movement may activate these currents.

REFERENCES

Adams, R. M., and Sorgnit, E. F., 1951, "Comparison of Summer and Winter Sea Temperatures, Gulf of Mexico," *Dept. Ocean., Texas A. and M. Tech. Rept. 3* (July, 1951). 4 pp., 3 figs.

Bates, C. C., 1953, "Rational Theory of Delta Formation," *Bull. Amer. Assoc. Petrol. Geol.*, Vol. 37, pp. 2119–62.

Bigelow, H. B., and Edmondson, W. T., 1947, "Wind Waves at Sea Breakers and Surf," *U. S. Navy Hydrographic Office Pub. 602.* 177 pp.

Blackman, B., and Lindner, C. P., 1952, "Harbor and Coastal Problems on the East Gulf Coast," *Proc. 2d Conf. Coastal Engineering*, Houston, 1951, pp. 226–35.

British Meteorological Office, 1939, "Quarterly Section Charts of Ocean Currents for the North Atlantic, Southwestern Portion, and the South Atlantic, Eastern Portion," *M. O. Misc. Pubs. 371/6, 7, 9.*

Cameron, W. M., 1953, "Hydrographic and Oceanographic Observations in the Beaufort Sea, 1952," *Progress Rept., Inst. Ocean., Univ. British Columbia.* 12 pp.

"Central American Water Current Chart," 1952, *U. S. Navy Hydrographic Office Misc. Pub. 10-690*, pp. 1–12 (January–December).

Clarke, F. W., 1920, "The Data of Geochemistry," *U. S. Geol. Survey Bull. 695.* 832 pp.

Crickmay, C. H., and Bates, C. C., 1955, "Delta Formation" (Discussion), *Bull. Amer. Assoc. Petrol. Geol.*, Vol. 39, pp. 107–14.

Dent, E. J., 1921, "Notes on the Mouths of the Mississippi River," *U. S. Engineers Office, ms.*, January 3.

———, 1928, "The Mouths of the Mississippi River," *Trans. Amer. Soc. Civil Engineers*, Vol. 87, pp. 997–1006.

Ellet, C. J., 1850, "Report on the Improvement of the Navigation Across the Bars at the Mouths of the Mississippi River," *31st Cong., 2d Sess.*, Sen. Doc. 17, Vol. 3, pp. 1–18.

Elliott, D. O., 1932, *The Improvement of the Lower Mississippi River for Flood Control and Navigation*, U. S. Waterways Experiment Station, Vicksburg, Mississippi, May 1, 3 Vols. 345 pp., 71 pls.

Escoffier, F. F., 1952, "Design and Performance of Sea Walls in Mississippi Sound," *Proc. 2d Conf. Coastal Engineering*, Houston, 1951, pp. 257–67.

Farmer, H. G., and Morgan, G. W., 1953, "The Salt Wedge," *Proc. 3d Conf. Coastal Engineering*, Cambridge, Massachusetts, October, 1952, pp. 54–64.

Fisk, H. N., 1952, *Geological Investigation of the Atchafalaya Basin and the Problem of Mississippi River Diversion*, Mississippi River Comm., Vicksburg, Mississippi. 145 pp.

Fjarlie, R. L. I., 1950, *The Oceanographic Phase of the Vancouver Sewage Problem*, Pacific Oceanographic Group, Nanaimo, B. C., File No. N 7-18. 21 pp.

———, and others, 1953, *Sewerage and Drainage of the Greater Vancouver Area, British Columbia*, Rept. Vancouver and Districts Joint Sewerage and Drainage Board, September, 1953. 278 pp.

Forshey, C. G., 1877, "Contributions to the Physics of the Gulf of Mexico, and Its Chief Affluent, the Mississippi River," *Proc. Amer. Assoc. Adv. Sci.*, Vol. 26, pp. 134–73.

Freeman, J. C., 1953, "Wind Mixing Currents," *Texas A. and M. College, Dept. Ocean. Tech. Rept. 6* (October). 6 pp., 4 figs.

———, 1954, "Wind Mixing Currents," *Jour. Marine Res.*, Vol. 13, pp. 157–65.

Fuglister, F. C., 1947, "Average Monthly Sea Surface Temperatures of the Western North Atlantic Ocean," *Papers in Phys. Ocean. and Meteor., Massachsetts Inst. Tech. and Woods Hole Ocean. Inst.*, Vol. 10, No. 2. 25 pp.

———, 1953, "Average Temperature and Salinity at a Depth of 200 Meters in the North Atlantic Ocean," *Woods Hole Ocean. Inst. Tech. Rept. 53-58.* 13 pp., 8 charts. (Unpublished manuscript)

Geyer, R. A., 1950, "The Occurrence of Pronounced Periodic Salinity Variations in Louisiana Coastal Waters," *Jour. Mar. Research*, Vol. 9, pp. 100–10.

———, 1955, "Effect of the Gulf of Mexico and the Mississippi River on Hydrography of Redfish Bay and Blind Bay, "*Pub. Inst. Mar. Sci.*, Vol. IV, No. 1, pp. 157–68.

Hachey, H. B., and Fothergill, N. O., 1953, "Wind Currents and Storm Effects on Water Movement at Sambro Lightship," *Trans. Roy. Soc. Canada*, 3d Ser., Vol. 47, pp. 1–14.

Hedgpeth, J. W., 1953, "An Introduction to the Zoogeography of the Northwestern Gulf of Mexico with Reference to the Invertebrate Fanua," *Pub. Inst. Marine Sci.*, Vol. III, No. 1, pp. 113–224.

Hilgard, E. W., 1871, "On the Geology of the Delta, and the Mudlumps of the Passes of the Mississippi," *Amer. Jour. Sci.*, 3d Ser., Vol. 1, pp. 238–46, 356–68, 425–34.

Hirsch, A. A., 1939, "Mississippi River Water Temperatures at New Orleans," *Monthly Weather Review* (November), p. 415.

Holle, C. G., 1952, "Sedimentation at the Mouth of the Mississippi River," *Proc. 2d Conf. Coastal Engineering*, Houston, Texas, pp. 111–129.

Humphreys and Abbot, 1876, "Report upon the Physics and Hydraulics of the Mississippi River," *U. S. Engineers Prof. Paper 13.* 691 pp., App. A–M, Pls. 1–25.

Jerlov, N. G., 1951, "Optical Studies of Ocean Waters," *Repts. of Swedish Deep-Sea Expedition, Vol. III, Physics and Chemistry*, No. 1. 69 pp.

Ketchum, B. H., 1951 a, "The Flushing of Estuaries," *Sewage and Industrial Wastes*, Vol. 23, No. 2, pp. 198–209.

———, 1951 b, "The Exchanges of Fresh and Salt Waters in Tidal Estuaries," *Jour. Mar. Research*, Vol. 10, pp. 18–38.

———, 1953, "Circulation in Estuaries," *Proc. 3d Conf. Coastal Engineering*, Cambridge, Massachusetts, October, 1952, pp. 65–76.

———, Redfield, A. C., and Ayers, J. C., 1951, "The Oceanography of New York Bight," *Papers in Phys. Ocean. and Meteor., Massachusetts Inst. Tech. and Woods Hole Ocean. Inst.*, Vol. 12, No. 1, pp. 3–46.

Lane, E. W., and Eden, E. W., 1940, "Sand Waves in the Lower Mississippi River," *Jour. Western Soc. Engineers*, Vol. 45, No. 6, pp. 281–91.

Leipper, D. F., 1954, "Physical Oceanography of the Gulf of Mexico," in "Gulf of Mexico, Its Origin, Waters, and Marine Life," *Fishery Bull. 89, U. S. Dept. Interior*, pp. 119–37.

Marmer, H. A., 1954, "Tides and Sea Level in the Gulf of Mexico," *ibid.*, pp. 101–18.

Mason, M. A., 1952, "Pertinent Factors in the Protection of the Gulf Coast," *Proc. 2d Conf. Coastal Engineering*, Houston, 1951, pp. 217–25.

Morgan, J. P., Van Lopik, J. R., and Nichols, L. G., 1953, "Occurrence and Development of Mud Flats Along the Western Louisiana Coast," *Trafficability and Navigability of Louisiana Coastal Marshes, Tech. Rept. 2*, Louisiana State Univ., Baton Rouge. 34 pp.

O'Neil, T., 1949, *The Muskrat in the Louisiana Coastal Marshes*, Louisiana Dept. Wildlife and Fisheries, New Orleans. 152 pp.

Parr, A. E., 1935, "Report on Hydrographic Observations in the Gulf of Mexico and the Adjacent Straits Made during the Yale Oceanographic Expedition on the Mabel Taylor in 1932," *Bull. Bingham Ocean. Collection*, Vol. 5, Art. 1. 93 pp.

Prandtl, L., 1952, *Essentials of Fluid Dynamics.* 452 pp. Hafner Publishing Company, New York.

Prichard, D. W., 1952, "Salinity Distribution and Circulation in the Chesapeake Bay Estuarine System," *Jour. Marine Res.*, Vol. 11, No. 2, pp. 106–23.

———, and Burt, W. V., 1951, "An Inexpensive and Rapid Technique for Obtaining Current Profiles in Estuarine Waters," *Chesapeake Bay Inst., Johns Hopkins Univ., Tech. Rept. 1.* 16 pp. See also *Jour. Marine Res.*, Vol. 10, pp. 180–89.

Rhodes, R. F., 1950, "Effect of Salinity on Current Velocities," *U. S. Eng. Com. on Tidal Hydraulics, Rept. 1*, pp. 41–100.

Riley, G., 1937, "The Significance of the Mississippi River Drainage for Biological Conditions in the Northern Gulf of Mexico," *Jour. Marine Res.*, Vol. 1, pp. 60–74.

Roelofs, E. W., and Bumpus, D. F., 1953, "The Hydrography of Pamlico Sound," *Bull. Mar. Sci. of Gulf and Caribbean*, Vol. 3, pp. 181–205.

Rouse, H., 1950, *Elementary Mechanics of Fluids.* 376 pp. John Wiley and Sons, New York.

Russell, R. J., 1936, "Physiography of Lower Mississippi River Delta," *Louisiana Geol. Survey, Geol. Bull. 8*, pp. 3–199.

———, and Russell, R. D., 1939, "Mississippi River Delta Sedimentation," in *Recent Marine Sediments*, P. Trask, ed., Amer. Assoc. Petrol. Geol., pp. 153–77.

Scruton, P. C., 1953, "Deposition of Evaporites," *Bull. Amer. Assoc. Petrol. Geol.*, Vol. 37, pp. 2498–2512.

———, 1955, "Sediments of the Eastern Mississippi Delta," *Soc. Econ. Paleon. and Min. Spec. Paper 3*, pp. 21–51.

———, and Moore, D. G., 1953, "Distribution of Turbidity off Mississippi Delta," *Bull. Amer. Assoc. Petrol. Geol.*, Vol. 37, pp. 1067–74.

Shaw, E. W., 1913, "The Mud Lumps at the Mouths of the Mississippi," *U. S. Geol. Survey Prof. Paper 85B*, pp. 11–27.

Shepard, F. P., 1955, "Delta-Front Valleys Bordering the Mississippi Distributaries," *Bull. Geol. Soc. America*, Vol. 66, pp. 1489–98.

———, and Moore, D. G., 1955, "Central Texas Coast Sedimentation: Characteristics of Sedimentary Environment, Recent History, and Diagenesis," *Bull. Amer. Assoc. Petrol. Geol.*, Vol. 39, pp. 1463–1593.

Simmons, H. B., 1952, "Salinity Problems," *Proc. 2d Conf. Coastal Engineering*, Houston, Texas, pp. 68–85.

Slocum, G., 1935, "Sea Surface Summary for the North-Central Gulf of Mexico, 1912–33," *Monthly Weather Review*, Vol. 63, p. 174.

Soley, J. C., 1914, "The Gulf Stream in the Gulf of Mexico Showing the Currents as They Exist during the Different Seasons," reprint from *Pilot Chart of the North Atlantic Ocean*, U. S. N. Hydrographic Office.

Stommel, H., 1953, "The Role of Density Currents in Estuaries," *Proc. Minnesota Internat. Hydraulics Conv.*, Minneapolis, September, pp. 305–312.

———, and Farmer, H. G., 1952, "Abrupt Change in Width in Two-Layer Open Channel Flow," *Jour. Marine Res.*, Vol. 11, pp. 205–14.

———, and ———, 1952a, "On the Nature of Estuarine Circulation," *Woods Hole Ocean. Inst.*, Pts. I, III, Ref. Nos. 52–51, 52–88, and 52–63.

Sverdrup, H. U., Johnson, M. W., and Fleming, R. H., 1946, *The Oceans, Their Physics, Chemistry, and General Biology*. 1060 pp. Prentice-Hall.

Tannehill, I. R., 1950, *Hurricanes*. 304 pp. Princeton Univ. Press.

Trowbridge, A. C., 1930, "Building of the Mississippi Delta," *Bull. Amer. Assoc. Petrol. Geol.*, Vol. 14, pp. 867–901.

Tully, J. P., 1937, "Oceanography of Nootka Sound," *Jour. Biol. Board Canada*, Vol. 3, pp. 43–69.

———, 1949, "Oceanography and Prediction of Pulp Mill Pollution in Alberni Inlet," *Bull. Fish. Res. Board Canada*. 169 pp.

———, 1952, "Notes on the Behavior of Fresh Water Entering the Sea," *7th Pacific Sci. Congress*, Vol. III, pp. 1–23.

U. S. Coast and Geodetic Survey, 1951, *Current Tables, Atlantic Coast, North America*.

———, 1952, *Tide Tables, Atlantic Coast, North and South America*.

U. S. Engineers, 1939, "Study of Materials in Transport, Passes of the Mississippi, River," *Tech. Memo. 158-1*, U. S. Engineers, New Orleans and Waterways Experiment Station, Vicksburg. 36 pp., 70 tables.

U. S. N. Hydrographic Office, "Current Charts of Central American Waters," *H. O. Misc. Pub. 10-690*, pts. 1–12.

van Andel, Tj., and Postma, H., 1954, "Recent Sediments of the Gulf of Paria," *Reports of the Orinoco Shelf Expedition*, Vol. I, Eerste Reeks, Deel XX, No. 5, Amsterdam: North-Holland Publishing Company. 245 pp.

Woods Hole Oceanographic Inst., 1946, *The Determination of Chlorinity by the Knudsen Method*, translation of *Chloruration par la Methode de Knudsen*, by Mieczyslaw Oxner, and reprint of *Hydrographical Tables*, by Martin Knudsen. 63 pp.

APPENDIX

After the galley for this paper had been returned to the editor, an unpublished Louisiana State University dissertation by F. A. Welder was obtained. Welder's report on hydraulic processes in the Cubits Gap area and the natural development there of distributary channels, bars, and other features is both thorough and complete. Where his report and this one overlap, there is excellent agreement between the two. Areas of overlapping are mostly in the descriptions of bar hydraulics, bar development and downstream migration, and channel constriction upstream from the bar. Welder's report, "Deltaic Processes in Cubits Gap Area, Plaquemines Parish, Louisiana," Baton Rouge, 1955, 119 pp., goes into other phases of channel development as well and should be consulted by any serious student of delta building.

THE GUADALUPE FUR SEAL STILL LIVES!

By Carl L. Hubbs, Ph.D.
PROFESSOR OF BIOLOGY,
SCRIPPS INSTITUTION OF OCEANOGRAPHY,
UNIVERSITY OF CALIFORNIA*

The Guadalupe Fur Seal is one of the animals that only the San Diego Zoo has exhibited alive. On several occasions it has been feared extinct, but each time a thread of continued existence has been discovered . . . and in this history of alternating fears and hopes the San Diego Zoological Society has played an important role. For seals long have been a specialty with our Zoo.

During the early years of the last century the Guadalupe Fur Seal was the object of extensive and profitable commercial hunting for its fur. They were found not only on Guadalupe Island, off Baja California and about 240 miles south of San Diego, but reportedly on the Farallon Islands also, off San Francisco and on the intervening Channel Islands.

On the bleak shores of Guadalupe can be seen the ruins of stone houses that reportedly were occupied by Aleuts brought there from Alaska by the Russians to slaughter the swarming fur seals. That the species had long

The Guadalupe Fur Seal. This splendid bull is one of two that made a unique exhibit at the Zoo in 1928.

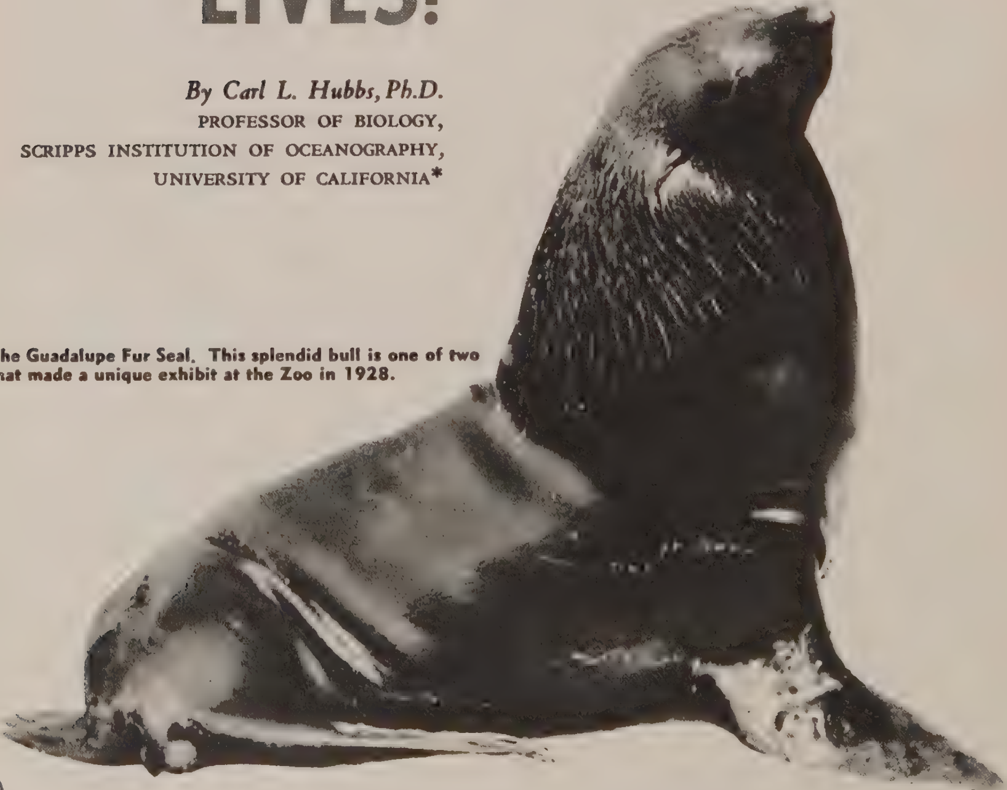

**Also a member of the Board of Directors and Research Council, San Diego Zoological Society.*

abounded on the Guadalupe rookeries is shown by the smoothed and polished lava rock over which countless generations of fur seals dragged their bodies and flippers.

Competing with the Russians in the greedy game were American sealers from New England seaports. There are a few historic records of the thousands they killed as well, particularly on the Farallons. On the largest and best preserved of the stone-house ruins on Guadalupe are carefully engraved the records of numerous visits by venturesome yankees, giving the dates 1834, 1835, 1837, 1839, 1849, 1851, 1861(?), 1869, 1873 and 1881 . . . but significantly, none since.

Around the middle of the century the species was thought to be near extinction and perhaps gone. However, it was found again and there are records of rather limited kills until 1894.

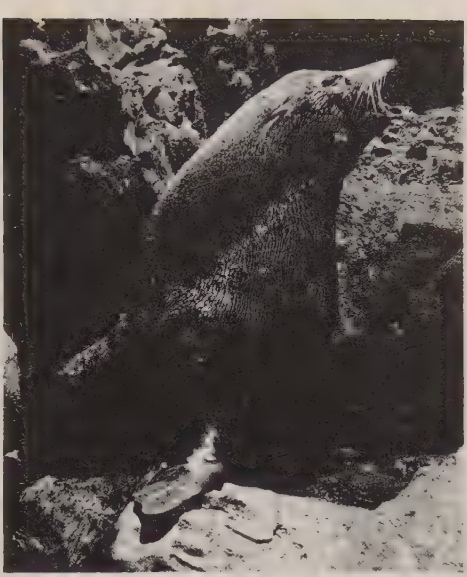

Another male Guadalupe Fur Seal photographed on Guadalupe Island in June, 1955, six months following the latest rediscovery of the species. The photographer was Dr. George E. Lindsay, director of the San Diego Museum of Natural History.

FIRST IDENTIFIED IN 1892

It was not known that the fur seals on the islands off California and Baja California were different from the Northern Fur Seal, until the first scientific specimens were collected on Guadalupe Island in 1892. These specimens represented a new species, *Arctocephalus townsendi,* oddly related to the Southern Hemisphere fur seals.

For the period between 1895 and 1925 we found (by hearsay) only a few records of Guadalupe Fur Seals having been seen alive. Again, it was generally feared that this rare species was extinct.

The history of the species was resumed in 1926 when two fishermen, William O. Clover and Harry Fisher, wandering to Guadalupe Island, found animals they thought to be fur seals. Clover reported their find to Dr. Harry Wegeforth, founder of the San Diego Zoological Society. Always on the lookout for exhibits for the rapidly growing Zoo, and hopeful that Clover's claim might be correct, "Doctor Harry" engaged him to capture specimens. Eventually Clover caught two bulls which he delivered in 1928. Dr. Wegeforth was highly elated upon identifying the handsome creatures as Guadalupe Fur Seals.

Fortunately, Dr. Charles Haskins Townsend, an authority on seals and the first to collect this species, was just then on his way to the Zoo, bringing a spectacular collection of giant land tortoises from the Galapagos. Dr. Townsend verified the identification, and the rediscovery of the species was promptly announced in ZOONOOZ of May - June 1928.

SLAUGHTERED FOR REVENGE

Clover, who might have been the hero of this rediscovery, turned out to be something of a villain. Following a quarrel with Dr. Wegeforth, he swore that he would slaughter the whole herd, which reportedly he did, taking the hides to Panama to sell, only to be killed there in a barroom brawl.

The story of the rediscovery by Clover was verified by Joseph W. Sefton, Jr. and me on January 9, 1950, when we visited Harry Fisher, Clover's companion of 22 years previous. Lying ill in the Navy Hospital, and perhaps realizing that his days were numbered, Fisher vividly described the spot where the fur seals had been encountered. Telling the story possibly overexcited him, for the poor fellow went to his fisherman's reward the very next day.

Reprinted, by permission, from Zoonooz, publication of the San Diego Zoological Society, Dec., 1956.

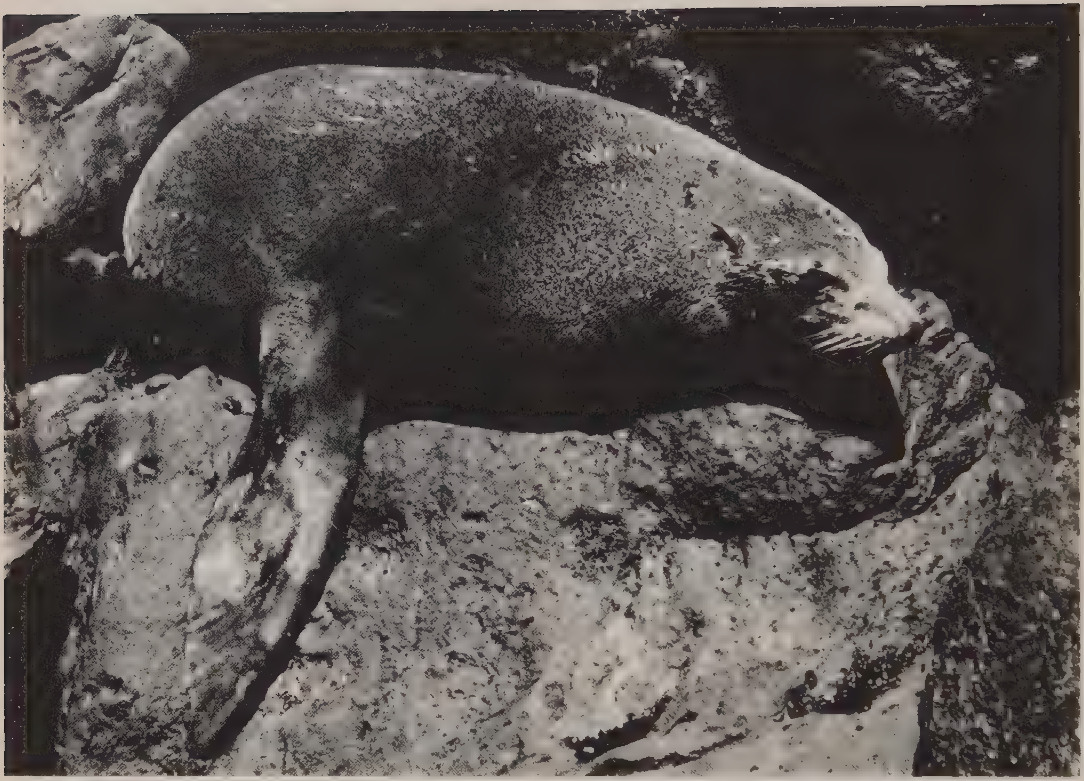

A female or cow Guadalupe Fur Seal, a mate of the bull pictured on preceding page, permitted Dr. Lindsay to take her picture as she lay basking in the sun.

Following the death of the two fur seals that had provided the Zoo with a unique and cherished exhibit, Belle Benchley, then executive secretary of the Zoo, arranged and accompanied an expedition to Guadalupe Island on the Valero II, Captain Allan Hancock's famous yacht, to locate the reported hiding place of the fur seals. The attempt failed, but during the 1930's a few were seen by Lewis Wayne Walker, well known naturalist and author, on each of several trips . . . always in the area where we have since rediscovered the species. Although I know of no subsequent records of finding the species on Guadalupe until I first saw them myself, in November of 1954, rediscovery was made on San Nicolas Island in 1949 by Dr. George A. Bartholomew of the University of California.

On four successive visits to San Nicolas Island (most remote of the famed Channel Islands of California), Dr. Bartholomew saw a bull Guadalupe Fur Seal. His field identification was confirmed by comparing his excellent close-up photographs with pictures of the specimens in the San Diego Zoo in 1928.

Dr. Bartholomew and I immediately planned to explore the shores of Guadalupe Island, the last stronghold of the species, to see if additional specimens might be living there. Joseph W. Sefton, Jr. graciously made available the good ship Orca. In February, 1950, we examined the rugged shores of this volcanic island, but found no trace of seals identifiable as *Arctocephalus townsendi*. Although disappointed on this score, we were pleased by other discoveries, including migrating Northern Fur Seals found as far south as between Guadalupe and San Benito Islands. On the San Benitos, however, not a single fur seal was detected among approximately 9,500 sea lions counted.

When Dr. Bartholomew could not find the old, emaciated and cantankerous bull he had seen on San Nicolas Island in 1949, it was thought that he had observed the last living example of a once flourishing race. As no others appeared, despite close watch up and down the coast during the following years, our hopes of finding the species alive kept failing . . . but not completely.

WAVERING HOPE REWARDED

Hope and vigilance finally brought reward in November, 1954. We were on another trip to Guadalupe on the Orca when, on the very last day, I asked Mr. Sefton for the privilege of running close along the shore in one of the ship's launches in the almost forlorn hope of seeing a fur seal. Ever eager to advance natural science, Mr. Sefton granted my request and the search was on.

Just before darkness and our rendezvous with the Orca, our straining eyes had failed to see anything resembling a fur seal, when the boatman, Eddie Arebalo, and I spotted a seal perched on a rock at the mouth of a cave. Knowing that the last of the sealing had been in caves, we expectantly turned in closer, to be greeted by a defiant roar quite unlike the voice of the sea lions and elephant seals. Edging still closer in the surf, I saw the sharp, almost collie-like snout, the course guard hairs overlying fur, oversized flippers and other characteristics of the species thought to be extinct.

Soon we heard also the belligerent bleat of fur-seal cows and the plaintive whimper of a pup. In the late afternoon shadows we saw in the cave at least two cows and three pups. These voices of bull, cow and pup were crisply reminiscent of the calls of the Northern Fur Seal that rang in my ears all through the days and nights I had spent on the Pribilof Islands in 1939. No trace of doubt remained. I had rediscovered the Guadalupe Fur Seal alive!

Along the nearby shore we saw other pups on a rock, with some half-grown fur seals disporting in the surf, as yearlings of the Alaska species are wont to do. At least 14 fur seals were counted before darkness set in.

MY FIND CONFIRMED LATER

In June, 1955, with famed seal specialist, Dr. Victor B. Scheffer, as collaborator, and Dr. George E. Lindsay, as photographer (now executive director of the San Diego Museum of Natural History), I returned on the Orca for more definite observations, counts and for a photographic record. This time we saw more than twice as many and took still and motion pictures. Subsequently Dr. Raymond M. Gilmore of the United States Fish and Wildlife Service and I each made two other trips, during which some reproduction was observed.

Even allowing for individual seals hiding, or absent at sea, we realize that only a thin thread of life holds from extinction this fine species that once crowded the island rookeries. With the aid and encouragement of national and international conservation agencies, as well as naturalists in the United States and Mexico, we are pleading for more secure protective measures for the Guadalupe Fur Seal. Like the Northern Fur Seal, the Elephant Seal, the Gray Whale, and to a lesser degree the Sea Otter, it may recover from perilously low populations to regain some measure of former abundance. We even dare hope that with such protection the increasing numbers may eventually justify adding this species again to the list of unique exhibits at the San Diego Zoo.

Contribution from Scripps Institution of Oceanography, New Series No. 893.

With dignity and decorum the bull fur seal poses in his "bubble bath" in the surf.

ISOTOPIC GEOCHEMISTRY OF THERMAL WATERS

by

Craig, Boato and White

Reprinted From

Proceedings of the Second Conference on
Nuclear Processes in Geologic Settings,
Publication 400 of the National Academy
of Science-National Research Council, 1956.

Reproduced by Permission

V

ISOTOPIC GEOCHEMISTRY OF THERMAL WATERS

Harmon Craig* and Giovanni Boato**
Enrico Fermi Institute for Nuclear Studies
University of Chicago
and
Donald E. White
U. S. Geological Survey
Menlo Park, California

It is by now well known that the isotopes of the lighter elements, especially hydrogen, carbon, oxygen, and sulfur, are fractionated by chemical and physical processes in natural systems. The most general application of such phenomena to geological problems is the use of what may be called "natural" isotopic tracer techniques to study the processes by which the earth has assumed its present heterogeneous composition. The use of such techniques requires as a starting point the assay of the isotopic composition of natural materials which serve as sources, sinks, and reservoirs of compounds of these elements, in order to establish the "natural" tagging of the elements and the patterns of variation. Such workers as Baertschi, Epstein, Friedman, Nier, Silverman, Thode, Wickman, the present writers, and others have established these basic patterns for the above elements, and are now beginning to exploit the accumulated data by studying specific problems. The present status of such work has recently been reviewed by two of us.[1]

The work described in this paper was begun with two main objectives. The first of these was the determination of the precise relationship between the variations in the deuterium and O^{18} concentrations in natural waters, since it was felt, as indeed proved to be the case, that this relationship might provide a natural "tag" for water, superior to data based on only one of these isotopes. The second objective was a general study of the isotopic geochemistry of water from areas of thermal activity, as a contribution to the problem of the excess volatiles on the earth's surface. This research was carried out in the laboratories of Dr. H. C. Urey, and his active interest and support are gratefully acknowledged. We are indebted to the Atomic Energy Commission, the Office of

---

* Present address: Scripps Institution of Oceanography, La Jolla, California. This paper is Contribution of the Scripps Institution of Oceanography, **New Series No.894.**

** Present address: Istituto di Fisica dell' Universita, Genova, Italy.

Naval Research, the National Science Foundation, and the Geological Society of America, which supported various phases of the work over the past two years. More specific acknowledgments will be made in the series of detailed papers which will be published in the near future. In the present paper no attempt is made to present detailed analytical data, since isolated analyses have little significance out of the context of the large amount of data accumulated for each of the areas studied. Rather, we wish to discuss briefly the basic concepts and some general conclusions, and to summarize some of the more important findings to date.

Table I shows the three most prominent members of the family of isotopic water molecules, their masses, relative abundances in average ocean water, and their vapor pressures at two temperatures. Other members of the family are much less abundant and can be neglected. One sees from the table that the vapor pressures are not a direct function of the molecular weight.

TABLE I

Vapor Pressures and Relative Abundances of the Isotopic Water Molecules

Species	Relative Abundance (ocean water)	Mass	p(mm Hg) 30°C	p(mm Hg) 100°C
H_2O	1	18	31.5	760
HDO	1/3230	19	29.4	741
H_2O^{18}	1/500	20	31.3	756

With increasing temperature the percentage deviation of the vapor pressures of the two heavier species from the vapor pressure of H_2O decreases. Thus at the higher temperature a vapor pressure dependent separation process will separate the isotopes less efficiently. However, the percentage deviation for p(HDO) decreases about 4 times as rapidly as the percentage deviation for p(H_2O^{18}), and so, with increasing temperature, the ratio of the separation efficiency for deuterium to the separation efficiency for O^{18} in such a process decreases.

When water molecules evaporate or condense in a system in which thermodynamic equilibrium is maintained, the concentrations of the isotopic species in the vapor and liquid phases are controlled by the respective vapor pressures, and the isotopic relationships are quite simply derived from the equations given long ago by Rayleigh for the process which has come to be known as Rayleigh distillation.

Defining:

$$\epsilon_D = \frac{p(HDO)}{p(H_2O)} - 1 ; \qquad \epsilon_O = \frac{p(H_2O^{18})}{p(H_2O^{16})} - 1$$

i. e., the fractional vapor pressure differences at a given temperature, and

$$E = \frac{R_2}{R_1} - 1$$

where E is, by standard terminology, the total phase enrichment in either heavy isotope, R_1 is the initial molecular ratio HDO/H_2O or H_2O^{18}/H_2O^{16} in the phase, and R_2 is the final ratio, then for the enrichments of deuterium and O^{18} in the liquid phase one readily derives

$$E_D = f^{\epsilon_D} - 1 \qquad E_O = f^{\epsilon_O} - 1$$

$$\frac{E_D}{E_O} \sim \frac{\epsilon_D}{\epsilon_O}$$

where f is the fraction of the liquid remaining. The enrichment ratio given by the last equation is a function of temperature alone and the approximation holds quite well for the small enrichments encountered in natural systems.

Now since H_2O^{16} is the most volatile species below temperatures of several hundred degrees, the liquid phase will become progressively enriched in the heavy isotopes during an equilibrium evaporation process, or the vapor phase will become progressively depleted in the heavy isotopes during an equilibrium condensation process, and according to the above equation the percentage enrichments or depletions in deuterium and O^{18} are related by the ratio of the fractional vapor pressure differences, the latter being known from experimental data. At room temperature the ratio is about 9, decreasing to about 5 at the boiling point of water. It appears, therefore, that if the meteoric water cycle of evaporation-condensation takes place under equilibrium conditions, the ocean waters should have about the highest concentrations of the heavy isotopes, while the terrestrial fresh waters should be relatively depleted in these isotopes, the extent of the depletion depending upon the fraction of the original water vapor remaining in the air mass from which their water has, on the average, been derived. The depletion ratio, taking the depletions relative to average ocean water, should be of the order of 9, independent of the extent of depletion of either isotope.

This relationship was first established experimentally by the work of Epstein and Mayeda[2] and Friedman,[3] who analyzed 36 marine and 9 terrestrial waters for both O^{18} and deuterium concentrations, and found a depletion ratio in the fresh waters corresponding to ordinary temperatures. Epstein and Mayeda further showed that the salinity-O^{18} variations in marine waters were consistent with a Rayleigh distillation process in which the oceanic precipitation is progressively depleted in the heavy isotopes as a function of the extent of precipitation from the local atmospheric reservoir. The surface layers of the oceans are enriched in the heavy isotopes relative to mean ocean water because of the net storage of H_2O^{16} in the stagnant and circulating fresh water and vapor; the extent of this enrichment reflects the hold-up at the boundary of the mixed surface layer.

In the course of the present study several hundred fresh water samples were analyzed for deuterium and O^{18} concentration. The deuterium concentration varies by about 30%, ranging from about 3% higher to 27% lower than in mean ocean water, while the O^{18} concentration varies by only 4%, ranging from 0.6% higher to 3.4% lower than mean ocean water. The linear correlation is good and the actual percentage depletions in the heavy isotopes show a general correlation with latitude or distance from the ocean. There is a general decrease in the heavy isotope concentration as the latitude varies from equatorial to polar, reflecting the continuous loss of vapor from the poleward moving air masses. In other words, the meteoric waters show a roughly constant ratio of deuterium depletion to O^{18} depletion, both taken relative to mean ocean water, while the individual percentage depletions, proportional to natural "plate numbers," vary widely, over a range corresponding to about four theoretical plates in a Rayleigh distillation.

The pattern of variation described above clearly provides a natural "labeling" of meteoric waters, which is twofold. A meteoric water unaffected by extensive evaporation (see below) is first of all labeled with a given ratio of deuterium to O^{18} depletion relative to ocean water, regardless of locality. This is our so-called "primary tag" which is provided by the vapor pressure ratios. However, the same analytical data yield also a "secondary tag," namely, the plate number, or the actual extent of the depletion of either isotope relative to ocean water, which is a function of the average local climatic conditions and varies with location. The primary tag provides an immediate identification of waters which have been derived from the oceans and precipitated over land as rain or snow; the variations in this tag are small and reflect the slight differences encountered in the isotopic composition of surface ocean waters and the variations in the temperatures encountered in the meteoric cycle of evaporation-condensation. The secondary tag is, however, of great significance, because it provides a variable factor which should be reflected in all waters of meteoric origin. Clearly, if all meteoric waters possessed the same concentration of deuterium and of O^{18}, then all thermal waters derived purely from meteoric waters would show isotopic variations related only to exchange phenomena occurring during passage through their aquifers. In this case it would be difficult, if not impossible, to identify waters resulting from the mixing of meteoric water with magmatic water or with any non-meteoric water of invariant isotopic composition. Thus the secondary tag, reflecting the natural variations in the multiple stage distillation cycle of meteoric waters, provides the frame of reference for a study of the geochemical cycle of water based on an independent variable.

The next step, then, is the investigation of thermal waters from areas of different "plate numbers," in order to see whether the local thermal waters show isotopic compositions correlated with the differences in the meteoric water composition, or whether they display some other pattern of variation. We have thus analyzed several hundred samples of thermal waters from such areas as Yellowstone Park, Wyoming; Lassen Park and The Geysers, California; Steamboat Springs, Nevada; Iceland; Kenya; New Zealand; Larderello, Italy; and various other localities, covering the spectrum of the natural variation in the isotopic composition of meteoric waters. For present purposes, we may roughly distinguish two main types of thermal springs, and, correspondingly, the isotopic data show a different pattern for each type. These types and their associated isotopic patterns may be briefly described as follows.

1. The normal chloride or near-neutral springs are tepid to hot, dilute, chloride waters with pH in the range of 5 to 9. These are often termed "alkaline" type springs, have a moderate to high discharge, shallow to deep circulation, and generally discharge from a large body of ground water. Well known examples are the springs of the Upper and Lower Geyser Basins of Yellowstone Park, and all true geysers discharge this type of water. Normal chloride springs are thought to be predominantly meteoric in origin, on the basis of the high rates of discharge, but may contain varying proportions of volcanic or connate water.

Isotopically, these springs are either identical in composition with the associated surface river or lake waters, or they have about the same deuterium concentration as the local meteoric waters, but are enriched in O^{18} with respect to these waters by amounts ranging up to about 0.4%. This enrichment is generally observed in the higher temperature, deeper circulating springs.

2. The acid hot springs range from pH 1 to 5, are relatively high in sulfate and low in chloride in comparison with the normal or alkaline springs, and generally possess lower temperatures and much smaller rates of discharge. For example, in Yellowstone Park, less than 2% of the total hot spring discharge comes from acid sulfate springs. The gas discharge in acid areas is, however, generally an order of magnitude greater than in alkaline areas. The acid springs are generally found on local topographic highs above the level of the normal water table. They have most generally been interpreted as resulting from superheated magmatic steam mixing into a shallow water table, with associated oxidation of hydrogen sulfide to sulfuric acid.

Isotopically the acid springs display a characteristic and unexpected pattern. There is a linear correlation between deuterium and O^{18} concentration such that the enrichment ratio E_D/E_O is about 3, the enrichments in this case being taken relative to the local surface water (rivers or lakes). These springs range up to 5% higher in deuterium, and up to 1.6% higher in O^{18}, than the local meteoric waters, and there is a general tendency for this enrichment to be associated with a progressive decrease in pH. Despite a 10% range in deuterium concentration of the surface waters of The Geysers, Lassen Park and Yellowstone Park, this enrichment ratio is essentially the same in all three areas, with no indication of a convergence of isotopic composition toward a unique deuterium and O^{18} concentration.

Thus both the normal and acid types of thermal waters show a strict dependence on the isotopic composition of the local surface water. They display a knowledge of the local climatic conditions on the earth's surface, knowledge of which magmatic waters should surely be ignorant. There is no single isotopic composition which a volcanic water could possess to produce the observed patterns by simply mixing with the surface waters in each area, and, in order to explain these patterns, we must look to some processes operating on the local meteoric waters. Two such processes in fact exist, one of which was discovered in the course of this work.

Silverman,[4] in a study of the oxygen isotopic composition of silicate rocks, has shown that the silicates are enriched in O^{18} with respect to ocean water, the enrichments ranging from about 0.7% for basalts, dunite, and stone meteorites, up to 1.0 to 1.5% for sandstones, shales, and schists. Limestones are known to be about 3% higher in O^{18} than ocean water. These rocks are about 50% oxygen by weight but contain only minute amounts of hydrogen; thus if isotopic exchange takes place between water and rock, we expect that the oxygen of the water will become enriched in O^{18} but that the hydrogen will not change significantly. If the exchange is an equilibrium phenomenon, this requires that the equilibrium constant at the contacting temperature be smaller than the difference in O^{18} concentration between the water and the rocks, and there is some indication from Silverman's data that this would be the case. Hutchison[5] has observed isotopic exchange between fused silica and water with a half-time of 100 minutes at 750°C. His data indicated a predominant surface rate-controlling reaction, with some evidence for a homogeneous reaction at about 1000°C. Since the normal types of hot springs have about the same deuterium concentration as their associated surface waters and show slight variable enrichments in O^{18} with respect to these waters, it appears that they are simply deep circulating meteoric waters which have undergone variable amounts of oxygen isotopic exchange with the local rocks. We know of no other process which could affect the oxygen isotopes in the local surface waters so markedly without also affecting the hydrogen isotopes.

It is interesting to note that our data on the steam fumaroles at Larderello, Italy, and The Geysers, California, show that the steam in these areas also has about the same deuterium concentration as the local surface water, but a slightly higher O^{18} concentration. The steam thus conforms isotopically to the normal chloride spring pattern, and presumably has a similar origin.

The isotopic pattern observed in the acid hot springs clearly reflects an isotopic enrichment process operating on the local meteoric waters, as shown by the ubiquitous E_D/E_O ratio of 3. As noted previously, this ratio should be about 5 at the boiling point of water for a process of equilibrium evaporation. The temperatures encountered in these springs generally range from about 70 to 90°C and thus such an evaporation process, which would seem, on a priori grounds, the most likely to produce the observed enrichments, should result in an enrichment ratio of the order of 6. We have found, however, that in the evaporation of natural waters, the isotopic effects are not those predicted for equilibrium distillation, and, in fact, are more closely allied to the effects predicted from simple theory for a molecular or kinetic distillation in which vapor and liquid are not in continuous equilibrium. This latter process operates with a single stage enrichment factor dependent both on the vapor pressure ratios and the inverse square roots of the molecular masses, and, since the mass difference between H_2O^{18} and H_2O^{16}

is twice that between HDO and H_2O, the enrichment of O^{18} in such a process, relative to the deuterium enrichment, is relatively much greater than in the equilibrium process. Thus the E_D/E_O ratios in such a process will always be lower than those in a Rayleigh distillation process.

We have observed this phenomenon in both laboratory experiments and in natural bodies of continental water evaporating at ordinary temperatures. In fact, we are able to duplicate isotopically the acid springs of a locality by simply evaporating down the local surface water in a pan. Sulfuric acid is, of course, also concentrated by the evaporation, explaining the general tendency for the pH to decrease as the enrichment of the heavy isotopes increases. Lakes and rivers evaporating at ordinary temperatures exhibit an E_D/E_O ratio of about 5, i.e., the ratio expected at the boiling point for an equilibrium process, and this ratio is also encountered in a flask of water evaporating at 25°C. The single stage enrichment factors for natural systems are difficult to determine, since the fraction of water evaporated is generally not well known, and a good deal of study will be necessary before we can be sure that the factors determined in the laboratory are precisely applicable in nature. However, the evaluation of these factors promises a tool of great intrinsic value for the general solution of the hydrologic equation, since evaporated waters are now distinguishable from unevaporated meteoric waters of lesser "plate numbers" because of this kinetic effect.

We have no positive isotopic evidence for any juvenile or magmatic water in any of the hot spring systems we have studied. The acid sulfate springs appear to be evaporated meteoric waters perched above the normal ground water table, acid because of superficial oxidation of H_2S by atmospheric oxygen available in the non-saturated ground, and exhibiting a general enrichment of sulfuric acid by the evaporation process. We have collected duplicate samples of some of these acid springs which were submitted to Dr. W. F. Libby for tritium determinations, and von Buttlar and Libby[6] have reported that such springs at The Geysers have the same tritium content as meteoric waters. It is thus in the normal chloride springs, products of a deeply circulating convective system, that we must look for small amounts of magmatic water possibly present.

It is probable that juvenile or magmatic water should have an O^{18} concentration similar to that of the oxygen in silicate rocks, since equilibrium at high temperatures may be expected. Moreover, on the basis that all but a small amount of the juvenile hydrogen which has emerged during geologic time has gone into the ocean as water, the hydrogen isotopic composition should be similar to that of mean ocean water. Considering that hydrogen should escape from the earth more readily than deuterium, and calculating a rough material balance for the free oxygen in the atmosphere, we may say that the hydrogen in magmatic water is probably a few percent depleted in deuterium with respect to the oceans, depending on whether the magmatic water is recycled connate water or truly juvenile. Thus we have a rough idea of the isotopic composition of magmatic water, and can look at the isotopic compositions of the normal chloride springs for any sign of a tendency toward conversion to such a unique value as a result of mixing of meteoric waters with magmatic water. Our data show no evidence of such mixing and fix an upper limit of several percent for the possible magmatic water content. The fixation of this upper limit depends on the isotopic composition of the springs in question, and we will publish detailed evaluations of this important point in the more extensive papers being prepared.

It should be noted that "magmatic water" is still only a concept as far as our evidence is concerned. We have not been able to prove that it even exists. The possibility that observations on heat flow, and assumed requirements for the transport of mineral matter of low volatility, require some such water is not discussed in this brief summary of the isotopic studies.

In conclusion, we wish to emphasize the obvious desirability of extending our investigation to other hot spring and fumarole areas in many different parts of the world. Communications from geologists and geochemists interested in furnishing samples of water, steam, and volcanic gases from such areas will be welcomed by the authors.

References

1. H. Craig and G. Boato, Ann. Rev. Phys. Chem. 6:403 (1955).
2. S. Epstein and T. Mayeda, Geochim. et Cosmochim. Acta 4:213 (1953).
3. I. Friedman, Geochim. et Cosmochim. Acta 4:89 (1953).
4. S. Silverman, Geochim. et Cosmochim. Acta 2:26 (1951).
5. D. A. Hutchison, J. Chem. Phys. 22:758 (1954).
6. H. von Buttlar and W. F. Libby, J. Inorganic and Nuclear Chem. 1:75 (1955).

Discussion

UREY: Why do you say hydrogen sulfide is rising?

CRAIG: H_2S is rising because I can smell it.

UREY: Then you mean it escapes, but do you know what the source is?

CRAIG: The point is that the oxidation can take place in the superficial zone above the water table.

EPSTEIN: Since igneous rocks have about the same oxygen isotopic composition as the water, would it not have to be exchanged with sediments in order that the water become enriched in O^{18}?

CRAIG: Basic igneous rocks are only about 0.7% higher in O^{18} than ocean water, but these are meteoric waters ranging down to 1.8% lower in O^{18} than ocean water, so the total difference can be 2.5%, depending on the area.

EPSTEIN: I wonder what temperature you would have to get in order to have such a small fractionation factor.

CRAIG: We have no data on that. As you say, the fractionation factor must be less than the difference between water and rock to get an enrichment in the water, if it is an equilibrium process. We don't know whether it reaches equilibrium at all. We do know that water can exchange oxygen with silicates and carbonates, and that there is essentially no hydrogen available for exchange, so that isotopic exchange can explain this pattern of normal chloride springs. Any other process should change the deuterium concentration as well as the O^{18} concentration.

EPSTEIN: I have a point on your assumption that juvenile water should have the same oxygen isotopic composition as basic igneous rock. Dr. Clayton, of our institute, has been analyzing the oxygen in pairs of calcite and silica, from formations which have undergone hydrothermal exchange. The higher the temperature of formation, the smaller the difference in isotopic composition, and the compositions approach a value about 0.3% higher in O^{18} than ocean water. If this is the value for juvenile water, you could tolerate more juvenile water in your chloride springs.

CRAIG: I don't know whether this water you speak of is juvenile water at all. It could be anything.

EPSTEIN: I wouldn't bet on it, but this composition fits a great deal of data on magmatic silica pairs from the Mesabi Range and other places.

CRAIG: We have studied carbonates deposited from various hot spring areas, and they all reflect just the composition of the meteoric water in the area. I don't know, it could even be that the ocean had that isotopic composition then. I don't think you can say what that 0.3% higher water means. I don't want to make any blanket statement about juvenile water but only to make a statement about what is in the springs we looked at. On the more sweeping statements we have to do a lot more work. The next phase is to concentrate on oceanic volcanoes.

FRIEDMAN: I have a comment about the deuterium content of juvenile water. I have been analyzing the water in obsidians, which may not be juvenile water, but I never find anything with more deuterium than Lake Michigan water, and Lake Michigan water has about 5% less deuterium than ocean water.

UREY: Just continuing this, the same thing is true about iron meteorites, but this may be atmospheric water that has entered the hydrated iron oxide or something, so we cannot be sure it is really water from out in space. But it is certainly true that whenever we get a sample from any source that we think might provide juvenile water, the deuterium content is always too low for us. We never can find anything as high in deuterium as the ocean water.

WICKMAN: Is this term "juvenile water" very clear?

CRAIG: I should define it by using Eduard Suess' original definition. It is water that has never been at the surface of the earth before. "Magmatic water" is a blanket term that I use to cover "juvenile water" or "recycled water," or, of course, a mixture of both. With our present knowledge we could not distinguish magmatic water of original oceanic origin from truly juvenile water. Furthermore, a low tritium count is not, of course, unequivocal, since one cannot thus distinguish between dead rain water and juvenile water mixing in. The most important thing is to combine stable and radioactive isotope studies on problems of this kind, and use as many isotopes in conjunction as you can. Then you really begin to hit hard at questions such as sources, rates, and so forth, and you have a really powerful tool.

Särtryck ur Tellus nr 1, 1957

The Natural Distribution of Radiocarbon and the Exchange Time of Carbon Dioxide Between Atmosphere and Sea

By HARMON CRAIG, Scripps Institution of Oceanography, University of California, La Jolla, California

(Manuscript received Oct. 4, 1956)

Abstract

Steady-state equations governing the transfer and distribution of a radioactive isotope between its various exchange reservoirs are applied to the natural distribution of carbon 14. The radiocarbon enrichment or depletion in each reservoir, relative to the hypothetical state in which mixing is infinitely faster than the decay rate, is evaluated as a quantitative function of the exchange rates between the reservoirs. From the observed distribution of C^{12}, C^{13}, and C^{14} in the atmosphere, biosphere, and sea, and from the estimated production rate of C^{14} by cosmic rays, the residence time of a carbon dioxide molecule in the atmosphere, before entering the sea, is found to be between four and ten years.

The atmospheric residence time may also be evaluated, independently of the estimated C^{14} production rate, by considering the functional dependence of the C^{14} concentration in the oceanic mixed layer on the residence times in the atmosphere and the deep sea. This second method of evaluation also leads to an atmospheric residence time of about seven years. The average annual exchange flux of carbon dioxide into the sea is thus about 2×10^{-3} moles per square centimeter of sea surface. The average residence time of carbon dioxide in the deep sea is estimated as probably not more than about 500 years.

Introduction

Some years ago, the writer made a study of the expected and observed relationships between C^{13} and C^{14} variations in natural materials (Craig, 1954). The ratio C^{13}/C^{12} varies by some 5 % in natural sources of carbon (Nier and Gulbransen, 1939; Craig, 1953), and it was shown that for isotopic fractionation processes, the C^{14} fractionation factors should be the square of the equivalent C^{13} fractionation factors. Since the fractionation factors are close to 1, then barring effects due only to the radioactivity of C^{14}, the percentage enrichment of C^{14} in any compound should be approximately twice the C^{13} enrichment relative to the same source material. Thus, since the carbonate shells of marine mollusks are enriched some 2.5 % in C^{13} relative to terrestrial wood, such shells should show a C^{14} enrichment, relative to wood, of about 5 %. The analytical data then available indicated, however, that wood and shell have about the same radiocarbon concentration, and it was concluded therefore, that the exchange rate of CO_2 between atmosphere and sea was slow enough to produce an apparent radiocarbon age of 400 years for the surface ocean bicarbonate, corresponding to 5 % of the radiocarbon mean life of 8,033 years. It was further pointed out that only slow

---

Contribution from the Scripps Institution of Oceanography, New Series, No. 895. This paper represents in part results of research carried out by the University of California under contract with the Office of Naval Research.

Reproduced by Permission

transfer of carbon across the ocean-atmosphere interface could account for this isotopic discrepancy between the concentrations of the stable and radioactive isotopes.

Recently, more detailed studies of the natural distribution of radiocarbon have established unequivocally the reality of this effect, and it appears that the apparent age of the surface ocean bicarbonate may be taken as 400 ± 100 years for the sake of general calculations (SUESS, 1954, 1955; RAFTER, 1955). It is therefore possible to present a more detailed discussion of the factors affecting the concentration of radiocarbon in its natural reservoirs, and to derive some quantitative values for the exchange rate of carbon dioxide between the atmosphere and the sea.

Recent estimates of the residence time of a molecule of carbon dioxide in the atmosphere, before entering the sea, range from 16 hours (DINGLE, 1954) to the order of 1,000 years (PLASS, 1956). It is, therefore, of considerable interest to determine how precisely this figure may be evaluated from the known distribution and properties of the carbon isotopes. In the following study, we evaluate the characteristics of the radiocarbon distribution in a model of the atmosphere—sea system which is constructed in accord with the known layered structure of the sea, and deduce the atmospheric exchange time by two different methods which are quasi-independent. Both of these methods are based on considerations of the steady state transfer phenomena; a third method of evaluating the CO_2 exchange time, based on the dilution of the atmospheric radiocarbon concentration by the combustion of coal, has been given by SUESS (1953), and recently in a more detailed treatment by REVELLE and SUESS (1957). As we shall see, all these methods lead to the same atmospheric exchange rate but yield essentially no new information on the rate of internal mixing in the sea. However, we shall derive an estimated upper limit for the internal mixing time of the sea, by consideration of the possible dilution of radiocarbon activity in the mixed layer of the sea by production of dead CO_2. (The steady-state radiocarbon balance and the Suess effect have both been treated in a recent study by Arnold and Anderson, in which the internal mixing time of the sea is taken as fixed from recent measurements of M. Rubin; their calculations differ considerably from those given here and are commented on under Acknowledgements.)

Distribution of the carbon isotopes within the exchangeable system

We shall denote the total carbon in the active reservoirs of the atmosphere, biosphere, and sea, as the *exchangeable system*, containing about 7.9 grams of carbon per square centimeter of earth surface (cm_e^2). Table 1 shows the amounts of carbon assumed for the various components of the exchangeable system, the characteristic carbon 13 concentration in each of the components (given as per mil enrichments relative to the Chicago isotopic standard), and the carbon 14 fractionation factor relative to modern wood, computed as the square of the equivalent factor for carbon 13. The values of α_{14} are the C^{14} concentration factors relative to modern wood which would be observed if carbon 14 were stable, i.e. if the relative concentrations were unaffected by radioactive decay.

Figure 1 shows the model used for calculation; the exchangeable system is divided into five reservoirs containing amounts of carbon relative to N_a, the amount in the atmosphere, as shown in the various boxes. For convenience the term *biosphere* is restricted to denote the living terrestrial plants. The transfer between units is assumed to be determined by first order rate constants, denoted as shown, except in the case of biosphere assimilation, where the uptake is probably proportional to $N_a^\varepsilon N_b$, ε being a number between 0 and 1.

The amounts of carbon in the atmosphere, biosphere, humus, and in the entire ocean, are taken directly from Table 1. However, in accord with observation, the ocean has been taken as consisting of two reservoirs, a mixed layer and the deep sea, separated by the thermocline. The average depth of the thermocline is a question of considerable geochemical significance with respect to problems where rates of uptake or mixing are concerned. We are here interested in the average depth as defining the volumes of material in the two more or less permanent layers of the sea, relative to the total volume of material in the sea. Dr. Warren Wooster of the Scripps Institution has kindly made a study of this important relationship, using most of the

(109 8)

Table 1. Amounts of carbon, characteristic C^{13} concentration, and C^{14} fractionation factor relative to terrestrial wood, of the various components of the exchangeable system of natural carbon

	δC^{13} (‰) (1)	α_{14} (2)	Carbon content grams/cm_e^2
Atmospheric CO_2.	— 7	1.037	0.126 (3)
Terrestrial biosphere (living)..	—25	1	0.06 (4)
Terrestrial humus	—25	1	0.215 (5)
Marine biosphere.	—13.5	1.024	0.002 (6)
Dissolved organic carbon in sea..	—13.5	1.024	0.533 (7)
Total inorganic carbon in sea..	— 1.5	1.049	6.94 (7)
Total exchangeable system ...			7.88

(1) Data from H. CRAIG (1953, 1954). $\delta = [(R \text{ sample}/R \text{ standard}) - 1] \times 1{,}000$, where $R = C^{13}/C^{12}$ and the standard is the Chicago isotopic standard. Data on the various isotopic reference standards in use are given by CRAIG (1957).

(2) Fractionation factor for C^{14} relative to terrestrial wood; i.e. the expected C^{14}/C^{12} ratio in the component material, divided by the C^{14}/C^{12} ratio of modern wood. From column 1, the C^{13} fractionation factors relative to modern wood (— 25 ‰) were computed for each component; these values squared give the values in column 2 (see text). α is the chemical fractionation factor which would give the observed C^{14} concentration relative to wood if the mixing between components were infinitely fast.

(3) Data from HUTCHINSON (1954).

(4) Data from SCHROEDER and NODDACK, as given by GOLDSCHMIDT (1954, p. 355). HUTCHINSON (1954) roughly estimates this figure as one order of magnitude lower; however he uses the estimates of Schroeder and Noddack for the rate of photosynthesis by terrestrial plants. Their calculated *rate* is based on their estimate of the size of the biosphere, and thus calculations of the atmosphere-biosphere flux cannot be consistent unless both (or neither) of their estimates are adopted.

(5) Mean of estimated values 0.29 by GOLDSCHMIDT (1954), and 0.14 by RUBEY (1951).

(6) Estimated upper limit from data of RILEY, STOMMEL, and BUMPUS (1949). Using their data for the Sargasso sea only, one obtains an order of magnitude less, and according to them the Sargasso crop is about the same as the mean temperate ocean water crop, exclusive of the spring flowering period. In our units, their highest recorded value is 0.007 in Long Island Sound; the bulk of their data indicate the average ocean crop is an order of magnitude less.

(7) Data from REVELLE and SUESS (1957).

available records of observation of the variations in temperature and density in the various seas. He concludes that the mean thermocline depth, averaged over an entire year and over all oceans, is certainly between 50 and 100 meters. We have thus adopted the figure 75 ±25 meters for the mean thermocline depth, for all calculations. The average depth of the ocean and all seas is taken as 3,800 meters (SVERDRUP *et al.*, 1942), and thus the mixed layer and the deep sea are taken as containing respectively 2 % and 98 % of the total carbon in the sea. (The marine biosphere was assumed to be entirely in the mixed layer.) The amounts of carbon relative to the amount in the atmosphere are then $N_m = 1.2\ N_a$ and $N_d = 58.3\ N_a$.

Figure 1 also shows the values used for the observed radiocarbon concentrations in the various reservoirs, relative to R_w, the ratio C^{14}/C^{12} in terrestrial wood. RAFTER (1955) has shown that the atmospheric ratio is about that expected on the basis of the C^{13} data, namely $1.037\ R_w$. The average radiocarbon activity in humus is not known, but must lie within limits of 0—1 R_w; the effect of this uncertainty on the following calculations is negligible. As discussed above, the activity in the mixed layer may be taken as equal to R_w; however the average activity in the deep sea is not known and we take this as a variable parameter. The absolute value of R_w is taken as 1.24×10^{-12} from the measurements of SUESS (1955) on 19th century wood normalized for time and isotopic fractionation.

Notation and symbols:

N_i = amount of $(C^{12}+C^{13})$ in reservoir i.

N_i^* = amount of C^{14} in reservoir i.

k_{i-j} = rate constant for transfer of carbon from reservoir i to reservoir j, (first order process assumed, i.e. flux from i to $j = k_{i-j} N_i$, except for transfer from atmosphere to biosphere), years^{-1}.

k_{i-j}^* = rate constant for transfer of C^{14}, used when $k^* \neq k$.

τ_{i-j} = $1/k_{i-j}$ = residence time (years) of a stable carbon atom in reservoir i before transfer to reservoir j.

τ_{i-j}^* = $1/k_{i-j}^*$ = residence time of a C^{14} atom in reservoir i before transfer to reservoir j.

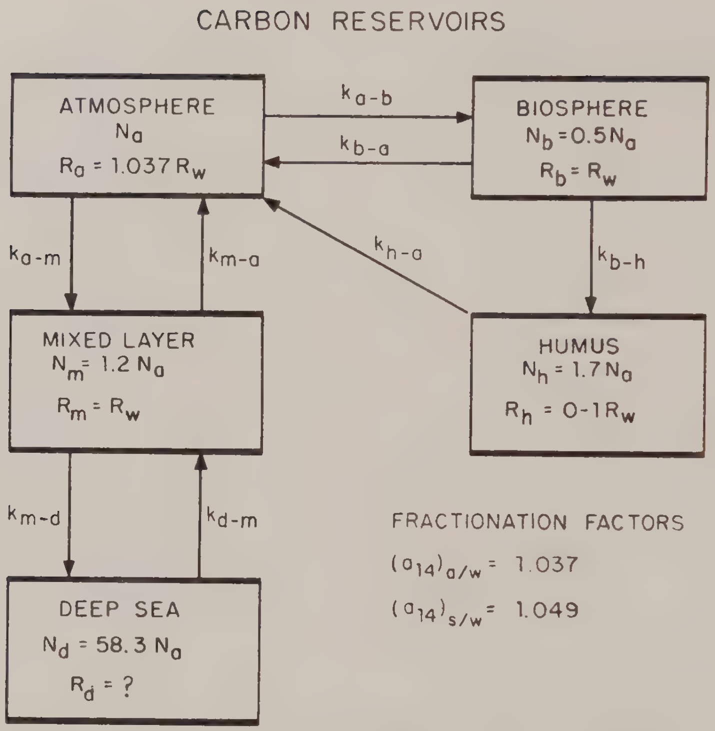
CARBON RESERVOIRS
ATMOSPHERE
N_a
$R_a = 1.037 R_w$
k_{a-b}
k_{b-a}
BIOSPHERE
$N_b = 0.5 N_a$
$R_b = R_w$
k_{a-m}
k_{m-a}
k_{h-a}
k_{b-h}
MIXED LAYER
$N_m = 1.2 N_a$
$R_m = R_w$
HUMUS
$N_h = 1.7 N_a$
$R_h = 0\text{-}1 R_w$
k_{m-d}
k_{d-m}
FRACTIONATION FACTORS
$(a_{14})_{a/w} = 1.037$
$(a_{14})_{s/w} = 1.049$
DEEP SEA
$N_d = 58.3 N_a$
$R_d = ?$

Figure 1. Carbon reservoirs in the exchangeable system. N_a = atmospheric carbon = 0.126 grams C/cm^2_e. R_w = C^{14}/C^{12} ratio in standard wood = 1.14×10^{-12}.

τ_r = $1/\lambda$ (λ = C^{14} decay constant) = radioactive mean life of C^{14} = 8,033 years.

R_i = N_i^*/N_i = C^{14}/C^{12} ratio in carbon in reservoir i.

$\bar{Q}$ = mean production rate of C^{14} from cosmic ray flux, atoms/cm^2 sec.

The meaning of τ:

We shall define τ rigorously and identify its particular meanings with specific subscripts, in order to avoid possible confusion with respect to the many usages of this symbol. Assume a reservoir with a steady-state fixed content of N molecules of a substance, and a continuous flux into and out of the reservoir of ϕ molecules/year. At a particular time, $t = 0$, we have N_0 particular molecules in the reservoir, and at some later time t, we have N' of these original N_0 molecules still present. Then we define the average life of a molecule in the reservoir in the usual way, as

$$\tau = \frac{\Sigma_i\, t_i n_i}{\Sigma_i\, n_i} \approx -\frac{1}{N_0} \int_{\substack{t=0 \\ N'=N_0}}^{\substack{t=\infty \\ N'=0}} t\, dN'$$

where n_i is the number of molecules of the original N_0 which remain in the reservoir for each time t_i, and dN' is the number of molecules removed in the interval t and $t+dt$, i.e. the number of molecules with a reservoir lifetime equal to t.

The number of molecules of the original particular set of N_0 which are removed in any interval dt is simply given by the concentration of such molecules in the reservoir, multiplied by the total flux from the reservoir, i.e.:

$$dN' = -\frac{N'}{N}\phi dt$$

which yields on integration $N' = N_0 \exp(-\phi t/N)$.

Substituting for dN' and then for N' in the integral expression for τ, and integrating between $t=0$ and infinity, we obtain:

$$\tau = \frac{N}{\phi}$$

and from the expression for N' one sees that τ, the average life, is also the time required for the original number of N_0 particular molecules to be reduced to $1/e$ times the initial number. τ is thus formally equivalent to a radioactive mean life.

In many cases, the rate of removal is dependent only on the total amount of substance, N, in the reservoir, and we can write the outgoing flux as the product of N and a first order rate constant, i.e. $\phi = kN$. In such cases we see that $\tau = 1/k$, just as the radioactive mean life is equal to $1/\lambda$.

We shall call τ, as rigorously defined above, the residence time or average reservoir life. In particular, we denote by subscripts i and j, as shown above under *Notation*, a particular residence time in reservoir i before removal to a specific reservoir j. When a reservoir exchanges with n different reservoirs, then we denote the *total* residence time in reservoir i, relative to removal by all routes, as τ_{i-T} where:

$$\frac{1}{\tau_{i-T}} = \sum_{j=1}^{j=n} \frac{1}{\tau_{i-j}}$$

For a radioactive isotope, the average reservoir life will not be the same as for the corresponding stable isotope, because of the following effects. (1) There may be isotopic fractionation in the removal process. This effect is of course independent of the radioactivity and dependent only on the isotopic mass difference; when it occurs it will cause the residence times of the isotopic species, relative to that specific removal process, to be slightly different. (2) Because of the radioactivity, the total removal rate of a radioactive species will be the sum of the physical removal rates plus λN_i, the decay rate. (3) In the steady state, after normalizing for effects (1) and (2), the residence times of the isotopic species will always be the same. However, it should be noted that in a *transient* state, the concept of residence time, as given above, may break down, and a somewhat different rigorous definition may be required. In particular, it is well known that, for transfer from a reservoir i to a reservoir j, the transfer process for an isotope in low concentration will always be a first order process (the exponential exchange law, based on the low probability of interaction) as long as the rate of mixing in reservoir j is fast relative to the transfer process, so that the isotope does not pile up at the boundary. (Humus, and the deep-sea carbon, represent reservoirs where such a pile-up might occur in the transient state.) On the other hand, the transfer process for the abundant isotopic species may or may not be first order, depending on the specific chemical and physical processes involved. Conversely, the more abundant isotope may pile up at the surface of reservoir j and mix backwards more rapidly than forward, if this is the isotope involved in the transient process. (An example of this might be the $C^{12}O_2$ produced by the combustion of fossil fuel, which might pile up in the surface layers of the deep sea or the humus.)

We shall not be concerned with the transient state in this study and thus the effects given under (3) above may be disregarded in this paper. Moreover, we shall consider only those processes in the carbon cycle which happen to be so fast, relative to the decay rate of C^{14}, that the effect of its radioactivity on the residence times is negligible. However, considering isotopic fractionation, as discussed under (1) above, we shall denote the residence times and rate constants for C^{14} as τ^*_{i-j} and k^*_{i-j} for processes in which isotopic separation may be involved (specifically for absorption and release of CO_2 by the sea).

Calculation of the CO_2 exchange time from the radiocarbon production rate

We consider the radiocarbon material balance, relative to cosmic-ray production, physical removal, and decay, in the atmosphere. Equating the flux of C^{14} entering the atmosphere, from production and from the sea and biosphere, to that leaving by physical means and decay, we write for the assumed steady state:

$$k^*_{a-m} N^*_a - k^*_{m-a} N^*_m = \bar{Q} - \lambda (N^*_a + N^*_b + N^*_h) \quad (1)$$

in terms of the isotopic rate constants for C^{14}. The steady state difference in the C^{14} flux between the atmosphere, and biosphere + humus, is simply $\lambda N^*_b + \lambda N^*_h$.

For $C^{12}O_2$ the steady state interaction of atmosphere and sea is:

$$k_{a-m} N_a = k_{m-a} N_m \quad (2)$$

and we then write the relation between the two sets of isotopic rate constants as:

$$\frac{k^*_{a-m}}{k^*_{m-a}} = \alpha_{s/a} \frac{k_{a-m}}{k_{m-a}} = \alpha_{s/a} \frac{N_m}{N_a} \quad (3)$$

where $\alpha_{s/a}$ is the ratio of the fractionation factor for C^{14} in the ocean bicarbonate, relative to wood, to the C^{14} factor in atmospheric CO_2 relative to wood; i.e. from table 1, $\alpha_{s/a} = 1.049/1.037 = 1.012$. (In these and the following derivations, we take all the factors relative to wood, which is the general radiocarbon standard.)

Substituting in (1) to eliminate k^*_{m-a}, and substituting $N^*_i = R_i N_i$, we obtain the expression for k^*_{a-m} in terms of the various R and N parameters, which may be written explicitly for the residence time of a $C^{14}O_2$ molecule in the atmosphere, before entering the sea, as:

$$\tau^*_{a-m} = \frac{\dfrac{\tau_r}{\alpha_{s/a}} \left[\alpha_{s/a} - \dfrac{R_m}{R_a} \right]}{\dfrac{\bar{Q}}{\lambda N^*_a} - \dfrac{R_b}{R_a} \dfrac{N_b}{N_a} - \dfrac{R_h}{R_a} \dfrac{N_h}{N_a} - 1} \quad (4)$$

wherein we note that the numerator of the expression is the fractional isotopic effect times the radiocarbon mean life. The denominator is the ratio of the total amount of radiocarbon in the sea to the amount in the atmosphere, $\bar{Q}/\lambda$ being equal to the total amount of radiocarbon in the world.

Using $\bar{Q}$ as 2 atoms/cm^2_e sec and $R_h/R_a = 0.5/1.037$ (see below for discussion of these values), setting $N^*_a = R_a N_a$, and using the various R and N values shown in Figure 1 and the other numerical values needed as given in the text, we find τ^*_{a-m} to be 6.2 years. The rate constant for absorption of $C^{12}O_2$ into the sea will be slightly greater than the rate constant for $C^{14}O_2$ because of an isotopic effect. For the case of absorption of $C^{12}O_2$ and $C^{13}O_2$ by barium hydroxide, the difference in rate is 1.5 % (CRAIG, 1953), and no significant error can be made by assuming a 3 % effect for the $C^{12} - C^{14}$ absorption by the sea. We thus find $\tau_{a-m} = .97\ \tau^*_{a-m} = 6$ years.

The range of possible error in the numerical values may be defined as follows. At present the most uncertain value is probably the cosmic ray production of C^{14}. Recent calculations of $\bar{Q}$ have yielded values of 2.6 (ANDERSON, 1953; LIBBY, 1955), and 2.4 (LADENBURG, 1952; KOUTS and YUAN, 1952). Anderson suggests these values may be systematically too high because of uncertainty in the calculation of the capture rate of cosmic ray neutrons in the energy range just above the sharp increase in the cadmium cross section at 0.4 ev. More recently, SOBERMAN (1956) has made a general study of the neutron intensity variations at high altitudes. With essentially the same experimental data, he calculates $\bar{Q}$ to be 1.1, neglecting the resonance capture, by nitrogen, of neutrons with energies greater than 0.5 Mev. KOUTS and YUAN (1952) found that the local production rate at Princeton was increased from $Q = 3.50$ to 4.13 by inclusion of the resonance capture rate. They also pointed out that the counters used in the slow neutron measurements are calibrated to no greater accuracy than 20 %, reflecting the uncertainty in the flux values of the Argonne standard reactor. All things considered, it appears that $\bar{Q}$ should be assigned an uncertainty of 25 %, and we shall assume the value 2 ± .5, though as noted below, it seems unlikely that the correct value can be greater than 2.

The apparent age of carbon in the mixed layer of the sea may be taken as 400 ± 100 years[1] (SUESS, 1954, 1955; RAFTER, 1955). The data by Suess represent the apparent age relative to a composite 19th century wood standard, corrected for isotopic fractionation and age, and thus the Suess effect, i.e. the slight dilution of the activity of modern wood and the atmosphere by combustion of coal during the past decades, does not affect this figure. However, there may be a slight dilution of the activity of the oceanic mixed layer samples. The average Suess effect over the world is probably of the order of 1 %, since the highest values found are near areas subject to local industrial contamination and are thus not representative. As pointed out below, the residence time of carbon in the mixed layer, before entering the deep sea, is probably about the same as the atmospheric residence time, and thus the dilution effect on the mixed layer is probably not more than 1 %.

---

[1] Suess' measurements on Atlantic shells and organic carbon average 430 years relative to his standard. Rafter's measurements on Pacific shells, organic carbon, and surface sea water, average 290 years relative to a modern wood standard (Rafter, 1955). Correction of his wood standard for the Suess effect adds 110 years to all the Pacific measurements (FERGUSSON and RAFTER, New Zealand C^{14} Age Measurements III, in press); thus the average age for Pacific samples, relative to age corrected 19th century wood, becomes 400 years, in exact agreement with the data of Suess. This age is obtained from the 5 % isotopic fractionation factor between wood and

This effect is well within the over-all uncertainty, and we shall use the 400 year figure, taking the activity ratio R_m/R_a as $(1 \pm .01)/1.037$, introducing an error of ±20 % in equation (4).

The counting error in the absolute value of R_w is 2 % (SUESS, 1955) and the value itself is based on a mass spectrometrically calibrated C¹⁴ standard for which the calibration data showed a range of 3 %. The error in the C^{14} decay constant can scarcely exceed 2 % (LIBBY, 1955, p. 42). Finally, one sees that the term $\bar{Q}/\lambda N_a^*$ in the denominator of equation (4) is about 60, while the remaining terms are of the order of 1. In particular, with the amount of humus assumed as $N_h = 1.7 \cdot N_a$, a possible range in R_h of 0 to R_w produces a range of only 3 % in τ_{a-m}^*. Thus we take $R_h = 0.5\ R_w$ for calculation, introducing an error of only ± 1.3 %. Even assuming that the humus value of 1.7 N_a is underestimated by a factor of 10, and that all humus has modern activity, would cause an error of only 1.6 years in τ_{a-m}.

A reasonable estimate of the maximum error possible is a range of ± 50 %. The value obtained from (4) is then: $\tau_{a-m} = 6^{+4}_{-2}$ years; the maximum value representing assumed values of 1.5 for $\bar{Q}$ and 500 years for surface ocean carbon, and the minimum value representing assumed values of 2.5 and 300 years. (The actual errors are not symmetrical because one enters in the numerator and one in the denominator.)

Distribution of carbon 14 in the atmosphere and sea

We now proceed to derive equations expressing the functional dependence of the amounts and specific activities of radiocarbon in the atmosphere, mixed layer, and deep sea, on the various rate constants or residence times involved. We assume that the residence time of C^{14} in the deep sea, relative to physical removal, is the same as that for C^{12}, i.e. that no isotopic fractionation is involved in the internal mixing in the sea. We shall then show how τ_{a-m}^* can also be calculated as an explicit function of the rate of mixing within the sea.

Writing out the expressions for steady state material balance of the radiocarbon flux in the mixed layer and in the deep sea, we have:

$$k_{a-m}^* N_a^* + k_{d-m} N_d^* = N_m^* \, (k_{m-a}^* + k_{m-d} + \lambda) \quad (5)$$

$$k_{m-d} N_m^* = N_d^* \, (k_{d-m} + \lambda) \quad (6)$$

where we have assumed, as stated above, that the isotopic rate constants for mixing within the sea are identical. The steady state C^{12} balance between the mixed layer and deep sea is given by:

$$k_{m-d} N_m = k_{d-m} N_d \quad (7)$$

For simplification, we shall now omit from the model the terrestrial biosphere and humus, i.e. we take the total radiocarbon balance as:

$$\bar{Q} = \lambda \, (N_a^* + N_m^* + N_d^*) \quad (8)$$

The effect of the biosphere could be included by substituting for $\bar{Q}$ in all equations in this section, the expression: $[\bar{Q} - \lambda(N_b^* + N_h^*)]$. This would change the calculated percentage changes in activity of the various reservoirs for a given change in mixing rates (δ values) by only 1 % of their numerical values, and thus the error introduced by this simplification is negligible. (The percentage error is actually variable and roughly equal to δ_a in percent divided by 30.)

From the above expressions and equation (3), one may derive the explicit relationships for the amounts of C^{14} in the three reservoirs as functions of the C^{14} decay constant, the rate

---

shell; the observed radiocarbon activities of wood and shell are about the same, but apparent ages are usually tabulated instead of relative activities.

constants k^*_{a-m} and k_{d-m} $(=1/\tau_{d-m})$, the production rate, and the known distribution of C^{12}, which are as follows:

$$N^*_a = \frac{\bar{Q}}{\lambda}\left[1+\frac{1}{\dfrac{\lambda}{k^*_{a-m}}+\dfrac{1}{\alpha_{s/a}F}}\right]^{-1} \qquad (9)$$

$$N^*_m = \frac{\bar{Q}}{\lambda}\frac{N_m}{N_a}\left[\frac{1}{F\left(1+\dfrac{\lambda}{k^*_{a-m}}+\dfrac{1}{\alpha_{s/a}F}\right)}\right] \qquad (10)$$

$$N^*_d = N^*_m\left[\frac{N_a}{N_m}F-1\right] \qquad (11)$$

$$F = \frac{N_m}{N_a}+\frac{N_d}{N_a}\left[\frac{1}{1+\dfrac{\lambda}{k_{d-m}}}\right] \qquad (12)$$

From these expressions one sees that N^*_a varies inversely with both rate constants, i.e. slow exchange between atmosphere and sea and slow internal mixing in the sea will both increase the radiocarbon concentration in the atmosphere. The reason of course is that the rate of decay is constant and proportional to the concentration, so that if the rate of physical removal is decreased more C^{14} is removed by decay with a consequent increase in the concentration. In the same way, N^*_m is seen to vary directly with k^*_{a-m} but inversely with k_{d-m}, while N^*_d varies directly with both rate constants. Setting k_{d-m}/λ equal to infinity in the above expressions gives the equations governing the simple model of an atmosphere and a uniform ocean, and if k^*_{a-m}/λ is then also set equal to infinity, one obtains the simple statistical partitioning of C^{14} corrected by the isotopic fractionation factor.

The function F is seen to be the "effective volume" or "effective carbon reservoir" of the sea, relative to the amount of carbon in the atmosphere. As k_{d-m}/λ varies from infinity to 0, F varies from $(N_m+N_d)/N_a$, i.e. the total amount of carbon in the sea relative to the atmosphere, to N_m/N_a, i.e. the carbon in the mixed layer only. In the derivation of the above equations, F falls out quite naturally as an algebraic entity; the physical significance of this function is discussed in the next section. Values of F as a function of the residence time of carbon in the deep sea are tabulated in the next section, and we shall use these values here to demonstrate the magnitude of the concentration changes in the various reservoirs as functions of the mixing rates.

Noting that for each reservoir, $R_i = N^*_i/N_i$, we denote by δ_i the percentage difference in radiocarbon activity (C^{14}/C^{12}), for any pair of rate constants k^*_{a-m} and k_{d-m}, from the state in which these rate constants are both infinitely greater than the decay constant, i.e. when the radioactivity of C^{14} has no effect on its natural distribution. Thus we define:

$$\delta_i\,(\%) = \left[\frac{R_i}{R_i\,(\tau_{i-j}=0)}-1\right]\times 100 \qquad (13)$$

where the notation $(\tau_{i-j}=0)$ signifies the hypothetical state in which the residence time in each reservoir before physical removal is essentially 0 relative to the residence time before radioactive decay (i.e. $k_{i-j}/\lambda=\text{infinity}$). The following equations give δ for the atmosphere, mixed layer, and deep sea, as explicit functions of the residence time in the atmosphere before entering the sea, the residence time in the deep sea before entering the mixed layer, the radioactive mean life τ_r, and the fixed amounts of carbon 12 in the various reservoirs.

$$\delta_a = \frac{\alpha_{s/a}\dfrac{N_s}{N_a}\dfrac{\tau^*_{a-m}}{\tau_r}+\dfrac{N_s}{N_a}\dfrac{1}{F}-1}{\dfrac{\tau^*_{a-m}}{\tau_r}+\dfrac{1}{\alpha_{s/a}F}+1} \qquad (14)$$

$$\delta_m = -\frac{\dfrac{\tau^*_{a-m}}{\tau_r}-\dfrac{N_s}{N_a}\dfrac{1}{F}+1}{\dfrac{\tau^*_{a-m}}{\tau_r}+\dfrac{1}{\alpha_{s/a}F}+1} \qquad (15)$$

$$\delta_d = \frac{\tau_r\delta_m-\tau_{d-m}}{\tau_r+\tau_{d-m}} \qquad (16)$$

In these expressions we have used N_s, the total stable carbon in the sea, $= N_m + N_d$. For the simpler model in which the ocean is taken as a single reservoir, uniformly mixed at a rate infinitely greater than the C^{14} decay rate, the function F is equal to N_s/N_a. The numerators of equations (14) and (15) are then reduced to containing the first term only, and one sees that, for a given atmospheric residence time, the percentage decrease in C^{14} activity in the mixed layer is approximately N_a/N_s or $^1/_{60}$ of the increase in the atmospheric activity, as of course it must be. In this case, of course, δ_d and δ_m are identical, as shown by (16).

In table 2 we tabulate the calculated δ_i values for atmospheric residence times, relative to the mixed layer, of 5, 10, and 20 years, and deep sea residence times, relative to the mixed layer, of 0 (rapidly mixed sea), 500, and 1,000 years. For the case of rapid mixing of the sea, the C^{14} activity in the atmosphere is increased by about 0.74 % for each year of atmospheric residence time, relative to the condition of rapid atmospheric exchange with the sea, while the activity in the sea is reduced by $^1/_{60}$ of the atmospheric increase. If the internal mixing within the sea is slow, corresponding to a deep-sea residence time of 500 years relative to the mixed layer, the effect is to increase the activity in both the atmosphere and the mixed layer by 6 %, while reducing the deep-sea activity by 0.28 %; thus the *difference* in the observed activities in the atmosphere and mixed layer remains about the same. As the table shows, the atmospheric and mixed-layer activities are each increased by about 1.2 %, relative to the condition of a rapidly mixed sea, for each 100 years of residence time in the deep sea, or "age" of the deep sea water.

Table 2. Effect of the residence times of CO_2 in the atmosphere and deep sea, both relative to exchange into the mixed layer, on the specific activity of radiocarbon in the atmosphere, mixed layer, and deep sea. δ = per cent difference in activity (C^{14}/C^{12} ratio) from the condition of infinitely fast mixing relative to the radioactive decay rate

		$\tau^*_{a-m} = 5$ y.	$\tau^*_{a-m} = 10$ y.	$\tau^*_{a-m} = 20$ y,
$\tau_{d-m} = 0$	δ_a	+ 3.7	+ 7.4	+ 14.7
	δ_m, δ_d	— 0.06	— 0.12	— 0.24
$\tau_{d-m} =$ 500 y.	δ_a	+ 9.7	+ 13.4	+ 20.7
	δ_m	+ 5.93	+ 5.86	+ 5.73
	δ_d	— 0.28	— 0.34	— 0.46
$\tau_{d-m} =$ 1,000 y.	δ_a	+ 15.6	+ 19.3	+ 26.6
	δ_m	+ 11.88	+ 11.81	+ 11.67
	δ_d	— 0.51	— 0.57	— 0.69

It is clear that the "apparent age" of the surface ocean bicarbonate does not reflect a simple decrease of activity due to slow transfer of radiocarbon into the sea, as is sometimes stated. The actual effect is a piling up of the radiocarbon in the atmosphere by the mixing barrier, amounting to several percent of the activity which would be observed in the case of very rapid exchange with the sea. The actual decrease in specific activity of the sea is seen to be an insignificant contribution to the observed difference of activity between the atmosphere and the sea. The "piling up" effect in the atmosphere and mixed layer, by slow internal mixing in the sea, is about the same for each of these reservoirs, because they contain about the same amounts of carbon (fixed by the chemical equilibrium between atmosphere and sea and the average depth of the thermocline); thus observations of the activity difference between the atmosphere and the mixed layer cannot yield much information about the rate of internal mixing in the sea.

Calculation of the CO_2 exchange time from the distribution of carbon 14

Table 2 shows that over the range of deep-sea residence time considered, the difference in activity between the atmosphere and mixed layer is practically unaffected by the internal mixing rate within the sea, and is essentially a function of the atmospheric residence time of CO_2 only. Thus we can estimate the atmospheric residence time rather closely by considering the atmosphere-mixed layer activity difference, if we have some idea of the order of magnitude of the mixing rate within the sea.

From equations (3), (5), (6), and (7), we derive the expression for the ratio of the radiocarbon activity in the atmosphere to the activity in the mixed layer, in terms of the mixing rate constants, as:

$$\frac{R_a}{R_m} = \frac{1}{\alpha_{s/a}} + \frac{\lambda F}{k^*_{a-m}} \tag{17}$$

where the function F was given by (12). For an infinite deep-sea residence time, i.e. no mixing between the layers of the sea, F reduces to N_m/N_a and the activity ratio is seen to become dependent on the size of the mixed layer reservoir only. It should be noted that (17) is derived from considerations of the steady state balance in the mixed layer and in the deep sea, and is *independent* of any assumptions about the terrestrial biosphere and humus.

Equation (17) may be rewritten as:

$$\tau^*_{a-m} = \frac{\tau_r}{F}\left[\frac{R_a}{R_m} - \frac{1}{\alpha_{s/a}}\right] \qquad (18)$$

and using R_a and R_m as given in figure 1, we now tabulate τ^*_{a-m} vs. τ_{d-m}, together with the function F and the ratio F/F_0 in percent, where $F_0 = N_s/N_a =$ the value of F for infinitely rapid mixing in the sea on the radiocarbon time scale.

τ_{d-m}(y)	F	F/F_0 (%)	τ^*_{a-m} (y)
0	59.5	100	6.54
100	58.8	98.8	6.62
300	57.4	96.5	6.78
500	56.1	94.3	6.93
1,000	53.0	89.1	7.34
5,000	37.1	62.4	10.5
10,000	27.2	45.7	14.3
20,000	18.9	31.8	20.6
50,000	9.3	15.6	41.8

By equating (18) with (4) we see that:

$$\frac{N_s^*}{N_a^*} = \frac{R_m}{R_a} F \qquad (19)$$

since, as noted in the discussion of (4), the denominator of (4) is equal to N_s^*/N_a^*. It is then easy to show rigorously the physical meaning which may be attached to F. For any given internal mixing rate in the sea, we may suppose the sea to be divided into two portions, the uppermost of which contains all the radiocarbon of the sea at a uniform concentration equal to that presently observed in the surface of the sea; i.e. the internal mixing in this portion is infinitely rapid on the radiocarbon time scale and the C^{14}/C^{12} ratio in this portion is $R_m (= R_w)$. The lowermost portion contains no radiocarbon. Then if X is the amount of C^{12} in the uppermost portion containing the radiocarbon, $X = FN_a$, and F is simply the ratio of the amount of stable carbon in the upper portion to the amount in the atmosphere. Moreover, $F/F_0 = X/N_s$, so that the ratio F/F_0 is simply the fraction of the total sea contained in the rapidly mixed upper portion.[1] Thus from the numerical values tabulated above, one sees that a deep-sea residence time of 5,000 years in the actual two-layer model assumed in this study, is equivalent to having 62 % of the sea, at C^{14} concentration R_m, rapidly mixed and functioning as an effective component of the exchangeable system, and 38 % of the sea completely isolated and containing no radiocarbon. This would correspond to complete mixing in the upper 2,400 meters of the sea and no communication with the bottom 1,400 meters.

The dependence of τ^*_{a-m} on τ_{d-m} is seen to be of such low order that a 5,000 year mixing time in the sea adds only 4 years to the atmospheric residence time calculated for a homogeneous sea with infinitely rapid internal mixing. This is simply the consequence of the long C^{14} half-life, coupled with the fact that one is dealing with a steady-state mixed system, rather than a case of simple exponential decay from an initial concentration.

Only one set of precise radiocarbon measurements on deep-sea water appears to exist at present. M. Rubin of the U.S. Geological Survey has found that in the area east of the Lesser Antilles, the water at 1,750 meters is only 200 years "older" than the surface water (personal communication). However, it appears to be well established that, in general, the internal mixing time of the sea is less than 1,000 years. WOOSTER and KETCHUM (1956) have calculated the mean displacement time of the deep water of the North Atlantic as 250 years, from oceanographic data. WORTHINGTON (1954) has studied the secular decrease of dissolved oxygen in these waters and estimates the age, relative to the surface water, as 140 years. His data indicate that the North Atlantic deep water may be formed sporadically, rather than replenished by a continuous mixing process. The deep Pacific water is probably older than the deep waters of the Atlantic. However, REVELLE and MAXWELL (1952) found that the heat flux through the floor of the Pacific is such that the deep Pacific water must be replenished in less than a thousand years.

From the figures tabulated above, one sees that a range in the deep sea residence time of

---

[1] Alternatively one could assume a model in which the uppermost portion of the sea, containing all the radiocarbon, grades from a C^{14}/C^{12} ratio of R_m at the surface to 0 at the lower boundary. In this case $X = (R_m/R_x)FN_a$ and $X/N_s = (R_m/R_x)\ (F/F_0)$, where $R_x = N_s^*/X =$ the average C^{14}/C^{12} ratio in the upper layer. The correspondence with our actual model would then depend on the type of activity gradient assumed.

0—1,000 years corresponds to a range in τ^*_{a-m} of only 0.8 years, an insignificant error. Thus we take τ^*_{a-m} as 6.8 years, corresponding to $\tau_{a-m} = 6.6$ years, with an estimated uncertainty of about 40 %, reflecting uncertainties of 5 % due to the internal mixing rate in the sea, 20 % in the measured percentage activity difference between the atmosphere and mixed layer, perhaps 10 % in the absolute amount of carbon in the sea, and 2 % in the decay constant. The error in F due to the uncertainty in the average depth of the thermocline is only 1 %, as the absolute amount of carbon in the mixed layer alone does not enter into the calculation. (Thus the possible error in estimating the size of the marine biosphere is seen to be entirely negligible.)

The value 6.6 years is in excellent agreement with the previous figure of 6 years, calculated by (4) from the radiocarbon production rate with a very minor dependence on the size of the biosphere and humus. Both calculations, however, require the measured "apparent age" of the mixed layer carbon, and thus they are not completely independent. The errors in each of these results are probably such as to make the values slightly higher, and $\bar{Q}$ is more probably less than, rather than greater than, 2.0. Weighting the errors, and using (2) we adopt the values:

$$\tau_{a-m} = 7 \pm 3 \text{ years} \qquad \tau_{m-a} = 8.4 \text{ years}$$

$$k_{a-m} = 0.14 \qquad k_{m-a} = 0.12$$

and the mixing rate constants are thus a thousand times larger than the radioactive decay constant.

Taking the amount of CO_2 in the atmosphere as 2.35×10^{18} grams, (HUTCHINSON, 1954) and k_{a-m} as 0.14, we find the exchange rate of CO_2 between atmosphere and sea to be 2×10^{-3} moles of CO_2 per square centimeter of sea surface, per year, or about 45 cc (STP) of CO_2.

$\bar{Q}$ and the radiocarbon content of the deep sea

Using Suess' value for $R_w^{\triangledown}$ and the data given in table 1 and figure 1, we can calculate the maximum amount of radiocarbon on the earth by assuming the average "age" of the ocean water to be 600 years and all the humus to have modern activity. In this way we can account for 57 metric tons of C^{14} on the earth, corresponding to 260 megacuries of activity. Using the $\bar{Q}$ value of 2.4 (LADENBURG, 1952), the predicted amount of C^{14}, corresponding to secular equilibrium with the production rate, is 72 metric tons. The discrepancy is thus about equivalent to the 20 % uncertainty assigned to the production rate by KOUTS and YUAN (1952).

We may write the relationship between τ_{d-m} and $\bar{Q}$ as:

$$\frac{\tau_{d-m}}{\tau_r} = \frac{N_d R_m}{\dfrac{\bar{Q}}{\lambda} - N^*_{a+b+h+m}} - 1 \tag{20}$$

and we calculate the following values of τ_{d-m} for the previously assumed mean and limits for $\bar{Q}$:

$\bar{Q}$	τ_{d-m} (y)
1.5	+2,580
2.0	− 265
2.5	−1,910

Thus from the uncertainty in $\bar{Q}$, the steady state conditions are consistent with any oceanic mixing time up to 2,500 years; however, the radiocarbon distribution data suggest that $\bar{Q}$ is actually about 1.8 and not greater than 2. In this calculation we have assumed all the humus to have modern activity; it seems unlikely that limestone can have acquired enough C^{14} by exchange to make up the balance required by the high value of $\bar{Q}$.

The relation between τ_{d-m} as defined for steady state mixing conditions, and t_c, the "age" of deep-sea water, relative to surface water, as calculated by the simple exponential decay relationship, is given by:

$$\frac{\tau_{d-m}}{t_c} = \frac{e^{\lambda t_c} - 1}{\lambda t_c} = 1 + \frac{1}{2}\frac{t_c}{\tau_r} + \frac{1}{6}\left[\frac{t_c}{\tau_r}\right]^2 \tag{21}$$

and thus τ_{d-m} will be greater than t_c, the "measured age", by about 0.6 % for each 100 years of t_c.

Summation and discussion

Using the empirical data on the relative distribution of C^{12}, C^{13}, and C^{14} in the exchangeable system of carbon, and a model for the sea consisting of a rapidly-mixed surface layer, coupled with the deep sea, a quantitative evaluation of the effects of the carbon transfer rates on the radiocarbon concentration in the various reservoirs has been made. Relative to the hypothetical state in which the various mixing rates are infinitely faster than the radiocarbon decay rate, we find that the specific activity of C^{14} in the atmosphere is increased about 5 %, while the activity in the mixed layer is decreased by about 0.08 %, by an atmospheric residence time, relative to the sea, of 7 years. However, slow mixing between the mixed layer and the deep sea increases the activity in both the atmosphere and the mixed layer, relative to the rapidly mixed state, by 1.2 % for each 100 years of deep-sea residence time of carbon. Thus, if the residence time in the deep sea is assumed to be about 250 years, as several lines of evidence indicate, the total effects of the mixing rates on the reservoir concentrations are: an 8 % increase in the atmospheric activity, a 2.9 % increase in the mixed-layer activity, and a 0.2 % decrease in the activity in the deep sea, all relative to the activities which would be observed if the transfer of carbon were so rapid that there were no effects from the radioactivity.

The exchange time of CO_2 between atmosphere and sea was found by two methods which are quasi-independent. The first method depends on the cosmic-ray production rate of radiocarbon, as calculated by various workers, on the C^{14} concentration in the mixed layer of the sea, and on the steady-state material balance in the atmosphere. The second method considers the steady-state material balance in the mixed layer, and the mixed-layer C^{14} concentration as a function of the exchange time between the mixed layer and the deep sea. Both these methods yield an atmospheric residence time of CO_2, relative to entrance into the sea, of 7 ± 3 years, corresponding to a rate constant $k_{a-m}=0.14$.

According to HUTCHINSON (1954) the flux of atmospheric CO_2 into the biosphere corresponds to about 3 % of the amount in the atmosphere per year. In our notation, with $\tau_{a-m}=7$ years, and $\tau_{a-b}=33$ years, the total residence time of a CO_2 molecule in the atmosphere is $\tau_{a-T}=6$ years, after which it goes either into the sea (9 chances out of 11) or into the terrestrial biosphere (2 chances out of 11). Thus the carbon dioxide flux into the sea is about 4.5 times larger than the flux into the biosphere, and about 82 % of the CO_2 leaving the atmosphere goes into the sea, while only 18 % goes into the terrestrial plants. This ratio represents a considerable departure from previous estimates, and indicates that the spatial distribution of plants and soils is probably not the dominant factor in determining the steady-state CO_2 concentration in the atmosphere, contrary to what has been supposed (HUTCHINSON, 1954, p. 391). In fact it appears more likely that the spatial pattern of absorption and release of CO_2 by the sea, and the seasonal variations in this pattern, are the dominant factors.

If the residence time of CO_2 in the Northern hemisphere atmosphere is even a few years, then the rapid rate of transfer into the sea should produce an appreciable difference in the observed Suess effects in the Northern and Southern hemispheres, because of the much greater industrial concentration in the Northern hemisphere. Thus, if the Northern hemisphere residence time, relative to cross-hemisphere mixing, is from 2 to 5 years, the Southern hemisphere Suess effect should be from 75 to 50 %, respectively, of the effect observed in the Northern hemisphere. There is some indication that the Southern effect may in fact be only about half the Northern effect (SUESS, 1955), but a great many precise measurements will be needed to establish the exact nature of the effect. Nevertheless, it is clear that the rapid exchange of CO_2 with the sea will allow one to make rather close estimates of the cross-hemispheric exchanges; the precision with which this can be done is of course a direct function of the exchange rate with the sea.

Turning to the mixed layer in the sea, we see that τ_{m-a}, the residence time of CO_2 relative to entrance into the atmosphere, is equal to N_m/N_a times τ_{a-m}, and is thus 8.4 years, corresponding to $k_{m-a}=0.12$. If the residence time in the deep sea, τ_{d-m}, is about 200 years, the residence time in the mixed layer, before transfer into the deep sea, is $\tau_{m-d}=$ about 4 years, corresponding to k_{m-d} about 0.25. The total residence time is then $\tau_{m-T}=2.7$ years, after which a CO_2 molecule can go into the deep sea (2 chances out of 3), or into the atmosphere (1 chance out of 3). Thus with τ_{d-m} about 200 years, about $^2/_3$ of the carbon cycled into and out of the mixed layer would exchange with the deep sea, and about $^1/_3$ with the atmosphere. The precise ratio depends of course on the actual residence time in the deep sea, but it is clear that for any reasonable mixing time of the deep sea, the exchange of the mixed layer is about equally proportioned between the atmosphere and the deep sea.

It should be emphasized that the indicated uncertainty in the atmospheric exchange time refers only to the rigorous model calculation; there is, of course, an additional uncertainty concerning the relationship of the model to the real physical situation. Our model does not exclude the existence of large horizontal gradients across the surfaces of the reservoirs, since we are dealing with steady-state average fluxes. However, the basic construction of the model assumes that the two reservoirs in the sea are each internally mixed over times comparable with their residence times, so that the material removed from each of these reservoirs has the average radiocarbon concentration of the reservoir as a whole.

Fortunately, the two methods of calculating τ_{a-m} depend on different assumptions. The calculation based on $\bar{Q}$ considers the material balance in the atmosphere only, and requires only that the CO_2 entering the atmosphere from the sea have the radiocarbon concentration corresponding to the measured activity of the mixed layer carbon; i.e. only a negligible amount of the CO_2 should be contributed directly from the deep sea to the atmosphere, without passing through the mixed layer first. Since the exchange of water between near-surface and deep waters takes place predominantly in high latitudes where the thermocline ceases to exist, there may well be some direct exchange of CO_2 between deep water and the atmosphere. On the other hand, inspection of equation (4) shows that decreasing R_m/R_a to correspond with *all* the CO_2 furnished to the atmosphere from a carbon source with an apparent age of 650 years relative to the atmosphere (i.e. $\tau_{d-m}=250$ years), increases the calculated value of τ_{a-m} to only 10 years. Since it is hardly likely that all the CO_2 released from the sea comes directly from the deep sea to the atmosphere, we conclude that the calculation of τ_{a-m} from $\bar{Q}$ cannot be significantly in error from the model assumption.

Our second calculation of τ_{a-m}, by equation (18) is more dependent on the actual model of oceanic mixing constructed; it assumes that the mixed layer is well mixed over times of the order of a few years, so that the bulk of the mixed layer has the same C^{14} concentration as the portions exchanging with the atmosphere and the deep sea, and that the deep sea is internally mixed over times of the order of the average reservoir life in the deep sea. The first assumption is fulfilled, for the mixed layer is known to mix by convection and wind action over times of the order of days. If the second assumption were not valid, the function F would be slightly changed because the C^{14} concentration in the carbon exchanged with the mixed layer would not represent the average reservoir concentration (as assumed in equation (6)). However, the very minor dependence of the value of τ_{a-m} on F was shown, and moreover, it seems not unlikely that in the mixing process by which exchange with the mixed layer is effected, the deep sea is itself mixed at least partially in a time equivalent to the residence time.

The close agreement of the two values of τ_{a-m}, based on the assumption that the deep-sea residence time is not more than several thousand years, indicates that the model approximates well enough the actual mixing conditions in the sea. The additional assumption of the steady state has of course also been made; from the close agreement between the historical ages and the radiocarbon dates on samples of known age, this assumption is clearly valid enough for our purposes. (For the most recent data on comparison of measured and historical ages, see Libby, 1955, p. 10.)

Suess (1953) has attacked the problem of the atmosphere-sea exchange rate from an entirely different viewpoint, namely the dilution of the atmospheric radiocarbon activity by the dead CO_2 from the combustion of fossil fuels, as recorded in the tree rings of the last 100 years. His measurements indicated a "Suess effect", as we shall indicate it for convenience, of about 3 %, from which he deduced an atmospheric CO_2 residence time, relative to the sea, of 20—50 years. The integrated amount of "dead" CO_2 which has been produced by human activity is equivalent to a constant production rate of 0.25 % of N_a for the past 40 years (REVELLE and SUESS, 1957), which is long enough for the atmosphere to have reached secular equilibrium (to a close enough approximation) with the production rate. Thus from our present figure of $\tau_{a-m} = 7$ years, the predicted Suess effect is 7×0.25 or 1.75 % dilution of the atmospheric radiocarbon activity.

More recent and extensive measurements by SUESS (1955) have shown that the observed effect is actually less than 3 %, and that effects of about 3 %, as previously observed, represent local effects in areas near industrial concentrations. As Revelle and Suess point out, the average figure obtained from the recent data of Suess turns out, by coincidence, to be 1.73 %. They reverse the present procedure, evaluating the atmospheric residence time from the Suess effect with a more detailed treatment than made previously by Suess, and conclude that, all things considered, the atmospheric CO_2 residence time is of the order of magnitude of 10 years relative to the sea. The close agreement of their value, obtained from considerations of the transient state and the measured changes in atmospheric radiocarbon activity over past decades, and the value found in this study of the steady-state distribution of C^{14}, is gratifying, and indicates that the factors governing the natural distribution of radiocarbon are now fairly well understood.

Some comment should be made on the differences between the treatment by REVELLE and SUESS (1957) and by the present writer. Their conclusions are based on a generalized evaluation of the interaction of all the following parameters: τ_{a-m}, the "apparent age" of surface ocean carbonate, and an "effective" sea reservoir, essentially as related by equation (18), an "effective" atmospheric reservoir (as a function of interaction with the biosphere and humus), and the Suess effect. The reason for the much larger uncertainty assigned to their estimate of τ_{a-m}, compared to the estimate of ± 3 years for the figure deduced in this paper, is twofold. First, their treatment involves the Suess effect, which, being very small, is not amenable to precise measurement, and moreover, is directly related to the interaction between atmosphere and biosphere. Thus given the exact magnitude of the Suess effect and the "apparent age" of surface sea carbon as fixed values, then e.g., if the CO_2 in the atmosphere is in rapid exchange with an equivalent amount of carbon in the biosphere, the value of τ_{a-m} deduced for no interaction is doubled. The amounts of carbon tied up in the biosphere and humus, and the rate and extent of their interaction with the atmosphere, are subject to order of magnitude uncertainty.

Secondly, they take the ocean as a single reservoir and deliberately refrain from attempting to construct a model of the sea to which physical significance must be attached. On the other hand, the model constructed for the present study is based on breaking the sea into two reservoirs, which correspond, more or less, to those actually observed in the sea. As was shown in the second calculation of the atmospheric residence time, the interaction of the deep sea with the atmosphere in the present model is so weak that a precise estimate of the atmospheric exchange time can be made, even though the internal mixing rate of the sea is not known to within several thousand years. In fact, the mixed layer of the sea functions as a buffer, both in nature and in the present model, serving to damp out almost completely the interaction between the atmosphere and the deep sea.

We turn, finally, to the question of the internal mixing rate in the sea, and to what one can say about this rate from the present knowledge of the distribution of radiocarbon. As pointed out in the previous section of this paper, the uncertainty in the production rate of C^{14} is consistent with deep-sea residence times up to about 2,500 years. Unfortunately, the Revelle-Suess analysis provides no closer estimate.

Revelle and Suess define an "effective sea reservoir", smaller than the actual amount of carbon in the sea because of incomplete mixing, but as noted above, do not attach a physical meaning to their definition. The reason for our discussion of the physical significance of the function F, in a previous section, is now apparent; this function is their "effective sea reservoir", and their ratio S^*/S, where S in our notation is N_s, the total amount of stable carbon in the sea, is simply the ratio F/F_0. Values of F and F/F_0 were tabulated as functions of the deep-sea residence time, τ_{d-m}, at the point where equations (18) and (19) were introduced. Revelle and Suess find that the interaction of their various parameters is such that ratios of S^*/S as low as 70 % are acceptable, and from the tabulated values of F/F_0 given with (18), we see that τ_{d-m} could then be as long as about 3,000 years and still be consistent with their requirements. Even if the effective sea reservoir can be restricted to 90 % of N_s, the deep-sea residence time can still be 1,000 years.

There is, however, one way in which the mixing rate of the sea can be defined more closely, from the radiocarbon data, than the 0—3,000 range obtained by the two methods discussed above. As mentioned above, the atmosphere can be considered to be essentially in secular equilibrium with a flux of dead CO_2 amounting to a constant input of 0.25 % of N_a over the past 40 years. From the discussion of τ_{a-T} given above, it appears that about 80 % of the CO_2 leaving the atmosphere goes into the sea, and thus we can assume a flux of about 0.2 % of N_a into the sea of dead CO_2. We may then ask what the maximum dilution of the radiocarbon activity in the mixed layer can have been.

The difference between the expected and observed radiocarbon activity of the mixed layer, relative to 19th century wood corrected for age, appears to be about 5 % and probably cannot be more than 6 % (SUESS, 1955). From the calculation based on $\bar{Q}$, equation (4), we found that τ_{a-m} is probably not less than 4 years; it is almost certainly not less than 3 years. These minimum figures for τ_{a-m} would account for 3 % and 2 %, respectively, of the observed 5 %, or maximum 6 %, mixed-layer effect, by virtue of the effect of the mixing rates on the atmospheric concentration, which was discussed in a previous section. Thus it appears that the maximum dilution of C^{14} activity the mixed layer can have suffered is most probably 2 %, and almost certainly not more than 4 %.

The forward mixing residence time in the mixed layer, τ_{m-d}, is found by dividing the percentage dilution by the percentage flux, assuming secular equilibrium (which is shown by the result to be valid enough). If τ_{a-m} is as low as 4 years, then actually 90 % of the atmospheric CO_2 goes into the sea, and the mixed layer carbon, N_m, is 1.2 times N_a, thus the dead CO_2 from industrial combustion has a flux rate through the mixed layer of approximately 0.2 % of N_m. Dividing the percentages given above, we find that τ_{m-d} is most probably not more than 10 years, and almost certainly not more than 20 years.

The residence time of a CO_2 molecule in the deep sea, τ_{d-m}, as given by (7) is about 50 times the residence time in the mixed layer before transfer to the deep sea. We thus find that τ_{d-m} is most probably not more than 500 years, and almost certainly not greater than 1,000 years.

The above statement on the mixing rate in the sea is the most precise limitation which can be put on the average mixing time in the sea by the present radiocarbon data. Direct measurements on deep waters should, of course, delineate the situation much more precisely. Nevertheless, it should be pointed out that measurements on 50 or 100 year old shells and seaweed to determine the Suess effect in the sea will give an independent check on the average mixing rates in the sea.

The detailed analysis of the steady-state distribution of a radioactive isotope is seen to be a powerful tool for the evaluation of rates of mixing in natural reservoirs. An analysis, similar to the present study of radiocarbon, has been made of the distribution of natural tritium in the atmosphere and the sea. The results indicate that the production rate of tritium from cosmic rays is probably five to seven times higher than the rates currently estimated by consideration of the cosmic-ray flux. Because of the short mean life of tritium (18 years), as contrasted with radiocarbon, a closer estimate of the internal mixing rate in the sea can be made from the steady-state distribution observed in the atmosphere and the mixed layer. The tritium distribution was found to indicate a deep-sea residence time of about 200—300 years, as a world average. Details of the tritium study will be published shortly.

Acknowledgements

This paper represents in part the results of a general study of the use of natural isotopic effects in the analysis of mixing rates in the atmosphere and the sea, begun while the writer was a member of a National Academy of Sciences Study Group on applications of

nuclear phenomena to oceanography; some of the material presented here is included in the final report of that group. It will be obvious from the text that I am greatly indebted to Drs. Hans Suess and Roger Revelle for discussion of many aspects of the subject, and that this paper has benefited in many ways from their own contribution (1957) and from the extensive radiocarbon studies of Suess. The present work was not aimed at duplication of their study, which is mainly concerned with the problem of the possible increase in the atmospheric carbon dioxide, and the limits which can be placed on this effect by knowledge of the CO_2 exchange rate between atmosphere and sea. Rather, the purposes of the writer's investigation were, first, to evaluate, on as quantitative a level as possible, the general factors affecting the distribution of natural radiocarbon in its various reservoirs, and second, to determine precisely what could be said, from the radiocarbon distribution, about the mixing of this isotope into the deep sea, because of the importance of this aspect relative to the study of the distribution of natural tritium.

Drs. James Arnold and Ernest Anderson had made calculations similar to some of the ones presented here, and I thank them for a preprint of their paper received during the early stages of this study. The present considerations were carried out independently of their work and we have not discussed our differences. Their estimate of the atmospheric residence time, as here defined, of about 14 years is obtained by a material balance calculation, independent of $\bar{Q}$, but they do not give their method of calculation and it is difficult to determine how their calculation differs from the method given by equation (18) above. They assume the flux of CO_2 into the sea to be proportional to the sum of $N_a + N_b + N_h$ as used in this paper, treating these three units as one large reservoir, and they assume the radiocarbon concentration in the deep sea to be given by Rubin's measurement, thus adopting a figure of 250 years for τ_{d-m}. Moreover, they use a figure for the amount of carbon in the marine biosphere 80 times higher than the maximum possible value estimated as an upper limit in the present study (see table 1); this essentially doubles the amount of carbon assumed to be in the mixed layer. (In the present study, the material balance for the mixed layer was derived in such a way that, as shown by (18), the calculated value of τ_{a-m} is decreased by only 2 % if the amount of carbon in the mixed layer is doubled.) It seems likely that our different results for τ_{a-m} are due to the interaction of these factors, and it is, in fact, gratifying, that with such serious differences in initial assumptions, the figures differ by no more than a factor of two.

Finally, I wish to thank Dr. Warren Wooster for extensive discussion of mixing phenomena in the sea, and for his efforts in examining the question of the average thermocline depth; and Dr. Meyer Rubin for the information on his radiocarbon measurements on deep-sea samples.

REFERENCES

Anderson, E. C., 1953: The production and distribution of natural radiocarbon. *Ann. Rev. Nuclear Science* **2**, pp. 63—78.

Craig, H., 1953: The geochemistry of the stable carbon isotopes. *Geochim. et Cosmochim. Acta* **3**, pp. 53—92.

Craig, H., 1954: Carbon 13 in plants and the relationships between carbon 13 and carbon 14 variations in nature. *Journ. Geol.* **62**, pp. 115—149.

Craig, H., 1957: Isotopic standards for carbon and oxygen and correction factors for mass spectrometric analysis of carbon dioxide. *Geochim. et Cosmochim. Acta* (in press).

Dingle, A. N., 1954: The carbon dioxide exchange between the North Atlantic Ocean and the atmosphere. *Tellus* **6**, pp. 342—350.

Goldschmidt, V. M., 1954: *Geochemistry* (A. Muir, ed.). Oxford: Clarendon Press, 730 pp.

Hutchinson, G. E., 1954: In *The Earth as a Planet* (G. Kuiper, ed.). Chicago: University of Chicago Press, Chapter 8.

Kouts, H. and Yuan, L., 1952: The production rate of cosmic-ray neutrons and C^{14}. *Phys. Rev.* **86**, pp. 128—129.

Ladenburg, R., 1952: The absorption rate of cosmic-ray neutrons producing C^{14} in the atmosphere. *Phys. Rev.* **86**, p. 128.

Libby, W. F., 1955: *Radiocarbon Dating*. 2nd edition, Chicago, University of Chicago Press, 175 pp.

Nier, A. O. and Gulbransen, E. A., 1939: Variations in the relative abundance of the carbon isotopes. *Journ. Am. Chem. Soc.* **61**, pp. 697—698.

Plass, G. N., 1956: Carbon dioxide theory of climatic change. *Tellus* **8**, pp. 140—154.

Rafter, T. A., 1955: C^{14} variations in nature and the effect on radiocarbon dating. *N. Zealand Journ. Sci. Tech. B* **37**, pp. 20—38.

Revelle, R. and Maxwell, A. E., 1952: Heat flow through the floor of the eastern North Pacific Ocean. *Nature* **170**, p. 199.

Revelle, R. and Suess, H. E., 1957: Carbon dioxide exchange between atmosphere and ocean and the question of an increase of atmospheric CO_2 during the past decades. *Tellus* **9**, p. 18.

Riley, G. A., Stommel, H., and Bumpus, D. F., 1949: Quantitative ecology of the plankton of the western North Atlantic. *Bull. Bingham Ocean. Coll.* **12**, Art. 3, 169 pp.

Rubey, W. W., 1951: Geologic history of sea water. *Bull. Geol. Soc. Amer.* **62**, pp. 1111—1147.

Soberman, R. K., 1956: High-altitude cosmic-ray neutron intensity variations. *Phys. Rev.* **102**, pp. 1399—1409.

Suess, H. E., 1953: Natural radiocarbon and the rate of exchange of carbon dioxide between the atmosphere and the sea. *Nuclear Processes in Geologic Settings*, National Academy of Sciences — National Research Council Publication, pp. 52—56,

Suess, H. E., 1954: Natural radiocarbon measurements by acetylene counting. *Science* **120**, pp. 5—7.

Suess, H. E., 1955: Radiocarbon concentration in modern wood. *Science* **122**, pp. 415—417.

Sverdrup, H. U., Johnson, M. W., and Fleming, R. H., 1942: *The Oceans*. New York: Prentice-Hall, Inc. 1087 pp.

Wooster, W. S. and Ketchum, B. H., 1956: Transport and dispersal of radioactive elements in the sea. Final report, *National Academy of Sciences Committee on Effects of Atomic Radiation on Oceanography and Fisheries* (in press).

Worthington, L. V., 1954: A preliminary note on the time scale n North Atlantic circulation. *Deep-Sea Research* **1**, pp. 244—251.

PRINTED IN SWEDEN ESSELTE, STHLM 57

Deep-Sea Research, 1957, Vol. 4, pp. 73 to 92. Pergamon Press Ltd., London

Reproduced by Permission

Light generation in a sonic-scattering layer

ELIZABETH M. KAMPA and BRIAN P. BODEN

Abstract—1. Luminescence at the depth of the sonic-scattering layer in the San Diego Trough has been recorded at various times of day and night with a telerecording bathyphotometer. The mean intensity of the luminescent flashes recorded is remarkably constant at a value near $1 \cdot 1 \times 10^{-4}$ microwatts per square centimetre throughout the diurnal cycle. The mean frequency of flashes varies widely, being least (10 to 24 per minute) at midday, greatest (42 per minute) during the twilight migration of the sonic-scattering layer, and at an intermediate level (32 per minute) during the night.

2. The colour of the luminescence from the sonic-scattering layer has been determined by using interference filters with the photometer. The independence of the light generated at depth from that incident on the sea surface has been established by a comparison of the colours of the two. The luminescence from the scattering layer is blue-green; the emission is maximal near 478 mμ.

3. Laboratory determinations have been made of the intensity and spectral distribution of the luminescence of two species, *Euphausia pacifica* and *Pyrosoma atlantica*, present in the water on the night when scattering-layer luminescence was measured. The emission spectra of both forms are bimodal. The primary peak of *Euphausia pacifica* luminescence is at about 476 mμ, and the secondary is near 520 mμ. The primary peak of *Pyrosoma atlantica* luminescence is near 482 mμ, and the secondary is near 525 mμ. The intensities of luminescence of both organisms are compatible with the range of intensities encountered in the measurements of light generated in the sonic-scattering layer.

4. The problems presented to the oceanographer and the biologist by the introduction of bioluminescence records are discussed, and the situation of *Euphausia pacifica* in particular is considered. The depth distribution of this euphausiid in the San Diego Trough is thought to be photoregulated and associated with the 1×10^{-4} microwatt per square centimetre isolume. At the same time the animal is apparently stimulating itself at intervals with light of a colour to which it should, by virtue of its photosensitive eye pigment, be most sensitive. The intensity of this intermittent stimulation is ten to one hundred times that of the constant environmental illumination with which *Euphausia pacifica* is oriented throughout the diurnal cycle.

THE generation of light *in situ* at various depths has been reported from the Atlantic Ocean by CLARKE and WERTHEIM (1956) and from the Pacific by BODEN and KAMPA (in press). In both oceans the light has been detected with underwater photometers which employ multiplier phototubes as sensors and which record continuously on electric recorders. The light is intermittent, and the intensity of the flashes is frequently as much as 1,000 times that of the background illumination. In some instances we have found that the frequency and intensity of the flashes are so great that the overall level of illumination actually increases, rather than decreases, with depth.

Luminescence is a common characteristic of the marine fauna (SVERDRUP, JOHNSON and FLEMING, 1942) and it has been suggested that this light in both oceans is of biological origin. This suggestion has been supported by our observation that there is a zone in which light increases with depth which corresponds with the depth of the sonic-scattering layer (DSL) in the San Diego Trough during the twilight migrations of the layer. JOHNSON (1948) and BODEN (1950) have demonstrated that this layer is associated with concentrations of plankton.

During the spring and summer of 1956 we have carried out a number of experiments, at sea and in the laboratory, in an attempt to determine (1) whether the degree of bioluminescent activity in the sonic-scattering layer varies diurnally, (2) the spectral character of the light produced, and (3) what species may be responsible for the phenomenon.

The characteristics of the photometer used in the work both at sea and in the laboratory have been described by SNODGRASS *et al.* (in press). A three-position strip shutter has been installed in the instrument immediately in front of the photocathode. The first shutter position obscures the cathode entirely, allowing us to observe the instrument's dark current at regular intervals. The second position is a pinhole, the geometry of which is such that the light admitted is 1/1,000 of the light admitted when the shutter is in the third, or " open " position. The shutter position is adjustable by the operator on deck. This mechanism has increased the useful intensity range of the instrument from 7 to 10 log cycles, and it is possible to measure light intensity from just beneath the surface to depths of several hundred metres.

Interference filters are placed in the light path when colour measurements are to be made, and a collimating tube restricts the angle of acceptance by the photocathode to the useful 5° cone of the filters. The integrating disc of opal plastic at the outer surface of the optical system has the characteristics of a true Lambert collector, that is, under a uniform sky the intensity I_θ, collected from the direction θ, is determined by

$$I_\theta = I_0 \cos \theta \qquad (1),$$

and the instrument measures irradiance.

Irradiance, H, is calculated from

$$n = kH = \int_0^\infty ETSd\lambda \qquad (2),$$

where n = recorder reading in millivolts, E = energy of the source, T = transmission of the interference filter, and S = relative spectral sensitivity of the photomultiplier through the wave-length interval $d\lambda$. The value of k was obtained by calibrating the entire instrument against a Bureau of Standards source.

The time constant of the photometer is established by the rate of response of the electric recorder, and the limitations imposed by it will be considered in the discussions of individual sets of results.

As has been pointed out before, this instrument is equipped with a pressure-sensitive element, and the depths mentioned here were determined directly, rather than by calculation.

The observations and collections on which this report is based were made at intervals between 18 January and 9 August 1956 in the San Diego Trough (Lat. 32°40'N., Long. 117°40'W.).

Experiment 1. During the daylight hours on 20 February, the photometer was lowered repeatedly with the sensor oriented upward. In the majority of these casts interference filters were used, and the results will be discussed elsewhere. At midday, however, total irradiance was measured by sending the instrument down without filters. Discrete flashes of light were detected at a depth corresponding to the depth at which sonic scattering was recorded by the EDO echo-sounder (Fig. 1). These burst were sufficiently separate in time that they appear as individual spikes.

An hour before sunset the photometer, without filters and with the sensor looking upward, was lowered to 200 metres. It was maintained at this depth for two hours. Portions of the record obtained are shown in Fig. 2. The smooth slope of the first (right side) section of the record is typical of what had gone before. As the sun approached the horizon the light intensity detected at 200 metres decreased regularly. During this time the scattering layer had risen from 260 to 225 metres, and at 1806 hours its depth on the fathogram was 200 metres. Concurrently, the photometer began to detect frequent flashes, and these persisted until the instrument was finally brought to the surface at 1855 hours.

Total irradiance was measured at 0430 hours (three hours after moonset and two hours before sunrise) and again at sunrise (0630 hours) on the following morning.

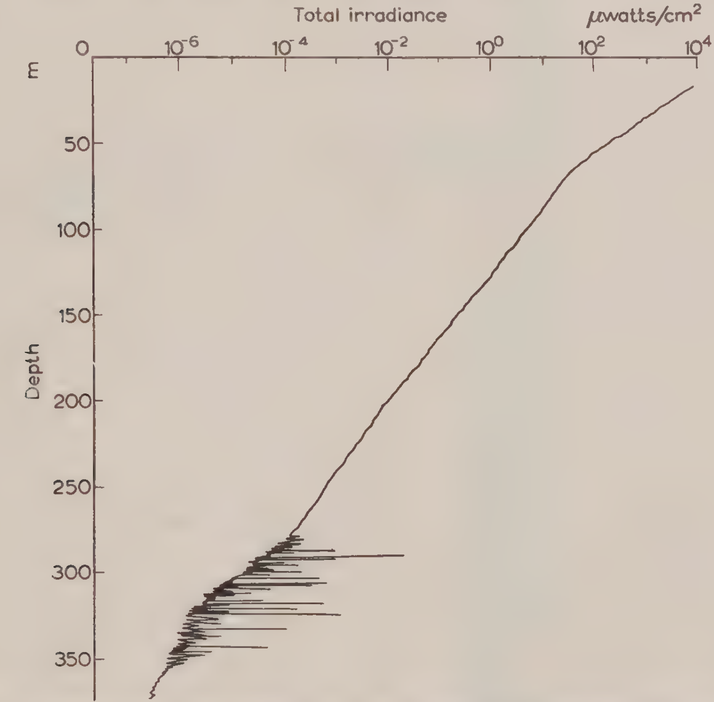

Fig. 1. Relation of light to depth in the San Diego Trough at 1215 hours on 20 February, 1956, obtained by applying equation (2).

Experiment 2. On 9 August records of luminescence were obtained from sonic-scattering layer depths at intervals throughout most of a 24-hour period. The photometer was lowered with its sensor oriented downward in order to reduce the masking of luminescent flashes by transmitted sunlight. On seven casts, the photometer was first lowered quickly to 100 metres below the sonic-scattering layer and then returned to the level of the layer and held at constant depth for several minutes.

DIURNAL VARIATION OF BIOLUMINESCENT ACTIVITY IN A SONIC-SCATTERING LAYER

A change in degree of any of the characteristics of luminescence – intensity and frequency of flashes are considered here – is indicative of a change in the degree of luminescent activity. The data at present at our disposal have been examined for evidence of any such change.

The findings, insofar as flash intensity is concerned, would lead us to believe that the animals in the sonic-scattering layer luminesce uniformly throughout the diurnal

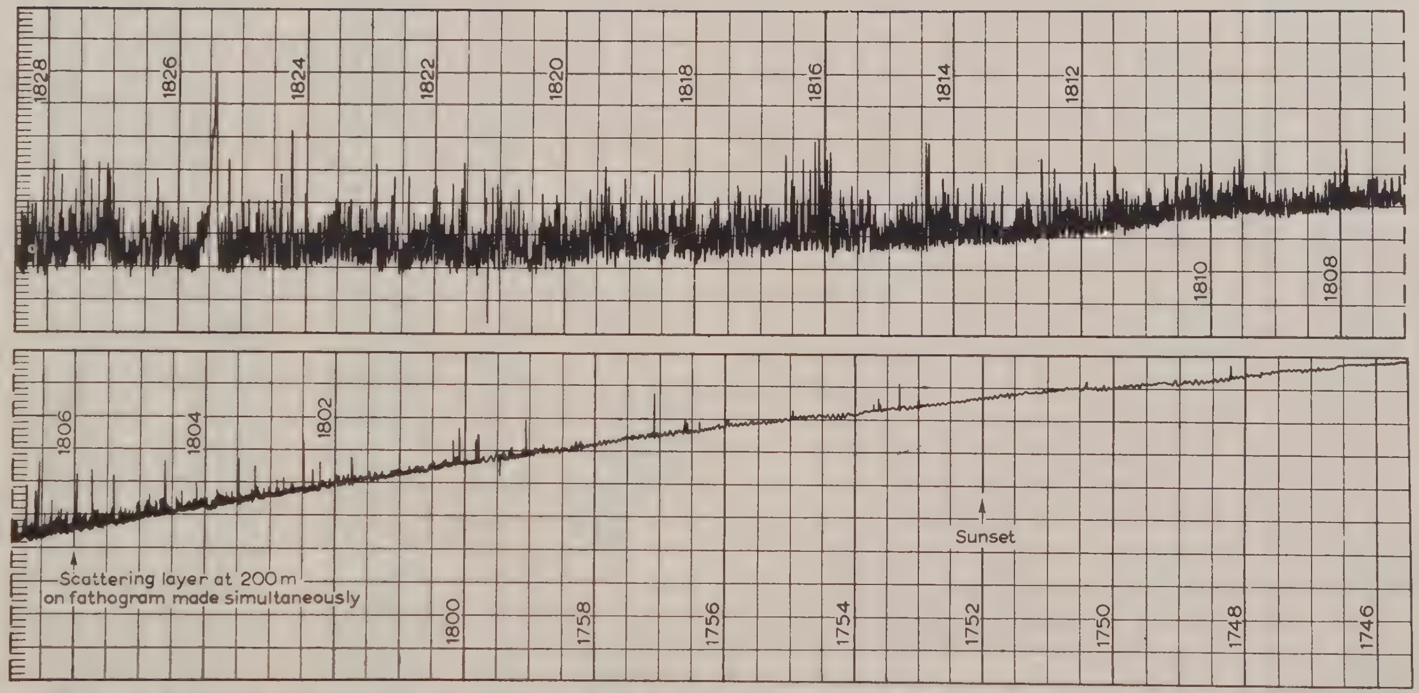

Fig. 2. Record obtained when photometer was maintained at 200 metres in the San Diego Trough during the sunset-twilight period on 20 February, 1956, showing the gradual reduction in the intensity of transmitted sunlight (upper right). The sonic-scattering layer reached 200 metres at 1806 hours, and luminescent from the layer may be seen.

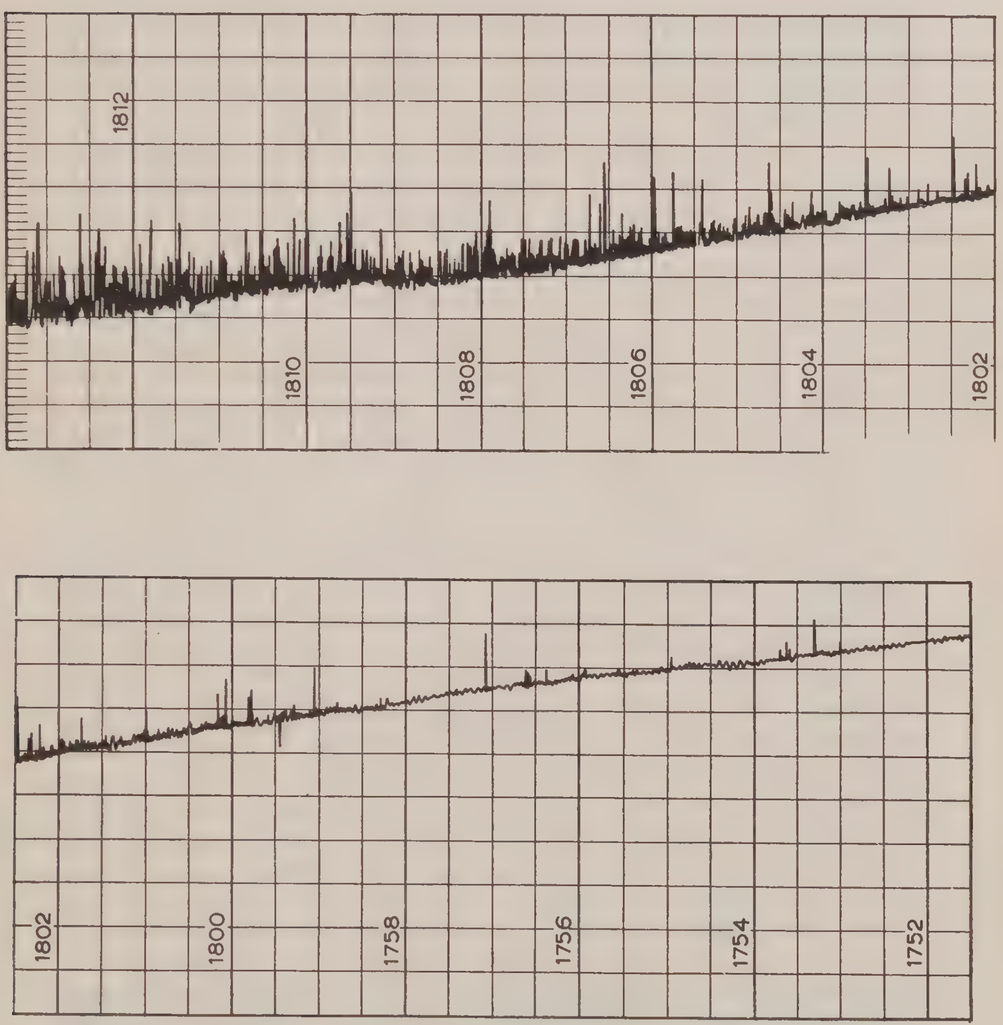

Fig. 2 *continued.* Enlargement of the section of the upper record between 1752 and 1812 hours.

cycle. Values of total irradiance indicated by the heights of individual spikes have been tabulated from records for various times of day and night, and, although a considerable varibaility is exhibited by each of the individual records, no significant difference has been found either in the range of intensities detected or in the mean intensity throughout a diurnal cycle.

The results obtained from analysis of the 20-21 February records are typical and show the following:

DSL Depth (metres)	*Time (hours)*	*Range of flash intensities (μ watts/cm^2)*	*Mean flash intensity (μ watts/cm^2)*
300	1215	1×10^{-6} to $1{\cdot}5 \times 10^{-2}$	$1{\cdot}1 \times 10^{-4}$
200	1800	2×10^{-5} to $2{\cdot}5 \times 10^{-2}$	$1{\cdot}1 \times 10^{-4}$
30	0230	$1{\cdot}3 \times 10^{-5}$ to 7×10^{-3}	$1{\cdot}1 \times 10^{-4}$

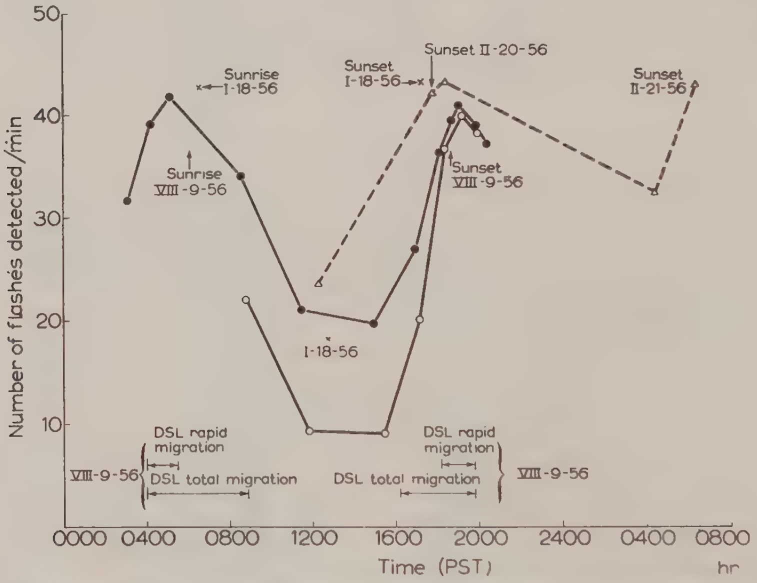

Fig. 3. Frequencies of luminescent flashes recorded at sonic-scattering layer depths at various times of day in January (×), February (Δ), and August (● and ○), 1956. The closed-circle values for August were recorded while the photometer moved at 35 metres per minute; the open circles when the photometer was held at constant depth for several minutes. Periods of scattering-layer (DSL) migration are indicated for August.

The frequency of the flashes detected, on the other hand, differs greatly with time of day (Fig. 3). In every set of observations so far, the number of flashes recorded per minute from a sonic-scattering layer is least near midday. This frequency (Fig. 3) has been approximately 20 flashes per minute in three sets of observations taken in three different months with the photometer moving rapidly (30 to 40 metres per minute) through the layer. During the periods of vertical migration of the layer, the number of flashes perceived by the photometer was about twice that recorded at midday.

When the photometer is held at a constant depth, the difference between the flash frequency at midday and that during the twilight migration is even greater. Although the number of bursts recorded with this procedure at twilight was not significantly lower than that detected by a rapidly moving photometer, the mean number (10 per minute) observed at midday with the photometer held as still as possible was about half that recorded when the photometer moved quickly through the layer.

The frequency of flashes increases gradually during the afternoon, and this increase appears to be associated with the onset of the scattering layer's migration. In this period the upward movement of the layer is slow but steady, and it is not until shortly before sunset that the animals attain their maximum upward velocity (KAMPA and BODEN, 1954). Concurrently, the frequency of luminescent flashes rises sharply, and a maximum number per minute may be observed in the hour after sunset. At the end of twilight, the upward migration has been completed. At about this time, the frequency of the luminescent flashes is diminished.

Because of technical difficulties the night-time relationship between sonic-scattering layers and luminescence is less readily established than are the daytime and twilight correlations. At the end of the evening migration, the trace of the scattering layer is frequently lost, either because the animals disperse to different depths in the water column and are perhaps no longer sufficiently concentrated to scatter sound, or because the layer has come so near the surface that its trace is obscured by that of the outgoing signal from the echo-sounder. Although luminescence – and most often luminescent strata – have been observed in the water column on every night when light measurements have been attempted, it cannot be said that these are related to sonic-scattering layers when no trace is distinguishable on the fathogram.

The most clear-cut evidence for a correlation between sonic scattering and luminescence during the middle of the night was obtained on 20 February. On that night both a scattering layer and a distinct luminescent stratum were present at about 30 metres. The mean frequency of flashes detected by the photometer was 32 per minute, a value midway between the minimum mean frequency (23 per minute) and the maximum mean (42 per minute) recorded from the same scattering layer at noon and at sunrise respectively on the following day.

Before even tentative conclusions can be drawn from these results, the limitations imposed by the methods and instruments used must be considered.

The importance of the procedure selected for gathering information to the interpretation of flash-frequency data has been stressed already. At the times when the degree of light generation in the sonic-scattering layer is high, as it is during the twilight migrations, the effect of the additional stimulus provided by dragging the 100-pound instrument with its attendant bridle and cable through the water at high speed seems negligible. When luminescent activity is lower, however, the method by which data are obtained becomes critical. Inasmuch as the photometer can never be entirely still, even when it is held at " constant " depth, we feel that the minimum frequencies are probably fallaciously high, and that nomral, spontaneous luminescence at scattering-layer depths at midday may be very slight indeed.

The time constant of the photometer, as it has been used so far, is established by the rate of response of the electric recorder. The limit of this response (about

50 distinct ½-inch cycles per minute) is approached in the records of flashes from the migrating sonic-scattering layer. At twilight the actual number of flashes per minute could well exceed the number detected. Even at midday, the number of spikes on the record may still be less than the true number of bursts of light to which the instrument is exposed, for, from what is known of luminescence in other organisms, the duration of an individual flash would be of the order of fractions of seconds rather than fractions of minutes. It is probable, therefore, that the " flashes " of which we are speaking here represent integrals of a number of flashes rather than individual bursts.

Estimates of flash intensity are without doubt similarly distorted by the time limitations of the photometer. Examination of the data at hand might lead us to believe that we are dealing with an " all or none " phenomenon in scattering-layer luminescence, for the mean intensity of the flashes detected remains constant throughout the day. The range of variation in a single set of observations could be explained on the basis of the inverse square law, and it could be said that if the photometer were equidistant from every flashing organism, every spike would be of the same height.

Individual flashes, by virtue of their short duration however, may more often than not reach a maximum intensity and then decay before the instrument can respond. The effect of this time limitation on the record becomes greater as the level of the background light decreases. It is probable, therefore, that the true intensity of the light generated at depth is best represented by the intensities calculated for flashes superimposed on high levels of background light. A definitive statement of the possible diurnal variation in intensity of the luminescent flashes must await the impending development of faster photometric techniques.

Diurnal fluctuations in the amount of light generated at the depth of the sonic-scattering layer in the San Diego Trough are evidenced, despite the limitations of the system, by the data presented here on the numbers of flashes that can be detected at the level of the layer at various times of day and night. A photosensor, placed in the layer, detects at least twice as many flashes of light during the twilight periods as it does at midday, and the temporal limits of the periods of greater light production seem to be associated with the beginnings and ends of the vertical migrations of the layer (Fig. 3).

From the biological standpoint, interpretation of this correlation of migration with light generation may proceed along any one of several lines. First, it can be assumed that, in order to produce a continuous trace on the fathogram, organisms must be present in some minimal concentration such that their numbers per unit area, if not their individual acoustic cross-sections, permit them to reflect sound. From this assumption one can continue to two alternatives, either that the concentration of the organisms remains fairly constant throughout the day, or that the concentration varies widely but is always great enough to permit sonic scattering.

The first of these alternatives would require a two- to four-fold increase in the average bioluminescent activity of individual planktonts during the twilight migratory periods to explain the observed changes in the frequency of flashes. The second alternative allows the argument that at midday the animals are dispersed, and consequently the flashes detected per minute are few, whereas at twilight the animals are packed more closely together, and the greater frequency of flashing is indicative of

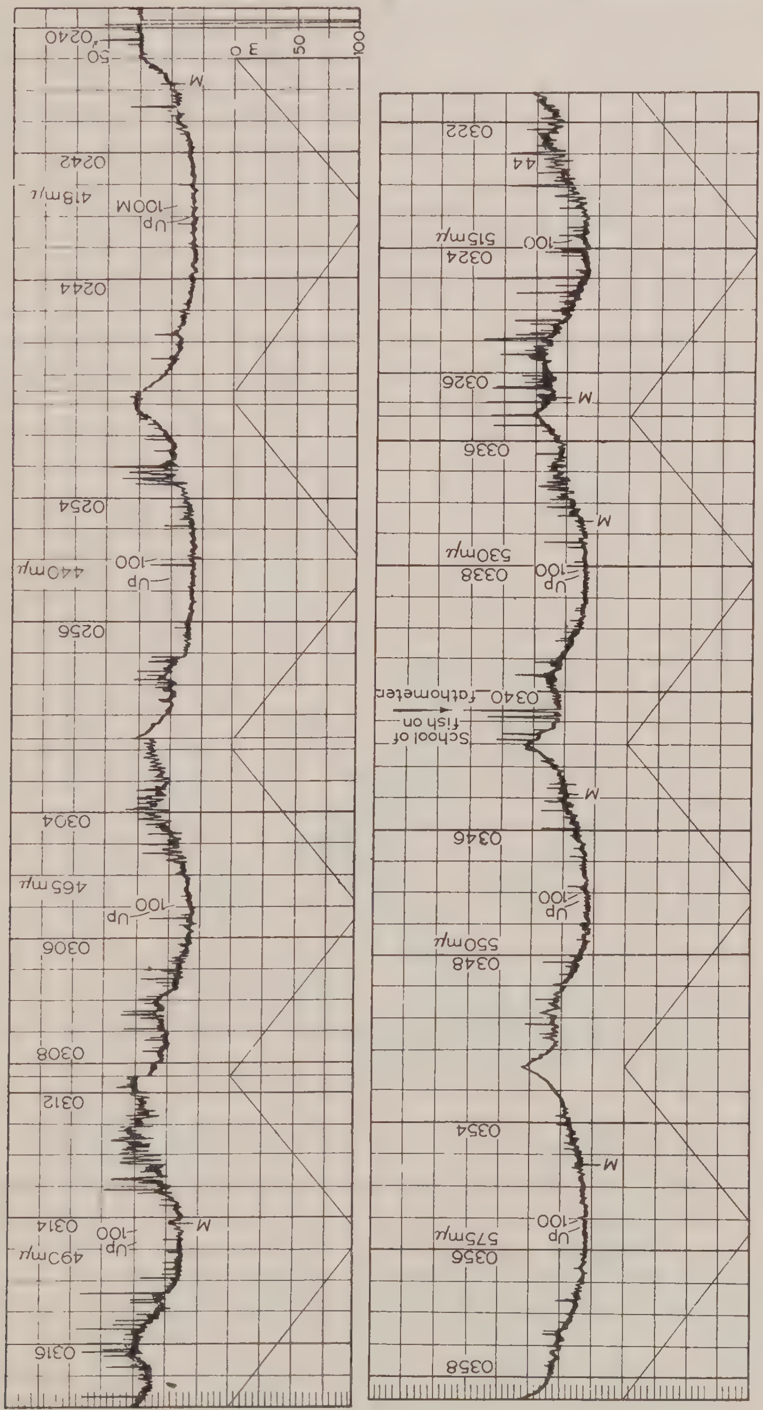

Fig. 4 *continued.*

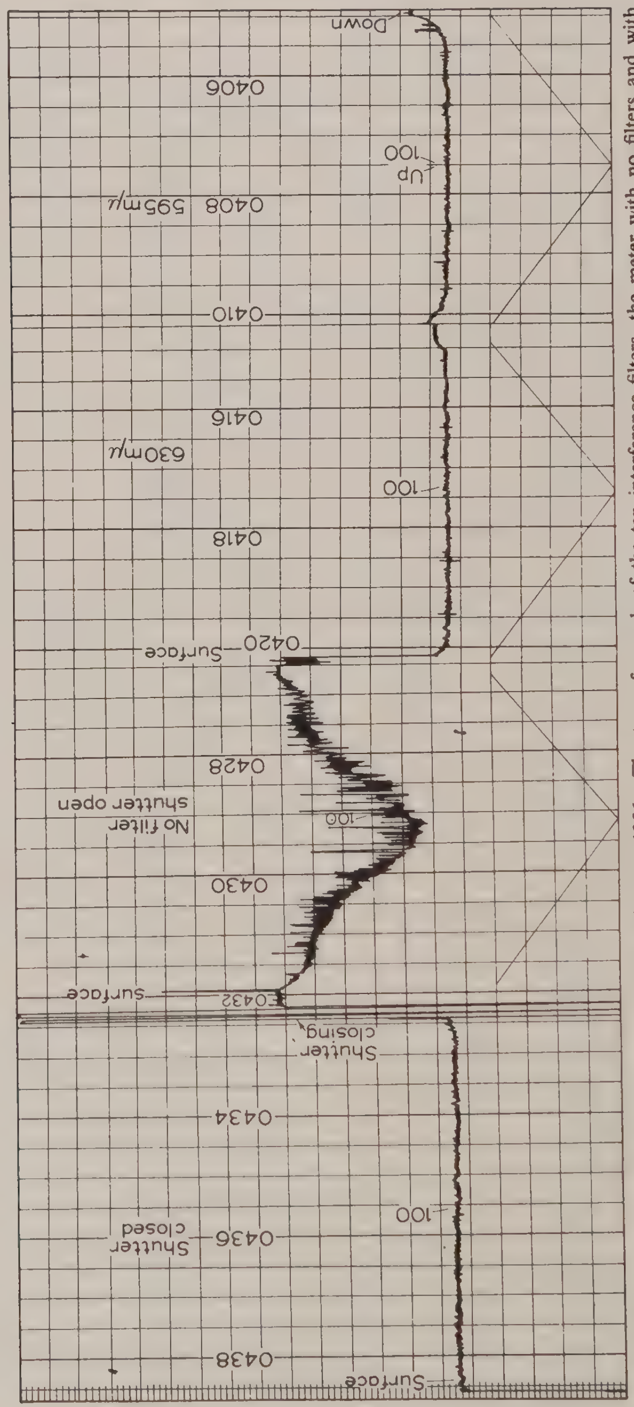

Fig. 4. Records obtained after moonset on 21 February, 1956. The trace for each of the ten interference filters, the meter with no filters and with the shutter closed, shows the photometer lowering to 100 metres (right half) and the return to the surface (left half).

higher concentration, rather than of greater luminescent activity, of individuals. It is probable that neither alternative is achieved and that changes in concentration and activity combine to produce the observed effect.

Support for the opinion that luminescent activity of the individual actually increases during the periods of vertical migration is offered by the direct correlation between luminescent activity and oxygen consumption established for other organisms whose luminescence has been studied (HARVEY, 1952). If the light-producing members of the scattering-layer fauna are not anomalous in this respect, one would predict that an increase in respiratory rate of the magnitude probably encountered during the rapid vertical migrations should be accompanied by an increase in luminescent output.

A third possibility exists – that the increment in light production is occasioned by the presence of other luminescent organisms in the water column. The acoustic dimensions of these other forms might be inadequate to cause detectable sonic scattering, and they need not migrate if their vertical distribution were uniform above the level of the layer. Their luminescent activity could be influenced by some stimulus provided by the migrating sonic scatterers. The critical stimulus could not be simple mechanical agitation, for we have been unable to detect such general luminescence in the water column above the sonic-scattering layer, even when the photometer was moved, sensor looking downward, at a rate of 35 metres per minute. Strength for such an argument may be derived from the work of BURGHAUSE (1914) with *Pyrosoma*. The luminescence of this colonial tunicate is suppressed by exposure to continuous sunlight, but stimulated by intermittent light. *Pyrosoma*, or any other form with a similar behaviour pattern, could be stimulated to luminesce by the approach of luminescent sonic scatterers, and the high frequencies of the flashes observed during the migratory periods may represent the sum of the luminescent activities of migrating and non-migrating organisms.

Experiment 3. At 0240 hours, one hour after moonset on 21 February, the ship's lights were reduced to a minimum, and a series of twelve photometer lowerings was begun. The sensor was oriented to look upward. In these casts ten interference filters were used, covering a spectral range from 418 to 630 mμ. One lowering without filters, and one with the shutter closed were made as well. The instrument was sent to 100 metres each time and then returned immediately to the surface (Fig. 4).

Throughout this period a scattering layer was detectable at a stable depth of about 30 metres. Flashes of light were detected from 25 metres downward. The spike heights (millivolts) recorded with each filter in the 25 to 60-metre layer of the water column were tabulated, and the intensity of irradiance corresponding to each spike height was calculated from equation (2).

SPECTRAL DISTRIBUTION OF LIGHT GENERATED IN A SONIC-SCATTERING LAYER

Examination of the individual records in Fig. 4 reveals that on every photometer lowering, except those casts with filters at the extreme red end of spectral range, an increase in the intensity of light was encountered as the instrument passed downward from 25 to about 40 metres. Similarly, as the photometer moved toward the surface (left half of each record) the intensity decreased in this water layer.

In the blue to green region of the spectrum, the intensity of one or more of the flashes recorded at depth was greater than the intensity of the light of the same wave length at the surface. In the 460 to 490 mμ range the intensity of the brighest flash was four to five times as great as the intensity at the surface.

The curve representing the spectral distribution of the brightest of the flashes recorded at each wave length (solid line, Fig. 5) is highest near 485 mμ and decreases quite regularly toward the blue and red. The spectrum derived from the mean values of irradiance of the flashes at each wave length (broken line, Fig. 5) peaks near 478 mμ and is similar in shape to the spectrum of the brighest flashes except at the extreme blue end where the mean spectrum shows no secondary rise. Each point on the mean curve is based on 30 to 48 individual flashes, and it is probably more representative of the distribution of colour in the light generated at depth than is the maximum intensity spectrum.

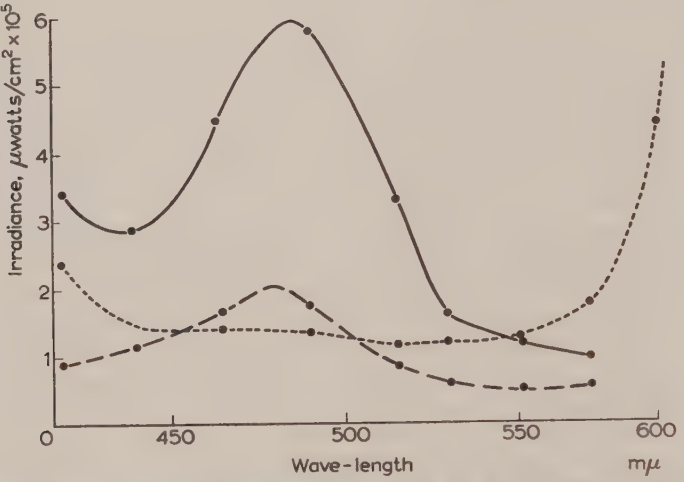

Fig. 5. Spectral distribution of light generated *in situ* at 25 to 60 metres (brightest flashes, solid line; mean intensity, broken line) and of light from sky and ship detected at the surface (dotted line) between 0240 and 0350 hours on 21 February, 1956. The three curves have been constructed from irradiance values obtained when equation (2) was applied to the data in Fig. 4.

The curve showing the spectral distribution of light from the ship and sky recorded at the surface (dotted line, Fig. 5) is low and quite flat in the 440 to 550 mμ range, but rises sharply in the red. A comparison of this curve with the other two obviates argument that the flashes recorded in the 25 to 60-metre water layer could have been artifacts produced by wave action or tilt of the photometer.

The time interval encompassed by the experiments on which the spectra are based was 77 minutes, and it is possible that during this period changes occurred in the character of the luminescent fauna of the scattering layer as well as in the excitability of individual organisms. No suggestion of such a change, however, could be found on the fathogram; the depth of the scattering layer and the intensity of the trace did not vary perceptibly. Dense, patchy scattering near the surface was recorded at 0340 to 0342 hours, and light flashes which may have been associated with these shallow sonic-scatterers were detected at a depth of 10 to 15 metres on the 515 mμ filter cast.

Downward movement of the scattering layer did not begin until 0540 hours, more than 100 minutes after the last observation used here to determine the colour of the light generated at depth.

The constancy of the fathogram record and the fact that the interval of the measurements was well separated from the onset of the twilight period during which the degree of luminescence increases, lend support to the assumption that the spectra in Fig. 5 – and particularly the mean spectrum – are valid estimates of the colour of the light which was generated by organisms associated with the sonic-scattering layer.

Experiment 4. Collection with a one-metre closing plankton net through the sonic-scattering layer yielded three forms: chaetognaths, euphausiids, and myctophids, whose swimming rates might have allowed them to take part in the rapid twilight migration. Of these, only the euphausiids and myctophids luminesced. *Pyrosoma* was also abundant in the surface waters, and, while it undoubtedly contributed to the light production, it could not have been a part of the migratory layer.

The myctophids died shortly after capture, but specimens of *Euphausia pacifica* and *Pyrosoma atlantica* survived transport to the laboratory where the luminescence of individuals could be measured.

Several methods (mechanical agitation, electric shock, chemical irritants) were tried to stimulate euphausiids to luminesce in the laboratory. Of the techniques tested so far, the most reliably reproducible results are obtained when dark-adapted specimens are treated with ammonia and the maximum intensity of the terminal or death glow is measured.

Adult specimens of *E. pacifica* were kept in darkness from 2100 hours, when they were captured at sea, until 0230 hours the following morning, when mesurements were begun. These animals were exposed subsequently onlv to the light from a Wratten No. 2 (red) safelight.

Three specimens were removed from the dark chamber to a one-centimetre absorption cell containing 3 millilitres of sea water. The cell was placed in front of the integrating plastic window of the photometer which had been used previously for measurements at sea. The red safelight was turned off, the shutter of the photometer was opened, and 0·3 millilitres of 40% NH_4OH was pipetted into the absorption cell. The animals emitted a bright glow which appeared blue-green to the human eye. The glow faded gradually over a period of 1½ to 2 minutes. A series of experiments showed that with specimens of uniform size the greatest difference between any two groups of three individuals was 0·15 millivolts in maximum recorder reading. In 50% of the tests the difference was less than 0·04 millivolts.

The process described above was repeated ten times with each of ten interference filters in the light path of the photometer (Fig. 6). Irradiance at each wave length was calculated from equation (2), using the maximum recorder reading after stimulation for the value of n.

Specimens of *Pyrosoma atlantica* were handled in a manner similar to that used for *E. pacifica*. A colony was placed in a beaker of sea water in front of the integrating plastic window of the photometer. After the safelight had been turned off and the photometer shutter opened, 40% NH_4OH was added in the ratio of 1 volume NH_4OH to 10 volumes of the sea water already in the beaker.

Preliminary experiments showed that following stimulation with ammonia the terminal glow was maintained for several minutes. The glow was long enough that a single specimen could be used for measurement at several wave lengths. The interference filter with maximum transmission at 490 mμ was used as a reference filter, and a measurement at this wave length was made before and after each other measurement (Fig. 7). By drawing a continuous line through each set of reference filter records it was possible to estimate the 490 mμ emission level at the time of each other measurement. Irradiance at each test level and at the corresponding 490 mμ reference level was calculated from equation (2).

The value $H\lambda_0$ for irradiance immediately after stimulation was computed for each wave length by

$$H\lambda_0 = \frac{H\lambda H_{r0}}{H_r} \qquad (3),$$

where $H\lambda$ is the observed irradiance at the test wave length at the time of measurement, H_r is the simultaneous irradiance level at the reference wave length, and H_{r0} is the maximum irradiance measured through the reference filter immediately after the animal had been treated with ammonia.

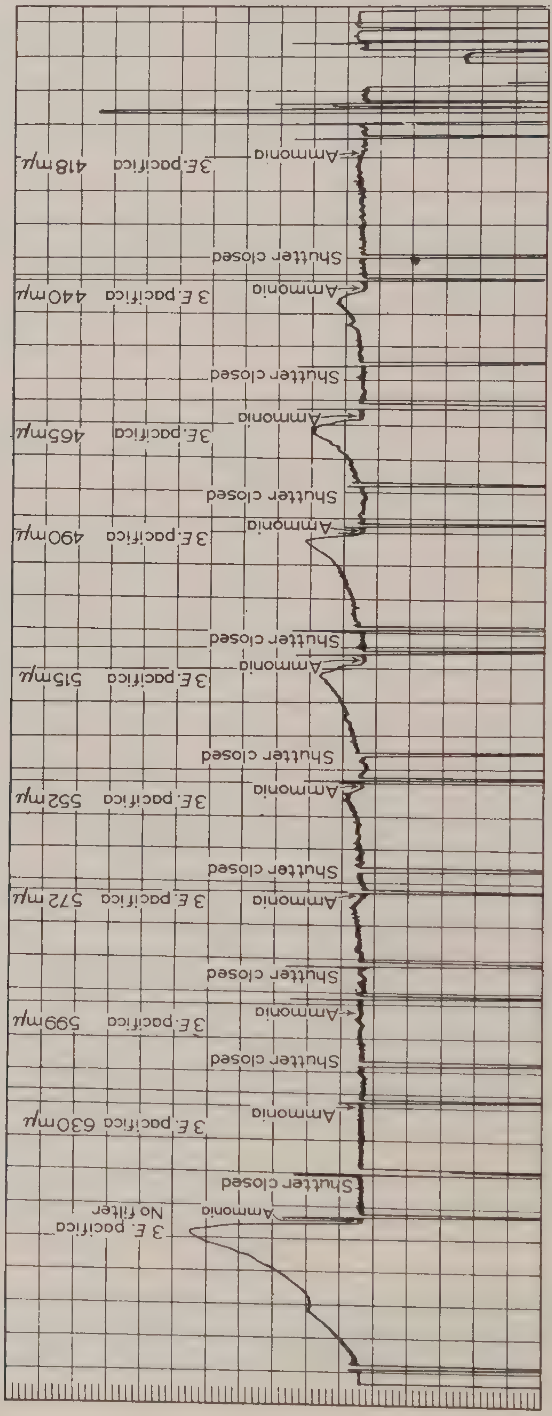

Fig. 6. Records of the terminal glows observed when specimens of *Euphausia pacifica* were treated with ammonia. One of ten series of tests with interference filters in the light path of the photometer and one test without filters are shown.

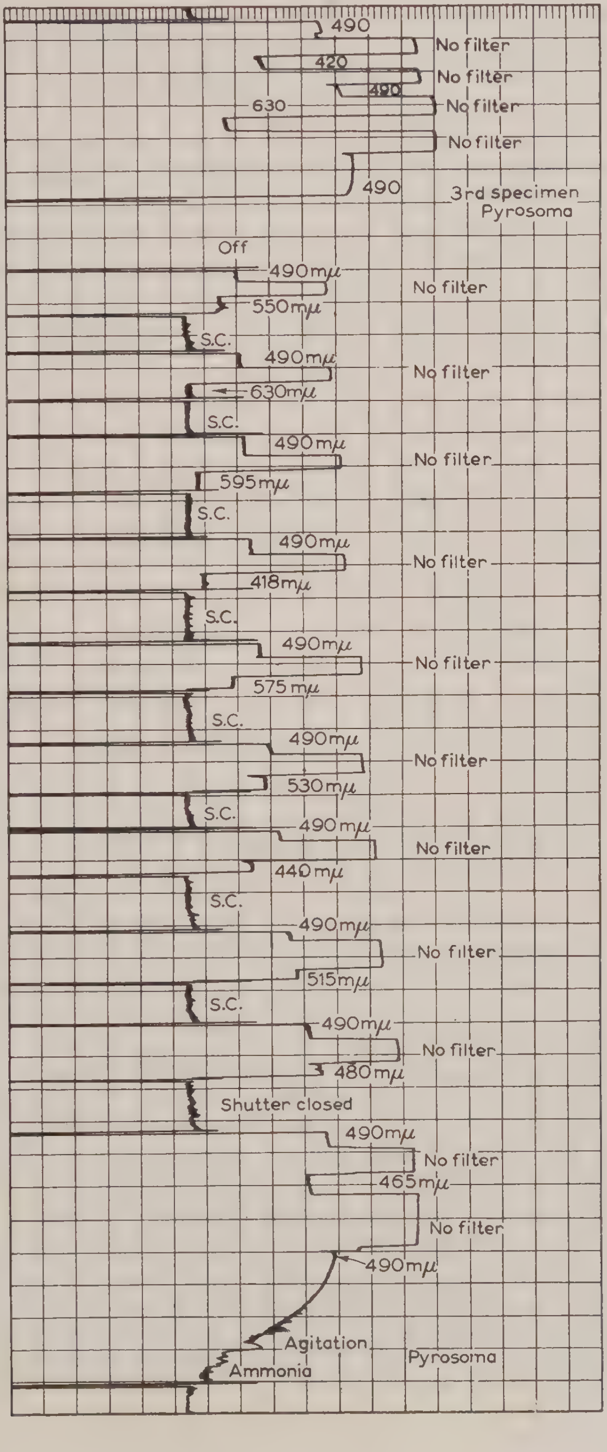

Fig. 7. Record of the terminal glow of a single *Pyrosoma atlantica* colony (one of 14 colonies measured) detected by the photometer when various interference filters were placed in the light path. Measurements through the reference filter (490 mμ) alternate with test measurements.

LUMINESCENCE OF *EUPHAUSIA PACIFICA* AND *PYROSOMA ATLANTICA*

The maximum intensity of total irradiance recorded during the terminal glow from individual adult specimens of *Euphausia pacifica*, killed with ammonia within eight hours of capture, was found to vary within narrow limits from 1·6 to 2·0 × 10^{-3} microwatts per square centimetre at a distance of one centimetre. It should be mentioned that the luminescent terminal glow is possibly composed of many flashes of such short duration and high frequency that the photometer, like the human eye, is incapable of resolving them. The recorded intensities of the terminal glows presented here, therefore, may be erroneously low. The mean of the values obtained in the experiments is 1·8 × 10^{-3} microwatts per square centimetre at a distance of one centimetre, and the relative spectral distribution of this discharge is represented by the curve (broken line) in Fig. 8. The spectrum is consistently bimodal with a primary peak at about 476 mμ and a lower, secondary peak between 515 and 530 mμ. The ratio between the heights of primary and secondary peaks is about 1 : 0·3.

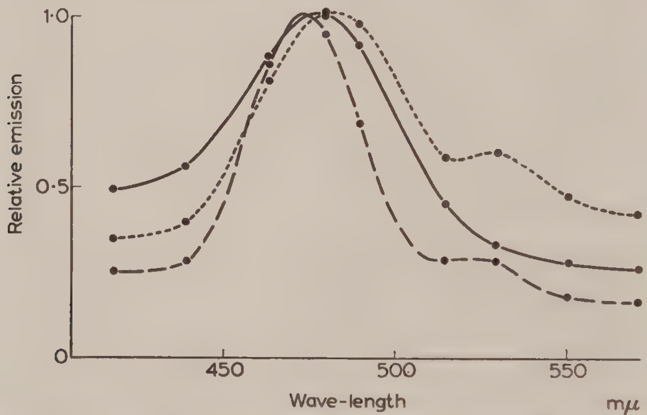

Fig. 8. Spectral distribution of luminescence from the sonic-scattering layer (solid line), *Euphausia pacifica* (broken line) and *Pyrosoma atlantica* (dotted line). Data on which the curves were based have been equated to 1·0 at the point of maximum emission.

E. pacifica, like most other euphausiids, possesses ten photophores, one on each eyestalk, one at the base of each of the paired second and seventh thoracic appendages, and a median one on each of the first four pleopods. When the animal is excited strongly by physical or chemical means, all of the photophores emit light, apparently simultaneously. Each light organ is quite distinct to the dark-adapted observer, and the glow may persist for as long as twenty seconds while the animal darts about its container looking like a miniature passenger train racing through the night.

Euphausiid luminescence is thought to be intracellular and under nervous control (HARVEY, 1952). The ability to luminesce is not lost with death, and the light organs of specimens which have been deep-frozen for several weeks will flash brightly when the dead animals are handled. If one cuts into a photophore, while dissecting out an eye for instance, the luminescent material is released, runs out in a bright stream and disperses in the water in the dissecting dish. In one instance, after 300 eyeless, discarded corpses had been collected on a bit of cheesecloth, the cloth was wrung out at the end of the dissections. The light emitted by the expressed fluid was bright enough that the outline of a microscope could be seen by it, and scissors and forceps on the bench could be distinguished readily in a room that was otherwise entirely dark.

The intensity of total irradiance recorded from *Pyrosoma atlantica*, killed with ammonia within eight hours of capture, varied with the size of the specimen. A colony 10 centimetres long emitted light having an initial maximum total irradiance of $2{\cdot}5 \times 10^{-2}$ microwatts per square centimetre at a distance of one centimetre. The relative spectral distribution of the light (dotted line, Fig. 8) was extremely constant from specimen to specimen. The emission spectrum, like that of *E. pacifica*, is bimodal with a primary peak at about 482 mμ and a secondary peak near 525 mμ. The ratio of the heights of primary to secondary is 1 : 0·6.

Luminescence in the genus *Pyrosoma* is thought to be caused by symbiotic bacteria located in the two or more light organs at the distal end of each member of the colony (HARVEY, 1952). The luminescence has been described from visual impressions, and much disagreement exists as to its colour. PÉRON (1804) reported that he saw it change from red through yellow and green to sky-blue. Such a change was not detected here during the 20- to 30-minute intervals through which the terminal glows persisted. The order in which filters were used was reversed on alternate specimens, and no differences could be found in the resulting relative spectral distributions of the emission.

The relative spectral distribution of light generated in the sonic-scattering layer on the night of 20-21 February (solid line, Fig. 8) peaks midway between the maximum for *E. pacifica* luminescence and that for *P. atlantica*, and neither organism can be disqualified as a contributor to the light produced at depth. It seems a certainty that *Euphausia pacifica*, a form commonly included in the sonic-scattering layer fauna in the San Diego Trough, was responsible, at least in part, for the flashes observed. The colour of the light emitted is consistent with this opinion, and the intensity of *E. pacifica*'s luminescence is within the intensity range of the light generated at depth.

Similarly, it seems likely that *Pyrosoma atlantica*, while it cannot have been part of the sonic-scattering layer during the rapid twilight migration, contributed to the light detected in the water column. Although the *P. atlantica* colonies appeared to be restricted to the water immediately below the surface on that night, the intensities of total irradiance (8×10^{-3} to 4×10^{-2} microwatts per square centimetre at a distance of one centimetre) recorded from individuals in the laboratory were from ten to fifty times the intensity (8×10^{-4} microwatts per square centimetre) of the light from the sky and ship recorded at the sea surface during the night of 20-21 February.

Emission spectra of *Gonyaulax*, obtained with a monochromator by Dr. Beatrice Sweeney of this Institution, are maximal near 470 mμ. Similar spectra obtained with our photometer peak near 480 mμ. This discrepancy may be occasioned by the difference between the widths of the spectral bands produced by the monochromator and those transmitted by the interference filters. It is possible that a difference might be observed between the emission spectra presented here for *E. pacifica* and *P. atlantica* and those which could be obtained by other methods. While such a difference would be important in determining the precise emission spectrum of any particular animal it cannot affect a comparison of the results presented here, for all observations were made with the same instrument.

GENERAL CONSIDERATIONS

The *in situ* generation of light in the sea at intensity levels high enough to be detected readily by modern photometric techniques presents a problem to the oceanographer who seeks to study the transmission of sunlight or moonlight in the oceans. Each discrepancy in an otherwise regular set of observations must be examined with redoubled caution before it can be evaluated as a physical characteristic of the water mass, an instrumental idiosyncracy, or a biological phenomenon. Often the appropriate classification will be impossible to determine.

One of us (KAMPA, 1955a) has described the extinction of sunlight with depth in the water off San Diego. Two inflections are commonly found in the extinction curve, one at about 100 metres – presumably associated with the lower margin of the euphotic zone, and a second regularly encountered at the level of the sonic-scattering layer. The curve in Fig. 1 of the present paper is typical of the pattern, if the spikes from about 250 metres downward are ignored. The two layers of higher extinction have been explained on the basis of concentrations of light-absorbing and light-scattering particles in the water.

Nothing in the bioluminescent data suggests that the upper inflection requires another interpretation, for the intensities of transmitted sunlight encountered between the surface and 100 metres are from one hundred to one million times as great as the brighest of the luminescent flashes ever recorded in the area.

Bioluminescence could affect the interpretation of the inflection at the level of the sonic-scattering layer, however. If on the cast represented by Fig. 1, the photometer had begun to detect luminescence from the layer at about 225 metres, and if this luminescence had been maximal near 290 metres, the apparently higher extinction from 290 to 350 metres could be caused simply by the instrument's retreat from the zone of greatest luminescent activity. The instrument used to collect the data on which KAMPA's (1955) conclusions were based employed a meter with a much slower response than that of the electric recorder, and flashes could conceivably have gone undetected.

The biologist is placed in an even greater quandary by the introduction of records of bioluminescence. It has been shown (KAMPA and BODEN, 1954) that when a photometer is held some 10 metres above the sonic-scattering layer in the San Diego Trough, the depth of the layer throughout the twilight migration can be correlated with the depth of an isolume. Observations over a two-year period have shown that the mean intensity of this isolume is 1×10^{-4} microwatts per square centimetre, and we have reasoned that at least some of the organisms in the layer move upward and downward in an attempt to keep their environmental light level constant. Such reasoning is clouded by the discovery that the layer itself is producing light of the same mean intensity as that with which the layer migrates and that individual flashes are commonly ten to one hundred times as intense.

A sonic-scatterer whose depth distribution is photoregulated, but which does not luminesce itself, would be exposed to conditions similar to those met by the photometer. If, as we believe, *Euphausia pacifica* is one of the photoregulated scatterers, the situation is even more complex, for the irrradiance level of the luminescence from an individual organism may be as high as 2 × 10^{-3} microwatts per square centimetre at a distance of one centimetre. This intensity seemingly represents the sum of the activities of ten photophores, and the light produced by the photophore in the eye stalk would then have an intensity of 2 × 10^{-4} microwatts per square centimetre at a distance of one centimetre. The distance from the centre of this photophore to the centre of the eye is about one millimetre in specimens of the size used here, and by the inverse square law, the intensity of a single flash must be of the order of 2 × 10^{-2} microwatts per square centimetre at eye-level.

Furthermore, the emission spectrum of this luminescence is maximal near 476 mμ, and the absorption of the photosensitive material extracted from *Euphausia pacifica* eyes (KAMPA, 1955b) is maximal near 465 mμ. If one assumes only 50 per cent efficiency in the system, the animal is still presenting its photosensor with intermittent stimuli of one hundred times the intensity of the constant environmental stimulus to which it is responding.

Acknowledgements—The authors are indebted to the U. S. Navy Electronics Laboratory, San Diego, for the use of the U.S.S. *Rexburg* from which certain of the observations were made, and to the American Philosophical Society for providing, through a grant from the Penrose Fund, the Beckman spectrophotometer used to calibrate parts of the bathyphotometer.

We should like to thank Professor ALISTER C. HARDY, F.R.S., Oxford University, England; Professors ROGER REVELLE, CARL ECKART, MARTIN W. JOHNSON, and CARL L. HUBBS, DR. FRANCIS T. HAXO, Dr. WHEELER J. NORTH, and Mr. JOHN E. TYLER of the Scripps Institution, for their continued interest in the work and for their stimulating criticism of the manuscript.

University of California
Scripps Institution of Oceanography
La Jolla, California

Contribution from the Scripps Institution of Oceanography, New Series, No. 896. *This paper represents results of research carried out by the University of California under contract with the Office of Naval Research. Reproduction in whole or in part is permitted for any purpose of the United States Government.*

REFERENCES

BODEN B. P. (1950) Plankton organisms in the deep scattering layer. *U. S. Navy Electronics Lab. Rept.* **186**, 1-29.

BODEN B. P. and KAMPA E. M. (in press) Records of bioluminescence in the ocean. *Pacific Science.* Accepted February, 1956.

BURGHAUSE F. (1914) Krieslauf und Herzschlag bei *Pyrosoma giganteum* nebst Bemerkungen zum Leuchtvermögen. *Zeit. Wiss. Zool.* **108**, 430-497.

CLARKE G. L. and WERTHEIM G. K. (1956) Measurements of illumination at great depths and at night in the Atlantic Ocean by means of a new bathyphotometer. *Deep-Sea Res.* **3**, 189-205.

HARVEY E. N. (1952) *Bioluminescence* pp. 649. Academic Press, New York.

JOHNSON M. W. (1948) Sound as a tool in marine ecology, from data on biological noises and the deep scattering layer. *J. Mar. Res.* **7**, 443-458.

KAMPA E. M. (1955a) A discrepancy between calculation and measurement of submarine illumination. *Proc. Nat. Acad. Sci.* **41**, 938-939.

KAMPA E. M. (1955b) Euphausiopsin, a new photosensitive pigment from the eyes of euphausiid crustaceans. *Nature* **175**, 996-997.

KAMPA E. M. and BODEN B. P. (1954) Submarine illumination and the twilight movements of a sonic scattering layer. *Nature* **174**, 869-870.

PÉRON F. (1804), Mémoire sur le nouveau genre *Pyrosoma. Ann. Mus. Hist. Nat. Paris*, **4**, 437-446.

SNODGRASS J. M., DEVEREUX R. F. and CAWLEY J. (in press) A telerecording bathyphotometer.

SVERDRUP H. U., JOHNSON M. W. and FLEMING R. H. (1942) *The Oceans* pp. 1087. Prentice-Hall, New York.

Printed in Great Britain by The Salisbury Press Ltd., Publicity House Wilton Road, Salisbury, Wilts. (8200)

(1134)

THE DOLOMITE QUESTION[1]

RHODES W. FAIRBRIDGE
Columbia University, New York, New York

ABSTRACT

Questions on dolomite were brought up at the S.E.P.M. Carbonate Symposium at St. Louis, 1954. New observations, techniques, and analyses published during the last few years provide grounds for a fresh review of the problem.

Apart from evaporite basins and intertidal concentration, the only important direct source of marine $MgCO_3$ is organic precipitation within the calcite crystal lattice (i.e., in solid solution) under warm-water conditions by the more primitive calcium-fixing plants and animals.

Dolomite, the double carbonate of Ca and Mg, is not precipitated directly during sedimentation today under the warm, shallow conditions suggested by the ecologic data of ancient marine dolomites. On the contrary, it appears that as a rule it begins to form initially very early in diagenesis. This may be due to the instability of both aragonite and high-magnesium calcite, and the presence of magnesium-rich solutions (sea or connate water), under special chemical and thermodynamic conditions existing beneath the surface of newly formed sediments. Dolomitization may go on discontinuously from time to time, before and after orogeny, until all the calcareous raw material has been metasomatically replaced.

From the evidence available it seems that dolomite is also formed today under deep-sea conditions and in cold water, but only in small, isolated crystals; even these may require organic, magnesium-rich calcite "starters." Marine dolomite is thus a most useful paleoecologic indicator. Nonmarine dolomites, hydrothermal and salt-pan precipitates, etc., are not considered here.

I. INTRODUCTION

It has sometimes been said that there has been nothing new on the dolomite question since van Tuyl produced his excellent review in 1916. It is true that van Tuyl treated most of the theoretical possibilities with equal care, including some of the features of the scheme now accepted. But recent observations, techniques, and analyses have made the picture much clearer. Many of the unrelated facts of forty years ago now fall logically into place.

Much work still remains to be done, and a satisfactory laboratory synthesis of dolomite under "natural," low-temperature and -pressure conditions has not yet been achieved. Nevertheless, a useful purpose may be served by stating the situation as it now exists. In this paper, however, very little attention will be paid to dolomites other than those found in normal marine sediments, for example, the hydrothermal products, evaporites. A fairly thorough study of the literature has been made, and the bibliography appended here represents merely a judicious selection; a more complete index of the older material was completed some years ago for the N.R.C. Committee on Sedimentation (Clee, 1950).

Questions on various aspects of dolomitization were asked at the panel discussion, and at the end of this paper an attempt will be made to arrange them in a logical order and to provide straightforward answers from the evidence marshalled below.

Warm appreciation must be expressed

---

[1] This paper was begun while the writer was Visiting Professor at the University of Illinois (1953-54) under a Fulbright Grant. Later it was continued at the University of California (Scripps Institution of Oceanography, La Jolla), and at the University of Western Australia, with the aid of an Australian Commonwealth research grant; and finally, it was completed at Columbia University, New York.

Reprinted from Regional Aspects of Carbonate Deposition, a Publication of the Society of Economic Paleontologists & Mineralogists, a Division of the American Association of Petroleum Geologists.

Contributions of the Scripps Institution of Oceanography, New Series No.897.

to the many geologists who have assisted —in the literature, in discussions, or with comments on the preliminary draft; they include: Gustav Arrhenius, F. W. Beales, W. M. Bradley, Keith Chave, C. W. Correns, K. O. Emery, Edward Goldberg, D. L. Graf, John F. Harris, F. R. S. Henson, N. D. Newell, J. B. Patton, R. R. Revelle, A. Rivière, K. Turekian, W. H. Twenhofel, C. J. Vitaliano, and others.

II. THE PROBLEM

In summing up the question, G. Linck (1937) concluded that dolomites had the following genesis:

1. By chemical precipitation from saturated solutions . . . only in ground water or under hydrothermal conditions (i.e., epigene).
2. By metasomatic replacement of $CaCO_3$ by $MgCO_3$
   a) before (i.e., early or contemporaneous) diagnesis: in calcareous sapropels of lagoon floors and evaporite basins;
   b) after (i.e., late or post-sedimentational) diagenesis: in all sorts of limestone.

Terms used in a similar summary by Cayeux (1935) are indicated above in parentheses; he added also a fourth way (by decalcification of magnesium-rich limestones, with consequent loss of volume). In this manner dolomitic sands may be produced (e.g., those of Belgium; see Moresée, 1921, and others). In general, however, this must be regarded as a special form, not usually encountered. Graf (personal communication) has noted that this is not really a means of dolomitization at all, since either scattered dolomite crystals are assumed to be present already in the limestone before leaching, or in the case of a magnesium-rich calcite, the Mg and Ca ions must still be crystallographically rearranged to form dolomite. A fifth, and also rather theoretical, possibility is noted by Thiel (1941), that is, by addition of $MgCO_3$. Here an almost insuperable space problem would be involved unless some of the $CaCO_3$ (e.g., by differential leaching of aragonite in an aragonite-calcite mixture) were removed to provide room for the $MgCO_3$; and even so, the formation of the double carbonate would still have to be explained.

It is with the metasomatic replacement that most of the dolomite "problems" are involved. Diagenesis begins immediately after deposition of a sediment and continues indefinitely. The earliest stages probably are the least understood, but recent researches are shedding some light on this aspect.

The first basic problem is the question of why no truly dolomitic sediments are found *in statu nascendi* on the sea floor today. Certainly no contemporary dolomites of the order of 40 percent $MgCO_3$ have yet been located in strictly Recent and normal marine sediments. In fact it seems most unlikely that they ever will be found so. Within the scope of "normal" environments may be included bathyal depths, continental shelves, shallow banks, bays, and coral-reef lagoons; and, in addition, more specialized environments such as coastal evaporite lagoons, even "euxinic" and "caspian" barred basins—all have failed to disclose the precipitation of the double carbonate, $CaMg(CO_3)_2$.

Rhombohedra of authigenic dolomite are, however, actually known in normal modern marine sediments, but as isolated crystals in low concentration, generally less than 2 percent (e.g., Böggild, 1912; Correns, 1937, 1939). Arnold Heim (1924) was of the opinion that deep-sea precipitation of dolomite actually took place, though possibly via contemporaneous metasomatism of organic material.

The "straight" compound, magnesium carbonate, is regularly being concentrated, along with calcium carbonate in neritic environments and even right on the seashore in warmer latitudes. It is not, however, as magnesite, which is unknown in the marine environment,[2] but in a solid solution with calcite. Since this "high magnesium-calcite" cannot exist long in stability, it is only a question of *time* before some sort of rearrangement should take place. The slow rate of the reaction is probably the reason why advanced dolomitization is not observed on the sea floor, except in buried sediments. And it is this slow reaction that is so difficult to match in any laboratory synthesis.

The ionic rearrangement of high-magnesium calcites to true dolomite does not, however, explain completely dolomitized rock formations. A very large additional supply of magnesium would be required, and only the ocean could supply it (Dana, 1849, 1872). Even from the sea, a great deal of water would have to be "processed" to extract the necessary Mg^{++} ions. If, following Clarke (1924), the oceans carry 17×10^{14} metric tons of Mg^{++}, and the annual addition is 93×10^{6} tons, the present balance would be reached within about 18 million years. A large-scale extraction seems inevitable, but how much is organic and how much is due to metasomatism is hard to say (Cayeux, 1935). The supply from ground water, on the other hand, is distinctly restricted even though *certain* ground waters and brines are richly magnesian.

From a calculation that the present average Ca/Mg ratio in marine sediments is 40:1, Chilingar (1956a) has determined that the annual precipitation of Mg^{++} is of the order of 13 million tons. Thus there is an excess of $93 - 13 = 80$ million tons of Mg^{++} entering the ocean annually, and Chilingar argues that a supersaturated condition may be ultimately achieved which should permit direct chemical precipitation. Why this condition does not apply today is not clear, but it may be due to an oscillating cycle of saturation—precipitation, in which the present time corresponds to some intermediate point; it may be that the present CO_2 concentration differs notably from that persisting in the older geological periods (see discussion under *Dolomite Chemistry,* sect. IV, pt. 2).

There is abundant geological evidence that dolomitization has in the past affected individual beds and formations penecontemporaneously. Worm tracks and tubes (with coarser filling), algal impressions and cavities, etc., have been dolomitized selectively. The aragonitic parts of fossils are less stable than the calcitic; they may invert to calcite, even within a few thousand years, though not necessarily so, or they may be preferentially dissolved, being 3-9 percent more soluble than calcite (Chilingar, 1956b). These aragonitic parts are thus susceptible to selective dolomitization, and the process of Mg^{++} interchange may have begun soon after burial. Evidence of porosity changes in some cases suggests that the time of dolomitization might also be separated from the time of deposition by a period of leaching and hardening (Howard and David, 1936; Landes, 1946; Hohlt, 1948). Such a period of exposure would require emergence (possibly eustatic) and in some cases need not be more than a few thousand years duration. It could, however, be of any duration.

Modern dolomitized reefs show gradation from magnesium-rich limestones (from less than 5 percent $MgCO_3$) to strict dolomites (over 40 percent $MgCO_3$). Most Paleozoic dolomites are completely altered, though they may interbed with low-magnesium, calcitic limestone. Thus a graph of Paleozoic carbonate rocks shows two peaks: low-magnesian limestones and true dolomites (see fig. 1). Intermediate gradations are rare (Lesley, 1879; Pfaff, 1907; Steidt-

---

[2] Gomez de Llarena (1951) recently described a magnesite (primary) from a Paleozoic laguno-marine environment in the Pyrenees.

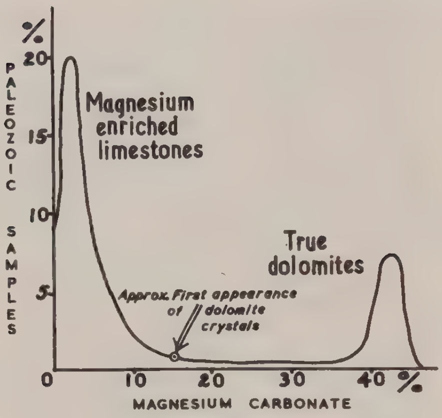

FIG. 1. Diagram to illustrate distribution of magnesium in Paleozoic sedimentary rocks, showing the two clear peaks of "magnesium enrichment" (1-15% $MgCO_3$) and complete dolomitization (40-45% $MgCO_3$). Extremely few and isolated analyses indicate intermediate stages (based on a histogram by Chave, 1954).

Note that Recent sediments show only the "magnesium-enriched" side of the curve, but true dolomite occurs already in the Pleistocene. It may be seen thus that most rocks in the geological column are either approaching true dolomites or else contain no dolomite crystals at all. Owing to the metastable character of magnesium-rich calcite (under normal pressures), there is a tendency in time to break up into low magnesian calcite, liberating Mg ions for dolomitization. Thus some dolomite crystals do appear in the older limestones below 15% $MgCO_3$. (See also fig. 2.)

mann, 1917; Scobey, 1940; Chave, 1954). These Paleozoic dolomites are often not directly related to reefs (although miscellaneous bioherms and biostromes are sometimes involved) and therefore, petrogenetically, we may say that they are not strictly identical in origin to the modern dolomitized atoll. The geographic environment cannot have been identical, but the essential chemical requirements may well have been the same, aided by such essentials as plentiful supply of Mg^{++} salts from sea water, slightly higher salinity, fairly warm temperature, reduced or elevated CO_2 pressure, high pH, reducing conditions, and presence of organic matter, hydrocarbons, and ammonia compounds.

The second great problem in connection with dolomite is the question of why it has proved so difficult to synthesize in the past. It is submitted here, that, with due respect to the learned chemists concerned, little real effort has been made to simulate the actual conditions that may reasonably be expected to exist at, say, a depth of 200-2000 fathoms beneath the floor of the modern ocean or in the core of an atoll. Many of the conditions have, in one way or another, been obtained, but the critical job has yet to be done.

III. CLASSIFICATION OF DOLOMITES

The classification of the magnesium-rich sediments, including dolomites, here adopted is essentially a spatial scheme, based upon the most recent conclusions of various authorities. Together with this geographic treatment, some attention is paid to the genetic problem, but it is hoped that, while doubts exist over the question of mode, the place of origin is nevertheless fairly clear. Some of these genetic deductions urgently require laboratory proof.

In this review the term dolomite is often used in a broad sense, including in some cases rocks that are strictly dolomitic limestones, but not in the extreme way of some European geologists, who may even call a 5-percent magnesium carbonate rock "dolomitic." According to the old system proposed by Forchhammer (1850) and popularized by Bischof (1854) and others, the following terms should be used:

"common limestone" . . less than 2% $MgCO_3$
"dolomitic limestone" more than 2% $MgCO_3$
"dolomite" . . . . more than 13% $MgCO_3$

Some later European workers have altered the last figure slightly (11 to 15 percent $MgCO_3$, etc.). Pfaff (1907) recommended that a class of "magnesian limestone" (less than 7 percent $MgCO_3$) be introduced, with "dolomitic limestone"

(7-11 percent), and "dolomite" for everything higher.

The generally accepted custom today is to say that a true dolomite carries over 40 percent $MgCO_3$, the pure mineral being 45.65 percent $MgCO_3$, 54.35 percent $CaCO_3$, a molecular ratio of 1:1 (Mitchell, 1923; Wyckoff and Merwin, 1924). Between 40 and 45 percent $MgCO_3$, the excess $CaCO_3$ is generally carried in solid solution or as minute calcite inclusions in the dolomite. In limestones with much less magnesia, however, there often are still recognizable dolomite crystals.

The scheme adopted by Cayeux (1935) and formalized by Pettijohn (1949, p. 312) and others (e.g., Carozzi, 1953; Rodgers, 1954) for the terminology of dolomitic rocks has much to commend it:

- "Limestone": containing over 95 percent calcite, less than 5 percent dolomite.
- "Magnesian limestone": 90-95 percent calcite, 5-10 percent dolomite.
- "Dolomite limestone": 50-90 percent calcite, 10-50 percent dolomite.
- "Calcitic dolomite": 10-50 percent calcite, 50-90 percent dolomite.
- "Dolomite": containing less than 10 percent calcite, more than 90 percent dolomite.

There is, however, a certain weakness in this plan, owing to the amounts of $MgCO_3$ normally in solid solution in the calcite of younger limestones. An attempt has been made to correct this diagrammatically (fig. 2). Since the carbonates may not form 100 percent of the rock composition, the diagram is drawn with diminishing proportions; thus the terms may be directly applied to the carbonate fraction, whatever it may be. A somewhat similar diagram has recently been worked out by Iurkevich (1953; see Chilingar, 1955) based upon CO_2 percent and insoluble residue.

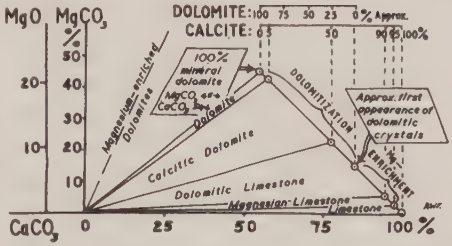
MgO
$MgCO_3$ %
20
10
50
40
30
20
10
DOLOMITE: 100 75 50 25 0 % Approx.
CALCITE: 0 5 50 90 95 100%
Magnesium-enriched Dolomites
100% mineral dolomite $MgCO_3$ 45.6 $CaCO_3$ 54.4
Dolomite
Calcitic Dolomite
Dolomitic Limestone
Magnesian-Limestone
Limestone
DOLOMITIZATION
Approx. first appearance of dolomitic crystals
ENRICHMENT
$CaCO_3$
0
25
50
75
100%
RWF.

FIG. 2. Classification of the younger magnesium-rich calcitic limestones and dolomites, following the basic scheme adopted by Cayeux (1935), Pettijohn (1949), and others. However the percentage of dolomite is NOT the reciprocal of the calcite. Note the first appearance of actual dolomite crystals at about 15% $MgCO_3$, thus straddling the class "dolomitic limestones;" below this level the magnesium is in solid solution in calcite and one should speak strictly of "magnesium enrichment," above it, of "dolomitization."

Rare cases of $MgCO_3$ over 45.6% are "magnesitic" or "magnesium-enriched dolomites."

The absence of true dolomite crystals below a certain concentration of $MgCO_3$ is due to the habit of calcite (but NOT aragonite) of taking up the related magnesium carbonate in isomorphous mixture. Thus, at Funafuti, Judd (1904) observed that recognizable rhombohedra of dolomite only start to appear when the $MgCO_3$ rises over 15 percent of the total.

The upward limiting amount of $MgCO_3$ in calcite is about 20-30 percent, but 15 percent is a fair mean for Recent sediments; in older rocks, dolomite crystals generally appear well below this figure. With older (e.g., Paleozoic and Mesozoic) rocks, dolomite rhombs may occur when the $MgCO_3$ is only 2-3 percent. Chave (1954) has shown that after considerable time, the high-magnesium calcites lose their Mg to form low concentrations of dolomite mineral. Under heat and pressure, such as during metamorphism, calcite with magnesium in solid solution is stable. At normal temperatures and CO_2 pressures, however, only the essentially Mg-free calcite is stable, and the magnesian calcites formed in nature or during metamorphism tend to lose their Mg (Graf and Goldsmith, 1955). The relationship is further complicated by the fact that dolomite in turn may take up calcite or magnesite in isomorphous solution (Foote and Bradley, 1914), possibly to about 10 percent.

Boardman (1953) has suggested that the Cayeux-Pettijohn nomenclature be applied also to calcium-magnesium cements in sandstones. Such distinctions may be very helpful, and are not difficult to make in the laboratory with new indicator methods of chemical analysis, by differential thermal analysis, or with X-ray equipment (see Diehl *et al.*, 1950; Tsvetkov, 1951; Rowland and Beck, 1952; Chave, 1954; Wohlmann, 1954).

Confusion over the rock "dolomite" and the mineral "dolomite" should not arise if the context is handled with reasonable care. Serious confusion can arise in analysis, however, if one refers to the calcite simply as $CaCO_3$, because of course there is another ion of this sort in the dolomite structure.

The terminology of genetic types of dolomite is complex. In the literature there are many references to "local" and "regional" dolomites, "primary" and "secondary" dolomites, "pre-emergent" and "post-emergent" dolomites, "complex" and "compound" dolomites, "contemporaneous," "penecontemporaneous," and "subsequent" dolomites, "chemical" and "metasomatic," "mechanical" and "biogenic," "clastic" and "leached," "diagenic," "dynamic," and "epigene," "pensedimentational" and "penemineralizational." It is not always clear just what is implied.

It is not just a question of black or white; every transition is known. In many cases there may be a superposition of one magnesium-building phase over another, in some places several phases, one after the other; but petrographic and fabric study should disclose the original conditions. Within each of these "environments" there may be more than one distinct genetic form.

The terms "primary" and "secondary" are most often employed to signify the suspected genesis of any dolomite. It is as well to consider what *most* people mean by such terms:

a) *Primary* implies that the dolomite in question has been laid down as such without alteration (see, for example, Twenhofel, 1932): (i) as a straight-out chemical precipitate, (ii) as an organic secretion, or (iii) as a clastic accumulation. As regards case (ii) there is no evidence in favor of a direct organic source of dolomite, but plenty in favor of organically precipitated magnesium-rich calcite. For case (iii) there is no problem, since dolomite sands and breccias presuppose an earlier dolomite; thus a clastic dolomite is not really primary at all, but is a detrital derived rock (see discussion: Sander, 1951; Rodgers, 1954). Finally for case (i) evidence below will be drawn up to indicate that although chemical precipitates of dolomite may occur in evaporites, and in continental and hydrothermal deposits, there is no clear evidence of it in the marine realm either now or in the past.

It has often been taken in the past (see, for example, Grabau, 1913) and still is, especially by some European and Russian geologists (e.g., Weynschenk, 1951a,b; Carozzi, 1953; Teodorovitch, 1946; Vischnjakov, 1951), that an alternation between thin beds of marine dolomite and relatively impervious limestones or shales is *ipso facto* evidence for primary deposition, that is, as a direct precipitate. Microbedding structure and lateral persistence are also taken to be proof of this contention. In the present writer's opinion, this is not satisfactory proof; while such an alternation is clearly enough a cyclic sedimentary sequence, the dolomitic beds may well have been magnesium-rich calcite muds of algal origin, which became contemporaneously or subsequently dolomitized from available Mg^{++} solutions. It cannot be a matter of certainty without detailed ecologic-petrographic investigation (see for example, Cloud and Barnes, 1948). Authigenic crystals of dolomite may be just as well produced by contemporary metasomatism as by primary precipitation.

b) *Secondary* is a term covering all

(1140)

other forms of dolomite genesis. For the marine realm, it may cover *all* dolomites. Within its scope, these are all the "metasomatic" or "diagenetic" and "epigene" dolomites, alternatively "replacement" and "leached" dolomites. The "metasomatic," "diagenetic," or "replacement" classes may be subdivided further into the "contemporaneous," "penecontemporaneous," and "subsequent" types. With a reasonably slow rate of accumulation, i.e., the time element, replacement can take place directly on the sea floor (Goldich and Parmelee, 1947).

Sander (1936; trans. 1951) in particular avoided the terms primary and secondary as "confusing," distinguishing not only the "chemical" (primary of earlier authors) and "metasomatic" (secondary of earlier authors), but also "mechanical" (i.e., accumulated by waves and currents) and "biogenic" (secreted by organisms). It should be understood, of course, that he accepted a very broad definition of dolomite or dolomitic: that is, any calcium carbonate rock especially rich in magnesium. There is, for example, no direct evidence to suggest that actual dolomite has ever been synthesized biogenically; magnesium-enrichment is something else.

The spatial or geographic approach to the classification of the magnesium-rich sedimentary rocks recommended here has certain advantages over a genetic scheme. It is felt that in this case the least confusion arises from identifying a rock from such observable characteristics as may disclose its original site and mode of deposition (see fig. 3). From the environmental conditions one may deduce the genesis of the rock, but the way is left open for multiple stages of metasomatism and differing interpretations.

1. *Marine*
    a) Clastic (mechanical)
    b) Organic (magnesium-rich calcite)
    c) Chemical and metasomatic (early diagenetic)
2. *Intermediate (i.e., littoral)*
    a) Intertidal
    b) Evaporite-lagoonal
3. *Continental*
    a) Late diagenetic (connate and other water)
    b) Leaching or "hard pan" formation (ground water)
    c) Lacustrine and playa evaporites

For completeness, igneous and hydrothermal sources may be added, but they will not be treated in this paper.

1. Marine Environments

There are three distinct sources of magnesium deposition, either on the sea floor, or recently buried in marine sediments but still having access to sea water by diffusion. Emphasizing that the process of alteration does not take place in the open-sea environment but in the newly buried sediments, Reuling (1934)

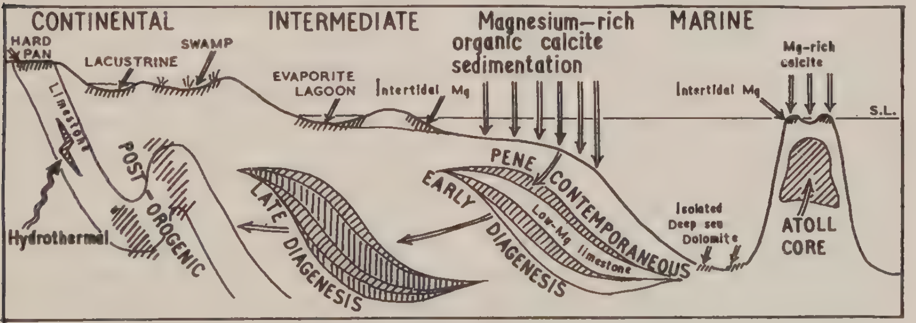
CONTINENTAL
INTERMEDIATE
Magnesium—rich organic calcite sedimentation
MARINE
HARD PAN
LACUSTRINE
SWAMP
EVAPORITE LAGOON
Intertidal Mg
Intertidal Mg
Mg-rich calcite
S.L.
Limestone
POST OROGENIC
Hydrothermal
LATE DIAGENESIS
EARLY DIAGENESIS
PENE CONTEMPORANEOUS
Low-Mg limestone
Isolated Deep sea Dolomite
ATOLL CORE

FIG. 3. Location of sedimentary magnesium deposition and sites of dolomite metasomatism.

has called it "Submarine Dolomitisierung"; Steidtmann (1917) called it "Pre-emergent"; Behre (1947) suggested "Pensedimentational."

a) *Clastic or mechanical.*—Clastic or mechanical magnesian or dolomitic rocks, essentially lime-sands or calcarenites, may be derived, at least in part, from erosion of a pre-existing dolomite (Lesley, 1879; Philippi, 1908; Grabau, 1913; Twenhofel, 1932). A consideration of them will not greatly assist the fundamental question. However, clastic debris of biogenic origin (see (b)) is common in the shallow water and along most of the beaches in warmer seas, and this may play a confusing role, especially in consideration of the intertidal enrichment (see Section V, 1).

b) *Organic.*—Numerous marine invertebrates and plants secrete quantities of $MgCO_3$ in solid solution within the calcite of their skeletal systems, but the crystalline development of dolomite in modern organisms has never been recognized. We may speak therefore only of "biogenic magnesium enrichment," though it may well be considered as a preliminary stage towards "dolomitization." Chave (1954) has shown that for any particular organism, the higher the environmental temperature, the more the magnesium secreted. Varying capacities are displayed by different groups of organisms. (See further discussion under Section IV, *Chemistry*.)

c) *Chemical and metasomatic.*—Chemical and metasomatic imply the processes of inorganic magnesium enrichment and replacement, i.e., metasomatism, that *are believed to take place* in recently deposited sediments at or not far below the present floor of the sea; not only is there sea water trapped in these sediments, but they must be sufficiently porous and permeable to allow free access of further sea water, saturated in Mg^{++} ions. If this is not taking place generally below the present sea floor, but only locally, such as in atoll floors, then, it is postulated, it must have taken place not far below the sea bottom during the Paleozoic, at which time, it is quite reasonable to suppose, the hydrologic conditions were somewhat different from those of today.

It is interesting that the rare dolomite crystals found in present deep-sea sediments are regarded as unquestionably authigenic, that is, formed *in situ* (see under *General Submarine Conditions* V, 4). Only in rare cases have idiomorphic gypsum crystals been found with them on the sea floor (these might be expected if von Morlot's theory operates: an interaction of $CaCO_3$ and $MgSO_4$ producing dolomite and gypsum, see under *Chemistry*).

The cones of semipervious coral rock that rise in oceanic regions and are called "atolls" possess hollow centers filled with clastic sediments and only scattered corals, thus presenting a very special environment that may be the *only sites* of large-scale Quaternary dolomitization. It is not necessary to regard the processes here as fundamentally different from what may have been the "normal" marine conditions of the Paleozoic.

It should be emphasized immediately that fossil "oceanic-type atolls" are never found in the parageosynclinal environments of the continents. "Shelf atolls" (cf. Fairbridge, 1950) are a restricted class forming today in epeiric seas, but they lack the deep foundations of the oceanic type; bores show them not to be dolomitized. Thus, only oceanic-type atolls are found to be dolomitized today; yet no atolls of this type occur in ancient epicontinental sequences.

In the core of the perfectly enclosed atolls it is believed that dolomitization takes place at a moderate depth (over 600 feet, according to Reuling, 1934) by one or more processes. Cullis (1904, p. 406) suggested that at first dolomite is precipitated directly from the sea water in cavities, but later (and deeper) it replaces the calcite "metasomatically."

The Paleozoic dolomites cannot be explained by assuming numerous atoll environments; their distribution is far too extensive. However, as will appear below, the supply of large quantities of organically fixed high-magnesium calcitic material at that time in broad and warm seas may have provided an adequate environment, even without assuming hydrologic changes.

2. Intermediate Environments

These are the areas periodically in contact with the sea, but greatly affected by exposure, heating, and evaporation.

a) *Intertidal environment.*—An enrichment of magnesium carbonate in any carbonate rock type is known to take place in the intertidal belt of the warmer oceans. It has been called "Gezeiten-Dolomitisierung" by Reuling (1934). This is, of course, a special and restricted environment. It cannot be regarded as an actual source of true dolomites, but it is interesting as indicating some of the processes of precipitation and replacement that may take place. Further, as will appear below, intertidal sediments can be used as "marker horizons" (indicating sea level) in relation to any postulated deep-operating dolomitization.

b) *Evaporite-lagoonal environments.*—By this heading a land-locked lagoon, liman, or effectively barred basin is implied, not the open lagoons of many coral reefs or barred basins of the continental borderland with a low sill. In true land-locked arms of the sea, evaporation takes place, leading to the precipitation of calcium and magnesium salts (with others). Even so, this is not necessarily as dolomite; the formation of the double carbonate rhombohedra, in fact, appears to be a secondary step *after* the primary precipitation. In the Permian reefs of the Guadalupe Mountains, the gypseous lagoon precipitates may antedate this second step (Newell *et al.,* 1953).

In the Paleozoic there is paleontological evidence to demonstrate that certain dolomites could not possibly have been genetically associated with evaporite lagoons, although it is true, as Twenhofel has pointed out, that some of the Paleozoic midcontinent basins could have had a restricted inflow, influencing the hydrology.

The theory of Dana (1849) that atoll lagoons form evaporite basins has not been substantiated, since the lagoons of this sort are never effectively sealed nowadays. Perhaps during the low sea levels of the Pleistocene some atoll lagoons would have become cut off completely, and this may have happened also during the Permian. But isolation in evaporite lagoons cannot be a general explanation for marine dolomites. What seems more likely is that the dolomites originate as magnesium-enriched limestones in shelf facies that are often followed in a normal sedimentational sequence by shallowing water and eventually evaporite facies (Fondeur *et al.,* 1954).

3. Continental Environments

Away from the marine realm, there are a number of special continental environments for magnesium precipitation which are well known and do not require very detailed discussion, for example, in connate water, in ground water, and in lake floors from solutions saturated in $MgSO_4$, $MgCl_2$, or $MgCO_3$. Continental dolomites are related to the topographic surface of the land and the processes of soil formation; thus their formation has been called "Gelände-Dolomitisierung" by Reuling (1934). They are essentially *epigene,* and Steidtmann (1917) has called them "post-emergent" to emphasize this character.

It is apparent that in any dolomitic or magnesium-rich rock there is a tendency toward leaching under saturation with waters of appropriate pH. Thus it is in no way surprising to find two or more generations of dolomite in many ancient deposits. The time between the first and the later generations may be considerable. There is strong evidence against an initial formation of the major dolomites by the leaching of magnesium-rich sediments. On the other hand, the major (but not the initial) dolomitization stage of some deposits may have been from saturated connate waters, provided various strict requirements were satisfied.

IV. DOLOMITE CHEMISTRY

This is not the place for a detailed examination of the calcium and magnesium carbonate systems. Those acquainted with the existing work on this subject realize that the question is still fraught with unsolved problems.

Such apparently simple things even as the solubility constants of $CaCO_3$ and $MgCO_3$ in sea waters of differing characters, under varying temperatures and pressures, are still not finally decided. However, certain basic observations may help to clarify the dolomite problem from the geological point of view.

Briefly, the data of geochemistry indicate that in the ocean today there are approximately 1.3 parts per thousand of magnesium, in contrast to 0.4 part for calcium (Sverdrup *et al.*, 1942). Thus, there is roughly three times as much magnesium. Expressed in gross quantities, there are about 5.5×10^{14} metric tons of calcium in the ocean, as against 17×10^{14} tons of magnesium. Judging from present rates of supply, such quantities could be built up in a matter of about 18 million years, so there must be certain limiting factors. Thus, the calcium is frequently supersaturated (especially in the warm surface waters), in fact about ten times more than magnesium at normal temperature, pressure, and pH. Calcium withdrawal can thus be physico-chemically controlled, but this does not seem applicable to magnesium, which does not approach saturation in sea water.

The question is, has the relationship always been like this? According to Clarke (1924), rivers today are constantly introducing calcium into the ocean at four times the rate of magnesium. If this may be taken as the geologically normal condition, then it is clear that calcium must be added and withdrawn at a much higher rate than magnesium. Is this a balanced condition? Rubey (1951) is of the opinion that, broadly speaking, this is true for post-Cambrian times. An interesting suggestion, however, has been put forward by Longchambon (1914) that the unmantling of orogenic fold-belts in the periods immediately following the orogenies may have provided extra magnesium so that dolomites (as in the Pyrenees) are specifically concentrated in time. However, Cayeux (1935) thinks that this generalization is possibly not universally applicable. It seems to be the case that an excess of calcium ions tends to inhibit magnesium deposition, so that the extra calcium salts available from weathering of orogenic belts might have the opposite effect on dolomite formation. Nevertheless, the varying CO_2 supplies from volcanic activity associated with orogenic revolutions may play a role, but not quite such a direct one. A quantitative study along the lines suggested by Longchambon would be illuminating.

A special condition may be sought to explain certain of the dolomites of the Precambrian and Paleozoic. Some of these rocks undoubtedly display rather peculiar features not found in Mesozoic-Cenozoic dolomites, notably their widespread occurrence in shallow, nonbiohermal facies. It is now accepted in some circles (Strakhov, 1953) that CO_2 pressure in the pre-Mesozoic atmosphere would have been considerably in excess of that today. Thus Chilingar's recent (1956a) demonstration of dolomite precipitation from evaporating sea water, saturated with $MgCO_3$ and $CaCO_3$, at a CO_2 pressure of 4 atmospheres, is highly suggestive. In a supersaturated ocean, with an atmosphere highly charged with CO_2, we might indeed expect primary dolomite precipitation (Chilingar, 1956a; Cooper, 1956). This prospect does not, of course, explain *all* marine dolomites, and the problem is to be pursued further.

The question of the removal of magnesium carbonate from sea water is complicated by its different associations. Anhydrous $MgCO_3$ (magnesite) will only precipitate from ordinary sea water at temperatures over 100°C, from 16°-100°C the association is as $MgCO_3 \cdot 3H_2O$ (nesquehonite), and below 16°C as the pentahydrate, $MgCO_3 \cdot 5H_2O$ (Wattenberg, 1937). None of these minerals is found associated with marine sediments. However, with a reduced CO_2 pressure, at a pH of about 9.5, the association is in the form of brucite, $Mg(OH)_2$. According to Wattenberg and Timmermann (1937) one could imagine such pH conditions being much more widespread at certain geological periods. Wattenberg and Timmermann (1937) believe that the undersaturation of normal sea water in $MgCO_3$ precludes any form of replacement *in situ* of $CaCO_3$, all the more as sea water is saturated in $CaCO_3$ already. High alkalinity may change the situation entirely.

A precipitation of $Mg(OH)_2$ as such may occur in warm sea water of high pH, but with the return of normal CO_2 pressure, Wattenberg believes that it will revert to $MgCO_3$; nevertheless, in spite of the lower pH, because the reaction is so sluggish, the $MgCO_3$ will not redissolve, but will crystallize onto any available nuclei, such as calcite (having the same crystal system) with or without Mg already in solid solution. Graf and Goldsmith (1956) have recently synthesized dolomite from brucite and calcite with an elevated CO_2 pressure, using relatively long periods of time and relatively high temperature. Thus:

$$CaCO_3 + Mg(OH)_2 + CO_2 \rightarrow CaMg(CO_3)_2 + H_2O$$

The reverse reaction was also obtained.

1. Early Work

The earliest work on dolimitization has been well summarized by van Tuyl (1916a), Clarke (1924), and Cayeux (1935). Over a century ago de Marignac, Durocher, and Deville had independently synthesized dolomite from $CaCO_3$ by treating it with $MgCl_2$ in various ways under considerable heat and pressure. As gypsum is sometimes associated with dolomite, Haidinger suggested that $CaCO_3$ could be treated with $MgSO_4$ to produce these minerals. This was demonstrated, again with heat and pressure, by von Morlot more than a century ago (1847).

Detailed experiments by Sterry Hunt (1859, 1866) on the precipitation of calcium and magnesium carbonates by alkaline carbonates from bicarbonate solutions generally resulted in only a mixture of the two carbonates, but on heating the wet mixture a dolomite was obtained.

Several series of experiments were then undertaken (in the late 19th century) in order to check Hunt's conclusions, and to see if any catalyst or other reagent would complete the formation of dolomite without employing heat or pressure. In this way, experiments by Hoppe-Seyler (1875), Bourgeois and Traube (1892), G. Linck (1909), Spangenberg (1913), and others all failed until heat was employed (Clarke, 1924).

Geologists have objected to all these earlier syntheses on the grounds that the younger dolomites could never have been subjected to such artificial conditions. On the other hand, there is not sufficient evidence available as yet to demonstrate to what extent *time* may replace *heat* and *pressure* in such reactions. Geological data show that in some cases, at least several thousand years are available for the reaction to advance materially toward completion.

2. Unstable Association of Calcite and Magnesite

A rather important line of thought was indicated in the last century by Sorby (1879, 1904), who exposed calcite crystals to a concentrated solution of $MgCl_2$, finding that magnesite became slowly encrusted on, and replaced, the calcite. No heat or pressure was employed.

It was next established that certain

carbonates cannot exist together in a stable relationship. Thus calcite and magnesite are unstable in association and, if brought together by some favorable circumstance of crystallization, will gradually tend to dissociate ionically and to recrystallize as dolomite (Baer, 1924).

Baer also described the stable "crystallization partners" of dolomite; a state of stable equilibrium can exist between calcite and dolomite, and likewise between magnesite and dolomite. This may explain the extraordinarily variable proportions of these two pairs of minerals when found together geologically in different dolomitic rocks.

The crystalline instability existing between calcite and magnesite shown by Baer was studied further by Franz Halla (1935, 1936) who claimed that at all normal pressures and temperatures existing in shallow seas today there should be a tendency for this dolomite-forming reaction to take place *spontaneously*. After considering the thermodynamic relations, he concluded that the *direction* of the reaction was controlled solely by the concentration of Ca^{++} and Mg^{++} ions available, as governed by the Law of Mass Action. Thus:

$$2CaCO_3 + Mg^{++} \rightleftharpoons CaMg(CO_3)_2 + Ca^{++}$$

However, he did not discuss the rate of the reaction, i.e., the time element, nor the "activation energy barriers," such as caused by the lack of magnesium saturation in normal sea water. Furthermore, sea water in the warm and tropical parts of the ocean is supersaturated in $CaCO_3$ (see Wattenberg, 1936, 1937; Revelle and Fleming, 1934). Thus the removal of $CaCO_3$ in solution is not facilitated in the shallow marine environment. On the other hand, the deeper water is undersaturated, sometimes being rich in CO_2, and, at a late diagenetic stage, the presence of unsaturated meteoric ground water would provide a ready vehicle for aiding progress of such a reaction. However, it should be kept in mind that magnesite ($MgCO_3$) is never found as such in the marine realm. Thus the classical concept of mixing calcite and magnesite in presence of catalysts or under special thermodynamic conditions to produce (primary) dolomite has little more than academic interest.

3. Carbon Dioxide and Magnesium Saturation

It has long been known that both fresh and sea water aerated by CO_2 increased the solubility of calcium and magnesium carbonates (Thoulet, 1888, 1890; Anderson, 1889; Murray and Irvine, 1891). The converse is, of course, also true; thus the removal of CO_2 increases alkalinity and may lead to the precipitation of calcium and magnesium carbonates. Treadwell and Reuter (1898), Baer (1924, 1932), Irving (1926), Kline (1929), Wattenberg and Timmermann (1937), Rivière (1941), Lucas (1948b), and Miller (1952) have produced detailed figures for the solubility of calcium and magnesium carbonates and bicarbonates in waters of varying CO_2 pressure and varying pH. The particular role of CO_2 in sea water is well reviewed in Buch, Harvey, Wattenberg, and Gripenberg (1932).

Baer, in particular, suggested an application of these data to the dolomite problem, claiming that the two solubility curves intersect at a certain CO_2 pressure. Direct precipitation of dolomite should theoretically occur at this point, magnesite above it and calcite below it. An increased CO_2 pressure in the ocean could be obtained in three ways:

i) By a simple increase in depth. Skeats (1905) realized that there was a basic significance of CO_2 in the dolomite reaction and postulated that dolomitization could take place in the ocean at depths from a little below sea level down to 150 feet, i.e., in water pressures ranging from 1 to 5 atmospheres, where CO_2 pressure might also be elevated. (It could also be reduced: see (iii) below). His idea was that the CO_2 would aid solution of $CaCO_3$ and when saturation was reached, at an even molecular ratio between the calcium and magnesium carbonates, precipitation would occur.

ii) Bottom circulation, introducing CO_2-rich water from the polar regions, is a second way in which high CO_2 pressure condition may be achieved. Wattenberg (1933) and Wüst (1933) have demonstrated this for the deep Atlantic, and Sverdrup *et al.* (1942) now recognize this as a general principle.

iii) CO_2 pressure can also be increased in microenvironments by organic activity; for example, by respiration of animals and plants, especially at night, when photosynthesis is interrupted (Chambers, 1912; Atkins, 1930); also by anaerobic bacteria, under certain conditions (Dorlodot, 1909; Jourdy, 1914; ZoBell, 1942; Débyser, 1954).

However, the solubility figures of Baer were not supported after further work by Wattenberg and Timmermann (1937), and it now seems more likely that a *reduced CO_2 pressure* would be necessary to obtain the necessary alkalinity to allow magnesium precipitation. This reduced CO_2 pressure and high pH are obtained in tide pools during photosynthesis. Only under certain conditions do bacteria elevate the CO_2 in buried sediments; at the deeper levels, the bacterial demand for oxygen and the sluggish circulation lead to the reduction of all oxygen-containing molecules, so that the CO_2 pressure drops and the pH rises. ZoBell (1942) recorded a pH of 8.9 at a sediment depth of 15 feet, and with longer cores, still higher figures might appear. Irving's (1926) experiments indicated that $MgCO_3$ would precipitate from alkalinized sea water at a pH of over 9, but for magnesium and calcium carbonates to precipitate simultaneously the pH of the sea water would need to rise nearly to 10; it is normally about 7.9-8.2, but will exceed 9 in the zone of intertidal photosynthesis and probably in buried sediments.

In 1894 Pfaff suggested that decay environments would favor dolomitization. Biological putrefaction products such as H_2S and NH_3 are freely produced in many marine muds. Experimentally treating $CaCO_3$ and magnesium salts in a saline solution with H_2S or ammonia compounds, he produced a wet mixture of the two carbonates, which on evaporation united as a product he took to be dolomite; however this was not confirmed by X-ray data. In a comprehensive review (1907) supported with many analyses, he came to the conclusion that only under highly alkaline conditions with an increase of pressure could dolomite be developed in marine sediments; this would be metasomatism and might be penecontemporaneous, preference going to the fine-grained calcareous muds. Udluft (1929) found considerable support for this theory in the Devonian dolomites of the Eifel with abundant evidence for bituminous hydrocarbons and ferrous iron. Similar observations were made on many North American dolomites (Twenhofel, 1932).

Reviewing the problem at this stage, Linck (1937) pointed out that since advanced dolomitization does not take place in the open sea or in sediments immediately on the sea floor, then special concentrations of Mg^{++} or abnormal pH conditions may be needed. Only marine salts offer the necessary Mg^{++} ions. Putrefaction conditions resulting in ammonia release were also tested. Koehler (1931) had already demonstrated that dolomite could be synthesized from $MgSO_4$ in the presence of ammonium sulfate, $(NH_4)_2SO_4$. Linck now repeated these experiments with both $MgCl_2$ and $MgSO_4$, using an elevated CO_2 pressure, a small amount of an ammonium salt, NH_4Cl or $(NH_4)_2SO_4$ and some organic material (as catalysts?), thus:

$$2CaCO_3 + MgCl_2 \rightarrow CaMg(CO_3)_2 + CaCl_2$$

or

$$2CaCO_3 + MgSO_4 + 2H_2O \rightarrow CaMg(CO_3)_2 + CaSO_4 \cdot 2H_2O$$

Gypsum is sometimes found in the dolomitized rocks, but normally it would be taken into solution.

In his last important paper Linck (1942) maintained this argument, suggesting that calcium and magnesium carbonate gels would be precipitated from sea water by the intermediary of organic activity. Diagenesis of these gel-containing sediments under increased pressure and free CO_2 would complete the process.

As may be seen from the succeeding discussions, the organic participation seems to be confirmed, but otherwise his concept may be very far from the truth.

4. Solid Solution of Magnesium in Calcite Lattice

An important principle, established by Sorby (1879, 1904), is that magnesium may replace calcium in calcite suspended in a solution of $MgCl_2$. This was developed by Klement (1895), who found that $MgSO_4$, which of course is abundantly present in sea water, will replace $CaCO_3$ as $MgCO_3$ when subjected to somewhat elevated temperature and pressure, and especially so in the presence of NaCl. In the case of aragonitic shell and coral material, some 34.6-41.9 percent $MgCO_3$ was taken up, but with calcite, only a trace. The curious thing is that in nature aragonite normally carries little or no magnesium, while organic calcite may carry large amounts in solid solution. It seems that it may be the metastable character of aragonite that favors its ionic rearrangement with Mg^{++} under elevated temperatures, etc.

One of the confusing elements of the general problem, not always faced in the past with sufficient caution by the chemists, has been the polymorphic crystallization habit of $CaCO_3$ (Graf and Lamar, 1955). It has long been recognized that the usual form, stable at moderate and low temperatures, is the rhombohedral calcite, while $CaCO_3$ precipitated at over about 80°F leads to the formation of the orthorhombic aragonite, and further, that in time, or with the application of heat and pressure, aragonite proves to be metastable and inverts to calcite (Bäckström, 1921; Jamieson, 1953).

Recent geochemical work (by Monaghan and Lytle, 1954) has demonstrated that in precipitating $CaCO_3$ from sea water, the addition of excess Mg^{++} ions favors aragonite rather than calcite crystallization. But this is not a simple control, and a more artificially controlled set of experiments by Zeller and Wray (1956) indicate that other trace elements may play a significant role. Thus aragonite precipitation may also be favored by the presence of high Sr^{++}, Ba^{++}, Pb^{++}, but low Mg^{++}, with a relatively high temperature and pH; in contrast, calcite is favored by lower Sr^{++}, Ba^{++}, Pb^{++}, but higher Mg^{++}, and at a lower temperature and pH.

The fact that many invertebrates and primitive marine plants contain $MgCO_3$ has long been known. Forchhammer (1850), Damour (1851), Högbom (1894), Nichols (1906), Bütschli (1908), Clarke and Wheeler (1917), Lipman and Shelley (1924), and others have provided a wealth of analytical data, but it was only lately that Chave (1954), using X-ray diffraction techniques, showed that the amount of $MgCO_3$ incorporated in the skeleton is dependent, firstly on the particular type of the animal or plant, and secondly on the environmental temperature in which the organism lived. The relationship of the Ca/Mg ratio to temperature was confirmed at the same time by Chilingar (1953).

Chave believed that he had demonstrated that the more primitive the plant or animal, the higher the magnesium; the higher the environmental temperature within any class of organisms, the higher the magnesium. This may not be a reliable rule, however, and should not be used indiscriminately. Nevertheless, the primitive plants, the calcareous algae such as *Lithothamnion*, range from about 7 to 30 percent $MgCO_3$ according to temperature, while the highly organized arthropods, the barnacles, range only from 2 to 4 percent; notice that the

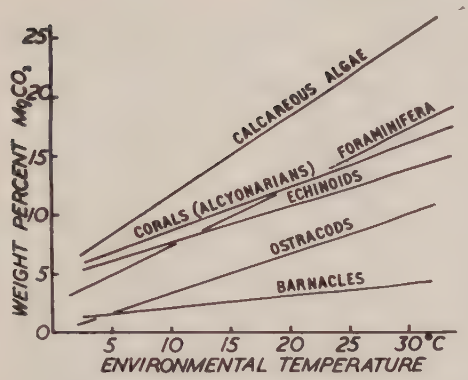

FIG. 4. Relationship of temperature-magnesium curve to phylogenetic level of magnesium-secreting organisms or plants. (Based on graphs by Chave, 1954.)

gradient is less the higher the class (see fig. 4).

Within these generalizations there are some gross exceptions and local variations; for example, certain foraminifera are low in magnesium; or, again, different parts of the skeleton contain varying amounts of $MgCO_3$, the useful effect of which is to strengthen the corresponding member (Vinogradov, 1953).

The capacity of the $CaCO_3$ lattice to take up trace elements in solid solution has been known or suspected for some time. For example, Vesterberg (1901, 1903) believed that there was a special form of $MgCO_3$ that could be dissolved from *Lithothamnion* with a weak acid, being more soluble than either magnesite or dolomite.

It was later suspected that this "special form" of $MgCO_3$ was fixed in the $CaCO_3$ lattice in solid solution (Foote and Bradley, 1914; Ford, 1917) and smaller amounts of $SrCO_3$, etc., may occur in a similar way.

That there existed a relationship between the crystal habit and the amount of magnesium in the hard parts of any organism was first suggested by Clarke and Wheeler (1917), a circumstance explained by Böggild (1930) who, in studying molluscan shell structure, determined that the aragonite layer was always low in magnesium, while two kinds of calcite existed, one high in magnesium, the other low.

A correlation between figures obtained by chemical analysis, X-ray diffraction, and D. T. A. treatment of these organic carbonates was first made by Spotts (1952, in a thesis, unfortunately not published though widely circulated), which convincingly demonstrated the capacity of calcite to take up magnesium in solid solution. At about the same time, Chave (1952) demonstrated a solid solution between calcite and dolomite.

Detailed analytical work by Chave (1954) has shown that in all lime-fixing marine organisms, appreciable amounts of magnesium will be taken into solid solution only in calcite crystals but very little in the aragonite. The significant feature of these magnesium-rich calcites is that they are also metastable at normal temperatures, like the nonenriched aragonite (Graf and Goldsmith, 1955; Goldsmith, Graf, and Joensuu, 1955).

As regards strontium carbonate impurities, the opposite relationship exists; that is, strontium prefers the aragonite lattice to the calcite (Noll, 1934). The quantity of strontium absorbed in this way is not directly related to temperature, according to work by Odum (1950) and by Kulp, Turekian, and Boyd (1952); but insofar as the aragonite precipitation is greater in the shallow parts of warmer oceans, it seems significant that the strontium content of the waters next to a coral reef is less than normal (Lowenstam, 1952).

Since aragonite is metastable, it is apparent that the strontium is likely to be set in motion during early diagenesis, but the present writer is not aware whether any relationship between dolomite minerals and the strontium carbonate has yet been demonstrated.

Of particular importance to the dolomite problems are the *rates* of breakdown of the unstable aragonite and high-magnesium calcites. Evidence from the coral reef bores at Funafuti, the Greater Barrier Reef, and elsewhere (summarized by Fairbridge, 1950) shows that the inversion from aragonite to calcite may take place rather quickly in nature. The aragonite in these bores disappears rapidly with depth and is almost gone by 150 feet; this probably represents part of the postglacial upgrowth of reef and may have been built up within a matter of a few thousand years. During their Pleistocene evolution, the reefs would have been exposed to subaerial leaching, so this may have contributed to the process of aragonite removal. Leaching is not a complete explanation, as may be seen from thin sections (Cullis, 1904). In the case of Funafuti atoll, the inversion to calcite (at about 80°F) may be said to reach completion within about 10,000 years (see further discussion under *Funafuti* and *Atoll Dolomitization*). A puzzling feature, however, is that some much older rocks still contain large amounts of aragonite.

Further light is shed on the problem of aragonite inversion by an analysis by Chave (1954), of the Timms Point silt of San Pedro, California; it is Pleistocene in origin, but a precise age is not available. Detailed examination of its content shows that aragonite is present in the coarse fraction, but has disappeared from the finer fraction, being apparently replaced by dolomite (see fig. 5). The failure of the aragonite to pass over to calcite before now may possibly be related to the lower prevailing water temperatures off southern California.

What of the unstable magnesium-rich calcite? It seems to possess greater stability than the aragonite, for high magnesium percentages (up to 5 or 6 percent of the *total* carbonates) appear here and there in all the bores into Quaternary carbonate sediments. In the Great Barrier Reef the bores run through the coral into continental shelf (terrigenous quartz) sands at 400-500 feet without any sign of dolomitization, but at Funafuti, dolomite is reached at 638 feet. At that depth some special condition appears to have been attained which led to the mobilization of the unstable magnesium-rich calcites. The nature of those special conditions will be discussed later.

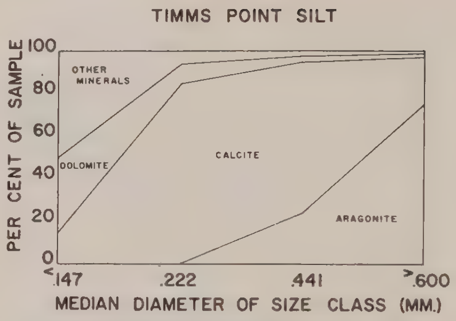

Fig. 5. Mineral composition of a Pleistocene part-dolomitized sediment. The Timms Point formation from San Pedro, California, is a calcareous silt, apparently in transformation from a lime clastic to a dolomite. Note how in the finer fraction the aragonite has disappeared, but seems to have been reciprocally replaced by the dolomite: at the same time a fraction (the Mg-rich part) of the calcite has also been replaced. (Reproduced, by permission, from Chave, 1954.)

The fixation of magnesium-rich calcite in nature seems to be essentially an organic process, but this may not always be so. Some experiments by Riviere (1939a, 1939b) shed light on the matter. Taking pure powdered $CaCO_3$ in circulating sea water, with its pH kept high by ventilation with air deprived of CO_2, for a period of nearly one year, he found there was an 8-percent absorption of magnesium carbonate into the calcite lattice. The process is accelerated by slightly increased salinity, and by the high pH. Such environments occur in coral-reef pools, on beaches and cliffs in the intertidal and splash ranges.

V. MODERN ENVIRONMENTS OF MARINE MAGNESIUM ENRICHMENT

1. Intertidal Magnesium Enrichment

The intertidal belt in calcareous rocks bounding warm oceans (say, roughly 30°N to 30°S) is a region of unstable microenvironments, largely associated with isolated tide pools and splash pits, where evaporation and large temperature changes take place. Biologic factors, such as photosynthesis and respiration, also play an important role. Observations on the pH in these specialized pools and droplets of sea water show interesting diurnal changes, ranging from about 7 to over 9 (Emery, 1946; and the writer). With the addition of rain water in the splash pools, the writer has observed the pH to reach as much as 10.6. Under these conditions *primary* precipitation of Ca and Mg salts may be expected within the interstitial spaces of the existing rock. It should be emphasized, however, that this filling must be called *secondary* in relation to the original rock. Further it will be strictly limited by the tidal range and splash limits. In no sense can such intertidal enrichment be regarded as a source of independent carbonate rocks. Nevertheless, it is a process that may be specially helpful in determining the *exact location* of former shorelines, and this in itself is important in the dolomite problem.

The process may be twofold:

a) Primary precipitation of $CaCO_3$ and $MgCO_3$ (possibly via $Mg(OH)_2$) from sea water solution, owing to evaporation.

b) Enrichment of the magnesium in solid solution with $CaCO_3$ (in the form of the skeletal parts of organisms) as $MgCO_3$ from the Mg^{++} of sea water.

Chave's work (1954) has shown that the warmer the temperature, the higher the organic magnesium secretion, so there is a natural impetus in favor of a considerable magnesium concentration in the intertidal belts, where higher temperatures are recorded than anywhere else in the marine realm. The widespread presence of calcareous algae (often *Lithothamnion*), the richest organic magnesium secreters, as a crust on the exposed surfaces of coral reefs, or even forming massive reef caps (Mayor, 1924), particularly help to accumulate high $MgCO_3$ deposits in the intertidal zone.

Not only are organic processes important, but inorganic action has also been demonstrated.

Some figures on this question may be interesting. On the Red Sea, Rivière (1940) claims that $MgCO_3$ forms in patches on the exposed reefs when the pH exceeds 9 during hours of protracted sunlight; there is no doubt whatever that

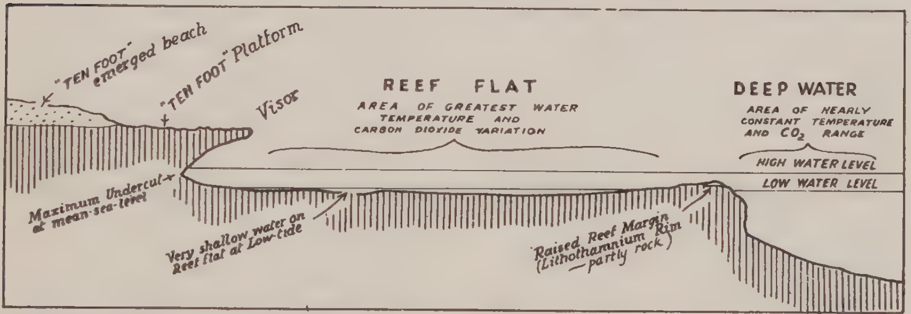
"TEN FOOT" emerged beach
"TEN FOOT" Platform
Visor
REEF FLAT
AREA OF GREATEST WATER TEMPERATURE AND CARBON DIOXIDE VARIATION
DEEP WATER
AREA OF NEARLY CONSTANT TEMPERATURE AND CO_2 RANGE
HIGH WATER LEVEL
LOW WATER LEVEL
Maximum Undercut at mean-sea-level
Very shallow water on Reef flat at Low-tide
Raised Reef Margin (Lithothamnium Rim — partly rock)

FIG. 6. Idealized section of a contemporary limestone reef flat such as occurs widely in all the warmer latitudes. Under intertidal conditions (climatic range, metabolism, photosynthesis, etc.), extreme ranges of temperature, salinity, alkalinity, pH, CO_2, and O_2 have been systematically recorded by the writer and collaborators (also Emery, 1946). Note that highest magnesium figures are obtained both organically in *Lithothamnion* (calcareous algae), invertebrate skeletons, etc., and inorganically in tide pool walls, in undercut cliffs, and on old (early Recent) eustatic marine platforms up to 10 feet above present low tide level. (From Fairbridge, 1950a.)

algal photosynthesis is an important factor in pH control (see fig. 6). Irving (1926) has indicated that in sea water the pH may have to reach 10 before both calcium and magnesium will precipitate together, but if calcium precipitates first, then magnesium will follow rapidly.

Experimental work by Rivière (1939a, b, 1941) at the Concarneau Marine Laboratory (reported above) showed that $CaCO_3$ exposed for a year to sea water of high pH revealed an 8-percent absorption of $MgCO_3$. Checked by field work in the Red Sea, where the reaction is accelerated by the high pH and high salinity, Rivière found elevated coral reefs enriched by magnesium to as much as 30-40 percent of the $CaCO_3$, thus clearly dolomitic, as Walther had pointed out more than half a century before (1888). The detailed geological history of those reefs has not, however, been worked out; thus it is not known to what extent they have been submerged and re-elevated. The early Recent reefs (elevated to 10 feet or so) have not been dolomitized (Macfadyen, 1930) so that Rivière's intertidal enrichment is not enough by itself.

Analyses of beach rocks and beach sands from many parts of the world, though always in the warmer to tropical belts, often display remarkably high magnesium figures (Gardiner, 1898; Branner, 1904; Thorp, 1935). Calcareous sands, consisting partly or even largely of magnesium-rich calcareous algae and foraminifera, quite naturally reflect their origin; e.g., 5 percent $MgCO_3$ from both Bahamas and Murray Island, Australia (Goldman, 1926), evidence, according to Goldman, that "would appear to be directly opposed to theory that ocean water tends to increase the magnesia of calcareous material exposed to its action." Unfortunately, his analyses did not take him quite far enough. These loose sands are only freshly accumulated. Analyses of beach rocks in similar locations often show figures ranging from 5 to 17 percent. However, there may be some unexplained feature of the Bahamas sands (largely oolitic) which gives exceptionally low figures, a feature recently checked by Turekian (personal communication).

It is particularly interesting that in borings through calcareous reefs and coastal lime-sands, wherever there is a hard rock corresponding in fabric and constitution to a beach rock, the $MgCO_3$ analysis jumps up; e.g., in the Key West bore Steiger analyzed 14 percent at 775 feet, while most of the rest was less than 5 percent (*in* Clarke, 1904). In Mayor's bores at Pago-Pago (Samoa), Bramlette (1926) showed 8 percent $MgCO_3$ at both 65 feet and 152 feet; it is perhaps significant that these depths correspond in depth to the 10-fathom and 25-fathom offshore eustatic platforms.

In the bores on the Great Barrier Reef of Australia, there is a similar coincidence of hard bands of what seems to be beach rock with high $MgCO_3$ figures (Fairbridge, 1950).

In the Bikini bore it was also observed that the only hard bands corresponded in depth to that of the present beach rock and to a 10-fathom offshore platform (evidence of a former sea level); at these horizons were found the *only* high-magnesium figures (Ladd, Tracey, and Lill, 1948). Similar hard bands were found in the Borneo Shelf bores (Kuenen, 1947) and in the Eniwetok bores (Ladd *et al.*, 1953).

This intertidal magnesium enrichment has been used with great effect by Reuling (1934) for the purpose of "marker horizons" in determining the rate and character of the subsidence of the Funafuti atoll.

In certain locations in warmer latitudes these intertidal concentrations take the form of a white to brownish or even black superficial plaster or varnish suggestive of chalcedony, ranging from 0.5 to 5 mm thick. It was first noted by Darwin encrusting basalt boulders on the island of Ascension, and was first named by Tschermak (1878) "pelagosite," under the false impression that it was a distinctive mineral, from specimens collected by K. Moser on the shores of the island Pelagosa, in the Adriatic Sea. It was later reported by Des Cloizeaux from Corsica and Oran, by Vélain from Réunion (again encrusting basalt), by many observers on the limestone coasts of Italy and Yugoslavia (Bellini, 1909; Gönner, 1917). The writer has noted it extensively along the limestone coasts of Australia and on many coral islands. Analyses show that it consists of about 90 percent $CaCO_3$, 1-2 percent $MgCO_3$, 1-2 percent SiO_2, and smaller amounts of iron, halite, gypsum, and organic matter.

In the "Coastal Limestones" of Western Australia (calcareous eolianites or eolian calcarenites of Pleistocene age), analyses have shown the *local* magnesium concentration in the intertidal belt to reach over 7 percent of the total carbonates although the amount elsewhere in the formation is generally 3-4 percent. Induration extends several feet back into the cliff, but not a great distance; in short, it is not a ground-water effect as believed by Hills (1949). Spotts (1952, unpublished thesis), by X-ray and differential thermal analysis (see Rowland and Beck, 1952), identified traces of both magnesite and dolomite in this indurated material. Further work should be done in this direction especially to determine the rate of the reactions, for it is significant that the rocks in question are almost certainly not over 50,000 years old, and these magnesium components both appear to belong to the intertidal cement; this is strictly "Recent" and subsequent to the formation of the parent rock. The possible dolomite indications are absent in the nonindurated calcarenite. Gypsum indications are also seen in the intertidal specimens.

If Spotts' identifications are confirmed, then the question of the source of this magnesium arises. The $MgSO_4$ and other salts in sea water are, of course, the most readily available, but there are also the disseminated fragments of Mg-rich character in the calcarenite itself. These fragments are mainly of algal origin. The dilution of such grains by debris of other organisms with such nonmagnesian material as molluscs and corals would appreciably reduce the possibility of their being a source of the magnesia (by means of solution and reprecipitation in the intertidal belt).

An interesting feature about the Australian calcarenites is that they are not only youthful (probably less than 50,000 years old), but also they have never been submerged beneath more than a few feet of sea water. Most of their existence has been subaerial. In no case have they been found to be dolomitized (that is to say with $MgCO_3$ exceeding 10-15 percent).

Further, studies of late Pleistocene and Recent coral reefs in relatively stable areas (Fairbridge, 1950), although often showing magnesium intertidal enrichment, have failed to disclose any tendency toward dolomitization. All those elevated atolls and coral limestone islands found to be even somewhat dolomitic by Skeats (1903), Marshall (1930), and others have clearly experienced submergence and emergence well beyond the limits of Pleistocene eustasy; that is to say, they have been subjected to tectonic oscillations as well.

It is concluded therefore that the type of dolomitization assumed to be submarine, if in any way penecotemporaneous, cannot be directly associated either with intertidal zones or partly open lagoons.

2. Evidence of Funafuti Atoll

Funafuti atoll, in the Gilbert Islands, was drilled in 1896-98 by the Royal Society of London in conjunction with Australian geologists headed by Sir Edgeworth David. The work was intended to test the Darwin subsidence theory of atolls, but in this direction it was not entirely conclusive, since some critics claimed that the bore had penetrated only the marginal talus of the reef and not the main core. Subsequent borings have decisively proved subsidence, but an unexpected result of the Funafuti hole was the light it shed on the problem of dolomitization.

The main Funafuti bore was located on one of the marginal islands of the atoll at 8 feet above low tide level (spring tide range: 7 feet). The first 638 feet consists of reef coral, lagoon limestone, and calcareous sands (Hinde, 1904). Below this to the bottom of the bore at 1114 feet, the same material is largely dolomitized. Aragonite is a common constituent in the top 100 feet, but is not found below 150 feet; below this level the core is very friable and cavernous, consisting largely of loose, foraminiferal sands. The cavernous nature of the limestone is not, however, apparently due entirely to the inversion of aragonite to calcite; it seems to have been actively removed by leaching, and must therefore have been subjected to circulation of *fresh* water.

Thin sections studied by Cullis (1904) show, in the upper 100-150 feet, the gradual buildup of secondary aragonite from the fine interstitial mud, but from 100 feet downwards, the aragonite becomes at first encrusted in calcite, and lower down entirely replaced by calcite. This seems to be clearly a matter of inversion. However, there is also a wholesale disappearence of aragonite below 100-150 feet, apparently due to solution, since large cavities are formed.

The evidence of corals, foraminifera, and sediments in the bore (summarized by Fairbridge, 1950, p. 384) suggests that the coral growth was initiated in shallow water, and as the foundation progressively sank, vertical growth took place, accompanied by a great deal of auxiliary sedimentation of coral sands, foraminiferal and algal debris, and talus. The upgrowth was irregular, as if stimulated by either subsidence of the basement or eustatic rise of sea level.

The nature of the basement has been recently demonstrated by seismic refraction observations by the new H. M. S. *Challenger* (Gaskell and Swallow, 1953). In the midlagoon area, unconsolidated coral and coral sands probably extend only to a depth of 400 feet, below which is a denser rock, probably dolomite, reaching to 1800 feet below the surface. Here there is a transition to medium velocity layers (10,200-13,000 ft/sec) which could be either consolidated limestones or possibly pyroclastics, and these continue to 12,000 feet (2000 fathoms) which must represent the massive volcanic stump that forms the core of the atoll and stands some 2000 feet or more above the floor of the surrounding Pacific.

In the bore itself the dolomite was not reached until 638 feet, which may be explained perhaps by the positions of the bore (on an island on the rim of the atoll). Its presence at this depth was interpreted by Judd (1904) as due to leaching, but by Skeats (1903, 1918) as evidence of shallow-water (0-150 feet) marine origin of dolomite, subsequently lowered by subsidence. Why no shallow-water dolomitization could be demonstrated today was not explained.

An entirely new set of observations from these old data were made later by a German geologist, Reuling (1934), who had been studying the Devonian dolomites of the Eifel. First he recognized the significance of intertidal magnesium enrichment as indicating a valuable marker horizon. Under stable conditions, a beach or shore reef deposit would become enriched in magnesium; under rapid subsidence there would be insufficient time for this enrichment to take place. In the Funafuti bore it has been observed that mostly the $MgCO_3$ is about 1-3 percent but at certain horizons there is a notable "jog" with a few feet of 5-6 percent. The writer (1950) observed in the bores of the Great Barrier Reef of Australia that there are similar "jogs" in the $MgCO_3$ and these correspond to *hard bands,* recorded by the drillers. Such hard bands represent indurated coral material or beach rock; the only level where such induration occurs today is just above sea level, where evaporation takes places.

Reuling's second observation on the Funafuti data was that there seems to be a correlation between the "jogs" of intertidal magnesium enrichment and peaks in the dolomitization curve at depth (see fig. 7). They always come 638 feet (±20 feet) apart. For example, there is contemporary enrichment at sea level today, and dolomitization begins at 638 feet; or again, there is a notable "jog" of magnesium enrichment at 210 feet, so at 638 feet (±20 feet) lower down, that is, at 855 feet (nearest sample), there is a high in the dolomitization.

The converse is also noted, that is, where there is little intertidal enrichment near the surface, then there is reduced dolomitization below 638 feet. Thus at 860 feet Reuling noticed a low dolomite figure (only 20 percent $MgCO_3$), at 860 less 638 feet, that is, 222 feet, there is only 1 percent intertidal magnesium.

These coincidences were explained by Reuling as follows: the dolomitization is assumed to take place within the closed lagoon floor of a coral atoll at a depth of approximately 638 feet. When the cone is stable or subsiding slowly there is time for the dolomitization process to be carried out to completion; at the same time the rocks and sands at sea level have time also to become enriched by intertidal $MgCO_3$. However, when the cone subsides rapidly, probably assisted by the eustatic rises of sea level, there is insufficient time for these chemical replacements to occur, and only low magnesium figures appear in the analyses.

3. Discussion of Atoll Dolomitization

It is evident that this hypothesis of Reuling's requires confirmation (see discussion, Fairbridge, 1950). It makes several assumptions:

a) A plentiful supply of magnesium-rich sea water; in the porous coral foundations of an atoll lagoon, this presents no difficulty. Even tidal rise and fall were measured in the Eniwetok holes (Ladd *et al.*, 1953).

b) Space within the $CaCO_3$ framework for Mg^{++} solutions to enter and substitute for Ca^{++} ions. This is favored by the normally loose branching nature of the coral reef and its clastic sediments, but is further aided by the metastable and more soluble nature of the aragonite which forms an important component in the upper part of each bore, but disappears below 100-150 feet.

c) Reducing conditions, presence of hydrocarbons, and an elevated pressure are requirements suggested by the chemical researchers. Such conditions are experienced today in the floor of those atolls that do not have open passes, samples from the lagoon floors being rich in organic matter and H_2S (Elschner, 1913; Seymour Sewell, 1935). Most of the present-day atolls, however, have deep-cut passes, owing to Pleistocene lowered sea levels, so are not very favorable environments. Only those atolls that are thus closed would provide the right environment. Other atoll lagoons might be well oxidized.

d) A human element, that can be rechecked, is the accuracy of Judd's chemical analyses of $MgCO_3$. It would be most helpful to have these figures recalculated using modern techniques, although a large margin of error seems most unlikely; what should be most interesting is to learn more of the crystal forms involved. Already the thin sections show a good deal.

e) In Reuling's scheme no serious consideration is given to the important eustatic factor in the Quaternary changes of relative level of land and sea. The glacial oscillations have not been equated against the movement of subsidence.

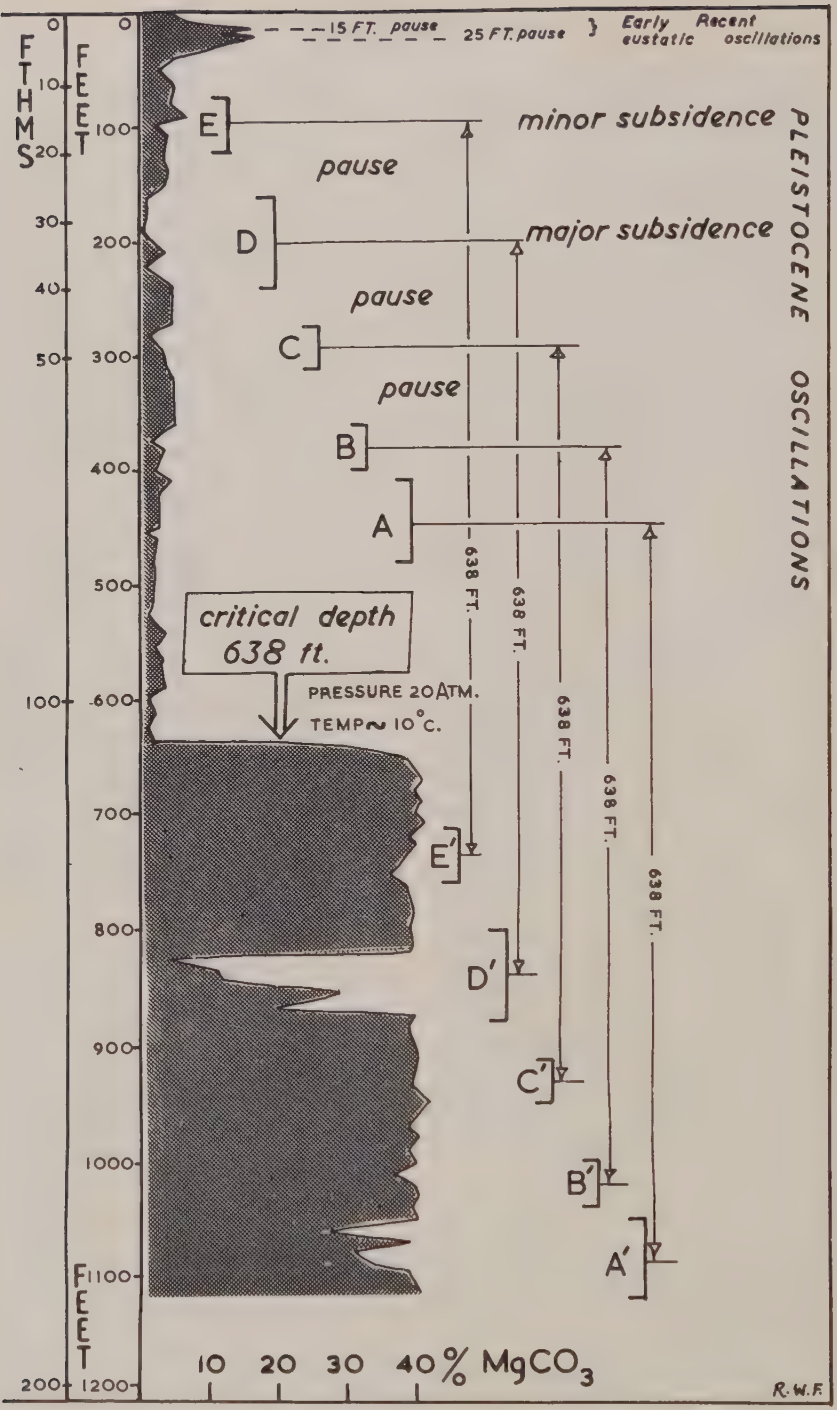

FIG. 7. Magnesium carbonate analyses of the Funafuti atoll bore, as interpreted by Reuling. Note how the $MgCO_3$ curve is under 16%, mostly under 5%, in the upper part of the bore, but below 638 ft. is mostly about 40%. Coincidences of minimal peaks of $MgCO_3$ are always separated by 638 ft. (± 20 ft., i.e., suspected range of dolomitization). Minima may correspond with times of most rapid subsidence, and maxima with times of stability or slow subsidence. The curious peaks at 15 and 25 ft. correspond to known low stands of the sea in early Recent time. (After Judd, 1904; Reuling, 1934.)

After reviewing all the evidence of Funafuti, Cayeux (1935) recently asked three basic questions:

a) Is the dolomitization completed in one rapid phase?
b) Is it a continuous process, or with variable phases?
c) Or is it connected in any way with discontinuous emergences?

Assuming that the maximum Pleistocene "low" was of the order of 300-350 feet, any prior coral upgrowth to near present level or higher (Pleistocene interglacial "highs") would have been subjected to ground-water leaching. This may help explain the aragonite disappearance from 100 to 150 feet to the dolomite level.

One of the first points that appears from the thin-section data of the Funafuti bore is that aragonite and dolomite are never found side by side. The aragonite, it is claimed (e.g., by Hatch, Rastall, and Black, 1938), could not have been dolomitized; it has all disappeared 500 feet above the dolomitic zone. But this was not necessarily the condition at the time when dolomitization began; perhaps the dolomitization of the lower zone was initiated early in the atoll growth, *before* the removal of the aragonite in the 100- to 600-foot levels. This zone could have leached out during a late Pleistocene emergence postdating the main dolomitization, the uppermost 100-150 feet being explained by post-Pleistocene growth.

There is evidence that the solution did not stop at the horizon where dolomite begins, because the traces of organisms below this level also show corroded outlines (Cullis, 1904, p. 408). This evidence of solution continues to a depth of 740 feet. From 638 to 660 feet there is a hard dolomitic "crust," but from 660 to 740 feet there is what Cullis called "soft dolomite," so friable that it could be scratched with a nail. From this it would seem that the whole crest of the atoll (the present 100- to 740-foot sequence) may have been briefly exposed as a mountainous island during one or more of the Pleistocene low sea levels. The hard crust may thus be in part a ground-water phenomenon, a hardening of the "softened" dolomite associated with the surface of the water table; another explanation is also possible.

Below 740 feet, cores rapidly became dense and hard, once more with no signs of excessive solution except between 1100 feet and the bottom (1114 feet). In the unleached cores it is not immediately apparent whether the original aragonite was still unaltered when dolomitization occurred, or whether inversion had already altered it to secondary calcite; it seems that some of the dolomite has directly replaced primary aragonite, and some had replaced it after inversion to secondary calcite. In any case the dolomite seems to show a preference for these parts or for the interstitial mud, rather than the primary calcites of the fossil corals. To the writer it seems likely that this is due to the lack of primary magnesium in the calcite lattices of the corals, thus the most stable elements in the reef complex. The muds regularly contain a great deal of magnesium, being derived largely from calcareous algae and foraminifera (see Chave's work, fig. 4, 1954). The tendency would always be for the Mg^{++} solutions to seek out the existing high-magnesium constituents, only later taking on the most stable calcites.

Finally the appearance of solution at 1100 feet may represent the trace of an earlier Pleistocene emergence (pre-Wisconsin, for example), but unfortunately the bore had to be stopped short at this point.

As regards the rate of dolomitization it would seem that as soon as the atoll was submerged to a certain depth, the process would continue, proceeding as the atoll gradually sank, to be interrupted periodically when there was a downward swing of sea level. The influence of lowered temperature associated with glacial stages is not regarded by the writer as of great significance in such equatorial latitudes. However, the emergence of the whole atoll by several hundred feet each time would institute a thorough leaching, particularly affecting the more soluble aragonites.

Reuling's argument implies that dolomitization is going on today at the appropriate depth and pressure. The sea level has been where it is today (±10 feet) only during the last 8000 years or so, i.e., since the postglacial rise. It is possible that the crust of hard dolomite from 660 to 638 feet developed during this Recent time, rather than as a subaerial "hard pan" during the preceding low sea-level period. Cullis (1904, p. 406) has remarked that near the top of this particular zone the dolomite crystals enclose the layers of the secondary calcite; the youngest dolomite is thus at the top (see fig 8).

Apart from Funafuti, in other bores of the Pacific region, the evidence is inconclusive. At Bikini there was no dolomitization, but in Eniwetok (bore F-1) some dolomitic material was found between 4300 and 4630 feet (where it bottomed apparently on basalt). At Kita-Daito-Jima there is an emerged and deeply eroded atoll, the upper part of which is completely dolomitized (Hanzawa, 1940).

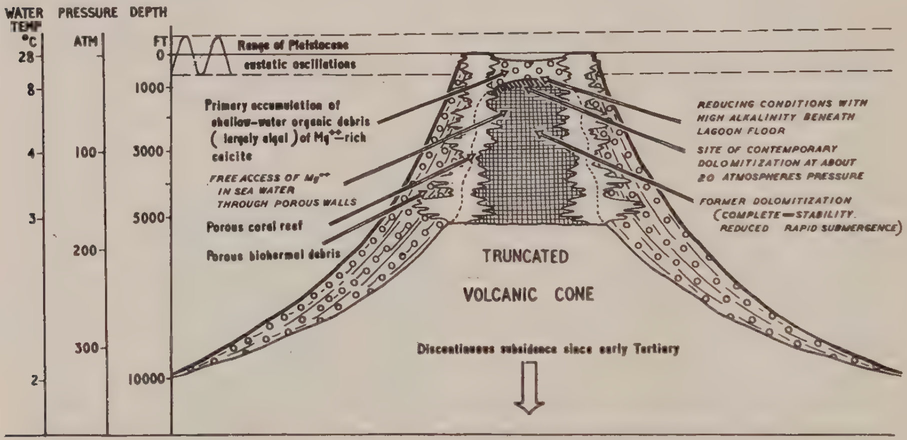
WATER TEMP °C
28
8
4
3
2
PRESSURE ATM
100
200
300
DEPTH FT
0
1000
3000
5000
10000
Range of Pleistocene eustatic oscillations
Primary accumulation of shallow-water organic debris (largely algal) of Mg⁺⁺-rich calcite
FREE ACCESS OF Mg⁺⁺ IN SEA WATER THROUGH POROUS WALLS
Porous coral reef
Porous biohermal debris
REDUCING CONDITIONS WITH HIGH ALKALINITY BENEATH LAGOON FLOOR
SITE OF CONTEMPORARY DOLOMITIZATION AT ABOUT 20 ATMOSPHERES PRESSURE
FORMER DOLOMITIZATION (COMPLETE—STABILITY. REDUCED RAPID SUBMERGENCE)
TRUNCATED VOLCANIC CONE
Discontinuous subsidence since early Tertiary

FIG. 8. Diagram to illustrate, in an idealized atoll, the suspected relationship of primary Mg-rich calcite (largely fixed by algae) to contemporary dolomitization, which may take place beneath the lagoon floor at a depth of 600-700 ft., where there is a pressure of about 20 atmospheres, a temperature of at least 10°C (possibly raised by organic activity), a free access of Mg^{++} ions from sea water, but a high alkalinity (pH about 9-10) due to reducing conditions brought about by organic activity both in the atoll walls and in the sediments themselves.

Below the level of contemporary dolomitization, the atoll core may have been dolomitized discontinuously, the process being affected by changes in depth (and pressure) due to eustatic oscillations of sea level and varying rates of atoll subsidence. Periods of stability permit complete dolomitization to be achieved, while rapid subsidence permits a quick buildup of sediment, partly sealing off the former zone of dolomitization, so that completion is not achieved (e.g., 5-20% $MgCO_3$ in some of the Funafuti analyses). Funafuti atoll stands as the sole prototype for this scheme; many other Tertiary dolomitized atolls in the Pacific and Indian Oceans have been partially elevated, so that the critical top 600 feet have been removed by erosion. Nondolomitized atolls, such as Bikini and Eniwetok may, for some reason or other, have failed to provide the necessary physico-chemical requirements, such as the reducing conditions (owing to freer circulation) or may have subsided too rapidly.

There are numerous other emerged atolls in the Indian and Pacific Oceans, some extensively dolomitized, a number of which were tested by Skeats (1903) and by Elschner (1913), but the most significant data were gathered by Marshall (1930), who systemically sampled the emerged lagoon and rim ("makatea") of Atiu Island, in the Cook Islands. He says: "Tests showed a definite and gradual decrease in dolomitization from the inner towards the outer side of the makatea." This is most interesting, because if—as Skeats and Reuling suggested—the dolomitization is a phenomenon of the restricted core of the atoll, this is exactly what one should expect. The interior of the island should be highly dolomitized, and the degree of dolomitization should decrease from the inner edge of the rim toward the outside, where open marine conditions would counteract the reducing environment of the interior. Curiously enough Reuling (1934) attributes these South Sea elevated reef dolomites to "continental dolomitization." Possibly there are subsequent crusts in places, but most of the metasomatism appears to be submarine.

Geology has relatively few examples to offer of atolls in the pre-Quaternary eras. Shelf-type atolls (e.g., the Marine Reef of Illinois) do not appear to have been dolomitized as a unit, but it is possible that the Triassic reefs of the Tyrol may have been. These were associated with the subsidence of the Alpine geosyncline and penecontemporaneously dolomitized. After the initial theory of von Buch, who conceived the idea of hydrothermal alteration, it was conclusively shown by von Richthofen (1860) that they were essentially organic marine reefs. He claimed in fact that only the atoll-type reefs of the Tyrol were strictly dolomitic, while barrier-type reefs only came into the class of dolomitic limestones.

In a similar case, but in the Upper Paleozoic geosyncline of Belgium, Dupont (1881, 1882) described many dolomites associated with reefs, in particular that of Roly, which he claimed had a dolomitized center, like those emerged atolls of the central Pacific observed by Dana. Latest studies of these Devonian reefs by Lecompte (1954) suggest however that all reef types here, coral, stromatoporoid, or other, may be dolomitized. The atoll or reef form generally may have acted as a nuclear center, but does not appear to be the *sine qua non* of dolomitization.

4. General Submarine Conditions for Dolomitization

If it is taken, as a working hypothesis, that dolomitization is going on under submarine conditions today, it may be possible to draw the limits of those environments from laboratory and geological evidence. As mentioned above, the basic chemical observation in this connection is that although $MgCO_3$ may be incorporated into the calcite lattice in ordinary warm sea water, the metasomatic changeover to dolomite requires a special environment of the marine realm, under a moderate pressure, and sufficiently in contact with the ocean to receive adequate Mg^{++} ions, but sufficiently isolated to permit elevated alkalinity and the concentration of catalytic agents such as the ammonia salts. All this, it seems, could be brought about soon after burial at relatively shallow depth in the sediments at a pressure corresponding to about 100 fathoms (20 atmospheres).

What is the evidence of contemporary dolomitization in open-sea sediments? Such a process would hardly be expected immediately on the surface, but curiously enough there are reports of contemporary authigenic dolomite right on the surface in certain localities. The crystals are isolated, but not rare, perfect rhombohedral idiomorphs, and are very generally the same size (about 10-20 mu). They are always found within about 300 miles of the coast, in fine-grained terrigenous or calcareous muds, in moderately deep water (500-2000 fathoms). They generally constitute less than 2 percent of the total sediment, so that there is no question of a true dolomite mud.

The occurrence of these isolated deep-sea dolomite crystals is interesting. They have been reported in the Mediterranean (Böggild, 1912) and off the coast of Africa (Correns, 1937, 1939, with Radczewski and Leinz), but not in any of the high latitudes. This fact may be significant in explaining their origin, for it may be suggested that they are due to *in situ* metasomatism of small pellets or fragments of magnesium-rich calcitic material, either of calcareous algal origin, washed out or transported in faeces from the shallow (and warm) shelf area, or of certain richly magnesian pelagic foraminifera. Those of the Mediterranean were often found associated with calcitic nodules. That they have certainly formed *in situ* is evidenced by Leinz' discovery (1937) of small inclusions in them of glauconite, another authigenic mineral derived from chemical alteration on the sea floor of terrigenous detritus. An essential condition for such processes seems to be slow accumulation, yet relative proximity to land. Some transportation from the warm shallows to greater depths may be achieved by turbidity currents.

As regards deeper operating metasomatism, it is difficult to judge in the absence of very much deep core-sampling. The longest deep-sea cores yet obtained do not exceed 65 feet. It is highly significant, however, that bacterial action has been observed in these deeper sediments, and at depth pH figures up to 8.9 have been recorded by ZoBell (1942), indicating an alkalinity approaching that required for inorganic magnesium precipitation.

Even surface samples or very short cores, of the type used by the *Challenger* Expedition, provide some interesting data. Murray and Renard (1891, p. xxviii, also p. 200) noted that the $MgCO_3$ proportions appeared "too high" in some of the terrigenous samples suggesting "incipient dolomitization." Actual dolomite was not found except in ice-rafted detritus. Högbom (1894) remarked on the fact that in the calcareous oozes of the *Challenger* collection, the deeper material tended to show a higher Mg/Ca ratio than the shallower samples. He claimed that these do not seem to be from such depths that differential removal of the calcium would be the cause. This appears to be true from his determinations of averages:

Carbonate Range	Average $CaCO_3$	Average $MgCO_3$	Percentage of $MgCO_3$ to $CaCO_3$
80-100%	86.7	0.7	0.8
60- 80	68.3	1.4	2.0
40- 60	52.0	1.2	2.4
20- 40	32.0	0.9	3.0
10- 20	16.2	1.6	10.0
5- 10	6.1	0.7	11.5
3- 5	3.7	1.6	43.0
1- 3	2.0	2.1	105.0

It is interesting to note that among the Recent deep-sea carbonate sands in the few cases where detailed analyses have been made, the finer fractions generally contain the largest Mg/Ca ratio. For example, in the case of a carbonate sand from station 271 of the *Meteor* Expedition (from 3504 m depth near the Cape Verde Islands, see Correns, 1937, p. 240), the fraction of less than 1 micron showed for Mg/Ca a ratio of 3.55:100, compared with about 0.4:100 in the coarse fractions (more than 55 microns). Considering the proportion of $MgCO_3$ in relation to its possible provenance, it is significant that the high figures correspond, at least in part, to their propinquity to reef-fringed islands; e.g., the above figures, close to the Cape Verde Islands. In the *Challenger* material the figures show 2.64 percent $MgCO_3$ near the Canary Islands, 2.42 percent near Fiji, whereas seaward, in comparable depths, analyses show about 0.5 to 1.00 percent.

There is no doubt that Högbom's determination of mean figures is useful in demonstrating the differential removal of $CaCO_3$ with depth and the stability of the $MgCO_3$. But it also tends to obscure another important fact. The writer has recalculated the $MgCO_3$ as a percentage of the $CaCO_3$ *for each individual area,* recognizing that the provenance, CO_2 pressure, and other factors vary from basin to basin. Within any typical basin these figures confirm that Högbom's generalization is correct, *but* also that the absolute value for $MgCO_3$ (determined as a percentage of the total sediment) increases with depth. Thus in the central North Atlantic the absolute values of $MgCO_3$ rise from 1.70 percent at 1900 fathoms to 3.75 at 2575 fathoms, even though the $CaCO_3$ has not dropped more than 25 percent. In the southeast Pacific the $MgCO_3$ rose from 0.33 percent at 1450 fathoms to 0.65 at 2025 fathoms. Some support is seen in more recent figures by Thorp (1935), and it is interesting that the highest Mg/Ca ratios occur in the deep-sea coprolite oozes and terrigenous blue muds. Proximity to neritic shelf areas seems to be an important factor. Insufficient figures are available for drawing general conclusions; but the trends are suggestive. Unfortunately most recent deep-sea expeditions have not found it necessary to determine $MgCO_3$, so that more data are not coming to hand. Increasing interest in this aspect may bring more light on this. Among other things, it has been noted that there may be a rather general increase in Mg in deep-sea clays (personal communication, Turekian).

In *shallow waters,* the same trend of Mg enrichment was pointed out by Mägdefrau (1933, 1942), who found that in the Bay of Naples, living calcareous algae (*Lithophyllum expansum*) near the surface contained an average of 2.5 percent $MgCO_3$: in dead specimens at 0-3 meters the figure rose to 4.8 percent, at 10-15 meters to 6.2 percent, at 40-70 meters to 9.5 percent, and at 90 meters eventually to 11.3 percent. Differential solution of $CaCO_3$ appears to be out of the question at such depths in the richly saturated Mediterranean.

There thus appears to be a progressive tendency with depth toward inorganic enrichment of magnesium involving presumably a replacement of the calcium, provided that high-magnesium calcite nuclei are initially present (developed essentially by organisms). However, these figures show two distinct gradients, (a) a steep one in magnesium-rich organic skeletal material in relatively shallow water, and (b) a rather gentle gradient, affecting coarse and fine clastic carbonate material in bathyal depths.

That warm-water conditions are particularly favorable is suggested by samples from the Red Sea, where in the Strait of Suakin, the *Pola* dredged samples of a calcareous crust exceeding 12 percent $MgCO_3$ (Natterer, 1898, p. 500; 1899). It is possible of course that some (or all) of these Red Sea samples might be reworked intertidal deposits, because extensive formation of high-magnesium muds is known to take place in the wide reef flats not far away (Rivière, 1939b, 1940, 1941).

Some other high-magnesium or dolomitic samples in relatively deep-sea environments may also have had a shallow-water origin. In the case of those reported from the East Indies, north of Australia, Böggild (1916) described three occurrences of dolomite concretions, the origin of which is obscure; it seems they were worm-bored, and thus may have been formed in shallow water; two of the occurrences are in depths (31 and 42 fathoms) that are within Pleistocene eustatic range and the third (266 fathoms) is on an active orogenic slope.

Somewhat similar nodules had been dredged by the *Challenger* from the Challenger and Argus Banks, near Bermuda, from depths of 24-30 fathoms (44-55 m). Nichols (1906) found that they consisted of fine-grained lime concretions of cemented coral and algal detritus, containing 4.98 percent $MgCO_3$ in the interior, but 10.7 percent on the outside. Again a submarine enrichment is implied.

Another case, reported by Murray and Philippi (1908) and discussed by Philippi (1907), was the discovery by the *Valdivia* on the Seine Bank (150 miles N.E. of Madeira) in depths of 70 fathoms (148 m) of idiomorphic rhombohedra of dolomite in the matrix associated with calcareous algae, corals, and shelly sands of shallow-water type, cemented into what appears to have been a beach rock (an intertidal phenomenon). The mean analysis ran 11-18 percent $MgCO_3$ and the presence of the pure dolomite in the cement suggests a penecontemporaneous metasomatism during formation or soon after the cement hardened. Clearly the whole bank has been reduced to its present depth by subsidence or a late Quarternary eustatic rise of sea level. Similar specimens of worm-bored concretions and corals, showing 10-12 percent $MgCO_3$, were dredged by Agassiz (1888) east of Florida.

In attempting to synthesize these data, it is suggested that in the ocean today the following processes are going on:

a) In shallow, warm water there occurs both organic and (localized) inorganic precipitation of $MgCO_3$ (in solid solution with calcite).
b) In shallow to intermediate depths round these nuclei further $MgCO_3$ is precipitated, apparently replacing $CaCO_3$ metasomatically, so that when the total $MgCO_3$ analysis approaches 15 percent, actual rhombohedra of dolomite are observable. This process also appears to be favored by warm water but may be assisted with increase in depth to some 200 fathoms or more. Complete dolomitization, however, has not yet been observed under 100 fathoms or without a considerable cover of sediment.
c) In deep water (bathyal depths of the order of 500-2500 fathoms), a similar downward increase of $MgCO_3$ is observed, but of a lower order, as a rule. However, in favored localities scattered rhombohedra of dolomite are actually found in the uppermost layers of sediment. There is a selective tendency for finer-grained material to be enriched first. It seems likely that with increasing depth the high CO_2 pressure (low pH) makes $CaCO_3$ more soluble and thus more easily replaced by $MgCO_3$. The presence, in modern deep-sea sediments, of biogenous silica gels, and the corroded nature of siliceous fossils (Arrhenius, 1952) suggest slow rates of accumulation under alkaline conditions at the surface. Beneath the surface, however, bacterial action may produce acid conditions alternating with alkaline. Chilingar (1953) considers that the usual absence of siliceous material from ancient dolomites is evidence for shallow-water origin, in contrast to the frequent presence of chert, etc. in the deeper limestones (Cooper, 1956).

  This authigenic silica is not to be confused with the clastic silica contained in the sandy dolomites such as those of the Lower Ordovician peripheral to the Canadian Shield; these are clearly evidence of shallow water (see section VI, pt. 1).

If the metasomatic processes noted under (b) and (c) increase progressively with depth beneath the sea floor, then they may surely represent an incipient dolomitization which must be essentially marine and penecontemporaneous. This process, however, lacks positive evidence of contemporary activity today, but Weynschenk (1951b) has suggested "it is to be expected that dolomites may be found of Recent and young geological date of large mass and extent in the sediment of tropical seas from a few hundred meters depth towards greater depths. These will furnish the most recent comparative material to the extensive dolomites of ancient times."

The only objection is that little trace

of such dolomites has yet been found. Still it must be clearly admitted that the longest deep-sea cores yet obtained do not exceed 65 feet even in soft areas, and in many places the depth of penetration is far less. In fact, in the northern Indian Ocean, the Kullenberg corers of the *Albatross* Expedition struck hard bottom again and again. Pettersson concluded (1949) that it was probably a basalt floor, but Weynschenk (1951b) suggested that it might be dolomite, and mentioned that either dolomite or chert might give the same seismic echoes as submarine lava flows. In the writer's opinion hard dolomite would scarcely be expected right at the surface, but it may possibly occur at some depth.

VI. REGIONAL DOLOMITIZATION

It has been suggested from geological evidence (e.g., dolomites of the Alps, Eifel, England, midcontinent U.S.A., of early Mesozoic and Paleozoic age) that there is a regional dolomitization that may affect broad areas, and will not be limited to the confines of an atoll stump (van Tuyl, 1916a).

The expression "regional dolomitization" is taken to include all those "dolomites of formational extent" (of Twenhofel, 1932) and those interbedded stratigraphically with other marine sedimentary rocks, but not those associated with evaporites. Such broad-scale dolomitization is believed to have taken place on the sea floor, either rapidly or in stages, to reach completion in many cases penecontemporaneously under essentially submarine sedimentary conditions, but, owing to one circumstance or another, in other cases may have been prematurely arrested or subsequently revived. As indicated by Steidtmann (1917), those in the Paleozoic are mostly complete, but some Quaternary examples are still apparently ***in statu nascendi*** (Chave, 1954).

It seems appropriate in this chapter to consider briefly the sedimentary and diagenetic relationships of such rocks, in order to determine their original environments, that is to say, their paleoecologic and paleogeographic significance.

1. Paleogeographic Indications

From the evidence of geology, it would appear that the marine dolomites of the early Mesozoic and Paleozoic originated, at least in large measure, in moderately shallow warm waters (Skeats, 1903, 1905; van Tuyl, 1916a,b, 1918; Steidtmann, 1911, 1917; Tarr, 1920; Udluft, 1929; Twenhofel, 1932, p. 364; Young, 1935; Linck, 1937, 1942). Associated fossil types are normal for such marine environments (Weller, 1911), but fossils are not always present, either because of primary sparsity or because of diagenetic obliteration. There is abundant sedimentary evidence of the shallow environments: sun cracks, intraformational breccias and conglomerates of the types generally associated with mud flats, ripples likewise of the tide-flat character, and even clastic dikes (fissure-filling) have been noted (Kramer, 1934).

The widespread presence of small quantities of iron and bitumen in these old marine dolomites suggests reducing conditions (Twenhofel, 1932; Beales, 1953; Osmond, 1954, 1956) which would mean that "moderately shallow" must be taken as well to mean below wave base and intertidal disturbance (Steidtmann, 1917). It does not mean, however, that normal benthonic life could not exist, as the reducing zone may well have been buried beneath a shallow cover of sediment.

Dolomitization associated with H_2S from putrefaction was suggested already by Pfaff (1895), so that associated FeS_2 would be expected. Udluft (1929) supported this idea with the evidence that the marine dolomites of the Eifel were iron-bearing, in contrast to the nonferruginous nature of the subsequent (epigene) dolomites. This is not an inflexible rule, however, because some epigene dolomitization is associated with the formation of ferruginous soils or ground waters and may thus also contain iron, but the latter is either zoned in or encrusted on the dolomite as hematite, whereas the primary iron is generally as interstitial limonite (Dixon, 1907/21; Parsons, 1918; Birse, 1928).

The "dolomite seas" were, on the evidence of fossils, warm and saline, perhaps highly saline (say about 4.0 percent) but not supersaline[3] or the normal biota would have been inhibited. The most interesting feature of that biota is the frequent dominance of algae, e.g., in the Oneota and Shakopee dolomitic limestones of the upper Mississippi valley, the Kona and Bad River rocks of the Huronian in upper Michigan, the Romanie formation of the Gulf of St. Lawrence. The high magnesium of some of the coralline algae is suggestive, but not all are rich in magnesium. The significance of algae may lie rather in their photosynthetic liberation of CO_2, creating microenvironments for the precipitation of (essentially inorganic) carbonates. Nevertheless certain other contemporary organisms, e.g., crinoids, are also noted for their magnesium enrichment, and further research in this direction seems to be indicated.

A relationship of the "dolomitic seas" to land masses and shorelines seems to be well established. Ulrich and Schuchert (1902) noticed that the dolomites cut out as one approached the Precambrian land masses, being replaced in part by clastics and apparently requiring a certain depth of water, this being suggested also by the relative scarcity of fossils.

Nevertheless, the geological evidence clearly shows that most dolomites were formed relatively close to land, certainly in neritic shelf facies (Sloss, 1947). It was suggested by Goetz (1921) that fluvial transport of Mg^{++} solutions or colloids from the land would naturally increase the magnesium concentration close to the continents; evidence, however, is lacking of especially high concentrations then as at the present time. *It may be that the warm shallow neritic seas particularly favored the growth of algae that aided the concentration of magnesium.* The diachronism of the Mississippian Greenbrier dolomite demonstrated by Rittenhouse (1949) seems to suggest a very precise relationship to the shoreline. The correlation between dolomitization and clastics showing nearness to the shore was indicated as early as 1879 by figures presented by Lesley. These have now been drawn up, firstly (fig. 9) to show the true scale section, and secondly (fig. 10) to bring out the rhythmic character of the near-shore (dolomitized) and offshore (nondolomitized) limestone facies.

In the offshore direction, as one goes seawards, the dolomitized sediments are generally replaced by nondolomitized limestones of colder and still deeper water character (Dixon, 1907; van Tuyl, 1918; Cloud and Barnes, 1948; Fondeur *et al.*, 1954). Evidence of silica in these nondolomitic limestones (Chilingar, 1953) suggests a lower alkalinity, favoring precipitation of silica, but not of magnesium (Chilingar, 1953, 1956c).

It seems to be an absolute rule that marine dolomites represent epicontinental shelf and shallow geosynclinal facies, and never bathyal or abyssal conditions.

The condition of the fossil contents is interesting. Even in the least altered dolomites, there are generally rather few shelly fossils, but worm borings and burrows are often widespread. These conditions suggest intermediate depths, generally well below wave base, where bottom conditions may not have been very favorable to the existence of shelly fossils. On the other hand, sun cracks, intraformational breccias, and ripple marks suggest occasional emergence, possibly rapid eustatic oscillations, as shortlived but widespread changes, and seem to be involved in rhythmic successions (Sander, 1951, etc.).

In fact, Raymond (1925) went so far

---

[3] Exceptional cases of halite and dolomite intergrowths are known in barred basin facies (Schwade, 1947).

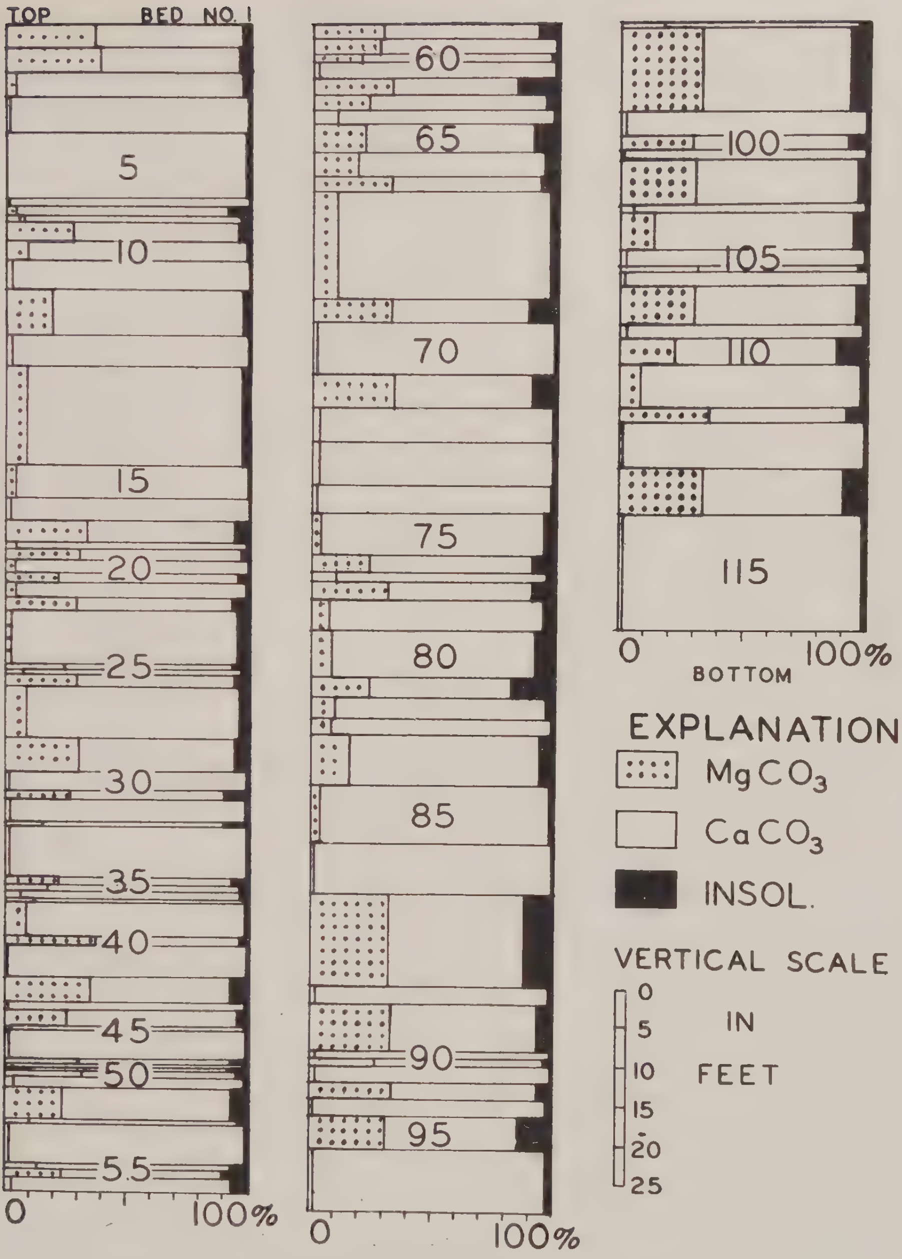

FIG. 9. True scale vertical section, with $MgCO_3$ and $CaCO_3$ analyses, of a sequence of Lower Ordovician rocks W. of Harrisburg, Pa. Note the apparently direct relationship between increase of insoluble material to increase of $MgCO_3:CaCO_3$ ratio. (Based on wet analyses by Lesley, 1879; no doubt the accuracy of this work could be improved by modern techniques, but the data are reliable enough to illustrate a principle.)

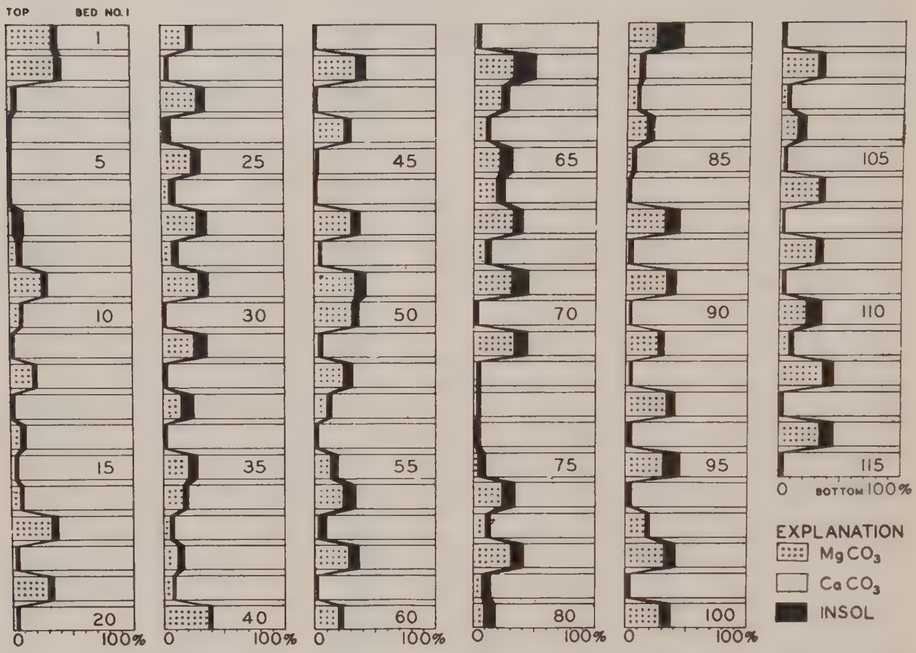

FIG. 10. Vertical section, with $MgCO_3$ and $CaCO_3$ analyses, reduced to beds of equal proportions, of a sequence of Lower Ordovician rocks W. of Harrisburg, Pa. Note the rhythmic alternation of dolomitized and nondolomitic limestones, the dolomitization coinciding always with the beds containing maximum terrigenous (insoluble) material, and therefore presumably closer to the original coastline. (Analytic data by Lesley, 1879.)

as to claim that one could almost predict the occurrence of diastems in many of the midcontinent Cambrian and Ordovician rocks by the presence of dolomites, although with the Silurian dolomites the emergence followed rather later (in mid-Devonian).

Fineness of grain is also apparently a primary feature of most sediments destined to become dolomites. In fact the finer-grained material is preferentially dolomitized. If these fine grains represented primary (chemical) aragonite of the "drewite" type, shallow banks would be indicated. However, if they represent organogenic clastics, an intermediate depth, located at a certain distance from the shore, would be implied (Lowenstam, 1952). The ready breakdown of primitive lime-secreting and lime-precipitating algae may be a factor in this connection, and the reduction of this material to an "algal dust" in the shallows would permit its distribution by wave and current action over extraordinarily wide areas (Wood, 1941). The pelagic secretion or precipitation of magnesium-rich calcite by microscopic free-floating algae is another explanation which is difficult to confirm owing to the alteration (by dolomitization) of the resultant formation. Distinctive shallow-water facies, such as oolites, however, are sufficiently durable that, even though completely dolomitized, traces of them can often be recognized (Lucas, 1948). In the older dolomites, however, neither the relationship to the shoreline nor the horizon or facies seems to make any difference to the grain size, the idiomorphic crystals being very uniformly about 0.02 mm (Daly, 1909).

If it is admitted that the parent sediments of normal marine dolomites consist of shallow-water limestones, rich in organically fixed magnesium, then the initial environments can only be the neritic shelves and shallow epicontinental (para-) geosynclines (see fig. 3). This is confirmed by geological observations on the paleofacies of the regional dolomites.

During geological time it is recognized that there have been systematic oscillations of sea level, considerably exceeding the glacio-eustatic swings, both in amplitude and in duration. During the high-level periods immense epicontinental seas spread out over the lowland areas and one has the concept of the "thalassocratic" phase (see fig. 11). Such epochs must have been immensely favorable to the formation of organic limestones (Steidtmann, 1911), and particularly to the magnesium-secreting algae, which flourish only in warm, shallow, well-illuminated water as required for photosynthesis.

Under the converse conditions, negative sea-level oscillations, regressions would occur and periods of "epeirocracy" would ensue. Not all the swings would be of major proportions, however, for it is evident that very minor oscillations have been superimposed on the major scheme. The effect on detailed sedimentation is often far-reaching (Fairbridge, 1954).

It is to be expected therefore that some geological periods are to be dominated by regional dolomitic sediments, while others are relatively free. And within any period, an alternation between dolomitic beds and nondolomitic beds is predictable. Reef dolomites form a special class, and may be favored by the special conditions of fairly rapid and continued subsidence that permit the buildup of atolls and other large bioherms.

Rhythmic subsidence and transgression is also a feature of coal-swamp development; thin marine bands are common

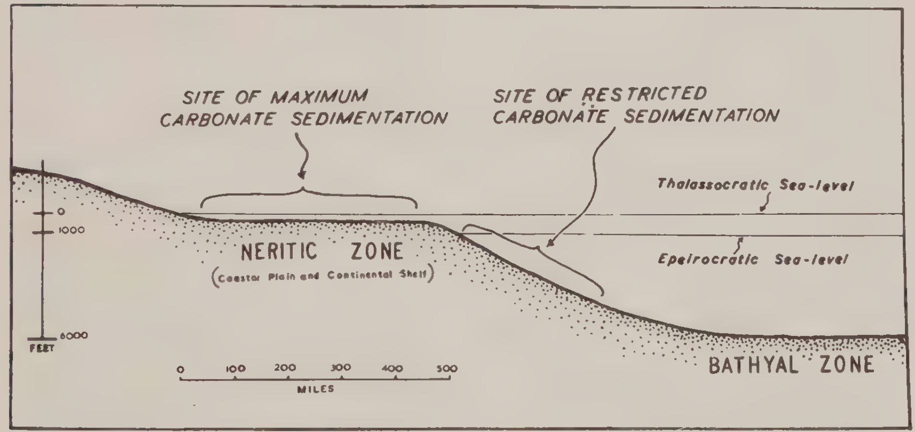
SITE OF MAXIMUM CARBONATE SEDIMENTATION
SITE OF RESTRICTED CARBONATE SEDIMENTATION
Thalassocratic Sea-level
Epeirocratic Sea-level
0
1000
6000
FEET
NERITIC ZONE
(Coastal Plain and Continental Shelf)
BATHYAL ZONE
0
100
200
300
400
500
MILES

FIG. 11. Maximum secretion of magnesium by primitive organisms and calcareous algae occurs in the warmest water (Chave, Chilingar, *et al.*). The neritic zone is also the site of maximum calcium carbonate sedimentation. During thalassocratic epochs, great transgressions will favor widespread formation of magnesium-rich carbonate rocks; epeirocratic epochs, when the sea level may have been hundreds of feet lower than at the maxima, would lead to widespread regressions, so that shallow seas were restricted to a narrow belt along the continental slope, which drops sharply away to the bathyal depths that were unfavorable to carbonate sedimentation prior to the Cretaceous.

in many of these basins. With such transgressions Teichmüller and Werner (1953) have correlated the dolomitic "coal balls" ("Torfdolomite") that occur in certain coalfields, e.g., the German Ruhr. A marine origin is generally admitted for the calcareous material of such "coal balls" (Stopes and Watson, 1908). Some other dolomitic formations in the coalfields, such as the fresh-water dolomitic limestones and sandstones, are of course continental (lacustrine) in origin.

2. Stages of Regional Dolomitization

From the primary deposition of the magnesium-rich sediments, to the ultimate folding of the rocks themselves, an evolutionary sequence of dolomitization may be deduced. Three principal stages are generally recognized:

a) *Early diagenetic (penecontemporaneous).*—With burial, gradual subsidence, and loading, a magnesium-rich lime-sand or -mud in a marine environment is predestined to dolomitization. Cayeux (1935) suggested that the organically fixed magnesium-rich calcite grains become the nuclei ("centres d'attraction") for further concentration of Mg^{++}. With an appropriate oscillation of pH, ending with high alkalinity, and with slight increase of pressure and temperature, early diagenetic dolomitization will set in. If supplies of magnesium ions from sea or connate waters are interrupted in any way or if other necessary conditions fail the metasomatism will terminate. Initially only the magnesium-rich calcites will be affected, but if the process continues, the alteration will pass without interruption into the late stage (see (b)).

A feature of the bedding is that thin bands of dolomitized rock and nonmagnesian limestone frequently alternate (see figs. 9 and 10), yet the lateral extent of the dolomitic beds and formations is often considerable, extending for hundreds of miles in some cases. Quite noteworthy is the case of the "varved" deposits of the Delaware basin. Laminae of dolomite are less than 1 mm thick (Newell *et al.*, 1953). There seems to be very little to support the hypothesis (e.g., by Bernauer, 1933) that the alternate banding could be explained by leaching of Mg^{++} from the adjacent limestones. On the contrary, there is often primary evidence of magnesium-rich material in the original sediments, for example, widespread algal colonies, and clastic algal debris, crinoidal stems. Autoclastic breccias may be due in part to mechanical (wave) breakup of algal crusts, recemented more or less *in situ*.

An interesting phenomenon is the occurrence of *mottled* limestones, in which it is apparent that the early diagenetic stage was arrested before even the dolomitization of the magnesium-rich beds was completed. For this, one may consider such things as rapid subsidence with impervious sediments sealing off further supplies of magnesium, or rapid emergence exposing the formation to oxidizing conditions, in fact any event that would upset the delicate balance of essential requirements for continued metasomatism. The characteristic features of the mottling seem to be an irregular development of pipes, tubes, and "nests" of dolomitized material in a groundmass of unaltered limestone. These pipes, etc., for the most part appear to be worm casts, often containing an initially coarser-grained sediment and, when altered, often appear yellowish against the greyish background. Sometimes they have a pseudo-brecciated appearance (see Wallace, 1927; Birse, 1928; Beales, 1953).

Another characteristic of the early diagenetic dolomites is the widespread presence of iron oxide, generally as limonitic grains, as noted earlier. According to Udluft (1929) this form of the iron must be due to the sulfate-reducing bacterial activity in the newly buried sediments, and thus can only be early diagenetic.

Even more emphatic perhaps is the foetid odor emitted by some of these early-stage dolomites. Preliminary studies by Lucas (1952) show that the smell is caused by the ammoniacal salt of a volatile acid containing phosphorous, probably organic, one of the phosphenate series; it is devoid of sulfur. The salt appears to be lodged as microscopic inclusions in the dolomite crystals. The possible role of ammoniacal salts in the basic dolomite reactions has already been mentioned (under *Chemistry*). The inclusion of such organic compounds in any late diagenetic reaction seems to be out of the question.

b) *Late diagenetic.*—With further loading and more extreme thermodynamic conditions, it appears now that dolomitic nuclei provide a trigger for further metasomatism, that even the low-magnesium calcites will become involved. Thus a late diagenetic stage is indicated. A feature of such dolomites is that the clear-cut primary bedding features will, to some extent, be cut across by the dolomitic boundaries.

Cases are known where the unaltered country rock is entirely surrounded by coarsely crystalline dolomite, and others where the latter passes laterally out into completely nondolomitized limestones. This may, of course, be due to a change of the original facies, passing say from shallow (Mg-rich) into deeper water (Mg-poor), but there is often internal evidence of constant primary facies, and it may be another condition of arrested development, but this time in the late diagenetic stage.

It would appear from Udluft's work (1929) that late-stage dolomites would also be free from ferruginous inclusions (as evidence of primary bacterial action).

Other features of late diagenetic metasomatism are generally the coarseness of the crystallization, the absence of fine interbedded limestones, the almost but not complete obliteration of many primary structures such as fossils, ripple marks, sun cracks, and oolites (see, for example, Lucas, 1948a).

In cases where a varied diagenetic history prior to dolomitization has allowed aragonitic fossils to be replaced by nonmagnesian calcite, the late-stage dolomites are observed to enclose the calcitic fossils, whereas in the early stage the aragonitic fossils would have been selectively dolomitized in preference to a low-magnesium calcite matrix (Cullis, 1904; Dixon, 1907; Elschner, 1913; Skeats, 1918; Newell *et al.*, 1953; Chilingar, 1956b).

c) *Postorogenic.*—Geologists in the field have often noticed that there is a dolomitization that tends to select joint planes and shear zones in the more disturbed regions. This is distinct from merely epigene caps (leaching downward) and from hydrothermal deposits. It often possesses a regional character, being located in the folded and faulted zones, and increases in importance from the plains to the orogenic belts.

In view of the chemical and physical work in synthesizing dolomite, it would seem logical that orogenic pressures, particularly shearing, would favor the action of such very late stage dolomitization. Relatively little work has been done on this aspect of the process as yet, but it seems that magnesium-rich solutions do not display the same selectivity here as in the unstressed rocks, attacking nonmagnesian limestones as freely as those rich in magnesium. Of course, it generally seems the case that the latter have already been dolomitized at an early stage, so that it is during the late stage and postorogenic metasomatism that the interbedded low-magnesium limestones become finally dolomitized over an irregular front.

3. Porosity and Stage of Development

Over a century ago Elie de Beaumont (1837) calculated that in the (then) theoretical replacement by magnesium for calcium to form dolomite there would be a volume reduction of 12.3 percent, and an actual porosity determination on one of the Alpine Triassic dolomites by von Morlot (1848) gave a figure of 12.9

percent which seemed to confirm the theory. This gave rise to an idea that secondary dolomites would all be porous, but compactly crystalline ones would be evidence of primary origin (e.g., Bischof, 1859). But this is not an acceptable criterion (van Tuyl, 1916a).

In studying the Bighorn dolomite, Blackwelder (1913) suggested that the dolomitization occurred penecontemporaneously in the soft sediments, so that no shrinkage is observable. Ground-water percolation is likely to increase the porosity, however, selectively removing nondolomitized calcite (Hardman, 1877; Moresée, 1921; Murray, 1930). Ground water may also take out clay minerals (Canal, 1947). Furthermore, in the case of biohermal replacement the semirigid framework is initially porous (by a nonstipulated amount); early diagenetic replacement is likely to increase the originally large porosity at first, but continued dolomitization (fed by incoming sea water with supplies of Ca^{++} and Mg^{++}) will contribute to a filling of the remaining spaces.

Brecciation is in part due to shrinkage of dolomitic muds during early diagenesis; upon cracking the openings are refilled with still mobile dolomitic mud and recemented as an autoclastic breccia or pseudobreccia.

Late-stage diagenetic dolomites may accordingly be regarded as more likely to be porous than the early, but only with certain reservations. Thus theoretically, the lower the Ca/Mg ratio, i.e., the more complete the replacement, the higher the porosity. Cloud and Barnes (1948) suggest that the greater porosity generally observed with late diagenetic (coarse-grained) dolomites may be related to the coarser fabric. This may permit the easy entrance of ground water (see also Chilingar, 1953). Here again subsequent ground-water percolation may open the pores and leach out less dolomitized parts of fossils; equally well induration may fill many of the pores, though the resultant rock will still tend to be vuggy. These vugs are often lined with dolomite crystals. Clearly, solution here must precede dolomite precipitation but often the two follow one another closely (Landes, 1946).

Although magnesium is less soluble than calcium, dolomites often disclose more solution porosity than limestone (Howard and David, 1936). Hohlt (1948) believes that the ground water moves more freely through formations where the crystals have a preferred orientation; and the calcite of limestones tends to crystallize with the bedding in adjustment to the load, whereas the dolomite crystals tend to have a random orientation.

4. Ca/Mg Ratio and Paleogeographic Significance

From the evidence now available, the proportion of magnesium in marine sediments may be used as a valuable paleoecologic and paleogeographic indicator. Warm shallow conditions are a primary necessity. Thus Chilingar (1953) proposes the use of the Ca/Mg ratio as a "geologic thermometer." The independent value of the calcareous algae as climatic indicators has also been stressed by Pia (1942).

The increasing Ca/Mg ratio with time was first demonstrated by Daly (1907, 1909), and this he believed was due to the different hydrology and higher bottom temperatures of the Precambrian seas. As mentioned earlier, his inorganic explanation of the magnesium precipitation is not now acceptable, but the basic accuracy of the Ca/Mg graph seems to be reliable though slightly modified by Chilingar (see fig. 12).

The curve itself, however, is susceptible to several interpretations. Clearly there seems to have been a progressive decrease in dolomitization from the late Precambrian to the late Mesozoic, but is this due to the possibility that (a) more *complete* dolomitization, through every generation, occurred in rocks that have been exposed to the most varied

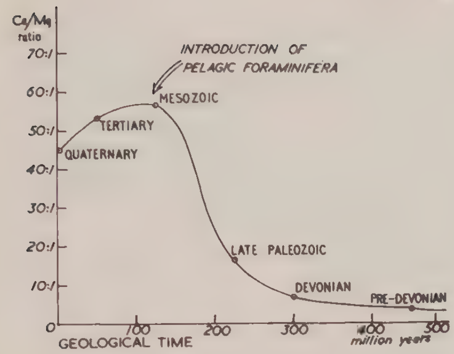

FIG. 12. Graph to illustrate the variation of the Ca/Mg ratio in geological time (based on figures by Daly and by Chilingar). Note that the proportion of dolomites to limestones as illustrated appears to be merely a function of age, though since late Mesozoic there has been a slight increase in the proportion of dolomites in the material available for analysis. This may or may not be due to the introduction of pelagic foraminifera at this stage (see discussion in text).

history? Or (b) that the deeper (? dolomitized) horizons of the younger mountain belts are not yet exposed to sampling? Or (c) that as orogenic belts increased in number and depth of weathering, saturation of the sea in calcium salts has tended to inhibit the precipitation of magnesium (the sea is still undersaturated in magnesium)?

As regards the Cretaceous peak in limestones and chalks, there seems no doubt that this was due to the appearance of pelagic calcareous foraminifera and coccoliths. But it should be noted that the Upper Cretaceous corresponded to one of the greatest thalassocratic (transgressive) epochs of all time. It would therefore automatically contain more limestones than any other epoch. Why are these not dolomitized for the most part? Was it that the foraminiferal oozes do not favor dolomitization owing to lack of porosity, insufficiency of magnesium-rich calcite, or some such "internal" feature? Perhaps the answer is that the greatest transgressions have covered the shield areas and other more stable parts of the crust: many of the resultant sediments have not been deeply buried or folded.

Finally, is not the Quaternary increase of dolomite completely illusory, owing to the incidence of coral atolls during this era? Clearly these are in a special location, and a contemporary regional open-sea dolomitization is not proven.

Utilized with caution, however, there seems no doubt that Ca/Mg ratios could be usefully employed in paleogeographic and paleoecologic reconstructions. The plotting of isodolomitic lines (of equal Ca/Mg ratio) proposed by Chilingar (1953) has much to commend it and may assist the determination of former bathymetry and the general configuration of sedimentary basins. However, care should be exercised not to include figures derived from late-stage and postorogenic dolomites, which will of course be influenced more by subsequent disturbances, structural deformation, etc. Additional caution would have to be applied to those involved in leaching.

5. Continental and Lacustrine Dolomitization

Some continental deposition of dolomite unquestionably takes place. It is often referred to as "Epigene" (e.g., Cayeux, 1935) or "Subsequent Dolomitization" (e.g., Hatch, Rastall, and Black, 1938, p. 193) and this implies subsequent to lithification and *emergence;* it is to be emphasized that "emergence" is a necessary part of the definition, as marine dolomitization may also be subsequent to lithification. In any case continental dolomitization is of little more than academic interest in a study of marine carbonates, and it may be regarded as a normal feature of the carbonate weathering cycle. Joint planes, bedding planes, and erosion surfaces are generally affected.

For example, in the Eifel district of Germany the dolomites were first considered epigene, but Quiring (1913) claimed that there were two generations

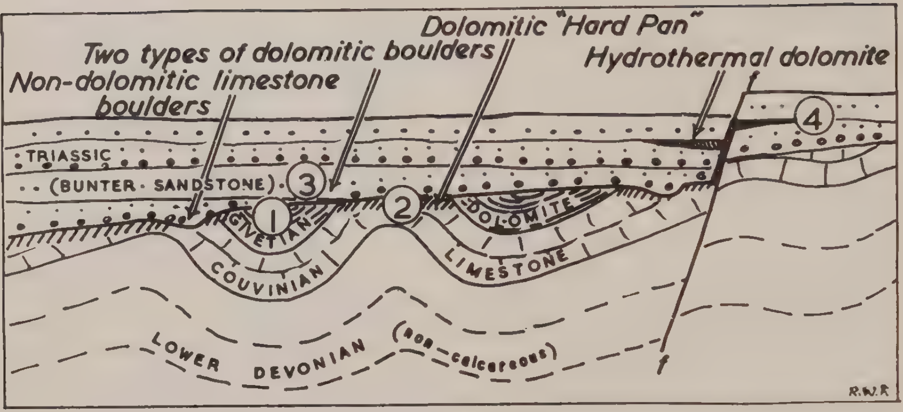

FIG. 13. Four generations of dolomite in the Eifel district of West Germany (adapted from work of Udluft, Reuling, *et al.*). Idealized section showing the Devonian sediments, consisting of noncalcareous Lower Devonian followed by the Middle Devonian Couvinian (low-magnesian) limestone and Givetian (penecontemporaneous) dolomite (1); these were broadly folded in Pennsylvanian-Permian times and peneplaned. During Permian soil formation, magnesium-saturated ground water (exposed to weathering of the Givetian dolomite) led to dolomitization of the bevelled surface layer of the Couvinian limestones, as a continental "hard pan" (2). Uplift led to some dissection of this peneplain, and locally the hard pan was stripped to expose nondolomitized Couvinian limestones. With the progressive invasion of the Triassic sea, (Bunter sandstone) sands were provided by the Lower Devonian, limestone boulders (now red from terra rossa soil formation) by the Couvinian, and dolomite boulders (3) of the two earlier generations. Penecontemporaneous and subsequent faulting, associated with further uplift, allowed hydrothermal solutions in places to introduce a fourth generation of dolomite (4), locally accompanied by ore formation.

of dolomite, the first being Middle Devonian (see fig. 13). Wilckens (1929) found boulders of it in the transgressive Triassic. After detailed surveys, Reuling (1931) confirmed that there is here an extensive (marine) dolomite in the Middle Devonian (Givetian); this sequence was folded during the late Pennsylvanian-early Permian and eroded almost to a peneplain. However, the whole landscape was then covered by a dolomitic cap rock prior to the Triassic transgression. In the synclines, one may observe then two dolomites, but over the anticlines, only the "unconformable" second dolomite capping. This cap is a feature of soil formation, perhaps analogous to laterite or "hard pan" in origin. Struve (1952) went so far as to argue that all the Eifel dolomite *could* be of this sort. Finally, hydrothermal solution, associated with faulting during the Jurassic, introduced local vein dolomites along with lead-zinc ores (Picard, 1954).

Two dolomite generations are observable also in the Carboniferous Limestone (Mississippian) districts of Britain where the subaerial or "subsequent" dolomite crystals show a zonation with hematite, apparently introduced during the weathering of the lateritic land surface of Permian and Triassic times (Dixon, 1907/21; Parsons, 1918, 1922). The similarity in time and environment with the German example suggests paleoclimatic control.

The association of dolomites with fault and fracture systems in this way has been widely reported. In some cases it is simply related to ground water, in others to a distinct disastrophic disturbance, involving both ground water and possible hydrothermal solutions. In most cases a local source of the Mg^{++}-rich solutions is to be found. Thus dolomite has been recently described along fault planes at Abu Roash in Egypt (Faris and Soliman, 1954), but this is only one of countless examples of up and down water-borne movement of Mg^{++} not directly related to the original conditions of sedimentation and concentration (Fondeur *et al.*, 1954).

Continental dolomitization may not be strictly a feature of normal ground-water and subaerial processes, but could be accomplished under swampy or ephemeral lacustrine conditions (Klähn, 1928; Gevers, 1930). Eardley (1938) has found a *double* magnesium calcium carbonate in the waters of the Great Salt Lake of Utah, which are strongly magnesian. Sherman and Thiel (1939) have described how in the floor of glacial Lake Agassiz, under poor drainage conditions, ground water saturated in $MgSO_4$ appears to be altering the calcareous sediments to magnesite and dolomite, leaving some gypsum crystals below. Strakhov (1953) has reported contemporary dolomite precipitation on the shores of Lake Balkash.

As regards the theory of a general origin of dolomites, however, by such subaerial processes as concentration by leaching, proposed by Apjohn (1838) and Grandjean (1844) and developed by Hardman (1877) and by Hall and Sardeson (1895), one can but echo the conclusions of Skeats (1905), Twenhofel (1932), and others, that there is little evidence in favor of it and very much against. Nevertheless, as recently as 1933, Bernauer ascribed alternately banded marine limestone and dolomite in the Alps to this differential leaching.

The suggestion by Judd (1904) that the 16-percent $MgCO_3$ concentrations on Funafuti at 15- to 25-foot depths were due to a marine leaching of the overlying sands is also unacceptable. First, the sands in question average 3-4 percent $MgCO_3$, which is *normal* for such atoll sands. Such sands show little evidence of leaching, according to the writer's observations, while the 16-percent band corresponds to a normal *beach-rock* horizon observed on almost all coral islets, where the $MgCO_3$ is explained by intertidal enrichment. Leaching (but subaerial, *not* marine) certainly occurs in the aragonite-impoverished parts of the bores at Funafuti and the Great Barrier Reef below 100 feet, but here again there is the serious difficulty that the normal concentrations of $MgCO_3$ for such coralline sediments (about 3-4 percent) is maintained. Further, a gigantic column of such rock would have to be leached clean to provide the 500-foot (minimum) thickness of dolomite at the foot of the Funafuti hole.

This rejection of leaching as a general theory of dolomitization is not to be taken as meaning that epigene leaching does not play an important role, but the evidence is rather in favor of a subsequent process, i.e., postdiagenetic dolomitization. It has been noted, for example, that many sediments and fossils normally rich in magnesia are leached without obvious disturbance to their general fabric. In some crinoidal limestones, the $MgCO_3$ is reduced to less than 1-2 percent although the unleached crinoid stems may run about 20 percent $MgCO_3$ (Clarke and Wheeler, 1917). Some interesting calculations might be made as to the total bulk removed in this way. The curious preference for what is normally less soluble $MgCO_3$ was discussed above (under *Regional Dolomitization*), and was studied by Hohlt (1948).

In consequence, ground water in existing dolomite terrains is always very rich in magnesium salts (Clarke, 1924), and it is a normal thing to find secondary magnesia precipitation. The same is true for hydrothermal solutions. Important differences in the form of the deposits may be expected, however, owing largely to the concentrations and temperatures of the magnesia-rich solutions. Quoting Faust and Callaghan (1948, p. 63): "The secondary origin of dolomite through the action of sea water or other cool magnesium-bearing waters on limestone is the result of the tendency to attain the equilibrium state. Slow reaction rates at near-surface temperatures, given sufficient time, produce the same end-product (dolomite) as hydrothermal solutions reacting over a relatively short time interval. Since the reactions proceed at such different speeds the structural and textural relations of the two types of replaced deposits may not be the same."

The reverse process, that is to say, *dedolomitization,* may also take place in special continental environments. According to Cayeux (1935) the term was probably first used by von Morlot (1848). It was used in an entirely different (metamorphic) sense by Teall (1903). Where the ground water is leaching existing saline deposits and becomes a brine, saturated, for example, in $CaSO_4$, according to von Morlot, the following reaction may be expected:

$$CaMg(CO_3)_2 + CaSO_4 \cdot 2H_2O \rightarrow 2CaCO_3 + MgSO_4 + 2H_2O.$$

Alternatively the ground water may carry $MgSO_4$ in the first place, leading to

$$CaMg(CO_3)_2 + MgSO_4 \rightarrow CaSO_4 + 2MgCO_3.$$

Magnesium carbonate liberated in this way would then be available for further epigene deposition (Skeats, 1905; Moresée, 1921; Faust, 1949). Weak acids, notably carbonic, will greatly assist this process (Murray, 1930). In general it seems likely that the CO_2 pressure will be the prime factor in controlling both dedolomitization as well as dolomitization itself (Sander, 1951).

Tatarski (1949) has recently surveyed examples of former dolomites now replaced by calcite; their fabrics were described by Teodorovich (1945). An interesting example was recently quoted by Stewart (1949) from the Eskdale No. 2 bore, in England, which penetrated Triassic evaporites and Permian dolomite. In thin section, a fine-grained anhydrite could be observed "eating" into the dolomite.

An important contribution to this subject has been made by Sander (1951) who noted that in the northern Alps the calcitization of dolomites was really more important than the dolomitization of calcites. Careful study of fabrics is thus of great significance in determining the former extent of regional dolomites.

VII. SUMMARY ON DOLOMITIZATION

1. The mineral dolomite, $CaMg(CO_3)_2$, is not found in rock-forming accumulations on the sea floor today, or at shallow depth in Recent marine sediments. Isolated euhedral rhombohedra of dolomite are apparently authigenic, since some contain inclusions of glauconite, another authigenic mineral formed by chemical alteration on the sea floor; these authigenic dolomite crystals are rather uniformly the same size (10-20 microns) and restricted to fairly deep sea environments (500-2000 fathoms) within 300 miles of the coast. Traces of dolomite are suspected from X-ray work on Recent intertidal deposits. In any case, a direct precipitation of the double carbonate is not proven.

2. The mineral magnesite, $MgCO_3$, is not found in the strictly marine environment, but only in intermediate facies, in the lagoonal evaporites. The hydrated form, nesquehonite, $MgCO_3 \cdot 3H_2O$, is generally restricted to mineralized areas.

3. Calcite, containing up to 30 percent magnesium carbonate in solid solution, is fixed organically on a large scale in shallow warm marine environments. Experimentally it has been fixed inorganically with up to 8 percent magnesium carbonate and this may take place in nature on coral reef flats, intertidal areas, etc. Aragonite carries little magnesium, but often appreciable strontium carbonate in solid solution.

4. Both high-magnesium calcite and aragonite are unstable or metastable. At normal temperatures (up to 80°F) and pressures (up to say 20 atmospheres), aragonite may, under favorable conditions, invert to calcite almost completely

in the course of 10,000 years. High-magnesium calcite breakdown is slower but is accelerated by pressures of the order of 20 atmospheres (corresponding to a depth of about 100 fathoms or 600 feet). With this instability the $MgCO_3$ is available for conversion to the mineral dolomite, which is 12 percent denser than calcite.

5. The formation of the mineral dolomite, if not by direct precipitation in the marine realm, must be by metasomatic replacement, in which an increase of the Mg^{++} ions takes place, either at the expense of some of the Ca^{++} ions or by filling primary cavities and space made available by the leaching of the more soluble aragonite component.

6. The source of the Mg^{++} ions is by diffusion from the sea, connate water, ground water, and so on.

  a) In the marine realm Mg^{++} ions are provided by sea water. This contains 1.3 parts per thousand of Mg^{++}, and 0.4 part of Ca^{++}. However, according to present beliefs regarding the solubility of these ions in sea water, magnesium is undersaturated, while calcium in warm surface waters is supersaturated. Mg^{++} and Ca^{++} solubility curves in sea water intersect under conditions such as increased alkalinity (pH 9 to 10), elevated temperature, elevated pressure. The alkalinity may be raised by various means such as removal of CO_2 and breakdown of bicarbonates by bacterial action.
  b) Further supply of Mg^{++} ions for late-stage diagenesis, postorogenic and continental dolomitization comes from connate water and ground water. Leaching, dedolomitization, and selective precipitation render many underground waters extremely high in magnesium.

7. The chemical, experimental data on dolomitization show that:

  a) Under normal temperatures and pressures:
    i) $CaCO_3$ and $MgCO_3$ may be precipitated from sea water by increasing the alkalinity.
    ii) As $CaCO_3$ is less soluble in sea water than $MgCO_3$, but $Ca(OH)_2$ is more soluble than $Mg(OH)_2$, the solubility curves intersect under increasing alkalinity, permitting both carbonates to precipitate together. With the pH at about 8.5, $CaCO_3$ precipitates, and at 9-10 $MgCO_3$ falls freely as well.
    iii) Calcite and magnesite, however, form an unstable association, and tend to dissociate (Baer, 1924), and with excess magnesium ions available should theoretically (not proven) tend to recombine as dolomite (Halla, 1935, 1936), even without added temperature or pressure.
    iv) Pure calcite, treated with $MgSO_4$ $MgCl_2$, or merely sea water (kept at a high pH by removal of CO_2), produces a high-magnesium calcite, without recourse to increased temperature or pressure (Rivière, 1939a,b).
    v) Analyses of marine carbonate-secreting plants and the more primitive invertebrates (together with the clastic sedimentary derivatives) suggest that biogenic fixation of high-magnesium calcite is far more important in nature than the inorganic compound.
  b) Under increased temperature and pressure:
    i) With considerable heat or pressure on a wet mixture of $CaCO_3$ and $MgCO_3$, the double carbonate, dolomite, may be synthesized (Sterry Hunt, 1859, 1866).
    ii) With considerable heat and pressure, $CaCO_3$, treated with $MgSO_4$, $MgCl_2$, and other salts, especially in the presence of NaCl, produces solid solutions of $CaCO_3$ and $MgCO_3$ and ultimately dolomite (theory of Haidinger; see von Morlot, 1847; Klement, 1895).

iii) High-magnesium calcite is unstable and with time and only very mild heat or pressure inverts to normal calcite, liberating $MgCO_3$, but as magnesite and calcite are unstable partners (see "(a) (iii)"), in the presence of Mg^{++} saturation, dolomite will form, leaving a residue of low-magnesium calcite if the Mg^{++} is insufficient to convert the entire carbonate available.

c) Under increased CO_2 pressure:
The solubility curves of $CaCO_3$ and $MgCO_3$ also intersect with increased CO_2 pressure, at which point dolomite is theoretically precipitated (Baer, 1924, 1932). This was recently repeated by Chilingar (1956a) and confirmed by X-ray analysis. Increased CO_2 may be obtained in the ocean by
- i) Increase in depth, by a simple hydrostatic pressure increase;
- ii) Bottom circulation, from cold CO_2-rich latitudes;
- iii) Organic activity, at depth, by benthonic organisms, including certain bacteria.

d) Other special environments:
- i) Decay environments in general, rich in CO_2, $(NH_4)_2CO_3$, $(NH_4)_2S$, H_2S, bituminous hydrocarbons, seem to favor dolomite formation (theory of Pfaff; also Udluft, 1929).
- ii) In the presence of small amount of ammonia salts, such as $(NH_4)_2SO_4$, NH_4Cl, etc. (liberated by bacteria in some marine sediments), it is said that dolomite can be precipitated directly from $MgSO_4$ and $MgCl_2$ (Koehler, 1931; Linck, 1937); it may be, however, that this is via the intermediary of magnesium-rich calcite, by rather rapid contemporary metasomatism.

8. Dolomitization by metasomatic replacement of $CaCO_3$ by Mg^{++} is therefore possible in the following environments (see fig. 14):

a) On the sea floor or sea shore:
No important dolomitization occurs at or near the surface of the sea floor, but considerable fixation of Mg-rich calcite occurs, that may become mobilized later (see (b)). However, two exceptional cases of probable dolomitization do occur in nature that may well be called "contemporaneous":
- i) In deep-sea environments, isolated crystals of authigenic dolomite are found at the surface or at shallow depth in Recent sediments that are difficult to explain. They may be derived from Mg-rich calcite fixed by floating (pelagic) algae or foraminifera or by neritic benthonic algae carried seaward after storms; or transported by turbidity flows; or alternatively from chemically (inorganically) fixed Mg-rich calcite, formed *in situ* from isolated bottom water characterized by low CO_2 and high pH. Metasomatism on the surface would be assisted by slow sedimentation. A direct precipitation of dolomite in this environment (increased pressure) does not seem to occur.
- ii) In the intertidal belt of warm shallow-sea environments, unconfirmed indications of isolated dolomite crystals suggest that organically fixed Mg-rich calcite (as grains in newly formed clastics) may become unstable in the presence of heat (from the sun) and high concentration of Mg^{++} owing to evaporation or other alkalinization of sea water (introduced by spray or diffusion from tide pools), leading to dolomite metasomatism.

b) In soft sediments (early diagenetic stage):
Metastable aragonite and Mg-rich calcite buried under a blanket of youthful sediments and subjected to increasing pressure, with adequate supplies of Mg^{++} ions from sea-water diffusion, seem to provide a primary

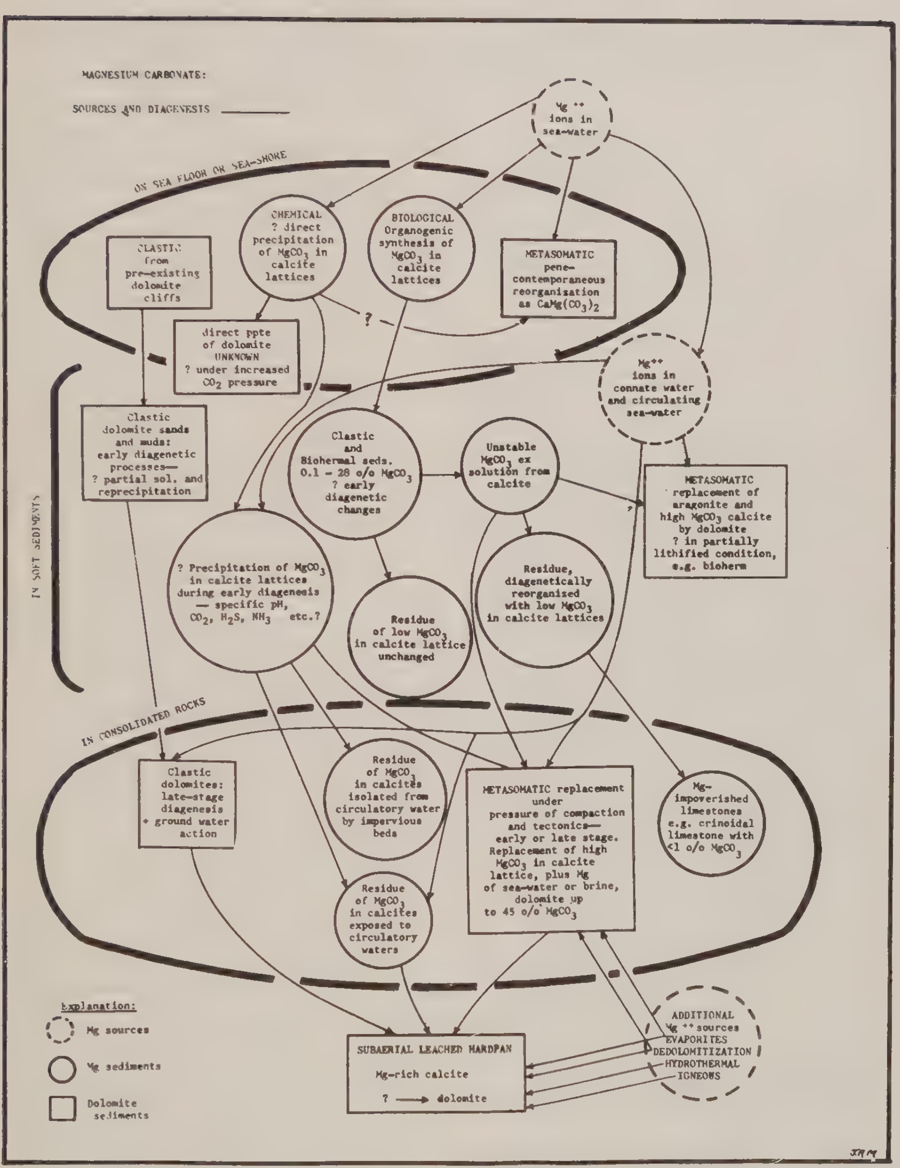
MAGNESIUM CARBONATE:
SOURCES AND DIAGENESIS
ON SEA FLOOR OR SEA-SHORE
IN SOFT SEDIMENTS
IN CONSOLIDATED ROCKS
Mg^{++} ions in sea-water
CLASTIC from pre-existing dolomite cliffs
CHEMICAL ? direct precipitation of $MgCO_3$ in calcite lattices
BIOLOGICAL Organogenic synthesis of $MgCO_3$ in calcite lattices
METASOMATIC pene-contemporaneous reorganization as $CaMg(CO_3)_2$
?
direct ppte of dolomite UNKNOWN ? under increased CO_2 pressure
Mg^{++} ions in connate water and circulating sea-water
Clastic dolomite sands and muds: early diagenetic processes— ? partial sol. and reprecipitation
Clastic and Biohermal seds. 0.1 – 28 o/o $MgCO_3$? early diagenetic changes
Unstable $MgCO_3$ ex solution from calcite
METASOMATIC replacement of aragonite and high $MgCO_3$ calcite by dolomite ? in partially lithified condition, e.g. bioherm
? Precipitation of $MgCO_3$ in calcite lattices during early diagenesis — specific pH, CO_2, H_2S, NH_3 etc.?
Residue of low $MgCO_3$ in calcite lattice unchanged
Residue, diagenetically reorganized with low $MgCO_3$ in calcite lattices
Clastic dolomites: late-stage diagenesis + ground water action
Residue of $MgCO_3$ in calcites isolated from circulatory water by impervious beds
METASOMATIC replacement under pressure of compaction and tectonics— early or late stage. Replacement of high $MgCO_3$ in calcite lattice, plus Mg of sea-water or brine, dolomite up to 45 o/o $MgCO_3$
Mg-impoverished limestones e.g. crinoidal limestone with <1 o/o $MgCO_3$
Residue of $MgCO_3$ in calcites exposed to circulatory waters
Explanation:
Mg sources
Mg sediments
Dolomite sediments
SUBAERIAL LEACHED HARDPAN
Mg-rich calcite
? ⟶ dolomite
ADDITIONAL Mg^{++} sources
EVAPORITES
DEDOLOMITIZATION
HYDROTHERMAL
IGNEOUS
JRM

FIG. 14. Four locations in the evolution of marine magnesian sediments to dolomite are: (i) on the sea floor (strictly marine), or on the seashore (and evaporite lagoons, i.e., Intermediate Class); (ii) in soft unconsolidated sediments (still marine, i.e., penecontemporaneous metasomatism or "early diagenetic"); (iii) in consolidated rocks (subsequent metasomatism or "late diagenetic"—may be pre- or postorogenic); (iv) continental (subaerial, leached "hard pan," a soil formation or ground water phenomenon). Not shown are special locations—evaporite lagoons, magnesian lakes, hydrothermal springs, etc.

raw material for dolomite metasomatism. Adequate supply of Mg^{++} depends on grain size or porosity of the initial formation.

Porous or clastic sediments are thus a *sine qua non*. However, the dolomitization process generally shows an initial preference for the finer-grained clastics.

An ideal site, providing a fairly rigid, but extremely porous and cavernous framework, is a coral reef foundation or similar biohermal structure. Within the core of a pervious atoll the following conditions may be provided: unstable raw material, unlimited Mg^{++} solutions in a saturated state owing in part to an increased pressure but also to high alkalinity, and reducing condition owing to removal of oxygen from the incoming water by organic activity in the outer atoll wall; bacterial action will remove further oxygen from the sulfates and bicarbonates of the sea water, further increasing the alkalinity. After the initial nuclei of dolomite develop from the Mg-rich calcites, complete dolomitization of the entire calcite formation may follow, provided the permeability is maintained.

As regards the impervious or extremely fine-grained sediments, it is difficult to see how the necessary supply of Mg^{++} ions could enter into such a formation as one of the pelagic ooze class, say, a globigerina ooze. Kullenberg core samples, even of great length, of globigerina oozes from many parts of the deep ocean have not disclosed the development of dolomite. With advanced diagenesis, elevation above sea level, jointing, and the availability of ground water, a totally different condition is developed (see under (c)).

c) In consolidated sediments (late diagenetic stages):

It is difficult to determine precise stages during later diagenesis, but broadly there may be distinguished pre- and postorogenic stages, and if there have been multiple movements then of course more.

i) "Preorogenic stage" implies that the sediment has become well cemented and probably elevated but not seriously folded or sheared. Since no orogenic disturbance may have occurred, this class is generally referred to as merely as "late diagenetic." Joint planes will have developed giving connate water mobility and ground water access to otherwise less pervious formations. In carbonate rocks solution effects provide additional access to waters possibly saturated in Mg^{++}. Dolomitization possibly initiated at stage (b) may now proceed. However, it appears unlikely that limestones originally very low in magnesium, such as those of cold deep-water facies, would become dolomitized; the nuclei provided by the unstable high-magnesium calcites would be absent and the supply of additional Mg^{++} in solution would not be assisted by leaching, unless located in the same stratigraphic column as magnesium-rich evaporites or neritic formations.

ii) "Postorogenic stage" implies that advanced deformation has led to much more extreme jointing, shearing, and faulting, thus opening up far more of the fine-grained sediments to artesian and ground-water circulation. Pressure effects, particularly shearing pressures, have been demonstrated to materially assist dolomitization. Thus, for any one formation of fairly uniform constituents the degree of dolomitization tends to be less away from any orogenic zone (theory of van Hise). Regional pressure often seems to have instituted a regional dolomitization that transcends the original high-magnesium limestone beds.

> In the most advanced stage where actual metamorphism takes place, recrystallization tends to inhibit further ground-water movement and thus dolomitization ceases.

9. Continental dolomitization is distinct from the marine class which has been the main subject of inquiry, but the Mg^{++} for epigene continental dolomites may be derived by leaching or dedolomitization of those dolomites due to diagenesis of marine sediments. Thus there are dolomitic "hard pans," which are developed during soil formation over peneplaned land areas containing magnesium-rich rocks, probably in the same way as laterite is formed under semitropical climatic conditions. Magnesium-rich terrains also lead to lake and swamp dolomites, as well as certain hydrothermal dolomites.

10. Ca/Mg ratio and paleogeographic implications. Dolomitization in stages (see "8," (a), (b), (c)) may explain in part Daly's (1907, 1909) fundamental statistics of the magnesium geoeconomy, i.e., that the oldest periods contain the most dolomite in proportion to limestone. The oldest rocks have had the greatest opportunity to suffer late diagenetic and postorogenic metasomatism. However, it should be added that paleogeographic studies show conclusively that the Proterozoic and Paleozoic epochs were marked by far wider epicontinental seas than exist today, and that calcareous algae, the most active secreters of magnesium-rich calcite, were infinitely more widespread. Both Chave and Chilingar have demonstrated that in marine organisms, for each particular class, the higher the temperature of the water, the higher the magnesium in solid solution in the skeletal calcite. Thus regional dolomitization is favored by the warm epicontinental seas of thalassocratic periods.

11. Unsatisfied problems regarding dolomite are still numerous; they include:

a) The hydrologic question: Was the salinity of sea water the same during the Proterozoic and Paleozoic as now? And was not the CO_2 pressure higher, as suspected by a number of workers (Strakhov, 1953; Chilingar, 1956a,b; Cooper, 1956)? In any case a contemporaneous metasomatism of unstable high-magnesium algal debris would be possible if the marine magnesium salts were near saturation close to the bottom.

b) The contemporary deep-sea problem: Weynschenk and some others suggest that dolomitization is going on today at some depth in deep-sea carbonate oozes. The overall depth satisfies the pressure requirement, but the fine-grained character of the sediment will not favor unlimited access by Mg^{++}-rich solutions. No deep-sea core of sufficient length has yet been able to test this hypothesis.

c) The problem of the primary precipitate: So far there is very little evidence to support the idea of any primary precipitation of dolomite in the marine realm, either now or in the past. All cases ultimately seem to come down to magnesium enrichment and metasomatic replacement. Modern spectrometric work on the carbon isotopes may ultimately solve the problem. Wickman, Blix, and Ubisch (1951) have determined from the C^{12}/C^{13} ratios of 45 carbonate samples that all the dolomites show an enrichment of the heavy carbon isotope (see discussion also in Craig, 1953). Paleotemperature work by means of oxygen isotopes may also assist the matter (Rankama, 1954; Urey, Lowenstam, *et al.*, 1950; Teis, 1951). Determination of Mg^{24}/Mg^{25} ratios may further indicate the extent of metasomatism (Ingerson, 1953).

d) What is the nature of the apparently inorganic enrichment of magnesium that seems to occur in organic debris after death in relatively shallow water (Mägdefrau's evidence), or in relatively deep-sea calcareous oozes (over 1000 fathoms)? Most recent deep-sea expeditions have ignored $MgCO_3$ analyses; it is possibly not too late for many core samples to be examined for $MgCO_3$. Does the Mg/Ca ratio rise as one goes down in each core? Or is the ratio increase merely a function of water depth? Cayeux (1935, p. 414) has suggested that the organically fixed magnesium-rich calcite nuclei form "centers of attraction" for further (inorganic) magnesium growth. Beales (1953) speaks of their "trigger effect."

e) More information is needed on the factors—especially pH, pressure, time—that control the stability/instability of aragonite and high-magnesium calcite.

f) If aragonite carries relatively large quantities of $SrCO_3$ in solid solution, as calcite carries $MgCO_3$, what becomes of the strontium when the aragonite is dolomitized? Only sparse traces of strontium are reported from dolomites (Odum, 1950). No significant trend is noted by Chilingar (1956a) in determining the Sr/Ca ratio of many ancient limestones and dolomites.

12. As promised at the beginning, an attempt should now be made to answer a number of questions on various aspects of dolomitization which were asked of different speakers at this symposium.

i) "Do we know of any calcium magnesium carbonates or dolomite being deposited in the oceans today?" . . . *Yes,* but in small quantities only. The isolated crystals are idiomorphic and may be primary precipitates, but are most likely formed by contemporary metasomatism, i.e., *before* burial.

ii) "What is the validity of the concept of 'penecontemporaneous' dolomitization?" . . . *True,* most metasomatism probably begins soon after burial at a critical depth in the ocean (several hundred feet below sea level), but *not all* dolomitization is of this sort, and in many formations several stages may be recognized (see (iii)).

iii) "At what phase of diagenesis does dolomitization begin?" . . . In some cases *soon after burial;* in others *after consolidation;* or, *after emergence and leaching;* again, in others they are *postorogenic.*

iv) "Are the modern 'dolomitized reefs' actually dolomite in the same sense as the ancient dolomite?" . . . Mineralogically and chemically, *yes.* Stratigraphically, *no.* Modern atoll reefs represent a special environment; the Paleozoic facies were probably neritic. Both cases involve essentially the metasomatism of organically fixed high-magnesium calcites.

BIBLIOGRAPHY

ADOLF, G., PULFRICH, M., and LINCK, G., 1921, Ueber die Darstellung des Dolomits und die Dolomit des Röt in der Umgebung von Jena: Centralbl. f. Min. Geol. Pal., pp. 545-558.

AGASSIZ, A., 1888, Three cruises of the "Blake": New York & London, 2 vols. (Also Bull. Mus. Comp. Zoo., vols. 14, 15.)

ANDERSON, W. S., 1889, The solubility of lime in fresh and sea water: Proc. Roy. Soc. Edin., v. 16 (1888-9), pp. 319-324.

APJOHN, J., 1838, Analysis of some Irish dolomites: Journ. Geol. Soc. Dublin, v. 1, pp. 368-381.

ARRHENIUS, G., 1952, Sediment cores from the East Pacific: Repts. Swedish Deep-Sea Exped. 1947-48, v. 5, no. 1.

ATKINS, W. R. G., 1930, Some geochemical applications of measurement of hydrogen ion concentration: Sci. Proc. Roy. Dublin Soc., n.s., v. 19, pp. 455-460.

BÄCKSTRÖM, H. L. J., 1921, Ueber die Affinität der Aragonit-Calcit-Umwandlung: Zeitschr. f. Physik. Chemie (Leipzig), v. 97, pp. 179-222.

BAER, O., 1924, Versuch einer Lösung des Dolomitproblems auf phasentheoretischen Grundlage: Senckenberg. Nat. Gesell., v. 6, pp. 116-118.
———, 1932, Beitrag zum Thema Dolomitentstehung: Centralbl. f. Min. Geol. Pal., Abt. A, pp. 46-62.
BEALES, F. W., 1953, Dolomitic mottling in Pallisser (Devonian) limestone, Banff and Jasper National Parks, Alberta: Bull. Amer. Assoc. Petr. Geol., v. 37, pp. 2281-2293.
BEAUMONT, E. de, 1837, Application du calcul à l'hypothèse de la formation par épigénie des anhydrites, des gypses et des dolomies: Bull. Soc. Geol. France, ser. 1, v. 8, p. 175.
BEHRE, C. H. Jr., 1947, Geochemistry and localization of dolomitization: Journ. Geol., v. 42, pp. 540-542.
BELLINI, R., 1909, Ueber das Vorkommen des Pelagosit auf der Insel Capri: Centralbl. f. Min. Geol. Pal., p. 667.
BERNAUER, F., 1933, Gebänderte Carbonatgesteine und ihre Umwandlung: Neues Jahrb. f. Min. Geol. Pal., B.B. v. 66 (Abt. A), pp. 319-380.
BIRSE, D. J., 1928, Dolomitization processes in the Paleozoic horizons of Manitoba: Trans. Roy. Soc. Canada, v. 22, pp. 215-221.
BISCHOF, G., 1854, Elements of chemical and physical geology: London, Cavendish Soc. (transl. of Lehrbuch der chemischen und physikalischen Geologie), 3 vols. 1854, '55, '59. (Also further in 3rd. German edition, v. 3, 1866, pp. 74-91.)
BLACKWELDER, E., 1913, Origin of the Bighorn dolomite of Wyoming: Bull. Geol. Soc. Amer., v. 24, pp. 607-624.
BOARDMAN, D. C., 1953, The determination of calcium-magnesium ratios in sedimentary rocks: Iowa Acad. Sci., v. 60, pp. 330-332.
BÖGGILD, O. B., 1912, The deposits of the sea-bottom: Report of the Danish Oceanographical Expeditions, 1908-1910, to the Mediterranean etc., v. 1, pt. 3, pp. 255-269.
———, 1916, Meeresgrundproben der Siboga-Expedition: Siboga-Expeditie (Leiden), v. 60, 50 pp.
———, 1930, The shell structure of the mollusks: Danske Vidensk. Selsk. Skr., v. 9, pt. II (2), pp. 235-326.
BOURGEOIS, L., and TRAUBE, H., 1892, Sur la reproduction de la dolomie: Bull. Soc. Franc. Mineralog., Paris, v. 15, pp. 13-15.
BRAMLETTE, M. N., 1926, Some marine bottom samples from Pago-Pago Harbor, Samoa: Carnegie Inst. Washington, Publ. 344 (Pap. Dept. Mar. Biol., v. 23, pp. 1-35).
BRANNER, J. C., 1904, The stone reefs of Brazil: Bull. Mus. Comp. Zoo. (Harvard), v. 44, 285 pp. (Also 1905, Bull. Geol. Soc. Amer., v. 14, pp. 1-12.)
BUCH, K., HARVEY, H. W., WATTENBERG, H., and GRIPENBERG, S., 1932, Ueber das Kohlensäuresystem im Meerwasser: Intern. Counc. Expl. Sea, Rapp. et Proc. Verb., v. 79, pp. 1-70.
BÜTSCHLI, O., 1908, Untersuchungen über organische Kalkgebilde: Abh. K. Gesell. Wiss. Göttingen, n.s., v. 6, pp. 1-164.
CANAL, P., 1947, Observations sur les caractères pétrographiques des calcaires dolomitiques et des dolomies: C. R. Somm. Soc. Géol. France, pp. 161-162.
CAROZZI, A., 1953, Pétrographie des roches sédimentaires: Lausanne (Rouge & Co.), 250 pp.
CAYEUX. L., 1935, Les roches sédimentaires de France. Roches carbonatées (calcaires et dolomies): Paris (Masson), 463 pp.
CHAMBERS, C. O., 1912, The relation of algae to dissolved oxygen and carbon dioxide: with special reference to carbonates: Ann. Rept. Missouri Bot. Garden (St. Louis), v. 23, p. 171.
CHAVE, K. E., 1952, A solid solution between calcite and dolomite: Journ. Geol., v. 60, pp. 190-192.
———, 1954, Aspects of the biochemistry of magnesium: Journ. Geol., v. 62, Pt. I. Calcareous marine organisms, pp. 266-283; Pt. 2. Calcareous sediments and rocks, pp. 587-599.
CHILINGAR, G., 1953, Use of Ca/Mg ratio in limestones as a geologic tool: The Compass of Sigma Gamma Epsilon, v. 30, pp. 203-209.
———, 1955, Soviet classification of carbonate rocks and chemically precipitated $CaCO_3$: a review: Bull. Amer. Assoc. Petr. Geol., v. 39, pp. 1885-1889.
———, 1956a, Relationship between Ca/Mg ratio and geologic age: Bull. Amer. Assoc. Petr. Geol., v. 40, pp. 2256-2266.
———, 1956b, Use of Ca/Mg ratio in porosity studies: Bull. Amer. Assoc. Petr. Geol., v. 40, pp. 2489-2493.
———, 1956c, Distribution and abundance of chert and flint as related to the Ca/Mg ratio of limestones: Bull. Geol. Soc. Amer., v. 67, pp. 1559-1561.

CLARKE, F. W., 1904, Analyses of rocks: U.S. Geol. Surv., Bull. 228.

———, 1924, The data on geochemistry: U.S. Geol. Surv., Bull. 770, 5th ed.

———, and WHEELER, W. C., 1922, The inorganic constituents of marine invertebrates: U.S. Geol. Surv., Prof. Paper 124, 2nd ed. (1st ed. 1917).

CLEE, V., 1950, Bibliography on Dolomite: Rept. Comm. on Sedimentation, N.R.C., Washington.

CLOUD, P. E., and BARNES, V. E., 1948, Paleoecology of the early Ordovician sea in central Texas: Rept. Comm. Mar. Ecology, no. 8, (1947-48), N.R.C., Washington, pp. 29-83. (See esp. Dolomite: pp. 45-50.)

COOPER, Byron N., 1956, Primary dolomite?: Min. Ind. Journ. (Va. Poly. Inst.), v. 3, pp. 5-7.

CORRENS, C. W., 1937, Die Sedimente des äquatorialen Atlantischen Ozeans: Wiss. Ergebn. Deutsch. Atlantisch. Exped. Meteor 1925-27, v. 3, Pt. 3, 298 pp.

———, 1939, Pelagic sediments of the North Atlantic Ocean; *In:* Trask, Recent Marine Sediments (Tulsa, Okla., Amer. Assoc. Petr. Geol., Sp. Publ.) pp. 373-395.

CRAIG, H., 1953, The geochemistry of the stable carbon isotopes: Geochim. et Cosmochim. Acta, v. 3, pp. 53-92.

CULLIS, C. G., 1904, The mineralogical changes observed in the cores of the Funafuti borings: The Atoll of Funafuti (Rept. Coral Reef Comm., Roy Soc.), pp. 392-420.

DALY, R. A., 1907, The limeless ocean of Pre-Cambrian time: Amer. Journ. Sci., v. 23, pp. 93-115.

———, 1909, First calcareous fossils and the evolution of limestone: Bull. Geol. Soc. Amer., v. 20, pp. 153-170.

DAMOUR, A., 1851, Note sur la composition des nullipores et quelques corallinées: C. R. Acad. Sci., Paris, v. 32, pp. 253-255.

DANA, J. D., 1849, United States Exploring Expedition, 1838-42: v. 10 (Geology).

———, 1872, Corals and coral islands: New York (2nd. ed. 1875; 3rd. 1890).

DEBYSER, J., 1954, Les horizons biochimiques dans les sédiments actuels: C. R. Somm. Soc. Géol. France, pp. 375-377.

DIEHL, H., GOETZ, C. A., and HACH, C. C., 1950, The versenate titration for total hardness: Journ. Amer. Water Works Assoc., v. 42.

DIXON, E. E. L., 1907-21, Notes on the geology of the South Wales Coalfield: Mem. Geol. Surv., England and Wales, (see esp. pts. 7, 8, 13).

DORLODOT, H. de, 1909, Description succincte des assises du calcaire carbonifère de la Belgique et de leurs principaux facies lithologique: Bull. Soc. Géol. Belg., v. 23, pp. 175-193 (Mem.).

DUPONT, E., 1881, Sur l'origine des calcaires dévoniens et carbonifères de la Belgique: Bull. Acad. Roy. Belg., v. 2, p. 264 (also v. 5, p. 211, 1883).

———, 1882, Les îles coralliennes de Roly et de Philippeville: Bull. Mus. Roy. Hist. Nat. Belg., v. 1, p. 89.

EARDLEY, A. J., 1938, Sediments of Great Salt Lake: Bull. Amer. Assoc. Petr. Geol., v. 22, pp. 1353-1359.

ELSCHNER, C., 1913, Corallogene Phosphat-inseln Austral-oceaniens: Lübeck (Verlag Schmidt), 118 pp.

EMERY, K. O., 1946, Marine solution basins: Journ. Geol., v. 54, no. 4, pp. 209-228.

FAIRBRIDGE, R. W., 1950a, The geology and geomorphology of Point Peron, Western Australia: Journ. Roy. Soc. West. Aust., v. 34 (for 1947-48), no. 3, pp. 35-72.

———, 1950b, Recent and Pleistocene coral reefs of Australia: Journ. Geol., v. 58, pp. 330-401.

———, 1954, Stratigraphic correlation by microfacies: Amer. Journ. Sci., v. 252, pp. 683-694.

FARIS, M. I., and SOLIMAN, S. M., 1954, Dolomitic rocks of Abu-Roash and the adjacent localities: C. R. Congr. Géol. Internat. (Algiers, 1952, XIX), sect. XIII, v. 15, pp. 441-456.

FAUST, G. T., 1949, Dedolomitization, and its relation to a possible derivation of a magnesium-rich hydrothermal solution: Amer. Mineralogist, v. 34, pp. 780-823.

———, and CALLAGHAN, E., 1948, Mineralogy and petrology of the Currant Creek magnesite deposits and associated rocks of Nevada: Bull. Geol. Soc. Amer., v. 59, pp. 11-74.

FONDEUR, C., GOTTIS, M., ROUIRE, J., and VATAN, A., 1954, Quelques aspects de la dolomitisation au Jurassique en France: C. R. Congr. Géol. Internat. (19th, Algiers, 1952), v. 15, pp. 471-491.

FOOTE, H. W., and BRADLEY, W. M., 1914, The isomorphism between calcite and dolomite: Amer. Journ. Sci., v. 37, p. 339.

FORCHHAMMER, G., 1850, On the formation of dolomite: Quart. Journ. Geol. Soc., v. 6, pt. 2, pp. 48-57. (Transl. from Kon. Danske Vidensk. Sels. Forh., 1849, pp. 83-96.)

FORD, W. E., 1917, Studies in the calcite group: Trans. Conn. Acad. Arts & Sciences, v. 22, pp. 211-248.

GARDINER, J. S., 1898, The coral reefs of Funafuti, Rotuma and Fiji, together with some notes on the structure and formation of coral reefs in general: Proc. Camb. Phil. Soc., v. 9, pp. 417-503.

GASKELL, T. F., and SWALLOW, J. C., 1953, Seismic experiments on two Pacific atolls: Occasional Papers, Challenger Soc. (London), no. 3, 8 pp.

GEVERS, T. W., 1930, Terrestrer Dolomit in der Etoscha-Pfanne, Südwestafrika: Centralbl. f. Min. Geol. Pal., Abt. B, pp. 224-230.

GOETZ, C., 1921, Ueber die Entstehung des Dolomits der Muschelkalkschluchten nördlich des Lothringer Hauptsatteis und über den Einfluss von kolloiden Phasen auf die Bildung von Dolomit überhaupt: Geol. Rundschau, v. 12, pp. 138-150.

GOLDICH, S. S., and PARMELEE, E. B., 1947, Physical and chemical properties of Ellenburger rocks, Llano County, Texas: Bull. Amer. Assoc. Petr. Geol., v. 31, pp. 1982-2020.

GOLDMAN, M. J., 1926, Proportions of detrital organic calcareous constituents and their chemical alteration in a reef sand from the Bahamas: Carnegie Inst. Washington, Publ. 344 (Pap. Dept. Mar. Biol., v. 23, pp. 37-66).

GOLDSMITH, J. R., GRAF, D. L., and JOENSUU, O. I., 1955, The occurrence of magnesian calcites in nature: Geochim. et Cosmochim. Acta, v. 7, pp. 212-230.

GOMEZ DE LLARENA, J., 1951, Die Lagerstätten des Sedimentären Magnesite im Paläozoikum der Westpyrenäen: Berg-und Hüttenmännische Monatsheften (Wien), v. 11, pp. 221-227.

GÖNNER, O., 1917, Ueber Pelagosite von der Insel Busi und einigen benachbarten Inseln und Scoglien: Denkschr. Wien. Akad. Wiss., Math.-nat. Kl., v. 92, pp. 29-34. (*In:* W. Ginzberger, Beitr. z. Naturgesch. d. Scoglien und kleineren Inseln Süddalmatiens.)

GRABAU, A. W., 1913, Principles of stratigraphy: New York (Seiler), 1185 pp. (2nd. ed. 1924, 1185 pp.).

GRAF, D. L., and GOLDSMITH, J. R., 1955, Dolomite-magnesian calcite relations at elevated temperatures and CO_2 pressures: Geochim. et Cosmochim. Acta, v. 7, pp. 109-128.

———, 1956, Some hydrothermal syntheses of dolomite and protodolomite: Journ. Geol., v. 64, pp. 173-186.

———, and LAMAR, J. E., 1955, Properties of calcium and magnesium carbonates and their bearing on some uses of carbonate rocks: Econ. Geol. (Fiftieth Ann. Vol.), pp. 639-713.

GRANDJEAN, Berg-Verw, 1844, Die Dolomite und Braunstein-Lagerstätten im unteren Lahn-Thale: Neues Jahrb. f. Min. Geol. Pal., pp. 543-552.

HALL, C. W., and SARDESON, F. W., 1895, The magnesian series of the northwestern states: Bull. Geol. Soc. Amer., v. 6, pp. 167-198.

HALLA, F., 1935, Eine Methode zur Bestimmung der Änderung freien Energie bei Reaktionen des Typus $A(s) + B(s) = AB(s)$ und ihre Anwendung auf das Dolomitproblem: Zeitschr. Phys. Chemie, Abt. A, v. 175, pp. 63-82. (Experimental part with F. Ritter.)

———, 1936, Bemerkungen zur kongruenten Löslichkeit des Dolomits: Nachtrag zu einer vorangegangenen Arbeit: Zeitschr. Phys. Chemie, Abt. A, v. 175, pp. 396-399.

HANZAWA, S., 1940, Micropalaeontological studies of drill cores from a deep well in Kita-Daito-Jima: H. Yabe Jubilee Publ., v. 2, pp. 755-802.

HARDMAN, E. T., 1877, On the Carboniferous dolomites of Ireland: Proc. Roy. Irish Acad., Dublin, ser. 2, v. 2 (1875-1877), pp. 705, 730, etc.

HATCH, F. H., RASTALL, R. H., and BLACK, M., 1938, The petrology of the sedimentary rocks: London (Allen and Unwin), 3rd. ed.

HEIM, Arnold, 1924, Ueber submarine Denudation und chemische Sedimente: Geol. Rundschau, v. 15, pp. 1-47.

HILLS, E. S., 1949, Shore platforms: Geol. Mag., v. 86, pp. 137-152.

HINDE, G. J., 1904, Report on the materials from the borings at the Funafuti Atoll: The Atoll of Funafuti (Rept. Coral Reef Comm., Roy. Soc.), pp. 186-361.

HÖGBOM, A. G., 1894, Ueber Dolomitbildung und dolomitische Kalkorganismen: Neues Jahrb. f. Min. Geol. Pal., v. 1, pp. 262-274.

HOHLT, R. H., 1948. The nature and origin of limestone porosity: Col. Sch. of Mines Quart., v. 43, no. 4, 49 pp.

HOPPE-SEYLER, E., 1875, Ueber die Bildung von Dolomit: Zeitschr. Deutsch. Geol. Gesell., v. 27, pp. 495-530.

HOWARD, W. V., and DAVID, M. W., 1936, Development of porosity in limestone: Bull. Amer. Assoc. Petr. Geol., v. 20, pp. 1389-1412.

HUNT, T. S., 1859, On some reactions of the salts of lime and magnesia and on the formation of gypsums and magnesian rocks: Amer. Journ. Sci., ser. 2, v. 28, pp. 170-187, 365-383.

———, 1866, Further contributions to the history of lime and magnesia salts: Amer. Journ. Sci., ser. 2, v. 42, pp. 49-67.

INGERSON, E., 1953, Nonradiogenic isotopes in geology; a review: Bull. Geol. Soc. Amer., v. 64, pp. 301-374.

IRVING, L., 1926, The precipitation of calcium and magnesium from sea water: Journ. Mar. Biol. Assoc., v. 14, pp. 441-446.

———, and BECKING, L. B., 1926, Observations on the metabolism of corallines: Proc. Soc. Exp. Biol. and Med., v. 22, pp. 162-166.

IURKEVICH, I. A., 1953, Lithologic-geochemical characteristics of carbonate rocks based on CO_2 and insoluble residue: Doklady Akad. Nauk U.S.S.R., v. 92, pp. 1031-1033. (English abstract, see CHILINGAR, 1955: Bull. Amer. Assoc. Petr. Geol., p. 1885.)

JAMIESON, J. C., 1953, Phase equilibrium in the system calcite-aragonite: Journ. Chem. Physics, v. 21, pp. 1385-1390.

JOHNSTON, J., MERWIN, H. E., and WILLIAMSON, E. C., 1916, The several forms of calcium carbonate: Amer. Journ. Sci., v. 41 (4th ser.), pp. 473-512.

JOURDY, E., 1914, Origine et genèse des dolomites sédimentaires: Bull. Soc. Géol. France, ser. 4, v. 14, pp. 279-309.

JUDD, J. W., 1904, The chemical examination of the materials from Funafuti: The Atoll of Funafuti (Rept. Coral Reef Comm., Roy. Soc.), pp. 362-389.

KLÄHN, H., 1928, Süsswasserkalkmagnesiagesteine und Kalkmagnesiasüsswasser: Chemie der Erde (Jean), v. 3, pp. 453-587.

KLEMENT, C., 1895, Sur l'origine de la dolomie dans les formations sédimentaires: Bull. Soc. Belg. de Géol., mém. v. 9, pp. 3-23 (see also: Tschermak's Min. und Petr. Mitth., n.s., v. 14, 1894, pp. 531 et seq.).

KLINE, W. D., 1929, The solubility of magnesium carbonate (nesquehonite) in water at 25° and pressures of carbon dioxide up to one atmosphere: Journ. Amer. Chem. Soc., v. 51, pp. 2093-2097.

KOEHLER, E., 1931, Ueber die Entstehung von Schaumspat und Dolomit: Chemie der Erde, v. 6, pp. 257-268.

KRAMER, W., 1934, Dolomite dikes in the Texas Permian: Journ. Geol., v. 42, pp. 193-196.

KUENEN, P. H., 1947, Two problems of marine geology: atolls and canyons: Proc. Kon. Nederl. Akad. Weten., Afd. Natuurk., sect. 2, v. 43, no. 3, pp. 1-69.

———, 1954, Eniwetok drilling results: Deep-Sea Research (London), v. 1, pp. 187-189.

KULP, J. L., TUREKIAN, K., and BOYD, D. W., 1952, Strontium content of limestones and fossils: Bull. Geol. Soc. Amer., v. 63, pp. 701-716.

LADD, H. S., INGERSON, E., TOWNSEND, R. C., RUSSELL, M., and STEPHENSON, H. K., 1953, Drilling on Eniwetok Atoll, Marshall Islands: Bull. Amer. Assoc. Petr. Geol., v. 37, pp. 2257-2280.

———, TRACEY, J. I., and LILL, G. G., 1948, Drilling on Bikini Atoll, Marshall Islands: Science, v. 107, pp. 51-55.

LANDES, K. K., 1946, Porosity through dolomitization: Bull. Amer. Assoc. Petr. Geol., v. 30, pp. 305-318.

LECOMPTE, M., 1954, Quelques données relative à la genèse et aux caractères écologiques des "recifs" du Frasnien de l'Ardenne: Volume Jubilaire V. van Straelen (Bruxelles, Inst. Roy. Sci. Nat. Belg.), v. 1, pp. 151-180.

LEINZ, V., 1937, Die Mineralfazies der Sedimente des Guinea-Beckens: Wiss. Ergebn. Deutsch. Atlantisch. Exped. Meteor 1925-27, v. 3, pt. 3, pp. 235-262.

LESLEY, J. P., 1879, Notes on a series of analyses of dolomitic limestone rocks of Cumberland County, Pa., . . . : Second Geol. Surv., Pennsylvania (1876-78), MM, pp. 311-362.

LINCK, G., 1909, Ueber die Enstehung der Dolomite: Monatsber. d. Deutsch. Geolog. Gesell. (Berlin), v. 61, pp. 230-241.

———, 1937, Bildung des Dolomits und Dolomitisierung: Chemie der Erde, v. 11, pp. 278-286.

———, 1942, Beobachtungen und ihre Ergebnisse an Gesteinen des mittleren Zechstein

(Hauptdolomit und Grauer Salzton) in Thüringen: Chemie der Erde, v. 14, pp. 312-357.

LINDGREN, W., 1912, The nature of replacement: Econ. Geol., v. 7, pp. 521-535.

LIPMAN, C. B., and SHELLEY, P. E., 1924, The chemical composition of Lithothamnium from various sources: Carnegie Inst. Washington, Publ. 340 (Pap. Dept. Mar. Biol., v. 19, pp. 193-199).

LONGCHAMBON, M., 1914, Sur la rôle de la magnésie dans les cycles sédimentaires: C. R. Acad. Sci., Paris, v. 158, pp. 267-269. (Also *ibid.*, 1914, v. 158, pp. 131-134.)

LOWENSTAM, H. A., 1952, Some new observations on Niagaran reefs in Illinois: Ill. Acad. Sci. Trans., v. 45, pp. 100-107.

LUCAS, G., 1948a, La sédimentation calcaire. Action du carbonate de sodium sur l'eau de mer: C. R. Acad. Sci., Paris, v. 226, pp. 937-939.

———, 1948b, La sédimentation calcaire: Quelques modalités de l'alcalinisation de l'eau de mer en présence d'ions carboniques: C. R. Acad. Sci., Paris, v. 226, p. 1023.

———, 1952, Premiers résultats d'une étude sur les produits odorants des calcaires fétides: C. R. Acad. Sci., Paris, v. 234, pp. 121-123.

MACFAYDEN, W. A., 1930, The undercutting of coral reef limestone on the coasts of some islands in the Red Sea: Geogr. Journ., v. 75, pp. 27-34.

MÄGDEFRAU, K., 1933, Ueber die Ca-und Mg-Ablagerung bei den Corallinaceen des Golfs von Neapel: Flora, n.s., v. 28, pp. 50-57.

———, 1942, Paläobiologie der Pflanzen: Jena (Fischer). See esp. p. 203.

MARSHALL, P., 1930, Geology of Rarotonga and Atiu: Bull. Bernice P. Bishop Mus. (Honolulu), no. 72.

MAYOR, A. G., 1924, Rose Atoll, American Samoa: Carnegie Inst. Washington, Publ. 340 (Pap. Dept. Mar. Biol., v. 19, pp. 73-91).

MILLER, J. P., 1952, A portion of the system calcium carbonate-carbon dioxide-water, with geological implications: Amer. Journ. Sci., v. 250, pp. 161-203.

MITCHELL, A. E., 1923, Studies on the dolomite system: Journ. Chem. Soc., v. 123, pp. 1055-1065, 1887-1904.

MONAGHAN, P. H., and LYTLE, M. L., 1954, Origin of calcareous oöliths: (Abstract) Bull. Geol. Soc. Amer., v. 65, p. 1287.

MORESÉE, G., 1921, Observations relatives a la grande dolomie (V. I by): Ann. Soc. Géol. Belg., v. 44 (1920-21), pp. B193-199.

MORLOT, A. von, 1847, Ueber die Dolomit und seine künstliche Darstellung aus Kalkstein: Haidinger, Nat. Abh., v. 1, p. 305. (Also: Sur l'origine de la dolomie: C. R. Acad. Sci., Paris, v. 26 (1848), pp. 311-315.)

MURRAY, A. N., 1930, Limestone oil reservoirs of the northeastern United States and of Ontario, Canada: Econ. Geol., v. 25, 452-469.

MURRAY, J., and IRVINE, R., 1891, On coral reefs and other carbonate of lime formations in modern seas: Proc. Roy. Soc. Edin. (A), v. 17, 1889/90), pp. 79-109.

———, and PHILIPPI, E., 1908, Die Grundproben der Deutsche Tiefsee-Expedition: Deutsch. Tiefsee-Exped. (Valdivia), 1898-1899, v. 10, pp. 79-206.

———, and RENARD, A. F., 1891, Deep-sea deposits. Rept. on the voyage of HMS Challenger 1873-1876, 525 pp.

NATTERER, K., 1899, Chemisch-Geologische Tiefseeforschung: Expeditionen der Schiffe *Pola* und *Taurus* in das östliche Mittelmeer, Marmara-Meer und Rote Meer: Geog. Zeitschr., v. 5, pp. 190-209, 252-260 (also: Denkschr. K.K. Akad. Wiss., Wien, vols. 59, 60, 61, 65; 1892, '93, '94, '98).

NEWELL, N. D., et al., 1953, The Permian reef complex of the Guadalupe Mountains region, Texas and New Mexico—A study in paleoecology: San Francisco (Freeman), 236 pp.

NICHOLS, H. W., 1906, Nodules from the Challenger and Argus Banks in the Atlantic Ocean: Field Columbian Mus. (Chicago), pub. 3, Geol. Ser. 3, pp. 40-50.

NOLL, W., 1934, Geochemie des Strontiums: Chemie der Erde, v. 8, pp. 507-600.

ODUM, H. T., 1950, Biogeochemistry of strontium: Yale Univ., Ph.D. Thesis. (See also: 1950. Strontium biogeochemistry, ecosystems, and paleoecological tools: Rept. Comm. Mar. Ecol. and Paleoecol., no. 10 (1949-50), N.R.C., Washington, pp. 55-58. Also: 1951. Notes on the strontium content of sea water: Science, v. 114, p. 214).

OSMOND, J. C., 1954, Dolomites in Silurian and Devonian of east-central Nevada: Bull. Amer. Assoc. Petr. Geol., v. 38, pp. 1911-1956.

———, 1956, Mottled carbonate rocks in the Middle Devonian of eastern Nevada: Journ. Sed. Petr., v. 26, no. 1, pp. 32-41.

PARSONS, L. M., 1918, Dolomitisation and the Leicestershire dolomites: Geol. Mag., v. 55, pp. 246-258.

———, 1922, Dolomitisation in the carboniferous limestone of the Midlands: Geol. Mag., v. 59, pp. 51-63, 104-117.

PETTERSSON, H., 1949, Exploring the bed of the ocean: Nature, v. 164, pp. 468-470.

PETTIJOHN, F. J., 1949, Sedimentary rocks: New York (Harper Bros.), 526 pp.

PFAFF, F. W., 1895, Beiträge zur Erklärung über die Entstehung des Magnesits und Dolomits: Neues Jahrb. f. Min. Geol. Pal., Beil.-Bd. 9, pp. 485-507.

———, 1907, Ueber Dolomit und seine Entstehung: Neues Jahrb. f. Min. Geol. Pal., Beil.-Bd., 23, no. 3, pp. 529-580.

PHILIPPI, E., 1907, Ueber Dolomitbildung und chemische Abscheidung von Kalk in heutigen Meeren: Neues Jahrb. f. Min. Geol. Pal., Festband, pp. 397-445.

———, 1908, Die kontinentale Trias; *In:* Lethaea geognostica. Stuttgart (Schweizerbartsche Verlag.), pt. 2, v. 1, pp. 1-105.

PIA, J., 1942, Uebersicht über die fossilen Kalkalgen und die geologischen Ergebnisse ihrer Untersuchung: Mitt. Alpenländ. Geol. Verein (Wien), v. 33 (1940), pp. 11-34.

PICARD, K., 1954, Beiträge zur Erforschung der Bleierzlagestätte bei Mechernich (Eifel): Geol. Jahrb., Hanover, v. 69, pp. 653-680.

QUIRING, H., 1913, Eifeldolomit und alttriadische Verebnung: Centralbl. f. Min. Geol. Pal., pp. 269-271.

RANKAMA, K., 1954, Isotope geology: London (Pergamon Press), 536 pp.

RAYMOND, P. E., 1925, A possible factor in the formation of dolomite: (Abstract) Bull. Geol. Soc. Amer., v. 36, p. 168.

REULING, H. T., 1931, Dolomit-Studien im Devon der Eifel: Senckenbergiana (Frankfurt), v. 13, pp. 271-293.

———, 1934, Der Sitz der Dolomitisierung: Versuch einer neuen Auswertung der Bohr-Ergebnisse von Funafuti: Abh. Senckenberg. Nat. Gesell. (Frankfurt), no. 428, 44 pp.

REVELLE, R. R., 1934, Physico-chemical factors affecting the solubility of calcium carbonate in sea water: Journ. Sed. Petr., v. 4, pp. 103-110.

———, and FLEMING, R. H., 1934, The solubility product constant of calcium carbonate in sea water: Proc. Fifth Pac. Sci. Congr. (Canada, 1933), v. 3, pp. 2089-2092.

RICHTHOFEN, F. von, 1860, Geognostische Beschreibung der Umgebung von Predazzo, St. Cassian und der Seisser-Alp in Süd-Tyrol: Gotha.

RITTENHOUSE, G., 1949, Petrology and paleogeography of Greenbrier formation; dolomite and dolomitic limestones: Bull. Amer. Assoc. Petr. Geol., v. 33, no. 10, pp. 1724-1728.

RIVIÈRE, A., 1939a, Sur la dolomitisation des sédiments calcaires: C. R. Acad. Sci., Paris, v. 209, pp. 597-599.

———, 1939b, Observations nouvelles sur le mécanisme de dolomitisation des sédiments calcaires: C. R. Acad. Sci., Paris, v. 209, pp. 691-92.

———, 1940, L'eau de mer et les sédiments calcaires: C. R. Somm. Soc. Géol. France, no. 5, pp. 40-42.

———, 1941, Sur le réserve alcaline et les carbonates de l'eau de mer: C. R. Somm. Soc. Géol. France, pp. 19-20.

RODGERS, J., 1954, Terminology of limestone and related rocks: An interim report: Journ. Sed. Petr., v. 24, no. 4, pp. 225-234.

ROWLAND, R. A., and BECK, C. W., 1952, Determination of small quantities of dolomite by differential thermal analysis: Amer. Mineralogist, v. 37, pp. 76-82.

ROZSA, M., 1926, Die Entstehung des Dolomits von Gesichtspunkt der Sedimentation von primären Magnesium Carbonats: Centralbl. f. Min. Geol. Pal., Abt. A, pp. 217-233.

RUBEY, W. W., 1951, Geologic history of sea water. An attempt to state the problem: Bull. Geol. Soc. Amer., v. 62, pp. 1111-1148.

SANDER, B., 1951, Contribution to the study of depositional fabrics (Rhythmically deposited Triassic limestones and dolomites): Amer. Assoc. Petr. Geol. (Tulsa), sp. publ., 207 pp. (transl. by E. B. Knopf from: Beiträge zur Kenntniss der Anlagerungsgefüge: (Rhythmische Kalke und Dolomite der Trias), publ. in 1936, Min. und Pet. Mitt., v. 48, pp. 27-139).

SCHWADE, I. T., 1947, Salt-dolomite intergrowths: Bull. Am. Assoc. Petr. Geol., v. 31, pp. 2208-2214.

SCOBEY, E. S., 1940, Sedimentary studies of the Wapsipinicon formation of Iowa: Journ. Sed. Petr., v. 10, pp. 34-44.

SEWELL, R. B. S., 1935, Studies on coral and coral-formations in Indian waters: Mem. Asiatic Soc. Bengal., v. 9, pp. 461-540.

SHERMAN, G. D., and THIEL, G. A., 1939, Dolomitization in glaciolacustrine silts of Lake Agassiz: Bull. Geol. Soc. Amer., v. 50, pp. 1535-1552.

SKEATS, E. W., 1903, The chemical composition of limestones from upraised coral islands with notes on their microscopical structures: Bull. Mus. Comp. Zoo. (Harvard), v. 42, pp. 53-126.

———, 1905, The chemical and mineralogical evidences as to the origin of the dolomites of Southern Tyrol: Quart. Journ. Geol. Soc., v. 61, pp. 97-141.

———, 1918, The formation of dolomite and its bearing on the coral reef problem: Amer. Journ. Sci., v. 45 (4th ser.), pp. 185-200.

SLOSS, L. L., 1947, Environments of limestone deposition: Journ. Sed. Petr., v. 17, pp. 109-113.

SORBY, H. C., 1879, Anniversary address: Quart. Journ. Geol. Soc., v. 35, Proc. pp. 56-95.

———, 1904, Note on the coral rock of Funafuti: The Atoll of Funafuti (Rept. Coral Reef Comm., Roy. Soc. London), pp. 390-391.

SPANGENBERG, K., 1913, Die künstliche Darstellung des Dolomits: Zeitschr. f. Kryst. u. Min., v. 52, pp. 529-567.

SPOTTS, J. H., 1952, X-ray studies and differential thermal analysis of some coastal limestones and associated carbonates of Western Australia: Univ. of West. Australia, unpubl. thesis.

STEIDTMANN, E., 1911, Evolution of limestone and dolomite: Journ. Geol., v. 19, pp. 323-345, 393-428.

———, 1917, Origin of dolomite as disclosed by stains and other methods: Bull. Geol. Soc. Amer., v. 28, pp. 431-450.

STEWART, F. H., 1949, The petrology of the evaporites of the Eskdale no. 2 boring, east Yorkshire, Pt. 1: Min. Mag., v. 28, pp. 621-675.

STOPES, M. C., and WATSON, D. M. S., 1908, On the present distribution and origin of the calcareous concretions in coal seams known as coal balls: Phil. Trans., Roy. Soc. (London), B, v. 200, pp. 167-218.

STRAKHOV, N. M., 1953, Diagenesis of sediments and its significance for sedimentary ore formation: Akad. Nauk. SSSR Izv., Ser. Geol., no. 5, pp. 12-49.

STRUVE, W., 1952, Zum Problem der Eifler Dolomite: Senckenbergiana, v. 33, no. 1/3, pp. 135-145.

SVERDRUP, H. U., JOHNSON, M. W., and FLEMING, R. H., 1942, The oceans; their physics, chemistry and general biology: New York (Prentice-Hall), 1087 pp.

TARR, W. A., 1920, A possible factor in the origin of dolomite: Science, v. 51, p. 521.

TATARSKI, V. B., 1949, Distribution of rocks in which dolomite is replaced by calcite: Doklady (C. R. Acad. Sci., U.S.S.R.), Moscow, v. 69, pp. 849-851 (See review by: Chilingar, 1956, Bull. Amer. Assoc. Petr. Geol., p. 762).

TEALL, J. J. H., 1903, On dedolomitization: Geol Mag., n.s. Dec. 4, v. 10, pp. 513-514.

TEICHMULLER, M. and R., and WERNER, H., 1953, Ein echter Torfdolomit in einem Flöz der mittleren Bochumer Schichten und die Frage nach der Herkunft der Karbonate im Ruhrkarbon: Geol. Jahrb., Hanover, v. 68, pp. 141-154.

TEIS, R. V., 1951, Isotopic method of determining the temperatures of formation of carbonate minerals: Doklady (C. R. Acad. Sci. U.S.S.R.), Moscow, v. 79, pp. 291-294.

TEODOROVICH, G. I., 1945, Principal types of chemogenous $CaCO_3$ in carbonate sedimentary rocks: Doklady Akad. Nauk S.S.S.R., v. 49, pp. 281-283. (English abstract, see CHILINGAR, 1955: Bull. Amer. Assoc. Petr. Geol., p. 1885.)

———, 1946, On the genesis of the dolomite of sedimentary rocks: Doklady (C. R. Acad. Sci. U.S.S.R.) Moscow, v. 53, pp. 817-820.

THIEL, G. A., 1941, Diagenetic changes in calcareous sediments: Rept. Comm. Sedimentation (for 1940-41), N.R.C., Washington, pp. 81-110.

THORP, E. M., 1935, Calcareous shallow-water marine deposits of Florida and the Bahamas: Carnegie Inst. Washington, Publ. 452, pp. 37-143.

THOULET, J., 1888, De la solubilité de divers minéraux dans l'eau de mer: C. R. Acad. Sci., Paris, v. 108, pp. 753-755.

———, 1890. De la solubilité de quelques substances dans l'eau de mer: C. R. Acad. Sci., Paris, v. 110, pp. 652-654.

TREADWELL, F. P., and REUTER, M., 1898, Ueber die Löslichkeit der Bikarbonate des Calciums und Magnesiums: Zeitschr. f. Anorgan. Chemie (Hamburg and Leipzig), v. 17, pp. 170-204.

TSCHERMAK, G., 1878, Neue Minerale: Pelagosit: (Tschermak's Mineralog. u. Petr. Mitth., n.s., v. 1, pp. 174-175).

TSVETKOV, A. I., 1951, A new fast, chemical and phase analysis of limestones and dolomites: Doklady (C. R. Acad. Sci. U.S.S.R.), Moscow, v. 79, pp. 295-298 (transl. in Petroleum Engineering).

TWENHOFEL, W. H., 1932, Treatise on sedimentation: Baltimore, 2nd. ed., 926 pp.

UDLUFT, H., 1929, Die Genesis der flächenhaft verbreiteten Dolomite des mitteldevonischen Massenkalkes: Jahrb. Preus. Geol. Landesanst. (Berlin), v. 50, pp. 396-436.

———, 1931, Ein neuer Beitrag zum Dolomitproblem: Zeitschr. Deutsch. Geol. Gesell., v. 83, pp. 1-13.

ULRICH, E. O., and SCHUCHERT, C., 1902, Paleozoic seas and barriers in eastern North America: N.Y. State Mus. Bull., v. 52, pp. 633-663.

UREY, H. C., LOWENSTAM, H. A., EPSTEIN, S., and McKINNEY, C. R., 1950, Measurement of paleotemperatures and temperature of the Upper Cretaceous of England, Denmark, and southeastern United States: Bull. Geol. Soc. Amer., v. 62, pp. 399-416.

VAN HISE, C. R., 1904, A treatise on metamorphism: U.S. Geol. Surv., Mon. 47.

VAN TUYL, F. M., 1916a, The origin of dolomite: Iowa Geol. Surv. Ann. Rept. (for 1914), v. 25, pp. 251-422.

———, 1916b, New points on the origin of dolomite: Amer. Journ. Sci., ser. 4. v. 42, pp. 249-260.

———, 1918, Depth of dolomitization: Science, v. 48, pp. 350-352.

VESTERBERG, A., 1901-03, Chemische Studien über Dolomit und Magnesit: Bull. Geol. Inst. Upsala, vols. 5 and 6, pp. 97 and 254.

VINOGRADOV, A. P., 1953, The elementary chemical composition of marine organisms: New Haven (Mem. Sears Foundation Mar. Res., 2), trans.

VISCHNJAKOV, S. G., 1951, Genetische Typen der Dolomitgesteine: Doklady (C. R. Acad. Sci., U.S.S.R.), Moscow, sect. 2, v. 76, pp. 111-114. (Abstract: Centralbl. für Geol. Pal., I, 1951.)

WALLACE, R. C., 1927, Recent work in dolomitization: Rept. Comm. on Sedimentation, N. R. C., Washington, pp. 64-70.

WALTHER, J., 1888, Die Korallenriffe der Sinaihalbinsel. Geologische und biologische Beobachtungen: Abh. K. Sächs. Gesell. d. Wiss. Leipzig, Math-Phys. Cl., v. 14, no. 10. pp. 437-506.

WATTENBERG, H., 1933, Ueber die Titrationsalkalinität und den Kalziumkarbonatgehalt des Meerwassers: Wiss. Ergebn. Deutsch. Atlantisch. Exped. Meteor 1925-1927, v. 8, part 2, pp. 122-231.

———, 1936, Kohlensäure und Kalziumkarbonat im Meere: Fortschr. d. Min. Kristal. u. Petrographie, v. 20, pp. 168-195.

———, 1937, Die Bedeutung anorganischen Factoren bei der Ablagerung von Kalziumkarbonat in Meere: Geol. d. Meere, u. Binnengew. (Berlin), v. 1, pp. 237-259.

———, and TIMMERMANN, E., 1937, Die Löslichkeit von Magnesiumkarbonat und Strontium Karbonat in Seewasser: Kieler Meeresforschungen, v. 2, pp. 81-94.

WELLER, S., 1911, Are the fossils of the dolomites indicative of shallow, highly saline, and warm water seas?: Bull. Geol. Soc. Amer., v. 22, pp. 227-231.

WEYNSCHENK, R., 1951a, The problem of dolomite formation considered in the light of research on dolomites in the Sonnwend mountains (Tirol): Journ. Sed. Petr., v. 21, pp. 28-31.

———, 1951b, A new sedimentary petrological interpretation of the results reported by the Swedish Albatross Deep-Sea Expedition 1947-48: Journ. Sed. Petr., v. 21, pp. 82-84.

WICKMAN, F. E., BLIX, R., and UBISCH, H., von., 1951, On the variations in the relative abundance of the carbon isotopes in carbonate minerals: Journ. Geol., v. 59, pp. 142-150.

WILCKENS, O., 1929, Die Dolomite der Eifel: Sitz.-ber. d. Nat. Abt. d. Niederrhein. Ges. f. Natur.-u. Heilk. (Bonn), for 1928, pp. 1-62.

WOHLMANN, E., 1954, Beitrag zur Kalk-, Dolomit-und Silikatanalyse: Geologie (Berlin), v. 3, no. 6/7, pp. 933-942.

WOOD, A., 1941, Algal dust and the finer-grained varieties of carboniferous limestone: Geol. Mag., v. 78, pp. 192-200.

WÜST, G., 1933, Das Bodenwasser und die Gliederung der Atlantischen Tiefsee: Wiss. Ergebn. Deutsch. Atlantisch. Exped. Meteor 1925-1927, v. 6, pt. 1.

WYCKOFF, R. W. G., and MERWIN, H. E., 1924, The crystal structure of dolomite: Amer. Journ. Sci., v. 8, pp. 448-461.

YOUNG, R. B., 1935, A comparison of certain stromatolitic rocks in the dolomite series of South Africa, with modern algal sediments in the Bahamas: Trans. Geol. Soc. S. Africa, v. 37, pp. 153-162.

ZELLER, E. J., and WRAY, J. L., 1956, Factors influencing precipitation of calcium carbonate: Bull. Amer. Assoc. Petr. Geol., v. 40, pp. 140-152.

ZOBELL, C. E., 1942, Changes produced by microorganisms in sediments after deposition: Journ. Sed. Petr., v. 12, pp. 127-136.

The Inter-American Tropical Tuna Commission
and conservation of the

TUNA & TUNA-BAIT RESOURCES

In the Eastern Tropical Pacific Ocean

by MILNER B. SCHAEFER

Director of Investigations, Inter-American Tropical Tuna Commissioner, Scripps Institution of Oceanography, La Jolla, California

Reprinted from PAN AMERICAN FISHERMAN, May 1956
Reproduced by Permission
Contributions from the Scripps Institution of Oceanography, New Series, No. 898

The Inter-American Tropical Tuna Commission and conservation of the

TUNA & TUNA-BAIT RESOURCES

In the Eastern Tropical Pacific Ocean

By MILNER B. SCHAEFER

THE fishery for tropical tunas, supported by the yellowfin tuna (*Neothunnus macropterus*) and the skipjack, or "barrilete (*Katsuwonus pelamis*) is the most valuable fishery in the Eastern Pacific Ocean. In 1954 it produced 139 million pounds of yellowfin and 174 million pounds of skipjack.

Most of the catch is taken by modern long-range fishing vessels based on the West Coast of the United States. A small but significant quantity is also taken by vessels based in Peru, while smaller quantities are landed in Costa Rica, Ecuador, Chile, Panama and Mexico. The landings in these countries are mostly transshipped frozen to the United States for canning, although small amounts are canned or otherwise used locally.

Over 80% of the catch of tunas is made by pole and line, live bait-fish being used to attract the tuna to the vessel and to induce them to bite. The remainder of the catch is made by purse-seine. Whereas most of the tuna are captured on the high seas, the various fishes used for tuna bait are mostly taken close inshore.

The growth of the fishery is illustrated in Figure 1, showing the landings of tunas, by species, from 1918 through 1954. In the beginning, fishing was conducted in waters not far from the canneries in Southern California. With the development of longer range vessels, and equipment for refrigerating the catch, the fishery expanded rapidly southward, reaching the equator by 1931. Subsequently, the fishery has expanded further southward, along the Peruvian and Chilean coasts, to about the southern limit of distribution of these species.

As may be seen from Figure 1, the growth of the fishery was interrupted during World War II, when many vessels were taken into Naval Service. With the end of the war, the catch rapidly recovered and increased to well above the prewar level. Since 1950, the total catch has fluctuated about 300 million pounds per year.

The Inter-American Tuna Commission

The very rapid post-war growth of the fishery gave rise to considerable concern as to the effects of fishing on the tuna resources and on the bait resources. Only very fragmentary scientific information was available respecting either the tunas or the important bait species, and no one had any information on the effects of the growing fishery on the fish stocks.

In order to make possible the gathering of scientific information respecting the tropical tunas, and the bait-fishes, there was signed in 1949 and ratified in 1950 a Convention between Costa Rica and the United States establishing an Inter-American Tropical Tuna Commission. The purpose of the Commission is to gather and interpret factual information to facilitate maintaining, at a level which will permit maximum sustainable harvests, the populations of tunas and bait-fishes.

The Commission is authorized and directed by the Convention to undertake various kinds of scientific investigations for this purpose, and, on the basis of these investigations, to make recommendations for joint action to the member governments.

The Convention provides that any other nations having an interest in this fishery may adhere by simple exchange of correspondence with existing members. Panama joined the Commission in the fall of 1953.

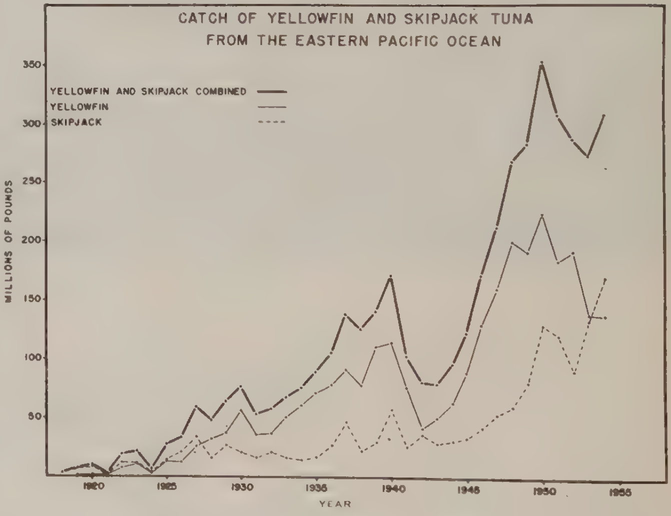

FIGURE 1.—Total landings, by species, of yellowfin and skipjack tunas from the Eastern Pacific 1918-1954.

Dr. Schaefer is Director of Investigations, Inter-American Tropical Tuna Commission, with offices at the Scripps Institution of Oceanography, La Jolla, California; and this article was prepared for a Conference in Ciudad Trujillo on the "Conservation of Natural Resources: the Continental Shelf and Marine Waters" under the sponsorship of the Organization of American States.

The Commission commenced its research in 1951 with a small scientific staff, which has since been increased by additional personnel. After five years of investigations, a great deal of progress has been made on gathering the basic scientific knowledge required for the conservation of the resources. Although much remains to be learned we have now sufficient knowledge to assess the general status of the fishery, and, through continuing observations, will be able to detect any overfishing. Studies of the life history, biology, ecology, behavior, and population dynamics of the species with which we are concerned are being vigorously pursued, in order to provide a sound basis for conservation action at such time as action is warranted.

The staff of the Tuna Commission has been particularly fortunate in having the opportunity to commence its research at a stage of development of the fishery prior to serious overfishing. Very often, scientific research is not commenced on a fishery resource until an economic crisis is brought on by overfishing. In this instance, we have a rather unique opportunity of maintaining the harvest of the fishery and preventing serious overfishing before it occurs.

Research on the Tropical Tunas

Geographical Distribution and Population Relationships

Yellowfin and skipjack tunas occur in all the warm oceans of the world. In the Pacific they are distributed in a wide belt along the equator between the isotherms of approximately 20° C. Off the shores of the Americas, these species are found in commercial abundance from approximately latitude 32° N. to 20° S., appearing seasonally during the summer months at the extremes of the range, but being present throughout the year in the central portion.

Skipjack, which tolerate somewhat lower temperatures than yellowfin, are found somewhat farther to the north and south than the latter species. The commercial fishery extends latitudinally over the entire range, and offshore from the mainland to a distance of some 300 miles, or farther where there are outlying islands such as the Rivella Gigedo Islands, Galapagos, and Clipperton.

The tunas are not found in equal abundance in all parts of this range, but are concentrated in localities where feeding conditions are most favorable, due to oceanographic factors. In Figure 2 is shown the region of the American fishery, with the localities of heaviest concentration shaded in more heavily.

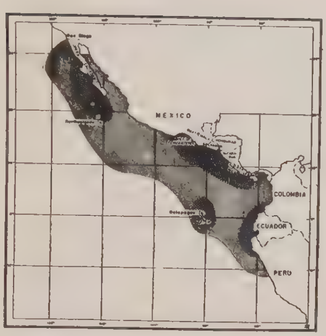

FIGURE 2.—Chart of the Eastern Tropical Pacific showing the region of the tuna fishery with areas of heaviest tuna concentration double cross-hatched.

It is of obvious importance to know whether the tunas found in the region of the American fishery are members of populations indigenous to this region, or whether they are members of larger, trans-oceanic populations. This must be known for considering the magnitude of the catch in relation to the sizes of the resources, determining the regions in which research must be conducted, and outlining areas which must be included in any management measures.

From several lines of evidence (morphometric studies, tagging results, and analysis of catch data) it has been concluded tentatively that the yellowfin tuna of the American fishery belong to a population distinct from those farther westward. So far as skipjack tuna are concerned, the factual information is as yet inadequate for drawing conclusions.

It is also of great importance to determine whether *within* the range of the American fishery there exist distinct or semi-distinct populations, which should be considered as independent biological units in conservation management.

The Commission staff is investigating this matter by means of morphometric comparison of series of specimens from different areas, by tracing migrations of tagged tunas, by analysis of size composition of catches, and by other means. Data are not yet sufficient for drawing firm conclusions. Pending solution of this problem, data on catch, fishing effort, and abundance are being collected by the smallest practical geographical subdivisions, so that they may be subsequently recombined according to whatever natural boundaries may exist.

Collection, analysis, and interpretation of catch statistics

The central problem of the Commission is to measure the effect of fishing on the abundance and yield of the tuna resources, and, in particular, to determine whether the current level of fishing effort is above or below that corresponding to maximum sustainable harvest. In order to accomplish this, it is necessary to measure over a considerable series of years the amount of fishing, the abundance of the tunas, and the magnitude of the catch, for each species.

This sort of data is best obtained from detailed records of the fishery. One of the first tasks of the Commission's staff was, therefore, to gather all available historical data of this sort, and to establish a continuing system of collecting such information on a current basis.

It has been possible to compile information respecting total catch of each tuna species since the early years of the fishery from the records of tuna canners and of governmental agencies in the United States and other countries, and we collect them on a continuing, current basis.

The relative abundance of each tuna species is measured by computing the average catch-per-day-of-tuna-fishing from logbooks, kept by masters of fishing vessels, in which are recorded for each day of fishing the locality and amount of catch.

Since 1951, when we commenced our researches, over 80% of all trips made by vessels landing in the United States have been covered by such logbook records. For earlier years, a number of vessel masters had kept logbooks for their own purposes which they kindly made available to us. An adequate sample of landings are covered by such logbook records since 1947, and some logs are available back to 1930.

For the entire series of years 1934-1954 there are available basic data for nearly the whole U.S. fleet to compute the catch-per-day's-absence-from-port. Fortunately, analysis of the logbook data for years 1936-1953 revealed that there is a fairly constant relationship between catch-per-day's-absence and catch-per-day-of-tuna-fishing, so it has been possible to convert these data fo rearly years, giving us a comparable series of estimates of abundance, as encountered by the fishermen, of each tuna species over the past 20 years.

Since efficiency of fishing varies with vessel size, we compile basic data on catch-per-unit-of-fishing-effort by six vessel-size categories. By comparing records of vessels of different sizes during the same years, we have arrived at correction factors, so that the catch-per-day's-fishing may be corrected to a standard vessel size, to eliminate effects of changes in the average vessel size over the years.

From the catch-per-day's-fishing and the total catch may be computed the total fishing intensity, in standard units, for each year.

Consideration of these series of statistical data leads to valuable conclusions respecting the effect of fishing on the resources of the two tuna species, considering as a whole the populations of each species in the Eastern Pacific.

Figure 3 shows for yellowfin tuna for the years 1934 to date: (1) *total catch* by all vessels of all types, (2) catch-per-day's-fishing of a large sample of U.S. clippers standardized to a particular vessel size, measuring *abundance* as encountered, on the average, by the vessels, and (3) calculated *total effort* in terms of number of fishing days of a standard clipper.

It is quite obvious that as the amount of fishing increased from 1934 to the beginning of World War II, the catch grew quite steadily, but the abundance declined rather steadily also. With a partial respite from fishing during World War II, the catch dropped sharply and the abundance increased. With the rapid postwar increase of fishing effort, the yield increased again but the abundance fell.

From this graph it appears that the intensity of fishing has been sufficiently great to influence the abundance of the yellowfin tuna of the Eastern Pacific. This indicates, of course, only that the amount of fishing is large enough to affect the average size of the standing crop of this species, which is an inevitable consequence of a significantly large fishery, and in itself tells nothing about the relation of present level of exploitation to level of maximum sustained yield. Information respecting this last point required further consideration of the data in the light of some theory of populations dynamics.

The results of such examination of the data have led to the conclusion that the indensity of fishing reached by 1953 was near, or perhaps even slightly beyond, the value corresponding to maximum sustainable catch of yellowfin tuna. The intensity of fishing dropped sharply in 1954, and even more in 1955, due to economic factors, so that there does not appear at this moment to be imminent danger of overfishing. The Commission is, however, keeping careful records of current developments so that recommendations for preventive action can be made if the fishing intensity again climbs rapidly and seems to be going beyond the level of maximum sustainable catch.

The picture for skipjack is quite different. Similar series of measurements of catch, apparent abundance, and fishing effort for this species are presented in Figure 4. It may be seen that during the past 20 years the apparent abundance has shown very wide fluctuations not correlated with amount of fishing effort. Average level of catch-per-day's-fishing in recent years, with very much greater effort and catch than pre-war, is as high as formerly. Ancillary biological and oceanographic data are not yet adequate to determine the causes of the wide fluctuations in apparent abundance, but it seems clear that they are not related to amount of fishing.

It appears that, at present levels of fishing effort, the effect of fishing on this resource is so small that it cannot be measured in the presence of large variations due to other factors. It may be concluded that the skipjack resource can support a much greater total catch than the present before reaching the maximum sustainable average yield.

Tuna life history, biology, and ecology

Although the collection, analysis, and interpretation of statistical catch data are a fundamental element in the research program, they are not, in themselves, adequate as a basis of fisheries conservation management. The detailed interpretation of the catch statistics, in particular the variations *not* related to amount of fishing, as well as the devising of effective and efficient regulatory measures when required, demands an adequate knowledge of the life history of the tunas, of their behavior, and of their relationship to their environment.

These species are creatures of the high seas, leading a completely pelagic existence, usually far out from shore, during their entire lives. Study of them is, therefore, costly and difficult, as a result of which little scientific study of their ways of life has been accomplished until recent years. During the past decade some fisheries scientists of the United States, Japan and other countries, have been able to devote considerable effort to this group of fishes, and our own staff has been conducting researches on them for four years, so that we are beginning to obtain some knowledge of the more important aspects of their biology.

The yellowfin and skipjack tunas, during early years of life at least, aggregate into schools near the sea

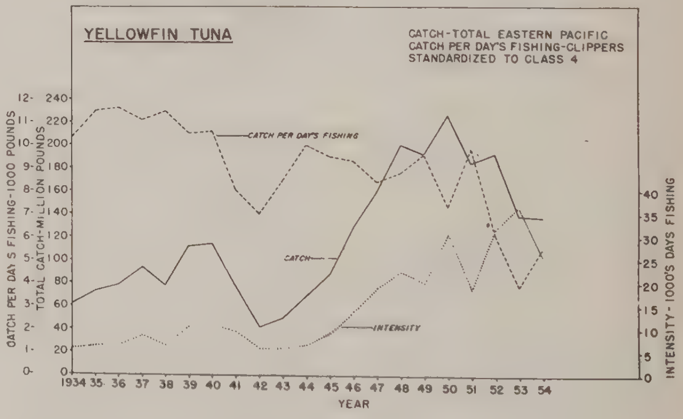

FIGURE 3.—Total catch, standardized catch-per-day's fishing, and calculated relative fishing intensity, for yellowfin tuna in the Eastern Pacific Ocean, 1934-1954.

surface. This habit is the basis of the American fishery, since both pole and line fishing and purse seining depend, for economical operation, on the occurrence of large, compact schools. Analysis of size frequencies of the commercial catch indicates that for both species the bulk of the catch consists of members of only two or three age classes, the youngest fish being probably in the first or second years of life.

In common with many other tropical fishes, the tunas appear to be very rapid-growing and subject to a high rate of natural mortality, so that the turnover of the standing crops of the resources is very rapid compared to that of many commercial fishes of high latitudes. The rapid growth of the tropical tunas, inferred from size frequency data, has been confirmed by direct measurement of the growth of tagged specimens, recovered after several months at liberty in the sea.

Spawning of the tropical tunas occurs over a wide geographical range and over a long season. Some of our recent studies, for example, indicate that yellowfin tuna spawn in waters off Baja California in the vicinity of the Revillo Gigedo Islands from at least May to September.

Off Central America, they spawn some throughout the whole year, with peak activity in the late winter and early spring. It is to be expected that, with a large spawning area and extended spawning season, large variations in year class strength will be less likely than for species having the spawning more concentrated in space and time.

The extent, however, to which variations in year class strength may cause fluctuations in abundance is being investigated by the continuing collection of extensive samples of the catch for measurement of size composition, from many different parts of the region of the American fishery.

This program of "market measurements" was commenced a little over a year ago and it will, of course, be several years before variations in year-class strength will be evident. The size frequency data thus collected are also valuable for inferring age and growth (as noted above), and as one approach to the problem of migrations and population structure, by comparison of the temporal sequence of modes in adjacent geographical areas.

A more direct approach to the problem of migrations and population structure is the employment of tagged fish, the recovery of which gives a direct measure of net movement. Preliminary attempts by scientists of the California State Fisheries Laboratory have yielded some valuable information, indicating movement of several hundred miles in some instances. Rates of recovery of tagged specimens have been so very low, however, that the data are quite inadequate for any firm conclusions as to migration patterns. The staff of the Tuna Commission is now engaged in an intensive effort to develop improved methods of tagging tunas in the hope of achieving a "break through" in this important line of research.

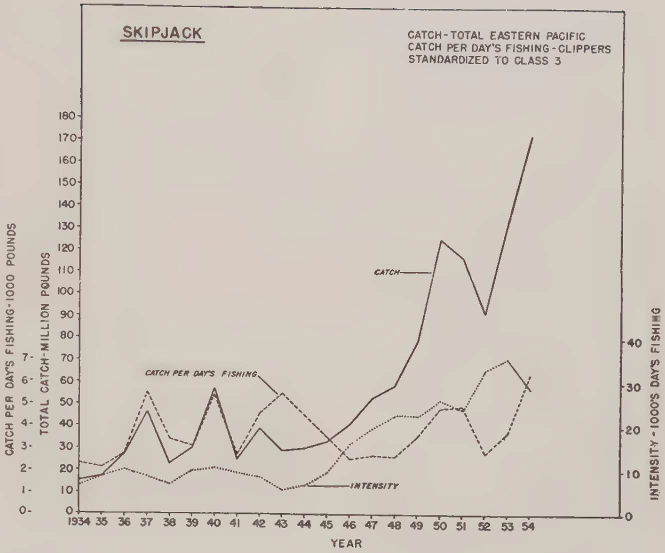

FIGURE 4.—Total catch, standardized catch-per-day's-fishing, and calculated relative fishing intensity, for skipjack tuna in the Eastern Pacific Ocean, 1934-1954.

Investigations of the feeding habits of the tunas by our staff and others in the Eastern Pacific, and by scientists of other agencies in other regions, indicate that the tunas feed quite omnivorously on all forms of pelagic animals encountered on the high seas which are of suitable size, ranging from Euphausids and Squilla larvæ to moderately large Cephalopods and fishes.

The logbook records of the tuna vessels indicate, as has been mentioned previously, that concentrations of tunas tend to be found in certain areas, for example off Baja California, off the Gulf of Tehuantepec (in the early spring), off the Coast of Central America, and in the areas off the northern part of Peru and Ecuador. These regions of concentration correspond, in general, with regions of high production of food organisms, which in turn depends on high production of the phytoplanton upon which all life in the sea depends. It further appears that these regions of high biological productivity are regions where the upper, sunlit layers of the sea are fertilized by the nutrients from the underlying deep waters, by upwelling, by mixing along current boundaries, and other physical processes. Since the circulation of the ocean which brings all this about is not constant, but is subject to variations between seasons and between years, it is probable that at least some of the fluctuations of the tuna fisheries may be cleared up by a better understanding of the oceanic circulation and the causes of its variations. This is a large problem upon which the Tuna Commission, in cooperation with the Scripps Institution of Oceanography and other agencies, has made only a small beginning, but which is being given high priority in our program.

Research on Bait Species

Important special and their distribution

The major share of the tuna catch is made with the use of live bait, taken mostly in inshore waters. Scientific information, to serve as a basis of conserving the bait resources, is therefore of great importance.

Figure 5 indicates the principal baiting areas for the important tuna-bait species, and Figure 6 shows the estimated catch, by species for the years 1947-1954, based on logbooks records of U.S. vessels.

As may be seen from Figure 6, only five species are taken in sufficient quantity to indicate even a remote possibility that the amount of fishing might adversely affect the continuing harvest. These are: The California sardine and northern anchovy taken off California and Baja California; the tropical anchoveta, *Cetengraulis,* taken in various bays from Almejas Bay in Baja California to the Gulf of Guayaquil; the Galapagos sardine; and the southern anchovy (called anchoveta in Peru) taken off the Peruvian Coast.

Of these five species, three are subject to other fisheries much greater in magnitude than the fishing for tuna bait (California sardine, northern anchovy, southern anchovy) and these species are also being studied by other agencies. In view of this, our staff has limited itself to gathering data on the amounts taken by the tuna boats, collecting samples, and otherwise cooperating with the other agencies studying them.

For the Galapagos sardine our studies have been confined to collecting catch data and limited biological examination of samples from tuna vessels. Detailed study of this species is not possible without work by scientists at Galapagos, which we cannot now undertake.

The remaining species, the anchoveta, *Cetengraulis mysticetus,* is the mainstay of the tuna fishery. Because of the importance of this deep-bodied, tropical anchovy to the fishery, and because of lack of knowledge concerning it prior to our reseach, we have concentrated our bait-fish investigations on this species.

Investigation of the anchoveta and other bait species are conducted not only at our headquarters laboratory, but also at regional laboratories in Costa Rica and Panama, which have been established for the purpose of studying the biology and ecology of the bait fishes of the Gulf of Nicoya and the Gulf of Panama, respectively.

Biology, ecology, and life history of anchovetas

Studies of meristic characters of anchoveta specimens from the several important baiting areas has indicated that there is little or no interchange of anchovetas among these areas. The lack of extensive migrations is probably related to restriction of suitable feeding areas for adult stages, which primarily feed by grazing on mud-flats, eating the microscopic plants, and perhaps the organic detritus, which are abundant there. In any event, it appears that the population of each major baiting area should be treated as a separate biological unit.

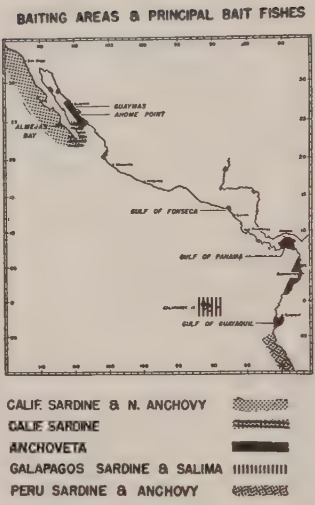

FIGURE 5.—Principal baiting areas in the Eastern Pacific.

In order to obtain some idea of the effect of fishing on the anchoveta populations we have gathered from tuna-vessel logbooks estimates of the amount of fishing in each baiting area for each year from 1947 to date, and the resulting catch, as well as the apparent abundance, measured by the catch-per-day-of-baiting. From these data it appears that the abundance of anchovetas in each of the major baiting areas is subject to wide variations from year to year, but that these are uncorrelated with amount of fishing, and so are probably due to natural factors. We are, of course, continuing to collect similar data currently. Such data are valuable not only for measuring fluctuations in abundance for correlation with possible natural causes, but also to enable us to detect any adverse changes in the anchoveta stocks due to fishing, so that corrective measures can be recommended when and if required.

Analysis of size-frequency data from several baiting areas has made it possible to follow model size-classes over long time periods and thus learn about the age and growth. It appears that this species is very rapid-growing in all areas, reaching 130 to 135 mm. at one year of age, at which time the fish are sexually mature and spawn.

The natural mortality rate is evidently very high, because no fish live very long, although in this respect there appears to be some differences between areas. In Panama most individuals live less than one year. Specimens are seldom taken in their second year of life, and those in the third year almost never. At Guaymas and Ahome Point in the Gulf of California, on the contrary, in some years a considerable share of the catch is composed of fish in their second year of life, and a significant number in their third year.

Since, even with these differences, the anchoveta is everywhere short-lived, and in some places is essentially an annual crop, the observed fluctuations in abundance are not too surprising, when we consider that these are inshore fishes of restricted habitat, the success of reproduction of which is likely to be heavily influenced by variable environmental conditions.

In order to rate the effects of environment on the anchovetas, and in order to work out the details of their life history and biology, continuous investigations of these matters are being conducted in the Gulf of Panama, as well as on the hydrography and the basic biological productivity of the Gulf. At the present time, a concentrated effort is being made to work out the details of the spawning and early larval development of the anchoveta there, as a basis of further

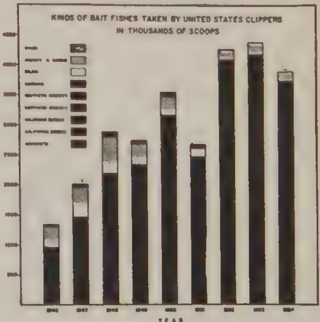

FIGURE 6.—Estimated total catch, by species, of bait-fishes by tuna fishing vessels based in the United States, 1947-1954.

investigations of the distribution and success of spawning in relation to hydrographic factors.

Investigations in the Gulf of Nicoya

The Gulf of Nicoya in Costa Rica was at one time an important bating ground for anchovetas, but the fishery failed after 1947—due, it is believed, to extensive occurrence of "red tides" which wiped out the population. During 1952 and 1953 extensive collecting and observing in all parts of the Gulf failed to produce a single specimen.

In an attempt to rehabilitate this population, the Commission in the fall of 1953 conducted an experimental transplantation of approximately half a million adult anchovetas from the Gulf of Panama. These fish apparently spawned successfully, because in the spring of 1954 we began to catch young, zero-year-class specimens in small numbers. The staff of our laboratory at Puntarenas is continuing to observe this re-established population and to collect hydrographic and other related data in the Gulf of Nicoya.

During 1954 the progeny of the transplanted fish reached maturity and commenced spawning. During 1955 increasing numbers of specimens have been taken in our collections. It appears that the anchovetas are living and reproducing in the Gulf of Nicoya, and that the population is increasing, but still far from sufficient to support any fishery. We shall continue to observe the increase of this population, and to study its ecology and biology.

It is hoped that in a few years the Gulf of Nicoya will again be able to support a fishery for this species. It is, of course, impossible to forecast the rate of increase of the population, but the initial results are most encouraging. It is not to be expected that the Gulf of Nicoya can ever support a bait fishery of the magnitude of the Gulf of Panama, because it lacks the physical conditions for the extremely rich biological productivity of the latter area, and is of smaller extent also.

Summary and Conclusion

It may be seen from the foregoing that the Inter-American Tropical Tuna Commission's research task is not, except in the case of the Gulf of Nicoya, in the nature of an emergency program to rebuild the fish stocks. Both for the tunas and for the bait species our mission is the continuing assessment of the condition of the fish stocks, and the gathering of extensive and adequate scientific information, to make possible the wise and effective regulation of the fishery at such times and places as regulations are shown to be required.

The Commission, in being able to conduct its scientific studies on an international basis, and in a careful, comprehensive, and orderly fashion, will be able to provide the necessary scientific information for effective management when it is required. This is, I believe, an almost unique example in fisheries conservation, and may well serve as an example for other similar problems in this hemisphere and throughout the world. ✶

THE END

EASTROPIC EXPEDITION

By **TOWNSEND CROMWELL**

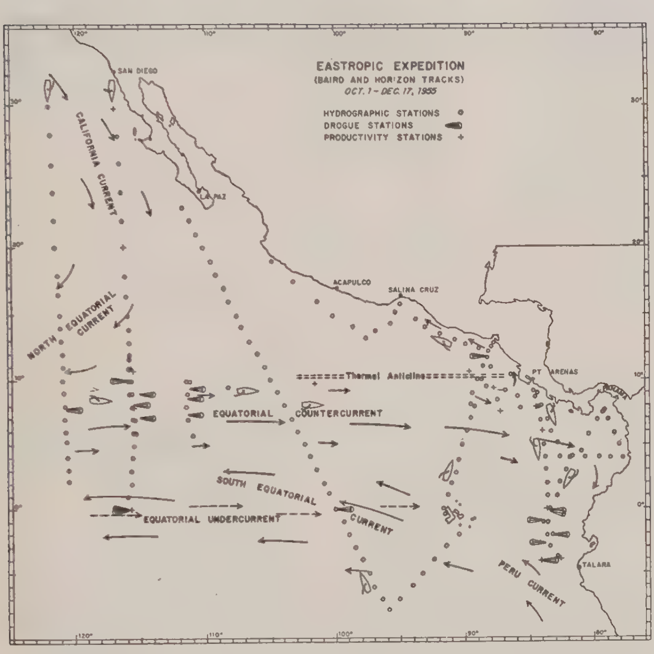

Figure 1

Positions of stations on EASTROPIC Expedition. Major currents shown by arrows.

What it Seeks, and Where it Fits Into Practical Industrial Fishing

● During the fall of 1955, five research vessels operated simultaneously in the eastern tropical Pacific. They were measuring ocean currents, the chemical fertility of the water, and the abundance of small plants and animal plankton which are the basic source of food for all the larger marine animals, including tunas. This effort has contributed to our understanding of the tuna resources in this part of the Pacific ocean.

Representatives of the tuna industry and scientists attending the Fifth Annual Tuna Conference at La Jolla in November of 1954, agreed that such studies should be made. Personnel of the Inter-American Typical Tuna Commission, together with Scripps oceanographers who were especially interested in the tropics, planned that two vessels, the *Baird* and *Horizon* would go south from San Diego to the equator and then in toward the coast, concentrating their measurements in areas of special interest including some well known tuna grounds. The Honolulu branch of the U. S. Fish and Wildlife Service planned to investigate the equatorial currents aboard the *Smith* during the same period, concentrating on the ocean to the west of the Scripps operation.

The California Fish and Game vessel *Scofield* fished longline gear in areas where the findings of the other vessels would help to explain their catches. Peru sent the naval vessel *Bondy* to work from the area between Galapagos and the mainland southward into the Peru Current. Each agency had its own particular interests but by getting data from the same and adjacent ocean regions simultaneously, the inter-relationships among the physics, chemistry and biology can be studied, and explanations for sterile and productive areas sought. This article is concerned mostly with Scripps' part in the work, and the area studied by the two Scripps' vessels is shown in Figure 1.

● It is well known that the ocean is not uniformly productive. In fact, the greater part of the oceans does not support fish in quantities great enough to make commercial fishing worthwhile. Part a. of Figure 2 is an attempt to show why this is so. The drawing illustrates temperature conditions as they are throughout most of the temperate and tropical ocean regions of the world. There is a warm "surface layer" and, just beneath, the "thermocline", a layer through which the temperature decreases rapidly. Below this, the temperature decreases slowly, through the deeper water and all the way to the bottom. There is an abundant supply of nutrients; phosphat, nitrate and the rarer trace elements essential to plant growth, in the thermocline and deep water. But sunlight does not penetrate these layers in sufficient strength for plant growth. On the other hand, there is plenty of sunlight near the sea surface, but lack of nutrients. The surface water is old in the sense that it has been at the surface a long time and plants have used up the nutrients to the extent that their own growth is limited. Plants and animals exist, but not in quantity. Unless the rich water is brought up to renew the sun-lighted zone, there is little biological production. In those places where a mechanism of renewal does exist, plankton thrive and so do fish because they have a source of food. Regions where there is upwelling, vertical mixing, or a thermal anticline, can be productive, and each of

---

Mr. Cromwell is an oceanographer on the staff of the Inter-American Tropical Tuna Commission.

Reprinted from PACIFIC FISHERMAN *July 1956*

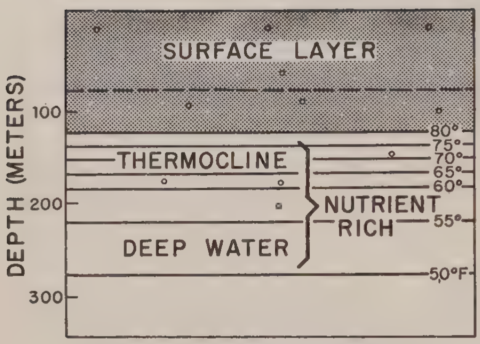

a. STERILE OR BARREN

Figure 2 (a).
See caption, Page 1145

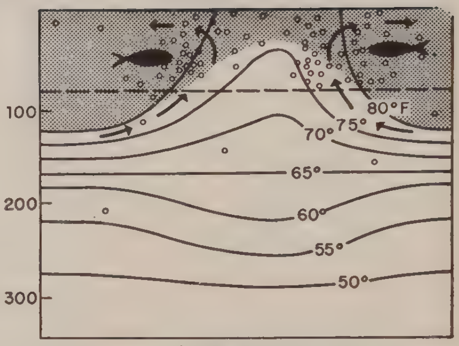

b. UPWELLING

Figure 2 (b).
See caption, Page 1145

these three situations was studied on the expedition.

- Upwelling occurs near the Galapagos Island and westward along the equator for several thousands of miles. In this equatorial band, water is impelled westward by the southeast trades. But the earth's rotation deflects this westward moving surface water northward and southward, away from the equator. Cool, nutrient-rich water comes up from below, as drawn in Figure 2, b., to replace that driven away, and this cool water is productive. Upwelling occurs also along the coast of Peru within the Peru Current which then turns westward toward Galapagos, and this brings up a question, as yet unanswered. Do the tunas, abundant in Galapagos waters, depend on feed developed in locally upwelled water or do they depend ultimately on water that upwelled off distant Peru? Data obtained on the *Baird* and *Horizon* will be studied in conjunction with that obtained close to the mainland by the *Bondy* and farther to the west by the *Smith*, in the hope of discovering the answer.

Furthermore, it is known that a narrow, strong current flows eastward along the equator, submerged beneath westward surface flow. This deeper current, the Equatorial Undercurrent, is nutrient-rich. It was found at two points west of Galapagos (See Fig. 1) by tracking floats attached by fine music wire to parachutes at various depths. This current did not exist at the equatorial station between Galapagos and the mainland. The undercurrent was discovered only recently and its significance to the behavior of tuna, if any, is not known.

- The tuna off Costa Rica live in a "thermal anticline", a place where the thermocline is elevated to a position close to the sea surface, where sunlight can reach it. As shown in Figure 2, c., the thermocline is "humped up" in the shape of a dome or ridge. It can't be detected by surface instruments because there is no continuing motion upward into the surface layer as there is in upwelling. The anticline just sits there, like a hill. Unlike a hill, however, it may move around and change shape, and the water composing it can be renewed by flow and mixing through it. This flow assures a continuing nutrient supply, in a lighted zone, for the phytoplankton to grow in. Measurements on *Eastropic* showed that large amounts of phytoplankton are produced in this region. The anticline extends westward from Costa Rica along roughly 10°N. Clippterton Island lies in it, and this may be one reason for the large tuna catches often made there.

A third situation which enriches the upper, lighted layer of the sea was studied, somewhat by accident, during *Eastropic*. The situation was a gale in the Gulf of Tehuantepec. The first station in the Gulf was occupied in a dead calm, but within a few hours a gale of sustained velocity of 40-50 knot had set in. The surface temperature dropped considerably during the gale, indicating that nutrient-rich waters were being mixed upward from the thermocline. This is a process that probably goes on to a small degree continually in the ocean, but a gale seems to result in a major "charge" of nutrients into the surface layer. Subsequently, phytoplankton, zooplankton and small animals for tuna forage, can develop in this water. In a place like Tehuantepec, where gales occur frequently, this mixing process may be of especial importance, by supporting an unusually large biological stock. One may curse a Tehuantepec Gale when he is running through it with a load of fish, but this same gale may be responsible for a future load. Maybe this is the first good word ever said for a Tehuantepecer.

There are other situations that cause tuna to congregate. The best known of these is a submarine bank, but it must be admitted that a completely convincing explanation for tuna abundance near banks has not been developed.

- At each of the hydrographic survey stations, shown in Figure 1 as circles, measurements were made of surface current and, from the sea surface down to 1000 meters, of temperature, salinity, dissolved oxygen, and inorganic phosphate. These measurements determine the locations of currents and of features like upwelling and the anticline. Zooplankton, also, was measured at each of these stations and the size of the crops was found to vary a great deal and in a manner consistant with the oceanography. High crops were found in the upwelling near the equator and in the termal anticline. The highest plankton catches were made in the Peru Current, near its nothern boundary. In this same region the California Fish and Game vessel *Scofield* made its highest longline catch, primarily of bigeye tuna.

The *Eastropic* expedition work was not confined entirely to these studies of direct bearing on fertility and productivity of the ocean. An intensive study of the Equatorial Countercurrent was made. The geomagnetic electrokinetograph (GEK) measured the surface current. Parachute drogues measured the current at various depths below the surface. The two Scripps ships worked together in this, crossing and recrossing the current for many days to learn

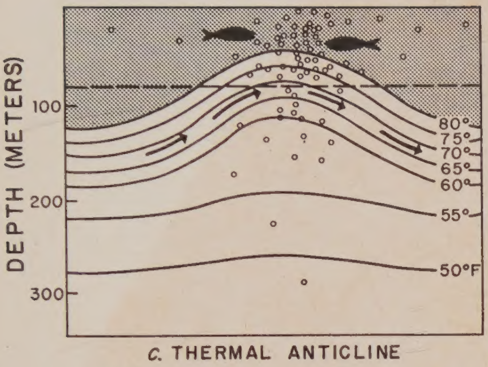

Figure 2 (c).
See caption below.

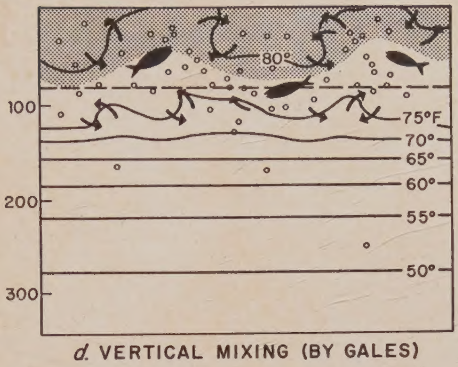

Figure 2 (d).
See caption below.

about its short term variations. The current was found to accelerate and decelerate from one day to the next. Sometimes the surface water was moving most rapidly and sometimes a layer below the surface was fastest. During the two weeks devoted to its study, it varied from a 2-knot current to one of a fraction of a knot. Along the vessel track going east at about 8°N, the Countercurrent stopped completely twice, or else swung to the north or south of the vessel.

A study like this one of the Countercurrent and that of the Undercurrent add to our knowledge of the currents of the tropics, knowledge which is essential to eventual understanding of the distribution of the tuna stocks.

Time is consumed in running from one area of interest to the next. It is frustrating to have to do this, but two important things can be accomplished, so that the steaming time is not wasted. In the first place, it is necessary to describe the extent of the features we're interested in. That upwelling occurs, for example, is important to know, but over how large an area it occurs, is also important. If waters upwell over an area of a few square miles, not as large a biological community can be supported as if the upwelling occurs over thousands of square miles. While running into and out of such an area, we get an idea of how large it is.

- Another value of the long runs is the opportunity to make measurements in the barren as well as the rich areas. This must be done to find reasons for the barrenness or richness. What is the difference between two areas, one productive and the other sterile? What currents or parts of currents are responsible? Some partial answers have been mentioned in terms of upwelling, anticlines and mixing. More complete answers are needed. Only by understanding the important features of the tuna's environment can we hope to understand, and eventually predict, the variations in their abundance due to such features.

A complete report of Sripps' participation in *Eastropic* would discuss numerous additional measurements, but only a few will be mentioned here. Bottom samples were obtained by coring off the Gulf of Fonseca. Prehistoric water conditions will be revealed by these cores. Water samples from 3000 meters will be analysed for content of radioactive carbon. It may be possible to tell, from these analyses, how long ago this deep water was at the surface and something of the rate of the deep circulation may be learned in this way. The distribution of particles suspended in the sea and of carbon dioxide in the atmosphere were measured.

Just what will be learned from some of these measurements is not really known. Unfortunately, nothing at all will be learned from some of them, except not to make the same mistake again. But this is no reason to abandon attempts to make new measurements. It has been said truly that we know less about the water beneath the sea surface than we do of the face of the moon. Efforts like *Eastropic* expedition, we hope, will remedy this situation.

Figure 2.

(a) The 3 major layers in the tropical & temperate ocean. 1.Surface layer (shaded) 2.Thermocline 3.Deep water. Dashed line indicates penetration of sunlight in strength sufficient for production of plankton (small circles). No mechanism exists to enrich the sunlighted zone. Plankton is sparse.

(b) Upwelling carries nutrient fertilizers into the sunlighted zone, plankton increase and larger fishes congregate to feed. It takes time for biological products to develop after water has upwelled, so that plankton are found displaced, downstream, from the center of the upwelling.

(c) The thermocline itself is elevated into strong sunlight, allowing plankton to develop.

(d) An exceptionally strong wind has mixed the surface water with that of the thermocline, making both layers irregular, and, at the same time, enriching the sunlighted zone. It may be weeks after a gale that the plankton develop and fish congregate.

(1200)